Polyhedron Vol. 1, No. 1, pp. 1–7, 1982
Printed in Great Britain.

0277–5387/82/010001–07$03.00/0
Pergamon Press Ltd.

COMPLETE SEPARATION OF THE ENANTIOMERS OF A TETRAORGANOTIN BY CHROMATOGRAPHY ON MICROCRYSTALLINE CELLULOSE TRIACETATE AND FRACTIONAL CRYSTALLIZATION

IVAN VANDEN EYNDE and MARCEL GIELEN*
Vrije Universiteit Brussel, TW-AOSC, Pleinlaan 2, B-1050 Brussel, Belgium

and

GEORGINE STÜHLER and ALBRECHT MANNSCHRECK
Universität Regensburg, Institut für Organische Chemie, Universitätsstrasse 31, D-8400 Regensburg, Germany

(*Received* 18 *May* 1981)

Abstract—Racemic methylneophylphenyltrityltin (**1**) could be resolved completely by chromatography on microcrystalline cellulose triacetate coupled with fractional crystallizations. The influence of temperature on the chromatographic separation of compound (**1**) and of *t*-butylmethylphenyltrityltin (**2**) is described.

INTRODUCTION

Racemic organotin compounds can be partially resolved by inclusion chromatography on microcrystalline cellulose triacetate.[2] In a preliminary work,[2] column *A* ($l = 35$ cm, $\phi = 2$ cm) filled with 55 g of microcrystalline cellulose triacetate (53–105 μ) had been used. On this column tetraorganotin compounds with a triphenylmethyl substituent could be partially separated.

Here we show that the use of a more efficient column coupled with recrystallizations can lead to the separation of racemic tetraorganotin compounds into the pure enantiomers.

EXPERIMENTAL RESULTS

A new column was made (column *B*: $l = 66$ cm, internal $\phi = 2.8$ cm) filled with 135 g of microcrystalline cellulose triacetate (43–53 μ) swollen in 95% ethanol; dead volume V_0: 120 ml; maximum allowed external pressure: *ca.* 780 torr; $T = 20$°C (thermostatized); flow ~250 ml/h; theoretical number of plates $N = 320$.

CHROMATOGRAPHIC RESOLUTION OF Me(PhMe$_2$CCH$_2$)Ph(Ph$_3$C)Sn (1)

Column *B* was used to separate the enantiomers of methylneophylphenyltrityltin (**1**). The UV-chromatogram ($A(v)$-curve) shows only 1 peak but the $\alpha(v)$-curve can be used to select five fractions N_2 (from 0° to α_N), N_1 (from α_N to −0.050°); R (from −0.050° to +0.050°), P_1 (from +0.050° to α_p) and P_2 (from α_p to 0°) see Fig. 1.

The influence of the temperature on the separation of the enantiomers of (**1**) has been studied and is described in Table 1.

At 0°C better resolution is obtained but chromatography takes place more slowly (see t_R in Table 1): the viscosity of ethanol, which is equal to 1.8 cP at 0°, is equal to 0.83 cP at 40°C.

A preparative separation of 1 g racemic (**1**) has been performed at 20°C by eluting successively 10 samples of 100 mg (**1**) on column *B*. The following fractions were obtained ($[\alpha]_D^{20}$, quantity (mg)): N_2 (−32.3, 220); N_1 (−7.0, 200); R (−0.6, 100); P_1 (+4.0, 250) and P_2 (+39.8, 200).

The extreme α-values were $\alpha_N \simeq -0.270°$ (±0.010°) and $\alpha_p \simeq +0.225°$ (±0.005°). Racemic (**1**) is a crystalline compound (m.p. 103–103.5°C). These five fractions were crystalline too and can be recrystallized from ethanol, yielding then, from N_2 like from P_2, crystals with a lower, and evaporated mother liquors with a higher optical rotation (see Fig. 2).

*Author to whom correspondence should be addressed.

Table 1. Influence of the temperature on the resolution of 75 mg (**1**) by chromatography on column *B*. (V'_R is retention volume; t_R is retention time). α_N and α_p, see Fig. 1

T(°C)	0	20	40
α_N (°, 365 nm)	−0.145	−0.138	−0.128
α_p (°, 365 nm)	+0.132	+0.126	+0.120
$V'_R = V_R - V_0$ (V_0 = 120 ml); t_R(min)	150; 102	156; 60	1145; 45
Fractions $[\alpha]_D^{20}$†; quantity(mg)			
N_2	−35.2; 14	−33.3; 15	−30.2; 13
N_1	−7.5; 16	−6.4; 19	−6.8; 20
R	−3.2; 7	−0.7; 11	+0.2; 10
P_1	+5.1; 21	+5.6; 16	+4.8; 17
P_2	+41.0; 13	+40.1; 13	+32.1; 14

†Measured in diethyl ether; $c = 0.6 - 1.6$ g/100 ml.

Chromatography on column *B* of crystals C_1N_2 (see Fig. 2) ($[\alpha]_D = -20$) gave an $\alpha(v)$-curve which showed at the end a small positive part (see Fig. 3a) whereas chromatography of the mother liquor M_1N_2, showing a much more negative $[\alpha]_D$ of -130, gave an $\alpha(v)$-curve which was characterized by negative α-values only (see Fig. 3b). However, M_1N_2 gave two fractions M_1N_4 ($[\alpha]_D = -155$) and M_1N_3 ($[\alpha]_D = -100$) see Fig. 2).

The enantiomeric purity P of the M_1N_2 fraction ($[\alpha]_D = -130$) was determined by a recently described method[3]: $P = 0.62$ (see Fig. 4) which would lead to $[\alpha]_D = -209$ for pure (−)-(**1**).

The first eluted fraction M_1N_4 has been crystallized from a 1:4 MeOH/EtOH mixture. The mother liquor M_2N_4 showed after evaporation of the solvent $[\alpha]_D = -199$, which would mean $P = 0.95$. Furthermore fraction M_1P_2 showed $[\alpha]_D = +201$, corresponding to $P = 0.96$. Unfortunately neither M_1P_2 nor M_2N_4 have been obtained yet as crystalline materials.

The enantiomeric purity of fraction M_1P_2 was determined by the method[3] used above for M_1N_2; the result being $P = 0.94$. We have now developed a novel procedure[9] related to the described one.[3] It determines $\alpha/A = C$ the same way[3] (cf. Fig. 4) but replaces the two manual area determinations (cf. Fig. 3b) by a second chromatographic run,[9] this time using an *achiral* sorbent but the *same* two detection instruments as for the above C measurement. This procedure resulted in $P = 0.98$. As the errors of both methods are not yet known quantitatively, their agreement is satisfactory. This means that fraction M_1P_2 represents almost pure (+)-(**1**).

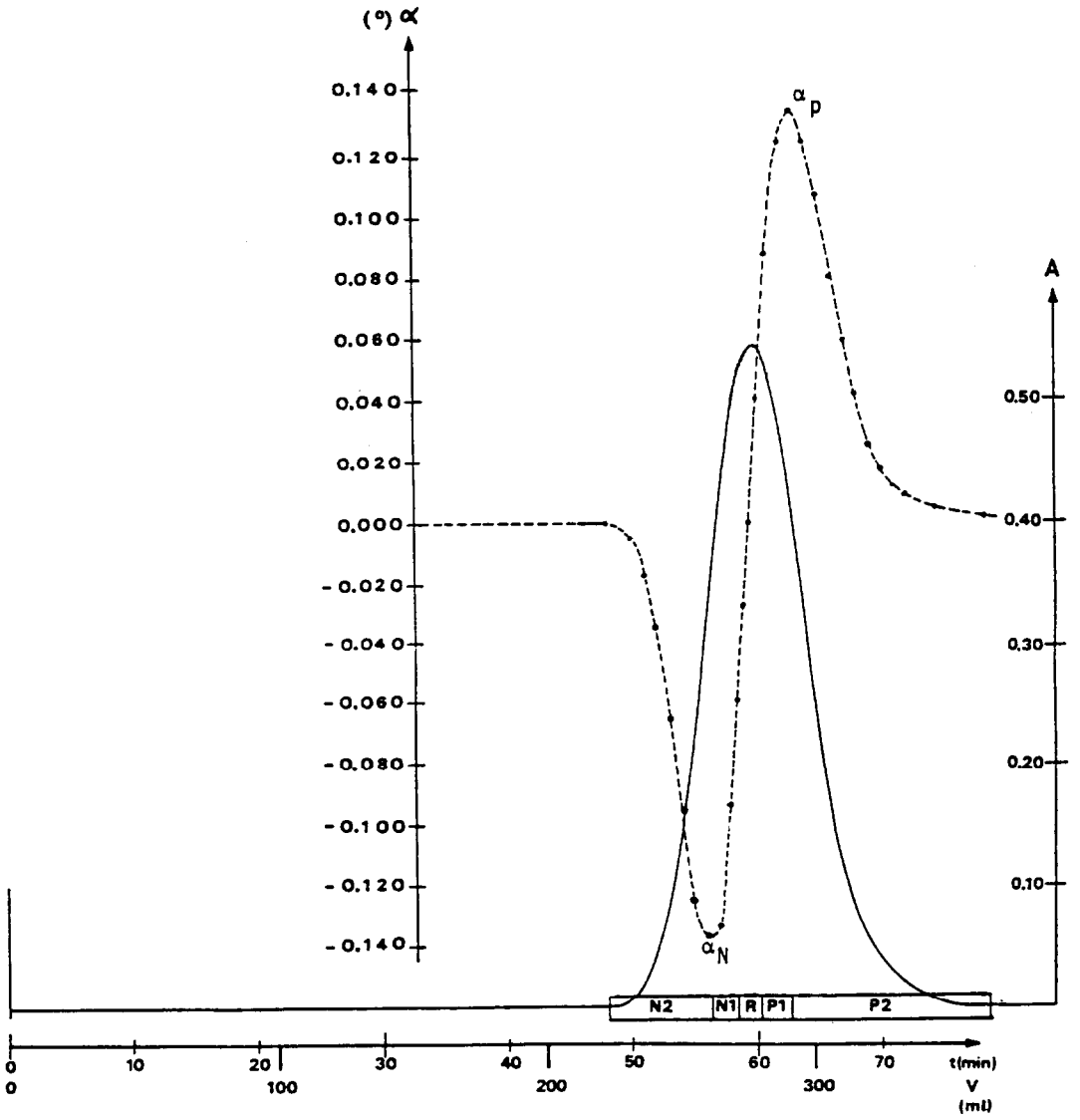

Fig. 1. Partial chromatographic resolution of 75 mg MeNeofPhTritSn (**1**) by chromatography on column *B*. Eluent: 95% ethanol: ——, UV absorption A in absolute units (AUFS (absolute units full scale) = 1), $\lambda = 275$ nm; -----, optical rotation α, $\lambda = 365$ nm; $\Delta p = 770$ torr; flowrate 277 ml/h; $T = 20$°C. (The solution of P_2 was allowed to crystallize for a longer period (3 days) than N_2 (1 day); this explains the better separation).

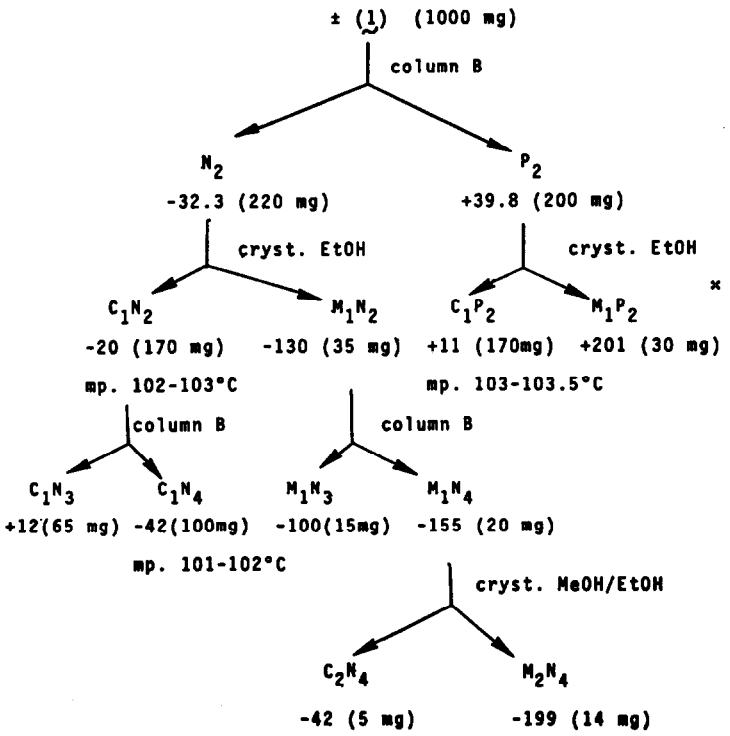

Fig. 2. Resolution of (1) by column chromatography on microcrystalline cellulose triacetate (column *B*) and by crystallization. *C* = crystals; *M*: mother liquor (the index following *C* or *M* gives the number of crystallizations the fraction has undergone). Positive and negative numbers are $[\alpha]_D$ values.

The enantiomeric purity of fraction M_2N_4 was determined by the same novel procedure.[9] The result was $P = 1.0$, its error again being unknown.

Chromatographic resolution of MePh(Me$_3$C)SnCPh$_3$ (2) *at different temperatures*

The influence of the column temperature on the resolution of *t*-butylmethylphenyltrityltin (2) is much more important than for (1). At 40°C there is no resolution at all on column *B*, whereas at −10°C important α_N and α_P values are measured (see Fig. 5). At lower temperatures however, (2) does not dissolve enough in ethanol for preparative separations. Maybe diethyl ether is a better eluent [it dissolves (2) much better than ethanol, it has a low viscosity (0.28 cP at 0°C), and it is acceptable for chromatography on cellulose triacetate].[2]

It may be noticed that the following compounds could *not* be resolved by chromatography on column *B at 20°C* PhMe(Np)SnH† (3)[4,6] PhMe(PhMe$_2$CCH$_2$)SnH (4)[4] [PhMe(Np)Sn]$_2$ (5),[18] [PhMe(PhMe$_2$CCH$_2$)Sn]$_2$ (6),[4,5,8] PhMe(PhMe$_2$CCH$_2$)SnSnPh$_3$ (7),[5] PhMe(Ph·Me$_2$CCH$_2$)-Sn–Co(CO)$_3$PPh$_3$ (8),[5] PhMe(Ph$_3$C)·SnCo(CO)$_3$[(S)Ph$_2$-PNMeCHMePh] (9),[5] PhMe·(PhMe$_2$CCH$_2$)SnFe(CO)$_2$Cp (10)[5] and PhMe(Np)·SnFe(CO)$_2$Cp (11) [Np = 1-naphthyl; Cp = η^5-C$_5$H$_5$].

It is worth mentioning that this column can be used to purify organotin compounds too: for instance, trityltriorganotins R_3SnCPh_3 can be easily separated from triphenylmethane [V'_R(Ph$_3$CH) ≃ 2 × V'_R(R_3SnCPh$_3$)] and from the hexaorganoditins often present (formed by a photochemical degradation of R_3SnCPh_3). Triorganotin halides are purified quite efficiently on cellulose triacetate, without redistributions or decompositions which are often observed on SiO_2 or Al_2O_3.

EXPERIMENTAL PART

Chromatography

For the UV-detection a DUPONT photometer equipped with the preparative cell coupled to a DUPONT recorder was used. The α-values were measured with a Perkin–Elmer 141 polarimeter. The 1,0 ml, 1,000 dm micro-cellule was used as flow-cell.

SYNTHESIS OF *t*-BUTYLMETHYLPHENYLTRITYLTIN (2)

1 g lithium was rasped under nitrogen into 150 ml extra dry THF; then a solution of 11.2 g trityl chloride in 250 ml THF was added in 2 hr under vigorous stirring. After 4 more hr, this solution was filtered into another flask through a polyethylene tubing filled with glasswool.

100 ml of this LiCPh$_3$ solution were added to 3.5 g *t*-BuMePhSnBr in 20 ml THF. After 2 hr, the reaction mixture was hydrolyzed and worked up. The obtained 5.9 g of a yellow viscous oil was purified by chromatography on SiO_2 (elution with benzene/p.e. 1/5). 3.5 g of a colourless oil were obtained and recrystallized twice from ethanol. (1 g/10 ml EtOH) yielding 2.5 g white crystals (49%), m.p. 115–115.5°C; ^{1}H NMR (60 MHz) (0.3 M/CCl_4): δ(MeSn): 0.22 ppm; ^{2}J(^{119}Sn^{1}H): 42.6 Hz; δ(MeC): 1.02 ppm; ^{3}J(^{119}Sn^{1}H): 75.8 Hz; δ(H$_{arom}$): 7.0–7.2 ppm; 70 eV monoisotopic mass spectrum (*m/e*, % BP, fragment ion): 512, 0.5, PhMe(Me$_3$C)(Ph$_3$C)Sn; 497, 0.05,

†The racemisation of chiral PhMe(Np)SnH (3) in ethanol cannot be excluded;[4] this could be an explanation why PhMe(Np)GeH can be separated[2] but not (3).

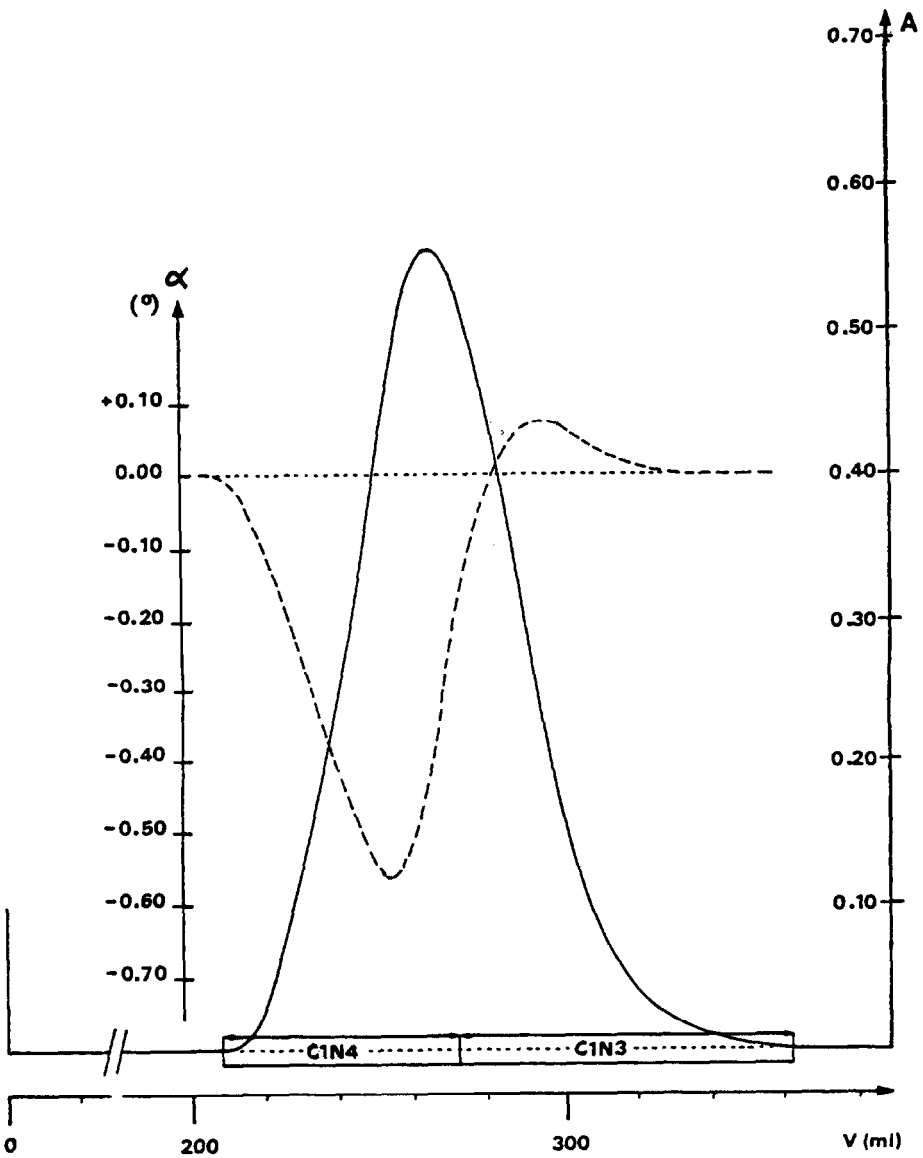

Fig. 3(a). Chromatogram of 170 mg MeNeofPhTritSn (1) fraction C_1N_2; $[\alpha]_D = -20$. ——, UV ($\lambda = 285$ nm) AUFS = 1; -----, α ($\lambda = 365$ nm); $\Delta p = 740$ torr; flowrate 244 ml/hr; $T = 20°C$.

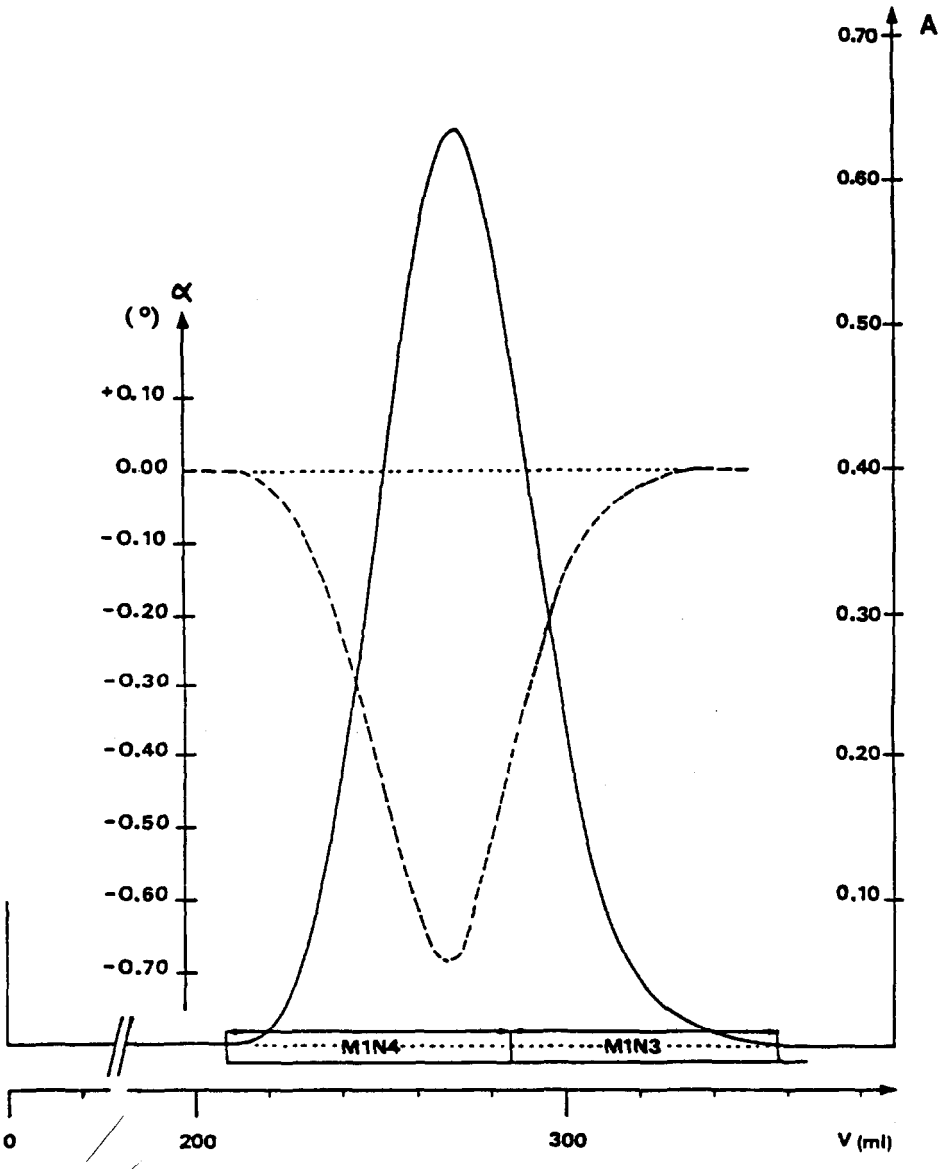

Fig. 3(b). Chromatogram of 35 mg MeNeofPhTritSn (1) fraction M_1N_2; $[\alpha]_D = -130$. ——, UV ($\lambda = 275$ nm) AUFS = 1; -----, α ($\lambda = 365$ nm); $\Delta p = 740$ torr; flowrate 244 ml/hr; $T = 20°C$; $\int \alpha dv = -26.5°$ ml; $\int A dv = 29.9$ ml.

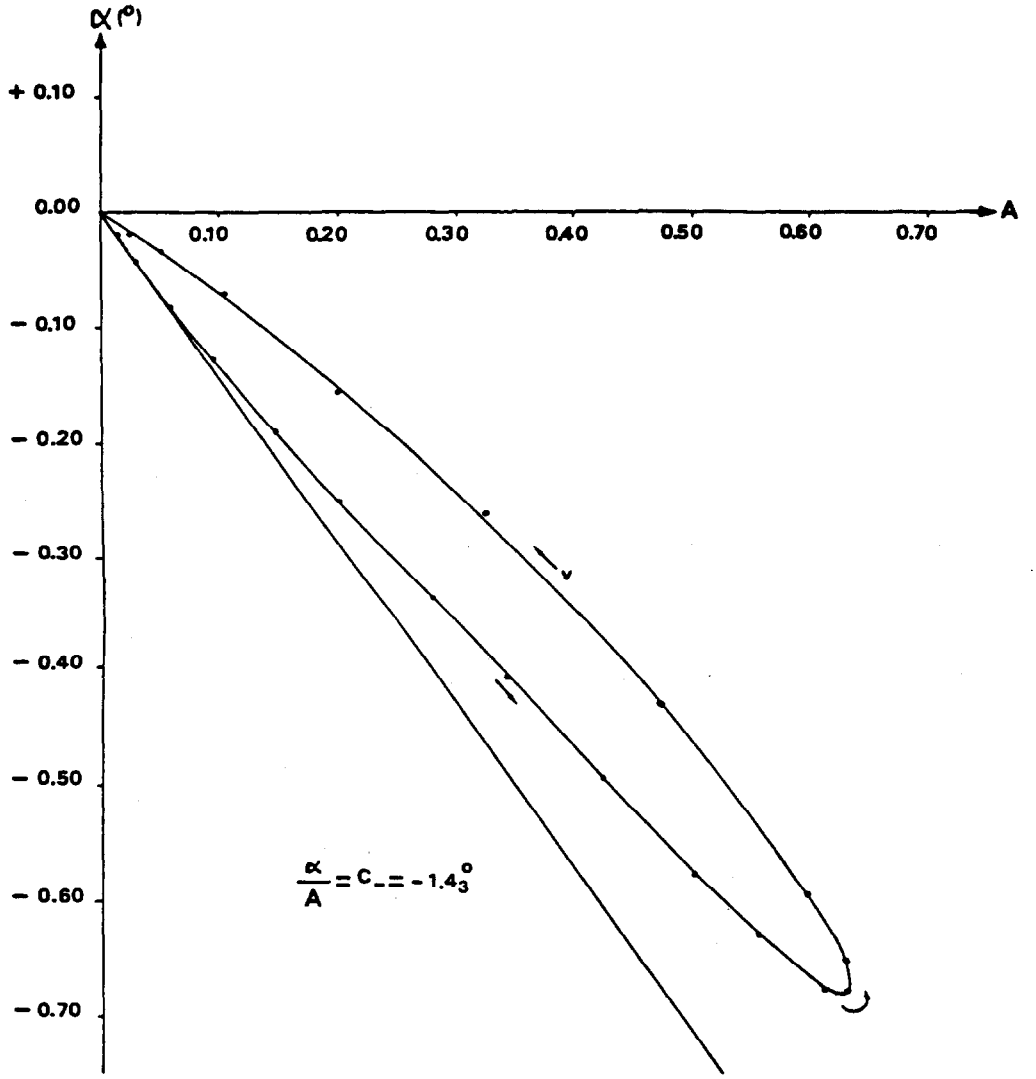

Fig. 4. $\alpha(A)$ diagram (see Ref. 3) drawn from the chromatogram, Fig. 3(b); (1) fraction M_1N_2

$$P = \frac{\int \alpha dv}{c_- \cdot \int A dv} = 0.62.$$

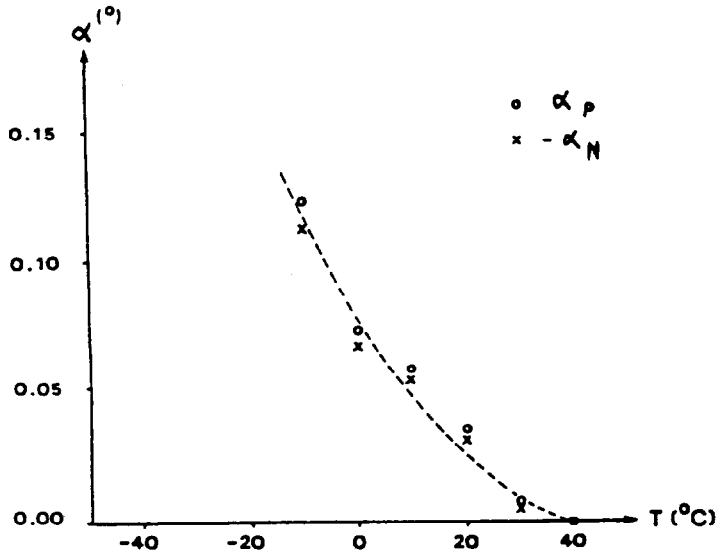

Fig. 5. Chromatography of 50 mg $MePh(Me_3C)SnCPh_3$ (2). Evolution of the extreme α-values α_N and α_p (see Fig. 1) as function of the column temperature $T \cdot (\Delta p = 770$ Torr).

$Ph(Me_3C)(Ph_3C)Sn$; 455, 0.05, $PhMe(Ph_3C)Sn$; 439, 0.06, $C_{25}H_{19}Sn$; 435, 0.08, $Me(Me_3C)(Ph_3C)Sn$; 351, 0.06, Ph_3Sn; 269, 43.7, $PhMe(Me_3C)Sn$; 213, 35, PhMeSnH; 197, 8.1, PhSn; 135, 6.3, MeSn; 121, 0.3, SnH; 120, 6, Sn.

SYNTHESIS OF METHYLNEOPHYLPHENYLTRITYLTIN (1)

Compound (1) was prepared like compound (2); yield: 37% white crystals; ^{1}H NMR (270 MHz) (0.05 M/CCl_4) δ(MeSn): 0.073 ppm; $^2J(^{119}Sn^1H)$: 49 Hz; $\delta(Me_AC)$: 1.167 ppm; $\delta(Me_BC)$: 1.204 ppm; $\delta(CH_AH_B)$: 1.668, 1.816 ppm, $^2J(H_AH_B) = 12.3$ Hz; δ H_{arom}: 6.85–7.20 ppm; UV (ethanol) λ_{max} (nm), log ϵ): 207, 3.98; 255, 3.45; 70 eV monoisotopic mass spectrum: 588, <0.1, $MePh(PhMe_2CCH_2)(CPh_3)Sn$; 573, 0.1, $Ph(PhMe_2CCH_2)(CPh_3)Sn$; 511, 0.1, $Me(PhMe_2CCH_2)(CPh_3)Sn$; 455, <0.1, $PhMe(CPh_3)Sn$; 407, 2.7, $Ph_2(PhMe_2CCH_2)Sn$; 345, 100, $PhMe(PhMe_2CCH_2)Sn$; 289, 4.7, Ph_2MeSn; 277, 7.1, Me_2PhSn; 213, 3.3, MePhSnH; 212, 0.8, MePhSn; 197, 26.6, PhSn; 145, 1.0, C_2HSn; 135, 5.4, MeSn; 121, 0.8, SnH; 120, 11.5, Sn.

SYNTHESIS OF DICARBONYLCYCLOPENTADIENYL(METHYL-1-NAPHTHYLPHENYLSTANNYL) IRON (11)

Compound (11) has been prepared by the usual method[7] from MeNpPhSnCl[4,6] and $Cp(CO)_2Fe \cdot Na$[7] in THF. Yield: 78% of orange crystals (recrystallized from *n*-hexane), m.p. 92–93°C; ^{1}H NMR (60 MHz) (0.43 M in CS_2): δ(MeSn): 0.75 ppm, $^2J(^{119}Sn^1H)$: 46 Hz; $\delta(C_5H_5Fe)$: 4.50 ppm; $\delta(H_{arom})$: 7.1–8 ppm; IR: ν(CO): 1945 cm^{-1} (s); 1995 cm^{-1} (s); 70 eV monoisotopic mass spectrum: 516, 1.5, $MeNpPhSnFe(CO)_2Cp$; 501, 6.0, $PhNpSnFe(CO)_2Cp$; 488, 3.8, $MeNpPhSnFe(CO)Cp$; 460, 1.1, MeNpPhSnFeCp; 445, 10.7, NpPhSnFeCp; 439, 1.8, $MeNpSnFe(CO)_2Cp$; 395, 3.6, MeNpPhSnFe; 389, 1.1, $MePhSnFe(CO)_2Cp$; 383, 0.4, MeNpSnFeCp; 339, 25.9, MeNpPhSn; 289, 6.8, $MePh_2Sn$; 247, 7.0, NpSn; 221, 0.8; 197, 5.0, PhSn; 185, 15.5, CpSn; 135, 0.6, MeSn; 121, 2.6, CpFe; 120, 5.9, Sn.

REFERENCES

[1] M. Gielen and I. Vanden Eynde, *J. Organometal. Chem.*, 1981, **218**, 315.
[2] I. Vanden Eynde and M. Gielen, *J. Organometal. Chem.*, 1980, **198**, C55.
[3] A. Mannschreck, M. Mintas, G. Becher and G. Stühler, *Angew. Chem.*, 1980, **92**, 490; *Angew. Chem. Int. Ed. Engl.*, 1980, **19**, 469.
[4] M. Gielen and Y. Tondeur, *J. Organometal. Chem.*, 1979, **169**, 265.
[5] M. Gielen and I. Vanden Eynde, *Transition Met. Chem.*, (Org. Met. Cpds 75).
[6] M. Gielen and I. Vanden Eynde, *J. Organometal. Chem.*, 1981, **217**, 205.
[7] M. Gielen and I. Vanden Eynde, *Israel J. Chem.*, 1980, **20**, 93.
[8] M. Gielen and Y. Tondeur, *J. Chem. Soc., Chem. Comm.*, 1978, 81.
[9] A. Mannschreck, R. Küspert and G. Stühler, Unpublished results.

Polyhedron Vol. 1, No. 1, pp. 9–12, 1982
Printed in Great Britain.

0277-5387/82/010009-04$03.00/0
Pergamon Press Ltd.

TRIS(DIFLUORO AND TRIFLUOROBUTANE-2,4-DIONATO) GALLIUM(III) AND INDIUM(III) COMPLEXES

DANIEL T. HAWORTH* and JAMES W. BEERY
Department of Chemistry, Marquette University, Milwaukee, WI 53233, U.S.A.

and

MANORANJAN DAS*
School of Chemistry, University of New South Wales, Kensington, N.S.W. 2033, Australia

(*Received* 20 *May* 1981)

Abstract—Eight *tris*(β-diketonate)gallium(III) and seven *tris*(β-diketonate)-indium(III) complexes M(RCOCHCOR')$_3$, with R' being difluoromethyl and trifluoromethyl substituents and R being methyl, phenyl, aryl, 2'-naphthyl and 2'-thienyl substituents have been studied by nuclear magnetic resonance spectroscopy. The complexes are all nonrigid (fluxional) and their ^{19}F NMR spectra show four resonances in the nonexchanging regions due to *cis* and *trans* isomers. A variable low temperature study of these complexes was done for the gallium chelates and activation parameters are calculated. The indium complexes all have nonexchanging regions below −100°C. The ^{13}C NMR data on the complexes are also reported.

INTRODUCTION

The classic ^{19}F NMR study of the aluminium, gallium and indium complexes containing the ligand trifluoroacetylacetonate (tfac–H) by Fay and Piper established the utility of nuclear magnetic resonance spectroscopy as a useful technique for the study of stereochemically nonrigid inorganic complexes.[1,2] Their ^{19}F NMR study showed that the spectra of the Ga(tfac)$_3$ complex below 50°C and the Al(tfac)$_3$ complex below 89° to have four resonances which coalesce into one resonance as the temperature is raised. The In(tfac)$_3$ complex showed only one resonance down to −57°. The four resonances of the Al(tfac)$_3$ and Ga(tfac)$_3$ complexes are attributed to the three nonequivalent CF_3 groups of the *trans* (meridional) isomer and to the equivalent CF_3 groups of the *cis* (facial) isomer. We have reported on a ^{13}C dynamic nuclear magnetic resonance study of *tris*(trifluoropentanedionato)aluminium(III).[3] More recently we also reported on the synthesis of a series of eight *tris*(difluoro and trifluoro-4-substituent-butane-2,4-dionato) aluminium(III) complexes whose fluxional behavior was followed by ^{19}F NMR spectroscopy.[4]

In continuation of our studies on fluxional molecules we have prepared the complexes of gallium and indium, M(RCOCHCOCHF$_2$)$_3$, where R is phenyl and 2'-thienyl. The fluxional behavior of these complexes along with the eight gallium and indium complexes of RCOCH$_2$COCF$_3$ where R is phenyl, 2'-naphthyl, *p*-fluorophenyl, *p*-methylphenyl and 2'-thienyl[5] and also the Ga(CH$_3$COCHCOCF$_3$)$_3$ complex are discussed in this report. The stereochemical β-diketones nonrigid behavior of these chelates was followed by ^{19}F NMR spectroscopy. ^{13}C NMR data on these complexes are also included in this study.

EXPERIMENTAL

The method of preparation of the gallium and indium complexes of the trifluoromethyl-β-diketones (RCOCH$_2$COCF$_3$) was reported in a separate communication[5]. The difluoromethyl-β-diketones (RCOCH$_2$COCHF$_2$) were prepared by the Claisen condensation of ethyl difluoroacetate (CHF$_2$COOC$_2$H$_5$) and the methyl ketones (ROCH$_3$) catalyzed by sodium methoxide.[6] The gallium and indium complexes (R is phenyl and 2'-thienyl) were prepared by the same method as those of the trifluoro-β-diketonates.[5] Analytical data for those complexes are presented in Table 1.

NMR Spectra were taken on a JEOL-FX60Q NMR Spectrometer. ^{19}F NMR spectra were run at 56.3 MHz with broad-band proton decoupling. A pulse width of 18 μs (90°) and a repetition time 10 sec were used in the accumulation. The spectra were accumulated as 4K data points and transformed as 16K data points over a 500 Hz sweep width for a digital resolution of 0.061 Hz/data point. The gallium complexes were run in $CDCl_3$ and the indium complexes in both $CDCl_3$ and CD_2Cl_2. ^{13}C NMR spectra were run in $CDCl_3$ using TMS as an internal standard. We have recently reported on the continuous recording of low temperature NMR spectra using the JEOL-FX60Q Spectrometer.[7]

RESULTS AND DISCUSSION

The ^{19}F NMR spectra of all the gallium complexes taken at ambient temperature showed four resonances indicating the presence of an equilibrium mixture of the *cis* and *trans* isomers for each complex. The least intense resonance is assigned to the *cis* isomer and the three resonances of about equal intensity are assigned to the *trans* isomers. In the *cis* isomer a C_3 axis of rotation is evident, whereas in the *trans* isomer this axis of symmetry is absent and the three fluoromethyl groups are magnetically nonequivalent.

As the temperature of the Ga(RCOCHCOR')$_3$ complexes is increased the four ^{19}F NMR resonances coalesce into one resonance. Table 2 shows the various gallium complexes studied, the coalescence temperature

*Authors to whom correspondence should be addressed.

Table 1. Analytical data for $Ga(RCOCHCOCHF_2)_3$ and $In(RCOCHCOCHF_2)_3$ complexes

Compounds	M.p.(°C)	Calc.			Found		
		C	H	metal	C	H	metal
$Ga(PhCOCHCOCHF_2)_3$[a]	176°	54.50	3.20	10.54	54.66	3.10	10.56
$In(PhCOCHCOCHF_2)_3$[a]	154°	51.01	3.00	16.25	50.77	3.01	16.19
$Ga(2'\text{-thienylCOCHCOCHF}_2)_3$[b]	200°	42.44	2.23	10.26	46.16	2.35	10.17
$In(2'\text{-thienylCOCHCOCHF}_2)_3$[b]	179°	39.81	2.09	15.85	39.68	2.09	15.83

[a] Ph, C_6H_5

[b] 2'-thienyl, C_4H_3S

(T_c) and the chemical shift difference ($\Delta\nu$). The chemical shift difference was taken as the average separation in hertz in the nonexchanging region between the low field resonance and the three resonances at high field.[2] From this data the rate constant (k_c) at the coalescence temperature (T_c) is obtained (eqn 1) and the free energy of activation (ΔG^+) is calculated (eqn 2).[8]

$$k_c = \frac{\Pi(\Delta\nu)}{\sqrt{2}} \tag{1}$$

$$\Delta G^+ = 4.57T_c(10.32 + \log T_c/k_c). \tag{2}$$

The stereochemical barrier is *ca.* 17.6 ± 0.7 kcal for all the gallium complexes studied. While the mechanism for this intramolecular rearrangement is unknown, a detailed topological analysis of aluminium β-diketone complexes having fluoro substituents suggests a bond rupture mechanism which takes place through a square pyramidal (SP) intermediate. The bond rupture is believed to take place at the fluoromethyl group end of the bidentate ligand.[9] The fluoro moieties, *p*-fluoro and CF_3, in $Ga(p\text{-}FC_6H_4COCHCOCF_3)_3$ gave the same free energy of activation, indicating that these fluorines are exchanging at the same rate.

Table 2 also shows the comparison of the activation energies of the gallium complexes with the aluminium complexes as previously reported.[4] A stereochemical barrier of *ca.* 20.8 ± 0.6 and 17.6 ± 0.7 kcal is observed for all the aluminium and gallium complexes, respectively. Our free energy of activation data for $Ga(CH_3COCHCOCF_3)_3$ agrees with that of Fay and Piper; however, we observed a slightly higher coalesecence temperature of 67° vs 61.5°.[2]

All of the indium complexes in CD_2Cl_2 gave a coalesence temperature (T_c) of *ca.* −95°C which is within the lower limit of our variable temperature accessory. Taking the average value of the separation ($\Delta\nu$) of the resonances of the isomer of the aluminium[4] and gallium complexes studied to be 9.32 ± 3.44 Hz and 12.36 ± 4.55 Hz respectively, one obtains on linear extrapolation a value of $\Delta\nu$ as 15.40 ± 7.30 Hz for the indium complexes. This yields an exchange rate constant of 34.2 ± 16.2 s^{-1} with a ΔG^+ of 9.0 ± 4.3 kcal/mol at the assumed coalescence temperature of −95°C. Error limits were calculated assuming a constant percentage error in the

Table 2. Exchange parameters for Ga(RCOCHCOR') complexes

R	R'	Δν(Hz)	$k_c(s^{-1})$	T_c(°C)	$\Delta G^{\ddagger}$ (kcal/mol)	$\Delta G^{\ddagger}$ (kcal/mol)[a]
phenyl	CHF_2	14.38	31.9	79	18.3	21.2
2'-thienyl	CHF_2	15.81	35.1	77.5	18.1	-
phenyl	CF_3	9.28	20.6	63	17.7	21.5
2'-thienyl	CF_3	8.67	19.3	56	17.4	20.3
methyl	CF_3	8.63	19.2	67	18.0[b]	20.3[c]
2'-naphthyl	CF_3	8.30	18.4	41	16.6	20.4
p-methylphenyl	CF_3	8.79	19.5	43	16.7	20.1
p-fluorophenyl	CF_3	17.29[d]	38.4	89	17.2	21.5
		20.03[e]	44.5	62.5	18.4	20.8

[a] Data for the corresponding Al chelates (kcal/mol) ref. 4

[b] $\Delta G^{\ddagger}$ is 17.2 ± 1.5 kcal/mol from ref. 2

[c] $\Delta G^{\ddagger}$ is 19.6 ± 1.7 kcal/mol from ref. 2

[d] p-FC_6H_4 fluorines

[e] CF_3 fluorines

Table 3. ^{13}C NMR chemical shift (ppm) data for the diketone ring carbons in $Ga(RCOCHOR')_3$ and $In(RCOCHCOR')_3$

R	R'	$Ga(RCOCHCOR')_3$			$In(RCOCHCOR')_3$		
		R-C-O	R'-C-O	C-H	R-C-O	R'-C-O	C-H
C_6H_5	CHF_2	190.9	180.2	92.3	193.2	181.7	92.8
2'-C_4H_3S[a]	CHF_2	184.2	179.7	92.4	187.7	180.7	92.6
C_6H_5	CF_3	192.3	173.0	92.6	194.7	174.6	93.2
2'-C_4H_3S[a]	CF_3	184.6	172.0	92.5	186.8	173.5	93.0
CH_3	CF_3	202.4	171.5	96.4	-	-	-
2'-$C_{10}H_7$[b]	CF_3	192.0	172.2	92.8	194.5	174.5	93.5
p-FC_6H_4	CF_3	190.8	172.7	92.2	193.0	174.8	92.8
p-$CH_3C_6H_4$	CF_3	191.9	172.7	92.0	194.3	174.0	92.8

[a] 2'-thienyl

[b] 2'-naphthyl

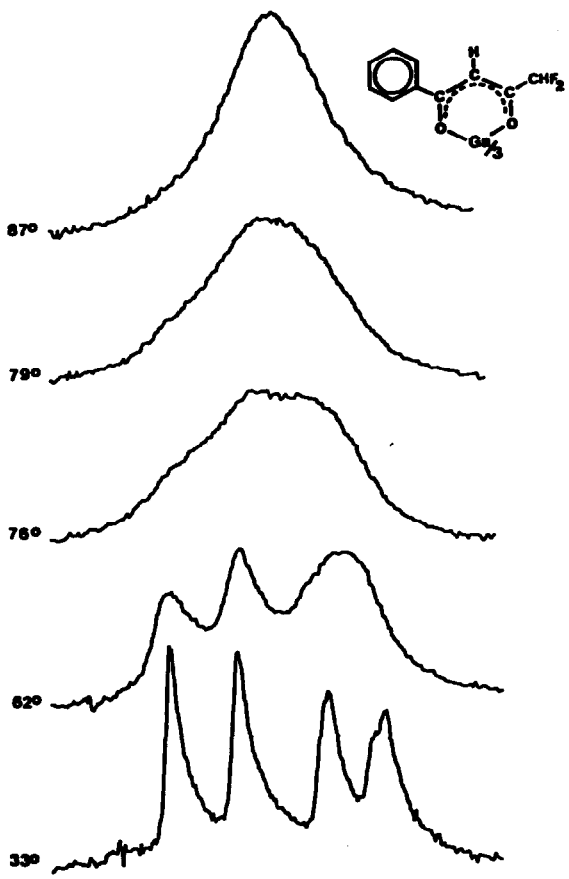

Fig. 1. Temperature dependence of the difluoromethyl region of the ^{19}F NMR spectra of $Ga(C_6H_5COCHCOCHF_2)_3$.

exchange rate constants of the aluminium and gallium complexes. If the rearrangement of these *cis* and *trans* isomers involve a bond rupture mechanism *via* a square pyramidal intermediate,[9] then the coalescence temperatures and the activation energies are not too surprising as the bond strengths of the metal oxygen bonds are Al–O > Ga–O > In–O.

Figure 1 shows the temperature dependence of the difluoromethyl region of the ^{19}F NMR spectra for $Ga(C_6H_5COCHCOCHF_2)_3$. The spectra were taken at 33, 62, 76, 79 and 87°C. Relative to the low field resonance the resonances occured at 0.00, 6.71, 15.50 and 20.94 Hz at 33°C.

The ^{13}C NMR spectra of all the aluminium complexes previously studied[4] showed nonexchanging behavior at *ca.* 31°, whereas the gallium and indium complexes all showed exchanging behavior at *ca.* 31° except for a phenyl carbon resonance of $Ga(C_6H_5COCHCOCHF_2)_3$ and a thienyl carbon resonance of $Ga(2'\text{-}C_4H_3SCOCHCOCF_3)_3$. Chemical shift data for the diketoneate ring carbons are presented in Table 3. In general the respective carbons in the indium complexes are more deshielded than those of the gallium complexes. The corresponding carbons in the aluminium complexes were the most shielded with the order of shielding for the diketone carbons being C–H > R'–C–O > R–C–O. It is interesting to note that the CHF_2 group gives the larger chemical shift on the R'–C–O carbon than the CF_3 group. The shieldings at this R'–C–O carbon show an upfield shift as the R' substituent is changed from CH_3[10] to CHF_2 to CF_3. These shifts have been explained by assuming the diketone ring to be quasi-aromatic and that the paramagnetic effect is dominant.[11] Also the methyl substituent gave a larger deshielding of the R–C–O carbon while the 2'-thienyl substituent had the largest shielding at this carbonyl carbon. The chemical shift of the R–C–O carbon having an aryl or phenyl substituent is intermediate between those of the methyl and 2'-thienyl substituents for the aluminium, gallium and indium complexes studied.

The data presented herein give further support that nuclear magnetic resonance spectroscopy can be a convenient method for the study of the stereochemically nonrigid metal β-diketonate complexes.[12,13]

Acknowledgement—D. T. H. thanks the Marquette University Committee on Research for financial assistance.

REFERENCES

[1]R. C. Fay and T. S. Piper, *J. Am. Chem. Soc.* 1963, **85**, 500.
[2]R. C. Fay and t. S. Piper, *Inorg. Chem.* 1964, **3**, 348.

[3]G. Y. Lin, C. A. Wilkie and D. T. Haworth, *J. Inorg. Nucl. Chem.* 1980, **42**, 1069.
[4]M. Das, D. T. Haworth and J. W. Beery, *Inorg. Chim. Acta.* 1981, **49**, 17.
[5]M. Das, *J. Inorg. Nucl. Chem.* In press.
[6]M. Das, *Transition Met. Chem.* 1980, **5**, 17.
[7]D. T. Haworth and J. W. Beery, *JEOL News Analytical Instrumentation*, 1981, **17A**, 8.
[8]H. Kessler, *Angew. Chem. Internat. Edit.* 1970, **9**, 219.
[9]M. Pickering, B. Jurado and C. S. Pringer, *J. Am. Chem. Soc.* 1976, **98**, 4503.
[10]C. A. Wilkie and D. T. Haworth, *J. Inorg. Nucl. Chem.* 1978, **40**, 195.
[11]C. A. Watkins and M. E. Harris, *J. Inorg. Nucl. Chem.* 1978, **40**, 1769.
[12]N. Serpone and D. G. Bickley, In *Progress in Inorganic Chemistry* (Edited by J. O. Edwards), Vol. 17, p. 391. Interscience, New York (1972).
[13]R. H. Holm, In *Dynamic Nuclear Magnetic Resonance Spectroscopy* (Edited by L. M. Jackman and F. A. Cotton), Chap. 19. Academic Press, New York (1972).

Polyhedron Vol. 1, No. 1, pp. 13–15, 1982
Printed in Great Britain.

0277-5387/82/010013-03$03.00/0
Pergamon Press Ltd.

TELLURONIUM SALT CHEMISTRY: SOME FLUORIDES AND CARBOXYLATES

WILLIAM R. MCWHINNIE* and JAHANGIR MALLAKI
Department of Chemistry, University of Aston in Birmingham, Birmingham B4 7ET, England

(*Received* 27 *May* 1981)

Abstract—Ph_3TeF is ionic and no evidence is obtained for a covalent form in solvents of relatively low polarity. By contrast significant covalent interaction is seen for $Ph_2(CH_3)Te(OOCR)$(R = Ph, *o*-$CH_3O{\cdot}C_6H_4$-, *m*-$NO_2{\cdot}C_6H_4$). Factors influencing the formation and stability of covalent forms of telluronium "salts" are discussed. Phenyl(methyl)telluronium-*ortho*-phthalate is shown to be a monomer in chloroform solution. The structure of the compound is discussed in relation to NMR and IR data and against the background of previous literature reports of both dimeric and monomeric diorganotellurium-*ortho*-phthalates.

INTRODUCTION

Our recent work[1] on the solution chemistry of telluronium salts, particularly the series $Ph_2(CH_3)TeX$(X = Cl, Br, I, NCS, OOCPh) led to the suggestion that, in solvents of low polarity a covalent form of the "salt" predominates. Reductive elimination of CH_3X may then occur from this species. In solvents such as DMSO however the ionic model, $Ph_2(CH_3)Te^+X^-$ seems valid, although considerable ion pairing occurs at high concentration. Recent crystallographic studies on triphenyltelluronium salts Ph_3TeX, e.g. X = NCS,[2] NCO[3] or Cl[4] have revealed that weak association occurs in the solid state. Our solution data for $Ph_2(CH_3)Te(OOCPh)$[1] and for a range of salts stable to reductive elimination of alkyl compounds[5] also indicate that the covalent form is at least a dimer.

In this paper we attempt to explore a little further some factors which affect the stability of the covalent form of the compounds. At the same time we seek to examine a difference between ourselves[6] and others[7] concerning the molecular complexity of Ph_2Te(*ortho*-phthalate). We include this discussion here since it appeared at one time that a telluronium salt model might account for the difference observed.

EXPERIMENTAL

Synthesis of compounds. The preparation of methyldiphenyl telluronium benzoate has been given[1] but some IR data is included here for comparative purposes.

Methyldiphenyltelluronium o-methoxy benzoate and m-nitrobenzoate. The freshly prepared silver salt of the appropriately substituted benzoic acid (0.001 mol.) was reacted with methyldiphenyltelluronium iodide[8] in distilled water (50 cm^3) contained in a r.b. flask fitted with a reflux condenser. The mixture was heated for 2 hr after which the (quantitative) yield of silver iodide was filtered. The filtrate was then allowed to stand in a desiccator over copious P_4O_{10} until crystallisation occured (attempts to evaporate off the water thermally led to loss of the methyl ester and to a residue of diphenyltelluride).

$Ph_2(CH_3)Te(o\text{-}CH_3OC_6H_4COO)$, white m.p. 98°C. Found: C, 56.3; H, 4.70%. $C_{21}H_{20}O_3Te$ requires C, 56.3; H, 4.47%. $Ph_2(CH_3)Te(m\text{-}NO_2{\cdot}C_6H_4COO)$, pale yellow m.p. 110°C. Found: C, 50.0; H, 3.50% $C_{20}H_{17}NO_4Te$ requires C, 51.8; H, 3.67%.

Triphenyltelluronium fluoride. Some difficulty was experienced with this preparation, however, the following method appeared to give satisfactory material: triphenyltelluronium chloride (3.3 g, 0.0086 mol), silver (I) oxide (1.0 g, 0.0043 mol) and distilled water were placed into a flask and stirred for 2 hr at ambient temperature. Filtration of silver chloride followed by treatment with hydrofluoric acid gave after evaporation, white triphenyltelluronium fluoride Ph_3TeF, white m.p. 180°C Found: C, 55.9; H, 3.80% $C_{18}H_{15}FTe$ requires: C, 57.2; H, 4.00%.

Methyl(phenyl)tellurium (IV) ortho-phthalate. Methyl(phenyl)telluride was prepared by potassium metabisulphite reduction of $Ph(CH_3)TeI_2$ prepared by the method of Morgan and Drew.[8] The telluride (0.02 mol) was dissolved in benzene (30 cm^3) and treated with thionyl chloride (0.02 mol) over 30 min under dinitrogen. Stirring at room temperature for 3 hr gave white methyl(phenyl)tellurium (IV) dichloride which was recrystallised from glacial acetic acid. Found: C, 28.9; H, 2.60; Cl, 23.0. Calc. $C_7H_8Cl_2Te$: C, 28.9; H, 2.70; Cl, 24.4%). Treatment of $Ph(CH_3)TeCl_2$ with sodium *ortho*-phthalate following the method of Dance[6] afforded $Ph(CH_3)Te(C_8H_4O_4)$ m.p. 102°C. Found: C, 45.3; H, 2.80%, M, 350. $C_{15}H_{12}O_4Te$ requires: C, 46.9; H, 3.10%; M, 383.

Physical measurements. Conductivity measurements in dimethylsulphoxide solution were carried out using a standard bridge and a Mullard type E7591/B cell of constant 1.46.

IR spectra (4000–250 cm^{-1}) were obtained for KBr discs and chloroform solutions with a Perkin–Elmer 457 spectrophotometer. ^1H NMR spectra were obtained at 60 MHz using a Perkin–Elmer R14 instrument. ^{19}F NMR data for Ph_3TeF were obtained via the University of Birmingham and a ^{125}Te NMR study of the same compound was undertaken by Prof. P. Granger of the Université de Rouen.

Molecular weights were measured using a Knauer vapour phase osmometer.

Mass spectral data were obtained at 70 eV with an AEI MS9 instrument.

RESULTS

The compounds considered in this paper gave satisfactory IR and ^1H NMR spectra. In particular correct ratios of aromatic to aliphatic protons were noted in the NMR. Thus, despite a tendency for the compounds to give low carbon figures, we are satisfied that they are pure. In Table 1 we gather together physical data relevant to our discussion and in Table 2 the major features of the mass spectrum of $Ph_2(Me)Te(OOCPh)$ are documented.

DISCUSSION

Our earlier paper[1] established the concept that "covalent" forms of telluronium salts could exist in solution when the solvent was of low polarity and, for $Ph_2(CH_3)TeX$, reductive elimination of CH_3X was from this associated species. The order of stability of the above compounds to reductive elimination was: X = PhCOO > Cl > Br ≃ NCS > I.

There is the implication within the series that the more electronegative ligand atoms are best able to stabilise the

*Author to whom correspondence should be addressed.

Table 1. Physical data for new tellurium (IV) carboxylates

Compound	IR data (cm^{-1}) ν(COO)	$\Delta\nu$	Methyl resonance (δ vs TMS) (initial)	(final)[a]	Λ_M(DMSO) (10^{-3} M)
$Ph_2(CH_3)Te(OOCPh)$	1600,1390 (solid)	210	2.96†	3.85†	20
	1600,1380 (soln)†	220			
$Ph_2(CH_3)Te(OOCC_6H_4{\cdot}OMe)$	1600,1385 (solid)	215	2.98†	3.85†	25
	1600,1385 (soln)†	215			
$Ph_2(CH_3)Te(OOCC_6H_4{\cdot}NO_2)$	1605,1234	260	2.80*	3.90*	23
$Ph(CH_3)Te(C_8H_4O_4)$	1645,1310 (solid)	335	3.28†		
	1645,1320 (soln)	325			

†Chloroform solution ($CDCl_3$ for NMR).
*DMSO solution.
(The methyl resonances initially observed showed weak satellite peaks with $J_{Te-H} = 25$ Hz).
[a]The "final" methyl resonance occurs at the same position as that observed for the appropriate methyl ester.

covalent form. If this is so it may be that the fluorides would be covalent in chloroform solution and stable to reductive elimination. We therefore attempted to synthesise $Ph_2(CH_3)TeF$, but to date have been unsuccessful.

Triphenyltelluronium fluoride has however been synthesised and has been subjected to study by both ^{19}F and ^{125}Te NMR spectroscopies. Neither technique revealed the presence of $J_{^{125}Te-^{19}F}$, each giving a single resonance in chloroform solution which is quite consistent with an ionic formulation. Not surprisingly therefore, in addition to the electronegativity of the ligand atom, the solvation energy of the anion also influences the relative stability of the covalent species. Whilst fluorine is the most electronegative of the ligand atoms considered, fluoride will undoubtedly have the largest solvation energy of the possible anionic groups used.

We have previously reported some data for $Ph_2(CH_3)Te(OOCPh)$.[1] The effect of introduction of *ortho*-methoxy-or *meta*-nitro-groups to the benzoate portion of the molecule is now considered. In the case of the *ortho*-methoxybenzoate the data in Table 1 are almost indistinguishable from those for the benzoate, also the release of the methyl ester in chloroform solution occurs at approximately the same rate in both cases. The *meta*-nitrobenzoate is insoluble in chloroform, hence complete comparison of data is not possible. In the solid state IR spectrum the separation of ν_s and ν_{as} (COO) ($\Delta\nu$-Table 1) is greater suggesting the possibility of stronger cation-anion interaction.[9] Even in DMSO solution the three benzoate derivatives slowly eliminate the appropriate methyl ester, but no significant difference in rate was noted. The single concentration conductivities (10^{-3} M) are similar and low for 1 : 1 electrolytes in DMSO; further all three compounds give curved plots of Λ_M vs (concentration)$^{1/2}$. On this basis it is not possible to argue for a strong electronic effect produced by substituents in the aromatic ring of benzoate; that the electron withdrawing *meta*-nitro-group should be the one to show a small difference in the solid state IR must not be over interpreted at this juncture since the effect may be other than electronic.

Table 2. Mass spectral data for $Ph_2(CH_3)Te(OOCPh)$

Species	*m/e*	Species	*m/e*
$Ph_2(CH_3)Te(OOCPh)^+$	420	Ph_2^+	154
$Ph_2(CH_3)Te^+$	299	$C_6H_5COOCH_3^+$	136
Ph_2Te^+	284	$PhCO_2^+$	121
$Ph(CH_3)Te^+$	222	Ph^+	77
$PhTe^+$	207	$C_4H_3^+$	51

(Relative to ^{130}Te, ^{16}O, ^{12}C, ^{1}H).

Molecular weight data for $Ph_2(CH_3)Te(OOCPh)$ and for a range of organotelluronium salts which are stable to reductive elimination[5] show these materials to be at least dimers in chloroform solution. Thus the stability in solution to reductive elimination and to ionisation of what we have termed the covalent form of the telluronium salt will be a function of the solvation energy of the anion, the electronegativity of the ligand atom and the ability to bridge two tellurium centres (this of course excludes consideration of kinetic factors). Within the series $Ph_2(CH_3)TeX$, benzoate has, to date, shown the most favourable combination of these factors.

It is of interest that the mass spectrum (Table 2) of $Ph_2(CH_3)Te(OOCPh)$ shows a peak at $m/e = 420$ (relative to ^{130}Te) showing the correct isotopic pattern for a tellurium containing fragment and corresponding to $Ph_2(CH_3)Te(OOCPh)^+$, although no fragments of higher m/e values were seen. The presence of the parent ion from methyl benzoate suggests that the mass spectrum observed includes contributions from the products of thermolysis which clearly follows the same pattern as does reductive elimination in solution.

The new compound phenyl(methyl)tellurium(IV) *ortho*-phthalate is reported in the experimental section and additional data are given in Table 1. This compound is apparently a little dissociated, but essentially monomeric in chloroform solution and is thus similar to the diaryl-derivatives reported by Tamagaki *et al.*[7] whereas we have found similar diaryl compounds to be dimers.[6] Our previous data were checked and confirmed after the appearance of Tamagaki's contribution,[10] thus it seems we may have monomeric and dimeric forms of some of those materials. The structure of the monomeric form is of some interest.

The IR data for $Ph(CH_3)Te(C_8H_4O_4)$ (Table 1) show single ν_{as} and ν_s(COO), hence the two carboxylate groups are equivalent in both the solid state and in solution; also from $\Delta\nu$ it may be concluded that both groups interact within tellurium. It is convenient to regard the structure of an organo-tellurium compound R_2TeX_2 (X is an electronegative group) as ψ-trigonal bipyramidal, however both crystallography[11] and, for example ^{125}Te Mössbauer spectroscopy[12] indicate that

the Te–C bonds have high tellurium *p*-character, although the XTeX angle is generally close to 180°. Reduction of the XTeX angle, which would presumably be necessary on steric grounds in the case of monomeric $Ph(CH_3)Te(C_8H_4O_4)$, is likely to increase the *s* character of the Te–C bonds.[13] Thus $J_{^{125}Te-H}$, the coupling constant between the methyl protons and ^{125}Te might be expected to be greater for $Ph(CH_3)Te(C_8H_4O_4)$ than for, say, $Ph(CH_3)TeCl_2$. In fact both compounds give the identical value of 25 Hz, thus given the implication of similar *s* and *p* character in bonds to tellurium in both compounds we must conclude that the electron density comprising the TeO bonds lies off the TeO axis.

An alternative view may be a zwitterionic telluronium formulation such as $Ph(CH_3)\overset{+}{T}e{\cdot}OCC{\cdot}C_6H_4{\cdot}C\bar{O}O$, but this appears to be ruled out by the IR data unless a fluxional situation exists in solution and a different (dimeric?) structure for the solid. If this is the case, greater differences between the solid and solution IR data might have been expected.

REFERENCES

[1]N. S. Dance, W. R. McWhinnie, J. Mallaki and Z. Monsef-Mirazi, *J. Organometal. Chem.*, 1980, **198**, 131.

[2]J. S. Lee, D. D. Titus and R. F. Ziolo, *Inorg. Chem.*, 1977, **16**, 2487.

[3]D. D. Titus, J. S. Lee and R. F. Ziolo, *J. Organometal. Chem.*, 1976, **120**, 381.

[4]R. F. Ziolo and M. Extine, *Inorg. Chem.*, 1980, **19**, 2964.

[5]A. Al-Rubaie, P. Granger, J. Mallaki and W. R. McWhinnie, unpublished data.

[6]N. S. Dance and W. R. McWhinnie, *J. Organometal. Chem.*, 1976, **104**, 317.

[7]S. Tamagaki, I. Hatanaka and S. Kozuka, *Bull. Chem. Soc. Japan*, 1977, **50**, 2501.

[8]G. T. Morgan and H. K. Drew, *J. Chem. Soc.*, 1925, 2307.

[9]N. F. Curtis, *J. Chem. Soc.*, 1969, 1579.

[10]N. S. Dance, personal communication.

[11]e.g. G. D. Christofferson and J. D. McCullough, *Acta Cryst.*, 1958, **11**, 249.

[12]C. H. W. Jones, R. Schultz, W. R. McWhinnie and N. S. Dance, *Can. J. Chem.*, 1976, **54**, 3234.

[13]M. M. L. Chin and R. Hoffman, *J. Am. Chem. Soc.*, 1976, **98**, 1647.

Polyhedron Vol. 1, No. 1, pp. 17–19, 1982
Printed in Great Britain.

0277-5387/82/010017-03$03.00/0
Pergamon Press Ltd.

THE CRYSTAL STRUCTURE OF AMMONIUM β-OCTAMOLYBDATE PENTAHYDRATE

TIMOTHY J. R. WEAKLEY
Chemistry Department, Dundee University, Dundee DD1 4HN, Scotland

(*Received* 29 *May* 1981)

Abstract—X-ray structure analysis (film data, R = 0.080 for 1568 reflections) has confirmed the structure of the anion in $(NH_4)_4[Mo_8O_{26}]$, $5H_2O$, deduced by Lindqvist in 1950 from the Mo coordinates alone. The compound is triclinic, $P\bar{1}$, $a = 9.769(16)$, $b = 9.832(13)$, $c = 7.848(11)$ Å, $\alpha = 99.11(4)$, $\beta = 101.03(11)$, $\gamma = 97.40(4)°$, $Z = 1$. Eight MoO_6 octahedra share edges in a compact grouping, with short terminal Mo–O bonds (1.69 to 1.75 Å), longer bonds (1.88–2.00 Å) to bicoordinate O atoms, and long bonds (2.18–2.39 Å) to multiply-shared interior atoms.

INTRODUCTION

A probable structure for the octamolybdate anion, $Mo_8O_{26}^{4-}$, in a salt reported by him to be a pentahydrate, $(NH_4)_4[Mo_8O_{26}]\cdot 5H_2O$ (I), was deduced by Lindqvist[1] from the approximate coordinates of the molybdenum atoms as given by the three-dimensional Patterson function. The oxygen atoms were not directly located. The proposed anion was based on eight edge-sharing MoO_6 octahedra. More complete X-ray studies, in which all non-hydrogen atoms were located, showed[2–4] that this anion is present in the tetrahydrate $(NH_4)_4[Mo_8O_{26}]\cdot 4H_2O$ (II) and also in $(3\text{-EtpyH})_4[Mo_8O_{26}]$.[5] It has been termed β-octamolybdate,[6] since an isomeric $\alpha\text{-}Mo_8O_{26}^{4-}$ anion, based on six MoO_6 octahedra and two MoO_4 tetrahedra,[7,8] has been characterised. While attempting to prepare crystalline citratomolybdates, we observed that a suspension of $MoO_3\cdot 2H_2O$ in hot water rapidly dissolved on the addition of small amounts of ammonium citrate, and that the solution on cooling deposited triclinic crystals of I (identified by chemical analysis and by the measurement of cell dimensions). Attempts to recrystallize I from warm water always afforded II (identified similarly). Our analyses indicated that I and II, although crystallographically distinguishable, were *both* $(NH_4)_4[Mo_8O_{26}]\cdot 4H_2O$. It seemed improbable that Lindqvist[1] had misinterpreted the Patterson function of I, or that I contained a new isopolymolybdate anion with the same Mo..Mo vector set as II. However, we have carried out a more complete determination of the structure of I.

EXPERIMENTAL

Ammonium citrate (3.5 g) was added in portions to a stirred suspension of $MoO_3\cdot 2H_2O$ (10.0 g) in hot water (80 ml, 70°). The slightly turbid solution (pH 3.1) was filtered and treated while hot with an equal volume of ethanol. Crystals of I separated rapidly on cooling, or overnight at 20° if no ethanol had been added. In the latter case another product, III, was sometimes obtained instead; the elongated prismatic crystals of III crumbled rapidly on exposure to air but were more stable if manipulated under Nujol and sealed into a capillary. After drying in air, compound I appeared to be a tetrahydrate, not a pentahydrate[1] (found, Mo 57.6, N 4.3, H 1.9, loss at 420° 13.4%; calculated for $(NH_4)_4[Mo_8O_{26}]\cdot 4H_2O$, 57.8, 4.2, 1.8, 13.3%). Crystals for X-ray study were taken directly from solution but were not protected after mounting; there was no evidence of deterioration during data collection.

Crystal data. Triclinic, $P\bar{1}$, $a = 9.769(16)$, $b = 9.832(13)$, $c = 7.848(11)$ Å, $\alpha = 99.11(4)$, $\beta = 101.03(11)$, $\gamma = 97.40(4)°$, $V = 720.6$ Å^{-3}, $D_m = 3.02$, $D_c = 3.06$ g cm^{-3}, $Z = 1$; Cu Kα radiation, $\lambda = 1.5418$ Å, $\mu = 292$ cm^{-1}. Cell dimensions were obtained from NaCl-calibrated Weissenberg photographs. The above cell is transformed into that of Ref. 1 by the matrix [0 0 1/0 1 0/1 0 0]. Compound III was found to be monoclinic, $P2_1/c$, with $a = 16.65(2)$, $b = 18.69(1)$, $c \sin\beta = 24.19(2)$ Å, from which it seemed likely that III was the ammonium isomorph of $K_8[Mo_{36}O_{112}(H_2O)_{12}]\cdot 36H_2O$ whose structure is known[9]; consequently it was not studied further. Because of the non-availability of a diffractometer, intensity data for I were collected via equi-inclination multi-film Weissenberg photographs (levels 0–2*kl*, *h*0–2*l* and *hk*0–6). Spot intensities and improved cell dimensions were measured by the S.R.C. Microdensitometer Service, Daresbury Laboratory. Absorption corrections were applied during data reduction. The Mo atoms were readily located by direct methods in the acentric space-group P1, and the structure was expanded by difference syntheses alternating with cycles of full-matrix least-squares refinement. Further refinement in the centric space-group P$\bar{1}$ converged at R 0.080 (1568 unique reflections above background, 99 parameters, anisotropic thermal parameters for Mo atoms only, unit weights for all data). The N and water O atoms were less sharply resolved than the anion O atoms. The N atoms were assigned from the requirement that the cations be well separated. Only one of the two independent water molecules could be located; its large thermal parameter and the presence of several weak peaks (*ca.* 2e Å^{-3}) in the final difference synthesis suggested that the water molecules were disordered. All calculations were carried out by use of the *SHELX*-76 program.[10] Atomic parameters have been deposited with the Editor as supplementary data;† derived dimensions are given in Tables 1–3.

DISCUSSION

The coordinates of the Mo atoms in I agree well with the values determined approximately by Lindqvist,[1] and his description of the structure of the $Mo_8O_{26}^{4-}$ anion in I (Fig. 1) is confirmed. The anion has crystallographic point symmetry $\bar{1}$ but approximates closely to $2/m(C_{2h})$ symmetry, and in Table 1 the equivalent bond lengths have been averaged accordingly and are compared with the results of two other determinations.[4,5] The bonds around each Mo atom fall into three groups (Table 2): a

†Atomic coordinates have also been deposited with the Institut für Anorganische Chemie, Bonn, FRG for inclusion in their Data Base. Copies are also available, on request, from the Editor at Queen Mary College.

Table 1. Molybdenum-oxygen bond lengths/Å

Anion point symmetry:	i[a]	2/m[b]	2/m[b] (ref.[4])	2/m[b] (ref.[5])
Mo(1)-O(2')	1.693(16)	1.69	1.70	1.68
Mo(1)-O(4)	1.751(18)	1.75	1.75	1.75
Mo(1)-O(6)	1.948(16)	1.94	1.95	1.95
Mo(1)-O(10)	1.929(14)			
Mo(1)-O(12)	2.381(14)	2.38	2.35	2.41
Mo(1)-O(12')	2.181(16)	2.18	2.18	2.42
Mo(2)-O(8')	1.705(16)	1.71	1.69	1.71
Mo(2)-O(13)	1.689(15)	1.69	1.69	1.69
Mo(2)-O(7)	1.911(16)	1.92	1.93	1.92
Mo(2)-O(11)	1.927(16)			
Mo(2)-O(4)	2.283(20)	2.28	2.32	2.29
Mo(2)-O(12)	2.394(13)	2.39	2.48	2.44
Mo(3)-O(3)	1.708(21)	1.70	1.71	1.69
Mo(4)-O(1)	1.688(21)			
Mo(3)-O(9')	1.714(16)	1.69	1.71	1.71
Mo(4)-O(5)	1.672(16)			
Mo(3)-O(10')	2.000(16)	2.00	2.00	1.98
Mo(4)-O(6)	1.999(14)			
Mo(3)-O(11)	1.881(15)	1.88	1.88	1.89
Mo(4)-O(7)	1.871(16)			
Mo(3)-O(6')	2.337(16)	2.35	2.33	2.34
Mo(4)-O(10)	2.354(15)			
Mo(3)-O(12)	2.328(13)	2.32	2.30	2.31
Mo(4)-O(12)	2.316(13)			

[a]Crystallographic symmetry [b]Ideal point symmetry

Table 2. Angles between (i) short, (ii) medium and (iii) long pairs of Mo–O bonds

(i)	O(4)–Mo(1)–O(2')	107.1(8)°	O(3)–Mo(3)–O(9')	107.0(8)°
	O(13)–Mo(2)–O(8')	105.3(8)	O(1)–Mo(4)–O(5)	106.0(9)
(ii)	O(10)–Mo(1)–O(6')	149.3(8)	O(11)–Mo(3)–O(10')	145.7(8)
	O(7)–Mo(2)–O(11)	142.9(7)	O(6)–Mo(3)–O(7)	144.6(7)
(iii)	O(12)–Mo(1)–O(12')	76.4(6)	O(12)–Mo(3)–O(6')	71.3(6)
	O(4)–Mo(2)–O(12)	70.4(6)	O(10)–Mo(4)–O(12)	71.8(5)

trans-pair of medium length, a short *cis*-pair, and a long *cis*-pair. As pointed out elsewhere,[4,8] the β-$Mo_8O_{26}^{4-}$ anion can be described either as an assemply of edge-linked MoO_6 octahedra, or alternatively (Fig. 1) as two cyclic Mo_4O_{12} units formed from distorted MoO_4 tetrahedra, cross-linked by long Mo–O bonds and by additional long bonds from Mo to two extra O^{2-} ions [O(12), O(12')]. The packing of the anions in I is a somewhat distorted version of the packing in II. The orientations of the anions in *c*-axis projection are similar

Table 3. Other interatomic distances/Å

Mo(1)..Mo(2)	3.452(3)	Mo(1)..Mo(4')	3.226(3)
Mo(1)..Mo(3)	3.544(2)	Mo(2)..Mo(3)	3.235(3)
Mo(1)..Mo(4)	3.523(2)	Mo(2)..Mo(4)	3.231(3)
Mo(1)..Mo(1')	3.589(4)	Mo(3)..Mo(4)	4.598(2)
Mo(1)..Mo(2')	4.530(4)	Mo(3)..Mo(4')	2.420(3)
Mo(1)..Mo(3')	3.218(3)		
N(1)..O(1)	3.04(3)	N(2)..O(8)	3.09(3)
N(1)..O(3)	2.98(3)	N(2)..O(9)	2.88(3)
N(1)..O(1')	3.00(3)	N(3)..O(3)	2.97(3)
N(1)..O(8')	3.01(3)	N(3)..O(13)	3.08(3)
N(1)..Aq	3.07(4)	Aq..O(2)	2.97(4)
N(2)..O(5)	2.92(3)	Aq..O(5)	2.99(4)

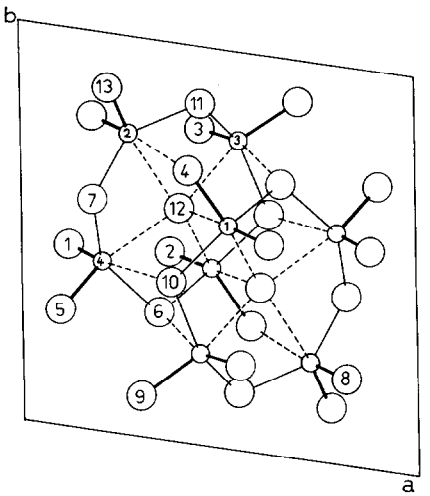

Fig. 1. The $Mo_8O_{26}^{4-}$ anion: *c*-axis projection. Heavy, light and dashed lines denote short, medium and long bonds.

(I, Fig. 1), but the cell of I is 4.6% larger; although its *a* and *b* axes are shorter, the interaxial angles are closer to 90°.

Lindqvist's analysis of I clearly implied that it was a pentahydrate; equally clearly, our analysis of the air-dried material imply it is a tetrahydrate. It seems likely that our product lost one molecule of water on exposure to air, with partial disordering of the remaining lattice water but without other loss of crystallinity. The circumstances under which I is obtained are not entirely clear. In the present work, we observed that I crystallises after $MoO_3 \cdot 2H_2O$ has been brought into solution by the addition of ammonium citrate or acetate, and we also obtained it in an attempt to prepare an acetyl analogue of $(HCO)_2Mo_8O_{28}^{4-}$ [11] by the addition of glacial CH_3COOH to a warm concentrated solution of $(NH_4)_6[Mo_7O_{24}] \cdot 4H_2O$. However, if the pH of a suspension of $MoO_3 \cdot 2H_2O$ is adjusted with aqueous NH_3 or if I is recrystallised from water, II is obtained. We tentatively conclude that the presence of excess ammonium ions during crystallization causes the deposition of I instead of II.

REFERENCES

[1] I. Lindqvist, *Arkiv. Kemi* 1950, **2**, 349.
[2] L. O. Atovmyan and O. N. Krasochka, *Zh. Strukt. Khim.* 1972, **13**, 342.
[3] B. M. Gatehouse, *J. Less-Common Metals* 1977, **54**, 283.
[4] H. Vivier, J. Bernard and H. Djomaa, *Rev. Chim. Minerale* 1977, **14**, 584.
[5] L. Giter, P. Roman, J. Jaud and J. Galy, *Z. Krist.* 1981, **154**, 59.
[6] W. G. Klemperer and W. Shum, *J. Am. Chem. Soc.* 1977, **98**, 8291.
[7] J. Fuchs and H. Hartl, *Angew. Chem.* 1976, **88**, 385.
[8] V. W. Day, M. F. Fredrich, W. G. Klemperer and W. Shum, *J. Am. Chem. Soc.* 1977, **99**, 952.
[9] I. Paulat-Boschen, *J. Chem. Soc. Chem. Comm.* 1979, 780.
[10] G. M. Sheldrick, *SHELX-76 Program for Crystal Structure Determination.* Cambridge University, England 1975.
[11] R. D. Adams, W. G. Klemperer and R.-S. Liu, *J. Chem. Soc. Chem. Comm.* 1979, 256.

Polyhedron Vol. 1, No. 1, pp. 21–30, 1982
Printed in Great Britain.

0277–5387/82/010021–10$03.00/0
Pergamon Press Ltd.

μ-PEROXODICOBALT(III) COMPLEXES CONTAINING AROMATIC LIGANDS

J. DALE ORTEGO* and MARK SEYMOUR
Department of Chemistry, Lamar University, Beaumont, TX 77710, U.S.A.

(*Received* 8 *June* 1981)

Abstract—A series of new μ-peroxodicobalt(III) complexes have been prepared and characterized. Studies of the chemical and physical properties of these complexes were carried out using IR, electronic and NMR spectroscopy along with conductivity, magnetic susceptibility and thermogravimetric measurements. The complexes $[Co_2(dpk \cdot dien)_2\ (dpk \cdot H_2O)O_2]\ (ClO_4)_4 \cdot H_2O$, $[Co_2(dpk)_4(py)_2O_2](ClO_4)_4 \cdot 4H_2O$, $[Co_2(dpk \cdot H_2O_4(py)_2O_2](ClO_4)_4$, and $[Co_2(dpk)_2(terpy)_2O_2](ClO_4)_4$ were prepared by bubbling oxygen through a solution containing $Co(NO_3)_2$, $NaClO_4$, and the appropriate ligand mixture. Electronic spectral studies are consistent with the formulation as binuclear peroxo complexes. Thermogravimetric studies reveal the stoichiometric loss of O_2 and H_2O below 100°C. The auxiliary ligands, pyridine (py), diethylenetriamine (dien) and terpyridine (terpy) are lost at higher temperatures. Molar conductance of these complexes is indicative of a 4:1 electrolyte while magnetic susceptibility measurements indicate the diamagnetic character of the above four complexes. Three additional complexes of Co(II) containing di-2-pyridyl ketone (dpk) and terpy were prepared to compare spectral changes upon oxygenation.

INTRODUCTION

It is well known that complexation of dioxygen plays a vital role in many biological systems. Extensive research has focused on the coordination chemistry of natrually occurring dioxygen complexes, i.e. haemoglobin, haemerythrin, haemocyanin and their model compounds.[1,2] The cobalt–dioxygen complexes have attracted considerable attention due to the extensive literature on cobalt chemistry. Recent studies involving pentadentate ligand systems have shed additional light on the stability and electronic spectra of $Co–O_2$ compounds.[3] However, very few dioxygen complexes of cobalt containing aromatic amine ligand systems have been isolated from aqueous solution.[2]

We wish to report here the isolation and characterization of μ-peroxodicobalt(III) compounds containing di-2-pyridyl ketone (dpk), 2, 2′, 2″-tripyridyl (terpy), pyridine (py) and diethylenetriamine (dien). Complexes with di-2-pyridyl ketone (dpk) have been previously characterized in our laboratory.[4,6] When di-2-pyridyl ketone is coordinated through the two nitrogen atoms, increased π back-bonding is possible (compared to pyridine) due to the presence of the carbonyl group. Also, the propensity of the CO group of dpk to undergo nucleophilic addition while coordinated allows one the opportunity to observe the effects of what is essentially a new ligand system on the dioxygen complex. The N, N-coordination mode of dpk in alcoholic and slightly acidic aqueous solutions has been established.[4,5] The carbonyl stretching frequency of dpk may serve to indicate the extent of π-delocalization of the aromatic system and also to determine whether or not nucleophilic addition occurs. The C = O group of coordinated di-2-pyridyl ketone has been found to be susceptible to attack by water, alcohols and certain amines.[6] Also carbonyl addition in aqueous solution is pH dependent, hydration occurring at pH values above about 6.5.[7] The base-catalyzed addition (in H_2O) results in the formation of a *gem*-diol which may deprotonate. This ionization in some Co(II) and Co(III) compounds results in a rearrangement of the binding sites of dpk from N, N- to N, N, O^--coordination (eqn 1).

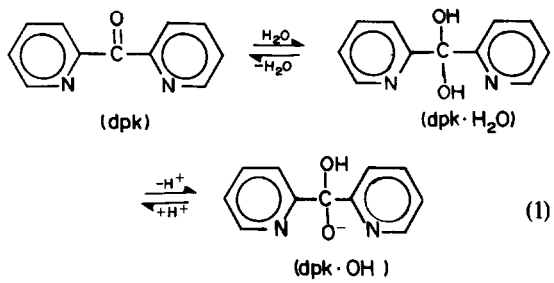

(1)

Our mixed-ligand systems were chosen such that each cobalt(II) center was initially provided with five nitrogen-donor atoms. The coordination of dioxygen has been shown to occur at low pH levels if the donor nitrogens are aromatic tertiary amines. For example, the complex $[Co_2(terpy)_2(bipy)_2O_2](ClO_4)_4$ forms at pH 4.[8] We were therefore confident that dioxygen complexes of dpk could be synthesized at pH levels low enough to prevent carbonyl addition. Also, by increasing the pH and allowing hydration of the carbonyl group, we were able to investigate the properties of dpk in its hydrated form. The μ-peroxodicobalt(III) complexes were all isolated from aqueous solution as the perchlorate salts. Attempts to produce dioxygen complexes with Co(II) and dpk in alcoholic solvents produced only Co(II) compounds. Mixed-ligand Co(II) complexes to dpk with pyridine and terpyridyl were prepared to compare spectral changes upon oxygenation.

EXPERIMENTAL

Spectral studies. IR spectra were recorded in the 200–4000 cm^{-1} range with a Beckman 4250 spectrophotometer. The complexes were prepared as Nujol mulls between CsI plates. Electronic spectra of the complexes and free ligands were recorded in the 200 nm to 1200 nm range using a Carey Model 171 spectro-photometer. The visible spectra of the aqueous solutions at room temperature were obtained using matched 1-cm

*Author to whom correspondence should be addressed.

quartz cells. NMR spectra of DMSO, *d*-6 solutions (~35 mg/mL) of the diamagnetic complexes were obtained on a Varian EM 90 MHz unit. TMS was used as an internal standard. The free ligand spectra were also recorded in DMSO *d*-6 solution. Signal averaging with an Ortec 547 Digital Signal Averager was used to resolve the complex spectra.

Magnetic susceptibility measurements. Magnetic susceptibility measurements for the compounds were obtained at room temperature by the Gouy method using mercury tetrathiocyanocobaltate(II) as calibrant. The apparatus employed a Cahn RH electrobalance and an Alfa Model 4600 electromagnet operating at 3600 gauss.

Conductivity. Measurements were made with a YSI Model 31 conductivity bridge using platinum electrodes. Cell constants were determined using standard 0.0200 M KCl solution. Solvents were purified by standard methods. Concentrations of $\sim 10^{-3}$ M were used.

Thermal studies. The thermal decomposition of the complexes was recorded on a Perkin Elmer TGS-2. Powdered samples of 3–8 mg were heated at 10°/min in a 5 mm platinum crucible under a nitrogen atmosphere at a controlled flow rate.

Elemental analysis. Analyses for cobalt were performed by atomic absorption using a Perkin–Elmer Model 303. Analysis for carbon, hydrogen and nitrogen were performed by Galbraith Labs, Inc., Knoxville, Tennessee.

Preparation of complexes. $[Co_2(dpk \cdot dien)_2(dpk \cdot H_2O)O_2](ClO_4)_4H_2O$. A solution of cobalt(II) nitrate hexahydrate (5 mmoles) and sodium perchlorate monohydrate (28 mmoles) in 25 mL of water was saturated with oxygen. A solution of dpk (7.5 mmoles) and diethylenetriamine (5 mmoles) in 10 mL of water was added dropwise to the cobalt solution as a rapid stream of oxygen was passed through the stirred solution. A pH of 6 was maintained by the dropwise addition of IN NaOH. The solution was stirred for 1 hr while continually bubbling oxygen through the mixture. After cooling the solution to about 4° for 1 hr a light brown solid was recovered, washed with *n*-propyl alcohol and ether and dried in a desiccator over calcium chloride at room temperature. Anal: Calcd. for $[Co_2(dpk \cdot dien)_2(dpk \cdot H_2O)O_2](ClO_4)_4 \cdot H_2O$: C, 37.9; H, 4.0; N, 12.5; Co, 8.1; found: C, 36.7; H, 4.0; N, 12.5; Co, 8.8%.

$[Co_2(dpk)_2(terpy)_2O_2](ClO_4)_4$. This complex was prepared in a manner similar to that described above, however the mixture of dpk (5 mmoles) and 2, 2′, 2″-tripyridyl (5 mmoles) was added as a suspension, and the pH of the reaction mixture was between 3 and 4. With the addition of the ligand mixture, the solution darkened and a brown powder was collected and dried as described. Anal: Calcd. for $[Co_2(dpk)_2(terpy)_2O_2](ClO_4)_4$ C, 45.2; H, 2.8; N, 10.1; Co, 8.5; found: C, 46.8; H, 3.2; N, 10.5; Co, 8.5%.

$[Co_2(dpk)_4(py)_2O_2](ClO_4)_4 \cdot 4H_2O$. This complex was prepared by the dropwise addition of a solution containing the appropriate ligand mixture to the cobalt(II) solution, and maintaining the pH between 3 and 4. A tan-brown powder was isolated from solution. Anal: Calcd. for $[Co_2(dpk)_4(py)_2O_2](ClO_4)_4 \cdot 4H_2O$: C, 42.8; H, 3.2; N, 9.2; Co, 7.8; Found: C, 41.9; H, 3.2; N, 8.7; Co, 7.9%.

$[Co_2(dpk \cdot H_2O)_4(py)_2O_2](ClO_4)_4$. When the above μ-peroxo complex remained in solution several days at 4°, a rust-red crystalline produce formed. The crystals were washed with ether and dried over $CaCl_2$. Anal: Calcd. for $[Co_2(dpk \cdot H_2O)_4(py)_2O_2](ClO_4)_4$; C, 42.8; H, 3.3; N, 9.2; Co, 7.8; found: C, 42.9; H, 3.9; N, 9.1; Co, 7.7%.

$[Co(dpk)_2(py)Cl]Cl \cdot 4H_2O$. This complex was prepared by addition of dpk (5 mmoles) and pyridine (2.5 mmoles) in deoxygenated ethanol to cobalt chloride hexahydrate in deoxygenated ethanol (30 mL). NaCl (12 mmoles) was added to the reaction mixture while it was stirred at room temperature. Upon cooling to ice bath temperature the paramagnetic peach-colored powder separated and was washed with ether and dried under nitrogen. Anal: Calcd. for $[Co(dpk)_2(py)Cl]Cl \cdot 4H_2O$: C, 49.9; H, 4.5; N, 10.8; found: C, 49.8; H, 3.9; N, 10.4%.

$[Co(dpk \cdot H_2O)(terpy)](ClO_4)_2$. A solution (10 mL) of dpk (10 mmoles) and terpy (10 mmoles) in 1:1 *n*-propyl alcohol-water was added dropwise to a 25 mL solution of cobalt nitrate (9 mmoles) and sodium perchlorate (25 mmoles). The pH of the reaction mixture was maintained at ~7.5 by the dropwise addition of IN NaOH. A red precipitate formed rapidly and was filtered on fritted glass, washed with *n*-proply alcohol and ether then dried over $CaCl_2$ at room temperature. If the solution pH is maintained above 7, this paramagnetic Co(II) complex forms even in the presence of oxygen.

$[Co(dpk \cdot OH)_2](ClO_4)_2 \cdot H_2O$. Oxygen was passed through a solution of cobalt perchlorate (4 mmoles) and dpk (8 mmoles) in 40 mL of water at pH 8. After cooling for several hours red crystals precipitated and were washed and dried as described above. This compound was first prepared in an attempt to synthesize the μ-peroxo complex using the 4dpk/2 imidazole ligand system. Anal: Calcd. for $[Co(dpk \cdot OH)_2](ClO_4) \cdot H_2O$: C, 45.7; H, 3.5; N, 9.7: Found: C, 45.7; H, 3.5; N, 9.6%. The unusual ability of the ligand dpk to exist in two forms, the geminal-diol and the ionized geminal-diol, has been observed in Cu(II) complexes and in the Co(III) complex $[Co(dpk \cdot OH^-)_2](NO_3)$.[10] This latter compound was prepared by bubbling air through an aqueous solution of $Co(NO_3)_2$ and dpk! It was evident that the addition of NaOH to maintain the pH had a profound effect on the stability of the μ-peroxo adducts. Optimum pH for the isolation of dpk μ-peroxo dicobalt(III) complexes is in the range from ~3.0 to 5.6. The higher pH makes the anionic form of dpk (dpk-OH^-) the predominant species.[7]

RESULTS AND DISCUSSION

Infrared, visible-ultraviolet data

Physical and spectral properties for the complexes are listed in Tables 1 and 2. Cobalt(II) complexes of the amine ligands used in this study react with oxygen to produce peroxo compounds of formula: $[(terpy)(dpk)Co\text{-}O_2\text{-}Co(dpk)(terpy)](ClO_4)_4$, $[(py)(dpk_2Co\text{-}O_2\text{-}Co(dpk)_2(py)](ClO_4)_4 \cdot 4H_2O$, $[(py)(dpk \cdot H_2O)_2Co\text{-}O_2\text{-}Co\text{-}(dpk \cdot H_2O)_2(py)](ClO_4)_4$ and $[(dpk \cdot dien)Co\text{-}O_2\text{-}(dpk \cdot H_2O)\text{-}Co(dpk \cdot dien)](dpk \cdot dien)](ClO_4)_4 \cdot 2H_2O$. In the latter complex there is, in addition to the peroxo bridge, a bridging dpk · H_2O ligand. The proposed structure for $[Co_2(dpk)_4(py)_2O_2]^{4+}$ is shown in Fig. 1.

The ligand dpk is basically a 2-substituted pyridine and extensive IR correlations are available[4, 9]. The infrared spectrum of the ligand dpk exhibits the ketocarbonly stretching, $\nu(C=O)$, at 1675 cm^{-1} which increases to

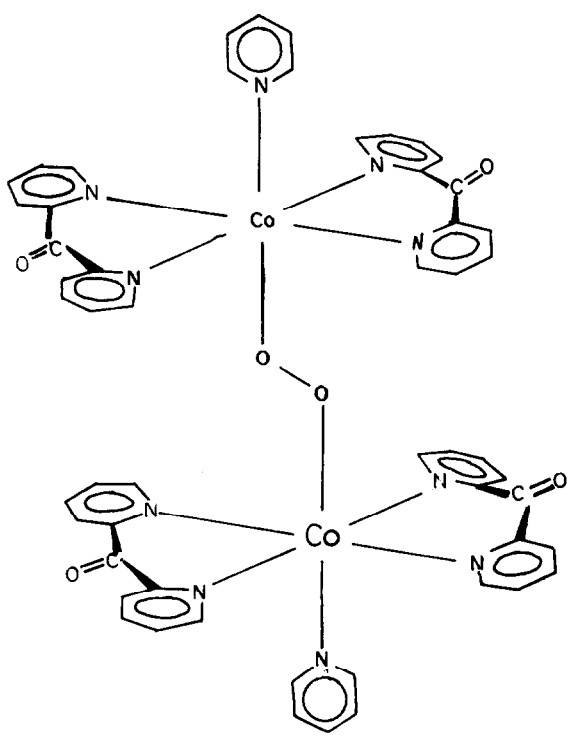

Fig. 1. The μ-peroxodicobalt(III) cation with di-2-pyridyl ketone and pyridine.

Table 1. Proposed band assignment for some μ-peroxodicobalt(III) complexes (λ in nm, ε in $1\,cm^{-1}\,mole^{-1}$)

Complex	$^1A_{1g} \rightarrow {}^1T_{1g}$		$\pi^*O_2 \rightarrow d_{z^2}$	intraligand bands	Ref.
$[Co_2(dpk\cdot dien)_2(dpk\cdot H_2O)O_2]^{4+}$		347(5200)		290(40,000) 235(60,000)	this work
$[Co_2(dpk)_4(py)_2O_2]^{4+}$	475(8800)	340(5500)		275(40,000) 230(65,000)	this work
$[Co_2(dpk\cdot H_2O)_4(py)_2O_2]^{4+}$	465(1400)	350(2700)	305(10,000)	285(40,000) 230(60,000)	this work
$[Co_2(dpk)_2(terpy)_2O_2]^{4+}$	465(4700)	350(8500)		320(30,000) 290(45,000) 275(39,000) 265(37,000)	this work
$[Co_2(en)_5O_2]^{4+}$		357(4100)			18
$[Co_2(dien)_2(en)_2O_2]^{4+}$	417(603)		300(9600)	227(22,000)	24
$[Co_2(pydien)_2O_2]^{4+}$	425(1000)	356(2500)	319(6000)	263(10,000) 232(18,000)	3
$[Co_2(pydpt)_2O_2]^{4+}$	454(1000)	350(6000)	319(6000)		3

pydien = 1,9-bis(2-pyridyl)-2,5,8-triazanonane pydpt = 1,11-bis(2-pyridyl)-2,6,10-triazaundecane

en = ethylenediamine

Table 2. Physical properties of complexes

	Decomposition Temp.*	Color	Magnetic Properties $\chi_g x10^6$	μ(B.M.)	Molar Conductance (25°C) mho cm^2M^{-1} CH_3NO_2	DMSO
$[Co_2(dpk\cdot dien)_2(dpk\cdot H_2O)O_2](ClO_4)_4\cdot H_2O$	212	light brown		diamagnetic	190	134
$[Co_2(dpk)_4(py)_2O_2](ClO_4)_4\cdot 4H_2O$	227	tan		diamagnetic	276	105
$[Co_2(dpk\cdot H_2O)_4(py)_2O_2](ClO_4)_4$	219	rust-red		diamagnetic	-	157
$[Co_2(dpk)_2(terpy)_2O_2](ClO_4)_4$	270	brown		0.4	316	128
$[Co(dpk)_2(py)Cl]Cl\cdot 4H_2O$	294	peach	15.17	4.54	77	48
$[Co(dpk\cdot H_2O)(terpy)](ClO_4)_2$	>320	red	8.67	3.53	179	62
$[Co(dpk)_2(ClO_4)_2]$	272	orange	8.76	3.62	—	69
$[Co(dpk\cdot OH^-)_2](ClO_4)\cdot H_2O$	>320	rust-red		diamagnetic	110	46

*The compounds darken above the temperature cited.

about 1695 cm^{-1} upon coordination. This change can be attributed to the shift of electron density when the ligand behaves as a bidentate N,N-donor. Another factor influencing $\nu(C=O)$ is the loss of conjugation of the keto carbonyl due to angle strain or loss of coplanarity with the pyridyl rings. The $\nu(C=O)$ at 1712 cm^{-1} and 1710 cm^{-1} in the complexes $[Co_2(dpk)_4(py)_2O_2](ClO_4)_4 \cdot 4H_2O$ and $[Co_2(dpk)_2(terpy)_2O_2](ClO_4)_4$ represent the highest carbonyl frequency reported for a dpk complex. The smaller ionic radius of the Co(III) ion could in some measure account for the introduction of added bond angle strain resulting in a higher frequency. In a series of dpk-chloride complexes with different transition metal ions, an inverse relationship between the ionic radii and $\nu(C=O)$ is observed. For example, in the complexes $[Ni(dpk)_2]Cl_2$, $[Zn(dpk)Cl_2]$, $[Cd(dpk)Cl_2]$, and $[Hg(dpk)Cl_2]$, $\nu(C=O)$ is located at 1687, 1680, 1676, and 1675 cm^{-1}, respectively.[6,10] The Pauling radii for those metal ions are 69, 74, 97 and 110 pm, respectively. However, the extremely high $\nu(C=O)$ in the dpk μ-peroxo complexes is only partially accounted for by the small ionic radius of Co(III). Extensive electron transfer via back-bonding in the coordinated pyridyl rings of dpk increases the electron density in the conjugated system thus raising the C–O bond order and stretching frequency.

Cobalt(II) complexes with suitable ligand systems undergo a dramatic color change when exposed to oxygen, due mainly to intense charge-transfer bands involving the dioxygen ligand. A major problem in the uv analysis of the complexes containing aromatic ligands is the differentiation between the very intense intraligand and charge-transfer bands and the relatively weak *d-d* transitions. A prominent feature of the spectra of μ-peroxodicobalt(III) complexes is a band between 300–360 nm which is assigned to the peroxide to cobalt charge-transfer.[2] Recent work has shown a direct relationship between the base strength (σ-donor) of the ligand system and the energy of this charge-transfer band.[11] As expected, our μ-peroxo complexes containing aromatic amines reveal comparatively lower energy charge-transfer bands than most μ-peroxodicobalt(III) aliphatic amine complexes (see Table 1).

The pyridine ring uv absorptions ($\pi \rightarrow \pi^*$) of aqueous solutions of dpk (10^{-4}M) below pH 10 occur at 278 nm ($\epsilon = 9140$).[7] Upon coordination of dpk in the peroxo complex a band at 275 nm ($\epsilon \sim 40{,}000$) appears in the spectrum. The $\pi \rightarrow \pi^*$ transitions of coordinated aromatic ligands are not significantly changed when compared to the free ligand.[12] It should be noted however, that in the dpk complexes that have undergone carbonyl addition the band at 275 nm is absent and an intense band at ~287 nm is present. The strong band at 250 nm (ϵ = 55,000) in $[Co_2(bipy)_4\text{-}\mu\text{-}NH\text{-}\mu O_2]^{3+}$ has been assigned to the $\pi \rightarrow \pi^*$ transition of the pyridyl ring.[13] The lower energy of the $\pi \rightarrow \pi^*$ transition in dpk is the result of substitution on the ring.[14] In the mixed-ligand complex, $[Co_2(dpk)_2(terpy)_2O_2](ClO_4)_4$ the free ligand bands of terpyridine are reproduced with only minor shifts. In the complex $[Co_2(dpk)_4(py)_2O_2](ClO_4)_4 \cdot 4H_2O$ the $\pi \rightarrow \pi^*$ transition of pyridine overlaps with more intense bands of the pyridyl rings from dpk. The free pyridine molecule exhibits the $\pi \rightarrow \pi^*$ transition at 256 nm ($\epsilon \sim$ 1860). The carbonyl intraligand band ($n \rightarrow \pi^*$) of dpk found at 356 nm ($\epsilon \sim 200$) in the free ligand was not observed in the spectra of our complexes.

Generally, two spin-allowed *d–d* transitions are observed in the electronic spectra of strong-field octahedral Co(III) ($^1A_{1g} \rightarrow {}^1T_{1g}$ and $^1A_{1g} \rightarrow {}^1T_{2g}$). The presence of the peroxo ligand raises the energy of these bands, with the typical five nitrogen-donor Co(III) complex absorbing near 500 and 365 nm. In many cases however, the high energy transition ($^1A_{1g} \rightarrow {}^1T_{2g}$) is totally obscured by intense charge-transfer bands. This was true of the μ-peroxo complexes prepared in our study. If tetragonal distortion of octahedral symmetry occurs the band at 500 nm is split into two components.[15] While the extinction coefficients of the *d–d* bands should fall in the range of 40 to 200, they often are much higher when located near intense charge-transfer bands. The intensities of the $^1A_1 \rightarrow {}^1T_1$ transition in our complexes are very high due to "intensity stealing". In addition, there is no splitting of this band to indicate significant tetragonal distortion.

Using mixed-ligand aromatic systems containing five donor nitrogen atoms per cobalt, reddish-brown diamagnetic μ-peroxo complexes were precipitated as perchlorates from aqueous solution at pH values ranging from 3 to 6. With the pH above 7, a mixed-ligand cobalt(II) complex of dpk/terpy was formed rapidly even in the presence of oxygen (eqn 2). Cobalt(II) complexes

$$\mathrm{Co(II)(dpk)(terpy)H_2O]^{2+} \xrightarrow{O_2} \begin{cases} \xrightarrow{pH=5} [(dpk)(terpy)Co(III)\text{-}O_2\text{-}Co(III)(terpy)(dpk)]^{4+} \\ \xrightarrow{pH=7} [Co(II)(dpk \cdot H_2O)(terpy)]^{2+} \end{cases} \quad (2)$$

formed under these conditions have no IR carbonyl absorption, indicating that dpk is present in the hydrated form. When the pH is above 7, the predominant form of dpk is the geminal diol which can deprotonate to form $dpk\text{-}OH^-$ (eqn 1). A likely mechanism for the inhibition of the oxygenation reaction at higher pH levels is the ability of the $dpk \cdot OH^-$ to coordinate through one of the hydroxyl oxygens, effectively blocking the sixth coordination site. IR analysis showed the presence of the characteristic bands for coordinated dpk and terpy. The red-brown solid $[Co(dpk \cdot H_2O)(terpy)](ClO_4)_2$ had a magnetic moment of 3.5 B.M. and behaved as a 2:1 electrolyte in nitromethane.

The complex $[Co(dpk)_2(py)Cl]Cl$ was prepared from degassed ethanol in order to test its reactivity with oxygen. The compound produced UV-visible spectra typical of a μ-peroxo complex after dissolving in oxygenated water. The distinctive charge-transfer band, arising from the electronic transition between the full $\pi^*(O_2^{-2})$ orbital and the empty dz^2 orbital of the metal, was located at 340 nm (ϵ = 5200) in the μ-peroxo complex prepared both by addition of $[Co(dpk)_2(py)Cl]Cl$ to water and by the titration of the ligand mixture into an oxygenated Co^{2+} solution at pH 4–6. If the complex $[Co_2(dpk)_4(py)_2O_2](ClO_4)_4$ is dissolved in a water–alcohol mixture the corresponding complex with the hydrated dpk will be formed after storage for several days at 4°

(eqn 3). In the IR spectrum of the

$$[Co(II)(dpk)_2(py)H_2O]^{2+} \xrightarrow[pH=6]{O_2}$$

$$(py)(dpk)_2Co(III)\text{-}O_2\text{-}Co(III)(dpk)_2(py)]^{4+} \xrightarrow[3\ days,\ 5°C]{pH\ 6.5}$$

$$(py)(dpk \cdot H_2O)_2Co(III)\text{-}O_2\text{-}Co(III)(dpk \cdot H_2O)_2(py)]^{4+}$$

complex so obtained, $\nu(C=O)$ is absent and the series of bands between 1600 cm^{-1} and 760 cm^{-1} have retained their shape and order but decreased slightly as compared to the parent compound having the carbonyl intact. Changes in the spectra are consistent with the addition of H_2O to the keto function. The IR spectra of the two compounds were quite similar, except for two new bands that appear at 689 cm^{-1} and 3510 cm^{-1} in $[Co_2(dpk \cdot H_2O)_4(ph)_2O_2](ClO_4)_4$. The low energy band is assigned to the out-of-plane deformation of the OH by analogy to a study of a Co(III) complex of tripyridyl carbinol and $CdBr_2$(dpk · piperidine)[16, 17]. The high energy band at 3510 cm^{-1} is assigned to ν(OH). This compound also has the distinctive charge transfer band in the UV-vis spectrum located at 350 nm (ϵ = 10,000) being shifted from 340 nm in the parent compound.

The μ-peroxo complex formed using the ligands dpk and terpy is isolated from aqueous solution at pH 4. A compound of analogous structure using terpy and bipyridyl, capable of binding O_2 at pH 3 was reported by Huchital and Martell.[8] Oxygenation usually occurs only under neutral or basic conditions. This feature of the oxygenation reaction is largely a function of the protonation constant of the amine. The aromatic amines, being weaker bases, are free to complex metal ions at pH levels where the typical aliphatic amine is protonated. Pyridine ring-stretching frequencies (of dpk and terpy in the μ-peroxo complex) are consistent with coordination through the pyridyl nitrogens. The following bands were observed between 1560 cm^{-1} and 1625 cm^{-1}: 1565 cm^{-1}, 1587 cm^{-1}, 1606 cm^{-1} and 1622 cm^{-1}. The free ligands of both dpk and terpy contain only two bands in this region, thus the presence of both ligands is indicated. The carbonyl band appeared at an unusually high value of 1710 cm^{-1}. The conductivity of the complex $[Co(dpk)_2(terpy_2O_2](ClO_4)_4$ in nitromethane is consistent with its formulation as a 4:1 electrolyte. The small magnetic moment of 0.4 B.M. is near that commonly found for temperature-independent paramagnetism for Co(III) complexes.[16]

Nucleophilic addition to dpk of the secondary amine nitrogen of dien results in the formation of an amine carbinol compound referred to as dpk · dien. Confirmation of this reaction was obtained by running successive IR spectra of a mixture of dpk and dien. The $\nu(C=O)$ disappeared concurrently with the appearance of bands at 3400 cm^{-1} and 790 cm^{-1}. These two bands are assigned to the new OH function. An analogous reaction was observed[17] between dpk and piperidine in the complex $CdBr_2$(dpk · pip), where ν(OH) was located at 3440 cm^{-1}. Further evidence for carbonyl addition comes from the integration of the NMR spectra which shows the disappearance of one of the amine protons.

The IR spectrum of the complex $[Co_2(dpk \cdot dien)_2\text{-}\mu\text{-}O_2\text{-}\mu\text{-}(dpk \cdot H_2O)](ClO_4)_4 \cdot 2H_2O$ revealed the pyridine ring absorptions split into multiple bands. It might be expected that since the complex contains only the dpk pyridine ring, the spectra might be simpler than the other complexes containing different pyridyl compounds. Overall, the IR suggests the non-equivalence of the pyridyl rings, thus supporting the dibridged structure. The pyridyl rings in a bridging dpk would certainly have different vibration modes. For example, four sharp peaks are obtained in the py ring stretching region compared to only two bands for the dpk/py complex (see Table 3). The characteristic bands of dien, ν(N–H), $\delta(NH_2)$ and ν(C–N) appear at 3460 cm^{-1}, 1600 cm^{-1} and 1350 cm^{-1}, respectively. Table 1 shows the similarity in the uv-vis spectrum of the dpk/dien complex to the spectrum of the bridged complex $[Co_2(en)_5O_2]^{+4}$.[18] The characteristic two band pattern in the uv-vis spectra of many mono-bridged μ-peroxo complexes changes to a single charge-transfer absorption at 350–360 nm upon the addition of a second bridging group. Our dpk/dien complex exhibits a single strong band at 347 nm (ϵ = 5200). Aqueous solutions of this brown complex, after several minutes, turn green, probably indicating decomposition to Co(II). Bridging ligands have been reported to result in unstable dimeric O_2 adducts.[18]

Thermogravimetric data

Table 4 lists the thermogravimetric data compiled in this study. This method has been applied to oxygen complexes having volatile axial ligands such as pyridine and DMF.[19] The lattice water and the coordinated oxygen appeared to be the most thermally labile, being lost below 100°C in all cases. Thermogravimetric data can be explained accurately in terms of the loss of H_2O, the O_2 ligand, and the auxiliary ligand group. During the analysis of the dpk/terpy complex, the vaporized terpyridyl was found sublimed on the glass walls of the furnace in the form of white needle-shaped crystals. The superior binding ability of dpk was demonstrated by its thermal stability in the TGA study. On several occasions 3–5 mg samples of the μ-peroxo perchlorate salts detonated at temperatures ranging from 190 to 220° during the TGA runs.

Proton magnetic resonance data

The extent of electron donation to a metal ion and the factors involved in back-donation or "π-acidity" of coordinated pyridine compounds is usually qualitatively accessible by NMR analysis. If electron density is added to the aromatic system, it might be expected that a chemical shift upfield could be observed for the ring protons. A downfield shift of all the ring protons of the dpk ligand is expected and has been observed[9] upon coordination of the pyridyl nitrogens, this being a result of electron withdrawal by the metal ion. The degree of this downfield shift can be interpreted in terms of back-donation to the pyridyl ring or the reaction of the carbonyl function of dpk. The effect of coordinate-covalent bonding between pyridyl type ligands and a metal ion would be greatest for the α-proton. The π-electron density at the various carbon atoms can be inferred from the chemical shift of the proton. Several authors have proposed methods for calculating π-electron densities from NMR data but they emphasize that the interpretations are tentative and depend upon factors not well understood.[20,21]

Solvent effects on the spectra of pyridine compounds have been widely studied. However, few researchers can agree on either the size or the nature of the effects of

Table 3. Tentative IR band assignments

Compound	Keto carbonyl ν(C=O)	Pyridyl ring stretching ν(C=N), ν(C=C)	$\nu_3(ClO_4)$	Pyridyl ring breathing	Pyridyl C-H out of plane bending	Pyridyl ring in plane vibration	Ref.
di-2-pyridyl ketone(dpk)	1675s	1578s 1565m		998m	753s 742s	662m	9
2, 2^1, 2^{11}-tripyridine(terpy)		1587s 1568s		990m	770s 760s 730w	654m	this work
$[Co_2(dpk\cdot dien)_2(dpk\cdot H_2O)O_2](ClO_4)_4\cdot H_2O$		1610s 1592s 1578w	1090br	1030s 1003w	768s 752w	680w 668m 662w	this work
$[Co_2(dpk)_4(py)_2O_2](ClO_4)_4\cdot 4H_2O$	1712m	1609s 1578w	1098br	1030s	770s 762w	672s	this work
$[Co_2(dpk\cdot H_2O)_4(py)_2O_2](ClO_4)_4$		1610s 1572w	1093br	1028s	768s 750w	668m	this work
$[Co_2(dpk)_2(terpy)_2O_2](ClO_4)_4$	1710m	1606s 1587m 1565m	1093br	1018w 1030m 1000w	770m 735s	680m 672m	this work
$[Co(dpk)_2(py)Cl]Cl\cdot 4H_2O$	1685s	1606s 1593m		1020s 1000m	770m 755s 737w	660m	this work
$[Co(dpk\cdot H_2O)(terpy)](ClO_4)_2$		1608s 1583m 1567m	1093br	1030m 1017m	770s 740w	670m 650m	this work
$[Co(dpk)_2Cl_2]$	1683s	1585s 1565w		1018s	758s 737s	664m	4
$[Co(dpk)_2(ClO_4)_2]$	1694s	1594s 1580w	1140br 1030br	1026m	762s 742w	668m	4
$[La(dpk)_4](ClO_4)_3\cdot 2H_2O$	1695m	1600s 1585m	1100br	1023m	758s 735w	670s	9

Table 4. Thermogravimetric data

Compound	Loss of	% Weight Loss Calculated	Found	Temperature
$[Co_2(dpk\cdot dien)_2(dpk\cdot H_2O)O_2](ClO_4)_4\cdot H_2O$	O_2, $2H_2O$	5.1	5.8	90°
	O_2, $2H_2O$, 2dien	20.4	21.0	210°
$[Co_2(dpk)_4(py)_2O_2](ClO_4)_4\cdot 4H_2O$	O_2, $4H_2O$	6.9	7.0	55°
	O_2, $4H_2O$, 2py	17.3	16.5	195°
$[Co_2(dpk\cdot H_2O)_4(py)_2O_2](ClO_4)_4$	O_2	2.0	1.8	70°
	O_2, $4H_2O$	6.4	6.6	93°
	O_2, $4H_2O$, 2py	16.2	16.0	209°
$[Co_2(dpk)_2(terpy)_2O_2](ClO_4)_4$	O_2	2.3	2.1	95°
	O_2, 2terpy	36.1	38.0	350°

solvent on the chemical shift of the ring protons. It is important, therefore, that to undertake a comparative NMR study one must select studies based on similar solvents.

One of the most notable features of the NMR spectra of pyridine compounds is the broadening of the proton signals, being most apparent in the protons adjacent to the nitrogen atom. A pyridine-containing ligand has sp^2 orbitals on the nitrogen atom, and low-energy antibonding π-orbitals associated with the aromatic ring system; therefore, it is possible for di-2-pyridyl ketone, for example, to act both as a donor and an acceptor of electrons. This synergistic effect in the bonding of aromatic ligands to metal ions plays a prominent role in explaining the enhanced stability of some dioxygen complexes. It has been noted that oxygen affinities for Co(II) complexes containing pyridyl ligands are unusually high, considering only the σ donor capacities of these groups.[11] To study the extent of electron transfer in our complexes, the chemical shifts of the ring protons in a number of mixed-ligand μ-peroxo complexes have been measured. The spectrum of the coordinated ligand was compared to the spectrum of the free ligand using the same solvent. While spectra were run in D_2O, CD_3CN and DMSO, limited solubility in all but the DMSO precluded extensive solvent comparison study. Literature data, assignments of proton resonances, and a summary of the observed spectra in this study are found in Table 5. To simplify the assignment of the mixed-ligand systems that contain two different pyridyl compounds, it is assumed that the positions α to the nitrogen are equivalent.

In an NMR study of tris-o-phenanthroline complexes of Co(III), Fe(II), Ru(II) and Zn(II), it was determined that a shift to higher fields of the protons adjacent to nitrogen increases as the metal-ion radii decrease. Miller and Prince also reported that the resonance frequencies for all the aromatic protons move to higher fields as *o*-phenanthroline is coordinated.[22] When the dpk molecule is coordinated, there are changes in the magnetic environment of ligands that are independent of the coordinate bond formation. Since ligands are being held in close proximity to one another, a multiplicity of magnetic perturbations might be expected. Specific solvation of the ligand would be changed due to the more limited access of solvent molecules to the ligand dipoles. The carbonyl group of dpk exerts a downfield shift on all the ring protons (compared to pyridine) with the effects most apparent at the proton adjacent to the substituent group.

Changes in the NMR spectrum of $[Co_2(dpk\cdot dien)_2(dpk\cdot H_2O)O_2]^{4+}$ can be explained in terms of the coordination of the dpk and the reaction of the carbonyl group. The shift of 0.42 ppm of the resonance of H(6) is indicative of coordination. The failure of H(5) to show any downfield shift may be a result of the reaction of the carbonyl. The resonance for H(3) also showed a much smaller shift than would be expected from comparison to the La/dpk complex listed in Table 5. It is proposed that the loss of the carbonyl electron-withdrawing effect is offset by the downfield shift of coordination. This would seem to be a reasonable proposal in that the major effects of the carbonyl substituent occur at positions ortho and para, and the same is true of the effects of the nitrogen in pyridine. The more subtle change brought about by π-bonding and solvent interaction cannot be separated from the more drastic effects of coordination and carbonyl addition. One readily apparent feature of the spectrum of the dpk/dien complex was the extreme complexity of the signal compared to the complex with the dpk/py ligands. This strongly implies that the dpk/dien complex has pyridyl rings in different magnetic environments, again suggesting a bridging ligand. The resonance bands of the dien ligand were located at 2.8 ppm and 5.5 ppm for the C–H and the NH_2, respectively. These assignments are consistent with data reported by Crawford *et al.*[18] involving the spectra of [trien Co(μ-en, O_2)Co trien]$^{4+}$ in which they assigned a broad peak at ~2.8 ppm to the ethylenic protons of coordinated trien. In another study of Co(III) chelates of trien, Japanese researchers assigned the protons of the NH_2 group to a broad band centered at 5.3 ppm.[23] The possibility of the peak at 5.5 ppm in the dpk/dien complex originating from an O–H proton is discounted on the basis that it does not appear in any of the other complexes containing the gem-diol. The O–H group in the hydrated dpk can act as a strong acid, with the equilibrium shown in eqn (1) accounting for the lack of OH proton resonances at ~5 ppm. This ionization also explains the rapid drop in pH upon addition of dpk to Co^{2+} solutions.

The proton spectrum of $[Co_2(dpk)_4(py)_2O_2]^{4+}$ was fairly well resolved allowing integration of the resonance

Table 5. NMR Data of some mixed-ligand Co(III) complexes in DMSO *d*-6

Assignments of Proton Resonances		dpk	py	terpy	dien	dpk/dien complex	dpk/py complex	dpk·H_2O/py complex	dpk/terpy complex	dpk·OH^- complex
dpk	H(3)	7.92				8.08	8.02	8.03	8.00	7.90
	H(4)	7.92				8.08	8.02	8.03	8.00	7.90
	H(5)	7.55				7.34	7.44	7.39	7.50	7.37
	H(6)	8.62				9.04	8.74	8.48	8.80	8.41
py	H(2)(6)		8.61				8.74	~		
	H(3)(5)		7.31				7.35	7.35		
	H(4)		7.79				8.44	8.48		
terpy	H(2)(12)			8.70					9.50	
	H(3)(11)			7.46					7.36	
	H(4)(10)			7.98					8.30	
	H(5)(6)(8)(9)			8.50					8.70	
	H(7)			8.35					8.46	
dien	C-H				2.51	2.80				
	N-H				1.48	5.50				

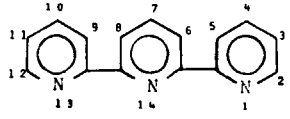

(terpy)

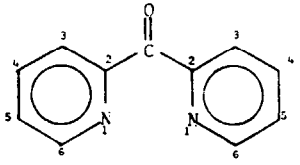

(dpk)

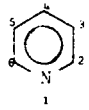

(py)

peaks. The H(6) protons of dpk produced a broad peak at 8.74 ppm. This downfield shift is expected if the pyridyl nitrogen adjacent to this proton is coordinated. A curious feature of the spectrum of the dpk/py complex was the presence of a sharp well-defined resonance peak at 8.44 ppm. The position and shape of this peak clearly places it in the range expected for the H(4) of pyridine. The calculated ratio in the complex (1:20) matches well with the determined integration of 1:22. The fact that the signal is not split conflicts with the known coupling constants for pyridine in D_2O, $J_{(24)} = 1.24$ Hz; $J_{(34)} = 2.95$ Hz.[20] Since the coupling constants are a function of protonation of the pyridine, it is possible that the sharp signal of H(4) in pyridine is the result of attenuation of the spin-spin coupling as a result of chelation.

The spectrum of $[Co_2(dpk \cdot H_2O)_4(py)_2O_2]^{4+}$ again showed a sharp well-defined peak near 8.5 ppm and the broad band far downfield that appeared in both of the previously discussed complexes is absent. The ratio of the resolved multiplets in the spectra is 4:21:13 for the peaks at 8.48 ppm, 8.03 ppm, and 7.39 ppm, respectively. No definitive assignment of this integration pattern was possible because of the overlap of the pyridine and dpk signals. The spectrum of this compound was run without signal averaging.

The extremely complex NMR spectrum of $[Co_2(dpk)_2(terpy)_2O_2]^{4+}$ was a result of the presence of ten different groups of equivalent aromatic protons. As in the case of the dpk/py complex a sharp spike in the spectra at 8.3 ppm appeared which is assigned to H(7). It appears that chelation of symmetrical nitrogen hetrocycles results in the decoupling of some signals. The extreme downfield shift of the α protons (9.5 ppm) sets this compound apart from the others.

Since the H(5) proton of dpk is most representative of π-electron density on the ring, its resonance position is significant.[20] A slight *upfield* shift is indicated in all the peroxo containing compounds. This behavior, along with the high carbonyl stretching frequencies, points to *increased* π-electron density on coordinated dpk, being only slightly less for the hydrated form. By contrast, in the La/dpk complexes, all the aromatic protons are shifted downfield[9].

Acknowledgements—The authors wish to thank the Robert A. Welch Foundation for financial support (JDO, grant V-368). We would also like to thank Todd McKenney for his help in obtaining the conductivity data.

REFERENCES

[1]G. McLendon and A. Martell, *Coord. Chem. Rev.* 1976, **19**, 1.
[2]D. Summerville, R. Jones, B. Hoffman and F. Basolo, *J. Chem. Ed.* 1979, **56**, 3.
[3]S. Pickens and A. Martell, *Inorg. Chem.* 1980, **19**, 15.
[4]J. D. Ortego, D. Waters and C. Steele, *J. Inorg. Nucl. Chem.* 1974, **36**, 751.
[5]I. Bakker, M. Feller and R. Robson, *J. Ibid.* 1971, **33**, 747.
[6]J. D. Ortego, S. Upalawanna and S. Amanollahi, *Ibid.* 1979, **41**, 595.
[7]B. Fischer and H. Siegel, *Ibid.* 1975, **37**, 2127.
[8]D. Huchital and A. Martell, *Inorg. Chem.* 1974, **13**, 2966.
[9]R. Jagannathan, *J. Inorg. Nucl. Chem.* 1980, **42**, 145.
[10]M. Feller and R. Robson, *Aust. J. Chem.* 1968, **21**, 2919.
[11]A. E. Martell *et al.*, *Inorg. Chem.* 1978, **17**, 2195.
[12]J. Hidaka and B. E. Douglas, *Inorg. Chem.* 1964, **3**, 1180.
[13]Y. Sasaki, J. Fujita and K. Saito, *Bull. Chem. Soc. Jpn.* 1970, **43**, 3462.
[14]G. Rao, *Ultra-Violet and Visible Spectroscopy*, p. 60. Butterworths, London 1961.
[15]B. Figgis, *Introduction to Ligand Fields.* Interscience, New York 1966.
[16]R. Bogges and S. Boberg, *J. Inorg. Nucl. Chem.* 1980, **42**, 21.
[17]S. Upalawanna, M. S. Thesis, Lamar University, 1978.
[18]M. Crawford, S. Bedell, R. Patel, L. Young and R. Nakon, *Inorg. Chem.* 1979, **18**, 2075.
[19]A. Crumbliss and F. Basolo, *J. Am. Chem. Soc.* 1970, **92**, 60.
[20]T. Batterman, *NMR Spectra of Simple Heterocycles.* Wiley-Interscience, New York 1973.
[21]T. Cobb and J. Memory, *J. Chem. Phy.* 1969, **50**, 4262.
[22]J. Miller and R. Prince, *J. Chem. Soc.* 1965, 3188.
[23]Y. Yamamoto and E. Toyota, *Bull. Chem. Soc. Jpn.* 1979, **52**, 2540.
[24]G. Lawrence and P. Lay, *J. Inorg. Nucl. Chem.* 1979, **41**, 301.

Polyhedron Vol. 1, No. 1, pp. 31–36, 1982
Printed in Great Britain.

0277–5387/82/010031–06$03.00/0
Pergamon Press Ltd.

SYNTHESIS AND REACTIONS OF PHENYLIMIDOTRIMETHYL-BIS(TRIMETHYLPHOSPHINE)-RHENIUM(V). SYNTHESIS AND X-RAY CRYSTAL STRUCTURE OF BIS(TRIMETHYLSILYLMETHYL)OXO-RHENIUM(V)-μ-OXO-TETRAKIS(TRIMETHYLPHOSPHINE)RHENIUM (I)-(TRIMETHYLSILYLMETHYL)DIOXORHENIUM(V), (Re–Re)

KWOK W. CHIU, WAI-KWOK WONG and GEOFFREY WILKINSON*
Chemistry Department, Imperial College, London SW7 2AY, England

and

ANITA M. R. GALAS and MICHAEL B. HURSTHOUSE
Chemistry Department, Queen Mary College, Mile End Road, London E1 4NS, England

(*Received* 12 *June* 1981)

Abstract—The interaction of phenylimidotrichloro*bis*(trimethylphosphine) with dimethylmagnesium gives the trimethyl compound, $Re(NPh)Me_3(PMe_3)_2$. Exchange reactions between the trichloro and trimethyl compounds are studied by ^1H nuclear magnetic resonance and the intermediates $Re(NPh)Me_2Cl(PMe_3)_2$ and $Re(NPh)MeCl_2(PMe_3)_2$ isolated.

The trimethyl reacts with fluoroboric acid to give a phenylamido complex $[Re(NHPh)Me_2F(PMe_3)_2]BF_4$, with acetic acid to give $Re(NPh)Me(CO_2Me_3)_2$, and with trityltetrafluoroborate to give $[Re(NPh)Me_2(PMe_3)_2]BF_4$.

The interaction of $Re(NPh)Cl_3(PMe_3)_2$ with excess of *bis*(trimethylsilylmethyl)magnesium and of trimethylphosphine in tetrahydrofuran gives an unusual tri-rhenium compound, $(Me_3SiCH_2)_3(O)Re$-μ-O-$Re(PMe_3)_4Re(O)_2(CH_2SiMe_3)$ whose structure as a thf solvate, has been determined by X-ray crystallography. Crystals of the latter are monoclinic, space group $P2_1/n$ with $a = 15.512(3)$, $b = 15.392(2)$, $c = 21.506(4)$Å, $\beta = 100.19(2)°$, $Z = 4$. The structure has been refined to an R of 0.07 for 5028 observed diffractometer data. The molecule is tri-nuclear with the central rhenium carrying four PMe_3 groups being bound to the second rhenium by a short Re–Re bond and to the third by an asymmetric oxygen bridge. The end rhenium bound to the bridge oxygen carries two CH_2SiMe_3 groups and an oxygen atom, while the other has one CH_2SiMe_3 group and two oxygen atoms.

The synthesis and reduction reactions of phenylimido trichloro*bis*(trimethylphosphine)rhenium(V) have been described.[1] We now report the synthesis of the trimethyl analogue, $Re(NPh)Me_3(PMe_3)_2$ and some of its reactions. NMR data for new compounds is collected in Table 1.

1. INTERACTION OF DIMETHYLMAGNESIUM AND $Re(NPh)Cl_3(PMe_3)_2$

The interaction of the trichloride with excess Me_2Mg in toluene gives dark green crystals of the air sensitive trimethyl $Re(NPh)Me_3(PMe_3)_2$ (**1**). Use of only one equivalent gives a similar dark green compound, $Re(NPh)ClMe_2(PMe_3)_2$ (**2**), while 0.5 equivalents leads to the light green $Re(NPh)Cl_2Me(PMe_3)_2$.

Intermolecular methyl transfer reactions between these species can be observed by NMR study (eqns 1–3).

$$Re(NPh)Me_3(PMe_3)_2 + Re(NPh)Cl_3(PMe_3)_2 \rightarrow Re(NPh)Cl_2Me(PMe_3)_2 + Re(NPh)ClMe_2(PMe_3)_2 \quad (1)$$

$$Re(NPh)Me_3(PMe_3)_2 + Re(NPh)Cl_2Me(PMe_3)_2 \rightarrow 2Re(NPh)ClMe_2(PMe_3)_2 \quad (2)$$

$$Re(NPh)ClMe_2(PMe_3)_2 + Re(NPh)Cl_3(PMe_3)_2 \rightarrow 2Re(NPh)Cl_2Me(PMe_3)_2. \quad (3)$$

Such transfer reactions are established in a number of cases, e.g. for Au, Pd and Pt compounds,[2] between $TaCl_4Me$ and $TaCl_2Me_3$,[3] and between Co and Rh complexes.[4] They have been considered as involving bi-molecular electrophilic substitution at the methyl group (S_E2).[5]

Between $Re(NPh)Cl_3(PMe_3)_2$ and $Re(NPh)Me_3(PMe_3)_2$ in d^8-toluene, there is no exchange at *ca.* 30°C but at 70°C the reaction is complete after *ca.* 36 hr and at 90°C after *ca.* 15 hr. Two new sets of doublets are observed in the ^1H NMR spectrum at δ 3.47 ($^3J_{P-H} = 7$ Hz) and 1.48 ($^2J_{P-H} = 8$ Hz) corresponding to the Re–Me and PMe_3 resonances of $Re(NPh)ClMe_2(PMe_3)_2$. Addition of an excess of $Re(NPh)Cl_3(PMe_3)_2$ to the solution causes no apparent change after 24 hr at 70°C, but on raising the temperature to 80°C the resonances due to (**2**) decrease in intensity and a new set of signals coincident with those for $Re(NPh)Cl_2Me(PMe_3)_2$ appear (δ 4.6 triplet, $^3J_{P-H} = 4.5$ Hz, Re–Me; δ 1.48 triplet, $^2J_{P-H} = 3.5$ Hz, PMe_3).

Methyl transfer is also observed between $Re(NPh)Me_3(PMe_3)_2$ and $Re(NPh)Cl_2Me(PMe_3)_2$ at 70°C and is again complete in *ca.* 36 hr. Since the monomethyl species can be observed (eqn 1), the rate of the second transfer to give $Re(NPh)ClMe(PMe_3)_2$ is probably not more than ten times that for the first transfer, whose activation energy must be greater. Also, since reaction (3) proceeds only at 80°C or above this must have the highest activation energy of the reactions 1–3.

2. REACTIONS OF PHENYLIMIDOTRIMETHYL-*BIS*(TRIMETHYLPHOSPHINE)RHENIUM(V)

Although the complex reacts with both NO and CO,

*Author to whom correspondence should be addressed.

Table 1. Nuclear magnetic resonance data[a]

Compound	^1H δ ppm	Assignment	$^{31}P\{^1H\}$ δ ppm	Assignment
1. $Re(NPh)Me_3(PMe_3)_2$	6.85 -7.25 m (5)	NPh	-59.7 d ($^2J_{P-P}$ = 6 Hz)	PMe_3
	3.42 d (6) ($^3J_{P-H}$ = 8 Hz)	Me		
	1.45 d (18) ($^2J_{P-H}$ = 8 Hz)	PMe_3		
	-1.08 t (3) ($^3J_{P-H}$ = 15 Hz)	Me		
2. $Re(NPh)C\ell Me_2(PMe_3)_2$	6.85-7.42 m (5)	NPh	-8.16 br,s	PMe_3
	3.52 d (6) ($^3J_{P-H}$ = 6 Hz)	Me		
	1.54 d (18) ($^2J_{P-H}$ = 8Hz)	PMe_3		
3. $Re(NPh)C\ell_2Me(PMe_3)_2$	6.6-7.4 m (5)	NPh	-39.6 br,s	PMe_3
	4.6 t (3) ($^3J_{P-H}$ = 4.5 Hz)	Me		
	1.48 t (18) ($^2J_{P-H}$ = 3.5 Hz)	PMe_3		
4. $[Re(NPh)Me_2(PMe_3)_2][BF_4]$[b]	7.4-7.6 m (5)	NPh	-25.3 d($^2J_{P-P}$ = 10 Hz)	PMe_3
	2.0 s (6)	Me		
	1.79 t (18)($^2J_{P-H}$ = 6 Hz)	PMe_3		
5. $[Re(NHPh)FMe_2(PMe_3)_2][BF_4]$[b,c]	7.6-8.1 m (5)	NPh	-26.7 d of d ($^2J_{P-P}$ = 11.0,	PMe_3
	3.7 br,s (1)	NH	$^2J_{P-F}$ = 57.2 Hz)	
	1.87 m (18)	PMe_3		
	2.18 d (6) ($^3J_{P-H}$ = 4.0 Hz)	Me		
6. $Re(NPh)(CO_2Me)_2Me(PMe_3)_2$	6.85-7.16 m (5)	NPh	-32.5 br,s	PMe_3
	3.39 t (3) ($^3J_{P-H}$ = 4 Hz)	Me		
	2.58 s (3) / 1.86 s (3)	CH_3CO_2		
	1.49 t (18) ($^2J_{P-H}$ = 4 Hz)	PMe_3		
7. $Re_2O_4(CH_2SiMe_3)_2(PMe_3)_4$	1.46 br,s (36)	PMe_3	-32.1 br,s	PMe_3
	0.38 s (18) / 0.18 s (9)	$SiMe_3$	-35.4 br,s	
	0.30 s (4) / 0.14 s (2)	CH_2		

[a] In $[^2H]_6$ benzene at 90 MHz, 35°C, Me_4Si, δ 0.0. Relative areas in parenthesis. ^{31}P to 85% H_3PO_4 external.

[b] In $[^2H]_6$ acetone at 90 MHz, 35°C, Me_4Si, δ 0.0. Relative areas in parenthesis.

[c] ^{19}F ; -156.45 s (4), BF_4; -167.59 t (1) ($^2J_{P-F}$ = 57.24 Hz), Re-F ; relative to $CFC\ell_3$, negative values to high field.

mixtures of products are obtained; there is no reaction with hydrogen at *ca.* 3 atm and 75°C.

(a) *Tetrafluoroboric acid*

In tetrahydrofuran the compound reacts with 48% aqueous HBF_4 undergoing protonation of the nitrogen and loss of one methyl group as methane to give white microcrystals of $[Re(NHPh)FMe_2(PMe_3)_2]BF_4$ (**4**). This salt is air-stable, diamagnetic and a 1 : 1 electrolyte in nitromethane. A precedent for this type of fluoro complex is $[Mo(N_2H)F(dppe)_2]BF_4$.[6,7]

(b) *Acetic acid*

In this case no protonation of the NPh group occurs although methane is lost and the acetate $Re(NPh)Me(CO_2Me)_2(PMe_3)_2$ (**5**) is obtained as a neutral purple air-stable compound. There is no N–H stretch in the IR spectrum which has bands characteristic of unidentate acetate[8] so that the compound is 6-coordinate.

(c) *Trityltetrafluoroborate*

Removal of a methyl group as Ph_3CMe by interaction with Ph_3CBF_4 in toluene–dichloromethane produces the purple air-stable salt $[Re(NPh)Me_2(PMe_3)_2]BF_4$ (**6**), which is a 1 : 1 electrolyte in nitromethane. Although possibly 5-coordinate, in d_6-acetone the ^1H NMR spectrum is unchanged from +40 to −80°C. In the solid state the BF_4 group may act as a unidentate ligand, since although IR evidence for BF_4^- coordination is somewhat ambiguous,[9] there is noticeable splitting of the bands at 1055 and 770 cm^{-1}.

A precedent for this reaction is the formation of $[(\eta^5\text{-}C_5H_5)_2TaMe_2]BF_4$ from $(\eta^5\text{-}C_5H_5)_2TaMe_3$.[10]

3. INTERACTION OF $Re(NPh)Cl_3(PMe_3)_2$ WITH $(Me_3SiCH_2)_2Mg$

The interaction of the phenylimido complex in the presence of excess trimethylphosphine with excess $(Me_3SiCH_2)_2Mg$ in tetrahydrofuran at 70°C for 2 days gives a complex that contains no nitrogen and has stoichiometry $Re_3O_4(CH_2SiMe_3)_3(PMe_3)_4$.

The IR and NMR data are in accord with the structure discussed below. Thus, in the IR there are terminal Re=O stretches at 1015, 910 and 890 cm^{-1} the first being ascribed to the stretch of the non-linear O=Re–O– group by comparison with other similar compounds.[11]

A drawing of the molecular structure is given in Fig. 1, whilst some of the more important molecular geometry parameters are given in Table 2. The molecule is structurally unique but it is possible to rationalise the bonding in terms both of common rhenium oxidation states and of electron counting. Representation of the structure by the single form (1) shows that the Re(1) and Re(3) atoms have formal oxidation states (V), whilst Re(2) has oxidation state (I). Furthermore, assuming a double Re(2)=Re(3) bond, these two metal atoms have 18-elec-

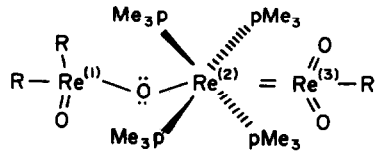

(i) R = CH_2SiMe_3

tron configurations. The atom Re(1) has 14 electrons as written but the electron number can be increased to 18 if the two lone pairs on the bridging oxygen atom are both donated to Re(1) in Re–O π-bonding. This would explain the large asymmetry in the Re(1)–O–Re(2) bridge, where

Table 2. Selected bond lengths and angles for $(Me_3SiCH_2)_2(O)Re(\mu\text{-}O)\text{-}Re(PMe_3)_4Re(O)(CH_2SiMe_3)$

a) Bond Lengths		b) Interbond Angles	
Re(1)-O(1)	1.78(1)	O(1A)-Re-O(1)	132.1(6)
Re(1)-O(1A)	1.71(2)	C(1B)-Re-C(1C)	85.5(8)
Re(1)-C(1B)	2.13(2)	Other angles at Re(1) are 104.2-	
Re(1)-C(1C)	2.13(2)	110.6(8)	
Re(2)-P(1)	2.419(6)	O(1)-Re(2)-Re(3)	175.0
Re(2)-P(2)	2.490(6)	O(1)-Re(2)-P	77.6-92.8(3)
Re(2)-P(3)	2.430(6)	P-Re(2)-P (cis)	89.4-91.2(2)
Re(2)-P(4)	2.427(6)	P(1)-Re(2)-P(2)	156.4(2)
Re(2)-O(1)	2.28(1)	P(3)-Re(2)-P(4)	177.8(2)
Re(2)-Re(3)	2.381(1)	Re(3)-Re(2)-P	88.7-106.0(2)
Re(3)-O(3A)	1.64(3)	O(3A)-Re(3)-O(3B)	108(1)
Re(3)-O(3B)	1.61(3)	O(3A)-Re(3)-C(3C)	103(1)
Re(3)-C(3C)	2.09(4)	O(3B)-Re(3)-C(3C)	112(2)
Si-C	1.65-1.97(9)		
P-C	1.81-1.88(3)		

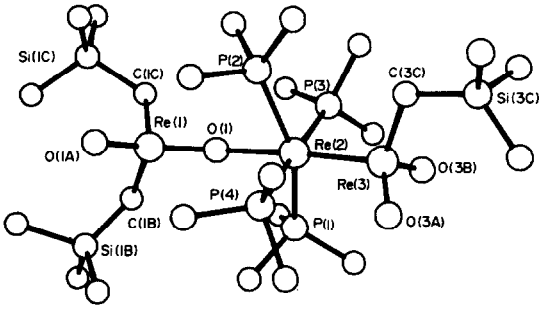

Re(1)–O is 1.781(2) Å and O–Re(2) is 2.28(2) Å, although the asymmetry could be due in part to the oxidation state differences. The remaining parameters are, for the most part in the ranges of expected values. Thus, the Re(2)–Re(3) distance of 2.381(1) Å is consistent with a double bond. The Re(2)–P distances show quite a large spread (2.42–2.49(1) Å) and the two Re(3)–oxo distances (1.61, 1.64(3) Å) differ from the Re(1)–oxo distance (1.71(2) Å) by more than might have been expected, although the difference is only 3σ. These inconsistencies are almost certainly due to deficiencies in the refinement, and indeed, our attempts at full anisotropic refinement indicated that the ligands on Re(3) undergo large thermal motion, (suggesting perhaps, some oscillation about the Re=Re bond).

The mechanism of formation of this unusual compound is not clear but the oxygen evidently comes from cleavage of the tetrahydrofuran since the reaction and work up were carried out in an inert atmosphere. The formation of a Re–Re bond in alkylation reactions has not previously been observed nor have Re–Re bonds involving, formally, a Re(V) atom been described. Four-coordination for Re(V) is also unique.[12]

EXPERIMENTAL

Microanalysis were by Pascher, Bonn and Imperial College Laboratories.

Spectrometers. IR: Perkin–Elmer 597; spectra in nujol mulls. NMR: Perkin–Elmer R32 (^{1}H, 90 MHz), Bruker WM–250 (^{1}H 250 MHz; ^{31}P{^{1}H} 101.27 MHz).

All operations were performed under oxygen-free nitrogen or argon or *in vacuo* and all solvents were dried over sodium (except dichloromethane which was dried over P_2O_5) and distilled from sodium/benzophenone under nitrogen immediately before use. Light petroleum had b.p. 40–60°C. Melting points were determined in sealed tubes (uncorrected). Analytical data are collected in Table 3.

(1) *Phenylimidotrimethyl*bis(*trimethylphosphine*)*rhenium*(*V*), (1)

To a solution of $Re(NPh)Cl_3(PMe_3)_2$[1] (5.4 g, 10 mmol) in toluene (100 cm^3) was added excess Me_2Mg (20 cm^3, 64 mmol, 3.2 M in Et_2O) at −78°C. The solution was slowly warmed to room temperature, then heated to 60–70°C for 24 hr. After removal of solvent under vacuum, the residue was extracted with petroleum (3 × 40 cm^3) to give a green solution. The combined extract was filtered through cellulose, the filtrate concentrated to *ca.* 40 cm^3 and cooled to −20°C to give green crystals. Yield, 3.3 g, 70%; m.p., 75–76°C.

IR cm^{-1}: 1584w, 1482s, 1424m, 1346s, 1306w, 1286m, 1263m, 1070m, 1024s, 988w, 958s, 948s, 938s, 850w, 800m, 770m, 720m, 692m, 672w, 554w, 496w, 483w.

(2) *Phenylimidochlorodimethyl*bis(*trimethylphosphine*)*rhenium*(*V*), (2)

To a solution of $Re(NPh)Cl_3(PMe_3)_2$ (1.0 g, 11 mmol) in toluene (40 cm^3) was added Me_2Mg (0.60 cm^3, 3.2 M in Et_2O, 2.0 mmol), at −78°C. The solution was stirred and slowly warmed to room temperature, then heated to 60–70°C for 24 hr. Solvent was removed under vacuum and the residue washed with petroleum (2 × 30 cm^3). It was then extracted with toluene (20 cm^3) and the solution filtered, concentrated to *ca.* 5 cm^3 and cooled to −20°C to give green crystals. Yield, 0.7 g, 75%; m.p. 122–3°C.

IR cm^{-1}: 1584w, 1482s, 1320s, 1300m, 1280s, 1260m, 1100w, 1070m, 1030m, 993w, 950vs, 850w, 760w, 725w, 697w, 670w.

(3) *Phenylimididichloromethyl*bis(*trimethylphosphine*)*rhenium* (*V*) (3)

To a solution of $Re(NPh)Cl_3(PMe_3)_2$ (1.5 g, 2.85 mmol) in toluene (50 cm^3) was added Me_2Mg (0.45 cm^3, 2.85 mmol, 3.2 M in Et_2O) at −78°C. The solution was stirred, warmed slowly to room temperature and then heated to 60–70°C for 24 hr. The solvent was removed under vacuum, the residue washed with petroleum (2 × 40 cm^3) and extracted with toluene (25 cm^3) which was filtered, concentrated to *ca.* 5 cm^3 and cooled to −20°C to give green crystals. Yield 0.6 g, 65%; m.p., 173–4°C.

IR cm^{-1}: 1580w, 1482s, 1420m, 1302w, 1284m, 1264w, 1072w, 1028m, 994w, 952s, 863w, 852w, 802w, 779m, 747m, 682m, 673w, 566w, 552w, 514w.

Table 3. Analytical data

Compound	Found (Required) %					
	C	H	N	P	Other	M[a]
1. $Re(NPh)Me_3(PMe_3)_2$	38.6 (38.0)	7.0 (6.8)	3.0 (3.0)	12.9 (13.1)		460 (474)
2. $Re(NPh)Cl^fMe_2(PMe_3)_2$	34.8 (34.0)	5.8 (5.9)	2.9 (2.8)	12.7 (12.5)	6.5(Cl^f) (7.2)	500 (495)
3. $Re(NPh)Cl^f_2Me(PMe_3)_2$	30.9 (30.3)	5.2 (5.1)	2.8 (2.7)	11.5 (12.0)	13.0(Cl^f) (13.8)	510 (515)
4. $[Re(NPh)Me_2(PMe_3)_2][BF_4]$	31.5 (30.8)	5.5 (5.3)	2.4 (2.6)	12.6 (11.4)	13.3(F) (13.9)	
5. $[Re(NHPh)FMe_2(PMe_3)_2][BF_4]$	28.8 (29.7)	5.1 (5.3)	2.5 (2.5)	10.4 (10.9)	16.7(F) (16.8)	
6. $Re(NPh)(CO_2Me)_2Me(PMe_3)_2$	36.5 (36.3)	5.8 (5.7)	2.5 (2.5)	11.4 (11.0)	11.6(O) (11.4)	540 (562)
7. $Re_2O_4(CH_2SiMe_3)_2(PMe_3)_4$. thf	26.5 (26.7)	6.1 (6.1)		10.0 (9.8)	6.5(O) (6.4) 7.1 (Si) (6.7)	1200 (1259)

[a] Cryoscopically in benzene.

(4) *Phenylamidofluorotrimethyl*bis(*trimethylphosphine*)*rhenium*(*V*) *tetrafluoroborate* (4)

To a solution of $Re(NPh)Me_3(PMe_3)_2$ (0.5 g, 1.05 mmol) in tetrahydrofuran (50 cm^3) was added aqueous HBF_4 (0.20 cm^3, 1.2 mmol, 40% HBF_4, *ca.* 6 mmol cm^{-3}) in tetrahydrofuran (5 cm^3) at −78°C. The solution was allowed to warm slowly to room temperature and stirred for 2 hr. The off-white precipitate was collected, washed with diethylether (2 × 20 cm^3) and then extracted into MeOH (40 cm^3). The solution was filtered, concentrated to *ca.* 10 cm^3 and cooled to give white crystals. Yield, 0.48 g, 80%; m.p., 93–4°C.

IR cm^{-1}: 3360w, 1584w, 1478s, 1420s, 1306m, 1286m, 1160br, s, 948s, 850m, 800w, 765m, 740m, 685m, 672m.

Conductivity. CH_3NO_2, 25°C, 105 Λ^{-1} cm^2 M^{-1}.

(5) *Phenylimidobis*(*acetato*)*methyl*bis(*trimethylphosphine*)*rhenium* (*V*) (5)

To a solution of $Re(NPh)Me_3(PMe_3)_2$ (0.4 g, 0.75 mmol) in toluene (50 cm^3) was added excess glacial acetic acid (2 cm^3, 35.0 mmol) at −78°C. The solution was warmed slowly, stirred at room temperature for 3 hr, then evaporated to dryness under reduced pressure and the residue extracted into toluene (2 × 20 cm^3). The solution was filtered, concentrated to *ca.* 15 cm^3 and cooled to −20°C to give pale brownish crystals. Yield, 0.34 g, 80%; m.p., 108–9°C.

IR cm^{-1}: 1649s, 1610s, 1584m, 1484m, 1418m, 1364s, 1357s, 1322m, 1301m, 1297s, 1210m, 1072w, 1031w, 1010m, 993w, 948s, 925m, 857m, 849m, 779m, 742m, 724w, 684m, 672w, 659w, 630w, 602w.

IR (Voltalef 35 oil), cm^{-1}: 1649s, 1610s, 1584m, 1484m, 1429w, 1418m, 1378m, 1368m, 1359m.

(6) *Phenylimidodimethyl*bis(*trimethylphosphine*)*rhenium*(*V*)*tetrafluoroborate* (6)

To a solution of $Re(NPh)Me_3(PMe_3)_2$ (0.68 g, 1.42 mmol) in diethylether (30 cm^3) was added Ph_3CBF_4 (0.47 g, 1.43 mmol) in diethylether (20 cm^3) at −20°C. The solution was warmed slowly to room temperature and stirred for 5 hr when the solvent was evaporated to dryness under *vacuo*. The oily residue was washed with diethylether (2 × 20 cm^3) and then extracted into tetrahydrofuran (30 cm^3) filtered, concentrated to *ca.* 10 cm^3 and diethylether diffused slowly into the tetrahydrofuran solution to give greenish red crystals. Yield, 0.5 g, 65%; m.p., 92–4°C.

IR cm^{-1}: 1584w, 1424m, 1310m, 1290s, 1210w, 1170w, 1162w, 1070br, s, 1030s, 988m, 948s, 855m, 780m, 745m, 730m, 690m, 670m.

Conductivity. CH_3NO_2, 25°C 100 Λ^{-1} cm^2 M^{-1}.

7. Bis(*trimethylsilylmethyl*)*oxorhenium*(*V*) - *μ* - *oxo* - *tetrakis* (*trimethylphosphine*)*rhenium*(*I*) (*trimethylsilylmethyl*)*dioxorhenium*(*V*) (*Re–Re*) *tetrahydrofuran* (7)

To a solution of $Re(NPh)Cl_3(PMe_3)_2$ (0.54 g, 1 mmol) and trimethylphosphine (1 cm^3, 10 mmol) in tetrahydrofuran (50 cm^3) was added $(Me_3SiCH_2)_2Mg$[13] (6 cm^3 of 0.6 M solution in Et_2O, 3.6 mmol) at −30°C. The solution was allowed to warm and then heated at 70°C for *ca.* 2 days. The solvent was removed, the residue extracted with petroleum (2 × 30 cm^3), the solution filtered, concentrated to *ca.* 10 cm^3 and cooled to −20°C to give dark red crystals. Yield 0.3 g, 70%; m.p., 118–119°C.

IR cm^{-1}: 1420m, 1368sh, 1298m, 1282ms, 1245sh, 1242s, 1090br, m, 1015m, 948vs, 910s, 890s, 865sh, 852s, 832s, 814s, 742m, 720s, 672m, 556m.

CRYSTALLOGRAPHIC STUDIES

The crystal used for X-ray study was obtained from tetrahydrofuran as the thf adduct and sealed under nitrogen in a Lindemann capillary. Unit cell and crystal orientation data were obtained using the search and index routines on a Nonius CAD4 diffractometer. Accurate values were obtained by least squares refinement using setting angles for 25 high angle reflections, automatically centred. Intensity data were recorded as described previously.[14] The crystal morphology was obscured by the vacuum grease used for mounting, and so no absorption correction could be applied.

Crystal data

$C_{24}H_{69}O_4P_4SiRe_3 \cdot C_4H_8O$, F. wt. = 1260.7, monoclinic, $a = 15.512(3)$, $b = 15.392(2)$, $c = 21.506(4)$ Å, $\beta = 100.19(2)°$, $U_A = 5053.8$ Å^3, space group $P2_1/n$, $Z = 4$, D_m not measured, $D_c = 1.64$ g cm^{-3} $F(000) = 2288$, μ(Mo–Kα) = 78.0 cm^{-1}.

Data collection

CAD4 diffractometer, graphite monochromated Mo–Kα radiation, $\omega/2\theta$ scan mode, 8467 reflections collected ($1.5 < \theta < 25°$), 7568 unique, 5028 observed [$I > 1.5\sigma(I)$].

Structure solution and refinement

Direct methods (Re positions), difference syntheses, full matrix least squares. Attempts to refine all non-hydrogen atoms anisotropically resulted in non-positive definite conditions or exceedingly anistropic ellipsoids for many atoms, especially the trimethylsilylmethyl carbons; additionally, the thf molecule is disordered over two neighbouring sites. Whilst high thermal motion or positional scatter for these atoms is likely to be the major cause of the refinement problem, the absence of an absorption correction may also contribute. Accordingly, only the Re and P atoms on Re(2) were refined anisotropically and the remainder were assigned isotropic thermal parameters. The final R values were $R = \Sigma|\Delta F|/\Sigma|F_o| = 0.070$ and $R\omega = [\Sigma|\omega\Delta F|^2/\Sigma\omega F_o]^{1/2} = 0.0698$ with $\omega = 1/[\sigma(F_o) + 0.0006\,F_o^2]$. Final atomic coordinates, thermal parameters and a list of F_o/F_c values have been deposited with the Editor as supplementary data.† Programs, computers and sources of scattering factor data are given in Ref. 14.

Acknowledgement—We thank the Science Research Council for support.

REFERENCES

[1]K. W. Chiu, W. K. Wong and G. Wilkinson, *J. Chem. Soc. Chem. Commun.* 1981, 451; W. K. Chiu, W. K. Wong, G. Wilkinson, A. M. R. Galas and M. B. Hursthouse, *Polyhedron*, 1982, **1**, 37.

[2]R. J. Puddephatt and P. J. Thompson, *J. Chem. Soc., Dalton Trans.* 1977, 1219; *J. Organomet. Chem.* 1979, **166**, 251.

[3]R. R. Schrock and G. W. Parshall, *Chem. Revs.* 1976, **76**, 243.

[4]D. Dodd and M. D. Johnson, *J. Chem. Soc., Chem. Commun.* 1971, 1371.

[5]See, M. H. Abraham, in *Comprehensive Chemical Kinetics* (Edited by C. H. Bamford and C. F. H. Tipper), Vol. 12, Chap. 3. Elsevier, Amsterdam (1973); J. K. Kochi, *Organometallic Mechanisms and Catalysis*, Academic Press, New York (1978); J. P. Collman and L. S. Hegedus, *Principles and Applications of Organotransition Metal Chemistry*. University Science Books, Mill Valley, California (1980).

[6]J. Chatt, A. J. Peerman and R. L. Richards, *J. Chem. Soc., Dalton Trans.* 1976, 1520.

[7]M. Hidai, T. Kodama, M. Sato, M. Harakawa, and Y. Uchida, *Inorg. Chem.* 1976, **15**, 2694.

[8]G. B. Deacon and R. J. Phillips, *Coord. Chem. Revs.* 1980, **33**, 227.

†Atomic co-ordinates have also been deposited with the Cambridge Crystallographic Data Centre, for inclusion in their Data Base. Copies are also available, on request, from the Editor at Queen Mary College.

[9]See, F. A. Cotton and G. Wilkinson, *Advanced Inorganic Chemistry*, 4th Edn, p. 193. Wiley, New York (1980).
[10]R. R. Schrock and P. R. Sharp, *J. Am. Chem. Soc.* 1978, **100**, 2389.
[11]K. Mertis, D. H. Williamson and G. Wilkinson, *J. Chem. Soc., Dalton Trans.* 1975, 607.
[12]Ref. [9], pp. 884–885.
[13]R. A. Andersen and G. Wilkinson, *J. Chem. Soc., Dalton Trans.* 1977, 809.
[14]M. B. Hursthouse, R. A. Jones, K. M. A. Malik and G. Wilkinson, *J. Am. Chem. Soc.* 1979, **101**, 4128.

Polyhedron Vol. 1, No. 1, pp. 37–44, 1982
Printed in Great Britain.

0277-5387/82/010037-08$03.00/0
Pergamon Press Ltd.

REACTIONS OF PHENYLIMIDOTRICHLOROBIS(TRIPHENYLPHOSPHINE)RHENIUM(V). REACTION WITH TRIMETHYLPHOSPHINE AND REDUCTION OF TRIMETHYLPHOSPHINE COMPLEX TO PHENYLAMIDO COMPLEXES OF RHENIUM(I, III). THE X-RAY CRYSTAL STRUCTURES OF PHENYLAMIDO-(DINITROGEN)TETRAKIS(TRIMETHYLPHOSPHINE)-RHENIUM(I) AND PHENYLAMIDO(BUTA-1,3-DIENE)-TETRAKIS-(TRIMETHYLPHOSPHINE)RHENIUM(I)

KWOK W. CHIU, WAI-KWOK WONG and GEOFFREY WILKINSON*
Chemistry Department, Imperial College, London SW7 2AY, England

and

ANITA M. R. GALAS and MICHAEL B. HURSTHOUSE*
Chemistry Department, Queen Mary College, Mile End Road, London E1 4NS, England

(*Received* 17 *June* 1981)

Abstract—The interaction of $Re(NPh)Cl_3(PPh_3)_2$ with PMe_3 gives $Re(NPh)Cl_3(PMe_3)(PPh_3)$ or $Re(NPh)Cl_3(PMe_3)_2$ depending on conditions. In the presence of excess PMe_3 the phenylimido compounds in tetrahydrofuran are reduced by sodium amalgam giving products whose nature depends on the atmosphere (Ar, N_2, H_2 CO, butadiene) used. The following compounds have been characterised: $Re(NHPh)(N_2)(PMe_3)_4$, $ReH(NHPh)(\eta'\text{-}CH_2PMe_2)(PMe_3)_4$, $Re(H)_2(NHPh)(PMe_3)_4$, $Re(NHPh)(CO)_2(PMe_3)_3$, $Re(NHPh)(CO)_3(PMe_3)_2$, $Re(NHPh)(\eta^4\text{-}C_4H_6)(PMe_3)_3$ and $Re(NPh)Cl_2(PMe_3)_3$. The structures of $Re(NHPh)(N_2)(PMe_3)_4$ (3) and $Re(NHPh)(C_4H_6)(PMe_3)_3$, (8) have been confirmed by single-crystal X-ray diffraction studies. (3) is monoclinic, space group $P2_1/n$ with $a = 9.574(2)$, $b = 19.528(3)$, $c = 14.385(3)$Å and $\beta = 99.06(2)°$; (8) is orthorhombic, space group $Pbc2_1$, with $a = 12.207(2)$, $b = 13.884(2)$, $c = 14.242(2)$Å. The structures were solved via the heavy atom method and refined by least squares to R values of 0.065 and 0.062 for 3249 and 2009 observed diffractometer data, respectively. In the dinitrogen complex the N_2 and NHPh ligands adopt a *cis* configuration with Re–N bond lengths of 1.955(13) and 2.200(14)Å, respectively. In the butadiene complex, whose structure is not well defined due to disorder and/or pseudo symmetry correlation effects, the Re–N (amido) distance is 2.13(3)Å.

INTRODUCTION

It has been noted[1] that although alkyl or arylimido complexes of rhenium have long been known few of their reactions have been studied. Reactions of $Re(NR)Cl_3(PPh_3)_2$ with sulphur and oxygen have been studied, the latter reaction generating arylnitroso species $ReCl_3(RNO)(OPPh_3)$. *t*-Butylimido alcoxo complexes, e.g. $Re(OSiMe_3)(NBu^t)_3$, have also been recently described.[2]

We now report the synthesis of trimethylphosphine phenylimido compounds and of species obtained from the sodium amalgam reduction of $Re(NPh)Cl_3(PPh_3)_2$ in the presence of PMe_3 and/or $Re(NPh)Cl_3(PMe_3)_2$ under atmospheres of Ar, N_2, H_2 and CO.

In Table 1 are collected the ^1H NMR data for new compounds; ^{31}P data is given in the text and experimental section.

RESULTS AND DISCUSSION

(1) *Interaction of phenylimidotrichlorobis(triphenylphosphine)rhenium(V) with trimethylphosphine*

Interaction of PMe_3 and $Re(NPh)Cl_3(PPh_3)_2$ in toluene at room temperature (20–25°C) leads to replacement of only one PPh_3 ligand and formation of the green crystalline solvate $Re(NPh)Cl_3(PMe_3)(PPh_3)$. C_7H_8 (1) in high yield. At 80–90°C the *bis*-trimethylphosphine complex $Re(NPh)Cl_3(PMe_3)_2$ (2) is obtained; the similar triethylphosphine complex is known.[3]

The IR spectrum of 1 shows a strong band at 760 cm^{-1} (Re=NPh) while the ^1H NMR spectrum has a PMe_3 doublet (δ 1.59 ppm, $^2J_{P-H} = 10$ Hz) indicating *cis* phosphorus atoms as in the *fac* structure (1). In the compound 2, there is a similar band at 769 cm^{-1} in the IR for Re=NPh but the ^1H NMR is a triplet (δ 1.48 ppm, $^2J_{P-H} = 4$ Hz), indicating *trans* phosphines as in (2).

(2) *Reductions by sodium amalgam*

The reduction of either $Re(NPh)Cl_3(PPh_3)_2$ or $Re(NPh)Cl_3(PMe_3)_2$ in the presence of excess PMe_3 gives similar products in all cases when Ar, N_2, H_2 and CO atmospheres are used and, except in one case, leads to phenylamido (NHPh) complexes since tetrahydrofuran as solvent can also act as a source of hydrogen.

(a) *Phenylamido(dinitrogen)tetrakis(trimethylphosphine)rhenium(I).*

The reduction using excess sodium amalgam leads to $Re(NHPh)(N_2)(PMe_3)_4$ (3) whose IR spectrum shows a weak band at 3390 cm^{-1} for the N–H stretch and a very strong band at 2000 cm^{-1} for coordinated N_2. The ^1H NMR spectrum has a broad resonance at δ 2.3 ppm

*Authors to whom correspondence should be addressed.

Table 1. ^{1}H nuclear magnetic resonance spectra[a]

Compound	^{1}H δ ppm	Assignment
1. $Re(NPh)Cl_3(PMe_3)(PPh_3)C_7H_8$	7.0-7.9 m (20)	PPh_3, PhN
	7.1 s (6)	$PhCH_3$
	2.3 s (3)	$PhCH_3$
	1.59 d (9) ($^2J_{P-H}$ = 10 Hz)	PMe_3
2. $Re(NPh)Cl_3(PMe_3)_2$	7.0-7.9 m (5)	PhN
	1.48 t (18) ($^2J_{P-H}$ = 4 Hz)	PMe_3
3. $Re(NHPh)(N_2)(PMe_3)_4$	6.4-7.5 m (5)	PhNH
	2.30 br,s (1)	NH
	1.22-1.40 m (18)	PMe_3
	0.98-1.10 m (18)	
4. $Re(NHPh)(H)_2(PMe_3)_4$	6.4-7.5 m (5)	PhNH
	2.85 br,s (1)	NH
	1.56 t ($^2J_{P-H}$ = 2 Hz)	PMe_3
	1.45 d ($^2J_{P-H}$ = 4 Hz)	
	-8.8 q of d (1)	$Re-H_A$
	($^2J_{P-H}$ = 21.0; $^2J_{H-H}$ = 2.4 Hz)	
	-7.8 q (1) ($^2J_{P-H}$ = 21.3 Hz)	$Re-H_B$
5. $Re(NHPh)(H)(CH_2PMe_2)(PMe_3)_4$	6.4-7.5 m (5)	Ph NH
	3.0 br,s (1)	NH
	2,3 d (9) ($^2J_{P-H}$ = 26.5 Hz)	PMe_3
	2.14-2,6 m (17)	PMe_3, CH_2PMe_2
	1,22 br,s (9)	PMe_3
	-3,30 br,s (1)	Re-H
6. $Re(NHPh)(CO)_2(PMe_3)_3$	6.4-7.5 m (5)	PhNH
	2.80 br,s (1)	NH
	1.35 d ($^2J_{P-H}$ = 4.0 Hz)	PMe_3
	1.14 m	
7. $Re(NHPh)(CO)_3(PMe_3)_2$	6.4-7.5 m (5)	PhN
	2.72 br,s (1)	N-H
	1.28 d ($^2J_{P-H}$ = 7.7 Hz)	PMe_3
	1.33 d ($^2J_{P-H}$ = 8 Hz)	
8. $Re(NHPh)(\eta^4-C_4H_6)(PMe_3)_3$	7.3-6.4 br,m (5)	N-Ph
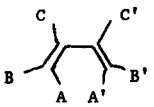	4.53 br,s (2)	CC'
	1.50 br,s (2)	BB'
	-0.35 br,s (2)	AA'
	1.21 d ($^2J_{P-H}$ = 6.6 Hz)	PMe_3
	1.15 d ($^2J_{P-H}$ = 5.9 Hz)	
	0.92 d ($^2J_{P-H}$ = 5.2 Hz)	
	2.74 br, s	N-H

[a] In $^2[H]_6$ benzene at 90 MHz, 35°C; Me_4Si δ 0.0. Relative areas in parenthesis.

(N–*H*) together with complex multiplets between δ 1.0–1.7 ppm for the PMe_3 groups. This complexity suggests different environments for the PMe_3 groups in solution similar to those confirmed in the solid state by X-ray diffraction study described below. The complex reacts with hydrogen and with carbon monoxide to displace dinitrogen as described later. Other rhenium(I) dinitrogen complexes, $ReX(N_2)(PR_3)_4$, and $ReX(N_2)(diphos)_2$, X = Cl, Br, are known.[4,5]

A diagram of the molecule is shown in Fig. 1 and some of the more important bond-lengths and angles are listed in Table 2. The compound is a direct relative of the Re^I chloro derivative $ReCl(N_2)(PMe_2Ph)_4$.[5] However, the two structures are significantly different in that in the chloro compound, the chlorine and dinitrogen ligands are *trans* (and, in fact, mutually disordered) whereas in our compound, the phenylamido and dinitrogen groups are *cis*.

Detailed comparison of the structures is quite revealing. In the chloro complex, the four "equatorial" Re–P bond lengths lie in the narrow range 2.413(4)–2.435(4)—the small differences being ascribed to steric crowding. In our complex we have three structurally different phosphines, and the Re–P distances vary accordingly. Two of the phosphines are mutually *trans* with equal Re–P distances [2.405(4), 2.408(4)Å], which are similar to those in the chloro complex. The phosphine *trans* to the N_2 ligand has an Re–P length of 2.397(3)Å—only slightly shorter than the first two, suggesting little if any *trans* influence for the dinitrogen ligand. This is understandable since, like two *trans* phosphines, we have in this situation, two *trans* π-acceptor ligands competing for *d* electron density. On the other hand, the phosphine *trans* to the phenylamido group has a very short Re–P bond, of length 2.334(4)Å. This again is understandable since *trans* to this phosphine we have the NHPh ligand, and repulsion of the metal *d* electrons by the nitrogen lone pair would tend to enhance the drift of *d* electron density from the metal to the phosphorus.

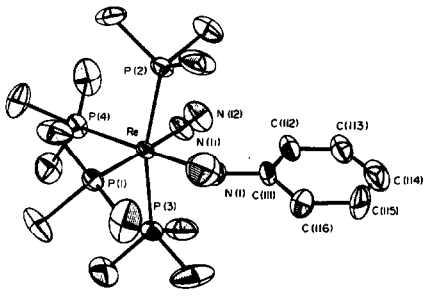

Fig. 1. The molecular structure of $Re(NHPh)(N_2)(PMe_3)_4$.

It may be noted that the metal achieves an 18-electron configuration without N⇄Re electron donation and this accounts for the relatively long Re–N(amide) bond length of 2.20(1)Å. Additionally, the nitrogen atom deviates significantly from planarity with the sum of the angles being 353°.

(b) *Phenylamido dihydridotetrakis(trimethylphosphine)-rhenium(III)*

The extremely air-sensitive complex $Re(NHPh)(H)_2(PMe_3)_4$ (**4**) can be obtained directly by reduction of $Re(NPh)Cl_3(PMe_3)_2$ in the presence of excess PMe_3 under hydrogen or by oxidative addition of hydrogen from compound (**3**). This reaction is reversible at room temperature

$$Re(NHPh)(N_2)(PMe_3)_4 + H_2 \rightleftharpoons Re(NHPh)(H)_2(PMe_3)_4 + N_2.$$

The complex has bands in the IR spectrum at 3382 (N–H str) and medium broad bands at 1925 and 1885 cm^{-1} (Re–H str). The ^1H NMR spectrum again confirms the N–H (δ 2.85 ppm) and in addition to PMe_3 resonances there are two Re–H resonances; H_A at δ −8.8 ppm, quintet of doublets ($^2J_{P-H}$ = 21 Hz, $^2J_{H-H}$ = 2.4 Hz), H_B at 7.8 ppm, a poorly resolved quintet ($^2J_{P-H}$ = 21 Hz). There is no change in these high field resonances between −100 and +90°C. The $^{31}P\{^1H\}$ spectrum has two broad singlets at δ −41.63 and −45.37 ppm. This seven-coordinate rhenium(III) complex can have isomers 4a, b; for 4a, the ^1H NMR spectrum should show two pseudo quintets of equal intensity for H_A and H_B provided J_{H-Re-H} is very small. For 5b, the two hydrides are equivalent giving a pseudo quintet. The observed spectrum is consistent with a mixture of isomers.

Table 2. Selected bond lengths and angles for $Re(NHPh)(N_2)(PMe_3)_4$

a) Bond Lengths (Å)		b) Bond Angles (°)	
Re-N(11)	1.955(13)	N(1)-Re-N(11)	94.9(6)
Re-N(1)	2.200(14)	N(11)-Re-P(1)	178.3(4)
Re-P(1)	2.397(5)	N(11)-Re-P(cis)	85.9-87.6(5)
Re-P(2)	2.405(6)		
Re-P(3)	2.408(6)	N(1)-Re-P(4)	178.8(4)
Re-P(4)	2.334(6)	N(1)-Re-P(cis)	83.4-86.8(5)
N(11)-N(12)	1.101(18)		
		Re-N(11)-N(12)	176.5(15)
P-C	1.79(2)-1.88(2)		
N(1)-C(111)	1.36(2)	Re-P-C	115-127(1)
C-C(Ph)	1.33(4)-1.47(3)	Re-N(1)-C(111)	141(1)

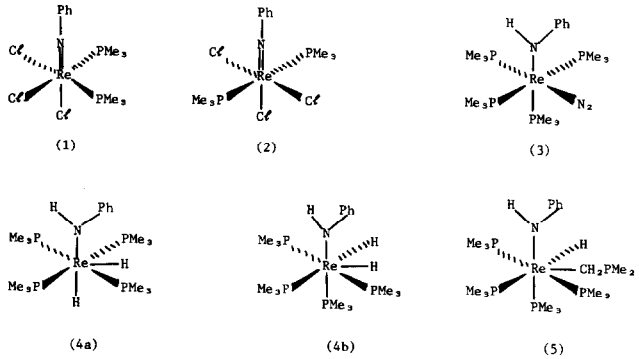

(1) (2) (3) (4a) (4b) (5)

(c) *Reduction under argon*

Reduction of $Re(NPh)Cl_3(PMe_3)_3$ with excess sodium amalgam under argon leads to a pale yellow extremely air sensitive crystalline complex that we must formulate as $Re(NHPh)(H)(\eta^1\text{-}CH_2PMe_2)(PMe_3)_4$ (**5**).

The IR spectrum shows a weak band at 3386 cm^{-1} for the N–H stretch and a weak broad band at 1900 cm^{-1} for the Re–H stretch. The ^1H NMR spectrum confirms the Re–H (δ −3.3 ppm) and also shows a singlet at δ 1.22 ppm, a doublet at δ 2.30 ppm ($^2J_{P-H}$ = 26.5 Hz) and a complex multiplet between δ 2.14–2.60 ppm for PMe_3. The $^{31}P\{^1H\}$ NMR spectrum shows a broad multiplet at δ −39.8 ppm that can be assigned to the $\eta^1\text{-}Me_2PCH_2$ group formed by hydride transfer from the methyl group of PMe_3. Although previously only $\eta^2\text{-}CH_2PMe_2$ groups have been formed in such reactions,[6] there is a precedent for an $\eta^1\text{-}CH_2PR_2$ group (as contrasted with the numerous examples of $\eta^1\text{-}CH_2PR_3$ groups) namely, the complex $(\eta^5\text{-}C_5H_5)_2ZrCl(\eta^1\text{-}CHPPh_2)$ whose structure has been determined by X-ray diffraction.[7] The compound **5** so formulated is thus a 7-coordinate complex of rhenium(III) and is an 18e species.

On passing nitrogen through a tetrahydrofuran solution of the complex a new intense IR band appears at 2000 cm^{-1} and when this reaction is done in an NMR tube the Re–H resonance disappears, suggesting that in solution $Re(NHPh)(N_2)(PMe_3)_4$ is formed. On passing hydrogen through a thf solution, two new IR bands at 1930 and 1890 cm^{-1} appear while the NMR spectrum shows high field lines, characteristic of the above dihydride.

We, therefore, appear to have the reactions shown in Scheme 1.

(d) *Carbon monoxide complexes*

Two carbonyl complexes have been obtained, one by the reaction

$$Re(NHPh)(N_2)(PMe_3)_4 + 2CO = Re(NHPh)(CO)_2(PMe_3)_3$$

and the other, $Re(NHPh)(CO)_3(PMe_3)_2$, by reduction of $Re(NPh)Cl_3(PMe_3)_2$ under CO atmosphere.

The complex $Re(NHPh)(CO)_2(PMe_3)_3$ (**6**) forms air-sensitive orange crystals. The solution (toluene) IR spectrum shows the N–H stretch at 3360 cm^{-1} and terminal CO stretches at 1891 and 1940 cm^{-1} for *cis* CO groups.

The ^1H NMR spectrum has a pseudo quintet centred at δ 1.14 ppm and a doublet (J = 4.0 Hz) centred at δ 1.35 ppm for the PMe_3 groups. The $^{31}P\{^1H\}$ NMR spectrum shows a doublet (J_{P-P} = 24.4 Hz) and triplet (J_{P-P} = 24.4 Hz) with relative intensity 2:1 at δ −64.97 and −70.94 ppm, respectively.

There are two possible isomers 6a, b. The *fac- cis* isomer should show either two doublets of relative intensity 2:1 or three doublets of relative intensity 1:1:1 for the ^1H NMR spectrum of the PMe_3 groups, whereas 6b should show either a triplet and a doublet of relative intensity 2:1 or two triplets and a doublet of relative intensity 1:1:1. The observed spectrum can be considered as having two overlapping triplets and a doublet suggesting a *mer* configuration of PMe_3 groups. Thus, the spectroscopic data fits best for the *mer- cis* isomer 6b.

The reduction of $Re(NPh)Cl_3(PMe_3)_2$ under carbon monoxide either at room temperature or in presence of two equivalents of PMe_3 at 60°C leads to the tricarbonyl complex $Re(NHPh)(CO)_3(PMe_3)_2$ (**7**) as air-sensitive orange crystals. The solution IR spectrum (benzene) shows the N–H stretch at 3360 cm^{-1} and terminal CO stretches (2006w, 1910m, 1850s). The ^1H NMR spectrum shows the N–H singlet (δ 2.72), two doublets at δ 1.28 ($^2J_{P-H}$ = 7.7 Hz) and δ 1.33 ppm ($^2J_{P-H}$ = 8 Hz) indicating non-equivalent PMe_3 groups as in (**7**) although the $^{31}P\{^1H\}$ spectrum has a broad singlet at δ −73.77 and some free PMe_3 at −62.8 ppm.

(e) *Phenylamido(buta-1,3-diene)tris(trimethylphosphine) rhenium(I)*

The reduction of $Re(NPh)Cl_3(PMe_3)_2$ by excess

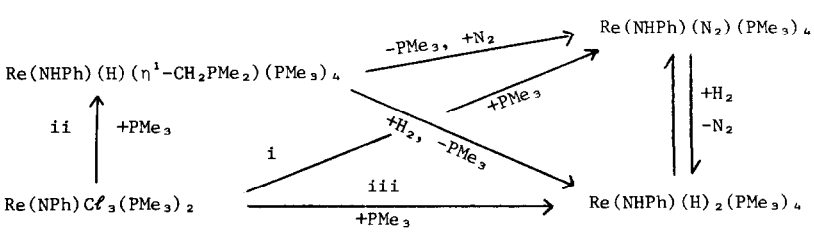

Scheme. Reduction by Na/Hg under (i) N_2, (ii) Ar, (iii) H_2.

sodium amalgam under an atmosphere of butadiene in tetrahydrofuran leads to pale yellow crystals of $Re(NHPh)(\eta^4\text{-}C_4H_6)(PMe_3)_3$ (**8**). The IR spectrum has the N–H stretch at 3423 cm^{-1} in addition to PMe_3 and butadiene bands. The ^1H NMR spectrum has the N–H resonance at δ 2.74 ppm, resonances for $\eta^4\text{-}C_4H_6$ at δ 4.53, 1.50 and −0.35 ppm, plus three doublets for PMe_3 groups. The ^{31}P NMR has a triplet and two doublets. The spectra are in accord with the structure (**8**) which has been confirmed by X-ray diffraction study.

The gross structural features of the compound are shown in Fig. 2, and although we experienced some problems in the refinement of this structure, there is no doubt in our minds that the complex is correctly identified. In view of the uncertainties in some atomic positions (see Experimental) the bond-lengths and angles in Table 3, must be regarded with some suspicion and where relevant the esd's have been artifically increased.

Accordingly, the discussion of the structure can only be in general terms. One of the main points of note is that the [Re(NHPh)$(PMe_3)_3$] unit has a very approximate mirror plane, defined by the NHPh group and containing P(3), so that P(1) and P(2) are ψ-mirror related. As far as we can tell, however, the butadiene group is *not* oriented

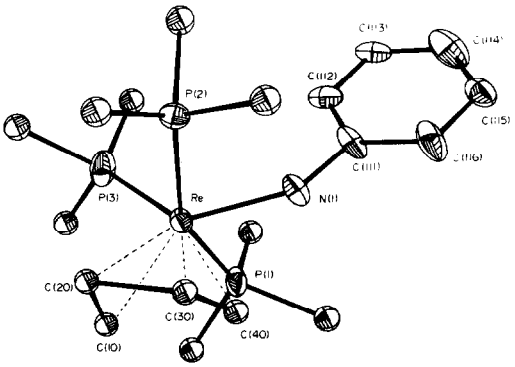

Fig. 2. The molecular structure of $Re(NHPh)(C_4H_6)(PMe_3)_3$.

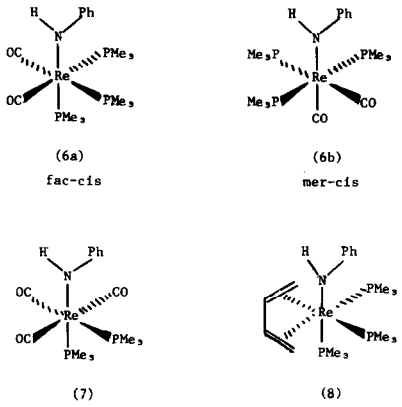

symmetrically with respect to this approximate plane, even though the P(1), P(2) PMe_3 groups are pushed back towards the (NHPh) group almost equally [P(1)–Re–N = 77°, P(2)–Re–N = 76°].

A second point of interest is that if the butadiene group is acting as a 4e donor, then, as in compound **3**, the Re atom achieves and 18e configuration without the need for any amido $p\pi$ donation; although the Re–N distance of 2.13(4)Å is smaller than the value found in compound **3**. The symmetrical orientation of the NHPh group may therefore be explained by intramolecular packing effects.

There are only few phosphine alkene complexes of rhenium. The complex $Re(H)_3(\eta^4\text{-}C_4H_6)(PPh_3)_2$ has been made from $ReH_7(PPh_3)_2$[8] while the latter complex in presence of 3,3-dimethylbut-1-ene dehydrogenates cyclopentane to $Re(H)_2(\eta^5\text{-}C_5H_5)(PPh_3)_2$.[9]

(f) *Phenylimido dichlorotris(trimethylphosphine)-rhenium(IV)*

The only case where a phenylamido group is not formed is when $Re(NPh)Cl_3(PMe_3)_2$ in tetrahydrofuran is reduced with exactly one equivalent of sodium amalgam. The air sensitive dark red crystalline rhenium(IV) complex $Re(NPh)Cl_2(PMe_3)_3$ has no N–H stretch in the IR

Table 3. Bond lengths and angles for $Re(NHPh)(\eta^4\text{-}C_4H_6)(PMe_3)_3$

a) Bond Lengths (Å)		b) Bond Angles (°)	
Re-N(1)	2.13(4)	N(1)-Re-P(1)	77(1)
Re-P(1)	2.404(10)	N(1)-Re-P(2)	76(1)
Re-P(2)	2.432(8)	N(1)-Re-P(3)	128(1)
Re-P(3)	2.205(14)	P(1)-Re-P(2)	152(1)
Re-C(10)	2.31(6)	P(1)-Re-P(3)	97(1)
Re-C(20)	2.28(6)	P(2)-Re-P(3)	95(1)
Re-C(30)	2.26(15)		
Re-C(40)	2.28(12)	Re-N(1)-C(111)	140(3)
C(10)-C(20)	1.46(10)		
C(20)-C(30)	1.72(20)		
C(30)-C(40)	1.18(20)		

P-Me – fixed at 1.84 ± 0.01Å

spectrum but shows a Re=NPh band at 739 cm^{-1}. It is also paramagnetic but the magnetic moment (1.66 BM) is low. No EPR signal was observed at room temperature but a frozen benzene solution gave a single broad line centred on $g = 1.74$ with a line width between points of maximum slope of 80 mT. These observations are consistent with a low spin rhenium(IV) species with a ligand field of low symmetry.

EXPERIMENTAL

Microanalyses were by Pascher (Bonn) and Imperial College.

Spectrometers: IR: Perkin–Elmer 597, NMR: Perkin–Elmer R32 (^1H 90 MHz), Bruker WM-250 (^1H 250 MHz and ^{31}P 101.2 MHz, 28°C). ^1H data referenced to Me_4Si, ^{31}P to external 85% H_3PO_4: epr Varian E12 (X-band).

All operations were performed under oxygen-free nitrogen or argon or *in vacuo* and all solvents were dried over sodium and distilled from sodium/benzophenone under nitrogen immediately before use. Light petroleum had b.p. 40–60°C. Melting points were determined in sealed tubes under nitrogen (uncorrected). Analytical data is collected in Table 4.

$Re(NPh)Cl_3(PPh_3)_2$ was prepared according to the literature.[10]

IR spectra were obtained in Nujol mulls, except where stated otherwise.

1. *Phenylimidotrichloro(trimethylphosphine) (triphenylphosphine)rhenium(V)-toluene* (1)

To $Re(NPh)Cl_3(PPh_3)_2$ (2.0 g, 2.2 mmol) suspended in toluene (50 cm^3) was added excess trimethylphosphine (2 cm^3, 20 mmol) and the suspension stirred overnight at room temperature. The green solution was filtered, concentrated to *ca.* 5 cm^3 and cooled at −20°C to give green crystals which were collected, washed with diethyl ether and recrystallised from toluene. Yield 1.5 g, 82%: m.p., 210°C with loss of toluene.

IR cm^{-1}: 3060w, 1480m, 1448m, 1434s, 1410m, 1302w, 1284m, 1278m, 1090s, 1024m, 990w, 947vs, 846m, 760s, 743s, 727s, 692vs, 626s, 560m, 521vs, 514s, 492s.

2. *Phenylimidotrichlorobis(trimethylphosphine) rhenium(V)*, (2)

A suspension of $Re(NPh)Cl_3(PPh_3)_2$ (20.0 g, 22 mmol) and excess trimethylphosphine (8.0 cm^3, 80 mmol) in toluene (100 cm^3) were placed in a pressure bottle and the solution heated at 80–90°C for 18 hr. The green solution was cooled and filtered and the volatile materials removed under vacuum. The residue was extracted with hot toluene (*ca.* 100 cm^3), filtered, concentrated to *ca.* 30 cm^3 and cooled at −20°C. The green crystals were collected and washed with diethylether (50 cm^3) and dried *in vacuo*. Yield 9.4 g (80%); m.p., 239–241°C.

IR (KBr disc), cm^{-1}: 2978w, 2908m, 1408s, 1382m, 1284s, 1260m, 1110br, m, 1026m, 948vs, 860w, 850w, 769s, 748s, 554m.

NMR: $^{31}P\{^1H\}$, δ-40.87 *s* (PMe_3).

3. *Phenylamido(dinitrogen)tetrakis(trimethylphosphine) rhenium(I)*, (3)

A suspension of $Re(NPh)Cl_3(PPh_3)_2$ (2.0 g, 2.20 mmol) in thf (50 cm^3) was added to a solution of trimethylphosphine (3 cm^3, 30 mmol) in thf (50 cm^3) containing excess sodium amalgam (0.78 g, Na in 5 cm^3 Hg) at −78°C under dinitrogen. The solution was allowed to warm slowly and was stirred at ambient temperature for 18 hr. The red solution was filtered, evaporated to dryness under reduced pressure and the residue washed with petroleum (2 × 40 cm^3), then extracted into toluene (*ca.* 30 cm^3), filtered, concentrated (*ca.* 15 cm^3) and cooled at −20°C to give yellow crystals. Yield 1.1 g, 80%: m.p., 98°C (decomp.)

IR cm^{-1}: 3390w, 2000vs, 1590s, 1556m, 1490s, 1340s, 1320m, 1302m, 1284m, 1276m, 1225w, 1174w, 1020w, 980m, 965m, 938s, 856m, 828w, 734s, 710m, 692s, 660s, 518m, 506m.

NMR: $^{31}P\{^1H\}$, δ −67.92 *d* ($^2J_{P-P}$ = 42.72 Hz), −70.72 br, s, −74.7br, s and −77.95br, s.

4. *Dihydrido(phenylamido)tetrakis(trimethylphosphine) rhenium(III)*, (4)

Method A. A suspension of $Re(NPh)Cl_3(PPh_3)_2$ (2.0 g, 2.2 mmol) in thf (50 cm^3) was added to excess trimethylphosphine (3.0 cm^3, 30 mmol) in thf (30 cm^3) with sodium amalgam (1.2 g Na in 5 cm^3 Hg) in a pressure bottle at −78°C. After pressurisation with hydrogen (3 atm) the solution was allowed to warm slowly; the bottle was repressurised and the solution stirred for 18 hr at room temperature. The solution was filtered, evaporated under reduced pressure and the residue was extracted with petroleum (40 cm^3), the solution filtered, concentrated to *ca.* 10 cm^3 and cooled to −20°C to give yellow crystals. Yield 0.83 g, 65%; m.p., 125–126°C (decomp.)

Method B. The complex $Re(NHPh)(N_2)(PMe_3)_4$ (0.85 g, 1.4 mmol) in toluene (50 cm^3) was stirred at room temperature for 12 hr under hydrogen (3 atm) with periodic repressurisation. The solution was filtered, evaporated in vacuum and the residue extracted into petroleum (25 cm^3). This solution was filtered, concentrated to *ca.* 10 cm^3 and cooled at −20°C to yield yellow crystals. Yield: 0.73 g, 90%.

IR cm^{-1}: 3380w, 1925br,w, 1885br,w, 1592s, 1487m, 1420w, 1335w, 1320w, 1298w, 1260s, 1085br,s, 1020br,s, 940vs, 851w, 800s, 732w, 700m, 658m.

NMR: $^{31}P\{^1H\}$, δ −41.63br, s; −45.39br,s (PMe_3).

Table 4. Analytical data

Compound	Analysis %[a]					M[b]
	C	H	N	P	Cℓ	
1. $Re(NPh)Cℓ_3(PMe_3)(PPh_3).C_7H_8$	50.3 (50.2)	4.6 (4.6)	1.7 (1.7)	7.6 (7.6)	13.0 (13.1)	
2. $Re(NPh)Cℓ_3(PMe_3)_2$	27.0 (26.9)	4.3 (4.3)	2.6 (2.6)	11.7 (11.6)	19.5 (19.9)	
3. $Re(NHPh)(N_2)(PMe_3)_4$	35.2 (35.4)	6.9 (6.9)	6.5 (6.9)	20.2 (20.3)		580 (610)
4. $Re(NHPh)(H)_2(PMe_3)_4$	36.9 (37.0)	7.5 (7.6)	2.4 (2.4)	20.4 (21.0)		550 (584)
5. $Re(NHPh)(H)(CH_2PMe_2)(PMe_3)_4$	38.3 (38.3)	7.9 (7.8)	2.3 (2.1)	23.5 (23.5)		620 (658)
6. $Re(NHPh)(CO)_2(PMe_2)_3$	36.2 (36.3)	5.9 (5.9)	2.7 (2.5)	16.5 (16.6)	[c]	530 (563)
7. $Re(NHPh)(CO)_3(PMe_3)_2$	35.4 (35.0)	4.8 (4.7)	2.6 (2.7)	12.1 (12.1)	[d]	510 (514)
8. $Re(NHPh)(C_4H_6)(PMe_3)_3$	40.4 (40.8)	7.0 (6.8)	2.6 (2.5)		16.5 (16.6)	540 (559)
9. $Re(NPh)Cℓ_2(PMe_3)_3$	31.9 (31.0)	5.4 (5.5)	1.9 (2.4)	16.3 (16.0)	11.9 (12.2)	600 (576)

[a] Calculated values in parenthesis

[b] Cryoscopically in benzene

[c] O, 6.1 (5.7)%

[d] O, 9.5 (9.3)%

5. *Phenylamidohydrido(η^1 - dimethylphosphidomethyl)tetrakis-(trimethylphosphine) rhenium(III)*, (5)

Excess trimethylphosphine (2.0 cm^3, 20 mmol) and a suspension of $Re(NPh)Cl_3(PPh_3)_2$ (2.0 g, 2.2 mmol) in thf (100 cm^3) was stirred with sodium amalgam (0.7 g, Na in 5 cm^3 Hg) under argon at −78°C. The solution was allowed to warm slowly and stirred at ambient temperature for 18 hr. The deep red solution was filtered, evaporated to dryness under reduced pressure and the residue extracted with toluene (50 cm^3) which was filtered, concentrated *ca.* 15 cm^3, and cooled at −20°C to give yellow crystals. Yield 1.15 g, 85%; m.p., 124–126°C (decomp.).

IR cm^{-1}: 3386w, 1980m, 1590s, 1550m, 1485s, 1430s, 1338s, 1330s, 1272s, 1265s, 1225w, 1162m, 1140m, 1062w, 1015w, 980m, 946vs, 850s, 828s, 725m, 690s, 640s.

NMR: $^{31}P\{^1H\}$, δ −39.8br,m; −43.89br, s; −52.70br,s.

6. *Phenylamidobis(carbon monoxide)tris(trimethylphosphine) rhenium(I)*, (6)

A solution of $Re(NHPh)(N_2)(PMe_3)_4$ (0.72 g, 1.18 mmol) in toluene (50 cm^3) was pressurised with CO (3 atm) in a pressure bottle and stirred at room temperature for 12 hr with occasional repressurisation.

The solution was filtered, evaporated and the residue extracted into toluene (35 cm^3). After filtering the solution was concentrated to *ca.* 20 cm^3 and cooled to −20°C to yield orange crystals which were washed with petroleum and dried. Yield 0.6 g, 90%; m.p., 172–173°C.

IR cm^{-1}: 3360w, 1908s, 1825s, 1590m, 1485m, 1422w, 1330m, 1312m, 1309m, 1287w, 1280w, 1171w, 1025w, 980w, 948s, 860w, 845w, 740m, 728m, 722m, 690m, 670m.

NMR: $^{31}P\{^1H\}$, δ −64.97 *d* ($^2J_{P-P}$ = 24.4 Hz); −70.94 t ($^2J_{P-P}$ = 24.4 Hz).

7. *Phenylamidotris(carbon monoxide)bis(trimethylphosphine) rhenium(I)*, (7)

To a solution of $Re(NPh)Cl_3(PMe_3)_2$ (0.6 g, 1.1 mmol) in thf (50 ml) was added sodium amalgam (1.1 g, Na in 5 ml Hg) in thf (50 ml) in a pressure bottle. After pressurising with carbon monoxide (2 atm) the solution was stirred at ambient temperature for 18 hr. The bottle was repressurised periodically. The solution was filtered and evaporated to dryness under reduced pressure. The residue was extracted with petroleum (2 × 40 cm^3), filtered, concentrated to *ca.* 50 cm^3 and cooled to −20°C to yield orange crystals which were washed with petroleum and dried. Yield 0.42 g (75%); m.p., 143–145°C.

IR cm^{-1}: 3360w, 1950w, 1874s, 1855s, 1590m, 1485m, 1335w, 1320w, 1312w, 1304w, 1285m, 1252w, 1160br,w, 1090br,w, 1020w, 982w, 964w, 948s, 858m, 804m, 739m, 724m, 692w, 672m, 630w, 600m.

IR (benzene) cm^{-1}. 3360w, 2006w, 1910m, 1850vs.

8. *Phenylamido(η^4 - buta - 1,3 - diene)tris(trimethylphosphine) rhenium(V)* (8)

The solution of $Re(NPh)Cl_3(PMe_3)_2$ (0.8 g, 1.5 mmol) in thf (50 cm^3) and excess sodium amalgam [0.8 g, 35 mmol in Hg (5 cm^3)] in a pressure bottle was pressurised with buta-1,3-diene slightly over atmospheric pressure and stirred overnight at room temperature. The solution was filtered and taken to dryness under vacuo. The residue was extracted into petroleum (2 × 30 cm^3), filtered, concentrated to *ca.* 10 cm^3 and cooled to −20°C, to give yellow crystals. Yield 0.5 g, 60%; m.p. 162–164°C (decomp.)

IR cm^{-1}: 3423w, 1588m, 1557w, 1487m, 1437m, 1418w, 1332w, 1320w, 1295m, 1280w, 1270w, 1209w, 1163w, 1141w, 1064w, 1040w, 1020w, 984m, 945s, 850m, 810m, 760m, 715m, 692m, 665m, 650m.

$^{31}P\{^1H\}$, δ −43.83 *t* ($^2J_{P-P}$ = 24.4 Hz), −39.98 d ($^2J_{P-P}$ = 24.4 Hz); −40.36 *d* ($^2J_{P-P}$ = 30.5 Hz) plus weak free PMe_3 at δ −61.85 ppm.

9. *Phenylimidodichlorotris(trimethylphosphine)rhenium(IV)*, (9)

A solution of $Re(NPh)Cl_3(PMe_3)_2$ (1.0 g, 1.87 mmol) in thf (70 cm^3) was added to a solution of trimethylphosphine (2 cm^3, 20 mmol) in thf (50 cm^3) containing exactly 1 equivalent of sodium amalgam (0.043 g in 2 cm^3 Hg) at room temperature. The mixture was stirred for 18 hr at ambient temperature. The red solution was filtered, evaporated to dryness under reduced pressure and the residue extracted with toluene (2 × 35 cm^3), filtered, concentrated to *ca.* 30 cm^3 and cooled to −20°C to give dark red crystals. Yield 0.87 g, 81%; m.p., 179–180°C.

IR cm^{-1}: 3032w, 3022w, 1560m, 1525w, 1475s, 1430m, 1415m, 1390w, 1340w, 1300m, 1280s, 1160w, 1148w, 1068w, 945vs, 856w, 800w, 739s, 722m, 680m, 665w, 650w, 500w.

10. *Crystallographic studies*

Crystal data. Compound 3. $C_{18}H_{42}N_3P_4Re$, M = 610.65, monoclinic, a = 9.574(2), b = 19.528(3), c = 14.385(3)Å, β = 99.06(2)°, U = 2655.9 Å; space group $P2_1/n$, Z = 4 D_c = 1.53 g cm^{-1}, D_M not measured, $F(000)$ = 1224, μ(Mo–Kα) = 48.5 cm^{-1}.

Compound 8. $C_{18}H_{39}NP_3Re$, M = 548.64 orthorhombic, a = 12.207(2), b = 13.884(2), c = 14.242(2)Å, U = 2413.7 Å^3; space group $Pbc2_1$, Z = 4, D_c = 1.509 g cm^{-3}, D_M not measured, $F(000)$ = 1096, μ(Mo–$K\alpha$) = 50.0 cm^{-1}.

Data collection.[11] CAD4 diffractometer, Mo–$K\alpha$ radiation, (λ = 0.71069 Å graphite monochromator), $\theta/2\theta$ scan mode.

Compound 3. $1.5 \leq \theta \leq 25.0$, 4662 data measured, 3249 observed [$I > 1.5\sigma(I)$]; uncorrected for absorption (crystal encapsulated by vacuum grease).

Compound 8. $1.5 \leq \theta \leq 25.0$, 3066 data measured, 2009 observed [$I > 1.5\sigma(I)$]; corrected for absorption and decay.

Structure solution and refinement

Heavy atom method, full matrix least squares. The structure of compound 3 was refined without problems to final R values of $R = \Sigma|\Delta F|/\Sigma|F_0| = 0.065$, $R_W = [\Sigma(\omega\Delta F_0)^2/\Sigma\omega F_0^2]^{\frac{1}{2}} = 0.064$ with $\omega = 1/[\sigma^2(F_0) + 0.006F_0^2]$. Non-hydrogen atoms were assigned anisotropic thermal parameters, hydrogen atoms were added in idealised positions but allowed to shift according to the movement of the parent C or N atoms and assigned a refineable overall isotropic thermal parameter. The structure of compound 8 was easily solved for the heavy atom position but developed with difficulty due to pseudo-symmetry correlation effects. Eventually enough of the structure was defined to confirm the adoption of the chosen space group, rather than the centrosymmetric alternative, *Pbcm*, but it was found impossible to select an acceptable model for the positions of the butadiene carbon atoms. Additionally, free refinement gave some rather abnormal parameters in the PMe_3 groups (e.g. Re–P(3) = 2.19(1) Å, P–C = 1.66(4) – 1.90(3) Å, although the R value was quite low (0.058). Close analysis of the structure showed that in fact some of the P(3) methyl groups were pseudo-mirror related (i.e. across Z = 0.25) to atoms thought to constitute the butadiene group. Unsure of how the Re–P distances may vary in this structure we felt only partially able to tackle the problem by fixing the P–Me bond lengths to well established values. This failed to remove the uncertainty surrounding the detailed identification of the butadiene unit and we can only presume that this group is affected not only by pseudo-symmetry correlation but also perhaps disorder. Attempts to refine using an idealised C_4 group were unsuccessful. The final model presented, therefore contains some residual uncertainties, and the esd's in the coordinates have been adjusted to signify this. The final R, R_W values (see above) are 0.0615 and 0.0583, respectively. Only the rhenium, phosphorus and phenyl amido group atoms were refined anisotropically, and the amido phenyl group was treated as an ideal C_6 hexagon.

Final atomic coordinates for both compounds, tables of anisotropic thermal parameters and lists of F_0/F_c have been deposited with the Editor as supplementary material.† Computers, programs and sources of scattering factor data are given in Ref. 11.

Acknowledgements—We thank the S.E.R.C. for support and Dr. J. F. Gibson for assistance with epr measurements.

†Atomic co-ordinates for these structures have also been deposited with the Cambridge Crystallographic Data Centre for inclusion in their Data Base. Copies are also available on request from the Editor at Queen Mary College.

REFERENCES

[1]G. La Monica and S. Cenini, *J. Chem. Soc. Dalton Trans.* 1980, 1145.
[2]W. A. Nugent and R. L. Harlow, *J. Chem. Soc. Chem. Commun.* 1979, 1105.
[3]J. Chatt, J. D. Garforth, N. P. Johnson and G. A. Rowe, *J. Chem. Soc. Dalton Trans.* 1964, 1012.
[4]J. Chatt, J. R. Dilworth and G. J. Leigh, *J. Chem. Soc. Dalton Trans.* 1973, 612.
[5]B. R. Davis and J. A. Ibers, *Inorg. Chem.* 1971, **10**, 578.
[6]H. Schmidbauer and G. Blaschke, *Z. Naturforsch. Teil B* 1980, **35**, 584; H. Werner and R. Werner, *J. Organomet. Chem.* 1981, **209**, C60.
[7]N. E. Schore and H. Hope, *J. Am. Chem. Soc.* 1980, **102**, 4251.
[8]D. Baudry and M. Ephritikhine, *J. Chem. Soc., Chem. Commun.* 1980, 249.
[9]D. Baudry, M. Ephritikhine, H. Felkin, Y. Jeannin and F. Robert, *J. Organomet. Chem.*, 1980, **220**, C7; see also M. A. Green, J. C. Huffman, K. G. Caulton, W. K. Rybak and J. F. Ziólkówski, *J. Organomet. Chem.* 1981, **218**, C39.
[10]J. Chatt, J. R. Dilworth and G. J. Leigh, *J. Chem. Soc.* (*A*) 1970, 2239.
[11]M. B. Hursthouse, R. A. Jones, K. M. A. Malik and G. Wilkinson, *J. Am. Chem. Soc.* 1979, **101**, 4128.

Polyhedron Vol. 1, No. 1, pp. 45–47, 1982
Printed in Great Britain.

0277-5387/82/010045-03$03.00/0
Pergamon Press Ltd.

PERMETALLOPLUMBANES: PREPARATION OF $[Pb\{Co(CO)_3(L)\}_4]$ AND $[Pb\{Fe(CO)_2(NO)(L)\}_4]$.

COMPLEXES CONTAINING FOUR TRANSITION METAL TO LEAD BONDS (L = TERTIARY ARSINE, PHOSPHINE OR PHOSPHITE).

PAUL HACKETT and A. R. MANNING*
Department of Chemistry, University College, Belfield, Dublin 4, Ireland

(*Received* 20 *June* 1981)

Abstract—The sole and unexpected products from the reactions of a variety of lead (II) and lead (IV) compounds with $[Co_2(CO)_6(L)_2]$ complexes (L = tertiary arsine, phosphine, or phosphite) in refluxing benzene solution are the blue, air-stable percobaltoplumbanes $[Pb\{Co(CO)_3(L)\}_4]$. These have also been obtained from the reaction of $Na[Co(CO)_3(L)]$ ($L = PBu^n_3$) with lead (II) acetate which with $Na[Fe(CO)_2(NO)(L)]$ forms the isoelectronic $[Pb\{Fe(CO)_2(NO)(L)\}_4]$ [$L = P(OPh)_3$]. The IR spectra of the complexes in the ν(CO) and ν(NO) regions are consistent with tetrahedral $PbCo_4$ or $PbFe_4$ fragments, trigonal bipyramidal coordination about the cobalt or iron atoms and linear Pb–Co–As, Pb–Co–P, or Pb–Fe–P systems. Unlike $[Pb\{Co(CO)_4\}_4]$, our complexes do not dissociate to $[Co(CO)_3(L)]^-$ or $[Fe(CO)_2(NO)(L)]^-$ ions when dissolved in donor solvents.

Our previous studies have shown that a wide variety of complexes containing tin–cobalt bonds may be obtained from the facile reactions of tin (II) and tin (IV) halides, and tin (II) sulphate with $[Co_2(CO)_6(PBu^n_3)_2]$ or $Na[Co(CO)_3(PBu^n_3)]$.[1] In view of the relatively high reactivity of the cobalt–cobalt bond, we felt that lead (II) compounds might undergo related reactions despite a previous report that lead (II) chloride did not insert into the metal–metal bond of $[Fe_2(\eta\text{-}C_5H_5)_2(CO)_4]$.[2]

We have found that lead (II) halides react with $[Co_2(CO)_6(PBu^n_3)_2]$ in refluxing benzene, but the only products were metallic lead and $[Pb\{Co(CO)_3(PBu^n_3)\}_4]$. This and related derivatives were the only products from similar thermal reactions of lead metal or a wide variety of lead (II) or lead (IV) compounds (ranging from $Pb(NO_3)_2$ to $PbEt_4$) with $[Co_2(CO)_6(L)_2]$ (L = tertiary arsine, phosphine or phosphite) or from the room temperature reactions of lead (II) acetate with $Na[Co(CO)_3(PBu^n_3)]$ or $Na[Fe(CO)_2(NO)\{P(OPh)_3\}]$.

Prior to our investigation, little work had been carried out on permetalloplumbanes. Spectroscopic evidence had been obtained for $[PbFe_4(CO)_{16}]$[3] and $[PbFe_3(CO)_{12}]$.[4] $[PbFe(CO)_4]_n$[5] and $[Pb\{Co(CO)_4\}_2]$[6] had been reported. Subsequently, Schmid and Etzrodt described the preparation of $[Pb\{Co(CO)_4\}_4]$ from $[Co_2(CO)_8]$ and lead metal, or from $Na[Co(CO)_4]$ and lead (II) nitrate, and its reaction with PPh_3 to give $[Pb\{Co(CO)_4\}\{Co(CO)_3(PPh_3)\}_3]$ and $[Pb\{Co(CO)_3(PPh_3)\}_4]$ complexes.[7] The last is analogous to our cobalt compounds.

EXPERIMENTAL

Literature methods were used to prepare $[Co_2(CO)_6(L)_2]$ (L = tertiary phosphine, phosphite or arsine),[8] $[Hg\{Fe(CO)_2(NO)[P(OPh)_3]\}_2]$,[9] $(C_5H_5)_2Pb$[10] and Ph_6Pb_2.[11] Other chemicals were purchased.

All solvents were dried over calcium hydride and distilled under an atmosphere of nitrogen prior to use. All reactions were carried out at room temperature in these purified solvents under an atmosphere of nitrogen unless it is stated otherwise.

IR spectra were obtained using a Perkin–Elmer 337 spectrometer fitted with a Hitachi-Perkin–Elmer readout recorder. They were calibrated using DCl or water vapour[12] so that peak positions are accurate to ±1 cm^{-1}. The spectra were measured in carbon disulphide solution. The frequencies of absorption bands due to ν(NO) and ν(CO) vibrations are quoted in cm^{-1} with relative peak heights in parentheses.

Compounds were analysed in the Analytical Laboratory of this Department (analyses are quoted as determined values with those calculated in parentheses). Their melting points were measured in sealed tubes and are given in °C; dec. indicates that the sample decomposed on melting.

A solution of $Na[Co(CO)_3(PBu^n_3)]$ in diglyme (40 ml) was prepared by the reduction of $[Co_2(CO)_6(PBu^n_3)_2]$ (1.7 g) with sodium amalgam. To it was added an aqueous solution of $Pb(O_2CMe)_2{\cdot}3H_2O$ (10 g in 150 ml). A metallic mirror, probably lead, was deposited on the walls of the reaction flask. After 10 min the mixture was shaken with ether (100 ml), washed with water, dried over anhydrous sodium sulphate, and the solvent removed at reduced pressure. The residue was recrystallized from acetone–methanol to give dark blue crystals of $[Pb\{Co(CO)_3(PBu^n_3)\}_4]$ in 70% yield [m.p. = 203–204. %C = 45.3 (45.4), %H = 7.2 (6.8), %P = 7.9 (7.8). ν(CO) = 1920 (0.6), 1946 (10), 1982 (7.3)].

If $Na[Co(CO)_3(PBu^n_3)]$ was replaced by $Na[Fe(CO)_2(NO)P(OPh)_3]$ (from 1.7 g of $[Hg\{Fe(CO)_2(NO)[P(OPh)_3]\}_2]$ and sodium amalgam), black crystals of $[Pb\{Fe(CO)_2(NO)[P(OPh)_3]\}_4]$ were isolated in 45% yield on recrystallization from toluene–hexane mixtures [m.p. = 142–145 (dec). %C = 47.2 (47.7), %H = 3.0 (3.0), %N = 2.6 (2.8). ν(NO) = 1740 (4.0), 1753 (4.3), ν(CO) = 1943 (8.8), 1956 (sh), 1990 (10), 2018 (2.9)].

When a solution of red $[Co_2(CO)_6(PBu^n_3)_2]$ (0.69 g) in benzene (50 ml) was refluxed with a lead compound (10 mmoles) such as $Pb(O_2CMe)_2{\cdot}3H_2O$, $Pb(O_2CMe)_2$, $Pb(NO_3)_2$, $PbCl_2$, PbI_2, Et_4Pb, Ph_6Pb_2, Ph_2PbCl_2 or $(C_5H_5)_2Pb$, the mixture turned blue. The reaction was monitored by IR spectroscopy. It was complete within 1 hr for $Pb(O_2CMe)_2$, but required 16 hr for Et_4Pb. The reaction mixtures were filtered and the solvents removed from the filtrates at reduced pressure. The residues were recrystallised from acetone–methanol to give blue $[Pb\{Co(CO)_3(PBu^n_3)\}_4]$ in yields of *ca.* 50%. This reaction was extended to other $[Co_2(CO)_6(L)_2]$ derivatives which gave analytically pure $[Pb\{Co(CO)_3(L)\}_4]$ complexes in comparable yields with L = $AsEt_3$ [m.p. 250 (dec.); ν(CO) = 1921 (1.1), 1948 (10), 1984 (7.3)], PEt_3 [m.p. = 250 (dec.); ν(CO) = 1924 (0.7), 1948 (10), 1983 (6.7)], PPr^n_3 [m.p. = 230 (dec.); ν(CO) = 1920 (0.6), 1947 (10), 1982 (7.8)],

*Author to whom correspondence should be addressed.

$PMePh_2$ [m.p. = 180-181; ν(CO) = 1927 (0.9), 1954 (10), 1991 (7.6)], PBu^nPh_2 [m.p. = 195–196; ν(CO) = 1929 (0.9), 1954 (10), 1991 (6.4)], and $P(OPh)_3$ [m.p. = 128 (dec.); ν(CO) = 1954 (10), 1981 (10), 2015 (6.7)].

A suspension of $[(Bu^n_3P)_2(Co(CO)_3][Co(CO)_4]$ (1 g) and Pb powder (11 g) in tetrahydrofuran (50 ml) were heated on a steam-bath for 3 hr. The purple solution was filtered, its solvent removed at reduced pressure, and the residue recrystallized from a methanol/acetone mixture to give purple crystals of $[Pb\{Co(CO)_3PBu^n_3\}_4]$ in 60% yield.

A suspension of $[Co_2(CO)_6(PBu^n_3)_2]$ (1 g) and Pb powder (10 g) in benzene (50 ml) were allowed to stand at room temperature for 6 hr whilst being stirred. There was no significant reaction, but when the mixture was heated on a steam bath, $[Pb\{Co(CO)_3(PBu^n_3)\}_4]$ was formed. It was isolated as above in 75% yield after 2 hr.

Both $[Hg\{Co(CO)_3[P(OPh)_3]\}_2]$ (0.5 g) and $[Hg\{Fe(CO)_2(NO)(PPh_3)\}_2]$ (1 g) failed to react with Pb powder (5 g) or PbI_2 (2 g) in tetrahydrofuran (50 ml) even after heating the mixtures to boiling on a steam bath for 6 hr.

A solution of $[Pb\{Co(CO)_3(PBu^n_3)\}_4]$ (0.7 g) in benzene (50 ml) was boiled with PbX_2 (10 mmoles X = Br or I) for 20 hr. The colour of the reaction mixture changed from purple to brown. The solvent was removed from the filtered reaction mixture at reduced pressure. The residue was recrystallized from aqueous methanol to give $[Co(PBu^n_3)_2(CO)_2X]$ in 15–20% yield [X = Br; m.p. = 50–51; %C = 51.1 (51.3), %H = 8.9 (8.9); ν(CO) = 1905 (10), 1969 (1.8). X = I; m.p. = 46–47; %C = 48.0 (48.3); %H = 8.1 (8.4); ν(CO) = 1906 (10), 1970 (2.9)].

To a solution of $[Pb\{Co(CO)_3(PBu^n_3)\}_4]$ (0.5 g) in chloroform (20 ml) was added (from a burette) a saturated solution of iodine in chloroform. The reaction was monitored by IR spectroscopy. The absorption bands at *ca.* 1950 and at 1980 cm^{-1} due to $[Pb\{Co(CO)_3(PBu^n_3)\}_4]$ were replaced by others at 1979 (10), 2018 (1.3) and 2074 (0.6) cm^{-1}. the reaction mixture was brown. This compound was very unstable and could not be isolated. The addition of more iodine solution resulted in the formation of a yellow precipitate and the disappearance of the intermediate compound.

RESULTS AND DISCUSSION

The $[Pb\{Co(CO)_3(L)\}_4]$ complexes are blue, air-stable crystalline solids which are soluble in hexane, benzene, chloroform and acetone, sparingly soluble in acetonitrile, dimethylsulphoxide and methanol, and insoluble in water. The closely-related $[Pb\{Fe(CO)_2(NO)[P(OPh)_3]\}_4]$ is black. All are more robust than $[Pb\{Co(CO)_4\}_4]$ towards heat and air.

These compounds are the sole and unexpected products from the reactions of a wide variety of ionic and covalent lead (II) and lead (IV) compounds as well as metallic lead with $[Co_2(CO)_6(L)_2]$ in boiling benzene. It is probable that the formation of $[Pb\{Co(CO)_3(PBu_3)\}_4]$ from $[Co(PBu^n_3)_2(CO)_3][Co(CO)_4]$ and Pb metal also proceeds via $[Co_2(CO)_6(PBu^n_3)_2]$.[8] There is no evidence for the formation of analogues of $[Co(CO)_3(L)SnX_3]$, $[\{Co(CO)_3(L)\}_2SnX_2]$, $[\{Co(CO)_3(L)\}_3SnX]$ and $[\{Co(CO)_3(L)\}_3SnH]$ which were obtained from the comparable reactions involving tin halides.[1] Furthermore compounds containing cobalt–cobalt as well as lead–cobalt bonds were not observed (the preparation of $[GeCo_4(CO)_{14}]$[13] and $[(CO)_4CoGeCo_3(CO)_9]$.[14] This particular subject has been reviewed recently.[15]

The reaction of lead (II) salts with $Na[Co(CO)_3(L)]$ or $Na[Fe(CO)_2(NO)(L)]$ to give $[Pb\{Co(CO)_3(L)\}_4]$ or $[Pb\{Fe(CO)_2(NO)(L)\}_4]$ resembles that of $PbCl_2$ with PhMgBr. This forms a mixture of Ph_6Pb_2 and Ph_4Pb with the former decomposing to the latter and lead metal at higher temperatures.[11] We have looked for the analogous percobaltodiplumbane, $[Pb_2\{Co(CO)_3(L)\}_6]$, but have not detected it.

The IR spectra of the $[Pb\{Co(CO)_3(L)\}_4]$ derivatives in the ν(CO) region are similar to those of their tin counterparts, e.g. $[Sn\{Co(CO)_3(PBu^n_3)\}_4]$.[1] The two most intense absorption bands at *ca.* 1950 and 1985 cm^{-1} when $L = PR_3$ or AsR_3 and *ca.* 1980 and 2015 cm^{-1} when $L = P(OPh)_3$ are probably due to the fundamental ν(CO) modes of all-^{12}CO species. The weaker feature at somewhat lower frequencies (*ca.* 1920 or 1950 cm^{-1}) is attributed to those molecules containing one ^{13}CO ligand. As these are relatively abundant (*ca.* 12%), they give rise to a relatively intense absorption band. The IR spectra are consistent with T_d molecular symmetry for the $[Pb\{Co(CO)_3(L)\}_4]$ complexes for which two IR active ν(CO) vibrations would be expected, each having T_2 symmetry.[16] Furthermore the observed four ν(CO) and two ν(NO) absorption bands in the IR spectrum of $[Pb\{Fe(CO)_2(NO)[P(OPh)_3]\}_4]$ are consistent with S_4 molecular symmetry. Thus it is probable that both series of compounds contain tetrahedral PbM_4 moieties (M = Co or Fe), trigonal bipyramidal coordination about M and linear Pb–M–P or Pb–M–As systems.

The spectra of solutions of our $[Pb\{Co(CO)_3(L)\}_4]$ complexes are virtually independent of the solvent employed when L is a tertiary arsine, phosphine or phosphite. On the other hand this is not the case for $[Pb\{Co(CO)_4\}_4]$ where L = CO. Schmidt and Ekrodt attributed this behaviour to the coordination of molecules of donor solvents such as ether or acetone to the lead atom whilst the Pb–Co bonds remained intact.[7] We feel that this explanation is unlikely to be correct, and that it is more probable that when $[Pb\{Co(CO)_4\}_4]$ is dissolved in such donor solvents it dissociates reversibly to give $[Co(CO)_4]^-$ ions which give rise to the IR absorption band reported[7] as having a frequency of 1867 cm^{-1} in ether. Such dissociations are a common feature of the chemistry of complexes possessing bonds between main group and transition metals. They are generally more extensive in ether than in acetone, and are inhibited by replacing CO ligands coordinated to the transition metal by arsines, phosphines or phosphites, as has been observed in the present instance (cf. the dissociation of $[Ph_2Pb\{Fe(CO)_2(NO)(L)\}_2]$ in donor solvents).[17]

Although it may not be surprising that neither $[Hg\{Co(CO)_3[P(OPh)_3]\}_2$ nor $[Hg\{Fe(CO)_2(NO)(PPh_3)\}_2]$ react with lead powder, one might have anticipated that they would react with PbI_2. The analogous reactions with SnX_2 have been shown to form $[SnX_2\{Co(CO)_3(PBu^n_3)\}_2]$ derivatives (X = halogen).[18]

Attempts to prepare stable compounds containing both lead–cobalt and lead–iodine bonds were not successful. Although $[Pb\{Co(CO)_3(PBu^n)\}_4]$ did react with iodine, the brown product decomposed readily. Its IR spectrum [ν(CO) = 1979 (10), 2018 (13), 2074 (0.6) cm^{-1}], when compared with those of analogous tin compounds, suggested that it could be $[PbI_2\{Co(CO)_3(PBu^n_3)\}_2]$ or $[PbI_3\{Co(CO)_3(PBu_3)\}]$ [for $[SnI_2\{Co(CO)_3(PBu^n_3)\}_2]$, ν(CO) = 1960 (2.6), 1975 (10), 2019 (2.1) cm^{-1}; and for $[SnI_3\{Co(CO)_3(PBu_3)\}]$, ν(CO) = 1984 (10), 2051 (1.0) cm^{-1}].[1]

REFERENCES

[1]P. Hackett and A. R. Manning, *J. Chem. Soc., Dalton Trans.* 1974, 2257.

[2]F. Bonati and G. Wilkinson, *J. Chem. Soc.* 1964, 179.

[3]J. D. Cotton, S. A. R. Knox, I. Paul and F. G. A. Stone, *J. Chem. Soc.(A)* 1967, 264.
[4]W. Hieber, J. Gruber and F. Lux, *Z. anorg. allgem. Chem.* 1959, **300**, 417.
[5]P. Krumholz and S. Bril, *Proc. Chem. Soc.* 1960, 116.
[6]A. Vizi-Orosz, G. Bor and L. Marko, *Acta Chim. Acad. Sci. Hung.* 1969, **59**, 417.
[7]G. Schmid and G. Etzrodt, *J. Organometallic Chem.* 1977, **131**, 477.
[8]A. R. Manning, *J. Chem. Soc.(A)* 1968, 1135.
[9]M. Casey and A. R. Manning, *J. Chem. Soc.(A)* 1970, 2258.
[10]L. D. Dane, D. F. Evans and G. Wilkinson, *J. Chem. Soc.* 1959, 3684.
[11]L. C. Willemsens and G. J. van der Kerk, *J. Organometallic Chem.* 1970, **21**, 123.
[12]*Tables of Wavenumbers for the Calibration of Infrared Spectrometers*, Butterworths, London, 1961.
[13]R. F. Gerlach, K. M. McKay and B. K. Nicholson, *J. Organometallic Chem.*, 1979, **178**, C30.
[14]G. Schmid and G. Etzrodt, *J. Organometallic Chem.* 1977, **137**, 367.
[15]G. Schmid, *Angew. Chem. Int. Ed., Engl.* 1978, **17**, 932.
[16]M. Bigorgne and A. Quintin, *Compt. rend.* 1967, **264**, 2055, and D. J. Patmore and W. A. G. Graham, *Inorg. Chem.* 1968, **7**, 771.
[17]M. Casey and A. R. Manning, *J. Chem. Soc.(A)* 1971, 256.
[18]F. Bonati, S. Cenini and R. Ugo, *J. Chem. Soc.(A)* 1967, 933.

Polyhedron Vol. 1, No. 1, pp. 49–51, 1982
Printed in Great Britain.

0277-5387/82/010049-03$03.00/0
Pergamon Press Ltd.

ION PAIR ASSOCIATION OF COMPLEXES OF La^{3+} AND Nd^{3+} WITH Br^- AND NO_3^- IN N,N-DIMETHYLACETAMIDE

CLAUDIO AIROLDI, PEDRO L. O. VOLPE and AÉCIO P. CHAGAS*
Instituto de Química, Universidade Estadual de Campinas, Caixa Postal 1170, 13100 Campinas, São Paulo, Brasil

(*Received* 23 *June* 1981)

Abstract—The formation constants and the respective variations of enthalpy were obtained by means of calorimetric titration of the lanthanides La^{3+} and Nd^{3+} with bromide and nitrate in N,N-dimethylacetamide. These thermochemical data were calculated for the 1:1 and 1:2 species which are less stable than the corresponding species obtained with chloride. The order of stability $Cl^- > Br^- > NO_3^-$ was established for both species of La^{3+}, and the order $Br^- > Cl^- > NO_3^-$ for 1:1 species of Nd^{3+}. $NdCl_2^+$ and $NdBr_2^+$ species were not detected. Our results support the view that the metal-anion interactions involve inner sphere species.

INTRODUCTION

In coordination chemistry studies N,N-dimethylacetamide (DMA) serves not only as a ligand, but also, as an excellent non-aqueous solvent.[1]

Although DMA is a polar non-hydrogen bonded solvent, it does not ionize to any significant extent. It is a good solvent for cations and its high donor property[2] permits coordination to the cation in many cases.[3] In contrast it is a relatively poor solvent for anions.[4,5] All these features favour the study of metal-anion interactions in solution. Indeed, this can be illustrated by calorimetric titrations of lanthanide (III) perchlorates with chloride[6]. The results show a clear evidence of the break of gadolinium and present a very close agreement with the P (M) function.[7,8]

In continuing, we report now the calorimetric titration of La^{3+} and Nd^{3+} with bromide and nitrate anions in DMA. The results are compared with our earlier results,[6] so as to understand better the nature of lanthanide (III)-anion interactions in this non-aqueous solvent.

EXPERIMENTAL AND CALCULATIONS

The preparations of the lanthanide compounds and solutions have been described previously.[6] Sodium bromide and nitrate (Carlo Erba) were dried at ~130°C under vacuum.

The calorimeter system, titrations and calculations are the same as in the preceding article.[6] La^{3+} and Nd^{3+} 5.000×10^{-2} M solutions were titrated with bromide and nitrate solutions. Each Ln^{3+} ion was titrated twice by employing ligand solutions 2.520×10^{-1} M and 3.600×10^{-1} M. The initial volume of solution in the calorimeter vessel was 90.00 ml and at the end of the titration was around 100 ml.

Data for a typical titration of Nd^{3+} with NO_3^- are summarized in Table 1. Q_A is the variation of enthalpy observed after the addition of each increment of volume. To correct the effect of dilution during the titration, pure DMA was added to Ln^{3+} solution and also to the anion solution. The thermal dilution effects Q_B and Q_C, respectively, are listed in Tables 2 and 3.

The variation of enthalpy due to the chemical reaction was obtained by subtracting the caloric effects of dilution from Q_A values, i.e. $Q_{obs} = Q_A - Q_B - Q_C$. In Fig. 1 are plotted the accumulated values of Q_A, Q_B, Q_C and Q_{obs} for $Nd^{3+} - NO_3^-$ interactions, against the volume of solution.

RESULTS AND DISCUSSION

The results are summarized in Table 4. Figure 2 shows

Table 1. Titration of 90.0 ml of Nd^{3+} solution 5.000×10^{-2} M with 3.600×10^{-1} M NO_3^- solution

V/ml	Q_{obs}/J	ΣQ_{obs}/J
90,00	0	0
90,24	0,32	0,32
90,81	0,83	1,15
91,34	0,68	1,83
91,92	0,84	2,67
92,46	0,73	3,40
92,97	0,71	4,11
93,48	0,67	4,78
94,11	0,83	5,61
94,64	0,67	6,28
95,21	0,70	6,98
95,71	0,61	7,59
96,24	0,63	8,22
96,87	0,72	8,94
97,38	0,52	9,46
97,95	0,60	10,06
98,55	0,58	10,64
99,11	0,49	11,13
99,60	0,35	11,48
100,02	0,26	11,74

Table 2. Dilution of 90.0 ml of Nd^{3+} solution 5.000×10^{-2} M with DMA

V/ml	Q_{obs}/J	ΣQ_{obs}/J
90,00	0	0
91,17	- 0,14	- 0,14
92,20	- 0,11	- 0,25
93,36	- 0,11	- 0,36
94,41	- 0,12	- 0,48
95,50	- 0,08	- 0,56
96,67	- 0,07	- 0,63
97,76	- 0,10	- 0,73
99,27	- 0,12	- 0,85
100,18	- 0,07	- 0,92

*Author to whom correspondence should be addressed.

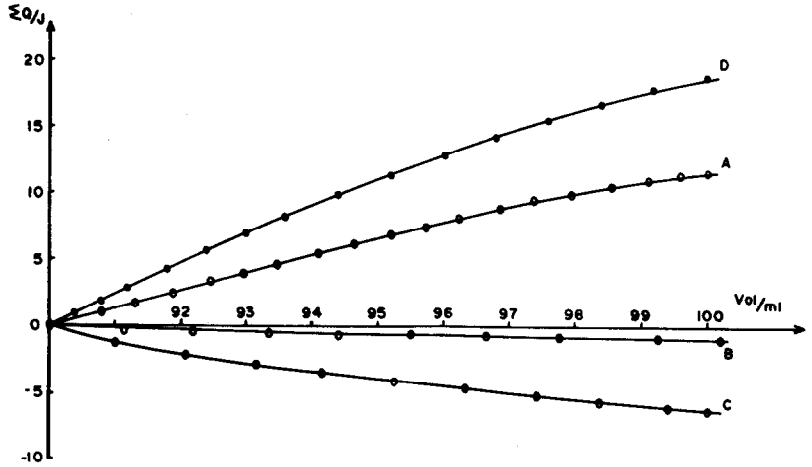

Fig. 1. Calorimetric titration of 90.0 ml of a 5.000×10^{-2} M solution of Nd^{3+} with 3.600×10^{-1} M NO_3^- solution. The experimental points in curves *A*, *B* and *C* represent the summation of Q_A's, Q_B's and Q_C's, respectively. The calculated points in curve *D* represent the summation of the Q_{obs}.

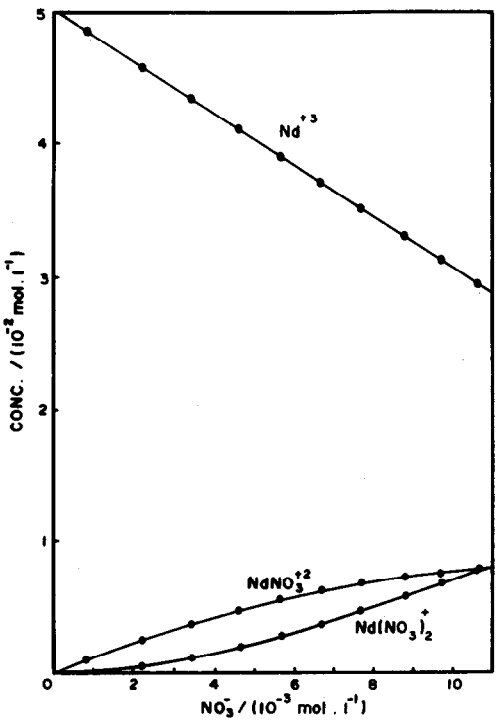

Fig. 2. Distribution curves of $NdNO_3^{2+}$ and $Nd(NO_3)_2^+$ species present in the Nd^{3+}–NO_3^- system in DMA at 298°K.

Table 3. Dilution of 90.0 ml of NO_3^- solution 3.600×10^{-1} M in DMA

V/ml	Q_{obs}/J	ΣQ_{obs}/J
90,00	0	0
91,03	- 1,18	- 1,18
92,08	- 0,87	- 2,05
93,19	- 0,74	- 2,79
94,18	- 0,62	- 3,41
95,27	- 0,59	- 4,00
96,34	- 0,57	- 4,57
97,41	- 0,50	- 5,07
98,39	- 0,47	- 5,54
99,41	- 0,43	- 5,97
100,01	- 0,23	- 6,20

the distribution curve of Nd^{3+}, $NdNO_3^{2+}$ and $Nd(NO_3)_2^+$ species during the titration at 298 K, calculated from the values of K_1 and K_2. From Table 4 one can observe that with La^{3+} the order of stability of the 1:1 species is $Cl^- > Br^- > NO_3^-$, while with Nd^{3+} the observed order is $Br^- > Cl^- > NO_3^-$.

The values of K and ΔH for the 1:2 species of La^{3+} are of the same order as with its 1:1 species. In the case of Nd^{3+} the species $NdCl_2^+$ and $NdBr_2^+$ were not detected in our experimental conditions. All species present low values of the constant of formation and are endothermic ($\Delta H > 0$).

Table 4. K_1, K_2, ΔH_1 and ΔH_2 values for the interactions of La^{3+} and Nd^{3+} with Cl^-, Br^- and NO_3^- at 298 K

Ln^{3+}	X^-	K_1/mol^{-1}.ℓ	K_2/mol^{-1}.ℓ	ΔH_1/kJ mol^{-1}	ΔH_2/kJ mol^{-1}
La^{3+}	Cl^- (a)	212 ± 1	62 ± 9	26,1 ± 0,1	36,0 ± 0,4
	Br^-	165 ± 1	48 ± 7	32,6 ± 0,2	45,6 ± 0,4
	NO_3^-	17 ± 1	16 ± 2	48,2 ± 0,2	23,1 ± 0,2
Nd^{3+}	Cl^- (a)	58 ± 1	—	24,1 ± 0,1	—
	Br^-	115 ± 1	—	33,6 ± 0,2	—
	NO_3^-	25 ± 1	92 ± 13	15,0 ± 0,1	8,3 ± 0,1

(a) These data, obtained from ref. (6) are included for comparation.

Choppin and Bertha[9] discussed the formation of lanthanide complexes in water with various anions and found the following sequence of stability $F^- > IO_3^- > SCN^- > NO_3^- > Cl^- > ClO_4^-$. The first two anions form preferentially inner sphere species. Otherwise outer sphere species for the others, in which the ionic pairs are separated by solvent. On the other hand, the complexes of lanthanides with Cl^-, Br^- and NO_3^- in DMA, are in our opinion predominantly inner sphere species and the arguments which support this view are the following:

(i) These anions present a low degree of solvation in DMA.[4,5] It was possible for literature data to calculate $\Delta G^\ominus$ for the process: $Cl^-_{(g)} + \infty DMA_{(l)} = Cl^-_{(solv)}$, which gave the value $-334\,kJ\,mol^{-1}$. This value is comparable to $-372\,kJ\,mol^{-1}$, which was obtained for the same process by applying the Born formula, $\Delta G^\ominus = -Ze^2L/2r\,(1-1/\epsilon)$, where Z = charge of the ion, e = elementary electrical charge, L = Avogadro's number, r = ion radius and ϵ = dielectric constant.[10] The low salvation of the anion makes it easy for the cation to compete with the solvent to interact with the anion.

(ii) $\Delta H_1^\ominus$ values obtained experimentally and $\Delta S_1^\ominus$ calculated by means of the usual expressions $\Delta G_1^\ominus = -RT \ln K_1^\ominus$ and $\Delta G^\ominus = \Delta H_1^\ominus - T\Delta S_1^\ominus$, considering $K_1 = K_1^\ominus$; indicate that both values are positive, and are in agreement with the application of Ahrland's model for water.[11,12] In that case, the outer sphere complexes produce $\Delta H_1^\ominus < 0$ and $\Delta S_1^\ominus \simeq 0$.

(iii) Prue[13] has developed an ion pair contact model of inner sphere. Applying this model to $LaCl^{2+}$ species gives the values $\Delta H_1^\ominus = 25\,kJ\,mol^{-1}$ and $\log K_1^\ominus = 2.3$, which are practically coincident with the experimental results $(26.1 \pm 0.1)\,kJ\,mol^{-1}$ and 2.32, respectively. For these calculations we used the expressions: $\Delta H_1^\ominus = -RTb\,(1 + d \ln \epsilon/d \ln T)$; $K^\ominus = \bar{v} \exp b$; $\bar{v} = 4/3\,\pi La^3$; $b = |Z + Z - |e^2/4\pi\epsilon_0\epsilon akT$; $a^3 = r_{La^{3+}} + r_{Cl^-}$(10). Where k is the Boltzmann's constant. Other symbols are of general use or have been already defined above.

(iv) Some ligands can affect the hypersensitive bands of Nd^{3+}. These effects are more evident with the band centered at 580 nm, as was pointed out by various authors.[14–17] These effects provide information about the nature of the metal-ligand interaction, indicating the formation of inner or outer sphere complexes. In the case of the interaction of Nd^{3+} with Cl^- in DMA,[18,19] a series of spectra are obtained which qualitatively suggest the presence of inner sphere species.

(v) Studies of X-ray diffraction in solution of $LaCl_3$ or $NdCl_3$ with 10 M HCl in water or in methan[20–22] show the presence of species where the anion is in the inner sphere, although water is more nucleophilic than chloride. This effect is more evident in methanol solution.

(vi) Recently, Johnson[23] generalised some conclusions of Cater,[24] to give the following principle "The lanthanide elements behave similarly in reactions in which the $4f$ electrons are conserved, and very differently in reactions in which the number of $4f$ electrons changes". The $K_1^\ominus$ and $\Delta H_1^\ominus$ results found for chloride ions with all lanthanides across the elements of the series follow the function P (M),[7,8] as shown previously.[6] The function is in good agreement with Johnson's principle. Therefore, this implies that the anions studied are close enough to the central atom to disturb the f orbitals. in contrast with other ligands where practically the thermodynamic parameters do not vary across the lanthanide series. In conclusion, the species formed through the interaction of Ln^{3+} with chloride, bromide and nitrate in DMA, in the range of the concentration studied, are all inner sphere complexes.

Acknowledgements—The authors are indebted to FINEP for financial support.

REFERENCES

[1] J. J. Lagowski, *The Chemistry of Non-Aqueous Solvents*, Vol. II. Academic Press, London, 1967.
[2] V. Gutmann, *Coordination Chemistry in Non-Aqueous Solutions*. Springer, New York, 1968.
[3] J. A. Simoni, C. Airoldi and A. P. Chagas, *J. Chem. Soc. Dalton* 1980, 156.
[4] U. Mayer, *Pure Appl. Chem.* 1975, **41**, 291.
[5] U. Mayer, *Coord. Chem. Rev.* 1976, **21**, 159.
[6] P. L. O. Volpe, A. P. Chagas and C. Airoldi, *J. Inorg. Nucl. Chem.* 1980, **42**, 1321.
[7] L. J. Nugent, J. L. Burnett and L. R. Morss, *J. Chem. Thermodynamics* 1973, **5**, 665.
[8] F. David, K. Samboon, R. Guillaumont and N. Edelstein, *J. Inorg. Nucl. Chem.* 1978, **40**, 69.
[9] G. R. Choppin and S. L. Bertha, *J. Inorg. Nucl. Chem.* 1973, **35**, 1309.
[10] W. E. Dassent, *Inorganic Energetics*. Penguin, London, 1970.
[11] S. Ahrland, *Helv. Chim. Acta* 1967, **50**, 306.
[12] S. Ahrland, *Struct. Bonding* 1973, **15**, 167.
[13] J. E. Prue, *J. Chem. Ed.* 1969, **46**, 12.
[14] C. K. Jørgensen and B. R. Judd, *Mol. Phys.* 1964, **8**, 281.
[15] G. R. Choppin, D. E. Henrie and K. Buys, *Inorg. Chem.* 1966, **5**, 1743.
[16] D. G. Karraker, *J. Chem. Ed.* 1970, **47**, 424.
[17] J. H. Forsberg, *Observations on the Rare Earths. Studies of Ethylenediamine Complexes of the Lanthanide Ions*, Ph.D. Thesis, University of Illinois, Microfilm Corp., 1968.
[18] G. Vicentini and C. Airoldi, *An. Acad. Brasil. Ciênc.* 1970, **42**, 431.
[19] C. Airoldi and G. Vicentini, *An. Acad. Brasil, Ciênc.* 1972, **44**, 427.
[20] L. S. Smith Jr. and D. L. Wertz, *J. Am. Chem. Soc.* 1975, **97**, 2365.
[21] L. S. Smith Jr., D. C. McCain and D. L. Wertz, *J. Am. Chem. Soc.* 1976, **98**, 5125.
[22] M. L. Steele and DL. L. Wertz, *Inorg. Chem.* 1977, **16**, 1225.
[23] D. A. Johnson, *J. Chem. Ed.* 1980, **57**, 475.
[24] E. D. Cater, *J. Chem. Ed.* 1978, **55**, 697.

Polyhedron Vol. 1, No. 1, pp. 53–56, 1982
Printed in Great Britain.

0277–5387/82/010053–04$03.00/0
Pergamon Press Ltd.

BINUCLEAR 2,2'-BIPYRIMIDINE COMPLEXES DERIVED FROM CHROMIUM, MOLYBDENUM AND TUNGSTEN CARBONYLS

COLIN OVERTON and JOSEPH A. CONNOR*
Department of Chemistry, The University, Manchester M13 9PL, England

(*Received* 15 *July* 1981)

Abstract—Reaction of 2,2'-bipyrimidine (bpym) with [$Mo(CO)_4$(diene)] gives [$Mo(CO)_4$(bpym)], which will react with [$M(CO)_4$(diene)] to form [$MoM(CO)_8$(bpym)] (M = Cr, Mo, W). The bipyrimidine complexes are characterised by microanalysis and spectroscopy (IR, ^1H and ^{13}C NMR, UV/vis). Reduction of [$Mo_2(CO)_8$(bpym)] produces an anion in which the unpaired electron is localised on the bridging bpym ligand.

INTRODUCTION

Binuclear transition metal complexes in which electronic interaction between the metals can occur through a common binucleating ligand have acquired interest recently in the context of intramolecular redox processes. We are interested in redox reactions of 2,2'-bipyridine (bpy) complexes of the group six metals in those formal oxidation states which are isoelectronic with the well-known complexes of ruthenium and osmium. The isosteric relation between 2,2'-bipyridine and 2,2'-bipyrimidine (bpym) suggested study of analogous simple derivatives of molybdenum hexacarbonyl. We report the synthesis of binuclear carbonyl complexes [$MoM(CO)_8$(bpym)] (M = Cr, Mo, W) and some of their properties. Ruthenium(II) complexes such as [Ru_2(bpy)$_4$(bpym)]$(PF_6)_2$ have been described recently,[1] and μ-bipyrimidyl heterobinuclear complexes containing iron(II) with either copper(II) or zinc(II) have been examined[2] as models of the active site of the enzyme cytochrome oxidase.

RESULTS

The mononuclear complex *cis*-[$Mo(CO)_4$(bpym)] was obtained in good yield from the reaction between *cis*-[$Mo(CO)_4(\eta^2,\eta^2\text{-}C_7H_8)$] ($C_7H_8$ is bicyclo [2.2.1]hepta-2,4-diene) in hexane and a slight excess of the ligand bpym in tetrahydrofuran at room temperature. Well-formed dark red crystals of the complex were obtained on recrystallisation of the reaction product from thf/petrol. The complex is soluble in a wide range of solvents including benzene, but it is insoluble in paraffins. The binuclear complex [$Mo_2(CO)_8$(bpym)] was prepared by the addition of solid ligand, bpym (1 mol) to a solution of *cis*-[$Mo(CO)_4(\eta^2,\eta^2\text{-}C_7H_8)$] (2 mol) in tetrahydrofuran at room temperature. The deep purple powder which had precipitated after 12 hr was washed with hot methylene chloride and dried. The solid is soluble in acetonitrile and dimethylsulphoxide and insoluble in solvents of lower polarity. The heterobinuclear complexes were prepared by the addition of a slight excess of solid *cis*-[$M(CO)_4(\eta^2,\eta^2\text{-}C_7H_8)$] (M = Cr,W) to a solution of *cis*-[$Mo(CO)_4$(bpym)] in tetrahydrofuran. No reaction was observed at room temperature after 4 days. The mixture was heated at reflux for 12 hr after which the black solid product was isolated and purified by reprecipitation with ether from solution in acetone or acetonitrile.

IR spectra

The spectra of the complexes in the region of the carbonyl ligand ν(CO) absorption (2100–1800 cm^{-1}) are similar, both in the solid state and in solution in acetonitrile (Table 1) and they are not significantly different from the spectra of [$M(CO)_4$(bpy)] (M = Cr, Mo, W)[3]. Comparison of the absorptions due to the bpym ligand in the complexes with those of the uncomplexed molecule shows more significant changes. The pattern of ν(CH) vibrations in bpym (3120m, 3060s, 3025m, 2980m cm^{-1}) appears as two very weak absorptions (3090, 2960 cm^{-1}) in the complexes. The strong bands (1560, 1550 cm^{-1}) in bpym, assigned to ring stretching modes (8a, 8b in benzene[4], are very weak and broad in the complexes. Another ring stretching mode (19b in benzene[4]), observed as a strong sharp band at 1400 in bpym, appears a single band of medium intensity (1406 cm^{-1}) in [$Mo(CO)_4$(bpym)] and as two bands, one of medium intensity (1400 cm^{-1}) and one of weaker intensity (1420 cm^{-1}) in [$MoM(CO)_8$(bpym)]. The band of medium intensity at 1140 cm^{-1} due to β-CH vibration (9a in benzene[4]) in bpym is observed as two absorptions of medium–weak intensity (1110, 1015 cm^{-1}) in [$Mo(CO)_4$(bpym)] and (1190, 1050 cm^{-1}) in [$MoM(CO)_8$(bpym)]. The antisymmetric γ-CH vibration (10b in benzene[4]) appears as two medium–weak absorptions in bpym, but in the complexes these appear as a single absorption of increased relative intensity at 810 cm^{-1}. The strong sharp absorption at 760 cm^{-1} in free bpym is observed as a much weaker band at 750 cm^{-1} in [$Mo(CO)_4$(bpym)] and at 740 cm^{-1} in [$MoM(CO)_8$(bpym)].

Nuclear magnetic resonance

(a) *Proton* (Table 2). The coordination shift [δ(complex–δ(free)] between bpym and [$Mo(CO)_4$(bpym)] is similar to that observed in the case of bpy, with the exception that 6-H is shifted less in the case of bpym. The ^1H NMR spectrum of [$Mo(CO)_4$(bpym)] recorded in benzene d_6 shows the expected aromatic solvent induced shift. The magnitude of this shift (138Hz, 1.73 ppm) in the case of 5-H is noteworthy, as is the difference in the shift (17 Hz, 0.21 ppm, 35 Hz, 0.42 ppm (C_6D_6)) between 6-H (which is close to the metal) and 4-H. Coordination of a second $Mo(CO)_4$-group to bpym forming

*Author to whom correspondence should be addressed.

Table 1. Carbonyl ligand stretching absorptions, ν(CO) cm^{-1} of 2,2'-bipyrimidine (bpym) complexes

Complex	ν(CO)/cm^{-1} in solution (MeCN)				ν(CO)/cm^{-1} solid (Nujol mull)			
$Mo(CO)_4$(bpym)	2023m	1925vs	1891m	1847m	2014m	1912m	1869vs	1833vs *
$CrMo(CO)_8$(bpym)	2015m	1922vs	1892m	1848m	2008m	1909s.sh	1879v	1831vs
$Mo_2(CO)_8$(bpym)	2020m	1922vs	1887m	1844m	2013m	1920s.sh	1896s	1837vs
$MoW(CO)_8$(bpym)	2013m	1919vs	1887m	1847m	2007m	1907s.sh	1882s	1836vs

* plus bands at (2009sh), 1886, 1858, (1812sh).

$[Mo_2(CO)_8(bpym)]$ increases the coordination shift of 5-H. The coordination shift of 4H/6H in $[Mo_2(CO)_8(bpym)]$ is approximately the mean of their values in $[Mo(CO)_4(bpym)]$. The effect of the metal on the proton chemical shifts in $[MoM(CO)_8(bpym)]$ is consistent: both signals move to lower field in the order M = Mo < W < Cr.

(b) *Carbon.* The shift of the ring carbon signals which occurs on coordination of bpym to molybdenum decreases as the distance between the particular carbon atom and the donor nitrogen atom increases. Qualitatively similar observations are made for bpy in $[Mo(CO)_4(bpy)]$, but in this case the decrease is more marked (see Table 2). Problems with the solubility of the compounds prevented measurement of the ^{13}C NMR spectra of $[MoM(CO)_8(bpym)]$ complexes within reasonable instrument time.

Electronic spectra

In the visible region, the spectrum of *cis*-$[Mo(CO)_4(bpym)]$ in solution consists of two absorptions which are absent from the spectrum of the free ligand. These absorptions (Table 3) are assigned to metal *d*-to-ligand π^* charge transfer transitions on the basis of their extinction coefficients ($\epsilon > 1000\,M^{-1}\,cm^{-1}$). The energy of the lower of these two bands exhibits marked solvent dependence (solvatochromism). The lower energy $d\pi^*$ absorption in $[Mo(CO)_4(bpym)]$ is shifted 35 nm to lower

Table 2. Proton and ^{13}C-NMR spectra of 2,2'-bipyrimidine and 2,2'-bipyridine and complexes of these ligands

A. Proton n.m.r spectra.

	Chemical shift,[a] δ/p.p.m.				
Molecule	3-H	4-H	5-H	6-H[b]	Solvent
bpy	8.49	7.80	7.28	8.68	$CDCl_3$
bpym	-	8.98d	7.43t	8.98d	CD_2Cl_2
$Mo(CO)_4$(bpy)	8.16	7.95	7.39	9.12	CD_2Cl_2
$Mo(CO)_4$(bpym)	-	9.10dd	7.52dd	9.32dd	$CDCl_3$
$Mo(CO)_4$(bpym)	-	7.93dd	5.79dd	8.36dd	C_6D_6
$Mo_2(CO)_8$(bpym)	-	9.24d	7.65t	9.24d	CD_3CN
$Mo_2(CO)_8$(bpym)	-	9.26d	7.79t	9.26d	C_2D_6SO
$CrMo(CO)_8$(bpym)	-	9.37m	7.88m	9.37m	C_2D_6SO
$MoW(CO)_8$(bpym)	-	9.33m	7.83m	9.33m	C_2D_6SO

B. ^{13}Carbon n.m.r spectra.

	Chemical shift[a], δ/p.p.m.					
Molecule	2-C	3-C	4-C	5-C	6-C[b]	Solvent
bpy	156.8	124.15	137.40	121.34	149.65	$CDCl_3$
bpym	161.0	-	156.7	120.3	156.7	$CDCl_3$
$Mo(CO)_4$(bpy)	155.5	125.80	138.02	122.73	153.68	$CDCl_3$
$Mo(CO)_4$(bpym)	161.0	-	158.0	122.3	160.1	$CDCl_3$

a. relative to tetramethylsilane, δ = 0

b. The coordinated nitrogen in mononuclear complexes is adjacent to 6-H/6-C

Table 3. Visible absorption spectra λ_{max} nm of 2,2'-bipyrimidine complexes

Complex	Benzene		Dichloromethane		Methylcyanide	
$Mo(CO)_4(bpym)$	381	517	379	508	368	468
$CrMo(CO)_8(bpym)$			450	670	400	562
$Mo_2(CO)_8(bpym)$ [a]			440	675	380	574
$MoW(CO)_8(bpym)$			450	700	394	580

[a] Solid state (MgO matrix) λ_{max} 460, 632 nm.

energy of the corresponding absorption in $[Mo(CO)_4(bpy)]$[5], in the same solvent. A similar difference (but in the opposite sense) was observed[1] between $[Ru(bpy)_3]^{2+}$ and $[Ru(bpy)_2(bpym)]^{2+}$. The absorption spectrum of $[Mo_2(CO)_8(bpym)]$ in the visible region in solution comprises two bands (Table 3), both of which are at lower energy than in $[Mo(CO)_4(bpym)]$. In methyl cyanide solution, the shift of the 468 nm band in $[Mo(CO)_4(bpym)]$ to a weaker, broad band at 574 nm in the binuclear complex can be compared with that observed[1] between $[Ru(bpy)_2(bpym)]^{2+}$ (420 nm) and $[Ru_2(bpy)_4(bpym)]^{4+}$ (592 nm) in the same solvent. The effect of changing the metal M on the position of the lower energy visible absorption in $[MoM(CO)_8(bpym)]$ (M = Cr, M, W) appears just significant. The absorption spectra of the binuclear complexes are also solvatochromic; once again it is the lower energy absorption which is more sensitive, moving to the near infrared (700 nm) in solvents of low polarity. In the solid state, both $d\pi^*$ absorptions of $[Mo_2(CO)_8(bpym)]$ move to lower energy, indicating that the polarity of the matrix has diminished.

Redox reactions

Reduction of the binuclear complex $[Mo_2(CO)_8(bpym)]$ with sodium amalgam in dimethoxyethane solution produces the anion, $[Mo_2(CO)_8(bpym)]^-$. The reduction reaction is accompanied by a change in the colour of the solution from dark green to orange. The electron spin resonance spectrum of the solution yields a value of $g_{av} = 1.977$ for the anion. The complex signal (Fig. 1) shows no evidence of molybdenum hyperfine interaction, even in the most concentrated solutions, unless interaction is very small ($a_{Mo} < 2G$). The ESR spectrum of the product obtained by reduction of the mononuclear

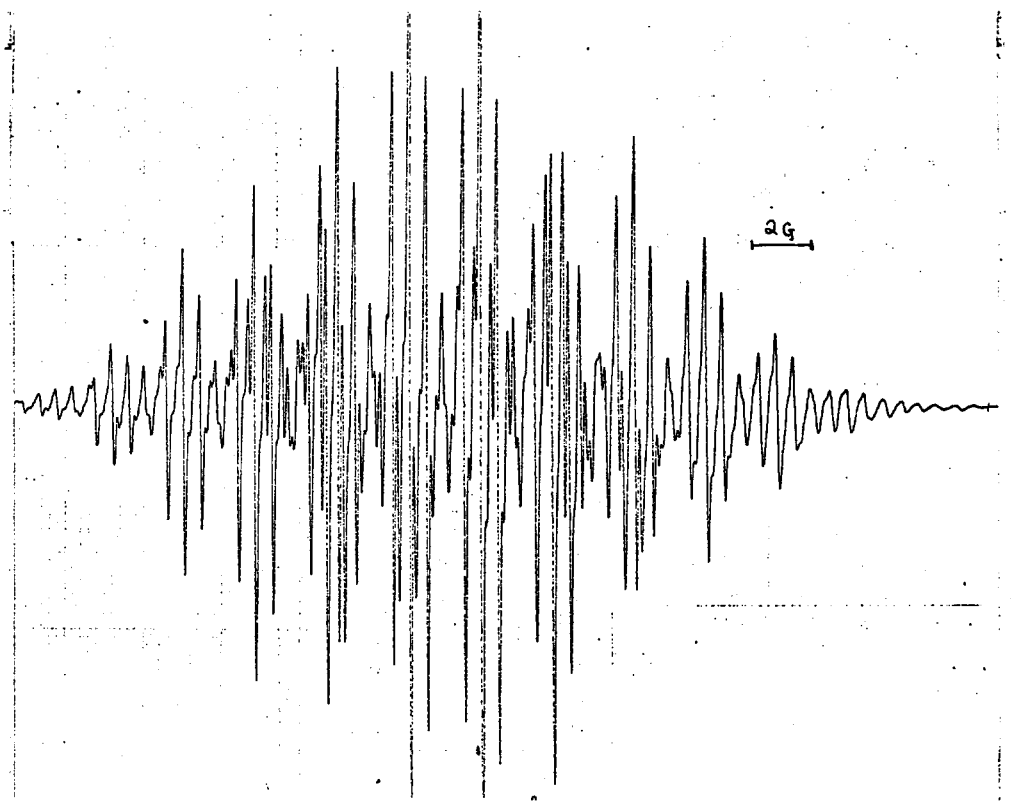

Fig. 1. ESR spectrum of $[Mo_2(CO)_8(bpym)]^-$ in dimethoxyethane solution.

complex $[Mo(CO)_4(bpym)]$ with sodium amalgam in dimethoxyethane (g_{av} 1.979) is very different in appearance from that of the binuclear complex. Again, there is no evidence of significant molybdenum hyperfine interaction. Both of these ESR spectra are distinct from that of the bipyrimidine radical anion[6] for which we measure $g_{av} = 2.0042$. Attempts to oxidise the binuclear complex, $[Mo_2(CO)_8(bpym)]$ with $AgBF_4$ or with iodine in methyl cyanide solution were unsuccessful; use of more vigorous oxidising agents led to decomposition of the complex.

DISCUSSION

The preparation of these new compounds proceeds in good yield using well-established methods. Evidence for the electronic interaction between the metals through the bridging bpym ligand is immediately apparent from the change in colour from the red mononuclear $[Mo(CO)_4(bpym)]$ to the deep purple–black binuclear $[MoM(CO)_8(bpym)]$ complexes. This is substantiated by spectroscopic measurements. Proton NMR spectra provide a sensitive indicator of electron density distribution in bpym. The chemical shift of the least biased proton in the bpym molecule, 5-H, moves to progressively lower field in the mononuclear and binuclear complexes. The clearest evidence of the interaction between the metal centres is provided by the visible spectra which show a large bathochromic shift of the lowest energy $d\pi^*$ absorption as interaction increases from the mononuclear to the bridged binuclear complexes.

We have not found a suitable one-electron oxidising agent for the homo-binuclear complex $[Mo_2(CO)_8(bpym)]$ which would permit a closer examination of the extent of intervalence transfer through the bridging bpym ligand. However, one electron reduction of the same complex gives an anion, $[Mo_2(CO)_8(bpym)]^-$, the ESR spectrum of which is consistent with localisation of the unpaired electron density on the bipyrimidine ligands; delocalisation onto the metal atom is not significant.

EXPERIMENTAL

All preparations were carried out in an atmosphere of oxygen-free dry nitrogen. Solvents were dried, deaerated and distilled under nitrogen immediately prior to use. Care was taken to shield reactions and their products from direct sunlight. IR spectra were recorded in solution using 1.0 mm solution cells and as mulls with Nujol and hexachlorobutadiene on PE257 or SP3-200 spectrometers. UV and visible spectra were recorded on a Unicam SP800 spectrometer. NMR spectra were recorded on a WP80 spectrometer using Fourier transform techniques. ESR spectra were recorded on a Varian E112 spectrometer operating at 9.238 GHz. Microanalyses were carried out by Mr. M. Hart and his staff in this Department. Metal hexacarbonyls were purchased from Pressure Chemical Co., and 2,2'-bipyrimidine was purchased from Aldrich. The complexes *cis*-$[M(CO)_4(\eta^2,\eta^2\text{-}C_7H_8)]$ were prepared, using freshly distilled bicyclo [2.2.1]hepta-2,4-diene, according to the literature.[7]

Preparation of Tetracarbonyl (2,2'-bipyrimidine)molybdenum

A solution of $[Mo(CO)_4(\eta^2,\eta^2\text{-}C_7H_8)]$ (0.38 g, 1.27 m mol) in hexane (20 cm^3) was added dropwise to a vigorously stirred solution of 2,2'-bipyrimidine (0.3 g, 1.9 m mol) in tetrahydrofuran (30 cm^3). The resulting red solution was stirred at room temperature for 1 hr, filtered (cannula), and concentrated. A layer of petroleum ether (40–60° fraction) was added to the concentrate and then set aside in the refrigerator. After 4 days the large, well-formed red crystals were isolated by filtration and dried. Yield 0.335 g, 72%. Analysis: Found; C, 39.8; H, 1.6; Mo, 25.6; N, 15.3. Calculated for $C_{12}H_6MoN_4O_4$; C, 39.3; H, 1.6; Mo, 26.2; N, 15.3%.

Preparation of μ-(2,2'-bipyrimidine)octacarbonyldimolybdenum

Solid 2,2'-bipyrimidine (0.2 g, 1.27 m mol) was added portionwise to a stirred solution of $[Mo(CO)_4(\eta^2,\eta^2\text{-}C_7H_8)]$ (0.76 g, 2.53 m mol) dissolved in tetrahydrofuran. The red colour changed immediately to purple and, after a few minutes, a greenish-brown colour developed. The mixture was stirred for 15 hr (overnight) at room temperature, after which time the reaction mixture appeared black. Solvent was removed by distillation under reduced pressure at room temperature leaving a black powder. The black powder was washed with hot dichloromethane and dried *in vacuo*. Yield 0.62 g, 86%. Analysis: Found. C, 33.8, H, 0.9; Mo, 34.2; N, 9.7. Calculated for $C_{16}H_6Mo_2N_4O_8$: C, 33.5; H, 1.0; Mo, 33.5; N, 9.8%.

Preparation of μ-(2,2'-bipyrimidine)octacarbonylchromium-molybdenum

A slight excess of *cis*-$[Cr(CO)_4(\eta^2,\eta^2\text{-}C_7H_8)]$ (0.25 g, 0.98 m mol) was added portionwise to a solution containing *cis*-$[Mo(CO)_4(bpym)]$ (0.33 g, 0.9 m mol) dissolved in tetrahydrofuran (25 cm^3). The mixture was heated at reflux for 12 hr, during which time the solution darkened. Evaporation of the solvent under reduced pressure gave a black solid which was reprecipitated from acetonitrile by the addition of ether. Yield 0.26 g, 54%. Analysis: Found C, 35.2; H, 1.5; Cr, 10.0; Mo, 16.7; N, 9.8. Calculated for $C_{16}H_6CrMoN_4O_8$; C, 36.2; H, 1.1; Cr, 9.8; Mo, 18.1; N, 10.9%.

Preparation of μ-(2,2'-bipyrimidine)octacarbonylmolybdenum-tungsten

A slight excess of *cis*-$[W(CO)_4(\eta^2,\eta^2\text{-}C_7H_8)]$ (0.32 g, 0.82 m mol) was added portionwise to *cis*-$[Mo(CO)_4(bpym)]$ (0.29 g, 0.79 m mol) dissolved in tetrahydrofuran (25 cm^3). The mixture was heated at reflux for 12 hr during which time the solution darkened. Evaporation of the solvent under reduced pressure gave a black residue. The black solid was extracted with acetone and reprecipitated by slow diffusion of a layer of ether. The black, air-stable powder is insoluble in non-polar solvents but fairly soluble in acetone, acetonitrile and other polar solvents. Yield 0.31 g, 59%. Analysis: Found C, 28.5; H, 1.0; Mo, 14.0; N, 8.2; W, 28.7. Calculated for $C_{16}H_6MoN_4O_8W$; C, 29.0; H, 0.9; Mo, 14.5; N, 8.4; W, 27.8%.

Acknowledgements—We thank the Science Research Council for support through a Studentship awarded to C.O. and Dr. D. Collison for help with recording some ESR spectra.

REFERENCES

[1]E. V. Dose and L. J. Wilson, *Inorg. Chem.* 1978, **17**, 2660; M. Hunziker and A. Ludi, *J. Am. Chem. Soc.* 1977, **99**, 7370.
[2]R. H. Petty, B. R. Welch, L. J. Wilson, L. A. Bottomley and K. M. Kadish, *J. Am. Chem. Soc.* 1980, **102**, 611.
[3]M. H. B. Stiddard, *J. Chem. Soc.* 1962, 4712.
[4]A. R. Katritzky and P. J. Taylor, *Physical Methods in Heterocyclic Chemistry* (Edited by A. R. Katritzky) 1971, **4**, 325.
[5]J. Burgess, *J. Organometallic Chem.* 1969, **19**, 218.
[6]D. H. Geske and G. R. Padmanabhan, *J. Chem. Phys.* 1965, **87**, 1651.
[7]E. B. Abel, M. A. Bennett, R. Burton and G. Wilkinson, *J. Chem. Soc.*, 1958, 4559; R. B. King and A. Fronzaglia, *Inorg. Chem.* 1966, **5**, 1837.

Polyhedron Vol. 1, No. 1, pp. 57–59, 1982
Printed in Great Britain.

0277-5387/82/010057-03$03.00/0
Pergamon Press Ltd.

EFFECTS OF CHEMICAL SHIFT ANISOTROPY AND ^{14}N COUPLING ON THE ^{1}H AND ^{195}Pt NUCLEAR MAGNETIC RESONANCE SPECTRA OF PLATINUM COMPLEXES

ISMAIL M. ISMAIL, S. JOHN S. KERRISON and PETER J. SADLER†
Department of Chemistry, Birkbeck College, Malet Street, London WC1E 7HX, England

(*Received* 20 *July* 1981)

Abstract—Broadening of the ^{195}Pt satellites in the ^{1}H NMR spectrum of *trans*-Pt(ethene)(2-carboxy-pyridine)Cl_2 at high field arises from relaxation of ^{195}Pt via the chemical shift anisotropy mechanism. We also demonstrate that well-resolved ^{14}N–^{195}Pt couplings can be observed in ^{195}Pt NMR spectra of Pt(II) and Pt(IV) amine complexes, including anti-tumour agents, at elevated temperature where scalar coupling contributions to ^{195}Pt relaxation are much reduced.

INTRODUCTION

There is much current interest in the mechanisms of relaxation of the heavier spin $\frac{1}{2}$ nuclei such as ^{113}Cd, ^{195}Pt, ^{199}Hg and ^{205}Tl.[1] The chemical shift anisotropy mechanism is of particular interest because its effect increases as the square of the applied field.[2] There are few detailed studies of this. In two recent papers Brady *et al.*[3] have clearly demonstrated that the relaxation of ^{205}Tl at high fields is dominated by chemical shift anisotropy relaxation and that this effect is reflected in the linewidths of coupled *proton* resonances. We demonstrate here that the same effect can occur for ^{195}Pt. This is of direct practical concern because 1 : 4 : 1 proton resonances are usually considered diagnostic of Pt-ligand bonds, the outer peaks arising from ^{1}H coupling to the 34% abundant isotope ^{195}Pt. This pattern will arise only when the linewidths of the components of the triplet are equal, and deviations are expected when the spin–spin relaxation times of ligand nuclei are significantly different in Pt (I = O) and ^{195}Pt species. Indications that such an effect could exist were first noted by Erickson *et al.*[4] in their ^{1}H NMR studies of 1,2-diaminoethane complexes of platinum, and recently by Lallemand *et al.*[5] for some platinum nucleoside and phosphine complexes. We show here that the linewidths of the ^{195}Pt satellites in the ^{1}H NMR spectrum of *trans*-[Pt(ethene)(2-carboxy-pyridine)Cl_2] are directly related to the relaxation rate of ^{195}Pt, which is dominated by the chemical shift anisotropy mechanism. In the second part of this paper we show that relaxation of ^{195}Pt via scalar coupling to ^{14}N decreases at elevated temperatures allowing direct measurement of ^{195}Pt–^{14}N couplings. Like their ^{195}Pt–^{15}N counterparts, these are sensitive to the nature of the *trans* ligand and therefore very useful in structure determination.

EXPERIMENTAL

^{1}H NMR spectra were recorded on JEOL FX 60, Bruker WP 80, JEOL MH 100, Varian XL 200, Bruker WH 270 and Bruker WH 400 spectrometers at 296 ± 1 K. ^{195}Pt NMR spectra were recorded on JEOL FX 60 (12.8 MHz) Varian XL 200 (43 MHz) and Bruker WH 400 (86 MHz) spectrometers. *Cis*-$[Pt(NH_3)_2(H_2O)_2](NO_3)_2$ was prepared by adding 1.95 molar equivalents of $AgNO_3$ to a suspension of *cis*-$Pt(NH_3)_2Cl_2$ in H_2O. The precipitate of AgCl was filtered off and an external D_2O lock was used for NMR to avoid deuteration of coordinated NH_3. *Cis, trans, cis*-Pt(isopropylamine)$(OH)_2Cl_2$ was kindly supplied by Johnson Matthey Ltd. *Trans*-Pt(ethene)(2-carboxypyridine)Cl_2 was kindly supplied by Dr. J. K. Sarhan and Dr. M. Green (York University).

†Author to whom correspondence should be addressed.

RESULTS AND DISCUSSION

Field dependence of ^{1}H NMR satellites

The ^{195}Pt satellites for the ethene proton resonance in the ^{1}H NMR spectrum of *trans*-Pt(ethene)(2-carboxy-pyridine)Cl_2 decrease in ratios of peak heights from 1 : 5 : 1 at 60 MHz to 1 : 16 : 1 at 270 MHz, to 1 : 27 : 1 at 400 MHz. The observed linewidth is given by eq. (1)[3b]

$$\Delta\nu_{1/2}(^{1}H) = (\Pi T_2'(H))^{-1} + (2\Pi T_1(Pt))^{-1} \qquad (1)$$

where $(\Pi T_2'(H))^{-1}$ is the sum of the natural proton linewidth and magnetic inhomogeneity broadening, and is conveniently estimated as the linewidth of the centre component of the triplet. Thus $\Delta\nu_{1/2}(H)$–$(\Pi T_2'(H))^{-1}$ should be proportional to the spin-lattice relaxation rate of ^{195}Pt, $(2\Pi T_1(Pt))^{-1}$. In the case of extreme narrowing and for axial symmetry the chemical shift anisotropy (c.s.a.) contribution to the relaxation is given by eq. (2)

$$(T_{1(Pt)})^{-1}(\text{C.S.A.}) = 6/7(T_{2(Pt)})^{-1}(\text{C.S.A.}) = (2/15)\gamma_{Pt}{}^2B_0{}^2(\sigma_{11} - \sigma_\perp)^2\tau_c. \qquad (2)$$

Hence a plot of corrected proton linewidth vs $B_0{}^2$ (applied field) should be linear, if c.s.a. provides the dominant spin-lattice relaxation mechanism for ^{195}Pt in this complex. Figure 1 shows that this is indeed the case.

If ^{195}Pt–^{1}H couplings are being sought, it will clearly *be a disadvantage* for some complexes if measurements are made at very high fields. It can be seen from eqn (2) that the c.s.a. contribution is likely to increase for highly anisotropic molecules ($\Delta\sigma$ term), at low temperatures and with increase in molecular weight (τ_c increases). However, it is clear that ^{195}Pt satellites in ^{1}H NMR spectra can be used to monitor changes in ^{195}Pt T_1 values. C.s.a. relaxation will decrease at higher temperature (and therefore satellites in ^{1}H NMR spectra should sharpen up) although relaxation via spin rotation will increase. The latter can be dominant in some Pt

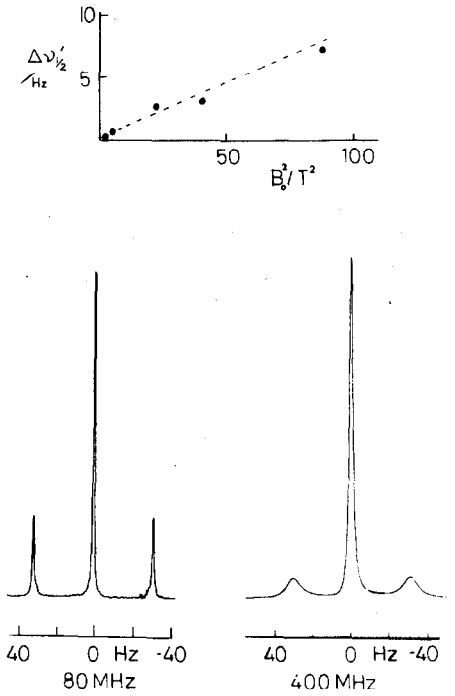

Fig. 1. The ethene ^1H NMR resonances of *trans*-Pt(ethene)(2-carboxy-pyridine)Cl_2 in $CDCl_3$ at 80 and 400 MHz and a plot of $\Delta\nu_{1/2}'$ (linewidth of satellite–linewidth of centre peak) vs the square of the applied filed.

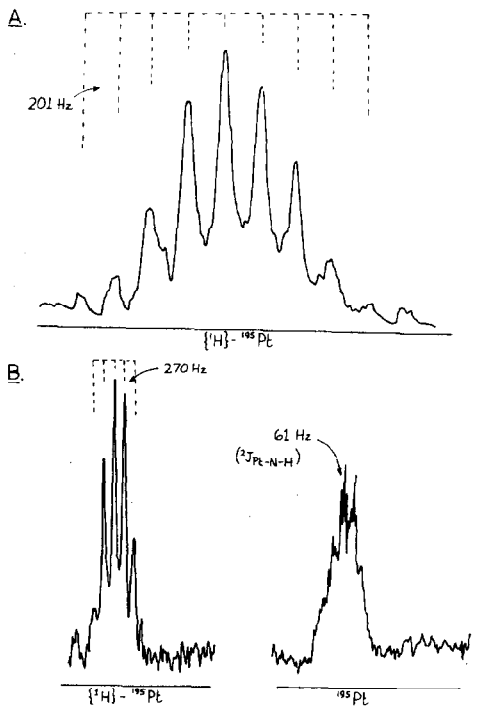

Fig. 2. 12.8 MHz {^{1}H}–^{195}Pt NMR spectra of 0.5 M solutions of (A) $Pt(NH_3)_4^{2+}$ and (B) *cis*-$Pt(NH_3)_2(H_2O)_2^{2+}$ at 343 K showing resolved ^{195}Pt–^{14}N couplings (1 : 4 : 10 : 16 : 19 : 16 : 10 : 4 : 1 nonet and 1 : 2 : 3 : 2 : 1 quintet respectively).

complexes.[6] Other mechanisms can contribute to the spin–spin relaxation of ^{195}Pt including scalar coupling to ^{14}N. At 1.4 T ^{195}Pt coupling to ^{14}N in the ethene complex is unresolved giving an overall linewidth of ca. 430 Hz for the ^{195}Pt resonance. The increasing use of Pt compounds containing nitrogen ligands as antitumour agents has added to the importance of ^{195}Pt NMR studies on platinum compounds with bonded ^{14}N ligands. We now describe a simple method of improving the resolution of ^{195}Pt–^{14}N couplings.

^{14}N couplings in ^{195}Pt NMR spectra

The {^{1}H}–^{195}Pt NMR spectrum of [*cis*-$Pt(NH_3)_2(H_2O)_2]^{2+}$ consists of a broad unresolved resonance at 12.8 MHz, 300 K, unlike that of [*cis*-$Pt(^{15}NH_3)_2(H_2O)_2]^{2+}$ which is a sharp triplet with $^1J(^{195}Pt–^{15}N)$ of 387 Hz.[7] With ^{14}N, a quadrupolar nucleus ($I = 1$), as a ligand, additional scalar relaxation of the second kind can occur for ^{195}Pt. The magnitude of the effect is determined by the quadrupolar relaxation time of ^{14}N, given by eqn (3), where χ is the nuclear quadrupole coupling constant ($e^2q_{22}\,Q/h$; q_{22} being the largest component of the electric field gradient at the nucleus) and η is the asymmetry parameter of the electric field gradient.

$$T_{1q}^{-1} = T_{2q}^{-1} = \frac{3\pi^2}{10}\frac{(2I+3)}{I^2(2I-1)}\chi^2(1+\tfrac{1}{3}\eta^2)\tau_c. \qquad (3)$$

At high temperatures the quadruploar relaxation rate decreases due to a decrease in the correlation time τ_c, which is dependent on the motion of the complex. Provided that the field gradients at the ^{14}N nucleus are small (and this is generally the case for tetravalent N atoms) then at high temperatures T_{1q} may become long enough to allow resolution of ^{195}Pt–^{14}N couplings in ^{195}Pt NMR spectra. Analogous observations were originally made by Roberts[8] in the ^{1}H NMR spectra of amides.

The predicted resolution of ^{195}Pt–^{14}N couplings at higher temperatures is confirmed for the Pt(II) complexes [*cis*-$Pt(NH_3)_2(H_2O)_2]^{2+}$ (**1**) and $Pt(NH_3)_4^{2+}$ (**2**) and the Pt(IV) complex *cis, trans, cis*-Pt(isopropylamine)$_2$(OH)$_2$(Cl)$_2$ (**3**) in Fig. 2. We had briefly described the spectra of the Pt(II) complexes previously[9] but this appears to be the first report of resolved ^{14}N coupling in the spectrum of a Pt(IV) complex. The latter is an important, potential second-generation Pt anti-tumour complex.[10] The measured $^1J(^{195}Pt–^{14}N)$ for (**1**), 270 Hz, compares favourably with the value from the ^{15}N-labelled complex, adjusted by the ratio of magnetogyric ratios: 387/1.402 = 276 Hz. The high value being typical of N *trans* to oxygen (low *trans* influence). The value for (**2**) 201 Hz, is lower, as expected, since NH_3 has a higher *trans* influence than H_2O. $^1J(^{195}Pt–^{14}N)$, 190 Hz in the Pt(IV) complex (**3**) can be compared to 222 Hz for *cis*-$Pt(NH_3)_2Cl_2$ in DMSO[7] a Pt(II) complex with Cl^- as a *trans* ligand (again adjusted from ^{15}N values). Pregosin *et al.*[11] have noted previously for a few halo-amine complexes that ^{195}Pt–^{15}N couplings in Pt(II) complexes are 1.41 times those in analogous Pt(IV) complexes. Our value of 1.17 suggests that *cis* effects may also influence couplings. The range of $^1J(^{195}Pt(II)–^{14}N)$ couplings will be expected to vary from *ca.* 121 Hz with *trans* ligands having a high *trans* influence (e.g. P), up to 228 Hz for those with a low *trans* influence (e.g. Cl). ^{15}N labelling is expensive and sometimes impracticable but, as we have shown here, with the use of elevated temperatures ^{14}N couplings can often be measured.

The resolution of ^{1}H–^{195}Pt couplings in the undecoupled spectrum of *cis*-$Pt(NH_3)_2(H_2O)_2^{2+}$ in H_2O,

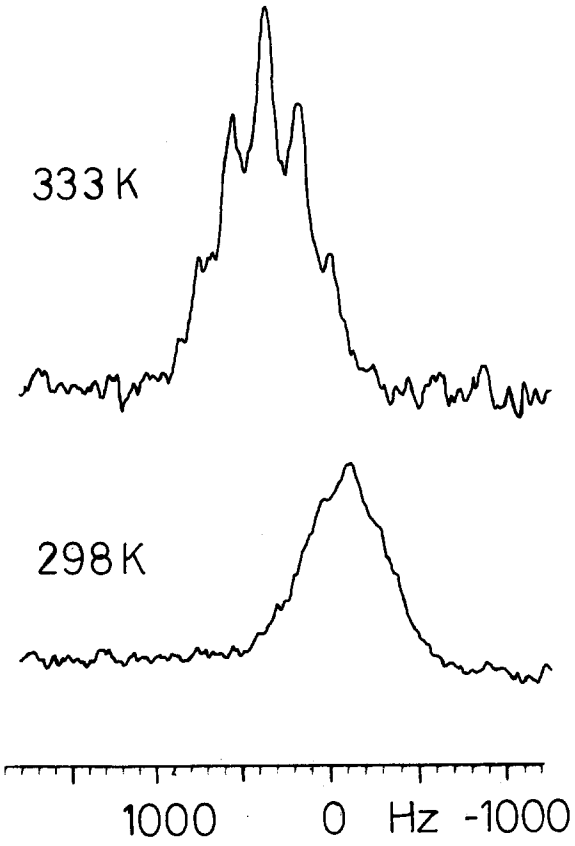

Fig. 3. 43 MHz $\{^1H\}$–^{195}Pt NMR spectra of 0.1 M *cis, trans, cis* Pt(IV)(isopropylamine)$_2$(OH)$_2$Cl$_2$ in D_2O at 298 and 333 K. A temperature dependent chemical shift is seen. (δ/ppm +880 at 298 K, rel. ext. Na_2PtCl_6).

Fig. 2, shows that proton exchange reactions of coordinated NH_3 molecules are slow on the NMR timescale ($\ll 60\,sec^{-1}$). However when D_2O is used, NH_3 deuteration readily occurs over a period of minutes, resulting in severe broadening of the ^{195}Pt resonance. Proton exchange on co-ordinated H_2O is normally very fast. In contrast the same $\{^1H\}$–^{195}Pt spectrum was observed for the Pt(IV) complex (3) in H_2O or D_2O at 343 K, suggesting that proton exchange on the coordinated isopropylamines is very slow.

Little change in the ^{195}Pt NMR spectrum of *cis, trans, cis*–Pt(isopropylamine)$_2$(OH)$_2$Cl$_2$ was observed on increasing the measurement field from 4.7 to 9.4 T (43 to 86 MHz), showing that the dominant broadening mechanism is quadrupolar relaxation of ^{14}N and not the chemical shift anisotropy of ^{195}Pt.

Acknowledgements—We thank the SRC, MRC and Johnson Matthey Ltd. for support and several workers, including the ULIRS High Field NMR service, who helped us to obtain NMR spectra at different frequencies. We acknowledge stimulating discussions with Dr. D. G. Gillies (Royal Holloway College) who kindly provided preprints of his studies on thallium relaxation.

REFERENCES

[1]R. Garth Kidd and R. J. Goodfellow, In *NMR and the Periodic Table* (Edited by R. K. Harris and B. E. Mann) p. 195. Academic Press, London (1978).
[2]G. A. Webb, In *NMR and the Periodic Table* (Edited by R. K. Harris and B. E. Mann) p. 49. Academic Press, London (1978).
[3a]F. Brady, R. W. Matthews, M. J. Forster and D. G. Gillies, *Inorg. Nuc. Chem. Lett.* 1981, **17**, 155; and [b]F. Brady, R. W. Matthews, M. J. Forster and D. G. Gillies *J.C.S. Chem. Comm.* 1981, 911.
[4]L. E. Erickson, J. E. Sarneski and C. N. Reilley, *Inorg. Chem.* 1975, **14**, 3007.
[5]J-Y. Lallemand, J. Soulié and J-C. Chottard, *J. Chem. Soc. Chem. Comm.* 1980, 436.
[6]J. J. Pesek and W. R. Mason, *J. Magn. Res.* 1977, **25**, 519.
[7]S. J. S. Kerrison and P. J. Sadler, *J.C.S. Chem. Comm.* 1981, 61.
[8]J. D. Roberts, *J. Amer. Chem. Soc.* 1956, **78**, 4495.
[9]S. J. S. Kerrison and P. J. Sadler, Poster presented at the International NMR Meeting, York University (1978).
[10]M. J. Cleare, P. C. Hydes, D. C. Hepburn and B. Malerbi in Cisplatin (Edited by A. W. Prestakyo, S. T. Crooke and S. K. Carter) p. 149. Academic Press, New York (1979).
[11]P. S. Pregosin, H. Omura and L. M. Venanzi, *J. Am. Chem. Soc.* 1973, **95**, 2047.

Polyhedron Vol. 1, No. 1, pp. 61–68, 1982
Printed in Great Britain.

0277-5378/82/010061-08$03.00/0
Pergamon Press Ltd.

LAMELLAR ZIRCONIUM PHOSPHONATES CONTAINING PENDANT SULPHONIC ACID GROUPS

PETER M. DiGIACOMO* and MARTIN B. DINES
Occidental Research Corporation, P.O. Box 19601, Irvine, CA 92713, U.S.A.

(*Received* 22 *July* 1981)

Abstract—The versatile sulphonic acid group has been introduced into the family of interlamellar anchored materials. Zirconium *bis*-3-sulphopropylphosphonate is an example of an aliphatic acid. Zirconium *bis*-2-(sulphophenyl)ethylphosphonate is an example with an aromatic sulphonic acid group. In general, the sulphonic acids are not as crystalline as the carboxylic acid analogs. This is probably due to the relatively large size of the sulphonic acid group compared to the available cross sectional area of the layer face. The aliphatic compounds are more crystalline than the aromatics, as is expected from size considerations. The sulphonic acid group in both crystalline and semi-crystalline examples is accessible to reaction with bases. A few preliminary experiments have demonstrated the utility of these compounds as both strong acid ion exchangers and Bronsted acid catalysts. The layered sulphonic acid—zirconium 3-sulphopropylphosphonate—is thermally stable to well over 200°C. This indicates good potential for applications in Bronsted catalysis. This stability compares favorably with organic resin based sulphonic acids.

INTRODUCTION

The preparation and structural characterization of a variety of lamellar metal phosphonates and phosphates have been reported in recent years.[1–4] These compounds are generally crystalline materials with the same layered structure as zirconium phosphate.[5] The lamellar surfaces contain a hexagonal array of attached groups spaced about 5.3 Å apart. Certain compounds can be prepared by derivatizing the interlamellar –OH groups of zirconium phosphate.[4] A more general method involves the direct reaction of tetravalent metal ions with phosphonic or organophosphoric acids (eqn 1). This reaction was first reported by Alberti *et al.*[2] In our laboratories we have demonstrated that this is a general, essentially

$$M(IV) + (HO)_2\overset{\overset{O}{\|}}{P}\text{—OR} \text{ or } (HO)_2\overset{\overset{O}{\|}}{P}\text{—R} \longrightarrow M(O_3POR)_2 \text{ or } M(O_3PR)_2 \quad (1)$$

quantitative reaction. Compounds have been prepared with a variety of tetravalent metal ions and organic substituents on phosphorus.[1] The sulphonic acid functionality has been widely used as strong acid cation exchangers as well as in Bronsted acid catalysis. In view of the broad scope of the expected chemistry, it was of interest to prepare lamellar sulphonic acids. The sulphonic acid group is quite large in relation to the approximately 24 Å^2 (Fig. 1) cross-sectional area available to each substituent of the layer face. Examination of CPK models indicates that the $-RSO_3H$ group (R = alkyl) will essentially fill the area available on each layer surface site. Where R = aryl, more crowding is evident. In this paper we report the synthesis and characterization of alkyl and aryl lamellar phosphonates containing sulphonic acid substituents.

*Author to whom correspondence should be addressed.

RESULTS AND DISCUSSION

Preparation of sulpho-phosphonate intermediates

As has been previously pointed out, the preparation of an appropriately substituted phosphonic acid or ester precursor is usually the main hurdle in the synthesis of lamellar phosphonates.[1] In the sulphonic acid system, relatively straightforward transformations yielded suitable intermediates. A convenient route to a sulpho-substituted phosphonate is afforded by reactions 2 and 3. The addition

$$(EtO)_2\overset{\overset{O}{\|}}{P}H + NaH \longrightarrow (EtO)_2PONa + H_2 \quad (2)$$

$$(EtO)_2PONa + \underbrace{CH_2CH_2CH_2SO_2O}\longrightarrow (EtO)_2\overset{\overset{O}{\|}}{P}CH_2CH_2CH_2SO_3Na \quad (3)$$

of the phosphorus centered nucleophile, sodium diethylphosphite, to propane sultone yields diethyl-3-sulphopropyl phosphonate.[6] This salt is a hygroscopic solid. It is soluble in water and ethanol, but insoluble in low polarity solvents such as toluene, ether and chloroform. Acid hydrolysis or cleavage of the phosphonate ester with aqueous HBr yields the required precursor to the lamellar phosphonate-3-sulphopropylphosphonic acid (eqn 4).

$$(EtO)_2\overset{\overset{O}{\|}}{P}CH_2CH_2CH_2SO_3Na + HBr(aq) \longrightarrow (HO)_2\overset{\overset{O}{\|}}{P}CH_2CH_2CH_2SO_3H + 2EtBr. \quad (4)$$

Preparation and characterization of lamellar sulphonic acids

The reaction of 3-sulphopropylphosphonic acid and

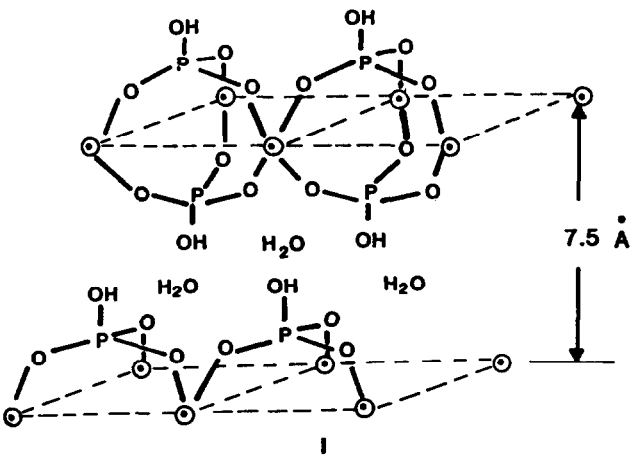

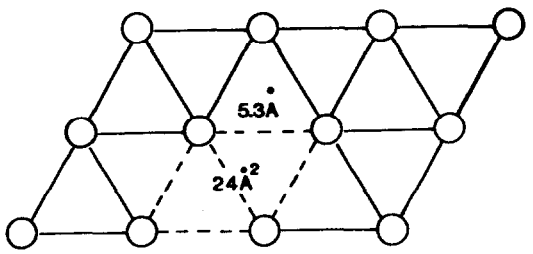

Fig. 1. Projection of hexagonal structure of Z-P.

zirconyl chloride in aqueous solution yields a white to off-white solid, as has been found for many of the other lamellar phosphonates. This material is a semi-crystalline solid with a broad X-ray powder diffraction pattern. The apparent layer-layer spacing, d_{001}, is 18.8 Å. If the reaction is carried out in the presence of HF, a more crystalline material is formed as evidenced by the sharper X-ray powder pattern. The layer-layer spacing is shifted somewhat to 17.3 Å. Extensive washing of the material with $d_{001} = 18.8$ Å with relatively concentrated aqueous acid (3N HCl) yields a material with $d = 17.3$ Å of essentially unchanged crystallinity. This difference in d-spacing probably reflects the degree of hydration of the strong acid groups in the isolated samples. X-Ray diffraction patterns are shown in Fig. 2.

The effect of added HF during preparation of these materials results in enhanced crystallinity. This effect has also been observed in the preparation of other lamellar zirconium phosphonates,[1] as well as for zirconium phosphate itself[7] and is attributable to the sequestering effect of the fluoride upon the metal ion. This enhancement of crystallinity can be observed by the increase in sharpness of the X-ray powder pattern. Table 1 presents a comparison of an empirical correlation of X-ray reflection sharpness and the HF/Zr^{4+} ratio during synthesis. The sharpness is defined as the ratio of counts (intensity) to line width at half height for the second X-ray line. The second line was chosen because there is no interference at small 2θ angles. By analogy to the carboxylic acid substituted zirconium phosphonates, the increase in sharpness of the powder pattern is attributed primarily to increased crystallinity rather than increased particle size. In the carboxylic derivatives, increased sharpness is accompanied by an increase in the pK_a of the carboxylic acid. The change in pK_a is not expected for a change in particle size, but is more reasonably attributable to environmental effects manifested in enhanced order of the structure. Similar effects have been observed spectroscopically.

The definitive presence of the sulphonic acid group is demonstrated by the titration of the acid with aqueous NaOH. The titration curves in water and saturated salt solution are given in Fig. 3. These curves show the presence of a strong Bronsted acid. The strong acid content ranges from about 70 to 80% of the theoretical value based on the product empirical formula $Zr(O_3PCH_2CH_2CH_2SO_3H)_2$.

The cause of the break in the curve in the pH 7–9 region is most likely due to hydrolysis of the metal phosphonate. Its magnitude correlates with the relative crystallinity of the product. In the more crystalline sample, this break is less pronounced than in the less crystalline material (0.7 meg. vs > 2.0 meg. of hydroxide per gram). In the carboxy analogs, hydrolysis of the metal phosphonate layer structure takes place rapidly enough to compete with the titration in the semi-crystalline case. (In these sulphopropyl compounds, the more crystalline modification does not have an X-ray powder pattern as sharp and resolved as high crystallinity zirconium 2-carboxyethyl phosphate.[1]) This high pH break can thus

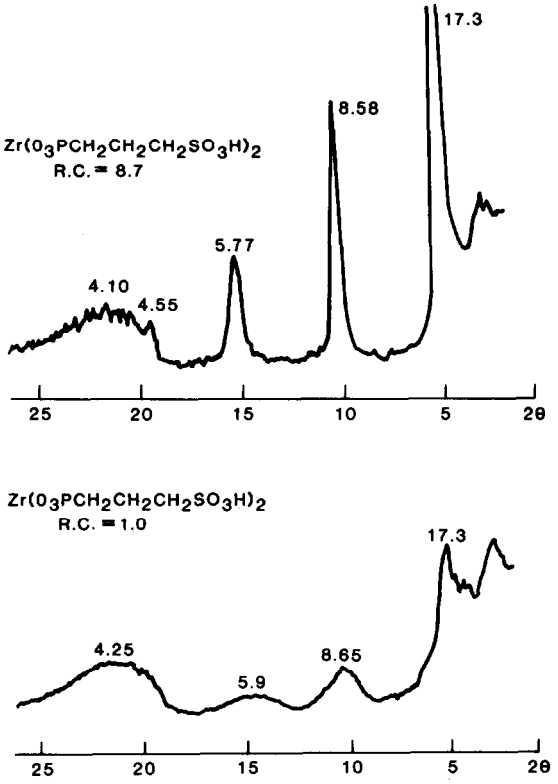

Fig. 2. XRD of zirconium 3-sulphopropylphosphonate. RC is the relative crystallinity (see Table 1).

be attributed to "zones" of amorphous or semi-crystalline structure in the material that hydrolyze rapidly enough to consume base during the titration. A separate experiment indicates that base consumption by hydrolysis is fast enough to cause the observed effect. This is discussed later.

The acid content in these materials is 70–80% of theoretical on a weight basis. There is undoubtedly some water of hydration in the material. The IR spectrum shows a broad band at 1650 cm^{-1} which can be attributed to the OH_2 deformation. This is a common band in hydrated salts and acids. Thermal analysis indicates about 20% weight loss just above 100°C. There is likely to be some contamination from other phosphonates in the preparative sequence. Nonsulphoalkylated derivatives of diethylphosphite will yield phosphorous acid on hydrolysis which will co-react with zirconium ion, thereby diluting the sulfonic acid content of the product.

The titration data and X-ray powder pattern analysis indicate the product is a sulphonic acid with an amorphous to layered crystalline structure. These materials are not stable to aqueous hydroxide solutions. The rate of hydrolysis is dependent on the degree of crystallinity. Hydrolysis experiments were carried out on the sodium salts of the materials in Table 1. The initial reaction with hydroxide is first order in hydroxide. The linearity of the pH vs time plot is maintained until about 90% of the hydroxide is consumed. The relative rates are presented in Table 2.

The relative rate data correlates with the degree of crystallinity. The less crystalline materials hydrolyze more rapidly. This data is consistent with the observation of partial hydrolysis during titration.

The accessibility of the sulphonic acid group can be measured by the rate at which it is neutralized by aqueous NaOH. It is anticipated that the rate-limiting step will be interlamellar diffusion for layered materials. The solid sulphonic acid (rel. crystallinity = 8.7) was added to an aqueous solution of NaOH and the pH measured as a function of time. This experiment was conducted in both water and saturated salt solution. The tendency of the sulphonic acid to swell and agglomerate before dispersal in low ionic strength aqueous solutions is avoided in salt solutions. In the high ionic strength media, the solid remains a discrete particulate. The data from these experiments are presented in Fig. 4. The rate is the same in both media with virtually complete reaction in less than 90 sec. This reaction rate is slower than the analogous reaction of crystalline zirconium 2-carboxyethylphosphonate. This probably indicates a more hindered environment in the interlamellar sulphonic acid leading to slower diffusion. Predispersal of the sulphonic acid in water results in extremely rapid reaction, with complete reaction in less than 5 sec. The dispersal in water appears to swell the sulphonic acid like a gel. This should serve to separate the layers and allow easier access through the interlamellar region.

The relative accessibility of the acid group for reaction can also be assessed from the neutralization rate profiles. Neutralization rate experiments were carried out with samples of zirconium 3-sulphopropylphosphonate of varying crystallinity. This data is presented in Fig. 5. The rapid rate reduction in the latter stages of the reaction of the sample with relative crystallinity 3.9 probably reflects "blocked" pores and/or inhibited edge access. The rapid reaction of the least crystalline material is expected. The correlations between interlamellar reactivity and crystal-

Table 1. Relative crystallinity depends on HF to Zr^{4+} ratio during synthesis

ENTRY	HF/Zr^{4+}	XRD RATIO cnts/width	RELATIVE CRYSTALLINITY
1	0	78	1.0
2	0.57	305	3.9
3	2.3	682	8.7

Table 2. Relative rate of hydrolysis

ENTRY	RELATIVE CRYSTALLINITY (Table 1)	REL. RATE OF HYDROLYSIS
1	1.0	1.0
2	3.9	0.49
3	8.7	0.25

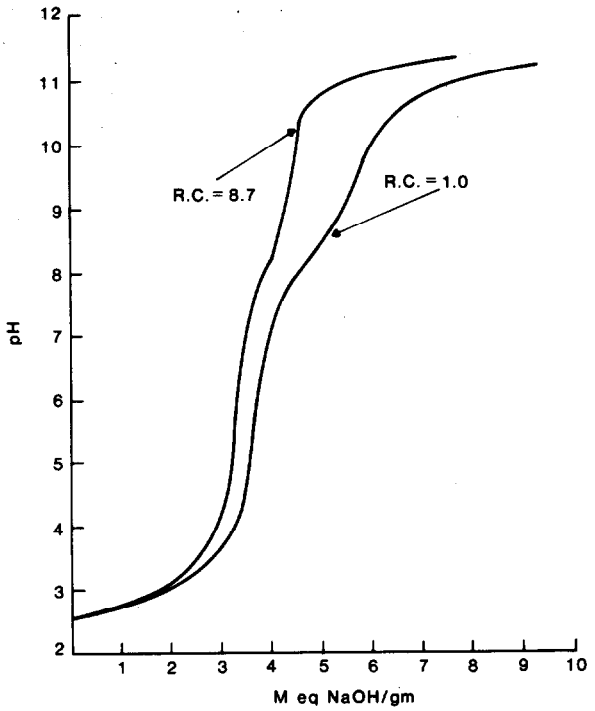

Fig. 3. The titration of zirconium 3-sulphopropyl phosphonate; samples of two crystallinities.

$$Zr(O_3PCH_2CH_2CH_2SO_3H)_2 + 2NaOH \longrightarrow Zr(O_3PCH_2CH_2CH_2SO_3Na)_2$$

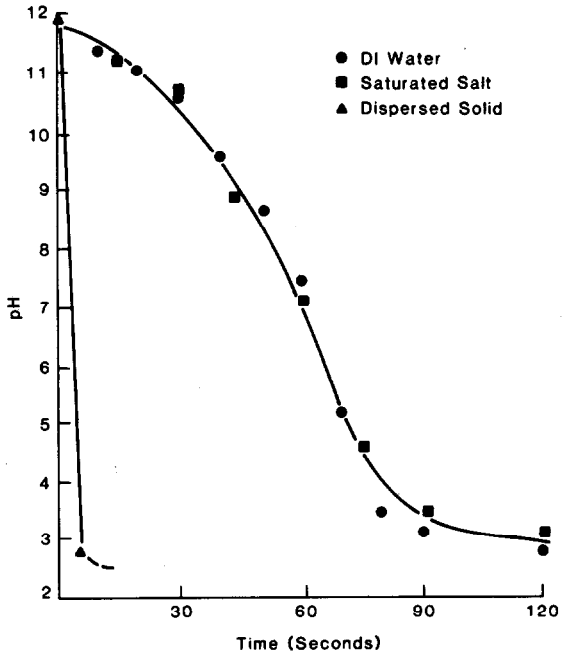

Fig. 4. The neutralization of zirconium 3-sulphopropyl phosphonate in aqueous suspension (RC = 8.7).

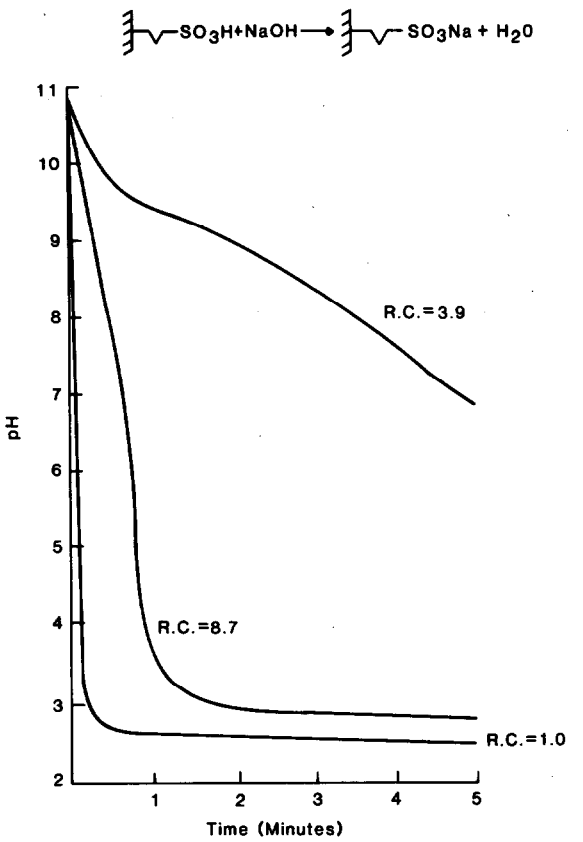

Fig. 5. The neutralization of zirconium 3-sulphopropylphosphonate of varying crystallinity. The rate and accessibility of acid group does not correlate with XRD crystallinity.

linity are not straightforward and will involve considerations of crystal agglomeration, packing, size, defects and distribution.

Thermal stability

The wide range of utility of solid sulphonic acids as catalysts might be considerably extended if enhanced thermal stability could be achieved. Most solid organic resin-based sulphonic acid catalysts are limited to use below 150°C. Thermal analysis of layered zirconium 3-sulphopropylphosphonate indicates stability to approximately 220°C before any weight loss other than water of hydration takes place. Loss of water of hydration occurs at 117°C. The maximum of the DTA peak is at 340°C. This data is presented in Fig. 6. The 220°C figure appears to be a conservative upper stability limit figure for these materials.

The reactions of layered sulphonic acids

In preliminary work both ion exchange and acid catalysis experiments were carried out. These two types of applications represent the area in which layered sulphonic acids are likely to find technological utility.

Ion exchange. A simple batch ion exchange experiment was carried out by contacting the layered sulphonic acid (semicrystalline) with an aqueous solution of cupric sulphate. The pH of the solution immediately decreased from 3.8 to 0.92 by reaction 4.

$$Zr(O_3PCH_2CH_2CH_2SO_3H)_2 + CuSO_4(aq) \longrightarrow$$
$$\longrightarrow Zr(O_3PCH_2CH_2CH_2SO_3Cu_{1/2})_2 + H_2SO_4(aq). \quad (4)$$

The characteristic blue color of the cupric sulphate solution markedly decreased in intensity. As expected, the white solid sulphonic acid was pale blue after the exchange reaction. A similar exchange experiment was carried out with the sodium salt form of the sulphonic acid. This exchange (reaction 5) did not reach equilibrium as far to the right as did reaction 4.

$$Zr(O_3P\text{-}CH_2CH_2CH_2SO_3Na)_2 + CuSO_4 \longrightarrow$$
$$\longrightarrow Zr(O_3PCH_2CH_2CH_2SO_3Cu_{1/2})_2 + Na_2SO_4. \quad (5)$$

These results conclusively demonstrate the utility of these materials as strong acid ion exchangers.

Acid catalysis. The esterification of carboxylic acids is a straightforward reaction subject to general Bronsted acid catalysis. The reaction of ethyl alcohol and acetic acid was selected as a model example (reaction 6).

$$CH_3CO_2H + EtOH \overset{H+}{\rightleftharpoons} CH_3CO_2Et + H_2O. \quad (6)$$

Equivalent amounts of ethyl alcohol and acetic acid were combined in a distillation apparatus. Zirconium 3-sulphopropylphosphonate ("high crystallinity") was added in such amounts so as to make an 8%/wt. slurry. The mixture was heated to very gently reflux and ethyl acetate distilled over slowly. The identity of ethyl acetate was confirmed by GC and IR comparison of an authentic sample. This experiment was repeated at 0.5%/wt. slurry. Reaction was run to 40% conversion with virtually quantitative yield of the ester.

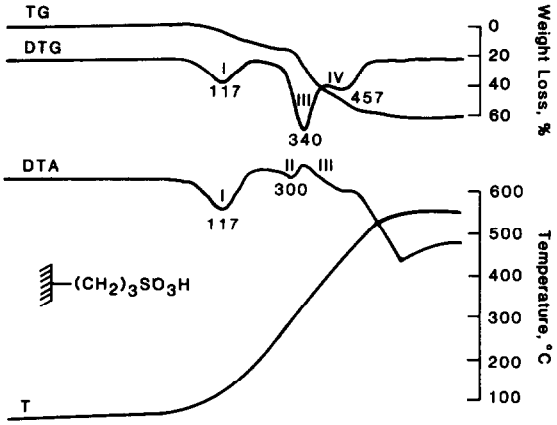

Fig. 6. Thermal analysis of zirconium 3-sulphopropylphosphonate.

Dehydration of alcohols is another reaction catalyzed by Bronsted acids. A 10% slurry of zirconium 3-sulphopropylphosphonate in cyclohexanol was heated to 125°C. Cyclohexene was evolved smoothly in virtually quantitative yield (by GC relative area) (reaction 7).

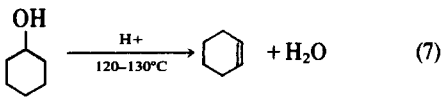

(7)

The above experiments demonstrate the use of interlamellar sulphonic acids in both ion exchange and acid catalysis experiments. While these experiments are both simple and straightforward, they establish the utility of these materials in applications relevant to the chemical industry.

Aromatic sulphonic acids

Molecular models indicate aromatic sulphonic acid groups are quite large with respect to the available area on the layer face. This may strain the limits of the stability of the layered modification. An example of an aromatic sulphonic acid was prepared in order to test this consideration.

A straightforward synthetic sequence yielded the precursor sulphonicphosphonic acid (eqns 11–13).

Zirconium 2-(sulphophenyl)ethylphosphonate was prepared in the normal manner via the HF moderated metathetical reaction of zirconyl chloride and the precursor sulphonic phosphonic acid (eqn 14). This product is an off-white solid. Its X-ray powder pattern is quite broad, indicating low crystallinity (Fig. 6). A d-spacing of about 20–25 Å is expected for this compound in the layered modification. The X-ray shows a shoulder in the appropriate region ($2\theta = 4.5°$; d 20 Å). A very broad second order peak also appears to be centered at about $2\theta = 9°$. This low crystallinity in spite of preparation by the HF modified route is probably the result of crowding in the structure.

The titration curve for zirconium 2(-sulphophenyl)ethylphosphonate is presented in Fig. 8. This curve shows the presence of the strong acid functional group and the hydrolysis of the metal phosphonate structure by hydroxide. Comparison of this curve to the titration of semicrystalline zirconium 3-sulphopropylphosphonate (Fig. 3) indicates that the hydrolysis takes place in the aromatic case at lower pH than in the aliphatic case. This means that the hydrolysis rate in the aromatic case is much faster since it impacts the titration curve at hydroxide concentrations about two orders of magnitude lower (pH 6.2 vs pH 8.2). This rate factor is a result of the lower crystallinity of the material. It has been demonstrated that the hydrolysis rate correlates

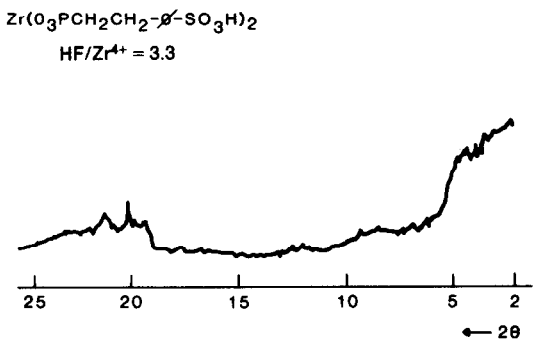

Fig. 7. XRD of zirconium 2-(sulphophenyl)ethyl phosphonate. Note the low degree of crystallinity even though prepared by the HF modified route.

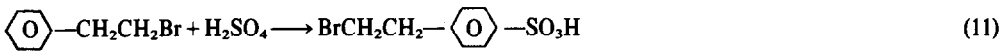

(11)

(12)

(13)

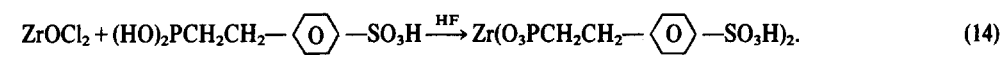

(14)

Table 3. Ion exchange reactions of zirconium 3-sulphopropylphosphonate

EXCHANGE[a]	Cu^{2+} meq/ml INITIAL	FINAL	pH EQUIL.	LOADING Cu^{2+} meq/g	% EXCHANGE
H+-Cu+2	0.215	0.093	0.92	2.46	77
Na+-Cu+2	0.215	0.135	2.88	1.62	51

a. 0.50 g of $Zr(O_3PCH_2CH_2CH_2SO_3H)_2$ or $Zr(O_3PCH_2CH_2CH_2SO_3Na)_2$ was reacted with 10ml of 0.215N $CuSO_4$.

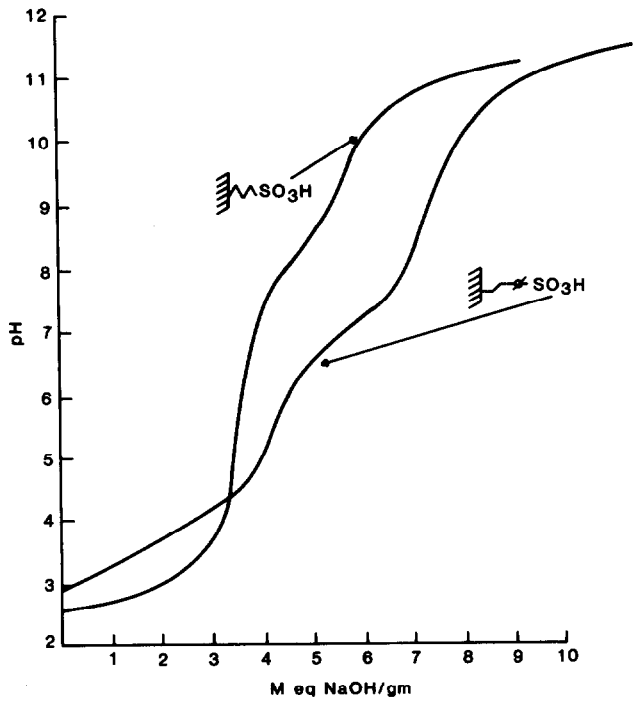

Fig. 8. Comparison of the titration curves of zirconium 3-sulphopropylphosphonate and zirconium 2-(sulphophenyl)ethyl phosphonate.

with the degree of crystallinity as evidenced by the X-ray powder pattern in the 3-sulphopropyl case. (The same correlation does not hold for neutralization rates.) These results are all consistent with the expectation that the crowding in the aromatic sulphonic acid case will result in inherently lower crystallinity.

SUMMARY

The sulphonic acid class of interlamellar anchored materials have now been established. Both aliphatic and aromatic examples have been prepared. The utility of the sulphonic acid has been demonstrated with the typical reactions of this functional group. Specifically, the acids have been shown to be strong acid cation exchangers and a Bronsted acid catalyst. In addition, we have begun to develop an insight into the structural ramifications of these compounds. The size constraints of the zirconium phosphate type backbone are evident. Further, the thermal stability of this group of compounds is encouraging relative to its applications potential.

EXPERIMENTAL

The experiments were carried out without extraordinary precautions to exclude oxygen or moisture. Reagents were usually used as received from the supplier. In most cases, elemental analyses of the products were not within rigorous limits, but purification was not possible since the products are insoluble in normal solvents and do not sublime. The combined weight of yield data, spectroscopy, TGA and powder diffraction results confirmed the compositions with good reliability. The X-ray powder patterns were run on a Phillips diffractometer using CuK_α radiation. Thermal analysis was carried out on a Mettler TA-2 instrument under N_2. IR spectra were obtained with a Beckman Acculab 10 Spectrometer.

Preparation of sulphoalkylphosphonates

I. 3-*Sulphopropylphosphonic acid via diethyl* 3-*sulphopropylphosphonate sodium salt.* To a 1 l., 3-necked flask fitted with a stirrer, addition funnel, reflux condenser and thermometer was charged 225 ml dry toluene. To this was added 17.2 g of 57% sodium hydride dispersion (9.8 g, 0.41 mole of NaH) with stirring. Diethylphosphite (56.5 g, 0.41 mole) was charged to the addition funnel and added dropwise to the toluene slurry over about 2 hr. Evolution of H_2 was smooth and began immediately. The addition rate was periodically adjusted to control the level of foam in the reactor. The reaction temperature was 30–40°C during the addition. After the addition of the phosphite was complete, a solution of 52 g propane sultone (0.43 mole) in 20 ml of toluene was charged to the addition funnel and added dropwise to the reaction mixture at a rate of about 1 ml/min. The temperature rose to about 60°C over the course of addition. The reaction mixture cooled to room temperature on standing overnight. At this point, the reaction mixture was two-phased. The upper toluene phase was decanted and the viscous lower product phase washed two times with diethylether (100 ml). The pasty product was then charged to a glass Soxhlet and continuously extracted with diethyl ether for about 40 cycles (7 cycles per hour). The product was removed from the Soxhlet and the residual ether removed under vacuum. The product—diethyl 3-sulphopropylphosphonate, sodium salt—is a hygroscopic solid, yield 73 g (63%). Hydrolysis of this ester salt in acid solution yields 3-sulphopropylphosphonic acid.

Hydrolysis of diethyl 3-*sulphopropylphosphonate, sodium salt.* To a 250 ml round bottom flask fitted with a reflux condenser and Dean–Stark trap was charged 7.7 g of diethyl 3-sulphopropylphosphonate, sodium salt and 30 ml of 48% hydrobromic acid. The solution was refluxed and ethylbromide removed in the Dean–Stark trap. The aqueous solution contains the required acid.

Preparation of zirconium 3-*sulphopropylphosphonate (high crystallinity).* The aqueous solution of 3-sulphopropylphosphonic acid from the above hydrolysis was charged to a 250 3-necked flask fitted with an addition funnel. To the addition funnel is charged a solution of 3.3 g of $ZrOCl_2 \cdot 8H_2O$ (0.010 mole) and 0.94 g of 48% aqueous HF in 10 ml of water. This solution was added dropwise to the aqueous phosphonic acid solution as the temperature was brought to gentle reflux. An immediate pre-

cipitate formed. The reaction mixture was heated at gentle reflux under a slow N_2 purge overnight. The reaction mixture was cooled to room temperature, the product isolated by filtration, washed 4 times with 25 ml of acetone, twice with 25 ml of ether and oven dried at 100°C-yield 4.3 g of zirconium-3-sulphopropylphosphonate.

Preparation of zirconium 3-sulphopropylphosphonate (semi-crystalline). The preparation was the same as above except the HF is omitted and the N_2 purge during reflux is unnecessary.

Zirconium 2-(4-sulphophenyl)ethylphosphonate: $Zr(O_3PCH_2CH_2C_6H_4SO_3H)_2$. To a 3-necked 100 ml round bottom flask fitted with a Dean–Stark trap and reflux condenser, magnetic stirrer and N_2 purge line was charged 1.1 g of diethyl 2-(sulphophenyl)ethylphosphonate sodium salt and 20 ml of 48% HBr. This mixture was refluxed until ethylbromide evolution was complete (as judged by its volume in the Dean–Stark trap). To the resultant aqueous acid phase 2-(sulphophenyl)ethylphosphonic acid was added 0.28 g of zirconium oxychloride ($ZrOCl_2$) and 0.20 g of 48% aqueous HF. A solid phase began to form and the slurry was refluxed under an N_2 purge for about 4 hr. The slurry was then cooled to room temperature and the solid product recovered by filtration. After washing with acetone (50 ml, 3 times) and ether (25 ml, 2 times), the white solid was dried under suction; yield was 0.58 g.

Diethyl 2-(sulphophenyl)ethylphosphonate sodium salt, $(EtO)_2P(O)CH_2CH_2C_6H_4SO_3Na$. To a 3-necked 100 ml flask, arranged for distillation of the product and fitted with a stirrer, and thermometer was charged 7.18 g of 2(sulphophenyl)ethyl bromide sodium salt, 16.6 g triethylphosphite and 30 g dimethylformamide. This mixture was stirred and heated to 120–130°C and ethyl bromide slowly distilled out. The reaction mixture was held at that temperature for about 2 hr, then cooled to room temperature. The pasty reaction mass was extracted 2 times with 75 ml portions, and dimethylformamide. The solid product was a mixture of diethyl 2-(sulphophenyl)ethylphosphonate sodium salt and 2-(sulphophenyl)ethylbromide sodium salt. Hydrolysis of the mixture in acid yielded an aqueous solution containing 2-(sulphophenyl)ethylphosphoric acid.

2-(Sulphophenyl)ethylbromide sodium salt, $BrCH_2CH_2H_6H_4SO_4Na$. To a 240 ml round bottom flask fitted with a reflux condenser, magnetic stirrer and thermometer was charged 18.5 g of phenethylbromide (Aldrich), 1.0 g dichlorobutane (GC std) and 25 ml of hexane. To this solution was added 14.2 ml of concentrated sulphuric acid with stirring. The mixture was raised to gently reflux for about 3 hr. The 2-phase mixture was cooled to room temperature and the lower acid phase separated and then slowly added to ethanolic NaOH (20 g NaOH in 200 ml ethanol) with vigorous stirring. The resulting slurry was filtered and the residue washed with a 150 ml portion of ethanol followed by a 75 ml portion of ethanol. The ethanol washing and the original filtrate was combined, concentrated to about 80 ml total volume and cooled to 0°C. The solid product 2-(sulphophenyl)-ethyl bromide sodium salt crystallized as a white solid and was recovered by filtration (9.70 g). As expected, the IR spectrum showed the presence of a strong band at 1185 cm^{-1} due to the $-SO_3Na$ group.

Acknowledgement—We are grateful to R. Cooksey for his very able assistance in this work.

REFERENCES

[1]M. B. Dines and P. M. DiGiacomo, *Inorg. Chem.* 1981, **20**, 92.
[2]G. Alberti, U. Constantino, S. Allulli and N. Tomassini, *Ibid.* 1978, **40**, 1113.
[3]G. Alberti, U. Constantino and M. L. Luciani Giovagnotti, *J. Chrom.* 1979, **180**, 45.
[4]S. Yamanaka, *Inorg. Chem.* 1976, **15**, 2811.
[5]G. Alberti, *Acc. Chem. Res.* 1978, **11**, 163; also A. Clearfield, G. H. Nancollas and R. H. Blessing, *Ion Exchange and Solvent Extraction* (Edited by J. H. Marinsky and Y. Marcus), Vol. 5. Marcel Dekker, New York (1973).
[6]R. F. Fischer, *Ind. Eng. Chem.* 1964, **56**(3), 41.
[7]G. Alberti and E. Torracca, *J. Inorg. Nucl. Chem.* 1968, **30**, 317.

Polyhedron Vol. 1, No. 1, pp. 69–75, 1982
Printed in Great Britain.

0277-5387/82/010069-07$03.00/0
Pergamon Press Ltd.

THE PROTONATION CONSTANTS AND ^{31}P NMR OF TETRA-, PENTA-, HEXA- AND HEPTAPOLYPHOSPHATES

HIROHIKO WAKI* and MASAO HATANO

Department of Chemistry, Faculty of Science, Kyushu University, Hakozaki, Fukuoka, 812 Japan

(*Received* 31 *July* 1981)

Abstract—The first and second protonation constants of linear polyphosphates at 25°C and ionic strength 0.1 have been evaluated: log $K_1 = 8.91$, log $K_{12} = 6.13$ for $P_2O_7^{4-}(P_2)$; log $K_1 = 8.88$, log $K_{12} = 5.86$ for $P_3O_{10}^{5-}(P_3)$; log $K_1 = 8.40$, log $K_{12} = 6.58$ for $P_4O_{13}^{6-}(P_4)$; log $K_1 = 8.15$, log $K_{12} = 7.03$ for $P_5O_{16}^{7-}(P_5)$; log $K_1 = 8.12$, log $K_{12} = 7.16$ for $P_6O_{19}^{8-}(P_6)$; log $K_1 = 8.07$, log $K_{12} = 7.18$ for $P_7O_{22}^{9-}(P_7)$. The variations of these values with the polyphosphate chain length have been discussed. A simple identification for polyphosphate species utilizing ^{31}P NMR signal ratio of middle to end P has been proposed. By applying a micro ion-exchange technique, a rapid concentration of each polyphosphate and the subsequent preparation of the magnesium salt have been accomplished.

INTRODUCTION

The studies on polyphosphates in various fields such as inorganic chemistry, biochemistry and medicine have been made. The important characteristics of the polyphosphates are the high stability towards hydrolysis compared with other water-soluble inorganic polymers such as polymers of silicate and borate and the high negative charge density compared with organic polyelectrolytes.

However, the linear polyphosphates longer than tetrapolyphosphate have been little investigated, although the shorter linear polymers such as pyro-, tripoly- and tetrapolyphosphate have been well studied. Griffith *et al.*[1] have determined rate constants of hydrolysis on tetra-through-octapolyphosphates. Glonek *et al.*[2] have measured ^{31}P NMR spectra on the sodium and tetra-*n*-butylammonium salt solutions of polyphosphates up to nonapolyphosphate. There are no reports on the protonation constants of linear polyphosphate anions longer than tetrapolyphosphate. The reason may be that the pure sample of each individual polyphosphate can be isolated only with difficulty.

In this work a sufficient amount of each polyphosphate was prepared by anion-exchange chromatographic separation and by anion-exchange sorption–desorption concentration technique, and the first and second protonation constants were determined. Also, an identification for each polyphosphate species was attempted using ^{31}P NMR spectroscopy.

EXPERIMENTAL

Chemicals

All the commercial chemicals used were of reagent grade. The purity of each polyphosphate obtained by ion-exchange chromatographic separation was confirmed by the end group pH-titration and by checking the NMR spectrum.

Chromatographic separations of polyphosphates

The glassy polyphosphate mixture with average polymerization number of about 6 was separated into its components by anion-exchange chromatography with a large column (Dowex 1-X4, Cl-form, 100 ~ 200 mesh, $\phi 2.6 \times 95$ cm). The solution containing 4 g of the glassy sodium polyphosphate was loaded on the column and the components were eluted with potassium chloride solution by gradient-elution technique. The initial eluent solution in the mixing bottle was 0.2 M KCl and the solution in the reservoir was 0.47 M KCl, both being adjusted to pH 4.5 by 0.02 M sodium acetate-acetic acid buffer contained. Elution was carried out with flow rate *ca.* 200 ml/hr at room temperature. The effluent was collected into 25 g fractions with an automatic fraction collector. The Mo(V)–Mo(VI) reagent was used for determining the phosphorus content in each fraction colorimetrically.

Ion-exchange concentration of the effluent

The effluent solution containing each particular component isolated was diluted to about 10 times in volume and one g of anion-exchange resin (Dowex 1-X4, Cl-form, 100 ~ 200 mesh) was added to the solution to resorb the polyphosphate component. The equilibration was done for a few hours, then the filtered resin was packed onto a small column ($\phi 0.5 \sim 0.6$ cm) and a very small volume of 1 M tetramethylammonium chloride solution was slowly passed to elute the sorbed polyphosphate. Thus each polyphosphate was concentrated to about 100 times by this procedure.

NMR measurements

The nmr spectra were recorded on a Hitachi high resolution nmr spectrometer Model R-20B with R.F. unit operating at 24.2793 MHz at 35°C for freshly prepared aqueous polyphosphate solutions (pH 7 or 12) containing 0.4 ~ 1 M as total phosphorus atom, using 5 mm spinning sample tubes. All chemical shifts were measured in comparison with a 85% orthophosphoric acid external standard, with positive shifts being downfield[2]. The measurements at pH 12 were made on the solutions pH-adjusted with tetramethylammonium hydroxide.

The signal area ratio of the middle to end P was determined by measuring directly the weights of tracing paper corresponding to each signal recorded.

The pH titrations

A Hitachi–Horiba pH meter with a Horiba pH glass electrode No. S764 and a calomel reference electrode was employed for pH titrations of polyphosphates. The pH reading was made on a 1 pH unit-full scale. The solution of 0.1004 M in HCl and 0.100 M in $(CH_3)_4NCl$ was added to the solution containing tetramethylammonium salt of each polyphosphate under continuous stirring and nitrogen atmosphere. The ionic strength was maintained close to 0.1 throughout the titration.

Preparation of magnesium salts of polyphosphates

2 ml of 1 M magnesium chloride was added to a 3 ml of polyphosphate solution which was prepared by the concentration of the effluent, then a few drops of acetone were added to form precipitation of the magnesium salt. The precipitate was stored in a desiccator after removing the adhering solution with filter paper.

*Author to whom correspondence should be addressed.

Evaluation of protonation constants

The amount of protons bound to polyphosphate anion was calculated as the difference between the amounts of the added protons and of the free protons measured. Dividing the amount of the bound protons, m_H, by the total amount of polyphosphates, m_P, the average proton number for each polyphosphate, $\bar{n}_H$, was obtained.

$$\bar{n}_H = \frac{m_H - [H^+]V}{m_P} \tag{1}$$

where V is the volume of the solution. The $\bar{n}_H$ is also described as Bjerrum's formation function as follows, when only the first two protonated species are present.

$$\bar{n}_H = \frac{K_1[H^+] + 2K_1K_{12}[H^+]^2}{1 + K_1[H^+] + K_1K_{12}[H^+]^2} \tag{2}$$

where K's are the stepwise protonation constants,

$$K_1 = \frac{[HP_nO_{3n+1}^{(n+1)-}]}{[H^+][P_nO_{3n+1}^{(n+2)-}]} \tag{3}$$

$$K_{12} = \frac{[H_2P_nO_{3n+1}^{n-}]}{[H^+][HP_nO_{3n+1}^{(n+1)-}]}. \tag{4}$$

Using the proton concentrations at half $\bar{n}_H$ values, $\bar{n}_H = 0.5$ and 1.5, K_1 and K_{12} were evaluated with the following equations derived from eqn (2).

$$K_1 = \frac{[H^+]_{\bar{n}_H=1.5} - 3[H^+]_{\bar{n}_H=0.5}}{[H^+]_{\bar{n}_H=0.5}[H^+]_{\bar{n}_H=1.5}} \tag{5}$$

$$K_{12} = \frac{1}{[H^+]_{\bar{n}_H=1.5} - 3[H^+]_{\bar{n}_H=0.5}} \tag{6}$$

RESULTS AND DISCUSSION

Preparation of polyphosphates

A typical elution curve on the preparative chromatographic separation is shown in Fig. 1. The isolation of each component was satisfactory. As a subsequent stage, an evaporation technique under reduced pressure for the concentration of the effluent has conventionally been applied. However, this procedure takes a lot of time and often leads to hydrolytic decomposition of polyphosphates.

By our anion-exchange sorption–desorption technique,[3] concentration and desalting take place simultaneously, and, therefore, the deduction to 1/100 in solution volume was attained within only 1 hr. The sorption rate can be seen from a typical curve for dodecapolyphosphate (Fig. 2). Thirty minutes was enough to absorb more than 90% of the polyphosphate. The subsequent desorption of the polyphosphate from the resin was

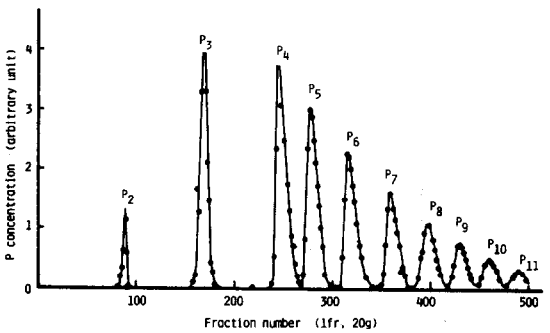

Fig. 1. Elution curve of linear polyphosphates at pH 4.5 from an anion-exchange column.

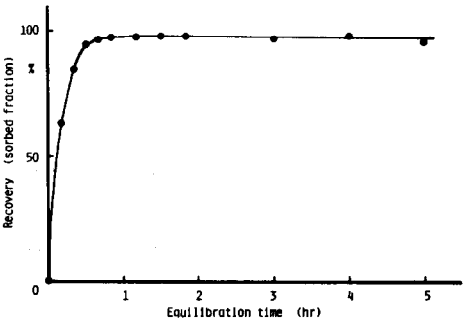

Fig. 2. Recovery curve of P_{12} by ion-exchange sorption at pH 5.5 and room temperature.

Table 1. Yields of the magnesium salt of polyphosphate

Polyphosphate P_n	Weight of salt (mg) (in air-dried)	Yield (%)[a]
P_5	105	3.0
P_6	134	3.3
P_7	102	2.1
P_8	48	0.9
P_{11}[b]	131	2.4

[a] Yields were calculated against the glassy sodium polyphosphate loaded on the column.

[b] P_{11} was obtained from a separate chromatographic run.

carried out in a very short time with a short column and only few milliliters of 1 M tetramethylammonium chloride eluent. Through these procedures no hydrolytic decomposition of the polyphosphate was observed.

When necessary, the magnesium salt of each polyphosphate was prepared by adding acetone to the concentrated solution obtained in the above procedure. The data of yield for each salt are summarized in Table 1.

NMR studies

The ^{31}P NMR signals for tetramethylammonium salt solutions of tetra- through-octapolyphosphates are shown in Fig. 3. The chemical shifts determined from the peak position of each signal are given in Table 2. The values by both the end and middle phosphorus groups tend to approach a constant respectively with the chain length of linear polyphosphate. This trend was similar to that from the tetra-*n*-butylammonium salts reported by Glonek.[2] The difference in chemical shifts among polyphosphates longer than tripolyphosphate were not appreciably recognized at pH 7 or 12. The pH dependence of chemical shifts is found to be much greater for end groups than for middle groups. This may result from the direct binding to end groups of the two protons. The absolute values of chemical shifts are, however, different from those by Glonek[2] because of employment of different conditions such as pH and the kind of counter cation. The chemical shifts at pH 12 may be recognized as those by the completely dissociated polyphosphate anions because of very weak complexibility of the tetramethylammonium ion. The identification of linear polyphosphate species utilizing the chemical shift of ^{31}P nmr was considered almost impossible by the fact that all

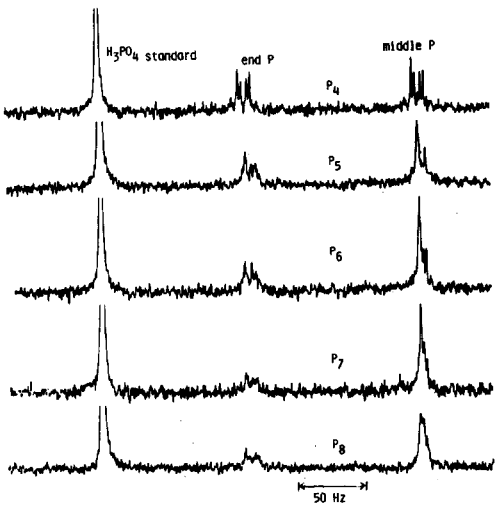

Fig. 3. ^{31}P NMR spectra of the tetra- through-octapolyphosphates at pH 7.

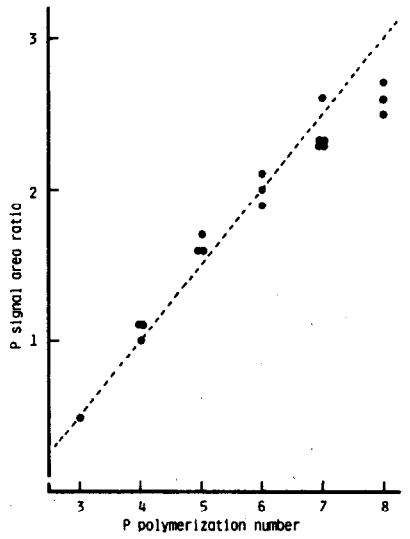

Fig. 4. ^{31}P NMR signal area ratio of middle to end P of tri- through-octapolyphosphates. Broken line is theoretical.

Table 2. ^{31}P nmr chemical shifts for the solutions of the pure tetramethylammonium polyphosphates at pH 7

Polyphosphate	Chemical shift (ppm)			
P_n	Middle P group		End P group	
P_3	-22.1		-6.9	
P_4	-23.3		-10.6	
P_5	-23.4	-22.4*	-10.8	-6.4*
P_6	-23.3	-22.4*	-10.9	-6.4*
P_7	-23.4		-10.9	
P_8	-23.3		-10.9	

The chemical shifts measured are referenced to "external" 85 % H_3PO_4.

*Measured at pH 12.

chemical shift values are indistinguishable from each other for long polyphosphates.

Instead, the measurement of the peak area ratio of ^{31}P nmr spectrum was thought to be more promising for such identification.[4] The ratios of the peak areas of middle to end P nuclei are plotted against chain length of polyphosphate in Fig. 4. It is seen that the ratios approximately agree with the practical ratios of the number of middle to end P nuclei. For P_8 the deviation to lower value may result from the experimental error by the measurement at too low concentration. This method seems more simple and useful than other identification methods, if a sufficient amount of polyphosphate is used.

Evaluation of protonation constants

Figures 5–8 show pH-titration curves for the tetra- through-heptapolyphosphate. All solutions contained tetramethylammonium chloride to keep ionic strength of 0.1. The concentrations of free proton and hydroxyl ion were calculated from the pH-reading through titration using activity coefficient $y_{H^+} = 0.83$ and the ion product of water $K_w = 1.096 \times 10^{-14}$.

The average protonation numbers $\bar{n}_H$ calculated by eqn (1) for P_4 to P_7 were plotted against logarithms of proton concentration in Figs. 9–12. The same experiment was carried out also for P_2 and P_3, in order to compare with the literature's results, but the details were omitted here. Next the proton concentrations at $\bar{n}_H = 0.5$ and $\bar{n}_H = 1.5$ were determined by the interpolation on several points in the range just around these half $\bar{n}_H$. Since the measurements in this range should give the minimum errors with respect to the protonation function, the protonation constants directly calculated by eqns (5) and (6) may be considered to be the most reasonable. The presence of tri- and further protonated species can be neglected completely at the pH conditions studied, since the corresponding stepwise protonation constants may be much less than 10^3.[5] The K_1 and K_{12} thus obtained are tabulated in Table 3. The reliability of the values was confirmed by fitting the original protonation function curves (Figs. 9–12).

An important result on these protonation constants may be that K_1 decreases monotonously while K_{12} increases after P_3 with increasing the chain length of polyphosphate, both tending to approach respective constant values. This trend of K_{12} except for P_3 may be

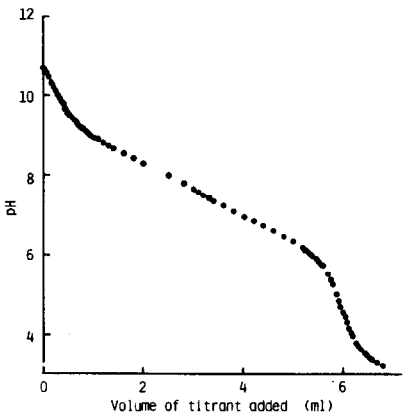

Fig. 5. Titration curve for tetrapolyphosphate. Original solution: 64 ml of 0.00445 M $P_4O_{13}^{6-}$ containing $N(CH_3)_4Cl$. Titrant: 0.1004 M HCl + 0.100 M $N(CH_3)_4Cl$.

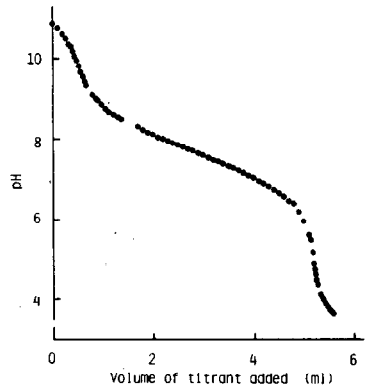

Fig. 6. Titration curve for pentapolyphosphate. Original solution: 64 ml of 0.00366 M $P_5O_{16}^{7-}$ containing $N(CH_3)_4Cl$. Titrant: 0.1004 M HCl + 0.100 M $N(CH_3)_4Cl$.

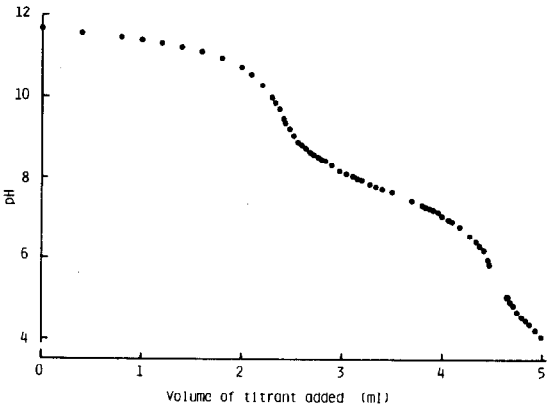

Fig. 7. Titration curve for hexapolyphosphate. Original solution: 64 ml of 0.00166 M $P_6O_{19}^{8-}$ containing $N(CH_3)_4Cl$. Titrant: 0.1004 M HCl + 0.100 M $N(CH_3)_4Cl$.

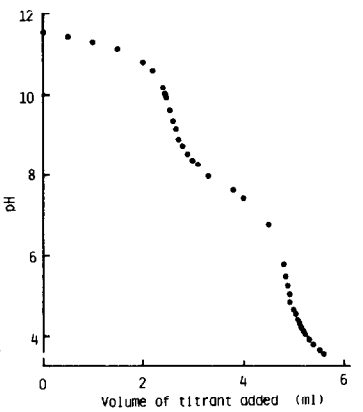

Fig. 8. Titration curve for heptapolyphosphate. Original solution: 64 ml of 0.00183 M $P_7O_{22}^{9-}$ containing $N(CH_3)_4Cl$. Titrant: 0.1004 M HCl + 0.100 M $N(CH_3)_4Cl$.

easily understood by considering the interaction between proton and the increased total anionic charge of a longer polyphosphate. In the case of K_1 the situation is more complicated. In P(V) polyphosphates, the anionic charge is localized within each PO_3 group and do not move across an oxygen atom linkage as shown by the fact that they do not have any appreciable light absorption in UV

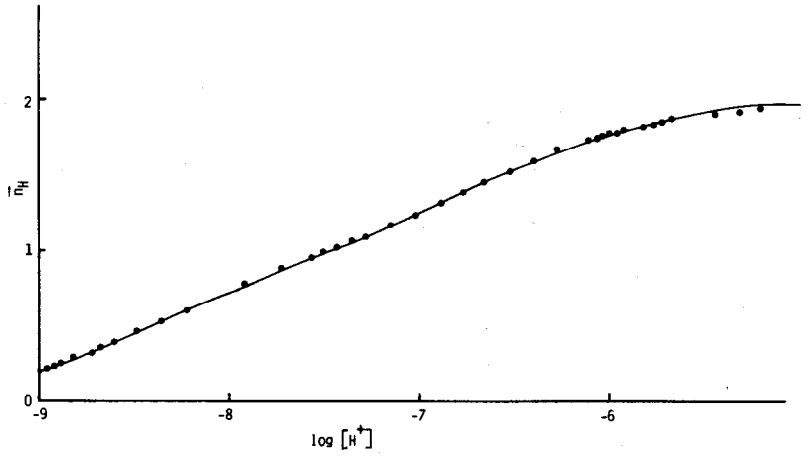

Fig. 9. Protonation function for tetrapolyphosphate. Solid line is the calculated curve with $\log K_1 = 8.40$ and $\log K_{12} = 6.58$.

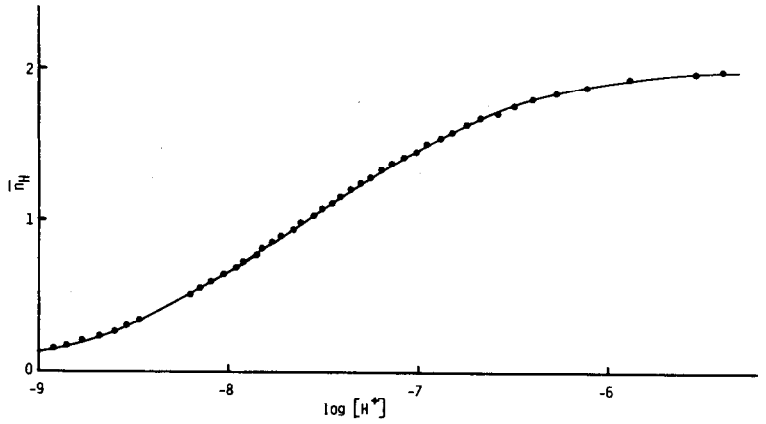

Fig. 10. Protonation function for pentapolyphosphate. Solid line is the calculated curve with $\log K_1 = 8.15$ and $\log K_{12} = 7.03$.

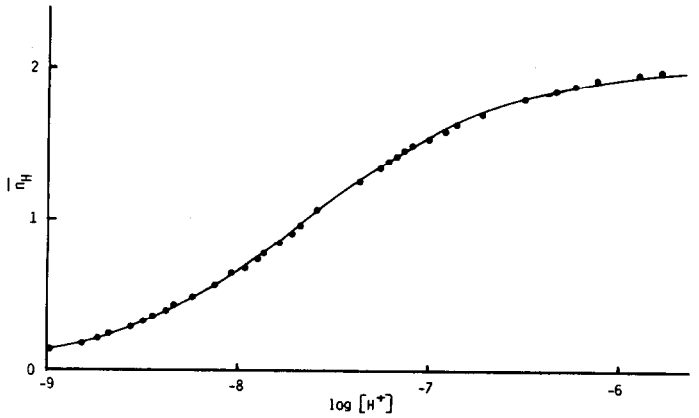

Fig. 11. Protonation function for hexapolyphosphate. Solid line is the calculated curve with $\log K_1 = 8.12$ and $\log K_{12} = 7.16$.

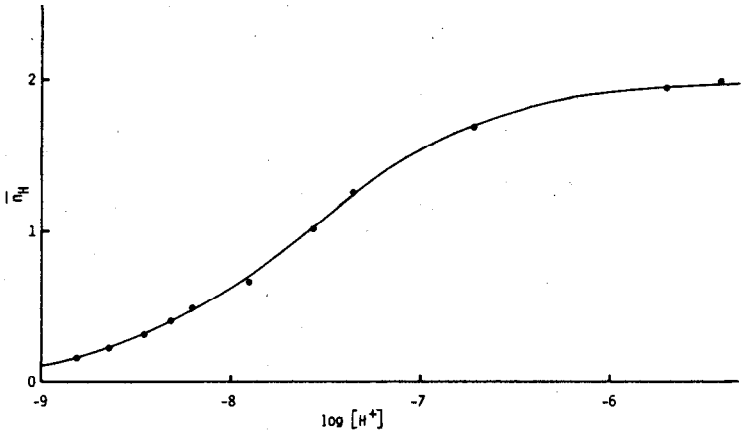

Fig. 12. Protonation function for heptapolyphosphate. Solid line is the calculated curve with $\log K_1 = 8.07$ and $\log K_{12} = 7.18$.

Table 3. Protonation constants of linear polyphosphates at 25°C and I = 0.1

polyphosphate P_n	log K_1	log K_{12}
P_2	8.91 ± 0.01	6,13 ± 0.01
	8.93 *	6.12 *
	9.00 **	6.23 **
P_3	8.88 ± 0.01	5.86 ± 0.02
	8.81 *	5.76 *
	8.74 **	6.02 **
P_4	8.40 ± 0.02	6.58 ± 0.02
	8.88 *	5.91 *
P_5	8.15 ± 0.02	7.03 ± 0.02
P_6	8.12 ± 0.01	7.16 ± 0.02
P_7	8.07 ± 0.04	7.18 ± 0.04

* ref. 6

** ref. 7

± value indicates the error caused by ± 0.01 error in pH reading around half $\bar{n}_H$.

and VIS regions. Therefore the interaction of proton with a polyphosphate anion can be considered as the sum of interactions with each PO_3 unit. Of these, the interaction with a binding site, i.e. one of the end PO_3 groups may be almost identical among different linear polyphosphates. Accordingly, the difference in K_1 should be the difference in the long range electrostatic interaction between a proton and PO_3 units not bound to the proton. A stronger electrostatic interaction is caused by higher charge, shorter distance and lower dielectric constant. The decreasing tendency of K_1 with chain length of linear polyphosphate in spite of increasing total anionic charge may be explained by the separation of the other doubly-charged end PO_3 group from the bound proton, and by the resultant increase of dielectric constant in the hydrated sphere around the polyphosphate anion. For the second protonation such unusual behavior should not be present since all PO_3 units are singly-charged. The reason for exceptional K_{12} in P_3 is not clear at present. A more quantitative explanation for protonation constants of polyphosphates will be reported elsewhere.

The protonation constants of P_2 and P_3 evaluated in

this work fairly agree with those in the literatures.[6,7] Though the constants of tetrapolyphosphate in this work differ from those in the literature,[7] our data seem to be more reliable by the employment of a more sensitive instrument and precisely established experimental conditions.

Acknowledgements—We thank Prof. Shigeru Ohashi for his valuable suggestion and encouragement and Mr. Yuzo Miyahara for his help in measuring ^{31}P nmr spectra.

REFERENCES

[1]E. J. Griffith and R. L. Buxton, *J. Am. Chem. Soc.* 1967, **89**, 2884.
[2]T. Glonek, A. J. Costello, T. C. Myers and J. R. Van Wazer, *J. Phys. Chem.* 1975, **79**, 1214.
[3]H. Waki *et al.*, Unpublished data.
[4]D. W. Matula, L. C. D. Groenweghe and J. R. Van Wazer, *J. Chem. Phys.* 1964, **41**, 3105.
[5]R. M. Smith and A. E. Martell (Editors), *Critical Stability Constants, Inorganic Complexes*, Vol. 4. Plenum Press, New York (1976).
[6]W. M. McNabb, J. F. Hazel and R. A. Baxter, *J. Inorg. Nucl. Chem.* 1968, **30**, 1585.
[7]G. G. Hammes and M. L. Morrell, *J. Inorg. Nucl. Chem.* 1964, **20**, 1497.

Polyhedron Vol. 1, No. 1, pp. 77–82, 1982
Printed in Great Britain.

0277-5387/82/010077-06$03.00/0
Pergamon Press Ltd.

SYNTHESIS OF π-(ARENE)METALLOCARBORANES CONTAINING IRON AND RUTHENIUM. CRYSTAL STRUCTURE OF 3,1,2-(η^6-1,3,5-$(CH_3)_3C_6H_3$)$FeC_2B_9H_{11}$

TIMOTHY P. HANUSA, JOHN C. HUFFMAN and LEE J. TODD*
Department of Chemistry, Indiana University, Bloomington, IN 47405, U.S.A.

(*Received* 8 *June* 1981)

Abstract—The reaction of *bis*(arene)iron(II) salts (arene = mesitylene or hexamethylbenzene) or benzenedichlororuthenium(II) dimer with Tl[3,1,2-$TlC_2B_9H_{11}$] in THF produces neutral, air-stable π-(arene)(Fe, Ru)$C_2B_9H_{11}$ complexes in low or moderate yields. The metallocarboranes are formal analogues of [π-(arene)(Fe, Ru)$^{n+}$(C_5H_5)] species, and a single crystal X-ray structure of the title compound has established the *closo* sandwich geometry expected for the molecule on the basis of electron counting rules. The carborane cage was found to be disordered in the crystal but the essential features of the molecular geometry were not obscured. The mesitylene is symmetrically bound to the iron, and the Fe-arene (centroid) distance of 1.60 Å is similar to that found in the previously-characterized [$(CH_3)_6C_6$]$Fe^I(C_5H_5)$ complex, despite the difference in the metal electronic configurations (d^6 vs d^7) and the change from the $B_9C_2H_{11}^{2-}$ cage to $C_5H_5^-$. Crystals of 3,1,2-(η^6-1,3,5-$(CH_3)_3C_6H_3$)$FeC_2B_9H_{11}$ are orthorhombic, space group $Pn2_1a$, with a = 12.638(4), b = 12.432(4), c = 9.686(3) Å.

INTRODUCTION

The remarkable structural and electronic similarities between the cyclopentadienide anion (Cp^-) and the five-membered open face of the undecahydro - dicarba - *nido* - undecaborate(2)-dianion ($B_9C_2H_{11}^{2-}$) have long been recognized.[1–3] Even though recent theoretical analyses have suggested that the carborane moiety is not a pure π-electron donor to transition metals,[4] it can often substitute isoelectronically for one or more π-cyclopentadienyl ligands in a metal complex. In some cases, the presence of the carborane cage enhances the thermal or hydrolytic stability of the complex,[5] or stabilizes the metal in a higher formal oxidation state than that in a Cp analogue.[6]

In recent years the study of mixed-sandwich transition metal compounds of the type [(arene)Fe^{n+}(Cp)] has provided numerous insights into the electronic and steric controls governing the synthesis and reactivity of metal-arene complexes.[7–9] The increasing interest being expressed in such systems should logically extend to the related [(arene)M^{n+}-$C_2B_9H_{11}$] (M = Fe, Ru, Os) species as well. No π-(arene)-carborane metal complexes containing "free" arene ligands have been reported in the literature,[10] however, although their likely existence was predicted soon after the discovery of the first metallocarboranes.[13] Whether only the requisite synthetic procedures were lacking, or whether an inherent instability of such complexes precluded their isolation, was not apparent at the beginning of our studies. We have, however, been able to prepare several π-(arene)$MC_2B_9H_{11}$ complexes containing iron and ruthenium, and have obtained crystals of 3,1,2-(η^6-1,3,5-$(CH_3)_3C_6H_3$)$FeC_2B_9H_{11}$ which were suitable for X-ray analysis. A low-temperature structural determination was then completed, both to confirm the *closo* sandwich geometry anticipated for the complex, and to establish general structural parameters to be expected in this new class of metallocarboranes.

*Author to whom correspondence should be addressed.

EXPERIMENTAL

Physical measurements

Boron (^{11}B) NMR spectra were obtained at 70.6 MHz with a Varian HR-220 spectrometer and were externally referenced to $BF_3{\cdot}O(C_2H_5)_2$ (positive values downfield). Proton NMR spectra were recorded on either a Varian HR-220 or a Varian T-60A spectrometer and were referenced to internal Me_4Si. IR spectra were obtained as KBr disks using a Perkin–Elmer 283 spectrometer. Low resolution mass spectral data were collected on a Varian CH-7 spectrometer. High resolution mass spectral data were obtained on a Hitachi Perkin–Elmer RMH-2 spectrometer interfaced to a Kratos DS50S data system at the University of Pennsylvania, Philadelphia, Pennsylvania. Melting points were determined in sealed, evacuated capillaries and are uncorrected. Elemental analysis was performed by Schwarzkopf Microanalytical Laboratories, Woodside, New York.

Materials

All reactions were performed under an atmosphere of prepurified nitrogen. Tetrahydrofuran (THF) was freshly distilled from sodium benzophenone ketyl. The *bis*(arene) iron salts,[14,15] benzenedichlororuthenium dimer,[16] and Tl[3,1,2-$TlC_2B_9H_{11}$][17] were prepared according to literature methods. All other commercially-available reagents were used as received.

Preparation of 3,1,2-[η^6-1,3,5-$(CH_3)_3C_6H_3$]$FeC_2B_9H_{11}$

To a slurry of *bis*(mesitylene)iron hexafluorophosphate, (1,3,5-$(CH_3)_3C_6H_3)_2Fe(PF_6)_2$[16] (1.99 g, 3.4 mmole) in dry tetrahydrofuran (50 mL) was added Tl[3,1,2-$TlC_2B_9H_{11}$] (0.61 g, 1.13 mmole) with stirring. The reaction mixture developed a dark red color within 15 sec after the addition of the thallium salt. Stirring under nitrogen was continued for 5 hr at room temperature, after which the reaction was opened to the air and silica gel (0.5 g, 60–200 mesh) added. The solvent was removed *in vacuo* and the solids chromatographed on a short (~13 cm) silica gel column packed under benzene. Elution with benzene produced an orange band; enrichment of the eluent with CH_2Cl_2 and finally acetonitrile yielded a dark purple–red band.

Removal of the solvent from the orange fraction yielded 3,1,2-[η^6-1,3,5-$(CH_3)_3C_6H_3$]$FeC_2B_9H_{11}$. Recrystallization from CH_2Cl_2/hexanes produced orange crystals (30 mg, 9%), m.p. 249–251°C(dec). The proton NMR spectrum (220 MHz, $CDCl_3$) contains sharp singlets at δ 5.66(3H) and 2.40(9H), and a broad resonance at δ 3.4(2H). The IR spectrum includes absorptions at 3346(w), 2568(vs, br), 1539(w), 1455(m), 1377(m), 1305(w),

1259(m), 1101(m), 1032(w), 1013(m), 983(m), 875(m, sharp), 799(m, br), 735(w) and 398(w).

On evaporation of the solvent, the purple chromatographic fraction yielded $TlPF_6$, identified by its IR spectrum, and after filtration, crude $Tl[(1,2\text{-}C_2B_9H_{11})_2Fe^{III}]$ (0.4 g), identified by its IR and paramagnetic ^{11}B NMR spectra.[2]

Preparation of $3,1,2\text{-}[\eta^6\text{-}(CH_3)_6C_6]FeC_2B_9H_{11}$

The procedure used was similar to that for the mesitylene analogue. *Bis*(hexamethylbenzene)iron (II) hexafluorophosphate,[17] $((CH_3)_6C_6)Fe(PF_6)_2$ (1.30 g, 1.94 mmoles) was slurried in THF (60 mL), and $Tl[3,1,2\text{-}TlC_2B_9H_{11}]$ (0.55 g, 1.0 mmole) was added with stirring. The reaction mixture darkened within 1 min after the addition of the thallium salt, and stirring of the reaction mixture under nitrogen was continued for 4 hr. The workup was as described previously; elution of the silica gel column with benzene produced an orange band, which on removal of the solvent yielded crude $3,1,2\text{-}[\eta^6\text{-}(CH_3)_6C_6]FeC_2B_9H_{11}$.

Heating the crude product (90°C, 10^{-2} torr) caused free hexamethylbenzene (22 mg) to collect on a water-cooled probe. The remaining unsublimed solids were dissolved in hot benzene/heptane (*ca.* 200 mL); on cooling, additional solids precipitated and were removed by filtration. The volume of the solution was reduced to 20 mL, and cooling in an ice bath produced reddish-orange crystals of $3,1,2\text{-}[\eta^6\text{-}(CH_3)_3C_6]FeC_2B_9H_{11}$ (9 mg, 3%), m.p. 299–302°C(dec). The proton NMR spectrum (220 MHz, $CDCl_3$) contains a sharp singlet at δ 2.27 (18H) and a broad resonance at δ 2.9(2H). The IR spectrum contains absorptions at 3028(w), 2906(w), 2527(vs, br), 1477(w), 1450(m, br), 1379(m), 1125(w), 1103(m, sharp), 1063(m), 1010(m), 984(m, sharp), 877(m), 717(w, br), 680(w), 605(w), 434(m) and 381(w) cm^{-1}.

Elution of the silica gel column with acetone yielded a purple band containing $Tl[(1,2\text{-}C_2B_9H_{11})_2Fe^{III}]$, yield not determined.

Reaction of $(C_6H_6)_2Fe(PF_6)_2$ *or* $[(CH_3)C_6H_5]_2Fe(PF_6)_2$ *with* $Tl[3,1,2\text{-}TlC_2B_9H_{11}]$

The hexafluorophosphate salts of *bis*(benzene)iron, $(C_6H_6)_2Fe(PF_6)_2$ or *bis*(toluene)iron, $[(CH_3)C_6H_5]_2Fe(PF_6)_2$ (2 or more equivalents) were treated with $Tl[3,1,2\text{-}TlC_2B_9H_{11}]$ (1 equiv.) in THF under conditions identical to those for the mesitylene analogue. The reaction mixtures were opened to air after stirring under nitrogen for 4–5 hr, and purified using silica gel columns. Elution of the columns with benzene produced orange-colored bands which on stripping of the solvent yielded small quantities (< 1 mg) of orange-brown oily residues.

Attempted recrystallizations from CH_2Cl_2/hexanes were not successful, and NMR spectra usually indicated the presence of mixtures, containing among other products, the symmetric and asymmetric isomers of $7,8\text{-}B_9C_2H_{11}(THF)$.[18] Occasionally, however, column chromatography produced a relatively clean sample, and from the reaction with $(C_6H_6)_2Fe(PF_6)_2$ a ^{11}B NMR (CH_2Cl_2) spectrum containing doublets in a 1:1:2:2:2:1 ratio centered at +1.3(166), −1.0(148), −8.3(127), −10.1(127), −19.6(151) and −24.9(178) ppm could be obtained. The proton NMR spectrum (220 MHz, $CDCl_3$) contained a singlet at δ 6.34. Samples from the reactions with $[(CH_3)C_6H_5]_2Fe(PF_6)_2$ could not be obtained sufficiently pure for detailed NMR study.

Large amounts of $Tl[(1,2\text{-}C_2B_9H_{11})_2Fe^{III}]$ (up to 50% based on $Tl[3,1,2\text{-}TlC_2B_9H_{11}]$) and $TlPF_6$ could be recovered from the silica gel columns by elution with polar organic solvents.

Preparation of $3,1,2\text{-}(\eta^6\text{-}C_6H_6)RuC_2B_9H_{11}$

To a slurry of benzenedichlororuthenium dimer,[16] $[(C_6H_6)_2RuCl_2]$ (0.54 g, 1.1 mmole) in dry tetrahydrofuran (100 mL) was added $Tl[3,1,2\text{-}TlC_2B_9H_{11}]$ (0.58 g, 1.1 mole) with stirring. The reaction mixture gradually turned brown over a 15-min interval. Stirring under nitrogen was continued for 4 hr at room temperature, after which the reaction was opened to the air and silica gel (0.5 g, 60–200 mesh) added. The solvent was removed *in vacuo* and the solids chromatographed on a short (~ 13 cm) silica gel column packed under CH_2Cl_2. Elution with CH_2Cl_2 produced a yellow band, which on stripping of the solvent yielded $3,1,2\text{-}(\eta^6\text{-}C_6H_6)RuC_2B_9H_{11}$. Recrystallization from acetone/hexanes produced canary yellow needles (108 mg, 32%), m.p. 308–309°C(dec). The proton NMR spectrum (60 MHz, $Me_2SO\text{-}d_6$) contains a sharp singlet at δ 6.29(6H) and a broad resonance at δ 4.3(2H). The IR spectrum includes absorptions at 3073(s), 2578(vs), 2541(vs), 1439(s, sharp), 1358(w, br), 1189(w), 1150(w), 1123(w), 1104(s, sharp), 1019(m), 991(m), 976(m), 877(m), 842(w), 814(s, sharp), 748(w), 721(w), 666(w), 416(w), 377(s, sharp) and 330(m) cm^{-1}.

Anal. calcd. for $C_8H_{17}B_9Ru$: C, 30.84; H, 5.50. Found (using V_2O_5 as a combustion catalyst): C, 29.59; H, 5.67.

Crystallography of $3,1,2\text{-}(\eta^6\text{-}1,3,5\text{-}(CH_3)_3C_6H)FeC_2B_9H_{11}$

Crystal data. $C_{11}H_{23}B_9Fe$, $M = 308.4$, Orthorhombic, $a = 12.638(4)$, $b = 12.432(4)$, $c = 9.686(3)$ Å, $U = 1521.9$ Å^3, $D_{calcd.} = 1.346$ g cm^{-3}, $Z = 4$, $\mu(M_0 - K_\alpha) = 9.7$ cm^{-1}. $F(000) = 640$, $\lambda(M_0 - K_\alpha) = 0.71069$ Å, space group $Pn2_1a$.

X-Ray data collection. Crystals were obtained by slow evaporation from a $CDCl_3$ solution. Because of the disorder problem encountered (*vide infra*), two different samples were examined. Crystal I of dimensions $0.19 \times 0.20 \times 0.38$ mm was mounted on a previously-described goniostat[19] and cooled to 110 K. Lattice parameters were determined from 32 reflections centered using automated top–bottom/left–right techniques. Intensity data were collected using θ–2θ scan techniques with a scan speed of 6°/min over a 2° + dispersion and 3 sec stationary background counts at each extreme of the scan. Statistics and the Patterson function indicated the proper space group to be the polar $Pn2_1a$ ($Pn2_1a$ is a non-standard setting of $Pna2_1$; No. 33, $C_2{}^9v$). The iron atom was located from a Patterson synthesis, and all remaining non-hydrogen atoms were located by standard Fourier techniques. Data reduction[19] and full-matrix least-squares refinement using anisotropic thermal parameters (no hydrogens located) converged to $R(F) = 0.095$ and $R_w(F) = 0.089$. Nearly all the atoms in the B_3C_2 face as well as several carbon atoms in the mesitylene refined to non-positive definite thermal parameters. In addition, there was an ambiguity in the occupancies of the atoms in the B_3C_2 face. Although it was apparent that disorder was present, it was not possible to determine a consistent set of occupancy parameters.

A second crystal (II) ($0.25 \times 0.35 \times 0.35$ mm) was then examined using a slower scan speed (4°/min, 4 sec background counts). The mosaicity of crystal II was better than that of I and data were collected in the range $5° \leq 2\theta \leq 45°$. Of 1290 reflections measured, 1053 were unique, and 869 with $F_0 > 2.33\ \sigma(F_0)$ were used in the solution and refinement. The data were reduced as before, but on refinement the partial occupancies of the B_3C_2 face were now found to be well-defined, and were fixed at C(2) = 100% C, B(4) and B(5) = 100% B, and C(3) and B(6) = 50% B, 50% C for all subsequent refinement. A difference Fourier synthesis located all hydrogen atoms, and final refinement using anisotropic thermal parameters for all non-hydrogen atoms and isotropic thermal parameters for the hydrogens ($1.0 + B_{iso}$ of the connecting atom) converged to the residuals of $R(F) = 0.040$ and $R_w(F) = 0.038$. Five atoms (C(2), B(6), B(10), B(12) and C(15)) refined to non-positive definite thermal parameters. We attribute this to the slight disorder forced upon the molecule by the B(6)-C(2)-C(3) disorder. A final difference Fourier synthesis was featureless, the largest peak being 0.42 e/Å^3.

Atomic co-ordinates, thermal parameters and a list of F_0/F_c values have been deposited with the Editor as supplementary material; copies are available on request. Atomic co-ordinates have also been deposited with the Cambridge Crystallographic Data Centre.

RESULTS AND DISCUSSION

The reaction of $Tl[3,1,2\text{-}TlC_2B_9H_{11}]$ with *bis*(arene)iron(II) hexafluorophosphates or benzenedichlororuthenium(II) dimer produces π-(arene)$MC_2B_9H_{11}$ metal complexes in low or moderate yields. Their synthesis provides evidence for the versatility of metal substitution reactions as convenient routes to metallocarboranes,[20] in this instance, a thallium atom is replaced by iron or ruthenium in the carborane cage icosahedron.

When $Tl[3,1,2\text{-}TlC_2B_9H_{11}]$ is mixed with $(1,3,5\text{-}(CH_3)_3C_6H_3)_2Fe(PF_6)_2$ in tetrahydrofuran, the reaction mixture after 4 hr yields $3,1,2\text{-}(\eta^6\text{-}1,3,5\text{-}(CH_3)_3C_6H_3)FeC_2B_9H_{11}$ in low yield. Electron-counting rules[21] suggest that the [(arene)Fe(II)] unit should function as a formal 2-electron donor to the carborane cage, producing an uncharged 12-membered *closo* molecule. These predictions for the complex are borne out by a variety of chemical and spectroscopic evidence. The π-(mesitylene)ferracarborane is a thermally-stable neutral orange solid, which shows no signs of decomposition after several month's exposure to the air. Its boron (^{11}B) NMR spectrum (Table 1) is consistent with an icosahedral geometry for the cage, and is similar to that found in related cobaltacarborane species.[22]

The proton NMR spectrum shows two sharp singlets at δ 5.66 and 2.40 in an intensity ratio of 1:3; these are assigned to the aromatic ring protons and methyl protons, respectively, and exhibit the upfield shift expected for the protons of a metal-complexed arene.[23] The IR C=C stretching frequencies at 1610 and 1475 cm^{-1} in uncomplexed mesitylene are shifted to 1455 and 1101 cm^{-1}, respectively, in the metallocarborane; shifts of such magnitude are typically encountered in π-arene complexes.[24] The low-resolution mass spectrum cuts off at m/e = 310, corresponding to the $^{11}B_9{}^{12}C_{11}{}^{1}H_{23}{}^{56}Fe^+$ molecular ion.

There is a dearth of published structural information on π-(arene)iron complexes of any kind, and almost none on sandwich π-(arene)iron species. A single-crystal X-ray diffraction study of the mesitylene complex was, therefore, completed, which both augments the structural data on π-(arene)iron compounds which does exist, and also permits comparison of the geometry of the carborane species with that of the related $[(CH_3)_6C_6]Fe^I(C_5H_5)$.[8c]

Solid state structure of 3,1,2-(η⁶-*mesitylene*)*dicarborayliron*(*II*)

The molecule crystallizes in monomeric units which possess a sandwich-type geometry, with the iron atom flanked by an η^6-mesitylene ring and by the open B_3C_2 face of the subicosahedral carborane cluster. There is no symmetry to the molecule as a whole. A view of the molecule indicating the coordination geometry and numbering scheme is presented in Fig. 1. Selected interatomic bond distances and angles are listed in Tables 2 and 3, respectively. In the carborane cage, all definite B–B distances are typical for this unit[25] (average of 15 bond lengths = 1.77(4) Å). The rotational disorder observed in the cage resulted in partial averaging of the distances on the B_3C_2 face, however; the expected short (*ca.* 1.60 Å)[25] C(2)–C(3) distance is lengthened to

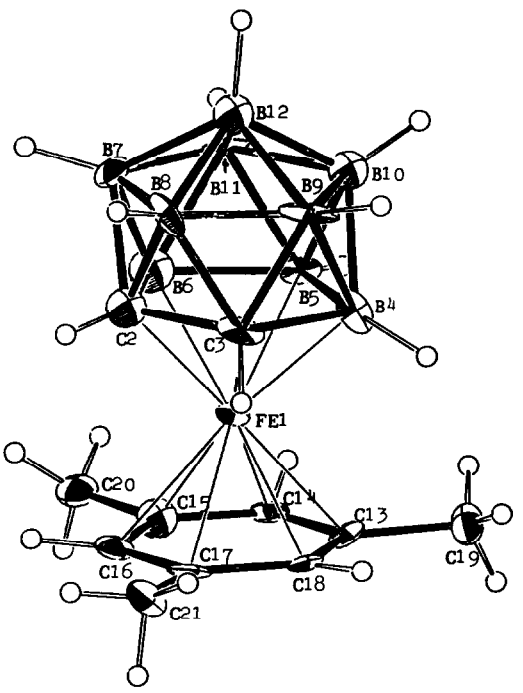

Fig. 1. ORTEP view of the 3,1,2 - (η⁶ - 1,3,5 - $(CH_3)_3C_6H_3)FeC_2B_9H_{11}$ molecule showing the atom numbering scheme used in the tables. Hydrogen atoms are represented as open circles.

1.65(2) Å, and the B–C lengths appear as 1.67 Å (av.) instead of the more common ~1.72 Å.[25] The B_3C_2 face itself is planar, and all atoms are within 0.012 Å of the least-squares plane.

The geometry of the mesitylene ligand is typical of a complexed arene. The six-carbon ring is highly planar; no atom deviates from the least-squares plane by more than 0.003 Å. Carbon–carbon bond lengths within the ring are equal within experimental error (average length = 1.41(2) Å) and there is no evidence for a significant two-fold or three-fold distortion of the ring. The methyl groups are attached to the ring via normal C–C bonds of average length 1.49(1) Å, and are displaced slightly out of the six-carbon plane and toward the metal by 0.05 Å ($\bar{\alpha} = 1.8°$). The three hydrogen–carbon bonds of the arene ring are also tilted toward the metal, but an examination of the packing in the crystal lattice reveals that there are no intermolecular contact distances significantly less than the sum of the appropriate van der Waals radii. Rather, the displacements of the ring substituents can be identified as another example of the effect of the rearrangement of arene e_1 orbitals which

Table 1. 70.6 MHz Boron (^{11}B) NMR data

COMPOUND (solvent)	RELATIVE AREAS	δ_B(ppm) [J_{BH}(Hz)]
$3,1,2\text{-}(\eta^6\text{-}1,3,5\text{-}(CH_3)_3C_6H_3)FeC_2B_9H_{11}$ ($CDCl_3$)	1:1:4:2:1	+2.9(129); -2.1(134); -8.5; -19.6(164); -24.8(181)
$3,1,2\text{-}(\eta^6\text{-}(CH_3)_6C_6)FeC_2B_9H_{11}$ ($CDCl_3$)	1:1:4:2:1	+3.6(139); -3.8(127); -8.3; -19.9(146); -24.7(173)
$3.1.2\text{-}(\eta^6\text{-}C_6H_6)RuC_2B_9H_{11}$ ($Me_2SO\text{-}d_6$)	2:2:2:2:1	+0.3(134); -8.5(127); -9.6(112); -19.8(154); -24.4(166)

Table 2. Bond distances (Å) for the 3,1,2-(η^6-1,3,5-$(CH_3)_3C_6H_3$)$FeC_2B_9H_{11}$ molecule

A	B	Distance
FE(1)	C(2)	2.049(12)
FE(1)	C(3)	2.071(10)
FE(1)	C(13)	2.125(9)
FE(1)	C(14)	2.103(14)
FE(1)	C(15)	2.145(12)
FE(1)	C(16)	2.140(12)
FE(1)	C(17)	2.134(10)
FE(1)	C(18)	2.089(10)
FE(1)	B(4)	2.126(12)
FE(1)	B(5)	2.147(11)
FE(1)	B(6)	2.083(13)
C(2)	C(3)	1.644(16)
C(2)	B(6)	1.625(25)
C(2)	B(7)	1.723(17)
C(2)	B(8)	1.699(18)
C(3)	B(4)	1.730(21)
C(3)	B(8)	1.708(17)
C(3)	B(9)	1.694(20)
C(13)	C(14)	1.422(17)
C(13)	C(18)	1.393(17)
C(13)	C(19)	1.491(16)
C(14)	C(15)	1.378(17)
C(15)	C(16)	1.429(17)
C(15)	C(20)	1.490(18)
C(16)	C(17)	1.422(15)
C(17)	C(18)	1.425(21)
C(17)	C(21)	1.480(16)
B(4)	B(5)	1.846(17)
B(5)	B(6)	1.809(29)

Table 3. Bond angles (deg) for the 3,1,2-(η^6-1,3,5-$(CH_3)_3C_6H_3$)$FeC_2B_9H_{11}$ molecule

A	B	C	Angle
C(2)	FE(1)	C(3)	47.0(5)
C(2)	FE(1)	B(6)	46.3(7)
C(3)	FE(1)	B(4)	48.7(6)
C(13)	FE(1)	C(14)	39.3(5)
C(13)	FE(1)	C(16)	83.7(4)
C(13)	FE(1)	C(18)	38.6(5)
C(14)	FE(1)	C(15)	37.8(5)
C(14)	FE(1)	C(17)	83.6(5)
C(15)	FE(1)	C(16)	39.0(5)
C(15)	FE(1)	C(18)	82.6(5)
C(16)	FE(1)	C(17)	38.9(4)
B(4)	FE(1)	B(5)	51.2(5)
B(5)	FE(1)	B(6)	50.6(9)
C(3)	C(2)	B(6)	111.5(12)
C(2)	C(3)	B(4)	110.4(9)
C(14)	C(13)	C(18)	117.0(11)
C(14)	C(13)	C(19)	122.2(10)
C(18)	C(13)	C(19)	120.7(11)
C(13)	C(14)	C(15)	122.5(12)
C(14)	C(15)	C(16)	119.6(11)
C(14)	C(15)	C(20)	121.4(12)
C(16)	C(15)	C(20)	119.0(12)
C(15)	C(16)	C(17)	120.2(11)
C(16)	C(17)	C(18)	117.3(11)
C(16)	C(17)	C(21)	120.3(10)
C(18)	C(17)	C(21)	122.4(10)
C(13)	C(18)	C(17)	123.5(11)
C(3)	B(4)	B(5)	105.8(9)
B(4)	B(5)	B(6)	102.1(9)
C(2)	B(6)	B(5)	110.1(11)

occurs on complexation to a transition metal. The theoretical basis for the effect has been discussed by Hoffmann,[26] and structural evidence for it has often been found, as in the orientation of methyl groups in $[(CH_3)_6C_6]Fe(C_5H_5)$[8c] and $[(CH_3)_6C_6]Cr(CO)_3$,[27] and in the ring hydrogens of $(C_6H_6)Cr(CO)_3$.[28]

The methyl group hydrogens are oriented so that one is pointed away from the metal. Such an arrangement is commonly encountered in complexed aromatic rings.[29] The planes containing the open face of the carborane cage and the mesitylene ring are essentially parallel, with a dihedral angle of 2.9°.

The Fe-B_3C_2 face (centroid) distance is 1.48 Å, which compares favorably with the value of 1.49 Å found for the analogous distances in both 3,1,2-$(C_5H_5)FeC_2B_9H_{11}$[30] and the $(1,2\text{-}C_2B_9H_{11})_2Co^-$ ion.[31] The Fe-arene (centroid) distance of 1.60 Å in the carborane complex is nearly coincident with the value of 1.58(1) Å reported for $[(CH_3)_6C_6]Fe^I(Cp)$.[8c] The relative constancy of the Fe-arene distance in 18-electron and 19-electron (arene)Fe^{n+}(Cp) complexes has been briefly mentioned before,[32] but the apparent insensitivity of the Fe-arene distance to the electronic configuration on the iron (d^7 vs d^6), the number of methyl groups on the arene, and to the nature of other ligands on the metal ($C_5H_5^-$ vs $B_9C_2H_{11}^{2-}$) in such structurally-distinct molecules as the cyclopentadienyl and metallocarborane complexes is still remarkable.[33] Molecular orbital studies and spectroscopic evidence have been used to argue that the HOMO in [(arene)FeCp]$^{n+}$ complexes (and presumably in (arene)$FeC_2B_9H_{11}$ species[4]) is largely metal-centered, and that the ligand character of the e† LUMO is weighted toward the Cp ring rather than toward the arene.[8d] Changes in the electronic environment of the metal should not therefore greatly affect the bonding of the arene ligand. Although more structural studies are needed to establish the Fe-arene distances in a variety of other complexes, our findings are supportive of this theoretical analysis of the metal-arene bonding in sandwich-type complexes.[34]

Reaction of other bis(arene)iron salts with Tl[3,1,2-$TlC_2B_9H_{11}$]

Attempts to prepare π-(arene)$FeC_2B_9H_{11}$ complexes with arenes other than mesitylene met with mixed success. Reaction of *bis*(HMB)iron hexafluorophosphate (HMB = hexamethylbenzene) with Tl[3,1,2-$TlC_2B_9H_{11}$] produced 3,1,2-(η^6-$(CH_3)_6C_6$)$FeC_2B_9H_{11}$ in low yield. Its spectroscopic properties are similar to those of the mesitylene analogue (see Table 1); the proton NMR spectrum contains one sharp singlet at δ 2.27 (methyl CH) and a broad resonance at δ 2.9 (carborane CH) in an intensity ratio of 9:1, consistent with a complexed η^6-HMB ring. The low-resolution mass spectrum cuts off at $m/e = 352$, corresponding to the $^{11}B_9{}^{12}C_{14}{}^{1}H_{29}{}^{56}Fe^+$ molecular ion.

In contrast to the results with mesitylene or HMB, however, isolable solid complexes could not be obtained from *bis*(benzene) or *bis*(toluene) salts using the present method. Despite repeated attempts, workup of the *bis*(arene)salt-Tl[3,1,2-$TlC_2B_9H_{11}$]-THF reaction mixtures left only small amounts of intractable oily residues. NMR spectra usually indicated the presence of complex mixtures, although in the case of the reaction with *bis*(benzene)iron hexafluorophosphate, a species could be identified whose ^{11}B NMR spectrum (see Experimental) was very similar to those of the mesitylene and HMB complexes (Table 1). The observance of a singlet at δ 6.34 in the proton NMR spectrum is consistent with the presence of an η^6-benzene ring, suggesting that the species is in fact 3,1,2-(η^6-C_6H_6)$FeC_2B_9H_{11}$. The reaction mixtures with *bis*(toluene)iron hexafluorophosphate proved even more difficult to purify, and the small quantity of material involved prevented the isolation of any complex.

Since both the free arene and $TlPF_6$ were found among the products of the various reactions, even

though not quantitatively accounted for, the following reaction scheme is plausible:

$$(\text{arene})_2\text{Fe}(\text{PF}_6)_2 + \text{Tl}[3,1,2\text{-TlC}_2\text{B}_9\text{H}_{11}] \rightarrow$$

$$(\text{arene})\text{FeC}_2\text{B}_9\text{H}_{11} + \text{arene} + 2\ \text{TlPF}_6. \quad (1)$$

The dominant reaction however, which seems to be almost exclusive with the *bis*(benzene)iron and *bis*(toluene)iron salts, is the simultaneous displacement of both arenes from the metal center, releasing the iron to react with $\text{Tl}[3,1,2\text{-TlC}_2\text{B}_9\text{H}_{11}]$ and forming $\text{Tl}_2[(1,2\text{-C}_2\text{B}_9\text{H}_{11})_2\text{Fe}^{\text{II}}]$;[35] subsequent aerial oxidation produces the $\text{Tl}[(1,2\text{-C}_2\text{B}_9\text{H}_{11})_2\text{Fe}^{\text{III}}]$ found in large amounts as a product in all the reactions. The inaccessability of the π-(benzene)- and π-(toluene)ferracarborane complexes by the present method may thus stem from the greater lability of the arene ligands in the *bis*(benzene)iron and *bis*(toluene) iron dications than in the more highly-substituted *bis*(mesitylene)iron and *bis*(HMB)iron salts.[36]

$3,1,2\text{-}(\eta^6\text{-C}_6\text{H}_6)\text{RuC}_2\text{B}_9\text{H}_{11}$

We hoped to begin exploring the chemistry of analogous second and third-row transition metal complexes by incorporating ruthenium into a π-(arene)metallocarborane.

Our initial efforts in this direction were successful, as the reaction of $\text{Tl}[3,1,2\text{ - }\text{TlC}_2\text{B}_9\text{H}_{11}]$ with benzenedichlororuthenium(II) dimer affords $3,1,2\text{ - }(\eta^6\text{ - }\text{C}_6\text{H}_6)\text{RuC}_2\text{B}_9\text{H}_{11}$ in moderate yield (32%). The ruthenium complex is a bright yellow, air-stable sublimable solid. Its ^{11}B NMR spectrum (Table 1) is similar to that of the isoelectronic *closo* iron analogues. The proton NMR spectrum contains a sharp spike at δ 6.29, as expected for the protons of an η^6-benzene ring. The low-resolution mass spectrum cuts off at $m/e = 316$, corresponding to the $^{11}\text{B}_9{}^{12}\text{C}_8{}^{1}\text{H}_{17}{}^{104}\text{Ru}^+$ molecular ion. The high resolution mass of this ion was determined to be $m/e = 316.1218$ (calcd. 316.1223).

Preliminary investigations of the reactivity of the ruthenium complex indicate that the arene is not highly labile; the molecule is unaffected by trimethyl phosphite or triphenylphosphine at room temperature, and photolysis of a THF solution of the complex for 4½ hr while under an atmosphere of CO does not result in arene displacement. Although no chemistry has been described for the analogous cyclopentadienyl complex $(\text{C}_6\text{H}_6)\text{Ru(Cp)}^+$,[37] such inertness has been noted for other d^6 arene-ruthenium complexes, and has been interpreted as an indication of the strength of the Ru-arene bond.[23]

CONCLUSION

The analogy between the $\text{B}_9\text{C}_2\text{H}_{11}^{2-}$ dianion and the cyclopentadienyl ligand extends also to complexes containing an arene π-bonded to a metal center. In contrast to the cationic $[(\text{arene})\text{Fe}^{\text{II}}(\text{Cp})]^+$ complexes, or the highly air-sensitive, often thermally unstable, reduced $[(\text{arene})\text{Fe}^{\text{I}}(\text{Cp})]^\circ$ species,[8d] neutral, air-stable 18-electron iron and ruthenium carborane complexes can be prepared which possess high thermal stability and solubility in a variety of organic solvents. As a formal 2-electron donor to carboranes, the [arene(Fe, Ru)(II)] unit is isoelectronic with the $(\text{C}_5\text{H}_5)\text{Co(III)}$ moiety, and hence some of the tremendously varied synthetic and isomerization reactions of (cyclopentadienyl)-cobaltacarboranes[38] may have parallels in π-(arene)ferra- and ruthenacarborane chemistry. We are exploring such possibilities in our continuing study of π-(arene)metallocarboranes.

Acknowledgement—This work was supported by the National Science Foundation through Grant No. CHE 78-08719.

REFERENCES

[1] M. F. Hawthorne, D. C. Young and P. A. Wegner, *J. Am. Chem. Soc.* 1965, **87**, 1818.

[2] M. F. Hawthorne, D. C. Young, T. D. Andrews, D. V. Howe, R. L. Pilling, A. D. Pitts, M. Reintjes, L. F. Warren and P. A. Wegner, *J. Am. Chem. Soc.* 1968, **90**, 879.

[3] M. F. Hawthorne, *Acc. Chem. Res.* 1968, **1**, 281.

[4a] D. A. Brown, M. O. Fanning and N. J. Fitzpatrick, *Inorg. Chem.* 1978, **17**, 1620; [b] *ibid.* 1980, **19**, 1822.

[5a] H. W. Ruhle, and M. F. Hawthorne, *Inorg. Chem.* 1968, **7**, 2279; [b] R. J. Wilson, L. F. Warren and M. F. Hawthorne, *J. Am. Chem. Soc.* 1969, **91**, 758; [c] Chris G. Salentine and M. F. Hawthorne, *J. Am. Chem. Soc.* 1975, **97**, 426.

[6] The $(1,2\text{-C}_2\text{B}_9\text{H}_{11})_2\text{Ni}$ and $[(1,2\text{-C}_2\text{B}_9\text{H}_{11})_2\text{Cu}]^{2-}$ species (Ref. 2) contain formal Ni(IV) and Cu(III), respectively, oxidation states which are inaccessible or unstable with Cp ligands; but see L. O. Pont, A. R. Siedle, M. S. Lazarus and W. L. Jolly, *Inorg. Chem.* 1974, **13**, 483.

[7a] W. H. Morrison, Jr., E. Y. Ho and D. N. Hendrickson, *J. Am. Chem. Soc.* 1974, **96**, 3603; [b] *ibid. Inorg. Chem.* 1975, **14**, 500, [c] R. G. Sutherland, S. C. Chen, W. J. Pannekock and C. C. Lee, *J. Organomet. Chem.* 1975, **101**, 221; [d] *ibid.* 1976, **117**, 61; [e] C. C. Lee, K. J. Demchuk and R. G. Sutherland, *Synth. React. Inorg. Metal. Org. Chem.* 1978, **8**, 361; [f] *ibid. Can. J. Chem.* 1979, **57**, 933.

[8a] D. Astruc, E. Roman, J.-R. Haman and P. Batail, *J. Am. Chem. Soc.* 1979, **101**, 2240; [b] A. Buet, A. Darchen and C. J. Moinet, *J. Chem. Soc., Chem. Commun.* 1979, 447; [c] D. Astruc, J.-R. Hamon, G. Althoff, E. Roman, P. Batail, P. Michand, J.-P. Mariot, F. Varret and D. Cozak, *J. Am. Chem. Soc.* 1979, **101**, 5445; [d] J.-R. Hamon, D. Astruc and P. Michand, *J. Am. Chem. Soc.* 1981, **103**, 758, and references cited therein.

[9a] J. F. Helling and G. C. Cash, *J. Organometal. Chem.* 1974, **73**, C10; [b] T. P. Gill and K. R. Mann, *Inorg. Chem.* 1980, **19**, 3007; [c] N. E. Murr, *J. Chem. Soc., Chem. Commun.* 1981, 251.

[10] Hawthorne and Leyden[11] have prepared a colbaltacarborane characterized as $3,1,2\text{-}(\text{C}_6\text{H}_5\text{–C}_5\text{H}_5\text{B})\text{CoC}_2\text{B}_9\text{H}_{11}$, in which the metal is apparently π-bonded to the η^6-borabenzene ring. For our purposes, however, a heterocyclic system such as this is not properly regarded as a true arene (π-carbocyclic) complex. While the present work was being refereed, Stone and Welch[12] reported the synthesis of several π-(arene)ferracarboranes and the crystal structure of $(\eta^6\text{ - }(\text{CH}_3)\text{C}_6\text{H}_5)\text{ - }2,4\text{ - }(\text{CH}_3)_2\text{ - }1,2,4\text{ - }\text{FeC}_2\text{B}_9\text{H}_9$. The spectroscopic properties of the toluene complex seem to be in general agreement with those of the $(\text{arene})\text{FeC}_2\text{B}_9\text{H}_{11}$ compounds reported here, although their synthetic method differs considerably from ours.

[11] M. F. Hawthorne and R. N. Leyden, *Inorg. Chem.* 1975, **14**, 2018.

[12] M. P. Garcia, M. Green, F. G. A. Stone, R. G. Somerville and A. J. Welch, *J. Chem. Soc., Chem. Commun.* 1981, 871.

[13] D. R. Scott, *J. Organometal. Chem.* 1966, **6**, 429.

[14] J. F. Helling, S. L. Rice, D. M. Braitsch and T. Mayer, *J. Chem. Soc., Chem. Commun.* 1971, 930.

[15] J. F. Helling and D. M. Braitsch, *J. Am. Chem. Soc.* 1970, **92**, 7207.

[16] R. A. Zelonka and M. C. Baird, *Can. J. Chem.* 1972, **50**, 3063.

[17] H. D. Smith, Jr. and M. F. Hawthorne, *Inorg. Chem.* 1974, **13**, 2312.

[18] D. C. Young, D. V. Howe and M. F. Hawthorne, *J. Am. Chem. Soc.* 1969, **91**, 859.

[19] J. C. Huffman, L. N. Lewis and K. G. Caulton, *Inorg. Chem.* 1980, **19**, 2755.

[20] R. N. Grimes in *Organometallic Reactions and Synthesis* (Edited by E. I. Becker and M. Tsutsui), Vol. VI, Chap. 2, p. 79. Plenum Press, New York, 1977.

[21]K. Wade, *Adv. Inorg. Chem. Radiochem.* 1976, **18**, 1.
[22]A. R. Siedle, G. M. Bodner and L. J. Todd, *J. Organometal. Chem.* 1971, **33**, 137.
[23]R. G. Gastinger and K. J. Klabunde, *Trans. Met. Chem.* 1979, **41**, 1.
[24]E. O. Fischer and H. P. Fritz, *Angew. Chem.* 1961, **73**, 353.
[25a]A. Zalkin, T. E. Hopkins and D. H. Templeton, *Inorg. Chem.* 1966, **5**, 1189; [b]P. T. Green and R. F. Bryan, *Inorg. Chem.* 1970, **9**, 1464; [c]A. J. Welch, *J. Chem. Soc. Dalton Trans.* 1975, 1473.
[26]M. Elian, M. L. Chen, M. P. Mingos and R. Hoffmann, *Inorg. Chem.* 1976, **15**, 1148.
[27]M. F. Bailey and L. F. Dahl, *Inorg. Chem.* 1965, **9**, 1298.
[28]B. Rees and P. Coppens, *Acta Crystallogr., Sect. B.* 1973, **29**, 2515.
[29a]M. R. Thompson, C. S. Day, V. W. Day, R. I. Mink and E. L. Muetterties, *J. Am. Chem. Soc.* 1980, **102**, 2979; [b]D. P. Freyberg, J. L. Robbins, K. N. Raymond and J. C. Smart, *J. Am. Chem. Soc.* 1979, **101**, 892; [c]R. G. Teller and J. M. Williams, *Inorg. Chem.* 1980, **19**, 2770.
[30]A. Zalkin, D. H. Templeton and T. E. Hopkin, *J. Am. Chem. Soc.* 1965, **87**, 3988.
[31]A. Zalkin, T. E. Hopkins and D. H. Templeton, *Inorg. Chem.* 1967, **6**, 1911.
[32]Reference 8d, footnote 67.
[33]It should be noted that, in contrast, Fe–Cp distances are highly dependent on the presence of other coordinated ligands on the metal and on electrons in excess of the noble gas configuration; crystallographically-determined values range from 1.64 to 1.79 Å. See: G. M. Reiner, I. Bernard, H. Brunner and M. Mushiol, *Inorg. Chem.* 1978, **17**, 783.
[34]Additional evidence for the insensitivity of Fe-(arene) distances to the number of methyl ring substituents is provided by the identical Fe–C (ring) distances of 2.12 Å (ave.) found in the structure of both the π-(toluene)-^{12} and π-(mesitylene)ferracarboranes.
[35]J. L. Spencer M. Green and F. G. A. Stone, *J. Chem. Soc., Chem. Commun.* 1972, 1178.
[36]M. Tsutsui and H. Zeiss, *Naturwissenschaften.* 1957, **44**, 420.
[37]R. A. Zelonka and M. C. Baird, *J. Organometal. Chem.* 1972, **44**, 383.
[38a]Ref. 20, Chap. 2. [b]K. P. Callahan and M. F. Hawthorne, *Adv. Organometal. Chem.* 1976, **14**, 145.

Polyhedron Vol. 1, No. 1, pp. 83–87, 1982
Printed in Great Britain.

0277–5387/82/010083–05$03.00/0
Pergamon Press Ltd.

TRIPHENYLPHOSPHONIUM AND TRIMETHYLPHOSPHONIUM HEXACHLOROOSMATES (IV) AND THEIR REACTIONS WITH ALKYLATING AGENTS; METHYL AND TRIMETHYLSILYLMETHYL OSMIUM COMPOUNDS; *TRANS*-DICHLOROTETRAKIS(TRIMETHYLPHOSPHINE)-OSMIUM(II); TETRAKIS(TRIMETHYLSILYLMETHYL)OXOOSMIUM(VI)

ALFREDO S. ALVES, DAVID S. MOORE, RICHARD A. ANDERSEN and GEOFFREY WILKINSON*
Chemistry Department, Imperial College, London, SW7 2AY, and Chemistry Department, University of California, Berkeley, CA 94721, U.S.A.

(*Received* 6 *August* 1981)

Abstract—The reported synthesis of tetrachlorobis(triphenylphosphine) osmium(IV) is shown to proceed via initial formation of a salt, $[Ph_3PH]_2[OsCl_6]$, from which the corresponding $[Me_3PH]^+$ salt can be obtained by exchange; the latter salt reacts with acetone to give $[Me_3PC(OH)Me_2]_2[OsCl_6]$. The action of methyl and trimethylsilylmethyl alkylating agents on the hexachloroosmates and on $OsCl_3(PPh_3)_3$ to give σ-alkyls is reported. The complex *trans*-$OsMe_2(PPh_3)_4$ reacts with carbon monoxide to give the corresponding bis acetyl. The complex *trans*-$OsCl_2(PMe_3)_4$ is resistant to attack by alkylating agents. The interaction of bis(trimethylsilylmethyl)magnesium with OsO_4 in pentane at −70°C yields $(Me_3SiCH_2)_4OsO$.

INTRODUCTION

Osmium compounds with metal–carbon σ bonds have been recently reviewed.[1] Relatively few tertiary phosphine complexes with alkyl or aryl groups are known: these are mainly chelating diphosphine complexes of the type $OsXR(diphos)_2$ (where X may be Cl, R = Me, Et, X, R = Me, Ph) hydrido, alkyl or aryl compounds derived from the halides by $LiAlH_4$ reduction,[2] and carbonyl compounds $OsClR(CO)(PPh_3)_2$.[3]

We now report some alkyls derived from phosphonium salts of the hexachloroosmate(IV) ion, from $OsCl_3(PPh_3)_3$ and from OsO_4.

A. OSMIUM(IV) HALIDE COMPLEXES AND THEIR ALKYLATION REACTIONS

1. *Triphenylphosphine complexes*

On attempting to prepare *trans*-$OsCl_4(PPh_3)_2$ by the method of Kahar *et al.*[4] a yellow solid was isolated and shown to be the salt $[Ph_3PH]_2[OsCl_6]$. Thus, the IR spectrum has a band at 2425 cm^{-1} [ν(P–H)] and a strong Os–Cl stretch at 301 cm^{-1}. The conductivity in nitromethane corresponded to that of a 2 : 1 electrolyte. X-ray crystallographic study[5] has confirmed the salt formulation; the two phosphonium ions are located at opposite faces of the octahedral ion and orientated so that the hydrogen bound to phosphorus points towards the face as in (**1**). The P–H bond length is 1.22Å. On crystallisation of this salt from *hot* acetone, the dark brown crystals of $OsCl_4(PPh_3)_2$, identical with those reported[4] are obtained and X-ray study[5] confirms the octahedral geometry with *trans*-PPh_3 groups. The conversion of the phosphonium salt to the neutral complex in acetone can be monitored by ^{13}C NMR spectra; there is no evidence of any stable intermediates.

The reaction of $[Ph_3PH]_2[OsCl_6]$ with an excess of MeLi and Ph_3P in benzene produces two products that can be separated either by low temperature extraction with petroleum or by chromatography. These compounds were identified spectroscopically and analytically as *trans*-$OsMe_2(PPh_3)_4$ and $OsH(Me)(C_6H_4PPh_2)(PPh_3)_2$. The presence of the ortho metallated group in the latter was confirmed by bands in the IR spectrum at 1590, 1085 and 740 cm^{-1}.[6]

The dimethyl compound reacts readily at ambient temperature with carbon monoxide (2 atm) and the reaction can be monitored by IR and NMR spectra. Thus, the ^1H NMR spectrum shows the disappearance of the Os–*Me* resonance at δ 0.02 ppm and the appearance of an acetyl resonance at δ 1.3 ppm. In the IR spectrum a new band at 1940 cm^{-1} (Os–CO) appears initially but disappears with the concommitant appearance of the acyl band at 1830 cm^{-1}. We have been unable to isolate the carbonyl or monoacyl intermediates, however, but it seems likely that the first species formed is $OsMe_2(PPh_3)_3(CO)$ resulting from dissociation of PPh_3 and coordination of CO to which methyl is then transferred. The two methyl groups are transferred successively since they are in *trans* positions and there is no evidence for the formation of acetone which might have been expected from a group transfer of methyl in *cis* positions.[7]

By contrast with the above alkylations giving Os^{II} and Os^{III} species the interaction of $[Ph_3PH]_2[OsCl_6]$ with MeMgI in diethylether gives a red-brown solution from which $OsMe_4(PPh_3)_2$ can be isolated as an air-sensitive solid.

The interaction of $[Ph_3PH]_2[OsCl_6]$ with Me_3SiCH_2MgCl in diethyl ether also produces an orthometallated osmium(III) species $OsH(CH_2SiMe_3)(C_6H_4PPh_2)(PPh_3)$ similar to the methyl compound noted

above; the IR spectrum again has typical bands at 1585, 1430, 1085 and 730 cm^{-1}.

2. *Trimethylphosphine complexes*

The interaction of $[Ph_3PH]_2[OsCl_6]$ with excess PMe_3 in toluene at 80°C produces the exchanged salt $[Me_3PH]_2[OsCl_6]$ which has a conductance corresponding to a 2 : 1 electrolyte. The IR spectrum shows the P–H stretch at 2470 cm^{-1} and an Os–Cl stretch at 305 cm^{-1}. The ^{31}P NMR spectrum has a main doublet [J(P–H) = 513 Hz] each line split into a 10 line multiplet [J(P–CH) = 10 Hz] due to coupling with the methyl group protons.

On recrystallisation from acetone, a second phosphonium salt is obtained. This shows IR bands at 3440 and 3394 cm^{-1}(OH); 1380–70, 1360–50, 1122 cm^{-1} (R_3COH); and 305 cm^{-1} (OsCl). The ^{31}P NMR spectrum has a multiplet at δ +41.3 ppm [J(P–CH) = 16.88 Hz] while the ^1H NMR spectrum has lines corresponding to Me_3P (δ 1.7, d, J = 11 Hz), $PCMe_2OH$ (δ 1.2, d, J = 12 Hz) and OH (δ 6.2, d, J = 3.8 Hz). The spectroscopic data suggests that the salt is $[Me_3PCMe_2OH]_2[OsCl_6]$ and this formulation has been substantiated by a full X-ray crystallographic study.[8] In the crystal the hydroxyl hydrogen is hydrogen-bonded to one of the chlorines of the $[OsCl_6]^{2-}$ anion [H ... Cl = 2.49Å] in which there is a corresponding lengthening of the Os–Cl bond [2.345Å compared to 2.270Å] as in (2). The interaction of P–H bonds with acetone has been suggested to proceed by nucleophilic attack at the carbonyl carbon followed by proton transfer in reactions of the type:[9]

$$Ph_2PH + R_1R_2C{=}O \rightarrow Ph_2P{-}C(OH)R_1R_2.$$

In the present case, the following reactions seem reasonable:

$$MePH^+ \rightleftharpoons Me_3P + H^+$$

$$Me_2CO + H^+ \rightleftharpoons Me_2C^+OH$$

$$MeC^+OH + :PMe_3 \rightarrow [Me_2C(OH)PMe_3]^+.$$

Unlike the case with triphenylphosphonium hexachloroosmate no neutral species is formed even on prolonged reaction. The failure of the $[Ph_3PH]^+$ ion to react is probably due to the lower basicity of Ph_3P. In anhydrous acetone $ReCl_5$ and PPh_3 react to give $[Ph_3PC(Me)_2CH_2C(O)Me]^+[ReCl_5PPh_3]^-$ and the cation was also obtained from K_2ReCl_6, PPh_3 and HCl in acetone but here the reaction was proposed to proceed via acid catalysed condensation of acetone to mesityl oxide followed by Michael addition to PPh_3.[10]

The interaction of $[Me_3PH]_2[OsCl_6]$ with Me_3SiCH_2MgCl produces two products. When the salt is in excess, $OsCl_3(CH_2SiMe_3)(PMe_3)_2$ is obtained and when the Grignard reagent is in excess, a dimer, $Os_2Cl(CHSiMe_3)_2(PMe_3)_5$. The latter appears to have lost a hydrogen from the Me_3SiCH_2 groups[11] to form bridges as in (3); the ^1H NMR spectrum has resonances at δ −0.1 and −0.3 ppm with a ratio of 1 : 9 (CH and SiMe_3) while the methyl groups of the non-equivalent PMe_3 groups have resonances at δ 1.8 t, 1.3 d and 1.15 ppm. The compound thus appears to have two five-coordinate osmium atoms in different (II, III) formal oxidation states wth a different number of PMe_3 groups on each atom. There are precedents for unusual asymmetric structures in PMe_3 complexes.[12] Unfortunately, we have been unable to obtain crystals suitable for X-ray crystallography.

B. REACTIONS OF TRICHLORO *TRIS*(TRIPHENYLPHOSPHINE) OSMIUM

The complex *fac*-$OsCl_3(PPh_3)_3$[4] and Me_3SiCH_2MgCl in toluene react to produce what is clearly according to analytical and spectroscopic data an orthometallated triphenylphosphine osmium(IV) complex, $OsHCl(CH_2SiMe_3)(C_6H_4PPh_2)(PPh_3)$, presumable via initial reduction to an Os^{II} intermediate which then undergoes oxidative addition.

On attempting to convert $OsCl_3(PPh_3)_3$ into $OsCl_2(PPh_3)_3$[13] by the same procedure used to prepare the latter from $(NH_4)_2OsCl_6$ and Ph_3P, namely refluxing in aqueous *t*-butanol, the product was a yellow solid, $OsCl_3(PPh_3)_2$. Neither this complex nor $OsCl_3(PPh_3)_3$ appear to undergo exchange with PMe_3 under conditions we have tried but $OsCl_2(PPh_3)_3$ does so quite readily to give *trans*-$OsCl_2(PMe_3)_4$. The structure of the latter has been confirmed by X-ray diffraction study;[5] the four PMe_3 ligands adopt a pseudo tetrahedral arrangement about the osmium atom. This complex is extremely resistant to attack and may be recovered unchanged after treatment in toluene, ether or tetrahydrofuran with Li, Mg and Al methyls, $NaBH_4$, $LiAlH_4$ and Na/K liquid alloy.

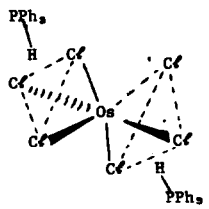

(1)

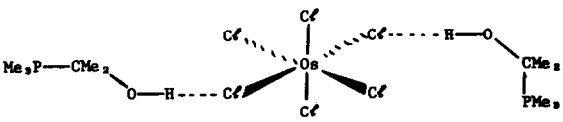

(2)

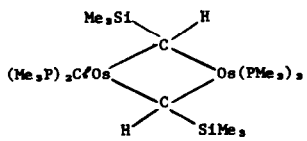

(3)

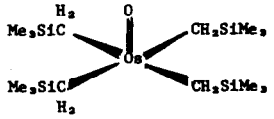

(4)

It is appropriate to note that although several of the above osmium compounds are odd electron species, sharp NMR spectra were obtained. Electron paramagnetic resonance spectra of $OsH(CH_2SiMe_3)(C_6H_4PPh_2)(PPh_3)$ and its methyl analogue, as well as some osmium(III) carboxylate complexes[14], gave only very weak signals at *ca.* 100°K in the $g = 2$ region. The weakness is probably a result of fast spin-lattices interaction at this temperature.

C. TETRAKIS(TRIMETHYLSILYLMETHYL) OXOOSMIUM(VI)

Addition of three molar equivalents of $(Me_3SiCH_2)_2Mg$ to a pentane solution of OsO_4 at −70°C yields a dark brown-red solution from which $(Me_3SiCH_2)_4OsO$ can be isolated as brown-yellow crystals which melt at *ca.* 15°C to a light brown liquid. The oxygen- and water-stable oxoalkyl is diamagnetic (by Evans' method) and monomeric (by mass spectroscopy). The IR spectrum shows an absorption at 1040 cm^{-1} assignable to the Os=O stretch, in addition to bands due to Me_3SiCH_2 groups.

The ^1H NMR spectrum, which is unchanged from +25 to −80°C, consists of single resonances at δ 4.00 and 0.42 ppm in an area ratio of 2:9. The $^{13}C\{^1H\}$ NMR spectrum has resonances at δ 38.7 and 1.76 ppm, the former due to CH_2 and the latter to the trimethylsilyl carbon atoms. Since the molecule appears to be rigid, the equivalence of the Me_3SiCH_2 groups indicate a square pyramidal structure (4). A similar geometry has been deduced by epr spectroscopy for the related oxoalkyl $(Me_3SiCH_2)_4ReO$.[15]

We suggest the mechanism of alkylation is similar to that found for nucleophilic substitution at an organic carbonyl group by Grignard reagents.[16] At some stage along the pathway, a reductive-elimination reducing Os^{VIII} to Os^{VI}, must also occur.[17] This alkylation mechanism also accounts for the earlier observation that hexamethylrhenium results from reaction of tetramethyloxorhenium(VI) and trimethylaluminum.[18]

The oxoalkyl does not react with trimethylaluminum, trimethylphosphine, or carbon monoxide (18 atm).

EXPERIMENTAL

Microanalyses by the Imperial College and Pascher Laboratories.

Instruments. IR: Perkin–Elmer 597. NMR: Perkin–Elmer R32 (^1H, 90 MHz), Bruker WM-250; ^1H referenced to Me_4Si, ^{31}P to 85% external H_3PO_4 (positive values to low field) in ppm. Epr: Varian E-12 (X-band). Molecular weights were determined cryoscopically in benzene.

Materials. Solvents were dried over sodium benzophenone or sodium and distilled before used; petroleum used had b.p. 40–60°C. The osmium starting materials were from Johnson Matthey Ltd. Reactions were carried out under nitrogen or argon.

PHOSPHONIUM SALTS

1 *Bis(triphenylphosphonium) hexachloroosmate(IV)*

The procedure of Ref. 4 was followed. $(NH_4)_2OsCl_6$ (0.8 g, 1.8 mmol) in 100 cm^3 conc. HCl-methanol (1:2) was refluxed for 30 min. To the hot solution was added Ph_3P (0.5 g, 1.9 mmol in 10 cm^3 MeOH) and the solution refluxed for 4 hr, when it was filtered hot and the yellow-brown solid collected, washed with hot MeOH (20 cm^3) and ether (20 cm^3) and dried in vacuum at 80°C. Recrystallisation from dichloromethane gave yellow crystals. Yield, 0.7 g, 42%; m.p., 280°C. [Found: C, 46.7 (47.0); H, 3.8 (3.5); Cl, 23.0 (22.5); P, 4.9 (5.5)%]. $\Lambda_M(MeNO_2)$, 180 ohm cm^2 mol^{-1}.

Tetrachlorobis(triphenylphosphine) osmium[4] was obtained from the salt (0.1 g) by dissolution in hot acetone (10 cm^3) which was concentrated to 5 cm^3 and then allowed to evaporate at room temperature leaving large diamond shaped black crystals, which were washed with hexane and air-dried. Yield *ca.* 50%. NMR (MeCN): ^1H δ 7.05 ppm; ^{31}P δ −2.23, s, ppm (*trans*-PPh_3). IR: Os–Cl, 305 cm^{-1}.

2 *Bis(trimethylphosphonium) hexachloroosmate(IV)*

The $[Ph_3PH]^+$ salt (0.8 g) was stirred with Me_3P (4 cm^3) in toluene (20 cm^3) in a pressure bottle at 80°C for 18 hr. The solution was filtered and the solid washed with toluene and light petroleum and dried in vacuum. Yield 0.48 g, 95%, m.p. 340°C. [Found: C, 13.3 (12.9); H, 3.6 (3.7); Cl, 38.3 (38.2); P 8.7 (10.0)%]. $\Lambda_M(MeNO_2)$, 200 Ω cm^2 mol^{-1}.

3 *Bis(propan-2-ol-2-trimethylphosphonium) hexachloroosmate(IV)*

The $[Me_3PH]^+$ salt was dissolved in 20 cm^3 of hot acetone–methanol (2:1) and the solution filtered, concentrated to 7 cm^3 and cooled at −17°C to yield orange-yellow crystals which were collected washed with methanol (3 × 1 cm^3) and hexane (5 cm^3) and air-dried. Yield *ca.* 70%, m.p. 298°C [Found: C, 21.3 (22.0); H, 4.7 (4.9); Cl, 32.1 (32.4)]. $\Lambda_M(MeNO_2)$, 170 ohm^{-1} cm^2 mol^{-1}.

4 *Interaction of* $[Ph_3PH][OsCl_6]$ *with Methyllithium: trans-Dimethyltetrakis(triphenylphosphine) osmium(II) and Hydrido(methyl)(η^2-diphenylphosphinophenyl) bis(triphenylphosphine) osmium(III)*

The salt $[Ph_3PH]_2OsCl_6$ (1.6 g, 2 mmol) in benzene (20 cm^3) containing excess Ph_3P (2.0 g, 7.6 mmol) was stirred until the solution was homogeneous, when methyl-lithium (10 cm^3 of 1.3 M solution in Et_2O) was added. After stirring for 3 hr at ambient temperature, 15 cm^3 degassed water was added at 0°C, the organic layer separated and the aqueous phase extracted with benzene (3 × 10 cm^3). The combined extracts were dried ($CaSO_4$), filtered, and evaporated in vacuum. The yellow residue was extracted with petroleum (3 × 20 cm^3) the extracts concentrated to *ca.* 15 cm^3 and cooled at −20°C for 12 hr to give a pale yellow solid which was recrystallised from petroleum as $OsMe_2(PPh_3)_4$. Yield 0.5 g, 27%, m.p. (decomp.) 130°C. [Found: C, 69.2 (69.8); H, 5.2 (5.2); P, 8.0 (7.9)%]. NMR: ^1H δ 0.02 (Me) 7.18, 7.49 m (Ph); ^{31}P δ 5.6. The *trans*-dimethyl formulation is confirmed by the *ortho* and *meta* separation of phenyl protons (0.3 ppm)[19].

The residue remaining after the petroleum extraction was washed with petroleum (3 × 10 cm^3) at −70°C dried in vacuum and recrystallised from toluene–petroleum (1:1) at −20°C as yellow-brown microcrystals of $OsH(Me)(\eta^2\text{-}C_6H_4PPh_2)(PPh_3)_2$. Yield: 0.4 g, 24%; m.p. (decomp.) 180°C. [Found: C, 65.4 (65.8); H, 5.8 (6.2); P, 8.9 (9.2)%]. NMR: ^1H δ 0.31 (4 × Me), −9.5 weak m (H), 7.09 m (Ph).

Both compounds are air-sensitive; they are soluble in hydrocarbons but decompose in MeOH, EtOH, $CHCl_3$, etc.

5 *Trans-bis(acetyl)tetrakis(triphenylphosphine) osmium(II)*

The above dimethyl compound (0.1 g) was dissolved in petroleum (5 cm^3) under argon and the solution then treated with CO (2 atm). Removal of solvent after *ca.* 12 hr left a white solid, which was recrystallised from

toluene. Yields are essentially quantitative. [Found: C, 68.0 (68.8); H, 5.1 (5.0); P, 9.4 (9.4)%]. The formulation as the *trans*-bis(acetyl) is confirmed by the *ortho* to *meta* separation of the phenyl protons (0.3 ppm)[19] in the ^{1}H NMR spectrum and by the ^{31}P NMR spectrum, δ − 4.22 ppm (s).

6 *Tetramethylbis(triphenylphosphine) osmium(IV)*

To a stirred solution of $[Ph_3PH]_2[OsCl_6]$ (0.21 g) in Et_2O (10 cm^3) at −70°C was added dropwise MeMgI (1.5 cm^3 of 1.3 *M* solution in Et_2O) and the mixture stirred at ambient temperature for 3 d. The solution was filtered and the solvent removed; extraction of the oily residue with petroleum (3 × 10 cm^3), concentration to 15 cm^3 and cooling at −20°C gave a brown-red crystalline solid which was collected, washed with petroleum and dried in vacuum. Yield 0.03 g, 17%; m.p. (decomp.) 80°C. [Found: C, 62.5 (62.2); H, 5.7 (5.4); P, 7.0 (8.0)%. *M* 700 (774)]. NMR: ^{1}H 0.31 (4 × Me), 7.09 m (6 × Ph); the *trans* formulation of PPh_3 groups is established by the same criterion[19] as above (0.65 ppm).

The compound is soluble in hydrocarbons decomposes in $CHCl_3$, CH_2Cl_2, Me_2CO and thf and is insoluble in pyridine, MeOH and EtOH.

7 *Hydrido (trimethylsilylmethyl) (η^2 - diphenylphos - phinophenyl) triphenylphosphine osmium(III)*

To $[Ph_3PH]_2[OsCl_6]$ (0.86 g) in Et_2O (20 cm^3) at −70°C was added Me_2SiCH_2MgCl (5 cm^3 of 1.6 *M* solution in Et_2O). After 1 hr the solution was allowed to warm to room temperature and after 12 hr stirring the solvent was removed and the residue extracted with petroleum (3 × 20 cm^3). The extract was filtered, concentrated (10 cm^3), and cooled to −20°C for 12 hr when the yellow-brown crystals were collected, washed with petroleum and dried in vacuum. Yield 0.3 g, 40%; m.p. 170°C. [Found: C, 59.4 (59.8); H, 5.1 (5.1); P, 7.6 (7.7)%]. NMR: ^{1}H; −10.6 m (H); 0.3 ($SiMe_3$), 0.75 (CH_2), 7.7–7.0 (Ph).

8 *Hydrido (chloro) (trimethylsilylmethyl) (η^2 - diphenyl phosphinophenyl) triphenylphosphineosmium(III)*

To *fac*-$OsCl_3(PPh_3)_3$ (0.84 g) in toluene (40 cm^3) was added Me_3SiCH_2MgCl (3.5 cm^3, 1.65 *M* in Et_2O) and the solution stirred for 30 min at −70°C and again at room temperature for 2 d. Work up as in 7, but extracting with toluene gave a microcrystalline brown solid. Yield 0.15 g (24%); m.p. (decomp.) 140°C. [Found: C, 56.9 (56.9); H, 4.8 (4.8); Cl, 3.8 (4.1); P, 7.1 (7.9)%. *M* 720 (836)]. NMR: ^{1}H, −9.2 m (H); 0.3 ($SiMe_3$); 0.7 (CH_2); 6.5–8.0 br (Ph). The compound is soluble in aromatic solvents and cyclohexane, slightly soluble in petroleum and reacts with Me_2SO, $CHCl_3$ and CH_2Cl_2.

9 *Trichloro(trimethylsilylmethyl)bis(trimethylphosphine) osmium(IV)*

To $[Me_3PH]_2[OsCl_6]$ (0.89 g) in thf (60 cm^3) at −70°C was added Me_3SiCH_2MgCl (3 cm^3 of 1.3 *M* solution in Et_2O) and the solution stirred for 20 min followed by 2 d at room temperature. The filtered solution was evaporated and the oily residue extracted with petroleum (2 × 20 cm^3) which was evaporated in vacuum and the residue crystallised from toluene at −40°C to give red-brown crystals. Yield, 0.42 g, 44%; m.p. > 340°C. [Found: C, 24.4 (24.0); H, 6.1 (5.8); Cl, 21.0 (21.0); P, 6.3 (8.3)%]. *M* 400 (535)]. NMR: −0.22 (CH_2); −0.1 ($SiMe_3$); 1.1 (PMe_3).

10 *Chloro bis (μ-trimethylsilylmethylidene) pentakis (trimethylphosphine) di - osmium(II, III)*

To $[Me_3PH]_2[OsCl_6]$ (1.0 g) in tetrahydrofuran (80 cm^3) at −70°C was added Me_3SiCH_2MgCl (6 cm^3 of 1.3 *M* solution in Et_2O) and the solution stirred for 3 min at −70°C and *ca.* 1 d at room temperature. After removal of solvent the residue was extracted with petroleum (50 cm^3) which was concentrated to *ca.* 5 cm^3. Elution from a cellulose column with toluene gave a yellow-red fraction which was collected, concentrated to *ca.* 3 cm^3 and cooled to −40°C to give red microcrystals which were washed with chilled petroleum and dried in vacuum. Yield 0.25 g, 30%; m.p. (decomp.) 130°C. [Found: C, 29.0 (28.5); H, 6.7 (6.9); Cl, 3.7 (3.7); P, 14.5 (15.4)%. *M* 880 (968)].

11 *Trichlorobis(triphenylphosphine) osmium(III)*

A solution of *fac*-$OsCl_3(PPh_3)_3$[4] (1 g) in Bu^{t}OH (25 cm^3) and water (1 cm^3) was refluxed for 3 d. The resulting yellow solid was collected, washed with water (3 × 5 cm^3), methanol (3 × 5 cm^3) and ether (2 × 10 cm^3) and dried in vacuum over NaOH pellets. Yield 0.7 g, 83% m.p. 160°C. [Found: C, 52.0 (52.5); H, 3.8 (3.8), Cl, 12.8 (12.8); P, 6.3 (6.8)%. *M* 800 (820)].

12 *trans-Dichlorotetrakis(trimethylphosphine) osmium(II)*

The complex $OsCl_2(PPh_3)_3$[13] (1.0 g, 1.8 mmol) and PMe_3 (2 cm^3) in toluene (20 cm^3) were dried at 80°C in a pressure bottle for 20 hr after which the solvent was removed and the yellow solid washed with petroleum (3 × 15 cm^3). Recrystallisation from toluene–petroleum (1 : 1) gave a yellow-gold crystals of quality suitable for X-ray study. Yield, 0.5 g, 83%; m.p. > 350°C. [Found: C, 25.8 (25.5); H, 6.4 (6.3); Cl, 12.6 (12.5); P, 20.6 (21.6)%. *M* 600 (565)].

13 *Tetrakis(trimethylsilymethyl) oxoosmium(VI)*

Bis(trimethylsilylmethyl) magnesium (6.7 cm^3 of a 1.0 *M* Et_2O solution, 0.0067 mol) was added to osmium tetraoxide (0.85 g, 0.0033 mol) in pentane (50 cm^3) at −70°C. The dark brown suspension was stirred for an additional 2 hr. The volatile material was removed in vacuum and residue was extracted with pentane (50 cm^3), filtered, and concentrated to *ca.* 10 cm^3. Chromatography on silica gel with pentane, elution followed by concentration to *ca.* 2 cm^3 and cooling to −70°C gave the brown-yellow *needles* which were collected and dried in vacuum. Yield: 0.45 g, 12%, m.p., *ca.* 15°C. [Found: C, 34.3 (34.5); H, 8.0 (7.9)%].

Acknowledgements—We thank the Brazilian Science Research Council (A.S.A.) and S.E.R.C. (D.S.M.) for support, Dr. J. F. Gibson for epr measurements and Johnson Matthey Ltd. for loan of osmium salts.

REFERENCES

[1]D. S. Moore, *Coord. Chem. Revs.* 1982, in press.
[2]J. Chatt and R. G. Hayter, *J. Chem. Soc.* 1963, 6017.
[3]W. R. Roper and L. J. Wright, *J. Organometal. Chem.* 1977, **142**, C1.
[4]M. M. T. Kahar, S. S. Ahamed and R. A. Levenson, *J. Inorg. Nuclear Chem.* 1976, **38**, 1135.
[5]A. C. Skapski, Imperial College, private communication.
[6]D. J. Cole-Hamilton and G. Wilkinson, *J. Chem. Soc., Dalton Trans.* 1977, 797; W. Keir, *J. Organometal. Chem.* 1968, **14**, 179.
[7]See, e.g. E. Carmona-Guzman and G. Wilkinson, *J. Chem. Soc., Dalton Trans.* 1978, 1139.

[8]M. B. Hursthouse, Queen Mary College, private communication.
[9]E. Evargelidou-Tsolis, F. Ramirez, J. F. Pilot and C. P. Smith, *Phosphorus* 1974, **4**, 109.
[10]H. Gerkke Jr., and G. Eastland, *Inorg. Chem.* 1970, **9**, 2722, *J. Inorg. Nuclear Chem.* 1970, **32**, 867.
[11]M. Bochmann, G. Wilkinson, A. M. R. Galas, K. M. A. Malik and M. B. Hursthouse, *J. Chem. Soc. Dalton Trans.* 1980, 1797.
[12]See, e.g., R. A. Andersen, R. A. Jones and G. Wilkinson, *J. Chem. Soc., Dalton Trans.* 1978, 466.
[13]P. R. Hoffman and K. G. Caulton, *J. Am. Chem. Soc.*, 1975, **15**, 4221.
[14]D. S. Moore, A. Alves and G. Wilkinson, *J. Chem. Soc., Chem. Commun.* 1982, in press.
[15]J. F. Gibson, K. Mertis and G. Wilkinson, *J. Chem. Soc., Dalton Trans.* 1975, 1093.
[16]E. C. Ashby, J. Laemmle and H. M. Neumann, *Accts. Chem. Res.* 1974, **7**, 272.
[17]P. S. Braterman and R. J. Cross, *Chem. Soc. Revs.* 1973, **2**, 271.
[18]K. Mertis and G. Wilkinson, *J. Chem. Soc., Dalton Trans.* 1976, 1488.
[19]D. S. Moore and S. D. Robinson, *Inorg. Chim. Acta* 1981, **53**, L171.

Polyhedron Vol. 1, No. 1, pp. 89–95, 1982
Printed in Great Britain.

0277–5387/82/010089–07$03.00/0
Pergamon Press Ltd.

SYNTHESIS AND ^{31}P NMR SPECTRA OF SOME PLATINUM(II) COMPLEXES OF THE PHOSPHA-ALKENE, (MESITYL)P=CPh$_2$

CRYSTAL AND MOLECULAR STRUCTURE OF *cis*-[PtCl$_2$(PEt$_3$)(C$_6$H$_2$Me$_3$P=CPh$_2$)]·CHCl$_3$

HAROLD W. KROTO, JOHN F. NIXON* and MICHAEL J. TAYLOR
School of Chemistry and Molecular Sciences, University of Sussex, Brighton BN1 9QJ, Sussex, England

and

AILEEN A. FREW and KENNETH W. MUIR
Chemistry Department, The University, Glasgow, G128QQ, Scotland

(*Received* 14 *August* 1981)

Abstract—Syntheses of the phospha-alkene complexes *cis*- and *trans*-[PtCl$_2$(PEt$_3$)(mesityl)P=CPh$_2$], and *cis*-[PtX$_2$\{(Mesityl)P=CPh$_2$\}$_2$](X=Cl, I, Me) complexes are reported. ^{31}P NMR spectra indicate that bonding of the phospha-alkene to the metal is via the phosphorus lone pair and this is confirmed by a single crystal X-ray diffraction study of *cis*-[PtCl$_2$(PEt$_3$)\{(mesityl)P=CPh$_2$\}]CHCl$_3$.

INTRODUCTION

There is current interest in the chemistry of trivalent phosphorus compounds in which phosphorus is one or two coordinate. Recently we and others[1–4] have developed synthetic routes to novel compounds containing carbon multiply bonded to phosphorus, viz. phospha-alkenes, R$_2$C=PR′, and phospha-alkynes, RC≡P.

In a preliminary report[5] we described a number of transition metal complexes of the phosphaalkene C$_6$H$_2$Me$_3$P=CPh$_2$,[3] (C$_6$H$_2$Me$_3$ = mesityl). NMR studies on complexes of tungsten(0), rhodium(I) and platinum(II) indicated that in all cases the bonding of the phospha-alkene to the transition metal was via the phosphorus lone pair as in (A) rather than as in (B).

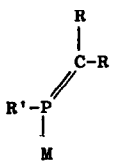

(A)

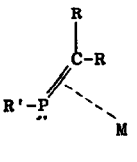

(B)

These results complemented observations by Niecke[6] and Scherer[7] on complexes containing the isoelectronic R′PNR and RPO ligands.

We now report details of a number of platinum(II) complexes of (mesityl)P=CPh$_2$ and the crystal and molecular structure of the chloroform solvate of *cis*-[PtCl$_2$(PEt$_3$) (mesityl)P=CPh$_2$] which confirms the nature of the metal–ligand bonding.

RESULTS AND DISCUSSION

Many amine and phosphine ligands, L, cleave the bridge of the dinuclear complex [Pt$_2$Cl$_4$(PEt$_3$)$_2$] to afford *trans*-complexes [PtCl$_2$(PEt$_3$)L]. The ^{31}P{^{1}H} NMR spectrum of a dichloromethane solution of [Pt$_2$Cl$_4$(PEt$_3$)$_2$] and (mesityl)P=CPh$_2$, shown in Fig. 1,

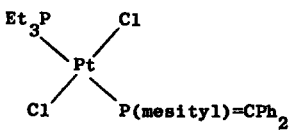

(I)

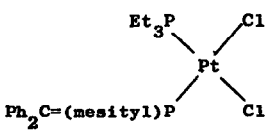

(II)

consists of two "triplets" from coupling to ^{195}Pt each line exhibiting a further large ^{2}J(PP′) coupling (544 Hz) typical of formation of the *trans*-isomer of [PtCl$_2$\{(mesityl)P=CPh$_2$\}(PEt$_3$)], (I), in which the phosphaalkene is coordinated via the phosphorus lone pair. Coupling constant data are listed in Table 1.

Removal of solvent from the solution of (I) gave a yellow oil from which a yellow solid, (II), can be obtained from pentane. The ^{31}P{^{1}H} NMR spectra of (II) shown in Fig. 2 indicated that it was the *cis*-isomer of (I) since the magnitude of ^{1}J(PtP) was greatly increased while ^{2}J(PP′) was only 23 Hz (Table 1). The IR spectrum of (II) exhibited two (Pt–Cl) bands at 315 and 290 cm^{-1} expected for a *cis*-complex. A solid sample of (I) could not be obtained pure but the IR of a mixture of (I) and (II) exhibited an additional band at 335 cm^{-1} which is assigned as ν(Pt–Cl) for (I).

The complex *trans*-[PtCl$_2$(PEt$_3$)\{PCl(mesityl)CHPh$_2$\}], (III), was also prepared from [Pt$_2$Cl$_4$(PEt$_3$)$_2$] and its reaction with dbu (dbu = 1,5 - diazabicyclo - [5,4,0]*trans* -

*Author to whom correspondence should be addressed.

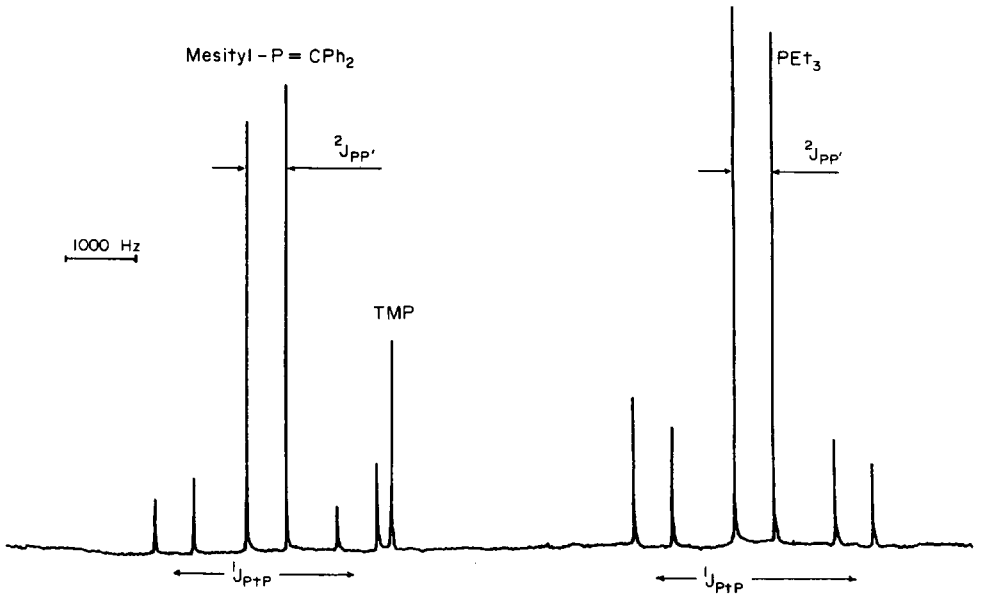

Fig. 1. ^{31}P NMR spectrum of *trans*-[$PtCl_2(PEt_3)$(mesityl)P=CPh_2)].

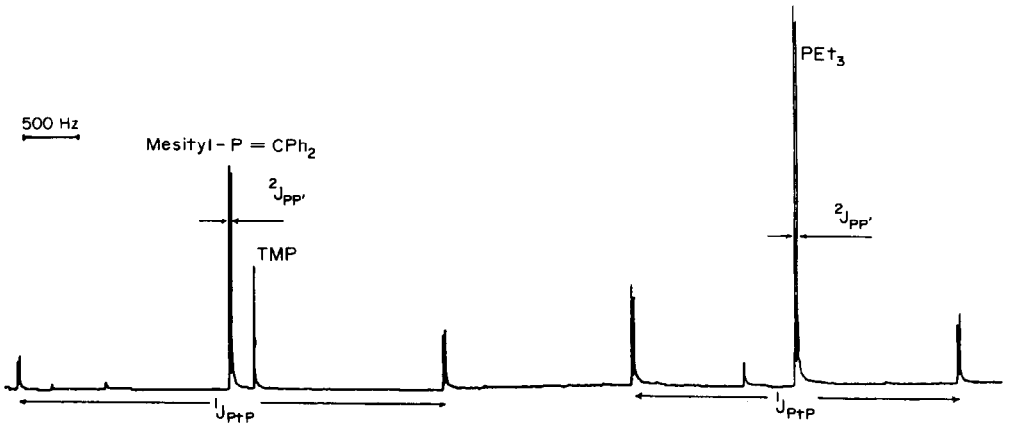

Fig. 2. ^{31}P NMR spectrum of *cis*-[$PtCl_2(PEt_3)$(mesityl)P=CPh_2)].

Table 1. ^{31}P NMR data for some $PtCl_2LL'$, complexes

L	L'		$^1J_{PtL}$ [c]	$^1J_{Pt(PEt_3)}$ [c]	$^2J_{PP'}$ [c]
(mesityl)P = CPh_2 [a]	PEt_3	cis	4294	3269	23
(mesityl)P = CPh_2 [a]	PEt_3	trans	2590	2844	544
PF_3 [b]	PEt_3	cis	7388	2869	19
$P(OPh)_3$ [b]	PEt_3	cis	6249	3197	22
$P(OPh_3)_2$ [b]	PBu_3	trans	4116	2570	715
PCl_3 [b]	PEt_3	cis	6054	2977	17
PPh_2Cl [b]	PEt_3	cis	5077	3164	17
PPh_3 [b]	PEt_3	cis	3815	3373	17
PEt_3 [b]	PEt_3	cis	3520	3520	17
P(Cl)(mesityl)($CHPh_2$) [a]	PEt_3	trans	2539	2647	547

(a) This work. (b) Data from refs. 8, 10, 20, 21. (c) In Hz.

undec - 5 - ene) was studied to see if hydrogen chloride could be eliminated from the coordinated chlorophosphine to afford (I). This type of reaction has been previously established by us for PCl(mesityl)$CHPh_2$ coordinated to zerovalent tungsten.[5]

The $^{31}P\{^1H\}$ NMR spectrum of the reaction mixture, however, showed only the presence of PCl(mesityl)$CHPh_2$, (mesityl)P=CPh_2 (+some phosphine oxide) and a platinum complex tentatively identified as *trans*-[$PtCl_2(PEt_3)$(dbu)], (IV), since the same product was obtained directly from [$Pt_2Cl_4(PEt_3)_2$] and dbu. In the presence of small amounts of moisture the complex hydro - 1,5 - diazabicyclo - [5,4,0] - undec - 1 - ene trichloro(triethylphosphine) platinate(II), [[dbuH] [$PtCl_3 \cdot (PEt_3)$]], is also formed.

Displacement of coordinated cyclo-octadiene (COD) from [PtX_2(COD)], (X=Cl, I, Me) by

$$[PtX_2(COD)] \rightarrow cis\text{-}[PtX_2\{(mesityl)P{=}CPh_2\}_2]$$

(mesityl)P=CPh_2 readily afforded the corresponding phospha-alkene complexes *cis*-[$PtX_2\{$(mesityl)P=$CPh_2\}_2$], (X=Cl, (V), X=I, (VI) and X=Me (VII)). The $^{31}P\{^1H\}$ NMR spectra of these complexes were simple "triplet" patterns as expected. Coupling constant data are listed in Table 2 the values of ^{1}J(PtP) being typical for *cis*-[PtX_2P_2] complexes.

^{1}J(PtP) for *cis*-[$PtCl_2\{$(mesityl)P=$CPh_2\}_2$], (V), (3950 Hz) is slightly greater than the value found in *cis*-[$PtCl_2(PEt_3)_2$], (3250 Hz), and much larger than that in *trans*-[$PtCl_2(PEt_3)_2$], (2500 Hz). The *cis*-geometry in (V) is also confirmed by the observation of two ν(Pt–Cl) stretching bands at 320 and 298 cm^{-1} in the IR spectrum. Substitution of chloride by iodide to form *cis*-[$PtI_2\{$(mesityl)R=$CPh_2\}_2$] (VI), results in an increase in ^{1}J(PtP) (4009 Hz) consistent with the poorer *trans*-influence of iodide. The *cis*-geometry for (VII), [$PtMe_2\{$(mesityl)P=$CPh_2\}_2$], is inferred by the very small value of ^{1}J(PtP) (1816 Hz) (see ^{1}J(PtP) for *cis*-[$PtMe_2(PEt_3)_2$], 1856 Hz). Bands at 550 and 522 cm^{-1} in the IR spectrum of (VII) are assigned to Pt–C stretching modes.

The magnitude of ^{1}J(PtP) in phosphine complexes of platinum is given by the expression[8]

$$^1J(PtP) = \gamma_P \gamma_{Pt} \frac{h}{2\pi} \frac{256\pi^2}{9} \beta^2 \frac{a^2(1-a^2)\alpha_P^2}{n} \times \frac{|S_P(O)|^2 |S_{Pt}(O)|^2}{^3\Delta E}$$

where γ_X is the magnetogyric ratio of nucleus X, $S_X(O)^2$ is the s-electron density of X evaluated at the nucleus, α_P^2 is the s-character of the phosphorus lone pair orbital, a^2 is the s-character of the metal hybrid orbital, n is the number of ligands and $^3\Delta E$ is an average triplet excitation energy. Changes in the magnitude of ^{1}J(PtP) within a series of platinum-phosphine complexes are largely dependent on changes in $|S(O)|^2$ and α_P^2.

Inspection of the coupling constant data in Tables 1 and 2 indicates that in complexes in which the (mesityl)P=CPh_2 is *trans* to a ligand of weak *trans* influence (e.g. in *cis*-[PtX_2L_2], X=Cl, I or *cis*-[$PtCl_2L(PEt_2)$]), the values of $^1J_{(PtP)}$ for (mesityl)P=CPh_2 are larger than those of PR_3 (or PAr_3) but lower than those of $P(OR)_3$ or PX_3 (X = halogen).

The former can be readily interpreted in terms of the greater s-character of the lone pair of (mesityl)P=CPh_2 (sp^2) compared with PR_3 (sp^3), which produces a larger α_P^2 term in the equation for ^{1}J(PtP). The s-character of the lone pair of PF_3, however, has been calculated to be *ca.* 35%[9] approximately the same as that expected for an sp^2 hybrid. Since $^1J_{(PtP)}$ for PF_3 complexes, and those of

Table 2. ^{31}P NMR data for some *cis*-[PtX_2L_2] complexes (X–Cl, Me)

L	$^1J_{(PtP)}$[a]	$^1J_{(PtCH_3)}$[a]	Ref
X = Cl			
PF_3	6462	-	22
$P(OPh)_3$	5793	-	23
(Mesityl) P = CPh_2	3950	-	This work
PPh_3	3684	-	8
$PBuPh_2$	3641	-	24
PBu_2Ph	3551	-	24
PBu_3	3500	-	24
PEt_3	3520	-	10
X = Me			
PPh_2Me	1851	68.0	25
PEt_3	1855	67.6	10
(mesityl) P = CPh_2	1816	75.0	This work

[a] In Hz.

$P(OR)_3$ where the lower electronegativity of the substituents reduces the s-character of the lone pair, are larger than those of (mesityl)P=CPh_2 it appears that the charge on phosphorus, and hence the $|\Psi_{S(P)}(O)|^2$ term also plays an important part in determining $^1J_{(PtP)}$.

In complexes where (mesityl)P=CPh_2 is *trans* to a ligand of high *trans*-influence (e.g. Me, PR_3) the magnitude of $^1J_{(PtP)}$ falls below those of the analogous PR_3 complexes. This would indicate that (mesityl)P=CPh_2 has a lower *trans* influence than PR_3, in line with their relative donor properties.[10,11]

Some support for this view comes from consideration of the Pt–Cl stretching frequencies in the complexes *cis*-$[PtCl_2L_2]$ and the magnitudes of $^2J_{(PtCH_3)}$ in the complexes *cis*-$[PtMe_2L_2]$. For *cis*-$[PtCl_2L_2]$ complexes the average νPt–Cl stretching frequency (in cm^{-1}) increases along the series:

$$L=PEt_3(294) < PPh_3(305) \sim \{(mesityl)P=CPh_2\}(309) < P(OPh_3)(322) < COD(327);$$

which is the *opposite* order of the *trans*-influence of these ligands. Likewise $^2J_{(PtCH_3)}$ (Hz) in the complexes *cis*-$[PtMe_2L_2]$ show a similar behaviour viz.

$$L=PEt_3(67.6) < PPh_3(69) < \{(mesityl)P=CPh_2\}(75) < COD(83.4).$$

SINGLE CRYSTAL X-RAY STUDIES

The results of a single-crystal X-ray analysis of the chloroform solvate of *cis*-$[PtCl_2(PEt_3)L]$, {L =(mesityl)P=CPh_2}, (II), are presented in Fig. 3 and in Table 3. Together with those recently reported for $[Cr(CO)_5L]$[12] they permit a tentative discussion of the nature of the bonding in L and of its properties as a ligand.

In both metal complexes L behaves as a mono-dentate P-donor ligand. The significant structural features of L in the two complexes are broadly similar and they are fully compatible with the proposed formulation of L as a phosphalkene with a localised P=C bond.[5] In the chromium complex the central $CrCP{=}CC_2$ skeleton deviates only slightly from planarity—the Cr–P=C–C(Ph) and C(mesityl)–P=C–C(Ph) torsion angles are 3 and 6°, respectively, whereas in the platinum complex the corresponding torsion angles are 12 and 22°. The greater distortions from planarity in the platinum complex arise both from slight deviations from planarity of the bonds radiating from P(1) and C(1) but also (and more seriously) from a twisting of the two coordination planes by *ca.* 17° about the P=C bond (see Table 3c). However, the P(1)–C(1) and P(1)–C(1C) bond lengths [1.660(9) and 1.794(10) Å] do not differ significantly from the corresponding values in the chromium complex [1.679(4) and 1.822(5) Å]. Valency angles at the donor phosphorus atom also show nearly identical distortions from an ideal trigonal-planar arrangement: in the platinum complex the C–P–C angle of 112.5(5)° is narrowed at the expense of the Pt–P–C angle of 127.5(3)° [see 109.8(2) and 130.8(2)° for corresponding angles in the chromium compound]. An implication of these narrow C–P–C angles is that the phosphorus lone pair has more s-character than would be expected from ideal sp^2-hybridisation; a not unexpected conclusion since the lone pair of a monotertiary phosphine is usually thought to have more s-character than would be expected from sp^3-hybridisation in view of the tendency for C–P–C angles in phosphine complexes to be less than 109.5° and M–P–C angles to be greater. In

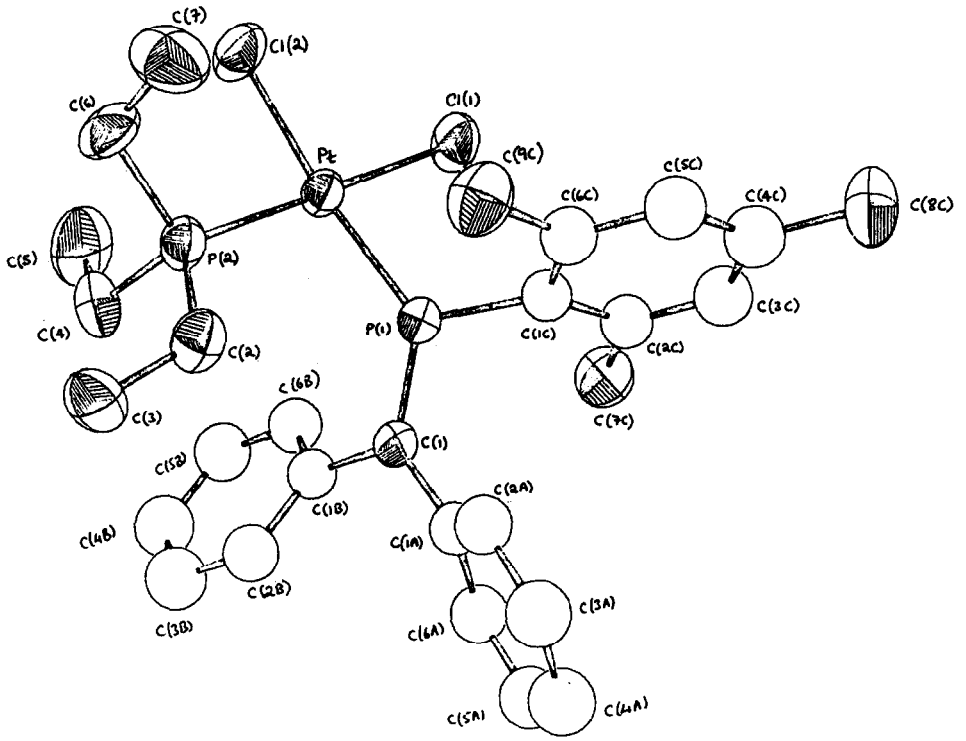

Fig. 3. A perspective view of the *cis*-$[PtCl_2(PEt_3)(C_6H_2Me_3P{=}CPh_2)]$ molecule showing the atom numbering and 50% probability ellipsoids. Anisotropic vibrational parameters were used only for shaded atoms.

Table 3. Selected distances (Å) and angles (°) in *cis*-[PtCl$_2$(PEt$_3$)(C$_6$H$_2$Me$_3$P=CPh$_2$)]

(a) Bond lengths			
Pt-Cl(1)	2.358(3)	C(4)-C(5)	1.51(2)
Pt-Cl(2)	2.335(3)	C(6)-C(7)	1.49(2)
Pt-P(1)	2.199(2)	C(1C)-C(2C)	1.42(2)
Pt-P(2)	2.256(3)	C(2C)-C(3C)	1.35(2)
P(1)-C(1)	1.660(9)	C(3C)-C(4C)	1.43(2)
P(1)-C(1C)	1.794(10)	C(4C)-C(5C)	1.38(2)
P(2)-C(2)	1.821(12)	C(5C)-C(6C)	1.39(2)
P(2)-C(4)	1.828(12)	C(6C)-C(1C)	1.41(2)
P(2)-C(6)	1.843(12)	C(2C)-C(7C)	1.53(2)
C(1)-C(1A)	1.50(2)	C(4C)-C(8C)	1.50(2)
C(1)-C(1B)	1.49(2)	C(6C)-C(9C)	1.52(2)
C(2)-C(3)	1.53(2)		

(b) Bond angles			
Cl(1)-Pt-Cl(2)	88.7(1)	Pt-P(1)-C(1)	127.5(3)
Cl(1)-Pt-P(1)	85.2(1)	Pt-P(1)-C(1C)	119.8(3)
Cl(2)-Pt-P(2)	89.6(1)	C(1)-P(1)-C(1C)	112.5(5)
P(1)-Pt-P(2)	96.6(1)	P(1)-C(1)-C(1A)	122.0(7)
Cl(1)-Pt-P(2)	177.9(1)	P(1)-C(1)-C(1B)	119.9(6)
Cl(2)-Pt-P(1)	173.4(1)	C(1A)-C(1)-C(1B)	117.9(7)
Pt-P(2)-C	111.9(4)-116.2(4)	P(2)-C-C	115(1) -117(1)
C-P(2)-C	103.8(5)-106.6(5)	At C(aromatic)	118(1) -122(1)

(c) Torsion angles			
Pt-P(2)-C(2)-C(3)	-166(1)	P(2)-Pt-P(1)-C(1)	53.7(5)
Pt-P(2)-C(4)-C(5)	-50(1)	Pt-P(1)-C(1)-C(1A)	-163(1)
Pt-P(2)-C(6)-C(7)	-56(1)	Pt-P(1)-C(1)-C(1B)	12(1)
P(1)-Pt-P(2)-C(2)	18.1(4)	C(1C)-P(1)-C(1)-C(1A)	22(1)

the platinum complex the olefinic carbon atom C(1) subtends valency angles which are all within 2 of 120°. In the chromium complex the corresponding angles are more variable with the C(Ph)–C–C(Ph) angles being narrowed to 114.8(4)°. The differences in the planarity of the central skeleton of L and in the valency angles at the olefinic carbon atom found between the platinum and chromium complexes probably have a steric origin. In the chromium complex the mesityl ring makes an angle of 81° to the central CrCP=CC$_2$ plane whereas the corresponding value in the platinum complex is 67°. The phenyl rings are tilted at 70 and 37° to the central plane in the chromium complex whereas the corresponding values are 47 and 51° in the platinum complex.

The Pt–PEt$_3$ and *trans* Pt–Cl (1) bond lengths of 2.256(3) and 2.358(3) Å are normal, being virtually identical to the mean values of 2.258(2) and 2.361(6) Å found in *cis*-[PtCl$_2$(PEt$_3$)$_2$].[13] These values may be compared with the Pt–P(1) and *trans* Pt–Cl(2) bond lengths of 2.199(2) and 2.335(3) Å. Differences in the nature of the phosphorus hybridisation would be expected to cause some shortening of the Pt–P(1) distance relative to the Pt–P(2) distance. This shortening is accompanied by a slight but detectable diminution of *trans*-influence as judged by the Pt–Cl bond lengths. The different *trans*-influences of the two P-donor ligands may reflect the different types of phosphorus hybridisation, although we have previously[14] shown that the *trans*-influences of C-donor ligands on Pt–Cl bond lengths are insensitive to the state of hybridisation of the donor carbon atom, a result in accord with current theories of σ-*trans*-influence. An alternative explanation for the slightly lower *trans*-influence of L relative to PEt$_3$ would be that L is a slightly better π-acceptor. This conclusion contrasts somewhat with the suggestion, based on the structural results for [Cr(CO)$_5$L], that L has fairly strong π-acid properties relative to other P-donor ligands.[12]

Whatever view is taken of the relative importance of σ- and π-effects in determining the platinum-ligand bond lengths in *cis*-[PtCl$_2$(PEt$_3$)L] it is interesting to note that the Pt–P and Pt–Cl distances are in accord with our previous discussion of bond lengths in complexes with *cis*-[PtCl$_2$P$_2$] donor sets.[13] The Pt–P(1) bond length is shorter than the Pt–P(2) bond length by 0.06 Å and as expected the *trans* Pt–Cl bond length is also shorter, but by roughly half this amount. Since the bond length variations can be related empirically to the electron-withdrawing of the P-donor ligand, in the sense defined by Tolman,[15] it would appear that L can be compared with P(OPh)$_3$ in terms of electron-withdrawing ability and *trans*-influence.

EXPERIMENTAL

All manipulations were carried out under an atmosphere of dry nitrogen gas or *in vacuo*. Solvents were dried by standard methods and freshly distilled before use and degassed by the repeated freeze–thaw method. ^{31}P NMR spectra were obtained using a JEOL PFT 100 Fourier transform spectrometer operating

at 40.49 MHz with broad band noise irradiation at 99.9984 MHz to decouple ^{1}H. Chemical shifts are quoted relative to H_3PO_4 with downfield positive. ^{1}H NMR spectra were recorded on Varian T60 or Varian EM360 instruments. IR spectra in the range 4000–250 cm^{-1} were recorded on a Perkin–Elmer 457 grating spectrometer. Elemental analyses were obtained by Mr. and Mrs. A. G. Olney of this laboratory.

(Mesityl)P=CPh$_2$ was prepared by a modification of the method of Ref. 3. It was imperative to dry dbu which is very hygroscopic. This was best done by adding benzene, removing the C_6H_6/H_2O azeotrope followed by distillation and storage under dry nitrogen over fresh 4 Å molecular sieve. The following platinum complexes were prepared by standard procedures, [PtCl$_2$(COD)],[16] [PtMe$_2$(COD)][16] and [Pt$_2$Cl$_4$(PEt$_3$)$_2$].[17]

Reaction of (mesityl)P=CPh$_2$ with [Pt$_2$Cl$_4$(PEt$_3$)$_2$]

(i) [Pt$_2$Cl$_4$(PEt$_3$)$_2$] (0.153 g, 0.2 mmol) in 5 cm^3 of CH_2Cl_2 was stirred for 1 hr at R.T. with (mesityl)P=CPh$_2$ (0.15 g, 0.474 mmol) to produce a solution of *trans dichloro (triethyl phosphine)(P-mesityl diphenylmethylene phosphine)platinum(II)*, (I), ^{31}P δ_p 186.9 (d of t, $^1J_{(PtP)}$ = 2590 Hz), 14.7 (d of t, $^1J_{(PtP)}$ = 2844 Hz), $^2J_{(PP')}$ = 544 Hz. Removal of solvent produced a yellow oil which was stirred with hexane to produce the *cis* isomer, (II), as a pale yellow solid. m.p. 210–212°. Found, C, 47.7; H, 5.2; $C_{28}H_{36}P_2Cl_2Pt$ requires C, 48.00; H, 5.18%. IR (KBr) 2970(m), 2940(m, br), 1650(m), 1605(m), 1490(m), 1450(s), 1410(m), 1380(m), 1260(w), 1075(w), 1035(s), 920(w, br), 890(w), 850(w), 800(w, br), 765(s), 759(s), 740(m), 695(s), 555(s), 461(m), 420(m), 315(m), 290(m) cm^{-1}. ^{1}H δ 0.8–3.0(m, 24H), 6.8–8.0(m, 12H). ^{31}P δp 149 (d of t, $^1J_{(PtP)}$ = 4294 Hz); 8.6 (d of t, $^1J_{(PtP)}$ = 3269 Hz), $^2J_{(PP')}$ = 23 Hz. A crystalline sample suitable for the x-ray diffraction study was obtained by recrystallisation from chloroform/hexane.

(ii) As above with THF as solvent. ^{31}P NMR spectrum revealed both *cis* and *trans* isomers. IR (KBr) was identical to the *cis* isomer above except for an extra ν(Pt–Cl) band at 335(m) cm^{-1}.

(iii) As in (i) above, except the phosphine was contaminated with dbu. Crystallisation from CH_2Cl_2/hexane yielded hydro - 1,5 - diazabicyclo[5,4,0] - undec - 1 - ene trichloro(triethylphosphine)platinate(II), (DBUH)(PtCl$_3$(PEt$_3$)] as yellow plates, m.p. 117–120°. Found C, 31.5; H, 6.0; N, 4.8; $C_{14}H_{30}N_2PCl_3Pt$ requires C, 31.51; H, 5.58; N, 4.91%. IR (KBr) 3270(s), 3140(w), 2935(m), 1645(s), 1580(m), 1105(w), 1039(w), 980(w), 780(s), 750(w), 728(w), 330(m). ^{1}H 3.8–1.0(m). ^{31}P δ_p10 (t, $^1J_{(PtP)}$ = 3747 Hz). (Lit. for [Et$_4$N](PtCl$_3$(PEt$_3$) 3704 Hz.[19]

Reaction of [Pt$_2$Cl$_4$(PEt$_3$)$_2$] with mesityl (CHPh$_2$)PCl

[Pt$_2$Cl$_4$(PEt$_3$)$_2$] (0.187 g, 0.243 mmol) in 5 cm^3 of CH_2Cl_2 was stirred at R.T. with mesityl (CHPh$_2$)PCl (0.18 g, = 0.51 mmol) for 2 hr. Removal of solvent yielded a yellow solid which was washed with 2 cm^3 of hexane, identified as *trans dichloro (triethylphosphine)(mesityl(diphenylmethyl)chlorophosphine platinum(II)*, (III), by ^{31}P NMR spectroscopy. ^{31}P δ_p 102.8 (d of t, $^1J_{(PtP)}$ = 2539 Hz); 15.2 (d of t, 2647 Hz), $^2J_{(PP')}$ = 547 Hz.

Reaction of trans-[PtCl$_2$(PEt$_3$)[PCl(CHPh$_2$)(mesityl)]] with dbu

Trans-[PtCl$_2$(PEt$_3$)[PCl(CHPh$_2$)(mesityl)] (0.15 g, 0.204 mmol) in 1 cm^3 of THF was stirred with dbu (0.03 g, 0.2 mmol) for 2 hr with the formation of a white precipitate. The ^{31}P NMR spectrum of the reaction mixture showed δ_p 235(s), 131(s), 120(s), 85(s), and (IV) 0.0 (t, $^1J_{(PtP)}$ = 3340 Hz).

Reaction of [Pt$_2$Cl$_4$(PEt$_3$)$_2$] with dbu

[Pt$_2$Cl$_4$(PEt$_3$)$_2$] (0.05 g, 0.065 mmol) in 1 cm^3 of CH_2Cl_2 was stirred with a few drops (excess) of dbu to yield *trans dichloro(triethylphosphine)(1,4 - diazabicyclo trans - unde - 1 - ene) platinum(II)*, δ_p 0.1 (t $^1J_{(PtP)}$ 3272 Hz).

Reaction of (mesityl)P=CPh$_2$ with PtX$_2$ (COD), (X=Cl, I)

[PtCl$_2$(COD)] (0.04 g, 0.11 mmol) in 2 cm^3 of CH_2Cl_2 was stirred overnight with (mesityl)P=CPh$_2$ (0.095 g, 0.3 mmol). The initial colourless solution became yellow and yielded a yellow oil on removal of solvent. This was washed with 2 × 2 cm^3 of Et$_2$O and recrystallised from CH_2Cl_2/pentane to produce *cis dichloro di(P-mesityldiphenylmethylene phosphine) platinum(II)*, (V), m.p. 230–233°. Found C, 55.9; H, 4.7; $C_{40}H_{42}P_2Cl_2Pt$ requires C, 58.80; H, 4.71%. IR (KBr) 2910(w), 1602(m), 1489(m), 1445(s), 920(w), 892(w), 853(w), 761(s), 691(s), 637(m), 600(m), 558(s), 530(w), 451(m), 425(m), 320(m), 298(m). ^{1}H δ 2.2(s, 3H), 2.45(s, 6H), 6.5–7.8(m, 12H). ^{31}P δ_p 131.5 (t, $^1J_{(PtP)}$ = 3950 Hz).

Similarly PtI$_2$(COD) gave (VI), δ_p 138.9 (t, $^1J_{(PtP)}$ = 4009 Hz).

Reaction of (mesityl)P=CPh$_2$ with [PtMe$_2$(COD)]

(Mesityl)P=CPh$_2$ (0.095 g, 0.3 mmol) in 2 cm^3 to toluene was stirred with [PtMe$_2$(COD)] (0.038 g, 0.12 mmol) for 2 hr. The initial colourless solution became yellow, which yielded a yellow oil on removal of solvent. This was washed with 2 cm^3 of pentane to produce *cis dimethyl di(P-mesityl diphenylmethylenephosphine)platinum(II)*, (VII), which could not be isolated analytically pure and was identified by NMR spectroscopy. m.p. 205–208°. IR (KBr) 2920(m, br), 1645(m), 1608(m), 1495(m), 1485(m), 1445(m), 1250(m, br), 1975(w), 1030(w), 910(w, br), 845(m), 755(s), 690(s), 630(s), 600(w), 550(m), 522(m, br), 435(m). ^{1}H δ 0.8 (t, $^2J_{(PtCH_3)}$ = 75 Hz), 2.35(s, 3H), 2.4(s, 6H), 6.8–7.8(m, 12H). ^{31}P δ_p 208.1 (t, $^1J_{(PtP)}$ = 1816 Hz).

X-Ray structure analysis of cis-[PtCl$_2$(PEt$_3$)(C$_6$H$_2$Me$_3$P=CPh$_2$)]·CHCl$_3$

Crystal data. $C_{28}H_{36}Cl_2P_2Pt{\cdot}CHCl_3$, M = 819.9, monoclinic, a = 10.904(2), b = 14.351(4), c = 21.560(4) Å, β = 91.01(2)°, U = 3373 Å, Z = 4, D_c = 1.614 g cm^{-3}, F(000) = 1615.8, space group P2$_1$/n, Mo-K$_\alpha$ radiation, λ = 0.71069 Å, μ = 44.6 cm^{-1}.

Measurements. The unit cell dimensions and the intensities of all independent reflections with θ(Mo–K$_\alpha$) < 28° were determined by standard experimental methods using an Enraf–Nonius CAD4F diffractometer equipped with a graphite monochromator. Corrections were applied for Lorentz, polarization, crystal decomposition, and absorption effects. The wide variation in the calculated transmission factors (0.19–0.96) is a consequence of the platy morphology of the specimen, which measured 0.94 × 0.25 × 0.08 mm. 4585 Reflections with $I \geq 3\sigma(I)$ were used in the subsequent analysis.

Structure analysis. The structure was solved by the heavy-atom method and the atomic parameters were refined by full-matrix least-squares. In the final calculations contributions for geometrically-positioned hydrogen atoms were included in the structure factors and phenyl rings A and B were constrained to be hexagons of side 1.395 Å. Anisotropic temperature factors were assigned to all atoms except the 18 phenyl ring carbon atoms and the hydrogen atoms. The refinement converged at R 0.050 and R$_w$ 0.068. Function values in the final difference synthesis did not exceed 1.0 eÅ^{-3} except close to the platinum atom. Final atomic coordinates and a list of F_0/F_c values have been deposited with the Editor as supplementary material.† Atomic scattering factors and anomalous dispersion corrections were taken from Ref. 17.

Acknowledgements—We thank the S.E.R.C. for financial support for this work and Mr. M. J. Maah for the synthesis of the [PtI$_2$((mesityl)P=CPh$_2$)$_2$ complex].

REFERENCES

[1]M. J. Hopkinson, H. W. Kroto, J. F. Nixon and N. P. C. Simmons, *J. Chem. Soc. Chem. Commun.*, 1976, 513; *Chem. Phys. Lett.* 1976, **42**, 460; H. W. Kroto, J. F. Nixon, N. P. C. Simmons and N. P. C. Westwood, *J. Am. Chem. Soc.* 1978, **100**, 446; N. P. C. Westwood, H. W. Kroto, J. F. Nixon and N. P. C. Simmons, *J. Chem. Soc., Dalton Trans.* 1979, 1405; H. W. Kroto, J. F. Nixon and N. P. C. Simmons, *J. Mol. Spectrosc.*, 1979, **77**, 270; H. Eshtiagh-Hosseini, H. W. Kroto, J. F. Nixon, S. Brownstein, J. R. Morton and K. F. Preston, *J. Chem. Soc. Chem. Commun* 1979, 653; T. A. Cooper, H. W. Kroto, J. F.

†Copies are available, on request from the Editor at Queen Mary College. Atomic co-ordinates have also been deposited with the Cambridge Crystallographic Data Centre.

Nixon and O. Ohashi, *J. Chem. Soc., Chem. Commun.* 1980, 333; H. Eshtiagh-Hosseini, H. W. Kroto, J. F. Nixon and O. Ohashi, *J. Organomet. Chem.* 1979, 181, C1; H. W. Kroto, J. F. Nixon and N. P. C. Simmons, *J. Mol. Spectrosc.* 1980, **82**, 185; H. W. Kroto, J. F. Nixon, K. Ohno and N. P. C. Simmons, *J. Chem. Soc. Chem. Commun.* 1980, 709.

[2]G. Becker, *Z. Anorg. Allg. Chem.* 1976, **423**, 242.

[3]T. C. Klebach, R. Lourens and F. Bickelhaupt, *J. Am. Chem. Soc.* 1978, **100**, 4886.

[4]K. Issleib, H. Schmidt and H. Meyer, *J. Organomet. Chem.* 1978, **160**, 47; R. Appel and V. Barth, *Angew. Chem., Int. Ed. Engl.* 1979, **18**, 469; R. Appel and A. Westerhaus, *ibid.* 1980, **19**, 556; G. Becker and O. Mundt, *Z. Anorg. Allg. Chem.* 1980, **462**, 130; G. Becker, G. Gresser and W. Uhl, *ibid* **463**, 144.

[5]H. E. Hosseini, H. W. Kroto, J. F. Nixon, M. J. Maah and M. J. Taylor, *J. Chem. Soc. Chem. Commun.* 1981, 199.

[6]E. Niecke, M. Engelmann, H. Zorn, B. Krebs and G. Henkel, *Angew. Chem. Int. Edn. Engl.* 1980, **19**, 710.

[7]O. J. Scherer, N. Kuhn and H. Jungmann, *Z. Naturforsch* 1978, **33b**, 1321.

[8]J. F. Nixon and A. Pidcock, *Ann. Rev. NMR Spectroscopy* 1969, **2**, 345.

[9]I. H. Hillier and V. R. Saunders, *Trans. Faraday Soc.* 1970, **66**, 2401.

[10]T. G. Appleton, H. C. Clark and L. E. Manzer, *Coord. Chem. Rev.* 1973, **10**, 335.

[11]E. Schustorovich, *Inorg. Chem.* 1979, **18**, 1030; 1039; 2108.

[12]T. C. Klebach, R. Lourens, F. Bickelhaupt, C. H. Stam and A. Van Herk, *J. Organometal. Chem.* 1981, **210**, 211.

[13]A. N. Caldwell, Lj. Manojlović-Muir and K. W. Muir, *J. Chem. Soc. (Dalton)* 1977, 2265.

[14]C. J. Cardin, D. J. Cardin, M. F. Lappert and K. W. Muir, *J. Chem. Soc. (Dalton)* 1978, 46.

[15]C. A. Tolman, *J. Amer. Chem. Soc.* 1970, **92**, 2953.

[16]H. C. Clark and L. E. Manzer, *J. Organometal Chem.* 1973, **59**, 411.

[17]A. C. Smithies, M. Rycheck and M. Orchin, *J. Organometal Chem.* 1968, **12**, 199.

[18]*International Tables for X-ray Crystallography*, Vol. IV. Kynoch Press, Birmingham, 1974.

[19]G. Mather, A. Pidcock and G. Rapsey, *J. Chem. Soc. (Dalton)* 1973, 2095.

[20]J. G. Verkade, *Coord. Chem. Rev.* 1972, **9**, 1.

[21]B. Jackobsen, D. Phil Thesis University of Sussex 1977.

[22]J. F. Nixon, Unpublished results.

[23]N. Ahmad, E. W. Ainscough, T. A. James and S. D. Robinson, *J. Chem. Soc. (Dalton)* 1973, 1148.

[24]S. O. Grim, R. L. Keiter and W. McFarlane, *Inorg. Chem.* 1967, **6**, 1133.

[25]T. G. Appleton, M. A. Bennett and I. B. Tomkins, *J. Chem. Soc. (Dalton)* 1976, 439.

Polyhedron Vol. 1, No. 1, pp. 97–103, 1982
Printed in Great Britain.

0277–5387/82/010097–07$03.00/0
Pergamon Press Ltd.

REACTIONS OF DICHLOROBIS(DITERTIARYPHOSPHINE)-RUTHENIUM(II) WITH CARBON MONOXIDE: PREPARATION OF DICARBONYLBIS(DITERTIARYPHOSPHINE) RUTHENIUM(II) CATIONS

GARRY SMITH, DAVID J. COLE-HAMILTON*

and (in part)

ANNE C. GREGORY and NANCY G. GOODEN

Department of Inorganic, Physical and Industrial Chemistry, University of Liverpool, P. O. Box 147, Liverpool L69 3BX, England

(*Received* 14 *September* 1981)

Abstract—Reactions of $RuCl_2(L\text{–}L)_2$ (L–L = dppm or dppe) with CO and silver salts of non coordinating anions produce $[Ru(CO)_2(L\text{–}L)_2]X_2$ which, once formed, are stable to CO loss. However, the fluxional five coordinate intermediates $[Ru(Cl)(L\text{–}L)_2]X$, which in some cases may contain ion pairs, are sufficiently electrophilic to abstract fluoride ion from $[BF_4]^-$ or to coordinate other ions in solution such as $[O_2PF_2]^-$ formed by hydrolysis of $[PF_6]^-$. A series of complexes of general formula $[Ru(CO)_2(dppm)_2AgY]X_2$ may also be isolated and are shown to contain a dppm ligand bridging ruthenium and silver, the bond between which is reversibly cleaved by nitromethane on the nmr timescale.

INTRODUCTION

Although polycarbonyl containing transition metal complexes holding charges from −2 to +1 are well known,[1] and charges as low as −3 have been reported,[2] very few such complexes with a dipositive charge have been isolated. This is presumably because there is insufficient electron density on the metal for back donation to the carbonyl ligand and hence the carbonyl groups in such complexes are labile.

The only complexes of this kind appear to be $[M(CO)_2(dppe)_2]^{2+}$ (M = Fe[3], Cr, Mo or W[4]) which are prepared electrochemically and, at least for M = Cr, Mo or W, are unstable; unstable $[Mo(CO)_2(dmpe)_2]^{2+}$,[5] and the more stable $[Os(CO)_n(NH_3)_{6-n}]^{2+}$ (n = 2 or 3).[6,7] Very recently, Connor has prepared[8] some stable molybdenum complexes $[Mo(CO)_2(N\text{–}N)_2L]^{2+}$ ((N–N) = 2,2-bipyridyl or 1,10-phenanthroline, L = H_2O or MeCN).

We now report the sucessful preparation of stable complexes of formula $[Ru(CO)_2(L\text{–}L)_2]^{2+}$, (L–L = $Ph_2P(CH_2)_nPPh_2$, n = 1 (dppm) or 2 (dppe)), together with other complexes obtained during these preparations. IR ^{31}P and ^{19}F nmr data for the new complexes are collected in Tables 1–3 and analytical data are in Table 4.

RESULTS AND DISCUSSION

The general synthetic approach that we have employed for $[Ru(CO)_2(L\text{–}L)_2]^{2+}$ has involved reaction of dichloro complexes, $RuCl_2(L\text{–}L)_2$ with silver salts of non-coordinating anions under 3 atmospheres† of CO. A similar method has been used for the preparation of other ruthenium dications, $[Ru(N\text{–}N)_2L_2]^{2+}$, (N–N = 1,10-phenanthroline or 2,2′-bipyridyl, L_2 = dppe[9] or norbornadiene[10]). It is already known[11] that $RuCl_2(dppm)_2$ reacts with CO to give $[RuClCO(dppm)_2]^+$.

Since the products obtained in the various reactions depend markedly upon the nature of the non-coordinating anion, the reactions for each silver salt will be described in turn.

(i) $AgSbF_6$

(a) $RuCl_2(dppm)_2$. Addition of $AgSbF_6$ to a solution of *cis* or *trans* $RuCl_2(dppm)_2$ in dichloromethane under CO causes the colour to change from yellow through deep red to colourless over a period of 4 hr at 50°C with concurrent precipitation of AgCl. The final solution yields white crystals of a 2:1 electrolyte[12] which analyse for $[Ru(CO)_2(dppm)_2][SbF_6]_2$. The IR spectrum of these crystals (nujol mull) shows three peaks at 2096, 2060 and 2040 cm^{-1} (see Table 1) which appear as two peaks, at 2085 and 2050 cm^{-1} in dichloromethane solution. Although initially we thought that this indicated that the *cis* isomer was the product obtained, ^{31}P NMR studies (see Table 2) clearly show both the *cis* and the *trans* isomers to be present. These can be separated with some difficulty by fractional crystallisation from methylene chloride-diethyl ether since the *trans* isomer is considerably less soluble in CH_2Cl_2 than the *cis*.

The high value of $\nu(C{\equiv}O)$ in these complexes is consistent with their being dicationic since the low electron density of the metal should allow little population of the π^* orbitals of CO and hence cause only a small drop in νCO from the value for free carbon monoxide (2143 cm^{-1}).

Clearly, the fact that both *cis* and *trans*-$RuCl_2(dppm)_2$ produce the same product distribution suggests a common, probably fluxional intermediate and this must give rise to the red colour of the solution‡ during the intermediate stages of the reaction. Although we have not isolated this five coordinate intermediate, we believe it to be $[RuCl(dppm)_2]^+$, analogous[14] to $[RuCl(dppp)_2]^+$

*Author to whom correspondence should be addressed.

†Throughout this paper 1 atmos = 101,325 kNm^{-2}.

‡Five coordinate complexes of ruthenium(II) are generally red or dark coloured.[13]

Table 1. IR data (cm^{-1}) for ruthenium carbonyl cations

Complex	νC≡O (solid)	νC≡O (CH_2Cl_2)	Other
cis$[Ru(CO)_2(dppm)_2][BF_4]_2$	2088, 2045	2080, 2040	
cis$[Ru(CO)_2(dppm)_2][PF_6]_2$	2093, 2060	2085, 2050[a]	
cis$[Ru(CO)_2(dppm)_2][SbF_6]_2$	2096, 2060	2085, 2050	
trans$[Ru(CO)_2(dppm)_2][SbF_6]_2$	2040	2050	
trans$[Ru(CO)_2(dppe)_2][BF_4]_2$	2022		
trans$[Ru(CO)_2(dppe)_2][SbF_6]_2$	2040	2032	
trans$[RuF(CO)(dppe)_2]BF_4$	1968	1959	
trans$[Ru(O_2PF_2)CO(dppm)_2]PF_6$	1971	1988	1290[b], 1125[c]
trans$[\{RuCO(dppm)_2\}_2O_2PF_2][PF_6]_3$	1975	1985	1312[b], 1157[c]
cis$[Ru(CO)_2(dppm)_2AgBF(OH)_3][BF_4]_2$	2060, 2000	2076, 2014	3675[d]
cis$[Ru(CO)_2(dppm)_2AgO_2PF_2][O_2PF_2]_2$	2078, 2018	2080, 2020	1318[b], 1296[b] 1146[c], 1138[c]
cis$[Ru(CO)_2(dppm)_2AgClO_4][ClO_4]_2$	2094, 2037	2090, 2030	
cis$[Ru(CO)_2(dppm)_2AgCl][AsF_6]_2$	2076, 2015	2078, 2018	

a) $MeNO_2$ solution

b) ν asym PO_2 of $[O_2PF_2]^-$

c) ν sym PO_2 of $[O_2PF_2]^-$

d) ν O-H

(dppp = bisdiphenylphosphinopropane) since a similar red colouration is obtained if $RuCl_2(dppm)_2$ is treated first with $AgSbF_6$ and then with CO; but not if $[RuCl(CO)(dppm)_2]^+$ is treated with $AgSbF_6$. This last result eliminates the possibility that the red species is $[Ru(CO)(dppm)_2]^{2+}$.

(b) $RuCl_2(dppe)_2$. An exactly similar reaction to that described above for $RuCl_2(dppm)_2$ occurs when *trans*-$RuCl_2(dppe)_2$ is treated with $AgSbF_6$ under CO. In this case, hovever, only *trans*-$[Ru(CO)_2(dppe)_2]$ $[SbF_6]_2$ is isolated despite the fact that a red and presumably five-coordinate intermediate is again formed. Once again,

Table 2. ^{31}P and ^{19}F NMR spectra for some cationic ruthenium complexes ($MeNO_2$, 25°C)

Compound	Phosphines δ[a] P_t	Phosphines δ[a] P_c	O_2PF_2- ^{31}P δ[a]	O_2PF_2- ^{19}F δ[b]	J_{PF} Hz
cis$[Ru(CO)_2(dppm)_2][PF_6]_2$[c]	-19.9t[d]	-32.7t			
trans$[Ru(CO)_2(dppm)_2][SbF_6]_2$	-17.5s				
trans$[Ru(CO)_2(dppe)_2][SbF_6]_2$	-41.1s				
trans$[Ru(CO)(O_2PF_2)(dppm_2)]PF_6$[c]	-13.7s		-16.8t	-76.8d	955
trans$[\{Ru(CO)(dppm)_2\}_2O_2PF_2][PF_6]_3$[c]	-14.1s		-15.3t	-89d	951
trans$[RuF(CO)(dppe)_2]BF_4$	-42.7d			-400q[e]	17

a) p.p.m to high frequency of external 85% H_3PO_4

b) p.p.m to high frequency of external $CFCl_3$.

c) All $[PF_6]^-$ salts have ^{31}P: δ-145(septet) and ^{19}F: δ-74d, J_{PF} = 708 Hz.

d) J_{PP} = 33 Hz.

e) Ru-F; BF_4: -153.5 ppm(s).

Table 3. ^{31}P NMR data for ruthenium-silver cations (25°C, $MeNO_2$)

Compound	Chemical shifts[a]				Coupling constants (JHz)			
	P_A	P_B	P_C	P_D	AB	AC	BC	DAg
$[Ru(CO)_2(dppm)_2Ag_2O_2PF_2][O_2PF_2]_2$[b]	13.4	-10.0	-26.7	-7.5	266	29.3	40.3	57
$[Ru(CO)_2(dppm)_2AgClO_4][ClO_4]_2$	13.1	-10.1	-26.9	8.2	268	29.3	41.5	64
$[Ru(CO)_2(dppm)_2AgCl][AsF_6]_2$[c]	12.0	-10.8	-27.2	8.9	268	29.3	42.5	39
$[Ru(CO)_2(dppm)_2AgCl][AsF_6]_2$[d,e]	12.1	-10.3	-27.3	5.6	264	29.4	43.9	59
$[Ru(CO)_2(dppm)_2AgCl(MeNO_2)][AsF_6]_2$[d]	10.1	-11.1	-26.9	7.1	268	29.3	44.0	24.4

a) ppm to high field of 85% H_3PO_4, for assignments see figure

b) $[O_2PF_2]^-$ poorly resolved triplets $\delta \sim -14$, $J_{PF} \sim 1000$ Hz.

c) ^{19}F: -66.82 ppm from $CFCl_3$ (1:1:1:1 quartet), ^{75}As 17.122705 MHz; (septet); J_{ASF} = 930 Hz; ^{109}Ag: 23.4(brs), -879(brs)ppm from $AgNO_3$.

d) -35°C.

e) J_{P_AAg} = 4.9 Hz, J_{P_BAg} = 7.4 Hz, J_{P_CAg} = 0 Hz.

Table 4. Analytical and conductivity data for ruthenium complexes

Compound	mpt °C	Found % (calculated)						Λ[a]
		C	H	P	F	Cl	Ag	
cis-$[Ru(CO)_2(dppm)_2][BF_4]_2$	315-8d	54.3(56.8)	3.9(4.0)	10.8(11.3)	14.0(13.8)	0.1(0)		193
cis-$[Ru(CO)_2(dppm)_2][PF_6]_2$		50.6(51.4)	3.7(3.6)					197
cis-$[Ru(CO)_2(dppm)_2][SbF_6]_2$	288d	44.0(44.7)	3.2(3.2)					175
trans-$[Ru(CO)_2(dppm)_2][SbF_6]_2$	276d	43.8(44.7)	3.5(3.2)	8.6 (8.9)[b]	16.2(16.3)[b]			180
trans-$[Ru(CO)_2(dppe)_2][SbF_6]_2$	208d	45.5(45.5)	3.5(3.4)	8.3(8.7)				175
trans-$[RuFCO(dppe)_2]BF_4$	338-45d	60.9(61.7)	5.0(4.3)		9.0(9.2)	0.5(0)		97
trans-$[RuCO(O_2PF_2)(dppm)_2]PF_6$		53.2(53.5)	3.8(3.9)	15.5(16.3)	13.9(13.3)			82
cis-$[Ru(CO)_2(dppm)_2AgBF(OH)_3][BF_4]_2$	200-202	48.5(48.3)	3.8(3.7)	9.8(9.6)	12.9(13.3)	0.9(0)	8.0(8.4)	193
cis-$[Ru(CO)_2(dppm)_2AgClO_4][ClO_4]_2$	150*	46.0(46.9)	3.5(3.3)	9.7(9.3)			9.6(8.1)	
cis-$[Ru(CO)_2(dppm)_2AgCl][AsF_6]_2$	198d	46.7(43.1)	3.4(3.0)	9.0(8.6)	16.3(15.8)	2.6(2.5)	8.1(7.5)	155

* DETONATES

a $\Omega^{-1}cm^2mol^{-1}$

b cis, trans mixture.

$\nu C{\equiv}O$ for this 2:1 electrolyte is $> 2000\,cm^{-1}$ (see Table 1).

We presume that the fact that only the *trans*-$[Ru(CO)_2(dppe)_2]$ $[SbF_6]_2$ is isolated is caused by steric effects since Chatt has shown[15] that space filling models of *cis*-$RuCl_2(dppe)_2$ are sterically hindered and has suggested this as the reason for the non-existence of this complex.

(ii) $AgClO_4$ and $AgAsF_6$ with *cis*-$RuCl_2(dppm)_2$

Under CO, $AgClO_4$ and $AgAsF_6$ react slowly with *cis*-$RuCl_2(dppm)_2$ to give a single white crystalline complex which, in the case of $AgClO_4$ *EXPLODES* on heating. These complexes show two $\nu C{\equiv}O$ near 2080 and $2020\,cm^{-1}$ suggesting that the metal ion is again dicationic but clearly cannot contain *cis*-$[Ru(CO)_2(dppm)_2]^{2+}$ since this has $\nu(C{\equiv}O$ at 2090 and $2060\,cm^{-1}$ (see above). Analytical data suggest the formulation $[Ru(CO)_2(dppm)_2AgX]Y_2$ (X = Cl, Y = AsF_6 or X = Y = ClO_4) and the exact nature of these complexes is discussed below, together with their complex ^{31}P NMR spectra.

(iii) $AgPF_6$

(A) $RuCl_2(dppm)_2$. The products of reactions of $AgPF_6$ with $RuCl_2(dppm)_2$ under CO depend markedly upon the age and purity of the silver salt, as well as on the reaction time. Thus, fresh $AgPF_6$ (which has not had contact with air or moisture) smoothly gives $[Ru(CO)_2(dppm)_2]$ $[PF_6]_2$ on reaction with *cis*-

$RuCl_2(dppm)_2$ after 0.5 hr under CO, although unlike the reaction with $AgSbF_6$, only the *cis* isomer is formed. This is somewhat surprising but the most likely explanation is that ion pairing occurs in $[RuCl(dppm)_2]$ $[PF_6]$ but not with the more bulky and less nucleophilic $[SbF_6]^-$. Thus, no fluxional 5-coordinate intermediate is formed (indeed we do not observe a red colouration) and hence the stereo chemical integrity of the complex is retained throughout the reaction.

With aged or partially hydrolysed $AgPF_6$, it is rather difficult to isolate any $[Ru(CO)_2(dppm)_2]^{2+}$ from *cis*-$RuCl_2(dppm)_2$ and there are two major types of product. One, which has a pinkish tinge, has $\nu C{\equiv}O$ at 1960 cm^{-1} suggesting a monocationic monocarbonyl complex as well as strong bands at 1290 and 1125 cm^{-1}. Room temperature, ^{31}P and ^{19}F NMR studies clearly show that this is a mixture of at least two species, both of which have the four dppm phosphorus atoms equivalent, PF_6^- and a PF_2 group. Taken with the IR stretches at 1290 ($\nu_{asym}PO_2$) and 1125 ($\nu_{sym}PO_2$) cm^{-1}, we propose that these complexes contain the $[PO_2F_2]^-$ group.

By careful recrystallisation from CH_2Cl_2-diethyl ether we have been able to obtain one of these complexes pure. It analyses for $[Ru(CO)(PO_2F_2)(dppm)_2]$-$[PF_6]$ and is a 1:1 electrolyte.

In view of the equivalence of the dppm phosphorus atoms in this complex at temperatures down to −35°C we suggest a *trans* stereochemistry with a mono-dentate $[PO_2F_2]^-$ group. The other similar complex we have not isolated pure but propose, on the basis of its similar spectroscopic properties, that it is $[\{Ru(CO)(dppm)_2\}_2(O_2PF_2)]$ $[PF_6]_3$ with a bridging O_2PF_2 ligand and *trans* stereochemistry at each ruthenium atom. Consistent with this, the main NMR difference is in the chemical shift of the fluorine atoms of the $[O_2PF_2]^-$ group and the higher positive charge on ruthenium should lead to a high field shift of the phosphorus atoms of the dppm ligand, as is observed. (δ − 14.1 ppm c.f. −17.5 for *trans* $[Ru(CO)_2(dppm)_2]^{2+}$ and −13.7 for *trans* $[Ru(CO)(O_2PF_2)(dppm)_2]^+$

Comparison of the IR spectra of these complexes with those of other $[O_2PF_2]^-$ complexes, in which the bonding is known,[16–18] supports these conclusions. Thus, although $\nu_{asym}PO_2$ varies over the range 1230–1290 cm^{-1} for bridging, chelating and monodentate bonding, $\nu_{sym}PO_2$ appears to fall in specific areas for the three different kinds of coordination.

For bridging $[O_2PF_2]^-$ ν_{sym} appears[17] at 1157–1175 cm^{-1}, for chelating it is[16,18] at 1165–1200 cm^{-1} and for monodentate coordination it lies[18] in the range 1130–1140 cm^{-1}. Clearly, the complex which we have obtained pure, which has $\nu_{sym}PO_2$ at 1125 cm^{-1} must, on this basis, contain monodentate $[O_2PF_2]^-$, in agreement with the conclusions reached on the basis of analytical data. For the other, similar complex, although we have not obtained it pure, $\nu_{sym}PO_2$ appears to be at 1157 cm^{-1}—in the region expected for bridging $[O_2PF_2]^-$, although in view of the rather high $\nu_{sym}PO_2$ (1312 nm^{-1}) we cannot unequivocally rule out the possibility that this complex contains ionic $[O_2PF_2]^-$ which has $^{17}\nu_{asym}PO_2$ at 1310 cm^{-1} and $\nu_{sym}PO_2$ at 1148 cm^{-1}.

We have been unable to assign the other fundamental vibrational modes of the $[O_2PF_2]^-$ ligand in any of these complexes, since they fall in regions in which vibrations of either dppm or $[PF_6]^-$ occur.

Small amounts of another complex, which contains a resonance at −138.9 ppm in the ^{19}F NMR spectrum, are present as an impurity in $[\{RuCO(dppm)_2\}_2(O_2PF_2)]$ $[PF_6]_3$ and we believe this to be $[Ru(CO)F(dppm)_2]PF_6$ by analogy with $[Ru(CO)F(dppe)_2]BF_4$ (see below).

The other product isolated from the reaction of *cis*-$RuCl_2(dppm)_2$ with aged $AgPF_6$ has $\nu C{\equiv}O$ at 2010 and 2078 cm^{-1}† and is very similar to the compounds formed with $AgClO_4$ and $AgSbF_6$. The presence of IR absorptions at 1296 and 1138 cm^{-1} again suggest the presence of an $(O_2PF_2)^-$ group and we, therefore, believe that this compound contains $[Ru(CO)_2(dppm)_2Ag(O_2PF_2)]^{2+}$. Since no resonances from $[PF_6]^-$ are observed in the ^{31}P NMR spectrum of this product, and since only medium intensity νP–F absorptions are observed in the IR spectrum, we assume that $[O_2PF_2]^-$ is also the counter anion, and peaks in the IR spectrum at 1310 and 1146 cm^{-1} are consistent with this.

To our knowledge, isolation of complexes of the $[O_2PF_2]^-$ ligand from reactions with aged $AgPF_6$ has not previously been reported, but the mechanism of its formation by silver promoted hydrolysis of the $[PF_6]^-$ anion is presumably related to that of formation[19] of POF_3 from PF_5 and Me_2O.

(iv) $AgBF_4$

(a) $RuCl_2(dppm)_2$. Like $AgPF_6$, fresh $AgBF_4$ reacts with *cis* $RuCl_2(dppm)_2$ to give only *cis*-$[Ru(CO)_2(dppm)_2]$ $[BF_4]$ consistent with the high nucleophilicity and low bulk of the $[BF_4]^-$ anion. Solution IR studies show that another complex ($\nu C{\equiv}O$ at 1992 cm^{-1}) is also formed after prolonged reaction, apparently from $[Ru(CO)_2(dppm)_2]$ $[BF_4]_2$. Although we have not isolated this complex, we believe it to be $[RuF(CO)(dppm)_2]$ $[BF_4]$ by analogy with the complex formed by a similar reaction using *trans*-$RuCl_2(dppe)_2$ (see below).

Aged samples of $AgBF_4$ again show different behaviour, the product being a silver-containing species similar to those obtained with $AgClO_4$, $AgAsF_6$ and aged $AgPF_6$. Full analytical data show that this 1:2 electrolyte does not have F^-, Cl^- or BF_4^- as the anion bound to silver but a sharp peak at 3675 cm^{-1} in the IR spectrum of CH_2Cl_2 solutions suggests the presence of hydroxide ion. The compound could be $[Ru(CO)_2(dppm)_2.AgOH]$ $[BF_4]_2$ but analytical data suggest that it contains some partially hydrolysed $[BF_4]^-$, such as $[BF(OH)_3]^-$.

(b) $RuCl_2(dppe)_2$. Reaction of *trans*-$RuCl_2(dppe)_2$ with $AgBF_4$ under one or three atmospheres of CO produces a mixture of two complexes, one of which is *trans*-$[Ru(CO)_2(dppe)_2]$ $[BF_4]_2$ ($\nu C{\equiv}O$, 2022 cm^{-1}). The other is a 1:1 electrolyte and has $\nu C{\equiv}O$ at 1968 cm^{-1}, consistent with its being a monocationic monocarbonyl species. Analytical data suggest the formulation $[RuF(CO)(dppe)_2]BF_4$, which is confirmed by ^{31}P and ^{19}F NMR studies (Table 2).

The abstraction of fluoride ion from $[BF_4]^-$ has previously been observed and we believe that it occurs via an ion paired intermediate, $Ru(BF_4)Cl(dppe)_2$, although it is possible that it forms from $[BF_4]^-$ attack on $[Ru(CO)_2(dppe)_2]^{2+}$, by analogy with the dppm complex (see above).

†We have also observed small amounts of a compound with $\nu C{=}O$ at 2035 and 2086 cm^{-1} and $\nu P{=}O$ at 1305 and 1240 cm^{-1}. We have not fully characterised this compound but believe it to be the $[PF_6]^-$ salt of the same cation, although we cannot rule out the possibility that it is $[Ru(CO)_2(dppm)_2AgCl][O_2PF_2]$.

The structure of $[Ru(CO)_2(dppm)_2.AgX]Y_2$

As indicated above, a major product from many of the reactions of $RuCl_2(dppm)_2$ with silver salts under CO is $[Ru(CO)_2(dppm)_2AgX]Y_2$. For $Y = AsF_6$, $X = Cl$ but in all other cases, X appears to be an oxo anion, $[O_2PF_2]^-$, $[ClO_4]^-$ or $[BF(OH)_3]^-$. IR data suggest a *cis* dicarbonyl formulation and conductivity measurements show the complexes to be 1:2 electrolytes.

The room temperature† ^{31}P NMR spectra of the $[O_2PF_2]^-$ and $[ClO_4]^-$ complexes are very similar and show four separate resonances from the phosphine phosphorus atoms which are not all mutually coupled (see Table 4). Three of the phosphorus atoms, P_A, P_B and P_C are coupled together in such a way that they must be meridionally orientated about the metal. Thus, $J_{P_AP_B} = 268$ Hz, typical[20] for non equivalent mutually *trans* phosphorus atoms on ruthenium, whilst $J_{P_BP_C} = 41.5$ Hz and $J_{P_AP_C} = 29$ Hz are both characteristic values for J_{PP} *cis*. The fourth resonance appears as a slightly broad doublet whose position is anion dependent with a coupling constant of ~60 Hz. Clearly this coupling is not to phosphorus, but, since silver is present in the complex (microanalytical data), we conclude that the phosphorus is coupled to the silver atom. In fact, since silver has ^{107}Ag (51.4%) and ^{109}Ag (48.6%), for both of which $I = 1/2$, the resonance should appear as two doublets ($\gamma 107_{Ag}/\gamma 109Ag = 1.14$), but we assume that the broadness of the lines obscures the small difference in coupling constants. The low solubility of these complexes has precluded the direct observation silver NMR spectra.

For $[Ru(CO)_2(dppm)_2.AgCl]$ $[AsF_6]_2$, the ^{31}P NMR spectrum is temperature dependent, although at high temperature (50°C) it is very similar to the spectra for $X = Y = [ClO_4]^-$ or $[O_2PF_2]^-$. On cooling, the resonances broaden, this occurring at high temperature for the lower field signals, and then sharpen again to show two sets of signals (see Table 4) which can be assigned to two distinct isomers of the compound which have the same basic stereochemistry and interconvert at higher temperatures. The major isomer clearly shows coupling between silver and three of the phosphine phosphorus atoms (P_A, P_B and P_D) whilst in the other isomer this coupling is absent and only coupling to P_D is observed.‡

These data taken together suggest that one dppm ligand chelates the ruthenium whilst the other bridges the silver and ruthenium in both isomers. Two structures which contain this basic framework are shown below in Iand II.

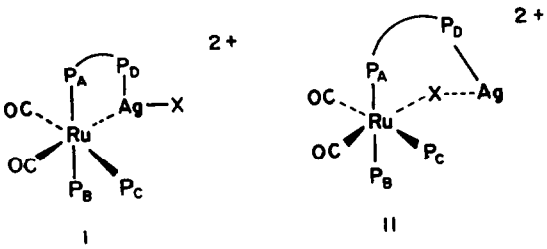

†The low solubility of these complexes has precluded low temperature measurements but we assume that their behaviour would be similar to that of $[Ru(CO)_2(dppm)_2AgCl]$ $[AsF_6]_2$ (see below).

‡The silver NMR spectrum shows two very broad peaks at 23.4 and −879 ppm from $AgNO_3$ suggesting that the two isomers have different silver environments but is otherwise uninformative.

P_A and P_B are then assigned as shown, since phosphorus atoms in a 4 membered metallacyclic ring are known[20] to resonate at higher field than those in larger rings. Assuming that one or both of these structures is correct, $J_{P_AP_D}$ must be close to 0. Although this is unuaual, $J_{PP'}$ in bridging dppm ligands usually being[21] ~ 50 Hz, the value of this coupling constant must depend on the angle at the bridging carbon atom and could be 0 under some circumstances.

Since for $X = [O_2PF_2]^-$, IR data support unidentate binding ($\nu_{sym}PO_2$, 1138 cm^{-1}) we favour structure I as being the most probable solid state structure for these complexes. This is also likely to be the structure of the major isomer in solution in view of the observation of direct Ag-P coupling to P_A and P_B. The minor solution isomer of $[Ru(CO)_2(dppm)_2AgCl]$ $[AsF_6]_2$ could have structure II although we think it unlikely since silver prefers linear coordination when 2 coordinate. The linearity would not be possible at least when $X = Cl^-$, although it may be possible when $X = [ClO_4]^-$ or $[O_2PF_2]^-$. We think the most likely explanation of the fluxionality of these complexes is that the Ru-Ag bond is solvolysed in nitromethane to give III, which is then the minor isomer observed at low temperature in the NMR spectrum and that at higher temperatures facile interconversion of I and III occurs on the NMR time scale.

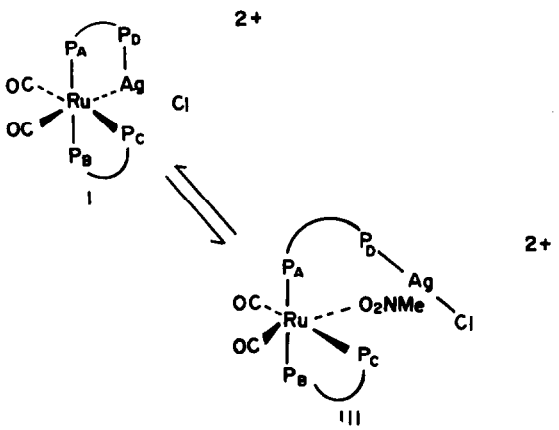

This process would also explain the lack of observable coupling between silver and phosphorus atoms other than P_D in the high temperature limiting spectra for these complexes.

Similar types of compound in which rhodium or iridium and silver are bridged by heteroallyl ligands have been reported.[22]

EXPERIMENTAL

Microanalyses are by Butterworth Laboratories Ltd. and Elemental Microanalysis Ltd. IR spectra were measured in nujol mulls between CsI plates or in 0.2 mm NaCl matched solution cells on a Perkin-Elmer PE 577 spectrometer. Multinuclear NMR spectra were recorded on a JEOL FX90Q spectrometer operating in the Fourier Transform mode, with noise proton decoupling for all nuclei other than fluorine. Conductivity measurements were performed on a Phillips PR9500 conductivity bridge with a Mullard E7591/B conductivity cell. Melting points were measured on an Electrothermal melting point apparatus and are uncorrected. Dichloromethane, nitromethane and acetone, G.P.R. grade, were used without purification, whereas diethyl ether was purified by distillation from sodium-benzophenone ketyl.

Silver salts (Lancaster Syntheses) were used without

purification. *cis*-$RuCl_2(dppm)_2$, *trans*-$RuCl_2(dppm)_2$ and *trans*-$RuCl_2(dppe)_2$ were prepared[11,14,15] by standard literature methods as well as the method described below.

Manipulations were carried out in air unless otherwise stated.

Alternative preparation of cis-$RuCl_2(dppm)_2$ (carried out under nitrogen)

trans-$RuCl_2(dppm)_2$ (3 g) was heated to 230°C in the solid state for 48 hr, during which time the colour changed from orange to yellow. The yellow product was identified as pure *cis*-$RuCl_2(dppm)_2$ by its IR spectrum. Yield 3 g (100%).

Carbonylation reactions

The following compounds were prepared by addition of the appropriate silver salt to carbon monoxide saturated CH_2Cl_2 solutions of $RuCl_2(L\text{–}L)_2$(1 g/80 cm^3), followed by pressurisation to three atmospheres with carbon monoxide and stirring for the stated time. The resulting pale solutions were filtered to remove silver chloride, combined with CH_2Cl_2 washings of the AgCl, evaporated to half volume and treated with diethyl ether. On cooling, the products crystallised, were collected and recrystallised from dichloromethane-ether.

cis - dicarbonylbis(bis(diphenylphosphino)methane) ruthenium(II) tetrafluoroborate from *cis*-$RuCl_2(dppm)_2$ (1 g, 1.06 mmol) and fresh $AgBF_4$ (2.0 g, 10.6 mmol) for 24 hr at 25°C as white crystals. Yield 0.8 g (69%).

IR max cm^{-1}† 2088s, 2045s, 1338w, 1313w, 1285w, 1270wsh, 1191 m, 1162s, 1134vs, 1098vsbr, 1060vsbr, 1025vsbr, 995vs, 975ssh, 925mbr, 850w, 788m, 752ssh, 733vs, 691s, 612vw, 539s, 520s, 508vs, 498vs, 471m, 449w, 428w, 400w, 375w.

cis - dicarbonylbis(bis(diphenylphosphino)methane)ruthenium(II) hexafluorophosphate from *cis*-$RuCl_2(dppm)_2$ (1.0 g, 1.06 mmol) and $AgPF_6$ (0.54 g, 2.14 mmol) for 1 hr at 25°C as pale purple plates. Yield 0.6 g (47%).

IR max cm^{-1} 2093s, 2060s, 1338wshbr, 1300wbr, 1190vw, 1167w, 1150sh, 1130w, 1095m, 995w, 875msh, 858ssh, 848vssh, 835vsbr, 782w, 750wsh, 735ssh, 728s, 692m, 553s, 540msh, 535msh, 520s, 505s, 497s, 470w, 423wbr, 418wbr, 375vwbr, 247vwbr.

cis and *trans-dicarbonylbis (bis(diphenylphosphino) methane) ruthenium(II) hexafluoroantimonate* from *trans*- or *cis*-$RuCl_2(dppm)_2$ (1 g, 1.06 mmol) and $AgSbF_6$ (0.8 g, 2.33 mmol) for 4 hr at 50°C or 24 hr at 25°C via a red intermediate, as a mixture of white cubes (*trans* isomer) and needles (*cis* isomer). These could be separated with difficulty by crystal picking or by careful fractional crystallisation from CH_2Cl_2-Et_2O, in which the *trans* isomer is less soluble. Total yield 1.0 g (67%) ^{31}P NMR studies suggest *ca.* 2.5:1 *cis*:*trans*.

IR max cm^{-1} *cis*: 2096s, 2060s, 1328wsh, 1309w, 1267w, 1190w, 1165w, 1127w, 1098s, 1022w, 998m, 971w, 845w, 773wsh, 754m, 740ssh, 631vs, 698s, 670ssh, 657vs, 640ssh, 547wsh, 540m, 520s, 506s, 495ssh, 470w, 428w, 368vw, 288vs, 280ssh.

trans: 2040vs, 1334wbr, 1263vwbr, 1193wbr, 1165wbr, 1122wsh, 1100w, 1000w, 760wsh, 750msh, 744ssh, 737s, 717s, 695s, 670wsh, 657s, 628mbr, 575wsh, 568m, 522m, 502s, 470m, 442w, 395wvbr, 285vs, 278vssh.

trans-dicarbonylbis (bis(diphenylphosphino)ethane) ruthenium(II) tetrafluoroborate from *trans*-$RuCl_2(dppe)_2$ (0.5 g, 0.517mmol) and fresh $AgBF_4$(1.07g, 5.49mmol) for 16 hr at 25°C. as white crystals from dichloromethane–methanol. Further addition of methanol to the filtrate after collection of *trans*-$[Ru(CO)_2(dppe)_2]$ $[BF_4]_2$ afforded pink crystals of *trans carbonylfluorobis(bis (diphenylphosphino)ethane) ruthenium(II) tetrafluoroborate* which were recrystallised from CH_2Cl_2-diethyl ether as pink micro crystals.

IR (*trans* dicarbonyl) max cm^{-1}. 2022s, 1340w, 1322wbr, 1286w, 1248vw, 1190w, 1162w, 1122msh, 1080sbrsh, 1040vsbr, 995s, 945msh, 880w, 802w, 744s, 719m, 690s, 669msh, 650msh, 615vw, 572s, 525s, 508s, 486m, 472msh, 440w, 415vwsh, 389w, 373msh; $\Lambda = 190\ \Omega^{-1}\ cm^2\ mol^{-1}$, m.p. 333–337°C.

IR (fluorocarbonyl) max cm^{-1}. 1968sbr, 1940msh, 1432s, 1412m, 1409msh, 1335vw, 1319w, 1282w, 1270w, 1242vw, 1190m, 1182wsh, 1168w, 1159m, 1140vw, 1127vw, 1095vsbr, 1070vssh, 1050vsbr, 1030vsbr, 995s, 980msh, 972msh, 940wsh, 920wsh, 878s, 860vw, 850vw, 840vw, 815s, 806m, 760msh, 751s, 742s, 715ssh, 702s, 693s, 688s, 668m, 651m, 648msh, 618m, 598s, 590s, 579w, 571w, 540s, 525vs, 518vssh, 509vs, 488vs, 472s, 445s, 435msh, 423m, 384w, 274w, 247w, 240wsh, 321vw, 268vw, 257vw.

trans - dicarbonyl(bis(diphenylphosphino)ethane) ruthenium(II) hexafluoroantimonate from *trans* $RuCl_2(dppe)_2$ (1.0 g, 1.03 mmol) and $AgSbF_6$ (0.78 g, 2.27 mmol) for 4 hr at 25°C via a shortlived red intermediate, as white crystals. Yield 1.1 g (74%).

IR max cm^{-1}. 2040vs, 2018wsh, 1312wbr, 1265wbrsh, 1245vwbrsh, 1190w, 1160m, 1155wsh, 1092s, 998m, 970vw, 870m, 850vwsh, 840vw, 825m, 808m, 748ssh, 740s, 715s, 700s, 689s, 668sh, 654vs, 642ssh, 570s, 526s, 504s, 490msh, 480m, 438w, 428w, 418wsh, 390w, 375w, 290vs, 282vssh.

trans - carbonylbis(bis(diphenylphosphino) methane) difluorophosphatoruthenium(II) hexafluorophosphate from *cis*-$RuCl_2(dppm)_2$ (0.8 g, 0.848 mmol) and aged (partially hydrolysed) $AgPF_6$ (0.432 g) for 2 hr. The resulting pink solid was recrystallised from CH_2Cl_2-diethyl ether to give the complex as grey plates.

IR max cm^{-1}. 1971vs, 1290vs, 1184wbr, 1143sh, 1125s, 1093s, 1022vw, 995w, 970vwsh, 885m, 875msh, 832vs, 777m, 735ssh, 725s, 715ssh, 688s, 583msh, 575m, 550m, 547w, 516s, 500s, 470m, 408vw, 375vw, 365vwsh.

Using slightly fresher $AgPF_6$ and a similar procedure, a complex believed to be *μ-difluorophosphatobis [bis(bis(diphenylphosphino)methane)carbonylruthenium(II)]hexafluorophosphate* contaminated with *trans*-$[RuCO(O_2PF_2)(dppm)_2]PF_6$ and $[RuF(CO)(dppm)_2]PF_6$[RuF(CO(dppm)$_2PF_6$(^{19}F – 138.9s) was obtained.

IR max cm^{-1}. 1975vs, 1965ssh, 1312w, 1300wsh, 1274w, 1187w, 1157w, 1112wsh, 1103msh, 1092s, 1022w, 997w, 970wbr, 888m, 860msh, 851msh, 838s, 790wsh, 780wbr, 767wsh, 748msh, 730s, 710m, 703msh, 689s, 651wsh, 574msh, 567m, 551m, 519s, 503s, 490wsh, 470m, 443m, 420w, 411wsh, 379w, 370w, 307w.

cis - bis(diphenylphosphino)methanedicarbonylruthenium(II)μ - bis(diphenylphosphino) methaneperchlorato silver(I)perchlorate from *cis*-$RuCl_2(dppm)_2$ (1 g, 1.06 mmol) and $AgClO_4$ (0.485 g, 2.12 mmol) for 6 days at 25°C as cream crystals. Yield 0.7 g (50%).

IR max cm^{-1}. 2094s, 2037s, 1310w, 1280vwbr, 1265vwbr, 1195wsh, 1170wsh, 1158w, 1095vsvbr, 1010s, 1008ssh, 998ssh, 975vw, 925w, 897wsh, 845s, 792w, 780vwbr, 762msh, 753msh, 740s, 728msh, 711m, 702msh, 690s, 663w, 648w, 620s, 615msh, 589vw, 580w, 565m, 532w, 513m, 501s, 483wsh, 479w, 471vw, 455vw, 441w, 435vw, 420wbr, 380w, 342w, 260w.

cis - bis(diphenylphosphino)methanedicarbonylruthenium(II)μ - bis(diphenylphosphino) methanechlorosilver(I) hexafluoroarsenate from *cis*-$RuCl_2(dppm)_2$ (1.0 g, 1.06 mmol) and $AgAsF_6$ (0.69 g, 2.3 mmol) for 24 hr at 25°C as off white crystals. Yield 0.95 g (62%).

IR max cm^{-1}. 2076s, 2015s, 1310wsh, 1306w, 1277w, 1190w, 1160w, 1093s, 1021w, 995m, 841w, 778msh, 745vssh, 701vs, 698vs, 695vs, 673ssh, 668ssh, 613vw, 577w, 560m, 530w, 515m, 502s, 485w, 470w, 420wsh, 392vs, 375msh.

cis - bis(diphenylphosphino)methanedicarbonylruthenium(II)μ - bis(diphenylphosphino) methane(fluorotrihydroxyborato) silver(I)tetrafluoroborate from *cis* - $RuCl_2(dppm)_2$ (1 g, 1.06 mmol) and aged (partially hydrolysed) $AgBF_4$ (2.07 g) for 24 hr at 25°C, as white microcrystals. Yield 0.6 g(42%).

IR max cm^{-1}. 2060s, 2000s, 1332vw, 1320w, 1280w, 1260w, 1189w, 1160mbr, 1050vsvbr, 850vw, 842vw, 768msh, 755ssh, 738vs, 712s, 690vs, 668msh, 612w, 580m, 561m, 532m, 518s, 503vs, 485m, 471m, 450wsh, 440wsh, 418wsh, 379w, 350vw, 342vwsh.

cis - bis(diphenylphosphino)methanedicarbonylruthenium(II)μ - bis(diphenylphosphino) methanedifluorophosphatosilver(I)difluorophosphate from *cis*-$RuCl_2(dppm)_2$ (0.5 g, 0.53 mmol) and aged (hydrolysed) $AgPF_6$ (0.405 g) in dichloromethane (50 ml) for 2 weeks as an off-white microcrystalline powder.

IR max cm^{-1}. 2078‡s, 2018‡s, 1318s, 1312ssh, 1296s, 1276w,

†All complexes have 3020wbr, 1580w, 1570w, 1478m, 1438m, in addition to those bands cited.

‡On occasions these peaks appear at 2086 and 2035 cm^{-1}.

1190w, 1146m, 1095m, 1025vw, 995w, 965wbr, 892ssh, 883s, 875ssh, 848s, 842s, 780m, 765m, 755m, 745ssh, 738ssh, 720wsh, 710s, 689m, 580w, 530wsh, 516m, 500s, 476m, 443m, 375w.

Acknowledgements—We thank Johnson Matthey Ltd. for loans of ruthenium, I.C.I. Ltd. and the S.R.C. for a CASE studentship (G.S.), Drs. W. McFarlane, C. McFarlane and B. V. Cheesman, City of London Polytechnic, for multinuclear NMR spectra carried out under the SRC low field multinuclear NMR service and Prof. J. A. Connor for a communication of his results prior to publication.

REFERENCES

[1]P. S. Braterman, *Metal Carbonyl Spectra.* Academic Press, London, 1975.
[2]J. E. Ellis, P. T. Barger and W. L. Winzenburg, *J. Chem. Soc. Chem. Commun.* 1977, 686 and references therein.
[3]G. Zotti, S. Zecchin and G. Pilloni, *J. Organometallic Chem.* 1979, **181**, 375.
[4]F. L. Wimmer, M. R. Snow and A. M. Bond, *Inorg. Chem.* 1974, **13**, 1617 and references therein.
[5]J. A. Conner and P. I. Riley, *J. Chem. Soc. Dalton Trans.* 1979, 1231.
[6]F. W. Johannsen, W. Preetz and A. Scheffler, *J. Organometallic Chem.* 1975, **102**, 527.
[7]H-C. Frickenschmidt and W. Preetz, *J. Organometallic Chem.* 1978, **146**, 285.
[8]J. A. Connor, E. J. James, C. Overton and N. Elmurr, *J. Organometallic Chem.* 1981, **218**, C13.
[9]B. P. Sullivan, D. J. Salmon and T. J. Meyer, *Inorg. Chem.* 1978, **17**, 3334.
[10]B. P. Sullivan, J. A. Baumann, T. J. Meyer, D. J. Salmon, H. Lehmann and A. Ludi, *J. Amer. Chem. Soc.* 1977, **99**, 7368.
[11]J. T. Mague and J. P. Mitchener, *Inorg. Chem.* 1977, **11**, 2714.
[12]W. J. Geary, *Coordination Chem. Reviews.* 1971, **7**, 81.
[13]B. N. Chaudret, D. J. Cole-Hamilton, R. S. Nohr and G. Wilkinson, *J. Chem. Soc. Dalton Trans.* 1977, 1546 and references therein.
[14]M. Bressan and P. Rigo, *Inorg. Chem.* 1975, **14**, 2286.
[15]J. Chatt and R. G. Hayter, *J. Chem. Soc.* 1961, 896.
[16]J. Weidlein, *Z. Anorg. Allg. Chem.* 1968, **358**, 13.
[17]T. H. Tan, J. R. Dalziel, P. A. Yeats, J. R. Sams, R. C. Thompson and F. Aubke, *Canad. J. Chem.* 1977, **50**, 1843.
[18]S. D. Brown, L. M. Emme and G. L. Gard, *J. Inorg. Nucl. Chem.* 1975 **37**, 2557.
[19]R. A. Goodrich and P. M. Treichel, *J. Amer. Chem. Soc.* 1966, **88**, 3509.
[20]D. J. Cole-Hamilton and G. Wilkinson, *Nouveau J. Chim.* 1977, **1**, 141 and references therein.
[21]M. P. Brown, J. R. Fisher, S. J. Franklin, R. J. Puddephatt and K. R. Seddon, *J. Organometallic Chem.* 1978, **161**, C46.
[22]P. I. van Vliet, G. van Koten and K. Vrieze, *J. Organometallic Chem.* 1979, **182**, 105.

Polyhedron Vol. 1, No. 1, pp. 105–107, 1982
Printed in Great Britain.

0277-5387/82/010105-03$03.00/0
Pergamon Press Ltd.

SYNTHESES OF SOME MIXED Au–Os AND Pt–Os CLUSTERS AND THE X-RAY STRUCTURE OF $[Os_4H_2(CO)_{12}(AuPPh_3)_2]$

BRIAN F. G. JOHNSON, DAVID A. KANER, JACK LEWIS,* PAUL R. RAITHBY and MICHAEL J. TAYLOR
University Chemical Laboratory, Lensfield Road, Cambridge CB2 1EW, England

(*Received* 14 *September* 1981)

Abstract—Some reactions of $[Os_4H_3(CO)_{12}AuPR_3]$ (R = Et, Ph) resulting in the formation of $[Os_4H_2(CO)_{12}(AuPR_3)_2]$ are presented. A single-crystal X-ray structure of $[Os_4H_2(CO)_{12}(AuPPh_3)_2]$ is reported and reveals a novel Ph_3PAu–$AuPPh_3$ unit asymmetrically bridging one edge of an Os_4 tetrahedron, the first example of a mixed gold–metal carbonyl cluster with an Au–Au bond.

Previously,[1–3] we have shown that the reaction of a carbonyl-metallate with a metal halide complex can be successfully applied to the synthesis of osmium–gold cluster species, e.g.

$$[Os_3H(CO)_{11}]^- + AuClPR_3 \longrightarrow Os_3H(CO)_{10}AuPR_3{}^1. \quad (1)$$

Such mixed metal clusters are of interest as they introduce polarity into the metal–metal bonds and also allow the introduction of $14e^-$ and (in the case of Pt) $16e^-$ centres into the cluster, both of which may result in an enhanced reactivity. We report here the synthesis and structure of $[Os_4H_2(CO)_{12}(Au\text{–}PPh_3)_2]$, a novel cluster containing two $AuPPh_3$ moieties.

We have recently demonstrated that $Os_4H_3(CO)_{12}AuPR_3$ (R = Et, Ph) can be prepared in high yields by reaction (2)[3]

$$[Os_4H_3(CO)_{12}]^- + AuClPR_3 \longrightarrow [Os_4H_3(CO)_{12}AuPR_3] \quad R = \text{Et or Ph}. \quad (2)$$

This complex contains a central tetrahedral core of osmium atoms with one edge bridged by an $AuPR_3$ group, which apparently acts as a one electron donor.[3] We have explored several reactions aimed at synthesising $[Os_4H_x(CO)_{12}(AuPR_3)_{4-x}]$ to investigate the mode of bonding of the $AuPR_3$ units in these clusters.

$[Os_4H_3(CO)_{12}AuPR_3]$ reacts cleanly with "$[AuPR_3]^+$" (generated by the action of $TlBF_4$ on $AuClPR_3$) in the presence of NEt_3 to produce two isomeric complexes, A and B, (3)

$$[Os_4H_3(CO)_{12}AuPR_3] + "[AuPR_3]^+" \longrightarrow [Os_4H_2(CO)_{12}(AuPR_3)_2] \quad (R = \text{Et, Ph}) \quad \text{Isomers A and B.} \quad (3)$$

Both isomers are air stable red crystalline solids and were isolated by TLC followed by recrystallation. The mass spectra of both A and B (R = Et) exhibit parent ions at $m/e = 1736$, consistent with the above formulation. The IR spectra (νCO) of each isomer are different, but there is no significant change whether R = Et or Ph).

[ν CO(95% hexane, 5% CH_2Cl_2); A, 2077(s), 2055 (sh), 2050 (s), 2026(s), 2013(m), 1999(m), 1991(m), 1941(w, br), 1903(w, br); B, 2057(s), 2020(s), 2011(s), 1994(m), 1969(w), 1939(w, br)]. In a control reaction $[Os_4H_3(CO)_{12}AuPPh_3]$ reacted with NEt_3 alone to produce both isomers of $[Os_4H_2(CO)_{12}(AuPPh_3)_2]$ and a mixture of cluster anions, which on protonation yielded $[Os_4H_4(CO)_{12}]$ and $[Os_4H_3(CO)_{12}AuPPh_3]$(4)

$$[Os_4H_3(CO)_{12}AuPPh_3] \xrightarrow{NEt_3} [Os_4H_2(CO)_{12}(AuPPh_3)_2] + \text{"anions"} \quad (4)$$

$$\text{"anions"} \xrightarrow{H^+} [Os_4H_4(CO)_{12}] + [Os_4H_3(CO)_{12}AuPPh_3]$$

The NEt_3 is, therefore, effectively disproportionating the $[Os_4H_3(CO)_{12}AuPPh_3]$ to $[Os_4H_4(CO)_{12}]$ and $[Os_4H_2(CO)_{12}(AuPPh_3)_2]$. These results can be rationalised in terms of nucleophilic attack by NEt_3 at the $AuPPh_3$ centre, which would produce a gold cation by heterolytic cleavage of the Au–Os bond. This could then attack $[Os_4H_3(CO)_{12}AuPPh_3]$ (or $[Os_4H_2(CO)_{12}AuPPh_3]^-$) to produce $[Os_4H_2(CO)_{12}(AuPPh_3)_2]$. Nucleophilic attack at the gold centres of $[Ph_3PAuCo(CO)_4]$ and $[Ph_3PAuFe(CO)_3NO]$ to produce gold cations has previously been demonstrated,[4] but this is the first report of such a reaction for a cluster species.

The reaction of a metal–alkyl with a metal–hydride, with the aim of eliminating RH and forming a metal–metal bond[5–7] has also been investigated (5).

$$M\text{–}R + M\text{–}H \longrightarrow M\text{–}M^1 + RH. \quad (5)$$

Reaction of $[PtR_2(dppe)\dagger]$ (R = Ph, Me) with $[Os_4H_4(CO)_{12}]$ (6) resulted in high yields (*ca.* 80%) of $[Os_4H_2(CO)_{12}Ptdppe]$ as dark red/black needles [νCO 2086(w, sh), 2079(s), 2067(w), 2057(s), 2046(w), 2026(s), 2012(sh), 2005(s), 1998(w, sh), 1977(m), 1964(w, br), 1917(w, br)].

*Author to whom correspondence should be addressed.
†dppe = diphenyl phosphino ethane.

$$[Os_4H_4(CO)_{12}] + [PtR_2(dppe)] \longrightarrow [Os_4H_2(CO)_{12}Pt(dppe)] \quad (6)$$
(R = Ph, Me).

$[Os_4H_4(CO)_{12}]$ also reacts with $AuMePPh_3$ to produce moderate yields of $[Os_4H_3(CO)_{12}AuPPh_3]$ (7).

$$[Os_4H_4(CO)_{12}] + [AuMePPh_3] \longrightarrow [Os_4H_3(CO)_{12}AuPPh_3]. \quad (7)$$

Further reaction of $[Os_4H_3(CO)_{12}AuPPh_3]$ with $[AuMePPh_3]$, however, produces only small quantities of $[Os_4H_2(CO)_{12}(AuPPh_3)_2]$.

To date, attempts to obtain crystals of isomer B of $[Os_4H_2(CO)_{12}(AuPR_3)_2]$ (R = Et, Ph) suitable for X-ray diffraction have been unsuccessful, but those of isomer A have been obtained. This complex crystallises in the monoclinic space group $C2/c$ with cell dimensions a = 38.239(15), b = 13.265(5), c = 23.447(10) Å, β = 113.41(3)°, and U = 10914(7) Å^3; D_c = 2.45 g cm^{-3} for Z = 8 and M = 2017.42 and $C_{48}H_{32}Au_2O_{12}Os_4P_2$. 4189 intensities were recorded on a Stoe four-circle diffractometer using graphite monochromated Mo-K_α radiation [μ(Mo-K_α) = 147.11 cm^{-1}]. The structure was solved by a combination of direct methods and Fourier difference techniques and refined by blocked full-matrix least squares to R = 0.078 and R_w = 0.073 for 2109 unique, observed, absorption corrected data [$F > 3\sigma(F)$].

The molecular structure of isomer A of $[Os_4H_2(CO)_{12}(AuPPh_3)_2]$ is shown in Fig. 1 together with some important bond parameters. The four Os atoms define a distorted tetrahedron one edge of which is bridged by two Au atoms which themselves are joined by an Au–Au bond. The metal skeleton may be described as two tetrahedra sharing a common edge, and can also be related to the structure of $[Os_6(CO)_{18}]$ which is a bicapped tetrahedron,[8] but in this case the Os(3)...Au(2) distance of 3.159(4) Å may be too long to be considered a formal bond. Each Au atom is coordinated to a triphenylphosphine group and each Os atom is coordinated to three terminal carbonyls. The two hydrides were not located directly but the carbonyl groups adjacent to the long Os(1)–Os(3) and Os(2)–Os(3) edges bend away from them (average *cis* Os–Os–C 117.5°) suggesting that this effect may be caused by the presence of the bridging hydrides along these edges.

Unlike the monogold complexes with Os_3 and Os_4 units, where the $AuPR_3$ unit behaves in a similar manner to a bridging hydride,[1,3] in $[Os_4H_2(CO)_{12}(AuPPh_3)_2]$ both Au atoms bridge the same Os(1)–Os(2) edge and the Au(1)–Au(2) bond is formed. It appears to be energetically favourable to form an Au–Au bond rather than have

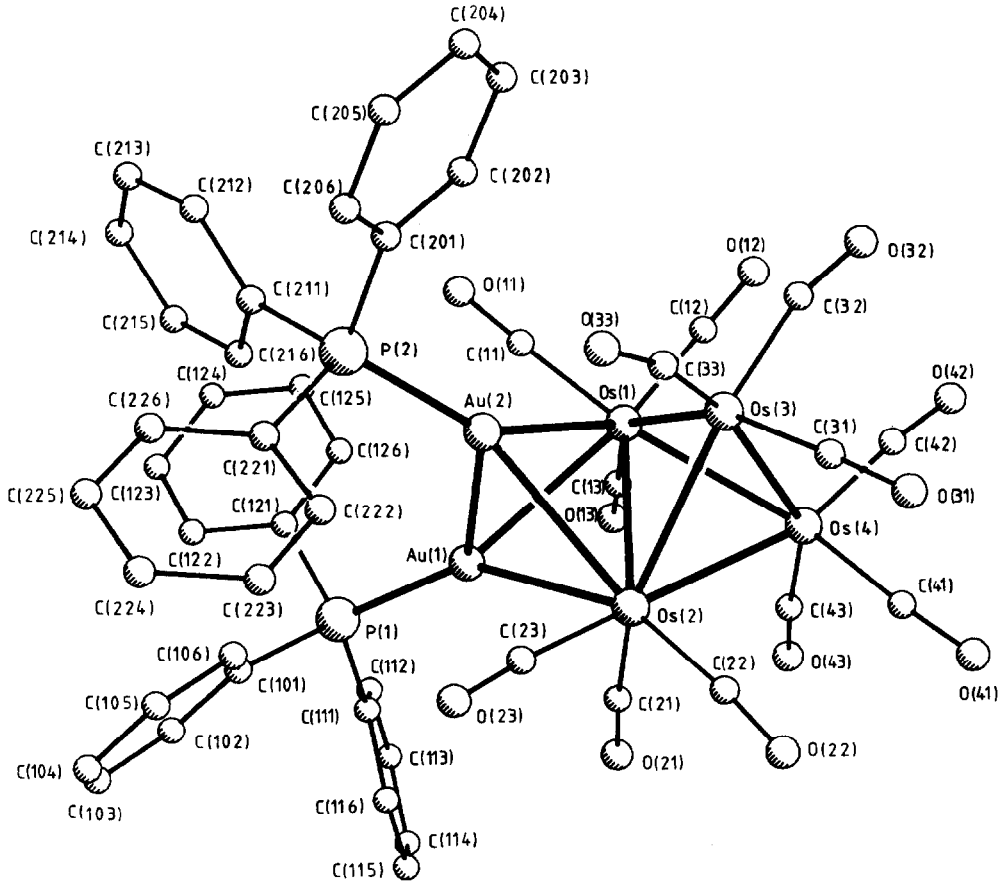

Fig. 1. The molecular structure of isomer A of $Os_4H_2(CO)_{12}(AuPPh_3)_2$. Bond lengths (Å) Os(1)–Os(2), 2.977(6); Os(1)–Os(3), 2.968(4); Os(1)–Os(4), 2.815(5); Os(2)–Os(3); 2.952(5); Os(2)–Os(4), 2.828(4); Os(3)–Os(4), 2.870(4); Os(1)–Au(1), 2.858(4); Os(2)–Au(1), 2.857(4); Os(1)–Au(2), 2.839(4); Os(2)–Au(2), 3.004(5); Os(3)...Au(2), 3.159(4); Au(1)–Au(2), 2.793(4) A. Bond angles (°): Os(1)–Au(1)–Os(2), 62.8(1); Os(1)–Au(1)–Au(2), 60.3(1), Os(2)–Au(1)–Au(2); 64.2(1); Os(1)–Au(1)–P(1), 147.3(6), Os(2)–Au(1)–P(1), 147.5(6); Au(2)–Au(1)–P(1), 132.2(4); Os(1)–Au(1)–Os(2), 61.2(1); Os(1)–Au(2)–Au(1), 61.0(1); Os(2)–Au(2)–Au(1), 58.9(1); Os(1)–Au(2)–P(2), 146.7(6); Os(2)–Au(2)–P(2), 152.1(6); Au(1)–Au(2)–P(2), 124.8(4)°.

a configuration in which two $AuPR_3$ groups bridge different Os–Os edges (a situation which may occur in isomer B). The Au(1)–Au(2) bond length is similar to the values reported for unsupported Au–Au single bonds in a number of Au clusters.[9] An analogy may be drawn between two Au atoms bridging an Os–Os bond and two hydrides bridging an Os–Os bond, as in $[Os_3H_2(CO_{10}]$,[10] since both types of ligand are considered to donate one electron. However, the presence of two hydrides bridging an unsaturated Os–Os edge is associated with a short Os–Os bond (2.683(1) Å) and in the case of the Au bridges there is no unsaturation and the Os(1)–Os(2) bond is longer. The donated electrons enter different orbitals in the two cases.

The geometry around the Au atoms indicates that they should be considered as *sp* hybridized Au(I). If the P(1)–Au(1) vector is projected, to establish the position of the other lobe of the *sp* orbital, it is found that it points to a location close to the centre of the Os(1)–Os(2)–Au(2) triangle. Similarly, the P(2)–Au(2) vector points in the region of the centre of the Os(1)–Os(2)–Au(1) triangle. The bonding of the Os(1)–Os(2)–Au(1)–Au(2) unit may then be described in terms of a four-centre delocalised bond.

The reactions outlined above offer a potential route for successively replacing hydrides by $AuPR_3$ units. We are currently extending these reactions to other systems and initial results indicate that $Os_4H(CO)_{13}AuPR_3$[3] is cleanly converted to $Os_4(CO)_{13}(AuPR_3)_2$ (R = Et, Ph). Other methods of introducing $AuPR_3$ units into clusters are also under investigation as is the general reactivity of these osmium–gold species.

Acknowledgements—We would like to thank the S.R.C. for financial support (to D.A.K.) and the "Tunku Abdul Raman" Foundation for the award of a Fellowship (to M.J.T.).

REFERENCES

[1]B. F. G. Johnson, D. A. Kaner, J. Lewis and P. Raithby, *J. Organomet. Chem.* 1981, **215**, C33.
[2]B. F. G. Johnson, D. A. Kaner, J. Lewis and P. Raithby, *Chem. Commun.* 1981, 953.
[3]B. F. G. Johnson, D. A. Kaner, J. Lewis, P. R. Raithby and M. J. Taylor, *J. Chem. Soc., Chem. Commun*, to be published.
[4]M. Casey and A. R. Manning, *J. Chem. Soc. A*, 1971, 2989.
[5]J. R. Norton, *Acc. Chem. Res.* 1979, **12**, 139.
[6]L. J. Farrugia, J. A. K. Howard, P. Mitrprachachon, J. L. Spencer, F. G. A. Stone and P. Woodward, *Chem. Commun.* 1978, 260.
[7]P. Renauet, G. Taintarier and B. Goutheron, *J. Organomet. Chem.* 1978, **150**, C9.
[8]R. Mason, K. M. Thomas and D. M. P. Mingos, *J. Am. Chem. Soc.* 1973, **95**, 3802.
[9]F. Demartin, M. Manassero, L. Naldini, R. Ruggeri and M. Sansoni, *J. Chem. Soc., Chem. Commun.* 1981, 222; J. W. A. van der Velden, J. J. Bour, B. F. Otterloo, W. P. Bosman and J. H. Noodik, *J. Chem. Soc., Chem. Commun.* 1981, 583.
[10]R. W. Broach and J. M. Williams, *Inorg. Chem.* 1979, **18**, 314.

Polyhedron Vol. 1, No. 1, pp. 109–111, 1982
Printed in Great Britain.

0277–5387/82/010109–03$03.00/0
Pergamon Press Ltd.

PREPARATION AND PROPERTIES OF A SOLUBLE POLYMERIC AQUO ION OF MOLYBDENUM(V)

FRASER A. ARMSTRONG and A. GEOFFREY SYKES*
Department of Inorganic Chemistry, The University, Newcastle upon Tyne, NE1 7RU, England

(*Received* 28 *October* 1981)

Abstract—An orange/brown ionic and polymeric Mo(V) ion (Mo to Na ratio 2.3:1), soluble in H_2O to give stable solutions at pH ~ 6, with UV visible spectrum λ_{max} 318 nm, ϵ(per Mo) 3300 M^{-1} cm^{-1}, has been prepared and partially characterised. Various properties are described, including the conversion to the well established Mo(V) aquo dimer, $Mo_2O_4^{2+}$, on adjustment of $[H^+]$ to 0.17–0.50 M, I = 0.50 M ($H/LiClO_4$). First-order rate constants, k_{obs}(25°C), determined by conventional spectrophotometry give a good fit to the empirical rate law,

$$k_{obs} = \frac{a[H^+]^2}{1 + b[H^+]}$$

and a reaction sequence consistent with this $[H^+]$ dependence is proposed.

INTRODUCTION

Although the orange–yellow aquo-ion $Mo_2O_4^{2+}$ is now well characterised, little is known about the nature of Mo(V) aquo-species in weakly acid through alkaline solutions. In contrast it has been established that the aqueous chemistry of Mo(VI) in the region pH 1–7 is characterised by the presence of oligomers such as $Mo_7O_{24}^{6-}$ and $Mo_8O_{26}^{4-}$, and that the molybdate ion MoO_4^{2-} predominates under more alkaline conditions.[1,2] The nature of Mo(VI) in solution at pH < 1 has also been investigated.[3,4]

UV visible absorbance changes occurring on addition of alkali to acidic solutions containing the ion $Mo_2O_4^{2+}$ have been reported, and the existence of a more condensed cationic species postulated.[5] However, as far as we are aware no well-defined crystalline solid has been isolated from these solutions. Further addition of alkali invariably results in precipitation of brown molybdenum(V) hydroxide $MoO(OH)_3$ which redissolves at higher pH's to give Mo(IV) and Mo(VI) by disproportionation[6]. It was, therefore, of some interest to investigate a new form of Mo(V) having the properties of a polymer which is obtained as a reproducible product by a procedure described herein. This species is stable in aqueous solution at pH ~ 6.

EXPERIMENTAL

Preparation

To a solution of sodium molybdate dihydrate (B.D.H., Analar grade, 9.7 g) in H_2O (20 ml) was added acetylacetone (B.D.H. Analar grade, 4 ml). A solution of sodium dithionite (B.D.H., Reagent grade, 4.0 g) in cold water (15 ml) was added and the mixture (pH *ca.* 5.5) was stirred for 15 min. The orange/brown precipitate obtained was collected by suction filtration then suspended in degassed H_2O (*ca.* 300 ml) and heated to 60° with stirring. The resulting red solution was cooled, filtered and an equal volume of ethanol added with stirring. The gelatinous precipitate was filtered off, washed with ethanol and ether then dried by suction.

Carbon analysis showed C < 1% thus indicating that no acetylacetone was contained in the product. Attempts to prepare the orange/brown solid in the absence of acetylacetone, by careful control of pH at *ca.* 5.5, resulted in the precipitation of a brown solid which was only very slightly (≪ 1%) soluble in hot water. The UV visible spectrum of the solution was very similar to that reported below in Fig. 1 although large increases in absorbance at < 280 nm were apparent. The IR spectrum was similar to that observed for the orange water-soluble solid obtained in the presence of acetylacetone displaying bands at 730, 960, 1625 and a broad absorption at 2500–3600 cm^{-1}. The function of the acetylacetone is not understood. Since this procedure has proved reproducible, it was left essentially unchanged.

Analyses

The solid obtained gave for Mo (gravimetric), 51.9%; and Na (flame photometry), 5.6%. Tests for S (which might result from oxidation products of $S_2O_4^{2-}$) were negative. Values obtained for H were not reproducible for different preparations, the range being 2.1 ± 0.6%. Water analysed by vacuum desiccation over P_4O_{10}, and thermo-gravimetrically using a Stanton Thermobalance was also variable. Typical values were H_2O, 6.6%(P_4O_{10}) and 15.6% (thermogravimetric, single stage dehydration 40–440°). A thermogravimetric analysis on a P_4O_{10}-desiccated sample gave H_2O, 9.9%. Thus, only about one-third of the H_2O is readily removable by vacuum desiccation and can be assigned as lattice H_2O (very likely a variable). From the reproducible Mo:Na of 2.3:1, the empirical formula $Na_3Mo_7O_{19}\cdot 12 \pm 4H_2O$ may be tentatively proposed, with the reservation that hydroxo groups might be present as opposed to

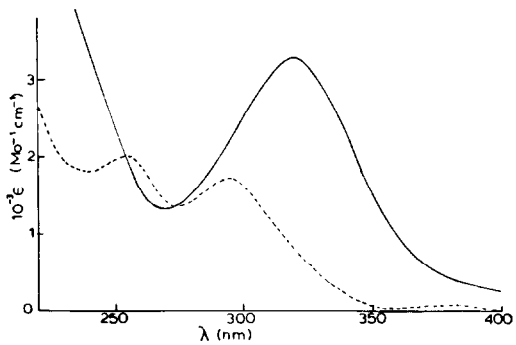

Fig. 1. Spectra of polymeric Mo(V) in H_2O (———) and of $Mo_2O_4^{2+}$ in 1.00 M $HClO_4$ (– – – –).

*Author to whom correspondence should be addressed.

coordinated H_2O. Incorporation of as little as 1 mole of acetylacetone per empirical formula would give ~4% C analysis which clearly does not apply. The oxidation state of the molybdenum, from titration with Ce(IV), was found to be Mo(V). The UV visible spectrum (determined for a sample purified by precipitation in 1:1 ethanol-H_2O until a constant spectrum was obtained) is shown in Fig. 1, where absorption coefficients (ϵ) per Mo (i.e. Mo atom^{-1} cm^{-1}) are at λ_{max} 318(3300) and λ_{min} 268(1300). The IR spectrum (KBr disc) shows bands at 960, 730 and 710 cm^{-1} consistent with a structure containing terminal oxo groups and bridging oxygens.[8] Bands at 1620 and 2500–3600 cm^{-1} (broad) can be assigned to loosely bound H_2O molecules.[9]

Other properties

The solubility of the soluble orange solid is *ca.* 20 g l^{-1} in distilled H_2O. The UV visible spectrum of a dilute solution is stable for >6 hr in the presence of air. Addition of salts such as LiCl, NaCl, $NaClO_4$, KCl, CsCl or $BaCl_2$ or the careful addition of ethanol result in the slow formation of red gelatinous precipitates which on filtration and drying in air are degraded to orange powders. Products precipitated by ethanol, LiCl, NaCl or $NaClO_4$ are readily soluble in distilled H_2O, whereas the KCl-, CsCl- and $BaCl_2$-precipitated products are insoluble.

The salt effects, strongly indicate that the species under investigation is an ionic polymeric form of Mo(V). This was supported by the quantitative formation of the di-μ-oxo Mo(V) dimer $Mo_2O_4^{2+}$ in 0.1–0.5 M $HClO_4$, the kinetics of which were studied briefly as described below.

An attempt was made to obtain polymeric Mo(V) by slow addition of dilute NaOH solution to a solution of $Mo_2O_4^{2+}$ in 0.1 M $HClO_4$ under oxygen-free conditions. The spectrum of $Mo_2O_4^{2+}$ (corrected for dilution) was stable up to pH 2.0. Changes then occurred, the absorbance >300 nm increasing to about twice the former value with smaller increases occurring below 280 nm. The spectral change was complete at pH 3.5 and addition of acid, in an attempt to reverse the process, resulted in little change over a period of 5 min. Addition of further alkali over the pH range 3.6–6.0 caused a general decrease in absorbance, the nature of which is uncertain. However, at no point in the addition of alkali was a spectrum corresponding to that of polymeric Mo(V) shown in Fig. 1 generated.

Conversion to $Mo_2O_4^{2+}$

Acidification of an aqueous solution of polymeric Mo(V) with perchloric acid results in the quantitative formation of the aquo-dimer, $Mo_2O_4^{2+}$, λ_{max} (ϵ, Mo atom^{-1} cm^{-1}) 293(1727) and 254(1950).[10,11] Isosbestic points are observed at 255 and 274 nm, Fig. 1.

Kinetic studies

The above conversion was followed at 25.0°, $[H^+] = 0.17$–0.50 M, I = 0.50 M ($LiClO_4$) by monitoring the decrease in absorbance due to polymeric Mo(V) at 318 nm (ϵ = 3300 Mo atom^{-1} cm^{-1}). Anaerobic conditions were used (N_2, Teflon tubing and nylon syringes) to minimise oxidation of $Mo_2O_4^{2+}$ during the course of each run. To initiate each reaction, typically a 5 ml aliquot of $HClO_4$ (0.20–1.00 M), I = 1.00 M ($LiClO_4$), was added to 5 ml of an aqueous solution of polymeric Mo(V) (*ca.* 1.8×10^{-4} M in Mo) in a 4 cm silica cell. Absorbance readings were taken at intervals of (usually) 2 min using a Unicam SP500 spectrophotometer.

Table 1. First-order rate constants for the formation of $Mo_2O_4^{2+}$ from polymeric Mo(V)

$[H^+]$ (M)	$10^3 k_{obs}$ (s^{-1})
0.17	0.52
0.30	1.12
0.33	1.34
0.40	1.61
0.50	2.14

[Mo] (total) = 9.0×10^{-5} M, I = 0.50 M ($LiClO_4$), T = 25.0°C.

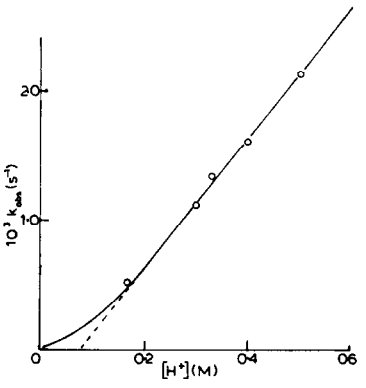

Fig. 2. The formation of $Mo_2O_4^{2+}$ from polymeric Mo(V). Dependence of first-order rate constants k_{obs} on $[H^+]$, [Mo] = 9.0×10^{-5} M, I = 0.50 M ($LiClO_4$), T = 25.0°.

Plots of absorbance (A) changes $\log(A_t - A_\infty)$ were linear to >90% and from the slopes (×2.303), first-order rate constants, k_{obs} as in Table 1 were obtained. The dependence of k_{obs} on $[H^+]$ is first order in the region $[H^+] = 0.17$–0.50 M as shown in Fig. 2. However an apparent negative intercept results which clearly has no meaning. The data give a good fit to the modified empirical expression (1),

$$k_{obs} = \frac{a[H^+]^2}{1 + b[H^+]} \quad (1)$$

which can be rewritten in the more useful linear form (2),

$$\frac{[H^+]}{k_{obs}} = \frac{1}{a} \cdot \frac{1}{[H^+]} + \frac{b}{a} \quad (2)$$

Thus a plot of $[H^+]/k_{obs}$ against $[H^+]^{-1}$ is linear with the slope = $1/a$ and intercept = b/a.

DISCUSSION

The appearance of gel-like precipitates on treatment with ethanol or inorganic salts, and the absence of any crystalline form is consistent with the Mo(V) species under examination being polymeric in nature. The suggested empirical formula for the solid, $Na_3Mo_7O_{19} \cdot 12 \pm 4H_2O$, implies that condensed species, possibly $Mo_7O_{19}^{3-}$ or related, perhaps multiple units, may exist in aqueous solution. Similar condensed species are a familiar feature in the aqueous chemistry of aquo-molybdenum(VI). The insolubility of polymeric Mo(V) in solutions containing other dissolved salts may explain why such species have not been previously identified in weakly acidic solutions. Brown precipitates (usually described as molybdenum(V) hydroxide) which are frequently formed during preparations of Mo(V) compounds, may in many circumstances be found to redissolve (perhaps only partially) in distilled H_2O to give stable solutions of the polymer. The function of acetylacetone in the formation of polymeric Mo(V) is uncertain. It may prohibit extensive condensation of Mo(V) which would ultimately lead to the formation of insoluble molybdenum(V) hydroxide, by initially coordinating to smaller Mo(V) units, and thus limiting the formation of Mo–O–Mo bridges. Stabilisation of the oligomer might then occur by intramolecular rearrangement. The coordination of acetylacetone appears to

be transient as little or no carbon is detectable by analysis of the product. Although the Mo:Na ratio of 2.3:1 appears to be constant for a variety of preparations, the assignment of a precise unambiguous formula is difficult due to variable amounts of associated H_2O molecules.

The quantitative formation in acid solution of the aquo-ion $Mo_2O_4^{2+}$, and excellent first-order kinetic behaviour suggests a single unique rate-determining step and very likely that a single unique polymeric species is present. The rate constants obtained give a good fit to (2) the mechanistic implications of which are now considered. Two mechanisms are proposed. The first involves formation of a small stationary-state concentration of intermediate by protonation, which then reacts with another proton to yield products. Such a scheme is described by eqns (3) and (4),

$$Mo(V)_n + H^+ \underset{k_2}{\overset{k_1}{\rightleftharpoons}} Mo(V)_n, H^+ \quad (3)$$

$$Mo(V)_n, H^+ + H^+ \xrightarrow{k_3} \text{products.} \quad (4)$$

Applying the stationary-state approximation for polymeric $Mo(V)_n,H^+$, eqn (5) is obtained,

$$k_{obs} = \frac{k_1 k_3 [H^+]^2}{k_2 + k_3 [H^+]} \quad (5)$$

in which $a = k_1k_3/k_2$ and $b = k_3/k_2$. From 1/intercept and the ratio of intercept/slope respectively $k_1 = (5.5 \pm 0.3) \times 10^{-3}\ M^{-1}\ s^{-1}$ and $k_3/k_2 = 7.6 \pm 1.1\ M^{-1}$ are obtained.

An alternative mechanism (6) and (7),

$$Mo(V)_n + H^+ \overset{K_4}{\rightleftharpoons} Mo(V)_n,H^+ \quad (6)$$

$$Mo(V)_n,H^+ + H^+ \xrightarrow{k_5} \text{products} \quad (7)$$

requires the rapid establishment of a large equilibrium concentration of intermediate by protonation followed by a rate-determining reaction of intermediate with another proton. This leads to the rate eqn (8),

$$k_{obs} = \frac{k_5 K_4 [H^+]^2}{1 + K_4 [H^+]}. \quad (8)$$

From (8) it follows that $a = k_5K_4$ and $b = K_4$, and the least squares fit gives $k_5 = 5.45 \pm 0.27 \times 10^{-3}\ M^{-1}\ s^{-1}$ and $K_4 = 7.58 \pm 1.12\ M^{-1}$. The value obtained for K_4 of $7.58\ M^{-1}$, gives an acid dissociation pK_a for the polymer of 0.88. Consequently, under conditions of $[H^+] = 0.17$–0.50 M, most of the polymeric Mo(V) will be protonated, the rate of $Mo_2O_4^{2+}$ formation being controlled by k_5. The spectrum of such a protonated species might be expected to differ from that of the unprotonated form, hence the observation of isosbestic points is relevant here. Previously attention has been drawn to the interpretation of isosbestic points and application to the analysis of chemical reactions.[12,13] For a consecutive reaction A→B→C, the presence of isosbestic points as defined in Fig. 1 throughout the reaction is indicative that the first stage A→B is rate determining with no measurable build-up of species B. Since two isosbestic points are observed throughout this reaction, sequence (3)–(4) involving a very small stationary-state concentration of intermediate seems preferable to (6)–(7). Since simple protonation reactions are known to be rapid, the rate constant k_1 ($5.5 \times 10^{-3}\ M^{-1}\ s^{-1}$) almost certainly corresponds to a proton-induced cleavage of an oxo bridge to produce a more reactive species which can either deprotonate to give the starting material, or protonate again to produce (finally) $Mo_2O_4^{2+}$.

Acknowledgement—F.A.A. is grateful to SERC for a post-graduate studentship.

REFERENCES

[1]J. Aveston, E. W. Anacker and J. S. Johnson, *Inorg. Chem.* 1964, **3**, 735.
[2]D. S. Honig and K. Kustin, *Inorg. Chem.* 1972, **11**, 65.
[3]J. J. Cruywagen, J. B. B. Heyns and E. F. C. H. Rohwer, *J. Inorg. Nucl. Chem.* 1978, **40**, 53.
[4]L. Krumenacker, *Ann. Chim.* 1972, **7**, 425.
[5]B. Viossat and M. Lamache, *Bull. Soc. Chim. France* 1975, 1570.
[6]P. Souchay, M. Cadiot and B. Viossat, *Bull. Soc. Chim. France* 1970, 892.
[7]A. I. Vogel, *Textbook of Quantitative Inorganic Analysis*, 3rd Edn, 1961.
[8]W. E. Newton and J. W. McDonald, *J. Less Common Metals* 1977, **54**, 51.
[9]K. Nakamoto, *Infra-red Spectra of Inorganic and Coordination Compounds*, 2nd Edn, p. 166, 1970.
[10]M. Ardon and A. Pernick, *Inorg. Chem.* 1973, **12**, 2484.
[11]Y. Sasaki and A. G. Sykes, *J. Chem. Soc. Dalt. Trans* 1974, 1469.
[12]M. D. Cohen and E. Fischer, *J. Chem. Soc.* 1962, 3044.
[13]T. Nowicka-Jankowska, *J. Inorg. Nucl. Chem.* 1971, **33**, 2043.

Polyhedron Vol. 1, No. 1, pp. 113–121, 1982
Printed in Great Britain.

0277–5387/82/010113–09$03.00/0
Pergamon Press Ltd.

PARAMAGNETIC ION BINDING TO AMINO ACIDS, STRUCTURAL AND DYNAMICAL INFORMATION ON A Mn(II) COMPLEX OF L-PROLINE FROM ^{13}C RELAXATION DATA

BERNARD HENRY, JEAN-CLAUDE BOUBEL and JEAN-JACQUES DELPUECH*
Laboratoire de Chimie Physique Organique, ERA CNRS 222, Université de Nancy I, C.O. No. 140, 54037 Nancy Cedex, France

(*Received* 28 *September* 1981)

Abstract—The ^{13}C relaxation times (T_1 and T_2) and isotropic contact shift ($\Delta\omega$) of 1.28 molar aqueous solutions of L-Proline at pH = 11 (or pD = 11.4) containing $10^{-4} - 10^{-5}$ M manganese perchlorate are measured at 62.86 MHz over a temperature range of 28–80°C. Under these conditions, the Mn^{2+} cation is bound to three L-Proline molecules in their dibasic form, and a fast exchange is occurring between bound and bulk L-Proline molecules. The longitudinal relaxation of carbons α, β, γ, δ of L-Proline molecules in this complex is shown to be purely dipolar, and is controlled by the rotational reorientation of the complex. The transverse relaxation of bound L-Proline molecules is mainly scalar and is controlled by the electronic relaxation. Overall relaxation rates and paramagnetic shifts also depend on the ligand exchange rate k_M (from bound to free sites) at lower temperatures. The measurement of these quantities allow us to determine (i) the structure of the complex: the Mn(II) cation may be positioned with respect to each proline ligand, the sites of coordination are the uncharged nitrogen and one carboxylic atom, the distance to the Mn^{2+} cation are respectively 2.08 and 1.97 Å; (ii) Hyperfine coupling constants: A = +0.16; 0.08; 0.25 and 0.22 MHz for carbons α, β, γ, δ, respectively. (iii) Electronic relaxation parameters: assuming that T_{1e} ($= 2.18 \times 10^{-8}$ s at 25°C) is controlled by the modulation of the quadratic crystalline zero-field splitting interaction allows us to estimate the trace of the corresponding tensor: $\Delta = 0.0305$ cm^{-1}, and a correlation time $\tau_v(25°C) = 1.32$ ps for the impact of solvent molecules against the Mn^{2+}-L-Proline complex (iv) Kinetic parameters for ligand exchange: $k_M(25°C) = 7.41 \times 10^4$ s^{-1}; $\Delta H^{\ddagger} = 15.6$ kcal. mol.$^{-1}$; $\Delta S^{\ddagger} = 16.1$ e.u.

INTRODUCTION

^{13}Carbon relaxation in paramagnetic systems is widely used to obtain structural and dynamical information on complexes of transition metal ions. In this respect the Mn(II) cation has gained a widespread use as a paramagnetic probe to study the binding site of metal ions to biological molecules, such as nucleic acids and bases, nucleosides and their phosphates, DNA, proteins and enzymes.[1–9] These binding sites have often been characterized by selective line-broadening of hydrogen and ^{13}C nuclei that are close to the presumed metal ion binding site. Theoretical treatments have been devised to obtain a quantitative description of the structure and dynamics of such complexes. A thorough analysis uses in fact, besides line-broadening measurements, the values of the chemical shift and the longitudinal relaxation time induced by the paramagnetic cation on the ^{13}C nuclei in the ligand.

Investigations using amino-acids as ligands are relatively rare in the literature[10–13] in spite of the importance of these compounds in the building of complex biochemical and biological molecules.

In a previous work,[14] we obtained structural parameters for a Mn(II) complex of L-Proline in water solution from the T_1 relaxation times of the α, β, γ, δ carbon-13 nuclei of the pyrrolidine ring at 60°C. Experiments were carried out in D_2O solution at pD = 11.4 using concentrations in the range $[Mn^{2+}] \simeq 10^{-4}$ M and [L-Proline] = 1.28 M. Under these conditions, the Mn(II) cation is bound to the amino-acid under the form of a tris-Proline complex $[Mn(L\text{-}PRO^-)_3]^-$ to an extent of 95%.[14–15] We have then considered that two species only are existing in solution, the free L-Proline molecules and the L-Proline molecules in the tris-L-Proline complex. Carbon nuclei may therefore exist either in a diamagnetic site or a paramagnetic site respectively. These two sites are denoted D and M in the following. These letters will also appear as subscripts in the denomination of experimental quantities, i.e. the molar fractions p of free and bound proline molecules, the T_1 and T_2 relaxation times and the chemical shifts ω (in rad. s^{-1}).

This paper reports a thorough NMR investigation of the above complex at several temperatures so as to obtain information on both the structure of the Mn^{2+}-L-Proline complex and the kinetic parameters for the ligand–metal ion reaction. The fast exchange approximation is no longer valid at lower temperatures and the measured nuclear parameters T_1, T_2 and ω therefore depend on the exchange rate $1/\tau_M$ of the bound proline molecules. The transverse relaxation rate $1/T_{2M}$ in the paramagnetic site is predominantly scalar in character and therefore mainly depends on the hyperfine coupling constant A and the electronic relaxation time T_{1e}. The longitudinal relaxation rate $1/T_{1M}$ is on the contrary exclusively dipolar, thus allowing to deduce the ion-to-ligand distances r_c and the reorientational correlation time τ_r in the complex. A great deal of structural, dynamical and kinetic information can therefore be extracted from the whole set of ^{13}C NMR measurements.

THEORY

The chemical shifts ω and relaxation rates $1/T_1$, $1/T_2$ of the observed nuclei depend on the nuclear and kinetic parameters which are necessary to describe the Mn^{2+}-L-Proline complex. Theoretical expressions which show this dependence are well-known at the present time.[16] They are summarized in Tables 1 and 2. We shall not

*To whom correspondence should be addressed.

Table 1. The full set of equations

$$\tau_M = \tau_M^{\circ} \exp(E_M/RT) \qquad (1)$$

$$\tau_R = \tau_R^{\circ} \exp(E_R/RT) \qquad (2)$$

$$\tau_V = \tau_V^{\circ} \exp(E_V/RT) \qquad (3)$$

$$\frac{1}{T_{1e}} = \frac{2}{50} \Delta^2 (4S(S+1)-3) \left(\frac{\tau_V}{1+\omega_e^2\tau_V^2} + \frac{4\tau_V}{1+4\omega_e^2\tau_V^2}\right) \qquad (4)$$

$$\frac{1}{T_{2e}} = \Delta^2 (4S(S+1)-3) \left(3\tau_V + \frac{5\tau_V}{1+\omega_e^2\tau_V^2} + \frac{2\tau_V}{1+4\omega_e^2\tau_V^2}\right) \qquad (5)$$

$$\frac{1}{\tau_{ci}} = \frac{1}{\tau_R} + \frac{1}{\tau_M} + \frac{1}{T_{ie}} \quad (i = 1 \text{ or } 2) \qquad (6)$$

$$\frac{1}{\tau_{ei}} = \frac{1}{\tau_M} + \frac{1}{T_{ie}} \quad (i = 1 \text{ or } 2) \qquad (7)$$

$$K_{DD} = \frac{2\times10^{-14}}{15} \frac{\mu_M^2\gamma_c^2}{r_c^6} \qquad (8)$$

$$K_{RS} = 8\pi^2A^2S(S+1)/3 \qquad (9)$$

$$1/T_{1M} = K_{DD}\left(\frac{\tau_{c2}}{1+(\omega_c-\omega_e)^2\tau_{c2}^2} + \frac{3\tau_{c1}}{1+\omega_c^2\tau_{c1}^2} + \frac{6\tau_{c2}}{1+(\omega_c+\omega_e)^2\tau_{c2}^2}\right)$$
$$+ K_{RS}\left(\frac{\tau_{e2}}{1+(\omega_c-\omega_e)^2\tau_{e2}^2}\right) \qquad (10)$$

$$1/T_{2M} = K_{DD}\left(2\tau_{c1} + \frac{0.5\tau_{c2}}{1+(\omega_c-\omega_e)^2\tau_{c2}^2} + \frac{1.5\tau_{c1}}{1+\omega_c^2\tau_{c1}^2}\right) + \frac{3\tau_{c2}}{1+\omega_e^2\tau_{c2}^2}$$
$$+ \frac{3\tau_{c2}}{1+(\omega_c+\omega_e)^2\tau_{c2}^2}) + \frac{K_{RS}}{2}\left(\tau_{e1} + \frac{\tau_{c2}}{1+(\omega_c-\omega_e)^2\tau_{e2}^2}\right) \qquad (11)$$

$$\frac{\Delta\omega_M}{\omega_c} = \frac{-2\pi A\mu_M\sqrt{S(S+1)}}{3kT\gamma_c} \qquad (12)$$

$$\frac{1}{T_{1r}} \equiv \left(\frac{1}{T_1} - \frac{1}{T_{1D}}\right)/p_M = \frac{1}{T_{1M}+\tau_M} \qquad (13)$$

$$\frac{1}{T_{2r}} \equiv \left(\frac{1}{T_2} - \frac{1}{T_{2D}}\right)/p_M = \frac{1}{\tau_M} \frac{1/T_{2M}^2 + 1/T_{2M}\tau_M + \Delta\omega_M^2}{(1/T_{2M}+1/\tau_M)^2 + \Delta\omega_M^2} \qquad (14)$$

$$\Delta\omega_r \equiv \Delta\omega/p_M = \frac{\Delta\omega_M}{(1/\tau_M/T_{2M})^2 + \tau_M^2\Delta\omega_M^2} \qquad (15)$$

Table 2. Simplified equations (eqns 1–5, 8 and 9, 12–15 are left unchanged and are not reproduced)

$$\frac{1}{\tau_{ci}} = \frac{1}{\tau_R} \quad (i = 1 \text{ or } 2) \qquad (6)$$

$$\frac{1}{\tau_{e1}} = \frac{1}{\tau_M} + \frac{1}{T_{1e}} \qquad (7)$$

$$T_{1M}^{-1} = 3K_{DD}\tau_R = \frac{2\times10^{-14}}{5} \mu_M^2\gamma_c^2 \cdot \frac{\tau_c}{r_c^6} \qquad (10)$$

$$T_{2M}^{-1} = \frac{7}{6} T_{1M}^{-1} + 8\pi^2A^2S(S+1)\tau_{e1}/6$$
$$\approx 8\pi^2A^2S(S+1)\tau_{e1}/6 \qquad (11)$$

comment upon these expressions, but rather explain how they have been used to extract structural and dynamical information.

We shall consider the experimental quantities $1/T_1$, $1/T_2$ and ω as functions of the variable T (temperature). These functions depend on a set of parameters, some of which are known data, and the other ones are unknown quantities to be adjusted by trial and error so as to obtain the best fit between experimental and theoretical $1/T_1$, $1/T_2$ and ω values.

Known parameters are: the magnetogyric ratios of the ^{13}C nuclei and of the unpaired electrons (γ_c and γ_e, respectively) or, alternatively, their resonance frequencies ω_c and ω_e in a given magnetic field B_0; the magnetic momentum and the spin number of the investigated cation; the molar fraction p_M of bound-L-Proline molecules $p_M = 3C_S/C_L$ (where C_S and C_L are the analytical concentrations of the salt and the amino-acid, respectively); the relaxation times T_{1D}, T_{2D} and the chemical shift ω_D of the diamagnetic site (i.e. of the amino-acid in water solution in the absence of salt).

Unknown parameters may refer to the whole complex (τ_M°, τ_v°, τ_R°, E_M, E_v, E_R, Δ) or to each ^{13}C nucleus (r_c and A values, see below). The dynamic behaviour of the complex is described by various correlation times which are themselves expressed as a function of the temperature according to Arrhenius equations (1)–(3) (see Table 1). These equations which express the rotational correlation time τ_R,[17–19] the electronic correlation time τ_v[20–21] and the mean lifetime of a bound L-Proline molecule τ_M[22–23] at a given temperature T, require the knowledge of two parameters for each of them, namely a preexponential factor (τ_R°, τ_v°, τ_M°) and an activation energy (E_R, E_v, E_M). Computation of the electronic relaxation times T_{1e}, T_{2e} (eqns 4 and 5) requires the knowledge of one more parameter, Δ, the mean squared value of the zero-field splitting tensor.[20–21] Each carbon nucleus is characterized by the electron-to-nucleus distance r_c and a hyperfine electron-nucleus coupling constant A.[24–25] These quantities will be further subscripted with letters α, β, γ, δ, when considering carbons α, β, γ, δ individually. It should be mentioned that the various distances $r_{c\alpha}$, $r_{c\beta}$, $r_{c\gamma}$, $r_{c\delta}$ are not independent parameters, since three distances only are necessary to position the Mn^{2+} cation with respect to the pyrrolidine ring of L-Proline molecules (see below).

The experimentally observed quantities $1/T_1$, $1/T_2$, ω can be expressed as a function of the (variable) temperature T and of the constant parameters listed above by the sequence of eqns (1)–(15) (rather than under the form of one compact equation for the sake of simplicity). This procedure introduces quantities which thus appear as computing intermediate variables. Some of them have in fact an important physical meaning: the correlation times, the electronic (T_{1e}, T_{2e}) and nuclear relaxation times (T_{1M}, T_{2M}) in the paramagnetic site, the contact shift $\Delta\omega_M = \omega_M - \omega_D$.[24–25]

As stated above, eqns (1)–(3) merely represent an empirical Arrhenius law for the temperature dependence of τ_M, τ_R and τ_v. Equations (4) and (5) express the electronic relaxation times for paramagnetic ions with $S > 1/2$, where the predominant electron spin relaxation mechanism is modulation of the zero-field tensor.[20–21] Equations (8) and (9) introduce coefficients K_{DD} and K_{RS} which are necessary to write down the dipolar and scalar contribution,[17–19] respectively, to the relaxation rates T_{1M}^{-1}, T_{2M}^{-1} in the paramagnetic site (eqns 10 and 11). Finally, the experimental quantities $y = 1/T_1$, or $1/T_2$, or ω, are rather expressed as the proportionality coefficients $(y - y_D)/P_M$ ($1/T_{1r}$, $1/T_{2r}$, $\Delta\omega_r$, respectively, eqns (13)–(15) of the variation $(y - y_D)$ (i.e. the variation of the function referred to its value y_D in the diamagnetic site) to the mole fraction of the paramagnetic site. Such a formulation recalls the necessity for actually observing such a proportionality. Theoretical expressions (14)–(15) giving $1/T_{1r}$, T_{2r} and $\Delta\omega_r$ also include a kinetic parameter, the exchange rate $k_M = 1/\tau_M$ between the free diamagnetic (D) and the bound paramagnetic (M) L-Proline molecules:[22–23]

$$M \overset{k_M}{\rightleftarrows} D.$$

These equations may be greatly simplified if we take into account the presumed order of magnitude of $\tau_R \simeq 10^{-11}$ s[14]; T_{1e}, $T_{2e} \simeq 10^{-8}$ s[26]; $\tau_M \simeq 10^{-6}$ s; $K_{RS} \leqslant 10^{13}$ s^2. Wr thus obtain that $1/\tau_{c1} = 1/\tau_{c2} \simeq 1/\tau_R$; $\tau_{e1} \simeq T_{1e}$; $\omega_e^2\tau_{c1}^2 \gg 1$ and $\omega_c^2\tau_R^2 \ll 1$ (with $\omega_c = 62.86$ MHz or 3.946×10^8 rad. s^{-1} and $\omega_e = 1.03 \times 10^{12}$ rad. s^{-1}). These approximations allow us to simplify the set of equations (1)–(15) as shown in Table 2. We then observe that the scalar contribution to the longitudinal relaxation rate T_{1M}^{-1} is negligible with respect to the dipolar contribution. The reverse is true for the transverse paramagnetic relaxation rate T_{2M}^{-1} since it may be seen that $T_{2M}/T_{1M} \ll 1$ in the course of the computation.[27]

COMPUTING STRATEGY

We have to adjust *fourteen unknown parameters*: τ_M°, τ_v°, τ_R°, E_M, E_v, E_R, Δ, r_α, r_β, r_γ, A_α, A_β, A_γ, A_δ, *knowing seventy-two experimental data*: two $1/T_{1r}$ (at 33° and 60°C), eight $1/T_{2r}$ and eight $\Delta\omega_r$ values (at 28°, 33°, 38°, 45°, 52°, 60°, 70° and 80°C) for each carbon C_α, C_β, C_γ, C_δ). The unknown parameters can thus be adjusted so as to obtain the best fit between the theoretical and experimental $1/T_{1r}$, $1/T_{2r}$, $\Delta\omega_r$ values according to a generalized least squares procedure.[28] However the great number of parameters to be adjusted makes this procedure rather hazardous: a convergence of the estimated parameters to limiting values from one iteration to the next one is difficult to obtain; optimization can lead to erroneous values if the guessed initial values of the unknown parameters to be introduced in the first iteration are too inaccurate.

We have therefore adopted the following stepwise procedure.

(a) *The hyperfine coupling constants* A (in fact A_α, A_β, A_γ, A_δ) are given a constant approximate value $A^{(1)}$. These values are obtained by taking $\Delta\omega_M = \Delta\omega_r$ as a limiting expression for eqn (15) at a sufficiently high temperature ($T \geqslant 60$°C), and then deducing A by means of eqn (12). Conversely the provisory adoption of $A^{(1)}$ values allow us to deduce an approximate set $\Delta\omega_M^{(1)}$ of contact shifts $\Delta\omega_M$ at any temperature.

(b) Approximate values $\tau_M^{(1)}$ and $T_{2M}^{(1)}$ of τ_M and T_{2M} (at any temperature) are obtained from eqns (14) and (15), which are recast under the following form

$$1/T_{2M} = \frac{\Delta\omega_M(1/\tau_M - 1/T_{2r}) - \Delta\omega_r/\tau_M}{\Delta\omega_r} \qquad (15\text{bis})$$

$$\Delta\omega_M = \frac{\Delta\omega_r}{\left(1 - \frac{\tau_M}{T_{2r}}\right)^2 + \tau_M^2\Delta\omega_r^2} \qquad (16\text{bis})$$

τ_M may be extracted from eqn (16bis) where $\Delta\omega_M$ is given the above value $\Delta\omega_M^{(1)}$. The computation is made still easier since in most cases $\tau_M^2\Delta\omega_r^2 \ll (1-\tau_M/T_{2r})^2$ so that

$$\tau_M^{-1} = T_{2r}^{-1}\cdot\left(1-\sqrt{\left(\frac{\Delta\omega_r}{\Delta\omega_M}\right)}\right)^{-1}.$$

Four τ_M values can be computed in this way, one for each carbon atom. However the expected accuracy over τ_M is much better for carbons γ and δ whose paramagnetic shifts and line-broadenings are the more intense. The τ_M value adopted at this stage thus results from an arithmetic mean over carbons γ and δ.

The relaxation rates T_{2M}^{-1} are then obtained by reporting the above approximate values $\tau_M^{(1)}$ and $\Delta\omega_M^{(1)}$ into eqn (15bis).

(c) We may then deduce the longitudinal relaxation rates $1/T_{1M}$ in the paramagnetic site using eqn (13)

$$(T_{1M}^{(1)})^{-1} = (T_{1r} - \tau_M^{(1)})^{-1}.$$

The computation is first performed at a temperature of 60°C for which the chemical exchange is fast and $\tau_M^{(1)}$ may be neglected as compared to T_{1r}. Values of the ratio $\lambda = \tau_R/r_c^6$ are then obtained for each carbon nucleus by means of eqn (9) and (10). The numerator and denominator of these ratios can be exactly computed provided that there exists a known rigid (or semi-rigid) basis of four non-equivalent ^{13}C atoms (at least) in the ligand molecule.[14] This is approximately the case for the carbon nuclei C_α, C_β, C_γ, C_δ of the pyrrolidine ring in the L-Proline molecule. The computing procedure has been fully described in a previous work.[14] Let us recall that we have to consider the ratio of λ (or T_{1M}^{-1}) values for couples of carbon nuclei, C_α and C_β, C_β and C_γ, C_γ and C_δ

$$\lambda_{\alpha\beta} = \frac{\lambda_\alpha}{\lambda_\beta} = \left(\frac{r_{c_\beta}}{r_{c_\alpha}}\right)^6;\ \lambda_{\beta\gamma} = \left(\frac{r_{c_\gamma}}{r_{c_\beta}}\right)^6 \text{ and } \lambda_{\gamma\delta} = \left(\frac{r_{c_\delta}}{r_{c_\gamma}}\right)^6.$$

The Mn^{2+} ion is therefore located on a sphere $S_{\alpha\beta}$ whose diameter $M_\alpha M_\beta$ is determined by the two points M_α and M_β which share the internuclear vector $C_\alpha C_\beta$ in a known ratio $(\lambda_{\alpha\beta})^{1/6}$. The position of the Mn(II) nucleus results from the intersection of three spheres $S_{\alpha\beta}$, $S_{\beta\gamma}$, $S_{\gamma\delta}$. Two positions are actually obtained in this way, which are symmetrical about the plane passing through the centers of the three spheres, but one of these positions can be discarded on account of a too close proximity of the Mn^{2+} cation to the pyrrolidine ring. All C–Mn(II) distances are computed after the position of the Mn(II) cation has been determined. This allows in turn to compute the correlation time τ_R from eqn (10).

Similar computations are also performed at 33°C, in which case τ_M is given the value $\tau_M^{(1)}$ at 33°C. They yield similar distances r_c (Table 3) and a new value of τ_R at 33°C, thus allowing us to deduce the Arrhenius parameters τ_R° and E_R. In the following the distances r_c will be taken equal to their values at 60°C, because they are presumably obtained with a higher degree of accuracy when the exchange rate $1/\tau_M$ does not intervene in eqn (10).

(d) The scalar contribution

$$(1/T_{2M})_{RS} = 8\pi^2A^2S(S+1)\tau_{e1}/6 \qquad (11bis)$$

to the paramagnetic transverse relaxation rate $1/T_{2M}$ may then be deduced by subtracting the dipolar contribution $(1/T_{2M})_{DD} = (7/6)(1/T_{1M})$ from $1/T_{2M}$ (eqn 11). This allows in turn to derive the correlation time $\tau_{e1}^{(1)}$ from eqn (10bis), and then the electron relaxation rate $1/T_{1e}$ by subtracting $(1/\tau_M)^{(1)}$ from $(1/\tau_{e1})^{(1)}$. We may then observe that a plot of $1/T_{1e}$ vs $1/T$ goes through a maximum when $1/T \sim 0.315\ K^{-1}$ (Fig. 1). At this temperature we should then have $\omega_e\tau_v \sim 1$ (in fact, $0.5 < \omega_e\tau_v < 1$) from an inspection of eqn (4). This allows to deduce an approximate value $\Delta^{(1)} \sim 0.03\ cm^{-1}$, and then an approximate value of $\tau_v^{(1)}$ at any temperature. Finally approximate values $\tau_v^{\circ(1)}$ and $E_v^{(1)}$ of the Arrhenius parameters τ_v° and E_v can be obtained from the set of $\tau_v^{(1)}$ values.

(e) A least-squares optimization procedure is then started so as to obtain the best fit between the experimental ($y_i^{exp.}$) and theoretical ($y_i^{th.}$) values of the function $y = 1/T_{2r}$, i.e. to minimize the sum of the squares of the residuals $S = \Sigma(y_i^{th.} - y_i^{th.})^2$. The parameters $A^{(1)}$, $r_c^{(1)}$, $\tau_R^{\circ(1)}$ and $E_R^{(1)}$ are kept constant, and the five remaining

Table 3. The relaxation times T_{1r} and T_{1M}(s) of ^{13}C nuclei in bound L-Proline molecules at 33° and 60°C; the distances (Å) between the Mn(II) cation and the atoms of L-Proline in the complex $[Mn(L\text{-}PRO^-)_3]^-$ (see Fig. 4), and the corresponding values for the Cu^{2+}–Proline complex in the solid state [34]

Atom	Mn^{2+}-L-Proline Complex 33°			Mn^{2+}-L-Proline Complex 60°		Cu^{2+}-L-Proline Complex
	T_{1r}	T_{1M}	r	T_{1r} ($=T_{1M}$)	r	r
C_α	10933 ±533	11769	2.93 ±0.20	4230 ±210	2.89 ±0.28	2.85
C_β	1704 ±78	1723	4.03 ±0.28	656 ±33	3.94 ±0.31	3.98
C_γ	1355 ±67	1367	4.19 ±0.25	509 ±22	4.11 ±0.28	4.12
C_δ	8967 ±447	9522	3.04 ±0.21	3625 ±181	2.96 ±0.23	2.95
N			2.01		2.08	1.95
C(O)			2.86		2.86	2.82
O_1			2.02		1.97	2.04
O_2			4.07		3.99	4.04

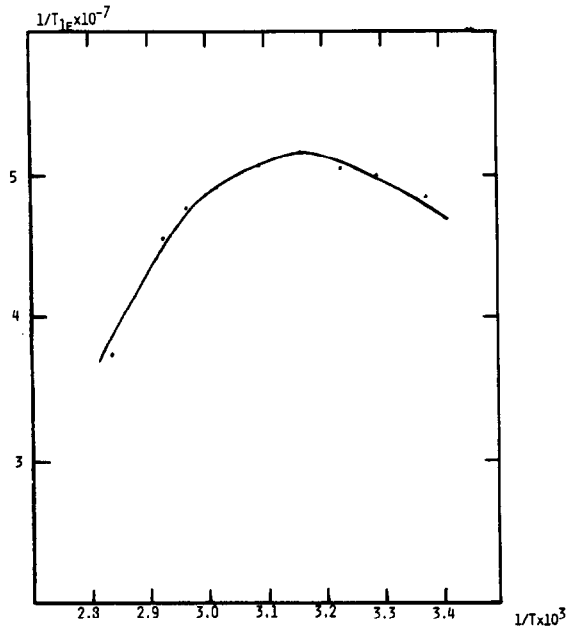

Fig. 1. Temperature variation of the electronic relaxation rate $1/T_{1e}$ for the Mn^{2+}-L-Proline complex in aqueous solution at pD = 11.4 with a magnetic field of 5.87 T. The points shown on the graph are approximate values of $1/T_{1e}$ derived in the first cycle of computation (see the text). The curve is drawn using the parameters in Table 4.

parameters τ_M°, E_M, τ_v°, E_v and Δ, are adjusted in the course of successive iterations, taking as initial values for the first iteration the above approximate set of parameters $\tau_M^{\circ(1)}$, $E_M^{(1)}$, $\tau_v^{\circ(1)}$, $E_v^{(1)}$ and $\Delta^{(1)}$. Let $\tau_M^{\circ(2)}$, $E_M^{(2)}$, $\tau_v^{\circ(2)}$ and $\Delta^{(2)}$ the set of adjusted parameters at the end of the least-squares computation.

(f) The whole cycle of computations is then started again using a slightly modified value of the hyperfine coupling constant A, until a best value is found by trial and error for A, which ensures an absolute minimum of the sum S of the squares of the residuals. Four sets of parameters are actually obtained in this way, since we may choose to optimize individual hyperfine coupling constants A_α, or A_β, or A_γ, or A_δ, of each carbon nucleus. They should have in common the C–Mn(II) distances r_c and the quantities which are necessary to define the correlation times (τ_R°, E_R, τ_v°, E_v, Δ) and the exchange rate (τ_M°, E_M). In fact, the parameters r_c, τ_R° and E_R, which determine the dipolar contribution to the relaxation rates $1/T_{1M}$ and $1/T_{2M}$ are almost independent on the rest of the computation (step f). This is due to the fact that the dipolar contribution to $1/T_{1M}$ is large compared to the scalar contribution, while the reverse is true for $1/T_{2M}$, i.e.: $(1/T_{2M})_{DD} \ll (1/T_{2M})_{RS}$. The remaining set of parameters τ_M°, E_M, τ_v°, E_v, and Δ is slightly different depending on the examined carbon nucleus. The differences however are reasonably small (Table 4), thus suggesting the validity of the computing procedure and of the experimental measurements. The final values of these parameters are then obtained as their arithmetic mean over the four carbon nuclei.

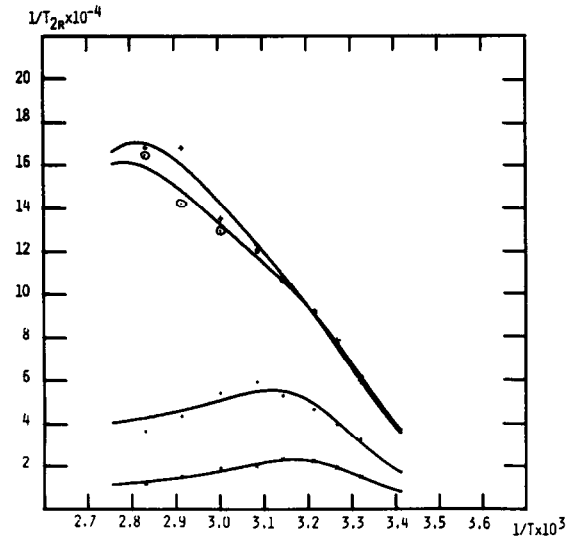

Fig. 2. Temperature variation of the specific relaxation rate $1/T_{1r} = (1/T_1^{obs.} - 1/T_{1D})/p_M$ for the L-Proline carbons at 62.86 MHz, obtained from 1.28 solutions of L-Proline in D_2O at pD = 11.4 and with $[Mn^{2+}] = 0.50 \times 10^{-4} - 5.00 \times 10^{-4}$ M: (●) C_α, (×) C_β, (○), C_γ, (+) C_δ. The curves were computed using the parameters in Tables 3 and 4 and correspond to the best fit.

EXPERIMENTAL

The preparation of solutions has been described in a previous work.[14] Concentrations $C_S = 0$; 5.0; 10.0; 20.0×10^{-5} M of the Mn(II) cation and a fixed concentration $C_L = 1.28$ M of L-Proline were used in this study. The magnetic susceptibility of the complex in water solution was measured according to the method first described by Evans,[29] and then by Crawford and Swanson.[30-31] The measured value $\mu_M = 5.70$ Bohr magnetons is in agreement with an octahedral configuration of the ligand and an electron spin number S = 5/2 in the Mn(II)-L-Proline complex. Longitudinal relaxation times of ^{13}C nuclei at 62.86 MHz are obtained from partially relaxed Fourier Transform spectra using a CAMECA 250 spectrometer, D_2O as an internal heteronuclear lock, and 180°-τ-90° pulse sequences with the fast inversion-recovery variant.[32] 128 FID's over 16 K points were accumulated in each run. Transverse relaxation times are obtained from linebroadenings $\Delta\nu$ (measured at half height on spectra) according to the formula: $1/T_2 = \pi\Delta\nu$. Specific relaxation rates $1/T_{1r}$ and $1/T_{2r}$ are obtained from the slope of the least squares lines representing the relaxation rates $1/T_1$, and $1/T_2$ measured as a function of $p_M = 3C_S/C_L$. They were determined at two (33° and 60°C) and eight (28°, 33°, 38°, 45°, 52°, 60°, 70° and 80°C) temperatures, respectively. All calculations were performed on a Texas Instruments 980A minicomputer equipped with a digital plotter, Hewlett-Packard 7210A.

RESULTS

The quality of the curve-fitting procedure used to extract theoretical parameters from the experimental

Table 4. Fitted values of the parameters $1/\tau_M^\circ(10^{16}\ s^{-1})$, $\tau_v^\circ(10^{-15}\ s)$, E_M and E_v (kcal. mol.$^{-1}$) and $\Delta(10^{-2}\ cm^{-1})$ for carbons α to γ and the corresponding mean values

	C_α	C_β	C_γ	C_δ	Mean
$1/\tau_M^\circ$	5.78 ±0.58	5.74 ±0.94	5.60 ±0.42	5.40 ±0.33	5.53 ±1.0
E_M	16.70 ±0.06	17.10 ±0.10	16.20 ±0.04	16.19 ±0.04	16.54 ±0.6
τ_v°	1.33 ±0.34	1.80 ±0.43	1.1 ±0.22	1.36 ±0.17	1.3 ±0.6
E_v	4.38 ±0.31	4.50 ±0.21	3.84 ±0.15	3.82 ±0.27	4.11 ±0.40
Δ	3.30 ±0.08	3.30 ±0.22	2.91 ±0.15	2.91 ±0.29	3.05 ±0.3

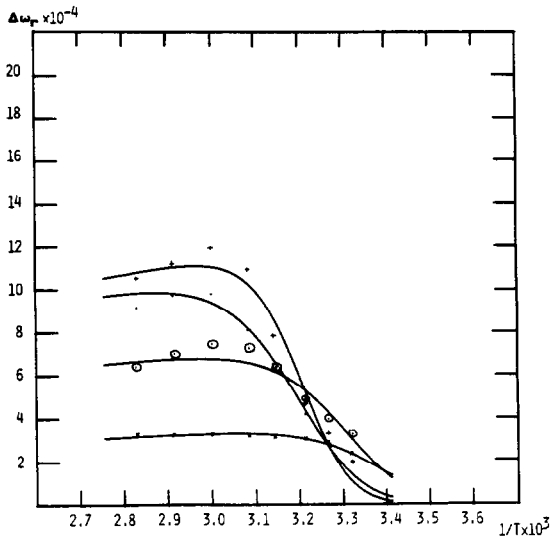

Fig. 3. Temperature variation of the specific paramagnetic shift $\Delta\omega_r = (\omega_{obs.} - \omega_D)/p_M$ of the L-Proline carbons at 62.86 MHz, using the same conditions and notations as in Fig. 2.

data can be appreciated by inspecting the curves of Figs. 3 and 4 which correspond to the best fit. The temperature range chosen for our investigations corresponds to large variations of the measured values of $1/T_{2r}$ and $\Delta\omega_r$ for each carbon C_α, C_β, C_γ, C_δ and to strong curvatures in the respective graphs, thus allowing us to check the theoretical models used with a good degree of confidence.

Values of the specific relaxation times T_{1r} and of the longitudinal relaxation times T_{1M} are displayed in Table 3, together with the Mn^{2+}–^{13}C distances in the complex obtained in the last iteration. The proline atomic coordinates which serve as a basis for the computation of these distances are taken from crystallographic data relative to the Cu^{2+}-Proline or Pd^{2+}-Proline complexes.[33–35] Specific relaxation rates are computed with an error of *ca.* 5%. Ratios such as $\lambda_{\alpha\beta}$ are then obtained with an error $\Delta\lambda_{\alpha\beta}/\lambda_{\alpha\beta} = 2 \times 5/6 = 1.5\%$. Values $\lambda_{\alpha\beta} \pm \Delta\lambda_{\alpha\beta}$, $\lambda_{\beta\gamma} \pm \Delta\lambda_{\beta\gamma}$, $\lambda_{\gamma\delta} \pm \Delta\lambda_{\gamma\delta}$ are then introduced into the compute program to derive all the possible sets of distances $r_{c\alpha}$, $r_{c\beta}$, $r_{c\gamma}$, $r_{c\delta}$ and the rotational correlation time τ_R. Each of these distances is finally given in Table 3 as the mean over the eight sets resulting from the combinations of the $\lambda_{\alpha\beta}$, $\lambda_{\beta\gamma}$, $\lambda_{\gamma\delta}$ ratios. The corresponding errors are estimated as the difference between the maximum and minimum values obtained for each parameter. A good agreement is observed between the distances shown in Table 3 and those obtained in the solid state for the Cu^{2+}-Proline complex.[34] The two values of the rotational correlation time $\tau_R = (1.28 \pm 0.40) \times 10^{-10}$ s and $(4.6 \pm 2.0) \times 10^{-11}$ s at 33° and 60°C allow us in turn to compute mean Arrhenius parameters, $\tau_R^\circ = 4.56 \times 10^{-16}$ s and $E_R = 7.6$ kcal. mol^{-1}, with a large uncertainty range.

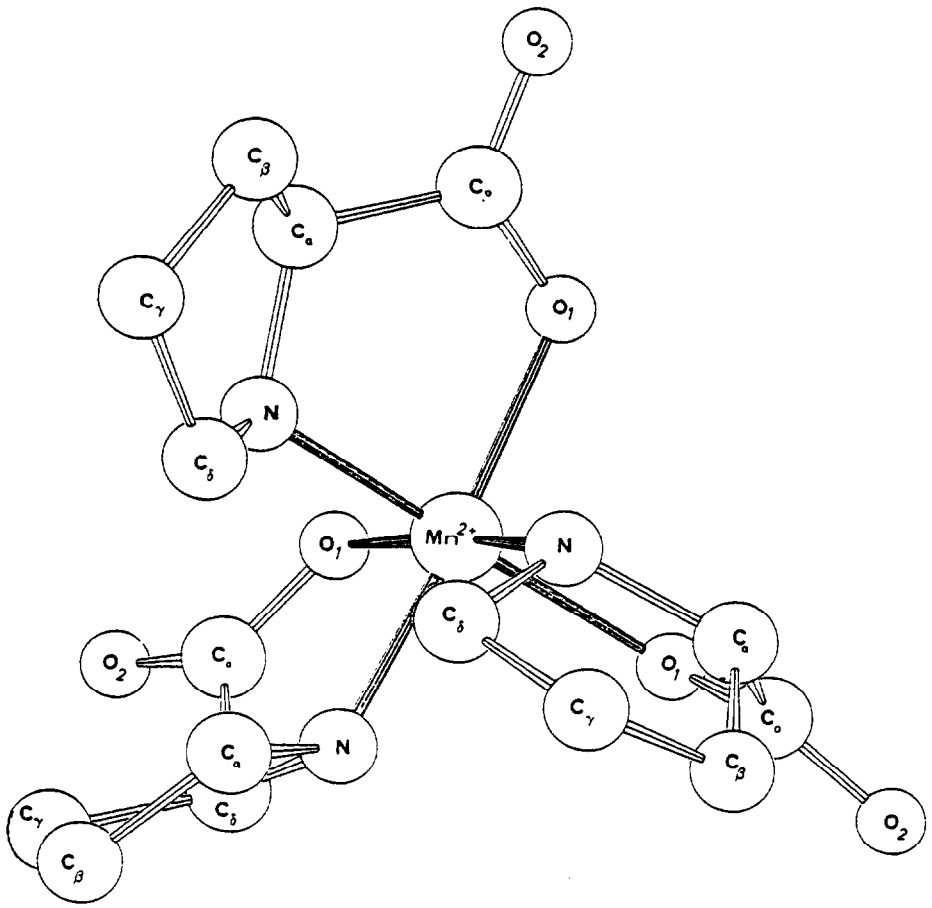

Fig. 4. The structure of the Mn(II)–L-Proline complex in D_2O solution at pD = 11.4 and T = 33°C.

Table 5. Parameters calculated from experimental and contact shift data

Hyperfine coupling constants (10^5 Hz)

$A_\alpha = 1.6\pm0.1$; $A_\beta = 0.8\pm0.1$; $A_\gamma = 2.5\pm0.1$; $A_\delta = 2.2\pm0.1$

Rotational correlation times

$\tau_R(25°C) = (1.28\pm0.60)\times10^{-10}$ s

$\tau_R^\circ = 4.56\times10^{-16}$ s ; $E_R = 7.6$ kcal.mol^{-1}

Electronic relaxation parameters

$T_{1e}(25°C) = (2.18\pm0.70)\times10^{-8}$ s

$\tau_v(25°C) = (1.32\pm0.60)\times10^{-12}$ s

$\Delta = 0.0305\pm0.30$ cm^{-1}

$\tau_v^\circ = (1.3\pm0.6)\times10^{-15}$ s and $E_v = 4.1\pm0.3$ kcal.mol^{-1}

Kinetic parameters

$\tau_M(25°C) = 1.35\times10^{-5}$ s or $k_M = 7.41\times10^4$ s^{-1}

$1/\tau_M^\circ = (5.6\pm1.0)\times10^{16}$ s^{-1}

$E_M = 16.2\pm1.0$ kcal.mol^{-1}

$\Delta H^\ddagger = 15.6\pm1.0$ kcal.mol^{-1}

$\Delta S^\ddagger = 16.1\pm3.0$ e.u.

Four sets of adjusted parameters τ_M°, E_M, τ_v°, E_v and Δ, are computed for each carbon atom, each one with its own uncertainty (Table 4). Final values of these parameters are given in Tables 4 and 5 as arithmetic means over the four sets of data. These values allow us in turn to extrapolate correlation times and exchange rates for a conventional temperature of 25°C (Table 5).

DISCUSSION

Structure of the complex

The value of the magnetic momentum $\mu_M = 5.70\pm0.20$ Bohr magnetons is in agreement with an octahedral configuration of the ligand and an electron spin number $S = 5/2$ in the Mn(II)-L-Proline complex over the entire observed temperature range. In our experiments, the contact shift and line broadening for the water protons are equal to zero, showing that L-Proline has replaced all water in the first coordination sphere of the Mn^{2+} ions. This is in sharp contrast with the Mn(II)–histidine complex,[11] or the Cu(II)-L-Proline complex (to be described in a next paper), in which two sites of coordination are occupied by a water molecule. We can therefore propose a hexacoordinated structure for the complex $Mn(L\text{-}PRO^-)_3^-$ by assembling three proline units where the six coordination sites are three nitrogen and three carboxylic oxygen atoms. Moreover we can position the Mn^{2+} cation with respect to carbons C_α, C_β, C_γ, C_δ of each proline ligand by the method explained above. The position of the other atoms of proline molecules, i.e. nitrogen and atoms C(0), O_1, O_2 of the carboxylate group is obtained by using the geometry of the proline molecule in the solid state (the ^{13}C carboxylate signal was too broad to allow us quantitative measurements even at the lowest Mn^{2+} concentrations). The structure of the whole complex is represented in Figure 4, obtained from a computer using program ORTEP.[36]

The internuclear distances N–Mn^{2+} and O_1–Mn^{2+} (2.08 and 1.97 Å) are slightly smaller than the sum of the corresponding Van der Waals or ionic radii (N: 1.5 Å; O_2: 1.32 Å; Mn^{2+}: 0.8 Å). This confirms that the coordination sites of the proline ligand are the uncharged nitrogen atom and an oxygen atom of the carboxylate anion, as in the solid state proline–Cu^{2+} complex[34] or in the histidine–Mn^{2+} complex in aqueous solution.[12] It should be observed that the hyperfine coupling constants of the carbon nuclei are not a reliable index to characterize the proximity of the central metal ion, since the most remote carbon C is endowed with the largest hyperfine coupling constant. In fact, hyperfine coupling constants depend primarily on electron spin delocalization onto the observed nucleus according to Fermi formula

$$A = \frac{8\pi}{3h} g_e \beta_e g_N \beta_N |\phi_0|^2$$

where g_e, g_N are the Landé factors, β_e and β_N the magnetons of the electron and of the observed nucleus, respectively, and $|\phi_0|^2$ the squared amplitude of the electronic wave function at the nucleus. According to these views, electron delocalization is expected to be higher on carbons α and δ, which are close to the coordinated nitrogen atom, and smaller on carbons β and γ. Effectively A_β is about one half A_α or A_δ as expected, but A_γ is larger than A_α and A_δ. Further explanation should require a complete and accurate calculation of molecular orbitals in the whole complex (the accuracy of CNDO calculations has proved to be not sufficient for this purpose). All four hyperfine coupling constants correspond to isotropic contact shifts toward lower field and are therefore positive. They have the same sign and order of magnitude as in the Mn^{2+}–histidine,[11] Mn^{2+}–ATP,[37] or the Mn^{2+}–DMSO[38] complexes.

Dynamics of the complex

The measured *rotational correlation time* $\tau_R(60°C) = 4.60\times10^{-11}$ s is clearly longer than that of the aquo-complex $Mn(H_2O)_6^{2+}$, $\tau_R(65°C) = 1.60\times10^{-11}$ s,[39] as expected from the different sizes of the two complexes (the larger complex is tumbling more slowly). On the same basis, it is reasonable that our value is not very far from the one obtained for the $Mn(DMSO)_6^{2+}$ complex (in DMSO): $\tau_R = 3.83$ and 1.53×10^{-10} s at 37° and 70°C, respectively[38] against 1.28 and 0.46×10^{-10} s at 33° and

60°C (this work). The value obtained for the Mn^{2+}–histidine complex[11] is however unexpectedly much larger: $\tau_R(25°C) = 5.64 \times 10^{-10}$ s (against 1.28×10^{-10} s).

Another interesting set of parameters results from the measured *electronic relaxation times*, namely the correlation time $\tau_v(25°C) = 1.32 \times 10^{-12}$ s, which characterizes the modulation of the quadratic zero field splitting (ZFS) interaction: $\Delta = 0.0305\ cm^{-1}$, or, in other units, $\Delta = 320$ G or 896 MHz. The ZFS parameter Δ is of the same order of magnitude as in the Mn^{2+}–histidine complex, $\Delta = 408$ G or $0.038\ cm^{-1}$,[11] but is clearly larger than in $Mn(DMSO)_6^{2+}$[38] or $Mn(H_2O)_6^{2+}$[20] ions, $\Delta = 0.0148$ and $0.014\ cm^{-1}$, respectively. The high spin Mn(II) ion with five unpaired electrons (S = 5/2) is orbitally non-degenerate and endowed with an unimportant spin–orbit coupling, and therefore a small ZFS. This splitting is smaller in octahedral undistorted complexes, such as $Mn(H_2O)_6^{2+}$ or $Mn(DMSO)_6^{2+}$, and is expected to become larger for complexes such as Mn^{2+}–L-Proline or Mn^{2+}–histidine which strongly deviate from a regular octahedral symmetry.[40] The calculated correlation time τ_v corresponds to a mechanism where the solvent molecules cause transient fluctuations in the first solvation shell which provide in turn fluctuating fields for the electronic relaxation.[41,42] The value obtained in our experiments is smaller than the one measured for the aquo-complex[19–20]: $\tau_v(25°C) = 1.32$ against 2.4×10^{-12} s, in accord with the picture of H_2O solvent molecules colliding with the complex molecules (the frequency of collisions is higher—and therefore τ_v is smaller—for the larger target molecule, $[Mn(L\text{-}PRO^-)_3]^-$ compared to $Mn(H_2O)_6^{2+}$). The corresponding activation energy $E_v = 4.1$ kcal. mol^{-1} lies in the range 2.5–4.3 kcal. mol^{-1} which is found for other Mn^{2+} complexes, e.g. $E_v = 3.9$ kcal. mol^{-1} for the $Mn(H_2O)_6^{2+}$[19,43] and the Mn^{2+}–histidine[11] complexes.

Kinetic parameters obtained for ligand exchange show a relatively low NMR site exchange rate

$$k_M(25°C) = 1/\tau_M = 7.41 \times 10^4\ s^{-1}$$

as compared to those of labile solvation complexes such as $Mn(DMSO)_6^{2+}$[38], $Mn(CH_3CN)_6^{2+}$[44], $Mn(DMF)_6^{2+}$[45], $Mn(H_2O)_6^{2+}$[19] ($k_M = 2.7$; 12.0; 2.3; $43.5 \times 10^6\ s^{-1}$, respectively), or to those of Mn^{2+}–AMP,[46] Mn^{2+}–ATP,[47] and Mn^{2+}–histidine[11] complexes (0.91; 0.15 and $1.2 \times 10^6\ s^{-1}$, respectively). This is due to the magnitude of the activation enthalpy $\Delta H^+ = 15.6$ kcal. mol^{-1}, which is clearly larger than the values obtained for the above-mentioned solvation complexes ($\Delta H^+ = 8.9$; 7.25; 9.1 and 8.1 kcal. mol^{-1}, respectively), and slightly larger than those for the second group of ligands quoted above ($\Delta H^+ = 14.0$; 11.0 and 13.2 kcal. mol^{-1}). This suggests a stronger coordination of the Mn^{2+} cation by the second group of ligands, presumably because of the chelate effect in these multidentate ligands and of the existence of an ionic extremity (phosphate or carboxylate) in each of them. These effects are also reflected in the magnitude of ΔS^+. The activation entropies are clearly positive for the latter group of ligands: $\Delta S^+ = 16.1$ and 13.8 e.u. for the Mn^{2+}–L-Proline (this work) and the Mn^{2+}–histidine[11] complexes, respectively. On the contrary, they are rather close to zero for the above-mentioned solvation complexes, $\Delta S^+ = 0.7$; −1.8; 0.7; 2.0 e.u., respectively. The positive value of ΔS^+ and the magnitude of ΔH^+ suggest a dissociative mechanism[48] for ligand exchange in which the rate-determining step consists in the detachment of one extremity of the bidentate L-Proline molecule from the central metal ion. Such a mechanism has already been described for the exchange of glycine on cations of transition metal ions[49] and the exchange of acetylacetonate[50] or nonamethylimidodiphosphoramide[51] ligands on cations of main metals.

In conclusion, these investigations show again the importance of the Mn(II) cation as a paramagnetic probe. This study also confirms the conclusions we drew a few years ago when using for the first time the relaxation of ^{13}C nuclei in a Mn(II) complex $Mn(DMSO)_6^{2+}$.[52] Contrary to the case of proton observation, the dipolar term is not predominant in the transverse ^{13}C relaxation. Moreover chemical exchange effects may intervene significantly in the relaxation rates. Selective line-broadening experiments are therefore not sufficient to extract complete and reliable information by NMR spectroscopy; they may even be completely misleading as shown in the present study. Another important conclusion is the possibility of extracting both the electron-to-nucleus distances and the rotational correlation time of the Mn^{2+} complexes, even in motional narrowing conditions, provided that there exista a known rigid basis of four ^{13}C atoms at least in the ligand molecule.

Acknowledgements—Financial support from the Centre National de la Recherche Scientifique is gratefully acknowledged. All NMR spectra were recorded on spectrometers of the Groupement Régional de Mesures Physiques de l'Académie de Nancy–Metz.

REFERENCES

[1]D. F. S. Natusch, *J. Amer. Chem. Soc.* 1973, **95**, 1688.
[2]M. Ihnat and R. Bersohn, *Biochem.* 1970, **9**, 4555.
[3]G. L. Eichborn, P. Clark and E. D. Becker, *Biochem.* 1966, **5**, 245.
[4]J. W. Emsley, J. Feeney and L. H. Sutcliffe, *High Resolution Nuclear Magnetic Resonance Spectroscopy*, Vol. 1. Pergamon Press, Oxford (1965).
[5]G. V. Fazakerley and G. E. Jackson, *J. C. S. Perkin II* 1975, 567.
[6]M. C. Donald and W. D. Philipps, *J. Amer. Chem. Soc.* 1963, **85**, 3736.
[7]A. M. Bowles, W. A. Szarek and M. C. Baird, *Inorg. Nucl. Chem. Lett.* 1971, **7**, 25.
[8]K. Kim and A. E. Martell, *J. Am. Chem. Soc.* 1969, **91**, 872.
[9]R. Marthur and R. B. Martin, *J. Phys. Chem.* 1965, **69**, 668.
[10]W. G. Espersen and R. B. Martin, *J. Phys. Chem.* 1976, **80**, 161.
[11]J. J. Led and D. Grant, *J. Amr. Chem. Soc.* 1975, **97**, 6962.
[12]J. J. Led and D. Grant, *J. Amr. Chem. Soc.* 1977, **99**, 5845.
[13]R. E. Viola, C. R. Hartzell and J. J. Villafranca, *J. Inorg. Bioch.* 1979, **10**, 281.
[14]B. Henry, M. Rappeneau, J-C. Boubel and J-J. Delpuech, *Adv. Mol. Relax. Inter. Process.* 1980, **16**, 29.
[15]C. W. Childs and D. Perrin, *J. Chem. Soc.* (*A*), 1969, 1039.
[16]For a review, see [a]R. A. Dwek, *NMR in Biochemistry; Applications to Enzyme Systems.* Clarendon Press, Oxford (1973). [b]The collection *Metal Ions in Biological Systems* (Edited by H. Sigel), especially the volume 4. Marcel Dekker, New York, (1974). [c]J-C. Boubel, Thesis, Nancy (1977).
[17]I. Solomon and N. Bloembergen, *J. Chem. Phys.* 1956, **25**, 261.
[18]N. Bloembergen, E. M. Purcell and R. V. Pound, *Phys. Rev.* 1948, **73**, 679.
[19]N. Bloembergen and L. O. Morgan, *J. Chem. Phys.* 1961, **34**, 842.
[20]M. Rubinstein, A. Baram and Z. Luz, *Mol. Phys.* 1971, **20**, 67.
[21]A. D. McLachlan, *Proc. R. Soc. London* 1964, **A280**, 271.
[22]T. J. Swift and R. E. Connick, *J. Chem. Phys.* 1962, **37**, 307.
[23]Z. Luz and S. Meiboom, *J. Chem. Phys.* 1964, **40**, 2686.
[24]N. Bloembergen, *J. Chem. Phys.* 1957, **27**, 595.

[25]H. M. McConnell and B. D. Chesnut, *J. Chem. Phys.* 1958, **28**, 107.
[26]W. B. Lewis and L. O. Morgan, In *Transition Metal Chemistry* (Edited by R. L. Carlin), Vol. 4. M. Dekker, New York (1968).
[27]J-C. Boubel, J. Brondeau and J-J. Delpuech, *Adv. Mol. Relax. Inter. Process.* 1977, **11**, 323.
[28]W. E. Deming, *Statistical Adjustment of Data.* Dover, New York (1938).
[29]D. F. Evans, *J. Chem. Soc.* 1959, 2003.
[30]T. H. Crawford and J. Swanson, *J. Chem. Educ.* 1971, **48**, 382.
[31]B. N. Figgis and J. Lewis, In *Modern Coordination Chemistry, Principles and Methods* (Edited by J. Lewis and R. Wilkins), Chap. 6. Academic Press, New York (1960).
[32]D. Canet, G. C. Levy and I. R. Peat, *J. Magn. Reson.* 1975, **18**, 199.
[33]R. L. Kaynshina and B. K. Vainhstein, *Sov. Phys. Cryst.* 1966, **10**, 698.
[34]N. Shamala, *Cryst. Struct. Commun.* 1973, **2**, 5.
[35]T. Ito, F. Marumo and Y. Saito, *Acta Cryst.* 1971, **B27**, 1062.
[36]C. K. Johnson, ORNL 3794 (Oak Ridge National Laboratory, Oad Rdige (Tennesse), ORTEP (1965).
[37]Y. F. Lam, G. P. P. Kuntz and G. Kotowycz, *J. Am. Chem. Soc.* 1974, **96**, 1834.
[38]J-C. Boubel, J. Brondeau and J-J. Delpuech, *Adv. Mol. Relax. Process.* 1977, **11**, 323.
[39]H. G. Hertz, In *Progress in Nuclear Magnetic Resonance Spectroscopy* (Edited by J. W. Emsley, J. Feeney and L. H. Sutcliffe), Vol. 3, Chap. 5. Pergamon Press, Oxford (1967).
[40]A. Carrington and A. D. McLachlan, *Introduction to Magnetic Resonance.* A. Harper International Edition (1967).
[41]G. H. Reed, J. S. Leigh and J. E. Pearson, *J. Chem. Phys.* 1971, **55**, 3311.
[42]G. H. Reed and M. Cohn, *J. Biol. Chem.* 1972, **245**, 662.
[43]A. W. Nolle and L. O. Morgan, *J. Chem. Phys.* 1962, **36**, 378.
[44]W. L. Purcell and R. S. Marianelli, *Inorg. Chem.* 1970, **9**, 1724.
[45]R. C. Philipps, quoted in T. M. Chen and L. O. Morgan, *J. Chem. Phys.* 1972, **76**, 1973.
[46]R. H. Henson, D.Phil. Thesis, Oxford (1972).
[47]F. F. Brown, I. D. Campbell, R. H. Henson, C. W. J. Hirst and R. E. Richards, cited in R. A. Dwek, *Nuclear Magnetic Resonance in Biochemistry*, p. 206. Clarendon Press, Oxford (1973).
[48]C. H. Langford and H. B. Gray, *Ligand Substitution Processes.* W. A. Benjamin, New York (1965).
[49]R. G. Pearson and R. D. Lanier, *J. Am. Chem. Soc.* 1964, **86**, 765.
[50]C. Chatterjee, K. Matsuzawa, H. Kido and K. Saito, *Bull. Chem. Soc. Jpn.* 1974, **47**, 2809.
[51]P. R. Rubini, L. Rodehüser and J-J. Delpuech, *Inorg. Chem.* 1979, **18**, 2962.
[52]J-C. Boubel and J-J. Delpuech, *Adv. Mol. Relax. Process.* 1975, **7**, 209.

Polyhedron Vol. 1, No. 1, pp. 123–127, 1982
Printed in Great Britain.

0277-5387/82/010123-05$03.00/0
Pergamon Press Ltd.

THE ^{31}P NMR SPECTRA AND STRUCTURE OF SOME COMPOUNDS CONTAINING PHOSPHONIUM IONS IN 25-OLEUM SOLUTION

KEITH B. DILLON,* MARTIN P. NISBET and THOMAS C. WADDINGTON✠
Chemistry Department, University of Durham, South Road, Durham DH1 3LE, England

(*Received* 13 *October*)

Abstract—25-oleum has proved to be an extremely useful solvent for recording the ^{31}P NMR spectra of a variety of compounds containing phosphonium ions. Not only have data in very good agreement with previous solid state and solution results been obtained, but the structures of some solids containing mixtures of phosphorus (V) species have been ascertained for the first time.

INTRODUCTION

Recent studies by ^{31}P NMR spectroscopy of the behaviour of phosphorus compounds in strongly acidic solvents such as $HSFO_3$, $HSFO_3$–SbF_5 ("magic acid"), 100% H_2SO_4, $HSClO_3$ and oleums of various strengths have given much useful information as to the nature of the species present in solution.[1–10] In particular, phosphorus (V) chloride dissolved in several of these solvents to yield a mixture of products, because of the instability of the PCl_6^- ion, whereas PCl_4BCl_4 gave the PCl_4^+ ion as the only phosphorus-containing species in 25 oleum, although halogen exchange took place in $HSFO_3$.[5] Similarly, phosphorus (V) bromide yielded the PBr_4^+ ion as the main initial product in 100% H_2SO_4, $HSClO_3$, $HSFO_3$, 25- and 65-oleum, but solvolysis took place rapidly in H_2SO_4 and very slowly in 25-oleum, while halogen exchange in both $HSFO_3$ (rapid) and $HSClO_3$ (slow) was observed.[5] The salt PBr_4BBr_4 gave a stable solution in 25-oleum with a single ^{31}P resonance due to PBr_4^+, but halogen exchange occurred in $HSFO_3$.[5] Furthermore, PCl_5 and PBr_5 did not undergo mutual halogen exchange in oleum solvents.[8] The feasibility of using strongly acidic solvents to obtain ^{31}P NMR spectra from species containing phosphonium ions, including both halo- and organo-derivatives, has therefore been investigated.

The most suitable solvent for this purpose appeared to be 25-oleum, since halogeno-species solvolyse in 100% H_2SO_4, while halogen exchange is possible in certain circumstances in both $HSClO_3$ and $HSFO_3$,[5–9] 65-oleum is a very powerful sulphonating and oxidising agent, and the behaviour of "magic acid" towards phosphonium compounds has been less extensively studied.[2,3] Side-reactions such as sulphonation, particularly of aromatic groups, are possible,[9–11] but these, too, should be reflected in the resultant NMR spectra. In practice, no difficulties were encountered from this source with freshly-prepared samples. Since halogen exchange in 25-oleum can be effectively ruled out,[8] the technique proved to be especially useful for studying "compounds" known or expected to contain mixtures of phosphonium ions with halogens among the substituents, for which other solvents are not readily available.[12–16] Good agreement has been obtained with literature data from both solid state and solution, where available.

EXPERIMENTAL

All manipulations, including sample preparation, were carried out under an inert atmosphere of dry nitrogen. Chemicals of the best available commercial grade were used, generally without further purification except for $PhPCl_2$ which was re-distilled before use. The preparations of several of the samples examined have been described previously.[14–19] Ph_2PBr was prepared by an adaptation of the method of Kuchen and Grünewald.[20] A mixture of 8.8 ml PBr_3 and 8 ml Ph_2PCl was stirred and heated to 413 K under nitrogen for about 1 hr. PCl_3 and excess PBr_3 were distilled off successively under water pump pressure and the bath temperature increased to 433 K. The flask was then transferred to a vacuum line and the liquid distilled; the first fraction was discarded, and the product collected between 401 and 403 K.

The reaction between $PhPCl_2$ and Br_2 (1 : 1) in CCl_4[21] initially gave a solid of approximate composition $PhPCl_2Br_4$; preparation of such a compound from $PhPCl_2Br_2$, obtained by an alternative route, and Br_2 has been described by Michaelis.[22] The experiment was repeated to yield the desired product $PhPCl_2Br_2$, and both samples were used for ^{31}P NMR studies. Ph_2PClBr_2, $PhPBr_4$, Ph_2PBr_3 and Ph_3PBr_4 were similarly obtained by reacting Ph_2PCl, $PhPBr_2$, Ph_2PBr and Ph_3PBr_2 respectively with an equimolar amount of bromine in a suitable halogenated hydrocarbon solvent. The solutions were concentrated if necessary to initiate precipitation of the solid products, which were isolated, washed with pentane and dried *in vacuo*. The salts $PhPBr_3^+BBr_4^-$, $Ph_2PBr_2^+BBr_4^-$ and $Ph_3PBr^+BBr_4^-$ were prepared by reacting the appropriate bromophosphorane with a slight excess of BBr_3. The compounds were separated and purified as above. Elemental analyses, carried out as described previously,[18] for products newly prepared by us are given in Table 1. Carbon and hydrogen results were very variable, particularly for tetrabromoborates where formation of carboranes may interfere with the analysis, and the phosphorus and halogen results were usually considered as more reliable.

^{31}P NMR spectra were recorded at 307.2 K as described in earlier papers,[5–10] using the Fourier transform spectrometer and sample tubes of either 5 or 8.4 mm. outside diameter. Chemical shifts were measured relative to external 85% H_3PO_4, and are quoted with the downfield direction taken as positive.

RESULTS AND DISCUSSION

The compounds may be conveniently grouped according to the substituents present; each group of compounds is discussed separately.

*Author to whom correspondence should be addressed.
✠Deceased.

Table 1. Analytical data for some phosphorus (V) compounds

Compound	Found (%):-					Calculated (%):-				
	C	H	P	Cl	Br	C	H	P	Cl	Br
$PhPCl_2Br_2$	19.13	1.63	9.06	20.10	47.60	21.27	1.49	9.14	20.93	47.17
$PhPCl_2Br_4$	16.48	1.25	7.91	13.10	66.54	14.45	1.01	6.21	14.22	64.10
Ph_2PClBr_2	37.88	2.68	8.22	8.50	41.75	37.88	2.65	8.14	9.32	42.01
$PhPBr_4$	15.37	1.67	6.08		75.40	16.85	1.18	7.24		74.73
$PhPBr_3^+BBr_4^-$	11.03	0.85	4.79		82.06	10.63	0.74	4.57		82.47
Ph_2PBr_3	32.50	2.37	7.32		56.30	33.92	2.37	7.29		56.42
$Ph_2PBr_2^+BBr_4^-$	16.78	1.33	5.17		71.10	21.34	1.49	4.59		70.98
Ph_3PBr_4	36.17	2.37	5.26		54.30	37.15	2.60	5.32		54.93
$Ph_3PBr^+BBr_4^-$	31.16	2.47	4.72		59.10	32.14	2.25	4.60		59.40

(a) *Phosphorus (V) derivatives with halogeno-substituents only*

Several solids containing mixtures of $PCl_nBr_{4-n}^+$ ions had been prepared by Drs. A. Finch, P. N. Gates *et al.* at Royal Holloway College, University of London, and studied by means of vibrational[12,14] and high resolution solid state ^{31}P NMR[13] spectroscopy. The existence of all the possible mixed species was clearly demonstrated, and their fundamental vibrational frequencies assigned. (These ions have since been identified in the solid state by broad line NMR spectroscopy also.[23]) Nine different samples thus prepared were dissolved in 25-oleum, with effervescence in most instances, which soon ceased, yielding clear solutions. Their ^{31}P spectra showed sharp peaks corresponding to the different ions. A typical spectrum is shown in Fig. 1. The chemical shifts, which remained constant for a particular ion within experimental error throughout the series of samples, are given in Table 2, and are in very good agreement with the only previous solution values for the mixed species, obtained in liquid HCl as solvent.[24] In the solid state, these same mixtures showed variations in chemical shift with counter-ion,[13] while similar variations were also found in their vibrational frequencies.[14] The constancy of shift in the present work presumably arises because the counter-ion is effectively constant in 25-oleum, probably either HSO_4^- or $HS_2O_7^-$. In agreement with this hypothesis, the shifts are as expected for a large counter-ion such as BX_4^- rather than a smaller ion such as X^-.[13,24] All the mixtures contained at least three halophosphonium ions; the 'purest' sample, which analysed as $PBBrCl_7$,[14] has

Table 2. ^{31}P NMR data for $PCl_nBr_{4-n}^+$ ions in 25-oleum solution

δ ^{31}P (p.p.m.)	Assignment
88 ± 1	PCl_4^+
50.5 ± 0.5	PCl_3Br^+
9 ± 1	$PCl_2Br_2^+$
-36 ± 1	$PClBr_3^+$
-85 ± 1	PBr_4^+

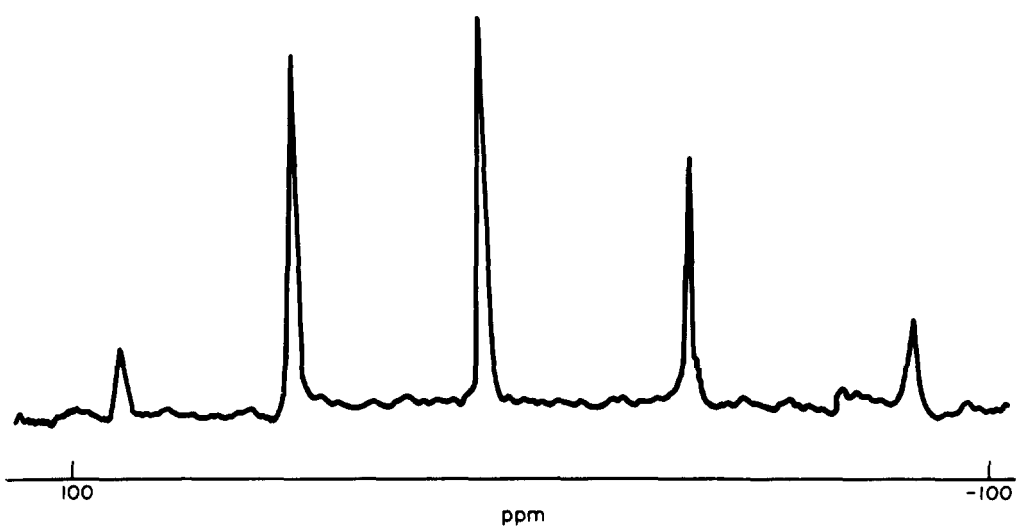

Fig. 1. The ^{31}P NMR spectrum of $[PCl_{4-n}Br_n]^+BCl_4^-$ ($0 \leq n \leq 4$) in 25-oleum.

PCl_3Br^+ as the main phosphorus constituent with small, approximately equal amounts of PCl_4^+ and $PCl_2Br_2^+$ also present.

Some other solids in this category were also examined. A product of composition $PSbBrCl_9$, the main components of which were deduced to be PCl_4^+ and $SbCl_5Br^-$ from vibrational[17] and solid state ^{31}P NMR spectroscopy, gave a strong PCl_4^- signal at 88 ppm, and a very weak resonance at 51 ppm due to PCl_3Br^+. The chief phosphorus-containing constituent of $PSbBrCl_9$ was thus confirmed as the PCl_4^+ ion. A small peak at 32 ppm, assigned to PCl_3OH^+,[5] was also found; this was probably caused by hydrolysis of the quite old sample prior to dissolution in 25-oleum, since the tetrahalophosphonium ions appear to be stable to solvolysis in this medium. The spectra of the mixtures described above remained unchanged for at least a month, and one solution was monitored for ten months, without detectable difference. A solid product obtained by Reeve[16] from reaction of PCl_5 with BBr_3 gave signals at 88(w), 51(m), 10(s) and −36(m) ppm, and thus contains a mixture of bromochlorophosphonium ions, with $PCl_2Br_2^+$ as the main constituent (Table 2).

From various physical measurements, a complex structure consisting of $6PCl_4^+$, $2PCl_3Br^+$, $4PCl_6^-$ and $4Br^-$ ions has been deduced[15] for the yellow solid of empirical formula P_2Cl_9Br, originally prepared by Kolditz and Feltz and thought by them to have the structure $PCl_4^+PCl_5Br^-$.[25] The ^{31}P NMR spectrum of this compound in 25-oleum showed signals at 88 (PCl_4^+) and 51 (PCl_3Br^+) ppm, in a *ca.* 3:1 intensity ratio, together with a signal at 25 ppm assigned to PCl_3OH^+.[5] The latter resonance arises from the instability of the PCl_6^- ion in 25-oleum, as found previously for both PCl_5 and Et_4NPCl_6.[5] The solution results are thus entirely compatible with the suggested solid state structure.

(b) *Phosphorus (V) derivatives with at least one aromatic group present*

The compound $PhPCl_3^+BCl_4^-$ gave a single ^{31}P resonance in 25-oleum solution at 103 ppm, in excellent agreement with the solid state value of 101 ± 2 ppm[18] and with previous solution results for the cation.[26,27] Both $PhPBr_4$ and the salt $PhPBr_3^+BBr_4^-$ gave single signals at 23 ppm in 25-oleum. No previous data are available for comparison, but the values are entirely as expected for an ionic structure containing the $PhPBr_3^+$ cation in both cases. Further confirmation of this assignment is provided by the results for the mixed monophenylphosphonium derivatives discussed below.

The preparation of "compounds" of composition $PhPCl_2Br_2$[21] and $PhPCl_2Br_4$[22] has been described (Experimental section). The solids dissolved in 25-oleum to give four ^{31}P NMR signals, as shown in Fig. 2 for $PhPCl_2Br_2$. The chemical shifts are given in Table 3, and the peaks are assigned to the series of ions $PhPCl_nBr_{3-n}^+$. These solids therefore contain mixtures of cations, similar to those found in the mixed halophosphonium systems. The counter-ion in the solid is presumably either X^- or (for $PhPCl_2Br_4$) a polyhalide such as X_3^- or X_2Y^-. Solid $PhPCl_4$ has a molecular structure,[18] but the replacement of

Table 3. ^{31}P NMR data for $PhPCl_2Br_2$ and $PhPCl_2Br_4$ in 25-oleum solution

δ ^{31}P (p.p.m.)	Assignment
103	$PhPCl_3^+$
80	$PhPCl_2Br^+$
54	$PhPClBr_2^+$
23	$PhPBr_3^+$

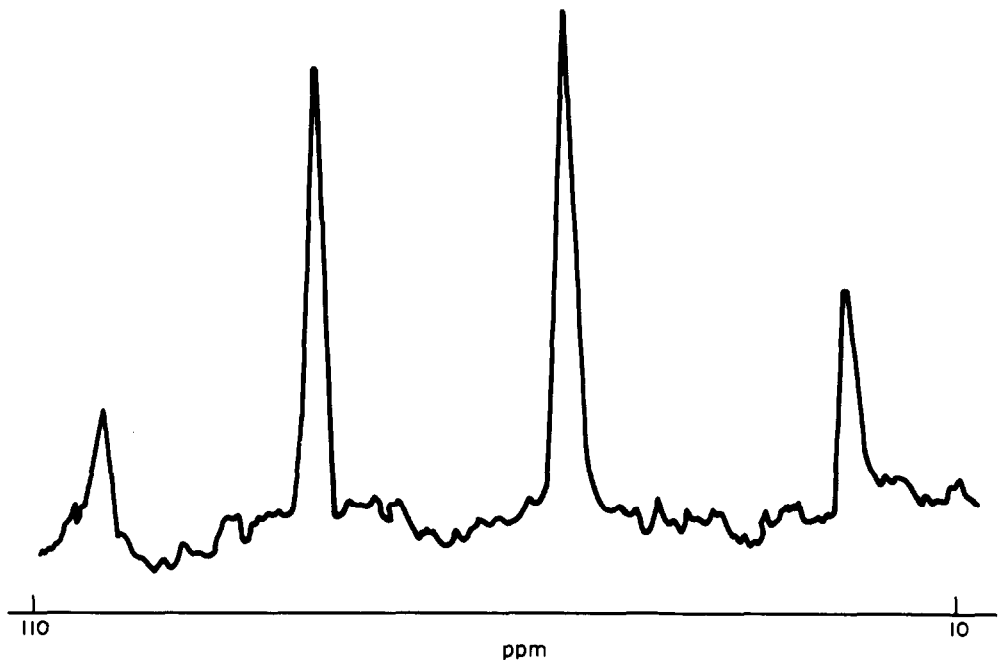

Fig. 2. The ^{31}P NMR spectrum of $PhPCl_2Br_2$ in 25-oleum.

one or more chlorines by bromine is expected to make an ionic structure more favourable, on both steric and electronic grounds.[28,29]

The salt $Ph_2PCl_2^+BCl_4^-$ produced a single peak at 95 ppm in 25-oleum, again in excellent agreement with the solid state value of 93.6 ± 5 ppm,[18] and with literature data from organic solvents.[26,27] The "compound" Ph_2PClBr_2 was also examined, and gave two strong signals, at 74 and 58 ppm. These are assigned to Ph_2PClBr^+ and $Ph_2PBr_2^+$ respectively, since the chemical shifts look very reasonable by comparison with the data for other phenyl-substituted derivatives, and with the literature value for the $Ph_2PBr_2^+$ cation in an organic solvent.[30] To confirm the latter assignment, the compounds Ph_2PBr_3 and $Ph_2PBr_2^+BBr_4^-$ were prepared. These gave single solid state ^{31}P NMR signals at 56 and 55 ppm respectively, and resonances in 25 oleum solution at 56.5 and 56.5 ppm respectively. Ph_2PBr_3 clearly has the expected ionic structure $Ph_2PBr_2^+Br^-$ in the solid state, and the identity of the higher field peak from Ph_2PClBr_2 was fully confirmed. Interestingly, the mixture in this instance appeared not to contain the $Ph_2PCl_2^+$ ion in detectable amount, possibly because of the preparative procedure used.

Some variation in shift with counter-ion has been observed in solid compounds containing the Ph_3PCl^+ cation,[18,31] but solution shifts in organic solvents all lie between 67 and 62 ppm[26,27,29,30,32] The tetrachloroborate salt gave a value of 65 ppm in 25 oleum. Like Ph_3PCl_2,[18] Ph_3PBr_2 has an ionic structure in the solid state, as shown by a ^{31}P NMR shift of 48.6 ppm.[28] Ph_3PBr_2, Ph_3PBr_4, and $Ph_3PBr^+BBr_4^-$ all gave single peaks at 49 ppm in 25-oleum solution, entirely as expected for compounds containing the Ph_3PBr^+ cation. $Ph_4P^+Br^-$ also gave the expected single peak at 23 ppm, in perfect agreement with data from organic solvents.[33]

It is interesting to note the effect of successive phenyl group substitution on the upfield shift caused by replacement of Cl by Br. In the phosphonium ions with halogeno-substituents only, the average upfield shift is 43 ppm (Table 2); it is 27 ppm in mono-phenyl derivatives (Table 3), 19 ppm in diphenyl-compounds, and 16 ppm for Ph_3PCl^+ and Ph_3PBr^+. ^{31}P NMR shifts in phosphonium ions thus depend on both the nature and number of the substituents present.

(c) *Phosphorus (V) derivatives with aliphatic groups*

The solid state spectra of several compounds containing ions of the type $R_nPCl_{4-n}^+$, where R = Me or Et and $1 \leq n \leq 3$, have been previously recorded, and show that the parent phosphorane R_nPCl_{5-n}, as well as derivatives with Lewis acids such as BCl_3 or $SbCl_5$, have ionic structures.[18] With the exception of the $EtPCl_3^+$[32] and Et_3PCl^+[34] cations, however, solution values for these species have not been reported. The chemical shifts for a number of these compounds in 25 oleum solution are collected in Table 4. The solid state data are included for comparison, and show very good agreement in each case, the maximum difference being *ca.* 4.6 ppm for $EtPCl_3^+AlCl_4^-$. The result for $Bu_4P^+Cl^-$ is also included, and again agrees well with previous solid state[19] and solution[19,33] values for the cation.

No evidence for sulphonation of the organic residue in compounds from groups (b) and (c) was found during the time of study, which was usually *ca.* 14 days. No solvolysis of P-halogen bonds in any of the samples was detected over this length of time either, although hydrolysis impurity peaks were occasionally found in the initial spectra, as mentioned in one or two cases. These invariably seemed to arise from impurities in the original samples, several of which were some years old. We therefore conclude that 25-oleum is likely to be a valuable solvent for recording ^{31}P NMR spectra of compounds containing phosphonium ions, particularly where other solvents are not readily available, or where mixtures of halogenated species may be present, since it does not appear to affect the proportions of these in any way.

Acknowledgements—We thank Drs. A. Finch, P. N. Gates and F. J. Ryan of the Chemistry Department, Royal Holloway College, University of London, and Dr. R. N. Reeve of the University of Durham, for gifts of chemicals, J. Lincoln for preparation of some compounds, Dr. M. G. C. Dillon and J. Lincoln for recording some of the ^{31}P NMR spectra, and the S.R.C. for the award of a maintenance grant (to M.P.N.).

REFERENCES

[1]K. B. Dillon and T. C. Waddington, *J. Chem. Soc. A* 1970, 1146.
[2]G. A. Olah and C. W. McFarland, *J. Org. Chem.* 1971, **36**, 1374.
[3]G. A. Olah and C. W. McFarland, *Inorg. Chem.* 1972, **11**, 845.

Table 4. ^{31}P NMR data for some phosphonium ions with aliphatic substituents in 25-oleum solution

Compound	Ion	δ ^{31}P (p.p.m.)	δ ^{31}P (p.p.m.) in solid[18]
$MePCl_4$	$MePCl_3^+$	120	119 ± 2
$MePCl_3^+AlCl_4^-$	$MePCl_3^+$	120	117 ± 1
Me_2PCl_3	$Me_2PCl_2^+$	123	124 ± 5
$Me_2PCl_2^+BCl_4^-$	$Me_2PCl_2^+$	123	119.5 ± 2
$Me_2PCl_2^+SbCl_6^-$	$Me_2PCl_2^+$	123	123 ± 4
$Me_3PCl^+BCl_4^-$	Me_3PCl^+	90	87 ± 1
$EtPCl_3^+AlCl_4^-$	$EtPCl_3^+$	129	124.4 ± 1
$Et_2PCl_2^+BCl_4^-$	$Et_2PCl_2^+$	138	137.4 ± 2
$Et_3PCl^+BCl_4^-$	Et_3PCl^+	108	105 ± 2
$Bu_4P^+Cl^-$	Bu_4P^+	31	35.1*

* Value for Bu_4PI from reference 19.

[4]L. J. Vande Griend and J. G. Verkade, *J. Am. Chem. Soc.* 1975, **97**, 5958.
[5]K. B. Dillon, M. P. Nisbet and T. C. Waddington, *J. C. S. Dalton* 1978, 1455.
[6]K. B. Dillon, M. P. Nisbet and T. C. Waddington, *J. C. S. Dalton*, 1979, 883.
[7]K. B. Dillon, M. P. Nisbet and T. C. Waddington, *J. C. S. Dalton* 1979, 1591.
[8]K. B. Dillon, M. P. Nisbet and T. C. Waddington, *J. Inorg. Nucl. Chem.* 1979, **41**, 1273.
[9]K. B. Dillon, M. P. Nisbet and T. C. Waddington, *J. C. S. Dalton* 1981, 212.
[10]K. B. Dillon, M. P. Nisbet and T. C. Waddington, *J. C. S. Dalton*, 1982, 465.
[11]R. J. Gillespie and E. A. Robinson, In *Non-Aqueous Solvent Systems*, (Edited by T. C. Waddington), Academic Press, New York (1965).
[12]F. F. Bentley, A. Finch, P. N. Gates and F. J. Ryan, *Chem. Commun*, 1971, 860.
[13]K. B. Dillon and P. N. Gates, *Chem. Commun.* 1972, 348.
[14]A. Finch, P. N. Gates, F. J. Ryan and F. F. Bentley, *J. C. S. Dalton* 1973, 1863.
[15]F. F. Bentley, A. Finch, P. N. Gates, F. J. Ryan and K. B. Dillon, *J. Inorg. Nucl. Chem.* 1974, **36**, 457.
[16]R. N. Reeve, Ph.D. Thesis, Durham (1975).
[17]F. F. Bentley, A. Finch, P. N. Gates and F. J. Ryan, *Inorg. Chem.* 1972, **11**, 413.
[18]K. B. Dillon, R. J. Lynch, R. N. Reeve and T. C. Waddington, *J. C. S. Dalton* 1976, 1243.
[19]K. B. Dillon and T. C. Waddington, *Spectrochim. Acta* 1971, **27A**, 1381.
[20]W. Kuchen and W. Grünewald, *Chem. Ber.* 1965, **98**, 480.
[21]J. Meisenheimer, *Annalen* 1913, **397**, 299.
[22]A. Michaelis, *Berichte* 1873, **6**, 817.
[23]A.-R. Grimmer, *Z. anorg. Chem.*, 1973, **400**, 105.
[24]K. B. Dillon, T. C. Waddington and D. Younger, *Inorg. Nucl. Chem. Lett.* 1973, **9**, 63.
[25]L. Kolditz and A. Feltz, *Z. Anorg. Chem.*, 1957, **293**, 286.
[26]A. Schmidpeter and H. Brecht, *Angew Chem.*, 1967, **79**, 535.
[27]D. B. Denney, D. Z. Denney and B. C. Chang, *J. Am. Chem. Soc.* 1968, **90**, 6332.
[28]K. B. Dillon and T. C. Waddington, *Nature Phys. Sci.* 1971, **230**, 158.
[29]G. A. Wiley and W. R. Stine, *Tetrahedron Lett.* 1967, 2321.
[30]A. Schmidpeter and H. Brecht, *Z. Naturforsch.* 1968, **23B**, 1529.
[31]K. B. Dillon, R. J. Lynch, R. N. Reeve and T. C. Waddington, *J. Inorg. Nucl. Chem.* 1974, **36**, 815.
[32]H. P. Latscha, *Z. Naturforsch.* 1968, **B23**, 139.
[33]V. Mark, C. H. Dungan, M. M. Crutchfield and J. R. van Wazer, *Topics Phosphorus Chem.* 1967, **5**, 227.
[34]D. D. Axtell and J. T. Yoke, *Inorg. Chem.* 1973, **12**, 1265.

Polyhedron Vol. 1, No. 1, pp. 129–130, 1982
Printed in Great Britain.

0277–5387/82/010129–02$03.00/0
Pergamon Press Ltd.

NOTES

Perfluoromethanamine ion

(*Received* 29 *May* 1981)

Perfluoroalkanamine ions are not well characterized, although they have been proposed as intermediates in chemical reactions.[1] A clear example is the $(CF_3)_2N^-$ ion, which is proposed as an intermediate in the dimerization of $CF_3N{=}CF_2$ by fluoride ions.[2]

$$CF_3N{=}CF_2 \xrightarrow{F^-} [(CF_3)_2N^-] \xrightarrow[-F^-]{CF_3N=CF_2} (CF_3)_2NCF{=}NCF_2.$$

During investigations of the chemistry of $CF_2{=}NF$[3, 4], it became obvious that the perfluoromethanamine ion, CF_3NF^-, is readily formed by attack of fluoride ion on $CF_2{=}NF$. The reaction chemistry of this ion resembles that of the pseudoisoelectronic species CF_3O^-, which is readily formed from $O{=}CF_2$ and fluoride.[1] However, the perfluoromethanamine ion is clearly the more reactive of the two.

The reaction of $CF_2{=}NF$ with KF results in dimerization of the imine to yield perfluoro-N-methylformamidine.

$$CF_2{=}NF \xrightarrow[22°]{KF} CF_3NF^- \xrightarrow[-F^-]{CF_2=NF} CF_3NF{-}CF{=}NF \quad (60\%).$$

The amidine is characterized by its ^{19}F NMR, IR and molecular weight. The NMR exhibits four resonances in the ratio of 3 : 1 : 1 : 1 with the expected chemical shifts. The $^3J_{FF}$ coupling of the imine group is only 16.0 Hz, indicating the fluorines are in the *syn* configuration. The IR shows a strong absorption at 1675 cm^{-1} due to $\nu(C{=}N)$.

The reaction of $CF_2{=}NF$ with CsF forms the amidine as an intermediate product but it undergoes further reaction with CsF forming perfluoro-1-methyldiaziridine.

$$CF_2{=}NF \xrightarrow{CsF} CF_3NF^- \xrightarrow[-F^-]{CF_2=NF} CF_3NF{-}CF{=}NF$$

$$CF_3NF{-}CF{=}NF \xrightarrow{CsF} [CF_3NFCF_2NF^-] \xrightarrow{-F^-} CF_3N(\text{–}CF_2\text{–})NF \quad (71\%).$$

The novel diaziridine is characterized by ^{19}F, NMR, IR and molecular weight.[5] The NMR exhibits 3 resonances in the ratio of 3 : 2 : 1 with appropriate chemical shifts. The signal of area 2 represents an AB spin system arising from the non-equivalence of the methylene fluorines due to slow inversion at nitrogen, with $^2J_{FF}$ = 41.5 Hz. The highest fundamental in the IR is at 1435 cm^{-1}. This may be taken as additional evidence for the ring system by analogy to the related compound $CF_3{-}N(\text{–}CF_2\text{–})O$, which exhibits a strong absorption at 1458 cm^{-1}.[6]

Nucleophilic substitution of $CF_3C(0)F$ may be achieved with CF_3NF^- by reaction of $CF_2{=}NF$ with $CF_3C(0)F$ over KF.

$$CF_2{=}NF \xrightarrow{KF} CF_3NF^- \xrightarrow[-F^-]{CF_3C(0)F} CF_3NFC(0)CF_3 \quad (60\%).$$

Perfluoro-N-methylacetamide exhibits a characteristic $\nu(C{=}0)$ at 1800 cm^{-1} in the IR. The ^{19}F NMR contains three resonances in the ratio of 3:3:1 with the expected chemical shifts and multiplicities. A surprising competition of $CF_2{=}NF$ and $CF_3C(0)F$ for fluoride ion is observed when the same reaction is carried out over CsF. In this case, the acid fluoride interacts more strongly with the CsF leading to nucleophilic substitution of the imine.

$$CF_3C(0)F \xrightarrow{CsF} CF_3CF_2O^- \xrightarrow[-F^-]{CF_2=NF} CF_3CF_2OCF{=}NF \quad (55\%).$$

Perfluoro-1-ethoxymethanimine exhibits the expected IR, ^{19}F NMR and molecular weight. The $\nu(C{=}N)$ is at 1685 cm^{-1} and $^3J_{FF}$ of the imine group is 38 Hz indicating that the fluorines are in the *syn* configuration.

The perfluoromethanamine ion can be oxidized by halogen (Cl_2, Br_2) to the corresponding N-haloamine. With bromine this provides the first example of an N-fluoro-N-bromoamine.

$$CF_2{=}NF \xrightarrow{KF} CF_3NF^- \xrightarrow{Br_2} CF_3NBrF \quad (50\%).$$

N-fluoro-N-bromotrifluoromethylamine exhibits the expected molecular weight. The IR and ^{19}F NMR are similar to CF_3NClF,[7] with a higher field chemical shift for the N–F in CF_3NFBr, as expected (– 16.5 vs – 6.5 ppm relative to $CFCl_3$)[8].

The reaction chemistry of $CF_2{=}NF$ clearly provides facile routes to novel organofluorine compounds. The five new compounds reported either represent new classes of chemical compounds ($CF_3C(0)NFCF_3$, $CF_3CF_2OCF{=}NF$ and CF_3NBrF) or the most readily available examples of existing classes of compounds ($CF_3NF{-}CF{=}NF$ and $CF_3N(\text{–}CF_2\text{–})NF$). In addition, these and other reactions of $CF_2{=}NF$ provide some of the best available evidence for the existence of perfluoroalkanamine ions.

Acknowledgements—The financial support of this research by U.S. Army Research Office (Grant No. DAAG 29-80-C-0102) is gratefully acknowledged. The Alexander von Humboldt Stiftung is also acknowledged for a research fellowship to D. D. D. during part of this work.

Department of Chemistry
Kansas State University
Manhattan,
KS 66506, *U.S.A.*

SHI-CHING CHANG
DARRYL D. DESMARTEAU

REFERENCES

[1] J. A. Young, *Fluor. Chem. Rev.* 1967, **1**, 359.
[2] J. A. Young, S. N. Tsoukalas and R. D. Dresdner, *J. Am. Chem. Soc.* 1958, **80**, 3604.
[3] A. Sekiya and D. D. Desmarteau, *J. Am. Chem. Soc.* 1979, **101**, 7640.
[4] A. Sekiya and D. D. Desmarteau, *J. Org. Chem.* 1981, **46**, 1277.
[5] The only reported compounds closely related to this diaziridine are

$CF_3N{-}CFNF_2$ and $F_2NCF_2N{-}CFNF_2$. R. A. Mitsch, *J. Org. Chem.* 1968m **33**, 1847, and W. C. Firth Jr., *J. Org. Chem.* 1968, **33**, 3489.

[6]E. R. Falardeau and D. D. Desmarteau, *J. Am. Chem. Soc.* 1976, **98**, 3529.

[7]J. B. Hynes, B. C. Bishop and L. A. Bigelow, *Inorg. Chem.* 1967, **6**, 417.

[8]In CF_3NHF the N–F chemical shift is at − 127.6 ppm ($CFCl_3$). A. Sekiya and D. D. Desmarteau, *J. Fluor. Chem.* 1980, **15**, 185 (note: high field chemical shifts relative to $CFCl_3$ are negative).

Polyhedron Vol. 1, No. 1, pp. 130–132, 1982
Printed in Great Britain.

0277–5387/82/010130–03$03.00/0
Pergamon Press Ltd.

Molybdenum-95 nuclear magnetic resonance studies of molybdenum-phosphorus compounds

(*Received* 6 *July* 1981)

The advent of Fourier Transform spectrometers makes possible the direct observation of metal nuclei at natural abundance in a wider variety of environments[1]. Potential applications of molybdenum-95 ($I = 5/2$, 15.8%) NMR have been recognized[1–3] but there is a paucity of data, particularly on coupling to molybdenum. In describing the most extensive series of compounds yet examined by molybdenum-95 NMR spectroscopy we report the first systematic study of chemical shifts and coupling constants in molybdenum-phosphorus compounds.

Table 1 summarizes the chemical shift (δ Mo) and coupling constant $^1J(^{95}Mo, ^{31}P)$ data for the species in this preliminary investigation. Some illustrative spectra are shown in Fig. 1. Known complexes were chosen to represent the different types of substituted molybdenum carbonyls, with their identification being checked via observation of the characteristic carbonyl stretching frequencies. Their synthesis followed standard literature procedures.[4,5] Relatively narrow signals are observed in the range of *ca.* −1090 to −1890 ppm for these types of Mo(O) compounds, allowing an assessment of degree of carbonyl replacement, nature of the replacing ligand, and substituent effects within the phosphorus ligands. Values of $^1J(^{95}Mo, ^{31}P)$ are sensitive to substituent effects, as observed earlier by Verkade for $Mo(CO)_5PR_3$ compounds by ^{31}P NMR spectroscopy[6]. The influence of concentration, solvent, and temperature on the spectral parameters is the subject of further work.

Some general conclusions can be made from the ^{95}Mo NMR spectral data. Replacement of carbonyl groups of $Mo(CO)_6$ with other ligands generally leads to a downfield chemical shift, with the greatest shift occurring for the nitrogen ligands, acetonitrile and piperidine. With acetonitrile, the trisubstituted species becomes the predominant species in solution after 75 min of reflux. Similarly, conversion of the *cis*-$Mo(CO)_4L_2$ species to the *trans*-isomers can readily be followed by ^{95}Mo NMR spectroscopy. In the case of $MePPh_2$ as the ligand, the presence of a quartet signifies the conversion to the trisubstituted $Mo(CO)_3(MePPh_2)_3$ complex in addition to the *trans*-isomer. The upfield trend in chemical shift in the order of $PPh_3 < AsPh_3 < SbPh_3$ is found for both the $Mo(CO)_5L$ and $Mo(CO)_4L_2$ series of compounds. A chelate effect may be operative in that the chemical shifts of the species containing dpe, diars and TRIPHOS are significantly upfield as compared to analogous compounds involving related monodentate ligands with the same donor atoms. As expected,[6] coupling constants are higher for the species containing $P(OPh)_3$ as ligand than those involving phosphine ligands. Values of $^1J(^{95}Mo, ^{31}P)$ are also relatively insensitive to the substituent or type of complex for the phosphines observed in this study, though δ Mo allows clear differentiation. A wider range of phosphine-substituted molybdenum carbonyls are under investigation, as are diamagnetic Mo(II) and Mo(IV) compounds. The relatively narrow bandwidths observed for the present compounds provides optimism for applications of molybdenum-95 NMR to a wide variety of molybdenum compounds.

Acknowledgements—Support of this research by the Natural Sciences and Engineering Research Council of Canada is gratefully acknowledged. The NMR spectra were obtained at the Southwestern Ontario NMR Center funded by a Major Installation Grant from N.S.E.R.C.

(GWC)[2], *Guelph Campus*
University of Guelph
Guelph, Ontario
Canada, N1G 2W1

E. C. ALYEA*
R. E. LENKINSKI
A. SOMOGYVARI

*Author to whom correspondence should be addressed.

REFERENCES

[1]R. G. Kidd and R. J. Goodfellow, In *NMR and The Periodic Table* (Edited by R. K. Harris and B. E. Mann). Academic Press, London, 1978.

[2](a) O. Lutz, A. Nolle and P. Kroneck, *Z. Naturforsch* 1976, **31a**, 454; (b) O. Lutz, A. Nolle and P. Kroneck, *Z. Naturforsch* 1977, **32a**, 505; (c) O. Lutz, A. Nolle and P. Kroneck, *Z. Physik* 1977, **282a**, 157; (d) A. Nolle, *Z. Physik* 1977, **280a**, 231; (e) K. U. Buckler, A. R. Haase, O. Lutz, M. Müller and A. Nolle, *Z. Naturforsch* 1977, **32a**, 126; (f) W. D. Kautt, H. Krüger, O. Lutz, H. Maier and A. Nolle, *Z. Naturforsch* 1976, **31a**, 351.

[3]A. F. Masters, R. T. C. Brownlee, N. J. O'Connor, A. G. Wedd and J. D. Cotton, *J. Organomet. Chem.* 1980, **C17-20**, 195.

[4]D. J. Darensbourg and R. L. Kump, *Inorg. Chem.* 1978, **17**, 2680.

[5]J. A. Connor, E. M. Jones and K. W. McEwen, *J. Organomet. Chem.* 1972, **43**, 357.

[6]D. S. Milbrath, J. G. Verkade and R. J. Clark, *Inorg. Nucl. Chem. Lett.* 1976, **12**, 921.

$CF_3N{-}CFNF_2$ and $F_2NCF_2N{-}CFNF_2$. R. A. Mitsch, *J. Org. Chem.* 1968m **33**, 1847, and W. C. Firth Jr., *J. Org. Chem.* 1968, **33**, 3489.

[6]E. R. Falardeau and D. D. Desmarteau, *J. Am. Chem. Soc.* 1976, **98**, 3529.

[7]J. B. Hynes, B. C. Bishop and L. A. Bigelow, *Inorg. Chem.* 1967, **6**, 417.

[8]In CF_3NHF the N–F chemical shift is at − 127.6 ppm ($CFCl_3$). A. Sekiya and D. D. Desmarteau, *J. Fluor. Chem.* 1980, **15**, 185 (note: high field chemical shifts relative to $CFCl_3$ are negative).

Polyhedron Vol. 1, No. 1, pp. 130–132, 1982
Printed in Great Britain.

0277–5387/82/010130–03$03.00/0
Pergamon Press Ltd.

Molybdenum-95 nuclear magnetic resonance studies of molybdenum-phosphorus compounds

(*Received* 6 *July* 1981)

The advent of Fourier Transform spectrometers makes possible the direct observation of metal nuclei at natural abundance in a wider variety of environments[1]. Potential applications of molybdenum-95 ($I = 5/2$, 15.8%) NMR have been recognized[1–3] but there is a paucity of data, particularly on coupling to molybdenum. In describing the most extensive series of compounds yet examined by molybdenum-95 NMR spectroscopy we report the first systematic study of chemical shifts and coupling constants in molybdenum-phosphorus compounds.

Table 1 summarizes the chemical shift (δ Mo) and coupling constant $^1J(^{95}Mo, ^{31}P)$ data for the species in this preliminary investigation. Some illustrative spectra are shown in Fig. 1. Known complexes were chosen to represent the different types of substituted molybdenum carbonyls, with their identification being checked via observation of the characteristic carbonyl stretching frequencies. Their synthesis followed standard literature procedures.[4,5] Relatively narrow signals are observed in the range of *ca.* −1090 to −1890 ppm for these types of Mo(O) compounds, allowing an assessment of degree of carbonyl replacement, nature of the replacing ligand, and substituent effects within the phosphorus ligands. Values of $^1J(^{95}Mo, ^{31}P)$ are sensitive to substituent effects, as observed earlier by Verkade for $Mo(CO)_5PR_3$ compounds by ^{31}P NMR spectroscopy[6]. The influence of concentration, solvent, and temperature on the spectral parameters is the subject of further work.

Some general conclusions can be made from the ^{95}Mo NMR spectral data. Replacement of carbonyl groups of $Mo(CO)_6$ with other ligands generally leads to a downfield chemical shift, with the greatest shift occurring for the nitrogen ligands, acetonitrile and piperidine. With acetonitrile, the trisubstituted species becomes the predominant species in solution after 75 min of reflux. Similarly, conversion of the *cis*-$Mo(CO)_4L_2$ species to the *trans*-isomers can readily be followed by ^{95}Mo NMR spectroscopy. In the case of $MePPh_2$ as the ligand, the presence of a quartet signifies the conversion to the trisubstituted $Mo(CO)_3(MePPh_2)_3$ complex in addition to the *trans*-isomer. The upfield trend in chemical shift in the order of $PPh_3 < AsPh_3 < SbPh_3$ is found for both the $Mo(CO)_5L$ and $Mo(CO)_4L_2$ series of compounds. A chelate effect may be operative in that the chemical shifts of the species containing dpe, diars and TRIPHOS are significantly upfield as compared to analogous compounds involving related monodentate ligands with the same donor atoms. As expected,[6] coupling constants are higher for the species containing $P(OPh)_3$ as ligand than those involving phosphine ligands. Values of $^1J(^{95}Mo, ^{31}P)$ are also relatively insensitive to the substituent or type of complex for the phosphines observed in this study, though δ Mo allows clear differentiation. A wider range of phosphine-substituted molybdenum carbonyls are under investigation, as are diamagnetic Mo(II) and Mo(IV) compounds. The relatively narrow bandwidths observed for the present compounds provides optimism for applications of molybdenum-95 NMR to a wide variety of molybdenum compounds.

Acknowledgements—Support of this research by the Natural Sciences and Engineering Research Council of Canada is gratefully acknowledged. The NMR spectra were obtained at the Southwestern Ontario NMR Center funded by a Major Installation Grant from N.S.E.R.C.

(GWC)[2], *Guelph Campus*
University of Guelph
Guelph, Ontario
Canada, N1G 2W1

E. C. ALYEA*
R. E. LENKINSKI
A. SOMOGYVARI

*Author to whom correspondence should be addressed.

REFERENCES

[1]R. G. Kidd and R. J. Goodfellow, In *NMR and The Periodic Table* (Edited by R. K. Harris and B. E. Mann). Academic Press, London, 1978.

[2](a) O. Lutz, A. Nolle and P. Kroneck, *Z. Naturforsch* 1976, **31a**, 454; (b) O. Lutz, A. Nolle and P. Kroneck, *Z. Naturforsch* 1977, **32a**, 505; (c) O. Lutz, A. Nolle and P. Kroneck, *Z. Physik* 1977, **282a**, 157; (d) A. Nolle, *Z. Physik* 1977, **280a**, 231; (e) K. U. Buckler, A. R. Haase, O. Lutz, M. Müller and A. Nolle, *Z. Naturforsch* 1977, **32a**, 126; (f) W. D. Kautt, H. Krüger, O. Lutz, H. Maier and A. Nolle, *Z. Naturforsch* 1976, **31a**, 351.

[3]A. F. Masters, R. T. C. Brownlee, N. J. O'Connor, A. G. Wedd and J. D. Cotton, *J. Organomet. Chem.* 1980, **C17-20**, 195.

[4]D. J. Darensbourg and R. L. Kump, *Inorg. Chem.* 1978, **17**, 2680.

[5]J. A. Connor, E. M. Jones and K. W. McEwen, *J. Organomet. Chem.* 1972, **43**, 357.

[6]D. S. Milbrath, J. G. Verkade and R. J. Clark, *Inorg. Nucl. Chem. Lett.* 1976, **12**, 921.

Table 1. ^{95}Mo NMR spectral data[a]

Compound[b]	Solvent	δMo(ppm)	$\Delta\nu_{\frac{1}{2}}$(Hz)	J(Mo-P)
$Mo(CO)_6$	THF	-1854.3	1	-
$Mo(CO)_5(MeCN)$	MeCN	-1439.7	39	-
$Mo(CO)_4(MeCN)_2$	MeCN	-1306.6	49	-
$Mo(CO)_3(MeCN)_3$	MeCN	-1113.8	10	-
$Mo(CO)_5P(OPh)_3$	CH_2Cl_2	-1819.1	36	234
$Mo(CO)_5P(p+O(C_6H_4OMe\text{-}p)_3$	CH_2Cl_2	-1744.7	66	156
$Mo(CO)_5(PPh_3)$	CH_2Cl_2	-1742.7	54	139
$Mo(CO)_5(PCy_3)$	CH_2Cl_2	-1824.5	46	129
$Mo(CO)_5(PBu^n_3)$	CH_2Cl_2	-1842.8	16	129
$Mo(CO)_5(PBu^t_3)$	CH_2Cl_2	-1710.7	67	127
$Mo(CO)_5(AsPh_3)$	CH_2Cl_2	-1756.5	112	-
$Mo(CO)_5(SbPh_3)$	CH_2Cl_2	-1863.9	117	-
$Mo(CO)_5(pip)$	CH_2Cl_2	-1433.3	76	-
$[Et_4N][ClMo(CO)_5]$	CH_2Cl_2	-1512.9	108	-
$Mo(CO)_4(dpe)$	CH_2Cl_2	-1781.1	90	128
$Mo(CO)_4(diars)$	CH_2Cl_2	-1807.4	43	-
$cis\text{-}Mo(CO)_4(P(OPh)_3)_2$	CH_2Cl_2	-1753.7	36	250
$cis\text{-}Mo(CO)_4(pip)[P(OPh)_3]$	CH_2Cl_2	-1362.0	109	257
$cis\text{-}Mo(CO)_4(PPh_3)_2$	CH_2Cl_2	-1556.1	46	140
$cis\text{-}Mo(CO)_4(MePPh_2)_2$	CH_2Cl_2	-1637.1	57	133
$cis\text{-}Mo(CO)_4(PBu^n_3)_2$	CH_2Cl_2	-1741.7	93	123
$cis\text{-}Mo(CO)_4(AsPh_3)_2$	CH_2Cl_2	-1576.9	187	-
$cis\text{-}Mo(CO)_4(SbPh_3)_2$	CH_2Cl_2	-1807.0	247	-
$cis\text{-}Mo(CO)_4(pip)_2$	DMF	-1092.6	94	-
$trans\text{-}Mo(CO)_4(P(OPh)_3)_2$	CH_2Cl_2	-1785.0	96	225
$trans\text{-}Mo(CO)_4(MePPh_2)_2$	$C_6H_5CH_3$	-1631.0	87	134
$Mo(CO)_3(TRIPHOS)$	CH_2Cl_2	-1759.5	43	129
$Mo(CO)_3(MePPh_2)_3$	CH_2Cl_2	-1427.1	7	126

a Spectra were obtained on naturally abundant samples with a multinuclear Bruker WH-400 NMR spectrometer operating in the pulsed Fourier Transform mode at 26.08 MHz. Samples were measured at ambient temperature in 10 mm diameter cylindrical tubes. Chemical shifts are expressed as δ values in ppm (positive values are downfield) relative to aqueous alkaline 2 M K_2MoO_4 as external standard (3). The signal to noise was 132/1 for 1 scan for the reference. Digital resolution was better than 0.02 ppm per data point. The concentrations and the number of transients varied widely but the signal to noise was always greater than 20/1.

b Abbreviations: pip = piperidine, TRIPHOS = bis(diphenylphosphino)phenylphosphine, DMF = dimethylformamide, MeCN = acetonitrile, dpe = bis(diphenylphosphino)ethane, diars = o-phenylenebis(dimethylarsine).

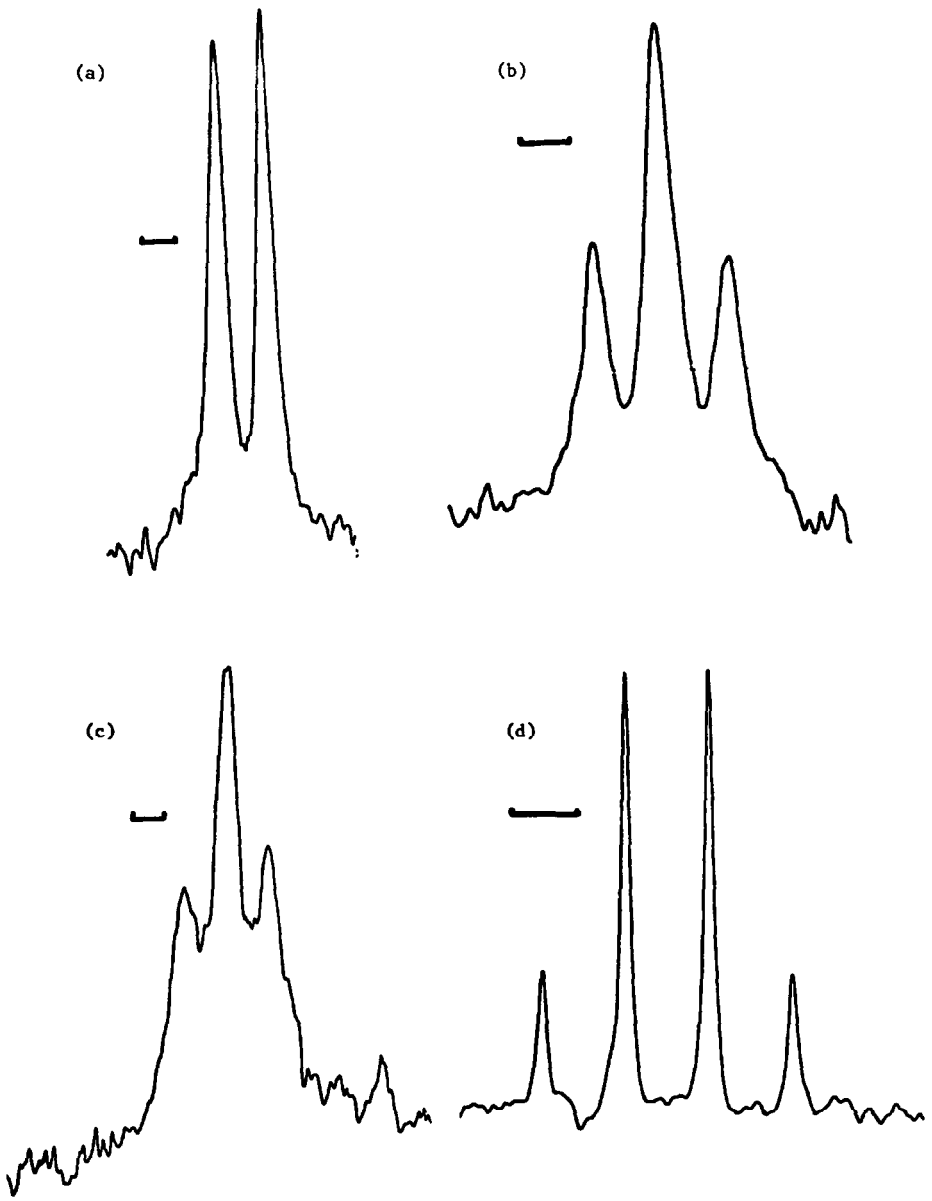

Fig. 1. ^{95}Mo NMR spectra of Ch_2Cl_2 solutions of (a) $Mo(CO)_5PPh_3$ (1293 transients), (b) *cis*-$Mo(CO)_4(MePPh_2)_2$ (944 transients), (c) *trans*-$Mo(CO)_4(MePPh_2)_2$ (1791 transients), and (d) $Mo(CO)_3(MePPh_2)_3$ (894 transients). Scales are different, but the bar represents 100 Hz in each case.

Polyhedron Vol. 1, No. 1, pp. 133–134, 1982
Printed in Great Britain.

0277-5387/82/010133-02$03.00/0
Pergamon Press Ltd.

Simple bonding schemes for eight-vertex D_{2d} dodecahedral clusters violating Wade's rules

(*Received* 16 *September* 1981)

The geometry of deltahedral eight-vertex clusters such as borane and carborane derivatives is based on the D_{2d} dodecahedron, the topology of which can be represented as a cube with six added diagonals (1).[1] Most such clusters (e.g. $B_8H_8^{2-}$ and $C_2B_6H_8$) contain the 18 (namely $2n+2$) skeletal electrons[2] expected from Wade's rules[3,4,5] and consistent with delocalized bonding models.[6] However, recently both an apparent 16 skeletal electron tetracobalt complex $(C_5H_5)_4Co_4B_4H_4$ (Ref. 2) and an apparent 20 skeletal electron tetranickel complex $(C_5H_5)_4Ni_4B_4H_4$ (Refs. 7 and 8) have been shown also to exhibit D_{2d} dodecahedral geometry thereby violating Wade's rules. Recent extended Hückel molecular orbital calculations[9] on these systems interpreted to

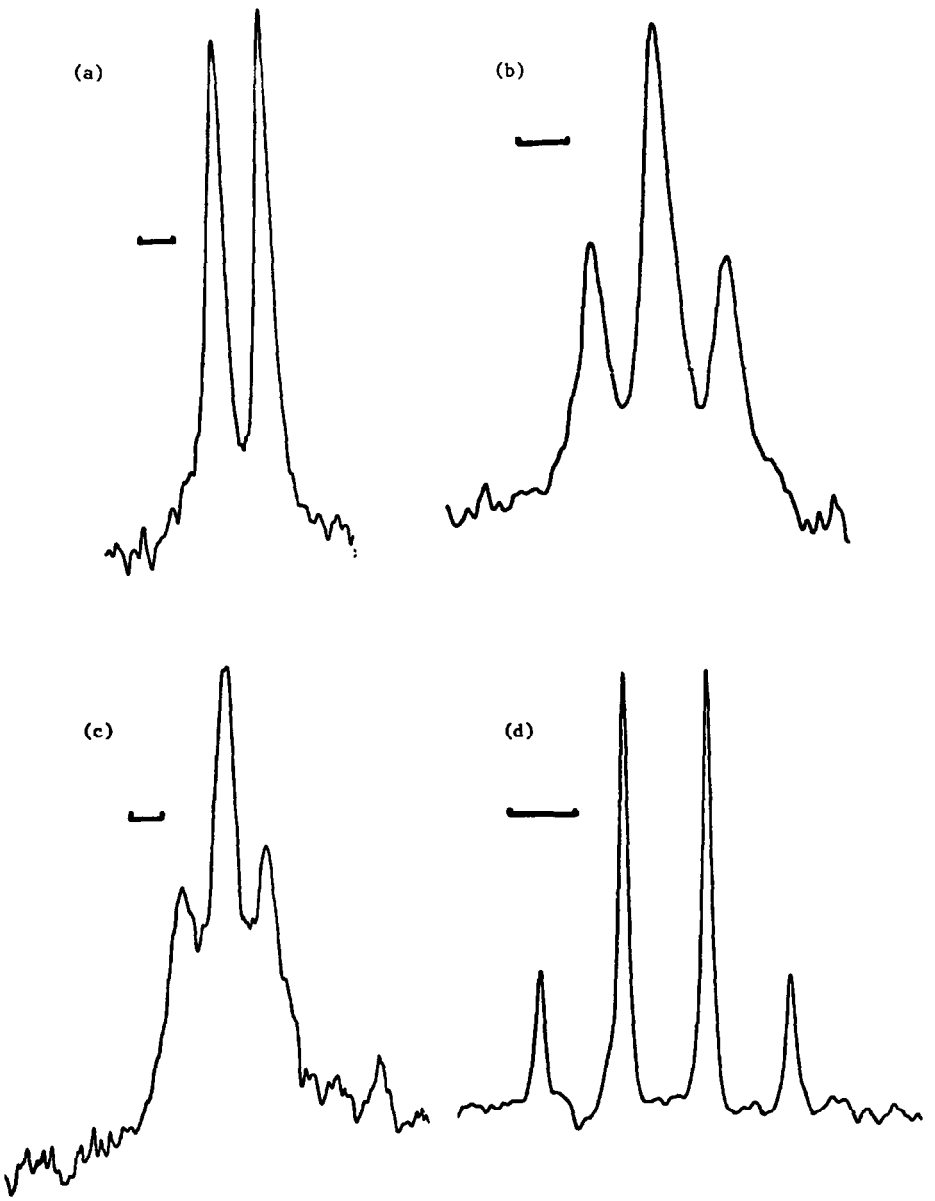

Fig. 1. ^{95}Mo NMR spectra of Ch_2Cl_2 solutions of (a) $Mo(CO)_5PPh_3$ (1293 transients), (b) *cis*-$Mo(CO)_4(MePPh_2)_2$ (944 transients), (c) *trans*-$Mo(CO)_4(MePPh_2)_2$ (1791 transients), and (d) $Mo(CO)_3(MePPh_2)_3$ (894 transients). Scales are different, but the bar represents 100 Hz in each case.

Polyhedron Vol. 1, No. 1, pp. 133–134, 1982
Printed in Great Britain.

0277-5387/82/010133-02$03.00/0
Pergamon Press Ltd.

Simple bonding schemes for eight-vertex D_{2d} dodecahedral clusters violating Wade's rules

(*Received* 16 *September* 1981)

The geometry of deltahedral eight-vertex clusters such as borane and carborane derivatives is based on the D_{2d} dodecahedron, the topology of which can be represented as a cube with six added diagonals (1).[1] Most such clusters (e.g. $B_8H_8^{2-}$ and $C_2B_6H_8$) contain the 18 (namely $2n+2$) skeletal electrons[2] expected from Wade's rules[3,4,5] and consistent with delocalized bonding models.[6] However, recently both an apparent 16 skeletal electron tetracobalt complex $(C_5H_5)_4Co_4B_4H_4$ (Ref. 2) and an apparent 20 skeletal electron tetranickel complex $(C_5H_5)_4Ni_4B_4H_4$ (Refs. 7 and 8) have been shown also to exhibit D_{2d} dodecahedral geometry thereby violating Wade's rules. Recent extended Hückel molecular orbital calculations[9] on these systems interpreted to

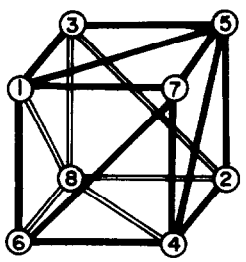

I

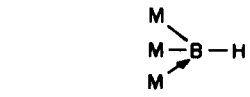

II

III

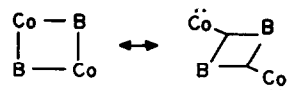

IV

contain two interpenetrating tetrahedra provide a basis for these violations of Wade's rules. This correspondence shows how much simpler bonding models are sufficient to account for these discrepancies.

Consider first the nickel complex $(C_5H_5)_4Ni_4B_4H_4$ shown by an X-ray structural determination[7,8] to have the C_5H_5Ni units at the vertices of degree 4 (namely 2, 3, 6 and 7 in 1) and the BH units at the vertices of degree 5 (namely 1, 4, 5, and 8 in 1). The Ni–Ni distances along the diagonals 23 and 67 (I) are 2.35 Å consistent with a Ni–Ni bond. The remaining Ni–Ni distances fall in the range 3.56–3.60 Å which are too long for Ni–Ni bonding. Both the nickel and boron atoms have the favoured electronic configuration of the next rare gas if there are localized covalent Ni–Ni bonds along the 23 and 67 diagonals and localized Ni–B bonds along each of the twelve original edges of the cube. Thus each boron atom is bonded to three nickel atoms and each nickel atom is bonded to three boron atoms. The environment around each boron atom can be represented as II (M = Ni) in which one of the three metal atoms forms a dative metal ⟶ boron bond and the other two metal atoms form normal metal–boron covalent bonds. Through resonance all three of these metal–boron two-center bonds can become equivalent. Each nickel atom acquires the 18-electron rare gas configuration as follows: (a) 10 electrons from neutral nickel; (b) 5 electrons from neutral C_5H_5; (c) 1 electron from the Ni–Ni bond across diagonal 23 or 67; (d) 1 electron each (total 2 electrons) from the two BH groups with which the nickel atom forms a normal two-centre covalent bond; (e) no electrons from the third BH group, namely the one with which the nickel atom forms the Ni⟶B dative bond.

This bonding model for $(C_5H_5)_4Ni_4B_4H_4$ consists of fourteen two-centre bonds and no three-centre bonds. The two-centre bonds are found on all of the eighteen edges of the D_{2d} dodecahedron (I) except for the 18, 84, 45 and 51 edges. This bonding model has the following difficulties:

(1) The 18, 84, 45 and 51 "non-bonding" edges in this model correspond to B–B distances which are found by X-ray crystallography[7,8] to be close enough (1.87–1.96 Å) to imply B–B bonding;

(2) The C_5H_5Ni vertices use four internal orbitals rather than the three internal orbitals normally used by C_5H_5Ni vertices in deltahedra[6] such as $(C_5H_5)_2Ni_2B_{10}H_{10}$ and related molecules.[8] This makes the C_5H_5Ni vertices in $(C_5H_5)_4Ni_4B_4H_4$ effective five skeletal electron donors rather than the more normal type of three skeletal electron donor found for a C_5H_5Ni vertex using three internal orbitals. By such electron counting rules $(C_5H_5)_4Ni_4B_4H_4$ would be a (4)(5) + (4)(2) = 28 skeletal electron system consistent with the fourteen two-centre bonds implied by this model.

These difficulties can be circumvented by applying operation III (M = Ni) four times. Each application of this operation trades two two-centre bonds for one three-centre bond and removes one electron pair of the C_5H_5Ni vertex from the skeletal electron system. We thus arrive at a $(C_5H_5)_4Ni_4B_4H_4$ polyhedron with 4 three-centre bonds and 14 − (2)(4) = 6 two-centre bonds requiring a total of twenty skeletal electrons for the ten bonds. This is exactly what is available since operation III restores a C_5H_5Ni vertex to the usual donor of three skeletal electrons and three internal orbitals.

An analogous situation applies to the cobalt complex $(C_5H_5)_4Co_4B_4H_4$. However, its structure determination by X-ray diffraction shows a completely different arrangement of metal and boron vertices in the D_{2d} dodecahedron. Thus the C_5H_5Co units now appear at the vertices of degree 5 (namely 1, 4, 5, and 8 in 1) and the BH units at the vertices of degree 4 (namely 2, 3, 6 and 7 in 1). There are now four bonding Co–Co distances (~2.48 Å), namely those along the four diagonals 15, 54, 48, and 81. The remaining two Co–Co distances (~3.18 Å) are much longer indicating no direct Co–Co bonding. Each cobalt atom is therefore directly bonded to two other cobalt atoms in ordinary two-electron localized bonds. The Co_4 unit may be considered as a quadrilateral which is puckered so that each of the four boron atoms can bond to a different set of three cobalt atoms. Each boron atom thus has the same rare gas electronic configuration (II) in both $(C_5H_5)_4M_4B_4H_4$(M = Co and Ni) complexes. Each cobalt atom in $(C_5H_5)_4Co_4B_4H_4$ acquires the 18 electron rare gas configuration as follows: (a) 9 electrons from the neutral cobalt; (b) 5 electrons from the neutral C_5H_5; (c) 1 electron each (total 2 electrons) from the two cobalt atoms to which it is directly bonded; (d) 1 electron each (total 2 electrons) from the two BH groups with which the cobalt forms a normal covalent bond; (e) no electrons from the third BH group, namely the one with which the cobalt forms a Co⟶B dative bond.

This bonding model for $(C_5H_5)_4Co_4B_4H_4$ consists of sixteen two-centre bonds and no three-centre bonds. The two-centre bonds are found on all of the eighteen edges of the D_{2d} dodecahedron (I) except for the 23 and 67 edges. This bonding model has difficulties analogous to those discussed above for the bonding model of $(C_5H_5)_4Ni_4B_4H_4$ containing only two-centre bonds. These difficulties can be circumvented by applying operation III (M = Co) four times and operation IV two times. Operation IV, like operation III converts 2T two-centre bonds of specified type into a group of T three-centre bonds (T = 1 for operation III and T = 2 for operation IV). We thus arrive at a $(C_5H_5)_4Co_4B_4H_4$ polyhedron with eight three-centre bonds and no two-centre bonds. The eight three-centre bonds, of course, are fully consistent with the observed sixteen skeletal electrons of $(C_5H_5)_4Co_4B_4H_4$ calculated on the basis of each C_5H_5Co vertex being a donor of two skeletal electrons and three internal orbitals in the conventional way.

Previous work[10] indicates that the relative energetics of alternative structures in eight-vertex deltahedral boranes are more delicate than those in deltahedral boranes of other sizes. The analysis in this paper suggests a new delicacy of the eight vertex deltahedral system, namely the replacement of light atom vertices (boron and carbon) by transition metal vertices leads eventually to a point where deltahedral bonding involving both surface and core interactions (namely a $2n+2$ skeletal electron system using three internal orbitals[6] of each vertex) is replaced by surface localized bonding. Furthermore, this paper shows how such surface localized bonding can be described either by using only two-center bonds and variable numbers of internal orbitals from different vertex atoms or by using three-centre bonds (and possibly some two-centre bonds as well) and three internal orbitals from each vertex atom. Such alternative bonding models can be related by applications of the relatively simple operations III and IV.

Acknowledgements—I am indebted to the U.S. Army Research Office for partial support of this work under Contract No.

DAAG29-80-K0030. I am also indebted to Dr. Stanislav Heřmanek of the Institute of Inorganic Chemistry, Czechoslovak Academy of Sciences, Dr. D. M. P. Mingos of the Inorganic Chemistry Laboratory, Oxford University (England), and Dr. Russell Grimes of the University of Virginia for useful suggestions and constructive criticisms of earlier versions of this paper.

Department of Chemistry R. B. KING
University of Georgia
Athens, GA 30602
U.S.A.

REFERENCES

[1]R. B. King, *Theor. Chim. Acta.*, 1981, **59**, 25.
[2]J. R. Pipal and R. N. Grimes, *Inorg. Chem.*, 1979, **18**, 257.
[3]K. Wade, *Chem. Comm.*, 1971, 792.
[4]R. N. Grimes, *Ann. N.Y. Acad. Sci.*, 1974, **239**, 180.
[5]K. Wade, *Adv. Inorg. Chem. Radiochem.*, 1976, **18**, 1.
[6]R. B. King and D. H. Rouvray, *J. Am. Chem. Soc.*, 1977, **99**, 7834.
[7]J. R. Bowser and R. N. Grimes, *J. Am. Chem. Soc.*, 1978, **100**, 4623.
[8]J. R. Bowser, A. Bonny, J. R. Pipal and R. N. Grimes, *J. Am. Chem. Soc.*, 1979, **101**, 6229.
[9]D. N. Cox, D. M. P. Mingos and R. Hoffmann, *J.C.S. Dalton*, 1981, 1788.
[10]E. L. Muetterties and B. F. Beier, *Bull. Soc. Chim. Belg.*, 1978, **84**, 397.

Polyhedron Vol. 1, No. 1, pp. 134–135, 1982
Printed in Great Britain.

0277–5387/82/010134–02$03.00/0
Pergamon Press Ltd.

New routes to halogenated B_8 and B_9 boron cages

(*Received 17th July* 1981)

Abstract—B_8Br_8 and B_9Br_9 are formed when B_8Cl_8 and B_9Cl_9 are heated with aluminium tribromide. Cage-size reduction occurs on heating $B_{10}Cl_{10}$ and $B_{11}Cl_{11}$ with hydrogen to give B_9Cl_8H and $B_9Cl_7H_2$, respectively. At least six bromine atoms in B_9Br_9 can be substituted for methyl groups using $SnMe_4$.

To date complete halogen exchange on boron cage compounds has not been achieved. However, we have found that B_8Cl_8 can be fully brominated under the relatively mild conditions of 100°C in the presence of aluminium tribromide using boron tribromide as solvent. B_9Cl_9 does not react under these conditions but is brominated completely by molten aluminium tribromide (which acts as a solvent) at 260°C.

Normally, B_8Cl_8 as isolated from decomposed diboron tetrachloride samples contains substantial amounts of B_9Cl_9 which are very difficult to remove;[1] the differing reactivities of the B_8 and B_9 systems towards bromine–chlorine exchange means that separation of the two chlorides is not required prior to reaction. The B_8Cl_8–B_9Cl_9 mixture was sealed under vacuum in a pyrex tube with freshly sublimed aluminium tribromide and vacuum distilled boron tribromide to give a very dark purple solution (the colour being due to B_8Cl_8). When the tube was heated to 100° the colour was observed to slowly change to dark brown; after 14 days the tube was opened under vacuum and the boron tribromide removed. The gentle heat of a hot air blower was sufficient to sublime the aluminium halides and unreacted B_9Cl_9 to a remote part of the apparatus leaving behind a dark red–brown solid. This solid sublimed cleanly on heating with a free flame and was identified as B_8Br_8 by mass spectrometry. On resealing the tube containing the yellow mixture of aluminium halides and B_9Cl_9 and heating to 260°C for 15 hr it was found that the colour slowly changed to deep red; fractional sublimation of the products allowed isolation of pure B_9Br_9 as dark red crystals.

To our knowledge B_8Br_8 has not been isolated previously although it has been detected as a minor component among the decomposition products of diboron tetrabromide.[2] It is a very dark reddish–brown, water-sensitive solid which is soluble in halogenated solvents and which sublimes without melting when heated under vacuum. The parent ion gives rise to the base peak of the mass spectrum, the next most intense peak being due to the loss of BBr_3 from the parent ion. An as yet unexplained phenomenon is that glass having been in contact with B_8Br_8 and then sealed with an oxygen–gas flame assumes a light green colour near the point of sealing; in contrast, glass previously used for handling B_8Cl_8 takes on a permanganate–purple colour at the seal. The other boron sub-halides do not exhibit this glass-colouring effect.

Previously we have described the reaction of $B_{10}Cl_{10}$–$B_{11}Cl_{11}$ mixtures with hydrogen.[3] To study the reaction of $B_{10}Cl_{10}$ alone with hydrogen the $B_{10}Cl_{10}$–$B_{11}Cl_{11}$ mixtures obtained from decomposed diboron tetrachloride were heated under vacuum at 350° to pyrolyse the less stable $B_{11}Cl_{11}$ leaving the $B_{10}Cl_{10}$ intact (small amounts of B_9Cl_9 sometimes formed in this procedure do not react with hydrogen below 300°C[3] and so do not affect the next stage of reaction). The red–orange $B_{10}Cl_{10}$ was sublimed into a clean piece of apparatus, sealed up with 10–20 cm pressure of hydrogen and heated to 150° overnight. On cooling a yellow, crystalline solid condensed out on the cooler parts of the glass tubing; mass spectral analysis showed this to be B_9Cl_8H contaminated with unchanged B_9Cl_9. The main fragmentation process in the mass spectrometer is loss of either BCl_3 or BCl_2H from the parent ion to give $B_8Cl_6^+$ and $B_8Cl_5H^+$; the next two most prominent ions were $B_6Cl_3^+$ and $B_7Cl_3^+$.

If, as seems likely, the $B_{10}Cl_{10}$ molecule possesses a bicapped square antiprismatic boron cage a possible mechanism for the exclusive formation of B_9Cl_8H may be as follows. Loss of one of the eight equatorial boron atoms from the cage (boron 2) would leave the pre-

DAAG29-80-K0030. I am also indebted to Dr. Stanislav Heřmanek of the Institute of Inorganic Chemistry, Czechoslovak Academy of Sciences, Dr. D. M. P. Mingos of the Inorganic Chemistry Laboratory, Oxford University (England), and Dr. Russell Grimes of the University of Virginia for useful suggestions and constructive criticisms of earlier versions of this paper.

Department of Chemistry R. B. KING
University of Georgia
Athens, GA 30602
U.S.A.

REFERENCES

[1]R. B. King, *Theor. Chim. Acta.*, 1981, **59**, 25.
[2]J. R. Pipal and R. N. Grimes, *Inorg. Chem.*, 1979, **18**, 257.
[3]K. Wade, *Chem. Comm.*, 1971, 792.
[4]R. N. Grimes, *Ann. N.Y. Acad. Sci.*, 1974, **239**, 180.
[5]K. Wade, *Adv. Inorg. Chem. Radiochem.*, 1976, **18**, 1.
[6]R. B. King and D. H. Rouvray, *J. Am. Chem. Soc.*, 1977, **99**, 7834.
[7]J. R. Bowser and R. N. Grimes, *J. Am. Chem. Soc.*, 1978, **100**, 4623.
[8]J. R. Bowser, A. Bonny, J. R. Pipal and R. N. Grimes, *J. Am. Chem. Soc.*, 1979, **101**, 6229.
[9]D. N. Cox, D. M. P. Mingos and R. Hoffmann, *J.C.S. Dalton*, 1981, 1788.
[10]E. L. Muetterties and B. F. Beier, *Bull. Soc. Chim. Belg.*, 1978, **84**, 397.

Polyhedron Vol. 1, No. 1, pp. 134–135, 1982
Printed in Great Britain.

0277–5387/82/010134–02$03.00/0
Pergamon Press Ltd.

New routes to halogenated B_8 and B_9 boron cages

(*Received 17th July* 1981)

Abstract—B_8Br_8 and B_9Br_9 are formed when B_8Cl_8 and B_9Cl_9 are heated with aluminium tribromide. Cage-size reduction occurs on heating $B_{10}Cl_{10}$ and $B_{11}Cl_{11}$ with hydrogen to give B_9Cl_8H and $B_9Cl_7H_2$, respectively. At least six bromine atoms in B_9Br_9 can be substituted for methyl groups using $SnMe_4$.

To date complete halogen exchange on boron cage compounds has not been achieved. However, we have found that B_8Cl_8 can be fully brominated under the relatively mild conditions of 100°C in the presence of aluminium tribromide using boron tribromide as solvent. B_9Cl_9 does not react under these conditions but is brominated completely by molten aluminium tribromide (which acts as a solvent) at 260°C.

Normally, B_8Cl_8 as isolated from decomposed diboron tetrachloride samples contains substantial amounts of B_9Cl_9 which are very difficult to remove;[1] the differing reactivities of the B_8 and B_9 systems towards bromine–chlorine exchange means that separation of the two chlorides is not required prior to reaction. The B_8Cl_8–B_9Cl_9 mixture was sealed under vacuum in a pyrex tube with freshly sublimed aluminium tribromide and vacuum distilled boron tribromide to give a very dark purple solution (the colour being due to B_8Cl_8). When the tube was heated to 100° the colour was observed to slowly change to dark brown; after 14 days the tube was opened under vacuum and the boron tribromide removed. The gentle heat of a hot air blower was sufficient to sublime the aluminium halides and unreacted B_9Cl_9 to a remote part of the apparatus leaving behind a dark red–brown solid. This solid sublimed cleanly on heating with a free flame and was identified as B_8Br_8 by mass spectrometry. On resealing the tube containing the yellow mixture of aluminium halides and B_9Cl_9 and heating to 260°C for 15 hr it was found that the colour slowly changed to deep red; fractional sublimation of the products allowed isolation of pure B_9Br_9 as dark red crystals.

To our knowledge B_8Br_8 has not been isolated previously although it has been detected as a minor component among the decomposition products of diboron tetrabromide.[2] It is a very dark reddish–brown, water-sensitive solid which is soluble in halogenated solvents and which sublimes without melting when heated under vacuum. The parent ion gives rise to the base peak of the mass spectrum, the next most intense peak being due to the loss of BBr_3 from the parent ion. An as yet unexplained phenomenon is that glass having been in contact with B_8Br_8 and then sealed with an oxygen–gas flame assumes a light green colour near the point of sealing; in contrast, glass previously used for handling B_8Cl_8 takes on a permanganate–purple colour at the seal. The other boron sub-halides do not exhibit this glass-colouring effect.

Previously we have described the reaction of $B_{10}Cl_{10}$–$B_{11}Cl_{11}$ mixtures with hydrogen.[3] To study the reaction of $B_{10}Cl_{10}$ alone with hydrogen the $B_{10}Cl_{10}$–$B_{11}Cl_{11}$ mixtures obtained from decomposed diboron tetrachloride were heated under vacuum at 350° to pyrolyse the less stable $B_{11}Cl_{11}$ leaving the $B_{10}Cl_{10}$ intact (small amounts of B_9Cl_9 sometimes formed in this procedure do not react with hydrogen below 300°C[3] and so do not affect the next stage of reaction). The red–orange $B_{10}Cl_{10}$ was sublimed into a clean piece of apparatus, sealed up with 10–20 cm pressure of hydrogen and heated to 150° overnight. On cooling a yellow, crystalline solid condensed out on the cooler parts of the glass tubing; mass spectral analysis showed this to be B_9Cl_8H contaminated with unchanged B_9Cl_9. The main fragmentation process in the mass spectrometer is loss of either BCl_3 or BCl_2H from the parent ion to give $B_8Cl_6^+$ and $B_8Cl_5H^+$; the next two most prominent ions were $B_6Cl_3^+$ and $B_7Cl_3^+$.

If, as seems likely, the $B_{10}Cl_{10}$ molecule possesses a bicapped square antiprismatic boron cage a possible mechanism for the exclusive formation of B_9Cl_8H may be as follows. Loss of one of the eight equatorial boron atoms from the cage (boron 2) would leave the pre-

viously apical boron 1 relatively coordinatively unsaturated in the open-cage intermediate; it is suggested that the chlorine on this unique boron atom is the one which is substituted by hydrogen. Cage closure to give B_9Cl_8H then occurs after substitution. The formation[4] of B_9Cl_8H in low yield from the pyrolysis of $(H_3O)_2B_{10}Cl_{10}$ may occur via the same route; hydrogen, formed by partial hydrolysis of the boron cages could attack small amounts of $B_{10}Cl_{10}$ produced by oxidation of some of the $B_{10}Cl_{10}^{2-}$ ions.

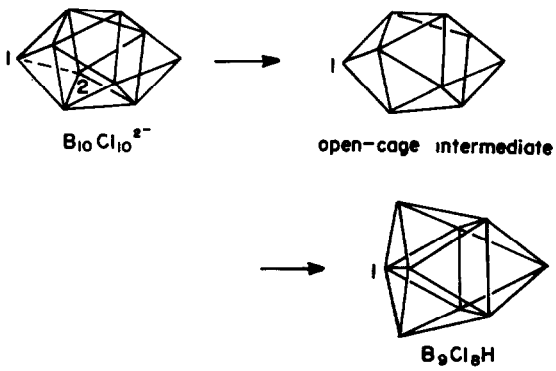

Dilute solutions of diboron tetrachloride in boron trichloride decompose slowly at room temperature to give $B_{11}Cl_{11}$ together with a few per cent of $B_{12}Cl_{12}$.[3] A sample of $B_{11}Cl_{11}$ prepared in this way was heated to 150°C with an excess of hydrogen; small yellow crystals, melting at 93–95°C under vacuum, appeared on cooling. In a larger mass the compound, shown by mass spectrometry to be mainly $B_9Cl_7H_2$, was red-orange in colour. The two largest peaks in the mass spectrum were due to the ions $B_8Cl_4H_2^+$ and $B_8Cl_5H^+$ (base peak) representing loss of BCl_3 and BCl_2H, respectively, from the parent ion. The compound $B_9Cl_6H_3$ was present as an impurity and possibly arises from the attack of hydrogen on $B_{12}Cl_{12}$. Hydrogen chloride and boron trichloride were identified by IR spectroscopy as the gaseous products.

Morrison has shown that B_9Br_8Me may be prepared in about 15% yield by the pyrolysis of $(Et_3NH)_2B_{10}Br_{10}$;[5] we have studied the thermal decomposition of the corresponding chloride $(Et_3NH)_2B_{10}Cl_{10}$ in an effort to make B_9Cl_8Me. Although the major sublimate product was found to be B_9Cl_8Me the yield was less than 1% and impurities, thought to be B_9Cl_9 and $B_9Cl_7Me_2$, were also present. The poor yield from the reaction caused us to abandon the study. The thermal decomposition of $(Et_3NH)_2B_{10}Cl_{10}$ in an atmosphere of chlorine, in an attempt to form B_9Cl_9, again gave B_9Cl_8Me as the main boron-containing sublimate.

It appears to be widely assumed that boron cages present in the sub-halides are stabilized by back-donation from halogen to the cage orbitals. Therefore an important question to ask is how many of the halogen atoms may be changed for groups which can't stabilize the cages by such back-donation. From the experiments described here it is evident that up to three hydrogen atoms or one methyl group may be substituted onto the B_9 cage. By heating B_9Br_9 with a large excess of tetramethyltin up to six bromine atoms could be replaced by methyl groups. The whole range of mixed methylbromides $B_9Br_{9-n}Me_n$ ($n = 0$–6) was formed and unfortunately proved impossible to separate into its components.

EXPERIMENTAL

Reactions were carried out under vacuum in Pyrex glass tubes which had previously been baked out in an atmosphere of either boron trichloride or boron tribromide. In the brominations the apparatus was designed so that the aluminium tribromide could be sublimed directly into the reaction vessel from a side-arm, which was then removed by sealing off a constriction.

We had occasion to heat a small sample of B_8Cl_8 in an open test-tube. In the dry, anaerobic conditions at the bottom of the tube the B_8Cl_8 sublimed to give a purple vapour which, on "pouring" into the air by inverting the tube, ignited spontaneously with a series of mild explosions.

A. J. MARKWELL
A. G. MASSEY*
P. J. PORTAL

Department of Chemistry,
University of Technology,
Loughborough, Leicestershire, LE11 3TU,
England

*Author to whom correspondence should be addressed.

REFERENCES

[1] A. G. Massey, *Chemistry in Britain* 1980, 588.
[2] J. Kane and A. G. Massey, *J. Inorg. Nucl. Chem.* 1971, **33**, 1195; N. A. Kutz and J. A. Morrison, *Inorg. Chem.* 1980, **19**, 3295.
[3] S. B. Awad, D. W. Prest and A. G. Massey, *J. Inorg. Nucl. Chem.* 1978, **40**, 395.
[4] J. A. Forstner, T. E. Haas and E. L. Muetterties, *Inorg. Chem.* 1964, **3**, 155.
[5] D. Saulys and J. A. Morrison, *Inorg. Chem.* 1980, **19**, 3057.

Polyhedron, Vol. 1, No. 1, pp. 135–137, 1982
Printed in Great Britain.

0277-5387/82/010136-03$03.00/0
Pergamon Press Ltd.

The thiocyanato adduct of chromium(II) acetate

(*Received* 30 *July* 1981)

Abstract—The first dichromium complex with axially bonded anions, $[NEt_4]_2[Cr_2(O_2CCH_3)_4(NCS)_2]$, was obtained by reaction of $[NEt_4]NCS$ with $[Cr_2(O_2CCH_3)_4(OH_2)_2]$ in ethanol.

INTRODUCTION

The axial water molecules in binuclear chromium(II) acetate $[Cr_2(O_2CCH_3)_4(OH_2)_2]$ can be replaced by various neutral bases, e.g. pyridine, pyrazine,[1] piperidine,[2] substituted pyridines[3] and ammonia.[4] The Cr–Cr ligands, and in the absence of axial ligands "supershort" quadruple bonds are formed.[5] Recently, it has been reported[6] that chromium(II) forms many thiocyanato-

viously apical boron 1 relatively coordinatively unsaturated in the open-cage intermediate; it is suggested that the chlorine on this unique boron atom is the one which is substituted by hydrogen. Cage closure to give B_9Cl_8H then occurs after substitution. The formation[4] of B_9Cl_8H in low yield from the pyrolysis of $(H_3O)_2B_{10}Cl_{10}$ may occur via the same route; hydrogen, formed by partial hydrolysis of the boron cages could attack small amounts of $B_{10}Cl_{10}$ produced by oxidation of some of the $B_{10}Cl_{10}^{2-}$ ions.

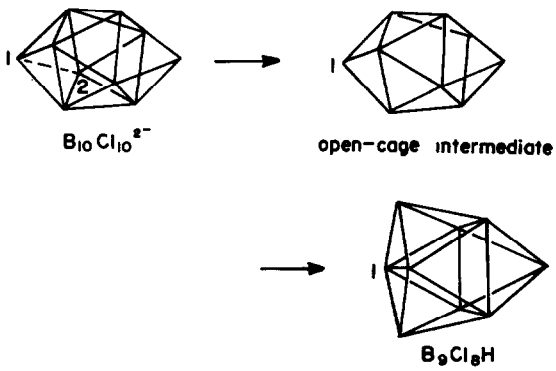

Dilute solutions of diboron tetrachloride in boron trichloride decompose slowly at room temperature to give $B_{11}Cl_{11}$ together with a few per cent of $B_{12}Cl_{12}$.[3] A sample of $B_{11}Cl_{11}$ prepared in this way was heated to 150°C with an excess of hydrogen; small yellow crystals, melting at 93–95°C under vacuum, appeared on cooling. In a larger mass the compound, shown by mass spectrometry to be mainly $B_9Cl_7H_2$, was red-orange in colour. The two largest peaks in the mass spectrum were due to the ions $B_8Cl_4H_2^+$ and $B_8Cl_5H^+$ (base peak) representing loss of BCl_3 and BCl_2H, respectively, from the parent ion. The compound $B_9Cl_6H_3$ was present as an impurity and possibly arises from the attack of hydrogen on $B_{12}Cl_{12}$. Hydrogen chloride and boron trichloride were identified by IR spectroscopy as the gaseous products.

Morrison has shown that B_9Br_8Me may be prepared in about 15% yield by the pyrolysis of $(Et_3NH)_2B_{10}Br_{10}$;[5] we have studied the thermal decomposition of the corresponding chloride $(Et_3NH)_2B_{10}Cl_{10}$ in an effort to make B_9Cl_8Me. Although the major sublimate product was found to be B_9Cl_8Me the yield was less than 1% and impurities, thought to be B_9Cl_9 and $B_9Cl_7Me_2$, were also present. The poor yield from the reaction caused us to abandon the study. The thermal decomposition of $(Et_3NH)_2B_{10}Cl_{10}$ in an atmosphere of chlorine, in an attempt to form B_9Cl_9, again gave B_9Cl_8Me as the main boron-containing sublimate.

It appears to be widely assumed that boron cages present in the sub-halides are stabilized by back-donation from halogen to the cage orbitals. Therefore an important question to ask is how many of the halogen atoms may be changed for groups which can't stabilize the cages by such back-donation. From the experiments described here it is evident that up to three hydrogen atoms or one methyl group may be substituted onto the B_9 cage. By heating B_9Br_9 with a large excess of tetramethyltin up to six bromine atoms could be replaced by methyl groups. The whole range of mixed methylbromides $B_9Br_{9-n}Me_n$ ($n = 0$–6) was formed and unfortunately proved impossible to separate into its components.

EXPERIMENTAL

Reactions were carried out under vacuum in Pyrex glass tubes which had previously been baked out in an atmosphere of either boron trichloride or boron tribromide. In the brominations the apparatus was designed so that the aluminium tribromide could be sublimed directly into the reaction vessel from a side-arm, which was then removed by sealing off a constriction.

We had occasion to heat a small sample of B_8Cl_8 in an open test-tube. In the dry, anaerobic conditions at the bottom of the tube the B_8Cl_8 sublimed to give a purple vapour which, on "pouring" into the air by inverting the tube, ignited spontaneously with a series of mild explosions.

A. J. MARKWELL
A. G. MASSEY*
P. J. PORTAL

Department of Chemistry,
University of Technology,
Loughborough, Leicestershire, LE11 3TU,
England

*Author to whom correspondence should be addressed.

REFERENCES

[1] A. G. Massey, *Chemistry in Britain* 1980, 588.
[2] J. Kane and A. G. Massey, *J. Inorg. Nucl. Chem.* 1971, **33**, 1195; N. A. Kutz and J. A. Morrison, *Inorg. Chem.* 1980, **19**, 3295.
[3] S. B. Awad, D. W. Prest and A. G. Massey, *J. Inorg. Nucl. Chem.* 1978, **40**, 395.
[4] J. A. Forstner, T. E. Haas and E. L. Muetterties, *Inorg. Chem.* 1964, **3**, 155.
[5] D. Saulys and J. A. Morrison, *Inorg. Chem.* 1980, **19**, 3057.

Polyhedron, Vol. 1, No. 1, pp. 135–137, 1982
Printed in Great Britain.

0277-5387/82/010136-03$03.00/0
Pergamon Press Ltd.

The thiocyanato adduct of chromium(II) acetate

(*Received* 30 *July* 1981)

Abstract—The first dichromium complex with axially bonded anions, $[NEt_4]_2[Cr_2(O_2CCH_3)_4(NCS)_2]$, was obtained by reaction of $[NEt_4]NCS$ with $[Cr_2(O_2CCH_3)_4(OH_2)_2]$ in ethanol.

INTRODUCTION

The axial water molecules in binuclear chromium(II) acetate $[Cr_2(O_2CCH_3)_4(OH_2)_2]$ can be replaced by various neutral bases, e.g. pyridine, pyrazine,[1] piperidine,[2] substituted pyridines[3] and ammonia.[4] The Cr–Cr ligands, and in the absence of axial ligands "supershort" quadruple bonds are formed.[5] Recently, it has been reported[6] that chromium(II) forms many thiocyanato-

Table 1. Magnetic behaviour of $[NEt_4]_2[Cr_2(O_2CCH_3)_4(NCS)_2]$

T/K	$10^6\chi_{Cr}$/c.g.s.	μ_{eff}/B.M.
293	273	0.80
263	232	0.70
230	219	0.63
198	201	0.56
167	172	0.48
136	175	0.43
104	224	0.42
89.5	258	0.43

(diamagnetic correction = -203×10^{-6}c.g.s.)

complexes, and it has now been found that the water molecule can be replaced by thiocyanate to give $[NEt_4]_2[Cr_2(O_2CCH_3)_4(NCS)_2]$. This seems to be the first example of an anionic adduct to the quadruply-bonded binuclear Cr_2 system.

EXPERIMENTAL

The chromium(II) complexes were prepared and investigated under nitrogen or *in vacuo*.

Preparation of bis(tetraethylammonium) tetra-μ-acetatodi-isothiocyanato di-chromate(II)

A solution of tetraethylammonium thiocyanate was obtained by mixing equimolar solutions of tetraethylammonium chloride monohydrate and potassium thiocyanate in ethanol. The mixture was centrifuged and the solution decanted from the precipitated chloride. Chromium(II) chloride was prepared by the reduction of chromium(III) chloride with zinc and hydrochloric acid, and the solution was filtered into a warm solution of sodium acetate to give red needles of chromium(II) acetate monohydrate. The monohydrate (1.9 g, 0.01 mole) was filtered off and extracted by boiling ethanol into a hot solution of tetraethylammonium thiocyanate (1.9 g, 0.01 mol.) in ethanol (80 cm^3). The mixture was refluxed for 30 m and after cooling the violet, microcrystalline precipitate was filtered off, washed with ethanol and dried by continuous pumping for 5 hr. Found: C, 44.0; H, 7.55; N, 8.6; Cr, 14.2. $C_{13}H_{26}N_2O_4SCr$ requires: C, 43.6; H, 7.3; N, 7.8; Cr, 14.5%.

Magnetic measurements were carried out by the Gouy method. Electronic spectra were recorded on a Beckman Acta MIV recording spectrophotometer provided with a diffuse reflectance attachment. A lithium fluoride reference was used. Infrared spectra of nujol mulls were recorded on a Perkin-Elmer 577 spectrophotometer.

RESULTS AND DISCUSSION

Although the values of molar susceptibility χ_{Cr} (Table 1) show that the compound is essentially diamagnetic, they are larger than those obtained for the ammine $[Cr_2(O_2CCH_3)_4(NH_3)_2]$ (*ca.* 120×10^{-6} c.g.s., almost independent of temperature, and ascribed[4] to temperature independent paramagnetism), and they increase after passing through a minimum at approx. 150K. The increase is what would be expected if a small amount of chromium(III) impurity were present.[7] The magnetic behaviour can be reproduced by substitution of $J\sim550$° and $g=2$ in the expression for a binuclear chromium(II) complex ($S=2$), with the assumptions that $\chi_{TIP}=100\times10^{-6}$ c.g.s., and that approx. 0.7% magnetically-dilute chromium(III) impurity is present. However, the errors in measurements on nearly diamagnetic compounds are considerable so it can be concluded only that there is a large singlet–triplet ($2J$) separation. The propionate $[NEt_4]_2[Cr_2(O_2CCH_2CH_3)_4(NCS)_2]$ has been isolated but unfortunately contaminated with several per cent of chromium(III) impurity as estimated from the magnetic behaviour.

The IR spectrum of $[NeT_4]_2[Cr_2(O_2CCH_3)_4(NCS)_2)]$ contains absorptions at $[NEt_4]_2[Cr_2(O_2CCH_3)_4(NCS)_2)]$ contains absorptions at 2070*s*, ν(CN), 790*m*, ν(CS), and 474*w*, δ(NCS), in regions characteristic of N-bonded thiocyanate.[8]

A detailed analysis of the electronic absorption spectrum of single crystals of $[Cr_2(O_2CCH_3)_4(OH_2)_2]$ at 6K has recently been carried out.[9] There are two main features in the spectrum in the regions of 21000 cm^{-1} (Band I) and 30000 cm^{-1} (Band II). Band I has been assigned to the $\delta\leftarrow\pi^*$ transition of the binuclear system intensified by vibronic coupling, and band II to charge transfer from a non-bonding π-orbital of the carboxylate ligand to the π^* metal orbital. The room temperature diffuse reflectance spectrum of the thiocyanate is as follows: 18700*s*, *vb*, 24900*sh*, 28700*s*, *b*, 33900*sh* and 38900*m*, *b*, and the strong absorptions near 19000 and 29000 cm^{-1} can be similarly assigned. In a series of carboxylates,[9] the energies of bands I and II decrease linearly with increasing Cr–Cr separation. Extrapolation of the published data to the energies of I and II for $[NEt_4]_2[Cr_2(O_2CCH_3)_4(NCS)_2]$ indicates that the Cr–Cr separation is likely to be among the longest known (~2.5 Å). The attachment of a negatively charged ligand would be expected to lengthen the Cr–Cr bond through donation of electron density into the d_z2-σ^* antibonding orbital.

L. F. LARKWORTHY*
A. J. ROBERTS

The Joseph Kenyon Laboratory,
University of Surrey,
Guildford,
GU2 5XH, England

*Author to whom correspondence should be addressed.

REFERENCES

[1]F. A. Cotton and T. R. Felthouse, *Inorg. Chem.*, 1980, **19**, 328.
[2]F. A. Cotton and G. W. Rice, *Inorg. Chem.*, 1978, **17**, 2004.
[3]S. Herzog and W. Kalies, *Z. anorg. Chem.*, 1966, **351**, 237.
[4]L. F. Larkworthy and J. M. Tabatabai, *Inorg. Nucl. Chem. Lett.*, 1980, **16**, 427.
[5]F. A. Cotton, W. H. Ilsley and W. Kaim, *J. Am. Chem. Soc.*, 1980, **102**, 3464.
[6]L. F. Larkworthy, A. J. Roberts, B. J. Tucker and A. Yavari, *J.C.S. Dalton*, 1980, 262.
[7]A. Earnshaw, *Introduction to Magnetochemistry*. Academic Press, London (1968).
[8]R. A. Bailey, S. L. Kozak, T. W. Michelsen and W. N. Miles, *Coordination Chem. Rev.*, 1971, **6**, 407.
[9]S. F. Rice, R. D. Wilson and E. I. Solomon, *Inorg. Chem.*, 1980, **19**, 3425.

Polyhedron Vol. 1, No. 1, pp. 137–138, 1982
Printed in Great Britain.

0277-5387/82/010137-02$03.00/0
Pergamon Press Ltd.

A new uninegative ligand, *tris*-(diphenylthiophosphinyl)methanide[1]

(*Received* 16 *October* 1981)

Abstract—The reaction of *tris*-(diphenylthiophosphinyl)methane, $[(C_6H_5)_2P(S)]_3CH$, with mercury(II) halides produces complexes of the type $[(C_6H_5)_2P(S)]_3CHgX$, where X is Cl, Br and I.

We report here the first coordination compound of *tris*-(diphenylthiophosphinyl)methanide, the prototype of a new class of uninegative ligands. Reaction of the neutral parent compound, *tris*-(diphenylthiophosphinyl)methane,[2–4] with mercuric halides in ethanol produces compounds with the stoichiometry $[(C_6H_5)_2P(S)]_3CHgX$, where X is Cl, Br and I. The compounds are air-stable, high-melting, diamagnetic, monomeric crystalline solids. The analogous cadmium halide complexes are prepared similarly except that the addition of triethylamine to the reaction medium facilitates removal of the methine proton from the neutral starting ligand. Molecular weight determinations establish the monomeric nature of the complexes and thus preclude the possibility of dimeric mercury(I) compounds.

The ^{31}P NMR spectrum of the chloro compound, for example, at room temperature consists of a singlet (δ_P = 44.1 ppm vs 85% H_3PO_4, coordination shift = 2.2 ppm) flanked by mercury-199 (I = 1/2, relative abundance = 16.4%) satellites with $^2J(Hg199–P31) = 91$ Hz. This indicates that the three phosphorus atoms are equivalent. The observation of two-bond ^{31}P–^{199}Hg coupling in phosphine sulphide complexes at room temperature is unusual since such ligands are labile[5] on the NMR time scale with the result that sharp mercury satellites in the phosphorus spectrum are not usually observed. The ^{31}P NMR spectra of the other complexes in this study are similar.

Additional evidence for the existence of the anion form of the ligand is (a) the failure to observe a signal for the methine proton in the ^1H NMR spectrum of the complexes, whereas the neutral parent ligand has an easily detectable methine proton signal at 6.04 ppm (quartet, $^2J(PCH) = 16.5$ Hz); and the failure to observe the methine carbon in the ^{13}C NMR spectra of the complexes, undoubtedly due to the long relaxation time of the protonless carbon.

These data are consistent with two possible structures: (a) a four-coordinate mercury (II) complex, approximately tetrahedral, with the ligand bonded in a tridentate fashion through the three sulphur atoms or (b) a two-coordinate mercury(II) complex, approximately linear, with the ligand bonded via the methine carbon to the mercury. We currently favor the tridentate ligand structure since space filling models of the neutral parent ligand indicate that the methine proton is sterically very crowded, and replacement of this small proton with a large mercury atom would be very difficult indeed. An X-ray structural determination of an analogue of these compounds is currently in progress.

We thank the National Science Foundation (CHE 78–09536), NATO, SRC, and the Sir John Cass's Foundation for financial support and Dr. Elizabeth M. Briggs for the magnetic susceptibility measurements.

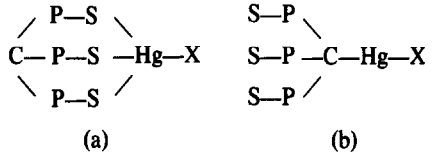

(a) (b)

Possible structures of $[(C_6H_5)_2P(S)]_3CHgX$ with phenyl groups omitted for clarity.

SAMUEL O. GRIM*
PATRICIA H. SMITH
LARRY C. SATEK

Department of Chemistry,
University of Maryland,
College Park,
MD 20742, *U.S.A.*

*Author to whom correspondence should be addressed.

REFERENCES

[1]F. A. Cotton and T. R. Felthouse, *Inorg. Chem.*, 1980, **19**, 328.
[2]F. A. Cotton and G. W. Rice, *Inorg. Chem.*, 1978, **17**, 2004.
[3]S. Herzog and W. Kalies, *Z. anorg. Chem.*, 1966, **351**, 237.
[4]L. F. Larkworthy and J. M. Tabatabai, *Inorg. Nucl. Chem. Lett.*, 1980, **16**, 427.
[5]F. A. Cotton, W. H. Ilsley and W. Kaim, *J. Am. Chem. Soc.*, 1980, **102**, 3464.
[6]L. F. Larkworthy, A. J. Roberts, B. J. Tucker and A. Yavari, *J.C.S. Dalton*, 1980, 262.
[7]A. Earnshaw, *Introduction to Magnetochemistry*. Academic Press, London (1968).
[8]R. A. Bailey, S. L. Kozak, T. W. Michelsen and W. N. Miles, *Coordination Chem. Rev.*, 1971, **6**, 407.
[9]S. F. Rice, R. D. Wilson and E. I. Solomon, *Inorg. Chem.*, 1980, **19**, 3425.

Polyhedron Vol. 1, No. 1, pp. 137–138, 1982
Printed in Great Britain.

0277-5387/82/010137-02$03.00/0
Pergamon Press Ltd.

A new uninegative ligand, *tris*-(diphenylthiophosphinyl)methanide[1]

(*Received* 16 *October* 1981)

Abstract—The reaction of *tris*-(diphenylthiophosphinyl)methane, $[(C_6H_5)_2P(S)]_3CH$, with mercury(II) halides produces complexes of the type $[(C_6H_5)_2P(S)]_3CHgX$, where X is Cl, Br and I.

We report here the first coordination compound of *tris*-(diphenylthiophosphinyl)methanide, the prototype of a new class of uninegative ligands. Reaction of the neutral parent compound, *tris*-(diphenylthiophosphinyl)methane,[2–4] with mercuric halides in ethanol produces compounds with the stoichiometry $[(C_6H_5)_2P(S)]_3CHgX$, where X is Cl, Br and I. The compounds are air-stable, high-melting, diamagnetic, monomeric crystalline solids. The analogous cadmium halide complexes are prepared similarly except that the addition of triethylamine to the reaction medium facilitates removal of the methine proton from the neutral starting ligand. Molecular weight determinations establish the monomeric nature of the complexes and thus preclude the possibility of dimeric mercury(I) compounds.

The ^{31}P NMR spectrum of the chloro compound, for example, at room temperature consists of a singlet (δ_P = 44.1 ppm vs 85% H_3PO_4, coordination shift = 2.2 ppm) flanked by mercury-199 (I = 1/2, relative abundance = 16.4%) satellites with $^2J(Hg199–P31) = 91$ Hz. This indicates that the three phosphorus atoms are equivalent. The observation of two-bond ^{31}P–^{199}Hg coupling in phosphine sulphide complexes at room temperature is unusual since such ligands are labile[5] on the NMR time scale with the result that sharp mercury satellites in the phosphorus spectrum are not usually observed. The ^{31}P NMR spectra of the other complexes in this study are similar.

Additional evidence for the existence of the anion form of the ligand is (a) the failure to observe a signal for the methine proton in the ^1H NMR spectrum of the complexes, whereas the neutral parent ligand has an easily detectable methine proton signal at 6.04 ppm (quartet, $^2J(PCH) = 16.5$ Hz); and the failure to observe the methine carbon in the ^{13}C NMR spectra of the complexes, undoubtedly due to the long relaxation time of the protonless carbon.

These data are consistent with two possible structures: (a) a four-coordinate mercury (II) complex, approximately tetrahedral, with the ligand bonded in a tridentate fashion through the three sulphur atoms or (b) a two-coordinate mercury(II) complex, approximately linear, with the ligand bonded via the methine carbon to the mercury. We currently favor the tridentate ligand structure since space filling models of the neutral parent ligand indicate that the methine proton is sterically very crowded, and replacement of this small proton with a large mercury atom would be very difficult indeed. An X-ray structural determination of an analogue of these compounds is currently in progress.

We thank the National Science Foundation (CHE 78–09536), NATO, SRC, and the Sir John Cass's Foundation for financial support and Dr. Elizabeth M. Briggs for the magnetic susceptibility measurements.

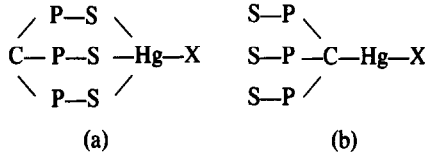

(a) (b)

Possible structures of $[(C_6H_5)_2P(S)]_3CHgX$ with phenyl groups omitted for clarity.

SAMUEL O. GRIM*
PATRICIA H. SMITH
LARRY C. SATEK

Department of Chemistry,
University of Maryland,
College Park,
MD 20742, *U.S.A.*

*Author to whom correspondence should be addressed.

IAN J. COLQUHOUN
WILLIAM McFARLANE

Department of Chemistry,
City of London Polytechnic,
London EC3N 2EY,
England

REFERENCES

[1](a) Part VI. Polydentate Ligands Containing Phosphorus. Part V. S. O. Grim and E. D. Walton, *Phosphorus Sulfur* 1980, **9**, 123; (b) presented at the *Int. Conf. on Phosphorus Chemistry.* Durham, North Carolina, June (1981).
[2]K. Issleib and H. P. Abicht, *J. Prakt. Chem.* 1970, 312, 456.
[3]S. O. Grim. L. C. Satek and J. D. Mitchell, *Z. Naturforsch.* 1980, **35b**, 832; I. J. Colquhoun, W. McFarlane, J.-M. Bassett and S. O. Grim, *J. Chem. Soc., Dalton Trans.* 1981, 1645.
[4](a) H. H. Karsch, *Z. Naturforsch.* 1979. **34b**, 1171; (b) private communication.
[5]S. O. Grim, E. D. Walton, and L. C. Satek, *Can. J. Chem.* 1980, **58**, 1476.

Polyhedron Vol. 1, No. 1, p. 139, 1982, Pergamon Press Ltd., Printed in Great Britain.

BOOK REVIEW

^{13}C NMR Data for Organometallic Compounds

B. E. Mann and B. F. Taylor

Academic Press, London. 1981. pp. viii and 326. £15.80/$32.50.

THE development of organometallic chemistry during the past 25 years has relied very heavily upon spectroscopic methods of analysis in general, and upon NMR spectroscopy in particular. Initially, the proton was by far the most commonly studied nucleus, but more recently instrumental developments such as the Fourier transform method have lead to a great deal of work being done on other nuclei of which ^{13}C is by far the most important. Already the literature contains an enormous quantity of ^{13}C NMR data relating to organometallic compounds, and the present volume performs a valuable service by making a large amount of it available in one place.

The first 30 pages of the book are a guide to ^{13}C NMR for the chemist who is already familiar with its straightforward organic applications. Given the amount of space available the choice of topics and their coverage is about right, although I should have liked to have seen rather more on exchange phenomena since some of the most attractive examples of the use of NMR in this area have come from organometallic chemistry.

The remainder of the book consists of a set of tables giving ^{13}C data mainly chemical shifts, but also couplings to the proton and other nuclei when available—for something like 8000 different organometallic compounds. In this context the term "metal" is interpreted very widely as any element other than hydrogen, carbon, nitrogen, oxygen, sulphur, a halogen or a noble gas. The grouping into tables, and the sub-divisions of the tables themselves are such that it was quite easy to find any desired compound, and in order to accommodate as many different compounds as possible data are presented mainly for those carbon atoms having a reasonably close association with the metal.

A sabbatical period spent in California during the writing has allowed some americanisms to creep into the text, but overall a high standard has been maintained. Direct reproduction of the authors' typescript has presumably reduced costs and cut down errors, although inevitably some remain, for example, extensive confusion of coupling constants and chemical shifts on p. 83. Some 1800 references are cited, the literature coverage being stated to be up to the end of 1979, (which appears to mean the beginning), and this can be recommended as a useful reference book for the practising organometallic chemist.

W. MCFARLANE

Polyhedron Vol. 1, No. 1, p. 141, 1982, Pergamon Press Ltd., Printed in Great Britain.

SYSTEMATICS AND THE PROPERTIES OF THE LANTHANIDES

A NATO ADVANCED STUDY INSTITUTE

Under the sponsorship of the NATO ASI an International Summer School on the Systematics and the Properties of the Lanthanides is planned to be held in Braunlage, Harz, Western Germany, from 11 to 25 July 1982. The topics of the School are divided in four general sections:

(1) Systematics (2) Structural Chemistry of the Lanthanide Complexes (3) Electronic, Spectroscopic and Magnetic properties of the Lanthanides (4) Lanthanides as Geochemical Indicators.

Several Plenary lectures will be delivered in each of the four sections. Participants will have ample opportunity to comment on and discuss the lectures and to take part in the Panel discussions.

Of interest to chemists, physicists, geochemists and biochemists. Participation is limited to 90 members.

For further information and application form please write to:

PROF. S. P. SINHA
Hahn-Meitner-Institut, Postfach 390128, D-1000 Berlin 39,
Fed. Rep. Germany.

Polyhedron Vol. 1, No. 2, pp. 143–144, 1982
Printed in Printed in Great Britain.

0277-5387/82/020143-02$03.00/0
Pergamon Press Ltd.

PREPARATION AND STUDY OF BIS(THEOPHYLLINATO) COPPER(II) COMPOUNDS

MILAN MELNÍK
Department of Inorganic Chemistry, Slovak Technical University, 812 37 Bratislava, Czechoslovakia

(*Received* 18 *June* 1981)

Abstract—*Bis*(theophyllinato) copper(II) dihydrate and its anhydrous form, were prepared. Their thermal, spectral and magnetic behaviours were investigated. Magnetic susceptibility studies show that the dihydrate form can be fitted to the Curie law. The magnetic behaviour of the anhydrous form is interpreted in terms of antiferromangetically exchange-coupled pairs of copper atoms. The change in magnetic properties as the dihydrate is dehydrated implies that structural rearrangement in first coordination sphere of copper accompanies the dehydration process. For *bis*(theophyllinato)copper(II) dihydrate we propose a pseudo octahedral coordination of copper(II) in a polymeric chain, and for the anhydrous form four-coordination in binuclear units.

INTRODUCTION

Theophylline (1,3-dimethyl-2,6-dioxopurine) which has the structure

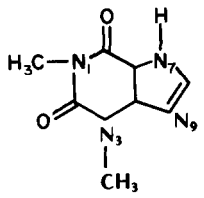

is a purine alkaloid, which is present in coffee beans and cocoa. The interaction of nucleic acids and their constituents with metal atoms are extensively studied.[1] Only a few crystal structures of copper(II) compounds with theophylline have been described.[2–4] Kistenmacher *et al.*[2,3] have reported the crystal and molecular structures of (*N*-salicylidene-*N*-methylethylenediamine) (theophyllinato)copper(II) monohydrate and of *bis* (theophyllinato)(diethylenetriamine)copper(II) dihydrate and found that the theophylline anions coordinated by $N_{(7)}$. Also in nitrato-diaquo-*bis*(1,3-dimethyl-2,6-dioxopurine)copper(II) nitrate,[4] two purine rings are bound to copper via $N_{(7)}$.

Some copper(II) compounds with the general formula $[(\text{purine})_2\text{Cu}(\text{N})_2].x\text{H}_2\text{O}$, where purine = the deprotonated form of theophylline, *N* = ammine, methylamine, ethylamine, *n*-propylamine, *n*-butylamine or benzylamine, were prepared and characterized by IR spectra.[5,6]

We here report the preparation, thermal, spectral and magnetic behaviours of *bis*(theophyllinato)copper(II) dihydrate and its anhydrous form.

EXPERIMENTAL

Preparation

$\text{Cu(tof)}_2 \cdot 2\text{H}_2\text{O}$ (tof = deprotonated form of theophylline) was prepared by treating theophylline (in excess) with copper (II) acetate monohydrate and a small amount of acetic acid in a hot ethanol solution. The filtered solution produced a grey-green product. The final complex was washed with ethanol. Its insolubility in all common organic solvents precluded recrystallization.

The $\text{Cu(tof)}_2 \cdot 2\text{H}_2\text{O}$ was also prepared by the reaction of theophylline with copper(II) trichloroacetate trihydrate in a similar way Calcd. for $\text{Cu(tof)}_2.2\text{H}_2\text{O}$: C, 36.72; H, 3.96; N, 24.47; Cu, 13.87. Found: C, 36.47; H, 3.9; N, 24.5; Cu, 14.06%.

The anhydrous Cu(tof)_2 was obtained by drying $\text{Cu(tof)}_2 \cdot 2\text{H}_2\text{O}$ at about 443 K for about 10 hr. The brown Cu(tof)_2 was found to be non-hygroscopic. Calcd. for Cu(tof)_2: C, 39.86; H, 3.34; N, 26.56; Cu, 15.06. Found: C, 40.0; H, 3.5; N, 26.42; Cu, 15.0%.

The thermal decomposition was studied on the derivatograph (MOM, Budapest). The apparatus and its operation was described by Paulik *et al.*[7] Platinum crucibles were of 14 mm in upper diameter. The powder samples were of 100 mg weight. The rate of temperature increase was 6 deg/min; the measurements were made in air.

Spectroscopic studies

IR spectra were recorded on a Perkin–Elmer 621 spectrophotometer. Electronic spectra were recorded on a Perkin–Elmer 450 spectrophotometer in the region 1.0–3.0 μm^{-1}. In both cases the Nujol suspension technique was applied. X-band EPR spectra of polycrystalline samples were measured at room temperature on the Varian E-4 spectrometer.

Magnetic susceptibility measurements

Magnetic susceptibility measurements were made over the temperature range 81–294 K by the Gouy method with the mercury tetrathiocyanatocobaltate (II) as calibrant.[8] Diamagnetic corrections were estimated from the Pascal constants[9] and effective magnetic moments were calculated from the equation

$$\mu_{\text{eff}} = 2.83(\chi_M^{\text{corr}} - N\alpha)^{1/2}$$

where $N\alpha$ equals 60×10^{-6} cm^3 mol^{-1}.

RESULTS AND DISCUSSION

It is interesting to note that the while copper(II) carboxylates with caffeine[10] gave solid products involving caffeine as a neutral ligand; with theophylline a solid copper(II) compound was obtained in which theophylline exists in an anionic form. The mechanism of reaction of theophyllinate with copper(II) has been proposed.[6]

The thermal decomposition of *bis*(theophyllinato) copper(II) dihydrate was carried out under air. The initial temperature of decomposition for $\text{Cu(tof)}_2 \cdot 2\text{H}_2\text{O}$ was 473 K. The compound between 473–503 K lost the bonded water molecules in one step, which gave in the DTA curve an endothermic peak at that temperature. In the temperature range 503–953 K the anions were evolved. At 703 K the DTA curve shows another endothermic peak. The TG curve at that temperature shows no break. The weight loss continued up to 953 K and a plateau on the TG curve is reached at a weight loss of 84% which corresponds to the formation of copper oxide. Above 600 K the oxidation of volatile organic product takes place, heat being emitted with strong exothermic peaks on the DTA curve at 673 and 773 K.

The IR spectrum of $Cu(tof)_2 \cdot 2H_2O$ shows a wide absorption band at about 3220 cm^{-1}. This frequency corresponds to the antisymmetric and symmetric OH stretching modes of the water molecules. The absorption band at 830 cm^{-1}, is probably due to the coordinated water molecules. Locating the "third" band of water is very difficult because there are bands of theophylline[6] in the region $\approx$ 1630 cm^{-1} where the band is expected. No bands in the regions of $\approx$ 3200 cm^{-1} and $\approx$ 830 cm^{-1}, were found in the case of the anhydrous form. In other regions the IR spectra of the compounds are very similar to each other.

It was proposed[3,6] that strong bands at 1500–1700 cm^{-1} and 1200–1250 cm^{-1} in some copper(II) compounds with theophylline can be attributed to theophylline coordination. IR spectra of the compounds studied show in these regions the peaks at 1700, 1640, 1535 and 1220 cm^{-1}, respectively. Some bands and especially that at 1220 cm^{-1} shift to higher frequencies than those in free theophylline[6]. This suggests coordination of theophylline to the copper.

The electronic spectrum of $Cu(tof)_2 \cdot 2H_2O$ in the visible region shows a band at 1.70 μm^{-1} with a shoulder at about 1.38 μm^{-1}. The band and shoulder may be assigned to the *d–d* transitions of the copper(II) ions, viz. $^2E_g \leftarrow {}^2B_{1g}$, $^2A_{1g} \leftarrow {}^2B_{1g}$ and $^2B_{2g} \leftarrow {}^2B_{1g}$. In the UV region, the compound shows an unsymmetrical shoulder with maximum at about 2.50 μm^{-1}, which may be assigned as a charge-transfer transition. The electronic spectrum of the anhydrous form exhibit wide shoulders with a maxima at 1.9 μm^{-1} and at $\approx$ 2.6 μm^{-1}.

The EPR spectra of the compounds obtained for the polycrystalline samples at room temperature show unsymmetrical isotropic bands with $g_i = 2.06$ for the hydrate form and $g_i = 2.07$ for the anhydrous form.

The magnetic behaviour of hydrated and anhydrous forms were studied in the temperature range 81–294 K. The μ_{eff} value of 1.85 B.M. observed for $Cu(tof)_2 \cdot 2H_2O$ at 294 K is temperature independent. The magnetic behaviour of the hydrate obeyed a Curie Law (C = 0.424 c.g.s.u.k. mol^{-1}). On the basis of experimental data of $Cu(tof)_2 \cdot 2H_2O$ can be assumed a pseudo-octahedral stereochemistry around copper(II) perhaps in a polymeric chain.

A drastic change in magnetic behaviour as the dihydrate is dehydrated was observed. Magnetic moment per copper atom is very low at room temperature ($\mu_{eff} = 0.56$ B.M. at 294 K), indicating that a fairly strong antiferromagnetic interaction is operating between copper(II) atoms. The magnetic susceptibility decreases with lowering of temperature but increases again below 200 K. This feature is most likely due to the binuclear structure and the presence of mononuclear paramagnetic impurity. Accordingly, the impurity term was added to the Bleaney–Bowers equation[11] giving,

$$\chi_M^{corr} - N_\alpha = \left\{\frac{g^2 N\beta^2}{3kT}[1 - 1/3(e^{-2J/kt})]^{-1}\right\}(1 - x) + \left(\frac{g^2 N\beta^2}{4kT}\right)x \qquad (1)$$

where x is the ratio of mononuclear copper(II) atoms to total copper(II) atoms, and other symbols have the usual meanings.[12] The magnetic susceptibility data were fitted using the BGD-2 programme on the ODRA 1305 computer. The criterion used to determine the best fit is the minimization of the sum of the squares of the deviation A, where

$$A = \sum_i (\chi_i^{calcd} - \chi_i^{exp})^2$$

with the value of 5.00×10^{-9}. The best fit parameters are: $J = -490$ cm^{-1} and $x = 5.2\%$. The drastic change in magnetic behaviour as the dihydrate is dehydrated implies that structural rearrangement in the first coordination sphere of copper accompanies the dehydration process. The compound shows very strong antiferromagnetic exchange interaction, which render it almost diamagnetic. The behaviour is closely similar to the magnetic properties of a series of binuclear copper(II) compounds with Schiff bases.[13,14] On the basis of such a similarity a binuclear structure of the type I[13,14] can be also proposed for $Cu(tof)_2$.

Acknowledgement—The author is indebted to Dr. J. Mroziński from Wroclaw University (Poland), for performing the magnetic susceptibilities and EPR spectra for this research.

REFERENCES

[1]D. J. Hodgson, *Progr. Inorg. Chem.* (Edited by S. J. Lippard), Vol. 23, Wiley, New York, 1977.
[2]T. J. Kistenmacher, D. J. Szalda and L. G. Marzilli, *Inorg. Chem.* 1975, **14**, 1686.
[3]T. Sorrell, L. G. Marzilli and T. J. Kistenmacher, *J. Am. Chem. Soc.* 1976, **98**, 2181.
[4]B. L. Kindberg, E. A. H. Griffith, E. L. Amma and E. J. Joner, Jr., *Cryst. Struct. Commun.* 1976, **5**, 533.
[5]W. J. Birdsall and M. S. Zitzman, *J. Inorg. Nucl. Chem.* 1979, **41**, 117.
[6]M. S. Zitzman, R. R. Krebs and W. J. Birdsall, *J. Inorg. Nucl. Chem.* 1978, **40**, 572; and refs. therein.
[7]P. Paulik, J. Paulik and L. Erdey, *Z. Anal. Chem.*, 1958, 160, 241.
[8]B. N. Figgis and R.. S. Nyholm, *J. Chem. Soc.* 1958, 4190.
[9]A. Earnshaw, *Introduction to Magnetochemistry.* Academic Press, London, (1968).
[10]M. Melník, *J. Inorg. Nucl. Chem.* 1981, **43**, 3035.
[12]B. Bleaney and K. D. Bowers, *Proc. Roy. Soc.* (London), Ser A, 1952, **214**, 451.
[12]T. R. Felthouse and D. N. Hendrickson, *Inorg. Chem.* 1978, **17**, 2636.
[13]E. Sinn, *Inorg. Chem.* 1976, **15**, 358.
[14]J. A. Davis and E. Sinnn, *J. Chem. Soc., Dalton Trans.* 1976, 165.

Polyhedron Vol. 1, No. 2, pp. 145–148, 1982
Printed in Great Britain.

0277–5387/82/020145–04$03.00/0
Pergamon Press Ltd.

^{13}C NMR STUDY OF DILUTE TERNARY SOLUTIONS: ACETONITRILE, SILVER NITRATE AND OTHER ELECTROLYTES IN WATER AT 25°C

MICHEL FROMON and CLAUDE TREINER*
Laboratoire d'Electrochimie, Université P. et M. Curie 4, place Jussieu, 75005 Paris, France

and

ODILE CONVERT,
Laboratoire de Chimie Organique Structurale, Université P. et M. Curie, 4, Place Jussieu, 75005 Paris, France

and

B. SUNDHEIM
University of New York, 4 Washington Place, Department of Chemistry, NY 10003, U.S.A.

(*Received* 29 *June* 1981)

Abstract—The ^{13}C NMR chemical shifts have been measured for dilute aqueous solutions of acetonitrile in presence of various electrolytes including silver nitrate. The two formation constants of the silver ion/acetonitrile complexes have been calculated assuming an additive contribution of each possible complex configuration. Under these conditions the values obtained for the formation constants are very close to those deduced from vapour pressure or electromotive force techniques. The other systems studied are discussed in relation to the salting phenomenon in aqueous electrolyte solutions.

INTRODUCTION

The interaction of the silver ion with acetonitrile in aqueous and non-aqueous media is a classical problem of physicochemical studies of ion + solvent interactions. Transference numbers,[1] spectroscopic data,[2,4] e.m.f. measurements[5,6] and vapour pressure data[7] are available for this system; from the thermodynamic methods one can deduce the formation constants of at least two complexes. It has been shown that in water both $(AgAN)^+$ and $[Ag(AN)_2]^+$ (AN = acetonitrile) occur, the values of the corresponding formation constants being very close to each other.

The spectroscopic studies, principally proton NMR, were used to determine solvation numbers assuming a chemical model and making use of the formation constants as evaluated by e.m.f. measurements. We felt it would be interesting to investigate the same system using ^{13}C NMR with two main objectives: firstly to examine the method of determination of formation constant by this spectroscopic method in a well documented but at the same time ambiguous case where several complexes are assumed formally without direct experimental proof of their existence; secondly to supplement with spectroscopic data, our recent study of the salting effect of a number of widely different electrolytes, including silver nitrate, by acetonitrile in water using a precise vapour pressure technique.[7] Comparisons of thermodynamic and spectroscopic studies have been made most extensively by Covington *et al.*[8,9] on a formal basis and also by Cox *et al.*;[3] other authors have attempted to do so more qualitatively.[10] In all these cases electrolytes were used as solutes in pure or mixed solvents in the whole range of composition. Here we report on a study of the interactions between acetonitrile and the ions under the same overall conditions as for our thermodynamic measurements, i.e. in relatively dilute solutions with respect to both components (acetonitrile and electrolytes) in water; in other words the Setchenov region.

EXPERIMENTAL AND MATERIALS

The NMR spectra were determined in a JEOL PS 100 in the Fourier transform mode working at 25.15 MHz. Two coaxial tubes (diameters: 8 and 10 mm) were used, the larger one with dioxane as a reference and D_2O for the lock and the smaller one with the solutions studied. The temperature was 23°C. The resolution of the chemical shifts was estimated to be 0.05 ppm.

All salts were from Merck ("of the highest purity") except for tetrabutylammonium bromide (nBu$_4$NBr) from O.S.I. which was recrystallized and dried before use. Acetonitrile from Merck ("zur analyze") was used for the most concentrated AN solutions. The experiments at 0.1 molar of AN were performed with ^{13}C enriched on the carbon of the nitrile group (Commissariat à l'energie atomique) in order to obtain acceptable signal to noise ratio.

PROCEDURE AND CALCULATIONS

The salting constants of acetonitrile by the electrolytes in aqueous solutions had been previously determined for dilute electrolyte solutions ($m \leq 0.05$ mole/kg), the acetonitrile concentration range between 0.3 and 1.5 mole/kg having been selected for technical reasons. The spectroscopic results however, could not be performed in the same electrolyte concentration range; here the molality had to be varied between 0.05 and 1.5 mole/kg in order to observe a significant chemical shift but the acetonitrile concentration could be maintained at a very low concentration by making use of ^{13}C labelling. The choice of concentration range of both solutes in the determination of the chemical shifts is important if one wants to obtain accurate formation constants from spectroscopic data as we shall see in the discussion section.

*Author to whom correspondence should be addressed.

We begin by summarizing the general features of the rigorous determination of formation constants by NMR spectroscopy.

Figure 1 presents the measured variation of chemical shift of the carbon atom of the nitrile group with electrolyte concentration. For silver nitrate a strong curvature is observed which is not seen for the other electrolytes; this curvature can be interpreted as an evidence for a strong ion/solvent interaction which may be described in terms of complex formation constants. We know from independent thermodynamic measurements in this case that the system behaves as though two complexes are formed and can be represented by the following equilibria:

$$Ag^+ + AN \rightleftharpoons (AgAN)^+ \tag{1}$$

$$Ag^+ + 2AN \rightleftharpoons (Ag(AN)_2)^+ \tag{2}$$

with the constants:

$$K_1 = \frac{(AgAN)^+}{(Ag^+)(AN)} \tag{3}$$

and

$$K_2 = \frac{(Ag(AN)_2{}^+)}{(Ag^+)(AN)^2}. \tag{4}$$

We assume here that the activity coefficients are unity which is a reasonable hypothesis when all ions involved bear the same charge.[11] The method most often used to obtain formation constants from spectroscopic data is the Benesi–Hildebrand plot which suffers from a number of well known approximations. Hence we shall use a more rigorous procedure, as follows:

We know that[12]

$$(Ag^+)_T = (Ag^+) \sum_{n=0}^{n=2} K_n(AN)^n \tag{5}$$

and

$$(AN)_T = (AN) + (Ag^+) \sum_{n=0}^{n=2} nK_n(AN)^n \tag{6}$$

(with $K_0 = 1$): subscript T means total concentration and no subscript refers to the unbound (free) ions or molecules, n being the number of formation constants. From these two relations we get:

$$\sum_{n=0}^{n=2} [n(Ag^+)_T + (AN) - (AN)_T]K_n(AN)^n = 0. \tag{7}$$

For simplicity we set:

$$(Ag^+)_T = M_T, \quad (AN)_T = A_T, \quad (AN) = A,$$
$$(AgAN)^+ = AM \quad \text{and} \quad (Ag(AN)_2) = A_2M.$$

Developing we obtain:

$$A - A_T = (M_T + A - A_T)K_1A + (2M_T + A - A_T)K_2A^2 = 0. \tag{8}$$

Rearranging, we get:

$$M_T = (A_T - A)\frac{1 + K_1A + K_2A^2}{K_1A + 2K_2A}. \tag{9}$$

The observed chemical shift relative to a given absorption peak (the reference) may be related to the various species in solution by the relation:[13]

$$\delta = \sum_n \delta_n(S_n) \tag{10}$$

where δ_n is the chemical shift due to each species of concentration S_n.

In the general case of two simultaneous complexes when the resonance is observed on the ligand then one can write:

$$\delta = \left(\frac{A}{A_T}\right)\delta_A + \left(\frac{AM}{A_T}\right)\delta_{AM} + \left(\frac{A_2M}{A_T}\right)\delta_{(1)_{A_2M}} + \left(\frac{A_2M}{A_T}\right)\delta_{(2)_{A_2M}} \tag{11}$$

where $\delta_{(1)_{A_2M}}$ and $\delta_{(2)_{A_2M}}$ are the resonance signals corresponding to the two possible sites of the acetonitrile molecules of the A_2M complex. If these two signals are independent from each other, then:

$$\delta_{(1)_{A_2M}} = \delta_{(2)_{A_2M}} = \delta_{AM},$$

We shall come back to this assumption in the discussion section:

$$\delta = \left(\frac{A}{A_T}\right)\delta_A + \left[\frac{AM + 2A_2M}{A_T}\right]\delta_{AM}.$$

Noting that $AM + 2A_2M = A_T - A$ represents the concentration of bound acetonitrile and:

$$\delta = \left(\frac{A}{A_T}\right\}\delta_A + \left[1 - \left(\frac{A}{A_T}\right)\right]\delta_{AM}. \tag{12}$$

We write:

$$\delta - \delta_{AM} = \left(\frac{A}{A_T}\right)(\delta_A - \delta_{AM})$$

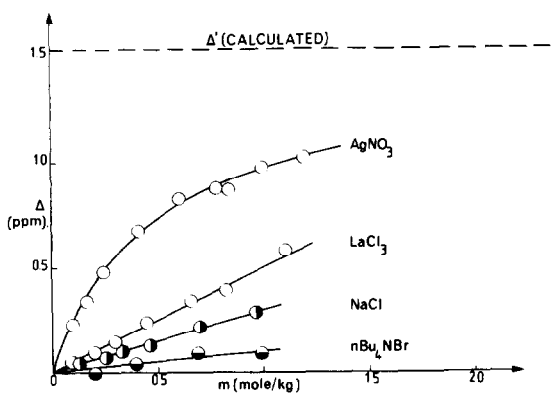

Fig. 1. Variation of the ^{13}C chemical shift on the nitrile group of 0.1 molal aqueous acetonitrile solutions with electrolyte concentration. Δ' is the saturation chemical shift.

let:

$$\delta_{AM} - \delta_A = \Delta'$$

and:

$$\delta - \delta_A = \Delta$$

we obtain the classical relationship:

$$\frac{A}{A_T} = \frac{\Delta' - \Delta}{\Delta'} \tag{13}$$

Δ' is the saturation chemical shift and Δ is the chemical shift relative to the acetonitrile resonance frequency without added salt.

Replacing A of eqn (13) in (9) one gets:

$$M_T = \Delta K_3 \cdot \frac{K_2K_3^2\Delta^2A_T^2 - A_T(K_1K_3 + 2K_2K_3A_T)\Delta + K_2A_T^2 + K_1A_T + 1}{2K_2K_3^2A_T\Delta^2 - (K_1K_3 + 4K_2K_3A_T)\Delta + 2K_2A_T + K_1} \tag{14}$$

with $K_3 = (\Delta')^{-1}$.

This equation contains three unknown quantities, K_1, K_2 and K_3.

In the case of a single complex we obtain an equation of the type used by Popov:[15]

$$M_T = \frac{A_TK_1K_3^2\Delta^2 - K_3(A_TK_1 + 1)\Delta}{K_1K_3\Delta - K_1} \tag{15}$$

with two unknowns, K_1 and K_3. Equation (15) contains no arbitrary assumption, and the additivity principle used to get eqn (14) will be justified in the next section. These equations should be employed in place of the Benesi–Hildebrand and related procedures, which in the present notation may be written as:

$$M_T = \frac{\Delta}{K_1K_3 - K_1}. \tag{16}$$

The constants K_1, K_2 and K_3 are adjusted using a mathematical technique derived from the simplex method. For programming convenience tests are performed on the total acetonitrile concentration rather than on the chemical shifts.

RESULTS AND DISCUSSION

1. *Silver nitrate and acetonitrile in water*

According to Deranleau[15] the value of the saturation fraction or in the present case of NMR measurements—the ratio of saturation chemical shift Δ/Δ'—should be between 0.2 and 0.8 in order to obtain accurate values of the formation constants. This point has also been stressed by Stockton and Martin[16] who determined formation constants in the same experimental regime as ours from proton NMR chemical shifts. They used, however, the Benesi–Hildebrand plot assuming only one complex between cations and different substrates at 0.1 molar in acetonitrile. This is the reason for our choice of the very small acetonitrile concentration used to determine the formation constants.

Table 1 presents the data used to calculate the formation constants. All chemical shifts are downfield. Table 2 collects the values obtained from thermodynamic sources, for the same processes as those described by the equilibria (1) and (2). The agreement between these data is remarkable and rather unexpected. It is noteworthy that the various formation constants were obtained in different concentration ranges with respect to all components for different experimental methods, namely dilute solution for the vapour pressure method, and concentrated $AgNO_3$ solution for e.m.f. and NMR determinations.

Table 1. Chemical shift of ^{13}C NMR for acetonitrile: CH_3–*C≡N (0.1 molar) in aqueous silver nitrate solutions

m	0	0.092	0.245	0.415	0.604	0.822	1.008
Δ	0	0.24	0.48	0.68	0.82	0.87	0.97

Table 2. Formations constants of AN/Ag^+ complexes in water according to thermodynamic and NMR methods

	K_1	K_2	Δ'
^{13}C NMR	1.45 ± 0.15	5.1 ± 0.5	1.54 ± 0.08
e.m.f.	(a) 2.0	4.4	—
	(b) 2.7 ± 0.2	3.0 ± 0.1	—

(a) Ref. 6.
(b) Ref. 1.

The same calculations were performed on the results of another series of experiments at a constant 1 molar acetonitrile concentration, within the same $AgNO_3$ concentration range. It was then found to be impossible to describe the experimental curve with the experimental error of 0.05 ppm contrary to the preceding case although a pair of formation constants could still be obtained. Thus the main test adopted for the adequacy of the chemical model used is the matching of the experimental curve of the required accuracy.

It seems that the procedure adopted is essentially sound and might be useful especially in the case of two or even more simultaneous equilibria when individual complexes cannot be observed. This is obtained at the cost of an additivity assumption (eqn 12); however Delpuech *et al.*[17] have shown that in the case of beryllium hydrates, for which a particular signal is observed for the replacement of each water molecule by an organic molecule (hexamethylphosphoric triamide: HMPT) in the solvation shell of the cation, the chemical shifts are indeed close to each other. This observation, the importance of which has been also stressed by Covington and Newman[18] cannot be generalized without further studies, but is a strong support in favour of our assumption.

In an attempt to detect the different possible complexes of the Ag^+ ion with acetonitrile, some experiments were performed under the same experimental conditions in pure methanol instead of water down to −55°C in order to decrease the exchange rate between free and bound acetonitrile molecules. The formation constants as determined by the e.m.f. method[6] are of the same order of magnitude, although somewhat larger than in water, so that the comparison between the results in the two solvents would have been meaningful; e.g. the values obtained in methanol for the processes (3) and (4)

are, respectively: $K_1 = 3.0$ and $K_2 = 9.0$ at 25°C. However, no splitting nor modification of the peak corresponding to the −C≡N group could be observed from +25 to −55°C.

2. *Case of other electrolytes*

Table 3 presents the chemical shifts for $LaCl_3$, NaCl and Bu_4NBr for the carbon atom of the nitrile group. All chemical shifts are again downfield but they show no curvature as a function of electrolyte concentrations. This is an interesting result in so far as it can be interpreted as an evidence for a rather weak ion + acetonitrile interaction. The salting constants of acetonitrile with $LaCl_3$, $BaCl_2$, Bu_4NBr—and evidently $AgNO_3$—display a pronounced non-ideal behavior. Henry's law is not attained for these salts at the lowest acetonitrile concentration investigated ($m \geq 0.3$ mole/kg) contrary to alkali halides for example.[7] This behavior may now be ascribed in the case of $LaCl_3$, $BaCl_2$ and presumably for *n*-Bu_4NBr as well—to structural features of the media (concerning a large number of solvent molecules) and not to any strong specific/ion + acetonitrile interaction, which would have shown up in the spectroscopic data.

Although it is most often difficult and sometimes even misleading to correlate ion + solvent interactions and solvent/solvent interaction, it is noteworthy that the excess enthalpies of the acetonitrile + water mixtures display a shallow minimum at $m_{AN} \simeq 1.4$ mole/kg at 25°C which is the region where the apparent salting constants of the multicharged electrolytes display their most non-ideal behavior.[19] These structural features would not have any influence on a strong ion + acetonitrile interaction such as occurs with the silver ion.

It is also interesting to note that it is for nBu_4NBr that the chemical shift of the carbon of the nitrile group is the smallest. Table 4 presents the chemical shifts obtained for a 1 molar acetonitrile solution and up to a 1 molar electrolyte concentration (in order to get fair signal/noise

Table 3. Chemical shifts of ^{13}C NMR for acetonitrile (0.1 m CH_3–*C≡N) in different aqueous electrolyte solutions

$LaCl_3$		NaCl		Bu_4NBr	
m (mole/kg)	Δ	*m* (mole/kg)	Δ	*m* (mole/kg)	Δ
0	0	0	0	0	0
0.103	0.05	0.148	0.05	0.200	0.0
0.203	0.10	0.299	0.10	0.402	0.05
0.309	0.15	0.678	0.19	0.692	0.10
0.448	0.24	1.002	0.29	1.011	0.10
0.666	0.34				
0.826	0.39				
1.11	0.53				

Table 4. Chemical shifts of ^{13}C NMR for acetonitrile (1 M: *CH_3–C≡N) in aqueous silver nitrate solutions

m	0	0.062	0.247	0.322	0.459	0.688	0.982
Δ	0	0.05	0.08	0.11	0.13	0.22	0.29

Note: For a 1 molar solution of nBu_4NBr in a 1 molar aqueous solution of acetonitrile, δ(*CH–C≡N) is equal to +0.23 (as compared to 0.30 for $AgNO_3$).

for the methyl group of the acetonitrile molecule as well as for the natural carbon of the nitrile group). The comparison of nBu_4NBr and $AgNO_3$ results shows that the chemical shift on the methyl group is twice that of the nitrile group with nBu_4NBr and only a third that of the same group for $AgNO_3$.

This behavior may be attributed to the more direct contact of the methyl group of the acetonitrile molecule with the hydrocarbon moieties of nBu_4NBr as compared to the interaction involving the carbon of the nitrile group in the case of the inorganic cations.

REFERENCES

[1]H. Strehlow and H. M. Koepp, *Z. Elektrochem.* 1958, **62**, 373.
[2]H. Schneider and H. Strehlow, *Z. Physik. Chem.* Neue Folge 1966, **49**, 45.
[3]B. G. Cox, A. J. Parker and W. E. Waghorne, *J. Phys. Chem.* 1974, **78**, 1731.
[4]H. Schneider, In *Solute-Solvent Interactions* (Edited by J. F. Coetzel and C. D. Ritchie), Vol. II, p. 155. Marcel Dekker, New York, 1976.
[5]H. M. Koepp, H. Wendt and H. Strehlow, *Z. Elektrochem.* 1960, **64**, 483.
[6]S. E. Manahan and R. T. Iwamoto, *J. Electroanal. Chem.* 1867, **14**, 213.
[7]C. Treiner and M. Fromon, *J. C. S., Far. Trans. I* 1980, **76**, 1062.
[8]A. K. Covington, T. H. Lilley, K. E. Newman and G. A. Porthouse, *J. C. S., Far. Trans. I* 1972, **68**, 963.
[9]A. K. Covington and K. E. Newman, In *Thermodynamic Behavior of Electrolytes in Mixed Solvents* (Edited by W. F. Furter), *Adv. in Chem. Ser.* No. 155, p. 153, 1976.
[10]E. A. Arnett, H. C. Ko and R. J. Minasz, *J. Phys. Chem.* 1972, **76**, 2474.
[11]F. M. D'Itri and A. I. Popov, *J. Inorg. Nucl. Chem.* 1969, **31**(4), 1069.
[12]F. J. C. Rossoti and H. Rossoti, *The Determination of Stability Constant.* McGraw-Hill, New York, p. 39, 1961.
[13]Ref. 12, p. 292.
[14]A. I. Popov, In Ref. 4, p. 324.
[15]D. A. Deranleau, *J. Am. Chem. Soc.* 1969, **91**, 4044.
[16]G. W. Stockton and J. S. Martin, *J. Am. Chem. Soc.* 1972, **94**, 6921.
[17]J. J. Delpuech, A. Peguy and M. R. Khaddar, *J. Magn. Res.* 1972, 325.
[18]A. K. Covington and K. E. Newman, *Modern Aspects of Electrochemistry* (Edited by J.O'M. Bockris), 1977.
[19]K. W. Morcom and R. W. Smith, *J. Chem. Thermodyn.* 1969, **1**, 503.

Polyhedron Vol. 1, No. 2, pp. 149–151, 1982
Printed in Great Britain.

0277–5387/82/020149–03$03.00/0
Pergamon Press Ltd.

INNER-SPHERE OXIDATION OF IRON(II) BY TRIS(MALONATO)COBALTATE(III)

YOUSIF SULFAB* and M. S. AL-OBADIE
Department of Chemistry, University of Kuwait, Kuwait

(*Received* 1 *July* 1981)

Abstract—The kinetics of oxidation of Fe^{2+} by $[Co(C_3H_2O_4)_3]^{3-}$ in acidic solutions at 605 nm showed a simple first-order dependence in each reactant concentration. The second-order rate constant dependence on $[H^+]$ is in accordance with eqn (i)

$$k_2 = k_2' + k_3[H^+] \quad \text{(i)}$$

where k_2' and k_3 have values of $73.4 \pm 14.0\ M^{-1}\ s^{-1}$ and $353 \pm 41\ M^{-2}\ s^{-1}$, respectively, at 1.0 M ionic strength ($NaClO_4$) and 25°C. At 310 nm the formation and decomposition of an intermediate, believed to be $[FeC_3H_2O_4]^+$, was observed. The increase in the rate of oxidation with increasing $[H^+]$ was interpreted in terms of a "one-ended" dissociation mechanism which facilitates chelation of Fe^{2+} by the carbonyl oxygens of malonate in the transition state.

INTRODUCTION

It is believed that iron(II) generally, reacts with cobalt(III) complexes containing bridging ligands via an inner-sphere mechanism.[1–3] Both spectrophotometric and kinetic evidence has been presented in support of this mechanism.[1,2] Oxidation of iron(II) by $[Co(C_2O_4)_3]^{3-}$ was shown to proceed in two stages corresponding to the formation and decomposition of the primary product $[FeC_2O_4]^+$ [1]. A long-lived intermediate was detected kinetically in the iron(II) reduction of nitrilotriacetatopentaamminecobalt(III), $[Co(NH_3)_5(nta)]$.[2] Following a previous report that oxidation of iron(II) by *tris*-(malonato)cobaltate(III), $[Co(C_3H_2O_4)_3]^{3-}$, proceeds via the formation of a bridged intermediate,[4] we report here a kinetic study of this reaction. The formation and decomposition of the initial product $[FeC_3H_2O_4]^+$ may thus be used as a criterion for ascertaining a bridged mechanism. This complex was reported to oxidize chromium(II) via an inner-sphere mechanism.[5]

EXPERIMENTAL

The complex $K_3Co(C_3H_2O_4)_3 \cdot 3H_2O$ was prepared according to Al-Obadie and Sharpe's method.[6] Iron(II) perchlorate solutions were prepared by dissolving fine iron powder (Reidel–DeHaen AG) in ~1 M perchloric acid and gently heating to increase the dissolution rate. The solution was filtered and standardized against a standard permanganate solution.[7] Fresh solutions were always prepared, flushed with nitrogen and cooled. The concentration of the total acid was determined by sodium hydroxide titration after passing a known volume of the iron(II) solution through a cation exchange column (Amberlite IR 120 (H)). The free acid concentration was obtained by subtracting twice the iron(II) concentration from that of the total. A stock solution of perchloric acid was prepared by dilution and standardized against sodium hydroxide. Sodium perchlorate solution was standardized by feeding on the cation-exchange column and titrating agsinst sodium hydroxide.

Pseudo first-order conditions were maintained in all kinetic runs with iron(II) and hydrogen ion concentrations being in vast excess of that of $[Co(C_3H_2O_4)_3]^{3-}$ concentrations. The ionic strength was maintained at 1.0 M by addition of $NaClO_4$. Fresh solutions of $[Co(C_3H_2O_4)_3]^{3-}$ were always prepared as this complex slowly decomposes on standing, and the acid was added to iron(II) solutions because hydrogen ions catalyse aquation of $[Co(C_3H_2O_4)_3]^{3-}$.[8]

The rate of oxidation of iron(II) by $[Co(C_3H_2O_4)_3]^{3-}$ was followed at 605 nm on a Durrum stopped-flow spectrophotometer. At this wavelength, a peak for the complex, only $[Co(C_3H_2O_4)_3]^{3-}$ absorbs. The formation and decomposition of the intermediate $[FeC_3H_2O_4]^+$ was monitored at 310 nm. This wavelength was selected because it was expected that the intermediate $[FeC_3H_2O_4]^+$ would have an absorption spectrum similar to that of $[FeC_2O_4]^+$. The concentration of iron(II) and hydrogen ions were varied over the range $(1.16–5.79) \times 10^{-2}$ M and 0.10–0.50 M, respectively.

RESULTS AND DISCUSSION

Loss of $[Co(C_3H_2O_4)_3]^{3-}$, at 605 nm, showed a simple first order dependence on its concentration. Plots of log $(A_t - A_\infty)$ vs time were linear up to ≥90% of reaction. The pseudo first-order rate constant, k_{obs}, at fixed $[H^+]$, temperature, and ionic strength varied linearly with $[Fe^{2+}]$ as shown in Table 1. The variation of k_2 with $[H^+]$ at fixed temperature, and ionic strength is shown in Fig. 1. From these results the dependence of k_2 on $[H^+]$ is given by eqn (1)

$$k_2 = k_2' + k_3[H^+]. \quad (1)$$

The values of k_2' and k_3 were calculated as $73 \pm 14\ M^{-1}\ s^{-1}$ and $353 \pm 41\ M^{-2}\ s^{-1}$, respectively, at 25.0°C and ionic strength 1.0 M, using a linear least-squares fit to eqn (1). The stopped-flow traces in Fig. 2 show the reaction between Fe^{2+} and $[Co(C_3H_2O_4)_3]^{3-}$, at 605 nm, to be simple. However, this same reaction when monitored at 310 nm showed that there are two steps similar to those observed in the reaction between Fe^{2+} and $[Co(C_2O_4)_3]^{3-}$. The two steps observed at 310 nm, most likely, correspond to the formation and decomposition of the intermediate $[FeC_3H_2O_4]^+$. The observation of this intermediate leads to the conclusion that malonate is bonded to both Co(III) and iron(II) in the transition state

*Author to whom correspondence should be addressed.

of the oxidation–reduction reaction. The malonate could either be monodentate or bidentate in the intermediate $[FeC_3H_2O_4]^+$. In the reaction between $[Co(C_3H_2O_4)_3]^{3-}$ and Cr^{2+} both chelated and monodentate malonate Cr^{3+} products were identified.[4] The ratio of these two products was found to be dependent upon $[H^+]$; the lower $[H^+]$ the higher is the amount of the chelated product. This was interpreted in terms of protonation of a carbonyl oxygen, the atom responsible for bridging the two metal ions. Chelation to Cr^{2+} by the two carbonyl oxygens, is believed, to be possible in the boat and chair conformers where both oxygens are on the same side. The two carbonyl oxygens are pointing in opposite directions and cannot bond to the same chromium in the "staggered" conformer. This explanation may also apply to the bonding of Fe^{2+} in the transition state.

The rate law obtained is consistent with the involvement of two Co(III) species in the oxidation process, protonated and unprotonated forms. The greater reactivity of the protonated form is, probably, due to a rapid "one-ended" dissociation of a malonate, assisted by H^+, that facilitates chelation to iron(II) in the transition state as in I.[9]

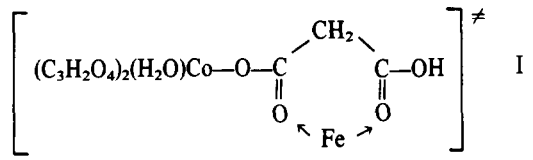

I

This is in agreement with the proposed mechanism of

Table 1. Kinetic data for the oxidation of Fe^{2+} by $[Co(C_3H_2O_4)_3]^{3-}$

$10^2 \times [Fe^{2+}]$, M	$[H^+]$, M	k_{obs}, s^{-1}	$10^{-2} x k_2$, $M^{-1}s^{-1}$
1.16	0.29	1.99 ± 0.01	1.72 ± 0.01
2.32	0.29	3.93 ± 0.02	1.69 ± 0.01
3.47	0.29	5.86 ± 0.05	1.69 ± 0.01
3.47	0.50	8.50 ± 0.06	2.45 ± 0.02
3.47	0.10	3.60 ± 0.02	1.04 ± 0.01
4.63	0.29	7.62 ± 0.43	1.65 ± 0.09
5.79	0.29	10.84 ± 0.11	1.87 ± 0.02

λ = 605 nm, ionic strength 1.0 M ($NaClO_4$), temperature 25.0°C, and $[Co(C_3H_2O_4)_3^{3-}] = 10^{-3}$ M.

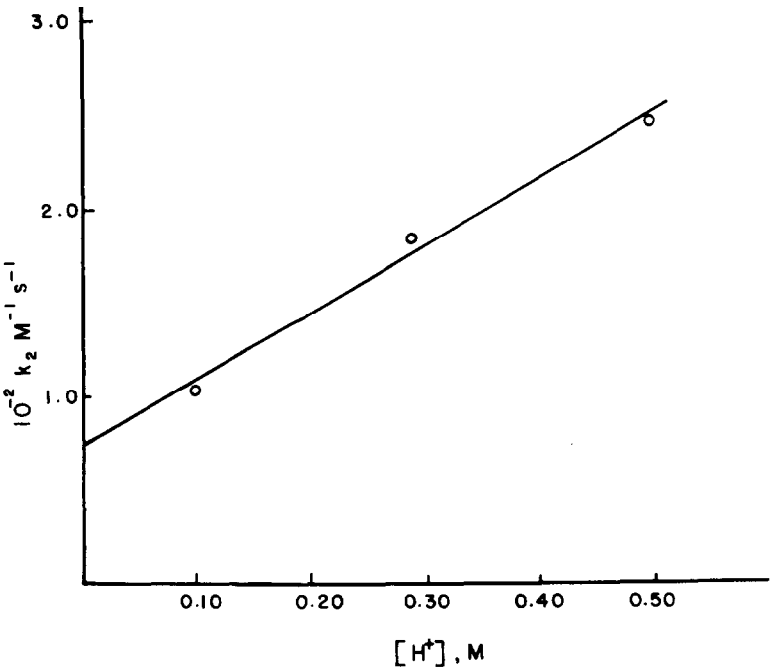

Fig. 1. Dependence of the second-order rate constant k_2 M^{-1} s^{-1} on $[H^+]$ M.

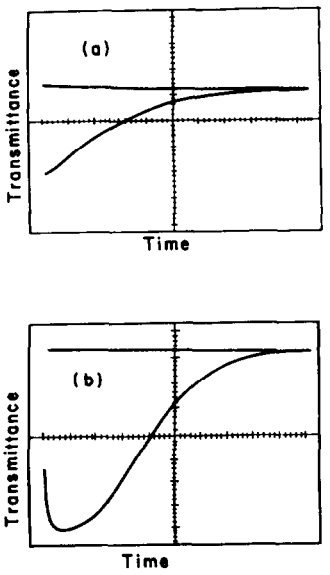

Fig. 2. Stopped-flow traces for the reaction between $[Co(C_3H_2O_4)_3]^{3-}$ and Fe^{2+}. $[Co(C_3H_2O_4)_3]^{3-} = 10^{-3}$ M, $[Fe^{2+}] = 3.47 \times 10^{-2}$ M, $[HClO_4] = 0.50$ M, ionic strength = 1.0 M ($NaClO_4$). Upper curve (a) shows the disappearance of $[Co(C_3H_2O_4)_3]^{3-}$; $\lambda = 605$ nm; abscissa scale 50 msec. per major division. Lower curve (b) shows the formation and disappearance of the intermediate $[FeC_3H_2O_4]^+$; $\lambda = 310$ nm; abscissa scale, 0.1 sec per major division. Vertical axis, in both traces, gives transmittance of 10% per major division.

aquation of $[Co(C_3H_2O_4)_3]^{3-}$.[8] A similar transition state was proposed in the reaction between Cr^{2+} and $[(NH_3)_5Co(C_3H_2O_4)]^+$.[10] An H^+-catalysed "one-ended" dissociation of the chelated malonate did not fit the data for the reaction between Cr^{2+} and $[Co(C_3H_2O_4)_3]^{3-}$, where an increase in $[H^+]$ leads to a decrease, not an increase, in the yield of the chelated product. A "one-ended" dissociation mechanism, probably, operates in the Fe^{2+} reaction, and not in the Cr^{2+} reaction, because in the reaction of the former, electron transfer rate is slower than the "one-ended" dissociation rate. The rate of oxidation of Cr^{2+} by $[Co(C_3H_2O_4)_3]^{3-}$ is too fast to follow by the stopped-flow technique and that $k_2 > 10^6$ M^{-1} s^{-1}.

The rate of decomposition of the intermediate $[FeC_3H_2O_4]^+$ seems to be comparable with its rate of formation as shown in Fig. 2. This points to the lower thermodynamic stability and higher kinetic liability of malonate complexes compared to those of oxalate. The rate of decomposition of $[FeC_2O_4]^+$ was observed to be considerably slower than its rate of formation.

It is, however, worth mentioning that a slower third reaction was also observed. This was accompanied by an increase in absorbance. The nature of this slower reaction has not been elucidated. A similar behaviour was also observed in the reaction between Cr^{2+} and $[Co(C_3H_2O_4)_3]^{3-}$ where two reactions follow the oxidation process.[5]

Acknowledgement—The authors would like to thank Mr. S. A. P. Abdussalam for helping in performing the experiments and in calculations.

REFERENCES

[1]A. Haim and N. Sutin, *J. Am. Chem. Soc.* 1966, **88**, 5343.
[2]R. D. Cannon and J. Gardiner, (a) *J. Am. Chem. Soc.* 1970, **92**, 3800; (b) *Inorg. Chem.* 1974, **13**, 390.
[3]K. Ohashi, *Bull. Chem. Soc. Japan* 1973, **46**, 1880.
[4]M. S. Al-Obadie, *Inorg. Chem.* 1980, **19**, 2897.
[5]J. D. Edwards, Y. Sulfab and A. G. Sykes, *Inorg. Chem.* 1975, **14**, 1474.
[6]M. S. Al-Obadie and A. G. Sharpe, *J. Inorg. Nucl. Chem.* 1969, **31**, 2963.
[7]A. I. Vogel, *A Text-book of Quantitative Inorganic Analysis*, 3rd Edn, p. 287, 1962.
[8]Y. Sulfab and M. S. Al-Obadie, *J. Inorg. Nucl. Chem.* 1974, **36**, 2067.
[9]K. R. Ashley and R. E. Hamm, *Inorg. Chem.* 1965, **4**, 1120.
[10]D. H. Huchital and H. Taube, *Inorg. Chem.* 1965, **4**, 1660.

Polyhedron Vol. 1, No. 2, pp. 153–155, 1982
Printed in Great Britain.

0277–5387/82/020153–03$03.00/0
Pergamon Press Ltd.

POTENTIOMETRIC INVESTIGATION OF SPARINGLY SOLUBLE METAL-LIGAND SYSTEMS USING METAL-ION BUFFERS

Z-X. HUANG,† H. S. AL-FALAHI, A. COLE, J. R. DUFFIELD, C. FURNIVAL, D. C. JONES, P. M. MAY, G. L. SMITH and D. R. WILLIAMS*

Department of Chemistry, University of Wales Institute of Science and Technology, Cardiff CF1 3NU, Wales

(*Received* 8 *July* 1981)

Abstract—A novel approach based on metal–ion buffers has been used to determine metal–ligand formation constants for a variety of sparingly soluble systems. It is suggested that the approach will be particularly useful in the study of metal binding by pharmaceuticals.

The passive diffusion of molecules through biochemical membranes depends on their charge density and so the distribution of administered agents throughout the body is often determined by the polarity and formal electrical charge of the species which they form *in vivo*.[1] Molecules having a low charge density tend to be readily absorbed through the gastrointestinal tract and are subsequently dispersed into a wide variety of tissues whereas more highly charged species are poorly absorbed and, when injected intravenously, are confined to extracellular space. Thus, the properties of therapeuticals which enable them to reach their site of action by passing through cell walls, are inherently apt to make them insoluble in water.

On the other hand, highly water-insoluble substances would be at a disadvantage because, in addition to the transport through membranes, drug species must also move through aqueous biofluids such as blood plasma. This dichotomy is resolved by agents which can change their stoichiometry (and thus also their electrical charge) according to the composition of the medium. Most commonly, the protonation of drug anions produces lower charged species.

However, even neutral molecules must be relatively nonpolar in order to cross the lipid bilayer of cell membranes. So it is not surprising that many therapeutic agents are found to be only sparingly soluble in water. This limits potentiometric analysis of these systems because the protonated species tend to precipitate as soon as they begin to form in the solution.

The difficulty is even more pronounced when metal-ion interactions with the drug are being investigated. With most anionic ligands, complexation will reduce the charge on the species so insolubility often becomes a problem as the pH is raised and the free concentration of the ligand increases.

This paper outlines a technique which has proved very useful in avoiding such precipitation during potentiometric titrations. Although straightforward in principle, it has not previously been described in the literature. It appears to have considerable potential in many areas of inorganic solution chemistry but particularly in the field of metal binding by pharmaceuticals.

THE TECHNIQUE

It has long been established that the problem of measuring very large formation constants can sometimes be overcome using the principle of ligand–ligand competition.[2,3] A secondary chelating agent is introduced to lower the free metal ion concentration in the solution and thus bring about some conditions under which the species being investigated can dissociate. This is tantamount to using a metal ion buffer.[4]

We have found that this kind of competition can also be used successfully to supress precipitation during potentiometric investigations of sparingly soluble systems where the solubility product of the metal-hydroxide or the metal-ligand species is exceeded.

The reason why this approach is effective is illustrated in Figs. 1 and 2 using the cadmium(II)–cystine system. Figure 1 shows the concentration of the binary species over a wide range of pH (i.e. including calculated extensions as they would have been obtained had they not been precluded by insolubility). Figure 2 shows the distribution for the real ternary system. The introduction of the secondary ligand (NTA) sufficiently lowers the free cadmium ion concentration to permit limited formation of the mono cadmium-cystine complex in a pH range where the species does not precipitate.

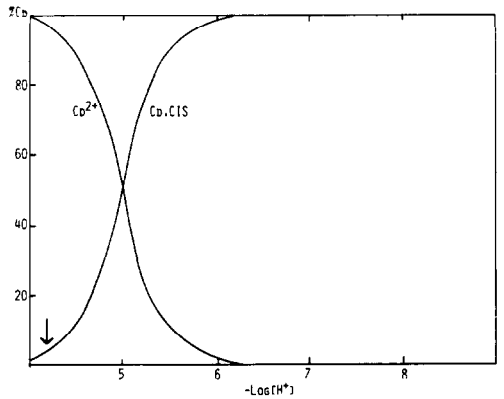

Fig. 1. Theoretical distribution of cadmium in the presence of cystine (Cd: Cystine = 1:2). The point at which the titration was prevented by precipitation is shown by the arrow.

*Author to whom correspondence should be addressed.

†On leave from the Chemistry Department, Fudan University, Shanghai, People's Republic of China.

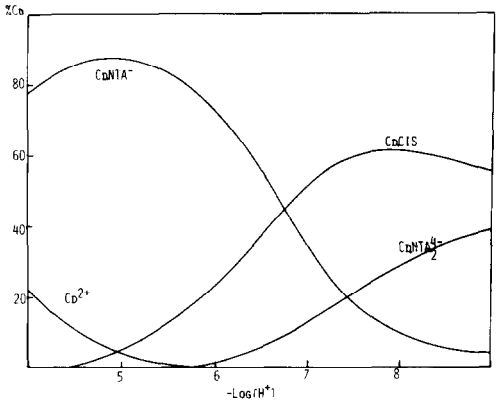

Fig. 2. Actual distribution of cadmium in the presence of cystine and nitrilotriacetate as buffering ligand (Cd: Cystine: NTA = 1:2:1). Note that the CdNTA complex suppresses $[Cd^{2+}]$ and allows the titration to be completed.

RESULTS AND DISCUSSION

Table 1 gives some examples of formation constants for poorly soluble systems which have been obtained using this buffering method. The mathematics for treating such competition has been available for many decades but the introduction of computer programs such as SCOGS[4] and MINIQUAD[5] has greatly facilitated potentiometric data assessment and treatment. Ideally, the same value for the ML constant ought to be obtained by using two or more buffering ligands. We have several examples of this check procedure, one of which, β_{1011} for Cu-guanosine, is shown in the Table.

The buffering ligands were chosen according to the following criteria.

If the formation constant for β_{ML} is required and if B is the buffering ligand,

1. The complexing ability of B ought not to be much greater than that of L, otherwise MB and MB_2 complexes will be formed (and vice versa in that only ML_2 complexes will be formed if B is considerably weaker than L as a complexing ligand this leads to precipitation of ML).

2. Preferably mixed ligand ternary complexes should be avoided. This may be achieved by having the sum of the number of donor groups for both ligands considerably in excess of the coordination number of the central metal ion.

3. Unfortunately, polydentate groups as defined under 2, because of the chelate effect, often bring about very

Table 1. Formation constants (at 37° and I = 150 mmol dm^{-3} NaCl) for the general reaction.

$$pL + qB + rM + sH \rightleftarrows L_pB_qM_rH_s; \quad \beta_{pqrs} = \frac{[L_pB_qM_rH_s]}{[L]^p[B]^q[M]^r[H]^s}$$

Complexes **underlined** are those determined by the new approach

Ligand, L	Complex pqrs	log β	Buffer, B	Binary complexes pqrs	log β
Metal ion = Cd^{2+}					
Cystinate	1001	8.602	NTA	0101	9.020
	2003	16.356		0102	11.449
	1003	18.407		0103	13.357
	1004	20.043		0110	8.253
				0210	12.238
	1010	8.22			
Cystinate			EDDA	0101	9.541
				0102	16.025
				0103	18.327
				0104	19.602
	as above			0110	8.629
				0210	12.991
	111-1	1.07			
Cystinate			Penicil-laminate	0101	10.244
				0102	17.921
				0103	19.827
				0110	10.742
	as above			0210	17.684
				0211	24.671
	111-1	5.41			
Cystinate			EDTA	0101	9.120
				0102	15.033
				0103	17.66
	as above			0104	19.66
				0110	13.790
				0111	16.515
	111-1	24.47			
Metal ion = Zn^{2+}					
Aminothi-azoline	1001	8.483	Thiazoli-dine car-boxylate	0101	6.104
				0102	7.829
				0110	3.19
				0210	5.75
	1010	3.15			

Ligand, L	Complex pqrs	log β	Buffer, B	Binary complexes pqrs	log β
Metal ion = Zn^{2+} (contd)					
Aminothiazoline			Alanine	0101	9.368
				0102	11.699
	as above			0110	4.44
				011-1	-3.18
	1110	7.25			
Cystinate	1002	8.602	Histidinate	0101	8.777
	1002	16.356		0102	14.601
	1003	18.407		0103	16.287
	1004	20.043		0110	6.30
				0210	11.45
	1010	6.688		0111	10.38
	1011	12.802		0211	16.67
Metal ion = Cu^{2+}					
Nalidixate	1001	5.94	Ethylene-diamine	0101	9.6
	1010	6.0		0102	16.43
				0110	10.14
				0210	18.84
				021-1	7.4
	2010	11.64			
	1010	6.0			
Guanosine	1001	8.91	Ethambutol	0101	9.05
	1002	10.97		0102	15.10
				0110	9.9
				011-1	3.26
				011-2	-5.05
	1111	20.77			
	1011	11.21			
Guanosine	as above		Nalidixate	0101	5.94
				0110	6.0
				0210	11.64
	1011	11.22			

*Full details of data treatment, standard deviations etc., will be published in full papers in due course

powerful complexing and this contravenes criterion number 1.

Competition between two ligands for a central metal ion has been used since the early days of solution coordination chemistry. However, the application described in this letter to sparing solubility is a new concept that has a widespread potential to the field of pharmaceutical metal-ion studies.

REFERENCES

[1] A. M. Fiabane and D. R. Williams, *The Principles of Bioinorganic Chemistry*. Royal Society of Chemistry, 1977.

[2] J. Bjerrum, Dissertation, Copenhagen, 1941.

[3] I. Leden, Dissertation, Lund, 1943.

[4] D. D. Perrin and B. Dempsey, *Buffers for pH and Metal Ion Control*, Chapman and Hall, London, 1974.

[5] A. Sabatini, A. Vacca and P. Gans, *Talanta* 1974, **21**, 53.

Polyhedron Vol. 1, No. 2, pp. 157–161, 1982
Printed in Great Britain.

0277-5387/82/020157-05$03.00/0
Pergamon Press Ltd.

COMPLEXES OF 1-METHYL-4-MERCAPTOPIPERIDINE WITH ZINC(II), CADMIUM(II) AND MERCURY(II) HALIDES

J. C. BAYON, I. CASALS, W. GAETE,* P. GONZALEZ-DUARTE and J. ROS
Departament de Química Inorgànica, Universitat Autónoma de Barcelona, Bellaterra (Barcelona), Spain

(*Received* 8 *July* 1981; *accepted for publication* 13 *August* 1981)

Abstract—The preparation of a series of complexes formed by 1-methyl-4-mercaptopiperidine (AH) and divalent zinc, cadmium and mercury halides is reported together with some spectral and physical properties. The results of a crystallographic study allows to establish the structure of those of formula $[M_2(AH)_2X_4]H_2O$ (M = Zn, Cd, Hg; X = Br, I) consisting of dimers and involving tetrahedral environment with sulphur-bridges for the metal atoms. Polymeric structures are proposed for the complexes of formulae $Cd(AH)Cl_2$ and $Hg_2Cl_4(AH)$.

INTRODUCTION

As a part of our work on the coordination of γ-mercaptoamines to metal ions we have reported some solid complexes formed by 1-methyl-4-mercaptopiperidine recently. The crystal structure of the complex formed with cadmium perchlorate show that it is polymeric[1] while the one formed with zinc chloride is dimeric.[2] Taking into account that information relative to metal complexes of γ-mercaptoamines is scarce and that mercury(II) and thiol ligands give rise to a great diversity of structures[3–6] and in order to better understand the differences in coordination chemistry of the IIB elements we have undertaken a systematic study of the complexes of 1-methyl-4-mercaptopiperidine with the halides of these elements. We present in this paper good evidence of dimeric sulphur bridged tetraco-ordinated zinc, cadmium and mercury atoms.

EXPERIMENTAL

Preparations

1-Methyl-4-mercaptopiperidine(AH) and its hydrohalides were synthesized following a previously reported method.[7] The complexes of empirical formula $[M_2(AH)_2X_4]\cdot H_2O$ (where M = Cd(II), Hg(II); X = Br, I and AH denotes the zwitterionic form of the ligand), $[Cd(AH)Cl_2]$ and $[Hg_2(AH)Cl_4]$ were obtained in 10% methanolic solution by adding the appropriate metal(II)-halide to the stoichiometric amount of the ligand. A slight excess of NaI was used in order to make HgI_2 soluble. The complexes $[M_2(AH)_2X_4]\cdot H_2O$ (where M = Zn(II) and X = Br, I) were prepared analogously to the chloride derivative.[2] In all cases the white crystalline products obtained (slightly yellow in the case of M = Hg(II) and X = I) were filtered off, washed with cold water, ethanol and ethyl ether and dried *in vacuo*. The complexes were analyzed as follows: S iodometrically or as barium sulphate; Zn as anthranilate; Cd with EDTA; Hg as $[Cu\ en_2][HgI_4]$; Cl as AgCl; Br and I potentiometrically with $AgNO_3$; C, H and N in a Perkin–Elmer 240 analyser. Results are given in Table 1.

Physical measurements

The water content was determined by thermal gravimetric analysis and differential thermal analysis with a Netzch S.T.A. model 429 apparatus. Conductivity measurements were made on fresh solutions (1.10^{-3} M) in DMF at 20°C with a Radiometer conductivity bridge type CDM3. The IR spectra were recorded in KCl, KBr or KI pellets or as Nujol mulls supported between thin polyethylene sheets on a Beckman IR-20A (4000–250 cm^{-1}) spectrophotometer. Powder diffraction patterns were recorded on a Philips X-ray Diffractometer using the CuK_α radiation. Mass spectra were recorded on a HP 5730 A spectrometer with a 70 eV beam and at approx. 10^{-7} mm Hg pressure.

RESULTS AND DISCUSSION

X-Ray powder patterns indicate that these complexes of formula $[M_2(AH)_2X_4]\cdot H_2O$ have the same structure as $[Zn_2(AH)_2Cl_4]\cdot H_2O$ already reported.[2] The unit-cell dimensions have been calculated by least-squares methods and are given in Table 2. The other physical measurements are consistent with the results of the crystallographic study. Consequently, there can be little doubt that these halide complexes prepared in this work have a dimeric structure such as

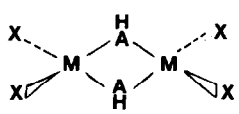

where the sulphur atoms of two ligand molecules in a zwitterionic form link two metal atoms. The co-ordination geometry around each metal atom is that of a distorted tetrahedron with two equivalent sulphur atoms and two non-equivalent halogen atoms. The water molecule is hydrogen bonded to two NH groups forming infinite chains in (010) directions and to two halogen atoms that belong to parallel chains.

In agreement with their structure the values of the molar conductivities of $[M_2(AH)_2X_4]\cdot H_2O$ complexes in N,N-dimethylformamide solutions (Table 1) indicate that they are not electrolytes,[8] except the complex $[Zn_2(AH)_2I_4]\cdot H_2O$ for which the value of Λ_M = 126.3 Ω^{-1} cm^2 mol^{-1} suggests that there is either some ionization or decomposition in this solvent.

The most significant bands of the IR spectra of all the complexes obtained in this work together with the assignments made is given in Table 3. The differences observed between these spectra and the one of the corresponding halohydrated ligand are small. In the hydrated complexes absorptions due to ν(OH) and ν(NH) vibrations appear between 3600 and 2600 cm^{-1}. We have postulated previously[2] that the band corresponding to ν(NH) vibration is split up in two bands owing to Fermi resonance with the first overtone of the $\delta(CH_2)$ vibration (1465 cm^{-1}). In the region mentioned $[Cd(AH)Cl_2]$ and $[Hg_2(AH)Cl_4]$ complexes show the ab-

*Author to whom correspondence should be addressed.

Table 1. Analytical results[a]

Compound		% C	% H	% N	% M	% S	% X	Λ_M[b]
$[Zn_2(AH)_2Br_4].H_2O$	Calcd.	19.72	3.83	3.83	17.89	8.77		38.8
	Found	19.75	3.93	3.80	17.46	8.54		
$[Zn_2(AH)_2I_4].H_2O$	Calcd.	15.69	3.05	3.05	14.23	6.98		126.3
	Found	15.52	3.10	3.08	14.35	6.80		
$[Cd(AH)Cl_2]$	Calcd.	22.91	4.17	4.45	35.74	10.19	22.54	insol.
	Found	23.27	4.18	4.47	35.62	10.20	22.48	
$[Cd_2(AH)_2Br_4].H_2O$	Calcd.	17.47	3.43	3.47	27.25	7.77	38.75	22.0
	Found	17.81	3.45	3.43	27.56	8.05	38.90	
$[Cd_2(AH)_2I_4].H_2O$	Calcd.	14.23	2.79	2.76	22.20	6.33	50.12	23.0
	Found	14.14	2.65	2.76	21.84	6.36	48.21	
$[Hg_2(AH)Cl_4]$	Calcd.	10.68	1.93	2.08	59.51	4.75	21.04	insol.
	Found	10.95	1.93	2.10	59.69	4.86	21.18	
$[Hg_2(AH)_2Br_4].H_2O$	Calcd.	14.39	2.82	2.80	40.07	6.40		44.5
	Found	14.10	2.73	2.75	40.36	6.39		
$[Hg_2(AH)_2I_4].H_2O$	Calcd.	12.12	2.38	2.36	33.73	5.39		37.5
	Found	12.34	2.31	2.36	34.17	5.11		

[a] X = halide, M = metal.

[b] Λ_M Molar conductance (Ω^{-1} cm^2 mole^{-1}) in 1.10^{-3}M N,N-dimethylformamide solutions at 20ºC. Molar conductance of $[Zn_2(AH)_2Cl_4].H_2O$ in the same conditions is 36.8.

Table 2. Unit-cell dimensions of $[M_2(AH)_2X_4]\cdot H_2O$ complexes

	a(Å)	b(Å)	c(Å)	β (deg)
$[Zn_2(AH)_2Cl_4].H_2O$	10.99	13.09	7.49	91.99
$[Zn_2(AH)_2Br_4].H_2O$	11.10	13.14	7.63	92.25
$[Zn_2(AH)_2I_4].H_2O$	11.41	13.30	8.02	92.39
$[Cd_2(AH)_2Br_4].H_2O$	11.42	13.12	7.81	92.52
$[Cd_2(AH)_2I_4].H_2O$	11.88	13.39	8.35	92.35
$[Hg_2(AH)_2Br_4].H_2O$	11.56	13.13	7.90	92.85
$[Hg_2(AH)_2I_4].H_2O$	11.72	13.22	8.22	92.61

$[Zn_2(AH)_2Cl_4].H_2O$ data included for comparison.

Table 3. Principal infrared frequencies (4000–250 cm^{-1}) of the solid complexes

Compound	ν (O–H)	ν (N–H)	δ (O–H)	γ (O–H)	ν (M–S)	ν (M–Cl)
$[Zn_2(AH)_2Cl_4].H_2O$	3340s, br	3050, 2770s, br	1630m	700m, br	290s	293, 280s
$[Zn_2(AH)_2Br_4].H_2O$	3350s, br	3050, 2750s, br	1610m	680m, br	290m	
$[Zn_2(AH)_2I_4].H_2O$	3360s, br	3060, 2750s, br	1600m	640m, br	287m	
$[Cd(AH)Cl_2]$	———	3060s	——	———	255m	
$[Cd_2(AH)_2Br_4].H_2O$	3340s, br	3080, 2790m, br	1610m	690m, br	285m	
$[Cd_2(AH)_2I_4].H_2O$	3450s, br	3090, 2790m, br	1600m	640m, br	280m	
$[Hg_2(AH)Cl_4]$	———	3060s	——	———	250–285w. br < 300br	
$[Hg_2(AH)_2Br_4].H_2O$	3340s, br	3090, 2750m, br	1620m	675m, br	282w	
$[Hg_2(AH)_2I_4].H_2O$	3460s, br	3090, 2800w, br	1600m	675m, br	282m	

Table 4. X-Ray powder patterns of $[Cd(AH)Cl_2]$ and $[Hg_2(AH)Cl_4]$

$[Cd(AH)Cl_2]$		$[Hg_2(AH)Cl_4]$	
d(Å)	I/I_o [a]	d(Å)	I/I_o [a]
7.49	60	8.58	10
6.93	40	7.79	100
5.82	100	7.49	5
5.43	20	6.91	2
4.84	35	4.88	20
4.76	65	4.67	20
4.68	25	4.41	4
4.35	20	4.27	1
4.19	25	3.95	10
3.95	60	3.91	10
3.85	70	3.81	5
3.70	80	3.75	3
3.66	45	3.46	15
3.63	25		
3.45	35		

[a] Intensities proportional to the peak heights.

sorption due to ν(NH) vibration at 3060 cm^{-1}. The hydrated complexes have between 800 and 600 cm^{-1} a broad band that can be attributed to libration modes of the water molecule.[9] In agreement with the literature those bands in the region of lowest frequencies that do not appear in the corresponding halohydrated ligand have been assigned to metal-ligand stretchings (ν(M–S) and ν(M–X)).

The stoichiometry and X-ray powder diffraction patterns of complexes $[Cd(AH)Cl_2]$ and $[Hg_2(AH)Cl_4]$ (Table 4) prove that they are not isomorphous with $[M_2(AH)_2X_4]\cdot H_2O$ complexes. The low solubility of these in DMF suggests a polymeric structure in both cases. One possibility could be to formulate the cadmium complex as $[Cd(AH)_2](CdCl_4)$ where the cation would be the same as the one found in the polymeric complex $[Cd(AH)_2]$ $(ClO_4)_2\cdot 2H_2O$ previously reported[1] and analogously the mercury complex as $[Hg(AH)][HgCl_4]$ where the cation would consist of zig-zag chains already known.[10–13] The IR spectrum of $[Cd(AH)Cl_2]$ shows a strong band at 260 cm^{-1} which could be assigned to ν(Cd–Cl) vibration of the $CdCl_4^{2-}$ anions.[14] However in the IR spectrum of $[Hg_2(AH)Cl_4]$ a broad band appears from 300 cm^{-1} up to the lowest frequency limit of the spectrophotometer used that would be better attributed to terminal Hg–Cl[15] than to $[HgCl_4]^{2-}$ modes.[14]

A serious drawback of this hypothesis is that the value of the formation constants for MX_4^{2-} species (M = Hg(II), Cd(II) and X = Cl, Br, I) follows the order I > Br > Cl,[16] which makes it difficult to postulate polymeric structures involving MX_4^{2-} units for the complexes formed with $CdCl_2$ and $HgCl_2$ while the complexes of known structure, where the existence of these species would be clearly favored, do not contain MX_4^{2-} groups.

Strong support for a polymeric structure for $[Cd(AH)Cl_2]$ and $[Hg_2(AH)Cl_4]$ involving a coordination number greater than four is based on the radius ratio. The values of covalent tetrahedral radii for Cd(II) and Hg(II) are practically identical and greater than for Zn(II).[17] Thus the smallest halogen to metal covalent radius ratio in the series studied corresponds to chlorine and cadmium or mercury. It is well known that zinc is tetrahedrally coordinated in $ZnCl_2$ while cadmium is octahedrally coordinated in $CdCl_2$.

According to that the structure of $[Cd(AH)Cl_2]$ could consist of distorted octahedra sharing two opposite faces as indicated:

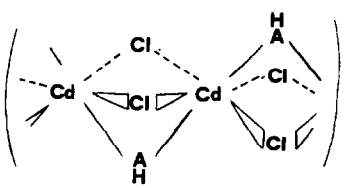

Consequently the band at 255 cm^{-1} in the IR spectrum should be assigned to the S–Cd vibration which has shifted to lower frequencies because of the increase in the coordination number. Frequencies assigned to Cd–Cl vibrations for chlorine-bridge atoms appear below 200 cm^{-1}.[15]

Based on the same argument $[Hg_2(AH)Cl_4]$ could be essentially an adduct $2HgCl_2 \cdot AH$ where mercury atoms would have a coordination number of five. The structure could be envisaged as consisting of $HgCl_2$ units linked together by chlorine bridges and also every two mercury atoms should be linked by one sulphur atom, as it is shown

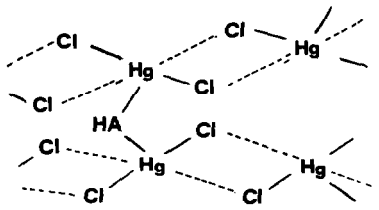

The fact that the thermogravimetric analysis shows the loss of two $HgCl_2$ molecules at approximately 250°C (theoretical loss of weight 80.5%; found: 77%), also that the fragments $HgCl_2^+$, $HgCl^+$ and Hg^+ are easily identified in its mass spectrum and that the strong band at 300 cm^{-1} in the corresponding IR spectrum could be assigned to the different Hg–Cl vibrations are in good agreement with the proposed structure. The absorption band corresponding to Hg–S vibration is probably masked by the ν(Hg–Cl) band.

Acknowledgements—This work was supported by financial aid from the Comisión Asesora Científica y Técnica of Spain.

REFERENCES

[1]J. C. Bayón, M. C. Briansó and P. González-Duarte, *Inorg. Chem.* 1979, **18**, 3478.
[2]M. C. Briansó, J. L. Briansó, W. Gaete, J. Ros and C. Suñer, *J. Chem. Soc. Dalton Trans.* 1981, 852.
[3]D. C. Bradley and N. R. Kunchur, *J. Chem. Phys.* 1964, **40**, 2258.
[4]N. R. Kunchur, *Nature* 1964, **204**, 468.
[5]D. C. Bradley and N. R. Kunchur, *Can. J. Chem.* 1965, **43**, 2786.
[6]D. Grdenić, *Quart. Rev.* 1965, **19**, 303.
[7]H. Barrera and R. R. Lyle, *J. Org. Chem.* 1962, **27**, 641.
[8]W. J. Geary, *Coord. Chem. Rev.* 1971, **7**, 81.
[9]J. V. Elsken and D. W. Robinson, *Spectrochim. Acta* 1961, **17**, 1249.
[10]H. Puff, R. Sievers and G. Elsner, *Z. Anorg. Allg. Chem.* 1975, **413**, 37.
[11]A. J. Canty, R. Kishimoto and R. K. Tyson, *Aust. J. Chem.* 1978, **31**, 671.
[12]A. J. Canty, C. L. Raston and A. H. White, *Aust. J. Chem.* 1978, **31**, 677.
[13]A. J. Canty, C. L. Raston and A. H. White, *Aust. J. Chem.* 1979, **32**, 311.
[14]D. M. Adams, J. Chatt, J. M. Davidson and J. Gerrat, *J. Chem. Soc.* (*A*) 1963, 2189.
[15]G. E. Coates and D. Ridley, *J. Chem. Soc.* (*A*) 1964, 166.
[16]F. A. Cotton and G. Wilkinson, *Advanced Inorganic Chemistry*, 4th Edn. Wiley, New York, 1980.
[17]L. Pauling, *The Nature of the Chemical Bond.* p. 246 Cornell University Press, Ithaca, New York, 1973.

Polyhedron Vol. 1, No. 2, pp. 163–167, 1982
Printed in Great Britain.

0277-5387/82/020163-05$03.00/0
Pergamon Press Ltd.

MOLYBDENUM (V) OXO-COMPLEXES OF 2-METHYL-8-QUINOLINOL

R. LOZANO*, A. DOADRIO and A. L. DOADRIO
Departamento de Química Inorgánica, Facultad de Farmacia, Universidad Complutense de Madrid, Madrid (3), España

(*Received* 14 *July* 1981)

Abstract—The synthesis and structure elucidation of the dimeric or monomeric nature of several molybdenum (V) oxo-complexes of 2-methyl-8-quinolinol (2-methyloxine) have been described, and we have compared these complexes with the molybdenum (V) oxo-complexes of 8-quinolinol (oxine). These complexes, were identified by IR and electronic spectra, magnetic susceptibility, differential scanning calorimetry, thermogravimetric analysis and the analytical data. The results permit us to assign the formulae: $(C_{10}H_8NO)_4Mo_2O_3$, $(C_{10}H_8NO)_2Mo_2O_4$ and $(C_{10}H_8NO)_2MoO(OH)$. We suggest that the low magnetic moments observed for the dimeric complexes $(C_{10}H_8NO)_4Mo_2O_3$ and $(C_{10}H_8NO)_2Mo_2O_4$ are due, at least in part to intramolecular metal–metal interactions. Monomeric molybdenum (V) species $(C_{10}H_8NO)_2MoO(OH)$, exhibits a magnetic moment *ca.* 1.75 Bohr magnetons.

INTRODUCTION

Mitchell and Williams[1] and Andruchow and Archer,[2] have prepared a series of 8-quinolinato complexes of molybdenum (V), which are either monomeric or dimeric with a Mo–O–Mo linear bridge. In previous studies[3,4] we have described the formation of monomeric Mo(V) complexes with 8-quinolinol and of dimers with oxo-bridges, to which we have assigned bands in the IR and electronic spectra.

The object of the present study, has been to obtain compounds of molybdenum (V) with a 2-methyl 8-quinolinol ligand, so as to observe the effects of steric impediment exercised by the methyl group in the formation of this complex, with respect to the ligand 8-quinolinol in the compounds obtained by us.

We have, in addition, prepared a new compound of 2-methyl-8-quinolinol with molybdenum (V) of dimeric structure with dioxo bridges $Mo\begin{matrix}O\\O\end{matrix}Mo$ having a structure which is uncommon in the complexes of Mo (V) penta-coordinated, having been obtained only in the case of dialkyldithiocarbamates.[5] This has permitted us also, to appreciate the effect exercised by the bridge on the bands of the IR and electronic spectra in this series of compounds, and on the direct spin–spin interaction of the dimeric forms by means of magnetic susceptibilities.

*Author to whom correspondence should be addressed.

EXPERIMENTAL

(a) *Materials*

$MoO_4Na_2 \cdot 2H_2O$ and $MoCl_5$ were Merck commercial products and the ligand 2-methyl 8-quinolinol (2-methyloxine), was Koch–Light Laboratories Ltd. commercial product used as supplied.

The solvents used to prepare and to recrystallize the complexes were Carlo Erba or Merck.

The solutions for absortion spectra were prepared using dimethylsulphoxide (DMSO) spectral grade (Merck-Uvasol).

(b) *Analytical procedures*

Elemental analysis were performed by "Instituto de Química Orgánica (C.S.I.C.)" Madrid, España.

Molybdenum was determined by Atomic Absorption with a Perkin–Elmer model 430 Atomic Absorption Spectrophotometer, after decomposing the complexes with a 1 : 1 mixture of concentrated nitric and sulphuric acids.

The analytical data are given in Table 1.

(c) *Methods*

Magnetic susceptibility was determined by the Gouy method at room temperature using a Mettler H-51 AR. balance and a type C Newport electromagnet. Molar susceptibilities have been corrected for diamagnetism.[6]

The magnetic moments were calculated according to the formula $\mu = 2.84\ (\chi'_M \cdot T)^{0.5}$ B.M. were $\chi'M$ is the corrected molar susceptibility.

Table 2 shows the results obtained.

The IR spectra have been measured on a Perkin–Elmer recording spectrophotometer model 283. The samples were run as KBr pellets.

Table 1. Elemental and molybdenum analyses

Compounds		Analysis C	N	H	Mo
$(C_{10}H_8NO)_4Mo_2O_3$	%Calcd.	55.05	6.42	3.67	22.01
	%Found.	54.94	6.47	3.60	22.04
$(C_{10}H_8NO)_2MoO(OH)$	%Calcd.	53.93	6.29	3.82	21.56
	%Found.	53.54	6.28	3.71	21.61
$(C_{10}H_8NO)_2Mo_2O_4$	%Calcd.	41.96	4.90	2.80	33.55
	%Found.	41.63	4.95	2.69	33.47

Table 2. Magnetic properties of molybdenum (V) oxo complexes of 2-methyl-8-quinolinol

Compound	χ_o (10^6cgs)	χ_M (10^6cgs)	χ'_M (10^6cgs)*	μ (BM)
$(C_{10}H_8NO)_4Mo_2O_3$	- 0.182365	- 159	108	0.51
$(C_{10}H_8NO)_2MoO(OH)$	2.459218	1094	1287	1.75
$(C_{10}H_8NO)_2Mo_2O_4$	- 0.279482	- 160	16	0.19

* The corrected χ'_M values of these dimers have been divided by two to give the χ'_M value/mole Mo.

Important IR absorption peaks for the compounds prepared in this study, are listed in Table 3.

The visible-nearUV spectra of the compounds, were measured, in the range 220-1000 nm, on a Beckman recording spectrophotometer model DK-2A, using solutions of the complexes in dimethylsulphoxide. The results obtained are given in Table 4.

TG and DSC have been carried out (Flow rate of 51 hr^{-1}) in synthetic air in a thermobalance Mettler HE-20 and Mettler T.A. 3000 system, with DSC 20 cell.

The conditions of the analysis have been:

TG Range = 20 mw.
DSC Range = 2 and 50 mw.
Heating rate = 2°C/min.
Reference = Aluminum.

(d) *Preparation of complexes*

$(C_{10}H_8NO)_4Mo_2O_3$: 2.05 g (10 mmol) of $MoO_4Na_2 \cdot Na \cdot 2H_2O$ was dissolved in 50 ml of water. Another solution, of 3.16 g (20 mmol) of 2-methyloxine in 75 ml of hot absolute ethanol Merck, is prepared. Once it is cold, this solution is added to the previous one. The resultant solution takes on a yellow colour, and to it is added a solution of 0.25 g of sodium dithionite in 30 ml of water. The solution takes on an orange colour. Drop by drop, and with vigorous stirring, glacial acetic acid is added, till reaching pH = 5.

The solution turns reddish and precipitates a brown solid,

Table 3. IR absorption maxima in cm^{-1} of molybdenum (V) oxo-complexes of 2-methyloxine

		$(C_{10}H_8NO)_4Mo_2O_3$	$(C_{10}H_8NO)_2MoO(OH)$	$(C_{10}H_8NO)_2Mo_2O_4$
ν_s	Mo=O	932-945	935-945	930-945
ν_a	Mo-O	690	-	688
ν_s	Mo-O	400	-	390
ν	Mo-OH	-	300	-
ν	Mo-N	348	345	350
ν	C-O-Mo	1110	1108	1114

Table 4. Electronic absorption spectra of molybdenum (V) oxo-complexes of 2-methyloxine

Compound	λ (nm)	$\tilde{\nu}$ (kK)	ε	Transition
$(C_{10}H_8NO)_4Mo_2O_3$	750	13.3	54	$^2B_2 \rightarrow {}^2E(I)$
	540	18.5	708	$^2B_2 \rightarrow {}^2B_1$
	350	28.6	17800	Charge transfer
	311	32.2	10832	" "
	256	39.1	123062	Intraligand
$(C_{10}H_8NO)_2MoO(OH)$	752	13.3	33	$^2B_2 \rightarrow {}^2E(I)$
	545	18.3	548	$^2B_2 \rightarrow {}^2B_1$
	354	28.2	3894	Charge transfer
	310	32.3	5118	" "
	255	39.2	50832	Intraligand
$(C_{10}H_8NO)_2Mo_2O_4$	700	14.3	275	$^2B_2 \rightarrow {}^2E(I)$
	350	28.6	12012	Charge transfer
	325	30.8	9724	" "
	255	39.2	115216	Intraligand

ε: molar extinction coefficient

which is separated by filtration *in vacuo*, and washed repeatedly with a boiling water–ethanol mixture (50%).

The residuum is filtered hot and *in vacuo*, so that one obtains a reddish powder which is dried over P_2O_5.

Yield: 82%.

$(C_{10}H_8NO)_2MoO(OH)$: 2.74 g (10 mmol) of $MoCl_5$ are dissolved in 20 ml of water, with instant hydrolysis and a brown solution is obtained, to which is added NH_3 concentrated to cause total precipitation. The brown precipitate, identified as $MoO(OH)_3$, is filtered *in vacuo* and washed repeatedly with boiling water. When dry, it is dissolved in 100 ml of boiling glacial acetic acid.

At the same time, a solution of 3.16 g (20 mmol) of 2-methyloxine in 40 ml of hot glacial acetic acid is prepared. This solution is added to the first, forming a dark solution. It is concentrated by boiling, till only 25 ml of the solution remain. It is left to grow cold, and precipitates a solid which is filtered *in vacuo* and is washed with a boiling acetic acid–water mixture (1 : 1).

Orange crystals are obtained and are dried over P_2O_5.

Yield: 74%.

$(C_{10}H_8NO)_2Mo_2O_4$: A solution of 2.05 g (10 mmol) of $MoO_4Na_2 \cdot 2H_2O$ in 50 ml of water is prepared. NaOH 2N is added till reaching pH = 10, and the solution is heated by boiling for 5 min.

At the same time, 1.58 g (10 mmol) of 2-methyloxine are dissolved in 40 ml of hot Merck absolute ethanol. The two solutions are combined, and the resulting solution takes on an orange colour, to which is added a solution of 0.3 g of sodium dithionite in 25 ml of water. The solution changes to a green colour. Lastly, HCl 2N is added drop by drop, and with vigorous stirring till reaching pH = 2, so that a precipitate of greenish color is obtained which is separated by filtration *in vacuo*.

The solid obtained is washed with a mixture of 20 ml of water and 20 ml of boiling ethanol, and is filtered hot and *in vacuo* so that a greenish solution is obtained, and is dried over P_2O_5.

Yield: 78%.

DISCUSSION

(a) *Structures of the complexes*

In this study, we have synthesized three different complexes of molybdenum (V) with 2-methyloxine as ligand. According to the results of the analytical and spectroscopic data, two of the complexes present a dimeric structure, while the other is a monomeric specie.

Starting with a $MoO_4Na_2 \cdot 2H_2O$ solution and reacting with a solution of the ligand in ethanol, followed by reduction of Mo(VI) to Mo (V) with sodium dithionite, a dimeric complex is precipitated in acid medium.

Carrying out the precipitation at pH = 5, with acetic acid, the complex of stoichiometry 2 : 1, obtained has a monoxo bridge and the molybdenum is six-coordinated. The formula which most closely fits the analyses is $(2\text{-methyloxine})_4Mo_2O_3$. We suggest that the structure for this complex should be as follows:

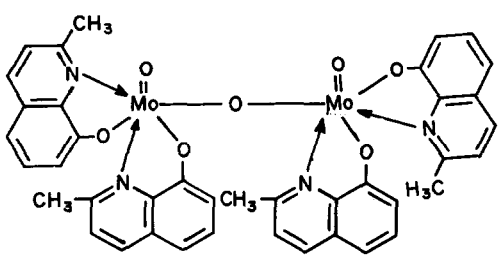

Mo⟨O⟩Mo, is less than the magnetic moment of the

However, at pH = 2(HCl 2N) the stoichiometry of the compound precipitated is 1 : 1, the molybdenum is five-coordinated, and the union between the two atoms of molybdenum is realized by means of a dioxo-bridge. The formula which we assign to this complex is $(2\text{-methyloxine})_2Mo_2O_4$ and we suggest that the compound presents the following structure:

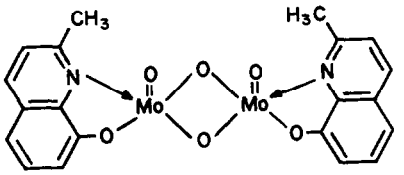

For the synthesis of the monomeric complex of formula $(2\text{-methyloxine})_2MoO(OH)$, a solution of $MoO(OH)_3$ in glacial acetic acid is made to react with another of the ligand, also in acetic acid. The stoichiometry of the compound is 2:1 and the molybdenum is six-coordinated.

We suggest that the structure for this complex should be as follows:

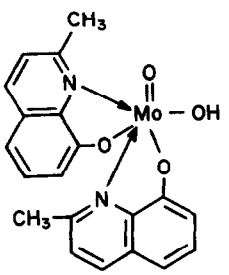

(b) *Magnetic properties*

The magnetic susceptibility measurements and calculated magnetic moments, suggested spin–spin interaction through the oxygen bridges in a dimeric complex $(2\text{-methyloxine})_4Mo_2O_3$ comparable to that found in other complexes of molybdenum (V) which have been studied.[7]

The magnetic moment found for the complex $(2\text{-methyloxine})_2Mo_2O_4$ ($\mu = 0.19$ BM), which presents a dimeric structure with dioxo bridge of the type Mo⟨O⟩Mo, is less than the magnetic moment of the dimeric complex of monoxo bridge of formula $(2\text{-methyloxine})_4Mo_2O_3$ and structure Mo–O–Mo, with a value of magnetic moment $\mu = 0.51$ BM. This is due to the possible formation of a direct metal–metal bond[8], which is more favourable to the dioxo bridge than to the monoxo bridge, due to the shorter distance between the molybdenum atoms, and the smaller bond angle, as has been proved by X-ray diffraction for Mo(V) complexes with dialkyldithiocarbamates (Mo–Mo = 2.58 Å, O–Mo–O = 91.9° and Mo–Mo = 3.70 Å, Mo–O–Mo = 178.1°, respectively).[5,9]

The compound of formula $(2\text{-methyloxine})_2MoO(OH)$ has a magnetic moment of 1.75 BM, which corresponds to the spin-only value for d^1 electron of the molybdenum (V) atom, being, therefore, a monomeric species.

(c) *IR spectra*

The IR spectra of the three complexes exhibit a very strong doublet at 930–945 cm^{-1}, which we attribute to the vibration of the symmetric stretching mode of the ter-

minal Mo = O bond. The antisymmetric mode has not been detected. However, the appearance of the symmetric stretching mode is sufficient to designate, in the dimeric complexes, a *cis* disposition of two terminal Mo = O bonds.[8]

The Mo = O bonds are very sensitive to the variations produced in the metal-donor atom as is usual in all oxocation complexes of metal-oxo group.

If we compare these complexes of 2-methyloxine with the Mo(V) complexes of oxine[3,4] we observe that the complexes of 2-methyloxine exhibit the band of the symmetric stretching mode of the Mo = O bond displaced to greater frequencies (930–945 cm^{-1}) than the analogous complexes with oxine (910–925 cm^{-1}). This difference is due to the steric effect of the methyl group, which weakens the union of the 2-methyloxine ligand with the molybdenum atom, strengthening the molybdenum terminal oxygen bond, as happens also in vanadium (IV)complexes with oxine and 2-methyloxine.[10]

Also, since the Mo = O bond is stronger in the 2-methyloxine complexes than in the oxine complexes, the bond order of the molybdenum atom to the oxygen-bridge atoms should be less in the dimeric 2-methyloxine complexes than in the dimeric oxine complexes.

In fact, the dimeric 2-methyloxine complexes exhibit an intense band in the 690 cm^{-1} region, which we attribute to the antisymmetrical stretching vibration of the Mo–O bridge bond, and another band of weak intensity at 400 cm^{-1} which corresponds to the symmetric stretching mode. Both bands appear at greater frequency in the oxine complexes (760 and 405 cm^{-1}, respectively).

Upon comparing the IR spectra of the 2-methyloxine mono-bridge complex, and of the 2-methyloxine dioxo bridge complex, one observes no differences for the vibration frequency of antisymmetrical stretching in constrast to what is claimed by other workers,[11] who have tried to resolve the problem of differentiating the monoxo and dioxo bridges by means of the IR spectra.

The IR spectrum of the monomeric 2-methyloxine complex of formula (2-methyloxine)$_2$MoO(OH) exhibits a band at 300 cm^{-1}, which we attribute to the stretching of the Mo–OH bond, as occurs in other molybdenum compounds with Mo–OH bonds.[12]

The IR spectra of the three 2-methyl-oxine complexes of molybdenum (V) studied, exhibit a very strong band in the 1105 cm^{-1} region and another band of lesser intensity in the 350 cm^{-1} region. We attribute the first band to a C–O–Mo, vibration, and this indicates the formation of a molybdenum chelate, while the second band corresponds to the stretching of the Mo–N bond, as happens also in other complexes that we have studied.[13]

(d) *Visible and UV spectra*

The visible and UV spectrum of dimeric complex with a monoxo bridge of formula (2-methyloxine)$_4$Mo$_2$O$_3$ and the spectrum of the monomeric complex of formula (2-methyloxine)$_2$MoO(OH) exhibits two bands at 13,300 and 18,500 cm^{-1} which we attribute to transitions $^2B_2 \leftarrow {}^2E(I)$ and $^2B_2 \leftarrow {}^2B_1$, respectively, according to the Balhausen–Gray scheme for an octahedral structure.[14] However, the dimeric complex, with a dioxo bridge of formula (2-methyloxine)$_2$Mo$_2$O$_4$ exhibits only a band in the visible at 14,286 cm^{-1} which corresponds to a transition $^2B_2 \leftarrow {}^2E(I)$ in accordance with the Gray–Hare diagram, for a possible square-pyramidal structure.[15]

On comparing the spectra of the dimeric complexes with monoxo bridge and dioxo bridge in the visible region, one observes the change produced in the d–d transitions, on varying the coordination and passing from an octahedral structure for the six-coordinated complex with monoxo bridge, to a square-pyramidal structure for the complex with a five-coordination index and dioxo bridge.

If we compare the transitions observed in the visible region for the dimeric 2-methyloxine complex with dioxo bridge of formula (2-methyloxine)$_2$Mo$_2$O$_4$ (14,286 cm^{-1}), with the transition observed for the analogous complex with oxine as ligand (13,698 cm^{-1}) no appreciable change in d–d transitions is observed and therefore, the structures of the two complexes are probably similar, in contrast to the monomeric vanadium (IV) complexes with oxine and 2-methyloxine of formula VOLL$_2$, (where LL = oxine and 2-methyloxine),[10] where there are appreciable differences in structure of the complexes: the 2-methyloxine complex having a trigonal-bipyramidal structure in which the steric impediment is less, while the oxine complex possessses a square-pyramidal structure.

The absence of this structural change in the dimeric molybdenum (V) complexes might be due to the existence of the bridge, that determines the structure of two square pyramids.

In the UV region, the three complexes produce three transitions at 350, 310 and 255 nm. The two first corresponding to charge-transfer transitions and the last corresponding to an intra-ligand transition.

(e) *Thermogravimetry and differential scanning calorimetry*

The DSC and TG of the dimeric complex with monoxo bridge and formula (2-methyl-oxine)$_4$Mo$_2$O$_3$ shows that, from 210 to 770°C, combustion of the complex is produced so as to form molybdenum (VI) oxide MoO_3, by an exothermic process. (% loss calculated: 66.97; % loss found: 67.00).

The DSC and TG of the monomeric complex (2-methyloxine)$_2$MoO(OH) (Fig. 1) shows the loss, between 90-°C and 130-°C, of a water molecule, (% loss calculated: 2.02; % loss found: 2.00) between two molecules of the complex, so as to form the dimeric complexes with a monoxo bridge identified by infrared spectrum, by the reaction:

$$2(\text{2-methyloxine})_2\text{MoO(OH)} \rightarrow (\text{2-methyloxine})_4\text{Mo}_2\text{O}_3 + \text{H}_2\text{O}\uparrow .$$

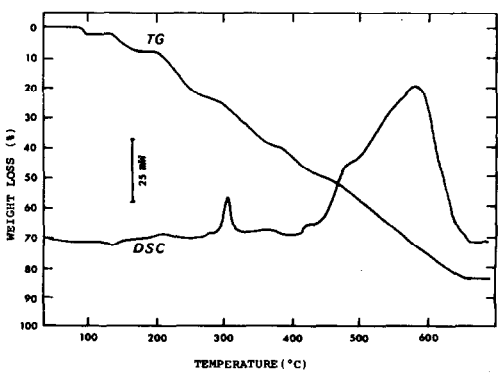

Fig. 1. DCS and TG curves of (2-methyloxine)$_2$MoO(OH).

This endothermic process presents a value of ΔH = 20.1 kJ/mol.

The dimeric complex formed continues the oxidation until formation of MoO_3 at 650°C. (% loss calculated: 66.97; % loss found: 66.90).

The dimeric complex of dioxo bridge and formula (2-methyloxine)$_2Mo_2O_4$ shows in the DSC and the TG, only one exothermic process untill 690-°C, in which MoO_3 is formed. (% loss calculated: 49.65; % loss found: 49.60).

REFERENCES

[1]P. C. H. Mitchell and R. J. P. Williams, *Inorg. Chem.* 1968, **882**, 4570.

[2]W. Andruchow and R. D. Archer, *J. Inorg. Nucl. Chem.* 1972, **34**, 3185.

[3]A. Doadrio, A. L. Doadrio and R. Lozano, *An. Quim.* 1978, **74**, 566.

[4]A. Doadrio, R. Lozano and A. L. Doadrio, *An. Quim.* 1980, **76**, **B**, 193.

[5]L. Ricard, C. Martin, R. Wiest and R. Weiss, *Inorg. Chem.* 1975, **14**, 9, 2300.

[6]P. W. Selwood, *Magnetochemistry.* Interscience, New York, 1956.

[7]H. B. Blake, F. A. Cotton and J. S. Wood, *J. Amer. Chem. Soc.* 1964, **86**, 3024.

[8]F. A. Cotton, D. L. Hunter, L. Ricard and R. Weiss, *J. Coord. Chem.* 1974, **3**, 259.

[9]L. Ricard, J. Estienne, P. Karagiannidis, P. Toledano, J. Fischer and A. Mitschler, *J. Coord. Chem.* 1974, **3**, 277.

[10]A. Doadrio and J. Martinez, *An. Quim.* 1977, **73**, 956.

[11]R. M. Wing and K. P. Callahan, *Inorg. Chem.* 1969, **8**, 871.

[12]D. M. Adams, *Metal ligand vibrations.* Arnold, London, 1967.

[13]R. Lozano, Thesis, Madrid, 1980.

[14]C. J. Ballhausen and H. B. Gray, *Molecular Orbital Theory.* Benjamin, New York, 1965.

[15]H. B. Gray and C. R. Hare, *Inorg. Chem.* 1962, 1, 363.

Polyhedron Vol. 1, No. 2, pp. 169–174, 1982
Printed in Great Britain.

0277-5387/82/020169-06$03.00/0
Pergamon Press Ltd.

THE NATURE OF Pb(II)-BROMIDE COMPLEXES IN PROPYLENE CARBONATE

A. R. JONES and D. A. AIKENS*

Department of Chemistry, Rensselaer Polytechnic Institute, Troy, NY 12181, U.S.A.

(*Received* 28 *July* 1981)

Abstract—The greatly increased solubility of $PbBr_2$ in propylene carbonate (PC) caused by addition of LiBr indicates that Pb(II) interacts strongly with bromide ion in propylene carbonate to form stable Pb(II)-bromide complexes. Solubility and spectrophotometric data for LiBr solutions saturated with $PbBr_2$ indicate the presence of two Pb(II)-bromide complexes whose bromide:lead ratios are respectively 3.00 and 2.75. The former, which predominates in dilute (< 0.03 m) solutions of LiBr saturated with $PbBr_2$, was shown by potentiometry and solubility data to be $PbBr_3^-$, a species also formed when $PbBr_2$ dissolves in PC in the absence of LiBr. The latter, which is predominant in more concentrated LiBr solutions saturated wih $PbBr_2$, was shown by spectrophotometry and solubility data to be the polynuclear complex $Pb_4Br_{11}^{-3}$. Both complexes are sufficiently stable that the free bromide ion concentration in these solutions corresponds to only a small fraction of the total bromide concentration. In LiBr solutions unsaturated with respect to $PbBr_2$, the major Pb(II) species are $PbBr_3^-$ and $PbBr_4^{-2}$.

INTRODUCTION

Its unique physical and chemical properties[1] make propylene carbonate (PC, 4-methyl-2-dioxolone) an interesting solvent for electrochemical studies, but a major impediment to many such studies is the lack of convenient, general purpose reference electrodes. This problem, of course, reflects the more general problem that we know relatively little of the fundamental chemistry in PC of heavy metal ions which might form the basis of such electrodes. In a survey of the solubilities of electrolytes in PC, Harris[2] showed that the solubility of lead iodide in PC is greatly increased by additon of lithium iodide, and he postulated formation of a polynuclear Pb(II) species. Brievogel and Eisenberg[3] also invoked the formation of polynuclear species to explain the conductance of concentrated equimolar LiCl–$AlCl_3$ solutions in PC. On the other hand, Butler's[4] careful potentiometric study of the solubility of AgCl in PC revealed only the mononuclear complexes AgCl, $AgCl_2^-$ and $AgCl_3^{2-}$. Earlier potentiometric studies in this laboratory[5] indicated that the lead amalgam-lead bromide couple showed promise as a reference electrode, but did not address the question of the nature of the Pb(II) species in solution. We report here the solubility of lead bromide and potentiometric and spectrophotometric studies of the solution chemistry of Pb(II) in PC solutions of lithium bromide, which establish the nature of the Pb(II)-bromide species in PC solutions containing LiBr.

EXPERIMENTAL

PC (98% pure by GLC) obtained from Matheson, Coleman and Bell was purified by vacuum distillation as described by Murry and Aikens[5] except that the pot and column temperatures were 100 and 65°C, respectively. The distillate was transferred to the controlled atmosphere box with minimal exposure and was analyzed by GLC as described by Jasinski and Kirkland[6] except that the column temperature was programmed from 105 to 200°C at 2°C/min. The purified PC which was used in the metal–metal halide cells contained less than 20 ppm water and all other experiments utilized PC which contained less than 1 ppm water. Thallium bromide was dried at 110°C for 24 hr, lead bromide and lithium bromide were dried under the same conditions in a vacuum oven and all were stored in the controlled atmosphere box. Solutions were prepared and stored in a controlled atmosphere box (Kewaunee Scientific Equipment Model 2C405R) filled with recirculating nitrogen whose moisture content was below 1 ppm, and maintained at 25.0 ± 0.1°C.

The total lead concentration was determined by the method of Suk and Malat,[7] and the total bromide concentration as described by Caldwell and Moyer[8] except that nitrobenzene was not used. The average coefficients of variation for these analyses were, respectively, 0.37 and 0.23%.

Potential measurements of thallium-lead electrode pairs utilized cells in which the two half cells were joined by a side arm with a teflon stopcock which was only opened during potential measurements. The cells, which were filled under vacuum, backfilled with nitrogen and sealed, were thermostatted at 25.00 ± 0.05°C. Potential difference measurements between lead half cells containing different concentrations of LiBr made use of a LiBr salt bridge.

Ultraviolet spectra were secured using a sealed thin layer cell with quaartz windows separated by a teflon spacer. The thickness, which could be selected to be between nominal values of 0.013 and 0.2 mm, was determined precisely by measuring the absorbance of a standard solution of acetophenone in methanol. All spectra were obtained using a Cary Model 14 spectrophotometer with the sample chamber thermostatted at 25.0 ± 0.1°C and were corrected for the absorption of the cell and solvent.

RESULTS AND DISCUSSION

Effect of solvent composition on cell potential

To establish qualitatively the manner in which PC affects the electrode potentials of interest, we measured the potential of cell I where Tl(Hg)

$$Tl(Hg)/TlBr(s)/LiBr(C_i)/PbBr_2(s)/Pb(Hg) \qquad (I)$$

and Pb(Hg) denote the saturated two phase amalgams and the solvent is one of the four in Table 1. The potential of the aqueous cell and the value of 375.3 mV which was calculated from standard free energies of formation[9] and the solvent independent potentials of the metal–metal amalgam cells[10,11] for eqn (1) agree within

$$2Tl(Hg) + PbBr_2(s) \rightleftarrows 2TlBr(s) + Pb(Hg) \qquad (1)$$

*Author to whom correspondence should be addressed.

Table 1. Average potentials and 90% confidence limits of metal amalgam-metal bromide cells. These are based upon the potential of three electrode pairs measured 3 times daily for 5 days

X_{H_2O}	X_{PC}	[LiBr]/M	E/mV
1.000	0.000	0.0389	376.4±0.2
0.998	0.002	0.0789	371.2±0.2
0.967	0.033	0.0683	376.3±0.1
0.000	1.000	0.0368	506.8±0.4

2 mV, confirming that eqn (1) describes the cell reaction in the aqueous cell. Replacing water by pure PC causes the measured potential to increase by approximately 130 mV, evidence that eqn (1) does not describe the cell reaction in PC. Table 1 shows that mixed solvent cells containing concentrations of PC up to that of the 2 phase boundary exhibit essentially the same potential as does the aqueous cell. This result indicates that the interaction of PC with the thallium and lead half cells is not stronger than that of water, which in turn suggests that the potential of the PC cell reflects more the absence of water than the presence of PC.

Dilute LiBr *solutions saturated with* $PbBr_2$

Although the solubility of $PbBr_2$ in concentrated LiBr solutions corresponds to considerably more than one mole of $PbBr_2$ per mole of LiBr, in dilute LiBr solutions it approaches a limiting value of one mole of $PbBr_2$ per mole of LiBr. This behaviour is reflected in the solubility data in Fig. 1, where the solid line defines a 1:1 mole ratio of $PbBr_2$ to LiBr, but it is more apparent in Fig. 2, where the solubility data have been transformed to show the dependence of the bromide:lead ratio on the lead concentration in these saturated solutions. As the lead concentration falls, the bromide:lead ratio increases steadily until at *ca.* 0.03 m Pb(II), it reaches a limiting value of 3.01 with a standard deviation of the sample of 0.013. This limiting bromide:lead ratio indicates that in such dilute solutions the predominant Pb(II) species corresponds to $PbBr_3^-$ or to some multiple thereof. Although in principle a bromide:lead ratio of 3.0 could also be compatible with equimolar concentrations of

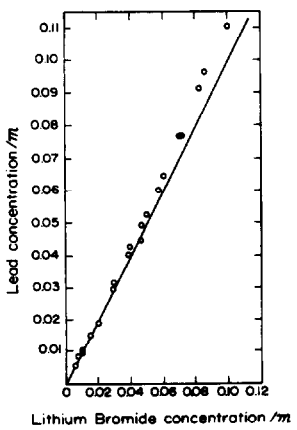

Fig. 1. Lead concentration versus lithium bromide concentration for LiBr solutions saturated with $PbBr_2$. The line defines a 1:1 mole ratio of $PbBr_2$ to LiBr.

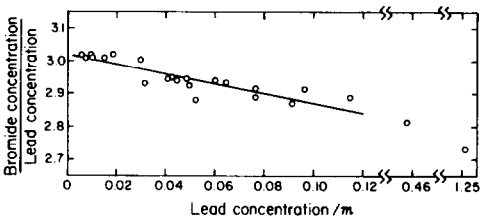

Fig. 2. Dependence of experimental bromide:lead ratio on lead concentration for LiBr solutions saturated with $PbBr_2$.

$PbBr_2$ and $PbBr_4^{2-}$, this would require that the solubility of $PbBr_2$ be at least 0.03 m, a value which is two orders of magnitude above the measured solubility (see spectrophotometric studies below).

The UV spectra of dilute LiBr solutions saturated with $PbBr_2$ provide additional and complementary information concerning the Pb(II) species in these solutions. Figure 3 reports the spectra of 4 such solutions which range in Pb(II) concentration from 0.0057 to 0.018 m. If the Pb(II) concentration is below 0.015 m, the spectra exhibit a single peak centered at 305 nm, whereas if the Pb(II) concentration is above 0.015 m, the spectra also exhibit a second peak centered at 327 nm, whose intensity relative to the 305 nm peak increases with increasing Pb(II) concentration. For Pb(II) concentrations between 0.0057 and 0.0098 m, the apparent molal absorptivity of the 305 nm peak remains constant at a value of 9790 $m^{-1}\,cm^{-1}$, which means that over this concentration range, the nature of the predominant Pb(II) species does not change. Knowledge of the apparent molal absorptivity of the 305 nm peak also permits one to estimate of the solubility of $PbBr_2$ in PC. The absorption spectrum of a saturated solution of $PbBr_2$ in PC and that of a dilute solution of LiBr saturated with $PbBr_2$ are virtually identical with respect to both the wavelength of maximum absorption and the band contour. This result indicates that dissolution of $PbBr_2$ in PC yields $PbBr_3^-$ and that any other Pb(II) products do not absorb significantly in this wavelength range. The most probable reactions which meet these conditions are those defined by eqns (2) and (3).

$$3\,PbBr_2(s) \rightarrow 2\,PbBr_3^- + Pb^{+2} \qquad (2)$$

$$2\,PbBr_2(s) \rightarrow PbBr_3^- + PbBr^+. \qquad (3)$$

The absorbance of a saturated solution of $PbBr_2$ is equivalent to that of a $PbBr_3^-$ concentration of 9.2×10^{-5} m, which in turn corresponds to a molal solubility of $PbBr_2$ of from 1.4×10^{-4} m (eqn 2) to 1.8×10^{-4} m (eqn 3).

Neither the spectrophotometric results nor the solubility data are sensitive to the degree of aggregation of the Pb(II) species in dilute LiBr solutions saturated with $PbBr_2$, that is, to whether this species is $PbBr_3^-$ or an oligimer $(PbBr_3^-)_N$. Because polynuclear Pb(II) complexes form in more concentrated LiBr solutions saturated with $PbBr_2$ it was necessary to determine the degree of aggregation of $(PbBr_3^-)_N$, i.e. the value of N. This was accomplished by analysis of the potential dependence of a Pb(II) concentration cell in which the predominant species is $(PbBr_3^-)_N$ and the spontaneous reaction is defined by eqn (4),

$$(PbBr_3^-)_N(C_r) \rightarrow (PbBr_3^-)_N(C_i) \qquad (4)$$

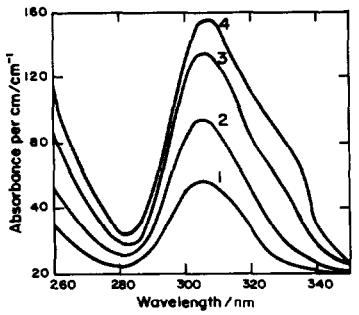

Fig. 3. UV spectra of dilute LiBr solutions saturated with $PbBr_2$. The spectra denoted as 1, 2, 3 and 4 correspond to solutions with lead concentrations of 0.005697, 0.00979, 0.01507 and 0.01832 m, respectively.

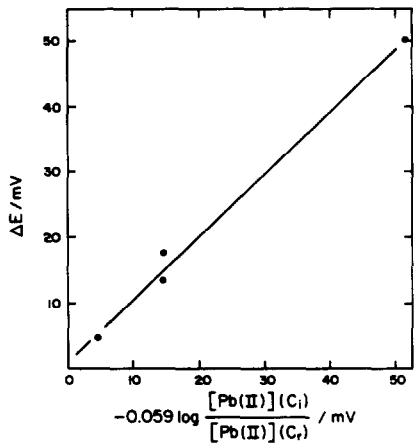

Fig. 4. Experimental test of eqn (7) for concentration cell II.

where the terms C_i and C_r denote the formal concentrations of Pb(II) in the two compartments, i.e. the concentrations of the complex assuming that N is unity. Experimentally, it is necessary to isolate the two $(PbBr_3^-)_N$ solutions with a salt bridge to prevent precipitation at the interface between the two solutions. The necessary isolation was accomplished using a LiBr salt bridge whose concentration was equal to the formal LiBr concentration in the reference half-cell, as in cell II.

$$^-Pb(Hg)/PbBr_2(s)/Li^+, (PbBr_3^-)_N(C_r)//LiBr(C_r)//$$
$$Li^+, (PbBr_3^-)_N(C_i)/PbBr_2(s)/Pb(Hg)^+. \quad (II)$$

In this cell there are two liquid junctions, whose potentials must be subtracted from the measured potential. To estimate the contribution of these two liquid junctions, it was necessary to make two approximations. First, the two liquid junctions in cell II can be approximated by a single junction between the two $(PbBr_3^-)_N$ solutions (cell III) whose liquid junction potential can be estimated using the method of MacInnes[12]. Second, the value of the transference number of Li^+ in this junction can be approximated by the value of 0.4 determined for $LiClO_4$ in PC by Gabano,[13]

$$^-Pb(Hg)/PbBr_2(s)/Li^+, (PbBr_3^-)_N(C_r)//$$
$$Li^+, (PbBr_3^-)_N(C_i)/PbBr_2(s)/Pb(Hg)^+. \quad (III)$$

The electrode reactions in cell II and the dissolution of $PbBr_2$ in LiBr solutions follow respectively eqns (5) and (6).

$$(PbBr_3^-)_N + 2N\,e^- \rightleftarrows N\,Pb(Hg) + 3N\,Br^- \quad (5)$$
$$N\,PbBr_2(s) + N\,Br^- \rightleftarrows (PbBr_3^-)_N. \quad (6)$$

Combining these reactions with the Nernst equation and solving for ΔE, the potential ofcell II yields eqn (7).

$$\Delta E = \frac{-0.059}{N} \log \frac{[Pb(II)](C_i)}{[Pb(II)](C_r)} \quad (7)$$

The plot of eqn (7) in Fig. 4, which covers values of C_i from 0.001 m to 0.008 m, has a slope of 0.96 showing that N is unity and thus the complex in dilute LiBr solutions saturated with $PbBr_2$ is the monomer $PbBr_3^-$.

Concentrated LiBr *solutions saturated with* $PbBr_2$

As Fig. 1 shows, increasing the LiBr concentration above 0.03 m causes the solubility of lead bromide to deviate progressively above the reference line which defines the quantity of lead bromide that corresponds to formation of $PbBr_3^-$. This excess solubility of lead bromide in concentrated lithium bromide is reflected in Fig. 2 as a continual decrease in the bromide:lead ratio with increasing lead concentration. From the limiting value of 3.01 which characterizes dilute solutions, the bromide:lead ratio falls to 2.85 in a solution whose lead concentration is 0.12 m. These data can only be interpreted as the formation of at least one polynuclear complex of the type Pb_XBr_Y where $Y < 3X$.

The spectral data in Fig. 5 which extend to much more concentrated solutions than do the data in Fig. 3, confirm the appearance of the second complex in more concentrated LiBr solutions. As the analytical concentration of Pb(II) increases, the 327 nm peak grows progressively in intensity relative to the 305 nm peak until the 305 nm peak becomes an ill defined shoulder on the 327 nm peak. The presence of an isobestic point in Fig. 6 which occurs at 315 nm indicates that only two lead species are present in these solutions. The systematic variation of the in-

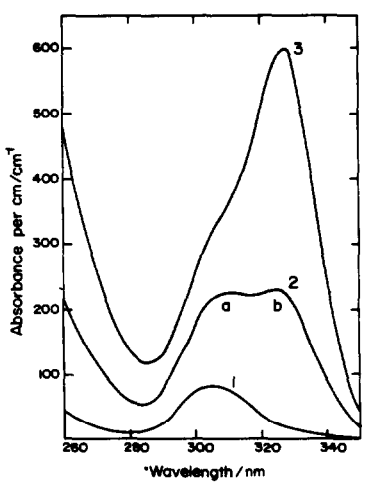

Fig. 5. UV spectra of solutions containing various concentrations of LiBr saturated with $PbBr_2$. The spectra denoted as 1, 2 and 3, correspond to solutions with lead concentrations of 0.06015, 0.03140 and 0.008152 m, respectively.

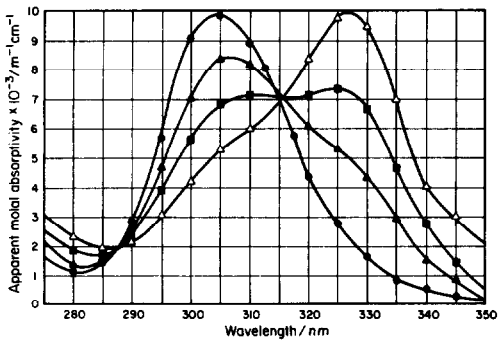

Fig. 6. UV spectra of solutions containing various concentrations of LiBr saturated with $PbBr_2$. The spectra correspond to lead concentrations as follows: ●, 0.008152 m; ▲, 0.01832 m; ■, 0.0314 m, and △, 0.06015 m.

tensities of the two peaks of course reflects the corresponding variation of the relative concentrations of the monoculear species $PbBr_3^-$ and the polynuclear species Pb_XBr_Y. In principle, the identity of Pb_XBr_Y can be established by systematic analysis of the spectrophotometric data for a series of solutions covering a range of concentrations. In practice, however, it is advantageous to apply spectral stripping to minimize the considerable overlap of the pertinent peaks which otherwise interferes with the spectrophotometric analysis.

The spectrophotometric analysis is based on the assumption that the formation of the Pb(II) solute species can be described by eqns (8) and (9).

$$PbBr_2(s) + Br^- \rightleftarrows PbBr_3^- \quad (8)$$

$$X\,PbBr_2(s) + (Y-2X)Br^- \rightleftarrows Pb_XBr_Y^{2X-Y} \quad (9)$$

the former predominating in dilute LiBr and the latter in concentrated LiBr solutions. At any wavelength where both species absorb, A/l, the total absorbance per unit cell thickness, follows eqn (10) where ϵ_i denotes the molal absorptivity of species i.

$$A/l = \epsilon_{PbBr_3^-}[PbBr_3^-] + \epsilon_{Pb_XBr_Y}[Pb_XBr_Y]. \quad (10)$$

Replacing the concentration of Pb_XBr_Y by its equivalent in terms of the concentration of $PbBr_3^-$ and K_8 and K_9, the equilibrium constants of eqns (8) and (9), and rearranging, yields eqn (11).

$$A/l - \epsilon_{PbBr_3^-}[PbBr_3^-] = K_9K_8^{(2X-Y)}\epsilon_{Pb_XBr_Y}[PbBr_3^-]^{(Y-2X)}. \quad (11)$$

All the terms on the l.h.s. can be evaluated experimentally, and the only unknown variable is the exponent $(Y-2X)$. To emphasize this aspect of eqn (11), we have rewritten it as eqn (12) where A' denotes the terms on the l.h.s. of eqn (11), and B the constant terms on the r.h.s. of eqn (11).

$$A' = B[PbBr_3^-]^{Y-2X}. \quad (12)$$

The molal absorptivity of $PbBr_3^-$, which is already known from spectrophotometric measurements at appropriate wavelengths of dilute LiBr solutions saturated with $PbBr_2$, is used to estimate the concentration of $PbBr_3^-$ in a series of concentrated LiBr solutions saturated with $PbBr_2$. The problem here is that in moderately concentrated LiBr solutions saturated with $PbBr_2$ there is no wavelength at which either the 327 nm peak or the short wavelength end absorption or both do not interfere significantly with estimation of the $PbBr_3^-$ concentration. We have dealt with this problem in two ways which collectively define a unique formula for Pb_XBr_Y. The first and simpler method, which assumes that spectral overlap does not seriously interfere with estimation of the $PbBr_3^-$ concentration, yields a lower limit for the value of the term $Y-2X$. This estimate of the exponent tends to fall below the true value because as the concentration of Pb(II) increases, the magnitude of the spectral interferences increases, thus causing the estimated concentration of $PbBr_3^-$ to deviate progressively above the true value. In the second method, an approximate spectral stripping method used to minimize the peak overlap probably tends to overcorrect the spectral interference, thus yielding an upper limit for the value of $Y-2X$. In both methods, the value of $Y-2X$ is evaluated at nine equally spaced wavelengths from 290 to 310 nm, the wavelength range corresponding to the $PbBr_3^-$ absorption band. To determine the best value of the term $Y-2X$ at each wavelength, we subjected eqn (12) to nonlinear regression analysis using the program BMDP3R from the Biomedical Computer Program Libraries.

Curve a in Fig. 7 reports the estimated value of $Y-2X$ at each of the nine experimental wavelengths. It is clear that the value of $Y-2X$ depends systematically on the wavelength, reaching a maximum value of 2.94 ± 0.17 at 300 nm and falling rapidly at both higher and lower wavelengths. This result shows that spectral interference is lowest at 300 nm and that it increases at both longer wavelengths because of the Pb_XBr_Y peak and at shorter wavelengths because of the strong end absorption. Because these peaks may still cause one to overestimate the $PbBr_3^-$ concentration somewhat at 300 nm, the value of 2.94 represents a lower limit of the term $Y-2X$.

To reduce the spectral interference by the Pb_XBr_Y peak and the short wavelength end absorption band, we applied the approximate spectral stripping technique outlined below. First, it was established that over the

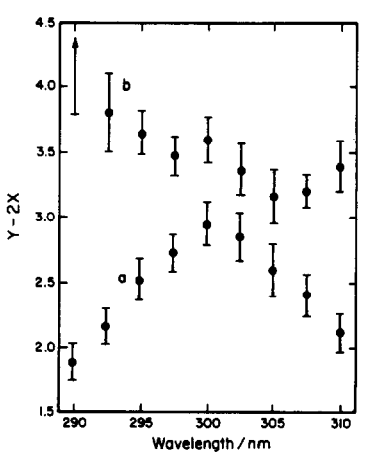

Fig. 7. Estimated values of $Y-2X$ in eqn (12) with bars showing 90% confidence limits: a, uncorrected; b, corrected by spectral stripping to reduce interference.

composition range and wavelength range of interest, the three absorption bands can be appoximated fairly well as Gaussian curves of absorbance vs frequency. This provided estimates of the spectral interference arising from the Pb_XBr_Y peak and the end absorption band at each of the 9 wavelengths of interest for each of the nine LiBr concentrations studied. Because the estimates of the total spectral interference at each wavelength obtained in this way exhibited considerable scatter when plotted against the observed absorbance they were smoothed by linear regression. Since at each wavelength the ratio of the total estimated interference to the observed absorbance was found to increase linearly with the observed absorbance, the individual correction terms were replaced by the smoothed values calculated from the regression line. Subtraction of the appropriate refined correction term from the measured absorbance of each LiBr solution at each wavelength then yields corrected $PbBr_3^-$ concentrations for substitution in eqn (12). In the most concentrated solution, which has a lead concentration of 0.0913 m, the correction estimated in this way corresponds to between 1 and 50% of the absorbance of the $PbBr_3^-$ peak. In the less concentrated solutions it is proportionately less, and at all concentrations it reaches a minimum at 302.5 nm. This result agrees well with the earlier finding that when the spectral overlap was not corrected the minimum interference was found at 300 nm.

Values of $Y-2X$ obtained in this manner are plotted against wavelength in curve *b* of Fig. 7. As is true of the uncorrected data, the estimated values of $Y-2X$ show a pronounced wavelength dependence but unlike the uncorrected data, the value of $Y-2X$ exhibits a minimum. This minimum value of 3.17 ± 0.21 thus represents an upper limit of the estimated value of $Y-2X$. As might be anticipated, this minimum value occurs at 305 nm, the wavelength at which $PbBr_3^-$ absorbs most strongly. The value of 2.94 ± 0.17 obtained without correction for spectral interference thus define 3.00 as the most probable value of $Y-2X$.

Combining the value of $Y-2X$ with the known composition of the $PbBr_2$ saturated solutions summarized in Fig. 2 limits the possible formulas of the species Pb_XBr_Y still further. Thus the values of X and Y must satisfy eqns (13) and (14),

$$Y < 3X \tag{13}$$

$$Y = 2X + 3 \tag{14}$$

the former constraint arising from the composition of concentrated solutions and the latter from the spectrophotometric analysis. The integral values of X and Y which meet both constraints limit the formula of Pb_XBr_Y to $Pb_4Br_{11}^{3-}$, $Pb_5Br_{13}^{3-}$, and $Pb_6Br_{15}^{3-}$, which correspond, respectively, to bromide : lead ratios of 2.75, 2.60 and 2.50. Of these, the species $Pb_4Br_{11}^{3-}$ gives by far the best agreement between calculated and observed values of the bromide: lead ratio. For solutions in which $PbBr_3^-$ and the polynuclear species Pb_XBr_Y are the only Pb(II) species, R, the bromide: lead ratio can be calculated from the spectrophotometrically estimated $PbBr_3^-$ concentration and the analytically determined total lead concentration through eqn (15).

$$R = \frac{Y}{X} + \left(3 - \frac{Y}{X}\right)\frac{[PbBr_3^-]}{[Pb]_t} \tag{15}$$

For a solution 0.09 m in Pb(II) in which the polynuclear species is $Pb_4Br_{11}^{3-}$, eqn (15) predicts a bromide : lead ratio of 2.85. If the polynuclear species is $Pb_5Br_{13}^{3-}$, the predicted bromide : lead ratio is 2.74, and if the polynuclear species is $Pb_5Br_{15}^{3-}$, the predicted bromide: lead ratio is 2.68. Comparison of these three values with the experimental bromide: lead ratio of 2.87 verifies that the polynuclear complex is indeed $Pb_4Br_{11}^{3-}$. Further evidence that the polynuclear complex is $Pb_4Br_{11}^{3-}$ is the experimental bromide: lead ratio of 2.73 of the 1.25 m Pb(II) solution Fig. 2), which agrees very well with the value of 2.75 assuming that essentially all the lead is present as $Pb_4Br_{11}^{3-}$. This value cannot be checked spectrophotometrically because it would be necessary to reduce the pathlength to less than 10 μm to obtain sufficient light transmission, but at this high concentration, nearly all the lead must be converted to the polynuclear species. Another significant result of these calculations is that they show that in LiBr solutions saturated with $PbBr_2$ the free bromide concentration is only a very small fraction of the total bromide concentration. For example, the free bromide concentration in a 0.09 m LiBr solution saturated with $PbBr_2$ is less than 0.002 m. Such low concentrations confirm the high stability of the Pb(II)–Br complexes in PC.

Unsaturated $PbBr_2$ *solutions in* LiBr

Relative to a solution of the same Pb(II) content which is saturated with $PbBr_2$, a solution which is unsaturated with respect to $PbBr_2$ contains a higher bromide concentration. That is, the bromide : lead ratio of an unsaturated solution is higher than that of a saturated solution of equal Pb(II) content, suggesting that the Pb(II) species in the saturated solution would be converted to higher complex(es) in the unsaturated solution. Figure 8, which compares the absorption spectra of two 0.0075 m Pb(II) solutions, the first of which is saturated with $PbBr_2$ while the second is unsaturated, shows that the spectra differ substantially. Most notable is the fact that the relatively symmetric peak of $PbBr_3^-$ in the spectrum of the saturated solution is replaced by a broad asymmetric peak in the spectrum of the unsaturated solution. The decrease in absorbance at 305 nm shows that some of the $PbBr_3^-$ has been converted to a higher Pb(II)-bromide complex, a process which is reported in more detail in Fig. 9. Covering a range of Pb(II) and bromide concentrations, these spectra clearly reveal the progressive conversion of $PbBr_3^-$ into a second complex which absorbs at longer wavelengths. That this second complex is not $Pb_4Br_{11}^{3-}$ is apparent if one compares its spectrum with that of $Pb_4Br_{11}^{3-}$ in Fig. 6. Although both spectra

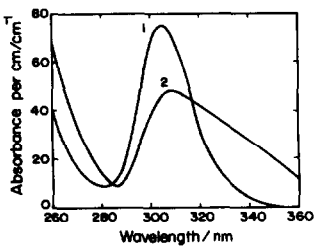

Fig. 8. UV spectra of a $PbBr_2$ saturated solution (curve 1) and a $PbBr_2$ unsaturated solution (curve 2). Both solutions have a lead concentration of 0.0075 m, but the saturated solution has a bromide : lead ratio of 3.0 whereas the unsaturated solution has a bromide : lead ratio of 5.0.

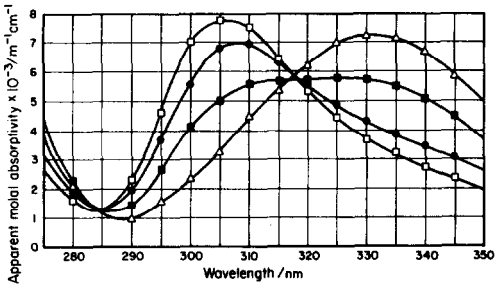

Fig. 9. UV spectra of unsaturated $PbBr_2$ solutions show conversion of $PbBr_3^-$ into $PbBr_4^{2-}$ with increasing bromide:lead ratios. Total bromide:lead ratios are as follows:

	[Br]/[Pb]
□,	4.5
●,	5.0
■,	8.0
△,	13.9.

exhibit maximum absorption at similar wavelengths, the $Pb_4Br_{11}^{3-}$ peak in saturated solutions is much narrower than is the peak of the second complex in unsaturated solutions. The isosbestic point at 318 nm in the spectra of the unsaturated solutions confirms that only two absorbing species are present, so that the equilibrium conforms to eqn (16)

$$R\,PbBr_3^- + (S-3R)\,Br^- = Pb_RBr_S^{(2R-S)}. \quad (16)$$

The identity of the species Pb_RBr_S is easily obtained from the dependence of the spectrum on the solution composition. Consideration of the equilibrium constant of eqn (16) shows that for two solutions *a* and *b*, the ratio of the concentrations of Pb_RBr_S obeys eqn (17) where the charges are omitted

$$\frac{[Pb_RBr_S]_a}{[Pb_RBr_S]_b} = \left(\frac{[PbBr_3]_a}{[PbBr_3]_b}\right)^R \left(\frac{[Br]_a}{[Br]_b}\right)^{S-3R} \quad (17)$$

and the subscripts *a* and *b* denote the two solutions. The concentration ratio for $PbBr_3^-$ can be replaced by the absorbance ratio at 295 nm and that for Pb_RBr_S by the absorbance ratio at 330 nm, leaving only the bromide concentration ratio which can be determined by mass balance. As an example, consider two unsaturated solutions denoted *a* and *b* with Pb(II) concentrations of 0.0075 and 0.0050 m, respectively, prepared by adding sufficient LiBr to appropriate saturated solutions so that the added LiBr concentration of each is 0.015 m. Since the free bromide concentration of a saturated solution is essentially zero, the free bromide concentration in an unsaturated solution equals the added bromide concentration corrected for the quantity which is consumed in eqn (16). This relatively small correction is easily accomplished by estimating spectrophotometrically the decrease in the $PbBr_3^-$ concentration which results from addition of the bromide and assuming a stoichiometry for eqn (16). Combining the fact that in solution a the $PbBr_3^-$ concentration falls by 0.00225 m while in solution *b* it falls by 0.00150 m with the assumption that in eqn (16) $PbBr_3^-$ and Br^- reacct in equimolar proportions yields the estimated bromide ion concentrations of solutions *a* and *b* as 0.01225 and 0.01350 m. To a first approximation, these are equal. Substitution of this result in eqn (16) along with the absorbances at 295 and 330 nm yields *R* equal to 0.95, and eqn (16) simplifies to eqn (18)

$$PbBr_3^- + (S-3)Br^- = PbBr_S^{(2-S)}. \quad (18)$$

Table 2. Concentration of $PbBr_3^-$ in unsaturated solutions

$[Pb]_t$/m	$[LiBr]_{added}$/m	$[PbBr_3^-]$/m
0.0050	0.010	0.0032
0.0050	0.015	0.0028
0.0050	0.025	0.0023
0.0075	0.015	0.0042
0.0057	0.062	0.0013
0.0065	0.010	0.0047

The stoichiometry and the equilibrium constant of eqn (18) can be determined by combining mass balance considerations with the spectrophotometrically measured concentration of $PbBr_3^-$ and the analytical total concentrations of bromide and lead. Application of this approach to the six solutions described in Table 2 yields 3.98 ± 0.13 as the value of *S* and $54 \pm 28\ m^{-1}$ as the equilibrium constant of eqn (18). Thus the product of eqn (16) is $PbBr_4^{-2}$ and its stepwise formation constant is $54 \pm 28\ m^{-1}$. This value, which in the molar concentration scale is $45\ M^{-1}$, is somewhat higher than the value of *ca.* $8\ M^{-1}$ determined potentiometrically by Matsura *et al.*,[14] but it is not clear to what extent the difference arises from the limitations inherent in the two methods. It is also clear that our estimate of the stepwise formation constant of $PbBr_4^{-2}$ in PC is substantially greater than corresponding values for aqueous solutions, which are *ca.* $0.2\ M^{-1}$.[15] Such enhanced stability relative to aqueous solutions appears to be a general charaacteristic of Pb(II)- bromide complexes in PC. For example, log β_4 is 21.8 in PC[14] as compared to 1.5 in water.[15] The extreme stability of $PbBr_4^{-2}$ in PC, which is consistent with that of other heavy metal halide complexes in this solvent, indicates that potentiometric methods will be necessary for full characterization of these complexes.

REFERENCES

[1]R. Jasinski, *Advances in Electrochemistry and Electro chemical Engineering*, p. 253. Wiley-Interscience, New York (1971).
[2]W. S. Harris, Thesis, University of California, Berkeley, California (1958).
[3]F. W. Breivogel and M. Eisenberg, *Electrochim. Acta* 1969, **14**, 459.
[4]J. N. Butler, *Anal. Chem.* 1967, **39**, 1799.
[5]R. C. Murry and D. A. Aikens, *Electrochim. Acta* 1975, **20**, 259.
[6]R. J. Jasinski and S. Kirkland, *Anal. Chem.* 1967, **39**, 1663.
[7]V. Suk and M. Malat, *Chem. Anal.* 1956, **45**, 30.
[8]J. R. Caldwell and H. V. Moyer, *Ind. Engng Chem. Anal. Edn*, 1935, **7**, 38.
[9]W. M. Latimer, *Oxidation Potentials*, 2nd Edn, pp. 152 and 164. Prentice-Hall, Englewood Cliffs, New Jersey (1952).
[10]T. W. Richard and F. Daniels, *J. Amer. Chem. Soc.* 1919, **41**, 1732.
[11]W. R. Carmody, *J. Am. Chem. Soc.* 1929, **51**, 2905.
[12]D. A. MacInnes, *The Principles of Electrochemistry*, p. 225. Dover, New York (1961).
[13]J. Gabano, Y. Jumel and J. Laurent, *Power Sources* 2 (Edited by D. Collins), p. 255. Pergamon Press, Oxford (1968).
[14]N. Matsuura, M. Takizawa, and Y. Sasaki, *Nippon Kagaku Kaishi* 1976, **9**, 1495.
[15]V. E. Mironov, F. Ya. Kul'ba, V. A. Fedorov, and O. B. Tikhomirov, *Zh. Neorg. Khim.* 1963, **8**, 2524.

Polyhedron Vol. 1, No. 2, pp. 175–177, 1982
Printed in Great Britain.

0277-5387/82/020175-03$03.00/0
Pergamon Press Ltd.

INVESTIGATIONS OF CHANGES IN THE OXIDATION STATE OF THE CATALYST DURING THE OsO_4-CATALYSED DECOMPOSITION OF HYDROGEN PEROXIDE

ZOLTÁN M. GALBÁCS, LÁSZLÓ NAGY and LÁSZLÓ J. CSÁNYI*
Institute of Inorganic and Analytical Chemistry, A. József University, P.O. Box 440, 6701 Szeged, Hungary

(*Received* 11 *August* 1981)

Abstract—By using different methods, such as spectrophotometry, potentiometric titration, polarography and extraction, it was found that at pH > 8.5 osmium (VIII) is reduced by hydrogen peroxide to osmium(VI) to various extents. At pH 10.6, where the rate of the OsO_4-catalysed decomposition of hydrogen peroxide reaches its maximum, the concentration ratio of osmium (VIII) and osmium (VI) was found to be nearly one. This favours the explanation that the maximum rate of hydrogen peroxide decomposition is found at the pH where the rate of reduction of osmium (VIII) by hydrogen peroxide just becomes equal to the rate of oxidation of osmium (VI) by hydrogen peroxide.

INTRODUCTION

The decomposition of hydrogen peroxide was recently investigated in the presence of osmium tetroxide.[1] The observed strong catalysis was interpreted in terms of a redox-cycle assuming that osmium (VIII) is reduced to osmium (VI) and the latter is reoxidised by hydrogen peroxide at rates governed by the pH. This paper attempts to collect direct evidence to support the mechanism of catalysis. The reaction was reinvestigated at about 1000 times higher concentration of catalyst to facilitate the estimation of osmium species [osmium (VIII), osmium (VI)] in the reaction mixture when the decomposition of hydrogen peroxide was complete.

EXPERIMENTAL

Sodium hydroxide solution was purified by the procedure of D'Ans and Mattner.[2] Other substances of reagent grade were used, without further purification. Triple distilled water was used to prepare solutions and reaction mixtures. Osmium (VI) was prepared by reduction of OsO_4 with ethanol. Freshly-prepared standard arsenite solution was used for osmium (VIII) titrations.[3]

The absorption spectra were taken with a Unicam SP 800 spectrophotometer. Pt-wire and saturated calomel electrodes were used for potentiometric titrations; the e.m.f. was measured with a Radiometer pH 22 pH-meter. A Radiometer Polariter PO4 was used to record polarograms. The bottom of the polarographic cell was fitted a small bulb, which served to collect the mercury drops in order to reduce the free contact of the solution to be determined with the mercury dropped. 0.1 mol dm^{-3} phosphate buffer solution served as supporting electrolyte.

The total dissolved osmium contents were determined by the spectrophotometric method of Ayres and Wells.[4]

Extraction experiments were carried out in two different ways. (i) Pure solutions of either osmium (VIII) or osmium (VI) were taken in ampoules and dioxygen was removed. Carbon tetrachloride, also freed from dioxygen, was then added in a 1:1 (V/V) ratio and the ampoules were closed. They were subsequently shaken in a thermostat for different periods (0.5–72 hr), after which the aqueous and organic phases were separated and analyzed by the Ayres and Wells' method. (ii) For investigations of reaction mixtures, an equilibration time of only 15 min was used. To the solution to be investigated carbon tetrachloride was added in a 1:1 ratio and the mixture was efficiently stirred with a magnetic stirrer. After 15 min the phases were separated and the spectrum of the organic phase was recorded in the range 400–250 nm.

RESULTS AND DISCUSSION

Figures 1 and 2 show the pH-dependence of the light absorption of osmium (VIII) and osmium (VI). It can be seen that at a given pH one can always find a wavelength where the absorbances of the two osmium species differ from each other sufficiently for the determination of Os (VIII) and Os (VI) separately. Further, it is also seen that there is a considerable difference in the acidic strengths of the osmium species. Osmium (VI) proved to be a stronger acid than osmium (VIII). The [Os (VIII)]/[Os_{total}] values obtained for the reaction mixtures with different pH's are plotted in Fig. 3.

The polarographic measurements

In alkaline medium osmium (VIII) is reduced in a stepwise manner at the dropping mercury electrode. The first step rises at zero applied e.m.f., showing that osmium (VIII) is spontaneously reduced to osmium (VI) by metallic mercury.[5–8] The second and third waves, with half-wave potentials of −0.61 and −1.51 V (vs SCE), respectively, have been correlated with the Os (VI)–Os (IV) and Os (IV)–Os (III) reductions. It has been repor-

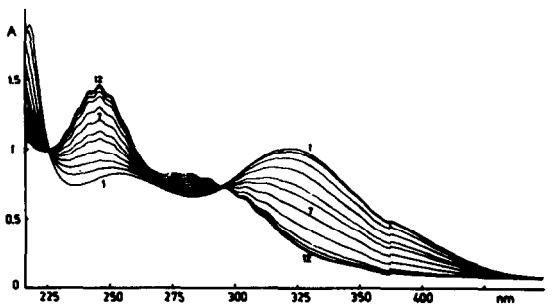

Fig. 1. Spectrum of OsO_4 as a function of pH. Conditions: 298 K. 4.05×10^{-4} mol dm^{-3} OsO_4; light pathlength = 1 cm; reference: water. 1: pH 13.47; 2: pH 13.28; 3: pH 13.00; 4: pH 12.73; 5: pH 12.46; 6: pH 12.19; 7: pH 11.96; 8: pH 11.73; 9: pH 11.36; 10: pH 11.02; 11: pH 10.47; 12: pH 9.93.

*Author to whom correspondence should be addressed.

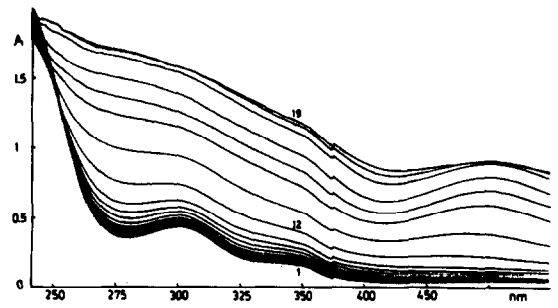

Fig. 2. Spectrum of Os (VI) as a function of pH. Conditions: 298 K; 2.47×10^{-4} M Os (VI) prepared by the reduction of OsO_4 with etanol; light pathlength = 1 cm; reference: water. 1: pH 13.36; 2: pH 13.00; 3: pH 12.54; 4: 12.06; 5: pH 11.41; 6: pH 10.99; 7: pH 10.39; 8: pH 10.03; 9: pH 9.76; 10: pH 9.50; 11: pH 9.33; 12: pH 9.08; 13: pH 8.82; 14: pH 8.50; 15: pH 8.36; 16: pH 7.99; 17: pH 7.05; 18: pH 6.16; 19: pH 5.32.

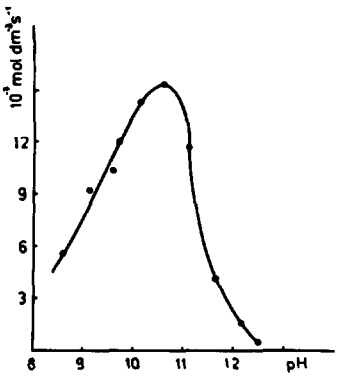

Fig. 4. Rate of oxidation of Os (VI) by dioxygen as a function of pH. Conditions: 0.1 mol dm^{-3} phosphate + std. borax buffer 1×10^{-3} mol dm^{-3} $K_2OsO_2(OH)_4$ 298 K; extraction of the Os (VIII) with CCl_4.

ted[9] that the polarographic determination of osmium (VIII) and osmium (VI) is disturbed by both hydrogen peroxide and dissolved dioxygen, as both substances are reduced to water near zero applied e.m.f. in the presence of osmium ($\geq 10^{-6}$ M). It follows that before the polarographic determination of the [Os (VIII)]/[Os (VI)] ratio one has to wait until the hydrogen peroxide has decomposed completely, and the dioxygen must also be expelled by bubbling N_2 through the solution.

Polarogram of a reaction mixture which contained osmium (VIII) and H_2O_2 at the beginning showed an increase of the second wave at the expense of the first one and the total diffusion current of the first two waves is also decreased. On the other hand, in the case of osmium (VI)–H_2O_2 reaction mixture the total diffusion current increased by the appearance of the first wave due to the partial oxidation of osmium (VI) by H_2O_2. Data obtained can be seen in Fig. 3.

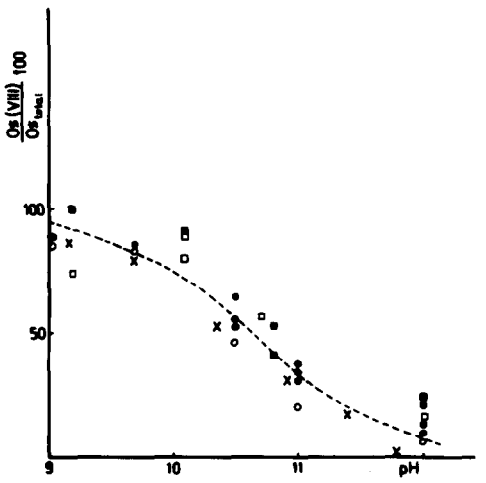

Fig. 3. Change in oxidation state of the osmium catalyst during the catalysed decomposition of H_2O_2 as a function of the pH. Osmium (VIII) + H_2O_2 reaction mixture: ■, spectrophotometric; ●, potentiometric and polarographic; ×, extraction method; Osmium (VI) + H_2O_2 reaction mixture; □, spectrophotometric; ○, potentiometric and polarographic; ×, extraction method.

Potentiometric arsenometry

After the quantitative decomposition of hydrogen peroxide the estimation of osmium (VIII) content of the reaction mixture can be carried out by potentiometric titration with standard arsenite solution in appropriately alkaline solution (>0.5 mol dm^{-3}).[3] Determination is not affected by dioxygen dissolved in the analyzed solution. Data obtained can be seen in Fig. 3.

It was checked separately that, [Os (VIII)]/[Os_{total}] concentration ratio is similarly not influenced by the presence of dioxygen, for the rate of oxidation of osmium (VI) by dioxygen is rather low, even at pH 10.6 where its rate maximum was found (Fig. 4). It is interesting to note that the rate maximum of the OsO_4-catalysed decomposition of hydrogen peroxide is also at pH 10.6.

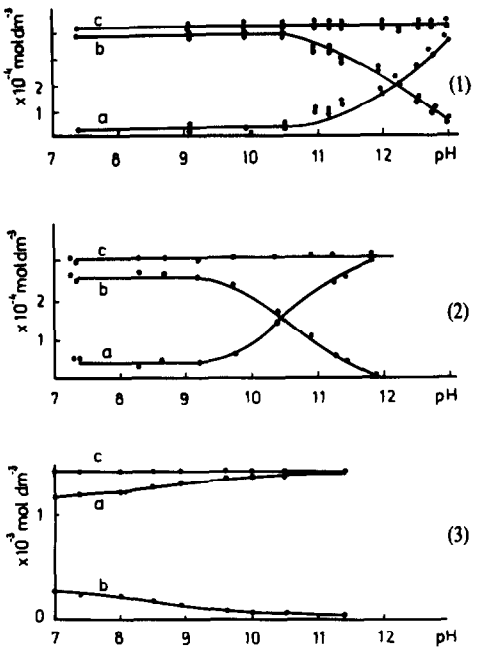

Fig. 5. Distribution between water and CCl_4 of Os (VIII) (1), Os (VI) (3) and the osmium species of the reaction mixture (2) as a function of pH. Curve a: aqueous phase; curve b: organic phase; curve c: osmium total.

Figure 5 shows extractabilities of osmium (VIII) (curve 1) osmium (VI) (curve 3) and the reaction mixture (curve 2) as a function of the pH. 50% distribution was found at pH 12.2 for osmium (VIII) and at pH 10.6 for the reaction mixture. In the case of osmium (VI) the distribution depends strongly on the duration of equilibrating. It can be seen from Fig. 5, curve 3 that osmium (VI) is hardly extracted from the aqueous phase in 15 min, i.e. the concentration of osmium in the organic phase can be considered as being due only to osmium (VIII) from the reaction mixture. At pH < 9 and at longer equilibration interval (> 10 hr) the total dissolved osmium concentration is decreased, as a result of the increasing rate of dismutation of osmium (VI) with the increase in the hydrogen ion concentration.

Figure 3 summarizes the results obtained with the different methods. It is seen that at pH < 9 osmium (VIII) is the dominating species, independently of whether the osmium was introduced in the form of osmium (VIII) or osmium (VI). At pH > 12 osmium (VI) is the main species.

As the maximum rate of decomposition was found at pH 10.6[1] while the concentration ratio [Os(VIII)]/[Os (VI)] is nearly 1 at the same pH, it is plausible to assume that the maximum rate of decomposition of hydrogen peroxide is found at the pH where the rate of reduction of osmium (VIII) by hydrogen peroxide and the rate of oxidation of osmium (VI) by hydrogen peroxide become equal. The present investigation does not give any information concerning the mechanism of these processes, i.e. nothing can be said about the formation of an osmium (VII) intermediate, which was observed when the concentration of alkali is 2 mol dm^{-3} or higher.[10,11]

REFERENCES

[1] L. J. Csányi, Z. M. Galbács, L. Nagy, *J. C. S. Dalton* 1982, 237.
[2] J. D'Ans and J. Mattner, *Angew. Chem.* 1952, **64**, 448.
[3] P. K. Norkus and J. J. Yankauskas, *Zhurn. Anal. Khim.* 1971, **26**, 1827.
[4] G. H. Ayres and W. N. Wells, *Anal. Chem.* 1950, **22**, 317.
[5] W. C. Crowell, J. Heyrovsky and D. W. Engelkemeir, *J. Am. Chem. Soc.* 1941, **63**, 2888.
[6] P. Zuman, *Coll. Czechoslov. Chem. Communs.* 1950, **15**, 1107.
[7] L. Meites, *J. Amer. Chem. Soc.* 1957, **79**, 4631.
[8] J. G. Connery and R. E. Cover, *Anal. Chem.* 1968, **40**, 87.
[9] K. Fülöp and L. J. Csányi, *Acta Chim. Hung.* 1963, **38**, 193.
[10] J. C. Bavay, G. Nowogrocki and G. Tridot, *Bull. Soc. Chim.* 1967, **6**, 2030.
[11] P. K. Norkus, G. J. Rozovsky and Yu. Yu. Yankauskas, *Zhurn. Anal. Khim.* 1971, **26**, 1561.

Polyhedron Vol. 1, No. 2, pp. 179–181, 1982
Printed in Great Britain.

0277–5387/82/020179–03$03.00/0
Pergamon Press Ltd.

CYCLOPALLADATION COMPOUNDS OF THE 2-PYRIDYLHYDRAZONE DERIVATIVES OF *p*-SUBSTITUTED ACETOPHENONES AND ACETYLTHIOPHENES

MATSUO NONOYAMA* and CHISATO SUGIURA
Department of Chemistry, Faculty of Science, Nagoya University, Chikusa, Nagoya, 464 Japan

Abstract—Cyclopalladation occurs for 2-pyridylhydrazones(HL) of *p*-methyl-, *p*-methoxy-, *p*-chloro-, and *p*-nitroacetophenone, and 3-acetyl- and 2-acetyl-thiophene with lithium tetrahalopalladate to give the complexes [PdXL] (X = Cl and Br) and some iodo complexes are prepared by metathesis of the chloro complexes with lithium iodide. These complexes are characterized spectroscopically. The hydrazones are coordinated to palladium through benzene or thiophene ortho-carbon, hydrazone-nitrogen, and pyridine ring-nitrogen atoms forming fused five-membered chelate rings.

INTRODUCTION

Hydrazone derivatives are versatile ligands in coordination chemistry and one of such ligands well studied is pyridine-2-aldehyde 2'-pyridylhydrazone(abbreviated as Hpaphy)[1]. The ligand Hpaphy is coordinated to metal ions either as a neutral or as an anionic terdentate ligand(Structures I and II, respectively) depending upon the conditions under which complexes are prepared. We are interested in the ligands in which one of the two pyridine rings of Hpaphy is substituted by a benzene ring. In a previous paper[2] we have reported that 2-acetylpyridine *p*-methylphenylhydrazone is cyclopalladated to give the complex III(X = Cl and Br) containing a Pd–C bond. In this paper we describe the

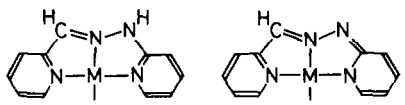

I II

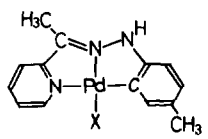

III

palladium(II) complexes of isomeric hydrazones(HL) obtained by condensation of 2-pyridylhydrazine with *p*-methylacetophenone(abbreviated as Hmap), *p*-methoxyacetophenone(Hmxp), *p*-chloroacetophenone (Hcap), *p*-nitroacetophenone(Hnap), 3-acetylthiophene(Ha3p), and 2-acetylthiophene(Ha2p) (Structures IV and V; X = Cl, Br and I; Y = CH_3, CH_3O, Cl and NO_2).

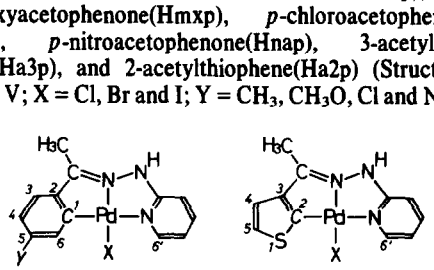

IV V

*Author to whom correspondence should be addressed.

EXPERIMENTAL

Measurements

Measurements were carried out by the methods reported previously[3].

Syntheses

The yields, melting points, and analytical results are given in Table 1. 2-Pyridylhydrazine was prepared by the method in the literature.[4] The hydrazones and complexes were prepared, respectively, by methods similar to those given below for Hmap and [PdX(map)](X = Cl, Br, I).

Hmap: An ethanol solution (30 ml) of 15 mmol of *p*-methylacetophenone and 15 mmol of 2-pyridylhydrazine containing a few drops of acetic acid was refluxed for 1 hr and concentrated to a small volume to give a precipitate. The product was recrystallized from acetone to form light yellow crystals.

[PdCl(map)]: To a solution of lithium tetrachloropalladate, prepared *in situ* from 1 mmol of palladium chloride and 2.5 mmol of lithium chloride in 30 ml of methanol, were added 1 mmol of Hmap and 1 mmol of sodium acetate. The mixture was stirred for 2 days at room temperature to form a yellow precipitate. The precipitate was recrystallized from acetone.

[PdBr(map)]: The yellow bromo complex was obtained similarly from lithium tetrabromopalladate prepared *in situ* by using 4 mmol of lithium bromide instead of lithium chloride.

[PdI(map)]: Metathesis reaction of [PdCl(map)] with an excess of lithium iodide in acetone gave the yellowish brown iodo complex.

RESULTS AND DISCUSSION

The reaction of the 2-pyridylhydrazones(HL) with lithium tetrahalopalladate in the presence of sodium acetate give the complexes [PdXL](X = Cl, Br)(Table 1). The IR spectra (Table 2) show the bands ν(N–H) suggesting that the hydrogen atoms of the hydrazone groups (–NH–N = $C(CH_3)$–) are present in the complexes. The ^{1}H NMR spectra of [PdXL] in dmso-d_6 also suggest the presence of the hydrogen atoms, since the signals due to –NH– remained. A proton should, therefore, be removed from other place than the hydrazone groups. A similar result has been reported for the palladium(II) complexes of isomeric 2-acetylpyridine *p*-methylphenylhydrazone.[2]

Upon formation of the complexes the ^{1}H NMR spectra change markedly in the region of aromatic ring proton resonances (Fig. 1). The acetophenone derivatives show a characteristic singlet in this region (Fig. 1 and Table 2). The chemical shifts of the singlet are sensitive to halide ions X and the singlet is assigned to 6-H(ph).[5] The doublets which shift similarly depending upon X is

Table 1. Melting points, yields, and analytical results of the complexes and hydrazones

Compound	M.P.[a] (°C)	Yield (%)	Analysis, found(calcd.), % C	H	N
Hmap	102-108	77	74.45(74.63)	6.78(6.72)	18.80(18.65)
[PdCl(map)]	222(dec)	83	45.58(45.93)	3.80(3.86)	11.36(11.48)
[PdBr(map)]	259(dec)	76	41.22(40.95)	3.20(3.44)	10.15(10.23)
[PdI(map)]	214(dec)	78	36.62(36.75)	3.12(3.08)	8.92(9.18)
Hmxp	105-107	57	69.70(69.69)	6.13(6.27)	17.17(17.41)
[PdCl(mxp)]	243(dec)	88	43.85(44.00)	3.70(3.69)	10.84(11.00)
Hcap	102-108	79	63.14(63.55)	4.82(4.92)	16.91(17.01)
[PdCl(cap)]	262(dec)	88	40.43(40.39)	2.82(2.87)	10.88(10.87)
[PdBr(cap)]	260(dec)	95	36.88(36.23)	2.50(2.57)	10.01(9.75)
[PdI(cap)]	245(dec)	63	32.62(32.67)	2.27(2.32)	8.54(8.79)
Hnap	156-163	76	60.70(60.93)	4.63(4.72)	21.73(21.86)
[PdCl(nap)]	238(dec)	80	39.04(39.32)	2.88(2.79)	14.09(14.11)
Ha3p	109-115	69	60.70(60.80)	4.93(5.10)	19.42(19.34)
[PdCl(a3p)]	226(dec)	87	37.05(36.89)	2.85(2.81)	11.87(11.73)
[PdBr(a3p)]	242(dec)	97	33.28(32.82)	2.54(2.50)	10.80(10.44)
[PdI(a3p)]	209(dec)	75	29.39(29.39)	2.22(2.24)	9.02(9.35)
Ha2p	98-101	62	60.90(60.80)	5.08(5.10)	19.56(19.34)
[PdCl(a2p)][b]	179(dec)	93	36.95(36.94)	3.55(3.62)	10.51(10.77)

a) dec = decomposition.

b) This complex was obtained as a methanol adduct, [PdCl(a2p)]·CH_3OH. The presence of one mole of methanol was confirmed by the ^1H nmr spectrum.

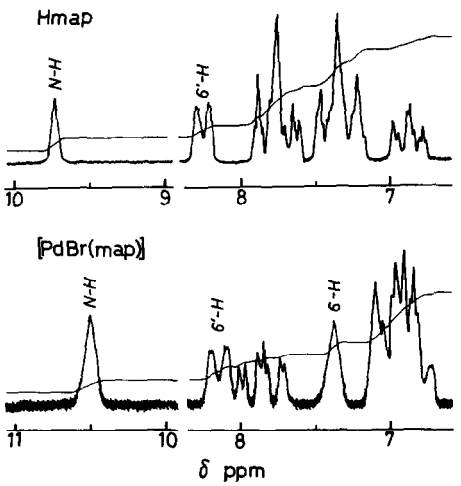

Fig. 1. 60 MHz ^1H NMR spectra of Hmap and [PdBr(map)] in dmso-d_6 (δ ppm from internal sodium 2,2-dimethyl-2-silapentane-sulfonate, DSS).

assigned to 6'-H(py). For these complexes is proposed Structure IV where both 6-H(ph) and 6'H(py) are situated in the proximity of X. This structure is closely related to Structure III of the cyclopalladated isomeric hydrazone. In accordance with Structure IV, the bands ν(Pd-X) are observed in the normal region (Table 2).[6]

Because of the low solubilities of the thiophene derivatives no satisfactory ^1H NMR spectra are obtained and it is difficult to observe fine splittings required for determination of the structures. The rough features of the spectra are similar to those of the cyclopalladated complexes of acetylthiophene acetylhydrazones previously reported.[7] Structure V is proposed for [PdX(a3p)](X = Cl, Br, I). [PdCl(a2p)] may have a structure where the position 3 of the thiophene ring is metallated.[8]

The signals due to 3-H and 4-H of p-substituted acetophenone moieties of the complexes(IV, Y = CH_3–, CH_3O–, Cl–) are observed near 7 ppm. The cyclopalladation results in upfield shifts of the signals compared with those of the free hydrazones. On the contrary, the signals of –NH– of the hydrazone groups shift to lower field. This indicates that electrons of the hydrazone group move toward the phenyl ring in the complexes. The contribution of Structure VI is presumed. The thiophene derivatives show a similar trend.

It is interesting that the phenyl and thienyl rings of the 2-pyridylhydrazones prepared here are easily cyclopalladated in preference to deprotonation of the

Table 2. Characteristic bands of IR and ^{1}H NMR spectra

Compound	IR(Nujol), cm^{-1}		NMR(dmso-d_6) δ, ppm(DSS)[a]		
	ν(N-H)	ν(Pd-X)	-NH-	6'-H(py)	6-H(ph)
Hmap	3160		9.73	8.25	7.82d, 7.28d(7.2)[b]
[PdCl(map)]	3280	337	11.43	8.05	7.12
[PdBr(map)]	3290	278	11.50	8.13	7.38
[PdI(map)]	3230		c)	8.22	7.72
Hmxp	3190		9.65	8.25	7.86d, 7.03d(8.9)
[PdCl(mxp)]	3150	301	11.42	8.02	6.95
Hcap	3170		9.88	8.25	7.93d, 7.51d(8.6)
[PdCl(cap)]	3250	321	11.70	8.08	7.33
[PdBr(cap)]	3280	265	11.70	8.20	7.57
[PdI(cap)]	3260		11.75	8.41	7.95
Hnap	3195		10.22	8.25	8.34d, 8.12d(8.8)
[PdCl(nap)	3215	343	12.08	ca. 8.42[d]	ca. 8.42[d]
					4,5-H(th)
Ha3p	3180		9.67	8.23	7.5 - 7.9m
[PdCl(a3p)]	3220	328	11.42	7.98	7.13s
[PdBr(a3p)]	3210		11.48	8.05	7.12s
[PdI(a3p)]	3200		11.67	8.27	7.13[e]
Ha2p	3180		9.83	8.25	7.0 - 7.8m
[PdCl(a2p)]	3210	333	11.52	7.95	7.53d, 6.99d(4.8)

a) Only major splitting patterns are given for the complexes because insufficient solubilities prevent observation of fine splitting patterns. The N-H and 6-H(ph) signals are a singlet and 6'-H(py) signal is a doublet (J = ca. 5 Hz). s = singlet, d = doublet, m = multiplet.

b) For free hydrazones are shown all signals of phenyl rings and figures in parentheses are coupling constants in Hz. c) Not observed.

d) Both the signals are overlapped as a complex multiplet.

e) The signal seems to be a quartet[7] but is partially hindered by pyridine ring signals.

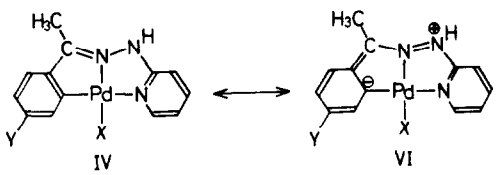

IV VI

hydrazone groups. This fact is a great contrast to the fact that Hpaphy is deprotonated at the hydrazone group.[1] Cyclopalladation has also been reported for other substituted hydrazones of aromatic ketones.[2,7,8] High electron density of the hydrazone group may facilitate cyclopalladation of aromatic rings by enhancing the electron density of the rings. The mechanism is difficult to be proposed at present.

REFERENCES

[1] C. Bell, *Rev. Inorg. Chem.* 1979, **1**, 133.
[2] M. Nonoyama, *Inorg. Chim. Acta* 1978, **28**, L163.
[3] T. Komatsu, M. Nonoyama and J. Fujita, *Bull. Chem. Soc. Jpn.* 1981, **54**, 186.
[4] R. G. Fargher and R. Furness, *J. Chem. Soc.* 1915, **107**, 688.
[5] Phenyl, pyridyl, and thienyl groups are indicated, respectively, as "ph", "py", and "th".
[6] T. G. Appleton, H. C. Clark and L. E. Manzer, *Coord. Chem. Rev.* 1973, **10**, 335.
[7] M. Nonoyama, *J. Inorg. Nucl. Chem.* 1980, **42**, 297.
[8] M. Nonoyama, *Inorg. Nucl. Chem. Lett.* 1978, **14**, 337.

Polyhedron Vol. 1, No. 2, pp. 183–186, 1982
Printed in Great Britain.

0277-5387/82/020183-04$03.00/0
Pergamon Press Ltd.

SYNTHESIS OF SILVER (II) OXIDE BY OXIDATION OF SILVER OR SILVER OXIDE BY MEANS OF OZONE

R. DALLENBACH†, J. PAINOT‡ and P. TISSOT*
Département de Chimie Minérale, Analytique et Appliquée, Sciences II, 30, quai E. Ansermet, CH-1211 Genève, Switzerland

(*Received* 26 *August* 1981)

Abstract—The oxidation by ozone of a suspension of silver or silver oxide in an aqueous solution of sodium hydroxide is described. It has been shown that the oxidation proceeds in two steps:

$$Ag \xrightarrow{O_3} Ag_2O \xrightarrow{O_3} AgO.$$

The experimental results are in good agreement with a mechanism of dissolution and precipitation. The silver (II) oxide obtained has remarkable properties of stability in alkaline solution and of reducibility to metallic silver. These special properties are probably due to the large size of the particles.

INTRODUCTION

Since the work of Marignac,[1] who was the first to observe the formation of AgO by reaction of O_3 on silver, some authors have studied this solid–gas reaction both on silver and on silver oxide.[2–5] The oxidation by ozone of the ion Ag^+ in solution has formed the subject of a greater number of studies with several silver salts in acid, neutral or alkaline solutions.[5–7] As far as we know, there has been no work on the oxidation by O_3 of an aqueous suspension of silver or silver oxide; this possibility to obtain the silver peroxide has been mentioned in the review published by McMillan[8] and in a patent application.[9] We describe in this paper a detailed study of the synthesis of AgO by oxidation of a suspension of silver or silver oxide in an aqueous solution of sodium hydroxide, and we compare the properties of the product obtained (named OSK) with those of a commercial silver (II) oxide (Merck suprapur, named Msp) obtained by oxidation of Ag^+ by persulphate.

EXPERIMENTAL

Equipment

All the runs were done in a 10 l. reactor, fitted with a double mantle, a stirrer, an input and an output for the gaseous mixture O_2–O_3. The ozone was produced by a brush-discharge device providing a maximum flow of 2.6 $gh^{-1}O_3$ with a total flow (O_2 + O_3) of 150 lh^{-1}. The 2N sodium hydroxide solution contained either 100 g of silver powder (mean dia. 20 μm) or 100 g of silver oxide (mean dia. 2 μm).

Analytical methods

During the course of the synthesis, we took samples and analysed the mixture Ag–Ag_2O–AgO. The titration of this mixture is complicated by the dismutation reaction (1)

$$Ag^{+2} + Ag^0 = 2\,Ag^{+1} \qquad (1)$$

which proceeds in solution and prevents the use of a chemical titration of the oxidizer power of AgO in the presence of metallic silver.[10] We used this method only for the samples taken at the end of the synthesis. In the other cases we used thermogravimetry; this method is well known[11–13] and is based on the loss of weight associated with the reactions (2) and (3):

$$2\,AgO \xrightarrow{\sim 120°C} Ag_2O + 1/2\,O_2 \qquad (2)$$

$$Ag_2O \xrightarrow{\sim 400°C} 2\,Ag + 1/2\,O_2. \qquad (3)$$

Unfortunately between the two steps, there is a continuous small weight loss, so that the accuracy of the method is not better than ±2% for AgO alone. In the presence of metallic silver, the solid–solid reaction (1')

$$AgO + Ag = Ag_2O \qquad (1')$$

proceeds at the same time as the reaction (2). However the reaction (1') is slow, and we have made a correction curve taking into account this phenomenon for several AgO–Ag ratios. The accuracy of the thermogravimetric method is ±5% in the case of the mixtures.

In addition each sample was checked by X-ray diffraction and with the scanning electron microscope.

STUDY OF THE SYNTHESIS

The stirring of the suspension and the flow of ozone are the main factors which influence the yield, calculated as the ratio of the silver oxidized (Ag_2O + AgO) over the total amount of ozone introduced. Figure 1 shows the results obtained for the maximum flow of ozone; with our experimental equipment, the optimum rotation speed of the stirrer is 480 rpm, which we used in all runs.

Figure 2 represents the change of the concentration during the course of a synthesis. All the runs show the same aspect, which is characteristic of two successive reactions; the oxidation proceeds then in two steps, $Ag^0 \rightarrow Ag^+ \rightarrow Ag^{+2}$.

The complete oxidation (to 96 ± 2% AgO) of 100 g of silver takes about 20 hr. A prolongation of the ozone

*Author to whom correspondence should be addressed.
†Present address: Union Carbide, 43, rue J. L. Chevrolet –CH-2301 La Chaux-de-Fond, France.
‡Present address: Thermocompact SA, 10 rue Richemont, CH-1202 Geneve, Switzerland.

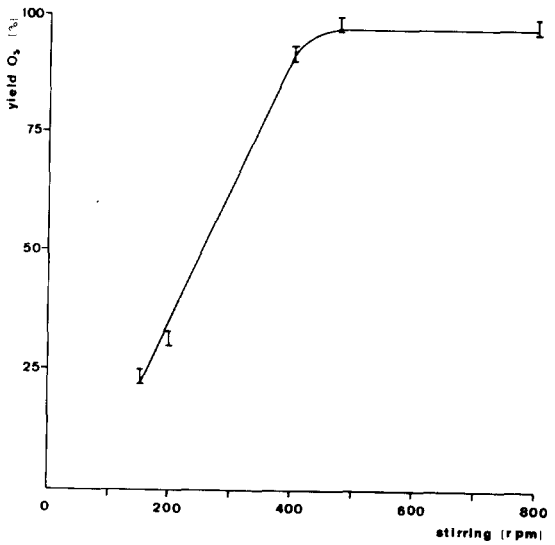

Fig. 1. Consumption of ozone as a function of stirring. Total flow (O_2+O_3), 150 l H^{-1}; flow of O_3, 2.6 gh^{-1}; temperature, 25°C; reaction mixture, 100 g of Ag in 10 l NaOH 2N.

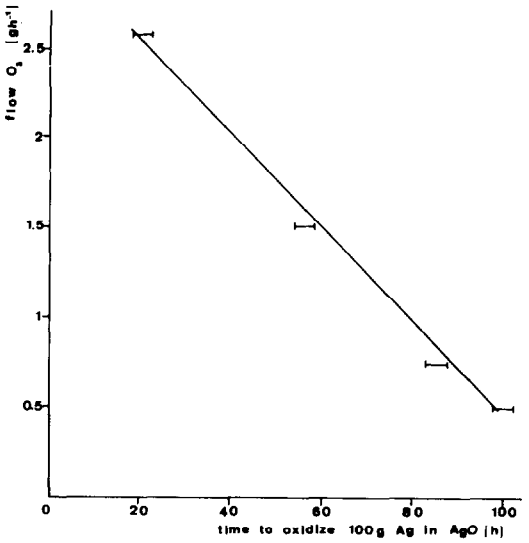

Fig. 3. Rate of oxidation as a function of ozone flow-rate. Temperature, 25°C.

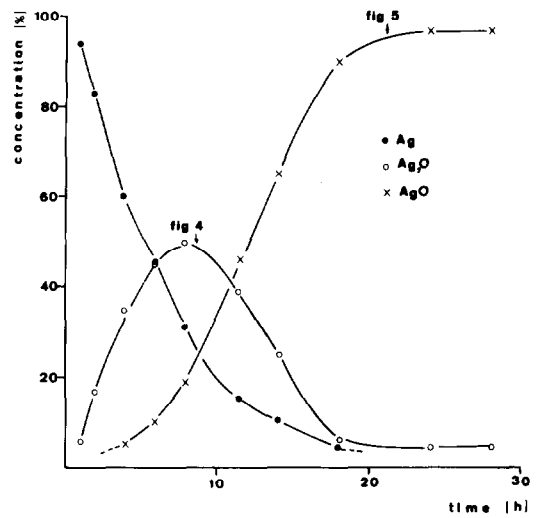

Fig. 2. Change of the concentration during the synthesis. Total flow (O_2+O_3), 150 lh^{-1}; flow of O_3, 2.6 gh^{-1}; temperature, 25°C; reaction mixture, 100 g of Ag in 10 l NaOH 2N.

bubbling does not change the percentage of AgO. With the same experimental conditions, we have observed the same rate of oxidation (100 g in 20 hr) with batches of 50–400 g of silver. The influence of the flow of ozone is shown in the Fig. 3, which represents the linear relation between the flow rate of ozone and the time required to oxidize 100 g of silver. It was not possible to test higher flow rates of ozone than 2.6 gh^{-1}, but it is likely that a linear relation exists for larger rates of flow.

All tests were made at 25°C; at O and 50°C we observed a slower rate of oxidation.

By starting with Ag_2O instead of Ag, we obtained the same product; in this case, the rate of oxidation is about two times greater. This is in good agreement with the hypothesis that the oxidation of silver proceeds in two steps. The examination with the SEM of the samples taken during the synthesis also confirms this hypothesis; as a matter of fact, one initially observes the formation of small protuberances of Ag_2O on the surface of the silver grains, whose sizes diminishes. We never observed the formation of a film over the surface of silver, and so we think that the Ag_2O is formed by a mechanism of dissolution and precipitation. After some hours AgO appears in the shape of flakes (Fig. 4); at the end of the oxidation, the AgO flakes enlarge and theAg_2O disappears (Fig. 5). The size of the particles obtained is exceptionally big, as compared with the usual AgO (Fig. 6). However, the two products shown in Fig. 5 and 6 have the same X-ray pattern, corresponding to the usual monoclinic form of AgO.

PROPERTIES OF THE SILVER (II) OXIDE

The main difference observed between AgO obtained by oxidation of silver by ozone and AgO obtained by oxidation of silver ions is the shape and the size of the particles. With the procedure described in this paper, we obtained large flakes of 10–30 μm of length and 0.1–1 μm of thickness. The specific area of this product is less than 0.1 m^2g^{-1}, when the specific area of Msp is 0.8 m^2g^{-1} as measured by the BET method. The thermal stability of the two kinds of silver oxide has been tested by thermogravimetry and differential thermal analysis. The starting temperature of decomposition according to the reaction (2) is about 10°C lower for the Msp sample.

We have also compared the stability of the two types of oxide in 7N KOH solution at 60°C, by measuring the volume of oxygen evolved. Figure 7 shows the remarkable stability of OSK; we have tested more than 15 types of AgO of different origins, and never obtained the same stability.

Another outstanding property of the OSK type AgO is the possibility to reduce it (by hydrogen or hydrazine for example) to metallic silver, well before the complete

Fig. 4. Scanning electron microscope photography of reaction-mixture after 8 hr (see Fig. 2) (1000×) Ag: 30%; Ag_2O: 50%; AgO: 20%.

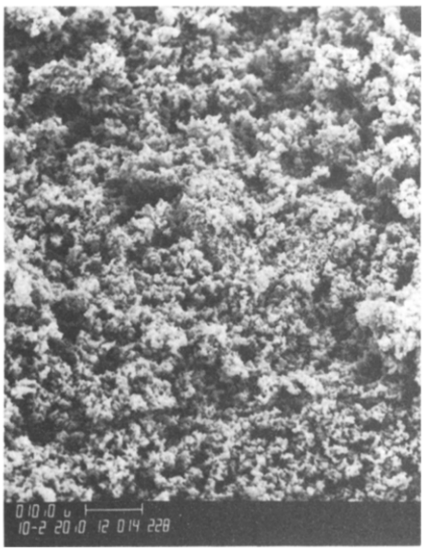

Fig. 6. SEM photography of AgO (type Msp) (1000×).

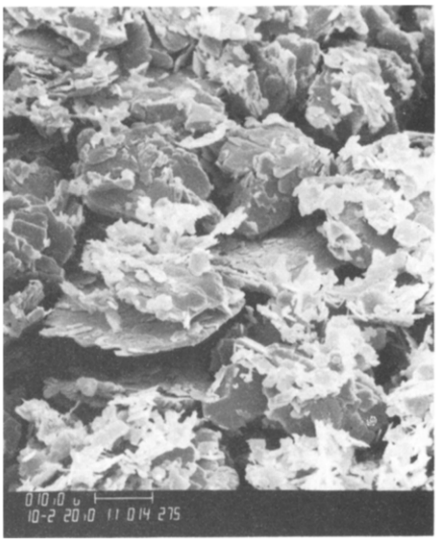

Fig. 5. SEM photography of AgO (types OSK) (1000×).

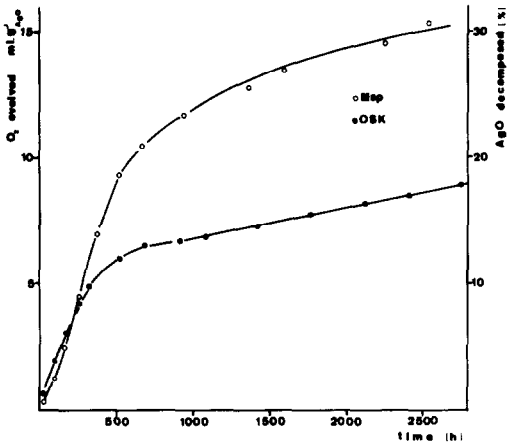

Fig. 7. Decomposition of AgO in 7N KOH at 60°C.

reduction of AgO to Ag_2O. This reduction proceeds in two steps:

$$2\,AgO + H_2 = Ag_2O + H_2O \quad (4)$$

$$Ag_2O + H_2 = 2\,Ag + H_2O. \quad (5)$$

With all samples tested except OSK, we did not detect silver by X-ray analysis until 90% of AgO had been transformed into Ag_2O; with OSK, on the other hand, we have detected metallic silver when only 30% of AgO had been reduced to Ag_2O. This property could be very useful in the preparation of the cathodic mass of electrical cells.

CONCLUSIONS

The overall reaction of formation of silver (II) oxide by oxidation of silver by ozone can be written as follow:

$$Ag + O_3 = AgO + O_2. \quad (6)$$

We have clearly demonstrated that this reaction takes place in two steps, with the intermediary formation of Ag_2O. Moreover, it seems that solid silver is not oxidized directly by gaseous ozone, but rather that we have a reaction between soluble species. The silver is not soluble in alkaline solution, and the first step must be the oxidation of silver. Silver oxides present some solubility, and several authors[5,11,14] have proposed $Ag(OH)_2^-$, AgO^-, $Ag(OH)_3^-$ and $Ag(OH)_4^-$ as the soluble species.

The solubility of ozone in alkaline solution has also been studied by several authors;[15,20] most of them have mentioned that the decomposition of O_3 goes through the ozonide ion and that the concentration of OH radicals is high.

All our experimental results are in good agreement

with a mechanism involving successive steps of dissolution-oxidation-precipitation. The slow rate of oxidation observed could be partly explained by one or the other of the two folowing reactions:

$$2\,Ag(OH)_3^- = 2\,Ag(OH)_2^- + H_2O + 1/2\,O_2 \qquad (7)$$

or

$$Ag(OH)_3^- + Ag = Ag_2O + OH^- + H_2O. \qquad (8)$$

Finally, the outstanding properties of the OSK type AgO is probably due to the size of the particles obtained by this synthesis.

Acknowledgements—We are grateful to Miss H. Lartigue and to Mr. R. Mercier for their technical assistance, and to the "Commission pour l'encouragement des recherches scientifiques" for financial support (Project No. 915).

REFERENCES

[1]J. C. G. de Marignac, *Comptes rendus* 1885, **20**, 87.
[2]F. Jirza and J. Jelinek, *Z. anorg. und allg. Chemie* 1926, **158**, 61.
[3]F. Jirza, *Coll. Czech. Chem. Commun.* 1949, **14**, 445.
[4]A. S. McKee and D. Clark, *Batteries. Proc. 3rd Int. Symp.* p. 285. Pergamon Press, Oxford, 1962.
[5]Gmelins, *Hanbuch der Anorg. Chemie Silber Teil* B1, p. 107. Verlag, Chemie, 1971.
[6]T. M. Franchuck and V. A. Lunekok-Burmakina, *Tezisy Dokl. Uses Savesh Khim. Neorg. Perekisnikh Svedin*, 1973, **114**, 28 (CA 1975, 83, 103902p).
[7]D. S. Gorbenko-Germanov and W. K. Baskova, *Zhur. Fis Khim.* 1974, **48**, 2225.
[8]J. A. McMillan, *Chem. Rev.* 1962, **62**, 65.
[9]German Patent Request No. 240910 Varta Batterie Ag, 3000 Hanover 1976.
[10]C. P. Lloyd, *Anal. Chimica Acta* 1968, **43**, 95.
[11]T. P. Dirks and B. Wiers, *J. Electrochem. Soc.* 1959, **106**, 284.
[12]J. C. Jack and T. Kennedy, *J. Thermal Analysis* 1971, **3**, 25.
[13]G. M. Arcand, NASA Report No. 68–379, 1968.
[14]A. Fleisher, *J. Electrochem. Soc.* 1968, **115**, 816.
[15]Gmelins, *Handbuch der Anorg. Chemie.* Sauerstoff Lief. 7, p. 2272. Verlag Chemie, 1966.
[16]G. Czapski, *Israël J. Chem.* 1968, **6**, 969.
[17]G. I. Rogozhkin, *Tr. Uses Naush. Issled Inst.* 1970, **25**, 76.
[18]V. I. Matrozov, *ZH, Prikl. Khim.* 1975, **48**, 1838.
[19]R. Hongue, *Water Res.* 1976, **10**, 377.
[20]L. Rizzuti, *Chem. Eng. Sci.* 1977, **31**, 877.

Polyhedron Vol. 1, No. 2, pp. 187–190, 1982
Printed in Great Britain.

0277-5387/82/020187-04$03.00/0
Pergamon Press

SYNTHESES, CHARACTERIZATION, AND MOSSBAUER STUDY OF Sn(II AND Sn(IV) COMPLEXES OF THE CYCLOPENTADIENEDITHIOCARBOXYLATE LIGAND

ROBERT D. BEREMAN*
Department of Chemistry, North Carolina State University, Raleigh, NC 27650, U.S.A.

MARY L. GOOD and JOHN BUTTONE
Department of Chemistry, University of New Orleans, New Orleans, LA 70122, U.S.A.

and

PAUL SAVINO
Department of Chemistry, SUNY at Buffalo, Buffalo, NY 14214, U.S.A.

(*Received* 1 *September* 1981)

Abstract—The preparation and physical characterization of the tetraethylammonium salts of *bis*(cyclopentadienedithiocarboxylate)stannate(II) and *tris*(cyclopentadienedithiocarboxylate)stannate(IV) are reported. The coupling constants for the ring protons of the coordinated and uncoordinated ligand indicate that the oxidation state variation of the metal has little effect on the electronic structure of the ligand. The Mössbauer parameters for the Sn(IV) complex ($\delta = 1.05 \pm 0.02$ mm/sec with respect to SnO_2, Line width = 1.05 mm/sec) are normal for a *pseudo*-octahedral complex. The values for the Sn(II) complex are somewhat abnormal for a Sn(II) complex ($\delta = 0.29$ mm/sec, Line width = 1.65 mm/sec) and are interpreted as indicative of metal–metal bonding in the molecular structure.

INTRODUCTION

In an effort to complete our studies of a new dithiolate ligand (cyclopentadienedithiocarboxylate, $cpdtc^{2-}$) which has been shown to produce novel electronic structures in many transition element complexes,[1–6] we have chosen to prepare and study a few examples of non-transition element compounds. This ligand was proposed to exist predominately in resonance form B (Scheme 1) since the five membered ring would be aromatic ($4n+2$, $n=1$). As such the dithio acid behaves as a strong π-acceptor for the "out-of-plane" orbitals available in coordinated metals. The requirement that any nontransition element has an extensive coordination chemistry and the requirement that some probe of the electronic structure of the metal centre be available clearly led us to consider Sn(II) and Sn(IV) complexes. In addition, Hoskins *et al.*[7] have reported a Mössbauer study on the *bis*(diethyldithiocarbamate)tin(II) compound and it seemed that a comparison between the Mössbauer parameters of tin(II) dithiolates and dithiocarbamates could also be of interest.

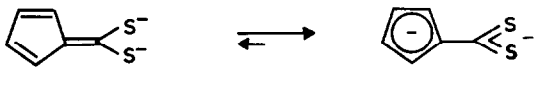

A ⟷ B

Scheme 1

EXPERIMENTAL

Materials. $SnBr_2$ and $SnBr_4$ were obtained from Research Organic/Inorganic Chemical Corp. Na_2(cpdtc) was obtained by a modification of the original procedure.[2] All other reagents were treated as before.[1]

Preparation of complexes. The tin complexes can be prepared by the reaction of $SnBr_2$ or $SnBr_4$ with stoichiometric quantitites of Na_2(cpdtc) and isolated by addition of tetraethylammonium bromide.

$[(C_2H_5)_4N]_2Sn(C_5H_4CS_2)_2$. Typically, 0.535 millimoles of $SnBr_2$ were mixed with 1.07 mmole of disodium cyclopentadienedithiocarboxylate in acetonitrile under argon at −30°C. The solution was stirred for 30 min and allowed to warm to room temperature. After stirring at ambient temperature for an additional 30 min, 1.07 mmole of tetraethylammonium bromide were added and the reaction mixture was stirred for 2 hr. The mixture was filtered under argon to remove solid sodium bromide, concentrated under vacuum, and chilled to −30°C. The resulting fine, air-sensitive, reddish-brown crystals were gathered and stored under argon. Analysis Calcd for $[(C_2H_5)_4N]_2Sn(C_5H_4CS_2)_2$: C, 50.98; H, 7.33; N, 4.25. Found, C, 50.80; H, 7.19; N, 4.33%.

$[(C_2H_5)_4Sn(C_5H_4CS_2)_3$. The Sn(IV) complex was prepared in a manner and scale similar to the Sn(II) complex, using three equivalents of the ligand. The resulting air-sensitive crystals were of a golden-brown color. Analysis Calcd for $[(C_2H_5)_4N]_2Sn(C_5H_4CS_2)_3$: C, 51.06; H, 6.55; N, 3.50; S, 24.05; Sn, 14.83. Found: C, 51.14; H, 6.64; N, 3.63; S, 23.93; Sn, 14.99%.

Analyses. All analyses were obtained from Galbraith Laboratories Inc., Knoxville, Tenn.

Spectroscopic measurements. IR spectra were obtained by use of Nujol nulls employing a Perkin-Elmer Model 457 spectrophotometer. The NMR spectra were obtained on a Jeolco 100 MHz instrument. Since high resolution data were required, sealed precision-bore sample tubes were run under conditions of high amplitude, high filter, and slow (40 min) scan times. J-coupling constants were obtained as previously explained[5] by use of a computer simulation program written by Bothner-By and Castellano.[8] The Mössbauer spectra were obtained using a drive unit and electronics package supplied by Austin Science Associates, Inc., Austin, Texas.[4] Samples were run at 78 and 298 K and are referenced against SnO_2.[9]

*Author to whom correspondence should be addressed.

RESULTS AND DISCUSSION

Mössbauer spectral results

Sn(cpdtc)$_3^{2-}$, The singlet shape of the Mössbauer spectrum at 78 K (Fig. 1) coupled with the stoichiometric ligand to metal ratio indicate the Sn(IV) is nearly octahedrally coordinated with three bidentate sulfur ligands.[10] Furthermore, the lack of a room temperature Mössbauer effect is consistent with the presence of a presumed symmetric complex with only van der Waals forces in the lattice.[11–13] The Mössbauer spectrum at 78 K is characterized by an isomer shift of $+1.05 \pm 0.02$ mm/sec with respect to SnO_2 and a line width of 1.05 ± 0.06 mm/sec. *Sn(cpdtc)*$_2^{2-}$. The somewhat broadened singlet in the Mössbauer spectrum for the Sn(II) complex (Fig. 2) indicates some unresolved quadrupole interaction. (line width = 1.65 ± 0.06 mm/sec at 78 k). Interestingly, however, a very low isomer shift of $+0.29 \pm 0.06$ mm/sec at 78 K with respect to SnO_2 is not typical of Sn(II) complexes but in fact is more in the range of Sn(IV) compounds. There is some evidence that diorganotin(II) compounds (R_2Sn) whiich are often found to have similarly low isomer shifts form metal–metal bonds leading to dimeric or polymeric systems.[14–17] The larger recoil free fraction observed at 298 K (isomer shift = $+0.12 \pm 0.12 \pm 0.07$ mm/sec with respect to SnO_2; line width = 1.30 ± 0.03 mm/sec) is consistent with some strong interaction between neighboring molecules.

Nuclear magnetic resonance results

The proton NMR spectra of both the Sn(II) and Sn(IV)

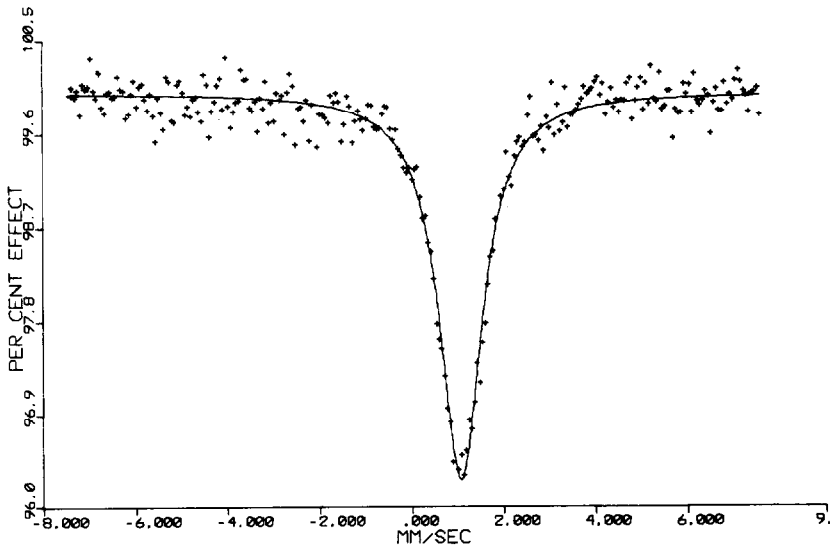

Fig. 1. Mossbauer spectrum of $[(C_2H_5)_4N]_2[Sn(C_5H_4CS_2)_3]$ at 78 K.

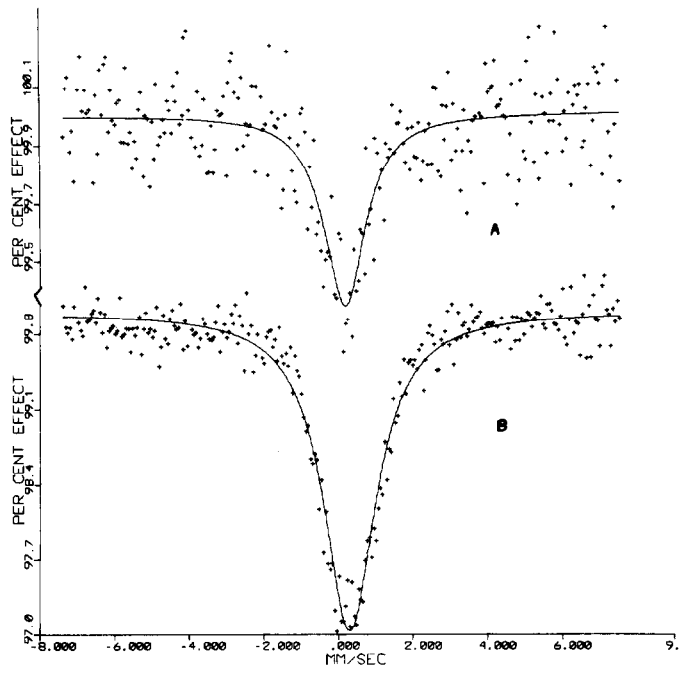

Fig. 2. Mossbauer spectra of $[(C_2H_5)_4N]_2[Sn(C_5H_4CS_2)_2]$ at 295 K (Curve A) and at 78 K (Curve B).

complexes are characteristic of an AA'BB' system. The detailed coupling constants for these complexes as well as those for the Na_2cpdtc compound are shown in Table 1. The J-coupling constants represent the best computer fit with a simulated spectrum.[5,8]

A relationship between proton NMR and degree of aromatic character in cyclopentadienides has been proposed by Smith, Watson and Chiranjeevi[18] and further examined by Ammon *et al.*[19,20] where the bond order (p) has been directly related to aromaticity. Streitwieser has proposed that in π systems, single bonds will have $p < 0.4$, aromatic bonds will have $p = 0.5$–0.7, and that double bonds will exhibit $p > 0.8$.[21] A plot of J-coupling constants vs bond order can be found in Fig. 3 for a number of selected compounds.[18] The J-coupling constants for $cpdtc^{2-}$, its Sn(II) and Sn(IV) complexes, and the derivative of $cpdtc^{2-}$, S,S'-ethylene-t,6'-dimercaptofulvene, are also plotted on the same graph and approximate bond orders can be obtained (Table 2). Two items are of immediate interest. It is apparent that the ligand alone has a great deal of aromatic character and the resonance structure B above weighs heavily in the overall bonding scheme. The Sn(II) and Sn(IV) NMR data indicate that the complexed ligand shows less aromatic character. Since we have previously shown that d^{10} [Zn(II) and Cd(II)] transition element complexes of this ligand result in a ligand

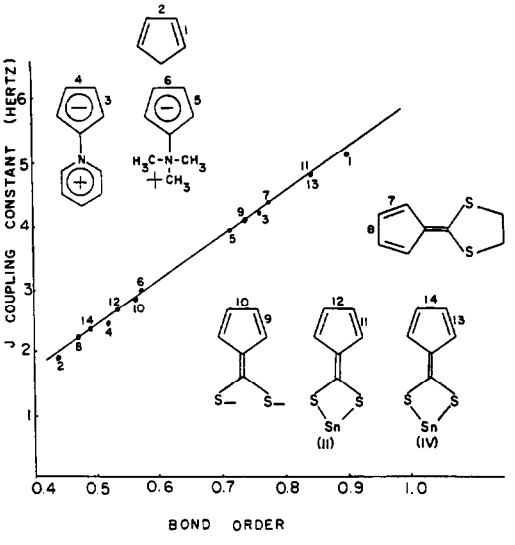

Fig. 3. A plot of bond order vs J coupling constant (Hz).

Table 2. Bond orders for $(cpdtc)^{-2}$, $Sn(II)(cpdtc)_2^{-2}$[a], $Sn(IV)(cpdtc)_3^{-2}$, and S,S'-ethylene-6,6'-dimercaptofulvene

	p^{1-2}	p^{2-3}
$cpdtc^{-2}$	0.73	0.56
$Sn(II)(cpdtc)_2^{-2}$	0.84	0.53
$Sn(IV)(cpdtc)_3^{-2}$	0.84	0.50
$C_5H_4CS_2C_2H_4$	0.78	0.48

[a]The J-coupling constants were plotted against bond orders for known compounds.[18] Experimentally derived coupling constants for the dithiolates were plotted on this same graph, bond orders were extrapolated, and are presented.

form with significant aromatic character,[5] the lack of a similar behaviour here is a little surprising. Yet, we may be observing an example of an energy mismatch of ligand orbitals and Sn orbitals.

In addition, the similarity of the NMR data for both the Sn(II) and Sn(IV) complexes would indicate that the ligand itself is probably not responsible for the unusually low isomer shift for the Sn(II) complex. These results suggest a strong metal–metal interaction in the Sn(II) complex. Hoskins *et al.*[7] have reported that the *bis*(diethyldithiocarbamate)tin(II) compound showed an isomer shift of 0.46 mm/sec (adjusted to SnO_2 standard). The crystal structure of that compound showed a *monomeric* structure with the bidentate ligands bridging one axial and one equatorial position of a pseudo-trigonal bipyramidal structure. The application of valence bond theory which has traditionally been very successful as a predictive tool in the main group elements, would also predict a trigonal-bipyramidal for a monomer or a pseudo-octahedral geometry for a dimer or polymer system. Again, the similarily of the NMR data for the Sn(II) and octahedral Sn(IV) complex taken together with the large recoil free fraction at 298 K observed in the Mössbauer spectrum suggest some polymeric system with metal–metal bonding. Attempts to obtain single crystals of the Sn(II) complex in order to obtain an X-ray crystal structure have not been successful to date.

Acknowledgement—We thank Prof. H. L. Ammon of the University of Maryland and Dr. J. J. Tufariello of State University of New York at Buffalo for the use of computer programs. R. D. B. gratefully acknowledges support from the Camille and Henry Dreyfus Foundation. R. D. B. also acknowledges some very useful suggestions by a referee.

Table 1. NMR parameters of disodium cyclopentadienedithiocarboxylate and its Sn(II) and Sn(IV) complexes[a]

	τ[b]	$\Delta A,B$	J_{12}	J_{23}	J_{13}	J_{14}
$Na_2(cpdtc)$[c]	4.02	.997	4.04	2.81	2.04	2.50
$Sn(cpdtd)_2^{2-}$	3.87	.638	4.77	2.65	1.94	2.65
$Sn(cpdtc)_3^{-2}$	3.88	.561	4.77	2.36	1.65	2.36

[a]values for Δ and J are presented in Hz
[b]centre of ring proton spectrum
[c]replaces less accurate data in reference 2

REFERENCES

[1]P. C. Savino and R. D. Bereman, *Inorg. Chem.* 1973, **12**, 173.
[2]B. J. Kalbacher and R. D. Bereman, *Inorg. Chem.* 1973, **12**, 2997.
[3]B. J. Kalbacher and R. D. Bereman, *Inorg. Chem.* 1975, **14**, 1417.
[4]R. D. Bereman, M. L. Good, B. J. Kalbacher and J. Buttone, *Inorg. Chem.* 1976, **15**, 618.
[5]B. J. Kalbacher and R. D. Bereman, *J. Inorg. Nucl. Chem.* 1976, **38**, 471.
[6]R. D. Bereman and D. N. Nalewajek, *Inorg. Chem.* 1976, **15**, 2981.
[7]B. F. Hoskins, R. L. Martin and N. M. Rohde, *Aust. J. Chem.* 1976, **29**, 213.
[8]A. A. Bothner-By and S. Castellano, LAOCN3, Mellon Institute, Pittsburgh, Pennsylvania, 1966.
[9]C. A. Clausen and M. L. Good, *Inorg. Chem.* 1970, **9**, 817.
[10]C. H. Stapfer and R. H. Herber, *Inorg. Nucl. Chem. Lett.* 1974, **10**, 161.
[11]J. D. Donaldson, *Progress in Inorganic Chemistry* (Edited by F. A. Cotton), Vol. 8, p. 287. Interscience, New York, 1976.
[12]R. C. Poller, J. N. R. Ruddick, B. Taylor and D. L. B. Toley, *J. Organometal. Chem.* 1970, **24**, 341.
[13]J. L. K. F. deVries and R. H. Herber, *Inorg. Chem.* 1972, **11**, 2458.
[14]V. S. Shpinel, V. A. Kryukhanov and N. N. Delyagin, *Sov. Phys. JETP* 1962, **14**, 1256.
[15]R. E. Rundle and D. H. Olson, *Inorg. Chem.* 1964, **3**, 596.
[16]D. H. Olson and R. E. Rundle, *Inorg. Chem.* 1963, **2**, 1310.
[17]V. I. Gol'danskii, V. Ya. Rochev and V. V. Khrapov, *Dokl. Akad. Nauk. SSSR* 1964, **156**, 909.
[18]W. B. Smith, W. H. Watson and S. Chiranjeevi, *J. Am. Chem. Soc.* 1967, **89**, 1438.
[19]H. L. Ammon and G. L. Wheeler, *Chem. Commun.* 1971, 1032.
[20]H. L. Ammon and L. A. Plastas, *Chem. Commun.* 1971, 356.
[21]A. Streitwieser, *Molecular Orbital Theory for Organic Chemists*, p. 172. Wiley, New York (1961).

Polyhedron Vol. 1, No. 2, pp. 191–193, 1982
Printed in Great Britain.

0277-5387/82/020191-03$03.00/0
Pergamon Press Ltd.

SOLVENT EFFECTS ON THE ELECTRONIC SPECTRUM OF THE HEXATHIOCYANATOCHROMATE (III) ANIONS. A REVISED OCTAHEDRAL CRYSTAL FIELD SPLITTING PARAMETER FOR THE THIOCYANATE ION

V. ALEXANDER, J. L. HOPPÉ and M. A. MALATI*
Mid-Kent College of Higher and Further Education, Chatham, ME5 9UQ, England

(*Received* 4 *September* 1981)

Abstract—An early report on the solvent dependence of the electronic spectra of complex ions considered the electrostatic effect of solvent molecules in the second coordination sphere, on the position of the absorption bands.[1] Solvent effects on the ligand field bands for solutions of $K[Cr(NH_3)_2(NCS)_4]$ have been discussed by Adamson[2] who emphasised a correlation between the solvent shifts in the spin-allowed bands and the shifts in the quartet-doublet bands. This work describes the effects of various solvents on the electronic absorption spectra of $[Cr(CNS)_6]^{3-}$.

INTRODUCTION

Using solutions of $[Cr(H_2O)_6]$ $(ClO_4)_3$ in alcohols, King *et al.* assigned maximum absorption peaks to partially solvated species.[3,4] The spectra of the latter complex in various solvents have been studied by Gutmann and Melcher who compiled the octahedral crystal field splitting parameter, Δ_0, for numerous ligands including solvent molecules.[5] Some mixed chromium (III) complexes containing coordinated solvent molecules have been obtained as solids.[6,7]

EXPERIMENTAL

$K_3[Cr(NCS)_6]\cdot 4H_2O$ was prepared by both the dry[8] and wet[9] methods. The solids obtained (I and II, respectively) were recrystallised from methanol.[8] By heating to constant weight at 110°C, the anhydrous solids: III and IV, respectively, were obtained and stored in a vacuum desiccator over conc. H_2SO_4. $(C_5H_6N)_3[Cr(NCS)_6]\cdot H_2O$ (preparation V) was prepared from solid II.[8] Heating at 60°C to constant weight produced the anhydrous solid VI. Preparation V and VI were kept in the dark in a vacuum desiccator since they are photosensitive.[8]

Because of their hygroscopic nature, the purity of preparations I–IV was ascertained not by chemical analysis but by the identical wavelengths of maximum absorption, λ_{max}, of their aqueous solutions with the published data.[1,10] Loss in weight of solid V at 60°C was 5.5% (calc. $H_2O = 5.5\%$). Chemical analysis of preparation VI[8] gave the following results: % C = 39.1 (39.3), % N = 19.4 (19.6), % H = 2.8 (2.8); the values between parentheses are the calculated percentages.

A. R. dimethylformamide, DMF, and A. R. dimethylsulphoxide, DMSO, were dried using recommended procedures.[11] The other A. R. solvents were used without further purification. The spectra of the filtered solutions were recorded in 10 mm quartz cells in a Unicam SP800 spectrophotometer and the values of λ_{max} were determined using a Perkin Elmer Coleman 55 spectrophotometer, checking the wavelength scale with standard K_2CrO_4 solution. Spectral data were obtained for freshly prepared solutions, for solutions aged for a week in the dark and for solutions heated at 80°C for different periods. The approximate concentrations were 0.012 and 0.003–0.006 M for the potassium and pyridinium salts, respectively. Solid state spectra of preparations III and IV were also recorded.

RESULTS AND DISCUSSION

The wavelengths, λ_{max}, of the lowest energy spin-allowed band for freshly prepared solutions are collected in Table 1, which includes Δ_0 values calculated from the energy of the responsible transition: $^4A_{2g} \rightarrow {}^4T_{2g}$. If it is assumed that Δ_0 for the thiocyanate ligand is 212.7 kJ mol^{-1} (corresponding to the confirmed literature value of λ_{max} in aqueous solution i.e. 564 nm[1,10]) and if the solvent shift in λ_{max} is ascribed to electrostatic effects, it is expected that the shifts would depend on the dipole moment and the size of the solvent molecule.[1]

However, λ_{max} in the five non-aqueous solvents was 554 ± 1 nm (Table 1) although their molecules have different dipole moments and/or sizes.

On the other hand, if the solvent shift is ascribed to the replacement of the thiocyanate ligand by solvent molecules, λ_{max} in the non-aqueous solvents is expected to shift to longer wavelengths (> 564 nm) on the basis of the published Δ_0 values for these solvents.[5]

It is suggested that the correct value of Δ_0 for the thiocyanate ligand is 216.5 ± 0.4 kJ mol^{-1} (corresponding to $\lambda_{max} = 554 \pm 1$ nm). This is confirmed by the diffuse reflectance spectra of preparations III and IV for which the recorded λ_{max} was ~ 550 nm, which is distinctly different from λ_{max} of the aqueous solution.

It can be argued that the literature Δ_0 and λ_{max}, obtained for aqueous solutions, are shifted from the true values as a result of the replacement of thiocyanate ligands by water molecules. The aquation of $[Cr(NCS)_6]^{3-}$ is reported to be rapid even in the dark and is further accelerated by light.[12] The small shifts in λ_{max} for the aqueous solution of complex IV heated at 80°C and for its solution in 7.7 M NH_4CNS (see Tables 1 and 2) are in agreement with this explanation. Δ_0 for a mixed complex $[MA_nB_{6-n}]$, containing the ligands A and B, may be calculated from the law of average environment:[13]

$$\Delta_0 = \frac{1}{6}[n\Delta_0{}^A + (n-6)\Delta_0{}^B] \qquad (1)$$

where the superscripts A and B refer to the two ligands. Equation (1) was used to calculate Δ_0 and hence λ_{max} for $[Cr(NH_3)_2(NCS)_4]^-$. Taking the literature values[5] for NH_3 and NCS^-, the calculated λ_{max} was 526 nm compared to the experimental value of 518 nm.[2] However, when the suggested revised value of Δ_0 for NCS^- is used, the computed λ_{max} was 520 nm, which is close to the experimental λ_{max}.

*Author to whom correspondence should be addressed.

Table 1. The absorption bands of $[Cr(NCS)_6]^{3-}$ in different solvents

Solvent	H_2O	7.7 M NH_4CNS	MeOH	EtOH	iso-PrOH	DMSO	DMF
λ_{max}/nm	*564	562 (560)	553	*555	553	554 (555)	554 (553)
$\tilde{\nu}$ /cm^{-1}	17730	17795	18085	18020	18085	18050	18050
Δ_o/kJ mol^{-1}	212.7	213.4	216.9	216.1	216.9	216.5	216.5
λ'/nm	*419	-	409	*410	415	408 (413)	407 (412)
λ(C.T.1)/nm	*309	-	309	308 (311)	308	-	-
λ(C.T.2)/nm	[a] 234	-	234	234	234	-	-
λ(C.T.?)/nm	218	-	210	211	211	-	-

Values in parentheses are for preparation VI. The remaining values refer to preparation IV.
*Identical values for the two preparations.
[a]Partially masked.

Table 2. The wavelengths of the absorption bands, λ_{max}, for solutions of $[Cr(NCS)_6]^{3-}$ in aged solutions in different solvents or after heating at 80°C and the approximate number, *n*, of thiocyanate ligands replaced by the solvent

Solvent	H_2O	MeOH	EtOH	iso-PrOH	DMSO	DMF
Aged soln.	564	568	568	564	554	554
n	3	2-3	2	1-2	0	0
1 hr. at 80°C	566 (567)	569	568 (562)	564	573 (565)	570 (573)
n	3-4	2-3	2	1-2	1-2	3
2 hrs. at 80°C	566	570	569	-	583	575
n	3-4	3	2	-	2-3	4
3 hrs. at 80°C	-	-	-	-	595	580
n	-	-	-	-	3-4	5
4 hrs. at 80°C	-	-	-	-	596	585
n	-	-	-	-	3-4	6

Values in parentheses are for preparation VI. The remaining values refer to preparation IV.

Table 2 contains the observed λ_{max}'s for solutions aged for one week or heated at 80°C for different intervals. The approximate† value of *n*, the number of solvent molecules replacing the thiocyanate ligand, is also given in Table 2. Equation (1) and the corrected Δ_0 for NCS^- were used for the calculation. When comparing Tables 1 and 2, it can be seen that the solvents used fall into two groups: those which replace the thiocyanate readily (water and alcohols) and those which replace the thiocyanate only on heating (DMSO and DMF).

The wavelengths λ' of the absorption bands ascribed to the transition: $^4A_{2g} \rightarrow {}^4T_{1g}$, are also included in Table 1. The values of λ' are less accurate than λ_{max} because the former were estimated from recorded spectra. However, the λ' values exhibit the same expected trend as found for λ_{max}. From the average λ' in the non-aqueous solvents, the configuration interaction parameter[13] was estimated as 97 kJ mol^{-1} using Δ_0 = 216.5 KJ mol^{-1}. λ' shifted to longer wavelengths on heating the solutions at 80°C in a similar way to the shift in λ_{max}.

The intense UV absorption bands: CT1 and CT2, also given in Table 1, are ascribed to charge transfer from ligand to metal.[14] The proximity of the values obtained in all the solvents studied is not surprising. The position and intensity of an absorption band at 210–218 nm, also included in Table 1, suggests that it is also a charge transfer band. Structured absorption in the region 250–

†Because the values of Δ_0 for the solvents[5] cluster near Δ_0 for the thiocyanate, the calculated figures for *n* are only approximate.

265 nm, found for solutions of the pyridinium but not the potassium salt in H_2O or EtOH, is due to the cation.

Acknowledgements—Thanks are due to Dr. R. Thomas for carrying out the reflectance spectra.

REFERENCES

[1]J. Bjerrum, A. W. Adamson and O. Bostrup, *Acta Chem. Scand.* 1956, **10**, 329.
[2]A. W. Adamson, *J. Inorg. Nucl. Chem.* 1966, **28**, 1955.
[3]D. W. Kemp and E. L. King, *J. Am. Chem. Soc.* 1967, **89**, 3433.
[4]C. C. Mills and E. L. King, *ibid* 1970, **92**, 3017.
[5]V. Gutmann and G. Melcher, *Mh. Chem.* 1972, **103**, 624.
[6]K. R. Ashley and R. E. Hamm, *Inorg. Chem.* 1966, **5**, 1645.
[7]J. Casabó, J. Ribas, V. Cubas, G. Rodriguez and F. J. Fernandez, *Inorg. Chim. Acta* 1979, **36**, 183.
[8]W. G. Palmer, *Experimental Inorganic Chemistry.* Cambridge University Press, Cambridge, 1962.
[9]G. Brauer, *Handbook of Preparative Inorganic Chemistry*, 2nd Edn, Vol. 2. Academic Press, New York, (1965).
[10]C. K. Jorgensen, *Advances in Chemical Physics* 1963, **5**, 33.
[11]*Vogel's Textbook of Practical Organic Chemistry*, 4th Edn. Longman, London (1978).
[12]E. E. Wegner and A. W. Adamson, *J. Am. Chem. Soc.* 1966, **88**, 394.
[13]D. Sutton, *Electronic Spectra of Transition Metal Complexes.* McGraw-Hill, Maidenhead (1968).
[14]H-H. Schmidtke, *Berichte der Bunsengesellschaft* 1967, **71**, 1138.

Polyhedron Vol. 1, No. 2, pp. 195–199, 1982
Printed in Great Britain.

0277–5387/82/020195–05$03.00/0
Pergamon Press

PFEIFFER EFFECT OPTICAL ACTIVITY DEVELOPED IN LANTHANIDE TRIS(PYRIDINE-2,6-DICARBOXYLATE) COMPLEXES BY CHIRAL TARTRATE SUBSTRATES

FANSHI YAN† and HARRY G. BRITTAIN*‡
Chemistry Department, Seton Hall University, South Orangs, NJ 07079, U.S.A.

(*Received* 18 *September* 1981)

Abstract—Optical activity has been induced in the title complexes through outer-sphere complexation with L-tartaric acid, and with several carboxyl and hydroxyl esters. The optical activity was studied in the Tb(III) and Eu(III) complexes by means of circularly polarized luminescence (CPL) spectroscopy, and the symmetry changes associated with the adduct formation were followed by examining the hypersensitive absorption of the Ho(III) complexes. Optical activity was found to be induced by each substrate, although the nature of the outer-sphere interaction was necessarily different in the various systems. It was found in every case that the presence of a (R,R)-tartrate substrate led to enrichment of the Λ-isomer of the lanthanide complexes.

INTRODUCTION

The Pfeiffer effect is the appearance of optical activity in a racemic mixture upon addition of some other optically active compound,[1,2] and can be used to obtain the chiroptical spectra of a metal complex which is too labile to be chemically resolved. This effect has primarily been investigated for positively charged transition metal complexes of aromatic polypyridines, although some work has been carried out on tetrahedral and negatively charged complexes.[3] Dissymmetric transition metal complexes have even been used to induce optical activity in racemic mixtures of other transition metal complexes.[4] All these studies appear to require the presence of either a hydrogen bonding or an electrostatic associative mechanism to account for the observed chirality, and the Pfeiffer effect is thought to reflect a perturbation of the enantiomer interconversion of the racemic mixture which results from complexation with the chiral environmental substance.

On the other hand, essentially no attention had been paid to possible Pfeiffer effect studies of lanthanide complexes until we demonstrated that such effects could be measured for the *tris*-derivatives of dipicolinic acid (DPA, or pyridine-2,6-dicarboxylic acid) with Tb(III). This particular complex is ideal for such studies in that it has essentially D_3 symmetry in solution[5] and thus consists of a pair of highly labile enantiomers, and also the chelate rings contain the aromatic rings which appear to be necessary for the Pfeiffer effect to be measured. In our previous studies, we have shown that the effect can be measured when $[Cr(en)_3]^{3+}$,[6] L-ascorbic acid,[7] proline-type amino acids,[8] or L-histidine[8] is present as the environmental substance. Thus, while the $[Tb(DPA)_3]^{3-}$ complex contains a 9-coordinate lanthanide ion, the full range of Pfeiffer effects is seen to be possible. Finally, we have examined a wide variety of monoamine- and diaminocarboxylic acids,[9] and have been able to correlate the sign of the induced optical activity with the absolute configuration of the preferred Tb(III) enantiomer.

In the present work, we present studies of the optical activity induced in $[Eu(DPA)_3]^{3-}$, $[Tb(DPA)_3]^{3-}$, and $[Ho(DPA)_3]^{3-}$ as a result of interactions with L-tartaric acid, and with several derivatives of this chiral environmental substance. Tartaric acid has been extensively employed for Pfeiffer effect studies of transition metal complexes,[10–13] and derivatives of this ligand have been used to determine the nature of the interactions.[12] In our work, we have studied the induced optical activity by means of circularly polarized luminescence (CPL) spectroscopy rather than the more conventional method of circular dichroism (CD) spectroscopy, since the Tb(III) and Eu(III) complexes are known to emit strongly (and the *f–f* absorption bands are extremely weak).

EXPERIMENTAL

The $[Ln(DPA)_3]^{3-}$ complexes (we shall use Ln to signify the members of the lanthanide series in general) were prepared by mixing stock solutions of Ln(III) and pyridine-2,6-dicarboxylic acid in a 1:3 stoichiometric ratio. The lanthanide ions were obtained as the 99.9% oxides (Kerr–McGee), and the stock solutions were prepared by dissolving the oxide in the minimum amount of 11.6 M $HClO_4$ and neutralizing to pH 3 with NaOH. The dipicolinic acid was used as received from Aldrich. In a previous work, $Na_3Tb(DPA)_3 \cdot 15H_2O$ was prepared and used for the induced optical activity studies, but no difference in results was noted when comparing the two methods of complex preparation.[8] The concentration of $[Ln(DPA)_3]^{3-}$ used in all spectroscopic studies was found to be 13 mM after all dilutions were performed.

The environmental substances used in the present study were L-tartaric acid, DL-tartaric acid, meso-tartaric acid, (+)-dimethyl tartrate, (+)-diethyl tartrate, Dibenzoyl-L-tartaric acid, and Di-*p*-toluoyl-L-tartaric acid; all substances were used as received from Aldrich. The absolute configurations of the two asymmetric atoms in the chiral substrates are available from the literature,[14] and the (R,R)-enantiomers were used in every case. Spot-checks using the (S,S)-enantiomers revealed no trace of stereoselectivity. All chiroptical spectra merely reversed sign if unnatural tartrate substances were used, but all quantitative results remained invariant.

The optical activity of the Tb(III) and Eu(III) complexes was monitored by studying the circular polarization within the luminescence bands. For the $[Tb(DPA)_3]^{3-}$ complex, the $^5D_4 \rightarrow {}^7F_5$ transition at 545 nm was studied to the greatest extent since it is now well established that this band represents the strongest Tb(III) emission and also shows the most intense CPL spectra. The other Tb(III) emission bands correspond to transitions from the $^5D_4$ level to the $^7F_6$ (490 nm), $^7F_4$ (582 nm), and $^7F_3$ (622 nm)

*Author to whom correspondence should be addressed.
†Visiting Scholar from the Department of Chemistry, Sichaun University, Chengdu, Sichaun, People's Republic of China.
‡Teacher–Scholar of the Camille and Henry Dreyfus Foundation, 1980–1985.

levels, but these were only examined briefly to compare to earlier work.[8] For the $[Eu(DPA)_3]^{3-}$ complex, the $^5D_0 \rightarrow {}^7F_1$ (595 nm) and $^5D_0 \rightarrow {}^7F_2$ (613 nm) transitions were studied in all cases. The relatively high symmetry of the $Ln(DPA)_3^{3-}$ complexes (D_3) in aqueous solution was shown by the lack of a measurable $^5D_0 \rightarrow {}^7F_0$ transition (this band is both electric and magnetic dipole forbidden, and is only seen if axial symmetry is absent in the complex).

All CPL and total luminescence (TL) spectra were obtained on a medium-resolution spectrometer constructed in our laboratory for this purpose, and whose operation has been described in detail.[15] The $[Tb(DPA)_3]^{3-}$ and $[Eu(DPA)_3]^{3-}$ complexes were excited at 295 nm, taking advantage of the fact that the DPA ligand absorbs quite strongly at this wavelength and is capable of sensitizing the lanthanide ion emission. The emission spectra were analyzed by a 0.5 m grating monochromator at 1 nm resolution, and further increases in spectral resolution did not lead to an improvement of the bandshape features. The TL and CPL spectra are obtained in proportional arbitrary units, with the TL being defined as $I = \frac{1}{2}(I_L + I_R)$ and the CPL as $\Delta I = (I_L - I_R)$; I_L and I_R represent the emitted intensities of left- and right-circularly polarized light. The ratio of these quantities, $\Delta I/I$, is termed the luminescence dissymmetry factor (g_{lum}), and this quantity is dimensionless. No other absolute quantal parameters were obtained. It was generally found that the TL intensity did not depend strongly on the nature or concentration of added tartrate substrate, and that the dissymmetry factor was an excellent measure of the degree of induced optical activity in the $[Ln(DPA)_3]^{3-}$ complex.

The interaction between the chiral substrates and the $[Ln(DPA)_3]^{3-}$ complexes was also investigated by examining the $^5I_8 \rightarrow {}^5G_6$ absorption of $[Ho(DPA)_3]^{3-}$ at 450 nm. This particular band is one of the "hypersensitive" lanthanide transitions which display intensity and wavelength variations as a function of the metal ion environment. Data were obtained on a Cary 11 UV/VIS recording spectrophotometer.

The pH of all solutions was obtained using an Orion model 701A pH meter, employing a glass microcombination electrode which could be directly inserted into the spectrophotometer and fluorescence cuvettes. The system was calibrated daily using phosphate buffers.

RESULTS AND DISCUSSION

Addition of any of the (R,R)-tartrate substrates to a solution of either $[Tb(DPA)_3]^{3-}$ or $[Eu(DPA)_3]^{3-}$ resulted in the appearance of CPL in the lanthanide ion emission bands. The CPL associated with the Eu(III) complexes tended to be more difficult to measure than for the corresponding Tb(III) complexes, but this difference can be ascribed to the much lower quantum yield of emission in the $[Eu(DPA)_3]^{3-}$ complex. In this paper, we shall detail the results of the Tb(III) complexes, but will refer to the Eu(III) complexes were necessary. It should be emphasized that the observed experimental trends are the same for both sets of complexes, and all differences can be traced to small variations in the association constants of the adduct complexes.

The CPL associated with the various Tb(III) emission bands is essentially the same as what we had presented before,[8] and, therefore, only the $^5D_4 \rightarrow {}^7F_5$ emission band is illustrated in Fig. 1. The invariance of the CPL lineshape in all transition bands during the course of all previous studies and in the present work is evidence that no inner-sphere complexation between the chiral substrates and the lanthanide ion takes place, and that we are dealing with a true Pfeiffer effect. The strong degree of optical activity within the $^5D_4 \rightarrow {}^7F_5$ transition (relative to the other Tb(III) emission bands) provides further support for the predictions of Richardson[16] regarding *f–f* optical activity.

Pfeiffer effect CPL in $[Eu(DPA)_3]^{3-}$ has been reported in one of our previous studies involving monoamino- and diaminocarboxylic acids,[9] and the representative spectra shown in Figs. 2 ($^5D_0 \rightarrow {}^7F_1$) and 3 ($^5D_0 \rightarrow {}^7F_2$) greatly resemble those previously published. As in the case of the Tb(III) complexes, all (R,R)-tartrate substrates led to the same set of CPL lineshapes. In our previous work, we presented correlations with solid-state CPL studies on chiral D_3 Eu(III) complexes, and these arguments enabled us to conclude that if the sign of the $^5D_0 \rightarrow {}^7F_1$ CPL band was negative in sign then the Δ-isomer of the $[Eu(DPA)_3]^{3-}$ complex was present in the greater excess. Examination of Fig. 2 reveals that using (R,R)-tartrates as environmental substances leads to positive CPL in the $^5D_0 \rightarrow {}^7F_1$ band region, and we, therefore, conclude that the Λ-isomer of the $[Ln(DPA)_3]^{3-}$ complexes is being enriched as a result of the outer-sphere interaction. It is highly likely that the same isomer would be preferred

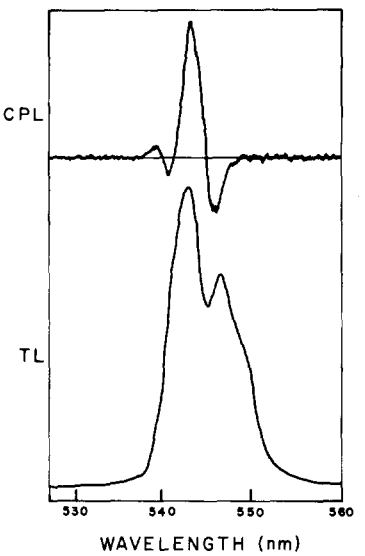

Fig. 1. Total luminescence (TL, lower trace) and circularly polarized luminescence (CPL, upper trace) of the $[Tb(DPA)_3]^{3-}$/(+)-dimethyl tartrate complex at pH 4.5. The data are shown in arbitrary units for the $^5D_4 \rightarrow {}^7F_5$ Tb(III) transition.

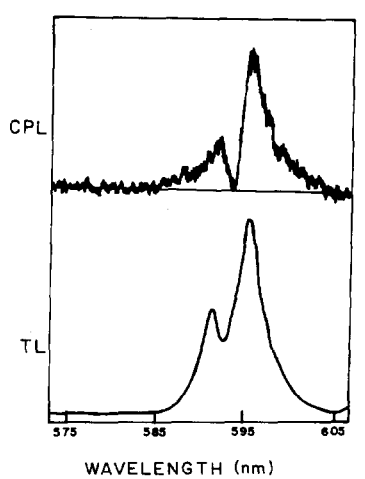

Fig. 2. TL (lower) and CPL (upper) spectra obtained for the $[Eu(DPA)_3]^{3-}$/(+)-dimethyl tartrate complex at pH 4.5 within the $^5D_0 \rightarrow {}^7F_1$ transition.

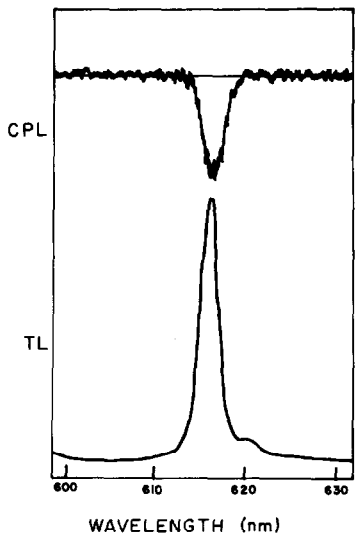

Fig. 3. TL (lower) and CPL (upper) spectra obtained for the $[Eu(DPA)_3]^{3-}$/(+)-dimethyl tartrate complex at pH 4.5 within the $^5D_0 \rightarrow {}^7F_2$ transition.

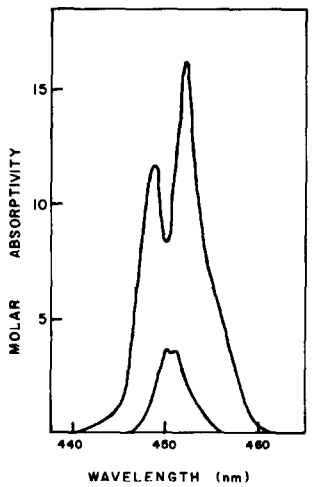

Fig. 4. Absorption spectra of Ho(III) within the hypersensitive $^5K_8 \rightarrow {}^5F_6$ transition. Data are shown for 15 mM solutions of Ho(III)/H_2O (lower trace) and $[Ho(DPA)_3]^{3-}$ (upper trace). The spectrum for $[Ho(DPA)_3]^{3-}$/(+)-dimethyl tartrate is identical with the upper trace.

with the $[Tb(DPA)_3]^{3-}$ adducts since the lanthanide complexes tend to have very similar patterns of reactivity, and we therefore conclude that positive CPL in the $^5D_4 \rightarrow {}^7F_5$ Tb(III) emission band signifies the presence of the Λ-isomer. This conclusion is in accord with our earlier observation that the Δ-isomer of $[Tb(DPA)_3]^{3-}$ led to the presence of negative CPL in this emission band.

Further information regarding the nature of the adduct complexes was obtained by examining the absorption spectra of the $^5I_8 \rightarrow {}^5G_6$ hypersensitive band in $[Ho(DPA)_3]^{3-}$. It is well known that certain *f–f* transitions of lanthanide ions are quite sensitive to environmental changes,[17] and any perturbation of the D_3 symmetry of the Ho(III) complex should be manifested by a change in the lineshape or magnitude of the hypersensitive transition. In Fig. 4 we show the absorption spectra obtained for Ho^{3+}/H_2O and $[Ho(DPA)_3]^{3-}$ within the $^5I_8 \rightarrow {}^5G_6$ absorption, and one notes that the absorption of this particular band increases by approximately 4.5 times when the Ho(III) ion is complexed. However, upon addition of 20-fold excesses of any of the tartrate substrates no change in either intensity or bandshape could be detected. We conclude that the environment of the lanthanide ion in the $[Ln(DPA)_3]^{3-}$ complexes remains approximately the same in the outer-sphere adduct. This symmetry must remain fairly high (at least axial), since examination of Fig. 2 reveals no trace of the $^5D_0 \rightarrow {}^7F_0$ Eu(III) emission band (this band is both electric and magnetic dipole forbidden in octahedral symmetries).

We now turn our attention to the chemical information revealed by the CPL studies, and will begin with the parent compound, tartaric acid. While no induced optical activity was ever observed at any pH values when *meso*- or DL-tartaric acid was employed as the environmental substance, CPL was observed at low pH when L-tartaric acid was used. This induced CPL was found to maximize at pH 2.2, and vanished if the solution pH was raised to 5. These trends are illustrated in Fig. 5, where the CPL of the $^5D_4 \rightarrow {}^7F_5$ Tb(III) transition is shown both as a function of pH and as a substrate concentration.

Since pK_a values associated with the two carboxyl proton ionizations of tartaric acid are known to be 3.95 and 2.82,[18] it would appear that production of the fully protonated ligand is necessary for the observation of the Pfeiffer effect. This trend is not at all surprising when one remembers that the $[Ln(DPA)_3]^{3-}$ complexes and the tartrate anion are of the same sign and would not interact as a result of the electrostatic repulsion. The lack of optical activity at higher pH values indicates that the simple existence of an asymmetric environment is not a sufficient condition for production of a Pfeiffer effect in the $[Ln(DPA)_3]^{3-}$ complexes.

In our previous works, we have outlined methods by which the association constant of the $[Ln(DPA)_3]^{3-}$/substrate adducts may be calculated.[8,9] These methods take advantage of our observations in

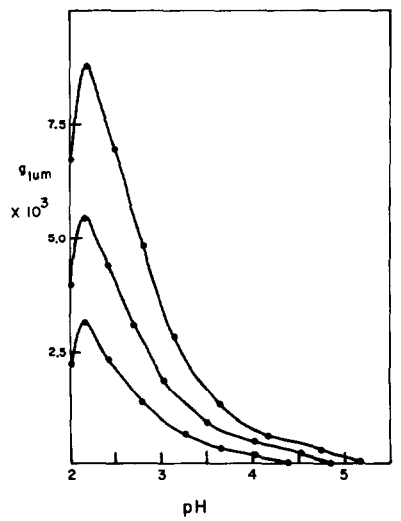

Fig. 5. Dependence of the luminescence dissymmetry factor of $[Tb(DPA)_3]^{3-}$/L-tartaric acid solutions upon solution pH. Data are shown for tartaric acid concentrations of 0.2 M (upper trace), 0.1 M (middle trace), and 0.05 M (lower trace).

Table 1. Formation constants of the $[Tb(DPA)_3]^{3-}$/L-tartaric acid adduct at various pH values

pH	K_1
2.0	2.26
2.2	3.44
2.5	2.36
3.0	0.98
3.5	0.42
4.0	0.24
4.5	0.12

Each formation constant is reliable to ± 0.05

several Pfeiffer systems involving $[Tb(DPA)_3]^{3-}$ which demonstrate that the limiting dissymmetry factor within the $^5D_4 \rightarrow {}^7F_5$ Tb(III) transition is 0.022,[6-8] with the sign of the CPL being determined by the absolute configuration of the environmental substance. Table 1 contains the association constants calculated for $[Tb(DPA)_3]^{3-}$/L-tartaric acid at various pH values. Analagous results for the $[Eu(DPA)_3]^{3-}$ adducts were not calculated due to the low values observed for the induced CPL, but are expected to be of similar magnitude. The trend toward lower assocation constants below pH 2.2 reflects destruction of the $[Tb(DPA)_3]^{3-}$ comples as a result of acid hydrolysis.

Quite different behaviour was noted when esters of L-tartaric acid were allowed to interact with the $[Ln(DPA)_3]^{3-}$ complexes. To avoid hydrolysis of the tartrate esters, all work was concentrated between pH values of 3.0 and 6.0. Within these pH ranges, the CPL induced in $[Tb(DPA)_3]^{3-}$ luminescence bands was independent in both sign and magnitude of the solution pH. The CPL within the $^5D_4 \rightarrow {}^7F_5$ emission band was always positive, indicating that only the Λ-isomer of the Tb(III) complex was preferred as a result of the outer-sphere interaction. The magnitude of the induced CPL depended critically on the concentration of chiral substrate, as is shown in Fig. 6 for dimethyl and diethyl tartrate (carboxyl esters) and in Fig. 7 for dibenzoyl-L-tartaric and di-*p*-toluyl-L-tartaric acid (hydroxyl esters).

For the carboxyl esters, it is clear that increasing the steric nature of the substrate results in decreased degrees of interaction with the $[Tb(DPA)_3]^{3-}$ complex, and the

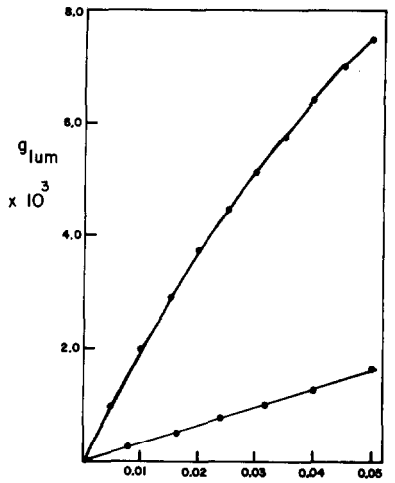

Fig. 6. Dependence of the luminescence dissymmetry factor with carboxyl ester concentration. Results are shown for (+)-dimethyl tartrate (upper trace) and (+)-diethyl tartrate (lower trace).

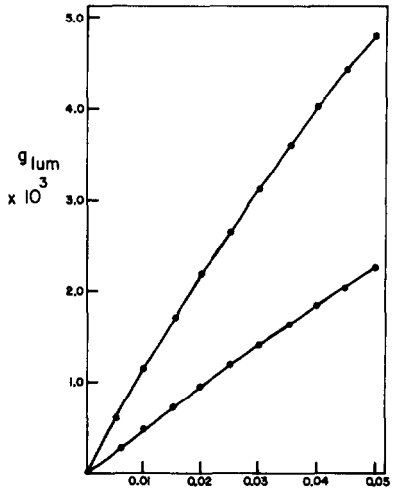

Fig. 7. Dependence of the luminescence dissymmetry factor on hydroxyl ester concentration. Data are shown for dibenzoyl-L-tartaric acid (lower trace) and di-*p*-toluyl-L-tartaric acid (upper trace).

Table 2. Formation constants of the $[Tb(DPA)_3]^{3-}$ and $[Eu(DPA)_3]^{3-}$ adducts with various tartrate substrates

Substrate	K_1 (Tb^{3+} complex)	K_1 (Eu^{3+} complex)
(+)-Dimethyl Tartrate	11.37	10.70
(+)-Diethyl Tartrate	1.64	(a)
Dibenzoyl-L-tartaric acid	2.37	(a)
Di-p-Toluyl-L-Tartaric Acid	5.95	5.59

(a) The CPL associated with these adducts was too weak to permit accurate calculation of the formation constant.

The error associated with all other constants is ±0.05.

association constants shown in Table 2 are proof of this trend. We postulate that in these complexes, the alcoholic -OH groups of the substrates are responsible for bonding to the $[Ln(DPA)_3]^{3-}$ complexes, as has been indicated for transition metal complexes.[12] Presumably, the bonding involves hydrogen bonding between the chelate and substrate, with solvent molecules bridging the two substances. It is quite likely that when L-tartaric acid binds to $[Ln(DPA)_3]^{3-}$ at low pH it does so by a similar mechanism.

On the other hand, the results obtained for the hydroxyl esters reveal a very different pattern, and the assoication constants shown in Table 2 confirm the trend. Unlike the transition metal Pfeiffer effects just mentioned,[12] esterification of the hydroxyl groups does not eliminate the Pfeiffer effect when the $[Ln(DPA)_3]^{3-}$ complexes are used. In addition, substitution on the benzoyl ring leads to a greater degree of interaction. These results point toward hydrophobic interactions between the substrate rings and the DPA chelate rings as being the mode of bonding by which the Pfeiffer effect develops in this situation, and may even involve charge transfer complexation. Such interactions have been noted in other transition metal Pfeiffer systems.[19] We have previously obtained strong evidence to indicate that hydrophobic interactions can be very important in the Pfeiffer effects of $[Ln(DPA)_3]^{3-}$ systems.[19]

Acknowledgement—This work was supported by the Camille and Henry Dreyfus Foundation, through a Teacher-Scholar Award to HGB.

REFERENCES

[1]P. E. Schipper, *Inorg. Chim. Acta* 1975, **12**, 199.
[2]S. Kirschner, N. Ahmad, C. Munir and R. J. Pollock, *Pure and Appl. Chem.* 1979, **51**, 913.
[3]R. J. Pollock, S. Kirschner and S. Policec, *Inorg. Chem.* 1977, **16**, 522.
[4]K. Miyoshi, Y. Wada and H. Yoneda, *Inorg. Chem.* 1978, **17**, 751.
[5]H. Donato and R. B. Martin, *J. Am. Chem. Soc.* 1972, **94**, 4129.
[6]J. S. Madaras and H. G. Brittain, *Inorg. Chem.* 1980, **19**, 3841.
[7]J. S. Madaras and H. G. Brittain, *Inorg. Chim. Acta* 1980, **42**, 109.
[8]H. G. Brittain, *Inorg. Chem.* 1981, **20**, 3007.
[9]F. Yan, R. A. Copeland and H. G. Brittain, *Inorg. Chem.*, 1982, **21**.
[10]S. F. Mason and B. J. Norman, *Chem. Comm.* 1965, 335.
[11]K. Ogino and V. Saito, *Bull. Chem. Soc. Jap.* 1967, **40**, 826; K. Ogino, *ibid.* 1969, **42**, 3043.
[12]Y. Kuroda, K. Miyoshi and H. Yoneda, *Inorg. Chim. Acta* 1978, **28**, 211; *ibid.* 1978, **31**, L453.
[13]K. Miyoshi, C. E. Oh and H. Yoneda, *Bull. Chem. Soc. Jap.* 1980, **53**, 2815.
[14]W. Klyne and J. Buckingham, *Atlas of Stereochemistry*, 2nd Ed. Oxford Press, New York, 1978.
[15]H. G. Brittain, *J. Am. Chem. Soc.* 1980, **102**, 3693.
[16]F. S. Richardson, *Inorg. Chem.* 1980, **19**, 2806.
[17]D. E. Henrie, R. L. Fellows and G. R. Choppin, *Coord. Chem. Rev.* 1976, **18**, 199.
[18]A. E. Martell and R. M. Smith, *Critical Stability Constants.* Plenum Press, New York, 1977.
[19]C. C. Lee and P. Hemmes, *Inorg. Chem.* 1980, **19**, 485.

Polyhedron Vol. 1, No. 2, pp. 201–202, 1982
Printed in Great Britain.

0277-5387/82/020201-02$03.00/0
Pergamon Press Ltd.

REACTIVITY OF *CIS* DICHLORODIAMMINEPLATINUM(II) (CISPLATIN) TOWARD SELECTED NUCLEOPHILES

C. M. RILEY, L. A. STERNSON*, A. J. REPTA and S. A. SLYTER
Department of Pharmaceutical Chemistry, The University of Kansas, Lawrence, KS 66045 U.S.A.

(*Received* 23 *September* 1981)

Abstract—Results are reported for the reaction of *cis*-dichlorodiammineplatinum(II) ("cisplatin") with various nucleophiles in aqueous solution at constant ionic strength ($\mu = 0.5$) and 30°C. The reactivity is described in terms of linear free energy relationships between the logarithm of the second order rate constants and two established indices of nucleophilicity, i.e. electrode potentials, $E°$ and nucleophilic reactivity constants, n^0_{Pt} (based on reactivity of *trans*-$[Pt(PY)_2Cl_2]$ in methanol). New nucleophilic reactivity constants, $(n^0_{Pt})'$ are reported based on "cisplatin" reactivity in water.

INTRODUCTION

Biomedical interest in *cis*-dichlorodiammineplatinum(II) ("cisplatin") (CDDP) has been stimulated by its proven clinical

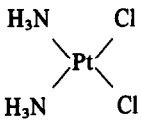

activity in the control of a variety of cancers which are difficult to treat.[1] On the molecular level, this activity appears to be related to replacement of the chloride ligands by endogenous nucleophiles incorporated in macromolecules. Accordingly, it was of interest to determine whether the reactivity of "cisplatin" toward a variety of nucleophiles could be described in terms of a linear free energy relationship.

EXPERIMENTAL

Crystalline "cisplatin" was obtained from the National Cancer Institute, Bethesda, Maryland and used as received. All other chemicals were of analytical grade. "Cisplatin" (3.3×10^{-4} M to 6.7×10^{-4} M) was incubated in aqueous solution containing the appropriate nucleophile at 30°C. Each nucleophile was studied at five or more concentrations in the presence of at least a fifteen fold molar excess of nucleophile. The nucleophiles were maintained in their anionic form by the use of a phosphate buffer (pH 6.5, 10^{-3} M) and the ionic strength was adjusted to 0.5 M with sodium nitrate.

The "cisplatin" concentration was determined by HPLC using an ODS Hypersil column pretreated with 0.5% hexadecyltrimethylammonium bromide (HTAB) and a mobile phase of 10^{-4} M HTAB in water. In all cases, the products of the reaction were well separated from "cisplatin". The chromatographic aspects of this study have been reported elsewhere.[2]

RESULTS AND DISCUSSION

We have investigated the reactivity of "cisplatin" towards a variety of nucleophiles (Nu) (Table 1) in aqueous solution at 30°C ($\mu = 0.5$). The loss of "cisplatin" followed the two term rate law

$$R = k_1 [CDDP] + k_2 [CDDP] [Nu] \quad (1)$$

involving a term for the solvent pathway (described by k_1) and a term, k_2, for the pathway involving direct reagent displacement. Excess reagent was used and the pseudo-first order rate constant, k_{obs}, was determined by HPLC following both "cisplatin" disappearance and product formation.[2] This experimentally determined value was related to k_1 and k_2 according to eqn (2).

$$k_{obs} = k_1 + k_2 [Nu]. \quad (2)$$

For each nucleophile k_{obs} was determined at ≥ 5 concentrations of nucleophile. In all cases, linear relationships between k_{obs} vs [Nu] were observed, as predicted. The values of k_2 were determined by linear regression analysis and are reported in Table 1. Attempts were made to correlate this kinetic data with extrakinetic properties (i.e. nucleophilicity indices) of the reagents. The oxibase scale of $E°$ values has been widely used in such relationships to predict reagent nucleophilicity.[3] The k_2 values (Table 1) correlated with $E°$ (Fig. 1) according to the relationship (eqn 3)

$$\log k_2 = 1.65\, E° + 1.75 \quad r = 0.966 \quad n = 7. \quad (3)$$

Omitting the point for thiocyanate which is an obvious outlier (as similarly observed by Belluco *et al.*[4] for *trans*-$[Pt(PY)_2Cl_2]$) the relationship becomes (eqn 4)

$$\log k_2 = 1.66\, E° + 1.59 \quad r = 0.997 \quad n = 6. \quad (4)$$

Table 1. Second order rate constants, k_2, for reaction of "cisplatin" with selected nucleophiles and calculated nucleophilicity indices

Nucleophile	k_2[a] ($M^{-1} hr^{-1}$)	$(n^0_{Pt})'$[b]	n^0_{Pt}[c]	E^{0}[d]
H_2O	2.27×10^{-3}[e]	0.00	0.00	−2.60
Br^-	0.42	2.27	4.18	−1.04
N_3^-	0.62	2.44	3.58	−1.02
I^-	8.04	3.55	5.42	−0.54
SCN^-	28.2	4.10	6.65	−0.77
$(NH_2)_2CS$	187	4.91	7.17	0.42
$S_2O_3^{2-}$	129	4.38	7.34	0.30

[a]As defined by eqn (1) and determined according to eqn (2).
[b]Defined by eqn (7).
[c]Defined by eqn (5) (Ref. 5).
[d]Electrode potentials (Ref. 3).
[e]k_2 determined as aquation rate ($0.126\ hr^{-1}$) divided by solvent concentration (55.51 M).

*Author to whom correspondence should be addressed.

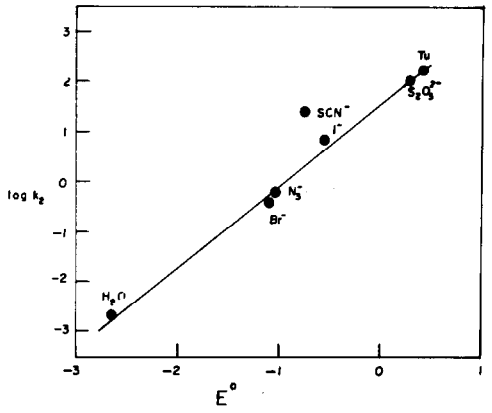

Fig. 1. Rates of reaction of "cisplatin" in water at 30°C with different nucleophiles as a function of their $E°$ values (eqn 3).

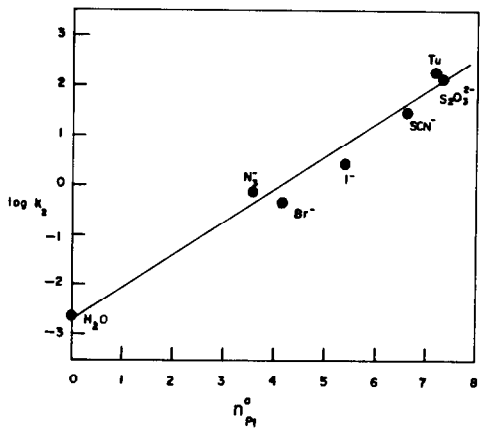

Fig. 2. Rates of reaction of "cisplatin" in water at 30°C with different nucleophiles as a function of their n^0_{Pt} values (eqn 6).

The existence of such outliers when correlating nucleophilicty with electrode potential led Belluco *et al.*[4] to the introduction of the nucleophilic reactivity constant, n^0_{Pt}, which is defined by eqn (5)

$$n^0_{Pt} = \log (k_y/k_s) \quad (5)$$

where k_y and k_s are the rate constants for the reaction of *trans*-$[Pt(PY)_2Cl_2]$ with nucleophile y and solvent, s, (in that study[4] methanol), respectively, at 30°C. Correlation of k_2 for "cisplatin" with n^0_{Pt} (Table 1) gave the relationship (eqn 6 and Fig. 2).

$$\log k_2 = 0.66\, n^0_{Pt} - 2.73 \quad r = 0.991. \quad n = 7. \quad (6)$$

The slope of the linear free energy relationship in eqn (6) is defined as the nucleophilic discrimination factor[4] and describes the sensitivity of the substrate to nucleophilic attack. The value for "cisplatin" in water (0.66) is similar to that previously described for $Pt(en)Cl_2$ in water[4] and indicates that these substrates behave similarly.

The slight scatter about the regression line (Fig. 2; eqn 6) confirms the conclusion of others[4,5] that substrate nature is important in determining reactivity. Accordingly, new reactivity constants, $(n^0_{Pt})'$ are defined according to eqn (7) using "cisplatin" as standard and water as solvent (where k_2 and k_1 are defined in eqn 1)

$$(n^0_{Pt})' = \log (k_2/k_1) + 1.74. \quad (7)$$

These values may prove more useful in linear free energy relationships involving compounds of biological interest since only divalent platinium compounds exhibiting *cis* geometry are biologically active[1] and n^0_{Pt} values[4,5] were determined with *trans* divalent platinum complexes, in organic media.

Acknowledgement—This work was supported by grants from the American Cancer Society (No. CH-149) and the National Institutes of Health (No. CA 24934).

REFERENCES

[1]A. W. Prestayko, In *Cisplatin: Current Status and New Developments* (Edited by A. W. Prestayko, S. T. Crooke and S. K. Carter), Chap. 1, pp. 1–7. Academic Press, New York (1980).
[2]C. M. Riley, L. A. Sternson, A. J. Repta and R. W. Siegler, *J. Chromatogr.*, 1982, in press.
[3]J. O. Edwards, *J. Am. Chem. Soc.* 1954, **76**, 1540.
[4]U. Belluco, L. Callalini, F. Basolo, R. G. Pearson and A. Tuns, *J. Am. Chem. Soc.* 1965, **87**, 241.
[5]F. Basolo and R. G. Pearson, *Mechanisms of Inorganic Reactions.* p. 395. Wiley, New York (1967).

Polyhedron Vol. 1, No. 2, pp. 203–208, 1982
Printed in Great Britain.

0277–5387/82/020203–06$03.00/0
Pergamon Press Ltd.

A STUDY OF SOME REACTIONS OF ACETYLACETONATOBIS(ETHYLENEDIAMINE)COBALT(III) ION IN SODIUM HYDROXIDE SOLUTION

L. STUART BARK
Chemistry Department, University of Salford, Salford, England

and

MICHAEL B. DAVIES* and STEVEN R. DAWSON
Science Department, Stockport College of Technology, Stockport, England

(*Received* 8 *June* 1981; *in revised form* 11 *November* 1981)

Abstract—The reactions of acetylacetonato cobalt (III) ion in sodium hydroxide solutions have been studied spectrophotometrically over a range of temperatures and hydroxide ion concentrations. The activation enthalpy, $\Delta H^{\neq}$ was 70.6 kJ mol^{-1} and the activation entropy, $\Delta S^{\neq}$ was -119 JK^{-1} mol^{-1}, with a rate law of $k_{obs} = k_2$ [OH$^-$]^2. A mechanism involving initial de-chelation of the acetylacetone ligand is suggested. The rate of exchange of methyl hydrogen of the acetylacetone ligand was studied, using proton nuclear magnetic resonance. The rate law was $k_{obs} = k$ [OH$^-$]. Initial de-chelation is also suggested as a mechanism for this process. The ^{13}C nuclear magnetic resonance spectrum of the complex is reported.

INTRODUCTION

The vast majority of studies of base hydrolysis reactions of octahedral cobalt (III) complexes have been on the loss of monodentate ligands in pentaammine-type complexes[1] or in the loss of monodentate ligands from *bis* (ethylenediamine) complexes where stereochemical information was required. There are comparatively few investigations of the base hydrolysis of bidentate complexes. The most detailed studies have been of the complex ion oxalato *bis*(ethylenediamine) cobalt (III). Several groups of workers have published the results of the base hydrolysis of this complex[2–4]. It is now well established that this reaction proceeds via a two-stage reaction and that the kinetics of the loss of oxalate involve terms which are first and second order in hydroxide concentration[2]. Farago *et al.* have investigated the base hydrolysis of the corresponding malonate complex and have found only a single stage reaction.[5] Anation reactions of diaqua *bis*(ethylenediamine) cobalt (III) ion and related complexes[6–8] have shown the existence of reasonably stable (isolatable from basic solution) monodentate oxalato complexes.[8] Similar studies of the reaction between acetylacetone and aquahydroxo *bis* (ethylenediamine) cobalt (III) ion[9] have shown that in basic solution there is no evidence for the formation of a monodentate acetylacetonato complex present in measurable quantities.

The proton nuclear magnetic resonance spectrum of acetylacetonato *bis*(ethylenediamine) cobalt (III) ion in deuterium oxide solution has been reported[10], but the ^{13}C nuclear magnetic resonance spectrum has not hitherto been determined. This paper reports the ^{13}C NMR spectrum in aqueous solution and a study of the proton NMR spectrum in basic deuterium oxide as well as a study of the rate-of-loss of acetylacetone in strongly alkaline aqueous solution at fairly high temperatures.

*Author to whom correspondence should be addressed.

EXPERIMENTAL

Reagents

Where available reagents were BDH Analar grade and were used without further purification unless otherwise stated. Water was distilled and passed down a column of Permutit "Biodeminrolit" mixed-bed resin.

Carbonate free sodium hydroxide solution was prepared as described by Vogel.[11] Solutions of the required concentrations were prepared by carefully withdrawing volumes from the stock solution and diluted with recently deionised water.

Acetylacetone was dehydrated with calcium sulphate and distilled under reduced pressure before use.

Acetylacetonato *bis*(ethylenediamine) cobalt (III) iodide was prepared using the method of Reid and Sargeson.[13] Analysis for $(C_2H_8N_2)_2Co(C_5H_7O_2)$; Calcd: Co 10.7 $C_2H_8N_2$ 21.8; Found: Co 11.2 $C_2H_8N_2$ 21.8%.

Instrumentation

UV-visible spectra were recorded on a Unicam SP 1800 or on a Perkin–Elmer 550 spectrophotometer, using stoppered silica cells of 1.0, 2.0 or 4.0 cm path length.

Proton nuclear magnetic resonance spectra were obtained using a Perkin–Elmer R12 spectrometer or a Varian CFT 20 spectrometer.

^{13}C nuclear magnetic resonance spectra were measured using a Jeol FX 90 Q spectrometer.

Kinetics were measured using a Perkin–Elmer 550 or a Unicam SP1800 spectrophotometer fixed at a wavelength of 402 or 510 nm where there was a large change in absorbance in each case. In some cases complete scans between 350 and 600 nm were obtained during the reaction.

The temperature was maintained using a Grant constant temperature bath with the liquid passing around the cell housing in the spectrometer. This gives temperature control which is in the region of ± 0.1 K of the desired temperature. The sodium hydroxide solution of the desired strength was made up to an ionic strength of 2.0 M using sodium perchlorate and thermostatted in the constant temperature bath. A sample of the solid complex was thermostatted at the same time in the same bath. 10 cm^3 of the sodium hydroxide solution was quickly withdrawn and transferred to the tube containing the solid complex. The solid dissolved rapidly on shaking and the mixture was then transferred to the thermostatted stoppered spectrophotometer

cell. The spectrometer at a fixed wavelength was then started and a trace of absorbance against time was automatically recorded. The runs at the two wavelengths gave the same rate constants, within experimental error. Good plots of $\ln(D_t - D_\infty)$ against t were obtained. The process was repeated over a range of temperatures and a number of hydroxide ion concentrations at each temperature.

Kinetics of isotope exchange was carried out by a similar procedure except that the constant temperature bath was maintained at the same temperature as the sample compartment of the NMR spectrometer and immediately on mixing the solutions of NaOD in D_2O with the complex ion, the solution was transferred in an NMR tube to the spectrometer. The solutions of NaOD were prepared by dissolving weighed amounts of sodium metal in the required volume of D_2O with dilution with D_2O if necessary.

RESULTS AND DISCUSSION

In 2.0 M sodium hydroxide solution, $[Coen_2(AcAc)]^{2+}$ ion undergoes a very slow reaction at room temperature. A conveniently measured rate is not achieved until about 60°C. The spectrum of this complex ion between 350 and 600 nm at room temperature does not vary significantly with variation of sodium hydroxide concentration. NMR studies have shown[10] that even in acid solution, the C–H proton exchanges with deuterium in D_2O and this change becomes very rapid in basic solution. However, the pK_a of the complexed acetylacetone must be very high, because of the absence of any change in the spectrum of the complex with variation of $[OH^-]$ up to 2.0 M. It is reasonable to suppose that the disturbance of the electronic system of the acetylacetone-metal ring, would result in significant spectral changes when a proton is removed.

The very slow reaction at room temperature indicates that there is no evidence for an initial rapid ring-opening reaction resulting in a monodentate acetylacetonato species, since the reaction is accurately first order in complex ion at higher temperature with no initial rapid absorbance change. This is not unexpected, because Sargeson *et al.*[9] in a study of the reaction between acetylacetone and $[Coen_2(H_2O)_2]^{3+}$, showed that there was no evidence for the initial formation of a stable monodentate acetylacetonato species.

The visible spectrum of the product is shown to be that of a *cis-trans* mixture of $[Coen_2(OH)_2]^+$ and compares well with that found in the literature and determined under similar conditions.[13] At the high temperatures used here, the *cis-trans* isomerism of $[Coen_2(OH)_2]^+$ is very fast[13] compared with the base hydrolysis of the complex. Thus, it is not expected that this will have any effect upon the kinetics of the reaction.

At the higher temperatures (65 and 70°C) small amounts of a brown precipitate were produced in the spectrophotometer cell, during reaction with the higher concentration of sodium hydroxide solution. This is a little surprising in view of the known stability of ethylenediamine complexes.[14] As a consequence of this effect the determination of the kinetics of the reaction at the highest concentration of hydroxide ion at 65 and 70°C was prevented. Under milder conditions, excellent first order plots of $\ln(D_t - D_{00})$ against t were obtained and

Table 1. Effect of variation of hydroxide ion concentration on the observed rate constant

Temperature/°C	Hydroxide Ion concentration/M	$10^5 k_{obs}/s^{-1}$
60.0	0.70	1.02±0.70
	1.00	2.88±0.63
	1.30	6.09±0.16
	1.50	7.89±0.01
	1.70	9.04±0.96
	1.80	10.6 ±0.8
	1.90	12.4 ±0.3
	2.00	14.2 ±0.2
65.0	1.00	5.64±0.22
	1.50	12.4 ±5.5
	1.80	16.2 ±2.7
71.0	0.30	1.37±0.41
	0.50	2.27±0.39
	0.70	3.10±0.38
	1.00	8.11±0.80
	1.50	16.8 ±5.4
	1.70	22.6 ±6.4

these were found to be linear for more than two half lives in every case. (D_t = absorbance at time t, D_∞ = final absorbance).

The hydroxide ion concentration was varied with the ion strength maintained at 2.0 up to 2.0 M. It can be seen from the results which are given in Table 1, that there is a rapid increase in observed rate constant (k_{obs}) with increasing [OH^-]. The rate of increase of k_{obs} is too fast to be due to a reaction which is first order in [OH^-]. Plots of k_{obs} against [OH^-]^2 at these temperatures are shown in Fig. 1. It can be seen from these that excellent linear plots are obtained which pass through the origin. This implies that the rate law for the reaction is:

$$k_{obs} = k_2[OH^-]^2. \quad (1)$$

Values of k_2 calculated from the slopes of the graphs shown in Fig. 1 are given in Table 2. These values were used to determine an activation enthalpy of 70.6 kJ mol^{-1} and an activation entropy of -119.0 JK^{-1} mol^{-1}.

This is an unusual rate law for the base hydrolysis of an octahedral cobalt (III) complex. There appear to be no other examples for the type of reaction though rate laws of the type

$$k_{obs} = k_1[OH^-] + k_2[OH^-]^2 \quad (2)$$

are common, particularly when the departing ligand is a carboxylate ion.[15] The above rate law bears some resemblance to that obtained for the base hydrolysis of the corresponding tetraammine oxalato complex ($[Co(NH_3)_4C_2O_4]^+$) in which the rate law at low temperature is

$$k_{obs} = k_1[OH^-] \quad (3)$$

and at high temperature is:

$$k_{obs} = k_2[OH^-]^2.$$

Table 2. Rate constants derived from plots of [OH^-]^2 against observed rate constants

Temperature/°C	$10^5 k_2/M^2s^{-1}$
60.0	3.30×10^{-5}
65.0	5.23×10^{-5}
71.0	7.73×10^{-5}

Various attempts have been made to interpret the mechanism of base hydrolysis involving second order terms in [OH^-].[15] Studies of fumarate, maleate and oxalate complexes among others have shown that in the monodentate complexes formed by these ligands the term second order in [OH^-] is the result of a pathway that involves O–C bond breaking. It is not easy to distinguish between O–C and O–Co bond breaking in the acetylacetonato complex, but the absence of two different dependences on [OH^-] concentration and the fact that no monodentate species is present in isolatable amounts suggest that the rate law for this reaction arises from an initial fast equilibrium forming the monodentate species.

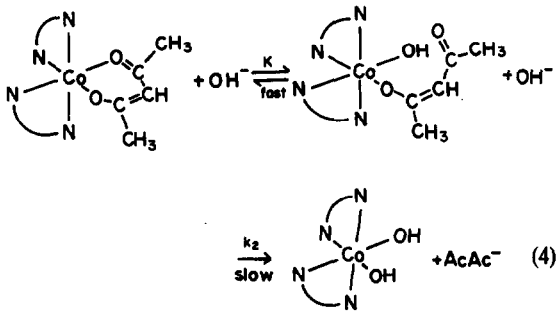

(4)

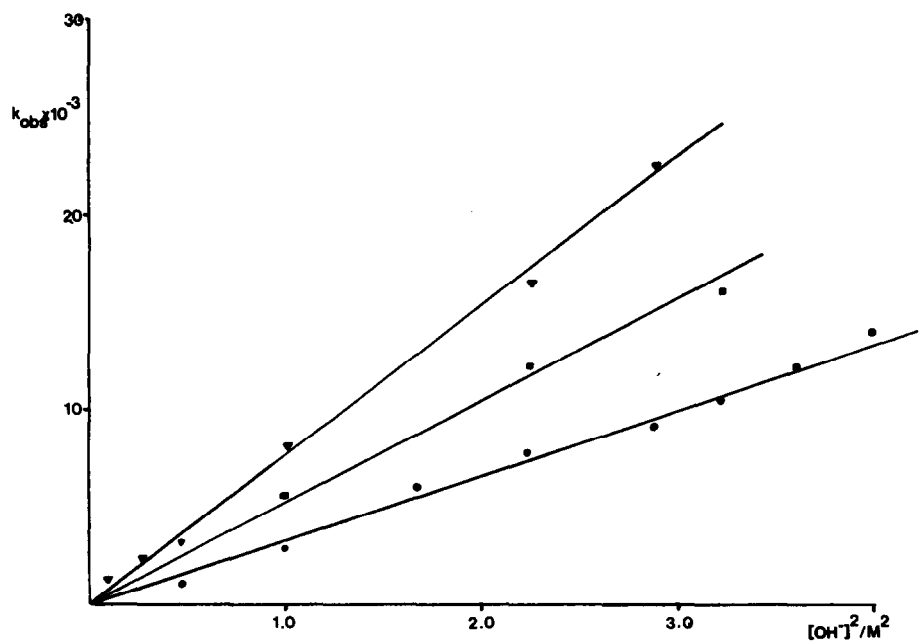

Fig. 1. Variation of observed rate constant with [OH^-]^2: ▼ = 344 K; ■ = 338 K; ● = 333 K.

The rate law corresponding to this mechanism can be shown to be:

$$k_{obs} = \frac{k_2 K[OH^-]^2}{1 + K[OH]}. \quad (5)$$

Thus, if the first reaction only occurs to a small extent, then this rate law becomes

$$k_{obs} = k_2 k [OH^-]. \quad (6)$$

The rate constants obtained from the graphs of k_{obs} against $[OH^-]^2$ are, therefore, composite rate constants. Some care has to be exercised, therefore on the interpretation of activation energy data derived from such graphs because the temperature dependence of k_2K will only reflect the true variation of k_2 if K remains effectively constant over the temperature range used. This does not appear to be a valid assumption and the variation of K with temperature depends on the sign of ΔH for the reaction, so that K may increase or decrease with temperature. This may account for the apparently low value of the activation enthalpy of this reaction if K varies in the opposite direction to k_2 with increasing temperature. The question of attack on carbon or cobalt remains a moot point, since either could give rise to an $[OH^-]^2$ term according to the above mechanism. Application of tracer techniques to this system which might resolve the above question would be complicated by the fact that under the harsh conditions used, the liberated acetylacetone undergoes rapid irreversible decomposition reactions.

The ^1H NMR spectrum of the acetylacetonatobis (ethylenediamine) cobalt (III) complex has been previously obtained in neutral and acid solution.[10] Under these conditions in D_2O, only exchange of the "active" CH hydrogen occurred. We have measured the proton NMR spectrum of the complex in a solution of NaOD in D_2O. There is no signal due to the CH proton in basic solution because this proton has already rapidly exchanged. Otherwise the spectrum compares well with the literature.[10] Scanning of this spectrum after various time intervals showed that the signal at 2.02 δ, which is attributed to the methyl protons, diminishes with time until it completely disappears. Thus, the methyl protons also exchange with deuterium. We felt that it was of interest to investigate the rate of disappearance of this signal and to see whether the rate was affected by the variation of deuteriooxide ion. There was no evidence over the time-scale used here for any exchange of the methylene protons of the ethylenediamine ligand (at 2.66 δ). These were, therefore, used as an internal standard to allow for instrumental variations in the area of the methyl protons peak. The variation in the intensity of these peaks was interpreted in terms of the ratio of the intensity of the methylene peak (I_{CH_2}) to the intensity of the methyl peak (I_{CH_3}). Plots of ln $(I_{CH_3}/I_{CH_2})^*$ are shown in Fig. 2 for four hydroxide ion concentrations. It can be seen that they are reasonably linear and it is, therefore, concluded that the disappearance of the CH_3 peak is a first-order reaction. The slopes of these graphs were used to determine the first order rate constant at each hydroxide ion concentrations. The values are given in Table 3. The rate increases with increasing hydroxide ion concentration in a way which suggest that the order with respect to OH^- is one. This is as expected for the mechanism:

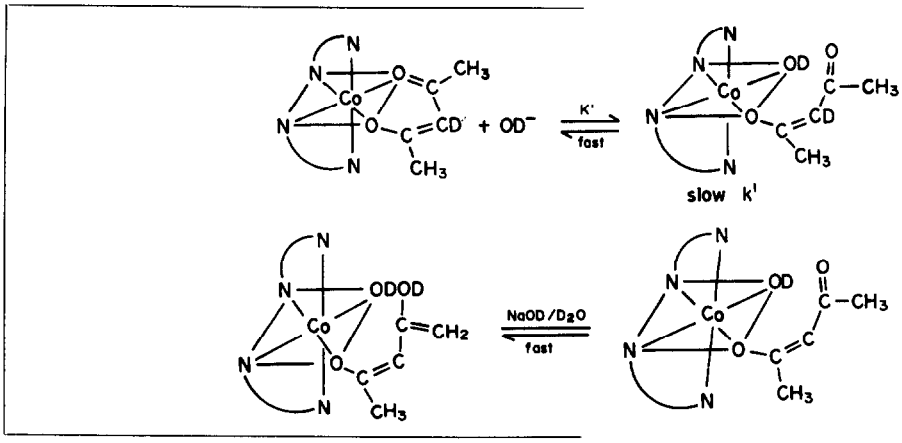

The observed rate constant for this reaction will be given by

$$k_{obs} = \frac{k' K[OH^-]}{1 + K[OH^-]} \quad (8)$$

and if K is small, this becomes:

$$k_{obs} = k' K [OH^-]. \quad (9)$$

It is not certain that de-chelation occurs before the keto-enol change followed by exchange takes place. However, observations of similar reactions with related complexes appear to support this mechanism. Farago *et al.*[16] have studied the ^{13}C and ^1H NMR spectra of malonato *bis*(ethylenediamine)-cobalt (III) complex in acid and basic solution and have concluded that dechelation occurs in basic solution and that in neutral solution the coordinated malonate group is stable. Furthermore, exchange of the methylene protons does not occur in neutral solution. In basic solution the malonato group

Table 3. Variation of isotope exchange rate constant with deuterooxide ion concentration at 308.6 K

OD^-/M	$10^3 k_{obs}/s^{-1}$
0.38	2.03±0.02
0.57	5.04±1.29
0.77	5.52±0.67
0.96	9.31±0.04

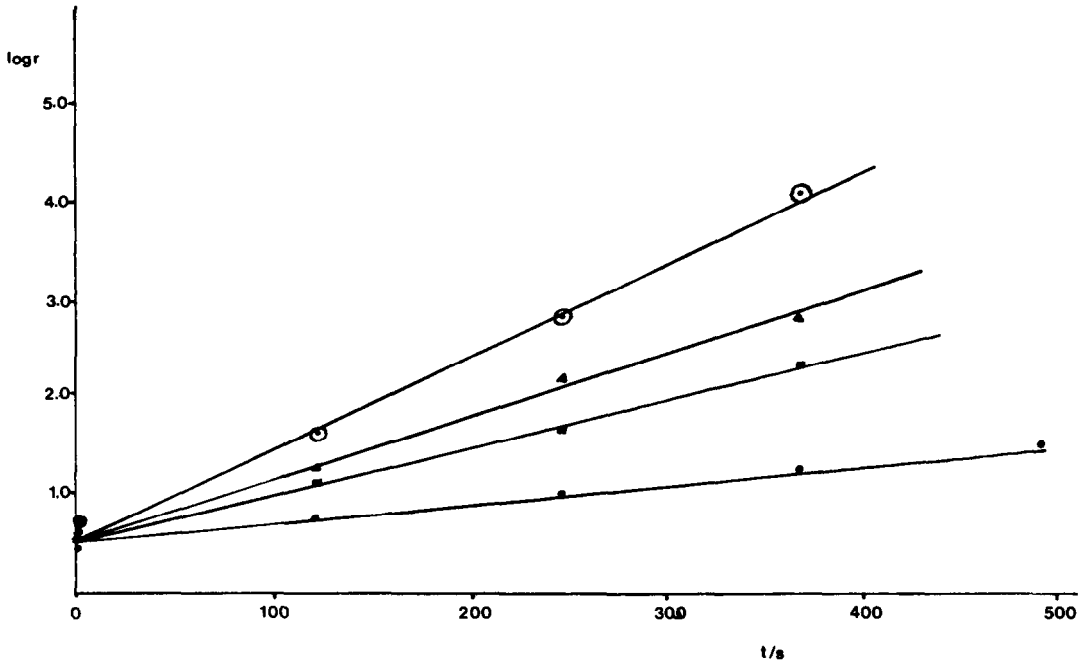

Fig. 2. Plot of log r (where $r = I_{cH_3}/I_{cH_2}$, see text) against time at 308.6 K for the NMR spectrum of acetylacetonato *bis*(ethylenediamine)-cobalt (III) ion in various concentrations of NaOD: ⊙ = 0.96 M NaOD; ▲ = 0.76 M NaOD; ■ = 0.57 M NaOD; ● = 0.38 M NaOD.

becomes de-chelated and they have shown that at the same time exchange of the methylene protons occurs.

The ^{13}C NMR spectrum of acetylacetonato *bis*(ethylenediamine) cobalt (III) ion in neutral 95% water, 5% deuterium oxide is shown in Fig. 3. By comparison with similar systems the signal at 27.6 ppm relative to trimethylsilane is assigned to the methyl carbons. Farago *et al.* have observed two signals from two non equivalent methylene groups in ethylenediamine in malonato *bis* (ethylenediamine) cobalt (III) ion. These were at 45.87 and 44.29 ppm and the values in this work at 44.75 and 46.62 ppm compare well with Farago's work. There is, thus, no evidence for de-chelation in neutral solution, where more than two ethylenediamine signals would be expected. The above mechanisms both depend upon only a small amount of de-chelated complex being formed in strongly basic solution and thus de-chelation in neutral solution is not expected. The shift at 99.76 ppm is attributed to the C–H carbon of acetylacetone. The value of 193.02 ppm for the carbonyl carbon which is coordinated to cobalt shows that it is considerably more shielded than the corresponding carbon in the malonato complex, which has a value of 179.5 ppm.[16] This additional shielding could possibly be due to the electron donating properties of the methyl group which is bonded directly to the carbonyl carbon.

CONCLUSION

In alkaline solution acetylacetonato *bis*(ethylenediamine) cobalt (III) ion is comparatively stable. However, at elevated temperatures it loses acetylacetone to form a *cis–trans* mixture of dihydroxo *bis*(ethylenediamine) cobalt (III) ion. NMR studies show that in addition to the well-known exchange properties of the C–H proton, the methyl protons are also active to exchange in strongly basic solutions. It is postulated that

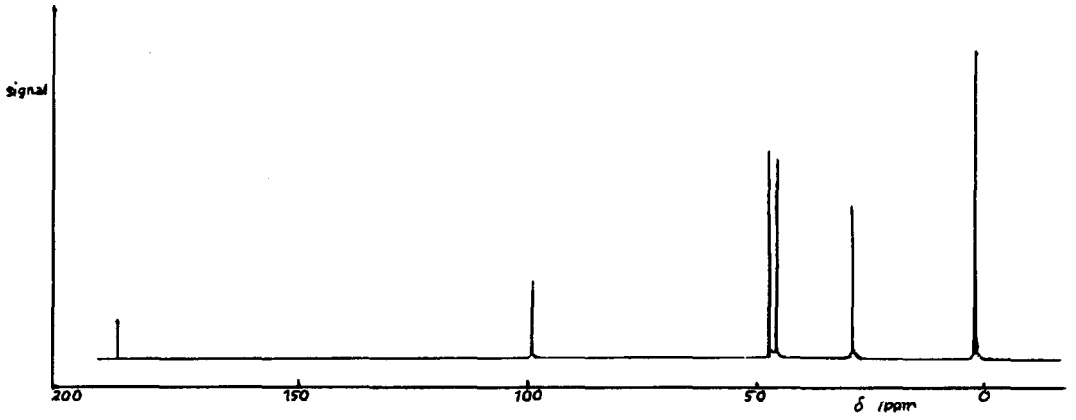

Fig. 3. ^{13}C NMR spectrum of aceylacetonato *bis*(ethylenediamine)-cobalt (III) ion in H_2O/D_2O (95:5).

many reactions in basic solution are usually preceded by reversible de-chelation of the acetylacetone which occurs only to a small extent.

Acknowledgements—The authors would like to thank Mr P. Hampson and I.C.I. Pharmaceuticals, Macclesfield for the ^{13}C NMR spectrum of acetylacetonato *bis*(ethylenediamine) cobalt (III) ion and Mr Hayes of Salford University for running ^{1}H NMR spectra. Also the extensive technical help of Mr D. Dawson is gratefully acknowledged. We would also like to thank a referee for useful comments.

REFERENCES

[1]F. R. Nordmeyer, *Inorg. Chem.* 1969, **8**, 2780, and references therein.
[2]C. Andrade and H. Taube, *J. Am. Chem. Soc.* 1964, **86**, 1328.
[3]M. E. Farago and C. F. V. Mason, *J. Chem. Soc.* (*A*) 1970, 3100.
[4]S. Sheel, D. R. Meloon and G. M. Harris, *Inorg. Chem.* 1962, **1**, 170.
[5]M. E. Farago, Coord. *Chem. Revs.* 1966, **1**, 66.
[6]M. B. Davies, *J. Inorg. Nucl. Chem.* in press.
[7]P. B. Brown and G. M. Harris, *Inorg. Chem.* 1968, **7**, 1872.
[8]S. C. Chan and G. M. Harris, *Inorg. Chem.* 1971, **10**, 1317.
[9]D. A. Buckingham, J. M. Harrowfield and A. M. Sargeson, *J. Amer. Chem. Soc.* 1973, **95**, 7281.
[10]R. J. Balahura and H. A. Lewis, *Can. J. Chem.* 1975, **53**, 1154.
[11]A. I. Vogel, Quantitative Inorganic Analysis, 3rd. Edn. Longmans–Green, London (1961).
[12]I. K. Reid and A. M. Sargeson, *Inorg. Synth. IX* 167.
[13]M. E. Farago, B. A. Page and C. F. V. Mason, *Inorg. Chem.* 1969, **8**, 2271.
[14]C. F. V. Mason and M. E. Farago, *J. Inorg. Nucl. Chem.* 1969, **42**, 131.
[15]L. S. Bark, M. B. Davies and M. C. Powell, *J. Inorg. Nucl. Chem.* 1978, **40**, 1661.
[16]S. Amirhaeri, M. E. Farago, J. A. P. Glucku, M. A. R. Smith and J. N. Wingfield, *Inorg. Chim. Act.* 1979, **33**, 57.

Polyhedron Vol. 1, No. 2, pp. 209–211, 1982
Printed in Great Britain.

0277–5387/82/020209–03$03.00/0
Pergamon Press

CONVENIENT SYNTHESES OF ZERO VALENT 2,2′-BIPYRIDINE AND RELATED COMPLEXES OF TRANSITION METALS

JENNIFER QUIRK and GEOFFREY WILKINSON*
Chemistry Department, Imperial College of Science and Technology, London, SW7 2AY, England

(*Received* 10 *December* 1981)

Abstract—The neutral *tris*-2,2′-bipyridine(bipy) and 1,10-phenanthroline(phen) compounds $Mbipy_3$ and $Mphen_3$ can be made conveniently in high yield by sodium amalgam reduction of the chlorides of Ti, Zr, Hf, V, Nb, Ta, Cr or better, for Mo, W and Re, the respective adducts $MoCl_4L$, WCl_4L and $ReCl_4(THF)$ in tetrahydrofuran containing the ligands. The Cr and Mo compounds can also be obtained from the dimeric acetates $M_2(CO_2Me)_4$. For vanadium, similar compounds have been obtained from 2,2′-dipyridylamine, 2,2′-dipyridyldisulfide and di-*t*-butyldiimine. Reduction of VCl_3 in THF containing one equivalent of 2,2′-bipyridine under CO gives the carbonyl $V(CO)_4bipy$. Interaction of $Vbipy_3$ with NO and CH_3I give respectively, $V(NO)bipy_3$ and $[V(CH_3)I(bipy)]$.

Although Herzog[1] has made a number of zero-valent transition metal complexes of 2,2′-bipyridine and 1,10-phenanthroline (L) by reduction using Mg, Li_2bipy, etc. of cationic $[ML_3]$ complexes or halides, in many cases the syntheses involved several steps and the yields were often low.[2] We find that the metal chlorides $TiCl_3$, $ZrCl_4$, $HfCl_4$, VCl_3, $NbCl_5$, $TaCl_5$ and $CrCl_3$ plus three equivalents of the ligand in tetrahydrofuran can be directly reduced by an excess of sodium amalgam at room temperature under an inert atmosphere for *ca.* 24 hr, to give deep purple to black solutions from which the highly air sensitive zerovalent complexes $Mbipy_3$ and $Mphen_3$ can be obtained in yields of 80% or more.

The direct reduction of the metal halides $MoCl_5$, WCl_6 and $ReCl_5$ did not proceed cleanly and gave a mixture of products. However, treatment of the adducts of the tetrachlorides, $MoCl_4L$, WCl_4L and $ReCl_4(THF)_2$ under identical conditions gave the respective ML_3 compounds.

The compounds $Crbipy_3$, $Crphen_3$, $Mobipy_3$ and $Mophen_3$ can also be prepared by the direct reduction of $M_2(CO_2Me)_4$, M = Cr, Mo, in THF by sodium amalgam. The cleavage of the metal–metal bond in such tetracarboxylates to give mononuclear species has been previously observed with isocyanide ligands.[3–5] The reductions probably proceed via interactions of the radical anions $bipy^-$.

The properties of the compounds, where known, are similar to those described by Herzog.[1] The new compounds $Zrphen_3$, HfL_3, $Nbphen_3$, TaL_3, $Mophen_3$, $Wphen_3$ and ReL_3 generally have similar properties being dark coloured, extremely air sensitive, and either diamagnetic or paramagnetic, according to whether the M^0 state has even or odd number of electrons. It may be noted that $Cobipy_2$ has recently been made by metal vapour synthesis,[6a] and Ru $bipy_3$ by electrolytic reduction of $[Ru\ bipy_3]^{2+}$ in MeCN.[6b]

For vanadium, the same reduction procedure allows synthesis of the corresponding complexes from 2,2′-dipyridylamine (1), 2,2′-dipyridyl disulfide (2) and di-*t*-butyldiimine (3); similar complexes of other metals can doubtless be made. So far only the zero-valent diazabutadiene complexes of nickel[7] and ruthenium[8] have been reported.

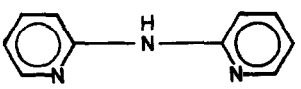

1

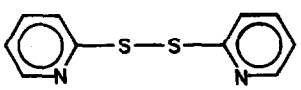

2

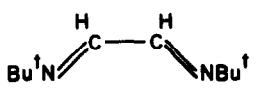

3

For vanadium, the reductions were also carried out under atmospheres of hydrogen, carbon monoxide and buta-1,3-diene, but only the VL_3 compounds were isolated. However, the reduction of VCl_3 under CO (2 atm) using only one equivalent of 2,2′-bipyridine gave the black microcrystalline compound $V(CO)_4bipy$.

Although $Vbipy_3$ does not react with CO or with H_2 at 100°C and 100 atm pressure, with methyl iodide it undergoes an oxidative-addition reaction to give an air-sensitive green solid $[V[Me)I(bipy)_2]$ and with nitric oxide to give a diamagnetic, white, 7-coordinate nitrosyl $V(NO)bipy_3$.

EXPERIMENTAL

Microanalyses were by Pascher (Bonn) and Imperial College Laboratories. All operations were performed under oxygen-free nitrogen or argon or *in vacuo*. Solvents were dried over sodium and distilled from sodium–benzophenone under nitrogen immediately before use. Petroleum had b.p. 40–60°C. Magnetic moments in solution were obtained using Evans' method and given as μ_{eff} in B.M. at 309 K. Analytical data are collected in the Table.

$MoCl_4(CH_3CN)_2$ and $WCl_4(CH_3CN)_2$,[9] and $ReCl_4(THF)_2$[10] were prepared by known methods.

Spectrometers: NMR Perkin–Elmer R32 (^1H, 90 MHz), Bruker WM 250 (^1H, 250 MHz). Data in ppm, referenced to $SiMe_4$. All the diamagnetic species had a rather complex spectrum centred the region 7.9–8.6 ppm due to the aromatic protons of the ligand. IR. Perkin–Elmer 597; spectra in Nujol mulls.

*Author to whom correspondence should be addressed.

Table 1. Analytical data for new compounds

Compound	Found (Required) %				M
	C	H	N	Other	
$Zrbipy_3$	64.5 (64.4)	4.3 (4.3)	15.3 (15.0)		530 (559)
$Zrphen_3$	68.9 (68.9)	3.8 (3.8)	13.1 (13.3)		600 (631)
$Hfbipy_3$	55.8 (55.7)	3.7 (3.7)	13.1 (13.0)		650 (646)
$Hfphen_3$	60.1 (60.1)	3.2 (3.3)	11.9 (11.7)		690 (718)
$Nbphen_3$	68.5 (68.3)	3.8 (3.8)	13.5 (13.3)		600 (633)
$Tabipy_3$	55.6 (55.5)	3.8 (3.7)	12.8 (12.9)		630 (649)
$Taphen_3$	59.8 (59.9)	3.4 (3.3)	16.1 (16.5)		750 (721)
$Mophen_3$	67.9 (67.9)	3.8 (3.8)	13.3 (13.2)		630 (634)
$Wphen_3$	59.5 (59.7)	3.3 (3.3)	11.7 (11.6)		690 (724)
$Rebipy_3$	55.0 (55.0)	3.6 (3.7)	12.9 (12.8)		620 (654)
$Rephen_3$	59.5 (59.5)	3.3 (3.3)	11.5 (11.5)		750 (726)
$V[C_5H_4N)_2NH]_3$	63.8 (63.8)	4.8 (4.8)	22.0 (22.3)		680 (711)
$V[(C_5H_4N)_2S_2]_3$	50.5 (50.6)	3.3 (3.4)	11.9 (11.8)	27.0 S (27.0)	520 (564)
$V[(Me_2C)NC_2H_2NCMe_2]_3$	65.0 (64.9)	10.8 (10.8)	15.3 (15.1)		520 (556)
$MoCl_4bipy$	30.6 (30.5)	2.2 (2.2)	7.1 (7.1)	36.1 Cl (36.0)	
$MoCl_4phen$	34.3 (34.5)	2.0 (1.9)	6.5 (6.7)	34.1 Cl (33.9)	
WCl_4bipy	24.9 (24.9)	1.7 (1.7)	5.7 (5.8)	29.7 Cl (29.4)	
WCl_4phen	28.5 (28.5)	1.7 (1.6)	5.5 (5.5)	28.0 Cl (28.0)	
$V(CO)_4bipy$	52.3 (52.7)	2.6 (2.5)	8.9 (8.8)	19.8 O (20.1)	
$V(Me)Ibipy_2$	50.0 (49.9)	3.8 (3.8)	11.0 (11.1)	24.6 I (25.1)	
$V(NO)bipy_2$	65.2 (65.6)	4.5 (4.4)	17.9 (17.9)	2.6 O (2.9)	

(1) *Standard procedure*

2,2'-Bipyridine (3.1 g, 20 mmol) was added to a suspension of $TiCl_3$ (1.0 g, 6.5 mmol) and sodium amalgam (1.0 g Na in 100 g Hg) in THF (80 cm^3). After stirring for 24 hr at room temperature and filtering, the solution was reduced to *ca.* 15 cm^3 under vacuum. Diethylether (25 cm^3) was slowly added to precipitate a dark blue solid which was collected, washed with petroleum (2 × 20 cm^3) and recrystallised from THF-diethylether (1 : 1). Yield, 3.0 g, 89%.

The compounds $Zrbipy_3$, 81%; $Hfbipy_3$, 81%; $Vbipy_3$, 92%; $Nbbipy_3$, 78%, μ_{eff} = 1.75 BM; $Tabipy_3$, 80%, μ_{eff} = 1.77 BM and $Crbipy_3$, 91% were also prepared from the respective chlorides, $ZrCl_4$, $HfCl_4$, VCl_3, $NbCl_5$, $TaCl_5$ and $CrCl_3$. The 1.10-phenanthroline analogues $Tiphen_3$, 86%; $Zrphen_3$, 78%; $Hfphen_3$, 79%; $Vphen_3$, 86%; $Nbphen_3$, 72%, μ_{eff} = 1.91 BM; $Taphen_3$, 81%, μ_{eff} = 1.81 BM and $Crphen_3$, 85%, have been similarly prepared. Good analytical data for the known compounds were obtained.

(2) *Tris-(2,2'-dipyridyldisulfide)vanadium(O) and related compounds*

2,2'-Dipyridyldisulfide (4.3 g, 20 mmol) was added to sodium amalgam (1.0 g, Na in 100 g Hg) and a suspension of VCl_3 (1.0 g, 6.4 mmol) in THF (80 cm^3) at room temperature. After stirring for 24 hr the volatile materials were removed under vacuum. The residue was extracted into toluene, (50 cm^3) which was filtered, reduced to *ca.* 15 cm^3 and cooled to 0°C to yield a purple solid which was collected, washed with petroleum (2 × 20 cm^3) and dried under vacuum. Yield, 4.0 g, 88%; μ_{eff} = 1.82 BM.

The compounds *tris(2,2'-dipyridylamine)vanadium(O)* (yield 74%), μ_{eff} = 1.71 BM, and *tris(di-tert-butyldiimine) vanadium (O)* (yield 61%), μ_{eff} = 1.79 BM, can be prepared by reacting VCl_3 with the corresponding ligand under identical conditions.

(3) *2,2'-Bipyridine and 1,10-phenanthroline adducts of molybdenum and tungsten tetrahalides*

The adducts were prepared by the same procedure given for $MoCl_4$(bipy). Excess 2,2'-bipyridine (2.0 g, 13 mmol) was added to $MoCl_4(MeCN)_2$ (2.0 g, 6.2 mmol) in dichloromethane (50 cm^3) at room temperature. After stirring the mixture for 24 hr, the solution was reduced to *ca.* 10 cm^3, filtered and the brown solid washed with diethylether (2 × 25 cm^3) and dried under vacuum. Yield, 2.3 g, 96%.

Similarly, $MoCl_4phen$, 93% and from $WCl_4(MeCN)_2$, WCl_4bipy, 97%, WCl_4phen, 96%.

(4) *Zero-valent compounds from adducts*

The following procedure for $Mobipy_3$ is representative. 2,2'-Bipyridine (1.0 g, 6.4 mmol) was added to $MoCl_4bipy$ (1.0 g,

2.5 mmol) and sodium amalgam (1.0 Na in 100 g Hg) in THF (80 cm^3). After stirring for 24 hr the solvent was reduced to *ca.* 20 cm^3 under vacuum. Diethylether (25 cm^3) was then added slowly to precipitate a dark purple solid. This was collected, washed with light petroleum (2 × 20 cm^3) and recrystallised from THF-diethylether (1 : 1). Yield, 1.2 g, 83%. Similarly $Wbipy_3$, 84%; $Mophen_3$, 80%; $Wphen_3$ 87%.

(5) *Chromium and molybdenum compounds from the acetate*

From $M_2(CO_2Me)_4$ the following is representative. 2,2'-Bipyridine (2.3 g, 15 mmol) was added to a suspension of $Mo_2(CO_2Me)_4$ (1.0 g, 2.3 mmol) and sodium amalgam (1.0 g, Na in 100 g Hg) in THF (80 cm^3) and the solution stirred for 24 hr at room temperature. The dark purple solution was filtered and the volatile materials removed under vacuum. The residue was extracted into toluene (60 cm^3) which was filtered, reduced to 15 cm^3 and cooled to 0°C to give purple crystals which were collected, washed with petroleum (2 × 15 cm^3) and dried under vacuum. Yield 2.0 g, 77%. Similarly $Mophen_3$, 85% and from $Cr_2(CO_2Me)_4$, $Crbipy_3$, 91%; $Crphen_3$ 89%.

(6) *Tris(2,2'-bipyridine)rhenium(O)*

To a suspension of $ReCl_4(THF)_2$ (1.0 g, 2.2 mmol) in THF (80 cm^3) and sodium amalgam (1.0 g, Na in 100 g Hg) was added 2,2'-bipyridine (1.2 g, 7.7 mmol). After stirring for 24 hr at room temperature and filtering, the solution was reduced to *ca.* 20 cm^3 under vacuum and diethylether (25 cm^3) was added slowly to precipitate a purple solid. The solid was collected, washed with petroleum (2 × 20 cm^3) and recrystallised from THF–Et_2O (1 : 1). Yield, 1.2 g, 83%, μ_{eff} = 4.1 BM. Similarly $Rephen_3$, 76%, μ_{eff} = 4.3 BM.

(7) *Tetracarbonyl 2,2'-bipyridine vanadium(O)*

2,2'-Bipyridine (1.0 g, 6.4 mmol) was added to a suspension of VCl_3 (1.0 g, 6.4 mmol) and sodium amalgam (1.0 g, in 100 g Hg) in THF (60 cm^3). The solution was stirred for 24 hr under CO (2 atm) at room temperature. The black solution was filtered and the volatile materials removed under vacuum. The residue was extracted into toluene (50 cm^3) which was filtered, reduced to *ca.* 20 cm^3 and cooled to 0°C to yield a black microcrystalline compound which was collected and dried under vacuum. Yield, 1.2 g, 57%. IR. 1850 cm^{-1} broad ν(CO).

(8) *Bis(2,2'-dipyridine)methyl(iodo)vanadium(II)*

The vanadium(O) complex $V(bipy)_3$ (0.5 g, 1.0 mmol) in THF (30 cm^3) was treated with an excess of methyl iodide (1.0 g, 7.0 mmol) in THF (20 cm^3) and the mixture stirred for 2 hr at room temperature. The solution was reduced under vacuum to *ca.* 10 cm^3. The green solid which was precipitated was collected, washed with petroleum (2 × 10 cm^3) and recrystallised from toluene (10 cm^3) at 0°C. Yield, 55 g, 87%.

(9) *Bis(2,2'-bipyridine)nitrosylvanadium*

Nitric oxide was bubbled slowly into $Vbipy_3$ (0.5 g, 1.0 mmol) in toluene (25 cm^3) at 0°C. A white solid was precipitated, collected, washed with light petroleum (2 × 10 cm^3) and dried under vacuum. Yield, 0.37 g, 71%.

IR. 1690 cm^{-1} ν(NO).

Acknowledgements—We thank the SERC for partial support and the NSF for a NATO postdoctoral fellowship (J.Q.).

REFERENCES

[1]For references see W. R. McWhinnie and J. D. Miller, *Adv. Inorg. Chem., Radiochem.* 1969, **12**, 135.
[2]See, e.g. S. Herzog, *Z. Anorg. Allg. Chem.* 1958, **294**, 155; *Naturwiss.* 1956, **43**, 35.
[3]G. S. Girolami and R. A. Andersen, *Inorg. Chem.* 1981, **20**, 2040.
[4]T. E. Wood, J. C. Deaton, J. Corning, R. E. Wild and R. A. Walton, *Inorg. Chem.* 1980, **19**, 2614.
[5]K. W. Chiu, C. G. Howard, G. Wilkinson, A. M. R. Galas and M. B. Hursthouse, *Polyhedron* 1982, in press.
[6a]T. G. Groshens, B. Henne, D. Bartak and K. J. Klabunde, *Inorg. Chem.* 1981, **20**, 3629; [b]H. D. Abruña, A. Y. Teng, G. J. Samuels and T. J. Meyer, *J. Am. Chem. Soc.* 1979, **101**, 6745.
[7]H. tom Dieck, M. Svoboda and T. Greiser, *Z. Naturforsch. Teil B.* 1981, **36**, 823.
[8]B. Chaudret, H. Köster and R. Poilblanc, *J. Chem. Soc., Chem. Commun.* 1981, 266.
[9]J. R. Dilworth and R. L. Richards, *Inorg. Syntheses* 1980, **20**, 119.
[10]E. A. Allen, N. P. Johnson, D. T. Roseveare and W. Wilkinson, *J. Chem. Soc. (A).* 1969, 788.

Polyhedron Vol. 1, No. 2, pp. 213–214, 1982
Printed in Great Britain.

0277–5387/82/020213–02$03.00/0
Pergamon Press Ltd.

NOTES

Tin–oxygen coordination in dimethyltin dichloride N-arylsalicylideneimine complexes

(*Received* 8 *June* 1981)

Abstract—Proton and ^{13}C NMR data indicate that in their complexes with dimethyltin dichloride, the N-arylsalicylideneimines behave as monodentate ligands with oxygen, rather than imine nitrogen, as donor atom.

INTRODUCTION

The coordination behaviour of N-salicylideneaniline and its substituted derivatives towards diorganotin dichlorides has been examined.[1,2] Based on IR[1] and Mössbauer[2] studies, two different modes of coordination, (I) and (II), were proposed for the 1:2 adducts.

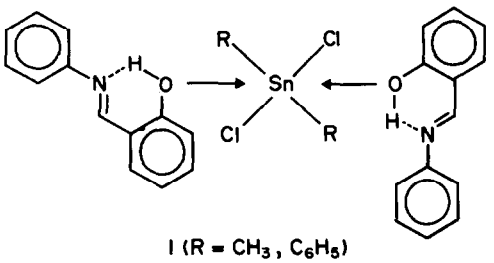

I (R = CH_3, C_6H_5)

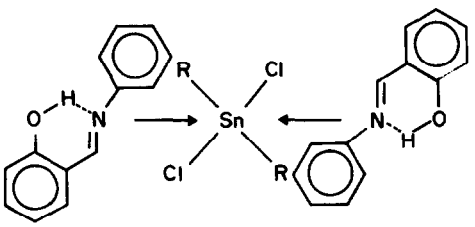

II (R = CH_3, C_6H_5)

With a view to resolving this discrepancy, we prepared the dimethyltin dichloride complexes of N-salicylideneaniline and N-salicylidene-p-methoxyaniline, and examined their ^{13}C and proton NMR spectra

EXPERIMENTAL

N-Salicylideneaniline and its derivatives were prepared by the direct condensation of salicylaldehyde with anilines in ethanol. The adducts were synthesized according to the procedures of Srivastava and Chauhan.[1]

The PMR spectra were obtained in $CDCl_3$ with TMS as internal reference on a Perkin–Elmer R12B spectrometer.

^{13}C NMR spectra were recorded on a Varian CFT-20 spectrometer with 8 mm tubes at 27°C. Generally 50,000 transients of 1s were accumulated after excitation pulses corresponding to "flip angles" of 20–40°. Spectra width were 4000 Hz with 4 K real data points in the transformed spectra. Peak assignments were made with the help of off-resonance and comparison of the spectra with those of the ligands.[3]

RESULTS AND DISCUSSION

The ^{13}C NMR spectra of the complexes and the ligands are recorded in Table 1.

The N-arylsalicylideneimine ligands could coordinate to the metal atom either through the oxygen atom, or through the imine nitrogen atom. Both modes of coordination have previously been reported.[4,5] Coordination through N as in (II) would be expected to lead to a downfield shift of the azomethine carbon (C-1). This is not in fact observed. Comparison of the ^{13}C NMR data of the ligands and complexes (Table 1) shows that ∂(C-1) remains unchanged. But, the value of ∂(C-2') for the complexes moves downfield (0.4–0.6 ppm) when compared with the ligand values. This is consistent with (I) because coordination through oxygen should result in a decrease in electron density and consequently a downfield shift for C-2'.

Further evidence in support of (I) can be obtained from the NMR of the azomethine and hydroxylic protons. As the ring formed by the intramolecular hydrogen bond of the Schiff base ligand is retained but distorted in the complex,[1,2] coordination through oxygen will result in the weakening of the O–H bond and the strengthening of the C=N...H hydrogen bond. This is reflected in the broadening (disappearance) of the hydroxylic proton which resonates at δ 13.3 ppm for the ligand.[6] However the OH protons reappear at δ13.2 ppm as a singlet when DMSO is added to the complex (DMSO, as expected, forms a stronger complex with Me_2SnCl_2 than Schiff bases). Similarly the azomethine proton (δ8.54 ppm for the ligand)[6] shows a small broadening (difference of $\Delta\nu_{1/2}$ between complex and ligand is *ca.* 2 Hz).[7] That this is due to strengthening of the C=N...H hydrogen bond is further substantiated by the fact that in the protonated spectra. of N-benzalaniline and its derivatives, the azomethine proton resonance (δ *ca.* 8 · 61 ppm)[8] is either very broad or exists as a doublet.[9]

The value of the coupling constant $^2J(^{119}SnCH)$ has also been used in the elucidation of the structures of methyltin derivatives.[10–12] An increase in the coordination number of the tin atom should give rise to an increase in the value of $^2J(^{119}SnCH)$. The coupling constants determined for dimethyltin dichloride N-salicylideneaniline and dimethyltin dichloride N-salicylidene-*p*-methoxyaniline are 70.8 and 71.2 cps respectively. An increase of 1.8–2.2 cps over the $^2J(^{119}SnCH)$ of 69.0 cps for Me_2SnCl_2[13] is of the order for tin–oxygen coordination. The $^2J(^{119}SnCH)$ values of Me_2SnCl_2 in phenol[14] and anisole[15] are 70.0 and 72.4 cps respectively. Thus, the NMR results provide quite strong evi-

Table 1. ^{13}C chemical shift (ppm) of N-salicylideneaniline and its dimethyltin dichloride complexes in $CDCl_3$

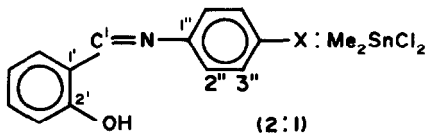

(2 : 1)

	δ(C—1)	δ(C—2')	δ(C—1'')	Other carbons
X=H				
Ligand	162.6	161.2	148.5	119.2; 117.3; 133.1; 118.9; 132.2; 121.1; 129.2; 126.8
Complex	162.6	161.6	148.5	119.2; 117.4; 133.3; 119.0; 132.3; 121.2; 129.4; 126.9 $\delta_{(CH_3Sn)}$6.6
X=OCH_3				
Ligand	160.4	161.0	141.3	119.4; 117.1; 131.9; 118.9; 132.6; 122.6; 122.3; 114.7; 158.9; $\delta_{(CH_3O)}$55.4
Complex	160.4	161.6	141.2	119.3; 117.3; 131.9; 118.9; 132.9; 122.3; 114.7; 158.9; $\delta_{(CH_3O)}$55.5 $\delta_{(CH_3Sn)}$6.8

dence for oxygen, rather than imine-nitrogen coordination in the N-arylsalicylideneimine complexes of diorganotin dichlorides.

Acknowledgements—We thank Universiti Sains Malaysia (Short Term Research Grant), Kenyatta University College and the International Tin Research Institute for financial assistance and Mr. Clement D'Silva for technical assistance.

LIAN E. KHOO

School of Chemical Sciences,
Universiti Sains Malaysia,
Penang, Malaysia

FRANK E. SMITH*

Department of Chemistry,
University of Prince Edward Island, Charlottetown, PEI
Canada

REFERENCES

[1]T. N. Srivastava and A. K. S. Chauhan, *J. Inorg. Nucl. Chem.* 1977, **39**, 371. *idem, Synth. React. Inorg. Met.-org. Chem.* 1977, **7**, 373.
[2]B. S. Saraswat, G. Srivastava and R. C. Mehrotra, *Inorg. Chimica Acta* 1979, **36**, 289; *Idem., J. Organomet. Chem.* 1979, **164**, 153.
[3]L. E. Khoo, to be submitted.
[4]T. N. Srivastava, A. K. S. Chauhan and M. Agarwal, *J. Inorg. Nucl. Chem.* 1979, **41**, 896.
[5]L. Randaccio, *J. Organometal. Chem.* 1973, **55**, C58.
[6]N. M. D. Brown and D. C. Nonhebel, *Tetrahedron* 1968, **24**, 5655.
[7]A larger difference, 8 Hz, was observed for dimethyltin dichloride N,2-hydroxynaphthylideneaniline adduct.
[8]L. E. Khoo, *Spectrochimica Acta* 1979, **35A**, 993.
[9]M. Holik, J. Belusa and J. Brichacek, *Coll. Czeth. Chem. Comm.* 1978, **43**, 610.
[10]G. Barbieri and F. Taddei, *J. Chem. Soc. Perkin Trans. II* 1972, 1327.
[11]T. F. Bolles and R. S. Drago, *J. Am. Chem. Soc.* 1966, **88**, 3921; 5730.
[12]T. Tanaka, *Inorg. Chim. Acta.* 1967, **1**, 217.
[13]J. Lorberth and H. Vahrenkamp, *J. Organometal. Chem.* 1968, **11**, 111.
[14]K. Kawakami, M. Miya-Uchi and T. Tanaka, *J. Inorg. Nucl. Chem.* 1971, **33**, 3773.
[15]G. Matsubayashi, Y. Kawasaki, T. Tanaka and R. Okawara, *Bull. Chem. Soc. (Japan)* 1967, **40**, 1566.

*Author to whom correspondence should be addressed.

Polyhedron Vol. 1, No. 2, pp. 215–216, 1982
Printed in Great Britain.

0277–5387/82/020215–02$03.00/0
Pergamon Press Ltd.

Thermogravimetric analysis and dissociation pressure of caesium trihalides

(*Received* 26 *June* 1981)

The relative stabilities of compounds containing polyhalide ions has for long been a subject of discussion. For example, Ephraim, on the basis of vapour pressure measurements arrived at the order, $CsI_3 > CsIBr_2 > CsICl_2 > CsI_2Br > CsBr_3$ for caesium trihalides.[1] Similar sequences have been compiled for the trihalide ions themselves, and in those sequences derived from measurements in solution it is found that the relative position of the trihalide ions depends on the particular solvent used.[2] In a recent paper Finch *et al.* correctly drew attention to the fact that several parameters contribute to the thermodynamic stability of a polyhalide ion and they suggested the rank order $IC1_2^- > IBr_2^- > I_3^-$ for the stabilities of these three trihalide ions.[3]

A convenient method for obtaining an "order of stability" of a series of compounds involves comparison of the procedural decomposition temperatures obtained from thermogravimetric analysis.[4,5] This has been used with some success as a rapid analytical technique for empirically assessing the apparent thermal stability of polymers.[6] We have, therefore, carried out a thermogravimetric study of caesium trihalides to obtain, from the procedural decomposition temperatures, an order of apparent thermal stability which could be compared with the order of thermodynamic stability obtained by Ephraim from vapour pressure measurements. Thermogravimetric analysis could also prove to be a useful method for rapid analysis of metal polyhalides.

RESULTS AND DISCUSSION

The thermograms of the caesium trihalides indicated a one-step decomposition for each compound; the procedural decomposition temperatures and percentage weight losses obtained are given in Table 1. The figures for percentage weight loss lie close to the theoretical values for the loss of one mole of halogen or interhalogen per mole of caesium trihalide. In the case of mixed trihalides it is known that dissociation takes place in such a way that the halogen or interhalogen molecules contain the heaviest halogen atoms.[7] Thus, thermogravimetric analysis affords a useful method for checking the purity of metal polyhalides provided the volatile dissociation products are known.

The values of procedural decomposition temperature lead to the following "stability" order: $CsIC1_2 > CsIBr_2 > CsI_3 > CsI_2Br > CsBr_3$. This order is at variance with that obtained by Ephraim from his vapour pressure studies and although agreement in the results obtained from the two different approaches (on the one hand, measurements in an open, dynamic system, and on the other, measurements in a closed system under equilibrium conditions) would not necessarily be expected, it was thought desirable to repeat the measurement of vapour pressure for the series of caesium trihalides. This was done using an all-glass system incorporating a spiral gauge null-meter.

Dissociation pressures were measured in the temperature range 17–162°C and for each compound the plot of $\log_{10}(p/\text{atm})$ vs T^{-1}/K^{-1} was a straight line represented by $\log_{10}(p/\text{atm}) = -AT^{-1}/K^{-1} + B$, the values of A and B for individual compounds being given in Table 2. Within the temperature range studied, the dissociation equilibrium for each compound is of the type: solid $\rightleftharpoons$ solid + gas for which the equilibrium constant (Kp) is $Kp = p$. Thus for each compound $\log_{10}(Kp/\text{atm}) = -AT^{-1}/K^{-1} + B$. Consequently values of equilibrium constant and enthalpy of dissociation may be calculated (Table 2). From the equilibrium constant values it is seen that the order of thermodynamic stability of the compounds is:- $CsIBr_2 > CsI_3 > CsIC1_2 > CsBr_3 > CsI_2Br$† (this order holds for other temperatures within the range studied).

It is noted that this sequence does not correspond exactly with that obtained in the thermogravimetric study described above; the difference can only be put down to the operation of kinetic factors in the latter case. Thus whilst the stability order obtained

†Our dissociation pressure measurements lead to a different order from that obtained by Ephraim. We cannot offer an explanation of this but suggest that vapour pressures measured in an all glass system are likely to be more reliable than those measured in an apparatus using sulphuric acid or $KNSO_4/H_2SO_4$ as manometer liquid in an isoteniscope.

Table 1. Thermogravimetric analysis of caesium trihalides

Compound	p.d.t* °C	weight loss† %
CsI_3	77	50.1 (49.4)
CsI_2Br	49	53.7 (54.4)
$CsIBr_2$	124	48.4 (49.3)
$CsBr_3$	38	42.4 (42.9)
$CsIC1_2$	139	48.9 (48.5)

*Procedural decomposition temperature

†Theoretical value in brackets

Table 2. Dissociation pressure, equilibrium constant and enthalpy of dissociation data for caesium trihalides

Compound	A	B	$\frac{Kp(298\ K)}{atm.}$	$\frac{\Delta H}{kJ\ mol^{-1}}$
CsI_3	2362	4.75	6.65×10^{-4}	45.23
CsI_2Br	2187	5.79	2.80×10^{-2}	41.87
$CsIBr_2$	2291	4.22	3.37×10^{-4}	43.87
$CsBr_3$	2160	5.39	1.38×10^{-2}	41.36
$CsICl_2$	1864	3.66	2.57×10^{-3}	35.69

from studies in the open, dynamic system (thermogravimetry) is a useful empirical guide to the "apparent thermal stability" of caesium trihalides, it is not the same as the order of thermodynamic stability of these compounds. These results emphasise the danger inherent in drawing conclusions about relative thermodynamic stabilities of any series of compounds on the basis of decomposition temperatures measured in an open system.

CONCLUSIONS

Thermogravimetric analysis provides a useful means of checking the composition of caesium trihalides. The procedural decomposition temperatures obtained give only an order of "apparent thermal stability" of caesium trihalides and do not lead to the order of thermodynamic stability (obtained from dissociation pressure measurements).

EXPERIMENTAL

Reagents used were of the best grade available and, if necessary, were purified before use. The caesium trihalides were prepared by standard methods involving reaction of caesium halide with the appropriate halogen or interhalogen.[8,9] The purity of the compounds was checked by halide analysis after reduction; the analysis was carried out potentiometrically using silver nitrate as precipitant.[10]

Thermogravimetric analysis was carried out using a Stanton TR1 balance with attachment OS12 which enabled temperature measurement to be made at the base of the sample. The compound (*ca.* 0.15 g) was contained in an open silica crucible and a slow stream of air (100 ml min^{-1}) was passed through the furnace which was heated at the rate of 4 K min^{-1}.

The dissociation pressures were measured by a static method in an all-glass system involving a spiral gauge with an optical lever which was used as a null-meter. Pressures were read on a cathetometer as a difference in mercury levels in a wide-tube manometer. The constant volume section of the apparatus (containing the compound) was kept at constant temperature in an electrically heated oil bath and dissociation pressures were recorded only after solid-vapour equilibrium had been established (after 1–2 hr); values of pressure for ascending and descending temperatures were recorded.

Acknowledgement—We thank Mr. Kenneth Harris, Madras College, St. Andrews for assistance.

Department of Chemistry
University of St. Andrews
Fife, KY 16 9*ST*
Scotland

G. S. HARRIS*
J. S. McKECHNIE

*Author to whom correspondence should be addressed.

REFERENCES

[1]F. Ephraim, *Chem. Ber.* 1917, **50**, 1069.
[2]E. H. Wiebenga, E. E. Havinga and K. H. Boswijk, *Adv. Inorg. Chem. Radiochem.* 1961, **3**, 133.
[3]A. Finch, P. N. Gates and S. J. Peake, *Thermochimica Acta* 1977, **19**, 213.
[4]A. E. Newkirk, *Anal. Chem.* 1960, **32**, 1558.
[5]C. J. Keattch and D. Dollimore, *An Introduction to Thermogravimetry*, pp. 25 and 51. Heyden, London, 1975.
[6]C. D. Doyle, *Anal. Chem.* 1961, **33**, 77.
[7]E. H. Wiebenga, E. E. Havinga and K. H. Boswijk, *Adv. Inorg. Chem. Radiochem.* 1961, **3**, 146.
[8]A. I. Popov and R. E. Buckles, *Inorg. Synth.* 1957, **5**, 167.
[9]L. R. Morss, *J. Chem. Thermodyn.* 1975, **1**, 709.
[10]J. J. Lingane, *Electroanalytical Chemistry*, p. 118. Interscience, New York, 1958.

Polyhedron Vol. 1, No. 2, p. 217, 1982 Pergamon Press Ltd. Printed in Great Britain.

ERRATUM

The List of Contributors that appeared in *Polyhedron* **1**(1), p. ii (1981) was shown incorrectly. The corrected list appears below. The printer regrets any inconvenience caused.

Contributors to Vol. 1, No. 1

Polyhedron Vol. 1, No. 3, pp. 219–223, 1982
Printed in Great Britain.

0277–5387/82/030219–05$03.00/0
Pergamon Press Ltd.

LANTHANIDE THERMODYNAMIC PREDICTIONS

STEVEN BRATSCH* and HERBERT B. SILBER
Division of Earth and Physical Sciences, The University of Texas at San Antonio (UTSA),
San Antonio, TX 78285, U.S.A.

(*Received* 26 *May* 1981)

Abstract—For the plus-two and plus-three lanthanide ions, ΔH_f is inversely related to the sums of the ionic radii by

$$\Delta H°_f = Q_n + A/(r_{Ln^{3+}} + r_X n -) + B.$$

This equation reproduces the known values for the plus-three oxides and the halides, and predicts the absolute hydration energies of the aqueous lanthanide(III) ions. The model is also used to calculate ΔH_f of the lanthanide(II) oxides and fluorides. Based upon the enthalpies of disproportionation, EuO, YbO, SmF_2, EuF_2 and YbF_2 are predicted to be stable.

INTRODUCTION

Although much thermodynamic information is available for the plus-three lanthanides in solution and in the solid state[1,2], the situation is much different for the plus-two lanthanides. Lanthanide dichloride enthalpies have been calculated[3] and several have been measured by Morss and associates[4–6]. Kim and Oishi have recently published calculated values for the enthalpies of formation of the dihalides[7]. Kim's cycle is based upon calculating the energies for the valence change from plus-three to plus-two. We have developed an alternate approach to the calculation of the plus-two lanthanide thermodynamic values, and this approach can be extended to other compounds in addition to the dihalides. Our approach utilizes a simple ionic model coupled to the known lanthanide contraction.

CALCULATIONS AND RESULTS FOR PLUS-THREE LANTHANIDES

Using a Born–Haber cycle, the enthalpy of formation of a crystalline lanthanide compound, LnX, is given by:

$$\Delta H°_f(LnX, c) = \Delta H°_f(Ln^{n+}, g) + \Delta H°_f(X^{n-}, g) - \Delta H°_{lat}(LnX). \quad (1)$$

Here $\Delta H°_{lat}(LnX)$ is the lattice energy of LnX, which can be estimated empirically by:

$$\Delta H°_{lat}(LnX) = A/(r_0) + k_2 \quad (2)$$

where r_0 is the sum of the ionic radii for the cation and anion. The constants are dependent upon the choice of Ln and X, and include the Madelung constant, the Born repulsion term, Van der Waals interactions, zero point energies, and heat capacity corrections to 25°C. The enthalpy of formation of the lanthanide cation, $\Delta H°_f(Ln^{n+}, g)$ is given by

$$\Delta H°_f(Ln^{n+}, g) = \Delta H°_{subl}(Ln) + \sum_1^n I_i + 5/2\,nRT \quad (3)$$

where $\Delta H°_{subl}(Ln)$ is the standard sublimation enthalpy of the lanthanide; $\sum_1^n I_i$ is the sum of the lanthanide ionization energies; and 5/2 nRT is the enthalpy change as a function of temperature from 0 K where I is calculated to the experimental temperature, assuming the lanthanide ion acts as an ideal gas. Combining eqns (2) and (3) with (1), results in the following expression:

$$\Delta H°_f(LnX, c) = \Delta H°_{subl}(Ln) + \sum_1^n I_i - A/(r_0) + B \quad (4)$$

where the new constant B includes $H°_f(X^{n-}, g)$, 5/2 nRT and k_2. We will utilize a new function called $Q_n(Ln)$ which will be defined as:

$$Q_n = \Delta H°_{subl}(Ln) + \sum_1^n I_i. \quad (5)$$

Thus, $\Delta H°_f(LnX, c)$ is simplified to:

$$\Delta H°_f(LnX, c) = Q_n(Ln) + A/(r_{Ln^{n+}} + r_X n -) + B. \quad (6)$$

We will establish the validity and utility of eqn (6) by applying it to known experimental data. The constants A and B will vary for different ligand systems. For our test systems we will correlate the results for the Ln_2O_3 cubic sesquioxides and for the hydrated lanthanide ions. Table 1 summarizes the data for the lanthanide oxides, with all units converted to kilojoules. Templeton and Dauben's lanthanide radii were utilized along with 1.380 Å for the radius of the O^{2-} ion in the oxides[10]. Since two lanthanides are contained in Ln_2O_3 and since $r_X n - = 1.380$ Å for O^{2-}, eqn (6) becomes:

$$\Delta H°(Ln_2O_3, c) = 2Q_3 + A/(r_{Ln^{3+}} + 1.380\ Å) + B. \quad (7)$$

If our simple electrostatic model is correct, a graph of $\Delta H°(Ln_2O_3, c) - 2Q_3$ should be a linear function of $1/(r_{Ln^{3+}} + 1.380$ Å). As shown in Fig. 1, the data for the lanthanide oxides are linear, with A calculated to be −25,072 KJ-Å/mol and B = 695 KJ/mol. The absence of significant crystal field stabilization energy for the lanthanide oxides is consistent with the general view that these stabilization energies are unimportant in lanthanide systems.

The derivation of a similar equation for the enthalpy of formation of the solvated lanthanide (III) ions is somewhat more complex and the following cycle is used.

*Author to whom correspondence should be addressed.

Table 1. Evaluation of Q_3 and $H_f(Ln_2O_3)$

Ln	$\Delta H°_{subl}$ KJ mol^{-1} [1, 8]	$\sum_1^3 I_i$ [9]	Q_3 KJ mol^{-1}	$r_{Ln^{3+}}$ Å [10]	$-\Delta H°_f(Ln_2O_3, c)$ KJ mol^{-1} [1, 8]
La	431.0	3455.6	3886.6	1.061	1799
Ce	421.3	3523	3944	1.034	1799
Pr	356.5	3627	3984	1.013	1819
Nd	327.2	3697	4024	0.995	1812
Pm	−318	−3739	−4057	0.979	—
Sm	206.7	3869	4076	0.964	1828
Eu	176.6	4036	4213	0.950	1663
Gd	397.5	3750	4148	0.938	1827
Tb	388.7	3790	4179	0.923	1865
Dy	290.4	3898	4188	0.908	1863
Ho	300.8	3923	4224	0.894	1881
Er	316.7	3934	4251	0.881	1898
Tm	232.2	4044	4276	0.869	1889
Yb	154.0	4194	4348	0.858	1815
Lu	427.6	3910	4338	0.848	1878

$$Ln(c) + nH^+(aq) \rightarrow Ln^{n+}(aq) + n/2H_2(g) \quad (8)$$

$$Ln(g) = Ln(c) \quad (9)$$

$$Ln^{n+}(g) + ne^- = Ln(g) \quad (10)$$

$$n/2H_2(g) = nH(g) \quad (11)$$

$$nH(g) = nH^+(g) + ne^- \quad (12)$$

$$nH^+(g) = nH^+(aq). \quad (13)$$

The net reaction is:

$$Ln^{n+}(g) = Ln^{n+}(aq) \quad (14)$$

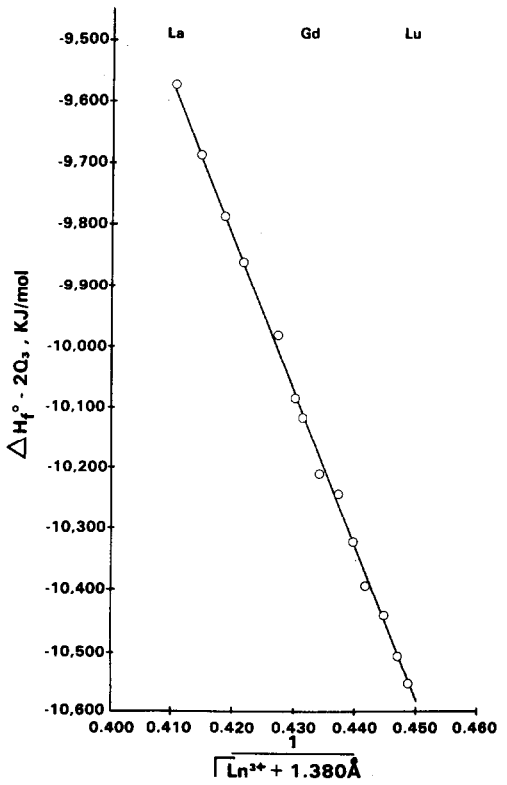

Fig. 1. The predicted and calculated values for the formation of Ln_2O_3.

For (8)–(14), the sum of the ΔH's equals the absolute hydration enthalpy of the Ln^{n+} ions. For $Ln^{3+}(aq)$,

$$\Delta H°_{hyd}(Ln^{3+}) = \Delta H°(Ln^{3+}, aq) - \Delta H°_{subl}(Ln) - \left(\sum_1^3 I_i + 5/2\, nRT\right) + 3/2\, D_{H-H} + (3I_H + 5/2\, nRT) + 3\Delta H°(H^+, aq) \quad (15)$$

where the bond dissociation, D_{H-H}, equals 435.9 KJ/mol[1]; the ionization energy at 0 K is 1312.0 KJ/mol[1] plus the correction to 25°C, 5/2 nRT; and $\Delta H°(H^+, aq)$ is the hydration energy. $\Delta H°(H^+, aq)$ has been estimated to be -260.7 ± 2.4[11], -263.7 ± 3[12], and -266[13], and we have utilized −263 Kcal/mol or −1110 KJ/mol in our calculations. Equation (15) simplifies to:

$$\Delta H°_{hyd}(Ln^{3+}) = \Delta H°_f(Ln^{3+}, aq) - Q_3 + 1284\ \text{KJ}. \quad (16)$$

In Table 2 we have summarized the known $\Delta H°_f(Ln^{3+}, aq)$ values and the hydration energy results calculated from eqn (16). In Fig. 2 we have plotted our calculated $\Delta H°(Ln^{3+}, aq)$ values as a function of the ionic radii, obtaining a straight line. Once again crystal field effects are absent.

The data for the hydrated lanthanide(III) ions can also be correlated in an equation similar to (7), calculated to be in units of joules:

$$\Delta H°(Ln^{3+}, aq) = Q_3(Ln) - 6053/(r_{Ln^{3+}} + 0.775) - 1289. \quad (17)$$

We will use the proposed ionic model to calculate $\Delta H°_f$ of the lanthanide triiodides. This series is chosen because covalent bonding has been postulated by Myers for the lanthanide trihalides in order to explain differences in the energy for the process

$$LnX_3(g) = Ln(g) + 3X(g) \quad (18)$$

between experimental and the calculated data[14]. The data for La[III], Gd[III] and Lu[III] are used to determine the constants for the LnI_3 system.

$$\Delta H°_f(LNi_3, s) = Q_3 - 14{,}644/(r_{Ln^{3+}} + 2.20\ \text{Å}) - 95. \quad (19)$$

Table 2. Hydration enthalpies for Ln(III) ions

Ln(III)	$-\Delta H°_f(Ln^{3+}, aq)$ KJ/mol [1, 8]	$-\Delta H°_{hyd}$ KJ/mol
La	708	3306
Ce	698	3353
Pr	705	3400
Nd	696	3432
Pm	—	—
Sm	691	3478
Eu	605	3527
Gd	687	3542
Tb	690	3579
Dy	697	3597
Ho	706	3637
Er	705	3663
Tm	702	3690
Yb	674	3733
Lu	684	3732

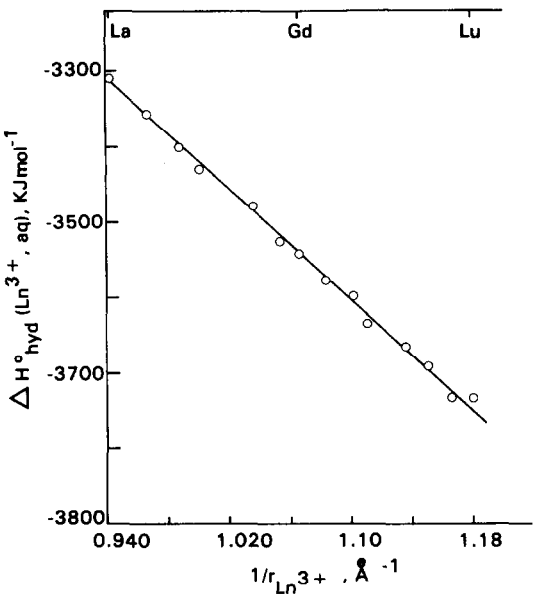

Fig. 2. The enthalpy of hydration for the lanthanide(III) ions as a function of the reciprocal of the ionic radii.

Table 3. Evaluation of $\Delta H°_f(LnI_3, c)$

Ln	Experimental $-\Delta H°_f$ KJ mol^{-1} [15, 16]	Calculated $-\Delta H°_f$ KJ mol^{-1}
La	699	699
Ce	686	679
Pr	678	669
Nd	665	654
Pm	—	—
Sm	640	647
Eu	615	531
Gd	619	614
Tb	598	605
Dy	603	619
Ho	594	604
Er	586	597
Tm	582	591
Yb	561	536
Lu	556	561

Except for EuI_3 the average deviation of the calculated enthalpies compared to the measured ones is 1.6%, an excellent result considering our model. Myers has pointed out that the Eu(III) discrepancies exist in all the halide calculations and is probably due to incorrect formation values[17]. The observation that our simple ionic model reproduces the experimental data not only confirms the validity of our calculations, but also indicates the lack of a significant covalent effect for lanthanide halide formation.

The calculated results for the known plus-three lanthanide ions are consistent with our simplified ionic model. We will now extend these results to selected plus-two lanthanide systems.

CALCULATIONS AND RESULTS FOR PLUS-TWO LANTHANIDES

The sizes of the plus-two lanthanides are not as well-established as for the plus-three lanthanides. We have developed empirical relations for the plus-three ions which agree within 0.001 Å for those given by Templeton and Dauben[10].

$$r_{Ln^{3+}} = 5.10\ Å/(q + 14) + 0.695\ Å \quad (La–Gd) \qquad (20)$$

$$r_{Ln^{3+}} = 7.65\ Å/(q + 14) + 0.575\ Å \quad (Gd–Lu) \qquad (21)$$

where q is the number of $4f$ electrons present in the Ln^{3+} ion. Two equations are necessary because of the gadolinium break. In order to correlate the lanthanide (II) data, the chemically similar Ba(II) ion is included in the series, resulting in the following equations:

$$r_{Ln^{2+}} = 8.40\ Å/(q + 14) + 0.750\ Å \quad (Ba–Eu) \qquad (22)$$

$$r_{Ln^{2+}} = 11.76\ Å/(q + 14) + 0.590\ Å \quad (Eu–Yb). \qquad (23)$$

Equations (22) and (23) allow for a structural break at f^7 and reproduce the ionic radii of Ba^{2+} (1.35 Å), Eu^{2+} (1.15 Å) and Yb^{2+} (1.02 Å)[8,18,19]. Here q is the sum of the $4f$ and the 5d electrons in the lanthanide(II) ion. The Q_2 values are summarized in Table 4. Using the known values for ΔH_f for BaO and EuO, the A and B constants can be calculated, resulting in the following equation for the lanthanide(II) oxides:

$$\Delta H_f(LnO, c) = Q_2 - 6851/(r_{Ln^{2+}} + 1.380\ Å) + 308. \qquad (24)$$

The calculated results are included in Table 4. The lanthanide(II) oxides of La, Ce and Gd are significantly less stable than those of the other lanthanides. Although each of the enthalpies is negative, the stabilities of the lanthanide(II) oxides must be measured in terms of their disproportionation into the metals and the metal (III) oxides, via

$$3LnO(c) = Ln(c) + Ln_2O_3(c). \qquad (25)$$

The enthalpy of disproportionation values, per mole of LnO, ΔH_{disp}, are summarized in Fig. 3. The only two

Table 4. Thermodynamic data for LnO

M^{2+}	$r_{Ln^{2+}}$, Å	Q_2 KJ mol^{-1}	$-\Delta H_f(LnO, c)$ KJ mol^{-1}	$-\Delta H_{disp}$ KJ mol^{-1}
Ba	1.350	1648	553.5 [1]	—
La	1.310	2036.2	203	397
Ce	1.275	1995	277	323
Pr	1.244	1898	405	201
Nd	1.217	1892	438	166
Pm	1.192	−1905	—	—
Sm	1.170	1818	561	48
Eu	1.150	1807.9	592.0 [1]	− 38
Gd	1.125	2157	270	339
Tb	1.101	2065	388	234
Dy	1.080	1988	489	132
Ho	1.060	2020	480	147
Er	1.042	2056	465	168
Tm	1.026	1991	548	82
Yb	1.010	1933	625	− 20
Lu		2316		

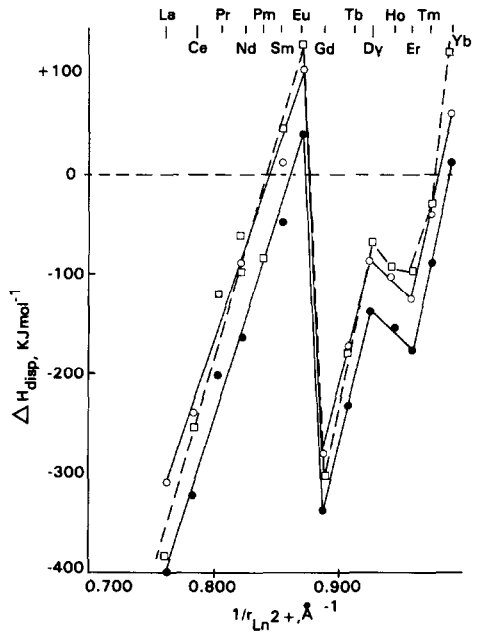

Fig. 3. The predicted enthalpies of disproportionation for LnO and LnF_2. ●, LnO; ○, LnF_2 (this work); □, LnF_2 Ref. [7].

oxides which have a positive ΔH_{disp} are EuO and YbO, a result consistent with the idea that the plus-two state is stabilized by half-filled or completely filled shells. Although EuO is known, YbO has not yet been isolated. The actual stabilities are based on the free energies of disproportionation rather than the enthalpies alone. The reactions involve similar solid substances only and the entropy differences should be relatively similar. Therefore, ΔH_{disp} should be a good measure of the compound stabilities.

Using a similar procedure, the enthalpies of formation of the difluorides can be calculated and compared to those calculated by Kim[7]. The starting point will be the known values for BaF_2, SmF_2, EuF_2 and YbF_2 summarized in Table 5. The best fit equation is:

$$\Delta H_f(LnF_2, c) = Q_2 - 4663/(r_{Ln^{2+}} + 1.330\ \text{Å}) - 1114. \quad (26)$$

Similarly, an equation can be derived fro the plus-three lanthanide fluorides using LaF_3, GdF_3 and LuF_3 as the known compounds, obtaining:

$$\Delta H_f(LnF_3, c) = Q_3 - 10{,}199/(r_{Ln^{3+}} + 1.33\ \text{Å}) - 1353. \quad (27)$$

The results for LnF_2 and LnF_3 are included in Table V along with the results from Kim's studies. The enthalpies of disproportionation are calculated by:

$$LnX_2(s) = 1/3\ Ln(c) + 2/3\ LnX_3(c) \quad (28)$$

and the results are also contained in Table 5. Subsequent to Kim's estimation of the enthalpies of the dihalides[7], Kim has measured ΔH_f for NdF_3 obtaining -1660.6 KJ/mol^{-1} rather than -1713 KJ mol^{-1} shown in Ref. [7], thereby modifying ΔH_{disp} to be -62 KJ mol^{-1} rather than the -97 KJ mol^{-1} shown in the Table. Although the two sets of data have some differences, these are sometimes less than the errors for the experimental measurements. The disproportionation results are summarized in Fig. 3. The only difluorides predicted to be stable are SmF_2, EuF_2 and YbF_2. The trends from both models are equivalent.

Table 6 summarizes the calculated constants for eqn (6) for all of the systems investigated. The elementary ionic model gives results consistent with experimental data for known systems and makes equivalent predictions to those from more complicated models. In the case of the triiodides, this simple model correctly reproduced the experimental data, indicating that the earlier sug-

Table 6. Summary of results

Species	r_x- Å	A KJ·Å mol^{-1}	B KJ mol^{-1}
$Ln_2O_3(c)$	1.380	−25,072	695
$Ln^{3+}(aq)$	0.775	−6,053	−1,289
$LnI_3(c)$	2.20	−14,644	−95
LnO(c)	1.380	−6,851	+308
$LnF_2(c)$	1.33	−4,663	−1,114
$LnF_3(c)$	1.33	−10,199	−1,353

Table 5. Thermodynamic data for the lanthanide fluorides

M^{2+}	$-\Delta H_f(LnF_2, c)$ measured KJ mol^{-1} [20]	$-\Delta H_f(LnF_2, c)$ calculated from eqn (26) KJ mol^{-1}	$-\Delta H_f(LnF_2)$ from [7] KJ mol^{-1}	$-\Delta H_f(LnF_3, c)$ calculated from eqn (27) KJ mol^{-1}	$-\Delta H_f(LnF_3, c)$ experimental KJ mol^{-1}	$-\Delta H_{disp}$ from eqn (28) KJ mol^{-1}	$-\Delta H_{disp}$ from [7] KJ mol^{-1}
Ba	1207	1206	1207 [20]	—	—	—	—
La		844	771	1732	1732 [20]	311	384
Ce		909	901	1723	1733 [20]	240	254
Pr		1028	1021	1722	1712 [20]	120	120
Nd		1053	1045	1716	1660.6 ± 4.9 [21]	91	97
Pm		—	1051	—	—	—	85
Sm	1160	1161	1160 [20]	1723	1669.0 ± 4.6 [22]	− 12	− 47
Eu	1188 ± 17	1186	1188 [20]	1613	1584 [20]	−111	−132
Gd		856	830	1702	1698.7 ± 7.1 [23]	279	303
Tb		967	962	1701	1707 [20]	167	177
Dy		1061	1056	1722	1678 ± 8 [24]	87	63
Ho		1045	1040	1715	1698 ± 6 [25]	98	92
Er		1024	1016	1715	1669 ± 6 [26]	119	97
Tm		1102	1097	1715	1689 [20]	41	29
Yb	1172 ± 29	1174	1172	1666	1569.8 ± 7.1 [23]	− 63	−125

gestion of significant covalent binding in the lanthanide halide systems is not necessary. These results should be useful to predict the thermochemical properties of additional systems.

Acknowledgements—The authors gratefully acknowledge the financial support of the Robert A. Welch Foundation of Houston, Texas through Grant AX-659.

REFERENCES

[1]*Selected Values of Chemical Thermodynamic Properties*, NBS TN 270-3 through 270-7, U.S. Government Printing Office, Washington, D.C., 1968–73.
[2]See, e.g. F. H. Spedding, J. A. Rard and A. Habenschuss, *J. Phys. Chem.* 1977, **81**, 1069.
[3]D. A. Johnson, *J. Chem. Soc. A.* 1969, 2578.
[4]L. R. Morss and H. O. Haug, *J. Chem. Thermo.* 1973, **5**, 513.
[5]L. R. Morss and M. C. McCue, *Inorg. Chem.* 1975, **14**, 1624.
[6]L. R. Morss and J. A. Fahey, *Proc. 12th Rare Earth Res. Conf.* 1976, **I**, 443.
[7]Y.-C. Kim and J. Oishi, *J. Less Common Metals* 1979, **65**, 199.
[8]L. R. Morss, *Chem. Rev.* 1976, **76**, 827.
[9]W. C. Martin, L. Hagan, J. Reader and J. Sugar, *J. Phys. Chem. Ref. Data* 1974, **3**, 771.
[10]D. H. Templeton and C. H. Dauben, *J. Am. Chem. Soc.* 1954, **76**, 5237.
[11]H. F. Halliwell and S. C. Nyburg, *Trans. Faraday Soc.* 1963, **59**, 1126.
[12]D. F. C. Morris, *Structure and Bonding*. Springer-Verlag. New York (1968).
[13]R. Jalenti and R. Caramuzza, *J. C. S. Faraday Trans. I.* 1976, **3**, 715.
[14]C. E. Myers, *Inorg. Chem.* 1975, **14**, 199.
[15]R. C. Ferber, *Heats of Dissociation of Gaseous Halides*, Los Alamos Scientific Laboratory Report No. LA-3164, USAEC No. TID-4500, 40th ed. Los Alamos Scientific Laboratory, Los Alamos, N. Mexico.
[16]D. Brown, *Halides of the Lanthanides and Actinides*, pp. 237–247. Wiley, New York (1968).
[17]C. E. Myers, *Inorg. Chem.* 1975, **14**, 2021.
[18]L. Pauling, *The Nature of the Chemical Bond*, 3rd edn. Cornell University Press, New York (1960).
[19]D. A. Johnson, *J. C. S. Dalton Trans.* 1974, 1671.
[20]Values quoted in Ref. [7].
[21]Y.-C. Kim and J. Oishi, *J. Chem. Thermodynamics* 1980, **12**, 407.
[22]Y.-C. Kim, J. Oishi and S.-H. Kang, *J. Chem. Thermodynamics* 1977, **9**, 973.
[23]Y.-C. Kim, J. Oishi and S.-H. Kang, *J. Chem. Thermodynamics* 1978, **10**, 975.
[24]Y.-C. Kim and J. Oishi, *Memoirs Fac. Engr. (Kyoto Univ.)* 1980, **62**, 13.
[25]Y.-C. Kim, M. Misumi, H.Yano and J. Oishi, *J. Chem. Thermodynamics* 1979, **11**, 657.
[26]Y.-C. Kim, H. Yano, M. Misumi and J. Oishi, *J. Chem. Thermodynamics* 1979, **11**, 429.

Polyhedron Vol. 1, No. 3, pp. 225–231, 1982
Printed in Great Britain.

0277-5387/82/030225-07$03.00/0
Pergamon Press Ltd.

BINDING OF SOME FIRST-ROW TRANSITION METAL IONS BY A POLY(IMINOETHYLENE)DITHIOCARBAMATE COPOLYMER

PHILIP C. H. MITCHELL* and MARINA G. TAYLOR†
Department of Chemistry, The University, Whiteknights, Reading RG6 2AD, England

(*Received* 31 *July* 1981)

Abstract—The binding of the transition metal ions VO^{2+}, Fe^{2+}, Fe^{3+}, Co^{2+}, Co^{3+}, Ni^{2+} and Cu^{2+} by a poly(iminoethylene)dithiocarbamate copolymer has been investigated by uptake studies and physical measurements (electronic, IR, and ESR spectra and magnetic susceptibility). Metal ions may be bound by both the dithiocarbamato and amino groups of the co-polymer. Binding to nitrogen (in addition to binding to sulphur) increases in the order Fe(II) < Ni(II) < Cu(II) and accounted for increasing metal ion uptake by the copolymer in the same order. Factors which determine the relative uptake of the metal ions by the copolymer are discussed.

INTRODUCTION

Poly(iminoethylene)dithiocarbamate copolymer (1) (abbreviated "copolymer" in the text and PIED in formulae) is a zwitterion with both nitrogen and sulphur sites.

$$\begin{array}{l} -CH_2CH_2-NH-CH_2CH_2-NH^+-CH_2CH_2-NH- \\ \qquad\qquad\qquad\qquad\quad | \\ \qquad\qquad\qquad\qquad CH_2CH_2-NHCS_2^-. \qquad (1) \end{array}$$

The copolymer is amorphous and is insoluble in water and organic solvents. It is of practical use as a scavenger of metal ions from solution.[1] In this paper we report a study of the reactions of the copolymer with aqueous solutions of the ions VO^{2+}, Fe^{2+}, Co^{2+}, Ni^{2+} and Cu^{2+} following our earlier work with molybdate.[2]

The object was to determine the uptake of metal ions, the binding sites and the stereochemistry of the copolymer complexes by comparisons with well characterised monomeric dithiocarbamato complexes.[3–5]

EXPERIMENTAL

Materials. Poly(iminoethylene) was obtained from B.D.H. Ltd. as a 50% aqueous solution. Iron(II) chloride was purified by heating under reflux with iron powder and hydrochloric acid.[6] Other chemicals were analytical or reagent grades.

Preparations. Poly(iminoethylene)dithiocarbamate copolymer. Carbon disulphide (10.2 g) in ethanol (50 cm³) was added to a stirred solution of poly(iminoethylene) (30 g) in ethanol (75 cm³) at *ca.* 20°C. The white precipitate, which formed immediately in quantitative yield, was filtered off, washed with ethanol and dried *in vacuo*. (Found: C, 40.6; H, 8.1; N, 20.4; S, 24.1. Calc. for $C_{38}H_{90}N_{16}S_8O_5$, i.e. $C_9H_{19}N_4S_2 \cdot H_2O, 0.25C_2H_5OH$: C, 41.2; H, 8.1; N, 20.3; S, 23.1%).

Metal–copolymer complexes. The copolymer (1 g, 3.6×10^{-3} mol dithiocarbamate), which is insoluble in water, was stirred with aq. solutions of the compounds $VOSO_4 \cdot 2H_2O$, $FeCl_2 \cdot 2H_2O$, $CoCl_2 \cdot 6H_2O$, $NiCl_2 \cdot 6H_2O$, $CuSO_4 \cdot 5H_2O$ (*ca.* 7.5×10^{-3} mol) in water (100 cm³) under air or nitrogen at 20°C for 0.5–1 hr. The metal–copolymer complexes were filtered off, washed with water and dried *in vacuo*. Analyses are given in Table 1.

Physical measurements. Electronic spectra were recorded in a Unicam SP1800 spectrophotometer. Diffuse-reflectance spectra of powdered solids were obtained relative to a magnesium oxide standard or the uncomplexed polymer on a Unicam SP700C spectrophotometer. IR spectra of compounds in KBr discs or Nujol mulls were recorded on a Perkin–Elmer 557 spectrophotometer. ESR spectra were obtained on a Varian E-3 spectrometer calibrated with 1,1-diphenyl-2-picrylhydrazyl (*g* 2.0037. Magnetic susceptibilities were measured on a Newport Instruments Gouy balance calibrated with $[Ni(H_2NCH_2CH_2NH_2)_3]S_2O_3$. Diamagnetic corrections were taken from Selwood[7] and determined by measurement for the copolymer.

Analyses. Carbon, hydrogen and nitrogen were determined by the microanalytical service of this Department and sulphur by Butterworth Microanalytical Consultancy Ltd. Metals were determined by standard gravimetric procedures and by atomic absorption after decomposing the complexes with 1.1 nitric–sulphuric acid.

RESULTS AND DISCUSSION

The copolymer

Structure of the copolymer. The dithiocarbamate copolymer (I) is prepared by CS_2 substitution at primary and secondary amino groups of poly(iminoethylene). The latter has an average molar mass of 40,000 g mol^{-1}. Chain branching occurs at nitrogen given a 1:2:1 ratio of primary:secondary:tertiary amino groups.[8] The maximum number of amino groups which undergo substitution with CS_2 is *ca.* 35%, the actual number depending on the CS_2/poly(iminoethylene) ratio in the preparation.[9] In the copolymer used in the present work *ca.* 25% of the amino groups were substituted. Thermal analysis showed substitution was predominantly at the primary amino sites and some water and ethanol was usually retained.

UV and IR spectra of the copolymer. Peak positions and assignments are given in Table 2. The UV spectrum of the copolymer was similar to that of $Et_2NCS_2^-Na^+$ in agreement with the zwitterion formulation (I). In the IR spectrum, by analogy with simple dithiocarbamate $R_2NCS_2^-$, we assign a strong broad band centred at 1460 cm^{-1} as $\nu(NCS_2) + \delta(CH_2)$.[10,11] The strong band at 965 cm^{-1} is assigned as $\nu_{as}(CNC) + \nu_{as}(CS_2)$.[12] For simple dithiocarbamates, $R_2NCS_2^-$, this band moves to lower wavenumbers as the number and size of the R groups increase. For our copolymers, the shift of the band to lower wavenumbers was greatest in copolymers with more than 25% substitution of amino groups, i.e. when secondary as well as primary amino groups had reacted with CS_2.[9] The presence of the band at 965 cm^{-1} is

*Author to whom correspondence should be addressed.
†Present address: Department of Zoology, The University, Whiteknights, Reading RG6 2AD, England.

Table 1. Formulation of metal copolymer complexes[a]

Formulation[b]	Analysis/wt.-% [c]			
	C	H	N	M
$VOSO_4$.1.24 PIED.3.5H_2O	25.1(25.3)	5.20(5.33)	12.7(13.1)	9.80(9.61)
$FeCl_3$.5.0 PIED.30H_2O	27.5(27.8)	7.00(8.24)	15.1(14.4)	2.80(2.88)
$FeCl_2$.3.0 PIED.3.0H_2O	30.6(30.8)	5.00(6.68)	15.6(16.0)	9.0(9.03)
$CoCl_3$.5.0 PIED.5.7H_2O	36.3(35.8)	7.00(7.39)	18.4(18.6)	3.90(3.90)
$CoCl_3$.4.6 PIED.27H_2O	27.9(27.7)	6.90(8.15)	14.6(14.4)	3.30(3.29)
$NiCl_2$.1.67 PIED 3.0H_2O	30.3(30.2)	6.20(6.59)	15.6(15.6)	10.0(9.86)
$NiCl_2$.1.55 PIED.3.9H_2O	28.8(28.7)	6.40(6.63)	14.3(14.8)	10.2(10.1)
$CuSO_4$.1.10 PIED.4.5H_2O	23.5(23.1)	4.70(6.04)	11.8(12.0)	12.6(12.4)

[a] Prepared as outlined in Table 3.

[b] PIED is the ideal copolymer repeating unit, $C_9H_{20}N_4S_2$.

[c] Found and, in parenthesis, calculated.

Table 2. IR and UV spectra of the copolymer and related compounds. (a) IR spectra ($\tilde{\nu}$/cm^{-1})[a]

Assignment	Copolymer	$Et_2NCS_2^-Na^+.3H_2O$
ν(OH)	3400 vs,b	3300 vs.b
ν(NH)	3240 vs	-
ν(CH)	2930 vs, 2830 vs	2915 vs, 2860 vs
δ(NH)	1615 mb,1505 sh	-
ν(N-CS_2) + δ(CH_2)	1460 vs	1478 vs
ν[(C)CN]	1215 w	1204 vs
ν(CNC+CS_2)	965 vs,b	988 vs,b

[a] In KBr discs. Peak maxima, relative intensities (vs, very strong; s, strong; m, medium; w, weak; b, broad, sh, shoulder) (ν, stretching; δ, bending).

(b) U.v. spectra ($\tilde{\nu}$/10^3 cm^{-1})

Phase	Copolymer	$Et_2NCS_2^-Na^+.3H_2O$
Solid [a]	44.5	45.0
	37.6	37.0
	33.4	33.4
	28.4	28.4
aqueous solution	47.4	48.5
	38.8	38.9
	34.7	35.5

[a] Reflectance relative to MgO.

Table 3. Uptake of metal ions by the copolymer[a]

Ion		Conditions [b]	Initial concentration[c] $10^2[M]_o$/mol ℓ^{-1}	Bound metal $10^3[M]_b$/mol(g polymer)$^{-1}$	Fractional coverage(θ) [d]
VO^{2+}	[e]	0.5h, air	8.272	3.09	0.81
Fe^{2+}	[f]	0.5h, air	7.603	0.675	0.177
		0.25h, N_2	6.753	2.10	0.551
Co^{2+}	[f]	0.5h, N_2	7.634	0.732	0.192
		0.5h, N_2	7.616 [g]	0.782	0.205
Ni^{2+}	[f]	1.0h, air	7.603	2.22	0.583
		1.0h, N_2	7.575	2.47	0.648
Cu^{2+}	[e]	0.75h, air	7.605	3.40	0.892

[a] Copolymer (1.0g, 3.813×10^{-3} mol CS_2^- Groups, 14.6×10^{-3} mol N) stirred with metal ion solution (100 cm^3) at ca. 20°C.

[b] Contact time, whether under air or nitrogen.

[c] In deionised water unless otherwise indicated.

[d] $[M]_b/[L]$ where [L] is the molar concentration of CS_2^- groups per g polymer (see text).

[e] As sulphate.

[f] As chloride.

[g] In hydrochloric acid (0.4 mol ℓ^{-1})

consistent with the $RNHCS_2^-$ structure formed by reaction of CS_2 at primary amine sites.[10]

Metal–copolymer complexes. Aqueous solutions of metal salts, at concentrations twice that of the dithiocarbamato groups in the copolymer, were stirred with the copolymer until reaction was complete (0.5–1 hr). The fractional coverage (θ) of dithiocarbamato binding sites by the metal ions is given in Table 3. For 1:1 coordination of metal ions by dithiocarbamato groups θ should be unity but this value was never attained. If *bis*- and *tris*-complexes were formed θ would take the value 0.5 and 0.33. With Fe(II) in air and with Co(II) in air and under nitrogen, $\theta \leq 0.2$ and the products consisted mainly of copolymer complexes of Fe(III) and Co(III) which are therefore, as in the monomeric complexes, stabilised by dithiocarbamate. For the other metal ions, and the anaerobic reaction with Fe(II), $0.5 < \theta < 1$ and θ increased $Fe^{2+} < Ni^{2+} < VO^{2+} < Cu^{2+}$. The capacity of the copolymer for metal ions depends therefore not only on the stoichiometry of the complexes formed but also on the accessibility of the ligating groups. Binding with the amino groups by individual metal ions is discussed below.

For nickel the quantity taken up by the solid copolymer was determined as a function of the concentration of nickel in solution. The resulting adsorption isotherm is shown in Fig. 1. The horizontal portion, which occurs when the surface is saturated with nickel, corresponds to a ratio of nickel to copolymer repeating unit of 0.65:1, i.e. 65% utilisation of binding groups. The inflexion in the isotherm shows that adsorption of the nickel is stepwise. Since, in general, S-donor ligands bind Ni(II) more strongly then N-donor ligands we expect the initial, steeper part of the isotherm to represent Ni(II)-dithiocarbamato binding and the second, shallower part, Ni(II)-N binding. If, as indicated by the horizontal portion of the isotherm, a fraction 0.65 of the potential binding sites is available, then the first inflexion corresponds to a Ni:dithiocarbamate ratio of 1:2. The presence of Ni bound to S and N is consistent with the physical measurements (see below).

IR spectra of the metal–copolymer complexes. Peak positions and assignments are given in Table 4. Coordination of dithiocarbamate causes $\nu(N–CS_2)$ to move to higher wavenumbers[13] owing to an increased contribution of the canonical form $R_2N^+=CS_2^{2-}$ with the precise value for each metal depending on the R group (e.g. R=Et, 1478; L-proline, 1458 cm^{-1}).[10]

In the IR spectrum of the copolymer a strong, broad band centred at 1460 cm^{-1} is assigned $\nu(N–CS_2)+\delta(CH_2)$. In the metal–copolymer complexes the $\nu(N–CS_2)$ component moved to higher wavenumbers leaving,

Table 4. Spectroscopic and magnetic properties of the metal–copolymer complexes[a]

Metal ion	VO^{2+}	Fe^{2+}	Fe^{3+}	Co^{3+} [b]	Ni^{2+} [b]	Cu^{2+}
I.r.spectra ($\tilde{\nu}$/cm^{-1}) [c]						
ν(N–CS_2)	1500	1495	1490	1480	1495	1495
ν(CNC+CS_2)	970	990	975–980	970	980	960
ν(MS)	370	352		355–360	384	355
others	985 [d]					1105 [f]
	875 [e]					613 [f]
	1105 [f]					
	613 [f]					
	460 [g]					
uv-visible spectra ($\tilde{\nu}$/10^3 cm^{-1}) [h]						
	28.5	25.0	25.0	25.4	23.0	24.0sh
	23.0	19.0	19.0	20.6	21.0	16.0sh
	10.6	17.0sh	17.0sh	15.6	15.8	
		7.0sh	10.0sh	12.0sh	10.0	
		5.0	7.00sh	9.4sh		
Esr spectra (g-values)						
	2.008		4.250	2.041	2.111	2.089
	1.993		2.186	2.010		
	2.899		2.140	1.870		
			1.982			
Magnetic moments (μ/μ_B)						
	1.39	5.40	5.19	0.87	1.86	2.26

[a] Complexes in Table I. [b] Identical data for the two cobalt and nickel complexes respectively of Table I. [c] In KBr discs, positions of structurally significant peaks and assignments (cf. Table I). [d] ν(V=O). [e] ν(VOV). [f] Sulphate. [g] ν (V-O) (cf. 480 cm^{-1} for [VO(acetylacetonate)$_2$] and 463 cm^{-1} for its pyridine adduct). [h] Reflectance spectra relative to MgO (sh. shoulder).

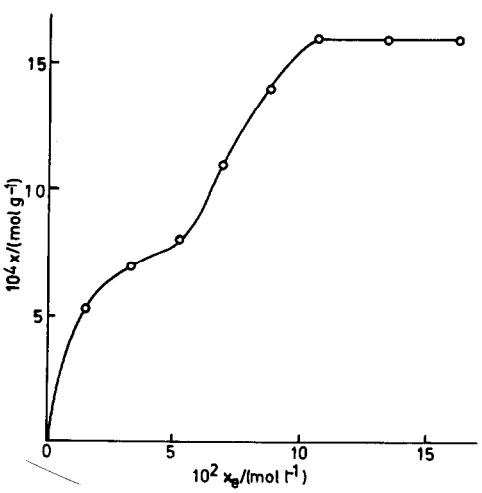

Fig. 1. Isotherm of concentration change at 20°C for the binding of Ni^{2+} ions by a poly(iminoethylene) dithiocarbamate copolymer: bound nickel [10^4x/mol (g copolymer)$^{-1}$] vs equilibrium concentration of Ni^{2+} ions [10^2x_e/mol l^{-1}] in water. The copolymer (0.2 g) was equilibrated with aqueous Ni(II) chloride (20 cm^3), the suspension filtered, and Ni determined in the filtrate by EDTA titration.

if any dithiocarbamato groups remained free, a medium intensity band at 1460 cm^{-1} [ν(NCS_2)] of free dithiocarbamate and a band at 1430 cm^{-1} [δ(CH_2)]. Therefore, for the metal copolymer complexes assignments may be complicated by the presence of bound and free dithiocarbamato groups. For the copolymer ν(N–CS_2) (1460 cm^{-1}) was 18 cm^{-1} lower than for $Et_2NCS_2^-Na^+$ (1478 cm^{-1}) (see p. 3). For our metal–copolymer complexes we found additional strong bands at wavenumbers consistently *ca.* 15 cm^{-1} less than for the Et_2NCS_2 complexes and so we assign these bands as ν(NCS_2) and they are evidence for the coordination of the dithiocarbamato groups of the copolymer.

The dithiocarbamato group can be bidentate or, less commonly, monodentate. In the case of monodentate binding the 950–1050 cm^{-1} band [ν_{as}(CNC) + ν_{as}(CS_2)] is split by about 25–30 cm^{-1}. Smaller splitting (<20 cm^{-1}) or broadening of the band may be observed for bidentate, unsymmetrical dithiocarbamates.[10] For our copolymer complexes, the band was fairly broad but was split only in the Cu complex and then by less than 20 cm^{-1}. Therefore binding of the dithiocarbamate is bidentate. Further evidence for metal coordination to sulphur is the weak to medium bands at 352–384 cm^{-1} assigned ν(M–S) by comparison with the low molecular weight complexes.

Vanadium. With $Et_2NCS_2^-$ the vanadium (IV) air sensitive complexes $[VO(Et_2NCS_2)_2]$ (grey)[11b,14] and $[V(Et_2NCS_2)_4]$ (red-brown)[15] are known. However, our vanadium–copolymer complex was green with a V : PIED ratio (0.81) indicative of 1 : 1 coordination. The electronic spectrum of the V-copolymer complex (Table 4) was different from that of $[VO(Et_2NCS_2)_2]$ (peaks at 17,200, 18,600, 23,500 and 27,400 cm^{-1}) and the magnetic moment (μ = 1.39) was in the range for VO^{2+} complexes having interactions between adjacent VO^{2+} groups (e.g. carboxylato and tridentate Schiff's base complexes).[16,17] The ESR spectrum was complex (g_{av} 1.99) and was not well enough resolved to establish whether there were fifteen lines, as would be expected for a complex with two interacting V(1V) atoms, or a monomer with very low symmetry. The IR spectrum showed the presence of some uncoordinated CS_2^- groups [$\nu(NCS_2)$, 1460 cm^{-1}]. Our data on the vanadium copolymer complex are, therefore, best interpreted by the structure 2 with dithiocarbamate bound to interacting vanadyl groups. Since ν(V=0) is in the range observed for the monomeric VO^{2+} complexes, the interaction does not involve terminal oxide. The stoichiometry (0.81 : 1 PIED) indicates predominantly 1 : 1 coordination of VO^{2+} and dithiocarbamate. The coordination sphere could be completed by H_2O or OH^- ligands, and in agreement with this proposal we can assign medium intensity IR bands (Table 4) to ν(V–O) and ν(VOV).[18] The relatively high uptake of vanadium by the copolymer is therefore to be attributed not to a high binding affinity but rather to the formation of a 1 : 1 complex.

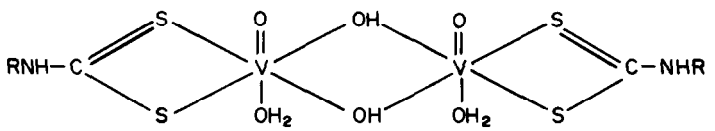

(2)

Iron. A solution of Fe(II) chloride with the copolymer gave a Fe(III) complex (I) in air and a Fe(II) complex (II) under nitrogen (Table 1). The Fe(III)–copolymer complex (I) was black; its electronic spectrum (Table 4) was similar to that of the *tris*-complexes,[19] e.g. $[Fe(Et_2NCS_2)_3]$ (absorption maxima at 7000, 17,100, 19,700, 25,700 and 28,900 cm^{-1}). These complexes, which have distorted prismatic structures,[20] show the phenomenon of spin cross-over;[19] the $^2T_{2g}$ state lies below $^6A_{1g}$ with a separation of the order of thermal energies and at room temperature the magnetic moment is less than the spin only value for high spin Fe(III) (5.9 B.M.). The magnetic moment of our Fe(III) copolymer complex (Table 4) was similarly less than the high spin value. The Fe(III) complex also gave an ESR spectrum at room temperature which compared with that of other dithiocarbamate Fe(III) complexes.[21] There were signals at $g = 4.25$, $g = 2$ and a five line signal at $g = 1.98$.

The UV-visible spectrum of our Fe(II) complex was similar to that of complex (I) except for a shoulder at *ca.* 10,000 cm^{-1} which corresponds with a peak in the spectra of Fe(II) dithiocarbamato complexes.[19a,22] The magnetic moment (5.40 B.M.) was in the range expected for high spin Fe(II) with a small orbital contribution and greater than the moments observed for simple iron (II) dithiocarbamates {see $[Fe(R_2NCS_2)_2]$ dimers, 4.8–4.2 B.M., and the *tris*-complex $[Fe(Et_2NCS_2)_2S_2C_2(CCF_3)_2]$, 2.25 B.M.}. Complex (II) was ESR inactive as expected for Fe(II). Both the simple iron (II) complexes and our iron (II) copolymer complex readily oxidise in air.

The question arises as to the number of dithiocarbamato groups bound to iron in complexes (I) and (II). The spectroscopic properties of the copolymer complexes are similar but not identical with those of simple iron dithiocarbamato complexes and the magnetic moments are greater. The NCS_2 vibrations in the IR spectra gave broad bands which can be atrributed to the presence of both bound and free NCS_2 groups. In complex (I) Fe(III) probably has distorted octahedral geometry (see the ESR spectrum) and is ligated only by NCS_2^- groups. In complex (II) the number of NCS_2^- groups bound to Fe(II) is one or two and the coordination sphere is completed by Cl^-, H_2O, or amino groups of the copolymer.

Cobalt. Co(II) chloride and the copolymer in the presence and absence of air gave green complexes which contained Co(III). Co(III) is strongly stabilised by dithiocarbamate; reaction of Co(II) with $Et_2NCS_2^-$ even in the absence of air is reported to give a Co(III) complex.[3] The IR spectrum of our cocopolymer complex was similar to that of the Fe(III) complex indicating the presence of both bound and free dithiocarbamate groups. The electronic spectrum was similar to that of $[Co(Et_2NCS_2)_3]$ (peaks at 15,500; 20,600; 25,000 and 27,000 cm^{-1})[3,9] but there were additional shoulders at 9400 and 12,000 cm^{-1}. The magnetic moment was greater than expected for diamagnetic low spin Co(III). Broad ESR signals ($g \sim 2$) observed at room temperature sharpened on cooling to 77 K. Such signals could arise from distorted octahedral Co(II). We conclude that the copolymer complexes contain mainly cobalt(III) bound to dithiocarbamate and some Co(II) in a distorted coordination environment.

Nickel. Ni(II) chloride and the copolymer gave green complexes in the presence and absence of air. Their IR spectra showed the absence of free NCS_2^- groups (no 1460 cm^{-1} band). The monomeric Ni(II) *bis*-(dithiocarbamates) are square planar[23] and, therefore, if Ni(II) is similarly coordinated in the Ni–copolymer complex (Ni : copolymer 0.63 : 1) some nickel must be bound to the amino groups. The electronic spectra of the monomeric Ni(II) dithiocarbamate and our copolymer complexes were similar. A peak at *ca.* 30,000 cm^{-1} has been assigned to charge transfer in monomeric Ni(II) dithiocarbamates.[24] A peak at 10,000 cm^{-1} is characteristic of

octahedral Ni(II) coordinated to amino groups. The copolymer complex was paramagnetic (1.86 B.M.) and gave a broad ESR signal. From the observed magnetic moment (1.86 B.M.) we calculate the ratio of planar ($\mu = 0$) to octahedral (typically $\mu = 3.2$ B.M.) species as 2:1.

Copper. Copper (II) sulphate and the copolymer gave a khaki complex with the highest metal content of all the complexes prepared. The IR spectrum showed that not all the dithiocarbamate groups had reacted. The main feature of the electronic spectrum was a peak at 16,000 cm^{-1} similar to a peak found for $[Cu(Et_2NCS_2)_2]$.[3,9] Absorbance extended into the near IR as in copper (II) amino complexes. The magnetic moment was close to the spin only value for one unpaired electron showing that the Cu was present as Cu(II). The ESR spectrum was isotropic with a g value (2.089) slightly higher than found for the analogous monomeric complex (2.052).[25] The ESR spectrum was quite similar to that of $[Cu(dien)_2(NO_3)]$.[26] Low molecular weight copper dithiocarbamato complexes occur in +1, +2, +3 and mixed oxidation states, and the complexes often have interacting copper atoms in dimeric or polymeric species.[4] There was no evidence of reduction or magnetic interactions in the copolymer complexes. We conclude that copper (II) is bound to NCS_2^- and also to amino groups of the copolymer rather like Ni(II).

CONCLUSIONS

All the metals combined with the dithiocarbamato groups of the copolymer as deduced from IR spectra, i.e. the shift in the $\nu(NCS_2)$ band and the metal sulphur vibrations. The electronic spectra, magnetic moments and ESR spectra, however, show that the structures were not always the same as found in the analogous low molecular weight complexes. Not all the dithiocarbamato groups of the copolymer were coordinated and the degree of reaction appears to depend on the number of dithiocarbamates bound in the low molecular weight species. Thus Co(III) and Fe(III) dithiocarbamates are coordinated to six sulphurs and so the degree of reaction depends on the accessibility of three dithiocarbamato groups for coordination whereas the requirements for VO^{2+}, Fe^{2+}, Ni^{2+} and Cu^{2+} are two dithiocarbamates. The evidence for the binding of amino groups is limited. The electronic spectra of the nickel and copper complexes both have bands characteristic of metal amino complexes. This was supported in the case of copper by the ESR spectrum.

The structure of the copolymer and the binding of metal ions

The shape of the polyethylene molecule has been described as "elliptical" similar to an American football.[8] The rapid and extensive reaction of the amino groups with CS_2 suggests that the reactive groups are on the outside of the polymer molecule and that the resulting dithiocarbamato groups are also on the outside. Consistent with this is our conclusion that *ca.* 80% of the dithiocarbamato groups are accessible to metal ions. The acid form of the copolymer prepared by us is insoluble in water but the copolymer dissolves readily in alkaline solutions. The insolubility of the polymer suggests an interaction between molecules (or particles) possibly through NH_2^+ and CS_2^- groups [see (1)]. This interaction is destroyed by deprotonation in alkali and so the polymer dissolves. Transition metal complexes of the copolymer were prepared in our work by reaction of an aqueous suspension of the acid form of the copolymer with solutions of metal salts. Copolymer complexes may also be prepared by reaction of aqueous *solutions* of the sodium salt of the polymer and metal ions. The complexes are insoluble and precipitate.[27] Therefore, the transition metal ions, like the proton, are effective in binding together polymer molecules or particles by forming *bis* and *tris* complexes with particles by binding dithiocarbamato groups and amino groups from different polymer molecules or particles. Such interactions must also occur when the complexes are prepared by interaction with suspensions of the polymer. The ligating groups on the copolymer are charged and distributed over the polymer surface. The initial reaction is electrostatic, cations binding to the negative sulphur and anions to the positive nitrogen. Davydova[28] has proposed a mechanism for metal binding with polymers whereby initial coordination of the metal ion is to one ligand on the polymer. Further coordination of the metal will depend on the proximity of neighbouring groups and the flexibility of the copolymer to change conformation. This treatment has usually been confined to soluble polymers but we have shown that our insoluble copolymer behaves similarly.

None of the copolymer complexes had properties identical with those of analogous low molecular weight compounds. Studies of binding of metal ions with proteins have shown that conformational changes in the protein occur following binding of the metal ion and the consequent redistribution of charge. Structural studies of metalloproteins have revealed that at the binding site the metal may have a distorted stereochemistry not found in complexes of simple ligands.[29] Our work has shown that in reactions of metal ions with a copolymer complexes with properties and probably structures different from those of analogous complexes with simple ligands are formed.

Acknowledgements—MGT thanks the Science Research Council for a research studentship. We have refined our script following helpful comments from the referee.

REFERENCES

[1]J. H. Barnes and G. F. Esselmont, *Die Makromol. Chem.* 1976, **177**, 307; C. O. Giwa and M. J. Hudson, to be published.
[2]P. C. H. Mitchell and M. G. Taylor, *J. Less Common Metals* 1977, **54**, 111; *Proc. Climax 2nd Int. Conf. on the Chemistry and Uses of Molybdenum* (Edited by P. C. H. Mitchell), p. 55. London (1976).
[3]D. Coucouvanis, *Prog. Inorg. Chem.* 1970, **11**, 234 and references therein.
[4]J. Willemse, J. A. Cras, J. J. Steggerda and C. P. Keijzers, *Structure and Bonding* 1976, **28**, 83 and references therein.
[5]D. Coucouvanis, *Prog. Inorg. Chem.* 1979, **26**, 301.
[6]D. D. Perrin, W. L. F. Armarego and D. R. Perrin, *Purification of Laboratory Chemicals.* Pergamon Press, Oxford (1966).
[7]P. W. Selwood, *Magnetochemistry*, 2nd Edn. Interscience, London (1956).
[8]L. E. Davis in R. L. Davidson and M. Sitha (Editors), *Water-soluble Resins.* Reinhold, New York (1968).
[9]M. G. Taylor, Ph.D. Thesis. University of Reading (1978).
[10]D. A. Brown, W. K. Glass and M. A. Burke, *Spectrochim. Acta* 1976, **32a**, 137.
[11a]S. Wajda and K. Drabent, *Bull. Acad. Polon Sci. Ser. Sci. Chim.* 1977, **25**, 963. [b]B. J. McCormick, *Inorg. Chem.* 1968, **7**, 1965. [c]S. Vigoe and J. Selbin, *J. Inorg. Nucl. Chem.* 1969, **31**, 3187.

[12]K. A. Jensen, B. M. Dahl, P. H. Nielsen and G. Borch, *Acta Chem. Scand.* 1971, **25**, 20, 29; *Ibid.* 1971, **25**, 2038; 1972, **26**, 2241.
[13]J. Chatt, L. A. Duncanson and L. M. Venanzi, *Nature* 1956, **177**, 1042.
[14]K. Henrick, C. L. Raston and A. H. White, *J. Chem. Soc. (Dalton)* 1976, 26.
[15a]D. C. Bradley and M. H. Gitlitz, *J. Chem. Soc.* (A), 1969, 1152. [b]D. C. Bradley, I. F. Rendall and K. D. Sales, *Ibid.* 1973, 2228.
[16]A. P. Ginsberg, E. Koubeck and H. J. Williams, *Inorg. Chem.* 1966, **5**, 1656.
[17]A. Syamal, *Co-ord Chem. Rev.* 1975, **16**, 309.
[18]A. Anagnostopoulos, D. Nichols and M. E. Pettifer, *J. Chem. Soc. Dalton* 1974, 569.
[19a]R. L. Martin and A. H. White, *Trans. Met. Chem.* 1968, **4**, 113. [b]S. A. Cotton, *Coord. Chem. Rev.* 1972, 8. [c]C. A. Tsipis, C. C. Hadjikostas and G. E. Manoussakis, *Inorg. Chim. Acta* 1977, **23**, 163.
[20]B. F. Hoskins and B. P. Kelly, *J. Chem. Soc. (Chem. Comm.)* 1968, 1517.
[21]C. Flick and E. Gelerinter, *Chem. Phys. Lett.* 1973, **23**, 422.
[22]L. F. Larkworthy, B. W. Fitzsimmons and R. R. Patel, *J. Chem. Soc. (Chem. Comm.)* 1973, 902.
[23]G. Peyronel and A. Pignedati, *Acta Cryst. Sect. A.* 1966, **21**, 156.
[24]D. Oktare, B. Siles, J. Stefanec, E. Korgara and J. Garoj, *Coll. Czech. Chem. Comm.* 1980, **45**, 791.
[25]T. R. Reddy and R. Srinivasan, *J. Chem. Phys.* 1965, **43**, 1404.
[26]B. J. Hathaway, M. J. Bew and D. E. Billing, *J. Chem. Soc.* (A) 1970, 1090.
[27]M. Okawara and T. Nakai, *Bull. Tokyo Inst. Technol.* 1966, **78**, 1.
[28]S. L. Davydova and N. A. Plate, *Co-ord. Chem. Rev.* 1975, **16**, 195.
[29]B. L. Vallee and R. J. P. Williams, *Proc. Natl. Acad. Sci. U.S.A.* 1968, **59**, 498.

Polyhedron Vol. 1, No. 3, pp. 233–238, 1982
Printed in Great Britain.

0277–5387/82/030233–06$03.00/0
Pergamon Press Ltd.

CONFORMATIONAL ANALYSIS IN DIASTEREOISOMER EQUILIBRIA OF SQUARE-PYRAMIDAL $[C_5H_5(CO)_2Mo$ PYRIDINE-2-IMINE$]PF_6$ COMPLEXES

DEVENDRA K. RASTOGI* and SHARAD RASTOGI
Department of Chemistry, Meerut College, Meerut-250001, India

(*Received* 3 *August* 1981)

Abstract—Synthesis and characterization of some new square-pyramidal pyridine-2-imine complexes $[C_5H_5(CO)_2MoNC_5H_4CX{=}NCH(R_1)(R_2)]PF_6$ with $X = CH_3$, C_6H_5 and chiral amine, 1-phenyl-isobutylamine and amino acid methyl ester $H_2NCH(COOCH_3)(R)$ with $(R) = (CH_2C_6H_5)$ and (C_2H_5) have been reported. In combination with Mo chirality (R) and (S), mixtures of two diastereoisomeric pairs of enantiomers with racemic amine and amino acids were obtained which were separated by fractional cystallization. The diastereoisomers differ in the chemical shift of most of their ^1H NMR signals and interconvert on heating in acetone-d_6 at 80°C for 80 hr and 40°C for 200 hr. On the basis of three conformational determining effects (i) C–H or C-alkyl of the asymmetric centre eclipses the ligand plane, (ii) MC_5H_5/C_6H_5 attraction and (iii) MC_5H_5/alkyl repulsion in order of decreasing significance, the chemical shifts of the C_5H_5 signals, their differences as well as the diastereoisomer ratio at equilibrium for all the complexes has been rationalised.

INTRODUCTION

Recently, the conformational analysis for a number of square-pyramidal pyridine-imine complexes $[C_5H_5(CO)_2MoNC_5H_4CX{=}NCH(R_1)(R_2)]PF_6$ with $X = H$, CH_3 and C_6H_5 was reported.[1,2] The asymmetric catalysis frequently makes use of such chelate ligands with optically active substituents.[3–6] We report herein synthesis, characterization and conformational analysis of some new complexes $[C_5H_5(CO)_2Mo$ pyridine-2-imine$]PF_6$ with methyl and phenyl substituents at the imine carbon atom. 1-Phenyl-isobutylamine (I, IV) and amino acid methyl esters $H_2NCH(COOCH_3)(R)$ with $(R) = CH_2C_6H_5$(II, V) and C_2H_5(III, VI) were taken to derive the Schiff bases NN′ used in these studies. This is an extension of the work described in an earlier communication[1] wherein our efforts to synthesize pyridine–imine complexes with $(R_1)(R_2) = (i\text{-}C_3H_7)(C_6H_5)$ and $X = CH_3$ or C_6H_5 failed, for these decomposed during preparation.

EXPERIMENTAL

All operations were carried out under nitrogen using freshly distilled and dry solvents. The amino acid ester hydrochlorides were converted into the free bases by literature method.[7]

Synthesis of $[C_5H_5Mo(CO)_2NN']PF_6$ *complexes I–IV*

Violet crystals of $[C_5H_5Mo(CO)_2NN']Cl$ of complexes I and II, carmine crystals of III and IV and dark red crystals of V and VI were obtained by refluxing a solution of 5 mmol of $C_5H_5Mo(CO)_3Cl$ and 7 mmol of Schiff base NN′ in 50 ml benzene at 80°C for about 1 hr for complexes II, III, V, VI and at 40° for about 50 hr for I, IV until the theoretical quantity of CO was liberated. These were filtered off and dissolved in the minimum quantity of EtOH. After again filtering about 100 mL of water was added to the filtrate. Now 7 mmol of NH_4PF_6 were added to the stirred solution which resulted in the precipitation of hexafluorophosphate salt of the cations $[C_5H_5Mo(CO)_2NN']^+$. These were filtered, washed with water, ether and purified on a sephadex LH-20 column. Complexes I and IV were very air sensitive and therefore, care was taken in their preparation by removing traces of oxygen. The analytical data are given in Table 1. The complexes are readily soluble in acetone, CH_2Cl_2, alcohols, sparingly soluble in benzene, THF, chloroform and almost insoluble in ether and pentane. Preparation of complexes VII–IX has been described earlier.[2] The Schiff bases NN′ were derived from 1-phenyl-isobutylamine $H_2NCH(C_6H_5)(i\text{-}C_3H_7)$(I, IV); the amino acid methyl esters $H_2NCH(COOCH_3)(R)$ with $(R) = CH_2C_6H_5$(II, V); C_2H_5(III, VI).

Diastereoisomer separation and equilibration

The diastereoisomers of complexes I–VI were separated on the basis of their different solubilities. In all the cases enrichments of the less soluble isomer in the crystallised fraction and of the more soluble isomer in the mother liquor were obtained. For the diastereoisomer separation of complexes I and IV, minimum quantity of a mixture of acetone:CH_2Cl_2:ethanol (10:5:1) needed for dissolution was used. On keeping the solution at −5°C for about 20 days, crystals of the less soluble diastereoisomer were obtained. The separation has been monitored by ^1H NMR spectroscopy as the diastereoisomers differ in the chemical shift of their signals. Fractionation of complex II was done by dissolving in the minimum quantity of acetone:CH_2Cl_2:ether (0.5:6:3) and those of III, V and VI from CH_2Cl_2:pentane (4:1.5). In all the diastereoisomer separation experiments, the less and more soluble isomers were distinguished by their high field and low field C_5H_5 signals, respectively in their ^1H NMR spectra.

The epimerization was carried out as described before.[2] The diastereoisomer equilibria were approached from both sides. To fully equilibrate, the fractions enriched in the more and less soluble diastereoisomers were heated in acetone-d_6 in sealed NMR tubes at 80°C for 80 hr (II, III, V, VI) and for about 200 hr at 40°C (I, IV). Interconversion that occurs was frozen by cooling. The room temperature ^1H NMR spectrum gives the diastereoisomer ratio at equilibrium from the C_5H_5 signals (I, II, IV, V) and from both the C_5H_5 and $COOCH_3$ signals (III, VI).

RESULTS AND DISCUSSION

In the reaction of $C_5H_5Mo(CO)_3Cl$ with Schiff base ligands NN′ (Schemes I and II), one mole of CO is liberated and the Cl ligand covalently bonded to Mo is displaced as Cl^-, thereby resulting in the formation of the salt $[C_5H_5Mo(CO)_2NN']Cl$, which by metathesis with NH_4PF_6 are converted into the sparingly soluble

*Author to whom correspondence should be addressed.

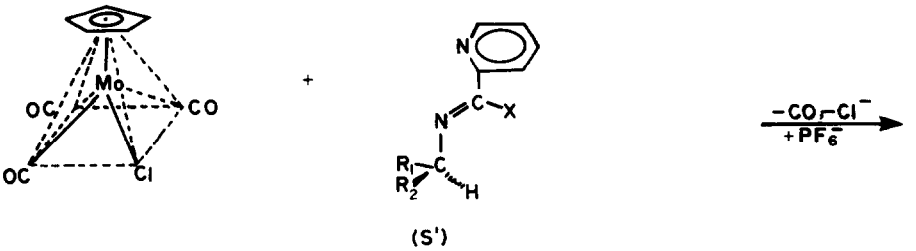

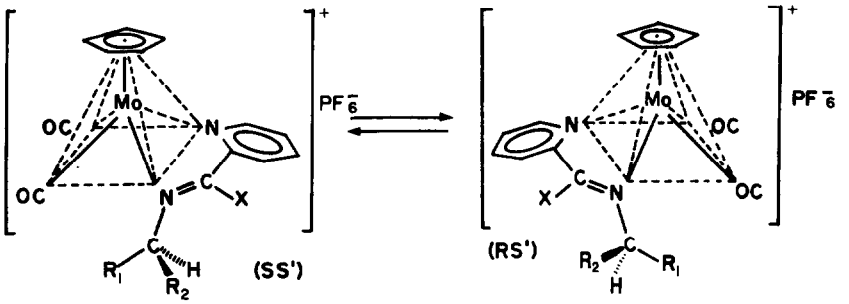

	I	II	III	IV	V	VI	VII	VIII	IX
R_1	i-C_3H_7	$COOCH_3$	$COOCH_3$	i-C_3H_7	$COOCH_3$	$COOCH_3$	i-C_3H_7	$COOCH_3$	$COOCH_3$
R_2	C_6H_5	$CH_2C_6H_5$	C_2H_5	C_6H_5	$CH_2C_6H_5$	C_2H_5	C_6H_5	$CH_2C_6H_5$	C_2H_5
X	C_6H_5	C_6H_5	C_6H_5	C_6H_5	CH_3	CH_3	H	H	H

Scheme 1.

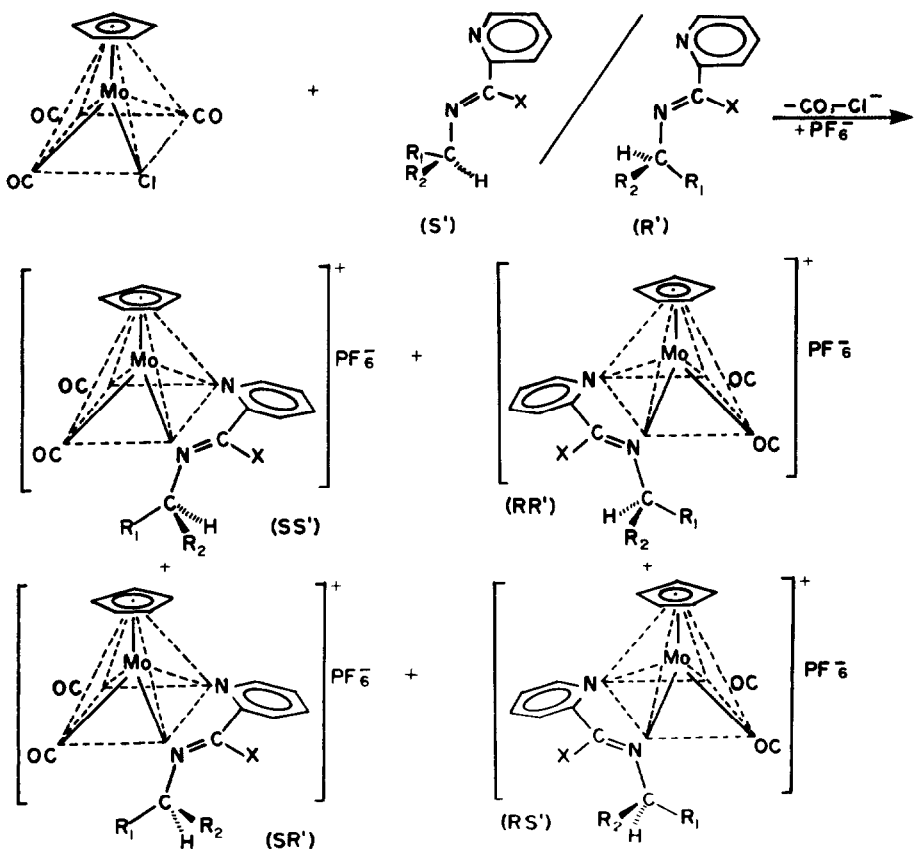

Scheme 2.

Table 1. Analytical data of $[C_5H_5Mo(CO)_2NN']PF_6$ complexes I–VI

Complex	Formula (mol.wt.)		C %	H %	N %	Yield %	m.pt./dec.pt.† °C
I	$[C_{29}H_{27}N_2O_2Mo]PF_6$	(676.4)	Calcd: 51.49	4.02	4.14	40	70–72†
			Found: 51.51	3.87	4.22		
II	$[C_{29}H_{25}N_2O_4Mo]PF_6$	(706.4)	Calcd: 49.31	3.57	3.96	75	155–160
			Found: 49.22	3.64	3.60		
III	$[C_{24}H_{23}N_2O_4Mo]PF_6$	(644.36)	Calcd: 44.74	3.56	4.35	75	176–180
			Found: 44.36	3.29	4.26		
IV	$[C_{24}H_{25}N_2O_2Mo]PF_6$	(614.38)	Calcd: 46.92	4.10	4.56	38	76†
			Found: 46.22	3.86	4.62		
V	$[C_{24}H_{23}N_2O_4Mo]PF_6$	(644.36)	Calcd: 44.74	3.56	4.35	60	140–142
			Found: 44.28	3.42	4.04		
VI	$[C_{19}H_{21}N_2O_4Mo]PF_6$	(582.29)	Calcd: 39.19	3.63	4.81	65	156
			Found: 38.60	3.28	4.44		

salts $[C_5H_5Mo(CO)_2NN']PF_6$. In this reaction the configuration[8,9] at the Mo atom is specified as (R) or (S). The introduction of a Schiff base ligand NN′ derived from an optically pure amine of stable configuration (S′) results in the formation of only two isomers, the diastereoisomers (RS′) and (SS′) ad depicted in Scheme 1. However, a Schiff base NN′ containing a chiral amine component in its racemic form (R′)/(S′) results in the formation of four isomers, the two diastereoisomeric pairs of enantiomers (RS′)/(SR′) and (SS′)/(RR′) as shown in Scheme 2.

Racemic amine was used for the synthesis of I and IV, whereas II, III, V and VI were prepared with optically pure (S)-amino acid esters. Even after fractional crystallization of these complexes, no optical activity was observed, which has been explained[2] due to racemization at the asymmetric centre during preparation. Therefore, the reaction mixture of complexes I–VI contain mixture of four isomers (SS′), (RS′), (SR′) and (RR′).

Two characteristic strong bands in the 1980–2000 and 1900–1920 cm^{-1} regions due to ν(C≡O) absorptions and a band of medium intensity due to ν(C=N) vibration between 1610–1625 cm^{-1}, are observed in the IR spectra of complexes I–VI. Besides this, the spectra of II, III, V and VI show a medium intensity band at 1735–1745 cm^{-1} due to ν(C=O) vibration of the ester group.

A perusal of Table 2, shows that in all the complexes both diastereoisomers differ appreciably in the chemical shifts of most of their ^{1}H NMR signals. As enantiomers under achiral conditions have identical ^{1}H NMR spectra, mixtures of two diastereoisomers (RS′)/(SS′) as well as two diastereoisomeric pairs of enantiomers (RS′)/(SR′) and (SS′)/(RR′) give the same ^{1}H NMR spectra. The ^{1}H NMR spectra of I–VI show singlets between $\delta = 5.20$–6.04 due to the C_5H_5 protons of the two diastereoisomers, suitable for the determination of the equilibrium ratio by integration. In III and VI, the chemical shift differences of both the C_5H_5 and $COOCH_3$ signals are sufficient enough to estimate this ratio at equilibrium. The equilibration with respect to the Mo configuration, brought about by heating the samples enriched in the more soluble and less soluble diastereoisomers in acetone-d_6 in sealed tubes, was periodically checked by recording their ^{1}H NMR spectra. It was confirmed that from both sides, i.e. enrichment in the more soluble and less soluble diastereoisomers, the same equilibrium ratio was obtained. The diastereoisomer ratio at equilibrium are shown in Table 3.

Interestingly, an examination of the value of diastereoisomeric ratios at equilibrium for square-pyramidal pyridine-2-imine complexes $[C_6H_5(CO)_2MoNC_5H_4CX{=}NCH(R_1)(R_2)]PF_6$ with X = C_6H_5(I, 80:20) and X = CH_3(IV, 67:33) $[(R_1)(R_2) = (i\text{-}C_3H_7)(C_6H_5)]$ indicates that asymmetric induction in these complexes is enhanced considerably as the molecular weight of the alkyl substituent increases in the alkyl phenyl derivatives with the ratios 56:44, 75:25 (X=C_6H_5) and 57:43, 63:37 (X=CH_3) $[(R_1)(R_2) = (CH_3)(C_6H_5); (C_2H_5)(C_6H_5)]$,[1] respectively and therefore, it can be stated that the equilibrium ratio of the diastereoisomers in such type of complexes depends essentially on the substituents at the chiral carbon atom. Brunner *et al.* have made similar observations in the corresponding square-pyramidal dicarbonylcyclopentadienylmolybdenum - pyridine - 2 - carbaldimine,[1] the thioamidato $C_5H_5(CO)_2MoSC(R)NR'$,[10–12] and the amidinato $C_5H_5(CO)_2MoN(R')C(R)NR'$ complexes.[3–5] However, the equilibrium ratios for the new complexes I–VI are comparatively low (Table 3).

Conformational analysis

The square pyramids of the diastereoisomers are

Table 2. ^{1}H NMR Spectra of $[C_5H_5Mo(CO)_2NN']PF_6$ complexes I–VI in acetone-d_6; assignments, multiplicities,[a] and values in ppm (internal Me_4Si)

Complex	$CH_2\underline{CH_3}$	$CH(\underline{CH_3})_2$	$\underline{CH_2}CH_3$[b]	$N{=}CC\underline{H_3}$	$\underline{CH_2}C_6H_5$	$COO\underline{CH_3}$	$C_5\underline{H_5}$	$C_6\underline{H_5}$[b]	$NC_5\underline{H_4}$[b]
I	–	^{2}1.08 ^{2}1.14	–	–	–	–	5.20 6.04	7.65	8.20, 7.35, 9.40[h]
II	–	–	–	–	3.60[f] 3.64[f]	3.79 3.84	5.30 6.00	7.67	8.40, 7.72, 8.38, 9.28
III	^{3}0.90[c] ^{3}1.04[c]	–	2.26	–	–	3.80 3.90	6.00 6.03	7.62	8.53, 7.48, 9.50[h]
IV	–	^{2}1.12 ^{2}1.19	–	2.98[e]	–	–	5.40 5.64	7.42	8.57, 7.60, 8.22, 9.32
V	–	–	–	2.92[e]	3.64[g] 3.66[g]	3.84 3.87	5.43 5.58	7.55	8.70, 7.64, 8.32, 9.44
VI	^{3}1.08[d] ^{3}1.22[d]	–	2.38	2.73[e]	–	3.86 3.98	6.00 6.02	–	8.65, 7.68, 8.42, 9.38

[a] Multiplicity is shown as superscript ; [b] multiplets ; [c] J=7.0 Hz ; [d] J=7.4 Hz ; [e] second isomer may be obscured by solvent signals ; [f] J=1.4 Hz ; [g] J=1.2 Hz ; [h] partly overlapped with C_6H_5 signal.

Table 3. Equilibrium ratios of the diastereoisomers of I–IX after equilibration in acetone-d_6

I	II	III	IV	V	VI	VII	VIII	IV
80:20	54:46	55:45	67:33	54:46	52:48	81:19	57:43	58:42

represented as projection formulas in which the chiral substituent is above the plane of the paper. It has been discussed[1] that the cations $C_5H_5Mo(CO)_2NN'$ of the pyridine–imine complexes are simple models for a conformational analysis of the arrangement of the chiral carbon substituent with respect to the ligand plane, although they contain a large number of atoms. From now onwards only the (S') configuration of the chiral carbon atom is considered (Scheme 1).

On the basis of experimental evidence, the following three effects which govern the conformation of such molecules have been elaborated: (1) C–H or C-alkyl of the asymmetric centre in the ligand plane is *most significant*, (2) phenyl/MC_5H_5 attraction is of *some significance*, (3) alkyl/MC_5H_5 repulsion is of *least significance*.

Large chemical shift differences of the C_5H_5 signals (0.84 and 0.70 ppm, Table 1) for the diastereoisomers (RS') and (SS') are observed for the alkyl,phenyl containing complex I and the ester derivative II containing aryl group, respectively. For the ester derivative III, which does not contain aryl group, the two C_5H_5 signals are isochronous, lying in the proximity of the signals of the low field isomer of I and II.

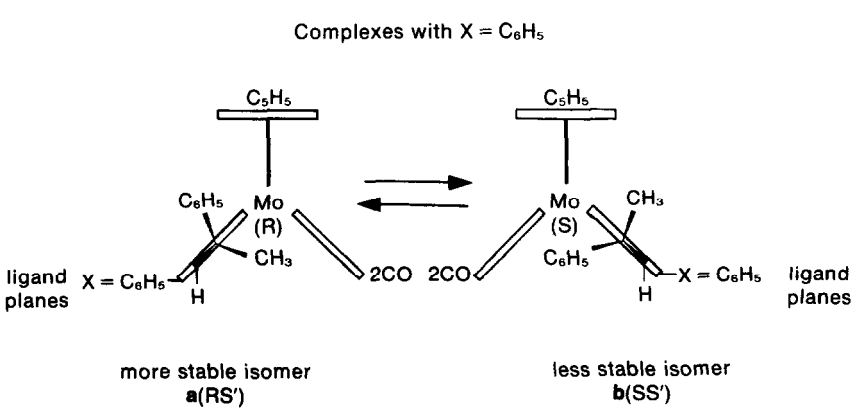

In all the three complexes with X = C_6H_5, the high field isomers are those which are thermodynamically favoured at equilibrium. The three effects, important for the determination of the conformation of the complexes under discussion, have been shown in the order of decreasing significance. Most important conformation determining factor for I–III is the effect number (1) C–H bond of the asymmetric centre coplanar with C–C_6H_5 bond of the chelate ring giving thereby conformations *a* and *b* to both the isomers. The reason for this arrangement is that all other substituents of the chiral carbon atom larger than hydrogen would suffer from severe steric hindrance with the large substituent X = C_6H_5 at the imine carbon atom. For I and II, effect (2), the phenyl orientation towards the C_5H_5 ligand is "β-phenyl effect" is the reason why the left diastereoisomer of configuration (RS′) and conformation *a* is thermodynamically more stable exhibiting the high field resonance than the right isomer of configuration (SS′) and conformation *b*, which is also destabilized by effect (3), i.e. MC_5H_5/alkyl repulsion. An upfield shift arises only if the C_5H_5 ligand is in the inner anisotropy region of the phenyl ring[3–5,13] as shown in the (RS′) isomer of conformation *a*, to which the high field signal must be ascribed. Because MC_5H_5/C_6H_5 interaction is not possible in isomer (SS′) of conformation *b*, it is thermodynamically less stable than (RS′). An interesting situation arises, if within the series of the square pyramidal pyridine-2-imine complexes $[C_5H_5Mo(CO)_2NN']PF_6$ with X=C_6H_5, the equilibrium ratios of the isopropyl derivative I (80:20) are compared with the ratios obtained for its corresponding methyl (56:44) and ethyl (75:25) derivatives,[1] the (SS′) isomer of type *b* is most destabilized in the isopropyl derivative than its corresponding methyl or ethyl derivatives owing to increasing MC_5H_5/alkyl repulsion. Further, on the basis of effect (3) the thermodynamically more stable isomer of complex III is assigned the configuration (SS′) and conformation *b* with the smaller alkyl group pointing towards MC_5H_5 moiety.

Complexes with X = H, VII and VIII containing aryl group exhibit chemical shift difference for the C_5H_5 signals 0.38 and 0.45 ppm, respectively, whereas for IX without an aryl group, the C_5H_5 chemical shift difference drops to 0.07 ppm.[2] Similar to the observations for I–III with X=C_6H_5, in the complexes VII–IX with X=H, the thermodynamically more stable complexes are the high field isomers. Here effect (1) determines that C-alkyl of the asymmetric centre eclipses the C–N bond yielding thereby conformations *c* and *d* to both the isomers. The analogy of this situation has often been seen in organic chemistry where, in the absence of steric hindrance, methyl rather than hydrogen usually eclipses double bonds like [13–27] C=N, C=O and C=C. According to conformation determining effect (2) –MC_5H_5/C_6H_5 attraction, the thermodynamically favoured high field isomers of VII and VIII can be assigned (SS′) configuration and conformation *c*. Effect (3) –MC_5H_5/alkyl repulsion, explains that the more stable diastereoisomer of IX has (RS′) configuration with the smaller alkyl group pointing towards the C_5H_5 ligand.

From the above discussion it can be concluded that conformations *a* and *b* prevail in complexes with X=C_6H_5 (I–III) and the thermodynamically more stable diastereoisomers of I and II dominating at equilibrium are (RS′). In complexes with X=H (VII–IX), conformations *c* and *d* are dominating and the more stable diastereoisomers of VII and VIII have (SS′) configuration. For complexes with X=CH_3 (IV–VI), an intermediate situation arises wherein all the conformations from *a* to *d* do exist.

For the aryl containing complexes IV and V with X=CH_3, chemical shift differences of C_5H_5 signals are 0.24 and 0.15 ppm, respectively. Interestingly, the position of C_5H_5 signals for these two complexes (Table 2) 5.40, 5.64δ (IV) and 5.43, 5.58δ (V) is intermediate between high and low field isomers of I and II and definitely closer to the high field isomer (RS′) of conformation *a*′ or the thermodynamically more stable isomer (SS′) of conformation *d*′, relative to the less stable isomer (SS′) of conformation *b*′ or (RS′) of conformation *c*′, respectively. Further, the position of these C_5H_5 signals is also upfield compared to both isomers of the dialkyl derivatives III and VI. Another important experimental result is the value of diastereoisomeric ratio at equilibrium for these complexes. Table 3 shows that for complexes with X=CH_3, the value of diastereoisomeric ratio at equilibrium 67:33 (IV), 54:46 (V), 52:48 (VI) is between those observed for complexes with X=C_6H_5 and X=H, except for V (X=CH_3) where this value is lower than that of VIII (X=H) but equal to that of II (X=C_6H_5).

The experimental results of (i) chemical shift difference of C_5H_5 signals and (ii) diastereoisomeric ratio at equilibrium point that in pyridine-2-imine complexes with X=CH_3, all the four conformations *a*′, *b*′, *c*′ and *d*′ are involved with the dominance of *a*′ and *d*′, which can possibly be explained by effect (2) and (3) making way for destabilization of conformations *b*′ and *c*′. This situ-

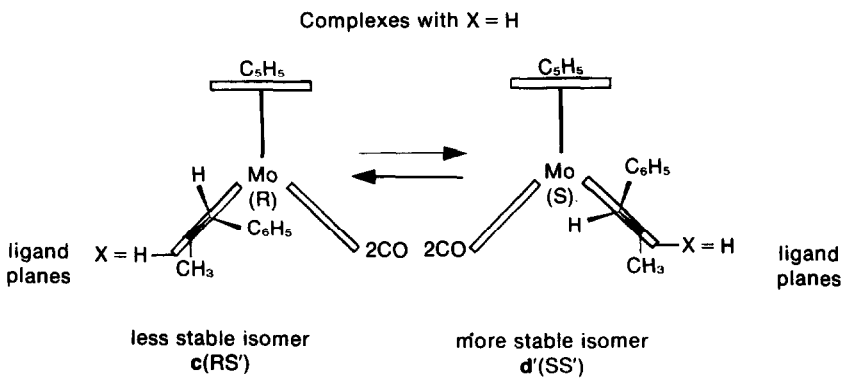

Complexes with X = CH_3

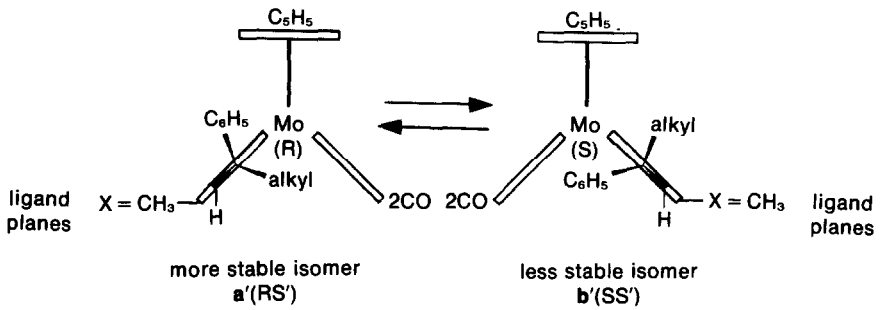

more stable isomer
a'(RS')

less stable isomer
b'(SS')

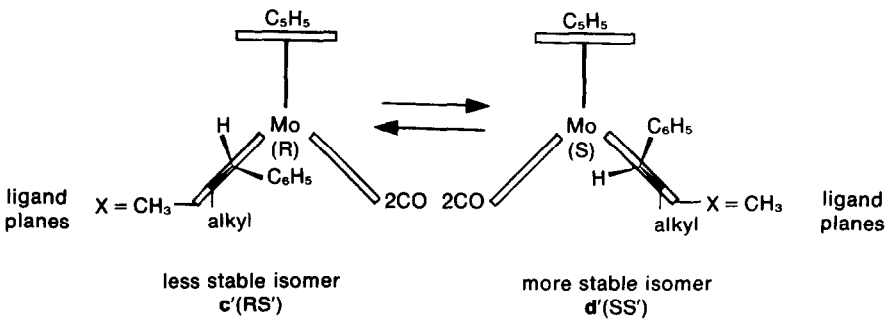

less stable isomer
c'(RS')

more stable isomer
d'(SS')

ation parallels to that observed in the conformational analysis of a large number of $C_5H_5(CO)_2Mo$ thioamidato,[8–10] amidinato[3–5] and pyridine-2-imine complexes[1,2] in which on the basis of these three conformational determining effects, it has been shown that the complexes with X=CH_3 are intermediate between X=H and X=C_6H_5, although closer to X=C_6H_5 than X=H.

Acknowledgement—One of the authors, Dr. D. K. Rastogi thankfully acknowledges the inspirations that he had derived from Prof. Dr. H. Brunner of Institut für Chemie, Universität Regensburg, West Germany, while he was working with him on problems of conformational analysis.

REFERENCES

[1]H. Brunner and D. K. Rastogi, *Bull. Soc. Chim. Belg.* 1980, **89**, 883.
[2]H. Brunner and D. K. Rastogi, *Inorg. Chem.* 1980, **19**, 891.
[3]I. Bernal, M. Creswick, H. Brunner and G. Agrifoglio, *J. Organometal. Chem.* 1980, **198**, C4.
[4]H. Brunner, J. Lukassek and G. Agrifoglio, *J. Organometal. Chem.* 1980, **195**, 63.
[5]H. Brunner, G. Agrifoglio, I. Bernal and M. W. Creswick, *Agew. Chem.* 1980, **92**, 645; *Agew. Chem. Int. Ed. Engl.* 1980, **19**, 641.
[6]H. Brunner and B. Pullman, *Catalysis in Chemistry and Biochemistry. Theory and Experiment*, p. 255. Reidel, New York, 1979.
[7]R. W. Chambers and F. H. Carpanter, *J. Am. Chem. Soc.* 1955, **77**, 1524.
[8]I. Bernal, S. J. LaPlaca, J. Corp, H. Brunner and W. A. Hermann, *Inorg. Chem.* 1978, **17**, 382.
[9]G. M. Reisner, I. Bernal, H. Brunner and J. Wachter, *J. Organometal. Chem.* 1977, **137**, 329.
[10]H. Brunner and J. Wachter, *Chem. Ber.* 1977, **110**, 721.
[11]H. Brunner and R. Lukas, *Chem. Ber.* 1979, **112**, 2528.
[12]H. Brunner, W. A. Hermann and J. Wachter, *J. Organometal. Chem.* 1976, **107**, C11.
[13]E. L. Eliel, N. L. Allinger, S. J. Angyl and G. A. Morrison, *Conformational Analysis*, p. 19. Wiley, New York, 1969.
[14]G. J. Karabatsos and D. J. Fenoglio, *Top. Stereochem.* 1970, **5**, 167.
[15]E. B. Wilson, *Chem. Soc. Rev.* 1972, **1**, 293.
[16]G. J. Karabatsos, *J. Am. Chem. Soc.* 1967, **89**, 1367.
[17]S. S. Butcher and E. B. Wilson, *J. Chem. Phys.* 1964, **40**, 1671.
[18]L. S. Bartell, B. L. Carroll and J. P. Guillory, *Tetrahedron Lett.* 1964, 705.
[19]M. J. T. Robinson, *Chem. Ind. (London)* 1964, 932.
[20]G. J. Karabatsos and N. Hsi, *J. Am. Chem. Soc.* 1965, **87**, 2864.
[21]Nguyên Trong Anh and O. Eisenstein, *Nouv. J. Chim.* 1977, **1**, 61.
[22]V. W. Suter, *J. Am. Chem. Soc.* 1979, **101**, 6481.
[23]F. Bernardi, N. D. Epiotis, R. L. Yates and H. B. Schlegel, *J. Am. Chem. Soc.* 1976, **98**, 2385.
[24]A. Cosse-Barbi and A. Massat, *J. Mol. Struct.* 1980, **63**, 31.
[25]D. Van Hemelrijk, L. Van den Enden, H. J. Geise, H. L. Sellers and L. Schäfer, *J. Am. Chem. Soc.* 1980, **102**, 2189.
[26]J. R. Durig and D. A. C. Compton, *J. Chem. Phys.* 1978, **69**, 2028.
[27]J. R. Durig and D. A. C. Compton, *J. Chem. Phys.* 1980, **84**, 773 and literature references therein.

Polyhedron Vol. 1, No. 3, pp. 239–241, 1982
Printed in Great Britain.

0277–5387/82/030239–03$03.00/0
Pergamon Press Ltd.

COMPLEX FORMATION OF TRACE ELEMENTS IN GEOCHEMICAL SYSTEMS—VI

STUDY ON THE FORMATION OF HYDROXO FLUORO MIXED LIGAND COMPLEXES OF THE LANTHANIDE ELEMENTS IN FLUORITE BEARING SYSTEM

B. A. BILAL* and V. KOß
Geochemical Group, Nuclear Chemistry Division, Hahn-Meitner-Institute für Kernforschung Berlin, FRG

(*Received* 26 *August* 1981)

Abstract—The complexation of the rare elements Ce, Eu, Tb and Yb in fluorite bearing model solution of the pH 5–9 and the pF 2–5 has been studied by means of the distribution method. Hydroxofluoro mixed ligand complexes were found to be the most important species formed at pH 7 and pF 3 which are the relevant values of hydrothermal fluorite bearing solutions. The stability constants and the distribution of these complexes as a function of pH and pF were determined.

INTRODUCTION

In previous publications[1–5] the complex formation between the lanthanide elements (Ln) and different ligands (Cl^-, F^-, SO_4^{2-}, OH^-) present in a fluorite bearing model system has been studied. Only fluoro and hydroxo complexes have such stability as to affect seriously the coprecipitation of the lanthanides during fluorite mineralization. At the pH and pF of hydrothermal solutions, mixed fluoro hydroxo complexes seem to play the most important role.

For the calculation of the stability constants of the mononuclear fluoro hydroxo mixed complexes, the following equations are evaluated taking into account that neither $[Ln(OH)_3]$ nor negative complexes are formed.[3,5] The total concentration of the Ln in the organic phase $(C_{Ln})_0$ and in the aqueous phase $(C_{Ln})_{aq}$ are expressed by the eqns (1) and (2)

$$(C_{Ln})_0 = [Ln(DEHP)_3] + [LnF(OH)_2]_0 + [LnF_2OH]_0 + [LnF_3]_0 \quad (1)$$

(HDEHP = the organic solvent di-2-ethyl-hexyl-phosphoric acid)

$$(C_{Ln})_{aq} = [Ln^{3+}] + [LnF^{2+}] + [LnOH^{2+}] + [LnF_2^+] + [Ln(OH)_2^+] + [LnF(OH)^+] \quad (2)$$

The distribution coefficient in the absence of F^- (Q_{laF}) is given by the equation

$$Q_{laF} = \frac{\beta_0[DEHP^-]}{1 + \beta_{01}[OH^-] + \beta_{02}[OH^-]^2}. \quad (6)$$

Equations (3) and (6) can be combined to give eqn (7) which is suitable for the calculation of the stability constants of the mixed ligand complexes from the sets of measurements in which the fluoride concentration was varied at a constant pH.

$$\frac{(Q - Q_{laF})(1 + \beta_{01}[OH^-] + \beta_{02}[OH^-]^2) + Q(\beta_{10}[F^-] + \beta_{20}[F^-])}{[F^-]} = \beta_{12}[OH^-]^2 - \beta_{11}[OH^-]Q + \beta_{21}[OH^-][F^-] + \beta_{30}[F^-]^2. \quad (7)$$

EXPERIMENTAL

The distribution of four selected lanthanides ^{144}Ce, ^{152}Eu, ^{160}Tb and ^{169}Yb between HDEHP and aqueous solutions having the pH 7.48 ± 0.03 and containing fluoride in increasing concentration as well as between HDEHP and aqueous solutions of the pF 3 and varying pH was investigated. A stock solution having the ionic strength 1 M (0.93 M NaCl, 0.05 M NaF and 0.02 M (NaH_2PO_4 + Na_2HPO_4, 1:100)) was prepared. This solutions was diluted with a similar one but fluoride free to obtain samples of different fluoride concentration which were equilibrated at 25 ± 0.5°C with 0.01% solution of HDEHP in benzene. Experimental details were reported previously.[3]

$$Q = \frac{(C_{Ln})_0}{(C_{Ln})_{aq}} = \frac{[Ln^{3+}](\beta_0[DEHP^-]^3 + \beta_{12}[F^-][OH^-]^2 + \beta_{21}[F^-]^2[OH^-] + \beta_{30}[F^-]^3)}{[Ln^{3+}](1 + \beta_{01}[OH^-] + \beta_{02}[OH^-]^2 + \beta_{10}[F^-] + \beta_{11}[F^-][OH^-] + \beta_{20}[F^-]^2)} \quad (3)$$

$$\beta_{ab} = \frac{[LnF_a(OH)_b^{3-a-b}]}{[Ln^{3+}][F^-]^a[OH^-]^b} \quad (4)$$

$$0 \leq a, b \leq 3$$

$$\beta_0 = \frac{[Ln(DEHP)_3]_0}{[Ln^{3+}][DEHP^-]^3}. \quad (5)$$

RESULTS AND DISCUSSION

Figure 1 shows the distribution coefficient Q of Yb (as example) as a function of the fluoride concentration at the constant pH of 7.48. More or less similar graphs are obtained for the other three lanthanides studied. Q decreases slightly with increasing fluoride concentration

*To whom correspondence should be addressed.

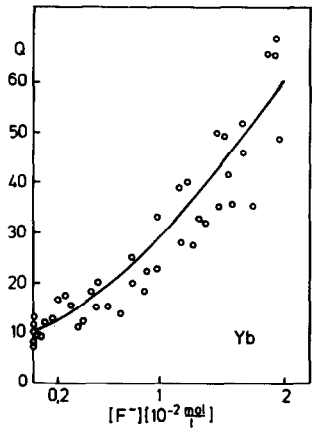

Fig. 1. Distribution coefficient of Yb as a function of fluoride concentration at pH 7.48.

up to $[F^-] \approx 2$ mM (due to the formation of additional cationic complexes) and then increases monotonously within the investigated range (up to $[F^-] \approx 20$ mM), indicating the increasing formation of neutral complexes. The still increasing slope of the curves excludes the formation of anionic complexes.

The calculation of β_{12} and β_{11} of Ce- and Tb complexes according to the eqn (7) resulted in negative values, due to the incomplete separation of the variables in this equation. For calculating the stability constants of the complexes of these two elements, the eqn (8) was therefore developed, which is suitable for deducing the values of β_{11} particularly at low values of $[F^-]$.

$$\frac{Q_{iaF}}{Q}(1+\beta_{01}[OH^-]+\beta_{02}[OH^-]^2) = 1+\beta_{01}[OH^-] + \beta_{02}[OH^-]^2+(\beta_{10}+\beta_{11}[OH^-])[F^-]. \quad (8)$$

The resulted β_{11} values were then used for the calculation of β_{ab} of the neutral complexes according to the eqn (9).

Figures 2 and 3 show the mole ratio of the different complexes of Ce and Tb (as example) as a function of the fluoride concentration at constant pH = 7 and as a function of the pH at constant $[F^-] = 10^{-3}$ M, respectively.

In Ref. 6 the hydrolysis constants of Ce^{3+}, $[CeF]^{2+}$ and $[CeF_2]^+$ ions were determined at various ionic strength, $0.034 \leq I \leq 0.06$ M ($Ce(NO_3)_3$, NaF), pH 5.75 and at a maximum total Ce concentration of 5.75 mM. Using $pK_w = 14$ the following values of the β_{ab} and K_{ab} ($K_{ab} = (\beta_{ab}/\beta_{(a-1)b})$) were calculated:

$$\beta_{01} = 5.2 \times 10^4\ M^{-1}$$
$$K_{11} = 3.2 \times 10^7\ M^{-2}$$
$$K_{21} = 4.1 \times 10^7\ M^{-2}.$$

The values of K_{11} and K_{21} are in good agreement with

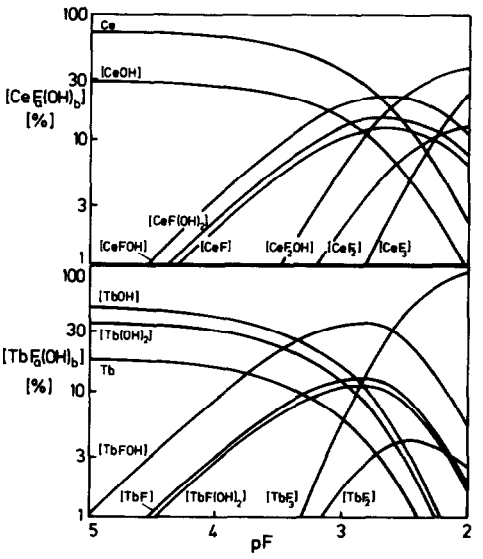

Fig. 2. Mole ratio of the different complexes as a function of fluoride concentration at pH = 7.

$$\frac{(Q-Q_{iaF})(1+\beta_{01}[OH^-]+\beta_{02}[OH^-]^2)+Q((\beta_{10}+\beta_{11}[OH^-])([F^-]+\beta_{20}[F^-]^2)}{[F^-]} = \beta_{12}[OH^-]^2+\beta_{21}[OH^-][F^-]+\beta_{30}[F^-]^2. \quad (9)$$

From eqns (7)–(9) the β_{ab} values, summarized in Table 1, are obtained. The error shown is the sum of the relative one time standard deviation (1σ) and the relative error of the constants β_{11}^{Ce}, β_{10}^{Eu}, β_{11}^{Tb} and β_{02}^{Yb} of the corresponding complexes present in the solution. β_{11}^{Eu}, β_{21}^{Eu}, β_{21}^{Tb}, β_{11}^{Yb} and β_{30}^{Yb} were not determinable under our experimental conditions.

our results, whereas β_{01} value is 2 orders of magnitude lower than that reported in Ref. 5. This deviation cannot be due to the different ionic strength only, but seems also to be due to the method of calculation used in Ref. 6 in which neither the possible formation of polynuclear complexes nor the complexation by the nitrate ion were considered.

Table 1. Stability constants of the complexes $LnF_a(OH)_b$

β_{ab}	Ce	Eu	Tb	Yb
β_{11}	(5.2±2.1) 10^9		(5.7±2.0) 10^{10}	
β_{21}	(1.7±1.0) 10^{12}			(4.1±2.3) 10^{12}
β_{12}	(3.5±2.3) 10^{16}	(5.0±0.7) 10^{16}	(1.8±1.2) 10^{17}	(9.8±5.3) 10^{18}

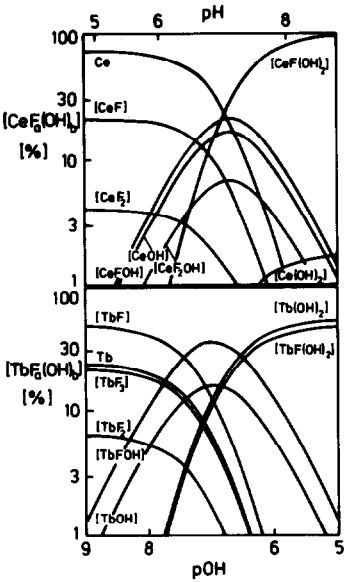

Fig. 3. Mole ratio of the different complexes as a function of the pH at pF = 3.

The results show that for the complexation of the lanthanides in fluorite bearing model system between pH 7–8, the fluoride and hydroxyl ions are the most significant complexing ligands (at least under normal *p*- and *T*-conditions). Sulphate plays no considerable role at the concentration in question.[4] The influence of chloride had to be examined, despite the very low formation constants reported in the literature for the lanthanide chloro complexes. An interference of Cl^- may take place because of the high NaCl concentration used for adjusting the ionic strength. The effect of Cl^- was investigated potentiometrically[1] and no measurable interference was found even at Cl^- concentration of 1 M.

Furthermore, we have studied a possible Cl^- effect using the method reported by Martin and Gillies,[7] in

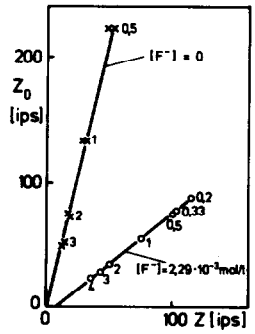

Fig. 4. $(C_{Yb})_{org}$ vs $(C_{Yb})_{aq}$ at different volume ratio (aqueous phase/organic phase).

which the volume ratio of the organic and the aqueous phase was varied in a set of distribution experiments. A linear function was found by plotting the metal concentration in the organic phase against that in the aqueous phase. The extrapolation of the line shown in Fig. 4 pass through the origin of the coordination system, indicating that in presence of Cl^- (even at 1 M) all Yb (as example) is presented as extractable species, which are likely to be Yb^{3+}. On running the experiment with aqueous phase containing 2.3 mM of fluoride a graph intersecting the *x* axis is obtained, indicating the formation of non-extractable, complexed, Yb species.

REFERENCES

[1]B. A. Bilal, F. Herrmann and W. Fleischer, *J. Inorg. Nucl. Chem.* 1979, **41**, 347.
[2]B. A. Bilal and P. Becker, *J. Inorg. Nucl. Chem.* 1979, **41**, 1607.
[3]B. A. Bilal and V. Koß, *J. Inorg. Nucl. Chem.* 1980, **42**, 629.
[4]B. A. Bilal and V. Koß, *J. Inorg. Nucl. Chem.* 1980, **42**, 1064.
[5]B. A. Bilal and V. Koß, *J. Inorg. Nucl. Chem.* 1981, **43**, 3393.
[6]S. J. Lyle and S. J. Naqvi, *J. Inorg. Nucl. Chem.* 1967, **29**, 2441.
[7]F. S. Martin and G. M. Gillies, A.E.R.E. Rep. No. C/R816, 1951.

Polyhedron Vol. 1, No. 3, pp. 243–245, 1982
Printed in Great Britain.

0277-5387/82/030243-03$03.00/0
Pergamon Press Ltd.

REACTIVITY OF POLYCHLOROPHENYLMERCURY COMPOUNDS WITH 1,10-PHENANTHROLINE

M. CRESPO, O. ROSSELL, J. SALES* and M. SECO
Departament de Química Inorgànica. Facultat de Química, Universitat de Barcelona, Diagonal 647. Barcelona 28, Spain

(*Received* 26 *August* 1981)

Abstract—The action of 1,10-phenanthroline (phen) on the THF solutions of RHgCl (R = 2,5-$C_6H_3Cl_2$; 2,3,4- and 2,4,6-$C_6H_2Cl_3$; 2,3,4,5-, 2,3,4,6-, and 2,3,5,6-C_6HCl_4 and C_6Cl_5) gives RHgCl (phen) when R contains two chlorine substituents in ortho (R = 2,4,6-$C_6H_2Cl_3$; 2,3,4,6-, and 2,3,5,6-C_6HCl_4 and C_6Cl_5), but the symmetrisation reaction occurs when R = 2,5-$C_6H_3Cl_2$; 2,3,4-$C_6H_2Cl_3$ and 2,3,4,5-C_6HCl_4. The action of phen on HgR_2 only gives HgR_2 (phen) when R = 2,3,4,5-C_6HCl_4. Compounds of the type RHgMe do not react with phen. These results indicate that steric effects are as important as the electronegativity of R in the formation of tetracoordinated mercury compounds.

INTRODUCTION

It is well known that organomercury derivatives show little tendency to increase their coordination number by interaction with donor molecules. However, the replacement of an organic group in HgR_2 either by more electronegative groups, such as the halogens, to form RHgX, or by other organic groups containing electron-withdrawing substituents, increases the positive charge on mercury thereby enhancing the stabilization of complexes, particularly with nitrogenous bases.

A large number of papers describe the action of donor molecules on organomercury derivatives, HgR_2, (R = hydrogenated or fluorinated organic ligands). In contrast to this, the corresponding reactions with organomercury derivatives containing chlorinated organic ligands has received little attention.[1] It is noteworthy in these compounds the low coordinating ability of $Hg(C_6Cl_5)_2$[2] as compared to $Hg(C_6F_5)_2$[3] or $(C_6Cl_5)HgCl$.[4] Since the electronegativity of the pentachlorophenyl and pentafluorophenyl groups must be similar, the different accepting behaviour of the two compounds could be related to the steric hindrance due to the presence of the bulky chlorine atoms in ortho positions to the Hg-C σ-bond.

In order to study this effect, we have examined the action of 1,10-phenanthroline on HgR_2, RHgX and RHgMe where R is a polychlorophenyl group with one or two ortho chlorine atoms.

EXPERIMENTAL

General

Microanalyses were carried out at the Institute of Bio-Organic Chemistry of Catalunya. IR spectra were recorded on a Beckman IR-20 A spectrophotometer; samples were examined as KBr disks or Nujol mulls. ^1H NMR spectra data were obtained on a Perkin–Elmer R-24 B in $CDCl_3$ solution with tetramethylsilane as the internal reference ($\delta = 0$).

Preparative methods

RHgCl (R = 2,5-$C_6H_3Cl_2$; 2,3,4-, *and* 2,4,6-$C_6H_2Cl_3$; 2,3,4,5-, 2,3,4,6-, *and* 2,3,5,6-C_6HCl_4 *and* C_6Cl_5)

The procedure is general for all of them. HgR_2 (1 mmol) and $HgCl_2$ (1 mmol) were dissolved in 50 ml of xylene, and the solution refluxed for 2 hr. On cooling, RHgCl precipitated. This was filtered and recrystallized twice from dichloromethane-methanol. Yields about 95%.

RHgMe

The procedure is also general. CH_3I (0.25 ml), Mg (0.36 g, 1.5 mmol) and dry ether (20 ml) were mixed in a flask under nitrogen. The mixture was stirred at room temperature for 30 min. After separating the excess of Mg, the solution was added slowly and with constant stirring onto RHgCl (1.5 mmol). The resulting solution was treated with ethanol (10 ml) and concentrated to dryness. The residue was treated with dichloromethane (25 ml) and concentrated to half volume. On adding methanol, RHgMe precipitated. Yields about 60%.

RHgCl (phen) (R = 2,4,6-$C_6H_2Cl_3$; 2,3,4,6-, *and* 2,3,5,6-C_6HCl_4) *and* HgR_2 (phen) (R = 2,3,4,5-C_6HCl_4)

These were prepared by mixing a solution of RHgCl or HgR_2 (1.0 mmol) in THF (5 ml), with another of phen (2 mmol) in THF (5 ml). The compounds RHgCl(phen) or HgR_2(phen) precipitated immediately with a 70% yield.

RESULTS AND DISCUSSION

Preparation of RHgCl *and* RHgMe

The compounds HgR_2 (R = 2,5-$C_6H_3Cl_2$; 2,3,4-, and 2,4,6-C_6Cl_3; 2,3,4,5-, 2,3,4,6-, and 2,3,5,6-C_6HCl_4) were obtained by metallation of the corresponding polychlorobenzenes with $Hg(O_2CCF_3)_2$[5]. $Hg(C_6Cl_5)_2$ was made by the action of a THF solution of C_6Cl_5MgCl on $HgCl_2$[6]. The compounds RHgCl were prepared with an almost quantitative yield by refluxing an equimolar solution of HgR_2 and $HgCl_2$ in xylene for 2 hr. The compounds RHgMe were obtained by treating the corresponding RHgCl with a solution of methylmagnesium iodide in ether.

The new compounds RHgCl and RHgMe are air-stable in solid and in solution. Analytical data and melting points are listed in Table 1. Values of the molar conductivity (10^{-4} M) in anhydrous acetone at 18°C are typical of non-electrolytes. They are soluble in benzene, chloroform, dichloromethane, and acetone, and scarcely soluble in ethanol and in ether. The IR spectra of the compounds RHgCl show the bands due to the ligands R.[5] As the electronegativity of the group R increases, the band corresponding to the ν(Hg-Cl) is shifted to larger frequencies (Table 1). The methyl protons of the derivatives RHgMe appear in the ^1H NMR spectra as a triplet,

*Author to whom correspondence should be addressed.

Table 1. Partial elemental analyses, melting points and ν(Hg–Cl) IR bands (cm^{-1}) of polychlorophenylmercury compounds

Compound	%C Found (Calcd)	%H Found (Calcd)	%N Found (Calcd)	Melting point (°C)	ν(Hg–Cl)
(2,3,4,6-C_6HCl_4)HgCl	15,1(15,98)	0,3(0,22)		185	330
(2,3,5,6-C_6HCl_4)HgCl	16,4(15,98)	0,3(0,22)		219	350
(2,3,4,5-C_6HCl_4)HgCl	16,1(15,98)	0,3(0,22)		210	320
(2,4,6-$C_6H_2Cl_3$)HgCl	17,4(17,30)	0,5(0,48)		180	330
(2,3,4-$C_6H_2Cl_3$)HgCl	17,4(17,30)	0,5(0,48)		224	325
(2,5-$C_6H_3Cl_2$)HgCl	18,9(18,86)	0,8(0,79)		205	310
(2,3,4,6-C_6HCl_4)HgMe	19,5(19,53)	1,0(0,94)		90	—
(2,3,5,6-C_6HCl_4)HgMe	20,4(19,53)	1,0(0,94)		127	—
(2,3,4,5-C_6HCl_4)HgMe	18,8(19,53)	1,1(0,94)		115	—
(2,4,6-$C_6H_2Cl_3$)HgMe	22,1(21,23)	1,3(1,27)		88	—
(2,3,4-$C_6H_2Cl_3$)HgMe	21,7(21,23)	1,3(1,27)		81	—
(2,5-$C_6H_3Cl_2$)HgMe	24,2(23,25)	1,7(1,67)		70	—
(2,3,4,6-C_6HCl_4)HgCl(phen)	34,4(34,24)	1,4(1,43)	4,5(4,44)	230(dec)	—
(2,3,5,6-C_6HCl_4)HgCl(phen)	34,1(34,24)	1,4(1,43)	4,7(4,44)	255(dec)	—
(2,4,6-$C_6H_2Cl_3$)HgCl(phen)	36,4(36,22)	1,7(1,68)	4,9(4,09)	290	—
(2,3,4,5-C_6HCl_4)$_2$Hg(phen)	35,5(35,55)	1,3(1,23)	3,5(3,46)	170	—

due to the coupling with the ^{199}Hg nucleus (natural abundance, 11.86%). $^2J(^1H\text{-}^{199}Hg)$ decreases in the order given in the Table 2; from which it may be concluded that the electronegativity of R decreases in the order C_6Cl_5 > 2,3,5,6-C_6HCl_4 > 2,3,4,6-C_6HCl_4 > 2,4,6-$C_6H_2Cl_3$ > 2,3,4,5-C_6HCl_4 > 2,3,4-$C_6H_2Cl_3$ > 2,5-$C_6H_3Cl_2$.

Reaction with 1,10-*phenanthroline*

The addition of an excess of 1,10-phenanthroline on a solution of RHgCl in THF leads to different results as a function of the identity of R. The following symmetrisation reaction takes place when R contains only one ortho chlorine atom (R = 2,5-$C_6H_3Cl_2$; 2,3,4-$C_6H_2Cl_3$ and 2,3,4,5-C_6HCl_4):

$$2RHgCl + phen \rightarrow HgCl_2(phen) + HgR_2.$$

On the other hand, when R contains two ortho chlorine atoms, the corresponding RHgCl(phen) (R = 2,4,6-$C_6H_2Cl_3$; 2,3,4,6- and 2,3,5,6-C_6HCl_4) are isolated.

Two mechanisms may account, according to Deacon *et al*,[4] for the symmetrisation reactions:

First mechanism

$$2RHgXL_2 \xrightarrow{slow} HgX_2L_2 + HgR_2 + L_2$$

Second mechanism

$$RHgXL_2 \xrightarrow{fast} RHgX + L_2$$

$$RHgXL_2 + RHgX \xrightarrow{slow} HgX_2L_2 + HgR_2.$$

Two molecules of organomercury derivative are involved in the symmetrisation reaction for either mechanism. The approach of the two molecules when R contains two ortho chlorine atoms will be strongly disfavoured due to steric congestion and this fact may explain the remarkable stability of those species. Thus, these compounds are recovered unaltered after refluxing in benzene for 12 hr. Although the stability of unsymmetrical mercurials RHgX towards disproportionation has been reported to increase as the electronegativity difference between the substituents increases,[4] our results show that the electronegativity difference is not the only factor and that the presence of two ortho chlorine atoms in the compounds RHgCl is the factor which prevents the symmetrisation reaction. Thus, the stability of C_6Cl_5HgCl(phen) towards the symmetrisation reaction attributed to the low solubility,[4] can be more properly interpreted in terms of the presence of two ortho chlorine atoms. The action of phen on HgR_2 gives only tetracoordinated HgR_2(phen) when R = 2,3,4,5-C_6HCl_4. The others do not react at all. These results agree both with the steric effects when R contains two ortho chlorine atoms and with the lower electronegativity of R for the other cases (R = 2,5-$C_6H_3Cl_2$ and 2,3,4-$C_6H_2Cl_3$).

Finally, the action of phen on RHgMe does not lead in any case to the formation of the corresponding tetracoordinate derivatives; the low electronegativity of the methyl group being the reason for the nonreactivity of these species.

All the new tetracoordinate species are pale pink solids, stable in the air and in the solution. They are non electrolytes in acetone. Analytical data and decomposition temperatures are listed in Table 1.

Table 2. Selected ^{1}H NMR spectra data for RHgMe

Compound	$\delta(CH_3)$(ppm)	$^2J(^1H\text{-}^{199}Hg)$(Hz)
(C_6Cl_5)HgMe	0,92	137
(2,3,5,6-C_6HCl_4)HgMe	0,83	135
(2,3,4,6-C_6HCl_4)HgMe	0,81	134
(2,4,6-$C_6H_2Cl_3$)HgMe	0,80	131
(2,3,4,5-C_6HCl_4)HgMe	0,80	128
(2,3,4-$C_6H_2Cl_3$)HgMe	0,78	125
(2,5-$C_6H_3Cl_2$)HgMe	0,77	123

REFERENCES

[1]N. A. Bell, I. W. Nowell and P. A. Reynolds, *J. Organometal. Chem.* 1980, **193**, 147; N. A. Bell, I. W. Nowell and D. J. Starkey, *Inorg. Chim. Acta* 1981, **48**, 139.
[2]G. B. Deacon and P. W. Felder, *Aust. J. Chem.* 1966, **19**, 2381.
[3]A. J. Canty and J. B. Deacon, *Aust. J. Chem.* 1971, **24**, 489.
[4]A. J. Canty and G. B. Dacon, *Aust. J. Chem.* 1968, **21**, 1757.
[5]J. Bertino, G. B. Deacon and F. B. Taylor, *Aust. J. Chem.* 1972, **25** 1645.
[6]F. E. Paulik, S. I. E. Green and R. E. Dessy, *J. Organometal. Chem.* 1965, **3**, 229.

Polyhedron Vol. 1, No. 3, pp. 247–251, 1982
Printed in Great Britain.

0277-5387/82/030247-05$03.00/0
Pergamon Press Ltd.

NITROSOLATES AND RELATED COMPOUNDS—IX[1]

COORDINATION COMPOUNDS OF DIVALENT COPPER, NICKEL AND COBALT WITH NITROACETATE(2–) IONS AS CHELATING LIGANDS

CRYSTAL AND MOLECULAR STRUCTURE OF POTASSIUM BIS[NITROACETATO(2–)]CUPRATE(II)–WATER (1/1)

K. VON DEUTEN, W. HINRICHS and G. KLAR*
Institut für Anorganische und Angewandte Chemie der Universität Hamburg, Martin-Luther-King-Platz 6, D-2000 Hamburg 13, Germany

(*Received* 26 *August* 1981)

Abstract—The syntheses of $K_2[Cu(nac)_2]\cdot H_2O$ (**4**), $[Cu(nac)(N\text{–}N)(H_2O)]\cdot H_2O$ (N–N = bpy, phen; **5**,**6**) and $[M(nac)(N\text{–}N)_2]\cdot xH_2O$ (M = Ni, Co; **7**–**10**) with nitroacetate(2–) ions (nac^{2-}) as chelating ligands are described.

The structure of **4** has been determined by single crystal X-ray diffraction and contains square planar $[Cu(nac)_2]^{2-}$ units in which the nitro and carboxyl groups of the two chelate ligands are in *cis* positions. Two of the units form a centrosymmetric dimer with a four-membered CuOCu'O'-ring, the dimers being connected by exo-oxygens of the ligands into two-dimensional layers. The water molecules and the potassium ions are arranged between the layers; there are two kinds of potassium ions with distorted (1+4+1) and (2+4+3) coordinations respectively.

INTRODUCTION

While the carboxyl and nitro groups of nitroacetic acid $O_2N\text{–}CH_2\text{–}COOH$[2,3] are arranged almost perpendicular to each other[4] they are coplanar in the potassium salt $K_2[(O_2N)CH(CO_2)]$[5] indicating π-interactions in the nitroacetate(2–) ion (nac^{2-}, **1**). We therefore became interested in **1** in the course of our investigations on ligands with extended π-systems. **1** combines in itself all structural elements of the different forms of nitrosolates **2** and 2,4-pentanedionates **3** and furthermore is isoelectronic with **3**. But in contrast to **3** with three planar configurations, only one planar form of **1** is possible since any rotation of the CO_2 and/or NO_2 groups around the CC and/or CN axes resp. leads to identical conformations so that **1** should readily act as bidentate ligand. However, no well defined coordination compounds of transition metals with **1** were known prior to the present investigations.

Since an aqueous solution of potassium nitroacetate(2–) reacts strongly alkaline only hydroxy salts are precipitated by adding solutions of metal ions. However, a *bis*-(nitroacetato) complex of copper(II), $K_2[Cu(nac)_2]\cdot H_2O$ (**4**), could be isolated when the reactants were added in the reverse order. A precipitation of hydroxy salts could also be prevented in the presence of

*Author to whom correspondence should be addressed.

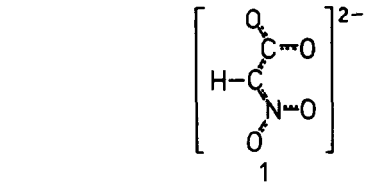

1

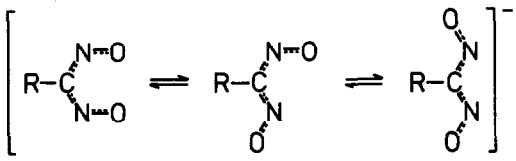

2a 2b 2c

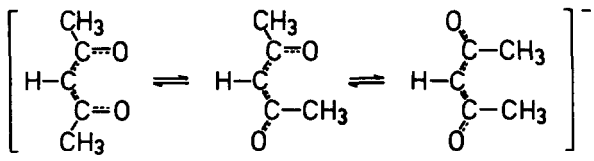

3a 3b 3c

chelating nitrogen ligands such as 2,2'-bipyridyl and 1,10-phenanthroline. In this case the compounds $[Cu(nac)(N-N)(H_2O)]\cdot H_2O$ (N-N = bpy, phen; **5**,**6**) and $[M(nac)(N-N)_2]\cdot xH_2O$ (M = Co, Ni; **7**–**10**) were obtained. To ascertain the coordination manner of the nitroacetate ligand we carried out X-ray structure determinations of $K_2[Cu(nac)_2]\cdot H_2O$ (**4**) and of $[Cu(nac)(bpy)(H_2O)]\cdot H_2O$ (**5**), the latter of which has been reported elsewhere.[6]

EXPERIMENTAL

Caution. Derivatives of nitroacetic acid are thermally unstable and may explode on heating to temperatures higher than 50°C as has been found for potassium *bis*-[nitroacetato(2−)]cuprate(II) (**4**).

Preparation of compounds

Potassium nitroacetate(2−) was prepared from nitromethane and potassium hydroxyde (50% in water) according to Feuer *et al.*[7]

Potassium bis[nitroacetato(2−)]cuprate(II)–water (1/1) (**4**). The aqueous solution of potassium nitroacetate(2−) (9.2 g, 51 mMol, 30 ml) was slowly added to the solution of $Cu(NO_3)_2\cdot 3H_2O$ in water (6.0 g, 25 mMol, 20 ml). Soon a crystalline blue green precipitate was produced (4.5 g, 49%) which had to be separated immediately since the second more voluminous fraction from the filtrate already contained hydroxy salts. Found: C, 13.07; H, 1.13; N, 7.30; Cu, 17.98; K, 21.07. $C_4H_4N_2O_9CuK_2$ requires C, 13.13; H, 1.10; N, 7.66; Cu, 17.37; K, 21.38. μ_{eff}: 1.90 (295.8 K), 1.86 (196.0 K), 1.80 BM (77.4 K). The compound is sparingly soluble in water; single crystals suitable for an X-ray structure determination were obtained only by chance when a solution was allowed to evaporate during several weeks.

Mixed ligand complexes with nitroacetate(2−) *and bipyridyl or phenanthroline.* Suspensions of 2,2'-bipyridyl or 1,10-phenanthroline monohydrate and solutions of the metal salts in water (10 ml for 5 mMol in each case) were combined, the solutions formed filtered and aqueous solutions of potassium nitroacetate(2−) (10 ml for 10 mMol) added dropwise. The precipitations (70–80% yield) were separated immediately, washed with water, acetone, toluene, ether and dried in air (for details see Table 1). The compounds are soluble in methanol and ethanol, sparingly soluble in water and insoluble in toluene, chloroform, ether or acetone.

Structure determination of $K_2[Cu(nac)_2]\cdot H_2O$

Crystal data. With Mo–K_α radiation (λ = 70.926 pm): monoclinic P; a = 854.4(1), b = 943.3(2), c = 1281.9(2) pm, β = 98.07(1)°; space group $P2_1/n$, Z = 4; $V = 1023.4\times10^6$ pm^3; MW = 365.8; D_c = 2.38 g/cm^3.

Intensity data, structure determination and refinement. Two thousand, nine hundred and ninety nine independent reflections with $1<2\theta<60°$ were collected on a Syntex $P2_1$ four-circle diffractometer and corrected for Lorentz and polarization factors. The structure was solved by the heavy atom method and subsequent difference Fourier syntheses, which also revealed hydrogen atom positions. Since carbon and nitrogen have similar scattering factors and since coordinated carboxyl and nitro groups have similar geometry, the possible ambiguity was resolved by inspection of a difference Fourier map phased on all heavy atoms expect C(carboxyl) and N(nitro). Full matrix least-squares refinement with all atoms included and, except for hydrogen, anisotropic led to a final conventional R = 0.058 for 2032 reflections having $F_0 > 3\sigma(F_0)$. All calculations were done using the SHEL 76 program system.[8]†

†Tables of atomic positional and thermal parameters and lists of F_0/F_C values have been deposited as supplementary data with the Editor, from whom copies are available on request. Copies of atomic positional parameters have also been submitted to the Cambridge Crystallographic Data Centre.

RESULTS AND DISCUSSION

As can be seen from Fig. 1 the nitroacetate(2−) ion acts as a chelating ligand in $K_2[Cu(nac)_2]\cdot H_2O$ (**4**), a bonding mode which has also been found in $[Cu(nac)(bpy)(H_2O)]\cdot H_2O$ (**5**).[6] From the similarity of IR data reported in Table 6 it can be concluded that the ligand is bonded in the same way also in complexes **6**–**10**. Due to the additional bipyridyl or phenanthroline ligands the IR spectra of the complexes are rich in structure, but by comparison with the spectra of these ligands the bands of the nitroacetate(2−) ion could be reasonably separated. The frequencies were assigned following Jensen[9] except for the ν_{as}ONO and νN–CH=C, the assignments of which we exchanged considering the predominance of the nitroalkene form in the mesomerism of the ion.[5]

Thus the coordination sphere of the central ions in the cobalt and nickel complexes **7**–**10** is quasi-octahedral in accordance with the measured magnetic moments (see Table 1). The electronic spectra of the nickel compounds **7** and **8** (reflectance spectra) show, besides CT bands above 20000 cm^{-1}, two distinct bands at *ca.* 10500 and 17600 cm^{-1} thus indicating octahedral geometry too. In the copper compounds **5** and **6** the coordination sphere is square-pyramidal, the coordinated water molecules occupying apical positions,[6] while in the crystal of **4** inner and outer coordination spheres of the copper ions must be distinguished. In the first sphere the copper(II) ion shows square planar coordination with the nitro and carboxyl groups of the two nitroacetate(2−) ligands in *cis* positions (Fig. 1). The four Cu–O distances are equal within experimental error and their value (average 192 pm) conforms well to the range of 190–195 pm typically found in similar complexes.[10–16] The coordination sphere of the copper(II) ion is completed in the usual (4+2) arrangement by weaker bonds to oxygen atoms of two further $[Cu(nac)_2]^{2-}$ units, one bond (254 pm) to 06″ of a carboxyl group and another (289 pm) to 03′ of a nitro group. The crystal structure thus formed can be described as polymer layers of centrosymmetric dimers with a four-membered CuO3Cu′O3′-ring connected by bridges of the exo-oxygens 06 of the dimers (Fig. 2). The resulting anisotropic surrounding of the copper(II) ion is also indicated by the unsymmetrical signal in the ESR spectrum of the powdered substance. The evaluation led to $g_\parallel = 2.249$ ($H_\parallel = 0.29263$ T) and $g_\perp = 2.078$ ($H_\perp = 0.31690$ T).

In **4** both nitroacetate(2−) ligands are almost planar, the distances and angles being typical for delocalized π-systems with bond orders between 1 and 2.[17] Some minor non-equivalence between the two ligands can,

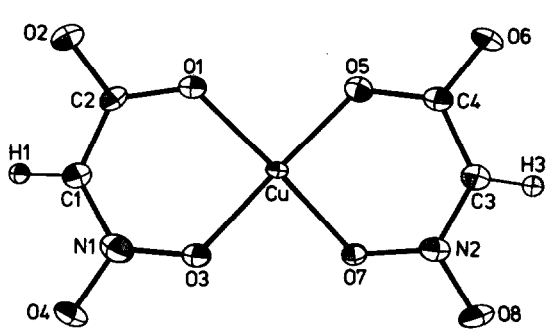

Fig. 1. ORTEP-plot and numbering scheme of atoms in the $[Cu(nac)_2]^{2-}$ unit of **4**.

Table 1. Preparative and analytical data of the mixed ligand complexes with nitroacetate(2−) ions and bipyridyl or phenanthroline

compound	starting material		analyses found (required)	μ_{eff}
$[Cu(nac)(bpy)(H_2O)]\cdot H_2O$ (5) (blue)	$Cu(NO_3)_2\cdot 3H_2O$	1.3 g (5.4 mMol)	C 39.94% (40.17)	2.06 BM (292.0 K)
	bpy	1.3 g (8.3 mMol)	H 3.56% (3.65)	2.01 BM (196.0 K)
	K_2nac	1.8 g (10.0 mMol)	N 11.63% (11.71)	1.58 BM (77.4 K)
			Cu 17.31% (17.71)	
$[Cu(nac)(phen)(H_2O)]\cdot H_2O$ (6) (blue)	$Cu(NO_3)_2\cdot 3H_2O$	1.0 g (4.1 mMol)	C 43.77% (43.93)	1.97 BM (293.0 K)
	$phen\cdot H_2O$	0.8 g (4.0 mMol)	H 3.33% (3.43)	1.96 BM (196.0 K)
	K_2nac	1.5 g (8.3 mMol)	N 10.85% (10.98)	1.86 BM (77.4 K)
			Cu 17.13% (16.60)	
$[Ni(nac)(bpy)_2]\cdot 3H_2O$ (7) (grey)	$NiCl_2\cdot 6H_2O$	1.2 g (5.0 mMol)	C 50.56% (50.03)	2.98 BM (293.1 K)
	bpy	1.1 g (7.0 mMol)	H 3.88% (4.39)	3.02 BM (165.0 K)
	K_2nac	1.7 g (9.4 mMol)	N 13.24% (13.26)	2.99 BM (102.4 K)
			Ni 10.82% (11.12)	
$2[Ni(nac)(phen)_2]\cdot 7H_2O$ (8) (grey)	$NiCl_2\cdot 6H_2O$	1.2 g (5.0 mMol)	C 53.24% (53.36)	3.18 BM (293.0 K)
	$phen\cdot H_2O$	2.0 g (10.1 mMol)	H 3.67% (4.13)	3.21 BM (166.0 K)
	K_2nac	1.0 g (5.5 mMol)	N 11.84% (11.97)	3.20 BM (104.8 K)
			Ni 9.93% (10.03)	
$[Co(nac)(bpy)_2]\cdot 2H_2O$ (9) (orange)	$Co(NO_3)_2\cdot 6H_2O$	1.0 g (3.4 mMol)	C 51.79% (51.77)	
	bpy	0.9 g (5.8 mMol)	H 3.97% (4.15)	
	K_2nac	1.8 g (10.0 mMol)	N 13.56% (13.72)	
			Co 11.63% (11.55)	
$[Co(nac)(phen)_2]\cdot 4H_2O$ (10) (red orange)	$CoCl_2\cdot 6H_2O$	1.2 g (5.0 mMol)	C 52.36% (52.53)	5.09 BM (292.7 K)
	$phen\cdot H_2O$	2.0 g (10.1 mMol)	H 3.50% (4.24)	4.98 BM (196.0 K)
	K_2nac	1.0 g (5.5 mMol)	N 11.43% (11.78)	4.53 BM (77.4 K)
			Co 9.80% (9.91)	

Table 2. Bond lengths (pm) in $K_2[Cu(nac)_2]\cdot H_2O$ (4) with estimated standard deviations in parentheses. For comparison the corresponding distances in $[Cu(nac)(bpy)(H_2O)]\cdot H_2O$ (5)[6] and K_2nac[5] are also given

	$K_2[Cu(nac)_2]\cdot H_2O$ (4)			5	K_2nac
C2-01	129.5(8)	C4-05	129.7(8)	131.8	133
C2-02	126.2(7)	C4-06	126.6(7)	125.7	127
C1-C2	142.4(9)	C3-C4	139.5(9)	136.2	138
C1-N1	136.0(8)	C3-N2	138.4(8)	136.3	139
N1-03	131.0(7)	N2-07	127.8(8)	132.6	128
N1-04	126.7(7)	N2-08	127.6(7)	126.6	126
Cu-01	192.6(4)	Cu-05	193.2(5)	191.7	
Cu-03	191.9(4)	Cu-07	191.6(4)	191.3	
Cu-03'	289.1	Cu-06"	253.9		

Table 3. Bond angles (°) in $K_2[Cu(nac)_2]\cdot H_2O$ (4) with estimated standard deviations in parentheses. For comparison the corresponding angles in $[Cu(nac)(bpy)(H_2O)]\cdot H_2O$ (5)[6] and K_2nac[5] are also given

	$K_2[Cu(nac)_2]\cdot H_2O$ (4)			5	K_2nac
01-C2-02	120.5(6)	05-C4-06	118.1(6)	117.2	117
01-C2-C1	122.3(5)	05-C4-03	122.9(5)	123.3	124
02-C2-C1	117.2(6)	06-C4-C3	119.0(6)	119.5	119
C2-C1-N1	126.9(6)	C4-C3-N2	125.3(6)	129.3	128
C1-N1-03	122.7(5)	C3-N2-07	124.5(5)	122.1	125
C1-N1-04	121.0(6)	C3-N2-08	117.7(6)	121.6	114
03-N1-04	116.3(5)	07-N2-08	117.8(6)	116.3	121
C2-01-Cu	124.2(4)	C4-05-Cu	126.9(4)	124.3	
N1-03-Cu	123.7(4)	N2-07-Cu	126.9(4)	125.3	
01-Cu-03	92.0(2)	05-Cu-07	92.0(2)	94.3	
01-Cu-05	89.8(2)	03-Cu-07	86.2(2)		
01-Cu-07	178.2(2)	05-Cu-03	169.5(2)		
01-Cu-03'	91.8	01-Cu-06"	92.8		
03-Cu-03'	86.8	03-Cu-06"	88.8		
05-Cu-03'	82.9	05-Cu-06"	101.5		
07-Cu-03'	88.2	07-Cu-06"	87.1		
06"-Cu-03'	173.7	C4"-06"-Cu	116.3		

Table 4. Dihedral angles (°) in $K_2[Cu(nac)_2]\cdot H_2O$ (4); for comparison the corresponding values are also given for $[Cu(nac)(bpy)(H_2O)]\cdot H_2O$ (5)[6] and K_2nac.[5] Best planes through the ligands of 4 with deviations (pm) of each of the defining atoms in parentheses; angle between planes

	$K_2[Cu(nac)_2]\cdot H_2O$ (4)			5	K_2nac
01-C2-C1-N1	5.6	05-C4-C3-N2	11.5	3.8	0
02-C2-C1-N1	-174.3	06-C4-C3-N2	-169.3	-176.2	0
C2-C1-N1-03	-2.0	C4-C3-N2-07	-9.8	-6.9	0
C2-C1-N1-04	178.1	C4-C3-N2-08	168.4	173.3	0

plane 1: 0.3361x + 1.1021y + 12.5263z - 5.8788 = 0

defined by: 01(-3.7), 02(5.0), C2(-1.0), C1(-4.4), N1(-0.1), 03(4.3), 04(-0.3)

plane 2: 1.1234x + 2.4817y + 11.8964z - 5.9738 = 0

defined by: 05(0.0), 06(-7.5), C4(1.1), C3(13.0), N2(2.4), 07(-1.9), 08(-7.1)

plane 1 / plane 2: 10.2°

Table 5. IR spectra of complexes. Assignment of frequencies due to the nitroacetate(2−) ion

K_2nac	4	5	6	7	8	9	10	assignment
1590	1570	1560	1580	1570	1570	1570	1570	ν_{as}OCO
1485	1525	1500	1500	1490	1480	1490	1480	νN-Ch=C
1430	1400	1405	1410	1415	1420	1410	1420	ν_{as}ONO
1325	1310, 1295	1295	1290	1310	1300	1310	1300	ν_{s}OCO
1165	1225	1220	1220	1190	1200	1190	1210	ν_{s}ONO
945	920	940	940	940	945	940	940	νN-CH-=C
770, 765	805	790	790	780	785	780	780	νONO

however, be detected in the NO distances of the nitro groups and the angles of twist at C1 and C3 (Tables 2, 3). This can be traced back to the crystal structure, viz. to the bridges between the monomer units formed by 03 and 06 and to an additional hydrogen bond (202 pm) between 08 and H91 of the crystal water.

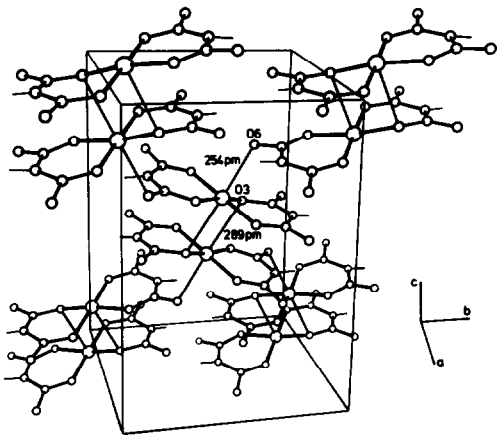

Fig. 2. 2D-layer with dimers of the $[Cu(nac)_2]^{2-}$ ions in 4. Not all ions of the unit cell have been plotted, the water molecules and potassium ions also have been omitted for clarity.

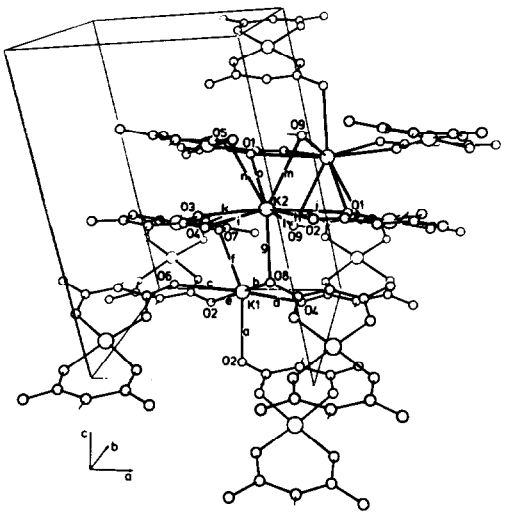

Fig. 3. Coordination spheres of the potassium ions in 4. Distances: a = 281.8, b = 269.9, c = 286.4, d = 280.5, e = 287.0, f = 277.3, g = 285.0, h = 276.2, i = 291.2, j = 308.9, k = 272.3, l = 260.2, m = 315.7, n = 294.3, o = 295.8 (pm); only contacts up to 320 pm have been considered and for reasons of clarity not all molecules and ions of the unit cell are plotted.

In the crystal structure of 4 the water molecules and potassium ions are found between the layers of the $[Cu(nac)_2]^{2-}$ ions. The two potassium ions of the asymmetric unit occupy different sites with distorted (1+4+1) and (3+4+2) coordinations for K1 and K2 respectively (all contacts up to 320 pm being considered). Two potassium ions K2 form a centrosymmetric arrangement with four asymmetric oxygen bridges (Fig. 3) leading to relatively short distances (348 pm) between each pair of K2 ions which are, however, longer than in potassium oxide (322 pm).[18]

Acknowledgements—We would like to thank Professor E. Weiss for granting the use of the single crystal diffractometer sponsored by the DFG. Furthermore we acknowledge useful suggestions by the referee.

REFERENCES

[1]Part VIII: M. Kastner, S. Jónsdóttir and G. Klar, *Chemiker-Ztg.* 1981, **105**, 232.
[2]W. Steinkopf, *Ber. Deut. Chem. Ges.* 1909, **42**, 2026 *and* 3925.
[3]K. J. Pedersen, *Trans. Faraday Soc.* 1927, **23**, 316.
[4]K. von Deuten und G. Klar, *Cryst. Struct. Commun.* 1980, **9**, 397.
[5]D. J. Sutor, F. J. Llewellyn and H. S. Maslen, *Acta Cryst.* 1954, **7**, 145.
[6]K. von Deuten and G. Klar, *Cryst. Struct. Commun.* 1980, **9**, 479.
[7]H. Feuer, H. B. Hass and K. S. Warren, *J. Am. Chem. Soc.* 1949, **71**, 3078.
[8]G. Sheldrick, *Programs for Crystal Structure Determination.* Cambridge, England (1975).
[9]K. A. Jensen, O. Buchardt and C. Lohse, *Acta Chem. Scand.* 1967, **21**, 2797.
[10]H. C. Freeman, J.E.W.L. Smith and J. C. Taylor, *Nature* 1959, **184**, 707.
[11]M. A. Jarski and E. C. Lingafelter, *Acta Cryst.* 1964, **17**, 1109.
[12]P. L. Orioli, E. C. Lingafelter and B. W. Brown, *Acta Cryst.* 1964, **17**, 1113.
[13]E. C. Lingafelter, G. L. Simmons, B. Morosin, C. Scheringer and C. Freiburg, *Acta Cryst.* 1961, **14**, 1222.
[14]C. Panattoni, G. Bombieri and R. Graziani, *Acta Cryst.* 1967, **23**, 537.
[15]J. A. J. Jarvis, *Acta Cryst.* 1961, **14**, 961.
[16]R. C. Hoy and R. H. Morriss, *Acta Cryst.* 1967, **22**, 476.
[17]G. Vetter, J. Kopf and G. Klar, *Z. Naturforsch.* 1973, **28b**, 293 and literature cited therein.
[18]E. Zintl, A. Harder and B. Dauth, *Z. Elektrochem.* 1934, **40**, 588.

Polyhedron Vol. 1, No. 3, pp. 253–256, 1982
Printed in Great Britain.

0277–5387/82/030253–04$03.00/0
Pergamon Press Ltd.

A STUDY OF LANTHANIDE *p*-TOLUENE SULPHONIC ACID COMPLEXES IN SOLUTION

B. S. NAKANI† and E. W. GIESEKKE*
University of Fort Hare, P.O. Alice, 5700, South Africa

(*Received* 14 *September* 1981)

Abstract—Lanthanide *p*-toluene sulphonic acid (ptsa) complexes were prepared for La, Pr, Nd, Sm, Eu, Dy, Ho, Er and Yb, and found to exist as $Ln(ptsa)_3$. Conductivity studies of $La(ptsa)_3$ in DMSO and DMF suggest 1 : 2 and, possibly, 1 : 1 electrolyte behaviour in these solvents, respectively. NMR lanthanide-induced chemical shifts (LIS) for aromatic protons in $(ptsa)^-$ and methyl protons in DMSO, were measured for all complexes as a function of the $[Ln^{3+}]/[DMSO]$ in a medium consisting of CCl_4, DMSO, and CH_3CN. Analysis of the LIS data suggests a change in $(ptsa)^-$ coordination round Ln^{3+} across the lanthanide series.

INTRODUCTION

Benzene–sulphonic acid groups are extensively used in cation-exchange resins of the polystyrene–divinyl benzene–sulphonic acid type to separate individual lanthanides[1,2]. The extraction of lanthanides by liquid cation exchangers, e.g., dinonylnaphthalene sulphonic acid, has been extensively studied.[3,4] There is therefore good reason for the nature of the interaction between lanthanide ions (Ln^{3+}) and benzene sulphonic acid to be characterized, not only in aqueous but in non-aqueous media.

It is of interest for an attempt to be made to assess to what extent the changes in coordination of sulphonic acid round the Ln^{3+}, across the lanthanide series, contribute to the selectivity that resins and liquid cation exchangers exhibit for the individual Ln^{3+}. Such changes in coordination can be deduced from the nuclear magnetic resonance (NMR) lanthanide-induced chemical shift (LIS), and have been reported for various ligands.[5–7]

The preparation of lanthanide methane sulphonate[8] and trifluoromethane sulphonate[9–11] complexes with various neutral donor ligands, was reported recently. No agreement has as yet been reached in these studies on the coordination of the sulphonate ligand round the Ln^{3+}. To the best of our knowledge, no complexes of *p*-toluene sulphonic acids have been reported in the literature.

*Address for correspondence: National Institute for Metallurgy, Private Bag X3015, Randburg, 2125, South Africa.

†Present address: Department of Chemistry, University of the Witwatersrand, 1 Jan Smuts Ave., Johannesburg 2000, S. Africa.

EXPERIMENTAL METHODS

The lanthanide *p*-toluene sulphonic acid complexes were prepared as follows. To an aqueous solution of *p*-toluene sulphonic acid monohydrate, $(Hptsa \cdot H_2O)$ a slight excess of the calculated amount of lanthanide oxide was added to give a molar ratio of 6 for $Hpsta \cdot H_2O$: Ln_2O_3. After boiling the mixture, the excess oxide in the resulting solution was removed by filtration, the filtrate then being reduced in volume to facilitate crystallization of the product. The crystals were dried to constant mass in a heated vacuum desiccator. Analyses of the complexes prepared, which all conform to the formula $Ln(ptsa)_3$, are given in Table 1. The analyses for C, H and S were determined at the National Chemical Research Laboratory, Pretoria. The metal analyses were determined with 0.01 M ethylenediaminetetraacetic acid (EDTA), xylenol orange being used as the indicator.[12]

The conductivity measurements of solutions were determined with a Metrohm E527 conductometer equipped with a micro-conductivity cell, of which the cell constant was 0.79 cm^{-1}. The dimethyl sulphoxide (DMSO) and dimethyl formamide (DMF) were purified in accordance with the procedure of Ramalingam and Soundarajan,[13] and the acetonitrile was purified in accordance with the procedure of Coetzee *et al.*[14]

NMR measurements were carried out with a Varian T-60A spectrometer operating at 34°C. The methyl proton shifts of DMSO and aromatic proton shifts of $(ptsa)^-C_6H_4$ were measured with reference to tetramethylsilane (TMS) in a mixture of DMSO, CH_3CN, and CCl_4. The solution, which contained 130 mg $Ln(ptsa)_3$ and 0.1 ml to 1.0 ml of DMSO, were prepared in a 5 ml volumetric flask. The Ln^{3+} concentration in these solutions remained constant at $\pm 4 \times 10^{-2}$ mol·l^{-1} depending on the atomic mass of the Ln. All solutions contained 1 ml of CH_3CN to promote the solubility of the complex in CCl_4, which was added to make up the solution to 5 ml. (In this manner, the observed DMSO and C_6H_4 proton chemical shifts could be determined as a function of the $[Ln^{3+}]/[DMSO]$ molar ratio and conserving the

Table 1. Analyses of $Ln(ptsa)_3$ complexes

Element	Ln, %		C, %		H, %		S, %	
	Found	Calc.	Found	Calc.	Found	Calc.	Found	Calc
La	21.07	21.29	38.57	38.66	3.36	3.24	13.93	14.74
Pr	21.18	21.43	38.40	38.59	3.37	3.24	14.58	14.71
Nd	22.14	21.93	37.69	38.34	3.43	3.22	14.23	14.62
Sm	22.49	22.65	36.78	37.99	3.43	3.19	13.74	14.48
Eu	22.83	22.83	—	37.90	—	3.18	—	14.45
Dy	23.94	24.04	36.82	37.31	3.52	3.13	13.27	14.23
Ho	23.35	24.31	36.73	37.17	3.61	3.12	14.14	14.18
Er	23.73	24.57	—	37.05	—	3.11	—	14.13
Tm	25.04	24.75	—	36.96	—	3.10	—	14.09
Yb	24.72	25.20	34.23	36.74	3.99	3.08	11.71	14.01

use of $Ln(ptsa)_3$). The solutions were analysed for their metal concentration by the titration of 1 ml of solution with EDTA.[12] The DMSO concentration of the solutions were determined by the titration of another 1 ml of solution with standardized $KMnO_4$, according to the procedure of Krishman and Patel.[15]

RESULTS AND DISCUSSION

The experimental molar conductance Λ_m, in $\Omega^{-1}\,mol^{-1}\,cm^2$, of dilute aqueous solutions of $La(ptsa)_3$ with a molar concentration of C_m could be represented by the relation

$$\Lambda_m = 304 - 1.23 \times 10^3\, C_m^{1/2},$$

obtained by a linear least-squares analysis of five experimental values in the concentration range 4×10^{-5} mol l^{-1} to 1×10^{-3} mol l^{-1}. Comparison of these values with similar values in the literature[16] for $La(ClO_4)_3$ and $La(NO_3)_3$ suggests that, at these concentrations, $La(ptsa)_3$ acts as a 1 : 3 electrolyte in aqueous solutions. The value for the limiting conductance at infinite dilution, $304\,\Omega^{-1}\,mol^{-1}\,cm^2$ for $La(ptsa)_3$, suggests that the $(ptsa)^-$ possesses an ionic conductance of $31.6\,\Omega^{-1}\,mol^{-1}\,cm^2$ at infinite dilution based on the independent migration of ions (if the ionic conductance of La^{3+} at infinite dilution is assumed to be $69.7\,\Omega^{-1}\,mol^{-1}\,cm^2$).[17]

In non-aqueous media, the observed molar conductance of a 10^{-3} mol l^{-1} $La(ptsa)_3$ was 108.9 and $88.1\,\Omega^{-1}\,mol^{-1}\,cm^2$ in DMF and DMSO respectively. According to Geary,[18] this implies that, in DMSO, $La(ptsa)_3$ tends to behave as a 1 : 2 electrolyte, whereas, in DMF, its behaviour is somewhere between that of a 1 : 2 and 1 : 1 electrolyte. Data in the literature[19,20] on molar conductance for $La(ClO_4)_3$ in these solvents suggest that DMSO and DMF displace three ClO_4^- per mole of $La(ClO_4)_3$. For $La(NO_3)_3$, data on molar conductance[13,21] suggest that DMSO displaces three NO_3^-, but that DMF displaces only one or two NO_3^- from the La^{3+} coordination sphere. By comparison, the observed molar conductances for $La(ptsa)_3$ in similar solvents suggests that $(ptsa)^-$ behaves as a coordinating anion for La^{3+}, which is much stronger than ClO_4^-, and as strong, if not stronger, than NO_3^-. In the presence of a coordinating solvent, S, the $(ptsa)^-$ competes with the solvent for coordination sites round the Ln^{3+}, i.e.,

$$Ln(ptsa)_3 + zS \rightleftharpoons Ln(ptsa)_3zS \qquad (1)$$

and

$$Ln(ptsa)_3zS + yS \rightleftharpoons \{Lnptsa)_{(3-x)}(z+y)S\}^{x+} + x(ptsa)^-, \qquad (2)$$

where $(z+y) = 8-2(3-x)$, and $z = 3$ or 4.

This implies a maximum coordination of eight DMSO molecules around the Ln^{3+}. Presumably this maximum number of DMSO molecules would be reduced to seven for the heavier lanthanides as has been found for DMSO solvation of $Ln(ClO_4)_3$[20].

Data have been reported[9–11] on the molar conductance for $Ln(CF_3SO_3)_3\cdot nS$, where S represents a neutral donor ligand, $4 < n < 9$, and also[8] for $Ln(CH_3SO_3\cdot 3(TSMO)$ [TMSO = tetramethylene-sulphoxide]. The methanesulphonate complexes behave as non-electrolytes in methanol. The data on molar conductance for trifluoromethanesulphonate complexes in acetonitrile and nitromethane indicate the existence of 1:1, 1:2 and 1:3 electrolytes, depending on the value of n. This is analogous to the results reported for $Ln(ptsa)_3$.

The variation in proton NMR shifts for DMSO and $(ptsa)^-$ C_6H_4 aromatic protons are shown as a function of the molar ratio, $[Nd^{3+}]/[DMSO]$, in Figs 1 and 2 respectively. The observed shift is a weighted average of the free and Ln-bound contributions, since the molecule in question is exchanged rapidly between these two states. The linear dependence of DMSO shift, i.e. δ_{DMSO}, on the $[Nd^{3+}]/[DMSO]$ ratio (Fig. 1) suggests that, with decreasing DMSO content in solution, a greater proportion of the latter is bound to the Nd^{3+}. On the other hand, the aromatic C_6H_4 proton shift, $\delta_{C_6H_4}$ shows a different trend (as can be seen in Fig. 2) with decreasing DMSO content. For $[Nd^{3+}]/[DMSO] > 0.04$, $\delta_{C_6H_4}$ remains constant, indicating that the same proportion of $(ptsa)^-$ is bound to Nd^{3+}, whether increasing amounts of DMSO are bound to the Nd^{3+} or not. The variation in

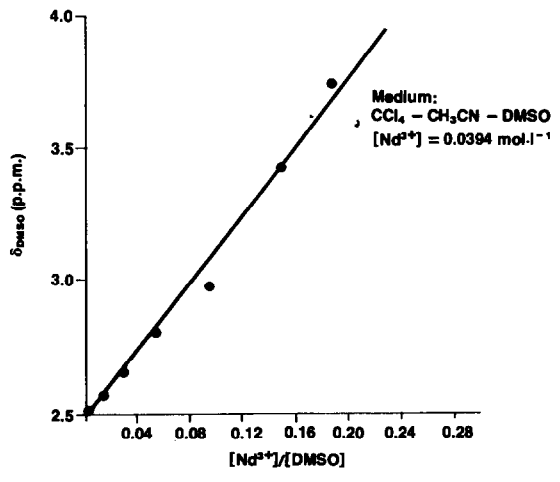

Fig. 1. Variation in the chemical shift of DMSO, δ_{DMSO}, as a function of $[Nd^{3+}]/[DMSO]$.

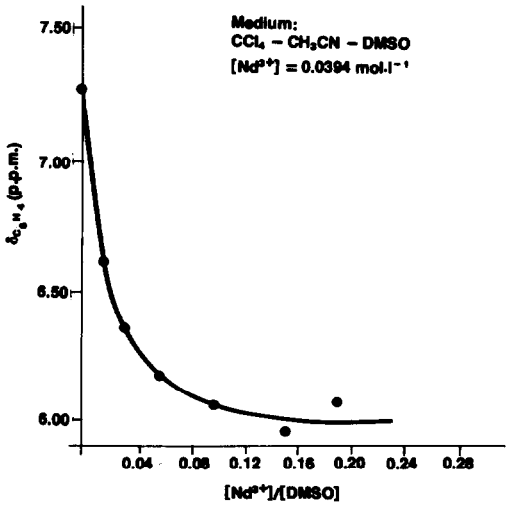

Fig. 2. Variation in the chemical shift of C_6H_4 PROTONS, $\delta_{C_6H_4}$, as a function of $[Nd^{3+}]/[DMSO]$.

molar conductance for these solutions follows a similar trend. The molar conductance remains low, but constant, at $< 2\,\Omega^{-1}\,mol^{-1}\,cm^2$ for $[Nd^{3+}]/[DMSO] > 0.04$, but increases rapidly for $[Nd^{3+}]/[DMSO] < 0.04$. The increase in molar conductance for $[Nd^{3+}]/[DMSO] < 0.04$ parellels the change in $\delta_{C_6H_4}$ (shown in Fig. 2). Thus, according to eqn (2), the replacement of $(ptsa)^-$ by DMSO in the inner coordination sphere occurs only in the presence of excessive amounts of DMSO, i.e. when $[Nd^{3+}]/[DMSO] < 0.04$. The replaced $(ptsa)^-$ contributes to the molar conductance which increases. Similarly, the observed $\delta_{C_6H_4}$ contains a greater proportion of free $(ptsa)^-$ and $\delta_{C_6H_4}$ approaches that of free $(ptsa)^-$ (7.276 ppm) as seen in Fig. 2. With smaller amounts of DMSO, the molar conductance and $\delta_{C_6H_4}$ shifts suggests that the conditions shown in eqn (1) predominate. Behaviour similar to that of Nd was observed for Pr, Sm, Eu, Ho, Er, Tm and Yb, although the $\delta_{C_6H_4}$ could not be measured for Ho due to excessive broadening.

It is assumed that the CH_3CN does not coordinate to the $Ln(ptsa)_3$ in the presence of DMSO because no apparent changes in CH_3CN proton chemical shifts were observed in these solutions. (The methyl proton signals of CH_3CN and $(ptsa)^-$ occur very close to each other.) If CH_3CN associates with $Ln(ptsa)_3 \cdot z(DMSO)$ it will occur in the outer coordination sphere, resulting in very small chemical shifts.

The δ_{DMSO} and $\delta_{C_6H_4}$ LIS for different lanthanides were analysed according to suggestions made by Reilley *et al.*,[5] so that any changes in coordination of the ligands round the Ln^{3+} could be detected. The true paramagnetic LIS was obtained by subtraction of the shift for lanthanum complexes from the observed shift, i.e. $\Delta\delta_i = \delta_{obs(i)} - \delta_{La(i)}$. If dipolar contributions to the observed LIS are predominant, a plot of $\Delta\delta_i/S_Z{}^G$ vs $C^D/S_Z{}^G$, for different Ln should be a straight line. $S_Z{}^G$ and C^D are theoretical constants that are mentioned in the literature[22,23] as reflecting the respective contact and dipolar contributions for individual lanthanides.

Values for $\Delta\delta_{DMSO}$ at [Ln]/[DMSO] = 1 were obtained for Nd from the slope of the straight line in Fig. 1. Similar plots for other Ln were also thus obtained. A plot of these values for $\Delta\delta_{DMSO}/S_Z{}^G$ vs $C_D/S_Z{}^G$ is shown in Fig. 3. The data all fall in a straight line with intercept 0.101 and slope 0.630. According to Reilley *et al.*,[5] this indicates a minimum dipolar contribution to $\Delta\delta_{DMSO}$ for Eu^{3+} of 70%. All other Ln have a larger proportion of dipolar contributions. There is no evidence of any change in DMSO coordination in the solvent species across the lanthanide series. $Ln(ptsa)_3$ therefore forms isostructural compounds with DMSO in this solvent mixture.

The $\Delta\delta_{C_6H_4}$ values were calculated from the observed shift at a ratio of [Ln] to [DMSO] of 0.1, which, according to the previous discussion, occur in a region where no dissociation of the complex, $Ln(ptsa)_3 \cdot z(DMSO)$, is found. A plot of $\Delta\delta_{C_6H_4}/S_Z{}^G$ vs $C^D/S_Z{}^G$ is shown in Fig. 4. Two straight lines, one for Pr, Nd and Sm with intercept -0.150 and slope -0.106, and the other for Eu, Er, Tm, and Yb with intercept -0.057 and slope -0.058, best fit the data. This suggests that there are two spatial arrangements of the $(ptsa)^-$ round Ln^{3+} across the lanthanide series. The non-zero intercepts of the straight lines are indicative of greater contact contributions to the LIS for $\Delta\delta_{C_6H_4}$. A minimum dipolar contribution of 21% was calculated for $\Delta\delta_{C_6H_4}$ in shifts induced by Eu^{3+}. The delocalization of electrons in aromatic systems is more likely to enhance contact contributions to aromatic protons. The excessive broadening observed for Ho^{3+} is probably due to contact contributions to the LIS. The interaction between $(ptsa)^-$ and Ln^{3+} is primarily ionic in nature with some contribution from covalent bonding, as judged from the contact contributions toward the LIS.

Although the two straight lines in Fig. 4 pass through few points, the indications are that the $(ptsa)^-$, which is presumably coordinated in a bidentate fashion, is more susceptible to changes in coordination with a decreasing Ln^{3+} radius. Hence, the detection of such changes is easier in the analysis of the LIS for $\Delta\delta_{C_6H_4}$ than it is in that for $\Delta\delta_{DMSO}$. The latter is bound in a monodentate mode to the Ln^{3+}, and is presumably more labile. The

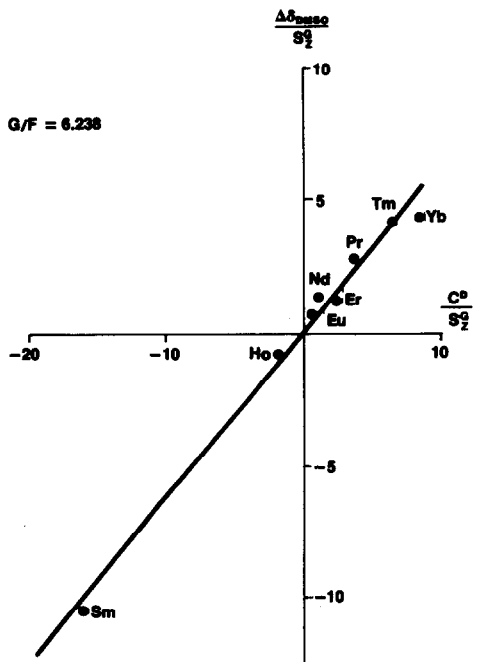

Fig. 3. Analysis of LIS for DMSO protons.

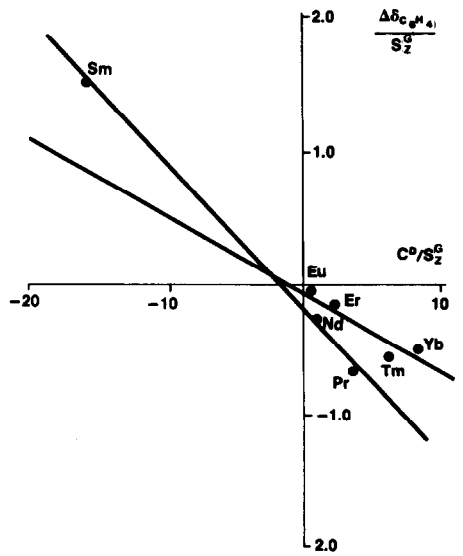

Fig. 4. Analysis of LIS for $C_6H_4(ptsa)^-$ protons.

change in DMSO coordination across the lanthanide series is less pronounced, and is not detected (Fig. 3).

Some of these conclusions can be used to elucidate the role of (sulphonate)$^-$ in the selective extraction of lanthanides. In aqueous media, the interaction between Ln^{3+} and (sulphonate)$^-$ is primarily electrostatic. The selective extraction of individual Ln^{3+} by ion-exchange resins with sulphonic acid groups is primarily due to process that are not based on the coordinating ability of the sulphonate group. However, in non-aqueous media, the (sulphonate)$^-$ acts to a greater extent as a coordinating ligand, since it is more covalent. Hence, for liquid cation exchangers, such as dinonylnaphthalene sulphonic acid dissolution in non-aqueous media, the selectivity of extraction for individual Ln^{3+} reported in the literature[4] is presumably due to changes in coordination of (sulphonate)$^-$ round the Ln^{3+}.

Acknowledgements—This paper is published by permission of the National Institute for Metallurgy, which also provided financial assistance in the form of a bursary to one of the authors. The financial assistance from the Council for Scientific and Industrial Research for the purchase of chemical is also gratefully acknowledged.

The authors wish to express their appreciation to one of the referees for the constructive criticism of the paper.

REFERENCES

[1]Y. Marcus, *Chem. Rev.* 1963. **63**. 193

[2]Y. Marcus and A. S. Kertes, *Ion Exchange and Solvent Extraction of Metal Complexes.* Wiley-Intersciences, New York (1969).

[3]G. W. Markovits and G. R. Choppin, *Solvent Extraction with Sulphonic Acids. Ion Exchange and Solvent Extraction* (Edited by J. A. Marinsky and Y. Marcus), Vol.3, p. 51. Marcel Dekker, New York (1973).

[4]R. Chiarizia, P. R. Danesi, M. A. Raieh and G. Sibona, *J. Inorg. Nucl. Chem.* 1975. **37**, 1495.

[5]C. N. Reilley, B. W. Good and R. D. Allendoerfer, *Anal. Chem.* 1976. **48**, 1446.

[6].A. D. Sherry, P. R. Yang and L. O. Morgan, *J. Am. Chem. Soc.* 1980. **102**, 5755.

[7]A. D. Sherry and E. Pascual, *J. Am. Chem. Soc.* 1977. **99**, 5871.

[8]L. B. Zinner and G. Vincentini, *J. Inorg. Nucl. Chem.* 1980. **42**, 1349.

[9]H. A. Friedman and L. M. Toth, *J. Inorg. Nucl. Chem.* 1980. **42**, 1510.

[10]L. B. Zinner and G. Vicentini, *J. Inorg. Nucl. Chem.* 1981. **43**, 193.

[11]A. Seminara and E. Rizzarelli, *Inorg. Chim. Acta.* 1980. **40**, 249.

[12]S. J. Lyle and MD. M. Rahman, *Talanta* 1963. **10**, 1177.

[13]S. K. Ramalingam and S. Soundarajan, *J. Inorg. Nucl. Chem.* 1967. **29**, 1763.

[14]F. Coetzee, *et al.*, *Analyt. Chem.* 1962. **34**, 1139.

[15]V. Krishnan and C. C. Patel, *J. Inorg. Nucl. Chem.* 1964. **26**, 2201.

[16]F. H. Spedding and H. S. Jaffe, *J. Am. Chem. Soc.* 1954. **76**, 882, 884.

[17]R. A. Robinson and R. H. Stokes, *Electrolyte Solutions*, 2nd Edn. Butterworths, London (1959).

[18]W. J. Geary, *Coord. Chem. Revs.* 1971. **7**, 81.

[19]D. K. Koppikar and S. Soudarajan, *J. Inorg. Nucl. Chem.* 1976. **38**, 174.

[20]V. N. Krishnamurty and S. Soundarajan, *J. Inorg. Nucl. Chem.* 1967.**29**, 517.

[21]S. N. Krishnamurthy and S. Soundarajan, *J. Inorg. Nucl. Chem.* 1966. **28**, 1689.

[22]R. M. Golding and M. P. Halton, *Austr. J. Chem.* 1972. **25**, 2577.

[23]R. M. Golding and P. Pyykkö, *Mol. Phys.* 1973. **26**, 1389.

Polyhedron Vol. 1, No. 3, pp. 257–262, 1982
Printed in Great Britain.

0277–5387/82/030257–06$03.00/0
Pergamon Press Ltd.

ON EXTRACTANT PROPERTIES OF β-KETOPHOSPHONATES—I

LANTHANIDES EXTRACTION FROM PERCHLORATE MEDIUM BY DIBUTYLPHENACYLPHOSPHONATE

BRUNO CECCAROLI,* JOROLF ALSTAD and MAURICE J. F. LEROY†
Division of Nuclear Chemistry, University of Oslo, P.O. 1033, Blindern, Oslo 3, Norway

(*Received* 13 *October* 1981)

Abstract—Liquid–liquid distribution of lanthanides was studied using dibutylphenacylphosphonate (HDBPP) in an aromatic diluent as organic phase and 1M sodium perchlorate as the aqueous phase. Appropriate radioactive isotopes of the elements were used as indicators in the determination of the distribution ratios. HDBPP was found to act both as a neutral and an acidic extracting agent, the extracted species having the general composition $[M\{H(DBPP)_{3-q}\}_x(ClO_4)_q]$. $x = 4$, $q = 1$ were found for M = La and $x = 3$, $q = 0$ for M = Eu, Gd, Tb and Tm. The separation factors of adjacent elements $\alpha_{z/z-1}$ and with respect to lanthanum $\alpha_{z/La}$ were determined for all elements, except cerium. In a plot of $\alpha_{z/La}$ as a function of z, the dividing of the series into subgroups is discussed in terms of ionic radius, coordination numbers and nephelauxetic effect.

INTRODUCTION

The β-ketophosphonates[1–7] with the composition $[R'C(O)CH_2P(O)(OR)_2]$ and related compounds having a carbonyl group and a phosphoryl group in β to each other such as carbamyl-methylenephosphonates[8–13] $[R_2^1NC(O)CH_2P(OR)_2]$ or hydrogen 2-ethylhexylphenacylphosphonate[14] $[C_6H_5C(O)CH_2P(O)(OH)(OC_8H_{17})]$ have been the subject of some recent studies because of their extraction abilities. Useful information about the metal complex formation by these ligands is also available from spectroscopic and structural investigations. Some of them have been reported concerning complexes of transition elements,[15–18] lanthanides,[19] thorium[7] and alkali metals.[20] The potential extraction abilities, which may be expected from these compounds are due to some particular structural properties. They have an asymmetric donor power due to the phosphoryl and carbonyl groups, while their enolic tautomerism gives them an acidic character. They are also potential chelating agents owing to the respective positions of the two oxygen atoms from PO and CO groups. Their behaviour in liquid–liquid systems should in part be governed by the inductive effects and the steric bulk of the substituents. Recent reports[3–6] have shown that dibutylphenacylphosphonate (HDBPP) behaves as an extracting reagent by using almost all these potential properties. HDBPP was found to be able to act both as a neutral adduct forming agent through the PO group and as a chelating anionic ligand. Also stoichiometries in agreement with mixed complexes have been found for the extracted species. The two kinds of extraction are identified by hydrogen-ion concentration dependencies. The neutral adduct forming is independent of hydrogen-ion concentration while the hydrogen-ion exchanging extraction has a negative power dependence. They will, therefore, be called, respectively, the *neutral* and the *acidic extraction*. The previous results[3–6] with HDBPP have easily shown the neutral extraction of a large range of metals (Th^{4+}, lanthanides, Ga^{3+}, In^{3+}, Fe^{3+}, VO_2^{2+}, UO_2^{2+}, Zn^{2+}) and of inorganic acids from various aqueous solutions (thiocyanate, nitrate, chloride, sulphate, perchlorate, tetrafluoroborate). Spectroscopic studies[3,7,21] of organic phases have proved that the adduct complexes with the neutral species are formed only through the PO group. In this case the quantitative and qualitative extraction behaviour of HDBPP is very similar to that observed for tri-*n*-butylphosphate (TBP). The low value that was found[5] for the dissociation constant of HDBPP ($pK_a = 12.30 \pm 0.03$) emphasizes the difficulty in observing the acidic extraction. Evidence for it must be investigated from low complexing aqueous solutions such as ClO_4^- or BF_4^- and/or at low hydrogen-ion concentrations. Even under those conditions the acidic extraction is often accompanied by the neutral one[3,5]. Spectroscopic investigations[7,21] of the organic phase and of complexes prepared by using a liquid–liquid extraction method show that β-ketophosphonates like HDBPP are chelating reagents when acting as anionic ligands. In this paper we will deal with the extraction stoichiometries and the separation factors of the lanthanoids for the extraction of these elements from molar perchlorate solutions by HDBPP. The present work completes a previous report[6] where we showed the neutral extraction of gadolinium from thiocyanate solution, the duality (neutral/acidic extraction) of HDBPP towards the extraction of gadolinium from BF_4^- and ClO_4^- media and the separation factors for lanthanides under conditions proper to the acidic extraction. The magnitude of the values obtained for the separation factors were encouraging and it seemed interesting to investigate the parameters influencing the separation. The study of the extraction stoichiometries and the study of the separation factors require two different methods of measurement. As previously pointed out[22] the former may be carried out by single element experiments while the latter requires multielement experiments. The presentation of the results and the discussion are, therefore, subdivided in two parts corresponding to the two experimental methods.

*Author to whom correspondence should be addressed.
†Laboratoire de Chimie Minérale de l'E.N.S.C.S., B.P. 296/R8, F.67008, Strasbourg, Cedex, France.

DEFINITIONS

The distribution ratio of an element Z is represented by D_z and defined by the ratio of the total analytical concentration in the organic phase to its total analytical concentration in the aqueous phase. The separation factor $\alpha_{z/z'}$ is the ratio of the respective distribution ratios of two extractable elements z and z' measured under the same conditions.

In this paper symbols with a bar above them refer to the organic phase and in brackets refer to the equilibrium concentrations. The total analytical molarity of reactants (moles per dm^3) is given by a numeric value followed by M and the symbol of the reactant.

EXPERIMENTAL

Radionuclides

^{153}Gd was obtained, as the aqueous chloride from the Radiochemical Centre Amersham. The other radionuclides ^{140}La, ^{142}Pr, ^{147}Nd, $^{149+151}Pm$, ^{153}Sm, $^{152+154}Eu$, ^{153}Gd, ^{160}Tb, ^{165}Dy, ^{166}Ho, ^{171}Er, ^{170}Tm, $^{169+175}Yb$, ^{177}Lu were produced by thermal neutron irradiation of the respective rare earths oxides in the reactor of Kjeller (Norway). The irradiated oxides and the aqueous chloride were converted to perchlorates and dissolved in diluted $HClO_4$.

Chemicals

HDBPP was obtained from the Laboratoire de Chimie Minérale de l'ENSCS, where it was prepared and purified as previously described.[3] Solvesso 150 was purchased from ESSO Company (Norway). This "carrier" diluent was chosen because of its high boiling point (180–210°C) and because its high aromaticity (97%) allowed us to avoid the polymerization of HDBPP in the organic phase. All other chemicals were of p.a. quality and used without further purifications.

Distribution measurements

Equilibrations were performed in a thermostated glass vessel at 20°, the two phases with the appropriate radionuclides added being shaken for 10 min and separated by gravity and centrifugation when necessary. Samples of each phase were then withdrawn and analysed by radiometry (γ-counting). When only one radionuclide was present in the extraction system, the distribution ratio D_z of the element Z was measured by using a NaI(Tl) well type scintillation detector. Such measurements were carried out in experiments whose aim was to investigate the extraction stoichiometries. But the determination of separation factors with a maximum of accuracy requires a simultaneous determination of the distribution ratios for several elements in extraction systems using admixtures of radionuclides. In this latter case the γ-counting was made by using a Ge(Li) detector and a 4096 analogue to digital converter interfaced to a NORD-1 computer. Procedure applying this latter counting method, choice of γ-rays and evaluation of data have been described in a previous paper.[22]

EXPERIMENTAL CONDITIONS

Single element experiments

Extractant (HDBPP) concentration (i) and hydrogen-ion concentration (ii) dependencies of the distribution ratios of La, Eu, Gd, Tb and Tm have been determined for each element under the following conditions:

(i) 20°C, 1 M (Na, M, H)ClO_4, $[H^+] = 10^{-5}$, $\sim(2\times10^{-2} - 10^{-7})$ M (metal) solvesso-150.

(ii) 20°C, 1 M (Na, M, H)ClO_4, $(4-1)\times10^{-3}$ M (metal), solvesso-150, 0.43 M HDBPP.

Multielement experiments

The determinations of the separation factors were made with $[H^+]$ as variable parameter by using the 10 following admixtures of elements.

1. Eu, Tb, Tm	6. Pr, Er, Tm
2. Eu, Tm	7. La, Pr, Nd, Sm
3. Eu, Gd	8. La, Pr, Nd, Sm, Lu
4. Dy, Tm	9. La, Pr, Nd, Sm, Ho, Lu
5. Er, Tm	10. La, Tm, Yb, Lu

under the following experimental conditions:

20°C, 1 M (Na, M, H)ClO_4, 2×10^{-3} M (metal/element), solvesso-150, 0.43 M HDBPP.

RESULTS AND DISCUSSION

Single element experiments

Dependencies of the hydrogen-ion concentration on the distribution ratios of La^{3+}, Eu^{3+}, Gd^{3+}, Tb^{3+} and Tm^{3+} by 0.43 M HDBPP diluted in solvesso-150 from 1 M (M^{3+}, Na^+, H^+, ClO_4^-) are presented in Fig. 1. Each curve itself is the result of several experiments at various metal concentrations represented by different symbols in Fig. 1. In most cases macroscopic amounts of metal were used in order to avoid any irregularity in the distribution ratio caused by possible organic impurities at very low concentration. A disadvantage of this procedure is the risk of formation of polynuclear metal complexes which would not occur at trace metal concentrations. The metal concentration, however, seems not to affect significantly the distribution ratio, in so far as the amount of metal remains low compared to the amount of the extractant in the system. According to the shape of the curve plotting $\log D_z$ vs $\log[H^+]$ the results are divided into 3 regions where the extraction mechanisms and the species involved either in the aqueous or organic phase may differ. The metal distribution is independent of the higher hydrogen-ion concentration, indicating that the dominating mechanism in this region is the neutral extraction. When decreasing $[H^+]$ a new region appears, where the

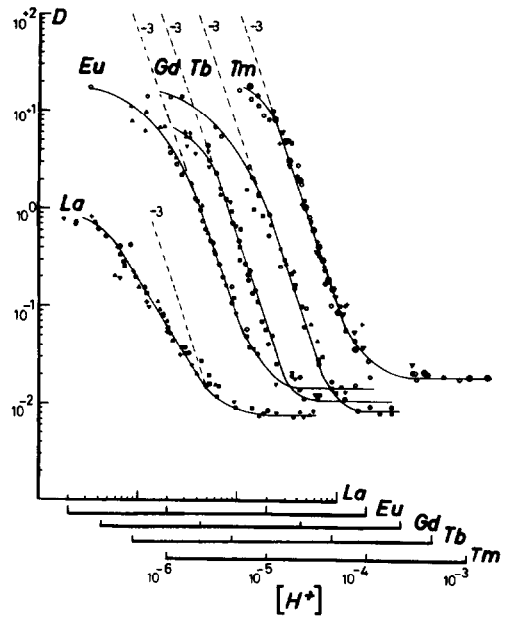

Fig. 1. Hydrogen-ion dependencies of the extractions of La, Eu, Gd, Tb and Tm as obtained by single element measurements. [20°C, 0.43 M HDBPP, solvesso-150, 1 M (Na, H, M)ClO_4]. Each symbol refers to one experiment.

La	+ ● ▼	4.5×10^{-3} M (La^{3+})
	■ ▲	2×10^{-2} M (La^{3+})
Eu	○ ◇ □ ▽	2×10^{-3} M (Eu^{3+})
Gd	● ▲ ▼	10^{-3} M (Gd^{3+})
	■	1.6×10^{-3} M (Gd^{3+})
Tb	○ □	Trace (Tb^{3+})
	△	10^{-2} M (Tb^{3+})
Tm	○	6×10^{-4} M (Tm^{3+})
	◑ + □	4×10^{-3} M (Tm^{3+})
	▽	7×10^{-3} M (Tm^{3+})

inversely third power hydrogen-ion concentration dependencies are observed except for lanthanum which seems to prefer a close to inversely second power dependence. The negative values of the $[H^+]$ power dependencies are interpreted as clear evidence for the acidic extraction. Since the valence of lanthanides is +3, the third power dependence is the highest that can be expected. The third power dependence, thus, implies that the metal is in uncomplexed free ion form in the aqueous phase and forms extractable complexes with 3 dissociated (anionic) ligands $DBPP^-$. The second power dependence observed in the case of lanthanum may be explained by several hypotheses and it is, therefore, necessary to fully determine the stoichiometries of the extractable complexes. At lower hydrogen-ion concentrations the curve $\log D_z$ vs $\log[H^+]$ steadily falls off from the linearity to approach a horizontal region. The deviation is often supposed to be caused by the ligation of the metal in the aqueous phase either by the hydroxilic ion (OH^-) or by the dissociated enolate form $DBPP^-$. But according to the values of the overall stability constants of $M(OH)_2^{2+}$—M representing a lanthanide—obtained by Guillaumont *et al.*[23] the metal hydrolytic character should not be very significant in the H^+-concentrations ($10^{-5}-10^{-6}$) where the deviation is observed. Guillaumont *et al.* used a solvent extraction method, which consists of deducing the constants from the deviation from the linear relationship between $\log D$ and $\log[H^+]$ when the extractant is HTTA. The comparison of our studies with theirs is, therefore, very relevant. The deviation from linearity is much more pronounced for extraction by HDBPP and may be attributed to the formation of aqueous species with the composition $M(DBPP)_i^{(3-i)+}$. When the extractable non-charged complexes are also dominating in the aqueous phase, the metal distribution becomes independent of hydrogen-ion concentration as the curves tend to suggest at the lower concentrations.

In order to determine the full stoichiometries of complexes involved in the organic phase by the acidic extraction the extractant dependencies had to be determined at an appropriate H^+-concentration. The extractant dependencies of single element extraction of La, Eu, Gd, Tb and Tm at $[H^+]=10^{-5}$ from 1 M ($Na^+ClO_4^-$) are presented in Fig. 2. Results give a +4.0 power dependence for lanthanum and a +3.0 power dependence for the others. A change in the coordination number is, however, not unusual throughout the 4f series and is, however, assumed to decrease from lanthanum to lutetium.

Taking into account the hydrogen-ion concentration and extractant concentration dependencies, the obtained stoichiometries are convenient with structural composition $M(DBPP)_3$ to the extracted complexes where M = Eu, Gd, Tb and Tm are surrounded by three dissociated enolic ligands. Since in this case the ligand was found[21] to be bidentate by IR spectroscopy, the coordination numbers are 6 provided that no water molecule are co-extracted. An excess of coordination sites is not unusual for lanthanide chelates as for instance substituted β-diketonates. The stoichiometries obtained for lanthanum are consistent with a mixed complex $La(DBPP)_2(HDBPP)_2ClO_4$ where La is chelated by 2 anionic ligands. $[La(DBPP)_2]^+$ is extracted as an ion pair by 2 donor neutral molecules HDBPP and the charge is neutralized by 1 inorganic anion ClO_4^-. If we assume that the neutral HDBPP is monodentate, the coordination number N_c is 6. The ClO_4^- anion is not taken into account because it is reasonable to assume that it is localized in the outer coordination sphere. But, the greater stability of the ion-pair formed by lanthanum compared to the other elements arises from the large size of La^{3+}, which is therefore able to accept 4 molecules in the inner coordination sphere instead of 3. In conclusion we propose to describe the extraction of lanthanides from 1 molar $NaClO_4$ solution by HDBPP by the following general equilibrium regardless of whether the mechanism is acidic or neutral.

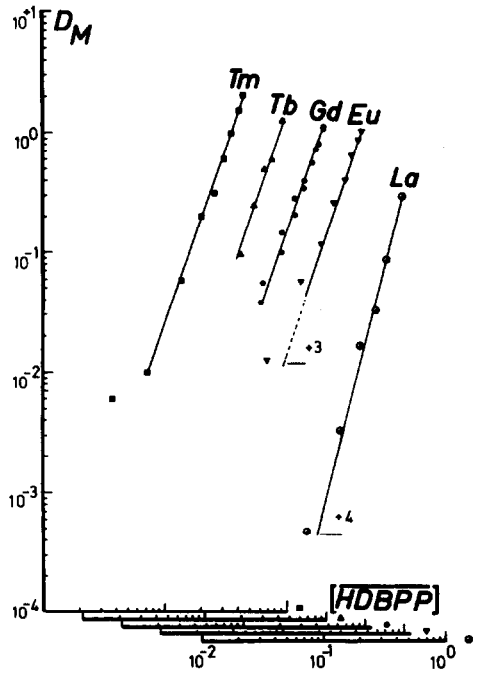

Fig. 2. Extractant dependencies of the extractions of La, Eu, Gd, Tb and Tm as obtained by single element measurements. [20°C, 1 M (Na, H)ClO_4, $[H^+]=10^{-5}$ ($10^{-3}-5\times10^{-3}$) M metal-ion].

$$M^{3+} + x\overline{HDBPP} + qClO_4^- \rightleftharpoons \overline{M\{H(DBPP)_{3-q}\}_x(ClO_4)_q} + (3-q)H^+.$$

The mechanism of the extraction is identified by the value of q.

M	x	q	Mechanism
Eu, Gd, Tb, Tm	3	0	Acidic
La	4	1	Mixed
Gd	3 and 4	3	Neutral (previous results)[6]

Multielement experiments

In an attempt to determine the separation factors with a maximum of accuracy multielement experiments have been carried out by using admixtures of radionuclides. The distribution ratios were measured at various hydrogen-ion concentrations, and the results led to a new study of this parameter dependence. The main originality of Fig. 3 compared to Fig. 1 consists of the fact that each curve is linked to the others by several

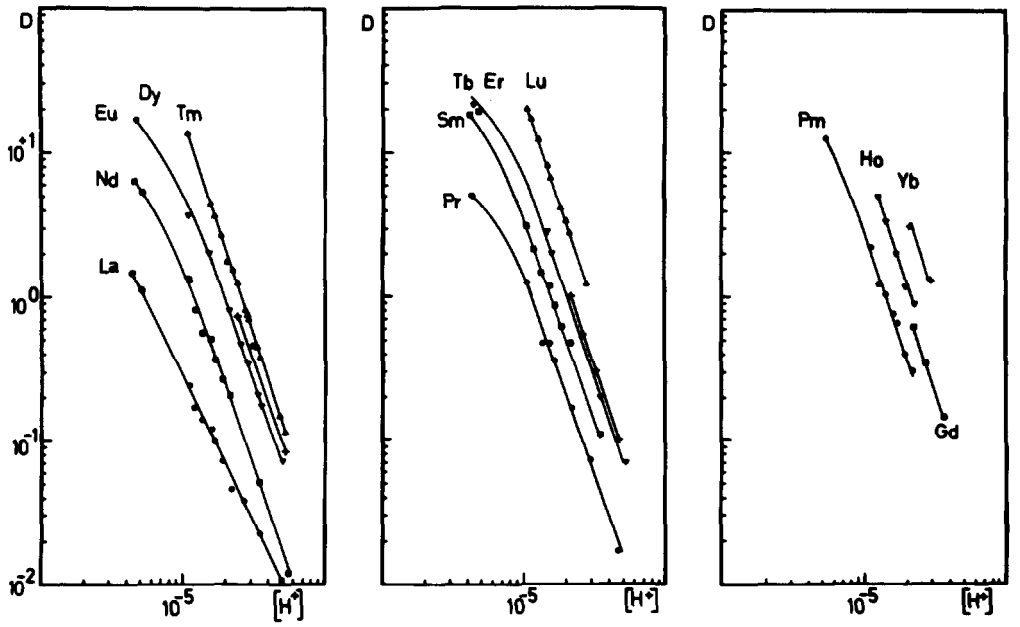

Fig. 3. Hydrogen-ion dependencies of the extractions of lanthanoids by HDBPP as obtained by multielement measurements. [20°C, 1 M (Na, H, M)ClO_4, 0.43 M HDBPP, solvesso-150].

experimental points simultaneously determined. The inverse third power dependencies are to a large extent confirmed for all elements except for lanthanum, for which the second power dependence also is confirmed. A regular slight decrease in the power dependence must, however, be pointed out from Lu(−3.0) to Pr(−2.7) as shown in Table 1.

Separation factors between two elements are, therefore, not constant but vary with the hydrogen-ion concentration, especially in regions far from that of a linear relationship between log D_z and log [H^+]. The separation factors $\alpha_{z/La}$ and $\alpha_{z/z-1}$ were graphically deduced from the Fig. 3 at 3 different hydrogen-ion concentrations (7.5×10^{-6}, 1.5×10^{-5} and 5×10^{-5}). They are reported in Table 2. Figure 4 presents a plot of log $\alpha_{z/La}$ vs Z as recommended by Peppard *et al.*[24] In an earlier work[22] we proposed to discuss the shape of such plot in terms of 3 intrinsic properties of the 4f elements. This discussion seems also to be relevant for the present extraction system.

(1) *The ionic radius.* According to the variations of the ionic radius through the 4f series the stability of a given complex is expected to increase almost linearly with the atomic number, z, because the chemical bond between the strong electropositive lanthanide ions and oxygen atoms from the ligands is mainly ionic. Although different complexes are involved in log $\alpha_{z/La}$, this general trend is observed at least from La to Sm and from Er to Lu. But many irregularities are also observed and obviously reveal the occurrence of other effects influencing the separation.

(2) *The change in the coordination number throughout the lanthanoid series* is a well known effect and may be interpreted as a consequence of both the large size that characterizes the lanthanide ions, and the decrease with z in ionic radius also called the lanthanide contraction. The coordination number N_c of trivalent lanthanides varies largely. In the solid state they form complexes with N_c ranging from 3 to 12, but 8 and 9 are most common. $N_c = 6$ and 7 are often found in tris-complexes where substituted β-diketones act as anionic bidentate ligands. In solution the coordination number is not well defined and varies with the chosen statistical model. Spedding *et al.*[5] have concluded from partial molal

Table 1. Hydrogen-ion concentration dependencies determined by multielement experiments. [20°C, 1 M (Na, M, H)ClO_4, 0.43 M HDBPP, solvesso-150]

La	2.0 ± 0.1	Gd	3.0 ± 0.2
Ce		Tb	2.9 ± 0.1
Pr	2.7 ± 0.1	Dy	
Nd	2.8 ± 0.1	Ho	2.9 ± 0.1
Pm	2.9 ± 0.1	Er	3.0 ± 0.1
Sm	2.9 ± 0.2	Tm	3.0 ± 0.1
Eu	2.8 ± 0.2	Yb	
		Lu	3.0 ± 0.1

Table 2. Separation factors $\alpha_{z/z-1}$ and $\alpha_{z/La}$ and extraction constant $K(Gd) = D_{Gd}\,[H^+]^{+3}[\overline{HDBPP}]^{-3}$ at various hydrogen-ion concentrations. [20°C, 1 M (Na, M, H)ClO_4, 0.43 M $\overline{HDBPP}$, solvesso-150]

$[H^+]$	7.5×10^{-6}		1.5×10^{-5}		5×10^{-5}	
log K(Gd)	-13.3		-13.2		-13.1	
Z	$\alpha_{z/z-1}$	$\alpha_{z/La}$	$\alpha_{z/z-1}$	$\alpha_{z/La}$	$\alpha_{z/z-1}$	$\alpha_{z/La}$
La	-	1.0	-	1.0	-	1.0
Ce	(3.5)	(3.5)	(2.5)	(2.5)	(1.45)	(1.45)
Pr	(1.49)	5.2	(1.56)	3.9	(1.10)	1.60
Nd	1.19	6.2	1.07	4.2	1.03	1.65
Pm	1.61	10	1.50	6.25	1.03	1.70
Sm	1.50	15	1.60	10.0	2.35	4.0
Eu	0.93	14	1.58	16	1.98	7.9
Gd	(0.89)	(12.5)	0.79	12.5	(0.75)	(5.9)
Tb	(1.68)	21	1.60	20	(1.44)	8.5
Dy	1.43	30	1.04	21	1.22	10.4
Ho	1.13	34	0.96	20	(1.00)	(10.4)
Er	1.24	42	1.19	24	(0.96)	(10.0)
Tm	1.52	64	1.51	36	(1.40)	14
Yb	1.56	100	1.63	58	1.18	16.5
Lu	1.26	126	1.16	65	0.88	14.5

volume data that the ions La^{3+} to Nd^{3+} are nine-coordinated, Tb^{3+} to Lu^{3+} are eight-coordinated and Sm^{3+}, Eu^{3+} and Gd^{3+} are mixtures of both coordination numbers. In the present work the changes in the hydrogen-ion and extractant concentrations, which have been observed especially for lanthanum to be different from those of other metal ions are an effect of the same kind. The formation of mixed complexes is easier for the largest ions, more able to accept an excess of neutral extractant molecules in the non occupied coordination sites. This effect should be correlated with the steric bulk of extractant.

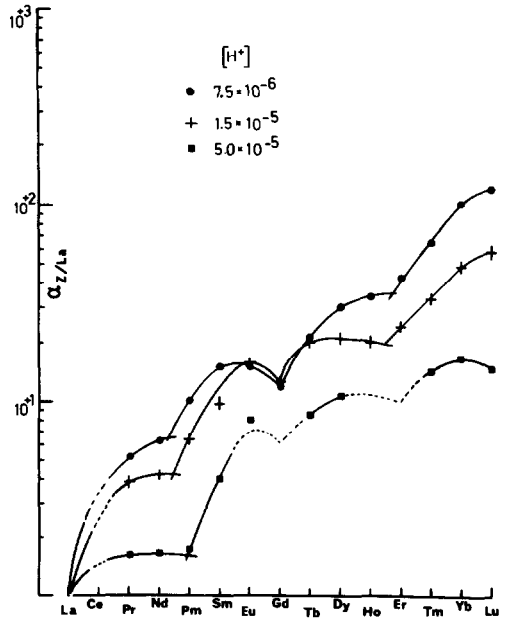

Fig. 4. Variation of the logarithm of the separation factor $\alpha_{z/La}$ with the atomic number z. [20°C, 1 M (Na, H, M)ClO_4, 0.43 M HDBPP, solvesso-150].

(3) *The nephelauxetic effect* in the 4f series is responsible, as independently explained by Jørgensen[26] and Nugent,[27] of the dividing of the series into 4 subgroups represented by 4 "tetrades" in a plot of log $\alpha_{z/La}$ vs z or by the "double-double effect" in a plot of $\alpha_{z/z-1}$ vs z as suggested respectively, by Peppard *et al.*[24] and Fidelis and Siekierski.[28]

CONCLUSION

Interesting differences with respect to the complex formation are observed between lanthanum and the other elements. The extracted lanthanum complex has the composition $La(\overline{DBPP})_2(\overline{HDBPP})_2ClO_4$ while the *tris*-enolate chelates $M(\overline{DBPP})_3$ are dominating species for the others.

The shape of the curve log $\alpha_{z/La}$ vs z gives a clear evidence of the division of the series into four branches as expected by the tetrade or double-double effect. This feature and the values of α_{zLa} agree well with our previous results[6] taking into account the different extractant concentrations. The most favourable conditions for high separation are found at low hydrogen-ion and extractant concentrations. The extraction constants, however, vary greatly from $-\log K(Gd) = 10.5 \pm 0.2$ in [6] to $-\log K(Gd) = 13.2 \pm 0.1$ in the present work. Some sporadic tests seem to indicate that HDBPP

efficiency continuously decreases with age. These constants should be determined by freshly prepared and purified product. The values of the extraction constants must, therefore, be very carefully considered.

Acknowledgements—The authors are grateful to the Royal Norwegian Council for Scientific and Industrial Research for the support of a postdoctorate fellowship to one of them (B.C.) during the period of this work.

REFERENCES

[1]D. Sevdić and H. Meider-Goričan, *J. Less. Common Metals* 1972, **27**, 403.
[2]P. Bronzan and H. Meider-Goričan, *J. Less. Common Metals* 1972, **29**, 407.
[3]J. L. Martin and M. J. F. Leroy, *J. Chem. Res.* 1978, S. 88 and M. 1113.
[4]J. P. Brunette, M. J. F. Leroy, B. Ceccaroli and J. Alstad, *Acta Chem. Scand.* 1978, **A32**, 415.
[5]U. Olofsson, J. P. Brunette, B. Allard and A. Selme, *Proc. Int. Solv. Ext. Conf.*, Liége, Art. 80–88, 1980.
[6]J. Alstad, B. Ceccaroli, J. P. Brunette and M. J. F. Leroy, *Proc. Int. Solv. Ext. Conf.*, Liége, Art. 80-48, 1980.
[7]J. P. Brunette, B. Allard, L. Jurdy and M. J. F. Leroy, *Spectrochimica Acta* 1981, **37A**, 991.
[8]R. R. Shoun, W. J. McDowell and B. Weaver, *Proc. Int. Solv. Ext. Conf.*, Montreal, 1977.
[9]W. W. Schulz and L. D. McIsaac, *Proc. Int. Solv. Ext. Conf.*, Montreal, 1977.
[10]T. H. Siddall, III, *J. Inorg. Nucl. Chem.* 1963, **25**, 883.
[11]T. H. Siddall, III, *J. Inorg. Nucl. Chem.* 1964, **26**, 1991.
[12]H. Petržilová, J. Blinka and L. Kuča, *J. Radioanal. Chem.* 1979, **51**, 107.
[13]N. C. Schroeder, L. D. McIsaac, D. H. Meikrantz, J. F. Krupa and J. D. Baker, *J. Inorg. Nucl. Chem.* 1980, **42**, 1029.
[14]G. G. Warren, *J. Inorg. Nucl. Chem.* 1961, **23**, 103.
[15]F. A. Cotton and R. A. Schunn, *J. Am. Chem. Soc.* 1963, **85**, 2394.
[16]C. N. Lestas and M. L. Truter, *J. Chem. Soc. A* 1971, 738.
[17]C. M. Mikulski, W. Henry, L. L. Pytlewski and N. M. Karayannis, *J. Inorg. Nucl. Chem.* 1978, **40**, 769.
[18]M. T. Youinou, J. E. Guerchais, M. E. Louër and D. Grandjean, *Inorg. Chem.* 1977, **16**, 872.
[19]W. E. Stewart and T. H. Siddall III, *J. Inorg. Nucl. Chem.* 1970, **32**, 3599.
[20]T. Bottin-Strzalko, J. Corset, F. Froment, M. J. Pouet, J. Seyden-Penne and M. P. Simonnin, *J. Org. Chem.* 1980, **45**, 1270.
[21]B. Ceccaroli and M. Burgard, to be published.
[22]B. Ceccaroli and J. Alstad, *J. Inorg. Nucl. Chem.* 1981, **43**, 1881.
[23]R. Guillaumont, B. Désiré and M. Galin, *Radiochem. Radioanal. Let.* 1971, **8**, 189.
[24]D. F. Peppard, C. A. A. Bloomquist, E. P. Horwitz, S. Lewey and G. W. Mason, *J. Inorg. Nucl. Chem.* 1970, **32**, 339.
[25]F. H. Spedding, M. J. Pikal and B. O. Ayers, *J. Phys. Chem.* 1966, **70**, 2440.
[26]C. K. Jørgensen, *J. Inorg. Nucl. Chem.* 1970, **32**, 3127.
[27]L. J. Nugent, *J. Inorg. Nucl. Chem.* 1970, **32**, 3485.
[28]I. Fidelis and S. Siekierski, *J. Inorg. Nucl. Chem.* 1971, **32**, 3191.

Polyhedron Vol. 1, No. 3, pp. 263–267, 1982
Printed in Great Britain.

0277-5387/82/030263-05$03.00/0
Pergamon Press Ltd.

MECHANISM OF FLUORIDE LOSS FROM FLUOROPOLYTUNGSTATES POSSESSING THE KEGGIN STRUCTURE

F. CHAUVEAU,* P. DOPPELT and J. LEFEBVRE
Laboratoire de Chimie des Polymères Inorganiques, Université Pierre et Marie Curie, 75230 Paris Cedex 05, France

(*Received* 13 *October* 1981)

Abstract—The fluoropolytungstates $[H_2W_{12}F_2O_{38}]^{4-}$ and $[HW_{12}F_3O_{37}]^{4-}$, which are of the metatungstate type with the fluoride ions occupying inner sites, lose fluoride ion and form more highly charged species $[H_2W_{12}FO_{39}]^{5-}$ and $[HW_{12}F_2O_{38}]^{5-}$ in aqueous solution about pH 3 in media of suitable ionic strength. Kinetic results are presented here consistent with a mechanism involving less condensed species containing 11 tungsten and 1, 2 or 3 fluoride atoms. Involvement of such species is supported by the isolation of the aluminotungstates $[HW_{11}AlF_3O_{36}(H_2O)](TMA)_5$†, $30H_2O$ and $[H_2W_{11}AlF_2O_{37}(H_2O)](TMA)_5$, $17H_2O$.

INTRODUCTION

In the dodecatungstoheteropolyanions with the general formula $[X^{(n)}W_{12}O_{40}]^{(8-n)-}$ the nature of the heteroelement X(X = Si, P, H_2...) has little or no effect on the structure of the molecule.[1–3] However, its role becomes very important when considering the charge of the polyanion. Hydrolysis mechanisms in aqueous solutions are affected by this charge. Accordingly, heteropolytungstates can be divided into two categories:

(i) those that undergo hydrolysis with no detectable intermediate: metatungstate or "tungstate X"[4] ($X=H_2^{2+}$) having a charge of −6 (pH hydrol. ~7–8).

(ii) Those that hydrolyse at pH ~4–5 by giving intermediates whose tungsten content per anion is 11 or 9 (X = B, Si, P; charges −3, −4, −5, respectively).[5–8]

We recently synthesised fluoropolytungstates with a metatungstic structure.[9] In accordance with their charges these can be divided into two groups:

(i) those that possess a 4(—) charge: $[H_2W_{12}F_2O_{38}]^{4-}$ and $[HW_{12}F_3O_{37}]^{4-}$,

(ii) those that possess a 5(—) charge: $[H_2W_{12}FO_{39}]^{5-}$ and $[HW_{12}F_2O_{38}]^{5-}$.

By ^{19}F and ^1H NMR studies the fluorine atoms were shown to be located in the central tetrahedron of the molecule.[10] However, an interesting phenomenon is observed in this series of compounds: above pH 3[11] fluoride is lost and the less highly-charged varieties convert to the highly charged ones. Fluoride exit from the central region of such a highly compact structure would seem most surprising were it not accompanied by a structural rearrangement of the molecule.

Our aim is to elucidate this point through the kinetic study of the transformations of the two varieties viz. $[H_2W_{12}F_2O_{38}]^{4-}$ and $[HW_{12}F_3O_{37}]^{4-}$.

EXPERIMENTAL

(A) *Preparation and analysis of fluoropolytungstic acids*

Procedures for the synthesis of the four fluoropolytungstates were reported in a previous article.[9] We shall briefly summarize the main steps involved in the preparation of the two varieties of compounds:

$$[HW_{12}F_3O_{37}]H_4 \quad (1)$$

Synthesis

In a polytetrafluoroethylene container, place successively 12 ml of hydrofluoric acid (40%), 110 ml of distilled water and 30 ml of hydrochloric acid (5 M).When hot and while stirring, add 160 ml of sodium tungstate (1 M). After cooling, add 16 ml of hydrofluoric acid (40%); after a few minutes still stirring, add 80 ml of concentrated hydrochloric acid. After cooling in ice, extract with ether (200 ml) using a plastic separatory funnel. The dense ether layer is collected and plunged into an aqueous solution previously saturated with potassium chloride. The potassium salt $[HW_{12}F_3O_{37}]K_4$ precipitates and is collected. The parent acid is generated from its salt by Drechsel's method[12] in HCl 3M medium. The maximum yield is 40%.

Analysis	%W	%F	% Central H	% Free H	% H_2O
Found	66.2	1.6	0.028	0.126	14.0
Calcd	66.3	1.7	0.030	0.120	—

$$[H_2W_{12}F_2O_{38}]H_4. \quad (2)$$

This variety is prepared indirectly starting with $[HW_{12}F_3O_{37}]H_4$: $[HW_{12}F_3O_{37}]H_4$ is dissolved in a 1M formic buffer with pH 3.2 in the presence of KCl (1M); its concentration is then W 0.1M. The hydrolysis reaction time is 24 hr when T = 25°C. The resulting solution which contains two varieties $[H_2W_{12}FO_{39}]^{5-}$ and $[HW_{12}F_2O_{38}]^{5-}$ is partially precipitated using excess KCl. The mixture of potassium salt obtained in the ratio of 40% of $[HW_{12}F_2O_{38}]K_5$ to 60% of $[H_2W_{12}FO_{39}]K_5$ is dissolved (total concentration W 0.2M) in a solution of 2.4N hydrochloric acid. The reaction $[HW_{12}F_2O_{38}]H_5 \rightarrow [H_2W_{12}F_2O_{38}]H_4$ which occurs in acidic medium is complete within 48 h at 50°C. $[H_2W_{12}F_2O_{38}]H_4$ is separated by four successive extractions using ether in HCl 2.4M medium.[12] It is obtained 95% pure. The yield is 10–15% of the initial mixture.

Analysis	%W	%F	% Central H	% Free H	% H_2O
Found	67.7	1.1	0.052	0.130	12.1
Calcd	67.8	1.2	0.061	0.122	—

(B) *Hydrolysis study*

The compounds analyzed were dissolved in acid form (concentration 5.10^{-3}M W) in 0.5M formic buffers at pH 3–4.2 with 1M NaCl at a temperature of 21°C.

*Author to whom correspondence should be addressed.
†TMA is the abbreviation of the tetramethylammonium cation.

The polarograms were recorded on a Tacussel type EPL 1B. The reference electrode was a saturated calomel electrode.

The liberated labile tungstate percentage was determined by polarography as follows:

The percentage of tungsten included in the substrate was determined at all stages of the reaction by measuring the height (at −0.3 V) of the first polarographic wave of the substrate (one electron wave).

The percentage of tungsten included in the fluoropolytungstates resulting from the hydrolysis ($HW_{12}F_2O_{38}^{5-}$ and $H_2W_{12}FO_{39}^{5-}$) was determined by measuring the height (at −0.5 V) of the first polarographic wave of the compounds (one electron wave). When the wave height does not reach its maximum, the difference is assumed to be indicative of W liberated as labile tungstate.

During the reaction, the liberated fluoride was determined by the use of a specific lanthanum fluoride electrode.[13]

(C) *Preparation and analysis of* $[HW_{11}AlF_3O_{36}(H_2O)](TMA)_5$ and $[H_2W_{12}AlF_2O_{37}(H_2O)](TMA)_5$.[14]

0.5 mmoles of $[HW_{12}F_3O_{37}]H_4$ were caused to react with 25 mmoles of $AlCl_3$ in 100 ml of pH 4 formic buffer containing 5 mmoles of NaCl. The mixture was kept at 21°C for 6 hr and precipitated by 5 g of tetramethylammonium chloride. The solid was filtered off, washed with water, ethanol, diethyloxide and vacuum dried.

Analysis	Compound	%W	%F	Al	%TMA
$[HW_{11}AlF_3O_{36}(H_2O)](TMA)_5, 30H_2O$ (M = 3344)	Found	60.4	0.014	0.88	10.6
	Calcd	—	0.017	0.81	11.1
$[H_2W_{11}AlF_2O_{37}(H_2O)](TMA)_5, 17H_2O$ (M = 3410)	Found	59.2	0.012	0.82	10.8
	Calcd	—	0.011	0.79	10.9

W was determined gravimetrically by the cinchonine method.

F was checked by the specific fluoride electrode after decomposition of the fluorinated compound.[13]

Al^{3+} was determined by atomic absorption spectroscopy with a Perkin-Elmer 373.

The tetramethylammonium in the fluoropolytungstates was determined by elemental analysis of carbon and nitrogen.

The Na salt was obtained from TMA salt by ion exchange. ^{19}F NMR showed that the anion was not modified during this experiment.

^{19}F NMR spectra were recorded on a Brüker W H 90.

RESULTS AND DISCUSSION

(A) *Products resulting from the hydrolysis of* $[H_2W_{12}F_2O_{38}]^{4-}$ and $[HW_{12}F_3O_{37}]^{4-}$

An analysis of the product formed at the end of the reaction shows that, in the pH range 3–4.2, the hydrolysis of $[H_2W_{12}F_2O_{38}]^{4-}$ and $[HW_{12}F_3O_{37}]^{4-}$ liberates only part of the combined fluoride (Tables 1 and 2). This fact is not the result of an incomplete transformation of the substrate, since the polarographic waves of the latter have completely disappeared by the end of the reaction.[15]* On the other hand, the appearance of a new wave with $E_{1/2} = -0.4$ V, agrees with the presence of fluoropolytungstates with charge −5, $[H_2W_{12}FO_{39}]^{5-}$ and $[HW_{12}F_2O_{38}]^{5-}$.

In both cases, raising the pH favours the formation of the $[H_2W_{12}FO_{39}]^{5-}$ variety to the detriment of the other species. It was also observed that above pH 3.4–3.6 a certain proportion of the initial fluoropolytungstate is totally destroyed to give fluoride and tungstate. The latter then condenses to give polytungstates.[15]

Table 1. Results of hydrolysis of $[H_2W_{12}F_2O_{38}]^{4-}$

pH	3	3.2	3.4	3.6	3.8	4	4.2
Disappearance $t_{1/2}$ of substrate (min)	176	28	12	6	4	2	1
Formation $t_{1/2}$ of fluorinated polyanions (min)				60	80	100	
% $[HW_{12}F_2O_{38}]^{5-}$ present at the end of the reaction	21	9	0	0	0	0	0
% $[H_2W_{12}FO_{39}]^{5-}$ present at the end of the reaction	79	91	95	85	64	41	25

(B) *An intermediate—evidence of its presence*

The question is to learn how the fluoride which is located in the central part of a relatively compact structure migrates from this site without a complete destruction of the structure. We wish to show that the mechanism of hydrolysis of the two varieties, which occurs with a loss of fluoride involves one and the same intermediate in both cases.

The mechanisms are easier to observe for $[H_2W_{12}F_2O_{38}]^{4-}$. For instance, at pH 3.6 the polarograms (Fig. 1) show that the half disappearance time of the initial compound (6 min) is clearly different from the half formation time of $H_2W_{12}FO_{39}^{5-}$ (60 min).

Hence both reactions occur consecutively and the determination of F^- enables us to assert that the conversion $[H_2W_{12}F_2O_{38}]^{4-} \rightarrow [H_2W_{12}FO_{39}]^{5-}$ involves a fluorinated intermediate which contains one fluorine per molecule. Similar measurements were taken at pH 3.8

Table 2. Results of hydrolysis of $[HW_{12}F_3O_{37}]^{4-}$

pH	3	3.2	3.4	3.6	3.8	4	4.2
Disappearance $t_{1/2}$ of substrate (min)	480	150	53	36	22	11	9
Formation $t_{1/2}$ of fluorinated polyanions (min)					70	95	
% $[HW_{12}F_2O_{38}]^{5-}$ present at the end of the reaction	57	47	25	18	13	0	0
% $[H_2W_{12}FO_{39}]^{5-}$ present at the end of the reaction	43	53	75	72	70	66	40

*The rate of disappearance of the fluorinated substrate is first order with respect to either $[H_2W_{12}F_2O_{38}]^{4-}$ or $[HW_{12}F_3O_{37}]^{4-}$, but it is of higher order with respect to OH^-.

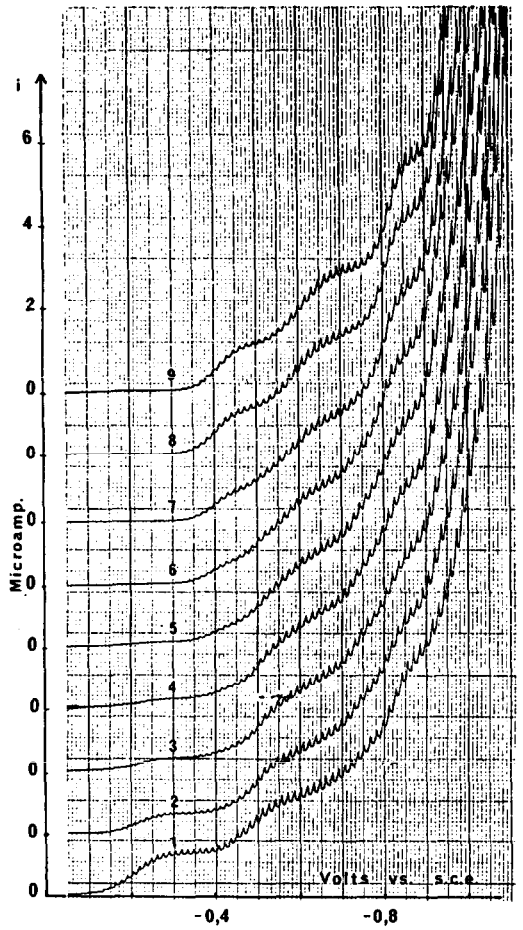

Fig. 1. Evolution of the $[H_2W_{12}F_2O_{38}]^{4-}$ polarogram as a function of time, for a 5×10^{-3}M solution in W, in a formic buffer pH 3.6 (0.5M), 1M NaCl at 21°C: t = (1) 4 min; (2) 11 min; (3) 18 min; (4) 26 min; (5) 39 min; (6) 63 min; (7) 125 min; (8) 300 min; (9) 1440 min.

and 4. Thus we can assume that the hydrolysis reaction involves at least two stages:

(1) $[H_2W_{12}F_2O_{38}]^{4-} \longrightarrow$ intermediate

(2) intermediate $\longrightarrow [H_2W_{12}FO_{39}]^{5-}$.

The existence of an intermediate is confirmed by a polarographic wave which develops around -0.5 V, and disappears when $[H_2W_{12}FO_{39}]^{5-}$ is formed (Fig. 1).

In the case of $[HW_{12}F_3O_{37}]^{4-}$, the disappearance time $t_{1/2}$ of the initial compound is higher. In spite of the lack of precision, the formation time $t_{1/2}$ of $[HW_{12}FO_{39}]^{5-}$ was determined (Table 2); the two stages of the reaction were still detectable by polarography, particularly the wave corresponding to the intermediate.

We did not succeed in separating a salt of the intermediate. However, the following experiments allow us to specify its nature.

(C) *Effect of some metal cations on hydrolysis*

A first series of kinetic experiments was carried out in the presence of metal ions at various concentration. The use of Co^{2+} and Al^{3+} is developed here.

(1) The presence of Co^{2+} in a concentration of 2.10^{-2}M (four times the concentration of W) at pH 4 did not disturb the kinetics of the first stage of the reaction,[15] but did modify the ratio of the expected products to yield new varieties. Only 10% of the mixture $[HW_{12}F_2O_{38}]^{5-}$ and $[H_2W_{12}FO_{39}]^{5-}$ was obtained instead of 41% in the absence of Co^{2+}, 26% of polytungstates and 64% of new varieties. The latter were characterized by a polarogram whose first wave appears at *ca.* -0.6 V followed by a second wave at *ca.* -0.8 V. The titration of liberated fluoride during the experiments showed that the complex formed from $[H_2W_{12}F_2O_{38}]^{4-}$ contains two fluorine atoms while the one corresponding to $[HW_{12}F_3O_{37}]^{4-}$ contains three fluorine atoms. These facts are interpreted later.

(2) Other experiments were conducted at lower pH (3.2 and 3.8). The Co^{2+} complex was much less stable and Co^{2+} slightly disturbed the kinetics. The same mechanisms were found with Al^{3+} as at pH 4, but the formation rates were slower; to obtain the same yield as at pH 4 it was necessary to increase the Al^{3+} concentration (for instance at pH = 3.6, $Al^{3+} = 3.3 \times 10^{-3}$M instead of 1.7×10^{-3}M at pH = 4).

(D) *Synthesis of two complexes with Al^{3+} and a suggested mechanism*

We conclude from these experiments that the mechanism is the same between pH 3.2–4 and the

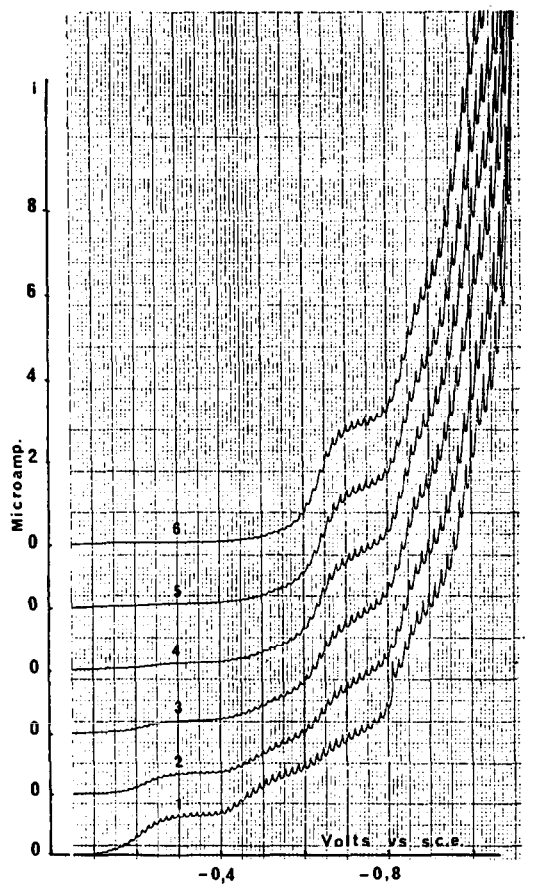

Fig. 2. The same solution as in Fig. 1, in the presence of $AlCl_3$, 3.3×10^{-3}M: t = (1) 4 min; (2) 11 min; (3) 18 min; (4) 28 min; (5) 39 min; (6) 63 min.

hydrolysis involves a series of compounds possessing a defect structure type.[5] We suggest that these compounds contain 11 tungsten atoms (Fig. 3). They are usually obtained by the removal of WO^{4+} from the structure composed of 12 W, during similar reactions: thus $SiW_{12}O_{40}^{4-}$ gives $SiW_{11}O_{39}^{8-}$ above pH 4.5.[5] Compounds of this type are not known in the case of the metatungstate: hence, they should not be expected in the hydrolysis of fluoropolytungstates. These molecules are open (see Schema Fig. 3) and, in our case, allow fluorine migration from the molecule. When the cations Al^{3+} and Co^{2+} are present in the solution, they fill the hole and effectively prevent fluorine migration. The formation reaction of the compound with a defect structure occurs partially (case of Co^{2+}) or is completely stopped (case of Al^{3+}).

Some experiments conducted with different metal cations enable us to classify the latter into two groups: (i) divalent cations (Cu^{2+}, Co^{2+}, Zn^{2+}) complex the fluorinated defect structure compounds if their concentration is very high in the medium ($M^{2+}/W = 4$, M is the cation); (ii) tri or tetravalent cations (Al^{3+}, Fe^{3+}, Zr^{4+}) complex the defect structure compounds at concentrations which practically correspond to stoichiometric conditions of the compound formation (M/W = 1/3–1/2).

These results are in agreement with those already obtained for $[SiW_{11}O_{39}]^{8-}$.[13,17,18] The stability of the substituted compounds increases with the charge of M. The substituted compounds of Al obtained from $[HW_{12}F_3O_{37}]^{4-}$ and $[H_2W_{12}F_2O_{38}]^{4-}$ which are quantitatively formed in solution have been isolated as TMA salts. The analytical data noted in the experimental section give a ratio Al/W = 1/11. This is in agreement with the formulas $[HW_{11}AlF_3O_{36}(H_2O)](TMA)_5$ and $[H_2W_{11}AlF_2O_{37}(H_2O)](TMA)_5$. However, there is a slight fluorine defect in the first compound that can be explained by incipient hydrolysis.

The hydrolysis of $[H_2W_{12}F_2O_{38}]^{4-}$ and $[HW_{12}F_3O_{37}]^{4-}$ to $[HW_{12}F_2O_{38}]^{5-}$ and $[H_2W_{12}FO_{39}]^{5-}$ appear to occur via fluorinated species containing 1, 2 or 3 fluorine atoms and 11 tungsten atoms. This hypothesis is substantiated by the composition of the isolated substituted compounds. In both cases, the intermediate observed by polarography in the absence of metal cations contains one fluorine per molecule $[H_xW_{11}FO_{38}]^{(11-x)-}$.

The ^{19}F NMR spectra of the Al substituted compounds were obtained with the sodium salts. The spectrum of the trifluorinated compound shows only a multiplet probably composed of two peaks about 90 ppm relative to the trifluorinated acetic acid. The difluorinated compound includes two main multiplets at 58.4 and 88 ppm. Resolution of the spectra is difficult for two reasons: the introduction of Al^{3+} into the molecule creates magnetic inequivalence of the fluorine atoms and on the other hand, the existence of several isomers is possible. The complexity of the spectra does not enable us to indicate the situation of the Al ion relative to the fluorine atom.

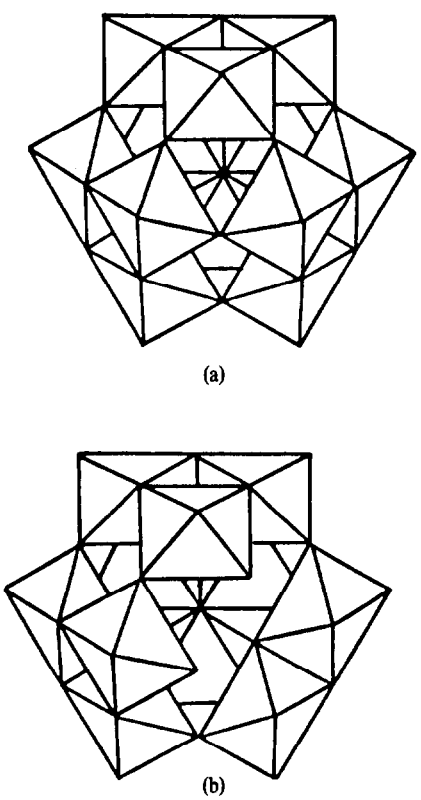

Fig. 3. (a) Keggin's structure. (b) Structure of 11-tungsto complex, derived from the former by removal of one W along with one of its oxygens. As a result, a more open structure is obtained, allowing the departure of F^-.

CONCLUSION

Detailed study of the hydrolysis of the two fluorinated polytungstates with charge—4 revealed the existence of defect structure varieties involved in the mechanism. The hydrolysis of the two varieties with charge—5, $[HW_{12}F_2O_{38}]^{5-}$ and $[H_2W_{12}FO_{39}]^{5-}$ is effective only above pH 5.8 (Table 3) and does not implicate other varieties detectable by polarography or by fluoride determination. At these pH, the defect structure variety observed by polarography is unstable and breaks down very rapidly. It is presumed that a similar type of mechanism occurs in the destruction reaction of $[HW_{12}F_2O_{38}]^{5-}$ and $[H_2W_{12}FO_{39}]^{5-}$.

Isolation of the two substituted compounds $[HW_{11}AlF_3O_{36}(H_2O)](TMA)_5, 30H_2O$ and $[H_2W_{11}AlF_2O_{37}(H_2O)](TMA)_5, 17H_2O$ showed the possibility of obtaining a new family of heteropolyanions.

Table 3. Degradation reaction kinetics of $[H_2W_{12}FO_{39}]^{5-}$ and $[HW_{12}F_2O_{38}]^{5-}$

pH	5.8[a]	6.2[a]	6.3[a]	6.7[b]	7.05[b]
$t_{1/2}$(min)	450	155	95	51	22

The reactions are followed polarographically under the same conditions as above: [a]succinic buffer, [b]phosphoric buffer.

REFERENCES

[1]A. Kobayashi and Y. Sasaki, *Bull. Chim. Soc. Jap.* 1975, **48**, 885.
[2]R. Allmann and H. D'amour, *Z. Kristallogr.* 1975, **141**, 161.
[3]J. Fuchs and E. P. Flindt, *Z. Naturforsch* 1979, **34b**, 412.
[4]B. Le Meur and P. Souchay, *Rev. Chim. Miner.* 1975, **12**, 69.
[5]P. Souchay, Ions minéraux condensés, Masson et Cie, Paris, 1969, p. 93.
[6]P. Souchay, B. Le Meur et F. Chauveau, *C.R. Acad. Sci. C* 1974, **279**, 1031.

[7]G. Herve and A. Teze, *Inorg. Chem.* 1977, **16**, 2115.
[8]G. Herve and A. Teze, *C.R. Acad. Sc. C* 1974, **278**, 1417.
[9]F. Chauveau, P. Doppelt and J. Lefebvre, *J. Chem. Res.* (S), 1981, 155; *J. Chem. Res.* (M), 1981, 1937–1944.
[10]F. Chauveau, P. Doppelt and J. Lefebvre, *J. Chem. Res.* (*S*) 1978, 130; *J. Chem. Res.* (*M*) 1978, 1727.
[11]F. Chauveau and P. Souchay, *J. Inorg. Nuclear Chem.* 1974, **36**, 1767.
[12]E. Drechsel, *Chem. Ber.* 1887, **20**, 1452.
[13]J. J. Lingane, *Analyt. Chem.* 1967, **39**, No. 8, 881.
[14]The formula includes one molecule of water according to published data. C. Tourne, *C.R. Acad. Sc. C* 1968, **266**, 702.
[15]P. Souchay, Ions minéraux condensés. Masson 1969; D. L. Kepert, *Prog. in Inorg. Chem.* 1962, **4**, 199.
[16]G. Salamon-Bertho, *Rev. Chim. Miner.* 1972, **9**, 683.
[17]A. Teze, Thèse d'Etat. Université P. M. Curie, Paris 1972.
[18]T. J. R. Weakley, *Structure and Bonding* 1974, **18**, 131.

Polyhedron Vol. 1, No. 3, pp. 269–275, 1982
Printed in Great Britain.

0277-5387/82/030269-07$03.00/0
Pergamon Press Ltd.

THERMODYNAMICS AND KINETICS OF COMPLEXATION OF IRON(III) ION BY PICOLINIC AND DIPICOLINIC ACIDS†

KEITH BRIDGER, RAMESH C. PATEL* and EGON MATIJEVIĆ*
Department of Chemistry and Institute of Colloid and Surface Science, Clarkson College of Technology, Potsdam, NY 13676, U.S.A.

(*Received* 22 *October* 1981)

Abstract—The complexation reactions of iron(III) with 2-pyridine carboxylic acid (picolinic acid) and 2,6-pyridine dicarboxylic acid (dipicolinic acid) in aqueous solutions have been studied by spectrophotometric and stopped flow techniques. Equilibrium constants were determined for the 1:1 complexes at temperatures between 25 and 80°C. The values obtained are:

Picolinic Acid (HL): $Fe^{3+} + H_2L^+ \rightleftharpoons FeHL^{3+} + H^+$ ($K_1 = 2.8$, $\Delta H = 2$ kcal mole^{-1} at 25°C, $\mu = 2.67$ *M*)

Dipicolinic Acid (H_2D): $Fe^{3+} + H_2D \rightleftharpoons FeD^+ + 2H^+$ ($K_1K_{1A} = 227$ *M*, $\Delta H = 3.4$ kcal mole^{-1} at 25°C, $\mu = 1.0$ *M*).

The rate constants for the formation of these complexes are also given. The results are used to evaluate the effects of these two acids upon the rate of dissolution of iron(III) from its oxides.

INTRODUCTION

Carboxylic acid derivatives of pyridine have found use in different applications, such as in chemical analysis[1] and corrosion inhibition.[2–4] Acids with a carboxylic group adjacent to the nitrogen atom exhibit strong complexation reactions with a variety of metal ions.[5–9]

Recently, vanadium(II) picolinate, which is a strong reducing agent, was tested as a possible decontamination agent for nuclear power plants.[10] It was shown that this complex dissolved iron oxides at a sufficiently rapid rate for the intended purpose. To explore the feasibility of using carboxylic acids of pyridine for decontamination of nuclear reactors, the interactions of nicotinic, picolinic, and dipicolinic acids with uniform, spherical colloidal particles of chromium hydroxide and of haematite were studied in detail.[11] It was found that the reactivity increased in the order nicotinic < picolinic < dipicolinic acid and that the uptake by the amorphous chromium hydroxide was considerably larger than by crystalline haematite particles. Furthermore, dipicolinic acid leached iron from haematite over a given pH range. In contrast, no significant dissolution of iron(III) oxide was observed in the presence of picolinic acid.[11] In order to develop a better understanding of the above findings, this work reports results on the thermodynamics and kinetics of the complexation reactions between iron(III) and the picolinic and dipicolinic acids in aqueous solution at low pH for temperatures up to 80°C. Spectrophotometry and stopped flow techniques were utilized. The latter offered an insight into the mechanism of the complexation reactions.

EXPERIMENTAL

(a) *Solutions*

Stock solutions of ferric perchlorate were prepared from the anhydrous salt (Baker), either in the highly concentrated state ($> 2M$) or with a large excess of added perchloric acid ($[H^+]/[Fe^{3+}] > 10$); these conditions provide solutions which are stable over extended periods of time.[12] The total concentration of ferric ion was determined spectrophotometrically as the thiocyanate complex in acidic media.[13]

Picolinic acid (Pfaltz and Bauer), dipicolinic acid (Aldrich), sodium perchlorate (G. F. Smith), and perchloric acid (Baker), all reagent grade, were used as supplied. All solutions were passed through 0.2 μm pore size Millipore filters before use.

Throughout this work the order of mixing was as follows: sodium perchlorate, perchloric acid, the ligand solution (if any), and doubly distilled water were mixed in a volumetric flask leaving just sufficient room for the ferric salt solution which was then added. The remaining volume was filled up with water. All solutions were allowed to equilibrate overnight at ambient temperature before any measurements were taken.

(b) *Methods*

(i) *Spectrophotometry.* Quantitative spectral measurements were performed on a single beam Zeiss MQ3 spectrophotometer equipped with a Zeiss PM1 photometer-indicator with digital readout. The latter device permitted the determination of absorbance values to 3 decimal places. The water-jacketted cell holder was temperature-controlled to ±0.1°C using a Haake Model FK external circulating water bath. Matched 1-cm quartz (Hellma) cells were tightly stoppered to prevent evaporation, especially at high temperatures. Since no mechanical agitation was employed, a minimum of 20 min was allowed for thermal equilibration.

In all cases the reference cell contained a solution of similar ferric perchlorate, sodium perchlorate, and perchloric acid concentrations to the sample solution. To the latter a known concentration of the ligand was added. Neither acid alone absorbed light at the wavelengths used and over the concentration and temperature ranges studied. The measured absorbance difference (ΔA) resulted, therefore, from the formation of complex(es).

(ii) *Stopped flow.* The kinetics of the complexation at 25°C was studied using a combined stopped flow/temperature jump apparatus described elsewhere.[14]

DATA TREATMENT AND CALCULATIONS

(a) *Spectrophotometry*

(i) *Graphical analysis.* The following set of equilibria

†Supported by the Electric Power Research Institute, Contract RP-966-2.

*Authors to whom correspondence should be addressed.

are proposed in aqueous solutions of picolinic and dipocolinic acids:

(a) Picolinic Acid (HL)

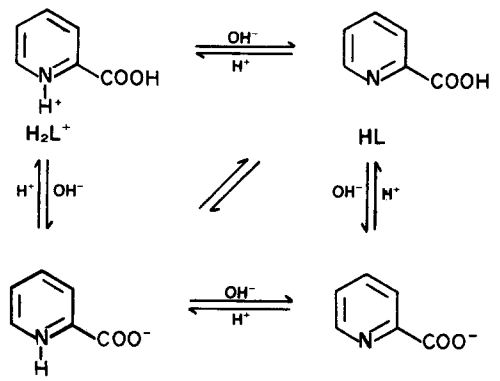

(b) Dipicolinic Adid (H_2D)

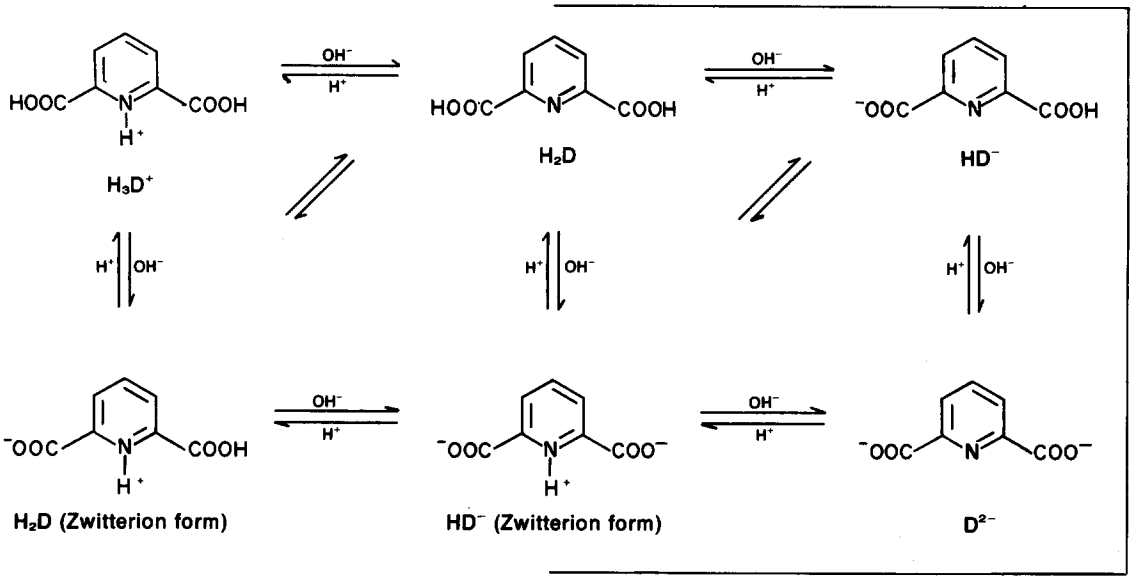

In acidic media both substances may be treated as biprotic ligands (H_2X). Various possible equilibria of these ligands with iron(III), are summarized as follows (ionic charges and displaced water molecules are omitted for simplicity):

H_2X	$\overset{K_{A1}}{\rightleftharpoons}$	$HX + H$	(1)
$M(H_2O)_6$	$\overset{K_H}{\rightleftharpoons}$	$M(H_2O)_5OH + H$	(2)
$M(H_2O)_6 + H_2X$	$\overset{K_1}{\rightleftharpoons}$	$M(H_2O)_5HX + H$	(3)
$M(H_2O)_5HX$	$\overset{K_{1A}}{\rightleftharpoons}$	$M(H_2O)_5X + H$	(4)
$2M(H_2O)_5OH$	$\overset{K_{22}}{\rightleftharpoons}$	$M_2(H_2O)_8(OH)_2$	(5)
$M(H_2O)_5HX$	$\rightleftharpoons$	$M(H_2O)_4OH(HX) + H$	(6)
$M(H_2O)_5X$	$\rightleftharpoons$	$M(H_2O)_4OH(X) + H$	(7)

†Note that ϵ_M' is constant only at a fixed proton concentration and at reasonably low ferric ion concentrations.

Several species [e.g. X, $M(H_2O)_4(OH)_2$] have been neglected since, under the high acid conditions studied, their concentrations are assumed to be vanishingly small.

The simplest analysis considers only equilibria (1–3). The mass balance conditions for metal and ligand then become:

$$C_M^\circ = C_M + C_{MOH} + C_{MHX} \quad (8)$$

$$C_M^\circ = C_{H_2X} + C_{HX} + C_{MHX} \quad (9)$$

where C_{MHX}, C_{H_2X}, C_M, C_{MOH}, and C_{HX} represent the equilibrium concentrations of the various moieties present. In large excess initial concentrations of the metal ion ($C_M^\circ > C_X^\circ$), the metal–ligand term, C_{MHX}, may be neglected in eqn (8), and if the added hydrogen ion concentration, C_H°, is large as compared to C_M° and C_X°, $C_H^\circ \simeq C_H$. With these approximations in mind a combination of eqns (8), (9) and (1)–(3) yields:

$$C_{MHX} = (K_1 C_M^\circ C_X^\circ / C_H^\circ) \times [(1 + K_H/C_H^\circ)(1 + K_{A1}/C_H^\circ) + (K_1 C_M^\circ / C_H^\circ)]^{-1} \quad (10)$$

In acidic media the absorbance change, ΔA, due to complexation reaction is given by:

$$\Delta A = (\epsilon_{MHX} - \epsilon_M')C_{MHX} \quad (11)$$

where ϵ_{MHX} is the extinction coefficient of the complex and ϵ_M' is the measured extinction coefficient† of the ferric solution in the absence of the organic acid, which includes contributions from Fe^{3+} and $FeOH^{2+}$. When C_H° is large the contribution from $FeOH^{2+}$ is a small and effectively constant fraction of the total. A combination of eqns (10) and (11) gives:

$$C_X^\circ/\Delta A = 1/\Delta\epsilon + (C_H^\circ/C_M^\circ \Delta\epsilon K_1)(1 + K_H/C_H^\circ)(1 + K_{A1}/C_H^\circ) \quad (12)$$

where $\Delta\epsilon = (\epsilon_{MHX} - \epsilon_M')$. The bracketted sums are close to unity at high acid concentrations so that a plot of $C_X^\circ/\Delta A$ versus C_H°/C_M° tests the validity of selecting eqns (1)–(3) above. Note that if the complex MX predominates then the C_H°/C_M° term in eqn (12) is replaced by $C_H^{\circ 2}/C_M^\circ$ with everything else unchanged.

(ii) *Quantitative numerical analysis.* (a) Picolinic Acid (HL). At elevated temperatures the extent of hydrolysis of the ferric ion increases and the simple analysis based on the assumptions made in eqn (11) breaks down. In more exact terms the measured absorbance difference is given by:

$$\Delta A = A^T - A^i \tag{13}$$

where A^i is the absorbance of a ferric solution prepared in the absence of ligand and A^T is the absorbance of the same ferric solution in the presence of a known concentration of ligand. The value of A^i is the sum of contributions from Fe^{3+}, $FeOH^{2+}$ and, at the highest total ferric concentrations studied, from $Fe_2(OH)_2^{4+}$. Changing the pH in the ferric solutions alters the relative concentrations of these species; since $\epsilon_{FeOH^{2+}} \gg \epsilon_{Fe^{3+}}$ over the wavelengths studied, the value of $\epsilon^i_{Fe^{3+}}$ changes. Equation (11) is, therefore, only valid when either A^i is small compared to A^T (in which case $\Delta\epsilon = \epsilon_{MHL}$) or when the values of C°_H are sufficiently large to yield negligible amounts of hydrolysis products.

Even with the correct expression for ΔA, the absorbance data could not be explained over the entire range of acid concentration and temperature by assuming only reactions (1)–(3). The final model incorporated equilibria (1)–(5) giving mass balance:

$$C^\circ_M = C_M + C_{MOH} + 2C_{M_2(OH)_2} + C_{MHL} + C_{ML} \tag{14}$$

$$C^\circ_L = C_{H_2L} + C_{HL} + C_{MHL} + C_{ML}. \tag{15}$$

Combination with the corresponding equilibrium expressions and assuming $C_H = C^\circ_H$ leads to the cubic equation:

$$\alpha C_M^3 + \sigma C_M^2 + \delta C_M + \kappa = 0 \tag{16}$$

$$\alpha = 2K_1K_{22}K_H^2(1 + K_{1A}/C^\circ_H)/C^{\circ 3}_H \tag{16a}$$

$$\sigma = [(K_1/C^\circ_H)(1 + K_H/C^\circ_H)(1 + K_{1A}/C^\circ_H)] + [2K_{22}K_H^2(1 + K_{A1}/C^\circ_H)/C^{\circ 2}_H] \tag{16b}$$

$$\delta = [K_1(1 + K_{1A}/C^\circ_H)(C^\circ_L - C^\circ_M)/C^\circ_H] + [(1 + K_H/C^\circ_H)(1 + K_{A1}/C^\circ_H)] \tag{16c}$$

$$\kappa = -C^\circ_M(1 + K_{A1}/C^\circ_H). \tag{16d}$$

The value for the absorbance difference is then

$$\Delta A = \epsilon_{MHL}C_{MHL} + \epsilon_{ML}C_{ML} + \epsilon_M(C_M - C^i_M) + \epsilon_{MOH}(C_{MOH} - C^i_{MOH}) + \epsilon_{M_2(OH)_2}(C_{M_2(OH)_2} - C^i_{M_2(OH)_2}) \tag{17}$$

where superscript i refers to concentrations in the absence of the added ligand.

The data were evaluated using the multiparametric curve-fitting program CFT4A[15] with 4 parameters (i.e. K_1, K_{1A}, ϵ_{MHL}, and ϵ_{ML}). Values for K_H and K_{22} were taken from the literature[12] and the extinction coefficients ϵ_M, ϵ_{MOH} and $\epsilon_{M_2(OH)_2}$ were obtained from the absorbance readings of the ferric perchlorate solutions alone. Values for K_{A1} were evaluated independently from the u.v. spectra of several picolinic acid solutions of varying hydrogen ion concentrations ($0.02 < [H^+] < 1.0M$). Equation (16) was solved numerically using the Newton–Raphson method and the species distribution calculated. Values for C^i_M, C^i_{MOH}, and $C^i_{M_2(OH)_2}$ were determined from the known hydrolysis constants for the corresponding ferric complexes.[12]

(b) Dipicolinic Acid (H_2D). The absorbance data for dipicolinic acid indicated that MD was the predominant species formed. The values for the equilibrium constants ($K_1 \cdot K_{1A}$) were larger than those for the picolinic–ferric complexes, so more dilute ferric solutions were employed. Under these conditions, the dimeric species, $Fe_2(OH)_2^{4+}$, could be neglected. The equilibria (1)–(4), with C_{MHD} taken to be vanishingly small, were used to formulate an expression for C_M:

$$\alpha C_M^2 + \sigma C_M + \gamma = 0 \tag{18}$$

where

$$\alpha = K_1K_{1A}(1 + K_H/C^\circ_H) \tag{18a}$$

$$\sigma = C^\circ_H(1 + K_H/C^\circ_H)(C^\circ_H + K_{A1}) + K_1K_{1A}(C^\circ_D - C^\circ_M) \tag{18b}$$

$$\gamma = -C^\circ_MC^\circ_H(C^\circ_H + K_{A1}). \tag{18c}$$

The absorbance difference was given by

$$\Delta A = \epsilon_{MD}C_{MD} + \epsilon_{MOH}(C_{MOH} - C^i_{MOH}) + \epsilon_M(C_M - C^i_M). \tag{19}$$

A two parameter ($K_1 \cdot K_{1A}$, ϵ_{MD}) fit was undertaken, using independently measured values for K_{A1} obtained by titration of the dipicolinic acid against standard sodium hydroxide solution in $1.0M$ sodium perchlorate medium.[16]

(b) *Stopped flow*

The time-voltage data obtained from the stopped flow experiments were considered to follow single exponential curves:

$$\Delta V = \Delta V_\infty(1 - e^{-t/\tau}) \tag{20}$$

in which ΔV is the voltage change at time t, ΔV_∞ is the total voltage change, and τ is the relaxation time. This equation is applicable when small absorbance changes are involved, as was the case in the investigated systems. Implicit in this equation is the assumption that the concentration of the complex is small compared to the concentrations of the metal and the ligand. In most cases this condition is realized by using only the initial part of the ΔV vs t curve.

Where the exponential levelled off to a suitable plateau value, V_f, the data were plotted as $\ln(V_f - V)$ vs t. If the final value was unknown, as was the case when the time scale was shortened to expand the initial portion of the curve, the data were treated according to the Swinbourne method,[17] which only required voltage values at constant time intervals. At least four curves were recorded for each solution and average values of the relaxation time and amplitude were estimated to within ± 10% accuracy limits. The relaxation times for solutions with similar $[H^+]$ follow the relation:

$$\tau^{-1} = k_{OBS} = k_f(C^\circ_M + C^\circ_X) + k_b \tag{21}$$

where k_f and k_b are the composite forward and backward

rate constants which may or may not vary with $[H^+]$ depending on the reaction mechanism. Values of ΔA for the complex formation were calculated from the relaxation amplitudes according to:[18]

$$\Delta A = (1/2.303\, l) \ln(1 + \Delta V_\infty / V_0) \qquad (22)$$

RESULTS

(a) *Picolinic acid*

(i) *Equilibrium data.* The equilibrium constants of the formation of $FeHL^{3+}$ were determined for temperatures of 25, 35, 50, 65 and 75°C at an ionic strength of 2.67*M*. Values of ΔA in the presence of 0.05*M* picolinic acid were recorded every 5 nm between 380 and 405 nm for solutions in which $[H^+]$ varied between 0.2 and 1.0*M*, and that of $[Fe^{3+}]_{TOT}$ between 0.04 and 0.40*M*.

Linear plots of $C_L^\circ/\Delta A$ vs C_H°/C_M° were obtained at 25°C confirming the predominance of the $FeHL^{3+}$ species under those conditions. A typical plot is shown in Fig. 1. Deviation from linearity was observed at $[H^+] < \sim 0.5M$ and at higher temperatures, as other complexes appeared in significant amounts. In these cases the rigorous analysis given in the section on data treatment was applied. The standard deviations between the measured ΔA and that calculated from eqn (17) did not exceed 0.005 absorbance units. Table 1 gives a compilation of the equilibrium constants for $FeHL^{3+}$ and the dissociation constants for H_2L^+ obtained over the temperature range studied. The errors quoted represent the total scatter based on the data obtained at seven different wavelengths. Values of K_1 calculated at 25° and 35°C were in excellent agreement with those determined by the graphical analysis.

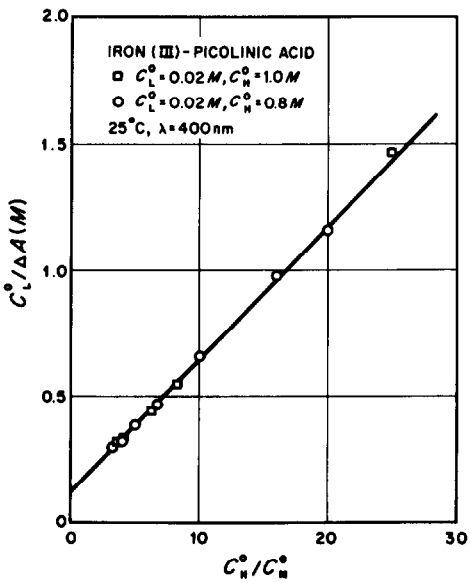

Fig. 1. Absorbance data for iron(III)-picolinic acid complex formation, plotted according to eqn (12) ($\mu = 2.67M$).

Although inclusion of the complex FeL^{2+} was necessary in order to accurately evaluate the data, insufficient amounts of the complex were formed to give a reliable value of K_{1A}. It is estimated that K_{1A} is in the order of 0.1*M*, which indicates the second species to be indeed FeL^{2+} and not $Fe(OH)HL^{2+}$. The latter complex, while giving a similar mathematical formulation, would lead to much lower value for the equilibrium constant ($\sim 10^{-3}M$) of its formation.

A van't Hoff plot of $\ln K$ vs $1/T$ gave a $\Delta H^\circ \approx 2$ kcal mole^{-1} both for the complexation step (3) and for the first dissociation of protonated picolinic acid (1) at an ionic strength of 2.67*M*. The reversibility of the reactions was checked by cooling samples from 75 to 25°C and then measuring again the absorbances after approx. 2 hr. In no case did the difference exceed 2% of the original value.

(ii) *Kinetic data.* The equilibrium data indicated that at high acidities the dominant complexation reaction involved binding of the picolinic acid to a ferric ion according to:

$$Fe^{3+} + H_2L^+ \rightleftharpoons FeHL^{3+} + H^+. \qquad (23)$$

The possible reaction paths for this process are as follows:

$$Fe^{3+} + H_2L^+ \underset{k_{-1}}{\overset{k_1}{\rightleftharpoons}} FeHL^{3+} + H^+ \qquad (24)$$

$$FeOH^{2+} + H_2L^+ \underset{k_{-2}}{\overset{k_2}{\rightleftharpoons}} FeHL^{3+} + H_2O \qquad (25)$$

$$Fe^{3+} + HL \underset{k_{-3}}{\overset{k_3}{\rightleftharpoons}} FeHL^{3+} \qquad (26)$$

$$FeOH^{2+} + HL \underset{k_{-4}}{\overset{k_4}{\rightleftharpoons}} FeHL^{3+} + OH^-. \qquad (27)$$

Stopped flow experiments have been conducted with solutions in which proton concentrations ($HClO_4$) were varied between 1.0 and 0.5*M*, picolinic acid between 0.01 and 0.04*M*, and iron(III) between 0.04 and 0.25*M*. In all cases the solute iron species were in excess over picolinic acid and the low equilibrium constant ensured that the concentration of complex formed was always small compared to that of Fe^{3+}. The values obtained for k_f and k_b (eqn 21) are shown in Table 2.

There is no obvious trend in the values of k_f signifying that path 1 (eqn 24) is rate determining for the forward

Table 1. Formation constants for $FePic^{3+}$ and acid dissociation constants for picolinic acid (H_2L^+) at various temperatures ($\mu = 2.67M$)

T°C	25	35	50	65	75
K_1	2.8 ± .1	3.1 ± .2	3.9 ± .1	3.8 ± .3	4.7 ± .4
K_{A1} (*M*)	.085 ± .007	.090 ± .009	.094 ± .018	.120 ± .014	.126 ± .013

$K_1 = [FeHL^{3+}][H^+]/[Fe^{3+}][H_2L^+]$ $\qquad$ $K_{A1} = [HL][H^+]/[H_2L^+]$

reaction, thus, $k_1 = k_f$. This finding is due to the very low concentration of $FeOH^{2+}$ present in the highly acidic media used in this work. The latter complex is known to be many times more reactive than Fe^{3+}.[19-21] The reverse rate constants, however, do not show the direct proton dependence as required by path 1. The discrepancy between the measured values of k_b and those calculated from the equilibrium constant, k_b', reflect the relatively large experimental errors in the measurements. It may be that k_b is also independent of $[H^+]$ in which case the reverse reaction proceeds via paths 2 or 3 (eqns 25 and 26) or both. It is recognized that the interchange of $FeOH^{2+}$ with Fe^{3+} and HL with H_2L^+ is very rapid.

The stopped flow data recorded for $[H^+] = 0.5\,M$ did not obey the single exponential formula (eqn 20). It was clear from the shape of the curves generated that a faster process, $\tau \sim 20$ ms, was present and was probably associated with the formation of FeL^{2+}. Owing to inherent difficulties, these curves with small amplitudes were not analyzed quantitatively.

(b) *Dipicolinic acid*

(i) *Equilibrium data.* To determine the equilibrium constant for the formation of the complex between the ferric and dipicolinate ions, FeD^+, absorbances were measured at 350, 345, 340 and 335 nm over the temperature range 25–80°C, for a series of solutions in which $[H^+]$ varied between 0.04 and 1.00M, $[Fe^{3+}]_{TOT}$ between 10^{-4} and $4\times10^{-3}M$, and $[H_2D]$ between 5×10^{-5} and $8\times10^{-4}M$. The ionic strength was kept constant at 1.0M with $NaClO_4$.

Excellent linear plots of $C_D^\circ/\Delta A$ vs $C_H^{\circ 2}/C_M^\circ$ (Fig. 2) were obtained at 25°C for the concentrations under investigation, indicating the formation of FeD^+. The rigorous analysis showed that the experimental data over the temperature range studied could be rationalized by considering only the FeD^+ complex; the values obtained for $K_1 \cdot K_{1A}$ are given in Table 3.

The large formation constant for FeD^+ could be measured with far greater precision than that for $FeHL^{3+}$. Consequently, the value of $\Delta H^\circ = 3.4 \pm 0.6$ kcal mole^{-1}, was also much more accurate than the enthalpy for the corresponding picolinate complex.

(ii) *Kinetic data.* The complexation reaction with dipicolinic acid may be represented as follows:

$$Fe^{3+} + H_2D \underset{k_{-1}}{\overset{k_1}{\rightleftharpoons}} FeD^+ + 2H^+ \quad (28)$$

$$FeOH^{2+} + H_2D \underset{k_{-2}}{\overset{k_2}{\rightleftharpoons}} FeD^+ + H^+ + H_2O \quad (29)$$

$$Fe^{3+} + HD^- \underset{k_{-3}}{\overset{k_3}{\rightleftharpoons}} FeD^+ + H^+ \quad (30)$$

$$FeOH^{2+} + HD^- \underset{k_{-4}}{\overset{k_4}{\rightleftharpoons}} FeD^+ + H_2O. \quad (31)$$

Stopped flow experiments were conducted for $1.0 > C_H^\circ > 0.625M$; $1.0\times10^{-3} > C_D^\circ > 0.5\times10^{-3}M$, and

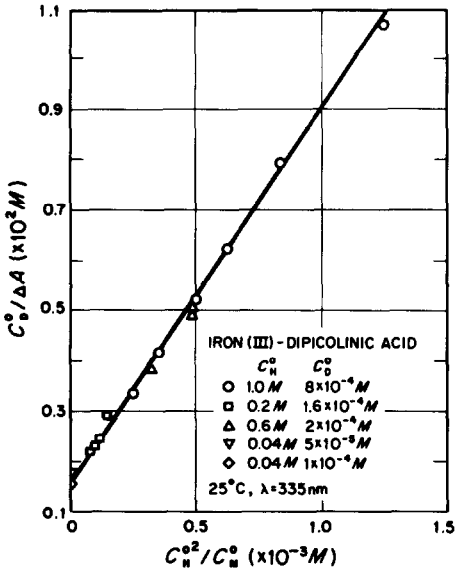

Fig. 2. Absorbance data for iron(III)-dipicolinic acid complex formation, plotted according to eqn (12) with $C_H^{\circ 2}$ dependence ($\mu = 1.0M$).

Table 2. Forward, $k_f(M^{-1}\,s^{-1})$ and reverse, $k_b(s^{-1})$ rate constants calculated from eqn (21) at 25°C, $\mu = 2.67M$, for different acidities

C_H° (M) :	1.000	0.875	0.750	0.625
k_f ($M^{-1}s^{-1}$) :	29 ± 5	21 ± 10	24 ± 6	22 ± 10
k_b (s^{-1}) :	5.3 ± .8	5.6 ± 1	6.6 ± .8	7.6 ± .6
$k_b' = k_f C_H^\circ/K_1$ (s^{-1}):	10.4	6.6	6.4	4.9

Table 3. Formation constants for FeD^+ at various temperatures, $\mu = 1.0M$

T°C :	25	35	50	65	80
$K_1 \cdot K_{1A}$ (M) :	227 ± 6	276 ± 5	326 ± 10	443 ± 8	560 ± 36

$pK_{A1} = 2.05 \pm 0.1$; $pK_{A2} = 4.47 \pm .05$ (at 25°C)

$K_1K_{1A} = [FeD^+][H^+]^2/[H_2D][Fe^{3+}]$

$0.015 > C_M^\circ > 1.0 \times 10^{-3} M$. In all cases only single exponential curves were observed with τ values ranging between 0.8 and 5 sec. Table 4 gives values for the observed forward and reverse rate constants, which show that k_f varies inversely with hydrogen ion concentration indicating a contribution from paths 2 and 3 (eqns 29 and 30) to path 1 (eqn 28). Of these two, 2 is the more likely since $[FeOH^{2+}]$ and $[HL^-]$ will be similar but the hydroxylated species is very much more reactive to ligand substitution than is the hexaquoiron(III) ion. Thus,

$$k_f \approx k_1 + k_2 K_H / C_H^\circ \qquad (32)$$

from which k_1 and k_2 are estimated to be $34 M^{-1} s^{-1}$ and $1.5 \times 10^4 M^{-1} s^{-1}$, respectively, using a value of $1.47 \times 10^{-3} M$ for K_H.[12] The k_b values increase with increasing hydrogen ion concentration which suggest that paths 1, 2 and 3 contribute to the reverse process. The error in k_b values is, however, too large for any reliable estimates of the individual rate constants to be made. In the case of dipicolinic acid the agreement between the experimental and calculated values of k_b is quite reasonable.

DISCUSSION

A compilation of various data for the dissociation constants of the two acids (Table 5) shows that the measurements in this work are in good agreement with the literature values. The proton independent formation

Table 4. Forward, $k_f(M^{-1} s^{-1})$ and reverse, $k_b(s^{-1})$, rate constants calculated from eqn (21) at 25°C, $\mu = 1.0 M$, for different acidities

C_H° (M)	1.000	0.875	0.750	0.625
k_f ($M^{-1}s^{-1}$)	53.1 ± 1.0	59.6 ± 2.7	65.3 ± 2.8	66.2 ± 7.3
k_b (s^{-1})	0.209 ± .014	0.171 ± .013	0.109 ± .013	0.099 ± .035
$k_b' = k_f C_H^2 / K_1$ (s^{-1}):	0.231	0.198	0.160	0.112

Table 5. Comparison of pK values for picolinic and dipicolinic acids in aqueous solutions

A. Picolinic Acid

Ionic Strength	Temp. (°C)	Method*	pK_{A1}	ΔH_1° (kcal/mole)	pK_{A2}	Ref.
0	25	gl,cal	1.01 ± .02	0.52 ± .07	5.32	22,23
0.1M $NaClO_4$	25	gl	1.03 ± .05	-	5.30 ± .01	24
0.5M $NaClO_4$	25	gl	0.86 ± .02	-	5.17 ± .01	25
0.5M $NaClO_4$	25	sp	1.43 ± .03	-	4.66 ± .02	8
2.67M $NaClO_4$	25	sp, T	1.07 ± .03	1.5 ± .7	-	This work

B. Dipicolinic Acid

Ionic Strength	Temp. (°C)	Method	pK_{A1}	ΔH_1° kcal/mole	pK_{A2}	ΔH_2° kcal/mole	Ref.
0	20	gl	2.24	-	5.07	-	26
0	20	sp	2.23	-	5.10	-	26
0	25	sp	2.22	-	5.22	-	27
0	25	gl	2.29	-	5.14	-	27
0.1M $NaNO_3$	20	gl	2.10	-	4.68	-	28
0.5M KNO_3	20	gl	2.27	-	4.55	-	26
0.5M $NaClO_4$	25	sp	2.15 ± .03	-	4.32 ± .02	-	7
0.5M $NaClO_4$	25	gl	2.092 ± .006	-	4.532 ± .004	-	29
0.5M $NaClO_4$	25	gl,cal	2.00 ± .02	1.1	4.50 ± .01	-0.2	30
1.0M $NaClO_4$	25	gl	2.18	-	4.62	-	31
1.0M $NaClO_4$	25	sp	-	-	4.60	6 ± 1	31
1.0M $NaClO_4$	25	gl	2.05 ± 0.1	-	4.47 ± .05	-	This work

* gl: glass electrode; sp: spectrophotometry; cal: calorimetry; T: temperature variation

constants, β_1, calculated from the tabulated pK, are: $\log\beta_1 = 1.52 \pm 0.05$ (MHL) and $\log\beta \approx 4.5$ (ML) for iron(III) picolinic acid at 25°C, $\mu = 2.67M$; and $\log\beta_1 = 8.88 \pm 0.17$ (MD) for iron(III) dipicolinic acid at 25°C, $\mu = 1.0M$. No data have been found for comparison with the picolinic acid values but the formation constant for FeD^+ has been quoted as $\log\beta_1 = 10.91$ at 20°C, $\mu = 0.1M$.[5] The discrepancy between the latter value and one found in the present work is quite large. The ionic strength is not the same, but it is not possible to say if the difference is due to this parameter alone.

In this study the protonated form of dipicolinic acid (H_3D^+) has been ignored; since $\log\beta \approx -1.0$[7,25] no significant amounts of H_3D^+ should form except at very high acid concentrations ($[H^+] > 2M$). Omitting this species from the analysis is further justified, because the data could be described over a wide range of $[H^+]$ values.

The kinetic experiments gave rise to single exponentials which is consistent with the formation of a single complex. The amplitudes (ΔV_∞) of these exponentials yielded similar stoichiometries and equilibrium constants to those evaluated from the equilibrium absorbance measurements. Thus, this work is internally consistent. The rate constants evaluated from the kinetic data conform very well to those expected for the rates of substitution of bound water in the coordination spheres of Fe^{3+} and $FeOH^{2+}$. The water exchange rates, k_{H_2O}, for these ions, have been measured by NMR and were found to be 160 and $1.4 \times 10^5\ s^{-1}$, respectively.[32] Values for the exchange rates of various 0 and 1− charged ligands, tabulated in Refs. [32, 33], fall in the range $1.2–1500\ s^{-1}$ for Fe^{3+} and $0.1–5 \times 10^4\ s^{-1}$ for $FeOH^{2+}$. The behavior of dipicolinic acid with $FeOH^{2+}$ is intermediate between that of a 0 and 1− ligand. This is quite reasonable since uncharged dipicolinic acid may exist in a zwitterionic form. In this case the ligand penetration will begin from the dissociated carboxylic group and the true charge seen by the metal will be between 0 and −1. The range of values of Fe^{3+} is very large, and a dependence upon the basicity of the ligand has been demonstrated for the series chloro-, dichloro-, trichloroacetate anions.[34] These observations suggest an associative mechanism for substitution at Fe^{3+}. The majority of ligands not having a particularly high basicity give values for the ligand–water exchange rate in the range $1.2–120\ s^{-1}$.

The comparison between the solution properties of the two acids and their interactions with metal (hydrous) oxides[10,11] can only be made in a qualitative manner. Dipicolinic acid is a stronger acid which binds iron(III) in solution more strongly than picolinic acid. Since the two acid molecules have similar structures, it is expected that dipicolinic acid could leach iron(III) from its oxides more rapidly than picolinic acid.

Finally, it is worthwhile noting that the measured enthalpy of complexation of iron(III) by picolinic acid is low and so it is to be expected that the interactions with metal oxides will be of similar nature at higher temperatures, as long as the surface of the solids does not change appreciably. The formation of FeD^+ has a moderate positive enthalpy change associated with it and this implies that the rate of dissolution of haematite by dipicolinic acid may increase with temperature.

Acknowledgement—The authors appreciate useful comments made by the referee.

REFERENCES

[1] I. Morimoto and S. Tanaka, *Anal. Chem.* 1963, **35**, 1234.
[2] P. Siegfried, GER. 946003, 19 July (1956).
[3] R. L Every and O. L. Riggs Jr., *Mater. Protect.* 1964, **3**, 46.
[4] L. Campanella and G. de Angelis, *Ann. Univ. Ferrara. Sez* 1970, **5**, 565.
[5] G. Anderegg, *Helv. Chim. Acta* 1960, **43**, 1530.
[6] C. F. Timberlake, *J. Chem. Soc.* 1964, 1229.
[7] E. Chiacchierini, G. d'Ascenzo, G. de Angelis, A. L. Magri and V. Petrone, *Ann. Chim. (Rome)* 1977, **67**, 195.
[8] L. Campanella, E. Chiacchierini, G. de Angelis and V. Petrone, *Ann. Chim. (Rome)* 1977, **67**, 385.
[9] I. Grenthe, *J. Am. Chem. Soc.* 1960, **83**, 360.
[10] C. Wood, Communicated at Electric Power Research Institute Contractors Meeting, Schenectady, N.Y., 1980; M. G. Segal and R. M. Sellers, *J. Chem. Soc. Chem. Commun.* 1980, 991.
[11] C. G. Pope, E. Matijević and R. C. Patel, *J. Colloid Interface Sci.* 1981, **80**, 874.
[12] R. S. Sapieszko, R. C. Patel and E. Matijević, *J. Phys. Chem.* 1977, **81**, 1061.
[13] P. H. Hsu, *Soil Sci. Soc. Am., Proc.* 1967, **31**, 353.
[14] R. C. Patel, *Chem. Instrum.* 1976, **7**, 83.
[15] L. Meites, *The General Multiparametric Curve Fitting Program CFT4.* Hard-copy listings of the basic program and a number of modifications of it that serve a variety of different but related purposes, together with a 220-page manual of instructions, explanation and documentation may be obtained by remitting $100 to the Computing Laboratory of the Department of Chemistry, Clarkson College of Technology, Potsdam, N.Y. 13676.
[16] H. H. Trimm and R. C. Patel, *Inorg. Chim. Acta* 1979, **35**, 15.
[17] E. S. Swinbourne, *J. Chem. Soc.* 1960, 2371.
[18] U. Strahm, R. C. Patel and E. Matijević, *J. Phys. Chem.* 1979, **83**, 1689.
[19] R. G. Wilkins, *The Study of Kinetics and Mechanism of Reactions of Transition Metal Complexes.* Allyn and Bacon, Boston (1974).
[20] E. Mentasti, E. Pelizzetti and G. Saini, *J. Chem. Soc., Dalton Trans.* 1974, 1944.
[21] E. Mentasti and E. Pelizzetti, *J. Chem. Soc., Dalton Trans.* 1973, 2605.
[22] R. W. Green and H. K. Tong, *J. Am. Chem. Soc.* 1956, **78**, 4896.
[23] J. J. Christensen, R. M. Izatt, D. P. Wrathall and L. D. Hansen, *J. Chem. Soc. (A)* 1969, 1212.
[24] N. K. Dutt, G. S. Sanyal and K. Nag, *J. Indian Chem. Soc.* 1968, **45**, 334.
[25] T. F. Gritmon, M. P. Goedken and G. R. Choppin, *J. Inorg. Nucl. Chem.* 1977, **39**, 2021.
[26] C. Petitfaux and R. Fournaise, *Bull. Soc. Chim. France* 1972, 914.
[27] C. Tissier and M. Agoutin, *J. Electroanal. Chem. Interfacial Electrochem.* 1973, **47**, 499.
[28] G. Anderegg, *Helv. Chim. Acta* 1960, **43**, 414.
[29] A. Napoli, *Talanta* 1968, **15**, 189.
[30] I. Grenthe and E. Hansson, *Acta. Chem. Scand.* 1969, **23**, 611.
[31] S. Funahashi, K. Haraguchi and M. Tanaka, *Inorg. Chem.* 1977, **16**, 1349.
[32] M. Grant and R. B. Jordan, *Inorg. Chem.* 1981, **20**, 55.
[33] E. Mentaoti, *Inorg. Chem.* 1979, **18**, 1512.
[34] B. Parmutter-Hayman and E. Tapuhi, *J. Coord. Chem.* 1976, **6**, 31.

Polyhedron Vol. 1, No. 3, pp. 277–281, 1982
Printed in Great Britain.

0277–5387/82/030277–05$03.00/0
Pergamon Press Ltd.

STRUCTURAL INFLUENCES ON THE LANTHANIDE–ACTINIDE SELECTIVITY OF SOME AMINOCARBOXYLATES

J. E. POWELL,* M. W. POTTER, H. R. BURKHOLDER, E. D. H. POTTER and P. K. TSE
Ames Laboratory and Department of Chemistry, Iowa State University, Ames, IA 50011, U.S.A.

(*Received* 9 *November* 1981)

Abstract—Data for the resolution of americium from europium and terbium using 2,2'-diaminodiethylether-N,N,N',N'-tetraacetate and 1,5-diaminopentane-N,N,N',N'-tetraacetate are reported along with values of the formation constants of the La–Lu and Y chelates of the latter. It is shown that the minimum single-stage separation factor for Am^{3+} from Ln^{3+} cations, using 2,2'-diaminodiethylether-N,N,N',-N'-tetraacetate with Dowex 50 resin, exceeds 1.7 for all Am–Ln pairs, and runs as high as 350 in the case of Am^{3+}, La^{3+}. The minimum of 1.7 occurs at Eu^{3+} in the lanthanon sequence. A novel separation of Am^{3+}, Cm^{3+} and heavier actinons from each other and from all the lanthanons and yttrium appears to be feasible.

INTRODUCTION

The partitioning of americium and curium from the fission products has been regarded by numerous authors as being advantageous in minimizing the long-term hazards associated with the geological disposal of nuclear waste.[1,2] Unfortunately, the isolation of these actinides is complicated by the presence of large quantities of the chemically similar lanthanide elements in the fission-product mixture. All known separation techniques for segregating Am and Cm from the lanthanides have proven deficient in some manner. The TRAMEX process, which exploits the preferential amine extraction of anionic actinide chloride complexes, requires the use of large quantities of highly corrosive chloride salt solutions (10 M LiCl).[3] Attempts at the use of analogous systems, which substitute thiocyanate for chloride, suffer from the instability of SCN^- in the presence of alpha radiation.[4] At present, the most effective Am, Cm–Ln separation processes utilize diethylenetriaminepentaacetic acid (DTPA) anions to preferentially complex the actinides. These systems suffer from the very high stability of the DTPA-metal complexes, which produces slow exchange rates in ion-exchange and Talspeak-type solvent-extraction systems.[5]

Most of the known reagents for Am, Cm–Ln separations share the common trait of forming their strongest lanthanide complexes with cations in the mid-lanthanon range. The necessity of a Ln stability constant maximum in this position can be divined from a consideration of the bonding characteristics of the lanthanide and actinide complexes. Since electrostatic interactions dominate the bonding in these complexes, and the charge of the cations in question is equal (+3), the paramount factor in determining the relative stability of the complexes formed by the Lns and Am and Cm, is the cationic radius. On this basis the difficulty of Ln–Am, Cm separation is apparent in the fact that Am and Cm have radii equivalent to Nd and Pm, and are, consequently, interspersed in the lanthanide sequence by reagents whose Ln complex stability constants steadily increase from La to Lu (e.g. hydroxycarboxylic acids).

Fortunately another more exploitable trend emerges from a comparison of the chemistry of the lanthanides and actinides. It has been observed[6] that for most ligands the trivalent An cations form more stable complexes than do Ln cations of the same radius. This phenomenon has long been attributed to increased covalence of the 5f actinide orbitals, but the continuation of the comparison to Er and Y of similar radius indicates that the effect may be a result of the increasing nuclear charge of the three series (Y < Ln < An). No matter what the origin of the excess stability seen in the An complexes, the result of its existence is that one would expect the most effective Ln–Am, Cm separation agent to form its strongest lanthanide complexes with Nd or Pm. A stability constant maximum in this position would allow the entire magnitude of the An "excess stability" to be reflected in the Ln–Am, Cm separation factors.

The problem of Ln–Am, Cm separation now becomes one of designing a ligand which exhibits a Ln maximum in the correct position, and maximizes the "excess stability" experienced by the An's. The few ligands which display relative maxima in the mid-lanthanon range appear to do so as a result of a decrease in dentate character which occurs in the lanthanide complexes of some multidentate ligands.[7]

This paper examines the ion-exchange elution behavior and Ln complex chemistry of two ligands, 2,2'-diaminodiethylether-N,N,N',N'-tetraacetic acid (EEDTA) and 1,5-diaminopentane-N,N,N',N'-tetraacetic acid (PMDTA), in hope of distinguishing the structural moieties necessary in producing an effective Ln–Am, Cm separation agent.

EXPERIMENTAL

2,2' - *Diaminodiethylether* - N,N,N',N' - tetraacetic acid

This reagent was prepared from 2,2'-dichlorodiethylether (Aldrich) via the method of Yashunskii *et al.*[8] The anhydrous EEDTA exhibited a formula weight of 334 (theoretical 336). Calc for $C_{12}H_{20}N_2O_9$: C, 42.9, H, 6.0, N, 8.3. Found: C, 43.0, H, 6.1, N, 8.3%

1,5 - Diaminopentane - N,N,N',N' - tetraacetic acid

Twenty-five g of 1,5-diaminopentane (Aldrich) was dissolved in 100 ml of water. To this solution 115 g of chloroacetic acid (Aldrich), which had been dissolved in 100 ml of water, cooled,

*Author to whom correspondence should be addressed.

and neutralized with NaOH, were added. The resulting mixture was warmed to 40°C, and maintained at pH 10 by timely additions of 10 M NaOH. Over a 24 hr period, 122 ml of base were added in this fashion. The reaction mixture was diluted to 2, 1 and loaded on five, (1"×4'), −40 +50 mesh, hydrogen-form, Dowex 50 cation-exchange columns. The resulting HCl and unreacted chloroacetic acid were flushed from the system with distilled water. A light-coloured, easily discernible band of PMDTA formed, and was displaced from the resin bed by elution with 0.2 M NH_4OH. The acidic fractions of the eluate were collected, evaporated to a hard glass, and recrystallized from water. The resulting white powder (59 g) was characterized by equivalent weight and C, H, N analyses, and determined to be PMDTA·H_2O. Calculated for $C_{13}H_{24}N_2O_9$: C, 44.3; H, 6.88; N, 7.95. Found: C, 44.2; H, 6.99; N, 7.95%. The anhydrous PMDTA was obtained by drying overnight at 108°C. Calc for $C_{13}H_{22}N_2O_8$: C, 46.7; H, 6.65; H, 8.38. Found: C, 45.6; H, 6.78; N, 8.17%.

Reagents

Lanthanide nitrates. Solutions of approximately 0.1 M in Ln $(NO_3)_3$ were made by dilution of stock solutions previously prepared from the corresponding oxides (greater than 99.9% purity) using the method described by Adolphson.[9]

Lanthanide tracers. Solutions of $^{241}Am(NO_3)_3$, $^{155}Eu(NO_3)_3$ and $^{160}TbCl_3$ were purchased from New England Nuclear and diluted to provide convenient activities.

Cation elution experiments

The Ln–An selectivities of EEDTA and PMDTA were investigated by elution of ^{241}Am, ^{155}Eu and ^{160}Tb mixtures from a 2-mm × 500-mm, cation-exchange column (Dowex 50W-8, 200–400 mesh). The eluents were prepared by dissolution of the respective purified aminocarboxylic acids followed by pH adjustment with NH_4OH. The eluents were also made 0.1 M in NH_4ClO_4 to insure a constant ionic strength. The effluent from the elution experiments was collected and counted by means of a Ge–Li detector. The discrete gamma energies used were: 59.5 KEV (^{241}Am), 105.3 KEV (^{155}Eu) and 298.6 KEV (^{160}Tb). The flow rate utilized was 2 drops per min (37 drops per ml).

Protonation constants of the PMDTA anion

The PMDTA anion protonation constants were obtained from pH_c measurements on a series of independently prepared PMDTA solutions, each containing a different amount of KOH or HNO_3, and enough KNO_3 to adjust the ionic strength to 0.1 M. The resulting values of the protonation constants are shown in Table 1.

Lanthanide–PMDTA stability constants

The stability constants for the ML^- ($\beta_1 = [ML]/[M][L]$) and MHL ($\beta_H = [MHL]/[M][HL^-]$) complexes formed by the various lanthanides and yttrium were determined potentiometrically at 25.0 C and 0.1 M ionic strength (KNO_3). These values were calculated from pH_c measurements on a series of independently prepared solutions of PMDTA, $M(NO_3)_3$, KNO_3 and KOH. The nonlinear calculation method which was employed, has been described in detail elsewhere.[11] The results of these calculations are shown in Table 2.

DISCUSSION

EEDTA elutions

Although the similarities between the lanthanide complex stability curves of DTPA and EEDTA have been recognized for some time[12] no attempt has been made to utilize EEDTA as a Ln–An separations agent. It had been shown previously that the maximum Ln–EEDTA complex stabilities occur at Eu and Tb, and that these were the leading elements in the lanthanide elution sequence.[13] In view of these results the elution chromatogram illustrated in Fig. 1 is quite encouraging. The desired elution order of Am, Tb and Eu is observed implying that EEDTA can indeed be used to separate Am from the entire lanthanide family. The equivalence of the Tb and Eu–EEDTA complex stabilities is again confirmed by the near coincidence of their elution peaks. By employing the Am–Tb separation factor calculated from the chromatogram (1.71) and the EEDTA stability constants reported in Ref. 12, the separation factor between americium and each of the lanthanides was calculated. These values appear in Table 3 along with the separation factors observed for DTPA cation-exchange systems at 70–80°C,[14,15] and values calculated from the DTPA stability constants reported previously.[16,17] The average separation factor actually measured for DTPA at 25°C is 2.35.[17] The α_{Ln}^{Am} values in parenthesis are normalized to this value and are probably more reliable than those calculated from the absolute magnitude of the Am–DTPA stability constant.

As seen in Table 3, EEDTA, like DTPA, exhibits excellent separation factors between Am and the light lanthanides. In the heavy lanthanide range EEDTA attains separation factors greater than 2.0 for the entire group from Dy to Lu. This behavior is clearly superior to that of DTPA which achieves a heavy-rare-earth separation factor of this magnitude only at Lu. It is clear that by exhibiting a minimum Am–Ln separation factor of 1.7, EEDTA promises to be a ligand of great utility in nuclear waste processing.

In addition to favorable separation factors, EEDTA has other attributes which may encourage its use. The acid form of EEDTA is quite soluble in water, allowing the use of hydrogen ion as a retaining ion in a displacement cation-exchange system. As evidenced by its isola-

Table 1.

$\alpha_N = [H_NL]/[H]^N[L]$	σ	pK_a Values	
		This Work	Ref. 10
$\alpha_1 = 0.157 \times 10^{11}$	2.02%	$\log [HL]/[H][L] = 10.20$	10.58
$\alpha_2 = 0.350 \times 10^{20}$	1.32%	$\log [H_2L]/[H][HL] = 9.35$	9.50
$\alpha_3 = 0.180 \times 10^{23}$	2.32%	$\log [H_3L]/[H][H_2L] = 2.71$	2.7
$\alpha_4 = 0.311 \times 10^{25}$	2.65%	$\log [H_4L]/[H][H_3L] = 2.24$	2.2

Table 2. Stability constants of rare earth PMDTA chelate species (25°; $I = 0.1$)

M	β_H	log β_H	β_1	log β_1
Y	$.663 \times 10^7$	6.82[a]	$.227 \times 10^{11}$	10.36[a]
La	$.123 \times 10^7$	6.09	$.910 \times 10^9$	8.96
Ce	$.218 \times 10^7$	6.34	$.321 \times 10^{10}$	9.51
Pr	$.282 \times 10^7$	6.45	$.510 \times 10^{10}$	9.71
Nd	$.334 \times 10^7$	6.52	$.588 \times 10^{10}$	9.77
Pm				
Sm	$.462 \times 10^7$	6.66	$.149 \times 10^{11}$	10.17
Eu	$.496 \times 10$	6.70	$.166 \times 10^{11}$	10.22
Gd	$.611 \times 10^7$	6.79	$.232 \times 10^{11}$	10.37
Tb	$.771 \times 10^7$	6.89	$.344 \times 10^{11}$	10.53
Dy	$.960 \times 10^7$	6.98	$.560 \times 10^{11}$	10.75
Ho	$.115 \times 10^8$	7.06	$.678 \times 10^{11}$	10.83
Er	$.137 \times 10^8$	7.14	$.106 \times 10^{12}$	11.03
Tm	$.172 \times 10^8$	7.24	$.154 \times 10^{12}$	11.19
Yb	$.207 \times 10^8$	7.32	$.213 \times 10^{12}$	11.33
Lu	$.214 \times 10^8$	7.33	$.231 \times 10^{12}$	11.36

[a]Values are estimated to be reliable to ±.05.

Table 3. α_{Ln}^{Am} for EEDTA and DTPA

M	EEDTA 25°	DTPA 25°		DTPA 70°–80°
La	349.14	(1907.75)	2630.26	1202.0
Cr	71.28	(269.48)	371.54	162.0
Pr	15.24	(49.04)	67.61	40.74
Nd	7.46	(14.47)	19.95	13.80
Pm				6.46
Sm	2.25	(2.63)	3.63	3.02
Eu	1.71 (measured 1.78)	(2.35)	3.24	2.04
Gd	2.59	(1.99)	2.75	2.00
Tb	1.71 (measured)	(1.12)	1.55	
Dy	2.15	(0.870)	1.20	
Ho	2.59	(0.957)	1.32	
Er	3.57	(1.052)	1.45	less than 1.00 at 70°C
Tm	5.16	(1.095)	1.51	
Yb	4.93	(1.385)	1.91	
Lu	6.21	(2.089)	2.88	

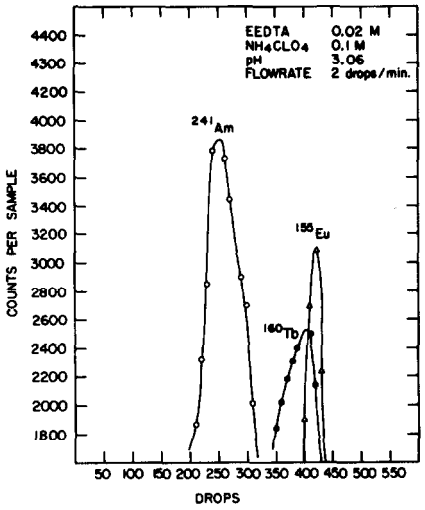

Fig. 1. Cation-exchange elution of a ^{155}Eu–^{160}Tb–^{241}Am mixture using an EEDTA solution.

tion after synthesis, EEDTA is protonated and sorbed by a hydrogen-form cation exchanger. This phenomenon will cause the formation of a sorbed EEDTA band immediately ahead of the Am band in a displacement system with H^+-cycle resin and will permit a convenient recovery and reuse of the ligand. Finally, the ten thousand-fold decrease in the magnitude of the stability constants of EEDTA, relative to DTPA, should translate into improved exchange kinetics for both ion-exchange and Talspeak-type, solvent-extraction methods which could be developed with EEDTA.

PMDTA investigations

The successful separation of Am from the lanthanides in the EEDTA cation-exchange experiments prompted an attempt to discover which structural properties common to EEDTA and DTPA were responsible for their peculiar selectivity. It was conjectured that the decline of the EEDTA and DTPA stability constant values for the heavy lanthanons (Tb or Dy–Lu) was essential to their preference for Am and Cm relative to all lanthanons and that this phenomenon was related to the gradual detachment of a ligand chelating group as the lanthanide radius decreased for steric reasons. Two possibilities for the failing chelating group are evident in a structural comparison of EEDTA and DTPA. Both ligands consist of two terminal imino-diacetate groups connected by a five-membered chain. It is possible that this particular chain length between the terminal nitrogen atoms is such that the coordination of one of the terminal carboxylates is compromised and gradually fails due to steric constraints resulting from the decreasing lanthanide radius. A second possible explanation of the decreasing heavy lanthanide stability constants would predict a gradual failure of the coordination of the EEDTA ether–oxygen atom and the corresponding failure of the DTPA mid-chain nitrogen atom or carboxylate group. An investigation into the Ln, An elution behavior and Ln complex stability constants of the PMDTA ligand was conducted to examine the importance of the mid-chain chelating moiety in producing Ln–An selectivity.

From the outset it was apparent that the behaviour of the PMDTA ligand was remarkably different than that of EEDTA. Preliminary ion-exchange experiments revealed that elutions with thirty column volumes of 0.02 M PMDTA solutions at pH's of 3.0 (optimum for EEDTA), 4.0, or 4.8 were insufficient to remove the Am, Eu and Tb tracers from the resin bed. An acceptable chromatogram was obtained only after the PMDTA concentration was increased to 0.04 M and the pH was increased to 5.1. These more severe conditions were indicative of the significant differences observed in the magnitude of the PMDTA and EEDTA protonation and lanthanide complex stability constants.

The PMDTA chromatogram depicted in Fig. 2 also revealed substantial differences in the PMDTA and EEDTA elution orders for the lanthanide and actinide tracers. Unlike EEDTA which eluted Am well ahead of a poorly separated Eu–Tb mixture, PMDTA eluted Tb first followed by an unresolved Am–Eu peak. The relative positions of these peaks showed that the PMDTA–Ln chelate system does not possess the decline in stability across the heavy lanthanons needed to allow the elution of Am ahead of Tb.

The values determined for the Ln stability constants of the protonated and unprotonated complexes confirmed the behaviour observed in the elution experiments. In both cases the stability constant sequence increases continuously across the entire lanthanide family. The complete reversal of the decreasing trend exhibited by the DTPA–Ln and EEDTA–Ln chelates in the heavy lanthanon region underscores the importance of the mid-chain chelating moiety which PMDTA lacks. Further comparisons are evident in Fig. 3, which displays the plots of $\log \beta_1$ vs lanthanide cationic radius for DTPA[16], EEDTA[12], 1,6 - diaminohexane - N,N,N',N' - tetraacetic acid (HMDTA)[18], diethylenetriamine-N'-propanoic-N,N',N'',N''-tetraacetic acid (DTPTA)[19], and PMDTA; and the $\log \beta_2$ values for N-methyliminodiacetic acid (MIDA)[20]. The most striking feature of this graph is the 10^7-fold decrease in β_1 value directly attributable to the replacement of the ether oxygen atom in EEDTA with a methylene group (PMDTA). The stability constants of PMDTA bear little resemblance to those of DTPA and EEDTA, and instead parallel the values exhibited by HMDTA and MIDA. It is evident from this phenomenon

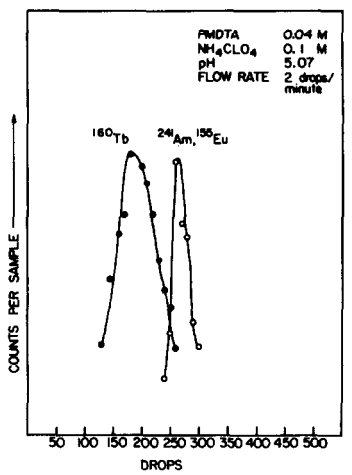

Fig. 2. Cation-exchange elution of a ^{155}Eu–^{160}Tb–^{241}Am mixture using a PMDTA solution.

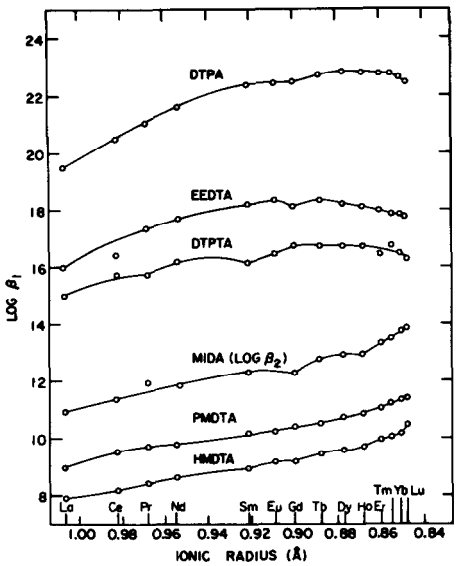

Fig. 3. Stability constants of the lanthanide chelates formed by several aminocarboxylates.

that the two additional five-membered chelate rings formed by the mid-chain chelating group are essential to the high stability and actinide selectivity shown by EEDTA and DTPA. Unfortunately, it is still impossible to determine the exact role played by this group in the decrease in complex stability displayed in the heavy lanthanides. Molecular models show that chelation of the mid-chain group introduces considerable strain in the coordination of the iminodiacetate groups, but the present data do not offer conclusive evidence as to which group fails as the cationic radius decreases.

The literature contains only two other citings which offer further evidence in deciphering the mode of chelation in these ligands. In 1979, Choppin, Baisden and Khan[21] published ^1H and ^{13}C NMR spectra for the DTPA complexes of La and Lu. They concluded that the middle carboxylate group was unbound, implying heptadentate coordination of the metal cation by three nitrogen atoms and an average of four carboxylate groups. If one accepts this view, however, it becomes difficult to rationalize the 10^4-fold increase in β_1 values of DTPA over those of EEDTA. The only other indication of the chelation mode of these aminocarboxylates appears in the stability constants reported for DTPTA.[19] This ligand has a structure equivalent to DTPA with one of the terminal acetate groups replaced by propanoate. Surprisingly, this minor change (one-CH_2-unit) reduced the stabilities of the lanthanide complexes to positions below those of EEDTA (i.e. approximately a factor of 10^5 below those of DTPA). The decline in chelate stability observed in the heavy lanthanon region for EEDTA and DTPA chelates seems to be retained in the case of DTPTA, although the published data in this region are poor. If one assumes that the remarkable decrease in the overall magnitude of the DTPTA stability constants, relative to the DTPA series, is due to the failure of the propanoate group to bond, the retention of the decreasing trend in the heavy lanthanon region might well be indicative of a gradual failure of the mid-chain donor atom to coordinate.

Acknowledgement—Operated for the U.S. Department of Energy by Iowa State University under contract no. W-7405-ENG-82. This work was supported by the Office of Basic Energy Sciences.

REFERENCES

[1]J. O. Blomek, J. P. Nichols and W. C. McClain, *Phys. Today* 1973, **26**, 36.
[2]G. I. Rochlin, *Science*, 1977, **195**, 23.
[3]R. E. Lueze, M. H. Lloyd. *Progress in Nuclear Energy*, Series III Process Chemistry 4 (Edited by C. E. Stevenson, E. A. Mason and A. T. Gresky), Vol. 4. Pergamon Press, New York, 1970.
[4]T. K. Keenan, *J. Inorg. Nucl. Chem.*, 1961, **20**, 185.
[5]Z. Kolarik, G. Koch and W. J. Kuhn, *J. Inorg. Nucl. Chem.*, 1974, **36**, 905.
[6]A. I. Moskvin, *Soviet Radiochem.*, 1967, **9**, 677.
[7]J. E. Powell and H. R. Burkholder, *J. Chromatogr.*, 1968, **36**, 99.
[8]V. A. Yashunskii, D. D. Smolin, V. G. Ermolaeva and M. N. Shchikina, *J. Gen. Chem. USSR*, 1960, **30**, 3872.
[9]M. Adolphson, Ph.D. Thesis, Iowa State University of Science and Technology, 1969.
[10]G. Schwarzenbach and H. Ackermann, *Helv. Chim. Acta*, 1948, **31**, 1029.
[11]M. W. Potter, Ph.D. Thesis, Iowa State University of Science and Technology (1981).
[12]J. L. Mackey, M. A. Hiller and J. E. Powell, *J. Phys. Chem.*, 1962, **66**, 311.
[13]F. H. Spedding and J. E. Powell, AEC Report ISC-1116, Ames, Iowa, April 1969.
[14]J. T. Lowe, W. H. Hale and D. F. Hallman, *Ind. Engng Chem. Process. Des. Develop.*, 1971, **10**, 131.
[15]J. A. Kelley, AEC Report DP-1308, Savannah River, Georgia, 1973.
[16]T. Moeller, L. C. Thompson, *J. Inorg. Nucl. Chem.*, 1962, **24**, 499.
[17]R. D. Baybarz, *J. Inorg. Nucl. Chem.*, 1965, **27**, 1381.
[18]E. Brücker, R. Kiraly and Z. Varga, *Magy. Kern. Folyoirat*, 1975, **81**, 339.
[19]V. F. Vasil'eva, O. Yu. Lavrova, N. M. Dyatlova and V. G. Yashunskii, *J. Gen. Chem. USSR*, 1966, **36**, 688.
[20]L. C. Thompson, B. L. Shafer, J. A. Edgar and K. D. Mannila. *Lanthanide/Actinide Chemistry* (Edited by P. R. Fields and T. Moeller). American Chemical Society Symposium Series 71, American Chemical Society, Washington, D.C., 1967.
[21]G. R. Choppin, P. A. Baisden and S. A. Khan, *Inorg. Chem.*, 1979, **18**, 1330.

Polyhedron Vol. 1, No. 3, pp. 283–287, 1982
Printed in Great Britain.

0277-5387/82/030283-05$03.00/0
Pergamon Press Ltd.

NEW MIXED HETEROPOLYTUNGSTATES CONTAINING Ge(IV) OR Sn(IV)

ANNA SCHOUTEN* and BERNARD CROS
Laboratoire de Chimie des Matériaux, Ecole Normale Supérieure, Takaddoum, BP 5118 Rabat, Morocco

(*Received* 16 *November* 1981)

Abstract—New mixed heteropolyanions with formulae $XZW_{11}O_{39}(OH)^{m-}$[X = Si, Ge, B, As(V), Ga, Co(II), Zn; Z = Ge(IV), Sn(IV)] and $X'_2ZW_{17}O_{61}(OH)^{7-}$[X' = As(V), P(V); Z = Ge(IV), Sn(IV)] were prepared. Crystal systems of the potassium salts were determined. The stability range of the anions is given in terms of the pH. The acids corresponding to the salts were obtained and their neutralization studied. Spectroscopic and polarographic reduction studies are reported.

INTRODUCTION

In the recent research developments in the field of molybdo- and tungsto-heteropolyanions an important step has been taken in proving that unsaturated hpa† of composition XW_{11}‡ or XMo_{11} and X'_2W_{17} or X'_2Mo_{17} react rapidly with transition metals Z to give anions of the XZW_{11} or $XZMo_{11}$ and X'_2ZW_{17} or X'_2ZMo_{17} series[1].

The anions XW_{11} and X'_2W_{17} have been described as unsaturated or incomplete hpa, in which one of the twelve (or eighteen) octahedral W atoms is missing[1]. These unsaturated hpa result from the controlled base attack of the complete anions XW_{12} (and X'_2W_{18}); most of the hpa XW_{11} can also be prepared by direct methods. The rapid reaction between a metallic element and an unsaturated hpa has been used in the prepation of mixed hpa XZW_{11}, where a transition metal occupies the empty octahedral site[2,3,4,5] and more recently in the preparation of mixed hpa where another element (Al^{III}, Ga^{III}, In^{III} or Tl^{III}) completes the unsaturated anion[6].

This paper gives the results of the preparation of mixed hpa XZW_{11} and X'_2ZW_{17} where Z is germanium (IV) or tin (IV). Germanium cannot be added to unsaturated hpa as Ge^{II}; in this oxidation state this element is oxidized instantaneously by the W atoms. An investigation on hpa containing tin (II) is in progress.

EXPERIMENTAL

Starting material

The commercial oxide GeO_2 used in this work is the hexagonal "soluble" variety, which is very reactive. GeO_2 is dissolved in concentrated base. The pH of the solution is adjusted to approx. 3 and this solution is used as Ge^{IV} reagent. A solution of $SnCl_4.5H_2O$ is the starting material of Sn^{IV}. The unsaturated hpa XW_{11} to which the Ge^{IV} or Sn^{IV} elements are going to be added, are prepared according to the methods described by Zonnevijlle[6]. The mixed hpa ($CoCoW_{11}$ and $ZnZnW_{11}$) used in the preparations involving the exchange reaction, are obtained with the methods elaborated by Bauchet *et al.*[7] and Baker *et al.*[8,9].

General method

An excess of Ge^{IV} or Sn^{IV} is added to solutions or suspensions of the potassium salts of unsaturated hpa, previously heated to 60–70°C. In the case of Sn^{IV} the pH of the final solution is adjusted to 4 with potassium bicarbonate. The excess of the reagent is filtered off and on cooling the potassium salt of the mixed hpa separates from the solution as long transparent needles. By adding potassium chloride or a saturated solution of potassium acetate in methanol to the reagent mixture, precipitation of the potassium salt is almost complete. The yield after recrystallisation is near 80%.

This method is applicable in the preparation of $SiGeW_{11}$, $GeGeW_{11}$, $SiSnW_{11}$, $GeSnW_{11}$, P_2SnW_{17}, P_2GeW_{17}, As_2SnW_{17} and As_2GeW_{17}.

The potassium salts of the anions $BGeW_{11}$, $BSnW_{11}$, $GaGeW_{11}$ and $GaSnW_{11}$ are obtained by applying the general method but at less elevated temperatures (30–40°C). They separate after several days on cooling (5°C) when treating the reagent mixture with a saturated solution of potassium acetate in methanol or ethanol.

Spectral studies and conductivity measurements made during the addition reaction show clearly the formation of the complexes in the ratio $Z/XW_{11} = 1$ (Figs. 1 and 2).

Since the unsaturated hpa corresponding to the complexes $Co^{II}GeW_{11}$ and $ZnGeW_{11}$ cannot be obtained because of their instability, we applied the exchange method to prepare these complexes starting from the mixed hpa containing an element in the oxidation state II in the octahedral site ($CoCoW_{11}$ and $ZnZnW_{11}$ in this case). The reaction is the following:

$$XZ^{II}W_{11}O_{40}H_2^{p-} + Z'^{IV} \rightleftharpoons XZ'^{IV}W_{11}O_{40}H_2^{(p-2)} + Z^{II}.$$

The higher the oxidation state of the element Z', the more complete is the substitution of the divalent element. For the elements Ge(IV) and Sn(IV) this reaction is quantitative in a limited pH range. For the preparation of the complexes $CoGeW_{11}$ and $ZnGeW_{11}$ the general method outlined above is followed, only the pH of the mixtures is adjusted to 2.5 to obtain a quantitative reaction. Because of the solubility of these complexes the yield doesn't exceed 30%.

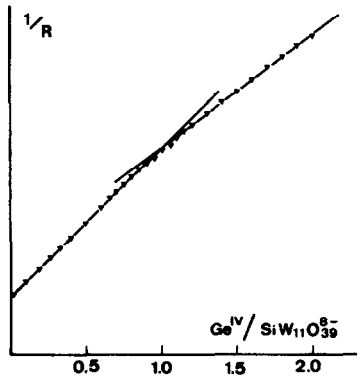

Fig. 1. Conductimetric study of the formation of the complex $SiGeW_{11}O_{39}(OH)^{5-}$ ($c_{hpa} = 5.10^{-3}$.M; 1/R in arbitrary units).

*Author to whom correspondence should be addressed.

†The abbreviation hpa stands for heteropolyanion.

‡As others, we refer to hpa by their symbolic formulae: for example SiW_{11} and P_2W_{17} are respectively the anions $SiW_{11}O_{39}^{8-}$ and $P_2W_{17}O_{61}^{10-}$.

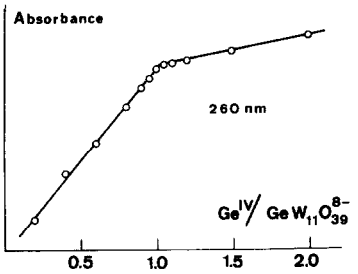

Fig. 2. Spectrophotometric study of the formation of the complex $GeGeW_{11}O_{39}(OH)^{5-}$ in a buffer solution of pH = 4.5 (c_{hpa} = 5.10^{-4} M).

The anion $AsSnW_{11}$ is obtained by adding to a solution of the sodium salt of AsW_{11} (the potassium salt being unstable) the stoichiometric quantity of $SnCl_4 \cdot 5H_2O$. This mixture is passed on a cation-exchanger in the hydrogen form (Amberlite IR-120) to obtain the acids corresponding to the salts in the solution. A passage on a weak base resin (Amberlite IR-45) eliminates all acids but the acid of the polyanion $AsSnW_{11}$. Addition of a solution of potassium bicarbonate to the mixture does not lead to a precipitation of the potassium salt of the anion, but an evaporation afterwards at room temperature results in the deposition of the potassium salt as a transparent amorphous material.

Chemical analyses

The elements K, W, Ga, Co(II) and Zn were estimated by the following classical methods:

—W and Ga by precipitation with 8-hydroxyquinoline;

—Co by biamperometry: oxidation by $K_3[Fe(CN)_6]$ and back-titration with a standard cobalt solution;

—K by precipitation with sodium tetraphenylborate.

The water content was evaluated by ignition at 600°C. Germanium and tin were estimated by a new method using the fluorescence X technique. This method is described in detail elsewhere[10].

Other measurements: for spectral, pH, conductivity, polarographic and X-ray studies the instruments already described were used[11].

RESULTS

Analytical results and formulation of the anions

Chemical analysis of the potassium salts of the new anions leads to the formulae indicated in Table 1, showing a OH^- ligand to complete the octahedral coordination of Ge(IV) or Sn(IV).

Crystal systems

The salts of mixed hpa belong to a limited number of crystallographic types, depending on the number of cations n_c per anion and on their nature[3]. The crystallographic types resulting from X-ray powder diffraction studies of the potassium salts of the mixed hpa containing Ge(IV) or Sn(IV) are in agreement with the value of n_c found by chemical analysis.

Thus the potassium salts of the anions $SiGeW_{11}$, $GeGeW_{11}$, $SiSnW_{11}$ and $GeSnW_{11}$ with formula $K_5XZW_{11}O_{39}(OH)$ belong to the hexagonal system and are isomorphous with $K_4SiW_{12}O_{40} \cdot 18H_2O$[3]. The potassium salts of $BGeW_{11}$, $BSnW_{11}$, $GaGeW_{11}$ and $GaSnW_{11}$ with general formula $K_6XZW_{11}O_{39}(OH)$ belong to the tetragonal system, $Q\beta$ type, isomorphous with $K_7PW_{11}O_{39} \cdot 15H_2O$[3] and the salts of P_2SnW_{17}, P_2GeW_{17}, As_2SnW_{17} and As_2GeW_{17} with formula $K_7X_2'ZW_{17}O_{61}(OH)$ belong to the rhombohedral series. The potassium salts of the new anions $Co^{II}GeW_{11}$ and $ZnGeW_{11}$ with general formula $K_7XZW_{11}O_{39}(OH)$ belong to the cubic system (c.f.c. type, space group Fm3m) and are isomorphous with $K_8Co^{II}Co^{II}W_{11}O_{39}(H_2O)$; the value of the lattice parameter (22.2 Å) is greater than the one found usually in this crystal system (21.5 ± 0.2 Å).

Stability

The stability of the new mixed hpa is studied in terms of the pH by spectrophotometry. The Figs. 3 and 4 show the results for $GeGeW_{11}$ and $GeSnW_{11}$. The sharp decrease of the absorbance at pH > 6 for the first one and at pH > 5 for the latter is due to the degradation of the hpa, which is confirmed by the appearence of a precipitate. The rapid change at pH < 2 agrees with the formation of polyacids. This stability in acidic medium allows the preparation of the free acids of the new anions by cation-exchange; analysis of the resins eluate revealed that none of the elements contained in the anion was retained on the resin during the preparation of the polyacids.

The results of the potentiometric study (Figs. 5 and 6) of the neutralization of the acids are in agreement with

Table 1. Analytical results for the new salts (calculated percentages in parentheses)

Salt	% K	% W	% Ge or Sn	% X
$K_5SiSnW_{11}O_{39}(OH).17H_2O$	6.30(5.90)	61.63(61.07)	3.50(3.58)	
$K_5SiGeW_{11}O_{39}(OH).16H_2O$	6.14(6.02)	63.02(62.26)	2.22(2.23)	
$K_5GeSnW_{11}O_{39}(OH).17H_2O$	6.26(5.83)	60.22(60.26)	3.40(3.54)	
$K_5GeGeW_{11}O_{39}(OH).12H_2O$	6.07(6.07)	62.67(62.81)	4.54(4.51)	
$K_6BSnW_{11}O_{39}(OH).14H_2O$	7.43(7.15)	62.33(61.67)	3.58(3.62)	
$K_6BGeW_{11}O_{39}(OH).15H_2O$	7.58(7.24)	61.27(62.38)	2.19(2.24)	
$K_4AsSnW_{11}O_{39}(OH).15H_2O$	4.76(4.77)	62.05(61.68)	3.76(3.62)	
$K_7P_2SnW_{17}O_{61}(OH).28H_2O$	5.54(5.59)	62.93(63.62)	2.50(2.42)	
$K_7P_2GeW_{17}O_{61}(OH).17H_2O$	5.52(5.66)	63.73(64.67)	1.51(1.50)	
$K_7As_2SnW_{17}O_{61}(OH).18H_2O$	5.45(5.50)	62.30(62.76)	2.28(2.38)	
$K_7As_2GeW_{17}O_{61}(OH).17H_2O$	5.62(5.56)	62.65(63.53)	1.44(1.48)	
$K_6GaSnW_{11}O_{39}(OH).15H_2O$	7.09(7.01)	60.35(60.42)	3.45(3.55)	2.09(2.08)
$K_6GaGeW_{11}O_{39}(OH).14H_2O$	7.23(7.13)	61.28(61.45)	2.05(2.21)	2.13(2.12)
$K_7CoGeW_{11}O_{39}(OH).15H_2O$	8.05(8.16)	61.04(60.45)	2.13(2.17)	1.75(1.76)
$K_7ZnGeW_{11}O_{39}(OH).13H_2O$	8.20(8.29)	61.80(61.25)	2.25(2.20)	1.95(1.98)

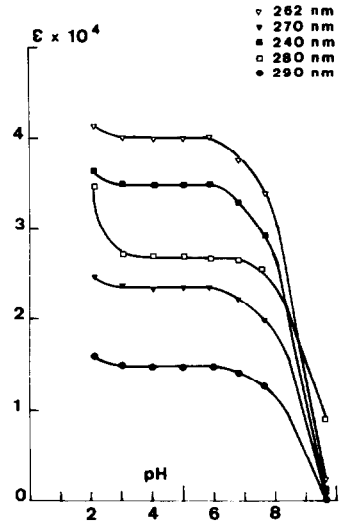

Fig. 3. Study of the stability of $K_5GeGeW_{11}O_{39}(OH)$: absorbance in terms of the pH ($c_{hpa} = 5.10^{-4}$ M).

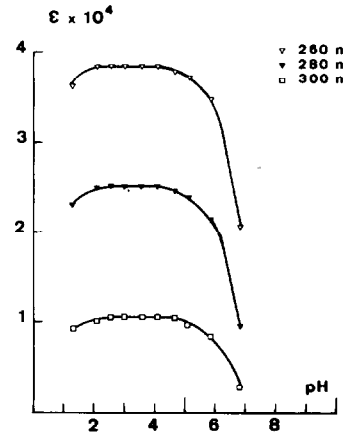

Fig. 4. Study of the stability of $K_5GeSnW_{11}O_{39}(OH)$: absorbance in terms of the pH ($c_{hpa} = 5.10^{-4}$ M).

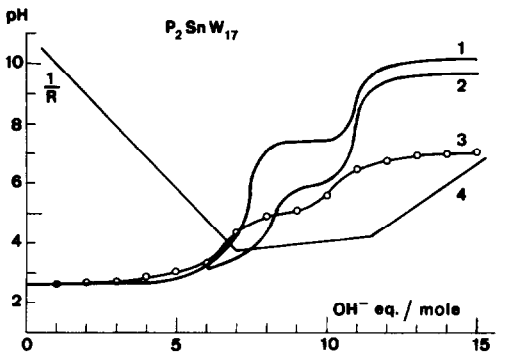

Fig. 6. Neutralization of the polyacid $H_7P_2SnW_{17}O_{61}(OH)$ ($c_{acid} = 5.10^{-3}$ M). (1) Potentiometric titration. (2) Potentiometric titration in 1M $NaNO_3$ as background electrolyte. (3) Potentiometric titration by allowing the mixtures to obtain their equilibrium (after 2 months). (4) Conductimetric titration.

those obtained from conductivity measurements: the first equivalence points on titration with base confirm the anion charges already given; yet the neutralization of the acids of the anions $SiSnW_{11}$ and $GeSnW_{11}$ shows the presence of one more proton than predicted by the charge of the anion; since no change in the acid strength is observed in the course of the reaction, equivalent hydrogens must be neutralized, so these acids are formulated as follows: $H_6XSnW_{11}O_{40}$.

A second equivalence point is correlated to a complex degradation reaction.

The presence of a background electrolyte destabilizes the acids of the hpa containing Sn(IV). The neutralization of these acids in solutions of high ionic strength shows equivalence points at 0.5 equivalents of OH^- after the inflexions found in the absence of background electrolyte (Figs. 6 and 7).

The results obtained from the different methods and the formulae of the acids derived from them are shown in Table 2.

Spectral study

All of these new hpa are colorless (except the compound containing Co(II) in the tetrahedral site); the spectral region of interest is to be found in the near UV

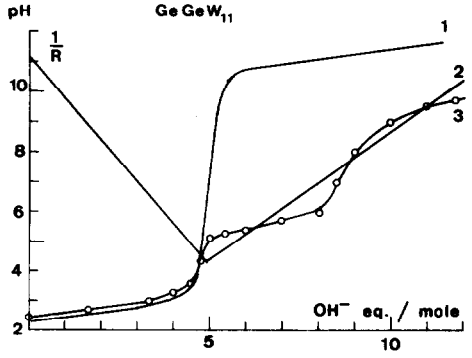

Fig. 5. Neutralization of the polyacid $H_5GeGeW_{11}O_{39}(OH)$ ($c_{acid} = 5.10^{-3}$ M). (1) Potentiometric titration in 1M $NaNO_3$ as background electrolyte. (2) Conductimetric titration. (3) Potentiometric titration by allowing the mixtures to obtain their equilibrium (after 2 days).

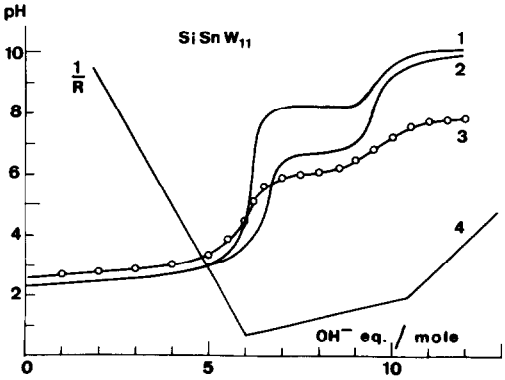

Fig. 7. Neutralization of the polyacid $H_6SiSnW_{11}O_{40}$ ($c_{acid} = 5.10^{-3}$ M). (1) Potentiometric titration. (2) Potentiometric titration in 1M $NaNO_3$ as background electrolyte. (3) Potentiometric titration by allowing the mixtures to obtain their equilibrium (after 2 months). (4) Conductimetric titration.

Table 2. Number of equivalents OH^- per mole deduced from the first equivalence points observed in the neutralization of the acids; the equivalence point for the complete degradation of the anions is not mentioned. Potentiometric measurements. (a) Without background electrolyte. (b) In $NaNO_3$ 1 M. (c) At equilibrium

Acids	Conduct. results	Potentiometric results a	b	c
$H_6SiSnW_{11}O_{40}$	6.0	6.1	6.5	6.0
$H_5SiGeW_{11}O_{39}(OH)$	5.0		4.9	
$H_6GeSnW_{11}O_{40}$	5.9	6.0	6.6	
$H_5GeGeW_{11}O_{39}(OH)$	5.0		4.9	4.8
$H_6BSnW_{11}O_{39}(OH)$	5.9	6.0	6.1	
$H_6BGeW_{11}O_{39}(OH)$	5.9		6.0	5.2
$H_4AsSnW_{11}O_{39}(OH)$	4.1			
$H_7P_2SnW_{17}O_{61}(OH)$	7.0	7.3	8.2	6.5
$H_7P_2GeW_{17}O_{61}(OH)$	6.3		7.1	
$H_7As_2SnW_{17}O_{61}(OH)$	7.0	7.0		
$H_7As_2GeW_{17}O_{61}(OH)$	6.5		7.2	
$H_6GaGeW_{11}O_{39}(OH)$	5.9		6.3	7.5
$H_7CoGeW_{11}O_{39}(OH)$	6.9		7.0	

from 210 to 300 nm (Fig. 8). In this range the hpa show a charge transfer band; at approx. 250 nm appears a characteristic maximum, separated from the whole of the band for the complete anions (XW_{12}), but reduced to a shoulder for most of the unsaturated hpa. This maximum reappears on filling the empty octahedral site by an element, all the more separated from the whole as the oxidation state of the element is higher. The absorption spectra of the hpa do not change very much whatever the element X may be. When the hpa are $X_2'ZW_{17}$ the appearance of a shoulder near 300 nm is observed which extends into the visible region, explaining the slightly yellow color of the salts.

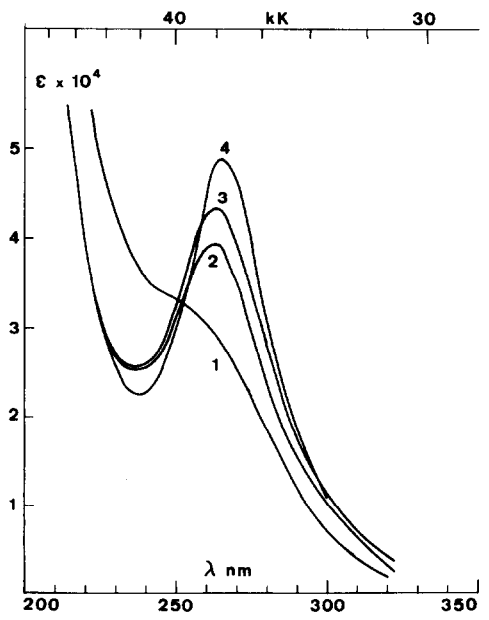

Fig. 8. UV absorption spectra of (1) $K_8GeW_{11}O_{39}$. (2) $K_5GeGeW_{11}O_{39}(OH)$. (3) $K_5GeSnW_{11}O_{39}(OH)$. (4) $K_4GeW_{12}O_{40}$.

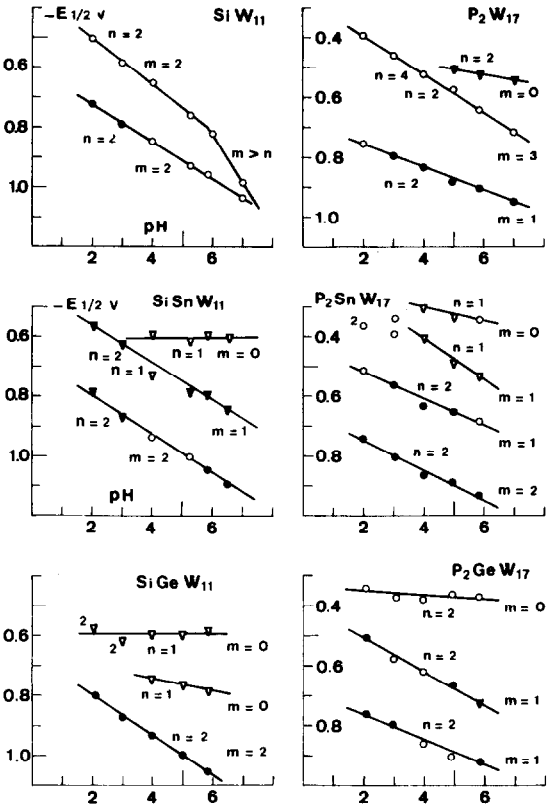

Fig. 9. *Left.* Half wave potentials in terms of the pH of $SiSnW_{11}$ and $SiGeW_{11}$ in comparison with SiW_{11}. *Right.* Half wave potentials of P_2SnW_{17} and P_2GeW_{17} in comparison with P_2W_{17}. $c_{hpa} = 10^{-3}$ M; $c_{buffer} = 0.5$ M; $c_{NaNO_3} = 0.5$ M. *n* represents the number of electrons observed in the reduction process. *m* represents the number of protons participating in the reduction reaction. ▽, represents a reversible reaction; ▼, a nearly reversible reaction; ●, a nearly irreversible reaction; ○, an irreversible reaction.

Polarographic study

The reducibility of the new hpa has been studied in terms of the pH and has been compared to the reducibility of the corresponding unsaturated hpa. Generally the half wave potentials of the unsaturated hpa are more negative than those of the mixed hpa, owing to the higher negative charge of the unsaturated hpa. The total number of electrons observed in the reduction process does not change by filling up the octahedral site in the unsaturated hpa with an element like germanium or tin. When the pH is raised the first bielectronic wave in the case of the hpa $XGeW_{11}$ is split into two pH independent monoelectronic waves associated with a reversible reduction reaction and into two reversible waves of which only the first one is pH independent in the case of the hpa $XSnW_{11}$ (Fig. 9).

For the anions $X_2'ZW_{17}$ this splitting up is observed over the whole pH range studied here (Fig. 9). In acidic medium (pH near 2) the solutions are slowly changing and after some days the presence of reduction waves due to the complete hpa is observed.

DISCUSSION

The results show that p^2 elements can replace one tungsten atom in the complete anions XW_{12} and $X_2'W_{18}$.

Substitutions by organometallic derivatives of tin(IV) and germanium(IV) have been reported[12-14] but until now no study of the purely inorganic mixed hpa has been undertaken. A polarographic study by Salomon-Bertho[15] showed that the reaction of Ge(IV) with the unsaturated hpa SiW_{11} gives the stable anion $SiGeW_{11}$.

Germanium belongs to the elements which are able to occupy the octahedral site Z as well as the tetrahedral site X in the hpa of symbolic formula XZW_{11}. Until now it is the only non-metallic element for which such a behaviour has been observed.

The mixed hpa of the XZW_{11} and $X_2'ZW_{17}$ type with Z = Ge(IV) or Sn(IV) have been isolated as their potassium salts and as their polyacids for X = Si, Ge, B, As(V), Ga, Co(II), Zn and for X' = As(V), P(V).

The mixed hpa with X = P(V) (Z = Ge, Sn) and X = As(V) (Z = Ge, Sn) have been detected but the occurence of secondary reactions at the pH of preparation prevents the formation of pure compounds. An indirect method has to be found for the preparation of these complexes.

The study of the acids, of the composition of the salts and of their crystallographic type leads to the conclusion that in XZW_{11} the anion XW_{11} acts as a pentadentate ligand towards Z(IV), the sixth coordination position being occupied by a OH^- ligand and to the general formulae of the anions:

$XGeW_{11}O_{39}(OH)^{(9-x)-}$ $\quad$ $X_2'GeW_{17}O_{61}(OH)^{(12-x)-}$

$XSnW_{11}O_{39}(OH)^{(9-x)-}$ $\quad$ $X_2'SnW_{17}O_{61}(OH)^{(12-x)-}$

where x stands for the oxidation state of the element X or X'.

Acknowledgements—This work is part of the Thesis of A. Schouten and was carried out in the Laboratoire de Chimie des Solides of the Université des Sciences et Techniques du Languedoc in Montpellier (France).

REFERENCES

[1]C. Tourne and G. Tourne, *Bull. Soc. Chim. Fr.* 1969, 1124.
[2]C. Tourne, *C. R. Acad. Sci. Paris*, 1968, **C266**, 702.
[3]C. Tourne and G. Tourne, *C. R. Acad. Sci. Paris* 1968, **C266**, 1363.
[4]C. Tourne, G. Tourne, S. A. Malik and T. J. R. Weakley, *J. Inorg. Nucl. Chem.* 1970, **32**, 3875.
[5]T. J. R. Weakley, H. T. Evans, J. S. Showell, G. Tourne and C. Tourne, *J. C. S. Chem. Comm.* 1973, 139.
[6]F. Zonnevijlle, Thesis Montpellier, 1976.
[7]M. Bauchet, C. Tourne and G. Tourne, *C. R. Acad. Sci. Paris* 1972, **C275**, 407.
[8]L. C. W. Baker and Th.P. McCutcheon, *J. Am. Chem. Soc.* 1956, **78**, 4503.
[9]L. C. W. Baker and V. E. Simmons, *J. Am. Chem. Soc.* 1959, **81**, 4744.
[10]A. Schouten and B. Cros, *C. R. Acad. Sci. Paris* 1981, **II 293**, 45.
[11]A. Schouten, Thesis Montpellier, 1980.
[12]F. Zonnevijlle and M. T. Pope, *J. Am. Chem. Soc.* 1979, **101**, 2731.
[13]W. H. Knoth, *J. Am. Chem. Soc.* 1979, **101**, 759.
[14]W. H. Knoth, *J. Am. Chem. Soc.* 1979, **101**, 2211.
[15]G. Salomon-Bertho, *C. R. Acad. Sci. Paris* 1975, **C280**, 1199.

Polyhedron Vol. 1, No. 3, pp. 289–298, 1982
Printed in Great Britain.

0277–5387/82/030289–10$03.00/0
Pergamon Press Ltd.

STRUCTURAL DEPENDENCIES OF PYRAMIDAL INVERSION AT SULPHUR AND SELENIUM IN THIO- AND SELENO- ETHER COMPLEXES OF PALLADIUM(II) AND PLATINUM(II)

A NUCLEAR MAGNETIC RESONANCE STUDY

E. W. ABEL, S. K. BHARGAVA, K. KITE, K. G. ORRELL,* V. ŠIK and B. L. WILLIAMS
Department of Chemistry, The University, Exeter EX4 4QD, England

(*Received* 17 *December* 1981)

Abstract—Total NMR band shape fitting methods have provided accurate energy data for inversion barriers at sulphur and selenium in complexes of types *cis*-$[MX_2L]$ (M = Pd^{II}, Pt^{II}; X = Cl, Br, I; L = $MeS(CH_2)_2SMe$, $MeS(CH_2)_3SMe$, o-$(SMe)_2C_6H_3Me$, *cis*-MeSCH=CHSMe) and $[PtXMe\{MeE(CH_2)_2E'Me\}]$ (E = E' = S or Se and E = S, E' = Se; X = Cl, Br, I). Barrier energies were found to decrease by 10–12 kJ mol^{-1} in going from aliphatic through aromatic to olefinic ligand back-bone. This can be explained in terms of $(3p-2p)\pi$ conjugation between the inverting centre and the ligand back-bone. The effects of ligand ring size, nature of halogen atom and the metal oxidation state on the barrier energies are discussed.

INTRODUCTION

The use of the NMR technique for studying sulphur inversion dates back to 1966 when Abel *et al.*[1] examined the Pt(II) chelate $[PtCl_2\{MeS(CH_2)_2SMe\}]$. Shortly afterwards, Haake and Turley[2,3] examined the effect of *trans* influence on inversion rates in complexes *cis* and *trans*-$[PtCl_2(SRR')_2]$ (R = Me, Et, Bz). More recently, Cross *et al.*[4–7] and Hunter *et al.*[8–10] have studied S, Se and Te inversion in a wide range of Pd(II) and Pt(II) complexes. Energy barriers to inversion were, in most cases, based only on coalescence temperature measurements in contrast to our own studies which utilised total band shape analysis. This method has been rigorously applied to the Pd(II) and Pt(II) complexes $[MX_2\{ER(CH_2SiMe)\}_2]$ (E = S, Se; R = CH_2SiMe_3, Me, Ph)[11,12] and $[MX_2\{S(CR_2)_n\}_2]$ (R = H and/or Me; n = 2–5).[13,14] Latterly, however, we have been examining chalcogen inversion in Pt(IV) complexes, in particular $[PtXMe_3\{MeE(CH_2)_nE'Me\}]$ (E = E' = S or Se, n = 2, 3)[15] and (E = S, E' = Se, n = 2, 3).[16] Since little is known about the influence of the oxidation state of platinum on the inversion rates of S and Se we have now prepared and examined Pt(II) complexes of general type $[PtXMe\{MeE(CH_2)_2EMe\}]$ (X = Cl, Br, I; E = S, Se, S/Se). Furthermore, in order to examine whether the chalcogen inversion rates depend on the electronic nature of the ligand back-bone, we have prepared the following complexes with aliphatic, aromatic and olefinic back-bones, *cis*-$[MX_2L]$(M = Pd(II), Pt(II); X = Cl, Br, I; L = $MeS(CH_2)_2SMe$, $MeS(CH_2)_3SMe$, o-$(SMe)_2C_6H_3Me$ and *cis*-MeSCH = CHSMe). Some of the complexes have been reported previously[4,5,17] but only limited inversion studies have been carried out. We report here accurate inversion energy data and discuss the major structural dependencies of these values.

EXPERIMENTAL

Materials. The ligands 1,3-bis(methylthio)propane, 1,2-bis(methylthio)ethane and *cis*-1,2-bis(methylthio)ethene were prepared by previously reported methods.[17] 3,4-Bis(methylthio)toluene was prepared by the methylation of toluene-3,4-dithiol (B.D.H.). 1,2-Bis(methylthio)benzene was isolated by the methylation of o-methylthiobenzene thiol.[18]

Preparations of complexes of the above ligands were based on standard general methods[19] with some improvements. A typical preparation was as follows. Potassium tetrachloroplatinate(II) (0.5 mmol) and the ligand (1.0 mmol) were refluxed in an ethanol/water (3:1) mixture for *ca.* 12 hr. The resulting precipitate was filtered, washed with water and ethanol, and further purified by recrystallisation from a suitable solvent depending on the ligand as follows: 3,4-bis(methylthio)toluene (dichloromethane or chloroform), 1,2-bis(methylthio)propane (acetonitrile), 1,2-bis(methylthio) ethane and 1,2-bis(methylthio)ethene (Soxhlet extraction using ethanol or dichloromethane as solvent).

The corresponding dibromide and diiodide complexes were prepared by refluxing the dichloride complex with lithium bromide or iodide in ethanolic solution.

The ligands 1,2-bis(methylseleno)ethane (b.p. 88°C/8 mmHg) and 1-methylthio-2-methylselenoethane (b.p. 82°C/10 mmHg) were prepared by literature methods.[20,16]

[*Chloro(methyl)* (η^4-1,5-*cyclooctadiene*)*platinum*(*II*)]. (m.p. 166–167°C) was prepared from [dimethyl(η^4-1,5-cyclooctadiene)platinum(II)].[21] The corresponding bromo- and iodo-complexes were obtained by adding excess of the appropriate potassium halide to an acetone solution of the chloro compound. Immediate precipitation was noted (white–bromide, yellow–iodide). After stirring for 1 hr, acetone was removed by rotary evaporation. The residue was collected on a frit, washed with distilled water followed by pentane and air dried (90–95°C) to give either white [*bromo*(*methyl*) (η^4-1,5-*cyclooctadiene*)*platinum*(*II*)], m.p. 170–171°C, or yellow [iodo(methyl) (η^4-1,5-cyclooctadiene)platinum(II)], m.p. 139–140°C.

The preparations of the complexes $[PtXMe\{MeE(CH_2)_2E'Me\}]$ were very similar, and only a representative method for one of the chloride complexes is given. An excess of 1-methylthio-2-methylseleno-ethane (0.1088 g; 0.64 mmol) in chloroform (3 cm^3) was added to a solution of [chloro(methyl) (η^4-1,5-cyclooctadiene)platinum(II)] (0.2114 g; 0.599 mmol) in chloroform (5 cm^3). After refluxing for 2 hr the solvent was removed. Recrystallisation from dichloromethane/hexane gave [*chloro*(*methyl*)(1 - *methylthio* - 2 - *methylselenoethane*)*platinum*(*II*)] as a pale yellow powder (0.141 g; 57%).

*Author to whom correspondence should be addressed.

Spectra. All ^1H NMR spectra (with one exception, see later) were recorded on a JEOL PS/PFT-100 spectrometer operating in the F.T. mode at 100 MHz. Complexes were studied in a variety of solvents (see later). A standard variable temperature unit was used to control the probe temperature. Temperatures were recorded immediately before and after running the spectra and were measured with a copper-constantan thermocouple with an accuracy of ≤1°C. Computer simulations of spectra were achieved with a program based on that of Binsch.[22]

RESULTS

Analytical data for the complexes are collected in Tables 1 and 2.

cis-[MX_2L] *complexes*

All these five and six membered ring complexes of palladium(II) and platinum(II) possess the same basic geometry and differ only in the ligand back-bone. At

Table 1. Characterisation of the *cis*-[MX_2L] complexes

No.	M	L	X	Colour	M.p/°C	Analysis*/% C	H
1	Pt	$MeSC_2H_4SMe$	Cl	Pale yellow	234	12.20 (12.35)	2.75 (2.60)
2			I	Yellow	242	8.50 (8.40)	1.65 (1.75)
3	Pt	$MeSC_2H_2SMe$	Cl	Yellow	208(d)	12.25 (12.40)	1.10 (1.10)
4			I	Dark yellow	189(d)	8.65 (8.45)	1.40 (1.40)
5	Pt	$o\text{-}(SMe)_2C_6H_3Me$	Cl	Yellow	230	23.85 (24.00)	2.50 (2.65)
6			Br	Orange-yellow	260(d)	20.30 (20.05)	2.10 (2.20)
7			I	Dark yellow	235(d)	17.35 (17.10)	1.80 (1.90)
8	Pt	$MeSC_3H_6SMe$	Cl	Pale yellow	239	14.80 (14.95)	2.95 (3.00)
9	Pd	$MeSC_2H_4SMe$	Cl	Dark yellow	242(d)	15.75 (16.00)	3.45 (3.35)
10			I	Purple	215(d)	10.00 (9.95)	2.00 (2.05)
11	Pd	$MeSC_2H_2SMe$	Cl	Light yellow	192	14.85 (16.05)	2.70 (2.70)
12			I	Dark red	175(d)	10.00 (10.00)	1.65 (1.65)
13	Pd	$o\text{-}(SMe)_2C_6H_3Me$	Cl	Yellow	240(d)	29.65 (29.80)	3.25 (3.30)
14			Br	Dark yellow	210(d)	23.90 (23.95)	2.55 (2.65)
15			I	Purple	195	19.90 (19.85)	2.05 (2.20)

*Calculated values in parentheses

(d) decomposes

Table 2. Characterisation of the *cis*-[PtXMeL] complexes

No.	L	X	Colour	M.p./°C	Analysis*/% C	H
16	$MeSC_2H_4SMe$	Cl	White	152 - 154	16.00 (16.35)	3.50 (3.55)
17		Br	Pale yellow	136 - 137	14.95 (14.55)	3.00 (3.15)
18		I	Yellow	133 - 135	12.90 (13.10)	2.70 (2.85)
19	$MeSeC_2H_4SeMe$	Cl	Light orange	144 - 146	12.85 (13.00)	2.80 (2.80)
20		Br	Orange	141 - 142	11.55 (12.20)	2.40 (2.65)
21		I	Dark orange	137 - 138	10.85 (11.15)	2.20 (2.40)
22	$MeSC_2H_4SeMe$	Cl	Pale yellow	139 - 140	14.55 (14.50)	3.10 (3.15)
23		Br	Pale yellow	144 - 146	13.25 (13.05)	2.80 (2.85)
24		I	Orange-yellow	132 - 133	11.60 (11.85)	2.45 (2.55)

*Calculated values in parentheses

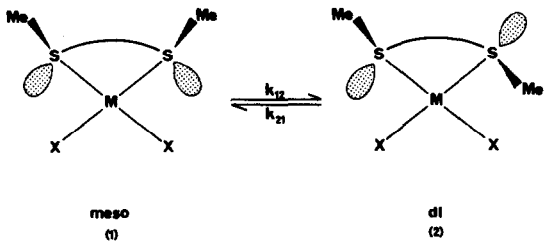

Fig. 1. Diastereoisomers of *cis*-[MX_2L] (L = homochalcogen ligands with aliphatic, aromatic or olefinic backbones) complexes.

ambient (Pt complexes) or lower temperatures (Pd complexes) the ^1H spectra were consistent with the presence of two diastereoisomers, *meso* and DL, generally in unequal abundances (Fig. 1) (Table 3). This is strikingly apparent in the 360 MHz spectrum of [PdI_2\{*o*-$(SMe)_2C_6H_3Me$\}] at −70°C (Fig. 2), where isomeric distinction is clearly observed in the -SMe, the -CMe and the three aromatic proton signals.

On warming the complexes in solution the spectra change in accord with an increasing rate of sulphur inversion such that at higher temperatures (*ca.* 60°C) time-averaged signals for the two isomers were observed. These changes were fully consistent with previous qualitative studies on certain of these complexes.[1,15,17] In order to evaluate the sulphur inversion barriers accurately in all the present complexes, we chose to study the band shape changes of the methyl and (where appropriate) olefinic protons. The spectra of [$PtCl_2$(MeSCH=CHSMe)] may be taken as typical (Fig. 3). At low temperatures the two olefinic signals for the *meso* and DL isomers (plus ^{195}Pt satellites) are clearly visible as sharp singlets. On raising the temperature, coalescence of the signals occurs, which is complete by *ca.* 60°C. Computation of the energy barrier for the inversion process was straightforwardly accomplished using the static parameters in Table 3 and the authors' version of the standard band shape program[22] for the spin problem

$$\underset{\text{(meso) (DL)}}{\underset{66.3\%}{A \rightleftharpoons B}} \qquad \underset{\text{(meso) (DL)}}{\underset{33.7\%}{AX \rightleftharpoons BX}} \qquad X = {}^{195}Pt$$

Table 3. Static parameters used in the computations of the SMe signals of *cis*[MX_2L] complexes

Complex No.	T/°C	Meso (syn) isomer			DL (anti) isomer			
		ν_A[a]/Hz	^3J(PtH)/Hz	p_1[b]	ν_B[a]/Hz	^3J(PtH)Hz	p_2[b]	T_2^*/s
1	54.0	271.7	48.3	0.44	259.6	49.3	0.56	0.320 0.240[c]
2	27.0	286.9	51.3	0.30	259.3	50.5	0.70	0.230
3	-11.3	287.4 679.0[d]	48.0 82.5	0.40 0.40	280.8 668.0	43.6 77.8	0.60 0.60	0.330 0.330
4	-25.8	296.4 654.8[d]	51.0 78.9	0.47 0.46	299.8 643.8	45.4 73.8	0.53 0.54	0.270 0.270
5	11.7	311.6 308.6	47.1 46.8	0.39 0.39	305.4 302.5	45.8 45.9	0.61 0.61	0.455[2]
6	-5.5	305.4 301.4	49.0 47.9	0.47 0.47	303.2 299.1	48.7 47.9	0.53 0.53	0.382 0.382
7	-38.6	315.2 312.6	48.3 48.7	0.50 0.50	312.6 310.3	48.7 49.2	0.50 0.50	0.286 0.208[c]
8	-1.9	270.0	45.4	0.49	262.9	48.1	0.51	0.180
9	1.8	266.4	-	0.50	259.3	-	0.50	0.340
10	-10.0	282.9	-	0.36	261.3	-	0.64	0.185
11	-32.8	284.4 672.4[d]	- -	0.23 0.23	275.5 662.6	- -	0.77 0.77	0.327 0.360
12	-74.0	310.8 694.0[d]	- -	0.32 0.32	317.1 683.9	- -	0.68 0.68	0.250 0.320
13	-36.2	304.7 302.5	- -	0.41 0.41	299.8 297.6	- -	0.59 0.59	0.509[e] 0.509[e]
14	-68.0	309.2 307.7	-	0.43 0.43	307.7 305.8	-	0.57 0.57	n n
15	-70.0	311.8 309.4	-	0.47 0.47	317.0 314.6		0.53 0.53	0.187[e] 0.187[e]

[a] Shifts measured at 100 MHz relative to Me_4Si

[b] Populations accurate to ± 0.005

[c] For ^{195}Pt satellite lines

[d] Olefinic protons

[e] Slightly temperature dependent

[n] Not measured

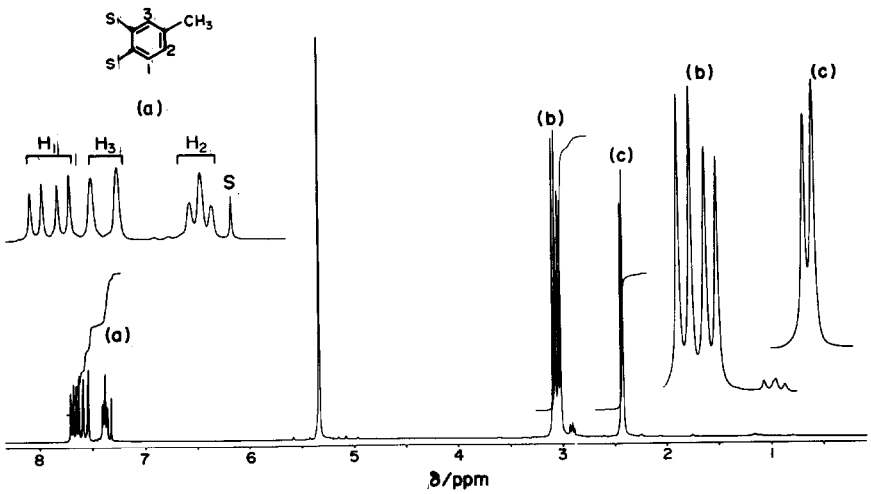

Fig. 2. 360 MHz ^{1}H spectrum at −70°C of $[PdI_2\{o\text{-}(SMe)_2C_6H_3Me\}]$ in CD_2Cl_2 showing isomeric distinction in (a) the aromatic, (b) the -SMe and (c) the -CMe regions. In the aromatic region $J_{12} = 7.5$ and $J_{23} \simeq 2$ Hz.

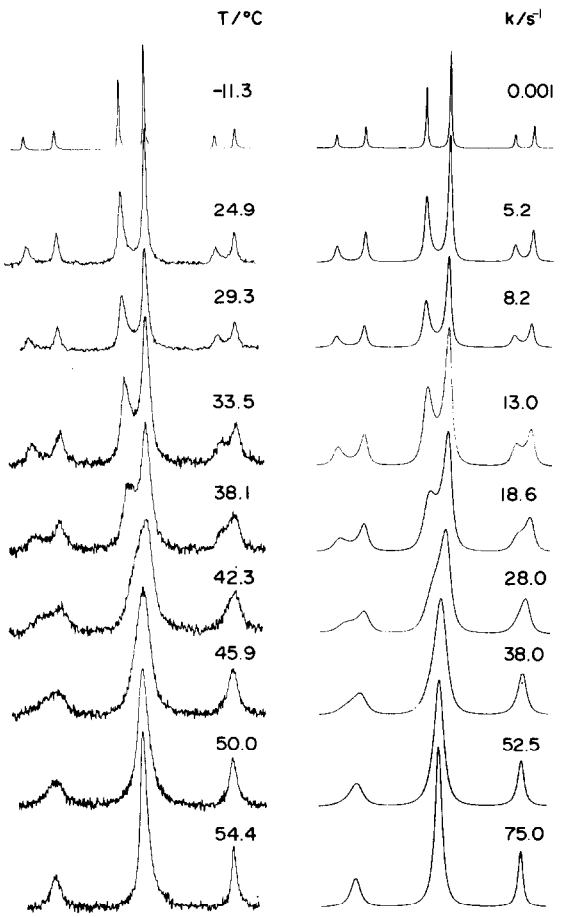

Fig. 3. Experimental and theoretical 100 MHz ^{1}H spectra of the olefinic region of $[PtCl_2(MeSCH{=}CHSMe)]$ showing the effects of pyramidal S inversion.

Activation parameters for the inversion process were calculated from the usual Arrhenius and Eyring plots (Fig. 4) and are reported in Table 4. The errors quoted are standard deviations, those for $\Delta G^{\ddagger}$ being quoted in the manner recommended by Binsch.[23] The energies are, in all cases, based on the rate constants k_{12} for the interconversion *meso* → DL. For the complexes with olefinic back-bone $[MX_2(MeSCH{=}CHSMe)]$, the band shape changes in both the SMe and -CH=CH- regions were computed. The two energies subsequently calculated were in excellent agreement (Table 4).

cis-[PtXMeL] complexes

In the complexes (L = $MeS(CH_2)_2SMe$ or $MeSe(CH_2)_2SeMe$) the chalcogen atoms are centres of chirality and thus, in the absence of any internal exchange process, two diastereoisomers may exist, one with *syn* chalcogen methyls and the other with *anti* chalcogen methyls (Fig. 5). At low temperatures (*ca.* −60°C) the spectra showed the presence of both isomers in solution, the more abundant species being attributed to the *anti* conformation (Table 5). Taking the complex $[PtClMe\{MeS(CH_2)_2SMe\}]$ as a representative case, the -SMe region exhibited four signals (plus ^{195}Pt satellites) at *ca.* −50°C whereas the methylene region was predictably complex. Two PtMe signals (plus ^{195}Pt satellites) were observed at lower frequencies. Chemical shift and coupling constant data for this and the other complexes have been collected in Table 5. On warming the sample, band broadening commenced and by *ca.* 20°C bands had coalesced and sharpened again to reveal two averaged SMe signals (one each for the SMe groups *trans* to the halogen and methyl groups) and one averaged PtMe signal. The methylene region absorption was still very complex and was not analysed. On heating the complex to its decomposition point, *ca.* 160°C, no further spectral changes were observed. Throughout this temperature range, −60°C to 160°C, ^{195}Pt-H coupling was retained, confirming the absence of any ligand dissociation.

In these complexes, in contrast to the complexes $[PtX_2\{MeS(CH_2)_2SMe\}]$, sulphur pyramidal inversion can proceed via two different transition states depending on whether the chalcogen *trans* to methyl (E_1) or *trans* to chalcogen (E_2) inverts (Fig. 5). Since there are only two chemically distinct species *syn* and *anti*, NMR will not be able to distinguish between these two inversion pathways. If, however, the two inversion barrier energies are substantially different (see later), the spectra will be

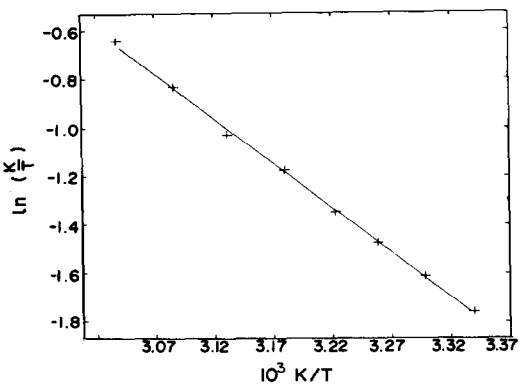

Fig. 4. Eyring plot for the olefinic band fittings of [$PtCl_2$(MeSCH=CHSMe)].

sensitive only to the lower energy process. Studies on [PtX_2{$MeS(CH_2)_2SMe$}] demonstrated band coalescences at *ca.* 100°C as a result of independent inversion of each sulphur atom. The much lower coalescences (*ca.* 0°C) in the [PtXMe{$MeS(CH_2)_2SMe$}] complexes imply that the spectral changes here are a consequence of inversion at sulphur *trans* to methyl (E_1 in Fig. 5) and are totally insensitive to the (presumably) higher energy inversion of the sulphur *trans* to halogen. Energy barriers for the former process were computed in the usual way and the data are reported in Table 6.

Complexes of this type involving mixed S/Se ligands, e.g. [PtXMe{$MeS(CH_2)_2SeMe$}], can exist as two geometrical isomers each of which occurs as a diastereoisomeric DL pair (Fig. 6). Interconversion between these DL pairs takes place by pyramidal inversion at either the sulphur or the selenium atoms. At low temperatures (*ca.* −50°C) the ^1H spectra clearly indicated the presence of all four DL isomers in unequal abundances (Complexes 22–24, Table 5). The variable temperature spectra of the complex (X = Br) are illustrated in Fig. 7. The line assignments in the lowest temperature spectrum follow the methyl labelling in Fig. 6 and are based on careful comparisons with the corresponding homochalcogen complexes. On raising the temperature of the sample, the expected band broadenings and coalescences occurred as the rates of pyramidal inversion at the chalcogen atoms increased. We show later that this may be ascribed to inversion at sulphur and selenium atoms *trans* to the Pt–Me group. In the spectra shown in Fig. 7, sulphur inversion has become rapid at 32.8°C and both sulphur and selenium inversions are rapid at 131.8°C. Total band shape analyses were not preformed on the spectra of these mixed chalcogen ligand complexes since the spectral changes were predictably more complex than for the homochalcogen complexes and did not war-

Table 4. Arrhenius and Eyring parameters for sulphur inversion[a] in *cis*-[MX_2L] complexes

No.	Solvent	T_c[b]/K	E_a/kJ mol^{-1}	$\log_{10}$ A	$\Delta H^{\ddagger}$/kJ mol^{-1}	$\Delta S^{\ddagger}$/JK^{-1} mol^{-1}	$\Delta G^{\ddagger}$(298.15K)/kJ mol^{-1}
1	$(CD_3)_2SO$	382	84.3 ± 0.5	13.3 ± 0.1	81.1 ± 0.5	-0.9 ± 1.3	81.40 ± 0.11
2	$(CD_3)_2SO$	361	77.2 ± 1.4	13.1 ± 0.2	74.3 ± 1.4	-3.4 ± 4.1	75.25 ± 0.24
3	CD_3CN	314	70.9 ± 0.9	13.2 ± 0.2	68.4 ± 0.9	-0.6 ± 3.0	68.61 ± 0.01
		319[c]	73.1 ± 0.9	13.5 ± 0.2	70.5 ± 0.9	5.5 ± 3.0	68.82 ± 0.04
4	CD_3CN	276	68.3 ± 1.1	13.8 ± 0.2	66.0 ± 1.1	10.5 ± 4.0	62.88 ± 0.08
		285[c]	66.3 ± 1.1	13.4 ± 0.2	63.9 ± 1.1	4.2 ± 3.9	62.76 ± 0.08
5	$CDCl_3$	320	74.7 ± 1.8	13.4 ± 0.3	72.0 ± 1.8	2.4 ± 5.7	71.29 ± 0.13
7	CD_2Cl_2	283					63.9 ± 0.5[d]
8	$(CD_3)_2SO$	295	68.8 ± 0.5	13.3 ± 0.1	66.3 ± 0.5	2.3 ± 1.6	65.61 ± 0.07
9	CD_3CN	320	74.5 ± 0.6	13.5 ± 0.1	71.9 ± 0.6	5.7 ± 2.0	70.24 ± 0.01
10	CD_3CN	293	72.0 ± 0.3	14.7 ± 0.05	69.7 ± 0.3	29.5 ± 1.0	60.88 ± 0.01
11	CD_3CN	269	60.3 ± 0.3	13.1 ± 0.1	58.1 ± 0.3	-0.7 ± 1.3	58.29 ± 0.01
		274[c]	60.7 ± 0.8	13.2 ± 0.2	58.4 ± 0.8	0.5 ± 3.0	58.28 ± 0.09
12	$(CD_3)_2SO$	228	53.0 ± 0.5	13.5 ± 0.1	51.1 ± 0.5	7.8 ± 0.2	48.73 ± 0.15
		230[c]	52.9 ± 0.6	13.5 ± 0.1	51.0 ± 0.6	7.3 ± 2.7	48.78 ± 0.18
13	CD_2Cl_2	269	66.0 ± 1.1	13.9 ± 0.2	63.8 ± 1.1	14.3 ± 4.1	59.50 ± 0.12
15	CD_2Cl_2	228	51.1 ± 1.5	12.9 ± 0.3	49.1 ± 1.5	-3.9 ± 6.5	50.3 ± 0.40

[a] Energy data derived from SMe region signals except where stated

[b] Coalescence temperature for SMe signals

[c] Coalescence temperature and associated energy data for olefinic proton signals

[d] Value based on a single fitting at 230.0 K

Table 5. *Static parameters for the complexes* [PtXMe{MeE$(CH_2)_2$E'Me}]

Complex No	T/°C	Solvent	Meso(syn) isomer							DL(anti) isomer						
			Pt-Me		E-Me				p^d	Pt-Me		E-Me				p^d
			ν^a	$^2J^b$	ν(trans Me)	$^3J^c$	ν(trans X)	^3J		ν	^2J	ν(trans Me)	^3J	ν(trans X)	^3J	
16	-49.8	CD_2Cl_2	62.9	71.9	262.9	18.2	261.6	74.0	0.33	70.1	71.4	238.6	19.0	248.0	73.1	0.67
17	-62.0	CD_2Cl_2	68.8	72.5	265.1	18.7	262.2	74.7	n	76.0	71.5	238.5	19.5	248.2	74.0	n
18	-50.9	CD_2Cl_2	79.8	73.0	266.8	20.5	262.0	71.8	0.31	87.2	72.5	238.3	21.0	244.6	71.3	0.69
19	-3.2	$CDCl_3$	82.5	70.8	250.2	15.1	248.3	59.8	0.43	90.1	70.6	230.2	15.6	237.3	59.1	0.57
20	-1.5	$CDCl_3$	87.9	71.5	250.0	15.9	250.0	60.1	n	95.5	71.0	230.2	16.1	237.8	59.8	n
21	-1.5	$CDCl_3$	100.1	73.0	252.4	16.6	250.2	61.0	0.39	107.2	72.5	230.2	17.1	235.6	56.6	0.61
22	-62.3	CD_2Cl_2	62.3[e]	70.1	263.9	17.8	247.8	61.1	0.14	69.6	70.3	236.6	18.6	236.1	60.5	0.26
			67.9[e]	73.2	245.4	15.1	262.0	73.3	0.23	75.9	72.5	225.1	16.1	246.6	73.0	0.37
23	-47.0	CD_2Cl_2	70.3[e]	70.6	266.2	18.3	249.0	61.9	0.14	77.1	70.3	237.2	19.8	235.8	61.0	0.25
			75.0	73.4	245.5	15.5	262.0	72.9	0.24	83.0	72.5	224.7	15.9	245.5	72.5	0.37
24	-62.0	CD_2Cl_2	81.7[e]	71.8	269.7	n	263.1	n	n	88.5	71.9	236.7	19.8	243.5	71.3	n
			84.2[e]	73.9	245.7	15.3	262.0	n	n	92.8	73.2	223.4	17.1	243.5	n	n

[a] Chemical shifts ν/Hz measured at 100 MHz relative to Me_3Si.

[b] $^2J_{(Pt\text{-}C\text{-}H)}$/Hz

[c] $^3J_{(Pt\text{-}E\text{-}C\text{-}H)}$/Hz

[d] Isomer populations

[e] In these mixed chalcogen ligand complexes there are two distinct syn(DL-1,4) isomers and two distinct anti(DL-2,3) isomers (Fig. 6).

n Not calculated

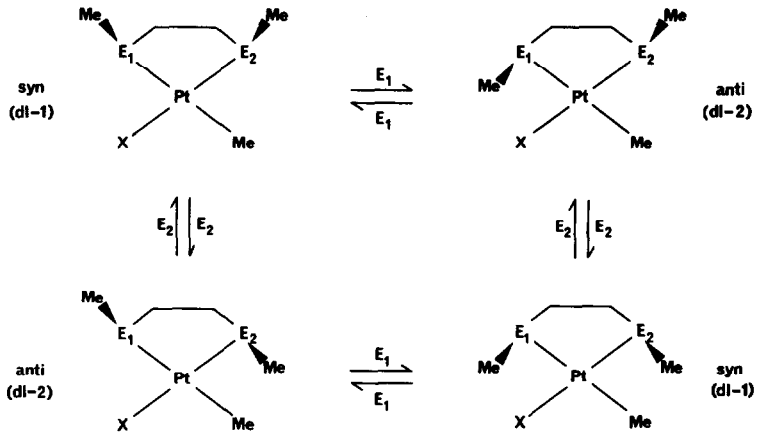

Fig. 5. Diastereoisomers of *cis*-[PtXMe{MeE(CH$_2$)$_2$EMe}] complexes showing the two possible E inversion pathways.

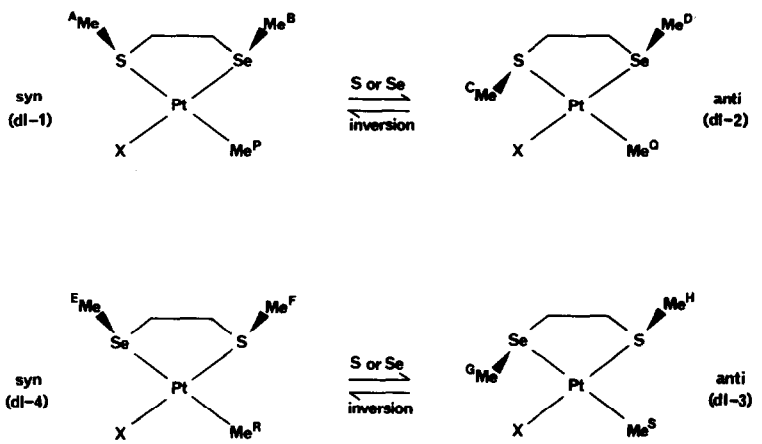

Fig. 6. Structural and diastereoisomers of [PtXMe{MeS(CH$_2$)$_2$SeMe}]. Only one of each DL pair is depicted.

Table 6. Energy parameters for the complexes [PtXMe{MeE(CH$_2$)$_2$Me}]

Complex No.	Complex	E_a/kJ mol^{-1}	$\log_{10}$ A	$\Delta H^{\ddagger}$/kJ mol^{-1}	$\Delta S^{\ddagger}$/J K^{-1}mol^{-1}	$\Delta G^{\ddagger}$/kJ mol^{-1}
16	[PtClMe{MeS(CH$_2$)$_2$SMe}]	61.9 ± 3.9	13.2 ± 0.8	59.7 ± 3.9	-0.2 ± 14.7	59.8 ± 0.5
18	[PtIMe{MeS(CH$_2$)$_2$SMe}]	60.3 ± 2.9	13.0 ± 0.6	58.1 ± 2.9	-3.4 ± 11.2	59.2 ± 0.5
19	[PtClMe{MeSe(CH$_2$)$_2$SeMe}]	66.0 ± 3.8	12.0 ± 0.6	63.3 ± 3.8	-24.6 ± 12.0	70.7 ± 0.2

rant the considerable computational efforts that would have been involved.

No further significant spectral changes were noted on heating these mixed chalcogen ligand complexes to their decomposition points. It thus appears that other fluxional rearrangements so characteristic of the Pt(IV) complexes of type [PtXMe$_3${MeE(CH$_2$)$_2$E'Me}][16] are absent in the Pt(II) complexes of type [PtXMeL].

DISCUSSION

Static NMR parameters

Considering first the [MX$_2$L] complexes (Table 3), the chemical shift assignments are based on the lower populated isomer being the *meso* form due to steric factors. On this assumption the SMe protons in this isomer appear at somewhat higher frequencies than their position in the DL isomer in most cases. A change in halogen

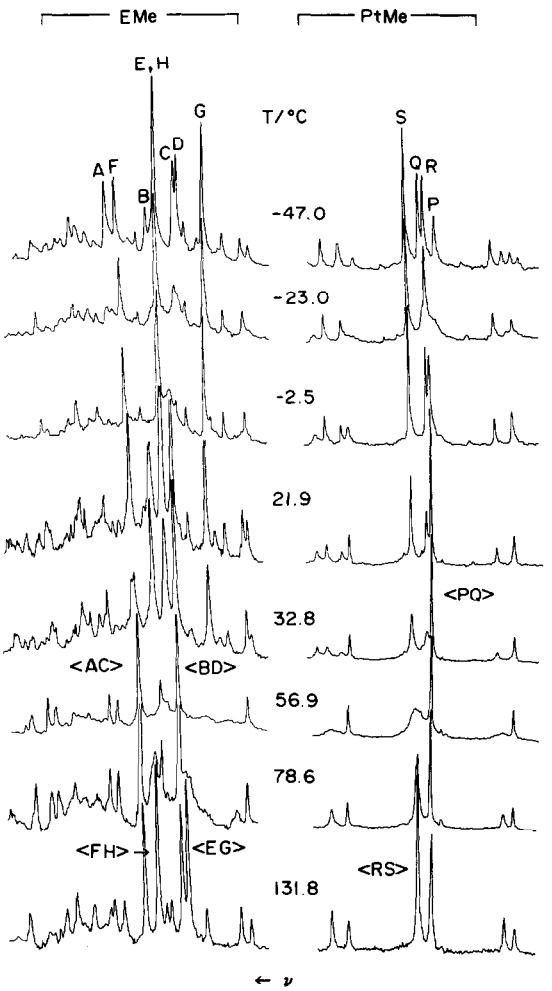

Fig. 7. Variable temperature 100 MHz H spectra of [PtBrMe{MeS(CH$_2$)$_2$SeMe}]. Lowest temperature lines are labelled according to Fig. 6. In the higher temperature spectra the labelling (AC), etc represents the shift of the averaged A and C signals, etc.

from Cl to I favours the *meso* isomer in the unsaturated ligand complexes but favours the DL form in the cases of saturated ligands. In all cases, however, sizeable high frequency shifts of the SMe protons occur. This is particularly apparent in the olefinic ligand complexes (Nos. 3, 4; 11, 12) where the DL isomer signals experience such large high frequency shifts that they occur at higher frequencies than the *meso* signals. The magnitude of the ^{3}J (PtH) coupling constants are also halogen dependent, increasing with halogen size for the SMe protons and decreasing for the olefinic protons. The higher values of ^{3}J(PtH) coupling for the olefinic protons (74–83 Hz) compared to the SMe protons (45–51 Hz) may be ascribed to the greater s character of the olefinic carbons compared to the methyl carbons.

In the case of the [PtMeXL] complexes, certain striking differences in the static parameters compared to those of [PtX$_2$L] complexes are apparent. For instance, ^{3}J(PtH) values for SMe protons *trans* to halogen lie in the range 56–75 Hz but, for these protons *trans* to methyl, values in the range 15–18 Hz were detected. This illustrates the large difference in the *trans* influence[24] of halogen and methyl groups. The ^{2}J(PtMe) values in the range 70–74 Hz are somewhat lower than those predicted from results obtained for the mononuclear complexes [PtMe$_3$X{MeE(CH$_2$)$_2$EMe}] in which the J values for Pt–Me *trans* to E–Me are of the order of 69–71 Hz. Now the magnitudes of coupling constants may, to a first approximation, often be related to the magnitude of the Fermi contact term, i.e. to the amount of *s* character in the bond. Oxidation from platinum(II) to platinum(IV) implies a change in hybridisation of platinum orbitals from dsp^2 to sp^3d^2 and a consequent reduction in the magnitude of ^{2}J(PtMe) values in platinum(IV) complexes to two thirds their values in the corresponding platinum(II) complexes. The fact that this was not observed here suggests that the above simple theoretical model is inadequate in this case.

Pyramidal inversion energies

These are listed in Tables 4 and 6. For the *cis*[MX$_2$L] (L = homochalcogen ligands) complexes, only one pyramidal inversion pathway is possible (Fig. 1). For the *cis*-[PtXMeL] (L = MeE(CH$_2$)$_2$EMe) complexes (Fig. 5) the energies calculated are lower by *ca.* 15–20 kJ mol^{-1} compared to the [MX$_2$L] complexes and are therefore attributed to inversion of the chalcogen *trans* to the methyl group rather than that *trans* to the halogen. This lowering of energy again reflects the different *trans* influences of halogen and methyl groups.

No inversion energies were calculated for the *cis*-[PtMeX{MeS(CH$_2$)$_2$SeMe}] complexes for reasons mentioned earlier. The spectral changes, however, can be qualitatively interpreted to give a relative ordering of the various possible inversion pathways (Fig. 6). There are four such pathways depending on whether inversion involves S or Se atoms situated either *trans* to X or *trans* to methyl. We have shown in earlier work on platinum(IV) systems[15], that, in general, S inversion occurs more readily than Se inversion (the energy difference is *ca.* 10 kJ mol^{-1}). In the present work we have shown that the strong *trans* influence of Me lowers the S inversion barrier by *ca.* 15–20 kJ mol^{-1}. Moreover, a ΔG^+ value of 70 kJ mol^{-1} has been calculated for Se inversion *trans* to methyl (Complex No. 19) whereas inversion at Se *trans* to halogen, as in the complexes [PtX$_2${MeSe(CH$_2$)$_2$SeMe}], was too slow to be measured by DNMR methods. In the complex [PtXMe{MeS(CH$_2$)$_2$SeMe}] we can therefore predict that the relative order of inversion energies will be S(*trans* Me) (~60 kJ mol^{-1}) < Se(*trans* Me) (~70 kJ mol^{-1} < S(*trans* X) (~75–80 kJ mol^{-1}) < Se(*trans* X) (~85–90 kJ mol^{-1}). The two coalescence phenomena at *ca.* 0° and 60°C observed in Fig. 7 can therefore be attributed with some certainty to inversion at S *trans* to methyl and at Se *trans* to methyl respectively.

(i) *Variation in metal.* The change of metal from Pt to Pd in the complexes [MX$_2$L] produces a decrease in the S inversion barrier of 10–15 kJ mol^{-1}. This trend, which has been observed previously,[11–13] may be explained in terms of the greater strength of the Pt–S bond compared with the Pd–S bond.

(ii) *Variation in metal oxidation state.* Since we have shown that in the complexes [PtXMeL] pyramidal inversion occurs at chalcogens *trans* to Me, these systems are well suited for comparison with the trimethylplatinum(IV) complexes [PtXMe$_3$\{MeE(CH$_2$)$_2$EMe\}][15]. Comparison of ΔG^+ values of the appropriate complexes reveals a consistent increase of the chalcogen barrier of 1.5–4.5 kJ mol^{-1} on going from platinum(II) to

platinum(IV). This trend, which may be primarily associated with a slight increase in platinum-chalcogen bond strength on oxidation from platinum(II) to platinum(IV), parallels that found for the complexes $[PtX_2\{MeS(CH_2)_2SMe\}]$ and $[PtX_4\{MeS(CH_2)_2SMe\}]$.[25]

(iii) *Variation of halogen.* The effects of the difference in *trans* influence between halogens and methyl groups have been discussed already. The relative *trans* influences of the three halogens themselves are reflected in the energy data in Table 4 for the *cis*$[MX_2L]$ complexes. When M = Pt(II) the energy barriers ($\Delta G^{\ddagger}$ values) show a consistent decrease by 6–7 kJ mol^{-1} from chloro to iodo complexes. When M = Pd(II) the decrease is by 9–10 kJ mol^{-1}. The relative order of $\Delta G^{\ddagger}$ values, namely X = Cl > Br > I is in accord with increasing *trans* influence, and a concomitant weakening of the M–S bonds.

(iv) *Variation in ligand ring size.* A comparison of the $\Delta G^{\ddagger}$ values of $[PtCl_2\{MeS(CH_2)_2SMe\}]$ and $[PtCl_2\{MeS(CH_2)_3SMe\}]$ in Table 4 shows a large decrease of *ca.* 16 kJ mol^{-1} as the heterocyclic ring increases from five to six members. This trend is in keeping with that found for inverting nitrogen atoms in various sized rings,[26] but differs somewhat from our earlier albeit not strictly analogous study[1] of the complexes *trans* $[MX_2\{S(CR_2)_n\}_2]$ (M = Pd(II), Pt(II), n = 2–5). Here sulphur inversion energies in the five and six-membered rings (n = 4, 5) were virtually the same and essentially no different from those of open-chain sulphide complexes. It is of interest to note that in the platinum(IV) complexes,[15] increasing the ring size from five to six caused a lowering of $\Delta G^{\ddagger}$ of 5–6 kJ mol^{-1}.

(v) *Variation in ligand back-bone.* The effect of varying the ligand back-bone from aliphatic to aromatic to olefinic produced consistent trends in both platinum and palladium complexes. The change aliphatic→aromatic (e.g. complexes 1→5 or 9→13, Table 4) caused a lowering of the S inversion barrier of 10–11 kJ mol^{-1}, whereas the change aromatic→olefinic (e.g. complexes 5→3 or 13→11, Table 4) caused a further lowering of 1–2 kJ mol^{-1}. These decreases in barrier height are clear examples of $(3p–2p)\pi$ conjugation effects between the chalcogen lone pair and the ligand back-bone, such interactions being more effective in the planar transition state than in the pyramidal ground state. These effects have already been observed in the case of Group VA elements.[27] The results are consistent with those of Mislow *et al.*[28,29] for phosphorus and arsenic inversion. In the former case replacement of an alkyl by an aryl group in acyclic dialkylarylphosphines lowers the phosphorus inversion barrier by *ca.* 9 kJ mol^{-1} due to $(3p–2p)\pi$ delocalisation.

Additional data supporting $(3p–2p)\pi$ conjugation effects have been obtained from appropriate complexes in the platinum(IV) series. For example, $\Delta G^{\ddagger}$ values for S inversion in the complexes $[PtClMe_3\{MeS(CH_2)_2SMe\}]$, $[PtClMe_3\{o\text{-}MeS(C_6H_4)SMe\}]$, and $[PtClMe_3\{MeSCH{=}CHSMe\}]$ are 63.3[15], 52.2[16] and 50.5[30] kJ mol^{-1} respectively. Similar trends will also be reported in rhenium(I) carbonyl complexes.[31]

FLUXIONAL REARRANGEMENTS

Since no further spectral changes occurred after pyramidal inversions became fast on the NMR time scale, it is apparent that the 180° ligand rotation movement ("pancake flip") we proposed for the mononuclear platinum(IV) complexes is *not* taking place in these platinum(II) complexes. Such a movement would only be observable in the [PtXMeL] complexes by virtue of their lower symmetry compared to the $[MX_2L]$ complexes. Its absence, however, in these former complexes in the temperature range studied calls for some explanation. In the Pt^{IV} complexes it would appear that the "pancake flip" mechanism requires inversion at *both* chalcogen atoms to be rapid in NMR terms before the fluxion can operate. In the complexes $[PtXMe\{MeE(CH_2)_2E'Me\}]$ (E = E' and E = S, E' = Se) the "pancake flip" mechanism would be expected to interchange the resonances due to EMe(*trans* X) and EMe(*trans* Me). In the particular case of $[PtBrMe\{MeS(CH_2)_2SeMe\}]$, for example, (Fig. 7), the fluxion would interconvert the two geometrical isomers and so produce averagings of the inversion-averaged S-methyls ⟨AC⟩ and ⟨FH⟩, the Se-methyls ⟨BD⟩ and ⟨EG⟩, and the Pt-methyls ⟨PQ⟩ and ⟨RS⟩. This was *not* observed at temperatures below decomposition, which suggests that the inversions at either or both E atoms *trans* to X (most likely Se *trans* X) were too slow to initiate the "pancake flipping".

The nature of the transient intermediates almost certainly has a strong influence on the ease of the fluxional motion. For platinum(II) complexes, the motion will involve a change from four to pseudo-six coordination at the metal, whereas the corresponding mechanism for platinum(IV) complexes requires a change in coordination number from six to pseudo-eight. This a proportionally smaller change in coordination but almost certainly other factors concerning the stabilities of the ground and transition states of these species will be important in finally determining the ease of the fluxional rearrangements in these complexes.

Acknowledgements—We thank the Commonwealth Scholarship Commission, U.K. and the University Grants Commission, India, for generous support (to S.K.B.). We thank the S.E.R.C. for use of the Edinburgh University 360 MHz NMR Service.

REFERENCES

[1]E. W. Abel, R. P. Bush, F. J. Hopton and C. R. Jenkins, *J. Chem. Soc. Chem. Commun.* 1966, 58.
[2]P. Haake and P. C. Turley, *J. Am. Chem. Soc.* 1967, **89**, 4611.
[3]P. C. Turley and P. Haake, *J. Am. Chem. Soc.* 1967, **89**, 4617.
[4]R. J. Cross and R. Wardle, *J. Chem. Soc. (A)* 1970, 840.
[5]R. J. Cross, I. G. Dalgleish, G. S. Smith and R. Wardle, *J. Chem. Soc., Dalton Trans.* 1972, 992.
[6]R. J. Cross, T. H. Green and R. Keat, *J. Chem. Soc., Dalton Trans.* 1976, 1150.
[7]R. J. Cross, T. H. Green, R. Keat and J. F. Paterson, *J. Chem. Soc., Dalton Trans.* 1976, 1486.
[8]G. Hunter and R. C. Massey, *J. Chem. Soc., Chem. Commun.* 1973, 797.
9. G. Hunter and R. C. Massey, *J. Chem. Soc., Dalton Trans.* 1976, 2007.
[10]J. C. Barnes, G. Hunter and M. W. Lown, *J. Chem. Soc., Dalton Trans.* 1976, 1227.
[11]E. W. Abel, G. W. Farrow, K. G. Orrell and V. Šik, *J. Chem. Soc. Dalton Trans.* 1977, 42.
[12]E. W. Abel, A. K. S. Ahmed, G. W. Farrow, K. G. Orrell and V. Šik, *J. Chem. Soc. Dalton Trans.* 1977, 47.
[13]E. W. Abel, M. Booth and K. G. Orrell, *J. Chem. Soc., Dalton Trans.* 1979, 1994.
[14]E. W. Abel, M. Booth and K. G. Orrell, *J. Chem. Soc., Dalton Trans.* 1980, 1582.
[15]E. W. Abel, A. R. Khan, K. Kite, K. G. Orrell and V. Šik, *J. Chem. Soc., Dalton Trans.* 1980, 1175.
[16]E. W. Abel, S. K. Bhargava, K. Kite, K. G. Orrell, V. Šik and B. L. Williams, *J. Chem. Soc. Dalton Trans.*, 1982, 583.

[17]F. R. Hartley, S. G. Murray, W. Levason, H. E. Soutter and C. A. McAuliffe, *Inorg. Chim. Acta* 1979, **35**, 265.
[18]S. E. Livingstone, *J. Chem. Soc.* 1956, 437.
[19]G. T. Morgan and W. Ledbury, *J. Chem. Soc.* 1922, 2882.
[20]E. E. Aynsley, N. N. Greenwood and J. B. Leach, *Chem. Ind. (London)* 1966, 379.
[21]H. C. Clark and L. E. Manzer, *J. Organomet. Chem.* 1973, **59**, 411.
[22]D. A. Kleier and G. Binsch, DNMR3 Program 165, *Quantum Chemistry Program Exchange.* Indiana University, 1970.
[23]G. Binsch and H. Kessler, *Angew. Chemie (Int. Edn)* 1980, **19** 411.
[24]T. G. Appleton, H. C. Clark and L. E. Manzer, *Coord. Chem. Rev.* 1973, **10**, 335.
[25]D. J. Gulliver, W. Levason, S. G. Murray, K. G. Smith and M. J. Selwood, *J. Chem. Soc. Dalton Trans.* 1980, 1872.
[26]J. B. Lambert, *Topics Stereochem.* 1971, **6**, 19.
[27]A. Rauk, L. C. Allen and K. Mislow, *Angew. Chem. (Int. Edn)* 1970, **9**, 400.
[28]W. Egan, R. Tang, G. Zon and K. Mislow, *J. Am. Chem. Soc.* 1971, **93**, 6205.
[29]R. H. Bowman and K. Mislow, *J. Am. Chem. Soc.* 1972, **94**, 2861.
[30]E. W. Abel, S. K. Bhargava, K. G. Orrell and V. Sik, to be published.
[31]E. W. Abel, S. K. Bhargava, M. M. Bhatti, K. Kite, M. A. Mazid, V. Šik, B. L. Williams, M. B. Hursthouse and K. M. A. Malik, *J. Chem. Soc., Dalton Trans.* 1982.

Polyhedron Vol. 1, No. 3, pp. 299–302, 1982
Printed in Great Britain.

0277-5387/82/030299-04$03.00/0
Pergamon Press Ltd.

COPPER(I) PHOSPHINE HYDROBORATE COMPLEXES: A STUDY INVOLVING HYDROBORATES CONTAINING A B–O BOND

P. G. EGAN and K. W. MORSE*
Department of Chemistry and Biochemistry, Utah State University, Logan, UT 84322, U.S.A.

(*Received* 24 *December* 1981)

Abstract—A study was made of the reactions between chloro*tris*(methyldiphenylphosphine)copper(I) and several hydroborates containing a boron-oxygen bond. The new complex ((acetoxy)trihydroborato)*tris*(methyldiphenylphosphine)copper(I) $(Ph_2MeP)_3CuH_3B(O_2CCH_3)$ was isolated and characterized by analysis, IR, and NMR data. Analogous reaction conditions using $HB(OR)_3^-$ anions did not give a B–H containing product nor did several other anions of the general type HBR_3^-. The ability of the hydroborate to complex is related to the Lewis acidity of the respective borane attached to H^-.

INTRODUCTION

A variety of complexes have resulted from the studies of hydroborate complexes of copper(I).[1–4] Interest in these complexes has been centred on the various bonding modes assumed by the hydroborate moiety[1–5] as well as the selective reducing capability exhibited by these complexes.[6] How various phosphine and phosphite ligands have influenced the former characteristics has been determined.[2,3] Also ascertained have been the bonding modes and various bond strengths of several hydroborates including tetrahydroborate, (ethoxycarbonyl)trihydroborate, (methoxycarbonyl)trihydroborate, and (carboxy)trihydroborate.[3] The latter complexes contain boron attached to only hydrogen and carbon. To our knowledge no hydroborate containing a B–O bond has been incorporated into a copper(I) complex analogous to those listed above. We wished to examine the effect this bond linkage might have on the ability of the hydroborate to coordinate to copper(I) phosphine complexes. In addition, the series of anions $H_3BO_2CCH_3^-$, $H_2B(O_2CCH_3)_2^-$ and $HB(O_2CCH_3)_3^-$[7–9] had been reported in the literature and we anticipated the possibility that the copper complexes of this series might afford a stepwise comparison of hydroborate complexes containing three, two, and one B–H respectively. We report the reactions of B–O containing hydroborate salts with $(Ph_2MeP)_3CuCl$ and the synthesis and characterization of the new complex ((acetoxy)-trihydroborato) *tris* (methyldiphenylphosphine)copper(I), $[CH_3(C_6H_5)_2P]_3CuH_3BO_2CCH_3$.

RESULTS

The general reaction studied was that used for the synthesis of copper(I) hydroborates:[1–4]

$$(Ph_2MeP)_3CuX + NaH_{4-n}BR_n \rightarrow (Ph_2MeP)_3CuH_{4-n}BR_n + NaX.$$

The reaction in which R = OCH_3, OPr^i did not give a B–H containing product as indicated by IR. The reaction in which R = acetoxy required more rigorous conditions than usually employed in making copper(I) hydroborate complexes since the mixture had to be refluxed for 24 hr and crown ether was required to solubilize the sodium salt reactant. In addition, rigorously anhydrous conditions must be used. However, these reaction conditions gave a compound which analysis, IR and NMR data indicated to be $(Ph_2MeP)_3CuH_3BO_2CCH_3$. We were unable to synthesize the $H_2B(O_2CCH_3)_2^-$ anion, a result substantiated by a recent report by Hiu.[8] However, the reaction using the $HB(O_2CCH_3)_3^-$ anion was studied using conditions analogous to that for the (acetoxy)trihydroborate, and no reaction was detected.

Characterization of $(Ph_2MeP)_3CuH_3BO_2CCH_3$

Analysis. Analysis supports the formulation shown, which is analogous to that found for the methyldiphenylphosphine copper complex of tetrahydroborate thereby suggesting the presence of a singly bridged M–H–B linkage since the latter complex was found using neutron diffraction techniques to have such a singly bridged M–H–B bond.[5]

IR spectra

IR data also support the proposed structure since the IR absorptions show coordination of the hydroborate moiety. Characteristic absorptions are seen in the B–H stretching region and in the carbonyl region (Table 1). Sodium (acetoxy)trihydroborate, prepared by the method of Gribble and Ferguson,[7] shows three absorptions in the B–H stretching region at 2500, 2225, and 2290 cm^{-1}. Potassium tetrahydroborate and potassium (ethoxycarbonyl)trihydroborate show B–H absorptions at 2260 cm^{-1} and 2320 cm^{-1}, respectively.[3b] The frequency shift of the B–H absorption of potassium (ethoxycarbonyl)trihydroborate compared to the analogous absorption in potassium tetrahydroborate was rationalized as being due to the decreased negative charge on the boron caused by the electron withdrawing effect of the ethoxycarbonyl group. It would be expected that a similar effect would be observed with sodium (acetoxy)trihydroborate only to a greater degree since the OC=O group with the oxygen bonded directly to the boron would be expected to result in a greater withdrawing effect than the carbon attached to boron as in the ethoxycarbonyl. The larger shift for the acetoxy salt is substantiated by the strong absorption at 2500 cm^{-1} in

*Author to whom correspondence should be addressed.

sodium (acetoxy)trihydroborate, an absorption that is not present in potassium tetrahydroborate or potassium (ethoxycarbonyl)trihydroborate.

Upon complexation with copper, the strong absorption at 2500 cm^{-1} disappears and a broad, weak absorption appears at 2060 cm^{-1} and is assigned to a B–H bridging stretch. FT-IR results in a more definite observation of this absorption. The other two B–H absorptions remain essentially the same at 2291 and 2221 cm^{-1}. The very small change in the latter frequencies is surprising and may be indicative of the influence of the oxygen directly bonded to boron and its strong withdrawing effect compared to the carbon directly bonded to boron in the B–C bond of the (alkoxycarbonyl)trihydroborates.

The separation between the B–H terminal and bridging stretches is considered to be a measure of the covalency of the M–H–B bond since, as Marks and Kolb[1] have pointed out, the difference between the frequencies should decrease as the B–H force constants become more equal and covalency decreases. Table 1 shows that this value is 290 cm^{-1} for the tetrahydroborate complex, 240 cm^{-1} for the ethoxycarbonyl complex and 230 cm^{-1} for the (acetoxy)trihydroborate complex indicating a weaker coordination or weaker covalent M–H–B bond in the (acetoxy)trihydroborate complex than for either the tetrahydroborate or ethoxycarbonyl complexes. The withdrawal of electron density from the boron and subsequently the hydrogens attached to it, is likely the cause for the weak bond and thus the difficulty encountered in preparation of this complex compared to the other hydroborates. The values for the B–H absorptions for the (acetoxy)trihydroborate along with the gradual decrease in the differences in the BH_t–BH_b values going from BH_4^- to $H_3BCO_2C_2H_5^-$ to $H_3BO_2CCH_3^-$ for the diphenylmethylphosphine complexes is consistent with the (acetoxy)hydroborate existing as a singly bridged hydroborate in analogy to the structure recently definitively determined by neutron diffraction for $(Ph_2MeP)_3CuBH_3$.[5] Coordination through the carbonyl group might also be a possibility, but coordination through this group would have the effect of lowering the C–O stretching frequency which occurs at 1683 cm^{-1} for the free anion. Upon complexation an increase of 8 cm^{-1} is observed indicating that no direct interaction occurs between the carbonyl oxygen and the metal. The increase in frequency is a logical consequence of the inductive effect as a result of complexation to a positive centre through the hydrogens of the borane group. The smaller shift (8 cm^{-1}) compared to that observed for analogous alkoxycarbonyl complexes[3] (30 cm^{-1}) is further evidence that the M–H–B bond is not as strong in the acetoxy complex.

^{1}H NMR. Proton nmr supports the structure assigned to this complex by IR and analysis data. The proton nmr consists of three peaks at 7.28, 2.18 and 1.55 ppm corresponding to the phenyl protons, the acetate methyl protons, and the phosphine methyl protons, respectively. The ratio of these peaks is 30:2.94:8.24 compared to the expected ratio of 30:3:9. The peak corresponding to the acetoxy methyl protons is shifted slightly downfield from acetic acid at 2.11 ppm indicating that some electron density is shifted from the acetoxy methyl group. The fact that B–H protons are not observed is characteristic of many B–H containing compounds, and is a result of partial decoupling of the boron from the hydrogens by quadrupole-induced ^{11}B and ^{10}B relaxation.

^{11}B NMR. The boron NMR of (acetoxy)(trihydroborato) *tris* (methyldiphenylphosphine)copper(I) also is consistent with the proposed formulation and shows a broad absorption centred at −0.7 ppm from boron trifluoride etherate. This absorption is broadened to the point where no fine structure can be seen. The broadness of the peak is comparable to other tetrahydroborate complexes and is indicative that thermal broadening is occurring at room temperature.[3a]

The boron chemical shifts of the *tris*(methyldiphenylphosphine)copper(I) complexes of tetrahydroborate and (ethoxycarbonyl)trihydroborate are reported as −39.0 ppm[2a] and −32.9 ppm[4] from boron trifluoride etherate. The large downfield shift in the acetoxy complex again reflects the large withdrawing effect of the acetoxy group as compared to hydrogen and ethoxycarbonyl and is completely consistent with observations in proton NMR and IR data.

DISCUSSION

Bommer and Morse[3a] prepared the (ethoxycarbonyl)trihydroborate complex of copper(I) and did not

Table 1. Characteristic IR frequencies[a] for $NaH_3B(O_2CCH_3)$ and $(Ph_2MeP)_3CuH_3B(O_2CCH_3)$ (cm^{-1})

Compound	B-H Terminal	B-H (Bridging)	C=O	(BH_b-BH_t)
$NaH_3B(O_2CCH_3)$	2500 s 2290 s 2225 m		1683 s	
$(Ph_2MeP)_3CuH_3B(O_2CCH_3)$	2291 s 2221 m	2060 w	1691 s	230
$(Ph_2MeP)_3CuH_3BCO_2C_2H_5$[3a]	2330 s 2260 sh	2090 s	1660	240
$(Ph_2MeP)_3CuBH_4$ [3a]	2335 sh 2310 s	2095 s		290

[a]All spectra are solid state.

experience the difficulty that was encountered in the preparation of the (acetoxy)trihydroborate complex. Our NMR data support the fact that the electron density around the boron is much less in the (acetoxy)trihydroborate than in the (ethoxycarbonyl)trihydroborate complex. Our IR data also show that the M–H–B bond is weaker in the (acetoxy)trihydroborate complex. These results clearly indicate that the withdrawal of electron density from the boron severely weakens the M–H–B bond. This is a logical conclusion in light of the fact that hydrogen has no *p* or *d* orbitals available for back bonding and so most of the electron density for the bond must come from the hydride iteslf.

Although the sodium salt containing the (acetoxy)trihydroborate anion was prepared by Hui[8], he reported that the di(acetoxy)dihydroborate anion could not be prepared. Our results confirm this. The tri(acetoxy)monohydroborate salt was prepared by Gribble.[7] We found that no reaction occurred between it and chloro*tris*(methyldiphenylphosphine)copper(I) under the conditions used. This may not be particularly surprising since the extensive withdrawal of electron density from the boron by the acetoxy group ($\sigma_I = 0.39$)[9] would be even more pronounced with three acetoxy groups. Upon this more extensive removal of electron density from the hydride hydrogens, it would be expected that they would become even poorer electron donors and therefore be less available for coordination to the metal. The bulky nature of the anion may also discourage complexation. Both properties are consistent with the remarkably weak reducing characteristics of $NaHB(OAc)_3$.[7]

Another hydroborate which contains a B–O bond is sodium trimethoxyhydroborate.[10] Reaction of this hydroborate with $(Ph_2MeP)_3CuCl$ resulted in the immediate formation of a coloured product and no B–H containing species resulted. Analogous results were obtained with potassium tri*iso*propoxyhydroborate.[11] A similar result was observed by Churchill[12] with the reaction between tetrameric chloro*tris*(triphenyl)phosphinecopper(I) with sodium trimethoxyhydroborate in which a hexameric copper hydride cluster was formed. It is logical to assume that such a reaction was taking place in this study and that such results indicated complete hydride transfer and breaking of the B–H bond. The fact that $HB(OMe)_3^-$ and $HB(OPr^i)_3^-$ did not form an isolable complex analogous to the acetoxy- or alkoxycarbonyl derivatives is consistent with their behaviour as strong reducing agents.[10] Similarly, strong reducing agents such as potassium triethylhydroborate[13] and potassium tri-*sec*butylhydroborate[14] gave results analogous to those when the trimethoxyhydroborate anion was used. The greater reactivity of the latter anions compared to BH_4^-, $H_3BOC(O)CH_3^-$ and $HB[OC(O)CH_3]_3^-$ may be attributable to the greater ease of removing a hydride ion from a weak Lewis acid such as $B(OCH_3)_3$ and $B(C_2H_5)_3$ as compared to a strong Lewis acid such as BH_3, $H_2BC(O)OR$, and $H_2BOC(O)R$. The ability of the carbonyl group to withdraw electron density has already been pointed out and results in the substituted boranes behaving as stronger Lewis acids toward H^- than BH_3.

One may conclude on the basis of these results with the (acetoxy)hydroborates that if the substituent group on the boron is strongly electron withdrawing that coordination is much more difficult to attain and once attained is much weaker. Furthermore, if the hydroborate acts as a strong reducing agent, the reaction with copper(I) phosphine complexes do not produce compounds containing M–H–B bonds.

EXPERIMENTAL

Chemicals. Commercially obtained samples were used except where indicated. All solvents were dried by reported procedures.[15]

Sodium (acetoxy)trihydroborate. This reagent was prepared by the method similar to that of Gribble.[7] An alternate synthesis is as follows: A sample of sodium tetrahydroborate (0.38 g, 0.01 mol) was magnetically stirred in 50 ml of dry benzene in a 250 ml round bottom flask under a stream of dry nitrogen. Acetic acid (0.19 g, 0.015 mol) dissolved in 25 ml of dry benzene, was added dropwise. The mixture was stirred until gas evolution stopped (about one hour), and the white solid product was collected by filtration and dried under vacuum. The product was slightly contaminated by sodium tetrahydroborate as indicated by a small amount of the tetrahydroborate complex isolated from the complexation reaction with $(Ph_3MeP)_3CuCl$.

((Acetoxy)trihydroborato)*tris*(methyldiphenylphosphine)copper(I). To a stirred solution of 15-crown-5 (0.44 g, 0.002 mol) in 50 ml of dry methylene chloride was added sodium (acetoxy)trihydroborate (0.19 g, 0.002 mol). When all of the salt dissolved, chloro*tris*(methyldiphenylphosphine)copper(I) (1.4 g, 0.002 mol) was added. The mixture was refluxed with stirring under an inert atmosphere for 24 hr. After this time the solution was filtered and the filtrate collected. The solvent was removed by flash evaporation and to the remaining oil was added 150 ml of hexanes. The hexanes caused the product to crystallize as a white solid which was then collected by filtration. Analysis: Calc. 66.8% C, 6.1% H, 1.49% B, 8.62% Cu; Found 66.9% C, 5.88% H, 1.41% B, 8.41% Cu.

The reactions using the alkoxy- and alkylhydroborate salts were carried out in an analogous manner except that the crown ether was not used. For example, to a stirred solution of $(Ph_2MeP)_3CuClO_4$ (1.53 g, 0.002 mol) in 50 ml methylene chloride was added $NaHB(O\text{-}iPr)_3$ (0.002 ml in THF). The solution immediately turned bright yellow. Removal of the solvents and an IR of the remaining solids showed no B–H present.

Acknowledgements—Acknowledgement is made to the donors of The Petroleum Research Fund, administered by the American Chemical Society, for the support of this research.

REFERENCES

[1]T. J. Marks and J. R. Kolb, *Chem. Rev.* 1977, **77**, 263 and references therein.
[2](a) J. C. Bommer and K. W. Morse, *Inorg. Chem.* 1981, **20**, 1731. (b) *Ibid.* 1978, **17**, 3708. (c) Submitted for publication.
[3](a) J. C. Bommer and K. W. Morse, *Inorg. Chem.*, 1980, **19**, 587. (b) *Ibid.*, 1979, **18**, 531. (c) J. C. Bommer and K. W. Morse, *Chem. Comm.* 1977, 137.
[4]J. C. Bommer, Ph.D. dissertation. Utah State University (1977).
[5]F. Takusagawa, A. Fumagalli, T. F. Koetzle, S. G. Shore, T. Schmitkons, A. V. Fratini, K. W. Morse, Chau-Yu Wei, and R. Bau, *J. Am. Chem. Soc.* 1981, **103**, 5156.
[6](a) T. N. Sorrell, R. J. Spillane, *Tetrahedron Lett.* 1978, 2473. (b) T. N. Sorrell, *Tetrahedron Lett.* 1978, 4985. (c) G. W. J. Fleet, C. J. Fuller, P. J. C. Harding, *Tetrahedron Lett.* 1978, 1437. (d) G. W. J. Fleet, P. J. C. Harding, *Tetrahedron Lett.* 1979, 975. (e) T. N. Sorrell, P. S. Pearlman, *J. Org. Chem.* 1980, **45**, 3449.
[7]G. W. Gribble and D. C. Ferguson, *Chem. Comm.* 1975, 535.
[8]B. C. Hui, *Ventron Alembic*, 1980, No. 20.
[9]R. W. Taft, N. C. Deno, and P. S. Skell, *Ann. Phys. Chem.* 1958, **9**, 287.
[10]H. C. Brown, E. J. Mead, and C. J. Shoaf, *J. Am. Chem. Soc.* 1956, **78**, 3616.
[11](a) H. C. Brown, E. J. Mead, and B. C. Subba Rao, *J. Am.*

Chem. Soc. 1955, **77**, 6209. (b) C. A. Brown, S. Krashnamurthy and S. C. Kim, *Chem. Commun.* 1973, 391.
[12]M. R. Churchill, S. A. Berman, J. A. Osborn, and J. Wormald, *Inorg. Chem.* 1972, **11**, 1818.
[13](a) H. C. Brown, H. I. Schlesinger, I. Sheft, and D. M. Ritter, *J. Am. Chem. Soc.*, 1953, **75**, 192. (b) H. C. Brown and S. Krashnamurthy, *Ibid.* 1972, **94**, 7159; 1973, **95**, 1669.
[14]C. A. Brown, *J. Am. Chem. Soc.* 1970, **92**, 709.
[15]A. J. Gordon and R. A. Ford, *The Chemists Companion.* Wiley, New York (1972).

Polyhedron Vol. 1, No. 3, pp. 303–306, 1982
Printed in Great Britain.

0277–5387/82/030303–04$03.00/0
Pergamon Press Ltd.

THE PREPARATION AND COORDINATION CHEMISTRY OF 2,2′:6′,2″-TERPYRIDINE MACROCYCLES—1

EDWIN C. CONSTABLE and JACK LEWIS*

University Chemical Laboratory, Lensfield Road, Cambridge CB2 1EW, England

(*Received* 3 *February* 1982)

Abstract—A range of 6,6″-disubstituted derivatives of 2,2′:6′,2″-terpyridine have been prepared with the intention of forming macrocycles incorporating the 2,2′:6′,2″-terpyridyl moiety. A high yield route to 6,6″-bis(methylhydrazino-4′-phenyl-2,2′:6′,2″-terpyridine is described, and a number of complexes of this novel pentadentate ligand have been prepared.

Although complexes of the "classic" diimine ligands 2,2′-bipyridine (1) and 1,10-phenanthroline (2) have been known for many years[1–3] it is only recently that such fragments have been incorporated into macrocycles[4–6]. We have demonstrated that macrocycles of type 3 form transition metal complexes which exhibit unusual coordination geometries about the metal, and, with a view to extending these observations, we have embarked upon the synthesis of derivatives of 2,2′:6′,2″-terpyridine (4) suitable for incorporation into such systems.

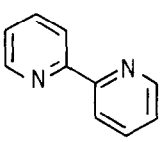

1

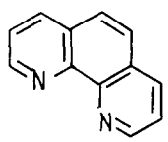

2

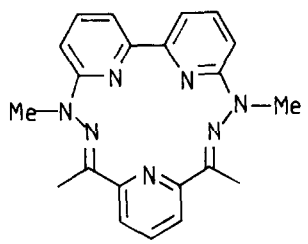

3

Our target molecule was a 6,6″-bishydrazino substituted compound, **4a**, which was expected to condense with a 1,2-dicarbonyl compound to give a macrocycle of type 5, which has a similar donor set to macrocycle 3.

We describe herein the synthesis of such derivatives using the Krohnke pyridine synthesis,[7] in which an α,β-unsaturated carbonyl compound is condensed with an active methylene species in the presence of ammonium acetate to form a 1,4-dihydropyridine (Scheme 1). By adopting the strategy in which the methylene group is additionally activated by an N-pyridinium group (i.e.

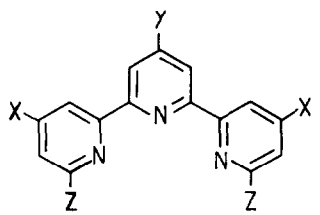

4

4a Z = $NRNH_2$
4b Z = Cl, Y = H, X = Ph
4c Z = $NHNH_2$, Y = H, X = Ph
4d Z = $NMeNH_2$, Y = H, X = Ph
4e Z = NH_2, Y = H, X = Ph
4f Z = Br, Y = Ph, X = H
4g Z = $NMeNH_2$, Y = Ph, X = H

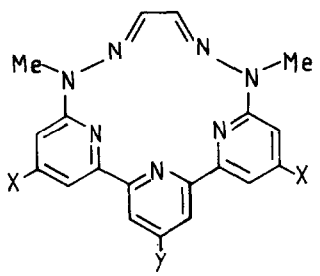

5

*Author to whom correspondence should be addressed.

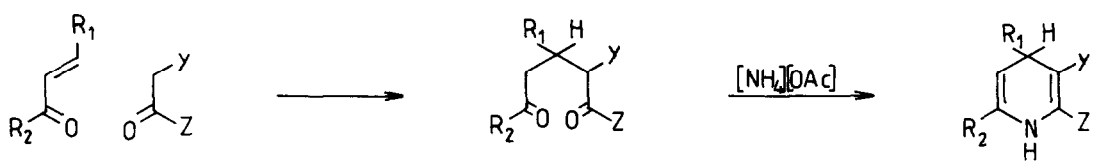

Scheme 1.

Y = $-NC_5H_5^+$), a pyridine is obtained directly by loss of $C_5H_5NH^+$. Obviously, if R and Z are pyridyl groups, the synthesis may be extended to terpyridines.[2,7]

2,6-diacetylpyridine reacted smoothly with benzaldehyde in methanol or n-propanol in the presence of diethylamine to form the *bis*chalcone **6** as a yellow crystalline solid, in 88% yield. The reaction of **6** with 1-ethoxycarbonylmethylpyridinium bromide (**7**) and ammonium acetate in n-propanol proceeded smoothly, with the precipitation of the 6,6″-*bis*pyridone **8** as a tan powder in 99% yield. Attempts to convert **8** to the 6,6″-dichloro derivative

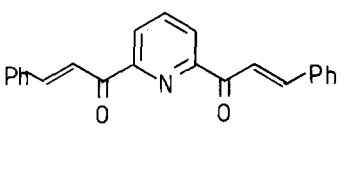

6

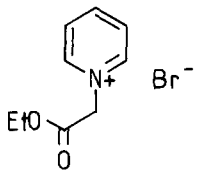

7

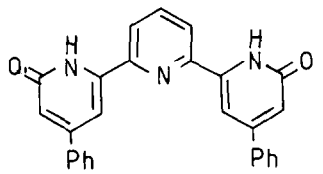

8

4b with $PCl_5/POCl_3$ led predominantly to a monochloro derivative, and only after four days at reflux could **4b** be obtained, and then only in poor yield. No improvement in yield was observed on using PCl_5, SO_2Cl_2, $SOCl_2$ or PBr_3/Br_2 as the halogenating agent. The dichloro compound reacted with hydrazine or methylhydrazine with difficulty to give the desired derivatives **4c** and **4d**.

We considered that diazotisation/bromination[8] of the 6,6″-diamino compound **4e** might provide an alternative route to the desired 6,6″-dihalo derivatives, but the yield of **4e** from the reaction of **6** with 1-cyanomethylpyridinium chloride and ammonium acetate was low (32%), and this route was not further investigated.

We therefore decided to investigate syntheses in which the halogen atom was carried through the synthesis, and the central pyridine ring was generated from acyclic precursors. 2,6-Dibromopyridine was prepared from 2,6-dichloropyridine in 80% yield[9], and then converted to 2-acetyl-6-bromopyridine by lithiation followed by reaction with Me_2NCOCH_3.[10] Attempts to convert 2,6-dichloropyridine directly to 2-acetyl-6-chloropyridine failed, the chlorine atoms appearing to be inert to metal exchange with either *n*-BuLi or PhLi at low temperature.

Although 2-acetylpyridine reacts smoothly with half an equivalent of benzaldehyde in the presence of base to form the 1,5-diketone **9**, (indeed it is difficult to stop the reaction at the chalcone stage) the reaction was nowhere near so facile with the 6-bromo derivative, the major product under a range of conditions being the chalcone **10**. The reaction of 2-acetyl-6-bromopyridine with benzaldehyde

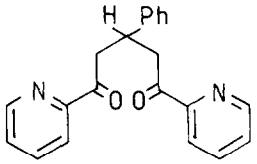

9

in aqueous methanolic KOH was optimised to give a yield of 92% of the pale yellow chalcone, **10**.

The Ortoleva-King reaction[7] of 2-acetyl-6-bromopyridine with iodine led to the formation of the very insoluble golden-yellow pyridinium salt **11** in 75% yield. Finally, the desired dibromo compound, **4f**, was prepared in 86% yield from the reaction of **10** and **11** with ammonium acetate in glacial acetic acid (Scheme 2). The reaction of **4f** with methylhydrazine at reflux led to a rapid, high-yield conversion to the desired *bis*(methylhydrazino)-derivative **4g**.

The *bis*(methylhydrazino) derivative **4g** is a potentially pentadentate ligand, and we have completed a preliminary investigation of its coordination chemistry. Coloured solutions are obtained on refluxing a suspension of **4g** with a methanolic solution of a transition metal salt, from which solid $[ML]^{n+}$ species may be obtained upon the addition of ammonium hexafluorophosphate of tetra-*n*-butylammonium tetrafluoroborate (See Table 1). We are at present investigating further examples of such complexes in an attempt to determine the mode of bonding of the ligand. Preliminary crystallographic studies indicate that **4g** acts as a planar pentadentate ligand. If this is the case it is a non-macrocyclic analogue to the macrocycles of type **3**, and certain observations on the electrochemical behavior of complexes of **4g** confirm this belief.

We have also demonstrated that macrocycles of type **5a** may be prepared by template condensations. Thus, the template reaction of $[Co(4g)]^{2+}$ with glyoxal-sodium bisulphite in aqueous methanol leads to the formation of $[Co(5a)]^{2+}$ which may be isolated as its $[BF_4]$ or $[PF_6]$ salts. Further synthetic, structural and electrochemical studies upon these systems are underway and will be reported shortly.

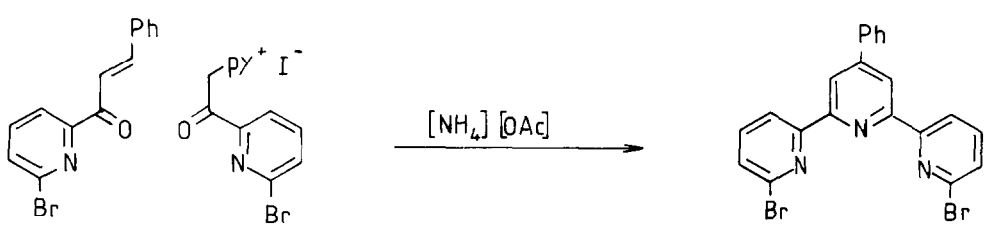

10 **11** **4f**

Scheme 2.

Table 1.

Compound	Colour	Calc. C	Calc. H	Calc. N	Found C	Found H	Found N
[Cr(4g)]Cl_3. HCl	Red	45.58	4.21	16.18	45.59	4.09	16.22
[Mn(4g)][PF_6]$_2$.H_2O	Orange	36.27	3.28	12.88	36.18	3.44	12.88
[Fe(4g)][BF_4]Cl.H_2O	Green	46.53	4.21	16.52	46.37	4.09	16.33
[Co(4g)][BF_4]$_2$.MeOH	Red	43.54	4.08	14.83	43.43	4.39	14.54
[Ni(4g)][BF_4]$_2$.$\frac{1}{2}H_2O$	Yellow	43.24	3.75	15.35	43.08.	3.63	15.34
[Co(5a)][PF_6]$_2$.$2H_2O$	Orange	37.32	3.11	12.19	37.52	3.53	11.98

EXPERIMENTAL

^{1}H NMR spectra were recorded on Bruker WH-400 or Varian CFT-20 spectrometers. Infrared spectra were recorded on a Perkin–Elmer 577 spectrometer. Mass spectra were recorded on an AEI MS-30 spectrometer. Elemental analyses were performed in the microanalytical section of the University Chemical Laboratory.

2,6-Dibromopyridine and 2-acetyl-6-bromopyridine were prepared by the literature methods[9,19].

2,6-Bis(cinnamoyl)pyridine (**6**): 2,6-Diacetylpyridine (5.00 g, 0.03 mol), benzaldehyde (15.0 ml, 0.148 mol) and diethylamine (20.0 ml) were dissolved in *n*-propanol (120 ml) and heated to reflux for 3 hr, and allowed to cool, when a yellow crystalline precipitate of the bischalcone **6** was obtained (9.03 g, 88%). $\bar{\nu}$(C=O str) 1671 cm^{-1}, MS 339 (M$^+$, 100%).

1-Ethoxycarbonylmethylpyridinium bromide (**7**): Ethyl bromacetate (14.0 ml, 0.126 mol) and pyridine (10.0 ml, 0.116 mol) were dissolved in acetone (35.0 ml) and left to stand overnight. The white crystal mass so obtained was collected by filtration, washed well with acetone, and stored over P_2O_5 until required (the product is *very* hydroscopic) (19.0 g, 92%) m.p. 135.5–136.5. $\bar{\nu}$(C=O str) 1754 cm^{-1}, ^{1}H NMR (dmso-d_6) δ1.24, *t*, 7.1 Hz (CH_3); 4.22, *q*, 7.1 Hz (CH_2); 5.73, *s*, (CH_2N); 8.24, *m*, ($H_{3,5}$); 8.73, *m*, (H_4); 9.10, *dd*, ($H_{2,6}$).

4,4″-Diphenyl-2,2′:6′,2″-terpyridine-6(1H), 6″(1″H)-dione (**8**). **6** (1.50 g, 4.5 mmol), **7** (3.00 g, 12.2 mmol) and ammonium acetate (6.0 g) were heated to reflux in *n*-propanol (110 ml) for 2 hr, after which period the suspension was cooled, and the tan precipitate of the dione **8** collected by filtration. Found: C, 77.46; H, 4.77; N, 10.26%. Calc. for $C_{27}H_{19}N_3O_2$; C, 77.69; H, 4.56; N, 10.07%.

6,6″-Dichloro-4,4″-diphenyl-2,2′:6′,2″-terpyridine (**4b**): **8** (1.36 g, 3.26 mmol), PCl_5 (5.00 g, 24 mmol) and $POCl_3$ (25.0 ml) were heated to reflux for 96 hr, after which period the dark brown suspension was allowed to cool, and quenched on ice (200 g). The yellow precipitate was extracted with chloroform (8 × 100 ml) and the extracts dried over $MgSO_4$. The dark coloured insoluble residue consisted predominantly of 6-chloro-4,4″-diphenyl-2,2′:6′,2″-terpyridin-6″(1″H)-one (MS 435,437). The $CHCl_3$ extract was evaporated to dryness *in vacuo*, and the pale yellow solid evaporated from aqueous methanol. Despite drying *in vacuo* the recrystallised solid always contained some water, as evidenced by the analysis and the i.r. spectrum. Found: C, 62.80; H, 4.71% Calc. for $C_{27}H_{17}N_3Cl_2$: 3.5 H_2O C, 62.67; H, 4.64%, MS 453, 455, 457.

6,6″ - Bis(methylhydrazino) - 4,4″ - diphenyl - 2,2′:6′,2″ - terpyridine (**4d**): **4b** (0.30 g, 0.58 mmol) was heated to reflux with methylhydrazine (10.0 ml) under nitrogen for 3 hr, after which period the yellow solution was allowed to cool, and the pale yellow crystals of **4d** collected by filtration. MS 473 (M$^+$ 100%). The 6,6″-bis(hydrazino) derivative, **4c**, was prepared in a similar manner on substituting hydrazine for methylhydrazine.

1-Cyanomethylpyridinium chloride: Chloroacetonitrile (10.0 ml, 0.158 mol) and pyridine (12.9 ml, 0.160 mol) were mixed and allowed to stand for three days at room temperature, after which period a pale brown crystalline mass had formed. This was dissolved in warm methanol (40 ml) and the solution so obtained quenched in ether (200 ml) to give the desired salt as an off-white solid (18.8 g, 77%). $\bar{\nu}$(C ≡ N str) 2260 cm^{-1}, ^{1}H NMR (dmso-d_6) δ 6.22, *s*, (CH_2N); 8.25, *m*, ($H_{3,5}$); 8.78, *m*, (H_4), 9.30, *dd*, ($H_{2,6}$).

6,6″-Diamino-4,4″-diphenyl-2,2′:6′,2″-terpyridine (**4e**). 1-Cyanomethylpyridinium chloride (1.85 g, 12 mmol), **6** (2.00 g; 5.9 mmol) and ammonium acetate (6.0 g) were heated to reflux in *n*-propanol (85.0 ml) for 1 hr after which period the deep red solution was allowed to cool, when yellow crystals of **4e** were precipitated (0.784 g, 32%). MS 415 (M$^+$ 100%).

1-(2-Bromopyridyl)-3-phenyl-2-propenone (**10**): 2-Acetyl-6-bromopyridine (5.0 g, 0.025 mol) and benzaldehyde (10.0 ml, 0.1 mol) were added to a solution of KOH (1.2 g) in water (10 ml) and methanol (50 ml), and the solution so obtained stirred at room temperature for 2 hr, after which time precipitation of the pale yellow chalcone **10** was complete (6.64 g, 92%). $\bar{\nu}$(C=O str) 1670 cm^{-1}, MS 287, 289 (M$^+$ 60%), 258, 260 (M − 29, 45%), 131 (M − C_5H_3NBr, 100%).

1-(2-Bromopyridylcarbonylmethyl)pyridinium iodide (**11**). 2-Acetyl-6-bromopyridine (10.00 g, 0.05 mol) and iodine (12.80 g, 0.05 mol) were heated to reflux in pyridine (60 ml) for 1 hr. The solution was cooled, and the yellow crystalline pyridinium salt **11** separated by filtration (15.26 g, 75%). ^{1}H NMR (dmso-d_6) δ 6.45, s, (CH_2), 8.00–9.04, m (aromatics).

6,6″-Dibromo-4′-phenyl-2,2′:6′,2″-terpyridine (**4f**). **11** (7.05 g, 0.0174 mol), **10** (5.0 g, 0.0174 mol) and ammonium acetate (7.7 g) were heated to reflux in acetic acid (50 ml) for 90 min, after which period the pale brown solution was cooled to give **4f** as off-white needles (6.95 g, 85.8%). MS 465, 467, 469 (M$^+$ 100%), 386, 388 (M − Br, 20%).

6,6″-Bis(methylhydrazineo)-4′-phenyl-2,2′:6′,2″-terpyridine (**4g**). **4f** (6.41 g, 0.01 mmol) was heated to reflux in methylhydrazine (25 ml) for 2 hr under nitrogen, after which a pale yellow suspension had been obtained. The suspension was cooled, and the yellow solid collected by filtration to give **4g** as yellow needles (4.87 g, 89%). MS 395 (M − H, 100%), 381 (M − CH_3, 50%).

Coordination compounds of **4g**

Typically, **4g** (0.2 mmol) and the metal salt (0.2 mmol) were heated to reflux in methanol (20 ml) under a nitrogen atmosphere for 1 hr, after which period a clear solution had been obtained [NH_4][PF_6] or [*n*-Bu_4N][BF_4] was added to the hot solution, which was allowed to cool slowly, when the complexes were obtained as crystalline or microcrystalline solids. The metal salts used were $CrCl_3.6H_2O$, $Mn(OAc)_2.4H_2O$, $FeCl_2.4H_2O$, $CoCl_2.6H_2O$, $Co(OAc)_2.4H_2O$ and $Ni(OAc)_2.4H_2O$ (See Table 1).

Formation of the macrocyclic complex [Co(**5a**)][PF_6].$2H_2O$. **4g** (0.22 g, 0.554 mmol) and $Co(OAc)_2.4H_2O$ (0.138 g, 0.554 mmol)

were heated to reflux in methanol (20 ml) for 5 min to give a clear orange solution. A solution of glyoxal–sodium bisulphite hydrate (0.138 g, 0.554 mmol) in water (10 ml) was added, and the mixture refluxed for a further 20 hr, after which period a deep orange solution had been obtained. This was filtered hot and treated with $[NH_4][PF_6]$ (1.0 g) and cooled, when orange needles of $[Co(\mathbf{5a})][PF_6]_2.2H_2O$ were obtained.

Acknowledgement—We thank the S.E.R.C. for the award of a Post-Doctoral Fellowship (to E.C.C.).

REFERENCES

[1]W. E. McWhinnie and J. D. Miller, *Adv. Inorg. Chem. Radiochem.* 1969, **12**, 135.
[2]L. A. Summers, *Adv. Heterocycl. Chem.* 1979, **22**, 1.
[3]E. C. Constable, *The Chemistry of Diimine Ligands*. Academic Press, New York (1983).
[4]E. Buhleier, W. Wehner and F. Vogtle, *Chem. Ber.* 1978, **111**, 200.
[5]G. R. Newkome, A. Nayak, F. Fronczek, T. Kawato, H. C. R. Taylor, L. Meade and W. Mattice, *J. Am. Chem. Soc.* 1979, **101**, 4472.
[6]J. Lewis, T. D. O'Donoghue, Z. P. Haque and P. A. Tasker, *J. Chem. Soc., Dalton Trans.* 1980, 1664.
[7]F. Krohnke, *Synthesis* 1976, 1.
[8]L. C. Craig, *J. Am. Chem. Soc.* 1934, **56**, 231.
[9]F. Mutterer and C. D. Weiss, *Helv. Chim. Acta* 1976, **59**, 1.
[10]J. E. Parks, B. E. Wagner and R. H. Holm, *J. Organomet. Chem.* 1973, **56**, 53.

Polyhedron Vol. 1, No. 3, pp. 307–310, 1982
Printed in Great Britain.

0277-5387/82/030307-04$03.00/0
Pergamon Press Ltd.

SOME TRIMETHYLPHOSPHINEOXIDE COMPLEXES OF LANTHANIDE AND INDIUM TRIS-(BIS-TRIMETHYLSILYLAMIDES)

D. C. BRADLEY* and YI CI GAO†
Department of Chemistry, Queen Mary College, Mile End Road, London E1 4NS, England

(*Received* 24 *February* 1982)

Abstract—The reactions of the 3-coordinated metal *tris*-(bis-trimethylsilylamides) $M[N(SiMe_3)_2]_3$ (ML_3; where M = La, Pr, Eu, Gd and In) with trimethylphosphineoxide $Me_3PO(L')$ have been studied. All of these metals gave 1:1 complexes $ML_3(L')$ which dissociated on heating *in vacuo*. The Pr and Eu complexes gave interesting pseudo-contact shifted ^1H NMR spectra which are qualitatively in accord with the expected molecular structure. Variable temperature NMR measurements proved the restricted rotation of the silylamide (L) ligands occurs around the M–N axes. Evidence is also presented for unstable 5-coordinated complexes $ML_3(L')_2$. The gadolinium 1:1 complex gave a very broad NMR spectrum and its ESR spectrum is being investigated.

INTRODUCTION

Previous research has shown that the lanthanide elements may be constrained to the exceptionally low coordination number of three by the steric effect of the bulky nitrogen donor ligand $N(SiMe_3)_2$.[1] An entirely unpredicted feature of these compounds was the pyramidal structure exhibited in the crystalline state[2,3] in contrast to the trigonal configuration favoured by transition metals and Group IIIB elements.[4]

The pyramidal configuration of $M[N(SiMe_3)_2]_3$ compounds suggested that coordination of a fourth ligand was feasible provided that it was sterically undemanding. This was confirmed by the addition of excess triphenylphosphine-oxide which gave the 1:1 complexes $M[N(SiMe_3)_2]_3(Ph_3PO)$, (M = La, Eu and Lu).[5] Furthermore it seemed worthwhile to try the addition of the less bulky ligand trimethylphosphineoxide since it was possible that 1:2 complexes containing 5-coordinated lanthanides might be obtained. This paper gives an account of our results in this area.

RESULTS AND DISCUSSION

It was decided to study reactions of Me_3PO with $M[N(SiMe_3)_2]_3$, where La, Pr, Eu, Gd and In, for the following reasons.

(i) Praseodymium and europium would give complexes which should yield interesting pseudo-contact shifted NMR spectra.

(ii) Lanthanum was selected because being the largest lanthanide element it was more likely to give a 1:2 complex than the smaller elements. In addition the diamagnetic chemical shift of the lanthanum complex was needed to evaluate the paramagnetic pseudo-contact shifts of the praseodymium and europium complexes.

(iii) Gadolinium was included because the $4f^7$ species would be expected to give an interesting ESR spectrum for comparison with the detailed ESR studies on $Gd[N(SiMe_3)_2]_3$.[6]

(iv) The indium complex was of interest in its own right but also in case it was required as a diamagnetic host for the ESR studies on the gadolinium complexes.

(a) 1:1-*Complexes* $M[N(SiMe_3)_2]_3(Me_3PO)$ (M = La, Pr, Eu, Gd, In)

The metal *tris*-(bis-trimethylsilylamide) (ML_3) and trimethylphosphineoxide (L') were combined in equimolecular proportions in benzene and the 1:1 complexes $ML_3(L')$ were eventually crystallized from pentane at low temperature.

$$M[N(SiMe_3)_2]_3 + Me_3PO \rightarrow M[N(SiMe_3)_2]_3(Me_3PO). \quad (1)$$

Some data on these complexes are listed in Table 1. Although the NMR and IR spectra confirmed the integrity of these 1:1 complexes they dissociated on heating *in vacuo* and mass spectral studies gave peaks only for the separate ML_3 and Me_3PO species and their fragment ions. However, the lowering of the ν_{PO} frequency (La, 46; Eu, 47; Gd, 42; In, 25 cm^{-1}) of the ligand on complexation suggested a significant interaction in the complex. Bands at *ca.* 380 and 360 cm^{-1} are probably the two NM_3 stretching frequencies expected for the OMN_3 system with local C_{3v} symmetry.

The ^1H NMR spectra showed some interesting features. In the lanthanum complex the silylamide methyls (δ0.53) were shifted slightly downfield compared with the parent LaL_3 (δ0.25)[1] and the Me_3PO methyls (δ0.85) were shifted slightly upfield compared with the free ligand (δ1.0). It is noteworthy that in $LaL_3(Ph_3PO)$ the silylamide methyls (δ0.07) were shifted slightly upfield compared with the parent LaL_3 compound but this may in part result from a ring-current effect due to the nearby phenyl groups on the phosphineoxide ligand.

The europium complex gave a highfield shift to the silylamide methyls ($\delta - 0.45$) and a very great downfield shift to the phosphineoxide methyls (δ23.0). Assuming that the diamagnetic contribution to these chemical shifts to be same as in the lanthanum compound the paramagnetic shifts in the europium complex are −0.98 ppm (L) and 22.15 ppm (L'). Extensive measurements on toluene (C_7D_8) solutions of $EuL_3(L')$ showed that these paramagnetic shifts increased markedly with decrease in temperature Table 2 (the plot of shifts vs $1/T$ was approximately linear). Simultaneously the silylamide methyl signal broadened and below *ca.* 220 K eventually split into two equal signals one upfield and the other downfield (e.g. at 193 K: δ +21.68, −28.64). Such

*Author to whom correspondence should be addressed.
†Department of Chemistry, Lanzhou University, Lanzhou, People's Republic of China.

Table 1. $M[N(SiMe_3)_2]_3(Me_3PO)$ compounds

M in $M[N(SiMe_3)_2]_3(Me_3PO)$	Colour	M.p. (°C)	^{1}H N.m.r. Chem. Shifts[a]		Infrared Bands (cm^{-1})	
			$N(SiMe_3)_2$	Me_3PO[g]	ν_{PO}[g]	ν_{MN}
La	White	189-191	0.53(s,6)[b]	0.85(d,1)[b,c]	1124	380,360
Pr	Pale Yellow	[f]	0.09(s,6)[b]	-22.81(d,1)[b,c]	[f]	[f]
Eu	Pale Orange	158-162	-0.45(s,6)[b,c]	23.0 (d,1)[b,c]	1123	380,365
Gd	White	168-172	[e]	[e]	1128	363,350
In	White	dec.137	0.42(s,6)[d]	0.90(d,1)[c,d]	1145	360

[a] Chemical shifts δ in ppm relative to TMS, downfield positive.

[b] In C_6D_6 at 306K.

[c] $^2J_{HP}$ = 16 Hz.

[d] In C_7D_8

[e] Very broad signals due to paramagnetism.

[f] This compound was studied in solution only.

[g] Free ligand: ν_{PO} = 1170 cm^{-1} ; δ = 1.0.

Table 2. ^{1}H NMR chemical shifts for $Eu[N(SiMe_3)_2]_3(Me_3PO)$

T(K)	$N(SiMe_3)_2$[a]	Me_3PO[a]	θ_L[b]
293	-0.42	23.78	124.8
253	-0.84	32.94	124.8
233	-1.68	40.84	124.6
223	v. broad	44.31	-
213	v. broad	49.16	-
203	-25.99, +20.00	56.51	(124.6)[c] ; 114.5, 132.2
193	-28.64, +21.68	61.15	(124.5)[c] ; 114.7, 132.3

[a] In C_7D_8, δ in ppm relative to TMS, downfield positive.

[b] Calculated angle from $K(\cos^2\theta-1)r^{-3}$ function (see text).

[c] Value calculated for averaged δ_L.

behaviour is consistent with the onset of restricted rotation of the silylamide ligands around the Eu–N bonds which would be expected in the frozen conformation to have for each $N(SiMe_3)_2$ ligand one $SiMe_3$ group proximal to the Me_3PO group and the other distal. This is in accordance with the crystal molecular structure determined for $LaL_3(Ph_3PO)$.[5] In this complex the PÔLa was 174° whilst the OLâN angles were 107.8, 105.2 and 104.8° (i.e. significantly less than the "tetrahedral" angle of 109.5°). Moreover each silylamide ligand had a planar Si_2NLa structure and these "ligand planes" subtended angles of 39.2, 43.9 and 48.6° with the N_3 plane of the molecule. If the origin of the paramagnetic chemical shifts in $EuL_3(L')$ lies in the pseudo-contact (dipolar) mechanism and the molecule has axial (3-fold) symmetry then these data should accord with the wellknown formula $K(3\cos^2\theta-1)r^{-3}$. Although we could not reliably calculate K from first principles we were able to make reasonable estimates of θ_L (~21°) and r_L (5.72 Å) for the Me_3PO protons by assuming with suitable adjustments that $Eu[N(SiMe_3)_2]_3(Me_3PO)$ has a structure analogous to that determined for $La[N(SiMe_3)_2]_3(Ph_3PO)$[5]. Thus a value of K was deduced and taking a reasonable estimate (4.89 Å) for the average value of r_L for the silylamide protons in freely rotating silylamide groups a value of θ_L was calculated. In fact two solutions to the equation are

obtained, namely θ and $180-\theta$, due to the $\cos^2\theta$ term. In our model only the $180-\theta$ value has any physical meaning and the values obtained at each temperature are listed in Table 2. It is reassuring to find that θ_L is practically independent of temperature (average 124.7°) although the chemical shifts are very sensitive to temperature. Moreover the value of θ_L is very close to one of the values (54.73° and 125.27°) at which the function $3\cos^2\theta - 1$ changes sign. However, this value of *ca.* 125° is considerably greater than which might have been expected on the basis of the structural model. Although it is difficult to visualize the average position of silylamide protons in such a complicated fluxional molecule, intuitively one would expect the angle θ_L to coincide with that of the Eu–N bond vector. In the structure of $LaL_3(Ph_3PO)$ the La–N bonds averaged 106° relative to the O–La axis and this is near the tetrahedral angle. It is possible that $Eu[N(SiMe_3)_2]_3(Me_3PO)$ has a more covalent interaction between metal ion and ligands than the lanthanum complex and that the silylamide ligands are pressed further away from the phosphineoxide ligand thus widening the OÊuN angle. Clearly a crystal structure is needed to settle the structural details of this interesting molecule. However, it must also be borne in mind that the above calculations are rather unsophisticated and assume a purely pseudo-contact mechanism for the paramagnetic shifts. If covalency is invoked this raises the possibility of some Fermi contact contribution due to transfer of 4*f* electron spin which would vitiate the above calculations. Further insight should be gained from the measurements in progress of ^{13}C NMR chemical shifts since agreement on geometrical parameters derived from ^1H and ^{13}C NMR shifts will only be obtained if a purely pseudo-contact mechanism is operative. Before leaving the europium complex it is worth pointing out that the limiting low temperature ^1H NMR spectrum showed restricted rotation of silylamide ligands around the Eu–N bonds. If the "frozen" structure of the molecule in solution is similar to that given by the crystal structure of $LaL_3(Ph_3PO)$ then the $SiMe_3$ groups proximal to the Me_3PO ligand should resonate at high field due to their θ_L becoming less than 124.7° and the distal $SiMe_3$ groups should shift downfield because their θ_L should exceed the limiting angle of 125.27°. Such is indeed the case as shown in Table 2 for the two lowest temperatures where θ_L values are approx. 115° and 132°.

The NMR spectra on the praseodymium complex $Pr[N(SiMe_3)_2]_3(Me_3PO)$ are consistent with those obtained for the europium complex although the paramagnetic shifts are opposite in sign. The data in Table 1 show that in $PrL_3(L')$ the Me_3PO protons experience a large upfield shift (−23.66 ppm) relative to the lanthanum complex and the silylamide protons give a small upfield shift (−0.44 ppm). Using the same structural model as for $EuL_3(L')$ the paramagnetic shifts for $PrL_3(L')$ predict an angle $\theta_L = 125.65°$ which is remarkably close to that predicted for Eu (124.7°). In fact the upfield shift for the praseodymium silylamide protons, which at first sight is surprising bearing in mind that the europium silylamide protons also give an upfield shift, is due to the change in sign of $3\cos^2\theta - 1$ on crossing the limiting angle of 125.27°. Thus there is remarkable agreement between structural parameters for $PrL_3(L')$ and $EuL_3(L')$ derived from ^1H NMR spectra based on pseudo-contact paramagnetic chemical shifts. The gadolinium complex $GdL_3(L')$ gave as expected very broad ^1H NMR peaks which will require further analysis as will the complex ESR spectra which have been obtained in preliminary experiments.

(b) 1:2 *Complex*: $Eu[N(SiMe_3)_2]_3(Me_3PO)_2$

The addition of Me_3PO (2 mols) to EuL_3 (1 mol) in benzene gave an unstable 1:2 complex $EuL_3(L')_2$ which had a red–orange colour and decomposed (>115°C) before melting. Its IR spectrum showed significant differences from that of the 1:1 complex; in particular the PO stretching frequency 1140 cm^{-1} (*cf.* 1123 cm^{-1}) suggested weaker bonding of the Me_3PO ligands to europium in the 1:2 complex. The ^1H NMR spectrum of the 1:2 complex was dramatically different from that of the 1:1 complex. Thus at 293 K in C_7D_8 the doublet ($^2J_{HP} = 16$ Hz) for the Me_3PO protons was shifted upfield ($\delta - 6.22$; *cf.* $\delta 23.78$ for 1:1 complex) and the silylamide protons downfield ($\delta 2.24$; *cf.* $\delta - 0.42$ for 1:1 complex). It would be premature to attempt any structural calculations based on these data bearing in mind the doubts expressed concerning the origin of the paramagnetic shifts for the 1:1 complex. Nevertheless it is reasonable to suppose that the 1:2 complex should have a structure based on a trigonal bipyramid with the phosphine oxide ligands occupying the axial positions with the silylamide ligands in equatorial positions. On this model the oxygen atoms would be axial and the nitrogens equatorial but the $SiMe_3$ groups might alternate above and below the equatorial plane to minimize interligand repulsions. This would imply a substantial dihedral angle between the EuN_3 plane and the $EuNSi_2$ planes but by symmetry the $SiMe_3$ groups would be equivalent. If the θ_L values for the $SiMe_3$ groups are between 54.73 and 125.27° then their ^1H pseudo-contact paramagnetic shifts will be opposite in sign from those of the Me_3PO protons. In fact the NMR data suggest values of *ca.* 60° (or 120°) which implies a considerable dihedral angle for the $EuNSi_2$ planes. It is hoped that a single crystal X-ray structural determination will be obtained in due course.

Preliminary work suggests that praseodymium forms $PrL_3(L')_2$ with ^1H NMR chemical shifts in C_6D_6 of −3.0 (L) and +5.8 (L').

EXPERIMENTAL

All of the compounds described in this work were extremely sensitive to moisture and operations were conducted *in vacuo* or under an atmosphere of de-oxygenated dry nitrogen, using vacuum-line and glove-box techniques as reported earlier.[1,5] The three-coordinated species ML_3 (M = La, Pr, Eu, Gd and In) were prepared by the literature method.[1,7] Trimethylphosphine oxide (m.p. 139–140°C) was prepared by a modification of Burg and Mekee's method[8] using THF as solvent.

ANALYTICAL METHOD

Elemental analysis for C, H, N and P were obtained commercially from Butterworth Laboratories and University College, London. Lanthanide elements were determined gravimetrically and *bis*-trimethylsilylamide ligand volumetrically by previously reported methods.[1]

Spectroscopic measurements

IR spectra were obtained as Nujol mulls using cells with CsI windows and Perkin–Elmer 577 and 225 spectrophotometers. Mass spectra were obtained by direct insertion in an MS902 machine. NMR spectra were obtained on a Bruker WP80 machine and on the ULIRS Bruker 400 MHz machine. For variable temperature studies solutions were kept in sealed off NMR tubes to avoid hydrolysis. Hydrolysis was indicated by the

presence of the methyl proton signal of the free amine $(Me_3Si)_2NH$ (δ0.19). All chemical shifts are relative to TMS and are reported in Table 1.

Lanthanum tris - (bis - trimethylsilylamide)mono - trimethylphosphine oxide

Trimethylphosphine oxide (0.17 g, 1.85 mmol) in benzene (15 cm^3) was added dropwise to a solution of $La[N(SiMe_3)_2]_3$ (1.14 g, 1.85 mmol) in pentane (40 cm^3). After standing for 14 hr the solvents were pumped off *in vacuo* and the residue purified by extraction and low temperature crystallization from pentane (60 cm^3) giving a white solid (0.7 g, 52% yield). Found: La, 19.16; P, 4.39; $N(SiMe_3)_2$, 66.58%. $La[N(SiMe_3)_2]_3(Me_3PO)$ requires: La, 19.50; P, 4.35; $N(SiMe_3)_2$, 67.47%. IR spectra: 1312(vs), 1300(vs), 1250(sh), 1240(vs), 1124(vs), 1110(sh), 980(vs), 947(vs), 867(vs), 825(vs), 770(m), 750(m), 665(vs), 595(vs), 380(vs), 360(sh).

Indium tris - (bis - trimethylsilylamide)mono-trimethylphosphine oxide

Me_3PO (0.33 g, 3.6 mmol) and $In[N(SiMe_3)_2]_3$ (2.12 g, 3.6 mmol) were allowed to react in benzene (100 cm^3) and after 12 hr the solvent was removed *in vacuo* and the residue extracted with pentane and crystallized to a white solid (1.95 g, 71% yield). Found: In, 16.87; C, 34.86; H, 9.28; N, 5.50; P, 5.2; $N(SiMe_3)_2$, 68.94%. $In[N(SiMe_3)_2]_3(Me_3PO)$ requires: In, 16.71; C, 36.69; H, 9.24; N, 6.12; P, 4.51; $N(SiMe_3)_2$, 69.91%. IR spectra: 1310(vs), 1300(vs), 1265(sh), 1250(vs), 1145(vs), 940(vs), 860(vs), 835(s), 665(sh), 630(sh), 620(s), 395(sh), 360(vs).

Europium tris - (bis - trimethylsilylamide) - mono - trimethylphosphine oxide

Me_3PO (0.18 g, 1.95 mmol) and $Eu[N(SiMe_3)_2]_3$ (1.23 g, 1.96 mmol) were added together in benzene (80 cm^3) and left overnight before pumping off the solvent. The residue was extracted with pentane concentrated to 20 cm^3 and cooled to −20°C. Yellowish-orange hexagonal plates were slowly deposited (0.92 g, 65% yield). Found: Eu, 20.67; Si, 23.1; P, 3.89; $N(SiMe_3)_2$ 65.32%. $Eu[N(SiMe_3)_2]_3(Me_3PO)$ requires: Eu, 20.95; Si, 23.22; P, 4.27; $N(SiMe_3)_2$, 66.25%. IR spectra: 1315(vs), 1300(vs), 1250(sh), 1240(vs), 1180(sh), 1123(vs), 960(vs), 950(sh), 865(m), 850(sh), 825(vs), 770(s), 690(sh), 670(vs), 600(vs), 380(vs), 365(sh).

Europium tris-(bis - trimethylsilylamide) - bis(trimethylphosphine oxide)

Me_3PO (0.31 g, 3.34 mmol) was allowed to combine with $Eu[N(SiMe_3)_2]_3$ (1.06 g, 1.67 mmol) in benzene (50 cm^3). Removal of the solvent *in vacuo* left an orange-red microcrystalline solid. It was noticed that during the addition of the Me_3PO solution to the orange solution of EuL_3 the colour first diminished until about equimolecular proportions were present and thereafter the reddish-orange colour was restored during the addition of the second mol of Me_3PO. The 1:2 complex was unstable and gave problems for analysis. Found: Eu, 19.97; $N(SiMe_3)_2$, 57.01%. $Eu[N(SiMe_3)_2]_3(Me_2PO)_2$ requires: Eu, 18.59; $N(SiMe_3)_2$, 58.79%. IR spectra: 1340(m), 1305(vs), 1290(vs), 1280(sh), 1245(vs), 1233(sh), 1140(vs), 1030(vs), 985(vs), 940(vs), 830(m), 820(sh), 762(m), 745(m), 730(sh), 680(w), 660(vs), 603(sh), 595(vs), 485(vs), 400(m), 363(vs), 350(sh), 275(vs), 245(vs), 215(s), 205(s).

Gadolinium tris-(bis-trimethylsilylamide)-mono-trimethylphosphine oxide

The complex was obtained in 65% yield from equimolar proportions of reactants added together in benzene as for the preparation of the lanthanum complex. Found: Gd, 21.12; P, 4.27; $N(SiMe_3)_2$, 66.73%. $Gd[N(SiMe_3)_2]_3(Me_3PO)$ requires: Gd, 21.52; P, 4.24; $N(SiMe_3)_2$, 65.89%. IR spectra: 1315(vs), 1300(vs), 1250(vs), 1240(sh), 1180(sh), 1128(vs), 1110(sh), 985(sh), 955(s), 940(sh), 775(m), 755(w), 725(sh), 670(vs), 600(vs), 385(vs), 365(sh), 290(w), 245(w).

Acknowledgements—We thank Mr. Greg Coumbarides for measuring NMR (WP80) and IR (PE225) spectra, Mr. Peter Cook for mass spectra, Dr. Halina Chudzynska for technical assistance and Dr. G. E. Hawkes for highfield NMR spectra (400 MHz ULIRS machine at Queen Mary College). Also we are grateful to the Chinese Ministry of Education for financial support.

REFERENCES

[1]D. C. Bradley, J. S. Ghotra and F. A. Hart, *Chem. Comm.* 1972, 349; *J. Chem. Soc. Dalton* 1973, 1021.
[2]J. S. Ghotra, M. B. Hursthouse and A. J. Welch, *Chem. Comm.* 1973, 669.
[3]R. A. Anderson, D. H. Templeton and A. Zalkin, *Inorg. Chem.* 1978, 17, 2317.
[4]D. C. Bradley and M. H. Chisholm, *Acc. Chem. Res.* 1976, 9, 273.
[5]D. C. Bradley, J. S. Ghotra, F. A. Hart, M. B. Hursthouse and P. R. Raithby, *J. Chem. Soc. Dalton* 1977, 1166.
[6]D. S. Katoch and K. D. Sales, *J. Chem. Soc. Dalton* 1980, 2476.
[7]H. Burger, J. Cichon, U. Goetze, U. Wannagat and H. J. Wismar, *J. Organomet. Chem.* 1971, 33, 1.
[8]A. B. Burg and W. E. Mekee, *J. Am. Chem. Soc.* 1951, 73, 4590.

Polyhedron Vol. 1, No. 3, pp. 311–312, 1982
Printed in Great Britain.

0277–5387/82/030311–02$03.00/0
Pergamon Press Ltd.

NOTES

The preparation and electrochemistry of complexes of 4′,4‴-diphenyl-2,2′:6′,2″:6″,2‴:6‴,2⁗ quinquepyridine

(*Received* 24 *November*, 1981)

INTRODUCTION

Although complexes of 2,2′-bipyridine and 2,2′:6′,2″-terpyridine have been widely studied,[1,2] the coordination chemistry of the higher oligopyridines has received little attention. A few complexes of quaterpyridines have been described[1,2,3], but apart from an uncharacterised 1:1 adduct with $Li[ClO_4]$[4], no coordination compounds of quinquepyridines are known. We report here the preparation and electrochemistry of the nickel(II), cobalt(II) and cadmium(II) complexes of 4′,4‴-diphenyl-2,2′:6′,2″:6″,2‴:6‴,2⁗-quinquepyridine (L), and the electrochemical generation of the corresponding nickel(I) and cobalt(I) species.

EXPERIMENTAL

The ligand was prepared by the method of Krohnke[5], the desired 2,6-*bis*(cinnamoyl)pyridine being obtained by the condensation of benzaldehyde with 2,6-diacetylpyridine in the presence of diethylamine. The complexes were prepared by the addition of one equivalent of L to a solution of metal(II) acetate in refluxing methanol. The suspension so obtained was refluxed for 1 h to give a clear solution. Addition of either $[NH_4][PF_6]$ or $Na[BPh_4]$ followed by cooling yielded the product as a microcystalline solid. Satisfactory elemental analyses (C, H, N) were obtained for the complexes $[NiL][PF_6]_2$, $[CoL][BPh_4]_2 4H_2O$ and $[CdL][PF_6]_2.2H_2O$.

Electrochemical measurements were recorded on a Princeton Applied Research Electrochemistry System Model 170. Cyclic Voltammetric studies were carried out using a three-electrode potentiostatic system with platinum wire as auxiliary and working electrodes and an Ag–$Ag[NO_3]$ reference electrode at a scan rate of 1 V sec^{-1}. All readings were taken in acetonitrile with 0.1 mol l^{-1} $[n\text{-}Bu_4N][BF_4]$ present as base electrolyte. Controlled potential electrolysis experiments were carried out using a platinum gauze as the working electrode, a salt bridge being incorporated to separate oxidised and reduced species. ESR spectra were measured as glasses in acetonitrile at 77 K. All solvents were distilled, dried and degassed before use. ^1H NMR spectra were recorded in $CDCl_3$ or CD_3CN solution at ambient temperature on a Bruker WH-400 spectrometer.

RESULTS AND DISCUSSION

Although complexes of L could be obtained under the conditions described above, no coordination occurred if water was used as the solvent, or if metal halide, nitrate or sulphate was used. These results suggest that the ligand in the above complexes is only weakly bound to the metal centre. This was confirmed by the liberation of free ligand upon the addition of halide, water, imidazole, pyridine or triphenylphosphine to solutions of $[NiL]^{2+}$. No complexes could be obtained with salts of Ti(III), Cr(II), Cr(III), Mn(II), Fe(III) or with second-row transition metals other than cadmium. Preliminary results have indicated that polynuclear species are obtained with Zn(II) and Hg(II), and that stable M(O) compounds may be formed with metal carbonyls.

Reductive cyclic voltammetry of $[NiL][PF_6]_2$ in acetonitrile shows a reversible primary reduction wave at $E_{1/2} = -1.14$ V, and a quasi-reversible secondary wave centred at $E_{1/2} = -1.62$ V. Controlled potential electrolysis of $[NiL][PF_6]_2$ in acetonitrile at -1.2 V gave a deep purple solution, the E.S.R. spectrum of which showed the characteristics of typical d^9 nickel(I) spectra $g_\parallel$ 2.197, $g_\perp$ 2.062.[6] The generation of Ni(I) in the system is of particular interest since relatively few examples are known with nitrogen donor ligands.[7] The paramagnetic nickel(II) starting material gave no ESR spectrum at 77 K, but gave a contact shifted ^1H NMR spectrum at ambient temperature. Reduction of $[NiL][PF_6]_2$ by controlled potential electrolysis at the secondary reduction potential, -1.7 V, led to the formation of a nickel(I) ligand radical species, as demonstrated by ESR spectroscopy, $g_\parallel$ 2.130, $g_\perp$ 2.088, isotropic g 2.0661, with the slow concomitant precipitation of L from solution. A similar ligand dissociation process also occurs on the reduction of $[Ni(bipy)_3]^{2+}$ at its secondary reduction potential, although the reduction potentials for this complex occur at significantly higher negative potentials than for $[NiL]^{2+}$. This presumably reflects a greater π-acceptor ability for L compared with bipy.

Reductive cyclic voltammetry of $[CoL][PF_6]_2$ in acetonitrile shows a reversible primary reduction wave at $E_{1/2} = -0.89$ V. Controlled potential electrolysis of $[CoL][PF_6]_2$ at -0.9 V led to the reduction of the cobalt(II) species with concommitant change of colour from orange to dark blue. The reduction was followed by ESR spectroscopy at 77 K which showed the gradual loss of the signal at g_{av} 2.542 assigned to the d^7 Co(II) starting material; on completion of the reduction no ESR signal could be detected at 77 K. This is consistent with the formation of a d^8 cobalt(I) complex with high zero-field splitting.[8]

Cyclic voltammetry of $[NiL]^{2+}$ and $[CoL]^{2+}$ shows a number of further reduction waves for each complex; however, these could not be investigated quantitatively due to the precipitation of the highly insoluble free ligand. The complex $[CdL][PF_6]_2$ gave an irreversible reduction wave at -1.62 V.

In order to elucidate the mode of coordination of the quinquepyridine ligand we have investigated the ^1H NMR spectra of $CDCl_3$, and CD_3CN solutions of L, and CD_3CN solutions of the diamagnetic cadmium(II) complex. In both cases the resonances due to the protons on the *A* and *A′* rings are equivalent, as are those on the *B* and *B′* rings. This indicates that the complex has a high symmetry on the NMR time-scale at ambient temperature, a result which is consistent with a planar quater- or quinquedentate ligand. The resonances due to H_3 $H_{3'}$, $H_{5'}$, H_3 and equivalent protons all experience a considerable downfield shift ($\sim 0.7\delta$) upon coordination, which may be interpreted in terms of Van der Waals deshielding resulting from the adoption of the *cis, cis, cis*-configuration.[9]

This work was undertaken as part of our study of polydentate ligands,[10] and further synthetic and electrochemical studies are underway to elucidate the similarities and dissimilarities between complexes of L and polydentate macrocycles.

Acknowledgements—We should like to thank the S.R.C. for the award of Post-Doctoral Fellowships to ECC and MS.

Department of Chemistry
Lensfield Road
Cambridge CB2 1EW
England

E. C. CONSTABLE,
J. LEWIS*
and M. SCHRÖDER

*Author to whom correspondence should be addressed.

REFERENCES

1. W. E. McWhinnie and J. D. Miller, *Adv. Inorg. Chem. Radiochem.* 1969, **12**, 135.
2. E. C. Constable, *The Chemistry of Diimine Ligands* (1983). Academic Press, New York.
3. W. W. Brandt, F. P. Dwyer and E. C. Gyarfas, *Chem. Rev.*, 1954, **54**, 959.
4. G. Orpen and F. Vogtte, *Annalen* 1979, 2114.
5. F. Krohnke, *Synthesis*, 1976, 1.
6. R. R. Gagne and P. M. Ingle, *J. Am. Chem. Soc.* 1980, **102**, 1444.
7. K. Nag and A. Chakravorty, *Coord. Chem. Rev.* 1980, **33**, 87.
8. B. A. Goodman and J. B. Raynor, *Adv. Inorg. Chem. Radiochem.* 1970, **13**, 136.
9. F. E. Lytle, *Anal. Chim. Acta* 1971, **57**, 239.
10. J. Lewis *et al.*, *J. Chem. Soc., Dalton Trans.* 1980, 1664.

Polyhedron Vol. 1, No. 3, pp. 313–318, 1982
Printed in Great Britain

0277–5387/82/030313–06$03.00/0
Pergamon Press Ltd.

POTENTIOMETRIC INVESTIGATIONS OF SOME ORTHO-DIPHENOLIC COMPLEXES OF ALUMINIUM

by Richard A. Hancock* and Stefan T. Orszulik

The Bourne Laboratory, Royal Holloway College (University of London),
Egham, Surrey TW20 OEX

(*Received* 18 *November* 1981)

Measurements of stability and equilibrium constants of catecholato and pyrogallolato complexes of aluminium have been assessed. They have been redetermined using iterative techniques and these have been applied to complexes of sulphonyl derivatives of these polyhydric phenols.

Water-soluble chelates of aluminium (III) with ortho-diphenolic compounds have been known for 75 years. More recently Dubey and Mehrotra[1] isolated the potassium salts of the mononuclear chelates, $K[Al\ R(OH)_2]\ 3.5\ H_2O$, $K[Al\ R_2].3H_2O$ and $K_3[Al\ R_3]3H_2O$ where R is the catecholate dianion. Similarly the three pyrogallolato complexes were prepared[2] in which the chelating ligand is again the ortho-dianionic species. These workers evaluated the stability constants for both the catecholato and pyrogallolato complexes by potentiometric methods but there are several reservations about their results, some of which have been noted by another worker[3] and others which will be discussed here.

EXPERIMENTAL

Potentiometric titrations were carried out in the temperature range 22-25° using a Pye-Unicam 290 pH meter fitted with an E07 401 HA combined electrode. Aqueous solutions, having an initial volume of 0.05 cm^3, containing nitric acid (4×10^{-3}M), potassium nitrate (2×10^{-1}M) and as appropriate the phenolic compound (6×10^{-3}M) and aluminium nitrate (6×10^{-3}M) were titrated with standardised potassium hydroxide (~1M) (initially by the addition of 0.02 cm^3 aliquots). Nitrogen was bubbled through the solutions to ensure adequate mixing and to maintain an inert atmosphere.

Aluminium-pyrogallolato complexes were isolated as their ammonium salts by the dropwise addition of aqueous ammonia to appropriate mixtures of pyrogallol (50, 100 and 150 mmol) and aluminium nitrate (50 mmol) in water (0.05 dm^3) which had been heated to 90° for 5 min under nitrogen. The products separated from the cold mixture (by the addition of ethanol in the latter two cases) were recrystallised from aqueous solution by the addition of acetone. Satisfactory analyses were obtained for each complex for aluminium[4] and pyrogallate.[5]

RESULTS AND DISCUSSION

As a preliminary to the determination of formation constants using the Irving-Rossotti potentiometric titration technique[6] an attempt was made to prepare the potassium salts of the pyrogallolato complexes of aluminium. Despite many approaches with the exclusion of oxygen, only black products could be obtained. However in contrast, the corresponding ammonium salts were white products, much easier to manipulate owing to their lower solubilities and analysed as $NH_4[Al\ R'(OH)_2].2H_2O$, $NH_4[Al\ R_2'].H_2O$ and $(NH_4)_3[Al\ R_3'].4H_2O$. where R' =

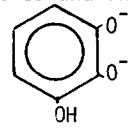

*Author to whom correspondence should be addressed.

Catechol

The proton-ligand formation curve ($\bar{n}_A$ vs. pH) (where $\bar{n}_A$ is the average number of protons bound to catechol) was determined from the titration curves[7] and from it approximate values of the proton-ligand stability constants (K_1 and K_2) obtained by "interpolation of the half $\bar{n}_A$ values" i.e. at $\bar{n}_A \sim 0.5$ and 1.5 respectively. The theoretical formation curve is symmetrical about $\bar{n}_A = 1$ for two proton ligands. Using the correction term method[8] mean proton-ligand stability constants were calculated and are given in Table 1.

Table 1. Proton-ligand stability constants

	$\log_{10} K_1$	$\log_{10} K_2$	$\log_{10} K_3$
Catechol	12.52 ± 0.13	9.46 ± 0.07	-
Pyrogallol	12.67 ± 0.12	11.72 ± 0.11	9.21 ± 0.09
3,3',4,4'-tetra-hydroxydiphenylsulphone	12.09 ± 0.07	7.83 ± 0.05	-
3,3',4,4',5,5'-hexa-hydroxydiphenylsulphone	12.66 ± 0.15	10.39 ± 0.08	7.46 ± 0.09
2,3-dihydroxybenzoic acid	12.4 ± 0.08	9.9 ± 0.03	3.01 ± 0.04
3,4-dihydroxybenzoic acid	11.89 ± 0.08	9.02 ± 0.05	4.67 ± 0.02

The formation curve for the catecholato complexes of aluminium ($\bar{n}$ vs. pL, where $\bar{n}$ is the average number of catecholate ligands (L) bound to aluminium) was obtained from the appropriate titration curves[7] and from it an estimate of the three metal-ligand stability constants (K_n) made by "interpolation of half $\bar{n}$ values". Beck[8] regards the Irving-Rossotti[9] requirement of ratios of successive stability constants $(K_n/K_{n+1}) > 10^{2.5}$ to be insufficiently demanding for reliance to be put on the "half $\bar{n}$ value" method and instead prefers the ratio to be $>10^4$. Previously determined (3, 10) values of K_2/K_3 meet the more exacting condition but values of K_1/K_2 do not and therefore the "half-$\bar{n}$ value" method would be expected to give inaccurate results. Dubey and Mehrotra[1] in using the correction term method have assumed symmetry in the formation curve for $0<\bar{n}<2$ at $\bar{n} = 1$ and similarly for $1<\bar{n}<3$ at $\bar{n} = 2$. However when there is overlapping of equilibria there cannot be these points of symmetry and so the correction term method must not be applied. In addition to this fundamental restriction, Slabbert[3] has pointed out that these workers have used data for their formation curve which is not consistent with the experimental titration curve. This we have now been able to apportion to their implied use of a value of $\bar{n}_A = 1$ for the calculation of $\bar{n}$ values rather than $\bar{n}_A \sim 2$ which is more appropriate for the pH range studied.

In this work rigorous values for the aluminium-ligand stability constants have been calculated using the approximation formula given by Beck[8], from which, for three successive equilibria, the following three equations may be derived:

$$\log_{10} K_1 = -\log_{10} [L] + \log_{10}\left\{\frac{\bar{n}}{(1-\bar{n}) + (2-\bar{n})[L] K_2 + (3-\bar{n})[L]^2 K_3 K_2}\right\} \qquad (1)$$

$$\log_{10} K_2 = -\log_{10} [L] + \log_{10}\left\{\frac{(\bar{n}-1)[L] K_1 + \bar{n}}{(2-\bar{n})[L] K_1 + (3-\bar{n})[L]^2 K_1 K_3}\right\} \quad (2)$$

$$\log_{10} K_3 = -\log_{10} [L] + \log_{10}\left\{\frac{(\bar{n}-2)[L]^2 K_1 K_2 + (\bar{n}-1)[L] K_1 + \bar{n}}{(3-\bar{n})[L]^2 K_1 K_2}\right\} \quad (3)$$

Thus, beginning with the estimated values of K_1, K_2 and K_3 an iterative method was applied to the equations 1-3 until the sum of the absolute differences between successive approximations of the three log K_n values was $<10^{-6}$. The values of log K_n, included in Table 2, are the arithmetic means for iterations commenced with several different values of [L] and $\bar{n}$ (three values of each of [L] and $\bar{n}$ being required for each approximation, one pair appropriate to each K_n such that $n>\bar{n}>n-1$).

Table 2. Aluminium-ligand stability constants

	$\log_{10} K_1$	$\log_{10} K_2$	$\log_{10} K_3$
Catechol	15.31 ± 0.10	12.36 ± 0.15	7.74 ± 0.18
3,3',4,4'-tetra-hydroxydiphenylsulphone	14.93 ± 0.08	12.65 ± 0.32	9.24 ± 0.20
3,4-dihydroxybenzoic acid	15.03 ± 0.08	12.61 ± 0.12	9.91 ± 0.35

3,3',4,4'-tetrahydroxydiphenyl sulphone[11]

Similar methods for the determination of proton and aluminium-ligand stability constants to those used for catechol were applied here. It was assumed that this sulphone could be treated as a pair of independent orthodiphenolic units and that electronic effects are not transferred from one ring to the other through the sulphonyl group. Only two proton-ligand stability constants were thus calculated (see Table 1) and these used to construct a theoretical formation curve (Fig. 1) from equation 4.

$$\bar{n}_A = \frac{K_1[H^+] + 2K_1K_2[H^+]^2}{1 + K_1[H^+] + K_1K_2[H^+]^2} \quad (4)$$

The experimental formation curve is also shown in Fig. 1 and the agreement supports the assumption made above. The relative concentrations of sulphone and aluminium was such as to prohibit the formation of polynuclear complexes. The three aluminium-ligand stability constants are shown in Table 2.

Pyrogallol The proton-ligand formation curves were determined as outlined for catechol. Equations 1-3 were used iteratively as before with H^+ and $\bar{n}_A$ replacing L and $\bar{n}$ respectively to determine the proton-ligand stability constants. The approximate values were first determined using "half $\bar{n}$ values".

To obtain the aluminium-o-pyrogallolate dianion formation curve it is necessary to know the proton stability constants of the ortho-dianion, thus it is a requirement to know the structures of species involved in the successive protonations of the trianion. If the dianion has the structure R' then from K_2,(Ka_2) and K_3,(Ka_1) the aluminium-o-pyrogallolate dianion formation curve may be deduced. However, if the dianion has the structure R" then this formation curve may not be deduced.

R" = 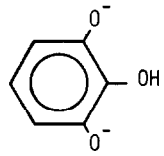

Evidence for the dianion structure being R" has been provided[12] on the basis of the similarity between the pKa_2 for resorcinol (11.06) and that for pyrogallol (11.19).

In their work with pyrogallol, Dubey and Mehrotra[2] did not acknowledge the existence of any difficulty with the assignment of a structure to the dianion. For the aluminium-ligand formation curve they simply used K_2 and K_3 (the second and third proton-ligand stability constants). Slabbert[3] attempted to overcome the difficulty by using the value of pKa_2 of 3-methoxycatechol in place of K_2, justifying this by the similarity of σ_{meta} for m-OH and m-OMe. We have devised the following approach for the determination of the aluminium-ligand formation curve when there is no direct access to [L] values. Since the equilibrium constant, Ke_n, is defined for equation 5 then [L] can be expressed by equation 6 (LH_2 is the protonated dianion).

$$AlL_{n-1}^{(2n-5)-} + LH_2 \xrightarrow{Ke_n} AlL_n^{(2n-3)-} + 2H^+ \qquad (5)$$

$$[L] = (Ke_n/K_n)\,[LH_2]\,/[H^+]^2 \qquad (6)$$

The quantity $[LH_2] / [H^+]^2$ has been used by us in place of [L] for both the construction of the aluminium-ligand formation curves and for the iterative treatment using equations 1-3. The constants so determined are equilibrium constants, defined by equation 6 and are given in Table 3. Potentiometric measurements were made in the pH range for which the hydroxyl group, not involved in chelation, remained undissociated. Thus, regarding pyrogallol as a dibasic acid (eqn. 6) the maximum value of $\bar{n}_A$ was taken as 2 for calculations of $\bar{n}$. Slabbert appears inadvertently to have applied this restriction but by virtue of having evaluated only Ka_1 and Ka_2 for pyrogallol.

Table 3. Aluminium-ligand equilibrium constants

	pK_1	pK_2	pK_3
Catechol	6.67 ± 0.10	9.62 ± 0.15	14.24 ± 0.18
Pyrogallol	6.00 ± 0.03	8.62 ± 0.42	14.67 ± 0.22
3,3',4,4'-tetra-hydroxydiphenylsulphone	4.99 ± 0.08	7.27 ± 0.32	10.68 ± 0.20
3,3',4,4',5,5'-hexa-hydroxydiphenylsulphone	4.73 ± 0.28	6.60 ± 0.07	9.57 ± 0.23
3,4-dihydroxybenzoate anion*	5.88 ± 0.08	8.30 ± 0.12	11.00 ± 0.35

*Carboxylate considered fully ionised in pH range studied

3,3'4,4',5,5'-hexahydroxydiphenylsulphone[11]

This sulphone may be considered to behave as a pair of independent pyrogallol units. The proton-ligand formation curve and the three proton-ligand stability constants were evaluated therefore as above (see Table 1). Again, without having access to [L] values, the aluminium-ligand formation curve was constructed as a plot of $\bar{n}$ vs. $p([H^+]^2/[LH_2])$, from which equilibrium constants were obtained. Use of these was made to construct a theoretical formation curve from eqn. 7.

$$\bar{n} = \frac{Ke_1 X + 2Ke_1Ke_2 X^2 + 3Ke_1Ke_2Ke_3 X^3}{1 + Ke_1 X + Ke_1 Ke_2 X^2 + Ke_1Ke_2Ke_3 X^3} \qquad (7)$$

$$X = \left[LH_2\right] / \left[H^+\right]^2$$

The good agreement between the theoretical and experimental formation curves (Fig. 2) supports the assumption that just one of the identical ortho diphenate groups is the effective ligand here.

3,4 and 2,3- dihydroxybenzoic acids

The proton ligand stability constants were determined as previously described and are given in Table 1. However, the aluminium-ligand formation curves yielded values for stability constants which were of the correct magnitude only in the case of 3,4-dihydroxybenzoic acid. In evaluating pL for these formation curves proton-ligand stability constants for the two phenolic groups were used. Preliminary studies indicate that chelation with the 2,3-dihydroxybenzoic acid is through the carboxylate and ortho phenate groups.

Hydroxides of aluminium chelates

The presence of hydroxides would be expected to interfere with the titrations of both di- and tri- hydroxyphenyl systems. However it has been shown by Dubey and Mehrotra[1,2] that titrations of 1:1,1:2 and 1:3 molar ratios of aluminium to phenolic compounds have inflexions for the formation of hydroxides but at higher pH than the formation of the next successive complex. Since we have used considerable excesses of phenolic compounds over aluminium nitrate, the formation of such hydroxides is thought not to have any significant effect.

Acknowledgements

The financial support of the British Leather Manufacturers' Research Association to one of us (S.T.O.) and experimental help with the dihydroxybenzoic acids by Miss F. M. Hardy and Miss K. S. Hartridge is acknowledged.

References

1 S. N. Dubey and R. C. Mehrotra, J. Inorg. Nucl. Chem. 26, 1543 (1964)

2 S. N. Dubey and R. C. Mehrotra, Indian J. Chem. 5, 327 (1967)

3 N. P. Slabbert, Ph.D. Thesis, Rhodes University (South Africa), 1972

4 A. I. Vogel, A textbook of quantitative inorganic analysis, 3rd edn., Longmans, London, 1931, P.516

5 W. Bottger, Newer methods of volumetric chemical analysis, Chapman & Hall, Lond.,1938,p.55

6 H. S. Rossotti, Chemical Applications of potentiometry, D. Van Nostrand, London, 1969

7 H. Irving and H. S. Rossotti, J. Chem. Soc., 2904 (1954)

8 M. T. Beck, Chemistry of complex equilibria, Van Nostrand Reinhold, London, 1970

9 H. Irving and H. S. Rossotti, J. Chem. Soc. 3397 (1953)

10 L. Havelkova and M. Bartusek, Coll. Czech. Chem. Comm. 34, 3722 (1969)

11 S. T. Orszulik, Ph.D. Thesis, University of London, 1978

12 M. Bartusek and J. Zelinka, Coll. Czech. Chem. Comm. 32, 992 (1967)

Figure 1: Proton-ligand formation curve of 3,3',4,4'-tetrahydroxydiphenyl sulphone

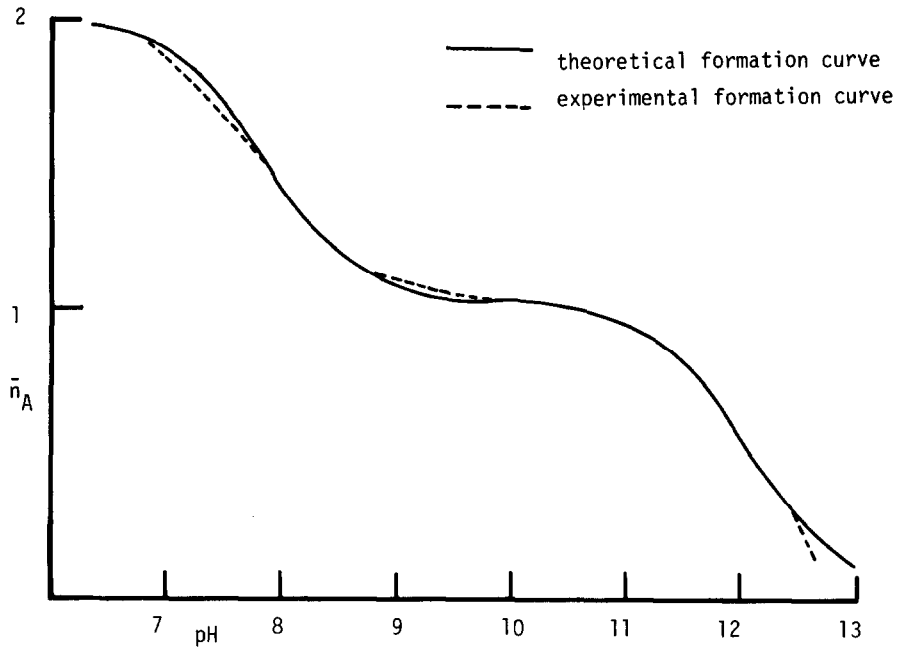

Figure 2: Metal-ligand formation curve of the aluminium-3,3',4,4',5,5'-hexahydroxydiphenyl sulphone complexes

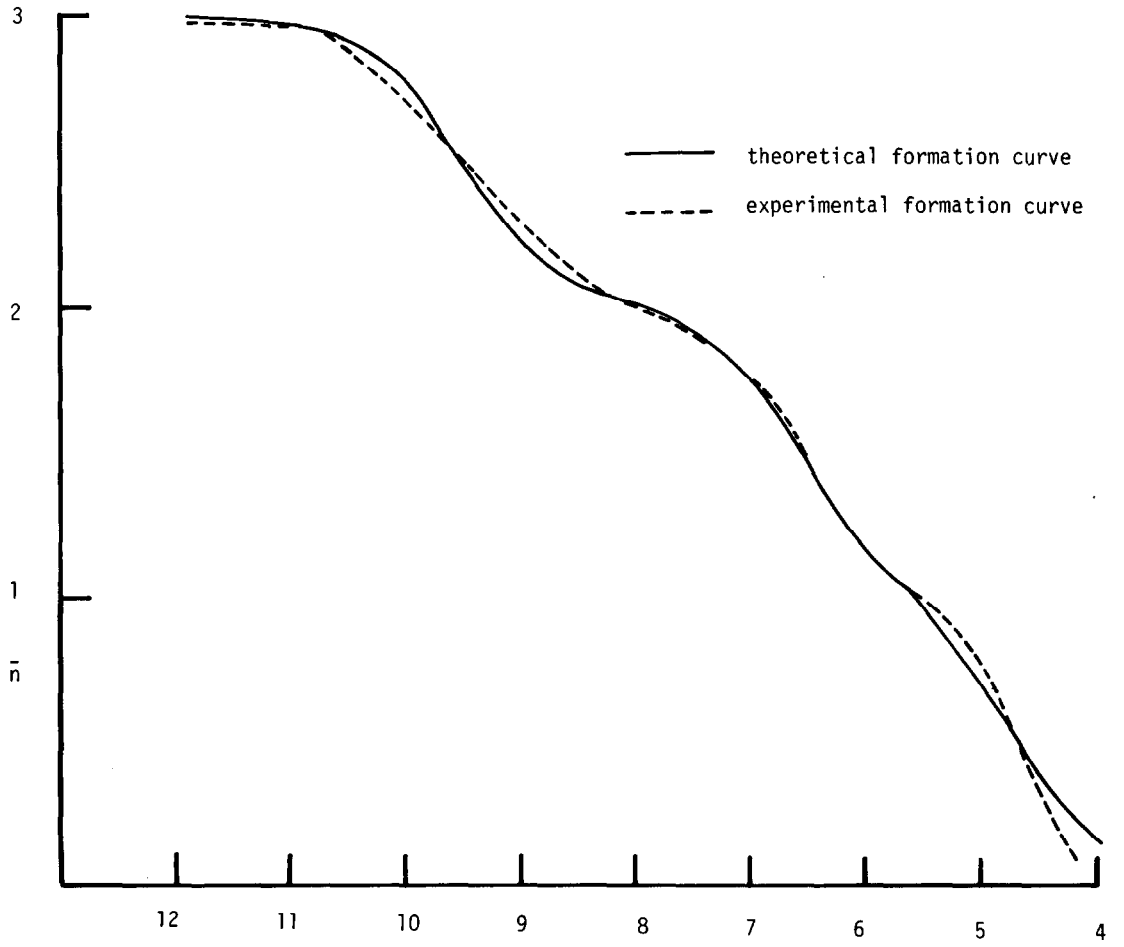

Polyhedron Vol. 1, No. 3, p. 319, 1982
Printed in Great Britain.

0277-5387/82/030319-01$03.00/0
Pergamon Press Ltd.

COMMUNICATION

Diboron tetraiodide and its decomposition

(*Received* 16 *October* 1981)

Schumb *et al.*,[1] in describing the preparation of diboron tetraiodide[1], reported that the compound did not melt and that it decomposed to give an involatile black solid. We have repeated the preparation, which involves passing boron triiodide vapour through a radiofrequency discharge, and found that B_2I_4 melts under vacuum reproducibly at 94–95°. A few degrees below the melting point the colour darkens from the original pale yellow and on melting the samples immediately begin to decompose giving a black-looking product and boron triiodide. At room temperature the decomposition is slow and only after some days do hexagonal crystals of BI_3 begin to appear; decomposition is more rapid in a solvent such as methylene chloride giving dark, red–purple solutions.

After decomposing samples of diboron tetraiodide at 100–400° and removing the boron triiodide it was found that the dark residue would sublime at temperatures in excess of 250° at 10^{-4} mm Hg pressure. Mass spectral analysis showed that the sublimate was mainly B_9I_9 with about 15% of B_8I_8. The B_9I_9 has very similar properties to those described by Wong[2]: solutions in CH_2Cl_2, $CHCl_3$, CCl_4, toluene and petrol ether were pink to red–purple depending on solubility whilst royal blue solutions were formed in methyl and ethyl alcohols and acetone. Wong[2] has shown that the latter blue colour is due to the presence of $B_9I_9^-$ ions.

The mass spectrum of B_9I_9 shows a continuation of the trend observed with B_9Cl_9 and B_9Br_9; the heavier the halogen the more stable is the parent ion towards loss of BX_3. The ratios $B_9X_9^+$: $B_8X_6^+$ are approximately, 0.4 (Cl), 1.3 (Br) and 8 (I). The stability of B_9I_9 is further indicated by the formation of the doubly-charged parent ion $B_9I_9^{2+}$; two other doubly-charged ions, $B_9I_3^{2+}$ and $B_9I_2^{2+}$, are also encountered in the mass spectrum.

The discharge vessel is coated with a mainly involatile black residue but, on strong heating with a hand torch, small amounts of B_9I_9 and B_8I_8 can be sublimed out. As the discharge zone gets very warm during operation it is probable that these two monoiodides arise from the thermal decomposition of some B_2I_4 and are not, therefore primary discharge products.

A. G. MASSEY*
P. J. PORTAL

Department of Chemistry
University of Technology,
*Loughborough, Leicestershire, LE*11 3*TU*
England

*Author to whom correspondence should be addressed.

REFERENCES

[1]W. C. Schumb, E. L. Gamble and M. D. Banus, *J. Am. Chem. Soc.* 1949, **71**, 3225.
[2]E. H. Wong, *Inorg. Chem.* 1981, **20**, 1300.

Polyhedron Vol. 1, No. 4, pp. 321–325, 1982
Printed in Great Britain.

0277-5387/82/040321-05$03.00/0
Pergamon Press Ltd.

^{1}H NMR STUDIES OF THE ISOMERS OF DICYANOCOBALAMIN AND DICYANOCOBINAMIDE

PRASANNA K. MISHRA and RAJ K. GUPTA*
The Institute for Cancer Research, The Fox Chase Cancer Center, PA 19111, U.S.A.

and

PRABHAT C. GOSWAMI, P. N. VENKATASUBRAMANIAN and AMAR NATH*
Department of Chemistry, Drexel University, PA 19104, U.S.A.

(*Received* 27 *April* 1981)

Abstract—An isomeric form of cyanocobalamin (cyanocobalamin') discovered earlier has been reported to exhibit conformational differences from the regular form, in the corrin ring, aminopropanol side chain, and the nucleotide base. In the present work, we have attempted to answer the question whether a variation in the puckering of the corrin ring in the new form brings about a conformational change in the nucleotide base or vice versa. Measurements of NMR chemical shifts and spin-lattice relaxation times for a large number of protons show that the two isomeric forms of dicyanocobalamin (where the benzimidazole base is detached from the cobalt atom) exhibit differences in conformation for all the three segments of the molecule, namely, the corrin ring, the amino-propanol chain, and the nucleotide base. NMR studies also indicate the existence of a conformationally different isomer of dicyanocobinamide (where the nucleotide base is completely cleaved off), namely dicyanocobinamide'. The existence of cobinamide' is confirmed by means of thin layer chromatography. Based on these observations, it is suggested that a significant variation in the puckering of the corrin ring occurs in the new form and brings about a consequent change in the conformation of the nucleotide base through the amino-propanol linkage.

INTRODUCTION

We have reported earlier a new naturally occurring isomeric form of cobalamins[1]. The UV-visible spectrum of any cobalamin' (the new form) is indistinguishable from that of its corresponding regular analog. The conversion of a cobalamin to cobalamin' is achieved by substituting the benzimidazole base by a small group like H_2O or CN^- and modest thermal treatment. The base can subsequently be re-attached to the cobalt atom by adjustment of pH of the solution with retention of the new form. It seems that the corrin ring becomes quite flexible in the "base-off" form, due to the absence of benzimidazole steric contacts, and it flips into a new conformation with modest thermal treatment. For instance, adenosylcobalamin tends to convert into adenosylcobalamin' in acidic aqueous solution (pH ~ 2) in the "base-off" state at 70°C, while the adenosylcobalamin' tends to back-convert into adenosylcobalamin at room temperature. The interconversion can be frozen by raising the pH and putting the base on.

The new form of cobalamin is inevitably present as an impurity in the pharmaceutical preparations of the corresponding regular analog; hydroxycobalamin' can even be present to the extent of 10% in commercially available hydroxycobalamin. This raises the question whether one of the forms could be anti-anemic factor while the other one could be anti-neurologic or whether the new form is biologically inactive.

Any cobalamin' can be separated from the corresponding regular analog using ion-exchange chromatography and each of the forms can be identified with the help of thin layer chromatography.

The conformational change in going from cobalamin to cobalamin' is borne out by subtle relative changes in chemical shifts of protons on the corrin ring and the nucleotide base. However, there are considerable differences in the Mössbauer parameters of the two forms for a large variety of derivatives. These differences are indicative of significant variation in the immediate environment of the cobalt atom. Both NMR and Mossbauer data would be consistent with a small out-of-plane upward displacement of the cobalt atom associated with variations in the puckering of the corrin ring and changes in the conformation of the nucleotide base[1].

The present work is an attempt to investigate the cause and effect relationship, namely, whether the conformational change in the corrin ring brings about a corresponding conformational change in the benzimidazole base or vice versa. To answer this question we have followed two approaches. Firstly, we have studied the chemical shifts and nuclear spin-lattice relaxation times, T_1, for protons in the corrin ring (including its substituents) and in the benzimidazole base when it is detached from the cobalt atom, for the two isomeric forms of dicyanocobalamin. Secondly, we have looked into the possibility of the existence of the conformational isomer of a cobinamide, where the benzimidazole base is completely cleaved off (Fig. 1). Some of the preliminary work was reported earlier[2].

MATERIALS AND METHODS

Preparation of dicyanocobalamin and dicyanocobalamin'

Cyanocobalamin' was prepared by thermal treatment of the dicyanocobalamin under controlled conditions[1]. About 5 mg each of cyanocobalamin and cyanocobalamin' were dissolved in approx. 0.5 ml of D_2O con-

*Author to whom correspondence should be addressed.

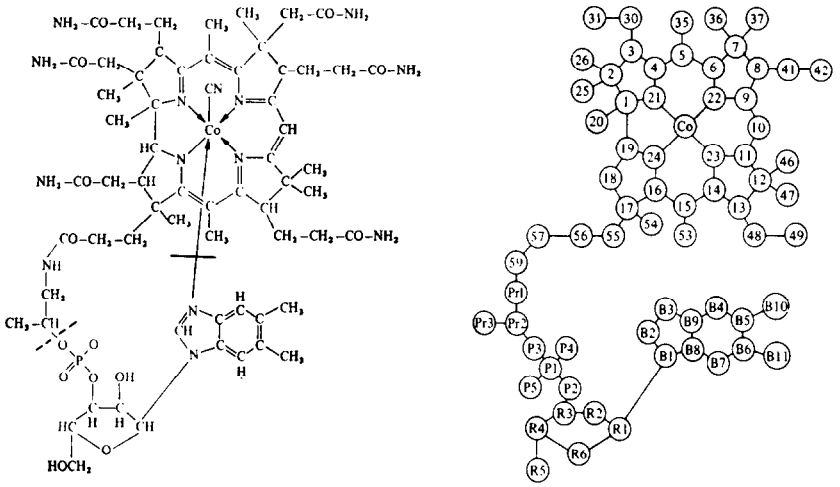

Fig. 1. Molecular structure formula of cyanocobalamin. (a) Rupture of the bond at ——— gives dicyanocobalamin. (b) Hydrolysis at ----- gives dicyanocobinamide.

taining 10 equivalents of KCN for NMR measurements (pH ~ 11.0).

Preparation of dicyanocobinamide and dicyanocobinamide'

The cobinamide and cobinamide' were prepared from the cyanocobalamin and cyanocobalamin', respectively, by treatment with concentrated HCl at 65°C for 5 min[3]. Under these conditions the nucleotide side chain is split off with little hydrolysis of the amides. Fifty milligrams of cyanocobalamin or cyanocobalamin' was treated with 10 ml of concentrated HCl at 65°C for 5 min and then the solution was chilled in ice–salt bath. The excess acid was neutralized by dropwise addition of chilled 6 M NaOH with constant stirring and finally the pH was adjusted to ~ 4 using 0.1 M NaOH. The corrinoid solution was desalted using phenol solution in methylene chloride[1].

The cobinamide was purified as follows. The solution was passed through SP–Sephadex C–25 and the effluent and washings were rejected. The absorbed corrinoids were eluted with 1% NaCl and the solution acidified with dilute HCl to adjust the pH of the solution to ~ 5. The solution was desalted with phenol and passed over DEAE–Sephadex A–25 (Cl^-). The effluent was collected and freeze-dried. Five milligrams of cyanoaquocobinamide was dissolved in approx. 0.5 ml of D_2O containing 2 equivalents of KCN for NMR studies (pH ~ 10.5).

The cobinamide' was purified by passing the solution through DEAE–Sephadex A–25 (Cl^-). The effluent was freeze-dried. The freeze-dried corrinoid was dissolved in a couple of millilitres of water and passed over SP–Sephadex A–25. The faster moving fraction is cyanoaquocobinamide'. Five milligrams of cyanoaquocobinamide' in about 0.5 ml of D_2O containing 2 equivalents of KCN was used for NMR studies.

Identification of cobinamides using thin layer chromatography (TLC)

TLC was carried out on cellulose plates at room temperature using s-butyl alcohol–ammonia ($\rho = 0.88$)–water–1.0 M KCN (250:0.4:100:0.3) as solvent[4]. The cobinamide' moves slowly as compared to the cobinamide. Moreover, two spots of unequal intensity were observed for the cobinamide' which is reminiscent of cyanocobalamin'[1]. The R_f values for the two components of cobinamide' were found to be 0.45 (more intense spot) and 0.55 respectively as compared to 0.62 for the cobinamide. The two components of cobinamide' were found to be genetically related. If one of the spots on the TLC plate was scraped and redeveloped on a fresh TLC plate, after keeping the solution for several weeks, the other spots also make their appearance.

NMR measurements

The chemical shifts (in parts per million (ppm) of the observing field) of the protons are measured at 360 MHz relative to the methyl resonance of the sodium salt of 2,2 dimethyl-2-silapentane sulfonic acid (DSS), used as an internal reference, using the Middle Atlantic NMR Facility at the University of Pennsylvania, Philadelphia. Parts of the 360 MHz NMR spectra with assignable lines, for the two isomeric forms of dicyanocobalamin and dicyanocobinamide, are given in Figs. 2–4.

Spin-lattice relaxation times, T_1, for several of the identifiable protons were measured at 21 ± 1°C at 100 MHz using the inversion recovery technique[5]. The values of T_1 are reported in Table 1. The errors in T_1 measurements are less than ± 5% for the longer values (>200 ms) and ±10% for the shorter values (<200 ms). Both, the least-squares fitting of the data points to a theoretical recovery curve for the magnetization and the observation of the magnetization null point in the inversion recovery sequence gave similar values for T_1. Because of overlap of DSS lines with C–47 (Fig. 1) methyl resonance of dicyanocobinamides at 100 MHz, the T_1 for C–47 methyl group could not be measured.

The line assignments were made with the help of earlier studies[6–8]. There are eleven methyl groups in the cobalamins and nine in cobinamides. In addition, in D_2O solution the cobalamins give rise to five assignable single proton resonances (Fig. 3) and the cobinamides give a single line attributable to C-10 vinyl proton (Fig. 4).

RESULTS AND DISCUSSION

One observes dramatic changes in chemical shifts for the benzimidazole base protons B–2, B–4 and B–7 in going from (the two isomeric forms of) cyanocobalamin to (the corresponding forms of) dicyanocobalamin. It seems that the B–2 and B–4 protons due to their closer proximity initially to the π-electron system of the corrin ring[9] than B–7 (Fig. 1) show a larger downfield shift when the benzimidazole base is detached from the cobalt atom (and replaced by CN^-) and presumably moves further away from the corrin ring. It is interesting to note that the chamical shifts for B–4 and R–1 protons exhibit significant changes in going from cyanocobalamin to cyanocobalamin' and dicyanocobalamin to dicyanocobalamin' in contrast to that of the B–7 proton. A slight change in the orientation and/or the distance of the benzimidazole base with respect to the corrin ring can account for these shifts. Similarly, B–2 chemical shift also shows significant change for the two isomeric forms of dicyanocobalamin.

The C–20 and C–47 methyls which are ring current-shifted by the benzimidazole base undergo substantial downfield shifts when the base is detached in the dicyanocobalamins. Even other methyl protons on the corrin ring show quite significant changes in the chemical shifts while going from cyanocobalamin to dicyanocobalamin.

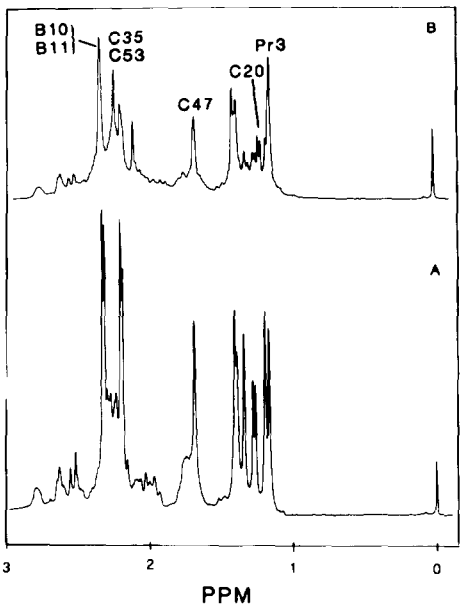

Fig. 2. The high field portion of 360 MHz proton NMR spectrum of (A) dicyanocobalamin and (B) dicyanocobalamin', both at pH 11.0, in D_2O solution and at 21 ± 1°C. The sample concentration in each case is approximately 10 mg/ml of the solution. The methyl resonance of 2,2-dimethyl-2-silapentane sulfonic acid (DSS) internal reference appears at 0.0 ppm.

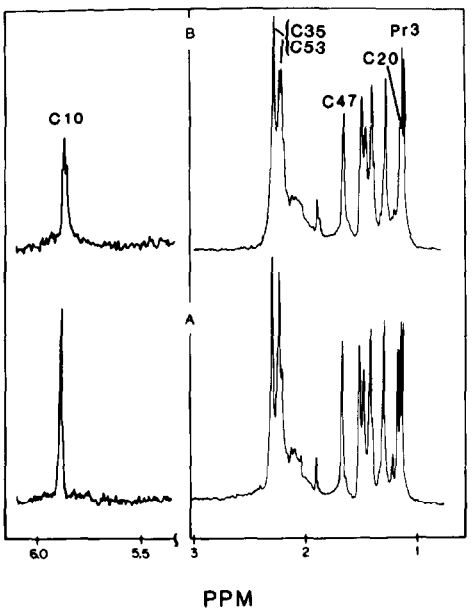

Fig. 4. The high and low field (aromatic) portions of 360 MHz proton NMR spectrum of (A) dicyanocobinamide (B) dicyanocobinamide' both at pH 10.5, in D_2O solution and at 21 ± 1°C. The sample concentration in each case is approx. 10 mg/ml.

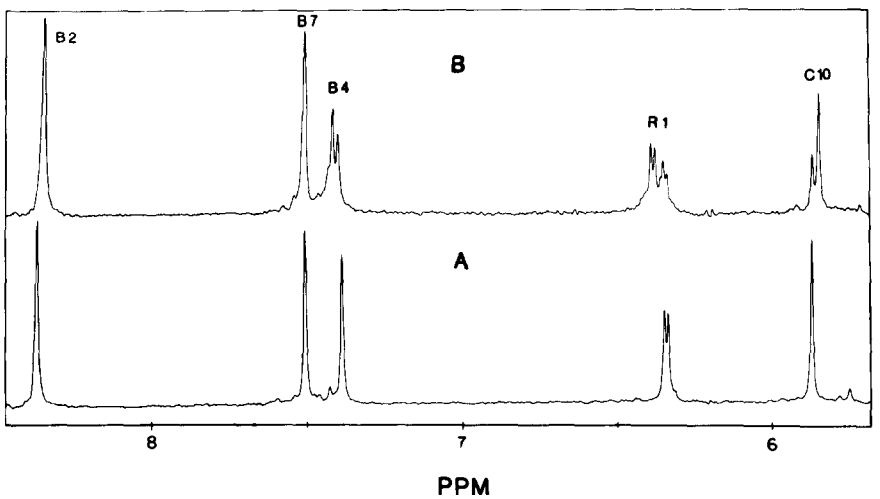

Fig. 3. The low field (aromatic) portion of 360 MHz proton NMR spectrum of (A) dicyanocobalamin and (B) dicyanocobalamin', both at pH 11.0, in D_2O solution and at 21 ± 1°C. The sample concentration in each case is approximately 10 mg/ml of the solution.

Table 1. Line position, T_1 and assignment

Assignment	Cyanocobalamin[a]		Cyanocobalamin'[a]		Δδ (ppm)[b]	Dicyanocobalamin		Dicyanocobalamin'		Δδ (ppm)[b]	Dicyanocobinamide		Dicyanocobinamide'		Δδ (ppm)[b]
	δ (ppm)	T_1 (ms)	δ (ppm)	T_1 (ms)		δ (ppm)	T_1 (ms)	δ (ppm)	T_1 (ms)		δ (ppm)	T_1 (ms)	δ (ppm)	T_1 (ms)	
B2	7.275	335	7.276	326	-0.001	8.380	850	8.348	526	0.032					
B4	6.503	294	6.532	219	-0.029	7.392	330	7.420	494	-0.028					
B7	7.081	298	7.088	278	-0.007	7.510	690	7.510	555	0.000					
B10	2.536	144	2.562	116		2.331	172	2.332	226						
B11	2.570					2.318									
R1	6.349	239	6.361	202	-0.012	6.349 6.337	220	6.392 6.380	234	-0.043 -0.043					
Pr3	1.253	195	1.259	180	-0.006	1.163	143	1.146	135	0.017	1.146 1.129	290	1.148 1.129	325	-0.002 0.000
C10	6.081	205	6.071	195	0.010	5.871	235	5.850	214	0.021	5.878	220	5.872	200	0.006
C20	0.448	55	0.473	56	-0.025	1.277 1.258	169	1.229			1.172	263	1.182	244	-0.010
C47	1.187	144	1.177	117	0.010	1.684	85	1.671	75	0.013	1.670		1.671		-0.001
C35	2.253	203	2.263	181	-0.010	2.208	117	2.239	112	-0.031	2.302	102	2.300	109	0.002
C53						2.192		2.197	122	-0.005	2.238	116	2.250 2.233	110	
Unassigned	1.380	132	1.372	134	0.008			2.107	138		1.519	56	1.510	61	0.009
	1.863	116	1.872	87	-0.009	1.406	105	1.410		-0.004	1.477		1.475		0.002
											1.417	79	1.422	65	-0.005
											1.299	157	1.297	195	0.002

[a] These results are from [1].

[b] Δδ (ppm) is the shift in the novel form of the molecule's line position. A positive number indicates a shift in the upfield direction, and a negative number indicates a shift in the downfield direction with respect to the line position in the regular form. The error in chemical shift measurements is ± 0.002 ppm.

[c] The errors in T_1 measurements are less than ± 5% for larger values (>200 ms) and ± 10% for shorter values (< 100 ms).

On the other hand, the differences in chemical shifts between dicyanocobalamins and cobinamides are relatively small. Detachment of the benzimidazole base removes the steric interactions with the corrin ring and so the puckering of the corrin ring is modified and is quite similar for the dicyanocobalamins and the cobinamides. However, small but significant differences in chemical shifts are observed between dicyanocobalamin and dicyanocobalamin', and between dicyanocobinamide versus dicyanocobinamide' (Table 1).

We observe very interesting changes in proton spin-lattice relaxation times, T_1, in going from cyanocobalamin to dicyanocobalamin and to dicyanocobinamide, and also between the two isomeric forms of these species. The changes in the magnitude of T_1 can be governed by the tumbling time of the molecule (correlation time, τ_c), localized segmental motion of a group (e.g. degree of hindrance to methyl rotation) and to changes in the magnetic environment. It is not possible at present to estimate the relative contribution of each of the above factors. However, we discuss the changes in T_1 in a more general and qualitative fashion. As seen from the relaxivity expression below (for a proton relaxing due to the direct dipolar interaction with another proton)

$$\frac{1}{T_1} = \frac{3}{2}\frac{\gamma_H{}^4\hbar^2}{r^6}$$

(where γ_H and $\hbar$ are the gyromagnetic ratio of proton and the Planck's constant respectively), very small changes in the magnetic environment, i.e. inter-proton distance, r, can bring about a large change in T_1. Furthermore, it is estimated that if a completely hindered methyl group becomes entirely free to rotate, one can observe an increase in T_1 of about a factor of four[10].

Doddrell and Allerhand[11] have observed for dicyanocobalamin that the T_1 values for all singly protonated ^{13}C nuclei in the nucleotide base viz., B–2, B–4 and R–1, are centered around 240 ms while for ^{13}C attached to a single proton on the corrin ring, namely C–10, the T_1 is 110 ms. From these observations we have obtained the effective correlation time at 21°C for the corrin ring as $\simeq 8\times10^{-10}$ s and for the nucleotide base as $\cong 4\times10^{-10}$ s. This clearly indicates that the nucleotide base is free to undergo some segmental motion once its linkage from cobalt is detached. This would in part explain the dramatic increase in T_1 for B–2 and B–7 in going from cyanocobalamin to dicyanocobalamin. The increase in T_1 for the same protons is not so impressive while going from cyanocobalamin' to dicyanocobalamin'. It would seem that the nucleotide base in dicyanocobalamin' may not have that much motional freedom and, moreover, it may be situated closer to the corrin ring. T_1 for the B–4 proton also shows an increase but to a lesser extent than for B–2 and B–7 presumably because of its closer proximity to some protons on the corrin ring. For the two methyls in the nucleotide base, namely B–10 and B–11, one observes relatively small increases in T_1, contrary to expectations, in going from cyanocobalamin' to dicyanocobalamin'. Perhaps the benzimidazole group moves closer to the propionamide group when detached from cobalt and the magnetic environment reduces the spin-lattice relaxation time. The methyl Pr3 on the aminopropanol side-chain shows a decrease in T_1 in going from cyanocobalamin to dicyanocobalamin presumably due to a change in the magnetic environment and shows a dramatic increase for the dicyanocobinamide. This is not surprising; one would expect considerable freedom of motion of the amino-propanol side chain after cleavage of the nucleotide base (Fig. 1).

The methyl groups on the corrin ring, C–35, C–53, C–47 and C–20 show changes, either an increase or decrease in T_1, while going from cyanocobalamin to dicyanocobalamin. The changes can be attributed to a combination of all three afore-mentioned factors.

We have also previously studied the ^{31}P nuclear relaxation times T_1 of the two isomeric forms of cyanocobalamin and dicyanocobalamin[12]. The observed differences in T_1 in their two isomeric forms were interpreted on the basis of structural changes arising from variations in the nature of puckering of the corrin ring. The ^{31}P chemical shifts for the two isomers were, however, the same, indicating that the structural differences in the isomeric forms do not alter the electronic environment of the phosphorus nucleus.

In conclusion, one may say that once the nucleotide base is detached from its linkage to cobalt, the corrin ring acquires a different puckering. The changes in T_1 and the chemical shifts clearly indicate that the aminopropanol side chain, the nucleotide base and the corrin ring have different conformations for the two isomeric forms of dicyanocobalamin. This rules out the possibility of the conformational change of the corrin ring or of the nucleotide base in cyanocobalamin' being transferred from one part of the molecule to the other by direct steric interactions. Differences in conformation of the corrin ring are apparent in the two isomeric forms of dicyanocobinamide. The existence of dicyanocobinamide' is also verified by thin layer chromatography. From these observations, one can perhaps infer that a change in the puckering of the corrin ring in the new forms of cyanocobalamin and dicyanocobalamin brings about a significant change in the nucleotide base through the aminopropanol linkage.

Acknowledgements—We are thankful to Mr. Sudhir Burman for the thin layer chromatography of cobinamides. This work has been supported by NIH Grant AM–19454, by Grants CA–06927 and RR–05539 to the Institute for Cancer Research from the National Institutes of Health, and by an appropriation from the Commonwealth of Pennsylvania. RKG is the recipient of a Research Career Development Award (NIH AM–00231) from the United States Public Health Service.

REFERENCES

[1]M. Katada, S. Tyagi, A. Nath, R. L. Petersen and R. K. Gupta, *Biochim. Biophys. Acta*, 1979, **584**, 149.
[2]R. K. Gupta, P. C. Goswami and A. Nath, *Vitamin B_{12}* (Edited by B. Zagalak and W. Friedrich), pp. 179–182. Walter de Gruyter & Co., Berlin (1979).
[3]J. M. Pratt, *Inorganic Chemistry of Vitamin B_{12}*, pp. 294. Academic Press, London (1972).
[4]R. A. Firth, H. A. O. Hill, J. M. Pratt and R. G. Thorp, *J. Chem. Soc.* (*A*), 1968, 453.
[5]R. L. Vold, J. S. Waugh, M. P. Klein and D. E. Phelps, *J. Chem. Phys.*, 1968, **48**, 3831.
[6]H. A. O. Hill, J. M. Pratt and R. J. P. Williams, *Methods in Enzymology*, 1971, **18C**, 5.
[7]J. D. Brodie and M. Poe, *Biochemistry*, 1971, **10**, 914; J. D. Brodie and M. Poe, *Biochemistry*, 1972, **11**, 2534.
[8]J. M. Wood and D. G. Brown, *Structure and Bonding*, 1972, **11**, 47.
9. H. A. O. Hill, B. E. Mann, J. M. Pratt and R. J. P. Williams, *J. Chem. Soc.* (*A*), 1968, 564.
[10]R. A. Dwek, *Nuclear Magnetic Resonances in Biochemistry: Applications to Enzyme Systems*, pp. 140–142. Oxford University Press, London (1975).
[11]D. Doddrell and A. Allerhand, *Proc. Nat. Acad. Sci. U.S.A.*, 1971, **68**, 1083.
[12]P. K. Mishra, R. K. Gupta, P. C. Goswami, P. N. Venkatasubramanian and A. Nath, *Biochim. Biphys. Acta*, 1981, **668**, 406.

Polyhedron Vol. 1, No. 4, pp. 327–330, 1982
Printed in Great Britain.

0277–5387/82/040327–04$03.00/0
Pergamon Press Ltd.

ELECTRON SPIN RESONANCE AND OPTICAL ABSORPTION SPECTRAL STUDIES ON SOME MANGANESE(II) COMPLEXES WITH 2,2′-BIPYRIDYL, 4,4′-BIPYRIDYL AND THEIR DIOXIDES

RAGHUVIR SINGH
School of Chemistry, University of Hyderabad, Hyderabad, 500 134, India

and

ISHAR SINGH AHUJA* and CHHOTE LAL YADAVA
Chemistry Department, Banaras Hindu University, Varanasi, 221 005, India

(*Received* 2 *May* 1981)

Abstract—Coordination compounds formed by the interaction of manganese(II) chloride, thiocyanate, acetate and sulphate with 2,2′-bipyridyl (2,2′-Bipy), 4,4′-bipyridyl (4,4′-Bipy) and their dioxides have been characterized by electron spin resonance and optical absorption spectral studies in solid and solution states to determine the spin-Hamiltonian constant for manganese(II), metal-ligand bond parameters and the tentative environments around manganese(II). The metal–ligand σ-bond in the compounds studied herein in formamide solution is found to be moderately covalent. The compounds seem to have an essentially axial symmetry with g-value close to 2.0. The magnetic moments, electronic and photoacoustic spectra of these complexes are also recorded and interpreted in the solid state.

INTRODUCTION

Although electron spin resonance spectra on the coordination compounds of manganese(II) have been studied[1–4] extensively the majority of these were on diluted single crystal where the metal ion geometry was only slightly distorted from cubic. The zero-field splitting parameters D were small and the g values were close to 2.0. Moveover, a few reports[5,6] have been published to use this ion as a stereo-chemical probe for other well-known divalent ions. Further, recently[7] the electron spin resonance studies on the manganese(II) ion have been recorded in a trigonal-prismatic coordination and parameters such as D and λ are correlated with distortion from regular octahedral symmetry. In the present study we have investigated the recently reported[8] coordination compounds of manganese(II) chloride, thiocyanate, acetate and sulphate with 2,2′-bipyridyl, 4,4′-bipyridyl and their dioxides by electron spin resonance, photoacoustic and electronic spectral studies in solid and solution state. The manganese(II) ions in these complexes are shown to achieve six-coordinate, high-spin octahedral environment through the ligand and/or anion bridging. Since the magnitude of the g and A values is likely to throw light on the nature of metal–ligand bond the ESR spectra of the compounds concerned are compared with similar chromophores like MnO_6, MnN_2O_4 and MnN_4O_2.

EXPERIMENTAL

Manganese(II) chloride, acetate and sulphate were obtained from B.D.H. and used as such. Manganese(II) thiocyanate was prepared by the literature method.[9] 2,2′-Bipyridyl and 4,4′-bipyridyl were obtained from Koch Light Labortories and used without further purification. These were oxidized to their dioxides as described by Simpson *et al.*[10] and Ochiai.[11] The complexes were prepared as described earlier[8] and chemical analyses were carried out to confirm their stoichiometries.

Electronic spectra of the complexes prepared were recorded in the solid state as nujol mulls in the range 33—6×10^3 cm^{-1}. The mulls were smeared on filter paper and run against a reference consisting of a similar piece of filter paper soaked in nujol. Magnetic susceptibilities were measured at room temperature with a Cahn R. G. Electrobalance Model 7550 using $HgCo(NCS)_4$ as the magnetic susceptibility standard. Diamagnetic corrections were estimated from Pascals' constants and magnetic moments were calculated using the equation

$$\mu_{eff} = 2.84\sqrt{(\chi_M^{corr}\,T)}$$

The photoacoustic spectra were recorded in the solid state on a Princeton Applied Research instrument Model 6001 in the range 50—6.5×10^3 cm^{-1} using carbon black as a reference. ESR spectra of the complexes studied were recorded as 4×10^{-3} M solutions in formamide and/or dimethylformamide at room temperature (296 K) and at low temperature (120 K) on a JOEL PE-3X spectrometer. The magnetic field homogenity is *ca.* ± 30 mG on the effective sample value. DPPH was used as a g-marker. The maximum error in g, hyperfine separation and hyperfine line width are ±0.001, ±2 G, ±3 G, respectively.

RESULTS AND DISCUSSION

The room temperature magnetic moments, electronic and photo-acoustic spectral bands are given in Table 1 and the ESR parameters are listed in Table 2.

Magnetic moments

Because of the additional stability of the half-filled d-shell manganese(II) generally forms high spin complexes which have an orbitally degenerate ^6S ground state term and the spin-only magnetic moment of 5.92 B.M. is expected which will be independent of the temperature and of the stereochemistry.[12] All the manganese(II) complexes reported here show magnetic moment values in the range 5.7–6.1 B.M. thereby indicating the presence of five unpaired spins and hence these are high spin complexes.

Electronic and photoacoustic bands and spectral parameters

In the case of manganese(II) complexes the intensity of the electronic transitions from the ground state (^6S)

*Author to whom correspondence should be addressed.

Table 1. Magnetic moments (B.M.), electronic and photoacoustic spectral data ($\times 10^3$ cm^{-1})*

Compound	μ_{eff}	ν_1	ν_2	ν_3	ν_4	ν_5
Mn(2,2'-Bipy)Cl$_2$	6.08	19.0 (17.8)	...	23.4	26.5 (27.0)	31.0 (31.2)
Mn(2,2'-BipyO$_2$)Cl$_2$	5.97	18.4	...	26.0 (25.6)	...	...
Mn(4,4'-Bipy)Cl$_2$	5.77	(18.5)	...	...	29.0 (29.4)	...
Mn(4,4'-BipyO$_2$)Cl$_2$	6.13	18.8 (19.5)	21.6 (21.6)	24.4	29.5 (29.5)	...
Mn(2,2'-Bipy)$_2$(NCS)$_2$	5.99	17.5 (16.4)	22.9	24.4	29.5 (29.8)	...
Mn(2,2'-BipyO$_2$)$_2$(NCS)$_2$	5.89	18.9 (17.5)	21.5 (22.4)	24.4	29.6 (28.9)	32.6 (32.7)
Mn(4,4'-Bipy)$_2$(NCS)$_2$	6.14	19.5	23.0	25.0	27.4 (29.4)	30.2
Mn(4,4'-BipyO$_2$)(NCS)$_2$	5.71	20.0 (20.0)	... (21.7)	23.5	27.6	31.2
Mn(2,2'-Bipy)(OAc)$_2$	5.77	18.3	21.9	...	27.7 (26.3)	... (31.2)
Mn(4,4'-Bipy)(OAc)$_2$	5.90	...	...	...	26.7 (27.3)	...
Mn(2,2'-Bipy)SO$_4$	5.90	19.2 (20.4)	...	23.1	26.6 (27.4)	30.1 (30.3)
Mn$_2$(4,4'-Bipy)(SO$_4$)$_2$	5.75	...	...	25.6	... (27.0)	...
Mn$_2$(4,4'-BipyO$_2$)(SO$_4$)$_2$	6.02	17.8	20.0	25.3	27.7	31.2

* Photoacoustic spectral bands are shown in parentheses.

to the states of four-fold multiplicity are rather weak and since the Mn(II) ion has a d^5 configuration the same type of energy level diagram applies whether the metal ion is in tetrahedral or octahedral environments. Out of the six electronic spectral bands of the $[Mn(H_2O)_6]^{2+}$ ion only four could be observed in the electronic spectra of the complexes studied here. The observed bands representing the corresponding transitions and energies in terms of Racah parameters are:

$$6A_{1g} \rightarrow {}^4T_{1g}({}^4G)(10\,B + 5\,C) \quad \sim 20 \times 10^3\ cm^{-1}$$
$$\rightarrow {}^4E_g, {}^4A_{1g}({}^4G)(10\,B + 5\,C) \sim 24 \times 10^3\ cm^{-1}$$
$$\rightarrow {}^4E_g\ ({}^4D)\ (17\,B + 5\,C) \quad \sim 27.5 \times 10^3\ cm^{-1}$$
$$\rightarrow {}^4T_{1g}\ ({}^4P)\ (7\,B + 5\,C) \quad \sim 33 \times 10^3\ cm^{-1}.$$

The observed electronic spectral transitions of practically all the manganese(II) complexes studied here are identical and typical[13] of octahedral environments around the metal ion. The energies of ${}^6A_{1g} \rightarrow {}^4E_g({}^4D)$ and ${}^6A_{1g} \rightarrow {}^4E_g$, ${}^4A_1({}^4G)$ transitions are known to be independent of Dq but depend[14] only on the values of B and C, and, therefore, these have been used to calculate the parameters B and C. The Dq values have been evaluated following the method of Preti.[15] The ligand field parameters Dq, B and C of the manganese(II) complexes studied here have values 1100–800, 920–730 and 3700–2900 cm^{-1}, respectively, and are in good agreement with similar data obtained for high spin octahedral manganese(II). In order to avoid errors due to mull technique we recorded photoacoustic spectra of

Table 2. Electron spin resonance parameters

Compound	$\langle g \rangle$	$\langle A \rangle$ (in G)
Mn(2,2'-Bipy)Cl$_2$	2.01	92.5
Mn(2,2'-BipyO$_2$)Cl$_2$	2.01	90.0
Mn(4,4'-Bipy)Cl$_2$	2.01	95.0
Mn(4,4'-BipyO$_2$)Cl$_2$	2.00	90.0
Mn(2,2'-Bipy)$_2$(NCS)$_2$	2.01	92.5
Mn(2,2'-BipyO$_2$)$_2$(NCS)$_2$	2.01	93.0
Mn(4,4'-Bipy)$_2$(NCS)$_2$	2.01	92.5
Mn(4,4'-BipyO$_2$(NCS)$_2$	2.01	90.0
Mn(2,2'-Bipy)(OAc)$_2$	2.01	92.5
Mn(4,4'-Bipy)(OAc)$_2$	2.01	92.0
Mn(2,2'-Bipy)SO$_4$	2.01	95.0
Mn$_2$(4,4'-Bipy)(SO$_4$)$_2$	2.00	92.5
Mn$_2$(4,4'-BipyO$_2$)(SO$_4$)$_2$	2.01	92.5

these complexes in the solid state. This technique is quite useful in studying the optical absorption spectra for almost all types of materials irrespective of whether the sample is crystalline, amorphous, powder, gel or gas.[16] The scattered light does not affect signals which is usually the case with the conventional methods dealing with solid samples. The photoacoustic spectra of all the complexes studied here show several bands in the range 50—6.5×10^3 cm^{-1} which are due to d–d spin allowed transitions and in a few cases the charge-transfer bands also appear in this region. The bands obtained are in good agreement with the electronic spectral bands and support the proposed octahedral geometries for the complexes.

Electron spin resonance spectra

The interpretation of the electron spin resonance spectra observed for high-spin d^5 complexes have been made in detail but it is important to mention a few of the principles. For the compounds under study the spectra could be fitted for an axial Hamiltonian. The high spin manganese(II) has an obrital $^6S_{5/2}$ ground state term which should not interact with the electric field in the first order case. However, the combined action of the electric field gradient and the spin–spin interaction produces splitting of the energy levels[17] due to second order spin-orbit coupling between the $^6A_1$ ground state and the lowest level of the manifold $^4A_{2g}$ state. The magnitude of the Zero-field splitting is expected by the axial field splitting parameter D in the case of an axially distorted octahedral field. The spin–Hamiltonian for manganese(II) can be defined as:

$$\mathcal{H} = g\beta \mathrm{H}s + \mathrm{D}[s_z^2 - 1/3s(s+1)] + \mathrm{A}s.\mathrm{I}$$

where H is the magnetic field vector, g is the spectroscopic splitting factor, β the Bohr magneton, A is the manganese hyperfine splitting constant, s is the electron spin vector, I is the nuclear spin vector, $s = 5/2$ and s_z is the diagonal spin operator.

For $s = 5/2$ and noting the selection rule $\Delta m_s = \pm 1$, five allowed transitions should arise when field separations are dependent on θ, the angle between the applied magnetic field and the symmetry axis. These transitions are:

$$\Delta m_s = \pm 5/2 \leftrightarrow 3/2;\ \mathrm{H} = \mathrm{H}_0 \pm 2\mathrm{D}(3\cos^2\theta - 1)$$
$$\Delta m_s = \pm 3/2 \leftrightarrow 1/2:\ \mathrm{H} = \mathrm{H}_0 \pm \mathrm{D}(3\cos^2\theta - 1)$$
$$\Delta m_s = \pm 1/2 \leftrightarrow -1/2:\ \mathrm{H} = \mathrm{H}_0$$

where $H_0 = h\nu/g\beta$ and θ is the angle between the applied magnetic field and the direction of the axial distortion. When the complex is very nearly octahedral only the central $\Delta m_s = -1/2 \leftrightarrow +1/2$ transition will be observed since it has only a second order dependence on D. This fine central line will of course be split into a sextet due to electron spin-nuclear spin hyperfine coupling (^{55}Mn, I = 5/2). If, however, the zero-field splitting is appreciable then the other electronic transitions will appear in the powder spectrum and the value of zero-field splitting can thus be evaluated. In addition to these allowed transitions the frozen solution spectra give low intensity pair of forbidden lines between each pair of allowed lines (Fig. 1b). These lines are due to simultaneous change of both the electron and nuclear spin by ± 1. From the intensity ratio (IR) of the forbidden lines to the allowed lines one can obtain an approximate value of the distortion parameter D by using the following equation:[18]

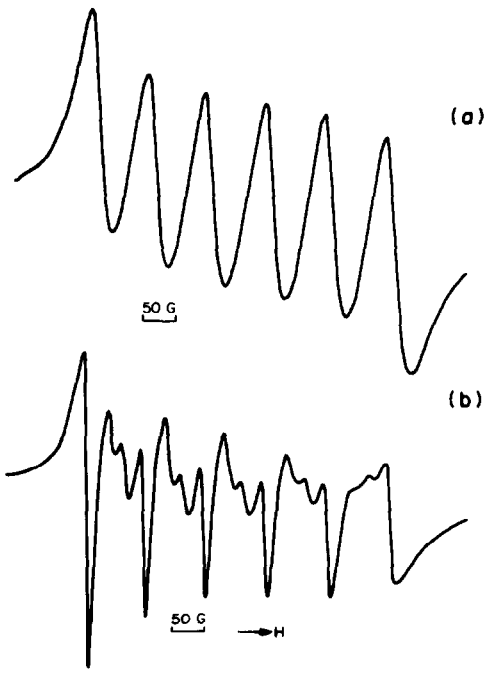

Fig. 1. ESR spectra of Mn(2,2'-Bipy)Cl_2 in formamide. (a) At 25°C. (b) At −170°C.

$$\mathrm{IR} = 8/15(3/4.\mathrm{D}/g\beta\ \mathrm{H})^2[1 + s(s+1)/3m_s(m_s+1)]^2$$
$$[\mathrm{I}(\mathrm{I}+1) - m^2 + m].$$

In an alternative method for the calculation of D, Allen's plots[19] (D vs IR) have been found useful. However, we could not succeed in evaluating D by this method for want of certain data. The electron spin-nuclear spin hyperfine coupling constant A in the present study has been calculated by taking average of all the observed lines (Fig. 1a). From the ESR spectra (in formamide solution) the values of g and A have been calculated for all the manganese(II) complexes studied here (Table 2). The observed values are consistent with the values obtained for chromophores like[1–5,20] MnO_6, MnN_2O_4 and MnN_4O_2. It is seen that the A values are somewhat lower than the pure ionic compounds and also when manganese(II) is coordinated to oxygen the metal–ligand bond seems to be more covalent as reflected by A values (Table 2).

Acknowledgements—We are grateful to the referee for his helpful suggestions and criticisms for the improvement of the manuscript and to Mr. C. Prabhakar Rao, University of Hyderabad, for recording the photoacoustic and ESR spectra.

REFERENCES

[1]R. D. Dowsing, J. F. Gibson, D. M. L. Goodgame, M. Goodgame and P. J. Hayward, *Nature (London)* **1968**, **219**, 1037.
[2]R. D. Dowsing and J. F. Gibson, *J. Chem. Phys.* 1969, **50**, 294.
[3]R. D. Dowsing, B. Nieuwenhuijse and J. Reedijk, *Inorg. Chim., Acta*, 1971, **5**, 301.
[4]C. J. O'Connor and R. L. Carlin, *Inorg. Chem.*, 1975, **14**, 291.
[5]R. D. Dowsing, J. F. Gibson, M. Goodgame and P. J. Hayward, *J. Chem. Soc.* 1970, **A**, 1133; M. Goodgame and P. J. Hayward, *J. Chem. Soc.* 1971, **A**, 3406.
[6]R. B. Birdy and M. Goodgame, *J. Chem. Soc., Dalton Trans.*, 1977, 461.

[7]R. B. Birdy and M. Goodgame, *Inorg. Chem.* 1979, **18**, 472.
[8]I. S. Ahuja, Raghuvir Singh and C. L. Yadava, *J. Molecular Struct.* 1981, **74**, 143.
[9]C. D. Flint and M. Goodgame, *J. Chem. Soc.* 1970, **A**, 442.
[10]P. G. Simpson, A. Vinciguerra and J. V. Quagliano, *Inorg. Chem.* 1963, **2**, 282.
[11]E. Ochiai, *J. Org. Chem.* 1953, **18**, 534.
[12]B. N. Figgis and J. Lewis, *Prog. Inorg. Chem.*, 1964, **6**, 37.
[13]L. J. Heidt, G. F. Koster and A. M. Johnson, *J. Am. Chem. Soc.* 1958, **80**, 6471.
[14]S. Olari and B. C. Harry, *Inorg. Chem.* 1974, **13**, 1185.
[15]C. Preti and G. Frost, *Aust. J. Chem.* 1976, **29**, 543.
[16]A. Rosencwaig, *Anal. Chem.* 1975, **47**, 592.
[17]A. S. Chakravorty, *J. Chem. Phys.*, 1963, **39**, 1004.
[18]B. Bleaney and R. S. Rubins, *Proc. Phys. Soc.* (*London*) 1961, **77**, 103; R. S. Rubins, *Phys. Revs.* 1964, **133**, 1099.
[19]B. T. Allen, *J. Chem. Phys.*, 1965, **43**, 3820.
[20]G. M. Woltermann and J. R. Wasson, *Inorg. Chem.* 1973, **12**, 7366; G. M. Wolterman and J. R. Wasson, *J. Magnetic Resonance* 1973, **9**, 486.

Polyhedron Vol. 1, No. 4, pp. 331–334, 1982
Printed in Great Britain.

0277–5387/82/040331–04$03.00/0
Pergamon Press Ltd.

VIBRATIONAL SPECTRUM OF NICKEL MOLYBDATE

S. SHEIK SALEEM and G. ARULDHAS*
Department of Physics, University of Kerala Kariavattam, 695 581, Trivandrum, India

(*Received* 16 *June* 1981)

Abstract—The IR and Raman spectra of gel grown nickel molybdate have been recorded. The group theoretical analysis has been carried out and a vibrational assignment proposed based on C_{2h} symmetry. The observed Mo–O stretching frequencies and the splitting suggest a tetrahedral coordination of oxygens around the molybdenum. Hence it has been concluded that the gel grown nickel molybdate is isomorphous with the *a*-form of cobalt molybdate.

INTRODUCTION

The vibrational spectra of molybdates and tungstates with scheelite structure have been investigated and discussed in detail by numerous authors.[1–7] However, not much work has been reported on metal molybdates and tungstates which form monoclinic crystals. The infrared spectra of these molybdates and tungstates have been reported.[8,9] The Raman spectra of $HgMoO_4$, $HgWO_4$ and $CdWO_4$ have been analysed by Blasse[10] and that of $MgMoO_4$ by Miller.[11]

There are two forms (*a* and *b*) of $CoMoO_4$ which is isomorphous with $NiMoO_4$.[12–16] According to Courtine *et al.*[12] the *a*-form of $CoMoO_4$ consists of CoO_6 octahedra and MoO_4 tetrahedra, whereas according to Lipsch and Schuit;[13] Plyasova and Karakchiev,[14] it consists of CoO_6 and MoO_6 octahedra. Clark and Doyle[8] ascribe the complexity of the observed infrared spectrum to the octahedral nature of the molybdenum oxygen network. However, no mention is made about the *a* and *b* forms in their study. A detailed infrared investigation of the $CoMoO_4$[17] has shown that in the *a*-form the molybdenum cations are surrounded by a tetrahedron of oxygen and in the *b*-form the coordination of oxygens is octahedral.

In the present investigation the vibrational spectroscopic study of the gel grown $NiMoO_4$ was taken up to find out to which form (*a* or *b*) it belongs.

EXPERIMENTAL

Gel grown $NiMoO_4$ has been used for the investigation. The details of the growth and morphology are given by Kurien and Ittyachen.[18] The infrared spectrum in the range 50–500 cm^{-1} was recorded using a FIR 30 Polytec and in the range 400–4000 cm^{-1} with a Perkin–Elmer 457 spectrometer. The Raman spectrum, Fig. 1, was recorded using a Spex Ramalog 1401 double monochromator equipped with a Spectra-Physics Model 165 argon ion laser operating at 4880 Å. The sample was placed in a capillary tube and spectral slit widths of 200 and 100 μ were employed for different regions of the spectrum.

FACTOR GROUP ANALYSIS

$NiMoO_4$, isomorphous with $CoMoO_4$, crystalizes in a monoclinic system with space group C2/m (C_{2h}^3) and has 8 molecules per unit cell.[15,16,19]. The primitive cell contains 4 molybdenum atoms surrounded by slightly distorted oxygen tetrahedra in $2C_2$ and $2C_s$ sites.

The standard group theory analysis to predict the correct number of active modes for each symmetry species of the crystal's factor group, can be carried out by correlation of the MoO_4^{2-} and Ni^{2+} ions even though discrete MoO_4^{2-} do not exist in the lattice. The analysis, however, is more easily done by correlating the site group of each atom in the unit cell individually to the factor group. In either case the same total number of modes is predicted for each symmetry species. The results of the analysis are summarized in Table 1.

RESULTS AND ASSIGNMENTS

The internal modes of the molybdate ion are expected to occur in the regions 800–950 cm^{-1} stretching and 275–400 cm^{-1} bending. For the external modes, the frequencies strongly depend on the type of motion (translation or rotation) and on the nature of the cation. Further, interactions are likely to occur between rotational, translational and low-lying internal modes. These features can be distinctly observed and the assignments of the bands to various classes of symmetry can be more correctly done with single crystal data.

As the crystal contains two pairs of molybdate ions in $2C_2$ and $2C_s$ sites there will be $4\nu_1$, symmetric ($2A_g + A_u + B_u$) and $12\nu_3$, asymmetric ($3A_g + 3B_g + 2A_u + 4B_u$) stretchings. In Raman, the totally symmetric line observed at 937 cm^{-1} has been assigned as one of the A_g components. It is presumed that there may be some accidental degeneracy between the ν_1 of C_2 and C_s site molybdate ions, or it would have mixed up with the asymmetric stretchings (i.e. ν_1 of C_2 mixing with ν_3 of C_s or vice versa). The lines at 915.5, 909, 898, 885, 881 and 876 cm^{-1} are assigned to the $3A_g$ and $3B_g$ components of ν_3 stretchings. In infrared, however, only three lines at 930, 904 and 878 cm^{-1} are observed in the Mo–O stretching region. This may be due to the poor resolution of the instrument.

The infrared frequencies 970, 690 and 610 cm^{-1} observed by Cord *et al.*[8] for $NiMoO_4$ are not observed. The observed spectrum is also different from that reported by Clark and Doyle[9] and the spectrum of *b*-form $NiMoO_4$.[17] In all these cases the molybdenum is coordinated octahedrally. The above frequencies are the characteristic ν_3 and ν_1 modes of a MoO_6 octahedra.

In Raman, the observed Mo–O stretching frequencies are in the region 937–876 cm^{-1} and further the splitting for the ν_3 degenerate stretching is about 40 cm^{-1}. For a distorted octahedron[11] the splitting is of the order of 150 cm^{-1}. The observed stretching frequencies are indicating a tetrahedral coodination except for a slight shift towards high wave number, which may be due to the distortion in the tetrahedra. Thus, the infrared and Raman spectra together indicate the presence of a distorted MoO_4 tetrahedra.

Discrepancies[20–24] exists in the assignments of ν_2 and ν_4. From single crystal data and UBFF analysis[2,23–25]

*Author to whom correspondence should be addressed.

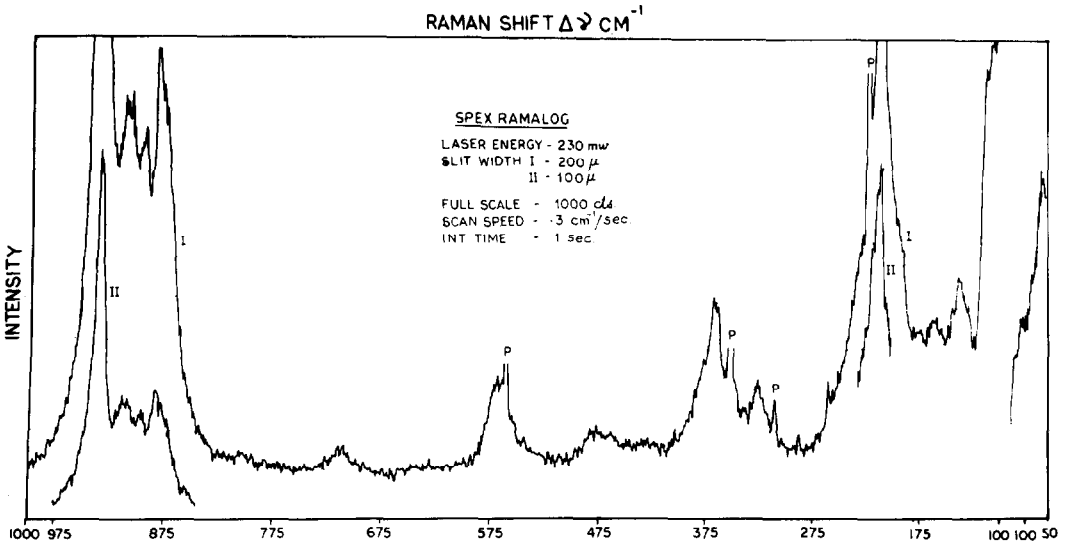

Fig. 1. Raman spectrum.

Table 1. Factor group analysis of $NiMoO_4$ space group $C2/m$ (C_{2h}^3); $Z=8$ $Z^B=4$

Free ion	Sites	Crystal	Activity
T_d	C_2	C_{2h}	
$2x2\nu_1$ A_1	A	A_g $2\nu_1, 3\nu_2, 3\nu_3, 3\nu_4$ 2R, 3T	R
$2x2\nu_2$ E	B	B_g $\nu_2, 3\nu_3, 3\nu_4$ 4R, 3T	R
$2x2R$ F_1	C_s A'	A_u $3\nu_1, 3\nu_2, 2\nu_3, 2\nu_4$ 3R, 2T	IR
$2x(2T, 2\nu_3, 2\nu_4)$ F_2	A"	B_u $\nu_1, \nu_2, 4\nu_3, 4\nu_4$ 3R, 4T	IR
For Ni^{2+} ions in C_2 Site	Γ_{Ni} =	$A_g+2B_g+A_u+2B_u$	
For Ni^{2+} ions in C_s Site	Γ_{Ni} =	$2A_g+B_g+A_u+2B_u$	
		$3A_g+3B_g+2A_u+4B_u$	
Acoustic modes		$-A_u-2B_u$	
Total active modes		$19A_g$, $17B_g$, $14A_u$, $19B_u$	

it has been established that $\nu_4 > \nu_2$. For the two different molybdate ions, group theory predicts eight ν_2 [$3A_g + B_g$(R); $3A_u + B_u$(IR)] and twelve ν_4 [$(3A_g + 3B_g$; $2A_u + 4B_u$(IR)]. In Raman, the strong band with factor group splitting at 368, 365 and 361 cm^{-1} has been assigned to three of the six ν_4 components. However, the asymmetric band contour present just below these three lines (around 350 cm^{-1}) superimposed by the plasma line of the argon ion laser, indicates the presence of one or two more ν_4 components. The lines at 340, 327 and 288 cm^{-1} have been assigned to three of the four expected ν_2 components. It is possible that the band at 327 cm^{-1} may also contain the fourth ν_2 component. In infrared the broad band appearing between 340 and 440 cm^{-1} with peaks at 410, 400, 386 and 365 cm^{-1} are assigned to four of the six ν_4 components and the band centering at 317 cm^{-1} with a shoulder at 305 cm^{-1} has been assigned to two of the four expected ν_2 components.

In the case of external modes it is difficult to distinguish between the twelve translations [$(3A_g + 3B_g$(R); $2A_u + 4B_u$(IR)] and twelve rotations [$(2A_g + 4B_g$(R); $3A_u + 3B_u$(IR)]. But in general the rotational modes are expected to have higher intensity than the translational

Table 2. Vibrational assignments of nickel molybdate

Raman in cm^{-1}	Infrared in cm^{-1}	Assignments
937	930 s	A_g, $\nu_1 MoO_4$
915.5		
909		
898	904 vs	$3A_g$ & $3B_g$ $\nu_3 MoO_4$
885	878 vs	
881		
876		
718		R H_2O or 2x361
	638 s, br	--
	598 m	R H_2O or C
	578 m	
570		365 + 207
	483 w	R H_2O or C
464	450 w	R H_2O or C
	410 m,br	
368	400 m,br	
365	356 m,br	A_g or B_g $\nu_4 MoO_4$
361	365 m,br	
340		
327	317 w,br	A_g or B_g $\nu_2 MoO_4$
258	305 sh	
233		
213	260 m	R MoO_4
207	200 w	
194		
174		
161		
142	162 w	T MoO_4
137		
110,104	112,79,72,	Lattice modes
96,73,54	70,65,60	

Abbrevations: vs, very strong; s, strong; m, medium; w, weak; br, broad; sh, shoulder; R, Rotation; T,Translation; C, Combination.

modes. The strong lines observed at 233, 213, 207 and 194 cm^{-1} have been tentatively assigned to the rotational modes and the frequencies at 174, 161, 142 and 137 cm^{-1} as the translational modes. Only three peaks 260, 200 and 162 cm^{-1} have been observed for the rotational and translational modes.

The bands observed at 712 and 464 cm^{-1} in Raman and the lines at 598, 578, 383 and 450 cm^{-1} in IR may be due to the librational modes of lattice water, if present in the crystal or due to some combinations.

The proposed assignments are shown in Table 2.

CONCLUSION

The mutual exclusion of frequencies to be obeyed under C_{2h} symmetry is observed (Table 2). The factor group splitting predicted by the group theoretical analysis for the stretching vibrations has been observed in the Raman spectrum; in the case of bending modes all the components could not be observed. The observed stretching frequencies and their splitting are characteristic of a tetrahedral coordination. Hence, it may be concluded from the vibrational spectroscopic study that the gel grown nickel molybdate is isomorphous with the *a*-form of cobalt molybdate.

Acknowledgements—The authors are thankful to Prof. P. S. Narayanan for making available the Spex Ramalog for recording the spectrum and for the cordiality shown to one of us (S.S.S.) during his stay in I.I.Sc., Bangalore. Thanks are also due to Mr. K. V. Kurien, Teacher fellow, department of Physics for providing the crystal. One of the authors (S.S.S.) is grateful to the CSIR for the award of a fellowship.

REFERENCES

[1]A. S. Barker, Jr., *Phys. Rev.*, 1964, **135A**, 742.
[2]R. K. Khanna and E. R. Lippincott, *Spectrochim. Acta*, 1968 **24A**, 905.
[3]J. F. Scott, *J. Chem. Phys.*, 1968, **49**, 98.
[4]M. Nicol and J. F. Durana, *J. Chem. Phys.*, 1971, **54**, 1436.
[5]P. Tarte and M. Liegeois-Duykagerts, *Spectrochim. Acta*, 1972, **28A**, 2029, and M. Liegeois-Duykagerts and P. Tarte, *Ibid*, 1972, **28A**, 2037.
[6]J. P. Russell and R. Loudon, *Proc. Phys. Soc. (London)*, 1965, **85**, 1029.
[7]S. P. S. Porto and J. F. Scott, *Phys. Rev.*, 1967, **157**, 716.
[8]P. P. Cord, P. Courtine and G. Pannetier, *Spectrochim. Acta*, 1972, **28A**, 1601.
[9]G. M. Clark and W. P. Doyle, *Spectrochim. Acta*, 1966, **22**, 1441.
[10]G. Blasse, *J. Inorg. Nucl. Chem.*, 1975, **37**, 97.
[11]P. J. Miller, *Spectrochim. Acta*, 1971, **27A**, 957.
[12]P. Courtine, P. P. Cord, G. Pannetier, J. C. Dumas and R. Montarnal, *Bull. Soc. Chim. France*, 1968, **12**, 4816.
[13]J. M. J. G. Lipsch and G. C. A. Schutt, *J. Catalysis*, 1969, **15**, 163.
[14]L. M. Plyasova and L. G. Karakchiev, *Izv. Akad. Nauk. SSSR. Neorg. Mater*, 1972, **1**, 117.
[15]G. W. Smith, *Acta. Cryst.*, 1962, **15**, 1054.
[16]G. W. Smith and J. A. Ibers, *Acta. Cryst.*, 1965, **19**, 269.

[17]N. I. Svinston, D. N. Timenov and L. P. Shapovaloua, *Z. Prikl. Spektrosk.*, 1975, **23**, 730.
[18]K. V. Kurien and M. A. Ittyachen, *Krist. Technik.*, 1980, **15**, 763.
[19]A. P. Young and C. M. Schwartz, *Science*, **141**, 348.
[20]R. H. Busy and O. L. Keller, *J. Chem. Phys.* 1965, **41**, 215.
[21]R. G. Brown, J. Denning, A. Hallet and S. D. Ross, *Spectrochim. Acta*, 1970, **26A**, 963.
[22]J. F. Scott, *J. Chem. Phys.*, 1968, **48**, 874.
[23]P. J. Miller, R. K. Khanna and E. R. Lippincott, *J. Phys. Chem. Solids*, 1973, **34**, 535.
[24]R. A. Johnson, M. T. Roberts and G. E. Legoi, *J. Chem. Phys.*, 1972, **56**, 789.
[25]L. J. Basile, J. R. Ferraro, P. La Bonville and M. C. Wall, *Coordination. Chem. Rev.*, 1973, **11**, 21.

Polyhedron Vol. 1, No. 4, pp. 335–338, 1982
Printed in Great Britain.

0277-5387/82/040335-04$03.00/0
Pergamon Press Ltd.

OSMIUM CARBOHYDRATE POLYMERS

C. C. HINCKLEY*, P. S. OSTENBURG and W. J. ROTH

Department of Chemistry and Biochemistry, Southern Illinois University at Carbondale, Carbondale, IL 62901, U.S.A.

(*Received* 24 *June* 1981)

Abstract—The preparation and characterization of osmium carbohydrate polymers derived from glucose are reported. The materials are polydisperse, anionic polyelectrolytes. Solution viscosity measurements indicate generally spherical shapes. Both gel electrophoresis and ultracentrifuge experiments show that each preparation contains a range of molecular sizes. Representative molecular weights determined for several preparations range from 13,000 to 77,000 daltons. Estimates of molecular diameters range from 27.3 to 41.5 Å.

We have prepared and partly characterized a new group of substances which are osmium carbohydrate polymers exhibiting a wide range of compositions. Typical preparations yield materials having from 10 to 40% osmium, although some materials outside this range have been prepared. These substances have a number of potentially useful properties. They are non-toxic when injected into synovial spaces, and are effective and long lasting stains of tissue surfaces there[1]. Studies by others[2] lead to the suggestion that osmium containing materials of this sort may be valuable as anti-inflammatory agents[1]. Research into this topic has led to the finding of unusual growth patterns in porcine articular cartilage stained by some of the compounds. In related work, the polymers are found to stain gluteraldehyde fixed tissue and appear to be generally useful in electron microscopy. Each of these applications is dependent upon the macromolecular character of the osmium compounds, with higher molecular weight preparations being the most effective.

In this paper we report the preparation and characterization of osmium carbohydrate polymers prepared from glucose. Methods of characterization include elemental analysis, visible UV spectroscopy, solution density and viscosity measurements, gel filtration, gel electrophoresis and ultracentrifugation experiments. These studies indicate that the compounds are polydisperse, anionic polyelectrolytes. Molecular weights vary from a few thousand daltons for the lower osmium percentages to nearly 1 million daltons for the higher osmium percentages. Although these materials have not been previously reported, there have been other studies of osmium–carbohydrate chemistry. They include Bahr's early survey of osmium tetroxide–biomolecule chemistry,[3] polarographic studies of osmium–sodium gluconate solutions,[4] and recent preparations of osmium polysaccharide complexes.[5] In this research, crystalline products have not been obtained nor have monomeric complexes. The compounds are characterized as macromolecules in terms of molecular size and weight. The picture that emerges is consistent with an osmium containing backbone for the polymer with monosaccharide ligands attached.

RESULTS AND DISCUSSION

Preparations

The polymers were prepared by the reaction of potassium triacetatodioxoosmium (VI) (TAKO) and glucose (or other carbohydrate). The relative proportions of osmium to carbohydrate, the nature of the carbohydrate, the nature of the solvent, and the temperature determines the composition of the product.

In Fig. 1, typical visible-UV spectra for black and brown compounds are presented. Although there are differences in band contours, the principal difference between the two is in the intensity of absorption in the visible range. Extinction coefficients, calculated on the basis of osmium present in the preparations, show that

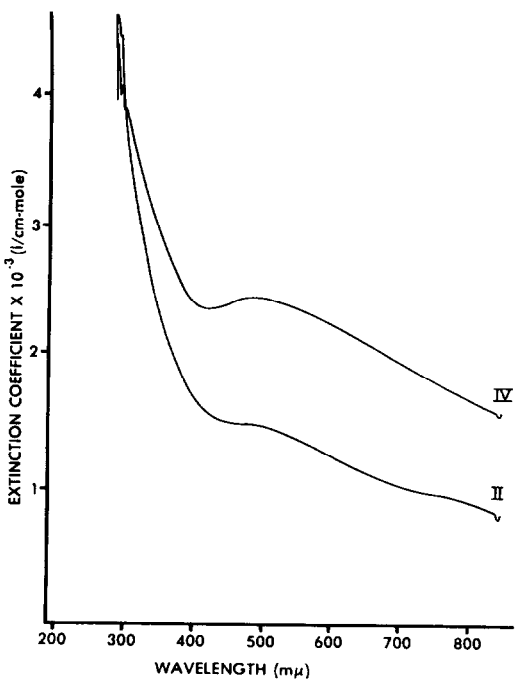

Fig. 1. Visible-UV spectra of black (IV) and Brown (II) polymer preparations. Extinction coefficients are plotted versus wavelength.

*Author to whom correspondence should be addressed.

the absorption of the black materials is approximately three times that of the brown. Direct comparisons with other materials are difficult, but the magnitude of visible light absorption is similar to that found in some charge transfer complexes.[7]

Composition

Carbon, hydrogen, and potassium were determined by Galbraith Laboratories.[8] Osmium was determined colorimetrically.[9] Compositions ranged from extremes of 6–35% osmium, with associated carbon percentages for these extremes of 30 and 13% respectively. Potassium percentages were irregular, and varied from 1 to 13%. Preparations containing more than 40% osmium have been prepared, but they were insoluble.

Titration with potassium permanganate and ceric ammonium nitrate indicated an average oxidation state for osmium in the compounds of +4. IR spectra showed broad bands in the regions 1610–1550, 1400–1300 cm and 1200–950 cm^{-1}. These spectra indicate the presence of glucose and gluconate in the compounds. The analyses were consistent with the empirical formula: $K_u OsO_v$ $(glucose)_x$ $(gluconate)_y$ $(H_2O)_z$. This formula embodies an interpretation of these materials as glucose and/or gluconate solubilized osmium dioxide, OsO_2, or a closely related salt, e.g. K_2OsO_3.

Gel filtration[10]

Gel filtration of the product mixtures demonstrated that the osmium–glucose complexes were relatively large molecules. When eluted on a Sepharose 6-B column, the black polymers eluted at, or near, the void volume. They were comparable in size to globular proteins that range in molecular weight up to 1 million daltons. The brown compounds generally eluted behind the void volume indicating smaller molecular size.

Density and viscosity[11,12]

Partial specific volumes, $\bar{v}$, were obtained from solution density measurements of a selection of polymer preparations. Intrinsic viscosities, $\{\eta\}$, were determined for the same preparations. Values in units of cm^3/g for these two determinations for the four preparations studied were: 0.454, 2.37; 0.505, 1.88; 0.492, 2.13; 0.292, 1.76; for $\bar{v}$ and $\{\eta\}$ in each case. Ratios of these numbers vary from 3.72 to 6.03, consistent with distorted spherical shapes for the molecules.

Gel electrophoresis[13,14]

Electrophoretic mobility relative to a standard substance, R_f, is given by, $R_f = d/d_B$ where d is the distance migrated by the sample, and d_B is the distance migrated by the standard under the same conditions. In these studies, the stationary phase was either agarose or polyacrylamide gel, and the reference standard for R_f calculations was bromophenol blue (BPB). Electrophoresis was through a glass tube filled with gel connecting conducting reserviors of trihydroxymethylamine-acetic acid buffer (0.1–0.4 M) solution in contact with platinum electrodes.

Osmium carbohydrate polymers were anionic polyelectrolytes and migrated towards the positive electrode. In a typical experiment, electrophoresis was continued for 2–4 hr. During this time, the osmium polymer migrated as a band 2–4 cm broad, at a rate, measured for the center of the band, comparable to or slightly greater than BPB in most cases. The broad band is due to the polydisperse nature of the preparations.

Electrophoretic mobility in a gel is dependent upon the concentration of the stationary phase,[14] as in, $\log R_f = \log R_f^0 - K_r C_g$, where C_g is the gel concentration, R_f^0 is the mobility extrapolated to $C_g = 0$, and K_r is the retardation coefficient. The latter is dependent upon the geometry of the migrating species and the nature of the gel. It is found experimentally, in some systems, to be linearly dependent upon the molecular weight of the migrating species. Determination of R_f^0 provides a measure of relative charge-carrying capacity, and K_r is an index of relative size.

In these polydisperse materials both R_f^0 and K_r differed within the mixtures, giving rise to migrating bands which broadened as the electrophoresis proceeded. For the osmium polymers studied here, R_f^0 values for the leading edges of the bands are smaller than those calculated for the trailing edges, consonant with the greater mobility of the smaller molecules. A typical range was 0.029–0.049 for K_r values reflecting a radius difference, after suitable assumptions,[14] of 30% between the smallest and largest particles in the mixture. Radius differences of this kind up to 50% have been measured. The maximum range for observed K_r values includes 0.029 and 0.108 for the smallest and largest measured respectively. The preparations are clearly mixtures containing molecules of different charge and size, but they migrate in continuous bands. Only rarely are there band separations.

Ultracentrifugation[15–18]

Sedimentation velocity experiments gave results which were broadly similar to those of electrophoresis. That is, the polymer preparations were polydisperse and of high molecular weight. Centrifugations through a 5–20 (or 25%) sucrose gradient resulted in broad bands with the most concentrated region of the band having sedimentation coefficients ranging from 3–10 svedbergs, in most cases.

In Table 1 molecular weights calculated for several cases are listed, together with the sedimentation coefficients from which they are derived. Values listed are for the concentration maxima of the sedimentation profiles. These molecular weights correspond to molecules which contain from 15 to 80 osmium atoms. They may be considered typical of the preparations they represent, but each preparation contains both smaller and larger components. Although the relationship is not smooth, there is a general correspondence between elemental composition of the preparations and molecular weights found in the mixtures; polymers with higher percentates of osmium have larger average molecular weights.

Molecular volume and molecular weight determinations may be combined to provide estimates of the diameters of the molecules. These are listed in Table 1, and are derived assuming that the molecules are spherical. The relatively large dimensions are consistent with the gel-filtration results which suggest large molecules in solution.

Conclusions

Compositions and properties of osmium carbohydrate polymers suggest that they may be considered carbohydrate solubilized OsO_2, or a closely related material. The polymers are anionic, and viscosity measurements indicate that the molecules are generally spherical in shape. This, together with the polydisperse character of

Table 1. Representative sedimentation coefficients and estimated molecular weights for polymer preparations[a]

Preparation	% Os	$S_{20,w}$(svedbergs)	M(daltons)	Particle diameter (Å)
I	6.7	3.5	13,000	27.3
II	9.7	3.5	12,400	27.0
III	23.0	5.0	20,000	30.6
IV	20.0	9.5	53,000	42.4
V	35.0	17.0	77,000	41.5

(a) $S_{20,w}$ values refer to the band midpoint of highest concentration.

the mixtures, suggests that the structure of these molecules may be described as coiled chains of varying length. The chains may be crosslinked or branched, but not linearly extended. The osmium containing links of the chain are most likely bridged via oxo or carbohydrate ligands.

Osmium dioxide polymers have been suggested as products of the reaction of OsO_4 with biological materials[19-21]. The materials reported in this study are analogous to those polymers, but unlike them, are soluble and characterizable as macromolecules. Pursuit of the analogy has produced a number of potential applications, all of which so far, are dependent upon the ability of the higher molecular weight preparations to bind to tissue surfaces. In the research reported in this paper, these compounds have been studied in aqueous or dilute buffer solutions. In these media they are near spherical in shape, but they are unlikely to remain so when bound to surfaces. A polymer molecule which contains a hundred osmium atoms, when uncoiled, would yield a filament several hundred Angstroms long. Molecules of this length could bind to extensive regions of membrane surface. It is likely that conformational changes of the kind described are involved in binding to biological surfaces.

EXPERIMENTAL

Preparation

The contents of one ampoule of OsO_4 (~0.5 g, 2 mmole) was dissolved in 5 mL of methyl alcohol. To this was added 10 mL of 1.0 M-KOH in methanol. The solution became orange and after about 30 minutes a precipitate of dipotassium tetramethyl osmate (DTMO) formed. DTMO was removed from the solvent and excess base by centrifugation. The supernant was removed and the precipitate dissolved in 100 mL of glacial acetic acid to form the blue triacetate compound, K $\{OsO_2(O_2CCH_3)_3\}$, (TAKO). D-glucose 4 mmole (0.72 g) was added to 100 ml of glacial acetic acid in a 1.0 L round bottom flask. The D-glucose did not completely dissolve. To this was added the acetic acid solution of TAKO. The reaction mixture turned brown in a few minutes and darkened after standing overnight after which the mixture was filtered to remove undissolved D-glucose and insoluble Os complexes. Acetic acid was removed by rotary evaporation leaving a viscous liquid. This liquid was dissolved in about 30 mL of distilled water and loaded on a Sephadex G-25 column (total volume about 600 mL) and eluted with distilled water. Water was removed from the product by rotary evaporation. This product is dried over phosphorus pentoxide under vacuum. Yield: 0.422 g. Anal. 35.0, Os; 14.6, C; 5.8, H; 4.9%, K.

The brown complexes were obtained in the same manner using 2.16 g (12 mMol) of D-glucose. Yield: 0.575 g. Analysis: 13.0% Os, 26.09% C, 4.3% H, 13.2% K.

Alternative preparation

A homogeneous reaction mixture was obtained by varying the procedure slightly. Instead of adding D-glucose to glacial acetic acid, the carbohydrate was dissolved in 10.0 mL of distilled H_2O in a 1.0 L RB flask. To this was added 100 mL glacial acetic acid, and then the blue solution of TAKO in acetic acid. The carbohydrate remained in solution. The synthesis was completed as described above. No major difference in physical or chemical properties of the complexes obtained from the two methods of synthesis has been found.

Osmium analysis

Five to ten milligrammes of the Os-glucose complex was dissolved in 10 mL of distilled water with 1 mL of 6N H_2SO_4. Standardized $KMnO_4$ was added dropwise until the black or brown color disappears and a faint pink color persist and the solution was transferred quantitatively to a volumetric flask. The flask was then filled to the mark with a solution of 1 M thiourea in 1N H_2SO_4. The absorbance of the rose-colored Os-thiourea complex was measured on a Perkin-Elmer model 340 spectrophotometer (480 nm). Osmium content was calculated using a previously determined calibration based upon freshly prepared OsO_4 solutions.

Gel filtration

For a Sepharose 6-B column (1 m long, O.D. = 15 mm), the void volume and total volume were determined by using a mixture blue dextran and $Co(NO_3)_2$ dissolved in water. Approximately 10 mg of the Os-glucose complex to be studied was dissolved in 0.5 mL H_2O and loaded on the column. Elution takes about 12 hr. Fractions of about 2.2 mL were collected using a Gilson FC-220 K fractionator. The absorbance of each fraction was determined using a Perkin-Elmer 340 spectrometer. A plot of fraction number (or total volume) vs. absorbance was then made.

Density and viscosity

The determinations of partial specific volumes and viscosities of solutions in water were carried out using the same solutions. Guy-Lussac (10 mL) and Moore-Van Slyke (2 mL) pycnometers, and an Ostwald dropping pipette were used, all supplied by Fisher Scientific Co., catalog numbers 3-24 A, 3-249 and 13-695 respectively. Starting solutions containing 0.035-0.10 weight fraction of the osmium compound in water were prepared and then diluted with water as less concentrated solutions were investigated. A water bath was used to maintain temperature at 20° ±0.02° C. Before measurement, solutions were kept in the bath for 20-30 min. Time flow in the viscosimeter was measured with an accuracy of ±0.05 sec.

Agarose and polyacrylamide gel tube electrophoresis

Electrophoretic chambers, constructed locally and similar to one described elsewhere[13], accommodating 15 or 8 tubes having i.d. of 6 mm were used. A Heathkit, model IP-32, power supply was used. 0.1–0.4 M TRIS (trihydroxymethyl amine) titrated with glacial acetic acid to pH = 7.4–7.5 constituted the buffer system for all experiments. Agarose gels were prepared by boiling a slurry of agarose (Calbiochem No. 121852) in the buffer. The hot solution was poured into the tubes closed at the bottom with conditioned Spectapor 5 dialysis membrane. After the gel set, a flat top on the gel column was obtained by cutting out the meniscus. Preparation of polyacrylamide gels is described elsewhere[13]. Electrophoretic purity reagents supplied by BIO-RAD were used. BIS constituted 5% of the total acylamide concentration and the final concentration of TEMED and ammonium persulphate were 0.006 v/v and 0.3 w/v respectively. Isobutyl alcohol was pipetted on top of the polymerizing gel to ensure its flat surface. Twenty to one-hundred micro-litres of 1-2% polymer solutions were delivered on the gels in buffer solution after pre-electrophorising the system for 0.5–1 hr. The potential applied was 60 ± 1 V, resulting in a current of 1–2 mA per tube. Positions of the front and trailing edge of a band after electrophoresis were determined visually on Polaroid pictures of gels, measured with an accuracy of ±0.5 mm, and then recalculated into real distances. Bromophenol blue, supplied by Fisher Scientific Co., was used as the reference, but since its band overlaps with bands of the investigated compounds, it was electrophoresed in a separate tube.

Sedimentation velocity in preformed sucrose gradients

Spinoco Model L and L5–50 preparative ultracentrifuges were used with either W 41 or SW 50.1 rotors. Preformed linear sucrose gradients of concentration 5–25 and 5–20% w/w were used. The gradients were prepared according to standard procedures[15]. Gradient maker, peristaltic pump, and "Densi-flow" layering devices, were manufactured by Buchler Instruments. Fifty to one-hundred micro litres solutions containing 1–2 mg of the polymer were layered on the top of a gradient, and within 15–30 min. centrifugation was begun. The temperature of the centrifuge was 20 ± 1°C. The centrifuged sample was fractionated immediately after the run. A glass capillary was lowered down to the bottom of the sample tube and the contents carefully pumped out. By measuring the refractive index with an Abbe-3L refractometer (Bausch & Lomb) and/or the absorbance (Perkin–Elmer Model 340 spectrophotometer) of the fractions, the gradient was calibrated and the sample distribution along the tube determined.

Acknowledgements—Helpful suggestions of a referee were incorporated in the final manuscript. This research has been supported by the Department of Chemistry and Biochemistry and the office of Research Development and Administration of Southern Illinois University. A gift of OsO_4 was gratefully received from Malinkrodt, Inc.

REFERENCES

[1]C. C. Hinckley, L. E. Strack and L. D. Russell, unpublished research.
[2]I. Boussina, R. Lagier, H. Ott and G. H. Fallet, *Scand. J. Rheumatology* 1976, **5**, 53.
[3]G. F. Bahr, *Exptl. Cell. Res.* 1954, **7**, 457.
[4]D. T. Sawyer and D. S. Tinti, *Inorg. Chem.* 1963, **2**, 796.
[5]J. Resch, D. Tunkel, C. Stoechert and M. Beer, *J. Mol. Biol.* 1980. **138**, 673.
[6](a)R. Criegee, *Ann. Chem.* 1936, **522**, 75; *Angewandte chem.* 1938, **51**, 519. b. R. Criegee, B. Marchand and H. Wannowins, *Ann. Chem.* 1942, **550**, 99.
[7]F. A. Cotton and G. Wilkinson *Advanced Inorganic Chemistry, 4th Edn*, p. 666. Wiley, New York (1980).
[8]Galbraith Laboratories, Inc., P. O. Box 4187, Knoxville, Tennessee, 37921.
[9]R. D. Sanerbrunn and E. B. Sandell, *Analytica Chimica Acta* 1953, **9**, 86.
[10]*Gel Filtration, Theory and Practice.* Pharmacia Fine Chemicals, Upsala, Sweden (1979).
[11]D. W. Kupke, *Physical Principles and Techniques of Protein Chemistry* (Edited by S. L. Leach), Part C, p. 1. Academic Press, New York (1973).
[12]B. Jergensons and M. E. Straumanis, *Colloid Chemistry* p. 143. Wiley, New York (1954).
[13]T. G. Cooper, *The Tools of Biochemistry*, p. 194. Wiley, New York (1977).
[14]D. Rosebard and A. Chrambach, *Anal. Biochem.* 1971, **40**, 95.
[15]Ref. 12, p. 309.
[16]R. G. Martin and B. N. Ames, *J. Biol. Chem.* 1961, **236**, 1372.
[17]C. R. McEuen, *Anal. Biochem.* 1967, **20**, 114.
[18]J. Eigner and P. Doty, *J. Mol. Biol.* 1965, **12**, 549.
[19]J. S. Hanker, F. Kasler, M. G. Bloom, J. S. Copeland and A. M. Seligman, *Science* 1967, **156**, 1737.
[20]A. M. Seligman, M. L. Wasserkrug, C. Deb, and J. S. Hanker, *J. Histochem. Cytochem* 1968, **16**, 87.
[21]A. J. Nielson and W. P. Griffith, J. Chem. Soc. Dalton 1979, 1084.

Polyhedron Vol. 1, No. 4, pp. 339-341, 1982
Printed in Great Britain.

0277-5387/82/040339-03$03.00/0
Pergamon Press Ltd.

TETRAPHENYLBORATE TETRA- AND PENTACOORDINATED COMPLEXES OF RHODIUM(I) WITH DIOLEFINS

M. ANGELES GARRALDA* and LOURDES IBARLUCEA
Department of Inorganic Chemistry, Facultad de Ciencias Químicas, San Sebastián, Universidad del País Vasco, Spain

(*Received* 31 *July* 1981)

Abstract—The synthesis and properties of complexes of the $[Rh(COD)L_2]BPh_4$ type (COD = 1,5-cyclooctadiene, L = monodentate N-donor ligand) and of mixed complexes of the general formula $[Rh(diolefin)L_nL']BPh_4$ (diolefin = COD or norbornadiene, L = monodentate N-donor ligand, L' = P- or As-donor ligand, n = 1 or 2) are described. The stoichiometry of the precipitated complexes depends upon the nature of the diolefin and group Vb donor ligands.

INTRODUCTION

Cationic rhodium(I) diolefin complexes containing group Vb ligands have been extensively studied during recent years and a review on their synthetic methods and properties has been published.[1]

Most of the interest has centred on the $[Rh(diolefin)L_2]A$ complexes while mixed complexes containing both N- and P-donor ligands have been studied to a much lesser extent.[1,2] Usually these mixed complexes are four-coordinate and no five-coordinate complexes containing N- and P-monodentate donor ligands have been described.

These compounds are usually isolated as the corresponding ClO_4^-, PF_6^- or BF_4^- salt, BPh_4^- being much less used as counterion due to its higher coordination capability to metals via π-interaction of an arene ring[3-8] which hinders the possibility of isolation of $[Rh(diolefin)L_2]BPh_4$ complexes when L are weak nitrogen-donor ligands such as nitriles or aniline.[2,9]

We describe below the preparation of new cationic rhodium(I) complexes containing norbornadiene or 1,5-cyclooctadiene and group VB donor ligands with BPh_4^-, formulated as $[Rh(diolefin)L_nL'_m]BPh_4$ (n = 1 or 2, m = 0 or 1) which can be either four- or five-coordinate depending on the ligands present in the complexes. Thus, we describe the preparation of three new pentacoordinated compounds when L = quinoline, L' = PR_3 and diolefin = NBD.

RESULTS AND DISCUSSION

The reaction of $[Rh(COD)Cl]_2$ with N-donor ligands such as pyridine, 2-ethyl-pyridine or quinoline in alcoholic medium followed by the addition of sodium tetraphenylborate yields the corresponding cationic complexes according to the reaction:

$$[Rh(COD)Cl]_2 + 2L + 2NaBPh_4 \longrightarrow 2[Rh(COD)L_2]BPh_4 + 2NaCl. \quad (1)$$

Similar complexes could be obtained by using other non-coordinating anions[10,11] but when trying to prepare the corresponding norbornadiene derivatives with 2-ethyl-pyridine or quinoline only the arene $Rh(NBD)BPh_4$ could be obtained.[9]

Mixed complexes could be obtained by addition of an excess of N-donor ligand and stoichiometric amount of P- or As-donor to the corresponding $[Rh(diolefin)Cl]_2$ dimers suspended in methanol. Precipitation occurs by addition of sodium tetraphenylborate.

The results are summarized in the scheme.

Then the diolefinic ligand present in the complex is norbornadiene, the complexes can be either four- or five-coordinate. Thus, when the N-donor ligand in the complex is pyridine or 2-ethyl-pyridine, displacement of one of the ligand molecules occurs (process i) yielding the corresponding four-coordinate complexes similar to those obtained when the anion was ClO_4^-[12].

If quinoline (pK_a = 4.89) with lower donor strength than pyridine (pK_a = 5.25) or 2-ethyl-pyridine (pK_a = 5.89) is used the added phosphine occupies the fifth coordination position on the metal, thus affording the corresponding five-coordinate complexes when triphenylphosphine or *p*-substituted phosphines are used (process ii). When using phosphines with larger steric hindrance such as $(m\text{-}MeC_6H_4)_3P$ it was not possible to isolate any pentacoordinated complex and only the corresponding tetracoordinated compound was obtained (process i). With $(o\text{-}MeC_6H_4)_3P$ no cationic complexes could be isolated and the only product obtained was the arene $Rh(NBD)BPh_4$ derivative (process iii).

When ligands weaker and with larger steric hindrance than triphenylphosphine, e.g. triphenylarsine are used, the arene complex was obtained in every case (process iii).

These results suggest that it is likely that the mechanism of ligand substitution in four-coordinate cationic diolefin rhodium(I) complexes proceeds via the formation of a five-coordinate species of the type $[Rh(NBD)L_2L']A$ with subsequent loss of one molecule of N-donor ligand to afford the four-coordinate mixed complexes.

All these complexes are stable in the solid state but when the triphenylphosphine complexes are suspended in pure methanol, they lose N-donor ligand as indicated in the following reaction:

$$2[Rh(NBD)L_n(Ph_3P)]BPh_4 \xrightarrow[\text{suspension}]{MeOH} [Rh(NBD)(Ph_3P)_2]BPh_4 + Rh(NBD)BPh_4 + nL \quad (2)$$

as proved by the IR spectra of the products that show

*Author to whom correspondence should be addressed.

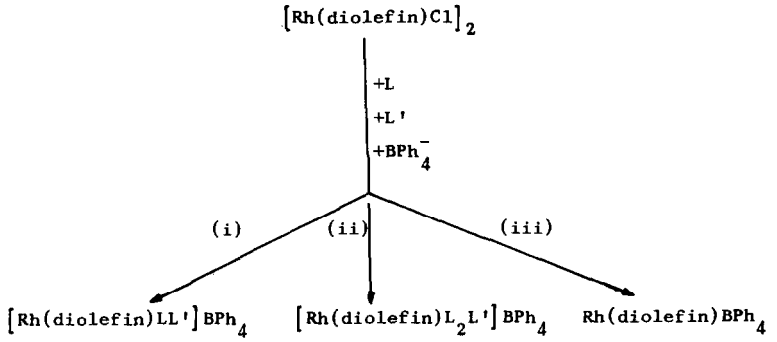

(i) diolefin=NBD; L=py, 2-et-py; L'=Ph_3P
L=quin; L'=$(\underline{m}\text{-MePh})_3P$
diolefin=COD; L=py, 2-et-py, quin; L'=Ph_3P
L=2-et-py, quin; L'=Ph_3As
(ii) diolefin=NBD; L=quin; L'=Ph_3P, $(\underline{p}\text{-FPh})_3P$, $(\underline{p}\text{-MePh})_3P$
(iii) diolefin=NBD; L=quin; L'=$(\underline{o}\text{-MePh})_3P$
L=py, 2-et-py, quin; L'=Ph_3As

Scheme 1.

Table 1. Analytical results for the $[Rh(diolefin)L_nL'_m]BPh_4$ complexes

Complex	Found. (calc.) (%) C	H	N	Λ_M ($ohm^{-1}cm^2mol^{-1}$)
$[Rh(COD)(py)_2]BPh_4$	73,64 (73,26)	6,10 (6,14)	4,03 (4,06)	27
$[Rh(COD)(2\text{-et-py})_2]BPh_4$	73,27 (74,19)	6,66 (6,76)	3,93 (3,76)	8
$[Rh(COD)(quin)_2]BPh_4$	74,80 (76,14)	5,90 (5,87)	3,25 (3,55)	16
$[Rh(COD)(py)(Ph_3P)]BPh_4$	75,77 (75,78)	6,34 (6,01)	1,68 (1,60)	56
$[Rh(COD)(2\text{-et-py})(Ph_3P)]BPh_4$	74,37 (76,87)	6,24 (6,27)	1,38 (1,55)	52
$[Rh(COD)(quin)(Ph_3P)]BPh_4$	75,05 (76,87)	6,16 (5,90)	1,64 (1,51)	44
$[Rh(COD)(2\text{-et-py})(Ph_3As)]BPh_4$	71,86 (72,54)	5,39 (5,98)	1,13 (1,48)	12
$[Rh(COD)(quin)(Ph_3As)]BPh_4$	72,53 (73,37)	5,47 (5,63)	1,53 (1,45)	20
$[Rh(NBD)(py)(Ph_3P)]BPh_4$	75,77 (75,79)	5,99 (5,65)	1,66 (1,63)	48
$[Rh(NBD)(2\text{-et-py})(Ph_3P)]BPh_4$	73,67 (76,11)	6,03 (5,96)	1,23 (1,58)	48
$[Rh(NBD)(quin)(\underline{m}\text{-}MeC_6H_4)_3P]BPh_4$	77,47 (77,30)	6,24 (5,95)	1,49 (1,47)	68
$[Rh(NBD)(quin)_2(Ph_3P)]BPh_4$	77,60 (77,76)	5,73 (5,55)	2,50 (2,70)	48
$[Rh(NBD)(quin)_2(\underline{p}\text{-}MeC_6H_4)_3P]BPh_4$	77,87 (78,06)	6,11 (5,89)	2,23 (2,60)	44
$[Rh(NBD)(quin)_2(\underline{p}\text{-}C_6H_4)_3P]BPh_4$	73,36 (73,90)	5,04 (4,99)	2,17 (2,57)	44

the presence of both cationic and arene complexes and no bands due to coordinated N-donor ligand.

When the diolefinic ligand present in the complex is 1,5-cyclooctadiene, only the four-coordinate derivatives could be isolated. These mixed complexes are analogous to those obtained with ClO_4^- as anion.[12] It is noteworthy that when using 1,5-cyclooctadiene as diolefinic ligand it has been possible to isolate mixed complexes containing both N- and As-donor ligands contrarily to what happened in the case of norbornadiene, while the isolation of five-coordinate species with COD was not possible. These observations could be in line with the higher π-acidity of norbornadiene which enhances pentacoordination ability.[13,14] The only mixed pentacoordinated complexes containing 1,5-cyclooctadiene described in the literature are $[Rh(COD)_2(Ph_3Sb)]BPh_4$[15] and those by Cocevar *et al.* containing bidentate N-donor ligands.[16]

The analytical data for these complexes are collated in the table.

The conductivities for all these complexes are much too low for the bulky anion BPh_4^- to be responsible,[17] therefore suggesting the existence of an equilibrium in acetone solution:

$$[Rh(diolefin)L_nL'_m]BPh_4 \rightleftharpoons Rh(diolefin)BPh_4 + nL + mL'$$

$$n = 1 \text{ or } 2,\ m = 0 \text{ or } 1$$

though in the solid state all these complexes contain the uncoordinated BPh_4^- anion as may be clearly seen from their IR spectra.

EXPERIMENTAL

$[Rh(COD)L_2]BPh_4$ complexes were prepared similarly to $[Rh(NBD)(py)_2]BPh_4$[9].

Synthesis of the $[Rh(NBD)L_nL']BPh_4$ *complexes*

To a methanol suspension of $[Rh(NBD)Cl]_2$ an excess of N-donor ligand (Rh:L = 1:50) was added upon which the dimer dissolved. The solution was then cooled to 0–10°C and an equimolar amount of phosphine (Rh:P = 1:1) was added, followed by the addition of an equimolar amount of $NaBPh_4$ upon which a yellow-orange solid precipitated that was immediately filtered at 0°C. The solid was washed with cold methanol/water and air dried.

Synthesis of the $[Rh(COD)LL']BPh_4$ *complexes*

Addition of N-donor ligand (Rh:L = 1:4) to methanol suspensions of $[Rh(COD)Cl]_2$ led to disolution of the dimer. The solution was then cooled to 10°C and an equimolar amount of Ph_3P or Ph_3As was added. After the addition of the stoichiometric amount of $NaBPh_4$ the compound precipitated. The solid was filtered, washed with cold methanol/water and air dried.

REFERENCES

[1] M. A. Garralda and L. A. Oro, *Transition Met. Chem.* 1980, **5**, 65.
[2] R. Usón, L. A. Oro, J. Artigas and R. Sariego, *J. Organometal. Chem.* 1979, **179**, 65.
[3] R. R. Schrock and J. A. Osborn, *J. Am. Chem. Soc.* 1971, **93**, 2397.
[4] R. R. Schrock and J. A. Osborn, *Inorg. Chem.* 1970, **9**, 2339.
[5] M. J. Nolte, G. Gafner and L. M. Haines, *J. Chem. Soc. Chem. Comm.* 1969, 1406.
[6] R. Usón, P. Lahuerta, J. Reyes and L. A. Oro, *Transition Met. Chem.* 1969, **4**, 332.
[7] P. Albano, M. Aresta and M. Manassero, *Inorg. Chem.* 1980, **19**, 1069.
[8] G. Mestroni, G. Zassinovich and A. Camus, *J. Organometal. Chem.* 1977, **140**, 63.
[9] L. A. Oro, E. Pinilla and M. L. Tenajas, *J. Organometal. Chem.* 1978, **148**, 81.
[10] B. Denise and G. Pannetier, *J. Organometal. Chem.* 1973, **63**, 431.
[11] R. Usón, L. A. Oro, C. Claver and M. A. Garralda, *J. Organometal. Chem.* 1976, **105**, 365.
[12] R. Usón, L. A. Oro, M. A. Garralda, C. Claver and P. Lahuerta, *Transition Met. Chem.* 1979, **4**, 55.
[13] K. Vrieze, H. C. Volger and A. P. Pratt, *J. Organometal. Chem.* 1968, **15**, 195.
[14] H. C. Volger, M. M. P. Gaasbeek, H. Hogeveen and K. Vrieze, *Inorg. Chim. Acta* 1969, **3**, 145.
[15] B. Denise and G. Pannetier, *J. Organometal. Chem.* 1978, **161**, 171.
[16] C. Cocevar, G. Mestroni and A. Camus, *J. Organometal. Chem.* 1972, **35**, 389.
[17] W. J. Geary, *Coord. Chem. Rev.* 1971, **7**, 81.

Polyhedron Vol. 1, No. 4, pp. 343–348, 1982
Printed in Great Britain.

0277–5387/82/040343–06$03.00/0
Pergamon Press Ltd.

SYNTHESES AND CHARACTERIZATION OF URANIUM CONTAINING APATITES

A. GIVAN†, I. MAYER and L. BEN-DOR*
Department of Inorganic and Analytical Chemistry, The Hebrew University, Jerusalem, 91904 Israel

(*Received September* 1981)

Abstract—Synthetic apatites containing uranium were prepared from solution by precipitation. The hydroxy apatite obtained contained up to ca. 1% uranium homogeneously dispersed in the apatite matrix. Carbonate–fluoride apatites were prepared from calcium carbonate via a heterogeneous reaction. The uranium content in the latter apatites was to low to check for distribution by EPMA. However, emission spectra and vibrational analysis proved that UO_2^{2+} was the species present in both apatites (HAP and CAP). XRD of pure and uranium containing apatites revealed no significant differences. When heated to 700°C most uranium-containing apatites, including natural Oron (Israel) apatite, lose the characteristic UO_2^{2+} emission and show an identical emission centered at *ca.* 18860 cm^{-1}, suggesting the transformation of UO_2^{2+} to another ion, possibly uranate.

INTRODUCTION

Many geochemical and archaeological studies[1–4] have pointed out, mainly by means of fission tracks counting, that the concentration and distribution of the uranium and the apatite phase in natural rocks are mutually dependent. The Israeli Negev phosphates contain about 100–150 ppm uranium and the concentration ratio U/P, is practically constant in all the fields. The microscopic distribution of uranium in these phosphates was determined by fission tracks counting[5] and it was clearly shown that uranium concentrates in the apatite phase. The exact location of uranium and the nature of its bonding with apatite is not yet well understood and the fact that uranium is present in the IV and VI oxidation states, complicates the problem. Part of the uranium (5–25%) is quite mobile, and is easily extracted by suitable complexing agents while most of it is strongly connected to the phosphates. Only by heating the rock to about 700°C (a process in which the uranium is oxidized) does the uranium become extractable and fission tracks analysis indicates that uranium no longer concentrates in the apatite phase[6].

Investigations of synthetic apatites containing uranium also reflect different approaches regarding the bond between the two components. Thompson[7] investigated the uranium distribution in hydroxyapatite crystals prepared by precipitation from a solution of $Ca(NO_3)_2$ and $(NH_4)_2HPO_4$ at pH = 12, and concluded that:

- Relatively large amounts of the uranyl ions are lost in washing, and are loosely associated with the hydroxy apatite crystals in the hydration shell.
- The uranium remaining in the final solid phase after washing, concentrates on preferred regions of the crystal surface.

On the other hand, Blasse[8] doubts the assumption that uranium is present in the apatite lattice, basing this on the identification of a new phase—$Ba_2UO_2(PO_4)_2$[BUP] in a study of the emission spectrum of UO_2^{2+} in $Ba_3(PO_4)_2$.

In this work uranium containing apatites were prepared in order to examine the location of the uranium in relation to the apatite lattice. Fluoro–apatite, $Ca_5(PO_4)_3F$(FAP), hydroxy–apatite $Ca_5(PO_4)_3OH$(HAP) and fluorohydroxy–carbonate apatite $Ca_5(PO_4, CO_3)_3$(OH, F) (CAP), were prepared both by solid state reactions and in solution, in the presence of variable amounts of uranium in the IV and VI oxidation states. The products were examined by activation analysis, x ray diffraction (XRD), E.P.M.A. (electron probe micro analysis), infrared, Raman and emission spectroscopy in order to estimate the uranium concentration, chemical composition, cell constants, homogeneity of uranium distribution in the host matrices, the nature of the chemical bonds and the exact species of uranium in these materials.

EXPERIMENTAL

1. *Syntheses*

(a) *Hydroxy apatites* (*HAP*). The method of preparation used is a modification of the method suggested by Tandy.[9] The method is based on the dropwise addition of a $Ca(NO_3)_2$ solution to a Na_3PO_4 solution, the pH being raised to 14 by addition of 6N NaOH. The $Ca(NO_3)_2$ solution contains the UO_2^{2+} ion added in the form of $UO_2(NO_3)_2.6H_2O$ in the required amounts. The product was washed several times with T.D.W. and dried overnight at 100°C.

Materials. $Na_3PO_4.12H_2O$–Merck; $Ca(NO_3)_2.4H_2O$–Baker; $UO_2(NO_3)_2.6H_2O$–Hopkin and Williams. (No steps were taken to avoid atmospheric CO_2 absorption.)

(b) *Fluoro (hydroxy) carbonate apatites* (*CAP*). This apatite was prepared by a method described by Deutch.[10] The heterogeneous reaction was carried out in an alkaline solution (initial pH approx. 13.5). The reactants are calcite ($CaCO_3$), Na_2HPO_4, NaOH and KF. The ratio $(F^-)/(OH^-)$ was chosen so as to enable the formation of apatite at a suitable rate.[11] Also, owing to the large excess of fluoride ions, the apatite obtained had a minimal hydroxy substitution. The required concentration of uranium in the form of $UO_2(NO_3)_2.6H_2O$ was added to the reaction mixture, in propylene vessels, and refluxed at 60–70°C for 1 week. Samples were checked for the extent of reaction by comparing the intensities of the (104) reflection of calcite and the (211) reflection of apatite in the XRD diagram. The precipitate was repeatedly washed with T.D.W. to remove the soluble salts. The unreacted calcite was removed using a solution of triammonium citrate.[12]

Materials. $CaCO_3$—BDH Analar; $Na_2HPO_4.12H_2O$–BDH Lab Reagent; NaOH–BDH Analar; KF–Merck.

(c) *Fluoro-apatites* (*FAP*). Samples were prepared by grind-

†Post doctoral fellow supported by the Atomic Energy commision of Israel.

*Author to whom correspondence should be addressed.

ing the starting materials in the appropriate ratios in an agate mortar. A quantity of *ca.* 250 mg was introduced into a 30 mm long platinum capsule which was closed but not sealed. The mixture was gradually heated to the required temperature for 8–24 hr and then cooled slowly to room temperature. The extent of reaction was determined by examination of powder diffraction patterns.

Attempts to prepare uranium containing apatites were carried out using various uranium compounds:

$$UO_2,\ UP_2O_7 \text{ and } U_3(PO_4)_4{}^{13},\ UO_3{}^{14}.$$

Materials. UO_2—Alpha Inorganics; $CaHPO_4.2H_2O$—BDH Lab. Reagents; Cao—Baker; CaF_2—BDH Lab. Reagents; NaF—Merck.

2. *Analyses*

(a) Uranium was determined by activation analysis.† (b) The distribution of U, Ca and P was examined by E.P.M.A. using a Jeol JXA-5. The simultaneous examination of three elements was carried out by its three wavelength dispersive spectrophotometers. Uranium concentration was also estimated by this method using Corning glass (0.68–0.76% UO_2) as a standard.

(c) Phase analyses was accomplished by XRD at room temperature (Phillips diffractometer), using Ni-filtered copper radiation and 1/4–1° 2θ/min scanning speeds. Calibration was checked using Si as internal standard.

(d) IR spectra were recorded on a P.E. 180 spectrophotometer. Samples were prepared both in a nujol mull and KBr pellets and calibrated against atmospheric CO_2 bands.

(e) Raman and emission spectra were recorded on a Spex 1401 double monochromator with a Spex 1442 third monochromator in tandem. The signal was detected by a thermoelectrically cooled C13034 Class II photomultiplier. The 5154, 4880 and 6471 Å lines from spectra physics 164 Ar^+ and Kr^+ lasers were used as excitation sources. Laser plasma lines were used for calibration.

RESULTS

1. *Solid state reactions*

(a) *Reactions with U(IV).* The first series of reactions was conducted in order to substitute Ca^{2+} by U(IV) and Na^+ in the apatite lattice of FAP, using UO_2 as the uranium source. The reactants were $Ca_3(PO_4)_2$; $CaHPO_4.2H_2O$; CaF_2; NaF and UO_2, and the estimated product was $Ca_{10-x}U_{x/3}Na_{2x/3}(PO_4)_6F_2$. Increasing the uranium concentration from 0.7 to about 20% gave rise to a deepening yellow colour in the product. XRD analysis gave characteristic FAP diagrams, the cell constants being almost identical with those of pure FAP (JCPDS 15–876). In addition to typical FAP pattern, the diagrams show a number of unassigned reflections which gain intensity with the concentration of uranium in the reaction mixture.

The products were washed with TDW, 0.1N HCl and 0.2N citric acid. Activation analysis of the precipitates and filtrates revealed that the amount of uranium in the filtrate was negligible. On the other hand XRD analysis of the precipitates showed the disappearance of the unassigned reflections of the original products.

The precipitates containing 1.4 and 2.9% uranium were examined by E.P.M.A., before and after the washings with HCl and citric acid. It must be emphasized that E.P.M.A. was carried out on several different areas of a large number of product particles. The patterns found showed two significant phases: the first was homogeneous in the Ca and P distribution, while the uranium counts were no higher than the background noise. The second was richer in uranium and contained in addition mainly Ca. A similar pattern of Ca, P and U distributions resulted from measurements of the precipitates after washing by T.D.W., 0.1N HCl and 0.2N citric acid.

In a second set of substitution reactions U(IV) phosphates were used as starting materials. The reactions examined were:

$$2Ca_3(PO_4)_2 + CaF_2 + CaO + UP_2O_7 \rightarrow Ca_8U(PO_4)_6F_2 \quad (1)$$

(heating the reaction mixture to about 1000°C for 12–18 hr in a closed platinum tube).

$$7Ca_3(PO_4)_2 + 3CaF_2 + U_3(PO_4)_4 \rightarrow 3Ca_8U(PO_4)_6F_2 \quad (2)$$

(same conditions as above).

The products obtained in these reactions were yellow and their XRD analyses gave diagrams and cell constants similar to those of FAP (JCPDS 15–876) with additional unassigned reflections. The E.P.M.A. patterns were essentially the same as in the products of the UO_2 reactions.

(b) *Reactions with U(VI).* The substitution reaction performed was:

$$0.25UO_3 + 2.75Ca_3(PO_4)_2 + 0.5CaHPO_4 + CaF_2 \rightarrow Ca_{9.75}(UO_2)_{0.25}(PO_4)_6F_2 + 0.25H_2O \quad (3)$$

(same conditions as in reactions 1 and 2 above).

Again, the results of XRD analyses and E.P.M.A. were the same as for the UO_2 reactions. However, when heating the reaction mixture in an induction furnace for several minutes (temperature of about 1500°C), the E.P.M.A. pattern, although nonhomogeneous, revealed for the first time that uranium is present not only in the unknown phases with calcium, but also in the apatite matrix in a concentration of about 0.5%. In spite of the observed distribution of uranium in apatite, XRD analysis did not show any deviation from the cell constants of pure FAP.

2. *Reactions in solution*

(a) *Hydroxy apatites.* A series of uranium containing hydroxy apatites was prepared. The molar concentration U/Ca in the initial solution ranged from 0 to 10.5%. The products with the higher uranium concentration were more intensely yellow. The concentration of the starting materials and products is given in Table 1. The precipitates and filtrates were examined by activation analysis for uranium. Most of the uranium was found in the solid phase (Table 1).

A detailed E.P.M.A. of all solid phases was carried out. The homogeneity of U, P and Ca distribution, as well as the approximate concentration of uranium were checked. The results are compared with the uranium concentration determined by activation analysis (Table 1). The significant conclusion of these measurements is that uranium is homogeneously distributed up to U/Ca starting concentrations of 2.1%. Higher U/Ca molar concentrations in the initial solutions resulted in nonhomogeneous distribution of uranium. The uranium rich particles were also rich in Ca and contained negligible

†We are grateful to Dr. H. Feldstein from Soreq Nuclear Research Center for performing these measurements.

Table 1. Concentration and distribution of uranium in precipitated hydroxy apatites {Initial $[Ca^{2+}]$ and $[PO_4^{3-}]$ was 2.10^{-3} mol/l in all samples}

Sample	UO_2^{2+} moles in solution ($\times 10^6$)	U/Ca molar ratio in solution ($\times 10^3$)	U distribution in solid product (EPMA)	U concentration in solid (%) (EPMA)	U concentration in solid (%) (Activation Analysis)
1	-	0	-	-	-
2	0.21	0.105	-	-	0.012
3	0.42	0.21	-	-	0.022
4	0.84	0.42	-	-	0.049
5	2.1	1.05	homogeneous	0.17	0.12
6	4.2	2.1	homogeneous	0.54	0.59
7	8.4	4.2	homogeneous	0.83	0.7
8	21	10.5	homogeneous	0.73	0.69
9	42	21	homogeneous	1.35	0.69
10	84	42	beginning of nonhomogeneity	0.81	0.92
11	168	84	nonhomogeneous	-	6.04
12	210	105	nonhomogeneous	-	8.09

amounts of P. The particles with homogeneous uranium distribution showed similar behaviour with Ca and P.

As XRD analysis, of the solid phases dried at 100°C, resulted in diagrams with high background and broad peaks, the samples were further heated to 300–400°C and reexamined. The products with molar concentrations of U/Ca (in the initial solutions) from 0 to 2.1%, indicated a single phase in the XRD diagrams–HAP. A single additional reflection (not found in JCPDS 9–432) had a d value of 2.66Å and its relative intensity was moderate. Precipitates from solutions with U/Ca molar concentrations higher than 2.1% demonstrated the existence of additional phases and much lower intensity of the HAP reflections in their XRD diagrams. Cell constants were calculated for both pure and uranium-containing hydroxy apatites. The calculations were based on sixteen chosen reflections and results are given in Table 2. Heat treatment of HAP, pure and containing 10%U did not change the cell constants.

The uranyl ion UO_2^{2+}, has a well known emission spectrum in the visible region, consisting of a progression in ν_1 (the symmetrical vibration of UO_2^{2+}). The emission spectra of pure and uranium containing hydroxy apatites are given in Fig. 1, and compared with spectra of several other uranyl containing compounds: $UO_2(NO_3)_2.6H_2O$; $UO_2(OAc)_2.2H_2O$; Na_3PO_4 glass containing 1% UO_2^{2+}, and Oron (Israel) natural apatite. Temperature effects on emissions are also shown.

Raman and IR spectra of pure and U-containing (1%) HAP, were also recorded and analyzed according to functional groups. The spectra are summarized in Figs. 2, 3 and compared with spectra of other uranium containing compounds.

The HAP containing 1%U was subjected to an extraction experiment† in a hot (70°C) solution of 1N Na_2CO_3. Two successive processes extracted about 62% of the uranium. No change was found, however, in the XRD diagram and the emission spectrum of the remaining HAP. Similar results were obtained after prolonged heating (700°C) of HAP (1%U) with KF or NaF.

†We are grateful to Dr. H. Feldstein from Soreq Nuclear Research Centre for these measurements.

(b) *Carbonate apatites.* Three samples were prepared, the molar U/Ca concentrations in the starting solutions being 0, 0.02 and 0.08%. The pure CAP is white, while the U-containing CAP is yellowish. Activation analysis showed the uranium concentration of the 2 yellow compounds to be 0.025 and 0.1%. These low uranium concentrations prevented the use of E.P.M.A. to determine uranium distribution in the compounds (the lowest limit of sensitivity is about 0.2%). XRD analysis was carried out for the three products after thermal treatment at different temperatures. At temperatures up to 300°C, the diagrams as well as the cell constants calculated from them were similar to literature values of a carbonate apatite (JCPDS 19–272). At higher temperatures several changes were found, namely, the appearance of additional reflections, shifts toward lower 2θ values and changes in intensity ratios. These changes were typical of both pure and uranium containing CAP, but appeared at lower temperatures in the higher uranium-containing apatite. Cell constants derived from XRD analyses at different temperatures are listed in Table 3.

Emission spectra of CAP were also recorded and are given in Fig. 1. Unlike the uranyl ion in the HAP matrix, the typical UO_2^{2+} emission in CAP disappeared as soon as the sample was heated to about 100°C. Raman and IR spectra are given in Figs. 2 and 3. Vibrations of the UO_2^{2+} ion could not be detected due to low concentration.

DISCUSSION

(1) *Solid state reactions*

From XRD diagrams, cell constants and E.P.M.A., the main product of the reactions in presence of UO_2^{2+} is clearly FAP. As E.P.M.A. is insensitive to low uranium concentrations (0.2% is the upper limit of the technique), the possibility that small amounts of uranium were incorporated into the apatite lattice cannot be neglected. E.P.M.A. measurements show, however, that most of the uranium exists in phases in which the main other constituent is calcium. The additional unassigned reflections in the XRD patterns of the products, their disappearance from the precipitates' diagrams after washings with 0.1NHCl and 0.2N citric acid, and the absence of

Table 2. Cell constants of hydroxy apatites containing uranium

Sample	U/Ca molar concentration (%) in solution	Uranium concentration (%) in hydroxy apatite	a_0(Å) ±0.003Å	c_0(Å) ±0.005Å
HAP	0	0	9.428	6.892
HAP	0.21	0.59	9.420	6.887
HAP	0.42	0.70	9.427	6.890
HAP	1.05	0.69	9.423	6.894
HAP	2.1	0.69	9.426	6.897
HAP	4.2	0.92 (nonhomogeneous)	9.401	6.879
JCPDS 9–432	0	0	9.418	6.884

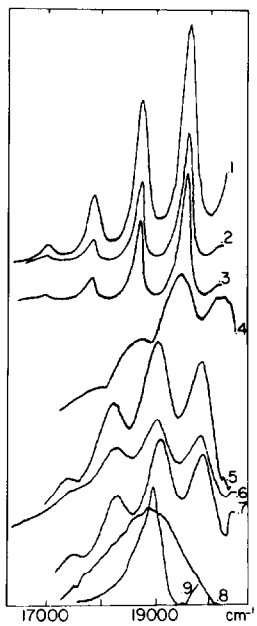

Fig. 1. Emission Spectra, excitation Ar^+ laser, 4880Å, 150 mW. (1) $UO_2(NO_3)_2.6H_2O$. (2) $UO_2(CH_3COO)_2.2H_2O$. (3) CAP mixed with 1% uranyl nitrate. (4) Na_3PO_4 glass containing 1% uranyl. (5) HAP containing 1% uranium. (6) No. 5 heated to 700°C. (7) CAP containing 1% uranium. (8) No. 7 heated to 700°C. (9) Oron Apatite heated to 800°C.

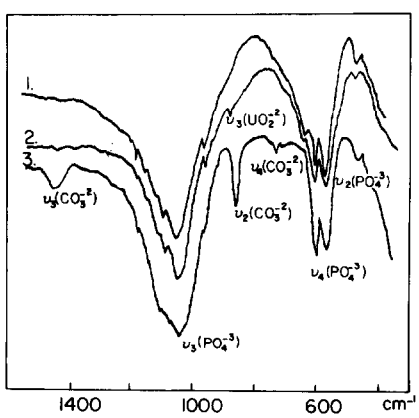

Fig. 2. IR spectra. (1) 0.2% HAP pure in KBr pellet. (2) 1.0% HAP containing 1% uranium in KBr pellet. (3) 0.3% CAP pure in KBr pellet.

uranium from the respective filtrate, suggest that uranium concentrates in a nonapatite phase, which is insoluble, and which has a very low-intensity XRD pattern. It might possibly be an imperfectly crystallized calcium uranate. Changing the uranium source from UO_2 to the U(VI) phosphates, UP_2O_7 and $U_3(PO_4)_4$, had no effect on the results. Uranium again concentrates in a nonapatite phase, but as previously mentioned a low distribution of uranium in the apatite lattice is possible.

In contrast, the reaction with UO_3-U(VI) leads, beyond doubt, to the incorporation of uranium in the apatite lattice. In addition to several undefined phases which are richer in uranium, the apatite matrix showed a homogeneous distribution in concentrations of approx. 0.5%.

(2) *Reactions in solution*

The fact that the HAP phase was indeed obtained is based on positive identification and on the absence of XRD reflections and IR bands characteristic of other phosphate phases[15–17]. The homogeneity of the phosphate matrix with respect to the distribution of Ca and P, as recorded by E.P.M.A. also rules out different phosphate phases.

In spite of the moderate accuracy of the determinations by E.P.M.A., very similar results were obtained for uranium concentration in the apatite solids both by this technique and activation analysis. The uranium was shown to be homogeneously dispersed in the apatite matrix at concentrations of up to 1%. The uranium concentration in the hydroxy apatites is almost a linear function of U/Ca molar ratios in solution for low values of U/Ca. At higher U/Ca values the uranium concentration reaches saturation (at about 1%) and at U/Ca molar ratios greater than 2.1% the crystallization of new, uranium containing phases begins. These phenonena are well demonstrated by E.P.M.A. and by additional reflections in the XRD. Most of these reflections are similar to those of $Ca_2U_2O_7$ (JCPDS 19–254) both in *d* values and relative intensities. This fact is in accordance with the qualitative E.P.M.A. picture, which indicated that the additional phases contain mainly Ca and U.

The uranium incorporation does not cause significant changes in HAP cell constants (Table 2). The deviation from literature values of these constants at high U/Ca molar ratios (Table 2, nonhomogeneous distribution of uranium in apatite), is of dubious character, since the appearance of new phases was associated with significant low intensity of the apatite reflections. Thus XRD alone cannot unequivocally determine the location of uranium in the apatite lattice. Additional data was supplied by other physical methods.

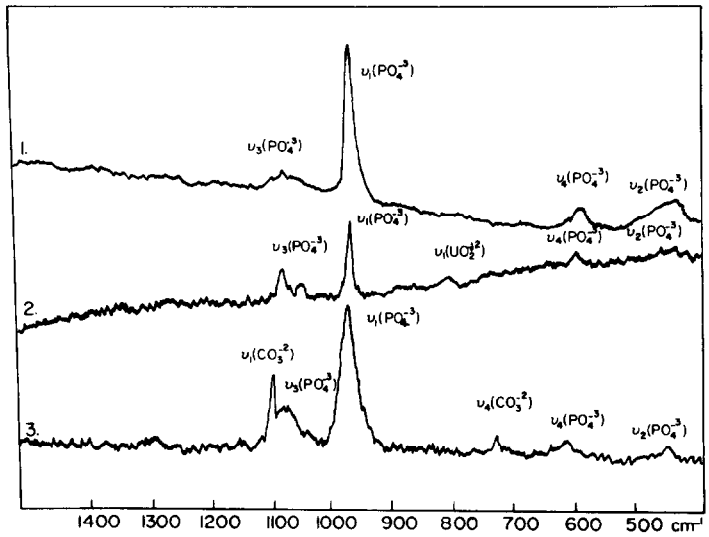

Fig. 3. Raman spectra. (1) HAP pure. (2) HAP containing 1% uranium. (3) CAP pure.

Table 3. Variation of lattice constants of carbonate apatites with temperature†

Temp.	CAP		CAP (0.025% U)		CAP (0.1% U)	
°C	a_0(Å)	c_0(Å)	a_0(Å)	c_0(Å)	a_0(Å)	c_0(Å)
150	9.292	6.929	9.290	6.915	9.291	6.899
300	9.287	6.900	9.294	6.900	9.303	6.893
500	9.315	6.894	9.318	6.892	9.336	6.896
700	9.369	6.892	9.369	6.905	9.443	6.950
900			9.443	6.951		

†Standard deviation—up to 0.009Å in c_0, and 0.007Å in a_0. Literature values (JCPDS 19-272): $a_0 = 9.309$Å; $c_0 = 6.972$Å.

Table 4. Force constants, bond order and bond length of the uranyl ion in various compounds

Sample	*fr* (md/Å)	frr (md/Å)	n†	r(Å)†	r(Å)‡
$UO_2(NO_3)_2.6H_2O$	7.180	−0.081	2.375	1.694	1.729
$UO_2(OAc)_2.2H_2O$	7.100	−0.099	2.351	1.699	1.732
Na_3PO_4(1% UO_2^{2+} glass)§	5.385	-	1.836	1.806	1.741
HAP (1% U)	6.180	−0.224	2.075	1.753	1.758
CAP (0.1% U)§	6.030	-	2.030	1.762	1.763
$Ba_2UO_2(PO_4)_2$‖	6.156	−0.276	2.068	1.754	1.759

†Calculated according to Ref. [23].
‡ Calculated according to Ref. [22].
§Calculation based only on ν_1 from emission spectrum.
‖Vibrational frequencies ν_1 and ν_3 from Ref. [8].

The identification of uranyl ions ion in the apatite matrix was determined by emission spectra (Fig. 1.). A comparison of these spectral splittings and intensity ratios with those of $UO_2(NO_3)_2.6H_2O$, $UO_2Ac_2.2H_2O$, Na_3PO_4 glass containing 1% UO_2^{2+} (Fig. 1), showed great similarity to the spectra of UO_2^{2+} in phosphate matrices. The fact that the emission spectrum changed neither after heating the sample to 700°C, nor when almost 2/3 of the uranium was extracted by 1N Na_2CO_3, nor after prolonged heating with KF, demonstrated the affinity of the UO_2^{2+} bonding to the host apatite matrix. On the other hand, the ease of only partial extraction of uranium, points out the possibility of the existence of several sites for the UO_2^{2+} in the lattice.

Assignment of Raman and infrared bands in the vibrational spectra of HAP and HAP containing 1% U was made on the basis of functional groups. The spectra identified the phosphate phase as HAP, and distinguished it from other phases (OCP, β-Ca_3PO_4). Despite the low intensity of the UO_2^{2+} bands of HAP (1%U), both in the

Raman and infrared spectra (due to the low UO_2^{2+} experimental concentration in the samples), they can be used to obtain further information about UO_2^{2+} in the apatite phase. Excellent agreement of the values of ν_1 (symmetric stretch vibration) was obtained from both Raman and emission spectra of $UO_2(NO_3)_2.6H_2O$, and $UO_2(OAc)_2.2H_2O$, facilitated the correct assignment of the ν_1 band of UO_2^{2+} in apatites, by comparison with the respective value from its emission spectrum.

The uranyl ion, of linear $D_{\infty h}$ symmetry, has four normal modes of vibration: ν_1 symmetric stretch mode, which is only Raman active, ν_3 antisymmetric stretch mode, only infrared active, and ν_2 the doubly-degenerate bending mode, again only IR active. Deviations from these activity rules[8], are usually assigned to environmental effects rather than to a change in the symmetry of the ion.[18,19] The frequencies ν_1 and ν_3 of UO_2^{2+} change in accordance with the ligands attached to the ion.[18,19] In principle, the more significant change is expected in the value of ν_3, a mode which includes motion of the centre of the ion relative to the centre of the trapping site, but due to the high atomic weight of the uranium, there can be no real difference between the effects on ν_1 and ν_3. Variations of the vibration frequencies imply respective changes in the force constants computed from them, and therefore also in the bonding strength within the ion. Several different empirical relationships between the stretching of the U–O bonds, force constants (fr) and the U–O bond length (r) and bond order (n) have been derived and have been checked for a series of UO_2^{2+} compounds with known U–O distances.[19–21] The Raman spectrum of HAP (1%U) showed a weak band at $795 \pm 3\ cm^{-1}$, which did not appear in the spectrum of pure HAP. This band was assigned to ν_1 (UO_2^{2+}) and is in excellent agreement with the value of $\nu_1(UO_2^{2+})$ from the emission spectrum of HAP (1%U) ($790\ cm^{-1}$). The IR spectrum of HAP (1%U), contains a weak band at $880 \pm 3\ cm^{-1}$ which is absent in the spectrum of pure HAP. This band was assigned to ν_3 (UO_2^{2+}). The two frequencies are quite similar to those of UO_2^{2+} in BUP[8]. The force constants calculated where used to compute the U–O bond lengths and bond orders for UO_2^{2+} in HAP (1%U) and several other compounds. The results of the calculations are listed in Table 4. Again, there is significant similarity in force constants, bond length and bond orders of UO_2^{2+} in various phosphate phases, excluding perhaps the Na_3PO_4 glass, the deviation of which is related to the broader and less resolved emission lines. Bond lengths computed for UO_2^{2+} in HAP are in the range attributed to stronger U–O bonds,[20] (1.69–1.76Å). Bonds in uranates, on the other hand, are weaker with bond lengths of around 2Å. It is noteworthy that the strength of the U–O bonds is anion dependent.

The emission and vibration spectra of CAP and HAP are very similar (except for the CO_3^{2-} bands). Although the vibrational bands of UO_2^{2+} in CAP could not be detected the ν_1 frequency was derived from the emission spectrum (Fig. 2). The value of ν_1 (UO_2^{2+}), namely $800 \pm 5\ cm^{-1}$ was used to calculate the force constant. The values listed in Table 4, are quite similar to those of UO_2^{2+} in HAP and of BUP.

Unlike HAP, CAP decomposed at temperatures higher than 500°C and CO_2 was released. The CO_3^{2-} ions which substitute part of the PO_4^{3-} ions, leave their sites and the lattice expands. This phenomenon was characterized by a shift toward lower 2θ and higher d values in the XRD diagrams, as well as by an increase of the respective cell constants. The presence of UO_2^{2+} evidently increased the ease of decomposition as it began at lower temperatures with higher uranium concentrations (Table 3). The disappearance of the typical UO_2^{2+} emission in the 0.1% uranium CAP system after heat treatment at 100°C suggests a different bonding of the UO_2^{2+} in this system as compared to HAP. Possibly, during heating *and* in the presence of F^- ions the uranyl radical is transformed to a different material, e.g. uranate. It is significant to note that natural Oron apatite, with no heat treatment also does *not* show the characteristic UO_2^{2+} emission although it certainly contains U(VI). When heated to *ca.* 700°C pure CAP, 0.1%U–CAP and Oron apatite have identical emission centered at 18860(3) cm^{-1}; the same as in pure HAP. Possibly the transformation of uranyl radical in synthetic apatites by heat treatment took place in the natural apatite in some past historical event.

Acknowledgements—This work was supported by a contract from the Atomic Energy Commission of Israel, to whom we are grateful. We thank Y. Marcus for his advice and interest, H. Feldstein for valuable help and cooperation and S. Cohen for helping with the XRD. The useful suggestions of the referee are kindly acknowledged.

REFERENCES

[1]S. Charalambus and C. Papastefanou, *Nucl. Instrum. Meth.* 1977, **142** 581.
[2]N. Bhandari, S. G. Bhat, D. Lal, G. Razagopalar, A. S. Tannhane and V. S. Venkatavaradan, *Earth and Planetary Sci. Lett.* 1971, **13** 191.
[3]H. M. Naguib, D. K. Murti, R. Kelley, *J. Mater. Sci.* 1976, **11** 406.
[4]D. W. Zimmerman, *Nature* 1971, **231** 818.
[5]Y. Avital, Geochemistry of Uranium in Phosphorites 1979. M.Sc. Thesis H.U.
[6]M. Stein, Geochemistry of Uranium in Calcination Process of Oron Phosphates 1979. M.Sc. Thesis H.U.
[7]R. C. Thompson, *Science* 1970, **167** 1494.
[8]G. Blasse and J.P.M. Van Den Dungen, *J. Inorg. Nucl. Chem.* 1978, **40** 2037.
[9]S. Tandy, Ph.D. Thesis. The Hebrew University of Jerusalem, 1977.
[10]Y. Deutch and S. Sarig, *J. Cryst. Growth* 1977, **42** 234.
[11]D. R. Simpson, *Am. Min.* 1968, **53** 1953.
[12]S. R. Silverman, R. K. Fuyat and J. P. Weiser, *Am. Min.* 1952, **37** 211.
[13]A. Burdese and M. L. Borleva, *Annali Di Chimia (Rome)* 1963, **53**, 344.
[14]F. A. Cotton and G. Wilkinson, *Advanced Inorganic Chemistry*, 3rd Edn. p. 1099. Interscience, New York (1972).
[15]E. C. Moreno, T. M. Gregory and W. F. Brown, *J. Res. NBS* 1968, **72A** 773.
[16]J. P. Feenstra and P. L. de Bruyn, *J. Phys. Chem.* 1979, **83** 475.
[17]H. Monmas, *J. Mater. Sci.* 1980, **15** 2428.
[18]S. D. Gabelnick, G. T. Reedy and M. G. Chasanov, *J. Chem. Phys.* 1973, **58** 4468.
[19]S. D. Gabelnick, G. T. Reedy and M. G. Chasanov, *J. Chem. Phys.* 1973, **57** 6397.
[20]J. I. Bullock, *J. Chem. Soc.* 1969, A781.
[21]L.H. Jones, *Spectrochim. Acta* 1959, **15** 409.
[22]R. M. Badger, *J. Chem. Phys.* 1935, **3** 710.
[23]N. Vdovenko, L. G. Mashirov and D. L. Suglobov, *Dokl. Akad. Nauk. SSR* 1969, **185** 824.

Polyhedron Vol. 1, No. 4, pp. 349–353, 1982
Printed in Great Britain.

0277–5387/82/040349–05$03.00/0
Pergamon Press Ltd.

STRONG Zn^{2+}/Mn^{2+} CATION ORDERING AMONG FIVE- AND SIX-COORDINATED SITES IN γ-$(Zn_{0.75}Mn_{0.25})_3(PO_4)_2$

ANDERS G. NORD*
Section of Mineralogy, Swedish Museum of Natural History, P.O. Box 50007, S-104 05 Stockholm 50, Sweden

and

THEODOR STEFANIDIS
Departments of Inorganic and Structural Chemistry, Arrhenius Laboratory, University of Stockholm, S-106 91 Stockholm, Sweden

(*Received* 13 *October* 1981)

Abstract—The solid solution γ-$(Zn_{0.75}Mn_{0.25})_3(PO_4)_2$ has been studied utilizing neutron powder diffraction data. The monoclinic ($P2_1/n$) structure has been refined by means of the Rietveld full-profile technique ($R_I = 0.051$, $R_p = 0.057$). The results clearly show that the cations are strongly ordered; Zn^{2+} at the five-, and Mn^{2+} at the six-coordinated sites. The "ZnO_5" polyhedra are somewhat distorted trigonal bipyramids, while the "MnO_6" octahedra are fairly regular.

INTRODUCTION

When zinc ions in α-$Zn_3(PO_4)_2$ are replaced by other M^{2+} cations, a solid solution called "γ-$Zn_3(PO_4)_2$", or more correctly γ-$(Zn_{1-z}M_z)_3(PO_4)_2$, may be formed;[1] it is henceforward abbreviated Zn/*M*. Such γ-phases were earlier studied owing to their potential use as components in colour television screens. It was then shown that the γ-phase could be stabilized by substituting Cd^{2+}, Mn^{2+} or Mg^{2+} for zinc.[2,3,4] (A metastable γ-phase with a few per cent Ca^{2+} exists above 1200 K.)[5] In addition, recent studies have shown that also Fe^{2+}, Co^{2+}, Ni^{2+} or Cu^{2+} can stabilize the γ-phase.[6] The crystal structure of "γ-$Zn_3(PO_4)_2$", stabilized by a small but unknown amount of manganese, was determined in 1963 by Calvo.[7] The monoclinic unit cell ($Z = 2$) contains four five-coordinated cations, M(1), and two six-coordinated cations, M(2). In his paper, Calvo suggested that the M^{2+} cations should preferentially enter the M(2) sites, thereby stabilizing the γ-phase with respect to α-$Zn_3(PO_4)_2$. Partly in order to verify this idea, we have carried out cation distribution studies of some Zn/*M* phases, utilizing various techniques.[8,9,10] The present investigation of γ-$(Zn_{0.75}Mn_{0.25})_3(PO_4)_2$ has been based on neutron powder diffraction data, because the neutron scattering amplitudes of the two metals in question are widely different.

$Mg_3(PO_4)_2$ is isomorphous with the "γ-$Zn_3(PO_4)_2$" phase,[11] and some cation distribution studies of various $(Mg_{1-z}M_z)_3(PO_4)_2$ solid solutions have been carried out.[12] These and the present investigation have been undertaken as part of a project on cation distributions in minerals and inorganic structures containing five-coordinated cation sites.[8–10,12–14]

EXPERIMENTAL

α-$Zn_3(PO_4)_2$ and $Mn_2P_2O_7$ were first prepared by conventional techniques (cf. Ref. 6). The solid solution γ-$(Zn_{0.75}Mn_{0.25})_3(PO_4)_2$ was then prepared by heating a mixture of α-$Zn_3(PO_4)_2$, $Mn_2P_2O_7$ and commercial MnO in the molar proportions 3:1:1 in evacuated and sealed silica tubes. The Mn content in the γ-phase (25 atom %) is close to the maximum solubility, which is 27% at 1070 K.[3,13] The heating continued at 1070 K (800 ± 10°C) for three months, whereupon the tubes were quenched in cool water. Eight samples so obtained were checked by means of X-ray powder diffraction (Guinier–Hägg camera, $CrK\alpha_1$ radiation: λ = 2.28975 Å; 50.00 mm camera radius, KCl internal standard). The photographs were evaluated by a film scanner and associated programs[15,16]. The dimensions of the monoclinic ($P2_1/n$) unit cell were refined to (mean values): $a = 7.563(2)$, $b = 8.553(1)$, c = 5.056(1) Å, $\beta = 94.78(2)°$, $V = 326.0(1)$ Å^3 ($Z = 2$). In some of the powder patterns a few weak reflections remained un-indexed. The three samples finally selected for the neutron diffraction study (combined volume about 3 cm^3, equivalent to ~ 10 g) had only one very weak un-indexed reflection (at $d = 4.076$ Å) in addition to the 33 indexed reflections. This batch sample was therefore judged to be sufficiently pure.

The neutron powder diffraction data were collected at room temperature at the Studsvik *R*2 nuclear research reactor (Studsvik, Nyköping, Sweden), with the sample kept in a vanadium cup, using a double monochromator in parallel setting (copper crystals). The average flux was 10^{10} neutrons m^{-2} s^{-1} for $\lambda \approx$ 1.52 Å. Accurate data were collected for $2° \leq \theta \leq 50°$, with a total scan time of 12 days ($\Delta\theta = 0.04°$).

THE PROFILE REFINEMENTS

For $\theta > 34.7°$ the reflections overlapped so much that it was quite impossible to fix the background level with satisfactory precision. Therefore only data with $2° \leq \theta \leq 34.7°$ were used. No evidence of superstructure could be detected in the intensity profile, nor extra reflections extinct in the centro-symmetric space group earlier reported for this structure type.[7,11,17,18] Peaks greater than 0.3% of the largest peak in the spectrum (comparing integrated intensity values) ought to be significantly observed in spite of the fact that the background was not so smooth. We therefore assume the space group symmetry for γ-$(Zn_{0.75}Mn_{0.25})_3(PO_4)_2$ to be $P2_1/n$ (No. 14).

After subtraction of the graphically determined background but without correction for absorption effects, the intensity data were processed by means of the full-profile refinement procedure of Rietveld.[19] In a preliminary step

*Author to whom correspondence should be addressed.

the scale factor, zero point and unit cell parameters were refined to fix the mean neutron wavelength. The crystal structure was then refined with 28 parameters: one scale factor C such that $I_{calc} = C \cdot I_{obs}$, three peak profile parameters, 18 atomic positional parameters, and six isotropic temperature factors (the two metal sites were given the same value for reasons discussed below, while phosphorus and the four oxygen atoms had individual temperature factors). Atomic coordinates from an X-ray single-crystal refinement of the γ-$(Zn_{0.97}Mn_{0.03})_3(PO_4)_2$ structure[18] were used as starting parameters.

The cation distribution was expressed by a parameter x, defined by the formula γ-$(Zn_{1-x}Mn_x)_2^{M(1)}(Zn_{0.25+2x}Mn_{0.75-2x})^{M(2)}(PO_4)_2$ with $0 \leq x \leq 0.375$. Thus $x = 0$ indicates an "ordered" model with M(1) occupied by zinc only, while $x = 0.25$ gives a random distribution such that all cation sites are occupied by 75% Zn and 25% Mn. The true value of x was determined through a series of ten-cycle refinements, with systematically shifted x values. The neutron scattering amplitudes were taken from the *International Tables of X-ray Crystallography*.[20] The discrepancy index R_I, defined as $\Sigma|I_{obs} - I_{calc}|/\Sigma I_{obs}$ and based on integrated reflection intensities, is given in Table 1 for the various refinements as a function of x, together with some further selected data from the respective refinements.

A distinct R_I minimum was soon found in the region $0 < x < 0.02$, and a computerized interpolation of the $R_I = f(x)$ curve located the minimum at $x = 0.0125$. Not only the R factors but also the standard deviations of the refined parameters obtained the smallest values for this final refinement with $x = 0.0125$; the R factors were $R_I = 0.051$, $R_p = 0.057$ and $R_{wp} = 0.073$ (cf. Ref. 19). The accuracy of x may be slightly affected by the fact that M(1) and M(2) were given the same temperature factor. This arrangement, though, was necessary because in the trial refinements M(2) sometimes had a scattering amplitude close to zero (cf. Table 1). However, an inspection of the results of other refinements of this structure type shows that this approximation may well be justified.[11,17,18] The observed and calculated intensity profiles are shown in Fig. 1. The refined atomic parameters are listed in Table 2. A table of observed and calculated integrated intensities for the $x = 0.0125$ refinement has been deposited with the Editor at Queen Mary College, London, from whom copies are available. (The refined atomic parameters have also been deposited with the Institut für anorganische Chemie, University of Bonn, F.R.G.).

The fact that three of the refined temperature factors (cf. Table 2) have acquired negative values, though close to zero, is somewhat curious. However, physically meaningless temperature factors sometimes occur with the profile-refinement procedure,[21] and even with single-crystal neutron diffraction data.[22] Our irrelevant temperature factors may be due to the rather high and not quite smooth background, and considerable overlapping among the reflections at higher θ values in the used part of the intensity profile. From the expression $\exp[-B \cdot (\sin\theta/\lambda)^2]$ it is clear that the temperature factors, B, are principally determined from reflections with higher θ values. Although slight, absorption effects also affect the temperature factors to some degree. However, the standard deviations of all positional parameters are quite small and do not suggest any deviations from $P2_1/n$ space group symmetry, or disorder in the structure. Neither are the standard deviations of the isotropic temperature factors very large, and they are also fairly equal. Moreover, the refinements with other values of the parameter x gave still worse B factors then those presented in Table 2. For instance, for $x = 0.10$ (i.e. still with a fairly strong cation ordering) the temperature

Table 1. Selected data from the Rietveld full-profile refinements of γ-$(Zn_{0.75}Mn_{0.25})_3(PO_4)_2$ for a series of x values ($0 \leq x \leq 0.375$). The value of x is defined according to the formula γ-$(Zn_{1-x}Mn_x)_2^{M(1)}(Zn_{0.25+2x}Mn_{0.75-2x})^{M(2)}(PO_4)_2$

x	b[M(1)][a]	b[M(2)][a]	R_I	R_p	R_{wp}	esd(B)[b]	esd(xyz)[b]
0	0.590	-0.120	0.053	0.058	0.074	0.15	0.001
0.0125[c]	0.578	-0.099	0.051	0.057	0.073	0.13	0.001
0.02	0.571	-0.084	0.053	0.058	0.074	0.14	0.001
0.025	0.566	-0.075	0.055	0.059	0.075	0.15	0.001
0.05	0.542	-0.028	0.068	0.067	0.083	0.16	0.001
0.10	0.500	0.070	0.111	0.103	0.121	0.23	0.002
0.15	0.448	0.162	0.157	0.150	0.174	0.33	0.002
0.20	0.400	0.258	0.197	0.198	0.230	0.44	0.003
0.25[d]	0.350	0.350	0.241	0.242	0.279	0.54	0.004
0.30	0.300	0.460	0.293	0.294	0.323	0.65	0.005
0.35	0.258	0.542	0.333	0.351	0.421	0.99	0.007
0.375	0.230	0.590	0.351	0.371	0.437	1.33	0.009

[a] Neutron scattering amplitudes in 10^{-12} cm units. [b] Definition: esd(B) denotes the mean e.s.d.'s of the six isotropic temperature factors (B) in a refinement, and esd(xyz) denotes the mean e.s.d.'s of the 18 atomic positional parameters (x,y,z) which were refined. [c] This is the "correct" model. [d] This is the random distribution model.

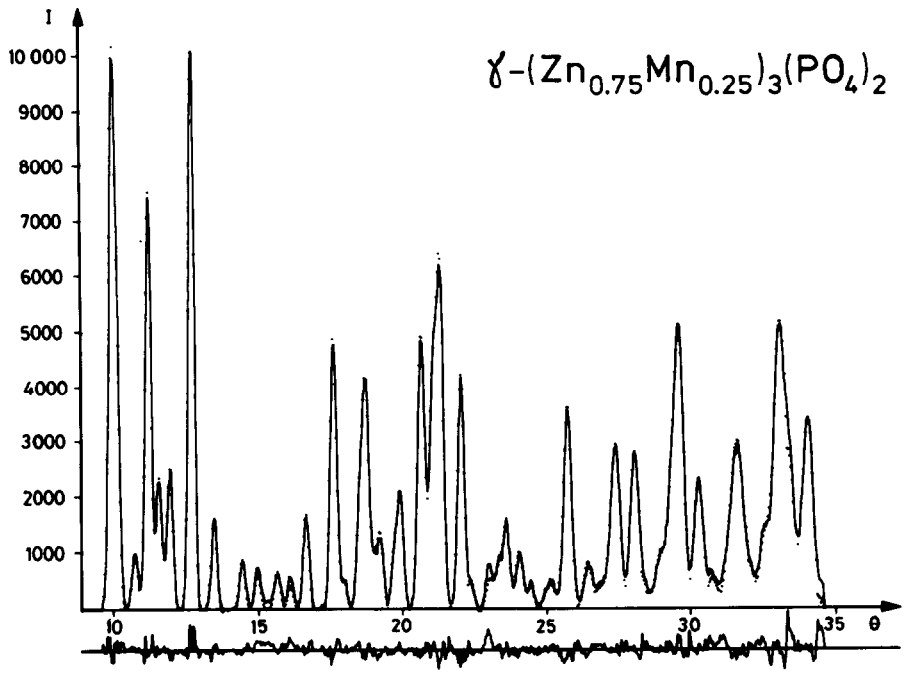

Fig. 1. The least-squares fit obtained between the observed intensities (continuous line) and calculated intensities (points) for γ-$(Zn_{0.75}Mn_{0.25})_3(PO_4)_2$ (neutron powder diffraction data). The discrepancy in the fit ($\Delta I = I_{obs} - I_{calc}$) is plotted below to the same scale.

Table 2. Atomic positional coordinates and temperature factors for the "$x = 0.0125$" refinement of γ-$(Zn_{0.75}Mn_{0.25})_3(PO_4)_2$ (see Table 1)

Atom	x	y	z	B /Å^2/
M(1)	0.622	0.134	0.081	0.46(12)
M(2)	0	0	1/2	0.46(12)
P	0.206	0.192	0.036	0.54(15)
O(1)	0.051	0.136	0.836	-0.31(14)
O(2)	0.135	0.205	0.304	-0.15(11)
O(3)	0.254	0.354	0.936	0.33(16)
O(4)	0.362	0.079	0.046	-0.34(10)

The estimated standard errors according to the fitting program were 0.001 or less for the positional parameters. Space group $P2_1/n$ (No. 14); equivalent positions (x,y,z), (-x,-y,-z), (1/2-x,1/2+y,1/2-z), (1/2+x,1/2-y, 1/2+z).

factors were in the region $-0.9(3) \leq B \leq 1.3(3)$ Å^2. We have also performed a series of refinements assuming the temperature factors of the four oxygen atoms to be equal, i.e. with 25 parameters instead of 28. The "best" refinement as regards low R factors, low standard deviations and reasonable temperature factors was obtained for $x = 0.0150$, i.e. quite close to $x = 0.0125$ earlier obtained. In this case we obtained B(metal) = 0.40(15), B(phosphorus) = 0.55(16), and B(oxygen) = −0.11(7) Å^2, with $R_I = 0.059$, $R_p = 0.058$, and $R_{wp} = 0.084$. The positional parameters deviated less than 1 σ from the respective values of the "$x = 0.0125$" refinement (Table 2); their standard deviations were always less than 0.001. We therefore conclude that the atomic parameters arrived at in the $x = 0.0125$ refinement are basically correct.

DISCUSSION

The crystal structure of γ-$(Zn_{0.75}Mn_{0.25})_3(PO_4)_2$ is built up of somewhat distorted $M(1)O_5$ trigonal bipyramids, and almost regular $M(2)O_6$ octahedra and PO_4 tetrahedra (see Fig. 2). Zinc orders strongly at the M(1), and manganese at the M(2) sites. This is interesting since Zn^{2+} ($3d^{10}$) as well as Mn^{2+} ($3d^5$, high-spin) yield zero CFSE (crystal field stabilization energy) in octahedral and in tetrahedral environments with oxygen ligands.[23] However, the most common state for manganese in mineral structures is high-spin, octahedrally coordinated Mn^{2+}, especially with O^{2-}, OH^- or H_2O ligands.[24] Its structural role seems to be controlled principally by local electric charge and ionic radius, so that relative to smaller divalent cations such as Zn^{2+}, Mn^{2+} preferentially occupies the largest cation sites. Zn^{2+} often occurs with lower coordination numbers, which may be explained by thermodynamic considerations.[25] This is in agreement with the observed Zn^{2+}/Mn^{2+} cation ordering.

Some interatomic distances and angles are summarized in Table 3, with corresponding values for γ-$(Zn_{0.97}Mn_{0.03})_3(PO_4)_2$ from an X-ray single-crystal study[7,18] added for comparison. The similarity between the two compounds is striking. According to our experience, the dimensions of the phosphate tetrahedra from the present neutron diffraction study are unusually good considering the fact that only powder data have been used in the structure refinement. It is also noteworthy that the metal–oxygen bond distances for the two compounds of Table 3 display a small but explicable difference: The M(2)–O mean distance in γ-$(Zn_{0.75}Mn_{0.25})_3(PO_4)_2$ has increased significantly from γ-

Table 3. Interatomic distances (Å) and angles (°)

	γ-$(Zn_{0.75}Mn_{0.25})_3(PO_4)_2$[a]	γ-$(Zn_{0.97}Mn_{0.03})_3(PO_4)_2$[b]
Distances		
M(1)-O(1)	2.43(1)	2.394(4)
M(1)-O(2)	1.97(1)	1.934(4)
M(1)-O(3)	1.98(1)	1.984(5)
M(1)-O(4)	1.94(1)	1.955(3)
M(1)-O(4′)	2.02(1)	2.007(4)
M(1)-O average	2.07(1)	2.055(4)
M(2)-O(1) (x2)	2.07(1)	2.010(5)
M(2)-O(2) (x2)	2.30(1)	2.201(3)
M(2)-O(3) (x2)	2.24(1)	2.227(4)
M(2)-O average	2.20(1)	2.146(4)
P-O(1)	1.56(1)	1.518(6)
P-O(2)	1.50(1)	1.551(4)
P-O(3)	1.53(1)	1.536(4)
P-O(4)	1.53(1)	1.555(3)
P-O average	1.53(1)	1.540(4)
Angles[c]		
O-M(1)-O range	66.2-163.1	67.4-163.7
O-M(1)-O average	104.8	104.9
O-M(2)-O range[d]	82.3-97.7	82.5-97.5
O-M(2)-O average[d]	90.0	90.0
O-P-O range	104.6-112.4	105.9-112.1
O-P-O average	109.5	109.8

[a]This work. [b]Data from Calvo [7, 18]. All atoms are numbered as in Table 2. [c]The estimated standard deviations of the angles are 0.4° or less for both studies. [d]The 180° angles are not included.

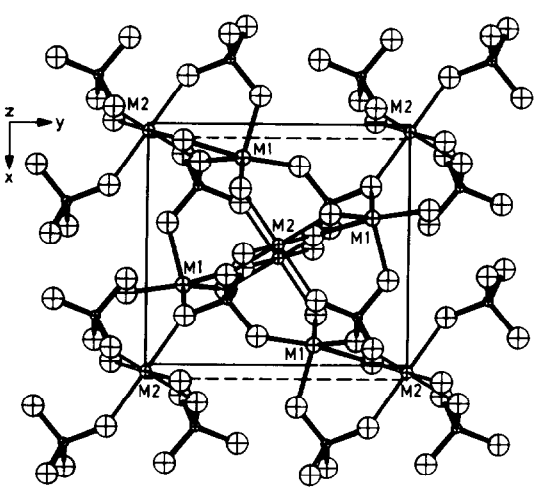

Fig. 2. An ORTEP plot of the "γ-$Zn_3(PO_4)_2$" structure. The smallest circles represent phosphorus atoms, the second largest are metal atoms [M(1) or M(2)], and the largest circles are oxygen atoms.

$(Zn_{0.97}Mn_{0.03})_3(PO_4)_2$, while the M(1)–O mean distance is almost unchanged. This reflects the situation that the larger Mn^{2+} cations concentrate at the M(2) sites, thereby increasing the M(2)–O distances. The converse effect for M(2)–O was in fact noticed in a former study of the isostructural γ-$(Zn_{0.70}Ni_{0.30})_3(PO_4)_2$ phase,[10] where nickel also preferentially entered the M(2) sites: the M(2)–O mean distance had in this case decreased to 2.12 Å as the smaller Ni^{2+} ions replaced zinc at the M(2) sites.

The observed cation ordering in γ-$(Zn_{0.75}Mn_{0.25})_3(PO_4)_2$ implies that Mn^{2+} prefers the octahedral M(2) positions, which comprise one third of all metal cation sites available. The maximum solubility of Mn^{2+} in "γ-$Zn_3(PO_4)_2$" is determined by this effect; however, it is not 33% but only 27% at 1070 K[3,13] so some additional factor, probably a size effect, must be involved. However, for γ-$(Zn, Ni)_3(PO_4)_2$ the maximum solubility of Ni^{2+} at 1070 K is close to 33%.[13]

The intra-crystalline Zn^{2+}/M^{2+} cation exchange in a γ-$(Zn_{1-x}M_x)_3(PO_4)_2$ solid solution may be expressed by means of the cation distribution factor $K_D = [X_{Zn}(M(1)) \cdot X_M(M(2))]/[X_{Zn}(M(2)) \cdot X_M(M(1))]$. Assuming equal activity factors for the cations, K_D may be regarded as the equilibrium constant at the temperature in question for the cation exchange reaction

$$Zn^{2+}[M(2)] + M^{2+}[M(1)] \rightleftarrows Zn^{2+}[M(1)] + M^{2+}[M(2)]. \quad (1)$$

A random distribution of the cations makes K_D equal to unity, while K_D increases as M^{2+} concentrates at the M(2) sites. For the solid solution γ-$(Zn_{0.75}Mn_{0.25})_3(PO_4)_2$ the cation distribution factor, as a function of the parameter x, is defined by the equation $K_D = (1-x)(0.75-2x)/x(0.25+2x)$, so that $x = 0.0125$ gives $K_D = 208$ and $x = 0.0150$ gives $K_D = 169$. Since the dis-

Table 4. Cation distribution K_D values (see text) and homogeneity ranges of M^{2+} (in atom%) for some γ-$(Zn_{1-z}M_z)_3(PO_4)_2$ solid solutions

Solid solution	Equilibrium temperature	K_D	Technique	Homogeneity range	Ref.
γ-$Zn_2Mg(PO_4)_2$	~1300 K	~20	X-ray	3-100 %	[8]
γ-$(Zn_{0.90}Fe_{0.10})_3(PO_4)_2$	1070 K	30	Mössbauer	3-40 %	[9,13]
γ-$(Zn_{0.80}Fe_{0.20})_3(PO_4)_2$					
γ-$(Zn_{0.70}Fe_{0.30})_3(PO_4)_2$					
γ-$(Zn_{0.65}Fe_{0.35})_3(PO_4)_2$					
γ-$(Zn_{0.70}Ni_{0.30})_3(PO_4)_2$	1070 K	40	Neutron	3-33 %	[10,13]
γ-$(Zn_{0.75}Mn_{0.25})_3(PO_4)_2$	1070 K	~200	Neutron	3-27 %	this work

tribution coefficient changes considerably with x, the factor for the Zn^{2+}/Mn^{2+} distribution at 1070 K should rather be given as $K_D \approx 200$. However, the fairly good R factors, the low standard deviations obtained in the $x = 0.0125$ refinement as well as the reasonable interatomic distances and angles certainly agree with the feasible result that Zn^{2+} strongly orders at the five- and Mn^{2+} at the six-coordinated sites. We therefore believe that our results are correct within the limitations set by the profile-refinement technique.

Corresponding K_D values, according to eq. (1), and homogeneity ranges for some γ-$(Zn_{1-z}M_z)_3(PO_4)_2$ solid solutions have been summarized in Table 4. Since $K_D > 1$ for all phases listed there, it is clear that Zn^{2+} has a much stronger preference for five-coordination than any of the cations Mg^{2+}, Fe^{2+}, Ni^{2+} or Mn^{2+}. Part of this result is in accordance with the results of an earlier study of isomorphous $(Mg_{1-z}M_z)_3(PO_4)_2$ solid solutions.[12] From recent studies of $(Fe_{1-z}M_z)_3(PO_4)_2$ graftonite-type solid solutions it is also evident that Zn^{2+} has a much greater tendency for five-coordination than has the Mn^{2+} cations.[26] In order to make this kind of cation distribution studies more complete, some further neutron diffraction investigations of γ-phases are in progress involving a number of other divalent-metal cations.

CONCLUSIONS

It is concluded that the divalent-metal cations of the solid solution γ-$(Zn_{0.75}Mn_{0.25})_3(PO_4)_2$ are strongly ordered, zinc at the five-, and manganese at the six-coordinated sites ($K_D \approx 200$ at 1070 K). This cation ordering agrees with the stabilizing effect of Mn^{2+} on the "γ-$Zn_3(PO_4)_2$" structure suggested by Calvo. It is also in accordance with the solubility of Mn^{2+} in the γ-phase. Finally, the observed changes in the metal–oxygen bond distances as Mn^{2+} substitutes for zinc correspond with the established cation ordering.

Acknowledgements—We are very grateful to Professor Peder Kierkegaard and Dr Sven Westman (both at the Arrhenius Laboratory, Stockholm) for their critical reading of the manuscript and for some valuable discussions concerning this work. Professor Eric Welin (Swedish Museum of Natural History) is cordially thanked for the excellent laboratory and computing facilities placed at our disposal. We are also indebted to Dr Roland Tellgren (University of Uppsala) for his willing help during the collection of the neutron diffraction data. The generous financial support from the Swedish Natural Science Research Council is gratefully acknowledged.

REFERENCES

[1]A. L. Smith, *J. Electrochem. Soc.* 1951, **98**, 363.
[2]J. J. Brown and F. A. Hummel, *J. Electrochem. Soc.* 1963, **110**, 1218.
[3]F. A. Hummel and F. L. Katnack, *J. Electrochem. Soc.* 1958, 105, 528.
[4]J. F. Sarver, F. L. Katnack and F. A. Hummel, *J. Electrochem. Soc.* 1959, **106**, 960.
[5]E. R. Kreidler and F. A. Hummel, *Inorg. Chem.* 1967, **6**, 524.
[6]A. G. Nord and P. Kierkegaard, *Chem. Scripta* 1980, **15**, 27.
[7]C. Calvo, *J. Phys. Chem. Solids* 1963, **24**, 141.
[8]A. G. Nord, *Mat. Res. Bull.* 1977, **12**, 563.
[9]H. Annersten, T. Ericsson and A. G. Nord, *J. Phys. Chem. Solids* 1980, **41**, 1235.
[10]A. G. Nord and T. Stefanidis, *Acta Cryst.* 1981, **B37**, 1509.
[11]A. G. Nord and P. Kierkegaard, *Acta Chem. Scand.* 1968, **22**, 1466.
[12]A. G. Nord and T. Stefanidis, *Mat. Res. Bull.* 1980, **15**, 1183.
[13]A. G. Nord and T. Stefanidis, *Mat. Res. Bull.* 1981, **16**, 1121.
[14]A. G. Nord, *Acta Chem. Scand.*, 1982, **A36**, 95.
[15]K. E. Johansson, T. Palm and P. E. Werner, *J. Phys. E.: Sci. Instrum.* 1980, **13**, 1289.
[16]T. Palm, S. Salomé and P. E. Werner, To be published.
[17]J. B. Anderson, E. Kostiner, M. C. Miller and J. R. Rea, *J. Solid State Chem.* 1975, **14**, 372.
[18]C. Calvo, Personal communication.
[19]H. M. Rietveld, *J. Appl. Cryst.* 1969 **2**, 65.
[20]*International Tables for X-Ray Crystallography*, Vol. III. Kynoch Press, Birmingham (1973).
[21]G. A. Mackenzie, R. W. Berg and G. S. Pawley, *Acta Cryst.* 1980, **B36**, 1001.
[22]M. Sakata, J. Harada, M. J. Cooper and K. D. Rouse, *Acta Cryst.* 1980, **A36**, 7.
[23]R. G. Burns, *Mineralogical Applications of Crystal Field Theory.* University Press, Cambridge (1970).
[24]D. R. Peacor, In *Handbook of Geochemistry* (Edited by K. H. Wedepohl), Vol. II/3, Chap. 25-A. Springer-Verlag, Berlin (1978).
[25]A. Navrotsky and O. J. Kleppa, *J. Inorg. Nucl. Chem.* 1967, **29**, 2701.
[26]A. G. Nord and T. Ericsson, *Am. Min.* 1982 (In press).

Polyhedron Vol. 1, No. 4, pp. 355–359, 1982
Printed in Great Britain.

0277–5387/82/040355–05$03.00/0
Pergamon Press Ltd.

PREPARATION, SPECTRAL PROPERTIES AND THE CRYSTAL STRUCTURE OF THE PENTACOORDINATED TRICHLOROBIS(HEXAMETHYLPHOSPHORAMIDE)-INDIUM(III) COMPLEX

SHYAMA P. SINHA*
Hahn-Meitner-Institut für Kernforschung, Glienicker Strasse 100, Postfach 390128, D-1000 Berlin 39, Federal Republic of Germany

and

T. T. PAKKANEN,† T. A. PAKKANEN† and L. NIINISTÖ
Department of Chemistry, Helsinki University of Technology, SF-02150 Espoo 15, Finland

(*Received* 26 *October* 1981)

Abstract—Trichlorobis(hexamethylphosphoramide)In(III), $InCl_3(OP(N(CH_3)_2)_3)_2$, was prepared by extraction of indium(III) chloride from aqueous solution into chloroform containing a slight excess of hexamethylphosphoramide and structurally characterized by X-ray methods. In this pentacoordinated complex, the central In(III) ion is bonded to two hexamethylphosphoramide molecules *via* the phosphoryl oxygens in the axial positions and to three chloride ions in the equatorial positions in a trigonal bipyramidal arrangement with average In–O and In–Cl bond distances of 2.18 and 2.36 Å respectively. The solid state infrared and Raman spectra of the complex are discussed. The observed spectra are consistent with those expected for the pentacoordinated structure of the complex.

INTRODUCTION

Recently the hexamethylphosphoramide [HMPA = $OP\{N(CH_3)_2\}_3$] complexes of the lanthanides have received particular attention from synthetic and spectroscopic points of view.[1–3] In our effort to systematize the synthesis of the HMPA complexes by special extractive methods,[1,2,4,5] we have prepared the In(III) complex of the composition $InCl_3(HMPA)_2$. Like the trivalent lanthanides, In(III) belongs to the class (*a*)-ions and readily forms complexes with oxygen donor ligands like HMPA. This paper describes preparative, identification, spectroscopic and structural studies of the $InCl_3(HMPA)_2$ complex.

EXPERIMENTAL

Preparation of the complex. The complex was prepared by an extractive method described previously.[1,2,4,5] 1 mMol of $InCl_3 \cdot 3H_2O$(BDH) was dissolved in a minimum quantity of water and the aqueous solution was extracted with 20 ml of $CHCl_3$ containing a slight excess than 2 mMol of HMPA. The chloroform layer was separated and dried by placing it in contact with molecular sieves for several days in a closed system. The solvent was then allowed to evaporate slowly in a vacuum desiccator when well formed crystals of $InCl_3(HMPA)_2$ were obtained. These crystals were washed with a small amount of CCl_4 to remove excess HMPA. The crystals were dried and kept in a desiccator until used.

Found C, 25.11; H, 6.33; N, 14.81; calc. for $InCl_3(C_6H_{18}N_3PO)_2$: C, 24.87; H, 6.26; N, 14.50% The absence of water peaks in the IR showed the sample to be anhydrous.

Spectroscopic measurements. The solid state absorption spectrum of the complex was recorded with a Beckman DBG spectrometer as thinly dispersed Nujol mull in a QS 81 sandwich type quartz cell. The IR spectrum of the complex in the solid state was measured by multiple internal reflection technique with a PE 283 instrument and as pellet (dispersed in RbI) with a Perkin–Elmer PE 580B instrument‡ from 4000–180 cm^{-1} (Fig. 1). Both spectra are essentially the same, indicating no exchange with RbI. Laser Raman spectrum of the solid sample was obtained with a Spex 1403 in combination with SCAMP data processing unit which allowed collection of spectra with considerable reduction of background noise. The 19435 cm^{-1} line of the Ar-ion laser (Spectra Physics) was used as excitation source.

Crystal structure determination. Unit cell parameters and orientation were determined and intensity data ($\theta_{min} < \theta < \theta_{max}$) recorded using conventional ω-scan methods on a crystal $1.0 \times 0.3 \times 0.3$ mm^3. Mo-K_α radiation ($\lambda = 0.71069$ Å) and a Syntex $P2_1$ diffractometer was used for structure determination.

The crystals of $InCl_3(HMPA)_2$ belong to the monoclinic space group $P2_1/c$. The unit cell parameters and other crystal data for $InCl_3(HMPA)_2$ (m.w. 579.6) are: $a = 16.986(3)$, $b = 10.214(2)$, $c = 16.254(3)$ Å and $\beta = 111.35(1)^0$, $V = 2626.3$ $Å^3$, $Z = 4$, $d_c = 1.47$ g/cm^3, $\mu = 13.37$ cm^{-1}, standard reflections 111, $20\bar{2}$. A total of 5335 independent reflections was measured, of which 3563 had intensities greater than three times their standard errors based on counting statistics and were considered as minimum useful intensity. Lorentz, polarization and absorption corrections were applied to the observed intensities. The structure was solved by direct methods (MULTAN 78). Isotropic least-squares refinement of all non-hydrogen atoms converged the conventional *R*-factor to 0.124. Subsequent anisotropic refinements with all hydrogen atoms in fixed and idealized positions with $U = 0.10$, yielded a final§ $R = 0.051$ and a weighted discrepancy factor $R_w = 0.052$ ($w = 1/\sigma^2(F_0^2)$).

RESULTS AND DISCUSSION

IR and Raman spectra. The IR spectrum of the $InCl_3(HMPA)_2$ complex in the water absorption region (Fig. 1a) showed the complex to be anhydrous. Direct evidence that all ligands (3 Cl^- and 2 HMPA) are bonded

*Author to whom correspondence should be addressed.

†Present address: Department of Chemistry, University of Joensuu, SF-80101 Joensuu, Finland.

‡We thank Perkin–Elmer Co., Bodenseewerk, Überlingen and especially Mr. Duelli for running the spectrum in their instrument.

§Tabulated data for final positional parameters and anisotropic thermal factors have been deposited as Supplementary Data with the Editor from whom copies are available on request. Atomic co-ordinates have also been deposited with the Cambridge Crystallographic Data Centre (CCDC).

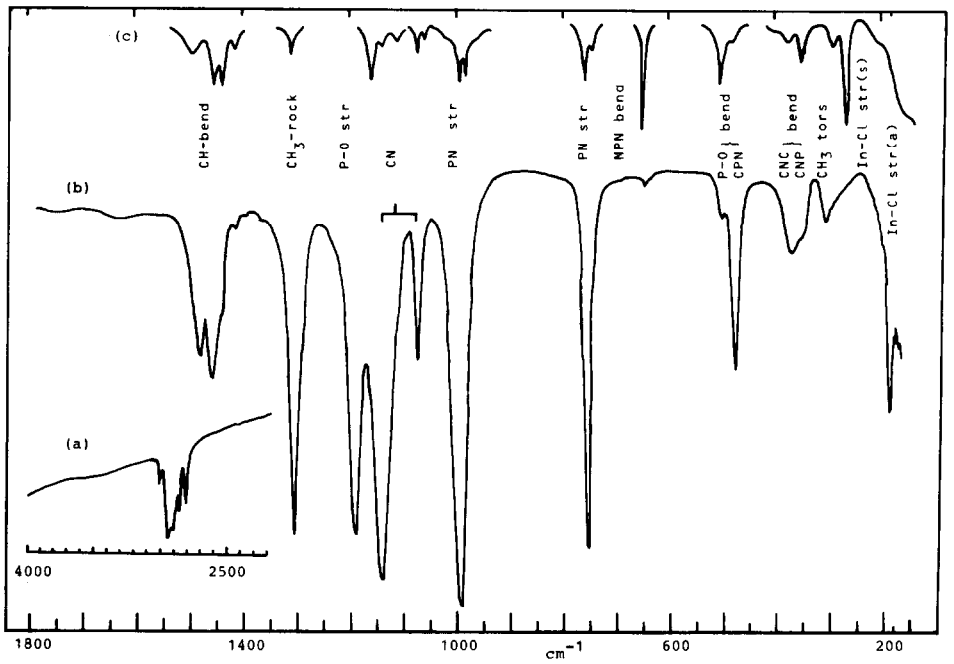

Fig. 1. (a, b) IR and (c) Raman spectra of $InCl_3(HMPA)_2$ complex with probable assignments.

to the central In(III) ion came from the crystal structure analysis of the complex. The main changes in the IR spectrum of the coordinated HMPA with respect to the free ligand are the lowering of the PO and raising of the PN peak frequencies[1,2] and these changes were observed (Fig. 1). The PO frequency (HMPA 1210 cm^{-1})[1,2] was lowered about 20 cm^{-1} and the PN frequencies at 982 and 740 cm^{-1} of HMPA[1,2] were raised to 992 and 755 cm^{-1} in the present complex. These changes are comparable to that observed for *a*-type trivalent cations like the lanthanides and Y(III).[1,3]

Complexation also brings about characteristic changes[1,2] of the peak centered at 1200 cm^{-1}. The CN stretching which is usually observed as shoulders (~1150, 1174 cm^{-1}) appears as a strong peak at 1142 cm^{-1} for the indium complex. Of the bending vibrations the NPN bending is IR inactive in HMPA and its complexes[1,2] and appears as a very weak peak at 645 cm^{-1} in our complex. However, in the Raman spectrum the complex showed the expected NPN bending as strong peak at 648 cm^{-1}.

The PO bending vibration of HMPA at 484 cm^{-1} (IR) showed the very small but expected lowering of frequency in our In-complex (476 cm^{-1}). The weak shoulder at ~500 cm^{-1} in the complex is probably the CNP bending vibration. A reversal of intensity of these peaks is usually observed in the Raman spectra of HMPA-complexes.[1,2] This is also the case with our In-complex (Figs. 1b, c). The weakly split peaks at 370 and 352 cm^{-1} (Raman 372 and 348 cm^{-1}) in the complex could be assigned to the CNC and CNP bending of the coordinated HMPA.[1,2]

Much has been said about In–Cl stretching vibrations[6–16] in different complexes. The chromophore $[InCl_3O_2]$ in *bis*-diethylether complex belonging to the D_{3h} symmetry showed[7,12] a strong IR band at 342 cm^{-1} due to In–Cl antisymmetric stretching. The symmetric In–Cl stretching which is IR inactive appeared as weak shoulder at 316 cm^{-1} in the IR and as strong polarized peak at 317 cm^{-1} in the Raman spectrum.[7] In a recent study of the matrix (Kr) isolated $InCl_3$ monomer, Givan and Loewenschuss[17] have assigned the observed triplet near 350 cm^{-1} as the symmetric In–Cl(A_2'') and the 394 cm^{-1} peak as the antisymmetric In–Cl(E') frequencies in the isolated molecule.

The structure of our $InCl_3(HMPA)_2$ complex with the same $[InCl_3O_2]$ chromophore (see later) can be approximated to D_{3h} symmetry. Within the range of our IR investigation (180 cm^{-1}), we are able to find only two bands with shoulders at 305 (sh. ~280) and 182 (sh. ~200) cm^{-1}. There is no indication of a strong absorption around 340 cm^{-1} in the infrared (see above CNC and CNP bending). The other weak intensity peak centered at 305 cm^{-1} is most probably the ligand CH_3 torsion, although some contribution from either In–Cl or In–O stretching vibrations to the intensity of this peak in this region cannot be completely ruled out.

In the Raman spectrum we observed (Fig. 1c) a strong and sharp peak at 265 cm^{-1} together with a peak of much weaker intensity at 286 cm^{-1}. The 265 cm^{-1} peak can be definitely assigned to the symmetric In–Cl stretching (A_1') frequency. The 286 cm^{-1} peak is provisionally assigned to the symmetric In–O stretching. Both these symmetric stretching frequencies being only Raman active are not observed in the IR.

The antisymmetric In–Cl stretching is, however, both infrared and Raman active (E'). The 182 cm^{-1} IR-peak with a shoulder at higher wavenumber corresponding to the broad peak at 150 cm^{-1} in the Raman is the antisymmetric In–Cl stretching vibration. We note that this antisymmetric stretching vibration is likely to be weak in the Raman.[7]

The assignment of the deformation modes at lower wavenumbers are very tentative as only the Raman data are available for the low wavenumber region. We have observed a strong and split peak around 80 cm^{-1} (not shown in Fig. 1) region. This peak is probably due to the deformation mode Cl–In–Cl. The splitting may have ori-

ginated due to the difference in the three <Cl–In–Cl angles (see later). The bending mode of O–In–Cl is also expected to occur in this region.

Unfortunately, we are unable to observe any charge transfer transition in the ultraviolet below 50 kK in the solid complex. In nonaqueous solutions the complex is found to dissociate. Thus for cyclohexane and chloroform solutions only solvent induced shifts of HMPA peak were observed. No broad charge transfer spectrum was evident.

Crystal structure. The crystal structure of trichloro*bis* - (hexamethylphosphoramide)In(III) complex consists of discrete monomeric units where the In(III) ion is coordinated to two HMPA molecules through the oxygen atoms and to three chloride ions as shown in Fig. 2. The chloride ions occupy the equatorial positions and the two HMPA molecules the axial positions in an approximately trigonal-bipyramidal arrangement around In(III) ion.

The three In–Cl bonds (Table 1) average 2.359 Å and none of the bonds deviates significantly from the mean value. The observed In–Cl bond length is only slightly smaller than that found in a similar pentacoordinated complex $InCl_3[(C_6H_5)_3P]_2$ (2.383 Å),[18] and may be compared to a calculated value obtained by summing the ionic radii of In^{3+} and Cl^-. Considering a linear relationship between the coordination numbers and the effective ionic radii,[19,20] we obtain a value of 0.71 Å for the

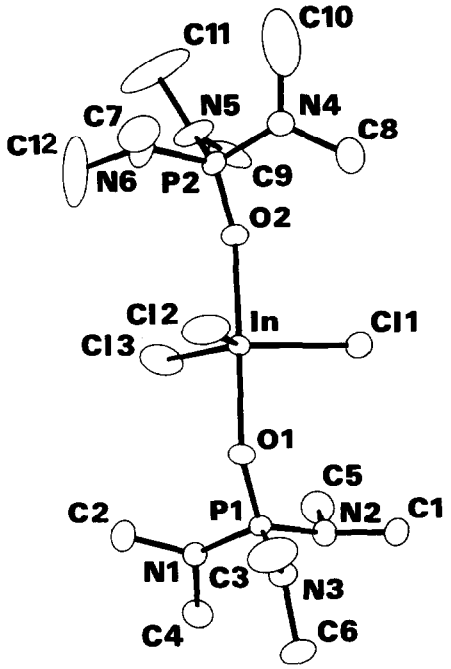

Fig. 2. Numbering scheme and perspective view of pentacoordination around In(III) ion in $InCl_3(HMPA)_2$ complex.

Table 1. Interatomic distances and angles in pentacoordinated $InCl_3(HMPA)_2$ complex. Estimated standard deviations are given in parentheses

Bond Lengths (Å)

In–Cl(1)	2.371(8)	P(1)–O(1)	1.498(6)	N(1)–C(2)	1.451(13)	N(4)–C(8)	1.439(14)
In–Cl(2)	2.358(3)	P(2)–O(2)	1.476(7)	N(1)–C(4)	1.454(10)	N(4)–C(10)	1.500(18)
In–Cl(3)	2.349(7)	P(1)–N(1)	1.631(7)	N(2)–C(1)	1.453(12)	N(5)–C(9)	1.470(15)
		P(1)–N(2)	1.638(9)	N(2)–C(5)	1.449(13)	N(5)–C(11)	1.469(19)
In–O(1)	2.175(10)	P(1)–N(3)	1.632(13)	N(3)–C(3)	1.423(12)	N(6)–C(7)	1.417(15)
In–O(2)	2.185(11)	P(2)–N(4)	1.636(9)	N(3)–C(6)	1.464(12)	N(6)–C(12)	1.405(21)
		P(2)–N(5)	1.638(13)				
		P(2)–N(6)	1.629(11)				

Bond Angles (Deg)

Cl(1)–In–Cl(2)	117.5(1)	Cl(1)–In–O(1)	91.4(2)	Cl(2)–In–O(2)	90.7(2)
Cl(1)–In–Cl(3)	118.1(1)	Cl(1)–In–O(2)	90.1(2)	Cl(3)–In–O(1)	90.7(1)
Cl(2)–In–Cl(3)	124.4(1)	Cl(2)–In–O(1)	87.4(1)	Cl(3)–In–O(2)	89.8(2)
O(1)–In–O(2)	178.0(2)	In–O(1)–P(1)	152.1(3)	In–O(2)–P(2)	154.4(4)
O(1)–P(1)–N(1)	108.8(3)	O(1)–P(1)–N(2)	118.3(3)	O(1)–P(1)–N(3)	107.3(3)
O(2)–P(2)–N(4)	108.8(4)	O(2)–P(2)–N(5)	107.1(4)	O(2)–P(2)–N(6)	118.1(4)
N(1)–P(1)–N(2)	103.4(3)	N(1)–P(1)–N(3)	114.3(3)	N(2)–P(1)–N(3)	105.0(3)
N(4)–P(2)–N(5)	115.0(4)	N(4)–P(2)–N(6)	105.5(5)	N(5)–P(2)–N(6)	102.5(4)
P(1)–N(1)–C(2)	120.9(5)	P(1)–N(1)–C(4)	124.3(6)	P(1)–N(2)–C(1)	121.2(6)
P(1)–N(2)–C(5)	120.2(6)	P(1)–N(3)–C(3)	124.6(5)	P(1)–N(3)–C(6)	121.1(5)
P(2)–N(4)–C(8)	122.4(7)	P(2)–N(4)–C(10)	120.7(8)	P(2)–N(5)–C(9)	120.1(7)
P(2)–N(5)–C(11)	123.8(8)	P(2)–N(6)–C(7)	125.0(8)	P(2)–N(6)–C(12)	120.3(10)
C(2)–N(1)–C(4)	111.4(7)	C(1)–N(2)–C(5)	111.0(8)	C(3)–N(3)–C(6)	112.4(6)
C(8)–N(4)–C(10)	114.4(11)	C(9)–N(5)–C(11)	113.3(9)	C(7)–N(6)–C(12)	109.9(12)

For numbering scheme of the atoms see Fig. 2.

pentacoordinated radius of In(III) ion. If we take the radius of chloride to be 1.81 Å[19]† the calculated In–Cl bond length would be 2.52 Å or clearly higher than the observed one. On the other hand, similar calculation for the In–O bond length (O^{2-} = 1.40 Å[19]) gives 2.11 Å which is somewhat smaller than the observed value (2.18 Å) (Table 1). The reason for these facts may be the steric requirements of the bulky HMPA ligands which cause the *trans*-In–O bands to lengthen while the equatorial In–Cl bonds are shorter than those predicted on the basis of ionic radii only. The effects of covalency should not be very prominent in case of trivalent indium.[19]

Least-squares analysis of the mean planes through the three equatorial chlorides, including the In(III) ion, shows that the central metal ion is only slightly (0.008 Å) above the plane of the chlorine atoms. The angle O(1)–În–O(2) being almost linear (178° ± 2), the In(III) site symmetry could be approximated to D_{3h}. This is borne out nicely by the observation of only one Raman active peak[7] for the symmetrical In–Cl stretching at 265 cm^{-1}. Probably the major distortion from the idealized trigonal bipyramidal geometry for our complex stems from the opening up of the angle between Cl(2) and Cl(3) (Cl(2)–În–Cl(3) = 124.4°) and closing up of the Cl(2)–În–O(1) angle (87.4°). It must be mentioned here that although the three equatorial angles (Table 1) are close to the idealized value of 120°, they differ somewhat amongst themselves. In the present complex, there is no drastic change in the interatomic distances in the coordinated HMPA ligand. The average P–O distance of 1.49 Å is similar to other coordinated complexes of HMPA (Table 2) which probably reflects on the similar order of decrease in the P–O stretching frequency (~20 cm^{-1}) in these complexes with respect to the free ligand. It may be noted that while X-ray structural data on the free HMPA molecule are lacking, CNDO/2 calculations have predicted a bond length of 1.51 Å for the free ligand.[35]

Interestingly enough in the uranyl complex $[UO_2Cl_2(HMPA)_2]$ the P–O stretching frequency is much lower than other HMPA complexes[30,31,36] although the P–O bond lengths are very similar 1.50 Å). This is possibly due to a unique feature of the uranyl complex, where the U–Ô–P angle is almost linear (178.5°).[30] The average P–N bond length (1.634 Å) in our indium complex is comparable to those found in other HMPA complexes. Vilkow *et al.*[37] have investigated by electron diffraction the structure of $P[N(CH_3)_2]_3$ and found the P–N bond length to be 1.70(±0.005) Å in this compound. Allowing for the tetracoordinated nature of phosphorus atom in HMPA, the PN bond lengths in the complexes reflect partial π-bond character. This is also evident from the almost planar nature of the nitrogen atoms in the

†See also: L. Pauling, *Nature of the Chemical Bond*, 3rd Edn. Cornell University Press, Ithaca (1960).

Table 2. Selected structural data on metal-HMPA complexes

Complex	P–O (Å)	<Metal–O–P (°)	Ref.
$MoO_5 \cdot HMPA \cdot H_2O$	1.52	173	21
$MoO_5HMPA \cdot Py$	1.47	159	21
$PrCl_3 \cdot 3HMPA$	1.49,1.48,1.48	159,164,173	22
$VOCl_2 \cdot 2HMPA$	1.46	154[a]	23
$UO_2 \cdot 4HMPA \cdot 2ClO_2$	1.52,1.48,1.55 1.51	153,164,152,158	24
$NbOCl_3 \cdot 2HMPA$	1.49,1.51	158,151	25
$MoOCl_3 \cdot 2HMPA$	1.50,1.50	148,156	26,27
α-$MoO_2Cl_2 \cdot 2HMPA$	1.48	159	28
β-$MoO_2Cl_2 \cdot 2HMPA$	1.48,1.48	144,149	29
$UO_2Cl_2 \cdot 2HMPA$	1.50	179	30,31
$SnCl_4 \cdot 2HMPA$	1.49	165	32
$NbCl_3(OR)_2 \cdot HMPA$[b]	1.52	158	33
$UCl_4 \cdot 2HMPA$	1.50	163	34
$UBr_4 \cdot 2HMPA$	1.53	166	34
$InCl_3 \cdot 2HMPA$	1.50,1.48	152,154	This work

[a]Disordered structure [b]R=i-Pr

coordinated HMPA molecules (the average of the sums of the three angles about the nitrogen atoms is 356°). Incidentally, the nitrogen atoms in $P[N(CH_3)_2]_3$ are also close to planar configuration.

REFERENCES

[1]S. P. Sinha, *Z. Anorg. Allg. Chem.* 1977, **434**, 277.
[2]S. P. Sinha and A. Bartecki, *Inorg. Chim. Acta* 1978, **28**, 145.
[3]R. P. Scholer and A. E. Merbach, *Inorg. Chim. Acta* 1975, **15**, 15.
[4]S. P. Sinha and H. Irving, *Anal. Chim. Acta* 1970, **52**, 193.
[5]S. P. Sinha, *J. Inorg. Nucl. Chem.* 1971, **33**, 2205.
[6]R. A. Walton, *J. Chem. Soc.(A)* 1967, 1485.
[7]M. J. Taylor, *J. Chem. Soc.(A)* 1967, 1462.
[8]D. M. Adams, A. J. Carty, P. Carty and D. G. Tuck, *J. Chem. Soc.(A)* 1968, 162.
[9]I. R. Beattie, T. Gilson and G. A. Ozin, *J. Chem. Soc.(A)* 1968, 1092.
[10]I. R. Beattie and G. A. Ozin, *J. Chem. Soc.(A)* 1968, 2373.
[11]I. R. Beattie and G. A. Ozin, *J. Chem. Soc.(A)* 1969, 542.
[12]C. A. Evans and M. J. Taylor, *J. Chem. Soc.(A)* 1969, 1343.
[13]I. R. Beattie, G. A. Ozin and H. E. Blayden, *J. Chem. Soc.(A)* 1969, 2535.
[14]A. J. Carty, *Coord. Chem. Rev.* 1969, **4**, 29.
[15]G. A. Ozin, *J. Chem. Soc.(A)* 1970, 1307.
[16]A. J. Carty, T. Hinsperger and P. M. Boorman, *Can. J. Chem.* 1970, **48**, 1959.
[17]A. Givan and A. Lowevenschuss, *J. Mol. Struct.* 1979, **55**, 163.
[18]M. V. Veidis and G. J. Palenik, *Chem. Comm.* 1969, 586.
[19]R. D. Shannon, *Acta Cryst. (A)* 1976, **32**, 751.
[20]S. P. Sinha, *Struct. Bonding* 1976, **25**, 69.
[21]J.-M. LeCarpentier, R. Schlupp and R. Weiss, *Acta Cryst. (B)* 1972, **28**, 1278.
[22]L. J. Radonovich and M. D. Glick, *J. Inorg. Nucl. Chem.* 1973, **35**, 2745.
[23]M. Laing, C. Nicholson and T. Ashworth, *J. Cryst. Mol. Struct.* 1975, **5**, 423.
[24]L. R. Nassimbeni and A. L. Rogers, *Cryst. Struct. Comm.* 1976, **5**, 301.
[25]L. G. Hubert-Pfalzgraf and A. A. Pinkerton, *Inorg. Chem.* 1977, **16**, 1895.
[26]P. Khodadad, B. Viossat and N. Rodier, *Acta Cryst. (B)*, 1977, **33**, 1035.
[27]D. Garner, P. Lambert, F. E. Mabbs and T. J. King, *J. Chem. Soc. Dalton Trans.* 1977, 1191.
[28]B. Viossat, P. Khodadad and N. Rodier, *Acta Cryst. (B)* 1977, **33**, 2523.
[29]B. Viossat, P. Khodadad and N. Rodier, *Acta Cryst. (B)* 1977, **33**, 3793.
[30]J. C. Russell, M. P. duPlessis and L. R. Nassimbeni, *Acta Cryst. (B)* 1977, **33**, 2062.
[31]R. Julien, N. Rodier and P. Khodadad, *Acta Cryst. (B)* 1977, **33**, 2411.
[32]L. A. Aslanov, V. M. Ionov, V. M. Attiya, A. B. Permin and V. S. Petrosyan, *Zh. Strukt. Khim. (Engl. Trans.)* 1977, **18**, 876.
[33]L. Hubert-Pfalzgraf, A. A. Pinkerton and J. G. Riess, *Inorg. Chem.* 1978, **17**, 663.
[34]J. G. H. duPreetz, B. J. Gellatly, G. Jackson, L. R. Nassimbeni and A. L. Rodbergs, *Inorg. Chim. Acta* 1978, **27**, 181.
[35]R. Dorshner and G. Kaufman, *Inorg. Chim. Acta* 1975, **15**, 71.
[36]S. P. Sinha, to be published.
[37]A. V. Vilkov, L. S. Khaikin and V. V. Evdokimov, *Zh. Strukt. Khim. (Engl. Trans.)* 1972, **13**, 4.

Polyhedron Vol. 1, No. 4, pp. 361-363, 1982
Printed in Great Briain.

0277-5387/82/040361-03$03.00/0
Pergamon Press Ltd.

THE KINETICS OF INTERACTION OF COPPER(II) SPECIES WITH APO-TRANSFERRIN

T. S. SHOUPE† and C. D. HUBBARD*
Department of Chemistry, University of New Hampshire, Durham, NH, 03824, U.S.A.

(*Received* 18 *November* 1981)

Abstract—The reaction between copper (II) species and human serum apo-transferrin has been studied spectrophotometrically using the stopped-flow method. An initial rapid step which is conveniently studied is first-order in concentration of both transferrin and copper (II) species under the experimental conditions; a pH near 8 was maintained by tris buffer and the solutions contained the synergistic bicarbonate ion. The rate of reaction appears to decrease in tris concentration. At 25°C second order rate constants of 2.1×10^4 and 2.9×10^4 $M^{-1} s^{-1}$ at pH 8.08 and 7.86 respectively (0.050 M tris and 0.050 M bicarbonate ion) can be determined The reaction appears to represent a principal binding of copper to the protein, and the results are discussed in the context of other kinetic data for substitution at copper (II).

INTRODUCTION

The two coordination sites of iron in the serum iron transport protein transferrin have yet to be characterized unequivocally. It has been established that in order for binding to occur at the specific sites by ferric ions or ions of other metals, bicarbonate ions or other appropriate substitute synergistic ions must be present.[1] There is reasonable certainty that one bicarbonate or replacement anion is required for each iron or other metal ion used.[2] Use of copper (II) ions for comparison with ferric ions in kinetic studies of metal ion binding to apo-transferrin was initially reported by Woodworth.[3] The spectrophotometric method was limited to the detection of reactions occurring in the conventional time range. Consequently, a study of the binding of cupric ions to human apo-transferrin employing a stopped-flow spectrophotometer was undertaken, in our laboratory. At the conclusion of the conduct of the experimental aspects of this work, an initial report of some results of a study of the kinetics of binding of cupric ions to apo-transferrin appeared,[4] but sufficient details for evaluation of the conclusions were not provided, and to our knowledge the study not formally published.[5] Therefore, we wish to report some results of a study of the interaction of copper (II) species with apo-transferrin employing the stopped-flow method. An objective of our work was to examine the direct interaction of a metal ion with the specific binding site in the presence of the synergistic ion. The difficulties associated with maintaining iron (III) in solution in the appropriate pH region have precluded use of uncomplexed ferric ions. A probable lower rate limit for copper (II) interaction is suggested by these results; however, exact interpretation of the observed reactions is thwarted by the existence of a multiplicity of possible copper (II) species in solution.

EXPERIMENTAL

Materials. Transferrin was purchased from Sigma, (104C-0141), or from Behring Diagnostics. Copper (II) ions were generated in solution from cupric perchlorate. All other materials were of reagent grade but were treated (*vide infra*) to remove any potential metal contaminants.[6] Distilled and deionized water was used for making up all solutions.

Methods. Transferrin samples were dissolved in approx. 0.1 M sodium perchlorate solution and dialyzed vs 0.1 M sodium perchlorate solution for 20 hr followed by two 10 hr dialyses against distilled and deionized water, all at 4°C. All containers and pipettes were washed with acid and rinsed before use.

Transferrin concentration was determined from measurement of the absorbance at 278 nm of aliquots of a stock diluted in 0.2 M hydrochloric acid ($\epsilon_{278} = 0.912 \times 10^5$ $cm^{-1} M^{-1}$)[6]. The molarity was calculated using the assumption of a molecular weight of 77,000 daltons.[7] Buffer materials, sodium bicarbonate and sodium perchlorate were extracted with a 0.001% chloroform solution of dithizone to remove potential contaminants which would interfere with kinetic studies. The aqueous layers were further washed with chloroform and stored in plastic bottles. Absorbance measurements on transferrin solutions in the absence or presence of metal ions were made using a Cary 14 spectrophotometer at 25.0°C. Kinetic runs were carried out in a Durrum–Gibson stopped-flow spectrophotometer. The reactant solutions do not contact metal surfaces in the version employed which has a Kel-F flow path and glass drive and stop barrels. Artefacts which possibly can arise due to temporary inhomogeneity of mixed solutions were eliminated by utilizing solutions of very similar ionic concentration in each drive syringe.

The stoichiometry of binding was studied at 430 nm at pH 8.1, 0.050 M sodium carbonate. To a solution of an appropriately diluted stock apo-transferrin solution, a stoichiometric amount of copper (II) ions was added (assuming two copper binding sites per molecule of transferrin). Upon addition of a further two equivalents of copper ions a slight increase in absorbance was observed, while a third two equivalent aliquot resulted in an absorbance change that was not outside of experimental error. It is conceivable that the very small absorbance change is a consequence of non-specific binding of copper following the saturation of the specific sites. Our observations are entirely consistent with results from spectrophotometric titrations reported earlier.[8]

RESULTS AND DISCUSSION

In all experiments about 80–85% of the total absorbance change occurs within about one tenth of a second, under the conditions employed, with a much slower reaction of the order of several seconds accounting for the remaining increase in absorbance at 430 nm. The reported results refer only to the first process since this may be regarded as the step involving the principal binding of copper ions to apo-transferrin. The second step is of such small amplitude that it cannot be charac-

†Present address: Department of Biochemistry and Drug Disposition, Revlon Health Care, Scarsdale Road, Tuckahoe, NY 10707, U.S.A.
*Author to whom correspondence should be addressed.

terized satisfactorily. The first step is analyzed to be first-order over at least three half-lives and the rate constants obtained, k_{obs}, for each of three series of experiments are compiled in Table 1.

Reaction of a solution of copper (II) ions with a solution of apo-transferrin each buffered with 0.050 M tris and containing 0.050 M sodium bicarbonate was studied as a function of copper ion concentration at both the pH of 8.08 and a pH of 7.86. The cited rate constants, k_{obs}, represent averages of typically, five to seven replicate determinations. The effect of concentration of the tris buffer was also studied at fixed copper ion and apo-transferrin concentrations. An unbuffered copper (II) solution, with no synergistic ion present was mixed with a buffered apo-transferrin solution (0.050 M tris, pH 8.08) containing 0.050 M sodium bicarbonate and the reaction monitored spectrophotometrically.

All reactions were run with an excess of copper (II) species. The observation of a first order reaction and the increase in k_{obs} with increase in copper (II) concentration imply that the rate of reaction is first order in the concentration of reacting apo-protein, viz, Rate = k_{obs} [Apo-transferrin]. At both pH values plots of k_{obs} vs total copper ion concentration are linear with the line passing through the origin, within experimental error. This indicates that the reaction is also first order in reacting Cu(II) species, and that the reverse reaction of dissociation of metal ion from the protein is unimportant under the experimental conditions. Second order rate constants at 25.0°C of 2.1×10^4 and 2.9×10^4 $M^{-1} s^{-1}$ can be derived from the slopes of these plots for the reaction at pH 8.08 and 7.86 respectively, in 0.050 M tris and 0.050 M bicarbonate medium. The first order rate constant at 25.0°C for the reaction of unbuffered copper ions (1.0×10^{-3} M) (pH ~ 5) with apo-transferrin in buffer, where the final solution has a pH of 8, and the final tris concentration is 0.025 M is 47 s^{-1} which yields an estimated second order rate constant of 4.7×10^4 $M^{-1} s^{-1}$. That this is approximately twice that for reaction of the buffered copper solution is most likely a reflection of the difference in final tris concentration since the Table shows the marked dependence of k_{obs} on tris concentration (~ 100 s^{-1} in the 2.5–5.0 mM region, with a tenfold reduction to ~ 9 s^{-1} observed at 50 mM tris). Converting our data to that which would pertain to a tris concentration of 2.5 mM yields a second order constant

Table 1. Kinetics of interaction of Cu(II) with apo-transferrin; k_{obs} for the initial phase under different conditions, at 25.0°C

	[Cu(II)]x10^{4}M	k^b_{obs} s^{-1}	
pH 8.08[a]	2.00	3.79	(0.07)
	5.00	12.2	(0.20)
	7.00	15.9	(0.13)
	10.0	20.1	(0.53)
	15.0	36.1	(1.0)
	20.0	42.1	(0.90)
pH 7.86[c]	0.75	2.82	(0.06)
	1.50	5.41	(0.20)
	3.0	11.0	(0.26)
	5.0	14.2	(0.44)
	10.0	30.0	(1.46)
pH 7.86[d]	[Tris]x10^{3}M		
	2.5	101	(3.1)
	3.5	112	(7.7)
	5.0	108	(2.7)
	10.0	58.9	(1.8)
	25.0	20.1	(0.9)
	50.0	9.2	(0.6)

a [Transferrin]$_0$ = 2.0 x 10^{-5}M; 0.050M tris and 0.050 bicarbonate in each syringe.

b Figure in brackets is the standard deviation.

c [Transferrin]$_0$ = 1.5 x 10^{-5}M; 0.050M tris and 0.050M bicarbonate in each syringe.

d [Transferrin]$_0$ = 1.5 x 10^{-5}M with 0.050M bicarbonate present.
[Cu(II)] = 2.5 x 10^{-4}M, no buffer or bicarbonate ion present.

of $4 \times 10^5\ M^{-1}\ s^{-1}$ at pH 7.86, which is not inconsistent with the reported value of $6.25 \times 10^5\ M^{-1}\ s^{-1}$ at pH 7.45 in 2.5 mM tris buffer, which was determined it appears from direct second order kinetics.[4]

The product of the overall reaction is a copper complex of apo-transferrin having two copper ion species in the specific sites and with possibly additional copper bound in non-specific locations, while the product of the reaction whose kinetics are reported is presumably apo-transferrin with its specific sites occupied by copper ions. Of necessity the kinetics were conducted using different concentrations from those used to verify the capacity of the apo-protein to accept two copper species (see experimental section and Ref. 8). Therefore, the stoichiometry of products has an attendant uncertainty.

An attempt to interpret these results requires both a knowledge of the copper (II) species in the solutions used and an appreciation of the lability of copper (II) species toward binding ligands with particular reference to the coordinating environment in the protein. A pH in the region of 8 is thought to be necessary for specific binding to be implemented;[9] the consequence is that a solution of copper (II) ions would be present as a mixture of the aquated 2+ ion and the $Cu(OH)^+$ species since a solution of aquo copper (II) ions is a weak acid (pK 6.3).[10] Proton transfer between these species would be rapid compared with observed processes and an analysis of data would be possible but copper hydroxide species precipitate in the pH range used. The buffering substance, tris hydroxyaminomethane is complexed by copper (II) ions. An inspection of the results of Bai and Martell[11] leads to the conclusion that virtually all of the copper in the kinetic runs will be in some tris complex form. The rate constants, therefore, represent composite terms for various copper-tris species of different aquation states reacting with the protein; tris is displaced by the stronger ligand sites within the protein which is supported by the fact that the rate constant is reduced by increased tris concentration.

Understanding of the kinetics of ligand binding to aquo copper (II) species within the framework of the Eigen–Wilkins' mechanism[12] has rested, in part, upon the versions of the value of the rate constant for water exchange from the aquated copper dication. Recently, an analysis of this area of research and further work would indicate that $2 \times 10^9\ s^{-1}$ at 25°C is a reasonable value.[13] For small ligands, in the absence of ligand steric effects, the second order rate constant for complex formation would be expected to be about $10^8\ M^{-1}\ s^{-1}$ at 25°C if outer sphere complex association constants are of comparable magnitude to those assumed for nickel (II) complex formation. The much lower value for copper (II) binding to apo-transferrin can be explained qualitatively.

In this study the macromolecular nature of the ligand, the range of incorrect orientations for binding, and the presence of adjacent hydrophobic groups giving rise to a lowered effective dielectric constant at the binding location are factors which could retard the rate of binding. A rate controlling conformational change of the protein would appear to be ruled out by the lack of any significant change in the circular dichroism spectrum upon the binding of copper.[14] The charge nature of both metal and ligand are important factors affecting the rate of formation of the outer sphere complex. Groups on the protein acting as ligands[2(c),9,15] are neutral under the experimental conditions and the charge of the synergistic ion is effectively neutralized.[14] However, a small rate retardation factor could result from the reduction in effective positive charge of the metal by bound tris or a hydroxy group. The observed rate constant is about three orders of magnitude reduced from that predictable for simple ligands; it is not possible to assess each factor quantitatively. In neutral solution tris would be very inert to displacement from copper (II) in the absence of apo-transferrin, by inference from the stability constant and expected formation rate constant. The closeness of the rate constants for formation of product from buffered copper (II) solution and from initially uncomplexed copper suggests that this may be displaced rapidly. Which species of copper actually reacts following the rapid increase in pH from 5 to 8 in the presence of a buffer and protein is not known. Therefore, it is conceivable that tris replacement is rate limiting.

The kinetics of copper (II) species binding to apo-transferrin are conveniently studied by the stopped-flow method; the reaction is complex. The first observed step which probably related to binding at the specific sites, is amenable to characterization. Subsequent steps, not characterized, may relate to additional binding of copper at other sites on apo-transferrin.

Acknowledgements—The Graduate School—Research Office of the University of New Hampshire is thanked for partial financial support of this work through a Central University Research Fund grant to T.S.S. We are pleased to acknowledge useful suggestions by a referee.

REFERENCES

[1]M. R. Schlabach and G. W. Bates, *J. Biol. Chem.* 1975, **250**, 2182.
[2]For example: (a) P. Aisen, R. Aasa and A. G. Redfield, *J. Biol. Chem.* 1969, **244**, 4628; (b) A. L. Schade and R. W. Reinhart, *Protides Biol. Fluids Proc. Colloq. Bruges*, 1966 **14**, 75; (c) and other references cited in N. D. Chasteen, *Coord. Chem. Rev.* 1977, **22**, 1.
[3]R. C. Woodworth, *Protides Biol. Fluids Proc. Colloq. Bruges* 1966, **14**, 37.
[4]G. W. Bates and M. R. Schlabach, In *Proteins of Iron Transport in Biochemistry and Medicine.* (Edited by R. R. Crichton), p. 51. North Holland, Amsterdam (1975).
[5]M. T. Cochran III. Ph.D. Thesis (1975). *Diss. Abs. Int. B* 1976, **36**, 3919.
[6]N. D. Chasteen is acknowledged for advice regarding solution preparation and procedures for handling transferrin.
[7]K. G. Mann, W. W. Fish, A. C. Cox and C. Tanford, *Biochemistry*, 1970, **9**, 1348.
[8]S. S. Lehrer, *J. Biol. Chem.* 1969, **244**, 3613.
[9]J. Zweier and P. Aisen, *J. Biol Chem.* 1977, **254**, 3512.
[10]R. M. Smith and A. E. Martell. *Stability Constants*, Vol. 4, p. 6. Plenum, New York (1976). A more recent report, A. J. Paulson and D. R. Kester, *J. Soln. Chem.* 1980, **9**, 269, has indicated that the first hydrolysis of aquo copper (II) ions is characterized by a pK of 5.9.
[11]K. S. Bai and A. E. Martell. *J. Inorg. Nucl. Chem.* 1969, **31**, 1967.
[12]M. Eigen and R. G. Wilkins, *Adv. Chem. Ser.* 1965, No. 49, 55.
[13]L. S. W. L. Sokol, T. D. Fink and D. B. Rorabacher, *Inorg. Chem.* 1980, **19**, 1263.
[14]Y. Tomimatsu and L. E. Vickery, *Biochim. Biophys. Acta* 1972, **285**, 72.
[15]Y. Tomimatsu, S. Kint and J. R. Scherer, *Biochemistry* 1976, **15**, 4918.

Polyhedron Vol. 1, No. 4, pp. 365–369, 1982
Printed in Great Britain.

0277–5387/82/040365–05$03.00/0
Pergamon Press Ltd.

THE CRYSTAL AND MOLECULAR STRUCTURES OF $[Co(NH_3)_6][CuCl_5]$ AS DETERMINED FROM SINGLE CRYSTAL X-RAY AND NEUTRON DIFFRACTION DATA

IVAN BERNAL* and JAMES D. KORP
Chemistry Department, University of Houston, Houston, TX 77004, U.S.A.

and

E. O. SCHLEMPER* and M. S. HUSSAIN
Chemistry Department, University of Missouri, Columbia, MO 65211, U.S.A.

(*Received* 23 *November* 1981)

Abstract—The crystal structure of the title compound was determined at room temperature (*ca.* 21°C) using single crystal *X*-ray and neutron diffraction data. The substance crystallizes in the cubic space group O_h^8–Fd3c in a unit cell whose edge is $a = 21.992(3)$Å. The X-ray data were refined to $R(F_0) = 0.026$ and $R_w(F_0) = 0.027$, while the neutron data refined to $R(F_0) = 0.055$. The two sets of coordinates obtained agree remarkably well even for the hydrogen atoms but, since the neutron results are more reliable for the hydrogen atom positions, our discussion is based on these.

The Co–N and ⟨N–H⟩ distances are, respectively, 1.968(2)Å and 0.953(5)Å. The most important result, namely the Cu–Cl(axial)/Cu–Cl(equat.) ratio, is 0.955; the individual values of these quantities being Cu–Cl(ax) = 2.301 and Cu–Cl(equat.) = 2.409. Thus, the $CuCl_5^{3-}$ anion is axially compressed by a substantial amount and, in this respect, resembles its octahedral CuF_6^{4-} relative.

INTRODUCTION

In 1968 Raymond *et al.* published the structure of $[Cr(NH_3)_6][CuCl_5]$ which is isostructural with the $[Co(NH_3)_6][CuCl_5]$ derivative we were studying at the time.[2] Inasmuch as our study was carried out with film techniques[2] while that of Raymond, *et al.*[1] was the product of data collected with a computer-controlled diffractometer, the data of Brennan and Bernal was never published except as Brennan's Ph.D. thesis.[3] Since that time, however, it has become evident that the system $[M(NH_3)_6][XCl_5]$ (M = Co(III), Cr(III); X = Cd(II), Hg(II), Cu(II), etc.) is more complex than was thought earlier. Major contributions to this interesting system were made by Clegg[4–6] who demonstrated that the cubic (Fd3c) lattice found for many of these salts was not as robust a system as previously thought. In fact, $[Cr(NH_3)_6][HgCl_5]$ was found[4] to be cubic (Fd3c) but the $Co(NH_3)_6^{3+}$ salt was reported to be monoclinic ($P2_1/c$).

Theoretical treatments due to Burdette[7] and to Rossi and Hoffmann[8] have predicted either no difference[7] between axial and equatorial bonds of the trigonal bipyramidal species or longer axial bonds,[8] when the central ion is d^{10}. The studies by Long, *et al.*[9] and by Epstein and Bernal[10] on the $CdCl_5^{-3}$ species and that by Clegg[4] on the $HgCl_5^{-3}$ ion demonstrated that they were axially compressed, as was the case for the $CuCl_5^{-3}$ ($3d^9$). Efforts to isolate a $ZnCl_5^{-3}$ ion failed in the cases of two independent studies,[9,11] the only species present being tetrahedral $ZnCl_4^{-2}$ and either Cl^- or NO_3^-, depending on whether the salt isolated was $[Co(NH_3)_6][ZnCl_5]$[9,11] or $[Co(NH_3)_6][ZnCl_4](NO_3)$[9].

In an effort to probe the electronic nature of the $CuCl_5^{-3}$ species, Epstein *et al.*[12] studied the ESR spectra of $[Co(NH_3)_6][CdCl_5]$ crystals doped with Cu(II) and found that as the temperature was lowered the spectra changed in a systematic manner indicating a drastic lowering of the point group symmetry at the previous trigonal bipyramidal (32) site such that full separation of the g_{xx}, g_{yy} and g_{zz} tensor components was evident at liquid nitrogen temperature. A differential scanning calorimetric study[12] was coupled with the above observations which indicated a first order phase trasition occuring at 280.8 K. In order to document the nature of this transition and the concomitant molecular rearrangement, we decided to study the crystal and molecular structue of $[Co(NH_3)_6][CuCl_5]$ at room temperature and at liquid nitrogen temperatures with X-ray and neutron diffraction data. The structures derived from single crystal, computer-controlled data obtained at *ca.* 21°C by both techniques is discussed in this paper.

EXPERIMENTAL

X-Ray data collection and refinement. A single crystal having nearly perfect octahedral geometry was selected for data collection. The size of the crystal along the square girth was approx. 0.15 mm. It was mounted on an Enraf–Nonius CAD-4 diffractometer and data were collected according to procedures we have described in detail already.[13] Crystallographic data collection and processing parameters are given in Table 1. The positional parameters of our previous X-ray determination were used as a trial set. After convergence, the thermal parameters of the heavy atoms were assumed anisotropic and refined. Hydrogens were found experimentally at excellent positions giving an average N–H distance of 0.90 Å but attempts to refine their positional and isotropic thermal parameters led to very large, and unreasonable, values of the latter. Thus, we decided to fix the thermal parameter at a value of U = 0.060 Å and to refine the

*Author to whom correspondence should be addressed.

Table 1. Summary of X-ray data collection and processing parameters

Space Group	Fd3c, cubic
Cell Constant	$a = 21.992(3)$ Å
Molecular Formula	$CoCuCl_5N_6H_{18}$
Formula Weight	389.826
Formula Weights per Cell	$Z = 32$
Density	$\rho = 1.947$ gm-cm^{-3}
Absorption Coefficient	$\mu = 32.8$ cm^{-1}
Radiation (MoKα)	$\lambda = 0.71073$ Å
Collection Range	$4° \leq 2\theta \leq 44°$
Scan Width	$\Delta\theta = (0.87+0.35 \tan\theta)°$
Maximum Scan Time	240s
Scan Speed Range	0.33 to 5.03° min^{-1}
Independent Data with $I>3\sigma(I)$	217
Total Variables	25
R.... $\Sigma\|\|F_o\| - \|F_c\|\|/\Sigma\|F_o\|$	0.026
R.... $[\Sigma_w(\|F_o - F_c\|)^2/\Sigma_w\|F_o\|^2]^{\frac{1}{2}}$	0.027
Weights	$\sigma(F)^{-2}$

positional parameters while restraining the entire $-NH_3$ ligand to a rigid, tetrahedral geometry. The success of this method is best illustrated by comparison of the value of the hydrogen atom fractional coordinates obtained by both methods (Table 2). One reflection, the (0, 0, 4), was eliminated from the refinement due to extinction since the crystal was mounted nearly exactly along the *c*-axis, and its measured value was only about 60% of that calculated.

Neutron diffraction data collection and refinement. An octahedral shaped crystal having dimensions *ca.* $1.4 \times 1.8 \times 1.9$ mm was mounted on a copper pin along the *a*-axis and optically centered inside the χ-circle of a PDP 11/03 computer controlled four-circle diffractometer interfaced to a PDP 11/40 computer. The whole neutron-diffraction system was developed at the University of Missouri Research Reactor Facility. A monochromatic neutron beam was obtained by reflection from (002) plane of beryllium. The neutron wave length, 1.058 Å was calibrated using a Si($a = 5.4308$ Å) crystal. The single lattice constant 21.992(3) Å was obtained by least-squares refinement of the setting angles of 17 automatically centred reflections. The neutron intensities of *hkl* reflections with all indices either even or odd having $4° < 2\theta < 95°$ were measured using $\theta/2\theta$ step scan method in which counts at each step were measured for a preset monitor count of the direct beam. Scan width of 1.95° was used with 39 steps of 0.05° each. Two standard reflections were measured after every 47 reflections and revealed no significant systematic fluctuation. The neutron intensity data are consistent with previously reported[9] space group: 0_h^6–Fd3c. The 1442 reflections were corrected for background and Lorentz effects. The neutron absorption corrections were applied using an analytical procedure. The linear absorption coefficient ($\mu = 2.97$ cm^{-1}) was calculated including an incoherent scattering cross section of 34×10^{-24} cm^2 for hydrogen. The resulting crystal transmission factors range from 0.646 to 0.705. The equivalent data were averaged yielding 658 unique reflections of which 334 having $I > 2\sigma(I)$ were used in the least-squares refinement. The variances of F_0^2 were calculated from $\sigma^2(F_0^2) = \sigma_c^2(F_0^2) + (0.01\,F_0^2)^2$ where $\sigma_c^2(F_0^2)$ is determined from the counting statistics and 0.01 is an empirical "ignorance factor."

The refinement of the structure was carried out by full-matrix least-squares techniques based on the minimization of $\Sigma w(F_0^2 - kF_c^2)^2$ with individual weights $w = 1/\sigma^2(F_0^2)$. The neutron scattering amplitudes were N(9.40), H(−3.723), Cl(9.58), Co(2.50) and Cu(7.60) all in fm.[2] All calculations were done on the University of Missouri Computer Network using an Amdahl 470/V7 computer and an IBM 3031 Processor with programs mentioned earlier.[14]

The initial parameters were those reported earlier for the analogous cobalt and chromium salts, $[Co(NH_3)_6][CdCl_5]$[9] and $[Cr(NH_3)_6][CuCl_5]$[1] which are isomorphous with the title compound. A difference-Fourier map phased upon isotropically refined X-ray positional parameters of the five independent non-hydrogen atoms revealed the positional parameters for hydrogen atoms. These parameters were in good agreement with those reported from the X-ray study of $[Cr(NH_3)_6][CuCl_5]$[1] when account is taken of the usual observation of X-ray shift of hydrogen atom positions. Several cycles of anisotropic least-squares refinement of all independent atoms with 50 variables, including an isotropic extinction parameter and a scale factor, converged to the final values of 0.080 for $R(F_0^2)$, 0.083 for $R_w(F_0^2)$ and 0.055 for the conventional R factor. The value of the secondary-extinction parameter (Zachariasen, 1963)[15] was 5.249×10^{-4}. The shifts in all refined parameters on the last cycle were below one-tenth of their standard deviations. Positional parameters along with their standard deviations are given in Table 2. The direction of vibration of thermal ellipsoids is shown in Figs. 1 and 2. Values of F_0 and F_c are available from the authors.

Analysis of thermal motion. The root-mean-square components of thermal motion along principal axes for all atoms are given in Table 2 and the directions of vibration are shown in Figs. 1 and 2. The minimum and maximum vibrational amplitudes for the equatorial chlorine atom vary by a factor of 4 indicating much larger anistropic vibration in this atom compared to the axial chlorine atom. The axial and equatorial Cu–Cl bond lengths corrected for the effects of thermal motion are 2.301Å and 2.409Å compared to 2.291 and 2.392 Å for uncorrected distances. The corrected Co–N distance is 1.973 Å compared to 1.968(2) Å for the corresponding uncorrected distance.

The amine hydrogen atoms have relatively larger amplitudes of vibration for which rigid body thermal motion analysis was carried out, and the amine group was treated as a hindered rotor.

Table 2. Positional parameters derieved from the X-ray and neutron diffraction data. There are two entries per atom, the top entry in each case is for the former. Estimated standard deviations are given in parentheses

Atom	Site Symmetry	x	y	z
Co	O_6-$\bar{3}$	0.0000(-)	0.0000(-)	0.0000(-)
		0.0000(-)	0.0000(-)	0.0000(-)
Cu	D_3-32	0.2500(-)	0.2500(-)	0.2500(-)
		0.2500(-)	0.2500(-)	0.2500(-)
Cl(ax)	C_3-3	0.1899(1)	x	x
		0.1899(1)	x	x
Cl(eq)	C_2-2	0.2500(-)	0.0765(1)	−y
		0.2500(-)	0.0769(1)	−y
N	Gen.	0.0690(3)	0.0479(3)	-0.0287(3)
		0.0690(1)	0.0489(1)	-0.0290(1)
H(1)*	Gen.	0.0989(3)	0.0457(3)	-0.0011(3)
		0.1041(4)	0.0474(5)	-0.0037(5)
H(2)*	Gen.	0.0553(3)	0.0862(3)	-0.0307(3)
		0.0585(4)	0.0899(4)	-0.0338(5)
H(3)*	Gen.	0.0834(3)	0.0367(3)	-0.0651(3)
		0.0822(5)	0.0371(5)	-0.0695(4)

*Atoms constrained to a rigid group in the X-ray refinement (see text).

The value for U'_{22} (amplitude of the difference ellipsoid in the direction of the hindered rotation axis × 10^3) was 132(29) Å^2. The average uncorrected N–H bond length is 0.953 Å. The root-mean-square amplitude of rotation, $\langle\theta\rangle$ (calculated by $\tan\langle\theta\rangle = (U'_{22})^{1/2}/r_{C-H}$) is 20.9°. On the basis of this, the N–H distance after correction for hindered rotaton is 1.020 Å.

DISCUSSION

As mentioned in the section on the refinement of the X-ray diffraction data, it was necessary to fix the thermal parameters of the hydrogens and since we also decided to use a rigid group refinement for the —NH_3 ligand, the current discussion will be based on the neutron diffrac-

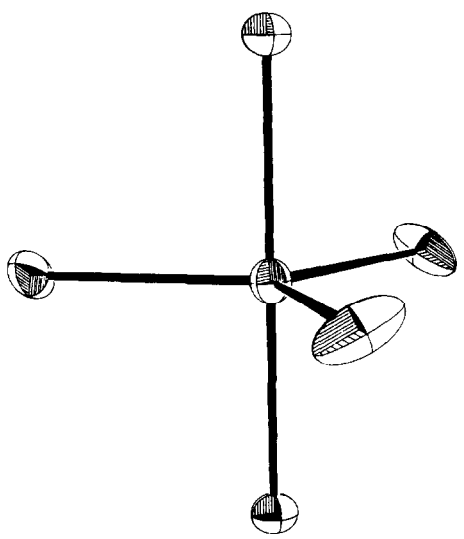

Fig. 1. A view of the $CuCl_5^{3-}$ ion in $[Co(NH_3)_6][CuCl_5]$. The shape of the thermal ellipsoids represent 30% probability contours of thermal motion.

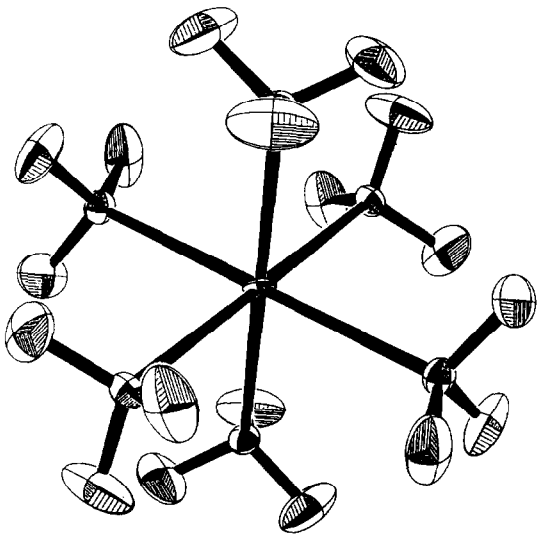

Fig. 2. A view of the $[Co(NH_3)_6]^{3+}$ ion in $[Co(NH_3)_6][CuCl_5]$ showing thermal motion of hydrogen atoms. The shape of the thermal ellipsoids represents 15% probability contours of thermal motion.

Table 3. Anisotropic thermal parameters for $[CO(NH_3)_6][CuCl_5]$ from X-ray and neutron diffraction

Atom	U_{11}	U_{22}	U_{33}	U_{12}	U_{13}	U_{23}
Co	0.0152(6) 0.0241(29)	U_{11}	U_{11}	-0.0009(8) -0.0094(35)	U_{12}	U_{12}
Cu	0.0252(7) 0.0287(11)	U_{11}	U_{11}	-0.0017(8) 0.0014(14)	U_{12}	U_{12}
Cl(ax)	0.0268(9) 0.0331(8)	U_{11}	U_{11}	-0.0028(11) -0.0037(8)	U_{12}	U_{12}
Cl(eq)	0.1111(33) 0.1220(35)	0.0219(12) 0.0285(11)	U_{22}	0.0149(17) 0.0116(15)	U_{12}	0.0048(16) 0.0058(13)
N	0.0228(41) 0.0244(12)	0.0233(45) 0.0345(14)	0.0238(37) 0.0352(13)	-0.0043(38)) -0.0037(8)	-0.0004(32) 0.0019(9)	-0.0010(36) 0.0026(9)
H(1)*	0.0521(47)	0.1483(89)	0.0825(64)	-0.0453(45)	-0.0251(45)	0.0542(59)
H(2)*	0.0680(55)	0.0503(53)	0.1320(95)	-0.0141(43)	0.0350(56)	0.0162(52)
H(3)*	0.0887(67)	0.1189(76)	0.0671(61)	-0.0554(53)	0.0418(49)	-0.0228(52)

The form of the thermal ellipsoid is $\exp[-2\pi^2(h^2U_{11}a^{*2} + k^2U_{22}b^{*2} + \ell^2U_{33}c^{*2} + 2hka^*b^*U_{12} + 2h\ell a^*c^*U_{13} + 2k\ell b^*c^*U_{23})]$.

*The x-ray refinement was carried out with a simple, isotropic, thermal parameter of 0.060 for all three hydrogen atoms (see text).

Table 4. Bond lengths and angles in $[Co(NH_3)_6][CuCl_5]$ from neutron diffraction results

	(a) Sym. Position	Distances(Å)		Sym. Position	Angle (deg)
Cu-Cl(ax)	-	2.291(1)	N-Co-N	9	89.7(4)
Cu-Cl(eq)	2	2.392(2)	N-Co-N	10	90.3(4)
Co-N	-	1.968(2)	H(1)-N-H(2)	-	107.4(8)
N-H(1)	-	0.952(10)	H(1)-N-H(3)	-	106.6(9)
N-H(2)	-	0.937(11)	H(2)-N-H(3)	-	103.3(8)
N-H(3)	-	0.971(11)	Co-N-H(1)	-	114.6(5)
Cl(ax)-H(1)	2,5,8	2.368(9)	Co-N-H(2)	-	111.8(5)
Cl(ax)-H(2)	3,6,7	3.016(11)	Co-N-H(3)	-	112.4(5)
Cl(ax)-H(2)	2,5,8	3.612(12)	Cu-Cl(ax)-H(1)	2,5,8	92.8(3)
Cl(ax)-H(2)	2	3.612(12)			
Cl(ax)-H(3)	2	3.740(11)			
Cl(ax)-N	2,5,8	3.312(3)			
Cl(ax)-Cl(eq)	2,5,8	3.312(1)			
Cl(eq)-H(2)	4	2.429(11)			
Cl(eq)-H(1)	6	3.128(10)			
Cl(eq)-N	4	3.297(3)			
Cl(eq)-H(3)	4	3.499(12)			
Cl(eq)-H(3)	6	3.552(12)			
Cl(eq)-N	6	3.647(3)			

(a) First atom is at the position corresponding to the coordinates listed in Table 1 while the last atom is at any of the symmetry related position. Where no symmetry position is listed, the last atom is also at the position defined by the listed coordinates.

(b) Symmetry positions are as follows:
$1 = X, Y, Z$; $2 = X, \frac{1}{4} - Y, \frac{1}{4} - Z$; $3 = \frac{1}{4} - X, Y, \frac{1}{4} - Z$; $4 = \frac{1}{4} - X, \frac{1}{4} - Y, Z$; $5 = \frac{1}{4} - Z, X, \frac{1}{4} - Y$;
$6 = \frac{1}{4} - Z, \frac{1}{4} - X, Y$; $7 = Y, \frac{1}{4} - Z, \frac{1}{4} - X$; $8 = \frac{1}{4} - Y, \frac{1}{4} - Z, X$; $9 = -Z, -X, -Y$; $10 = Z, X, Y$.

tion results only. This, in reality, corresponds to using the X-ray data as well since the results are extremely close, as shown on Table 2. In fact, it is remarkable how close the hydrogen fractional coordinates obtained in the X-ray study agree with those obtained by neutron diffraction.

Table 5 was prepared in order to compare the results of our work with those structures reported earlier which are of high precision. The worst agreement is associated with the N–H distance found in $[Co(NH_3)_6][CdCl_5]$, which is not surprising since it is remarkable that the authors[10] were even able to find the hydrogen atoms experimentally in a structure containing all those heavy atoms. The other parameters associated with the heavier atoms are in excellent agreement, however. All in all, correlations are very good and the very precise,

Table 5. A comparison of distances (Å) and Angles (°) between compounds containing the species $[Co(NH_3)_6]^{3+}$

Structural Parameter	I[a]	II[b]	III[c]	IV[d]
Co-N	1.968(2)	1.960(6)	1.968(1)	1.970(3)
<N-H>	0.953	0.79	0.88	0.86
N-Co-N	89.7(4)	89.51(12)	89.84(3)	89.47(3)
<Co-N-H>	112.9	107	111.5	112.7
<H-N-H>	105.8	not given	107.7	105.8
Reference	This study	10	17	18

(a) $[Co(NH_3)_6][CuCl_5]$; neutron data.

(b) $[Co(NH_3)_6][CdCl_5]$; x-ray data

(c) $[Co(NH_3)_6][Co(CN)_6]$; x-ray data

(d) $[Co(NH_3)_6][Cr(CN)_6]$; x-ray data

low temperature, study (X-ray) by Iwata[18] is impressive even when dealing with the geometrical parameters associated with the hydrogen atoms. Thus, this portion of the sturcture is obviously in very good company.

In so far as the Cu moiety is concerned, the results obtained by neutron diffraction, corrected for thermal motion (*vide supra*), give Cu–Cl(axial) = 2.301 and Cu–Cl(equat.) = 2.409 or a ratio of axial/equat. = 0.955, which is a clear case of an axial compression. Given the geometry of the complex anion $[CuCl_5]^{-2}$ (D_3–32), if one is to invoke a Jahn–Teller effect, the unpaired electron must reside in either of the pair of degenerate 3*d* orbitals (x^2-y^2; *xy*) or (*xz*; *yz*). Perhaps we will have more to say on this subject when the structure of the compound is redetermined at low temperature where, according to our esr spectrum orbital degeneracy seems to have been removed.

One more point on the question of axial/equatorial distances in Cu(II) complexes: In 1959, Knox[19] published the crystal structure of K_2CuF_4 which crystallizes in a tetragonal space group and consists of $[CuF_6]^{4-}$ anions having D_{4h} symmetry. Here, there are two axial Cu–F bonds of 1.95 Å and four equatorial Cu–F bonds of 2.08 Å. The axial/equatorial ratios is 0.938, which is, if anything, somewhat more compressed than ours. Therefore, as far as Cu(II)-halide systems are concerned, the occurrence of axial compression appears to be common, and relatively independent of the point group of the system or the number of bonds, provided it is of sufficiently high symmetry.

Acknowledgement—IB and JDK thank the US National Science Foundation and the Robert A. Welch Foundation, and EOS the National Science Foundation (NSF–CHE77–08325) for support of this study.

REFERENCES

[1]K. N. Raymond, D. W. Meek and J. A. Ibers, *Inorg. Chem.* 1968, **7**, 1111.
[2]Our results were presented at the *XIth Int. Cong. of Coordination Chemistry, Haifa and Jerusalem* (1968) and were published in *Coordination, Chemistry* (Edited by M. Cais), p. 518. Elsevier, Amsterdam (1968).
[3]T. F. Brennan, Ph. D. Thesis, State University of New York at Stony Brook, (Apr. 1970).
[4]W. Clegg, D. A. Greenhalgh and B. B. Straughan, *J. Chem. Soc.*, Dalton Trans, 1975, 2591.
[5]W. Clegg, *Acta Cryst.* 1976, **B32**, 2907.
[6]W. Clegg, *Acta Cryst.* 1978, **B34**, 3328.
[7]J. K. Burdett, *Inorg. Chem.* 1975, **14**, 931.
[8]A. R. Rossi and R. Hoffmann, *Inorg. Chem.*, 1975, **14**, 365.
[9]T. V. Long, II, A. W. Herlinger, E. F. Epstein and Ivan Bernal, *Inorg. Chem.* 1970 **9**, 459.
[10]E. F. Epstein and Ivan Bernal, *J. Chem. Soc.* **A**, 1971, 3628.
[11]D. W. Meek and J. A. Ibers, *Inorg. Chem.* 1970, **9**, 465.
[12]E. F. Epstein, Ivan Bernal and W. P. Brennan, *Inorg. Chim. Acta* 1976, **20**, L47.
[13]G. M. Reisner, I. Bernal and G. Dobson, *J. Organomeal. Chem.* 1978, **157**, 23.
[14]M. S. Hussain and E. O. Schlemper, *Inorg. Chem.* 1979, **18**, 2275.
[15]W. H. Zachariasen, *Acta Cryst.* 1963, **16**, 1139.
[16]V. Schomaker and K. W. Trueblood, *Acta Cryst.* 1968, **B24**, 63.
[17]M. Iwata and Y. Saito, *Acta Cryst.* 1973, **B29**, 822.
[18]M. Iwata, *Ibid.*, 1977, **B33**, 59.
[19]K. Knox, *J. Phys. Chem.* 1959, **30**, 991.

Polyhedron Vol. 1, No. 4, pp. 371–376, 1982
Printed in Great Britain.

0277-5387/82/040371-06$03.00/0
Pergamon Press Ltd.

HISTAMINE AS A LIGAND IN BLOOD PLASMA—II

STABILITY CONSTANTS FOR ITS TERNARY COMPLEXES OF Cu(II) WITH L-HISTIDINE, L-GLUTAMINE AND L-THREONINE†

AYCIL KAYALI‡ and GUY BERTHON*
Laboratoire de Chimie I. Electrochimie et Interactions 40, Avenue du Recteur Pineau, 86022 Poitiers, France

(*Received* 3 *December* 1981)§

Abstract—A preliminary study of the simulated distribution of histamine in blood plasma at different pathogenic levels has drawn attention to the importance of some copper ternary complexes with respect to the possible pathological activity of this metal.

The next stage of investigation required the calculation of the formation constants of the species that the simulation pointed out as the most concentrated in plasma.

The present work reports the determination of the formation constants for the ternary systems Cu–histamine–histidine, Cu–histamine–glutamine and Cu–histamine–threonine together with the parent binary systems Cu–histidine, Cu–glutamine and Cu–threonine under the proper experimental conditions (37°C, $I = 0.15$ M).

INTRODUCTION

For a long time it has been known that low-molecular-weight ligands can effectively compete with albumin for Cu(II) ion in blood plasma,[1–3] the amino-acid bound fraction of this ion being proposed to play a physiological role in the biological transport of the metal.[4]

The low-molecular-weight fraction as well as the free ion concentration have thus been proved to be of great interest from a general point of view, more especially in terms of the distribution of the metal ion amongst the different involved ligands.[4].

Accordingly, the computer simulation of the complex formation of equilibra between the low-molecular-weight ligands and the metal ions in blood plasma was subsequently pioneered by Perrin and his coworkers, their model including Cu(II) and Zn(II) together with initially seventeen,[5] and later twenty-two amino-acids.[6]

Clearly such distribution simulations can help to discern the specificity of metal ions implicated in biological processes.[7] Thus, the computer technique of the modelling of plasma complex equilibria has been improved by the achievement of a new more sophisticated model which takes account of eight metals and forty ligands.[8,9] Concerning the complexation of copper, this model points out the predominance of histidine, cystine and threonine as the main amino-acids to be bound to Cu(II) ions.

Histamine is a ligand normally present in blood plasma, but its concentration in the normal state[10] is so low that it is not expected to influence the distribution of the low-molecular-weight bound metal fraction and on account of this, it had not originally been included in the above model.[8]

Nevertheless, this concentration is known to increase dramatically when anaphylactic or anaphylactoid release of histamine occurs from mast cells in the blood stream.[10–12]

A recent work of ours, developing in more detail the different possible mechanisms of such an increase, has drawn attention to the fact that some metal–histamine–amino-acid ternary complexes could well become non-negligible in the pathogenic state.[13] In support of this suggestion, many physiological studies have produced evidence that metal ions interfere with the histamine release process and also with its biological activity.[14–20]

In that respect, whereas Zn(II) ion is widely known to inhibit the histamine release[14–18] and its pharmacodynamic activity,[21] Cu(II) ion has been proved to seriously aggravate the pathological effects of histamine in mice.[21].

In our last study on the topic,[13] we reported a simulation of the metal histamine complexes in plasma which denoted some ternary complexes of copper as potentially having pathological activity. As the stability constants on which this simulation was based were only estimated from the combination of the binary metal-histamine ones, especially determined for this occasion, and from literature data, there was an urgent need for the calculation of the ternary constants pertaining to the species appearing as the most predominant in the quoted distribution. The present work deals with the study of the ternary systems Cu(II)–histamine–L-histidine, Cu(II)–histamine–L-glutamine and Cu(II)–histamine–L-threonine; this involving the preliminary study of the binary systems Cu(II)–L-histidine, Cu(II)–L-glutamine and Cu(II)L-threonine under the same experimental conditions (37°C, I = 0.15 M $NaClO_4$).

EXPERIMENTAL

Reagents

L-histidine, L-glutamine and L-threonine were supplied by Merck as biochemical grade products and their purity was checked potentiometrically before use.

The stock solution of copper perchlorate in perchloric acid was prepared from crystals supplied by G. Frederick Smith Chemical Co. The metal content of the solution was determined volumetrically by complexometric titration against ethylenediaminetetraacetate,[22] the strong acid one from direct potentiometric measurements.

Perchloric acid was supplied by Prolabo R.P. as a "Nor-

†Part I: Ref. [13].

‡Permanent address: Istanbul Üniversitesi Kimya Fakültesi Bayazit, Istanbul, Turkey.

*Author to whom correspondence should be addressed.

§Originally submitted to The *Journal of Inorganic and Nuclear Chemistry* 23 May 1979.

matom" grade product. Sodium perchlorate was Merck reagent grade. Sodium hydroxide solutions were prepared from B.D.H. concentrated volumetric solutions with freshly boiled deionised water; their titre was systematically checked against potassium hydrogenophtalate Prolabo R.P.p.a.

Experimental procedure

A Corning digital type 113 mV meter was used, equipped with a Beckman glass electrode (cat. no. S39301) and a saturated sodium chloride calomel electrode arranged as below.

$$\text{G.E.}|\text{Ligand, } Cu^{2+}, NaClO_4\ 0.15\ M\|NaCl_{(satd)}|Hg_2Cl_2\text{-Hg.} \quad (1)$$

The reaction cell system (Ingold) was thermostatted at 37.00 ± 0.02°C by circulating water and maintained under an atmosphere of thermostatted, scrubbed, oxygen-free nitrogen. The ionic background to hold activity coefficients constant was I = 0.15 mol. dm^{-3}, this being isotonic with blood plasma.

The standard alkali solution was stored in and delivered from a Radiometer Autoburette ABU 12. The electrode system was calibrated as in Ref. [9].

The initial overall concentrations of the reactants used for the titrations pertaining to each binary or ternary system under consideration are summarized in Table 1.

Calculation of formation constants

All the potentiometric titration data were treated with the MINIQUAD program,[23] SCOGS[24] being used only additionally for a ternary system in view of a comparison as it can be seen further.

For each binary or ternary system, the optimization of the formation constants took account of the several sets of constants arising from the combination of all the possibly existing species.

As it has been emphasized in an earlier paper,[9] the use of only numerical criteria (the sum of squared residuals for instance) to test the given models capacity to describe the experimental measurements may sometimes be misleading. So the selection of the presumably best set of constants for each system was finally done on the basis of the graphical comparison between experimental and simulated data.

In that view, the following variables were looked at: (1) for the binary systems, we chose to use the formation function $\bar{r}$ on account of its particular sensitivity to be modified by the existence of species other than simple and mononuclear ones. Indeed, the experimental or simulated formation function is calculated in the usual way according to the relation

$$\bar{r} = \{C_L - ([L] + [HL] + [H_2L] + \cdots)\}/C_M. \quad (2)$$

This relation, in which C_L and C_M represent the total ligand and total metal concentrations, is established independently of the metal complex species existing in the solution. Thus, the formation curves obtained for different total ligand and total metal concentrations are superimposable as long as exclusively simple and mononuclear species are formed; any modification of this normal shape is therefore attributed to the existence of protonated, hydrolysed or polynuclear species. (ii) for the ternary

Table 1. Initial total concentrations of the reactants used for the potentiometric titrations (hsn = histamine, C_{OH} = 100.0 mM)

System	C_{hsn}/mM	C_X/mM	C_{Cu}/mM	C_H/mM
Proton-glutamine		10.00		25.03
		10.00		30.03
		20.00		45.05
Proton-threonine		20.02		42.85
		5.00		10.71
		10.01		21.43
		10.01		21.43
Copper-histidine		20.00	4.96	40.48
		10.00	4.96	20.46
		5.00	9.93	15.89
		5.00	4.96	15.45
		10.00	9.93	25.90
Copper-glutamine		20.00	4.96	40.48
		10.00	4.96	20.46
		5.00	9.93	15.89
		5.00	4.96	15.45
		10.00	9.93	20.89
Copper-threonine		20.02	4.96	32.57
		10.01	9.93	16.94
		5.00	9.93	11.58
		10.01	4.96	21.86
		5.00	4.96	11.15
Copper-histamine-histidine	9.29	10.00	9.93	40.91
	9.29	10.00	4.96	40.48
	9.29	5.00	4.96	30.47
	4.65	10.00	4.96	30.47
	4.65	5.00	4.96	20.46
	4.65	5.00	9.93	20.89
Copper-histamine-glutamine	9.29	10.00	9.93	40.91
	9.29	5.00	4.96	30.47
	4.65	10.00	4.96	30.47
	4.65	5.00	4.96	20.46
	4.65	5.00	9.93	20.89
Copper-histamine-threonine	8.58	10.01	9.93	43.72
	8.58	10.01	4.96	43.29
	8.58	5.00	4.96	32.57
	4.29	10.01	4.96	32.57
	4.29	5.00	4.96	21.86
	4.29	5.00	9.93	22.30

systems, we based our graphical comparisons on the average number of protons bound to both of the ligands under consideration, as defined in relation (3)

$$\bar{s} = \frac{C_H + NDP_L \times C_L + NDP_X \times C_X - C_{OH} + [OH] - [H]}{C_L + C_X} \quad (3)$$

where C_H, C_L, C_X, C_{OH} respectively stand for the total concentrations of strong acid, first ligand L, second ligand X and sodium hydroxide introduced in the solution and NDP for the number of dissociable protons of each ligand.

This calculation necessitated the modification[25] of the PSEUDOPLOT program.[26] Let us note on this occasion that, as has been previously explained in more detail,[9] the calculation of the theoretical variables to be compared with the experimental ones is a real simulation of the experiments. In point of fact, it is not based on the recalculation of the variable under consideration from the new total concentrations pertaining to a particular set of formation constants, but on the contrary it consists of the iterative calculation of the new values of [H] derived from this set of constants and the analytically known total concentrations. The calculation of the simulated variables $\bar{r}$ or $\bar{s}$ then performed exactly as in the case of the experimental curves.

RESULTS AND DISCUSSION

All the results are summarized in Table 2. Setting aside the proton–ligand equilibria which have already been well defined under other experimental conditions, let us examine the formation of the complexes for each system under study.

Cu-histidine

Among the copper–amino-acid systems, the Cu–histidine one has certainly been the most investigated during the past decade .[27–35] Nevertheless, as there was no available data under the proper experimental conditions, we had to redetermine the formation constants for this system. In particular, we compared the fitting of the different sets of constants proposed by the previous authors.[28–30,32,33,35]

As can be seen in Table 2, apart from Perrin and Sharma's results,[28] all the other authors were in close agreement about the identity of the species which are formed in acidic and neutral media, as our results confirm. As for the hydrolysed species, however, our "best" model excludes the existence of ML (OH) in favour of $M_2L_2(OH)_2$. Besides, the addition of $ML_2(OH)_2$ to this model or the replacement of $ML_2(OH)$ by $ML_2(OH)_2$ did not improve either the numerical or the graphical fits with the experimental data.

Figures 1 and 2 for example, show the comparison of the experimental curves with the simulated ones corresponding to our "best" model, both of them being defined as in the above chapter.

Cu–glutamine

There is nothing special to note on this system. The experimental formation curves were found superimposable and characteristic of the existence of the two simple species ML and ML_2 formerly evidenced.[36–38]

Cu–threonine

According to earlier studies, Cu–threonine is essentially composed of the two complexes ML and ML_2,[39–41] the species MLH_{-1} and ML_2H_{-2} being also previously characterised.[29,42]

Together with the simple species ML and ML_2, our results also establish the existence of MLH_{-1} and the fact that MLH_{-1} is preferred to $M_2L_2H_{-2}$ (see Table 2, V–A, V–B) indicates that the formation of this species arises from the dissociation of the hydroxide group of the amino-acid rather than from the bonding of a free hydroxide ion on the solvent.[41]

We also characterised the species ML_2H_{-1}, but not ML_2H_{-2} which did not improve the fits when introduced in the "best" model (see Table 2, V–C, V–D). This is probably because the pH range investigated $2 \leq pH \leq 9$) was not basic enough for the concentrations of this species to be significant under the present conditions of medium and temperature.

Let us finally note that we could not find out under these conditions the MLH species which had been pre-

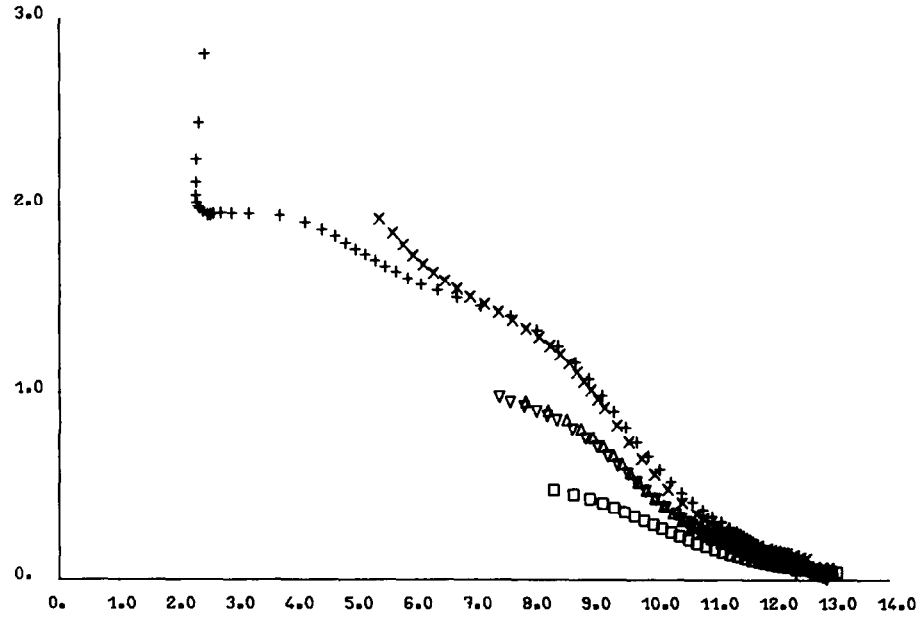

Fig. 1. Experimental formation curves of the CU–histidine system (37°C, I = 0.15 M $NaClO_4$) Experiment: (i) +; (ii) ×; (iii) □; (iv) △; (v) ▽. See corresponding concentrations in Table 1.

Table 2. Formation constants obtained from these studies. The formula of the general complex is Cu_r (histamine)$_p X_q H_s$ where X represents histidine, glutamine and threonine respectively. n = number of experimental observations, S = sum of squares of residuals. The results are obtained from MINIQUAD when not specified

	System	p	q	r	s	logβ	S	n	Notes
I	Proton-glutamine	0	1	0	1	8.680 ± 0.002	0.146E-05	227	
		0	1	0	2	10.864 ± 0.003			
II	Proton-threonine	0	1	0	1	8.573 ± 0.003	0.277E-05	288	
		0	1	0	2	10.721 ± 0.004			
III-A	Copper-histidine	0	1	1	0	9.896 ± 0.006	0.197E-05	300	Same model as ref.33
		0	2	1	0	17.499 ± 0.021			
		0	1	1	1	13.842 ± 0.008			
		0	2	1	1	23.166 ± 0.015			
		0	2	1	2	26.551 ± 0.055			
III-B	Copper-histidine	0	1	1	0	9.894 ± 0.007	0.230E-05	300	Same model as ref.28
		0	2	1	0	17.505 ± 0.024			
		0	1	1	1	13.883 ± 0.007			
		0	2	1	1	23.217 ± 0.015			
		0	1	1	-1	3.079 ± 0.109			
		0	2	2	-2	$\beta < 0$			
III-C	Copper-histidine	0	1	1	0	9.893 ± 0.006	0.191E-05	300	Same model as ref.29, 30, 35.
		0	2	1	0	17.498 ± 0.021			
		0	1	1	1	13.843 ± 0.007			
		0	2	1	1	23.172 ± 0.014			
		0	2	1	2	26.546 ± 0.053			
		0	1	1	-1	$\beta < 0$			
		0	2	2	-2	9.207 ± 0.158			
III-D	Copper-histidine	0	1	1	0	9.893 ± 0.006	0.179E-05	300	Same model as ref.32
		0	2	1	0	17.498 ± 0.021			
		0	1	1	1	13.843 ± 0.007			
		0	2	1	1	23.172 ± 0.014			
		0	2	1	2	26.546 ± 0.054			
		0	1	1	-1	$\beta < 0$			
		0	2	2	-2	9.204 ± 0.154			
		0	2	1	-1	6.422 ± 0.107			
III-E	Copper-histidine	0	1	1	0	9.893 ± 0.006	0.179E-05	300	'Best' model
		0	2	1	0	17.498 ± 0.021			
		0	1	1	1	13.843 ± 0.007			
		0	2	1	1	23.172 ± 0.014			
		0	2	1	2	26.546 ± 0.054			
		0	2	2	-2	9.204 ± 0.154			
		0	2	1	-1	6.422 ± 0.107			
IV	Copper-glutamine	0	1	1	0	7.475 ± 0.006	0.180E-05	232	
		0	2	1	0	13.586 ± 0.021			
V-A	Copper-threonine	0	1	1	0	7.793 ± 0.004	0.281E-05	300	
		0	2	1	0	14.272 ± 0.016			
		0	2	1	-2	7.142 ± 0.065			
V-B	Copper-threonine	0	1	1	0	7.791 ± 0.004	0.267E-05	300	
		0	2	1	0	14.249 ± 0.016			
		0	1	1	-1	2.036 ± 0.050			
		0	2	2	-2	$\beta < 0$			
V-C	Copper-threonine	0	1	1	0	7.789 ± 0.003	0.190E-05	300	'Best' model
		0	2	1	0	14.299 ± 0.013			
		0	1	1	-1	1.599 ± 0.122			
		0	2	1	-1	4.693 ± 0.049			
V-D	Copper-threonine	0	1	1	0	7.789 ± 0.003	0.189E-05	300	
		0	2	1	0	14.299 ± 0.012			
		0	1	1	-1	1.599 ± 0.113			
		0	2	1	-1	4.599 ± 0.144			
		0	2	1	-2	-5.303 ± 0.535			
V-E	Copper-threonine	0	1	1	0	7.789 ± 0.003	0.199E-05	300	Same model as ref.29, 42.
		0	2	1	0	14.321 ± 0.012			
		0	2	1	-1	4.676 ± 0.126			
		0	2	1	-2	-5.291 ± 0.558			
VI-A	Copper-histamine-histidine	1	1	1	0	17.336 ± 0.012		300	SCOGS (deviation in titre=0.0341 ml)
		1	1	1	1	22.853 ± 0.016			
		1	1	1	2	26.857 ± 0.055			
VI-B	Copper-histamine-histidine	1	1	1	0	17.341 ± 0.015	0.193E-05	300	
		1	1	1	1	22.842 ± 0.022			
		1	1	1	2	26.876 ± 0.064			
VII	Copper-histamine-glutamine	1	1	1	0	15.971 ± 0.016	0.664E-05	300	
		1	1	1	1	20.112 ± 0.097			
VIII	Copper-histamine-threonine	1	1	1	0	16.433 ± 0.014	0.527E-05	300	
		1	1	1	1	20.360 ± 0.113			
		1	1	1	-1	6.464 ± 0.057			

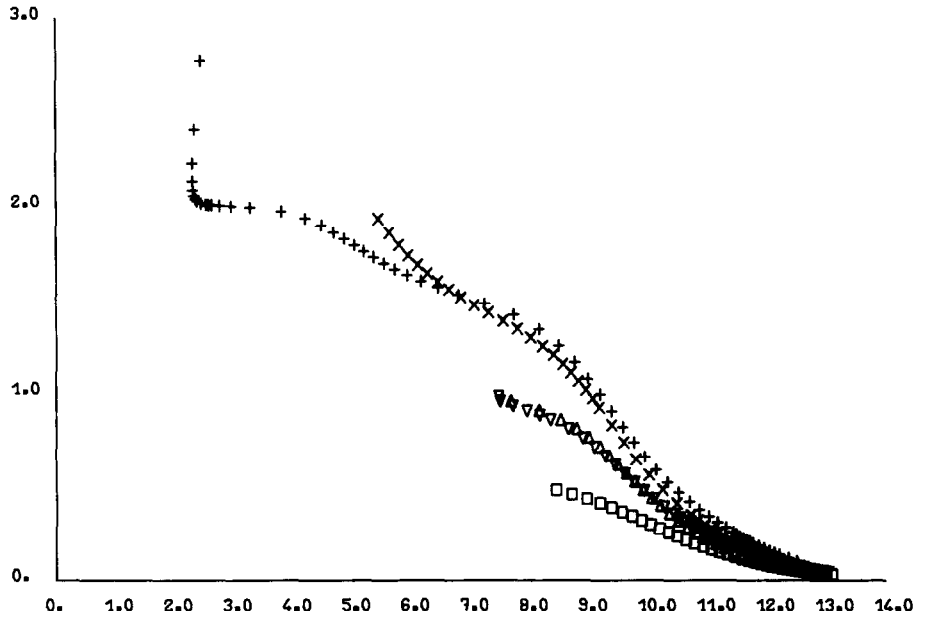

Fig. 2. Formation curves of the Cu–histidine system, simulated on the basis of the results shown in Table 2, III-E.

viously mentioned by Pettit and Swash in the acidic medium.[41]

Cu–histamine–histidine

The two MLX† and MLXH complexes had already been characterised for this system under different experimental conditions.[35,43] Our study confirmed them as the main ternary species (see Table 2, VI).

According to Williams' hypothesis based on thermodynamic considerations[30] the MX_2 complex involves a tridentate and a bidentate (histamine-like) histidine molecules, but it is more generally expected to be doubly-bound through the imidazole and the amino groups of histidine.[29,34] Whatever be the structure of this parent species, it seems logical that the histamine molecule replaces the histamine-like bonded histidine in the ternary species MLX.

In the MX_2H complex, a molecule of histidine is bound through the carboxyl and imidazole groups, while the bond of the second is histamine-like.[30] It is thus most likely that the structure of MLXH is based on the same bonding modes.

Besides MLX and MLXH, we also characterised the $MLXH_2$ species in the acidic range. The molecule of histidine in this complex is probably bound as in MLXH, whereas the histamine has the same structure as LH in the ML_2H complex. In that case, the histamine molecule is thought to be protonated either through its imidazole-group[44] or through its amino-group.[32]

Cu–histamine–glutamine

The two MLX and MLXH species were found for this system (see Table 2, VII).

Concerning the parent complex MX_2, spectroscopic studies made in the solid state assigned a third bond between copper and glutamine through the amido group of the latter.[45] On the contrary, Gergely *et al.*[38] concluded that this group did not bind copper in this complex. Thus it is not easy to predict a possible structure for MLX, which nevertheless might be similar to that of the Cu–(histamine)–(glycine) species.[35]

As for MLXH, the histamine molecule must once more be protonated through its imidazole[44] or its amino-group[32].

Cu–histamine–threonine

Three species were characterised for this system: MLX, MLXH and $MLXH_{-1}$ (see Table 2, VIII).

Although the bonding of the MX_2 species is generally thought to be glycine-like,[42] some authors lately suggested the possible interaction of the unionised hydroxy-group of the threonine molecule.[40,41] Nevertheless, the fact that the threonine in Cu–(histidine)–(threonine) does not coordinate through the hydroxy-group in the solid state[46] tends to suggest that the MLX structure is of the Cu–(histamine)–(glycine) type[35].

The structure of MLXH can reasonably be expected to arise from the bonding of a protonated histamine and a glycine-like molecule of threonine.

Finally, it is probable that the $MLXH_{-1}$ species is formed, as the species of same stoechiometry in the Cu–histidine–threonine system,[29] by the dissociation of the hydroxy-group of the threonine. Thus, it can be thought to have a similar structure.

†M = Cu, L = histamine, X = histidine in the present case and generally stands for the second ligand.

REFERENCES

[1]P. Z. Neumann and A. Sass-Kortsak, *Vox Sanguinis* 1963, **8**, 111.
[2]B. Sarkar and T. P. A. Kruck In *The Biochemistry of Copper* (Edited by J. Peisach, P. Aisen and W. E. Blumberg), p. 183. Academic Press, New York, (1966).
[3]B. Sarkar and T. P. A. Kruck, *Can J. Biochem.* 1967, **45**, 2046.
[4]P. Z. Neumann and A. Sass-Kortsak, *J. Clin. Invest.* 1967, **46**, 646.
[5]P. S. Hallman, D. D. Perrin and A. E. Watt, *Biochem. J.* 1971, **121**, 549.
[6]D. D. Perrin and R. P. Agarwal In *Metal Ions in Biological Systems* (Edited by H. Sigel), Vol. 2. Marcel Dekker, New York.
[7]R. Österberg, *Coord. Chem. Rev.* 1974, **12**, 309.

[8]P. M. May, P. W. Linder and D. R. Williams, *J. Chem. Soc. Dalton Trans.* 1977, 588.
[9]G. Berthon, P. M. May and D. R. Williams, *J. Chem. Soc. Dalton Trans.* 1978, 1433.
[10]A. Doenicke and W. Lorenz, *Ann. Anesth. Franc.* 1976, **17** (2), 219.
[11]J. C. Foreman, L. G. Garland and J. L. Mongar, *Symp. Soc. Exp. Biol.* 1976, **30**, 193.
[12]A. Doenicke and W. Lorenz, *Ann. Anesth. Franc.* 1977, **18** (7–8), 691.
[13]A. Kayali and G. Berthon, (to be published).
[14]R. Keller and E. Sorkin, *Experientia* 1970, **26**/1, 30.
[15]B. Uvnas, C. H. Aborg and U. Bergqvist, *Acta Physiol. Scand.* 1975, **93**, 401.
[16]W. Kazimierczak, B. Adamas and C. Maslinski, *Biochem. Pharm.* 1978, **27**, 243.
[17]C. W. Ogle and C. H. Cho, *Pharm. Res. Comm.* 1977. **9** (8), 679.
[18]W. Kazimierczak and C. Maslinski, *Agents and Actions* 1974, **4** (5), 320.
[19]J. L. Mongar, J. C. Foreman and M. Hallett, *Agents and Actions* 1978, **8** (4), 400.
[20]J. C. Foreman, M. B. Hallett and J. L. Mongar, *J. Physiol.* 1977, **271**, 193.
[21]W. R. Walker, R. Reeves and D. J. Kay, *Search* 1975, **6** (4), 134.
[22]G. Schwarzenbach, *Complexometric Titrations.* Methuen and Co, London (1957).
[23]A. Sabatini, A. Vacca and P. Gans, *Talanta* 1974, **21**, 53.
[24]I. G. Sayce, *Talanta* 1968, **15**, 1397.
[25]T. Alemdaroglu and G. Berthon, *Bioelectrochem. Bionerg.* 1981 **8**, 49.
[26]A. M. Corrie, G. K. R. Makar, M. L. D. Touche and D. R. Williams, *J. Chem. Soc. Dalton* 1975, 105.
[27]B. Sarkar and Y. Wigfield, *J. Biol. Chem.* 1967, **242**, 5572.
[28]D. D. Perrin and V. S. Sharma, *J. Chem. Soc. (A)* 1967, 724.
[29]H. C. Freeman and R. P. Martin, *J. Biol. Chem.* 1969, **244**, 4823.
[30]D. R. Williams, *J. Chem. Soc. Dalton* 1972, 790.
[31]A. C. Baxter and D. R. Williams, *J. Chem. Soc. Dalton* 1975, 1757.
[32]P. G. Daniele and G. Ostacoli, *Ann. Chim.* 1976, **66**, 387.
[33]G. Brookes and L. D. Pettit, *J. Chem. Soc. Dalton* 1977, 1918.
[34]N. Camerman, J. K. Fawcett, T. P. A. Kruck, B. Sarkar and A. Camerman, *J. Am. Chem. Soc.* 1978, **100** (9), 2690.
[35]I. Sovago, T. Kiss and G. Gergely, *J. Chem. Soc. Dalton* 1978, 964.
[36]R. C. Tewari and M. N. Srivastava, *J. Inorg. Nucl. Chem.* 1973, **35**, 2441.
[37]D. R. Williams, *J. Chem. Soc. Dalton* 1973, 1064.
[38]A. Gergely, I. Nagypal and E. Farkas, *J. Inorg. Nucl. Chem.* 1975, **37**, 551.
[39]A. Gergely, I. Sovago, I. Nagypal and R. Kiraly, *Inorg. Chim. Acta* 1972, **6**, 435.
[40]A. Gergely, J. Mojzes and Z. S. Kassai-Bazsa, *J. Inorg. Nucl. Chem.* 1972 **34**, 1277.
[41]L. D. Pettit and J. L. M. Swash, *J. Chem. Soc. Dalton* 1976, 2416.
[42]P. Grenouillet, R. P. Martin, A. Rossi and M. Ptak, *Biochim., Biophys. Acta* 1973, **322**, 185.
[43]P. G. Daniele and G. Ostacoli, *Ann. Chim.* 1978, **68**, 129.
[44]A. Gergely and I. Sovago, *Inorg. Chim. Acta* 1976, **20**, 19.
[45]M. N. Srivastava, R. C. Tewari, U. C. Srivastava, G. B. Bhargava and A. N. Vishnoi, *J. Inorg. Nucl. Chem.* 1976, **38**, 1897.
[46]H. C. Freeman, J. M. Guss, M. J. Healy, R. P. Martin, C. E. Nockholds and B. Sarkar, *Chem. Comm.* 1969, 225.

Polyhedron Vol. 1, No. 4, pp. 377–381, 1982
Printed in Great Britain.

0277-5387/82/040377-05$03.00/0
Pergamon Press Ltd.

DIVALENT NICKEL, COBALT AND COPPER COMPLEXES OF TETRADENTATE MACROCYCLE, DIBENZO (*f*, *n*) 2, 4, 10, 12- TETRAMETHYL-1, 5, 9, 13-TETRAZACYCLOHEXADECA [16] 1, 3, 9, 11-TETRAENE

V. B. RANA*, PRABHA SINGH, D. P. SINGH and M. P. TEOTIA
Department of Chemistry, Meerut College, Meerut-250001, India

(*Received* 3 *December* 1981)

Abstract—Metaphenylenediamine and acetylacetone react in presence of divalent nickel, cobalt and copper salts to form complexes of a 16-membered N_4 tetradentate macrocycle, dibenzo-(f, n)-2, 4, 10, 12-tetramethyl-1, 5, 9, 13-tetrazacyclohexadeca-[16]-1, 3, 9, 11-tetraene. The complexes are characterised to be distorted octahedral of the type [M(Me_4[16] 1, 3, 9, 11-tetraene N_4)X_2] where M = Ni(II), Co(II) and Cu(II); X = Cl, Br, NO_3 or NCS. The ligand coordinates through azomethine or imine nitrogen atoms which are bridged by acetylacetone moieties. The electrical conductance, molecular weight, magnetic, electronic and IR spectra are discussed.

INTRODUCTION

Complexes of metal ions with synthetic macrocyclic ligands are of great importance, in part because of their resemblance with many natural systems, e.g. porphyrins and cobalamines. These ligands are also of theoretical interest since they are capable of furnishing an environment of controlled geometry and ligand field strength. Curtis *et al.*[1] produced the first of many new synthetic macrocyclic ligands and their recent work has formed the basis of work in this field. Many of the macrocyclic ligands have been synthesised by the reaction of amines with 2,6-diacetylpyridine or dicarbonyl compounds,[2] however, a very few have been prepared from aromatic diamines and dicarbonyl compounds. A few complexes of benzene 1, 2-diamine with β-diketones have recently been reported[3–5] and their structures have been established by X-ray crystallography but similar compounds with benzene 1, 3-diamine have not been synthesised so far. In continuation of our efforts to study the metal chelates of macrocyclic ligands,[6–8] we report here the synthesis and characterisation of six-coordinate tetragonal complexes of tetradentate N_4 ligand dibenzo-(f, n)-2, 4, 10, 12-tetramethyl 1, 5, 9, 13-tetrazacyclohexadeca-[16]-1, 3, 9, 11-tetraene abbreviated as [Me_4[16] tetraene N_4]. Attempts to isolate the free ligand failed.

EXPERIMENTAL

All the chemicals and solvents used were of reagent grade. The ligand *m*-phenylenediamine acetylacetone was synthesised by refluxing methanolic solutions of diamine (0.01 mol) and acetylacetone (0.02 mol) on a water bath for 6 hr. The condensation product so obtained on cooling was recrystallised from methanol, yield ~ 45%.

Preparation of complexes

(a) [$M(m\text{-}PDA)_2X_2$]. A general procedure of two step reaction was adopted for synthesising the metal chelates.

m-Phenylenadiamine (0.02 mol) dissolved in the minimum amount of methanol was added to a methanolic solution of anhydrous metal salt (0.01 mol) (pH ~ 3.0–3.5) and refluxed on a water bath for 4–7 hr. The mixture was concentrated, cooled and the precipitate of the complex was filtered, recrystallised from methanol, and dried, yield ~ 60%.

(b) [$M(Me_4$[16] *tatene* $N_4)X_2$]. The metal complex of diamine obtained by the above method was dissolved in warm methanol and 2 ml of acetylacetone added to it. The resulting solution was stirred mechanically for 4 hr, refluxed for 12 hr and left for three weeks. The dark fine crystals which separated were filtered, recrystallised from DMF and dried at 110° *in vacuo* yield ~ 35%.

The nitrato complexes were prepared by taking metal nitrates. Bromo and thiocyanato salts were prepared by stirring and slowly adding KBr or NH_4CNS solution to ethanolic solution of metal chloride and filtering off KCl or NH_4Cl.

The colours and analyses of the complexes are given in Table 1. These are insoluble in common organic solvents but are all soluble in dimethylformamide. The nickel (II) complexes are also soluble in nitrobenzene. The nickel (II) and copper (II) complexes are stable up to 250° while those of cobalt (II) decompose ~ 250°C.

The metal contents were determined by standard EDTA titration using Eriochrome black T as indicator while halides were estimated by Volhard's method and nitrate as nitron salt. The micro-analyses of C, H and N were done at the Instrumentation Centre, Department of Chemistry, Aligarh Muslim University, Aligarh, U.P., India.

The magnetic susceptibility measurements were carried out using Gouy's method and $CuSO_4.5H_2O$ as calibrant. The IR spectra in 4000–625 cm^{-1} range in KBr pellets were recorded on a Perkin–Elmer 621 instrument and in the range 100–650 cm^{-1} in nujol mull on a Polytec FIR-30 spectrophotometer. The electronic spectra were recorded in nujol mull and DMF solution. 6660–33300 cm^{-1} (300–1500 nm) range on DMR-21, UV-VIS near IR spectrophotometer. The conductivity measurements were made in DMF solutions on Toshniwal type CL 01/01 conductivity bridge. The molecular weights of soluble nickel complexes were determined cryoscropically in nitrobenzene.

RESULTS AND DISCUSSION

The analytical data of these complexes show their formulae to be [M(Me_4-[16]-tetene N_4)X_2] where M = Ni(II), Co(II) or Cu(II) and X = Cl, Br, NO_3 or NCS. The electrical conductance of soluble complexes measured in nitrobenzene show their non-electrolytic nature. The molecular weight determination of nickel (II) complexes are consistent with their proposed formulae. The isomorphism of nickel (II) to those of cobalt and copper complexes indicate their similar nature. The compounds are stable to water but are hydrolysed by dilute mineral acids by the formation of a brown insoluble precipitate.

The reactions of acetylacetonato complexes with

*Author to whom correspondence should be addressed.

Table 1. Analytical data of complexes

Complex	Colour	Found %							Calculated %					
		M	C	H	N	X	Λ_M Mhos cm^{-2} mol^{-1}	Mol. Wt.	M	C	H	N	X	Mol. Wt.
$[Ni(C_{22}H_{24}N_4)Cl_2]$	Green	12.05	55.92	5.20	12.00	15.20	8.50	492	12.26	55.83	5.08	11.83	15.01	473
$[Ni(C_{22}H_{24}N_4)Br_2]$	Dark green	10.28	-	-	9.80	28.75	9.20	583	10.32	46.94	4.27	9.96	28.82	562
$[Ni(C_{22}H_{24}N_4)(NO_3)_2]$	Brownish-green	11.15	50.40	4.42	16.00	-	8.00	531	11.06	50.38	4.58	16.03	-	526
$[Ni(C_{22}H_{24}N_4)(NCS)_2]$	Light-green	11.04	-	-	15.82	-	10.50	529	11.19	55.60	4.61	16.21	-	518
$[Co(C_{22}H_{24}N_4)Cl_2]$	Greenish-black	12.62	56.0	5.20	11.50	15.10	-	-	12.44	55.69	5.06	11.80	14.98	474
$[Co(C_{22}H_{24}N_4)Br_2]$	Greenish-black	10.22	-	-	-	-	-	-	10.47	46.79	4.26	9.94	28.41	563
$[Co(C_{22}H_{24}N_4)(NO_3)_2]$	Black	11.30	55.80	4.72	16.30	-	-	-	11.19	50.09	4.55	15.93	23.52	527
$[Co(C_{22}H_{24}N_4)(NCS)_2]$	Black	13.16	-	-	16.22	-	-	-	13.36	55.48	4.62	16.18	-	519
$[Cu(C_{22}H_{24}N_4)Cl_2]$	Black	13.00	54.92	5.05	11.82	15.00	-	-	13.17	55.02	5.02	11.71	14.88	478
$[Cu(C_{22}H_{24}N_4)Br_2]$	Black	11.23	46.40	4.20	9.72	28.58	-	-	11.11	46.56	4.23	9.87	28.83	567
$[Cu(C_{22}H_{24}N_4)(NO_3)_2]$	Dark-brown	12.00	-	-	16.0	-	-	-	11.86	49.71	4.50	15.81	23.35	531
$[Cu(C_{22}H_{24}N_4)(NCS)_2]$	Brown	12.30	-	-	15.82	-	-	-	12.04	50.47	4.58	16.06	22.17	523

Table 2. Important IR bands and their assignments

Complexes	ν_{NH}	δ_{NH}	$\nu_{C=N} + \nu_{C=C}$	$\nu_{asymC-CH_3}$	$\nu_{symC-CH_3}$	$\delta_{CH} + \nu_{C-CH_3}$	$\rho_r CH_3$	Anions
$[Ni(L)\ Cl_2]$	3230 3200	1450 840	1610 1595	1440	1380	1190	1020	285
$[Ni(L)\ Br_2]$	3260 3200	1440 845	1615 1595	1430	1380	1175	1025	220
$[Ni(L)(NO_3)_2]$	3240 3200	1430 840	1610 1590	1440	1360	1190	1015	1240,870, 1010,230
$[Ni(L)(NCS)_2]$	3280 3200	1430 845	1610 1595	1435	1370	1165	1015	2110,810, 480, 285.
$[Co(L)Cl_2]$	3250 3200	1430 840	1600 1590	1440	1390	1175	1020	300
$[Co(L)Br_2]$	3240 3200	1640 835	1610 1595	1430	1380	1190	1025	215
$[Co(L)(NO_3)_2]$	3260 3180	1650 830	1615 1595	1435	1375	1180	1020	1240,1010, 870, 225.
$[Co(L)(NCS)_2]$	3260 3160	1640 840	1610 1590	1430	1365	1190	1020	270
$[Cu(L)Cl_2]$	3240 3180	1635 840	1600 1590	1440	1360	1185	1020	270
$[Cu(L)Br_2]$	3220 3180	1640 835	1610 1590	1435	1380	1190	1015	-
$[Cu(L)(NO_3)_2]$	3280 3180	1640 840	1615 1595	1440	1390	1190	1020	1240,1010, 865 ,235
$[Cu(L)(NCS)_2]$	3240 3160	1630 840	1610 1595	1435	1385	1190	1020	2110,815, 480, 260.

diamine and template synthesis of macrocyclic complexes fail in many solvents. However, the complexes are isolated by reaction of acetylacetone with diamine metal complexes in anhydrous methanol.

IR spectra

The assignment of important bands in the IR spectra are tabulated in Table 2. The strong bands ~3200 cm^{-1} are due to the presence of the NH group, however, these bands appear at higher or lower energies depending upon interaction of the anions.[9] The assignment is based on the fact that the macrocyclic ligands[10] which have coordinated secondary amine group have bands in the vicinity of 3200 cm^{-1}. This contention finds support from the appearance of strong bands ~1640 and 840 cm^{-1} assignable to NH deformation coupled with NH out-of-plane bending.[6,11] The strong bands appearing as doublets in the spectra of all the complexes ~1590–1610 cm^{-1} may be assigned to $\nu C=N$ vibrations and these bands indicate the presence of coordinated azomethine groups.[7,11] The absence of absorptions ~3400 cm^{-1} show that amino groups of the diamine have reacted with acetylacatone. This observation is substantiated by the appearance of bands ~2920, 1360, 1240–1260, 1190 and 660 cm^{-1} characteristic of acetylacatone moiety and may be assigned to νCH_3, $\delta sym\ CH_3$, $\nu C\text{–}CH_3$, $\delta CH + \nu C\text{–}CH_3$ and ring vibrational modes, respectively.[6,7,12] The absence of stretching and bending vibrations of (C–O) group ~1525 and 1280 cm^{-1} indicate the absence of this group in these complexes.

The spectra of nitrato complexes exhibit new bands at ~1240, 1015 and 865–870 cm^{-1} which are consistent with the monodentate nature of this group and is substantiated by the small splitting of bands appearing ~1760 and 1745 cm^{-1}. Thiocyanato complexes show bands ~2110, 815 and 480 cm^{-1} assignable to νCN, νCS and NCS bending,[13] respectively, and are in accordance with the monodentate N-bonded nature of this group.[14]

Magnetic and electronic spectral studies

The magnetic moments (Table 3) of nickel, cobalt and copper complexes lie in 3.05–3.25, 4.85–5.15 and 1.75–1.82 B.M. range at room temperature. The values are consistent with high- spin nature of the nickel and cobalt compounds and show the presence of a pseudooctahedral environment around the metal atom.[19]

The nujol mull absorbance spectra of nickel complexes show a broad band around ~ 8130–8530 cm^{-1} with a shoulder ~10000–10650, and ~15380–16700 and 26310–26700 cm^{-1}. The position of these bands is consistent with the postulation that the nickel ion has essentially an octahedral environment about it and can be interpreted in terms of D_{4h} symmetry of these complexes.[16] The spectra do not show any regular pattern except that the thiocyanato complex does not show any splitting of the first band perhaps due to the small difference among the ligand field strengths of nitrogen atoms of azomethine, secondary amine and thiocyanate group. The spectra of cobalt complexes exhibit bands ~7930–8920, 15380–17540 with a broad band envelope ~19000 cm^{-1} showing almost two bands ~18200 and 19500 cm^{-1}. The spectra are comparable to those reported to be distorted octahedral. The assignment of spin-allowed band (Table 2) to $4_{T_{1g}} \rightarrow 4_{A_{2g}}$ is justified since the first band appears approximately at half the energy of the visible band.[7,16] The spectra of copper complexes show a broad band maxima ~18200–19000 cm^{-1} with a shoulder on low energy side ~15280–16220 cm^{-1} and show that these complexes are

Table 3. Magnetic and electronic spectral data[a]

						μ_{eff} (B.M.)
[Ni(L)Cl_2]	8130sh,	11000,	15380,	26310,	30700	3.22
[Ni(L)Br_2]	8530sh,	10580,	16660,	26660,	30760	3.05
[Ni(L)$(NO_3)_2$]	8200sh,	10280,	15850,	26320,	30720	3.25
[Ni(L)$(NCS)_2$]	-	10600,	16520,	26700,	30680,	3.15
[Co(L)Cl_2]	7950,	15650,	18540,	19320,	30650,	4.92
[Co(L)Br_2]	7935,	15385,	18000,	18850,	30760,	5.15
[Co(L)$(NO_3)_2$]	8930,	17540	18250,	19000,	30700	4.88
[Co(L)$(NCS)_2$]	8220,	16050,	18320,	19210,	30580	4.85
[Cu(L)Cl_2]	15320,	18280,	30640			1.82
[Cu(L)Br_2]	16200,	19000,	30620			1.76
[Cu(L)$(NO_3)_2$]	15550,	18620,	30600			1.75
[Cu(L)$(NCS)_2$]	16000,	18720,	30750			1.80

(a) Nickel (II); $^3B_{1g} \rightarrow {}^3E_g$, $^3B_{1g} \rightarrow {}^3B_{2g}$, $^3B_{1g} \rightarrow {}^3A_{2g(F)}$, $^3B_{1g} \rightarrow {}^3A_{2g(P)}$. and charge-transfer; Cobalt(II); $^4T_{1g} \rightarrow {}^4T_{2g}$, $^4T_{1g} \rightarrow {}^4A_{2g}$, $^4T_{1g} \rightarrow {}^4T_{1g(P)}$ and charge-transfer. Copper(II); $^2B_{1g} \rightarrow {}^2B_{2g}$, $^2B_{1g} \rightarrow {}^2E_g$ or $^2A_{2g}$ and charge-transfer. The assignments are in increasing order of energy.

distorted octahedral.[7,16,17] The band separation of about ~3000 cm^{-1} is consistent with the proposed geometry of these complexes. All the complexes exhibit invariably strong absorptions 30700 cm^{-1} region which may be associated with the intraligand charge transfer involving imine functions.[18]

Far IR spectra

The far IR spectra in the region ~100–650 cm^{-1} show various bands characteristic of metal–ligand vibrations. The halocomplexes exhibit bands ~300, 285, 270 cm^{-1} νCo–Cl, νNi–Cl, νCu–Cl, respectively and ~220, 215 cm^{-1} assignable to νCo–Br and νNi–Br vibrations, respectively. The appearance of single bands and their regions are consistent with a *trans*- octahedral nature of these complexes.[19] The presence of bands ~430–495 cm^{-1} in all the complexes originates from νM–N (azomethine) vibration and substantiate this coordination. The coordination of nitrate and thiocyanate is further supported by the appearance of new bands at ~225–240 cm^{-1} assignable to νM–O of ONO_2 group and at 260–285 cm^{-1} to νM–NCS of NCS group,[13,21] respectively.

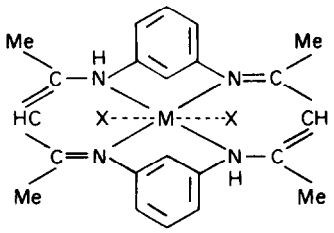

M = Ni(II), Co(II), Cu(II)

X = Cl, Br, NO_3, NCS.

Based on analyses, conductance, molecular weights, electronic and IR spectral studies structure (1) may be proposed for these complexes.

Acknowledgements—The authors are thankful to C.S.I.R., New Delhi, for financial assistance and to Head RSIC, I.I.T., Madras for recording electronic and IR spectra.

REFERENCES

[1]N. F. Curtis, *Coord. Chem. Rev.* 1968, **3**, 3.
[2]D. H. Busch, *Record. Chem. Progr.* 1964, **25**, 107.
[3]E. Jager, *Z. Chem.* 1968, **8**, 392.
[4]E. Jager, *Z. Anorg. Allg. Chem.* 1969, **364**, 177.
[5]D. P. Riley, J. A. Stone and D. H. Busch, *J. Am. Chem. Soc.* 1976, **98**, 1752.
[6]V. B. Rana and M. P. Teotia, *Ind. J. Chem.* 1980, **19A**, 267.
[7]V. B. Rana, D. P. Singh, (Mrs) P. Singh and M. P. Teotia, *Transition Met. Chem.* 1981, **6**, 36.
[8]V. B. Rana and M. P. Teotia *Proc. XX. I.C.C.C. Inorg III* 1979, 196.
[9]M. M. Blight and N. F. Curtis, *J. Chem. Soc.* 1962, 2016.
[10]D. A. House and N. F. Curtis, *J. Am. Chem. Soc.* 1964, **86**, 1331.
[11]V. B. Rana, S. K. Sangal, S. P. Gupta and S. K. Sahni *J. Ind. Chem. Soc.* 1977, **54**, 200.
[12]M. Mikami, I. Nagakawa and T. Shimanouchi, *Spectrochim Acta* 1967, **23A**, 1037.
[13]K. Nakamoto, *Infrared Spectra of Inorganic and Coordination Coordination Compounds.* Wiley Interscience, New York, (1970).
[14]A. B. P. Lever, E. Mantovani and B. S. Ramaswamy *Inorg. Chem.* 1969, **8**, 107.
[15]B. N. Figgis and J. Lewis, *Progr. Inorg. Chem.* 1964, **6**, 37.
[16]A. B. P. Lever, *Inorganic Electronic Spectroscopy.* Elsevier, Amsterdam, (1968).
[17]A. S. Bull, R. B. Martin and R. J. P. Williams, *Electronic Aspects of Biochemistry*, (Edited by B. Pullman), p. 524. Academic Press, New York (1964).
[18]A. M. Tait and D. H. Busch, *Inorg. Chem.* 1976, **15**, 197.
[19]R. J. H. Clark and C. S. Williams, *Inorg. Chem.* 1965, **4**, 350.
[20]B. Beecroft, M. J. M. Campbell and R. Grezeskoviak, *J. Inorg. Nucl. Chem.* 1974, **36**, 55.
[21]D. A. Baldwin, A. B. P. Lever and R. V. Parish, *Inorg. Chem.* 1969, **8**, 107.

Polyhedron Vol. 1, No. 4, pp. 383–386, 1982
Printed in Great Britain.

0277-5387/82/040383-04$03.00/0
Pergamon Press Ltd.

LIQUID–LIQUID PARTITION COEFFICIENTS OF *CIS*- AND *TRANS*-TRIS(1,1,1-TRIFLUORO-2,4-PENTANEDIONATO)CHROMIUM(III) BETWEEN DODECANE AND VARIOUS POLAR SOLVENTS

NOBUO SUZUKI,* MUTSUKO ITOH and HITOSHI WATARAI
Department of Chemistry, Faculty of Science, Tohoku University, Sendai 980, Japan

(*Received* 8 *December* 1981)

Abstract—Partition coefficients of *cis*-$Cr(tfa)_3$ and *trans*-$Cr(tfa)_3$ between dodecane and 12 polar solvents immiscible with dodecane were determined at 25°C. The partition coefficients of the *trans* isomer were slightly larger than those of the *cis* isomer. Solvent effect on the order of magnitude of the partition coefficient was discussed in terms of cavity formation energy.

INTRODUCTION

The liquid–liquid partition coefficient of metal chelate is one of the principal factors governing the extraction constant in chelate extraction and a systematic study on the liquid–liquid partition coefficient is necessary for the elucidation of the extraction mechanism. However, reliable partition coefficient data are not much in evidence at present. In particular, the partition coefficient of a geometric isomer of metal chelate has not yet been given. On the role of solvents composing two-phase systems, many studies have been reported, but most of them have concerned the solvent effect of the inert solvent phase.[1] Systematic studies on the role of the polar solvent phase is necessary for the meaningful discussion of the solvent effect of partition system. Recently, we have investigated the polar solvent effect of aqueous mixed solvent such as water–dimethyl sulfoxide, water–ethylene glycol and water–acetonitrile, on the partition equilibrium of β-diketone and its metal chelate, and reported the correlation of the partition coefficient with the internal pressure of the mixed solvent.[2] In this approach the importance of a solvophobic effect in the polar phase was clearly demonstrated.

In the present study, we determined the partition coefficients of *cis* and *trans* isomers of *tris*(1,1,1-trifluoro - 2,4 - pentanedionato)chromium(III) or *tris*(trifluoroacetylacetonato)chromium(III), $Cr(tfa)_3$, between dodecane and 12 polar solvents immiscible with the inert solvent. The purpose of this study is to examine (1) the solvent effect of the polar solvent phase and (2) the partition behaviour of two different geometric isomers, *cis* and *trans* forms.

EXPERIMENTAL

Chemicals. $Cr(tfa)_3$ was synthesized from chromium chloride and trifluoroacetylacetone according to the method reported by Fay *et al.*[3] The crude product was purified by chromatography on silica gel-benzene system. Mutual separation of *cis*- and *trans*-$Cr(tfa)_3$ was made by utilizing the differences in solubility in organic solvent and in elution volume in adsorption chromatography of the isomers. Reversed-phase chromatography on LiChrosorb RP-8 (Varian, E. M. Lab.) column was not effective for the separation of the isomers. *cis*-$Cr(tfa)_3$, which is present to *ca.* 20% in the synthesized product, was extracted with benzene from the solid mixture since it was more soluble than the *trans* isomer, and purified on silica gel column eluting with hexane–benzene (7:3) mixture. But a complete removal of *trans* isomer from *cis* isomer was difficult. The residual solid was recrystallized in hexane–benzene mixture, and *trans* isomer was obtained pure. The yield of *cis* isomer was highly improved through transformation by refluxing *trans* isomer dissolved in *o*-dichlorobenzene at 180°C for several hours. The compounds obtained were identified by means of elemental analysis. The purity of the isomers was determined by the silica-gel chromatography. Figure 1 shows the elution curves of the final products of the *cis* and *trans* isomers. The purity of the *trans* isomer was satisfactory but the *cis* isomer was found to contain 10.8% *trans* isomer. In the partition experiment of *cis* isomer, the contamination of *trans* isomer was corrected. Dodecane (Kanto, G. R.) was treated with fuming sulphuric acid and then distilled under reduced pressure or purified by passing through activated alumina column. N,N-Dimethylacetamide, acetonitrile, dimethyl sulfoxide, dimethyl formamide, propylene-1,2-carbonate, methanol, ethylene glycol and formamide, all G.R. grade reagent, were purified by distillation under reduced pressure after drying

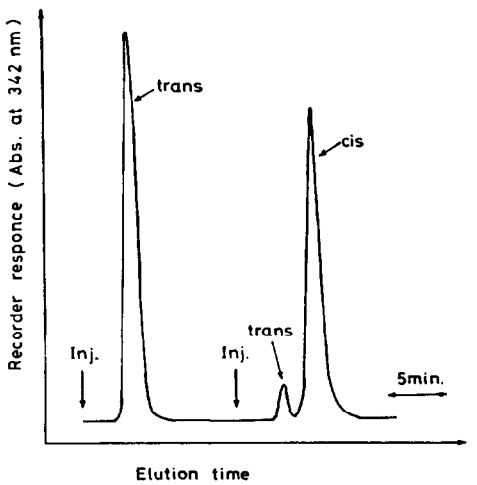

Fig. 1. Analysis of *cis*- and *trans*-$Cr(tfa)_3$ by liquid chromatography. Column; 17.5 cm × 4 mm I.D. packed with silica gel. Solvent; 7:3 hexane–benzene. Flow rate; 1.0 ml/min.

*Author to whom correspondence should be addressed.

on calcium hydride or molecular sieves 4A. Diethylene glycol, triethylene glycol and benzyl alcohol, G.R. grade reagent, were used without further purification. Redistilled water was used.

Measurement of partition coefficient. Partition experiment was carried out by stirring dodecane solution of $Cr(tfa)_3$ with polar solvent by magnetic stirrer in a glass stoppered vessel immersed in thermostated water bath at 25 ± 0.1°C. Within 5 min, the equilibrium was essentially attained, so that the stirring time of 1.5–3 hr was usually adopted. The volume ratio of the two phases was varied from 5/8 to 8/1 depending on the partition coefficient in order to facilitate the photometric determination of dodecane phase. For methanol, ethylene glycol and benzyl alcohol systems, in which volume change of a few per cent was observed in a preliminary partition experiment, the solvents mutually saturated with dodecane were used. Decomposition or *cis-trans* isomerization of $Cr(tfa)_3$ in the polar solvents was not observed even after 1 day. After centrifugation, the absorbance of the dodecane phase was measured at the absorption maximum wavelength of 343 nm at which *cis* and *trans* isomers show the equal molar extinction coefficient of $1.18 \times 10^4\ mol^{-1}\,l\,cm^{-1}$.

Partition coefficients of *trans*-$Cr(tfa)_3$ and *cis*-$Cr(tfa)_3$ in the presence of minute amounts of *trans* isomer were calculated from the next equations, respectively,

$$K_{D,trans} = \frac{A_{dod}}{A_{init} - A_{dod}} \cdot \frac{V_{polar}}{V_{dod}} \qquad (1)$$

$$K_{D,cis} = \frac{0.108K_{D,trans}A_{init} - \{K_{D,trans} + (V_{polar}/V_{dod})\}A_{dod}}{\{1 + K_{D,trans}(V_{dod}/V_{polar})\}(A_{dod} - 0.892A_{init}) - 0.108K_{D,trans}(V_{dod}/V_{polar})\}A_{init}} \qquad (2)$$

where A_{init} and A_{dod} are the absorbance of dodecane solution before and after partitioning, and V_{dod} and V_{polar} are the volumes of dodecane phase and polar phase.

For dodecane/water system, the partition coefficient was estimated as the ratio of the solubilities of the complex in dodecane and in water because of large partition coefficient and low solubility of the complex. Solubility was determined from photometric measurement of $Cr(tfa)_3$-saturated solution. Spectrophotometric measurement was carried out by means of Hitachi 356 or JASCO UVIDEC-2 spectrophotometer.

RESULTS

The observed partition coefficients of *cis*- and *trans*-$Cr(tfa)_3$, average values of at least four measurements, are listed in Table 1. In almost solvent systems, the partition coefficients are less than unity; this suggests higher solute-solvent interaction in polar phase. The partition coefficients for *trans* isomer is slightly larger than those for *cis* isomer in most systems. It is interesting that the difference in the partition coefficients of the *cis* and *trans* isomers is not so remarkable in every solvent pair and this must be compared with the quite large difference in the solubility of two isomers into a solvent; solubilities of *trans* isomer, 5.14×10^{-4} M in dodecane and 1.33×10^{-7} M in water, solubilities of *cis* isomer, 1.11×10^{-3} M in dodecane and 3.75×10^{-7} M in water.

DISCUSSION

Solvent effect on the partition coefficient

The partition coefficient does not show any satisfactory correlation with the solvent properties relating to solvent polarity, such as dielectric constant and dipole

Table 1. Partition coefficients of *trans*-$Cr(tfa)_3$ and *cis*-$Cr(tfa)_3$ at 25°C

No.	Solvent	Surface tension[a]	Partition coefficient[b]	
			trans	cis
1.	Triethylene glycol	45.2	0.317 ± 0.020	0.276 ± 0.022
2.	N,N-Dimethylacetamide	32.43	0.00870 ± 0.00077	0.00898 ± 0.00070
3.	Acetonitrile	29.3	0.00491 ± 0.00029	0.00436 ± 0.00021
4.	Dimethyl sulfoxide	46.2	0.0139 ± 0.0004	0.0106 ± 0.0004
5.	Dimethylformamide	35.2	0.00526 ± 0.00018	0.00321 ± 0.00044
6.	Benzyl alcohol	39.96	0.0682 ± 0.0015	0.0729 ± 0.0016
7.	Diethylene glycol	48.5	0.489 ± 0.019	0.433 ± 0.032
8.	Propylene-1,2-carbonate	38.3	0.0215 ± 0.0005	0.0128 ± 0.0007
9.	Methanol	22.6	0.0178 ± 0.0005	0.0150 ± 0.0001
10.	Ethylene glycol	46.49	10.1 ± 0.9	8.35 ± 0.79
11.	Formamide	58.2	13.6 ± 2.45	3.65 ± 0.09
12.	Water	72.8	3.86×10^3 [c]	2.96×10^3 [c]

a) Dynes cm^{-1}. For dodecane, 24.91 dynes cm^{-1}.

b) $K_D = C_{dod} / C_{polar}$.

c) Calculated from solubility, $3.86 \times 10^3 = 5.14 \times 10^{-4}$ M / 1.33×10^{-7} M for trans isomer and $2.96 \times 10^3 = 1.11 \times 10^{-3}$ M / 3.75×10^{-7} M for cis isomer.

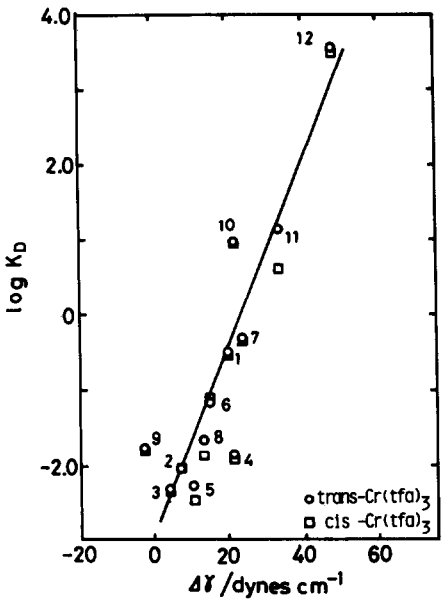

Fig. 2. Correlation between partition coefficient and the difference in surface tension, $\Delta\gamma = \gamma_{polar} - \gamma_{dod}$. Numbers in this figure correspond to those in Table 1.

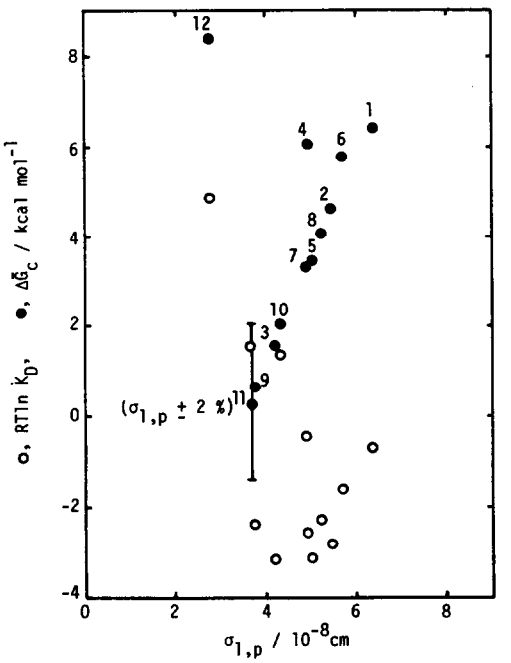

Fig. 3. Free energy changes for the partition of $Cr(tfa)_3$ and hard sphere cavity of $\sigma_2 = 9.48 \times 10^{-8}$ cm in dodecane(n)/polar solvent(p) systems; $\sigma_{1,n} = 7.57 \times 10^{-8}$ cm. The range in $\Delta\bar{G}_c$ indicated in the figure corresponds to 2% error in $\sigma_{1,p}$. Solvent numbers shown in this figure correspond to those in Table 1.

moment. But, with the surface tension of the polar solvent a good linear correlation was obtained. In Fig. 2, log K_D of the complexes are shown against the difference in surface tension between dodecane and polar solvent. The surface tension data used are listed in Table 1. The partition coefficient increases with increase in surface tension of the polar phase. This strongly suggests the contribution of cavity formation work in the partition process.[4]

The free energy change accompanied by the partition of the complex from dodecane to polar solvent can be represented by,

$$RT \ln K_D = (\bar{G}_c + \bar{G}_i)_{polar} - (\bar{G}_c + \bar{G}_i)_{nonpolar} = \Delta\bar{G}_c + \Delta\bar{G}_i \quad (3)$$

where $\bar{G}_c$ and $\bar{G}_i$ refer to the free energy contributions of cavity formation energy and interaction energy. In the present study, $\bar{G}_c$ was calculated according to the Scaled Particle theory[5,6] and was compared with $RT \ln K_D$. The equation for $\bar{G}_c$ has been given as[5],

$$\bar{G}_c = -RT\ln(1-y) + RT\frac{3y}{1-y}\left(\frac{\sigma_2}{\sigma_1}\right) + RT\left[\frac{3y}{1-y} + \frac{9}{2}\left(\frac{y}{1-y}\right)^2\right]\left(\frac{\sigma_2}{\sigma_1}\right)^2 + \frac{NyP}{\rho}\left(\frac{\sigma_2}{\sigma_1}\right)^3 \quad (4)$$

$$y = \pi\rho\sigma_1^3/6$$

where ρ is the number density of the solvent, σ the molecular diameter, and subscripts 1 and 2 refer to solvent and solute. For the calculation of $\Delta\bar{G}_c$, the data of hard sphere diameters of polar and nonpolar solvent molecules, σ_1, and solute molecule, σ_2, are required. The values of σ_1 for solvent used in the present study were estimated from an empirical linear relation between literature values of σ_1 for commonly used solvent and (molar volume)$^{1/3}$.[7] The value of $\sigma_2 = 9.48 \times 10^{-8}$ cm for $Cr(tfa)_3$ was calculated using the approximated relation between the potential minimum distance, r_0, and molecular diameter σ in Lennard-Jones potential function, $r_0 \simeq 1.122\ \sigma$[8] with the estimated molar volume of 379 cm^3 mol^{-1}.[9] The calculated $\Delta\bar{G}_c$, which is identical value for the two isomers, are shown in Fig. 3 as a function of σ_1, along with $RT \ln K_D$ of *trans* isomer. It is noted in Fig. 3 that $\Delta\bar{G}_c$ and $RT \ln K_D$ show a similar dependence on σ_1 of polar solvent. This indicates the importance of the cavity formation energy, that is, the order of magnitude of the partition coefficient is governed by that of cavity formation energy. The energy difference of about 5 kcal mol^{-1} between $\Delta\bar{G}_c$ and $RT \ln K_D$, noted in Fig. 3 irrespective of polar solvents, is ascribable to a solvation of $Cr(tfa)_3$ in polar solvent phase. Preferential solvation of polar solvents such as methanol, dimethyl sulfoxide and acetonitrile to *tris*(acetylacetonato)chromium(III) through its octahedral face was reported recently by means of NMR line broadening experiments.[10]

Stereochemical effect of cis *and* trans *isomers.* It is interesting that the difference in the partition coefficients between *cis* and *trans* isomers is only slight, nevertheless the solubility of *cis* isomer into dodecane or water are about 2–3 times higher than that of *trans* isomer into the same solvent. From the solubilities of isomer into dodecane determined in the present study and the partition coefficients, solubilities into the other polar solvents and solution free energy difference, $\Delta G_{s,cis-trans}$, were calculated according to the next equations,

Table 2. Estimated solubilities of *trans*-$Cr(tfa)_3$ and *cis*-$Cr(tfa)_3$ at 25°C.

No.	Solvent	Solubility, mol/l		$\Delta G_{s,cis-trans}$ kcal/mol
		trans	cis	
1	Triethylene glycol	1.62×10^{-3}	4.02×10^{-3}	-0.538
2	N,N-Dimethylacetamide	5.91×10^{-2}	1.24×10^{-1}	-0.437
3	Acetonitrile	1.05×10^{-1}	2.25×10^{-1}	-0.526
4	Dimethyl sulfoxide	3.70×10^{-2}	1.05×10^{-1}	-0.617
5	Dimethylformamide	9.77×10^{-2}	3.45×10^{-1}	-0.749
6	Benzyl alcohol	7.54×10^{-3}	1.52×10^{-2}	-0.419
7	Diethylene glycol	1.05×10^{-3}	2.56×10^{-3}	-0.528
8	Propylene-1,2-carbonate	2.39×10^{-2}	8.67×10^{-2}	-0.763
9	Methanol	2.89×10^{-2}	7.40×10^{-2}	-0.557
10	Ethylene glycol	5.09×10^{-5}	1.33×10^{-4}	-0.569
11	Formamide	3.78×10^{-5}	3.04×10^{-4}	-1.235
12	Water	1.33×10^{-7a}	3.75×10^{-7a}	-0.613
13	Dodecane	5.14×10^{-4a}	1.11×10^{-3a}	-0.456

a) Observed value in this work.

$$S_p = S_{dod}/K_D \quad (5)$$

$$\Delta G_{s,cis-trans} = RT \ln (S_{p,trans}/S_{p,cis}) \quad (6)$$

where S_p and S_{dod} correspond to solubilities into polar solvent and dodecane. The calculated results are listed in Table 2. Solvent effect in $\Delta G_{s,cis-trans}$ is found to be less important nevertheless the solubility varies over the range of 10^{-7}–10^{-1} M depending on the solvent. This result is consistent with ΔG_s for another set of different metal chelate and solvents estimated from solubility data of $Co(tfa)_3$ available in literature,[3] which gives $\Delta G_{s,cis-trans}$ at 25°C (kcal mol^{-1}); −0.553 in cyclohexane, −0.572 in benzene and −0.772 in ethanol. Difference in dipole moments of *trans* and *cis* isomers, reported as 3.80D and 6.48D for $Co(tfa)_3$,[11] seems not to play a dominant role in $\Delta G_{s,cis-trans}$. When we recall that $\Delta G_{s,cis-trans}$ is the sum of the differences in sublimation energy and in solution energy between *cis* and *trans* isomers, the slight solvent dependence of $\Delta G_{s,cis-trans}$ seems to reflect the difference in sublimation energy of the isomers (see m.p. of *trans* isomer is higher than that of *cis* isomer) as well as that in electrostatic interaction energy expected from the difference in dipole moment.

The present discussion gives also an explanation to the small solvent dependence observed in *cis–trans* equilibrium in solution;[12,13] the reported *cis–trans* equilibrium constants of *tris*-trifluoroacetylacetonates defined as [*trans*]/[*cis*] are in the range of 4–6 slightly depending on the solvent and the central metal ion. The fact that *trans* isomer is more stable than *cis* in equilibrium is not consistent with the solubility data which suggests *cis* isomer to be more stable. The equilibrium constant is governed by intermolecular energy as well as intermolecular energy in general. Hence, it is proposed that the *cis–trans* equilibrium is primarily governed by the difference in intermolecular free energy which includes entropy of geometric conformation favourable to *trans* isomer. In addition, the present results may explain the reason why the separation of *cis* and *trans* isomers may be achieved on silica gel, but not on a chemically bonded C-8 column. The latter system will be essentially similar to a liquid–liquid partition system and the separation between isomers may be difficult. It will be more promising for the separation to utilize the stronger afinity to silica surface expected for the *cis* isomer because it possesses the most hydrophilic octahedral face including three acetyl groups.

REFERENCES

[1] H. Irving, *Ion Exchange and Solvent Extraction* (Edited by J. A. Marinsky and Y. Marcus), Vol. 6, p. 139. Marcel Dekker, New York (1974).

[2] H. Awano, H. Watarai and N. Suzuki, *J. Inorg. Nucl. Chem.* 1979, **41**, 124; *Ibid.* 1980, **42**, 1516.

[3] R. C. Fay and T. S. Piper, *J. Am. Chem. Soc.* 1963, **85**, 500.

[4] N. Suzuki, T. Yoshida and H. Watarai, submitted for publication to *Bull. Chem. Soc. Jpn.*

[5] R. Pierotti, *Chem. Rev.* 1976, **76**, 717. *J. Phys. Chem.* 1963, **67**, 1840; 1965, **69**, 281.

[6] H. Watarai, M. Tanaka and N. Suzuki, to be published.

[7] E. Wilhelm and R. Battino, *J. Chem. Phys.* 1971, **55**, 4012.

[8] J. E. Lennard-Jones, *Proc. Roy. Soc.* 1924, **A106**, 463.

[9] W. R. Walf, R. E. Sievers and G. H. Brown, *Inorg. Chem.* 1972, **11**, 1995.

[10] G. S. Vigee and C. L. Watkins, *Inorg. Chem.* 1977, **16**, 709.

[11] R. A. Palmer, R. C. Fay and T. S. Piper, *Inorg. Chem.* 1964, **3**, 875.

[12] M. Yamazaki and T. Takeuchi, *Nippon Kagaku Zasshi* 1970, **91**, 965.

[13] C. Kutal and R. Sievers, *Inorg. Chem.* 1974, **13**, 897.

Polyhedron Vol. 1, No. 4, pp. 387–392, 1982
Printed in Great Britain.

0277-5387/82/040387-06$03.00/0
Pergamon Press Ltd.

SYNERGIC EFFECT OF SOME HETEROCYCLIC BIDENTATE AMINES ON THE EXTRACTION OF ZINC WITH 2-THENOYLTRIFLUOROACETONE

CORRELATION BETWEEN FORMATION CONSTANTS OF AMINE-COMPLEX IN ORGANIC AND AQUEOUS PHASES

YOSHIKAZU KIKUTA, HITOSHI WATARAI and NOBUO SUZUKI*
Department of Chemistry, Faculty of Science, Tohoku University, Sendai, 980 Japan

(*Received* 8 *December* 1981)

Abstract—Synergistic effects of seven bidentate amines S; 2,2'-bipyridyl, 1,10-phenanthroline and its derivatives, on the extraction of zinc(II) with 2-thenoyltrifluoroacetone, HTTA, in benzene were investigated at 25°C. Addition of the amines even at low concentration ($<10^{-5}$ M) caused a remarkable improvement in distribution ratio, while at higher concentration a lowering of the distribution ratio was observed because of masking effect of amines in aqueous phase. Slope analysis of the distribution curves, taking into account free amine concentration in the organic phase, showed that the dominant extracted species is $Zn(TTA)_2S$ in every system. The adduct formation constants obtained was found to be correlated with the formation constant of ZnS^{2+} in aqueous solution rather than the acid dissociation constant of the conjugate acid of the amine.

INTRODUCTION

Since a synergistic effect was observed in the extraction of uranyl ion,[1] many investigations have been carried out on this subject.[2] Synergistic ligands commonly investigated are phosphoric esters and pyridine derivatives acting as monodentate ligands. General properties common to these synergistic ligands seems to be their strong coordination ability to metal ions and high lipophilicity or hydrophobicity. However, we have not enough information on the factors governing the synergism, except reaction stoichiometry or qualitative discussion on ligand basicity. Recently a large synergistic effect of bidentate amines such as 2,2-bipyridyl and 1,10-phenanthroline was observed,[3] but not thoroughly investigated compared with monodentate ligand systems. Further investigation to assess the advantages of bidentate amines seemed worthwhile.

In the present study, synergistic effects of a series of bidentate amines on the extraction of zinc(II) with 2-thenoyltrifluoroacetone (HTTA) were systematically investigated. Our main interest concerned which property, basicity or hydrophobicity, of the amine plays a dominant role in the synergistic effect. Adduct formation constants were determined and discussed in comparison with the acid dissociation constants of the conjugate acid of the amines and the formation constant of metal-amine complex which are considered as measure of basicity of amine and with the liquid–liquid partition constants of amines as measure of hydrophobicity.

EXPERIMENTAL

Chemicals. 2-Thenoyltrifluoroacetone (Dotite, G.R.) was purified by vacuum sublimation at 36°C. 1,10-Phenanthroline (phen) (Dotite, G.R.) was purified as monohydrate form by recrystallization from aqueous solution. Bipyridyl (bipy), 5-methylphenanthroline (5MP), 4,7-dimethylphenanthroline (4,7DMP), 2,9-dimethylphenanthroline (2,9DMP), 2,9-dimethyl-4,7-diphenylphenanthroline (2,9DM4, 7DPP), and 4,7-diphenylphenanthroline (4,7DPP) (Tokyo Kasei and Dotite, G.R.) were used without further purification. Benzene, used as the organic solvent, was purified by distillation after acid washing. $^{65}Zn(II)$ tracer was obtained from New England Nuclear Corporation as a solution of $ZnCl_2$ in 0.5 M HCl. Stock solution of $^{65}Zn(II)$ was prepared by repeated evaporation with 0.1 M $HClO_4$ to eliminate HCl and the resulting $^{65}Zn(II)$ tracer was diluted with 0.1 M $HClO_4$. The resulting tracer concentration was 2×10^{-7}–10^{-6} M and the total concentration of Zn^{2+} was kept 3.5×10^{-6} M or less by the addition of an inactive Zn^{2+} solution. Sodium perchlorate commercially available as G.R. grade was purified by recrystallization three times from aqueous solution and dried at 260°C for 2 days. Sodium chloride (Wako, G.R.) was used as purchased form. All experiments was run at constant ionic strength, 1.0 or 0.5 M adjusted with sodium perchlorate and sodium chloride respectively. Aqueous phase was buffered with 0.004 M sodium acetate.

Distribution of Zn(II). Five ml of organic solution of TTA and an amine was shaken with an equal volume of the aqueous solution of zinc adjusted to desired pH in a thermostated room at 25 ± 0.5°C over 13 hr. After centrifugation, 2 ml portion of each phase was removed into a polyethylene tube and the radioactivity was counted to at least 1% accuracy on a NaI(Tl) scintillation counter. The equilibrium pH of the aqueous phase was carefully measured by a glass electrode.

Distribution of the amines. Distribution ratios of the amines between benzene and aqueous phase were obtained by batch method in the same experimental condition with zinc distribution. From distribution ratio observed as a function of pH, a partition coefficient was determined together with an acid dissociation constant of a conjugate acid.

RESULTS

The extraction processes of the zinc–TTA chelate may be expressed as follows:

$$Zn^{2+} + pA^- + qS \overset{\beta_{pq}}{\rightleftharpoons} ZnA_pS_q^{(2-p)+} \quad (1)$$

$$ZnA_2 \overset{K_{DC}}{\rightleftharpoons} ZnA_2(o) \quad (2)$$

*Author to whom correspondence should be addressed.

$$S \overset{K_{DS}}{\rightleftharpoons} S(o) \quad (3)$$

$$ZnA_2(o) + mS(o) \overset{\beta_{s,m}}{\rightleftharpoons} ZnA_2S_m(o) \quad (4)$$

where A^- and S stand for the enolate ion of HTTA and the amine, respectively. The mark of (o) refers to organic phase. In eqn (1) which includes all of the dominant complex formation reactions in aqueous phase, β_{p0} and β_{0q} correspond to the formation constants of $ZnA_p^{(2-p)+}$ and ZnS_q^{2+} respectively.

The distribution ratio of zinc in the absence of the amine, D_M, is given by:

$$D_M = \frac{K_{DC}\beta_2[A^-]^2}{1+\sum \beta_{p0}[A^-]^p}. \quad (5)$$

The distribution ratio in the presence of the amine, D_{MS}, is written as follows under the assumption that the formation of an additional complex with excess TTA, e.g. ZnA_2jHA or ZnA_2jHAS_m, is negligible,

$$D_{MS} = \frac{K_{DC}\beta_2[A^-]^2(1+\Sigma\beta_{s,m}[S]_o^m)}{1+\sum_{p,q} \beta_{pq}[A^-]^p[S]^q}. \quad (6)$$

Under the same concentration of $[A^-]$, the ratio of D_{MS}/D_M is written in logarithmic form as:

$$\log \frac{D_{M,S}}{D_M} = \log\left(1+\sum \beta_{s,m}[S]_o^m\right) + \log\left(\frac{1+\sum \beta_{p0}[A^-]^p}{1+\sum \beta_{pq}[A^-]^p[S]^q}\right). \quad (7)$$

The second term in the right hand side of eqn (7) is a correction term for a water soluble complex formation of Zn^{2+} including a competitive masking of Zn^{2+} with S.

Distribution of zinc chelate. Distribution ratio of zinc with 0.5 M HTTA in the absence of the amine was measured varying pH of aqueous phase in the range from 3.9 to 5.0. Slope analysis of log D_M vs pH plot indicated $Zn(TTA)_2$ to be extracted and a contribution of $ZnTTA^+$ to be negligibly small; this is consistent with the previous result.[4]

In the presence of amine, the distribution of zinc was greatly improved. Figure 1 shows the distribution ratio of zinc with HTTA against the initial amine concentration, $[S]_{o,init}$, in logarithmic scale. It is noteworthy that in phen, bipy and 5MP systems, the rapid increase of the distribution ratio in the low concentration region of amines is followed by the lowering of the distribution ratio in higher concentration of amine.

Extraction of zinc with amine alone was done in order to check the possible contribution of ion-pair extraction to the observed enhancement of the distribution ratio in the synergistic systems. With bipy alone no observable amount of zinc was extracted from 1.0 M $NaClO_4$ into the organic phase. For phen system, 3% of zinc was extracted with organic phase containing 10^{-4} M phen, but, from the mass balance examination by radiocounting measurement, over 70% of zinc was removed from the aqueous phase as insoluble compounds. Influence of $NaClO_4$ concentration, in the synergic system of HTTA-phen or -bipy, was examined; no appreciable change in

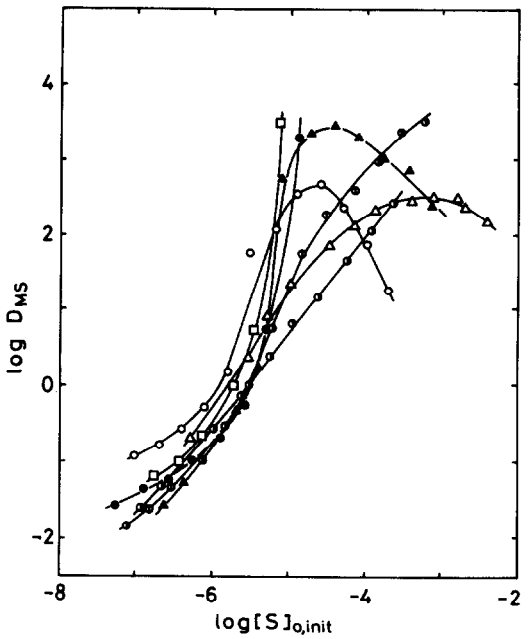

Fig. 1. Improvement of the distribution ratio of zinc with HTTA by addition of bidentate amines; ○, phen (pH = 4.0); △, bipy (pH = 4.1); □, 4.7DPP (pH = 3.7); ◑, 2.9DMP (pH = 3.9); ●, 4,7DMP (pH = 3.8); ▲, 5MP (pH = 3.7); ⊕, 2,9DM4,7DPP (pH = 3.7). [HTTA] = 0.05 M.

the distribution ratio of zinc in the concentration range of 10^{-6}–10^0 M $NaClO_4$ was observed. With the more hydrophobic amine of 4,7DPP, a quantitative ion-pair extraction was observed at the same $NaClO_4$ concentration and amine concentration above 3×10^{-5} M, but in another salt anion system, Zn^{2+} – 4,7DPP – 0.5 M NaCl, the extraction of zinc was depressed about two orders of magnitude. From these results it was concluded that the remarkable increase of the distribution ratio shown in Fig. 1 was due to a synergistic effect rather than ion-pair extraction.

Partition coefficients of the amines. The distribution ratio of the amine, D_S, in benzene/water system was observed as a function of pH of aqueous phase. The results for bipy, phen, 5MP, 4,7DMP and 2,9DMP are plotted in Fig. 2. The curves show a typical distribution profile for a monoacidic base and represented by the next equation:

$$\log D_S = \log K_{DS} - \log(1+[H^+]/K_{HS}) \quad (8)$$

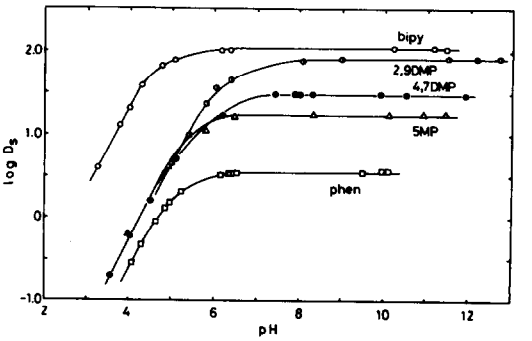

Fig. 2. Distribution curves of the amines in benzene/aqueous phase system.

where K_{HS} is dissociation constant of the conjugated acid of amine. Analysis of the distribution data based on eqn (8) gave $\log K_{DS}$ and pK_{HS} ($= -\log K_{HS}$), which are listed in Table 1. For 4,7DPP, because of its very low solubility in the aqueous phase, the partition coefficient was estimated by introducing the distribution ratio at low pH and literature value of K_{HS} into eqn (8).

Data analysis of synergic extraction. The dependencies of pH and HTTA concentration on the synergic extraction of zinc were examined. The experimental results for bipy and phen systems are shown in Figs. 3 and 4. The slopes in these figures are close to two in every case and this suggests, according to eqn (6), the mole ratio of TTA and zinc incorporated in the extracted species to be 2:1.

In the synergistic system provided that $[S]_o + [S] \gg q[ZnA_pS_q^{(2-p)+}] + m[ZnA_2S_m]_o$ holds, it is expected from eqn (6) that a linear correlation between $\log D_{MS}$ and $\log [S]_{o,init}$ should be observed and the slope correspond to the number of S molecules incorporated in the adduct complex. But, the rapid increase of the distribution ratio observed in Fig. 1 does not show a straight line corresponding simply to a limited number of amine molecules coordinated to $Zn(TTA)_2$ in the organic phase. Then, to suppress the formation of $ZnA_pS_q^{(2-p)+}$ and ZnA_2S_m, the synergistic extraction at low pH and HTTA concentration than the condition of Fig. 1 was examined. The results are shown in Figs. 5(a) and (b) for phen and 4,7DPP systems, respectively. These figures clearly show that the slopes of $\log D_{MS}$ vs $\log [S]_{o,init}$ are close to unity at low pH and low HTTA concentration. This means the adduct complex in the organic phase to be $Zn(TTA)_2S$ in these regions. Adduct formation constants were obtained, according to eqn (7), from $\log (D_{MS}/D_M) - \log \alpha$ vs $\log [S]_o$ plot, where $\log \alpha$ refer to the correction

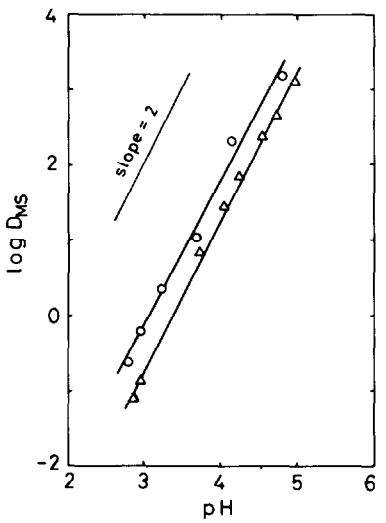

Fig. 3. Correlation between the distribution ratio of zinc and pH in the presence of bipy (△) and phen (○); [bipy] = 1.46×10^{-5} M, [phen] = 3.1×10^{-6} M, [HTTA] = 0.05 M, I = 1.0 M by (Na, H)ClO_4.

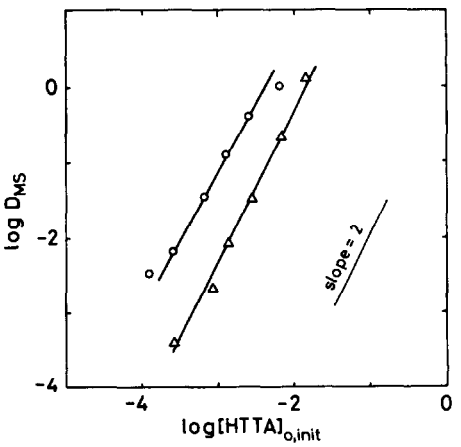

Fig. 4. Correlation between the distribution ratio of zinc and initial concentration of HTTA in the presence of bipy (△) and phen (○); [bipy] = 1.46×10^{-5} M, [phen] = 3.1×10^{-6} M. Aqueous phase; pH = 3.85, I = 1.0 M by (Na, H)ClO_4.

Table 1. Equilibrium data in synergistic extraction system of Zn-TTA-amine-benzene

Amine	$\log \beta_{s,1}$	$\log K_{DS}$	pK_{HS}	$\log K_S^{ex}$	V_M[a] ($cm^3\ mol^{-1}$)	$\log \beta_{01}$
bipy	8.38	2.03	4.72	5.52	92	4.89[d]
phen	10.2	0.57	5.15	4.41	151	6.36[e]
5MP	10.6	1.24	5.35	5.22	165	6.62[f]
4,7DMP	10.9	1.49	5.65	5.49	178	6.90[g]
4,7DPP	10.3	5.7[b]	4.84	10.31	243	5.69[h]
2,9DMP	8.15	1.83	6.25	5.88	178	4.1 [i]
2,9DM4,7DPP	9.2	(ca. 7.0)[c]	---	---	270	--

a) Estimated molar volume from V_M of phenanthrene (151 $cm^3\ mol^{-1}$) and van der Waals volume of phenyl (45.84 $cm^3\ mol^{-1}$) and methyl (13.67 $cm^3\ mol^{-1}$) groups.

b) Estimated value from D_S at low pH.

c) Estimated value based on the linear relationship between $\log K_{DS}$ and V_M for phen derivatives.

d) Ref. 5. e) Ref. 6. f) Ref. 7. g) Ref. 8 h) Ref. 9. i) Ref. 10.

term in the equation. The correction term for masking effect by the amine was calculated by the use of available data of formation constant between zinc ion and amine in aqueous solution.[5-10] Adduct formation constants for the seven amines are listed in Table 1 together with other equilibrium data.

DISCUSSION

Mechanism of the synergistic extraction. The distribution ratio of zinc with TTA was extremely enhanced by addition of the amines; bipy, phen and its derivatives (see Fig. 1). The synergistic effect is expected to be caused by a formation of more soluble complex in the organic phase than the simple complex $Zn(TTA)_2$. So, the determination of composition of the adduct complex is necessary in order to elucidate the synergistic extraction mechanism.

On the composition of adduct complex of $Zn(TTA)_2$ with monodentate base, only $Zn(TTA)_2S$ complex has been reported previously and this is different from the cases of $Co(TTA)_2$ and $Ni(TTA)_2$, in which $Co(TTA)_2S_2$ and $Ni(TTA)_2S_2$ were observed.[11] On the adduct with bidentate base, Kassierer and Kertes reported a formation of $Zn(TTA)_2$bipy complex in benzene/water system.[3] Concerning the Zn-phen system, although no extraction data was available, some spectral data of $Zn(TTA)_2$phen was reported.[12]

In the present study, the adduct complex in the organic phase was concluded to be $Zn(TTA)_2S$ for every amine system. In Fig. 5(a), $\log D_{MS}$ of phen system decreases over 10^{-5} M amine concentration, through a maximum value, with a slope of nearly two with respect to $\log [S]_{o,init}$. Since ZnS_3^{2+} is formed in aqueous phase at the higher concentration of amine,[6] the slope of -2 strongly supports the presence of mono-coordinated species in the organic phase. The structure of $Zn(TTA)_2S$ is expected to be octahedral from the IR spectral data.[12] Then, the adduct formation reaction of eqn (4) will be accompanied by a structural change of TTA coordination from square planar to octahedral.

Factors governing the synergistic effect. To symplify the discussion, when the formation of water soluble complex in the synergic extraction system is neglected, eqn (7) is transformed to,

$$D_{MS}/D_M = 1 + \beta_{s,1}[S]_o \qquad (9)$$

where D_{MS}/D_M is considered as a measure of synergic effect. If $[S]_o \gg [Zn(TTA)_2S]_o$, $[S]_o$ is nearly equal to $[S]_{o,init}/(1+K_{DS}^{-1})$. Then, eqn (9) is rewritten by,

$$D_{MS}/D_M = 1 + \beta_{s,1}[S]_{o,init}/(1+K_{DS}^{-1}). \qquad (10)$$

When $\beta_{s,1}[S]_o \gg 1$ in eqn (9), eqn (10) is simplified as,

$$\frac{D_{MS}}{D_M} = \frac{\beta_{s,1}}{1+K_{DS}^{-1}}[S]_{o,init}. \qquad (11)$$

From eqn (11), the order of D_{MS}/D_M for different amines can be compared with the order of $\beta_{s,1}(1+K_{DS}^{-1})^{-1}$ under the same initial concentration of amines. This provides a general principle that the larger $\beta_{s,1}$ and K_{DS} of the amine is, the greater the synergistic effect occurs. In the present systems where $\beta_{s,1} \gg 10^8$ and $K_{DS} > 1$, the ordering of the synergic effect of the amines is determined primarily by $\beta_{s,1}$; 4,7DMP > 5MP > 4,7DPP, phen > 2,9DM4,7DPP > bipy > 2,9DMP. The adduct formation

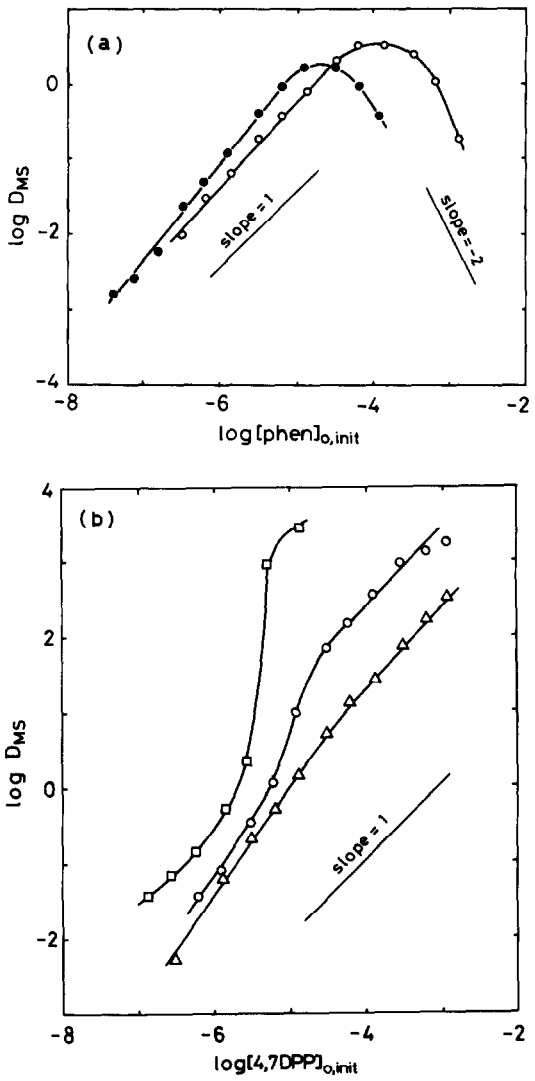

Fig. 5. Normal synergistic extraction curves at low pH or at low HTTA concentration. (a) Effect of phen: ●, [HTTA] = 0.002 M, pH = 3.8; ○, [HTTA] = 0.05 M, pH = 2.5. (b) Effect of 4,7DPP: □, [HTTA] = 0.05 M, pH = 3.70; ○, [HTTA] = 0.002 M, pH = 3.70; △, [HTTA] = 0.0004 M, pH = 3.70.

constants obtained for the bidentate amines are larger than those for TOPO ($\log \beta_{s,1} = 6.2$ in Zn–TTA-benzene[13]) known as a great synergistic ligand. The large adduct formation constant with the amine, especially with phen derivatives, may be due to the =N–C–C–N= grouping which tends to form five-membered rings with the central ion. Of the phen derivatives, 2,9DMP and 2,9DM4,7DPP give smaller adduct formation constants than other derivatives. This is explicable by considering a steric hindrance of the methyl groups at 2,9-carbon nearest to nitrogen atoms in the adduct formation reaction. The smaller complex formation constant reported for Zn-2,9DMP system in aqueous solution (see Table 1) supports this explanation.

The relative magnitude of $\beta_{s,1}$ for different amines is expected to relate to its basicity. It is pointed out that the increasing order of $\log \beta_{s,1}$ for different bases corresponds with the increasing basicity of the bases, and usually pK_{HS} of the conjugate acid of the base is compared with $\log \beta_{s,1}$.[14] Comparison of $\log \beta_{s,1}$ and pK_{HS}

shows only a slight proportionality between them, except for 2,9DMP system (Fig. 6a). A satisfactorily linear relationship between $\log \beta_{s,1}$ and $\log \beta_{01}$ in Table 1 was clearly obtained for the six amines including 2,9DMP as shown in Fig. 6(b). The empirical relationship is represented as,

$$\log \beta_{s,1} = 1.03 \log \beta_{01} + 3.80 \quad (12)$$

where $\beta_{s,1}$ and β_{01} refer to the formation constants for the next relations,

$$Zn(TTA)_2(o) + S(o) \rightleftharpoons Zn(TTA)_2S(o) \quad (13)$$

$$Zn^{2+} + S \rightleftharpoons ZnS^{2+}. \quad (14)$$

Equation (12) clearly shows the parallel relationship between the reactivities of amine in organic phase reaction of eqn (13) and in aqueous phase reaction of eqn (14). In addition, after an appropriate transformation $\beta_{s,1}$ can be related to β_{01} through the next type of equation:

$$\log \beta_{s,1} = \log \beta_{01} + \log \frac{[Zn(TTA)_2S]_o[Zn^{2+}]}{[Zn(TTA)_2]_o[ZnS^{2+}]} - \log K_{DS} \quad (15)$$

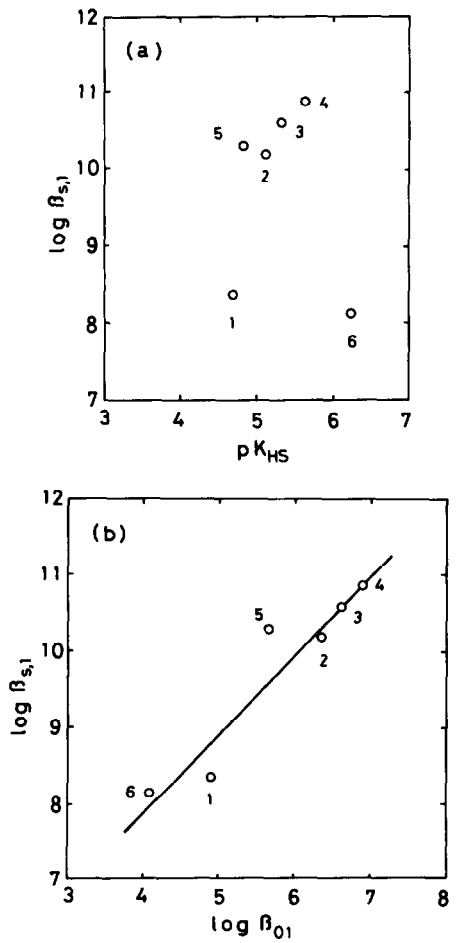

Fig. 6. Correlation of adduct formation constant with basicity of amine; (a) $\log \beta_{s,1}$ vs pK_{HS} and (b) $\log \beta_{s,1}$ vs $\log \beta_{01}$. Amines; (1) bipy, (2) phen, (3) 5MP, (4) 4,7DMP, (5) 4,7DPP, (6) 2,9DMP.

in which the second term in the right hand side can be replaced with exchange–extraction constant, K_S^{ex}, defined for the next equation,

$$Zn(TTA)_2(o) + ZnS^{2+} \rightleftharpoons Zn(TTA)_2S(o) + Zn^{2+}. \quad (16)$$

Equation (15) implies that $\beta_{s,1}$ is determined by β_{01} and K_S^{ex}/K_{DS}; the former reflects the basicity of S and the latter the difference in free energy of the processes of eqns (3) and (16). It is interesting to note that eqn (15) clearly supports the previously reported result that the organic solvent giving large K_{DS} is not always favourable to adduct formation.[15] The values of K_S^{ex} were calculated from eqn (15) as listed in the last column of Table 1.

Comparison of eqns (12) and (15) gives the next relation,

$$\log K_S^{ex} - \log K_{DS} = 3.8. \quad (17)$$

This relation indicates that the constant term in eqn (12) must be compared with $\log (K_S^{ex}/K_{DS})$.

Energetic consideration on the two processes of the partition and the exchange–extraction of amine gives the next free energy expression approximately,

$$-RT \ln K_{DS} = \Delta G(S)_o - \Delta G(S) \quad (18)$$

$$-RT \ln K_S^{ex} = \Delta G(ZnA_2S)_o + \Delta G(Zn^{2+}) - \Delta G(ZnA_2)_o - \Delta G(ZnS^{2+}) + \Delta G_v^{ex} \quad (19)$$

where ΔG refers to energy of solution of a given compound shown in parenthesis, ΔG_v^{ex} to the difference in bonding energy of S in eqn (16) in vapor phase and subscript o to organic phase. Assuming that the difference in number of water molecules hydrated to Zn^{2+} and ZnS^{2+} is 2, the energy difference of $\Delta G(Zn^{2+}) - \Delta G(ZnS^{2+})$ can be approximated by,

$$\Delta G(Zn^{2+}) - \Delta G(ZnS^{2+}) = 2\Delta G_h - \Delta G(S_c) \quad (20)$$

where ΔG_h and $\Delta G(S_c)$ refer to the hydration energy of Zn^{2+} per hydrated water molecule and the solution energy of the coordinated amine denoted as S_c, respectively. The difference of $\Delta G(ZnA_2S)_o - \Delta G(ZnA_2)_o$ will be approximated by,

$$\Delta G(ZnA_2S)_o - \Delta G(ZnA_2)_o = \Delta G(ZnA_2{}^a)_o + \Delta G(S_c)_o - \Delta G(ZnA_2)_o \quad (21)$$

where $\Delta G(ZnA_2{}^a)_o$ is the solution energy of ZnA_2 in adduct complex. If $\Delta G(ZnA_2{}^a)_o = \Delta G(ZnA_2)_o$ is assumed, eqn (19) is simplified as,

$$-RT \ln K_S^{ex} = 2\Delta G_h + \Delta G(S_c)_o - \Delta G(S_c) + \Delta G_v^{ex}. \quad (22)$$

From eqns (18) and (22), the next equation is derived,

$$RT \ln (K_S^{ex}/K_{DS}) = -2\Delta G_h + \Delta G(S)_o - \Delta G(S_c)_o - \Delta G(S) + \Delta G(S_c) - \Delta G_v^{ex}. \quad (23)$$

Assuming $\Delta G(S)_o = \Delta G(S_c)_o$ and $\Delta G(S) - \Delta G(S_c) =$

$\Delta G_h(S)$ where $\Delta G_h(S)$ is the hydration energy of the nitrogen atoms of the amine, we get the final equation,

$$\log K_S^{ex} - \log K_{DS} = -(2\Delta G_h + \Delta G_h(S) + \Delta G_v^{ex})/2.3RT. \quad (24)$$

Equation (24) shows that the constant value in eqn (17) is due to the hydration energies of zinc ion and amine and the bonding energy difference. From eqns (17) and (24), we can obtain the value of about -5 kcal/mol for $(2\Delta G_h + \Delta G_h(S) + \Delta G_v^{ex})$ at 25°C irrespective of amines. The present discussion gives additional suggestion that the effect of organic solvent on the adduct formation constant will be mainly caused from $\Delta G(ZnA_2^a)_o - \Delta G(ZnA_2)_o$ and $\Delta G(S)_o - \Delta G(S_c)_o$ which may be neglected in the present rough discussion.

From the present study, it is concluded that synergistic ligand having larger β_{01} and larger K_S^{ex}/K_{DS} is more promising for the effective synergistic extraction of zinc. Further investigation on the relationship developed in this study for the various other systems is worthwhile to elucidate factors governing synergistic effects.

REFERENCES

[1]C. A. Blake, C. F. Baes, K. B. Brown, C. F. Coleman and J. C. White, *Proc. the 2nd Int. Conf. Peaceful Uses of Atomic Energy Geneva* 1958, Vol. 28, pp. 289. IAEA, Vienna (1959).

[2]Y. Marcus and A. S. Kertes, *Ion Exchange and Solvent Extraction of Metal Complexes*, p. 815. Wiley-Interscience, London (1969).

[3]E. F. Kassierer and A. S. Kertes, *J. Inorg. Nucl. Chem.* 1972, **34**, 3221.

[4]K. Akiba, N. Suzuki and T. Kanno, *Bull. Chem. Soc. Jpn.* 1969, **42**, 2537.

[5]G. Atkinson and J. E. Bauman, Jr., *Inorg. Chem.* 1962, **1**, 900.

[6]C. V. Banks and R. Bystroff, *J. Am. Chem. Soc.* 1959, **81**, 6153.

[7]W. A. E. McBryde, D. A. Brisbin and H. M. Irving, *J. Chem. Soc.* 1962, 5245.

[8]D. A. Brisbin and W. A. E. McBryde, *Can. J. Chem.* 1963, **41**, 1135.

[9]Y. Bokra and G. Berthon, *J. Chim. Phys. Physiochim. Biol.* 1972, **69**, 1159.

[10]H. M. Irving and D. H. Mellor, *J. Chem. Soc.* 1962, 5222.

[11]*Equilibrium Constants of Liquid–Liquid Distribution Reactions—Part IV. Chelating Extractions.* Pergamon Press, Oxford (1975).

[12]A. S. Kertes and Y. Marcus, *Solvent Extraction Research.* Wiley-Interscience, New York (1969).

[13]T. Shigematsu, M. Tabuchi, M. Matsui and K. Utsunomiya, *Bull. Inst. Chem. Rev. Kyoto Univ.* 1967, **45**, 290.

[14]H. Irving, *Solvent Extraction Chemistry* (Edited by D. Dyrssen, J.-O. Liljenzin and J. Rydberg), p. 105. North-Holland, Amsterdam (1967).

[15]M. S. Bhatti, J. F. Desreux and G. Duyckaerts, *J. Inorg. Nucl. Chem.* 1980, **42**, 767.

Polyhedron Vol. 1, No. 4, pp. 393–396, 1982
Printed in Great Britain.

0277-5387/82/040393-04$03.00/0
Pergamon Press Ltd.

A CRYSTAL STRUCTURE DETERMINATION OF TITANIUM(II) TETRACHLOROALUMINATE BY VIBRATIONAL CORRELATION METHODS AND POWDER DIFFRACTION

A. JUSTNES and E. RYTTER*
Institute of Inorganic Chemistry, University of Trondheim, N-7034 Trondheim-NTH, Norway

and

A. F. ANDRESEN
Institute for Energy Technology, Box 40, N-2007 Kjeller, Norway

(*Received* 23 *December* 1981)

Abstract—The crystal structure of α-$TiAl_2Cl_8$, the low-temperature modification of titanium(II) tetrachloroaluminate, has been determined by vibrational frequency correlations and neutron powder diffraction. The infrared spectra of α- and β-$TiAl_2Cl_8$ and $TiAl_2Cl_8 \cdot C_6H_6$ are discussed.

INTRODUCTION

A number of divalent transition metal chlorides form solid compounds of the composition 1:2 with aluminum chloride. Belt and Scott[1] characterized several of the $MCl_2/AlCl_3$ (M = Cd, Co, Cr, Cu, Fe, Mn, Ni, Pd and V) mixtures by X-ray powder diffraction. Only two complete crystal structure determinations, however, have been performed. Ibers[2] found that the cobalt atoms in $CoAl_2Cl_8$ are octahedrally coordinated and linked together by $AlCl_4$ units in infinite chains. In contrast, $CuAl_2Cl_8$ consists of discrete molecules with a square planar coordination of the transition metal.[3] The same conclusion has been reported for $PdAl_2Cl_8$, while $NiAl_2Cl_8$ is isostructural with the cobalt compound.[5]

Brynestad *et al.*[6] isolated the title compound in two different crystal modifications. The high-temperature modification, which we denote as β-$TiAl_2Cl_8$, is isostructural with $CoAl_2Cl_8$. The *c*-axis is equal to the repetition length of the chain in this structure. Since the low-temperature modification, α-$TiAl_2Cl_8$, forms needle shaped crystals along an axis of half this repetition value, it is unlikely that both modifications contain the same type of chains. It follows that the α-modification probably has a chain with half the repetition length compared to β-$TiAl_2Cl_8$. This model is at variance with the suggestion of Brynestad *et al.*[6] that the chains are of the same kind, but differently stacked. The present study was undertaken in order to clarify the situation and give further insight into the crystallization and bonding of MAl_2Cl_8 compounds.

EXPERIMENTAL

The greenish-blue low-temperature modification of $TiAl_2Cl_8$ was prepared at 225°C by the reaction between aluminum chloride (Fluka, 99%; distilled 3 times) and bits of titanium metal wire (Koch-Light, 99.99%, ϕ = 3 mm) in excess:

$$Ti(s) + 4/3Al_2Cl_6(l) = TiAl_2Cl_8(s) + 2/3Al(s).$$

To ensure complete consumption of the aluminum chloride, the reaction time was about one month. Chemical analysis gives 12.8% Ti compared to the theoretical value 12.4%. The difference may be due to unseparated metal. Green crystals of the high-

*Author to whom correspondence should be addressed.

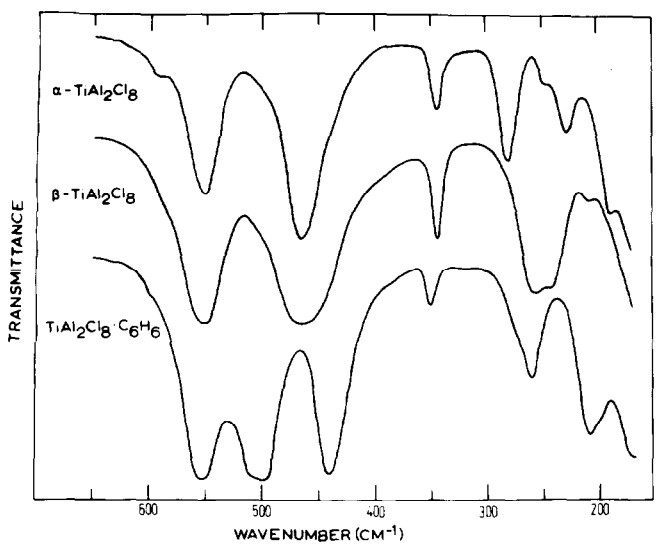

Fig. 1. IR spectra of $TiAl_2Cl_8 \cdot C_6H_6$ and the two crystal modifications of $TiAl_2Cl_8$.

Table 1. Positional parameters with estimated standard deviations for α-$TiAl_2Cl_8$

Atom	x	y	z
Ti	0	0	0
Al	0.119(7)	0.286(14)	0.380(9)
Cl(1)	0.930(4)	0.254(9)	0.253(11)
Cl(2)	0.144(2)	0.014(10)	0.266(5)
Cl(3)	0.180(3)	0.543(3)	0.245(9)
Cl(4)	0.066(4)	0.210(4)	0.747(8)

temperature modification were obtained by sublimation of α-$TiAl_2Cl_8$ over the temperature gradient 230–240°C. Both reactions were carried out in sealed quartz tubes. Large, dark violet crystals of $TiAl_2Cl_8 \cdot C_6H_6$ were synthesized by dissolving α-$TiAl_2Cl_8$ in benzene at 70°C with subsequent slow cooling until room temperature.

Spectra of Nujol mulls between CsI-windows were scanned with a Perkin-Elmer 580B spectrophotometer.

Neutron powder diffraction data were recorded by the OPUS II diffractometer at the JEEP II reactor equipped with a Ge monochromator and a BF_3 detector. The incident wavelength was 1.877 Å, step scan size 0.1° and angular resolution $\Delta d/d = 9.5 \cdot 10^{-3}$. The specimen was kept in an aluminum cylinder of I.D. 12 mm and length 40 mm.

RESULTS

The cell constants were obtained from the 2θ values of 78 reflections. With the literature data as starting point,[6] ($a = 13.17$, $b = 14.94$, $c = 5.982$ and $\beta = 90$) the refinement converged at $a = 13.161(3)$ Å, $b = 7.477(2)$ Å, $c = 5.981(1)$ Å and $\beta = 90.48(3)°$. No evidence was found for doubling of the b-axis. From the systematic extinctions, the space group was determined to be $P\ 2_1/a$ (monoclinic).

The cell parameters strongly indicate a hexagonal close packing of chlorine and $z = 2$ formula units. Besides, the spectra (Fig. 1) confirm the assumption of chain structures for the α- and β-modifications. Taking this information into account, only one trial structure is consistent with the space group.

Using the Rietveld least square profile refinement program, we arrived at a final R-factor of 0.061 for the 78 reflections ($R = \Sigma|I(obs) - I(calc)/C|/\Sigma I(obs)$). Because of the needle like shape of the powder, it was necessary to include a preferred orientation parameter in the refinement. Scattering factors were taken from standard tables.[7] The final positions of the atoms are given in Table 1. They correspond to an overall temperature factor of $B = 0.99$ Å^2, scale f. C = 0.65 and half-width parameters $u = 13852$, $v = -1605$ and $w = 932$. A list of observed and calculated structure factors may be obtained from the authors. Figure 2 illustrates a part of the chain, and a stereographic view of the unit cell is shown in Fig. 3.

DISCUSSION

The structure may be described as a slightly distorted hexagonal close packing of chlorine with titanium octahedrally and aluminum tetrahedrally coordinated in every second layer. The atoms are bonded in such a way that they form chains of the type shown in Fig. 4(a), parallel to the c-axis. It is clearly seen from the figure that the $AlCl_4$ tetrahedra are placed on top of each other in α-$TiAl_2Cl_8$, while they in β-$TiAl_2Cl_8$ are rotated $\pm 120°$ about the chain axis from one aluminum layer to the next. Thus, the Al–Al repulsions are minimized in the latter type.

The magnitude of the estimated standard deviations of the bond distances and angles (Table 2) does not permit a detailed discussion of bonding properties. It is evident, however, that the bridging Cl–Al–Cl angles are considerably smaller than the corresponding angles involving the terminal chlorine. Such a difference may be explained in terms of longer bridging bonds and smaller van der Waals radii of bridging atoms. Similar angles were observed in $CoAl_2Cl_8$ and $CuAl_2Cl_8$.[2,3]

The cobalt and copper compounds have distances

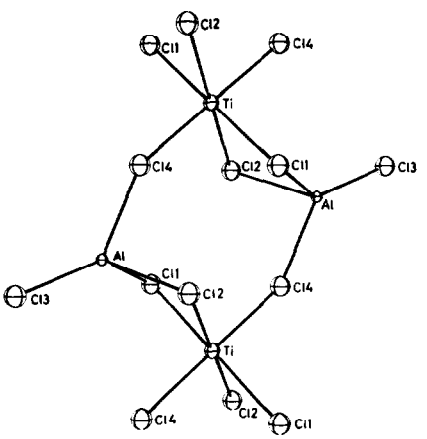

Fig. 2. Part of a chain in α-$TiAl_2Cl_8$.

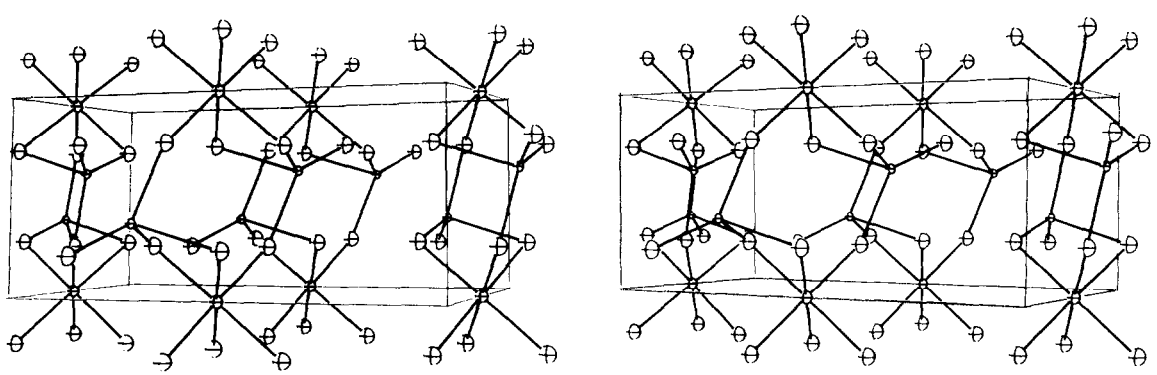

Fig. 3. Stereographic view of the unit cell of α-$TiAl_2Cl_8$. The unit cell has been translated ($\frac{1}{2}$00) compared to the positions given in Table 1. The axes are oriented with x horizontally to the right, y inwards into the page and z vertical.

Table 2. Interatomic distances and bond angles in α-$TiAl_2Cl_8$. Only the shortest non-bonding distances have been included

Distances (Å)	Angles (°)	
Ti–Cl(1) 2.60(6)	Cl(1)–Ti–Cl(2)	83(2)
Ti–Cl(2) 2.47(3)	Cl(1)–Ti–Cl(4)	89(2)
Ti–Cl(4) 2.35(4)	Cl(2)–Ti–Cl(4)	84(2)
Al–Cl(1) 2.61(10)	Cl(1)–Al–Cl(2)	88(4)
Al–Cl(2) 2.17(12)	Cl(1)–Al–Cl(3)	108(4)
Al–Cl(3) 2.23(11)	Cl(1)–Al–Cl(4)	88(3)
Al–Cl(4) 2.38(8)	Cl(2)–Al–Cl(3)	130(4)
	Cl(2)–Al–Cl(4)	96(4)
	Cl(3)–Al–Cl(4)	130(4)
Non-bonding within the chain		
	Ti–Cl(1)–Al	84(3)
Cl(2)–Cl(4) 3.23(6)	Ti–C(2)–Al	97(3)
Cl(1)–Cl(2) 3.35(7)	Ti–Cl(4)–Al	150(3)
Between chains		
Cl(2)–Cl(3) 3.55(8)		
Cl(3)–Cl(4) 3.57(6)		

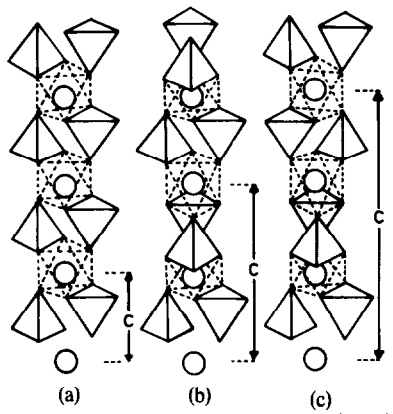

Fig. 4. Chains of composition $(MAl_2Cl_8)_n$ within a hexagonal close packing of chlorine atoms. The tetrahedra illustrate $AlCl_4$ units, and the circles indicate the transition metal, M. (a) Present in α-$TiAl_2Cl_8$, (b) present in $CoAl_2Cl_8$ and β-$TiAl_2Cl_8$ and (c) chain type not yet found.

from aluminum to the terminal chlorines of 2.06–2.11 Å and to bridging chlorines of 2.15–2.20 Å. Compared with the present investigation, it seems to be significant that the Al–Cl(1) bridge bond is longer than those reported previously. Further indications of perturbation of the ideal coordination polyhedra are found in the Ti–Cl distances and Ti–Cl–Al angles. The distortions may create a torsional force around the chain axis which may be relieved when the structure is changed to the β-modification.

This conclusion is in agreement with the IR frequencies summarized in Table 3. All bands between 200 and 300 cm^{-1} are assigned to Ti–Cl stretching modes. A regular $TiCl_6$ octahedron has only one IR active fundamental, situated at ~320 cm^{-1} for $TiCl_6^{2-}$.[8] This value is expected to be lower for a divalent complex with chlorine bridges. One strong band in the correct position was found for β-$TiAl_2Cl_8$, although some splitting was detected (Fig. 1). The observed much more distinct splitting for the α-modification is consistent with a more distorted structure.

Very interesting results may be deduced from the Al–Cl stretching region. The IR spectra of both α-and β-$TiAl_2Cl_8$ show three strong absorptions at 552, 466 and 344 cm^{-1}. Brinkmann and Gerding[9] showed that the probably isotructural[1] $FeAl_2Cl_8$ has three similar bands. They attributed bands at 350 and 560 cm^{-1} to oxide contaminations, while a peak at 480 cm^{-1} was assigned to the single infrared stretching mode of an $AlCl_4$ tetrahedron. However, it is shown below that all three frequencies nicely are explained by reduction of the symmetry.

The main perturbation of the $AlCl_4$ group is from T_d to C_{3v} symmetry, since the aluminum atom is attached to one terminal and three bridging chlorines. As shown in Table 4, the stretching fundamental $\nu_3(F_2)$ splits into the IR active modes A_1 and E. Furthermore, the totally symmetric stretching vibration, which belongs to A_1 (T_d), also is activated. This procedure leads to three IR active Al–Cl stretching modes, as observed for both the titanium(II) tetrachloroaluminates. The interpretation is confirmed by the positions of the fundamental frequencies for unperturbed $AlCl_4^-$ (in NH_4AlCl_4):[10] $\nu_1(A_1)$ = 356, $\nu_2(E)$ = 126, $\nu_3(F_2)$ = 485 and $\nu_4(F_2)$ = 184 cm^{-1}. An additional verification of the assignment is found in the Raman spectrum. It contains the expected prominent peak at 343 cm^{-1} (α-mod.).

Another example which provides further support to the vibrational model, is found in the IR spectrum of

Table 3. IR frequencies (cm^{-1}) of titanium(II) chloroaluminates

α-$TiAl_2Cl_8$	β-$TiAl_2Cl_8$	$TiAl_2Cl_8 \cdot C_6H_6$	Mode	
591 w	590 sh	598 sh		
552 s	552 s	554 vs	Al–Cl	$\nu_3(F_2)$ in $AlCl_4^-$
		504 vs	Al–Cl	
466 vs	466 vs	442 vs	Al–Cl	
344 m	344 m	350 m	Al–Cl	$\nu_1(A_1)$
280 s	256 s	275 sh	Ti–Cl	
246 sh	243 s	260 s	Ti–Cl	
227 m	209 w	209 s	Ti–Cl	
		200 sh	Ti–Cl	
188 m			Cl–Al–Cl	

w = weak, m = medium, s = strong, vs = very strong and sh = shoulder.

Table 4. Perturbation of the $AlCl_4$ group from T_d to C_{2v} and C_{3v} symmetries

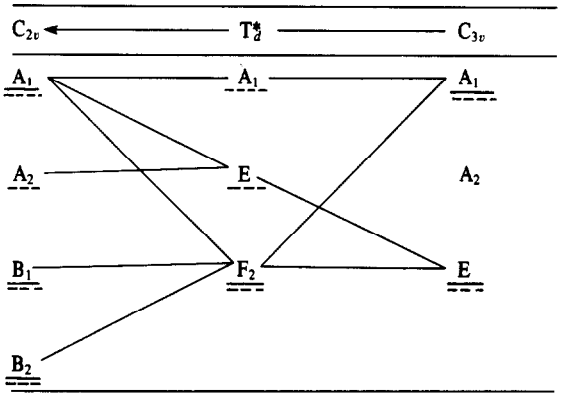

*Selected irreducible representations.
— IR active modes.
- - Raman active modes.

$TiAl_2Cl_8 \cdot C_6H_6$. This compound probably has the molecular structure:[11]

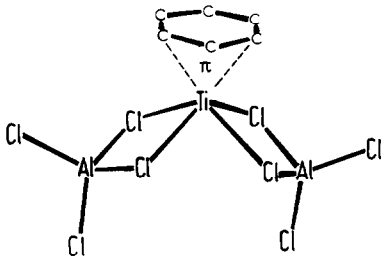

The symmetry of each $AlCl_4$ group is reduced from T_d to C_{2v}, since aluminum in this case is bonded to two terminal and two bridging chlorines. It is shown in Table 4 that $F_2(T_d)$ split into A_1, B_1 and $B_2(C_{2v})$. Together with the transformation $A_1(T_d) \rightarrow A_1(C_{2v})$, the correlations lead to four IR active Al–Cl stretching fundamentals. They are observed at 350, 442, 504 and 554 cm^{-1}. The bands in the range 200–300 cm^{-1} all can be assigned to the Ti–Cl modes of a square pyramid distorted from C_{4v} to C_{2v}. Thus, the proposed molecular structure of $TiAl_2Cl_8 \cdot C_6H_6$ is supported nicely by the IR data.

Finally, it is pointed out that two of the three natural arrangements of $(MAl_2Cl_8)_n$ chains in a hcp lattice now have been found (Fig. 4). We suggest that the third one, the helix structure, may exist in a crystal stable at elevated temperatures.

Acknowledgement—Financial support from Norges Tekniske Høgskoles Fond gratefully is acknowledged.

REFERENCES

[1]R. F. Belt and H. Scott, *Inorg. Chem.* 1964, **3**, 1785.
[2]J. A. Ibers, *Acta Cryst.* 1962, **15**, 967.
[3]H. Schäfer, M. Binnewies, R. Laumanns and H. Wächter, *Z. Anorg. Allg. Chem.* 1980, **461**, 31.
[4]*G. N. Papatheodorou, Inorg. Nucl. Chem. Lett.* 1974, **10**, 115.
[5]J. Brynestad, H. L. Yakel, and G. P. Smith, *Inorg. Chem.* 1970, **9**, 686.
[6]J. Brynestad, S. von Winbush, H. L. Yakel and G. P. Smith, *Inorg. Nucl. Chem. Lett.* 1970, **6**, 889.
[7]G. E. Bacon, *Neutron Diffraction*, p. 38. Clarendon Press, Oxford (1975).
[8]S. D. Ross, *Inorganic Infrared and Ramon Spectra*, p. 250, McGraw-Hill, London (1972).
[9]F. J. Brinkmann and H. Gerding, *Rev. Chim. Min.* 1971, **8**, 501.
[10]G. Mairesse, P. Barbier and J. P. Wignacourt, *Can. J. Chem.* 1978, **56**, 764.
[11]U. Thewalt and F. Österle, *J. Organomet. Chem.* 1979, **172**, 317.

Polyhedron Vol. 1, No. 4, pp. 397–403, 1982
Printed in Great Britain.

0277–5387/82/040397–07$03.00/0
Pergamon Press Ltd.

VIBRATIONAL SPECTRA OF $(CD_3)_3MX$ AND NORMAL COORDINATE CALCULATIONS FOR $(CH_3)_3MX$ AND $(CD_3)_3MX$ (M = Ge, Sn; X = Cl, Br)

YOSHIKA IMAI*, KOYO AIDA, KEN-ICHI SOHMA† and FUMIO WATARI‡
Department of Engineering Science, Faculty of Engineering, Tohoku University, Sendai 980, Japan

(*Received* 18 *February* 1982)

Abstract—IR (4000–30 cm^{-1}) and Raman (4000–0 cm^{-1}) spectra of $(CH_3)_3MX$ (M = Ge, Sn; X = Cl, Br) have been recorded, together with those of $(CD_3)_3MX$. By assuming the C_{3v} molecular symmetry, all the active fundamentals except an internal torsion have been assigned and normal coordinate calculations have been carried out to confirm the proposed assignments by a symmetry force field for $(CH_3)_3MX$ and $(CD_3)_3MX$.

INTRODUCTION

Numerous studies have been reported on the vibrational spectra of $(CH_3)_3GeX$ (X = F, Cl, Br, I)[1–5] and $(CH_3)_3SnX$ (X = F, Cl, Br).[6–9] However, all of them relate to the vibrational spectra of the undeuterated compounds, thus the normal coordinate calculations for these compounds have also been made by using only the data of the undeuterated compounds. Further, those calculations for $(CH_3)_3SnX$ have been made by assuming the methyl group as a point mass.[6,9] In order to obtain the more reliable force constants, it is desirable to carry out the normal coordinate calculations for these compounds by using the vibrational data of $(CD_3)_3MX$ as well as those of $(CH_3)_3MX$, and without assuming the methyl group as a point mass.

The aim of this study is to obtain the vibrational spectra of $(CD_3)_3MX$ (M = Ge, Sn; X = Cl, Br) and to make normal coordinate calculations by using the vibrational data of $(CH_3)_3MX$ and $(CD_3)_3MX$.

EXPERIMENTAL

$(CH_3)_3GeCl$ and $(CH_3)_3GeBr$ were prepared by the reaction of $(CH_3)_4Ge$ with acetyl chloride in the presence of $AlCl_3$[10] and by the reaction of $(CH_3)_3GeH$ with mercuric bromide,[11] respectively. $(CD_3)_3GeCl$ and $(CD_3)_3GeBr$ were prepared in the same manner, by using $(CD_3)_4Ge$ and $(CD_3)_3GeH$, respectively. The crude compounds were purified by trap-to-trap distillation in a conventional vacuum line.

$(CH_3)_3SnCl$ and $(CD_3)_3SnCl$ were synthesized by the reaction of $(CH_3)_4Sn$ and $(CD_3)_4Sn$ with $SnCl_4$, while $(CH_3)_3SnBr$ and $(CD_3)_3SnBr$ were prepared by bromination of $(CH_3)_4Sn$ and $(CD_3)_4Sn$, respectively.[12] The crude compounds were purified by sublimation under vacuum.

The purity of all the compounds was checked by their IR and Raman spectra. The spectra of the light compounds were identical with those reported in the previous papers.[2–4,6,7]

Infrared spectra in the range 4000–300 cm^{-1} were recorded on a Hitachi 345 spectrophotometer and far-infrared spectra in the range 400–30 cm^{-1} on a Hitachi FIS-III spectrophotometer. The spectra for the germanium compounds were recorded in the gas phase (path length: 10 cm). The spectra for the tin compounds were measured in carbon tetrachloride (4000–1300 cm^{-1}), carbon disulfide (1300–400 cm^{-1}) and hexane (400–30 cm^{-1}) solutions, by using fixed cells (thickness: 0.099 mm in the range 4000–400 cm^{-1} and 0.5 mm in the range 400–30 cm^{-1}).

Raman spectra in the range 4000–0 cm^{-1} were recorded in the liquid state on a JEOL JRS-S1 laser Raman spectrophotometer equipped with a NEC GLG 5800 He–Ne laser and qualitative polarizations were also obtained.

RESULTS

If each methyl group in $(CH_3)_3MX$ is staggered to the M–X bond and the neighbouring M–C bonds, the molecule will have a C_{3v} symmetry. Under this symmetry, the 24 fundamental modes are divided into eight non-degenerate A_1 vibrations, 12 doubly-degenerate E vibrations and four non-degenerate A_2 vibrations. The A_1 and E modes should be active in both the IR and Raman spectra and the former modes exhibit polarized bands and the latter depolarized bands in the Raman spectrum. The A_2 modes are inactive in both the infrared and Raman spectra. The 24 fundamentals can be divided into 19 modes which are largely associated with motions of the methyl groups and five modes which can be considered as C_3MX skeletal vibrations. Symmetry coordinates which are used to describe these fundamentals, are classified in Table 1. Figures 1 and 2 show the IR and Raman spectra of the deuterated compounds, respectively. Observed fundamental frequencies are listed in Tables 2–4.

The vibrational assignments for the light compounds were almost the same as those reported in the previous papers.[3,4,6] The assignments of the CD_3 stretching and CD_3 deformation modes of $(CD_3)_3MX$ can easily be made, by taking into consideration the isotopic shift and the polarization of Raman bands as well as data for related compounds.[13] Therefore, the assignments will be discussed only on the vibrations except the CD_3 stretching and CD_3 deformation modes for the deuterated compounds.

There should be one A_1 and two E methyl rocking modes in the region 700–550 cm^{-1}. For $(CD_3)_3GeCl$ two infrared bands due to these modes were observed at 656 and 588 cm^{-1} in this region. For $(CH_3)_3GeCl$[3] and $(CD_3)_3GeCF_3$[13], two corresponding bands have also been observed at 836, 762 cm^{-1} and 660, 595 cm^{-1}, respectively, in their infrared spectra. For each compound the higher frequency band has been assigned to the overlap of the A_1 mode and one of the E modes. Therefore, we assigned the 656 cm^{-1} bands for $(CD_3)_3GeCl$ to the A_1 rocking mode and one of the E modes. Thus the 588 cm^{-1} band should be assigned to the remaining E rocking mode. For $(CD_3)_3GeBr$ these modes were observed at 656 and 586 cm^{-1} in the IR spectrum and assigned in the same manner as $(CD_3)_3GeCl$.

For $(CD_3)_3SnCl$ and $(CD_3)_3SnBr$, the CD_3 rocking

*Author to whom correspondence should be addressed.
†Present address: Hitachi Research Laboratory of Hitachi Ltd., Kuji, Hitachi, Ibaraki 319-12, Japan.
‡Present address: Department of Resource Chemistry, Faculty of Engineering, Iwate University, Morioka, Iwate 020, Japan.

Table 1. Description of the symmetry coordinates for $(CH_3)_3MX$

Vibrational mode*	Coordinate		
	A_1	A_2	E
Stretching $(CH_3)_a$ or $(CD_3)_a$	S_1	S_9	S_{13}, S_{14}
Stretching $(CH_3)_s$ or $(CD_3)_s$	S_2		S_{15}
Deformation $(CH_3)_a$ or $(CD_3)_a$	S_3	S_{10}	S_{16}, S_{17}
Deformation $(CH_3)_s$ or $(CD_3)_s$	S_4		S_{18}
Rocking (CH_3) or (CD_3)	S_5	S_{11}	S_{19}, S_{20}
Stretching (MC_3)	S_6		S_{21}
Stretching (MX)	S_7		
Deformation (MC_3)	S_8		S_{22}
Rocking (MC_3)			S_{23}
Torsion		S_{12}	S_{24}

* Abbreviations used: a, asymmetric; s, symmetric.

Table 2. Observed and calculated frequencies (cm^{-1}) and potential energy distributions for $(CH_3)_3GeCl$ and $(CD_3)_3GeCl$*

No	$(CH_3)_3GeCl$				$(CD_3)_3GeCl$			
	IR	Raman	Calcd	PED	IR	Raman	Calcd	PED
1	2985	2998	2993	$100S_1$	2242	2239	2231	$99S_1$
2	2911	2913	2913	$99S_2$	2129	2124	2127	$96S_2$
3	1413	1410	1419	$96S_3$	1033	1032	1025	$97S_3$
4	1251	1253	1255	$82S_4$ $14S_2$	980	972	975	$72S_4$ $17S_2$ $11S_6$
5	837	832	846	$95S_5$	656	657	644	$92S_5$
6	569	576	577	$96S_6$	522	519	512	$82S_6$ $12S_4$
7	391	364	391	$93S_7$	390	364	385	$90S_7$
8	190	194	190	$94S_8$	169	171	170	$93S_8$
13	2985	2992	2994	$87S_{13}$ $13S_{14}$	2242	2239	2230	$75S_{13}$ $24S_{14}$
14	2985	2992	2993	$87S_{14}$ $13S_{13}$	2242	2239	2231	$75S_{14}$ $24S_{13}$
15	2911	2913	2912	$99S_{15}$	2129	2124	2128	$96S_{15}$
16	1413	1410	1418	$90S_{16}$	1033	1032	1026	$85S_{16}$ $13S_{17}$
17	1413	1410	1419	$88S_{17}$	1033	1032	1025	$83S_{17}$ $14S_{16}$
18	1251	1253	1253	$82S_{18}$ $15S_{15}$	980	972	977	$70S_{18}$ $17S_{15}$ $13S_{21}$
19	837	832	847	$96S_{19}$	656	657	642	$91S_{19}$
20	760	764	768	$94S_{20}$	588	590	576	$90S_{20}$
21	616	620	619	$96S_{21}$	553	558	550	$73S_{21}$ $13S_{18}$
22	190	194	191	$99S_{22}$	169	171	169	$95S_{22}$
23	172	168	165	$100S_{23}$	144	150	153	$98S_{23}$

* The weighted sum of squared deviations, $\sum(\lambda_{obsd} - \lambda_{calcd})^2/\lambda_{obsd}$: A_1, 1.78×10^{-3}; E, 2.75×10^{-3}. Average error: A_1, 0.71%; E, 0.75%.

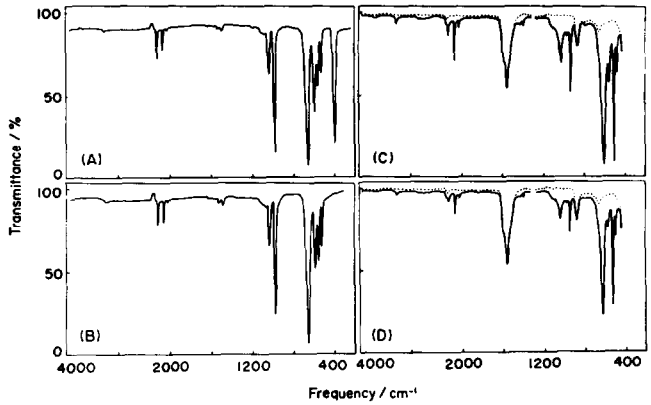

Fig. 1. Gas-phase IR spectra of (A) $(CD_3)_3GeCl$ (1870 Pa pressure) and (B) $(CD_3)_3GeBr$ (2000 Pa pressure), and solution infrared spectra of (C) $(CD_3)_3SnCl$ and (D) $(CD_3)_3SnBr$(—, solution; -----, solvent).

modes were observed at *ca.* 600 cm^{-1} and at *ca.* 550 cm^{-1} in the infrared spectra. Taking the assignments for the light compound[6] and $(CD_3)_3SnCF_3$[13] into consideration, we assigned the ca. 600 cm^{-1} bands to the overlap of the A_1 rocking mode and one of the E modes, and the *ca.* 550 cm^{-1} bands to the other E rocking mode.

The skeletal stretching vibrations are expected to appear in the region 560–200 cm^{-1}. For $(CD_3)_3GeCl$ three Raman bands were observed at 558, 519 and 364 cm^{-1} in this region. Of these bands, the 519 and 364 cm^{-1} bands are intense and strongly polarized, while the 558 cm^{-1} band is weak and depolarized. In $(CH_3)_3GeCl$ the 558 and the 519 cm^{-1} bands shift to 620 and 576 cm^{-1}, respectively, while the 364 cm^{-1} band remains at the same

Table 3. Observed and calculated frequencies (cm^{-1}) and potential energy distributions for $(CH_3)_3GeBr$ and $(CD_3)_3GeBr$*

No	$(CH_3)_3GeBr$					$(CD_3)_3GeBr$					
	IR	Raman	Calcd	PED		IR	Raman	Calcd	PED		
1	2983	2988	2990	$100S_1$		2238	2240	2228	$99S_1$		
2	2911	2910	2913	$99S_2$		2127	2122	2125	$96S_2$		
3	1413	1407	1419	$96S_3$		1033	1031	1025	$97S_3$		
4	1248	1249	1252	$83S_4$	$13S_2$	979	970	974	$72S_4$	$15S_2$	$12S_6$
5	836	828	845	$95S_5$		656	655	643	$92S_5$		
6	569	572	577	$97S_6$		520	518	511	$84S_6$	$13S_4$	
7	283	261	287	$71S_7$	$27S_8$	281	261	278	$77S_7$	$19S_8$	
8	182	189	178	$71S_8$	$28S_7$	160	165	162	$77S_8$	$21S_7$	
13	2983	2988	2991	$85S_{13}$	$15S_{14}$	2238	2240	2227	$73S_{13}$	$26S_{14}$	
14	2983	2988	2990	$85S_{14}$	$15S_{13}$	2238	2240	2228	$73S_{14}$	$26S_{13}$	
15	2911	2910	2912	$99S_{15}$		2127	2122	2126	$96S_{15}$		
16	1413	1407	1418	$91S_{16}$		1033	1031	1026	$88S_{16}$	$10S_{17}$	
17	1413	1407	1419	$90S_{17}$		1033	1031	1025	$86S_{17}$	$11S_{16}$	
18	1248	1249	1250	$83S_{18}$	$13S_{15}$	979	970	976	$71S_{18}$	$16S_{15}$	$13S_{21}$
19	836	828	846	$96S_{19}$		656	655	641	$93S_{19}$		
20	760	761	767	$94S_{20}$		586	589	575	$90S_{20}$		
21	614	618	618	$96S_{21}$		553	557	549	$73S_{21}$	$13S_{18}$	
22	182	189	182	$98S_{22}$		160	165	161	$97S_{22}$		
23		152	151	$100S_{23}$			137	138	$99S_{23}$		

* The weighted sum of squared deviations, $\sum(\lambda_{obsd} - \lambda_{calcd})^2/\lambda_{obsd}$: A_1, 1.82×10^{-3}; E, 2.54×10^{-3}. Average error: A_1, 0.94%; E, 0.65%.

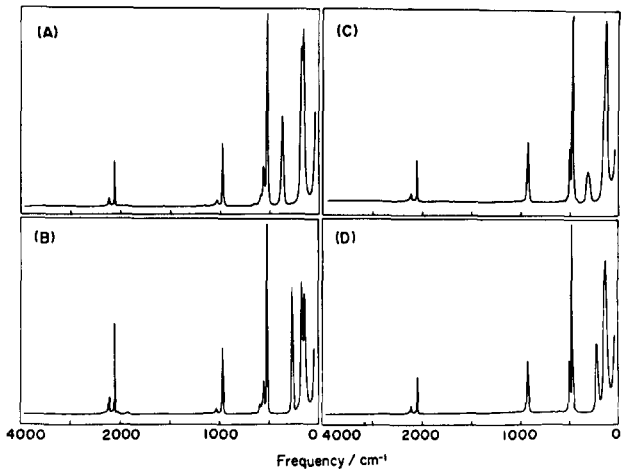

Fig. 2. Raman spectra of (A) $(CD_3)_3GeCl$, (B) $(CD_3)_3GeBr$, (C) $(CD_3)SnCl$, and (D) $(CD_3)_3SnBr$ in the liquid.

position. Therefore, the 558 and 519 cm^{-1} bands are assigned to the E and the A_1 GeC_3 stretching modes, respectively, and the 364 cm^{-1} to the Ge–Cl stretching mode. For $(CD_3)_3GeBr$ these skeletal stretching modes were observed at 557, 518 and 261 cm^{-1} in the Raman spectrum. The 557 and 518 cm^{-1} bands were assigned to the E and the A_1 GeC_3 stretching modes, respectively, and the 261 cm^{-1} to the Ge–Br stretching mode.

For the tin compounds, two Raman bands at *ca.* 500 cm^{-1} and *ca.* 470 cm^{-1} are assigned to the E and the

Table 4. Observed and calculated frequencies (cm^{-1}) and potential energy distributions for $(CH_3)_3SnCl$ and $(CD_3)_3SnCl$*

No	$(CH_3)_3SnCl$				$(CD_3)_3SnCl$			
	IR	Raman	Calcd	PED	IR	Raman	Calcd	PED
1	2987	2997	2995	$100S_1$	2241	2247	2231	$99S_1$
2	2911	2921	2912	$99S_2$	2118	2121	2117	$97S_2$
3	1395	1401	1402	$97S_3$	1023	1028	1013	$97S_3$
4	1200	1201	1202	$86S_4$ $10S_2$	926	923	924	$78S_4$ $12S_2$ $10S_6$
5	780	785	786	$96S_5$	599	600	590	$97S_5$
6	515	513	519	$99S_6$	471	469	466	$94S_6$
7	343	312	344	$98S_7$	343	312	342	$97S_7$
8	145	142	145	$97S_8$	130	128	130	$98S_8$
13	2987	2997	2995	$85S_{13}$ $15S_{14}$	2241	2247	2231	$65S_{13}$ $34S_{14}$
14	2987	2997	2995	$85S_{14}$ $15S_{13}$	2241	2247	2230	$65S_{14}$ $34S_{13}$
15	2911	2921	2912	$99S_{15}$	2118	2121	2117	$97S_{15}$
16	1395	1401	1402	$95S_{16}$	1023	1028	1013	$93S_{16}$
17	1395	1401	1401	$96S_{17}$	1023	1028	1014	$94S_{17}$
18	1191	1201	1193	$87S_{18}$ $10S_{15}$	926	923	922	$77S_{18}$ $13S_{15}$ $11S_{21}$
19	780	785	788	$97S_{19}$	599	600	587	$97S_{19}$
20	722	730	725	$97S_{20}$	548	550	544	$91S_{20}$
21	542	544	548	$99S_{21}$	499	498	493	$86S_{21}$
22	145	142	147	$76S_{22}$ $24S_{23}$	130	128	129	$91S_{22}$
23	145	142	141	$76S_{23}$ $24S_{22}$	130	128	133	$92S_{23}$

* The weighted sum of squared deviations, $\sum(\lambda_{obsd} - \lambda_{calcd})^2/\lambda_{obsd}$: A_1, 1.12×10^{-3}; E, 2.23×10^{-3}. Average error: A_1, 0.48%; E, 0.85%.

A_1 SnC_3 stretching modes, respectively, and Raman bands at 312 cm^{-1} for $(CD_3)_3SnCl$ and at 215 cm^{-1} for $(CD_3)_3SnBr$ were assigned to the tin–halogen stretching vibrations, in the same manner as the germanium compounds.

The remaining three skeletal bending modes are expected to appear below 200 cm^{-1}. For $(CD_3)_3GeCl$, two Raman bands were observed at 171 and 150 cm^{-1}. Considering the assignments of the light compound, we assigned the former band to the A_1 and E GeC_3 deformation modes and the latter to the E GeC_3 rocking mode. For $(CD_3)_3GeBr$, a Raman band at 165 cm^{-1} was assigned to the A_1 and E GeC_3 deformation modes and that at 137 cm^{-1} to the E GeC_3 rocking mode. The infrared band due to the E GeC_3 rocking mode was very weak and its frequency is indefinite for $(CD_3)_3GeCl$, while for $(CD_3)_3GeBr$ no corresponding band was observed even at the saturated vapour pressure: it will be probably too weak to be observed.

For $(CD_3)_3SnCl$, these A_1 and E SnC_3 skeletal bending modes were not resolved and were assigned to a common band at 128 cm^{-1} in the Raman spectrum. However, for $(CD_3)_3SnBr$ two Raman bands were observed at 115 and 126 cm^{-1}. In the previous study[6] for $(CH_3)_3SnBr$ two corresponding bands have been observed at 148 and 122 cm^{-1}. The 148 cm^{-1} band has been assigned to the A_1 and E SnC_3 deformation modes and the 122 cm^{-1} to the E SnC_3 rocking mode. Therefore, we assigned the 128 cm^{-1} band for $(CD_3)_3SnBr$ to the A_1 and E SnC_3 deformation modes and the shoulder at 115 cm^{-1} to the E SnC_3 rocking mode.

One methyl torsional mode should be expected. However, no band ascribable to this mode was observed in both the IR and Raman spectra for these compounds.

NORMAL COORDINATE CALCULATIONS AND DISCUSSION

Normal coordinate calculations were carried out by Wilson's GF-matrix method on an ACOS 77/900 computer at the Computer Center, Tohoku University, using the iterative least-squares refinements in the same manner as with an acetonitrile-borane adduct[14] and $(CH_3)_4M$ and $(CD_3)_4M$ (M = Si, Ge, Sn, Pb).[15]

Molecular parameters used in the calculations were based on the microwave data for $(CH_3)_3GeCl$[16] and $(CH_3)_3GeBr$[17] and on the electron-diffusion data for $(CH_3)_3SnCl$.[18] For lack of the structural data for $(CH_3)_3SnBr$, the molecular parameters were transferred from $(CH_3)_3SnCl$ and $SnBr_4$.[19]

The least-squares refinements were carried out in terms of the symmetry force constants, which were fitted

Table 5. Observed and calculated frequencies (cm^{-1}) and potential energy distributions for $(CH_3)_3SnBr$ and $(CD_3)_3SnBr$*

No	$(CH_3)_3SnBr$				$(CD_3)_3SnBr$			
	IR	Raman	Calcd	PED	IR	Raman	Calcd	PED
1	2985	2997	2993	$100S_1$	2240	2246	2229	$99S_1$
2	2909	2920	2910	$99S_2$	2118	2119	2117	$97S_2$
3	1391	1400	1399	$97S_3$	1022	1030	1011	$97S_3$
4	1200	1201	1202	$86S_4$ $11S_2$	925	922	923	$77S_4$ $14S_2$
5	780	785	786	$96S_5$	598	600	590	$97S_5$
6	514	512	518	$100S_6$	469	469	465	$94S_6$
7	237	217	238	$89S_7$ $11S_8$	236	215	235	$91S_7$
8	145	145	143	$89S_8$ $11S_7$	124	126	129	$91S_8$
13	2985	2997	2993	$72S_{13}$ $28S_{14}$	2240	2246	2229	$56S_{13}$ $43S_{14}$
14	2985	2997	2993	$72S_{14}$ $28S_{13}$	2240	2246	2229	$56S_{14}$ $43S_{13}$
15	2909	2920	2910	$99S_{15}$	2118	2119	2117	$97S_{15}$
16	1391	1400	1399	$96S_{16}$	1022	1030	1011	$94S_{16}$
17	1391	1400	1398	$97S_{17}$	1022	1030	1012	$95S_{17}$
18	1191	1201	1193	$86S_{18}$ $11S_{15}$	925	922	922	$76S_{18}$ $13S_{15}$ $11S_{21}$
19	780	785	788	$97S_{19}$	598	600	587	$97S_{19}$
20	721	730	723	$97S_{20}$	546	550	543	$92S_{20}$
21	540	543	545	$99S_{21}$	496	497	490	$86S_{21}$
22	145	145	143	$97S_{22}$	124	126	127	$98S_{22}$
23	120	125	120	$98S_{23}$	109	115	110	$98S_{23}$

* The weighted sum of squared deviations, $\sum(\lambda_{obsd} - \lambda_{calcd})^2/\lambda_{obsd}$: A_1, 1.19×10^{-3}; E, 2.33×10^{-3}. Average error: A_1, 0.77%; E, 0.71%.

Table 6. Symmetry force constants and their uncertainties*

		$(CH_3)_3GeCl$	σ	$(CH_3)_3GeBr$	σ	$(CH_3)_3SnCl$	σ	$(CH_3)_3SnBr$	σ
A_1	F_1	4.765	0.029	4.754	0.029	4.773	0.023	4.766	0.024
	F_2	4.660	0.152	4.677	0.149	4.721	0.116	4.697	0.122
	F_3	0.517	0.007	0.517	0.007	0.535	0.006	0.532	0.006
	F_4	0.522	0.046	0.513	0.044	0.502	0.035	0.507	0.038
	F_5	0.486	0.011	0.485	0.011	0.452	0.009	0.451	0.009
	F_6	2.832	0.127	2.844	0.128	2.339	0.073	2.329	0.076
	F_7	2.146	0.061	1.608	0.133	1.897	0.072	1.502	0.059
	F_8	0.595	0.078	0.649	0.143	0.479	0.045	0.517	0.096
	$F_{2,4}$	-0.457	0.164	-0.434	0.167	-0.390	0.151	-0.413	0.153
	$F_{4,6}$	-0.090	0.084	-0.091	0.082	-0.147	0.071	-0.145	0.073
E	F_{13}	4.768	0.038	4.758	0.038	4.773	0.041	4.766	0.035
	F_{14}	4.765	0.038	4.755	0.038	4.773	0.041	4.767	0.035
	F_{15}	4.641	0.156	4.663	0.147	4.729	0.132	4.705	0.137
	F_{16}	0.520	0.008	0.520	0.007	0.535	0.007	0.532	0.007
	F_{17}	0.517	0.008	0.517	0.007	0.537	0.007	0.534	0.007
	F_{18}	0.523	0.011	0.513	0.043	0.488	0.039	0.492	0.041
	F_{19}	0.492	0.047	0.492	0.010	0.460	0.010	0.460	0.010
	F_{20}	0.409	0.010	0.408	0.011	0.383	0.009	0.382	0.009
	F_{21}	2.697	0.120	2.697	0.115	2.263	0.085	2.244	0.088
	F_{22}	0.440	0.040	0.401	0.037	0.300	0.040	0.287	0.032
	F_{23}	0.532	0.055	0.557	0.061	0.497	0.065	0.439	0.058
	$F_{15,18}$	-0.478	0.162	-0.451	0.160	-0.380	0.175	-0.403	0.176
	$F_{18,21}$	-0.065	0.074	-0.070	0.071	-0.115	0.073	-0.109	0.075

*The stretching force constants are given in 10^2 N m^{-1}, the deformation force constants in 10^{-18} N m rad^{-2}, and the stretching-deformation interaction constants in 10^{-8} N rad^{-1}. The subscript number i in F_i corresponds with that in S_i in Table 1.

Table 7. Comparison of force constants (10^2N m^{-1}) and bond distances (nm)

Compound	f(M-C)	r(M-C)	f(M-X)	r(M-X)
$(CH_3)_4Ge$	2.65[15]	0.1945[22]		
$(CH_3)_3GeCl$	2.74[a]	0.1940[16]	2.15[a]	0.2170[16]
CH_3GeCl_3	3.01[21]	0.1893[23]	2.52[21]	0.2132[23]
$GeCl_4$			2.68[25]	0.2113[26]
$(CH_3)_3GeBr$	2.75[a]	0.1936[17]	1.61[a]	0.2323[17]
$GeBr_4$			2.14[25]	0.2272[27]
$(CH_3)_4Sn$	2.19[15]	0.2144[24]		
$(CH_3)_3SnCl$	2.29[a]	0.2106[18]	1.90[a]	0.2351[18]
$SnCl_4$			2.47[25]	0.2281[28]
$(CH_3)_3SnBr$	2.27[a]		1.50[a]	
$SnBr_4$			2.00[25]	0.246[19]

a) This work.

to the observed fundamental frequencies, for the two isotopic species of each compound, simultaneously. The observed frequencies used in the refinements were taken from the IR spectra except for the E GeC_3 rocking frequencies for the germanium compounds, which were taken from the Raman spectra. The observed frequencies were weighted by $(1/\lambda)$. The torsional mode was neglected in the E class. In order to improve the fit between the calculated and the observed frequencies, it was necessary to include two interaction constants, $\nu_s(CH_3)$-$\delta_s(CH_3)$ interaction and $\delta_s(CH_3)$-ν(C-M) interaction in the A_1 and the E blocks, in addition to the diagonals. Calculations were tried including other off-diagonal force constants but no reasonable results were obtained. Therefore, all the interaction constants, except for the above two constants in the A_1 and the E blocks, were constrained to zero in the least-squares refinements. Symmetry force constants from the last cycle in the least-squares refinement are given in Table 6, together with their uncertainties. Calculated frequencies are also given in Tables 2–5, together with potential energy distributions[20] expressed as $100F_{ii}L_{ij}^2/\Sigma F_{ii}L_{ij}$.[2]

The M-C and M-X valence stretching force constants calculated from the symmetry force constants are compared with those of the related compounds in Table 7. The M-C and M-X bond distances are also shown in Table 7. Although there is only a limited number of the data, it is seen from the table that both the M-C and M-X stretching force constants progressively increase with increasing halogen substitution. This is in agreement with what might be expected from the bond distances. The same trend of the force constants has been found in a series of $(CH_3)_{4-n}GeF_n (n = 0-4)$.[1]

Acknowledgement—This work was partly supported by a grant from the Asahi Glass Foundation for Industrial Technology to which authors' (Y. I. and K. A.) thanks are due.

REFERENCES

[1]J. W. Anderson, G. K. Barker, A. J. F. Clark, J. E. Drake and R. T. Hemmings, *Spectrochim. Acta, Part A*, 1974, **30**, 1081.
[2]D. F. Van de Vondel and G. P. Van der Kelen, *Bull. Soc. Chim. Belg.*, 1965, **74**, 453.
[3]J. R. Durig, K. K. Lau, J. B. Terner and J. Bragin, *J. Mol. Spectrosc.* 1969, **31**, 419.
[4]D. F. Van de Vondel, G. P. Van der Kelen and G. Van Hooydonk, *J. Organomet. Chem.* 1970, **23**, 431.
[5]J. W. Anderson, G. K. Barker, J. E. Drake and R. T. Hemmings, *Can. J. Chem.* 1971, **49**, 2931.
[6]Von H. Kriegsmann and S. Pischtschan, *Z. Anorg. Allg. Chem.* 1961, **308**, 212.
[7]W. F. Edgell and C. H. Ward, *J. Mol. Spectrosc.* 1962, **8**, 343.
[8]P. Taimsalu and J. L. Wood, *Spectrochim. Acta* 1964, **20**, 1357.
[9]P. Taimsalu and J. L. Wood, *Spectrochim. Acta* 1964, **20**, 1043.
[10]H. Sakurai, K. Tominaga, T. Watanabe and M. Kumada, *Tetrahedron Lett.* 1966, 5493.
[11]H. H. Anderson, *J. Am. Chem. Soc.* 1957, **79**, 326.
[12]C. A. Kraus and W. V. Sessions, *J. Am. Chem. Soc.* 1925, **47**, 2361.
[13]R. Eujen and H. Bürger, *Spectrochim. Acta, Part A* 1979, **35**, 1135.
[14]F. Watari, *J. Phys. Chem.* 1980, **84**, 448.
[15]F. Watari, *Spectrochim. Acta, Part A* 1978, **34**, 1239.
[16]J. R. Durig and K. L. Hellams, *J. Mol. Struct.*, 1975, **29**, 349.
[17]Y. S. Li and J. R. Durig, *Inorg. Chem.* 1973, **12**, 306.
[18]B. Beagley, K. McAloon and J. M. Freeman, *Acta Crystallogr., Sect. B* 1974, **33**, 444.
[19]L. E. Sutton, *Tables of Interatomic Distances and Configuration in Molecules and Ions.* Chemical Society, London (1958).
[20]K. Nakamoto, *Infrared Spectra of Inorganic and Coordination Compounds*, 2nd Edn. Wiley, New York, (1970).
[21]J. R. Durig, P. J. Cooper and Y. S. Li, *J. Mol. Spectrosc.* 1975, **57**, 169.
[22]J. L. Hencher and F. J. Mustoe, *Can. J. Chem.* 1975, **53**, 3542.
[23]J. E. Drake, J. L. Hencher and Q. Shen, *Can. J. Chem.* 1977, **55**, 1104.
[24]M. Nagashima, H. Fujii and M. Kimura, *Bull. Chem. Soc. Jpn.* 1973, **46**, 3708.
[25]H. Siebert, *Anwendungen der Schwingungsspektroskopie in der Anorganischen Chemie.* Springer-Verlag, Berlin (1966).
[26]Y. Morino, Y. Nakamura and T. Iijima, *J. Chem. Phys.* 1960, **32**, 643.
[27]G. G. B. Souza and J. D. Wieser, *J. Mol. Struct.* 1975, **25**, 442.
[28]H. Fujii and M. Kimura, *Bull. Chem. Soc. Jpn.* 1970, **43**, 1933.

Polyhedron Vol. 1, No. 4, pp. 405–408, 1982
Printed in Great Britain.

0277–5387/82/040405–04$03.00/0
Pergamon Press Ltd.

EQUILIBRIA OF ALUMINIUM (III) COMPLEXES WITH METHYLTHYMOL BLUE

SADAAKI MURAKAMI* and TAKASHI YOSHINO
Department of Industrial Chemistry, Faculty of Engineering Yamaguchi University, Tokiwadai, Ube 755, Japan

(*Received* 1 *February* 1982)

Abstract—A potentiometric and spectrophotometric study of aluminium (III) complexes with methylthymol blue has been performed in aqueous solutions. Evidence was found for the formation of 1:1 and 2:1 (metal:dye) complexes and it was concluded that protonated and hydroxo complexes of both 1:1 and 2:1 complexes were formed in addition to the neutral complexes. The formation constants were determined and possible structures for the complexes were discussed.

INTRODUCTION

Methylthymol blue, 3,3′-*bis*[[*bis*(carboxymethyl)-amino]methyl]thymolsulphonephthalein (Formula I, abbreviated as MTB or H_6mtb) has been used as an indicator in direct chelatometric determination of aluminium[1] and also as a sensitive reagent in spectrophotometric determination of aluminium.[2–7] Many reports have been published regarding both equilibria[3,5,8–12] and kinetics[13–15] of the Al(III) complex formation with MTB in acidic aqueous media. However, nothing has been published for the complexes formed in neutral to alkaline media. As to the complexes even in the acid solutions, despite the investigations above, there still remains uncertainty because of serious discrepancies among the conclusions by different authors. As far as the compositions of the complexes are concerned, the conclusions may be classified into the two groups: (i) only 1:1 (Al:MTB) complex[3,12] and (ii) both 1:1 and 1:2 complexes[5,8,10,11]. Based on these conclusions, the equilibrium[3,5,8,10,11] or rate[13–15] constant of each complex formation has been determined. Such discrepancies were primarily caused by the use of the reagents of low purity[16]. Another reason might be for the fact that these investigations have been performed only by spectrophotometry within the visible range.[17]

This paper deals with the results of a potentiometric and spectrophotometric study on the equilibria of Al(III)-complex formation with MTB in acidic to alkaline media.

EXPERIMENTAL

The MTB was purified using a cellulose column.[18] The other reagents, apparatus, and procedures were the same as described previously,[19] except for preparing test solutions. After the complex formation of Al(III) and MTB had been completed by heating the solutions at 80°C for at least 30 min (the pH's of the solutions were around 2.5), the reagents for the pH buffer and ionic strength were added. All the measurements were performed at 25 ± 0.1°C: the ionic strength of the solutions was maintained at 0.1 with sodium perchlorate.

The formation constants of the complexes were calculated in the same manner as described previously.[19] The acid dissociation constants of MTB used in the calculations were those determined previously[19] (pK_i: 12.94, 11.14, 6.85, 3.04, 2.0, and 1.8 for i = 1–6, respectively).

RESULTS AND IDSCUSSION

Complex formation equilibria

Potentiometric tititrations of the MTB solutions containing 1:2, 1:1, 2:1, and 3:1 molar ratios of Al(III) to MTB were performed, and hereafter the molar ratios of Al(III) to MTB are referred to as 1/2, 1/1, 2/1 and 3/1, respectively. The titration curves are shown in Fig. 1, together with those for Al(III) alone and for MTB alone. The 3/1 curve (Curve 6) is the same as the 2/1 curve (Curve 5) up to $a = 6$, but this a value up to 9 there is another buffer region where aluminium hydroxide was precipitated. This region is in the same pH as that of the Al(III) curve at a = 0–3, and the extent of this buffer region over three units of a indicates that there exists one mole of free Al(III) per mole of MTB in the 3/1 solution and that no more than two Al(III) ions can combine with a MTB molecule. Both 1/1 and 2/1 curves (Curves 4 and 5) have two inflections: at a = 5 and 6, and at a = 6 and 8, respectively. One proton in the MTB molecule remains undissociated at a = 5 for the 1/1 solution, and all the available protons of MTB are dissociated

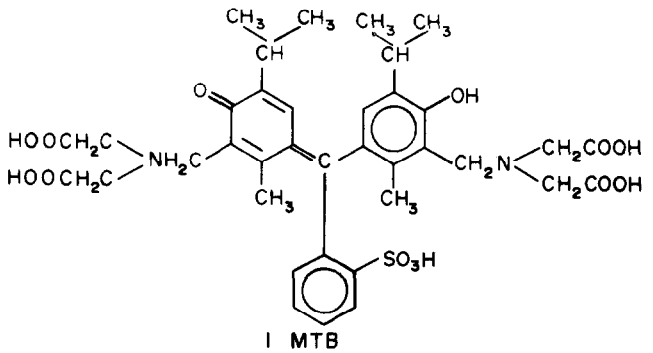

I MTB

*Author to whom correspondence should be addressed.

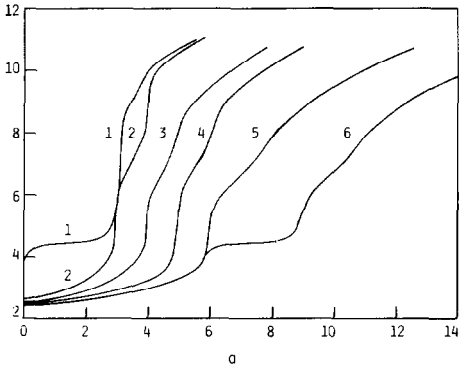

Fig. 1. Potentiometric titration curves of MTB solutions containing various molar ratios of Al(III) to MTB. a = number of moles of base added per mole of MTB. 1—Al(III) alone, 2—MTB alone, 3–6—1/2, 1/1, 2/1 and 3/1 solutions, respectively. [MTB] = 1×10^{-3} mol dm^{-3} and [Al(III)] is varied.

at $a = 6$ for the 2/1 solution. This indicates the formation of 1:1 and 2:1 complexes, $[AlHmtb]^{2-}$ and Al_2Hmtb, at respective a values. The extent of the buffer region at $a = 6$–8 for the 2/1 solution is just twice as much as that at $a = 5$–6 for the 1/1 solution. These facts suggest that each Al(III) ion in the 1:1 and 2:1 complexes is hydrolyzed to liberate one proton from the water molecule in its inner coordination sphere. Thus, formation of the hydroxo complexes, $[Al(OH)(Hmtb)]^{3-}$ and $[Al_2(OH)_2mtb]^{2-}$, may be complete at $a = 6$ and $a = 8$ in the 1/1 and 2/1 solutions, respectively.

The visible absorption spectra of 1/1, 2/1, and 3/1 solutions at various pH values (pH 0–14) were measured between 350 and 700 nm, and those of the 1/1 and 2/1 solutions are shown in Figs. 2 and 3. The spectra of the 3/1 solutions were the same as those of the 2/1 solutions but aluminium hydroxide was precipitated at pH 5–9. The variations in absorbances as a function of pH at 588 nm for the 1/1 and 2/1 solutions are shown in Fig. 4. The spectra of the MTB alone, 1/1, and 2/1 solutions around pH 0 (acidic media of 1 mol dm^{-3} perchloric acid) were the same and had an absorption maximum at 435 nm (Spectrum 1 in Figs. 2 and 3), indicating no complex formation taking place in such strongly acidic media. With increasing pH from 1, a new absorption band appeared around 590 nm for both 1/1 and 2/1 solutions (Spectrum 2 in Figs. 2 and 3), and either absorbance reached its maximum at pH 3–5 (the extent of their pH range is sightly wider in the 1/1 than in the 2/1 solution) as seen on each curve of variation in absorbance at

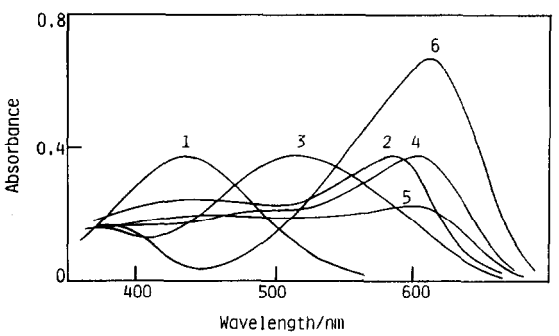

Fig. 2. Visible absorption spectra of the 1/1 solutions at various pH values. pH: 1—0.26, 2—4.53, 3—8.00, 4—9.75, 5—12.08, and 6—13.66. [MTB] = 1.92×10^{-5} mol dm^{-3}.

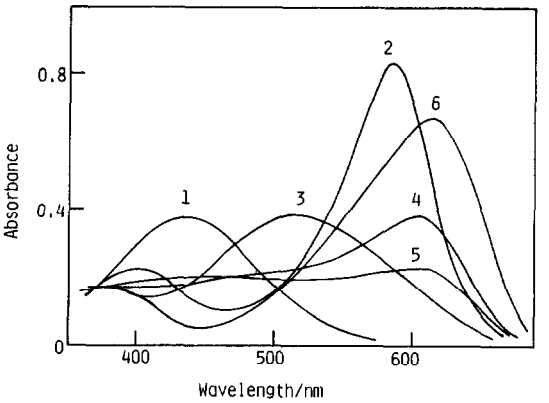

Fig. 3. Visible absorption spectra of the 2/1 solutions at various pH values. pH: 1—0.13, 2—4.46, 3—8.09, 4—10.12, 5—01, and 6—13.61. [MTB] = 1.92×10^{-5} mol dm^{-3}.

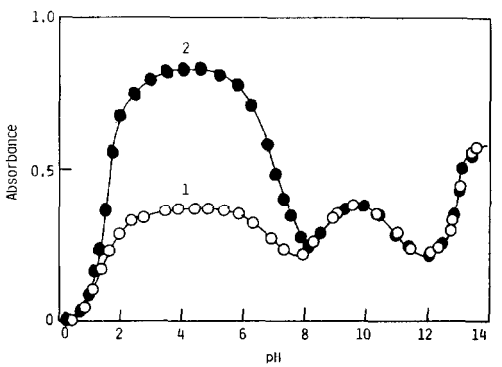

Fig. 4. Variations of the absorbances of the 1/1 and 2/1 solutions at 588 nm as a function of pH. 1—1/1 and 2—2/1, solutions, respectively.

588 nm in Fig. 4. These pH regions correspond to those for the first inflection points of 1/1 and 2/1 titration curves, respectively. This indicates the absorption bands around 590 nm being attributable to the complexes, $[AlHmtb]^{2-}$ and Al_2mtb, respectively. With further increase in pH, each spectrum shifted to 513 and 517 nm around pH 8 and became broad as seen on Spectrum 3 in Figs. 2 and 3, respectively. At much higher pH values (over 8), both 1/1 and 2/1 solutions showed three different spectra as shown on Spectra 4–6 in Figs. 2 and 3. These spectrum bands were exactly the same as those of the MTB alone solutions[19] at the respective pH's; being attributable to the acid species, H_2mtb^{4-}, $Hmtb^{5-}$ and mtb^{6-}, respectively. These facts suggest that the complexes, $[Al(OH)(Hmtb)]^{3-}$ and $[Al_2(OH)_2mtb]^{2-}$, are dissociatecd into $Al(OH)_4^-$ and H_2mtb^{4-} over pH 10. Two spectrum changes over pH 10 may correspond to the successive proton-dissociations from H_2mtb^{2-}.

No previous author has pointed out the formation of the 2:1 complex. However, the formation of this complex may be valid because precipitation did not occur in the 2/1 solution throughout the pH range investigated, while one mole of Al(III) ion per mole of MTB was hydrolyzed and precipitated in the 3/1 solution. Some authors[5,8,10,11] pointed out the formation of 1:2 complex. However, this is contradictory to the following fact. Two inflection points at $a = 4$ and $a = 5$ on the 1/2 curve (Curve 3 in Fig. 1) are just between each first and second

inflection points for the MTB and 1/1 curves. This fact can be explained reasonably as indicated below providing that a half mole of MTB reacts with Al(III) and another half mole of MTB remains being free.

$a = 0$–4:

$$\frac{1}{2}Al^{3+} + \frac{1}{2}H_6mtb \rightleftharpoons \frac{1}{2}[AlHmtb]^{2-} + \frac{5}{2}H^+$$

$$\frac{1}{2}H_6mtb \rightleftharpoons \frac{1}{2}H_3mtb^{3-} + \frac{3}{2}H^+$$

$a = 4$–5:

$$\frac{1}{2}[AlHmtb]^{2-} + \frac{1}{2}H_2O \rightleftharpoons \frac{1}{2}[Al(OH)(Hmtb)]^{3-} + \frac{1}{2}H^+$$

$$\frac{1}{2}H_3mtb^{3-} \rightleftharpoons \frac{1}{2}H_2mtb^{4-} + \frac{1}{2}H^+.$$

The results of molar-ratio and continuous-variation methods for the Al(III) complex suggested the formation of only 2:1 complex at pH 4.5 and of only 1:1 complex at pH 8, though both 1:1 and 2:1 complexations in either media were found by potentiometric titrations. Such results have been often observed in sulphonephthalein dyes;[17] one of the explanations for this problem is that the 1:1 and 2:1 complexes formed in solutions of the same pH have absorption maximum at almost the same wavelength, such as listed in Table 1.

Summarizing the discussion, the equilibria of complex formations for the Al(III) and MTB system are indicated in Scheme 1.

The formation constant and λ_{max} of each complex species are summarized in Table 1.

Structures

The MTB molecule has two chelating groups on each side of its large sulfonephthalein nucleus; each chelating group reacts with a metal ion independently.[20] Thus, the proton in the 1:1 complexes, $[AlHmtb]^{2-}$ and $[Al(OH)(Hmtb)]^{3-}$, may be attached to the amino nitrogen of another [*bis*-(carboxymethyl)amino]methyl (BCA) group which is not coordinating to the Al(III) ion, because the amino hydrogen may dissociate in more alkaline media.[19] The colour or spectral change of MTB, accompanying the proton dissociation or the complex formation, arises from the change in the π-electronic system in the sulphonephthalein nucleus. Thus, the proton dissociation from the phenolic group or the coordination of the phenolic oxygen leads to an important change in the absorption spectrum.[21] However, the spectral change is obscure when groups other than the phenolic one dissociate the proton or coordinate to metal ion.[22] Two carboxylic groups of the uncoordinated BCA group in $[AlHmtb]^{2-}$ are considered to be protonated successively in acidic media below pH 4, but the change in spectrum is obscure. Thus, highly protonated complexes, $[AH_nmtb]^{-3+n}$ with the maximum n-value of 3, may exist in strongly acidic media, although appreciable spectral changes were not observed. All available protons of a MTB molecule are dissociated at $a = 6$ in the 2/1 solution (Curve 5 in Fig. 1); this may be explained by the fact that the phenolic or quinoyl oxygen and all the donors of either BCA group coordinate to an Al(III) ion.

Evidence was found for the formation of 1:1 monohydroxo complexes in the other metal-sulphonephthalein or EDTA systems, e.g. $\{[Cu(OH)sxo]^{3-}\}$,[23] $\{[Fe(OH)Hxo)]^{3-}\}$,[24] and $\{[Fe(OH)edta]^{2-}\}$[25,26] (SXO or H_4 sxo, 3 - [[*bis*(carboxymethyl)amino]methyl] - *o*) cresolsulphonephthalein; XO or H_6xo, 3,3'-*bis*-[[*bis*-(carboxymethyl)amino]methyl - *o* - cresol-

The 1/1 or less solution:

$$Al^{3+} + H_6mtb \underset{pH<1}{\rightleftharpoons} [AlH_nmtb]^{-3+n}(n = 3-1) \underset{pH\,3-6}{\rightleftharpoons} [Al(OH)(Hmtb)]^{3} \underset{pH>10}{\rightleftharpoons} Al(OH)_4^- + H_mmtb^{-6+m}(m = 2-0) \quad (pH\ 8)$$

The 2/1 or more solution:

$$2Al^{3+} + H_6mtb \underset{pH<1}{\rightleftharpoons} Al_2mtb \underset{pH\,3.5-5.5}{\rightleftharpoons} [Al_2(OH)_2mtb]^{2-} \underset{pH>10}{\rightleftharpoons} 2Al(OH)_4^- + H_mmtb^{-6+m}(m = 2-0) \quad (pH\ 8)$$

Scheme 1.

Table 1. Formation constants and absorption spectra of Al(III) complexes with MTB at 25°C and $\mu = 0.1$ ($NaClO_4$)

Reaction	Log K	λ_{max} / nm	$\varepsilon \times 10^{-4}$ / $cm^{-1}mol^{-1}l$
$Al^{3+} + Hmtb^{5-} \rightleftharpoons *[AlHmtb]^{2-}$	16.2	587	1.96
$2Al^{3+} + mtb^{6-} \rightleftharpoons *Al_2mtb$	26.8	588	4.39
$H^+ + *[Al(OH)(Hmtb)]^{3-} \rightleftharpoons [AlHmtb]^{2-} + H_2O$	6.7	513	1.97
$2H^+ + *[Al_2(OH)_2mtb]^{2-} \rightleftharpoons Al_2mtb + 2H_2O$	13.8	517	1.95

*The complexes corresponding to the λ_{max} and ε values

sulphonephthalein). On the basis of potentiometric, magnetic susceptibility, NMR, ESR, IR or electronic spectral data, $\{[Cu(OH)sxo]^{3-}\}$[23] and $\{[Fe(OH)edta]^{2-}\}$[27,28] were found to undergo dimerization to form an hyroxo or oxo bridge structure, and the monomer and dimer are in equilibrium. Although no evidence was found regarding the structure of $[Al(OH)(Hmtb)]^{3-}$ in the present work, this complex is expected to be dimerized with oxo or hydroxo bridge. With regard to the 2:1 hydroxo complex, $[Al_2(OH)_2mtb]^{2-}$, a possible polymerized structure, e.g. $[_{HO}\diagdown\!\!\diagup Al.mtb.Al\diagdown\!\!\diagup^{OH}]_n^{2n-}$ ($n \geq 2$), could exist, as a result of dehydration (olation) of two $Al(OH)^{2-}$ ions attached to each side of the sulphonephthalein nucleus, as discussed in detail for $\{[Fe_2(OH)_2xo]^{2-}\}$.[24] However, a detailed discussion of the structures of the hydroxo complexes of the Al(III)–MTB system must await further investigation.

REFERENCES

[1]R. Geyer and R. Borman, *Z. Chem.* 1967, **7**, 30.
[2]V. N. Tikhonov and M. Ya. Grankina, *Zavod. Lab.* 1966, **32**, 278.
[3]V. N. Tikhonov, *Zh. Anal. Khim.* 1966, **21**, 275.
[4]M. A. Arshad, P. M. Huang and St. R. J. Arnaud, *Soil Sci.* 1972, **144**, 115.
[5]N. D. Lukomskaya, *Izv. Vyssh. Ucheb. Zaved., Khim. Khim. Tekhnol.* 1973, **16**, 1157.
[6]V. N. Tikhonov, *Khim. Khim. Tekhnol*, 1973, 92.
[7]N. M. Zolotukhina and T. M. Erenpreis, *Zavod. Lab.* 1979, **45**, 297.
[8]T. V. Mal'kova, N. D. Medvedeva and K. B. Yatsimirskii, *Zh. Neorg. Khim.* 1964, **9**, 2347.
[9]A. I. Cherkesov and B. I. Kazakov, *Novye Issle. Anal. Primen. Org. Reagentov* 1967, 3.
[10]V. A. Nazarenko and E. M. Nevskaya, *Zh. Anal. Khim.* 1969, **24**, 839.
[11]T. V. Mal'kova, V. D. Ovchinnikova and T. B. Boloshina, *Izv. Vyssh. Ucheb. Zaved., Khim. Khim. Tekhnol.* 1971, **14**, 1635.
[12]V. A. Malevannyi, *Zh. Obshch. Khim.* 1972, **42**, 1785.
[13]T. V. Mal'kova, N. D. Medvedeva and K. B. Yatsimirskii, *Zh. Neorg. Khim.* 1965, **10**, 72.
[14]T. V. Mal'kova, V. D. Ovchinnikova and G. V. Ryzhalova, *Zh. Neorg. Khim.* 1972, **17**, 372.
[15]*T. V. Mal'kova and V. D. Ovchinnikova, Zh. Neorg. Khim.* 1972, **17**, 1574.
[16]S. Nakada, M. Yamada, T. Ito and M. Fujimoto, *Bull. Chem. Soc. Jpn.* 1977, **50**, 1887.
[17]S. Murakami, K. Ogura and T. Yoshino, *Bull. Chem. Soc. Jpn.* 1980, **53**, 2228.
[18]T. Yoshino, H. Imada and T. Kuwano, *Talanta* 1969, **16**, 151.
[19]T. Yoshino, H. Imada, S. Murakami and M. Kagawa, *Talanta* 1974, **21**, 211.
[20]M. Otomo, *Japan Analyst* 1972, **21**, 436.
[21]S. Murakami and T. Yoshino, *Talanta* 1981, **28**, 623.
[22]K. Ogura, S. Murakami and K. Seno, *J. Inorg. Nucl. Chem.* 1981, **43**, 1243.
[23]S. Murakami, *J. Inorg. Nucl. Chem.* 1981, **43**, 335.
[24]T. Yoshino, S. Murakami and K. Ogura, *J. Inorg. Nucl. Chem.* 1979, **41**, 1011.
[25]G. Schwarzenbach and J. Heller, *Helv. Chim. Acta* 1951, **34**, 576.
[26]R. L. Gustafson and A. E. Martell, *J. Phys. Chem.* 1963, **67**, 576.
[27]H. Schugar, C. Walling, R. B. Jones and H. B. Gray, *J. Am. Chem. Soc.* 1967, **89**, 3712.
[28]S. J. Lippard, H. Schugar and C. Walling, *Inorg. Chem.* 1967, **6**, 1825.

Polyhedron Vol. 1, No. 4, pp. 409–412, 1982
Printed in Great Britain.

0277-5387/82/040409-04$03.00/0
Pergamon Press Ltd.

CROWN ETHER COMPLEXES OF TRANSITION METALS

SYNTHESIS AND CHARACTERIZATION OF COMPLEXES FORMED BETWEEN HYDRATED NICKEL (II) CHLORIDE AND THE CYCLIC POLYETHER 18 CROWN 6

JACQUES JARRIN* and FRANÇOIS DAWANS
Direction de Recherche Matériaux et Chimie Organique Appliquée, Institut Français du Pétrole 1,4 Avenue de Bois Préau, 92506 Rueil Malmaison, Paris, France

and

FRANCIS ROBERT and YVES JEANNIN
Laboratoire de Chimie des Métaux de Transition ERA 608, 4 Place Jussieu 75230 Paris, France

(*Received* 7 *July* 1981)

Abstract—When hydrated nickel (II) chloride reacts with 18-crown-6, two products are yielded: $Ni_2Cl_2(H_2O)_8\ Cl_2$. 18 C6 (compound I) and 2 $NiCl_2$. $2H_2O$. 18C6 (compound II). These complexes were separately isolated and characterized by infrared spectroscopy. The crystal structure of compound I is described. It crystallizes in the triclinic system with $a = 8{,}828$ (4), $b = 9{,}693$ (4), $c = 10{,}616$ (4) Å, $\alpha = 55{,}74$ (3), $\beta = 67{,}47$ (3), $\gamma = 63{,}62$ (3), $V = 648{,}1$ Å^3, space group $P\bar{1}$. This structure shows an unusual conformation of the 18 crown 6 polyether (all the atoms of the crown are divided into two parallel planes separated by 1.1 Å) and a $Ni_2Cl_2(H_2O)_8$ unit containing the nickel atoms in the form of a bridged dinuclear unit. The cohesion of the structure is given by hydrogen bonds between the crown ether and the water molecules surrounding the dinickel unit. In a previously reported structure involving crown ether the hexa-aquo metal ions were present as monometallic units.

INTRODUCTION

In previously described structures of complexes between alkali and alkaline earth metal cations and cyclic polyethers,[1,2] the metal cation is generally located at the centre of the hole. In more recently described complexes of actinides and lanthanides[3,5] the metal is outside of the hole.

Some structures have been determined for complexes of the transition metal cations within the first series. Sandwich-type structures are proposed when the metal is directly bonded to the crown[6,7]. Coordinated water molecules give more complicated structures in which the metal is not bonded to the crown. The cohesion of the structure is then give by hydrogen bonds between the water molecules in the aquated cation and the crown polyether.[8–10]

The synthesis of $(NiCl_2)_2$ 18C6 was briefly described by D. de Vos,[7] but the experimental conditions were not given in detail. We obtained different reaction products using the below-mentioned conditions. So we are giving herein the synthesis of two new complexes of hydrated nickel (II) chloride with 18-crown-6. The infrared spectra of both products are compared with that of the crown polyether in the free state. Further, the structure of compound I is determined by X-ray diffraction.

EXPERIMENTAL

Synthesis of the complexes

Triethylorthorformate, used by De Vos[7] as a drying agent, reacts with water to yield ethanol and ethyl formate. According to the conditions described, we always obtained compounds containing coordinated methanol and ethanol molecules. In all cases these compounds were isolated as powders. By varying the crystallization conditions we succeeded in obtaining two new crystalline complexes as follows: $NiCl_2{,}6H_2O$ (2.38 g, 10 mmol) and 18C6 (2.64 g, 10 mmol) were mixed in 30 ml of an methanol/ethyl formate mixture (5:1 volume ratio). With the addition of dried diethyl ether (about 75 ml) the green solution became muddy.

After several days, two different products are obtained: yellow–orange crystals (compound II) which are formed on the walls of the reaction vessel and a green oil (compound I) which is decanted and slowly crystallized from diethyl ether at room temperature. The use of ethyl formate is necessary, but the methanol/ethyl formate ratio, if it is between 5:1 and 2:1, does not influence the nature of the reaction products.

Table 1 shows the elemental analysis of the separately isolated complexes. Both compounds I and II are sensitive to atmospheric moisture and thus must be carefully stored under an argon atmosphere. The slight variations observed between the experimental and the theoretical values, particularly for compound I, are presumably due to the above-mentioned instability of the complexes.

CHARACTERIZATION OF THE COMPLEXES

IR spectroscopy

The IR spectra of the compounds are determined by a Perkin–Elmer 457 recording spectrophotometer as dry nujol mulls between potassium bromide plates.

X-Ray diffraction

The cell constants were determined directly on a diffractometer and refined from the least-squares fit of 2θ, χ, ϕ for 36 high Bragg angle reflections. This gave the triclinic lattice parameters: $a = 8.828$ (4), $b = 9.693$ (4); $c = 10.616$ (4) Å; $\alpha = 55.74$ (3); $\beta = 63.47$ (3); $\gamma = 63.62$ (3)°; $V = 648.1$ Å^3. The space group is $P\bar{1}$.

Data were collected by an automatic CAD-3 Enraf-Nonius Diffractometer with $Mo_{k\alpha}(\lambda = 0.71069$ Å$)Zr$ filtered radiation in the $\theta - 2\theta$ scan mode up to $2\theta_{max} =$

*Author to whom correspondence should be addressed.

Table 1. Elemental analysis of compounds I and II

	%	C	H	Cl	O	Ni
$[Ni_2Cl_2(H_2O)_8]Cl_2.18C6$	Found	21.8	5.9	23.6	31.2*	17.5
compound I	Calc.	21.6	6.0	21.2	33.6	17.6
$2NiCl_2.2H_2O.18C6$	Found	24.1	5.0	28.5	24.6	21.4
compound II	Calc.	25.7	5.0	25.4	22.9	21.0

*Calculated by difference.

50°. The scan range varied according to $\Delta\theta = 0.70 + 0.34 \text{ tg } \theta$. I301 reflections with $I \geq 3\sigma(I)$ were used for further calculations. The intensities were corrected for the Lorentz and polarization factors but not for absorption ($\mu\lambda_{Mo} = 19.3 \text{ cm}^{-1}$)

The structure was solved by direct methods (Multan[11])—isotropic and then anisotropic full matrix least-squares refinement gave R = 0,086. At this stage, alternate Fourier syntheses and least-squares refinement were used to locate all hydrogen atoms. In the last least-squares cycles a weighting scheme is used with the form $w = (325.0 - 1.857 \text{ Fo})^{-1}$ for Fo < 85.0 and $w = (100.0 + 0.7 \text{ Fo})$ for Fo ≥ 85.0. The final R values are $R = (\Sigma \| \text{Fo} | - | \text{Fc} \|) / \Sigma | \text{Fo} | = 0.045$ and $Rw = (\Sigma w(|\text{Fo}| - |\text{Fc}|)^2 / \Sigma w \text{ Fo}^2)^{1/2} = 0.059$.†

The atomic scattering factors were taken from *International Tables for X-Ray Crystallography.*[12] The real and imaginary parts of the anomalous dispersion were taken into account for nickel and chlorine atoms.

RESULTS AND DISCUSSION

IR spectroscopy

The spectra of compounds I and II are compared with the one of the pure 18-crown-6 polyether previously described by Charpin.[13]

As shown in Fig. 1, the absorptions at 3500–3150 and 1635 cm^{-1} frequencies are attributed to water molecules involved in a complicated set of hydrogen bonds.[14] The spectra of both compounds show the characteristic absorptions of 18-crown-6, but the absorption frequencies are slightly displaced, thus proving complex formation.

The absorptions between 1030 and 1080 cm^{-1} in the spectrum of complex II probably indicate a crown ether configuration similar to that observed with the free state. They are not mentioned in the previously described complexes. The spectrum of compound I in the 1250–1350 cm^{-1} frequency range is similar to that of $(MnX_2)_2$. 18C6. $8H_2O$ described by M.E. Farago.[15]

X-Ray diffraction

This compound presents a chain structure. The $[Ni_2Cl_2(H_2O)_8]^{2+}$ and 18C6 groups are alternatively bonded by hydrogen bonds. Free chloride ions are also hydrogen bonded to the water molecules surrounding two neighbouring dinickel units (Fig. 2).

Since the space group is centrosymmetric with one $[Ni_2Cl_2(H_2O)_8]Cl_2.18C6$ group in the unit cell, this implies that both the ether and the $[Ni_2Cl_2(H_2O)_8]^{2+}$ group lie on inversion centers (Fig 2).

†Atomic co-ordinates, thermal parameters and lists of Fo/Fc values have been deposited as supplementary material with the Editor, from whom copies are available on request. Atomic co-ordinates have also been deposited with the Cambridge Crystallographic Data Centre.

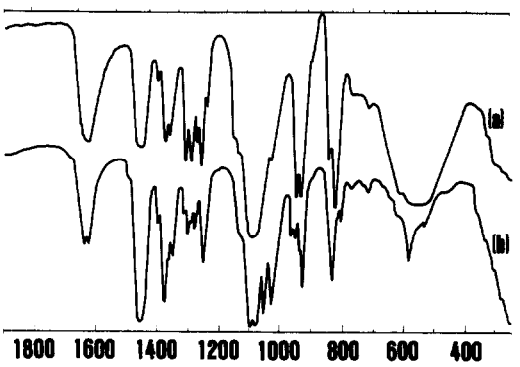

Fig. 1. IR spectra of; (a) compound I $[Ni_2Cl_2(H_2O)_8]Cl_2 \cdot 18C6$. (b) compound II $2NiCl_2 \cdot 2H_2O \cdot 18C6$.

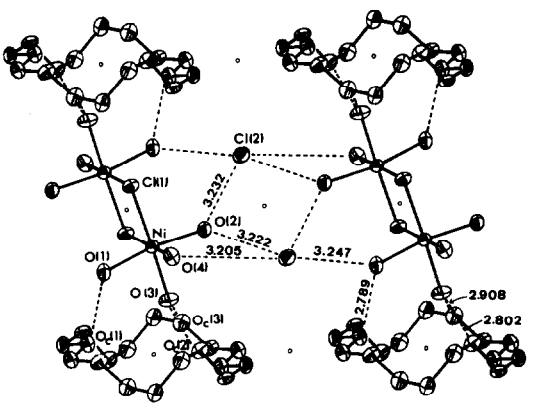

Fig. 2. Hydrogen bonding.

The $[Ni_2Cl_2(H_2O)_8]^{2+}$

This unit is formed by two edges sharing octahedra around Ni with the chlorine atoms at each end of the common edge. Four water molecules on each nickel atom complete the octahedron. The Ni–Cl distances are respectively 2.403 Å and 2.420 Å, which agree with those found in the $[Ni_2Cl_8]^{4-}$ ion[16,17] No significant variance is observed concerning bond angles and distances (Table 2 and 3). The water molecules are repelled by the Cl atoms, with Cl–Ni–O bond angles higher than O–Ni–O ones (93.3 and 87.1° respectively). All hydrogen atoms of the water molecules participate in the hydrogen bonds.

The hydrogen atoms of the water molecules which are not involved in hydrogen bonds with the crown have hydrogen bonds with the free chlorine atom (Fig. 2).

The 18-crown-6 polyether.

The bond angles and the distances do not differ from those usually found in other similar structures.[13,18–22] On the contrary a conformational analysis shows some big

Table 2. Interatomic distances in Å (the e.s.d.) in parentheses refer to last decimal places)

Ni–Cl(1)	2.403(2)	Oc(1)–C(2)	1.433(12)
Ni–Cl'(1)	2.420(3)	Oc(1)–C(3)	1.425(14)
Ni–O(1)	2.068(8)	Oc(2)–C(4)	1.425(12)
Ni–O(2)	2.067(7)	Oc(2)–(C(5)	1.432(12)
Ni–O(3)	2.050(6)	Oc(3)–C(l)	1.424(11)
Ni–O(4)	2.076(7)	Oc(3)–(C(6)	1.430(14)
		C(1)–C(2)	1.485(16)
		C(3)–C(4)	1.498(15)
		C(5)–C(6)	1.502(14)

Table 3. Bond angles in (°) (The e.s.d. in parentheses refer to last decimal places)

Cl(1)–Ni–Cl'(1)	85.12(8)	Cl'(1)–Ni–O(4)	176.1(2)
Cl(1)–Ni–O(1)	93.2(2)	O(1)–Ni–O(2)	170.9(3)
Cl(1)–Ni–O(2)	94.8(2)	O(1)–Ni–O(3)	85.0(3)
Cl(1)–Ni–O(3)	178.3(2)	O(1)–Ni–O(4)	85.3(3)
Cl(1)–Ni–O(4)	91.9(2)	O(2)–Ni–O(3)	86.9(3)
Cl'(1)–Ni–O(1)	92.3(2)	O(2)–Ni–O(4)	90.2(3)
Cl'(1)–Ni–O(2)	92.5(2)	O(3)–Ni–O(4)	87.9(3)
Cl'(1)–Ni–O(3)	95.0(2)	Ni–Cl(1)–Ni'	94.88(9)
C(1)–C(2)–O_c(1)	109.4(8)	O_c(2)–C(5)–C(6)	112.7(8)
C(2)–O_c(1)–C(3)	111.1(7)	C(5)–C(6)–O_c(3)	115.4(8)
O_c(1)–C(3)–C(4)	108.7(8)	C(6)–O_c(3)–C(1)	112.1(7)
C(3)–O_c(4)–O_c(2)	108.5(8)	O_c(3)–C(1)–C(2)	109.5(8)
C(4)–O_c(2)–C(5)	113.2(7)		

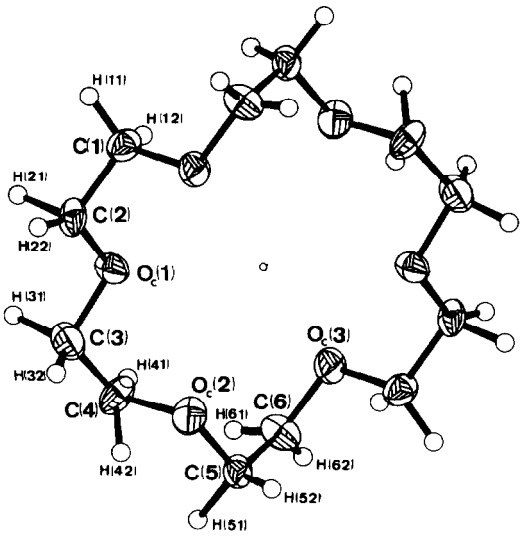

Fig. 3. The 18-crown-6 polyether.

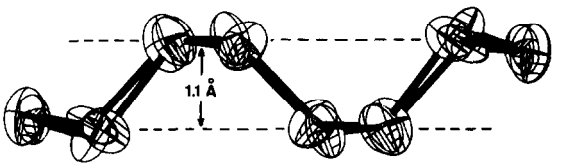

Fig. 4. Crown viewed perpendicular to the mean plane.

differences (Table 4). The atoms are not alternately above and below the mean plane of the crown. It can be described (Fig. 4) as a sequence of five atoms below (C(1), C(2), Oc(1), C(3), C(4)), two above (Oc(2), C(5)) and two below (C(6), Oc(3)), and the reverse for the symmetry related ones. In this way, all the atoms of the crown are in two parallel planes, and the distance between these planes is 1.10 Å (Fig. 4). The crown is thicker than in other similar structures.

The 6 oxygen atoms of the crown have hydrogen bonds with the water molecules of the $[Ni_2Cl_2(H_2O)_8]^{2+}$ units (Fig. 2). These bonds are alternately below and above the plane of the crown and roughly perpendicular to this plane. This may explain the unusual thickness of the crown and its peculiar conformation.

The unusual conformation of the crown ether is related to the strong hydrogen network which assumes crystal packing in the three directions

Table 4. Torsional angles in the crown (°)

O_c(3)–C(1)–C(2)–O_c(1)	72.6
C(1)–C(2)–O_c(1)–C(3)	−173.7
C(2)–O_c(1)–C(3)–C(4)	173.3
O_c(1)–C(3)–C(4)–O_c(2)	−65.4
C(3)–C(4)–O_c(2)–O(5)	−176.9
C(4)–O_c(2)–C(5)–C(6)	−75.5
O_c(2)–C(5)–C(6)–O_c(3)	−56.1
C(5)–C(6)–O_c(3)–C(1)	−68.4
C(6)–O_c(3)–C(1)–C(2)	177.1

CONCLUSIONS

The presence of polar oxygenated ligands such as water molecules around the metal causes an unfavorable competition with respect to crown ether ligation. So, 18-crown-6, which is a very flexible crown ether, is not bonded to the nickel atoms but is hydrogen bonded to the aquated cation $[Ni_2Cl_2, (H_2O)_8]$.[2+] The dinuclear unit were not observed in the previous reported structures of complexes between hydrated cations and crown ethers.[8–10]

This investigation shows, once again, that the solvent-metal interaction strongly influences the complexing.

The IR spectrum of compound II is quite different, and if suitable crystals are prepared their crystal structure will be solved.

Acknowledgements—The authors wish to thank Professors E. Marechal and S. Boileau (University of Paris VI) for fruitful discussions.

REFERENCES

[1]M. R. Truter, In *Structure and Bonding* Vol. 16. Springer-Verlag, Berlin (1973).
[2]J. J. Christensen, J. Delbert, D. J. Eatough and R. M. Izatt, *Chem. Rev.* 1974, **74**, 351.
[3]G. Folcher, P. Charpin, R. M. Costes, N. Keller and G. C. de Villardi, *Inorg. Chim. Acta* 1979, **38**, 87.
[4]C. Bombieri and G. de Paoli, *Inorg. Chim Acta* 1976, **L23**, 18.
[5]M. Ciampolini and N. Nardi, *Inorg. Chim. Acta* 1979, **L9**, 32.
[6]A. C. L. Su and J. F. Weiher, *Inorg. Chem.* 1968, **7**, 176.
[7]D. DeVos, J. Van Daalen, A. C. Knegt, Th. C. Van. Heyningen, L. P. Otto, M. W. Vonk, A. J. M. Wijsman and W. L. Driessen, *J. Inorg. Nucl. Chem.* 1975, **37**, 1319.
[8]A. Knogel, J. Kopf, J. Oehler and G. Rudolf, *Inorg. Nucl. Chem. Lett.* 1978, **14**, 61.
[9]T. B. Vance Jr, E. M. Holt, C. G. Pierpont and S. L. Holt, *Acta Cryst.* 1980, **B36**, 150.
[10]T. B. Vance Jr, E. M. Holt, C. G. Pierpont and S. L. Holt, *Acta. Cryst.*, 1980, **B36**, 153.
[11]MULTAN: G. Germain, P. Main and M. M. Woolfson, *Acta Cryst.* 1971, **A27**, 368.
[12]*International Tables for X-Ray Crystallography* Vol. 4, p. 71. Kynoch Press, Birmingham (1974).
[13]P. Charpin, R. M. Costes, G. Folcher, P. Plurien, A. Navaza and C. de Rango, *Inorg. Nucl. Chem. Lett.* 1977, **13**, 341.
[14]K. Nakamoto in *Infrared and Raman Spectra of Inorganic and Coordination Compounds.* Wiley New York (1978).
[15]M. E. Farago, *Inorg. Chim. Acta* 1977, **25**, 71.
[16]V. L. Gocken, L. M. Vallarino and J. V. Quagliano, *J. Am. Chem. Soc.* 1970, **92**, 303.
[17]F. K. Rass and G. D. Shucky, *J. Am. Chem. Soc.* 1970, **92**, 4538.
[18]J. D. Dunitz and P. Seiler, *Acta Cryst.* 1974, **B30**, 2739.
[19]M. Dobler, J. D. Dunitz and P. Seiler, *Acta Cryst.* 1974, **B30**, 2741.
[20]P. Seiler, M. Dobler and J. D. Dunitz, *Acta Cryst.* 1974, **B30**, 2744.
[21]M. Dobler and P. Phizackerley, *Acta Cryst.* 1974, **B30**, 2746.
[22]M. Dobler and P. Phizackerley, *Acta Cryst.* 1974, **B30**, 2748.

Polyhedron Vol. 1, No. 4, pp. 413–415, 1982
Printed in Great Britain.

0277-5387/82/040413-03$03.00/0
Pergamon Press Ltd.

NOTES

QUANTUM MECHANICAL INTERPRETATION OF PHOTODECOMPOSITION OF DI-TERTIARYBUTYL MERCURY

M. S. SOLIMAN* and A. M. EL-WAKIL
Department of Chemistry, Faculty of Science, Mansoura University, Mansoura, Egypt

(*Received* 19 *August* 1981)

Abstract—The quantum mechanical "Extended Hückel Theory" is applied to the electronic structure calculation of compounds containing heavy elements like mercury. Di-tertiarybutyl mercury, which deposits elementary mercury when irradiated, shows an absorption band at 242 nm ($\epsilon = 4070$). A quantitative discussion of the molecular orbitals calculated by the Extended Hückel Method, using a basis set of *s*-, *p*- and *d*-functions was made. The calculations indicate that the absorption band at 242 nm is attributed to a charge transfer between the Highest Occupied Molecular Orbital (HOMO) and the Lowest Occupied Molecular Orbital (LUMO). It was found to be a symmetry allowed transition and its calculated energy is in good agreement with that observed. A quantitative discussion of the coefficients of different atomic orbitals of both the HOMO- and LUMO-calculated wave functions and calculation of bond orders between Hg- and C-atoms for the ground and first excited states explained reasonably, that it is this transition which is responsible for the decomposition of di-tertiarybutyl mercury with the liberation of elementary mercury.

INTRODUCTION

Di-tertiarybutyl mercury is known to be sensitive to light, it absorbs light and decomposes to give the elementary mercury and the corresponding alkane. It was widely used for many chemical preparations, where different light radiation sources are used to initiate the reactions.[1,2]

$$(CH_3)_3C\text{–}Hg\text{–}C(CH_3)_3 \rightarrow 2(CH_3)_3C^{\cdot} + Hg. \qquad (1)$$

The literature pertaining to these reactions concentrated on the mechanisms of these reactions. However, no attention has been devoted to determine the proper wavelength of radiation that is responsible for the decomposition of t-Bu_2Hg. This stimulated the authors to study this particular point from the quantum mechanical point of view. The calculated energy states and their corresponding functions with their symmetry are the key for this study.

The Extended Hückel Molecular Orbital Method "EHMO"[3,4] employing the *s*-, *p*- and *d*-Slater orbitals was used to perform this study.

THEORETICAL BASIS OF CALCULATION

The EHMO method is based on the solution of the Linear Combination of Atomic Orbital Self Consistent Field "LCAO–SCF" equation:

$$\sum_{\mu=1}^{n} (F_{\mu\nu} - ES_{\mu\nu})\, C_{\mu\nu} = 0 \quad \nu = 1, 2, \ldots, n \qquad (2)$$

where $F_{\mu\nu}$ is the Coulomb- or resonance-integral, $S_{\mu\nu}$ is the overlap integral, E is the energy eigenvalue and $C_{\mu\nu}$ is the coefficient of atomic orbital. The diagonal matrix-elements $F_{\mu\mu}$ (Coulomb integral) will be taken as the negative value of the atomic orbital ionization energy, $F_{\mu\mu} = -I$. The out-of-diagonal elements $F_{\mu\nu}$ (resonance integral), is calculated from Wolfsberg–Helmholtz empirical equation:[5]

$$F_{\mu\nu} = 0.5k(F_{\mu\mu} + F_{\nu\nu})S_{\mu\nu} \qquad (3)$$

where k is a constant parameter, having a value between 1.5 and 2.0. In this study the k-value of 1.68 was used, as it gives the minimum total energy. $S_{\mu\nu}$ is the overlap integral, $S_{\mu\nu} = \int \phi_\mu \phi_\nu \, d\tau$. The functions ϕ_μ and ϕ_ν are the radial part of the electron wave functions, where they are a polynom of the radius r, multiplied by an exponential function $\phi = r^{n-1} e^{-\{(z-s)/nr\}}$, where n is the principal quantum number, z is the atomic charge and s is a shielding constant.[7] The value $(z - s)/n$ is termed the orbital-exponent ρ, and has a value for every atom depending on the shielding constant s.[8] These functions have no nodes and are known as the Slater functions.[6]

A molecular orbital will be considered as formed from a linear combination of all the atomic orbitals over all the molecule.

$$\psi_j = \sum_i C_{ji}\phi_i. \qquad (4)$$

EXPERIMENTAL

Di-tertiarylbutly mercury was prepared following the method described by Neumann.[9] It was isolated as colourless crystals (mp. 58–60°C) and gave an NMR singlet at $\tau = 8.8$. The UV-absorption spectrum was recorded using *n*-hexane as a solvent. A Perkin–Elmer UV–VIS spectrophotometer 200 was utilized with a 1 cm cell width for a duration not longer than 15 min.

To perform the calculation, t-Bu_2Hg was considered to be a linear molecule belonging to the D_{3d} symmetry group, all the angles at the carbon are exactly tetrahedral with bond lengths: C–H = 1.09, C–C = 1.54 and C–Hg = 2.07 Å.[10] The minimum basis set for atoms taken into consideration were: for the H-atoms, only the 1*s*-orbital; for the carbon atoms, 2*s*-, $2p_x$, $2p_y$, $2p_z$; for the mercury atom, 6*s*-, $6p_x$-, $6p_y$-, $6p_z$-, $6d_{z^2}$, $6d_{x^2-y^2}$-, $6d_{xy}$-, $6d_{yz}$- and $6d_{xz}$-orbitals. So a basis set of 59 atomic orbitals was considered in the calculations. The ionization energies used to evaluate the Coulomb integrals are given in Table 1. The orbital-exponents used to calculate the resonance integrals are summarised in Table 2.

*Author to whom correspondence should be addressed.

Table 1. Ionization energies after Skinner[11]

Atomic orbital	I, ev	Atomic orbital	I, ev
H (1s)	13.60	Hg (6s)	8.69
C (2s)	21.01	Hg (6p)	3.03
C (2p)	11.27	Hg (6d)	0.60

Table 2. Orbital exponents after Slater[6]

Atom	H	C	Hg
$= \frac{s-z}{n}$	1.0	1.625	1.036

The calculations were performed with the aid of FORTRAN IV computer programme using the IBM 370/158 computer system.

RESULTS AND DISCUSSION

The UV-absorption spectrum ot t-Bu_2Hg gave two absorption bands at 216 nm ($\epsilon = 21804$) and 242 nm ($\epsilon = 4070$). The present study is devoted to the latter band (at 242 nm) which is expected to be responsible for the decomposition of the compound under investigation. Evidence for this expectation is based on the work of Rebbert[12] where similar molecular (dialkyl mercury) was reported to decompose at 254 nm.

Having 59 atomic orbitals, the same number of eigenvalues assigned to 59 molecular orbitals should be obtained from Hückel equation. Also an eigenvector, whose components are the coefficients of the atomic orbitals, belongs to every eigenvalue.

In the molecule under investigation, 52 valence electrons are present. These electrons will occupy 26 molecular orbitals of lowest energies from ψ_{59} to ψ_{34}. Table 3 shows the energies and symmetries of the calculated molecular orbitals. A transition from the 26 occupied molecular orbitals to the unoccupied orbitals is expected. However, the probable transition is that from the Highest Occupied Molecular Orbital (HOMO) to the lowest Unoccupied Molecular Orbital (LUMO). To determine the probability of LUMO ← HOMO transition, their eigenvectors should be thoroughly investigated. Table 4 shows the eigenvectors of the HOMO (ψ_{34}) and the LUMO (ψ_{33}) molecular orbitals. The graphical presentation of these molecular orbitals, based on the coefficients in Table 4, for the s- and p-orbitals, are shown in Fig. 1. This figure shows that ψ_{34} transformed as species A_{2u} of the D_{3d} point group, while ψ_{33} will transform as species A_{1g}.

The direct product of irreducible representation to which ψ_{33}, dipole moment operator and ψ_{34} gave rise to a totally symmetric representation and consequently the LUMO ← HOMO is a symmetry allowed transition. The calculated coefficients of the s- and d_{z^2}- orbitals on the mercury atom in ψ_{33} (LUMO) are higher than the corresponding values for ψ_{34} (HOMO). This means a higher electron density on mercury atom in ψ_{33} than in ψ_{34}. This increase is consequently associated with a decrease in the electron density at the p_z-orbital (in the direction C–Hg bond).

The bond order between Hg- and C-atoms was deter-

Table 3. The molecular orbitals of t-Bu_2Hg, their energies and symmetry

Orbital ψ	Energy, eV		Symmetry
1	82.744		a_{1g}
2	68.407		a_{2u}
	o		
	o		
	o		
31,32	-02.277		e_u
33 (LUMO)	-04.859	↑ 5.566 eV	a_{1g}
34 (HOMO)	-10.425		a_{2u}
35	-10.547		a_{1g}
36,37	-12.970		e_u
38,39	-12.986		e_g
40	-13.818		a_{2g}
41	-13.830		a_{1u}
42,43	-14.286		e_u
44,45	-14.315		e_g
46,47	-15.089		e_u
48,49	-15.324		e_g
50	-15.495		a_{2u}
51	-15.734		a_{1g}
52	-18.183		a_{1g}
53	-18.329		a_{2u}
54,55	-23.741		e_u
56,57	-25.969		e_g
58	-30.902		a_{2u}
59	-30.909		a_{1g}

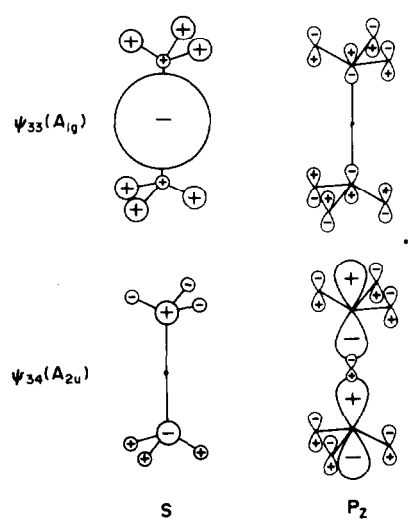

Fig. 1. Representation of s- and p-atomic orbitals in the molecular orbitals ψ_{34} (HOMO) and ψ_{33} (LUMO) according to their calculated coefficients.

Table 4. Eigenvectors of the molecular orbitals ψ_{34} and ψ_{33} given for the Hg- and C-atoms only

Atom	Orbital	Coefficients in ψ_{33} (LUMO)	Coefficients in ψ_{34} (HOMO)
1	Hg(6s)	−0.7674	0.0000
	$(6p_z)$	0.0000	0.0480
	$(6p_x)$	0.0000	0.0000
	$(6p_y)$	0.0000	0.0000
	$(6d_{z^2})$	0.4837	0.0000
	$(6d_{xz})$	0.0000	0.0000
	$(6d_{x^2-y^2})$	0.0000	0.0000
	$(6d_{yz})$	0.0000	0.0000
	$(6d_{xy})$	0.0000	0.0000
2	C(2s)	0.0290	0.1359
	$(2p_z)$	0.0366	−0.6680
	$(2p_x)$	0.0000	0.0000
	$(2p_y)$	0.0000	0.0000
3	C(2s)	0.0290	−0.1359
	$(2p_z)$	−0.0366	−0.6680
	$(2p_x)$	0.0000	0.0000
	$(2p_y)$	0.0000	0.0000

mined for both the ground and first excited states according to the equation:

$$P = 2\sum_{k}\sum_{\mu}\sum_{\nu} b_k C_{k\mu} S_{\mu\nu} \qquad (5)$$

where b_k is the occupation number of the molecular orbital, $C_{k\mu}$ is the atomic orbital coefficients and $S_{\mu\nu}$ is the overlap integral. The summation was performed over the HOMO and LUMO molecular orbitals.

For the ground state the bond order was calculated to be 0.1230, whereas for the first excited state the bond order is −0.0232. This indicates that LUMO ← HOMO excitation leads to a transition from a positive value of bond order which is a bonding state to a negative value which is antibonding state.

These changes in the electron density on the mercury and carbon atoms and this destructive change of the bond order indicates the breakage of the Hg–C bond and the consequent decomposition of di-tertiarybutyl mercury.

REFERENCES

[1] V. Balzani and V. Carassiti, *Photochemistry of Coordination Compounds*. Academic Press, London (1970).
[2] U. Blaukat and W. P. Neumann, *J. Organometal. Chem.* 1973, **49**, 323.
[3] R. G. Parr, *The Quantum Theory of Molecular Electronic Structure*. Benjamin, Amsterdam (1964).
[4] R. Hoffmann, *J. Chem. Phys.* 1963, **39**, 1397; 1963, **40**, 2474.
[5] M. Wolfsberg and L. Helmholtz, *J. Chem. Phys.* 1952, **20**, 837.
[6] J. S. Slater, *Phys. Rev.* 1930, **36**, 57.
[7] J. A. Pople and D. L. Beveridge, *Approximate Molecular Orbital Theory*. McGraw-Hill, New York (1970).
[8] E. Clementi and D. L. Raimondi, *J. Chem. Phys.* 1967, **38**, 2686.
[9] W. P. Neumann and U. Blaukat, *Angew. Chem.* 1969, **81**, 625.
[10] *International Tables for X-Ray Crystallography*, Vol. III. The Kynoch Press, Birmingham, England (1968).
[11] H. A. Skinner and H. O. Pritchard, *Trans. Far. Soc.* 1953, **49**, 1254.
[12] P. E. Rebbert and P. Ausloos, *J. Am. Chem. Soc.* 1963, **85**, 3086.

Polyhedron Vol. 1, No. 4, pp. 417–419, 1982
Printed in Great Britain.

0277-5387/82/040417-03$03.00/0
Pergamon Press Ltd.

THE SYNTHESIS AND CHARACTERIZATION OF $(UCp_3)_2$ (PYRAZINE) AND $[U(MeCp)_3]_2$(PYRAZINE): π-BRIDGED DIMERS OF U^{3+}

CHARLES W. EIGENBROT, Jr. and KENNETH N. RAYMOND*
Contribution from the Department of Chemistry, University of California, and the Materials and Molecular Research Division, Lawrence Berkeley Laboratory, Berkeley, CA 94720, U.S.A.

(*Received* 14 *September* 1981)

Abstract—The title compounds are formed by the reaction of $U(C_5H_5)_3(C_4H_8O)$ and $U(C_6H_7)_3(C_4H_8O)$ with pyrazine ($C_4H_4N_2$) and characterized by elemental analysis mass, IR, ^1H NMR and electronic spectra, and by X-ray powder patterns. The $[U(C_6H_7)_3]_2(C_4H_4N_2)$ exhibits anomalous magnetic behaviour that remains under investigation.

INTRODUCTION

Since the resurgence of interest in the organometallic chemistry of the lanthanide and actinide elements in the 13 yr since the synthesis of uranocene,[1] a continuing question has been the role of *f*-electrons in the bonding in these compounds.[2] As part of a programme to create, examine, and explain structural and magnetic probes of this bonding,[3,4] we have sought the synthesis of appropriate dimeric species of uranium for detailed magnetic characterization. A previous report on the synthesis and characterization of $(YbCp_3)_2$(pyrazine) led to the conclusion that as low as 4 K no spin-pairing took place.[4] The behaviour of pyrazine in *d*-metal dimers has demonstrated that, in the covalent extreme, it can facilitate spin-pairing between the metal ion paramagnets. The fact that no pairing was apparent in the Yb complex is convincing evidence of the predominantly ionic bonding in this compound, consonant with the known core-like properties of the 4*f* shell.

However, in the early actinides the 5*f* shell electrons make a greater contribution to the chemical environment, and so dimeric compounds of uranium have been sought. A few other uranium dimers have been reported,[5] but their magnetic characterization has not been complete. This study represents the completion of the investigation of the *f*-dimer complexes of pyrazine that began with $(YbCp_3)_2$(pyrazine) compound.

EXPERIMENTAL

All manipulations were accomplished using a Schlenk or vacuum line with high purity Argon or in a Vacuum Atmospheres HE-93 glove box with a recirculating oxygen and moisture-free Argon atmosphere. All solvents were dried by distillation from potassium benzophenone ketyl and were degassed prior to use. Pyrazine (Aldrich 99+%) was dried over BaO at 60°C. Infrared spectra were recorded on a Perkin–Elmer 597 spectrophotometer, the visible-near IR spectra on a Cary 14M spectrophotometer, NMR spectra on the UCB 250 MHz spectrometer, and mass spectra on an AEI-MS12 spectrometer. The magnetic behavior was measured as described elsewhere.[3] Elemental analyses were performed by the Microanalytical Laboratory at the University of California, Berkeley; or Mallissa and Reuter Analytische Laboratorien, Engelskirchen, West Germany. The X-ray power patterns were collected with Cu radiation. The NaCp(DME)[6] (DME is 1, 2-dimethoxyethane) and UCl_4[7] were prepared by the literature techniques. Naphthalene was sublimed before use. The K(MeCp) was produced by the reaction between the diene (after cracking) and KH in THF (tetrahydrofuran) at 0°C.

UCp(THF) *and* $U(MeCp)_3$(THF). To small pieces of sodium weighing 0.30 g (13 mmol) in 100 mL THF was added 1.70 g (13 mmol) of naphthalene. The resulting dark green mixture was stirred at room temperature overnight. It was then filtered through a glass frit onto 5.00 g (13 mmol) of UCl_4 in 150 mL THF. The mixture of green solutions turned immediately to a deep purple. This mixture was stirred at room temperature for one hour. Next, the NaCp(DME) or KMeCp (39.5 mmol) (solution and slurry, respectively) in 100 mL THF was added, the purple changing to brown immediately. The mixture was stirred at room temperature for another hour, at which time the THF was removed under vacuum. Care was taken to retain a slight dampness of THF. The brown residue was Soxhlet extracted with benzene overnight. Next the benzene was removed under vacuum and the residue subjected to room temperature vacuum for 12 hours to remove the naphthalene. The product thus obtained (90% based on UCl_4) is crystalline. Its composition was confirmed by the IR spectrum,[8] PMR spectrum [for the methylated compound at 21°C in d^8-toluene shifts in δ ppm vs TMS: −8.1 (*s* ~7 H, 102 Hz); −14.5 (*s*, ~12 H, 49 Hz); −21.4 (*s*, ~8 H, 73 HZ)], and elemental analysis. Found: C, 48.91; H, 5.53%; $UC_{22}H_{29}O$ requires: C, 48.26; H, 5.30%.

$(UCp_3)_2$(pyrazine). This compound can be synthesized by the combination of stoichiometric amounts of UCp_3(THF) and pyrazine in benzene, toluene, DME, or THF. The blue-grey product precipitates immediately upon addition of pyrazine to a brown solution of UCp_3(THF). It is most soluble in THF, but only sparingly so. The supernatant from a THF preparation, if cooled quickly to −78°C and held there for a few days, yields black microcrystalline material. This material was used for the X-ray powder pattern. Found: C, 43.40; H, 4.07; N, 2.22%; $U_2C_{34}H_{34}N_2$ requires: C, 43.13; H, 3.59; N, 2.96%. IR spectrum (Nujol mull) (cm^{-1}) 3080, 1422, 1279, 1261, 1068, 1018, 960, 809, 782, 737, 619, 602, 470.

Mass spectral data (70 eV) are included in Table 1(a).

The low solubility of this compound hampered further characterization.

$[U(MeCp)_3]_2$(pyrazine). To a dark brown solution of $U(MeCp)_3$(THF) in toluene was added a stoichiometric amount of pyrazine in a small volume of toluene. The color changed immediately to a deep blue–black. Stirring at room temperature for a few minutes, followed by filtration yielded a very strongly colored filtrate. Cooling to −15°C overnight yielded black crystals shaped like needles. Found: C, 46.60; H, 4.47; N, 2.72%; $U_2C_{40}H_{46}N_2$ requires: C, 46.29; H, 4.28; N, 2.81%. IR spectrum (Nujol mull) (cm^{-1}) 1420, 1279, 1057, 1048, 1030, 950, 880, 849, 840, 805, 770, 758, 742, 728, 694, 611, 463.PMR spectrum (20°C, d^8-toluene, δ ppm vs TMS) −2.15 (*s*, 18 H, 9 Hz, Me); −11.5 (*s*, 11 H, 15 Hz, ring); −13.4 (*s*, 12 H, 15 Hz, ring); −67.0 (*s*, 4 H, 15 Hz, pyrazine).

Mass spectral data (70 eV) are in Table 1 (b).

Electronic spectrum (in toluene vs toluene) (nm) 1510, 1360, 1220, 1180, 1020, 910, 680. The maxima are quite broad.

Single crystals suitable for diffraction studies have not been

Table 1 (a). Mass spectrum of $(UCp_3)_2$(pyrazine)

RA (%)[a]	m/e	Assignment[b]
0.8	883	U_2L_5X
1.5	817	U_2L_4X
0.8	620	U_2LX
1.1	514	UL_3X
1.4	512	-
15	433	UL_3
16	403	-
25	387	-
22	368	UL_2
16	338	-
23	322	-
4	303	UL
72	80	X
73	66	L
100	44	-

[a]Relative abundance.

[b]L = C_5H_5 and X = $C_4H_4N_2$.

Table 1 (b). Mass spectrum of $[U(MeCp)_3]_2$(pyrazine).

RA (%)[a]	m/e	Assignment[b]
0.2	966	U_2L_5X + 15
0.1	952	U_2L_5X
0.7	887	U_2L_4X + 15
0.4	873	U_2L_4X
0.3	726	-
0.6	647	-
0.7	602	-
0.7	568	-
2.0	556	UL_3X
1.5	523	-
30	494	-
20	475	UL_3
25	431	-
88	415	-
40	336	-
70	80	X
100	79	L

[a]Relative abundance.

[b]L = C_6H_7 and X = $C_4H_4N_2$.

obtained. Both this and the previous compound sublime with some decomposition at 10^{-3} torr and 120°C.

DISCUSSION

The dimeric formulation of these compounds is based primarily on: (a) the X-ray power pattern of $(UCp_3)_2$(pyrazine); (b) the mass spectra of both compounds; and (c) the PMR of the methylated compound.

The crystal and molecular structure of $(YbCp_3)_2$(pyrazine) has been determined,[4] and consists of a dimer located about a crystallographic inversion center. Two ytterbium atoms, each with three η^5-Cp rings, are nearly linearly bridged by a pyrazine ring coordinated through its nitrogens. Because $(UCp_3)_2$(pyrazine) exhibits low solubility, and $[U(MeCP)_3]_2$(pyrazine) forms only thin needles during crystal growth, a single crystal X-ray structure of these compounds has eluded us. However, it is reasonable to assume that substitution of U^{3+} for Yb^{3+} would lead to isomorphic structures, and if so, that powder patterns of the two compounds should be quite similar. Indeed this is so, the similarity of the patterns extending to the general pattern of the lines and their relative intensities.

The mass spectra of both compounds reveal the presence of dimeric species (Table 1). Both spectra contain several prominent peaks that are not easily assigned, but that are included for completeness. The intensity of the high-mass peaks in rather low, consistent with the decomposition observed during sublimation. In the spectrum of the methylated compound, peaks appear that correspond to $[U_2L_{6-x}(\text{pyrazine})+15]^+$, which suggests that perhaps uranium–methyl bonds are formed in the spectrometer.

The PMR spectrum of the methylated compound includes one singlet resonance for the four pyrazine protons. This supports the dimer formulation since in the monomer the chemical shifts should be two sets of two. This spectrum also exhibits resonances one expects for the mono-methyl Cp ligands—the methyl groups shifted the least, while the inequivalent sets of ring protons are shifted more by the uranium ion.

One use of the liquid helium apparatus is predicated on the expectation that any covalent effects would be of particularly low energy and necessitate the use of very low temperatures. For this reason neither the room temperature moment nor the temperature dependence of the NMR spectrum has been determined. The magnetic behavior of the methylated compound has been investigated four times. Three times the data indicate the compound is only weakly paramagnetic, and that the paramagnetism varies slowly with temperature. The fourth investigation produced results that suggest an abrupt spin-state change at very low temperature. Any further interpretation of the magnetic behavior of this compound will require further investigation.

Acknowledgements—We wish to thank Helena Ruben for her assistance with the X-ray powder patterns. This work was supported by the Director, Office of Energy Research, Office of Basic Energy Sciences, Chemical Sciences Division of the U.S. Department of Energy under Contract Number W-7405-ENG-48.

REFERENCES

[1]A. Streitwieser and U. Mueller-Westerhoff, *J. Am. Chem. Soc.* 1968, **90**, 7364.
[2]K. N. Raymond and C. W. Eigenbrot, Jr., *Acc. Chem. Res.* 1980, **13**, 726. and references therein.
[3]C. W. Eigenbrot, Jr. and K. N. Raymond, *Inorg. Chem.* in press.
[4]E. C. Baker and K. N. Raymond, *Inorg. Chem.* 1977, **16**, 2710.
[5]M. Tsutsui, N. Ely and A. Gebala, *Inorg. Chem.* 1975, **14**, 78.
[6]J. C. Smart and C. J. Curtis, *Inorg. Chem.* 1977, **16**, 1788.
[7]J. A. Hermann and J. F. Suttle, *Inorg. Syn.* 1957, **5**, 143.
[8]B. Kanellapopulos, E. O. Fischer, E. Dornberger and F. Baumgartner, *J. Organomet. Chem.* 1970, **24**, 507.

Polyhedron Vol. 1, No. 4, pp. 421–422, 1982
Printed in Great Britain.

0277-5387/82/040421-02$03.00/0
Pergamon Press Ltd.

DINITROGEN COMPLEX OF MAGNESIUM

K. C. PATIL,* C. NESAMANI and V. R. PAI VERNEKER
Department of Inorganic and Physical Chemistry, Indian Institute of Science, Bangalore, 560012, India.

(*Received* 11 *January* 1982)

INTRODUCTION

Since Allen and Senoff[1] reported the first dinitrogen complex of ruthenium in 1965, over one hundred and fifty dinitrogen complexes have been prepared. Dinitrogen complexes are generally formed by transition metals[2–5]. Linke *et al.*[6,7] have claimed the formation of dinitrogen complexes of calcium, strontium and barium during the incomplete solvolysis of the corresponding metal pernitrides (M_3N_4) with water, acetic acid and hydrazine. The route for the formation of dinitrogen complexes by the indirect method[5] involves, oxidation of hydrazine, thermolysis or acid catalysed decomposition of an azide complex. The source of the molecular nitrogen thus appears to be either azide or hydrazine. So it was thought interesting to see if thermolysis of hydrazine complexes of metal azides $[M(N_3)_2(N_2H_4)_2]$ which contain both hydrazine and azide can give rise to a dinitrogen complex. Since, transition metal azide hydrazinates are highly explosive, alkaline earth metal complexes were chosen. Thermolysis of calcium azide hydrazinate, $Ca(N_3)_2(N_2H_4)_2$ and barium azide hydrazinate $Ba(N_3)_2(N_2H_4)$, did not yield any dinitrogen complex probably because the hydrazine was lost initially giving anhydrous metal azides which exploded violently. However thermolysis of magnesium azide dihydrazinate, $Mg(N_3)_2(N_2H_4)_2$, gave a blue coloured compound which showed strong infrared absorption $\sim 2100\,cm^{-1}$ indicating the formation of a dinitrogen complex. The object of this communication is therefore to report a new route for the formation of dinitrogen complexes by the solid state decomposition of metal azide hydrazine complexes.

EXPERIMENTAL

Magnesium azide dihydrazinate, $Mg(N_3)_2(N_2H_4)_2$–I was prepared by a novel reaction of magnesium metal powder with ammonium azide dissolved in hydrazine hydrate (99%). Magnesium metal dissolves in the solution of hydrazinium azide formed metathetically[8] with the evolution of hydrogen. The reaction can be represented as follows:

$$NH_4N_3 + N_2H_4H_2O \rightarrow N_2H_5N_3 + H_2O + NH_3 \quad (1)$$

$$Mg^{O} + 2N_2H_5N_3 \rightarrow Mg(N_3)_2(N_2H_4)_2 + H_2 \quad (2)$$

$$Mg + 2NH_4N_3 + 2N_2H_4H_2O \rightarrow Mg(N_3)_2(N_2H_4)_2 + 2H_2O + 2NH_3 + H_2 \quad (3)$$

Magnesium azide dihydrazinate, $Mg(N_3)_2(N_2H_4)_2$–I was characterized by chemical analysis (Found: Mg, 14.00; N_3, 48.97; N_2H_4, 37.03. $Mg(N_3)_2(N_2H_4)_2$ requires: Mg, 14.11; N_3, 48.75; N_2H_4, 37.14%). Azide content was determined by ceric ammonium nitrate solution using N-phenylanthranilic acid as an indicator.[9] Magnesium content was determined by EDTA titration and hydrazine by the titration against 0.05 M potassium iodate solution under Andrew's condition.[8] Infrared spectra of I and its decomposition products were recorded as nujol mulls using Perkin-Elmer 599 spectrophotometer. UV spectrum was recorded using Cary-14 spectrophotometer. Thermal analysis was carried out using Stanton-Redcroft TG 750 and DTA instruments.[10] All experiments were done both in air and N_2. The heating rate employed was 10°C/min. both in TG and DTA. Platinum cups were used as sample holders. Mass spectral analysis was done using MS 10 spectrophotometer.

RESULTS AND DISCUSSION

Although calcium azide mono- and dihydrazinates are reported[11] there appears to be no mention in the literature about the preparation of magnesium azide hydrazinate. Presently we seem to have obtained magnesium azide dihydrazinate $Mg(N_3)_2(N_2H_4)_2$ by the novel method described above. The compound has been characterized by chemical analysis and infrared spectra (Table 1). The characteristic i.r. absorptions of the azide observed at $2080\,cm^{-1}$, 1310 and $640\,cm^{-1}$ have been assigned.[12] Hydrazine absorptions at 3400, 3300, 1600, 1400, 1100, 965, 820 and $530\,cm^{-1}$ are similar to those reported for $M(N_2H_4)_2X_2$.[13] The γ_{N-N} of N_2H_4 appears at $965\,cm^{-1}$ indicating the presence of bridged hydrazine.[13]

Differential thermal analysis (DTA) of $Mg(N_3)_2(N_2H_4)_2$ shows an exotherm at 217°C followed by an endotherm at 350°C. Thermogravimetry (TG) shows a two step decomposition corresponding to the DTA peaks. The weight loss for the first step is 51% and 77% for the second step (Table 2).

The observed weight loss (77%) corresponds to the formation of magnesium imide, MgNH (77.18%). The magnesium content of MgNH also shows good agreement (Found: 60.85; Calc. 61.85%). Ir spectrum of the residue shows characteristic absorptions of imide in the region 3700–3100 cm^{-1}, 860 cm^{-1} and 600–300 cm^{-1}.[14] On strong heating MgNH decomposes to Mg_3N_2 with the evolution of ammonia.

However the focal point of the present investigation is the intermediate obtained during the thermal decomposition of $Mg(N_3)_2(N_2H_4)_2$–I. The decomposition product after the exotherm at 217°C corresponding to 51% weight loss is blue coloured and sensitive to moisture and air. Observed weight loss (51%) is in good agreement with the formula $Mg(NH_2)_2N_2$–II. The in-

Table 1. IR absorption frequencies of $Mg(N_3)_2(N_2H_4)_2$–I and $Mg(NH_2)_2(N_2)$–II (cm^{-1})

$Mg(N_3)_2(N_2H_4)_2$–I	$Mg(NH_2)_2N_2$–II
3400 s JN_2 asym. stretching	3600 s —
3300 s NH_2 sym. stretching	3300 w NH_2 asym. stretching
2080 s N_3^- asym. stretching	3200 m NH_2 sym. stretching
1600 s NH_2 bending	2160 s N ≡ N stretching
1310 s N_3^- sym. stretching	2040 sh N ≡ N stretching
1170 s NH_2 twisting	1630 s NH_2 bending
1080 s NH_2 twisting	1200 s NH_2 wagging
965 s N–N stretching of N_2H_4	1080 s NH_2 twisting
820 w NH_2 rocking	600 vb NH_2 rocking
640 s N_3^- bending	400 s Mg–N_2 stretching
530 s NH_2 rocking	
400 m Mg–W stretching of N_3	
350 w Mg–N stretching of N_2H_4	

s—strong, m—medium, w—weak, sh—shoulder, vb—very broad.

*Author to whom correspondence should be addressed.

Table 2. Thermal analysis data of $Mg(N_3)_2(N_2H_4)_2$

Step No.	Thermogravimetry† Temp. range	% Wt. loss Obsd.	Reqd.	DTA‡ peak temp.	Reaction
1	25–217	51.00	51.06	217 (exo)	$Mg(N_3)_2(N_2H_4)_2 \rightarrow Mg(NH_2)_2N_2$
2	217–350	77.00	77.18	350 (endo)	$Mg(N_3)_2(N_2H_4)_2 \rightarrow MgNH$

†TG-N_2 atmosphere.
‡Air.

frared spectrum of II shows characteristic absorptions at 3660, 3300, 3200, 1630, 1200, 1080, 600 cm^{-1} have been assigned similar to those reported for $M(NH_2)_2$.[14,15] The absorptions at 2160 (s), 2040 (sh) cm^{-1} and 410 (s) cm^{-1} have been assigned to $\nu_{N=N}$ and ν_{Mg-N_2} respectively (Table 1). Presence of N_3^- in the residue which is known to show $\nu_{N=N}$ 2100 cm^{-1} as in the parent compound is ruled out by the qualitative analysis of the residue (-ve test with $FeCl_3$ solution; no blood red colour) as well as absence of N_3^- IR bands at 1310 and 640 cm^{-1}. Chemical analysis of the residue showed the presence of Mg^{2+} (Found: 28.59; Calc. 28.84%) and amide. Acid hydrolysis of the residue gave ammonium salt (+ve test with Nessler's reagent). The blue coloured compound showed an absorption at 240 nm in UV spectrum. On further heating $Mg(NH_2)_2(N_2)$ decomposes 350°C with the evolution of ammonia and nitrogen to magnesium imide, MgNH. Evolution of NH_3 and N_2 was confirmed by the mass spectrometric analysis of the evolved gases at above 350°C, which showed peaks at m/e = 14, 15, 16, 17 and 28.

It is not surprising that the thermolysis of $Mg(N_3)_2(N_2H_4)_2$ yields $Mg(NH_2)_2N_2$ since the hydrazine moiety is known[15] to disproportionate to amide and coordinated nitrogen.

REFERENCES

[1]A. D. Allen and C. V. Senoff, *Chem. Commun.* 1965, 621.
[2]J. Chatt, J. R. Dilworth and R. L. Richards, *Chem. Rev.* 1978, **78**, 589.
[3]W. Newton, J. R. Postgate and C. Rodriguez-Berrueco, *Developments in Nitrogen Fixation Proc. 2nd Int. Symp. Nitrogen Fixation.* Academic Press, New York (1977).
[4]M. M. Taquikhan and A. N. Martell, *Homogeneous Catalysis by Metal Complexes*, Vol. I. Academic Press, New York (1974).
[5]G. J. Leigh, *Preparative Inorganic Reactions*, 1971, 7, 165.
[6]K. H. Linke and R. Taubert, *Z. Anorg. Allgem. Chem.* 1971, **74**, 383.
[7]K. H. Linke, R. Taubert and T. H. Kruck, *Z. Anorg. Allgem. Chem.* 1973, **1**, 396.
[8]K. C. Patil, R. Soundararajan and V. R. Pai Verneker, *Proc. Indian Acad. Sci.* 1978, **87A**, 281. *Ibid.* 1979, **88A**, 211.
[9]I. M. Kolthoff and R. Belcher, *Volumetric Analysis* III. p. 139. Interscience, New York (1957).
[10]K. C. Patil, R. Soundararajan and V. R. Pai Verneker, *Inorg. Chem* 1979, **18**, 1969.
[11]A. L. Dresser and A. W. Browne, *J. Am. Chem. Soc.* 1931, **53**, 4235.
[12]S. D. Ross, *Inorganic Infrared and Raman Spectra* 119 (1972).
[13]L. Sacconi and A. Sabatini, *J. Inorg. Nucl. Chem.* 1963, **25**, 1389.
[14]G. Linde and R. Juza, *Z. Anorg. Allgem. Chem.* 1974, **409**, 199.
[15]J. J. Molewyn Hughes and A. W. B. Garner, *Chem. Commun.* 1969, 1309.

Polyhedron Vol. 1, No. 4, pp. 423–424, 1982
Printed in Great Britain.

0277–5387/82/040423–02$03.00/0
Pergamon Press Ltd.

COMMUNICATION

REACTIONS OF LANTHANIDE ELEMENTS WITH THALLOUS CYCLOPENTADIENIDE—A NEW ROUTE TO CYCLOPENTADIENYLLANTHANIDES

G. B. DEACON*, A. J. KOPLICK, and T. D. TUONG
Chemistry Department, Monash University, Clayton, Victoria 3168, Australia

(*Received* 15 *January* 1982)

Abstract—The cyclopentadienyllanthanides, $(C_5H_5)_2Yb$, $(C_5H_5)(C_5H_5)_2Yb(dme)$ (dme = 1,2-dimethoxyethane), and $(C_5H_5)_3M(thf)$ (M = Sm or Nd; thf = tetrahydrofuran) have been obtained from reactions of lanthanide elements with thallous cyclopentadienide, and $(C_5H_5)_3Yb$ has been prepared by oxidation of $(C_5H_5)_2Yb$ with $Tl(C_5H_5)$.

Transmetallation reactions between lanthanide elements and di(organo)mercurials provide a convenient synthesis of organolanthanides in which the organic group contains electron withdrawing substituents.[1–3] This route does not appear attractive for cyclopentadienyllanthanides, since *bis*-(cyclopentadienyl)mercury has low thermal and unsatisfactory storage stability,[4] and since the effect of the fluxional η^1-cyclopentadienyl groups of the mercurial[5] on transmetallation is uncertain. The readily prepared and more stable thallous cyclopentadienide[6] is a more attractive reagent, and we now report that cyclopentadienyllanthanides can be prepared by reaction of lanthanide elements with this compound. Although thallous cyclopentadienide is commonly used in the synthesis of cyclopentadienyls by reaction with metal halides,[6] reaction with free elements is novel.

Details of some reactions of thallous cyclopentadienide with lanthanide elements are given in Table 1. With an excess of metal, which enhanced reaction, samarium and neodymium gave *tris*-cyclopentadienyls) whereas ytterbium gave divalent species [eqn (1);

$$M + nTl(C_5H_5) \rightarrow (C_5H_5)_nM + nTl \qquad (1)$$

M = Sm or Nd, n = 3; M = Yb, n = 2]. Reactions were carried out in the presence of a little metallic mercury, which was not necessary for reaction to occur but reduced the induction time. After filtration of the reaction mixtures to remove suspended metals, the products were isolated by evaporation to small volume and addition of petrol (M = Yb) or by evaporation to dryness (M = Sm or Nd). The resulting compounds (Table 1) were identified by analysis, infrared absorption characteristic[7,8] of η^5-cyclopentadienyllanthanides, $(C_5H_5)_nM^+$ (n = 1 – 3; M = Sm or Nd) ions in the mass spectra of the $(C_5H_5)_3M(thf)$ complexes, and a ^1H NMR resonance in agreement with that reported[9] for $(C_5H_5)_2Yb$.

Monitoring the ytterbium/thallous cyclopentadienide reactions by visible/near IR spectroscopy (see[9] for background) has shown that *tris*-(cyclopentadienyl)ytterbium is formed as an intermediate [eqn (1), M = Yb, $n = 3$] and is then reduced to *bis*-(cyclopentadienyl)ytterbium (eqn 2) by the excess of metallic ytterbium used (Table 1). To this stage it has not been possible to isolate $(C_5H_5)_3Yb$ from transmetallation in preparatively useful

$$2(C_5H_5)_3Yb + Yb \rightarrow 3(C_5H_5)_2Yb \qquad (2)$$

yield even with adjusted stoichiometry. However, reaction of equimolar amounts of $(C_5H_5)_2Yb$ and $Tl(C_5H_5)$ in tetrahydrofuran at room temperature for 10 h, followed by filtration, evaporation to dryness, and sublimation gave *tris*-(cyclopentadienyl)ytterbium (32%) (eqn 3),

$$(C_5H_5)_2Yb + Tl(C_5H_5) \rightarrow (C_5H_5)_3Yb + Tl\downarrow \qquad (3)$$

which was identified by visible/near infrared spectroscopy[9] and $(C_5H_5)_nYb^+$ ($n = 1 - 3$) ions in the mass spectrum. Thus, transmetallation (1) and the oxidation (3) provide convenient halide-free routes to cyclopentadienyllanthanides.

*Author to whom correspondence should be addressed.

Table 1. Reactions of lanthanide metals with thallous cyclopentadienide in tetrahydrofuran (thf) or 1,2-dimethoxyethane (dme)[a]

Metal	mg at	$Tl(C_5H_5)$ mmol	Solvent ml	Temp (°C)	Time (h)	Product[b]	Yield[c] (%)
Yb	14.2	8.66	dme 45	85	16	$(C_5H_5)_2Yb(dme)$	42
Yb	13.3	6.39	dme 30	25	120	$(C_5H_5)_2Yb(dme)$	53
Yb	13.8	8.55	thf 50	65	72	$(C_5H_5)_2Yb$[d]	68
Sm	16.0	7.39	thf 30	65	18	$(C_5H_5)_3Sm(thf)$	59
Nd	11.2	5.99	thf 50	65	60	$(C_5H_5)_3Nd(thf)$	42

[a]Reactions were carried out under dry oxygen-free nitrogen in the presence of mercury (*ca.* 0.1 g). [b]Compounds were isolated and manipulated under purified nitrogen. [c]Based on $Tl(C_5H_5)$. [d]After drying the product at 140–150°C under vacuum for 2 h; the thf solvate is unstable.[9]

Acknowledgement—We are grateful to the Australian Research Grants Committee for support.

REFERENCES

[1]G. B. Deacon, W. D. Raverty and D. G. Vince, *J. Organomet. Chem.* 1977, **135**, 103.
[2]G. B. Deacon and A. J. Koplick, *J. Organomet. Chem.* 1978, **146**, C43.
[3]G. B. Deacon, A. J. Koplick, W. D. Raverty and D. G. Vince, *J. Organomet. Chem.* 1979, **182**, 121.
[4]G. Wilkinson and T. S. Piper, *J. Inorg. Nucl. Chem.* 1955, **2**, 32.
[5]A. J. Campbell, C. E. Cottrell, C. A Fyfe and K. R. Jeffrey, *Inorg. Chem.* 1976, **15**, 1326.
[6]F. A. Cotton and G. Wilkinson, *Advanced Inorganic Chemistry*, 4th Edn. Wiley, New York, 1980 p. 1163.
[7]E. O. Fischer and H. Fischer, *J. Organomet. Chem.* 1965, **3**, 181.
[8]T. J. Marks, *Prog. Inorg. Chem.* 1978, **24**, 51.
[9]F. Calderazzo, R. Pappalardo and S. Losi, *J. Inorg. Nuclear Chem.* 1966, **28**, 987.

Polyhedron Vol. 1, No. 5, pp. 425–428, 1982
Printed in Great Britain.

0277-5387/82/050425-04$03.00/0
Pergamon Press Ltd.

A KINETIC STUDY ON THE AMMONOLYSIS OF TRIMETAPHOSPHATE

TOHRU MIYAJIMA*, YASUHIKO MIYAHARA and SHIGERU OHASHI
Department of Chemistry, Faculty of Science, Kyushu University 33, Hakozaki, Higashiku, Fukuoka 812, Japan

(*Received* 14 *September* 1981)

Abstract—The rate constants for the ammonolysis of trimetaphosphate in aqueous solution were determined by measuring the disappearance of trimetaphosphate by use of high-performance liquid chromatography (HPLC). The rate of the reaction was of first order in the concentration of trimetaphosphate. It was found that metal cations added increased the reaction rate. The activation energy and the activation entropy were determined to be 13.6 kcal/mole and about −25 eu, respectively.

INTRODUCTION

It is well known that small cyclic phosphates such as trimetaphosphate, P_{3m}, react with various amine compounds to open their rings and form phosphorus–nitrogen compounds in aqueous solution.[1–4] Even though new compounds which contain a P–N bond in their molecules have been synthesized by utilizing these reactions,[5–7] fundamental consideration on the reaction mechanism has not sufficiently been made up to the present. This may be due to the lack of the analytical tools available for characterizing the reactions. HPLC developed in our laboratory allows us to separate and determine these phosphate compounds speedily and routinely.[8–10] By use of the HPLC device, a kinetic study was carried out in order to determine the reaction rates of the fundamental reaction, i.e. ammonolysis of P_{3m} to form monoamidotriphosphate, MATP.

EXPERIMENTAL

Chemicals. Trisodium trimetaphosphate trihydrate, $Na_3P_3O_9 \cdot 3H_2O$, was prepared according to the literature.[11] The purity was checked by the HPLC to be higher than 99%. Other reagents used in this study were of analytical grade.

NMR measurement. A Hitachi Model R-20B high resolution NMR spectrometer operating at 24.3 MHz for ^{31}P was used. Analyses were performed in 8 mm spinning sample tubes at 25°C. 85% orthophosphoric acid in a 1 mm capillary inserted in the sample tube was used as an external reference. Chemical shifts are reported positive downfield from the standard. For adequate signal-to-noise ratios, it was necessary to limit measurements to relatively high concentrations (higher than 0.1 M as P).

HPLC analysis. A Hitachi 635 liquid chromatograph was used for the separation of phosphates. The separation column (ϕ2.6 × 500 mm) was packed with an anion exchanger (TSK-GEL, IEX-220 SA). A portion of the effluent was introduced to the AutoAnalyzer detector in order to monitor continuously the total phosphate concentration in an effluent. Details of the chromatographic system have been described previously.[8–10] Potassium chloride solution of an appropriate concentration was used as an eluent for isocratic elution. Each eluent contained 0.1% EDTA · 4Na (pH 10.7) in order to obtain a well-resolved chromatogram with good reproducibility. The retention times and the areas of the peaks were determined and recorded automatically with a Shimadzu Chromatopac C-R1A data processor.

Rate measurement. The kinetic experiments were conducted at temperatures between 10 and 50°C in a thermostated bath controlled within ±0.1°C. The pH of the reaction mixture solution was between 11 and 12. Both ^{31}P NMR measurement and the HPLC analysis are available for the quantitative kinetic study. In this study, ^{31}P NMR measurement was carried out in order to identify the reaction products and the rate constant determination was performed mainly by HPLC. In order to separate P_{3m} and MATP by HPLC, 0.5 M potassium chloride solution was used as an eluent. 100-μl portions of the reaction mixtures were withdrawn at proper time-intervals and were poured into 100-ml measuring flasks containing an ice cold eluent. The flasks were surrounded by water at 0°C. This procedure "freezes" the reaction at the noted time intervals. 100-μl portions of the diluted sample solution were applied to the column. Good linearity was found for the plots of the peak area vs the amount of P_{3m} or MATP. The slopes of both the plots were consistent with each other.

RESULTS AND DISCUSSION

The mixed solution of sodium trimetaphosphate (0.28 M) and ammonia (4.9 M) was allowed to stand at 30°C for 30 hr. ^{31}P NMR spectrum of the mixed solution gave doublets at −0.2 and −5.2 ppm, attributable to the end PO_2NH_2 and the end PO_3 phosphorus atoms respectively, and a triplet at −20.5 ppm attributable to the middle PO_3 phosphorus atoms. The chemical shifts of the signals are consistent with the values of MATP in the literature[1]. Since the areas of the signals corresponding to each phosphorus atoms were found to be equal, it was concluded that the mole ratio of each phosphorus atom was equal to each other. This indicates that P_{3m} reacts with ammonia to form MATP predominantly in these experimental conditions. The mixed solution was analyzed by HPLC using 0.21 M potassium chloride solution as an eluent (Fig. 1). For comparison purposes, the chromatogram of a mixture of orthophosphate, P_1, diphosphate, P_2, and triphosphate, P_3, is also shown. Since no peak appeared at the peak positions of P_1, or

*Author to whom correspondence should be addressed.

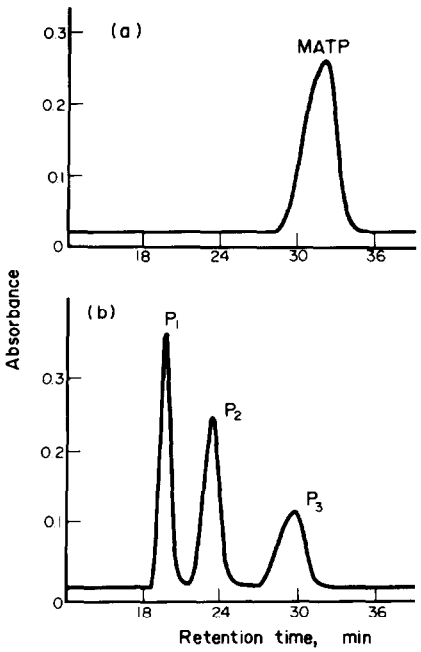

Fig. 1. Elution profiles of (a) monoamidotriphosphate and (b) a mixture of ortho-, di- and triphosphate.

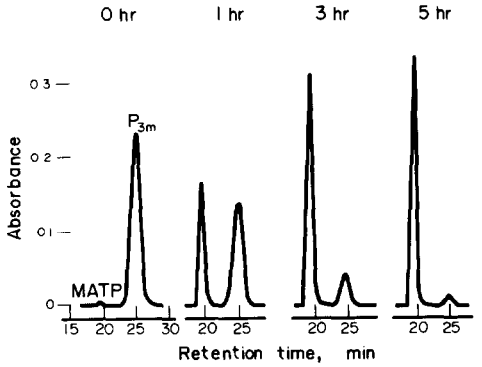

Fig. 2. Elution patterns for the ammonolysis of trimetaphosphate. $C^0_{P_{3m}} = 0.28$ M, $C^0_{NH_3} = 4.9$ M.

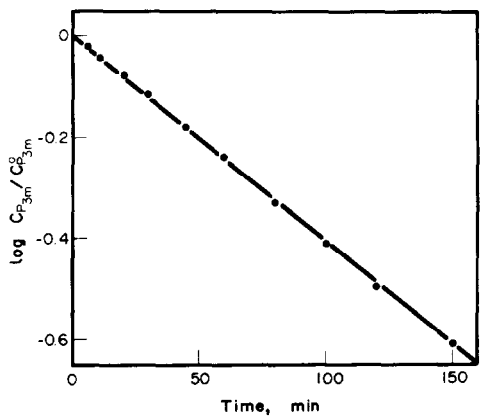

Fig. 3. The first-order disappearance of trimetaphosphate in aqueous ammonia at 30°C $C^0_{P_{3m}} = 0.28$ M, $C^0_{NH_3} = 4.9$ M.

P_2, it was concluded that ammonolysis reaction of MATP to diphosphate and diamidomonophosphate[3] did not occur in these experimental conditions.

A solution of P_{3m} whose pH was adjusted to be *ca.* 12 by adding sodium hydroxide was allowed to stand at 50°C for 12 hrs. By the ^{31}P NMR measurement and the chromatographic analysis, formation of P_3 was not detected, which excludes the possibility of hydrolysis reaction of P_{3m} under the present experimental conditions.

The ^{31}P NMR spectra of the mixed solution indicated the progress of the reaction. In order to determine the reaction rate accurately, HPLC analysis was carried out. In Fig. 2, representative elution patterns for the ammonolysis of P_{3m} are shown. The rate of disappearance of P_{3m} can be expressed as a first order equation with respect to a concentration of P_{3m}, $C_{P_{3m}}$, because the initial ammonia concentration, $C^0_{NH_3}$, is much higher than $C_{P_{3m}}$.

$$-\frac{dC_{P_{3m}}}{dt} = k \cdot CP_{3m} \qquad (2)$$

where k is the pseudo first-order rate constant depending on concentration of ammonia and temperature. Equation (2) can be rewritten as

$$-\log\frac{C_{P_{3m}}}{C^0_{P_{3m}}} = \frac{k}{2.303}t \qquad (3)$$

where $C^0_{P_{3m}}$ is the initial concentration of P_{3m} in reaction solution. Since the concentration of P_{3m} was determined by measuring the peak area of the chromatograms, the ratio $C_{P_{3m}}/C^0_{P_{3m}}$ can be calculated from the peak area ratio.

The data for the ammonolysis of P_{3m} were in accord with eqn (3) as shown in Fig. 3. The rate constants thus obtained are summarized in Tables 1–4 together with the results of all the kinetic experiments. For all the experiments, the reaction was followed for at least one half-life.

Effect of ammonia concentration. Figure 4 shows the relationship between the rate constant and the concentration of ammonia. Since the reaction was expected to be of first-order in the concentration of ammonia, linearity was expected for the plots of k vs $C^0_{NH_3}$. However, as can be seen from Fig. 4, the rate constant does not always increase with an increase in ammonia concentration. This phenomenon should be attributed to the change in the property of the solvent. Water as solvent may play an important role in this reaction.

Effect of cations. When ammonia concentration is kept constant, a higher value of $C^0_{P_{3m}}$ leads to a greater rate. This phenomenon indicates the catalytic effect of sodium ions in the sample. In Table 2, the rate constants are shown, where sodium chloride of various concentrations was added to the reaction solution. It is obvious that the rate constant increases with increasing sodium ion in the reaction solution. Sodium ions are known to bind the trimetaphosphate anions to form ion-pairs[12,13]. Ion-pairing may change the water structure around the trimetaphosphate anions and/or may decrease the negative potential near the anions, which may facilitate approach by nucleophile, NH_3.

In order to compare the catalytic effect of cations, the same amounts of chloride salts of several monovalent

Table 1. Summary of rate data (I)

Run	$C^0_{NH_3}$(M)	$C^0_{P_{3m}}$(M)	$kx10^3$ (min^{-1})
1	0.98	0.028	1.46
2	2.94	0.028	3.04
3	4.90	0.028	3.52
4	6.86	0.028	3.40
5	8.82	0.028	2.98
6	10.8	0.028	2.70
7	12.7	0.028	2.46
8	0.98	0.11	2.06
9	2.94	0.11	4.53
10	4.90	0.11	5.64
11	6.86	0.11	5.76
12	8.82	0.11	5.30
13	10.8	0.11	5.01
14	0.98	0.28	3.09
15	2.94	0.28	7.35
16	4.90	0.28	9.54
17	6.86	0.28	9.99
18	8.82	0.28	9.99

Temp. = 30°C

Table 2. Summary of rate data (II)

Run	C_{NaCl}(M)	C_{Na} (M)	$kx10^3$ (min^{-1})
19	0.33	0.41	6.82
20	0.83	0.91	11.5
21	1.51	1.59	18.8

$C^0_{P_{3m}}$ = 0.028 M, $C^0_{NH_3}$ = 4.9 M, Temp. = 30°C

C_{NaCl} : Concentration of sodium chloride added.

C_{Na} : Total concentration of sodium ion.

Table 3. Summary of rate data (III)

Run	Salt*	$kx10^3$(min^{-1})
22	LiCl	14.8
20	NaCl	11.5
23	KCl	10.5
24	$(CH_3)_4NCl$	0.99

$C^0_{P_{3m}}$ = 0.028 M, $C^0_{NH_3}$ = 4.9 M, Temp.= 30°C

* Concentration of salt added was 0.83 M.

Table 4. Summary of rate data (IV)

Run	$C^0_{P_{3m}}$(M)	C^0_{NaCl}(M)	C_{Na}(M)	Temp.(°C)	$kx10^3$(min^{-1})
25	0.28	0	0.84	10	1.75
26	0.28	0	0.84	20	4.19
27	0.28	0	0.84	40	17.0
28	0.28	0	0.84	50	35.7
29	0.028	0	0.084	10	0.68
30	0.028	0	0.084	20	1.60
31	0.028	0	0.084	40	7.32
32	0.028	0	0.084	50	14.4
33	0.028	0.83	0.91	10	2.31
34	0.028	0.83	0.91	20	5.08
35	0.028	0.83	0.91	40	22.6
36	0.028	0.83	0.91	50	43.7

$C^0_{NH_3}$ = 4.9 M

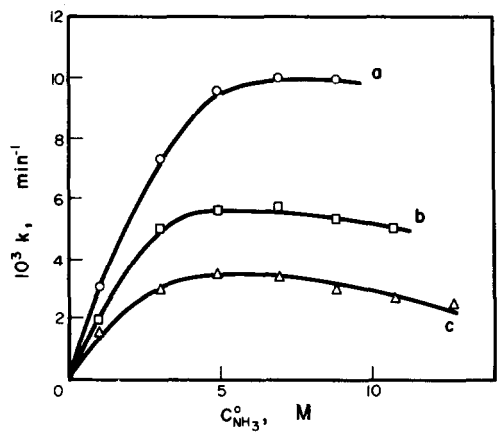

Fig. 4. Plots of rate constant vs. ammonia concentration $C^0_{P_{3m}}$ (M); (a) 0.28. (b) 0.11. (c) 0.028.

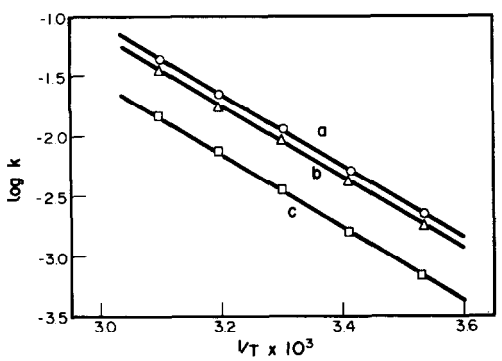

Fig. 5. Arrhenius' plots for the ammonolysis of trimetaphosphate. C_{Na} (M); (a) 0.91. (b); 0.84. (c) 0.084.

cations were added to the reaction system (Table 3). The order of the rate constant was found to be $(CH_3)_4N^+ < K^+ < Na^+ < Li^+$, which is consistent with the order of the stability constants of the ion-pairs. It should be noted that by adding tetramethylammonium ions to the system, the reaction was inhibited. One of the possible explanations is the decrease in the stability constant of sodium trimetaphosphate ion-pair with increasing ionic strength.

Table 5. Activation parameters for the ammonolysis of trimetaphosphate

	C_{Na}(M)	E_a(kcal/mole)	ΔS^* (eu)
a)	0.91	13.6	-24
b)	0.84	13.6	-24
c)	0.084	13.6	-26

$C^0_{NH_3}$ = 4.9 M

Activation parameters. The influence of temperature on the reaction rate is shown in Fig. 5 and Table 4, and the activation parameters obtained are listed in Table 5. Activation energies, E_a, were constant in spite of appreciable variation in the concentration of sodium ion. This may indicate that only one kind of activated complex may participate in the process. Since the formation of $NaP_3P_9^{2-}$ complex has been reported, the stage that $NaP_3O_9^{2-}$ is attacked by ammonia molecule may be the transition state.

Use of the value of ΔS^* has been suggested by Long as a criterion for the role of water in hydrolysis reactions.[14] Small values of ΔS^* about zero are expected for unimolecular reactions. Larger negative values, generally −15 to −30 eu are expected for bimolecular reactions. ΔS^* values for this reaction are about −25 eu which may indicate the bimolecular mechanism.

Acknowledgements—The authors wish to express their appreciation to Dr. M. Tsuhako for his interest in this work and for many useful suggestions. This work was partially supported by a Grant-in-Aid for Scientific Research No. 574224 from the Ministry of Education, Science and Culture of Japan.

REFERENCES

[1]O. T. Quimby and T. J. Flautt, *Z. Anorg. Allgem. Chem.* 1958, **296**, 220.
[2]W. Feldmann and E. Thilo, *Z. Anorg. Allgem. Chem.* 1964, **327**, 159.
[3]W. Feldman and E. Thilo, *Z. Anorg. Allgem. Chem.* 1964, **328**, 113.
[4]W. Feldman, *Z. Chem.* 1965, **5**, 26.
[5]M. Tsuhako, N. Fujita, A. Nakahama, T. Matsuo, M. Kobayashi and S. Ohashi, *Bull. Chem. Soc. Jpn.* 1980, **53**, 1968.
[6]M. Tsuhako, N. Fujita, A. Nakahama, T. Matsuo, M. Kobayashi and S. Ohashi, *Bull. Chem. Soc. Jpn.* 1981, **54**, 289.
[7]M. Tsuhako, M. Fujimoto and S. Ohashi, *Chem. Lett.* 1981, 849.
[8]Y. Hirai, N. Yoza and S. Ohashi, *J. Liq. Chromatogr.* 1979, **2**, 677.
[9]H. Yamaguchi, T. Nakamura, Y. Hirai and S. Ohashi, *J. Chromatogr.* 1980, **172**, 131.
[10]N. Yoza, K. Ito, Y. Hirai and S. Ohashi, *J. Chromatogr.* 1980, **196**, 471.
[11]G. Brauer *Handbuch der Präparativen Anorganischen Chemie*, p. 495. Ferdinand Enke Verlag, Stuttgart (1960).
[12]G. L. Gardner and G. H. Nancollas, *Anal. Chem.* 1969, **41**, 202.
[13]C. B. Monk, *J. Chem. Soc.* 1949, 413.
[14]L. L. Schaleger and F. A. Long, *Advances in Physical Organic Chemistry* (Edited by V. Gold), Vol. 1, p. 1. Academic Press, New York (1963).

Polyhedron Vol. 1, No. 5, pp. 429–436, 1982
Printed in Great Britain.

0277–5387/82/050429–08$03.00/0
Pergamon Press Ltd.

CHARGE TRANSFER SPECTRA, KINETICS AND THERMODYNAMICS FOR THIOUREA, THIOACETAMIDE AND DITHIOOXAMIDE COMPLEXES OF PENTACYANOFERRATE(II)

HENRIQUE E. TOMA* and MARIA S. TAKASUGI
Instituto de Química, Universidade de São Paulo, Caixa Postal 20780, São Paulo, Brazil

(*Received* 2 *December* 1981)

Abstract—The importance of π-backbonding in the pentacyanoferrate(II) complexes of thioamides has been demonstrated by a systematic study on the electronic spectra, kinetics and equilibrium, and on the electrochemistry of the thiourea (*tu*), thioacetamide (*ta*) and dithiooxamide (*dto*) derivatives. The complexes exhibit a characteristic absorption band at 305 nm (*tu*), 367 nm (*ta*) and 550 nm (*dto*), which was assigned to a metal-to-ligand charge transfer transition involving the thioamide group. The kinetics of formation of the complexes starting from the aquopentacyanoferrate(II) ion, and of substitution reactions in the presence of dimethyl sulphoxide or isonicotinamide, were consistent with a dissociative mechanism. From cyclic voltammetry, the E° values were evaluated as 300 mV (*tu*), 405 mV (*ta*) and 520 mV (*dto*), while the pKa of the coordinated cyanides in the complexes were respectively, 2.56, 2.38 and 2.13. The trends in the thermodynamic parameters of the iron(II) complexes followed the acceptor properties of the ligands; however, they were reversed in the oxidized state, where the major role is played by σ and π-donor interactions.

INTRODUCTION

Among the cyano complexes of the transition metals,[1] the pentacyanoferrates are probably the most well behaved series suitable for systematic studies of structure and reactivity. Because of the π-donor properties of the $Fe(CN)_5^{3-}$ group,[2] a special affinity is expected for unsaturated bases, as in the case of ruthenium(II) ammines.[3] Consequently, the study of charge transfer interactions becomes essential to understand the chemistry of $[Fe(CN)_5L]^{n-}$ and related complexes.

In this work, we have investigated the role of π-backbonding in cyanoiron complexes of thiourea, thioacetamide and dithiooxamide in aqueous solutions. These thioamide ligands have been selected because of their expected differences of acceptor properties,[4] and of their interest in analytical[5] and biological chemistry.[6] Thiourea was already known to coordinate to the pentacyanoferrate(II) ion.[7,8] However, for comparison purposes, it was found necessary to repeat and extend the previous work in order to include a detailed analysis of the electronic spectra and to evaluate fundamental thermodynamic and electrochemical parameters. Dithiooxamide has been used[9] in the presence of the amminepentacyanoferrate(II) complex as a spot test reagent for transition metal ions. In spite of this important application, little has been known about the nature of the dithiooxamide complex. Also, to our knowledge, no complex of thioacetamide with the pentacycnoferrate(II) ion has ever been reported in the literature.

EXPERIMENTAL

The complex $Na_3Fe(CN)_5NH_3 \cdot 3H_2O$ was prepared from sodium nitroprusside (Carlo Erba), as described in the literature.[10] Lithium perchlorate was prepared from perchloric acid (Merk) and lithium hydroxide (Fisher) or lithium carbonate (Carlo Erba). The solid was recrystallized several times from alkaline solutions to remove iron(III) impurities, then from acidic solutions to eliminate carbonate ions, and finally from a neutral solution. Dithiooxamide was recrystallized from ethanolic solutions; thioacetamide and thiourea (Baker) were used as supplied. Isonicotinamide was recrystallized from aqueous solution, after a treatment with activated charcoal. Dimethyl sulphoxide and other reagent grade chemicals were used as supplied.

The solutions of the complexes and of the ligands were always freshly prepared, with argon saturated, deionized water. In the case of thioacetamide (a possible carcinogen) the solutions were previously filtered to remove traces of colloidal sulfur present in the samples. The thioamide complexes were prepared in solution, from the amminepentacyanoferrate(II) complex, in the presence of a large excess of the free ligand. When concentrated solutions were required (e.g. 10^{-3} M), the free ammonia was neutralized with acetic acid. Attempts of isolating the thioamide complexes as solids by evaporating the solutions under vacuum, or by adding ethanol in the presence of sodium iodide, produced oily materials. After drying under vacuum, with calcium chloride, they convert into hygroscopic solids of very difficult manipulation. For this reason, all the experiments were carried out with the complexes directly prepared in aqueous solution. The oxidized thioamidepentacyanoferrate(III) complexes were generated by careful titrations with sodium hexachloroiridate(IV).

The electronic spectra of the complexes in the visible and near-UV region were recorded on a Cary-14 spectrophotometer, fitted with thermostatted cell compartments. The measurements were carried out under argon, in the presence of an excess of the ligands, to prevent the dissociation of the complexes. The absorption of the free ligands in the UV region was compensated with a blank, under identical conditions as the sample.

The kinetics of formation of the thioamide complexes were investigated with a Durrum model D-110 stopped-flow apparatus, equipped with a Kel-F flow system. The aquopentacyanoferrate(II) complex was generated at concentrations smaller than 10^{-4} M, by dissolving the appropriate amount of $Na_3Fe(CN)_5NH_3 \cdot 3H_2O$ in argon saturated water. The ligand solutions, containing 0.20 M lithium perchlorate, were always freshly prepared under argon, and kept in the dark. The kinetics were monitored at 440 nm for the thiourea and thioacetamide complexes, and at 550 nm, in the dithiooxamide case. A possible source of error influencing the kinetics of formation of the substituted pentacyanoferrate(II) complexes is the contribution of the starting $Fe(CN)_5NH_3^{3-}$ ion which becomes less dissociated as the pH increases. This kind of effect may be responsible for a gradual shift of the infinite time absorbance, but can be minimized by using Guggenheim's method,[11] for a first order behavior.[12] This also eliminates the contribution of dimeric spe-

*Author to whom correspondence should be addressed.

cies which can be present in the solutions of the aquopentacyanoferrate(II) ion.[13] The thiourea complex is air sensitive, and the presence of oxygen may be another source of error. The hydrolysis of the thioamides is also critical, specially at high pH. The kinetics of dissociation of the complexes were investigated in the presence of dimethyl sulphoxide or isonicotinamide, with a Cary-14 spectrophotometer. The solutions were transferred and mixed up with thermostatted syringes.

Cyclic voltammetry measurements were carrried out with a Princeton Applied Research Corporation instrument, consisting of a 173 potentiostat and a 175 universal programmer. A carbon paste electrode was employed for the measurements, with Ag/AgCl (1 M KCl) as the reference electrode, using the conventional Luggin capillary arrangement to minimize the ohmic drop. A platinum wire was used as the auxiliary electrode.

RESULTS AND DISCUSSION

Electronic spectra

The electronic spectra of a number of thioamides have been examined by Persson and Sandstrom.[4] In addition to a weak band associated to a $n \rightarrow \pi^*$ transition (Table 1) there is a strong band at 235, 260 and 305 nm in thiourea, thioacetamide and dithiooxamide, respectively. These bands have been assigned to a $\pi \rightarrow \pi^*$ transition, reflecting the trends in the energies of the empty, low lying π^* orbitals centered on the thioamide chromophore. On the other hand, the characteristic spectra of pentacyanoferrate(II) complexes containing σ-donor ligands (e.g. $Fe(CN)_5NH_3^{3-}$) consists of a ligand field band, of moderate intensity ($\epsilon = 200 - 450\ M^{-1}\ cm^{-1}$) in the visible-near UV region, and of a strong absorption below 240 nm associated to a $d_\pi \rightarrow p_\pi$, iron-to-cyanide, charge transfer transition.

In the thiourea complex, the ligand transitions are superimposed to the strong metal-to-cyanide CT bands in the ultraviolet region. The $\pi \rightarrow \pi^*$ transition can be detected as a shoulder at 240 nm in the thioacetamide complex, and as a peak at 300 nm in the dithiooxamide analog. The ligand field band can be seen at 407 nm in Fig. 1, for the thiourea complex. It is supported by Gaussian analysis, around 400 and 395 nm, in the thioacetamide and dithiooxamide complexes, respectively. In addition to the internal transitions in the ligand and in the pentacyanoferrate(II) moiety, there is a new band appearing at 305, 367 and 550 nm in the *tu*, *ta* and *dto* complexes, respectively.

The new band is relatively strong. Its energy is very sensitive to the substituent at the thioamide group, and correlates linearly with the energies of the $\pi \rightarrow \pi^*$ transition of the ligands. This and other observations to be described, support a charge transfer assignment, involving the highest occupied orbitals of iron(II) and the low lying, empty π^* orbitals of the thioamides.

The calculated oscillator strengths, assuming a Gaussian behavior for the charge transfer bands, are shown in Table 1. By assuming a simplified MO function, like

$$\Psi = (1 - \alpha^2)^{1/2}\Psi_{Fe} + \alpha\Psi_L$$

it is possible to estimate the resonance integral, β, in terms of the perturbation theory,[14] according to the equation

$$\frac{\alpha}{(1-\alpha^2)^{1/2}} = \frac{\beta}{E_{CT}}.$$

The values of α were obtained from the oscillator strengths data,[15] by using an approximate Fe–L distance of 2.5 Å. The calculations show that the charge transfer

Table 1. Spectral data of thioamides and of substituted pentacyanoferrate(II) and (III) complexes

Free Ligands	Thioamide	Thioacetamide	Dithiooxamide
$n \rightarrow \pi^*$, λ_{max}(log ϵ)[a]	280 (2)	327 (1.71)	483 (1.34)
$\pi \rightarrow \pi^*$, λ_{max}(log ϵ)[a]	242 (4.11)	266 (4.10) 210 (3.63)	312 (4.05)
$\pi \rightarrow \pi^*$, λ_{max}(log ϵ)[b]	235 (4.08)	260 (4.01)	305 (3.96)
$Fe(CN)_5(thioamide)^{3-}$			
LF, $^1A_1 \rightarrow {}^1E(1)$, λ_{max}(log ϵ)	407 (2.60)	400[c] (2.6)	395 (2.70)
CT, $\pi_{Fe} \rightarrow \pi^*_L$, λ_{max}(log ϵ)	305 (3.11)	367 (3.30)	550 (3.35)
Oscillator strength, P	0.037	0.045	0.070
Resonance integral, β ($10^3 cm^{-1}$)	4.2	4.3	4.5
$Fe(CN)_5(thioamide)^{2-}$			
CT, $\pi_L \rightarrow \pi_{Fe}$, λ_{max}(log ϵ)	595 (3.4)	565 (3.4)	560 (3.3)

a) in ethanol, ref. 4, b) in water c) Gaussian analysis

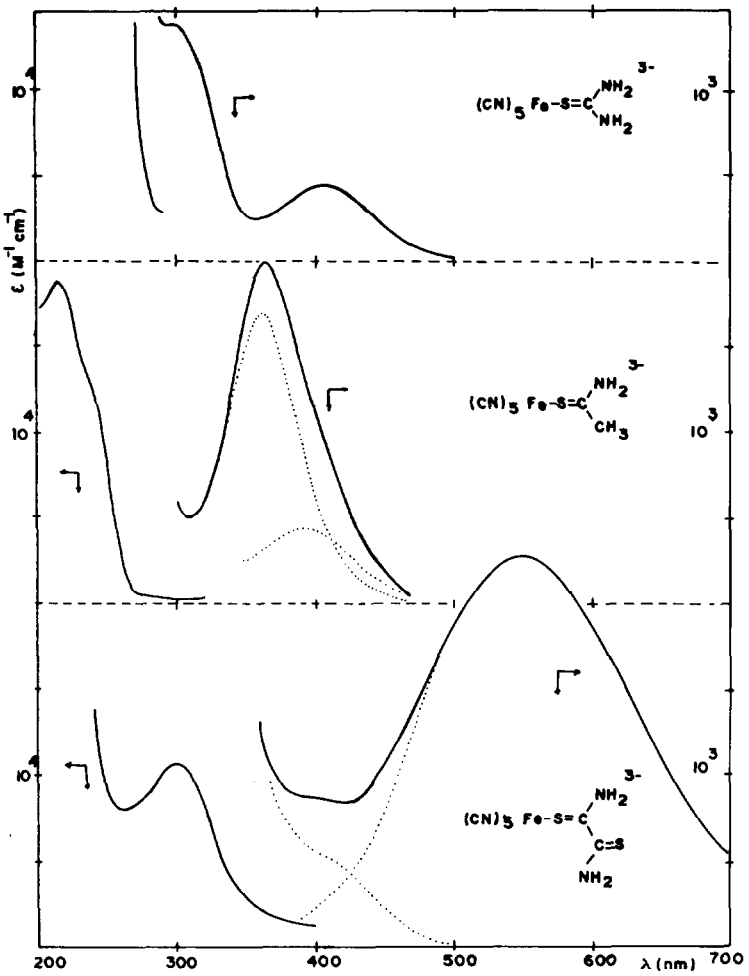

Fig. 1. Electronic spectra of thiourea, thioacetamide and dithiooxamide complexes of pentacyanoferrate(II).

interaction increases from thiourea to dithiooxamide, and provide a good comparison of the acceptor properties of the ligands.

The ligand field band observed in the pentacyanoferrates can be assigned to the $^1A_1 \rightarrow {}^1E(1)$ transition, in analogy with the related complexes reported in the literature.[16] The energy of this transition is a function of 10 Dq and of the tetragonal distortion parameter, Dt,

$$E_{^1A_1-{}^1E(1)} = 10\,Dq - (35/4)Dt - C$$

$$Dt = \frac{2}{7}(Dq_{CN} - Dq_L).$$

Since Dq_{CN} is nearly constant, the relative energies of the ligand field transition in a series of $[Fe(CN)_5L]$ complexes express the magnitude of Dq associated to the ligand L. In this way, the thioamides should be placed after imidazole and methionine, in the spectrochemical series, $NO^+ > CO > CN^- > dmso > P(C_6H_5)_3 \sim SO_3^{2-} > As(C_6H_5)_3 > Sb(C_6H_5)_3 >$ pyrazine > pyridine > imidazole ~ S-methionine > *dto* > $NH_2R \sim ta \sim tu > H_2O$.

Despite their electron acceptor properties, the thioamides actually provide a very weak ligand field strength. The situation seems rather anomalous, and may be a consequence of the presence of filled π-orbitals in the thioamides, interacting with the metal d_π orbitals. This kind of interaction has been detected in the oxidized pentacyanoferrate(III) complexes with π-donor ligands, like[17,18] SCN^- and N_3^-. The main evidence is a strong absorption band in the visible, associated to a ligand-to-metal, charge transfer transition. The pentacyanoferrate complexes with the thioamides possess a deep blue color in the oxidized state, with a strong absorption band at 560 nm (*dto*), 565 nm (*ta*) and 595 nm (*tu*). Analogously to the complexes previously reported in the literature, we have assigned it as a charge transfer transition from the highest occupied π orbitals of the thioamides to the d_π orbitals of the pentacyanoferrate(III) ion.

Kinetics of substitution

The formation of the thioamide complexes from the aquopentacyanoferrate(II) ion was observed to take place according to a first order kinetics for at least three half lives, in the presence of excess of the ligand. The reaction can be represented by

$$Fe(CN)_5H_2O^{3-} + \text{thioamide} \rightarrow Fe(CN)_5(\text{thioamide})^{3-} + H_2O.$$

The typical dependence of the observed rate constants on the ligand concentration can be seen in Fig. 2. From the slope of those linear plots we have obtained the

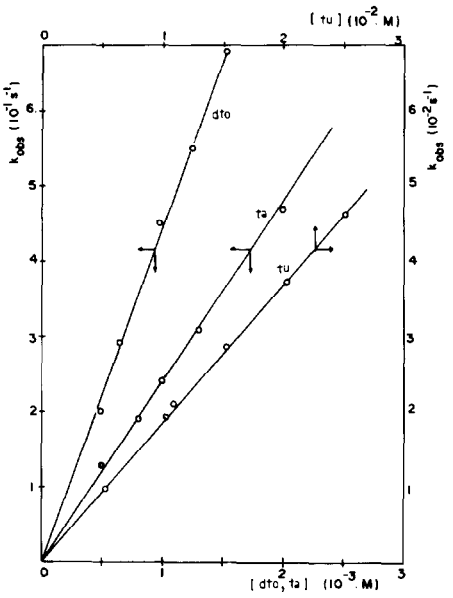

Fig. 2. Observed rate constants of formation of the pentacyanoferrate(II) complexes of thiourea, thioacetamide and dithiooxamide, versus the concentration of the ligands, at 25°C, μ = 0.100 M lithium perchlorate, $[Fe(CN)_5H_2O]^{3-} \leq 5 \times 10^{-5}$ M.

specific rates of formation of the complexes, at several temperatures, as shown in Table 2.

For the thiourea complex, previous work[8] has raised the question about the magnitude of the pKa of the coordinated water molecule in the $Fe(CN)_5H_2O^{3-}$ ion. Because of some inconsistent results in that work, as discussed by Davies and Garafalo,[19] we have also repeated the thiourea kinetics in order to invalidate definitely the proposed values of pKa of 7.86 for the $[Fe(CN)_5H_2O]^{3-}$ ion. Our typical results for k_{obs} at pH 3.6, 8.8 and 11.0 (25°C, $\mu = 0.100$ M lithium perchlorate, $[tu] = 9.9 \times 10^{-3}$ M) were essentially identical, namely 1.92, 1.95 and 1.95 s^{-1}. This kind of behavior is consistent with the work of Davies and Garafalo.[19] In another parallel study, using dimethyl sulphoxide as the ligand, we demonstrated that k_{obs} does not depend on the pH, over the pH range 5–13. The specific rates (in M^{-1} s^{-1}) in that case were 382 (pH 5.6), 382 (pH 6.80), 379 (pH 8.80), 378 (pH 11.9) and 382 (pH 13). In acidic solutions, however, there was a systematic decrease of the specific rates, for instance, 310 (pH 3.23), 187 (pH 2.5), 58 (pH 2.0) and 11.4 M^{-1} s^{-1} (pH 1). The cause of this variation is the protonation of the cyanides.[20,21] with a pKa around 2.50.

According to our results, the pKa of the coordinated water molecule in the $[Fe(CN)_5H_2O]^{3-}$ complex should be higher than 13. There are many reasons to believe that

Table 2. Specific rates of formation and dissociation of pentacyanoferrate(II) complexes of thioamides[a]

	k_f, $M^{-1}s^{-1}$ (T, K)[b]	k_d, s^{-1} (T, K)[c]
thiourea	8.2 x 10 (288.1)	4.4 x 10^{-3} (283.1)
	1.27 x 10^2 (293.1)	7.0 x 10^{-3} (286.1)
	1.94 x 10^2 (298.1)	1.26 x 10^{-2} (290.1)
	2.79 x 10^2 (303.1)	2.04 x 10^{-2} (294.1)
	4.4 x 10^2 (308.1)	3.30 x 10^{-2} (298.1)
thioacetamide	1.64 x 10^2 (293.1)	5.4 x 10^{-4} (288.1)
	2.71 x 10^2 (298.1)	1.18 x 10^{-3} (293.1)
	3.85 x 10^2 (302.1)	2.84 x 10^{-3} (298.1)
	5.7 x 10^2 (306.1)	6.1 x 10^{-3} (303.1)
		9.1 x 10^{-3} (306.1)
dithiooxamide	1.75 x 10^2 (288.1)	5.5 x 10^{-4} (288.1)
	2.80 x 10^2 (293.1)	8.2 x 10^{-4} (291.1)
	4.6 x 10^2 (298.1)	1.22 x 10^{-3} (293.1)
	6.7 x 10^2 (303.1)	1.85 x 10^{-3} (295.1)
	1.08 x 10^3 (308.1)	2.70 x 10^{-3} (298.1)
		5.4 x 10^{-3} (303.1)
		1.14 x 10^{-2} (308.1)

a) 0.100 M lithium perchlorate b) second order rate constants, measured at 440 nm (tu, ta) or 550 nm (dto), $[Fe(CN)_5H_2O^{3-}] \leq 5 \times 10^{-5}$ M
c) observed rate constants at the saturation point.

Table 3. Activation parameters of formation and dissociation of pentacyanoferrate(II) complexes of thioamides[a]

		thiourea	thioacetamide	dithiooxamide
$\Delta H_f^{\ddagger}$	($kJ.mol^{-1}$)	60	65	65
$\Delta S_f^{\ddagger}$	($J.mol^{-1}.deg^{-1}$)	0.8	21	22
$\Delta H_d^{\ddagger}$	($kJ.mol^{-1}$)	88	106	108
$\Delta S_d^{\ddagger}$	($J.mol^{-1}.deg^{-1}$)	21	64	70

a) 0.100 M lithium perchlorate.

the pKa of the complex cannot be as low as 7.86. For example, this value is smaller than the pKa of the oxidized $[Fe(CN)_5H_2O]^{2-}$ complex, namely[22] 8.4. By lowering the oxidation state, one would expect an increase of pKa accompaning the loss of acidity of the metal ion. This point is also supported by a comparison with pentaammineruthenium complexes,[3] which are closely related to the pentacyanoferrates.[2] Considering that the pKa of the $Ru(NH_3)_5H_2O^{3+}$ complex increases from 4.1 to 13.1 in the lower oxidation state, a pKa as high as 17 would be expected for $Fe(CN)_5H_2O^{3-}$ ion.

The activation parameters associated to the formation of the thioamide complexes are shown in Table 3. The activation enthalpies around 65 kJ . mol^{-1}, and the small, positive activation entropies are typical of substitution reactions in the aquopentacyanoferrate(II) ion with neutral ligands. Dithiooxamide reacts twice as faster than thiourea or thioacetamide, because of the statistical effect associated to the presence of two coordinating groups in the molecule. The fact that the specific rates and the activation parameters are practically independent on the nature of the ligand is consistent with a dissociative mechanism, as in most reactions of the cyanoferrates in aqueous solutions.[23,24]

The dissociation of the thioamide complexes can be conveniently investigated in the presence of dimethyl sulfoxide or isonicotinamide, which form stable complexes with the $Fe(CN)_5^{3-}$ ion. The reaction can be represented by

$$Fe(CN)_5(\text{thioamide})^{3-} + dmso \rightarrow$$

$$Fe(CN)_5 dmso^{3-} + \text{thioamide}.$$

By working with a constant, excess amount of the thioamide ligand, the kinetics of ligand exchange were typically of first order, with a saturation behavior of k_{obs} vs the concentration of dimethyl sulfoxide, as shown in Fig. 3. This kind of behaviour can be interpreted in terms

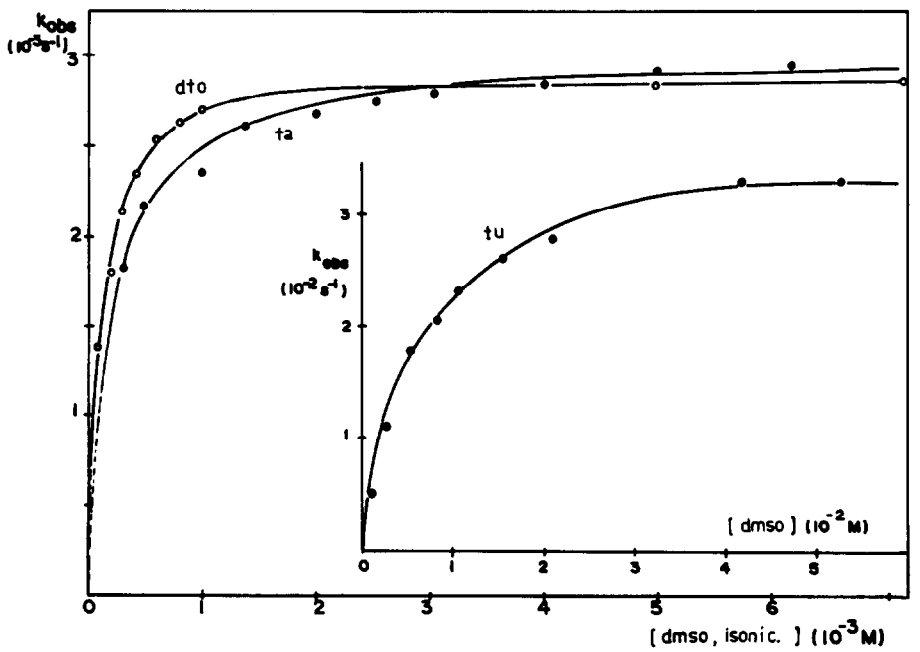

Fig. 3. Observed rate constants of substitution in the pentacyanoferrate(II) complexes of dithiooxamide (O O O) and thioacetamide (● ● ●) vs the concentration of dimethyl sulfoxide and isonicotinamide, respectively. The internal figure refers to the substitution in the thiourea complex by the dimethyl sulfoxide ligand, at 25°C and μ = 0.100 M lithium perchlorate.

of the dissociative mechanism,

$$Fe(CN)_5(thioamide)^{3-} \underset{k_L}{\overset{k_{-L}}{\rightleftharpoons}} Fe(CN)_5^{3-} + thioamide$$

$$Fe(CN)_5^{3-} + H_2O \overset{K}{\rightleftharpoons} Fe(CN)_5H_2O^{3-}$$

$$Fe(CN)_5^{3-} + A \underset{k_{-A}}{\overset{k_A}{\rightleftharpoons}} Fe(CN)_5A^{3-}$$

where L is the thioamide ligand, and A is the attacking ligand.

The rate law for this mechanism can be expressed by

$$-d[Fe(CN)_5L^{3-}] = d[Fe(CN)_5A^{3-}] = k_{obs}dt$$

were

$$k_{obs} = \frac{k_{-L} \cdot k_A[A] + k_L \cdot k_{-A}[L]}{k_A[A] + k_L[L]}.$$

The saturation profile of k_{obs} in Fig. 3 is generated by the terms involving $k_A[A]$ which predominate over the corresponding $k_L[L]$ terms, as the concentration of A increases. In this case, one can see that k_{obs} approaches k_{-L}, which is the rate constant of dissociation of the thioamide ligand from the complex.

The experimental values of k_{-L} at several temperatures are shown in Table 2. By carrying out independent kinetics in the presence of isonicotinamide instead of dimethyl sulphoxide, we have observed that k_{-L} does not depend on the nature of the attacking ligand. It was also possible to fit the experimental plots shown in Fig. 3, with the specific rates of formation of the thioamides and the *dmso* or isonicotinamide complexes, and the corresponding rates of dissociation previously reported in the literature.[25] The activation parameters shown in Table 3 are comparable to those of pentacycnoferrate(II) complexes of aromatic N-heterocycles[2,26] and amino-acids,[27,28] exhibiting analogously an isokinetic behavior between $\Delta H^{\neq}$ and $\Delta S^{\neq}$.

For some pentacyanoferrate(II) complexes of aromatic N-heterocycles, a limiting dissociative mechanism have been postulated[24] based on the corresponding volumes of activation. Considering that our activation parameters are similar to those obtained for those complexes, and that there is a general tendency of correlation[29] between $\Delta S^{\neq}$ and $\Delta V^{\neq}$, it seems reasonable to extend the mechanism to the present work.

From the rate constants of formation and dissociation of the thioamide complexes, one can obtain the stability constant, K_{II}, and the thermodynamic parameters ΔH_{II} and ΔS_{II} shown in Table 4. The trends in K_{II} parallel the π-backbonding stabilization predicted by the analysis of the charge transfer spectra. Dithiooxamide, which is more effective than thiourea in delocalizing the π-electrons of the pentacyanoferrate(II) group, also forms the most stable complex.

Electrochemistry

The electrochemistry of the pentacyanoferrate(II) complexes of the thioamide was investigated in aqueous solution, and 0.10 M KCl, using cyclic voltammetry. Of the several electrodes which we have tested, the best results were obtained with a carbon paste one. Platinum or gold electrodes exhibited only poorly reversible waves, and may be susceptible to the adsorption of the sulphur containing ligands, present in high excess in solutions.

Typical cyclic voltammograms can be seen in Fig. 4 for the thioacetamide complex, as a function of pH. The electrochemical behavior was practically reversible, following closely the Randles–Sevcik equation, with the ratio of anodic and cathodic peaks very close to one. The half wave potentials, measured at the center of the anodic and cathodic peak separation, are shown in Table 4. Within the experimental error, they can be taken as the formal potentials for the complexes, since the diffusion coefficients of the cyanoferrates do not vary substantially with the oxidation state.[30]

The results shown in Table 4 indicate that the dithiooxamide complex is the most resistant to oxidation, with an E^0 of 0.520 V vs NHE. In contrast, the thiourea complex can be easily oxidized ($E^\theta = 0.300$ V vs NHE), even by air, to deep blue $[Fe(CN)_5(tu)]^{2-}$ product. The electrochemical data parallel the kinetics and spectral properties, reinforcing the conclusion that d_π-backbonding should play an important role in the chemistry of the thioamide complexes.

By lowering the pH, we have observed that the complexes can be protonated reversibly, producing anodic shifts in the cyclic voltammograms, as shown in Fig. 4.

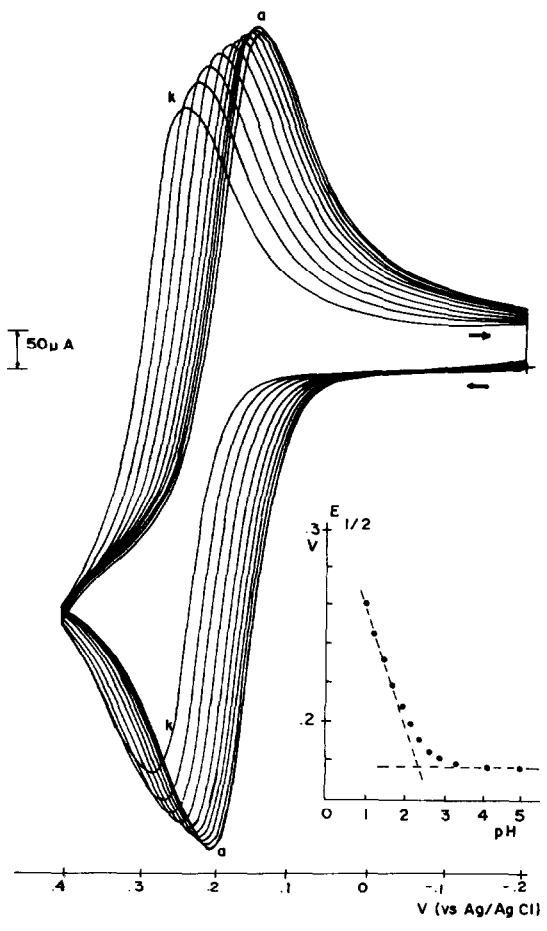

Fig. 4. Cyclic voltammograms of the pentacyano(thioacetamide) ferrate(II) complex, at 10^{-2} M, 0.10 M KCl, 25°C, scan rate = 100 mV . s^{-1}, obtained with a carbon paste, electrode. The pH is varying from 4.16 (a) to 0.92 (k). The internal figure shows the plot of $E_{1/2}$ vs pH for this complex.

Table 4. Thermodynamic parameters of pentacyanoferrate complexes of thioamides in aqueous solution[a]

	Thiourea	Thioacetamide	Dithiooxamide
K_{II} (M^{-1})	5.6×10^3	9.7×10^4	1.6×10^5
ΔH ($kJ.mol^{-1}$)	-2.8×10	-4.1×10	-4.3×10
ΔS ($J.mol^{-1}.deg^{-1}$)	-2.0×10	-4.4×10	-4.8×10
$E^{\ominus'}$ (V, vs NHE)	0.300	0.405	0.520
$\Delta H^{\ominus}$ ($kJ.mol^{-1}$)	-5.7×10	-7.3×10	-7.6×10
$\Delta S^{\ominus}$ ($J.mol^{-1}.deg^{-1}$)[b]	-9.5×10	-1.15×10^2	-8.7×10
K_{III} (M^{-1})	9.2×10^4	2.7×10^4	4.6×10^2
ΔH ($kJ.mol^{-1}$)	-4.0×10	-3.7×10	-2.8×10
ΔS ($J.mol^{-1}.deg^{-1}$)	2.33×10^2	2.14×10^2	1.47×10^2
pKa	2.56	2.38	2.13

a) 25.0 °C, μ = 0.100 M b) experimental reaction entropy of redox couple ($S^{\circ}_{red} - S^{\circ}_{ox}$) measured by using nonisothermal electrochemical cell with the reference electrode held at a fixed temperature. It can be related to the overall cell reaction ox + $\frac{1}{2}$ H_2 → red + H^+ by adding 20.5 eu[32], or 85.7 $J.mol^{-1}.deg^{-1}$.

$$[(CN)_5Fe(\text{thioamide})]^{3-} + H^+(aq) \overset{K_a}{\rightleftharpoons} [HNC(CN)_4Fe(\text{thioamide})]^{2-}.$$

The dependence of the redox potentials on the pH is illustrated internally in that figure. The initial curve, of slope ~0, intersects the second curve possessing a slope close to the theoretical value of 0.059, at a pH corresponding to the pKa of the complex.[31] The values of pKa obtained in this way are shown in Table 4. As one would expect, the basicity constants increase from the dithiooxamide to the thiourea complex, and are close to the pKa values of the pentacyanoferrate(II) complexes of aromatic N-heterocyclic ligands.[2]

The temperature dependence of the redox potentials was also investigated, in order to evaluate the corresponding values of ΔH and ΔS, as shown in Table 4. By solving the thermodynamic cycle at several temperatures, we have calculated the values of K_{III}, ΔH and ΔS.

$$\begin{array}{ccc} Fe(CN)_5H_2O^{2-} + L & \overset{K_{III}}{\rightleftharpoons} & Fe(CN)_5L^{2-} + H_2O \\ \Big\downarrow +e & & \Big\downarrow +e \\ Fe(CN)_5H_2O^{3-} + L & \overset{K_{II}}{\rightleftharpoons} & Fe(CN)_5L^{3-} + H_2O. \end{array}$$

The results, shown in Table 4, reveal an inverse trend for the association constants of the oxidized complexes, with the thiourea ligand forming the most stable complex. Dithiooxamide, which is the strongest π-acceptor of the series, behaves as a poor electron donor toward the pentacyanoferrate(III) ion. On the other hand, thioacetamide seems to act in both ways, stabilizing the two oxidation states in a comparable extent.

Acknowledgement—A fellowship from CAPES to M.S.T. is gratefully acknowledged.

REFERENCES

[1] A. G. Sharpe, *The Chemistry of Cyano Complexes of the Transition Metals.* Academic Press, New York (1976).
[2] H. E. Toma and J. M. Malin, *Inorg. Chem.* 1973, **12**, 1039.
[3] H. Taube, *Pure Appl. Chem.* 1979, **51**, 901.
[4] B. Persson and J. Sandstrom, *Acta Chem. Scand* 1964, **18**, 1059.
[5] R. N. Hurd and G. De LaMater, *Chem. Rev.* 1961, **61**, 41.
[6] W. Walter and J. Voss, *The Chemistry of Amides* (Edited by J. Zabick), Chap. 8. Interscience, London (1970).
[7] A. R. Garafalo and G. Davies, *Inorg. Chem.* 1976, **15**, 1787.
[8] D. H. Macartney and A. McAuley, *Inorg. Chem.* 1979, **18**, 2891; *Ibid* 1981, **20**, 748.
[9] A. I. Vogel, *Quantitative Inorg. Analysis*, 3rd Edn, p. 727. Longmans, London (1961).
[10] G. Brauer, *Handbook of Preparative Inorg. Chem.*, V II, 2nd Edn, p. 1511. Academic Press, New York (1965).
[11] E. A. Guggenheim, *Phil. Mag.* 1926, **2**, 538.
[12] A. A. Frost and R. G. Pearson, *Kinetics and Mechanism*, 2nd Edn, p. 49. Wiley, New York (1961).
[13] G. Emschwiller, *Comptes Rendus Acad. Sci. Paris* 1964, **259**, 4281.
[14] R. S. Mulliken, *J. Am. Chem. Soc.* 1952, **74**, 811.
[15] P. Day and N. Sanders, *J. Chem. Soc.* (A), 1967, 1536.

[16]H. E. Toma, E. Giesbrecht, J. M. Malin and E. Fluck, *Inorg. Chim. Acta* 1975, **14**, 11.
[17]R. Gale and A. McCaffery, *J. Chem. Soc., Dalton* 1973, 1344.
[18]D. Gutterman and H. B. Gray, *Inorg. Chem.* 1972, **11**, 1727.
[19]G. Davies and A. R. Garafalo, *Inorg. Chem.* 1980, **19**, 3543.
[20]H. E. Toma, *Inorg. Chim. Acta* 1975, **15**, 205.
[21]J. M. Malin and R. C. Koch, *Inorg. Chem.* 1978, **17**, 752.
[22]J. H. Espenson and D. G. Wolenuk Jr., *Inorg. Chem.* 1972, **11**, 2034.
[23]H. E. Toma and J. M. Malin, *Inorg. Chem.* 1973, **12**, 2080.
[24]A. Haim, A. P. Szecsy and S. S. Miller, *Inorg. Chim. Acta* 1978, **6**, 189.
[25]H. E. Toma, J. M. Malin and E. Giesbrecht, *Inorg. Chem.* 1973, **12**, 2084.
[26]D. R. Stranks, T. R. Sullivan, J. Burgess and R. I. Haines, *J. Chem. Soc., Dalton* 1977, 1460.
[27]H. E. Toma, J. M. Martins and E. Giesbrecht, *J. Chem. Soc., Dalton* 1978, 1610.
[28]A. A. Batista and H. E. Toma, *An. Acad. Brasil. Cienc.* 1980, **52**, 703.
[29]M. W. Twigg, *Inorg. Chim. Acta Lett.* 1977, **9**, 184.
[30]K. D. Schleinitz and G. von Louis of Menar, *Z. Chem.* 1975, **15**, 493.
[31]S. Wawzonek, In *Physical Methods of Chemistry*, Part II, *Electrochemical Methods* (Edited by A. Weissberger and B. W. Rossiter). Wiley, New York (1971).
[32]E. L. Yee and M. J. Weaver, *Inorg. Chem.* 1980, **19**, 1077.

Polyhedron Vol. 1, No. 5, pp. 437–440, 1982
Printed in Great Britain.

0277-5387/82/050437-04$03.00/0
Pergamon Press Ltd.

THE INTERACTION OF MORPHOLINE WITH METAL IONS—I

COPPER COMPLEXES

NORMA H. PIACQUADIO and MIGUEL A. BLESA*

Departamento Química de Reactores, Comisión Nacional de Energía Atómica, Avenida del Libertador 8250, 1429 Buenos Aires, Argentina

(*Received* 1 *February* 1982)

Abstract—The synthesis and electronic and IR spectra of $CuL_2(NO_3)_2$ and $CuL_4(NO_3)_2$, where L stands for morpholine, are described. The thermal behaviour of the complexes is also discussed. The solids contain distorted octahedral Cu(II) bonded to morpholine through nitrogen only. In aqueous solutions only the species $CuL_3(aq)^{2+}$ is stable in the concentration range $0.5 < [L] < 2$ mol dm^{-3}, its stability constant being $\log K_3 = 14.64 \pm 0.15$ at 25.00°C and ionic strength 1 mol dm^{-3}; at very high morpholine concentrations, $3.4 < [L] < 6$ mol dm^{-3}, evidence is also found for $CuL_4(aq)^{2+}$, the value $\log K_4 = 15.5$ being estimated. The aggressiveness of morpholine–H_2O_2 towards metallic copper is compared with that of ammonia–H_2O_2, both on thermodynamics and kinetics grounds; experimental results seems to be dominated by kinetics factors. The relevance of these results to water treatment in secondary systems of nuclear power reactors is discussed.

INTRODUCTION

Morpholine (perhydro-1,4-oxazine, O s NH) is used in secondary systems of nuclear power plants to control pH and at the same time avoid unwanted concentration of additives in steam generators. Due to its volatility, it is distributed throughout the secondary system,[1] and is frequently in contact with copper alloys in the condenser. It is well known that ammonia is detrimental towards copper in the presence of oxygen, partially because of the shift of the redox potential of the couple Cu(II)/Cu(0) associated with the formation of $Cu(NH_3)_4^{2+}$ and related species. In view of the lack of information on the complexation chemistry of morpholine in aqueous solutions, it was considered of interest to evaluate this system. In this paper, we report some aspects of the basic chemistry of the morpholine-copper system in aqueous solution, together with the complexation chemistry in solid phase in the absence of halide ions. Also, an estimation of the aggressiveness of morpholine-water mixtures of metallic copper in the presence of oxygen is given. Related previous work refers mainly to the structure of ML_2X_2 complexes (L = morpholine, X = halide ion),[2–5] a brief mention of the aqueous morpholine-copper system occurs in the literature.[6]

EXPERIMENTAL

Reagent grade chemicals without further purification and doubly-distilled water were used. Morpholine was purified by distillation through a multiple-plate column under nitrogen. Constant boiling point hydrochloric acid was prepared as usual.[7]

Elementary analyses were performed by the Department of Organic Chemistry, Facultad de Farmacia y Bioquímica; Cu(II) was determined using an Orion specific electrode, by titration with EDTA; morpholine solutions were standardized by potentiometric titration.

Complexes reported in this paper were prepared by dissolving 15 g $Cu(NO_3)_2 \cdot 3H_2O$ in 30 cm^3 morpholine, heating to 80°C and removing $Cu(OH)_2$ by centrifugation and filtration at high temperature. The solid complexes precipitate upon standing at 5°C; they were filtered off, washed with $(CH_3CH_2)_2O$ and dried on fritted glass *in vacuo* over morpholine.

UV and visible spectra were obtained in a Shimadzu UV-210A spectrophotometer; for solids, a reflectance accessory for the same equipment was used. IR spectra were recorded in the range 4000–600 cm^{-1} using a Beckman IR33 spectrophotometer, either as KBr pellets or as Nujol mulls.

Thermogravimetric analyses (weight, DTA and DTG) were obtained using a Mettler Recording Vacuum Thermoanalyzer Mod. 1; runs were performed between 25 and 550°C, at 4°C min^{-1} under N_2.

Polarograms were recorded on a PAR Polarographic Analyzer Model 174A in two operating modes, dc sampled and differential pulse. For these measurements, oxygen was excluded by purging with N_2, and temperature was kept at 25.00 ± 0.05°C. KNO_3 (1 mol dm^{-3}) was the supporting electrolyte; for the dropping electrode, $m = 2{,}625$ mg s^{-1}; $t = 2$ s; $h = 47$ cm.

Copper coupons used were 99.9% Cu, polished with 600 emery paper; aggressiveness of reagents was determined in the form of weight loss of the coupon, and copper (II) concentration increase in the solution.

RESULTS AND DISCUSSION

Characterization of solid phases. Whilst it is relatively easy to prepare morpholine complexes under rigorously anhydrous conditions,[2–5] the solid phases formed in the presence of water and especially in the absence of halide ions often show irreproducible compositions reflecting mixtures of copper hydroxide and morpholine containing solids. After several attempts in various H_2O–HNC_4H_8O mixtures it was apparent that water had to be kept at low concentrations, and that it was not included in the solid complexes formed by copper and morpholine. In practice, it was found that any water in excess to hydration water from $Cu(NO_3)_2 \cdot 3H_2O$ gave rise to basic precipitates. By the technique described in the experimental section it was possible to obtain a solid showing the composition $CuL_2(NO_3)_2$, as shown by elemtary analysis and thermal decomposition behaviour.

In some experiments carried out at lower Cu(II) concentrations, a different solid was also obtained, which lost morpholine easily on standing, and had to be stored in a desiccator saturated with morpholine. Elementary analysis indicated it to be $CuL_4(NO_3)_2$.

A tentative assignment of the most intense bands of the IR spectrum of $CuL_2(NO_3)_2$ is shown in Table 1. For comparison, bands of the free ligand are also shown.[2–

*Author to whom correspondence should be addressed.

Table 1. IR spectra of $CuL_2(NO_3)_2$ and L

Assignement	Frequency in $CuL_2(NO_3)_2$/cm^{-1}	Frequency in L/cm^{-1} *
ν_1 NH stretch.	3235s 3190s	3340s
$\nu_2;\nu_{3axial};\nu_{22}$ ν_{23} CH_2 stretch.	2910m	2910s
$\nu_4;\nu_5;\nu_{25axial}$	2860m	2860s
ν_5; combination	2710sh	2710sh
ν_3 NO_2 stretch.	1380vs,b	-
ν_{12}	1255s	1256s
ν_{31} C-N stretch.	1225m	1225m
ν_{32} C-O stretch and out-of-plane	1190m	1200m
$\nu_{13axial}$	1099s	1099s
ν_{14}stretch C-O	1030s	1030s
ν_{37}	872s	870s
ν_{16}	820m	820

* For the spectrum of pure L, see Refs [10-11].

[5,8,9] The spectrum of $CuL_4(NO_3)_2$ is very similar, except for the position of the higher frequency component of the N–H stretch (see below).

In liquid morpholine, the N–H stretching occurs at 3340 cm^{-1}; upon complexation this band is shifted to lower values[2–5] and sometimes it is split due to solid state effects.[4] In good agreement in $CuL_x(NO_3)_2$ complexes, there are two components located at 3190 and 3270 ($x = 4$) and 3190 and 3235 cm^{-1} ($x = 2$). The antisymmetric and symmetric C–O–C stretching bands appear at the same frequency as in the free ligand; this suggests that there are no Cu–L–Cu bridges in the structure, but that rather the polyhedron around Cu(II) in $CuL_2(NO_3)_2$ includes the nitrate ions. The strong band at 1380 cm^{-1}, which we assign to γ_3 (E')NO_2 stretch, indicates however that Cu–ONO_2 bands are highly ionic;[7] a similar behaviour is found in $CuNO_3 \cdot 1{\cdot}5H_2O$, the structure of which also involves NO_3- ions in the Cu(II) coordination sphere.[8]

The electronic spectrum of $CuL_2(NO_3)_2$ shows a broad maximum centered around 590 nm, which is consistent with the expected distorted octahedral configuration. The value of the energy of the band maximum is lower than for the aqueous ion, as expected for a crystal-field *d–d* transition when nitrate ions are replaced by H_2O. The electronic spectrum of $CuL_4(NO_3)_2$ also shows its maximum shifted to lower wavelengths, indicating the replacement of NO_3^- coordination by morpholine coordination.

Thermograms of $CuL_2(NO_3)_2$ are composed of three weight losses, two endothermic at 94 and 119°C, and the third exothermic at 200°C. The overlap of the two first steps precludes the quantification of the individual weight losses; the overall loss is in agreement with the weight of two morpholine molecules per copper atom (Found: 47.1; Calc., 48.1%). The last transition is consistent with the decomposition to copper oxide (Found: 55%, Calc. 57.6%). The loss of the four morpholine molecules in $CuL_4(NO_3)_2$ gives rise to a very broad weight loss amounting to 30% (Calc. 32.7%), followed by an exothermic transition at 210°C, which finally yields copper oxide (total Found, 85; Calc., 84.8%).

Species in aqueous solution. At pH values higher than 6, a single broad band centered at 547 nm is observed in the visible spectrum; there are no large expected differences between the various possible (morpholine–water–hydroxide)-copper complexes, but on the basis of the polarographic results described below, we attribute this band to the species $CuL_3(H_2O)_3^{2+}$; other minor species might contribute to the spectrum, but cannot be identified spectroscopically. An average values for $10Dq = 18{,}000$ cm^{-1} is calculated for the above complex.

On lowering the pH below 6, the band at 547 is replaced by the spectrum of aqueous Cu^{2+}, without any indication of other species with less than three coordinated morpholine molecules. All measurements were carried out at morpholine concentrations higher than 0.5 mol dm^{-3} (and usually equal to 2 mol dm^{-3}) because the range of stability of morpholine complexes is rather limited by the hydrolytic behaviour of Cu(II) and the protonation of morpholine.

Polarographic reduction of the morpholine complexes shows a single reversible wave yielding Cu(0); no evidence for Cu(I) is found. Reversibility was checked by the value of the slope of plots of $\log (i_d - i)/i$ vs E_{de} and values of $E_{3/4} - E_{1/4}$. Corrections were made for residual currents. The value of the overall dissociation constant of the prevailing complex, K_c was calculated from eqn (1).[10,11]

$$(E_{1/2})_c - (E_{1/2})_s = (2.3RT/nF)(\log K_c - \log (f_s k_c / f_c k_s) - p \log (L) f_L) \quad (1)$$

where (L) is the concentration of free ligand; f_c and f_s are the activity coefficients for Cu(II) with and without

added morpholine; f_L the activity coefficient of the ligand; p the number of L molecules bound to Cu(II); k_c and k_s the ratios of the cathodic diffusion current to Cu(II) concentration, with and without morpholine respectively. From the plot of $(E_{1/2})_c$ vs log (L) (see Fig. 1), the value of p can be calculated to be 3 in the range $0.5 < M < 2$, and seems to reach the value of 4 at very high amine concentrations. Measurements at different pH values indicate that the main species do not contain OH^- ions in the coordination sphere. This is shown in Table 2.

Estimation of (k_c/k_s) from Ilkovic's eqn (2) indicates the ratio to be always larger than 0.92, and we have therefore taken it as unitary in order to calculate K_c; the error thus introduced I.D. less than 0.04 units in log K_c.

$$(k_c/k_s) = (D_c/D_s)^{1/2} = (I_c/I_s). \quad (2)$$

In eqn (2), D_c and D_s are the diffusion coefficients of complexed and aqueous Cu(II).

Similarly, $(f_s/f_c) = 1$, as the ligand is non-ionic and the ionic strength was kept constant.

On these grounds, we obtain the value log K_3 = 14.64 ± 0.15 at ionic strength 1 mol dm^{-3} (KNO_3) and

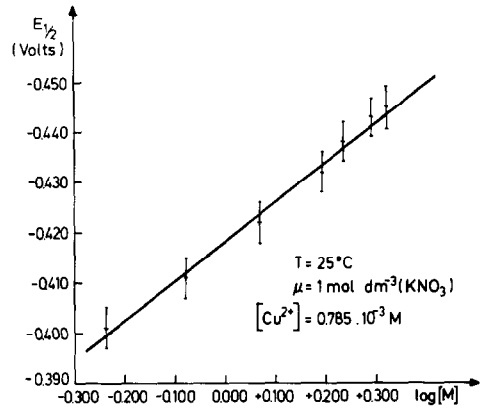

Fig. 1. Half wave potentials for the reduction of complex copper ions vs log M ([M] = 0; $E_{1/2}$ = +0.015V).

Table 2. Polarographic half-wave potentials at different pH values (25°C)

log L	pH	$E_{1/2}$ /V
0.293	10.89	-0.468
0.293	11.36	-0.472
0.293	12.12	-0.475
0.293	12.24	-0.474
0.662	11.89	-0.527
0.662	13.38	-0.530
0.662	11.98	-0.527

25.00°C, where K_3 is the overall stability constant, $K_3 = K_c^{-1}$.

As mentioned above, measurements performed in the morpholine concentration range 3.4–6 mol dm^{-3} yield the value $p = 4.4 \pm 0.7$ within the 75% confidence limits. These experiments were carried out at ionic strength of 0.5 mol dm^{-3} (KNO_3) and only a few points could be measured, giving rise to a rather large scatter of data. Assuming $p = 4$, the value log K_4 = 15.5 can be calculated.

The oxidation of Cu(0) in the presence of morpholine. From the value of K_3 the standard redox potential of the couple Cu(II)/Cu(0) is calculated to be −0.096V in the presence of 1 mol dm^{-3} morpholine. This value should be compared with the potentials for the aqueous couple, +0.337V and for the couple in 1 mol dm^{-3} ammonia, −0.120V. The corresponding $\Delta G°$ values for the reaction with hydrogen peroxide according to eqn (3)

$$pL + Cu(0) + H_2O_2 \rightarrow CuL_p^{2+} + 2OH^- \quad (3)$$

are −187.8 and −192.4 kJ for L = morpholine and ammonia respectively.

Table 3. Dissolution of metallic copper by morpholine/H_2O_2 and ammonia/H_2O_2 mixtures

t/°C	Reaction Medium	Coupon Weight Loss/ μg cm^{-2}h^{-1}	[Cu(II)] Increase in Solution/mol dm^{-3}h^{-1} x 10^4
60	Morpholine	8.2	0.39
60	Morpholine/H_2O 50%v/v	14	0.72
60	Ammonia	190	8.6
60	Ammonia/H_2O 40%v/v	780	39
60	Water	0.9	< 0.03
70	Morpholine	55	2.1
70	Morpholine/H_2O 50%v/v	60	3.0
70	Ammonia	900	38
70	Ammonia/H_2O 40%v/v	1800	74
70	Water	17	0.66

Thus, on thermodynamic grounds alone, morpholine is expected to be practically as dangerous as ammonia towards copper alloys in the presence of O_2 at least at high ligand concentration. (It is possible, although not very probable, that in more dilute solutions there might be larger differences determined by the values of the lower stability constant $k_n (n < 3)$ of morpholine and ammonia complexes). In practice, the aggressiveness of morpholine is much lower, probably due to kinetic effects. Table 3 shows that the rate of weight loss of copper coupons by oxidation with H_2O_2 is much faster in the presence of ammonia than in the presence of morpholine, although the latter system dissolves copper much faster than hydrogen peroxide alone. These observations, together with the lower volatility of morpholine,[1] makes this amine less dangerous to copper than ammonia for the condenser tubes in power plants.

It should be emphasized that the different aggressiveness is not a pH effect, as measurements similar to those included in Table 3 but at different fixed pH values showed that in the whole range $9 < pH < 12.5$ ammonia dissolved more copper than morpholine in the presence of 10^{-2} mol dm^{-3} H_2O_2.

Acknowledgements—We thank J. Magallanes and A. Caridi for assistance with the polarographic measurements. MAB is a member of CONICET.

REFERENCES

[1]P. V. Balakrishnan, *Canad. J. Chem.* 1978, **56**, 20, 2620.
[2]I. S. Ahuja, *J. Inorg. Nucl. Chem.* 1967, **29**, 2091.
[3]E. A. Allen and W. Wilkinson, *J. Inorg. Nucl. Chem.* 1973, **35**, 3135.
[4]E. A. Allen, N. P. Johnson, D. T. Rosevear and W. Wilkinson, *J. Chem. Soc. (A)* **1971**, 2141.
[5]R. A. Walton, *Inorg. Chem.* 1966, **5**, 4, 643.
[6]B. R. James and R. P. J. Williams, *J. Chem. Soc.* **1961**, 2007.
[7]C. C. Addison and B. M. Gatehouse, *J. Chem. Soc.* **1960**, 613.
[8]K. Dornberger and J. Leciejewicz, *Acta Cryst*, 1958, **11**, 825.
[9]A. I. Vogel, *Quantitative Inorganic Analysis*, 2nd Edn, Longmans, London (1958).
[10]D. Vedal, O. H. Ellestad, P. Klaboe and G. Hagen, *Spectrochim. Acta* 1976, **32A**, 4, 877.
[11]K. Nakamoto, *Infrared Spectra of Inorganic and Coordination Compounds*. Wiley, London (1963).
[12]L. Meites, *Polarographic Techniques*, 2nd Edn. Interscience Publishers (1965).
[13]I. M. Kolthoff and J. J. Lingane, *Polarography*, 2nd Edn. Interscience Publishers (1952).

Polyhedron Vol. 1, No. 5, pp. 441–451, 1982
Printed in Great Britain.

0277–5387/82/050441–11$03.00/0
Pergamon Press Ltd.

TRIMETHYL AND DIETHYLPHENYLPHOSPHINE COMPLEXES OF RHENIUM(I, III, IV, V) AND THEIR REACTIONS. X-RAY CRYSTAL STRUCTURES OF A BIS(η^5-CYCLOPENTADIENYL)-ETHANE-BRIDGED DIRHENIUM(I) COMPLEX OBTAINED FROM PHENYLACETYLENE, TETRAKIS-(DIETHYLPHENYLPHOSPHINE) (DINITROGEN) HYDRIDORHENIUM (I), TETRAKIS(TRIMETHYL-PHOSPHINE) (η^2-DIMETHYLPHOSPHINOMETHYL) RHENIUM(I) AND TETRAKIS(TRIMETHYL-PHOSPHINE) (IODO)METHYL RHENIUM(III) IODIDE-TETRAMETHYLPHOSPHONIUM IODIDE

KWOK W. CHIU, CHRISTOPHER G. HOWARD, HENRY S. RZEPA, RICHARD N. SHEPPARD and GEOFFREY WILKINSON*

Chemistry Department, Imperial College of Science and Technology, London, SW7 2AY, England

and

ANITA M. R. GALAS and MICHAEL B. HURSTHOUSE*

Chemistry Department, Queen Mary College, London, E1 4NS, England

(*Received* 1 *March* 1982)

Abstract—A number of trimethyl- and diethylphenylphosphine complexes of rhenium have been obtained by sodium amalgam reduction of $ReCl_4(THF)_2$ on from $Re(NPh)Cl_3(PMe_3)_2$ and their reactions studied. The following compounds have been isolated and characterised by infrared and nuclear magnetic resonance spectroscopy. $ReCl(PMe_3)_5$ (**A**), $ReH(PMe_3)_5$ (**B**), $[ReHCl(PMe_3)_5]BF_4$ (**C**), $[Re(N_2)(PMe_3)_5]Cl \cdot MeOH$ (**D**), and the corresponding BF_4^- salt, $[Re(PMe_3)_5]Cl$ (**E**), $ReMe(PMe_3)_5$ (**F**), $ReCl(CO)_2(PMe_3)_3$ (**G**), $[(Me_3P)_3Re(\eta^5\text{-}C_5H_2Ph_2)]_2C_2H_2Ph_2$ (**H**), $ReCl(N_2)(PEt_2Ph)_4$ (**I**), $ReH(N_2)(PEt_2Ph)_4$ (**J**), $[Re(NHPh)I(PMe_3)_4]I$ (**K**), $Re(NHPh)(\eta^2\text{-}CO_2)(PMe_3)_3$ (**L**), $Re(\eta^2\text{-}CH_2PMe_2)(PMe_3)_4$ (**M**), $ReH_3(PMe_3)_4$ (**N**), $[ReH_4(PMe_3)_4]BF_4$(**O**) and $[ReI(Me)(PMe_3)_4]I \cdot [Me_4P]I$ (**P**).

For $Re(\eta^2\text{-}CH_2PMe_2)(PMe_3)_4$ computer simulated and two dimensional δ/J resolved $^{31}P\{^1H\}$ NMR spectra have been obtained; the spectra are fully consistent with the structure determined by X-ray diffraction.

The X-ray structures of compounds **H**, **J**, **M** and **P** have been determined. Preliminary data for compound **C** have also been obtained.

Trimethylphosphine complexes of rhenium have been made by reduction of $Re(NPh)Cl_3(PMe_3)_2$ with sodium amalgam under different atmospheres, N_2, Ar, CO, etc.[1] Here we describe additional compounds of PMe_3, and also of PEt_2Ph, obtained by reduction of $ReCl_4(THF)_2$. The reduction in presence of Bu^tNC is described separately;[2] the reduction in presence of $P(OMe)_3$ leads[3] to the dimer $Re_2[P(OMe)_3]_{10}$, unlike the reductions described here which give mononuclear species.

Further studies on the reactions of $Re(NPh)Cl_3(PMe_3)_2$ are also described. X-Ray diffraction studies on four of the molecules have been made. The various reactions are summarised in Schemes 1 and 2. Infrared and nuclear magnetic resonance (^1H, ^{13}C and ^{31}P) data are given in the Experimental Section.

*Authors to whom correspondence should be addressed.

A. TERTIARY PHOSPHINE COMPLEXES DERIVED FROM RHENIUMTETRACHLORIDEBIS(TETRAHYDROFURAN)

(1) *Pentakis(trimethylphosphine)chloro- and hydrido-rhenium(I)*

The sodium amalgam reduction of $ReCl_4(THF)_2$ in tetrahydrofuran containing excess PMe_3 under nitrogen provides both $ReCl(PMe_3)_5$ (**A**) and $ReH(PMe_3)_5$ (**B**) where the hydride arises from the solvent. We have been unable to convert (**A**) into (**B**) by $LiAlH_4$ or $NaBH_4$. Both compounds are moderately air stable and can be handled briefly in air. The yellow chloride and white hydride can be separated by crystallisation from petroleum, or better, by sublimation of the hydride at 120°C and 10^{-3} cm Hg. The ^1H and $^{31}P\{^1H\}$ NMR spectra confirm the octahedral geometry. Analogues of the hydride with PR_3 ligands are $ReH[P(OMe)_3]_5$[3] and $ReH(PF_3)_5$,[4] while related hydrido species with chelating phosphines, e.g. $ReH(N_2)$-

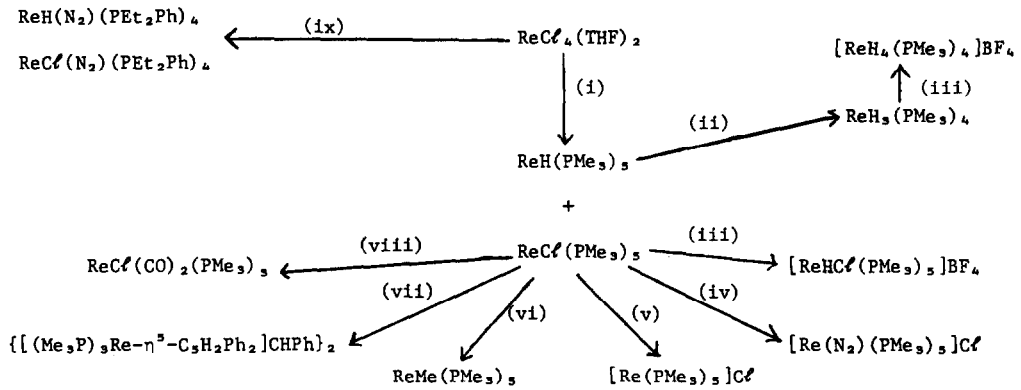

Scheme 1. (i) PMe_3, Na/Hg, N_2; (ii) H_2; (iii) HBF_4; (iv) N_2, MeOH; (v) Ar, MeOH; (vi) MeLi; (vii) PhC_2H; (viii) CO; (ix) PEt_2Ph, N_2.

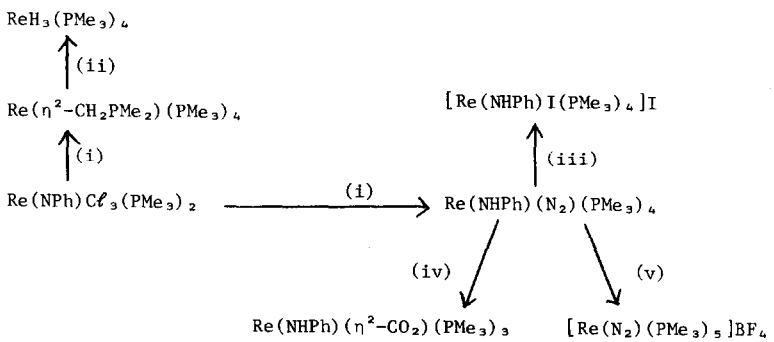

Scheme 2. (i) Na/Hg, PMe_3, N_2; (ii) H_2; (iii) I_2; (iv) CO_2; (v) HBF_4.

$(diphos)_2$ are known.[5,6] The hydride slowly reacts with hydrogen (4 atm) in benzene to give the trihydride $ReH_3(PMe_3)_4$ described later.

The chloride in methanol slowly dissociates to give $[Re(PMe_3)_5]Cl$ (see below) which on heating in toluene re-forms the neutral chloride.

(2) *Reactions of pentakis(trimethylphosphine)chlororhenium(I)*

(a) *Fluoroboric acid and trityltetrafluoroborate.* The interaction of $ReCl(PMe_3)_5$ with one equivalent of aqueous 48% HBF_4, or with two equivalents of Ph_3CBF_4 in THF, produces the yellow, air sensitive salt, $[ReH(Cl)(PMe_3)_5]BF_4$ (**C**). This is soluble in polar solvents and is a 1:1 electrolyte in $MeNO_2$.

The IR and ^1H NMR spectra confirm the presence of hydride but the high field line is poorly resolved and the 7-coordinate cation is presumably non-rigid in solution. Protonations by Ph_3CBF_4 in THF, where the H† evidently comes from the triphenylmethyl ion, have been recognised previously.[6] Protonation—or oxidative addition—to octahedral rhenium(I) complexes to give 7-coordinate species is rare but is known for *trans*-$ReH(N_2)(dppe)_2$.[4] The structure of compound (**C**) has been investigated by X-ray crystallography. Although the main features have been identified, confirming the nature of the compound, complete refinement has not yet been achieved due to disorder and/or pseudo symmetry correlation problems (see Experimental). Full details will be reported when the refinement has been completed.

(b) *Dinitrogen.* In methanol, the chloride reacts with N_2 to give an air-stable white salt $[Re(N_2)(PMe_3)_5]Cl.MeOH$ (**D**) which is a 1:1 electrolyte in methanol. In addition to the terminal $Re(N_2)$ stretch there is a band at 3350 cm^{-1} in the IR spectrum due to methanol. The fluoroborate salt of this cation has also been obtained by action of HBF_4 on $Re(NHPh)(N_2)(PMe_3)_4$ (see later).

(c) *Methanol.* From the reaction in methanol under argon a white crystalline solid can be isolated. According to analytical and spectroscopic data this is $[Re(PMe_3)_5]Cl$ (**E**). The spectroscopic data suggest that the cation, which is presumably 5-coordinate in solution, is non-rigid.

In methanol, the salt reacts readily with dinitrogen at 1 atm and the dinitrogen complex (**D**) can be isolated quantitatively from the solution. Surprisingly, however, it does not react with CO under the same conditions (1 atm), nor does it react with CO_2 or N_2O; it can be recrystallised unchanged from MeCN and pyridine. There is also no reaction with hydrogen, and under hydrogen, alk-1-enes are not isomerised or hydrogenated even at 120° at 30 atm.

(d) *Methyllithium.* The chloride is readily methylated by methyllithium in diethylether to give $ReMe(PMe_3)_5$ (**F**) whose isocyanide analogue, $ReMe(CNBu^t)_5$ has been described.[2]

(e) *Carbon monoxide.* In diethylether, $ReCl(PMe_3)_5$ reacts with CO (3 atm) to give the white crystalline $ReCl(CO)_2(PMe_3)_3$ (**G**) for which IR and NMR data indicates a structure with *cis*-CO and *mer*-PMe_3 groups. Similar compounds of the class $ReCl(CO)_n(PR_3)_m$, $n+m=5$, with different tertiary phosphines are well known.[7]

(f) *Phenylacetylene.* Interaction of $ReCl(PMe_3)_5$ with PhC_2H at 110°C in toluene gives the unusual η^5-cyclopentadienyl derivative (**H**) whose structure, shown diagramatically (1), has been determined by X-ray diffraction. Knowing the structure the NMR data can be interpreted. Although a wide variety of unusual

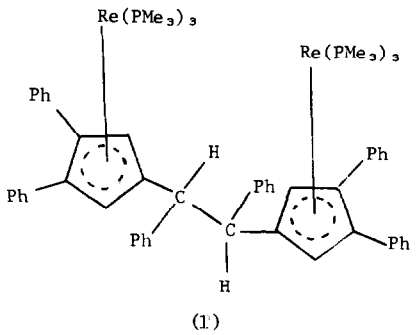

(1)

organometallic compounds may be made by linking of acetylenes[8] a derived molecule of the present type appears to be unique. Suitable crystals for X-ray study were obtained from petroleum.

The structure of the complex is shown in Fig. 1 and selected geometry parameters in Table 1. The terminal η^5-C_5R_5 rings are coordinated to $Re(PMe_3)_3$ groups and although such a system is uncommon, it is closely related to the more frequently found $(\eta^5$-$C_5H_5)Re(CO)_3$ systems. How the compound is formed from six phenyl acetylenes is unknown, but some sort of metal-mediated process involving hydrogen transfer from two acetylenes and C-C bond formation must occur.

3. *Tetrakis(diethylphenylphosphine)dinitrogen chloro- and hydrido rhenium(I)*

By contrast with the PMe_3 case, reduction of $ReCl_4(THF)_2$ in THF containing excess PEt_2Ph gives a yellow air-stable dinitrogen complex, $ReCl(N_2)(PEt_2Ph)_4$

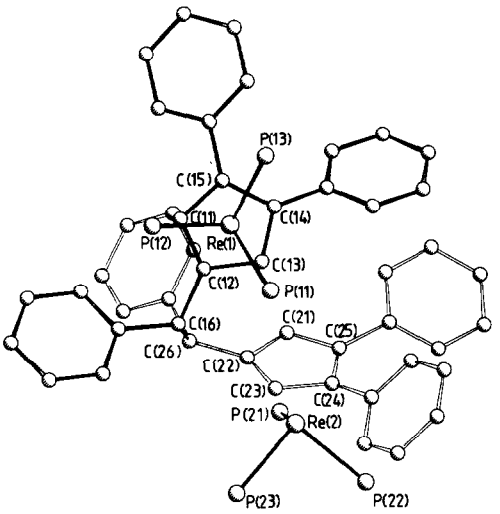

Fig. 1. Molecular structure of the complex derived from reaction of phenylacetylene with $ReCl(PMe_3)_5$.

(I). This is similar to other well known compounds such as $ReCl(N_2)(PMe_2Ph)_4$[9] and has Cl *trans* to N_2 with equatorial phosphines.

In addition, a small amount of petroleum soluble yellow hydride $ReH(N_2)(PEt_2Ph)_4$ (J) was isolated; this has Re–H and Re–N_2 stretches in the IR at 1890 and 1945 cm^{-1} respectively. Chelating phosphine dinitrogen hydrides are known.[4,5] A diagram of the molecular structure, which has crystallographic 2-fold symmetry coincident with the H–Re–N_2 axis, is shown in Fig. 2,

Table 1. Selected bond parameters for the complex derived from reaction of phenylacetylene with $ReCl(PMe_3)_5$

a) Bond Lengths (A)

Re(1)-P(11)	2.312(5)	Re(2)-P(21)	2.318(4)
Re(1)-P(12)	2.321(4)	Re(2)-P(22)	2.325(4)
Re(1)-P(13)	2.332(4)	Re(2)-P(23)	2.303(5)
Re(1)-C(11)	2.29(1)	Re(2)-C(21)	2.29(1)
Re(1)-C(12)	2.31(1)	Re(2)-C(22)	2.30(1)
Re(1)-C(13)	2.26(1)	Re(2)-C(23)	2.27(1)
Re(1)-C(14)	2.32(1)	Re(2)-C(24)	2.30(1)
Re(1)-C(15)	2.30(1)	Re(2)-C(25)	2.29(1)
P-C(Me)	1.82(2) - 1.92(2)	Avge 1.86	
C(12)-C(16)	1.56(2)	C(22)-C(26)	1.51(2)
C(16)-C(26)	1.62(2)		
C(11)-C(12)	1.38(2)	C(21)-C(22)	1.43(2)
C(12)-C(13)	1.46(2)	C(22)-C(23)	1.42(2)
C(13)-C(14)	1.40(2)	C(23)-C(24)	1.43(2)
C(14)-C(15)	1.44(2)	C(24)-C(25)	1.48(2)
C(15)-C(11)	1.43(2)	C(25)-C(21)	1.43(2)

b) Bond Angles (deg).

P(11)-Re(1)-P(12)	92.8(2)	P(21)-Re(2)-P(22)	90.6(2)
P(11)-Re(1)-P(13)	93.6(2)	P(21)-Re(2)-P(23)	96.4(2)
P(12)-Re(1)-P(13)	91.3(2)	P(22)-Re(2)-P(23)	91.4(2)
C(11)-C(12)-C(13)	108(1)	C(21)-C(22)-C(23)	108(1)
C(11)-C(12)-C(16)	129(1)	C(21)-C(22)-C(26)	127(1)
C(13)-C(12)-C(16)	122(1)	C(23)-C(22)-C(21)	123(1)
C(12)-C(16)-C(26)	112(1)	C(22)-C(26)-C(16)	110(1)

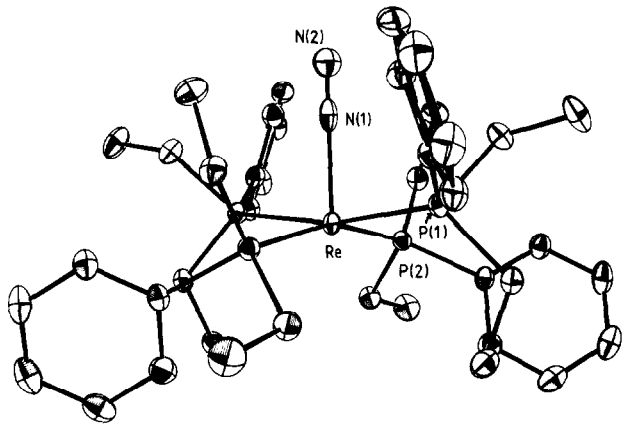

Fig. 2. Molecular structure of *trans*-ReH(N_2)(PEt_2Ph)$_4$.

and some of the more significant bond lengths and angles are given in Table 2.

The molecule is octahedral with an equatorial set of four, tetrahedrally distorted phosphines and mutually *trans* H and N_2 ligands. Since no structure of a *trans* hydrido dinitrogen rhenium complex has been determined (although *trans*-HRe(N_2)(dppe)$_2$ has been made and unidentate tertiary phosphine compounds of other metals are known[4,9c]) the molecular geometry parameters are most usefully compared with those of the [N_2–ReClP$_4$] unit found in the structures of ReCl(N_2)(PMe_2Ph)$_4$,[10] the ortho-metallated complex, *fac*-Re(N_2)(η^2-$C_6H_4PMe_2$)(PMe_2Ph)$_3$,[11] $MoCl_4[N_2ReCl(PMe_2Ph)_4]_2$[12] and (MeO)$Cl_4MoN_2ReCl(PMe_2Ph)_4$.[13] In the two μ-N_2 bridged species the Re–N distances are short (1.88, 1.81 Å) whereas in the mononuclear chloro complex[10] the distance is 1.97 Å, and in the ortho-metallated species[11] 1.960 Å. The considerably longer Re–N distance in the present complex indicates a significantly larger *trans* weakening influence by the hydride compared to chloride ligand.

An additional feature is that the shorter Re–N distances in the bridged molecules are associated with much longer Re–P distances [2.433(9) to 2.486(6) Å]. Values in ReCl(N_2)(PMe_2Ph)$_4$, the ortho-metallated species[11] and the hydride are all close to 2.400 Å. This suggests that the bonding characteristics of the bridging dinitrogen ligand, which appear to be those of a π-acceptor, at least at rhenium, are significantly modified when the ligand is terminal.

B. ADDITIONAL REACTIONS OF TETRAKIS(TRIMETHYLPHOSPHINE)DINITROGEN PHENYLAMIDORHENIUM(I).

(a) *Iodine.* Interaction of Re(NHPh)(N_2)(PMe_3)$_4$ with iodine in benzene solution leads to loss of N_2 in an oxidative addition reaction giving a quantitative yield of the salt [Re(NHPh)I(PMe_3)$_4$]I (**K**). This is a 1:1 electrolyte in nitromethane; the spectra are consistent with the NHPh and I groups being *cis*.

(b) *Fluoroboric acid.* With HBF_4 in THF the phenylamido complex reacts to give the fluoroborate salt of the same cation, [Re(N_2)(PMe_3)$_5$]$^+$ described above. The phenylamido group has been lost, presumably as $PhNH_3^+$ and the additional PMe_3 must be derived from a second molecule of the starting material since the yield is only *ca.* 45%; we have been unable to characterise what must be a more soluble species with less than four PMe_3 per Re.

(c) *Carbon dioxide.* Interaction of CO_2 with Re(NHPh)(N_2)(PMe_3)$_4$ in toluene leads to air sensitive orange crystals of Re(NHPh)(η^2-CO_2)(PMe_3)$_3$ (**L**). We have been unable to obtain crystals suitable for X-ray study; only three examples of η^2-CO_2 complexes are confirmed by X-ray diffraction.[14] The η^2-CO_2 formulation is based on spectra.[15–17] Thus, the IR spectrum has bands at 1620 and 1605 cm^{-1} similar to those in Ni(η^2-CO_2)(PBu_3^n)$_2$,[15] while the $^{13}C\{^1H\}$ NMR peak for CO_2 occurs at 163.4 ppm [in (η^5-C_5H_4Me)$_2$Nb(CH_2SiMe_3)(η^2-CO_2)[14] the value is given as −200.5 ppm and we presume this should be +200.5 since ^{13}C resonances of

Table 2. Selected bond parameters for *trans*-ReH(N_2)(PEt_2Ph)$_4$

a) Bond Lengths (A).

Re -P(1)	2.412(1)	Re -P(2)	2.404(1)
P(1)-C(11)	1.852(4)	P(2)-C(21)	1.856(4)
P(1)-C(13)	1.854(4)	P(2)-C(23)	1.849(5)
P(1)-C(111)	1.852(4)	P(2)-C211)	1.856(4)
	Re-N(1)	2.055(5)	
	N(1)-N(2)	1.018(8)	

b) Bond Angles (deg).

N(1)-Re-P(1)	83.8(1)	N(1)-Re-P(2)	99.6(1)
	P(1)-Re-P(2)	90.8(1)	
	Re-N(1)-N(2)	180	

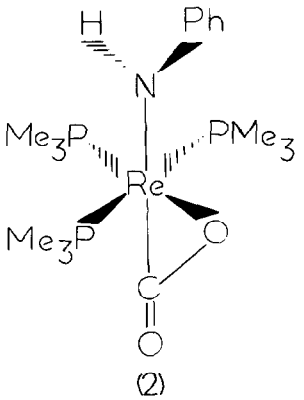

(2)

metal carbonyls are in the positive region up to 300 ppm]. The $^{31}P\{^1H\}$ spectrum indicates two phosphorus environments. The structure is probably of the type 2.

C. SYNTHESIS AND REACTIONS OF TETRAKIS(TRIMETHYLPHOSPHINE) (η^2-DIMETHYLPHOSPHINOMETHYL)RHENIUM(I)

Although the reduction of $Re(NPh)Cl_3(PMe_3)_2$ in presence of trimethylphosphine by sodium amalgam in THF under nitrogen leads[1] to $Re(NHPh)(N_2)(PMe_3)_4$ a prolonged reaction time gives the latter as minor product, the major one being $Re(\eta^2\text{-}CH_2PMe_2)(PMe_3)_4$ (**M**), as yellow, air-sensitive petroleum soluble crystals. The structure has been determined by X-ray crystallography. The structure of one of the two crystallographically independent molecules, which are identical within the limits of experimental error, is given in Fig. 3, whilst

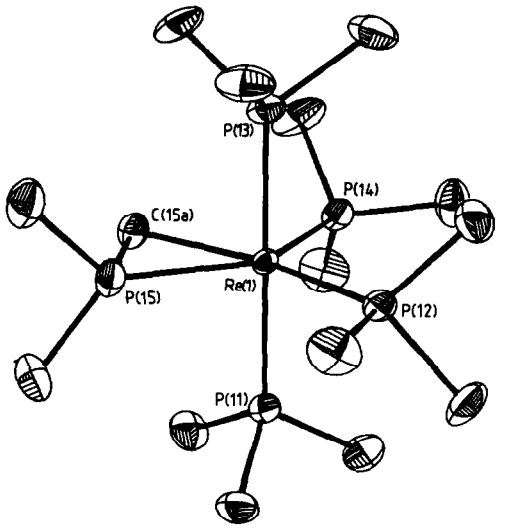

Fig. 3. Molecular structure of $Re(\eta^2\text{-}CH_2PMe_2)(PMe_3)_4$.

some of the more important geometry parameters are given in Table 3. The rhenium coordination geometry is distorted octahedral, with the main distortion arising from the presence of the three atom metallocycle. Interestingly, most of the angular distortion occurs in movement of the phosphorus atom in the ring from an idealised octahedral position, with P(12)–Re–C(14) = 160° and P(14)–Re–P(15) = 137°. A second point of interest is the distribution of the Re–P bond lengths into two groups, which might be termed axial [e.g. Re(1)–P(11), Re(1)–

Table 3. Selected bond parameters for $Re(\eta^2\text{-}CH_2PMe_2)(PMe_3)_4$

a) Bond Lengths (A).

Molecule 1		Molecule 2	
Re(1)-P(11)	2.378(1)	Re(2)-P(22)	2.376(2)
Re(1)-P(13)	2.379(2)	Re(2)-P(24)	2.374(2)
Re(1)-P(14)	2.326(2)	Re(2)-P(21)	2.331(1)
Re(1)-P(12)	2.334(2)	Re(2)-P(23)	2.322(2)
Re(1)-P(15)	2.332(2)	Re(2)-P(25)	2.321(2)
Re(1)-C(15A)	2.277(8)	Re(2)-C(25A)	2.280(6)
P(15)-C(15A)	1.755(7)	P(25)-C(25A)	1.756(8)
P(15)-C(15B)	1.846(11)	P(25)-C(25B)	1.844(11)
P(15)-C(15C)	1.842(9)	P(25)-C(25C)	1.847(12)
Other P-C(Me)	1.84-1.88(1)		1.83-1.88

b) Bond Angles (deg).

P(11)-Re(1)-P(13)	177.3(1)	P(22)-Re(2)-P(24)	176.7(1)
P(11)-Re(1)-P(12)	89.1(1)	P(22)-Re(2)-P(21)	88.5(1)
P(11)-Re(1)-P(14)	91.8(1)	P(22)-Re(2)-P(23)	91.5(1)
P(11)-Re(1)-P(15)	89.5(1)	P(22)-Re(2)-P(25)	89.6(1)
P(11)-Re(1)-C(15A)	91.0(2)	P(22)-Re(2)-C(25A)	90.6(2)
P(15)-Re(1)-C(15A)	44.8(2)	P(25)-Re(2)-C(25A)	44.9(2)
P(15)-Re(1)-P(12)	115.7(1)	P(25)-Re(2)-P(21)	115.5(1)
P(15)-Re(1)-P(14)	136.9(1)	P(25)-Re(2)-P(23)	137.0(1)
C(15A)-Re(1)-P(14)	92.2(2)	C(25A)-Re(2)-P(23)	92.1(2)
C(15A)-Re(1)-P(12)	160.4(2)	C(25A)-Re(2)-P(21)	160.4(2)
C(15A)-P(15)-C(15B)	113.0(5)	C(25A)-P(25)-C(25B)	111.3(5)
C(15A)-P(15)-C(15C)	110.2(5)	C(25A)-P(25)-C(25C)	113.3(5)
C(15B)-P(15)-C(15C)	97.0(5)	C(25B)-P(25)-C(25C)	96.5(5)
Re(1)-P(15)-C(15A)	66.0(3)	Re(2)-P(25)-C(25A)	66.3(2)
Re(1)-P(15)-C(15B)	130.8(3)	Re(2)-P(25)-C(25B)	130.4(3)
Re(1)-P(15)-C(15C)	130.8(4)	Re(2)-P(25)-C(25C)	131.1(4)

P(13)] and equatorial [Re(1)–P(12), Re(1)–P(14), Re(1)–P(15)]. In the former group all distances are 2.375–2.378(2) Å whilst in the latter the range is 2.321–2.337(2) Å. The equatorial group contains the metallocycle phosphorus atoms for which the Re–P bond lengths are unaffected by the ring formation. These features make interesting comparisons with results found for molecules containing equivalent $M<\begin{matrix}P\\|\\C\end{matrix}$ rings. In $IrCl_2(\eta^2\text{-}CH_2PMePh)(PMe_2Ph)_2$[18] the angular deformation is similar to that in our complex, with the Ir–C bond less distorted from the octahedral position than the Ir–P bond, but the latter is significantly shorter (~0.025 Å) than the other two equatorial Re–P bonds. In the distorted planar Pt^{II} complexes $Pt[\eta^2\text{-}CHPhP(CH_2Ph)_2](C_2B_{20}H_{20}Me)P(CH_2Ph)_3$[19] and the related PEt_3 and PPr^n_3[20] complexes, the deformations of the Pt–C and Pt–P bonds in the ring away from the orthogonal planar positions are about equal, but now the Pt–P distance in the ring is considerably less (~0.07 Å) than the other Pt–P bond length. A common feature of all structures, however, is a significant shortening of the metallocycle P–C bond.

The NMR data which is generally consistent with the solid state structure indicates that the molecule is non-rigid in solution. The ^1H NMR spectrum contains, in the δ 1.5–1.3 ppm region, doublets and doublets of doublets due to PMe_3 plus a broad multiplet at *ca.* δ 1.4 for the PMe_2 protons of the metallocycle similar to that observed in $HM(\eta^2\text{-}CH_2PMe_2)(PMe_3)_3$, M = Fe,[21] Ru.[22] The methylene protons, δ −0.51 ppm are equivalent and give a triplet [$^3J(P_{c,d}\text{–}H) = 9.09$ Hz] of triplets, [$^3J(P_b\text{–}H) = 3.78$ Hz] of doublets, [$^2J(P_a\text{–}H) = 1.95$ Hz] (for numbering see Diagram 3). Although at +36°C the $^{31}P\{^1H\}$ spectrum has four broad peaks, the molecule is non-rigid; at −60°C sharp multiplets are observed. This spectrum could not be assigned completely by normal methods. However, non-linear, least squares iterative computer simulation yielded all the phosphorus–phosphorus coupling constants. The standard deviation in the calculated line positions was 1.5 Hz, well within the resolution of the spectrometer at −60°C. Figure 4 shows the excellent agreement between the observed ($4a_1$, $4b_1$, $4c_1$, $4d_1$) and simulated ($4a_2$, $4b_2$, $4c_2$, $4d_2$) spectra. The resonance of P_a (Fig. 4a) occurs at δ −73.6 ppm as a doublet $^2J(P_a - P_d) = 89.6$ Hz of doublets $^2J(P_a - P_c) = 32.3$ Hz of triplets $^2J(P_a - P_b) = 19.9$ Hz. The two equivalent atoms P_b (Fig. 4b) at δ −40.6 ppm give rise to a doublet $^2J(P_b - P_d) = 21.2$ Hz, of doublets $^2J(P_b - P_a) = 19.9$ Hz, of doublets $^2J(P_b - P_c) = 19.2$ Hz. The resonance of P_c (Fig. 4c) at δ −45.5 ppm consists of an incompletely resolved doublet of triplets of doublets $^2J(P_c - P_d) = 13.4$ Hz; P_d (Fig. 4d) at δ −36.0 ppm is a doublet of triplets of doublets.

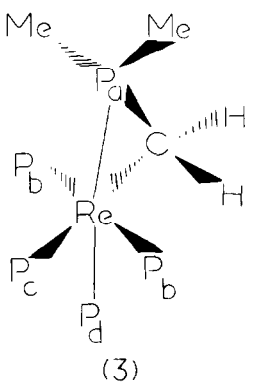

(3)

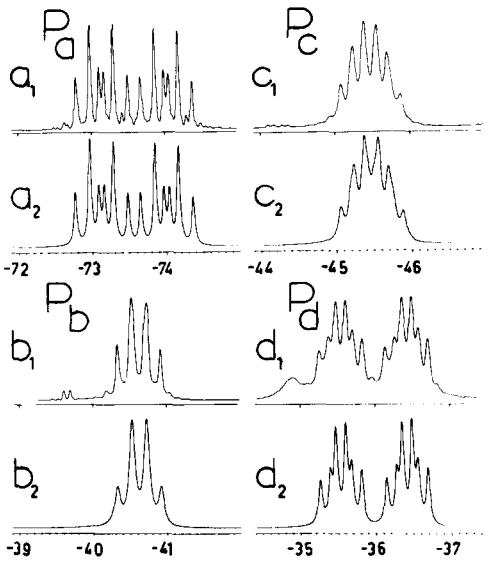

Fig. 4. Observed (a_1, b_1, c_1, d_1) and computer simulated (a_2, b_2, c_2, d_2) $^{31}P\{^1H\}$ NMR spectra of $Re(\eta^2\text{-}CH_2PMe_2)(PMe_3)_4$ in toluene at 213 K.

The two dimensional[23] δ/J resolved, proton decoupled, 101 MHz ^{31}P spectrum obtained at 213 K is also fully consistent with the crystal structure, showing four distinct phosphorus sites (Fig. 5). A cross section in the J axis through each resonance shows the ^{31}P homonuclear coupling patterns, identical, with one exception, with those observed in the conventional one dimensional spectrum (Fig. 4). The cross section through the peak at δ −36 ppm shows a broad singlet, compared with the well resolved 12 line multiplet observed in the one dimensional spectrum. The reasons for this are not well understood, but may be connected with the chemical exchange at this site that occurs on the time scale of the experiment.

The $^{13}C\{^1H\}$ spectrum of the compound is very com-

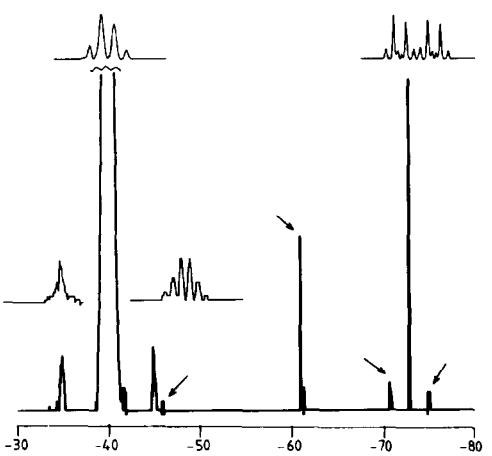

Fig. 5. Two dimensional δ/J resolved ^{31}P spectrum of (M), at 213 K showing a projection of the δ axis. Cross sections through each ^{31}P resonance, corresponding to the J axis, are shown above the peaks. Those peaks marked with an arrow are due to machine artifacts such as quadrature spikes, etc., except for the peak at δ −63 which is due to free PMe_3.

plex. A multiplet at δ −34.8 ppm can be assigned to the CH_2 group—this is at a much lower frequency than that in $IrCl_2[\eta^2\text{-}CH_2P(MePh)](PMe_2Ph)_2$[18] ($\delta$ −8.6 ppm), and in $Ru(\eta^2\text{-}CH_2PMe_2)[(CH_2)_2PMe_2](PMe_3)_2$[24] ($\delta$ +42 ppm); the ^{13}C spectrum of $HRu(\eta^2\text{-}CH_2PMe_2)(PMe_3)_4$[22] was not reported.

Interaction with hydrogen. In tetrahydrofuran with *ca.* 3 atm H_2 for 3 days, $Re(\eta^2\text{-}CH_2PMe_2)(PMe_3)_4$ reacts to give $ReH_3(PMe_3)_4$ (N) as the major product. This white crystalline compound can also be obtained (as noted above) from $ReH(PMe_3)_5$ and indeed the latter can be detected by NMR initially in the reaction mixture and is presumably an intermediate in the formation of the trihydride. The ^1H NMR spectrum is similar to that for $ReH_3(diphos)_2$[25] with a high field quintet at δ −7.84 ppm, $^2J(P\text{–}H) = 20.8$ Hz. The $^{31}P\{^1H\}$ spectrum consists only of an unresolved broad band δ −41.24 ppm even down to −60° indicating non-rigidity.

The trihydride reacts with one equivalent of tetrafluoroboric acid in THF at −78° to give the white air stable crystalline salt $[ReH_4(PMe_3)_4]BF_4$ (O). In addition to PMe_3 resonances at δ 1.78 ppm, the high field region has two sharp outer and three broad isomer lines which at +60° resolve to a quintet δ −5.40 ppm, $^2J(P\text{–}H) =$ 23 Hz, similar to the spectra of $MH_4(PMe_3)_4$, M = Mo,[26] W[27]; the $^{31}P\{^1H\}$ spectrum is also temperature dependent being a singlet at +50° and two broad overlapping singlets at +36°.

Interaction with methyl iodide. The addition of methyl iodide to $Re(\eta^2\text{-}CH_2PMe_2)(PMe_3)_4$ in THF gives an orange solid. On recrystallisation from methanol, both white and orange crystals are obtained which can be separated manually. The former were identified by NMR and analysis as $[PMe_4]I$.[28] The nature of the orange crystals was determined by X-ray diffraction study as the double salt $[ReI(Me)(PMe_3)_4]I\cdot[PMe_4]I$ (P). The structure of the complex rhenium cation, which has octahedral geometry with *trans* methyl and iodide ligands is given in Fig. 6 and some of the more important bond lengths and angles are listed in Table 4.

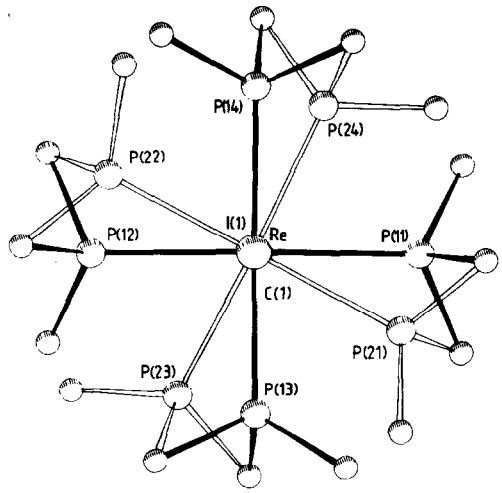

Fig. 6. Structure of the cation in the double salt $[ReI(Me)(PMe_3)_4]I\cdot[Me_4P]I$. Each cation site is occupied by two enantiomeric forms of the ion which are present in unequal amounts (60:40). The dominant form is shown with heavy bonds.

The reaction differs from those of methyl iodide with the hydride species $MH(\eta^2\text{-}CH_2PMe_2)(PMe_3)_3$, M = Ru,[23] Fe,[29] in producing a cation; the $\eta^2\text{-}CH_2PMe_2$ group is lost, presumably as PMe_2Et. Few examples of cationic phosphine complexes of rhenium(III) are known, namely $[ReX_2(dppe)_2]X$, X = Cl, Br.[25,30–32]

EXPERIMENTAL

Microanalyses by Pascher, Bonn, and Imperial College Laboratories. Molecular weights by cryoscopy in benzene. Melting points (uncorrected) in sealed tubes under nitrogen.

All operations were carried out under oxygen-free argon or nitrogen or in vacuum. Solvents were dried over sodium and distilled from sodium–benzophenone under nitrogen; methanol was dried over magnesium and distilled from magnesium methoxide under N_2. Petroleum had b.p. 40–60°C unless otherwise stated.

Table 4. Selected bond parameters for $[Re(I)(Me)(PMe_3)_4]I\cdot[Me_4P]I$

a) Bond Lengths (A)

Re	-I(1)	2.744(1)	Re	-C	2.13(2)
Re	-P(11)	2.442(7)	Re	-P(21)	2.458(14)
Re	-P(12)	2.461(7)	Re	-P(22)	2.476(13)
Re	-P(13)	2.463(8)	Re	-P(23)	2.396(14)
Re	-P(14)	2.440(7)	Re	-P(24)	2.472(14)
	P-C(Me)	1.83 - 1.87	(Range Fixed)		
P(111)-C(111)		1.79(2)	P(111)-C(112)		1.82(2)
P(111)-C(113)		1.81(2)	P(111)-C(114)		1.78(2)

b) Bond Angles (deg).

I(1)-Re-C	178.3(5)		
I(1)-Re-P(11)	98.7(2)	C-Re-P(11)	80.2(1)
I(1)-Re-P(12)	98.0(2)	C-Re-P(12)	83.1(6)
I(1)-Re-P(13)	83.9(2)	C-Re-P(13)	94.8(6)
I(1)-Re-P(14)	83.6(2)	C-Re-P(14)	97.8(6)
I(1)-Re-P(21)	81.7(3)	C-Re-P(21)	96.7(6)
I(1)-Re-P(22)	82.4(3)	C-Re-P(22)	99.1(6)
I(1)-Re-P(23)	97.2(3)	C-Re-P(23)	82.0(6)
I(1)-Re-P(24)	99.4(3)	C-Re-P(24)	81.3(6)

C(Me)-P(111)-C(Me) 107.3-111.7(1.5)

Spectrometers. NMR: Perkin–Elmer R32 (^{1}H, 90 MHz), Bruker WM 250 (^{1}H 250; ^{13}C{^{1}H}, 62.9; ^{31}P{^{1}H}, 101.27 MHz); data in δ ppm referenced to $SiMe_4$ and 85% H_3PO_4 (external) at 36°C in deuteriobenzene unless otherwise stated.

The two dimensional δ/J resolved ^{31}P spectrum was recorded at 213 K on the WM 250 with broad band proton decoupling and using a preliminary version of the Bruker 2D software. A relaxation delay of 30s between pulse cycles was used (T_1 = 10s) and half cosine window functions were used in the Fourier transformations in both dimensions.

IR: Perkin–Elmer 683; spectra in Nujol mulls unless otherwise stated; data in cm^{-1}; PMe_3 bands not listed.

(1) *Pentakis(trimethylphosphine) chlororhenium(I)*, **(A)**

To sodium amalgam (1 g in 5 cm^3 Hg) and PMe_3 (3 cm^3, 30 mmol) in THF (50 cm^3) was added a suspension of $ReCl_4(THF)_2$[33] (2.0 g, 4.2 mmol) in tetrahydrofuran (100 cm^3) and the mixture stirred 18 hr at room temperature. The solution was filtered, evaporated in vacuum after first subliming out the *hydride* at 120°C 10^{-3} cm Hg, and the residue extracted into petroleum (2 × 40 cm^3). The solution was filtered through cellulose, concentrated to *ca.* 5 cm^3 and cooled at −20°C to yield pale yellow crystals which were collected and dried in vacuum. A second batch was obtained by evaporation and cooling of the filtrate. Yield 1.5 g, 60%; m.p., 231–2°C (decomp). [Found: C, 29.8 (29.9); H, 7.8 (7.5); Cl, 5.8 (5.9); P, 25.6 (25.8)%. *M*, 580 (601.5)]. The compound is fairly air stable and readily soluble in hydrocarbons.

NMR. ^{1}H: 1.4 s (36) PMe_3; 1.2 d (9), ^2J(P–H) = 6 Hz, PMe_3 *trans* to Cl.

^{13}C{^{1}H}: 3.37 d, J(P–C) = 24 Hz; 24.7 m, PMe_3.

^{31}P{^{1}H}: −36.6 br, s (4); −43.8 br, s (1), PMe_3. At −60° the spectrum is sharper: −34.7 d (4), ^2J(P–P) = 9 Hz; −42.0 quin. (1) ^2J(P–P) = 8 Hz PMe_3. The broadening at 35°C is presumably due to some dissociation of PMe_3.

(2) *Pentakis(trimethylphosphine)hydridorhenium(I)*, **(B)**

Sublimation from the solid as above gave analytically and spectroscopically pure white crystals which could be crystallised from petroleum. Yield, *ca.* 0.7 g, 30%; m.p., 205–206°C. [Found: C, 31.8 (31.7); H, 8.1 (8.1); P, 27.5 (27.3)%. *M*, 530 (567).]

NMR. ^{1}H: 1.54 s (36), 1.41 s (9), PMe_3: −8.8 doublet of quintets, ^2J(P–H) = 13.4 Hz, ^2J(P–H) = 23.8 Hz.

^{31}P{^{1}H}: −44.5 s (4), −52.0 s (1) PMe_3.

IR. 1940 w (Re–H).

(3) *Pentakis(trimethylphosphine)chlorohydridorhenium(III) tetrafluoroborate*, **(C)**.

To $ReCl(PMe_3)_5$ (0.86 g, 1.43 mmol) in THF (30 cm^3) was added either one equivalent of HBF_4 (48% aqueous) or more conveniently, two equivalents of Ph_3CBF_4 (1.0 g, 3.0 mmol) in THF (30 cm^3). After 12 hr at room temperature the green solution was filtered, evaporated in vacuum and the residue washed with Et_2O (2 × 20 cm^3). After extraction into MeOH (30 cm^3) the solution was filtered, concentrated to *ca.* 5 cm^3 and cooled at −20°C to give orange crystals. Yield, 0.6 g, 60%; m.p., 162–163°C. [Found: C, 25.5 (26.1); H, 6.5 (6.7); Cl, 4.9 (5.2); F, 12.1 (11.0); P, 22.7 (22.5)%]. Λ_M($MeNO_2$, 25°C), 105 Ω^{-1} cm^2 mol^{-1}.

NMR. ^{1}H: 1.70 d, ^2J(P–H) = 3 Hz; 1.84 d, ^2J(P–H) = 9 Hz; 1.53 d, ^2J(P–H) = 7 Hz, PMe_3. −9.7 br (half height width 38 Hz) Re–H.

^{31}P{^{1}H}: −45.5 d (4), ^2J(P–P) = 24.4 Hz; −43.8 m (1), PMe_3.

IR. 2004 (Re–H).

(4) *Pentakis(trimethylphosphine) dinitrogen rhenium(I) chloride/methanol (1/1)*, **(D)**

To $ReCl(PMe_3)_5$ (0.5 g, 0.83 mmol) under N_2 at room temperature was added methanol (50 cm^3) and the mixture stirred for 2 hr. After evaporation under vacuum the residue was washed with petroleum (2 × 30 cm^3) and extracted into MeOH (20 cm^3); the solution was filtered, concentrated to *ca.* 2 cm^3, Et_2O (0.2 cm^3) added and cooled at −20°C to give white crystals which were washed with ether and dried. Yield, 0.44 g, 80%; m.p., 218–219°C. [Found: C, 28.9 (29.1); H, 7.2 (7.4); Cl, 5.6 (5.4); N, 4.0 (4.2); O, 2.6 (2.4); P, 24.0 (23.5)%]. Λ_M (MeOH, 25°C) = 83 Ω^{-1} cm^2 mol^{-1}.

NMR. ^{1}H (in d^4 MeOH): 1.64 s (36), 1.49 d (9), ^2J(P–H) = 7 Hz, PMe_3.

^{31}P{^{1}H}: −47.0 br, s(4), −40.3 br, s (1) PMe_3.

IR. 3350 br, m (OH), 2030 s (ReN_2).

(5) *Pentakis(trimethylphosphine)rhenium(I) chloride*, **(E)**

As in the above, but under argon for *ca.* 12 hr to give white crystals. Yield, 0.35 g (70%), m.p., 201–203°C. [Found: C, 29.6 (29.9); H, 7.6 (7.5); Cl 6.2 (5.9); P, 24.9 (25.7)%]. Λ_M (MeOH, 25°C), 96 Ω^{-1} cm^2 mol^{-1}.

NMR. ^{1}H: 1.45 s (36), 1.28 s (9).

^{31}P{^{1}H}: −47.08 (36°C).

(6) *Pentakis(trimethylphosphine)methyl rhenium(I)*, **(F)**

Methyllithium (0.62 cm^3, 1.1 M) was added to $ReCl(PMe_3)_5$ (0.41 g, 0.68 mmol) in Et_2O (70 cm^3) at −20°C. The mixture was allowed to warm slowly to room temperature and stirred for another 4 hr. The volatile materials were removed under reduced pressure and the residue extracted into petroleum (40 cm^3), which was filtered, concentrated to *ca.* 5 cm^3 and cooled at −20°C to give a yellow solid. Recrystallisation gave yellow crystals. Yield, 0.30 g, 82%; m.p., 185–6°C. [Found: C, 33.1 (33.0); H, 8.2 (8.3); P, 27.6 (26.7)%. M, 550 (581)].

NMR. ^{1}H: 1.37 s (36), 1.44 s (9), PMe_3; −0.22(3) quin. of doublets, $^3J(P_{cis}–H)$ = 7.4 Hz, $^3J(P_{trans}–H)$ = 3.0 Hz, Re-Me.

^{31}P{^{1}H}: −44.34 (4) br, s, −50.43 (1) br, s. Some free PMe_3 was observed at δ −62.0 ppm.

IR. 1430 m, 1392 m, 1370 m, 1360 sh, 1200 w, 1150 w, 1100 w, 1020 w, 932 s, 850 m, 800 w, 720 w, 682 m, 670 m, sh, 650 m, 640 m.

(7) *a,b-Bis(carbonyl)-c,d,e-tris(trimethylphosphine)chlororhenium(I)*, **(G)**

$ReCl(PMe_3)_5$ (1.0 g, 1.7 mmol) in Et_2O (50 cm^3) was stirred under CO (3 atm) in a pressure bottle at room temperature for 18 hr. The filtered solution was evaporated, the residue washed with petroleum (2 × 30 cm^3) and extracted into toluene (30 cm^3). The filtered solution was concentrated to *ca.* 10 cm^3 and cooled at −20°C to give off-white crystals. Yield, 0.7 g, (80%); m.p., 174–175°C. [Found: C, 26.4 (26.1); H, 5.4 (5.3); Cl, 6.6 (7.0); O, 6.6 (6.3); P, 19.0 (18.4)%. *M*, 490 (505.5)].

NMR. ^{1}H: 1.54 t (18), ^2J(P–H) = 3 Hz, 1.27 d (9), ^2J(P–H) = 9 Hz, PMe_3.

^{13}C{^{1}H}: 18.1 d, J(P–C) = 24.4 Hz; 18.9 t, J(P–C) = 17.1 Hz, PMe_3. 199.5, CO.

^{31}P{^{1}H}: −35.8 d(2), ^2J(P–P) = 24.4 Hz, −38.9 t (1), ^2J(P–P) = 24.4 Hz, PMe_3.

IR. 1920 vs, 1830 vs (CO).

(8) *μ-[1,2-Bis(3,4-diphenylcyclopentadienediyl)-1,2-diphenylethane-$C^{1'-5'}$ (Re^1), $C^{1''-5''}$ (Re^2)]-bis[tris(trimethylphosphine)]rhenium(I)*, **(H)**

To $ReCl(PMe_3)_5$ (1.0 g, 1.66 mmol) in toluene (70 cm^3) was added phenylacetylene (1 cm^3) and the mixture refluxed for 16 hr. The dark red solution was filtered and evaporated in vacuo. The residue was extracted with petroleum (2 × 40 cm^3), the solution filtered, concentrated to *ca.* 50 cm^3 and cooled at −20°C to give orange crystals. Yield, 0.7 g, 60%; m.p., 300°C. [Found: C, 55.8 (55.0); H 6.4 (6.4); P, 12.7 (12.9)%. *M* 1390 (1440)].

NMR. ^{1}H: 1.25 d, ^2J(P–H) = 4 Hz, PMe_3; 4.73, 5.03, 5.21 s, CH; 7.0–7.3 m, 7.58, 7.9 Ph.

^{31}P{^{1}H}: −41.6 br, s, PMe_3.

IR. 3065 w, 3015 w, 1600 m, 1500 m, 1450 m, 1425 m, 1290 m, 1275 m, 1155 w, 1140 w, 1080 w, 1070 w, 1040 w, 1030 w, 955 s, 935 vs, 895 w, 844 m, 755 m, 710 m, 705 m, 694 s, 656 m, 589 w, 560 w, 535 w, 510 w, 485 w.

(9) *Tetrakis(diethylphenylphosphine)(dinitrogen)chlororhenium (I)*, **(I)** *and Tetrakis(diethylphenylphosphine)(dinitrogen) hydridorhenium (I)*, **(J)**

To PEt_2Ph (1.5 cm^3, 9 mmol) and Na/Hg (0.8 g, in 8 cm^3 Hg) in THF (50 cm^3) was added a suspension of $ReCl_4(THF)_2$ (0.5 g,

1.1 mmol) in THF (100 cm^3) and the mixture stirred 18 hr under N_2. After filtration the solution was evaporated, the residue extracted into petroleum (2 × 30 cm^3), the solution filtered, concentrated to *ca.* 10 cm^3 and cooled at −20°C to give yellow crystals of the *hydride.* Yield, *ca.* 15%; m.p., 115–116°C. The hydride can also be sublimed at 100°C, 10^{-3} mm Hg. [Found: C, 54.0 (54.6); H, 6.5 (6.9); P, 13.7 (14.1)%. M, 840 (880)].

NMR. ^{1}H: 1.68 m, 1.10 m, P*Et*$_2$PH; 7.32 M, 7.65 m, PEt$_2$*Ph*; −7.43 quint, ^2J(P–H) = 2.22 Hz, Re-H.

^{31}P{^{1}H}: −23.6 br, s.

IR. 1945 (ReN_2); 1890 (Re–H).

The residue after sublimation or petroleum extraction was washed with petroleum and extracted into toluene (2 × 30 cm^3), the solution filtered, concentrated to 15 cm^3 and cooled at −20°C to give yellow crystals of the dinitrogen *chloro complex.* Yield, 0.6 g, (60%); m.p., 131–132°C. [Found: C, 52.2 (52.5); H, 6.3 (6.6); Cl, 3.7 (3.9); N, 2.8 (3.1); P, 13.1 (13.6)%. M 870 (913.5)].

NMR. ^{1}H: 0.9 m, 1.48 m Et; 7.45 m, 7.12 m Ph.

^{13}P{^{1}H}: −15.5 br, s, PEt$_2$Ph.

IR. 1918 (ReN_2).

(10) *Tetrakis(trimethylphosphine)iodo(phenylamido)rhenium (III)iodide* (**K**)

To Re(NHPh)$(N_2)(PMe_3)_4$ (0.5 g, 0.82 mmol) in benzene (40 cm^3) was added iodine (0.21 g, 0.9 mmol) in benzene (30 cm^3) and the mixture stirred for 4 hr at room temperature. The red precipitate was collected, washed with Et_2O (2 × 40 cm^3) and then recrystallised from MeOH–Et_2O (4 : 1) to give red crystals. Yield, 0.6 g, 86%; m.p., 284–5°C. [Found: C, 25.6 (25.8); H, 4.9 (5.0); N, 1.6 (1.7); P, 14.6 (14.8); I, 28.6 (30.3)%]. Λ_M (CH_3NO_2, 25°C) 100 Ω^{-1} cm^2 mol^{-1}.

NMR. ^{1}H: 7.4–6.8 m (5) Ph, 3.65 brs (1) N–H, 1.86 m and 2.31 m (36) PMe$_3$.

^{31}P{^{1}H}: −56.25 d, ^2J(P–P) = 12.1 Hz; −61.90 d ^2J(P–P) = 24.4 Hz; −86.26 t, ^2J(P–P) = 24.4 Hz, PMe$_3$.

IR. 3400 w, 1590 m, 1485 m, 1415 w, 1308 w, 1285 m, 1275 w, 1160 br, w, 1020 w, 980 w, 946 s, 945 vs, 918 m, 860 m, 760 w, 720 m, 710 m, 700 w, 682 m, 660 m.

(11) *Pentakis(trimethylphosphine)(dinitrogen)rhenium(I) tetrafluoroborate*

One equivalent of aqueous 48% HBF_4 (0.14 cm^3, 0.82 mmol) was added to Re(NHPh)$(N_2)(PMe_3)_4$ (0.5 g, 0.82 mmol) in THF (50 cm^3) at −78°C. The mixture was allowed to warm to room temperature and was stirred for 4 hr. The precipitate was collected, washed with petroleum (2 × 20 cm^3). After extraction into MeOH (20 cm^3), the solution was filtered, concentrated to *ca.* 2 cm^3 and Et_2O (1 cm^3) was slowly added to give, on cooling at −20°C white crystals. Yield, 0.25 g, 45% m.p., 203–205°C (decomp). [Found: C, 26.9 (26.4); H, 6.8 (6.6); N, 3.9 (4.1); P, 23.1 (22.7); F, 11.6 (11.2)%]. Λ_M (MeOH, 25°C), 80 Ω^{-1} cm^2 mol^{-1}.

NMR. ^{1}H(d^4-MeOH); 1.90 s (36), 1.73 s (9), PMe$_3$.

^{31}P{^{1}H}: −46.3 brs (4), −39.8 brs (1), PMe$_3$.

IR. 2005 s, 1460 m, 1420 m, 1310 m, 1289 m, 1085 s, 1050 vs, 1035 vs, 940 vs, 865 m, 715 m, 695 m, 662 m, 444 w.

(12) *Tris(trimethylphosphine) (η^2-carbon dioxide)phenylamidorhenium(I),* (**L**)

Dry CO_2 (conc. H_2SO_4) was passed through a solution of Re(NHPh)$(N_2)(PMe_3)_4$ (1 g) in toluene (40 cm^3) for 2 hr when the solution was evaporated and the residue extracted into petroleum (100 cm^3). On reducing the volume (50 cm^3) and cooling at −20°C, yellow-orange needles were obtained which were washed with petroleum and dried in vacuum. Yield, 0.41 g, (50%); m.p., 188°C. [Found: C, 36.8 (36.4); H, 6.8 (6.8); N, 2.3 (2.2); O, 5.5 (5.1); P, 21.0 (19.7)%. M, 600 (550)].

NMR. ^{1}H: 6.2–7.4 m *Ph*NH, 1.46 d, ^2J(P–H) = 7.4 Hz; 1.34 t, ^2J(P–H) = 3.0 Hz PMe$_3$.

^{31}P{^{1}H}: −14.13 s; −30.94 s.

^{13}C{^{1}H}: 163.4 s CO_2; 117.0–140.1 m Ph; 30.21 d, J(P–C) = 24.0 Hz, 19.75 t J(P–C) = 11.1 Hz, PMe$_3$.

IR. 1620 m, 1605 m (CO_2).

((13) *Tetrakis(trimethylphosphine)(η^2-dimethylphosphinomethyl) rhenium(I),* (**M**)

To Re(NHPh)$Cl_3(PMe_3)_2$ (4.0 g, 7.5 mmol) in a pressure bottle was added trimethylphosphine (4.0 cm^3, 40 mmol), sodium amalgam (*ca.* 20 fold excess of Na) and tetrahydrofuran (100 cm^3). The solution was stirred for 3 d under nitrogen (2 atm) when it was a yellowish green. The solution was evaporated in vacuum and the residue extracted with toluene (100 cm^3). After filtration and concentration to *ca.* 15 cm^3, cooling to −20°C gave a mixture of Re(NHPh)$(N_2)(PMe_3)_4$ and Re(η^2-CH_2PMe_2)$(PMe_3)_4$. This solid was collected and treated with petroleum (40 cm^3) in which the latter compound is soluble; cooling the petroleum extract gave the pure product as crystals. Yield, 2.1 g, 50%. [Found: C, 31.9 (31.8); H, 7.9 (7.8); N, <0.2 (0); P, 30.1 (27.4)%].

NMR. ^{1}H: 1.57 dd, ^2J(P–H) = 5.49, 0.98 Hz, 1.52 d, ^2J(P–H) = 1.10 Hz, 1.48 d, ^2J(P–H) = 1.22 Hz, PMe$_3$; 1.40 broad multiplet, PMe$_2$; 1.35 dd, ^2J(P–H) = 7.08, 1.95 Hz, PMe$_3$; −0.51 ttd, ^2J(P–H) = 9.09, 3.78 Hz, ^2J(P–H) = 1.95 Hz, C*H*$_2$PMe$_2$.

^{31}P{^{1}H} (−60°C): −73.6 ddt (1), ^2J (P_a–P_d) = 89.6 Hz, ^2J (P_a–P_c) = 32.7 Hz, ^2J(P_a–P_b) = 19.9 Hz, P_a; −45.5 dtd (1), ^2J(P_c–P_b) = 19.2 Hz, ^2J(P_c–P_d) = 13.4 Hz, P_c; −40.6 ddd (2), ^2J (P_b–P_d) = 21.2 Hz, P_d; −36.0 dtd (1), P_d.

^{13}C{^{1}H}: 35.05 d ^2J(C–P) = 7.93 Hz; 34.76 d, ^2J(C–P) = 6.71 Hz; 29.2 dt, ^2J(C–P) = 22.58, 3.36 Hz; 15.70 d ^2J(C–P) = 1.22 Hz, P(CH_3)$_3$; −34.8 broad multiplet (*C*H$_2$PMe$_2$).

IR. 1300 m, 1286 m, 1272 m, 1262 m, 935 s, 890 m, 745 m.

(14) *Tetrakis(trimethylphosphine)trihydridorhenium(III),* (**N**)

A tetrahydrofuran (25 cm^3) solution of compound (**M**) (1.6 g, 2.8 mmol) in a 100 cm^3 pressure bottle was stirred for 3 d under hydrogen (7 atm). The solution was then evaporated in vacuum and the residue extracted into petroleum (50 cm^3). This solution was filtered, reduced to 10 cm^3 and cooled at −20°C to yield white crystals. Yield, *ca.* 100%; m.p., 147°C. [Found: C, 29.8 (29.9); H, 8.0 (7.9); N, <0.2 (0); P, 27.3 (25.1)%].

NMR. ^{1}H: 1.54 s, 1.51 s, PMe$_3$; −7.85 quin. ^2J(P–H) = 20.84 Hz, ReH.

^{31}P{^{1}H}: −41.24 br, s.

IR. 1915 w, 1887 w, 1785 m, 1758 s (Re–H); 1290 s, 1270 s, 930 br, vs, 852 m.

(15) *Tetrakis(trimethylphosphine)tetrahydridorhenium(IV)tetrafluoroborate,* (**O**)

To a solution of $ReH_3(PMe_3)_4$ (0.2 g, 0.4 mmol) in tetrahydrofuran (50 cm^3) at −78°C, was added fluoroboric acid (0.067 cm^3 of 40% aqueous, 0.4 mmol). The white precipitate was collected and dried under vacuum. After dissolving in methanol (50 cm^3), and reducing the volume to *ca.* 15 cm^3, cooling to −20°C gave white crystals in essentially quantitative yield; m.p., dec. 210°C. [Found: C, 24.8 (24.8); H, 7.0 (6.9); N, <0.2 (0); P, 22.1 (21.3); F, 13.2 (13.0)%]. Λ_M (MeOH, 25°C) 115 Ω^{-1} cm^2 mol^{-1}.

NMR. ^{1}H: 1.78 s, PMe$_3$; −5.40 broad quintet ReH. At +60°C, −5.40 quin. ^2J(P–H) = 23.6 Hz, ReH.

^{31}P{^{1}H}: −42.53 br, s, −42.75 br, s; at +50°C, −42.83 s, PMe$_3$.

IR. 2005 w, 1948 m, 1930 bm (Re–H).

(16) *Tetrakis(trimethylphosphine)(a-Iodo)(f-methyl)rhenium(III) iodide—Tetramethylphosphonium iodide* (**P**).

To a solution of Re(η^2-CH_2PMe_2)$(PMe_3)_4$ (0.8 g, 1.4 mmol) in THF (50 cm^3) was added excess MeI (0.5 cm^3). The orange precipitate was collected, dissolved in methanol (30 cm^3) and the filtered solution concentrated to *ca.* 10 cm^3. On cooling at −20°C white and orange crystals respectively of [PMe_4]I and the rhenium complex were formed. These were hand picked. The orange crystals have m.p., 240–245°C.

NMR. ^{1}H (d^4-MeOH): 2.16 s, Re-Me; 1.92 s, PMe$_3$.

^{31}P (d^4-MeOH): −50.7 s RePMe$_3$; +25.2 s PMe$_4$.

CRYSTALLOGRAPHIC STUDIES

(a) *Crystal data*

Compound C. [ReH(Cl)$(PMe_3)_5$](BF_4), M = 689.87; orthorhombic, space group $Pca2_1$, a = 15.812(2), b = 9.982(4), c = 17.731(4) Å, Z = 4, D_c = 1.64 g cm^{-3}, μ–Mo–$K\alpha$) = 45.3 cm^{-1}.

Compound H. $[Re(PMe_3)_3]_2(C_{48}H_{36})$, M = 1441.7; monoclinic, space group $P2_1/a$, $a = 14.352(4)$, $b = 34.781(9)$, $c = 13.521(3)$ Å, $\beta = 105.34(2)°$, $Z = 4$, $D_c = 1.47\ g\ cm^{-3}$, $\mu(Mo\text{–}K\alpha) = 39.5\ cm^{-1}$.

Compound J. $ReHN_2(PEt_2Ph)_4$, M = 880.04; monoclinic, space group I2, $a = 15.830(4)$, $b = 8.174(2)$, $c = 15.914(4)$ Å, $\beta = 90.45(2)°$, $Z = 2$, $D_c = 1.42\ g\ cm^{-3}$. $\mu(Mo\text{–}K\alpha) = 29.8\ cm^{-1}$.

Compound M. $Re(\eta^2\text{-}CH_2PMe_2)(PMe_3)_4$, M = 565.59; triclinic, space group $P\bar{1}$, $a = 9.470(2)$, $b = 16.942(1)$, $c = 17.076(2)$ Å, $\alpha = 110.00(2)$, $\beta = 103.91(1)$, $\gamma = 89.27(1)°$, $Z = 4$, $D_c = 1.51\ g\ cm^{-3}$, $\mu(Mo\text{–}K\alpha) = 49.6\ cm^{-1}$.

Compound P. $[ReI(Me)(PMe_3)_4](PMe_4)(I)_2$, M = 977.39, orthorhombic, space group $P2_12_12_1$, $a = 8.775(2)$, $b = 14.038(2)$, $c = 27.884(4)$, $Z = 4$, $D_c = 1.89\ g\ cm^{-3}$, $\mu(Mo\text{–}K\alpha) = 64.9\ cm^{-1}$.

(b) *Data collection*

All data were recorded on a Nonius CAD4 diffractometer using graphite monochromated Mo–$K\alpha$ radiation ($\lambda = 0.71069$ Å) and an $\omega/2\theta$ scan mode, with the ω scan width at a constant $0.85 + 0.35 \tan\theta$ deg.[34] An empirical absorption correction[35] was applied in all cases. Additional data collection parameters are as follows:-

Compound	θ Range	ω scan speed	Temperature	Collected/ observed data*
C	$1.5 \le \theta < 30°$	1.27–6.77 deg min^{-1}	263 K	4195/2850
H	$1.5 \le \theta < 23°$	1.27–6.77 deg min^{-1}	293 K	9036/7619
J	$1.5 \le \theta < 27°$	1.27–6.77 deg min^{-1}	268 K	2412/2412
M	$1.5 \le \theta < 23°$	1.27–10.15 deg min^{-1}	268 K	6933/6132
P	$1.5 \le \theta < 28°$	1.27–6.77 deg min^{-1}	293 K	4806/3421

*Observed data have $I > 1.5\sigma(I)$.

(c) *Structure solution and refinement*

All five structures were solved via the heavy atom method. For compounds **H**, **J** and **M**, the structure development and refinement was routine and proceeded without problems. For compounds **J** and **M**, most methyl hydrogen atoms were determined experimentally; the remainder were inserted in expected positions. Unfortunately the metal hydride atom in **J** was not located, in spite of the apparent high quality of the data (*vide infra*). For compound **H**, the six phenyl rings were refined as rigid groups.

The structure development for compound **C** was problematical due to pseudosymmetry, with the metal atom, the chlorine and one phosphorus atom all lying in the same plane, perpendicular to z, thus imposing strong ψ-mirror symmetry on the electron density maps. Attempts to achieve stable refinement have so far been unsuccessful and so we defer presenting the final results until this problem has been overcome. However, with an R value of 0.10 with contributions from all heavy atoms expected for the proposed structure (albeit with a wide spread of temperature factor coefficients and several unreasonable bond lengths and angles), the proposed structure is felt to be reasonably confirmed in outline.

The development and refinement of structure **P** also gave problems. Electron density syntheses continually showed ghost peaks for the *P* atoms and some methyl carbons. At first it was assumed that these were occurring due to pseudo-symmetry, but when we found that a basically complete structure would not refine below $R \sim 0.20$, and the ghosting still occurred, we realised that the problem was one of disorder, with the complex cation site occupied by two enantimeric forms of the cation, in non-equal amounts. The two images have a common Me–Re–I axis, and both images have equatorial PMe_3 orientations such that one Me group lies in the equatorial plane with the other two above and below, and the four PME_3 groups in each image having a four-fold axis relationship, (see Fig. 6). Refinement of this model was then completed successfully, although to achieve stability, some fixing of P–C distances to standard values was necessary. The final $R(= \Sigma\Delta F/\Sigma F_0)$ and $R^1(= \Sigma\omega^{1/2}\Delta F/\Sigma\omega^{1/2}F_0)$ values are 0.053 and 0.054, adequately confirming the chosen model.

R and R^1 values for the other three structures are as follows: Compound **H**, $R = 0.066$, $R^1 = 0.070$; Compound **J**, $R = 0.0197$, $R^1 = 0.020$; Compound **M**, $R = 0.0314$, $R^1 = 0.0316$.

Final atomic coordinates, thermal parameters and lists of F_0/F_c values have been deposited with the Editor as supplementary data.† Computers, programs and sources of scattering factor data are given in Ref. 34.

Acknowledgements—We thank the SERC for support of this work and Dr. W. McFarlane for discussions.

†Copies are available on request from the Editor at Queen Mary College. Tables of atomic coordinates have also been deposited with the Cambridge Crystallographic Data Centre.

REFERENCES

[1]K. W. Chui, K. W. Wong, G. Wilkinson, A. M. R. Galas and M. B. Hursthouse, *J. Chem. Soc., Chem. Commun.* 1981, 451; *Polyhedron*, 1982, **1**, 37.
[2]K. W. Chiu, C. G. Howard, G. Wilkinson, A. M. R. Galas, M. B. Hursthouse, *Polyhedron* 1982, **1**, in press.
[3]H. W. Choi and E. I. Muetterties, *Bull. Soc. Chim. Belg.* 1980, **89**, 809.
[4]M. E. Tully and A. P. Ginsberg, *J. Am. Chem. Soc.* 1973, **95**, 2042.
[5]M. G. Bradley, D. A. Roberts and G. L. Geoffroy, *J. Am. Chem. Soc.* 1981, **103**, 379.
[6]R. A. Jones, G. Wilkinson, A. M. R. Galas, M. B. Hursthouse and K. M. A. Malik, *J. Chem. Soc., Dalton Trans.*, 1980, 1771.
[7]C. A. Heitzer and R. A. Walton, *J. Organometal. Chem.* 1977, **124**, C15; J. Chatt, J. R. Dilworth, H. P. Gunz and G. J. Leigh, *J. Organometal. Chem.* 1974, **64**, 245.
[8]F. A. Cotton and G. Wilkinson, *Advanced Inorganic Chemistry*, 4th Edn., pp. 1156, 1285. Wiley, New York (1980).
[9](a) J. Chatt, J. R. Dilworth and G. J. Leigh, *J. Chem. Soc. Dalton Trans.* 1973, 612;
(b) J. Chatt, J. R. Dilworth and R. L. Richards, *Chem. Rev.* 1978, **78**, 589.
[10]B. R. Davis and J. A. Ibers, *Inorg. Chem.* 1971, **12**, 578.
[11]M. A. Green, J. C. Huffman, K. G. Caulton, W. K. Rybak and J. J. Ziolkowski, *J. Organometal. Chem.* 1981, **218**, C39.
[12]P. D. Cradwick, *J. Chem. Soc., Dalton Trans.* 1976, 1934.

[13]M. Merzer, *J. Chem. Soc., Dalton Trans.* 1974, 1637.
[14]G. S. Bristow, P. B. Hitchcock and M. F. Lappert, *J. Chem. Soc., Chem. Commun.* 1981, 1145.
[15]M. Aresta and C. F. Nobile, *J. Chem. Soc., Dalton Trans.* 1977, 708.
[16]See R. A. Andersen, *Inorg. Chem.* 1979, **18**, 2928.
[17]See M. G. Bradley, D. A. Roberts and G. L. Geoffroy, *J. Am. Chem. Soc.*, 1981, **103**, 379.
[18]S. Al-Jibori, C. Crocker, W. J. McDonald and B. L. Shaw, *J. Chem. Soc. Dalton Trans.* 1981, 1572.
[19]S. Bresadola, N. Bresciani-Pahor and B. Longato, *J. Organometal. Chem.* 1979, **179**, 73.
[20]N. Bresciani, M. Calligaris, P. Delise, G. Nardin and L. Randaccio, *J. Am. Chem. Soc.* 1974, **96**, 5642.
[21]T. V. Harris, J. W. Rathke and E. L. Muetterties, *J. Am. Chem. Soc.* 1978, **100**, 6966; H. H. Karsch, H.-F. Klein and H. Schmidbauer, *Chem. Ber.* 1977, **110**, 2200.
[22]H. Werner and R. Werner, *J. Organometal. Chem.* 1981, **209**, C60.
[23]W. P. Aue, J. Karhan and R. R. Ernst, *J. Chem. Phys.* 1976, **64**, 4226; K. Nagayama, P. Bachmann, K. Wüthrich and R. R. Ernst, *J. Magn. Reson.* 1978, **31**, 1333.
[24]H. Schmidbauer and G. Blaschke, *Z. Naturforsch, Teil B.* 1980, **35**, 584.
[25]M. Freni, R. Demichelis and D. Guisto, *J. Inorg. Nuclear Chem.* 1967, **29**, 1433.
[26]K. W. Chiu, R. A. Jones, G. Wilkinson, A. M. R. Galas, M. B. Hursthouse and K. M. A. Malik, *J. Chem. Soc., Dalton Trans.* 1981, 1204.
[27]P. Meakin, L. G. Guggenberger, N. G. Peet, E. L. Muetterties and J. P. Jesson, *J. Am. Chem. Soc.* 1973, **95**, 1467.
[28]H. Schmidbauer, W. Büchner and D. Scheutzow, *Chem. Ber.* 1973, **106**, 1251.
[29]H. H. Karsch, *Chem. Ber.* 1977, **110**, 2699.
[30]J. Chatt and G. A. Rowe, *J. Chem. Soc. (A)*, 1962, 4019.
[31]F. A. Cotton, N. F. Curtis and W. R. Robinson, *Inorg. Chem.* 1965, **4**, 1496.
[32]M. Freni, D. Guisto and P. Romiti, *Gazz. Chim. Ital.* 1967, **97**, 833.
[33]E. A. Allen, N. P. Johnson, D. T. Roseveare and W. Wilkinson, *J. Chem. Soc. (A)*, 1969, 788.
[34]M. B. Hursthouse, R. A. Jones, K. M. A. Malik and G. Wilkinson, *J. Am. Chem. Soc.* 1979, **101**, 4128.
[35]A. C. T. North, D. C. Phillips and F. S. Mathews, *Acta Cryst.* 1968, **A24**, 351.

Polyhedron Vol. 1, No. 5, pp. 453–455, 1982
Printed in Great Britain.

0277-5387/82/050453-03$03.00/0
Pergamon Press Ltd.

MOLECULAR INTERACTION IN A MIXED α-HYDROXYOXIME-SULFONIC ACID SOLVENT EXTRACTION SYSTEM

MARK E. KEENEY and K. OSSEO-ASARE*
Departments of Mineral Engineering and Materials Science and Engineering, The Pennsylvania State University, University Park, PA 16802, U.S.A.

(*Received* 18 *May* 1982)

Abstract—The molecular interaction between dinonylnaphthalenesulphonic acid (HDNNS) and 5,8-diethyl-7-hydroxy-6-dodecanone oxime (HOx) was examined based on variations in the critical micelle concentration (CMC) of HDNNS in the presence of HOx. The CMC values were obtained from interfacial tension *vs* concentration isotherms measured at the hexane/aqueous interface. The interaction appears to involve hydrogen bonding between the HOx and HDNNS polar functional groups to form a dimeric structured complex.

INTRODUCTION

In previous papers[1,2] it has been shown that 5,8 - diethyl - 7 - hydroxy - 6 - dodecanone oxime (HOx) has the ability to alter the critical micelle concentration (CMC) of dinonylnaphthalenesulphonic acid (HDNNS), presumably through a specific oxime–sulphonic acid interaction in the bulk organic phase. Spectroscopic evidence has been presented which indicates that the specific interaction involves an intermolecular hydrogen bonding between HOx and HDNNS molecules.[2]

The purpose of this work is to examine quantitatively the effect of HOx on the interfacial and micellar behavior of HDNNS and to propose a specific complex involving the interaction between the polar functional groups of the oxime and the sulphonic acid.

EXPERIMENTAL

Reagents Dinonylnaphthalenesulphonic acid was obtained from King Industries, Inc. as SYNEX 1040 (Lot #146-32) and was purified according to the method of Danesi *et al.*[3] LIX63 was purchased from Henkel Corp. and was purified as described elsewhere.[2] All other chemicals were reagent grade and were used without further purification.

Measurements. Interfacial tensions were measured using the du Nouy ring method. Details of the experimental procedure for determining the interfacial tension vs concentration isotherms are presented elsewhere.[1,2]

RESULTS AND DISCUSSION

Variation of the CMC *and the* CAC *with oxime concentration*

Figure 1 shows the interfacial tension vs log [HDNNS] isotherm in the absence of HOx. The isotherm shows that a certain critical concentration is required before any significant interfacial adsorption occurs. This concentration, denoted CAC (critical adsorption concentration), is defined as the intersection of the extrapolated slope and the horizontal as shown in Fig. 1. It has been shown previously[1,2] that addition of HOx shifts the interfacial tension isotherms to the right. The variation in the CMC and the CAC of HDNNS in the presence of HOx, shown in Fig. 2, appears to be directly proportional to the concentration of HOx. The results of the effect of HOx on the CMC and the CAC are given in Table 1.

Normalization of the interfacial tension isotherms

The similarity of the form and the apparent proportionality to the oxime concentration of the various interfacial tension vs log [HDNNS] isotherms[1] suggest that a normalization might be accomplished with the proper mathematical manipulation. Consider the reaction between the oxime (HOx) and the sulfonic acid (HD) in the system free of HDNNS micelles:

$$HD + nHOx = HD \cdot nHOx. \quad (1)$$

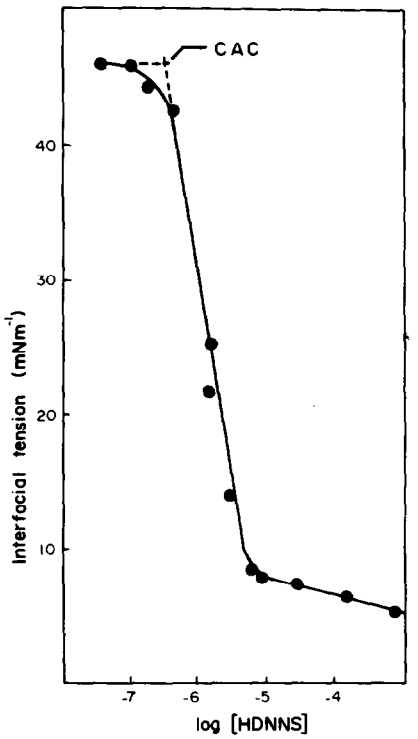

Fig. 1. Interfacial tension vs log [HDNNS](mol dm^{-3}) isotherm at the hexane/water interface (0.5 mol dm^{-3} KNO_3; pH = 2.5, 25°C).

*Author to whom correspondence should be addressed.

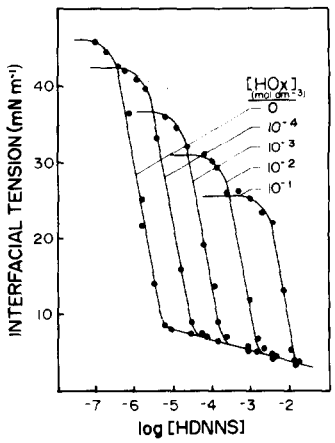

Fig. 2. Effect of HOx on the interfacial tension vs log [HDNNS] isotherms at the hexane/water interface.

Table 1. Effect of HOx on HDNNS CMC and CAC[a]

$[HOx]_0$	CMC	CAC
1.0×10^{-4}	2×10^{-5}	3×10^{-6}
1.0×10^{-3}	2×10^{-4}	3×10^{-5}
1.0×10^{-2}	2×10^{-3}	3×10^{-4}
1.0×10^{-1}	2×10^{-2}	3×10^{-3}

[a]All values in mol dm^{-3}.

The equilibrium constant for reaction (1) is given by

$$K = [HD \cdot nHOx]/[HD][HOx]^n \quad (2)$$

where [HOx] and [HD] represent the monomeric concentrations of HOx and HDNNS, respectively. If $[HOx]_0$ and $[HD]_0$ represent the total analytical concentrations of HOx and HDNNS in solution, then a mass balance gives

$$[HOx]_0 = [HOx] + n[HD \cdot nHOx] \quad (3)$$

$$[HD]_0 = [HD] + [HD \cdot nHOx]. \quad (4)$$

In the presence of HOx, the concentration of HDNNS available for adsorption at the organic/water interface is decreased from $[HD]_0$ to [HD] as a result of the formation of the complex $HD \cdot nHOx$. It shall be assumed that in each mixed reagent system, the same critical value of effective HDNNS monomer concentration, CAC_0, is needed in order for interfacial adsorption to become significant. Furthermore, it shall be assumed that for each HOx-HDNNS mixture, the monomer concentration of HDNNS between the CAC and the CMC is the same as the monomer concentration in the HDNNS-alone system at corresponding positions on the interfacial tension isotherms. Thus, at a given CAC, the monomer concentration is given by

$$[HD] = CAC_0 \quad (5)$$

where CAC_0 is the critical adsorption concentration for HDNNS in the oxime-free system.

In the mixed extractant system, the CAC also signifies the concentration at which the oxime–sulfonate complex formation is complete. Therefore,

$$[HD \cdot nHOx] = CAC. \quad (6)$$

Equations (2)–(6) can be rearranged to give

$$\log K = \log CAC - \log CAC_0 - n \log \{[HOx]_0 - nCAC\}. \quad (7)$$

With the exception of n, all the terms on the r.h.s. of eqn (7) can be obtained from the experimental data previously presented. By choosing values of n and solving eqn (7) under the condition that K must be constant for all isotherms, a value of $n = 1$ was found to give the best fit. Thus it appears that a 1:1 HOx-HDNNS complex is formed with $\log K = 4.8$. The results of the calculations are summarized in Tables 2 and 3 and indicate that for $CAC \ll [HOx]_0$, eqn (7) can be rewritten as

$$\log CAC_0 = \log CAC - \log [HOx]_0 - \log K. \quad (8)$$

Substitution of $\log K = 4.8$ into eqn (8) gives

$$\log CAC_0 = \log CAC - \log [HOx]_0 - 4.8. \quad (9)$$

Equation (9) can be used to normalize the interfacial tension vs log [HDNNS] isotherms at various HOx concentrations by assuming that the form of the equation holds for all points on the isotherm and not just at the CAC. Therefore, eqn (9) becomes

$$\log [HD]^* = \log [HD]_0 - \log [HOx]_0 - 4.8 \quad (10)$$

Table 2. Experimental data for the evaluation of the HOx-HDNNS complex stoichiometry[a]

$[HOx]_0$	CAC	CAC_0
1.0×10^{-4}	3×10^{-6}	5×10^{-7}
1.0×10^{-3}	3×10^{-5}	5×10^{-7}
1.0×10^{-2}	3×10^{-4}	5×10^{-7}
1.0×10^{-1}	3×10^{-3}	5×10^{-7}

[a]All values (in mol dm^{-3})

Table 3. Calculated values for the evaluation of the HDNNS–HOx complex stoichiometry

$\log\{[HOx]_0 - CAC\}$	logCAC	$\log CAC_0$	logK[b]
-4.0	-5.5	-6.3	4.8
-3.0	-4.5	-6.3	4.8
-2.0	-3.5	-6.3	4.8
-1.0	-2.4	-6.3	4.8

[a]All values calculated using data from Table 2.

[b]logK calculated from equation 8.

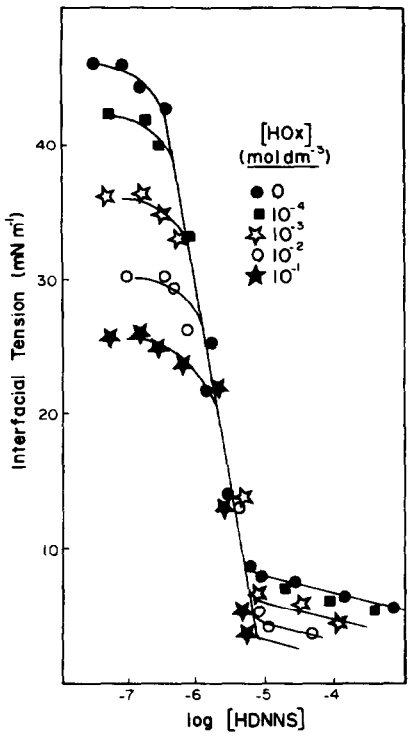

Fig. 3. Normalization of the interfacial tension vs log [HDNNS] isotherms at various HOx concentrations.

Table 4. Typical free energy values for hydrogen bond formation[a]

Bond Type	$-\Delta G$(kJ mol^{-1})
N---HO	0.62
=O---HO	0.35

[a]Values from Ref. [4].

where [HD]* is the effective sulphonic acid concentration and $[HD]_0$ and $[HOx]_0$ are the analytical concentrations of HDNNS and HOx, respectively. The results of the application of eqn (10) to the interfacial tension vs log [HDNNS] isotherms presented in Fig. 2 are shown in Fig. 3. The equation works remarkably well and convincingly supports the argument for a specific interaction between HOx and HDNNS in the organic phase.

Proposed HOx–HDNNS *complex structure*

Using the value of K evaluated from Table 3 the free energy change for the formation of the 1:1 HOx–HDNNS complex has been calculated according to the relation

$$\Delta G = -RT \ln K \tag{11}$$

and gives $\Delta G = -1.4$ kJ mol^{-1}. This is a typical value for the formation of multiple hydrogen bonds and suggests that the dimerization may be of a structure such as (I). This model of the oxime–sulphonate interaction involves two H---O hydrogen bonds and one N---H hydrogen bond.

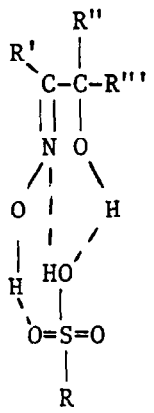

(I)

Based on structure (I) the free energy change can be calculated from tabulations of hydrogen bond types given by Vinogradov and Linnel.[4] As shown in Table 4, the free energy is calculated as approx. -1.3 kJ mol^{-1}, in remarkable agreement with the results calculated from the experimental data of this work.

Acknowledgement—This work was supported by the National Science Foundation under Grant Nos. ENG 76-82141 and CPE 8110756.

REFERENCES

[1]K. Osseo-Asare and M. E. Keeney, *Separation Sci.* 1980, **15**, 999.
[2]K. Osseo-Asare and M. E. Keeney, *Met. Trans. B.*, 1980, **11B**, 63.
[3]P. R Danesi, R. Chiarizia and G. Scibona, *J. Inorg. Nucl. Chem.* 1973, **35**, 3926.
[4]S. Vinogradov and R. Linnel, *Hydrogen Bonding*, p. 150. Van Nostrand Reinhold, New York (1971).

Polyhedron Vol. 1, No. 5, pp. 457-460, 1982
Printed in Great Britain.

0277-5387/82/050457-04$03.00/0
Pergamon Press Ltd.

EXTRACTION OF INDIUM(III) FROM CHLORIDE MEDIUM WITH 1-PHENYL-3-METHYL-4-ACYLPYRAZOL-5-ONES. SYNERGIC EFFECT WITH HIGH MOLECULAR WEIGHT AMMONIUM SALTS.

J.P. BRUNETTE*, M. TAHERI, G. GOETZ-GRANDMONT and M.J.F. LEROY.

Laboratoire de Chimie Minérale, Ecole Nationale Supérieure de Chimie, 1 rue Blaise Pascal, 67008 STRASBOURG CEDEX (France).

(Received 22 April 1982)

ABSTRACT : The extraction of In(III) from 1M (Na,H)(Cl,ClO_4) media with 4-acylpyrazol-5-ones (HL) in toluene at 25°C is described by equilibria $In^{3+} + 3\ \overline{HL} \rightleftharpoons \overline{InL_3} + 3\ H^+$ (log K = 1.48, 1.03, 0.87 with acyl = benzoyl, lauroyl, 2-thenoyl), $InCl^{2+} + 2\ \overline{HL} \rightleftharpoons \overline{InClL_2} + 2\ H^+$ (log K = 0.26, -0.45, -0.35 respectively) and $In^{3+} + m\ Cl^- \rightleftharpoons InCl_m^{(3-m)+}$ (log β_m available from literature). The extraction from 1M (Na,H)(Cl,NO_3) medium is enhanced by addition of aliquat ($\overline{TOMA^+,Cl^-}$) and the following synergic equilibrium takes place : $\overline{InClL_2} + \overline{(TOMA^+,Cl^-)} \rightleftharpoons \overline{(TOMA^+,InCl_2L_2^-)}$ (log K = 5.49, 5.25, 5.21 respectively). Cl^- of ($TOMA^+,Cl^-$) is exchanged by NO_3^- with the equilibrium constant log K = 1.50. If ($TOMA^+,Cl^-$) is replaced by tri-n-octylammonium chloride, the synergic effect is largely reduced (log K = 4.17 with acyl = benzoyl). The extraction from chloride solutions containing ClO_4^- remains unchanged by addition of ammonium salts.

INTRODUCTION

Since the discovery of the synergic effect by Cuninghame et al.[1] in 1954, numerous studies have been reported on metal extractions by mixtures of an acidic extractant plus a neutral extractant, an acidic extractant plus an acidic extractant, a neutral extractant plus a neutral extractant, but a relatively poor number of papers on the extractions of metals by mixtures of an acidic extractant and a cationic extractant (i.e."onium" salts) is available : they mainly concern the extraction of rare earths and cobalt[2-8]. To point out some extractant properties of this kind of mixture, the indium(III) extractions from chloride medium with 1-phenyl-3-methyl-4-acylpyrazol-5-ones (respectively noted HPMBP, HPMLP and HPMTP with acyl = benzoyl, lauroyl and 2-thenoyl) and "aliquat" ($TOMA^+,Cl^-$) or tri-n-octylamine (TOA) are investigated.

EXPERIMENTAL

REAGENTS AND SOLUTIONS : 4-acylpyrazol-5-ones were prepared as described previously[9]. Their initial concentrations in toluene varied from 0 to 0.04M whereas the total "$TOMA^+$" or TOA concentrations were 0 or 0.016M. The total "$TOMA^+$" concentration has been determined by potentiometric determination of stripped Cl^- in a 1M acidic nitrate solution from a toluene solution containing a well-known weight of Fluka "aliquat". Organic solutions were systematically pre-equilibrated against an aqueous solution, free of metal, of the same composition as the one used in the corresponding metal extraction procedure. Aqueous solutions were prepared by dissolution of the appropriate indium salt in perchlorate, nitrate and chloride solutions of 1M ionic strength. The total initial metal concentration was $4.35\ 10^{-3}$M. pH were

adjusted by addition of 0.1M NaOH solutions of suitable composition.

EXTRACTION AND ANALYTICAL PROCEDURES : The distribution measurements were performed in a thermostated vessel (25.0 ± 0.2°C) using a batch technique. Equal volumes of the organic and aqueous phases were shaken for at least 15 minutes, which was sufficient to reach equilibria, and then separated by gravity. For each experimental point, aliquots of the two phases were withdrawn and analysed. Metal concentration determinations were done with a IL 453 atomic absorption spectrophotometer. The withdrawn organic samples were previously diluted in a water-ethanol mixture.

RESULTS AND DISCUSSION

EXTRACTION OF In(III) FROM PERCHLORATE-CHLORIDE SOLUTIONS WITH HPMBP IN TOLUENE : Though the In(III) extraction from perchlorate medium has been given earlier some attention[10,11], new experiments have been performed because of our slightly different experimental conditions i.e. metal concentration, nature of diluent. As expected, plots of logD vs pH at constant $[\overline{HPMBP}]$ and of logD vs log $[\overline{HPMBP}]$ at constant pH are straight lines of slope 3 according to equilibrium {1} (D designs $[\overline{In}][In]^{-1}$)

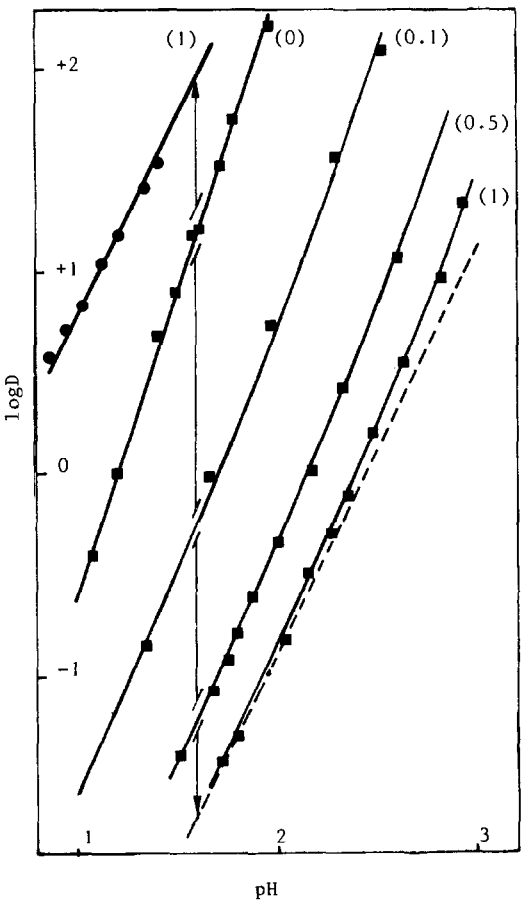

FIG.1 : In(III) extraction from 1M(H,Na) (Cl,ClO_4) medium with toluene solutions of: $[\overline{HPMBP}] = 0.02M$

$[\overline{HPMBP}] = 0.02M + [TOMA^+Cl^-] = 0.016M$

continuous lines: calculated extraction curves; broken line : extraction of $InCl(PMBP)_2$; parentheses values: $[Cl^-]$.

{1} $In^{3+} + 3\ \overline{HPMBP} \overset{K_1}{\rightleftharpoons} \overline{In(PMBP)_3} + 3\ H^+$

($\log K_1 = 1.48 \pm 0.03$).

The extraction of In from perchlorate-chloride aqueous solutions of constant ionic strength ($\mu = 1$) with HPMBP in toluene is drastically reduced compared with the extraction performed from pure perchlorate solutions : as shown on Fig.1, when ClO_4^- is progressively changed with Cl^-, the curves logD vs pH at constant $[Cl^-]$ and $[\overline{HPMBP}]$ are not anymore straight lines but curves the slopes of which increase from 2 at low pH to more than 2.5 at high pH. The mean slopes vary from 3 ($[ClO_4^-] = 1M$) to ∿ 2 ($[Cl^-] = 1M$). These experimental facts are consistent with the coextraction of $In(PMBP)_3$ and $InCl(PMBP)_2$ following the equilibria {1} and {2}

{2} $InCl^{2+} + 2\ \overline{HPMBP} \overset{K_2}{\rightleftharpoons} \overline{InCl(PMBP)_2} + 2\ H^+$

($\log K_2 = 0.26 \pm 0.03$).

K_2 determination : Assuming that $In(PMBP)_3$ and $InCl(PMBP)_2$ are the only extracted species, the distribution coefficient is

$$D = \frac{[\overline{In(PMBP)_3}] + [\overline{InCl(PMBP)_2}]}{\sum_{m=0}^{3} [InCl_m^{(3-m)+}]}$$

$D = a\ D_1 + b\ D_2$ with

$a = [In^{3+}] \left(\sum_{m=0}^{3} [InCl_m^{(3-m)+}]\right)^{-1}$

$b = [InCl^{2+}] \left(\sum_{m=0}^{3} [InCl_m^{(3-m)+}]\right)^{-1}$

$D_1 = [\overline{In(PMBP)_3}][In^{3+}]^{-1}$; $D_2 = [\overline{InCl(PMBP)_2}][InCl^{2+}]^{-1}$

For each experimental point, D_1 is determined from log K_1 expression whereas a and b coefficients are entirely determined by considering the β_m values of equilibria {3}

{3} $In^{3+} + m\ Cl^- \rightleftharpoons InCl_m^{(3-m)+}$ (β_m)

Then, D_2 is calculated and K_2 is obtained from the equation :

$\log K_2 = \log D_2 - 2pH - 2 \log [HPMBP]$

In fact, experimental D values are corrected because of the lack of extractant due to In complexation in the organic phase. The log β_m values considered in this paper are those of FERRI[12] (2.58, 3.84 and 4.20 for n = 1, 2 and 3) determined in $Cl^- - ClO_4^-$ medium at 25°C with μ = 3 and those of CARLESTON and IRVING[13] (2.36, 3.63 and 3.95) in the same medium at 20°C with μ = 0.69. The two series of values have been checked in our calculations and they are in good agreement with our experimental work. Nevertheless, the latter values are slightly better. The logD values, calculated with log K_1 = 1.48 and log K_2 = 0.26 are in good agreement with the corrected experimental ones. One may conclude that $In(PMBP)_3$ and $InCl(PMBP)_2$ are the only extracted species. Though $InCl_2^+$ and $InCl_3$ are the predominating aqueous species under the experimental conditions, $InCl_2(PMBP)$ remains too hydrophilic to be extracted.

EXTRACTION OF In(III) FROM PURE CHLORIDE (AND NITRATE-CHLORIDE) SOLUTIONS WITH HPMBP + $(TOMA^+,Cl^-)$: The addition of $(TOMA^+,Cl^-)$ largely enhances the In extraction from pure Cl^- aqueous solutions with HPMBP (fig.1). After an accurate correction of logD to counterbalance the lack of extractants due to the indium extraction, plots of logD vs pH at constant $[\overline{HPMBP}]$ and $[\overline{(TOMA^+,Cl^-)}]$ and of logD vs log $[\overline{HPMBP}]$ at constant pH and $[\overline{(TOMA^+,Cl^-)}]$ are straight lines of slopes $\sim$ 2 which is consistent with the extraction equilibrium {4}

{4} $InCl^{2+} + 2\ \overline{HPMBP} + n\ \overline{(TOMA^+,Cl^-)} \rightleftharpoons \overline{(n\ TOMA^+, InCl_{n+1}(PMBP)_2^{n-})} + 2\ H^+$ ($K_{4,n}$)

In this hypothesis, $\log D = \log K_{4,n} + \log b + 2 \log [\overline{HPMBP}] + 2\ pH + n \log [\overline{(TOMA^+,Cl^-)}]$.

A variation of $R = [NO_3^-][Cl^-]^{-1}$ permits to vary $[\overline{(TOMA^+,Cl^-)}]$ at constant "$[\overline{TOMA^+}]$" which limits aggregation effects. In view to evaluate $[\overline{(TOMA^+,Cl^-)}]$ for $0 < R < 9$ ("$[\overline{TOMA^+}]$"$_{total}$ = 0.016M) the constant of equilibrium {5}

{5} $\overline{(TOMA^+,Cl^-)} + NO_3^- \rightleftharpoons \overline{(TOMA^+,NO_3^-)} + Cl^-$ (K_5)

has been determined by potentiometric determination of the stripped Cl^- in $Na(NO_3,Cl)$ 1M solution from a $(TOMA^+,Cl^-)$ toluene solution : log K_5 = 1.50 ± 0.02.

Plots of (logD - logb) vs log $[\overline{(TOMA^+,Cl^-)}]$ at constant $[\overline{HPMBP}]$ and pH are straight lines of slope 1 which shows that n = 1. According to this result, log $K_{4,1}$ = 5.75 ± 0.05 has been calculated and the following synergic equilibrium is established :

{6} $\overline{InCl(PMBP)_2} + \overline{(TOMA^+,Cl^-)} \rightleftharpoons \overline{(TOMA^+, InCl_2(PMBP)_2^-)}$ (K_6)

with log K_6 = 5.49 ± 0.08

It must be noted that the extraction of In with $(TOMA^+,Cl^-)$ alone under the herein experimental conditions is negligible towards the synergic extraction.

EXTRACTION OF In(III) FROM CHLORIDE SOLUTIONS CONTAINING PERCHLORATE WITH HPMBP + $(TOMA^+,Cl^-)$: Since $(TOMA^+,Cl^-)$ is nearly fully changed into $(TOMA^+,ClO_4^-)$ under the experimental conditions, no synergic effect is observed in this case. However, it has been shown previously that $(TOMA^+,ClO_4^-)$ is a synergistic agent in the extraction of Co(II) with HPMBP[14] and it is noticeable that no similar effect is observed in the case of In. Then, the constant of the expected equilibrium {7} is negligible,

{7} $InCl_2^+ + 2\ \overline{HPMBP} + \overline{(TOMA^+,ClO_4^-)} \rightleftharpoons \overline{(TOMA^+, InCl_2(PMBP)_2^-)} + 2\ H^+ + ClO_4^-$

and the formation of ($TOMA^+$,$InCl_2(PMBP)_2^-$) is rather poor though $InCl_2^+$ is the predominating species in the aqueous phase.

EXTRACTION OF In(III) FROM PURE PERCHLORATE AND PURE CHLORIDE SOLUTIONS WITH OTHER ACYLPYRAZOLONES AND AMMONIUM SALTS : The constants of equilibria {1}, {2}, {4} and {6} have been also determined for the HPMLP - ($TOMA^+$,Cl^-), HPMTP - ($TOMA^+$,Cl^-) and HPMBP - ($HTOA^+$,Cl^-) systems (($HTOA^+$,Cl^-) = tri-n-octylammonium chloride) : the results are reported on table 1. It appears clearly that ($HTOA^+$,Cl^-) is not so an efficient synergic agent than ($TOMA^+$,Cl^-) in the extraction of In(III) from chloride medium by HPMBP. It appears that HPMBP is a better extractant of In(III) than HPMLP and HPMTP (see log K_1 and log K_2) in the same experimental conditions, and it is noticeable that the synergic effect is quite similar whatever the acylpyrazolone is.

Table 1 :

extractants	log K_1	log K_2	log $K_{4,1}$	log K_6
HPMBP + ($HTOA^+$,Cl^-)	1.48 ± 0.03	0.26 ± 0.03	4.43 ± 0.04	4.17 ± 0.07
HPMBP + ($TOMA^+$,Cl^-)	1.48 ± 0.03	0.26 ± 0.03	5.75 ± 0.05	5.49 ± 0.08
HPMLP + ($TOMA^+$,Cl^-)	1.03 ± 0.05	-0.45 ± 0.05	4.80 ± 0.03	5.25 ± 0.08
HPMTP + ($TOMA^+$,Cl^-)	0.87 ± 0.05	-0.35 ± 0.05	4.86 ± 0.05	5.21 ± 0.10

REFERENCES

(1) J.G. CUNINGHAME, B. SCARGILL and H.M. WILLIS, U.K. AERE Rept C/M 215 (1956).

(2) G. DUYCKAERTS and J.F. DESREUX, Proc.Int.Solv.Ext.Conf.-ISEC 77 - CIM Special Volume 21, 73 (1977) and included references.

(3) J.P. BRUNETTE, M. LAKKIS, G. GOETZ-GRANDMONT and M.J.F. LEROY, *Polyhedron*, to be published.

(4) M. KAWASHIMA and H. FREISER, *Anal.Chem.*, 1981, 53, 284.

(5) O. TOCHIYAMA and H. FREISER, *Anal.Chem.*, 1981, 53, 874. *Anal.Chim.Acta*, 1981, 131, 233.

(6) I. DUKOV and L. GENOV, *J.Inorg.Nucl.Chem.*, 1981, 43, 412.

(7) H. KAWAMOTO and H. AKAIWA, *Bunseki Kagaku*, 1975, 24, 127. CA 83 : 33426.

(8) S. NORIKI, *Anal.Chim.Acta*, 1975, 76, 215.

(9) B.S. JENSEN, *Acta Chem.Scand.*, 1959, 13, 1668.

(10) Y.A. ZOLOTOV and L.C. GAVRILOVA, *Zh.Neorg.Khim.*, 1969, 14, 2157.

(11) O. NAVRATIL and A. MALACH, *Coll. Czec.Chem.Com.*, 1978, 43, 2890.

(12) D. FERRI, *Acta Chem.Scand.*, 1972, 26, 733.

(13) B.G.F. CARLESTON and H. IRVING, *J.Chem.Soc.*, 1954, 4390.

(14) M. LAKKIS, Thèse de 3ème cycle, Strasbourg (1981).

Polyhedron Vol. 1, No. 5, pp. 461–466, 1982
Printed in Great Britain.

0277-5387/82/050461-06$03.00/0
Pergamon Press Ltd.

EXTRACTION OF COBALT(II) AND NICKEL(II) WITH MIXTURES OF 1-PHENYL-3-METHYL-4-BENZOYL-PYRAZOL-5-ONE (HPMBP) AND TRI-N-OCTYLAMINE (TOA)

J.P. BRUNETTE*, M. LAKKIS, G. GOETZ-GRANDMONT and M.J.F. LEROY.

Laboratoire de Chimie Minérale, Ecole Nationale Supérieure de Chimie, 1, rue Blaise Pascal 67008 STRASBOURG CEDEX (France).

(Received 30 March 1982)

ABSTRACT : The extraction of Co(II) with mixtures of 1-phenyl-3-methyl-4-benzoyl-pyrazol-5-one ((H)PMBP) and tri-n-octylamine (TOA) is investigated in order to explore the influence of diluents and inorganic anions with synergistic acidic extractant + liquid anion exchanger systems. Although it is proved that the same species $[HTOA]^+ [Co(PMBP)_3]^-$ is extracted from various inorganic media, with toluene as the diluent, the presence of ClO_4^-, SO_4^{2-} or Cl^- anion modifies the distribution of the anions which are associated to $(HTOA)^+$ in the organic phase, leading to different synergistic equilibria; with Cl^- or SO_4^{2-} :

$\overline{Co(PMBP)_2} + \overline{(HTOA^+,PMBP^-)} \rightleftharpoons \overline{(HTOA^+,Co(PMBP)_3^-)}$ (log K = 6.10) and with ClO_4^- :

$\overline{Co(PMBP)_2} + \overline{HPMBP} + \overline{(HTOA^+,ClO_4^-)} \rightleftharpoons \overline{(HTOA^+,Co(PMBP)_3^-)} + H^+ + ClO_4^-$ (log K = 2.34)

The same synergistic equilibrium is observed for the extraction of Ni(II) from ClO_4^- medium, with a comparable value of the constant (log K = 2.45).
The synergistic effect is cancelled in n-octanol.

INTRODUCTION

Previous investigations have shown that chelating acidic extractants in combination with cationic extractants (ammonium, arsonium, phosphonium salts) can produce synergism on the extraction of metal ions[1-19]. Most of the papers deal with the extraction of cobalt(II) and rare earths with mixtures of 2-thenoyltrifluoracetone (HTTA) and nitrogen bases or quaternary ammonium salts[1-11]. In the latter case, the extraction is enhanced by formation of metal anionic species $M(TTA)_3^-$ or $M(TTA)_4^-$ which are coordination-saturated and found in the organic phase in association with a lipophilic cation (i.e. R_4N^+). The conclusions are less obvious if one considers the HTTA-nitrogen bases system : the difficulties to explain the extraction curves are connected with the fact that nitrogen bases may form tertiary ammonium salts with the aqueous inorganic acid or with the acidic extractant (i.e. HTTA[1]); thus, they act as cationic extractants. Nitrogen bases may also remain neutral and act as common neutral extractants. In order to evaluate the importance of the nature of aqueous inorganic anions on such extraction systems, the extraction of cobalt(II) from perchlorate, sulphate and chloride media with 1-phenyl-3-methyl-4-benzoyl-pyrazol-5-one (HPMBP) in combination with tri-n-octylamine (TOA) is investigated.

EXPERIMENTAL

REAGENTS AND SOLUTIONS : HPMBP was prepared as described previously[20] and purified by several recrystallizations in a 1:10 toluene-ethanol mixture. Solutions of HPMBP and of HPMBP + TOA

in toluene or 1-octanol were prepared from Fluka or Merck chemicals. The HPMBP and TOA initial concentrations were varied between 0 and 0.04 M. Organic solutions were systematically pre-equilibrated against an aqueous solution, free of metal, of the same composition as the one that is used in the corresponding metal extraction procedure. Aqueous solutions were prepared by dissolution of the appropriate cobalt salt in sodium perchlorate, sulphate or chloride acidic solutions of 1M ionic strength(0.1M in a few but expressly noted cases). The total initial metal concentration was 1.7 10^{-3}M. pH was adjusted by addition of 0.1M NaOH solutions of suitable composition.

EXTRACTIONS AND ANALYTICAL PROCEDURES : The distribution measurements were performed in a thermostated vessel (25.0 ± 0.2°C) using a batch technique. Equal volumes of the organic and aqueous phases were shaken for a least 10 minutes, which was sufficient to reach equilibria, and then separated by gravity. For each experimental point, aliquots of each phase were withdrawn and analysed. Metal concentration determinations were done with a IL 453 spectrophotometer; the withdrawn organic samples were previously diluted in a water-ethanol mixture (water : ethanol : sample = 5:14:1) : it has to be noted that the sensitivity of Co absorption is slighty enhanced in such a medium.

RESULTS AND DISCUSSION

EXTRACTION OF COBALT(II) WITH HPMBP OR TOA : Zolotov *et al.*[21] accurately described the cobalt(II) extraction with HPMBP in benzene or isoamyl alcohol but new experiments were needed because of our slightly different experimental conditions i.e metal concentration, nature of diluents and inorganic anions, ionic strength. Plots of log D vs pH and log D vs log $[\overline{HPMBP}]$ at constant $[\overline{HPMBP}]$ and pH respectively (D = cobalt distribution ratio) have been performed to study the extraction of cobalt(II) from ClO_4^-, Cl^- and SO_4^{2-} aqueous solutions in HPMBP-toluene and HPMBP-1-octanol solutions; straight lines of slope 2 are obtained showing that the extractions are well described with equilibrium (1) :

(1) $$Co^{2+} + 2\ \overline{HPMBP} \rightleftharpoons \overline{Co(PMBP)_2} + 2\ H^+$$

The corresponding equilibrium constants K_1 are given in the following table :

Diluent	Inorganic anion	Ionic strength	log K_1	Ref.
benzene	ClO_4^-	0.1	-7.25 ± 0.08	21
isoamyl alcohol	ClO_4^-	0.1	-1.87 ± 0.07	21
toluene	ClO_4^-	1	-7.25 ± 0.05	this work
toluene	Cl^-	1	-7.00 ± 0.03	"
toluene	SO_4^{2-}	1	-7.78 ± 0.10	"
1-octanol	ClO_4^-	1	-1.98 ± 0.03	"
1-octanol	SO_4^{2-}	1	-2.87 ± 0.10	"

Two points have to be noted : - when the organic Co concentrations in toluene solutions are greater than ∿ 0.2 10^{-3}M, third phases appear; they disappear if alcohols are added; in this case, the extraction is largely enhanced and this synergistic effect is usually explained by the replacement of water molecules in the extracted species by alcohol molecules.

- the extraction is lower when it is performed from SO_4^{2-} aqueous solutions, whatever the diluent is. No detectible extraction of Co(II) from ClO_4^-, SO_4^{2-} and Cl^- aqueous solutions with TOA alone in toluene or 1-octanol has been observed under herein experimental conditions.

EXTRACTION OF COBALT(II) FROM PERCHLORATE MEDIA WITH A MIXTURE OF HPMBP AND TOA :

-Toluene as diluent : The extraction curves log D vs pH for $[ClO_4^-] = 1M$, $[\overline{HPMBP}]_i = 0.02M$ and various $[\overline{TOA}]_i$ (i denotes initial concentrations) are shown on Fig.1 : if TOA is added to the HPMBP-toluene solution, the cobalt extraction is enhanced, the third phase disappears and the slopes of the observed straight lines increase from 2 to 2.7 approximately. This last fact shows clearly that TOA is not merely a neutral synergistic agent in this extraction system : since $HClO_4$ is highly extracted with amines[22], the cobalt extraction from perchlorate aqueous solutions with HPMBP + TOA can be described by equilibrium (2) :

$$(2)\quad Co^{2+} + 3\,\overline{HPMBP} + \overline{(HTOA^+,ClO_4^-)} \rightleftharpoons \overline{(HTOA^+,Co(PMBP)_3^-)} + 3\,H^+ + ClO_4^-$$

In this hypothesis, experimental curves can be corrected using the following equations, $[\overline{HPMBP}] = [\overline{HPMBP}]_i - 3\,[\overline{Co}]$ and $[\overline{(HTOA^+,ClO_4^-)}] = [\overline{TOA}]_i - [\overline{Co}]$ where $[\overline{Co}]$ denotes the cobalt concentration in the organic phase. After corrections, the slopes of the curves log D vs pH are closed to 3 and are well-consistent with equilibrium (2). Accordingly, log-log plots of D vs $[\overline{HPMBP}]$ at constant pH and $[\overline{(HTOA^+,ClO_4^-)}]$ are straight lines of slope 3. A little more surprising is the slope 1 of the corrected curves log D vs log $[\overline{(HTOA^+,ClO_4^-)}]$ at constant pH and $[\overline{HPMBP}]$ if one considers that the aggregation of perchlorate ammonium salts in toluene is not negligible[22]. Assuming arbitrarily that ammonium cations and salts are monomers and taking log $[ClO_4^-] = 0$, log $K_2 = -4.91 \pm 0.06$ (K_2 = constant of equilibrium (2)). According to equilibrium (2) the extraction of Co is increased when $[ClO_4^-] = -1$; log $K_2 = -5.15 \pm 0.05$.

-1-octanol as diluent : when the diluent is 1-octanol, the addition of TOA has no effect on the extraction of cobalt with HPMBP. It must be concluded that $\overline{(HTOA^+,Co(PMBP)_3^-)}$ is not formed under herein experimental conditions.

EXTRACTION OF COBALT(II) FROM SULPHATE MEDIUM WITH A MIXTURE OF HPMBP AND TOA :

-Toluene as diluent : Extraction curves log D vs pH for $[\overline{HPMBP}]_i = 0.02M$ and various $[\overline{TOA}]_i$ are shown on Fig.2 : if TOA is added to HPMBP, the extraction of Co is enhanced and the previously observed third phase disappears; nevertheless, two facts are quite different from the extraction performed from perchlorate medium : the slope of the curves remains approximately 2, and the extraction does not increase regularly with increasing $[\overline{TOA}]_i$.

A maximum of extraction is observed for $[\overline{TOA}]_i . [\overline{HPMBP}]_i^{-1} \simeq 1/3$ (Fig.3) which is most probably the ratio of the two extractants in the extracted species. On the opposite to $HClO_4$, H_2SO_4 extraction with TOA is rather poor under the experimental conditions (less than 5% TOA are combined with H_2SO_4). Two equilibria explain the experimental facts :

$$(3)\quad \overline{HPMBP} + \overline{TOA} \overset{K_3}{\rightleftharpoons} \overline{(HTOA^+,PMBP^-)}$$

$$(4)\quad Co^{2+} + 2\,\overline{HPMBP} + \overline{(HTOA^+,PMBP^-)} \overset{K_4}{\rightleftharpoons} \overline{(HTOA^+,Co(PMBP)_3^-)} + 2\,H^+$$

with log $K_3 = 2.45$ (see Co extraction from Cl^- medium) and log $K_4 = -1.68 \pm 0.10$

The synergistic equilibrium is :

$$(5)\quad \overline{Co(PMBP)_2} + \overline{(HTOA^+,PMBP^-)} \overset{K_5}{\rightleftharpoons} \overline{(HTOA^+,Co(PMBP)_3^-)}$$

with log K_5 = log K_4 - log $K_1 = 6.10 \pm 0.10$

-1-octanol as diluent : the extraction of Co(II) from sulphate medium with HPMBP in 1-octanol is weakened if TOA is added to the organic phase. As observed with perchlorate medium, $\overline{(HTOA^+,Co(PMBP)_3^-)}$ is not formed : the antagonistic effect is explained by a decrease of HPMBP activity due to the TOA-HPMBP interactions described by equilibrium (3) with log $K_3 = 2.15 \pm 0.15$. This antagonistic effect is not observed with perchlorate medium because TOA exists mostly as $\overline{(HTOA^+,ClO_4^-)}$ and consequently its interactions with HPMBP are very weak.

EXTRACTION OF COBALT(II) FROM CHLORIDE MEDIUM WITH A MIXTURE OF HPMBP AND TOA IN TOLUENE :

-Extraction of HCl with TOA in toluene : for $[\overline{TOA}]_i = 0.001M$ to 0.02M and $pH_i = 1.5$ to 3,

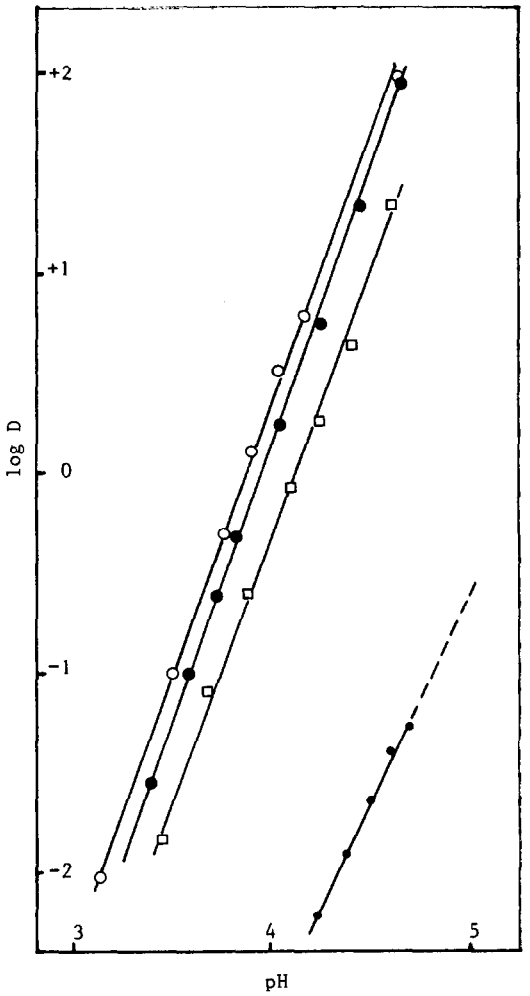

FIG. 1 : Extraction of Co(II) from ClO_4^- medium $[ClO_4^-]$ = 1M; $[HPMBP]_i$ = 0.02M; from the right to the left $[TOA]_i$ = 0, 0.0066, 0.02, 0.04; diluent : toluene.

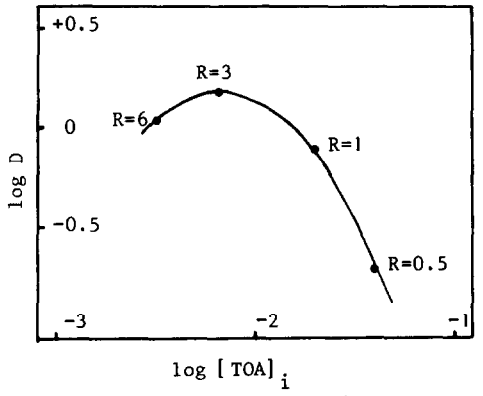

FIG. 3 : Influence of $R = [TOA]_i^{-1}[HPMBP]_i$ on the extraction of Co(II) from sulphate medium; diluent : toluene, pH = 4.00.

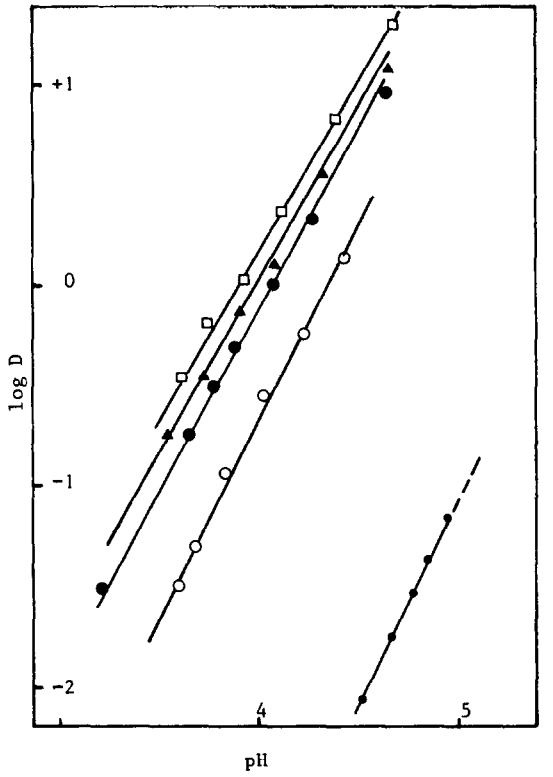

FIG. 2 : Extraction of Co(II) from $SO_4^=$ medium $[SO_4^=]$ = 0.33M; $[HPMBP]_i$ =0.02M; from the right to the left $[TOA]_i$ = 0, 0.04, 0.02, 0.0033, 0.0066; diluent : toluene.

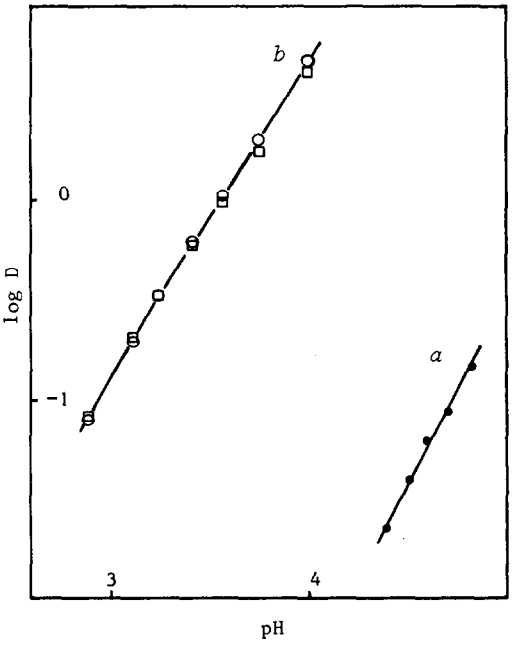

FIG. 4 : Extraction of Co(II) from Cl^- medium (diluent:toluene); $[Cl^-]$=1M; $[HPMBP]_i$ = 0.02M $[TOA]_i$ = 0^a and $[TOA]_i$ = 0.02M^b;
□ : calculated points; ●○ experimental points.

constants of equilibria (6) and (7) have been determined with pH and $[Cl^-]$ measurements and conventional calculations :

(6) $\overline{TOA} + H^+ + Cl^- \overset{K_6}{\rightleftharpoons} \overline{(HTOA^+,Cl^-)}$

(7) $2\overline{(HTOA^+,Cl^-)} \overset{K_7}{\rightleftharpoons} \overline{(HTOA^+,Cl^-)_2}$

with $\log K_6 = 3.57 \pm 0.03$ and $\log K_7 = 1.06 \pm 0.05$ $(\log[Cl^-] = 0)$
These results are in good agreement with previous determinations [22-23].

-HPBMP-TOA interactions in toluene : the addition of HPMBP to the organic phase TOA-toluene decreases the extraction of HCl from a 1M (Na,H)Cl aqueous solution. Equilibrium (3) can be considered to explain this fact. Using the following procedure based on pH measurements, the corresponding constant K_3 has been determined : $\log K_3 = 2.45 \pm 0.05$.

Procedure : A (TOA + HPMBP) toluene solution is shaken with an equal volume of 1M (Na,H)Cl aqueous solution. pH are measured before and after shaking and $\Delta[H^+]$ is calculated. Considering that the observed increase of pH is only due to HCl extraction (equilibria (6) and (7)), $[\overline{TOA}]$, $[\overline{(HTOA^+,PMBP^-)}]$ and $[\overline{(HPMBP)}]$ are obtained from the following equations :

$$\Delta[H^+] = K_6 [\overline{TOA}] [H^+] + 2 K_6^2 K_7 [\overline{TOA}]^2 [H^+]^2;$$

$$[\overline{(HTOA^+,PMBP^-)}] = [\overline{TOA}]_i - [\overline{TOA}] - \Delta[H^+] \text{ and } [\overline{HPMBP}] = [\overline{HPMBP}]_i - [\overline{(HTOA^+,PMBP^-)}]$$

$K_3 = [\overline{(HTOA^+,PMBP^-)}] [\overline{TOA}]^{-1} [\overline{HPMBP}]^{-1}$ has been determined with $pH_i = 2$, $[\overline{TOA}]_i = 0.01M$ and $0.05M < [\overline{HPMBP}]_i < 0.03M$

-Cobalt(II) extraction from 1M chloride medium : it has been performed with $[\overline{TOA}]_i = [\overline{HPMBP}]_i = 0.02M$; it can be described by equilibria (1), (3), (5), (6) and (7) with their respective constants $\log K_i = -7.00$, 2.45, 6.10, 3.57 and 1.06. A calculated curve log D vs pH obtained from these values is in quite good agreement with the experimental one (Fig.4). Each calculated value, $\log D_{cal.}$, has been determined through the following equations :

$$[\overline{TOA}]_i - [\overline{Co}] = [\overline{TOA}] + [\overline{(HTOA^+,PMBP^-)}] + [\overline{(HTOA^+,Cl^-)}] + 2[\overline{(HTOA^+,Cl^-)_2}]$$

$$[\overline{HPMBP}]_i - 3[\overline{Co}] = [\overline{HPMBP}] + [\overline{(HTOA^+,PMBP^-)}]; [\overline{(HTOA^+,Cl^-)_2}] = K_7 K_6^2 [H^+]^2 [\overline{TOA}]^2$$

$$[\overline{(HTOA^+,Cl^-)}] = K_6 [H^+][\overline{TOA}]; [\overline{(HTOA^+,PMBP^-)}] = ([\overline{HPMBP}]_i - 3[\overline{Co}])(1 + K_3[\overline{TOA}]^{-1})K_3[\overline{TOA}].$$

$$\log D_{cal.} = \log K_1 + \log K_5 + 2\,pH + 2 \log[\overline{HPMBP}] + \log[\overline{(HTOA^+,PMBP^-)}]$$

EXTRACTION OF NICKEL(II) WITH A MIXTURE OF HPMBP AND TOA IN TOLUENE : The extraction of nickel(II) from $(H,Na)ClO_4$ 1M medium with HPMBP in toluene is described by the equilibrium (1')

(1') $Ni^{2+} + 2\,\overline{HPMBP} \rightleftharpoons \overline{Ni(PMBP)_2} + 2\,H^+$ with $\log K_{1'} = -6.71$

if TOA is added to the organic phase, the equilibrium (2') takes place :

(2') $Ni^{2+} + 3\,\overline{HPMBP} + \overline{(HTOA^+,ClO_4^-)} \rightleftharpoons \overline{(HTOA^+,Ni(PMBP)_3^-)} + 3\,H^+ + ClO_4^-$

with $\log K_{2'} = -4.26$. Thus the synergistic equilibrium is :

(3') $\overline{Ni(PMBP)_2} + \overline{HPMBP} + \overline{(HTOA^+,ClO_4^-)} \rightleftharpoons \overline{(HTOA^+,Ni(PMBP)_3^-)} + H^+ + ClO_4^-$

with $\log K_{3'} = 2.45$

It noticeable that $K_{3'}$ is quite similar to K_3 ($\log K_3 = 2.45$) observed in the same conditions for Co(II); hence, it can be concluded that the Ni-Co separation remains unchanged with the formation of $\overline{(HTOA^+,M(PMBP)_3^-)}$ ion-pair. The slow extraction of Ni(II) from Cl^- and SO_4^{2-} media have not been extensively studied.

CONCLUSION

Whatever the nature of the inorganic aqueous anions is (ClO_4^-, Cl^- or SO_4^{2-}), a synergistic extraction of Co(II) and Ni(II) with a mixture of HPMBP and TOA in toluene is observed. In all cases, the extracted species is ($\overline{HTOA^+,M(PMBP)_3^-}$). It may be formed according to two different but thermodynamically equivalent ways. The first one is the phase transfer of the hydrated aqueous complex $M(PMBP)_2$,aq. followed by its water molecules substitution by the $PMBP^-$ anion of the organic ion pair ($\overline{HTOA^+,PMBP^-}$). The second way is consistent with the formation of the $M(PMBP)_3^-$ anion in the aqueous phase followed by an interfacial anionic exchange such as

$$M(PMBP)_3^- + \overline{(HTOA^+,X^-)} \rightleftharpoons \overline{(HTOA^+,M(PMBP)_3^-)} + X^-$$

where X^- represents the aqueous inorganic anion.

An accurate study of the extraction rates would be necessary to definitively conclude; however, the extraction rate of Ni(II) is higher from ClO_4^- medium than from Cl^- and SO_4^{2-} media, which suggests that the anionic exchange is the metal phase-transfer mechanism for the extraction from ClO_4^- medium.

REFERENCES

(1) L. Newman and P. Klotz, *J.Phys.Chem.*, 1963, 67, 205; *Inorg.Chem.*, 1966, 5, 461; *ibid.*, 1972, 11, 2151.

(2) E.V. Melent'eva, L.I. Kononenko and N.S. Poluektov, *Ukr.Khim.Zh.*, 1966, 32, 1147.

(3) L.I. Kononenko and R.A. Vitkun, *Russ.J.Inorg.Chem.*, 1970, 15, 690.

(4) M.S. Rahaman and H.L. Finston, *Anal.Chem.*, 1968, 40, 1709; *ibid.*,1969, 41, 2023.

(5) B. Kuznick, L. Genov and G. Georgiev, *Monatsh.Chem.*, 1974, 105, 1190; *ibid.*, 1975, 106, 1543.

(6) L. Genov, I. Dukov and G. Kassabov, *Acta Chim.Acad.Sc.Hung.*, 1977, 95, 361.

(7) I. Dukov and L. Genov, *Acta Chim.Acad.Sc.Hung.*,1980, 104, 329; *J.Inorg.Nucl.Chem.*,1981, 43, 412.

(8) S. Noriki, *Anal.Chim.Acta*, 1975, 76, 215.

(9) H. Kawamoto and H. Akaiwa, *Bunseki Kagaku*, 1975, 24, 127. (C.A. 83:33426).

(10) P.K. Khopkar and J.N. Mathur, *J.Inorg.Nucl.Chem.*, 1977, 39, 2063.

(11) J.F. Desreux, J. Massaux and G. Duyckaerts, *J.Inorg.Nucl.Chem.*, 1978, 40, 1159.

(12) W. Bacher and C. Keller, *J.Inorg.Nucl.Chem.*, 1973, 35, 2945.

(13) S. Noriki and M. Nishimura, *Anal.Chim.Acta*, 1974, 72, 339;*ibid.*, 1977, 94, 57.

(14) M. Nishiruma, S. Noriki and S. Muramoto, *Anal.Chim.Acta*, 1974, 70, 121.

(15) H. Hoshino, T. Yotsuyanagi and K. Aomura, *Anal.Chim.Acta*, 1976, 83, 317.

(16) Lj. Maric, M. Siroki, Z. Stephanac and M.J. Herak, *Microchem.J.*, 1979, 24, 536.

(17) D. Nonova and S. Pavlova, *Anal.Chim.Acta*, 1981, 123, 289.

(18) M. Kawashima and H. Freiser, *Anal.Chem.*, 1981, 53, 284.

(19) O. Tochiyama and H. Freiser, *Anal.Chem.*, 1981, 53, 874; *Anal.Chim.Acta*, 1981, 131, 233.

(20) B.S. Jensen, *Acta Chem.Scand.*, 1959, 13, 1668.

(21) Ju. A. Zolotov and L.G. Gavrilova, *Radiokhimiya*, 1969, 11, 389.

(22) J.F. Desreux, *Ind.Chim.Belg.*, 1972, 37, 637.

(23) R.R. Grinstead, "Solvent Extraction Chemistry ", Eds D. Dyrssen, J.O. Liljenzin and J. Rydberg, Amsterdam (1967) p.426.

Polyhedron Vol. 1, No. 5, pp. 467–470, 1982
Printed in Great Britain.

0277–5387/82/050467–04$03.00/0
Pergamon Press Ltd.

REDUCTION OF THE COPPER(II) CATION IN ACETONITRILE BY TRIMETHYL PHOSPHITE. EVIDENCE FOR AN INTERMEDIATE COPPER(II) COMPLEX

GERARD M. ANDERSON, JAMES H. CAMERON,
A. GRAHAM LAPPIN, AND JOHN M. WINFIELD*
Chemistry Department, University of Glasgow, Glasgow G12 8QQ, Scotland

and

ALEXANDER McAULEY
Chemistry Department, University of Victoria, Victoria B.C., Canada

(Received 12 July 1982)

Abstract - Reduction of the solvated copper(II) cation by trimethyl phosphite in acetonitrile occurs via a short-lived purple intermediate, believed to be a copper(II)-phosphite complex.

INTRODUCTION

Trialkyl(aryl)-phosphane and phosphite complexes of copper(I) are conveniently synthesised from reactions between the ligands and copper(II) salts in alcoholic media.[1] When a mixture of copper(II) hexafluorophosphate, pentakis-(acetonitrile) and trimethyl phosphite in acetonitrile $[Cu^{II}]:[P(OMe)_3] = 1:10$, is allowed to warm from 77K, a deep purple colour develops as $P(OMe)_3$ melts. The colour fades rapidly even below 230K, and at room temperature the identified products are the tetrakis(trimethyl phosphite)copper(I) and trimethoxymethylphosphonium cations, the hexafluorophosphate anion, and dimethyl methylphosphonate. Minor amounts of other organo-phosphorus compounds are formed also but were not identified. Spectrophotometric titration, monitoring $Cu(NCMe)_6^{2+}$ absorbance at 13,400 cm^{-1}, indicates that rapid, quantitative reduction of copper(II) occurs only when $[Cu^{II}]:[P(OMe)_3] < 1:6$. Below this ratio the stoicheiometry remains 1:6 and partial copper(II) reduction results.

Formation of the purple transient from solutions of $Cu(PF_6)_2 5MeCN$ and excess $P(OMe)_3$ in MeCN is complete within the time of mixing at 297±0.1K, but its decay is within the stopped-flow range providing $[P(OMe)_3]$ does not exceed 0.1 mol dm^{-3}. The electronic spectrum obtained by point-by-point determination over the range 22,200–32,800 cm^{-1}, $[Cu^{II}]:[P(OMe)_3] = 1:10$ or 1:100, consists

* Author to whom correspondence should be addressed

the difference in coordination number. As expected, substitution of MeCN by 2,2'-bipyridyl (bipy) reduces the oxidising ability of Cu^{II} ($E_{\frac{1}{2}}$ = ca. -0.24V vs Ag^{+}/Ag) and reduction of $Cu(bipy)_3^{2+}$ by $P(OMe)_3$ is not observed. Electrochemical oxidation of $Cu\{P(OMe)_3\}_4^{+}$ in MeCN is irreversible and occurs at a potential significantly higher than that of $Cu(NCMe)_4^{+}$. It is reasonable to conclude therefore that a species $Cu\{P(OMe)_3\}_n(NCMe)_{6-n}^{2+}$ is directly involved in the redox step.

The limited kinetic data obtained do not allow a definitive mechanism to be formulated, however equation (1), N = MeCN, P = $P(OMe)_3$, is plausible.

$$CuN_2P_4^{2+} + P \overset{K_5}{\rightleftharpoons} CuNP_5^{2+} + N$$
$$CuNP_5^{2+} + P \xrightarrow{k} CuP_4^{+} + P_2^{+} + N \qquad (1)$$

This will lead to the rate law, Rate = $kK_5[CuN_2P_4^{2+}][P]^2$, which is consistent with the observed behaviour, providing K_5 is small compared with the stepwise formation constants K_1---K_4. By analogy with complexation of Cu^{II} in water,[5] this is a reasonable assumption. The dimeric radical cation, $(MeO)_3P\text{-}P(OMe)_3^{\cdot+}$, postulated as the other product, has been observed from the γ-irradiation of $P(OMe)_3$ at 77K.[6] We suggest that one of its decomposition products is $MeP(OMe)_3^{+}$. This is known to be an intermediate in the autocatalytic Arbuzov rearrangement of $P(OMe)_3$,[7] and accounts for the presence of $MeP(O)(OMe)_2$ as the major organo-phosphorus product.

EXPERIMENTAL

Preparation of $Cu(PF_6)_2$5MeCN and $Cu(PF_6)$4MeCN and the spectroscopic and stopped flow techniques used to study the reactions under anerobic conditions have been described previously.[8,9] 2,2'-Bipyridyl (bipy) complexes were prepared by stoicheiometric reactions between bipy (B.D.H. Analar) and the copper salts in MeCN using standard vacuum techniques. Their vibrational spectra indicated that MeCN and free bipy were absent. Products from the reaction of $Cu(PF_6)_6$5MeCN with trimethyl phosphite (purified as described previously[9]) were identified by comparison of their ^1H, ^{19}F, and ^{31}P n.m.r. and i.r. spectra with those of authentic samples.

Solution concentrations used were as follows: for stopped flow $[Cu^{II}] = 5\times10^{-4}$, $[P(OMe)_3] = 7.5\times10^{-3}$-$7.5\times10^{-2}$ mol dm^{-3}; for spectrophotometric titration $[Cu^{II}] = 0.06$, $[P(OMe)_3] = 0.03$-0.45 mol dm^{-3}; for n.m.r. typically $[Cu^{II}] = 0.09$, $[P(OMe)_3] = 0.90$ mol dm^{-3}.

Cyclic voltammetry was carried out in a Pyrex cell contained in an Ar atmosphere glove box, H_2O<5p.p.m., coupled to a potentiostat (CV-1A, Bioanalytical

of an asymmetric band, ν_{max} 29,000 cm^{-1}, ϵ = $3x10^3 dm^3 mol^{-1} cm^{-1}$. The decrease in absorbance at 29,000 cm^{-1} is pseudo-first order in $[Cu^{II}]$ providing $[P(OMe)_3]:[Cu^{II}]$ >15:1, and the pseudo-first order rate constants at 297±0.1K, Figure 1, indicate a second order dependence on $[P(OMe)_3]$. The derived overall third order rate constant is $3.7\pm0.8x10^3$ $dm^6 mol^{-2} s^{-1}$.

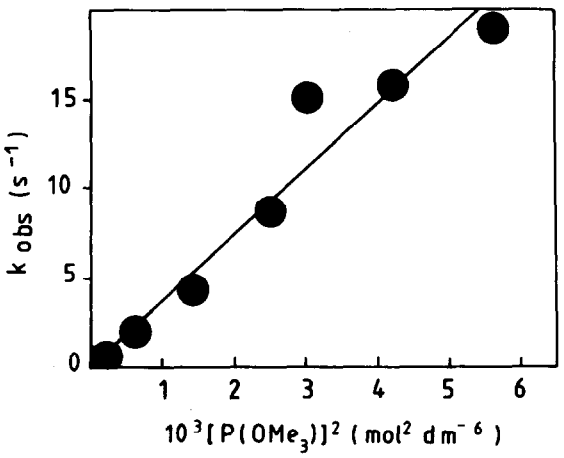

Fig. 1. Dependence of pseudo-first order rate constants, k_{obs} on $[P(OMe)_3]^2$.

The decrease in absorbance is slower when $[Cu^{II}]$ is in excess, but reproducible results were not obtained. On standing at room temperature, these solutions became brown suggesting attack of the solvent.

Substitution of MeCN by $P(OMe)_3$ at Cu^{II} is expected to be rapid by analogy with solvent exchange at $Cu(NCMe)_6^{2+}$.[2] The observed electronic spectrum is therefore assigned to a d-d transition in a species of the type $Cu\{P(OMe)_3\}_n(NCMe)_{6-n}^{2+}$, the relatively high molar absorption coefficient possibly being the result of intensity borrowing from charge transfer bands occurring >40,000 cm^{-1}. No e.p.r. signals could be observed from reaction mixtures quenched to 77K, however a paramagnetic Cu^{II}, tetramethylthiourea-(Me_4tu) complex, ν_{max} 19,600 and 25,000 cm^{-1}, has been observed as a relatively long-lived intermediate in the Me_4tu reduction of Cu^{II} in MeCN.[3]

$Cu(NCMe)_6^{2+}$ is a moderately good oxidising agent in MeCN due to the effective solvation of Cu^I by MeCN.[4] The $Cu^{II/I}$ couples determined by cyclic voltammetry using $Cu(NCMe)_6^{2+}$ and $Cu(NCMe)_4^+$ salts are quasi-reversible, peak-to-peak separations 0.070 and 0.170V respectively. The slight difference in mid-point potential, +0.710(Cu^{II}) and +0.750V(Cu^I) vs. Ag^+/Ag observed probably reflects

Systems Inc.) and XY recorder. The working and auxiliary electrodes were Pt wires and the reference electrode was $Ag/AgNO_3$, 0.1 mol dm^{-3} in MeCN. Et_4NBF_4 (0.1 mol dm^{-3}) was the supporting and bridging electrolyte. Reference, bridge, and sample compartments were separated by unfired Vycor tips sealed to the glass by heat-shrunk P.T.F.E. tubing. Acetonitrile (Rathburn Chemical Co., HPLC-S grade), purified[10] and dried over molecular sieves in vacuo, had limiting potentials +2.4 and -2.7V vs. Ag^+/Ag. Reproducible voltammograms (±0.005V) were obtained from at least three samples of each compound studied, [solute] = $3x10^{-4}$ mol dm^{-3}, scan rate 0.100 Vs^{-1}.

Acknowledgement - We thank the S.E.R.C. and N.A.T.O. for financial support.

REFERENCES

[1] J. G. Verkade and T. S. Piper, Inorg. Chem., 1962, 1, 453; K. J. Coskran, T. J. Huttemann, and J. G. Verkade, Adv. Chem. Ser., 1967, 62, 590; D. J. Gulliver, W. Levason, and M. Webster, Inorg. Chim. Acta, 1981, 52, 153.

[2] R. J. West and S. F. Lincoln, J. Chem. Soc., Dalton Trans., 1974, 281.

[3] D. A. Zatko and B. Kratochvil, Anal. Chem., 1968, 40, 2120.

[4] A. J. Parker, Electrochim. Acta, 1976, 21, 671; I. D. MacLeod, D. M. Muir, A. J. Parker, and P. Singh, Aust. J. Chem., 1977, 30, 1423.

[5] B. J. Hathaway and A. A. G. Tomlinson, Coord. Chem. Revs., 1970, 5, 1.

[6] T. Gillbro, C. M. L. Kerr, and F. Williams, Mol. Phys., 1974, 28, 1225.

[7] D. H. Brown, K. D. Crosbie, G. W. Fraser, and D. W. A. Sharp, J. Chem. Soc.A, 1969, 872.

[8] A. C. Baxter, J. H. Cameron, A. McAuley, F. M. McLaren, and J. M. Winfield, J. Fluor. Chem., 1977, 10, 289.

[9] C. J. Barbour, J. H. Cameron, and J. M. Winfield, J. Chem. Soc., Dalton Trans., 1980, 2001; J. H. Cameron, A. G. Lappin, J. M. Winfield, and A. McAuley, ibid., 1981, 2172.

[10] M. Walter and L. Ramaley, Anal. Chem., 1973, 45, 165.

Polyhedron Vol. 1, No. 5, pp. 471–474, 1982
Printed in Great Britain.

0277-5387/82/050471-04$03.00/0
Pergamon Press Ltd.

The Synthesis and Structure of trans-Bis(methylnicotinate)aquatrichlorochromium(III).

James V. McArdle*, Eric de Laubenfels,
A. Lee Shorter, and Herman L. Ammon*

Department of Chemistry
University of Maryland
College Park, MD 20742

(Received 1 June 1982)

Abstract

The title complex was synthesized and its structure was determined by single crystal X-ray diffraction. There are four molecules per unit cell and the space group is $P\bar{1}$. The methyl nicotinate ligands are bound in trans positions through the nitrogen atoms. The average Cr-N distance is 2.094 Å and the average N-Cr-N angle is 177.4 degrees. The average Cr-Cl and Cr-O bond lengths (2.317 Å and 2.011 Å, respectively) are typical of many other structures. The coordination between methyl nicotinate and chromium may serve as a model for the proposed complex between nicotinic acid and chromium in glucose tolerance factor.

Chromium has been recognized as an essential trace element since 1957.[1] Mertz first described chromium dependence in rats and later showed that chromium is an essential co-factor for insulin and is required for normal glucose tolerance in rats.[2] He has recently reviewed the status of chromium as an essential trace element in animals and in man.[3]

The compound of chromium responsible for insulin potentiation is called glucose tolerance factor (GTF). Much effort has gone into the purification and characterization of GTF but little success has been achieved.[4,5] Various preparations have been found to contain chromium, nicotinic acid, glycine, glutamic acid, and systeine.[4] Likewise, efforts at synthesizing and characterizing model compounds of GTF have not been successful.[4,6] Polarographic studies of the interaction between insulin, chromium and mitochondria have been performed.[7] These and other studies have led to a model for the mode of action of GTF in which two nicotinic acids are coordinated in trans positions to a chromium atom.[6] However, in these models the nicotinic acids are coordinated through the nitrogen atom. It is this feature of nitrogen-coordinated nicotinic acid that is of interest in the present work. There are no well-characterized model complexes to support this assignment, but there are, of course, many chromium carboxylic acid complexes. In order to study the chromium-nitrogen bond proposed for GTF, we prepared the title compound and determined its structure by single crystal X-ray diffraction.

The compound was prepared by dissolving 5.0 g (1.9×10^{-2} mol) $CrCl_3 \cdot 6H_2O$ and 7.0 g (5.1×10^{-2} mol) methyl nicotinate in 250 mL ethanol and refluxing over type 4A molecular sieves in a Soxhlet extractor for twenty-four hours. The product was evaporated to dryness, washed with water and a small amount of ethanol, and re-crystallized from ethanol/water

by slow evaporation at 0°. Dull green plate-like crystals were obtained. The compound has a distinct shoulder in the untraviolet spectrum measured in ethanol at about 265 nm. Preparations of GTF show an absorbance maximum at 262 nm.[4]

A 0.05 x 0.2 x 0.4 mm specimen was used for all X-ray work. The cell dimensions and intensity data were measured on a Picker FACS-I diffractometer with graphite-monochromated Cu radiation. The space group and cell data are: triclinic, $P\bar{1}$; a = 7.2917(5), b = 17.198(2), c = 17.893(2) Å; α = 91.76(1), β = 98.764(6), γ = 92.698(1)°; V = 2213.6 Å^3; d_{obsd} = 1.515 g cm^{-3}, d_{calc} = 1.514 g cm^{-3} for $Cr(H_2O)(C_7H_7NO_2)_2Cl_3 \cdot 3H_2O$ and z = 4. A total of 8055 diffraction intensities, measured to a 2Θ maximum of 127° with the 2Θ-Θ scan technique, yielded 7221 unique data after averaging, of which 6047 $\geq 3\sigma$ above background. An 8x8x8 grid Gaussian quadrature absorption correction was applied (μ = 96.5 cm^{-1}). The positions of the two chromium atoms in the asymmetric unit were obtained from an E^2-1 Patterson synthesis, and the remaining atoms were located in subsequent electron density and difference maps. Block-diagonal least-squares refinement with anisotropic temperature factors for the non-hydrogen atoms gave R = 0.106.[8]

The asymmetric unit contains two essentially identical molecules of $Cr(H_2O)(C_7H_7NO_2)_2Cl_3$ and six waters of hydration. The chromium atoms (Figure) are coordinated octahedrally with the methyl nicotinates bound through the nitrogen atoms in *trans* positions. The average Cr-N distance of 2.094 Å (see Table) found in this structure is similar to other Cr-N distances. For example, the corresponding distance in the complex $[CrCl_2(H_2O)_2en]^+$ is 2.09 Å,[9] in di-μ-hydroxo-tetraglycinatodichromium(III) it is 2.064 Å,[10] and in the ion bis(isopropyliminodiacetato)chromate(III) it is 2.118 Å.[11] Significantly shorter Cr-N bond distances have also been measured.[12,13] The 1.974 Å distance in bis(pyridine-2,6-dicarboxylato)chromate(III) clearly is due to the tridentate nature of the ligand. The Cr-Cl and Cr-O distances are typical of other structures.[9,13] The pyridine ring atoms are planar with all atoms less than 0.02 Å from the mean plane. The equatorial planes containing chromium, oxygen, and three chlorides are similarly well-defined with all atoms within 0.06 Å of the mean plane. It is also interesting to note that the methyl nicotinate planes are nearly parallel to each other. If $d\pi$-$p\pi$ bonding were important, the methyl nicotinate planes would be perpendicular to each other. Crystal-packing forces are probably responsible for the observed conformation.

Acknowledgements. We thank Prof. Carl Rollinson for many helpful discussions and the University of Maryland Computer Science Center for the use of its facilities.

Supplementary Material Available. Lists of observed and calculated structure factors, atomic coordinates, thermal parameters, bond lengths and angles, and cell dimension.

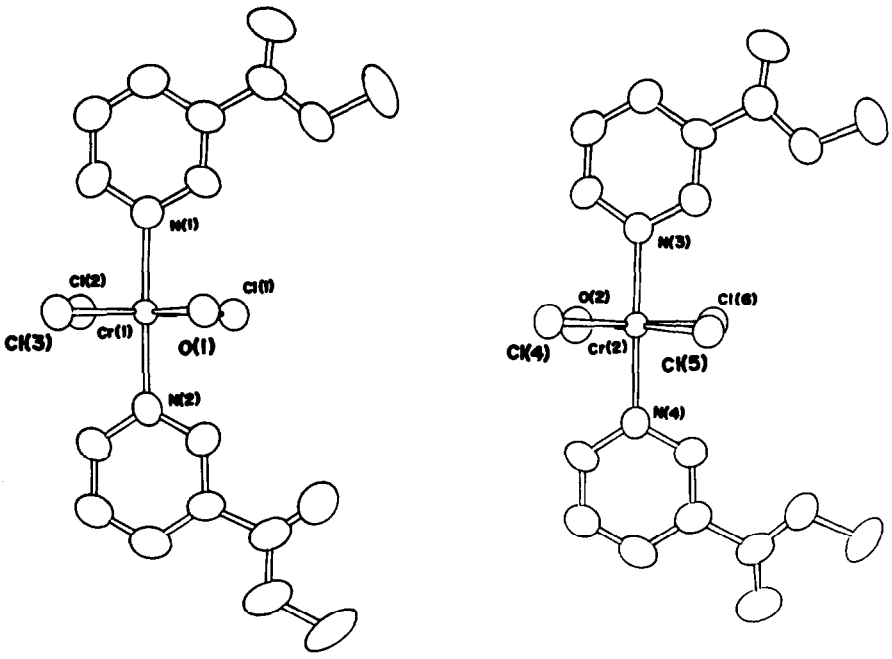

Figure. ORTEP plot of the nonhydrogen atoms of the two molecules of $Cr(me\text{-}nic)_2(H_2O)Cl_3$ in the asymmetric unit. Note the positions of the carbonyl oxygens.

Table: Selected Bond Lengths and Angles in $Cr(Me\text{-}nic)_2(H_2O)Cl_3$.[a]

	Bond Lengths (Å)		
Cr(1)-N(1)	2.119 (9)	Cr(2)-N(3)	2.100 (9)
Cr(1)-N(2)	2.071 (9)	Cr(2)-N(3)	2.084 (9)
Cr(1)-Cl(1)	2.328 (3)	Cr(2)-Cl(4)	2.324 (3)
Cr(1)-Cl(2)	2.324 (3)	Cr(2)-Cl(5)	2.308 (4)
Cr(1)-Cl(3)	2.303 (4)	Cr(2)-Cl(6)	2.316 (3)
Cr(1)-O(1)	2.016 (9)	Cr(2)-O(2)	2.006 (9)
	Bond Angles (deg)		
N(1)-Cr(1)-N(2)	175.8 (4)	N(3)-Cr(2)-N(4)	178.9 (3)
Cl(1)-Cr(1)-N(1)	90.5 (2)	Cl(4)-Cr(2)-N(3)	92.3 (3)
O(1)-Cr(1)-N(2)	88.0 (3)	O(2)-Cr(2)-N(4)	91.4 (4)

[a]Standard deviations in the least significant digit are given in parentheses.

References

1. K. Schwarz and W. Mertz, Arch.Biochem.Biophys., 1957, 72, 515.

2. K. Schwarz and W. Mertz, Arch.Biochem.Biophys., 1959, 85, 292.

3. W. Mertz, Science, 1981, 213, 1332.

4. E. W. Toepfer, W. Mertz, M. M. Polansky, E. E. Roginshi, and W. R. Wolf, J. Agric. Food Chem., 1977, 25, 162.

5. N. Mirsky, A. Weiss, and Z. Dori, J. Biochem., 1980, 13, 11.

6. W. Mertz, E. W. Toepfer, E. E. Roginshi, and M. M. Polansky, Federation Proc., 1974, 33, 2275.

7. G. D. Christian, E. C. Knoblock, W. C. Purdy and W. Mertz, Biochim. Biophys. Acta, 1963, 66, 420.

8. The function minimized was $\Sigma(|F_o|-|F_c|)^2$. $R = \Sigma||F_o|-|F_e||/|F_o|$.

9. R. Stomberg, I. Larking, Acta Chem. Scand., 1969, 23, 343.

10. J. T. Veal, W. E. Hatfield, D. Y. Jeter, J. C. Hempel and D. J. Hodgson, Inorg. Chem., 1973, 12, 342.

11. D. Mootz and H. Wunderlich, Acta Cryst., 1980, B36, 721.

12. W. Furst, P. Gouzerk and Y. Jeannin, J. Coord. Chem., 1979, 8, 237.

13. S. J. Cline, S. Kallesoe, E. Pedersen, and D. J. Hodgson, Inorg. Chem., 1979, 18, 796.

Polyhedron Vol. 1, No. 5, pp. 475-477, 1982
Printed in Great Britain.

0277-5387/82/050475-03$03.00/0
Pergamon Press Ltd.

VIBRATIONAL SPECTRA OF ANHYDROUS CHROMIUM(III) CHLORIDE

*R.E. Sowden, J.M. Orza, S. Montero
Instituto de Estructura de la Materia, C.S.I.C., Serrano 119, MADRID-6, Spain
Issued as C.S.I.C. No. FM 44. Running title: Infrared and Raman spectra of $CrCl_3$

(Received 7 June 1982)

ABSTRACT

The vibrational structure of anhydrous chromic chloride, $CrCl_3$, has been investigated at room temperature in the spectral range 240 - 500 cm^{-1} by means of Raman and infrared absorption spectroscopy.

INTRODUCTION

Although the spectra of many chromium complexes have been studied in depth, data on the vibrational spectra of the layer compound anhydrous chromium(III) chloride, $CrCl_3$, appear to rather scarce. Only one band, at 315 cm^{-1}, in the infrared absorption spectrum has been mentioned by Clark[1]; this band was attributed to the ν(Cr-Cl) bridge. Inview of the present day interest in the industrial uses of anhydrous chromic chloride[2-4] we have therefore undertaken a review of the vibrational structure of this compound in greater detail.

The crystal structure of $CrCl_3$ has been established by Morosin and Narath[5] as being unambiguously monoclinic (C2/m ; C_{2h}^3) with two $CrCl_3$ groups in the primitive cell at room temperature, and rhombohedral ($R\bar{3}$; C_{3i}^2) with six $CrCl_3$ units at ~225°K.

Factor group analysis of the room temperature phase of $CrCl_3$ yields the following information:

Optical branch, $\Gamma(C_{2h}^3, z=2) = 6A_g + 6B_g + 4A_u + 5B_u$

Acoustic branch, $\Gamma(C_{2h}^3, z=2) = 1A_u + 2B_u$

The optical branch can be observed using Raman and infrared spectroscopy. The two spectra have no bands in common, in principle, since only the A_g and B_g modes are Raman active and only the A_u and B_u modes are infrared active. None the less, both spectra occur in the same low frequency range, say 100 - 500 cm^{-1}.

EXPERIMENTAL

The vibrational spectra of micaceous, polycrystalline samples of anhydrous chromic chloride prepared by sublimation were investigated at room temperature.

Raman spectra of pure samples of the deep violet $CrCl_3$ were obtained with several different exciting lines using a double Czerny-Turner monochromator. Although no spectra were recorded with exciting lines of wavelengths 514.5 or 488.0 nm owing to the intensity of absorption in this region of the spectrum, good Raman spectra were obtained relatively easily with exciting lines of wavelengths 632.8, 465.8 and 475.9 nm using exciting radiation of powers below 100 mW.

Infrared absorption spectra were recorded as $CrCl_3$ pellets using a Perkin Elmer 225 spectrophotometer.

RESULTS AND DISCUSSION

The Raman and infrared spectra obtained for anhydrous chromic chloride are presented in Figure 1. At least five broad absorption bands can be observed in the infrared spectrum in the region between 240 and 500 cm^{-1}. Nevertheless no possible assignments

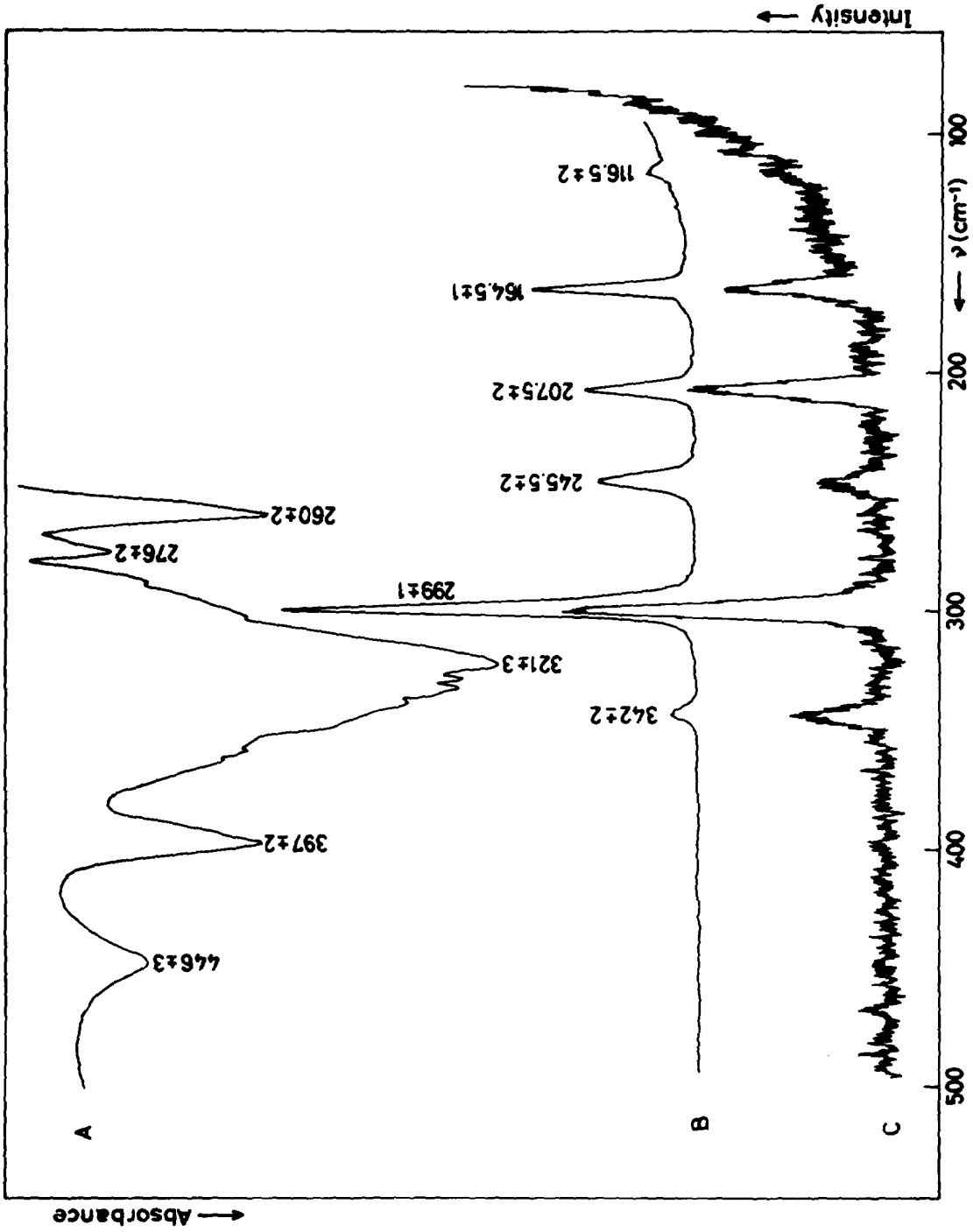

Fig. 1. Raman and infrared spectra of $CrCl_3$. A: KBr pellet, infrared spectrum of $CrCl_3$, B: Raman spectrum with 488.0 nm exciting line, C: Raman spectrum with 632.8 nm exciting line.

to the A_u or B_u modes can be made. On the basis of group theoretical arguments one would expect to be able to identify four or five strong $A_u + B_u$ doublets that could not be resolved at room temperature. The observed infrared spectrum is therefore not in contradiction with theoretical predictions based on the x-ray structure of $CrCl_3$ at room temperature.

No strong changes in the Raman spectrum as a function of the frequency of the exciting wavelength were noted in the present work, although the 245 cm^{-1} band was noticeably weaker when observing with an exciting line of wavelength 632.8 nm. The six bands in the Raman spectrum predicted by the above factor group analysis were all clearly visible and were probably $A_g + B_g$ doublets. Indeed, shoulders could be observed on the low frequency side of the bands at 299, 245 and 164 cm^{-1}. This aspect of the work, however, could be clarified only by recording single crystal spectra.

REFERENCES

1. R.J.H. Clark, Spectrochim. Acta, 1965, 21, 955.
2. R.E. Sowden and T. Rigg, Brit. Pat. 1567841.
3. R.E. Sowden, Comm. Fac. Sci. Ankara Univ., 1978, 26B(9), 61.
4. R.E. Sowden, Doctoral Thesis, E.T.S. Ing. Ind., Madrid Polytechnic University, Spain (1981).
5. B. Morosin and A. Narath, J. Chem. Phys., 1964, 40(7), 1958.

Polyhedron Vol. 1, No. 5, pp. 479–482, 1982
Printed in Great Britain

0277-5387/82/050479-04$03.00/0
Pergamon Press Ltd.

PURIFICATION OF MOLYBDENUM : VOLATILISATION PROCESSES USING MoO_3

D.A. JOHNSON#, J.H. LEVY#, J.C. TAYLOR# and A.B. WAUGH*#

Chemical Technology Division

and

J. BROUGH

Isotope Division

Australian Atomic Energy Commission Lucas Heights Research Laboratories
Private Mail Bag, Sutherland, 2232, NSW, Australia

ABSTRACT

Various volatilisation processes for the purification of MoO_3 were investigated. Of these, fusion of MoO_3 with NaCl at 600°C gave the best results. Thermal analysis of the MoO_3/NaCl and WO_3/NaCl systems illustrates details of the processes involved.

INTRODUCTION

This study arose from an investigation into the purification of MoO_3 for production of radiopharmaceutical technetium. Rhenium and tungsten are the impurities of major concern since their high neutron absorption cross sections produce excessive activity. Rhenium is a particularly undesirable contaminant as it exhibits similar chemistry to the final radionuclide required, its group VII partner, Tc. Tungsten is difficult to remove because of its chemical similarity to molybdenum. We felt that a volatilisation process using simple molybdenum compounds could result in a suitable purification procedure.

RESULTS AND DISCUSSION

Four likely processes were tested and their results are summarised in the table which also shows the results of analysis for rhenium and tungsten by spark source mass spectrometry.

The first two processes involve sublimation of MoO_3 from a tube furnace at 800°C to room temperature, in silica apparatus. Both processes result in significant reductions in rhenium content because volatility of rhenium oxides is higher than that of molybdenum and tungsten oxides. The high rhenium result observed in the MoO_3 fraction furthest from the furnace illustrates this convincingly.

Sublimation under vacuum does not lower the tungsten content but this cannot be explained by volatilisation. The crystal structures of MoO_3 and WO_3 are quite different. MoO_3 is layered[1] and volatilises as polynuclear species, whereas WO_3[1] exhibits an infinite lattice structure and hence is non-volatile. It is possible that WO_3 is physically carried over in the process. Sublimation in oxygen flow rates at 100-200 mL/min would be less likely to carry particulate matter and may explain the lower result for tungsten in process 2.

Current address : Division of Energy Chemistry, CSIRO, Lucas Heights Research Laboratories, Private Mail Bag 7, Sutherland, NSW, 2232, Australia.

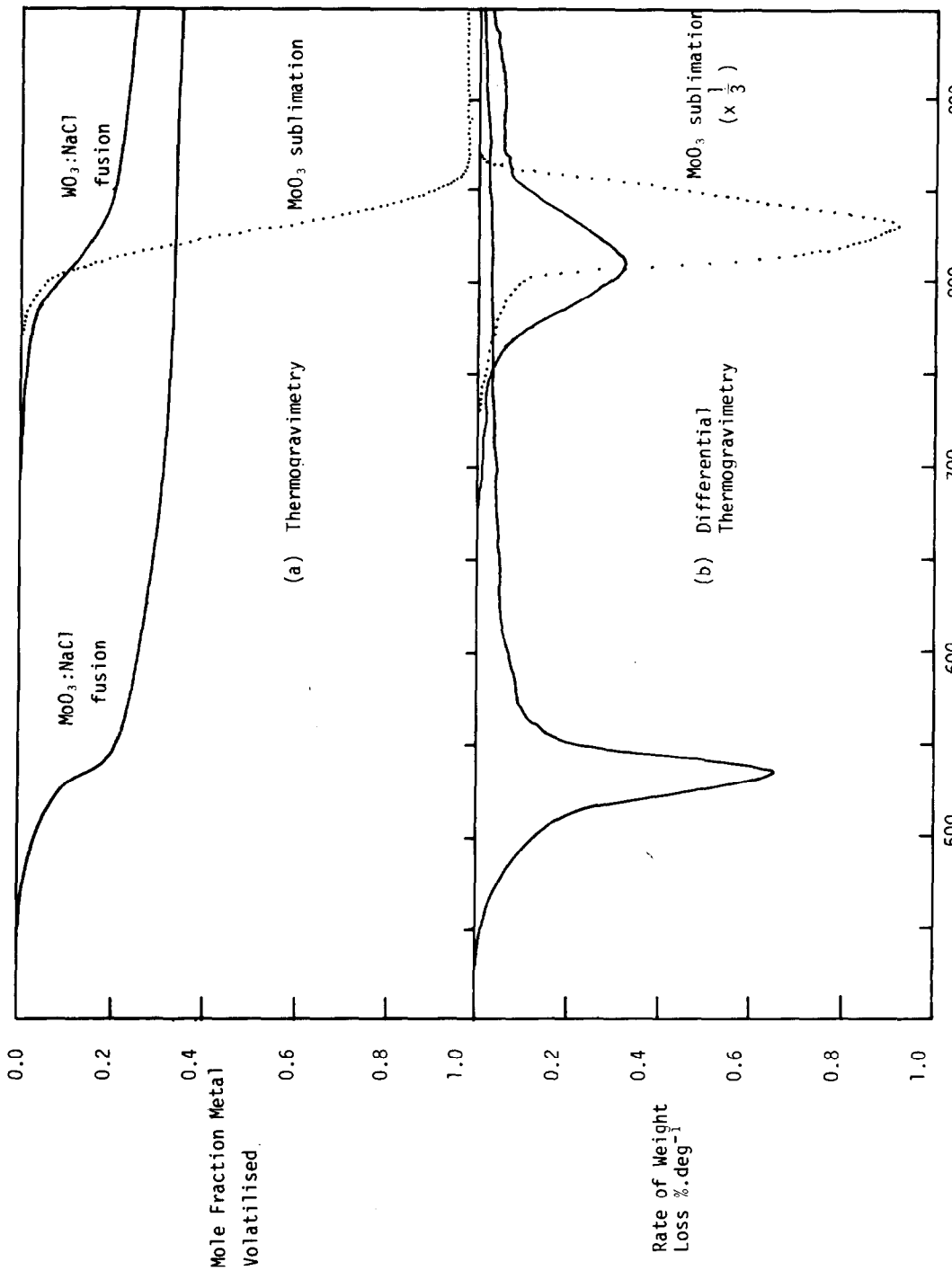

FIGURE 1 Thermograms and differential thermograms for the reaction of MoO_3 and WO_3 with NaCl and for the sublimation of MoO_3.

TABLE

PURIFICATION PROCESSES AND RESULTS FOR MOLYBDENUM TRIOXIDE

PURIFICATION PROCESS *SAMPLE ANALYSED*	ANALYSIS Re (ppm) †	 W (ppm) †
0. Starting Material		
Ampere Bulk MoO_3	*5.5*	*83*
1. Sublimation of MoO_3 at 800°C (in vacuum)		
Residue	*<0.2*	*170*
MoO_3 closest to furnace exit	*<0.4*	*130*
MoO_3 furthest from furnace exit	*42*	*110*
2. Sublimation of MoO_3 at 800°C in flowing O_2 ($\sim$150 cm^3 min^{-1})		
MoO_3	*<0.9*	*26*
3. MoO_3 refluxed in $SOCl_2$ to produce $MoOCl_4$		
*$MoOCl_4$ sublimed at 100°C**	*2.3*	*75*
4. Fusion of MoO_3 with NaCl at 600°C		
*MoO_2Cl_2 sublimate**	*<0.6*	*<0.6*

*Molydenum oxide chloride samples were hydrolysed, washed and dried then analysed as MoO_3

†Analysis by spark source mass spectrometry, estimated accuracy : ±25%

Unlike the processes 1 and 2 which involve high temperatures, process 3 uses low temperatures. MoO_3 is refluxed in thionyl chloride, producing $MoOCl_4$[2] which is subsequently sublimed at 100°C. However, no significant purification occurs because of formation of rhenium and tungsten oxide halides which have similar volatilities to $MoOCl_4$ at this temperature.

The fourth process utilised the fusion of MoO_3 with NaCl to form MoO_2Cl_2 which volatilises immediately. This product has greatly reduced concentrations of both rhenium and tungsten. A more thorough investigation of the process by thermochemical and X-ray diffraction techniques was carried out to determine the reactions involved. Thermogravimetry was carried out on a Cahn RH Electrobalance with hanging platinum sample cup in quartz tubing inside a vertical furnace. In an atmosphere of flowing nitrogen, samples were heated at 5 C° per minute. Amplified mass and temperature signals were processed and stored by an LSI-11 computer. Differential thermograms were calculated from TG data by computing the smoothed first derivative as described by Whittem, Stuart and Levy[3]. X-ray diffraction apparatus consisted of a 114 mm dia. Debye-Scherrer powder camera, attached to a Philips X-ray generator producing Ni-filtered copper radiation.

In the preparation of MoO_2Cl_2 by the fusion process[4], the reaction has been claimed to be

$$2\ MoO_3 + 2\ NaCl \longrightarrow Na_2MoO_4 + MoO_2Cl_2$$

However thermogravimetric studies on this system, using a range of MoO_3 to NaCl ratios from 1:2/3 to 1:3, gave the stoichiometry

$$3\ MoO_3 + 2\ NaCl \longrightarrow Na_2Mo_2O_7 + MoO_2Cl_2$$

A thermogram for this reaction is shown in Figure 1a. Powder X-ray diffraction studies did not show the presence of Na_2MoO_4. Sodium dimolybdate was confirmed as the sole non-volatile product.

Thermogravimetry on the WO_3/NaCl fusion system indicated the same stoichiometry as the MoO_3/NaCl system. A comparison of derivative thermograms (Figure 1b) shows that the reaction in the tungsten system occurs 300°C higher. We believe that it is this temperature difference of the solid state fusion reactions which results in the excellent separation observed for these two metals in impure MoO_3.

If increased yields of purified molybdenum are desired, the residue may be dissolved in hydrochloric acid solution, dried, and recycled through the fusion process,

$$Na_2Mo_2O_7 + 2\ HCl \longrightarrow 2\ NaCl + 2\ MoO_3 + H_2O$$

The MoO_3/NaCl fusion system at 600°C probably represents the simplest, most effective method of purifying MoO_3 for technetium production.

REFERENCES

1. Advanced Inorganic Chemistry. 2nd Edition, F.A. Cotton and G. Wilkinson, Interscience, Great Britain, 1966.
2. R. Colton, I.B. Tomkins and P.W. Wilson, Aust. J. Chem. 18, 447 (1965).
3. R.N. Whittem, W.I. Stuart and J.H. Levy, Thermochimica Acta, in press (1982).
4. A.N. Zelikman and N.N. Gorovits, Zh. Obshsh. Khim. 24, 1916 (1954).

Polyhedron Vol. 1, No. 5, pp. 483–486, 1982
Printed in Great Britain.

0277–5387/82/050483–04$03.00/0
Pergamon Press Ltd.

STRUCTURAL CHANGES IN $UO_2(hfa)_2\ NH_3$ NEAR THE MELTING POINT

D.A. Johnson, J.C. Taylor*, and A.B. Waugh

Energy Chemistry Division, CSIRO, Lucas Heights
Research Laboratories, Private Mail Bag 7,
Sutherland, NSW, 2232, Australia.

(Received 28 June 1982)

ABSTRACT

A reversible colour change from lemon-yellow to orange was observed for polycrystalline $UO_2(hfa)_2\ NH_3$ at 100°C (hfa = (1,1,1,5,5,5-hexafluoro-2, 4-pentanedione)). The changes in the X-ray powder pattern between -196° and 130°C were followed with a Guinier-Simon focussing camera. The colour change was not due to an $\alpha \longleftrightarrow \beta$ type structural transition as found earlier in α and β-$UO_2(hfa)_2$ tmp (tmp = trimethyl phosphate), but was considered to be due to changes in the hydrogen bonding of the ammonia molecules.

INTRODUCTION

The crystal structure of $UO_2(hfa)_2\ NH_3$ was recently determined[1]. At room temperature, this crystal is monoclinic, space group Cm, with a = 6.665(1), b = 24.428(4), c = 5.613(2) Å, β = 92.964(5)°, with two molecules per cell. The ammonia, coordinated to uranium, also serves to bind the molecules into sheets perpendicular to b by hydrogen bonding. During vapour pressure studies of $UO_2(hfa)_2\ NH_3$ under vacuum, it was noticed that, at around 100°C, a reversible colour change from lemon-yellow to orange occurred, with no loss of ammonia. It was thought that this might be caused by a phase transition similar to the $\alpha \longleftrightarrow \beta$ phase transition in $UO_2(hfa)_2tmp$[2,3] (tmp = trimethyl phosphate) which also has a yellow-orange colour change. We were thus led to follow the structure of $UO_2(hfa)_2\ NH_3$ from -196° to 130°C using a Guinier-Simon focussing camera, in order to ascertain the cause of the colour change.

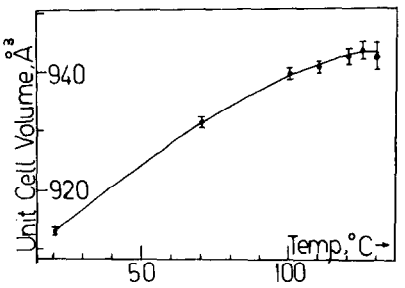

Fig 2. Variation of Cell Volume

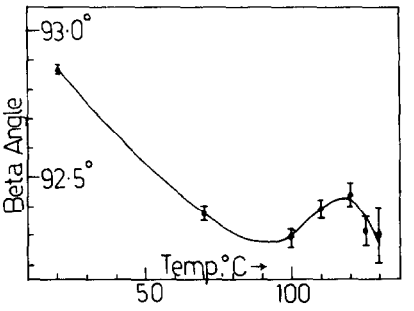

Fig 3. Variation of Beta Angle

The structural changes observed at 100°C were probably caused by weakening of the intermolecular hydrogen bond system involving the ammonia hydrogen atoms. These forces link the $UO_2(hfa)_2\ NH_3$ molecules into sheets perpendicular to $\underset{\sim}{b}$ at room temperature, as shown in Figure 4. The ammonia molecule is near the uranyl

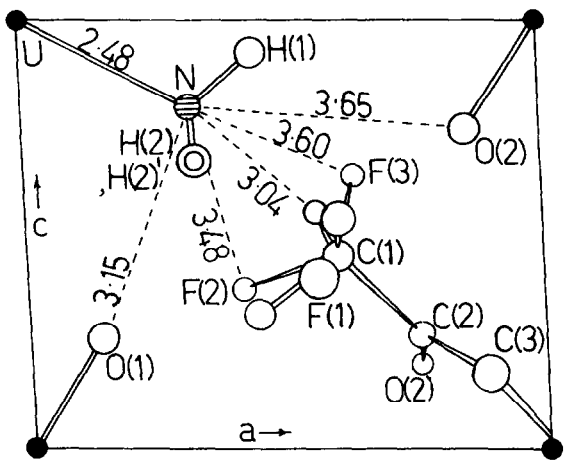

Fig.4 Possible Hydrogen Bonding Scheme in $UO_2(hfa)_2NH_3$.

oxygen atoms O(1) and O(2) and the partial fluorine atoms of the disordered $C(1)F_3$ group. Uranium, nitrogen, O(1) and O(2) lie in the plane of the paper (the mirror plane m) while there are two $C(1)F_3$ groups, one above and one below the mirror. In this configuration, the U-N-O and U-N-F angles are favourable for hydrogen bonding. Figure 4 shows that the hydrogen bond attractions are downward towards the $C(1)F_3$ group; the $C(1)F_3$ group in the next unit cell in the $\underset{\sim}{c}$-direction is too far away for any further attractions to occur. Thus, the bonding environment around the

EXPERIMENTAL

X-ray photographs of $UO_2(hfa)_2 NH_3$, in sealed glass capillaries, were taken at -196, 20, 70, 100, 110, 120, 125 and 130°C with the Guinier-Simon camera, using $Pb(NO_3)_2$ as the 2θ standard. Unit cell dimensions were determined at each temperature by least-squares analysis of the diffraction line positions (34, 59, 77, 51, 48, 58, 44 and 19 lines respectively). At 130° the pattern became weak, because the melting point was near. The results are given in Figures 1 to 3, except for -196°, when a = 6.485(4), b = 24.297(13), c = 5.470(3) Å, β = 93.74(3)° and the unit cell volume = 860(1) $Å.^3$

RESULTS AND DISCUSSION

The X-ray photographs could all be indexed on the C-centred monoclinic unit cell found at room temperature[1]. The relative intensities of the lines did not change greatly over the range, nor did the lines show splitting or fusion characteristic of a change in symmetry. Thus, the change in colour was not due to a phase transition, such as was found earlier in the tmp complex[2,3], but was a consequence of bonding changes within the Cm structure itself.

Figure 1 shows that irregularities in the expansion of the unit cell edges

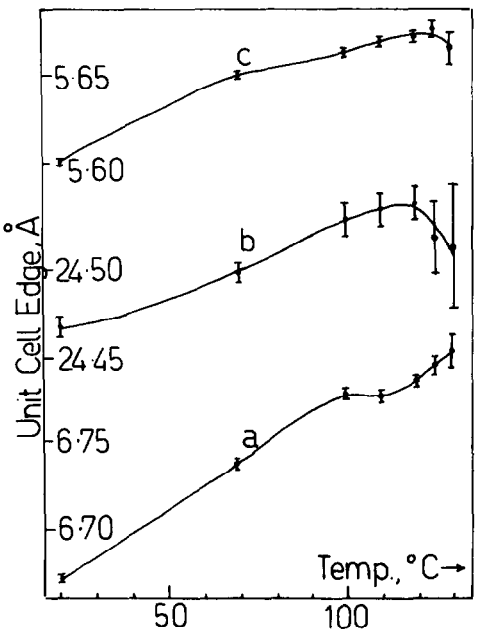

Fig.1 Unit Cell Dimensions of $UO_2(hfa)_2NH_3$ with Temperature.

commenced at 100°C. The unit cell volume increased steadily to 100°C and then levelled off (Figure 2). The β-angle also showed unusual behaviour (Figure 3).

ammonia molecule is asymmetric, which agrees with the above observations that the structural changes at 100°C are irregular.

Possible favoured positions of the ammonia hydrogen atoms H(1), H(2) and H(2)' are given in Figure 4. The ammonia molecule is most likely, in fact, to be disordered, like the CF_3 group. However, the main hydrogen bond forces are likely to be in the diagonal direction ($\underset{\sim}{a}$ - $\underset{\sim}{c}$). When the structure is heated above room temperature, the thermal motions increase and the mainly diagonal intermolecular attractions are weakened; this is consistent with the increase in $\underset{\sim}{a}$ and the β-angle. The expansion along $\underset{\sim}{a}$ may permit the sheets to stack together more closely (see Figure 1) causing the reduction in $\underset{\sim}{b}$.

These changes are more subtle than the expected α,β-type phase transition and a full high temperature structural analysis would be needed for further clarification of the atomic shifts.

REFERENCES

1. D.A. Johnson, J.C. Taylor and A.B. Waugh, J. Inorg. Nucl. Chem., 1979, 41, 827.

2. J.C. Taylor and A.B. Waugh, J. Chem. Soc. Dalton, 1977, 1630.

3. J.C. Taylor and A.B. Waugh, J. Chem. Soc. Dalton, 1977, 1636.

Polyhedron Vol. 1, No. 5, pp. 487–496, 1982
Printed in Great Britain.

0277-5387/82/050479-10$03.00/0
Pergamon Press Ltd.

BIS(N,N'-DISALICYLIDENE-3,4-PHENYLENEDIAMINE-1-ETHYLBENZOATO)ZIRCONIUM(IV), AN EIGHT-COORDINATE CHELATE WITH LINEAR POLYMERIZATION POSSIBILITIES

M. L. ILLINGSWORTH† and R. D. ARCHER*
Department of Chemistry, University of Massachusetts, Amherst, MA 01003

(Received 19 April 1982)

Abstract- Synthesis of the Schiff-base complex bis(N,N'-disalicylidene-3,4-phenylenediamine-1-ethylbenzoato)zirconium(IV), which has two, linearly disposed, uncoordinated ester groups, has been accomplished from the reaction of a zirconium alkoxide with the new Schiff ligand N,N'-disalicylidene-3,4-phenylenediamine-1-ethylbenzoate. The ligand itself was isolated in two forms, yellow and orange, which are believed to be tautomers based on infrared data. Elemental analyses, IR, NMR, and UV-Visible data are included for all new compounds, as well as mass spectral data for the complex. Broadening of ^{1}H NMR resonances in the complex spectrum, relative to TMS and ethanol of solvation resonances, may be indicative of a slow molecular motion. Preliminary attempts to polymerize the complex with aromatic amines failed, however, due to decomposition of the metal chelate unit at the high temperatures (>300°C) required.

INTRODUCTION

As part of our research program to prepare coordination polymers of high thermal stability, we are currently investigating ligand-centered polymerization reactions that will link eight-coordinate metal chelates. Ligand-centered polymerization has been extensively used in organometallic chemistry for the preparation of thermally stable polymers[1] and pendant polymers[2] (including heterogeneous and homogeneous catalysts); however, the application to eight-coordinate systems is virtually unknown. The use of reactions analogous to well-known organic polymerizations will hopefully lead to high degrees of polymerization, while problems associated with previous methods (e.g., the low solubility of delocalized diquadridentate ligands[3] and the hydrolytic reactivity of suitable zirconium(IV) reactants[4]) should be avoided.

The title compound, 1, derived from the new Schiff-base N,N'-disalicylidene-3,4-phenylenediamine-1-ethyl benzoate, H_2dspeb, contains two uncoordinated ester groups suitable for

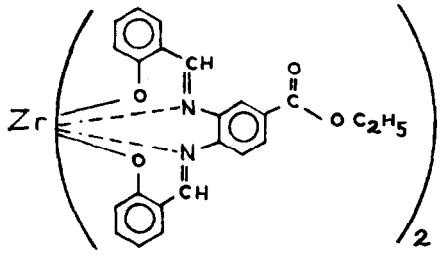

further reaction. The preparation and characterization of this chelate, as well as both of the yellow and orange forms of this new Schiff-base ligand, are reported herein. Preliminary polymerization reaction results with aromatic amines are also discussed.

EXPERIMENTAL

Preparation of the Free Schiff-base Ligand, H_2dspeb. In a 200 mL round bottom flask,

*Author to whom correspondence should be addressed at the University of Massachusetts.
†Current address: University of Delaware, Newark, Delaware 19711.

2.0 g (.011 mol, Eastman) 4-amino-3-nitrobenzoic acid was covered with 100 mL of absolute ethanol, and 3 mL of conc. H_2SO_4 was then added dropwise with concurrent magnetic stirring of the solution. Heating resulted in a clear burgundy-colored solution after several minutes, and reflux conditions were maintained overnight. After 24 hours the clear solution was thoroughly chilled with ice, neutralized with concentrated ammonium hydroxide with rapid stirring, immediately poured into an excess (approx. 400 mL) of ice-water slurry, and suction filtered. When dry, 2.3 g, a quantitative yield, of dark-yellow ethyl-4-amino-3-nitrobenzoate resulted, mp 135-136°C, in agreement with one literature source.[5] Hydrogenation was accomplished by dissolving the entire amount in a slurry of 150 mL of dry ethyl acetate (CaH_2) containing 1.0 g of 10% Pd/powdered charcoal (MCB) in a Parr bottle, and applying a one atmosphere pressure of hydrogen gas for approximately 5 hours.[6] [The end point was confirmed by TLC using a 10 hexane:4 ether:1 acetic acid eluent on silica gel. The yellow spot due to starting material was absent, and only one low R_f white spot remained which darkened upon standing in air.] Droplets of water, if apparent, were physically separated at this point, and the ethyl acetate was further dried with anhydrous calcium chloride. After standing covered for 10 to 15 minutes with occasional swirling, the mixture was filtered through a dry ethyl acetate-Celite pad or a fine-glass frit with suction, and the pad was further rinsed with dry ethyl acetate. The solvent was removed by rotary evaporation to give a quantitative amount of slightly impure ethyl-3,4-diaminobenzoate; mp, 107-109°C (lit.[7], 112-114°C). Without further purification approximately 2.0 g (.011 mol) of the diamine was dissolved in 150 mL of absolute ethanol, was treated with a slightly greater than stoichiometric amount of salicylaldehyde, 3.0 g (.025 mol), which gives a clear orange solution, and was heated at reflux for 12 hours overnight. The resulting solution was concentrated, then chilled to near 0°C, at which point both yellow and orange modifications of the free Schiff-base ligand precipitated. After a petroleum ether (61-70°C) washing, suction, filtering and drying, the combined weight of these products was indicative of quantitative yield. Subsequent recrystallization of the mixture from petroleum ether (61-70°C) or methylene chloride-petroleum ether (61-70°C) gives the orange powder, while absolute ethanol recrystallization of the mixture gives mostly soft yellow needles. Heating some of the small yellow needles in a melting point capillary causes a gradual color change to orange, followed by sharp melting at 164-165°C if conversion to the orange form is complete.

Anal. Calcd for $C_{23}H_{20}N_2O_4$: C, 71.1; H, 5.15; N, 7.22. Found (yellow needles): C, 71.0; H, 5.41; N, 7.31. Found (orange powder): C, 71.1; H, 5.34; N, 7.40.[8]

Preparation of $Zr(dspeb)_2$·Ethanol Solvate. Approximately 250 mL of absolute ethanol containing 80 mL of zirconium tetra-n-butoxide butanol solvate (Alfa) was heated under reflux conditions under a drying tube (anhydrous calcium sulfate) for one hour, and then distilled into oven-baked glassware. For the first 100 mL collected, 2.0 g (.0052 mol) of Schiff-base ligand was added and dissolved with gentle warming under a dry nitrogen stream. A slightly less than stoichiometric amount of $Zr(OBu^n)_4$·Bu^nOH (1.0 mL, 1.06 g, 0.0023 mol) was pipetted into the magnetically stirred ligand solution, and the solution was heated to reflux under a drying tube as described above. After one hour a yellow solid began to appear; after 16 hours at reflux the hot reaction mixture was filtered immediately through a hot glass frit, washed with petroleum ether (61-70°C), dried with suction; and further dried *in vacuo*; yield, 1.64 g of bright yellow 1, a 32% yield.

Anal. Calcd for $C_{48}H_{42}N_4O_9Zr$: C, 63.4; H, 4.62; N, 6.16. Found: C, 63.38; H, 4.73; N, 6.07.

Despite recrystallization from dry benzene-petroleum ether (61-70°C) 1 appears to remain solvated. Also, additional products with infrared spectra very similar to 1 were obtained upon the addition of petroleum ether (61-70°C) to the reaction filtrate; but these products darkened upon heating in melting point capillaries in contrast to 1, which shows no sign of discoloration to 270°C.

Spectral Measurements. Infrared, electronic, ^{1}H NMR, and mass spectra were obtained using instrumentation and accessories described previously.[4]

RESULTS AND DISCUSSION

Zr(dspeb)$_2$. To the best of our knowledge, Zr(dspeb)$_2$ is the first zirconium eight-coordinate chelate containing two uncoordinated functional groups to be successfully prepared. The choice of a zirconium alkoxide as the starting material rather than zirconyl chloride[4,9] or tetrakis(salicylaldehydato)zirconium(IV)[4] was based upon the almost quantitative yields of bis(quadridentate Schiff-base)zirconium(IV) products obtained from a similar reaction with the analogous ethylenediamine Schiff-base ligand.[10] Due to the more rigid aromatic ligand structure being used here along with the necessity of breaking apart the trimeric nature of the lower zirconium alkoxides,[11] our yields were somewhat lower. As a diester derivative of Zr(dsp)$_2$,[4] it retains the good solubility in benzene and methylene chloride which is displayed by the unsubstituted parent compound. It can be recrystallized from undried solvents without hydrolytic decomposition, and it is isolated in a pure enough form to be used directly in subsequent reactions.

Spectral characterization data for the new Schiff-base ligand, both forms, and the corresponding bis-zirconium chelate are given in the Table. For comparison, data for the known Schiff-base free acid, H_2dspba, are also included.[12]

Zr(dspeb)$_2$·EtOH. The spectral changes upon complexation are almost perfectly analogous with those observed for the H_2dsp/Zr(dsp)$_2$ system,[4] with subtle differences. In the infrared spectrum the phenolic C-O stretch shows the largest change in frequency, gaining about 25 cm^{-1}, while the imine stretching frequency remains almost unchanged as previously noted.[4] However, the broad hydroxy stretching resonance observed in the spectra of the free Schiff-base does not disappear upon complexation due to the presence of ethanol in the Zr(dspeb)$_2$ lattice.

The presence of solvated ethanol is further corroborated by comparing the ^{1}H NMR spectra of ethanol vs. Zr(dspeb)$_2$·C_2H_5OH in deuterated methylene chloride. Identical quartets appear at 6.15-6.60τ and identical triplets appear at 8.65-9.00τ in both spectra. These multiplets are easily distinguished from the ester chemical shifts in three ways: first of all, the ester carboxyl group deshields the ethyl protons to a different extent than does the hydroxyl group of ethanol, so a slightly different chemical shift is observed; secondly, the integrated relative intensities of the ethyl ester signals compare favorably with other ligand signals; and thirdly, all signals due to ligand moieties are considerably broadened in contrast to the very sharp ethanol and internal standard (TMS) signals in the same Zr(dspeb)$_2$ spectrum. However, no hydroxyl peak is observed in this spectrum, presumably due to fast proton exchange.

One explanation for the broadened NMR signals noted above is that a physical motion occurring within the chelate is slow enough at the probe temperature to allow the NMR instrument to detect differences in the chemical environments around protons affected by

TABLE. SPECTRAL DATA FOR $Zr(dspeb)_2$ AND APPROPRIATE PRECURSORS.

$Zr(dspeb)_2 \cdot C_2H_5OH$	Yellow H_2dspeb	Orange H_2dspeb	H_2dspba	Assignment
3455 m, br, smooth (C_2H_5OH)	3405 m, br 3300 m	3410 w, br	3420 w, br	(O-H)ν, H-bonding
3080	3054 w, br	3053 w, br	3050 w, cmplx.	(C-H)ν
2990	2960 mw	2990 mw	2800	
	2933 w	2978		
	2906	2941 w		
	2868 w	2929		
		2900 w		
		2860 vw, br		
1714 m	1708 m	1716 s	1680 s	acid/ester (C=O)ν
	1686 s	1684 w		
	1624 sh			quinoid (C=O)ν
1611 s	1614 s	1610 s	1615 s	(C=N)ν
1588 m	1596 m	1589 m	1590 w	(C=C)ν
1468 m	1484 m,d	1487 m,d	cmplx.	1,2-disubstituted aromatic
1337 m	1368 m	1364 m		aliphatic C-Hδ
1314 m				M(O-ϕ)ν
1287 m	1286 s br	1292 sh	1298 m	(ester C-O)ν and (O-ϕ)ν
1244 m	1250 m	1277 s	1275 m	
		1259 s		
1221 m	cmplx. m	cmplx. m	1230 m	(C-C)ν
1022 m	1017 m	1019 m	1145 m	
748 s	754 s	754 s,d	750 s	(C-H)δ

Ultraviolet/Visible Spectra, cm^{-1},[b,c]

$Zr(dspeb)_2 \cdot C_2H_5OH$		Yellow H_2dspeb		Orange H_2dspeb	
Abs C_2H_5OH	CH_2Cl_2	Abs C_2H_5OH	CH_2Cl_2	Abs C_2H_5OH	CH_2Cl_2
40,300	39,500(4.85)	40,300 sh			
38,900 sh	~38,800	38,800 sh			
		35,300(4.26)	36,200	36,100	36,000(4.43)
33,900	33,900(4.77)	33,600 sh	34,500	33,300 w,sh	33,300 w,sh
31,200 sh		31,100(4.5)			
29,700		29,900 sh	29,500	29,800	29,700(4.32)
26,700 w,sh		~26,700 sh	~27,000	26,700 sh	
25,700	25,600(4.49)				

^1H Nuclear Magnetic Resonance Spectra, τ,[b,f]

$Zr(dspeb)_2 \cdot C_2H_5OH$[h]	Yellow H_2dspeb(?)[h]	Orange H_2dspeb[h]	H_2dapba[g]	Assignment
	-2.40	-2.80 br		O-H
1:1		1.2-1.34(2) d	0.95-1.05 ud	H-C:N
1.40-1.65 ud		1.85-2.05(2) ud	1.85-2.05 br	ortho-
2.0 si or ud				aromatic

the motion. Presuming chelation analogous to that observed by X-ray diffraction for $Zr(dsp)_2$,[4] there are two such fluxional motions possible in this chelate, a stereochemical rearrangement of donor atoms around the eight-coordinate metal ion,[4] and an inverting motion of the puckered ligand backbones (*vide infra*). Since all signals in the ^1H NMR of $Zr(dsp)_2$ are sharp, it is the addition of the ester groups that causes one, or both, of these motions to be considerably slowed. Intuitively, one would predict that the relatively large mass of an ester group on the perimeter of a puckered dsp(2-) ligand is most likely to decrease the rate of ligand backbone inversion as shown in Figure 1.

Despite this broadening in the NMR spectrum, changes in chemical shifts resulting from chelation of the free ligand are still readily evident. Several aromatic proton signals are shifted upfield by as much as 1.2 ppm, which is comparable to the changes observed for the analogous signals in the unsubstituted $Zr(dsp)_2$ system. The imine protons and aromatic protons *ortho* to the ester group, which appear as two doublets downfield from the usual aromatic region for the free ligand, are also dramatically rearranged in the complex, but here the changes are unlike the simple upfield shift observed upon going from $H_2(dsp)$ to $Zr(dsp)_2$. A low temperature NMR study of $Zr(dspeb)_2$ would help elucidate these structural changes.

Band shifts observed in the electronic spectra due to chelation are also basically similar to the unsubstituted system. Although more shoulders are apparent in the spectra of H_2dspeb compared to H_2dsp, only two λ_{max}'s are observed for each of these ligands over the 43.5 to 14.3 kK (230 to 700 nm) range. Comparable, their chelates $Zr(dspeb)_2 \cdot EtOH$ and $Zr(dsp)_2$ both display three λ_{max}'s of slightly increased intensity over this same range; several shoulders due to vibronic coupling[15] adorn the "middle" λ_{max} of both chelates at about 33.9 and 36.9 kK (295 and 271 nm) respectively, and the lowest energy chelate maxima occur further toward the visible region than do the low energy ligand λ_{max}. While it is tempting to assign these low energy transitions as CT(L→M), metal ion perturbation of the low energy shoulders apparent in the free ligand spectra must also be considered as a possible explanation.[16]

Two subtle differences between the electronic spectra of $Zr(dspeb)_2$ and $Zr(dsp)_2$ should now be pointed out as they may assist in the further interpretation of these spectra. In the cascading sequence of vibronically induced shoulders mentioned above, one less shoulder is observed in the diester complex *vs.* the unsubstituted complex. Also, the low energy λ_{max} of $Zr(dsp)_2$ at 27.0 kK (370 nm) has a pronounced shoulder at 23.8 kK (420 nm) in contrast to the shoulderless λ_{max} of $Zr(dspeb)_2$, which falls equidistant between the two, at 25.6 kK (390 nm).

If the approximately 35.7 kK (280 nm) or 25.6 kK (390 nm) electronic bands are to be considered as possible CT(L→M), and if one uses an $\chi_{opt}(M)$ of 1.6 for Zr(IV), then the estimated value of $\chi_{opt}(L)$ would be either 2.8 or 2.4,, respectively, according to Jorgensen's empirical formulation.[18] Considering that the χ_{opt} of the delocalized acetylacetonate ligand, 2.7, is substantially lower than the typical oxygen donor ligands, 3.5, neither χ_{opt} (L) possibility can superficially be eliminated; however, in view of the dsp(2-) bond distances and angles in $Zr(dsp)_2$, extensive delocalization does not seem likely except within the benzene rings. Using typical χ_{opt} values for N and O donors, the lowest energy CT(L→M) bond is estimated to be near or higher in energy than the methylene chloride cut-off. The basic question of how easily the substituted and unsubstituted dsp(2-) anions are oxidized, which affects χ_{opt} (L), merits further consideration.

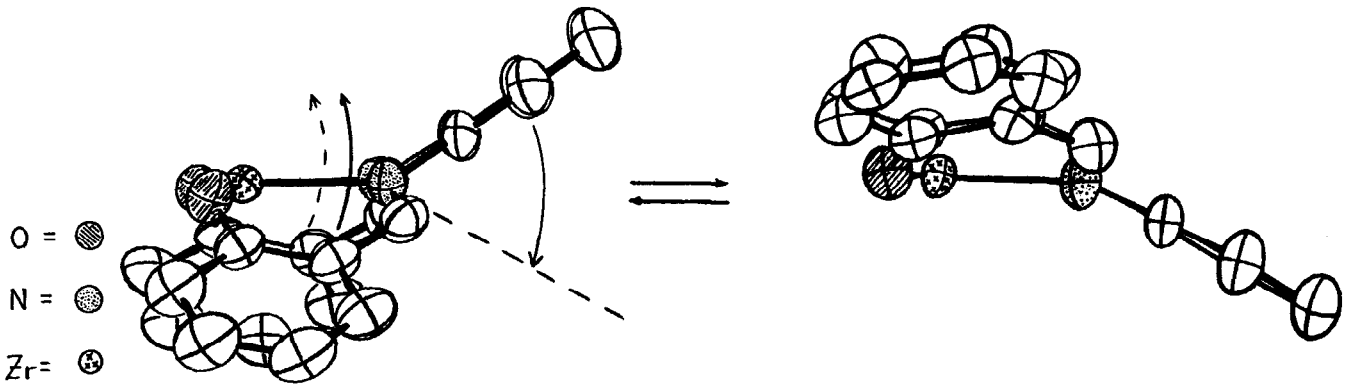

Figure 1. The possible inverting motion of puckered ligand backbones in $Zr(dsp)_2$ and dsp(2-). Only one ligand of the known structure[4] is shown for clarity.

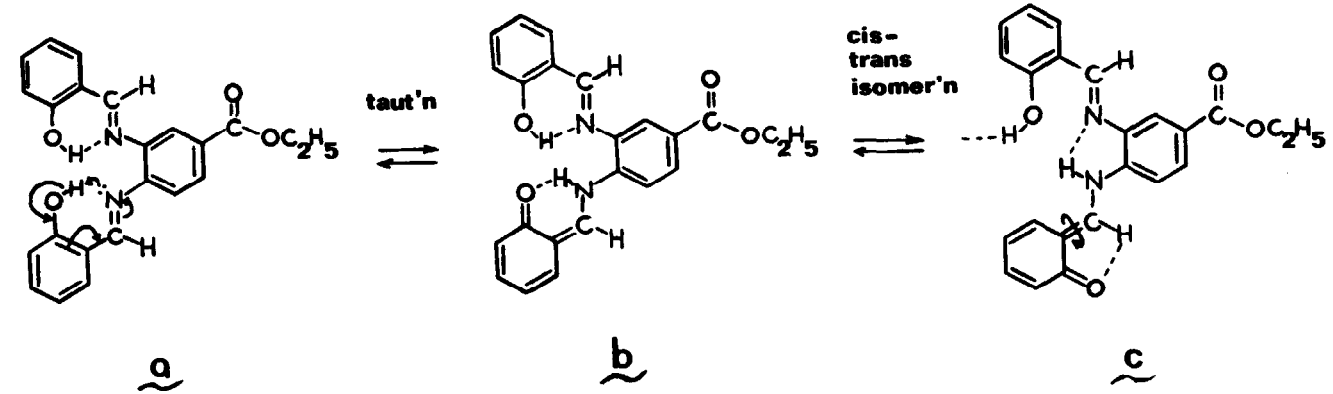

Figure 2. The "enol-imine" structure a is assigned to the orange form of H_2dspeb, whereas quinoid carbonyl and N-H infrared resonances, in addition to hydroxyl and imine infrared resonances, indicate the presence of both ket-amine and enol-imine tautomers for the yellow form, structures b and c. Neither a nor b is expected to be planar due to proton-proton repulsions noted previously for H_2dsp[22], while c can be planar.

The mass spectrum of $Zr(dspeb)_2 \cdot EtOH$ provides some final evidence for formulation 1 in that the parent peak at 862 m/e (only 4 m/e down from the 866 m/e peak of the tris-perfluoroheptyl-s-triazine standard) corresponds to the $^{90}Zr(dspeb)_2$ molecular ion. As with $Zr(dsp)_2$[4] the parent peak is also the base peak in the spectrum; the P-17 (loss of OH) is prevalent; and all zirconium-containing species display the distinctive pattern of peaks arising from its variety of isotopes. The P-280 peak can be interpreted as loss of an $OC_6H_4CH{:}MC_6H_3{-}(N)COOC_2H_5$ ligand fragment while the major ligand peak (no zirconium pattern) at 149 m/e corresponds to the $H_3COC_6H_3CH{:}N^+$ fragment.

The two Forms of H_2dspeb. The isolation of two forms of this Schiff-base ligand is not surprising since dimorphism,[19] thermochromism[20] and photochromism[20,21] have often been found for Schiff-base species. In this particular case, the recrystallization solvent appears to play a pivotal role. Whereas H_2dsp can be recrystallized from absolute ethanol or benzene-petroleum ether (61-70°C) without dimorphism, recrystallization of H_2dspeb from ethanol or salicylaldehyde leads primarily to the yellow modification, while recrystallization from petroleum ether (61-70°C) or methylene chloride-petroleum ether (61-70°C) leads to the orange powder.

Small but significant differences between these two forms are apparent in their room temperature electronic spectra in solution, thus ruling out solid state packing effects as the sole explanation. The absolute ethanol spectrum of the yellow form, especially, shows an extra band at 31.1 kK (322 nm) among the low energy transitions, and two additional high energy shoulders at 40.3 and 3.88 kK (248 and 258 nm) that do not correspond to any bands apparent in the other ligand spectra. In contrast, the spectrum of yellow H_2dspeb in methylene chloride actually bears a stronger resemblance to the electronic spectra of orange H_2dspeb, which shows no distinct solvent shifts in changing from absolute ethanol to methylene chloride.

Preliminary assignments of the corresponding structures are possible based on infrared results. In the KBr spectrum of yellow H_2dspeb, the broad peak at 3300 cm^{-1} and the shoulder at approximately 1624 cm^{-1} are tentatively assigned as an N-H stretch and a quinoid carbonyl stretch,[22] respectively, which suggests that a "ket-amine" structure is present. The fact that both ligand forms display hydroxyl stretches near 3400 cm^{-1} and C=N imine stretches near 1610 cm^{-1}, leads us to conclude that enol-imine structures must therefore be displayed by the opposite "arm" of the yellow form, and both arms of the orange form. See Figure 2.

Two other resonances common to both spectra, near 1710 and 1685 cm^{-1}, are assigned as free and hydrogen-bonded ester carbonyl stretching modes. This latter assignment is based upon analogy to the free acid, H_2dspba, in which hydrogen-bonding lowers the carboxyl carbonyl stretching frequency to 1680 cm^{-1}.[24] The yellow form, which is recrystallized from hydrogen-bonding solvents such as ethanol, shows a predominance of this hydrogen-bonded ester carboxyl resonance relative to the free ester carbonyl resonance in the solid state. This observation is consistent with the "external" hydrogen bonding of structure 2, although the enol-imine has been found to predominate for other Schiff-bases derived from salicylaldehyde.[26]

Upon heating the yellow form in a melting point capillary, however, an orange compound which retains an N-H stretch is obtained. Such thermochromic changes for similar Schiff-base species have also been attributed to tautomerism,[20a] although cis-trans isomerism and solid state effects have not been ruled out.

Both H_2dspeb forms give almost identical H^1 NMR in deuterated methylene chloride at 38°C probe temperature, the difference being a few anomolous signals at -2.40, 6.15, and 8.8-9.0τ in the spectrum of the yellow form. The remaining enol-imine spectrum, which predominates, can be interpreted as follows: The hydroxyl proton signals of H_2dsp remain almost unchanged in the ester derivative; the imine proton signals, while also in the same proximity as those for H_2dsp, are separated or otherwise split perhaps due to slight chemical differences or coupling via delocalization; signals derived from the aromatic protons ortho to the electron withdrawing group, in a manner analogous to the free acid H_2dspba, are shifted even further downfield from the usual aromatic region and remain unequal due to the Schiff-base substituents; and of course, signals assigned as ester protons are absent in the spectra of H_2dsp and H_2dspba.

Several preliminary reactions designed to augment the conjugated ligand system via condensation of aromatic amines with the free chelate ester groups were attempted. However, due to the high reaction temperatures required, approximately 280°C for aromatic amides and 360°C for benzimidazoles,[27] side reactions of the metal chelate unit predominate. Unexpected color changes, and the absence from the infrared of the distinctive metal coordinated C-O stretching resonance anticipated for the desired reaction products substantiate this conclusion. In spite of these observations, use of more reactive organic reagents, use of more reactive chelate derivatives and/or use of an appropriate catalyst[28] should permit these ligand-centered reactions to occur under milder conditions, and thus may still eventually lead to interesting polymerizations of these eight-coordinate species.

Acknowledgement. The authors wish to thank the University of Massachusetts Materials Research Laboratory for funding this research, the University of Massachusetts Microanalysis Laboratory for elemental analyses, and Mr. Eugene Guzik for the mass spectrum of $Zr(dspeb)_2 \cdot$-EtOH.

REFERENCES AND NOTES

1. C. E. Carraher, Jr., J. E. Sheats and C. U. Pittman, Jr., Eds., Organometallic Polymers, Academic Press, New York (1978), p. 53, p. 87, p. 107.
2. Ibid., p. 1, p. 13, p. 25, p. 39, p. 67, p. 181.
3. a. R. D. Archer, W. H. Batschelet and M. L. Illingsworth, Organic Coatings and Plastics Chem., (1979), 41, 191.
   b. M. L. Illingsworth and R. D. Archer, to be submitted for publication.
   c. P. H. Merrell and R. A. Osgood, Inorg. Chem. Acta, (1975), 14, L33.
4. R. D. Archer, R. O. Day and M. L. Illingsworth, Inorg. Chem., (1979), 18, 2908.
5. P. Thieme, J. prakt. Chem., (1891), [2], 43, 451.
6. P. R. Thomas and G. J. Tyler, J. Chem. Soc., (1957), 2197.
7. J. A. Silk, J. Chem. Soc., (1956), 2058.
8. University of Massachusetts Microanalysis Laboratory provided the analyses.
9. N. S. Biradar and A. L. Locker, J. Karnatak Univ. Science, (1972), 17, 1.
10. S. R. Grupta and J. P. Tandon, Monatsh. Chem., (1973), 104, 128.
11. D. C. Bradley and A. M. Thomas, J. Chem. Soc., (1969), 3857.
12. P. Pfeiffer, T. Hesse, H. Pfitzner, W. Scholl and H. Thielert, J. prakt. Chem., (1937), 149, 243.
    Note: Coordination through the carboxylate group was observed for H_2dspba, analogous to the known $Zr(RCOO)_4$[13] and the appearance of this compound is identical to the orange form of its ethyl ester H_2dspeb. Calcd for $C_{21}H_{16}N_2O_4$: C, 70.0; H, 4.44; N, 7.78. Found: C, 70.27; H. 4.34; N, 7.61.
13. J. Ludwig and D. Schwartz, Inorg. Chem., (1970), 9, 607.
14. R. C. Fay and J. K. Howie, J. Am. Chem. Soc., (1979), 101, 1115; and references therein; cf., C. J. Donahue and R. D. Archer, ibid., (1979), 99, 782 and S. L. Hawthorne, A. H. Bruder and R. C. Fay, Inorg. Chem., (1978), 17, 2114.
15. The regular spacing of the shoulders at approximately 1.5 kK intervals is possibly consistent with C=C vibronic coupling for $Zr(dsp)_2$ and $Zr(dspeb)_2$.
16. K. K. Chatterjee and B. E. Douglas, Spectrochim Acta, (1965), 21, 1625.
    Note: The appearance of prominent low energy shoulders is also seen in hydrogen bonding solvents.[17]
17. a. J. J. Charette, Spectrochim Acta, (1967), 21, 1625.
    b. A. V. Kiss, G. Bacskai and E. Varga, Acta Phys. Chem. Szeged., [N.S.], (1947), 41, 7256g.
18. C. K. Jorgensen, Progr. Inorg. Chem., (1970), 12, 101.
19. cf. A. Senier, F. Shepeard and R. Clarke, J. Chem. Soc., (1912), 101, 1955.
20. a. C. K. Jorgensen, Progr. Inorg. Chem., (1970), 12, 101.
    b. G. Smets, Pure and Appl. Chem., (1972), 30(1), 1.
21. Hydrogen bonding may contribute to the lowering of this quinoid carbonyl frequency; cf., L. J. Bellamy, The Infra-red Spectra of Complex Molecules, Wiley and Sons, New York, 1960, p. 143 and p. 151.
22. N. B. Pahor, M. Calligaris, P. Delise, G. Dodic, L. Randaccio, J. Chem. Soc., Dalton, (1976), 2478.
23. Note: The low carbonyl stretching frequency of the carboxylate group in the Hdspba, 1680 cm^{-1}, is probably due to resonance and the existence of hydrogen bonding dimers in the solid state.[24]

24. R. M. Silverstein and G. C. Bassler, Spectrometric Identification of Organic Compounds, Wiley, New York, (1967), p. 89-90.

25. a. G. C. Percy and D. A. Thornton, J. Inorg. Nucl. Chem., (1972), 34, 3557.
b. G. O. Dudek and E. P. Dudek, J. Am. Chem. Soc., (1964), 86, 4283.
c. P. Teyssie and J. J. Charette, Spectrochim Acta, (1963), 19, 1407.
d. G. O. Dudek and R. H. Holm, J. Am. Chem. Soc., (1962), 84, 2691.

26. cf., H. Vogel and C. S. Marvel, J. Polymer Sci., (1961), 50, 511.

27. a. cf., Ref. 1, p. 95.
b. M. Ueda, A. Sato and Y. Imai, J. Polym. Sci., Polym. Chem. Ed., (1979), 17, 783.

^{1}H Nuclear Magnetic Resonance Spectra, τ, [b,f]

$Zr(dspeb)_2 \cdot C_5H_5OH$[h]	Yellow H_2dspeb(?)[h]	Orange H_2dspeb[h]	H_2dapba[g]	Assignment
2.35-3.55(7)		5.40-5.80(2) q	2.10-3.55 m	
3.8-4.1(1) d				aromatic
4.2-4.5(1) d				
5.40-5.90(2) q		5.40-5.80(2) q		$-CH_2$ ester
6.15-6.60 q	6.15			$-CH_2$ C_2H_5OH
8.30-9.00 tt	8.8-9.0	8.45-8.73(3) t		$-CH_3$ ester and C_2H_5OH

Mass Spectrum of $Zr(dspeb)_2$, m/e and Assignment[i]

862 P	$^{90}Zr(dspeb)_2^+$	582 (P-280)	Loss of $OC_6H_4CH{:}NC_6H_3(N)COOC_2H_5$
845 (P-17)	Parent minus OH	149	$H_3COC_6H_3(O)CH{:}N^+$ fragment

[a]AS KBr pellets. [b]Abbreviations: w = weak, br = broad, s = strong, sh = shoulder, m = medium, si = singlet, ud = unsymmetrical doublet, d = doublet, cmplx = complex, d = doublet, mu = multiplet, q = quarter, t = triplet, tt = 2 overlapping triplets. [c]Log molar extinction coefficient ($M^{-1}cm^{-1}$) is in parentheses. [d]A λ_{max} occurs below the solvent cut-off. [e]Qualitative. [f]Relative intensities in parentheses. [g]d_6DMSO. [h]CD_2Cl_2. [i]Only the ^{90}Zr component is listed for the three Zr containing fragments.

Polyhedron Vol. 1, No. 5, pp. 497-499, 1982
Printed in Great Britain.

0277-5387/82/050497-03$03.00/0
Pergamon Press Ltd.

COMMUNICATIONS

Carcinogenic Chromium(VI) forms Chromium(V) with Ribonucleotides but not with Deoxyribonucleotides.

D.M.L. Goodgame,*[†] P.B. Hayman,[†] and D.E. Hathway,[‡]

[†]Chemistry Department, Imperial College, London, SW7 2AY,

[‡]Imperial Chemical Industries, P.L.C., Central Toxicology Laboratory, Alderley Park, Cheshire, SK10 4TJ.

Compounds of chromium(VI) present an industrial hazard because of their mammalian carcinogenicity and toxicity.[1,2,3] There is, therefore, appreciable interest in determining the biological transport and the mode of action of chromium species derived from the initial chromium(VI) compounds taken into the body.[4,5]

Chromium(VI) (as chromate or dichromate) is readily taken up by cells but can be easily reduced to chromium(III) by biological reductants (e.g., NADPH, ascorbic acid, etc.).[6,7] The fact (i) that chromium(III) is much more potent than chromium(VI) in causing infidelity of DNA synthesis in vitro[8] and (ii) that Cr^{III} may represent the state of oxidation involved in the chromate-induced DNA cross-linking, which was observed[7,9] in rat liver and kidneys, suggests that Cr^{III} may be the ultimate form of the metal that is bound in cells. However, chromium(III) penetrates cell membranes less effectively than does chromium(VI).[10]

During our studies on the interaction of a range of chromium compounds with nucleic acids and their components we have observed the formation of long-lived chromium(V) species derived from chromate(VI). In view of the recent report[11] that incubation of chromate(VI) with rat liver microsomes and NADPH produces an e.p.r. signal characteristic of chromium(V) we are prompted to summarise our own complementary observations in this area.

In a typical set of experiments, sodium chromate and the sodium salt of 5'-AMP were mixed in equimolar proportions in water in the pH range 6-7 and stored at room temperature (22°C) for ca. two months. At various times, portions of the solution were frozen and studied by e.p.r. spectroscopy (X-band, ∿ 9.2 GHz, and Q-band, ∿ 35.8 GHz, at ∿ 80 K). Within a few minutes of mixing the components a sharp (∿ 2.5 mT breadth) anisotropic signal (g = 1.982 and 1.976) characteristic[12,13] of chromium(V) was observed (Figure 1). The signal was better resolved at Q-band (Figure 1A) than at X-band frequency (Figure 1B) and the form of the spectrum is consistent with an axial ligand geometry about the metal ion. The signal increased in intensity over ∿ 1 hour but then remained essentially unchanged for several weeks.

Parallel studies using the sodium salts of 5'-GMP, 5'-IMP, 5'-CMP, 5'-UMP, 5'-ATP, D-ribose 5-phosphate, and also with adenosine, guanosine, cytidine, inosine, uridine, and D-ribose also gave chromium(V) signals very closely resembling those with 5'-AMP under the same conditions.(There were small variations in the observed g-values but the differences were barely outside experimental error).

In contrast to the above, corresponding experiments in which sodium chromate was reacted with the sodium salts of 2'-deoxyadenosine 5'-monophosphate (d-AMP), d-CMP, d-GMP, d-ATP, TMP, 2-deoxyribose 5-phosphate, or with thymidine, gave no evidence for chromium(V) even after periods of up to two months.

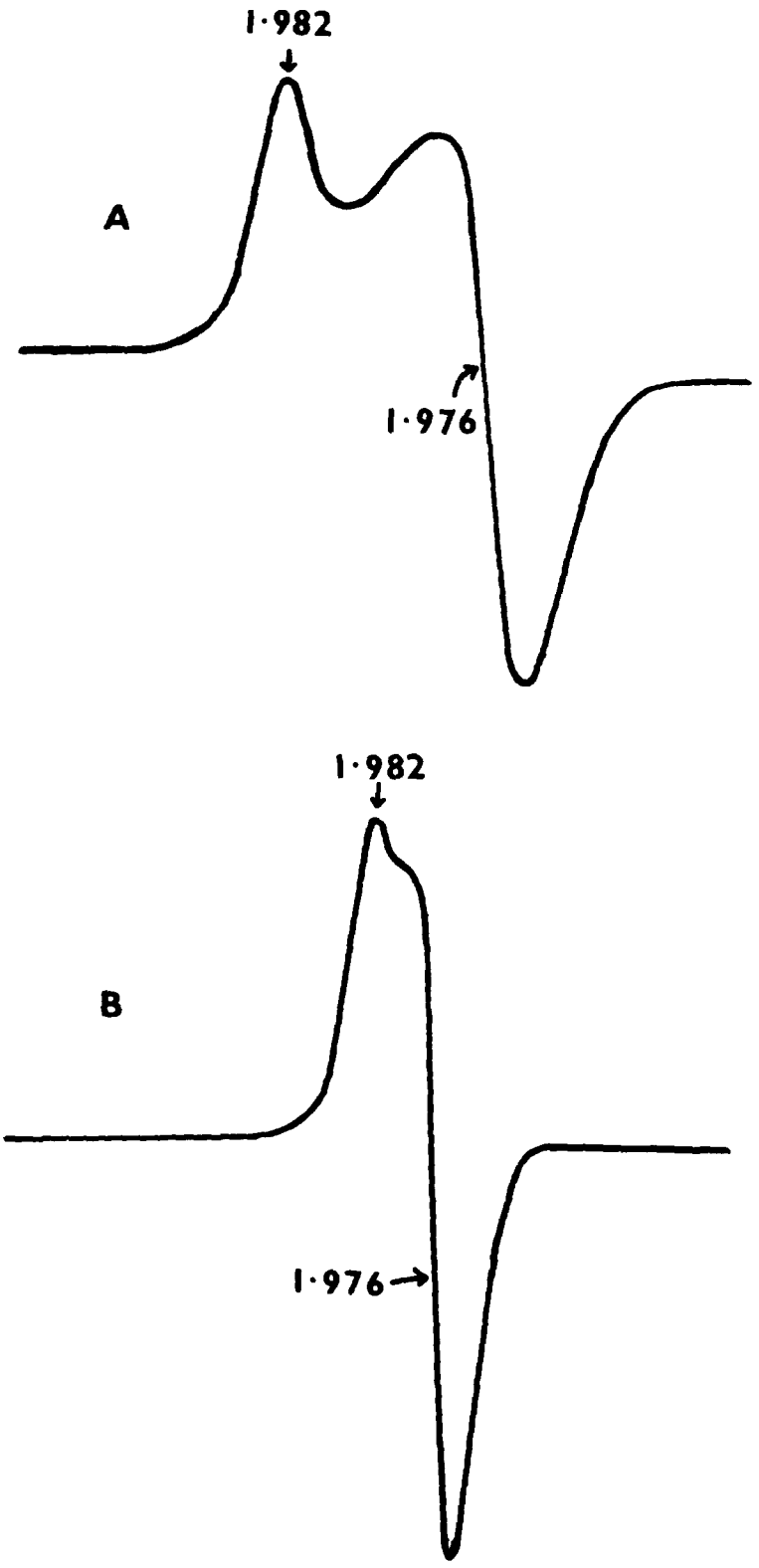

1. E.P.R. spectra of the Cr^{V} species obtained from aqueous solutions of sodium te and the sodium salt of 5'-AMP at ca. 80 K: A) at Q-band frequency; B) at X-band ncy.

It appears therefore that chromate(VI) differentiates between ribonucleotides and deoxyribonucleotides, and related molecules, in that the cis-diol grouping in the former is required for the formation of the chromium(V) species. Unfortunately, we have been unsuccessful, so far, in isolating the chromium(V) species present in such solutions. However, their ready formation from some of these fundamental units of nucleic acids suggests that further, more detailed, consideration should be given to the role of water soluble, long-lived chromium(V) species in the problem of chromium(VI) carcinogenicity and toxicity. Further studies in this direction are in progress.

Acknowledgement:- We thank the S.E.R.C. and Imperial Chemical Industries, P.L.C., for a CASE Studentship to P.B.H.

REFERENCES

1 J.M. Davies, *Lancet*, 1978, 384.
2 J.M. Davies, *J. Oil Col. Chem. Assoc.*, 1979, *62*, 157.
3 A. Furst, M. Schlauder and D.P. Sasmore, *Cancer Res.*, 1976, *36*, 1779.
4 T. Norseth, *"Origins of Human Cancer"*, Cold Spring Harbor Laboratory, 1977, pp. 159-167.
5 S. Langard and T. Norseth, *"Handbook on the Toxicology of Metals"*, ed. L. Friberg, *et al*, Elsevier/North Holland Biomedical Press, 1979, pp. 383-397.
6 F.L. Petrilli and S. De Flora, *Mutat. Res.*, 1978, *54*, 139.
7 J.E. Gruber and K.W. Jennette, *Biochem. Biophys. Res. Commun.*, 1978, *82*, 700.
8 M.A. Sirover and L.A. Loeb, *Science*, 1976, *194*, 1434.
9 M.J. Tsapakos, T.H. Hampton and K.W. Jennette, *J. Biol. Chem.*, 1981, *256*, 3623.
10 K.W. Jennette, *Biol. Trace Element Res.*, 1979, *1*, 55.
11 K.W. Jennette, *J. Am. Chem. Soc.*, 1982, *104*, 874.
12 H. Kon, *J. Inorg. Nucl. Chem.*, 1963, *25*, 933.
13 V. Srinivasan and J. Rocek, *J. Am. Chem. Soc.*, 1974, *96*, 127.

Polyhedron Vol. 1, No. 5, pp. 501-502, 1982
Printed in Great Britain.

0277-5387/82/050501-02$03.00/0
Pergamon Press Ltd.

Substituent Effects on Metal-Proton Interactions in 1-Tetralone Oxime Complexes of Rhodium(I)

By C.A. Johnson and A.J. Nielson*

Department of Chemistry, University of Auckland,

Auckland, New Zealand.

Complexes containing metal-proton interactions are important intermediates in aromatic C-H bond activation by d^8 transition metals[1]. The interactions, which may be detected by ^1H nmr spectroscopy[2], are of specific interest in that they represent orientated precursors to any σ intermediates formed during the electrophilic or nucleophilic processes involved[3,4]. We report here preliminary results showing apparent aromatic ring substituent effects on metal proton interactions in 1-tetralone oxime complexes of rhodium(I).

The complexes (1) to (4) were prepared by reacting 1-tetralone oximes with $Rh(CO)_2Cl$ dimer and were characterised by elemental and spectroscopic analysis. The ^1H nmr spectra showed coordinated nitrogen by shifts in the hydroxy and α-carbon proton resonances compared with the free ligand and the metal-proton interaction confirmed by a downfield shift of H_8.

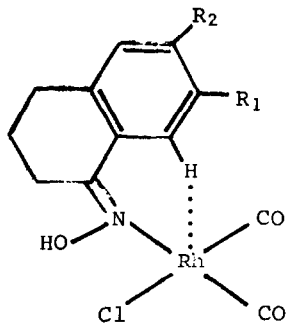

(1) $R_1 = R_2 = H$
(2) $R_1 = H$, $R_2 = OMe$.
(3) $R_1 = OMe$, $R_2 = H$.
(4) $R_1 = NO_2$, $R_2 = H$.

Thus for complex (2) δ($CDCl_3$) 1.76, m†, 2H, C_3-methylene; 2.64, t, 2H, C_2-methylene; 2.92, t, 2H, C_4-methylene; 3.83, s, 3H, C_6-methoxy; 6.78, d (J_m = 2Hz), 1H, C_5-aromatic; 6.91, dd (J_m = 2Hz, J_o = 8.1Hz), 1H, C_7-aromatic; 8.56, d (J_o = 8.1Hz), 1H, C_8-aromatic; 8.92, b, 1H, OH. 6-Methoxy-1-tetralone oxime, 1.88, m, 2H, C_3-methylene; 2.85, m, 4H, $C_{2,4}$-methylenes; 3.85, s, 3H, C_6-methoxy; 6.85, d (J_m = 2Hz), 1H, C_5-aromatic; 6.95, dd (J_m = 2Hz, J_o = 8.1Hz), 1H, C_7-aromatic; 8.05, d (J_o = 8.1Hz), 1H, C_8-aromatic; 9.28, b, 1H, OH.

For (1) to (4) ligand planarity imposes close proximity of H_8 to the filled metal dz^2 orbital, the HOMO available for overlap with a σ* CH orbital (LUMO) at an incipient stage in nucleophilic attack expected for rhodium(I)[3]. Ligand rigidity allows minimum distortion to remove proximity effects and anisotropy associated with the dz^2 orbital will be invariant in the series as ligands are similar in each case. With lack of backbonding ability the donor

† m, multiplet, t, triplet, s, singlet, b, broad, d, doublet, dd, double doublet.

power of nitrogen will be little affected by aromatic ring substituents[4]. As attractions or repulsions within the interaction vary the metal-proton distance, the C_8 shift will be sensitive to substituent effects as a result of differing anisotropy experienced by H_8. Metal-proton distances of *ca.* 2.6 to 2.9 Å have been determined by x-ray crystallography in other d^8 complexes containing metal-proton interactions[5].

Results from substituents studied so far (Table 1) show apparent greater sensitivity to inductive effects than resonance contributions.

Table 1 ^{1}H nmr Data for H_8 in 1-Tetralone Oximes (60 MHz)

Oxime	free ligand[a]	complex[a]	shift[b]
1-Tetralone	8.00	8.55	0.55
6-Methoxy-1-tetralone	8.07	8.61	0.54
7-Methoxy-1-tetralone	7.63	8.31	0.67
7-Nitro-1-tetralone	8.65	9.40	0.75

a, ppm from TMS; b, ppm.

Both effects can reduce electron density at H_8 in (4) but resonance contributing electron density to H_8 in (3) is not reflected in the proton shift. No effect is observed for (2). The shifts are in accord with the greater inductive effect of NO_2 over OMe groups. In terms of ^{1}H nmr shifts, for the Hammet equation D.S.P. extension, $\delta = \rho_I\sigma_I + \rho_R\sigma_R$, then $\rho_I >> \rho_R$. The magnitude of the inductive effect gauged from shift comparison of (3) and (4) shows contributions of 0.12 and 0.20 ppm for 7-methoxy and nitro groups respectively. The values are significantly large when compared with the downfield shift of (1).

References

1. A.J. Nielson, *J.Chem.Soc.Dalton*, 1981, 205.
2. See for example A.J. Nielson, *Transition Met.Chem.*, 1981, 6, 180; J.F. van Baar, K. Vrieze, and D.J. Stufkens, *J.Organometallic Chem.*, 1974, 81, 247; N.J. De Stefano, D.K. Johnson, and L.M. Venanzi, *Helv.Chim.Acta*, 1976, 59, 2683.
3. J.F. van Baar, K. Vrieze, and D.J. Stufkens, *J.Organometallic Chem.*, 1975, 97, 461.
4. M.I. Bruce, B.L. Goodall, and F.G.A. Stone, *Chem.Commun.*, 1973, 558.
5. J.M. Williams, R.K. Brown, A.J. Schultz, G.D. Stucky, and S.D. Ittel, *J.Amer.Chem.Soc.*, 1978, 100, 7407.

Polyhedron Vol. 1, No. 6, pp. 503–510, 1982
Printed in Great Britain.

0277–5387/82/060503–08$03.00/0
Pergamon Press Ltd.

EXTRACTION OF Cu(II) AND Ni(II) BY CAMPHORQUINONE DIOXIME

L. R. M. PAPING,* T. P. M. BEELEN, C. P. J. RUMMENS and R. PRINS
Department of Inorganic Chemistry, Eindhoven University of Technology, P.O. Box 513, 5600 MB Eindhoven, The Netherlands

(*Received* 26 *January* 1982)

Abstract—The extraction properties of three geometrical isomers (α-, β- and δ-) of D-camphorquinone dioxime (H_2CQD) with copper and nickel are described. Under extraction conditions isomerization occurred from α- and β-H_2CQD into δ-H_2CQD. The expected selectivity of δ-H_2CQD for nickel could not be established. On the contrary, copper formed complexes with lower $pH_{1/2}$ values than nickel. An ESR study showed that this was due to the fact that copper did not form a NN coordinated complex, but just like nickel a NO coordinated complex. UV spectroscopy proved that besides the $Cu(HCQD)_2$ complex a $Cu_2(HCQD)_2CQD$ complex is involved in copper extraction.

INTRODUCTION

The development of hydroxyoximes as commercial solvent extraction reagents for copper has prompted much research in the chemistry of such systems.[1,2] Many attempts have been made to find a reagent that is selective for nickel above copper. In order to from stronger complexes with nickel than with copper, a reagent must be found that does not follow the normal Irving–Williams order of stabilities. This is only possible if nickel forms a different kind of complex with the reagent than copper does. Aliphatic α-dioximes[3,4] did indeed extract nickel at lower pH than copper and this was explained[3] by assuming that nickel formed a square planar complex with a low spin d^8 configuration, while copper formed an octahedral complex by binding two additional water molecules. However, the extremely low rate of extraction does not make this system very attractive for commercial use.

Here we report on the separation properties of another kind of α-dioxime, camphorquinonedioxime H_2CQD. H_2CQD is known to exist in four isomeric forms (Fig. 1) which differ by the orientations of the OH groups. The rigid bicyclic skeleton is responsible for a larger NN distance than in aliphatic α-dioximes. NN coordination is the normal mode of coordination for vicinal dioximes but the large N ... N distance in H_2CQD makes this kind of coordination less attractive. Recently it was reported[5] that for copper only a NN coordinated H_2CQD complex could be isolated: $Cu(\beta\text{-}HCQD)_2 \cdot H_2O \cdot \frac{1}{2}$ dioxane (Fig. 2b).

In contrast to this it was published[5–8] that nickel forms stable NO coordinated complexes with α-, γ- and δ-H_2CQD (Fig. 2a) and an unstable NN coordinated com-

*Author to whom correspondence should be addressed.

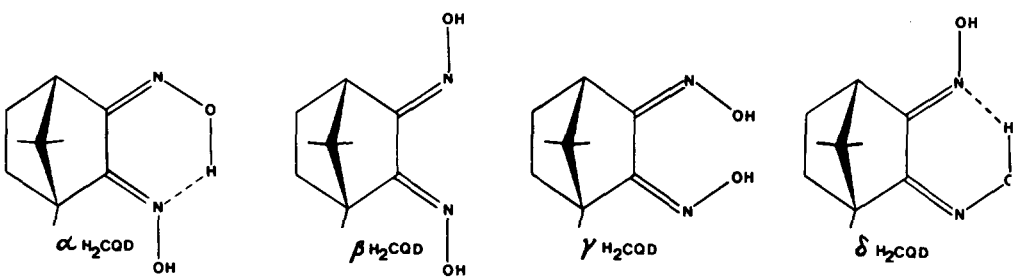

Fig. 1. The four isomeric forms of camphorquinone dioxime.

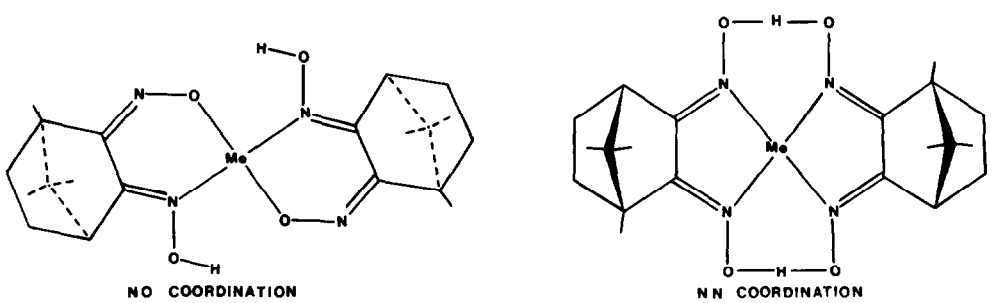

Fig. 2. Two possible ways of coordination of camphorquinone dioxime with copper or nickel.

plex with β-H_2CQD. α- and δ-H_2CQD are likely to form NO coordinated complexes (Fig. 1) and if no isomerization takes place into β-H_2CQD it is to be expected that these two isomers react better with nickel than with copper. In this way the Irving–Williams order of stabilities might be broken.

For this reason we have studied the extraction properties of the camphorquinone dioxime isomers for copper and nickel and the kind of complexes which are responsible for the extraction.

EXPERIMENTAL

The optically active camphorquinone dioxime ligands were prepared from (+) camphor according to the procedures of Forster.[9]

α-H_2CQD: $[\alpha]_D$ (in 2 per cent sodium hydroxyde) = −99.1 (−98.3[9]); β-H_2CQD: $[\alpha]_D$ = −25.7 (−24.1[9]); γ-H_2CQD could not be isolated pure. δ-H_2CQD: $[\alpha_D]$ = +85.2 (+83.6[9]).

Optical rotations were obtained at 20°C with a Kreis-Polarimeter 0.01/400 mm from Zeiss Winkel, while ESR measurements were done with a Varian E15 spectrometer at room temperature and UV-visible spectra were obtained on a Unicam SP.800D. Aqueous metal ion concentrations were measured with the Perkin–Elmer 300 Atomic Absorption Spectrophotometer.

The extraction experiments were carried out in a three stoppered flask with a stirring device and continuous pH measurements. The starting volumes of water and organic solvent were both 250 ml. Stirring was stopped when no further change of the pH was noticed, indicating that equilibrium was reached. For analysis equally small volumes of water layer and organic layer were withdrawn from the system. To measure the distribution coefficient as a function of pH thereafter a small quantity of 4N acid or base was added, and the process of stirring until equilibrium and withdrawal of small portions of the aqueous and organic solutions was repeated at a different pH. Care was taken to keep the volumes of the aqueous and organic solutions equal. Although in this procedure the electrolyte concentration does not stay constant we referred this method because it is convenient to execute and because in a separate experiment it was shown that in the applied concentration range the influence of the electrolyte concentration is negligible. As organic solvents used were chloroform, pentanol and tributylphosphate and inorganic salts used were metal chlorides, nitrates or sulphates. NAOH was used as base and HCl, HNO_3 or H_2SO_4 as acids.

TREATMENT OF EXTRACTION DATA

The extraction is expected to follow eqn (1):

$$M^{2+} + \overline{2H_2CQD} \rightleftarrows \overline{M(HCQD)_2} + 2H^+ \quad (1)$$

where M^{2+} represents the aquo metal ion, $M(HCQD)_2$ the extractable complex and bars indicate the organic layer. The equilibrium constant K_E and the distribution coefficient D are defined as:

$$K_E = \frac{[M(HCQD)_2][H^+]^2}{[M^{2+}][H_2CQD]^2} \quad (2)$$

$$D = \frac{[M(HCQD)_2]}{[M^{2+}]}. \quad (3)$$

Combination of (2) and (3) gives

$$\log D = \log K_E + 2pH + 2 \log [H_2CQD]. \quad (4)$$

When taking a large excess H_2CQD, so that H_2CQD is constant, it follows that

$$\left(\frac{\partial \log D}{\partial pH}\right)_{[H_2CQD]} = 2. \quad (5)$$

Introducing $pH_{1/2}$ as the pH value at which 50% of the metal is extracted (log D = 0) eqn (4) leads to:

$$\log K_E = -2 \log [H_2CQD] - 2pH_{1/2}. \quad (6)$$

Finally the value of $pH_{1/2}$ at 1.0 M equilibrium concentration of extractant in the organic phase, denoted by $(pH_{1/2})_{1.0}$ can be obtained from eqn (6) as

$$(pH_{1/2})_{1.0} = -\frac{\log K_E}{2}. \quad (7)$$

RESULTS

Figure 3 shows the results for the extraction of Ni^{2+} with δ-H_2CQD. The $pH_{1/2}$ value of 5.20 means a $(pH_{1/2})_{1.0}$ value of 3.60. The slope (1.93) of the log D-pH curve agrees with the theoretical expected value of 2 for the $Ni(HCQD)_2$ complex. The H_2CQD recovered after the extraction experiment did not show a significant change in specific rotation (Table 1).

The extraction properties of α-H_2CQD for Ni^{2+} are

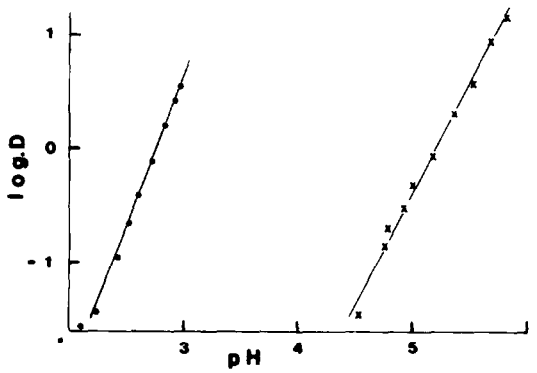

Fig. 3. Log D as a function of pH for the extraction of Cu(II) (O) or Ni(II) (X) with δ-camphorquinone dioxime. Concentration of δ-H_2CQD in pentanol 0.025 M. Initial aqueous metal sulphate concentration 0.001 M.

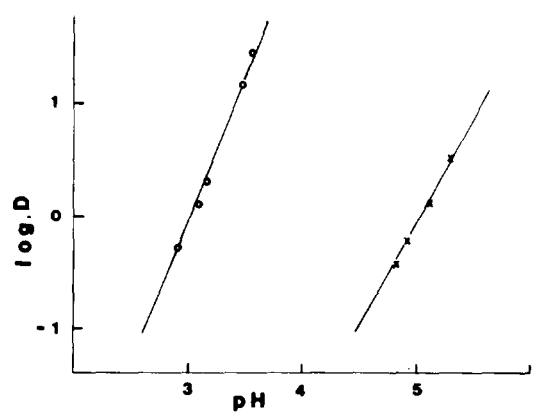

Fig. 4. Log D as a function of pH for the extraction of Cu(II) (O) or Ni(II) (X) with α-camphorquinone dioxime. Concentration of α-H_2CQD in pentanol 0.025 M. Initial aqueous metal sulphate concentration 0.001 M.

Table 1. Specific rotation

H_2CQD	fresh solution	after 7 days	after 45 days	after Cu extraction	after Ni extraction
α^a	-63.8	-64.3	-63.3	+51.9	+47.1
β^b	+ 3.7	+21.2	+23.9	+59.4	+45.5
δ^a	+78.6	+71.1	+70.2	+67.5	+67.8

a: pentanol as solvent b: t.b.p. as solvent

quite analogous to those of δ-H_2CQD (Fig. 4) with a $pH_{1/2}$ value of 5.03 and a slope of 1.96. The recovered H_2CQD had a specific rotation of $= +47.1$ (Table 1) indicating that isomerization had taken place.

The only solvent that we could find which dissolves β-H_2CQD and is not soluble in water was tributylphosphate (TBP). In Fig. 5 a pronounced difference is seen between results from experiments with fresh solutions and results from extractions performed with solutions after contact times of two days. In the latter case the results correspond to those of the Ni δ-H_2CQD system: $pH_{1/2} = 6.16$, slope 1.99 and the recovered H_2CQD showed a specific rotation of +45.5, indicating that isomerization had occurred. Fresh solutions, however, show a slope of 0.97 and a slightly higher $pH_{1/2}$ value of 6.33.

In contrast to the results obtained in the extraction of nickel a value of 2.50 is found (2 was expected on ground of eqn 1) for the slope of the extraction curve for copper with δ-H_2CQD (Fig. 3). A clearly lower $pH_{1/2}$ value of 2.75—leading to a $(pH_{1/2})_{1.0}$ of 1.15—is found. Also for copper no significant change in the specific rotation of δ-H_2CQD could be noted (Table 1).

As with the Ni α-H_2CQD system the Cu α-H_2CQD system gives almost the same figures as found for Cu δ-H_2CQD (Fig. 4). In this case also isomerization had taken place (Table 1). a $pH_{1/2}$ value of 3.08, a slope of 2.67 and a change in specific rotation from −63.8 to +51.9 are found.

With a fresh solution of β-H_2CQD in TBP (Fig. 6) a $pH_{1/2}$ value of 4.21 is obtained for the copper extraction, quite larger than with the Cu δ-H_2CQD pentanol system. The slope of 1.47 indicates that the extraction chemistry

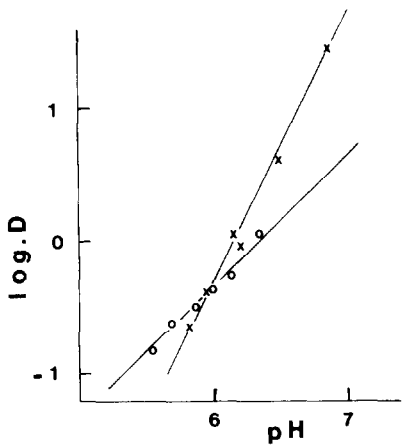

Fig. 5. Log D as a function of pH for the extraction of Ni(II) with β-camphorquinone dioxime. Concentration of β-H_2CQD in tributyl phosphate 0.025 M. Initial aqueous nickel chloride concentration 0.001 M O: fresh solution X: after two days of contact.

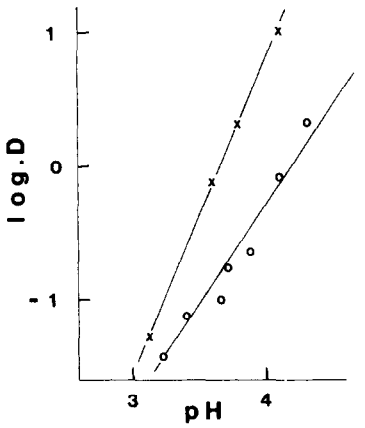

Fig. 6. Log D as a function of pH for the extraction of Cu(II) with β-camphorquinone dioxime. Concentration of β-H_2CQD in tributyl phosphate 0.025 M. Initial aqueous copper chloride concentration 0.001 M. O: fresh solution X: after two days of contact.

must deviate considerably from that represented by the extraction eqn (1). Just as in the experiment with nickel and β-H_2CQD, after two days the picture had dramatically changed. The $pH_{1/2}$ value was lowered to 3.66 and the slope had increased to 2.37. Specific rotation measurement from the recovered H_2CQD showed that most of the β-H_2CQD had isomerized. This isomerization was more pronounced than the isomerization that occurred without contact with the aqueous copper solution (Table 1).

The slopes of the log D-pH curves for the copper extraction deviate from 2 and point to an extraction chemistry which is different from that assumed in eqn (1). To find out which stoichiometry the copper camphorquinone dioxime complex had during extraction an experiment was carried out with equivalent moles of copper and δ-H_2CQD. If $Cu(HCQD)_2$ would be the only extraction complex at most 50% of the copper can be extracted. Figure 7 shows that definitely more than 50% of the copper can be extracted, but that even at high pH 100% extraction is not reached. At pH 5.0 65% of the copper was extracted.

VIS-spectroscopy (Fig. 8) shows that two different copper complexes are present in the organic phase after extraction. When the pH is relatively low a complex is formed with a maximum absorbance at 25,300 cm^{-1}. At higher pH's a new band appears with a maximum at 22,400 cm^{-1} and the corresponding complex becomes prevalent at pH is 3.20.

Also ESR measurements, correlated with the two different Cu–HCQD complexes are carried out. The ESR spectrum of the complex with λ_{max} 25,300 cm^{-1} is presented in Fig. 9. It is exactly the same as that found

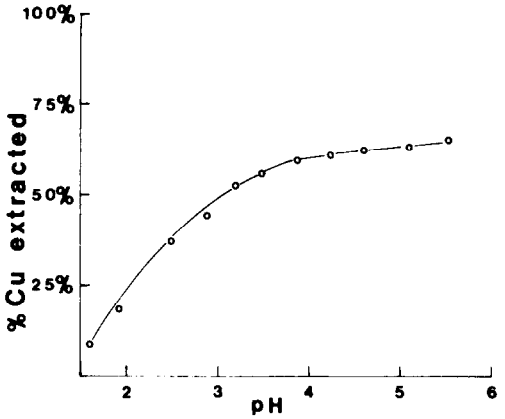

Fig. 7. % copper extraction as a function of pH for the extraction of Cu(II) with δ-camphorquinone dioxime. The initial concentration of δ-H_2CQD in chloroform and the initial copper nitrate concentration in H_2O are both 0.002 M.

by Ma[5] for Cu(β-HCQD)$_2$·H_2O·½ dioxane. For the complex with λ_{max} at 22,400 cm^{-1} no ESR signal could be observed.

DISCUSSION

From Table 1 it can be clearly seen that under extraction conditions isomerization takes place when α- or β-H_2CQD are used.

Without contact with an aqueous solution containing metal ions α-H_2CQD does not isomerize at all and β-H_2CQD isomerizes only to a certain extent.

This phenomenon can be readily explained by the bonding of metal ions or protons to the dioxime; by this interaction the double bond character of the CN bond will be weakened and thus the rotation barrier of this bond will be lowered. δ-H_2CQD is the only isomer which possesses hydrogen bridge stabilization and no steric repulsion (Table 2). Therefore it is not surprising that it is the most stable isomer.

Pedersen and Larsen[6] found isomerization of Ni(α-HCQD)$_2$ in chloroform to an equilibrium mixture of 85–90% Ni(δ-HCQD)$_2$ 5–10% Ni(α-HCQD)$_2$ and 5% Ni(β-HCQD) (δ-HCQD). This means that after recovering of H_2CQD a specific rotation is expected of $0.90 \times (+78.6) + 0.075 \times (-63.8) + 0.025 \times (+3.7) = +66.0$.

In Table 1 it is seen that after extraction with α-, β- or

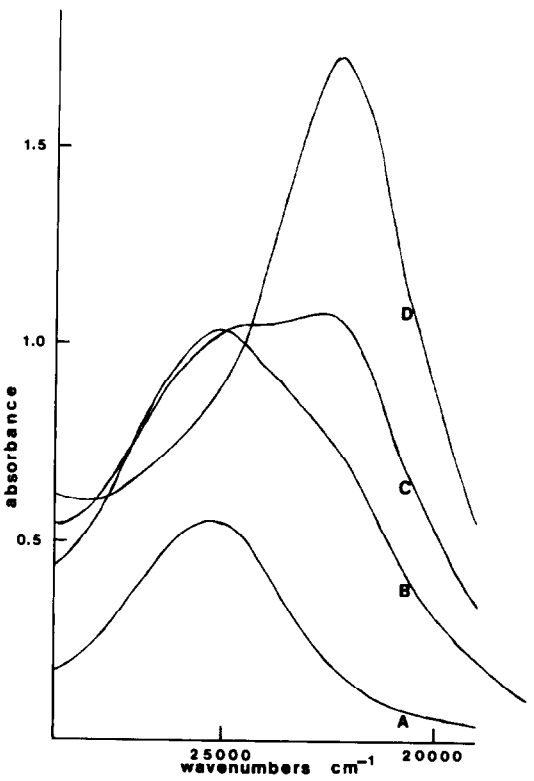

Fig. 8. VIS spectra of the organic phase for the extraction of copper(II) with δ-camphorquinone dioxime. A: pH = 1.93; B: pH = 2.87; C: pH = 3.20; D: pH = 5.00. For initial concentrations: see Fig. 7.

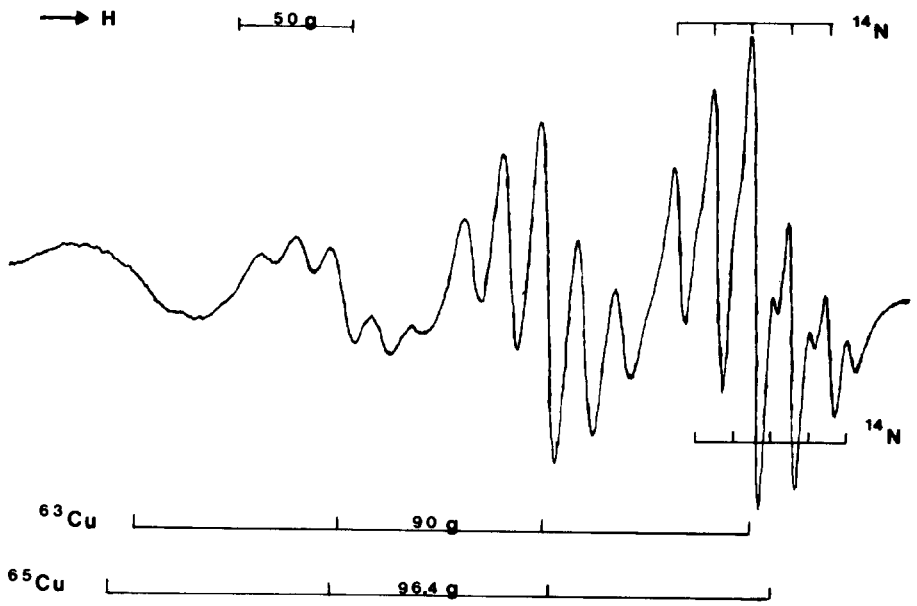

Fig. 9. ESR spectrum of copper H_2CQD complex (λ_{max} 25300 cm^{-1}) in chloroform at room temperature.

Table 2. Stabilization and repulsion of the four different H_2CQD isomers

H_2CQD	OH... CH_3 repulsion	OH... OH repulsion	OHO stabilization
α	yes	no	yes
β	yes	no	no
γ	no	yes	no
δ	no	no	yes

δ-H_2CQD the specific rotation had changed into the direction of this figure, but apparently equilibrium had not been reached.

The expected selectivity of δ-H_2CQD could not be established. On the contrary, copper was extracted at a much lower pH than nickel (Fig. 3). This result is surprising because if copper forms a NN complex as suggested by Ma[5] then rotation around the CN double bond is necessary. Furthermore it might have been expected that copper extraction with β-H_2CQD, for which no rotation is needed would have a lower $pH_{1/2}$ value than copper extraction with δ-H_2CQD. However, in Fig. 6 it can be seen that after a contact time of two days, in which isomerization from β- to δ-H_2CQD has taken place, the $pH_{1/2}$ value is lowered and not raised.

These results can only be explained if we assume that copper does not form a NN complex but a NO complex just like nickel.

To investigate this possibility we took a closer look at the ESR spectrum of the extracted complex, which is completely identical with the ESR spectrum found by Ma[5] for Cu(β-HCQD)$_2$·H_2O·$\frac{1}{2}$ dioxane. Ma has interpreted the ESR spectrum of Cu(β-HCQD)$_2$ by assigning the four main lines to copper (^{63}Cu, ^{65}Cu: I = 3/2) nuclear hyperfine interactions and the extra lines as being due to the nitrogen (^{14}N: I = 1) superhyperfine interaction. By counting 9 nitrogen superhyperfine lines he concluded that four nitrogen atoms are attached to copper. Because of the line broadening on the low field side of the spectrum the nitrogen superhyperfine lines are only clearly observed on the high field side.

Our interpretation of the superhyperfine structure is completely different from that of Ma. Natural copper is composed of 69.1% ^{63}Cu and 30.9% ^{65}Cu both with spin 3/2 but with a slightly different magnetic moment (0.70904×10^{-4} vs 0.75958×10^{-4} rad. sec^{-1} gauss^{-1}). The ESR signal of most copper compounds in liquid solution shows four lines with fairly large linewidths and as a consequence no separate peaks can be observed for the two Cu isotopes. However, whenever ligand nitrogen superhyperfine structure is observed one has to take into account[10,11] that extra lines may become observable as a result of the different magnetic moments of ^{63}Cu and ^{65}Cu. At the high field side of the spectrum (see Fig. 9) two overlapping hyperfine splitting patterns with intensity ratios of 1:2:3:2:1 can be seen with a splitting of 16.5 gauss. Computer simulation gave an excellent fit with an intensity ratio between ^{63}Cu and ^{65}Cu of 76:24. From the complete ESR spectrum a hyperfine splitting of 90 gauss is obtained for ^{63}Cu. The copper hyperfine splitting for ^{65}Cu can now be calculated to be $0.75958/0.70904 \times 90 = 96.4$ gauss. The predicted separation between ^{63}Cu and ^{65}Cu of the nitrogen superhyperfine splitting on the high field side of the ESR spectrum is $3/2(96.4 - 90) = 9.6$ gauss, and is in very good agreement with the observed separation of 9.5 gauss. With this interpretation it becomes clear why this extra hyperfine splitting of ^{65}Cu cannot be seen on the other copper hyperfine line with nitrogen superhyperfine structure, because for that line the calculated separation between ^{63}Cu and ^{65}Cu would be $\frac{1}{2}(96.4 - 90) = 3.2$ gauss and with such a small difference no separate peaks can be detected. A further argument in favour of our interpretation of the ESR spectrum is the fact that the nitrogen superhyperfine structure on the high field copper line does not have an intensity ratio of 1:4:10:16:19:16:10:4:1 and that the superhyperfine lines are not equidistant either, as would be required if four nitrogen atoms were bonded to copper. We therefore conclude that only two instead of four nitrogen atoms are bonded to copper, and so an intensity ratio of 1:2:3:2:1 occurs in the nitrogen superhyperfine structure. As a consequence the Cu(β-HCQD)$_2$ complex of Ma and the extracted complex with λ_{max} at 25,300 cm^{-1} do not have the NN structure but just like nickel a NO structure (Fig. 2).

The results found in the extraction experiments are in good agreement with this interpretation. For, when copper and nickel form the same kind of complex with H_2CQD, copper will have a lower $pH_{1/2}$ value than nickel according to the Irving and Williams law.

The low values of the slopes of the log D vs pH curves found in the extraction of copper and nickel by fresh β-H_2CQD (1.47 for Cu and 0.97 for Ni) can now also be explained if we assume that β-H_2CQD is not active in the extraction. Only the small portion of the δ-H_2CQD that is present will be active. As a consequence the extractant concentration in eqn (4) is not a constant when the equilibrium is changed by adding acid or base. This means that the slope of log D vs pH will not give a value of two, but will give a value which is considerably lower. After two days, during which most of the β-H_2CQD is isomerized to δ-H_2CQD, excess δ-H_2CQD will be present and indeed the slopes are increased to values (2.37 for Cu and 1.99 for Ni) which are almost equal to the values found in the extraction by δ-H_2CQD. Also the change of the $pH_{1/2}$ value (4.21–3.66 for Cu and 6.33–6.16 for Ni) can be explained by the fact that isomerization of β-H_2CQD to δ-H_2CQD increases the extractant concentration. For according to eqn (6) an increase in the extractant concentration leads to a decrease in the $pH_{1/2}$ value. For α-H_2CQD such a phenomenon was not observed. This is not surprising because α-H_2CQD itself can form a NO complex and thus is active in the extraction. As a consequence, during isomerization of α-H_2CQD to δ-H_2CQD the extractant concentration does not change.

The result of the slope analysis of 1.93 for the extraction of nickel(II) by δ-H_2CQD is consistent with the theoretically expected value of 2 (eqn 5) and thus the extraction equation can be represented by

$$Ni^{2+} + 2H_2CQD \rightleftarrows Ni(HCQD)_2 + 2H^+.$$

With copper(II), on the contrary, a deviating value of 2.50 was found for the extraction by δ-H_2CQD.

According to Fig. 8 it was shown that two different complexes are involved during the extraction: complex A with $\lambda_{max} = 25300\,cm^{-1}$ and complex B with $\lambda_{max} = 22400\,cm^{-1}$. Their ratio is strongly pH-dependent; at low pH the spectrum is dominated by A, at relatively high pH values B is more important. Since the spectrum of A correlates with the presence of the copper ESR described above, complex A may be assumed to be $Cu(HCQD)_2$.

Figure 7 shows that at pH = 5, 65% of the copper is extracted and from Fig. 8 it can be concluded that at this pH complex B is almost exclusively responsible for the extraction. The value of about 65% extraction at high pH can be explained if a complex with a copper:H_2CQD=2:3 ratio is assumed to be present during extraction. In that case the maximum concentration of copper in the organic phase is expected to be 66.7%. To check the hypotheses on the stoichiometry of the two copper complexes accurate values of the intensities of both (overlapping) bands were necessary. The separation at different pH values was carried out by means of computer simulation.

The best fit was obtained by using a corrected Lorentz function with the general form $y = a(1 + bx^2 + cx^4)^{-1}$ as used by Baker *et al.*[12] for IR band simulation. A strong absorption near $35000\,cm^{-1}$ with some overlap around $25000\,cm^{-1}$ has been taken into account. In Fig. 10 one of the simulations is shown, and the excellent fit is noteworthy. In this way the real intensities of the bands at λ_{max} could be obtained and these values are according to Lambert-Beer's law proportional to the concentrations of complex A ($25300\,cm^{-1}$) and B ($22400\,cm^{-1}$). By using the trial and error method the best extinction coefficients for A and B could be determined. These extinction coefficients are 4940 for A and 8700 for B. In Fig. 11 it is shown what happens with the different species as a function of pH.

For complex A we assume that the same reaction equation applies as used in eqn (1) and k_A is then given by eqn (8)

$$k_A = \frac{[Cu(HCQD)_2][H^+]^2}{[Cu^{2+}][H_2CQD]^2} = \frac{[A][H^+]^2}{[Cu^{2+}][H_2CQD]^2}. \quad (8)$$

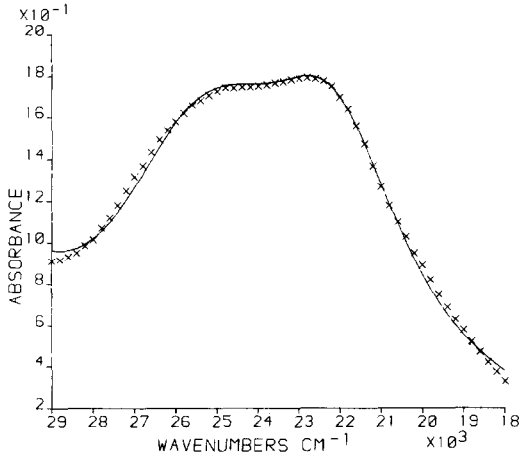

Fig. 10. VIS spectrum of the organic phase after the extraction of copper(II) with δ-camphorquinone dioxime at pH 3.20. X: experimental, —: calculated by computer simulation. For initial concentrations see Fig. 7.

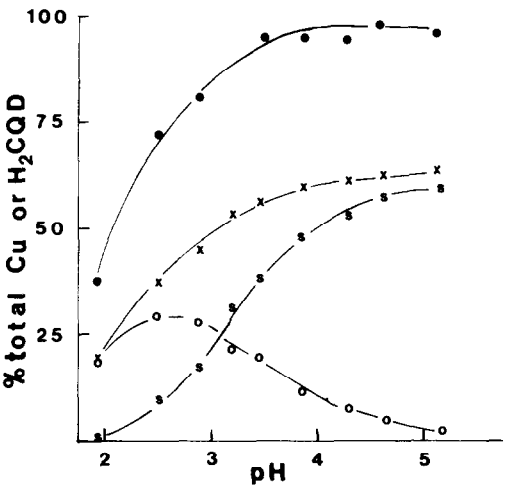

Fig. 11. Extraction of copper(II) with δ-camphorquinone dioxime as a function of pH. ●: % reacted δ-H_2CQD, X: % Cu extracted into the organic phase, O: % Cu extracted by complex A with λ_{max} $25300\,cm^{-1}$; S: % Cu extracted by complex B with λ_{max} $22400\,cm^{-1}$. For initial concentrations see Fig. 7.

The composition of complex B is more complicated. It is very likely that complex B is neutral in the organic phase, and in combination with the results of Fig. 7 this suggests its formula to be $Cu_2(HCQD)_2CQD$. In that case the reaction equation is

$$2Cu^{2+} + 3H_2CQD \rightleftarrows Cu_2(HCQD)_2CQD + 4H^+ \quad (9)$$

with an equilibrium constant k_B:

$$k_B = \frac{[Cu_2(HCQD)_2CQD][H^+]^4}{[Cu^{2+}]^2[H_2CQD]^3} = \frac{[B][H^+]^4}{[Cu^{2+}]^2[H_2CQD]^3}. \quad (10)$$

In eqns (8) and (10) all concentrations can be measured ($[H^+]$ with pH measurements $[Cu^{2+}]$ with atomic absorption, [A] and [B] with UV/visible spectroscopy) with the exception of $[H_2CQD]$. To eliminate $[H_2CQD]$ we combine (8) and (10)

$$\frac{[k_A]^3}{[k_B]^2} = \frac{[A]^3[Cu^{2+}]}{[B]^2[H^+]^2} \quad (11)$$

resulting in

$$\frac{\partial(\log[B] - 3\log[A] - \log[Cu^{2+}])}{\partial pH} = 2. \quad (12)$$

In Fig. 12 we see that a plot of $2\log B - 3\log A - \log[Cu^{2+}]$ vs pH indeed gives a straight line with a slope of 1.99 confirming our assumptions concerning complex B. However, the requirements of a neutral complex with a copper ligand ratio of 2/3 are also fulfilled with the assumption of the complex $Cu_2(HCQD)_3OH$, replacing the double negative charge of CQD by $HCQD^-$ plus OH^-:

$$2Cu^{2+} + 3H_2CQD + H_2O \rightleftarrows Cu_2(HCQD)_3OH + 4H^+. \quad (13)$$

Because $[H_2O]$ can be assumed to be constant, replacing (9) by (13) gives no difference in expressions (11) and

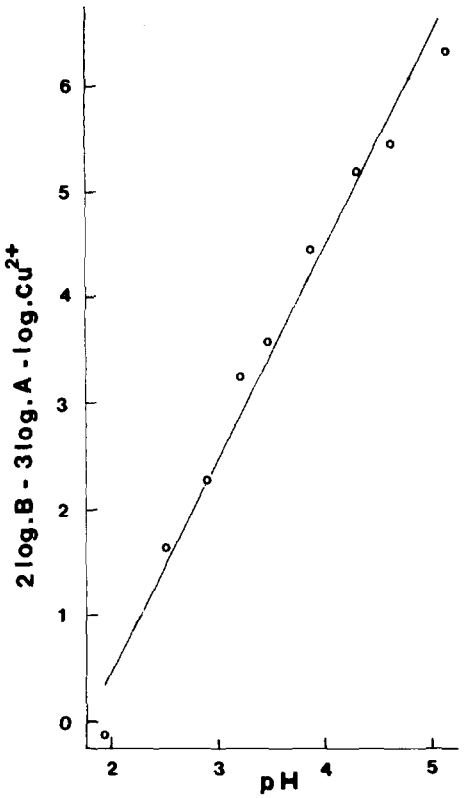

Fig. 12. 2 log B − 3 log A − log [Cu^{2+}] as a function of the pH for the extraction of copper(II) with δ-camphorquinone dioxime. A and B are the calculated values of the maxima of the complex with $\lambda_{max} = 25300\,cm^{-1}$ and of the complex with $\lambda_{max} = 22400\,cm^{-1}$ respectively. For initial concentrations see Fig. 7.

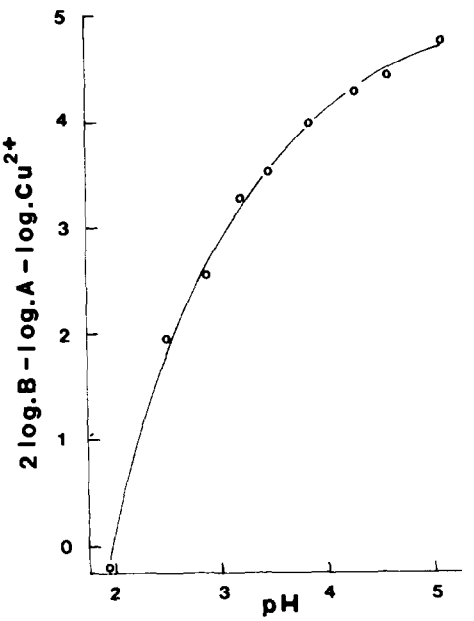

Fig. 13. 2 log B − log A − log [Cu^{2+}] as a function of the pH for the extraction of copper(II) with δ-camphorquinone dioxime. A and B are the calculated values of the maxima of the complex with $\lambda_{max} = 25300\,cm^{-1}$ and of the complex with $\lambda_{max} = 22400\,cm^{-1}$ respectively. For the initial concentrations see Fig. 7.

(12) so complex B might also be represented by $Cu_2(HCQD)_3OH$.

If OH^- is replaced by another anion, for example NO_3^- (to adjust pH HNO_3 is used), elimination of [H_2CQD] from the expressions for k_A and k_B gives:

$$\frac{k_A^3}{k_B^2} = \frac{[A]^3}{[B]^2}[NO_3^-]^2[Cu^{2+}]. \qquad (14)$$

This would mean that $[A^3]/[B]^2$ would be independent from the pH, which does not fit with Fig. 11. We therefore conclude that this reaction does not take place.

Although the extraction experiments strongly point to the formation of a 2:3 Cu:HCQD complex, we checked if a 1:1 complex could explain the extraction results

$$Cu^{2+} + H_2CQD \rightleftarrows Cu(CQD) + 2H^+. \qquad (15)$$

In combination with eqn (8) and by eliminating the [H_2CQD] we obtain

$$\frac{k_A}{k_B^2} = \frac{[A]}{[B^2]} \cdot \frac{[Cu^{2+}]}{[H^+]^2}. \qquad (16)$$

Therefore a plot of 2 log B − log A − log [Cu^{2+}] vs pH must give a straight line with slope 2. From Fig. 13 it is clear that this is not the case so we may safely reject eqn (15). Also Cu(HCQD) (NO_3) could be rejected by this way of analysis. Because of all these arguments for complex B we conclude that complex B must have the composition $Cu_2(HCQD)_2CQD$ or $Cu_2(HCQD)_3OH$.

In agreement with this conclusion no ESR signal could be observed for complex B. This is not an unknown phenomena[13,14] for binuclear Cu(II) complexes in which the antiferromagnetic coupling between the two copper ions is so large that the singlet ground state has a very pronounced energy difference from the triplet state. As a result the complex is diamagnetic at room temperature. Since only binuclear copper(II) complexes can have such an antiferromagnetic coupling and mononuclear copper(II) complexes always have an unpaired electron, this confirms the conclusion that the composition of complex B must be $Cu_2(HCQD)_3OH$ or $Cu_2(HCQD)_2CQD$.

CONCLUSIONS

The expected selectivity of δ-H_2CQD for the extraction of nickel above copper has not been confirmed. On the contrary, copper was found to have a $pH_{1/2}$ value that was much lower (2.75 vs 5.20) than that of nickel. This expected selectivity of camphorquinone dioxime for nickel above copper was based on a publication of Ma, claiming that the dioxime in $Cu(\beta\text{-}HCQD)_2 \cdot H_2O \cdot \frac{1}{2}$ dioxane, had a NN coordination around copper.

Our analysis of the ESR spectrum showed, however, that this product does not have a NN coordination but a NO coordination like nickel. With the knowledge that there is no difference in coordination of H_2CQD around copper and nickel, it is not surprising that δ-H_2CQD has no selectivity for nickel above copper, and that the normal order of stabilities according to Irving and Williams is followed.

Under extraction conditions isomerization occurred from α- and β-H_2CQD into δ-H_2CQD. Without contact with metal ions or protons the α-H_2CQD is stable in solution. We therefore conclude that metal ion or proton attaches on the nitrogen atoms and lowers the double

bond character of the CN bond, thus making rotation around this bond more easy.

Analysis of the slope of log D vs pH confirmed the expected reaction equation for nickel: $Ni^{2+} + 2H_2CQD \rightleftarrows Ni(HCQD)_2 + 2H^+$.

With copper two different complexes are involved in the extraction which is clearly seen by UV spectroscopy. Computer simulation showed that these two complexes are $Cu(HCQD)_2$, with an absorption at 25300 cm^{-1} and $Cu_2(HCQD)_2$ CQD or $Cu_2(HCQD)_3OH$ with an absorption at 22400 cm^{-1}. ESR spectroscopy proved the $Cu(HCQD)_2$ complex to have an NO structure. For the Cu:HCQD = 2:3 complex no ESR signal could be observed, which is not uncommon for binuclear copper(II) complexes with a very strong antiferromagnetic coupling.

REFERENCES

[1]A. W. Ashbrook, *Chem. Rev.* 1975, **16**, 285.
[2]D. S. Flett, *Chem. Ind.* 1977, 706.
[3]A. R. Burkin and J. S. Preston, *J. Inorg. Nucl. Chem.* 1975, **37**, 2187.
[4]M. L. Navtanovich, L. S. Lutova and V. L. Kheifets, *Russ. J. Inorg. Chem. (Engl. Transl.)* 1979, **24**, 243.
[5]M. S. Ma and R. J. Angelici, *Inorg. Chem.* 1980, **19**, 363.
[6]S. B. Pedersen and E. Larsen, *Acta Chem. Scand.* 1973, **23**, 3291.
[7]M. S. Ma, R. J. Angelici, D. Powell and R. A. Jacobson, *J. Am. Chem. Soc.* 1978, **100**, 7068.
[8]A. Nakamura, A. Konishi and S. Otsuka, *J. Chem. Soc. Dalton*, 1979, 488.
[9]M. O. Forster, *J. Chem. Soc.* 1903, **83**, 514.
[10]H. M. Swartz, J. R. Bolton and D. C. Borg, *Biol. Appl. Elec. Spin Reson.* 1972, 461.
[11]L. E. Warren, J. M. Flowers and W. E. Hatfield, *J. Chem. Phys.* 1969, **51**, 1270.
[12]C. Baker, J. P. Cockerell, J. E. Kelsey and W. F. Maddams, *Spectrochim. Acta*, 1978, **34A**, 673.
[13]D. E. Fenton and R. L. Lindtvedt, *J. Am. Chem. Soc.* 1978, **100**, 6367.
[14]J. A. Bertrand, J. H. Smith and P. G. Eller, *Inorg. Chem.* 1976, **13**, 1649.

Polyhedron Vol. 1, No. 6, pp. 511–519, 1982
Printed in Great Britain.

0277-5387/82/060511-09$03.00/0
Pergamon Press Ltd.

B-HALOGEN DERIVATIVES OF THE BIS(1,2-DICARBOLLYL)COBALT(III) ANION

Ľ. MÁTEL,* F. MACÁŠEK and P. RAJEC
Department of Nuclear Chemistry, Comenius University 842 15 Bratislava, Czechoslovakia

and

S. HEŘMÁNEK and J. PLEŠEK
Institute of Inorganic Chemistry, Czechoslovak Academy of Sciences, 250 68 Řež near Prague, Czechoslovakia

(*Received* 1 *February* 1982)

Abstract—The halogenation of $(C_2B_9H_{11})_2Co^-Cs^+$ by elemental halogens in alcohol and γ-radiation-induced halogenation by $CHBr_3$, $CHCl_3$ or CCl_4 in polar solvents proceeds alternatively in both ligands yielding successively 8-; 8,8'-; 8,9,8'-; 8,9,8',9'-; 8,9,12,8',9'- and 8,9,12,8',9',12'-halogen derivatives. The stepwise introduction of halogen was monitored by UV spectrometry, individual compounds were isolated by gel chromatography and identified by NMR. Thirteen halogen derivatives are described. γ-radiation-induced chlorination of $(C_2B_9H_{11})_2Co^-Cs^+$ by CCl_4 proceeds by reaction with liberated chlorine whereas the chlorination by $CHCl_3$ probably results from reactions with chlorine-containing intermediates.

INTRODUCTION

A study of the radiation stability of the $(C_2B_9H_{11})_2Co^-Cs^+$ species (I) (Fig. 1) in the $CHBr_3$-nitrobenzene mixture has proved not only an extraordinary resistance of this skeleton to degradation or structural changes, but also a transformation of (I) to its 8-Br-(IIb) and 8,8'-Br_2-(IIIb) derivatives,[1–3] the latter being the final product.[3] In contrast to the last fact, preliminary experiments have shown that the radiolysis of (I) in the CCl_4-nitrobenzene mixture can also afford more chlorinated compounds.[4]

To date, little was known on halogen substitution of the anion (I). Whilst the hexabromo derivative (VIIb) was prepared by a direct bromination of I in boiling acetic acid,[5] the 9,9'-dibromo (VIIIb) and 9,12,9',12'-tetrabromo derivatives (IXb) were obtained by a general synthesis from the appropriate bromo-o-carboranes.[6] In the chloro-series, only a chlorination of (I) to B-polychloro derivatives has been claimed in a recent patent application.[7] No iodinated derivatives of (I) were known.

Due to the fact that the halogenation of (I) during the radiolysis was considered to be a result of the reaction of (I) with an elemental halogen generated by the radiolysis of the polyhalomethane present,[3] a direct halogenation of (I) has been studied and the results compared with those of radiolysis, carried under various conditions.

EXPERIMENTAL

Physical measurements

UV-spectra were measured with Specord UV-VIS spectrophotometer (GDR). IR spectra were determined using a Perkin–Elmer Model 567 and Model 598 spectrophotometers (U.S.A.). NMR spectra in acetone were recorded on a Varian XL-200 spectrometer (^{1}H: 200 MHz, ^{11}B: 64.2 MHz) and Bruker WH-270 spectrometer (^{1}H: 270 MHz, ^{11}B: 86.6 MHz). The ^{11}B chemical shifts were externally referenced to $BF_3.O(C_2H_5)_2$, with the value signifying the signal to higher field.

Conductivity measurements were carried out using a Radelkis OK-102 conductometer at 80 Hz (0–150 μS) and 3 kHz (0.5–500 mS) at 22°C. They were analyzed by Gauss–Newton–Levenberg optimization method on a HP 8925 A calculator to obtain parameters of Debye–Hückel–Onsager equation in the Robinson–Stokes modification[8] $\lambda = \alpha(\lambda_0 - (a_1\lambda_0 + a_2)\sqrt{\alpha c}/(1 + B\sqrt{\alpha c}))$ where λ and λ_0 are molar conductivities at given concentration c and at infinite dilution, respectively, and α is the degree of dissociation. Thermodynamic dissociation constant K_T was included into calculations so that $K_T = \alpha^2 c^2 f_\pm^2/(1-\alpha)$ and $f_\pm = -A\sqrt{(\alpha c)}/(1 + B\sqrt{(\alpha c)})$, in order to optimize the λ_0, B and K_T values.

Analyses; separation

The elemental analyses were carried out by the Laboratory of elemental analysis, Chemical Institute of Comenius University, Bratislava.

Halogenation of I was followed by purification of samples, removed at intervals, on the Sephadex LH-20 column (100 × 4, 300 × 15 mm), methanol being used for both the swelling and

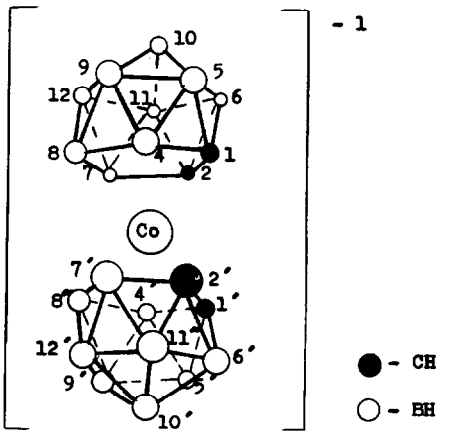

Fig. 1. Structure of compound I.

*Author to whom correspondence should be addressed.

elution. The progress of halogenation was monitored by UV spectra of eluted fractions, treated by linear regression analysis using a HP 9825 A calculator. The fractions exhibiting identical spectra were examined by isotachophoresis in Laboratory of Separation Methods, Chemical Institute of Comenius University and showed an absence of ionic impurities.

For the isolation of halogen derivatives, the methanol–water 60:40 v/v mixture has been found to be the most suitable eluent. The elution volumes for I and IIIb using the 90 × 4 mm column were 16.5 and 30 ml respectively. VIIb did not move under these conditions and pure methanol was required for its elution.

Irradiation

Solutions were irradiated with ^{60}Co γ-rays at 2 Gy.s^{-1} dose rate (determined by Fricke dosimeter) at 32 ± 2°C in sealed glass ampoules.

Chemicals

Caesium salt of *bis*(1,2-dicarbollyl) cobalt(III) has been prepared according to Hawthorne *et al.*[5] When necessary, it was converted to a free acid by passing the 0.1 mol dm^{-3} solution in methanol through a cation-exchange resin Dowes 50 × 8 in H^+-form (35 × 13 mm column for 100 ml of the solution) swelled in methanol. VIIb has been synthetized according to the literature.[5]

Sephadex LH-20 (Pharmacia Uppsala) was used for gel chromatography. All other chemicals were of the analytical grade purity.

Syntheses

Results of analysis of the products are summarized in Table 1. In order to obtain correct analytical data and pure substances, only the first crystallizate was isolated and recorded as the yield. As a rule, the actual yield of halogenation of polyhedral skeleton was quantitative.

$(8\text{-}BrC_2B_9H_{10})Co(C_2B_9H_{11})^-Cs^+$ (IIb)

(a) Elemental bromine (1.6 g, 10 mmol) was added to I (4.57 g, 10 mmol) in methanol. After evaporation of the solvent an orange product was purified twice by the gel chromatography and recrystallized from the ethanol–acetone–water (50:20:30 v/v) mixture. Yield: 4.01 g, (75%).

(b) Compound I (0.045 g) in 10 ml of the methanol–$CHBr_3$ (80:20 v/v) mixture was irradiated by 5 kGy dose. The product was isolated as described in (a). Yield: 0.035 g (66%).

$(8\text{-}BrC_2B_9H_{10})_2Co^-Cs^+$ (IIIb)

(a) Elemental bromine (3.2 g, 20 mmol) was added to the solution of 4.57 g (10 mmol) of I in methanol. After the evaporation of the solvent, the precipitated dark-orange crystals were recrystallized at 50°C in ethanol–water (70:30 v/v) mixture, yielding 4.74 g (77%) of needle shaped crystals of IIIb.

(b) A solution of 0.045 g of I in 10 ml of the methanol–$CHBr_3$ (80:20 v/v) mixture was irradiated by 12 kGy dose; higher doses may be applied as well. After a removal of the solvent, the product was purified as in (a). Yield: 0.054 g, (88%) of IIIb.

$(8\text{-}ClC_2B_9H_{10})Co(C_2B_9H_{11})^-Cs^+$ (IIa)

(a) Gaseous chlorine was bubbled through the solution of 4.57 g (10 mmol) of I in the mixture of ethanol–CCl_4 (70:30 v/v) under cooling. The reaction was stopped after an absorption of 0.75 g of Cl_2 (about 10 mmol). White crystals of CsCl were removed by filtration and after evaporation of the solvent, the product was purified and isolated like in the case of IIb. Yield: 3.68 g (75%).

(b) A solution of 0.045 g of I in 10 ml of the nitrobenzene–CCl_4 (70:30 v/v) mixture was irradiated by 40 kGy dose. After removal of the solvent, the product was purified as in (a). Yield: 0.039 g (80%) of IIa.

$(8\text{-}ClC_2B_9H_{10})_2Co^-Cs^+$ (IIIa)

(a) The synthesis was performed as with IIa–procedure (a), but with the absorption of 1.42 g of Cl_2 (about 20 mmol). Yield: 4.09 g (78%).

(b) A solution of 0.045 g of I in 10 ml of the nitrobenzene–CCl_4

Table 1. Analytical data of halogenated I (%)

Comp.	C		H		B		Cl,Br,I		Co	
	Calc.	Fd.	Calc.	Fd.	Calc.	Fd.	Calc.	Fd.	Calc.	Fd.
Parent	10.53	10.59	4.86	4.91	42.67	42.42			12.90	13.05
IIa	9.78	9.85	4.31	4.40	39.62	39.70	7.22	7.54	11.99	12.08
IIb	8.97	9.05	3.95	4.13	36.34	36.25	14.92	14.22	11.00	11.12
IIc	8.25	8.34	3.81	3.95	33.40	33.31	21.78	21.91	10.12	10.25
IIIa	9.14	9.21	3.78	3.83	37.03	37.10	13.49	13.62	11.21	11.41
IIIb	7.82	7.95	3.32	3.39	31.67	31.45	26.00	27.58	9.59	9.72
IIIc	6.78	6.80	2.84	2.47	27.47	27.52	35.82	35.68	8.32	8.45
IVa	8.58	8.69	3.42	3.53	34.75	34.81	18.99	19.12	10.52	10.62
Va	8.08	8.17	3.05	3.14	32.74	32.80	23.86	23.95	9.91	9.98
VIIa	7.24	7.29	2.43	2.38	29.34	29.44	32.07	32.13	8.88	8.94
VIIc	3.96	3.99	1.33	1.42	16.06	16.15	62.82	62.95	4.86	4.93
VIIIa	9.14	9.23	3.78	3.82	37.03	37.11	13.49	13.60	11.21	11.40
IXa	8.08	8.13	3.05	3.10	32.74	32.79	23.86	23.92	9.91	9.97

a -Cl, b -Br, c -I

(70:30 v/v) mixture was irradiated by 75 kGy dose. After the removal of the solvent, the product was purified as in IIb/(a). Yield: 0.041 g (78%).

$(8,9\text{-}Cl_2C_2B_9H_9)Co(8'\text{-}ClC_2B_9H_{10})^-Cs^+$ (IVa)

(a) Gaseous chlorine was bubbled through the solution of 4.57 g (10 mmol) of I in the mixture of nitrobenzene–CCl_4 (70:30 v/v) under cooling. The reaction was stopped after an absorption of 2.20 g of Cl_2 (about 30 mmol). After removal of the solvent, the product was purified as in (a). Yield: 4.58 g (82%).

$(8,9\text{-}Cl_2C_2B_9H_9)_2Co^-Cs^+$ (Va)

(a) The synthesis was performed as with IVa, but with the absorption of 2.92 g of Cl_2 (about 40 mmol). Yield: 5.05 g (85%).

$(8,9,12\text{-}Cl_3C_2B_9H_8)_2Co^-Cs^+$ (VIIa)

(a) It was used the same procedure as in IIa/(a) but with the absorption of 4.61 g of Cl_2 (about 60 mmol). Further absorption of chlorine led to the formation of chloro derivatives of I with more than six chlorine atoms in the molecule. Yield: 4.18 g (63%).

(b) A solution of 0.045 g of I in 10 ml of the nitrobenzene–CCl_4 (70:30 v/v) mixture was irradiated by 100 kGy dose. After the removal of the solvent, the product was purified as in IIb/A. Yield: 0.045 g (67%).

$(8\text{-}IC_2B_9H_{10})Co(C_2B_9H_{11})^-Cs^+$ (IIc)

Elemental iodine (0.25 g) was added to I (0.46 g) in methanol. After evaporation of the solvent an orange product was purified twice by the gel chromatography and recrystallized from the ethanol–acetone–water (70:20:10 v/v) mixture. Yield: 0.48 g (84%).

$(8\text{-}IC_2B_9H_{10})_2Co^-Cs^+$ (IIIc)

Iodine (15 g, 60 mmol) was added to the solution of I (9.2 g, 20 mmol) in 50 ml of ethanol. When an exothermic reaction ceased, the reaction mixture was left to stand overnight at room temperature and then was heated at 80°C for 2 hr. The excess iodine was decomposed by the addition of 12.6 g (50 mmol) of $Na_2SO_3.7\ H_2O$ in 100 ml of water, the whole solution was boiled for a while and then was left to stand for 2 days. The compound IIIc crystallized very slowly in the form of orange prisms 12.1 g (85%).

$(8,9,12\text{-}I_3C_2B_9H_8)_2Co^-Cs^+$ (VIIc)

To the suspension of I (4.6 g, 10 mmol) and $AlCl_3$ (3.0 g, 20 mmol) in 40 ml of benzene heated at 50°C was added iodine (16.5 g, 65 mmol) during 1 hr. The vigorously escaping HI was collected in a polyethylene bag connected with the reaction apparatus. After the addition of the all iodine, the reaction mixture was heated for additional 2 hr to 80°C until the colour of I_2 disappeared. To the reaction mixture was added 200 ml of water, benzene was evaporated *in vacuo* and the remnant was extracted by two 100 ml portions of diethyl ether. Excess iodine in the combined ether extracts was decomposed by an addition of a small amount of aqueous solution of Na_2SO_3, ether was evaporated *in vacuo* and the brown thick water-insoluble remainder was neutralized with 3.0 g of K_2CO_3 in 100 ml of water and dissolved by the addition of 40 ml of ethanol. The orange-brown liquor was filtered, 2.5 g of Cs_2SO_4 in 100 ml of water was added, the mixture was heated until turned homogeneous and was left to stand for 3 days to yield during a slow crystallization 10.3 g (84.4%) of heavy brown prisms of VIIc.

$(9\text{-}ClC_2B_9H_{10})_2Co^-Cs^+$ (VIIIa)

To the suspension of 9-chloro-o-carborane (3.6 g, 20 mmol) in 30 ml of methanol was added 6.0 g of KOH pellets. When a violent reaction (moderated by occasional cooling) ceased, the resulting solution was heated for additional 30 min till the end of a hydrogen evolution. After the evaporation of a part of methanol *in vacuo*, the remainder was diluted with 50 ml of water, the mixture was concentrated by evaporation *in vacuo* to the volume of 30 ml, and $CoCl_2.6H_2O$ (3.8 g, 15 mmol) in 10 ml of hot water, followed by 12 g of KOH pellets were successively added. The mixture was intensively shaken for 10 min, heated under stirring to 80°C and kept at this temperature for the additional 10 min. The resulting orange solution got turbid by separated particles of grey-black elemental cobalt and of hydrated cobalt oxides. The suspension was filtered, the precipitate was washed twice with 20 ml of hot water, the combined clear filtrates were heated to 90°C and mixed with 2.0 g of Cs_2SO_4 in 10 ml of water. The yellow precipitate was dissolved by an addition of ethanol under heating and the solution was left to stand overnight at room temperature. The precipitated yellow-orange leaflets were sucked off, washed with 20% aqueous ethanol and water, and dried in air yielding 4.5 g (85.5%) of VIIIa.

$(9,12\text{-}Cl_2C_2B_9H_9)_2Co^-Cs^+$ (IXa)

9,12-Cl_2-1,2-$C_2B_{10}H_{10}$ (4.3 g, 20 mmol) treated in the same manner as in the preparation of VIIIa afforded 5.1 g (85.6%) of IXa.

RESULTS AND DISCUSSION

Reaction of halogens with $(C_2B_9H_{11})_2Co^-Cs^+$ in various polar solvents (CH_3OH, C_2H_5OH, CCl_4/nitrobenzene) has been found to proceed successively with the main path represented by the following steps:

$$\underset{\text{I}}{(C_2B_9H_{11})_2Co^-Cs^+} \rightarrow \underset{\text{II}}{8\text{-X-}} \rightarrow \underset{\text{III}}{8,8'\text{-}X_2\text{-}} \rightarrow \underset{\text{IV}}{8,9,8'\text{-}X_3\text{-}}$$

$$\underset{\text{VII}}{8,9,12,8',9',12'\text{-}X_6\text{-}} \leftarrow \underset{\text{VI}}{8,9,12,8',9'\text{-}X_5\text{-}} \leftarrow \underset{\text{V}}{8,9,8',9'\text{-}X_4\text{-}}$$

$a = Cl \quad b = Br \quad c = I$

Scheme 1.

In accord with the estimation of electron densities which drop with I in the order B(8) > B(9,12) > B(10) > etc.,[9] the first product is always the 8-halogeno derivative (II), followed by the 8,8'-dihalogeno species (III). As it has been found by kinetic measurements,[10] the introduction of the second halogen atom is distinctly slower, which indicates an easy transmission of substituent effects from one carborane ligand through the cobalt atom to the opposite ligand. This fact allows control of the substitution by the reactants ratio. While the mono- and dihalogenation are easy to perform by using the appropriate molar amount of halogen, a further halogenation to a higher degree, as to the compounds (IV), (V) or (VI) results always in mixture of these compounds.

The substitution at the B(8) and B(8') positions brings distinct changes both in the ^1H NMR chemical shifts of the carborane C–H signals and in the HPLC relative retention times (Table 2) which had allowed a relatively easy identification and separation of mixtures, composed of compounds (I), (II) and (III). Surprisingly, in the case of the hexachloro derivative (VIIa), the presence of further four chlorine atoms did not differentiate these important characteristics from those of 8,8'-dichloro derivative (IIIa). A suspicion that chlorine atoms in positions B(9) and B(12) do not change properties governing these characteristics has been confirmed with $(9\text{-}ClC_2B_9H_{10})_2Co^-Cs^+$ (VIIIa) and $(9,12\text{-}Cl_2C_2B_9H_9)_2Co^-Cs^+$ (IXa) compounds, the discussed characteristics of which differ nly slightly from those of the parent compound (I) (see Table 1). This causes great difficulties in identification and separation of individual polychlorinated derivatives of (I) by HPLC on chemically bonded silica gel (controlled largely by dipole

Table 2. A comparison of ^{1}H NMR[a] and HPLC[b] characteristics of some chloro derivatives of I

Substituent/s and Their Position/s in I	Relative retention time[c]	^{1}H δ (ppm)
Parent	100	3.95
8-Cl	135	4.30 4.18
8,8′-Cl_2	235	4.29
9,9′-Cl_2	100	4.03 3.90
9,12,9′,12′-Cl_4	86	4.04
8,9,12,8′,9′,12′-Cl_6	230	4.31

[a] 200 MHz, CD_3COCD_3, TMS ; [b] Silanized silica gel; column : length 300 mm, I.D. 3.8 mm; eluent: 2.7 mM n-$C_{12}H_{25}NH_2$.HCl in methanol - water 6:4, pressure: 7.5 MPa; flow rate: 1.1 ml/min.; ; UV detector at 254 nm; relative retention time of I = 300 sec.; [c] Dr.Z. Plzák of the Institute of Inorganic Chemistry, Řež, is thanked for the kind permission to use these data prior publication.

moments) and of the successful separation by the gel chromatography on Sephadex which is governed preferentially by the molecular size of compounds to the separated. In this way, the practically pure chloroderivatives (IVa) and (Va) were isolated.

As demonstrated in the Scheme 1, the successive alternating entry of halogen atoms into both dicarbollide ligands is consistent with the suggestion that each halogen atom decreases the electron density both on single vertices in the same ligand, and although somewhat less distinctly, in the opposite ligand.

Going from chlorine to iodine, the reaction rate of halogenation of (I) distinctly decreases. This follows from the fact that, without catalysis, chlorine can afford not only hexachloro compound (VIIa) but also more chlorinated species even at ambient temperature, bromine does not react to (VIIb) before heating, and iodine in excess yields under prolongued heating only diiode compound (IIIc) while (VIIc) is formed in almost quantitative yield from (I) only in the presence of $AlCl_3$ and in a benzene slurry.

GAMMA-RADIATION-INDUCED HALOGENATION OF I IN THE PRESENCE OF $CHBr_3$, $CHCl_3$ OR CCl_4

The gamma-radiation-induced halogenation of the bis (dicarbollyl) cobalt (III) skeleton performed under various conditions is summarized in the Scheme 2.

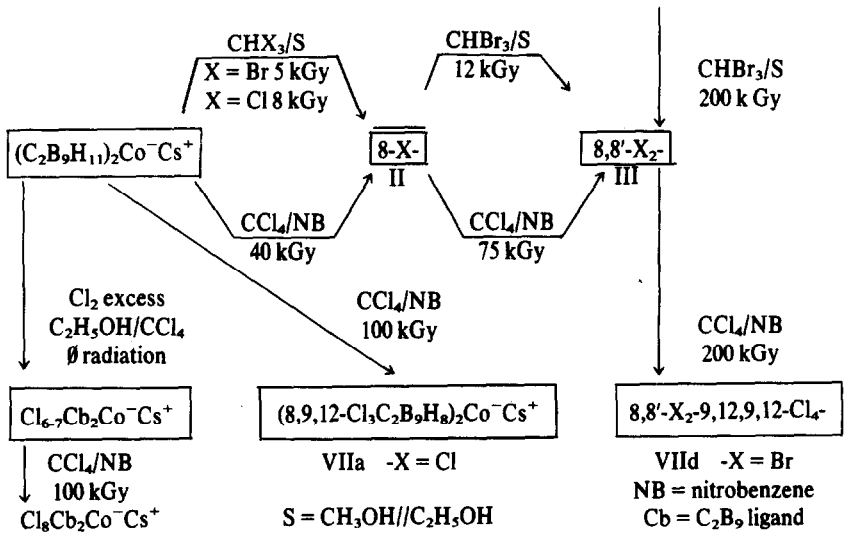

Scheme 2.

The Scheme 2 shows that the radiation-induced halogenation parallels in many respects the direct halogenation. The difficulty in the introduction of the third bromine atom during the radiation of (IIIb) in the presence of $CHBr_3$ is easy to understand since (IIIb) was also found unchanged in the presence of excess bromine under comparable conditions. The absence of further chlorination of (IIIa) under analogous conditions (200 kGy) in the presence of $CHCl_3$ is, however, more obscure, especially in the light of the fact that in the presence of CCl_4 a further chlorination proceeds until (VIIa) is reached even at lower doses (100 kGy). This indicates that the radiation-induced chlorination by $CHCl_3$ is probably of a different course than that evoked by CCl_4. A possible reason may be found in different results of radiolytical dissociation of $CHCl_3$ and CCl_4, of which the latter decomposes merely to Cl_2 and C_2Cl_6, while $CHCl_3$ changes to a variety of products with no chlorine among them.[11] If this consideration holds, the radiation-induced chlorination by $CHCl_3$ is likely to transfer the most hydridic H atom from the B(8) vertex to some of radiation intermediates, followed by the transfer of a chlorine atom to the released B(8) position.

As demonstrated in the Scheme 2, an introduction of more than six chlorine atoms into (I) is successful by a direct halogenation, the products of which can, in some cases, be again CCl_4-radiolytically chlorinated. The fact that no further radiation-induced chlorination can be achieved starting from the pure hexachloro derivative (VIIa) indicates that such a halogenation can probably be operative only with compounds in which during a violent chlorination also less negatively charged vertices were substituted leaving some B(9,12) positions untouched.

The above observations indicate that the γ-radiation-induced chlorination by CCl_4 is likely a result of a direct reaction of (I) (which reacts as an excellent halogen scavenger) with the elemental chlorine while the chlorination by $CHCl_3$ has a different course.

IDENTIFICATION OF HALOGENATED DERIVATIVES OF I

The main characteristics of the isolated halogen derivatives of (I) are gathered in Tables 3–6.

A combination of the gel chromatography on the Sephadex LH-20 column and of the electronic spectra of halogenated products (Table 3) treated by regression coefficient techniques were found to be a useful tool for tracking reaction steps to mono, di-, hexahalogenated compounds.

The IR spectra (Table 4) show four main groups of signals.

Table 3. UV spectra of halogenated I

Substituted I	λ_{1max}, nm	ε_1, $M^{-1}cm^{-1}$	λ_{2max}, nm	ε_2, $M^{-1}cm^{-1}$
Parent	287	30,980		
8-Cl	308	26,111	260	8,570
8-Br	315	30,000	273	8,830
8-I	295	35,200	318	34,700
8,8′-Cl_2	313	30,170	263	8,590
8,8′-Br_2	322	27,660	277	9,000
8,8′-I_2	291	17,000	335	15,500
8,9,8′-Cl_3	318	33,050	274	7,667
8,9,8′,9′-Cl_4	320	33,600	278	8,250
9,9′-Cl_2[x]	283	39,300		
9,12,9′,12′-Cl_4[x]	284	47,500		
8,9,12,8′,9′,12′-Cl_6	325	34,650	284	8,170
8,9,12,8′,9′,12′-I_6[x]	351	2,640	276	1,340

METHANOL SOLUTION, [x]-ACETONITRILE SOLUTION

Table 4. IIR spectra of halogenated I (cm^{-1}, Nujol mulls, x-KBr tablets)

Substituted I	
Parent	3040m,2595-2540br-s,1205m,1185w,1150m,1140m, 1100s,1115m,1080w,1050s,1010m,990s,950m,930w, 920m,895m,760w,730m
8-Cl	3040m,2580-2540br-s,1200m,1180w,1140m,1110m, 1100s,1080w,1020m,980s,940w,920m,900w,880m, 850s,830s,795w,780m,750s,690m
8-Br	3040m,2580-2540br-s,1219w,1200m,1180w,1140m, 1113m,1100s,1080w,1018m,990m,975s,940w,915m, 900w,880m,820m,802s,790s,750s,735w
8-I^{x}	3040m,2620-2520br-s,2480s,1200m,1135m,1108w, 1100s,1075w,1030m,1010m,990-980br-s,940w,910w, 900w,880m,(810w,765s,755s,730m)br,690w,650m
8,8'-Cl_2	3040m,2580-2540br-s,1185m,1105s,1080m,1040w, 1028m,990s,980s,940m,925w,915m,900w,880s,855m, 840s,810w,790w,750-744br-m
8,8'-Br_2	3040m,2600-2540br-s,1185m,1108s,1080m,1008m, 990m,980s,940w,915w,900m,880m,(830s,810s,790s) br,750m,735m,715w,690m,650m
8,8'-I_2^{x}	3040m,2600-2540br-s,1180m,1108s,1080m,1010m, 990w,980m,940w,920w,900m,880m,(820m,805s,775s, 750m,730s,710w)br,690m
8,9,8'-Cl_3^{x}	3035m,2590-2520br-s,1175m,1095s,1033m,1048w, 1030m,990s,978s,945m,930m,915m,878s,850s,835s, 785w,745m,695w,655w,610w,575w
8,9,8',9'-Cl_4	3040m,2600-2530br-s,1185m,1097s,1080m,1045m, 1025s,972s,945m,930m,920m,880vs,855vs,810m,
9,12,9',12'-Cl_4	785w,750s,700w,677w,750w,625w-sh,615w, 585w,500w,395w
8,9,12,8',9',12'-Cl_6	3065m,3030m,3010m,2610-2520br-s,1210w,1195w, 1140w,1108m,1090m,1075w,1048m,1032m,1003m, 975w,945s,890s,858vs,820m-sh,760m,710w,685w
8,9,12,8',9',12'-Br_6	3040m,2540br-s,1180m,1103s,1080w,1040m,1020s, (980s,940m,930m,910w,880s,860s,850s)br,810w, 790w,750s
8,9,12,8',9',12'-I_6	3040m,2560-2540br-s,1180m,1120w,1100s,1080m, 1008m,980m,955s,940m,910w,890w,(865s,850s, 830m)br,790m,750m,690w
9,9'-Cl_2	3020s,2610s,2595s,2560s,2530s,1175m,1095m, 1075m,976w,940m,930w,910w,840s,815s,805s, 763m,743m,678w,617w,590w,
	3040m,3010m,2600-2540br-s,1195m,1133w,1105m, 1090s,1072w,1040w,1023m,997m,975s,955m,935m, 920w,900w,875m-sh,860s,758m,728w,695w,620w

Table 5. NMR spectra of halogenated I (^{11}B: 64.2 MHz, acetone, related to $BF_3.O(C_2H_5)_2$, -sing: upfield from standard, *s* = singlet, ^1H: 200 MHz, CD_3COCD_3, TMS)

Substituted I	^{11}B δ in ppm (relative intensity higher than 1)	^1H δ CH-cage
Parent	6.5 1.5 -7.1(4) -16.9(2) -22.3	3.95
8-Cl	14.4[s] 6.8 -4.8(8) -12.3(4) -24.6(2)	4.30 4.18
8-Br	7.9[s] 6.8 2.9 0.0 -2.4(2) -5.8(6) -16.3(2) -18.5(2) -21.2 -24.8	4.45 4.33
8-I	6.2 3.2 0.9 -2.0(2) -5.1[s](5) -5.8(2) -16.3(2) -17.8(2) -21.2 -23.4	4.54 4.29
8,8′-Cl_2	12.9[s] 0.4 -4.8(4) -18.5(2) -24.8	4.29
8,8′-Br_2	7.8[s] 1.7 -4.2(4) -17.4(2) -23.4	4.33
8,8′-I_2	2.8 -3.3(4) -5.1[s] -17.0(2) -22.6	4.40
9,9′-Cl_2	6.5 5.0[s] 1.6 -5.6(2) -7.5 -17.4 -18.0 -23.4	4.03 3.90
8,9,8′-Cl_3	13.4[s] 11.4[s] 4.0[s] 1.0 0.6 -4.7(6) -6.8 -18.3(3) -19.9 -24.8(2)	4.39 4.28 4.24 4.16
8,9,8′,9′-Cl_4	11.8 4.1[s] 1.0 -4.7(2) -6.7 -18.4 -19.6 -24.9	4.38 4.26
9,12,9′,12′-Cl_4	6.3 4.4[s](2) 1.9 -7.6(2) -17.8(2) -24.4	4.04
8,9,12,8′,9′,12′-Cl_6	10.1[s] 3.1[s](2) -4.4(2) -19.4(2) -25.8	4.32
8,9,12,8′,9′,12′-Br_6	6.2[s] 2.7 -2.1[s](2) -3.8(2) -18.1(2) -24.1	4.58
8,9,12,8′,9′,12′-I_6	6.0 -3.5(2) -4.2[s] -13.4[s](2) -15.1(2) -21.4	5.00

Table 6. Electrolytical parameters of $(8\text{-}BrC_2B_9H_{10})_2Co^-Cs^+$ and $(8\text{-}BrC_2B_9H_{10})_2Co^-H^+$ solutions (22°C)

Solvent	nitrobenzene		nitrobenzene-CCl_4 (1:2 v/v)
Reference values:			
a_1 ($S^{-1}dm^{-1/2}$)	776		475
a_2 ($dm^{3/2}mol^{-1}$)	44.37		125
A ($dm^{3/2}mol^{-1}$)	1.72		9.67
Estimated:	IIIb(H^+)	IIIb(Cs^+)	IIIb(H^+)
λ_o ($Smol^{-1}dm^2$)	0.306	0.314	0.324
B ($dm^{3/2}mol^{-1/2}$)	4.3	2.7	11.8
K_T ($mol.dm^{-3}$)	$> 10^7$	$> 10^9$	$6.1x10^{-2}$

(1) ν CH vibrations at 3040 cm^{-1} which do not practically change with substitution.

(2) Strong ν BH vibration bands at about 2600 cm^{-1} exhibiting a refinement of the broad signal with 8,8′-disubstituted species.

(3) Substituent influenced bands in the 950–1200 cm^{-1} region

(4) B–X vibrations which are shifted to lower frequencies in order B–Cl (840–890 cm^{-1}) > B–Br (790–830 cm^{-1}) > B–I (750–800 cm^{-1}), i.e. similarly as it was observed with halogenated *o*-carboranes.[13–15]

The structures of all compounds described were proposed on the grounds of the ^{11}B and ^1H NMR spectra (Table 5). Line-narrowed ^1H decoupled and undecoupled ^{11}B spectra (at 64 or 86 MHz) revealed practically all signals present with the accuracy better than 0.1 ppm.

The constitutions of compounds substituted symmetrically in both C_2B_9-ligands, i.e. of $8,8'X_2$(III), $9,12,9',12'\text{-}X_4$ and $8,9,12,8',9',12'\text{-}X_6$ (VII) derivatives were deduced from the ^{11}B spectra which have shown in all cases the main features of the spectrum of the parent anion[12] with one singlet of relative area 2 with $8,8'\text{-}X_2$, one singlet of relative area 4 with $9,12,9',12'\text{-}X_4$ and two singlets of 2:4 area ratio with X_6-derivatives. In all cases, the signals belonging in the parent spectrum to the substituted atoms were changed to singlets and were shifted by 4–12 ppm to the lower field with chlorine, by 2 to −2 ppm with bromine and by −10 to −12 ppm (i.e. to the higher field) with iodine substitution. Analogously, the ^1H spectra have exhibited with all these compounds only one C–H carborane signal, which is in the full agreement with the preservation of symmetry in each C_2B_9-fragment and with an identity of both ligands.

The constitution of the 8-monosubstituted compounds (IIa–c), isolated as the first intermediate in the halogenation of the $(C_2B_9H_{11})_2Co^-$ anion follows both from the fact that a further halogenation converts them to the $8,8'\text{-}X_2$-derivatives and from the NMR spectra. The ^{11}B spectra are composed of two sets: one set containing 6 doublets in a 1:1:1:2:2:2 area ratio and of chemical shifts close to those of the parent anion (I), and another set consisting of a singlet of area one and five doublets of relative area 1:1:2:2:2, having chemical shifts rather similar to those of 8,8′-disubstituted compounds (IIa–c). In an agreement with this, the ^1H spectrum exhibits two slightly different C–H carborane signals belonging to the substituted and the unsubstituted ligand.

The ^{11}B spectrum of $8,9,8',9'\text{-}Cl_4$ derivative of (I) has confirmed both the identity of the two C_2B_9-ligands and unsymmetrical substitution in them, showing two different singlets and seven further doublets of intensity one (doublet of intensity 2 at −4.7 is a result of an insufficient resolution). The position of singlets corresponds to the substitution in the positions B(8) and B(9).

The position of the chlorine atoms in the $8,8',9\text{-}Cl_3$ derivative of (I) has been proposed on the ground of the ^{11}B spectrum which has the figure similar to that of (I), and in which it is possible to trace one set belonging to the B(8), i.e. symmetrically substituted ligand (area ratio $1^s:1:1:2:2:2$; s = singlet) and a second set appertaining to the B(8), B(9), i.e. unsymmetrically substituted ligand (2 singlets and 7 doublets of relative area one).

A more detailed discussion of ^{11}B spectra and assignments of most signals will be published elsewhere.

All the compounds should be highly dissociated in polar solvents which we used, as it ensues from electrolytical properties (Table 6). Even in the nitrobenzene–CCl_4 1:2 mixture, having relative permitivity $\epsilon = 11.0$. the dissociation constant of $(8\text{-}BrC_2B_9H_{10})_2Co^-H_3O^+$ is high enough to ensure high dissociation (>90%) even in 0.15 $mol.dm^{-3}$ solutions. Thus, the halogenation of (I–VI) can proceed as ion-molecular reactions.

Acknowledgement—Elemental analysis and IR spectra were performed by Dipl. Ing. Eva Greiplova, and Dr. A. Perjessy from the Chemical Institute of the Comenius University, Bratislava. We are also grateful to Professor Donald Gaines for NMR spectra measured on a Bruker WH-270 spectrometer. IR spectra in KBr tablets were performed by Dr. F. Haruda Institute of Inorganic Chemistry, Czechoslovak Academy of Sciences, Řež.

REFERENCES

[1]Ľ. Mátel, R. Čech, F. Macášek, S. Heřmánek and J. Plešek, *Radiochem. Radioanal. Lett.* 1977, **29**, 317.

[2]Ľ. Mátel, R. Čech, F. Macášek, S. Heřmánek and J. Plešek, *Radiochem. Radioanal. Lett.* 1978, **35**, 241.

[3]Ľ. Mátel F. Macášek and H. Kamenistá, *Radiochem. Radioanal. Lett.* 1981, **46**, 1.

[4]Ľ. Mátel, H. Kamenistá and R. Čech, XVI. Nat. Symposium on Radiation Chemistry, 2–6 May, 1979. Dvur Králové, Czechoslovakia.

[5]M. F. Hawthorne, D. C. Young, T. D. Andrews, D. V. Howe, R. L. Pilling, A. D. Pitts, M. Reintjes, L. F. Warren Jr. and P. A. Wegner, *J. Am. Chem. Soc.* 1968, **90**, 879.

[6]A. R. Siedle, G. M. Bodner, A. R. Garber, D. C. Beer and L. J. Todd, *Inorg. Chem.* 1974, **13**, 2321.

[7]P. Selucký, K. Baše, J. Plešek, S. Heřmánek and J. Rais, Czechoslov. Pat. Appl. PV 6892-79.

[8]Yu. A. Fialkov, A. N. Zhitomirskii, Yu. A. Tarasenko, Fiz icheskaya khimiya nevodnych rastvoroch, Khimiya, Leningrad (1973).

[9]J. Plešek, K. Baše and S. Heřmánek, II. *Int. Meeting on Boron Compounds, Abstracts*, p. 46, 25–29 March 1974. Leeds, England.

[10]Ľ. Mátel, F. Macášek, P. Rajec, S. Heřmánek and J. Plešek. *Polyhedron* to be published.

[11]J. W. T. Spinks and R. J. Wood, *An Introduction to Radiation Chemistry*, p. 401. Wiley, New York, (1976).

[12]A. R. Siedle, G. M. Bodner and L. J. Todd, *J. Organometal. Chem.* 1971, **33**, 137.

[13]L. A. Lejtes, L. E. Vinogradova, V. N. Kalinin and L. I. Zakharkin, *Izv. Akad. Nauk SSSR, Ser. Khim.* 1968, 1016.

[14]V. I. Stanko, A. I. Klimova and T. P. Klimova, *Zh. Obshch. Khim.* 1967, **9**, 2236.

[15]R. Freyman, A. Bullier, Mmes G. Capderroque and M. Selim, *Analusis* 1976, **4**, 258.

Polyhedron Vol. 1, No. 6, pp. 521–523, 1982
Printed in Great Britain.

0277-5387/82/060521-03$03.00/0
Pergamon Press Ltd.

ON THE VALIDITY OF THE ISOLOBAL PRINCIPLE: PENTABORANE(9) AND ITS FERRABORANE DERIVATIVES

ROGER L. DEKOCK*
Department of Chemistry, Calvin College, Grand Rapids, MI 49506, U.S.A.

and

THOMAS P. FEHLNER
Department of Chemistry, University of Notre Dame, Notre Dame, IN 46556, U.S.A.

(*Received* 11 *March* 1982)

Abstract—We have completed Fenske–Hall LCAO–MO–SCF calculations on B_5H_9, 1-$Fe(CO)_3B_4H_8$, 2-$Fe(CO)_3B_4H_8$, and 1,2-$[Fe(CO)_3]_2B_3H_7$. Comparison of orbital contour diagrams of the a_1 and e cluster MO's for B_5H_9 and 1-$Fe(CO)_3B_4H_8$ demonstrates the validity of the isolobal principle. In addition it is found that the apical and basal BH units of B_5H_9 have practically identical Mulliken overlap populations for framework cluster-type interactions. Further, in all the ferraboranes the 1-$Fe(CO)_3$ (apical) units have a larger cluster-type Mulliken overlap population than do the 2-$Fe(CO)_3$ (basal) units. The $Fe(CO)_3$ units have less electronic charge than do the BH units. The cluster-type Mulliken overlap population for an $Fe(CO)_3$ group is much less than that of the isolobal BH unit, but this may result from an artifact of the Mulliken overlap population analysis.

1. INTRODUCTION

The use of boranes as models for the geometric and electronic structures of metal clusters has received significant attention in recent years. In earlier studies an empirical correlation of geometric structures was noted and is commonly referred to as the "borane analogy".[1] A more complete understanding of the borane analogy has resulted from recognition that the pertinent molecular fragments [e.g. BH and $Fe(CO)_3$] have similar spatial and energetic distribution of their valence orbitals. The latter is referred to as the "isolobal principle".[2] Recently, the results of self-consistent charge extended Hückel molecular orbital calculations on metalloboranes have been used to suggest that, although there are similarities between BH and $Fe(CO)_3$, there is a significant difference as well.[3] Namely, that whereas the BH fragment contributes 3 atomic orbitals and 2 electrons in cluster bonding, the $Fe(CO)_3$ fragment is seen to effectively contribute only 2 orbitals and 1 electron. The purpose of this work is to reexamine the validity of the isolobal principle for B_5H_9 and some of its ferraborane derivatives, i.e. 1-$Fe(CO)_3B_4H_8$, 2-$Fe(CO)_3B_4H_8$, and 1,2-$[Fe(CO)_3]_2B_3H_7$, using a non-parameterized method.

2. METHOD OF CALCULATION

Our calculation technique is the LCAO–MO–SCF Fenske–Hall method[4] with use of the usual basis functions that are employed for this method. For Fe(+1) the atomic wave functions of Richardson *et al.*[5] were employed except that the 4*s* and 4*p* exponents were set to 2.00 to make them slightly more contracted than the free atom functions. The boron, carbon, and oxygen functions are those that have been used often in Fenske–Hall calculations and are essentially Clementi[6] double-zeta or curve-fit thereto. For hydrogen 1*s* we used an exponent of 1.16.

The geometry of B_5H_9 was taken from the reported microwave spectroscopic results,[7] and of 1,2-$[Fe(CO)_3]_2B_3H_7$ from the reported X-ray diffraction study[8] with slight adjustments for C_s symmetry as described in our study of diiron ferraboranes.[9] The structures of 1-$Fe(CO)_3B_4H_8$ and 2-$Fe(CO)_3B_4H_8$ were estimated based on the known structures of B_5H_9 and 1,2-$[Fe(CO)_3]_2B_3H_7$.

3. RESULTS AND DISCUSSION

The calculated electronic structures of B_5H_9 and 1-$Fe(CO)_3B_4H_8$ are in agreement with other theoretical results,[10–12] and with the interpretation of the UV-photoelectron spectra of these compounds.[11–14] Briefly, the HOMO of B_5H_9 is an e orbital, and the penultimate orbital is an a_1 orbital; both of these orbitals are involved in cluster bonding between the apical boron atom and the basal B_4H_8 group. The a_1 orbital also contains significant $(B–H)_{apical}$ character. The electronic structure of 1-$Fe(CO)_3B_4H_8$ is very similar in terms of the cluster e and a_1 orbitals; in addition there are three "nonbonding" orbitals that are predominantly localized on $Fe(CO)_3$ and characterized as "d^6". A summary of this qualitative orbital description is presented in Fig. 1. The existence

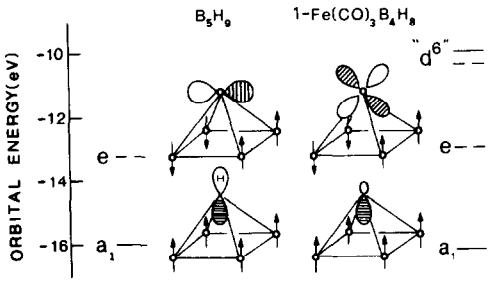

Fig. 1. Energy level diagrams for the upper MO's of B_5H_9 and 1-$Fe(CO)_3B_4H_8$ with qualitative sketches for the e and a_1 cluster MO's. The arrows represent 2*p* orbitals on boron. The eigenvalues of B_5H_9 were shifted to less negative values by 2.5 eV. Only one of each degenerate e orbital is shown.

*Author to whom correspondence should be addressed.

of analogous a_1 and e orbitals for both compounds is expected on the basis of the isolobal principle.

Orbital contour diagrams for both the e and the a_1 orbitals of B_5H_9 and 1-$Fe(CO)_3B_4H_8$ are presented in Fig. 2. These diagrams provide a more quantitative assessment of the isolobal principle. It is clear from the similarity of the contours that the predictions of the isolobal principle are indeed valid for these compounds. This conclusion contradicts the results obtained from self-consistent charge extended Hückel theory (SCC-EHT) calculations on 1-$Fe(CO)_3B_4H_8$ wherein the e orbital *only* was involved in cluster bonding.[3]

In order to further examine our results on B_5H_9 and the ferraboranes we tabulate relevant Mulliken overlap

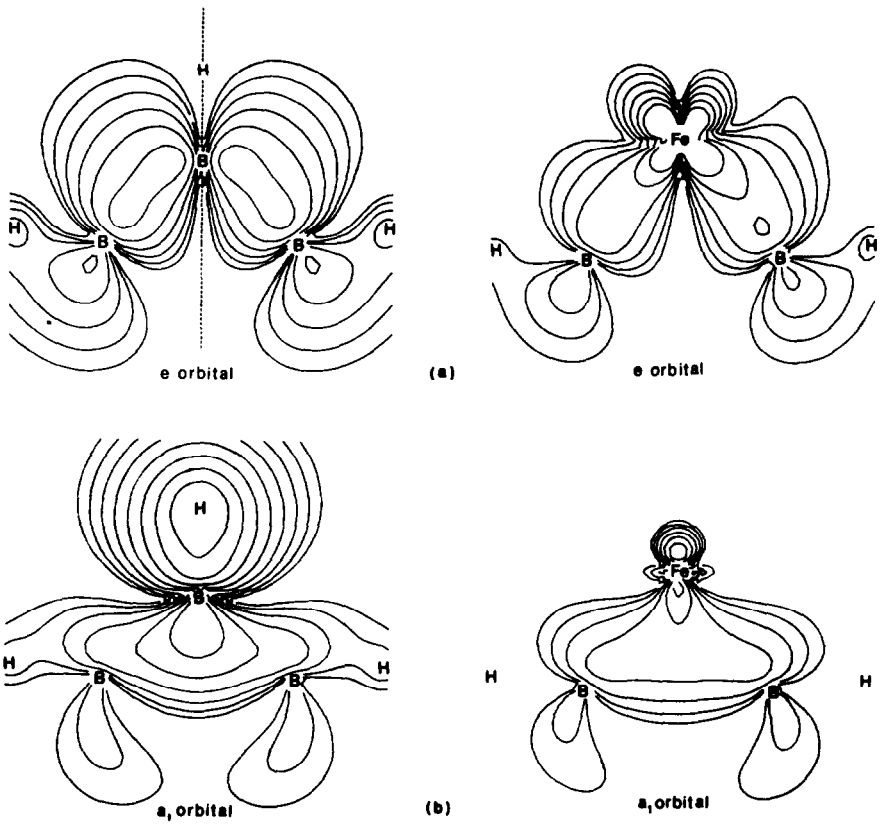

Fig. 2. Orbital contour diagrams for the e and a_1 MO's of B_5H_9 and 1-$Fe(CO)_3B_4H_8$. The contours are shown in the plane of B_1–B_2–B_4 (see sketch in Table 2). The contours are for the square of the appropriate wavefunction and succeeding contours decrease by a factor of two with units of electrons per cubic atomic unit (Bohrs). The largest contour value of all four diagrams is 0.05 except for the e set of B_5H_9 where it is 0.025. Notice that there is some distortion of the two-fold symmetry in 1-$Fe(CO)_3B_4H_8$ due to the local C_3 axis on the $Fe(CO)_3$ group.

Table 1. Total Mulliken overlap population between the specified cluster atom and the remainder of the cluster atoms

Molecule	Cluster Atom	Overlap Population Fenske-Hall	SCC-EHT[a]
B_5H_9	apical B	1.922	2.080
	basal B	1.901	1.785
1-$Fe(CO)_3B_4H_8$	apical Fe	0.357	1.066
	basal B	1.821	1.879
2-$Fe(CO)_3B_4H_8$	basal Fe	0.299	0.701
1,2-$[Fe(CO)_3]_2B_3H_7$	apical Fe	0.532	0.667
	basal Fe	0.234	0.794

[a]Ref. 3.

Table 2. Calculated atomic charges on BH, $Fe(CO)_3$, μ_2-H, and Fe atoms on sites shown in the diagram

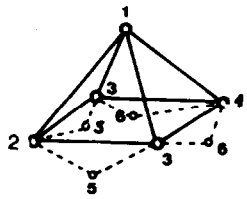

Molecule	Site						
	1	2	3	4	5	6	Iron atom
B_5H_9	-0.330	0.041	0.041	0.041	0.041	0.041	----
1-$Fe(CO)_3B_4H_8$	0.482	-0.219	-0.219	-0.219	0.098	0.098	0.405
2-$Fe(CO)_3B_4H_8$	-0.493	0.853	-0.161	0.123	-0.117	0.037	0.589
1,2-$[Fe(CO)_3]_2B_3H_7$	0.298	0.596	-0.410	-0.177	-0.074	0.126	0.295*

*Charge on the apical Fe Atom. The basal Fe atom has a calculated charge of 0.442.

population (o.p.) values in Table 1 and compare our values with those obtained in the extended Hückel calculations.[3] These o.p. values refer to the total cluster bonding of a given cluster atom to the remainder of the cluster atoms. Excluded are interactions with the terminal B–H hydrogen atoms and the three CO ligands on the iron atoms. Several conclusions result from these o.p. values. First, the apical and basal BH units of B_5H_9 have nearly the same cluster o.p. for the Fenske–Hall calculation in contrast to the SCC–EHT calculation which shows the basal BH unit to have a somewhat smaller o.p. than the apical unit. Second, in all three ferraboranes the 1-$Fe(CO)_3$ units have a larger cluster o.p. than do the 2-$Fe(CO)_3$ units. This also is borne out by the SCC–EHT calculations on 1-$Fe(CO)_3B_4H_8$ but not for 1,2-$[Fe(CO)_3]_2B_3H_7$. Third, in both the Fenske–Hall and SCC–EHT calculations the o.p. for the $Fe(CO)_3$ group is much less than that of the isolobal BH group. Due to the inherent limitations in the Mulliken overlap population analyses,[15] we do not feel that it is appropriate to conclude from this that the $Fe(CO)_3$ group is less tightly bound to the cluster than are the isolobal BH units.

The calculated atomic charges for pertinent cluster units are given in Table 2. These values illustrate that the $Fe(CO)_3$ group has less electron density associated with it than does the isolobal BH group that it replaces. This result is in agreement with the calculated atomic charges from the SCC–EHT calculations.[3]

Acknowledgements—The support of the National Science Foundation (CHE 79-15220) is gratefully acknowledged.

REFERENCES

[1]K. Wade, in *Adv. Inorg. Chem. Radiochem.* (Edited by H. J. Emeleus and A. G. Sharpe), p. 1. Academic Press, New York (1976); R. W. Rudolph, *Acc. Chem. Res.* 1976, **9**, 446.
[2]For leading references to the isolobal principle see D. N. Cox, D. M. P. Mingos and R. Hoffman, *J. Chem. Soc. Dalton* 1981, 1788.
[3]P. Brint and T. R. Spalding, *J. Chem. Soc. Dalton*, 1980, 1236; P. Brint, K. Pelin and T. R. Spalding, *Inorg. Nucl. Chem. Lett.* 1980, **16**, 391.
[4]M. B. Hall and R. F. Fenske, *Inorg. Chem.* 1972, **11**, 768; M. B. Hall, Ph.D. Thesis, University of Wisconsin, Madison, Wisconsin, 1971; R. F. Fenske, *Pure Appl. Chem.* 1971, **27**, 61.
[5]J. W. Richardson, W. C. Nieuwpoort, R. R. Powell and W. F. Edgell, *J. Chem. Phys.* 1962, **36**, 1057.
[6]E. Clementi, *J. Chem. Phys.* 1964, **40**, 1944.
[7]D. Schwock, A. B. Burg and R. A. Beaudet, *Inorg. Chem.* 1977, **16**, 3219.
[8]K. J. Haller, E. L. Andersen and T. P. Fehlner, *Inorg. Chem.* 1981, **20**, 309.
[9]E. L. Andersen, R. L. DeKock and T. P. Fehlner, *Inorg. Chem.* 1981, **20**, 3291.
[10]E. Switkes, I. R. Epstein, J. A. Tossell, R. M. Stevens and W. N. Lipscomb, *J. Amer. Chem. Soc.* 1970, **92**, 3837.
[11]D R. Lloyd, N. Lynaugh, P. J. Roberts and M. F. Guest, *J. Chem. Soc. Faraday II* 1975, **71**, 1382.
[12]D. R. Salahub, *J. Chem. Soc. Chem. Commun.* 1978, 385.
[13]J. A. Ulman, E. L. Andersen and T. P. Fehlner, *J. Am. Chem. Soc.* 1978, **100**, 456.
[14]T. P. Fehlner, in *Boron Chemistry* (Edited by R. W. Parry and G. Kodama), p. 95. Pergamon Press, New York (1980).
[15]A. Streitwieser, Jr., C. M. Berke, G. W. Schriver, D. Grier and J. B. Collins, *Tetrahedron* 1981, **37** Suppl. No. 1, 345.

Polyhedron Vol. 1, No. 6, pp. 525–534, 1982
Printed in Great Britain.

0277–5387/82/060525–10$03.00/0

ADDUCTS OF COORDINATION COMPOUNDS—12†

NEW HYDROGEN DINITRATES AND THEIR STRUCTURES

NABILA S. AL-ZAMIL, E. H. M. EVANS, R. D. GILLARD*, DAVID W. JAMES, TUDOR E. JENKINS, ROBERT J. LANCASHIRE, and P. A. WILLIAMS*

Department of Chemistry, University College, P.O. Box 78, Cardiff, CF1 1XL, Wales

(*Received* 14 *May* 1981)

Abstract—The new compounds *trans*-$[Ru(pyr)_4Cl_2][H(ONO_2)_2]$ and $[C_{13}H_9NH][H(ONO_2)_2]$ have been characterised (where pyr is pyridine and $C_{13}H_9N$ is phenanthridine) and these, with the known compounds *trans*-$[Ir(pyr)_4Cl_2][H(ONO_2)_2]$, $C_{13}H_9N]2HNO_3{\cdot}2H_2O$ and $[phenH][H(ONO_2)_2]$, shown to involve the hydrogen dinitrate ion. The crystal and molecular structure of the Ru complex has been determined. The orthorhombic unit cell, space group *Pbcn* has $a = 7.54$, $b = 21.83$, $c = 14.86(\pm 0.01)$ Å, $Z = 4$. The compound is isomorphous with the analogous Rh(III) complex, but has additional disorder involving the nitrate groups owing to loss of nitric acid with time to yield an isostructural mono-nitrate compound. The complexes *trans*-$[Ru(pyr)_4Cl_2][H(ONO_2)_2]$ and *trans*-$[Pt(pyr)_4Cl_2](NO_3)_2$ were obtained under conditions previously described as giving rise to nitration of the pyridine ring. In fact, no evidence for the formation of 3-nitro-pyridine has been found during these studies.

INTRODUCTION

Hydrogen-bonded species of the type $(XHX)^-$ are fairly common and new examples occur frequently.[2,3] Although derivatives including the caesium salt were made in 1862,[4] the hydrogen dinitrate anion was not fully characterised as such until the mid-1960's. At that time, two series of its salts with singly charged cations were deliberately synthesised. These were, first,[5] with complex cations of the general type *trans*-dihalo-*tetrakis*-pyridinerhodium(III), (*trans*-$[Rh(pyr)_4X_2][H(ONO_2)_2]$) and secondly,[6] with tetrahedral cations of the tetraphenylarsonium type, such as $[(AsPh_4)][H(ONO_2)_2]$.

Although the spectroscopic properties[5] of these species suggested that the hydrogen-bonded anion contained a short linear hydrogen bond with an oxygen–oxygen contact of about 2.5 Å, this was almost immediately contradicted[7,8] by a crystal structure, using X-ray diffraction, performed upon the original sample[5] of *trans*-dichloro-*tetrakis*-pyridinerhodium(III) hydrogen dinitrate, which was found to contain a quasi-tetrahedral anion, in which the hydrogen atom was essentially four-coordinate with respect to two oxygen atoms of two nitrate groups. The linear structure for the hydrogen bond was further discredited when the crystal structure of caesium hydrogen dinitrate was determined,[9] again by X-ray diffraction.

The structure of the anion was rather similar to that found earlier for the rhodium compound, although, in the interim period, one crystallographic study[10] had indicated that in $[Ph_4As][H(ONO_2)_2]$ despite some random occupancy of equivalent sites (disorder of $[H(ONO_2)_2]^-$), there was, undoubtedly a linear, short hydrogen bond as shown in (I). This situation is rather like that found[11] in the doubly hydrogen-bonded dimers of phenylpropiolic acid.

The debate has now, in part, been settled by a study of the caesium salt, using neutron diffraction. This shows[12] that the structure of its hydrogen dinitrate ion, (II), is as originally suggested, dominated by a short linear

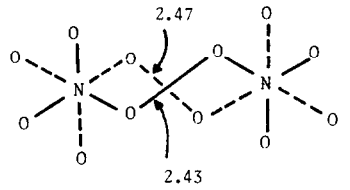

hydrogen bond. The controversy is well summarized in a recent short report.[13] However, there, an average O···O distance of 2.43 Å was attributed to the tetraphenylammonium rather than the tetraphenylarsonium salt.

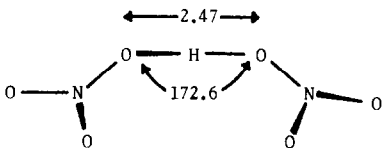

That the hydrogen dinitrate salt is not tetrahedral in the metal complexes was confirmed by a neutron diffraction study[14] of *trans*-$[Rhpyr_4Cl_2][H(ONO_2)_2]$. Contrary to the tetrahedrally coordinated ion suggested by earlier X-ray studies,[7,8] the hydrogen dinitrate ion is linear but disordered between two sites in the lattice. Undoubtedly this disorder was responsible for the unusually large anisotropic thermal parameters and apparent tetrahedral geometry observed[7,8] in the X-ray analysis.

However, there are still some complications which seem not to have been considered in detail. The spectroscopic properties (even the frequencies arising from the NO vibrations) which might be expected not to be particularly sensitive to the environment of the hydrogen dinitrate ion, are, in fact, rather variable. The suggestion was therefore made,[5] some years ago, that there may well be a number of possible conformations for this *ennea*-atomic anion, and the structures determined so far appear to confirm this. The structure found by the neutron study of the Cs^+ salt consists of two almost planar

*Author to whom correspondence should be addressed.
†Part 11 is Ref. 1.

nitrate groups. The geometry of the hydrogen bond and individual nitrate groups agree fully with those found in the tetraphenylarsonium salt. However, the entire hydrogen dinitrate ion is planar in the latter whilst in the Cs^+ salt the dihedral angle between the planes of the two nitrate groups is approx. 75°. It seemed of interest therefore to collect further examples of the existence of the ion.

This paper reports the syntheses of new hydrogen dinitrates and comments on two known ones,[15–17] which have not previously been characterized in detail. The compounds studied are of two kinds: first, the two compounds *trans*-dihalo-*tetrakis*-pyridinemetal(III) hydrogen dinitrate, where the metal is ruthenium (a new compound entirely) and iridium[15] (which we mentioned briefly 10 yr ago), and secondly, two salts of the phenanthridinium cation, $[PH]^+$, which are its new anhydrous hydrogen dinitrate, and the known compound[16] of composition phenanthridinium nitrate, nitric acid, dihydrate, together with the results of infrared studies of the hydrogen dinitrate of 1,10-phenanthroline, (V).

EXPERIMENTAL

Analytical results are given in Table 1

Preparation of trans-$[Ru(pyr)_4Cl_2]\cdot H_2O$: Commercial grade ruthenium trichloride (2.5 g) was dissolved in concentrated hydrochloric acid (5–10 cm^3) and the solution taken to dryness at 100° on a steam bath. The resulting solid was then added slowly with stirring to an aqueous solution of pyridine (10 cm^3) in hydrochloric acid. Zinc powder (about 1.5 g in lots of 0.3 g) was cautiously added to the gently boiling solution until the solution became green–yellow. At this stage, a greenish powder precipitated which when treated again with zinc powder/HCl yielded an orange–yellow solid. This was collected and washed with water, ethanol and finally ether.

Preparation of the hydrogen dinitrate salts: (a) *Ruthenium.* 0.5 g of the previously prepared $[Ru(pyr)_4Cl_2]\cdot H_2O$ was dissolved in 5 cm^3 of concentrated nitric acid. The solution was then warmed on a steam bath for no more than three minutes. On cooling the solution large orange crystals of *trans*-$[Ru(pyr)_4Cl_2][H(ONO_2)_2]$ were deposited. Prolonged heating leads to an as yet unidentified product, as shown by a change of colour to blue-green. X-ray powder photographs show that the new hydrogen dinitrate salt is isomorphous with the rhodium and iridium complexes, and the crystal and molecular structure of the Ru complex is mentioned below. (b) *Rhodium.* The method followed was essentially that of Poulenc.[18] An ethanolic solution of *trans*-$[Rh(pyr)_4Cl_2]Cl\cdot 5H_2O$ was treated with aqueous nitric acid (8M) and the product, which precipitates immediately, was collected. (c) *Iridium.* The method described by Gillard and Heaton[15] was used. (d) *Caesium.* 9–10 mm long crystals were grown from a saturated solution of caesium nitrate in concentrated nitric acid when it was slowly cooled from 70 to 25°. The colourless crystals were collected and dried in a desiccator over silica gel. For the Raman study, to avoid the possibility of decomposition, the sample was used immediately.

Preparation of trans-$[Pt(pyr)_4Cl_2][NO_3]_2$: The method of Grinberg *et al.* was followed.[19] A mixture of *cis*-$[Pt(pyr)_2Cl_2]$ (2 g), water (10 cm^3) and pyridine (3.5 cm^3) was heated on a boiling water bath until all the solid had dissolved. It was cooled to room temperature, and filtered. After reheating 5–10 min on a boiling water bath, the solution of $[Pt(pyr)_4]Cl_2$ thus prepared was poured into a hot solution of 20 cm^3 of conc. HNO_3 in 10 cm^3 water and heating was continued for another 30–40 min. The solution was cooled to room temperature, filtered and mixed with 2 volumes of alcohol and a large volume of ether. The mixture was cooled in ice–water for 2 hr, the precipitate filtered off, and washed with a mixture of alcohol and ether (1:3) until there was no acid reaction to methyl orange (this required a long time!), then finally with ether. Yield: 2.3 g.

Phenanthridine dinitric acid dihydrate: Phenanthridine (Aldrich Chemical Co.) was recrystallized twice from petroleum ether (60–80°) before use. MP 105–106°; Lit[16,17] 105–106°. It has been reported[16] that when a solution of phenanthridine in hot 3M HNO_3 is cooled, transparent pale yellow prisms of a dinitrate separated. This preparation is not reliably reproducible and on only one occasion could such a sample be isolated. We have found however that quite different thermogravimetric analyses are obtained from this dihydrate compared with the anhydrous compound (below). In the former, 2 molecules of water are lost at 94° prior to continuous sublimation of phenanthridine with the loss of HNO_3. By contrast, the latter compound begins to decompose at 75°. In both cases the yellow crystals which had sublimed had a melting point of 105–6°. All other attempts have so far led to a new anhydrous dinitrate. However, other workers have found[17] in the case of the various salts (including "acid nitrates") of (N,N-dimethyl)-di-acridylium doubly-charged cations (crystallized from nitric acid of differing strengths) that salt formation is extremely complicated and that several series of nitrates may exist. This may well be equally the case for the phenanthridinium nitrates.

Phenanthridinium hydrogen dinitrate: Phenanthridine (*ca.* 0.5 g) was dissolved in hot concentrated HNO_3 (5 cm^3) and left to cool. Fine acicular crystals, which were removed and air-dried, separated from the deep-yellow solution. These on keeping (2 yr) lost nitric acid, leaving chiefly $C_{13}H_9N\cdot HNO_3$. No nitration of the phenanthridine ring is observed in this preparation. During titration of the proton of the hydrogen dinitrate, a white solid precipitated which was recrystallized with 60–80 petroleum ether and proved to be pure phenanthridine (m.p., IR).

Phenanthridinium nitrate: If either of the above salts was treated with water, acetone or alcohol, the crystals changed from yellow to white as the hydrogen dinitrate decomposed to the nitrate salt.

1,10-*Phenanthrolinium hydrogen dinitrate*: 1,10-Phenanthroline monohydrate (Lancaster Synthesis Ltd.; *ca.* 0.5 g) was dissolved in hot concentrated HNO_3 (5 cm^3), and left to cool. During 1 month large elongated prisms separated which were collected and air-dried.

1,10-*Phenanthrolinium nitrate*: 1,10-Phenanthroline monohydrate (*ca.* 0.2 g) was dissolved in hot 3 M HNO_3 (5 cm^3) and the solution then concentrated to about 2 cm^3. A slightly hygroscopic powder separated.

Thermogravimetric analyses were carried out under a nitrogen atmosphere using a Stanton Redcroft TG 750. Infrared spectra were recorded as nujol mulls with a Perkin–Elmer 257 spectrometer.

Raman spectra of all the salts containing the hydrogen dinitrate ion were recorded at room temperature and, in addition, those samples with good signal-to-noise ratio were recorded at several temperatures between 10 and 300 K. Details of the apparatus have been given elsewhere.[20] Room temperature spectra on powder specimens were recorded at very low incident laser power (<30 mW) and in a spinning cell to reduce the possibility of sample decomposition. Resolution was typically 1.5 cm^{-1}.

X-Ray powder photographs were taken with either Debye–Scherrer or Guinier cameras using CuK radiation.

For the collection of single crystal X-ray data for *trans*-$Ru(pyr)_4Cl_2H(ONO_2)_2$, a 2θ scanning technique was employed using a Hilger and Watts Y290 four-circle diffractometer and MoK_α radiation, at 25°. The crystal used was of dimensions $0.2\times0.2\times0.3$ mm. Each reflection in the $0\text{–}5_{kl}$ layers was collected for $2\theta<70°$. 864 *unique reflections gave counts for which* $I>2\sigma(I)$ and these were used for the structure analysis. The scattering factors for all atoms are those given[21] in International Tables for X-ray Crystallography, the ruthenium and chlorine atoms being corrected for anomalous dispersion. All calculations were carried out on an ICL 472 computer using the X-RAY72 package[22] of programmes.

Crystal data: $C_{20}H_{21}N_6O_6Cl_2Ru$, $M=613.4$, $Z=4$, Orthorhombic, $a=7.54$, $b=21.83$, $c=14.86\pm0.01$ Å, $U=2444.2$ Å^3, $D_m=1.72$ (by flotation), $D_c=1.70$ g cm^{-3}, $F(000)=1236$: *space group Pbcn* (No. 60), $\mu(MoK_\alpha)=8.97$ cm^{-1}.

Initial refinement and analysis of difference Fourier maps showed that the site of the nitrate group of the asymmetric unit is not fully occupied and that for the crystal involved the compound is a mixture of the hydrogen dinitrate and the nitrate with disorder between the symmetry-allowed sites for the nitrate group of the latter. A population parameter of 0.70 was chosen

Table 1. Analytical results

Compound	M.P.(°)		C	H	N	H^+ [a]	M [b]
trans-$[Rh(pyr)_4Cl_2][H(ONO_2)_2]$	165	calc.	39.05	3.41	13.65	-	16.7
		found	39.65	3.41	13.65	-	18.5
trans-$[Rh(d5pyr)_4Cl_2][H(ONO_2)_2]$	-		37.80	-	13.23	-	16.2
			37.78	-	12.20	-	17.0
trans-$[Ru(pyr)_4Cl_2.H_2O]$	-		47.44	4.38	11.06	-	20.69
			46.88	4.12	10.43	-	20.1
trans-$[Ru(pyr)_4Cl_2][H(ONO_2)_2]$	-		39.16	3.45	13.70	-	16.5
			39.12	3.48	13.42	-	16.0
trans-$[Pt(pyr)_4Cl_2](NO_3)_2$	-		34.01	2.85	11.90	-	27.62
			34.20	3.07	11.95	-	28.5
$[Pt(pyr)_4](NO_3)_2$	-		37.81	3.14	13.22	-	30.7
			37.79	3.34	13.12	-	31.2
$C_{12}H_8N_2.HNO_3$	-		59.26	3.73	17.28	-	-
			59.50	3.69	17.35	-	-
$C_{12}H_8N_2.2HNO_3$	-		47.06	3.29	18.30	-	-
			47.11	3.15	18.08	-	-
$C_{13}H_9N.HNO_3$	170 [c]		64.40	4.13	11.57	0.39	-
			64.39	4.47	11.99	0.44	-
$C_{13}H_9N.2HNO_3$	[d]		51.17	3.60	13.76	0.66	-
			50.48	3.29	12.93	0.64	-
$C_{13}H_9N.2HNO_3.2H_2O$	[d]		45.77	4.39	12.30	0.59	-
			46.82	3.19	12.33	0.64	-

[a] from acid-base titration

[b] from the percentage residue in the thermogravimetric analysis

[c] literature m.p. 170° (ref. 15)

[d] decomposes

for all the atoms in the nitrate group of the asymmetric unit. This value gave rise to values of anisotropic thermal parameters for the atoms of the nitrate group which were comparable to those reported[8] for the isomorphous Rh(III) analogue. In the final refinement anisotropic thermal parameters for all atoms were used. Hydrogen atoms were not included in the calculation. Full-matrix least-squares refinement was terminated when the maximum shift in any parameter was less than 0.05σ, not including the atoms of the nitrate group whose maximum shifts at termination were less than 1σ. The final R based on all 864 reflections was 0.060.†

†Full lists of observed and calculated structure factors, atomic positions, bond lengths, angles and thermal parameters have been deposited as supplementary material with the Editor, from whom copies are available on request. Atomic co-ordinates have also been deposited with the Cambridge Crystallographic Data Centre.

RESULTS AND DISCUSSION

Details of the geometries of the cation and anion are given in Table 2.

Before discussing the vibrational spectrum for the hydrogen dinitrate anion, it is worthwhile comparing the known vibrations of the nitrate group,[23,24] and of nitric acid.[25]

In compounds in which the NO_3 group is covalently bonded through one of the oxygen atoms, the symmetry of the group will be lower than for the free nitrate ion (D_{3h}), and is expected to be C_{2v}. Consequently, six fundamental vibrations are expected; these will be both infrared and Raman active. The position of these bands has been reviewed by Field and Hardy[23] and are given in Table 3.

The hydrogen dinitrate ion can be envisaged as a nitrate ion that has been involved in a very strong

Table 2. *Trans*-$[Ru(py)_4Cl_2][O_2NOHONO_2]$

Final bond lengths and Angles (in Å and ° respectively), with Estimated Standard Deviations in Parentheses.

Ru - Cl	2.326(4)	C(7) - C(8)	1.436(30)
Ru - N(1)	2.091(12)	C(8) - C(9)	1.402(26)
Ru - N(2)	2.088(13)	C(9) - C(10)	1.399(24)
N(1) - C(1)	1.376(15)	C(10) - N(2)	1.353 (25)
C(1) - C(2)	1.413(22)	N(3) - O(1)	1.136(29)
C(2) - C(3)	1.373(24)	N(3) - O(2)	1.208(23)
C(3) - C(4)	1.407(21)	N(3) - O(3)	1.055(31)
C(4) - C(5)	1.411(22)	O(2) - O(2)'	2.879(24)*
C(5) - N(1)	1.322(19)	O(1) - O(1)'	3.104(23)*
N(2) - C(6)	1.371(23)	O(1) - O(2)'	3.097(23)*
C(6) - C(7)	1.432(25)		
Cl - Ru - Cl''	179.7(6)	O(1) - N(3) - O(2)	118.0(20)
Cl - Ru - N(1)	90.1(3)	O(1) - N(3) - O(3)	121.1(23)
Cl - Ru - N(2)	89.8(4)	O(2) - N(3) - O(3)	120.9(26)
N(1) - Ru - N(2)	89.0(5)		
C(1) - N(1) - C(5)	119.4(12)	C(6) - N(2) - C(10)	120.9(14)
N(1) - C(1) - C(2)	119.2(13)	N(2) - C(6) - C(7)	120.8(17)
C(1) - C(2) - C(3)	122.3(12)	C(6) - C(7) - C(8)	117.4(17)
C(2) - C(3) - C(4)	116.9(15)	C(7) - C(8) - C(9)	119.8(16)
C(3) - C(4) - C(5)	119.1(15)	C(8) - C(9) - C(10)	119.3(17)
C(4) - C(5) - N(1)	123.1(12)	C(9) - C(10) - N(2)	121.7(15)

* Contact distances

Relative to the atoms at x, y, z, the primed atoms are at 1-x, y, ½-z and the double primed atoms are at -x, y, ½-z.

symmetric hydrogen bond with nitric acid. Under these circumstances it is expected that the spectra should be more closely related to a coordinated nitrate group than a free nitrate ion.

It was pointed out in 1932[15] that an "abnormal" nitrate salt was a product of the reaction of dilute nitric acid with phenanthridine. The abnormality was that the compound was formulated as containing two molecules of nitric acid, i.e. $C_{13}H_9N{\cdot}2HNO_3{\cdot}2H_2O$. Such "abnormal" or acid nitrates are known[17] for other *N*-heterocyclic cations.

If instead of 3M HNO_3, hot concentrated nitric acid is used to crystallize phenanthridine, then a new compound is formed which has the formula $C_{13}H_9N{\cdot}2HNO_3$. The salt contains a labile acid molecule which is readily lost by washing. No nitration of the aromatic ring is observed during the preparation.

Since we could not synthesise the compound described[16] by Morgan and Walls except on one occasion, we restrict our discussion of the phenanthridinium salts to the anhydrous dinitrate and the simple nitrate. These two salts $P{\cdot}HNO_3$ and $P{\cdot}2HNO_3$ are most clearly distinguished by their characteristic X-ray powder patterns (Table 4). Upon prolonged exposure to X-radiation, lines of the simple nitrate salt appear in the spectrum of $P{\cdot}2HNO_3$, indicating decomposition. In the vibrational spectrum of this latter compound however, absorptions due to free HNO_3 are absent and on this basis we conclude that a $P{\cdot}2HNO_3$ contains the $[H(ONO_2)_2]^-$ anion.

It is intriguing that slow crystallization of 1,10-phenanthroline from 3 M nitric acid has very recently[3] been shown to give $C_{12}H_8N_2{\cdot}2HNO_3$ which is made up of a singly charged 1,10-phenanthrolinium cation and an anionic assembly $[H(ONO_2)_2]^-$ described as containing an unsymmetrical O–H–O bond with an oxygen–oxygen contact of 2.54 Å (III).

The vibrational spectral details of $C_{12}H_8N_2{\cdot}2HNO_3$ and the simple nitrate salt are shown in Table 3.

In the phenanthridine and 1,10-phenanthroline salts it

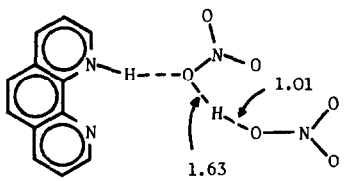

is not easy to determine which peaks are due to the anion owing to the large number of peaks for the organic cation.

The reaction of $[Ru(pyr)_4Cl_2]$ with nitric acid has previously been claimed to give rise to nitration of the pyridine ring.[26] However, our sole product under conditions identical to those cited[26] was the new hydrogen dinitrate salt *trans*-$[Ru(pyr)_4Cl_2][H(ONO_2)_2]$. It has also been claimed[27] that $[Pt(pyr)_4]Cl_2$ gives nitro-pyridine by treatment with nitric acid. However, this too is incorrect. The product is actually *trans*-$[Pt(pyr)_4Cl_2][NO_3]_2$ which we have used for comparison in the Raman studies. Thermogravimetric runs on the same compound after recrystallization from conc. HNO_3 were superimposable.

Infrared spectra for the three salts *trans*-$[M(pyr)_4Cl_2][H(ONO_2)_2]$ are superimposable and the relevant peak positions are recorded in Table 3. The salient features of these spectra are the broad bands centred on 1500 cm^{-1} and 750 cm^{-1} typical of hydrogen-bonded species and the extremely sharp peak at 866 cm^{-1} which shows the "window of absorption" noted[28] for Speakman's Class A of hydrogen bonds. Changes with perdeuteration of the pyridines in the infrared spectrum are also listed in Table 3.

The infrared bands at frequencies above 625 cm^{-1} attributed to the anion can be determined by considering which bands remain unchanged on deuteration of the pyridine ring. In practice, these are the bands at 1510, 1330, 1240, 1025, 987, 780 and 690 cm^{-1}, and of these, the peak at 690 cm^{-1} cannot be unambiguously assigned to the anion, since it may be due to a vibration of the *N*-heterocyclic ring which is relatively insensitive to deuteration.

The presently available vibrational information on the differing types of salts of the hydrogen dinitrate anion is collected in Table 3 (which chiefly relates to infrared spectra) and Table 5 (Raman spectra).

The overwhelming feature of the Raman spectra due to *trans*-$[M(pyr)_4Cl_2][H(ONO_2)_2]$ is the strength of the light scattering from internal modes associated with the pyridine ring. No strong features associated with the hydrogen dinitrate ion could be seen at very low temperature, although 21 fundamental vibrations are predicted.

In suitable crystals and with low signal-to-noise ratio it has been found that several broad weak features are present at 1335, 1080 and 700 cm^{-1} which are not observed in either *trans*-$[Rh(pyr)_4Cl_2]Cl{\cdot}5H_2O$ or *trans*-$[Pt(pyr)_4Cl_2][NO_3]_2$. We assign these peaks to the hydrogen dinitrate anion.

A recent Raman study of caesium hydrogen dinitrate immersed in CCl_4 has reported[9] bands above 600 cm^{-1} which were attributed to the hydrogen dinitrate ion. A band near 1400 cm^{-1} was said to shift to 1010 cm^{-1} upon deuteration. We have been unable to confirm all the details of that work since we find that the bands at 1382, 1050, 720 and 705 cm^{-1} in freshly prepared single crystals of caesium hydrogen dinitrate are, with the exception of the band at 1382 cm^{-1}, all present in $CsNO_3$ itself. To avoid decomposition of the caesium hydrogen dinitrate crystals, attempts were made to cool the freshly isolated product rapidly. However, this made no significant difference and all the bands of caesium nitrate were still observed.

The ready decomposition has previously been noted by Tuck *et al.*,[29] and no infrared spectrum could be obtained on mulling at room temperature. Saturated solutions of potassium nitrate in various concentrations of nitric acid (2–16 M) have also been examined by Raman spectroscopy, but no evidence was obtained for the existence of the $[H(ONO_2)_2]^-$ species in any of the solutions investigated.

The band at 1335 cm^{-1} in the Raman spectra of *trans*-$[M(pyr)_4Cl_2][H(ONO_2)_2]$ can be assigned by comparison with previous work. Williams *et al.*,[9] attributed the band close to this at 1382 cm^{-1} in the caesium salt to an O–H–O deformation since they found a shift to 1010 cm^{-1} on deuteration. Our infrared results for the metal complexes all show a strong band at 1340 cm^{-1} which can be assigned to an NO_2 symmetric stretch.

Raman studies[25] on anhydrous nitric acid attributed the band at 1303 cm^{-1} to the NO_2 symmetric stretch and ascribed that at 1395 cm^{-1} to a H–O–N bonding mode. The corresponding infrared band assigned to the H–O–N bonding mode at 1331 cm^{-1} in the vapour phase was found to shift to 1014 cm^{-1} upon deuteration. In addition the Raman studies[25] of anhydrous nitric acid assigned the bands at 926, 771, 677 and 612 cm^{-1} to ONO angle deformation, NO_2 out-of-plane bend, NO′ stretch and ONO′ bend respectively. The weak bands at 1059 cm^{-1} and 644 cm^{-1} were not assigned, but were considered to be due to ionized nitric acid.

It is not possible at present to assign the weak bands at 1080 and 700 cm^{-1} in the metal complexes of the hydrogen dinitrate anion, but they are close to those just mentioned as appearing in anhydrous nitric acid.

Room temperature spectra of *trans*-$[Ru(pyr)_4Cl_2][H(ONO_2)_2]$ were recorded, but owing to the poor signal-to-noise ratio, bands were observed only at 1030, 650, 360 and 300 cm^{-1}. It was not possible to isolate the broad weak bands from the background noise. Difficulty in locating bands due to $[H(ONO_2)_2]^-$ does not prove that the ion is not there, but merely that its Raman spectrum is elusive.

Our results and observations concerning the structure determination of the isomorphous Ru(III) complex complement these findings. We also find a pseudo-tetrahedral position of nitrate oxygen atoms but of special importance to the correct description of the structure is the fact that during the data collection HNO_3 was lost from the crystal even when this was sealed in a Lindemann tube.

Examination of difference Fourier syntheses with full occupancy of the nitrate positions of the asymmetric unit (viz. fully hydrogen dinitrate) disclosed holes at those positions. Assuming that all the HNO_3 of the hydrogen dinitrate had been lost resulting in the formation of an isostructural nitrate compound, difference Fourier syntheses were calculated with a population parameter of 0.5 for the nitrate atoms. Peaks were observed at the relevant atomic position. No extra peaks could be found in the Fourier map and thus it was evident that the structure as determined was a mixture of the hydrogen dinitrate and an isostructural simple nitrate with fractional occupancy of almost crystallographically equivalent

Table 3. Vibrational spectra (cm^{-1}) for nitrates, isotopic nitric acids and hydrogen-dinitrates

Assignments [a]	$\nu_2(\nu_4)$ [b] 	ν_4 (ν_1) 	ν_5 (ν_2) NO_2 angle deformation or	$\nu_8(\nu_6)$ NO_2 out of plane rock	$\nu_6(\nu_3)$ NO' Stretch or NO_2 symmetric	(OHO)	References
Compound	Asymmetric Stretch	Symmetric Stretch	NO' Stretch		Stretch		
Nitrates	1481 - 1531	1253 - 1290		781 - 800	739		23
$H^{14}NO_3$ (g)	1711.8 vs 1705.6 vs	1324.9 vs	878.6 s	762.2 s	646.6 w		25
$D^{14}NO_3$ (g)	1691.0 vs 1683.1 vs	1308.4 vs	888.0 s	762.8 s	641.0 s		25
$H^{15}NO_3$ (g)	1675.4 vs 1668.6 vs	1320.6 s	870.8 s	743.6 s	646.6 w		25
$D^{15}NO_3$ (g)	1657.5 vs 1653.5 vs	1290.7 s	876.3 s	743.4 s	640.9 s		25
HNO_3 (l)	1708.2 vs	1324.9 vs	878.6 s	762.2 s	646.6 w		25
HNO_3 (l) R	1675 W	1303 vs	926 s	(771) [c]	677 s		25
HNO_3 (s) (-193°C)	1646 vs	1256 vs	958 s	773 s	722 s		25
trans-$[Rh(pyr)_4Cl_2][D(ONO_2)_2]$	1515 br	1340 s	960 [d]	810 m	-	750 br	5

trans-$[Rh(d5pyr))_4Cl_2][H(ONO_2)_2]$	1510 br	1330 s	987 s	-	-	780 br	this work		
trans-$[Rh(pyr)_4Cl_2][H(ONO_2)_2]$	1510 br	1329 s	960	-	-	785 br	this work		
trans-$[Ru(pyr)_4Cl_2][H(ONO_2)_2]$	1515 br	1329 s	960 d	-	-	785 br	this work		
trans-$[Ir(pyr)_4Cl_2][H(ONO_2)_2]$	1510 br	1330 s	960 d	-	-	785 br	this work		
trans-$[Co(pyr)_4Cl_2][H(ONO_2)_2]$	1500 br	1320	-	-	-	750 br	5		
$[C_{13}H_9NH][H(ONO_2)_2]$	1670 br	1335 s	970 br	-	-	750 br	this work		
$[Ph_4P][H(ONO_2)_2]$	1670 br	-	-	-	-	750 br	6		21
cis-$[Rh(bipy)_2Cl_2][H(ONO_2)_2]$	1600 br	1340 s	945–1000 d	-	-	900 br	5		
trans-$[Pt(pyr)_4Cl_2][NO_3]_2$	-	1350 br	970 w	-	-	-	this work		
$[C_{12}H_8N_2][H(ONO_2)_2]$	1610 s	1320 s	1010 br			850 br	this work		
	1620 s		950 br	-	-				

[a] Infrared spectra except for the Raman spectrum designated R for nitric acid,

[b] Assignments outside brackets refer to the nitrate ion with the C_s symmetry of HNO_3[25], and those inside to C_{2v} symmetry.[24]

[c] *Calculated from a weak polarized overtone*[25] *observed at* 1542 cm^{-1}.

[d] Observed as characteristic quartet.

Table 4. *d*-Values[a] for phenanthridine and its salts

$C_{13}H_9N$[b]	$C_{13}H_9N.HNO_3$	$C_{13}H_9N.2HNO_3$
7.368	12.517	10.394
6.458	9.816	9.816
5.711	6.304	5.711
5.063	4.791	5.063
4.328	4.129	4.435
4.226	3.490	3.490
3.704	3.424	3.360

[a] Cu-K_α radiation.

[b] Obtained by crystallization from petroleum ether.

Table 5. Raman band frequencies (cm^{-1}) for nitrate and hydrogen dinitrate salts

Assignment	A	B	C	D	E	F	G
		30		30			30
					37	37	35
	58				55	55	60
							65
			70				67.5
Lattice		100	76	80			70
	120	120			120	120	120
							125
				130			130
			135				135
	140						140
	180	145					145
M-N	210	198	220		-	-	-
	225	205		235	-	-	-
	252	238	240	238	-	-	-
M-Cl	298	298	298	320	-	-	-
	302	301	302	320	-	-	-
	318	320	-	340	-	-	-
ring deformation	650	625	660	653	-	-	-
nitrate				665	705	705	705
hydrogen dinitrate	700				720	720	720
symmetric stretch of nitrate and pyridine ring	1028	980	1025	1032			
	1050	985	1050	1051	1050	1050	1052

Table 5 (Contd.)

hydrogen dinitrate	1080	1080	-	-	-	-	-
out of plane deformation	1215	845					
	1220	895	1220	1212	-	-	-
hydrogen dinitrate	1335	-	-	-	-	1385	1382
	1575	1500	1575	-	-	-	-
					-	-	-
	1610	1480	1610	1610	-	-	-

A: trans- $[Rh(pyr)_4Cl_2][H(ONO_2)_2]$

B: trans- $[Rh(d5pyr)_4Cl_2][H(ONO_2)_2]$

C: trans- $[Rh(pyr)_4Cl_2]Cl.5H_2O$

D: trans- $[Pt(pyr)_4Cl_2](NO_3)_2$

E: $CsNO_3$

F: $Cs[H(ONO_2)_2]$ (A - F all recorded at room temperature)

G: $Cs[H(ONO_2)_2]$ (recorded at 28K)

sites. A population parameter of 0.70 was finally chosen as such a value gave magnitudes of thermal vibration ellipsoids comparable with those of the isomorphous Rh(III) complex.[8] Such a choice of population parameter implies a mixture of 40% hydrogen dinitrate and 60% nitrate with the nitrate group of the latter distributed between the two equivalent positions in the lattice.

Roziere *et al.*[14] refined two sets of atomic positions in the Rh(III) neutron-diffraction determination but found it necessary to protect the sample in a sealed silica-glass tube. The loss of nitric acid would make it necessary to refine the crystal structure of the Ru(III) complex with two sets of positions for both the hydrogen dinitrate ion and the nitrate ions. Such a strategy was not considered worthwhile (if indeed possible) in the light of the more recent work.[14] The average disposition of the nitrate groups in the Ru(III) structure is shown in (IV).

Given these results, it is clear that hydrogen dinitrate ions of these types are linear as proposed[5] as confirmed above and in the analysis[9] by neutron diffraction of $Cs[H(ONO_2)_2]$.

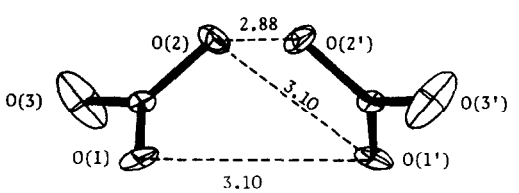

CONCLUSION

It is quite obvious, from the careful thermodynamic work using the vapour pressures of nitric acid and solutions in it by Dawber,[30,31] and from the ready isolation of salts of the general composition $[C][H_n(NO_3)_{n+1}]$ ($0 \leq n \leq 4$ is a typical range) that nitric acid/water mixtures contain at some equilibrium level such species as hydrogen dinitrate. Despite some early French work,[32,33] using Raman spectroscopy, which was interpreted in terms of such hydrogen bonded ions, no other spectroscopic work has supported the involvement, in aqueous solutions, of the equilibrium

$$[H\text{–}ONO_2]^\circ + [ONO_2]^- \rightleftharpoons [H(ONO_2)_2]^-.$$

However, distribution studies of nitrate species between aqueous and organic phases do indicate the importance of this equilibrium since $[R_3NH^+][H(ONO_2)_2^-]$ is a commonly extracted species,[34] and it may be necessary to reinterpret several other observations in these terms. For example, the "monohydrated dimer" of nitric acid[35] extracted into benzene, toluene, carbon tetrachloride or *n*-dodecane from its 6–16 M aqueous solutions might well be $[H_3O^+][H(ONO_2)_2^-]$.

Acknowledgements—We wish to thank the University of Kuwait for a studentship (N.S.A-Z), the SERC for a fellowship (T.E.J.) and I.C.I. for a grant under the Joint Research Scheme (D.W.J. and R.J.L.).

REFERENCES

[1]Part XI: R. D. Gillard and M. F. Pilbrow, *J.C.S. Dalton*, 1974, 2320.
[2]M. P. Hancock, J. Josephsen and C. E. Schaffer, *Acta. Chem. Scand.*, 1976, **A30**, 79.
[3]G. Thevenet and N. Rodier, *Acta Cryst.*, 1978, **B34**, 880.
[4]C. Schultz, *Z. Chem.*, 1862, **5**, 531.
[5]R. D. Gillard and R. Ugo, *J. Chem. Soc.* (*A*), 1966, 549.
[6]B. D. Faithful, R. D. Gillard, D. G. Tuck and R. Ugo, *J. Chem. Soc.* (*A*), 1966, 1185.

[7]G. C. Dobinson, R. Mason and D. R. Russell, *J. Chem. Soc. Chem. Comm.*, 1967, 62.
[8]G. C. Dobinson, Ph.D. Thesis, University of Sheffield (1970).
[9]J. M. Williams, N. Dowling, R. Gunde, D. Hadzi and B. Orel, *J. Am. Chem. Soc.*, 1976, **98**, 1581.
[10]B. D. Faithful and S. C. Wallwork, *J. Chem. Soc., Chem. Comm.*, 1967, 1211.
[11]J. S. Rollett, *Acta Cryst.*, 1955, **8**, 487.
[12]J. Roziere, M. Roziere-Bories and J. M. Williams, *Inorg. Chem.*, 1976, **15**, 2490.
[13]Annual Report of the Chemical Society, 1976, **73A**, 149.
[14]J. Roziere, M. S. Lehmann and J. Potier, *Acta Cryst.*, 1979, **B35**, 1099.
[15]R. D. Gillard and B. T. Heaton, *J. Chem. Soc. Chem. Comm.*, 1968, 75.
[16]G. T. Morgan and L. P. Walls, *J. Chem. Soc.*, 1932, 2225.
[17]K. Gleu and S. Nitzsche, *J. prakt. chem.*, 1939, **153**, 241.
[18]P. Poulenc, *Ann. Chim.*, 1935, **4**, 643.
[19]A. A. Grinberg, Kh. I. G. L'dengershel and V. F. Budanova, *Russ. J. Inorg. Chem.*, 1966, **11**, 1351.
[20]T. E. Jenkins, L. T. H. Ferris, A. R. Bates and R. D. Gillard, *J. Phys. C* 1977, **10**, L521.
[21]International Tables for X-ray Crystallography, 1962, **111**, 202.
[22]J. M. Stewart, G. J. Kruger, H. L. Ammon, C. Dickinson and S. R. Hall, *Computer Sci. Centre Rep.* University of Maryland, Technical Report TR172 (1972).
[23]B. O. Field and C. J. Hardy, *Quart. Rev.*, 1964, **18**, 361.
[24]B. M. Gatehouse, S. E. Livingstone and R. S. Nyholm, *J. Chem. Soc.* 1957, 4222.
[25]G. E. McGraw, D. L. Bernitt and I. C. Hisatune, *J. Chem. Phys.*, 1965, **42**, 237.
[26]J. Soucek, *Coll. Czech. Chem. Comm.*, 1962, **27**, 1645.
[27]L. A. Nazarova and T. N. Leonova, *Dokl. Akad. Nauk. SSSR*, 1968, **183**, 116.
[28]J. Clare Speakman, *Structure and Bonding*, 1972, **12**, 141.
[29]D. G. Tuck, *Progress in Inorg. Chem.*, 1971, **12**, 161; and references therein.
[30]J. G. Dawber, *J. Inorg. Nucl. Chem.*, 1975, **37**, 1043.
[31]J G. Dawber, *J. Chem. Soc. Faraday Transaction I*, 1976, **72**, 2125.
[32]J. Chedin and S. Fencant, *Compt. Rend.*, 1947, **224**, 930.
[33]J. Chedin and S. Fencant, *Compt. Rend.*, 1949, **228**, 242.
[34]J. I. Bullock, S. S. Choi, D. A. Goodrick, D. G. Tuck and E. J. Woodhouse, *J. Phys. Chem.*, 1964, **68**, 2687.
[35]C. J. Hardy, B. F. Greenfield and D. Scargill, *J. Chem. Soc.*, 1961, 90.

Polyhedron Vol. 1, No. 6, pp. 535–537, 1982
Printed in Great Britain.

0277–5387/82/060535–03$03.00/0
Pergamon Press Ltd.

NOTES

Triethylhydrazinium chloride and triphenylaminophosphonium chloride as aminating reagents for diphenylchlorophosphine

(*Received* 25 *May* 1982)

INTRODUCTION

Over the past four decades work in this laboratory[1–3] and others[4,5] has clearly established the utility of NH_2Cl as a synthetic reagent as a result of the numerous reactions of the type

$$B: + NH_2Cl \longrightarrow B{:}NH_2^+Cl^- \quad (B: = \text{Lewis base})$$

that it undergoes. However, NH_2Cl is an unstable chemical and may not be stored. We were, therefore, interested in determining whether or not adducts of the type $[B{:}NH_2]Cl$ can be used as sources of NH_2Cl in chloramination reactions.

Gilson and Sisler[6] have previously shown that ammonia-free NH_2Cl reacts with $(C_6H_5)_2PCl$ to produce the two adducts $(C_6H_5)_2P(Cl)NH_2Cl$ and $(C_6H_5)_2P(Cl)(NH_2)$–NH–$PCl_2(C_6H_5)_2$. These have been shown to form diphenylphosphazene trimer and tetramer when pyrolyzed. We report herein the results obtained in a study of the reaction of the adducts $[Et_3NNH_2]Cl$ and $[(C_6H_5)_3PNH_2]Cl$, respectively, when heated with $(C_6H_5)_2PCl$. Both these reactions resulted in the formation of diphenylphosphazene trimer and tetramer.

EXPERIMENTAL

Materials. Diphenylchlorophosphine was obtained from Victor Chemical Company and vacuum distilled at 0.15–0.20 Torr and 104–114°C. 1,1,1-Triethylhydrazinium chloride was prepared by the reaction of a solution of $(C_2H_5)_3N$ in benzene with NH_2Cl mixed with NH_3. This procedure is similar to that reported by Omietanski and Sisler.[7] The reaction mixture was filtered off, extracted with $CHCl_3$ and the product reprecipitated from the $CHCl_3$ extract by the addition of ether. Analysis: Calcd. for $[(C_2H_5)_3NNH_2]Cl$: N, 18.35; Cl, 23.23. Found: N, 18.34; Cl, 23.23. M.p. 189–190°C. (lit 177–178°C).[7]

Triphenylaminophosphonium chloride[8] was prepared by treating an ether solution of $(C_6H_5)_3P$ with a gaseous mixture of NH_2Cl and NH_3[9]. The reaction mixture was filtered off and extracted with $CHCl_3$. The product was reprecipitated by addition of ether to the extract. M.p. 232–235°C (lit. 236°C).[10]

All solvents used were dried and stored over CaH_2. All reactions were carried out in the absence of O_2 and H_2O. Infrared spectra were measured either on a Perkin–Elmer Model 137 spectrometer using sodium chloride optics, or on a Perkin–Elmer Model 337 grating spectrometer. Solid samples were examined as KBr pellets, as Nujol or Kel-F mulls between KBr plates, or in solution in CCl_4 in a NaCl cell of thickness 0.518 mm. Melting points were determined with a Thomas Hoover melting point apparatus.

Chloride analyses were performed by hydrolyzing the samples in 20 ml of water and 25 ml of 10% aquaous NaOH solution and then following the Volhard procedure. Nitrogen analyses were done on a Coleman Model 29 nitrogen analyzer.

Procedure. Equimolar mixtures of $[(C_2H_5)_3NNH_2]Cl$ and $(C_6H_5)_2PCl$ were heated for varying periods of time at temperatures in the range of 140–270°C, both without solvent and in $Cl_2CHCHCl_2$. Typical procedures follow.

The reaction of diphenylchlorophosphine with triethylhydrazinium chloride in the absence of solvent at 190°C

$$(C_6H_5)_2PCl + [(C_2H_5)_3NNH_2]Cl \longrightarrow [(C_2H_5)_3NH]Cl + HCl + 1/3\,[(C_6H_5)_2PN]_3$$

Under a flow of dry N_2 1.003 g (7.225 mmoles) of $[(C_2H_5)_3NNH_2]Cl$ was placed in a 50-ml flask with a magnetic stirring bar and 1.35 mL (7.28 mmoles) of diphenylchlorophosphine pipetted onto it. A water-cooled condenser was fitted into the top, and into the top of the condenser was fitted a nitrogen bubbler to maintain a constant small positive pressures of dry nitrogen in the system, and to flush out any evolved gases. From the nitrogen bubbler, gases passed into a trap containing 50 mL of 0.2 M NaOH solution to trap the evolved HCl. The reactants were heated together at 190–195°C for 48 hr with stirring. The material in the flask, including long white needles and a yellow mass, was digested in 40 mL of boiling benzene in two portions, filtered hot, and the filtrates combined. The residue was identified as $[(C_2H_5)_3NH]Cl$ by melting point (244–246°C with sublimation) and its infrared spectrum. The benzene extract was evaporated to dryness, leaving 1.393 g of tan solid, m.p. 203–214°C. The infrared spectrum indicated this material to be $[(C_6H_5)_2PN]_3$ in a crude yield of 96.7%. Recrystallization from hot benzene raised the melting point to 228–230°C (lit. 230–232°).[11] Other runs of the reaction of $[(C_2H_5)_3NNH_2]Cl$ with $(C_6H_5)_2PCl$ are summarized in Table 1.

The reaction of triphenylaminophosphonium chloride with diphenylchlorophosphine

$$(C_6H_5)_2PCl + [(C_6H_5)_3PNH_2]Cl \longrightarrow (C_6H_5)_3P + 1/n[(C_6H_5)_2PN]_n \quad (n = 3, 4).$$

Ten and one-tenth grams (32.2 mmoles) of $[(C_6H_5)_3PNH_2]Cl$ was weighed into the bottom of a sublimation apparatus, and under dry nitrogen flow 6.0 mL (32.4 mmoles) of $(C_6H_5)_2PCl$ added by pipette. The cold finger and seal were immediately fitted to the base of the sublimation apparatus and vacuum applied. The line was then switched to dry nitrogen and the apparatus left exposed to the dry nitrogen line during the reaction. The pot was heated with a silicone oil bath at 160°C for 24 hr, then at 210–240°C for 75 hr. When the pot had cooled, the base was removed under a stream of dry N_2 and the small portion of viscous oil (0.3 g) scraped from the cold finger and discarded. The apparatus was reassembled, evacuated, and heat applied. At 157–159°C and 0.2–0.6 mm, over a period of 6 hr, 3.43 g of white crystalline sublimate was obtained and discarded.

A tan, yellow and white amorphous residue remained, most of which dissolved when digested with hot $CHCl_3$. The small amount of undissolved material was NH_4Cl. Fractional crystallization of the dissolved material from $CHCl_3$ yielded 2.1 g of $[(C_6H_5)_2PN]_4$, m.p. 318–319°C (lit. 320–321°C).[12] Further fractional crystallization yielded 0.79 g of $[(C_6H_5)_2PN]_3$, m.p. 225–228°C (lit. 230–232°C).[11] The total phosphazene yield (tetramer plus trimer) was 44.8%. Further runs of the reaction of $(C_6H_5)_2PCl$ with $[(C_6H_5)_3PNH_2]Cl$ are listed in Table 2.

DISCUSSION

The results reported herein confirm that, as postulated and similarly to $[NH_3NH_2]Cl$, $[(C_2H_5)_3NNH_2]Cl$ and $[(C_6H_5)_3PNH_2]Cl$ act as *in situ* sources for NH_2Cl and serve as aminating agents toward $(C_6H_5)_2PCl$, converting this substance to diphenylphosphazene trimer and tetramer. Under some circumstances some amounts of the intermediate $(C_6H_5)_2PCl{=}N{-}P(NH)(C_6H_5)_2$[6] are also obtained. The reactions with

Table 1. Further runs of $[(C_2H_5)_3NNH_2]Cl + (C_6H_5)_2PCl$

$(C_6H_5)_2PCl$ (mmoles)	$(C_2H_5)_3NNH_2Cl$ (mmoles)	Conditions	Yield of Product $[(C_6H_5)_2PN]_3$	Yield of Product $[(C_6H_5)_2PN]_4$	Remarks*
54	45.7	no solvent; 140-198°C, 48 hrs	3.76g, 41.3%	---	M.p. 230-232°C.
29.1	13.9	At reflux of 4 ml of $(C_2H_5)_3N$, until it was consumed. 90°C for 48 hrs.	0.54g, 20%	---	M.p. 223-228°C.; 7.51% N: calcd. for $(C_6H_5)_2PN$, 7.03% N.
53.9	54.4	no solvent; 150°C., 15 hrs 200°C., 12 hrs 215°C., 108 hrs 270°C., 24 hrs	1.52g, 14.2%	1.32g, 12.3%	Separated from black tar by elution from a silica gel column with benzene.
11.9	11.71	no solvent; 197-237°C., 60 hrs	---	1.028 g, 44.1%	Separated by extraction with boiling benzene. M.p. 317-319°C.

*Literature: M.p. $[(C_6H_5)_2PN]_3$, 230-232°C; $[(C_6H_5)_2PN]_4$, 320-321°C

Table 2. Further runs of $[(C_6H_5)_3PNH_2]Cl + (C_6H_5)_2PCl$

$(C_6H_5)PCl$ (mmoles)	$[(C_6H_5)_3PNH_2]Cl$ (mmoles)	Conditions	Yield of Product $[(C_6H_5)_2PN]_3$	Yield of Product $[(C_6H_5)_2PN]_4$	Remarks
32.3	31.36	no solvent; 160°C., 52 hrs.	0.32g, 5.1%	---	Some $(C_6H_5)_3P$ also obtained major amounts of tar from which $[(C_6H_5)_2PN]_3$ was extracted with benzene. Identified by m.p. and spectrum.
10.8	11.2	no solvent; 73-150°C., 48 hrs.	0.17g, 7.9%	0.405g, 18.8%	Overall yield of $[(C_6H_5)_2PN]n$ material 26.7% of theory. Extracted with benzene. Identified by m.p. and spectrum.
32.4	32.2	no solvent; 160°C., 24 hrs.	0.79g, 12.3%	0.21g, 3.2%	Identified by m.p. and spectrum.

$[(C_2H_5)_3NNH_2]Cl$ may be considered to proceed by such steps as the following:

$$(C_6H_5)_2PCl + [(C_2H_5)_3NNH_2]Cl \longrightarrow [(C_6H_5)_2P(NH_2)Cl]Cl + (C_2H_5)_3N$$

$$2[(C_6H_5)_2P(NH_2)Cl]Cl + 3(C_2H_5)_3N \longrightarrow (C_6H_5)_2P(Cl)=N-P(=NH)(C_6H_5)_2 + 3[(C_2H_5)_3NH]Cl$$

$$(C_6H_5)_2P(Cl)=N-P(=NH)(C_6H_5)_2 + [(C_6H_5)_2P(NH_2)Cl]Cl \longrightarrow [(C_6H_5)_2PN]_3 + 3HCl$$

or

$$3[(C_6H_5)_2P(NH_2)Cl]Cl + 3(C_2H_5)_3N \longrightarrow [(C_6H_5)_2PN]_3 + 3HCl + 3[(C_2H_5)_3NH]Cl$$

The adduct $[(C_6H_5)_2P(NH_2)Cl]Cl$ has been isolated in the reaction of $(C_6H_5)_2PCl$ with ammonia-free NH_2Cl.[6] The fact that this compound was not isolated in the present instance may be attributed to the presence of the base $(C_2H_5)_3N$ formed by the thermal dissociation of $[(C_2H_5)_3NNH_2]Cl$. The adduct $[(C_6H_5)_2P(NH_2)Cl]Cl$ tends to undergo condensation with the loss of HCl even at room temperature, and appreciable quantities of this adduct would not accumulate in the presence of $(C_2H_5)_3N$. Similarly, the basic character of the system would account for the absence of the intermediate $(C_6H_5)_2P(NH_2)ClNHPCl_2(C_6H_5)_2$, which had been isolated from the reaction product of ammonia-free NH_2Cl with $(C_6H_5)_2PCl$ by Gilson and Sisler[6] and shown to form diphenylphosphazene trimer and tetramer upon pyrolysis.

An analogous series of steps is probable for the $[(C_6H_5)_3PNH_2]Cl$ reactions. The tars and oils obtained as by-products in these reactions were shown by their infra spectra to contain N-H, tetra-coordinated P-C_6H_5, P-C_6H_5, P=N-P and P-NH-P linkages (Table 3). Thus, intermediates of the types

Table 3. Principal bands in the IR spectra of the by-products of the $[(C_6H_5)_3PNH_2]Cl$-$(C_6H_5)_2PCl$ reaction

N-H	3.3-3.4 μ
tetracoordinated P-C_6H_5	9.0 μ
P-C_6H_5	6.9 μ
P=N-P	7.6-8.3 μ
P-NH-P	10.4 μ

discussed above are probably present in considerable quantity. This is not surprising since $(C_6H_5)_3P$ is much less basic that $(C_2H_5)_3N$.

HARRY H. SISLER*
JAMES CLINTON BARRICK

Department of Chemistry
University of Florida
Gainesville, FL 32611
U.S.A.

REFERENCES

[1]H. H. Sisler, F. Neth and F. R. Hurley, *J. Am. Chem. Soc.* 1954, **76**, 3909.
[2]G. Omietanski, A. D. Kelmers, R. W. Shellman and H. H. Sisler, *J. Am. Chem. Soc.* 1956, **78**, 3874.
[3]H. H. Sisler, G. Omietanski and B. Rudner, *Chem. Rev.* 1957, **57**, 1021.
[4]R. A. Rowe and L. F. Audrieth, *J. Am. Chem. Soc.* 1956, **78**, 563.
[5]L. F. Audrieth and L. H. Diamond, *J. Am. Chem. Soc.* 1954, **76**, 4860.
[6]I. T. Gilson and H. H. Sisler, *Inorg. Chem.* 1965, **4**, 273.
[7]G. Omietanski and H. H. Sisler, *J. Am. Chem. Soc.* 1956, **78**, 1211.
[8]H. H. Sisler, A. Sarkis, H. Ahuja, R. S. Drago and N. L. Smith, *J. Am. Chem. Soc.* 1959, **81**, 2982.
[9]H. Prakash and H. H. Sisler, *Allgem. u. prakt. Chem.* 1970, **21**(4), 123.
[10]R. Appel and A. Hauss, *Chem. Ber.* 1960, **93**, 405.
[11]C. P. Haber, P. L. Herring and E. A. Lawton, *J. Am. Chem. Soc.* 1958, **80**, 2116.
[12]H. H. Sisler, H. S. Ahuja and N. L. Smith, *Inorg. Chem.* 1962, **1**, 84.

*Author to whom correspondence should be addressed.

Polyhedron Vol. 1, No. 6, pp. 537-539, 1982
Printed in Great Britain.

0277-5387/82/060537-03$03.00/0
Pergamon Press Ltd.

Complex Formation Between Uranium(VI) Ion and some α-Aminoacids

(*Received* 18 *December* 1981)

Abstract—The formation constants for the complexation of the VO_2^{2+} by a number of C-substituted glycines have been determined by potentiometric titrations.

INTRODUCTION

Although there have been some reports on aminopolycarboxylic acid complexes with uranyl ion using solvent extraction or spectrophotometric methods[1] little work has been published on α-aminoacid complexes of uranium using a potentiometric titration technique.

Typical of the formation constants found are those for uranyl complexes of nitrilotriacetic acid and glycine reported as Log K = 9.56 ± 0.03 and 7.53 respectively.[2,3]

We report here the results of a study for UO_2^{2+} complexes of a series of α-aminoacids containing sulphur and oxygen atoms, having certain affinity to chelate with metal ions in cooperation with the aminoacid's nitrogen. The aminoacids studied were a series of C-substituted glycines of general formula R–CH(NH_2)COOH, where R = $-CH_2OH$, $-CH_2SH$, $-CH_3$, $-CH_2CH_2SCH_3$, $(CH_3)_2CH-$, $(CH_3)_2CHCH_2-$ and $C_2H_5CH(CH_3)$ all able to form five membered chelate rings. For comparison, complexes of serine and cysteine were investigated. Concurrently complexes of serine showed greater stability than those of alanine due to the presence of an OH group in serine which also showed an affinity to form an extra bond with the metal ion. In contrast to valine or leucine, methionine must therefore form more stable complexes due to its molecule containing a sulphur atom.

The only example of a related investigation so far reported has been by Cefola *et al.*[2] who studied complexes of glycine and UO_2^{2+} ions. Studies of mixed ligand complexes of uranyl ion with aminoacids and carboxylic acids or monocarboxylates have been published recently[3-5] each suggesting relatively strong bond formation between uranyl ion and oxygen donors.

EXPERIMENTAL

Measurement of protonation and complex formation constants; For the hydrogen and metal ions, formation constants were calculated from potentiometric titration curves[4] obtained using a combined electrode calibrated in terms of hydrogen ion concentration, [H] at 25°C. The electrode was also calibrated by 0.05 M KHP before and after each titration and agreement was always better than 0.005 PH units.

Potentials were measured with a Mettler DK31 digital pH meter. All solutions were made up in a background of KNO_3 (total I = 0.1 M). The aminoacids under experiment were converted to the fully protonated form by adding the calculated amount of standard nitric acid. The titration cell was thermostatically controlled (25 ± 0.1°C). Carbonate free alkali were added by means of a Mettler DV 210 automatic burette dispensing 0.02 ± 0.001 ml of alkali at each reading. The titrations were reproducible to 0.007 pH unit throughout. Solutions of 1:2 or 1:5 metal to ligand concentration were titrated with alkali and at the beginning of each titration total volume of solution in the cell was always kept at 30 ml. At higher pH values, when ligands titrated in the presence of a metal ion precipitation occured. In such instances therefore, data before precipitation only were considered and used to calculate KML_1 and KML_2 values.

Throughout this study uranyl nitrate (Analar) was used for the preparation of metal ion solutions. The aminoacids alanine, methionine, serine, leucine, valine, isoleucine and cycteine were obtained from Merck (Germany).

The proton and metal complex formatiom constant were calculated using a Fortran program.

RESULTS AND DISCUSSION

Calculated proton and uranyl complex formation constants are given in Table 1 with those for comparable ligands.

The obtained results for proton complex formation constants show the trends expected from inductive effects of the substituents. This effect is more noticable with the protonation of the amino group (Log βHL) than the carboxyl group—(Log βH_2L), since the amine nitrogen is closer to the substituent. The replacement of an α-hydrogen atom with an alkyl is seen to produce a small regular increase in proton complex formation

discussed above are probably present in considerable quantity. This is not surprising since $(C_6H_5)_3P$ is much less basic that $(C_2H_5)_3N$.

HARRY H. SISLER*
JAMES CLINTON BARRICK

Department of Chemistry
University of Florida
Gainesville, FL 32611
U.S.A.

REFERENCES

[1]H. H. Sisler, F. Neth and F. R. Hurley, *J. Am. Chem. Soc.* 1954, **76**, 3909.
[2]G. Omietanski, A. D. Kelmers, R. W. Shellman and H. H. Sisler, *J. Am. Chem. Soc.* 1956, **78**, 3874.
[3]H. H. Sisler, G. Omietanski and B. Rudner, *Chem. Rev.* 1957, **57**, 1021.
[4]R. A. Rowe and L. F. Audrieth, *J. Am. Chem. Soc.* 1956, **78**, 563.
[5]L. F. Audrieth and L. H. Diamond, *J. Am. Chem. Soc.* 1954, **76**, 4860.
[6]I. T. Gilson and H. H. Sisler, *Inorg. Chem.* 1965, **4**, 273.
[7]G. Omietanski and H. H. Sisler, *J. Am. Chem. Soc.* 1956, **78**, 1211.
[8]H. H. Sisler, A. Sarkis, H. Ahuja, R. S. Drago and N. L. Smith, *J. Am. Chem. Soc.* 1959, **81**, 2982.
[9]H. Prakash and H. H. Sisler, *Allgem. u. prakt. Chem.* 1970, **21**(4), 123.
[10]R. Appel and A. Hauss, *Chem. Ber.* 1960, **93**, 405.
[11]C. P. Haber, P. L. Herring and E. A. Lawton, *J. Am. Chem. Soc.* 1958, **80**, 2116.
[12]H. H. Sisler, H. S. Ahuja and N. L. Smith, *Inorg. Chem.* 1962, **1**, 84.

*Author to whom correspondence should be addressed.

Polyhedron Vol. 1, No. 6, pp. 537-539, 1982
Printed in Great Britain.

0277-5387/82/060537-03$03.00/0
Pergamon Press Ltd.

Complex Formation Between Uranium(VI) Ion and some α-Aminoacids

(*Received* 18 *December* 1981)

Abstract—The formation constants for the complexation of the VO_2^{2+} by a number of C-substituted glycines have been determined by potentiometric titrations.

INTRODUCTION

Although there have been some reports on aminopolycarboxylic acid complexes with uranyl ion using solvent extraction or spectrophotometric methods[1] little work has been published on α-aminoacid complexes of uranium using a potentiometric titration technique.

Typical of the formation constants found are those for uranyl complexes of nitrilotriacetic acid and glycine reported as Log K = 9.56 ± 0.03 and 7.53 respectively.[2,3]

We report here the results of a study for UO_2^{2+} complexes of a series of α-aminoacids containing sulphur and oxygen atoms, having certain affinity to chelate with metal ions in cooperation with the aminoacid's nitrogen. The aminoacids studied were a series of C-substituted glycines of general formula R–CH(NH_2)COOH, where R = $-CH_2OH$, $-CH_2SH$, $-CH_3$, $-CH_2CH_2SCH_3$, $(CH_3)_2CH-$, $(CH_3)_2CHCH_2-$ and $C_2H_5CH(CH_3)$ all able to form five membered chelate rings. For comparison, complexes of serine and cysteine were investigated. Concurrently complexes of serine showed greater stability than those of alanine due to the presence of an OH group in serine which also showed an affinity to form an extra bond with the metal ion. In contrast to valine or leucine, methionine must therefore form more stable complexes due to its molecule containing a sulphur atom.

The only example of a related investigation so far reported has been by Cefola *et al.*[2] who studied complexes of glycine and UO_2^{2+} ions. Studies of mixed ligand complexes of uranyl ion with aminoacids and carboxylic acids or monocarboxylates have been published recently[3-5] each suggesting relatively strong bond formation between uranyl ion and oxygen donors.

EXPERIMENTAL

Measurement of protonation and complex formation constants; For the hydrogen and metal ions, formation constants were calculated from potentiometric titration curves[4] obtained using a combined electrode calibrated in terms of hydrogen ion concentration, [H] at 25°C. The electrode was also calibrated by 0.05 M KHP before and after each titration and agreement was always better than 0.005 PH units.

Potentials were measured with a Mettler DK31 digital pH meter. All solutions were made up in a background of KNO_3 (total I = 0.1 M). The aminoacids under experiment were converted to the fully protonated form by adding the calculated amount of standard nitric acid. The titration cell was thermostatically controlled (25 ± 0.1°C). Carbonate free alkali were added by means of a Mettler DV 210 automatic burette dispensing 0.02 ± 0.001 ml of alkali at each reading. The titrations were reproducible to 0.007 pH unit throughout. Solutions of 1:2 or 1:5 metal to ligand concentration were titrated with alkali and at the beginning of each titration total volume of solution in the cell was always kept at 30 ml. At higher pH values, when ligands titrated in the presence of a metal ion precipitation occured. In such instances therefore, data before precipitation only were considered and used to calculate KML_1 and KML_2 values.

Throughout this study uranyl nitrate (Analar) was used for the preparation of metal ion solutions. The aminoacids alanine, methionine, serine, leucine, valine, isoleucine and cycteine were obtained from Merck (Germany).

The proton and metal complex formatiom constant were calculated using a Fortran program.

RESULTS AND DISCUSSION

Calculated proton and uranyl complex formation constants are given in Table 1 with those for comparable ligands.

The obtained results for proton complex formation constants show the trends expected from inductive effects of the substituents. This effect is more noticable with the protonation of the amino group (Log βHL) than the carboxyl group—(Log βH_2L), since the amine nitrogen is closer to the substituent. The replacement of an α-hydrogen atom with an alkyl is seen to produce a small regular increase in proton complex formation

Table 1. Proton and uranyl complex formation constants for the amino acids at 25° and I = 0.1 M. Standard deviation (σ values) in parentheses

	LH_2		UO_2^{2+}	
	log β HL	log β H_2L	log β 1	log β 2
D-Serine	9.16 (4) 9.12*	11.509 (9)	8.66 (3)	14.66 (5)
D-Cysteine	8.244 (4) 8.33†	10.552 (8) 10.50†	5.84 (2)	11.85 (5)
D-Methionine	8.921 (3) 9.052‡	11.271 (7) 11.203‡	6.41 (1)	13.38 (2)
DL-Alanine	9.592 (3)	12.067 (8)	7.33 (2)	14.97 (4)
DL-Valine	9.603 (2)	12.242 (9)	7.10 (1)	14.72 (2)
L-Leucine	9.621 (2)	12.266 (6)	7.13 (3)	14.36 (7)
L-Isoleucine	9.652 (4)	12.350 (9)	7.02 (3)	14.66 (8)

*Ref. [6].
†Ref. [7].
‡Ref. [8].

constant. This increase is to be expected as a result of the positive inductive effect of the alkyl groups causing electron repulsion and therefore tending to make the α-carbon atom negatively charged.

This effect will be transmitted to both the nitrogen atom and the carboxyl group resulting a decrease in acidity. The amino acids containing a sulphur or oxygen donor atom have lower proton complex formation constants than those of the other amino acids investigated in this work; even α-alanine with a simillar molecular structure forms a stronger proton complex than serine Δ Log βHL = 0.43) with cysteine having a (Δ Log βHL = 1.35).

This is due to the large negative inductive effect of the attached corboxyl or sulphydryl groups. The possibility of a steric effect has been demonstrated by Martell *et al.*[9] for L-Cysteine with Log βHL = 8.13 and DL-penicillamine Log β = 7.88 in 0.1 M potassium nitrate. For methionine the values are higher than those of cysteine due to a lower negative inductive effect of -SMe group. The proton complex formation constants for the series was found to be D-cysteine < D-methionine < D-serine < DL-α-alanine < DL valine < L-leucine < L-isoleucine, respectively.

With UO_2^{2+} all ligands produced a light yellow coloured solution and the solubility decreased as the alkyl chain increased in length. Mixtures of UO_2^{2+} and serine were found to be the most soluble of all. The degree of formation ($\bar{n}$) of the amino acid complexes with uranyl ion generally approached values 0.2–1.5 and complexes of serine were found to be markedly more stable, with $\bar{n}$ values approaching 1.85 and formation constants comparable to those previously reported for iminodiacetic acid[10] (Log β = 8.93).

Above $\bar{n}$ = 1.5 there was some evidence of the formation of *tris*-complexes but since the maximum M:L ratio used was 1:3 the formation constants calculated were not sufficiently reliable.

A maximum coordination number of 8 has been suggested for uranium ion,[11] therefore a maximum of three bidentated ligand molecules are sufficient to coordinate with UO_2^{2+} to reach the specified coordination number.

A quantitative comparison of the values for log βH_2L-log $\beta 2$ shows that the affinity of the ligands for protons and uranyl ion is comparable whether the ligand contains extra donor atoms (S or O) or not. The existing small differences can be explained in terms of steric factors and the fact that formation of a metal complex involves chelate formation of the N–U–O type while the proton complexes involve formation of separate N–H and O–H bonds.

In comparing the results for serine with those of alanine the proton complexes of serine (log βH_2L) tend to be weaker than those of alanine by 1.26 log units while the metal complexes are only marginally weaker (e.g. Δ Log β = 0.31). This can be regarded as an indication of extra bonding in serine. A similar comparison of results for cysteine and those for alanine suggests only limited bonding between the metal ions and the sulphur atom. Methionine forms complexes more stable than cysteine, this could be explained in terms of the difference of inductive effects in the two molecules.

Uranyl complex formation constants for other amino-acids, investigated in this work are also given in Table 1 followed by the pattern expected from the varying inductive effects of the substituent groups.

Acknowledgement—The authors should like to thank Mrs. A. Elhami for her assistance during the course of the investigation.

M. NOURMAND*
N. MEISSAMI

Nuclear Research Centre,
P.O. Box 3327 *Tehran*
Iran

*Author to whom correspondence should be addressed.

REFERENCES

[1]M. J. C. Nastasi and F. A. Lima, *J. Radioanalytical Chem.* 1972, **35**, 289.
[2]M. Cefola, R. C. Taylor, P. S. Gentile and A. V. Celiano, *J. Phys. Chem.* 1962, **66**, 790.
[3]P. V. Selvaraj and M. Santappa, *J. Inorg, Nucl. Chem.* 1977, **39**, 119.
[4]P. V. Selvaraj and M. Santappa, *J. Inorg. Nucl. Chem.* 1977 **38**, 837.
[5]L. Magon, R. Protanova, B. Zarli and A. Bismondo, *J. Inorg. Nucl. Chem.* 1972, **34**, 1971.
[6]E. V. Raju and M. B. Mathur, *J. Inorg. Nucl. Chem.* 1968, **30**, 2181.
[7]D. D. Perrin and I. J. Sayce, *J. Chem. Soc.* (*A*), 1968, 53.
[8]M. Israeli and L. D. Pettit, *J. Inorg. Nucl. Chem.* 1975, **37**, 999.
[9]G. R. Lenz and A. E. Martell, *Biochem. J.* 1964, **3**, 745.
[10]K. S. Rajan and A. E. Martell, *J. Inorg. Nucl. Chem.* 1964, **26**, 789.
[11]S. H. Ebele, Komplexverbindungen der Acticiden mit organishen liganden. K.F.K 1136, Karlsruher, Oct. (1970).

Polyhedron Vol. 1, No. 6, pp. 539–541, 1982
Printed in Great Britain.

0277–5387/82/060539–03$03.00/0
Pergamon Press Ltd.

Preparation of cationic (keto-stabilized phosphonium or sulphonium ylide)(η^5-cyclopentadienyl)(triphenylphosphine)palladium(II) complexes

(*Received* 30 *June* 1981)

Abstract—In the presence of $AgClO_4$, chloro(η^5-cyclopentadienyl)(triphenylphosphine)palladium(II) was treated with triphenylphosphonium benzoylmethylide triphenylphosphonium acetylmethylide, and dimethylsulphonium benzoylmethylide to yield the corresponding ylide complexes, [Pd(η^5-cyclopentadienyl)(ylide)(triphenylphosphine)]ClO_4 with ylidic carbon-metal σ bonds. When $NaClO_4$ was used in place of $AgClO_4$, the ylide complexes were not obtained.

Some keto-stabilized phosphonium and sulphonium ylides exhibit well-known interaction[1,2] with various electrophiles through the nucleophilic ylidic carbon next to onium atoms. The nucleophilic ylides displaced labile ligands in $[PdCl_2(SR_2)_2]$[3], $[Pd_2Cl_4(CH_2=CHPh)_2]$[4,5], and $[PdCl_2(NCR)_2]$[4,5], and cleaved chloro-bridges in $[Pd_2Cl_4(PR_3)_2]$[6] to give stable ylide complexes with ylidic carbon–palladium σ bonds. However, no attempt seems to have been described on the reaction of the ylides with (η^5-cyclopentadienyl)halo(tertiary phosphine)palladium(II) compounds. This note deals with the reaction of some ylides with chloro(η^5-cyclopentadienyl)(triphenylphosphine)palladium(II) (I) in the presence of silver perchlorate. Recently Kurosawa[7] reported that a bromo analogue of I was treated with silver perchlorate in the presence of olefins or carbon monoxide to replace bromine with these incoming ligands and to yield respective cationic complexes retaining the η^5-cyclopentadienyl moiety.

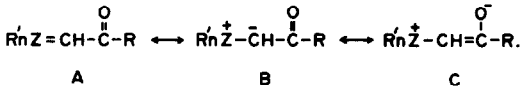

RESULTS AND DISCUSSION

(η^5-Cyclopentadienyl)palladium complex I was prepared in a very low yield from the reaction of thallium cyclopentadienide with a halogen-bridged complex $[Pd_2Cl_4(PPh_3)_2]$, owing to the low solubility of the reactants, as described by Cross and Wardle[8]. However, sodium cyclopentadienide is soluble in THF and reacted readily with $[Pd_2Cl_4(PPh_3)_2]$ to afford I in a high yield.

Complex I was treated with some keto-stabilized phosphonium and sulphonium ylides, which included triphenylphosphonium benzoylmethylide ($\mathbf{II_a}$), triphenylphosphonium acetylmethylide ($\mathbf{III_a}$), and dimethylsulphonium benzoylmethylide ($\mathbf{IV_a}$). These

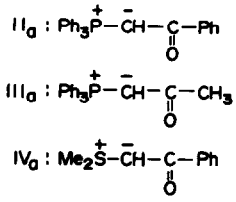

ylides could not displace chlorine coordinated to palladium in the presence of sodium perchlorate, implying low nucleophilicity of these ylides and fair stability of the palladium-chlorine bond. On the other hand, silver perchlorate, a strong halogen-trapping reagent could remove the chlorine from palladium, leading to the coordination of the ylides to palladium. Actually, the ylides $\mathbf{II_a}$, $\mathbf{III_a}$, and $\mathbf{IV_a}$ formed stable η^5-cyclopentadienyl ylide complexes $[Pd(\eta^5\text{-}C_5H_5)(PPh_3)\{CH(COR)ZR'_n\}]ClO_4$ ($ZR'_n = PPh_3$, R = Ph, $\mathbf{II_b}$; $ZR'_n = PPh_3$, R = Me, $\mathbf{III_b}$; $ZR'_n = SMe_2$, R = Ph, $\mathbf{IV_b}$), respectively, as shown in Tables 1 and 2.

These ylide complexes exhibited a $\nu(C=O)$ band in the range of 1620 to 1640 cm^{-1}, and the shift of the bands towards higher

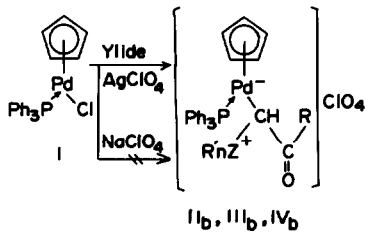

$\mathbf{II_b}$, $\mathbf{III_b}$, $\mathbf{IV_b}$

Table 1. Yields and properties of the palladium complexes

Complex	Yield[b] %	Mp[d] °C	Color	Found(Calcd), % C	H
I	80[c]	136-138	Dark green	59.03(58.87)	4.40(4.30)
II_b[a]	22	127-131	Yellowish green	62.45(62.18)	4.48(4.42)
III_b	25	151-162	Pale green	62.20(62.06)	4.75(4.62)
IV_b	9	113-133	Brown	55.45(55.55)	4.61(4.52)

a) Isolated as a hemisolvate of CH_2Cl_2. b) Based on I, unless noted elsewhere. c) Based on $Pd_2Cl_4(PPh_3)_2$. d) With decomposition.

Table 2. Spectroscopic properties of free ylides and their palladium complexes

	^{1}H-NMR[a], δ Value from TMS			IR[d], cm^{-1}	
	δ (CH)	δ (CH_3)	δ (Cp)[b]	ν(C=O)	ν(Cl-O)
I			5.48(d,3.0)		
II_a	4.57(d,24.3)[c]			1524	
II_b	4.25(ad,4.0)		5.00(d,2.0)	1620	1090
III_a	3.69(d,27.0)[c]	2.08(d,1.8)[c]		1530	
III_b	3.07(ad,1.1)	2.01(ad, 2.2)	5.19(d,2.2)	1640	1090
IV_a	4.29(s)	2.91(s)		1515	
IV_b	4.10(d,6.00)[b]	2.77(s), 2.69(s)	5.37(d,2.2)	1620	1085

a) In $CDCl_3$. Signal shape and coupling constant are given in the parentheses. Abbreviations used : s=singlet, d=doublet, ad=apparent doublet. b) Coupled with ^{31}P in triphenylphosphine. c) Coupled with onium ^{31}P nucleus. d) In KBr disk.

wave numbers upon coordination indicates larger contribution of the canonical structure B and smaller one of C, compared with those in free ylides. These results and the lack of an enolate C=O stretching band[9] suggest that the bonding mode of the ylides to palladium is through the ylidic carbon rather than through an enolate oxygen. Similar high-wavenumber shifts were observed in some keto-stabilized ylide complexes[3-6] upon coordination through the nucleophilic carbon. The chemical shifts of the ylide methine protons of these cationic complexes are at comparatively higher fields than those of free ylides and of reported neutral palladium ylide complexes[4-6]. The high-field resonances in the present complexes are possibly attributed to the electron donation to palladium from triphenylphosphine and η^5-cyclopentadienyl groups. Saito *et al.*[10] noticed similar highfield resonances of the methine protons in cationic ylide complexes. It is noteworthy that magnetic non-equivalence of two methyl groups on sulfur in $\mathbf{IV_b}$ was observed, due to the presence of the neighboring dissymmetric carbon which was induced by the σ-bond formation between the carbon and the palladium atoms.

In sharp contrast to the cases of $\mathbf{II_a}$, $\mathbf{III_a}$, and $\mathbf{IV_a}$, analogous cyclopentadienyl ylide complexes were not isolated from triphenylphosphonium methoxycarbonylmethylide (**V***a*) and dimethylsulphonium diacetylmethylide ($\mathbf{VI_a}$). ^{1}H NMR spectra of unidentified products from $\mathbf{V_a}$ and $\mathbf{VI_a}$ suggested loss of the cyclopentadienyl group.

EXPERIMENTAL

General procedures. IR and ^{1}H NMR spectra and melting points were measured according to the methods described in the previous paper.[11] Ylide compounds were prepared by the literature methods.[1,2]

Preparation of chloro(η^5-cyclopentadienyl)(triphenylphosphine)palladium(II) **I**. Complex **I** was prepared essentialy by the method described by Cross and Wardle[8], except that sodium cyclopentadienide was used in place of the thallium salt at temperatures lower than 0°C.

Reaction of phosphonium or sulphonium ylides with **I** *in the presence of $AgClO_4$.* To a mixture of triphenylphosphonium benzoylmethylide and **I** in THF, an equivalent quantity of $AgClO_4$ in benzene was added slowly. The precipitates formed were collected and recrystallized from dichloromethane, diethyl ether, and *n*-hexane to afford yellowish green powder of η^5-cyclopentadienyl)(triphenylphosphonium benzoylmethylide) (triphenylphosphine)palladium(II) perchlorate $\mathbf{II_b}$. (η^5-Cyclopentadienyl)(triphenylphosphonium acetylmethylide) (triphenylphosphine)palladium(II) perchlorate $\mathbf{III_b}$ and (η^5-cyclopentadienyl)(dimethylsulphonium benzoylmethylide) (triphenylphosphine)palladium(II) perchlorate $\mathbf{IV_b}$ were prepared similarly.

REFERENCES

[1] A. W. Johnson, *Ylid Chemistry*. Academic Press, New York (1966).
[2] B. M. Trost and L. S. Melvin, Jr., *Sulfur Ylides*. Academic Press, New York (1975).
[3] H. Koezuka, G. Matsubayashi and T. Tanaka, *Inorg. Chem.* 1974, **13**, 443.
[4] P. Bravo, G. Fronza, C. Ticozzi and G. Gaudiano, *J. Organomet. Chem.* 1974, **74**, 143.
[5] P. Bravo, G. Fronza and C. Ticozzi, *J. Organomet. Chem.* 1976, **111**, 361.
[6] H. Koezuka, G. Matsubayashi and T. Tanaka, *Inorg. Chem.* 1976, **15**, 417.
[7] H. Kurosawa, T. Majima and N. Asada, *J. Am. Chem. Soc.* 1980, **102**, 6996.
[8] R. J. Cross and R. Wardle, *J. Chem. Soc.* (*A*) 1971, 2000.
[9] J. Buckle and P. G. Harrison, *J. Organomet. Chem.* 1973, **49**, C-17.
[10] M. Kato, H. Urabe, Y. Oosawa, T. Saito and T. Sasaki, *J. Organomet. Chem.* 1976, **121**, 81.
[11] M. Onishi, K. Hiraki, K. Maeda and T. Itoh, *J. Organomet. Chem.* 1980, **188**, 245.

MASAYOSHI ONISHI*
YUSHICHIRO OHAMA
KATSUMA HIRAKI
HIROSHI SHINTANI

Department of Industrial Chemistry
Faculty of Engineering
Nagasaki University
Nagasaki
Japan

*Author to whom correspondence should be addressed.

Polyhedron Vol. 1, No. 6, pp. 541–542, 1982
Printed in Great Britain.

0277-5387/060541-02$03.00/0
Pergamon Press Ltd.

Molecular size and orientation of dinonylnaphthalenesulphonic acid at the hexane/water and air/water interfaces

(*Received* 10 *May* 1980)

During our investigation of the inverse micellization phenomenon of dinonylnaphthalenesulfonic acid (HDNNS) in the presence of an aliphatic α-hydroxyoxime[1], it came to our attention that the literature contains contradictory opinions of the molecular area (A_0) occupied by HDNNS at the organic/water interface.[2,3] Chiarizia *et al.*[2], calculated the size of HDNNS micelles in toluene by using a value of A_o derived from toluene/water ($HClO_4$) interfacial tension data. However, van Dalen *et al.*[3] determined A_o for HDNNS at the air/water interface and then utilized the value in a manner similar to Chiarizia *et al.*[2] to determine the size of the micelle. The purpose of this note is to present our work on the interfacial area measurements of HDNNS at both the hexane/water interfaces and to reconcile the disparity of opinion based on consideration of the probable interfacial orientations of HDNNS in each system.

EXPERIMENTAL

Materials. HDNNS was obtained from King Industries as SYNEX 1040 reported to be a 38% solution in heptane. HDNNS was purified according to the method of Danesi *et al.*[4] Purity was checked by IR and NMR spectroscopy. Water used in the experiments was twice distilled from potassium permanganate in an all-glass still.

Measurements. Interfacial tensions were measured at the hexane/water interface using the du Nouy ring method. Details are presented elsewhere.[1] In the case of the air/water interface, determinations of spreading pressure ($\pi = \gamma_o - \gamma$) vs area isotherms and the limiting area per molecule for HDNNS were made using a Langmuir trough apparatus (Cenco Hydrophic Balance). Samples of the sulfonic acid dissolved in hexane ($\sim 12\ \mu l$ of 6×10^{-3} mol dm^{-3}) were dispensed slowly onto the surface of an aqueous phase (ionic strength 0.5 mol dm^{-3} (KNO_3)) using a chromatographic syringe and the hexane was allowed to evaporate prior to measurement. Measurements were made by slow, stepwise compression of the surface material. All measurements were conducted at room temperature.

RESULTS AND DISCUSSION

Figure 1 shows the results obtained for the hexane/water interfacial activity of HDNNS from interfacial tension data. By using the Gibbs adsorption isotherm in the form

$$\frac{1}{A} = -\frac{1}{2.3RT}\frac{d\gamma}{d \log C} \qquad (1)$$

where A is the effective interfacial area occupied by an HDNNS molecule, γ is the interfacial tension and C is the bulk organic phase concentration of HDNNS, values for A (area in Å^2/molecule) can be obtained at any value of C. The results of the application of eqn (1) to Fig. 1 were used to construct the spreading pressure (π) vs. area isotherm shown in Fig. 2. Spreading pressure is defined as $\gamma_o - \gamma$, where γ_o is the interfacial tension in the surfactant-free system. The curve gives a limiting area/molecule (A_o) of 38Å^2 in agreement with the A_o value of approximately 40Å^2 determined at the toluene/aqueous interface by Chiarizia *et al.*[2]

The π versus area plot obtained with the air/water film balance is also shown in Fig. 2. According to this figure, the limiting area for HDNNS at the air/water interface is about 100Å^2. Using a different technique (measurement of the surface area of a monomolecular layer on water made visible by lycopodium), van Dalen *et al.*[3] have reported a value of 95 ± 7Å^2 for the interfacial area of an HDNNS molecule at the air/water interface.

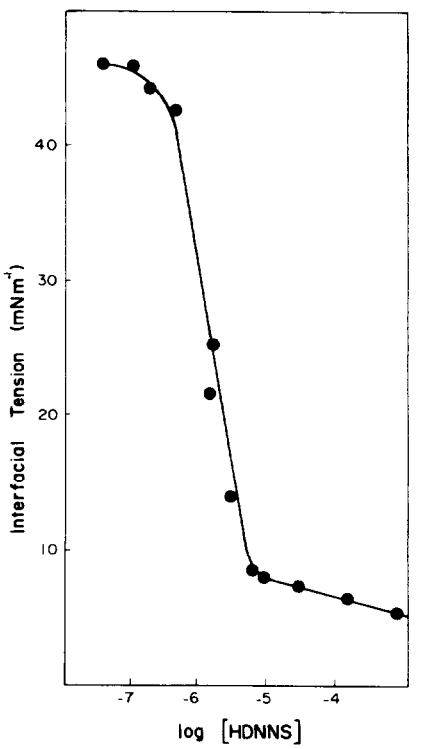

Fig. 1. Interfacial tension versus log[HDNNS] (mol dm^{-3}) isotherm at the hexane/water interface. (0.5 mol dm^{-3} KNO_3; pH 2.5; 25°C).

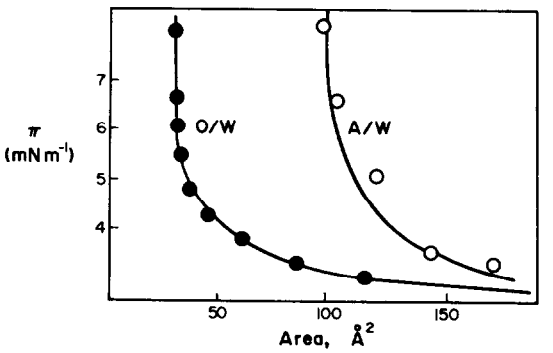

Fig. 2. Spreading pressure (π) versus area isotherms at the hexane/water interface (0/W) and the air/water interface (A/W). (Aqueous phase: 0.5 mol dm^{-3} KNO_3; pH 2.5; 25°C.)

The different values obtained for the interfacial areas at the air/water and the oil/water interfaces in identical aqueous systems indicate that HDNNS molecules are oriented differently at the two interfaces. The 100 $Å^2$ value for the air/water system suggests that the bulky dinonylnaphthalene group is lying adjacent to the aqueous phase at the air/water interface rather than being extended perpendicularly, if an organic phase were present. On the other hand, the value of 38$Å^2$ for HDNNS at the hexane/water interface indicates that HDNNS is oriented perpendicularly to the interface with the alkaryl group extended into the organic phase and the sulphonic acid group extended into the aqueous phase. HDNNS is known to hydrate extensively[4]; indicative of the favourable energy situation if the ($-SO_3^-$) group is hydrogen bonded.

In inverse micellar systems, the surfactant aggregate is in the organic phase and is known to contain an aqueous core.[2,3] Thus the inner micellar surface is actually an organic/aqueous interface and any physical properties of the surfactant molecule would probably reflect organic/aqueous interfacial characteristics. Therefore, in treating HDNNS micellar systems, the organic/aquous interfacial area is the appropriate quantity to use.

Acknowledgement—This work was supported by the National Science Foundation under Grant Nos. ENG 76–82141 and CPE 8110756.

MARK E. KEENEY
K. OSSEO-ASARE*

Departments of Mineral Engineering and Materials Science and Engineering
The Pennsylania State University
University Park, PA 16802
U.S.A.

*Author to whom correspondence should be addressed.

REFERENCES

[1]K. Osseo-Asare and M. E. Keeney, *Met. Trans. B.* 1980, **11B**, 63.
[2]R. Chiarizia, P. R. Danesi, G. D'Alessandro and B. Scuppa, *J. Inorg. Nucl. Chem.* 1976, **38**, 1367.
[3]A. van Dalen, K. Gerritsma and J. Wijkstra, *J. Colloid Interface Sci.* 1974, **48**, 122.
[4]P. R. Danesi, R. Chiarizia and G. Scibona, *J. Inorg. Nucl. Chem.* 1973, **35**, 3926.

Polyhedron Vol. 1, No. 6, pp. 543-548, 1982
Printed in Great Britain.

0277-5387/82/060543-06$03.00/0
Pergamon Press Ltd.

NOVEL COMPLEXES OF 2,6-(DIBENZOTHIAZOL-2-YL)PYRIDINE AND RELATED LIGANDS

A. S. Salameh and H. A. Tayim*

Department of Chemistry, American University of Beirut, Beirut, Lebanon

and

B. C. Uff

Department of Chemistry, University of Technology, Loughborough-Leicestershire, U.K.

(Received 26 February 1982)

ABSTRACT

The coordination chemistry of 2,6-pyridinedicarboxaldehyde (Dial) has been recently reported[1]. The Schiff base derived from Dial and o-aminobenzenethiol has also been reported and its reactions with transition metal ions have been investigated[2]. The condensation product derived from Dial and o-aminobenzenethiol rearranges into a poly-heterocyclic compound, 2,6-(dibenzothiazol-2-yl)pyridine (DBTP). We now report on the synthesis and reaction of DBTP with some transition metal ions.

EXPERIMENTAL

2,6-(Dibenzothiazol-2-yl)pyridine (DBTP): This ligand was prepared by two routes:

a) The method of Livingstone and Nolan[3] whereby a mixture of 2,6-lutidine and iodine with dimethylsulfoxide was treated with o-aminobenzenethiol; yield: 9%.

b) The condensation of Dial with o-aminobenzenethiol: To a solution of Dial[2] (1.00 g, 7.4 mmole) in ethanol (12 ml), o-aminobenzenethiol (4.35 g, 35 mmole) was added. The mixture was refluxed for 2½ hrs, then left to stand overnight at room temperature. A pale yellow precipitate was formed. It was recrystallized from chloroform. Yield: 1.6 g, 49%. M.P. 275-277° (lit. 273-275)[3]. Anal. calcd for $C_{18}H_{11}N_3S_2$: C, 66.1; H, 3.3; N, 12.2; S, 18.5. Found: C, 65.9; H, 3.3; N, 12.0; S, 18.6. No band occurred between 2300 and 2800 cm^{-1} in the spectrum (the region containing the ν S-H).

Reactions of DBTP With Metal Ions: Except for $RuCl_3.3H_2O$, the reactions of DBTP with various metal ions were carried out by the following general procedure:

A solution of DBTP (0.230 g, 0.67 mmole) in hot chloroform (40 ml) was added to a stirred solution of the metal salt (0.67 mmole) in hot ethanol (10-15 ml). The product which separated was filtered off, washed with hot chloroform, hot ethanol and ether, respectively. It was dried in vacuo over P_2O_5.

The above general method was thus applied to the reactions of $CuCl_2.2H_2O$, $CuBr_2$, $FeCl_3.6H_2O$, $Ni(ClO_4)_2.6H_2O$, $Pd(C_6H_5CN)_2Cl_2$, $ZnCl_2$, $HgBr_2$, $HgCl_2$, $CoI_2.2H_2O$, $RhCl_3.3H_2O$ and $AgClO_4$.

In the case of $RuCl_3.3H_2O$, a solution of DBTP (0.230 g, 0.67 mmole) in hot dioxane (60 ml) was added to a solution of the metal salt (0.176 g, 0.67 mmole) in hot ethanol (20 ml) and the reaction mixture was refluxed for 2 hrs. The brownish-black precipitate that separated was filtered off, washed with hot dioxane, hot ethanol and ether, respectively. It was then dried in vacuo over P_2O_5.

Elemental analyses were run by Pascher, Mikroanalytisches Laboratorium, Bonn, W. Germany.

The infrared spectra were recorded using a Perkin-Elmer 621 Grating Spectrophotometer. Potassium bromide pellets were used.

The melting points were taken using a Mel-Temp apparatus and are uncorrected.

RESULTS AND DISCUSSION

It is well established now that the condensation of o-aminobenzenethiol with an aldehyde does not normally lead to the isolation of the corresponding Schiff base but rather a benzothiazoline or its oxidation product, a benzothiazole. Benzothiazoline may rearrange to the Schiff base in a basic medium[3]. 2,6-(Dibenzothiazole-2-yl)pyridine (DBTP) I, originally reported by Livingstone and Nolan was synthesized by them by the condensation of o-aminobenzenethiol with 2,6-pyridinedicarboxaldehyde (Dial) which was prepared in situ by the facile reaction of 2,6-lutidine with iodine in DMSO. We improved the yield appreciably (from 10% to about 50%) by the condensation of o-aminobenzenethiol with presynthesized Dial[2]. The isolation of Dial from the 2,6-lutidine-I_2 reaction mixture was not possible.

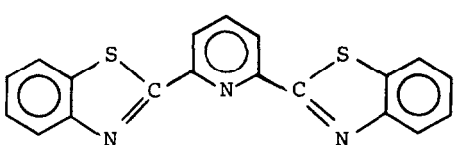

I

DBTP reacted with several metal salts; the products are listed in table I; their elemental analysis are listed in table II.

Table I

Reactions of DBTP With Some Metal Ions

Metal Salt	Product	Color	M.P. °C with decomposition	% Yield
$CuCl_2.2H_2O$	$Cu(DBTP)Cl_2.H_2O$	Yellow	245-248	71
$CuBr_2$	$Cu(DBTP)Br_2$	Yellow	>360	63
$FeCl_3.6H_2O$	$Fe(DBTP)_2Cl_3.H_2O$	Orange	283-285	62
$Ni(ClO_4)_2.6H_2O$	$Ni(DBTP)_2(ClO_4)_2.2H_2O$	Pale-Yellow	253-257	92
$Pd(C_6H_5CN)_2Cl_2$	$Pd_2(DBTP)Cl_4$	Brown	>360	78
$ZnCl_2$	$Zn(DBTP)Cl_2$	Pale-Yellow	>360	81
$RuCl_3.3H_2O$	$Ru(DBTP)Cl_3.C_2H_5OH$	Brownish-Black	>360	70
$HgBr_2$	$Hg(DBTP)Br_2$	Pale-Yellow	322-324	74
$HgCl_2$	$Hg(DBTP)Cl_2$	Pale-Yellow	326-331	69
$CoI_2.2H_2O$	$Co(DBTP)I_2$	Brown	>360	72
$RhCl_3.3H_2O$	$Rh(DBTP)Cl_3.2H_2O$	Yellow	>360	77
$AgClO_4$	$Ag(DBTP)ClO_4$	Pale-Yellow	311-313	73

Table II

Elemental Analyses of DBTP-Metal Complexes

Compound		C	H	N	S	X	Metal
$Cu(DBTP)Cl_2.H_2O$	Calcd	45.80	2.63	8.44	12.88	14.24	12.76
	Found	45.65	2.52	8.09	13.01	13.68	12.71
$Cu(DBTP)Br_2$	Calcd	40.12	1.95	7.39	11.27	28.15	11.17
	Found	39.82	1.98	7.40	11.80	27.84	10.86
$Fe(DBTP)_2Cl_3.H_2O$	Calcd	52.40	2.81	9.60	14.70	12.21	6.41
	Found	52.50	2.63	9.52	13.78	12.60	6.60
$Ni(DBTP)_2(ClO_4)_2.2H_2O$	Calcd	46.35	2.66	8.54	13.00	7.20	5.96
	Found	45.86	2.54	8.08	12.91	6.92	6.40
$Zn(DBTP)Cl_2$	Calcd	47.37	2.30	8.72	13.31	14.72	13.57
	Found	47.08	2.21	8.42	13.30	15.00	13.28
$Hg(DBTP)Cl_2$	Calcd	36.99	1.80	6.81	10.39	11.49	
	Found	37.07	1.80	6.94	9.96	11.49	
$Hg(DBTP)Br_2$	Calcd	32.33	1.57	5.95	9.08	22.64	
	Found	32.32	1.56	6.00	8.88	22.01	
$Co(DBTP)I_2$	Calcd	34.67	1.68	6.39	9.74	38.56	
	Found	34.72	1.73	6.37	9.74	37.96	
$Ag(DBTP)ClO_4$	Calcd	41.28	2.00	7.60	11.60	6.41	19.52
	Found	41.38	2.07	7.60	11.33	7.32	19.89
$Pd_2(DBTP)Cl_4$	Calcd	32.60	1.58	6.00	9.16	20.26	
	Found	33.20	1.60	6.00	9.40	19.98	
$Ru(DBTP)Cl_3.C_2H_5OH$	Calcd	42.11	2.86	7.02	10.55	17.76	
	Found	42.41	2.82	6.85	11.60	17.90	
$Rh(DBTP)Cl_3.2H_2O$	Calcd	38.63	2.56	7.11	10.85	18.01	
	Found	37.76	2.28	7.20	10.26	17.47	

The ligand reacted readily upon mixing with most of the ions reported. Some required refluxing for 2-3 hrs. The complexes are practically insoluble in water or common organic solvents. They are slightly soluble in DMF and DMSO.

The IR spectra of the complexes differed only slightly from that of the ligand. The presence of H_2O in some of the complexes is confirmed by the appearance of ν O-H in their IR spectra around 3400-3440 cm^{-1}. The band characteristic of uncoordinated perchlorate ion appeared at 1090 and 1080 cm^{-1} in the Ni(II) and Ag(I) complexes, respectively.

Although the ligand is potentially tridentate, it may very well behave as a mono- or bidentate, especially since the three donor nitrogen atoms are not equally basic. The pyridyl nitrogen is a stronger donor than the other two benzothiazole nitrogen atoms. Thus, the complexes $Zn(DBTP)Cl_2$, $Hg(DBTP)Cl_2$ and $Hg(DBTP)Br_2$ are most likely tetrahedral with DBTP behaving as a bidentate ligand bonded to the metal atom through the pyridyl and one of the benzothiazole nitrogens. The ligand may be bidentate resulting in tetracoordinate $Cu(DBTP)Br_2$ and $Co(DBTP)I_2$ or tridentate resulting in the complexes being pentacoordinate. $Co(DBTP)Br_2$ has been previously reported[3] to be five coordinate. The octahedral complexes $Cu(DBTP)Cl_2.H_2O$, $Fe(DBTP)_2Cl_3.H_2O$, $Ni(DBTP)_2(ClO_4)_2.2H_2O$, $Ru(DBTP)Cl_3.C_2H_5OH$ and $Rh(DBTP)Cl_3.2H_2O$ are most likely octahedral, involving the ligand as a tridentate. The palladium(II) complex, $Pd_2(DBTP)Cl_4$ involves Pd-Cl-Pd bridges as suggested in II.

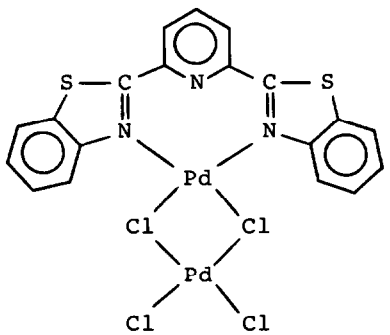

II

The IR spectrum showing two medium bands at 335 and 260 cm^{-1} assigned to terminal and bridging Pd-Cl, respectively, supports structure II.

Since the condensation of Dial and o-aminobenzenethiol did not afford the Schiff base III, we tried to prepare it by effecting the

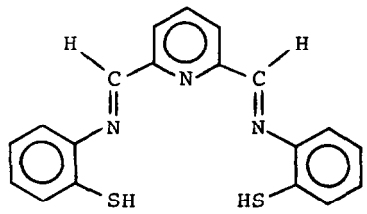

III

condensation in a basic medium. No Schiff base was obtained. Attempts to react metal salts with a mixture of Dial and o-aminobenzenethiol in a basic medium resulted in the isolation of the metal complexes of the o-aminobenzothiazolate ion. Thus, palladium(II) afforded bis(o-aminobenzenethiazolate)palladium(II). It was identified by comparison of its properties with authentic sample prepared by a known method[4].

REFERENCES

1. A.S. Salameh, B.C. Uff, Y. Saykali and H.A. Tayim, J. Inorg. Nucl. Chem. 42, 43 (1980).
2. H.A. Tayim, M. Absi, A. Darwish and S.K. Thabet, Inorg. Nucl. Chem. Lett. 11, 395 (1975).
3. S. Livingstone and J. Nolan, J. Chem. Soc. Dalton, 218 (1972).
4. L. Lindoy, S. Livingstone and T. Lockyer, Aust. J. Chem. 20, 471 (1967).

Polyhedron Vol. 1, No. 6, pp. 549–552, 1982
Printed in Great Britain.

0277-5387/82/060549-04$03.00/0
Pergamon Press Ltd.

Studies of Cyclic Indium Species Derived from 1,2,3,4-Tetraphenylbutadiene

Clovis Peppe and Dennis G. Tuck*

Department of Chemistry, University of Windsor
Windsor, Ontario, Canada N9B 3P4

(Received 29 March 1982)

Abstract. The reactions of 1,4-dilithio-1,2,3,4-tetraphenylbutadiene with indium(III) species have been investigated. The neutral compound $InCl_3.3py$ (py = pyridine) yields the pyridine adduct of a cyclo-C_4In-Cl molecule; with $InCl_4^-$, the spiro anion $[C_4InC_4]^-$ is obtained. It was not possible to detect any indium(I) or (II) derivatives in the decomposition products of these compounds.

INTRODUCTION

Alkyl and aryl derivatives of indium(III) are well known, and we now report the first synthesis of two related compounds containing the unsaturated C_4In heterocycle. The preparation of organometallic heterocyclic molecules formally derived by the ring closure of tetraphenylbutadiene onto a hetero atom was first described some years ago,[1,2] and synthesis via the dilithiated diene has been carried out with a variety of elements. It is appropriate to note here that the only reported derivative of a Group III element is $(C_6H_5)_4C_4BC_6H_5$; there are references to a thallium(III) compound, but no experimental details have been published. The present work has yielded the neutral $(C_6H_5)_4CInCl$, as the 1:1 adduct with pyridine, and the spiro anion $[(C_6H_5)_4C_4InC_4(C_6H_5)_4]^-$, as the tetraphenylarsonium salt. The latter compound reacts smoothly with two moles of maleic anhydride.

In addition to the synthetic problem, the decomposition of this type of indium heterocycle is of interest as providing a possible route to organo-indium(I) compounds, few of which are known. Although Neumann and co-workers[3] have reported the generation of free stannylenes R_2Sn by the decomposition of Diels-Alder derivatives of the corresponding tin(IV) compound, we were unable to identify any analogous reactions with the indium compounds prepared in this work.

*Author to whom correspondence should be addressed.

EXPERIMENTAL

General

Indium(III) starting materials were prepared by standard methods. Other materials were used as supplied; solvents were dried over sodium or calcium hydride before use. All experiments were carried out in an atmosphere of dry nitrogen.

Analytical methods and spectroscopic procedures were as described in previous papers.[4]

Preparative

(i) 1,4-dilithio-1,2,3,4-tetraphenylbutadiene (I). A slight excess of lithium metal was added to a solution of diphenylacetylene in diethylether. The mixture was stirred for ca. 6 h, at which time a yellow suspension separated from a red liquid. This suspension was used without further treatment.

(ii) Chloro(pyridine)(1,2,3,4-tetraphenyl-1,3-butadiene-1,4-diyl) indium(II). A preparation of I made from 1.25 g (7 mmol) diphenylacetylene in 20 mL diethylether was diluted to 100 mL; 1.60 g (3.5 mmol) of indium(III) chloride tris-pyridine[5] ($InCl_3$.3py) was added, and the mixture stirred for 30 h. The yellow product was collected and recrystallised from methylene chloride/petroleum ether. Yield 1.02 g, 50%, based on $InCl_3$.3py. Found: C, 66.0; H, 4.5; N, 2.2; In, 19.8; Cl, 6.5. $C_{33}H_{25}NClIn$ requires: C, 67.6; H, 4.3; N, 2.4; In, 19.6; Cl, 6.1%. The ^1H nmr spectrum in CD_2Cl_2 was a set of complex multiplets at δ 6.6 - 8.6 ppm.

(iii) Tetraphenylarsonium bis(tetraphenyl-1,3-butadienylene)indate(-1) (III). A suspension of I from 4.93 g (27.7 mmol) of diphenylacetylene was treated with 4.46 g (6.92 mmol) of tetraphenylarsonium tetrachloroindate(III)[6] for 48 h. The yellow insoluble product was recrystallised from dichloromethane/petroleum ether. Found: C, 79.0; H, 5.1; In, 9.6. $C_{80}H_{60}AsIn$ requires: C, 79.3; H, 5.0; In, 9.5%. The ^1H nmr spectrum (CD_2Cl_2) consisted of multiplets at 7.45 - 7.80 ppm (C_6H_5 of cation) and 6.75 - 6.90 ppm (C_6H_5 on C_4In ring), with the integrated intensity ratio 1:2. Yield 5.1 g, 61%.

(iv) Reaction of III with maleic anhydride. A solution of maleic anhydride (0.14 g) in 20 mL of dichloromethane was slowly added to 0.87 g (0.7 mmol) of III in the same solvent. The red solution which immediately formed was stirred overnight; solvent was then partially removed and petroleum ether was added, throwing down the Diels-Alder adduct in quantitative yield. Found: In, 8.3. $C_{88}H_{64}O_6AsIn$ requires: In, 8.2%. ^1H nmr spectrum (CD_2Cl_2); δ 0.75 - 1.5 multiplet (sp^3C-H); 6.75 - 6.90 multiplet, (C_6H_5 on C_4In ring); 7.45 - 7.80 multiplet,cation. The integrated ratio of phenyl proton to C-H was 16:1 (Calc. 15:1).

DISCUSSION

The reaction between I and $InCl_3.3py$ or $InCl_4^-$ proceeds smoothly, if slowly, under the conditions described to give the products II and III. Compound I did not yield identifiable products with uncomplexed indium(III) halides, giving rather a complicated mixture which we were unable to resolve. Similar conclusions applied to the reaction between I and CH_3InCl_2. We suggest that these difficulties arise because of the dimeric structure of these indium(III) species in solution[7]

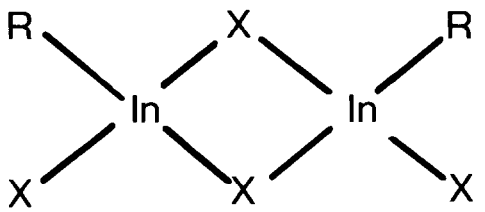

R = X,CH_3

which results in the presence of a number of pairs of halogens which can be eliminated by reaction with the 1,4-dilithiotetraphenylbutadiene, giving a variety of different products. The use of the mononuclear $InCl_3.3py$, or of $InCl_4^-$, obviates such difficulties.

The characterisation of the products depends on elemental analysis, on ^1H nmr, and in the case of the spiro anion III on ^{13}C nmr, which shows the predicted fourteen line spectrum in the region 151.6 - 121 ppm. We have not attempted to assign these resonances, but note that for the structure shown below one expects four resonances from the cation phenyl groups, two from the C_4In rings and eight from the two different types of phenyl rings attached to the C_4In rings. The reaction of III with two moles of maleic anhydride is also consistent with the structure proposed, which is isolectronic with that of the compound $Sn[C_4(C_6H_5)_4]_2$ reported earlier.[3]

The structures are then

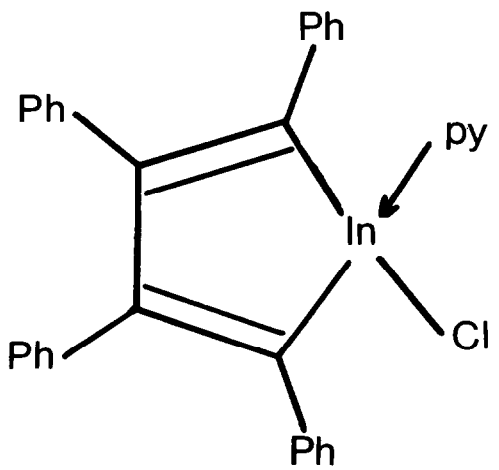

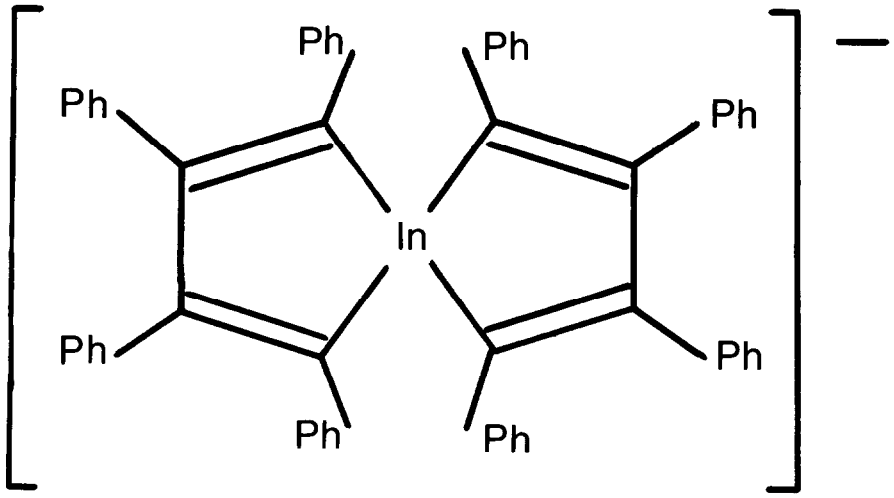

As noted in the Introduction, Diels-Alder decomposition of II or III did not yield any identifiable products, and these compounds do not therefore represent synthetic routes to organoindium(I) species.

Acknowledgement

This work was supported in part by Operating Grants (to DGT) from the Natural Sciences and Engineering Research Council of Canada. One of us (CP) thanks the Conselho Nacional de Desenvolvimento Cientifico e Tecnologico (Brasil) for a scholarship.

References

1. (a) F.C. Leavitt, T.A. Manuel, F. Johnson, J. Am. Chem. Soc., 1959, 81, 3163.
(b) F.C. Leavitt, T.A. Manuel, F. Johnson, L.U. Matternas, D.S. Lehman, J. Am. Chem. Soc. 1960, 82, 5099.
2. E.H. Braye, W. Hübel, I. Caplier, J. Am. Chem. Soc., 1961, 83, 4406.
3. C. Grugel, W.P. Neumann, M. Schriewer, Angew. Chem., Int. Ed., 1979 18, 543.
4. J.J. Habeeb, F.F. Said, D.G. Tuck, J. Organometal. Chem., 1980, 190, 325.
5. R.N. Ivanov-Emin, Y.I. Rabovik, Zhur. Neorg. Khim., 1959, 4, 2228.
6. J. Gislason, M.H. Lloyd, D.G. Tuck, Inorg. Chem. 1971, 10, 1907.
7. A.J. Carty, D.G. Tuck, Prog. Inorg. Chem., 1975, 19, 245.

Polyhedron Vol. 1, No. 6, pp. 553–555, 1982
Printed in Great Britain.

0277–5387/82/060553–03$03.00/0
Pergamon Press Ltd.

SYNTHESIS OF ALKALI OXYDIPEROXYFLUOROVANADATES(V)

M.K. CHAUDHURI* and S.K. GHOSH
Department of Chemistry, North-Eastern Hill University,
Shillong 793003, India

Abstract — The reaction of vanadium pentoxide with hydrogen peroxide in an alkaline medium in the presence of alkali fluorides AF (A = NH_4, Na, K, Rb or Cs) gives alkali oxydiperoxyfluorovanadates(V), $A_2[VO(O_2)_2F]$ in very high yields. Characterisation of the compounds was made from the results of chemical analyses, magnetic susceptibility measurements and i.r. spectral studies. IR spectrometry showed the peroxy ligands to be triangular bidentate.

INTRODUCTION

Although there has been a continued interest in the study of peroxyvanadium(V) chemistry,[1-6] the synthesis, characterisation and structural assessment of peroxy and mixed peroxyvanadium(V) compounds have received relatively less attention to date. This is presumably owing to the uncertain nature of peroxyvanadium(V) in solution of varying p^H. As a sequel of our studies mainly aimed at the synthesis of fluoro compounds of transition metals,[7-9] we undertook the synthesis of peroxyfluorovanadium(V) compounds. The present paper reports the first general synthesis of the title compounds along with their characterisation.

EXPERIMENTAL

Vanadium pentoxide, alkali metal fluorides and hydrogen peroxide were reagent grade products. Infrared spectra were recorded on a Perkin-Elmer model 125 spectrophotometer. Magnetic measurements were carried out by Gouy method using $Hg[Co(NCS)_4]$ as the calibrant.

Synthesis of alkali oxydiperoxyfluorovanadates(V)

$A_2[VO(O_2)_2F]$ (A = NH_4, Na or K) — A finely mixed powder of vanadium pentoxide (5.5 mmol) and alkali metal fluoride, AF (11 mmol) was dissolved in 9% hydrogen peroxide (79.4 mmol) by slightly warming over a steam-bath and a red solution was obtained. A concentrated solution of the corresponding alkali hydroxide (50 mmol) was slowly added with constant stirring whereupon the solution became yellow. An excess of alcohol was added to the solution with stirring until an yellow coloured microcrystalline product was obtained. The reaction container was then cooled in an ice-bath for ca 40 min. The compound was separated by centrifugation and purified by washing with alcohol and finally dried in vacuo over phosphorous pentoxide. The yields of $(NH_4)_2[VO(O_2)_2F]$, $Na_2[VO(O_2)_2F]$ and $K_2[VO(O_2)_2F]$ were 1.6g (78%), 1.8g (84%) and 2.1g (84%) respectively.

The $Rb_2[VO(O_2)_2F]$ and $Cs_2[VO(O_2)_2F]$ compounds were prepared in a manner similar to that described above, however, the solution of V_2O_5 (5.5 mmol) and AF (A = Rb or Cs) (11 mmol) in 9% hydrogen peroxide (79.4 mmol) was made alkaline by the addition of 25% solution of ammonium hydroxide (50 mmol). The yield of $Rb_2[VO(O_2)_2F]$ was 2.6g (74%) and that of $Cs_2[VO(O_2)_2F]$ was 3.5g (77%).

Table 1. Analytical data and structurally significant i.r. bands of $A_2[VO(O_2)_2F]$ (A = NH_4,Na,K,Rb or Cs)

Compound	Analysis[a] (%)				$\tilde{\nu}$/cm^{-1}	Assignments
	A	V	O^b_A	F		
$(NH_4)_2[VO(O_2)_2F]$	14.9[c] (15.06)	27.7 (27.40)	34.2 (34.41)	10.1 (10.22)	970s 870s 885s 472s	$\tilde{\nu}_{V-O}$ $\tilde{\nu}_{O-O}$ $\tilde{\nu}_{V-F}$
$Na_2[VO(O_2)_2F]$	23.6 (23.47)	26.2 (26.01)	32.3 (32.66)	9.5 (9.70)	935s 880s 895s 474s	$\tilde{\nu}_{V-O}$ $\tilde{\nu}_{O-O}$ $\tilde{\nu}_{V-F}$
$K_2[VO(O_2)_2F]$	34.5 (34.29)	22.6 (22.33)	27.5 (28.04)	8.2 (8.33)	965s 870s 890s 470s	$\tilde{\nu}_{V-O}$ $\tilde{\nu}_{O-O}$ $\tilde{\nu}_{V-F}$
$Rb_2[VO(O_2)_2F]$	53.5 (53.28)	16.1 (15.88)	19.7 (19.94)	5.7 (5.92)	970s 885s 895s 472s	$\tilde{\nu}_{V-O}$ $\tilde{\nu}_{O-O}$ $\tilde{\nu}_{V-F}$
$Cs_2[VO(O_2)_2F]$	63.7 (63.94)	12.4 (12.25)	15.1 (15.39)	4.6 (4.57)	945s 870s 885s 476s	$\tilde{\nu}_{V-O}$ $\tilde{\nu}_{O-O}$ $\tilde{\nu}_{V-F}$

[a]Calculated values in parentheses, [b]Peroxy oxygen, [c] Analysis for N.

RESULTS AND DISCUSSION

It has long been recognised that vanadium forms yellow diperoxyvanadate(V) in alkaline medium[10] and is converted to red monoperoxy species in acidic solution.[5] The reaction of V_2O_5 with alkali fluoride, AF and hydrogen peroxide in an alkaline medium gave alkali oxydiperoxyfluorovanadates(V), $A_2[VO(O_2)_2F]$ in very high yields. A report on the synthesis of $K_2[VO(O_2)_2F]$ appeared[11] while our work was in progress. However, the reaction condition of the present synthesis is different from the one previously reported.[11] An alkaline condition is found to be more conducive to the synthesis.

The $A_2[VO(O_2)_2F]$ compounds are all yellow coloured microcrystalline products. They are soluble in water with slow decomposition. Estimation of peroxide content[12] showed the presence of two peroxy groups in each of the compounds. This result and the diamagnetic nature of the compounds suggest that the complex ion contains two peroxy groups per vanadium atom and that the vanadium has an oxidation state of +5.

The occurrence of sharp vibrations around 880cm^{-1} (Table 1) in the IR spectra of the compounds imply the presence of triangularly bonded peroxy ligands, and in keeping with this there are two readily identifiable ν(-O-O-) bands at ca 895 and at ca 870 cm^{-1} [cf. the analysis of ν(-O-O-) in transition metal complexes].[13] Another characteristic feature of the spectra is the absorption at 935-970 cm^{-1}, which has been assigned as the ν(V-O) mode of terminal V-O multiple bonds.[9,14,15] The strong absorption at 470-480 cm^{-1}, in each spectrum, has been assigned as the ν(V-F) mode owing to the presence of F^- ligand bonded to vanadium(V) centre and compare very well with those observed for many fluorovanadate species.[9,16,17]

Acknowledgement - We thank the Council of Scientific and Industrial Research (New Delhi) for award of a fellowship (S.K.G.).

REFERENCES

[1] N. Vuletic and C. Djordjevic, J. Chem. Soc., 1973, 1137.

[2] S. Yamada, Y. Ukei and H. Tanaka, Inorg. Chem., 1976, 15, 964.

[3] S. Funahashi, K. Harraguchi and M. Tanaka, Inorg. Chem., 1977, 16, 1349.

[4] K. Weighardt, Inorg. Chem., 1978, 17, 57.

[5] U. Quilitz and K. Weighardt, Inorg. Chem., 1979, 18, 869.

[6] S. Funahashi, K. Ishihara and M. Tanaka, Inorg. Chem., 1981, 20, 51.

[7] M.K. Chaudhuri and N. Roy, Synth. React. Inorg. Met-Org. Chem., 1981, 11, 677.

[8] M.N. Bhattacharjee, M.K. Chaudhuri, H.S. Dasgupta and D.T. Khathing, J. Chem. Soc. Dalton Trans., 1981, 2587.

[9] M.K. Chaudhuri, H.S. Dasgupta, S.K. Ghosh and D.T. Khathing, Synth. React. Inorg. Met-Org. Chem., 1982, 12, 63.

[10] J.A. Connor and E.A.V. Ebsworth, 'Advances in Inorganic and Radiochemistry', Vol. 6, Ed. H.J. Emeléus and A.G. Sharpe, Academic Press, New York, p. 279, 1964.

[11] G.V. Jere and S.M. Kaushik, Synth. React. Inorg. Met-Org. Chem., 1980, 10,255.

[12] A.I. Vogel, 'A Text Book of Quantitative Inorganic Analysis', Longman Green, p. 295, 1962.

[13] W.P. Griffith, J. Chem. Soc., 1963, 5345; ibid., 1964, 5248.

[14] J. Selbin, L.H. Holmes, Jr., and S.P. McGynn, J. Inorg. Nucl. Chem., 1963, 25, 1359.

[15] J. Selbin, Chem. Rev., 1965, 65, 153.

[16] M. Goldstein, R.J. Hughes and W.D. Unsworth, Spectrochim. Acta, 1975, 31A, 621.

[17] H. Reiskamp and R. Mattes, Z. Naturforsch., 1976, 31b, 537.

Polyhedron Vol. 1, No. 6, pp. 557-560, 1982
Printed in Great Britain

0277-5387/82/060557-04$03.00/0
Pergamon Press Ltd.

COMMUNICATIONS

COMPLEXES OF N-BENZOTHIAZOLYL-N'-ALKYL THIOUREAS

(Received 5th August, 1982)

N'-substituted N-benzothiazolyl thioureas are of great biological and chemical interest [1-3]. Investigations on transition metal complexes have been carried out with the N'-phenyl derivate [4,5]. The ligand acts as a bidentate donor with nitrogen (from thiazole) and sulfur (from thiourea) as coordinating centres.

EXPERIMENTAL

Synthesis of the ligands

Equimolar amounts of 2-aminobenzothiazole and methyl (ethyl) isothiocyanate in pyridine were refluxed under N_2 for 3 hrs. After cooling to 30°C the reaction mixture was added to 10% HCl, the precipitated product was filtered and recrystallized from aqueous ethanol (ethyl (BETU): m.p. 198°C; methyl (BMTU): m.p. 209°C) [6].

Preparation of the complexes

A solution of the appropriate metal acetate (0,001 mol) (Cu, Ni, Co, Cd, Zn) in methanol was added to a hot methanolic solution of the ligand (0,003 mol). The copper complexes precipitated at once, the other compounds were obtained by concentrating the solutions on a water bath. The solids were filtered, washed with ether and dried in vacuo.

Analysis and physical measurements

Sulfur was evaluated as sulfate by titration with barium perchlorate. Analysis of C,H and N were performed at the Institut of Organic Chemistry, Graz. The IR spectra were recorded on a Perkin-Elmer 580B, the UV/VIS measurements were carried out with a Perkin-Elmer Lambda 3 and a Zeiss PMQ 3 spectrophotometer. Thermograms in nitrogen atmosphere were obtained using a Mettler Thermo Analyser with samples of approximately 15 mg and a heating rate of 6°C/min for all runs. Conductivities were measured with a Metrohm conductometer.

RESULTS AND DISCUSSION

The complexes isolated are listed in Table 1 with their analytical data.

Electronic spectra and conductivity data

All measurements were carried out with 5.10^{-3} M ethanolic solutions. Nevertheless the very slow solubility of the copper complexes precluded their solution spectra. To investigate the equilibria conditions in the solutions sets of spectra were recorded for constant metal and various ligand concentrations. The occurence of an isosbestic point for each compound indicates that only two species in equilibrium are present over the appropriate range of conditions. Plots of Job's curves at several wavelengths confirm the formation of 1:2 complexes [7].

Table 1. Characterisation data of the metal complexes

Compound	Colour	C (%)	H (%)	N (%)	S (%)	decomp. temp.°C	Λ_m [c] ($\Omega^{-1}cm^2mol^{-1}$)
$Cu(BMTU)_2$	green	42,63[a] 42,55[b]	3,19 3,17	16,42 16,54	25,39 25,24	174	23
$Co(BMTU)_2$	bluish	43,04 42,93	3,28 3,20	16,70 16,69	25,63 25,47	250	24
$Ni(BMTU)_2$	brown	43,87 42,95	3,33 3,20	16,94 16,70	25,73 25,48	242	19
$Cd(BMTU)_2$	yellow	39,24 38,81	2,93 2,90	14,80 15,09	23,41 23,03	193	22
$Zn(BMTU)_2$	white	42,92 42,35	3,18 3,14	16,70 16,47	25,12 25,09	177	23
$Cu(BETU)_2$	green	44,62 44,80	3,83 3,76	15,90 15,67	24,12 23,92	204	23
$Co(BETU)_2$	bluish	45,04 45,19	3,79 3,79	15,79 15,81	24,35 24,13	226	24
$Ni(BETU)_2$	brown	45,77 45,21	3,87 3,79	16,09 15,82	24,32 24,14	222	21
$Cd(BETU)_2$	yellow	41,61 41,06	3,50 3,45	14,52 14,36	22,27 21,92	208	21
$Zn(BETU)_2$	white	44,84	3,85	15,57	23,90	204	24

[a] found values [b] calculated values [c] 10^{-3} M in DMF, 25° C

Table 2. Selected IR bands[a] (in KBr)

Compound	ν (N-H)	thiazol I [ν (C=N)]	thiazol II + N-C=S I	N-C=S II	N-C=S III
BMTU	3180 st,sp 3050 st,sp	1600 sp	1510 st,sp	1351 m	1230 st,sp
$Cu(BMTU)_2$	3450 st,sp 3380 st,sp	1579 sp	1480 st,b	1310 st	1180 st
$Ni(BMTU)_2$	3400 m,b 3220 st,sp	1582 sp	1480 st,b	1310 st	1183 st
$Co(BMTU)_2$	3380 st,sp 3270 m,b	1587 m	1480 st,b	1309 st	1190 m
$Cd(BMTU)_2$	3200 m,b 3060 m,sp	1590 sp	1475 st,sp	1333 st	1180 m,sp
$Zn(BMTU)_2$	3260 m,b 3095 m,sp	1591 sp	1477 st,b	1330 m	1195 m
BETU	3180 st,sp 3020 st,sp	1597 sp	1525 st,sp	1379 st	1205 st
$Cu(BETU)_2$	3400 m,b 3200 w,b	1595 sp	1473 st,sp	1340 st	1180 m,sp
$Ni(BETU)_2$	3340 st,sp 3060 w,b	1580 sp	1475 st,b	1340 st	1178 st,sp
$Co(BETU)_2$	3380 m,b 3030 w,b	1590 sp	1480 st,sp	1337 st	1172 st,sp
$Cd(BETU)_2$	3420 st,b 3180 w,b	1592 sp	1485 st,sp	1350 st	1175 sp,m
$Zn(BETU)_2$	3315 st,sp 3040 m,sp	1590 st	1495 st,b	1345 st	1178 st

[a] st - strong, m - medium, w - weak, sp - sharp, b - broad
ν - stretching vibration

Effective stability constants were determined by the method of equimolar dilution [8]. According to the stability series of Irwing and Williams [9]the stability of the complexes increase namely in the order Zn < Cd < Ni < Co. The low conductivity data indicate that the complexes are non-electrolytes.

Thermogravimetric study

All thermograms show constant loss of weight without defined steps from the decomposition temperature up to 750°C. Analysis of the resulting products gave non stochiometric ratios of metal, carbon and sulfur.

Considerations about the dependence of the thermal stability of metal complexes on their stability in solution have been carried out earlier [10]. In our study the order of thermal stability is different from spectroscopic data and increases as follows : Cu < Zn < Cd < Ni < Co. Moreover the stability sequence is exchanged for Ni and Co. The decomposition temperatures are listed in Table 1.

IR spectra

From literature it is known that strong vibrational coupling effects prevent unambiguous assignments of bands in the spectra of thioureas and thio amides. Especially the ν (C=S) vibration is often not to be localized [11,12]. However three bands seem to consistently appear and may tentatively designed as the " N-C=S I, II and III " bands. In the complexes these bands shift to lower wavenumbers indicating a weakening of the C=S double bond. The band at ∿ 1600 cm^{-1} in the ligand spectra corresponding to the ring C=N stretching (thiazol I vibration [13]) occurs slightly at lower frequencies in the complexes. The ν (N-H) vibrations shift to higher wavenumbers with respect to the free ligand. These facts suggest that coordination occurs through the basic nitrogen of thiazole and the sulfur of the thiocarbonyl group.

Institut für Analytische Chemie
Karl-Franzens-Universität Graz
A-8010 Graz

H. GRESCHONIG

REFERENCIES

1. R. M. Hoskinson and I. M. Russell, J. Text. Inst. 64, 146 (1973).
2. T. Hirayama and M. Watanabe, Yakugaku Zhasshi 100, 1225 (1980).
3. K. Abdullaev, Farmakol. Prir. Veschestv 139 (1978).
4. M. R. Chaurasia, J. Inorg. Nucl. Chem. 37, 1547 (1975).
5. M. R. Chaurasia, S. V. Saxena and S. D. Khattri, Indian J. Chem. 20A, 741 (1981).
6. Farbenfabriken Bayer, N 6,500,844; Chem. Abstr. 64, P 4191f
7. M. Beck, Chemistry of Complex Equilibria. Van Nostrand-Reinhold, London (1970).
8. B. W. Budesinsky, Anal. Chem. 47, 560 (1975).
9. H. Irwing and R. J. P. Williams, Nature 162, 756 (1948).
10. P. B. Bowman and L. B. Rogers, J. Inorg. Nucl. Chem. 28, 2215 (1966).
11. L. J. Bellamy, The Infra-red Spectra of Complex Molecules, Chapman & Hall, London (1968).
12. C. N. R. Rao and R. Venkataraghavan, Spectrochimica Acta 18, 541 (1962).
13. P. Bassignana, C. Cogrossi and M. Gandino, Spectrochim. Acta 19, 1885 (1963).

Polyhedron Vol. 1, No. 6, pp. 561-562, 1982
Printed in Great Britain.

0277-5387/82/060561-02$03.00/0
Pergamon Press Ltd.

Phenylimido Tungsten(VI) Alkoxides

By A.J. Nielson and J.M. Waters

Department of Chemistry, University of Auckland,

Auckland, New Zealand.

(Received 3 June 1982)

There are many examples of early transition metal alkoxides[1] yet few complexes have been prepared which additionally contain the multiply bonded imido function, M≡NR. Those reported to date usually contain the trimethylsiloxy ligand and result from reactions of metal halides or oxyhalides with silylamines which incorporate both imido and siloxy ligands[2]. We report here preliminary results of the synthesis of phenylimido complexes of tungsten(VI) containing aliphatic alkoxide ligands.

Reaction of phenylimido tungsten tetrachloride[3] with methanol in the presence of ^{t}butylamine leads to a yellow complex analysing as $PhNW(OMe)_4$. An x-ray crystallographic determination[4] shows the dimeric structure (1) with the bridging methoxides *trans* to the phenylimido moiety.* The tungsten-tungsten separation is 3.47 Å indicating no metal-metal interaction as expected for tungsten(VI).

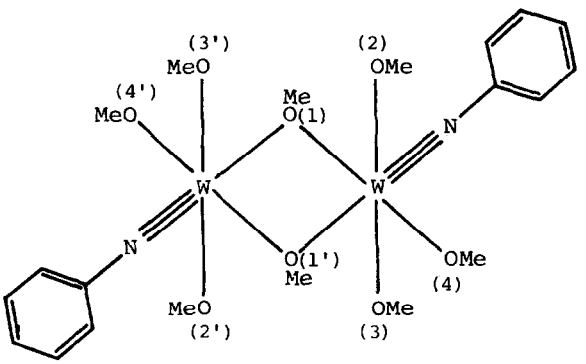

(1)

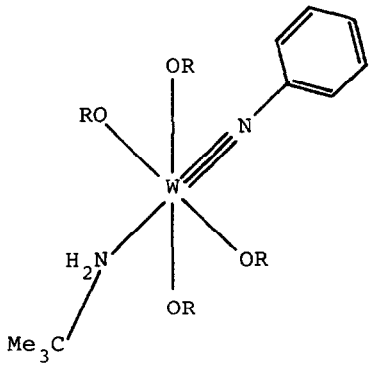

(2)

a) R = $-CHMe_2$

b) R = $-CH_2CMe_3$

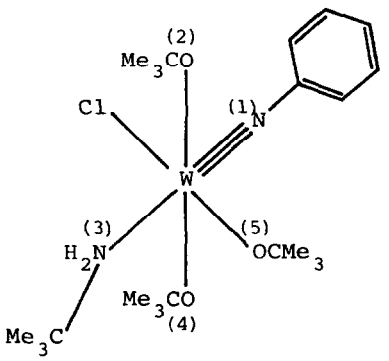

(3)

Figure. Complex (1): W-N, 1.65(2) Å; W-O(1), 2.04(1); W-O(1'), 2.14(1); W-O(2), 1.92(1); W-O(3), 1.97(1); W-O(4), 2.02(1). Complex (3): W-Cl, 2.500(4), W-N(1), 1.70(1); W-O(2), 1.87(1); W-N(3), 2.40(1); W-O(4), 1.87(1); W-O(5), 1.82(1).

* Lists of atomic coordinates and bond lengths and angles have been deposited as supplementary data with the Editor, from whom copies are available on request. Atomic coordinates have also been deposited with the Cambridge Crystallographic Data Centre.

Other alcohols were reacted by this method, to examine the effect of increasing size of ligand on coordination geometry. Thus ethyl alcohol gives a similar complex to (1) but samples appear to polymerise on attempted recrystallisation. *iso*-Propyl or *neo*-pentyl alcohols gave complexes (2a) and (2b), the structures being proposed on the basis of ^{1}H and ^{13}C nmr spectra. With ^{t}butyl alcohol phenylimido tungsten tetrachloride reacts to give complex (3) retaining one chloride ligand, presumably the result of steric constraint imposed by the bulky ^{t}butyl groups which surround it. An x-ray crystallographic structure determination[4] confirmed the amine *trans* to the phenylimido group and one ^{t}butoxy ligand *trans* to chloride.

These complexes show that for tungsten(VI), a bridging alkoxide or coordinating amine is preferred *trans* to the phenylimido function. A similar effect has been observed for the trimeric oxo bridged complex $[PhNW(\mu\text{-}O)(Me)_2PMe_3]_3$ which shows a lengthened W-O bond *trans* to the phenylimido group[3]. Thus localised π donation is possible only for ligands *cis* to the imido moiety, presumably since the multiply bonded function competes more successfully for metal d_π orbitals than any ligand *trans* to it.

References

1 D.C. Bradley, R.C. Mehrotra and D.P. Gaur, "Metal Alkoxides", Academic Press, 1978.

2 W.A. Nugent and B.L. Haymore, Coord.Chem.Rev., 1980, 31, 123.

3 D.C. Bradley, M.B. Hursthouse, K.M.A. Malik and A.J. Nielson, Chem.Commun., 1981, 103.

4 *Crystal data*: (1) Triclinic: a = 8.473(7), b = 10.776(5), c = 7.683(3) Å, α = 102.26(3), β = 102.68(4), γ = 71.13(5), space group $P\bar{1}$, Z = 2. MoK_α radiation.
(3) Monoclinic: a = 9.341(2), b = 29.608(7), c = 10.257(2) Å, β = 106.28(2)°, space group $P2_1/c$, Z = 4, CuK_α radiation.
Intensity data were collected on an ENRAF-NONIUS CAD-4 diffractometer (decomposition occurred during collection for (1)) and the two structures were solved by Patterson and Fourier methods. Full-matrix least-squares refinement has returned present values of R as .076 (1082 observed data) and .066 (2015 observed data) for molecules (1) and (3) respectively.

Polyhedron Vol. 1, No. 6, pp. 563-566, 1982
Printed in Great Britain.

0277-5387/82/060563-04$03.00/0
Pergamon Press Ltd.

REACTIONS OF ALLYLIC AND PROPARGYLIC AMINES AND ETHERS WITH $Zn[Co(CO)_4]_2$

(Received 13 August 1982)

Abstract - The allylic C-N bond of $CH_2=CHCH_2NEt_2$ is cleaved by $Zn[Co(CO)_4]_2$, producing π-$C_3H_5Co(CO)_3$. The propargylic amine, $HC\equiv CCH_2NEt_2$, undergoes an unusual catalytic dimerization to $Et_2NCH_2C\equiv CCH(Me)N(Et)$-$CH_2CH=CH_2$, which implies activation of an ethyl C-H bond. Comparison with the reactions of the corresponding ethers indicates that Zn-N coordination plays an important role in these reactions.

Transition metal compounds play a very important role as activators of carbon-carbon multiple bonds in many catalytic processes. Zinc, on the other hand, behaves as a typical main group metal in activating mainly carbon-hetero atom single and multiple bonds. We decided to investigate whether compounds containing a direct zinc-transition metal bond would exhibit selective and unexpected catalytic properties in reactions with substrates containing both of the above-mentioned functionalities. To this end, allylic and propargylic amines and ethers were selected as substrates. These compounds contain an isolated carbon-carbon multiple bond and a carbon-hetero atom single bond. As a catalyst, the reactive and easily accessible[1] zinc-*bis*-tetracarbonylcobaltate, $Zn[Co(CO)_4]_2$, was used. The only catalytic reaction of $Zn[Co(CO)_4]_2$ described so far is the dimerization of bicycloheptadiene to "Binor-S" (*endo*,*cis*,*endo*-heptacyclo[5.3.1.$1^{2,6}$.$1^{4,12}$.$1^{9,11}$.$0^{3,5}$.$0^{8,10}$]tetradecane)[2], which is believed to be just a function of the cobalt carbonyl moiety[3-5]. When zinc cobalt carbonyl was treated with a slight excess of 3-diethylamino-propene, allylcobalt tricarbonyl was obtained in a stoichiometric reaction :

$$Zn[Co(CO)_4]_2 + 2\ CH_2=CHCH_2NEt_2 \rightarrow Zn(NEt_2)_2 + 2\ CO + 2\ \pi\text{-}C_3H_5Co(CO)_3 \quad (1)$$

When a larger excess of the amine was used, the ex-

cess was converted to a polymer which was not studied further. 3-Methoxy-propene did not yield any isolable allylcobalt derivative on similar treatment with zinc cobalt carbonyl ; rather, a slow catalytic isomerization to the *cis*- and *trans*-isomers of 1-methoxy-propene was observed :

$$CH_2{=}CHCH_2OMe \xrightarrow{Zn[Co(CO)_4]_2} CH_3CH{=}CHOMe \qquad (2)$$

This was considered remarkable because a methoxy group normally is a much better leaving group than a diethylamino group. However, treatment of 3-phenoxy-propene with zinc cobalt carbonyl did yield the expected allyl cobalt tricarbonyl. It seems reasonable to correlate these results with the fact that the affinity of zinc for nitrogen donors is greater than that for oxygen donors[6]. Apparently, the coordination of the hetero atom to zinc can assist the nucleophilic substitution. In the absence of a strong coordination interaction, as in the case of the allyl ethers, a much better leaving group (i.e. phenoxy) is required to make the substitution possible. Two mechanisms can be visualized for the coordination-assisted nucleophilic substitution (1) :

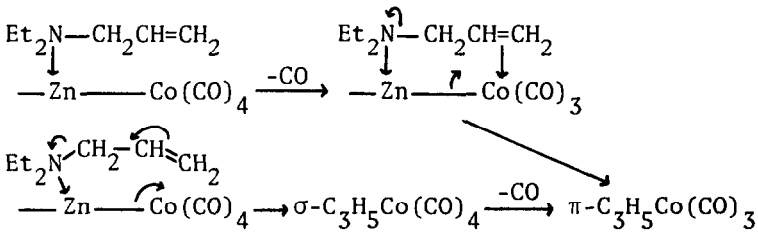

At the moment, we are unable to distinguish between these alternatives. It is apparent, however, that both the zinc atom and the transition metal group play a direct role in this reaction. On the other hand, it seems likely that only the cobalt atom is important in the isomerization reaction (2). Similar reactions are catalyzed by other cobalt compounds, e.g. the isomerization of allyl alcohol to propanal[7] :

$$CH_2{=}CHCH_2OH \xrightarrow{HCo(CO)_4} [CH_3CH{=}CHOH] \longrightarrow CH_3CH_2CHO$$

In the propargyl series, a marked difference was again observed between ethers and amines. 3-Methoxy-propyne and 1-methoxy-2-butyne slowly formed cyclotrimers on

refluxing with $Zn[Co(CO)_4]_2$ in benzene :

$$RC{\equiv}CCH_2OMe \xrightarrow[\text{or } Co_2(CO)_8]{Zn[Co(CO)_4]_2}$$

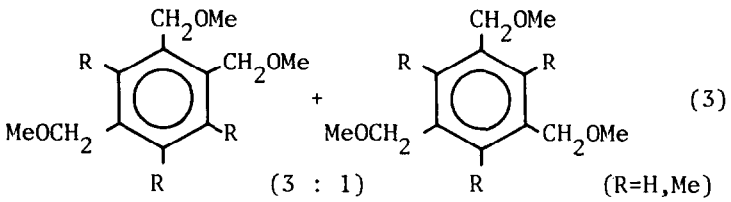

(3 : 1) (R=H,Me) (3)

The zinc atom probably plays no direct role in this reaction. Indeed, it was found that dicobalt octacarbonyl catalyzes the same reaction more efficiently, giving the same ratio of isomers in the product. Cyclotrimerization was also observed when 3-diethylamino-propyne was refluxed with dicobalt octacarbonyl in benzene. When, however, the same amine was treated with zinc cobalt carbonyl, the main organic product was a linear dimer formed by a very unusual "substitution" of one of the hydrogen atoms of an ethyl group bound to nitrogen:

$$2\ HC{\equiv}CCH_2NEt_2 \xrightarrow{Zn[Co(CO)_4]_2} Et_2NCH_2C{\equiv}CCH(Me)N(Et)CH_2{=}CHCH_2 \qquad (4)$$

This unexpected product was characterized by ^1H and ^{13}C NMR spectroscopy (table 1) and GC/MS. The mechanism of this curious reaction has not yet been elucidated. In particular, it is not clear why the methylene carbon atom of an ethyl group is attacked in preference to the usually much more reactive propargylic methylene group. It seems safe to state, however, that both metals are important in this catalytic dimerization. We are currently investigating the mechanism and the scope of the reaction.

Table 1. ^1H and ^{13}C NMR data for

$(CH_3CH_2)_2NCH_2C{\equiv}CCH(CH_3)N(CH_2CH_3)CH_2CH{=}CH_2$
1 2 3 4 5 6 7 8 9 10 11 12

	1	2	3	4	5	6	7	8	9
^1H	1.11	2.62	3.52			3.84	1.40	2.62	1.11
^{13}C	13.1	47.6	41.0	78.6	84.1	48.1	21.0	45.1	14.1

	10	11	12
^1H	3.43,3.13	6.01	5.14,5.34
^{13}C	54.5	138.0	116.2

(in C_6D_6, δ in ppm relative to internal TMS)

EXPERIMENTAL

All reactions were carried out in an atmosphere of dry, oxygen-free nitrogen. Solvents were carefully dried and distilled prior to use. In a typical experiment, 1 g (2.5 mmol) $Zn[Co(CO)_4]_2$ and 25-50 mmol substrate were dissolved in 40 ml benzene. The solution was kept at 50-80° C (depending on the reaction rate) for 10-100 hours, and the reaction was followed by ^1H NMR spectroscopy. Benzene and volatile components were drawn into a cold trap. Dimers and trimers were distilled from the reaction mixture at 10^{-4} mm Hg. All products were identified by NMR and/or GC/MS.

P.H.M. Budzelaar
H.J. Alberts-Jansen
J. Boersma*
G.J.M. van der Kerk

Department of Organic Chemistry,
University of Utrecht,
Croesestraat 79
3522 AD Utrecht
The Netherlands

REFERENCES

[1]P. Chini, M.C. Malatesta and A. Cavalieri, *Chim. Ind. (Milan)* 1973,55,120

[2]G.N. Schrauzer, B.N. Bastian and G.A. Fosselius, *J. Amer. Chem. Soc.* 1966,88,4890

[3]M. Ennis and A.R. Manning, *J. Organomet. Chem.* 1976,116,C31

[4]M. Ennis, R.M. Foley and A.R. Manning, *J. Organomet. Chem.* 1979,166,C18

[5]H.J. Langenbach, E. Keller and H. Vahrenkamp, *J. Organomet. Chem.* 1979,171,259

[6]K. NÜtzel in Houben-Weyl, "Methoden der Organischen Chemie", 4th ed., E. MÜller Ed., Georg Thieme Verlag Stuttgart, 1973,XIII/2a,p 661

[7]R.W. Goetz and M. Orchin, *J. Amer. Chem. Soc.* 1963,85,1549

Polyhedron Vol. 1, No. 6, p. 567, 1982
Printed in Great Britain.

0277-5387/82/060567-01$03.00/0
Pergamon Press Ltd.

ERRATUM

Elizabeth Gebert, Selmer W. Peterson, Arthur H. Reis, Jr. and Evan H. Appelman, The crystal structure of cesium perbromate. *J. Inorg. Nucl. Chem.* **43**, 3085 (1981).

The bond lengths and angles given in Table 4 are incorrect because of a computational error. A corrected Table 4 follows. Bond lengths and angles from Table 4 that are quoted in the body of the article are similarly incorrect and should be replaced by the corrected values presented here.

We wish to thank Dr. Dieter Wald of the Justus Liebig Universität, Giessen, for calling these errors to our attention.

Table 4. Bond lengths and angles based on data corrected for absorption empirically

Bond	Length (Å)
4 (Br–O)	1.610(7)†
4 (Cs–O)	3.194(7)
4 (Cs–O)	3.390(7)
4 (Cs–O)	3.392(7)
4 (O–O)	2.616(10)
2 (O–O)	2.654(9)
Atoms	**Angles (°)**
2 (O–Br–O)	111.0(4)
4 (O–Br–O)	108.7(4)

†Numbers in parentheses are the standard deviations.

Polyhedron Vol. 1, No. 7–8, pp. 569–605, 1982
Printed in Great Britain.

0277-5387/82/070569-37$18.50/0
Pergamon Press Ltd.

POLYHEDRON REPORT NUMBER RE 1

CARBONYLHYDRIDO*TRIS*(TRIPHENYLPHOSPHINE)RHODIUM(I)

F. H. JARDINE
Department of Chemistry, North East London Polytechnic, Romford Road, London E15 4LZ, England

CONTENTS

I. INTRODUCTION

Carbonylhydrido*tris*(triphenylphosphine)rhodium(I) is a Cinderella compound. Although it has proved to be one of the most commercially important homogeneous catalysts it has long been overshadowed by complexes of lesser importance.

Its preparation was initially essayed[1] in an attempt to isolate a crystalline analogue of tetra(carbonyl)hydridocobalt(I). At that time the cobalt complex was an important catalyst in hydrogenation and hydroformylation processes. It is ironic that the useful catalytic properties of the rhodium complex were ignored for several years, particularly as it has now virtually displaced the cobalt complex as an industrial catalyst. However, once the crystal structure of the rhodium complex had been determined interest in its properties subsided.

It was not recognised for some time that the title complex was the true hydroformylation catalyst in triphenylphosphine stabilized rhodium(I) systems. The catalyst was successively believed to be $RhCl(PPh_3)_3$[2] and *trans*-$RhCl(CO)(PPh_3)_2$[3] before it was realised that these complexes were precursors of $RhH(CO)(PPh_3)_3$ under hydroformylation conditions. Since its overdue recognition as a very important homogeneous catalyst many investigations of its catalytic behaviour, particularly in hydroformylation reactions, have been made. This has resulted in a copious patent literature dealing with minor changes in operating conditions and catalyst recovery.

Nevertheless, interest in the catalytic reactions of the complex has never been fully reflected in the stoicheiometric reactions of $RhH(CO)(PPh_3)_3$. These reactions have been much less studied than those of dichloro*tris*(triphenylphosphine)ruthenium(II) or chloro*tris*(triphenylphosphine)rhodium(I)[4] which are also important homogeneous catalysts. This review will deal with both stoicheiometric and catalytic reactions of $RhH(CO)(PPh_3)_3$.

II. PREPARATION

Preparative routes to the complex are summarised in Fig. 1.

The complex was first prepared by reacting hydrazine with *trans*-carbonylchloro*bis*(triphenylphosphine)rhodium(I) in ethanolic solution.[1] This is the safest route to the complex. Preparations direct from hydrated rhodium trichloride using aqueous formaldehyde as the source of the carbonyl ligand are

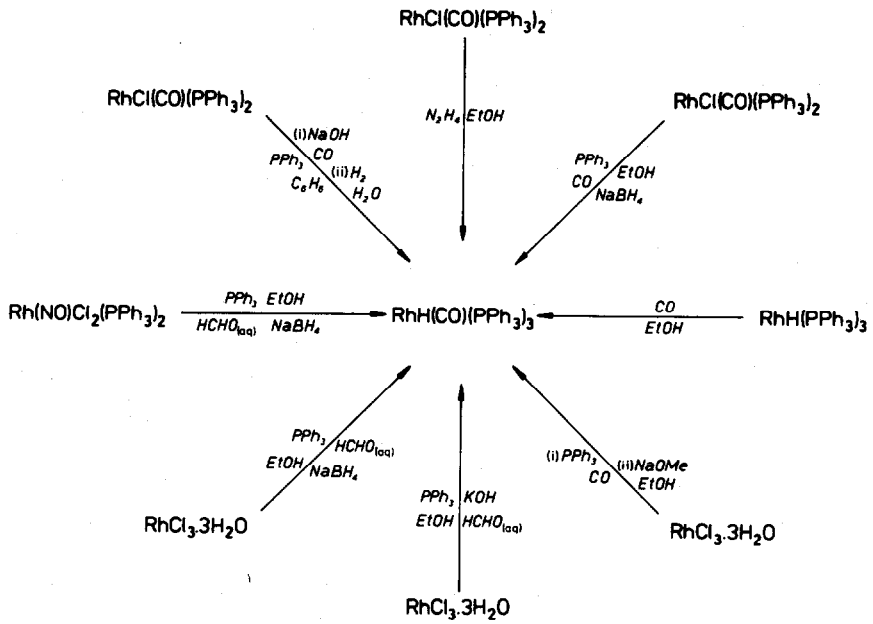

Fig. 1. Preparative routes to carbonylhydrido*tris*(triphenylphosphine)rhodium(I).

best avoided. Reduction of rhodium trichloride by either triphenylphosphine[5,6] or tetrahydroborate[7] produces hydrogen chloride. In the gas phase hydrogen chloride reacts with formaldehyde to form the potent carcinogen *bis*(chloromethyl)ether.[8]

Besides hydrazine reduction of *trans*-$RhCl(CO)(PPh_3)_2$ tetrahydroborate reduction of this complex will also yield $RhH(CO)(PPh_3)_3$.[9] Effectively, *trans*-$RhCl(CO)(PPh_3)_2$ is formed in the reaction between hydrated rhodium trichloride, carbon monoxide, and triphenylphosphine; the *trans*-complex is then reduced by sodium methoxide in refluxing methanol.[10] A similar reduction of Vaska's compound with sodium propoxide requires further reduction with hydrogen before $RhH(CO)(PPh_3)_3$ can be isolated. The triethyl-, tributyl-, diethylphenyl-, and methyldiphenylphosphine analogues may also be prepared by this method.[11]

An alternative to introducing a hydrido ligand into a carbonyl complex is to react either *tetrakis*- or *tris*(triphenylphosphine)hydridorhodium(I) with carbon monoxide.[12] It is possible that the reaction between hydrated rhodium trichloride, formaldehyde, triphenylphosphine, and sodium tetrahydroborate proceeds by this route, since if formaldehyde is omitted $RhH(PPh_3)_4$ is formed.[7]

Most preparative reactions have been carried out in ethanolic solution since $RhH(CO)(PPh_3)_3$ is insoluble in this solvent. It has been suggested that preparations on the decagram scale or above are preferable since small batches are often impure due to contamination with $RhH(PPh_3)_3$.[13]

Preparations from nitrosyl complexes,[14] or azido or cyanate complexes,[15] are not feasible due to the inaccessibility of the starting materials. Nor is the tetrahydroborate reduction of $[Rh(CO)(PPh_3)_3]BF_4$ ever likely to become a major preparative reaction.[16]

III. PHYSICAL PROPERTIES

Carbonylhydrido*tris*(triphenylphosphine)rhodium(I) is isolated from ethanol solutions as yellow monoclinic crystals. In a nitrogen atmosphere these melt at 172–174°; in air, reaction with oxygen lowers the melting point to 120–122°.[5,6]

In the IR spectrum of $RhH(CO)(PPh_3)_3$ the carbonyl stretch frequency has been reported as 1926[1] or 1918 cm^{-1}.[6] For the deuterio complex the carbonyl absorption occurs between 1923 and 1954 cm^{-1}.[17] The weak absorption attributable to the Rh–H stretch has been reported at 2004[1] or 2041 cm^{-1}.[6] The absorption of the Rh–D stretch is obscured by a band due to triphenylphosphine.[17]

A similar discrepancy between the two sources is noticed in the τ-values reported for the hydrido ligand in the high field ^1H NMR spectrum, these being 19.9[1] or 19.30[6] respectively. If the solution is cooled to −30° the exchange of the triphenylphosphine ligands is slowed. The small coupling constant ($J \leq 1$ Hz) and the splitting pattern imply that the triphenylphosphine ligands occupy equatorial sites in a trigonal bipyramidal complex.[12] This structure has been confirmed by X-ray crystallography.[18,19] The crystals belong to the monoclinic space group $P2_1/n$, and there are four molecules per unit cell. The unit

cell has the dimensions $10.11 \times 33.31 \times 1.33$ Å. The calculated density of 1.36 g cm^{-3} agrees well with the observed density of 1.33 g cm^{-3}. Unfortunately the intensity of the reflections was obtained by visual estimation of photographic records. The low accuracy and paucity of the data has required the phenyl rings to be treated as rigid hexagonal groups, and only the rhodium atom has been refined anisotropically.

As a consequence the hydrido ligand is difficult to locate. The preliminary report gave the Rh–H distance as 1.72 Å.[18] In the full report this was corrected to 1.60 Å.[19] The other molecular dimensions are essentially the same in both papers and are shown in Fig. 2.

The uncertainty of the Rh–H distance has been remarked on elsewhere.[20] It is difficult to locate the hydrido ligand in other rhodium(I) complexes, and the position of this ligand in $RhH(PPh_3)_3$ has only been inferred.[21] Accordingly the exact location of the hydrido ligand in $RhH(CO)(PPh_3)_3$ must await an improved structure determination.

The rhodium–phosphorus bond lengths of 2.337, 2.317, and 2.314 Å are longer than those found in many rhodium(I) triphenylphosphine complexes. Thus, in the five coordinate complex $\{RhCl(PPh_3)_2SO_2\}_2$ the Rh–P bond lengths are 2.298 and 2.308 Å.[22] In RhCl(triphos) [triphos = $PhP\{(CH_2)_3PPh_2\}_2$] the relevant bond lengths are 2.28 Å (twice) and 2.201 Å;[23] whilst in $RhBr\{P(C_6H_4CH{=}CH_2)_3\}$ the Rh–P bond is 2.176 Å long.[24] In $RhH(PPh_3)_3$ the bond lengths are 2.262, 2.274, and 2.316 Å (the last being for the phosphorus *trans* to hydrogen).[21] In the three coordinate cation $[Rh(PPh_3)_3]^+$ bond lengths of 2.21 and 2.24 Å have been quoted.[25]

Nevertheless, the Rh–P bond lengths found in $RhH(CO)(PPh_3)_3$ agree well with those found for *trans* triphenylphosphine groups in other complexes. Thus in $RhCl(PPh_3)_3$ these bond lengths are 2.304 and 2.338 Å (orange isomer) and 2.315 and 2.327 Å (red isomer);[26] in *trans*-$RhCl(CS)(PPh_3)_2$ the mean bond length is 2.336 Å;[27] in *trans*-$RhCl(C_2F_4)(PPh_3)_2$ the bond lengths are 2.347 and 2.370 Å.[28] Undoubtedly the longer than usual rhodium–phosphorus bonds in $RhH(CO)(PPh_3)_3$ result from the presence of four π-acid ligands in the complex.

Despite being *trans* to the hydrido ligand, known to have a high *trans* effect (see $RhH(PPh_3)_3$[21]), the Rh–C bond in $RhH(CO)(PPh_3)_3$ given as 1.81 Å[18] or 1.829 Å[19] is shorter than that found in *trans*-$RhCl(CO)(PPh_3)_2$ (1.86 Å).[29] It is, however, longer than the Rh–C bond in *trans*-$RhCl(CS)(PPh_3)_2$ (1.787 Å).[27]

The ESR spectrum of $RhH(CO)(PPh_3)_3$ shows no trace of any paramagnetic impurity, nor is any generated after exposure to air.[30] This may be contrasted with the small quantities of these impurities revealed in $RhCl(PPh_3)_3$ by this technique.[4]

Cryoscopy on solutions of $RhH(CO)(PPh_3)_3$ in benzene (m.pt. 5°) or *o*-xylene (m.pt. −29°) show the complex to be undissociated.[31] This is in accordance with NMR studies which show no dissociation of triphenylphosphine ligands at the latter temperature.[12] However, osmometry on benzene solutions of the complex, under nitrogen at 38°, indicate extensive dissociation at this temperature.[32] The following equilibria have been proposed for the system

$$RhH(CO)(PPh_3)_3 \underset{+PPh_3}{\overset{-PPh_3}{\rightleftharpoons}} RhH(CO)(PPh_3)_2 \underset{+PPh_3}{\overset{-PPh_3}{\rightleftharpoons}} RhH(CO)(PPh_3). \qquad (1)$$

Lack of change in the frequency of the carbonyl absorption band in solution IR spectra suggests that the *bis*(triphenylphosphine) complex is *trans*-square planar.[31] It will be seen later that the dissociation of at least one triphenylphosphine ligand is essential to the catalytic activity of the complex.

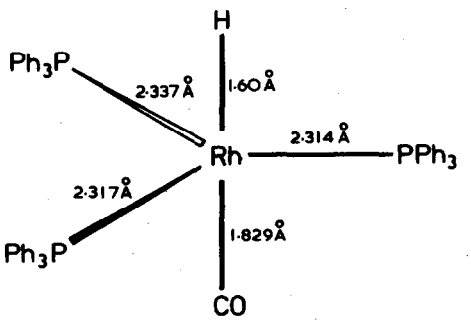

Fig. 2. X-ray crystal structure of carbonylhydrido*tris*(triphenylphosphine)rhodium(I). (Redrawn with permission from S. J. LaPlaca and J. A. Ibers, *Acta Cryst.* 1965, **18**, 511.)

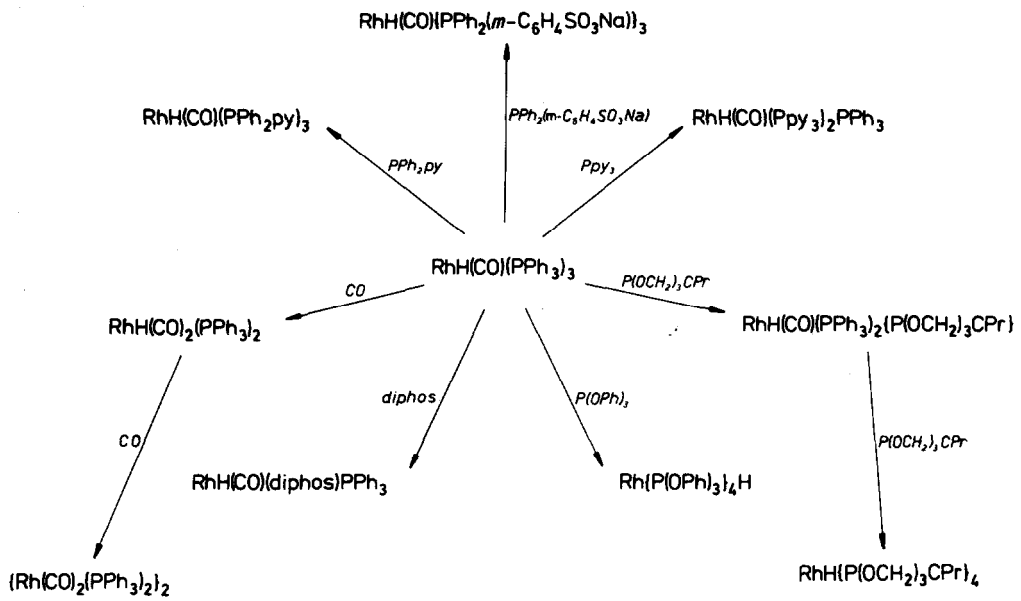

Fig. 3. Some triphenylphosphine displacement reactions of carbonylhydrido*tris*(triphenylphosphine)-rhodium(I).

IV. STOICHEIOMETRIC REACTIONS

A. *Triphenylphosphine displacement*

As was noted in Section III triphenylphosphine ligands are easily lost from the complex in solution (eqn 1). A chemical consequence of this reaction is that triphenylphosphine is preferentially displaced by neutral ligands. Reactions of this type are summarized in Fig. 3.

The stepwise replacement of triphenylphosphine ligands is best illustrated by the reactions of 4-propyl-2,6,7-trioxa-1-phosphabicyclo[2.2.2]octane, **1**, with carbonylhydrido*tris*(triphenylphosphine)-rhodium(I). In ethanolic solution at a 1.1:1 ratio the ligand displaces one triphenylphosphine ligand to form yellow $RhH(CO)(PPh_3)_2\{P(OCH_2)_3CPr\}$

$$RhH(CO)(PPh_3)_3 + P(OCH_2)_3CPr \longrightarrow RhH(CO)(PPh_3)_2\{P(OCH_2)_3CPr\} + PPh_3. \quad (2)$$

Under similar conditions excess phosphite ligand **1** displaces the remaining triphenylphosphine ligands and the carbonyl ligand forming white $RhH\{P(OCH_2)_3CPr\}_4$[33]

$$RhH(CO)(PPh_3)_3 + 4P(OCH_2)_2CPr \longrightarrow RhH\{P(OCH_2)_3CPr\}_4 + 3PPh_3 + CO \quad (3)$$

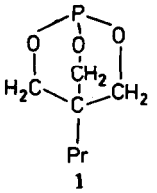

1

In ethanol at 25° triphenylphosphite also displaces all the neutral ligands from $RhH(CO)(PPh_3)_3$ to form pale yellow $RhH\{P(OPh)_3\}_4$.[34] *Tris*(2-pyridyl)phosphine displaces two triphenylphosphine ligands from $RhH(CO)(PPh_3)_3$ in benzene solution. Yellow $RhH(CO)(PPh_3)\{P(2\text{-}C_5H_4N)_3\}_2$ is the product. However, the closely related ligand diphenyl(2-pyridyl)phosphine is capable of displacing all three triphenylphosphine ligands from $RhH(CO)(PPh_3)_3$ upon reaction in tetrahydrofuran solution.[35]

$$RhH(CO)(PPh_3)_3 + 3Ph_2P(2\text{-}C_5H_4N) \longrightarrow RhH(CO)\{Ph_2P(2\text{-}C_5H_4N)\}_3 + 3PPh_3. \quad (4)$$

Similar behaviour is observed with the ligands $Ph_2P(CH_2)_{14}P^+Me(CH_2CHMe_2)_2$–4-$C_{12}H_{25}C_6H_4SO_3^-$[36] or $PPh_2(m\text{-}C_6H_4SO_3\cdot Na)$.[37] Both the $RhH(CO)L_3$ products act as water soluble alkene hydroformylation catalysts. Not surprisingly the bidentate ligand $Ph_2P(CH_2)_2PPh_2$ displaces two triphenylphosphine

ligands to yield yellow grey $RhH(CO)(PPh_3)$(diphos). The latter complex is an active but unselective hydroformylation catalyst[38]

$$RhH(CO)(PPh_3)_3 + Ph_2P(CH_2)_2PPh_2 \longrightarrow RhH(CO)(PPh_3)\{Ph_2P(CH_2)_2PPh_2\} + 2PPh_3. \quad (5)$$

This reaction implies that related complexes, so far unisolated, are formed when $RhH(CO)(PPh_3)_3$ reacts with other ditertiaryphosphine ligands. When the ditertiaryphosphine is chiral, the resulting complexes may function as homogeneous chiral catalysts (see Section VII.C). Substitution of a triphenylphosphine ligand may also be accomplished by using resin bound tertiary phosphines[39–46]

$$RhH(CO)(PPh_3)_3 + \mathfrak{R}—PPh_2 \longrightarrow \mathfrak{R}—PPh_2RhH(CO)(PPh_3)_2 + PPh_3. \quad (6)$$

The complex may also be bound to phosphinated silica supports in an analogous reaction.[47] These bound complexes function as heterogenised catalysts. The displacement of triphenylphosphine by carbon monoxide is better dealt with in Section VII which covers hydroformylation reactions.

B. *Hydrido ligand reactions*

In some instances the hydrido ligand reacts preferentially. In many of these reactions (Fig. 4) a triphenylphosphine ligand is also lost and four coordinate complexes result.

The complex is eventually destroyed by *t*-butyl hydroperoxide, but the order of ligand loss is hydrido, triphenylphosphine, and finally carbonyl.[48]

Triazenido complexes are precipitated by the addition of methanol after the reaction between carbonylhydrido*tris*(triphenylphosphine)rhodium(I) and 1,3-diaryltriazenes

$$RhH(CO)(PPh_3)_3 + ArNNNAr \xrightarrow[\text{reflux}]{MeOCH_2CH_2OH} Rh(ArNNNAr)(CO)(PPh_3)_2. \quad (7)$$

Their colours range from red for the diphenyl derivative to yellow for the di(*p*-tolyl) or di(*p*-chlorophenylene) complexes. The complex of the unsymmetric triazene, **2**, is brown.[49]

2

In the reaction between $RhH(CO)(PPh_3)_3$ and trifluoromethane sulphonic acid no triphenylphosphine ligand is displaced and an ionic complex results[50]

$$RhH(CO)(PPh_3)_3 + CF_3SO_3H \longrightarrow [Rh(CO)(PPh_3)_3]SO_3 \cdot CF_3. \quad (8)$$

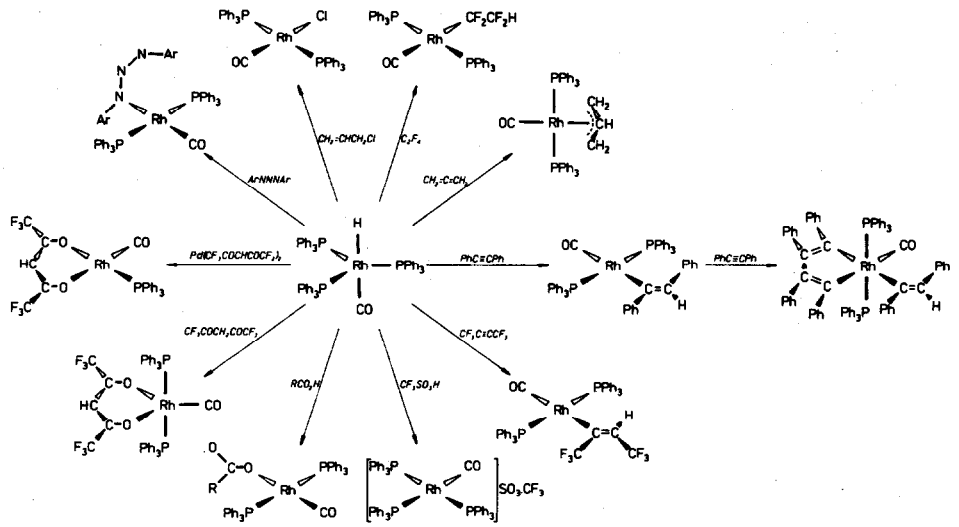

Fig. 4. Some hydrido replacement reactions of carbonylhydrido*tris*(triphenylphosphine)rhodium(I).

The yellow trifluoromethane sulphonate can be further characterised by conversion to the tetraphenylborate salt

$$[Rh(CO)(PPh_3)_3]SO_3{\cdot}CF_3 + NaBPh_4 \xrightarrow{MeOH/Me_2CO} [Rh(CO)(PPh_3)_3]BPh_4. \quad (9)$$

On the other hand, reactions with carboxylic acids (often perfluorocarboxylic acids), result in the formation of *bis*(triphenylphosphine) carboxylato complexes

$$RhH(CO)(PPh_3)_3 + RCO_2H \longrightarrow \textit{trans}\text{-}Rh(OCOR)(CO)(PPh_3)_2 + PPh_3 + H_2 \quad (10)$$

($R = CF_3$;[50-52] C_2F_5, C_6F_5;[51] Me, Et, *p*-MeC_6H_4, *p*-ClC_6H_4, *p*-$O_2NC_6H_4$, *p*-$MeOC_6H_4$[53]).

There has been some controversy over the structures of the yellow carboxylato-complexes. This has resulted from the failure to observe certain characteristic carboxylato absorptions in their IR spectra. Some of the complexes can be isolated containing carboxylic acid of crystallization. This molecule of carboxylic acid is hydrogen bonded to the carboxylato ligand, thus altering the IR spectra.[53] They are considered to contain monodentate carboxylato ligands. There is also a report of a very similar reaction occurring with a maleic acid/vinyl ether copolymer whereby rhodium is bound to the carboxylate group of the copolymer.[54]

Although much weaker acids can liberate hydrogen from carbonylhydrido*tris*(triphenylphosphine)iridium(I), for example *p*-nitrophenol, the limit appears to be reached at hexafluoroacetylacetone for the rhodium complex

$$RhH(CO)(PPh_3)_3 + (CF_3CO)_2CH_2 \xrightarrow[80°]{C_7H_8} Rh\{(CF_3CO)_2CH\}(CO)(PPh_3)_2 + PPh_3 + H_2. \quad (11)$$

Yellow needles of the five-coordinate product are obtained from this reaction.

A quite dissimilar orange product is obtained if the title complex is reacted at a lower temperature with *bis*(hexafluoroacetylacetonato)palladium(II)

$$RhH(CO)(PPh_3)_3 + Pd\{(CF_3CO)_2CH\}_2 \xrightarrow[50°]{C_7H_8} Rh\{(CF_3CO)_2CH\}(CO)(PPh_3). \quad (12)$$

Some reduction to palladium metal is also observed. A further side reaction between the palladium complex and triphenylphosphine

$$Pd\{(CF_3CO)_2CH\}_2 + PPh_3 \longrightarrow Pd\{(CF_3CO)_2CH\}_2(PPh_3) \quad (13)$$

probably assists in the removal of the ligand from rhodium.[55]

The most interesting reactions of the hydrido complex are those with alkenes or alkynes. Most alkenes are believed to form alkyls. Indeed, it will be seen later that the formation of such alkyls is essential in the catalytic reactions of $RhH(CO)(PPh_3)_3$. However, like most important, reactive, catalytic intermediates they are not isolable. The sole example so far prepared results from the reaction with tetrafluoroethene[56,57]

$$RhH(CO)(PPh_3)_3 + C_2F_4 \xrightarrow[5\text{ atm. }25°]{C_7H_8} \textit{trans}\text{-}Rh(C_2F_4H)(CO)(PPh_3)_2 + PPh_3. \quad (14)$$

The yellow complex can be reconverted to $RhH(CO)(PPh_3)_3$ by adding triphenylphosphine and treating the solution with hydrogen at 50 atm. pressure[56]

$$Rh(C_2F_4H)(CO)(PPh_3)_2 + PPh_3 + H_2 \longrightarrow RhH(CO)(PPh_3)_3 + HCF_2CF_2H. \quad (15)$$

Allene gives the yellow η^3-allyl complex $Rh(C_3H_5)(CO)(PPh_3)_2$ which can be precipitated from the reaction mixture by addition of ethanol and cooling to 0°[58]

$$RhH(CO)(PPh_3)_3 + H_2C{=}C{=}CH_2 \xrightarrow[C_7H_8]{N_2} Rh(\eta^3\text{-}C_3H_5)(CO)(PPh_3)_2 + PPh_3. \quad (16)$$

In this complex the allyl group is believed to be *trans* to the carbonyl group since the latter has a high IR stretch frequency of 1989 cm^{-1}.

Many alkynes, however, give stable isolable vinyl complexes

$$RhH(CO)(PPh_3)_3 + RC{\equiv}CR \longrightarrow Rh(CR{=}CHR)(CO)(PPh_3)_2 \quad (17)$$

$$(R = Ph;^{59,60}\ CO_2H,\ CO_2Et;^{59}\ CO_2Me^{59,61}).$$

As shown in Fig. 4 the geometry around the metal is *trans*. Varying opinions have been expressed about the geometry of the vinyl groups. The phenyl and carboxymethyl derivatives are believed to be *trans*, since cleavage of these vinyl complexes with dry hydrogen chloride gives *trans*-alkenes (Scheme 1). Nevertheless, the ^1H and ^{19}F NMR spectra of the *bis*(trifluoromethyl) derivative support a *cis* arrangement of trifluoromethyl groups in the complex. This structure is proposed to result from the formation of a relatively stable π-complex **3** which favours the eventual formation of the *cis*-vinyl complex.[59]

It has also been proposed that $MeO_2CC{\equiv}CCO_2Me$ forms a *cis*-vinyl complex upon reaction with $RhH(CO)(PPh_3)_3$. The vinyl complex oxidatively adds methyl iodide (Scheme 2). Vacuum pyrolysis of the resulting methyl complex gives predominantly the *Z* isomer. However, as a slower rate of heating gives a greater proportion of the *E* isomer, the structure of the initial vinyl complex[60] is still open to doubt.

Reaction of $RhH(CO)(PPh_3)_3$ with a ten-fold excess of diphenylacetylene results in the formation of a rhodacycle. The metallocycle arises from the oxidative addition of two further molecules of alkyne after initial formation of the vinyl complex.[61]

Chlorine is abstracted from allyl, methallyl, or vinyl chlorides to yield *trans*-$RhCl(CO)(PPh_3)_2$.[62] In view of the preceding reaction it is a little surprising that the reaction between $RhH(CO)(PPh_3)_3$ and $TlBr(C_6F_5)_2$ yields the perfluorophenyl rather than the bromocomplex[63]

$$RhH(CO)(PPh_3)_3 + TlBr(C_6F_5)_2 \xrightarrow[80°]{C_6H_6} Rh(C_6F_5)(CO)(PPh_3)_2. \quad (18)$$

In the absence of alkenes $RhH(CO)(PPh_3)_3$ has been shown to react with dioxygen, however, no rhodium products have been identified. Further, the two reports from the same workers disagree on the quantity of dioxygen reacting with the complex.[64,65] If alkene is present then a small proportion is oxidised to ketones.[65]

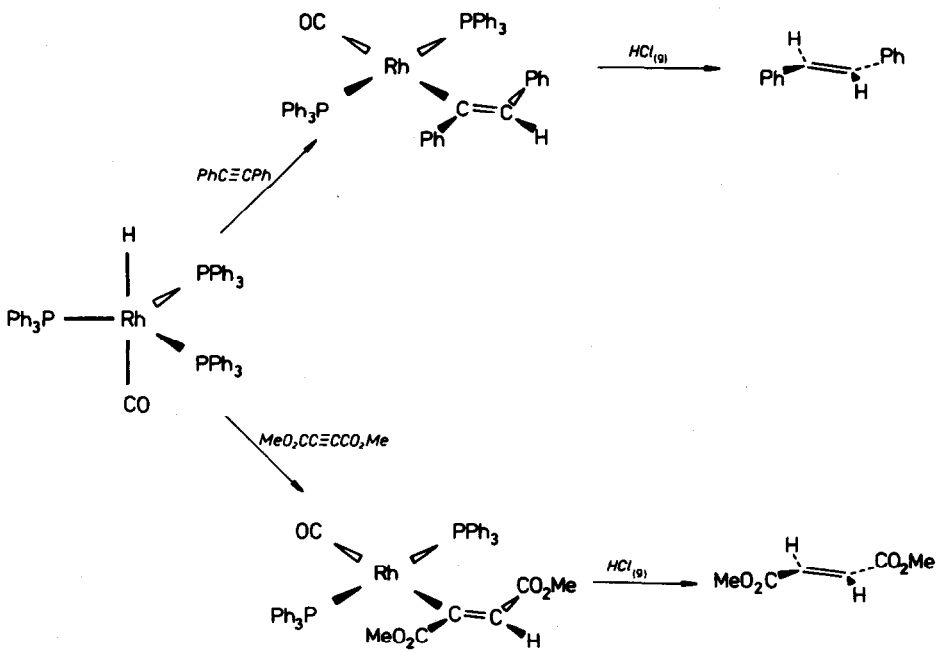

Scheme 1. Degradation of *trans*-$Rh(PhC{=}CHPh)(CO)(PPh_3)_2$.

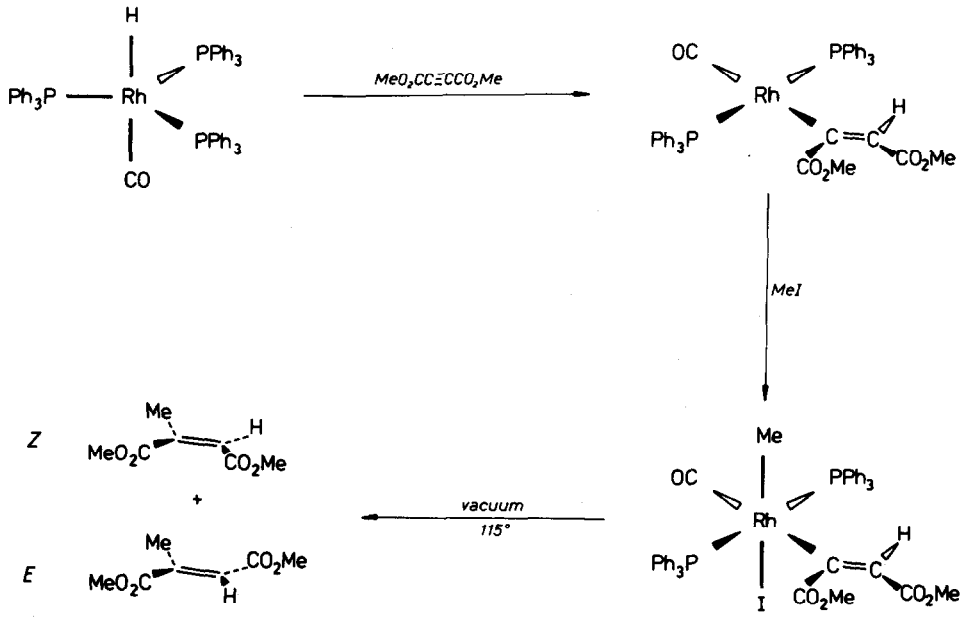

Scheme 2. Degradation of *trans*-Rh($MeO_2CC{=}CHCO_2Me$)(CO)(PPh_3)$_2$.

If *N*-chlorothioformyldimethylamine is allowed to react with the title complex *trans*-RhCl(CO)-(PPh_3)$_2$ is formed together with the six-coordinate complex RhCl(η^2-$SCNMe_2$)$_2$(PPh_3)

$$RhH(CO)(PPh_3)_3 + Me_2NC(S)Cl \xrightarrow{C_6H_6} RhCl(\eta^2\text{-}SCNMe_2)_2(PPh_3) + RhCl(CO)(PPh_3)_2. \quad (19)$$

The monotriphenylphosphine product is easily photolysed, so no X-ray structure was attempted. The coordination of the thiocarbonyl group, **4**, is believed to be simillar to that found in other rhodium and iridium complexes.[66]

Oxidative addition also occurs in the reaction between trichlorocyclotrithiazine and RhH(CO)-(PPh_3)$_3$. The chlorobridged dimer, **5**, is first formed

$$RhH(CO)(PPh_3)_3 + (NSCl)_3 \xrightarrow[25°]{CHCl_3/CCl_4} \{RhCl_2(NS)(CO)(PPh_3)\}_2. \quad (20)$$

Excess triphenylphosphine first cleaves the dimer

$$\{RhCl_2(NS)(CO)(PPh_3)\}_2 + PPh_3 \xrightarrow{CH_2Cl_2} RhCl_2(NS)(CO)(PPh_3)_2 \quad (21)$$

and on refluxing in dichloromethane reduces the monomer to a rhodium(I) complex

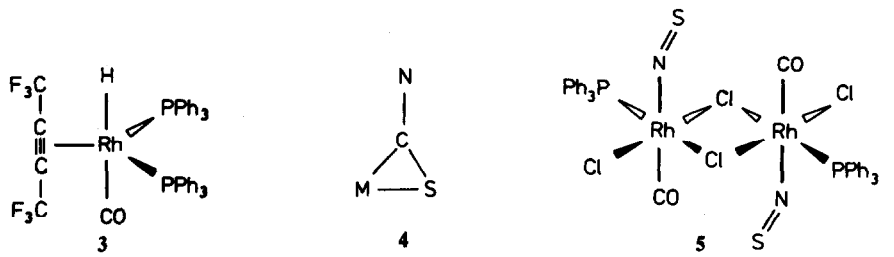

$$RhCl_2(NS)(CO)(PPh_3)_2 + PPh_3 \xrightarrow[40°]{CH_2Cl_2} RhNS(CO)(PPh_3)_2. \quad (22)$$

In all these complexes the thionitrosyl group is believed to be bound as NS^-.[67]

Nitrosyltribromide also adds oxidatively and forms an orange nitrosyl and a brown hyponitrite

$$RhH(CO)(PPh_3)_3 + NOBr_3 \xrightarrow{CH_2Cl_2} RhBr_2(NO)(CO)(PPh_3)_2 + \{RhBr_2(PPh_3)_2\}_2N_2O_2. \quad (23)$$

The IR spectrum of the nitrosyl complex suggests it contains NO^- bound *trans* to CO. The identity of the hyponitrite is confirmed by the formation of nitrous oxide upon treatment with mineral acids[68]

$$\{RhBr_2(PPh_3)_2\}_2N_2O_2 + HCl + PPh_3 \longrightarrow N_2O + RhBr(PPh_3)_3. \quad (24)$$

Anionic nitrosyl groups also coordinate when $RhH(CO)(PPh_3)_3$ is allowed to react with dinitrogen trioxide

$$RhH(CO)(PPh_3)_3 + N_2O_3 \xrightarrow{CH_2Cl_2} RhNO_2(NO)_2(PPh_3)_3. \quad (25)$$

The yellow product's IR spectrum shows it to contain a nitro group.[69]

The simple nitrosyl complex $Rh(NO)(CO)(PPh_3)_2$ may be prepared by two routes[70]

$$RhH(CO)(PPh_3)_3 + p\text{-}MeC_6H_4SO_3N(NO)Me \longrightarrow Rh(NO)(CO)(PPh_3)_2 \quad (26)$$

$$RhH(CO)(PPh_3)_3 + Co(NO)(dmg)_2{\cdot}MeOH \longrightarrow Rh(NO)(CO)(PPh_3)_2 \quad (27)$$

(dmg = dimethylglyoxime anion).

Surprisingly the title complex is not totally destroyed by treatment with concentrated nitric acid, instead yellow crystals of a *tri*(nitrato)rhodium(III) complex are formed[71]

$$RhH(CO)(PPh_3)_3 + HNO_3 \longrightarrow Rh(NO_3)_3(PPh_3)_2. \quad (28)$$

Electrochemical oxidation of $RhH(CO)(PPh_3)_3$ results in elimination of hydrogen from the $[RhH(CO)(PPh_3)_3]^+$ cation[72]

$$RhH(CO)(PPh_3)_3 \underset{+e}{\overset{-e}{\rightleftharpoons}} [RhH(CO)(PPh_3)_3]^+ \longrightarrow Rh(CO)(PPh_3)_3 + \tfrac{1}{2}H_2. \quad (29)$$

In toluene/acetonitrile mixtures coordination of acetonitrile increases the number of complexes that are formed (Scheme 3).[73]

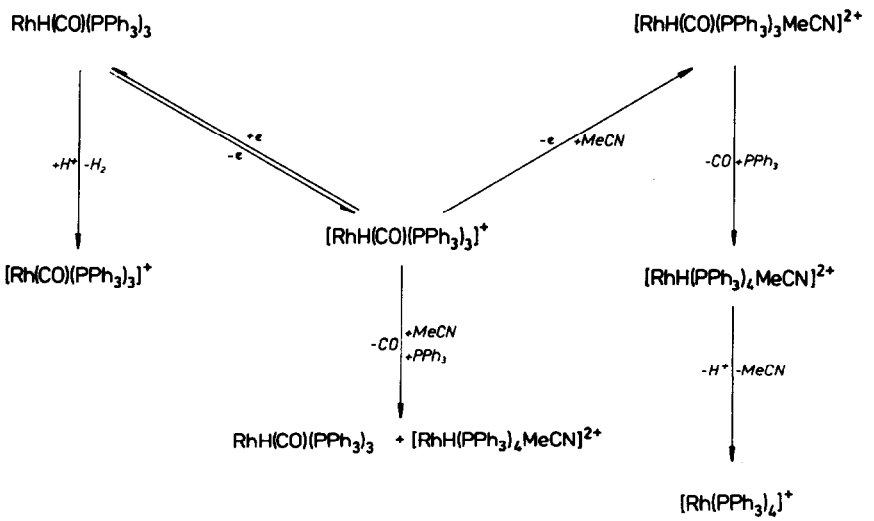

Scheme 3. Electrochemical reactions of $RhH(CO)(PPh_3)_3$. (Redrawn with permission from G. Pilloni, G. Schiavon, G. Zotti and S. Zecchin, *J. Organometal. Chem.* 1977, **134**, 305.)

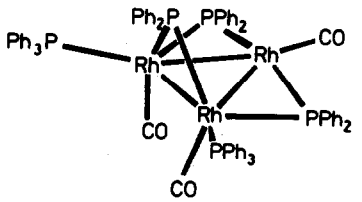

Fig. 5. Structure of $Rh_3(\mu\text{-}PPh_2)_3(CO)_3(PPh_3)_2$. (Redrawn with permission from E. Billig, J. D. Jamerson and R. L. Pruett, *J. Organometal. Chem.* 1980, **192**, C49.)

Carbonylhydrido*tris*(triphenylphosphine)rhodium(I) decomposes in many solvents at temperatures above 80°. Pyrolysis of a suspension of $RhH(CO)(PPh_3)_3$ in nonane at 120° gives a green, air-sensitive solid. The structure of this trimeric diphenylphosphido-complex is shown in Fig. 5.[74] A different brown product is obtained in the presence of carbon monoxide and hydrogen. Reactions of $RhH(CO)(PPh_3)_3$ with carbon monoxide and hydrogen or carbon monoxide are best dealt with in Section VII. A devoted to catalytic hydroformylation.

V. CATALYSIS OF ISOTOPE EXCHANGE AND ISOMERIZATION

Since carbonylhydrido*tris*(triphenylphosphine)rhodium(I) can form alkyl complexes upon reaction with alkenes (eqn 14) it acts as a powerful catalyst for isotope exchange and double bond migration. "Naked" transition metal surfaces function in a similar way and the parallel between these surfaces and monohydrido homogeneous systems has been noted.[75,76] Carbonyldeuterio*tris*(triphenylphosphine)rhodium(I) is, therefore, an unsatisfactory deuteration catalyst. Dideuterio systems in which alkyl complexes have very short lifetimes are far superior.[4] The mechanisms of isotope exchange and double bond migration are shown in Scheme 4. Both processes depend upon the formation of an alkyl complex and the subsequent reversal of this reaction by β-hydride or β-deuteride abstraction as the case may be. Formation of a 1-alkyl complex cannot result in isomerization but isotope exchange is possible. Isotopic exchange or isomerization or both may result from initial formation of a 2-alkyl complex. The relative rates of isotope exchange by different alkenes reflects the ease of formation and stability of their alkyl complexes. Thus, pent-1-ene rapidly incorporates deuterium whilst *trans*-pent-2-ene barely reacts. The rate of isotope exchange for *cis*-pent-2-ene is intermediate.[32,77]

The formation of alkyl complexes in both isotope exchange and isomerization reactions is inhibited by addition of triphenylphosphine, resulting in slower rates of both reactions in the presence of excess ligand.[32]

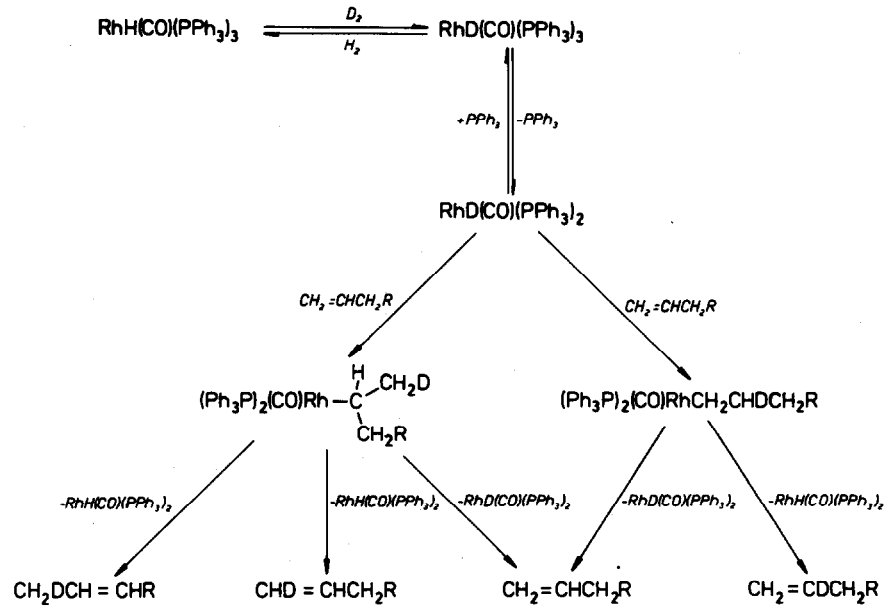

Scheme 4. Mechanisms of isotopic exchange and isomerization.

Scrambling of the deuterium atoms in *trans*-$C_2H_2D_2$ is catalysed by $RhH(CO)(PPh_3)_3$. The product distribution is shown in Fig. 6. Despite a slight loss of deuterium overall, no deuterium was found to have been incorporated into the phenyl groups of the catalyst.[78] Exchange takes place between perdeuteroethene and $RhH(CO)(PPh_3)_3$. The rate of exchange increases with temperature in benzene solution. The product distribution is shown in Fig. 7. The rhodium complex, however, undergoes extensive decomposition before the reaction is complete.[79]

In the catalytic isomerization of terminal alkenes the double bond migrates into the chain since internal alkenes are of greater thermodynamic stability

$$\text{Alk-1-ene} \longrightarrow \textit{cis}\text{-Alk-2-ene} \longrightarrow \textit{trans}\text{-Alk-2-ene}. \tag{30}$$

Thus, but-1-ene,[79] pent-1-ene,[32,77] and hept-1-ene[80] eventually give rise to the *trans*-alk-2-ene when allowed to react with $RhH(CO)(PPh_3)_3$ at either room temperature or above. For both pent-1-ene[32,77] and hept-1-ene[81] isomerization to the *cis*-alk-2-ene is more rapid than the second stage of the isomerization to the *trans*-alk-2-ene.

The relative tendency of double bonds to migrate is shown by the isomerization of 3,7-dimethylocta-1,6-diene.

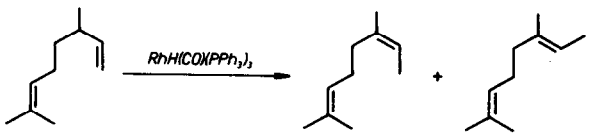

(31)

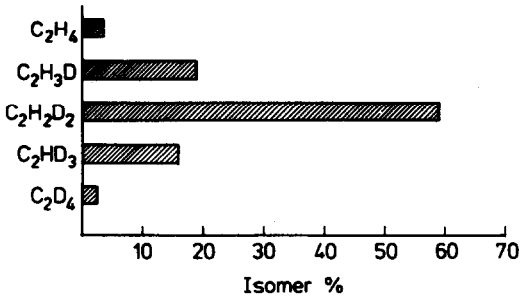

Fig. 6. Isotopic product distribution from *trans*-$C_2H_2D_2$.

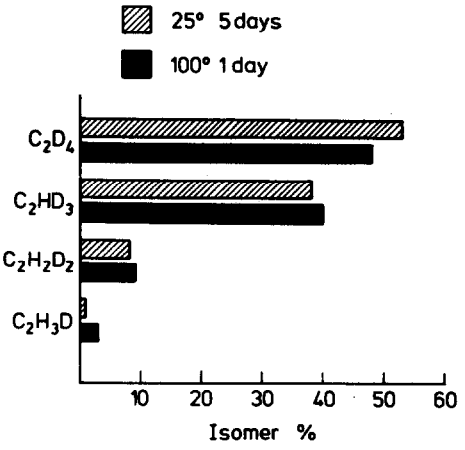

Fig. 7. Isotopic product distribution from C_2D_4.

The related compound 3,7-dimethyl-7-methoxyoctene isomerizes similarly during hydroformylation.[82]

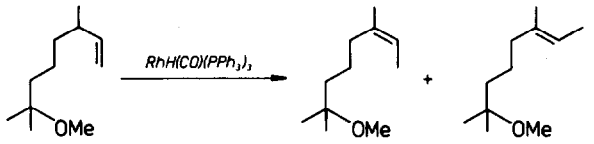

(32)

Double bond migration in nitrogen heterocycles is also catalysed by $RhH(CO)(PPh_3)_3$.[83]

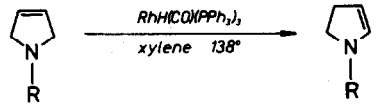

(33)

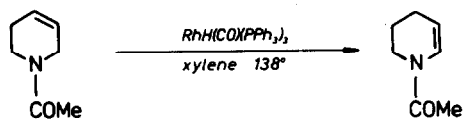

(34)

UV light reputedly assists the $RhH(CO)(PPh_3)_3$ catalysed isomerization of hept-1-ene to *trans*-hept-2-ene.[84] The isomerization of pent-1-ene is also catalysed by heterogenized derivatives of $RhH(CO)(PPh_3)_3$.[54]

The isomerization of allylbenzene

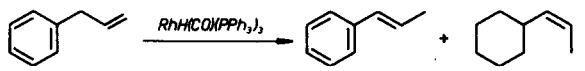

(35)

proceeds much more slowly when catalysed by $RhH(CO)(PPh_3)_3$ than when either chloro*tris*(triphenylphosphine)rhodium(I) or dichloro*tris*(triphenylphosphine)ruthenium(II) are the catalysts. Similarly 4-phenylbut-1-ene is only slowly isomerized to 1-phenylbut-2-enes in the presence of $RhH(CO)(PPh_3)_3$. In both these cases allylic complexes rather than simple alkyl complexes are believed to be the intermediates.[85] Formation of relatively stable allyl intermediates would also explain the poorer yield obtained in the isomerization of the allyl ether

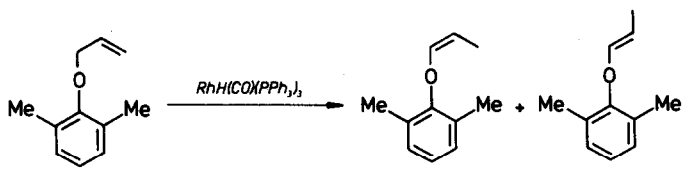

(36)

when $RhH(CO)(PPh_3)_3$ replaces $RuCl_2(PPh_3)_3$ as the catalyst.[86]

Allylic alcohols are eventually isomerized to aldehydes in the presence of $RhH(CO)(PPh_3)_3$[87]

$$CH_3{=}CMeCH_2OH \xrightarrow[CF_3CH_2OH]{RhH(CO)(PPh_3)_3} Me_2C{=}CHOH \longrightarrow MeCHCHO. \qquad (37)$$

If a chiral ditertiary phosphine (e.g. (−)-DIOP) is added to the reaction mixture—presumably forming $RhH(CO)(DIOP)(PPh_3)$—chiral aldehydes result[88]

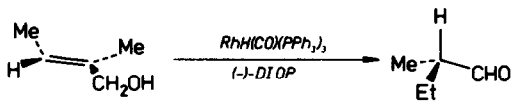

(S)

(38)

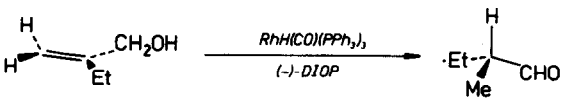

(R)

(39)

Other isomerizations catalysed by $RhH(CO)(PPh_3)_3$ include the 1,3-sigmatropic rearrangement of 3-chlorobutene

$$CH_2{=}CHCHClMe \xrightarrow{RhH(CO)(PPh_3)_3} MeCH{=}CHCH_2Cl. \quad (40)$$

However, this is almost a trivial catalysis since a very large number of transition metal complexes can catalyse the reaction which also takes place uncatalysed in dioxan solution at 70°.[89]

A rare instance of catalytic isomerization not involving double bond migration is provided by *cis*-1,2-epoxycyclohexan-3-ol. This compound is converted to the *trans*-isomer in the presence of $RhH(CO)(PPh_3)_3$ at 110°.[90,91]

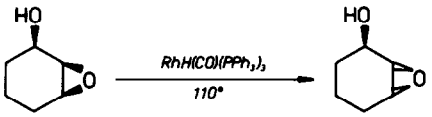

(41)

The above isomerization is also catalysed by *trans*-$RhCl(CO)(PPh_3)_2$ or $RuCl_2(PPh_3)_3$.[90]

VI. CATALYTIC HYDROGENATION

Despite the limitations outlined in the preceding section on isomerization and isotopic exchange processes carbonylhydrido*tris*(triphenylphosphine)rhodium(I) is a moderately useful catalyst for the hydrogenation of terminal alkenes under mild conditions. Its regioselectivity in favour of terminal alkenes can be exploited in reactions of the type

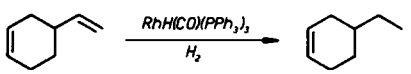

(42)

since at hydrogen pressures of one atmosphere or less internal alkenes are not reduced. Further, the complex does not catalyse the reduction of keto, cyano, chloro, hydroxyl, carboxyl, or aldehyde groups.[92] Alkynes react with $RhH(CO)(PPh_3)_3$ to form vinyl complexes (eqn 17). The vinyl complexes appear to be unable to activate molecular hydrogen, hence alkynes are not hydrogenated in the presence of the catalyst under mild conditions.[92] However, there is one claim that phenylacetylene can be hydrogenated when $RhH(CO)(PPh_3)_3$ is the catalyst.[93]

It was seen in Section IV above that tetrafluoroethene forms the alkyl complex $Rh(CF_2CF_2H)(CO)(PPh_3)_2$ (eqn 14). This alkyl complex reacts with hydrogen and regenerates $RhH(CO)(PPh_3)_3$ (eqn 15). The organic product is 1,1,2,2-tetrafluoroethane. Accordingly the alkyl route has been proposed for the hydrogenation of alkenes when $RhH(CO)(PPh_3)_3$ is the catalyst.[92] Scheme 5 shows the mechanism of catalytic hydrogenation. The upper loop of this scheme involves a 1-alkyl complex. This loop is favoured by the presence of two *trans* triphenylphosphine ligands. For steric reasons formation of a 2-alkyl complex (lower loop) is much less likely, and the equilibrium will lie on the side of the alkene hydrido complex. Since internal or cyclic alkenes must form complexes of this type, their rates of hydrogenation will be very much smaller than those of terminal alkenes.

Deuteration of alkenes offers some insight into the formation of metal alkyls despite potential complications arising from isotope exchange outlined in the previous section. Propene undergoes exchange with $RhD(CO)(PPh_3)_3$, as a result about 9% of the propane formed in the deuteration contains only one deuterium atom. The deuteration is not random since some two thirds of the d_1-propane is the 2-deutero isomer and only one third the 1-deutero product. This unequal distribution comes about because the stability of the primary alkyl complex, **6**, is greater than that of the secondary alkyl complex, **7**.[94]

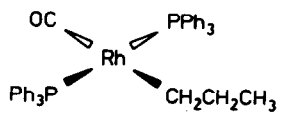

6

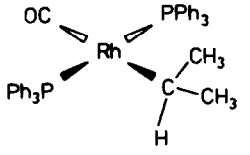

7

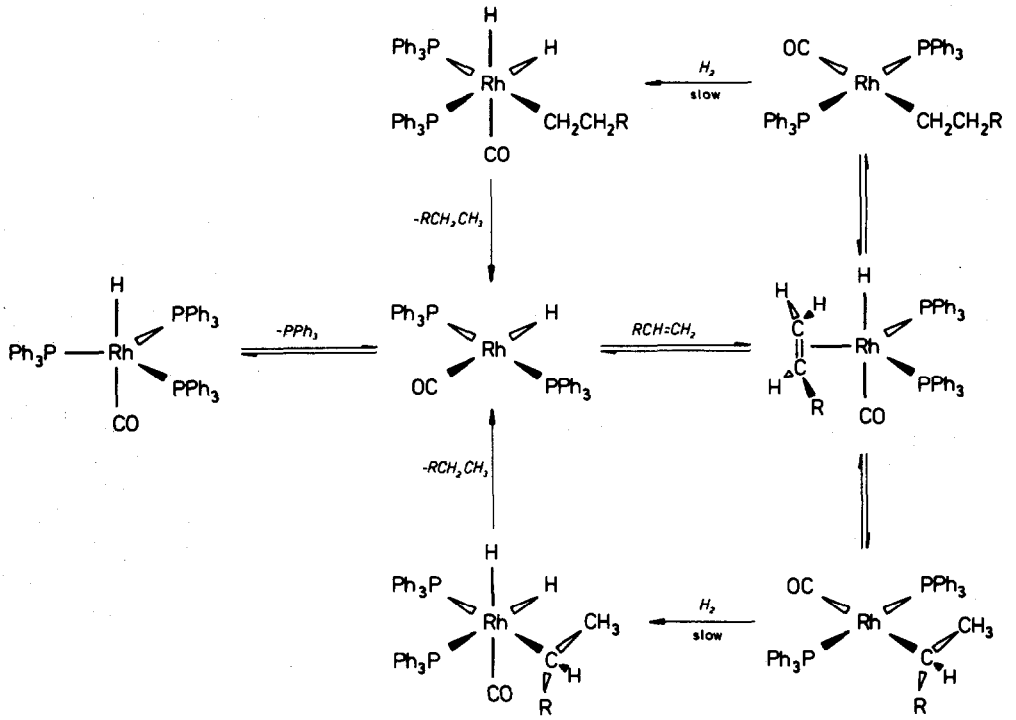

Scheme 5. Mechanism of catalytic hydrogenation.

This effect is even more marked in the catalytic deuteration of 2-methylpropene using RhD(CO)-$(PPh_3)_3$ (Scheme 6). The *tert*-butyl complex is too unstable to undergo deuteration or hydrogenation and decomposes to yield either monodeuterated or unchanged 2-methylpropene. The alternative, stable, primary, alkyl complex can be either deuterated or hydrogenated to form $CH_2DCD(CH_3)_2$ or $(CH_3)_3CD$ respectively.[95]

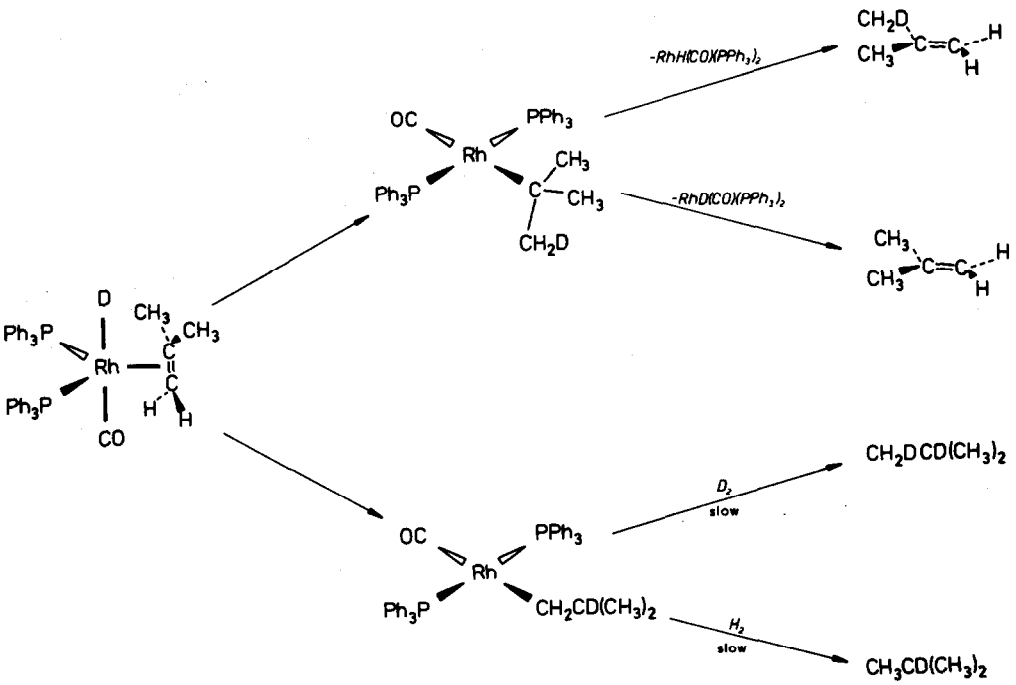

Scheme 6. Catalytic deuteration of 2-methylpropene. (Redrawn with permission from E. Hirota, M. Ito and T. Ueda, *Proc. 6th. Int. Cong. Catal.* 1977, 1, 518.)

It is believed the rate determining step in both loops of the cycle is the attack of hydrogen upon the alkyl complex. This view is supported by the work of Siegel and Ohrt[96] who studied the product distribution from the catalytic hydrogenation of 4-*tert*-butylmethylenecyclohexane.

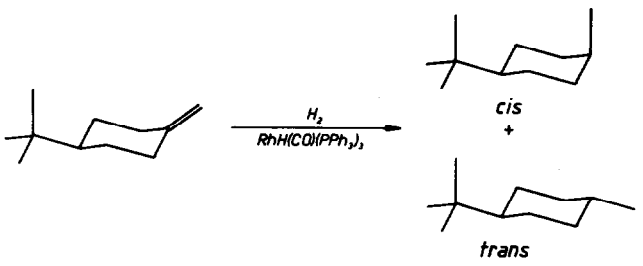

(43)

The steric bulk of the *tert*-butyl substituent requires that it is always equatorial. If hydrogen attack on the alkyl complex is the rate determining step then the major product is *trans*-4-*tert*-butylmethylcyclohexane. At low hydrogen pressures this is found to be the case. At higher hydrogen pressures hydrogenolysis of the intermediate alkyl complex is no longer the rate determining step since the concentration of hydrogen in solution is greater. As a consequence the proportion of *cis*-4-*tert*-butylmethylcyclohexane in the product increases. This is consistent with the rate of alkene attack on the original hydrido complex becoming of increasing importance. The proportion of *cis*-4-*tert*-butylmethylcyclohexane at high hydrogen pressures was found to approach that occurring when chloro*tris*(triphenylphosphine)rhodium(I) is used as the catalyst. The rate determining step in catalytic hydrogenation using the latter catalyst is known to be alkene coordination.[4]

Under similar conditions $RhH(CO)(PPh_3)_3$ is a less effective catalyst than $RhCl(PPh_3)_3$.[92] Amongst terminal alkenes there are some marked differences in relative hydrogenation rates (Table 1). However, it should be borne in mind that the efficiency of the rhodium(I) alkyl complexes in activating molecular hydrogen is the rate determining step in $RhH(CO)(PPh_3)_3$ catalyses. In $RhCl(PPh_3)_3$ catalysis the steric properties of the alkene determine its rate of attack on chlorodihydrido*bis*(triphenylphosphine)-rhodium(III).[4]

The dissociation of one triphenylphosphine ligand from $RhH(CO)(PPh_3)_3$ (eqn 1) before alkene coordination is essential on both steric and electronic grounds—six coordinate rhodium(I) complexes are 20-electron compounds. Other rhodium(I) and iridium(I) complexes which do not dissociate are catalytically inactive. However, at higher temperatures when thermal dissociation of a ligand occurs both carbonylhydrido*tris*(triphenylphosphine)iridium(I) and *trans*-carbonylchloro*bis*(triphenylphosphine)-rhodium(I) function as hydrogenation catalysts.[97,98] Care should be taken in comparing the activities of $RhH(CO)(PPh_3)_3$ and $IrH(CO)(PPh_3)_3$ since the latter complex alone reacts directly with molecular hydrogen in solution[99]

$$IrH(CO)(PPh_3)_3 + H_2 \longrightarrow IrH_3(CO)(PPh_3)_3. \quad (44)$$

Table 1. Relative rates of hydrogenation of alkenes catalysed by $RhH(CO)(PPh_3)_3$[92] and $RhCl(PPh_3)_3$[4]

Alkene	Rate, mmole H_2 min^{-1} [a]	
	$RhH(CO)(PPh_3)_3$	$RhCl(PPh_3)_3$
Allyl alcohol	0.905	3.02
Hex-1-ene	0.745	0.857
Undec-1-ene	0.637	---
Dodec-1-ene	---	1.01
Allyl cyanide	0.248	0.453
Styrene	0.062	2.56
cis-Pent-2-ene	0	1.01
Cyclohexene	0	0.800
Penta-1,3-diene	0	0.059

[a] Under standard conditions:- alkene 1.25M, catalyst 1.25mM, volume 80cm^3, H_2 pressure 50 cm Hg, 25°C.

It should be noted that the proposed iridium(III) product is a seven coordinate 20-electron compound!

At higher temperatures $RhH(CO)(PPh_3)_3$ itself becomes active towards a wider range of substrates. At 80° internal alkenes (e.g. cycloheptene, *cis*- and *trans*-hept-2-ene, and *trans*-hept-3-ene) can be hydrogenated.[97] Whilst it is possible that hydroisomerization to terminal alkenes[80,81] is taking place followed by hydrogenation, such a process is unavailable to cyclohexene[100] or cycloheptene.[97] Cyclohexene can be catalytically hydrogenated using low concentrations of $RhH(CO)(PPh_3)_3$ in benzene solution at 50° under ten atmospheres of hydrogen. However, at $RhH(CO)(PPh_3)_3$ concentrations above 0.25 m*M* the rate of hydrogenation tails off and the reaction virtually ceases at catalyst concentrations above 0.75 m*M*. These observations suggest that under these conditions further dissociation of $RhH(CO)(PPh_3)_3$ to the more active mono-triphenylphosphine complex $RhH(CO)PPh_3$ is taking place (eqn 1). At higher catalyst concentrations such dissociation is inhibited by the triphenylphosphine displaced in the first step

$$RhH(CO)(PPh_3)_3 \rightleftharpoons RhH(CO)(PPh_3)_2 + PPh_3. \quad (45)$$

The lower selectivity of the mono-triphenylphosphine complex follows from the less crowded nature of the alkyl intermediates. These cycloalkyl or 2-heptyl complexes are much less likely to revert to alkene and hydrido complex before they undergo the slow oxidative addition of hydrogen en route to alkane formation. It would also appear that at higher temperatures the vinyl intermediates formed by addition of alkynes undergo hydrogenolysis. At 80° both hex-1-yne and phenylacetylene are hydrogenated.[97,98]

The wider catalytic activity of $RhH(CO)PPh_3$ may also explain certain discrepancies in claims that substituted alkenes can be hydrogenated. Generally, impure substituted alkenes can be hydrogenated but this may arise from the traces of hydroperoxides they contain forming triphenylphosphine oxide from one or more triphenylphosphine ligands

$$RhH(CO)(PPh_3)_3 + ROOH \longrightarrow RhH(CO)(PPh_3)_2 + OPPh_3 + ROH \quad (46)$$

$$RhH(CO)(PPh_3)_2 + ROOH \longrightarrow RhH(CO)PPh_3 + OPPh_3 + ROH. \quad (47)$$

Further quantities of hydroperoxides will destroy the catalyst. Failure to purify the substrate may account for the observation that the activity of the catalyst decreases with time during hydrogenation.[101,102] In the hydrogenation of ethyl acrylate it was claimed that weak irradiation by UV light preserved the activity of the catalyst.[102]

One of the great advantages of a homogeneous hydrogenation catalyst is that it can be employed in the hydrogenation of insoluble substrates. This useful property has been combined with the regioselectivity of $RhH(CO)(PPh_3)_3$ in specifically reducing the pendant and external double bonds in rubber polymers.[103,104]

Very few attempts seem to have been made to employ heterogenised varieties of $RhH(CO)(PPh_3)_3$ as hydrogenation catalysts. The formation of heterogenised derivatives of the catalyst was discussed in Section IV.A. The majority of these derivatives have been used as hydroformylation catalysts, but there is one report of $RhH(CO)(PPh_3)_3$ being introduced into the pores of a polystyrene/divinylbenzene polymer and used as a hydrogenation catalyst.[105]

Transfer hydrogenation is another neglected area of study. This is surprising since another monohydrido system $RuHCl(PPh_3)_3$ has been widely investigated in transfer hydrogenation reactions. However, the results from the two studies that have been published are not encouraging, $RhH(CO)(PPh_3)_3$ is not very active in catalysing transfer hydrogenation. Hydrogen has been transferred from formic acid to oct-1-ene at temperatures between 60 and 100°. Unlike other systems the addition of lithium formate to the mixture decreases the yield of octane rather than increasing it.[106] Analogues of $RhH(CO)(PPh_3)_3$ containing aryl or mixed alkyl aryl tertiary phosphines function as poor hydrogen transfer complexes at 130°. Using these hydrogen has been transferred from benzyl alcohol to oct-1-ene. A further disadvantage that became apparent in these systems was the isomerization of oct-1-ene to *trans*-oct-2-ene.[11]

VII. CATALYTIC HYDROFORMYLATION

Hydroformylation is effectively the addition of formaldehyde across an alkene double bond. It is

usually achieved by reacting an alkene with a mixture of hydrogen and carbon monoxide in the presence of a suitable heterogeneous or homogeneous catalyst

$$RCH{=}CH_2 + H_2 + CO \longrightarrow RCH_2CH_2CHO. \quad (48)$$

In particular the hydroformylation of propene to butyraldehyde is of great industrial importance.[107] This reaction can be catalysed by rhodium metal or by various cobalt compounds.[108] The latter probably form tetra(carbonyl)hydridocobalt(I) which is the true catalyst. However, this catalyst typically requires pressures of 90 atmospheres and operating temperatures of 180°.[109] Carbonylhydrido*tris*(triphenylphosphine)rhodium(I) can bring about the reaction at sub-atmospheric pressure and room temperature.[62] As a consequence $RhH(CO)(PPh_3)_3$ has virtually displaced $CoH(CO)_4$ as a commercial hydroformylation catalyst. Currently plants with an actual or projected capacity of 1.1 Mtonnes use $RhH(CO)(PPh_3)_3$ to catalyse the hydroformylation of propene.[110] The butyraldehyde produced is converted to 2-ethylhexanol

$$2CH_3(CH_2)_2CHO \xrightarrow[150°\ 180\ atm]{H_2/Ni} CH_3(CH_2)_3CH(C_2H_5)CH_2OH. \quad (49)$$

The 2-ethylhexanol is used to esterify phthalic acid. *Bis*(2-ethylhexyl)phthalate is used as the plasticiser for polyvinyl chloride plastics. Some 10% of the 2-ethylhexanol is converted into 2-ethylhexyl acrylate which is an intermediate for surface coatings and adhesives.[107]

In most hydroformylations the yield of the desired terminal aldehyde is reduced by sundry side reactions. Possibly the most unwelcome side reaction is the formation of an isomeric branched aldehyde by addition of the CHO group to the second carbon atom of the chain

$$RCH{=}CH_2 + H_2 + CO \longrightarrow \underset{\displaystyle CHO}{\overset{\displaystyle |}{RCH}}{-}CH_3. \quad (50)$$

Double bond migration in the alkene (see Section V) followed by hydroformylation would also produce the 2-aldehyde.

Competitive hydrogenation of the alkene—most hydroformylation catalysts are also hydrogenation catalysts—will also reduce the yield of aldehyde. In many industrial plants a large throughput is achieved by using high temperatures and gas pressures. Under these conditions the product aldehyde can be reduced to an alcohol

$$RCH_2CH_2CHO + H_2 \longrightarrow RCH_2CH_2CH_2OH. \quad (51)$$

A stoicheiometric reaction of tetra(carbonyl)hydridocobalt(I) illustrates the reductive properties of many hydroformylation catalysts[111]

$$CH_2{=}CHCHO + CoH(CO)_4 \longrightarrow CH_3CH_2CH_2OH. \quad (52)$$

It is apparent that in any practically useful hydroformylation system the above side reactions should be of minimal importance. It will be seen in Section VII.B below that various features of the $RhH(CO)(PPh_3)_3$ catalysed hydroformylation system minimize the effects of the side reactions.

A. *Reactions with carbon monoxide and hydrogen*

Carbon monoxide and hydrogen in concert are capable of bringing about profound changes in the catalyst. The reactions amongst $RhH(CO)(PPh_3)_3$, carbon monoxide and hydrogen are complex and not all the species believed to be involved in the system have been fully characterized. If the reactions are carried out at high temperatures the ultimate products are catalytically inactive, polynuclear, diphenylphosphido complexes.

Solutions of $RhH(CO)(PPh_3)_3$ react with carbon monoxide to give two products[31,112]

$$RhH(CO)(PPh_3)_2 + CO \longrightarrow RhH(CO)_2(PPh_3)_2 + \{Rh(CO)_2(PPh_3)_2\}_2. \quad (53)$$

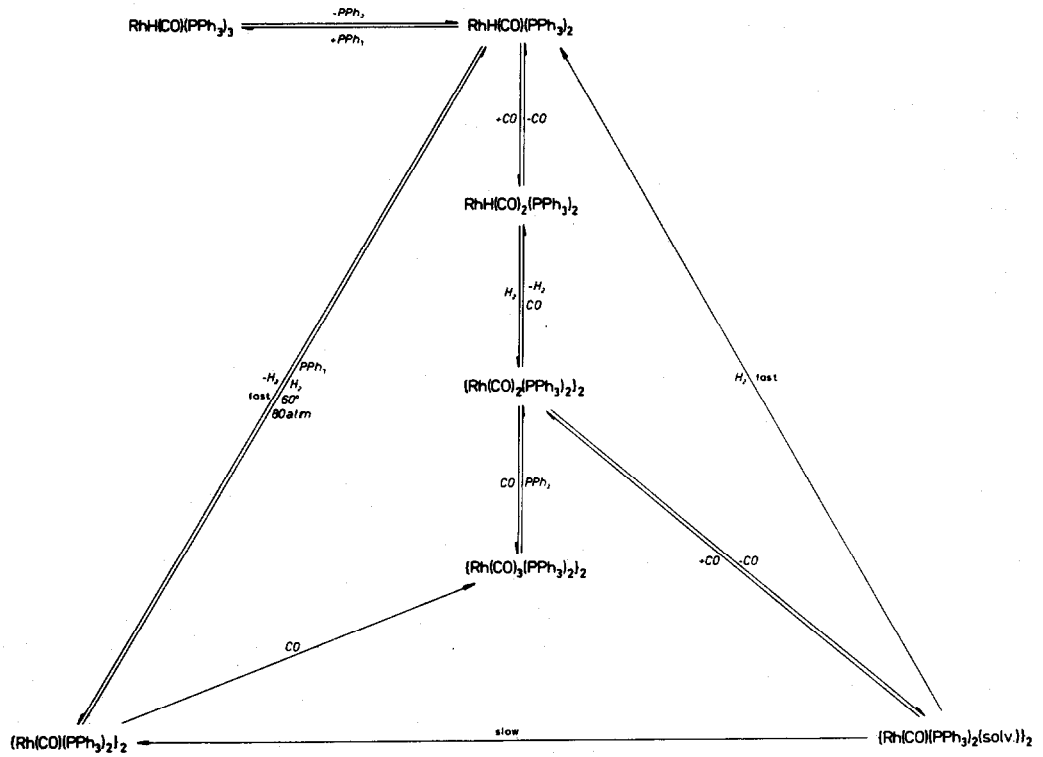

Scheme 7. Reactions of $RhH(CO)(PPh_3)_3$ with CO and H_2. (Redrawn with permission from M. Yagupsky, C. K. Brown, G. Yagupsky and G. Wilkinson, *J. Chem. Soc.* (*A*) 1970, 937.)

The yellow, dinuclear rhodium(0) complex is believed to have structure **8** on the basis of its IR spectrum.

In the presence of both hydrogen and carbon monoxide the variety of products increases (Scheme 7). In particular loss of carbon monoxide from 8 yields a red solvated dimer **9**, which in turn slowly forms

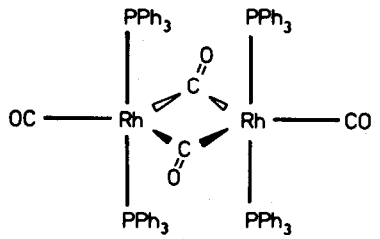

8

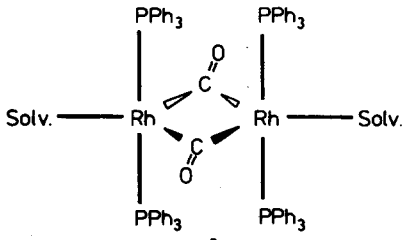

9

the catalytically inactive dimer **10**. The latter orange dimer can, however, react with triphenylphosphine and carbon monoxide to reform **8**. Under severe conditions oxidative addition of hydrogen to **10** occurs giving the un-isolable species $RhH(CO)(PPh_3)_2$.[113] The relative quantities of $RhH(CO)_2(PPh_3)_2$, $RhH(CO)(PPh_3)_2$, and **8** in solution under carbon monoxide and hydrogen at 25° have been estimated at 55, 25, and 20% respectively.[114]

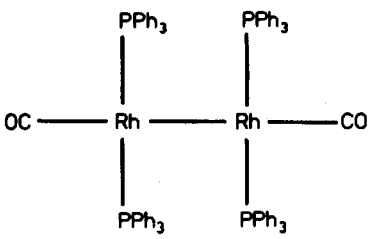

10

Using a pressurised, variable temperature, IR cell it has been proposed that the major species in solution are $RhH(CO)_2(PPh_3)_2$ and **8**. At high hydrogen pressures in the presence of triphenylphosphine

$RhH(CO)_2(PPh_3)_2$ reforms $RhH(CO)(PPh_3)_3$.[115] That **8** should be present in the red solutions is surprising, since solutions of this colour are usually associated with the red dimeric complex **9**.[113] Both groups agree that eventually brown solutions are formed.

The brown solutions presumably contain the brown, tetrameric, diphenylphosphido complex $Rh_4(\mu\text{-}PPh_2)_4(CO)_5PPh_3$. Crystals of this complex are obtained as virtually the sole product from nonane solutions of $RhH(CO)(PPh_3)_3$ which have been stored overnight at 120° under 4 atmospheres of carbon monoxide and hydrogen. The structure of the complex has been determined by X-ray crystallography,[116] and is shown in Fig. 8. This tetramer may be contrasted with the green trimer obtained in the absence of the gases (see Fig. 5).

The equilibria between dissociated mononuclear species and dimeric species adds to the difficulty of determining the mechanism of hydroformylation. Thermal degradation of the catalyst becomes important when the system is operated at high temperatures

B. *Mechanism of hydroformylation*

There are three reactants in hydroformylation reactions—as opposed to the two reactants in hydrogenations—and the catalyst must be capable of activating the reactants in the correct order. In this system hydrogen is the last reactant to be activated. This minimizes alkane by-product formation, and hydrogenation is only important at H_2:CO ratios above 1:1.[114]

1. *Linear aldehyde production.* The dinuclear complexes **8**, **9**, and **10** are not directly involved in the hydroformylation catalysis. However, Scheme 8 indicates that three mononuclear species are all capable of initiating hydroformylation cycles. In the relatively dilute catalytic solutions $RhH(CO)(PPh_3)_3$ dissociates to form $RhH(CO)(PPh_3)_2$ (eqn 1). The *bis*(triphenylphosphine) complex reacts rapidly with carbon monoxide to form the dicarbonyl complex **13**. Nevertheless, some reaction of $RhH(CO)(PPh_3)_2$ with alkene must take place since small quantities of alk-2-enes and alkane are formed even at low hydrogen pressures. These by-products must arise from the β-hydride abstraction and hydrogenation reactions respectively of the alkyl complex **12**. The dicarbonyl complex **15** could isomerize the alkene upon reverting to the hydrido alkene complex **14**, but it is believed to be unable to add hydrogen oxidatively and bring about alkene reduction.

The dicarbonyl complex **13** rapidly adds alk-1-ene to form $RhH(CO)_2(PPh_3)_2(RCH{=}CH_2)$, **14**. The latter complex is a 20-electron species but is believed to be a genuine, if undetectable, short-lived

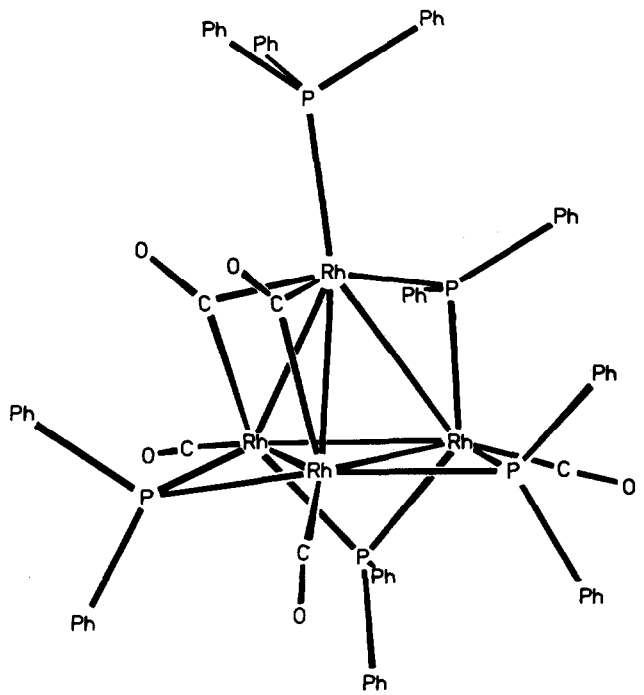

Fig. 8. Structure of $Rh_4(\mu\text{-}PPh_2)_4(CO)_5PPh_3$. (Redrawn with permission from J. D. Jamerson, R. L. Pruett, E. Billig and F. A. Fialto, *J. Organometal. Chem.* 1980, **193**, C43.)

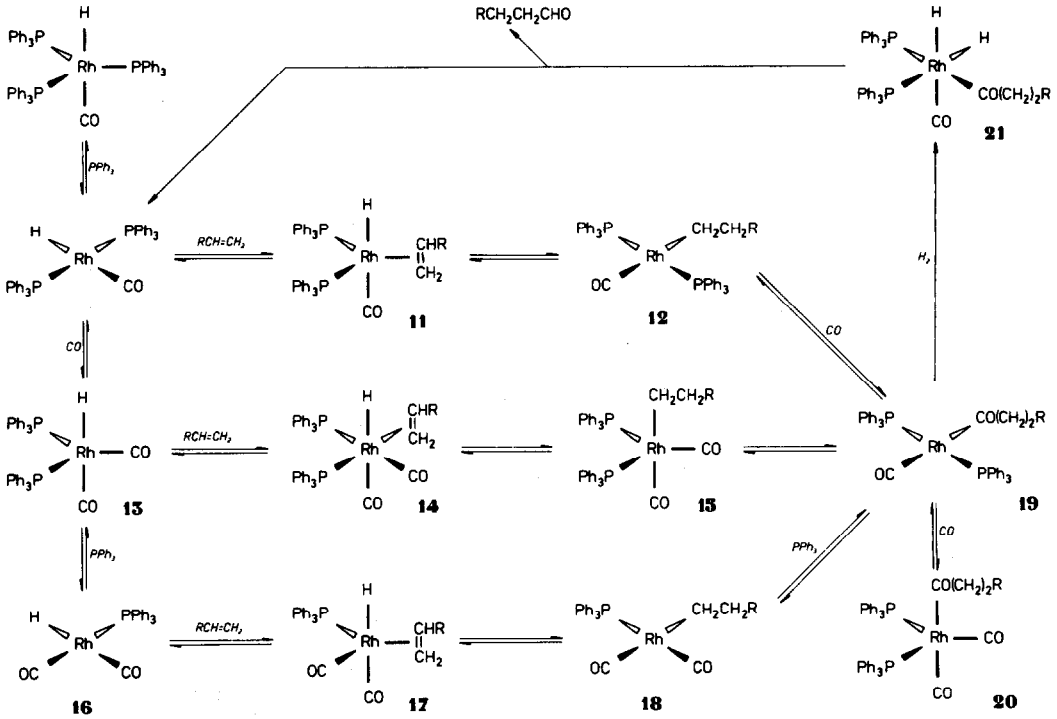

Scheme 8. Mechanism of catalytic hydroformylation.

intermediate that rapidly rearranges to the five-coordinate alkyl complex **15**. The *bis*(triphenylphosphine) complexes **14** and **15** participate in the "associative route".

At low catalyst concentrations when no triphenylphosphine has been added to the catalytic system, there is evidence for the "dissociative route" involving the mono-triphenylphosphine complexes **16–18** (see catalytic hydrogenation[100]). The participation of this route persists at much higher catalyst concentrations than in catalytic hydrogenation, possibly because the much greater π-acidity conferred by the additional carbonyl ligand enhances the lability of triphenylphosphine. The "dissociative route" avoids invoking a 20-electron intermediate such as **14**, but requires recoordination of triphenylphosphine

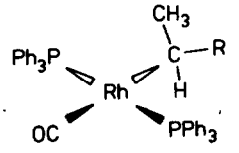

12a

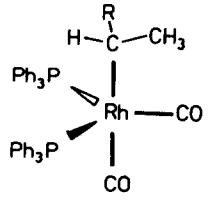

15a

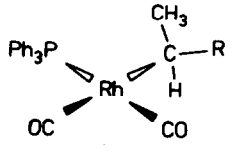

18a

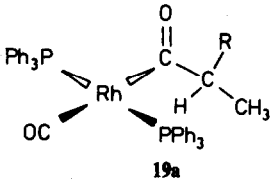

19a

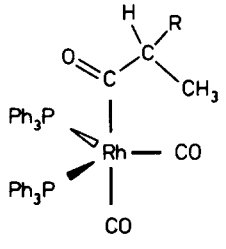

20a

upon formation of Rh(acyl)(CO)$(PPh_3)_2$, **19**.[114,117] This acyl complex can also arise from alkyl migration in **15** or carbonylation of **12**. Formerly it was believed that the alkyl complex **12** and particularly the secondary alkyl complex **12a** could not undergo carbonylation. This has now been shown to be erroneous since the reaction with carbon monoxide is much more rapid than that with hydrogen.[118] Secondary alkyls such as **12a** eventually lead to branched chain aldehydes (see below).[119]

The acyl complex may react with either carbon monoxide or hydrogen. Addition of the former forms the catalytically inactive five-coordinate dicarbonyl complex **20**. Thus excess carbon monoxide can poison the catalysis. As in catalytic hydrogenation oxidative addition of hydrogen to give a dihydridorhodium(III) complex is slow and rate determining. Although the rate determining step in both catalytic hydrogenation and hydroformylation is reaction with hydrogen, the rates themselves are not comparable since in the former process an alkyl complex activates hydrogen and in the latter an acyl complex is involved.

Hydrogen transfer to the acyl ligand followed by rapid elimination of aldehyde reforms RhH(CO)-$(PPh_3)_2$ and permits the catalytic cycle to continue.

2. *Branched chain aldehyde production.* Branched chain aldehydes result from the hydrogenolysis of branched acyl complexes **19a** which in turn may be derived from one of the branched alkyl complexes **12a**, **15a** or **18a**. The branched alkyl complexes play a much more important role in hydroformylation than they do in catalytic hydrogenation.

The generation of the 2-alkyl complex **15a** from alk-1-enes is much more likely that of **12a** during hydrogenation. In each system both Markownikov

$$L_nMH + RCH{=}CH_2 \rightarrow L_nM{-}\underset{\displaystyle CH_3}{\overset{\displaystyle |}{CHR}} \qquad (54)$$

and anti-Markownikov addition

$$L_nMH + RCH{=}CH_2 \rightarrow L_nM{-}CH_2CH_2R \qquad (55)$$

can occur. Markownikov addition is more favoured by the dicarbonyl complex **13** since in this complex the polarity of the metal hydride bond is $M^{\delta-}$–$H^{\delta+}$. Substitution of triphenylphosphine by a carbonyl ligand leads to this polarity—in the limit $CoH(CO)_4$ ionises to H^+ and $[Co(CO)_4]^-$.

Once formed the 2-alkyl complex **15a** is more stable than the monocarbonyl complex **12a**. The different dispositions of the large triphenylphosphine ligands in the four-coordinate alkyl **12a** and the five-coordinate dicarbonyl complex **15a** result in the latter experiencing less interligand repulsion. As a consequence it has a lower tendency to revert to a hydridoalkene complex and an increased possibility of reacting with carbon monoxide to form the branched acyl **19a**.

Obviously in the "dissociative route" where mono-triphenylphosphine complexes are involved there is very little steric destabilization of the intermediate alkyl complex **18a**. At low catalyst concentrations the proportion of branched chain product is increased.[114]

In catalytic hydrogenation the participation of the secondary alkyl complex **12a** was very limited since it tended to decompose before it could undergo the slow oxidative addition of hydrogen. It has been demonstrated that due to the greater rapidity of reaction with carbon monoxide secondary alkyl complexes are sufficiently long lived for hydroformylation to be competitive with alkene elimination. Scheme 9 shows the products of the deuterioformylation of *E*-3-methylpent-2-ene.[118] The secondary alkyl complex undergoes both carbonylation en route to *threo*-2,3-dimethylpentanal and decomposition to 3-methylpent-2-ene or 3-methylhex-1-ene the precursor of 4-methylhexanal. Indeed, even tertiary alkyl complexes are involved in the cycle. Since no 2-ethyl-2-methylbutanal could be detected amongst the products, carbonylation of the tertiary alkyl complex is not competitive with its decomposition to 3-methylpent-2-enes or 2-ethylbutene the precursor of 3-ethylpentanal.

It would seem, therefore, that the participation of tertiary alkyl complexes in hydroformylation rivals that of secondary alkyl complexes in hydrogenations. The ready formation of branched chain aldehydes as minor products implies that complexes such as **12a** take part in the hydroformylation cycle.

Further information can be obtained from the deuteroformylations shown in Scheme 9. It had been

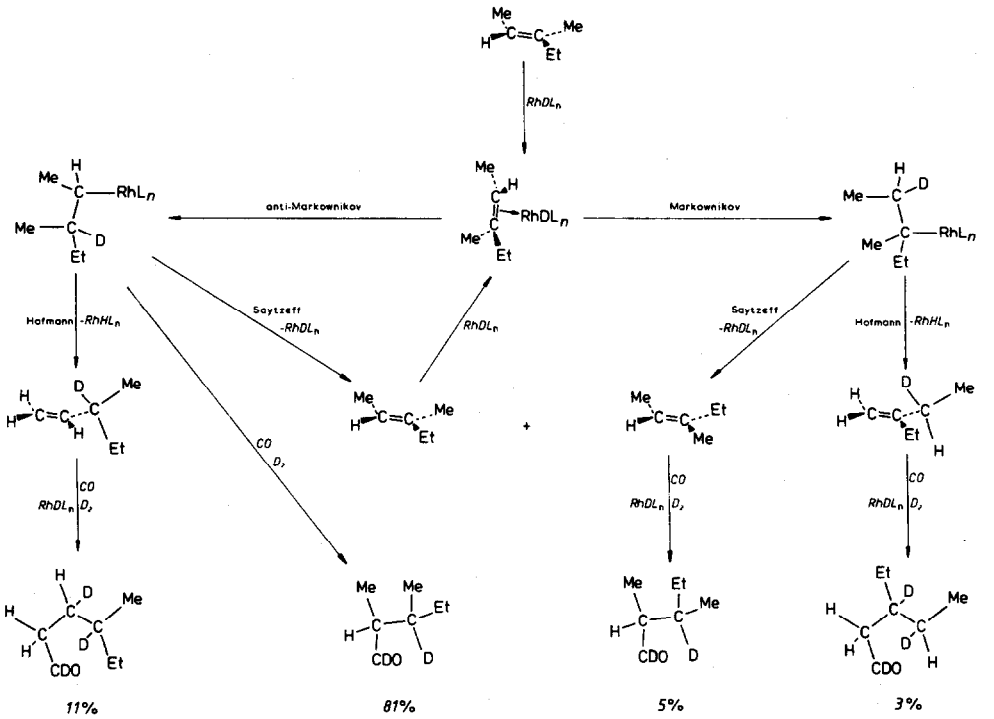

Scheme 9. Deuteroformylation of *E*-3-methylpent-2-ene.

demonstrated earlier that little deuterium scrambling occurred in the reaction.[120] Also, *Z*-3-methylpent-2-ene forms *erythro*-2,3-dimethylpentanal on catalytic hydroformylation.

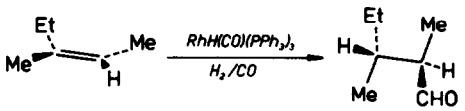

(56)

Thus the overall addition of deuterium and CDO is *cis*. Additionally the single deuterium atom in the alkyl group shows just one catalyst molecule to be involved. It is noteworthy that the deuteroaldehydes resulting from isomerization contained two deuterium atoms in their alkyl groups. The two atoms are present because two catalyst molecules have been involved in their production.[118]

Apart from the steric interactions between the ligands the electronic properties of the alkene are of some importance. Analysis of the reaction mixtures during the hydroformylation of styrene showed that although only small amounts of the inactive dicarbonyl complex **20a** (R = Ph) compared to **20** were present the bulk of the product consisted of 2-phenylpropanal.[114]

To summarize, branched chain aldehyde production arises from the relatively facile formation of secondary alkyl and acyl complexes from alk-1-enes during hydroformylation; the participation of such intermediates permits the hydroformylation of internal alkenes, even though they are hydroformylated much less rapidly than alk-1-enes.[62]

3. *Selectivity in hydroformylation.* Sub-sections 1 and 2 above have shown how both linear and branched chain aldehydes can result from the hydroformylation of alk-1-enes. Linear aldehydes are more desirable commercially than branched aldehydes. Accordingly many modifications have been made to hydroformylation systems, particularly those using propene, with a view to increasing the proportion of the linear product.

High catalyst concentrations minimize the contribution from the unselective "dissociative route". Alternatively this can be achieved by the addition of triphenylphosphine to the system. This additive also inhibits alkane production. It was shown in Section VI that excess triphenylphosphine retards the rate of catalytic hydrogenation of alkenes by $RhH(CO)(PPh_3)_3$. Similarly, addition of triphenylphosphine in high concentrations greatly retards the rate of hydroformylation. This may result from supression of the dissociation of $RhH(CO)(PPh_3)_3$ and thereby inhibiting the formation of the dicarbonyl complex **13**.

The increased selectivity of triphenylphosphine rich systems undoubtedly arises from the reaction proceding via *trans-bis*(triphenylphosphine) species.[117] Similar effects upon the product ratio are observed if other bulky tertiary phosphines are added to the system. Tributylphosphine, triphenyl phosphite, or pyrazine fail to bring about an improvement in the product ratio but still retard the rate of butyraldehyde production from propene,[3] as does diphos.[121]

The much lower rates observed in the presence of excess triphenylphosphine can be offset by increasing the reaction temperature and/or the gas pressure. The proportion of heptanal in the catalytic hydroformylation of hex-1-ene increases with temperature.[114,122,123] Elsewhere, it has been claimed that an increase in temperature had a neutral effect,[124] or even decreased the proportion of linear aldehyde.[3] However increasing the reaction temperature degrades the catalyst since it is pyrolysed to catalytically inactive diphenylphosphido complexes.

The other factor that has a major effect upon the product ratio is the partial pressure of carbon monoxide. Low carbon monoxide partial pressures favour the formation of linear aldehyde. However, hydrogenation and hydroisomerization are also increased.[114] Again increased selectivity comes about because of the lower concentration of the dicarbonyl complex $RhH(CO)_2(PPh_3)_2$. Low total gas pressures also increase the proportion of linear aldehyde. This results from a lower concentration of carbon monoxide in solution and a lower tendency to follow the less selective "associative route".

Hjortkjaer[125] is of the view that changes in carbon monoxide or triphenylphosphine concentrations affect the selectivity by increasing the participation of sterically selective routes rather than decreasing the participation of unselective ones. He concludes that there is a small range of carbon monoxide and triphenylphosphine concentrations that gives maximum aldehyde production rates. Other workers have reported a maximum in the rate of butyraldehyde production at moderate triphenylphosphine concentrations (Fig. 9).[3]

In laboratory systems the best selectivity for linear aldehydes in the reaction can be obtained at low gas pressures, and a 1:1 H_2:CO ratio. Triphenylphosphine should be added to the solution.

4. *Alkene hydrocarbon hydroformylation.* Linear terminal alkenes up to C_{12} have been hydroformylated.[126] Table 2 shows typical rates of hydroformylation under mild conditions. All terminal alkenes, save ethene, form some 2-methylalkanal as a minor product.[127] Propanal is the sole product from ethene hydroformylation.[128] The lean gas from oil cracking contains ethene, hydrogen, and carbon monoxide, and is a convenient feedstock for this reaction.[129]

The hydroformylation of propene is discussed separately in sub-section 6 below. In the hydroformylation of but-1-ene at high temperatures and pressures the catalyst $RhH(CO)(PPh_2CH_2SiMe_3)_3$ produces mainly dimeric products from pentanal condensation.[130] Carbonylhydrido*tris*(triphenylphosphine)rhodium(I), on the other hand, gives a 96.2% selectivity to pentanal.[131]

Under mild conditions the ratio of hydrogen to carbon monoxide in the reactants has a profound effect in the hydroformylation of pent-1-ene to hexanal. The ratio of linear to branched aldehyde increases greatly with an increasing proportion of hydrogen in the reactants.[132]

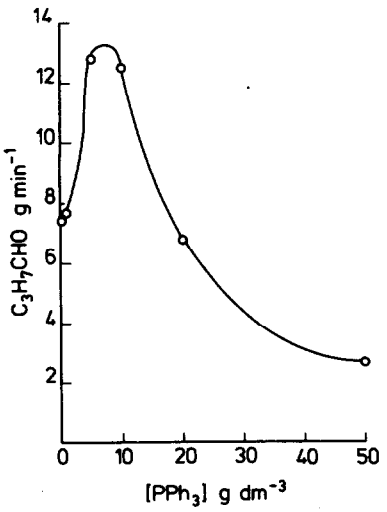

Fig. 9. Effect of added triphenylphosphine upon rate of butyraldehyde production.

Table 2. Alkene hydroformylation rates[62]

Alkene	Gas consumption $cm^3\ min^{-1}$ [a]
Styrene	4.32
Hexa-1,5-diene	4.26
4-Vinylcyclohexene	4.21
Pent-1-ene	3.74
Allyl benzene	3.56
Hex-1-ene	3.52
Hept-1-ene	3.50
Dodec-1-ene	3.18
Cyclooctene	0.26
Pent-2-ene [b]	0.15
cis-Hept-2-ene	0.12
dl-Limonene	0.10
2-Methylpent-1-ene	0.06

[a] Under standard conditions. 2.5 mM $RhH(CO)(PPh_3)_3$, 1.0 M alkene, 1:1 H_2/CO mixture total gas pressure 50 cm Hg, 25°, benzene solution volume 80 cm^3.

[b] Mixture of cis- and trans-isomers.

Several groups have investigated the hydroformylation of hex-1-ene. At high pressures in the presence of triphenylphosphine the isomer ratio (linear:branched) is 4.3:1,[133] but at one atmosphere pressure under similar conditions the ratio is 11.5:1.[114] Using synthesis gas (47% H_2, 52% CO) the activity of $RhH(CO)(PPh_3)_3$ is superior to its triphenylarsine or triphenylstibine analogues. The relative activities of the three catalysts were the same in the hydroformylation of oct-1-ene.[134] At high temperatures the ratio of nonanal to 2-methyloctanal formed from oct-1-ene was found to be 7.3:1 if triphenylphosphine was present.[135] The presence of oxygen in this hydroformylation gives rise to ketonic by-products and also degrades the catalyst.[136]

The hydroformylation of styrene is unusual in that the main product is the branched aldehyde 2-phenylpropanal.

$$PhCH{=}CH_2 + H_2 + CO \xrightarrow{RhH(CO)(PPh_3)_3} PhCH_2CHO + PhCH(CH_3)CH_2CHO \qquad (57)$$

Even upon addition of triphenylphosphine the branched aldehyde is still the major product.[114] There is evidence that the Markownikov addition of styrene predominates, both here and in hydrosilylation.

As shown in Table 2 internal alkenes are catalytically hydroformylated much more slowly than terminal alkenes. Preferential hydroformylation of but-1-ene in a mixture of other butenes results in an enrichment of the gas in the latter components.[137]

As internal alkenes inevitably form branched aldehydes, metal carbonyls or $Pt(PPh_3)_4$ have been used as co-catalysts to promote alkene isomerisation and thereby obtain some linear aldehyde from internal alkenes.[138] Palladium on charcoal is also a co-catalyst.[139]

Cyclohexene can be hydroformylated under mild conditions[114] but apart from cyclooctene[62] no other hydroformylations of cyclic monoalkenes have been attempted.

Alkadienes react in a stepwise fashion. Both mono- and *bis*-hydroformylation products are obtained from bicyclo[2.2.1] hepta-2,5-diene (norbornadiene).[140] Unsymmetric dienes illustrate the regioselectivity

of $RhH(CO)(PPh_3)_3$ catalysed hydroformylations. Thus, 3-methylocta-2,6-diene is hydroformylated only at the disubstituted double bond.[141]

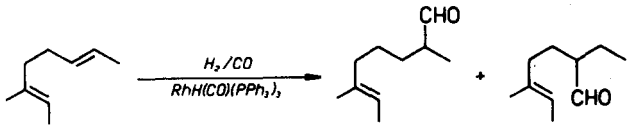

(58)

Only the vinyl group is hydroformylated in vinyldimethylcyclohexene.[142]

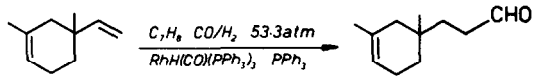

(59)

Hydroformylation of the least hindered double bond in *endo*-tricyclo[5.2.1.$0^{2,6}$]deca-3,8-diene takes place.

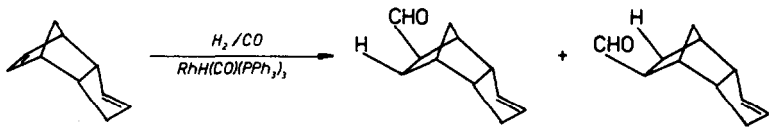

(60)

The products are intermediates in the preparation of the viricide 4-homoisotwistane.[143]

At gas pressures of up to 30 atmospheres a large proportion of the residual double bonds in a high molecular weight polypentenamer can be hydroformylated. Carbonylhydrido*tris*(triphenylphosphine)rhodium(I) can catalyse this reaction at 40°, but the temperatures required if dicobalt octacarbonyl is the catalyst are too high.[144]

The hydroformylation of alkynes is difficult.[2] This is now known to be due to the formation of vinyl complexes with the catalyst.[59-61] No aldehyde is formed unless triphenylphosphine is added to the system. With this addition the hydroformylation of but-2-yne produces both pentenal and 2-methylbutanal.[145]

5. *Hydroformylation of substituted alkenes.* The majority of functional groups are not affected during hydroformylation using $RhH(CO)(PPh_3)_3$ as catalyst, and therefore substituted alkenes can be used as the precursors of substituted aldehydes. The main difficulty encountered in the hydroformylation of substituted alkenes occurs when they react chemically with the catalyst. For example chloroalkenes form *trans*-$RhCl(CO)(PPh_3)_2$ which is inactive in the catalysis under mild conditions.[62,114] Allyl amine also poisons the catalyst, presumably by displacing two triphenylphosphine ligands. Other allyl compounds can be hydroformylated as can be seen in Table 3 which gives rates of substituted alkene hydroformylation under mild conditions.

Table 3. Substituted alkene hydroformylation rates[62]

Substrate	Gas consumption $cm^3\ min^{-1}$ [a]
Allyl alcohol	7.05
Allyl phenyl ether	5.78
2-Allylphenol	4.03
Allyl cyanide	3.72
Vinyl acetate	0.75
Ethyl vinyl ether	0.20

[a] Under standard conditions. 2.5mM $RhH(CO)(PPh_3)_3$, 1.0 M substrate, 1:1 H_2/CO mixture total gas pressure 50 cm Hg, 25°, benzene solution volume 50 cm^3

Allyl alcohol has been shown to form both linear[146–149] and branched[146,147] aldehydes. Another report quotes hydroxytetrahydrofuran as the product.[150] Pittman and Honneck have shown how four products may arise (Scheme 10).[46] Other allylic alcohols such as linalool[151]

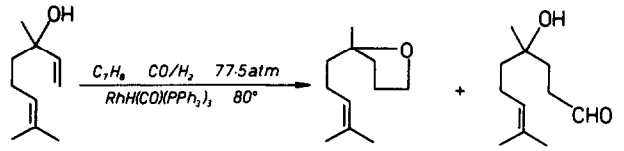

(61)

or nerolidol[152]

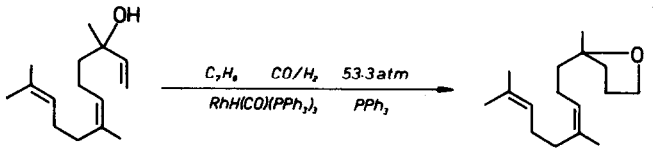

(62)

form substituted tetrahydrofurans upon catalytic hydroformylation.

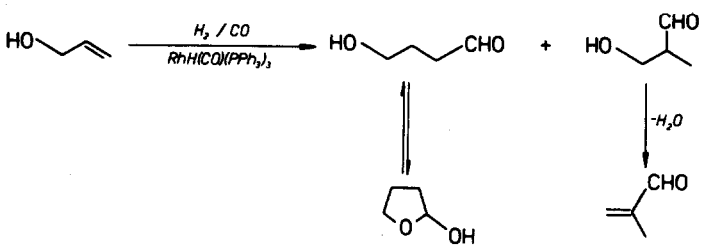

Scheme 10. Hydroformylation of allyl alcohol.

Non-allylic unsaturated alcohols merely undergo hydroformylation. Thus the trimethyloctenol[153]

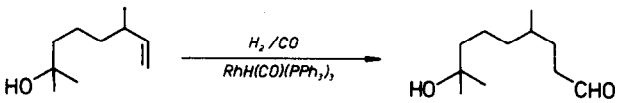

(63)

and the cyclic alcohols[154,155]

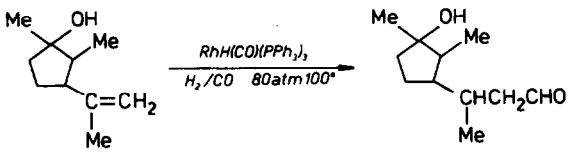

(64)

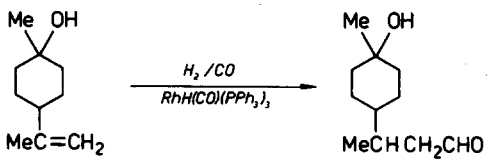

(65)

form terminal aldehydes.

But-2-en-1,4-diol does not undergo cyclization on hydroformylation.[156]

Unsaturated ethers are readily hydroformylated. Allyl *tert*-butyl ether has been shown to form the terminal aldehyde as the main product[157,158] and some branched aldehyde.[159] 2-Methoxy-2,6-dimethyloct-7-ene forms only the linear aldehyde.[160]

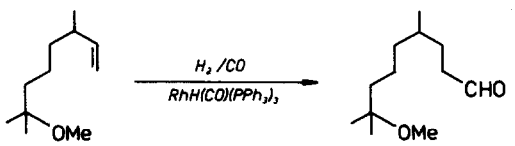

(66)

Vinyl esters on the other hand form mainly the branched aldehyde.[161,162]

$$RCO_2CH{=}CH_2 + CO + H_2 \xrightarrow{RhH(CO)(PPh_3)_3} RCO_2CHCHO \quad (67)$$
$$\qquad\qquad\qquad\qquad\qquad\qquad\qquad\qquad\qquad\qquad\quad |$$
$$\qquad\qquad\qquad\qquad\qquad\qquad\qquad\qquad\qquad\qquad\quad CH_3.$$

Methallyl acetate also preferentially forms the branched aldehyde but addition of triphenylphosphine increases the quantity of terminal aldehyde.[163] But-2-enylene diacetate has also been hydroformylated.[164]

Cyclic acetals of acrolein with various 1,3-diols, **22**, can be hydroformylated using either $RhH(CO)(PPh_3)_3$ or an alkylphosphine derivative as catalyst.[165]

It can be seen from the above hydroformylations that $RhH(CO)(PPh_3)_3$ is a useful hydroformylation catalyst for many alkene hydroformylations. However, the selectivity in many instances is low and limits the preparative applications of the reaction.

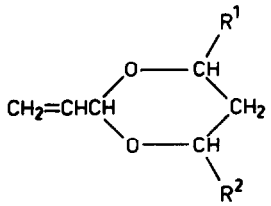

22

6. *High pressure propene hydroformylation.* The commercial hydroformylation of propene uses molten triphenylphosphine as solvent, gas pressures of 14 atmospheres, and temperatures of about 120°.[166] Since excess alkene encourages decomposition of the catalyst the system is saturated with carbon monoxide before admitting propene.[167] A high percentage conversion to butyraldehyde also seems to degrade the catalyst,[168] so the unreacted gases and butyraldehyde are removed from the reactor. The butyraldehyde product is condensed and the gases recycled.[169,170]

About 95% selectivity to butyraldehyde results from the choice of molten triphenylphosphine as solvent. However, the solvent soon becomes contaminated by condensation products of butyraldehyde and the minor product 2-methylpropanal. Some of the possible condensation products are shown in Scheme 11. The actual product mix reflects the 19:1 ratio of isomers and the sterically hindered reactions of 2-methylpropanal.[171] The condensation products do not appear to affect the catalysis adversely.

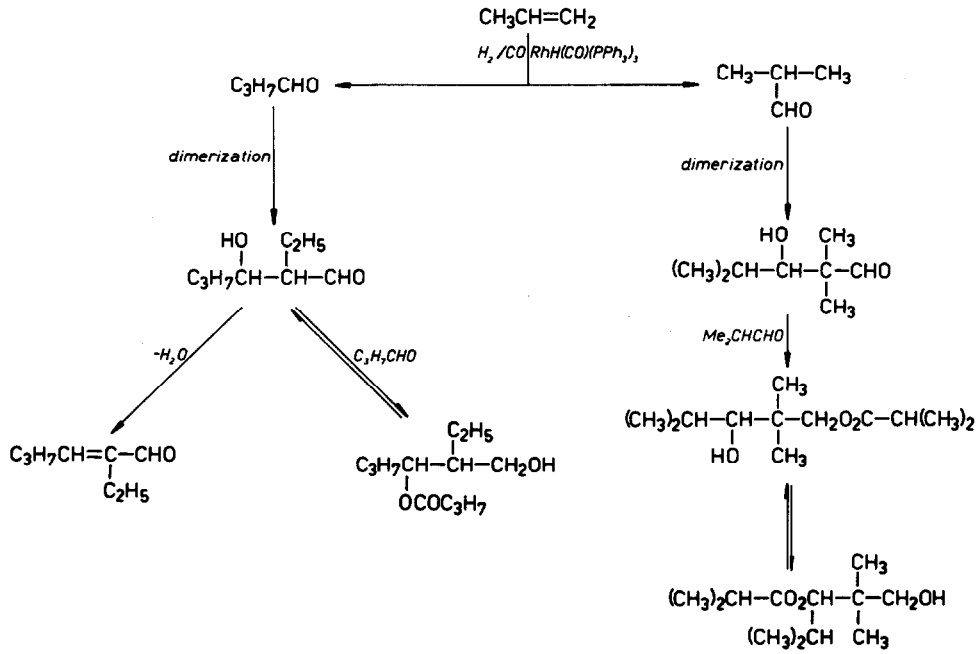

Scheme 11. Formation of aldehyde condensation products.

The catalyst is slowly degraded during the hydroformylation. Investigations on batch processes have revealed that the average yield in the first ten cycles of the catalyst's life is 89%. By the 31st–40th cycles the average yield has decreased to 82%, while in the 61st–70th cycles it has fallen to only 58%.[172,173]

The catalyst can be degraded in many ways. First, it has been shown earlier that its pyrolysis yields inactive diphenylphosphido complexes.[116] Further evidence for diphenylphosphido complex formation comes from the appearance of diphenylpropylphosphine in the hydroformylation of propene.[168] The formation of this tertiary phosphine is not rapid, nor does it have any serious effects on the catalytic reaction.

Fortunately, traces of oxygen in the system do not deactivate the catalyst since any oxygen–rhodium compounds react with the vast excess of triphenylphosphine and form inert triphenylphosphine oxide.[168] Under the more severe conditions encountered in the industrial process low concentrations of allene, buta-1,3-diene, or propyne—which all poison the catalyst under mild conditions—have no effect.[174] More serious is the contamination of feedstocks by chloride, even chloride concentrations as low as 12 ppm greatly reduce the yields of butyraldehyde.[175]

Although it has been stated that small concentrations of hydrogen sulphide in the gaseous feedstock does not poison the catalyst, this compound is probably the most serious poison.[176] Hydrogen sulphide forms rhodium sulphide compounds which besides being catalytically inactive make rhodium recovery from the spent catalyst difficult.[168]

The high price of rhodium makes it essential to recover at least the rhodium metal present after the catalyst has become degraded and unable to satisfy the operational demands of large scale industrial processes. Regeneration of an active catalyst showing high selectivity is difficult. In what is probably the simplest method of separation the spent catalyst, triphenylphosphine, and attendant organic material are dissolved in benzene and absorbed on a magnesium silicate column. The organic material can be stripped off the column by benzene. Finally the catalyst is eluted by tetrahydrofuran.[177]

A further method of regeneration involves distilling off all volatile material and adding a 100-fold excess of triphenylphosphine.[178] Another course is to add aldehyde and blow air or oxygen through the slurry before removing the solid and adding more triphenylphosphine.[179] The addition of dicobalt octacarbonyl or cobalt acetate to the spent catalyst[180] seems an unlikely method of regenerating an active, selective catalyst.

Schemes advanced for rhodium recovery show many gradations between the drastic method of burning the catalyst mixture with excess oxygen in an underwater combustion device[181] and conversion of the catalyst to other rhodium(I) complexes.[182,183] Several methods favour conversion to bromocarbonyl*bis*(triphenylphosphine)rhodium(I). Spent catalyst may be converted to the latter complex by oxidizing the organic matter with peroxides and then treating the inorganic residue with alkali metal bromides and triphenylphosphine, finally heating with carbon monoxide yields the bromo complex.[184] Bromocarbonyl*bis*(triphenylphosphine)rhodium(I) can be obtained similarly from aqueous rhodium solutions derived from the spent catalyst.[185]

Other methods of rhodium recovery involve extraction of rhodium ions from the above aqueous solutions by alkaline potassium cyanide solution,[186] or by ion exchange.[187] Carbon pretreated with nitric acid has also been used to extract the rhodium ions.[188] In other separation procedures rhodium compounds are recovered from organic solvents. Activated charcoal may again be used as an absorbent.[189,190] Alternatively the rhodium compounds may be absorbed by thiol groups incorporated into polystyrene resins.[191] Polyimide membranes are claimed to be impermeable to rhodium compounds and they have been used to retain rhodium from the catalyst.[192]

7. *Heterogenized catalysts.* As in all homogeneous systems, particularly on an industrial scale[193] there is the problem of separating the catalyst from the products. The operating temperatures of the butyraldehyde plants are such that the product is gaseous and can easily be separated from the catalyst solution. Other processes may, however, encounter problems due to heat sensitive or involatile products. If the catalyst and products cannot easily be separated continuous industrial processes are impossible and batch processes which are inconvenient and less economic must be used.

There are two approaches to the problem of catalyst separation. In the first the catalyst is physically absorbed on an inert support. This is known as a supported catalyst. The second method binds an active fragment of the catalyst to an inert polymer by a chemical bond. These catalysts are said to be polymer bound. Both these methods have been adopted to assist the separation of $RhH(CO)(PPh_3)_3$ from hydroformylation media.

The most widely used support for $RhH(CO)(PPh_3)_3$ is silica.[194] Normally the catalyst is dissolved in a

suitable solvent and applied to the support. Only the catalyst molecules at the phase boundary are catalytically active[195] and the results obtained are very dependent upon the type of support and the degree of pore filling.[196] The solvents used have included ethanol, ethylene glycol, polyethylene glycol, glycerol, pinacol, benzene, toluene, or xylenes.[193] Other workers have dissovled $RhH(CO)(PPh_3)_3$ in tertiary phosphines before applying it to the support. It has been claimed that this method gives good catalyst stability and selectivity.[196–198] The selectivity is achieved by coordinative saturation of the complex by the excess tertiary phosphine[195] which also inhibits the competing hydrogenation reaction.[199]

Other supports used include α, β,[193] or γ-alumina[58,200–202] alumina–silica,[201] aluminosilicates and granulated carbon.[193] There is even one report that a catalyst can be prepared by physically incorporating $RhH(CO)(PPh_3)_3$ into the pores of a non-substituted polystyrene resin.[105]

The most usual way of binding $RhH(CO)(PPh_3)_n$ fragments to polystyrene resins is to incorporate a tertiary phosphine ligand group into the resin. The preparation of these catalysts has been described in Section IV.A above.

The selectivity of the bound catalysts towards linear aldehyde production is commonly slightly less than that of the free catalyst.[38,40] There is, however, one claim that a highly phosphinated resin with a low ratio of rhodium: diphenylphosphine groups gives improved selectivity in the hydroformylation of pent-1-ene to hexanal.[42] The low selectivity in linear aldehyde production is offset by the bound catalysts' greater activity towards internal and polysubstituted alkenes.[38]

The tertiary phosphine catalysts prepared from previously chloromethylated polymers are inferior to those prepared from polymers which have been metallated unless the residual chlorine in the former has been carefully removed.[39] Presumably the chlorine they contain reacts with $RhH(CO)(PPh_3)_3$ to form polymer bound versions of $RhCl(CO)(PPh_3)_2$. It has been shown that the latter complex is at best only weakly active at low pressures.[117]

The resin bound catalysts exhibit good thermal stability.[39,42] It has been found that those containing tertiary phosphine groups were deactivated less rapidly at high temperatures than those catalysts containing phosphonite groups. This was ascribed to the greater stability of the five membered rings formed in the *o*-metallation reactions of the latter **23**. The former type yield four membered rings **24** in this reaction.[39]

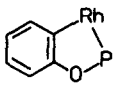

23

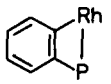

24

C. *Chiral hydroformylation*

It has been demonstrated that the addition of 1,2-*bis*(diphenylphosphino)ethane to solutions of $RhH(CO)(PPh_3)_3$ results in a more active but less selective catalytic system.[38] Since many chiral ligands are di-tertiary phosphines it is possible to devise catalytic systems that can bring about chiral hydroformylation. Obviously $RhH(CO)(PPh_3)_3$ is not the true catalyst in these systems. It is probable that species of the type RhH(CO)(L–L*) are involved.

The lower selectivity suggests that hydroformylation takes place by the "associative route" and that the acyl complex formed has *cis*-tertiary phosphine groups **25**. The lower selectivity both towards

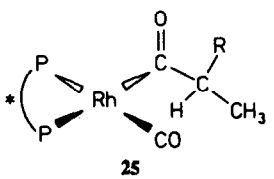

25

substrates and towards linear aldehyde production is important since the straight chain aldehydes prepared from achiral alk-1-enes cannot themselves be chiral.

$$RCH{=}CH_2 + H_2 + CO \rightarrow RCH_2CH_2CHO + RC^*H{-}CH_3 \quad (68)$$

$$\qquad\qquad\qquad\qquad\qquad\qquad\qquad\qquad\qquad\qquad\qquad\qquad\quad |$$

$$\qquad\qquad\qquad\qquad\qquad\qquad\qquad\qquad\qquad\qquad\qquad\qquad\quad CHO.$$

Both products from suitable internal alkenes are chiral

$$RCH{=}CHR' + H_2 + CO \rightarrow \underset{\underset{CHO}{|}}{RC^*H{-}CH_2R'} + \underset{\underset{CHO.}{|}}{RCH_2{-}C^*HR'} \qquad (69)$$

Many chiral ligands have been found to be effective. The most widely used has been (−)-DIOP, **26**, others have included *trans*-1,2-*bis*(diphenylphosphinomethyl)cyclobutane, 1,1′-*bis*(diphenylphosphino)-ferrocene,[203] (+)- or (−)-DIPHOL **27**,[204] (−)-2,2-dimethyl-4,5-*bis*(diphenylphosphinomethyl)-1,3-dioxolane **28**,[205] and 1,2,2-trimethyl(1*R*, 3*S*)-1,3-*bis*(diphenylphosphinomethyl)-cyclopentane **29**,[206]

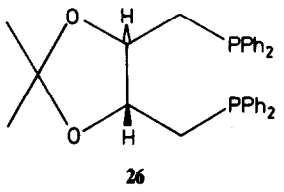

26

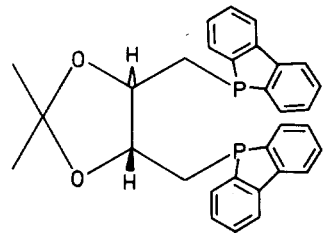

27

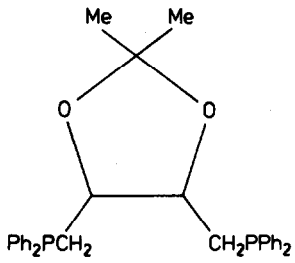

28

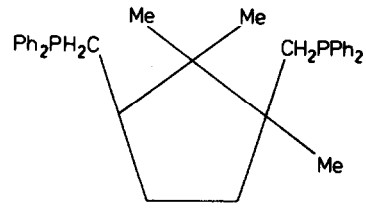

29

In sub-section B above it was seen that styrene was one of the few terminal alkenes to form significant quantities of branched aldehyde upon hydroformylation. Accordingly, its chiral hydroformylation has received considerable attention. Optical yields of 2-phenylpropanal as high as 25% have been obtained.[207] Using (−)-DIOP it was found that the prevailing chirality of the 2-phenylpropanal was *R*. The hydroformylation of α-deuterostyrene in the presence of (−)-DIOP yields *S*-2-phenyl-2-deutero-propanal but *R*-3-phenyl-2-deuteropropanal [208]

$$PhCD{=}CH_2 + H_2 + CO \xrightarrow[RhH(CO)(PPh_3)_3]{\text{(−)-DIOP}} \underset{\underset{CH_3.}{|}}{PhCD{-}CHO} + PhCHDCH_2CHO. \qquad (70)$$

The products are believed to arise from preferential attack upon one face of styrene.

The formation of two aldehydes of differing chirality according to the location of the aldehyde group has also been noted in the reactions of alk-2-enes

$$RCH{=}CHMe + H_2 + CO \xrightarrow[RhH(CO)(PPh_3)_3]{\text{(−)-DIOP}} \qquad (71)$$

$$(S)\text{-}\underset{\underset{Me}{|}}{RCH_2{-}CHCHO} + (R)\text{-}\underset{\underset{CHO.}{|}}{RCH{-}CH_2Me}$$

(R = Me, C_3H_7)[13]

Low overall and optical yields of 2-methylalkanals have been obtained from C_4 to C_8 alk-1-enes.[13]

Poor optical yields have also been obtained from α-alkylstyrenes, but the optical yields from allylbenzene or *trans*-β-methylstyrene are about 15%.[207]

Although 4-phenylpentanal forms the bulk of the product from the catalytic hydroformylation of

3-phenylbut-1-ene in the presence of (−)-DIOP, careful examination of the small quantity of 2-methyl-3-phenyl-butanal shows there to be twice as much *erythro* as *threo* isomer present.[209]

Internal alkenes used as substrates in chiral hydroformylation have included *cis*-but-2-ene,[13,210,211] hex-2-ene,[13] norbornene,[211] and bicyclo[2.2.2]oct-2-ene.[210]

But-1-en-3-ol represents one of the few substituted alkenes to have been chirally hydroformylated. As in normal hydroformylation of allyl alcohol cyclization occurs. The product is 2-hydroxy-5-methyltetrahydrofuran.[212] The other substituted alkenes are usually nitrogenous compounds.

Hydroformylation of *N*-vinylsuccinimide always gave the (*R*)-aldehyde no matter which hand of the DIOP was added. Addition of (+)-DIPHOL did form the (*S*)-isomer.

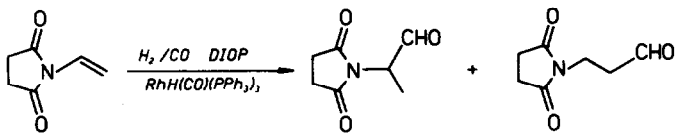

(72)

Using the latter additive *N*-vinylphthalimide could also be hydroformylated.

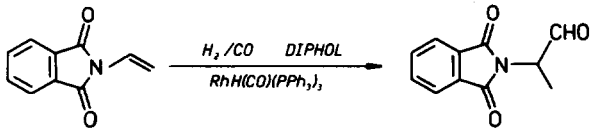

(73)

Although *N*-acyl-2,3-dihydropyrroles are rapidly hydroformylated

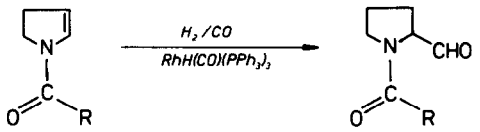

(74)

N-prop-2-enylacetamide reacted slowly

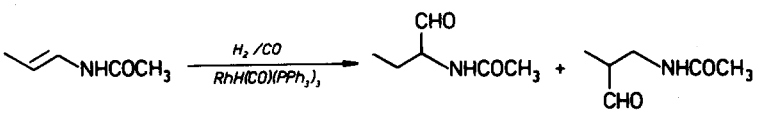

(75)

and *N*-2-methylpropenylacetamide did not react.[204]

The chiral hydroformylation of 2,5-dihydrofuran under mild conditions is not very successful. Under harsh conditions 98% conversion has been achieved.

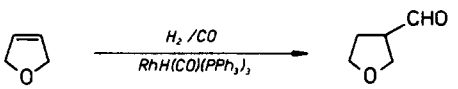

(76)

Unfortunately the harsh conditions greatly decrease the optical yields.[210] It is a general rule that harsh conditions reduce optical yields.

Alkynes can also be chirally hydroformylated in the presence of (−)-DIOP. But-2-yne forms some *E*-2-methylbut-2-enal

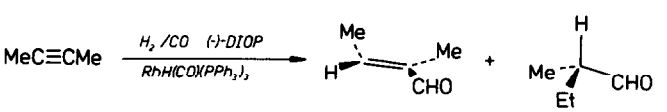

(77)

but no alkenal intermediates could be detected in the chiral hydroformylations of oct-1-yne or phenylacetylene. Not surprisingly the optical yield of (*S*)-2-methylbutanal was lower than that obtained from but-2-ene.[213]

It has also proved possible to bind fragments of the chiral ligands into polystyrene polymers. These polymers have been allowed to react with $RhH(CO)(PPh_3)_3$ to form polymer bound chiral catalysts.

Dibenzophosphole groups bound to the polymer greatly favour the formation of 2-phenylpropanal from styrene, but the optical yields are lower than when DIOP is added to the homogeneous catalyst.[45]

In all it would seem that chiral hydroformylation is a promising preparative method. The aldehydes so formed can be oxidized to carboxylic acids or reduced to alcohols by methods of known chirality.

VIII. CATALYTIC HYDROSILYLATION

Carbonylhydrido*tris*(triphenylphosphine)rhodium(I) is a disappointing hydrosilylation catalyst. Further, only alkenes and alkynes have been used as substrates. Surprisingly, in view of the utility of chiral hydroformylation, there have been no attempts to investigate chiral hydrosilylation which has proved a popular field with other transition metal complex catalysts.[4]

The performance of $RhH(CO)(PPh_3)_3$ in catalytic hydrosilylations is poor both in respect of regioselectivity and overall yields. Moreover the yields tend to decrease with increasing severity of the reaction conditions.[214,215]

A possible mechanism which accounts for the lack of regioselectivity is shown in Scheme 12. Unlike hydroformylations catalysed by $RhCl(PPh_3)_3$,[4] no intermediates have been isolated. An oxidative addition of one molecule of hydrosilane giving the catalytically inactive species $RhH_2(SiX_3)(CO)(PPh_3)_2$ may account for the low activity of the catalyst. As will be seen below alkynes are much more readily hydrosilylated than alkenes. Vinyl complexes (eqn 17) may be formed in preference to the dihydridorhodium complex. The vinyl complexes would then undergo oxidative addition of hydrosilane.

Vinyl cyanide can be catalytically hydrosilylated in the presence of $RhH(CO)(PPh_3)_3$. Normally,

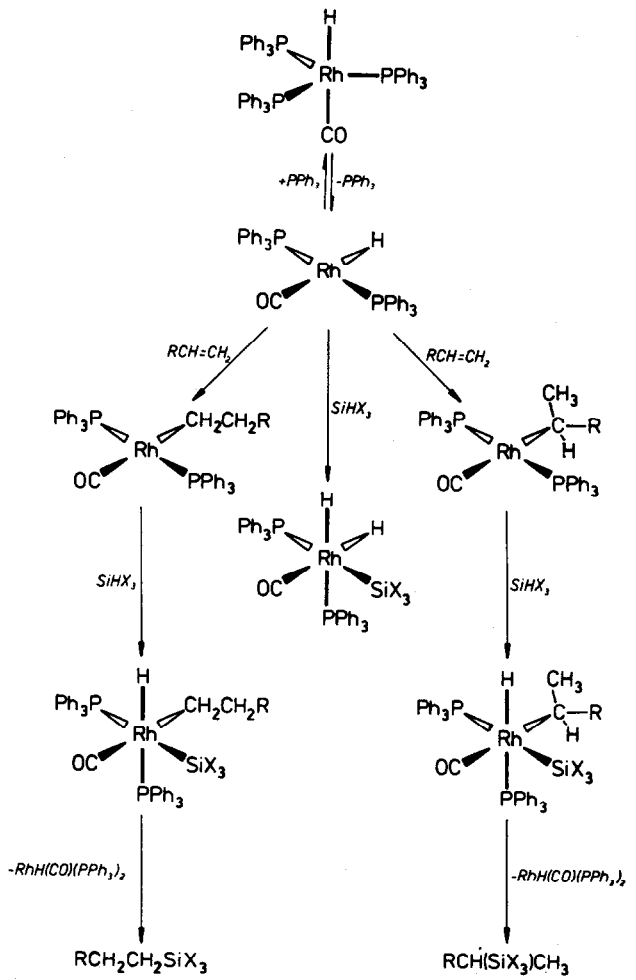

Scheme 12. Mechanism of catalytic hydrosilylation.

hydrosilylation of the conjugated cyanoalkene is difficult. The product is usually $(SiX_3)CH_2CH_2CN$. Catalysis by $RhH(CO)(PPh_3)_3$ forms the β-isomer[216]

$$CH_2{=}CHCN + HSiX_3 \xrightarrow{RhH(CO)(PPh_3)_3} CH_3{-}\underset{\displaystyle SiX_3}{\underset{|}{C}}HCN \qquad (78)$$

($X_3 = ClMe_2$, $PhMe_2$).

Similarly the conjugated alkadiene buta-1,3-diene gives yields in $RhH(CO)(PPh_3)_3$ catalysed hydrosilylations at least as good as in reactions using other transition metal complex catalysts.[217]

Alkynes are readily hydrosilylated. The products can include both *cis*- and *trans*-silylalkenes.[218,219] A

$$PhC{\equiv}CH \xrightarrow[RhH(CO)(PPh_3)_3]{SiHX_3} \underset{H}{\overset{Ph}{\diagdown}}\!\!=\!\!\underset{H}{\overset{SiX_3}{\diagup}} + \underset{H}{\overset{Ph}{\diagdown}}\!\!=\!\!\underset{SiX_3}{\overset{H}{\diagup}} \qquad (79)$$

small proportion of the product is formed by $PhC(SiX_3){=}CH_2$, the result of α-addition. The yield of this by-product is less than when $RhCl(PPh_3)_3$ or $H_2[PtCl_6]$ is the catalyst.[219]

The reactivity of ethyne is so high that a disilyl compound can be formed.[220]

$$HC{\equiv}CH + Et_3SiH \xrightarrow{RhH(CO)(PPh_3)_3} Et_3SiCH{=}CH_2 + Et_3SiCH_2CH_2SiEt_3. \qquad (80)$$

It would seem that alkyne silylations are the only area where $RhH(CO)(PPh_3)_3$ can compete with other well established hydrosilylation catalysts.

IX. MISCELLANEOUS CATALYSES

It has been claimed that $RhH(CO)(PPh_3)_3$ catalyses the carbonylation of butylamine at high temperatures and pressures. Monobutyl- and dibutylformamide are obtained in approximately equal quantities.[221]

$$BuNH_2 + CO \xrightarrow[C_6H_6,\ 70\ atm.,\ 150^\circ]{RhH(CO)(PPh_3)_3} (BuNH)_2CO + HCONHBu. \qquad (81)$$

Under very similar conditions ethene forms pentan-3-one [222]

$$C_2H_4 + CO \xrightarrow[MeOH/H_2O,\ 72\ atm.\ 170^\circ]{RhH(CO)(PPh_3)_3} C_2H_5COC_2H_5. \qquad (82)$$

A less practical method of preparing ketones is by reacting an acyl chloride and ethene in the presence of $RhH(CO)(PPh_3)_3$. The products from the stoicheiometric reaction are ketone and $RhCl(CO)(PPh_3)_2$. No clear indication was given as to how the chlororhodium complex was to be reconverted to the hydrido complex in the catalysis.[223]

In a complex reaction aromatic nitro compounds can be converted into the corresponding isocyanate. In the presence of $MoCl_5$ as co-catalyst yields of 4.2% have been reported. The reaction is believed to proceed via reduction to an aryl nitrene

$$ArNO_2 + 2CO \rightarrow ArN + 2CO_2 \qquad (83)$$

which is then carbonylated to the isocyanate [224]

$$ArN + CO \rightarrow ArNCO. \qquad (84)$$

The exact catalytic function of $RhH(CO)(PPh_3)_3$ in this reaction is not clear.

Hydroformylation of formaldehyde would form glycolaldehyde. This reaction is commercially attrac-

tive since the glycolaldehyde could be reduced to ethylene glycol. Catalysis by $RhH(CO)(PPh_3)_3$ gives disappointing yields of glycolaldehyde.[225] Methanol is the main product.[226]

Addition of carbon monoxide to methanol followed by hydrogen reduction could produce ethanol

$$CH_3OH + CO + 2H_2 \rightarrow CH_3CH_2OH + H_2O. \quad (85)$$

Unfortunately the main products when the reaction is catalysed by $RhH(CO)(PPh_3)_3$ are methyl acetate and acetic acid.[227] As methyl iodide is used as a promoter the similarity to the acetic acid synthesis is obvious.

Tertiary amines can be produced by allowing a secondary amine, carbon monoxide, and hydrogen to react in the presence of the catalyst.[228]

Very poor yields of diacetylenes are obtained in the attempted dimerization of pent-1-yne using $RhH(CO)(PPh_3)_3$ as catalyst at 100° in chloroform solution. The stoicheiometric reaction of $RhH(CO)(PPh_3)_3$ and excess alkyne was mentioned in Section IV.B. It would appear that elimination of dialkyne from the complex is quite difficult.[229]

In carbon tetrachloride solution $RhH(CO)(PPh_3)_3$ allows the polymerization of methyl methacrylate to proceed.[230,231] Free radical scavengers inhibit the polymerization.[230]

X. CONCLUSION

The preceding Sections have shown that while $RhH(CO)(PPh_3)_3$ is supreme as a hydroformylation catalyst it is a disappointing catalyst in many other reactions. Chloro*tris*(triphenylphosphine)rhodium(I) is probably a more generally useful hydrogenation catalyst, and dichloro*tris*(triphenylphosphine)ruthenium(II) is probably a more effective isotope exchange catalyst. The last complex is certainly a better hydrogen transfer catalyst.

Future advances in catalysis by $RhH(CO)(PPh_3)_3$ would appear to lie with a better understanding of the neglected coordination chemistry of the complex.

REFERENCES

[1]S. S. Bath and L. Vaska, *J. Am. Chem. Soc.* 1963, **85**, 3500.
[2]F. H. Jardine, J. A. Osborn, G. Wilkinson and J. F. Young, *Chem. and Ind. (London)* 1965, 560.
[3]K. L. Oliver and F. B. Booth, *Prepr. Am. Chem. Soc. Div. Petrol. Chem.* 1969, **14**, A7.
[4]F. H. Jardine, *Prog. Inorg. Chem.* 1981, **28**, 63.
[5]N. Ahmad, S. D. Robinson and M. F. Uttley, *J. Chem. Soc. (Dalton)* 1972, 843.
[6]N. Ahmad, J. J. Levison, S. D. Robinson and M. F. Uttley, *Inorg. Synth.* 1974, **15**, 45.
[7]J. J. Levison and S. D. Robinson, *J. Chem. Soc. (A)* 1970, 2947.
[8]L. Bretherick, *Hazards in the Chemical Laboratory*, 3rd. Edn, p. 339. Royal Society of Chemistry, London (1981).
[9]Toyo Soda Manufacturing Co. Ltd., *Jap. Pat.* 1980, 80 94,390; through *Chem. Abstr.* 1981, **94**, 5532.
[10]F. B. Booth, D. M. Fenton and K. L. Oliver, *U.S. Pat.* 1972, 3,644,446; through *Chem. Abstr.* 1972, **76**, 99822.
[11]G. Gregorio, G. Pregaglia and R. Ugo, *Inorg. Chim. Acta* 1969, **3**, 89.
[12]K. C. Dewhirst, W. Keim and C. A. Reilly, *Inorg. Chem.* 1968, **7**, 546.
[13]P. Pino, G. Consiglio, C. Botteghi and C. Salomon, *Adv. Chem. Ser.* 1974, **132**, 295.
[14]K. K. Pandey and U. C. Agarwala, *Ind. J. Chem.* 1980, **19A**, 805.
[15]W. Beck and K. von Werner, *Chem. Ber.* 1973, **106**, 868.
[16]P. Legzdins, R. W. Mitchell, G. L. Rempel, J. D. Ruddick and G. Wilkinson, *J. Chem. Soc. (A)* 1970, 3322.
[17]L. Vaska, *J. Amer. Chem. Soc.* 1966, **88**, 4100.
[18]S. J. LaPlaca and J. A. Ibers, *J. Am. Chem. Soc.* 1963, **85**, 3501.
[19]S. J. LaPlaca and J. A. Ibers, *Acta Cryst.* 1965, **18**, 511.
[20]N. Kasai, *Kagaku (Kyoto)* 1969, **24**, 45; through *Chem. Abstr.* 1969, **70**, 100647.
[21]S. H. Strauss, S. E. Diamond, F. Mares and D. F. Shriver, *Inorg. Chem.* 1978, **17**, 3064.
[22]G. J. Kubas and R. R. Ryan, *Cryst. Struct. Commun.* 1977, **6**, 295.
[23]T. Napier, D. W. Meek, R. M. Kirchnev, and J. A. Ibers, *J. Am. Chem. Soc.* 1973, **95**, 4194.
[24]C. Nave and M. R. Truter, *Chem. Commun.* 1971, 1253.
[25]Y. W. Yared, S. L. Miles, R. Bau and C. A. Reed, *J. Am. Chem. Soc.* 1977, **99**, 7076.
[26]M. J. Bennett and P. B. Donaldson, *Inorg. Chem.* 1977, **16**, 658.
[27]J. L. de Boer, D. Rogers, A. C. Skapski and P. G. H. Troughton, *Chem. Commun.* 1966, 756.
[28]P. B. Hitchcock, M. McPartlin and R. Mason, *Chem. Commun.* 1969, 1367.
[29]S. F. Watkins, J. Obi and L. F. Dahl, quoted in Ref. 27.
[30]G. Braca, G. Sbrana, G. Valentini, A. Colligiani and C. Pinzino, *J. Mol. Catal.* 1980, **7**, 457.
[31]D. Evans, G. Yagupsky and G. Wilkinson, *J. Chem. Soc. (A)* 1968, 2660.
[32]P. S. Hallman, D. Evans, J. A. Osborn and G. Wilkinson, *Chem. Commun.* 1967, 305.
[33]E. M. Hyde, J. R. Swain, J. G. Verkade and P. Meakin, *J. Chem. Soc. (Dalton)* 1976, 1169.
[34]J. J. Levison and S. D. Robinson, *Inorg. Synth.* 1972, **13**, 105.
[35]K. Kurtev, D. Ribola, R. A. Jones, D. J. Cole-Hamilton and G. Wilkinson, *J. Chem. Soc. (Dalton)* 1980, 55.
[36]A. A. Oswald, *PCT Int. Appl.* 80 01692, 1980; through *Chem. Abstr.* 1981, **94**, 157091.

[37]A. F. Borowski, D. J. Cole-Hamilton and G. Wilkinson, *Nouv. J. Chim.* 1978, **2**, 137.
[38]C. U. Pittman and A. Hirao, *J. Org. Chem.* 1978, **43**, 640.
[39]N. A. De Munck, M. W. Verbruggen, J. E. De Leur and J. J. F. Scholten, *J. Mol. Catal.* 1981, **11**, 331.
[40]E. Bayer and V. Schurig, *Angew. Chem. Int.* 1975, **14**, 493.
[41]C. U. Pittman, L. R. Smith and R. M. Hanes, *J. Am. Chem. Soc.* 1975, **97**, 1749.
[42]C. U. Pittman and R. M. Hanes, *J. Am. Chem. Soc.* 1976, **98**, 5402.
[43]N. De Munck, M. W. Verbruggen and J. J. F. Scholten, *J. Mol. Catal.* 1981, **10**, 313.
[44]A. R. Sanger and L. R. Schallig, *J. Mol. Catal.* 1977, **3**, 101.
[45]S. J. Fritschel, J. J. H. Ackerman, T. Keyser and J. K. Stille, *J. Org. Chem.* 1979, **44**, 3152.
[46]C. U. Pittman and W. D. Honnick, *J. Org. Chem.* 1980, **45**, 2132.
[47]Z. M. Michalska, *J. Mol. Catal.* 1977, **3**, 125.
[48]I. J. Harvie and F. J. McQuillin, *Chem. Commun.* 1977, 241.
[49]K. R. Laing, S. D. Robinson and M. F. Uttley, *J. Chem. Soc. (Dalton)* 1974, 1205.
[50]C. K. Brown, D. Georgiou and G. Wilkinson, *J. Chem. Soc. (Dalton)* 1973, 929.
[51]A. Dobson, S. D. Robinson and M. F. Uttley, *J. Chem. Soc. (Dalton)* 1975, 370.
[52]D. C. Andrews, A. Dobson, S. D. Robinson and M. F. Uttley, *Proc. 16th. Int. Conf. Coord. Chem.* 1974, 4.10.
[53]S. D. Robinson and M. F. Uttley, *J. Chem. Soc. (Dalton)* 1973, 1912.
[54]G. Valentini, G. Sbrana and G. Braca, *J. Mol. Catal.* 1981, **11**, 383.
[55]A. R. Siedle, *Inorg. Chem.* 1981, **20**, 1318.
[56]G. Yagupsky, C. K. Brown and G. Wilkinson, *Chem. Commun.* 1969, 1244.
[57]G. Yagupsky, C. K. Brown and G. Wilkinson, *J. Chem. Soc. (A)* 1970, 1392.
[58]T. G. Spek and J. J. F. Scholten, *J. Mol. Catal.* 1977, **3**, 81.
[59]B. L. Booth and A. D. Lloyd, *J. Organometal. Chem.* 1972, **35**, 195.
[60]J. Schwartz, D. W. Hart and J. L. Holden, *J. Am. Chem. Soc.* 1972, **94**, 9269.
[61]R. A. Sanchez-Delgado and G. Wilkinson, *J. Chem. Soc. (Dalton)* 1977, 804.
[62]C. K. Brown and G. Wilkinson, *Tetrahedron Lett.* 1969, 1725.
[63]P. Royo and F. Terreros, *An. Univ. Murcia, Cienc.* 1977, **30**, 139.
[64]C. Dudley and G. Read, *Tetrahedron Lett.* 1972, 5273.
[65]C. W. Dudley, G. Read and P. J. C. Walker, *J. Chem. Soc. (Dalton)* 1974, 1926.
[66]A. W. Gal, H. P. M. M. Ambrosius, A. F. M. J. van der Ploeg and W. P. Bosman, *J. Organometal. Chem.* 1978, **149**, 81.
[67]K. K. Pandey, K. C. Jain and U. C. Agarwala, *Inorg. Chim. Acta* 1981, **48**, 23.
[68]K. K. Pandey, S. Datta and U. Agarwala, *Trans. Met. Chem.* 1979, **4**, 337.
[69]K. K. Pandey and U. C. Agarwala, *Z. Anorg. Allg. Chem.* 1979, **457**, 235.
[70]C. B. Ungermann and K. G. Caulton, *J. Am. Chem. Soc.* 1976, **98**, 3862.
[71]P. B. Critchlow and S. D. Robinson, *Inorg. Chem.* 1978, **17**, 1896.
[72]S. Valcher, G. Pilloni, and M. Martelli, *J. Electroanal. Chem. Interfacial Electrochem.* 1973, **42**, App. 5.
[73]G. Pilloni, G. Schiavon, G. Zotti and S. Zecchin, *J. Organometal. Chem.* 1977, **134**, 305.
[74]E. Billig, J. D. Jamerson and R. L. Pruett, *J. Organometal. Chem.* 1980, **192**, C49.
[75]S. Siegel, *J. Catal.* 1973, **30**, 139.
[76]S. Siegel, J. Outlaw and N. Garti, *J. Catal.* 1978, **52**, 102.
[77]M. Yagupsky and G. Wilkinson, *J. Chem. Soc. (A)* 1970, 941.
[78]B. Hudson, D. E. Webster and P. B. Wells, *J. Chem. Soc. (Dalton)* 1972, 1204.
[79]R. A. Schunn, *Inorg. Chem.* 1970, **9**, 2567.
[80]W. Strohmeier, R. Fleischmann and W. Rehder-Stirnweiss, *J. Organometal. Chem.* 1973, **47**, C37.
[81]W. Strohmeier and W. Rehder-Stirnweiss, *J. Organometal. Chem.* 1970, **22**, C27.
[82]F. J. McQuillin and D. G. Parker, *J. Chem. Soc. (Perkin I)* 1975, 2092.
[83]J. K. Stille and Y. Becker, *J. Org. Chem.* 1980, **45**, 2139.
[84]W. Strohmeier, *J. Organometal. Chem.* 1973, **60**, C60.
[85]J. Blum and Y. Pickholtz, *Isr. J. Chem.* 1969, **7**, 723.
[86]P. Goldborn and F. Scheinmann, *J. Chem. Soc. (Perkin I)* 1973, 2870.
[87]W. Strohmeier and L. Weigelt, *J. Organometal. Chem.* 1975, **86**, C17.
[88]C. Botteghi and G. Giacomeli, *Gazz. Chim. Ital.* 1976, **106**, 1131.
[89]W. Strohmeier and E. Eder, *Z. Naturforsch. B*, 1974, **29**, 280.
[90]J. E. Lyons, *5th Conf. Catal. Org. Synth.* (Edited by P. N. Rylander and H. Greenfield), pp. 235–53. Academic Press, New York (1976).
[91]J. E. Lyons, *U.S. Pat.* 1978, 4,123,445; through *Chem. Abstr.* 1979, **90**, 168426.
[92]C. O'Connor and G. Wilkinson, *J. Chem. Soc. (A)* 1968, 2665.
[93]W. Strohmeier and S. Hohmann, *Z. Naturforsch. B* 1970, **25**, 1309.
[94]T. Ueda, *Proc. 5th. Int. Cong. Catal.* 1973, **1**, 431.
[95]E. Hirota, M. Ito and T. Ueda, *Proc. 6th. Int. Cong. Catal.* 1977, **1**, 518.
[96]S. Siegel and D. W. Ohrt, *Tetrahedron Lett.* 1972, 5155.
[97]W. Strohmeier, W. Rehder-Stirnweiss and R. Fleischmann, *Z. Naturforsch. B* 1970, **25**, 1481.
[98]W. Strohmeier and W. Endres, *Z. Naturforsch. B* 1972, **27**, 1415.
[99]L. Vaska, *Inorg. Nucl. Chem. Lett.* 1965, **1**, 89.
[100]J. Hjortkjaer and Z. Kulicki, *J. Catal.* 1972, **27**, 452.
[101]W. Strohmeier and W. Rehder-Stirnweiss, *Z. Naturforsch. B* 1971, **26**, 193.
[102]W. Strohmeier and G. Csontos, *J. Organometal. Chem.* 1974, **67**, C27.
[103]V. S. Shagov, A. I. Yakubchik, A. M. Sagulenko and L. Y. Lanina, *Vysokomol. Soedin. Ser. A* 1973, **15**, 10.
[104]J. W. Kang, *U.S. Pat.* 1976, 3,993,855; through *Chem. Abstr.* 1977, **86**, 56558.
[105]L. A. Gerritsen and J. J. F. Scholten, *Dutch Pat.* 1980, 79 02,964; through *Chem. Abstr.* 1981, **94**, 163360.
[106]M. E. Vol'pin, V. P. Kukolev, V. O. Chernyshev and I. S. Kolomnikov, *Tetrahedron Lett.* 1971, 4435.
[107]F. A. Lowenheim and M. K. Moran, *Faith, Key's, and Clark's Industrial Chemicals*, 4th Edn, p. 413. Wiley, New York (1975).
[108]R. L. Pruett and J. A. Smith, *J. Org. Chem.* 1969, **34**, 327.
[109]R. F. Heck, *Adv. Organometal. Chem.* 1968, **6**, 119.

[110]J. C. Chaston, *Platinum Metals Rev.* 1982, **26**, 3.
[111]R. W. Goetz and M. Orchin, *J. Org. Chem.* 1962, **27**, 3698.
[112]S. F. Hossain, K. M. Nicholas, C. L. Teas and R. E. Davis, *Chem. Commun.* 1981, 268.
[113]M. Yagupsky, C. K. Brown, G. Yagupsky and G. Wilkinson, *J. Chem. Soc.* (*A*) 1970, 937.
[114]C. K. Brown and G. Wilkinson, *J. Chem. Soc.* (*A*) 1970, 2753.
[115]D. E. Morris and H. B. Tinker, *Chem. Technol.* 1972, **2**, 554.
[116]J. D. Jamerson, R. L. Pruett, E. Billig and F. A. Fiato, *J. Organometal. Chem.* 1980, **193**, C43.
[117]D. Evans, J. A. Osborn and G. Wilkinson, *J. Chem. Soc.* (*A*) 1968, 3133.
[118]A. Stefani, G. Consiglio, C. Botteghi and P. Pino, *J. Am. Chem. Soc.* 1977, **99**, 1058.
[119]C. U. Pittman and C. C. Lin, *J. Org. Chem.* 1978, **43**, 4928.
[120]A. Stefani, G. Consiglio, C. Botteghi and P. Pino, *J. Am. Chem. Soc.* 1973, **95**, 6504.
[121]A. R. Sanger, *J. Mol. Catal.* 1978, **3**, 221.
[122]W. Strohmeier and M. Michel, *Z. Phys. Chem.* (*Wiesbaden*) 1981, **124**, 23.
[123]W. Strohmeier and M. Michel, *Proc. Symp. Rhodium Homogeneous Catal.*, 1978, p. 104; *Chem. Abstr.* 1979, **90**, 71705.
[124]P. Cavalieri d'Oro, L. Raimondi, G. Pagani, G. Montrasi, G. Gregorio and A. Andreetta, *Chim. Ind.* (*Milan*) 1980, **62**, 572.
[125]J. Hjortkjaer, *J. Mol. Catal.* 1979, **5**, 377.
[126]J. H. McCracken and R. C. Williamson, *Canad. Pat.* 1976, 992,101; through *Chem. Abstr.* 1977, **86**, 54975.
[127]R. L. Pruett and J. A. Smith, *U.S. Pat.* 1975, 3,917,661; through *Chem. Abstr.* 1976, **84**, 30433.
[128]G. Biale, *U.S. Pat.* 1973, 3,733,362; through *Chem. Abstr.* 1973, **79**, 41873.
[129]R. Kummer and R. Platz, *Ger. Pat.* 1975, 2,354,217; through *Chem. Abstr.* 1975, **83**, 78602.
[130]I. D. Huang and R. Drogin, *PCT Int. Appl.* 1980, 80 01,691; through *Chem. Abstr.* 1981, **94**, 156313.
[131]T. F. Shevels and N. Harris, *Eur. Pat. Appl.* 1980, 16285; through *Chem. Abstr.* 1981, **94**, 83610.
[132]G. Wilkinson, *Ger. Pat.* 1970, 1,939,322; through *Chem. Abstr.* 1970, **73**, 14195.
[133]G. Wilkinson, *French Pat.* 1971, 2,072,146; through *Chem. Abstr.* 1972, **77**, 4914.
[134]M. Polievka, L. Uhlar and V. Macho, *Petrochemia* 1978, **18**, 9; through *Chem. Abstr.* 1978, **89**, 146328.
[135]R. L. Pruett and J. A. Smith, *Ger. Pat.* 1971, 2,058,814; through *Chem. Abstr.* 1971, **75**, 109844.
[136]M. Polievka, V. Macho and L. Uhlar, *Petrochemia* 1979, **19**, 5; through *Chem. Abstr.* 1979, **91**, 91084.
[137]A. J. Dennis, T. F. Shevels and N. Harris, *Eur. Pat. Appl.* 1980, 16286; through *Chem. Abstr.* 1981, **94**, 83609.
[138]P. J. Davidson and R. R. Hignett, *U.S. Pat.* 1980, 4,200,592; through *Chem. Abstr.* 1980, **93**, 113966.
[139]R. R. Hignett and P. J. Davidson, *Belg. Pat.* 1978, 868,279; through *Chem. Abstr.* 1979, **90**, 103416: *ibid.*, *Brit. Pat* 1980, 2,028,793; through *Chem. Abstr.* 1980, **93**, 167640.
[140]M. J. Mirbach, N. Topalsavoglu, Tuyet Nhu Phu, M. F. Mirbach and A. Saus, *Angew. Chem. Int.* 1981, **20**, 381.
[141]A. J. De Jong, *Ger. Pat.* 1977, 2,719,735; through *Chem. Abstr.* 1978, **88**, 89113.
[142]M. Takeda, H. Iwane and T. Hashimoto, *Jap. Pat.* 1980, 80 28,969; through *Chem. Abstr.* 1980, **93**, 114041.
[143]Y. Inamoto, Y. Fujikura and H. Ikeda, *Ger. Pat.* 1977, 2,654,799; through *Chem. Abstr.* 1978, **88**, 6432.
[144]K. Sanui, W. J. MacKnight and R. W. Lenz, *Macromolecules* 1974, **7**, 952.
[145]B. Fell and M. Beutler, *Tetrahedron Lett.* 1972, 3455.
[146]T. Saito, Y. Tsutsumi and S. Arai, *Ger. Pat.* 1980, 3,017,682; through *Chem. Abstr.* 1981, **95**, 42342.
[147]T. Shimizu, *Ger. Pat.* 1976, 2,538,364; through *Chem. Abstr.* 1976, **85**, 45962.
[148]M. Matsumoto, S. Moriya, N. Tsunumaru, Y. Fuchigami, T. Shimizu and M. Tamura, *Jap. Pat.* 1978, 78 68,715; through *Chem. Abstr.* 1978, **89**, 146424.
[149]N. Saito, S. Arai and Y. Tsutsumi, *Jap. Pat.* 1980, 80 45,646; through *Chem. Abstr.* 1980, **93**, 204061.
[150]J. W. Kang and W. L. Hergenrother, *Ger. Pat.* 1977, 2,649,900; through *Chem. Abstr.* 1977, **87**, 135015.
[151]M. Takeda, H. Iwane and T. Hashimoto, *Jap. Pat.* 1980, 80 27165; through *Chem. Abstr.* 1981, **94**, 65899.
[152]Mitsubishi Petrochemical Co. Ltd., *Jap. Pat.* (*Tokkyo Koho*) 1981, 81 16482; through *Chem. Abstr.* 1981, **95**, 81276.
[153]A. J. de Jong, *Ger. Pat.* 1977, 2,707,108; through *Chem. Abstr.* 1977, **87**, 151706.
[154]R. T. Gray and A. J. de Jong, *Ger. Pat.* 1978, 2,753,644; through *Chem. Abstr.* 1978, **89**, 108350.
[155]A. J. de Jong and R. T. Gray, *Ger. Pat.* 1978, 2,753,639; through *Chem. Abstr.* 1978, **89**, 169670.
[156]H. B. Copelin, *Canad. Pat.* 1976, 983,942; through *Chem. Abstr.* 1976, **85**, 93803.
[157]A. J. Dennis, *Eur. Pat. Appl.* 1980, 18,162; through *Chem. Abstr.* 1981, **94**, 156338.
[158]N. Harris, A. J. Dennis and G. E. Harrison, *Eur. Pat. Appl.* 1980, 18,163; through *Chem. Abstr.* 1981, **94**, 156295.
[159]N. Harris, A. J. Dennis and G. E. Harrison, *Eur. Pat. Appl.* 1980, 18161; through *Chem. Abstr.* 1981, **94**, 156315.
[160]F. J. McQuillin, *Brit. Pat.* 1979, 1,555,331; through *Chem. Abstr.* 1980, **93**, 12948.
[161]H. B. Tinker, *Ger. Pat.* 1976, 2,623,673; through *Chem. Abstr.* 1977, **86**, 105957.
[162]K. Schwirten, H. W. Schneider and R. Kummer, *Ger. Pat.* 1978, 2,643,205; through *Chem. Abstr.* 1978, **89**, 5946.
[163]C. U. Pittman, W. D. Honnick and J. J. Yang, *J. Org. Chem.* 1980, **45**, 684.
[164]P. Fitton and H. Moffet, *Ger. Pat.* 1976, 2,621,224; through *Chem. Abstr.* 1977, **86**, 105966.
[165]R. Kummer, *Ger. Pat.* 1975, 2,401,553; through *Chem. Abstr.* 1975, **83**, 178295.
[166]G. Wilkinson, *Ger. Pat.* 1971, 2,064, 471; through *Chem. Abstr.* 1971, **75**, 109848.
[167]F. B. Booth, *U.S. Pat.* 1974, 3,801,646; through *Chem. Abstr.* 1974, **80**, 145418.
[168]G. Gregorio, G. Montrasi, M. Tampieri, P. Cavalieri d'Oro, G. Pagani and A. Andreetta, *Chim. Ind.* (*Milan*) 1980, **62**, 389.
[169]E. A. Brewester and R. L. Pruett, *U.S. Pat.* 1981, 4,247,486; through *Chem. Abstr.* 1981, **95**, 24271.
[170]R. Fowler, *Brit. Pat.* 1975, 1,387,657; through *Chem. Abstr.* 1975, **83**, 58122.
[171]G. Montrasi, G. Pagani, G. Gregorio, A. Andreetta and P. Cavalieri d'Oro, *Chim. Ind.* (*Milan*) 1980, **62**, 737.
[172]R. Tarao, S. Sakano, K. Miyazaki, F. Saito and S. Miyajima, *Jap. Pat.* 1973, 73 40,326; through *Chem. Abstr.* 1974, **81**, 13118.
[173]R. Tarao, S. Sakano, K. Miyazaki, K. Fujita, C. Saito and S. Miyajima, *Jap. Pat.* 1973, 73 43,799; through *Chem. Abstr.* 1974, **81**, 82836.
[174]T. Onoda, Y. Tsunoda, Y. Koyama, T. Kawatsu and K. Tano, *J. Pat.* 1975, 75 49,215; through *Chem. Abstr.* 1975, **83**, 96429.
[175]T. Onoda, Y. Tsunoda, Y. Koyama, T. Kawatsu and K. Tano, *Jap. Pat.* 1978, 78 24,928; through *Chem. Abstr.* 1978, **89**, 163068.
[176]T. Onoda, Y. Tsunoda, Y. Koyama, T. Kawatsu and K. Tano, *Jap. Pat.* 1975, 75 41,805; through *Chem. Abstr.* 1975, **83**, 78606.
[177]B. Fell and U. Hartig, *Ger. Pat.* 1974, 2,311,388; through *Chem. Abstr.* 1975, **82**, 3740.
[178]W. Otte, W. H. E. Müller and M. zur Hausen, *Ger. Pat.* 1980, 2,912,230; through *Chem. Abstr.* 1981, **94**, 21133.
[179]J. L. Dawes and T. J. Devon, *U.S. Pat.* 1980, 4,196,096; through *Chem. Abstr.* 1980, **93**, 32415.
[180]C. Demay, *Ger. Pat.* 1981, 3,023,025; through *Chem. Abstr.* 1981, **94**, 174281.

[181]T. Onoda, Y. Tsunoda, T. Nomura, T. Nonaka, O. Kurashiki and T. Masuyama, *Ger. Pat.* 1975, 2,438,847; through *Chem. Abstr.* 1975, **82**, 174055.
[182]B. Fell and W. Dolkemeyer, *Ger. Pat.* 1978, 2,637,262; through *Chem. Abstr.* 1978, **88**, 152032.
[183]K. L. Oliver, *U.S. Pat.* 1970, 3,547,964; through *Chem. Abstr.* 1971, **74**, 66299.
[184]R. Kummer, K. Schwirten and H. D. Schindler, *Ger. Pat.* 1976, 2,448,005; through *Chem. Abstr.* 1976, **85**, 77622.
[185]R. Kummer, K. Schwirten and H. D. Schindler, *Canad. Pat.* 1979, 1,055,512; through *Chem. Abstr.* 1979, **91**, 140340.
[186]K. L. Oliver, *U.S. Pat.* 1970, 3,530,190; through *Chem. Abstr.* 1970, **73**, 132733.
[187]R. Kummer, H. W. Schneider and K. Schwirten, *Ger. Pat.* 1977, 2,614,799; through *Chem. Abstr.* 1977, **87**, 207275.
[188]Y. Hayashi, H. Imai and Y. Iwatani, *Jap. Pat.* 1975, 75 49,189; through *Chem. Abstr.* 1975, **83**, 101307.
[189]Y. Hayashi, H. Imai and Y. Iwatani, *Jap. Pat.* 1975, 75 49190; through *Chem. Abstr.* 1975, **83**, 101308.
[190]Y. Hayashi, H. Imai and Y. Iwatani, *Jap. Pat.* 1975, 75 49188; through *Chem. Abstr.* 1975, **83**, 83133.
[191]T. Onoda, T. Masuyama and Y. Konami, *Jap. Pat.* 1975, 75 62,936; through *Chem. Abstr.* 1976, **85**, 5888.
[192]L. W. Gosser, W. H. Knoth and G. W. Parshall, *J. Mol. Catal.* 1977, **2**, 253.
[193]G. C. Bond, *Ger. Pat.* 1971, 2, 047,748; through *Chem. Abstr.* 1971, **75**, 25968.
[194]G. C. Bond, *Brit. Pat* 1973, 1,332,894; through *Chem. Abstr.* 1974, **80**, 36704.
[195]L. A. Gerritsen, J. M. Herman, W. Klut and J. J. F. Scholten, *J. Mol. Catal.* 1980, **9**, 157.
[196]L. A. Gerritsen, J. M. Herman and J. J. F. Scholten, *J. Mol. Catal.* 1980, **9**, 241.
[197]L. A. Gerritsen, W. Klut, M. H. Vreugdenhil and J. J. F. Scholten, *J. Mol. Catal.* 1980, **9**, 257.
[198]L. A. Gerritsen, W. Klut, M. H. Vreugdenhil and J. J. F. Scholten, *J. Mol. Catal.* 1980, **9**, 265.
[199]J. Hjortkjaer, M. S. Scurrell and P. Simonsen, *J. Mol. Catal.* 1979, **6**, 405.
[200]J. Hjortkjaer, M. S. Scurrell and P. Simonsen, *J. Mol. Catal.* 1980, **10**, 127.
[201]L. A. Gerritsen, A. van Meerkerk, M. H. Vreugdenhil and J. J. F. Scholten, *J. Mol. Catal.* 1980, **9**, 139.
[202]G. C. Bond, *Ger. Pat.* 1971, 2,055,539; through *Chem. Abstr.* 1971, **75**, 48429.
[203]O. R. Hughes, *U.S. Pat.* 1980, 4,201,728; through *Chem. Abstr.* 1980, **93**, 149796.
[204]Y. Becker, A. Eisenstadt and J. K. Stille, *J. Org. Chem.* 1980, **45**, 2145.
[205]P. Pino, C. Botteghi, G. Consiglio and C. Salomon, *Ger. Pat.* 1974, 2,359,101; through *Chem. Abstr.* 1974, **81**, 90644.
[206]W. Beck and H. Menzle, *J. Organometal. Chem.* 1977, **133**, 307.
[207]C. Salomon, G. Consiglio, C. Botteghi and P. Pino, *Chimia* 1973, **27**, 215.
[208]A. Stefani, D. Tatone, *Helv. Chim. Acta* 1977, **60**, 518.
[209]A. Stefani, D. Tatone and P. Pino, *Helv. Chim. Acta* 1976, **59**, 1639.
[210]C. Botteghi, M. Branca, G. Micera, F. Piacenti and G. Menchi, *Chim. Ind.* (*Milan*) 1978, **60**, 16.
[211]F. Piacenti, G. Menchi, P. Frediani, U. Matteoli and C. Botteghi, *Chim. Ind.* (*Milan*) 1978, **60**, 809.
[212]C. Botteghi, *Gazz. Chim. Ital.* 1975, **105**, 233.
[213]C. Botteghi and C. Salomon, *Tetrahedron Lett.* 1974, 4285.
[214]J. Rejhon and J. Hetflejš, *Collect. Czech. Chem. Commun.* 1975, **40**, 3680.
[215]H. Watanabe, M. Aoki, N. Sakurai, K. Watanabe and Y. Nagai, *J. Organometal. Chem.* 1978, **160**, C1.
[216]A. J. Chalk, *J. Organometal. Chem.* 1970, **21**, 207.
[217]J. Rejhon and J. Hetflejš, *Collect. Czech. Chem. Commun.* 1975, **40**, 3190.
[218]V. B. Pukhnarevich, L. I. Kopylova, E. O. Tsetlina, V. A. Pestunovich, V. Chalovsky, J. Hetflejš and M. G. Voronkov, *Proc. Acad. Sci. USSR* 1976, **231**, 764.
[219]V. B. Pukhnarevich, L. I. Kopylova, M. Čapka, J. Hetflejš, E. N. Satsuk, M. V. Sigalov, V. Chvalovsky and M. G. Voronkov, *J. Gen. Chem. USSR* 1981, **50**, 1259.
[220]M. G. Voronkov, V. B. Pukhnarevich, I. I. Tsykhanskaya and Y. S. Varshavskii, *Proc. Acad. Sci. USSR* 1981, **254**, 449.
[221]C. Lassau, Y. Chauvin and G. Lefeburo, *Ger. Pat.* 1969, 1,902,560; through *Chem. Abstr.* 1970, **72**, 21358.
[222]H. Hara, *Ger. Pat.* 1973, 2,321,191; through *Chem. Abstr.* 1974, **80**, 26757.
[223]J. Schwartz and J. B. Cannon, *J. Am. Chem. Soc.* 1974, **96**, 4721.
[224]L. V. Gorbunova, I. L. Knyazeva, E. A. Davydova and G. A. Abakumov, *Bull. Acad. Sci. USSR Div. Chem. Sci.* 1980, **29**, 761.
[225]R. W. Goetz, *U.S. Pat.* 1980, 4,200,765; through *Chem. Abstr.* 1980, **93**, 113951.
[226]A. Spencer, *J. Organometal. Chem.* 1980, **194**, 113.
[227]H. Dumas, J. Levisalles and H. Rudler, *J. Organometal. Chem.* 1979, **177**, 239.
[228]G. Biale, *U.S. Pat.* 1970, 3,513,200; through *Chem. Abstr.* 1970, **73**, 34776.
[229]S. Yoshikawa, J. Kiji and J. Furukawa, *Makromol. Chem.* 1977, **178**, 1077.
[230]N. Kameda, *Nippon Kagaku Kaishi* 1976, 682; through *Chem. Abstr.* 1976, **85**, 47144.
[231]N. Kameda and E. Ishii, *Kobunshi Ronbunshu* 1979, **36**, 347; through *Chem. Abstr.* 1979, **91**, 39979.

Polyhedron Vol. 1, No. 7–8, pp. 607–610, 1982
Printed in Great Britain.

0277–5387/82/070607–04$03.00/0
Pergamon Press Ltd.

ELECTRON SPIN RESONANCE STUDIES ON COMPLEXES OF COPPER(II) WITH *o*-PHENOLIC OXIMES

V. SURESH BABU, A. RAMESH, P. RAGHURAM and R. RAGHAVA NAIDU*
Department of Chemistry, School of Mathematics & Physical Sciences Sri Venkateswara University, Tirupati-517502, A.P., India

(*Received* 14 *October* 1981)

Abstract—Copper(II) forms 1:2 complexes with *o*-hydroxyacetophenone-, resacetophenone-, peonol- and 2-hydroxy-1-naphthaldoximes. Thermogravimetric analysis indicate that all the chelates are anhydrous. All the complexes are found to be non-electrolytes in nitrobenzene. Magnetic and electronic spectral data show planar geometry for all the complexes. Based on ESR studies all possible parameters have been determined. The g, A and G values for all the complexes are consistent with the fact that copper is involved in a square planar coordination with oxime ligands. The metal–ligand bonding parameters evaluated showed substantial in plane σ-bonding covalency and a small amount of in-plane as well as out-of-plane π-bonding.

INTRODUCTION

Oximes have various insecticidal, miticidal and nematocidal activities.[1] They were employed as antidotes against organophosphorus poisons.[2] Oximes were employed as inorganic analytical reagents for separation and determination of many metal ions. Considering their biochemical and analytical importance and with a view that metal ions may enhance their biochemical activity we have prepared the copper complexes of *o*-hydroxyacetophenone-, resacetophenone-, peonol- and 2-hydroxy-1-naphthaldoxime and characterised them by spectral, ESR and magnetic studies.

EXPERIMENTAL

The copper complexes of *o*-hydroxyacetophenoneoxime, resacetophenoneoxime, peonoloxime and 2-hydroxy-1-naphthaldoxime were prepared according to the procedures described in the literature.[3–6]

The copper–oxime complexes used in ESR spectral studies were diluted in their respective diamagnetic nickel oxime complexes (Cu to Ni 5:95 and 2:98 respectively) and were prepared as follows.

An aliquot of copper(II) ion solution (containing 2.5 mg of copper) and nickel(II) ion solution (containing 47.5 mg of nickel) were transferred to a 400-ml beaker and diluted to about 150 ml with distilled water. The solution was heated to about 60°C and a slight excess of the oxime solution (1% in rectified spirit) was added. The pH of the solution was adjusted to 6.5–7.5 with sodium acetate solution (10%) set aside for about 20 minutes and then filtered through a sintered glass crucible. The precipitate was washed with hot water and dried in a vacuum desiccator over fused calcium chloride.

Electronic spectra of the complexes in Nujol mull were obtained with Unicam SP-700 Spectrophotometer. ESR spectra of the solid complexes were recorded using Varian E-4X-band Spectrometer which was operated in the range 8.8–9.6 GHz. DPPH was used as the g-marker.

RESULTS AND DISCUSSION

All the complexes are powders which are insoluble in water and soluble in dioxan, 2-ethoxyethanol and acetone.

The complexes were stable in air and non-hygroscopic. All the complexes were analysed for the metal, carbon, hydrogen and nitrogen and the results showed a 1:2 metal–ligand composition. Nitrobenzene solutions of the complexes gave low conductance values (Table 1) in the range of 0.28–0.38 indicating a non-electrolytic nature. Elemental analysis, IR and thermogravimetric studies[7] revealed that all the four complexes were anhydrous. IR studies also revealed that the complexes involved the replacement of the hydrogen of the phenolic-OH group by copper with nitrogen of the oxime group coordinating to it.

The values of room temperature magnetic moments (μ_{eff}) for the complexes are given in Table 1. These are essentially spin only values, normally found for square planar copper(II) complexes in the absence of any antiferro-magnetic coupling. The values are consistent with an orbitally non-degenerate ground state for the copper(II) ion and indicate that the complexes are mononuclear in nature.

The electronic spectra of copper oxime complexes showed absorption peaks in the 16.0 and 19.0 kK regions, the bands observed around 16.0 kK are assigned to $^2B_{1g} \rightarrow {}^2B_{2g}$ transition of square planar copper(II) by analogy with the spectra of other square planar copper(II) species. The bands observed around 19.0 kK are attributed to $^2B_{1g} \rightarrow {}^2E_g$ transition (Table 1).

The electron spin resonance spectra of the polycrystalline specimens of the four copper–oxime complexes (diluted in the respective nickel oxime complex, Cu–Ni 5:95) showed interesting features of resolution of the copper hyperfine structure. The ESR spectra determined with copper–oxime chelates diluted in nickel complex (Cu-Ni 2:98) are found to be similar with those of the above but the hyperfine lines are slightly smaller for this concentration. In all the complexes, the low field part of the spectrum consisted of three of the four expected hyperfine lines (the fourth line overlapping with the high field line) (Cu^{2+}, $S = \frac{1}{2}$ and nuclear spin $I = \frac{3}{2}$). These spectra are characteristic of axial symmetry. The spectrum is composed of two parts, the $\theta = 0°$ ($g_\parallel$) part and the $\theta = 90°$ ($g_\perp$) part, where θ is the angle between **H** and the axis perpendicular to the coordinating plane formed by the ligand. Therefore, the copper hyperfine line of the $m_I = -(3/2)$ of the $g_\parallel$ absorption overlapped

*Author to whom correspondence should be addressed.

Table 1. Analytical, molar conductance, magnetic moment and electronic absorption spectral data of the complexes

Complex	Color	Metal (%)	Carbon (%)	Hydrogen (%)	Nitrogen (%)	Molar conductance ($Ohm^{-1}cm^2$ $mole^{-1}$ nitrobenzene)	Absorption maxima, kK $^2B_{1g} \rightarrow {}^2B_{2g}$	Absorption maxima, kK $^2B_{1g} \rightarrow {}^2E_g$	μ_{eff} (B.M.)
1.Copper-o-hydroxyacetophenoneoxime	Brown	17.31 (17.48)	52.90 (52.80)	4.39 (4.40)	7.71 (7.70)	0.30	15.9	18.9	1.79
2.Copper-resacetophenoneoxime	Brown	16.10 (16.07)	48.85 (48.85)	4.11 (4.05)	7.14 (7.08)	0.34	15.8	19.2	1.80
3.Copper-peonoloxime	Light Brown	15.00 (15.00)	51.00 (51.00)	5.10 (4.80)	6.70 (6.60)	0.38	15.8	18.7	1.70
4.Copper-2-hydroxy-1-naphthaldoxime	Light Brown	14.42 (14.57)	60.80 (60.60)	3.70 (3.70)	6.37 (6.40)	0.38	14.9	19.2	1.74

with the $g_\perp$ part. The spectra are fitted into an axial spin Hamiltonian given below.[8,9]

$$\mathbf{H} = \beta[g_\parallel \mathbf{H}_z S_z + g_\perp(\mathbf{H}_x S_x + \mathbf{H}_y S_y)] + A_\parallel I_z S_z + A_\perp(I_x S_x + I_y S_y). \quad (1)$$

With $S = \frac{1}{2}$ and nuclear spin $I = \frac{3}{2}$, the parameters in the spin-Hamiltonian as calculated from the spectra are given in Table 2. The analysis of ESR spectra of copper-oxime complexes is straight-forward when we compare these spectra with that of the ESR spectra of several copper complexes reported in the literature.[10–13] In the spectra of the present complexes the line-widths are larger and the resolution is sufficient to measure all the ESR parameters accurately. Table 2 gives the g, A values, optical absorption frequencies and orbital reduction factors $k_\parallel$ and $k_\perp$. Hathaway[14] pointed out that for pure σ bonding $k_\parallel \approx k_\perp \approx 0.77$, for in-plane pi-bonding $k_\parallel < k_\perp$ and for out of plane pi-bonding $k_\perp < k_\parallel$. In all the present complexes $k_\parallel < k_\perp$ which suggests that in these chelates in-plane pi-bonding is present. The parameters in Table 2 show some interesting trends. The $g_\parallel$ values are almost the same for all the complexes indicating that the type of bonding is the same in all the complexes and that Cu–N and Cu–O bond lengths do not vary from complex to complex. Kivelson and Neiman[15] have shown that $g_\parallel$ is a moderately sensitive function for indicating covalency. Normally $g_\parallel$ is 2.3 or more for ionic environment and it is less than 2.3 for more covalent environment. The present ESR results show that $g_\parallel$ is less than 2.3 in all the cases suggesting that the copper oxime complexes are more covalent in nature. Similar observations are reported by Wasson and Trapp.[16] Massacesi *et al.*[13] reported that $g_\parallel$ is 2.3–2.4 for copper-oxygen bonds (octahedral and planar respectively); 2.2–2.3 for copper-nitrogen bonds and mixed copper-nitrogen and oxygen system (with variation in the point symmetry from octahedral and planar among them) and 2.1–2.2 for copper-sulfur bonds. For copper-selenium bonds it is below 2.05. For the present copper-oxime complexes $g_\parallel = 2.200$–2.204, in conformity with the presence of mixed copper-nitrogen and oxygen bonds in these chelates. The data presented in Table 2 also reveal that there is not much variation in values of $A_\parallel$ and

Table 2. Spin Hamiltonian and orbital reduction parameters of copper-oxime complexes

	T(K)	g_{av}	A^a_{iso}	$g_\parallel$	$g_\perp$	$A^a_\parallel$	$A^a_\perp$	ΔE^b_1	ΔE^b_2	$k^2_\parallel$	$k^2_\perp$	
1.Cu-o-hydroxy-acetophenone-oxime	301	2.102	95.15	2.204	2.051	200.6	42.13	15880	18870	0.49	0.58	4.00
2.Cu-resaceto-phenoneoxime	301	2.099	97.61	2.200	2.048	200.4	44.98	15750	19280	0.48	0.56	4.17
3.Cu-peonoloxime	301	2.097	94.17	2.202	2.045	200.4	41.71	15750	18690	0.48	0.51	4.49
4.Cu-2-hydroxy-1-naphthald-oxime	301	2.096	95.26	2.200	2.044	202.9	41.44	14920	19230	0.45	0.51	4.54

[a]Units, $x10^{-4}cm^{-1}$, [b]In cm^{-1}

isotropic $g[(g_0 = 1/3(g_\parallel + 2g_\perp)]$ and $A[A_0 = 1/3(A_\parallel + 2A_\perp)]$ values. Furthermore, the high field "Perpendicular" transition shows no signs of any further resolution into the individual compounds to yield g_x and g_y (where $g_\perp = \frac{1}{2}(g_x + g_y)$ and hence suggest an effective "D_{4h}" point symmetry. This would mean that in all the chelates the nitrogens and oxygens provide effectively the same ligand field strength. Under this symmetry the unpaired electron is considered to be in the $^2B_{1g}[|x^2 - y^2\rangle]$ ground state orbital.[11,13]

Hathaway[10,11] stated that two types of axial spectra are observed depending on the value of lowest g-factor. (1) Lowest g 2.04—such a spectrum can be observed for a copper(II) ion in axial symmetry with all the principal axes aligned parallel and would be consistent with elongated tetragonal, octahedral or square planar stereochemistries. In these axial spectra the g values are related by the expression,

$$G = \frac{g_\parallel - 2}{g_\perp - 2} \approx 4.0 \qquad (2)$$

and is evidence that a $d_x^2 - y^2$ ground state is present. If $G > 4.0$, then the local tetragonal axes are aligned parallel or only slightly misaligned; if $G < 4.0$, significant exchange coupling is present and the misalignment is appreciable. Consequently the value of G is a useful indication of the extent of exchange coupling in tetragonal systems. (2) Lowest $g < 2.03$—such spectra can be observed for a copper(II) ion in: axial symmetry with all the principal axes aligned parallel and would be consistent with compressed tetragonal–octahedral or trigonal–bipyramidal stereochemistries. Further, if the g value is less than 2.03 it is an indication that the unpaired electron is present in the d_{z^2} ground state orbital and in these compressed stereochemistries the value of G has no significance. For the present four copper–oxime complexes $g_\perp = 2.044$–2.051, $G_\parallel = 2.200$–2.2034 and $G = 4.00$–4.54 (Table 2). These values suggest that all these chelates have symmetry lower than tetragonal. Further, for these complexes the lowest g value is greater than 2.04 and $G \geq 4.0$ consistent with a $d_{x^2-y^2}$ ground state and with an elongated axial symmetry.

Electron spin resonance and optical absorption spectra have been used many times to determine the covalent bonding parameters for the Cu^{2+} ion in various ligand field environments. The ESR parameters $g_\parallel$, $g_\perp$, $A_\parallel$ and $A_\perp$ and the separation of the d-orbitals ($^2B_{1g} \rightarrow {}^2B_{2g}$ corresponding to $|x^2 - y^2\rangle$ to $|XY\rangle$ transition and $^2B_{1g} \rightarrow {}^2E_g$ corresponding to $|x^2 - y^2\rangle \rightarrow |xz, yz\rangle$) are used to evaluate the bonding parameters α^2, $\beta_1{}^2$, β^2 and the Fermi contact hyperfine interaction term "K". α^2 measures the covalency of the in-plane σ bonds, $\beta_1{}^2$ of the in-plane pi-bonds and β^2 of the out-of-plane pi-bonds. These parameters are close to 1.0 for ionic bonds and become smaller with increasing covalent bonding.

For a Cu^{2+} complex with D_{4h} symmetry the ground state can be expressed by the molecular orbital[13,15]

$$B_{1g} = \alpha|x^2 - y^2\rangle - \frac{1}{2}\alpha^1|-\sigma^1 x + \sigma^2 y + \sigma^3 x - \sigma_y{}^4\rangle \qquad (3)$$

where α^1 is the ligand group orbital coefficient for the ground state and α is the metal d-orbital coefficient. The larger the square of the α^1, the more covalent is the bonding.

The magnitude of α^2 can be estimated using the following approximate formula[15]

$$\alpha^2 = \frac{A_\parallel}{P} + (g_\parallel - 2.0023) + \frac{3}{7}(g_\perp - 2.0023) + 0.04 \qquad (4)$$

where $P = 0.036\,cm^{-1}$ for Cu^{2+} free ion,[15] and $A_\parallel$ is expressed in cm^{-1}. The α^2 values obtained by this expression (Table 3) tend to be slightly less than those obtained using the more elaborate and exhaustive molecular orbital theory. This leads to a small discrepancy in the value of $(\alpha^1)^2$ derived from α^2 using the expression for normalisation of the B_{1g} orbital

$$\alpha^2 + (\alpha^1)^2 - 2\alpha(\alpha^1)S = 1 \qquad (5)$$

where S is the overlap integral between the metal and the normalised ligand orbitals. We have assumed the overlap integral value calculated by Assour[17] $S = 0.092$ and the values of $(\alpha^1)^2$ are presented in Table 3.

In order to estimate the molecular orbital coefficients (α, β and β_1), Hathaway and Tomlinson[10] assumed the value of β_1 as one and calculated α and β for several copper(II) ammonia complexes employing the expressions $k_\parallel \approx \alpha\beta_1$ and $k_\perp \approx \alpha\beta$. The present authors deter-

Table 3. Spin Hamiltonian and bonding parameters of copper(II) oxime complexes

Complex	$g_\parallel$	$g_\perp$	$A_\parallel^a$	$A_\perp^a$	α^2	$(\alpha^1)^2$	β^2	$P(cm^{-1})$	K
1.Cu-o-hydroxy-acetophenone-oxime	2.204	2.051	200.6	42.13	0.82	0.27	0.71	0.024	0.30
2.Cu-resaceto-phenoneoxime	2.200	2.048	202.9	47.04	0.82	0.27	0.68	0.023	0.33
3.Cu-peonoloxime	2.202	2.045	200.4	41.71	0.82	0.27	0.62	0.024	0.30
4.Cu-2-hydroxy-1-naphthaldoxime	2.200	2.044	202.9	41.44	0.82	0.27	0.62	0.024	0.30

[a]Units, $x10^{-4}cm^{-1}$

mined the values of α for the four copper–oxime complexes from the expression (4). Substituting the values of α in the expression $k_\perp \approx \alpha\beta$ the parameter β is obtained and these values are also given in Table 3. The estimated values of the bonding coefficients indicate a large amount of in-plane σ bonding and very little out of plane pi-bonding.

Giordano and Bereman[18] have treated the free ion dipolar term P as a variable to absorb the effect of electron delocalization by the use of the expression

$$P = \frac{(A_\parallel - A_\perp)}{\left[(g_\parallel - 2) - \frac{5}{14}(g_\perp - 2) - \frac{6}{7}\right]} \quad (6)$$

They suggested that identification of bonding groups may be obtained from values of P, e.g. for bonding to four sulfur atoms they found that P lies in the range 0.026–0.016 cm^{-1} and for bonding to two nitrogen and two oxygen atoms the value of P is in the range 0.022–0.029 cm^{-1}. The values of P obtained for the copper–oxime complexes by using the above expression are given in Table 3. These values are found to be between 0.023–0.024 cm^{-1} and are consistent with bonding of copper to two nitrogens and two oxygens. Smaller values for P also indicate slightly stronger in-plane pi-bonding in the systems agreeing with a higher ligand field.

The Fermi contact hyperfine interaction term K may be obtained from the expression[19]

$$K = -\frac{A_{iso}}{P\beta_1^2} + \frac{g_{av} - 2.0023}{\beta_1^2} \quad (7)$$

where the free ion dipolar term $P = g_e g_N \beta_e \beta_N \langle r^{-3} \rangle \simeq 0.036$. K is a dimensionless quantity which is a measure of the contribution of "s" electrons to the hyperfine interaction and is generally found to have a value of about 0.3. Substituting the values of A_{iso}, g_{av} and P in the above expression the value of K for the four complexes were obtained which are also given in Table 3. In these calculations β_1^2 is assumed as one. The values obtained for K are in good agreement with those estimated by Assour[17] and Abragam and Pryce.[20]

REFERENCES

[1]D'Silva, D. J. Themistocles (Union Carbide Corp.), June 1977, US 4,029,688 (Cr 260,465,4; CO7C 121/00); June 1974, Appl. 483,882.

[2]E. S. Rachaman, Y. Ashani, H. Leader, I. Granoth, H. Edery and G. Porath, *Arzneim-Forsch* 1979, **29**, 875 (Eng.).

[3]N. A. Raju and K. Neelakantam, *Curr. Sci.* 1950, **19**, 383.

[4a]S. N. Poddar, *Z. Anal. Chem.* 1957, **154**, 254; [b]S. N. Poddar, *Indian J. Appl. Chem.* 1963, **26**, 56.

[5]G. Raja Reddy, *Oximes as Inorganic Analytical Reagents.* Ph.D. Thesis. Sri Venkateswara University, Tirupati, India (1970).

[6]R. Seshadri Naidu, *o-Hydroxy-Carbonyl Compounds and Their Derivatives as Inorganic Analytical Reagents.* Ph.D. Thesis. Sri Venkateswara University, Tirupati, India (1979).

[7]V. Seshagiri and S. Brahmaji Rao, *Z. Anal. Chem.* 1972, **262**, 275.

[8]C. M. Guzy, J. B. Raynor and M. C. R. Symmons, *J. Chem. Sec.* (*A*) 1969, 2299.

[9]Y. Hsu, *Mol. Phys.* 1971, **21**, 1087.

[10]B. J. Hathaway and A. A. G. Tomlinson, *Coord. Chemi. Rev.* 1970, **5**, 1–43.

[11]B. J. Hathaway and D. E. Billing, *Coord. Chem. Rev.* 1970, **5**, 143–207.

[12]J. Subramanian, J. H. Fuhrhop, A. Salek and A. Gossauer, *J. Magn. Reson.* 1974, **15**, 19.

[13]M. Massacesi and G. Ponticelli, V. Buddha Addepali and V. G. Krishnan, *J. Mol. Struct.* 1978, **48**, 55; 1979, **51**, 27.

[14]B. J. Hathaway, *Structure and Bonding*, Vol. 4, p. 60. Springer-Verlag, Berlin (1973).

[15]D. Kivelson and R. Neiman, *J. Chem. Phys.* 1958, **29**, 35.

[16]J. R. Wasson and C. Trapp, *J. Phys. Chem.* 1969, **73**, 3763.

[17]J. M. Assour, *J. Chem. Phys.* 1965, **43**, 2477.

[18]R. S. Giordano and R. D. Bereman, *J. Am. Chem. Soc.* 1974, **96**, 1019.

[19]S. H. Laurie, T. Lund and J. B. Raynor, *J. Chem. Soc.* Dalton Trans. 1975, 1389.

[20]A. Abragam and M. H. L. Pryce, *Proc. Roy. Soc.* (London) 1961, **A206**, 164.

Polyhedron Vol. 1, No. 7-8, pp. 611-615, 1982
Printed in Great Britain.

0277-5387/82/070611-05$03.00/0
Pergamon Press Ltd.

THE KINETICS OF THE COPPER(II)–IODINE(–I) REACTION IN THE PRESENCE OF CHLORINE(–I) IONS

J. READMAN and D. A. HOUSE*
Department of Chemistry, University of Canterbury, Christchurch, New Zealand

(*Received* 9 *November* 1981)

Abstract—The kinetics of the reaction between Cu(II) and I^- to give Cu(I) and I_2 have been investigated in acidic solution in the presence of high chloride ion concentration ($\mu = 3.13$ M). Under such conditions the precipitation of CuI is avoided. The rate of I_2 production was followed using a "clock" technique, by addition of increments of thiosulphate and noting the time of appearance of the blue I_2-starch complex. At a constant chloride ion concentration 1500 times that of the initial $[Cu^{2+}]$, the reaction is second order in both Cu^{2+} and I^-, and is independent of $[H^+]$. The rate is almost independent of $[Cl^-]$, but CuI precipitates when the initial $[Cl^-]$ is less than 750 times that of the initial $[Cu^{2+}]$. The rate constant in the expression: Rate $= k_4[Cu^{2+}]^2[I^-]^2$ has a value of 5.6×10^4 M^{-3} s^{-1} at 298.2 K ($[Cl^-] = 2.73$ M, $\mu = 3.13$ M) with activation parameters: $E_a = 54.8$ kJ mol^{-1}, log PZ = 14.347 and $\Delta S^*_{298} = 21.4$ J K^{-1} mol^{-1}. The rate determining step is characterised by a large positive salt effect and a mechanism is proposed consistent with these observations.

INTRODUCTION

The reaction between Cu^{2+} and I^- is used extensively in the iodometric analysis of Cu(II)[1]. As the $[I^-]$ is reduced, the reaction occurs at a conveniently measurable rate.[2-4] Previous kinetic studies have been complicated by the precipitation of CuI, which gives rise to the characteristic autocatalytic behaviour of an heterogenous system, and reaction orders are not well established. To avoid these difficulties, we have investigated the kinetics of the reaction in the presence of excess chloride ion which effectively complexes the Cu(I) product and the system remains homogeneous.

EXPERIMENTAL

Stock solutions of $CuSO_4$ (2.06×10^{-2} M), NaI (0.123 M), $HClO_4$ (2.11 M), NaCl (5.00 M), $Na_2S_2O_3$ (2.05×10^{-2} M) and $NaClO_4$ (2.0 M, 5.0 M) were prepared and standardised by conventional volumetric techniques. The "standard run" conditions were Cu^{2+} (5 mL), I^- (5 mL), Cl^- (30 mL) and starch (freshly prepared, 1%, 5 mL) to give the following initial concentrations: $[Cu^{2+}] = 1.87 \times 10^{-3}$ M, $[I^-] = 1.13 \times 10^{-2}$ M, $[H^+] = 0.384$ M, $[Cl^-] = 2.73$ M, and an ionic strength, $\mu = 3.13$ M. All solutions, except Cu^{2+}, were added to a cylindrical reaction vessel fitted with a magnetic stirrer and jacketed with circulating water at the desired temperature. A 5 mL microburette containing $S_2O_3^{2-}$ solution was mounted above the reaction chamber. An appropriate volume of $S_2O_3^{2-}$ was added from the burette and, after temperature equilibration, the reaction was initiated by addition of the Cu^{2+} solution. The time of appearance of the blue I_2-starch complex was noted, and a further aliquot of $S_2O_3^{2-}$ added. The extent of reaction vs time was thus recorded (Table 1). In much of the preliminary investigation, the calculated (3/4)-life, (1/2)-life and (1/4)-life volumes of $S_2O_3^{2-}$ were used as aliquots. Under the above conditions, the (1/2)-life for the consumption of Cu^{2+} was 51 ± 2 s at 298.2 K.

The use of the "standard run" conditions allowed a systematic variation of $[Cu^{2+}]$ ($7.49 - 18.7 \times 10^{-4}$ M), $[I^-]$ ($4.52 - 11.3 \times 10^{-3}$ M), $[H^+]$ (0 – 0.384 M), $[Cl^-]$ (0.910 – 2.73 M), and μ (1.31 – 3.13 M), by varying the initial volumes. Appropriate amounts of $NaClO_4$ solution were added to maintain constant ionic strength where necessary. At least two, and usually three, kinetics runs were performed after the variation of any particular reaction parameter. Replacement of Cl^- by Br^- as complexing agent resulted in a much faster reaction. Stock solutions used under these conditions were: $[Cu^{2+}] = 1.01 \times 10^{-2}$ M, 5 mL: $[Cu^{2+}]_i = 9.16 \times 10^{-4}$ M, $[I^-] = 6.32 \times 10^{-2}$ M at $\mu = 0.126$ M, $NaClO_4$, 5 mL: $[I^-]_i = 2.30 \times 10^{-3}$ M, $[H^+] = 2.11$ M, 10 mL: $[H^+]_i = 0.384$ M, $[Br^-] = 5$ M, 30 mL: $[Br^-]_i = 2.73$ M and starch (5 mL), $[S_2O_3^{2-}] = 2.07 \times 10^{-2}$ M, $\mu = 3.13$ M.

*Author to whom correspondence should be addressed.

RESULTS

Some 100 kinetic runs allowed us to determine the variation of reaction rate with respect to $[Cu^{2+}]$, $[I^-]$, $[H^+]$, $[Cl^-]$, ionic strength and temperature. In most cases, the order with respect to a particular reagent was determined by the fractional life method.[5]

The reaction rate is independent of $[H^+]$ in the range 0.073–0.364 M, and even with no added acid, essentially the same (1/2)-life is observed (Table 2).

A slight decrease in reaction rate is observed (Table 2) with decreasing chloride ion in the range 1.36–2.73 M. Below this value, a more marked decrease is observed, and with $[Cl^-] < 1.0$ M, CuI precipitation occurs. A further set of reaction rates were measured in non-standard conditions ($\mu = 4.04$ M, $NaClO_4$), with $[Cl^-]$ varying from 3.64–1.82 M. These data (Table 2) confirm that the rate is independent of $[Cl^-]_i$ in the range 2.0–3.6 M and the small rate variation observed in the 1.0–2.0 M range may be due to the presence of colloidal CuI. Decreasing the $[Cl^-]$ without maintaining constant ionic strength shows that the reaction is characterised by a marked positive salt effect (Table 2).

Table 2 also presents the kinetic data obtained to determine the variation of rate with respect to $[Cu^{2+}]$ and $[I^-]$. The reaction is found to be second order in both reagents and can thus be represented as:

$$\frac{-d[Cu^{2+}]}{dt} = k_4[Cu^{2+}]^2[I^-]^2 \qquad (1)$$

($[Cl^-] = 2.73$ M, $\mu = 3.11$ M). The order with respect to $[Cu^{2+}]$ was confirmed[6] from a linear plot of $[Cu^{2+}]^{-1}$ *vs* t obtained from the "standard run" conditions by $S_2O_3^{2-}$ *vs* t data (Table 1). Pseudo-second-rate constants, k_2, M^{-1} s^{-1}, were obtained from the slope of such plots and are presented in Table 3. The fourth order rate constant,

Table 1. Volume of $S_2O_3^{2-}$ vs time data for the Cu^{2+}/I^- reaction.[a] T = 298.2 K, $[Cl^-]_i$ = 2.73 M, $[H^+]_i$ = 0.384 M, = 3.13 M, $S_2O_3^{2-}$ = 20.5 mM, $[Cu^{2+}]_i$ = 1.87 mM

Volume $S_2O_3^{2-}$	$10^4[Cu^{2+}]$	$[Cu^{2+}]^{-1}$	$[I^-]_i$, (mM)			
			11.3	9.05	6.79	4.52
(mL)	(M)	(M^{-1})	Mean time (s)			
0.75	15.9	629	-	-	-	24.5
1.00	15.0	668	8	11	16.7	50
1.25	14.0	714	-	-	34.3	78
1.50	13.1	763	21.6	28.8	54	115
1.75	12.1	826	-	45.3	77.3	151
2.00	11.2	893	41.6	61.7	100.3	220
2.25	10.3	971	55.3	81.7	132.5	-
2.50	9.36	1068	70.3	104	163	-
2.75	8.42	1188	88.6	127.7	195.5	-
3.00	7.48	1337	110	153.3	-	-
3.25	6.55	1527	132.3	-	-	-
3.50	5.61	1782	157.3	221	-	-
3.75	4.68	2137	184.6			

[a] Total volume of reaction mixture is 55 mL.

k_4 in eqn (1) was then calculated from the initial $[I^-]$ using the expression

$$k_4 = k_2[I^-]_i^{-2}. \quad (2)$$

The constancy of k_4 (Table 3) over a 1.7 fold variation in $[I^-]$ confirms the reaction order established by the fractional life method. Activation parameters[7] were obtained from the variation in k_4, using the "standard run" conditions, over the 13–25°C temperature range.

The use of bromide rather than chloride ion as a complexing agent resulted in a more rapid reaction and, in contrast to the chloride media, the rate showed a marked dependence on $[Br^-]_i$ (Table 4). At the same initial halide ion concentration of 2.73 M, the reaction is about 50 times faster in bromide media.

The use of CH_3CN as a complexing agent (without added halide ion) was also investigated. While water-CH_3CN (18%) mixtures were effective in maintaining an homogeneous medium, the starch-I_2 indicator complex could not be used as an indicator. Meaningful orders with respect to Cu^{2+} and I^- were not obtained (although the reaction under these conditions is approximately second order in Cu^{2+}) probably because the rate is very sensitive to $[CH_3CN]$.

DISCUSSION

Copper(II) oxidations of halide or pseudohalide ions have several synthetic [e.g. $(CN)_2$ formation] or analytical applications. From a kinetic aspect, the Cu^{2+}/CN^- system has been the subject of several investigations[8–11] as this is an homogeneous reaction in the presence of excess cyanide ion.

$$2Cu^{2+} + 6CN^- \rightarrow 2[Cu(CN)_2]^- + (CN)_2. \quad (3)$$

Although the relationship between the order and the coefficients in eqn (3) is coincidental, Baxendale and Westcott[8] found the rate law to have the form

$$\frac{-d[Cu^{2+}]}{dt} = k[Cu^{2+}]^2[CN^-]^6 \quad (4)$$

and a rate determining step of

$$2Cu(CN)_3^- \rightarrow 2Cu(CN)_2^- + (CN)_2 \quad (5)$$

was proposed.[8]

Despite less attention, it is obvious that the Cu^{2+}/I^- system must also be of high order in iodide ion, but the exact factor has been difficult to determine[4] because of the autocatalytic nature of the heterogenous reaction (6)

$$2Cu^{2+} + 4I^- \rightarrow 2CuI\downarrow + I_2. \quad (6)$$

For this reaction, Kemp and Rohwer[4] report the rate law:

$$\frac{-d[Cu^{2+}]}{dt} = k[CuI][Cu^{2+}]^{2.62}[I^-]^{6.2} \quad (7)$$

and it is this high power in $[I^-]$ that enables the iodometric estimation of Cu^{2+} to be performed in a reasonable time.

In the present system, Cu(I) is stabilised in the presence of Cl^- (or Br^-) and CuI precipitation is prevented. Precipitation of CuI is also prevented if the $[I^-]$ is sufficiently high[12,13] but under these conditions the reaction rate is too rapid for conventional techniques.

In principle, it should be possible, from a knowledge of the Cu^{2+}/halide ion stability constants[14] and the variation in rate with respect to the halide ion, to estimate which $Cu(II)X_n^{2-n}$ species is involved in the rate determining step. Unfortunately, the results of our calculations are inconclusive but it is obvious that Cu^{2+}, CuX^+ and CuX_4^{2-} are unlikely candidates for the active Cu(II)-halide species.[15] We have chosen CuX_2 as the reactive Cu(II) species in strong halide media to illustrate the possible mechanism, but CuX_3^- cannot be discounted. CuX_2 has the advantage of providing the appropriate Cu:X ratio for the most stable form of the Cu(I) halide complex.

The following equilibria fit the observed rate laws and

are analogous to those proposed for the Cu^{2+}/CN^- system:[15]

$$Cu^{2+} + 2X^- \rightleftharpoons CuX_2 \quad (8)$$

$$CuX_2 + I^- \rightleftharpoons CuX_2I^- \quad (9)$$

$$2CuX_2I^- \rightarrow CuX_2^- + I_2. \quad (10)$$

The positive salt effect suggests a rate determining step between two ions of the same charge (eqn 10), and the choice of equilibria has been made on the basis of reactants that will give the least unfavourable electrostatic interactions. We believe that the electron transfer is rate determining rather than substitution of a coordinated water molecule, as all observations suggest that such substitution processes are very rapid in Cu(II) systems.[16]

Although Cu(I)-halide complexes are known to be very sensitive to air oxidation, kinetic runs performed in the open atmosphere, and under N_2 were identical. Deli-

Table 2. Variation of rate with respect to initial concentrations. T = 298.2 K, μ = 3.13 M

Variation of $[Cu^{2+}]$[a]

$[Cu^{2+}]_i$ (mM)	$t_{\frac{3}{4}}$[c] (s)	$t_{\frac{1}{2}}$ (s)
1.87	12.3	49.7
1.50	13.8	53.3
1.12	20.3	67.7
0.75	31.5	98.5
n[d]	2.0 ± 0.2	1.8 ± 0.2

Variation of $[I^-]$[b]

$[I^-]_i$ (mM)	$t_{\frac{3}{4}}$[c] (s)	$t_{\frac{1}{2}}$ (s)
11.3	12.3	49.7
9.05	15.8	60
6.79	22	88.3
4.52	35	150
n[d]	2.1 ± 0.2	2.0 ± 0.2

Variation of $[H^+]$[e]

$[H^+]_i$ (M)	$t_{\frac{3}{4}}$[c] (s)	$t_{\frac{1}{2}}$ (s)
0.383	12.5	52.7
0.307	12	51
0.230	12	51.5
0.153	11.5	51.5
0.077	11.8	51.5
– [g]	11	53

Variation of μ[f]

$[Cl^-]_i$ (M)	μ (M)	$t_{\frac{3}{4}}$[c] (s)
2.73	3.13	12.7
2.27	2.65	23
1.82	2.20	55
1.36	1.74	113
0.91	1.29	195

Variation of $[Cl^-]$[h]

$[Cl^-]_i$ (M)	$t_{\frac{3}{4}}$[c] (s)	$t_{\frac{1}{2}}$ (s)
2.73	12.5	52.6
2.27	13	56
1.82	14	63
1.36[k]	16.3	94

Variation of $[Cl^-]$ (μ = 4.04)[i]

$[Cl^-]_i$ (M)	$t_{\frac{2}{5}}$[j] (s)
3.64	20
3.18	19.5
2.73	20
1.82	22.5

a $[I^-]_i = 1.13 \times 10^{-2}$ M, $[Cl^-]_i = 2.73$ M, $[H^+]_i = 0.384$ M.

b $[Cu^{2+}]_i = 1.87 \times 10^{-3}$ M, $[Cl^-]_i = 2.73$ M, $[H^+]_i = 0.384$ M.

c $t_{\frac{3}{4}}$ is the time taken for the initial concentration to decay to $\frac{3}{4}$ of its original value, i.e. at least two half-lives.

d The order, n, with respect to the varied reagent, X, calculated from the plot of ln $t_{\frac{3}{4}}$ (or ln $t_{\frac{1}{2}}$) vs ln $[X]_i$ where the slope = (1-n) [5].

e $[Cu^{2+}]_i = 1.87 \times 10^{-3}$ M, $[I^-]_i = 1.13 \times 10^{-2}$ M, $[Cl^-]_i = 2.73$ M.

f $[Cu^{2+}]_i = 1.87 \times 10^{-3}$ M, $[I^-]_i = 1.13 \times 10^{-2}$ M, $[H^+]_i = 0.384$ M.

g No added acid.

h $[Cu^{2+}]_i = 1.87 \times 10^{-3}$ M, $[I^-]_i = 1.13 \times 10^{-2}$ M, $[H^+]_i = 0.384$ M, μ = 3.13 M, $NaClO_4$.

i $[Cu^{2+}]_i = 1.87 \times 10^{-3}$ M, $[I^-]_i = 1.13 \times 10^{-2}$ M, $[H^+]_i = 0$.

j $t_{\frac{2}{5}}$ = time taken for the initial $[Cu^{2+}]$ to decay to two-fifths of its original value.

k Observable precipitation of CuI.

Table 3. Rate constants for the Cu^{2+}/I^- Reaction. $[Cl^-]_i = 2.73$ M, $[H^+]_i = 0.384$ M, $\mu = 3.13$ M, $[Cu^{2+}]_i = 1.87$ mM

T °C	[K]	$[Cu^{2+}]_i$ (mM)	$[I^-]_i$ (mM)	k_2[a] ($M^{-1}s^{-1}$)	$10^4 k_4$[b] ($M^{-3}s^{-1}$)	$10^4 k_4$ calc.[c] ($M^{-3}s^{-1}$)
25.0	[298.2]	1.87	11.3	6.7_4	5.2_7	5.63
		1.87	9.05	4.2_0	5.1_3	
		1.87	6.79	2.7_1	5.8_8	
		1.87	4.52	1.3_7	6.7_4	
		1.83	11.3	7.0_5	5.5_8	
22.0	[295.2]	1.83	11.3	5.7_0	4.4_6	4.50
19.0	[292.2]	1.83	11.3	4.6_4	3.6_3	3.58
16.0	[289.2]	1.83	11.3	3.7_4	2.9_4	2.83
13.0	[286.2]	1.83	11.3	2.7_5	2.1_6	2.23

a Estimated from the slope of the linear plot of $[Cu^{2+}]^{-1}$ vs t (Table 1).

b $k_4 = k_2[I^-]_i^{-2}$

c Calculated from the activation parameters

$E_a = 54.8 \pm 2.3$ kJ mol^{-1}, log PZ = 14.347,

$\Delta S^{\#}_{298} = 21 \pm 4$ J K^{-1} mol^{-1}, $\Delta H^{\#} = 52.3 \pm 2.2$ kJ mol^{-1}.

Table 4. Volume of $S_2O_3^{2-}$ vs time data for the Cu^{2+}/I^- reaction in the presence of bromide ion. $[Cu^{2+}]_i = 9.16 \times 10^{-4}$ M, $[I^-]_i = 2.30 \times 10^{-3}$ M, $[H^+]_i = 0.384$ M, $\mu = 3.13$ M,[a] T = 298.2 K, $[S_2O_3^{2-}] = 2.07 \times 10^{-2}$ M

Vol. $S_2O_3^{2-}$ (mL)	$10^4[Cu^{2+}]$ (M)	$[Cu^{2+}]^{-1}$ (M^{-1})	$[Br^-]_i$ (M) 2.73	2.27	1.82	1.36
			Mean time (s)			
0.8	6.06	1650	4	8	18.5	50
1.0	5.30	1890	-	-	-	100
1.1	4.92	2030	-	-	-	157
1.2	4.54	2200	-	-	-	205
1.3	4.17	2400	-	-	59.5	-
1.4	3.79	2640	-	-	-	258
1.5	3.42	2920	18	37	104.5	-
1.6	3.05	3280	-	-	143.5	-
1.7	2.68	3730	-	64	188	-
1.8	2.31	4330	34.5	82.5	242.5	-
1.9	1.94	5150	-	113	-	-
2.0	1.58	6350	60	146	-	-
2.1	1.21	8260	85	195	-	-
2.2	0.85	11800	123.7	268	-	-
2.3	0.48	20700	191	-	-	-

Calculated Rate Constants[b]

$[Br^-]_i$ (M)	k_2 ($M^{-1}s^{-1}$)	$10^5 k_4$[d] ($M^{-3}s^{-1}$)
2.73	$99._8$	$30._2$
2.27	$35._8$	$10._8$
1.82	$12._4$	3.7_4
1.36	3.4_7	1.0_5

a Ionic strength maintained with $NaClO_4$

b T = 298.2 K, μ = 3.13 M, $[H^+]$ = 0.384 M.

c Footnote a, Table 3.

d Footnote b, Table 3.

berate addition of an air or oxygen stream did, however, result in a catalytic system[17] (eqns 11, 12), dioxygen being about 50% more effective than air.

$$2CuCl_2 + 2I^- \rightarrow 2CuCl_2^- + I_2 \quad (11)$$

$$2H^+ + 2CuCl_2^- + (1/2)O_2 \rightarrow 2CuCl_2 + H_2O. \quad (12)$$

Under these conditions, I_2 production is much greater than the stoichiometric amount indicated by eqn (6) and the possibility of using this system for the recovery of iodine from iodide waste is under investigation.

REFERENCES

[1]A. I. Vogel, A Textbook of Quantitative Analysis, 2nd Edn, p. 343. Longmans (1951).
[2]M. Traube, *Ber.* **1884**, **17**, 1064.
[3]E. Oliveri-Mandala, *Gazz. Chim. Ital.* 1910, **40I**, 107. *J. Chem. Soc., Abstracts* 1910, **98ii**, 490.
[4]D. M. Kemp and E. F. C. H. Rohwer, *Sth. African Chem. Inst. J.* 1956, **9**, 12.
[5]A. A. Frost and R. G. Pearson, *Kinetics and Mechanism*, 2nd Edn, p. 32. Wiley, New York (1961).
[6]Ref. 5, p. 13.
[7]A. J. Cunningham, D. A. House and H. K. J. Powell, *J. Inorg. Nucl. Chem.* 1971, **33**, 572.
[8]J. H. Baxendale and D. T. Westcott, *J. Chem. Soc.* 1959, 2347.
[9]F. R. Duke and W. G. Courtney, *J. Phys. Chem.* 1952, **56**, 19.
[10]N. Tanaka, M. Kamada and T. Murayama, *Bull. Chem. Soc. Japan* 1959, **31**, 895.
[11]G. Nord and H. Matthes, *Acta. Chem. Scand.* 1974, **28**, 13.
[12]G. Bodlander and O. Storbeck, *Z. Anorg. Allgem. Chem.* 1902, **31**, 469.
[13]C. Herbo and J. Sigalla, *J. Chim. Phys.* 1958, **55**, 403.
[14]H. L. Riley and H. C. Smith, *J. Chem. Soc.* 1934, 1448.
[15]Coordinated water molecules are omitted from the complexes discussed in this section.
[16]F. Basolo and R. G. Pearson, *Mechanisms of Inorganic Reactions*, 2nd Edn, p. 222, 421. Wiley, New York (1967).
[17]J. Sigalla and C. Herbo, *J. Chim. Phys.* 1958, **55**, 407.

Polyhedron Vol. 1, No. 7-8, pp. 617-621, 1982
Printed in Great Britain.

0277-5387/82/070617-05$03.00/0
Pergamon Press Ltd.

ON THE ABSOLUTE CONFIGURATIONS OF ORGANOMETALLIC COMPOUNDS—XII†

THE CRYSTAL STRUCTURE AND ABSOLUTE CONFIGURATION OF $[+]_{579}$-(η^5-C_5H_5)Mo(CO)$_2$(C_4H_3N-CH)(=N-R*) WITH R* = (*S*)-CH(CH_3)(C_6H_5)

JAMES D. KORP and IVAN BERNAL*
Chemistry Department, University of Houston, Houston, TX 77004, U.S.A.

(*Received* 23 *November* 1981)

Abstract—The X-ray crystal structure and absolute configuration of $[+]_{579}$-(η^5-C_5H_5)Mo(CO)$_2$[C_4H_3N-CH(=NR*] for R* = (*S*)-CH(CH_2)$_3$(C_6H_5) have been determined from single crystal diffraction data. The compound crystallizes in the orthorhombic space group $P2_12_12_1$ with four molecules in a unit cell of dimensions a = 8.631(4), b = 12.973(5), and c = 15.948(7) Å. The structure was solved by the Patterson method and refined to a final R value of 2.3% using 2620 independent data. The Mo atom has square pyramidal coordination, and the configuration at Mo is found to be (*R*) for the $[+]_{579}$ diastereoisomer. The Mo–Cp distances average 2.330 Å, with the two carbons of the ring closest to the Schiff base being the most eclipsed by the other ligands on Mo. The Mo–C(O) and Mo–N bond lengths and associated angles are contrary to previous cases where a "*trans* effect" was thought to be seen. Instead, the disparate Mo–N lengths are due to the greater affinity of the formally charged, deprotonated pyrrole nitrogen for Mo. Discrepancies between bonding properties of the present compound and its pyridine analogue are similarly explained. The phenyl ring of the optically active Schiff base is directed away from the Mo atom, which is characteristic of the non-preferred diastereoisomers of the other compounds in this series. The configuration of the optically active carbon is found experimentally to be (*S*), as expected from the absolute configuration of the (*S*)-α-phenylethylamine used.

INTRODUCTION

In a series of papers on the structures and absolute configurations of organometallics having metals as chiral centers,[1-10] we have dealt principally with X-ray determinations of what we have labelled "the preferred diastereoisomers." That is, crystals studied were largely those of substances which (a) were the predominant species at equilibrium in solution and (b) crystallized first during a fractional crystallization experiment. However, in the case of one CpMO(CO)$_2$(thioamide)[10] and one CpMo(CO)$_2$(Schiff base)[3] we were able to determine the absolute configuration of non-preferred diastereoisomers. As shown in our previous studies,[1-10] the most prominent structural difference between the preferred and non-preferred diastereoisomers is the orientation of the phenyl ring of the optically active carbon with respect to the Cp ligand; i.e.

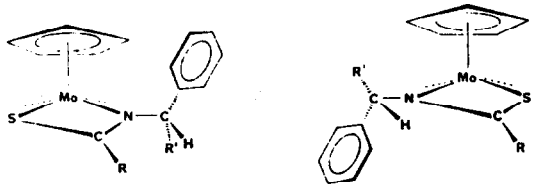

we found the preferred diastereoisomer to have the phenyl ring facing the edge of the Cp ligand whereas the non-preferred species has the phenyl ring pointing away from the Cp, as shown in the above sketches. We also designed molecules such as CpMo(CO)$_2$(L) with L = N(CH_2Ph)CPhN(CHMePh), in which two phenyl rings can, potentially, interact with the Cp ring and found that they behave as expected; that is, the preferred diastereoisomer has both phenyls close to and interacting edgewise with the Cp ring,[11] whereas the non-preferred species has one ring up and one down.[12]

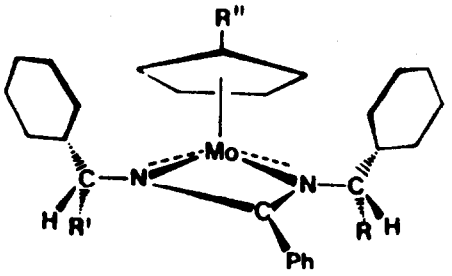

In this report, we discuss the structure and absolute configuration of another Schiff base derivative, obtained from pyrrole carbaldehyde and (*S*)-α-phenylethylamine, with the non-preferred configuration. With this study, we expected to be able to establish the relationship of the signs of the optical rotations at various wavelengths and the absolute configuration for the cases of two related Schiff base non-preferred diastereoisomers (that described in Ref. 3 and this one). Details are given below.

DISCUSSION

As can be seen in Fig. 1, the molecule consists of a central Mo atom in a square pyramidal coordination polyhedron. Distortions from ideal geometry are caused by the different bonding characteristics of the carbonyls and the Schiff base nitrogens. The cap of the pyramid is the polyhapto-cyclopentadiene ring, which can be thought of as a single binding point to the metal. The Mo

*Author to whom correspondence should be addressed.
†For paper 11 of this series see Ref. 12 of this paper.

atom is a chiral center, along with C13 in the ligand, and the correct absolute configuration (Fig. 1) was determined from analysis of 10 Bijvoet pairs of reflections.[13] Applying the extension of the *R, S* system[14] for polyhapto ligands in organometallic compounds,[15] the configuration at Mo is designated (*R*). This assumes that the ranking priority of the binding points is C_5H_5 > N(imine) > N(pyrr.) > CO. The configuration of the pyridyl analogue has also been shown to be (*R*),[7] although it was reported incorrectly in the original communication.[3] Circular dichroism measurements have shown that both compounds have the same sign of the optical rotation at the wavelengths sampled, positive at 579 nm and negative at 404 nm, and this correlates well with the observed equality of configuration.

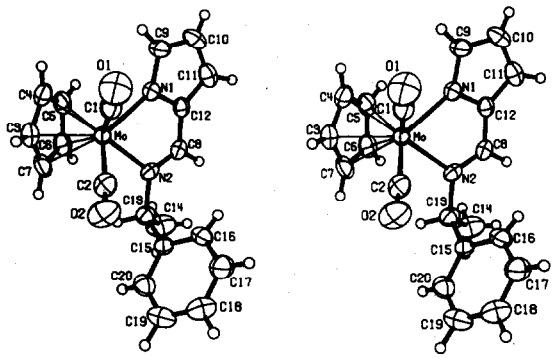

Fig. 1. Stereoscopic view of the molecule showing the atom labeling scheme. The thermal ellipsoids are 50% equiprobability envelopes, with hydrogens of arbitrary size. Note the (*R*) configuration about Mo, and (*S*) about C13.

The Mo–C(Cp) distances range from 2.257 to 2.399 Å, with an average of 2.330 Å. Bonding of Mo to a η^5-C_5H_5 ring has been shown to be influenced somewhat by the nature of the other ligands involved,[5,6] but the present values are in good agreement with those previously reported.[3,5,7] It is also found that the two longest Mo–C(Cp) distances are those to C5 and C6, the carbons closest to the Schiff base. If one considers the torsional angles X–Mo–Cent–C(Cp), where Cent is the midpoint of the cyclopentadienyl ring and X is each one of the four basal plane atoms, one finds the smallest values of the torsional angles when C(Cp) = C5 and C6. That is to say, C5 and C6 are the most eclipsed of the Cp carbons and, as pointed out earlier,[16,17] these minima almost never occur for X = C(CO) in complexes of the type *cis*-$(OC)_2MCp(L_1)(L_2)$. Since molecular orbital calculations predict the Cp rotational barrier in such compounds to be fairly low,[18] the reason for this obviously preferential orientation is unclear.

The Mo–C–O geometrical parameters are in accord with previous results,[1–10] although it may appear a bit unusual to find a significant difference between the two Mo–C(CO) bond lengths. A previously observed case was attributed to "the *trans* effect,"[7] even though similar cases[5] shown no such discrepancy. This situation is similar to that found in studies of Werner coordination

Table 1. Summary of data collection and processing parameters

Space Group	$P2_12_12_1$, orthorhombic
Cell Constants	a = 8.631(4) Å
	b = 12.973(5)
	c = 15.948(7)
	V = 1786Å^3
Molecular Formula	$MoC_{20}H_{18}N_2O_2$
Molecular Weight	414.32
Molecules per Cell	4
Density	1.54 g-cm^{-3}
Absorption Coefficient	6.6 cm^{-1}
Radiation (MoKα)	0.71073 Å
Collection Range	4° ≤ 2θ ≤ 70°
Scan Width	Δθ = (0.95+0.35 sin θ)°
Maximum Scan Time	90 sec.
Scan Speed Range	1.0 to 10.0° min^{-1}
Total Data Collected	4329
Independent Data with I>3σ(I)	2620
Total Variables	298
$R...\Sigma\|\|F_o\|-\|F_c\|\|/\Sigma\|F_o\|$	0.023
$R...\Sigma_w(\|F_o\|-\|F_c\|)^2/\Sigma_w\|F_o\|^2]^{1/2}$	0.021
Weights	$\sigma(F)^{-2}$
Goodness-of-fit	1.05

Table 2. Intramolecular bond distances (Å)*

Mo - C1	1.938(4)	N1 - C9	1.354(4)
Mo - C2	1.977(4)	N1 - C12	1.372(4)
Mo - C3	2.257(4)	N2 - C8	1.297(4)
Mo - C4	2.306(4)	N2 - C13	1.472(4)
Mo - C5	2.389(4)	C8 - C12	1.413(5)
Mo - C6	2.399(4)	C9 - C10	1.375(6)
Mo - C7	2.298(4)	C10 - C11	1.384(6)
Mo - N1	2.150(3)	C11 - C12	1.397(5)
Mo - N2	2.220(3)	C13 - C14	1.507(6)
C1 - O1	1.169(4)	C13 - C15	1.520(5)
C2 - O2	1.156(4)	C15 - C16	1.386(5)
C3 - C4	1.420(6)	C15 - C20	1.380(5)
C3 - C7	1.398(6)	C16 - C17	1.383(6)
C4 - C5	1.410(5)	C17 - C18	1.370(6)
C5 - C6	1.398(5)	C18 - C19	1.376(7)
C6 - C7	1.425(6)	C19 - C20	1.375(6)

* The average C-H distance is 0.95 (4) Å.

Table 3. Intramolecular bond angles (°)

C1-Mo-C2	73.3(2)	C10-C11-C12	105.7(4)
C1-Mo-N1	81.9(1)	C11-C12-C8	134.7(4)
C1-Mo-N2	126.2(1)	C11-C12-N1	110.2(4)
C2-Mo-N1	128.4(1)	N1-C12-C8	115.0(3)
C2-Mo-N2	86.1(1)	N2-C13-C14	115.7(4)
N1-Mo-N2	73.2(1)	N2-C13-C15	111.1(3)
C1-Mo-Cent*	119.4(1)	C14-C13-C15	111.4(4)
C2-Mo-Cent*	115.9(1)	C13-C15-C16	121.8(4)
N1-Mo-Cent*	115.7(1)	C13-C15-C20	120.3(4)
N2-Mo-Cent*	114.4(1)	C16-C15-C20	117.8(4)
Mo-C1-O1	178.5(4)	C15-C16-C17	121.1(4)
Mo-C2-O2	173.8(3)	C16-C17-C18	120.2(4)
Mo-N1-C9	136.9(3)	C17-C18-C19	119.2(4)
Mo-N1-C12	117.3(2)	C18-C19-C20	120.6(4)
C9-N1-C12	105.8(3)	C19-C20-C15	121.1(5)
Mo-N2-C8	116.1(2)	C4-C3-C7	107.2(4)
Mo-N2-C13	123.3(2)	C3-C4-C5	107.8(4)
C8-N2-C13	120.3(3)	C4-C5-C6	109.1(4)
N2-C8-C12	118.1(3)	C5-C6-C7	106.6(4)
N1-C9-C10	110.9(4)	C6-C7-C3	109.3(4)
C9-C10-C11	107.4(4)		

*Cent refers to the geometric center of the cp ring.

compounds in which structural determinations appear to show the *trans* effect in certain derivatives but not in closely related ones. At any rate, our values of Mo–N1 = 2.150(3) Å, N1–Mo–C2 = 128.4(1)° and of Mo–N2 = 2.220(3) Å, N2–Mo–Cl = 126.2(1)° show that attempts to correlate the Mo–N distances with the opposite N–Mo–C angle in the expectation that the shorter Mo–N distance is associated with the smaller angle is not very general even if in some cases[17] such a relationship exists.

As noted above and as found in the pyridyl Schiff base analogue,[1,3] the two Mo–N distances are quite different. Unfortunately, for the sake of comparison, the two cases give exactly opposite results. In the case of the pyridine derivative, the Mo–N(pyridine) bond is longer than the Mo–N(imine) whereas the Mo–N (pyrrole) bond is shorter than the Mo–N(imine). The reason for this apparent discrepancy is probably as follows: the pyrrole nitrogen, once deprotonated, can not only bond Mo as effectively in the sigma and pi sense as the pyridine nitrogen but, bearing a negative charge, binds more strongly the charged Mo (formally + 1). The bonding within the two imine moieties is probably very close judging by the values of the two C=N distances (pyrrole = 1.297(4) and pyridine = 1.270(16) Å).

The plane of the Cp is almost paralled with that defined by the basal atoms C1, C2, N1 and N2. The molybdenum atom is 1.99 Å from Cp and only 0.92 Å above the basal plane. For comparison, the values in the pyridyl analog are 2.00 Å and 0.95 Å. The N1–C12–C8–N2 torsion angle in both compounds is essentially 0°, which is a structural characteristic distinguishing these compounds from the thioamide series.[7] The phenyl rings in both Schiff base complexes are directed away from the Cp ring, which is the most prominent difference between the preferred and non-preferred diastereoisomers. [The present structure is referred to as "non-preferred" because it is not the predominant species in solution at equilibrium.] The configuration about the optically active carbon, C13, is (*S*). The remaining bond distances and angles in the current structure are as expected based on previous investigations.[1–10] The packing of the molecules in the crystal lattice is illustrated in Fig. 2, which shows the alternating rows of molecules characteristic of this space group.

Table 4. Least squares planes and atomic deviations

A. C3-C7 (Max. deviation 0.005Å)

-.2098x - .8832y - .4195z + .815 = 0

Mo	-1.992Å	N1	-3.033Å
C1	-2.848	N2	-3.022
C2	-2.751		

B. C15-C20 (Max. deviation 0.006Å)

-.9339x + .0506y -.3540z +7.812 = 0

C. N1, C9-C12 (Max. deviation 0.003Å)

.3061x -.7462y -.5912z +1.350 = 0

Mo	0.067Å	C8	-0.045Å
N2	-0.097	C13	-0.120

D. N1, N2, C1, C2 (Max. deviation 0.020Å)

-.1379x -.8748y -.4645z +3.589 = 0

Mo	0.915Å	C5	3.007Å
C3	2.814	C6	2.981

Interplanar Angles:

A, C	32.6°	B, C	96.6°
A, D	4.9	B, D	75.6
		C, D	27.7

Table 5. Selected torsion angles

C1-Mo-N1-C9	-46.52°
C2-Mo-N2-C13	48.90
Mo-N2-C13-C15	-85.45
N1-C12-C8-N2	- 0.84
C8-N2-C13-C14	-27.25
C8-N2-C13-C15	101.10
N2-C13-C15-C16	-38.79
C14-C13-C15-C16	91.81

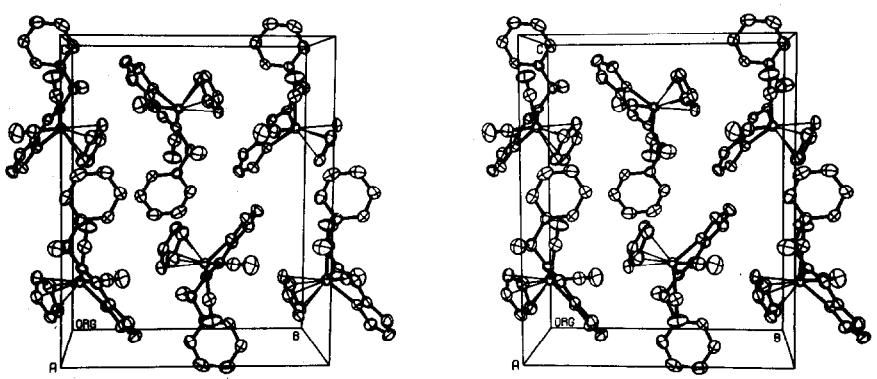

Fig. 2. Stereoscopic view of the molecular packing in the unit cell, with hydrogens omitted for clarity.

EXPERIMENTAL

The synthesis and resolution of $(\eta^5\text{-}C_5H_5)Mo(CO)_2(NN^*)$ has been published elsewhere.[19] The crystal used for all measurements was an irregular brownish-orange fragment of approximate dimensions $0.6 \times 0.4 \times 0.2$ mm. An Enraf-Nonius CAD-4 automatic diffractometer was used with MoKα radiation monochromatized by a dense graphite crystal assumed for all purposes to be ideally imperfect. Final cell constants, as well as other information pertinent to data collection and refinement, are listed in Table 1.

The structure was solved by interpretation of the Patterson map, which gave the position of the molybdenum atom. The remaining non-hydrogen atoms were found in subsequent difference Fourier syntheses. The usual sequence of isotropic and anisotropic refinement was followed, after which the hydrogens all were easily located. After shift/esd ratios were less that 0.1 for all refinable parameters, the refinement converged to the agreement factors listed in Table 1. There were no unusually high correlations between any of the variables in the final cycle. The atomic scattering factors for the non-hydrogen atoms were computed from numerical Hartree–Fock wave functions;[20] for hydrogen those of Stewart, Davidson, and Simpson were used.[21] The anomalous dispersion coefficients of Cromer and Liberman[22] were used for molybdenum. Bond lengths, angles, least squares planes, and torsion angles are presented in Tables 2–5. Final atomic parameters and lists of F_o/F_c values have been deposited as supplementary data with the Editor.† The atomic labeling scheme is shown in Fig. 1, with hydrogens numbered the same as the atom to which each is bonded.

Acknowledgement—We wish to thank the R. A. Welch Foundation for operational support through research grant E-594.

†Copies are available on request from the Editor at Queen Mary College. Atomic co-ordinates have also been deposited with the Cambridge Crystallographic Data Centre.

REFERENCES

[1]S. J. LaPlaca, I. Bernal, H. Brunner and W. A. Herrmann, *Angew. Chem.* 1975, **87**, 379.
[2]M. G. Reisner, I. Bernal, H. Brunner and M. Muschiol, *Angew. Chem.* 1976, **88**, 847.
[3]I. Bernal, S. J. Laplaca, J. Korp, H. Brunner and W. A. Herrmann, *Inorg. Chem.* 1978, **17**, 382.
[4]H. Brunner and J. Doppelberger, *Chem. Ber.* 1978, **111**, 673.
[5]M. G. Reisner, I. Bernal, H. Brunner and J. Wachter, *J. Organomet. Chem.* 1977, **137**, 329.
[6]M. G. Reisner, I. Bernal, H. Brunner and J. Doppelberger, *J. Chem. Soc., Dalton Trans.* 1979, 1664.
[7]G. M. Reisner and I. Bernal, *J. Organomet. Chem.* 1979, **173**, 53.
[8]G. M. Reisner and I. Bernal, *J. Organomet. Chem.* 1981, **220**, 55.
[9]J. D. Korp and I. Bernal, *Cryst. Struc. Comm.* 1980, **9**, 821.
[10]M. W. Creswick and I. Bernal, *Inorg. Chim. Acta*, 1982, **57**, 171.
[11]H. Brunner, G. Agrifoglio, I. Bernal and M. W. Creswick, *Angew. Chem.* 1980, **92**, 645.
[12]I. Bernal, M. Creswick, H. Brunner and G. Agrifoglio, *J. Organomet. Chem.* 1980, **198**, C4.
[13]J. M. Bijvoet, A. F. Peerdeman and A. J. Van Bommel, *Nature* 1951, **168**, 271.
[14]R. S. Cahn, C. Ingold and V. Prelog, *Angew. Chem.* 1966, **78**, 413.
[15]K. Stanley and M. C. Baird, *J. Am. Chem. Soc.* 1975, **97**, 6599.
[16]M. J. Bennett and R. Mason, *Proc. Chem. Soc. London* 1963, 273.
[17]M. W. Creswick, Ph.D. Thesis, University of Houston, 1981.
[18]T. A. Albright, R. Hoffman, Y. Tse and T. D'Ottavio, *J. Amer. Chem. Soc.* 1979, **101**, 3812.
[19]H. Brunner and W. A. Herrmann, *J. Organomet. Chem.* 1973, **63**, 339.
[20]D. T. Cromer and J. B. Mann, *Acta Crystallogr.* 1968, **A24**, 321.
[21]R. F. Stewart, E. R. Davidson and W. T. Simpson, *J. Chem. Phys.*, 1965, **42**, 3175.
[22]D. T. Cromer and D. J. Liberman, *J. Chem. Phys.* 1970, **53**, 1891.

Polyhedron Vol. 1, No. 7–8, pp. 623–627, 1982
Printed in Great Britain.

0277–5387/82/070623–05$03.00/0
Pergamon Press Ltd.

MUTUAL INFLUENCE OF METALS IN THE EXTRACTION OF THEIR CHLORIDE COMPLEXES WITH TRI-*n*-OCTYLAMINE AND ALIQUAT 336 IN NITROBENZENE

V. V. BAGREEV,* C. FISCHER,† L. M. KARDIVARENKO and YU. A. ZOLOTOV

Vernadsky Institute of Geochemistry and Analytical Chemistry, U.S.S.R. Academy of Sciences, Moscow, U.S.S.R.

(*Received* 6 *January* 1982)

Abstract—The simultaneous extraction of the micro- and macroamounts of In, Fe, Ga, Zn and Co from HCl with solution of tri-*n*-octylamine (TOA) and Aliquat 336 in nitrobenzene has been studied. A decrease in the extraction of the microelements in the presence of extractable macroelements (i.e. suppression of the microelement extraction) has been shown to occur. The conductivities, dielectric constants and viscosities of the nitrobenzene solutions of metal-containing and simple TOA and Aliquat salts have been measured. Their dissociation constants in nitrobenzene extracts have been calculated. Some features connected with mutual influences of metals are reported. The mechanism of this phenomenon is discussed.

INTRODUCTION

The extraction of certain elements can be affected by others being present and extracted in a given system. This effect is particularly noticeable when microamounts of the former elements are extracted in the presence of relatively large amounts of the latter. This has been shown for the extraction systems with long-chain amines and quarternary ammonium salts (QAS).[1–4] The influence of the macroelements, observed in this case, may be of two kinds; it may either decrease (extraction suppression) or, conversely, increase (co-extraction) the microcomponent extraction. A detailed study of the mutual influence of metals during their extraction from chloride solutions with tri-*n*-octylamine (TOA) and Aliquat 336 (trialkylmethyl ammonium chloride with alkyl radicals C_8–C_{10}) solutions in benzene[4] has led to a conclusion that suppression of microelement extraction can be principally due to the dissociation of alkylammonium salts in the extracts and a related common ion mechanism. Equations describing the extraction of the microelement in the presence of the macroelement have been derived.[3] Their analysis indicated that in a number of cases the dielectric constant of the organic solvent (amine diluent) may be important in the developing of the mutual influence of the metals in their extraction. In this connection it would be interesting to study the simultaneous extraction of metals by using a high-polar solvent, viz. nitrobenzene.

In the present paper the influence of large amounts of Fe, Ga, In, Zn and Co upon the extraction of microamounts of the same elements (except for gallium) from HCl solutions with TOA and Aliquat 336 is represented. The influence of HCl and the macrocomponent and extractant concentrations were studied. Moreover, the extraction of the microcomponents in the absence of the macroelements, as well as, of the macroelements themselves with the same extractants were investigated in parallel. The conductivities, dielectric constants and also the viscosities of the simple and metal-containing salts of TOA or Aliquat 336 were measured and plotted against their concentrations.

*Author to whom correspondence should be addressed.
†Central Institute of Solid State Physics and Material Research, Academy of Sciences of the GDR, Dresden, GDR.

EXPERIMENTAL

A procedure for the preparation of the solutions, experimental techniques and equipment for the conductivity measurements have been described earlier.[4] The dielectric constants of the nitrobenzene extracts were measured with an EIO–7 instrument (USSR). A contactless cell[5] and a data processing technique described in[6] where used. Their viscosities were measured with a capillary glass viscosimeter VPZh–I (U.S.S.R.) with a capillary diameter $d = 0.34$ mm.

RESULTS

Influence of hydrochloric acid on the microelements extraction

Figure 1 shows the results obtained for In(III), Fe(III), Zn(II) and Co(II) (microelements) in the absence and in the presence of the macrocomponents as a plot of log D microcomponent vs the initial concentration of HCl (1–8 M). The same metals and Ga were used as the macrocomponents. The influence of the macroelements on the extraction of the microelements will be considered below. A measure of such influence is the extent of the extraction suppression, i.e. the ratio of the microelement distribution coefficient in the absence of the macrocomponent to the corresponding value in its presence (D_1/D_2).

Indium. Indium was extracted in the presence of 0.4 M iron and 0.2 M zinc. In the case of TOA both macroelements suppress the extraction of indium. In the presence of iron D_{In} decreases more than by five orders of magnitude at 6–8 M HCl. In the presence of zinc this decrease is not strong, the factor is only 10–15. The extent to which the indium extraction is suppressed by iron increases with increasing HCl concentration, and it remains essentially constant for zinc in the acidity range investigated. The influence of iron and zinc occurs when metals are extracted with Aliquat 336 although this extraction suppression is still smaller and practically the same for both macroelements.

Iron. The influence of gallium (0.4 M), indium (0.4 M) and zinc (0.2 M) on the extraction of iron microamounts was investigated. There is a noticeable decrease in the

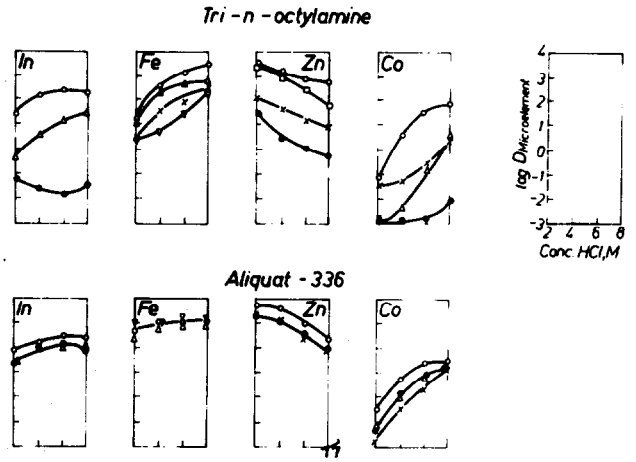

Fig. 1. Extraction of In, Fe, Zn and Co in dependence of the HCl concentration by 0.5 M solutions of TOA and Aliquat-336 in nitrobenzene in absence of the macrocomponent and in presence of In (⊗), Fe (●), Ga (▽), Zn (△) and Co (□). In, Fe, Ga = 0.4 M; Zn, Co = 0.2 M.

extraction of iron in the presence of Ga and In for TOA as extractant: D_{Fe} decreases by one to two orders of magnitude at 6–8 M HCl. The influence of zinc on the extraction of iron is less pronounced. In the extraction of iron with Aliquat 336 there is practically no influence of the macroelements.

Zinc. Macroamounts of iron (0.4 M) influence the extraction of zinc by TOA: D_{Zn} decreases by two to three orders of magnitude in comparison with D_{Zn} in its extraction alone as HCl concentration increases. In the presence of indium the degree of the extraction suppression of zinc is smaller (the factor is only about 50). Cobalt influences the extraction of zinc by TOA when HCl concentrations are over 6 M: for 8 M HCl the D_1/D_2 ratio is close to 10. In the case of Aliquat 336 the influence of macrocomponents is smaller, the D_{Zn} decreases by 3–4 times in comparison with its individual extraction in the acidity range investigated.

Cobalt. The cobalt extraction with TOA is strongly suppressed in the presence of 0.4 M iron and indium or 0.2 M zinc. Iron decreases D_{Co} by four to five orders of magnitude, indium and zinc approximately by two to three orders at the acid concentration 4–6 M. In the extraction with Aliquat 336 this effect, as in the above cases, is not strong—the factor is only 4–10.

Extraction of macroelements

We have studied the behaviour of the macroelements themselves under these conditions, when their extraction together with the microelements was carried out. Distribution coefficients of Fe(III), In(III), Ga(III), Co(II) and Zn(II) with both extractants, depending on the HCl concentration, are shown in Fig. 2. Aliquat 336 extracts Fe, Ga, In and Zn by 95–100%. The cobalt extraction increases from 28% at 2 M HCl to 93% at 8 M HCl. The percentage extractions of metals using TOA for 2 M and 8 M HCl are as follows: 50 and 98% for Fe, 46 and 66% for In, 2 and 97% for Co, 60 and 99% for Ga respectively. Zinc is extracted practically completely in the acidity range investigated. There seem to be no previous studies on the extraction of such large amounts of these elements by using TOA and Aliquat 336 in nitrobenzene.

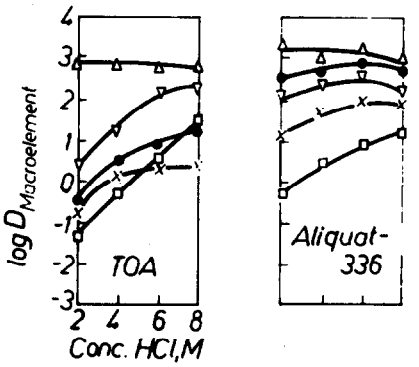

Fig 2. Extraction of macroelements with 0.5 M solutions of TOA and Aliquat in nitrobenzene (designations vs Fig. 1).

Conductivity, dielectric constant and viscosity measurements

To elucidate the reasons for the extraction suppression in systems containing amines and QAS it is necessary to know the state of the extractants themselves and compounds to be extracted in the organic phase. For this purpose the conductivities and dielectric constants of the extracts of simple and metal-containing salts of TOA and Aliquat 336 in nitrobenzene were measured. The preparation conditions of the extracts for the measurements of the conductivities and dielectric constants of these salts are summarized in Table 1. The initial extracts were adjusted to the desired metal or simple salt concentration by dilution with nitrobenzene. The conductivities of the nitrobenzene extracts are summarized in Fig. 3 as plots the equivalent conductivity λ vs the metals concentration in the organic phase. The same figure shows similar dependencies for the extracts of TOA HCl and Aliquat 336 themselves together with the latter's bromide and iodide analogues at various concentrations. The λ values decrease with increasing metal concentration in the organic phase (a picture differing from that for benzene extracts).[4-7] As in the case of benzene the conductivities of Ga-, Fe- and In-containing salts at equal con-

Table 1. Extraction of metals with 0.25 M solutions of TOA and Aliquat 336 in nitrobenzene

Metal	Aqueous phase	D	Molar ratio metal/extractant	Compound to be extracted*
		Trioctylamine		
Fe	0.30 M $FeCl_3$	3.90	0.96	R_3NHMCl_4
Ga	0.30 M $GaCl_3$	4.76	0.99	R_3NHMCl_4
Ih	0.30 M $InCl_3$	0.90	0.57	$R_3NHInCl_4$,R_3NHCl
Z_n	0.25 M $ZnCl_2$	0.91	0.48	$(R_3NH)_2MCl_4$
Co	0.25 M $CoCl_2$	0.66	0.40	$(R_3NH)_2MCl_4$
		Aliquat 336		
Fe	0.30 M $FeCl_3$	2.74	0.88	$R_3R'NMCl_4$
Ga	0.30 M $GaCl_3$	3.57	0.94	$R_3R'NMCl_4$
In	0.30 M $InCl_3$	2.33	0.84	$R_3R'NMCl_4$
Z_n	0.25 M $ZnCl_2$	0.96	0.49	$(R_3R'N)_2MCl_4$
Co	0.25 M $CoCl_2$	0.73	0.42	$(R_3R'N)_2MCl_4$

*The molar ratio metal/extractant for all the alkylammonium salts studied was determined.

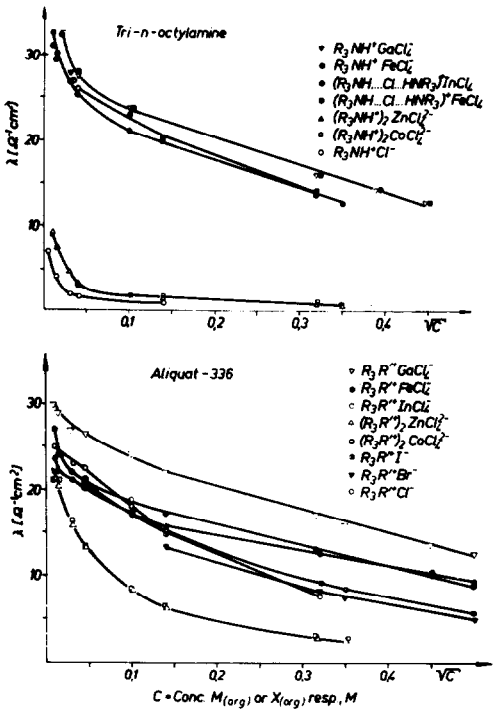

Fig. 3. Equivalent conductivity λ of metal-bearing and simple salts of TOA and Aliquat-336 in nitrobenzene vs concentration of $M_{(org)}$ or $X_{(org}$, resp.

centrations, which suggests a higher dissociation of the former. This is true for both TOA and Aliquat 336. The conductivities of extracts of the simple salts of TOA are substantially smaller than those of the solutions containing comparable amounts of its metal-containing salts. The conductivities of extracts of Aliquat 336 and its bromide and iodide analogues occupy and intermediate position between the λ values of the above mentioned two metal groups.

A sharp increase in dielectric constant of extracts of metal-containing alkylammonium salts is observed in solutions with salt concentrations higher than ~0.05 M (Table 2). The ϵ values increase in the case of the Fe-, Ga- and In-containing salts of both extractants more

Table 2. Dielectric constants of the extracts of the metal-containing and simple salts of TOA and Aliquat 336 in nitrobenzene ($t = 25°$, $\in$ of nitrobenzene 34.8)

Concentration of metal (M)	Dielectric constant: Iron	Indium	Gallium	Zinc	Simple salt
		Trioctylamine			
0.031	—	41 ± 4	—	—	—
0.050	44 ± 4	—	—	—	—
0.0625	—	42 ± 4	—	41 ± 4	—
0.100	—	—	—	42 ± 4	—
0.125	51 ± 5	51 ± 5	48 ± 5	47 ± 5	—
0.200	55 ± 5	—	—	—	—
0.250	64 ± 6	—	64 ± 6	—	—
		Aliquat 336			
0.057	—	—	—	—	44 ± 4
0.0625	45 ± 4	—	—	—	—
0.125	75 ± 7	—	—	50 ± 5	51 ± 5
0.25	63 ± 6	52 ± 5	67 ± 7	—	52 ± 5

sharply than for both Zn-containing salts studied. It can be noted that an increase of the dielectric constants of extracts should be accompanied probably by stronger dissociation of the compounds in the organic phase.

The viscosities of the extracts of Fe-, Ga- and In-containing salts of TOA and Aliquat 336 depending on their concentration in nitrobenzene were also measured. The viscosities of the extracts also show a marked increase with increasing salts concentration (Fig. 4).

On the basis of the conductivities, dielectric constants and viscosities data obtained the values of the dissociation constants of the corresponding salts of both extractants were calculated. Fuoss–Kraus' and Shedlovsky's equations allow the determination of K_{diss} to a good approximation when the degree of dissociation of the ion pairs is under 10^{-2}.[8] The reasonably high dielectric constants and conductivities of the extracts (Table 2) indicate that the salts R_3NHMCl_4 and $R_3R'NMCl_4$ studied are electrolytes whose dissociatiod degrees are over 0.01. Therefore Fuoss–Onsagers method[9] which is suitable for finding the K_{diss} values of weakly associated electrolytes was used for calculations. The precision of the method of conductivity measurements which we used (~0.1%) permit us also to

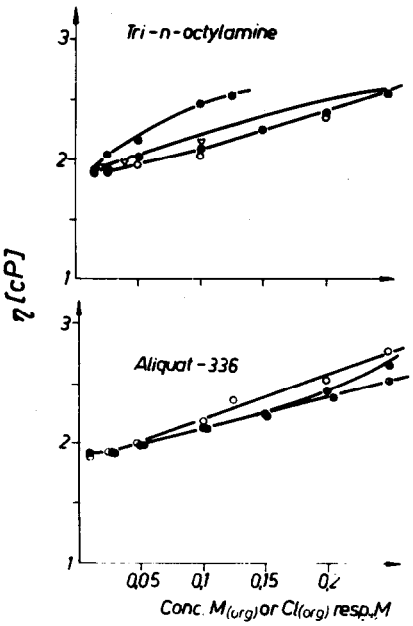

Fig. 4. Viscosity η of metal-bearing and simple salts of tri-*n*-octylamine and Aliquat-336 in nitrobenzene vs concentration of $M_{(org)}$ or $Cl_{(org)}$, resp. (designations vs Fig. 3).

apply this method. It is well known that large alkylammonium ions tend to strongly increase the viscosity of their solutions, therefore the viscosities were introduced into the equations for calculating the K_{diss} values. The initial values of the limiting equivalent conductivities (λ_0) for all the salts, except for TOA chloride, were found by extrapolating the C plots to infinitely diluted solutions ($C = 0$). The λ_0 value for TOA chloride was calculated from the data $\lambda_0^+ = 10.8$ *g*-ion^{-1} Ohm^{-1} cm^2 and $\lambda_0^- = 22.2$ *g*-ion^{-1} Ohm^{-1} cm^2 in nitrobenzene[10] and was found to be equal to 33 *g*-equiv^{-1} Ohm^{-1} cm^2. The dissociation constants were calculated in the interatomic distances 3–10 Å range through the 0.5 Å interval and the final K_{diss}, limiting equivalent conductivity and interatomic distance values were taken as the minimum values of the function $\delta(\lambda) = (\Sigma(\Delta\lambda)^2/N-3)^{1/2}$. The program developed for the computer 15-BSM-5 (USSR) was applied for the treatment of the results. The dissociation constant obtained are listed in Table 3. There are shown all the alkylammonium salts investigated, except for TOA chloride, are rather strongly dissociated in the nitrobenzene extracts. Our data for TOA chloride correspond within an order of magnitude to the data previously described.[10]

Some results concerning the IR-spectroscopic investigation of extracts which could confirm the stronger dissociation of salts studied in nitrobenzene can be represented. The IR-spectra of the investigated metal-containing TOA salts show one strong ν_{NH}-band at about 3160 cm^{-1}. There is a remarkable shift of 40–50 cm^{-1} to higher frequencies compared with the ν_{NH}-bands for the benzene extracts of the same salts (ν_{NH} = 3110...3120).[11,12] This shift is indicative of the weaker interaction of the alkylammonium cation with the complex metal-containing anion and, hence, the higher degrees of their dissociation in the nitrobenzene solutions as compared with benzene solutions.

The trends of the λ–C_M plots for the Zn- and Co salts of both extractants, i.e. $(R_3NH)_2MCl_4$ or $(R_3R'N)_2MCl_4$ indicate that these salts can be considered as medium-strong electrolytes. Therefore their dissociation constants can be calculated by using Shedlovsky's method on the assumption that these salts are dissociating mainly at the first stage whereas their dissociation at the second stage is very low. The dissociation constant thus calculated for the TOA zinc salt, $(R_3NH)_2ZnCl_4$ is equal to 4.0×10^{-4}. The corresponding constant for the cobalt-containing salt can be assumed to be close to this value.

Table 3. Dissociation constants (K_{Dis}) of the metal-containing and simple salts of TOA and Aliquat 336 in nitrobenzene

Element	Dissociation constant	
	Trioctylamine	Aliquat 336
In	$(1.9 \pm 0.9)10^{-2}$	—
Fe	$(1.5 \pm 0.9)10^{-2}$	$(1.2 \pm 0.5)10^{-3}$
Ga	$(4 \pm 1)10^{-3}$	$(1.2 \pm 0.5)10^{-3}$
Cl	$(6 \pm 1)10^{-5}$	$(1.4 \pm 0.9)10^{-2}$

DISCUSSION

Thus, the data obtained show that the extractable macroelements had a considerable effect on the extraction of microelements: extraction suppression of the microelements was observed in the majority of the systems investigated. In principle, the extent of this influence may be controlled by various parameters of the extraction system, such as nature and concentration of the acid, type of the extractant and the nature and extractability of the macroelement as well as the dielectric constant and other characteristics of the extracts. Generally, the character of the influence of these factors on the bahaviour of the microelement in the presence of the macrocomponent during the extraction by amine salts and QAS can be analysed by application of the following equation:[3]

$$D_{micro} = K_{ex} \cdot q \cdot \frac{[R_3R'NCL]_0}{\alpha_{micro}(\alpha_{R_3R'NCl} \cdot C_{Cl(0)} + \alpha_{macro} \cdot C_{macro})} \quad (1)$$

where D_{micro} is the coefficient of the microelement distribution, K_{ex} is the constant of its extraction, q is the fraction of the microcomponent complexes to be extracted in the aqueous phase, $[R_3R'NCl]_0$ is the concentration of the free extractant in the organic phase, $C_{Cl(0)}$ is the total concentration of the dissociated and nondissociated simple amine salt, C_{macro} is the concentration of the macroelement in the organic phase, α is the extent of dissociation of the corresponding alkylammonium salts in the organic phase, R'–H or CH_3.

TOA. In most cases an increase in the concentration of hydrochloric acid leads to an increase in the degree of the suppression of the microelement extraction. This can be attributed to the fact that extraction of the macrocomponents studied increases, as a rule, with the acidity increasing of the aqueous phase (Fig. 2). For example, the extraction of macroamounts of iron with TOA increases as HCl concentration varies from 2 to 8 M–D_{Fe} increases by one to two orders of magnitude. The degree of suppression of the In, Zn and Co amounts in the presence of iron also increases with the acid concentration.

The influence of concentration of the macroelements themselves on the behaviour of the microelements must show the more complicated character. In addition to the

fact that this parameter enters into the denominator of the eqn (1), the macroelement concentration produces a significant effect on the dielectric constant of the organic phase (as seen from Table 2). The latter in turn, affect the other parameters of the equation, such as the initial extractant concentration and the degrees of dissociation of the metal-containing alkylammonium salts in the organic phase. Hence the distribution coefficients of the microelements, D_{micro}, are expected to be the lower the higher is the degree of dissociation. In fact, the suppression of extraction is considerably stronger in the presence of Fe and Ga than in the presence of Zn and Co, nevertheless at reasonably high HCl concentrations all macroelements, except for indium, are extracted into the organic phase practically completely. There is analogous behaviour during extraction of the chloride complexes with TOA in benzene.[4] Thus suppression of microelement extraction can be connected not only with the macrocomponent concentration. The dissociation of their extractable compounds in the organic phase must be the principal cause of the suppression. As seen from Fig. 3 and Table 2, the Fe- and Ga- containing salts of TOA are more dissociated than its Zn- and Co-containing salts.

Aliquat 336. Mutual effects for Aliquat 336 are not so strongly pronounced as in the case of TOA (again the picture is analogous to that in the Aliquat 336–benzene system);[4] at the same time, the degree of suppression of microamounts of Zn and Co extraction with the macrocomponents in the case of nitrobenzene is higher by 10 times than in the benzene system. This could be expected from the analysis of the above eqn (1). The studied metal-containing salts of Aliquat 336 are dissociated less than the corresponding salts of TOA (Table 3). But the dissociation constant of Aliquat itself is higher by three orders of magnitude than that of TOA chloride. In such a case our equation could be expected to show that an extent of the microelement extraction suppression in the case of Aliquat 336 would be higher than that in the case of TOA or commensurate to it. In reality, however, the suppression effects observed for the systems with Aliquat are poorer (Fig. 1).

In our opinion one possible explanation of this phenomenon can be a very high extraction power of unsymmetrical QAS, containing a short alkyl chain, including Aliquat 336. In this connection the very large values of extraction constant in the numerator of the equation are likely to "smooth out" the probable influence of the variation in the other parameters of the eqn (1), which, in turn, obscures the action of the common ion mechanism as the principal cause of the extraction suppression. In Fig. 5 the influence of the iron concentration on the extraction of cobalt microamounts with TOA and Aliquat 336 is shown. The character of dependencies for TOA and Aliquat 336 is quite different. The iron concentration range where the cobalt distribution coefficients are constant, is wider during extraction with Aliquat–D values are constant up to iron concentrations of approximately 0.2 M and then fall. In the case of TOA cobalt extraction begins to be reduced

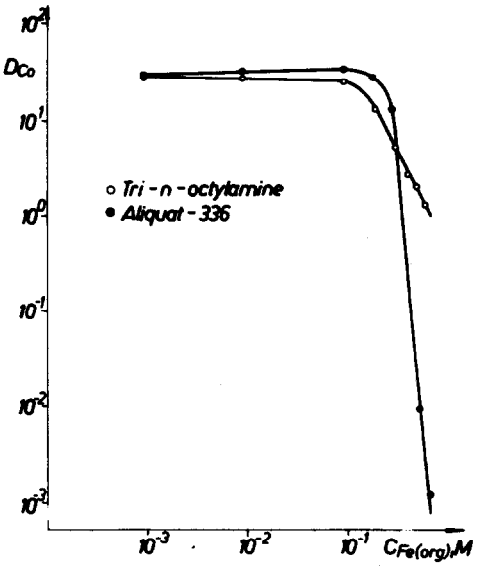

Fig. 5. Influence of $C_{Fe(org)}$ on the extraction of microamounts of Co (extractant concentration 0.5 M in nitrobenzene; C_{HCl} 6 M).

at the substantially lower iron concentration, i.e. 0.1M. But both for TOA and Aliquat 336 the microelement extraction suppression is begun long before the organic phase has been saturated with the macrocomponent. Therefore probably the conditions for the common ion effect are more favourable in the TOA system compared with the Aliquat system.

The data reported in this paper, concerning the mutual influence of metals during extraction, have been used to improve the conditions of their estractive separation.[13,14]

REFERENCES

[1]V. V. Bagreev, Yu. S. Tseryuta, N. A. Agrinskaya and Yu. A. Zolotov, *Izv. Akad. Nauk SSSR, Ser. Khim.* 1973, **10**, 2183.
[2]Yu. A. Zolotov, V. V. Bagreev and V. G. Revenko, *Zhurn. Analit. Khim.* 1972, **27** 185.
[3]Yu. I. Popandopulo, V. V. Bagreev and Yu. A. Zolotov, *J. Inorg. Nucl. Chem.* 1977, **39**, 2257.
[4]V. V. Bagreev, C. Fischer, L. M. Yudushkina and Yu. A. Zolotov, *J. Inorg. Nucl. Chem.* 1978, **40**, 553.
[5]F. Oehme, *Dielektrische Messmethoden.* Verlag Chemie, GmbH, Weinheim/Bergstr. (1966).
[6]V. A. Zarinsky and V. I. Ermakov, *Vysokochastotnyi Khimicheskyi Analiz* (*High-Frequency Chemical Analysis*), p. 65. Nauka, Moscow, 1970.
[7]C. Fischer and V. V. Bagreev, *Z. Chem.* 1974, **14**, 247.
[8]N. A. Izmailov, *Elektrokhimiya Rastvorov* (*Electrochemistry of Solutions*), p. 129. Khimiya, Moscow (1976).
[9]R. M. Fuoss and L. Onsager, *J. Phys. Chem.* 1957, **61**, 668.
[10]M. Gerin and J. Fresco, *Anal. Chim. Acta* 1978, **97**, 155.
[11]C. Fischer, H. Wagner, V. V. Bagreev and E. S. Stojanov, *J. Inorg. Nucl. Chem.* 1977, **39**, 513.
[12]Yu. I. Popandopulo, unpublished results.
[13]M. S. Milyukova, L. M. Yudushkina, V. V. Bagreev and B. F. Myasoyedov, *Chim. Anal.* (*Poland*) 1976, **21**, 51.
[14]V. V. Bagreev, C. Fischer, L. M. Yudushkina, P. Mühl and Yu. A. Zolotov, *Zhurn. Neorg. Khim.* 1978, **23**, 130.

Polyhedron Vol. 1, No. 7–8, pp. 629–631, 1982
Printed in Great Britain.

0277–5387/82/070629–03$03.00/0
Pergamon Press Ltd.

ACTIVATION OF CARBON–HYDROGEN BONDS: THERMOLYSIS OF BIS-η-CYCLOPENTADIENYL-HYDRIDOMETHYLTUNGSTEN IN *p*-METHOXYMETHYLBENZENE FORMS BIS-η-CYCLOPENTADIENYL-METHYL(PHENOXYMETHYL)TUNGSTEN

MASSIMO CANESTRARI and MALCOLM L. H. GREEN*
Inorganic Chemistry Laboratory, South Parks Road, Oxford OX1 3QR, England

(*Received* 2 *April* 1982)

Abstract—Thermal decomposition of $[WH(Me)(\eta\text{-}C_5H_5)_2]$ in 1 - methyl - 4 - methoxybenzene unexpectedly gives $[WMe(CH_2OPh)(\eta\text{-}C_5H_5)_2]$. Isomers of this compound, namely $[WR(R')(\eta\text{-}C_5H_5)_2]$, where R, R' = Me, C_6H_4OMe; OMe, C_6H_4Me; and Me, OC_6H_4Me have been prepared and characterised.

The insertion of a transition metal centre into carbon–hydrogen bonds under homogeneous conditions is a general reaction which is of interest since, for example, it could be envisaged to lead to the selective functionalisation of C–H systems. In a search for transition metal compounds which will insert a metal centre into C–H bonds under mild *thermal* conditions we found that the compound $[WH(Me)(\eta\text{-}C_5H_5)_2]$, **1**, decomposed at *ca.* 50°C giving methane and, presumably, the 16-electron compound tungstenocene $[W(\eta\text{-}C_5H_5)_2]$.[1] Tungstenocene formed in this way has been shown to insert into a range of carbon–hydrogen bonds where the carbon atom may be either saturated (sp^3) or unsaturated (sp^2).[1] Tungstenocene may also be formed by the photolysis of the compounds $[W(H)_2(\eta\text{-}C_5H_5)_2]$ and $[W(\eta\text{-}C_5H_5)_2CO]$[2] and it has been isolated and characterised spectroscopically in an argon matrix.[3]

Recently, striking advances have been made in the activation of fully saturated hydrocarbons using iridium and rhenium systems.[4]

As part of a continuing systematic study of C–H activation by high energy transition metal centres we have investigated the thermolysis of **1** in 1 - methyl - 4 - methoxybenzene. As described below an unexpected reaction occurred.

RESULTS AND DISCUSSION

A solution of $[WH(Me)(\eta\text{-}C_5H_5)_2]$ **1** in *p*-methylanisole was heated for fifteen hours at 70°C. Chromatography of the reaction mixture gave a small yield of the dihydride $[W(H)_2(\eta\text{-}C_5H_5)_2]$ and a very small quantity of orange crystals **3**. Elemental analysis and the mass spectrum of **3** were consistent with the stoichiometry $C_{18}H_{20}OW$. Treatment of **3** with dilute hydrochloric acid followed by chromatography of the more volatile products showed that methane and anisole were formed (glc). In an attempt to isolate intermediates in the formation of **3** the decomposition of **1** in 1 - methyl - 4 - methoxybenzene was carried out, in the presence of added dimethylphenylphosphine. Aqueous extraction of the involatile reaction products followed by addition of aqueous ammonium hexafluorophosphate gave the compound $[W(H)(\eta\text{-}C_5H_5)_2(PMe_2Ph)]PF_6$, **2**.

The ^1H NMR spectrum of **3** is entirely consistent with the structure shown in Scheme 1. This structure is so unexpected that it was thought worthwhile to attempt a synthesis of the compound by an alternative route, in order to obtain a greater quantity than could be obtained by the above method. It was also thought sensible to synthesise other isomers of the compound to confirm that they had different spectroscopic properties.

Unfortunately, thermolysis of **1** in anisole gave none of the compound **3** and no other tractable products could be isolated from the reaction mixture.

Treatment of the compound $[W(Me)_2(\eta\text{-}C_5H_5)_2]$ **4** with *p*-methylphenol gave a smooth reaction and orange crystals of the compound $[WMe(OC_6H_4Me\text{-}4)(\eta\text{-}C_5H_5)_2]$ **5** were formed in high yield. Similarly treatment of **4** with phenol yielded the compound $[WMe(OC_6H_5)(\eta\text{-}C_5H_5)_2]$ **6**.

The known compound $[WI(Me)(\eta\text{-}C_5H_5)_2]$, **7**,[5] was prepared by a new and more convenient route, namely the metathetical exchange by iodide of the benzoato group in the previously described[1] compound $[W(O_2CPh)Me(\eta\text{-}C_5H_5)_2]$, **8**, using lithium iodide in acetone. This reaction proceeded in 84% yield.

Treatment of **7** with *p*-methoxyphenylmagnesium bromide gave the expected compound $[WMe(C_6H_4OMe\text{-}4)(\eta\text{-}C_5H_5)_2]$, **9**.

The known compound $[WCl(C_6H_4Me\text{-}4)(\eta\text{-}C_5H_5)_2]$[2], **10**, was treated with sodium methoxide giving the compound $[W(OMe)(OC_6H_4Me\text{-}4)]$ **11**.

The data for the new compounds **3**, **5**, **6**, **9** and **11** are given in Table 1 and are entirely consistent with the proposed formulations. The proposed structures are illustrated in Scheme 1. The data in Table 1 shows that the compound **3** is clearly different from any of the other isomers prepared. The structure given for **3** is supported not only by the spectroscopic data but also by the reaction with hydrogen chloride which gives methane and anisole as volatile products. Clearly the compound **3** is a most unexpected product for which we are unable to envisage any simple mechanism of formation. We have put forward a speculative mechanism elsewhere[6] invoking a binuclear system in which the key step for the required cleavage of the methyl-ring carbon–carbon bond proceeds by migration of the aromatic ring of a tungsten–CH_2-C_6 system giving a carbene derivative $W(=CH_2)(\sigma\text{-}C_6)$.

EXPERIMENTAL

All the reactions and manipulations were carried out under dinitrogen or *in vacuo*. All solvents were thoroughly dried and

*Author to whom correspondence should be addressed.

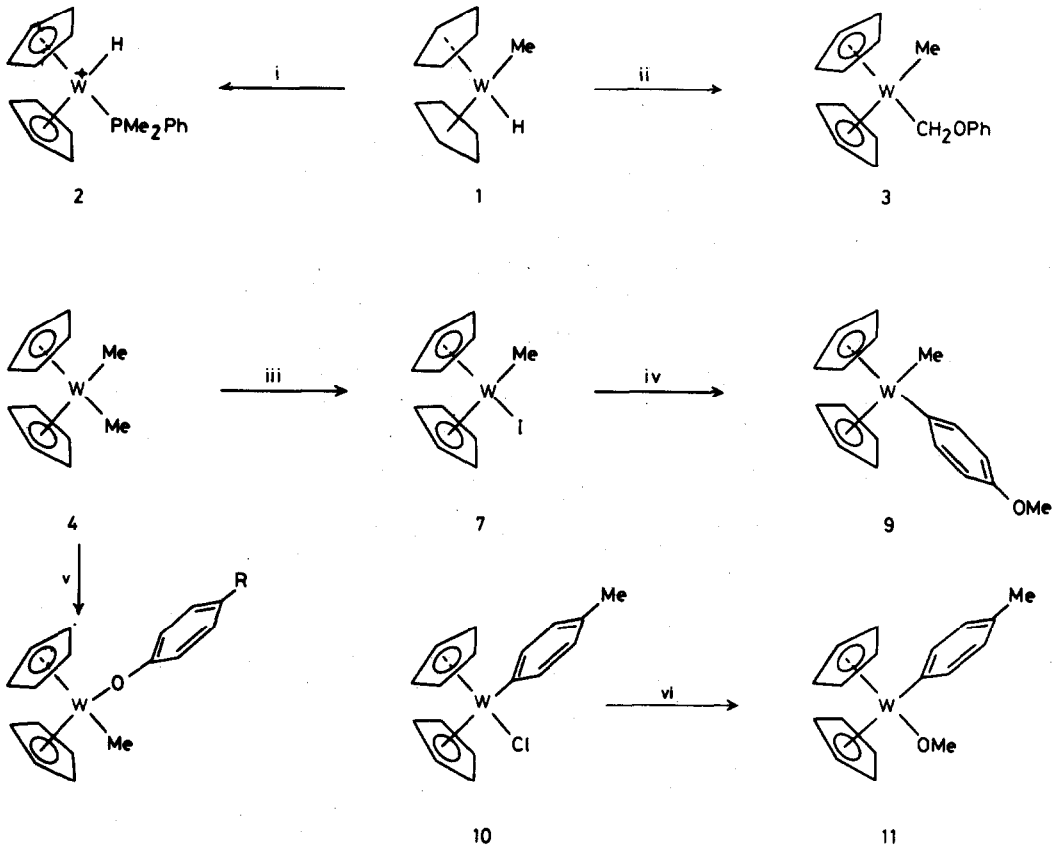

Scheme 1. (i) Me_2PhP in *p*-methylanisole at 70°C for 14 hr, 21%. (ii) *p*-Methylanisole at 70°C for 15 hr, 3%. (iii) Benzoic acid giving $[W(O_2CPh)Me(\eta\text{-}C_5H_5)_2]$; then LiI in acetone at 50°C for 12 hr. (iv) *p*-$MeOC_6H_4MgBr$ in Et_2O at 45°C for 1.5 hr, 35%. (v) *p*-HOC_6H_4R, R = H or Me, in petroleum ether (60–80°C) at r.t. for 15 hr, >90%. (vi) NaOMe in methanol at 40°C for 12 hr, 65%.

Table 1. Analytical and spectroscopic data

Compound	Colour	Analytical data (%)[a] C	H	^{1}H NMR data[b]
3 $[WMe(CH_2OC_6H_5)(\eta\text{-}C_5H_5)_2]$	Orange	49.8 (49.6)	5.0 (4.6)	2.88, **5**, *m*, Ph; 5.07, **10**, *s*, 2Cp; 5.53, **2**, *s*, CH_2; 9.73, **3**, *s*, Me[c]
5 $[WMe(CC_6H_4Me\text{-}4)(\eta\text{-}C_5H_5)_2]$	Red	49.8 (49.6)	4.7 (4.6)	3.05–3.65, **4**, *c* (AA'XX' J(AX) 38 J(A'X') 9) C_6H_4; 4.99, **10**, *s*, 2Cp; 7.78, **3**, *s*, Me; 9.51, **3**, *s*, WMe[d]
6 $[WMe(OC_6H_5)(\eta\text{-}C_5H_5)_2]$	Red	48.6 (48.3)	4.2 (4.3)	2.75–3.55, **5**, *m*, Ph; 5.07, **10**, *s*, 2 Cp; 9.49, **3**, *s*, Me[e]
9 $[WMe(C_6H_4OMe\text{-}4)(\eta\text{-}C_5H_5)_2]$	Yellow-orange		[f]	2.40–3.65, **4**, *c* (AA'XX' J(AX) 96.5, J(A'X' 9), C_6H_4, 5.41, **10**, *s*, 2 Cp; 6.34, **3**, *s*, OMe; 9.89, **3**, *s*, WMe[d]
11 $[W(OMe)(C_6H_4Me\text{-}4)(\eta\text{-}C_5H_5)_2]$	Orange		[f]	2.2–3.4, **4**, *c* (AA'XX' J(AX) 83 J(A'X') 8), C_6H_4; 5.03, **10**, *s*, 2 Cp; 6.51, **3**, *s*, OMe; 7.77, **3**, *s*, Me[d]
2 $[W(H)(\eta\text{-}C_5H_5)_2(PMe_2Ph)]PF_6$	Yellow	37.2 (36.2)	3.8[g] (3.7)	2.4, **5**, *m*, Ph; 4.84, **10**, *d* (J(P–H) 2.7) 2 Cp; 7.92, **6**, *d* (J(P–H) 9) PMe_2; 21.9, **1**, *d* (J(P–H) 28.8) W–H[d]

[a]Calculated values given in parenthesis. [b]Given as: chemical shift ( ), **relative intensity**, *multiplicity* (J in Hz), assignment Cp = η-C_5H_5. [c]In CS_2. [d]In $(CD_3)_2CO$. [e]In CD_2Cl_2. [f]Stoichiometry from the mass spectrum. [g]W–H stretch 1945 cm^{-1}.

distilled before use. Chromatography was carried out using aluminium oxide (100–120 mesh) supplied by East Anglia Chemicals Ltd. Celite 545 was supplied by Koch-Light Ltd. Microanalyses were by A. Bernhardt or by the microanalytical laboratory of this department. IR spectra were recorded as mulls on a Perkin-Elmer 457 instrument and were calibrated with polystyrene film. Hydrogen-1 NMR spectra were determined using a Bruker WH-90, JNM-PMX60 or Bruker WH-300 spectrometer. Mass spectra were recorded on an A.E.I. M.S. 902 spectrometer. Gas–liquid chromatography (glc) was carried out on a Pye 104 chromatograph using a 10% KCl-alumina column. The compounds $[WX_2(\eta\text{-}C_5H_5)_2]$, where X = Cl, Br or I[7], $[WI(Me)(\eta\text{-}C_5H_5)_2]$[5], $[WH(Me)(\eta\text{-}C_5H_5)_2]$[1] were prepared as previously described.

Bis(η - cyclopentadienyl)methyl(phenoxymethyl)tungsten

The compound $[WH(Me)(\eta\text{-}C_5H_5)_2]$ (0.57 g, 1.73 mmol) in redistilled *p*-methylanisole (150 cm^3) was heated for 15 hr at 70°C. The mixture was allowed to cool and was filtered and the solvent was removed under reduced pressure at 55°C. The resulting red–brown residue was dissolved in a minimum of benzene was placed on an alumina column made up on petroleum (40–60°C). Elution with benzene gave a yellow band which was shown from the IR spectrum to contain the compound $[W(H)_2(\eta\text{-}C_5H_5)_2]$. Further elution of the alumina column with dichloromethane gave an orange band which was collected, and the solvent was removed under reduced pressure giving a red–orange oil. This was extracted with petroleum (40 cm^3, 60–80°C) and the extract was filtered, then concentrated under reduced pressure and cooled to −78°C for 1 hr. Orange crystals separated. The crystals and their solutions in non-polar solvents were slowly decomposed on exposure to air. Yield 0.02 g, 3%. The mass spectrum showed bands corresponding to the isotope ^{184}W at 436 $[P]^+$; 421 $[P\text{–}Me]^+$; 329 $[P\text{–}C_6H_4OMe]^+$ and 314 $[W(\eta\text{-}C_2H_5)_2]^+$, where P = the parent ion.

Bis(η - cyclopentadienyl)(4 - methylphenoxy)methyltungsten

The compound $[W(Me)_2(\eta\text{-}C_5H_5)_2]$ (0.46 g, 1.33 mmol) in petroleum (150 cm^3, b.p. 60–80°) was treated with *p*-methylphenol (0.14 g, 1.33 mmol) and the mixture was stirred at 25°C for 15 hr. The solvent was removed under reduced pressure and the orange residue was dissolved in the minimum volume of toluene and was chromatographed on an alumina column made up in petroleum (30–40°C). Elution with toluene gave an orange band which was collected and shown to contain unreacted $[W(Me)_2(\eta\text{-}C_5H_5)_2]$. Further elution with dichloromethane gave a second orange band. This was collected and the solvent was removed under reduced pressure. The resulting red–orange solid was extracted with petroleum ether (60–80°C) and concentration and cooling gave red crystals. These were recrystallised from diethyl ether at −20°C. The resulting red crystals were dried *in vacuo*, yield 0.55 g, 94%. The mass spectrum showed bands at 436 $[P]^+$; 421 $[P\text{–}Me]^+$; 329 $[P\text{–}OC_6H_4Me]^+$ and 314 $[W(\eta\text{-}C_5H_5)_2]^+$.

Bis(η - cyclopentadienyl)(phenoxy)methyltungsten

The compound $[W(Me)_2(\eta\text{-}C_5H_5)_2]$ (0.51 g, 1.48 mmol) was reacted with phenol (0.14 g, 1.48 mmol) as described for the *p*-methoxyphenol analogue above. Chromatography on an alumina column made up in light petroleum ether and elution with toluene:diethyl ether (3:1) gave a red band. After removal of the solvent, the resulting red oil was extracted with petroleum (40–60°C). Concentration and cooling gave orange–red crystals which were dried *in vacuo*, yield 0.57 g; 91%. Mass spectrum: 422 $[P]^+$; 407 $[P\text{–}Me]^+$; 314 $[W(\eta\text{-}C_5H_5)_2]^+$.

Improved synthesis of bis(η-cyclopentadienyl)iodomethyltungsten

The compound $[W(O_2CPh)Me(\eta\text{-}C_5H_5)_2]$ (0.5 g, 1.11 mmol), prepared as described,[1] in acetone (150 cm^3) was treated with dried lithium iodide (1.5 g, 1.2 mmol) and the mixture was stirred at 50°C for 12 hr giving a dark green solution. The solvent was then removed under reduced pressure and the resulting dark green solid was extracted with benzene. The solution was filtered and petroleum (100–120°C) was added. Slow concentration under reduced pressure gave green needles which were collected and dried *in vacuo*, yield 0.43 g, 85%. The compound was identified as the title compound by comparison of the IR spectrum with that of an authentic sample.

Bis(η - cyclopentadienyl)(4 - methoxyphenyl)methyltungsten

The compound $[WI(Me)(\eta\text{-}C_5H_5)_2]$ (0.56 g, 1.23 mmol) in diethyl ether (50 cm^3) was treated with *p*-methoxyphenyl magnesium bromide (3.15 cm^3 of a 0.39 M solution in diethyl ether, 1.23 mmol). The mixture was stirred at 45°C for 1.5 hr. The solvent was removed from the resulting red–orange solution giving a red–orange oil. Toluene (60 cm^3) and water (50 cm^3) were then added and the mixture was vigorously shaken. After filtration through a Celite bed the orange organic layer was separated and the solvent was removed under reduced pressure. The oily red–orange residue was extracted with a minimum volume of diethyl ether and placed on an alumina column made up in petroleum (40–60°C). Elution with petroleum (40–60°C) gave a yellow–orange band which was collected and the solvent was removed under reduced pressure. The residue was extracted with petroleum (40–60°C) and the extract was filtered and then concentrated until it was observed to be saturated. The mixture was then cooled to −78°C for 12 hr giving yellow–orange crystals which were collected, washed with cold petroleum (30–40°C) and finally dried *in vacuo*, yield 0.18 g, 35%. Mass spectrum: 436 $[P]^+$; 421 $[P\text{–}Me]^+$; 329 $[P\text{–}C_6H_4OMe]^+$ and 314 $[W(\eta\text{-}C_5H_5)_2]^+$.

Bis(η - cyclopentadienyl)(4 - methylphenyl)methoxytungsten

The compound $[WCl(C_6H_4Me\text{-}4)(\eta\text{-}C_5H_5)_2]$ (0.46 g, 1.04 mmol) in methanol (50 cm^3) was treated with sodium metal (0.03 g, 1.30 mmol) and the mixture was stirred at 40°C for 12 hr giving a clear red solution. The solvent was removed under reduced pressure then toluene (60 cm^3) and water (30 cm^3) were added. The mixture was filtered through a bed of Celite and the toluene layer was separated. The solvent was removed under reduced pressure and the orange–red residue was dissolved in a minimum of dichloromethane and placed on an alumina column made up in petroleum (30–40°C). Elution with toluene:diethyl ether (3:1) gave a red–orange band which was collected. The solvent was removed under reduced pressure and the residue was extracted with petroleum (60–80°C). The extract was concentrated and cooled giving orange crystals, 0.29 g, 65%. Mass spectrum: 436 $[P]^+$; 421 $[P\text{–}Me]^+$; 405 $[P\text{–}OMe]^+$; and 314 $[W(\eta\text{-}C_5H_5)_2]^+$.

Bis(η - cyclopentadienyl)(dimethylphenylphosphine) - hydridotungsten hexafluorophosphate

The compound $[WH(Me)(\eta\text{-}C_5H_5)_2]$ (0.66 g, 2.0 mmol) in *p*-methylanisole (100 cm^3) was treated with dimethylphenylphosphine (1.93 g, 14 mmol) and the mixture was stirred at 70°C for 14 hr. The resulting yellow precipitate was collected and washed with petroleum (2 × 20 cm^3, 40–60°C). The residue was extracted with water (75 cm^3) and aqueous ammonium hexafluorophosphate was added to the extract giving a yellow precipitate. This was collected, washed with water and dried *in vacuo*. It was then recrystallised from acetone:diethyl ether mixture as yellow crystals which were dried *in vacuo*, 0.25 g, 21%.

Acknowledgements—We thank the Venezuelan Government for financial support (to M.C.) and the Petroleum Research Fund administered by the American Chemical Society for partial support.

REFERENCES

[1]N. J. Cooper, M. L. H. Green and R. Mahtab, *J. Chem. Soc. Dalton Trans.* 1979, 1557.
[2]M. Berry, K. Elmitt and M. L. H. Green, *J. Chem. Soc. Dalton Trans.* 1979, 1950.
[3]P. Grebenik, A. J. Downs, M. L. H. Green and R. N. Perutz, *J. Chem. Soc. Chem. Comm.* 1979, 742.
[4]R. H. Crabtree, J. Mihelcic and J. Quirk, *J. Am. Chem. Soc.* 1982, **104**, 107; D. Baudry, M. Ephritikhine and H. Felkin, *J. Chem. Soc. Chem. Comm.* 1980, 1243; A. H. Janowicz and R. Bergman, *J. Am. Chem. Soc.* 1982, **104**, 352.
[5]N. J. Cooper and M. L. H. Green, *J. Chem. Soc. Dalton Trans.* 1979, 1121.
[6]M. Canestrari, D.Phil thesis. Oxford (1981).
[7]M. L. H. Green and R. L. Cooper, *J. Chem. Soc.* (A) 1967, 1155.

Polyhedron Vol. 1, No. 7–8, pp. 633–635, 1982
Printed in Great Britain.

0277-5387/82/070633-03$03.00/0
Pergamon Press Ltd.

COPPER(I) AND SILVER(I) COMPLEXES OF N-METHYL-RHODANINE AND N-AMINO-RHODANINE

ANTONIO C. FABRETTI, GIANCARLO FRANCHINI, GIORGIO PEYRONEL* and MARCO FERRARI

Istituto di Chimica Generale e Inorganica, Università di Modena, 41100 Modena, Italy

(*Received* 26 *May* 1982)

Abstract—The following copper(I) and silver(I) complexes of N-methyl-rhodanine (MeRd, L) and N-amino-rhodanine (H_2NRd, L') have been prepared and studied by infrared and conductometric methods: CuXL (X = Cl, Br, I), $CuClO_4L_4$, CuXL' [X = Cl($\frac{1}{4}$HAc), I($\frac{1}{4}$DMF)], $Cu_2Br_2L' \cdot \frac{1}{4}HAc$, $Cu_2X_2L'_{2.25} \cdot \frac{1}{4}DMF$ (X = Cl, Br), $CuClO_4L'_2 \cdot HAc$, $AgNO_3L$, $AgNO_3L'$, $AgClO_4L_2$, $AgClO_4L'_2$. The MeRd is coordinated through the thiocarbonyl sulphur atom and in most of its complexes through the ring-notrogen atom. The H_2NRd is coordinated through the amine nitrogen and the thiocarbonyl sulphur atoms. Most of the complexes have a tetrahedral coordination.

INTRODUCTION

Rhodanine and its derivatives are used as analytical reagents. N-methyl-rhodanine (MeRd, L) and N-amino-rhodanine (H_2NRd, L') have two endocyclic (N, S) and two (O, S) or three (O, S, NH_2) potentially coordinating sites, respectively. Their coordination behaviour toward the copper(I) and silver(I) ions has been investigated in this work.

EXPERIMENTAL

The ligands and all the reagents were of the best chemical grade. The complexes were prepared by adding a solution of the metal salt to a solution of the ligand using the millimoles (mM) and milliliters (ml) indicated below.

CuClL *and* CuBrL. From the corresponding cupric halide (0.5 mM) in EtOH (3.5 ml) and L (1 mM) + hydroquinone (1 mM) in EtOH (3 ml).

CuIL. From cupric nitrate (0.5 mM) in water (1 ml) and L (2 mM) + hydroquinone (1 mM) + KI (0.8 mM) in EtOH (9 ml) + water (8 ml).

$CuClO_4L_4$. From cupric perchlorate (0.5 mM) in EtOH (3 ml) and L (2 mM) + hydroquinone (1 mM) + $NaClO_4$ (0.5 mM) in EtOH (10 ml). $AgNO_3L$. From silver nitrate (0.25 mM) in EtOH (3 ml) + HNO_3 (10 drops) and L (0.25 mM) in EtOH (3 ml) + HNO_3 (15 drops). $AgClO_4L_2$. From silver perchlorate (0.5 mM) in EtOH (5 ml) and L (1 mM) in EtOH (5 ml).

$AgNO_3L'$. From silver nitrate (0.25 mM) in EtOH (3 ml) + HNO_3 (4 drops) and L' (0.5 mM) in EtOH (25 ml) + HNO_3 (8 drops). $AgClO_4L'_2$. From silver perchlorate (0.25 mM) in EtOH (2 ml) and L' (0.5 mM) in EtOH (25 ml). $CuCl_2L'\frac{1}{4}HAc$ and $Cu_2Br_2L'\frac{1}{4}HAc$. A suspension of CuX (1 mM) in a solution of L' (1.2 mM) + hydroquinone in HAc (10 ml) was refluxed for 3 h. $Cu_2X_2L'_{2.5} \cdot \frac{1}{4}DMF$(X = Cl, Br) and CuIL'-$\frac{1}{4}$DMF:CuX (0.5 mM) was dissolved in a solution of L' (1 mM) in DMF (3 ml) and the complexes precipitated with $CHCl_3$ (12 ml). $CuClO_4L'_2 \cdot HAc$. From cupric perchlorate (0.5 mM) in HAc (2 ml) and L' (1.5 mM) + hydroquinone (0.5 mM) in HAc (8 ml) saturated with $NaClO_4$.

All the compounds were washed with the solvents used in the preparation.

The compounds were analysed by standard methods (Table 1). For some H_2NRd complexes the solvent percentage resulting from the elemental analysis was independently confirmed by determining thermogravimetrically the weight loss of the substance with a Mettler thermobalance. Infrared spectra (Table 2) were recorded with a Perkin–Elmer 180 spectrophotometer in KBr disks, or as Nujol mulls on KBr for the nitrates, in the range 4000–250 cm^{-1} and as Nujol mulls on polythene in the range 600–60 cm^{-1}. Molar conductivities were determined with a WTW conductivity bridge.

The silver halides dissolve in a DMF solution of MeRd or H_2NRd giving soluble silver complexes; by adding $CHCl_3$ to the solution only the silver halides precipitate.

RESULTS AND DISCUSSION

The very strong ν(CO) band observed at 1725 cm^{-1} for both the ligands is shifted to higher frequencies, at 1753–1727 cm^{-1} for the MeRd and 1748–1733 cm^{-1} for the H_2NRd complexes, excluding the coordination of these ligands through the carbonyl oxygen atom. Some ligand bands observed in the ν(C–S) frequency range[1] assignable to ring deformation modes may contain an important contribution from the ν(C–S) mode. Their frequency increase in the complexes excludes coordination of the ligands through the ring sulphur atom:

	Ligand	complexes
MeRd	774 (m)	782–770 (ms–mw) cm^{-1}
	612 (s)	624–620 (vs)
H_2NRd	630 (s)	642–633 (s)

The ν(NH) bands observed for the H_2NRd ligand in $CHCl_3$ solution at 3320 (vs) and 3245 (m) cm^{-1} are shifted in the complexes to lower frequencies (3280–3250, 3230–3160, 3175–3120 cm^{-1}) indicating a coordination through the amine nitrogen atom.

The H_2NRd band at 1050 (mw)cm^{-1} assignable to a ν(C=S) mode[2] is shifted in the complexes to lower frequencies (1026–1012 (*s–w*) cm^{-1}) indicating a coordination of the ligand through its thiocarbonyl sulphur atom.

For the H_2NRd complexes the ν(MN) and ν(MS) bands are clearly identifiable in the 499–403 cm^{-1} and 323–291 cm^{-1} region, respectively, close to the frequencies observed for other H_2NRd complexes.[2–4]

For the MeRd complexes the ν(MS) bands are clearly identified at 312–298 cm^{-1} in the same spectral region in which these bands were observed for the copper(I) (308–270 cm^{-1})[5] and silver(I) (296–280 cm^{-1})[6] complexes of rhodanine. Some bands observed at about 200 cm^{-1}, with intensities much higher than that of the weak band observed at 199 cm^{-1} for the free ligand, may be assigned to $\nu(MN_{ring})$ modes even if superimposed on or

*Author to whom correspondence should be addressed.

Table 1. Analytical data, Found % (Calc. %), molar conductivities Λ_M (Ω^{-1} mol^{-1} cm^2) in 10^{-3} M DMF solution and colour of the N-methyl-rhodanine (L) and N-amino-rhodanine (L') complexes

	N	C	H	M	S	Solvent	Colour	Λ_M
CuClL	5.58(5.69)	19.52(19.51)	1.92(2.05)	25.69(25.81)			light brown	35
CuBrL	4.86(4.82)	16.90(16.52)	1.65(1.73)	21.45(21.86)			yellow	36
CuIL	4.16(4.15)	14.48(14.23)	1.41(1.49)	18.61(18.82)			yellow	33
$CuClO_4L_4$	7.32(7.45)	25.61(25.56)	2.57(2.68)	8.15(8.45)			yellow brown	69
$AgNO_3L$	8.79(8.83)	15.15(15.15)	1.58(1.59)				orange	32
$AgClO_4L_2$	5.59(5.58)	19.34(19.15)	1.92(2.00)				light brown	62
$CuClL'.\frac{1}{4}HAc$	10.31(10.68)	16.05(16.03)	1.72(1.92)	24.38(24.23)	24.03(24.46)	5.53(5.73)	brown green	34
$Cu_2Cl_2L'_{2.5}.\frac{1}{4}DMF$	12.55(12.53)	16.83(16.89)	1.91(2.02)		27.46(27.33)	3.02(3.11)	light brown	32
$Cu_2Br_2L'.\frac{1}{4}HAc$	6.53(6.22)	9.21(9.34)	1.02(1.12)	28.19(28.23)	14.70(14.25)	2.83(3.33)	brown	31
$Cu_2Br_2L'_{2.5}.\frac{1}{4}DMF$	10.81(10.88)	14.60(14.67)	1.71(1.75)		23.24(23.73)	2.96(2.70)	light brown	26
$CuIL'.\frac{1}{4}DMF$	8.76(8.83)	12.68(12.62)	1.48(1.62)	17.47(17.80)	17.58(17.97)	4.89(5.12)	red brown	26
$CuClO_4L'_2.HAc$	10.68(10.79)	18.48(18.50)	2.24(2.33)			11.07(11.55)	yellow	66
$AgNO_3L'$	13.03(13.21)	11.81(11.33)	1.29(1.27)				yellowish	52
$AgClO_4L'_2$	10.97(11.12)	14.28(14.31)	1.50(1.60)				light yellow	61

(*) referred to one metal salt equivalent.

Table 2. Principal for IR bands (cm^{-1}) of the N-methyl-rhodanine (L) and N-amino-rhodanine (L') complexes

	ν(MN)	ν(MS)	ν(MX)	δ(ML')
CuClL	198msb	312mw	198msb,154vs	
CuBrL	198ms	304mw	145vs,115sb	
CuIL	199mw	298ms	101vs,85ms	
$CuClO_4L_4$		311m		
$AgNO_3L$	200s	307mw	301wm,261sm	
$AgClO_4L_2$	199ms,169mw	312m,305mw		
$CuClL'.\frac{1}{4}HAc$	494ms	304sm	262sm	198m,167m
$Cu_2Cl_2L'_{2.25}.\frac{1}{4}DMF$	495sm	300mb	263vs,(174vs)	198ms,168s
$Cu_2Br_2L'.\frac{1}{4}HAc$	493m	303w	(173vs,136ms)	198sm,165s
$Cu_2Br_2L'_{2.25}.\frac{1}{4}DMF$	493sm	322wm,(259sh)	(173vs)	198sm,167vs
$CuIL'.\frac{1}{4}DMF$	493ms	299m	148sm	199m,165vs
$CuClO_4L'_2.HAc$	499vs,409sh	323m,302sh		193vs,168s
$AgNO_3L'$	470sb	302vs	(302vs),201s	198s,167vs
$AgClO_4L'_2$	450mb,403m	307m,291w		199m,155vs

coupled with the ligand band. In this spectral region the ν(MN) bands due to metals bonded to endocyclic nitrogen atoms appear and very often these ν(MN) modes are coupled with ring vibration modes.

All the halide complexes have molar conductivities (Λ_M = 36–26) much lower than those characteristic for 1 : 1 electrolytes (Λ_M = 65–90)[7] in DMF solution. The CuX · MeRd (X = Cl, Br, I) complexes showing one ν(CuS), one ν(CuN) and two ν(CuX)$_b$ bands clearly have a (S, N, 2X$_b$) pseudotetrahedral coordination presumably with non-equivalent bridging Cu–X bond lengths. Their ν_{Br}/ν_{Cl} (0.73, 0.75) and ν_I/ν_{Cl} (0.51, 0.55) ratios are normal for isostructural coordination environments.[8]

The H_2NRd copper(I) halide complexes contain a certain amount of the solvent (HAc, DMF) used for their preparation, the presence of which in the solid complexes was ascertained by the analytical results and the thermogravimetric determinations. These solvent molecules may be considered as hydrogen bonded to the ligand molecules rather than coordinated to the metal ion.

The CuCl · H_2NRd · $\frac{1}{4}$HAc and CuI · H_2NRd · $\frac{1}{4}$DMF complexes show besides one ν(CuN) and one ν(Cus) band due to the presumably (N, S) chelating ligand molecule one ν(CuX) band with a ν_I/ν_{Cl} (0.56) ratio in agreement with an isostructural coordination environment.[8] The higher ν(CuX) frequencies observed in these complexes with respect to those of the corresponding MeRd complexes indicate shorter Cu–X bonds corresponding to a prevailing trigonal coordination probably in a pyramidal structure with some longer axial interaction probably with halide ions.

The H_2NRd complexes $Cu_2Cl_2L'_{2.25}\cdot\frac{1}{4}DMF$, $Cu_2Br_2L'\cdot\frac{1}{4}HAc$ and $Cu_2Br_2L'_{2.25}\cdot\frac{1}{4}$ DMF have fractional Cu/L ratios. Their bands at 173 and 136 cm^{-1} are tentatively assigned to ν(CuX) modes because in these complexes they are stronger than in the other H_2NRd complexes but may be superimposed to or coupled with the ligand bands at 177 (sm) and 134 (ms) cm^{-1}. These complexes have certainly a polynuclear structure and their rather high ν(CuX) frequencies seem to indicate as for the previous CuXL' complexes a prevailing trigonal pyramidal coordination.

The MeRd perchlorate complexes show a single ν_3 band of the perchlorate ion, this anion being clearly not coordinated in agreement also with their molar conductivities in the range given for 1 : 1 complexes.[7] A single ν(CuS) band clearly indicates a (4S) tetrahedral coordination for the $CuClO_4(MeRd)_4$ complex; two ν(AgN) and two ν(AgS) bands a (2N, 2S) tetrahedral coordination for the $AgClO_4(MeRd)_2$ complex 9.

For the $CuClO_4(H_2NRd)_2\cdot HAc$ and $AgClO_4(H_2NRd)_2$ complexes a splitting of the ν_3 band of the perchlorate anion indicates a distortion from the T_d symmetry very likely attributable to hydrogen bonds with the H_2N group of the ligand or with the HAc molecules in the copper(I) complex.

The molar conductivities, in the range given for 1 : 1 electrolytes[7], agree well with an uncoordinated perchlorate anion. Two ν(MN) and two ν(MS) bands indicate a (2N, 2S) tetrahedral coordination due to chelating ligand molecules.

The infrared spectra of the $AgNO_3(MeRd)_2$ and $AgNO_3(H_2NRd)_2$ complexes, recorded in Nujol mulls in order to avoid exchange reaction with KBr, show several bands not present in the other complexes of the same ligand:

$AgNO_3(MeRd)_2$ 1305 ms, 1073 sm, 1038 w, 1025 m, 815 vw, 808 mw, 720 mw $AgNO_3(H_2NRd)_2$ 1348 w, 1208 s, 1115 w, 1018 m, 818 mw, 734 w, 720 wm. Some of them more or less correspond to those given for monodentate nitrate ions[10], but their multiplicity may indicate as asymmetric chelating or bridging coordination.

For these complexes single ν(AgN) and ν(AgS) bands are observed and two bands may be assigned to ν(Ag–ONO_2) modes in agreement with other literature values[10] supporting a (N, S, 2O) tetrahedral coordination. The molar conductivity of the MeRd nitrate complex agree well with a non-ionic constitution of this complex; the greater molar conductivity of the H_2NRd nitrate complex, close to the 1 : 1 electrolyte values, may be due to solvolysis in DMF solution.

Acknowledgements— The infrared spectra were recorded in the Centro Strumenti of the University of Modena.

REFERENCES

[1]C. N. R. Rao, *Chemical Applications of Infrared Spectroscopy*, p. 297. Academic Press, New York (1963).
[2]A. C. Fabretti, G. C. Franchini and G. Peyronel, *J. Inorg. Nucl. Chem.* 1981, **43**, 2559.
[3]A. C. Fabretti, G. C. Franchini and G. Peyronel, *Inorg. Chim. Acta* 1981, **52**, 11.
[4]A. C. Fabretti, G. C. Franchini and G. Peyronel, *Transition Met. Chem.* 1980, **5**, 350.
[5]A. C. Fabretti, G. Peyronel and G. C. Franchini, *Transition Met. Chem.* 1978, **3**, 125.
[6]A. C. Fabretti and G. Peyronel, *Transition Met. Chem.* 1977, **2**, 224.
[7]W. J. Geary, *Coord. Chem. Rev.* 1971, **7**, 81.
[8]A. Brodie and C. J. Wilkins, *Inorg. Chim. Acta* 1974, **8**, 13.
[9]A. Finch, P. N. Gates, K. Radcliffe, F. N. Dickson and E. F. Bentley, *Chemical Applications of Far Infrared spectroscopy*, p. 168. Academic Press, London (1970).
[10]J. R. Ferraro, *Low Frequency Vibrations of Inorganic and Coordination Compounds* pp. 79–80. Plenum Press, New York (1971).

Polyhedron Vol. 1, No. 7-8, pp. 637-639, 1982
Printed in Great Britain.

0277-5387/82/070637-03$03.00/0
Pergamon Press Ltd.

METAL COMPLEXES OF ALKYLATING AGENTS—III

COMPLEXES BY CYCLOPHOSPHAMIDE

MELVIN D. JOESTEN,* RENATO NAJJAR† and GREGORY HEBRANK
Department of Chemistry, Vanderbilt University, Nashville, TN 37235, U.S.A.

(*Received* 3 *June* 1982)

Abstract—Complexes of cyclophosphamide (L)* which have been synthesized include $Rh_2(acetate)_4(L)_2$, $Rh_2(propionate)_4(L)_2$, $Rh_2(butyrate)_4(L)_2$, and $SbCl_3(L)$. Spectral data are consistent with coordination of both axial P = O and ring NH in the rhodium(II) carboxylate complexes of (L) and coordination of only axial P = O in $SbCl_3(L)$. Preliminary antitumour tests gave negative results for these complexes.

INTRODUCTION

The goal of our investigations of metal complexes of alkylating agents is to determine whether the effectiveness of known antitumour agents can be enhanced through coordination with metal ions.[1] Such enhancement might result if the metal complex (1) reduces toxicity and harmful side effects of the alkylating agent, (2) enhances delivery to the tumour cell, or (3) delivers a metal species also capable of blocking DNA base sites in tumour cells.

Previous papers in this series[2,3] reported the synthesis and testing results for metal complexes of aziridinyl phosphine oxides and aziridinyl phosphine sulphides. Three of the complexes had T/C values larger than 125, but the results were not sufficiently promising to justify further testing.

One of the most effective antitumour drugs is cyclophosphamide(L)[4] which reacts *in vivo* to give a number of active metabolites such as 4-hydroxycyclophosphamide, 4-ketocyclophosphamide and phosphoramide mustard. The latter is generally regarded as the ultimate DNA cross-linking reagent. The clinical success of cyclophosphamide both as a single-agent drug and in connection with *cis*-$Pt(NH_3)_2Cl_2$[5] prompted us to investigate whether complexes of cyclophosphamide could be prepared.

The present paper describes the synthesis and characterization of several coordination complexes of cyclophosphamide.

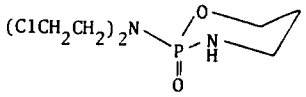

EXPERIMENTAL

Analyses

Carbon, hydrogen, and nitrogen analyses were performed by Galbraith Laboratories, Knoxville, TN.

Spectral measurements

IR spectra of Nujol mulls and KBr disks were recorded in the 4000–600 cm^{-1} region with a Perkin–Elmer 727 spectrophotometer. Electronic spectra of complexes dissolved in acetone were recorded with a Cary 14 recording spectrophotometer. Proton NMR spectra were recorded on a JEOL MH-100 spectrometer, and ^{13}C NMR spectra were recorded with a JEOL FT90XQ spectrometer. ^{31}P NMR spectra were obtained with an XL-100-15 spectrometer which is equipped with a Transform Technology Inc. (TT-100) Fourier-transform unit. Deuterated chloroform was used as solvent for all NMR spectra.

Starting materials

(1) Cyclophosphamide. We are grateful to Mead and Johnson for providing the cyclophosphamide used in the early stages of this work. Additional cyclophosphamide was purchased from Sigma and Aldrich.

(2) Rhodium(II) carboxylates. The rhodium(II) carboxylates were prepared by following literature methods.[6,7]

Preparation of complexes

(1) Adducts of rhodium(II) carboxylates. All adducts were prepared by following the same procedure. Approximately 1 mmole of rhodium(II) carboxylate was dissolved in a minimum amount of ethanol and mixed with 3 mmoles of cyclophosphamide dissolved in a minimum amount of ethanol. The solution was refluxed for one hour, and the solvent was removed under a nitrogen blanket. The residue was washed several times with ether, filtered, and dried under vacuum at room temperature.

(a) Found; C, 27.1; H, 4.42; N, 5.75. Calc. for $Rh_2(OOCCH_3)_4 \cdot 2C_7H_{15}Cl_2N_2O_2P$; C, 27.4; H, 4.40; N, 5.81%. Yield: 60% (b) Found; C, 30.4; H, 5.02; N, 5.56. Calc. for $Rh_2(OOCCH_2CH_3)_4 \cdot 2C_7H_{15}Cl_2N_2O_2P$; C, 30.6; H, 4.95; N, 5.49. Yield: 57%. (c) Found; C, 33.9; H, 5.52; N, 5.09. Calc. for $Rh_2(OOCCH_2CH_2CH_3)_4 \cdot 2C_7H_{15}Cl_2N_2O_2P$; C, 33.5; H, 5.43; N, 5.20%. Yield: 55%.

(2) Adduct of $SbCl_3$. Solid $SbCl_3$ (3.5 mmole) and solid cyclophosphamide (4.3 mmole) were mixed together. After about one minute, the solid mixture became gummy. Anhydrous ether (50 ml) was added and the mixture was stirred for twenty minutes. The mixture was filtered and the white powder was washed several times with ether and dried under vacuum at room temperature. Found; C, 17.2; H, 3.17; H, 5.73. Calc. for $SbCl_3 \cdot C_7H_{15}Cl_2N_2O_2P$; C, 17.2; H, 3.10; N, 5.72%. Yield: 88%.

RESULTS AND DISCUSSION

Although platinum(II) complexes of phosphine derivatives of cyclophosphamide have been reported,[8,9] no previous reports of cyclophosphamide complexes could be found. Cyclophosphamide apparently does not coordinate readily with metal ions in contrast to other phosphoryl donors such as a variety of substituted R_3PO donors.[10,11] The same procedures which were successful for isolation of metal complexes of R_3PO ligands[10] were used in the attempted synthesis of cyclophosphamide complexes with a wide variety of metal ions. However, the only type of complex we have been able to isolate

*Author to whom correspondence should be addressed.
†On leave from University of Sao Paulo, Brazil.

and characterize are those which require only one or two ligands to complete the coordination sphere of the metal. Isolated complexes include $Rh_2(acetate)_4(L)_2$ $Rh_2(propionate)_4(L)_2$, $Rh_2(butyrate)_4(L)_2$ and $SbCl_3(L)$.

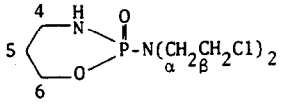

The structure of cyclophosphamide and its optical isomers have been reported.[12,14] The ring has the chair conformation with P = O in an axial position and the racemic form is stable as a hydrate. The water molecule holds cyclophosphamide molecules together by two O–H···O = P hydrogen bonds and one N–H···O hydrogen bond.[12] Solution stereochemical studies[15] with the lanthanide shift reagent, $Eu(dpm)_3$, have been interpreted in terms of coordination of europium to the axial P = O site along with chelation to the NH lone pair. Hence coordination is expected to stabilize the conformer with P = O in the axial position because of the greater basicity of axial P = O,[16] and both P = O and NH donor sites may be involved in coordination.

Spectral data for the complexes isolated in the present study are in agreement with P = O coordination. The IR bands for the complexes are listed in Table 1. Although the complexity of the IR spectra do not permit definitive assignments for P = O, the 1190–1260 cm^{-1} region for hydrated cyclophosphamide does show modest shifts to lower frequency. For example, the band at 1190 cm^{-1} shifts to 1175 cm^{-1} for rhodium(II) carboxylate adducts and to 1110 cm^{-1} for $SbCl_3(L)$. This suggests the coordination of rhodium to (L) is very similar to that found in the hydrogen bonded structure. The rhodium(II) carboxylate adducts also have broad NH bands at 3250–3275 cm^{-1} which is characteristic of bound NH. Hence the IR data are consistent with rhodium(II) chelate bonds to P = O and NH.

The $SbCl_3(L)$ adduct has a sharp NH band at 3375 cm^{-1} which is characteristic of free NH. This together with the decrease in the P = O band from 1190 cm^{-1} to 1110 cm^{-1} is evidence for coordination of Sb(III) to only the P = O site.

All of the rhodium(II) carboxylate adducts with cyclophosphamide have the same green colour as the parent compound or the water adduct.[17,18] The electronic spectral data in Table 2 illustrate that the visible absorption band at 617 nm for anhydrous rhodium(II) acetate follows the spectrochemical series for increased d-orbital splitting reported previously for $Rh_2(acetate)_4$ adducts.[17,18] The value of 604 nm for the cyclophosphamide adduct indicates weak Rh-(L) coordination comparable to acetone and THF. The similarity with oxygen donors rather than nitrogen donors supports assignment of P = O as the primary coordination site in cyclophosphamide.

The ^1H NMR of cyclophosphamide in $CDCl_3$ is complex.[19,20] Peaks have been assigned as follows: C-5,

Table 1. IR Data

Compound	Bands, cm^{-1}
cyclophosphamide(L)[a]	740, 770, 845, 875, 955, 980, 995, 1050, 1090, 1135, 1190, 1220, 1230, 1250, 1260, 1280, 1340, 1370, 1430, 1460, 1650, 2900, 2950, 2975, 3000, 3200, (broad), 3450 (broad)
$SbCl_3(L)$[a]	735, 770, 890, 945, 980, 1040, 1100, 1110, 1125, 1200, 1220, 1250, 1320, 1350, 1380, 1410, 2875, 2950, 3375
$Rh_2(acetate)_4(L)$[a]	740, 835, 870, 940, 970, 1040, 1090, 1120, 1175, 1205, 1340, 1425, 1690, 2750, 3275 (broad)
$Rh_2(propionate)_4(L)_2$[a]	740, 780, 800, 840, 880, 920, 945, 975, 1015, 1045, 1095, 1130, 1175, 1205, 1300, 1420, 1460, 1590, 2950, 2975, 3250 (broad).
$Rh_2(butyrate)_4(L)_2$[b]	800, 840, 875, 945, 970, 995, 1040, 1050, 1090, 1130, 1175, 1210, 1260, 1310, 1375, 1590, 3275 (broad)

[a] KBr pellet
[b] Nujol mull

Table 2. Electronic spectral data[a]

Adduct	$^{\lambda}$nm	ϵ	$^{\lambda}$nm	ϵ	Ref.
$Rh_2(acetate)_4$	617	*b*	442	*b*	18
$Rh_2(acetate)_4(H_2O)_2$	584	197	441	102	18
$Rh_2(acetate)_4\{(CH_3)_2SO\}_2$	497	317			
$Rh_2(acetate)_4(NH_3)_2$	528	*b*			18
$Rh_2(acetate)_4\{(CH_3)_2CO\}_2$	603	260	440	115	17
$Rh_2(acetate)_4(THF)_2$	597	235	441	110	17
$Rh_2(acetate)_4(CH_3CN)_2$	552	235	437	125	17
$Rh_2(acetate)_4(L)_2$	604	224	441	97	this work
$Rh_2(propionate)_4(L)_2$	606	270	438	178	this work
$Rh_2(butyrate)_4(L)_2$	607	267	442	113	this work

[a] Solution data from Refs. 17 and 18 were recorded for adducts dissolved in the ligand.
[b] Reflectance spectra.

Table 3. ^{13}C Decoupled NMR data[a]

Peaks/cpd	L	$SbCl_3 \cdot (L)$	$Rh_2(OAc)_4$[b] $(L)_2$	$Rh_2(O_2CEt)_4$[b] $(L)_2$	$Rh_2(O_2CPr)_4$[b] 2cp
C-5	25.56	25.26	25.54	25.56	25.56
	25.83	25.54	25.81	25.82	25.83
C-4	41.27	41.49	41.47	41.56	41.60
	41.35	41.62	41.62	41.69	41.76
C_β	42.15	42.06	42.38	42.54	42.57
	42.22		42.44		
C_α	48.72	48.69	49.16	49.36	49.43
	48.91	48.91	49.37	49.56	49.64
C-6	67.47	68.28	67.79	67.77	67.79
	67.79	68.60	68.09	68.09	68.09

[a]ppm at 22.5 MHz, solvent $CDCl_3$, calibrated relative to TMS, ppm downfield from TMS.
[b]Only cyclophosphamide peaks are listed.

1.84 m; C–4, 3.35 m; C-α, 3.48 m; C-β, 2.56 m; C–6, 4.3 m (m = multiplet; N–H and H_2O, variable). These peaks are not shifted or changed in appearance in the complexes.

The ^{13}C NMR data are given in Table 3. The peaks agree with those reported previously.[21] All the peaks are doublets because of splitting by ^{31}P. Some of the ^{13}C peaks are shifted in the complexes, and the changes for the rhodium(II) carboxylate adducts are not the same as those for $SbCl_3(L)$. C–5 is constant for the rhodium(II) compounds, but is shifted upfield 0.3 ppm in $SbCl_3(L)$. C–4 and C_β show small, downfield shifts of 0.2 ppm. C_α shifts 0.5–0.7 ppm downfield in the rhodium(II) compounds but is not changed in the $SbCl_3(L)$ adduct. C-6 shifts 0.8 ppm downfield in the $SbCl_3(L)$ adduct, and 0.3 ppm downfield in the rhodium(II) compounds. The ^{13}C shifts are not large and probably are caused by slight changes in the conformation of the cyclophosphamide ring. Upfield shifts wound be expected if steric crowding were present.

The ^{31}P NMR proton-decoupled spectra show a downfield shift of 4 to 6 ppm for the rhodium(II) carboxylate adducts and no shift for $SbCl_3(L)$. The downfield shifts relative to 85% H_3PO_4 are $L \cdot H_2O$, 12.7 ppm; $SbCl_3(L)$, 12.7 ppm; $Rh_2(acetate)_4(L)_2$, 16.9 ppm; $Rh_2(propionate)_4(L)_2$, 18.4 ppm; $Rh(butyrate)_4(L)_2$, 18.6 ppm. A downfield shift would be expected for P = O coordination, but the absence of a shift for $SbCl_3(L)$ relative to $(L) \cdot H_2O$ is puzzling in view of the IR data. Since ^{31}P chemical shifts are affected by bond angles of phosphorus, electronegativities, and *d*-orbital occupation per phosphorus atom,[22] it is possible that a configurational change has influenced the ^{31}P chemical shift in this adduct. In addition, the $SbCl_3(L)$ ^{31}P nmr shift is the same as $(L) \cdot H_2O$ which does have P = O · · · H hydrogen bonds. Therefore, the P = O - - - Sb bond can be considered comparable to the P = O · · · HOH bond.

All of the complexes isolated in this study are being tested by National Cancer Institute. Since the parent rhodium(II) carboxylates have shown antitumour activity against L1210 leukemia and Ehrlich ascites tumours in mice,[23,24] screening was requested to determine whether the cyclophosphamide adducts would have higher activity. The preliminary screening results for $Rh_2(propionate)_4(L)_2$(NSC 301994), $Rh_2(butyrate)_4 \cdot (L)_2$ (NSC 342722), and $SbCl_3(L)$ (NSC 342672) indicate the compounds are not active. These results are surprising in view of the activity shown previously by the parent compound.

Acknowledgement—This research was supported in part by an institutional grant from the NIH Biomedical Research Support Program. We also wish to acknowledge a fellowship to R. N. (Fundacão de Amparo á Pesquisa do Estade de São Paulo) and a summer fellowship to G. H. (Stephen Harris Cook Fellowship).

REFERENCES

[1]M. D. Joesten In *Metal Ions in Biological Systems* (Edited by H. Sigel), Vol. 11, Chap. 6. Marcel Dekker, New York (1980).
[2]R. O. Inlow and M. D. Joesten, *J. Inorg. Nucl. Chem.* 1975, **37**, 2353.
[3]R. O. Inlow and M. D. Joesten, *J. Inorg. Nucl. Chem.* 1976, **38**, 359.
[4]D. L. Hill, *A Review of Cyclophosphamide*, (Edited by C. C. Thomas), Springfield, IL (1975).
[5]R. J. Woodman, A. E. Sirica, M. Gang, I. Kline and J. M. Venditti, *Chemother.* 1973, **18**, 169.
[6]G. A. Rempel, P. Legzdins, H. Smith and G. Wilkinson, *Inorg. Syn.* 1972, **13**, 90.
[7]J. Kitchens and J. L. Bear, *Thermochim. Acta*, 1970, **1**, 537.
[8]A. Okruszek and J. G. Verkade, *Phosphorus and Sulfur* 1979, **7**, 235.
[9]A. E. Wroblewski, S. M. Socol, A. Okruszek and J. G. Verkade, *Inorg. Chem.* 1980, **19**, 3713.
[10]M. F. Prysak and M. D. Joesten, *Inorg. Chim. Acta*, 1970, **4**, 383.
[11]N. M. Karayannis, C. M. Mikulski and L. L. Pytlewski, *Inorg. Chim. Acta Rev.* 1971, **5**, 69.
[12]S. Garcia-Blanco and A. Perales, *Acta Cryst.* 1972, *B*28, 2647.
[13]J. C. Clardy, J. A. Mosbo and J. G. Verkade, *J. Chem. Soc. Chem. Commun.* 1972, 1163.
[14]I. L. Karle, J. M. Karle, W. Egan, G. Zon and J. A. Brandt, *J. Am. Chem. Soc.* 1977, **99**, 4803.
[15]D. W. White, D. E. Gibbs and J. G. Verkade, *J. Am. Chem. Soc.* 1979, **101**, 1937.
[16]J. G. Verkade, *Phosphorus and Sulfur* 1976, **2**, 251.
[17]S. A. Johnson, H. R. Hunt and H. M. Neumann, *Inorg. Chem.* 1963, **2**, 960.
[18]J. Kitchens and J. L. Bear, *J. Inorg. Nucl. Chem.* 1969, **31**, 2415.
[19]G. Zon, S. M. Ludeman and W. Egan, *J. Am. Chem. Soc.* 1977, **99**, 5785.
[20]W. Egan and G. Zon, *Tetrahedron Lett.* 1976, 813.
[21]R. F. Struck, M. C. Thorpe, W. C. Coburn, Jr. W. R. Laster, Jr., *J. Am. Chem. Soc.* 1974, **96**, 313.
[22]J. H. Letcher and J. R. Van Wazer In *Topics in Phosphorus Chemistry*, (Edited by M. Grayson and E. J. Griffith), Vol. 5, Chaps. 2 and 3. Wiley-Interscience, New York (1967).
[23]A. Erck, L. Rainen, J. Whileyman, I. M. Chang, A. P. Kimball and J. L. Bear, *Proc. Soc. Exp. Biol. Med.* 1974, **145**, 1278.
[24]J. L. Bear, H. B. Gray, Jr., L. Rainen, I. M. Chang, R. Howard, G. Serio, and A. P. Kimball, *Cancer Chemother. Rep., Part I* 1975, **59**, 611.

Polyhedron Vol. 1, No. 7-8, pp. 641-646, 1982
Printed in Great Britain.

0277-5387/82/070641-06$03.00/0
Pergamon Press Ltd.

SYNTHESIS OF THE HEXAPHENOXOTUNGSTATE(V) ION; THE X-RAY CRYSTAL STRUCTURES OF THE TETRAETHYLAMMONIUM AND LITHIUM SALTS

J. IWAN DAVIES, JOHN F. GIBSON, ANDRZEJ C. SKAPSKI,*
GEOFFREY WILKINSON* and WAI-KWOK WONG
Chemistry Department, Imperial College of Science and Technology, London, SW7 2AY, England

(*Received*, 25 *June* 1982)

Abstract—The interaction of metallic lithium, sodium and potassium with tungsten(VI) hexaphenoxide in tetrahydrofuran leads to salts of the hexaphenoxotungstate(V) ion, $[W(OPh)_6]^-$. Electron paramagnetic resonance spectra of the salts in frozen tetrahydrofuran suggests that for the Li^+, Na^+ and K^+ salts there are ion pairs with interaction between the cation and the oxygen atom of the phenoxo groups.

X-ray diffraction study of the tetraethylammonium salt confirms the octahedral nature of the $[W(OPh)_6]^-$ ion; for the lithium salt coordination of the oxygen atom of two phenoxo groups to Li^+ occurs.

INTRODUCTION

Tungsten(VI) hexaphenoxide is a surprisingly stable species[1] but it can be reduced by Raney nickel to give tungsten(V) pentaphenoxide.[2] During attempts to use the hexaphenoxide as starting material for the synthesis of hydrido tungsten species, we observed that it is readily reduced by alkali metals in tetrahydrofuran to give the hexaphenoxotungstate(V) ion. The yields depend upon the reaction conditions but we have isolated the salts $[Li(THF)_2][W(OPh)_6]$, $Na[W(OPh)_6]$. NaOPh, $K[W(OPh)_6]$ and $[Et_4N][W(OPh)_6]$ and the X-ray crystal structures of the tetraethylammonium and lithium salts have been determined.

SYNTHESES

(a) *Lithium and potassium salts*

The interaction of excess lithium or potassium metal with the dark red $W(OPh)_6$ in THF in presence of an excess of phenol leads to yellowish solutions from which orange-yellow salts of the stoichiometry $[Li(THF)_2][W(OPh)_6]$ and $K[W(OPh)_6]$ respectively can be isolated. If an excess of phenol is not present, complex mixtures from which no crystalline products could be isolated, are obtained. The optimum yield is obtained with mole ratios of metal, $W(OPh)_6$ and PhOH of 2.5:1:1. The lithium salt can be crystallised from toluene as air-sensitive orange crystals. The potassium salt is insoluble in toluene but forms air-sensitive yellow crystals from tetrahydrofuran.

(b) *Sodium salt*

The optimum yield of the sodium salt is obtained using a ratio of $Na:W(OPh)_6$:PhOH of 4:1:1:. It crystallises from THF with one mole of sodium phenoxide as solvated air sensitive cubic orange crystals which very readily lose THF on drying under a nitrogen atmosphere or under vacuum. Analysis of the unsolvated complex indicates the stoichiometry $Na_2(OPh)_7$ but since the epr data of frozen solutions of the salt are similar to those of the other salts is seems most likely that the composition is $Na[W(OPh)_6]$.NaOPh and not a 7-coordinate dianion. It is soluble in most polar organic solvents but is insoluble in petroleum, toluene and diethylether. Preliminary X-ray data on the THF solvate (see Fig. 3) confirm the presence of $[W(OPh)_6]^-$.

(c) *Tetraethylammonium salt*

The interaction of methanol solutions of the sodium salt with excess tetraethylammonium bromide in methanol gives the Et_4N^+ salt as air sensitive golden yellow crystals from methanol.

X-RAY STRUCTURAL STUDIES

(a) *The tetraethylammonium salt*

Within the crystal structure there are two crystallographically independent anions which lie on centres of symmetry, while the tetraethylammonium cation lies on a general position without any crystallographically imposed symmetry. One of the $[W(OPh)_6]^-$ ions shows the presence of disorder among the phenoxide ligands but both anions have the same structure. The $[W(OPh)_6]^-$ ion is shown in Fig. 1, while Table 1 lists the more important bond lengths and angles.

As expected the ion has a closely octahedral geometry. Within the accurately determined non-disordered anion the mean W–O distance is 1.943Å and O–W–O *cis* angles are within one degree of the ideal value. The mean W–O–C angle is 139.0°. In a tungsten(VI) compound *trans*-$WCl_2(OPh)_4$ the mean W–O distance is 1.82Å,[3] but the large standard deviations and scatter of individual bond lengths suggest that this is not an accurate structure.

The tetraethylammonium ion has the expected geometry with mean C–N of 1.50Å and mean C–C of 1.53Å and an approximate $\bar{4}2m(D_{2d})$ point symmetry.

(b) *The lithium salt*

In this crystal the $[W(OPh)_6]^-$ anion, the Li^+ ions and the tetrahydrofuran molecules are associated in the $[Li(THF)_2]-[W(OPh)_6]$ entity shown in Fig. 2. Table 2 gives the more important bond lengths while selected bond angles are listed in Table 3. As can be seen from Fig. 2 in contrast to the almost undistorted octahedral arrangement of the anion in the Et_4N^+ salt (Fig. 1), the anion is now distorted by the adjacent lithium atom which binds to two of the phenoxo-oxygen atoms. This causes a clear differentiation in bond lengths between the four W–O bonds of mean length 1.918Å and the other two W–O distances with an average of 2.012Å where the oxygens bind to both tungsten and lithium. The latter distances are very similar to those found[4] in the $\{[Na(THF)_3][W(OPh)_6]Na(THF)_3\}^+$ moiety in the solvated sodium salt which has the structure shown in Fig. 3 where the mean W–O bond length is 1.995Å. In the lithium containing ion pair the four short bonds are

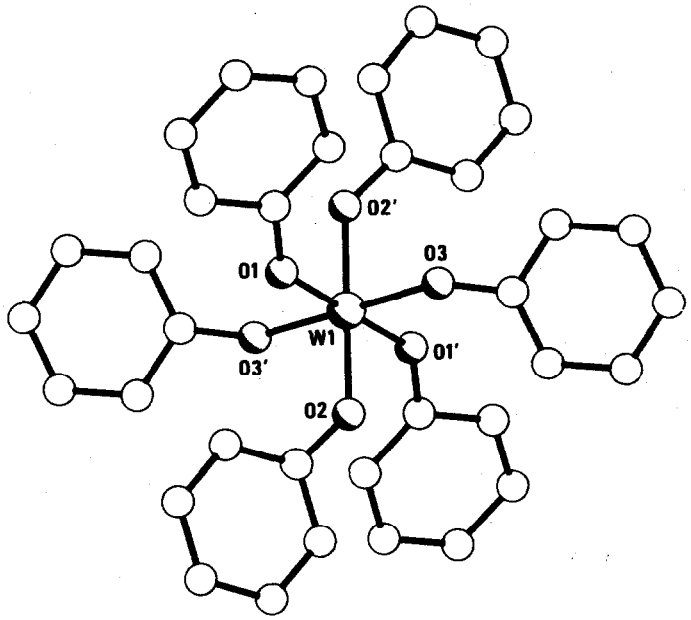

Fig. 1. Structure of the centrosymmetric hexaphenoxotungstate(V) ion.

shorter than those in the $[W(OPh)_6]^-$ ion (1.943Å), but these four are balanced by the two lengthened ones so that the overall mean W–O distance is 1.949Å.

Similarly, the angles at the phenoxo oxygen atoms show this differentiation. The four W–O–C angles have a mean of 139.9° (very similar to that in $[W(OPh)_6]^-$) while the other two have a mean W–O–C angle of 131.9°.

The lithium atom has a distorted tetrahedral environment with a mean Li–O distance of 1.94Å. Within the

segment the acute O(2)–W–O(5) (79.6°) and O(2)–Li–O(5) angles (82.8°) are clearly a consequence of the bridging oxygen atoms requiring reasonably obtuse

Table 1. Selected bond lengths (Å) and bond angles (°) in $(Et_4N)[W(OPh)_6]$

W(2)-O(4)	1.932(5)	W(2)-O(5)	1.956(4)
W(2)-O(6)	1.940(5)		
Average W-O 1.943			
O(4)-C(41)	1.351(10)	O(5)-C(51)	1.335(7)
O(6)-C(61)	1.334(7)		
Average O-C 1.340			
O(4)-W(2)-O(5)	89.2(2)	O(4)-W(2)-O(6)	90.4(2)
O(5)-W(2)-O(6)	90.0(2)		
All O-W-O trans angles 180 by symmetry			
W(2)-O(4)-C(41)	142.1(4)	W(2)-O(5)-C(51)	135.9(5)
W(2)-O(6)-C(61)	139.1(4)		
Average W-O-C	139.0		
Within disordered $[W(OPh)_6]^-$ moiety:			
Average W-O	1.936	Average O-C	1.332
O-W-O cis angles in range 88.1 - 91.9			

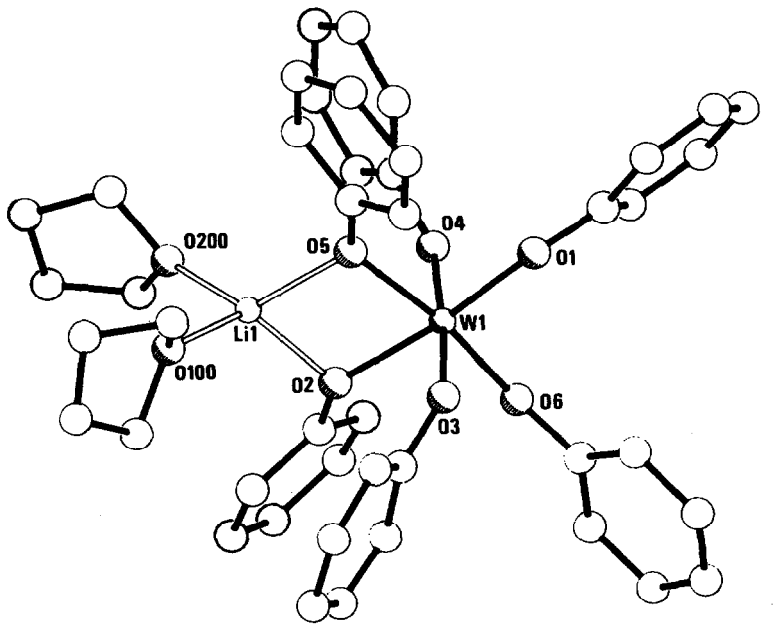

Fig. 2. Structure of $Li(THF)_2[W(OPh)_6]$.

bonding angles. This requirement appears to override the tendency of the lithium atom for tetrahedral bond angles.

It is pertinent to note that although a variety of "double metal alcoxides" have been characterised on the basis of stoichiometry, molecular weights and spectroscopic data, X-ray structural data on such complexes is notably lacking.[5]

Structural data is available for the lithium salts, $\{Li[Re^{VI}O(OPr^i)_5].LiCl(THF)_2\}_2$,[6] $Li\{Cr^{III}[OCH(CMe_3)_2]_4\}.THF$,[7] and $Li\{Fe[OCH(CMe_3)_2]_4.2(Me_3C)_2CHOH$,[7] and for some sodium salts (see Ref. 7). These lithium salts show similar interaction with the oxygen atoms of the alcoxo group to that found here for the phenoxo group and all the compounds can be considered as strongly associated ion pairs. In $LiCr[OCH(CMe_3)_2]_4.THF$ for example there is a CrO_2Li ring which severely distorts the symmetry about the chromium(III) ion just as the symmetry of the $[W(OPh)_6]^-$ ion is distorted in the present case.

Electron paramagnetic resonance spectra

The g values for the $[W(OPh)_6]^-$ ion in frozen tetrahydrofuran solutions of the salts are given in Table 4. These are low relative to comparable data for six-coordinate oxotungstate(V) species[8] in which, of course, there is a well defined symmetry axis along the W = O

Table 2. Selected bond lengths (Å) in $Li(THF)_2[W(OPh)_6]$

W(1)-O(1)	1.921(7)	W(1)-O(3)	1.928(6)
W(1)-O(4)	1.906(6)	W(1)-O(6)	1.915(6)
Average	1.918		
W(1)-O(2)	2.012(7)	W(1)-O(5)	2.012(7)
Average	2.012		
Average overall W-O distance	1.949		
O(1)-C(11)	1.362(12)	O(2)-C(21)	1.365(11)
O(3)-C(31)	1.358(13)	O(4)-C(41)	1.366(12)
O(5)-C(51)	1.350(12)	O(6)-C(61)	1.354(12)
Average O-C	1.359		
Li(1)-O(2)	1.92(2)	Li(1)-O(100)	1.89(2)
Li(1)-O(5)	1.98(2)	Li(1)-O(200)	1.98(2)
Average Li-O	1.94		

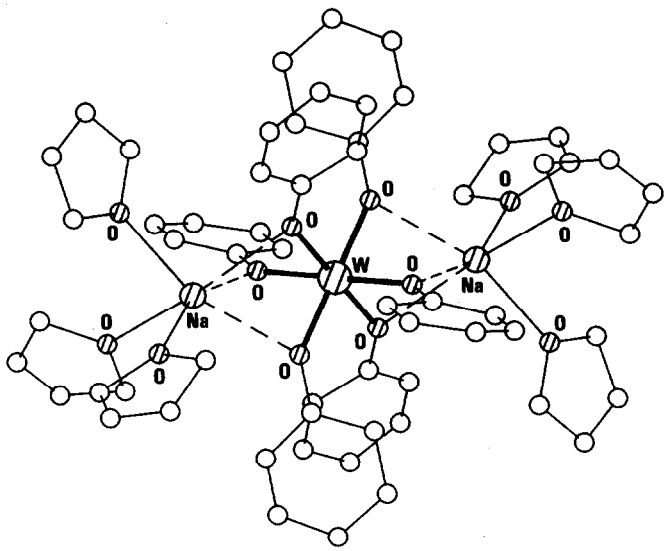

Fig. 3. The $\{Na(THF)_3[W(OPh)_6]Na(THF)_3\}^+$ moiety in the sodium salt.

bond direction. The values suggest that the orbital contributions to g are higher and hence that the t_{2g} orbitals are less widely split which is compatible with weaker axial fields than in the compounds with W = O bonds.

For the sodium salt, the asymmetry due to binding of the sodium ions (see Fig. 3) is retained in solution as indicated by the strictly axial nature ($g_x = g_y$). For the lithium salt the axial symmetry is lost and the g_x and g_y values are the same as for the octahedral $[W(OPh)_6]^-$ ion in the Et_4N^+ or K^+ salts. This does not mean, however, that the lithium ion is a free solvated ion since if the two fold axis defined by the W... Li direction as found in the crystal (Fig. 2) is retained in solution, rhombic g values would be expected. The g values for the Et_4N^+ salt also indicated octahedral geometry with a near axial distortion but g_z is noticeably lower in this case, suggesting a near octahedral geometry. There is no obvious distortion in the solid (Fig. 1) and it seems unlikely that distortion should arise in solution. We take this as indirect evidence that in the lithium salt, the Li^+ ion is still in a strong ion pair in solution. In view of the similarity in g values this probably applies also to the potassium salt.

Thus, for all three alkali metal ions, binding of M^+ to

Table 3. Selected bond angles (°) in $Li(THF)_2[W(OPh)_6]$

O(1)-W(1)-O(2)	171.6(3)	O(1)-W(1)-O(3)	91.5(3)
O(2)-W(1)-O(3)	87.9(3)	O(1)-W(1)-O(4)	91.2(3)
O(2)-W(1)-O(4)	88.9(3)	O(3)-W(1)-O(4)	175.7(3)
O(1)-W(1)-O(5)	92.0(3)	O(2)-W(1)-O(5)	79.6(3)
O(3)-W(1)-O(5)	88.4(3)	O(4)-W(1)-O(5)	88.2(3)
O(1)-W(1)-O(6)	96.3(3)	O(2)-W(1)-O(6)	92.0(3)
O(3)-W(1)-O(6)	90.0(3)	O(4)-W(1)-O(6)	93.0(3)
O(5)-W(1)-O(6)	171.5(3)		
W(1)-O(1)-C(11)	138.5(6)	W(1)-O(4)-C(41)	143.7(6)
W(1)-O(3)-C(31)	138.2(6)	W(1)-O(6)-C(61)	139.3(6)
Average 139.9			
W(1)-O(2)-C(21)	131.6(6)	W(1)-O(5)-C(51)	132.1(7)
Average 131.9			
W(1)-O(2)-Li(1)	99.7(6)	W(1)-O(5)-Li(1)	97.6(7)
Average 98.7			
Li(1)-O(2)-C(21)	121.1(8)	Li(1)-O(5)-C(51)	127.7(9)
Average 124.4			
O(2)-Li(1)-O(5)	82.8(9)	O(2)-Li(1)-O(100)	123.3(1.0)
O(2)-Li(1)-O(200)	113.4(1.0)	O(5)-Li(1)-O(100)	113.2(1.0)
O(5)-Li(1)-O(200)	125.2(1.0)	O(100)-Li(1)-O(200)	100.5(1.1)

Table 4. Electron paramagnetic resonance spectra of hexaphenoxotungstate salts. Tetrahydrofuran solution, *ca.* 100 K, X-band

Compound	g_x	g_y	g_z
$[Li(THF)_2][W(OPh)_6]$	1.21	1.29	1.62
$Na[W(OPh)_5].NaOPh$	1.28	1.28	1.62
$K[W(OPh)_6]$	1.21	1.28	1.60
$[Et_4N][W(OPh)_6]$	1.21	1.29	1.56
$W(OPh)_5$	1.20	1.28	1.63

the oxygen atoms of the phenoxo groups seems to be indicated.

Table 4 also gives data for $W(OPh)_5$ where the g values suggest that in THF the structure resembles that of the lithium salt, with a near axial distortion of the octahedron. It seems most likely that in THF we have $W(OPh)_5(THF)$ and indeed the compound is quite soluble in tetrahydrofuran although it is insoluble in methanol, benzene, etc.; the molecular weight by the Rast method in camphor was said to correspond to the monomer,[2] which is also confirmed by cryoscopic measurement in DMSO. In the solid it is probably polymeric with phenoxo bridges.

Mechanism of formation. It seems unlikely that the formation of the $[W(OPh)_6]^-$ ion is one involving simple one-electron reduction. As noted earlier unless additional phenol is present, the ion is not obtained. It is more likely that a hydride transfer is involved.

$$M + PhOH \rightarrow M^+ + OPh^- + H \quad (1)$$

$$H + W(OPh)_6 \rightarrow W(OPh)_5 + PhOH \quad (2)$$

$$W(OPh)_5 + OPh^- \rightarrow [W(OPh)_6]^-. \quad (3)$$

The reaction 2 was indeed proposed to occur in the synthesis of $[W(OPh)_5]_n$ using "nascent" hydrogen from Raney nickel.[2] We have shown that $W(OPh)_5$ could be an intermediate as the tetrahydrofuran solution reacts with excess lithium phenoxide as in eqn (3) to give $(Li(THF)_2][W(OPh)_6]$.

Interaction of $W(OPh)_6$ in THF with Red-Al or similar hydridic reagents gives yellow solutions which probably contain $[W(OPh)_6]^-$.

The $[W(OPh)_6]^-$ ion behaves as mild one-electron reducing agent, being oxidised to $W(OPh)_6$. Thus, the sodium salt reduces $(\eta^5-C_5H_5)Fe(CO)_2Br$ to $[\eta^5-C_5H_5Fe(CO)_2]_2$, $MnBr(CO)_5$ to $Mn_2(CO)_{10}$, and $Co_2(CO)_8$ to $Co_4(CO)_{12}$. Air oxidation produces $W(OPh)_6$.

EXPERIMENTAL

Microanalyses by Pascher, Bonn.

Spectra

IR; Perkin–Elmer 597, in Nujol mulls. Epr; Varian E12 (X-band) in THF at ca. 100 K. NMR; Bruker WM-250, data in δ ppm references to Me_4Si.

Syntheses

All operations were carried out under oxygen-free argon or nitrogen or in vacuum. THF was dried over sodium-benzophenone and distilled under nitrogen. Hexaphenoxo-[9] and pentaphenoxotungsten[2] were prepared by published methods. Melting points (uncorrected) were determined in sealed tubes. Petroleum had b.p., 40–60°.

(1) *Lithium bis(tetrahydrofuran)hexaphenoxotungstate(V)*

Lithium (0.07 g, 10 mmol) was added to a tetrahydrofuran (100 cm^3) solution of $W(OPh)_6$ (3.0 g, 4 mmol) and phenol (0.38 g, 4 mmol) at room temperature and the deep red solution stirred for 18 hr. The resulting yellowish green solution was filtered and evaporated to dryness under vacuum. The residue was washed with petroleum (2×30 cm^3) and extracted into toluene (2×30 cm^3) to give an orange solution which was concentrated to ca. 20 cm^3 and cooled to −20°C to give air-sensitive orange crystals of $[Li(THF)_2][W(OPh)_6]$.

Yield: 3.0 g, 85%; m.p., 260–266° decomp. [Found: C, 59.7 (59.0); H, 5.2 (5.1); O, 13.8 (14.3)].%

IR. 3070w, 1590s, 1490vs, 1485vs, 1280w, 1242vs, 1228vs, 1162s, 1069m, 1046m, 1023m, 1000m, 890m, 863s, 845m, 827m, 758s, 751s, 689s, 631s, 625m, 600m, 549w, 521w, 508w, 450m.

NMR. ^1H (d_6-Acetone); 1.77 m, (8); 3.62 m, (8); 5.06 t (6), $J = 6.7$ Hz; 9.20 br,s (12); 7.08 br, s, (12).

(2) *Potassium hexaphenoxotungstate(V)*

Potassium (0.39 g, 10 mmol) was added to a 100 cm^3 THF solution of $W(OPh)_6$ (3.0 g, 4 mmol) and phenol (0.38 g, 4 mmol) at room temperature and the solution stirred for 18 hr. After filtering, and evaporating to dryness under vacuum, the residue was washed with petroleum (2×30 cm^3) and toluene (2×30 cm^3) and extracted into tetrahydrofuran (2×30 cm^3). The solution was concentrated to *ca.* 30 cm^3 and cooled to −20°C to give 2 g of $KW(OPh)_6$ as yellow air-sensitive crystals. Yield, 2.0 g, 64% m.p., 255–260°C [Found: C, 55.6 (55.3); H, 4.1 (3.8); O, 11.9 (12.3)%.]

IR. 3070w, 1585s, 1480vs, 1450s, 1308w, 1228vs, 1169m, 1162m, 1146m, 1070m, 1024m, 1000m, 987w, 989m, 854s, 840s, 774s, 754s, 703m, 692s, 632s, 617m, 606m, 536w, 517w, 472m, 452w, 415m.

NMR. ^1H (d_6-Acetone): 5.05 br, s, (6); 7.12 br, s (12); 9.18 br, s (12).

(3) *Sodium hexaphenoxotungstate(V).sodium phenoxide* (1:1)

As above from sodium (0.37 g, 16 mmol) 100 cm^3 THF solution of $W(OPh)_6$ (3.0 g, 4 mmol) and phenol (0.38 g, 4 mmol). After solvent removal the residue was washed with petroleum (2×30 cm^3) and toluene (2×30 cm^3) and extracted into tetrahydrofuran (2×30 cm^3). The solution was concentrated to ca. 30 cm^3 and cooled to −20°C to give solvated orange crystals. The solvent of crystallisation was removed under vacuum leaving $NaW(OPh)_6.NaOPh$ as yellow crystals. Yield: 3.0 g, 85%; m.p., 260°C decomp. [Found: C, 55.7 (57.1); H, 4.0 (4.0); O, 13.1 (12.7)%.]

IR. 3060w, 1590s, 1484vs, 1466vs, 1260s, 1222vs, 1170s, 1151w, 1070w, 1043w, 1027w, 1001w, 886m, 853s, 764w, 753s, 722w, 700w, 689m, 633m, 623m, 607m, 596m, 520w, 495w, 472w.

NMR. ^1H (d_5-THF): 11.22 br,s (4); 9.33 br,s (24); 6.44 br,s (21); 5.03 br,s (12); 3.62 br,s (8); 1.76 br,s (8); 1.22 br,s (4); −2.19 br,s (2).

(4) *Tetraethylammonium hexaphenoxotungstate(V)*

A solution of tetraethylammonium chloride (0.2 g, 1.2 mmol) in 40 cm^3 of methanol was added dropwise to a solution of $NaW(OPh)_6.NaOPh$ (0.9 g, 1 mmol) in 30 cm^3 of methanol. The solution was cooled at −20°C to give golden-yellow crystals which were filtered and dried under vacuum to give 0.2 g of $[Et_4N][W(OPh)_6]$ The filtrate was concentrated to ca. 30 cm^3 and cooled to −20°C to give a further crop of crystals. Yield, 0.7 g, 80%; m.p., 190–1°C.

[Found: C, 60.5 (60.0); H, 5.8 (6.3); 0, 11.2 (10.9); N, 1.6 (1.6)%.]

IR. 3060w, 1587s, 1575m, 1480vs, 1393w, 1279w, 1240ws, 1162m, 1067m, 1021m, 998m, 890m, 857s, 833s, 692s, 632s, 604s, 520w, 476w.

NMR. ^1H (d_6-Acetone): 1.19 t (12), J = 7 Hz; 3 17 (8), J = 7 Hz; 5.09 t (6), J = 6.8 Hz; 7.18 br,s (12); 9.21 br,s (12).

(5) *Interaction of tungsten pentaphenoxide with lithium phenoxide*

Tungsten pentaphenoxide (1 g, 1.5 mmol) and lithium phenoxide (0.5 g, 5 mmol) were dissolved in 100 cm^3 of tetrahydrofuran at room temperature and the solution stirred for 2d. After solvent removal the residue was ashed with petroleum (2 × 30 cm^3) and extracted into toluene (2 × 30 cm^3). The orange solution was concentrated to ca. 20 cm^3 and cooled to −20°C to give $[Li(THF)_2][W(OPh)_6]$ identical with the product from $W(OPh)_6$. Yield: 0.8 g, 60%.

Crystallographic studies

X-ray intensity data collection was carried out using a Nicolet R3m/Eclipse S140 diffractometer system. Graphite monochromated Cu-$K\alpha$ radiation was used with the ω scan technique. The SHELXTL program system[10] was used throughout the calculations, and the atomic scattering factors and the anomalous dispersion corrections were taken from Ref. 11. Least-squares refinement was by the block cascade method, typical of the SHELXTL system. For both compounds an empirical absorption correction was applied,[10] based on 36 psi scan measurements for each of eleven representative reflections for each crystal.

(a) *Crystal data for* $(NEt_4)[W(OPh)_6]$

$C_8H_{20}N.C_{36}H_{30}O_6W$, mol. wt. = 872.7, triclinic, space group $P\bar{1}$, a = 10.734(2), b = 11.580(3), c = 17.998(3)Å, α = 80.85(2), β = 86.42(1), γ = 65.79(1)°, U = 2014.4 $Å^3$ (at 20°C), Z = 2, D_c = 1.44 g cm^{-3}, F(000) = 886, μ(Cu-$K\alpha$) = 57.3 cm^{-1}.

Unit-cell dimensions and orientation matrix based on 25 automatically centred reflections for a crystal sealed in a Lindemann tube under dry argon. Intensity data collected for 4432 reflections ($2 < 2\theta < 100°$), 4143 unique, 3333 observed [$I > 3\sigma(I)$].

Structure solution and refinement. A Patterson synthesis was used to locate the tungsten atom, and the remaining non-hydrogen atoms were found from subsequent difference Fourier syntheses. Because of the special positions of the tungsten atoms on centres of symmetry, progress was very slow. While the tetraethylammonium cation, and the $[W(OPh)_6]^-$ anion centred on $(0, \frac{1}{2}, \frac{1}{2})$ showed no disorder, the other crystallographically independent anion centred on (0, 0, 0) was present in two different orientations. Best agreement was obtained when the phenoxo ligands of the two orientations were given occupancy factors of 0.64 and 0.36 respectively. The non-hydrogen atoms of the ordered moieties were refined anisotropically. In the disordered $[W(OPh)_6]^-$ ion the tungsten atom was anisotropic and all remaining non-hydrogen atoms isotropic, with the phenyl rings refined as rigid bodies. The R values were $R = \Sigma||\Delta F|/\Sigma|F_0| = 0.044$ and $R_\omega = [\Sigma_\omega|\Delta F|^2/\Sigma_\omega|F_0|^2]^{1/2} = 0.047$, with $\omega = 1/[(\sigma F_0)^2 + 0.0012F_0^2]$

(b) *Crystal data for* $Li(THF)_2[W(OPh)_6]$

$C_{44}H_{46}O_8LiW$, mol. wt. = 893.6, monoclinic, space group $P2_1/n$, a = 18.230(3), b = 16.988(4), c = 13.249(3)Å, β = 99.18(2)°, U = 4050.5$Å^3$ (at 19°C), Z = 4, D_c = 1.46 g cm^{-3}, F(000) = 1808, μ(Cu-$K\alpha$) = 57.4 cm^{-1}.

Unit-cell dimensions and orientation matrix based on 18 automatically centred reflections for a crystal sealed in a Lindemann tube under dry argon. Intensity data collected for 4514 reflections ($2 < 2\theta \leq < 100°$), 4164 unique, 3193 observed [$I > 3\sigma(I)$].

Structure solution and refinement. The tungsten atom position was located from a Patterson synthesis, and all other non-hydrogen atoms were found from subsequent difference Fourier syntheses. All non-hydrogen atoms were refined anisotropically, except the carbons of one THF unit. It is clear from the relatively high thermal parameters that a degree of disorder/high thermal motion affects one or both THF rings. The final R values were R = 0.052 and R_ω = 0.048, with $\omega = 1/[(\sigma F_0)^2 + 0.0006F_0^2]$.

For both structures, the final atomic coordinates, thermal parameters, full lists of bond lengths and bond angles, and lists of F_0/F_c values have been deposited with the Editor as supplementary material.†

Acknowledgements—We thank the SERC for the diffractometer system and financial support. One of us (J.I.D.) thanks the Mid Glamorgan County Council for a maintenance grant.

REFERENCES

[1]D. L. Kepert, *The Early Transition Metals*, p. 273. Academic Press, New York (1972).
[2]H. Funk, H. Matschiner and H. Naumann, *Z. Anorg. Allg. Chem.* 1965 **340**, 75.
[3]L. B. Handy and C. K. Fair, *Inorg. Nucl. Chem. Lett.* 1975, **11**, 497.
[4]Details of this structure will be published separately by A. C. Skapski.
[5]D. C. Bradley, R. C. Mehrotra and D. P. Gaur, *Metal Alkoxides*, Chap. 5. Academic Press, New York.
[6]P. G. Edwards, G. Wilkinson, M. B. Hursthouse and K. M. A. Malik, *J Chem. Soc., Dalton Trans.* 1980, 2467.
[7]G. B. Young, M. Bochmann, G. Wilkinson, M. B. Hursthouse and K. M. A. Malik, *J. Chem. Soc., Dalton Trans.* 1980, 1863.
[8]W. Levason, C. A. McAuliffe and F. P. McCullough, Jr., *Inorg. Chem.* 1977, **16**, 2911.
[9]P. I. Mortimer and M. A. Strong, *Austral. J. Chem.* 1965, **18**, 1579.
[10]G. M. Sheldrick, SHELXTL–an integrated system for solving, refining and displaying crystal structures from diffraction data. Revision 3, July, 1981, Nicolet Instruments Ltd., Warwick, England.
[11]*International Tables for X-ray Crystallography*, Vol. 4. The Kynoch Press, Birmingham, England, (1974).

†Copies are available on request from the Editor at Queen Mary College. Tables of atomic coordinates have also been deposited with the Cambridge Crystallographic Centre, University Chemical Laboratory, Lensfield Road, Cambridge CB2 1EW, England.

Polyhedron Vol. 1, No. 7-8, pp. 647-654, 1982
Printed in Great Britain.

0277-5387/82/070647-08$03.00/0
Pergamon Press Ltd.

SYNTHESIS AND VIBRATIONAL SPECTRA OF $[RSHg^{II}]^{2+}(ClO_4)_2$ COMPLEXES. CRYSTAL AND MOLECULAR STRUCTURE OF BIS(N-METHYLPIPERIDINIUM-4-THIOLATO)-MERCURY(II) PERCHLORATE.

HERIBERT BARRERA, JOAN CARLES BAYON,
PILAR GONZALEZ-DUARTE,* JOAN SOLA and JOSEP M. VIÑAS
Departament de Química Inorgànica, Universitat Autònoma de Barcelona,
Bellaterra, Barcelona, Spain.

and

JOSE LUIS BRIANSO, MARIE CLAIRE BRIANSO and XAVIER SOLANS
Departament de Cristal.lografia, Universitat Autònoma de Barcelona,
Bellaterra, Barcelona, Spain.

(Received 9 June 1982)

Abstract-Hg(II) complexes have been prepared with *p*-mercaptoamine ligands 1-methyl-4-mercaptopiperidine (4-MP), 1-methyl-3(mercaptomethyl)piperidine (3-MMP) and 1-methyl-2(2-mercaptoethyl)piperidine (2-MEP) with 1:1 and 1:2 metal to ligand ratios. Infrared and Raman spectra for all these compounds have been recorded and discussed. The spectral features agree with a linear S-Hg-S structure and with the characteristic two-coordination of mercury in all the complexes. The structure of $[Hg(4\text{-}MP)_2](ClO_4)_2$ has been determined by X-ray crystallography. The crystals are orthorhombic, space group $C222_1$ (Z=4) in a unit cell of dimensions a= 13.161 (3) Å, b= 6.589 (2) Å and c= 24.740 (4) Å. Solution of the structure by direct methods led to a final weighted R factor of 0.057 for 1339 independent reflections. The crystal structure consists of discrete $[Hg(4\text{-}MP)_2]^{2+}$ cations and ClO_4^- anions packed in layers paralell to the (100) plane.

INTRODUCTION

Despite of the fact that the affinity of RSH compounds towards mercury has been well known for a long time it is not yet clear which factors determine the structure of mercury(II) mercaptides. The crystal structure of some di(alkylthio)mercury(II) compounds indicates that the coordination number of mercury depends strongly on the nature of the alkyl group. Thus, while the coordination around mercury is essentially linear in $Hg(SMe)_2$ [1] and $Hg(SEt)_2$, [2] it is tetrahedral in $Hg(SBu^t)_2$, [3] the framework of this structure being very similar to the one found in the cadmium complex of 1-methyl-4-mercaptopiperidine [4] which is one of the ligands studied here. It should also be noted that different assignments of the S-Hg-S stretchings have been

made for $Hg(SR)_2$ compounds. [5-8]

The aim of this work is that of contributing to clarify the nature of mercury(II) thiolate bond and to correlate the vibrational spectra of several mercury(II)-thiol complexes with their molecular structure. Accordingly we have synthesized and studied the complexes formed with mercury(II) perchlorate and the following ligands: 1-methyl-4-mercaptopiperidine (4-MP), 1-methyl-3(mercaptomethyl)piperidine (3-MMP) and 1-methyl-2(2-mercaptoethyl)piperidine (2-MEP).

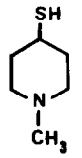

4-MP

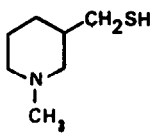

3-MMP

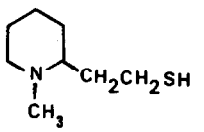

2-MEP

Owing to the zwitterionic behaviour of these ligands [4] the perchlorate anion has been used in order to prevent coordination of the mercury atom with the anion of its salt.

EXPERIMENTAL

The composition of the complexes was determined as follows: Hg gravimetrically as HgS, S iodametrically and C, H and N with a Carlo Erba analyser by the Instituto de Química Bio-Orgánica (Barcelona). Analytical data are collected in Table 1.

TABLE 1. Analytical Results

Compound		% C	% H	% N	% S	% Hg
3-MMP.HCl	Calcd.	46.26	8.87	7.71	17.64	--
	Found	46.38	8.94	7.78	17.50	--
2-MEP.HCl	Calcd.	49.09	9.27	7.16	16.38	--
	Found	49.20	9.38	7.26	15.98	--
$[Hg(4\text{-}MP)](ClO_4)_2$	Calcd.	13.58	2.46	2.64	6.04	37.79
	Found	13.54	2.47	2.65	5.90	37.40
$[Hg(4\text{-}MP)_2](ClO_4)_2$	Calcd.	21.77	3.96	4.24	9.69	30.30
	Found	22.03	3.99	4.20	9.47	30.49
$[Hg(3\text{-}MMP)](ClO_4)_2.H_2O$	Calcd.	14.94	3.05	2.49	5.70	35.65
	Found	15.24	3.11	2.52	5.80	35.50
$[Hg(3\text{-}MMP)_2](ClO_4)_2$	Calcd.	24.38	4.38	4.06	9.30	29.08
	Found	24.55	4.27	4.25	9.23	29.24
$[Hg(2\text{-}MEP)](ClO_4)_2.1/2H_2O$	Calcd.	16.92	3.20	2.47	5.65	35.33
	Found	16.95	3.36	2.38	5.66	35.69
$[Hg(2\text{-}MEP)_2](ClO_4)_2$	Calcd.	26.76	4.77	3.90	8.93	27.93
	Found	26.68	4.77	4.18	8.72	27.81

Spectrophotometers. IR: Perkin-Elmer 180, spectra in KBr pellets (4000--500 cm^{-1}) or in nujol mulls (500-150 cm^{-1}) between polythene plates. Raman: Dilor equipped with a Tracor multichannel using 514.5 nm excitation and samples run as powders in spinning capillary tubes.

Preparation of ligands

4-MP was synthesized according to the literature. [9] 3-MMP and 2-MEP were obtained from their isothiouronium salts that were formed after N-methylation [10] of 3-hydroximethylpiperidine and 2-hydroxiethylpiperidine respectively, following a reported method. [11, 12] $Hg(ClO_4)_2.6H_2O$ was prepared from analytical grade HgO and $HClO_4$.

Preparation of complexes

1) $[Hg(4\text{-}MP)](ClO_4)_2$

A methanolic solution of 4-MP (7.5 mmol in 50 ml) was slowly added to a stirred clean methanolic solution of $Hg(ClO_4)_2.6H_2O$ (6.7 mmol in 200 ml). The complex precipitated slowly as the ligand was being added.

2) $[Hg(4\text{-}MP)_2](ClO_4)_2$

A white crystalline solid was formed while adding slowly 15 mmol of 4-MP dissolved in 75 ml of 0.1 M $HClO_4$ aqueous solution to 75 ml of the same solvent where $Hg(ClO_4)_2.6H_2O$ (8 mmol) had been dissolved. Crystals suitable for x-ray diffraction were grown in 0.1 M $HClO_4$.

3) $[Hg(3\text{-}MMP)](ClO_4)_2.H_2O$

Using the same procedure of the related compound described above, a yellow oil formed. It was left in the freezer overnight and then washed with absolute ethanol several times. The oil became a white solid by staying under vacuum.

4) $[Hg(3\text{-}MMP)_2](ClO_4)_2$

An oil formed when $NaClO_4$ concentrated solution was added to 60 ml of a solution 0.1 M in $HClO_4$ containing 1.58 mmol of $Hg(ClO_4)_2.6H_2O$ and 3.27 mmol of 3-MMP. This oil was placed in the freezer where it turned to a white solid.

5) $[Hg(2\text{-}MEP)](ClO_4)_2.1/2H_2O$

While slowly adding an aqueous solution of 2-MEP in 0.1 M $HClO_4$ to a stirred solution of $Hg(ClO_4)_2.6H_2O$ in the same medium in 1:1 mole ratio an oil formed, which became a white solid through continuous stirring for several hours. This solid was collected, washed with 0.1 M $HClO_4$ solution and water, and dried under vacuum over P_2O_5.

6) $[Hg(2\text{-}MEP)_2](ClO_4)_2$

The same procedure as that used for the 1:1 analog was followed. In this case, the $Hg(ClO_4)_2.6H_2O$ solution was added to that of the ligand in 2:1 mole ratio. The oil formed was treated with methanol several times and finally dried under vacuum over P_2O_5. The white solid obtained is highly hygros-

copic.

Crystallographic studies

A small crystal of $[Hg(4\text{-}MP)_2](ClO_4)_2$ was chosen and mounted on a Philips PW-1100 four-circle diffractometer (Department of Mineralogy and Crystallography of Paris VI University), where crystal data and intensity measurements were carried out. Only Lorentz and polarization effects were corrected. *Crystal data.* $(Hg[SC_5H_9NH(CH_3)]_2)(ClO_4)_2$, orthorhombic, a = 13.161 (3), b = = 6.589 (2), c = 24.740 (4), U = 2145.4 $Å^3$, space group $C222_1$, Z = 4, D_m = = 2.03 g cm^{-3} (flotation in bromoform-carbon tetrachloride), D_c = 2.05 g cm^{-3}, F(000) = 1280.

Data collection. Philips PW-1100 diffractometer, graphite monochromated Mo-Kα radiation, θ-2θ scan mode, scan speed of 2°/min in 2θ, 1741 reflections collected, 1339 observed $[I \geq 2.5\,\sigma(I)]$.

Structure solution and refinement. The structure was solved by direct methods, using the MULTAN system of computer programs. [13] An E-map computed from the set of phases with the highest combined figure of merit revealed peaks for all atoms, except hydrogen and oxygen atoms of perchlorate groups. Isotropic and anisotropic refinements by full-matrix least-squares method were made with the SHELX76 program. [14] The function minimized was $w||F_o|-|F_c||^2$, where $w = (\sigma^2(F) + 0.0067|F|^2)^{-1}$. A difference synthesis at R = 0.093 revealed 7 non-symmetric equivalent peaks linked to chlorine atoms. The integration of these maxima from a Fourier synthesis at this point, gave an electronic number of 8 for one and about 4 for the rest of oxygen atoms, therefore, disorder in the localization of perchlorate ions was considered. Isotropic refinement of O atoms and anisotropic of the other atoms gave a final R factor of 0.057. Bond distances and angles are given in Table 2. Final atomic coordinates, thermal parameters and a list of F_o/F_c values have been deposited with the Editor as supplementary data.

TABLE 2. Bond lengths and angles for $(Hg[SC_5H_9NH(CH_3)]_2)(ClO_4)_2$.

a. Bond Lengths (Å)			b. Bond Angles (deg)		
Hg-S	2.329	(0.004)	S-Hg-S	176.9	(0.1)
S-C(1)	1.795	(0.015)	Hg-S-C(1)	102.1	(0.6)
C(1)-C(2)	1.511	(0.023)	C(1)-C(2)-C(3)	110.5	(1.3)
C(2)-C(3)	1.633	(0.022)	C(2)-C(3)-N	103.6	(1.4)
C(3)-N	1.485	(0.019)	C(3)-N-C(6)	105.0	(1.6)
N-C(6)	1.586	(0.024)	C(6)-N-C(4)	111.1	(1.8)
N-C(4)	1.448	(0.023)	C(3)-N-C(4)	115.7	(1.2)
C(4)-C(5)	1.444	(0.028)	N-C(4)-C(5)	113.2	(1.6)
C(5)-C(1)	1.547	(0.019)	C(4)-C(5)-C(1)	112.9	(1.5)
			C(2)-C(1)-S	109.0	(1.1)
			C(5)-C(1)-S	112.5	(1.1)
			C(5)-C(1)-C(2)	108.3	(1.3)

DESCRIPTION OF THE STRUCTURE OF $[Hg(4\text{-}MP)_2](ClO_4)_2$.

The crystal structure of this complex consists of discrete $[Hg(4\text{-}MP)_2]^{2+}$ cations, Figure 1, the ligands being in zwitterionic form, and of perchlorate anions packed in layers parallel to the (100) plane, Figure 2. These layers are linked together by weak hydrogen bonds. All the cations are crystallographically equivalent while there are two crystallographically independent anions.

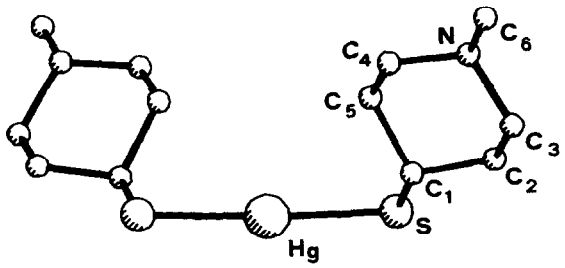

Fig. 1. The molecular structure of $\left(Hg[SC_5H_9NH(CH_3)]_2\right)^{2+}$.

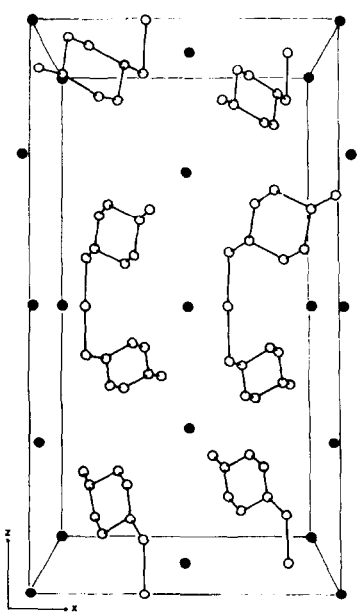

Fig. 2. Crystal structure of $\left(Hg[SC_5H_9NH(CH_3)]_2\right)(ClO_4)_2$. Shaded circles denote ClO_4^- anions.

The mercury atom is on a binary axis and its coordination is linear. Thus, there is only one type of piperidinic rings which are in chair conformation. The methyl group as well as the sulfur atom are in equatorial positions.

The Hg-S distance is 2.329(0.004) Å, which agrees very well with the sum of covalent radii [15] and is shorter than those reported for two mercury mercaptides with essentially digonal coordination, 2.36 Å in $Hg(SMe)_2$ [1] and 2.45 Å in $Hg(SEt)_2$. [2] The distance between mercury and its closest non-bonded atom, which is an oxygen atom, is 3.08(2) Å corresponding exactly to the sum of their van der Waals radii if taking the value of 1.73 Å for mercury as recently reported. [16]

The shortest interatomic distances between consecutive layers range between 2.9(1) and 3.2(1) Å indicating that weak hydrogen bonds between protonated amine groups and perchlorate anions should be considered. This is also in agreement with the disorder found for the perchlorate anions. It is clear that as both

chlorine atoms are on binary axes only two independent oxygen atoms should be found around each of them if it were not disorder.

IR AND RAMAN SPECTRA OF THE COMPLEXES

A significant feature of the IR spectra of all the complexes is a strong and broad band in the region of 3100 cm^{-1} showing that the amine group is protonated and linked by a very weak hydrogen bond to the anion [17] and thus indicating that the ligand is in zwitterionic form.

The spectra of $[Hg(4\text{-}MP)_2](ClO_4)_2$ of known structure show strong bands at 395 cm^{-1} (IR) and 372 cm^{-1} (Raman) that have been ascribed to S-Hg-S asymmetric and symmetric stretchings respectively. These assignments are quite clear because the rest of the bands in this region of the spectrum are only slightly shifted or remain in the same position as those of 1-methyl-4-mercaptopiperidine hydrochloride. They are also in agreement with previously reported assignments, 405 cm^{-1} (IR) and 394 (Raman), for the linear $Hg(SEt)_2$.[2] Further evidence provides the fact that in the case of the complex $[Hg(4\text{-}MP)](ClO_4)_2$ appears one band at 400 cm^{-1} (IR) and another at 379 cm^{-1} (Raman), which also indicate a linear coordination for the mercury atom. This suggests that a zigzag polymeric chain(-S-Hg-S-Hg-) is the backbone of the structure of this complex. Similar frameworks have been found in complexes of the type $CH_3COOHgSR$. [18-20] However in these cases coordination around mercury is greater than two (SHgS angles ranging from 140 to 160°) because of the coordinating carboxylate groups. Therefore it is not surprising that the corresponding S-Hg-S stretching bands have been assigned at lower frequencies. According to our results it does not seem likely that important interactions exist between Hg and S atoms of different chains in $[Hg(4\text{-}MP)](ClO_4)_2$ since the S-Hg-S stretching bands appear practically in the same position as in the "pure" digonal $[Hg(4\text{-}MP)_2](ClO_4)_2$.

Table 3 shows the assignments made for the S-Hg-S stretchings for all the complexes reported here.

TABLE 3. Mercury-Sulfur vibrations (cm^{-1})

Complex	ν_{as}(Hg-S) (IR)	ν_s(Hg-S) (Raman)
$[Hg(4\text{-}MP)](ClO_4)_2$	400 (s)	379 (m)
$[Hg(4\text{-}MP)_2](ClO_4)_2$	395 (s)	372 (s)
$[Hg(3\text{-}MMP)](ClO_4)_2.H_2O$	360 (s)	318 (s)
$[Hg(3\text{-}MMP)_2](ClO_4)_2$	350 (s)	326 (s)
$[Hg(2\text{-}MEP)](ClO_4)_2.1/2H_2O$ (*)	350 (s)	302 (s)
$[Hg(2\text{-}MEP)_2](ClO_4)_2$ (*)	360 (s)	326 (s)

(*) J.M.V. Doctoral thesis

s, strong; m, medium

In view of these data, linear coordination for the mercury atom has to be proposed for the complexes formed with 3-MMP and 2-MEP and thus, structures similar to those discussed above for the corresponding complexes formed with the 4-MP ligand should be expected for them. The assignment of ν(S-Hg-S) modes for 3-MMP and 2-MEP complexes indicates, however, the presence of very weak intermolecular Hg...S interactions. It must be pointed out that the values reported for the S-Hg-S bands in $Hg(SBu^t)_2$ are 172 cm^{-1}(asym.) and 188 cm^{-1}(sym.) [7](see this reference for discussion of other values reported previously).

The $Hg(SBu^t)_2$ complex is the only known mercury thiolate with tetrahedral coordination. However, it seems reasonable to think that this unique coordination around mercury cannot be explained if only considering the size of the alkyl substituent as on the one hand there is good evidence that bulky ligands such as substituted piperidines lead to linear Hg(II) complexes and on the other it is known that the crystal structure of the cadmium complex of 4-MP [4]is very similar to that of $Hg(SBu^t)_2$. According to Grdenić, [15]digonal coordination around mercury is favoured for atoms with electronegativity greater than 2.5(Pauling's) while for atoms with values smaller than 2.5 the tetrahedral one is preferred. Sulfur has a limiting position because of the value of 2.5 of its electronegativity and so a variation in its substituents can cause a change in the coordination number of mercury. The different coordination around Hg in $Hg(SBu^t)_2$ and in the γ-mercaptoamine-Hg(II) complexes described here could thus be rationalised in terms of a decrease and an increase respectively of the "effective electronegativity" of the sulfur atom. The fact that a positive charge on the nitrogen atom enhances the acidity of the thiol group, as it is shown in the following pK_a values [21]

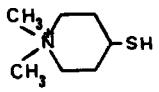

pK_a = 9.62

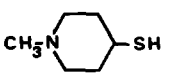

pK_a = 10.60

gives support to the previous argument.

Acknowledgement-We thank the Comisión Asesora Científica y Técnica for support and Prof. A. Potier, Prof. J. Potier and Dr. G. Bonnet from the Laboratoire des Acides Minéraux, Univ. Scien. Tech. Languedoc (Montpellier, France) for measurement of Raman-spectra.

REFERENCES

1 D.C. Bradley, N.R. Kunchur; *J. Chem. Phys.*, 1964, 40, 2258.
2 D.C. Bradley, N.R. Kunchur; *Can. J. Chem.*, 1965, 43, 2786.
3 N.R. Kunchur; *Nature*, 1964, 204, 468.
4 J.C. Bayón, M.C. Briansó, J.L. Briansó, P. González-Duarte; *Inorg. Chem.*, 1979, 18, 3478.
5 N. Iwasaki, J. Tomooka, K. Toyoda; *Bull. Chem. Soc. Jap.*, 1974, 47, 1323.
6 P. Biscarini, L. Fusina, G. Nivellini; *J. Chem. Soc.*, Dalton, 1974, 2140.
7 A.J. Canty, R. Kishimoto, G.B. Deacon, G.S. Farquharson; *Inorg. Chim. Acta*, 1976, 20, 161.

[8] P. Biscarini, L. Fusina and G. Nivellini; *Spectrochim. Acta*, 1980, 36A, 593.
[9] H. Barrera, R.R. Lyle; *J. Org. Chem.*, 1962, 27, 641.
[10] A. Kaluszyner and A.G. Galun; *J. Org. Chem.*, 1961, 26, 3536.
[11] R.L. Frank and P.V. Smith; *J. Am. Chem. Soc.*, 1946, 68, 2103.
[12] B.C. Cossar, J.O. Fournier, D.L. Fields and D.D. Reynolds; *J. Org. Chem.*, 1962, 27, 93.
[13] M.M. Wolfson, P. Main, L. Lessinger, G. Germain, J.P. Declerq (1976) MULTAN. A system of computer programs for crystal structure determination from X-ray diffraction data. Univ. York (England) and University of Louvain (Belgium).
[14] G.M. Sheldrick (1976) SHELX. A computer program for crystal structure determination. Univ. Cambridge (England).
[15] D. Grdénić; *Quart. Rev.*, 1965, 19, 303.
[16] A.J. Canty and G.B. Deacon; *Inorg. Chim. Acta*, 1980, 45, L 225.
[17] R.H. Nuttal, D.W.A. Sharp, T.C. Wadington; *J. Chem. Soc.* (A), 1960, 4965.
[18] H. Puff, R. Sievers, G. Elsner; *Z. Anorg. Allg. Chem.*, 1975, 413, 37.
[19] A.J. Canty, R. Kishimoto, R.K. Tyson; *Aust. J. Chem.*, 1978, 31, 671.
[20] A.J. Canty, C.L. Raston, A.H. White; *Aust. J. Chem.*, 1978, 31, 677.
[21] H. Barrera, J.C. Bayón, P. González-Duarte and J. Sola; *J. Chim. Phys. Chim. Biol.*, 1979, 76, 987.

Polyhedron Vol. 1, No. 7-8, pp. 655-658, 1982
Printed in Great Britain.

0277-5387/82/070647-04$03.00/0
Pergamon Press Ltd.

NOTES

Antimony(III) and Bismuth(III) Trihalide Complexes of 2-aminobenzothiazole

Aleardo Giusti, Giorgio Peyronel* and Elisa Giliberti

Istituto di Chimica Generale e Inorganica, Università di Modena
41100 Modena, Italy

(Received 7 May 1982)

Abstract

The following antimony(III) and bismuth(III) trihalide complexes of 2-aminobenzothiazole (L) were prepared and investigated by infrared spectroscopy: $SbCl_3.2L$, $SbBr_3.1.5L$, $MX_3.L$ (M=Sb,X=I; M=Bi,X=Cl,Br,I).The ligand is coordinated through its endocyclic nitrogen atom. The MX_3 point group has a C_{2v} or C_s symmetry in the SbX_3 and $BiCl_3$ and a C_{3v} symmetry in the $BiBr_3$ and BiI_3complexes.

Introduction

Few complexes of 2-aminobenzothiazole (L) with cobalt(II), nickel(II) (1) and iron(III) (2) have been studied. The crystal structure of the polymeric (2-aminobenzothiazolato)nitratotin(II) was determined by X-ray diffraction methods (3). Up to now no complexes of this ligand with the VA group elements have been investigated. As the activities of many enzymes depend upon the interaction of an imidazole or thiazole group with a metal ion, the coordination behaviour of the benzothiazole derivatives may have some interest. The 2-aminobenzothiazole complexes of antimony(III) and bismuth(III) halides have been investigated in this work.

Experimental

The ligand and all the reagents were of the best chemical grade. The complexes were prepared by adding a solution of the salt (0.5 mmol) in acetone (2 cm^3 for $SbCl_3$, 20 cm^3 for $BiCl_3$), benzene (1.5 cm^3 for $SbBr_3$) or acetic acid (10 cm^3 for SbI_3, 5 cm^3 for $BiBr_3$, 20 cm^3 saturated with KI for BiI_3) to a solution of the ligand (1 mmol) in the same solvent (2 cm^3 for acetone and acetic acid, 8 cm^3 for benzene) and washing the compounds with the solvent used for the preparation. All the compounds are white except the SbI_3 (yellow) and BiI_3 (orange) complexes. The ligand was deuteriated in MeOD solution and the hydrobromide derivative L.HBr was precipitated with Et_2O from an ethanolic solution of the ligand containing HBr.

The N,C,H,S elemental analyses are reported in Table 1 with the molar conductivities determined with a WTW conductivity bridge. Infrared spectra

were recorded in KX (X=Cl,Br,I) disks (4000-250 cm^{-1}) and as nujol mulls on polythene (600-60 cm^{-1}) with a Perkin Elmer 180 spectrophotometer.

Results and discussion

The ν(NH) bands of the ligand (3395s, 3350sh, 3265m, 3090sh, 3050s cm^{-1}) identified through the ν_D/ν_H ratio (0.74-0.76) of the corresponding bands of the deuteriated derivative appear for the complexes in about the same spectral regions (3380-3340, 3290-3280, 3170-3150, 3120-3050 cm^{-1}) while the $\delta(NH_2)$ band (1605-1600 cm^{-1}) has the frequency observed in the L.HBr derivative.

In the complexes the ν(C=N) band shows a frequency decrease of about 5-20 cm^{-1} while the bands assignable to ν(C-N) and ν(C-S) modes (4) show a frequency increase of 30-40 cm^{-1} and 20-25 cm^{-1}, respectively. These frequency changes are consistent with the electronic shifts

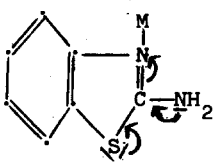

due to a coordination of the ligand through the endocyclic nitrogen atom, as occurs in other complexes of this ligand (1,3).

The ligand band at 302 cm^{-1}, observed in all the complexes of this series, was assigned (1) to a $\delta(C\text{-}NH_2)$ mode and its presence was considered to exclude a coordination through the exocyclic amino group.

The bands assigned to ν(MX) modes (Table 2) have frequencies in the range of terminal MX stretching modes (5-11). The antimony complexes have equal ν_{Br}/ν_{Cl} (0.79, 0.80, 0.81) and close ν_I/ν_{Cl} (0.51; 0.54, 0.61) ratios. The ν_{Bi}/ν_{Sb} ratios are for all the ν(BiX) frequencies, except for the ν(BiCl) band at 247 cm^{-1}, close to their average value of 0.91.

For the SbX_3 and $BiCl_3$ complexes three ν(MX) bands indicate that the MX_3 point group has a C_{2v} or C_s symmetry (12,13). For the SbX_3 group of the $SbCl_3$.2L and $SbBr_3$.1.5L complexes a C_{2v} symmetry may be given by a square pyramidal structure with the stereochemically active electron pair in the sixth position; two nitrogen atoms in cis position give the two ν(SbN) bands observed. In the antimony bromide complex one of the ligand molecules may bridge two metal ions.

For the MX_3 group of the SbI_3.L and $BiCl_3$.L complexes a C_s symmetry may be given by a trigonal pyramidal structure with the stereochemically active electron lone pair in the fifth position and the ligand molecule bonded as monodentate. The $BiBr_3$.L and BiI_3.L complexes show only two ν(BiX) bands corresponding to a C_{3v} symmetry of the BiX_3 group (12,13) which may be given by a trigonal pyramidal structure with the stereochemically active electron lone

pair in the fifth position and the N-monodentate ligand molecule in the apical position.

Table 1

Analytical data, found% (calcd.%), and molar conductivity Λ_M (Ω^{-1} mol^{-1} cm^2) in 10^{-3} M DMF solution at 25° of the 2-aminobenzothiazole (L) complexes.

	N	C	H	S	Λ_M
$SbCl_3$.2L	10.54(10.60)	32.06(31.82)	2.50(2.29)	11.76(12.13)	23.1
$SbBr_3$.1.5L	6.95(7.16)	21.07(21.49)	1.43(1.55)	7.89(8.20)	75.2
SbI_3.L	4.23(4.29)	12.52(12.88)	0.81(0.93)	4.62(4.91)	195.5
$BiCl_3$.L	5.63(6.02)	18.49(18.06)	1.40(1.30)	6.58(6.84)	11.2
$BiBr_3$.L	4.54(4.68)	13.82(14.04)	0.97(1.01)	5.12(5.35)	47.9
BiI_3.L	4.05(3.79)	11.58(11.36)	1.05(0.82)	4.48(4.33)	68.7

Table 2

Principal infrared bands (cm^{-1}) of the 2-aminobenzothiazole complexes.

	L	L.HBr	$SbCl_3$ 2L	$SbBr_3$ 1.5L	SbI_3 L	$BiCl_3$ L	$BiBr_3$ L	BiI_3 L
ν(C=N)	1640vs	1645vs	1635sh	1630vs	1627vs	1636vs	1630vs	1620s
ν(C-N)	1115sm	1120vw	1158vw	1156w	1155mw	1157w	1155w	1152w
ν(C-S)	620m	623sm	640s	648m	640ms	643m	645sm	640mw
δ(C-NH_2)	302vs	303s	306s	298s	307wm	308s	310s	306w
ν(MX)			310vs	245vs	157vs	281s	223s	133s
			247s	198vs	133sm	247s	179vs	125vs
			202vs	163vs	124vs	184vs		
ν(MN)			222s	222vs	221w	222sm	223s	220w
			184vs	192s				
δ(MX)			164s	(146m)	118s	164s		
			(143s)	114s	92sm	(146s)		
			114s		83ms	114sm		
other	280wm	278w	287wm	285s	284sm	288s	285s	284m
bands	212m	212m	279wm	279wm	276w		264w	
	202w	200wm	264w	264w	261w	252sh	246s	242wm
	155w	164wb	254w	254w	242w		204sh	200w
	148w	148vs		185sm	188ms		184sh	182sh
	138w	131vs			166sh			165w
	126w	92s	143s	146m	148ms	146s		146w
	97w				100w	106w	112wb	120sh

The ν(MN) bands of the (ring)nitrogen-metal bonds were located for the cobalt(II) and nickel(II) complexes of this ligand (1) at about 240 and 220 cm^{-1} with some contributions by ν(MN) modes to bands at about 170 and 140 cm^{-1}.

In the 280-240 cm^{-1} region the antimony and bismuth complexes of 2-amino-benzothiazole show new but mostly weak bands to which a ν(MN) contribution might be assigned. The bands at 222-184 cm^{-1} assigned to ν(MN) modes (Table 2) because of their mostly high intensities, even if they may be coupled with the medium or weak bands observed at 212 and 200 cm^{-1} for the ligand. Some mostly strong bands are tentatrively assigned to δ(MX) modes. Those at 146-143 cm^{-1} may correspond to or be coupled with the ligand band at 148 cm^{-1} having a very high intensity in the L.HBr derivative.

Acknowledgments. Infrared spectra were recorded in the Centro Strumenti of the University of Modena.

References

(1) M.J.M.Campbell, D.W.Card, R.Grzeskowiak and M.Goldstein, J.Chem.Soc.(A) 672 (1970).

(2) M.J.MCampbell, R.Grzeskowiak and G.S.Juneja, J.Inorg.Nucl.Chem. 40, 1247 (1978).

(3) M.Nardelli, C.Pelizzi and G.Pelizzi, J.Chem.Soc.Dalton 1595 (1975).

(4) C.N.R.Rao, Chemical Applications of Infrared Spectroscopy, p.250,297, Academic Press, New York (1963).

(5) C.Preti and G.Tosi, J.Mol.Struct. 50, 7 (1978).

(6) G.C.Allen and R.F.McMeeking, Inorg.Chim.Acta 23,185 (1977).

(7) P.B.Bevan and S.K.Madan, J.Inorg.Nucl.Chem. 36, 983 (1974).

(8) S.T.Yuan and S.K.Madan, Inorg.Chim.Acta 6, 463 (1972).

(9) S.Milicev and D.Hadzi, Inorg.Nucl.Chem.Letters 7, 745 (1971).

(10) G.Y.Ahlijah and M.Goldstein, J.Chem.Soc. (A) 2590 (1970).

(11) R.P.Oertel, Spectrochim. Acta 26A, 659 (1970).

(12) J.E.D.Davies and D.A.Long, J.Chem.Soc. (A) 1758, 1761 (1968).

(13) A.Finch, P.N.Gates, K.Radcliffe, F.N.Dickson and E.F.Benton, p.170,171, Academic Press, London (1970).

Polyhedron Vol. 1, No. 7–8, pp. 659–662, 1982
Printed in Great Britain.

0277–5387/82/070659–04$03.00/0
Pergamon Press Ltd.

Ethylenediamine rhodium(III) complexes of ethylenediamine-N,N′-di-S-α-propionic acid

(*Received* 24 *May* 1982)

Abstract—Ethylenediamine rhodium(III) complexes of ethylenediamine-N,N′-di-S-α-propionate ligand have been prepared and the absolute configurations of these complexes have been assigned based on pmr and CD data.

The optically active tetradentate ligand, ethylenediamine-N,N′-di-S-α-propionate (SS-EDDP) was shown to possess high stereospecificity in its coordination to cobalt(III) ion which yielded the Δ-*cis*-α, Λ-*cis*-α, and Δ-*cis*-β isomers. Schoenberg *et al.*[1] showed how pmr spectra could be utilized to assign the absolute configurations of those complexes. We have been interested in synthesizing rhodium(III) complexes of the SS-EDDP ligand, and in this paper wish to describe pmr and CD spectra of the ethylenediamine rhodium(III) complexes of this ligand.

EXPERIMENTAL

Physical measurements. Electronic absorption spectra were obtained with a Unicam SP 800A spectrophotometer. ORD and CD spectra were measured with a Jasco ORD/CD-5 spectrophotometer. Pmr spectra were recorded on a Varian A-60 or a Brucker 90 mHz spectrometer. Infrared spectra were taken with a Perkin–Elmer Model 337 spectrophotometer. Elemental analyses were performed by Spang Microanalytical Laboratories, Ann Arbor, Michigan.

Ethylenediamine - N,N′ - di - S - α - propionic acid (SS-EDDP). This was prepared according to the known method.[1] Found: C, 46.85; H, 7.92; N, 13.68. Calc. for $C_8H_{16}N_2O_4$; C, 46.90; H, 7.89; N, 13.70.

Δ-*cis*-α-[*Rh*(*SS-EDDP*)(*en*)]*Cl.* To a solution of 0.40 g of *trans*-[Rh(py)$_4$Cl$_2$] Cl·5H$_2$O (py = pyridine) in 25 ml of water was added to a 5 ml aqueous solution of 0.02 g of SS-EDDP and 0.025 g of LiOH·H$_2$O. The mixture was refluxed for two hours. The pyridine was removed by ether extraction. The solution was evaporated under a moving air until crystals started to form. The mixture was cooled in an ice bath and crystals were collected by filtration and dried. The ORD curve of the mother liquor indicated no other isomers present. The dried product was dissolved in freshly distilled DMF and three drops of ethylenediamine were added. The solution was refluxed for three hours, and cooled in an ice bath for 1 hr. The creamy white product was filtered and washed with ethanol and ether. Yield: 0.18 g (80%). Found: C, 29.90; H, 5.63; N, 13.99; Cl, 8.87. Calc. for $RhC_{10}H_{22}O_4Cl$; C, 29.96; H, 5.49; N, 13.98; Cl, 8.86%.

Λ-*cis*-β-[*Rh*(*SS-EDDP*)(*en*)] Cl·H$_2$O. Three drops of pure ethylenediamine were added to 0.216 g of Λ-*cis*-β-H[Rh(SS-EDDP)Cl$_2$]·3H$_2$O[2] dissolved in freshly distilled DMF. After thirty minutes of refluxing, the product began to precipitate out of solution and after three hours of refluxing the mixture was cooled in an ice bath for several hours. The creamy white product was filtered and washed with ethanol and ether. Yield: 0.14 g (70%). Found: C, 29.00; H, 5.84; N, 18.48; Cl, 8.60. Calc. for $RhC_{10}H_{22}N_4O_4Cl·H_2O$; C, 28.85; H, 5.77; N, 13.46; Cl, 8.50%.

RESULTS AND DISCUSSION

Two isomers were yielded out of the four possible isomers as shown in Fig. 1. The reaction of *trans*-[Rh(py)$_4$Cl$_2$]$^+$ with SS-EDDP and en yielded only the Δ-*cis*-α-[Rh(SS-EDDP)(en)]$^+$. The Λ-*cis*-β isomer was prepared from the reaction of Λ-*cis*-β-[Rh(SS-EDDP)Cl$_2$]$^-$ with en in DMF.

Although the electronic absorption spectra (Figs. 5 and 6) are not particularly helpful in distinguishing the geometric isomers, they are clearly distinguished in the PMR spectra. The *cis*-α complex shows a single methyl doublet at 1.5 ppm and the H$_b$ proton quartet at 3.62 ppm (Fig. 2), while the *cis*-β isomer has two methyl doublets as well as two very clear H$_b$ proton quartets at 3.60 and 4.02 ppm (Fig. 3).

Fig. 4 shows portions of the PMR spectra of *cis*-α-[Co(EDDA)(en)]$^+$, Λ-*cis*-α- and Δ-*cis*-α-[Co(SS-EDDP)(en)]$^+$, and *cis*-α-[Rh(SS-EDDP)(en)]$^+$. The chemical shifts of the α-protons of EDDA (labelled H$_a$ and H$_b$) can be distinguished

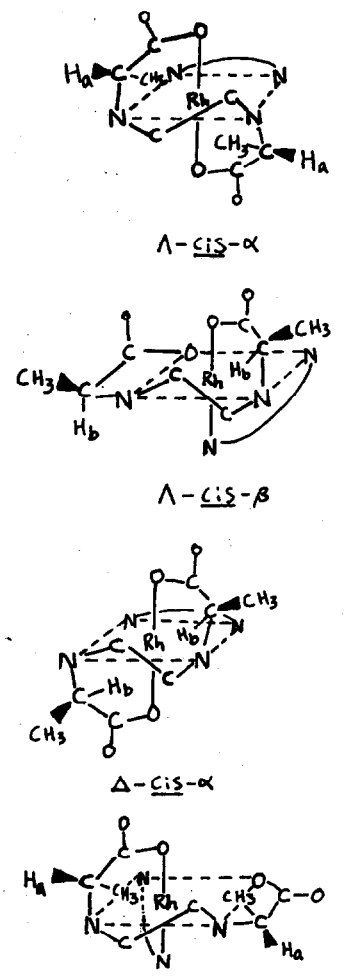

Fig. 1. The four possible isomers of [Rh(SS-EDDP)(en)]$^+$ ion.

*Author to whom correspondence should be addressed.
†Present address: Department of Chemistry, University of California, Berkeley, CA 94720, U.S.A.

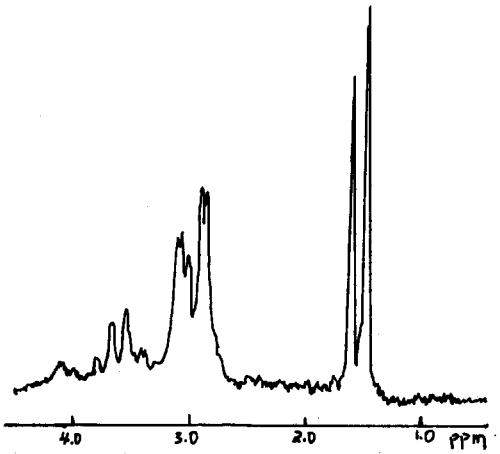

Fig. 2. The 60 mHz PMR spectrum of Δ-*cis*-α-[Rh(SS-EDDP)(en)]Cl.

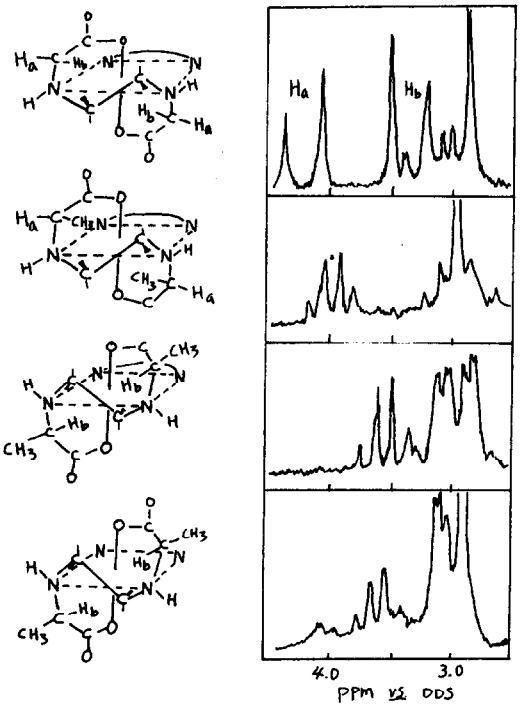

Fig. 4. The 60 mHz PMR spectra of (from top to bottom): *cis*-α-[Co(EDDA)(en)]$^+$, Λ-*cis*-α-[Co(SS-EDDP)(en)]$^+$, Δ-*cis*-α-[Co(SS-EDDP)(en)]$^+$, and Δ-*cis*-α-[Rh(SS-EDDP)(en)]$^+$. Stereochemical representations are shown at left.

because of the magnetic anisotropic shielding of the C–N bond.[1,3-5] Only an H_a proton is exhibited in the Λ-*cis*-α-[Co(SS-EDDP)(en)]$^+$ at 3.99 ppm and only an H_b proton signal in the Δ-*cis*-α-[Co(SS-EDDP)(en)]$^+$ at 3.53 ppm.[1,5] The *cis*-α-[Rh(SS-EDDP)(en)]$^+$ showed only the H_b proton signal at 3.62 ppm and a Δ absolute configuration has been assigned to this complex. The resonance of the Rh(III) complexes are shifted donwfield from the Co(III) isomers due to the different electronic environment of the Rh(III) complex ion.

The *cis*-β isomer has only C_1 symmetry and the propionate arms are no longer equivalent. The facial arm of the Λ-*cis*-β isomer is almost identical to one arm of the Δ-*cis*-α isomer (Fig. 1). The protons of these similar arms should resonate at nearly the same value. The H_b proton in the planar carboxylate arm no longer lies in the shielding area of the C–N bond: such loss of shielding causes it to resonate at lower fields (4.02 ppm in this work). An Λ absolute configuration may, therefore, be assigned to this isomer.

The region between 2.8-3.2 ppm is mainly a superimposition of the signals due to the methylene protons of the en and the en backbone of the tetradentate ligand. Interference from the methyl groups causes the en of Δ-*cis*-α isomer to adopt a particular conformation and a complicated pattern results. In the case of the Λ-*cis*-β complex the sharp peak at 2.86 ppm would imply that the en is free of interference from the methyl groups and can oscillate back and forth between its possible conformations.

Douglas, *et al.*[6] has shown that the $(-)_D$-[Rh(en)aa]$^{2+}$ and the $(+)_D$-[Co(en)$_2$aa]$^{2+}$ (aa = amino acid) have the same absolute configuration of Λ from the positive Cotton effect shown by

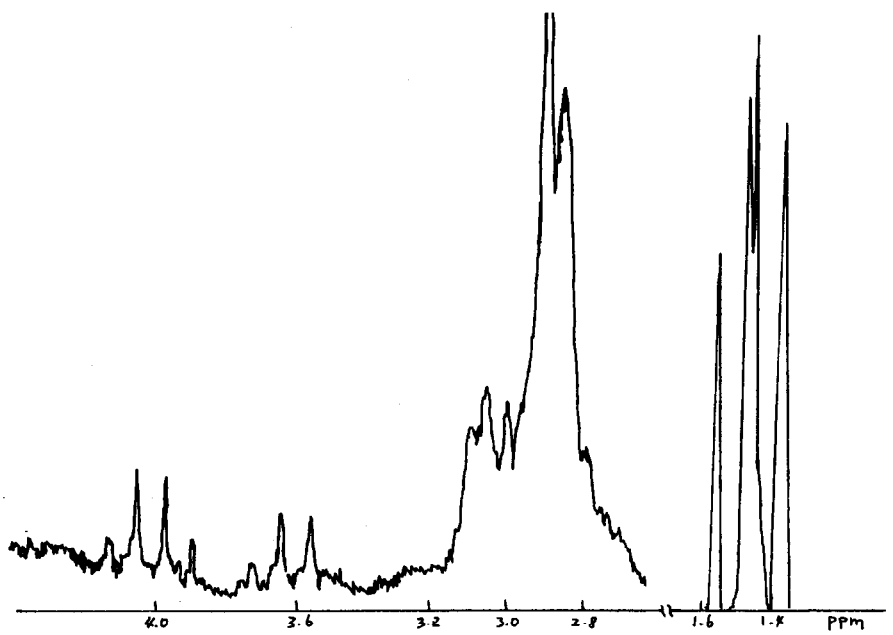

Fig. 3. The 90 mHz spectrum of Δ-*cis*-β-[Rh(SS-EDDP)(en)]Cl.

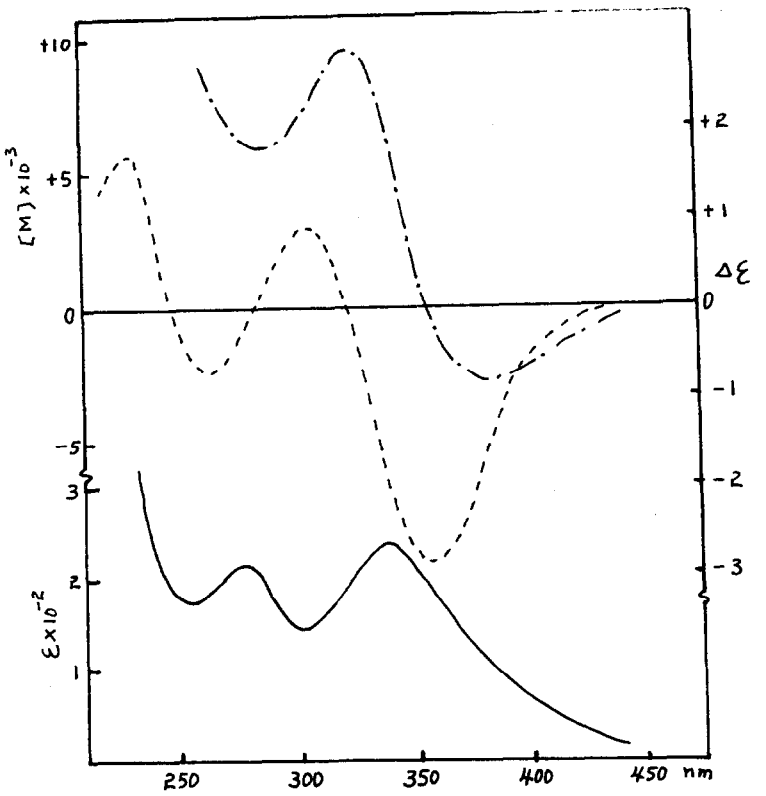

Fig. 5. The electronic absorption (———), ORD (—·—·—), and CD (------) spectra of Δ-*cis*-α-[Rh(SS-EDDP)(en)]$^+$.

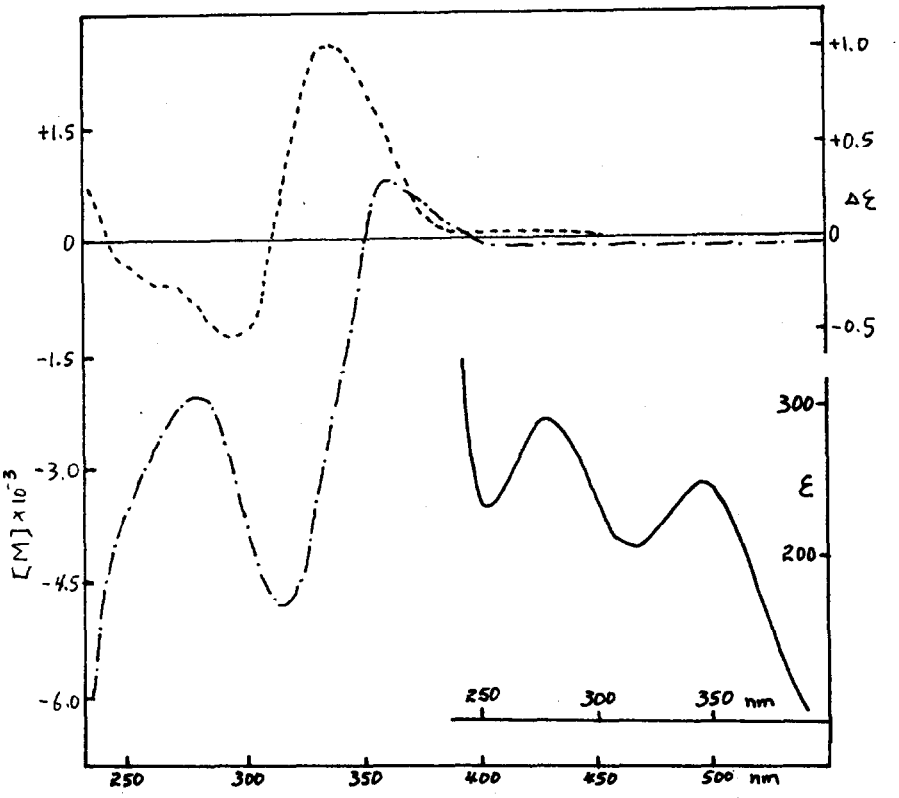

Fig. 6. The electronic absorption (———), ORD (—·—·), and CD (------) spectra of Λ-*cis*-β[Rh(SS-EDDP)(en)]$^+$.

those complexes, while the $(+)_D$-$[Rh(en)_2aa]^{2+}$ complex which showed a negative Cotton effect has been assigned a Δ absolute configuration. As expected from the PMR spectra, the negative Cotton effect seen in the long wavelength absorption band of the *cis*-α-[Rh(SS-EDDP)(en)]$^+$ complex (Fig. 5) indicates a Δ absolute configuration also. The positive Cotton effect observed in the *cis*-β-[Rh(SS-EDDP)(en)]$^+$ complex (Fig. 6) shows a Λ absolute configuration.

Acknowledgement—We thank the National Institute of Health for support. One of the authors (M.J.J.) wishes to thank the Korea Science and Engineering Foundation for support.

REFERENCES

[1]L. N. Scheonberg, D. W. Cooke and C. F. Liu, *Inorg. Chem.* 1968, 7, 2386.
[2]Synthesis of this complex is to be published elsewhere.
[3]J. I. Legg and D. W. Cooke, *Inorg. Chem.* 1968, 4, 1576.
[4]W. A. Freeman, *J. Coord. Chem.* 1978, 7, 197.
[5]L. N. Schoenberg, Ph.D. Thesis. University of Michigan (1966).
[6]S. Hall and B. E. Doulglas, *Inorg. Chem.* 1968, 7, 530.

MARY ELLEN FOSS SHERIDAN
MOO-JIN JUN*†
CHUI FAN LIU*

Department of Chemistry,
University of Illinois at Chicago
Chicago, IL 60680, U.S.A.
and
Department of Industrial Chemistry,
Kyungpook National University,
Daegu, Korea

Polyhedron Vol. 1, No. 7-8, pp. 663-665, 1982
Printed in Great Britain.

0277-5387/82/070663-03$03.00/0
Pergamon Press Ltd.

COMMUNICATION

Pentamethylcyclopentadiene and the carbaborane $B_9C_2H_{11}^{2-}$ as analogous ligands in transition metal complexes

(*Received* 26 *April* 1982)

Abstract—A variety of experimental evidence suggests that both the electron donor abilities and the steric requirements of η^5-pentamethylcyclopentadiene and the $B_9C_2H_{11}^{2-}$ carbaborane cluster are roughly equivalent, and are clearly greater than those of unsubstituted cyclopentadiene.

Metallocarbaborane chemistry originated with the recognition that the undecahydro-dicarba-*nido*-undecaborate(2−) anion ($B_9C_2H_{11}^{2-}$) could formally substitute for the η^5-cyclopentadienyl ligand (Cp^-) in a variety of transition metal complexes.[1] Despite acknowledged similarities between the two species, the $Cp^-/B_9C_2H_{11}^{2-}$ analogy is flawed on several theoretical[2] and experimental[3] counts; in particular, many compounds of $B_9C_2H_{11}^{2-}$ (and the closely related $B_{10}C_2H_{12}^{2-}$) are readily synthesized which have no similarly-stable counterparts in cyclopentadienyl chemistry. The neutral $(C_2B_9H_{11})_2Ni(IV)$ complex, for example, stands in contrast to the isoelectronic but highly reactive $Cp_2Ni(IV)^{2+}$ molecule, which has yet to be isolated.[4] The recent report[5] that stable salts can be prepared from the decamethylnickelocene dication, $(Me_5Cp)_2Ni^{2+}$, however, prompted us to consider whether in general *pentamethylcyclopentadiene* might be superior to unsubstituted Cp^- as an analogue for the $B_9C_2H_{11}^{2-}$ cage in transition metal complexes. A survey of the relevant literature in fact suggests that both the effective electron donor abilities and the steric requirements of coordinated Me_5Cp^- and $B_9C_2H_{11}^{2-}$ are roughly equivalent and clearly greater than those of Cp^-.

As evidence of their donor abilities, we note first that the oxidative susceptibility , and hence the metal center electron density, of first-row group VIII $(Me_5Cp)_2M$ and $(C_2B_9H_{11})_2M$ complexes is greater than that for the corresponding metallocenes. Both decamethylferrocene and $(C_2B_9H_{11})_2Fe(II)^{2-}$ can be spontaneously oxidized by air,[3a,6] and the rate of oxidation of the latter with $Fe(OH_2)_6^{3+}$ is at least four orders of magnitude more rapid than that of ferrocene under similar conditions.[7] In addition, cyclic voltammetric redox potentials for the Cp_2Ni, $(Me_5Cp)_2Ni$, and $(C_2B_9H_{11})_2Ni^{2-}$ molecules indicate that substitution of either Me_5Cp^- or $B_9C_2H_{11}^{2-}$ for Cp^- lowers the redox potential by approximately 0.5 eV for the Ni(IV)→Ni(III) reduction, and by over 0.6 eV in the Ni(III)→Ni(II) case.[3a,5] The M(III)→M(II) reduction potential in the analogous cobalt complexes is ~0.6 eV higher in cobaltocene than in decamethylcobaltocene or the metallocarbaborane.[3a,5]

The relative electronic properties of the ligands are also mirrored in the carbonyl infrared absorption frequencies for a variety of related complexes including $LCo(CO)_2$, $LMn(CO)_3$, $LRe(CO)_3$, $LMo(CO)_3CH_3$, and $LW(CO)_3CH_3$ (L = Cp^-, Me_5Cp^-, and $B_9C_2H_{11}^{2-}$).[3a,8-10] The frequencies are consistently lower by ~15–20 cm^{-1} and ~20–40 cm^{-1} in the Me_5Cp complexes and metallocarbaboranes, respectively, than in their Cp counterparts. Such reductions can be traced to greater M→CO backbonding, which stems ultimately from an electron-enriched metal center.

Although the literature data are still limited, the charge transfer spectra of cyclopentadienyl, pentamethylcyclopentadienyl, and metallocarbaborane complexes may provide another means of evaluating the donor capabilities of the three ligands. The data available[3a,8] reveal red shifts in the ligand-to-metal absorption bands of the latter two species relative to Cp compounds. The strong absorption at 200 nm (ϵ = 51,000) in the spectrum of ferrocene, for instance, assigned to the L→M transfer $1e_{1u}\rightarrow 2e_{1g}$,[11] has its equivalent at 222 nm (ϵ = 35,000) in $(Me_5Cp)_2Fe$,[8] and at 229 nm (ϵ = 28,000) in $(C_2B_9H_{11})_2Fe^{2-}$.[3a] The red shifts reflect the lower energy required for the charge transfers and thus the greater oxidizability of the ligands.

It must be stressed that the electronic effects of Me_5Cp^- and $B_9C_2H_{11}^{2-}$, although phenomenologically-similar, do not share a common origin. The higher charge of $B_9C_2H_{11}^{2-}$ relative to Cp^-, and perhaps the "focusing" of the orbitals on the open face of the carbaborane,[12] would be expected to increase the net charge on the metal, with a consequent reduction in redox potentials, IR stretching frequencies, etc. In the case of the uninegative Me_5Cp^-, however, recent evidence[13] suggests that the enhanced energy of the e_1'' orbitals of the permethylated ring may be responsible for the additional electron donation to the metal center.

In conjunction with the parallelisms in their electronic behavior, Me_5Cp^- mimics $B_9C_2H_{11}^{2-}$ (and $B_{10}C_2H_{12}^{2-}$) in its steric requirements as well. A semi-quantitative comparison of the bulkiness of the ligands based on their cone angles[14] in several cyclopentadienyl and metallocarbaborane complexes[15-18] is presented in Table 1. The comparable angles of Me_5Cp^- and $B_9C_2H_{11}^{2-}$ are found to be significantly greater (> 8%) than those subtended by Cp^-.[19] Such differences in ligand steric demand find qualitative expression in the stoichiometries of various metal complexes; note that the reaction of an excess of either Me_5Cp^- or $B_9C_2H_{11}^{2-}$ with UCl_4 generates species of the form L_2UCl_2,[20,21] whereas the use of the smaller Cp^- produces tetrakis (η^5-cyclopentadienyl)uranium, Cp_4U.[22] Similarly, Me_5Cp^- or $B_{10}C_2H_{12}^{2-}$ can be used to synthesize $(Me_5Cp)_2ZrH_2$[23] and $(C_2B_{10}H_{12})_2Zr^{2-}$,[24] respectively; with Cp^-, either the insoluble polymeric $[(Cp)_2ZrH_2]_n$[25] or the highly-coordinated $(\eta^5\text{-}Cp)_3Zr(\eta^1\text{-}Cp)$[26] is formed. Other examples could be cited.[24,27,28]

More important, however, is the influence the steric bulk of coordinated Me_5Cp^- and $B_9C_2H_{11}^{2-}$ may exert on the reactivity of their associated complexes. It has long been recognized that, presumably by shielding the metal center from attack, the presence of sterically-demanding substituents can dramatically reduce the reactivity of peralkylated cyclopentadienyl metal complexes, suppressing ligand exchange,[29] hindering decomposition,[30] and stabilizing otherwise transient reaction intermediates.[31] The sterically-generated inertness of peralkylated Cp complexes may have a parallel in the celebrated chemical stability of $(C_2B_9H_{11})_2M$ species. The $(C_2B_9H_{11})_2Fe^-$ ion, for example, is stable towards mineral acids,[3a] and unlike the isoelectronic ferricinium cation,[32] can be refluxed in aqueous KOH for days without change. Even more strikingly, the formally 15-electron complex $(C_2B_9H_{11})_2Cr(III)^-$ may be recrystallized from water and is unaffected by molecular oxygen or hot concentrated H_2SO_4,[36] in stark contrast to the readily hydrolyzed, highly air-sensitive $Cp_2Cr(III)^+$ ion.[33] Some indication of the degree to which the boron cage shields the metal center in this metallocarbaborane is provided by space-filling drawings (Fig. 1) generated[34] from the single crystal X-ray data reported for the $Cs[(1,2\text{-}(CH_3)_2C_2B_9H_9)_2Cr]\cdot H_2O$ complex.[35] The extent to which the encapsulation of the metal is responsible for the resistance of the molecule to chemical attack is of course difficult to gauge, but is should be pointed out that many metallocarbaboranes without a *bis*-cage construction possess no more oxidative or hydrolytic

Table 1. Ligand cone angles[14] in various cyclopentadienyl and metallocarbaborane complexes

Ligand	Cone Angle[a]	Complex	Ref.
Cp^-	127°	Cp_2Fe	15
	125°	$CpFeC_2B_9H_{11}^-$	16
	127°	$CpCoC_2B_{10}H_{12}^-$	17
Me_5Cp^-	138°	$(Me_5Cp)_2Fe$	18
$B_9C_2H_{11}^{2-}$	136°	$CpFeC_2B_9H_{11}^-$	16
$B_{10}C_2H_{12}^{2-}$	142°	$CpCoC_2B_{10}H_{12}^-$	17

[a]Distances from the metal to the ring centroid or to the best plane of the open face of the carborane were derived from crystal structure data (ref. 14-17). When necessary, the following bond distances were assumed: C-C (ring) = 1.42 Å, C-H = 1.08 Å, B-H = 1.19 Å, van der Waals radius of hydrogen = 1.00 Å.

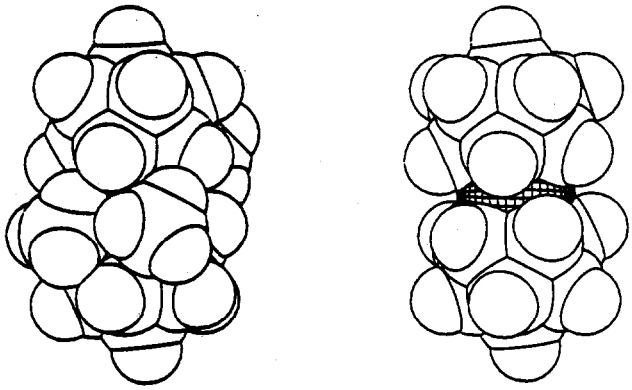

Fig. 1. Space-filling drawings generated from crystal structure data for the $Cs[(1,2\text{-}CH_3)_2C_2B_9H_9)_2\text{-}Cr]\cdot H_2O$ molecule.[35] On the left is a view of the original complex containing the dimethylated carborane cages; the methyl groups of the lower cage are in front. In order to illustrate more accurately the enclosure of the metal center (crosshatched sphere), the methyl groups were removed and replaced with hydrogens in calculated positions (C-H = 1.08 Å) for the drawing on the right.

stability than their Cp counterparts; the half-sandwich complexes $CpCo(CO)_2$,[36] $(Me_5Cp)Co(CO)_2$,[8] and $(C_2B_9H_{11})Co(CO)_2^-$,[37] for example, are all highly air-sensitive.

The relationship of Me_5Cp^- to $C_2B_9H_{11}^{2-}$ suggests that perhaps a larger role exists for the $B_9C_2H_{11}^{2-}$ ion in synthetic organometallic chemistry than has been generally appreciated. With a steric bulk comparable to that of Me_5Cp^-, it has a higher formal negative charge, which may aid the stability of unusual metal oxidation states.[3] Existing metallocarbaboranes might also serve as prototypes for the synthesis of organometallic species of currently unavailable types: based on the existence of $(C_2B_9H_{11})_2Cu^{2-}$,[3a] and $(C_2B_9H_{11})Pd^{2-}$,[3c] for example, "decamethylcupricene" $(Me_5Cp)_2Cu$, and "decamethylpalladocene" $(Me_5Cp)_2Pd$, would seem to be reasonable synthetic targets, even though the analogous unsubstituted metallocenes are not presently known.[38]

In brief, we believe the extent of the chemical interchangeability of Me_5Cp^- and $B_9C_2H_{11}^{2-}$ as ligands in transition metal complexes deserves at least exploratory experimental investigation—both metallocarbaborane and traditional organometallic chemistry could gain from it.

Acknowledgement—The author would like to thank Prof. K. G. Caulton for helpful suggestions, Dr. J. C. Huffman for generating the space-filling drawings, and the M. H. Wrubel Computing Center for an allotment of computer time.

REFERENCES

[1a]M. F. Hawthorne, D. C. Young and P. A. Wagner, *J. Am. Chem. Soc.* 1965, **87**, 1818. [b]M. F. Hawthorne, *Acc. Chem. Res.* 1968, **1**, 281.

[2a]D. A. Brown, M. O. Fanning and N. J. Fitzpartick, *Inorg. Chem.* 1978, **17**, 1620. [b]*Ibid.* 1980, **19**, 1822.

[3a]M. F. Hawthorne, D. C. Young, T. D. Andrews, D. V. Howe, R. L. Pilling, A. D. Pitts, M. Reintjes, L. F. Warren, Jr. and P. A. Wegner, *J. Am. Chem. Soc.* 1968, **90**, 879.[b]H. W. Ruhle and M. F. Hawthorne, *Inorg. Chem.* 1968, **7**, 2279. [c]L. F. Warren, Jr. and M. F. Hawthorne, *J. Am. Chem. Soc.* 1968, **90**, 4823.

[4a]R. J. Wilson, L. F. Warren, Jr. and M. F. Hawthorne, *J. Am. Chem. Soc.* 1969, **91**, 758. [b]S. P. Gubin, S. A. Smirnova and L. I. Denisovich, *J. Organometal. Chem.* 1971, **30**, 257. [c]R. P. Van Duyne and C. N. Reilley, *Anal. Chem.* 1972, **44**, 158.

[5]U. Koelle and F. Khouzami, *Angew. Chem. Int. Ed. Engl.* 1980, **19**, 640.

[6]A. N. Nesmeyanov, R. B. Materikova, I. R. Lyatikov, T. K. Kurbanov and N. S. Kochetkova, *J. Organometal. Chem.* 1978, **145**, 241.

[7]J. R. Pladziewicz and J. H. Espenson, *J. Am. Chem. Soc.* 1973, **95**, 56.
[8]R. B. King and M. B. Bisnette, *J. Organometal. Chem.* 1967, **8**, 287.
[9]M. F. Hawthorne and H. W. Ruhle, *Inorg. Chem.* 1969, **8**, 176.
[10]R. B. King and A. Efraty, *J. Am. Chem. Soc.* 1972, **94**, 3773.
[11]Y. S. Sohn, D. N. Hendrickson and H. B. Gray, *J. Am. Chem. Soc.* 1971, **93**, 3603.
[12a]E. B. Moore, L. L. Lohr and W. N. Lipscomb, *J. Chem. Phys.* 1961, **35**, 1329. [b]D. M. P. Mingos, *J. Chem. Soc., Dalton Trans.* 1977, 602. [c]M. J. S. Dewar and M. L. McKee, *Inorg. Chem.* 1980, **19**, 2662.
[13a]J.-R. Hamon, D. Astruc and P. Michaud, *J. Am. Chem. Soc.* 1981, **103**, 758. [b]D. C. Calabro, J. L. Hubbard, C. H. Blevins, II, A. C. Campbell and D. L. Lichtenberger, *J. Am. Chem. Soc.* 1981, **103**, 6839.
[14]C. A. Tolman, *Chem. Rev.* 1977, **77**, 313.
[15]F. Takusagawa and T. F. Koetzle, *Acta Cryst.* 1979, **B35**, 1074.
[16]A. Zalkin, D. H. Templeton and T. E. Hopkins, *J. Am. Chem. Soc.* 1965, **87**, 3988.
[17]M. R. Churchill and B. G. Deboer, *Inorg. Chem.* 1974, **13**, 1411.
[18]D. P. Freyberg, J. L. Robbins, K. N. Raymond and J. C. Smart, *J. Am. Chem. Soc.* 1979, **101**, 892.
[19]Although the cone angle for $B_9C_2H_{11}^{2-}$ was calculated from the formal iron (III) complex $CpFeC_2B_9H_{11}$, a comparison of the η^5-Cp angle in this molecule with that in Cp_2Fe(II) suggests that any error introduced by the change of oxidation state was not large.
[20a]J. M. Manriquez, P. J. Fagan and T. J. Marks, *J. Am. Chem. Soc.* 1978, **100**, 3940. [b]P. J. Fagan, J. M. Manriquez, E. A. Maatta, A. M. Seyam and T. J. Marks, *J. Am. Chem. Soc.* 1981, **103**, 6650.
[21a]F. R. Fronczek, G. W. Halstead and K. N. Raymond, *J. Chem. Soc., Chem. Commun.* 1976, 279. [b]*Ibid. J. Am. Chem. Soc.* 1977, **99**, 1769.
[22a]E. O. Fischer and Y. Hristidu, *Z. Naturforsch. B* 1962, **17**, 275. [b]J. H. Burns, *J. Am. Chem. Soc.* 1973, **95**, 3815.
[23]J. M. Manriquez, D. R. McAlister, R. D. Sanner and J. E. Bercaw, *J. Am. Chem. Soc.* 1978, **100**, 2716.
[24a]C. G. Salentine and M. F. Hawthorne, *J. Am. Chem. Soc.* 1975, **97**, 426. [b]*Ibid. Inorg. Chem.* 1976, **15**, 2872.
[25a]B. D. James, R. K. Nanda and M. G. H. Wallbridge, *Inorg. Chem.* 1976, **6**, 1979. [b]P. C. Wailes and H. Weigold, *J. Organomet. Chem.* 1970, **24**, 405.
[26]R. D. Rogers, R. V. Bynum and J. L. Atwood, *J. Am. Chem. Soc.* 1978, **100**, 5238.
[27]For Ti, see: F. Y. Lo, C. E. Strouse, K. P. Callahan, C. B. Knobler and M. F. Hawthorne, *J. Am. Chem. Soc.* 1975, **97**, 428 and References therein.
[28]For Hf, compare the $(C_2B_{10}H_{12})_2Hf^{2-}$ complexes described in Ref. 8 with the structure determined for the $(\eta^5\text{-Cp})_2Hf(\eta^1\text{-Cp})_2$ molecule: R. D. Rogers, R. V. Bynum and J. L. Atwood, *J. Am. Chem. Soc.* 1981, **103**, 692.
[29a]D. E. Bublitz, *J. Organomet. Chem.* 1969, **16**, 149. [b]D. W. Slocum and C. R. Ernst, *Adv. Organomet. Chem.* 1972, **10**, 79. [c]A. N. Nesmeyanov, O. V. Nogina, B. V. Lokshin and V. A. Dubovitskii, *Doklady Akademii Nauk SSSR* 1968, **182**, 844.
[30a]H. Rohl, E. Lange, T. Gossl and G. Roth, *Angew. Chem. Int. Ed. Engl.* 1962, **1**, 117. [b]A. N. Nesmeyanov, O. V. Nogina, N. A. Lazareva and V. A. Dubovitskii, *Izv. Akad. Nauk. SSSR Ser. Khim.* 1967, 803. [c]A. Z. Rubezhov and S. P. Gubin, *Adv. Organomet. Chem.* 1972, **10**, 347.
[31a]J. L. Thomas and H. H. Brintzinger, *J. Am. Chem. Soc.* 1972, **94**, 1386. [b]J. L. Thomas, *J. Am. Chem. Soc.* 1973, **95**, 1838. [c]J. E. Bercaw, R. H. Marvich, L. G. Bell and H. H. Brintzinger, *J. Am. Chem. Soc.* 1972, **94**, 1219.
[32]J. D. Smith, *J. Inorg. Nucl. Chem.* 1960, **14**, 290.
[33]E. O. Fischer and K. Ulm, *Chem. Ber.* 1962, **95**, 692.
[34]Using the *SPACE* program [G. M. Smith and P. J. Gund, *J. Chem. Inf. Comput. Sci.* 1978, **18**, 207].
[35]D. St. Clair, A. Zalkin and D. H. Templeton, *Inorg. Chem.* 1971, **10**, 2587.
[36]T. S. Piper, F. A. Cotton and G. Wilkinson, *J. Inorg. Nucl. Chem.* 1955, **1**, 165.
[37]M. F. Hawthorne and H. W. Ruhle, *Inorg. Chem.* 1969, **8**, 176.
[38]The reactions of CpH or Cp^- with various palladium salts produce a variety of complexes, none of which are believed to possess the classic $(Cp)_2M$ geometry. See: E. O. Fischer, P. Meyer, C. G. Kreiter and J. Müller, *J. Chem. Ber.* 1972, **105**, 3014.

Department of Chemistry T. P. HANUSA
Indiana University
Bloomington, IN 47405, U.S.A.

Polyhedron Vol. 1, No. 9–10, pp. 667–671, 1982
Printed in Great Britain.

0277-5387/82/090667-05$03.00/0
Pergamon Press Ltd.

METAL COMPLEXES OF HYBRID OXYGEN-ARSENIC LIGANDS—III

COMPLEXES OF 2-TERTIARYARSINOBENZOIC ACIDS WITH ZINC(II), CADMIUM(II) AND MERCURY(II). DISCOVERY OF A NOVEL CHELATING SYSTEM

SWARN S. PARMAR* and HARKEERAT KAUR
Chemistry Department, Guru Nanak Dev University, Amritsar-143005, India

(*Received* 3 *November* 1981)

Abstract—This paper describes the preparation of the halogeno complexes, $HgX_2(o\text{-}R_2AsC_6H_4CO_2H)$ (X = Cl, Br, I, and R = Et; X = Br, I, and R-C_6H_{11}) and the carboxylate complexes, $M(o\text{-}R_2AsC_6H_4CO_2)_2nL$(M = Cd, R = Et, C_6H_{11} and n = O; M = Zn; R = Et; $nL = H_2O$; M = Zn, R = C_6H_{11}, $nL = 3H_2O$; M = Hg, R = *p*-tolyl, $nL = 2H_2O$; M = Hg, R = Me, Ph; C_6H_{11} and nL = EtOH). The structures already reported for the halogeno complexes with R = Ph, Me, *p*-tolyl and X = Cl, Br, I, have been revised on the basis of detailed scrutiny of the IR spectral data and all these complexes have been divided into four structural types out of which three retain the acid dimer unit of the free ligand. In the carboxylate complexes the lowering of ν_s CO_2 band and the marginal change in the ν_{as} CO_2 band with respect to those of the corresponding ligand sodium salts have been attributed to the existence of a novel resonating chelating system with the possibility of having a ring current.

INTRODUCTION

In our earlier communications[1,2] it has been shown that the hybrid oxygen-arsenic ligands, arsinobenzoic acids (1, R = Me, Ph and *p*-tolyl) react with zinc(II) acetate dihydrate, cadmium(II) acetate dihydrate and mercury(II) halides to yield the complexes, $M(o\text{-}R_2AsC_6H_4CO_2)_2$ (M = Zn, R = Ph and *p*-tolyl, M = Cd, R = Me, Ph and *p*-tolyl), $Zn(o\text{-}Me_2AsC_6H_4CO_2)_2$ ($o\text{-}Me_2AsC_6H_4CO_2H$) and $HgX_2(o\text{-}R_2AsC_6H_4CO_2H)$ (X = Cl, Br, I) while their reactions with mercury(II) acetate fail to give the desired complexes $Hg(o\text{-}R_2AsC_6H_4CO_2)_2$.

The present investigation, in continuation, is an attempt to examine the influence of inductive and steric effects on the nature of complex formed by studying the complexes of zinc(II), cadmium(II) and mercury(II) with two analogous ligands(1) having R = Et and C_6H_{11} and to reinvestigate the reported failure to obtain carboxylate complexes, $Hg(o\text{-}R_2AsC_6H_4CO_2)_2$. The reported, structure(2) and (3) assigned to the halogeno complexes $HgX_2(o\text{-}R_2AsC_6H_4CO_2H)$ have also been revised.

EXPERIMENTAL

Preparation of the ligands, their sodium salts and the details of the physical measurements are the same as reported elsewhere.[3] In addition, halogens were estimated by the Volhard's method.[4] PMR spectra of the soluble samples were recorded in $CDCl_3$ on TESLA BS 487 (80 MHz) using TMS as internal standard.

$Zn[o\text{-}C_6H_{11})_2AsC_6H_4CO_2]_23H_2O$

The addition of a solution (20 ml) of the ligand (1.45 g, 4 mmol) in 95% ethanol to an ethanolic solution (10 ml) of zinc(II) acetate dihydrate (0.44 g, 2 mmol) resulted in the separation of a white solid which was filtered, washed with 95% ethanol and dried *in vacuo*. Yield 78%.

$M(o\text{-}Et_2AsC_6H_4CO_2)_2nH_2O$[M = Zn, n = 1; M = Cd, n = 0]

Solvent was completely removed from the reaction mixture containing metal(II) acetate dihydrate (2 mmol) in methanol (10 ml) and the ligand (1 g, 4 mmol) in methanol (20 ml) under reduced pressure. The solution of the residue, thus obtained, in 2–3 ml chloroform gave a white solid on treatment with pet. ether (60–80°C, 30–35 ml), which was filtered, washed with ether and dried *in vacuo*. Yield 75–78%.

$Cd[o\text{-}(C_6H_{11})_2AsC_6H_4CO_2]_2$

Boiling of a reaction mixture obtained by mixing a solution of cadmium(II) acetate dihydrate (0.53 g, 2 mmol) in 95% ethanol (10 ml) with that of the ligand (1.45 g, 4 mmol) in 95% ethanol (20 ml) under reflux for *ca* 6 h resulted in the separation of white crystals which were filtered, washed with 95% ethanol and dried *in vacuo*. Yield 80%.

$Hg(o\text{-}R_2AsC_6H_4CO_2)_2EtOH$(R = Me, Ph, C_6H_{11}) *and* $Hg[o\text{-}(p\text{-}tolyl)_2AsC_6H_4CO_2]_22H_2O$

The dropwise addition of a cold (−4 to −6°C) ethanolic solution (15–20 ml for R = Me, Ph or C_6H_{11} and 40 ml for R = *p*-tolyl) of the ligand (4 mmol) to a cold (−4 to −6°C) stirred suspension of mercury(II) acetate (0.64 g, 2 mmol) in ethanol (5 ml) resulted in the formation of a clear solution which yielded a white solid on subsequent sitrring for 5–10 min. It was filtered, washed with ethanol and dried *in vacuo*. Yield 80–90%.

Excess of ligand and traces of water resulted in the formation of black particles which were also obtained during the futile attempt to prepare a complex in the case of ligand with R = Et under similar conditions.

$HgX_2(o\text{-}R_2AsC_6H_4CO_2H)$ (R = Et, X = Cl, Br; R = C_6H_{11}, X = Br)

The dropwise addition of a cold (0°C) ethanolic solution (15 ml for R = Et; 25 ml for R = C_6H_{11}) of the ligand (4 mmol) to a cold (0°C) stirred ethanolic solution (10 ml) of mercury(II) halide (4 mmol) resulted in the formation of a white solid which was filtered, washed with ethanol and dried *in vacuo*. Yield 70–80%. A similar attempt to prepare a complex of the ligand with R = C_6H_{11} with mercury(II) chloride resulted in the formation of a compound with ill defined stoichiometry.

*Author to whom correspondence should be addressed.

$HgI_2(o\text{-}R_2AsC_6H_4CO_2H)$ (R = Et, C_6H_{11})

Mixing of a cold (0°C) solution of a ligand (2 mmol) in dry tetrahydrofuran (15 ml) with a cold (0°C) solution of mercury(II) iodide in dry tetrahydrofuran (15 ml) did not yield any solid product. The reduction in volume to 5 ml and subsequent treatment with ethanol (10 ml) yielded a white compound which was filtered, washed with ethanol and dried *in vacuo*. Yield 85–90%.

RESULTS AND DISCUSSIONS

A reaction of zinc(II), cadmium(II) and mercury(II) acetates (dihydrate in the first two cases) with the ligand ($o\text{-}R_2AsC_6H_4CO_2H$) in 1:2 molar ratio in ethanol yields the complexes $Zn(o\text{-}R_2AsC_6H_4CO_2)_2nH_2O$ (R = Et, n = 1; R = C_6H_{11}, n = 3), $Cd(o\text{-}R_2AsC_6H_4CO_2)_2$ (R = Et or C_6H_{11}), $Hg(o\text{-}R_2AsC_6H_4CO_2)_2EtOH$(R = Me, C_6H_{11}, Ph) and $Hg[o\text{-}(p\text{-tolyl})_2AsC_6H_4CO_2]_22H_2O$ while a reaction of mercury(II) halide with the ligand in 1:1 molar ratio gives the halogeno complexes $HgX_2(o\text{-}R_2AsC_6H_4CO_2H)$ (R = Et, X = Cl, Br, I; R = C_6H_{11}, X = Br, I) (Table 1). The presence of water or ethanol is supported by the TGA data (Table 1). The TGA curves for the complexes $Zn(o\text{-}R_2AsC_6H_4CO_2)_2nH_2O$ [R = Et, n = 1; R = C_6H_{11}, n = 3] show the loss of water molecule at 100–260°C and 100–140° which indicate that water molecule are deep seated in the crystal lattice since the IR data show their non-coordination to the metal ion. All the mercury(II) complexes are completely destroyed upto 500–600°C. For the complexes $Hg(o\text{-}R_2AsC_6H_4CO_2)_2EtOH$ (R = C_6H_{11} or Ph) soluble in $CDCl_3$ the presence of ethanol has been supported by the appearance of signals due to CH_2(δ = 1.95) and CH_3(δ = 1.25), protons in their PMR spectra. The PMR spectra of the zinc(II) and cadmium(II) are consistent with the absence of ethanol as suggested by the analytical data.

*All the efforts to prepare the methiodide of the ligand with R = Et failed.

$HgX_2(o\text{-}R_2AsC_6H_4CO_2H)$

In our earlier communication[2] the appearance of νC=O bands below 1700 cm^{-1}, i.e. at 1660, 1680 and 1675 cm^{-1} in the IR spectra of the ligands with R = Me, Ph and *p*-tolyl respectively was attributed to the internal hydrogen bonding between the carboxyl hydrogen and arsenic lone pair but recently[5] in the case of the ligand with R = Me, it has been proved to be rather due to arsenic lone pair conjugation with the aromatic ring. These studies when further extended to the ligands with R = Et (νC=O, 1665), Ph, C_6H_{11} (νC=O, 1675) and *p*-tolyl reveal the presence of lone pair conjugation in the first case and its absence in the remaining three cases. The absence of such conjugation has also been reported[6] for *para* and *meta* isomers of the ligand with R = Ph. The raising of νC=O value to about ~1700 cm^{-1} in the methiodides* (4, R = Me, Ph, *p*-tolyl, C_6H_{11}) can now be explained in terms of the electron withdrawing nature of the arsonium ion rather than the reported[2] absence of internal hydrogen bonding. While discussing the nature of the bonding in the halogeno complexes $HgX_2(o\text{-}R_2AsC_6H_4CO_2H)$ (X = Cl, Br, I and R = Me, Ph and *p*-tolyl) the emphasis was laid only on the lowering of δOH band of the COOH group on complex formation while the position of νOH band was completely ignored.[2] A comparison of the IR spectra of $HgX_2(o\text{-}Me_2AsC_6H_4CO_2H)$ with those of $Hg(o\text{-}Me_2AsC_6H_4CO_2)_2$ EtOH, the ligand and its sodium salt

Table 1. Elemental analysis and TGA data of zinc(II), cadmium(II) and mercury(II) complexes

Complex (mp°C)	Found (Calcd)% C	H	M[a]/X	Dec. range °C	Stepwise % Loss Found (Calcd)
$Zn(o\text{-}Et_2AsC_6H_4CO_2)_2H_2O$ (120)	43.2 (44.8)	4.5 (5.1)	11.1[a] (11.1)	100–260	3.5 (3.0, H_2O)
$Zn[o\text{-}(C_6H_{11})_2AsC_6H_4CO_2]_23H_2O$ (217)	54.4 (54.2)	6.7 (6.9)	7.8[a] (7.8)	100–140	6.5 (6.3, $3H_2O$)
$Cd(o\text{-}Et_2AsC_6H_4CO_2)_2$ (140)	41.6 (42.7)	4.4 (4.5)	18.7[a] (18.8)		
$Cd[o\text{-}(C_6H_{11})_2AsC_6H_4CO_2]_2$ (220)	54.9 (54.6)	5.8 (6.2)	12.8[a] (13.5)		
$Hg(o\text{-}Me_2AsC_6H_4CO_2)_2C_2H_5OH$ (150)	35.1 (34.5)	3.6 (3.8)	—	60–240	6.5 (6.6, C_2H_5OH)
$Hg[o\text{-}(C_6H_{11})_2AsC_6H_4CO_2]_2C_2H_5OH$ (225)	50.3 (49.5)	6.4 (6.0)	—	60–200	4.0 (4.5, C_2H_5OH)
$Hg(o\text{-}Ph_2AsC_6H_4CO_2)_2C_2H_5OH$ (155d)	49.7 (50.8)	3.3 (3.1)	—	80–200	6.0 (4.0, C_2H_5OH)
$Hg[o\text{-}(p\text{-tolyl})_2AsC_6H_4CO_2]_22H_2O$ (165d)	50.7 (50.9)	3.9 (4.0)	—	100–200	4.0 (2.0, $2H_2O$)
$HgCl_2(o\text{-}Et_2AsC_6H_4CO_2H)$ (175d)	25.6 (25.1)	2.9 (2.9)	13.4 (13.5)		
$HgBr_2(o\text{-}Et_2AsC_6H_4CO_2H)$ (200d)	22.4 (21.5)	2.8 (2.4)	26.8 (26.1)		
$HgI_2(o\text{-}Et_2AsC_6H_4CO_2H)$ (199)	18.9 (18.6)	2.1 (2.1)	36.0 (35.9)		
$HgBr_2[o\text{-}(C_6H_{11})_2AsC_6H_4CO_2H]$ (215d)	31.5 (31.6)	4.0 (3.7)	22.7 (22.2)		
$HgI_2[o\text{-}(C_6H_{11})_2AsC_6H_4CO_2H]$ (180d)	28.0 (27.9)	3.4 (3.3)	30.9 (31.3)		

*Estimation of arsenic by iodometric method and of mercury(II) by EDTA method did not give reproducible results.
d, decomposition.

clearly indicate that the ρCH_3 bands[5] present at 856 and 890 cm^{-1} in the latter two spectra respectively shift to 888 and 920 cm^{-1} in both the types of mercury(II) complexes. Thus the assignment of 920 cm^{-1} band present in the halogeno complexes should be revised as ρCH_3 from δOH assigned[2] earlier which means that the δOH band in these halogeno complexes is either missing or overlaid by the ρCH_3 bands. The same conclusion can be drawn on the basis of a similar conparison in the case of complexes of the ligands with R = Et and C_6H_{11}. However, the reported appearance of the δOH band in the IR spectra (Table 2) of five complexes HgX_2(*o*-$R_2AsC_6H_4CO_2H$) (X = Cl, Br, I, R = *p*-tolyl; X = Br, I, R = Ph) remains valid in terms of a similar scrutiny of the bands in the 850–950 cm^{-1} region.

The IR spectra of all the five ligands and their halogeno complexes show νC=O and νOH bands characteristic of the carboxylic acid dimers with the exception of the complex $HgCl_2$(*o*-$Ph_2AsC_6H_4CO_2H$) whose νOH band appears as a single broad band at 3170 cm^{-1} instead of a weak doublet of dimer bands, at 2500–2700 cm^{-1}. Except this complex the acid dimer unit of the ligand remains intact in all the halogeno complexes which can accordingly be divided into the following four types:

(a) $HgCl_2$(*o*-$Ph_2AsC_6H_4CO_2H$) which contains a monomeric COOH group showing νC=O value higher than in the dimeric ligand.

(b) HgX_2(*o*-$R_2AsC_6H_4CO_2H$) (X = Cl, Br, I and R = *p*-tolyl. X = Br, I and R = Ph) which contain COOH dimer unit with (i) a lower δOH value and (ii) same or lower νC=O value as compared to that of the corresponding ligand.

(c) HgX_2(*o*-$R_2AsC_6H_4CO_2H$) (X = Cl, Br, I and R = Me; X = I and R = Et; X = Br, I and R = C_6H_{11}) which contain CO_2H dimer unit with a slightly lower or higher νC=O value as compared to that of the ligand.

(d) HgX_2(*o*-$Et_2AsC_6H_4CO_2H$) (X = Cl, Br) which contain CO_2H dimer unit with (i) νC=O band split into two components.

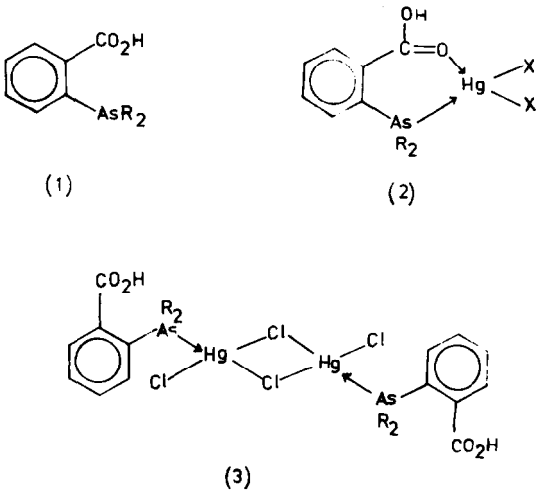

The appearance of νC=O band at 1700 cm^{-1} and the respective absence of δOH and acid dimer bands at 900–950 and 2500–2700 cm^{-1} suggests the coordination of the carbonyl oxygen to mercury(II) as shown in structure (2) since otherwise it is expected to absorb at 1750–1800 cm^{-1} (see νC=O in monomeric $PhCO_2H$, 1785 cm^{-1}).[8,9] This is further supported by the presenc of a strong monomer νC–O band at[7] 1200 cm^{-1} which is missing in the spectra of the ligand and its bromo and iodo complexes.

Only the slight difference (−10 to +15 cm^{-1}) observed in the νC=O values of the type-b and -c complexes from those of the respective ligands suggest the absence of the coordination of carbonyl group of the acid dimer unit to mercury(II) as shown in structure (5), since its coordination is expected to lead to a much lower value of νC=O.[5]

Table 2. IR spectral data (cm^{-1}) of mercury(II) halide complexes

Complexes	νOH	C=O(reported)	δOH(reported)[2]
o-$Me_2AsC_6H_4CO_2H$	2530, 2660	1665(1660)	895
$HgCl_2$(*o*-$Me_2AsC_6H_4CO_2H$)	2500, 2610	(1670)	— (920)
$HgBr_2$(*o*-$Me_2AsC_6H_4CO_2H$)	2515, 2650	(1670)	— (920)
HgI_2(*o*-$Me_2AsC_6H_4CO_2H$)	2500, 2620	(1670)	— (920)
o-$Et_2AsC_6H_4CO_2H$	2530, 2675	1665	916
$HgCl_2$(*o*-$Et_2AsC_6H_4CO_2H$)	2510, 2640	1640	
		1690	
$HgBr_2$(*o*-$Et_2AsC_6H_4CO_2H$)	2490, 2620	1640	
		1690	
HgI_2(*o*-$Et_2AsC_6H_4CO_2H$)	2530, 2650	1680	
o-$(C_6H_{11})_2AsC_6H_4CO_2H$	2550, 2660	1675	942
$HgBr_2$[*o*-$(C_6H_{11})_2AsC_6H_4CO_2H$]	2530, 2660	1690	
HgI_2[*o*-$(C_6H_{11})_2AsC_6H_4CO_2H$]	2520, 2640	1690	
o-$Ph_2AsC_6H_4CO_2H$	2550, 2650	1680	934(934)
$HgCl_2$(*o*-$Ph_2AsC_6H_4CO_2H$)	3170, —	1700(1700)	
$HgBr_2$(*o*-$Ph_2AsC_6H_4CO_2H$)	2485, 2650	1670(1670)	890(890)
		(1700)	
HgI_2(*p*-$Ph_2AsC_6H_4CO_2H$)	2500, 2650	1675(1675)	885(885)
o-(*p*-tolyl)$_2AsC_6H_4CO_2H$	2550, 2650	1675	934
$HgCl_2$[*o*-(*p*-tolyl)$_2AsC_6H_4CO_2H$]	2500, 2635	(1675)	(892)
$HgBr_2$[*o*-(*p*-tolyl)$_2AsC_6H_4CO_2H$]	2500, 2635	(1675)	(900)
HgI_2[*o*-(*p*-tolyl)$_2AsC_6H_4CO_2H$]	2580, 2600	(1675)	(910)

Table 2 shows that the νC=O, value of the ligand with R = Ph is lowered only by 10 cm^{-1} in type-b complexes whereas the δOH value is lowered from 934 to 890 cm^{-1}. It has been observed that on dilution in carbon tetrachloride solution the νC=O and δOH frequencies of these ligands show an upward shift which suggests that the weakening of the hydrogen bond of the acid dimer unit is accompanied by the increase in the δOH value. The observed low νC=O value of 1665 cm^{-1} for the ligands (1, R = Me and Et) has been explained in terms of the arsenic lone pair conjugation with the aromatic ring which due to the increased negative charge on the carbonyl oxygen increases the strength of the hydrogen bond and is consistent with lower δOH values of 895 and 916 cm^{-1} as compared to that of 934 cm^{-1} observed for (1, R = Ph) in which lone pair conjugation is absent. The effect of lone pair conjugation introduced by the attachment of the methyl group to arsenic(III) on the νC=O and δOH values in the ligand (1; R = Me) is thus the same as caused by the coordination of ligand with R = Ph through arsenic(III) to mercury(II) that can be only explained in terms of structure (5) since π-donation from mercury(II) to arsenic(III) is more pronounced than the σ-donation of arsenic(III) to mercury(II) which increases the electron density around arsenic(III) on coordination and compensates for the electron withdrawing nature of the phenyl group as compared to the electron releasing nature of the methyl group. It is, therefore, evident that the increase in the electron density around arsenic(III) on coordination is reflected by the increased strength of the hydrogen bond of the acid dimer unit which is manifested by a large downward shift of the δOH and a small one in νC=O. The attachment of *p*-tolyl group in the ligand (1, R = *p*-tolyl) makes arsenic(III) a slightly better σ donor and a poorer π-acceptor[10] as compared to the ligand with R = Ph. However, in all the three complexes the νC=O value is the same as in the case of the free ligand but as expected the lowering in the δOH frequency is slightly less than the case of $HgX_2(o\text{-}Ph_2AsC_6H_4CO_2H)$.

In the complexes $HgX_2(o\text{-}Me_2AsC_6H_4CO_2H)$ the presence of two methyl groups makes arsenic(III) a better σ donor as well as better π-acceptor than the ligand with R = Ph.[10] In contrast to the ligand with R = Ph, the coordination of arsenic(III) to mercury(II) affects the νC=O of the ligand with R = Me in two steps:

(i) The $\nu_{C=O}$ value of the free ligand (1665 cm^{-1}) is to be raised upto the extent it was lowered by lone pair conjugation since in the complexes the lone pair is involved in coordination to mercury(II).

(ii) If it is assumed that in the absence of lone pair conjugation the $\nu_{C=O}$ value were the same, i.e. 1680 cm^{-1} as in ligand with R = Ph the appearance of $\nu_{C=O}$ band at 1670 cm^{-1} in all the three complexes can be explained in terms of structure (5) on the assumption that arsenic(III) like the phenyl analog is a better π-acceptor than a σ donor.

It is noteworthy to point out here that in the free ligands with R = Me and Et, the conjugation takes place between $p\pi$ electrons of the aromatic ring and the sp^3 hybrid orbital of the arsenic(III) containing the lone pair whereas in the case of the halogeno complex it is the $d\pi$ orbital on arsenic(III) which is overlapping simultaneously with $p\pi$ orbital of the aromatic ring and the $d\pi$ orbital of mercury(II). Similar arguments assign the same structure (5) to the complexes $HgI_2(o\text{-}Et_2AsC_6H_4CO_2H)$ and $HgX_2[o\text{-}(C_6H_{11})_1AsC_6H_4CO_2H]$ where the higher $\nu_{C=O}$ values suggest the lack of conjugation of the $d\pi$ electrons of the coordinated arsenic with the aromatic ring probably due to steric factors. However in the case of type-*d* complexes the $\nu_{C=O}$ present in the ligand at 1665 cm^{-1} splits into two components at 1640 and

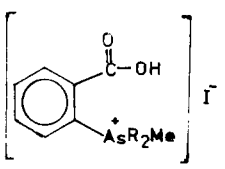

(4)

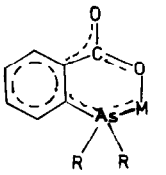

(7)

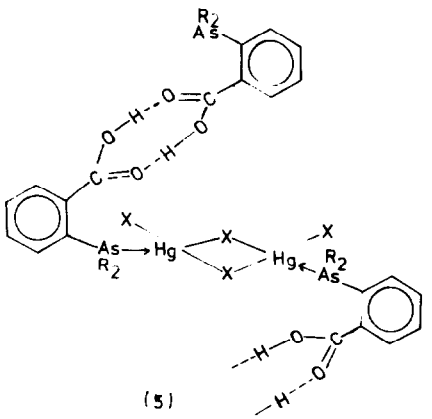

(5)

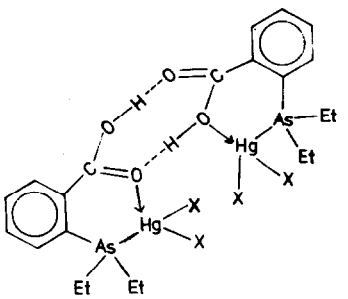

(6)

Table 3. IR spectral data (cm^{-1}) of zinc(II), cadmium(II) and mercury(II) complexes

Complexes	νOH (δHOH)	ν_{as} CO_2 (reported)	ν_s CO_2
o-$R_2AsC_6H_4CO_2Na$	—	1595	1400
$Zn(o\text{-}Me_2AsC_6H_4CO_2)_2$ -(o-$Me_2AsC_6H_4CO_2H$)	—	1615(1605)	1400
$Zn(o\text{-}Et_2AsC_6H_4CO_2)_2H_2O$	3380 (1625)	1610	1400
$Zn[o\text{-}(C_6H_{11})_2AsC_6H_4CO_2]_2 3H_2O$	3380	1595	1410
$Zn(o\text{-}Ph_2AsC_6H_4CO_2)_2$	—	1605(1610)	1400
$Zn[o\text{-}(p\text{-tolyl})_2AsC_6H_4CO_2]_2$	—	1602(1617)	1415
$Cd(o\text{-}Me_2AsC_6H_4CO_2)_2$	—	1602(1602)	1387
$Cd(o\text{-}Et_2AsC_6H_4CO_2)_2$	—	1590	1380
$Cd[o\text{-}(C_6H_{11})_2AsC_6H_4CO_2]_2$	—	1590	1380
$Cd(o\text{-}Ph_2AsC_6H_4CO_2)_2$	—	1590(1590)	1395
$Cd[o\text{-}(p\text{-tolyl-}_2AsC_6H_4CO_2]_2$	—	1595(1595)	1395
$Hg(o\text{-}Me_2AsC_6H_4CO_2)EtOH$	3380	1610	1365
$Hg[o\text{-}(C_6H_{11})_2AsC_6H_4CO_2]_2EtOH$	3420	1605	1380
$Hg(o\text{-}Ph_2AsC_6H_4CO_2)_2EtOH$	3380	1598	1350
$Hg[o\text{-}(p\text{-tolyl-}_2AsC_6H_4CO_2]_2 2H_2O$	3410 (1630)	1590	1360

1690 cm^{-1}. The lower νC=O value of the first component may be attributed to the coordination[5] of the carbonyl oxygen of the acid dimer unit to mercury(II) while the higher $\nu_{C=O}$ value of the second component may be ascribed to the coordination of enolic oxygen to mercury(II) in structure (**6**). The doublet of bands present in the IR spectrum of the ligand R = Et in the range 1270–1305 cm^{-1} spreads with the lower end shifting to 1230 cm^{-1} from 1270 cm^{-1} in the spectra of these two complexes and not in the third which supports the proposed coordination of the enolic oxygen and raising of the $\nu_{C=O}$ value.[11]

$M(o\text{-}R_2AsC_6H_4CO_2)_2(L)n$

The IR spectra of all the complexes of these ligands with zinc(II), cadmium(II) and mercury(II) (Table 3) show that in zinc(II) complexes the ν_s-CO_2 either remains the same as in the case of sodium salt or is raised by ~15 cm^{-1} whereas in the case of cadmium(II) and mercury(II) complexes this frequency decreases but the magnitude of this lowering is more pronounced in the case of mercury(II) complexes. This order is very much consistent with the expected order (Zn < Cd(II) < Hg(II)) of the strength of the covalent bond between metal ion and the carboxylate ion. The ν_{as}-CO_2 values in these complexes are slightly higher than those of the corresponding sodium salt. It has been seen in the case of all the complexes studied in present investigation that even if ν_s-CO_2 is lowered appreciably as in the case of mercury(II) complexes the changes in the ν_{as}-CO_2 are marginal. This makes the assignment of the type of the bonding mode difficult. However, this limitation can be easily understood if we consider the exceptional status of these complexes in which arsenic(III) is coordinated to the metal ion having $d\pi$ filled orbitals which take part in back bonding whose strength is increased by the flow of electrons from carboxylate oxygen to the metal ion. Thus this increased electron density around arsenic(III) lowers the C=O bond order of the carboxylate ion through conjugation with the π electron system of the benzene ring.

These metal complexes thus contain a highly stable hybrid chelate system (**7**) which is not only comparable in terms of the electron delocalisation with the chelating acetylacetonate system[12] but also shows a possibility of the presence of ring current in the complexes of metal ion having $d\pi$ electrons whose π donor power surpasses the σ donor power of arsenic(III).

REFERENCES

[1]S. S. Sandhu and S. S. Parmar, *Z. Anorg. Allgem. Chem.* 1968, **363**, 207.

[2]S. S. Sandhu and S. S. Parmar, *Z. Anorg. Allgem. Chem.* 1970, **373**, 64.

[3]S. S. Parmar and H. Kaur, *Trans. Met. Chem.* 1981, **7**, 79.

[4]A. I. Vogel, *A Text Book of Quantitative Inorganic Analyses*, 3rd Edn. ELBS and Longman, London (1973).

[5]S. S. Parmar, T. S. Basra, R. M. Malhotra and S. S. Sandhu, *Ind. J. Chem.* 1981, **20**, 235.

[6]E. N. Tsevetksov, D. I. Labanov, G. Kh. Kamai, N. A. Chandaeva and M. I. Kabachink, *Zh. Obsch, Khim.* 1969, **39**, 2670.

[7]L. J. Bellamy, *The Infrared Spectra of Complex Molecules*, p. 183. Chapman & Hall, London (1975).

[8]M. D. Taylor, C. P. Carter and C. I. Wynter, *J. Inorg. Nucl. Chem.* 1968, **30**, 1503.

[9]C. J. W. Brookes, G. Eglinton and J. F. Norman, *J.C.S.* 1961, 106.

[10]S. S. Sandhu, S. Baweja and S. S. Parmar, *Trans. Met. Chem.* 1980, **5**, 299.

[11]H. Muso, *Chem. Ber.* 1955, **88**, 1915.

[12]D. W. Thompson, *Structure and Bonding* 1971, **9**, 27.

Polyhedron Vol. 1, No. 9-10, pp. 673-678, 1982
Printed in Great Britain.

0277-5387/82/090673-06$03.00/0
Pergamon Press Ltd.

HYDROLYSIS OF HYDRO(PYRROLYL-1)BORATES

JÓZSEF EMRI* and BÉLA GYÖRI
Department of Inorganic and Analytical Chemistry, Lajos Kossuth University, H-4010 Debrecen, Hungary

(*Received* 4 *January* 1982)

Abstract—The hydrolysis of hydro(pyrrolyl-1)borates ($[BH_n(NC_4H_4)_{4-n}]^-$, $n = 1, 2, 3$) can be treated as a kinetically one-step reaction outside of the mildly acidic region. In strongly acidic medium the hydrolysis takes place in a stepwise manner; the intermediates (boranes and the cationic boron compounds) being hydrolyzed more slowly than the borate anion. In the first step of the hydrolysis of $[BH_3(NC_4H_4)]^-$ the B–H bond, while in case of $[BH_2(NC_4H_4)_2]^-$ and $[BH(NC_4H_4)_3]^-$ the B–N bond is breaking.

In neutral and mildly alkaline medium, the hydrolysis is a general acid catalyzed reaction (A-S_E2 mechanism). It becomes to a special H^+-ion catalyzed reaction (A-1 mechanism) in strongly alkaline region since the protonated intermediate can be reversed to the original borate upon reaction with the OH^- ion. The hydrolysis presumably takes place through an intermediate which is protonated on the pyrrolyl nitrogen. Concomitant to the hydrolysis an isotopic exchange reaction was observed on the C_α and C_β atoms of the pyrrolyl group in heavy water. In the hydrolysis of the $[BH_3(NC_4H_4)]^-$-anion the N-protonated intermediate is assumed to be able to reverse to the original borate even in acidic or neutral region, at least in part.

INTRODUCTION

In a previous paper[1] we established that the hydrolysis of phenyl(pyrrolyl-1)borates ($[B(C_6H_5)_nPyl_{4-n}]^-$, $n = 1$, 2, 3) and of the tetra(pyrrolyl-1)borate is a hydrogen-ion catalyzed reaction and the rate-determining step of the hydrolysis is the reaction between the pyrrolyl-borate and the hydrogen ion:

$$[(B(C_6H_5)_n(NC_4H_4)_{4-n}]^- + H^+ \overset{\text{slow}}{\rightleftharpoons} [H^+B(C_6H_5)_n(NC_4H_4)^-_{4-n}]$$

$$\longrightarrow B(C_6H_5)_n(NC_4H_4)_{3-n} + HNC_4H_4 \qquad (1)$$

$$B(C_6H_5)_n(NC_4H_4)_{3-n} + (3-n)H_2O \xrightarrow{\text{very fast}}$$

$$B(C_6H_5)_n(OH)_{3-n} + (3-n)HNC_4H_4 \qquad n = 0, 1, 2, 3. \qquad (2)$$

In the present communication we wish to report on the study of the kinetics and mechanism of the hydrolysis of hydro(pyrrolyl-1)borates ($[BH_n(NC_4H_4)_{4-n}]^-$, $n =$ 1, 2, 3). In contrast to the phenyl(pyrrolyl)borates, the hydrolytic stability of the two different bonds (B–H and B–NC_4H_4) is almost identical in the former compounds.[1] Similar to the BH_4^--ion[2] and the phenyl(pyrrolyl)borates[1] the hydro(pyrrolyl-1)borates are quickly hydrolyzed in mildly alkaline buffers[3,5] according to eqn (3):

$$[BH_n(NC_4H_4)_{4-n}]^- + H^+ + 3H_2O = B(OH)_3 + nH_2 + (4-n)HNC_4H_4. \qquad (3)$$

The light absorption at 220–270 nm of the hydro(pyrrolyl-1)-borates is considerably more intensive than that of the hydrolysis products so that the kinetics of hydrolysis can be conveniently followed spectrophotometrically.

*Author to whom correspondence should be addressed.

EXPERIMENTAL

The preparation of the borates utilized, $Na[BH_3(NC_4H_4)]\cdot C_4H_8O_2$; $K[BH_2(NC_4H_4)_2]$; $Na[BH(NC_4H_4)_3]$ and $Na[BH(NC_4H_4)_3]\cdot 1.5\ C_4H_8O_2$ has been described previously.[4,5] The buffers used have been prepared in the usual manner using analitical grade chemicals from Reanal and Merck. The ionic strengths of the buffers was adjusted to 0.1 with NaCl. pH-values were determined with Radiometer model PHM-4 pH-meter. The concentration of OH^- ions was determined by acid-alcalimetric titrations and the pH was calculated using the relationship $pH = 13.783 + \log [OH^-]$.

The 99.5 atom % heavy water used for the deuteration experiments.^{1}H NMR spectra were recorded on a Jeol model MH-100 NMR spectrometer.

Kinetic measurements

The rate of hydrolysis of hydro(pyrrolyl-1)borates was followed by spectrophotometry. The measurements were performed at 235 nm ($Na[BH_3(NC_4H_4)]$), 240 nm ($K[BH_2(NC_4H_4)_2]$) and 246 nm ($Na[BH(NC_4H_4)_3]$) wavelengths at borate concentrations between $2\cdot10^{-4}$ and $4\cdot10^{-4}$ mol/dm^3 at 25°C using samples thermostatted to ±0.1°C.

(a) In the acidic pH range the measurements were performed using a stopped flow apparatus developed at the Physical Chemistry Laboratory of the Lajos Kossuth University. Dead-time of the apparatus was 5 ms. Equivalent amounts of borate and buffer solutions were quickly transferred into the cuvette of a single beam UV-VIS spectrophometer (Hitachi-Perkin-Elmer 139) using a quick mixer. The change in absorption was recorded on a storage oscilloscope (Phillips PM-3220).

(b) In the neutral and alkaline pH range the borates were dissolved in a solution containing 0.01 mol/dm^3 NaOH and 0.09 mol/dm^3 NaCl. The borate solutions were diluted to 1:50 before measurements with rapid stirring and the light absorption of the samples were determined using a Beckman Acta M-IV spectrophotometer. The absorption of the hydrolysis products was measured when eight times the half-life of the reaction has elapsed.

When the half-lifetime exceeded 6 hr (alkaline medium) the measurements were performed with oxygen-free solutions and the samples were kept under nitrogen.

Hydrolysis in the presence of pyridine

1.2 cm^3 pyridine was added to 25 cm^3 of a solution containing

2.5 mmoles of borate then a HCl solution (1 mol/dm^3) was added dropwise, under vigorous stirring, until it became acidic with respect to methyl orange. After cooling to 0–5°C the crystalline material was filtered out, washed with a small amount of cold water, alcohol and ether and dried in a stream of dry nitrogen gas. The products were identified through their IR spectra.[5] The following products were obtained: $C_5H_5N \cdot BH_2(NC_4H_4)$ (0.123 g, 31%, from $Na[BH_3(NC_4H_4)]$; 0.152 g, 38%, from $Na[BH_2(NC_4H_4)_2]$ and $C_5H_5N{\cdot}BH(NC_4H_4)_2$ (0.045 g, 8%, from $Na[BH(NC_4H_4)_3]$).

Hydrolysis in deuterium oxide

The borates were dissolved in deuterium oxide containing 0.12 mol/dm^3 of $(CH_3)_3COD$ and 0.1 mol/dm^3 of dioxane. The concentration was 0.5 mol/dm^3 with respect to the pyrrolyl group. The relative amounts of hydrogens in the pyrrolyl and tert-butyl groups were measured from the ^{1}H NMR spectra, then the borate solution was reacted with CH_3COOD (2 mol/dm^3) in deuterium oxide. After hydrolysing the borate the hydrogen ratio in the pyrrolyl- and tert-butyl groups was measured again. The extent of deuteration in α- and β-positions of the pyrrolyl group was calculated from the difference of the hydrogen ratios.

Hydrogen-deuterium exchange studies

The borates were dissolved in deuterium oxide containing 1 mol/dm^3 of NaOD. The solutions were kept at room temperature and the relative amounts of hydrogens in the pyrrolyl group with respect to the HDO was measured from the ^{1}H NMR spectra at regular intervals. The exchange reaction was followed ultil 15% conversion level in the case of the $[BH(NC_4H_4)_3]^-$ anion and to 50–75% conversion level in the other cases. The exchange rate constants for the α and β hydrogens (k_α^{ex} and k_β^{ex}) were calculated from the following expression:

$$-\ln f_\alpha = \frac{k_\alpha^{ex}}{n} t - \ln f_\alpha^0$$

where f_α (or f_β) is the ratio of the α (or β) hydrogens, respectively, to the total amount of hydrogens in the pyrrolyl group and n is the number of equivalent hydrogens (2, 4, or 6) in the pyrrolylborates.

RESULTS AND DISCUSSION

The hydrolysis of hydropyrrolylborates—according to eqn (3)—in mildly acidic buffers can be described as a kinetically pseudo-first-order reaction:

$$-\frac{d[B^-]}{dt} = k_1^{hydr}[B^-] \qquad (4)$$

B^- denotes the hydro(pyrrolyl-1)borate ($[BH_n(NC_4H_4)_{4-n}]^-$, $n = 1, 2, 3$) and k_1^{hydr} is the pseudo-first-order rate constant. The rate of hydrolysis is proportional to the hydrogen ion concentration (see Table and Fig. 1), but in the pH range between 2 and 4 it increases more slowly than in the weakly acidic region with simultaneous formation of the end-product in—at least—two consecutive first-order reactions with nearly identical rates (Fig. 1). According to the data of Fig. 1 it can be assumed that in the region pH < 3 the hydrolysis of hydropyrrolylborates—like that of the tetrahydroborate[6]—takes place stepwise, and the hydrolysis of the borate anion as well as that of the intermediates formed from the borate may occur with nearly identical rates. One of the intermediates which is relatively stable in acidic solution may be a borane, $BH_n(NC_4H_4)_{3-n}$ (n = 1, 2) since, when the hydrolysis is performed in acidic solution in the presence of pyridine, the following reactions take place:

$$[BH_3(NC_4H_4)]^- + H^+ + C_5H_5N = C_5H_5N{\cdot}BH_2(NC_4H_4) + H_2 \qquad (5)$$

$$[BH_2(NC_4H_4)_2]^- + H^+C_5H_5N = C_5H_5N{\cdot}BH_2(NC_4H_4) + HNC_4H_4 \qquad (6)$$

$$[BH(NC_4H_4)_3]^- + H^+ + C_5H_5N = C_5H_5N{\cdot}BH(NC_4H_4)_2 + HNC_4H_4. \qquad (7)$$

The same reactions take place in ethereal solution as well.[5] The products of eqns (5)–(7) were identified. The formation of these products indicates that in the first step of the hydrolysis of $[BH_3(NC_4H_4)]^-$ the B–H bond, while in case of $[BH_2(NC_4H_4)^2]^-$ and $[BH(NC_4H_4)_3]^-$ the B–N bond is breaking. According to our observations the formation of pyridine-borane complexes in aqueous solution is possible only in those pH range where the borate hydrolysis is a stepwise process. When the hydrolysis of hydropyrrolylborates is conducted in 0.02–0.1 mol/dm^3 HCl solution the rate of product formation decreases with increasing HCl concentration (Fig. 1). This trend could be explained by the formation of a hydrolytically very stable boron(1+) cation (e.g. $[BH(NC_4H_4)(H_2O)_2]^+$ cation) or a species containing a protonated pyrrolyl group (e.g. $[(C_4H_5N)B(OH)_2]^+$ cation). The k_1^{hydr} values of the hydropyrrolylborates vary proportionally with the H^+ ion concentration in the weakly acidic pH range. In the more alkaline range, the hydrolysis of the hydropyrrolylborates may also proceed through a reaction which is independent of the H^+ ion concentration (Table 1). Since the rate of hydrolysis in buffers with different boric acid concentrations but identical pH is proportional with the boric acid concentration (Table 2), this H^+ ion-independent hydrolysis may be regarded as a water-catalyzed reaction and the hydroly-

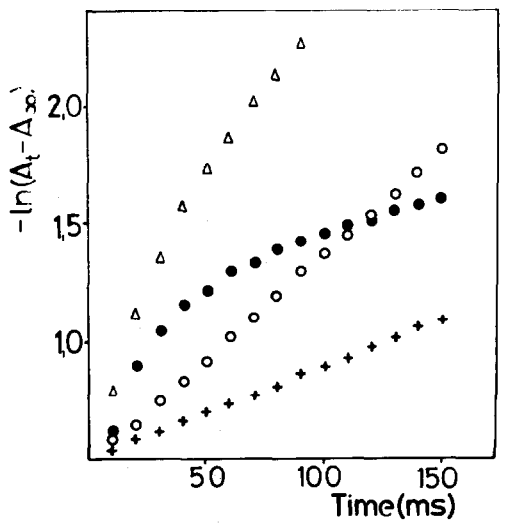

Fig. 1. Function of $\ln(A_t - A_\infty)$ vs time at the hydrolysis of $[BH_3(NC_4H_4)]^-$ in acidic buffers (●●● $[H^+] = 0.10$ mole/dm^3; △△△ $[H^+] = 0.02$ mole/dm^3; ○○○ pH = 4.147; +++ pH = 4.419).

Table 1. First-order hydrolysis rate constants (k_1^{hydr}) of hydro(pyrrolyl-1)borates in aqueous buffers at 25°C (a = measured by stopped flow method)

pH	k_1^{hydr} [s^{-1}]		
	$[BH_3(NC_4H_4)]^-$	$[BH_2(NC_4H_4)_2]^-$	$[BH(NC_4H_4)_3]^-$
3.182			7.0 [a]
3.429			3.6 [a]
3.713			1.9 [a]
4.147	8.7 [a]		0.72 [a]
4.419	3.9 [a]		0.37 [a]
4.561	2.9 [a]	7.7 [a]	
6.575			$2.7 \cdot 10^{-3}$
6.809			$1.6 \cdot 10^{-3}$
7.130			$7.3 \cdot 10^{-4}$
7.335			$4.6 \cdot 10^{-4}$
8.127	$8.9 \cdot 10^{-4}$	$2.3 \cdot 10^{-3}$	$8.5 \cdot 10^{-5}$
8.433	$4.5 \cdot 10^{-4}$	$1.2 \cdot 10^{-3}$	
8.636	$3.2 \cdot 10^{-4}$	$7.2 \cdot 10^{-4}$	$1.8 \cdot 10^{-5}$
8.840	$1.9 \cdot 10^{-4}$	$4.5 \cdot 10^{-4}$	
9.050	$1.1 \cdot 10^{-4}$		
9.203	$1.0 \cdot 10^{-4}$	$1.9 \cdot 10^{-4}$	$6.6 \cdot 10^{-6}$
9.583	$3.9 \cdot 10^{-5}$		
9.986	$1.6 \cdot 10^{-5}$	$3.4 \cdot 10^{-5}$	$1.2 \cdot 10^{-6}$
10.056	$1.4 \cdot 10^{-5}$		
10.234	$9.6 \cdot 10^{-6}$		
10.647	$4.9 \cdot 10^{-6}$	$7.2 \cdot 10^{-6}$	$2.5 \cdot 10^{-7}$
10.741	$3.6 \cdot 10^{-6}$		$2.1 \cdot 10^{-7}$
10.921	$2.7 \cdot 10^{-6}$		$1.5 \cdot 10^{-7}$
11.320	$1.1 \cdot 10^{-6}$		$7.5 \cdot 10^{-8}$
11.453			$5.9 \cdot 10^{-8}$
11.855	$3.1 \cdot 10^{-7}$		$3.6 \cdot 10^{-8}$
12.084		$3.2 \cdot 10^{-7}$	
12.362	$9.8 \cdot 10^{-8}$	$1.8 \cdot 10^{-7}$	
12.582		$1.4 \cdot 10^{-7}$	
12.810		$8.4 \cdot 10^{-8}$	
13.144		$4.3 \cdot 10^{-8}$	

Table 2. First-order hydrolysis rate constants (k_1^{hydr}) of hydro(pyrrolyl-1)borates at various concentrations of aqueous borate buffers at 25°C (ionic strength = 0.25)

$c_{H_3BO_3}$	k_1^{hydr} [s^{-1}]		
mole·dm^{-3}	$[BH_3(NC_4H_4)]^-$	$[BH_2(NC_4H_4)_2]^-$	$[BH(NC_4H_4)_3]^-$
0.000	$6.7 \cdot 10^{-5}$ [a]	$1.86 \cdot 10^{-4}$ [a]	$5.7 \cdot 10^{-6}$ [a]
0.029	$7.3 \cdot 10^{-5}$	$1.91 \cdot 10^{-4}$	$6.2 \cdot 10^{-6}$
0.087	$9.7 \cdot 10^{-5}$	$2.13 \cdot 10^{-4}$	$6.8 \cdot 10^{-6}$
0.175	$1.14 \cdot 10^{-4}$	$2.28 \cdot 10^{-4}$	$8.4 \cdot 10^{-6}$

[a] extrapolated value

sis of hydropyrrolylborates may be taken as a general-acid catalyzed reaction:

$$-\frac{d[B^-]}{dt} = [B^-]\sum_{HA} k_{HA}[HA] \qquad (8)$$

HA denotes the acid (H^+, H_2O, H_3BO_3, etc.), k_{HA} is the second-order rate constant of the acid-catalyzed reactions. The k_{HA} values for the hydropyrrolylborates are summarized in Table 3. On the basis of the general acid-catalysis mechanism one would expect the k_1^{hydr} values of the hydropyrrolylborates to approach to a constant value in the strongly alkaline range. In contrast to this expectation it was observed that when the measurements were performed in the absence of oxygen and transition metal ions, the k_1^{hydr} values (Table 1) approximated the zero. This was most conspicuous in the case of the $[BH_3(NC_4H_4)]^-$ anion (Fig. 2). This observation can be rationalized by assuming the formation—like the hydrolysis of the BH_4^- anion[9]—in the reaction between the hydropyrrolylborates and acids of an intermediate which can revert to the original borate upon the action of OH^- ions in the alkaline pH range. Thus the hydrolysis of the hydropyrrolylborates can be described by the following equations if only the H^+ ion and the H_2O molecule are being considered as acids:

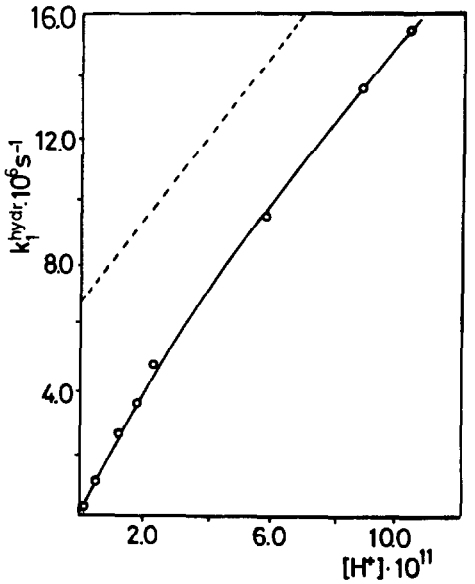

Fig. 2. Pseudo-first-order rate constants (k_1^{hydr}) for the hydrolysis of $[BH_3(NC_4H_4)]^-$ in strong alkaline buffers. (OOO measured values; --- calculated from eqn (8); —— calculated from eqn 15.)

$$[BH_n(NC_4H_4)_{4-n}]^- + H^+ \underset{k_{-H}}{\overset{k_H}{\rightleftharpoons}} [HBH_n(NC_4H_4)_{4-n}] \qquad (9)$$

$$[BH_n(NC_4H_4)_{4-n}]^- + H_2O \underset{K_{-H_2O}}{\overset{k_{H_2O}}{\rightleftharpoons}} [HBH_n(NC_4H_4)_{4-n}] + OH^- \qquad (10)$$

$$[HBH_3(NC_4H_4)] \xrightarrow{k_2} BH(NC_4H_4) + H_2 \qquad (11)$$

$$[HBH_n(NC_4H_4)_{4-n}] \xrightarrow{k_2} BH_n(NC_4H_4)_{3-n} + HNC_4H_4 \qquad (12)$$

$$n = 1, 2$$

$$BH_n(HC_4H_4)_{3-n} + 2H_2O \xrightarrow{\text{very fast}} B(OH)_3 + nH_2 + (3-n)HNC_4H_4 \qquad (13)$$

$$n = 1, 2, 3$$

$$B(OH)_3 + OH^- \xrightleftharpoons{\text{very fast}} [B(OH)_4]^-. \qquad (14)$$

Since the hydropyrrolylborate is only weakly basic it can be assumed that the concentration of the protonated intermediate ($[HBH_n(NC_4H_4)_{4-n}]$), formed in the reaction between the acid (H^+ and H_2O) and the borate, remains small all the time during the reaction.

Applying the Bodenstein principle

$$\left(\frac{d[HBH_n(NC_4H_4)_{4-n}]}{dt} \simeq 0\right)$$

and assuming that $k_2 \gg k_{-H}$ results in the following formula for k_1^{hydr}:

$$k_1^{hydr} = \frac{k_H[H^+]^2 + k_{H_2O}[H^+]}{[H^+] + K_w k_{-H_2O}/k_2}. \qquad (15)$$

Equation (15) includes the two limiting cases of the acid-catalysis: the general-acid catalysis ($A\text{-}S_E2$ mechanism) and the specific H^+ ion catalysis (A-1 mechanism). According to eqn (15) in acidic or less basic solutions ($[H^+] \gg K_w k_{-H_2O}/k_2$) the reaction is $A\text{-}S_E2$ type but it is A-1 type in more basic solutions ($k_H[H^+] \ll k_{H_2O}$; $[H^+] \ll K_w k_{-H_2O}/k_2$).

The rate constants in eqn (15) were determined in the following way. From the k_1^{hydr} value measured in the neutral and weakly alkaline region (Table 1) the k_H values were determined then, from the data obtained in the more alkaline range (Table 1) and from the known k_H the k_{H_2O} and $K_w(k_{-H_2O}/k_2)$ values could be obtained. The $[(k_1^{hydr} - k_1^{calcd})/k_1^{hydr}]$ values were minimized in these calculations (k_1^{calcd} means the right side of eqn 15). The calculated values obtained in this manner are summarized in Table 3. (In the case of the $[BH(NC_4H_4)_3]^-$ anion the value of k_{H_2O} is very small and uncertain therefore the $K_w \cdot k_{-H_2O}/k_2$ value was not calculated.)

Due to the general-acid catalysis, the rate-determining

step in the hydrolysis of the hydropyrrolylborates is the protonation of the borate anion (eqns 10 and 9). The borate anion may be protonated on the pyrrolyl group or—like the BH_3CN^-[10] and BH_4^-[9]—on the boron as well.

The hydrolysis of hydropyrrolylborates with deuteroacetic acid in D_2O resulted in the formation of 1, 2- and 1,3-dideuteropyrroles (Table 4). This finding indicates that the reaction between borate and acids gives rise to the formation of a product protonated at the pyrrolyl carbon as well as another one protonated at the pyrrolyl N atom since the rate of hydrogen exchange at the nitrogen is 1000-fold greater in D_2O than either at α- or β-carbons of pyrrole.[7,8] Accordingly, the formation of the following intermediates may be taken into consideration in the course of the reaction between the borates and H^+ ion (R denotes pyrrolyl group or H):

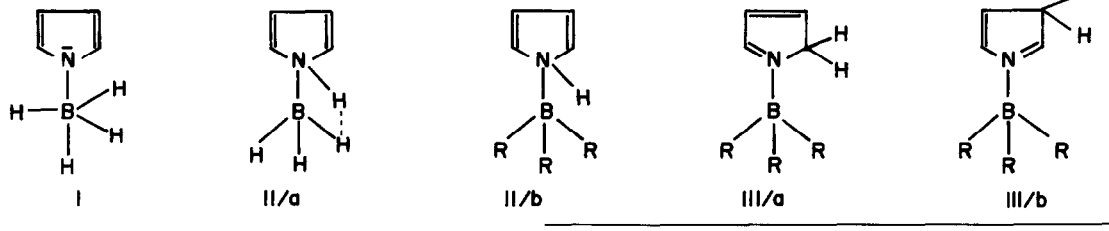

The formation of the intermediate I could not be demonstrated experimentally. The reaction of acetone with the residual borate anion after partial hydrolysis of the hydropyrrolyl-borates in D_2O did not result in the formation of $(CH_3)_2CDOD$ in measurable amounts; $(CH_3)_2CHOD$ was obtained instead. On the other hand, considerable hydrogen exchange at the B-atom was observed in the hydrolysis of BH_4^-,[9] BH_3CN^-[10] and amine boranes[11,12] in D_2O.

In the course of the hydrolysis of $[BH_3(NC_4H_4)]^-$ anion H_2 evolution was observed following the protonation reaction (eqns 5 and 11) indicating the appearance of intermediates I or II/a. The lack of B–H exchange makes intermediate II/a more likely but the formation of II/a can also be assumed in the reaction between the borate and H^+ ion followed by conversion to an intermediate type I which, in turn, decomposes into $BH_2(NC_4H_4)$ and H_2-gas.

The hydrolysis of $[BH_2(NC_4H_4)_2]^-$ and $[BH(NC_4H_4)_3]^-$ anions results in the formation of pyrrole in the reaction between the borate and acids (eqns 6, 7 and 12). It is to be expected in the case of the pyrrolylborates that the rate of protonation is faster at the N atom than at the C atom so that the hydrolysis can be assumed to occur through the intermediate type II/b.

We suggest that the hydrolysis of hydropyrrolylborates takes place through an intermediate protonated at the N-atom (II/a and II/b) and the observed exchange reactions of the C–H hydrogens may occur as parallel, nonproductive exchange reactions. However, since the

Table 3. Rate constants of hydrolysis of hydro(pyrrolyl-1)borates at 25°C

Rate constants	$[BH_3(NC_4H_4)]^-$	$[BH_2(NC_4H_4)_2]^-$	$[BH(NC_4H_4)_3]^-$
k_H ($mole^{-1}\cdot dm^3\cdot s^{-1}$)	$(1.25\pm0.09)\cdot10^5$	$(3.10\pm0.06)\cdot10^5$	$(1.00\pm0.02)\cdot10^3$
k_{H_2O} (s^{-1})	$(7.5\pm1.3)\cdot10^{-6}$	$(1.5\pm0.2)\cdot10^{-7}$	$(2.4\pm0.2)\cdot10^{-8}$
$K_w k_{-H_2O}/k_2$ ($mole\cdot dm^{-3}$)	$(3.0\pm0.6)\cdot10^{-11}$	$(2.1\pm0.3)\cdot10^{-13}$	-
$k_{H_3BO_3}$ ($mole^{-1}\cdot dm^3\cdot s^{-1}$)	$(2.8\pm0.4)\cdot10^{-4}$	$(2.4\pm0.7)\cdot10^{-4}$	$(1.5\pm0.2)\cdot10^{-5}$

Table 4. Deuterium contents (f_α, f_β) of pyrrole obtained in acidic hydrolysis (AcOD/D_2O). C_α-H and C_β-H exchange rate constants (k_α^{ex}, k_β^{ex}) of the hydro(pyrrolyl-1)borates in alkaline medium (0.1 mole · dm^{-3} NaOD in D_2O)

Borate	f_α [%]	f_β [%]	$k_\alpha^{ex}[s^{-1}]$	$k_\beta^{ex}[s^{-1}]$
$[BH_3(NC_4H_4)]^-$	34.2±4.0	37.6±2.4	$8.6\cdot10^{-7}$	$3.8\cdot10^{-7}$
$[BH_2(NC_4H_4)_2]^-$	5.1±0.5	5.1±0.5	$4.6\cdot10^{-7}$	$1.8\cdot10^{-7}$
$[BH(NC_4H_4)_3]^-$	5.4±0.5	5.6±0.5	$1.3\cdot10^{-7}$	$7.5\cdot10^{-8}$

protonations at the N- and the C_α- and C_β-atoms of the pyrrolyl group are parallel reactions, the study of C–H exchange may yield useful informations concerning the mechanism of hydrolysis reactions. In the case of hydropyrrolylborates (similarly to the observations[7,8] made with pyrrole derivatives) the relative rates of the hydrogen exchange at the α- and β-C atoms depend strongly on the soft or hard character of the acid that catalyses the deuteration reaction. In the weakly acidic and neutral region (where the hydrogen exchange occurs in the reaction catalyzed by D_2O^+ which, itself, can be considered as a hard acid) the rates of H-exchange are almost identical at the C_α- and C_β-atoms. In alkaline media, however (where the hydrogen exchange is a reaction catalyzed by the soft acid D_2O), the exchange is considerably faster at the C_α-atom than at the C_β-atom (Table 4).

The D/H ratio in the pyrrole obtained from the hydrolysis in D_2O of the hydropyrrolylborates in weakly acidic or neutral regions does not depend on the acidity of the medium, i.e. the ratio of the hydrolysis and the C–H exchange rate is constant. In the strongly alklaine range (0.01–0.1 mol/dm^3 NaOD–D_2O) the exchange rates are practically identical but the exchange rate exceeds considerably that of the hydrolysis and the D/H ratio in the hydrolysis products increases regularly with increasing alkalinity of the medium.

These findings can be rationalized by assuming that the intermediate that occurs in the reaction between the borate and D_2O may revert, upon the action of the OD^- anion, into the original borate to a considerable extent so that the conclusions readed upon from the kinetic measurements are supported by the exchange studies as well.

The pyrrole obtained through the acidic hydrolysis of the $[BH_3(NC_4H_4)]^-$ anion in D_2O contains much more deuterium than in the cases of other borates (Table 4). At the same time, the k_H value of the $[BH_3(NC_4H_4)]^-$ anion is much smaller (Table 3) than expected. Both the relatively small k_H value and the increased deuterium content of the hydrolysis product (pyrrole) indicate that the intermediate that occurs in the reaction between the $[BH_3(NC_4H_4)]^-$ anion and the H^+ ion (eqn 9) reverts partially into the original borate even in acidic media.

REFERENCES

[1]J. Emri, B. Györi and P. Szarvas, *Z. Anorg. Allg. Chem.* 1973, **400**, 321.
[2]R. E. Davis, E. B. Bromels and C. L. Kibby, *J. Amer. Chem. Soc.* 1962, **84**, 885.
[3]P. Szarvas, J. Emri and B. Györi, *Acta Chim Acad. Sci. Hung.* 1970, **64**, 203.
[4]P. Szarvas, B. Györi and J. Emri, *Acta Chim. Acad. Sci. Hung.* 1971, **70**, 1.
[5]B. Györi, J. Emri and P. Szarvas, *Acta Chim. Acad. Sci. Hung.* 1975, **86**, 235.
[6]F. T. Wang and W. L. Jolly, *Inorg. Chem.* 1972, **11**, 1933.
[7]D. M. Muir and M. C. Whiting, *J. Chem. Soc., Perkin II.* 1975, 1316; 1976, 388.
[8]G. P. Bean and T. J. Wilkinson, *J. Chem. Soc., Perkin II.* 1978, 72.
[9]M. M. Kreevoy and J. E. C. Hutchins, *J. Amer. Chem. Soc.* 1972, **94**, 6371.
[10]M. M. Kreevoy and J. E. C. Hutchins, *J. Amer. Chem. Soc.* 1969, **91**, 4329.
[11]R. E. Davis, A. E. Brown, R. Hopmann and C. L. Kibby, *J. Amer. Chem. Soc.* 1963, **85**, 487.
[12]H. C. Kelly, F. R. Marchelli and M. B. Giusto, *Inorg. Chem.* 1964, **3**, 431.

Polyhedron Vol. 1, No. 9-10, pp. 679-681, 1982
Printed in Great Britain.

0277-5387/82/090679-03$03.00/0
Pergamon Press Ltd.

PREPARATION AND STUDY OF COPPER(II) PROPRIONATE COMPLEX WITH PAPAVERINE

MILAN MELNÍK
Department of Inorganic Chemistry, Slovak Technical University, 812 37 Bratislava, Czechoslovakia

(*Received* 6 *January* 1982)

Abstract—The synthesis and characterization of $Cu(CH_3CH_2COO)_2 \cdot$papaverine is reported. The characterization of the compound was based on elemental and thermal analysis, on electronic and EPR spectra, as well as magnetic measurements over the temperature range. The available evidence supports a binuclear structure. The EPR spectrum is consistent with spin $S = 1$. The exchange interaction parameter $-2J = 362\ cm^{-1}$. Correlation between the $-2J$ values in familiar copper(II) proprionates and pKa values of the axial ligands was found and discussed.

INTRODUCTION

Copper(II) proprionates with nitrogen donor ligands have attracted increasing interest in recent years. This interest largely derives from the discovery that the proprionate groups possess a pronounced tendency to serve as a bridge between copper(II) atoms with a nitrogen donor ligand in the terminal position.[1,2] The binuclear copper(II) compounds formed in this way exhibit superexchange interaction, which becomes larger as the ligands supply more electron density to the metal atom. It has been reported that the pyridine and isomeric picoline compounds of copper(II) proprionate follow this trend, and that there exists a direct correlation between the $2J$ values of the compounds and the pKa values of the terminal ligands.[3] However, it must be noted that the lutidine compounds of copper(II) proprionate do not appear to follow this trend.[4] Therefore, it appears that beyond a certain point, the effect of the pKa of the terminal ligand on the $2J$ value of the compound are inconsequential.[4] One of the important trends which has been noted for copper(II) carboxylates is the sensitivity of the $2J$ value to the Cu–O–C–O–Cu bridged distance and angle, through which demagnetization operates.[5]

In order to examine further the nitrogen donation effect on the super-exchange interaction in copper(II) proprionate, we synthesized binuclear copper(II) proprionate with papaverine [1-(3′,4′-dimethoxybenzyl)-6,7-dimethoxy-isoquinoline], which has the structure represented as follows:

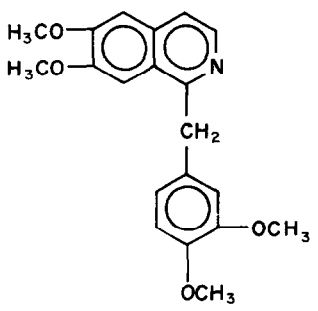

and investigated its thermal, spectral and magnetic behaviours in comparison with those found in familiar copper(II) proprionates. To our knowledge, papaverine as a ligand had not previously been studied, this is the first example.

EXPERIMENTAL

Preparation of copper(II) proprionate monopapaverine

A slightly acidified dilute methanol solution of $Cu(CH_3CH_2COO)_2 \cdot H_2O$ (1 mol) was added to a near boiling dilute methanol solution of papaverine (1 mol). The solution was allowed to stand at room temperature to give green microcrystals, which were collected and dried at room temperature. When the product was recrystallized from hot methanol green crystals of the composition $Cu(CH_3CH_2COO)_2$pap (pap = papaverine) were separated (Found: C, 56.68; H, 5.56; N, 2.8; Cu, 11.64. Calc. for $Cu(CH_3CH_2COO)_2$pap: C, 56.87; H, 5.69; N, 2.55; Cu, 11.57.)

Thermal study

The thermal decomposition was studied by means of a derivatograph (MOM, Budapest). The apparatus and its operation have been described by Paulik *et al.*[6] Platinum crucible with an upper diameter of 14 mm was used, and thermocouples were Pt, Pt–Rh. Powder sample used had a weight of 100 mg. The rate of temperature was 6°/min; the measurement was made in air atmosphere.

Spectral studies

Electronic spectrum in the region 1.0–2.8 μm^{-1} was measured with a Perkin–Elmer 450 spectrophotometer and IR spectrum in the region 400–3600 cm^{-1} with the UR 10 spectrophotometer. In both cases the nujol suspension technique was used. EPR spectrum of the powdered sample was run on a Varian Model E 4 spectrometer at room temperature.

Magnetic studies

Magnetic susceptibility measurements of the compound were made over the temperature range 81–293 K. At each temperature, measurements were obtained at 5 different field strengths by the Gouy method, with mercury tetrathiocyanatocobaltate(II) as calibrant.[7] Diamagnetic correction was calculated from Pascal's constants.[8] The effective magnetic moments were calculated from the expression

$$\mu_{eff} = 2.83\ (\chi_M^{corr} \times T)^{1/2}.$$

RESULTS AND DISCUSSION

Thermal decomposition of $Cu(CH_3CH_2COO)_2pap$ was carried out in aerobic conditions. The compound in air begins decomposing at about 423 K. At 523 K, the TG curve shows a pseudopause corresponding to the weight-loss of about 25%. In the temperature range 523–943 K slackening is registered on the TG curve with the weight-loss of another 61%, which probably corresponding to the loss of a papaverine molecule (theoretical weight-loss 61.81%), to give at 943 K copper(II) oxide. On the DTA curve, there are two endothermic peaks whose maxima are respectively at 423 and 603 K, and a strongly exothermic asymmetric peak with the maximum at about 743 K.

The IR spectrum of $Cu(CH_3CH_2COO)_2pap$ is very complicated. Locating the bands of "active" groups (COO^-, –C=N–) is very difficult because there is several bands of papaverine[9] in the region 1300–1600 cm^{-1} where the bands are expected.

The electronic spectrum in Nujol of $Cu(CH_3CH_2COO)_2pap$ exhibits two absorption bands, a main band at about 1.40 μm^{-1} and a shoulder at about 2.7 μm^{-1}. The band positions are comparable to those reported for binuclear copper(II) acetate monohydrate.[10] The band at lower energy may be assigned to a spin-allowed *d–d* transitions and the band at higher energy may be due to a copper–copper linkage. The spectrum corroborated the conclusions based on the magnetic behaviours (see below).

EPR spectrum obtained for the powdered sample at room temperature contained the absorption bands of axially-symmetric binuclear species.[11] The values obtained for the spin Hamiltonian parameters are: $g_\perp = 2.09_6$; $g_\parallel = 2.41_0$; $g_{av} = 2.20_6$; $|D| = 0.364\ cm^{-1}$ and $E = 0.003\ cm^{-1}$. The values are comparable to those found in binuclear copper(II) carboxylates.[12] The compound also displays a line which can be attribute to a mononuclear impurity ($g_\perp = 2.04_5$; $g_\parallel = 2.17_8$; $g_{av} = 2.09_0$).

The molar susceptibilities corrected for diamagnetism and magnetic moments for the compound are reported at various temperatures in Table 1. The temperature-susceptibility data can be described by the equation:

$$x_M^{corr} = \left\{\frac{Ng^2\beta^2}{3kT}\left[1 - 1/3(\exp^{-2j/kT})\right]^{-1}\right\}(1 - X) + \left(\frac{Ng^2_{imp}\beta^2}{4kT}\right)X$$

where x_M^{corr} was also corrected for t.i.p. equals $60 \times 10^{-6}\ cm^3\ mol^{-1}$ per Cu atom; X, is molar fraction of the mononuclear impurity; the other symbols have their usual meaning.[13] The least-squares fitting was performed using a new version of the minimization computer program BGD-2. The spectroscopic splitting factors g_{av} and g_{imp} were obtained from the EPR spectrum and used as constants in the least-squares fitting process. The criterion used to determine the best fit is the minimization of the sum of the squares of the deviation A, where

$$A = \sum_i (x_i^{calc} - x_i^{exp})^2.$$

The best fit parameters are: $2J = -362\ cm^{-1}$, $X = 0.81\%$ and $A = 1.485 \times 10^{-8}$.

The molar fractions of singlet and triplet states were calculated from the observed magnetic susceptibilities, by the method of Hatfield *et al.*[14] The singlet–triplet equilibrium constants (Table 1) obtained from the molar fractions were used for calculations of enthalpy ($\Delta H°$) and entropy ($\Delta S°$). The calculated values are: $\Delta S° = 2.7$ e.u. and $\Delta H° = 348\ cm^{-1}$. The enthalpy value is in good agreement with the value of electron spin coupling constant, $2J$.

Table 1. Magnetic data of $Cu(CH_3CH_2COO)_2pap$ ($-\Delta \times 10^6 = 294.4$)

T, K	$x_M^{corr} \times 10^6$	μ_{eff}, B.M.	K_{eg}
81	179	0.34	0.024
101	190	0.39	0.032
112	255	0.48	0.049
122	286	0.53	0.061
132	294	0.56	0.069
143	338	0.62	0.086
153	382	0.68	0.105
164	475	0.79	0.147
175	519	0.85	0.174
185	590	0.93	0.216
195	629	0.99	0.252
206	678	1.06	0.300
216	706	1.105	0.335
226	717	1.14	0.364
239	728	1.18	0.401
251	739	1.22	0.440
262	750	1.25	0.473
282	766	1.315	0.551
293	766	1.34	0.584

From the above observation it may be suggested that the $Cu(CH_3CH_2COO)_2pap$ has binuclear structure similar to that of copper(II) proprionate monopyridine.[1] Copper(II) atoms in the structural units $Cu_2(CH_3CH_2COO)_4(pap)_2$ are bridged in pairs by carboxylic groups of $CH_3CH_2COO^-$, while the molecules of papaverine are bonded through nitrogen atoms in axial positions.

It is known, that the value of exchange coupling constant, $-2J$, to vary according to several factors.[5] One of the important factors is terminal ligand. As the terminal ligand becomes stronger electron donor thus the $-2J$ value tends to increase. Since the pKa value of the terminal ligands reflects the σ-electron density on the nitrogen atom, such an increase in the value results in an increase in the Cu–N σ-bond strength, leading to a greater contribution to magnetic interaction. Although

Table 2. Values of $-2J$ for the copper(II) proprionates and pKa values of the terminal ligands

Compound	$-2J$ (cm^{-1})	pKa	Ref.
CuX_2py	350	5.25	15
$CuX_2$3-pic	364	5.68	16
CuX_2pap	362	5.90	This work
$CuX_2$2-pic	364	5.97	17
$CuX_2$4-pic	376	6.02	3
$CuX_2$3,5-lut	371	6.15	4
$CuX_2$3,4-lut	367	6.46	4
$CuX_2$2,4-lut	365	6.77	4
CuX_2nic	354	7.85	18

X, $CH_3CH_2COO^-$; py, pyridine; pic, picoline; pap, papaverine; lut, lutidine; nic, nicotine.

the $-2J$ value of $Cu(CH_3CH_2COO)_2$nic is to be expected in view of the pKa value of the terminal ligand being larger than that of the $Cu(CH_3CH_2COO)_2 \cdot 3$-pic complex (Table 2), just the opposite was observed.

As we can see in Table 2 the value of $-2J$ increases with increasing pKa value of the terminal ligand with maximum at pKa = 6.02, and although the pKa value increases up to this value, the $-2J$ value is decreasing. A possible explanation lies in the different charge densities and charge distributions in the hetero-ring. It is a well-known fact that in the hetero-ring involves σ- and π-electron system. It is, however, difficult to evaluate the effects of the σ- and π-paths separately at present. Further studies along this line will be needed to clarify this situation.

Acknowledgement—The author is indebted to Dr. J. Mroziński from Wroclaw University (Poland) for performing the magnetic susceptibilities measurements for this research.

REFERENCES

[1]M. M. Borel and A. Leclaire, *Acta Crystallogr. B* 1976, **32**, 1273; 1976, **32**, 3333; 1978, **34**, 99.
[2]M. M. Borel, A. Busnot and A. Leclaire, *J. Inorg. Nucl. Chem.* 1976, **38**, 1557.
[3]W. E. Marsh, G. O. Carlisle and M. V. Hanson, *J. Inorg. Nucl. Chem.* 1977, **39**, 1839.
[4]M. V. Hanson, G. O. Carlisle and W. E. Marsh, *J. Inorg. Nucl. Chem.* 1978, **40**, 1684.
[5]M. Melník, *Coord. Chem. Rev.* 1982, **42**, 259.
[6]F. Paulik, J. Paulik and L. Erdey, *J. Anal. Chem.* 1958, **160**, 241.
[7]B. N. Figgis and R. S. Nyholm, *J. Chem. Soc.* 1958, 4190.
[8]A. Earnshaw, Introduction to Magnetochemistry, pp. 4–8. Academic Press, London (1968).
[9]B. Hampel, Collection of E. Merck A. G., Darmstadt, DMS cards No. 6647.
[10]R. Tsuchida and S. Yamada, *Nature* 1955, **176**, 1171.
[11]B. Bleaney and K. D. Bowers, *Proc. Roy. Soc. (London) A* 1952, **214**, 451.
[12]M. Melník, *Coord. Chem. Rev.* 1981, **36**, 1; and refs. therein.
[13]T. R. Felthouse and D. N. Hendrickson, *Inorg. Chem.* 1978, **17**, 2636.
[14]W. E. Hatfield, T. S. Piper and V. Klabunde, *ibid* 1963, **2**, 629.
[15]M. V. Hanson, G. O. Carlisle and W. E. Marsh, *J. Mol. Struct.* 1977, **37**, 329.
[16]W. E. Marsh, G. O. Carlisle and M. V. Hanson, *Inorg. Chim. Acta* 1977, **21**, L 19.
[17]W. E. Marsh, G. O. Carlisle and M. V. Hanson, *J. Mol. Struct.* 1977, **40**, 153.
[18]M. Melník, *J. Inorg. Nucl. Chem.* 1979, **41**, 779.

Polyhedron Vol. 1, No. 9–10, pp. 683–688, 1982
Printed in Great Britain.

0277-5387/82/090683-06$03.00/0
Pergamon Press Ltd.

STUDY OF THE EXTRACTION OF URANIUM (VI) BY BIS-(DI-*n*-BUTYLPHOSPHATE) COMPOUNDS INCLUDING A POLYHETEROATOMIC CHAIN FROM NITRATE SOLUTIONS

ELISABETH ARCHELAS, GÉRARD BUONO* and BERNARD WAEGELL
Ecole Supérieure de Chimie de Marsielle—Faculté des Sciences, St. Jérôme, rue Henri Poincaré, 13397 Marseille Cédex 4, France

(*Received* 11 *January* 1982)

Abstract—Compounds **1–4** with two di-*n*-butylphosphate groups linked by a polyheteroatomic chain $(BuO)_2P(O)OCH_2(CH_2XCH_2)_nCH_2OP(O)(OBu)_2$ (**1**: $n = 0$; **2**: $n = 1$, X = O; **3**: $n = 2$, X = O; **4**: $n = 1$, X = S) were prepared respectively by action of chlorodi-*n*-butylphosphate on ethyleneglycol, di and triethyleneglycol, and thiodiethyleneglycol under phase transfer conditions.

The extraction of uranium (VI) from aqueous nitrate phase with these compounds, in toluene diluent, was studied. Distribution ratios with compounds **1–3** are somewhat greater than those obtained with tri-*n*-butylphosphate. Extraction studies reveal that polyoxygenated chain of these compounds takes part in U(VI) complexation. The general expression for the complexes is assumed to be $UO_2(NO_3)_2L_m$ in which L is extractant compound and *m* the number of molecules coordinated to uranyl cation. Extraction stoichiometry is dependent upon extractant compound and its concentration in organic phase. For the compounds **1–3**, $m = 1.5$ when extractant concentration is higher than 0.1 M; *m* takes the different values 0.5, 1.0 and 1.5 when extractant concentration is lower than 0.1 M For the compound in which X is sulfur atom, $m = 2.0$ over all studied concentration range.

It was found that in the solvent extraction of uranium (VI) with these compounds, di-*n*-butylphosphoric acid exhibits a synergistic effect increasing the distribution ratio of U(VI) by a factor of 100.

INTRODUCTION

Tri-*n*-butylphosphate (TBP) and related esters such as di-*n*-butylphosphoric acid (HDBP), *bis*-(2-ethylhexyl)phosphoric acid and other phosphoric compounds find important applications in the solvent extraction of lanthanides, actinides and other heavy metals from mineral sources and their recovery from waste products of the atomic energy industry.[2]

A solution of TBP in dodecane or kerosene diluent can be used for solvent extraction of uranyl nitrate.[1–3] Recently much attention has been paid essentially to some neutral extracting molecules containing two P=O groups. These molecules could be considered as bidentate ligands and extractant properties could be improved by an entropic factor. Among the different molecules so far studied we can mention tetra-*n*-butylpyrophosphate TBPP,[4] octaethyltetraamidopyrophosphate OETAPP,[5] tetra-*n*-butylethylenediphosphonate TBEDP.[6]

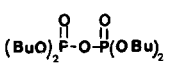

TBPP

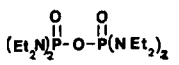

OETAPP

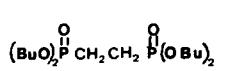

TBEDP

Cyclic polyethers or crown ethers form stable complexes with a large set of metallic salts including uranyl nitrate and other uranium salts.[7–9] In the present study we examined the extraction properties of compounds **1–4** in which two di-*n*-butylphosphate groups are connected by a polyheteroatomic chain. Both of these structural moieties could give particular extraction properties toward uranyl salts. Thus it might be expected that these compounds would coordinate better to uranyl cation than TBP does.

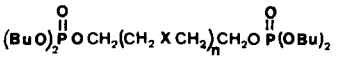

1 : n = 0

2 : n = 1 X = O

3 : n = 2 X = O

4 : n = 1 X = S

The compounds **1–4** are readily prepared by action of chlorodi-*n*-butylphosphate on ethyleneglycol, di and triethyleneglycol and thiodiethyleneglycol by using transfer phase techniques. The extraction properties of these compounds have been studied in order to establish the composition of the extractable species and the relation between the distribution ratios and the extraction system parameters.

EXPERIMENTAL

General: Infrared spectra were obtained on a Perkin–Elmer Model 457 IR spectrometer. ^{1}H NMR spectra were recorded on a Perkin–Elmer R-32 spectrometer at 90 MHz. Samples were studied in $CDCl_3$. Chemical shifts are reported in parts per million downfield from TMS. ^{13}C NMR spectra were recorded in C_6D_6 on a Varian CFT-20 pulse Fourier transform NMR instrument;

*Author to whom correspondence should be addressed.

chemical shifts are reported in parts per million downfield from TMS. ^{31}P NMR spectra were recorded on a Varian FT-80 pulse Fourier transform NMR spectrometer. The ^{31}P NMR signals are given in parts per million vs 85% H_3PO_4 (positive values are downfield from the reference). Splitting patterns are designated as *s*, singlet; *d*, doublet; *t*, triplet; *m*, multiplet. Coupling constants are given in hertz.

pH was determined with a Tacussel Minisis pH-meter. A Beckman DB-GT spectrophotometer was used for spectrophotometric determinations. Concentrations C are defined as the number of formula weights of solute contained in one litre of solution. The distribution ratio, D, for UO_2^{2+} is defined as the concentration of this cation in the organic phase divided by that in the aqueous phase.

MATERIALS

"Pure grade" toluene, ethyleneglycol and diethyleneglycol were obtained from Carlo Erba; di-*n*-butylphosphite, thiodiethyleneglycol, triethyleneglycol and uranyl nitrate were purchased from Fluka.

Preparation of $(Buo)_2P(O)OCH_2(CH_2XCH_2)_nCH_2OP(O)(OBu)_2$

Chlorodi-*n*-butylphosphate was prepared from di-*n*-butylphosphite as described by Walsh.[10] The compounds **1–4** were prepared as described by Moshkina *et al.*[11] but under these experimental conditions ^{31}P NMR spectra revealed the presence of di-*n*-butylphosphoric acid as side product. This can be overcome by using phase transfer catalysis reaction, indeed only this method gives rise to the pure compounds **1–4**. A solution of chlorodi-*n*-butylphosphate (100 mmol), glycol (50 mmol) and benzyl triethyl ammonium chloride (5 mmol) in CH_2Cl_2 (30 ml) was added to 50% NaOH solution (60 ml) under vigorous stirring, at 5–10°C. The mixture was then allowed to stand at room temperature with stirring for 24 hr. Water (40 ml) was added and the mixture was extracted. The organic layer was then washed with water and dried with magnesium sulphate. The solvent was removed under vacuum leaving a viscous product in 60–70% yield. The compounds were not further purified but their structure and purity are in accordance with ^1H, ^{13}C and ^{31}P NMR analysis. These compounds can be also obtained in pure form and in 70% yield by action of chlorodi-*n*-butylphosphate on disodium salt of glycols. The latter were prepared by action of NaH on glycols in THF. However the former procedure was generally prefered for convenience.

1 IR: 2950(C–H), 1280(P=O), 1030(P–O–C) cm^{-1}. ^1H NMR δ: 0.95(12H, *t*, J = 6 Hz), 1.25–1.80(16H, *m*), 4.00–4.30 (12H, *m*). ^{13}C NMR δ: 13.71, 18.99, 32.66 ($^3J_{CP}$ = 6.7 Hz), 66.73 ($^2J_{CP}$ = 5.8 Hz), 67.44 ($^2J_{CP}$ = 5.8 Hz). ^{31}P NMR δ: −3.56.

2 IR: 2950, 1275, 1025 cm^{-1}. ^1H NMR δ: 0.95(12H, *t*, J = 6 Hz), 1.30–1.80(16H, *m*), 3.65–3.80(4H, *m*) 4.00–4.30(12H, *m*). ^{13}C NMR δ: 13.71, 19.00, 32.69 ($^3J_{CP}$ = 6.8 Hz), 66.63 ($^2J_{CP}$ = 5.5 Hz), 67.28 ($^2J_{CP}$ = 5.8 Hz), 70.30 ($^3J_{CP}$ = 6.7 Hz). ^{31}P NMR δ; −3.45.

3 IR: 2950, 1265, 1025 cm^{-1}. ^1H NMR δ: 0.90(12H, *t*, J = 6 Hz), 1.25–1.75(16H, *m*), 3.60–3.80(8H, *m*), 3.90–4.30(12H, *m*). ^{13}C *NMR* δ: 13.59, 18.72, 32.35 ($^3J_{CP}$ = 6.8 Hz), 66.53 ($^2J_{CP}$ = 5.7 Hz), 67.53 ($^2J_{CP}$ = 5.9 Hz), 70.19 ($^3H_{CP}$ = 6.8 Hz), 70.72, ^{31}P NMR δ: −0.85.

4 IR: 2950, 1270, 1010 cm^{-1}. ^1H NMR δ: 0.95(12H, *t*, J = 6 Hz), 1.25–1.80(16 H, *m*), 2.82(4H, *t*, J = 7 Hz), 4.00–4.30(12H, *m*). ^{13}C NMR δ; 13.66, 18.96, 32.47 ($^3J_{CP}$ = 6.9 Hz), 32.61 ($^3J_{CP}$ = 6.6 Hz), 66.70 ($^2J_{CP}$ = 5.7 Hz), 67.38 ($^2J_{CP}$ = 6 Hz). ^{31}P NMR δ: −1.06.

Preparation of complexes

Complexes are readily prepared by action of uranyl nitrate on extractant in chloroform solution. Water was separated by decantation and organic solution was dried. The solvent was removed under vacuum, leaving the crude complex as a green viscous oil.

Several uranyl nitrate-extractant (U:L) stoichiometric ratios corresponding with those determined during extraction studies were used.

We have noted below the principal variations of IR and NMR spectra of these complexes with regard to those of free ligands:

1 U:L = 1:0.5, IR: 1190 cm^{-1}(P=O), ^{31}P NMR δ: 0.15.
U:L = 1:1.5, IR: 1190 cm^{-1}, ^{31}P NMR δ: −3.15.
2 U:L = 1:1, IR: 1185 cm^{-1}, ^{31}P NMR δ: −0.10.
U:L = 1:1.5, IR: 1190 cm^{-1}, ^{31}P NMR δ: 0.26.
3 U:L = 1:1.5, IR: 1180 cm^{-1}, ^{31}P NMR δ: −3.15.
4 U:L = 1:2, IR: 1200 cm^{-1}, ^{31}P NMR δ: −0.71.

DETERMINATION OF DISTRIBUTION RATIOS

Toluene solutions of extractant with a concentration from 0.025 M to 0.5 M were used. Uranyl nitrate solution (4.2×10^{-3} M) was prepared from a $NaNO_3$–HNO_3 solution and ionic strength of the aqueous phase was maintained equal to 1. Equal volumes of the two phases were mixed and shaken together during fifteen minutes. Preliminary experiments have shown that after 5 minutes the thermodynamic equilibrium for the extraction was established. After decantation and separation the pH of aqueous phase was measured and uranyl nitrate concentration in aqueous phase determined spectrophotometrically by complexing with 8-hydroxyquinoline. All distribution ratios (D) were determined at 20 ± 2°C, in all the pH range from 0.6 to 2.7.

EXTRACTION OF NITRIC ACID

Extraction of nitric acid into organic phase with a 0.2 M extractant concentration was studied from various concentrations in aqueous phase. Titrations were made according to the method described by Sato *et al.*[12]

RESULTS AND DISCUSSION

Nitric acid extraction

Figure 1 shows variations of nitric acid concentration in organic phase against its initial concentration in aqueous phase for 0.2 M extractant concentration at 20°C. We can note the closely similar curves for the compounds **1–4** consistent with their identical structure. Acid content in organic phase is higher than extractant concentration when initial HNO_3 concentration in aqueous phase exceeds 4 M. Generally, HNO_3 extraction is related with the properties of phosphoryl groups[13] therefore extraction with compounds **1–4** including two phosphoryl groups is twice as important as TBP extraction.

However the polyheteroatomic chain probably takes part in the complexation, this is supported by the fact that the substitution of a hard oxygen atom[14] by a soft sulphur atom in the chain (compound **4** vs **2**) results in a slight diminution of the extraction of HNO_3 in organic phase.

All studies of uranyl nitrate extraction have been made at nitric acid concentration in aqueous phase below 1 M; as shown the Fig. 1 for this value, HNO_3 concentration is lower than 0.045 M in organic phase.

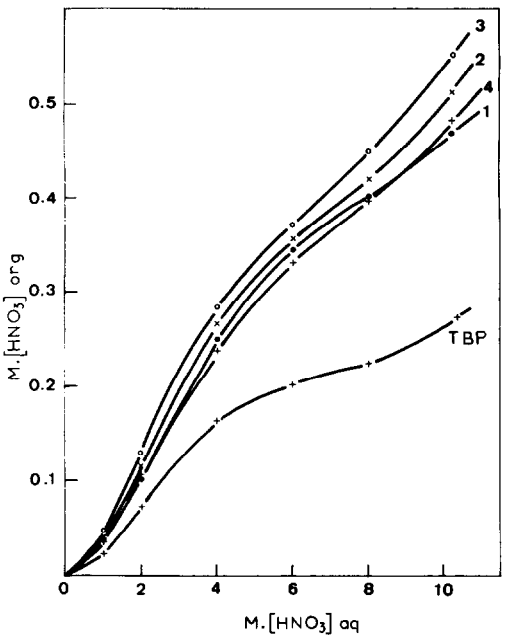

Fig. 1. Nitric acid concentration in the organic phase as a function of HNO_3 concentration in the aqueous phase after extraction.

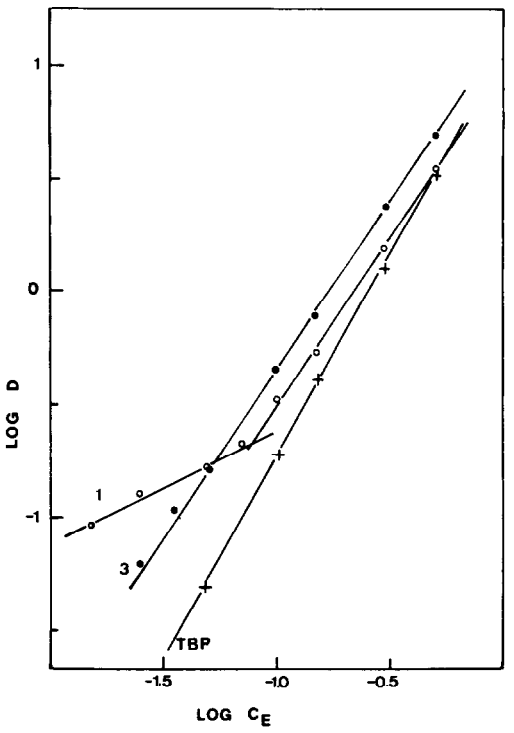

Fig. 2. Distribution coefficient of uranyl nitrate as a function of extractant concentration for the compounds 1, 3 and TBP.

Uranyl nitrate extraction

Distribution ratios obtained with compounds **1–4** do not depend upon the aqueous phase pH within all the studied pH range. Table 1 reports the D values at different pH extraction carried out with 0.5, 0.3 and 0.1 M concentrations of the compound **1**. Similar behaviour was noted for the compounds **2–4**. Therefore, we can consider these compounds as neutral extractants.

Figures 2 and 3 show the plots of log D for uranium against log C_E, C_E is the extractant concentration for the compounds **1–4** and TBP. The distribution ratios with the compounds **1–3** are somewhat greater than those obtained with TBP but this difference is more important at low concentrations for the compounds **1** and **2**. For the compound **4** the distribution ratios are lower than those of the analogous compound **2**. The difference particularly marked at low extractant concentration is due to the presence of the sulfur atom in the chain attaching the two phosphate groups. This result accounts for the participation of the heteroatomic chain in the extraction of uranyl nitrate in which the UO_2^{2+} cation is generally classified as a hard acid according to Pearson[14] and as A-type acceptor according to Ahrland *et al.*[15] Furthermore the interaction of the UO_2^{2+} cation with different donor atoms may be expected to follow the order O > S.

Table 1. Distribution ratios D with compound **1** at different concentrations (C_E) as a function of pH

	Distribution ratios D		
pH	C_E = 0.5 M	C_E = 0.3 M	C_E = 0.1 M
0.65	3.50	1.53	0.321
1.19	3.56	1.56	0.339
1.61	3.52	1.57	0.346
1.87	3.59	1.58	0.325
2.29	3.58	1.61	0.342
2.61	3.62	1.53	0.323

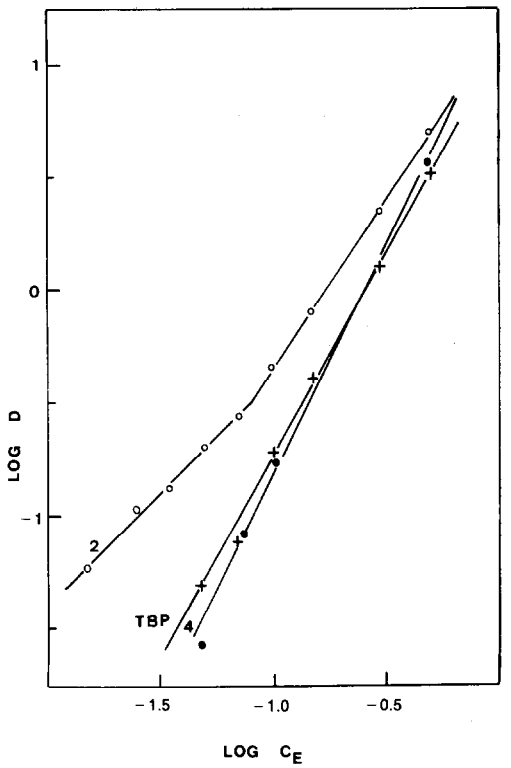

Fig. 3. Distribution coefficient of uranyl nitrate as a function of extractant concentration for the compounds **2**, **4** and TBP.

We can note that these compounds have different behaviours toward uranyl extraction within the extractant concentration range. A linear relationship is found for compounds **3**, **4** and TBP and two linear relationships describe the dependence of the log D against the log C_E for the compounds **1** and **2**.

Table 2 gives the slope values which correspond to the number of molecules coordinated to the uranyl nitrate. It was assumed that two nitrate ions are extracted with the uranyl cation as neutral extractant molecules, and the composition of the complex can be represented as follows $UO_2(NO_3)_2L_m$ in which L and *m* are respectively the extractant molecule and their number coordinated to the uranyl cation. As it was recently reported for tri-*n*-octylphosphine oxide[16] and octaethytetraamidopyrophosphate[5] this coordination number depends upon extractant molecular structure and extractant concentration in organic phase. Without further information about the molecular structure of such complexes, the

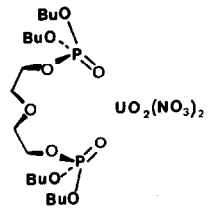

slope values could represent the average between two or more structures in equilibrium.

IR and NMR studies were made on complexes as oily compounds. ^1H, ^{13}C and ^{31}P NMR data were not very informative about the structure of the complexes since the spectra were practically unaffected by the presence of uranyl cation. In contrast we noted a marked reduction (80 cm^{-1}) in frequency at the P=O stretch band accompanying the complexation of uranyl cation.

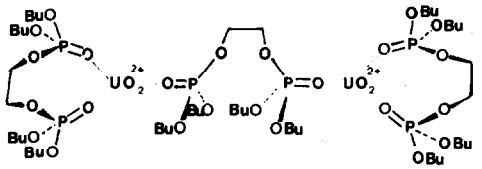

For the 0.025–0.07 M extractant concentration range, uranyl nitrate is extracted by compound **2** in the molar

Table 2. Number of extractant molecules coordinated with uranyl nitrate

Compound	C_E = 0.025 - 0.07 M		C_E = 0.1 - 0.5 M	
	Slope	Complex	Slope	Complex
TBP	1.8[a]	$UO_2(NO_3)_2L_2$	1.8[a]	$UO_2(NO_3)_2L_2$
1	0.5	$UO_2(NO_3)_2L_{0.5}$	1.5	$UO_2(NO_3)_2L_{1.5}$
2	1.0	$UO_2(NO_3)_2L$	1.5	$UO_2(NO_3)_2L_{1.5}$
3	1.5	$UO_2(NO_3)_2L_{1.5}$	1.5	$UO_2(NO_3)_2L_{1.5}$
4	2.0	$UO_2(NO_3)_2L_2$	2.0	$UO_2(NO_3)_2L_2$

a : value found in our experiment and that reported in reference (17)

ratio 1:1. The complex might be a chelate between uranyl nitrate and the two phosphoryl groups of extractant. This model is consistent with previous results obtained by Saisho,[6] Parker *et al.*[18] and Mikulski *et al.*[19] about neutral organophosphorus compounds containing two phosphoryl groups.

Only the compound **1** gives rise to a complex ratio 1:0.5 within the 0.025–0.07 M extractant concentration range and this might be represented as a dimer.

Complexes with stoichiometry $UO_2(NO_2)_2L_{1.5}$ are obtained with the compounds **1–3** for 0.1–0.5 M extractant concentrations and with compound **3** for 0.025–0.1 M extractant concentrations. The structure of such complexes could be dimeric as those of lanthanide nitrate complexes with *bis*-(di-disopropoxyphosphinyl)alkanes.[20] However the slope value 1.5 could also be analysed as an equilibrium between two complexes 1:1 and 1:2. Unlike compound **2**, a complex ratio 1:2 occurs with the analogous compound **4**. The present study illustrates that no important difference between distribution ratios of the compounds **1–4** and TBP was observed particularly at high extractant concentration. These results are supported by previous works about compounds behaving like bidentate ligands with respect to uranyl cation. Actually, it is difficult to draw comparisons between the extractant properties of various reported ligands such as TBPP,[4] OETAPP[5] and TBEDP,[6] since these studies have been carried out under different experimental conditions. However we can note that the distribution ratios obtained with the mentioned ligands stay relatively low.[5–7] For instance, a distribution ratio equal to 1 was reported with TBEDP ligand[6] at C = 0.1 M and 0.5 M HNO_3. Moreover this compound includes two phosphonate groups and it is well known that the extractant properties of these groups are far better than those of the less basic corresponding phosphate groups. It is worth mentioning that at low extractant concentrations, the heteroatomic chain of the compounds **1–4**. could be involved in the U(VI) complexation. This would explain the difference between the distribution ratios of the compounds **1–3** and TBP and the variation of the coordinated extractant number for the molecules **1–4**. The intramolecular complexation involving two phosphoryl groups of the same molecule could be more important at high extractant concentrations.

Synergism

Compounds **1–4** synthesized according to Moshkina's method[11] provide high distribution ratios and an influence of the aqueous phase acidity upon the distribution coefficients of uranium. Such effects can be easily explained by the presence of di-*n*-butylphosphoric acid (HDBP) as shown ^{31}P NMR spectra. It was already reported that a HDBP–TBP mixture[17] gives distribution ratios higher than the sum of those obtained with each of them under the same conditions. It was also found that in the solvent extraction of uranium (VI) with dialkylphosphorodithioic acids in benzene, TBP exhibits a synergistic effect.[21] As shown in the Table 3 a strong synergistic effect is observed with a mixture of compound **3** and HDBP.

The other compounds **1**, **2** and **4** lead to similar results. The data reported in Table 3 afford some evidences about the effect of HDBP upon the partition of the metal. We can note that compound **3** alone in toluene and 0.1 M concentration extracts in moderate amount the uranium from aqueous solution. Under the same condtions, toluene solutions of HDBP in 0.005, 0.01, 0.02 and 0.05 M and compound **3** in 0.1 M concentration extract the uranium with distribution coefficients which are respectively 14, 160, 350 and 280 times those obtained with compound **3** alone in 0.1 M concentration. An analogous effect is observed but less important when the HDBP concentration is maintained constant and different amounts of compound **3** are added. In both experiments the presence of large amounts of either added compound **3** or added HDBP produce an antagonistic effect. The latter must be assumed to be a strong interaction between HDBP and compound **3**.

Table 3. Distribution coefficients of uranyl nitrate with HDBP-compound **3** mixture[a]

Molar Concentration of compound 3	Molar concentration of HDBP 0	0.005	0.01	0.02	0.05
0	0	0.656	7.40	81.65	51.63
0.025	0.104	2.99	48.04	127.40	119.48
0.05	0.166	4.29	53.25	141.02	132.33
0.1	0.458	6.38	73.54	162.93	130.58
0.2	1.33	11.52	90.74	150.52	100.01

[a]All studies were carried out with an initial pH of aqueous phase equal to 2.1. This value decreases during the extraction, for instance the final pH of aqueous phase is 1.35 for a 0.05 M concentration of HDBP.

REFERENCES

[1a]G. M. Ritcey and A. W. Ashbrook, Solvent extraction. *Principles and Applications to Process Metallurgy.* Elsevier, Amsterdam (1979); [b]S. Gusmini and R. Nonnenmacher, Rep. CEA-R-4004 (1970); [c]G. W. Mason, S. McCarthy Lewey, D. M. Gilles and D. F. Peppard, *J. Inorg. Nucl. Chem.* 1978, **40**, 683. [d]G. W. Mason H. E. Griffin and D. F. Peppard, *J. Inorg. Nucl. Chem.* 1978, **40**, 677. [e]D. K. Koppikar, P. V. Sivapullaiah, L. Ramakrishnan and S. Soundararajan, Complexes of the lanthanides with neutral oxygen donor ligands. *Structure and Bonding*, Vol. 34, pp. 155–160, Springer-Verlag, Berlin Heidelberg (1978).

[2]G. Petrich and Z. Kolarik, Kernforschungszentrum Karlsruhe [Ber.], 1977, KFK 2536.

[3]D. Dryssen, J. O. Liljenzin and J. Rydberg, Solvent extraction chemistry. *Proc. Int. Conf. in Gothenburg*, Sweden. North Holland, Amsterdam (1967).

[4]J. Mikulski and K. A. Gravilov, *Kernenergie* 1966, **9**, 289.

[5]N. Jankowska, J. Kulawik and J. Mikulski, *J. Radional. Chem.* 1976, **31**, 9.

[6]H. Saisho, *Bull. Chem. Soc. Japan*, 1961, **34**, 1254.

[7]P. G. Eller and R. A. Penneman, *Inorg. Chem.* 1976, **15**, 2439.

[8]V. V. Yakshin, E. A. Filippov, V. A. Belov, G. G. Arkhipova, V. M. Abashkin and B. N. Laskorin, *Dokl. Akad. Nauk SSSR* 1978, **241**, 159.

[9]D. L. Williams and L. E. Deacon, *J. Inorg. Nucl. Chem.* 1977, **39**, 1079.

[10]E. N. Walsh, *J. Amer. Chem. Soc.* 1959, **81**, 9023.

[11]I. M. Moshkina and N. Pudovick, *Zh. Obshch. Khim.* 1962, **32**, 1671.

[12]T. Sato, H. Watanabe and M. Yamatake, *J. Appl. Chem. Biotechnol.* 1976, **26**, 697.

[13]D. G. Tuck, *J. Chem. Soc.* 1958, 2783.

[14]R. G. Pearson, *J. Am. Chem. Soc.* 1963, **85**, 3533.

[15]S. Ahrland, *Structure and Bonding*, Vol. 1, p. 207. Springer Verlag, Berlin-Heidelberg (1966).

[16]M. H. Konstantinova, *Dokl. Bolg. Akad. Nauk.* 1977, **30**, 1431.

[17]P. Moszkowicz, Rep. CEA-R-4735 (1976).

[18]J. R. Parker and C. V. Banks, *J. Inorg. Nucl. Chem.* 1965, **27**, 583.

[19]J. Mikulski and J. Vetulani, *J. Inorg. Nucl. Chem.* 1967, **29**, 209.

[20]W. E. Steward and T. H. Siddall III, *J. Inorg. Nucl. Chem.* 1968, **30**, 1513.

[21]I. Haiduc, G. H. Marcu, M. Curtui, *Rev. Roum. Chim.* 1977, **22**, 625.

Polyhedron Vol. 1, No. 9-10, pp. 689-692, 1982
Printed in Great Britain.

0277-5387/82/090689-04$03.00/0
Pergamon Press Ltd.

THE REACTION OF CARBON MONOXIDE WITH PLATINUM YLIDS

ROBERT D. GILLARD and MALCOLM F. PILBROW
Department of Chemistry, University College, Cardiff CF1 1XL, Wales

and

SUZANNE LEONARD, MELVYN C. RENDLE and CHARLES F. H. TIPPER*
Donnan Laboratories, The University, Liverpool L69 3BX, England

(*Received* 19 *February* 1982)

Abstract—The platinum(II) ylids $[X_2Pt\{CH(py)CH_2CH_3\}(py)]$ (X = Cl, Br; py = pyridine) react with carbon monoxide to give the platinum carbonyls $[CO(X_2)Pt\{CH(py)CH_2CH_2CH_3\}]$ which lose CO on heating or in solution. The platinum(IV) ylids $[Cl_4Pt\{CH(py)CH_2CH_3\}(py)]$ and $[Cl_2I(CH_3)Pt\{CH(py)CH_2CH_3\}(py)]$ also react with CO to give Pt(CO)-ylid compounds.

INTRODUCTION

Platina(IV)cyclobutane compounds readily isomerise to platinum ylids under appropriate conditions.[1] This reaction was established some years ago by Gillard *et al.*[2] They found that, on refluxing a solution of $[Cl_2PtCH_2CH_2CH_2(pyridine)_2]$ (I, Cl) in benzene for 10–15 min., the isomeric platinum(II) ylid $[Cl_2Pt\{CH(py)CH_2CH_3\}(py)]$ (I Cl) was formed. With $CHCl_3/CCl_4$ as solvent, refluxing for about 2 hr gave the platinum(IV) ylid $[Cl_4Pt\{CH(py)CH_2CH_3\}(py)]$ (III, Cl). However, on prolonged refluxing in $CHCl_3/CCl_4$, a solid (A) could be extracted, the IR spectrum of which was similar to those of the two ylids [2a] but which showed a strong absorption at about 2060 cm^{-1}. The elemental analyses for different samples were somewhat variable, but it was tentatively suggested that it was a platinum hydride $[H(Cl_3)Pt\{CH(py)CH_2CH_3\}(py)]$ contaminated with Cl_2Ptpy_2,[2a,3] the hydrogen coming from ethanol impurity in the trichloromethane, although no characteristic Pt–H signal in the ^{1}HNMR spectrum could be observed despite diligent search. We have now done further work to elucidate the nature of A, which in fact appears to be a Pt–CO(ylid) compound, and this has led us to investigate the reaction of carbon monoxide with the ylids. The compounds and the reactions involved are summarised in Scheme 1.

RESULTS AND DISCUSSION

Refluxing (I, Cl) in $CDCl_3/CCl_4$ for about 5 hr gave a solid which showed no IR absorption which could be attributed to Pt–D. On repeating in the presence of a little CD_3OD ($CDCl_3$ contains no alcohol impurity), the IR of the solid extracted was identical with that of A, including the absorption at 2060 cm^{-1}. Thus A can hardly be a platinum-hydride.

Platinum carbonyls with terminal CO groups show strong IR absorptions between 2050 and 2150 cm^{-1}.[4] The presence of CO in A is supported by the mass spectrum, which includes two sets of peaks (of the same pattern) centred on M/e 344 and 372, probably due to $[Cl_2Ptpy]^+$ and $[CO(Cl_2)Ptpy]^+$, respectively. On heating solid A *in vacuo* to about 130°C, both carbon monoxide and propene were detected in the gas phase. Thus, A is almost certainly an ylid related to (II, Cl) and [III, Cl] containing a Pt–CO moiety, but owing to the variables analyses, no more definite structure can be given. A compound (A, Br) similar to A is produced on prolonged refluxing of $[Br_2PtCH_2CH_2CH_2(py)_2]$ (I, Br) in $CHCl_3/CCl_4$. The IR spectrum again shows adsorption at 2060 cm^{-1}, and also at 330 cm^{-1} (Pt–Cl). Presumably (III, Cl) or $[Cl_2Br_2Pt\{CH(py)CH_2CH_3\}(py)]$ (III, Br) are first formed and react with CO produced slowly in the mixture at the boiling point.

On passing carbon monoxide through a solution of the ylid (II, Cl) in benzene at room temperature, the yellow colour faded rapidly and a pale-yellow solid (IV, Cl) eventually precipitated. This compound appears to have the structure:

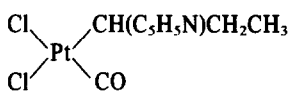

where CO has replaced the pyridine attached to the metal in (II, Cl) and the chlorines are now *cis* to each other (*trans* in (II, Cl)[2b]). Thus, the elemental analysis agrees with the formula $PtC_9H_{11}NCl_2O$. The IR spectrum of (IV, Cl), compared to that of (II, Cl)[2a], showed a very strong absorption at about 2080 cm^{-1} (PtC–O stretching[4]) and absorptions at 487, 497, 508, 556 and 568 cm^{-1} (Pt–CO stretching and Pt–C–O deformation[5]). The absorption at about 1600 cm^{-1} (C=C and C=N stretching vibrations of the pyridine attached to the platinum atom) is absent and there are two absorptions due to Pt–Cl stretching 330 and 280 cm^{-1}) indicating that the chlorine ligands are *cis* to each other.[-6] The mass spectrum includes two sets of peaks centred at M/e 344 and 372 (see A, above) and, on heating the solid, carbon monoxide was evolved. The *trans-cis* configurational change is not unexpected if the ylid ligand has some π-bonding character.[7]

The solid was soluble in methyl cyanide and dimethylsulphoxide giving greenish solutions. These were unstable, CO (but no hydrocarbons) being evolved slowly in the dark and very rapidly in daylight, the colour changing to a yellow brown. The ^{1}H NMR spectrum in $(CD_3)_2SO$ was nearly the same before and after photolysis (ylid hydrogens: CH, $\delta = 5.20$ [triplet, J(Pt-H) 103 Hz]; CH_2, $\delta = 2.4$ [Multiplet, partly obscured by H in

*Author to whom correspondence should be addressed.

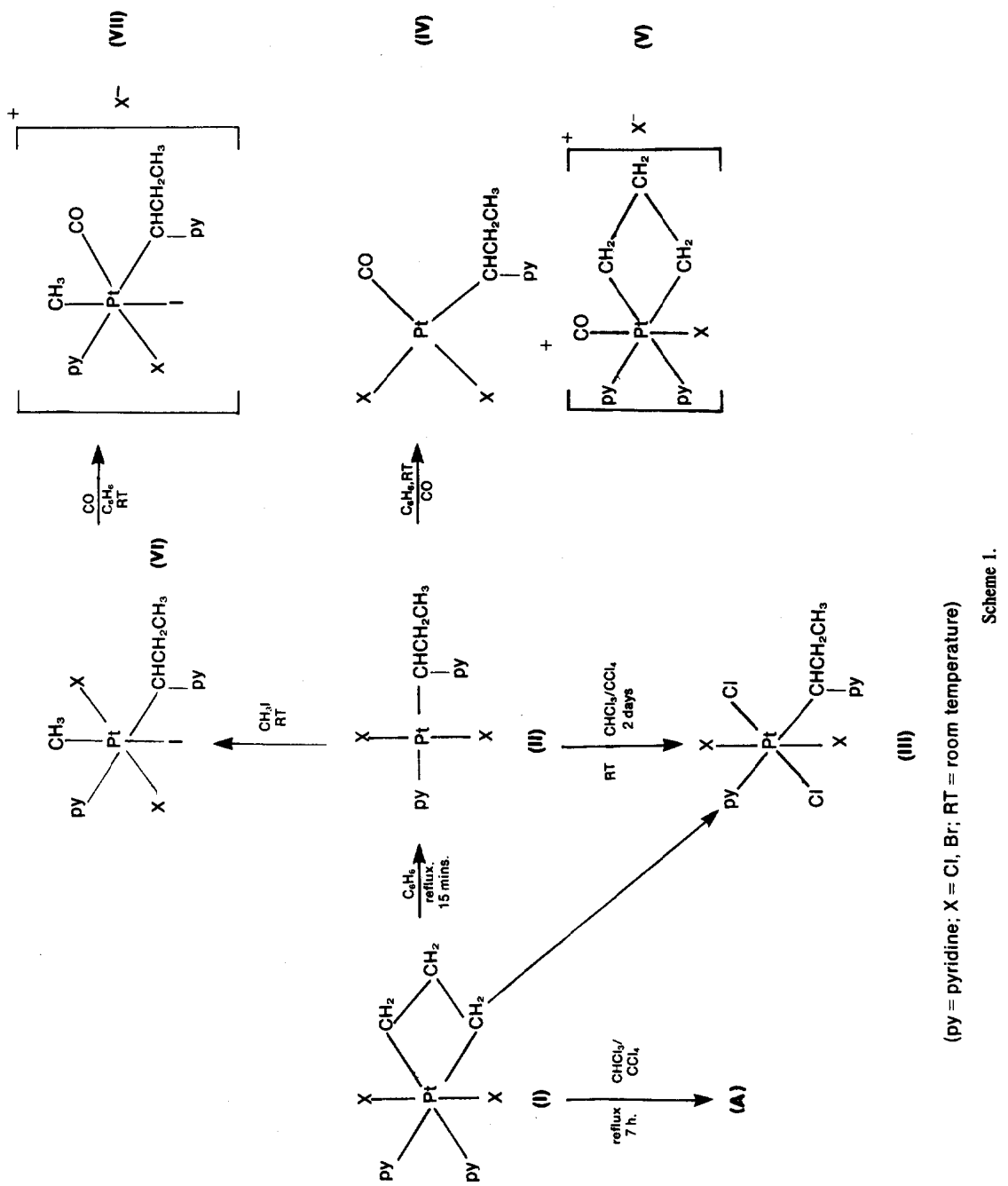
(VII)
(IV)
(V)
(VI)
(II)
(III)
(I)
(A)
CO
C6H6
RT
C6H6,RT
CO
CH3I
RT
C6H6
reflux
15 mins.
CHCl3/CCl4
2 days
RT
CHCl3/
CCl4
reflux
7 h.
py = pyridine; X = Cl, Br; RT = room temperature)

Scheme 1.

solvent]; CH_3, $\delta = 0.79$ [triplet] – c.f. (II, Cl) in $CDCl_3$:[2a] CH, $\delta = 5.57$ [$J(Pt\text{-}H)$ 115 Hz]; CH_2 $\delta = 2.43$ and 1.92; CH_3 $\delta = 1.07$) suggesting that the ligand trans to the ylid moiety (i.e. Cl) had not changed.

The ylid $[Br_2Pt\{CH(py)CH_2CH_3\}(py)]$ (II, Br) can be prepared from the corresponding platnacyclobutane (I, Br). Reaction with carbon monoxide gives the CO compound (IV, Br) corresponding to (IV, Cl).

On continuing to pass carbon monoxide through the solutions left after the carbonyls (IV, Cl) and (IV, Br) had been removed (see above) until all the benzene was driven off and then drying *in vacuo*, yellow-brown solids, (V, Cl) or (V, Br) were obtained. Reacting these with triphenyl-phosphine in dimethylsulphoxide gave large yields of cyclopropane, at least 50 times that from any traces of unchanged (I, Cl) or (I, Br) present. This indicates that at least most of the ylid left has been reconverted into a platinacyclobutane: the action of HI on (II, Cl) in benzene also gives a platinacyclobutane.[8] The IR spectra showed more than one absorption due to PtC–O stretching [(V, Cl): 2120, 2070 and 2035 cm^{-1}; (V, Br): 2115 and 2070 cm^{-1}] and a strong absorption at 1600 cm^{-1} (pyridine attached to platinum, see above) with no or weak absorption at 1625 cm^{-1} (ylid pyridine). There was also only one absorption due to Pt–Cl stretching (330 cm^{-1}). The elemental analysis of (V, Cl) indicated the presence of two pyridines. The results suggest that (V, Cl) and (V, Br) contain mainly platina(IV)cyclobutane carbonyls, probably $[X(CO)PtCH_2CH_2CH_2(py)_2]^+$ X^- (X = Cl, Br) which has three structural isomers with respect to PtCO, mixed with some (IV, Cl) or (IV, Br) (and probably X_2Ptpy_2[2]), the composition of the mixture depending on how much platinum was removed in the (IV, Cl) or (IV, Br) precipitate.

On passing CO through a benzene solution of the platinum(IV) ylid (III, Cl) at room temperature (see preparation of A above), the bright-yellow colour again faded and precipitation with pentane gave a solid, the IR and mass spectra of which are very similar to those of A. Unfortunately, the elemental analysis does not correspond to any simple formula.

Iodomethane oxidatively adds to the ylid (II, Cl) to give $[Cl_2I(CH_3)Pt\{CH(py)CH_2CH_3\}(py)]$(VI).[8] This platinum (IV) ylid reacts with CO in benzene solution to give the addition compound, presumably $[ClI(CH_3)(CO)Pt\{CH(py)CH_2CH_3\}(py)]^+Cl^-$(VIII). Until now platinum(IV) carbonyls have only been obtained in solution.[6,9]

EXPERIMENTAL

The ylids $[Cl_2Pt\{CH(py)CH_2CH_3\}(py)]$ (II, Cl) and $[Cl_4Pt\{CH(py)CH_2CH_3\}(py)]$ (III, Cl) were prepared by the method of Gillard *et al.*[2]

$[Br_2Pt\{CH(C_5H_4N)CH_2CH_3\}(C_5H_5N)]$(II, Br)

$[Br_2PtCH_2CH_2CH_2(py)_2]$ (I, Br) was prepared as previously described.[10] On refluxing a solution in benzene for 15 min. the colour turned yellow-brown. Addition of excess pentane gave a yellow brown solid: yield, 70%, m.pt 143°C with decomposition. Found; C, 28.12; H, 2.95; N, 4.18. Calc. for $C_{13}H_{16}N_2Br_2Pt$ C, 28.11; H, 2.88; N, 5.05%. The infra-red spectrum showed bands at (cm^{-1}); 3060m, 3030w, 2950m, 2915w, 2860w, 2840w, 1618m, 1589s, 1492s, 1477vs, 1444vs, 1370w, 1348w, 1273w, 1247w, 1238m, 1211s, 1190w, 1161m, 1149m, 1098w, 1068s, 1043m, 1011m, 945w, 936w, 913w, 882w, 848w, 817m, 768vs, 735w, 700vs, 675vs, 639w, 612w, 479w, 445w (see II, Cl[2a]). The mass spectrum included sets of perks centred on (M/e): 273 $[PtC_5H_4N]^+$, 352 $[pyPtC_5H_4N]^+$ and/or $[BrPtC_5H_4N]^+$, 432 $[BrPtpy_2]^+$ and/or $[Br_2Ptpy]^+$, 511 $[Br_2Ptpy_2]^+$, 553 (mol. ion).

(A, Br)

A solution of (I, Br) in a mixture of $CHCl_3/CCl_4$ (1:1 by vol) was refluxed for 6 hr. Addition of hot petroleum ether (40–60) to the hot solution gave a pale brown solid. Infra-red bands at (cm^{-1}): similar to (II, Br) above plus 2070s, 538w, 497w, 325m (broad). The mass spectrum included peaks centred on (M/e): 273 $[PtC_5H_4N]^+$, 352 $[pyPtC_5H_4N]^+$ and/or $[BrPtC_5H_4N]^+$, 353 $[Ptpy_2]^+$ and/or $[BrPtpy]^+$ and/or $[Br_2Pt]^+$, 381[(CO)$Ptpy_2$]$^+$ and/or $[(CO)BrPtpy]^+$, 432 $[BrPtpy_2]^+$ and/or $[Br_2Ptpy]^+$, 460 $[(CO)Br_2Ptpy]^+$ and/or $[(CO)BrPtpy_2]^+$, 511 $[Br_2Ptpy_2]^+$.

cis-$Cl_2(CO)Pt\{CH(C_5H_5N)CH_2CH_3\}$(IV,Cl)

A yellow solution of the ylid (II, Cl) was prepared from 0.1g $[Cl_2PtCH_2CH_2CH_2(py_2)]$ dissolved in the minimum volume of warm benzene (10–20 cm^3) by refluxing for 10 min.[2] Carbon monoxide was passed through the solution at room temperature for 2 hr. The colour faded and after leaving the solution saturated with CO overnight, a very pale yellow solid precipitated. This was filtered off, washed with pentane and dried in vacuo: yield, 70–80%; m.pt. 145°C with decomposition. Found: C, 26.4; H, 2.64; N 3.38. Calc. for $C_9H_{11}NCl_2OPt$: C, 26.0; H, 2.65; N, 3.37% IR bands (cm^{-1}): 3120w, 3075m, 3065m, 3030w, 2960m, 2935m, 2870m, 2080vs (tails), 2030w, 1625s, 1579w, 1482s, 1461s, 1414w, 1384w, 1375w, 1338w, 1321w, 1286w, 1245w, 1214w, 1187m, 1167m, 1132m, 1110m, 1069w, 1057w, 1029w, 1013w, 972w, 945w, 916w, 859w, 827m, 781s, 758w, 749w, 698s, 678s, 633w, 568m, 556s, 508m, 497m, 487m, 433w, 400w, 330s, 280s (broad). The mass spectrum included peaks centred on (M/e): 273 $[PtC_5H_4N]^+$, 308 $[ClPtC_5H_4N]^+$, 344 $[Cl_2Ptpy]^+$, 372 $[(CO)Cl_2Ptpy]^+$. Thermal decomposition of the solid at about 130°C gave CO and propene.

$Br_2(CO)Pt\{CH(C_5H_5N)CH_2CH_3\}$(IV, Br)

This was prepared in the same way as (IV, Cl); yield 60–70%; m.pt. 158°C with decomposition. Found: C, 21.8; H, 2.22; N. 2.78. Calc. for $C_9H_{11}NBr_2OPt$: C, 21.5; H, 2.18; N, 2.78%. IR similar to (IV, Cl) above but bands below 400 cm^{-1} missing. The mass spectrum includes peaks centred on (M/e): 273 $[PtC_5H_4N]^+$, 301 $[(CO)PtC_5H_4N]^+$, 352 $[BrPtC_5H_4N]^+$, 381 $[(CO)BrPtpy]^+$, 432 $[Br_2Ptpy]^+$, 460 $[(CO)Br_2Ptpy]^+$.

Reaction of CO *with* $[Cl_4Pt\{CH(C_5H_5N)CH_2CH_3\}(C_5H_5N)]$ (III, Cl)

The ylid (III, Cl) was dissolved in the minimum volume of benzene and carbon monoxide passed through at room temperature for 5 h. The bright yellow colour of the solution faded. The product, extracted by precipitation with pentane, was a light yellow-brown solid; yield 40–50%; m.pt. 148°C with decomposition. Found: C, 31.9; H, 3.39; N, 4.58%. IR: similar to (A, Br) above. The mass spectrum includes sets of peaks centred on (M/e). 230 $[ClPt]^+$, 273 $[PtC_5H_4N]^+$, 308 $[ClPtC_5H_4N]^+$, 344 $[Cl_2Ptpy]^+$, 372 $[(CO)Cl_2Ptpy]^+$, 388 $[ClPtpy_2]^+$, 422 $[Cl_2Ptpy(C_5H_4N)]^+$.

$[ClI(CH_3)(CO)Pt\{CH(py)CH_2CH_3\}(py)]^+Cl^-$(VII)

A solution of the ylid (II, Cl) in benzene was prepared as above and excess CH_3I added (~1 cm^3), CO was passed through the solution until all the volatiles appeared to have been driven off. The solid remaining was dried *in vacuo*, washed with benzene and again dried *in vacuo* giving a yellow powder. Found: C, 28.5; H, 3.13; N, 4.50. Calc. for $C_{15}H_{19}N_2OCl_2IPt$: C, 28.3; H, 2.99; N, 4.40%. The IR spectrum was almost the same as that of $[Cl_2I(CH_3)Pt\{CH(py)CH_2CH_3\}(py)]$,[8] except for a strong adsorption at 2060 cm^{-1}.

ANALYSIS

The IR spectra of the solids in KBr discs were obtained using a Perkin–Elmer grating spectrometer 577, and mass spectra using a VG micromass/2 with solid probe.

The solids were decomposed *in vacuo* and the reactions with PPh_3 performed in an apparatus which was a slight modification

of that already described.[11] The hydrocarbons were determined by GLC using a squalane column[11] and CO using a molecular sieve 5A column.

Acknowledgements—We wish to acknowledge the early work of M. Keeton and one of us (M.C.R.) thanks the Science Research Council for a maintenance grant.

REFERENCES

[1]R. J. Puddephatt, *Coord. Chem. Rev.* 1980, **33**, 149.
[2a]R. D. Gillard, M. Keeton, R. Mason, M. F. Pilbrow and D. R. Russell, *J. Organometal. Chem.* 1971, **33**, 247; [b]M. Keeton, R. Mason and D. R. Russell, *J. Organometal. Chem.* 1971, **33**, 259.
[3]M. Keeton, Thesis, University of Sheffield, 1967; M. F. Pilbrow, Thesis, University of Kent, 1970.
[4]P. S. Braterman, *Metal Carbonyl Spectra.* Academic Press, New York (1975).
[5]P. L. Goggin and R. J. Goodfellow, *J. Chem. Soc., Dalton,* 1973, 2355.
[6]U. Belluco, *Organometallic and Coordination Chemistry of Platinum.* Academic Press, New York (1974).
[7]See, for example, J. Chatt, N. P. Johnson and B. L. Shaw, *J. Chem. Soc.* 1964, 1662.
[8]R. J. Puddephatt, M. C. Rendle and C. F. H. Tipper, to be published.
[9]C. Crocker, P. L. Goggin and R. J. Goodfellow, *J. Chem. Soc. Chem. Comm.* 1978, 1056.
[10]S. E. Binns, R. H. Cragg, R. D. Gillard, B. T. Heaton and M. R. Pilbrow, *J. Chem. Soc.* 1969, 1227.
[11]D. C. L. Perkins, R. J. Puddephatt and C. F. H. Tipper, *J. Organometal. Chem.* 1980, **186**, 419.

Polyhedron Vol. 1, No. 9-10, pp. 693-699, 1982
Printed in Great Britain.

0277-5387/82/090693-07$03.00/0
Pergamon Press Ltd.

OPTICAL ACTIVITY IN MIXED-LIGAND TERBIUM COMPLEXES CONTAINING 5-SULFOSALICYCLIC ACID AND CHIRAL HYDROXYCARBOXYLIC ACIDS

ROBERT A. COPELAND and HARRY G. BRITTAIN*†
Chemistry Department, Seton Hall University, South Orange, NJ 07079, U.S.A.

(*Received* 15 *March* 1982)

Abstract—The optical activity associated with the *f–f* emission bands of Tb(III) complexes which contain chiral hydroxycarboxylic acids has been studied by means of circularly polarized luminescence (CPL) spectroscopy. Complexes having the general formula $Tb(SSA)_2(L)$ were studied (where SSA signifies 5-sulphosalicylic acid), with the chiral ligand (L) being L-lactic acid, L-mandelic acid, L-aspartic acid, and L-malic acid. The CPL spectra were found to be sensitive to the mode of bonding between the metal and the chiral ligand and therefore allowed predictions to be made regarding how the hydroxycarboxylic acid ligands attach to the Tb(III) ion. Also, the degree of optical activity varied systematically with the concentration of chiral ligand, and we have used this dependence to calculate formation constants for the addition of a hydroxycarboxylic acid ligand to the Tb/SSA complex. Finally, the line shape and magnitudes of the CPL spectra provide information regarding the type of chirality experienced by the Tb(III) ion.

INTRODUCTION

In recent years the study of optical activity in transition metal complexes has been greatly facilitated by the emergence of such techniques as circular dichroism, and optical rotatory dispersion. These techniques are of great utility in studying optical activity associated with the *d–d* bands of these complexes, but are of little use in studying *f–f* optical activity in chiral lanthanide complexes. Recently, however, the technique of circularly polarized luminescence (CPL) has received a great deal of attention as a convenient method for studying optical activity in lanthanides.[1-4]

Unlike the other aforementioned chiroptical techniques CPL allows one to study, directly, the chirality associated with the molecular emitting states rather than ground state phenomena.[2] This is quite advantageous for the study of the highly luminescent lanthanide complexes. As a result, many papers have appeared in which the technique of CPL spectroscopy has been utilized to observe optical activity of various mixed ligand complexes of Tb(III) and Eu(III).[3-7]

In an earlier paper we have detailed the complexation of chiral hydroxycarboxylic acids with complexes of Tb(DPA) (where DPA is pyridine - 2,6 - dicarboxylic acid), and have shown how the optical activity of the complex can be influenced by the addition of the hydroxycarboxylic acids and other chiral ligands.[6]

With the exception of glycolic acid (hydroxyacetic acid) all α-hydroxycarboxylic acids can be resolved into optical isomers, and one would anticipate that the interactions between lanthanide ions and these ligands could best be studied by chiroptical techniques. Circular dichroism studies revealed that the spectra associated with Pr(III) complexes were complicated and that the overlapping nature of the *f–f* absorptions prevented effectual use of the data.[8]

In the present work we have used CPL spectroscopy to study mixed-ligand Tb(III) complexes of sulphosalicylic acid (SSA) with chiral hydroxycarboxylic acids. The sulphosalicylic acid ligand, shown in Fig. 1, binds in a bidentate fashion to Tb(III), forming a *bis*-complex which leaves room for additional ligands to complete the coordination sphere.[9] Normally the extra ligating sites are filled by solvent molecules, but in the presence of the hydroxycarboxylic acids mixed ligand complexes are formed. The hydroxycarboxylic acids used in the present investigation were; L-lactic acid, L-malic acid, L-mandelic acid, and L-aspartic acid. The structures of these ligands are shown in Fig. 2.

Also, a method for evaluating the equilibria associated with mixed-ligand complexes of Tb(III) has been reported in an earlier paper.[6] We have made use of this method for the mixed-ligand complexes investigated here, and report formation constants for them.

EXPERIMENTAL

Tb(III) solutions were prepared by dissolving a weighed amount of Tb_4O_7 (99.96% pure, Kerr-McGee) in the minimum amount of 70% $HClO_4$, neutralizing to pH 3 with NaOH, and then diluting to the desired volume. A sufficient amount of $NaClO_4$ was then added to ensure that the final ionic strength was 0.1 M. L-lactic acid (LAC) was purchased from Eastman, as were L-malic acid (MAL), L-mandelic acid (MAN), and L-aspartic acid (ASP). The sulpho-salicylic acid was obtained from Aldrich. All materials were used as received.

Solutions containing 1:2 ratio of Tb(III) and SSA prepared from concentrated stock solutions, with the final Tb(III) concentration being 17 mM. For each system, varying amounts of each hydroxycarboxylic acid was added in turn, with ratios of Tb(III): carboxylic acid ranging from 1:0.5 to 1:10.

All CPL spectra were recorded on a high-resolution luminescence spectrometer constructed in our laboratory, whose operation and features have been previously reported.[7] All samples were excited at 303 nm (obtained from a 200 W Hg-Xe arc lamp and selected by a 0.1 m grating monochromater), corresponding to irradiation of the SSA ligand. Very strong Tb(III) emission was observed, and CPL spectra could be recorded for a varying number of Tb(III) luminescence bands depending on the attached chiral ligand. An emission bandpass of 10 A was used for all

*Author to whom correspondence should be addressed.

†Teacher-Scholar of the Camille and Henry Dreyfus Foundation, 1980-85.

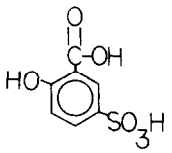

Fig. 1. Structure of 5-Sulphosalicylic acid.

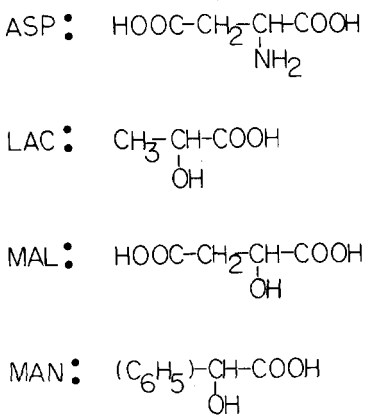

Fig. 2. Structures of the carboxylic acid substrates.

work. All studies were obtained in aqueous solution at room temperature.

pH adjustment of the solutions was carried out by adding microliter amounts of standard NaOH or $HClO_4$ directly to the fluorescence cuvette, with pH being read on an Orion 701A pH meter. The pH was obtained by inserting a glass microcombination electrode directly into the cuvette, and this electrode was calibrated daily with phosphate buffers.

RESULTS

The addition of any of the hydroxycarboxylic acids, shown in Fig. 2, to a solution containing 1:2 Tb:SSA results in the appearance of CPL in the terbium emission bands. All of the emissions originate in the $^5D_4$ excited state, and transitions to the $^7F_3$(620 nm), $^7F_4$(580 nm), $^7F_5$(545 nm) and $^7F_6$(490 nm) J levels of the ground state can be observed. Of the above transitions, the $^5D_4 \rightarrow {}^7F_5$ transition is the most intense and was found to exhibit the greatest degree of CPL. The $^5D_4 \rightarrow {}^7F_3$ and $^5D_4 \rightarrow {}^7F_4$ transitions were extremely weak; so much so that except for solutions of malic acid, no meaningful data could be obtained at these wavelengths. The $^5D_4 \rightarrow {}^7F_6$ transition appears at 490 nm. Unfortunately, this overlaps with emission from the sulphonsalicylic acid and as a result no meaningful data could be obtained at this wavelength for any of the chiral ligands investigated. Therefore, the bulk of the data presented here is that of the $^5D_4 \rightarrow {}^7F_5$ transition.

Simple mixing of 1:2 mol ratios of Tb(III) and SSA resulted in the formation of the $Tb(SSA)_2$ complex since the formation constants associated with the addition of each ligand are log K_1 8.42 and log K_2 6.19.[9] Addition of L-lactic, L-mandelic acid, L-malic acid, or L-aspartic acid led to the observation of strong CPL. Spectra were taken in the pH range of 2.0–10.0. For L-lactic and L-mandelic acid the CPL intensity was nearly constant at low pH, but then started to decrease rapidly above pH 6.0. In the case of aspartic acid, the opposite pattern was observed. That is, at low pH the CPL intensity was again constant, but above pH 6.0 the intensity rapidly increased up to about pH 7.5 where it once again leveled off. This pattern suggests that at high pH the aspartic acid is binding in a bidentate fashion (through its second carboxylic acid group) to the Tb/SSA complex in much the same manner as has been reported for the aspartic acid complexes of Tb/DPA.[7]

While the intensity of the CPL signal varied with pH for these ligands, the line shape remained invariant over the entire pH range. This was not true, however, in the case of L-malic acid. With malic acid we observed some rather peculiar behavior. At low pH the line shape of the malic acid complexes resembled, very closely, that of complexes of aspartic acid. However, at high pH (above 7.0) the sign of the CPL signal inverted. This is not the first time that such behavior has been noted. In previous papers we have observed CPL sign inversion, at high pH, in complexes of malic acid with Tb(DPA), and $Tb(DPA)_2$.[1,10] We have shown that this anomalous behaviour can be attributed to a change from bidentate binding (at low pH) to terdentate binding (at high pH) of the malic acid in complexes with Tb/DPA.[1,10] It now seems likely that the same binding pattern can be assigned to the malic acid complexes with Tb/SSA.

Examples of typical CPL spectra are presented here for the mixed ligand complexes of; lactic acid (Fig. 3), mandelic acid (Fig. 4), aspartic acid (Fig. 5), and malic acid (Figs. 6–9).

We generate two observables during the course of a CPL determination. One of these is the total luminescence (TL) intensity, given by eqn (1), and the other is the CPL intensity, given by eqn (2), where I_L and I_R represent the emitted intensities of the left- and right-circularly polarized light, respectively

$$I = \frac{1}{2}(I_L + I_R) \quad (1)$$

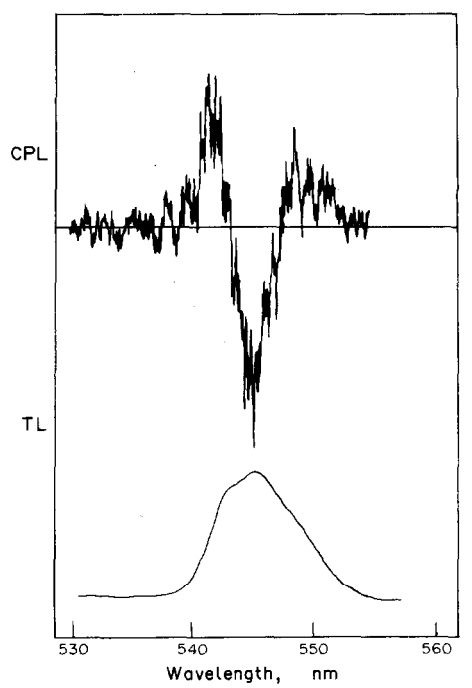

Fig. 3. TL (lower) and CPL (upper) spectra obtained for $Tb(SSA)_2$/L-lactic acid complex at pH 4.00 within the $^5D_4 \rightarrow {}^7F_5$ transition.

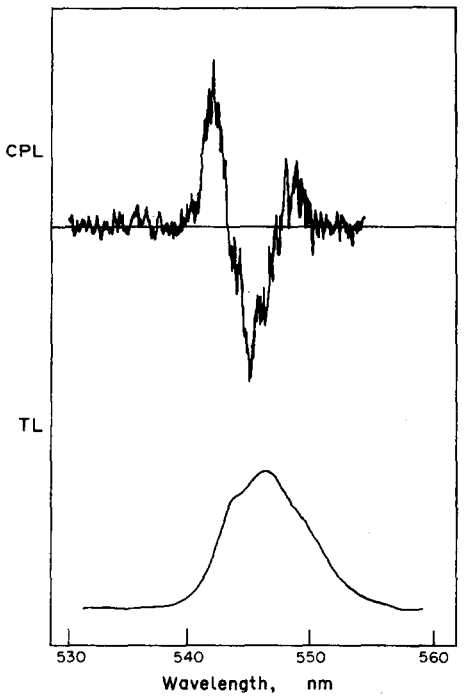

Fig. 4. TL (lower) and CPL (upper) spectra obtained for $Tb(SSA)_2$/L-mandelic acid complex at pH 2.60 within the $^5D_4 \rightarrow {}^7F_5$ transition.

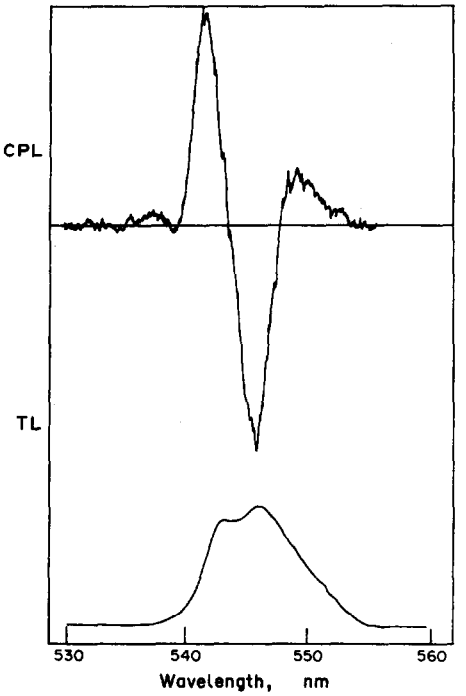

Fig. 6. TL (lower) and CPL (upper) spectra obtained for $Tb(SSA)_2$/L-malic acid complex at pH 8.80 within the $^5D_4 \rightarrow {}^7F_5$ transition.

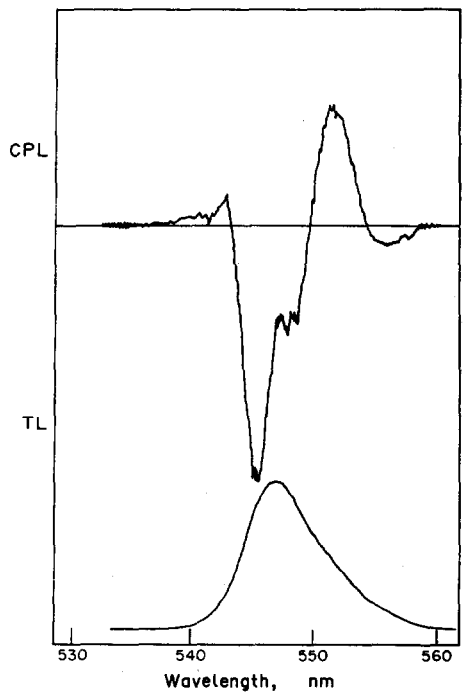

Fig. 5. TL (lower) and CPL (upper) spectra obtained for $Tb(SSA)_2$/L-aspartic acid complex at pH 9.00 within the $^5D_4 \rightarrow {}^7F_5$ transition.

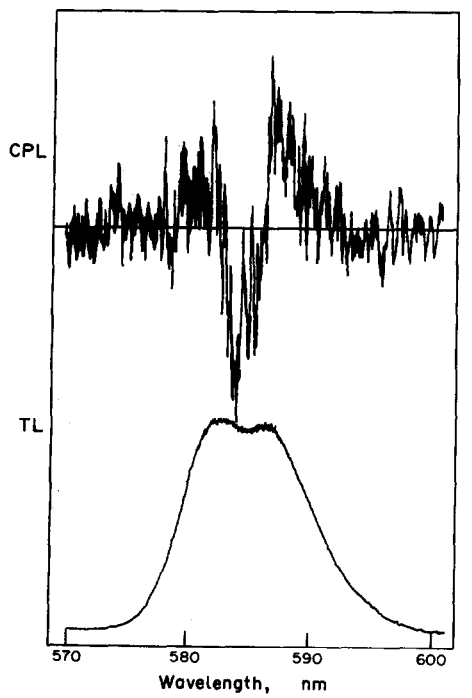

Fig. 7. TL (lower) and CPL (upper) spectra obtained for $Tb(SSA)_2$/L-malic acid complex at pH 8.80 within the $^5D_4 \rightarrow {}^7F_4$ transition.

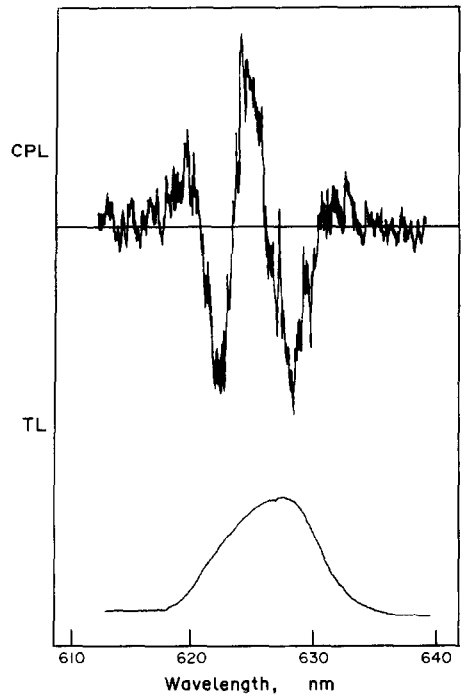

Fig. 8. TL (lower) and CPL (upper) spectra obtained for $Tb(SSA)_2$/L-malic acid complex at pH 8.80 within the $^5D_4 \rightarrow {}^7F_3$ transition.

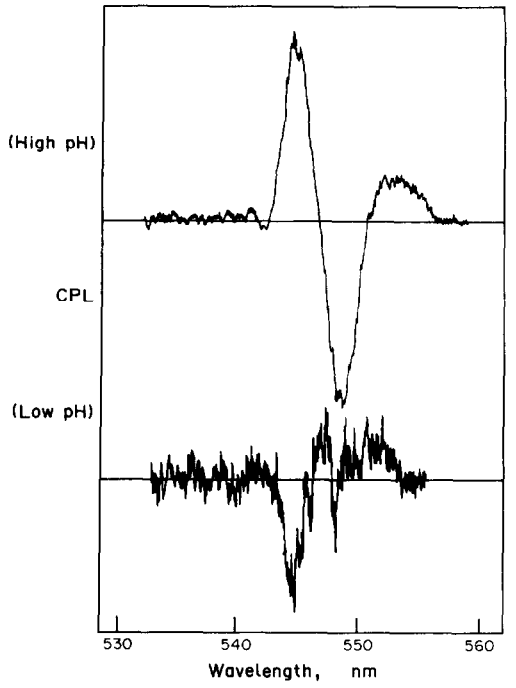

Fig. 9. CPL spectra of $Tb(SSA)_2$/L-malic acid complex at high pH (8.80) (upper) and low pH (5.12) (lower) within the $^5D_4 \rightarrow {}^7F_5$ transition.

$$\Delta I = I_L - I_R. \quad (2)$$

It is possible to eliminate the unit dependence associated with these two quantities by taking their ratio; this results in a parameter which is termed the luminescence dissymmetry factor (eqn 3)

$$g_{lum} = \Delta I/I. \quad (3)$$

This dissymmetry factor has both theoretical and experimental significance, as it may be related to the rotational strength of the transition.[2]

Values of g_{lum} were calculated for each Tb/SSA complex at several pH values. These results are presented in Tables 1–4 for complexes with L-lactic, L-mandelic, L-aspartic and L-malic acids, respectively.

In a previous paper we have outlined a method for calculating the formation constants for mixed ligand complexes of Tb(III).[6] We can take advantage of this method for the mixed ligand complexes described here. Knowing the large values of the association constants of Tb(III) and SSA,[9] and the low values for the association constants of Tb(III) and α-hydroxycarboxylic acids (ranging from 300 to 800),[11] it becomes clear that the chiral ligands investigated here would not be able to displace a SSA ligand. Therefore, the magnitude of the CPL intensity must be proportional to the extent of complexation between the Tb/SSA complexes and the chiral ligands. Clearly no CPL can be associated with the unbound Tb/SSA complex, and so it is apparent that if one molecule of chiral ligand is bound per molecule of complex, the mol. fraction of unbound Tb/SSA complex is given by eqn (4)

$$X_{LN} = (g_F - g_i)/g_F \quad (4)$$

where g_F is the dissymmetry factor value reached after addition of excess chiral ligand, and g_i is the dissymmetry factor value at the concentration of interest. Knowing this mol. fraction, and the starting concentrations for all materials, one can calculate the association constant for the following reaction:

$$Tb(SSA)_2^+ + L^- \longrightarrow Tb(SSA)_2L. \quad (5)$$

These association constants, for the mixed ligand complexes investigated here are presented in Table 5.

DISCUSSION

Review of Figs. 3–9 illustrates the dependence of the CPL line shape on the mode of binding of the chiral ligand to the Tb(III) ion. One notes immediately that the line shape for complexes with lactic acid and mandelic acid are identical to one another and indicative of the bidentate binding which must occur in these complexes. The line shape of these ligands contrasts sharply with that obtained for aspartic acid complexes (at all pH). This difference can be attributed to the ability of aspartic acid to form bidentate chelate rings through the two carboxylic acid groups on the molecule, rather than through one carboxylic acid group and one hydroxide group as is the case with lactic and mandelic acids. This distinction becomes important when one draws attention to the Tb/SSA complexes of malic acid.

Referring to Fig. 9 one notes that at low pH the CPL line shape for the malic acid complexes is practically identical to that obtained for aspartic acid. At high pH, however, the line shape changes drastically (inverts) and in fact has some resemblance to the line shapes obtained for the complexes of lactic, and mandelic acid. Now, as we mentioned earlier the anomalous behavior of the

Table 1. g_{lum} values for various mol. ratios of $Tb(SSA)_2$/L-lactic acid at varying pH

LAC/Tb Ratio	pH	g_{lum}
1.0	1.99	-0.0081
1.0	2.42	-0.0081
1.0	3.05	-0.0087
1.0	5.85	-0.0150
1.0	6.48	-0.0055
1.0	7.07	-0.0058
1.0	9.55	-0.0044
2.0	1.95	-0.0116
2.0	2.48	-0.0099
2.0	2.98	-0.0110
2.0	3.94	-0.0117
2.0	5.60	-0.0094
2.0	6.40	-0.0083
2.0	7.40	-0.0045
2.0	9.03	-0.0054
3.0	1.85	-0.0153
3.0	2.35	-0.0125
3.0	3.01	-0.0118
3.0	5.16	-0.0115

Table 2. g_{lum} values for various mol. ratios of $Tb(SSA)_2$/L-mandelic acid at varying pH

MAN/Tb Ratio	pH	g_{lum}
1.0	1.98	-0.0116
1.0	2.53	-0.0116
1.0	3.09	-0.0149
1.0	3.90	-0.0155
1.0	5.42	-0.0118
1.0	5.97	-0.0092
1.0	7.18	-0.0050
1.0	8.16	-0.0026
1.0	9.98	-0.0029
2.0	1.95	-0.0157
2.0	2.57	-0.0211
2.0	3.20	-0.0233
2.0	4.70	-0.0237
2.0	6.07	-0.0173
2.0	7.09	-0.0092
2.0	8.05	-0.0045
2.0	9.65	-0.0036
3.0	1.89	-0.0135
3.0	2.28	-0.0245
3.0	3.07	-0.0231

Table 3. g_{lum} values for various mol. ratios of $Tb(SSA)_2$/L-aspartic acid at varying pH

ASP/Tb Ratio	pH	g_{lum}	ASP/Tb Ratio	pH	g_{lum}
0.50	3.04	0.0000	3.00	6.30	-0.0131
0.50	5.20	0.0000	3.00	7.27	-0.0254
0.50	7.11	-0.0079	3.00	8.23	-0.0331
0.50	7.30	-0.0098	3.00	9.02	-0.0387
0 50	7.52	-0.0107	5.00	3.45	0.0000
0.50	7.65	-0.0096	5.00	3.77	0.0000
0.50	7.81	-0.0098	5.00	4.22	0.0000
0.50	7.95	-0.0101	5.00	4.65	0.0000
0.50	8.27	-0.0122	5.00	5.38	-0.0057
0.50	8.42	-0.0075	5.00	6.18	-0.0084
0.50	8.53	-0.0071	5.00	7.36	-0.0248
0.50	8.79	-0.0084	5.00	7.54	-0.0268
0.50	8.89	-0.0069	5.00	7.72	-0.0270
0.50	8.99	-0.0120	5.00	7.82	-0.0283
0.50	9.30	-0.0081	5.00	8.02	-0.0270
0.50	9.43	-0.0076	5.00	8.20	-0.0296
0.50	9.51	-0.0078	5.00	8.40	-0.0287
0.50	9.60	-0.0090	5.00	8.60	-0.0287
0.50	9.76	-0.0062	5.00	8.74	-0.0292
0.50	10.10	-0.0066	5.00	9.02	-0.0305
1.00	2.16	-0.0106	5.00	9.23	-0.0290
1.00	3.52	-0.0080	5.00	9.35	-0.0286
1.00	4.52	-0.0047	5.00	9.44	-0.0222
1.00	5.38	-0.0063	5.00	9.62	-0.0199
1.00	5.90	-0.0075	5.00	9.72	-0.0293

Table 3. (*Contd*)

ASP/Tb Ratio	pH	g_{lum}	ASP/Tb Ratio	pH	g_{lum}
1.00	6.44	-0.0100	5.00	9.95	-0.0158
1.00	7.23	-0.0197	10.00	3.61	-0.0130
2.00	2.68	-0.0060	10.00	5.43	-0.0242
2.00	3.16	-0.0059	10.00	7.20	-0.0623
2.00	4.01	-0.0066	10.00	7.71	-0.0462
2.00	4.61	-0.0062	10.00	8.12	-0.0513
2.00	5.60	-0.0085	10.00	8.43	-0.0505
2.00	6.06	-0.0101	10.00	8.60	-0.0462
2.00	7.18	-0.0212	10.00	8.70	-0.0523
2.00	9.60	-0.0299	10.00	8.95	-0.0439
3.00	2.37	-0.0079	10.00	9.36	-0.0360
3.00	2.99	-0.0053	10.00	9.60	-0.0375
3.00	3.94	-0.0084	10.00	9.78	-0.0288
3.00	5.63	-0.0116	10.00	9.92	-0.0350

Table 4. g_{lum} values for various mol. ratios of Tb(SS-)$_2$/L-malic acid at varying pH

MAL/Tb Ratio	pH	g_{lum}	MAL/Tb Ratio	pH	g_{lum}
0.50	2.25	-0.0073	2.50	9.07	0.0586
0.50	2.96	-0.0058	2.50	9.96	0.0416
0.50	3.18	-0.0101	5.00	2.44	-0.0122
0.50	3.41	-0.0117	5.00	3.28	-0.0245
0.50	4.70	-0.0123	5.00	4.39	-0.0271
0.50	5.84	-0.0091	5.00	5.95	-0.0268
0.50	6.02	-0.0064	5.00	7.19	-0.0118
1.25	3.11	-0.0137	5.00	7.31	0.0042
1.25	4.30	-0.0206	5.00	7.38	0.0076
1.25	5.64	-0.0200	5.00	7.48	0.0174
1.25	6.79	0.0159	5.00	7.55	0.0214
1.25	7.08	0.0271	5.00	7.75	0.0254
1.25	7.30	0.0394	5.00	7.95	0.0403
1.25	7.55	0.0438	5.00	8.20	0.0506
1.25	7.73	0.0458	5.00	8.35	0.0603
1.25	8.00	0.0470	5.00	8.67	0.0548
1.25	8.28	0.0450	5.00	8.85	0.0592
1.25	8.50	0.0412	5.00	8.99	0.0573
1.25	8.82	0.0387	5.00	9.17	0.0581
1.25	9.14	0.0323	5.00	9.43	0.0579
1.25	9.58	0.0322	10.00	2.46	-0.0076
2.50	2.50	-0.0146	10.00	3.13	-0.0272
2.50	3.61	-0.0409	10.00	4.07	-0.0256
2.50	5.15	-0.0306	10.00	5.12	-0.0230
2.50	6.54	0.0076	10.00	6.56	-0.0325
2.50	6.60	0.0056	10.00	7.03	-0.0315
2.50	6.69	0.0162	10.00	7.27	-0.0131
2.50	6.79	0.0146	10.00	7.32	-0.0133
2.50	6.88	0.0231	10.00	7.34	0.0116
2.50	6.91	0.0248	10.00	7.36	0.0094
2.50	7.38	0.0700	10.00	7.38	0.0330
2.50	7.53	0.0521	10.00	7.78	0.0429
2.50	7.78	0.0608	10.00	8.50	0.0656
2.50	7.98	0.0598	10.00	8.80	0.0886
2.50	8.23	0.0639	10.00	9.00	0.0853
2.50	8.43	0.0611	10.00	9.31	0.0765
			10.00	9.70	0.0549

Table 5. Formation constants of the mixed ligand complexes formed between the $Tb(SSA)_2$ species and various carboxylate ligands

Ligand	K_1
L-lactic acid	341
L-mandelic acid	308
L-malic acid	110
L-aspartic acid	42

malic acid complex, at high pH, can be attributed to terdentate binding to the Tb(III) ion. However, what is significant here is that by careful inspection of the CPL line shapes of these four ligands, one can deduce the order in which the possible sites of attachment, on the malic acid ligand, are complexing.

By comparison of the line shapes of aspartic acid and malic acid, at low pH, it becomes apparent that these two ligands (under the stated conditions) are binding in the same manner, via the two carboxylic acid groups at either end of the molecules. As the pH is increased, the hydroxide group of malic acid can begin to take part in the binding, and thus we see the CPL sign inversion as terdentate binding becomes predominant. This CPL change reflects the new ligand configurational changes which accompany the bidentate to terdentate bonding change.

Interestingly, these findings are quite different from the data collected on the corresponding complexes with Tb/DPA. In previous papers[6,7,10] we have contrasted the CPL line shapes of the $Tb(DPA)_2(ASP)$ and $Tb(DPA)_2(MAL)$ complexes (at high and low pH) and have concluded that the mode of binding was radically different. This leads us to conclude that the mode of attachment of malic acid to the Tb(III) ion is quite sensitive to the identity of the other ligand(s) involved in the complex. Further, in substituting SSA for DPA in the complex we have observed a drastic change in the order of binding of the possible attachment sites on this chiral ligand.

In our previous work on mixed ligand carboxylic acid complexes we have observed that the optical activity associated with these complexes was due to a mixture of vicinal (chirality due to the presence of an asymmetric atom bound to the metal ion), and conformational (chirality due to the presence of an asymmetric atom in a chelate ring bound to the metal) effects.[1] In the present work we have once again observed the double-signed CPL line shape, characteristic of a conformational effect, in all of the complexes studied. We therefore conclude that these complexes of Tb/SSA also derive their optical activity from a combination of vicinal and conformational effects.

The results reported here further demonstrate the usefulness of CPL spectroscopy as a probe of lanthanide ion stereochemistry. While our discussions have been of a qualitative nature (due to the current state of CPL theory), they have demonstrated that by varying the functional groups on the chiral ligands, in a systematic fashion, one can obtain significant information regarding the formation of chiral lanthanide complexes via CPL spectroscopy

REFERENCES

[1] H. G. Brittain, *Inorg. Chem.* 1981, **20**, 959.
[2] F. S. Richardson and J. P. Riehl, *Chem. Rev.* 1977, **6**, 773.
[3] X. Yang and H. G. Brittain, *Inorg. Chem.* 1981, **20**, 4273.
[4] F. Yan, R. A. Copeland and H. G. Brittain, *Inorg. Chem.* 1982, **21**, 1180.
[5] J. S. Madaras and H. G. Brittain, *Inorg. Chima. Acta* 1980, **42**, 109.
[6] H. G. Brittain, *Inorg. Chem.* 1981, **20**, 4267.
[7] H. G. Brittain, *J. Am. Chem. Soc.* 1980, **102**, 3693.
[8] L. I. Katzin, *Inorg. Chem.* 1968, **7**, 1183.
[9] C. R. Kanekar, N. V. Thakur and S. M. Jogdeo, *Bull. Chem. Soc. Jap.* 1968, **41**, 759.
[10] H. G. Brittain, *Inorg. Chem.* 1980, **19**, 2136.
[11] A. E. Martell and R. M. Smith, *Critical Stability Constants.* Plenum Press, New York (1974).

Polyhedron Vol. 1, No. 9-10, pp. 701-706, 1982
Printed in Great Britain.

0277-5387/82/090701-06$03.00/0
Pergamon Press Ltd.

BOND-ORDER DEPENDENT BOND ENTHALPY TERMS IN SIMPLE COMPOUNDS OF BORON

JACK B. HOLBROOK and BARRY C. SMITH*
Department of Chemistry, Birkbeck College, University of London, Malet Street, London WC1E 7HX, England

and

CATHERINE E. HOUSECROFT and KENNETH WADE*
Department of Chemistry, Durham University Science Laboratories, South Road, Durham DH1 3LE, England

(*Received* 24 *March* 1982)

Abstract—Published enthalpy data for simple boron compounds, mostly containing trigonally-coordinated boron atoms, have been used to calculate bond enthalpy terms E(B–X), for their B–X bonds (X = N, O, F, Cl or Br) that vary with their bond order, n(B–X), according to the relationship $E(B–X) = A[n(B–X)]^m$. Values of the constants A (the bond enthalpy term for a single bond) and m depend on X as follows:

X	N	O	F	Cl	Br
A (kJ mol^{-1})	385	434	606	419	347
m	0.32	0.65	0.21	0.21	0.21

Analysis of published thermochemical data for compounds with boron–hydrogen and boron–carbon single bonds affords single bond enthalpy terms $E(B–H) = 371 \pm 12$ kJ mol^{-1} and $E(B–C) = 350 \pm 10$ kJ mol^{-1}. These bond enthalpy terms have been used to estimate enthalpies of atomisation and standard heats of formation of gaseous mixed boranes $BR^1R_2^2$, $BR^1R^2R^3$, BRX_2 and BR_2X which have not yet been measured experimentally.

INTRODUCTION

This paper explores ways of rationalising and predicting enthalpies of atomisation and standard heats of formation of simple covalent compounds containing boron[1] by considering relationships between bond enthalpy terms and bond orders.

Boron forms trigonal covalent compounds, BR_3, with single bonds to subsitutents (e.g. R = H, Alk) which are not capable of π-bonding. In addition, boron forms trigonal covalent compounds, BX_3, in which the p_Z orbital perpendicular to the molecular plane can accept π-electronic charge from substituents with suitable lone pairs of electrons (e.g. X = Hal, OR, NR_2) or which form part of a π-bonded system (e.g. X = Ar, alkenyl, alkynyl). It is recognised that these bonds have some multiple character associated with dative $p_X \rightarrow p_B$ π-bonding.[2]

An attempt is made here to assign bond enthalpy terms, E(B–R) and E(B–X), to mixed derivatives, e.g., $BR_{(3-x)}X_x$, where bond orders, n(B–X), depend on the number of π-bonding substituents. A subsequent paper will consider other mixed derivatives, e.g. $BX^1X^2X^3$, where the substituents have different π-bonding potentials.

Our method of deriving bond orders assumes that boron uses four valence shell orbitals when attached to π-bonding substituents, so that the sum of the bond orders is four. In boron trihalides where all three bonds are equivalent, the bond order is taken as n(B–X) 1.33. In dihalogenoboranes, BRX_2, the π-bonding capacity of boron is shared between two bonds which are assigned bond orders n(B–X) 1.5. Monohalogenoboranes, BR_2X, contain a double boron-halogen bond because the p_Z orbital on boron is available exclusively for one π-bonding substituent. A similar approach is used in comparisons of boron-nitrogen compounds with isoelectronic carbon–carbon systems:[3] borazenes are assumed to contain double bonds $\rangle B{=}N\langle$, cf. alkenes; and borazynes are assumed to contain triple bonds —B≡N—, cf. alkynes.

The pioneering work of Pauling[4] was followed by various empirical equations[5–12] relating bond order, bond length, and bond strength. We shall use the relationship:

$$E(B–X) = A[n(B–X)]^m$$

where A and m are constants characteristic of the type of compound, because plots of log[E(B–X)] vs log[n(B–X)] give good straight lines for many covalent inorganic and organic systems.[13–15]

RESULTS AND DISCUSSION

Enthalpy changes refer to 298 K. The conversion factor 1 cal = 4.184 J has been used. Standard heats of formation of gaseous atoms[16] (enthalpies of atomisation of elements) are listed in Table 1.

Boron–hydrogen

The boron–hydrogen bond enthalpy term is derived from the standard heat of formation of borane:[17] $\Delta H_f^\circ(BH_3, g)$ 100.4 kJ mol^{-1}.

$$3E(B–H) = \Delta H_f^\circ(B, g) + 3\Delta H_f^\circ(H, g) - \Delta H_f^\circ(BH_3, g).$$

*Authors to whom correspondence should be addressed.

Table 1. Standard heats of formation of gaseous atoms[16]

Atom (g)	$\underline{\Delta H_f^\ominus}$ / kJ mol^{-1}	Atom (g)	$\underline{\Delta H_f^\ominus}$ / kJ mol^{-1}
H	218.0 (< 1)	O	249.2 (1)
C	716.7 (4)	F	79.1
B	560 (12)	Cl	121.3 (< 1)
N	472.7 (4)	Br	111.9 (1)

The resulting value, E(B–H) 371.2 ± 12 kJ mol^{-1}, is consistent with a bond length[18,19] of d(B–H) 116 pm, using the relationship discussed elsewhere:[14]

$$E(\text{B–H}) = 4.476 \times 10^{11}[d(\text{B–H})]^{-4.4}.$$

It is assumed that this bond enthalpy term can be transferred to other compounds containing boron-hydrogen bonds, e.g. BH_2X or BHX_2.

Boron–carbon

There are two principal methods of estimating the strengths of boron–carbon bonds in organoboranes. Mean bond dissociation energies,[1] $\bar{D}$(B–C), can be obtained from heats of dissociation into boron atoms and free radicals, R$^\cdot$.

$$3D(\text{B–C}) = \Delta H_f^\circ(\text{B, g}) + 3\Delta H_f^\circ(\text{R}^\cdot, \text{g}) - \Delta H_f^\circ(\text{BR}_3, \text{g}).$$

Bond enthalpy terms are derived from heats of disruption into boron atoms and hypothetical organic groups, R*, having bond enthalpy terms which are the same as in the parent hydrocarbon, RH.

$$3E(\text{B–C}) = \Delta H_f^\circ(\text{B, g}) - \Delta H_f^\circ(\text{BR}_3, \text{g}) - 3\Delta H_f^\circ(\text{H, g}) + 3\Delta H_f^\circ(\text{RH, g}) + 3E(\text{C–H}).$$

Table 2 contains standard heats of formation of some triorganoboranes,[20] free radicals,[21] and hydrocarbons,[20] and carbon–hydrogen bond enthalpy terms, E(C–H), which are taken as proportional to isolated C–H stretching frequencies in the hydrocarbons.[22] The difference between mean bond dissociation energy and bond enthalpy term, $\bar{D}$(B–C) − E(B–C), is equal to the reorganisation enthalpy for R*(g)→R$^\cdot$(g), which is greater for methyl than for other alkyl groups, and greatest for phenyl.

The bond enthalpy terms are similar for trialkylboranes, mean E(B–C) 350.0 kJ mol^{-1}. Table 3 contains estimated enthalpies of atomisation, ΔH_a°, and standard heats of formation of gaseous mixed boranes for which experimental data are not yet available. The bond enthalpy term is significantly greater in the case of triphenylborane which contains trigonal carbon and where the release of electronic charge from phenyl may lead to a higher bond order approaching n(B–C) 1.33, as in trivinylborane which has a similar boron-11 chemical shift.[23,24]

Boron–halogen

Standard heats of formation for halogenoboranes,[1,17,20,25] $BR_{(3-x)}X_x$ (R = H, Alk; X = F, Cl, Br), are used to derive boron–halogen bond enthalpy terms in Table 4.

Table 2. Mean bond dissociation energies and bond enthalpy terms for triorganoboranes

BR_3 (g)	$\underline{\Delta H_f^\ominus}$ / kJ mol^{-1} BR_3	R$^\cdot$	RH	$\underline{E}$(C–H) / kJ mol^{-1}	$\bar{D}$(B–C) / kJ mol^{-1}	$\underline{E}$(B–C) / kJ mol^{-1}
BMe_3	-122.8	142.3	-74.5	415.8	369.9	350.9
BEt_3	-148.8	108.4	-84.0	410.0	344.7	344.3
BPr^n_3	-236.7	94.6	-104.5	410.0	360.2	353.1
BPr^i_3	-252.1	76.2	-104.5	405.8	346.9	354.0
BBu^n_3	-290.6	71.1	-126.5	(410.0)	354.6	349.0
BPh_3	+129.9	325.1	+82.9	425.9	468.5	434.2

In this and subsequent tables, $\underline{E}$ and $\underline{D}$ values are given to the nearest 0.1 kJ mol^{-1} for arithmetrical convenience and do not imply this accuracy.

Table 3. Predicted thermochemical data for some gaseous trialkylboranes

Compound (g)	$\Delta H_a^\ominus$ / kJ mol^{-1}	$\Delta H_f^\ominus$ / kJ mol^{-1}
BMe_2Et	5956.3	-131.5
$BMeEt_2$	7117.6	-140.1
$BMeEtPr^n$	8299.6	-169.4
$BMePr^n_2$	9481.6	-198.7
$BMePr^i_2$	9491.9	-209.0
$BMeBu^n_2$	11823.0	-234.7
$BPr^nPr^iBu^n$	13000.8	-259.8

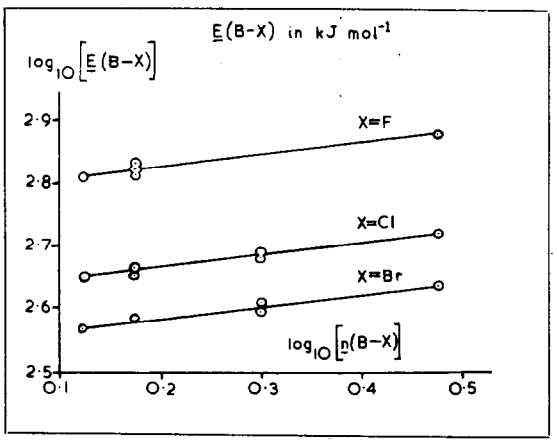

Fig. 1. Boron–halogen bonds.

$$6E(B\text{–}X) = 2\Delta H_f^\circ(B,g) + 6\Delta H_f^\circ(X,g) - \frac{6}{x}\Delta H_f^\circ(BR_{(3-x)}X_x,g) + \left(\frac{6}{x}-2\right)\Delta H_f^\circ(BR_3,g).$$

Data for diatomic boron halides[17,25] are included.

$$E(\text{B–X}) = \Delta H_f^\circ(B,g) + \Delta H_f^\circ(X,g) - \Delta H_f^\circ(BX,g)$$

Plots of $\log_{10}[E(\text{B}-\text{X})]$ vs $\log_{10}[n(\text{B}-\text{X})]$ in Fig. 1 give parallel straight lines of gradient 0.21:

$$E(\text{B–X}) = A[n(\text{B–X})]^{0.21}$$

(X = F, Cl, Br; A = 606, 419, 347 kJ.mol^{-1} respectively.) Bond enthalpy terms derived in this way are used to predict standard heats of formation for some halogenoboranes in Table 5 which have not yet been measured experimentally

Boron–oxygen

Orthoborates. Gaseous orthoboric acid and trialkyl borates contain trigonal BO_3 groups with n(B–O) 1.33. Table 6 contains standard heats of formation[17,20] of some triorthoborates, water, and dialkyl ethers. Bond enthalpy terms, E(B–O), are derived on the assumption that bond enthalpy terms in hydroxy or alkoxy groups are the same as those in water or the corresponding dialkyl ether.

Table 4. Bond enthalpy terms and bond orders for halogenoboranes

Halide (g)	$\Delta H_f^\ominus$(g) / kJ mol^{-1}	E(B-X) / kJ mol^{-1}	n(B-X)
BF_3	-1135.6	644.3	1.33
BHF_2	-733.9	649.4	1.5
$BMeF_2$	-832.6	661.6	1.5
$BEtF_2$	-874.5	678.2	1.5
BPr^iF_2	-887.0	667.2	1.5
BF	+122.0	761.3	3.0
BCl_3	-403.0	442.3	1.33
$BHCl_2$	-248.1	448.7	1.5
$BPhCl_2$	-266.0	462.6	1.5
BBu^n_2Cl	-368.8	483.0	2.0
BPh_2Cl	-95.3	489.7	2.0
BCl	+149.5	531.8	3.0
BBr_3	-205.6	367.1	1.33
$BPhBr_2$	-129.3	384.9	1.5
BBu^n_2Br	-305.2	410.0	2.0
BPh_2Br	-9.4	394.6	2.0
BBr	+234.3	437.6	3.0

Table 5. Predicted thermochemical data for some gaseous halogenoboranes, $BR_{3-x}X_x$

Compound (g)	$\underline{\Delta H_a^\ominus}$ / kJ mol^{-1}	$\underline{\Delta H_f^\ominus}$ / kJ mol^{-1}
Bu^nBF_2	6432.1	-885.1
H_2BF	1443.4	-368.3
Me_2BF	3897.6	-517.1
$Bu^n{}_2BF$	10925.6	-628.9
$MeBCl_2$	2510.7	-337.4
Bu^nBCl_2	6024.7	-393.3
H_2BCl	1227.1	-109.8
Me_2BCl	3681.3	-258.6
$HBBr_2$	1126.8	-125.0
$MeBBr_2$	2353.9	-199.4
Bu^nBBr_2	5867.9	-255.3
H_2BBr	1143.8	-35.9
Me_2BBr	3598.0	-184.7

$$6E(\text{B–O}) = 2\Delta H_f^\circ(\text{B, g}) + 3\Delta H_f^\circ(\text{0, g}) + 3\Delta H_f^\circ(\text{R}_2\text{O, g}) - 2\Delta H_f^\circ[\text{B(OR)}_3\text{, g}].$$

Their values increase slightly with increasing inductive effect of the alkyl group along the series Me ≈ Et < Pr^n < Bu^n.

Boron oxides. Table 7 contains standard heats of formation,[25] boron–oxygen bond enthalpy terms, and probable bond orders for various boron oxides.

The bond enthalpy term for crystalline diboron trioxide, neglecting van der Waals attractions, falls within the range for orthoborates (Table 6).

$$6E(\text{B–O}) = 2\Delta H_f^\circ(\text{B, g}) + 3\Delta H_f^\circ(\text{O, g}) - \Delta H_f^\circ(\text{B}_2\text{O}_3\text{, g})$$

Gaseous diboron monoxide has bond angle[25] BÔB 150°, consistent with n(B–O), *ca.* 1.75. A bent molecule having bond angle BÔB 120° and a nonbonding pair of electrons on each atom, or a linear molecule having a nonbonding pair of electrons on each boron would have bond orders n(B–O) 1.5 or 2.0 respectively

$$2E(\text{B–O}) = 2\Delta H_f^\circ(\text{B, g}) + \Delta H_f^\circ(\text{O, g}) - \Delta H_f^\circ(\text{B}_2\text{O, g}).$$

Gaseous boron dioxide, an odd-electron molecule, is linear[26] like carbon dioxide but contains one less electron. The highest occupied molecular-orbital of carbon dioxide is a nonbonding orbital and the bond order is unchanged by the removal of one electron. Hence boron dioxide has bond order n(B–O) 2.0.

$$2E(\text{B–O}) = \Delta H_f^\circ(\text{B, g}) + 2\Delta H_f^\circ(\text{0, g}) - \Delta H_f^\circ(\text{BO}_2\text{, g}).$$

A simple molecular-orbital picture for boron monoxide, another odd-electron molecule, indicates bond order n(B–O) 2.5.

$$E(\text{B–O}) = \Delta H_f^\circ(\text{B, g}) + \Delta H_f^\circ(\text{O, g}) - \Delta H_f^\circ(\text{BO, g}).$$

Gaseous diboron dioxide is linear[26] and isoelectronic with cyanogen. The boron–boron bond enthalpy term is

Table 6. Bond enthalpy terms for triorthoborates

Borate (g)	$B(OR)_3$	$\underline{\Delta H_f^\ominus(g)}$ / kJ mol^{-1} R_2O	$\underline{E(B\text{-}O)}$ / kJ mol^{-1}
$B(OH)_3$	-994.1	-241.8	521.7
$B(OMe)_3$	-900.1	-184.0	519.3
$B(OEt)_3$	-1001.7	-251.7	519.3
$B(OPr^n)_3$	-1076.4	-292.3	523.9
$B(OBu^n)_3$	-1147.0	-333.9	526.6

Table 7. Bond enthalpy terms for boron oxides

Oxide	$\underline{\Delta H_f^\ominus}$ / kJ mol^{-1}	$\underline{E(B\text{-}O)}$ / kJ mol^{-1}	$\underline{n(B\text{-}O)}$
B_2O_3(s)	-1270.4	523.0	1.33
B_2O(g)	+96.2	636.5	1.75
BO_2(g)	-284.5	671.5	2.0
BO(g)	0.0	809.2	2.5
B_2O_2(g)	-456.1	885.2	3.0

Table 8. Bond enthalpy terms for trigonal boron–nitrogen compounds

Compound (g)(ref. 1)	ΔH_f°(g) kJ mol^{-1}	E(B-N) kJ mol^{-1}	n(B-N)
$B(NMe_2)_3$	-245.6	422.9	1.33
$B_3H_3N_3H_3$	-513.4	438.9	1.5

assumed to have the same value as the single bond in diboron,[25] $\Delta H_f^\circ(B_2, g)$ 815.9 ± 26.8 kJ.mol^{-1}.

$$2E(B\text{–}O) = \Delta H_f^\circ(B_2, g) + 2\Delta H_f^\circ(O, g) - \Delta H_f^\circ(B_2O_2, g).$$

These boron–oxygen bond enthalpy terms increase with increasing bond order. Figure 2 shows that a plot of $\log_{10}[E(B\text{–}O)]$ gives a straight line of gradient 0.65:

$$E(B\text{–}O) = 434[n(B\text{–}O)]^{0.65}.$$

This relationship can be used to rationalise bond orders in other boron oxides, e.g. gaseous diboron trioxide,[25] $\Delta H_f^\circ(B_2O_3, g)$ −833.2 kJ mol^{-1}, which has bond angles[27] OBO 180° and BOB 120°. The heats of atomisation of a linear molecule having bond orders n(B–O) 2.0, or of a bent molecule having bond orders n(B–O) 3.0 (terminal) and 1.0 (bridging) would be 2724 or 2460 kJ.mol^{-1} respectively. The heat of atomisation of a bent molecule having bond orders n(B–O) 2.5 (terminal) and 1.5 (bridging) is 2704 kJ.mol^{-1}, which agrees well with 27 kJ.mol^{-1} derived from the standard heat of formation.

Boron–nitrogen

The boron–nitrogen bond enthalpy term for *tris*-dimethylaminoborane, n(B–N) 1.33, is derived on the assumption that bond enthalpy terms within the dimethylamino group are the same as those in dimethylamine,[20] $\Delta H_f^\circ(Me_2NH, g)$ − 185 kJ mol^{-1}; and that nitrogen–hydrogen bond enthalpy terms are the same in dimethylamine and ammonia:[20]

$$\Delta H_f^\circ(NH_3, g) - 45.9 \text{ kJ mol}^{-1}.$$

$$3E(B\text{–}N) = \Delta H_f^\circ(B, g) + \Delta H_f^\circ(N, g) + 3\Delta H_f^\circ(Me_2NH, g) - \Delta H_f^\circ(NH_3, g) - \Delta H_f^\circ[(Me_2N)_3B, g].$$

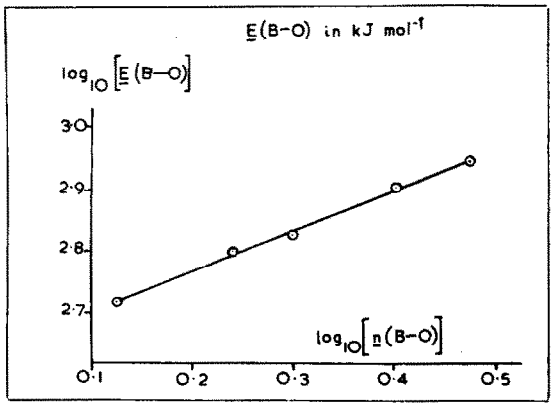

Fig. 2. Boron–oxygen bonds.

We have reinvestigated the heats of hydrolysis of borazine and *NN'N''*-trimethylborazine. The resulting standard heats of formation of the liquid compounds,[28] −516.6 and −563.4 kJ mol^{-1} respectively, suspersede earlier values,[29,30] and the value for borazine agrees well with that obtained from the heat of combustion.[31] The boron–nitrogen bond enthalpy term is derived on the assumption that E(B–H) and E(N–H) are the same as in borane and ammonia.

$$6E(B\text{–}N) = 2\Delta H_f^\circ(B, g) + 2\Delta H_f^\circ(N, g) + \Delta H_f^\circ(BH_3, g) + \Delta H_f^\circ(NH_3, g) - \Delta H_f^\circ(B_3H_3N_3H_3, G).$$

Consideration of the data in Table 8 for these two compounds[1] leads to the following relationship for trigonal boron–nitrogen compounds:

$$E(B\text{–}N) = 385[n(B\text{–}N)]^{0.32}.$$

REFERENCES

[1] A. Finch and P. J Gardner, *Prog. Boron Chem.* 1969, **3**, 177.
[2] N. N. Greenwood, *Comprehensive Inorganic Chemistry* (Edited by A. F. Trotman-Dickenson), Vol. 1, p. 665. Pergamon Press Oxford (1973).
[3] G. E. Coates, M. L. H. Green, P. Powell and K. Wade, *Principles of Organometallic Chemistry*, p. 86. Methuen, London (1971).
[4] L. Pauling, *Nature of the Chemical Bond*, 3rd Edn, Chap. 7. Cornell, New York (1970).
[5] W. Condy, *J. Chem. Phys.* 1947, **15**, 305.
[6] H. O. Jenkins, *J. Am. Chem. Soc.* 1955, **77**, 3168.
[7] J. C. Earl, *Tetrahedron*, 1960, **9**, 65.
[8] J. P. Fackler, D. Coucouvanis, *Inorg. Chem.* 1968, **7**, 181.
[9] A. Julg, *J. Chim. Phys. Physico-Chim. Biol.* 1968, **65**, 541.
[10] J. Stals, *Rev. Pure Appl. Chem.* 1970, **20**, 1.
[11] G. Haefelinger, *Tetrahedron* 1970, **26**, 2469; *Chem. Ber.* 1970, **103**, 2902, 2922, 2941, 3289.
[12] P. A. Koz'min, *Dokl. Akad. Nauk SSSR* 1972, **206**, 1384.
[13] C. E. Housecroft, K. Wade and B. C. Smith, *J. Chem. Soc. Chem. Comm.* 1978, 765; *J. Organometal. Chem.* 1979, **170**, Cl.
[14] C. E. Housecroft and K. Wade, *Inorg. Nucl. Chem. Lett.* 1979, **15**, 339.
[15] C. E. Housecroft, R. Snaith and K. Wade, *Inorg. Nucl. Chem. Lett.* 1979, **15**, 343.
[16] J. A. Kerr, and A. F. Trotman-Dickenson, *Handbook of Chemistry and Physics* (Edited by R. C. Weast and M. J. Astle), 59th Edn, p. F-236. Chemical Rubber Company, Cleveland, Ohio, (1978–79).
[17] D. D. Wagman, W. H. Evans, V. B. Parker, I Halow, S. M. Bailey, and R. H. Schumm, *Selected values of Thermodynamic Properties.* National Bureau of Standards Technical Note 270–3, U.S. Department of Commerce, Washington, D.C. (1968).
[18] J. D. Dill, P. von R. Schleyer and J. A. Pople, *J. Am. Chem. Soc.* 1975, **97**, 3402.
[19] M. J. S. Dewar, and M. L. McKee, *J. Am. Chem. Soc.* 1977, **99**, 5231.
[20] J. B. Pedley, J. Rylance, *Sussex-N. P. L. Computer Analysed Thermochemical Data: Organic and Organometallic Compounds.* University of Sussex (1977).

[21]Ref. 16, p. F-244.
[22]D. C. McKeen, *Chem. Soc. Rev.* 1978, **7**, 399.
[23]C. D. Good and D. M. Ritter, *J. Am. Chem. Soc.* 1962, **84**, 1162.
[24]H. Nöth and B. Wrackmeyer, *Nuclear Magnetic Resonance Spectroscopy of Boron Compounds.* Springer, Heidelberg (1978).
[25]D. R. Stull, and H. Prophet, *JANAF Thermochemical Tables.* NSRDS-NBS 37, U.S. Department of Commerce, Washington, D.C., 2nd Edn, (1971).
[26]A. Sommer, D. White, M. J. Linevsky and D. R. Mann, *J. Chem. Phys.* 1963, **38**, 87.
[27]W. Weltner, and J. R. W. Warn, *J. Chem. Phys.* 1962, **37**, 292.
[28]J. B. Holbrook, Ph.D. Thesis. University of London, (1975).
[29]B. C. Smith and L. Thakur, *Nature (London)* 1965, **208**, 74.
[30]B. C. Smith L. Thakur and M. A. Wassef, *J. Chem. Soc. (A)* 1967, 1616.
[31]M. V. Kilday, W. H. Johnson and E. J. Prosen, *J. Res. Nat. Bur. Stand.* 1961, **65A**, 101.

Polyhedron Vol. 1, No. 9-10, pp. 707-709, 1982
Printed in Great Britain.

0277-5387/82/090707-03$03.00/0
Pergamon Press Ltd.

THE KINETICS OF CATION EXCHANGE REACTION OF EUROPIUM PROPYLENEDIAMINETETRAACETATE WITH YTTERBIUM ION

INN HOE KIM and SOCK SUNG YUN†

Department of Chemistry, Chungnam National University, Daeduk 300-31, Korea

(*Received* 21 *April* 1982)

Abstract—The kinetics of cation exchange reaction of Eu(III) propylenediaminetetraacetate with Yb(III) has been studied in an aqueous solution by the polarographic procedure. The measurements were made at 25°C and at an ionic strength of 0.5 M KCl. The dissociation of the europium complex has been found to be catalyzed by hydrogen ions. The influences of the inductive effect and the steric hindrance of a C-methyl group on the ethylene of PDTA are discussed by comparing it to analogous EDTA and CyDTA system.

INTRODUCTION

The cation exchange reactions of the metal polyaminocarboxylate chelate complexes have been continuously interested by a number of groups.[1-11] It has been generally known that the reactions between lanthanide cations and lanthanide ethylenediaminetetraacetate complexes are catalyzed by the proton concentration in aqueous solution.[1-3]

Nyssen and Margerum[4] proposed, in the study of cation exchange reactions of Ln(III) *trans*-1,2-diaminocyclohexane-N, N, N′, N′-tetraacetate with Cu(II), a mechanism in which the association of a proton on the nitrogen of the ligand is the slow process followed by a fast cleavage of the bond between the lanthanide cation and carboxylate of the ligand. On the other hand, Ryhl[6] insisted that a proton associates primarily to the non-coordinated carbonyl oxygen atom of a carboxylate in the lanthanide exchange reactions of Ln(III) EDTA.

Propylenediaminetetraacetate has higher pK_4 value, because of the inductive effect of C-methyl group on the ethylene of the ligand, and thus forms more stable complexes with the metal ions than EDTA ligand.[12] It would be expected that the C-methyl group in the PDTA might be an important role on the rates of cation exchange reactions of its metal complexes. In the present paper, we report the results of a study of the cation exchange reaction between Eu(III) PDTA and Yb(III) ion through the polarographic method.

EXPERIMENTAL

Chemicals. Stock solutions of $EuCl_3$ and $YbCl_3$ were prepared by dissolving the corresponding oxides (American Potash and Chemical Co., 99.99% purity) in HCl and then adjusted to pH values below 3.5 to prevent the hydrolysis of the metal ions. The stock solutions were standardized by EDTA titration with EBT indicator in the presence of ammonia buffer. The stock solution of PDTA (Aldrich Chemical Co.) was prepared by dissolving it in the basic solution and standardized by the complexometric titration with the standard Zn solution. The working solutions were buffered with 1.25×10^{-2} M sodium acetate/acetic acid. The ionic strength were adjusted to 0.5 M with KCl. The deionized water was used for the preparation of all solutions.

Apparatus. A Beckman Model 4500 Digital pH meter with a Fisher standard combination electrode was used for pH measurements. A Yanaco Model P8-D DC Polarograph was used to record the variation of the free Eu(III) concentration with time in the reaction mixture.

†Author to whom correspondence should be addressed.

Procedure. The procedure is similar as described elsewhere.[5,6] The reaction was initiated by the injection of $EuCl_3$-Na_2PDTA solution into $YbCl_3$ solution. The cation exchange rate between Eu(III) and Yb(III) in the mixture was measured by recording the variation of the diffusion current of free Eu(III) with time at constant voltage of -0.85 V. The mixing time was less than about 4 sec. The reactions were followed for at least four half-life periods. All the measurements were made in the medium of 0.5 M KCl at 20°C ± 0.2. The pH was adjusted to desired value with 1.25 mM sodium acetate and varying amounts of acetic acid. The pH range of the solution studied was between the values of 4 and 5. The 0.01% gelatin was used to eliminate the polarographic maxima.

RESULTS AND DISCUSSION

The cation exchange reaction between $Eu(PDTA)^-$ and Yb(III) ion is written as

$$Eu(PDTA)^- + Yb^{3+} \underset{k_{-1}}{\overset{k_1}{\rightleftharpoons}} Yb(PDTA)^- + Eu^{3+}. \quad (1)$$

The equilibrium constants of the reaction is

$$K_{eq} = K_{Yb(PDTA)}/K_{Eu(PDTA)}.$$

Since $\log K_{Yb(PDTA)} = 20.25$, $\log K_{Eu(PDTA)} = 18.26$[12] and the concentration of Yb(III) ion is about a hundred times greater than that of $Eu(PDTA)^-$, the pseudo-first order rate equation is written as

$$R = -\frac{d[Eu(PDTA)^-]}{dt} = \frac{d[Eu^{3+}]}{dt} = k_0[Eu(PDTA)^-]. \quad (2)$$

The pseudo-first order rate constants (k_0) were calculated using Gugenheim's method.[13] The observed rate constant (k_0) is related to the diffusion currents (A) of the free Eu(III) ion as eqn (3):

$$k_0 t_i + \ln (A_i' - A_i) = \text{const.} \quad (3)$$

where A_i and A_i' are the series of the diffusion currents at times t_i and $t_i + t'$, respectively, with an exactly constant time interval of t'. A plot of $\ln (A_i' - A_i)$ against t_i gives a straight line of a slop equal to $-k_0$. Fig. 1 is a typical plot of $\ln (A_i' - A_i)$ vs t_i. The observed first order rate constants obtained at the various hydrogen ion concentrations are given in Table 1.

Table 1. Rate constants for the exchange reaction of Eu(III) PDTA with Yb(III). $T = 20°C$, $\mu = 0.5$ M (KCl)

$[H^+] \times 10^5$	$k_0 \times 10^3$ (sec^{-1})	$[H^+] \times 10^5$	$k_0 \times 10^3$ (sec^{-1})
0.99	3.38 ± 0.07	5.69	18.23 ± 0.15
1.58	5.88 ± 0.06	6.32	23.26 ± 0.22
1.92	5.40 ± 0.18	6.76	22.22 ± 0.29
2.48	9.96 ± 0.09	6.76	24.19 ± 0.33
3.13	12.09 ± 0.10	7.64	27.24 ± 0.29
4.05	13.83 ± 0.15	8.15	28.06 ± 0.38
5.13	15.09 ± 0.42	8.15	29.79 ± 0.36
5.57	18.30 ± 0.19		

$[Eu^{3+}]_0 = 3.45 \times 10^{-4}$ M, $[PDTA]_0 = 1.38 \times 10^{-4}$ M, $[Yb^{3+}]_0 = 1.08 \times 10^{-2}$ M, [acetate] = 1.25×10^{-2} M.

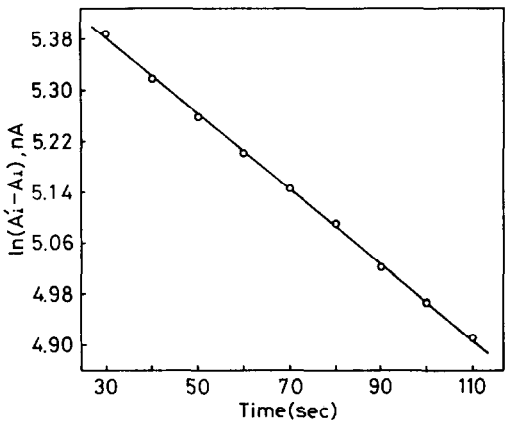

Fig. 1. Plot of $\ln(A_i' - A_i)$ vs time for exchange of Eu(PDTA)$^-$ with Yb(III) at 20°C, $\mu = 0.5$ M KCl and [acetate] = 1.25×10^{-2} M, $[Eu^{3+}]_0 = 3.45 \times 10^{-4}$ M, $[PDTA]_0 = 1.38 \times 10^{-4}$ M, $[Yb^{3+}]_0 = 1.08 \times 10^{-2}$ M.

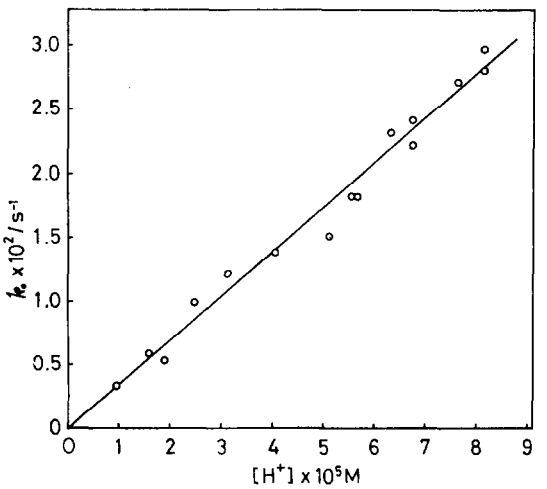

Fig. 2. Plot of k_0 vs $[H^+]$ for exchange of Eu(PDTA)$^-$ with Yb(III).

When k_0 is plotted against the hydrogen ion concentration, a linear relationship is obtained as;

$$k_0 = k_d^{Eu(PDTA)} + k_H^{Eu(PDTA)}[H^+] \quad (4)$$

where $k_d^{Eu(DPTA)}$ and $k_H^{Eu(PDTA)}$ are acid independent and acid dependent rate constants, respectively. Figure 2 shows the linear relationship of k_0 vs $[H^+]$. The least square analysis of the straight line of Fig. 2 gives $k_H^{Eu(PDTA)} = 3.50 \times 10^2\ M^{-1}\ sec^{-1}$ and $k_d^{Eu(PDTA)} = -1.93 \times 10^{-4}\ sec^{-1}$. The fact that the intercept is slightly negative and small would mean that the acid independent dissociation process in negligible and thus, $k_d^{Eu(PDTA)} \simeq 0$ within experimental error. Therefore, the reaction would proceed mostly through the acid dependent mechanism and eqn (4) could be reduced to

$$k_0 = k_H^{Eu(PDTA)}[H^+]. \quad (5)$$

The first order dependence on the hydrogen ion concentration has also been found for the dissociation processes of Ln(EDTA)$^-$ and Ln(CyDTA)$^-$ complexes in aqueous solution.[1,4] The acid dependent dissociation rate constants of several europium polyaminocarboxylate complexes are listed in Table 2, along with their stability constants taken from Ref. [12].

The cation exchange rate would be influenced by the structure of the ligand. The acid dependent dissociation constants decrease with the increase of the stability constant. However, it does not like that there is any regular relationship between K_{ML} and k_H^{ML} with the variation of the ligand. The stability constant of Eu(PDTA)$^-$ is about a ten times larger than that of Eu(EDTA)$^-$ because of the inductive effect of C-methyl group of PDTA ligand.[12] The dissociation rate of Eu(EDTA)$^-$ is only about twice faster than that of Eu(PDTA)$^-$, where as more than a hundred times faster than that of Eu(CyDTA)$^-$, even the stability of Eu(CyDTA)$^-$ is comparable to Eu(PDTA)$^-$. Thus, it seems like that the structural hindrance is more important factor affecting to the rate of the dissociation of the lanthanide polyaminocarboxylate complexes.

Table 2. Stability constants and proton catalyzed dissociation rate constants of some Eu(III) complexes

Complexes	log K_{ML} (ref. 12)	k_H^{ML} ($M^{-1}sec^{-1}$)	Ref.
$Eu(EDTA)^-$	17.51	6.0×10^2	2, 7
$Eu(PDTA)^-$	16.26	3.5×10^2	This work
$Eu(CyDTA)^-$	18.62	2.2	4

There have been the disagreements in the mechanism how the proton attacks the ligand of the complex in the acid dependent dissociation process. Ryhl[5] has suggested that the dissociation of $Ln(EDTA)^-$ complexes in aqueous solution presumably proceeds through the fast association of a proton to the non-coordinated oxygen atom of a carboxylate group of the ligand, followed by slow cleavage of the coordinative bond between the metal and the other oxygen atom. However, Nyssen and Margerum[4] have proposed a mechanism, in the study of $Ln(CyDTA)^-$ complexes, in which the meta stable complex is formed by the slow association of the proton on the nitrogen atom of the ligand and then the fast dissociation of the protonated complex is followed. In this mechanism, the structure of the ligand can have a large influence on the reaction rate.[4] Choppin *et al.*[8] have suggested that the rapid protonation equilibrium involves carboxylate oxygen protonation and the second step may involve the transfer of the proton from the carboxylate oxygen to the nitrogen atom. Once the nitrogen is protonated, the ligand can dissociate rapidly.

At this stage, it can not be definitely said how the proton associates to the ligand of the complex. However, if the metal-nitrogen bond is labilized by the protonation on the nitrogen atom and the protonation is the rate determining step, the steric environment around the nitrogen atom of the ligand would be an important factor for the dissociation process. The steric hindrance to the nitrogen atom in the CyDTA would be the largest and next in the PDTA, because of the cyclohexane group and C-methyl group of the ligands, respectively. Thus, it is expected that the dissociation rate of the complexes would be slower in the order of $Eu(CyDTA)^-$, $Eu(PDTA)^-$, and $Eu(EDTA)^-$. This agrees well with the results on Table 2.

REFERENCES

[1]P. Glentworth, B. Wiseall, C. L. Wright and A. J. Mahmood, *J. Inorg. Nucl. Chem.* 1968 **30**, 967.
[2]W. D'olieslager and G. R. Choppin, *J. Inorg. Nucl. Chem.* 1971 **33**, 127.
[3]P. Glentworth and D. A. Newton, *J. Inorg. Nucl. Chem.* 1971 **33**, 1701.
[4]G. A. Nyssen and D. W. Margerum, *Inorg. Chem.* 1970 **9**, 1814.
[5]T. Ryhl, *Acta Chem. Scand.* 1972 **26**, 3955.
[6]T. Ryhl, *Acta Chem. Scand.* 1972 **26**, 4001.
[7]T. Ryhl, *Acta Chem. Scand.* 1973 **27**, 303.
[8]G. R. Choppin and K. R. Williams, *J. Inorg. Nucl. Chem.* 1973 **35**, 4255.
[9]K. R. Williams and G. R. Choppin, *J. Inorg. Nucl. Chem.* 1974 **36**, 1849.
[10]R. K. Stimhous and S. H. Erickson, *Inorg. Chem.* 1980 **19**, 1913.
[11]W. D'olieslager, M. Wevers and M. De Jonghe, *J. Inorg. Nucl. Chem.* 1981 **43**, 423.
[12]H. Irving and J. P. Conesa, *J. Inorg. Nucl. Chem.* 1964 **26**, 1945.
[13]E. A. Guggenheim, *Phil. Mag.* 1926 **1**, 538.

Polyhedron Vol. 1, No. 9–10, pp. 711–722, 1982
Printed in Great Britain.

0277-5387/82/090711-12$03.00/0
Pergamon Press Ltd.

STUDIES ON $(SCN)_2M(NCS)_2Hg_2(p\text{-TOLYL})_2$ AND $(SCN)_2M(NCS)_2Hg_2(\alpha\text{-NAPHTHYL})_2$ AND THEIR COMPLEXES

P. P. SINGH* and KSHIPRA ATREYA
Department of Chemistry, M.L.K. College, Balrampur-271201, India

(*Received* 17 *May* 1982)

Abstract—*p*-Tolyl mercury thiocyanate and α-naphthyl mercury thiocyanate react with $Co(NCS)_2$2py and form a bimetallic pink compound of formula $(py)_2(SCN)_2Co(NCS)_2Hg_2R_2$ (R = *p*-tolyl and α-naphthyl group). On heating this compound in vacuum a blue compound $(SCN)_2Co(NCS)_2Hg_2R_2$ is formed. Nickel analogues $(SCN)_2Ni(NCS)_2Hg_2R_2$ are formed by direct reaction of *p*-tolyl or α-naphthyl mercury thiocyanate with nickel thiocyanate. $(SCN)_2Co(NCS)_2Hg_2R_2$ and $(SCN)_2Ni(NCS)_2Hg_2R_2$ act as Lewis acids and form complexes with bases. The Lewis acids and their complexes with various bases have been characterized by elemental analyses, molar conductance, molecular weight, magnetic moment, infrared and electronic spectral studies. These studies reveal that both the Lewis acids are monomers. In $(SCN)_2Co(NCS)_2Hg_2R_2$ the Co(II) has tetrahedral geometry, where as in $(SCN)_2Ni(NCS)_2Hg_2R_2$ the Ni(II) has octahedral geometry through elongated axial bondings with SCN-groups of other molecules. Thiocyanate bridging of the type R–Hg–SCN–M [M = Co(II), Ni(II)] is present in the compounds. Pyridine and dimethylsulphoxide form adducts with these compounds by coordinating at Co(II) or Ni(II). The thiocyanate bridge is retained in these complexes. 2-2'bipyridyl ruptures the thiocyanate bridging in both the Lewis acids and forms cationic–anionic complexes of the type $[M(L\text{–}L)_3][RHg(SCN)_2]_2$. In both the type of complexes Co(II) and Ni(II) possess octahedral environment. The "softness" values have been used in a novel manner in proposing the structure of the complexes.

INTRODUCTION

A new class of organobimetallic compounds and their Lewis acid behaviour has been recently published by us.[1] In this communication we report the synthesis and studies of few more such compounds in which phenyl has been changed by α-naphthyl and *p*-tolyl group.

EXPERIMENTAL

Reagent grade solvents were purified before use. Cobalt and nickel thiocyanates were prepared by reacting their respective nitrates with potassium thiocyanate in ethanol. $Co(NCS)_2(py)_2$ was prepared by the method described elsewhere.[2] Dimethylsulphoxide (dmso), 2-2'bipyridyl (bipy) and pyridine (py) were used as received. *p*-Tolyl mercury chloride and α-naphthyl mercury chloride were prepared by diazotization method[3–5] as described below:

143 g (1 mmole) of α-naphthylamine was added to a mixture of 450 ml of hydrochloric acid and 500 ml of water. To the mixture 500 g of ice was added and vigorously stirred. When the temperature reached 5°C solid sodium nitrite (about 69 g) was added. After stirring for about half-an-hour, the whole mass was filtered and any residue was rejected. To the clear filtrate a cold solution of 271 g (1 mmole) of mercuric chloride in 300 ml of hydrochloric acid was slowly added with vigorous stirring. Yellow precipitate of $RN_2Cl{\cdot}HgCl_2$ was formed which was filtered after stirring for an hour. The compound was washed with water followed by acetone and dried in air. Yield 417 g. The whole compound was mixed with 114 g of copper powder in 2 l. acetone and cooled to 0°C, stirred for an hour, allowed to stand overnight and filtered. The residue was boiled with xylene, and filtered. On cooling the filtrate crystals of RHgCl were obtained. Yield 30 g.

p-Tolyl mercury chloride was similarly prepared by using *p*-toluidine in place of α-naphthylamine.

α-Naphthyl and *p*-tolyl mercury chloride were converted into their respective thiocyanates by reaction with potassium thiocyanate (BDH) in 1:1 molar ratio in acetone. KCl was filtered off, and the filtrate was concentrated by evaporation. On addition of water to the concentrate *p*-tolyl mercury thiocyanate or α-naphthyl mercury thiocyanate precipitated, which was filtered, washed with solvent, recrystallized from acetone and dried in vacuum. Yield 28 g. The purity of compounds was tested by elemental analyses and IR spectral band positions.

p-Tolyl mercury thiocyanate m.p. 210°C. (Found: *N*, 3.96; *S*, 9.12; Calc.: *N*, 4.01; *S*, 9.16%). α-Naphthyl mercury thiocyanate m.p. 155°C. (Found: *N*, 3.42; *S*, 8.29. Calc.: *N*, 3.42; *S*, 8.31%).

PREPARATION OF COMPLEXES

$(py)_2(SCN)_2Co(NCS)_2Hg_2R_2$(R = *p-tolyl and α-naphthyl*)

p-Tolyl mercury thiocyanate (6.98 g, 2 mmole) and α-naphthyl mercury thiocyanate (7.7 g, 2 mmole) were separately dissolved in 100 ml of ethanol. To each solution an ethanolic solution of $Co(NCS)_2(py)_2$ (3.33 g, 1 mmole) was added and stirred for 72 hr. A pink precipitate appeared in each case, which was filtered, washed with ethanol and dried in vacuum. Both the complexes were crystallized from a mixture of acetone and ethanol.

$(py)_2(SCN)_2Co(NCS)_2Hg_2(p\text{-tolyl})_2$—m.p. 215°C.
$(py)_2(SCN)_2Co(NCS)_2Hg_2(\alpha\text{-naphthyl})_2$—m.p. 204°C

$(SCN)_2Cl(NCS)_2Hg_2R_2$ *and* $(dmso)_2(SCN)_2Co(NCS)_2Hg_2R_2$.

On heating the pyridine complexes in vacuum the pyridine is given off and blue compounds are formed, which were recrystallized from acetone. They have the general formula $(SCN)_2Co(NCS)_2Hg_2R_2$. On reaction with pyridine their parent compounds $(py)_2(SCN)_2Co(NCS)_2Hg_2R_2$ were again formed. When ethanolic solutions of RHgSCN and $Co(NCS)_2$ were directly reacted $(SCN)_2Co(NCS)_2Hg_2R_2$ was not formed but $CoHg(SCN)_4$ was formed instead.

The dmso complexes were prepared by stirring $(SCN)_2Co(NCS)_2Hg_2$ (*p*-tolyl)$_2$ and $(SCN)_2Co(NCS)_2Hg_2$ (α-naphthyl)$_2$ in 50 ml of dimethylsulphoxide separately for 24 hr. Pink complexes were formed, which were filtered and dried in vacuum.

$(dmso)_2(SCN)_2Co(NCS)_2Hg_2(p\text{-tolyl})_2$ m.p. 215°C
$(dmso)_2(SCN)_2Co(NCS)_2Hg_2(\alpha\text{-naphthyl})_2$ m.p. 204°C.

*Author to whom correspondence should be addressed.

$[Co(bipy)_3][RHg(SCN)_2]_2$

$(SCN)_2Co(NCS)_2Hg_2$ (*p*-tolyl)$_2$ (0.873 g, 1 mmole) and $(SCN)_2Co(NCS)_2Hg_2$ (α-naphthyl)$_2$ (0.945 g, 1 mmole) were separately dissolved in 50 ml of ethanol. To each solution an ethanolic solution of 2-2'-bipyridyl (0.468 g, 3 mmole) was added and stirred for about 24 hr. Pink precipitate in each case appeared, which was filtered, washed with ethanol and dried in vacuum. The complexes were recrystallized from acetonitrile.

$[Co(bipy)_3][p\text{-tolyl } Hg(SCN)_2]_2$ m.p. 146°C.
$[Co(bipy)_3][\alpha\text{-naphthyl } Hg(SCN)_2]_2$ m.p. 135°C.

$(SCN)_2Ni(NCS)_2Hg_2R_2$. *p*-tolyl mercury thiocyanate (6.987 g, 2 mmole) and α-naphthyl mercury thiocyanate (7.7 g, 2 mmole) were separately dissolved in acetone. To each solution a methanolic solution (1.75 g, 1 mmole) of $Ni(NCS)_2$ was added and stirred for 72 hr. A bluish-green precipitate appeared in each case which was filtered washed with methanol and dried in vacuum. The complexes were recrystallized from acetone.

$(SCN)_2Ni(NCS)_2Hg_2(p\text{-tolyl})_2$ m.p. 238°(*d*)
$(SCN)_2Ni(NCS)_2Hg_2(\alpha\text{-naphthyl})_2$ m.p. 217°(*d*).

$(py)_2(SCN)_2Ni(NCS)_2Hg_2R_2$ *and* $[Ni(bipy)_3][RHg(SCN)_2]_2$

$(SCN)_2Ni(NCS)_2Hg_2$ (*p*-tolyl)$_2$ (0.873 g, 1 mmole) and $(SCN)_2Ni(NCS)_2Hg_2$ (α-naphthyl)$_2$ (0.945 g, 1 mmole) were separately dissolved in 50 ml of ethanol. To each solution an ethanolic solution of pyridine (0.2 ml, 2 mmole) was added, and stirred for 36 hr. Green precipitate appeared in each case and was filtered, washed with solvent and dried in vacuum. Complexes were recrystallized from acetone.

$(py)_2(SCN)_2Ni(NCS)_2Hg_2$ (*p*-tolyl)$_2$ m.p. 230°(*d*)
$(py)_2(SCN)_2Ni(NCS)_2Hg_2$ (α-naphthyl)$_2$ m.p. 255°(*d*).

The bipyridyl complexes were similarly prepared by reacting ethanolic solutions of 2,2'-bipyridyl (0.468 g, 3 mmole) in place of pyridine.

$[Ni(bipy)_3][p\text{-tolyl } Hg(SCN)_2]_2$ m.p. 162°C.
$[Ni(bipy)_3][\text{naphthyl } Hg(SCN)_2]_2$ m.p. 166°C.

The dmso complexes were prepared by the method adopted for corresponding cobalt complexes.

Analyses of the complexes. The complexes were analysed for cobalt as anthranilate, nickel as dimethylglyoximate, sulphur as sulphate and mercury gravimetrically as sulphide. Nitrogen was estimated by semi-micro Kjeldahl's method. Analytical results along with melting points are presented in Table 1.

Physical measurements. The molar conductances of the complexes were measured in dimethylformamide using a Philips conductivity bridge model PR-9500. The molecular weights were determined in dmso solution by the cryoscopic method. The magnetic susceptibility measurements were made at room temperature by Gouy's method using $CoHg(SCN)_4$ as standard. The diamagnetic correction were made using Pascal's constants. Infrared spectra of the complexes were recorded as nujol mulls or as KBr pellets on a Perkin–Elmer 621 spectrophotometer in the range 4000–200 cm^{-1} and as polyethylene disc in the range 500–50 cm^{-1} on a polytech F.I.R. 30 Fourier spectrophotometer. Electronic spectra in the range 250–1800 nm were recorded on a Carl–Zeiss DMR-21 spectrophotometer.

RESULTS AND DISCUSSION

$M(NCS)_2(py)_2$ or $M(NCS)_2(dmso)_2$ reacts with RHgSCN and forms an adduct of general formula $L_2(SCN)_2M(NCS)_2Hg_2R_2$ (L = py, dmso). The pyridine or dmso is given off when the adducts are heated in vacuum, leaving behind a compound of general formula $(SCN)_2M(NCS)_2Hg_2R_2$ which is termed as Lewis acid. The Lewis acids when reacted with pyridine or dmso again form the adducts. On reaction with a strong base like 2-2'bipyridyl, the Lewis acids form cationic–anionic complexes. The structure of these complexes are discussed below.

1. *Adducts.* $L_2(SCN)_2M(NCS)_2Hg_2R_2$ *and Lewis acids*—$(SCN)_2M(NCS)_2Hg_2R_2$ (L = py, dmso; M = Co, Ni and R = *p*-tolyl, α-naphthyl)

Both the adducts and the Lewis acids are non-conducting in dimethylformamide. The molecular weight data (Table 2) of $(py)_2(SCN)_2M(NCS)_2Hg_2R_2$ indicate that they are monomeric. The molecular weight of $(SCN)_2M(NCS)_2Hg_2R_2$ could not be determined on account of insufficient solubility, however, the cobalt complex may be assumed to be monomeric, on the basis of the tetrahedral coordination of the cobalt atom but the octahedral nickel complex is presumably polymeric. The adducts can be formed by reaction of pyridine or dmso with the Lewis acids which in turn can be reformed by heating the adducts in vacuum.

For deriving structural information the spectra of RHgSCN have been first studied. The solid phase spectra shows the presence of νC–N band at 2182, νC–S at 729, νHg–S at 235, δSCN at 446, and νHg–C at 459 cm^{-1}. On the basis of this information the unit cell of RHgSCN has been considered to have a dimeric centrosymmetric model, where a four membered Hg_2S_2 ring is formed.[6] The position of these bands is considerably changed when the spectrum is recorded in methanol. The νC–N is observed at 2136 and νHg–S at 283 cm^{-1}. This indicates that bridging through sulphur of thiocyanate is destroyed in solution. It has been considered safer to derive shifts from the spectral data in solution phase. On comparison of the various bands of RHgSCN with the corresponding bands of $L_2(SCN)_2M(NCS)_2Hg_2R_2$, changes are observed in νC–N, νC–S and νHg–S bands (Table 3). The νC–N

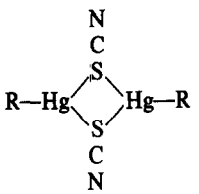

band is observed in the region 2125–2170 cm^{-1} and νC–S in the region 720–795 cm^{-1}. These changes indicate that the thiocyanate of RHgSCN becomes bridging probably by coordination to M through its N-end.

A band in νC–N region in the range 2060–2080 cm^{-1} is also observed, which is assigned to N-bonded terminal thiocyanate arising from M–NCS and can be supported from its analogy to the reported band in $M(NCS)_22L$.[7] In the case of Lewis acids the bands assigned to νC–N, νC–S and δNCS are present almost in the same region in which they are present in their corresponding adducts.

Table 1. Analytical data of the complexes

Complexes	Colour	M.P. °C	% Sulphur		% Mercury		% Cobalt/Nickel		% Nitrogen	
			cal.	obs.	cal.	obs.	cal.	obs.	cal.	obs.
$(SCN)_2Co(NCS)_2Hg_2(p\text{-tolyl})_2$	Blue	215	14.72	14.6	44.98	45.8	6.36	6.7	6.16	6.4
$(py)_2(SCN)_2Co(NCS)_2Hg_2(p\text{-tolyl})_2$	Pink	215	12.8	12.4	37.9	38.7	5.37	5.7	5.28	5.4
$(dmso)_2(SCN)_2Co(NCS)_2Hg_2(p\text{-tolyl})_2$	Violet pink	215	12.89	12.5	37.91	38.8	5.54	5.8	5.36	5.5
$[Co(bipy)_3][p\text{-tolyl Hg}(SCN)_2]_2$	Orange pink	146	9.87	9.5	28.9	29.02	4.12	4.3	3.87	4.1
$(SCN)_2Co(NCS)_2Hg_2(\alpha\text{-naphthyl})_2$	Blue	204	13.6	13.5	41.96	42.3	5.98	6.2	5.85	5.9
$(py)_2(SCN)_2Co(NCS)_2Hg_2(\alpha\text{-naphthyl})_2$	Pink	204	11.8	11.6	36.08	36.2	5.21	5.3	5.12	5.0
$(dmso)_2(SCN)_2Co(NCS)_2Hg_2(\alpha\text{-naphthyl})_2$	Violet pink	204	11.73	11.6	36.1	36.2	5.15	5.3	5.2	5.0
$[Co(bipy)_3][\alpha\text{-naphthyl Hg}(SCN)_2]_2$	Pink	135	9.25	9.0	28.15	28.3	4.01	4.1	4.1	3.9
$(SCN)_2Ni(NCS)_2Hg_2(p\text{-tolyl})_2$	Bluish green	238(d)	14.72	14.58	44.98	44.6	6.36	6.27	6.16	6.21
$(py)_2(SCN)_2Ni(NCS)_2Hg_2(p\text{-tolyl})_2$	Grey	230(d)	12.8	12.6	37.9	37.81	5.37	5.21	5.28	5.31
$(dmso)_2(SCN)_2Ni(NCS)_2Hg_2(p\text{-tolyl})_2$	Green	214(d)	12.89	12.62	37.91	36.98	5.54	5.14	5.36	5.12
$[Ni(bipy)_3][p\text{-tolyl Hg}(SCN)_2]_2$	Pink	162	9.87	9.5	28.9	28.54	4.12	4.25	3.87	3.75
$(SCN)_2Ni(NCS)_2Hg_2(\alpha\text{-naphthyl})_2$	Yellowish green	217(d)	13.6	13.38	41.96	41.76	5.98	5.73	5.85	5.75
$(py)_2(SCN)_2Ni(NCS)_2Hg_2(\alpha\text{-naphthyl})_2$	Grey	255(d)	11.8	11.54	36.08	36.0	5.21	5.3	5.12	4.96
$(dmso)_2(SCN)_2Ni(NCS)_2Hg_2(\alpha\text{-naphthyl})_2$	Green	226(d)	11.73	11.6	36.1	35.92	5.15	4.98	5.2	4.91
$[Ni(bipy)_3][\alpha\text{-naphthyl Hg}(SCN)_2]_2$	Pink	166	9.25	9.12	28.15	27.94	4.01	4.03	4.1	4.01

M.P. = melting point; d= decompose.

Table 2. Molar conductance and molecular weight data of the complexes

Complexes	cm^{-1} mhos/mole M/512	Molecular weight cal.	obs.
$(SCN)_2Co(NCS)_2Hg_2(p\text{-tolyl})_2$	42.63	-	-
$(py)_2(SCN)_2Co(NCS)_2Hg_2(p\text{-tolyl})_2$	58.015	1031	976
$(dmso)_2(SCN)_2Co(NCS)_2Hg_2(p\text{-tolyl})_2$	65.53	1029	936
$[Co(bipy)_3][p\text{-tolyl Hg}(SCN)_2]_2$	136.39	-	-
$(SCN)_2Co(NCS)_2Hg_2(\alpha\text{-naphthyl})_2$	48.47	-	-
$(py)_2(SCN)_2Co(NCS)_2Hg_2(\alpha\text{-naphthyl})_2$	62.08	1103	907
$(dmso)_2(SCN)_2Co(NCS)_2Hg_2(\alpha\text{-naphthyl})_2$	66.77	1101	1035
$[Co(bipy)_3][(\alpha\text{-naphthyl Hg}(SCN)_2]_2$	136.11	-	-
$(SCN)_2Ni(NCS)_2Hg_2(p\text{-tolyl})_2$	57.07	-	-
$(py)_2(SCN)_2Ni(NCS)_2Hg_2(p\text{-tolyl})_2$	53.62	1031	892
$(dmso)_2(SCN)_2Ni(NCS)_2Hg_2(p\text{-tolyl})_2$	52.04	1029	947
$(SCN)_2Ni(NCS)_2Hg_2(\alpha\text{-naphthyl})_2$	70.7	-	-
$(py)_2(SCN)_2Ni(NCS)_2Hg_2(\alpha\text{-naphthyl})_2$	69.39	1103	1012
$(dmso)_2(SCN)_2Ni(NCS)_2Hg_2(\alpha\text{-naphthyl})_2$	68.05	1101	986
$[Ni(bipy)_3][\alpha\text{-naphthyl Hg}(SCN)_2]_2$	132.03	-	-
$[Ni(bipy)_3][p\text{-tolyl Hg}(SCN)_2]_2$	136.39	-	-

Table 3. Assignment of IR spectral bands

Complexes	ν C–N (cm^{-1})	ν C–S (cm^{-1})	δ NCS (cm^{-1})
$(SCN)_2Co(NCS)_2Hg_2(p\text{-tolyl})_2$	2140(s), 2060(s) 2125(sh)	760(s), 700(s)	435(s)
$(py)_2(SCN)_2Co(NCS)_2Hg_2(p\text{-tolyl})_2$	2170(s), 2080(sh)	780(s), 690(w)	430(s)
$(dmso)_2(SCN)_2Co(NCS)_2Hg_2(p\text{-tolyl})_2$	2130(vs), 2060(sh)	755(m), 715(w)	440(s)
$[Co(bipy)_3][p\text{-tolyl Hg}(SCN)_2]_2$	2110(sh), 2090(s)	720(vs), 705(sh)	438(s)
$(SCN)_2Co(NCS)_2Hg_2(\alpha\text{-naphthyl})_2$	2145(s), 2070(sh)	785(m), 690(s)	445(s)
$(py)_2(SCN)_2Co(NCS)_2Hg_2(\alpha\text{-naphthyl})_2$	2160(sh), 2065(s)	790(w), 700(m)	425(s)
$(dmso)_2(SCN)_2Co(NCS)_2Hg_2(\alpha\text{-naphthyl})_2$	2130(s), 2080(s)	770(vs), 745(w)	440(s)
$[Co(bipy)_3][\alpha\text{-naphthyl Hg}(SCN)_2]_2$	2090(s), 2110(sh)	715(vs), 700(sh)	430(w)
$(SCN)_2Ni(NCS)_2Hg_2(p\text{-tolyl})_2$	2170(s), 2080(m)	785(w), 745(s)	442(s)
$(py)_2(SCN)_2Ni(NCS)_2Hg_2(p\text{-tolyl})_2$	2145(s), 2070(s)	790(vs), 690(s)	425(s)
$(dmso)_2(SCN)_2Ni(NCS)_2Hg_2(p\text{-tolyl})_2$	2150(s), 2075(sh)	790(w), 725(w)	450(b)
$[Ni(bipy)_3][p\text{-tolyl Hg}(SCN)_2]_2$	2100(sh), 2095(s)	720(vs), 695(sh)	430(w)
$(SCN)_2Ni(NCS)_2Hg_2(\alpha\text{-naphthyl})_2$	2140(sh), 2080(s)	790(w), 740(vs)	440(s)
$(py)_2(SCN)_2Ni(NCS)_2Hg_2(\alpha\text{-naphthyl})_2$	2165(s), 2065(m)	795(w), 710(s)	434(s)
$(dmso)_2(SCN)_2Ni(NCS)_2Hg_2(\alpha\text{-naphthyl})_2$	2150(s), 2070(sh)	790(sh), 725(s)	445(w)
$[Ni(bipy)_3][\alpha\text{-naphthyl Hg}(SCN)_2]_2$	2105(s), 2095(sh)	705(w), 695(s)	430(s)

s= strong; sh= shoulder; m= medium; w= weak; b= broad and v= very.

The slight changes in band positions are due to change in stereochemistry around M. The change in νC–N stretching band positions due to change in stereochemistry is well described elsewhere.[8] The νM–NCS bands in the case of cobalt Lewis acids are observed at about 308 cm^{-1}, which on adduct formation shift to 240 cm^{-1}. This negative shift shows the change from tetrahedral configuration to octahedral on adduct formation.[7,9] Such a change is not observed in nickel analogues because of the presence of octahedral configuration in both the Lewis acids and their adducts. A band assigned to νM–N (py) is observed at about 270 cm^{-1} in pyridine adducts and at 378 cm^{-1} in dmso adducts which is assigned[10,11] to νM–O. These bands are absent in the Lewis acids.

The electronic spectra of the Lewis acids and the adducts as discussed later indicate that cobalt in $(SCN)_2M(NCS)_2Hg_2R_2$ is in tetrahedral coordination and the nickel is octahedral. The octahedral geometry in case of nickel is perhaps acquired by axial coordination through sulphur of the thiocyanate group of the adjacent layer.[12] In the case of $L_2(SCN)_2M(NCS)_2Hg_2R_2$ both nickel and cobalt acquire the octahedral configuration. The magnetic moment values of $(SCN)_2Co(NCS)_2Hg_2R_2$ are 4.1–4.2 B.M. and of $L_2(SCN)_2Co(NCS)_2Hg_2R_2$ are 4.92–5.1 B.M. In the case of $(SCN)_2Ni(NCS)_2Hg_2R_2$ and their adducts these values are in the range 2.85–3.31 B.M. On the basis of above results the following structures (Figs. 1–3) can be proposed, pending confirmation by single crystal X-ray analysis. These structures are further supported by:

(I) The far IR spectra of the Lewis acids and their adducts show the presence of bands in the region 450–470, 210–220, 160–190 and 79–91 cm^{-1}, which can be

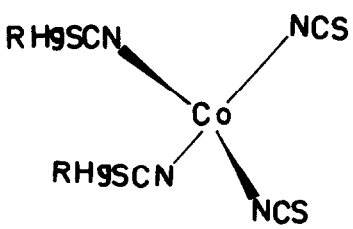

(R = *p*-tolyl and α-naphthyl.)

Fig. 1.

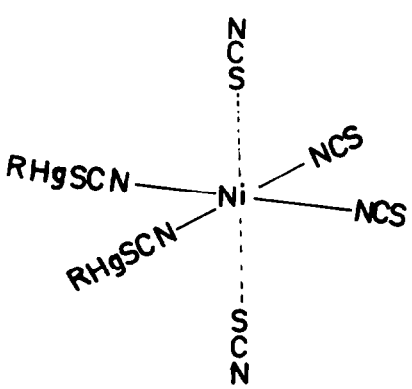

(R = *p*-tolyl and α-naphthyl.)

Fig. 2.

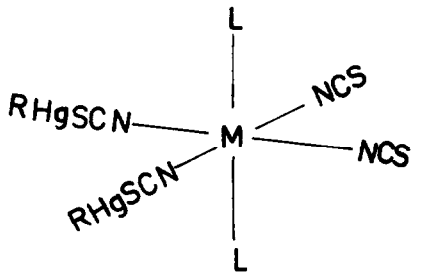

(M = Co, Ni; L = py, dmso and R = *p*-tolyl and α-naphthyl.)

Fig. 3.

assigned to νHg–C, νHg–SCN, δN–M–N and δS–Hg–C vibrations respectively.[12,13] The presence of these bands support the proposed structure.

(II) All the linkages shown in the structures are consistent with the requirements of HSAB principle.

(III) Quantitative softness values as discussed later also support various linkages.

(IV) Local symmetries around cobalt and nickel show that cobalt in $(SCN)_2M(NCS)_2Hg_2R_2$ has T_d symmetry and in $L_2(SCN)_2M(NCS)_2HgR_2$ has D_{4h} symmetry. The nickel in its Lewis acids and adducts have D_{4h} symmetry. The number of IR active bands calculated for these symmetries and the observed number of bands are in good agreement (Table 4).

(V) The cobalt and nickel are in their preferred coordination geometries in Lewis acids and in their adducts. Mercury, too has the preferred linear structure.

(VI) Organomercury halides have been shown to have poor acceptor properties,[14] hence the linkage of pyridine and dimethylsulfoxide to cobalt or nickel instead of mercury is more justified.

2. *Cationic–anionic complexes.* $[M(bipy)_3][RHg(SCN)_2]_2$

The bipyridyl complexes of both the Lewis acids show a different behaviour. Their molar conductance values (132–136 cm^{-1} mhos/moles) in dimethylformamide show that they are 1:2 electrolyte. The IR spectra of the complexes indicate the absence of bridging and N-bonded thiocyanate. Two bands in the νC–N and νC–S regions are observed which are in the range of S-bonded thiocyanate[15] (Table 3).

The electronic spectra of the complexes as discussed later indicate that cobalt and nickel are in octahedral configurations. The magnetic moment values also support this configuration. The Dq values of the complexes are close to the reported Dq values of $[Co(bipy)_3]^{2+}$ ion. The far IR spectra shows the presence of bands at 260 and 285 cm^{-1} for νCo–N and νNi–N respectively. On the basis of these observations we can suggest that the cation has cobalt or nickel duly coordinated with three molecules of bipyridyl. The anion possibly has a tri-coordinated mercury linked with two S-bonded thiocyanate ions and one aryl group. The tri-coordinated structure of mercury is also supported by the number of bands in the νC–N and νC–S regions. The anion has C_{2v} symmetry and is expected to give two bands in these regions. Two bands against each are actually present. Tricoordinated mercury compounds have been reported by earlier workers also.[16,17] The preference of bipyridyl for cobalt or nickel in comparison to mercury is in conformity with the HSAB principle[18] and ΔE_{nm}^{2+} [19] requirements. The far IR spectra show the presence of

Table 4. IR spectral band assignments in the far IR region

Complexes	νHg–C (cm^{-1}) A_1+B_2	νHg–SCN (cm^{-1}) A_1+B_2	μM–NCS (cm^{-1}) $2A_1+B_1+B_2$	νM–L (cm^{-1}) A_1+B_2	δL–M–L (cm^{-1}) $2A_1+B_1+B_2$	δN–M–N (cm^{-1}) $2A_1+B_1+B_2$	δS–Hg–C (cm^{-1}) $2A_1+B_1+B_2$
$(SCN)_2Co(NCS)_2Hg_2(p\text{-tolyl})_2$	450(s)	220(s)	308(s)	–	–	178(s)	91(s)
$(py)_2(SCN)_2Co(NCS)_2Hg_2(p\text{-tolyl})_2$	452(vs)	216(b)	240(m)	285(s)	140(m)	186(m)	86(s)
$(dmso)_2(SCN)_2Co(NCS)_2Hg_2(p\text{-tolyl})_2$	452(b)	210(b)	242(m)	378(m)	162(w)	178(m)	82(s)
$[Co(bipy)_3][p\text{-tolyl Hg(SCN)}_2]_2$	468(w)	210(m)	–	260(b)	135(w)	–	84(s)
$(SCN)_2Co(NCS)_2Hg_2(\alpha\text{-naphthyl})_2$	452(vs)	220(b)	306(b)	–	–	186(s)	79(b)
$(py)_2(SCN)_2Co(NCS)_2Hg_2(\alpha\text{-naphthyl})_2$	450(s)	218(m)	239(s)	280(b)	160(m)	180(vs)	80(s)
$(SCN)_2Ni(NCS)_2Hg_2(p\text{-tolyl})_2$	468(s)	216(s)	242(s)	–	–	190(m)	80(s)
$(SCN)_2Ni(NCS)_2Hg_2(\alpha\text{-naphtyl})_2$	470(vs)	220(w)	238(b)	–	–	160(m)	79(s)
$(py)_2(SCN)_2Ni(NCS)_2Hg_2(\alpha\text{-naphtyl})_2$	468(vs)	215(b)	242(m)	270(s)	132(w)	182(w)	82(w)
$[Ni(bipy)_3][p\text{-tolyl Hg(SCN)}_2]_2$	458(vs)	210(m)	–	285(vs)	125(b)	–	86(s)

s= strong; m= medium; b= broad; w= weak; and v= very.

Hg–SCN band at 210 cm^{-1} and absence of νCo–NCS or νNi–NCS band.

On the basis of these results the following structure (Fig. 4) can be proposed to cationic–anionic complexes.

Electronic spectra. The electronic spectra of the complexes have been recorded as nujol mulls in order to avoid the effect of solvolysis in solution. In the case of $(SCN)_2Co(NCS)_2Hg_2$ two intense bands assigned to $^4A_2 \rightarrow {}^4T_2(F)$ (ν_3), and $^4A_2 \rightarrow {}^4T_1(P)$ (ν_2) transitions were observed at about 16,400 and 7850 cm^{-1} respectively. The ν_2 band was not split showing the presence of T_d symmetry around cobalt. The Dq values derived from ν_3 and ν_2 bands are about 480 cm^{-1}. This value is higher than the reported[20] Dq value of $[Co(NCS)_4]^{2+}$. This increase in ligand field strength is consistent with the Cotton's observation.[20] It has been reported that when the free sulphur end of N-coordinated thiocyanate ions become bound to other ions such as Hg^{2+} the contribution of the N-coordinated thiocyanate to the ligand field around the first metal is enhanced. In $L_2(SCN)_2Co(NCS)_2Hg_2R_2$, three bands in the region 20,830–21,600, 16,500–17,800 and 8000–8900 cm^{-1} are observed assignable to $^4T_{1g} \rightarrow {}^4T_{1g}(P)$ (ν_3), $^4T_{1g} \rightarrow {}^4A_{2g}(\nu_2)$ and $^4T_{1g} \rightarrow {}^4T_{2g}(\nu_1)$ transitions respectively. The ν_2 band being two-electron transition is very weak. The spectral parameters Dq, B′ and β have been calculated from ν_2 and ν_3 bands. The Dq values so obtained have been compared with ν_1 band position and both are very close. The band position, spectral parameters and the magnetic moment values (Table 5) support octahedral configuration around cobalt in the adducts. In case of cationic–anionic complexes three bands are also observed which are assigned to $^4T_{1g} \rightarrow {}^4T_{1g}(P)(\nu_3)$, $^4T_{1g} \rightarrow {}^4A_{2g}(\nu_2)$ and $^4T_{1g} \rightarrow {}^4T_{2g}(\nu_1)$ transitions. These bands are present in the region 21,260–21,600, 16,490–17,710 and 8920–9300 cm^{-1} respectively. The position of the bands in case of the cationic–anionic complexes have higher value as compared to corresponding band positions of the pyridine adducts. The Dq value (945 cm^{-1}) of the cation$[Co(bipy)_3]^{2+}$ is higher than the Dq values (890 cm^{-1}) of the adducts. $[Co(bipy)_3]^{2+}$ is expected to have higher value than $L_2(SCN)Co(NCS)_2Hg_2R_2$. The higher Dq value supports the existence of such a cation.

The electronic spectra of the nickel Lewis acids, their adducts and cationic–anionic complexes show the presence of three bands in the region 25,640–28,570, 15,870–18,500 and 9010–11,360 cm^{-1} which are assigned to $^3A_{2g} \rightarrow {}^3T_{1g}(P)(\nu_3)$, $^3A_{2g} \rightarrow {}^3T_{1g}(F)(\nu_2)$ and $^3A_{2g} \rightarrow {}^3T_{2g}(F)(\nu_1)$ respectively. The Dq values derived from ν_2 and ν_3 bands or from ν_1 bands show that Lewis acid has the lowest value and the cationic–anionic complexes have the highest value. This difference in Dq values is perhaps due to the difference in moieties around nickel in all the three cases. In the Lewis acid the nickel has $(NCS)_2Ni(NCS)_2$ moiety and in the adducts has $L_2Ni(NCS)_4$ and in the cationic–anionic complexes has $[Ni(bipy)_3]$ moiety. The thiocyanate being at the weaker and of the spectrochemical series will have a lower Dq value than bipyridyl which is at the stronger end of the spectrochemical series. The highest Dq value in case of cationic–anionic complexes and its closeness to the reported[21] Dq value of $[Ni(bipy)_3]^{2+}$, indicates that nickel is linked only with bipyridyl.

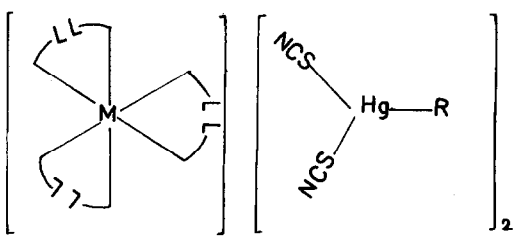

(M = Co, Ni; L = bipyridyl- and R = p-tolyl and α-naphthyl).

Quantitative "softness" values

Quantitative "softness" values of metal ions in different compounds and of ligands, have recently been used in deriving choice of linkages in a complex, its structures and relative metal ligand bond strength.[18,19,22,23] The "softness" of metal ions has been denoted by E_n^{2+} and of bases by E_m^{2+}, and the difference between the two by ΔE_{nm}^{2+}. The "softness" values of various metal ions and bases involved in the present series have also been calculated by the method described elsewhere,[19] and are presented in Table 6. These values have been applied in the following manner:

(1) The pyridine, dmso or bipyridyl when reacted with any of the Lewis-acids has two sites for linkage, one at M[Co(II) or Ni(II) or Zn(II)] and the other at mercury. The ΔE_{nm}^{2+} values derived for M–py linkage and Hg–py linkage show that the former will be preferred because of higher value of ΔE_{nm}^{2+} (Table 7). The experimental results also support this linkage.

(2) The difference in total "softness" ΔTE_n^{2+}(M–Hg) values of M and Hg has been indicative of the stability of thiocyanate bridge between M and Hg.[23] The difference in total "softness" between M(II) and Hg(II) of the three Lewis acids of the alkyl series (Table 8) shows the following order of the stability of the thiocyanate bridge: Ni–Hg > Co–Hg > Zn–Hg.

The difference in total "softness" values in Zn–Hg Lewis acids is the lowest, hence the thiocyanate bridge between these two metal ions is the weakest. On reaction with pyridine Co–Hg Lewis acids form adducts, whereas in case of Zn–Hg Lewis acid the thiocyanate bridge in between Zn–Hg is broken. This may be on account of lower ΔTE_n^{2+}(Zn–Hg) value. It is interesting to note that Zn–Hg Lewis acid of *p*-tolyl forms adducts with pyridine. The ΔTE_n^{2+}(Zn–Hg) derived for this Lewis acid is 14.449 which is, higher as compared to alkyl series, and it is perhaps on this account the thiocyanate bridge between Zn–Hg is stable.

(3) Metal ligand bond strength has recently been represented in terms of matching constant.[19] The matching constant data in case of Lewis acids and their adducts have been calculated by the following equation and are presented in Table 9.

$$\text{Matching constant} = |E_n^{2+} - E_m^{2+}| + \text{CFSE}.$$

A reference to Table 9 shows that the complexes where M = Ni(II) have higher value than the corresponding cobalt complexes. The zinc analogues have the lowest value. The sequence of stability is in consonance with the Irving–Williams stability sequence.[24] The matching constant value also indicate that the -naphthyl complexes are comparatively more stable than the *p*-tolyl complexes.

Table 5. Selected electronic bands and their spectral parameters

Complexes	ν_3 (cm^{-1})	ν_2 (cm^{-1})	ν_1 (cm^{-1})	Dq (cm^{-1})	B' (cm^{-1})	β	μ_{eff} (B.M.)
$(SCN)_2Co(NCS)_2Hg_2(p\text{-tolyl})_2$	16,400	7,850	-	480	642	.66	4.1
$(py)_2(SCN)_2Co(NCS)_2Hg_2(p\text{-tolyl})_2$	20,830	16,680	8,900	890	941	.97	4.92
$(dmso)_2(SCN)_2Co(NCS)_2Hg_2(p\text{-tolyl})_2$	21,600	17,800	8,010	801	806	.83	4.94
$[Co(hipy)_3][p\text{-tolyl } Hg(SCN)_2]_2$	21,260	16,490	8,920	890	941	.97	4.99
$(SCN)_2Co(NCS)_2Hg_2(\alpha\text{-naphthyl})_2$	16,390	7,840	-	475	757	.78	4.2
$(py)_2(SCN)_2Co(NCS)_2Hg_2(\alpha\text{-naphthyl})_2$	21,270	17,000	8,800	908	961	.99	5.1
$(dmso)_2(SCN)_2Co(NCS)_2Hg_2(\alpha\text{-naphthyl})_2$	21,270	16,500	8,000	755	728	.75	5.1
$[Co(hipy)_3][\alpha\text{-naphthyl } Hg(SCN)_2]_2$	21,600	17,710	9,300	945	961	.99	5.04
$(SCN)_2Ni(NCS)_2Hg_2(p\text{-tolyl})_2$	27,790	16,650	9,620	1,020	906	.87	3.07
$(py)_2(SCN)_2Ni(NCS)_2Hg_2(p\text{-tolyl})_2$	28,570	17,390	10,530	1,073	916	.88	2.99
$(dmso)_2(SCN)_2Ni(NCS)_2Hg_2(p\text{-tolyl})_2$	26,315	16,130	9,010	1,005	812	.78	3.18
$[Ni(hipy)_3][p\text{-tolyl } Hg(SCN)_2]_2$	27,200	17,800	11,360	1,114	770	.74	2.85
$(SCN)_2Ni(NCS)_2Hg_2(\alpha\text{-naphthyl})_2$	27,780	16,670	9,610	1,085	906	.87	3.14
$(py)_2(SCN)_2Ni(NCS)_2Hg_2(\alpha\text{-naphthyl})_2$	25,640	18,500	10,860	1,057	958	.92	3.08
$(dmso)_2(SCN)_2Ni(NCS)_2Hg_2(\alpha\text{-naphthyl})_2$	26,300	15,870	9,170	1,007	729	.70	3.31
$[Ni(hipy)_3][\alpha\text{-naphthyl } Hg(SCN)_2]_2$	26,940	16,500	10,900	1,057	698	.67	3.08

Table 6. Effective "softness" values of metals and ligands

Complexes	$E^{\ddagger}_{n(eff)}$ (Co)	$E^{\ddagger}_{n(eff)}$ (Ni)	$E^{\ddagger}_{n(eff)}$ (Zn)	$E^{\ddagger}_{n(eff)}$ (Hg)	$E^{\ddagger}_{m}$ (py) N-end	$E^{\ddagger}_{m}$ (dmso) O-end	$E^{\ddagger}_{m}$ $(SCN)^{-}$ N-end	$E^{\ddagger}_{m}$ $(NCS)^{-}$ S-end	$E^{\ddagger}_{m}$ (RHgSCN) N-end
$(SCN)_2M(NCS)_2Hg_2(p\text{-tolyl})_2$	-3.34	-4.062	-5.003	-6.431	-	-	-12.65	-8.22	-11.412
$(SCN)_2M(NCS)_2Hg_2(\alpha\text{-naphthyl})_2$	-3.269	-4.032	-	-6.414	-	-	-12.65	-8.22	-11.393
$(py)_2(SCN)_2M(NCS)_2Hg_2(p\text{-tolyl})_2$	-3.297	-4.067	-5.102	-6.431	-11.49	-	-12.65	-8.22	-11.412
$(py)_2(SCN)_2M(NCS)_2Hg_2(\alpha\text{-naphthyl})_2$	-3.281	-3.956	-	-6.414	-11.49	-	-12.65	-8.22	-11.393
$(dmso)_2(SCN)_2M(NCS)_2Hg_2(p\text{-tolyl})_2$	-3.217	-3.979	-	-6.431	-	-10.87	-12.65	-8.22	-11.412
$(dmso)_2(SCN)_2M(NCS)_2Hg_2(\alpha\text{-naphthyl})_2$	-3.202	-3.965	-	-6.414	-	-10.87	-12.65	-8.22	-11.393

The softness values of the metals and the ligands have been calculated in the solvent ethanol.

Table 7. Matching (ΔE^{2+}_{nm}) between metals and ligands

Ligands	ΔE^{+}_{nm}(Co–L)	E^{+}_{nm}(Ni–L)	ΔE^{+}_{nm}(Zn–L)	ΔE^{+}_{nm}(Hg–L)
pyridine	10.75	10.97	7.171	6.14
dmso	10.49	10.71	6.552	5.88
2-2′ bipyridyl	11.06	11.28	7.121	6.45

The matching (ΔE^{+}_{nm}) has been derived from the difference in softness values of metal ions and the ligand.[19] The higher is the value of ΔE^{+}_{nm} the better is the matching. E^{2+} of *metal ions*:—$Co^{+2} = -0.38$, $Ni^{2+} = -0.16$, $Zn^{2+} = -4.318$ and $Hg^{2+} = -4.99$.

Table 8. Total "softness" difference "ΔTE^{2+}_{n}(M(Hg)" values

Lewis acids	ΔTE_n^{+}(Co–Hg)	ΔTE_n^{+}(Ni–Hg)	ΔTE_n^{+}(Zn–Hg)
$(SCN)_2M(NCS)_2Hg_2(CH_3)_2$	14.48	16.65	13.10
$(SCN)_2M(NCS)_2Hg_2(C_2H_5)_2$	14.34	16.47	12.97
$(SCN)_2M(NCS)_2Hg_2(C_3H_7)_2$	11.94	12.77	11.46
$(SCN)_2M(NCS)_2Hg_2(C_4H_9)_2$	14.24	16.33	12.97

ΔTE_n^{+}(M–Hg) have been calculated by adopting the equation reported elsewhere.[22]

Table 9. Matching constant values of the complexes

Complexes	Dq (cm^{-1})	CFSE (cm^{-1})	CFSE (e.v)	ΔE^{+}_{nm}	Matching constant (ΔE^{+}_{nm} + CFSE)
$(SCN)_2Co(NCS)_2Hg_2(p\text{-tolyl})_2$	480	39,840	4.939	9.309	14.248
$(SCN)_2Co(NCS)_2Hg_2(\alpha\text{-naphthyl})_2$	475	39,900	4.946	9.380	14.327
$(SCN)_2Ni(NCS)_2Hg_2(p\text{-tolyl})_2$	1020	53,760	6.665	8.587	15.252
$(SCN)_2Ni(NCS)_2Hg_2(\alpha\text{-naphthyl})_2$	1026	53,668	6.656	8.618	15.274
$(SCN)_2Zn(NCS)_2Hg_2(p\text{-tolyl})_2$	-	-	-	7.548	7.546
$(py)_2(SCN)_2Co(NCS)_2Hg_2(p\text{-tolyl})_2$	890	38,480	4.770	8.193	12.963
$(py)_2(SCN)_2Co(NCS)_2Hg_2(\alpha\text{-naphthyl})_2$	908	38,336	4.753	8.208	12.961
$(py)_2(SCN)_2Ni(NCS)_2Hg_2(p\text{-tolyl})_2$	1073	53,124	6.586	7.428	14.014
$(py)_2(SCN)_2Ni(NCS)_2Hg_2(\alpha\text{-naphthyl})_2$	1057	53,688	6.656	8.618	15.274
$(py)_2(SCN)_2Zn(NCS)_2Hg_2(p\text{-tolyl})_2$	-	-	-	6.422	6.422
$(dmso)_2(SCN)_2Co(NCS)_2Hg_2(p\text{-tolyl})_2$	794	39,248	4.866	7.653	12.519
$(dmso)_2(SCN)_2Co(NCS)_2Hg_2(\alpha\text{-naphthyl})_2$	756	39,552	4.904	7.667	12.571
$(dmso)_2(SCN)_2Ni(NCS)_2Hg_2(p\text{-tolyl})_2$	1,005	53,940	6.687	6.89	13.577
$(dmso)_2(SCN)_2Ni(NCS)_2Hg_2(\alpha\text{-naphthyl})_2$	1,007	53,316	6.609	7.533	14.142

Comparison with alkyl mercury thiocyanate complexes

(1) Alkyl mercury thiocyanate RHgSCN–[R = CH_3, C_2H_5, C_3H_7, C_4H_9, C_5H_{11}] react with $Co(NCS)_2$ and form the Lewis acids of general formula $(SCN)_2Co(NCS)_2Hg_2R_2$. The aryl mercury thiocyanates ArHgSCN–[Ar = C_6H_5, $CH_3C_6H_4$, $C_{10}H_7$] do not react with $Co(NCS)_2$, to form the corresponding Lewis acids. They however, react with $Co(NCS)_2(py)_2$ and form adducts of general formula $(py)_2(SCN)_2Co(NCS)_2Hg_2(Ar)_2$. On heating these adducts in vacuum, the pyridine is given off and Lewis acids are formed.

(2) The dimethylsulphoxide forms stable complexes with aryl derivatives whereas the dmso complexes of alkyl derivatives are very unstable.

(3) The Dq values of $(SCN)_2Ni(NCS)_2Hg_2R_2$ (R = methyl, ethyl, propyl, butyl, amyl, *p*-tolyl and α-naphthyl) as presented in parentheses indicate th at *n*-amyl mercury thiocyanate has the highest ligand field strength and the *n*-propyl mercury thiocyanate has the lowest. The spectrochemical series can be drawn in the following order.

$n\text{-}C_5H_{11}HgSCN(1070) > \alpha\text{-}C_{10}H_7HgSCN(1026) > \alpha\text{-}CH_3C_6H_4HgSCN(1020) > C_2H_5HgSCN(1018) > CH_3HgSCN(1016) > n\text{-}C_4H_9HgSCN(1015) > C_3H_7HgSCN(1014)$.

(4) When Co(II) and Ni(II) are replaced by Zn(II) in the Lewis acids the behaviour become entirely different in alkyl and aryl analogs. On reaction with pyridine the alkyl derivative-$(SCN)_2Zn(NCS)_2Hg_2R_2$ decompose

whereas the aryl analogs $(SCN)_2Zn(NCS)_2Hg_2Ar_2$ forms well defined complexes.

Acknowledgements—The authors are grateful to the C.S.I.R., New Delhi for financial support and I.I.T., Madras for providing instrumentation facilities.

REFERENCES

[1]P. P. Singh, Subir Kumar and M. P. Reddy, *Inorg. Chem.* 1981, **20**, 2711.
[2]Koshits Porai, *Kristallografica*, 1959, **4**, 239 and references therein.
[3]A. N. Nesmeyanov, *Zh. Russ. Fiz. Khim. Obshch.* 1929, **61**, 1393.
[4]A. N. Nesmeyanov, *Chem. Ber.* 1929, **62**, 1010.
[5]R. Beattic and F. C. Whitmore, *J. Amer. Chem. Soc.* 1933, **55**, 1567.
[6]Kurt Dehnicke, *J. Organo. Chem.* 1967, **9**, 11.
[7]R. J. H. Clark and C. S. Williams, *Spectro. Chim. Acta.* 1966, **22**, 1081.
[8]S. M. Nelson and T. M. Shepherd, *J. Inorg. Nucl. Chem.* 1965, **27**, 2123.
[9]R. Makhija, L. Pazdernik and R. Rivest, *Can. J. Chem.* 1973, **51**, 2987.
[10]J. R. Ferraro, *Low Frequency Vibrations of Inorganic and Coordination Compounds*, Chaps. 5 and 7. Plenum Press, New York.
[11]R. J. H. Clark, *J. Chem. Soc.* 1962, 1377.
[12]D. Forster and D. M. L. Goodgame, *Inorg. Chem.* 1965, **4**, 715.
[13]R. A. Bailly, S. L. Kozak, T. W. Michelsen and W. N. Mills, *Coord. Chem. Rev.* 1977, **6**, 407.
[14]G. Schwavzenbach and M. Schellenberg, *Helv. Chem. Acta.* 1965, **48**, 28.
[15]I. S. Ahuja and A. Garg, *J. Inorg. Nucl. Chem.* 1972, **34**, 1929.
[16]R. C. Makhija, A. L. Beauchamp and R. Rivest, *J. Chem. Soc.* 1972, 1043.
[17]A. J. Canty and A. Marker, *Inorg. Chem.* 1976, **15**, 425.
[18]G. Klopman, *J. Amer. Chem. Soc.* 1968, **90**, 223.
[19]P. P. Singh, S. K. Srivastava and A. K. Srivastava, *J. Inorg. Nucl. Chem.* 1980, **42**, 521.
[20]F. A. Cotton, D. M. L. Goodgame, M. Goodgame and A. Sacco, *J. Amer. Chem. Soc.* 1961, **83**, 4157.
[21]P. P. Singh and A. K. Gupta, *Inorg. Chem.* 1978, **17**, 1.
[22]P. P. Singh, Lallan P. Pathak and Sharad K. Srivastava, *J. Inorg. Nucl. Chem.* 1980, **42**, 533.
[23]P. P. Singh, *Coordination Chemistry Rev.* 1980, **32**, 33.
[24]J. E. Huheey, *Inorganic Chemistry. Principles of Structure and Reactivity*, p. 229. Harper & Row, New York (1972).

Polyhedron Vol. 1, No. 9-10, pp. 723-734, 1982
Printed in Great Britain.

0277-5387/82/090723-12$03.00/0
Pergamon Press Ltd.

PREPARATION OF SOME NEW PENTAFLUOROSULFUR FLUOROETHANES; THE VIBRATIONAL SPECTRUM OF 1-HYDRO-1-PENTAFLUOROSULFUR-F-ETHANE AND ITS DEUTERIUM ISOTOPOMER

H. F. Efner[1], R. Kirk, R. E. Noftle*, and M. Uhrig*

Department of Chemistry, Wake Forest University
Winston-Salem, N. C. 27109, U.S.A.

(Received 20 July 1982)

Abstract - The preparation of 1-hydro-pentafluorosulfur-F-ethylsilver is described. $AgCH(SF_5)CF_3$ reacts with HCℓ and DCℓ to form $HCH(SF_5)CF_3$ and $DCH(SF_5)CF_3$. 1-Pentafluorosulfur-F-ethylsilver reacts with $Cℓ_2$ and DCℓ to form $CℓCF(SF_5)CF_3$ and $DCF(SF_5)CF_3$. $AgCH(SF_5)CF_3$, $DCH(SF_5)CF_3$, $CℓCF(SF_5)CF_3$ and $DCF(SF_5)CF_3$ have not been reported previously.

The vibrational spectra of $HCF(SF_5)CF_3$ and its deuterated analog were investigated, and a tentative assignment was made.

INTRODUCTION

Miller and coworkers have found that perfluoralkyl-silver compounds are highly reactive and can serve as useful intermediates for the synthesis of polyfluorocarbons,[2-4]. We have recently reported the first synthesis of a perfluoroalkylsilver complex which contains the pentafluorosulfur group[5]. Since it was of interest to determine whether or not other pentafluorosulfur containing alkylsilver complexes could exist, we undertook the present work in which the compound $AgCH(SF_5)CF_5$ was prepared and some of its reactions were studied.

The vibrational spectra of pentafluorosulfur compounds are of considerable interest, and much attention has been given to their interpretation in recent years[6-10]. Therefore, as part of this work, we obtained high resolution infrared and Raman spectra of $HCF(SF_5)CF_3$ and its deuterated analogue, $DCF(SF_5)CF_3$, in order to attempt a vibrational assignment.

EXPERIMENTAL

Silver fluoride (Ozark-Mahoning) was stored and transferred in a drybox under subdued light. Acetonitrile (J. T. Baker Reagent grade) was dried over calcium hydride and distilled prior to use.

1-Pentafluoro-F-ethylsilver was prepared from silver fluoride and pentafluorosulfur-F-ethene as described previously[5]. All manipulations involving fluoroalkylsilver compounds were carried out under vacuum in carefully dried glassware, and light was excluded from the photosensitive reaction mixtures. 1-Hydro-1-pentafluorosulfur-F-ethane, $HCF(SF_5)CF_3$, was prepared as described previously[5]. High resolution infrared and Raman data are presented in Table I.

Anhydrous DCℓ (99.5% isotopic purity) was prepared from Tridom 20% aqueous DCℓ by carefully drying the gas above the solution over P_4O_{10}.

Preparation of 1-hydro-1-pentafluorosulfur-F-ethene

$SF_5CH=CF_2$ was prepared by the dehydrohalogenation of $SF_5CH_2CF_2Br$ using NaOH suspended in mineral oil[11,12]. $SF_5CH_2CF_2Br$ was prepared by the addition of SF_5Br to $CF_2=CH_2$[11] and purity was checked by infrared spectroscopy[12]. $SF_5CH=CF_2$: Infrared spectrum, vapor

phase, cm^{-1}: 3130(w), 1730(s), 1350(s), 1245(w), 1210(s), 1085(w), 1010(s), 885(vs), 780(s), 680(m), 600(s), 560(m). M. Calcd.: 190. Found: 188.

Preparation of 1-hydro-1-pentafluorosulfur-F-ethyl silver

In a typical experiment, a dry 100 ml vessel was charged with silver fluoride (0.709 g, 5.59 mmol) and evacuated. Acetonitrile (1.85 g) and 1-hydro-1-pentafluorosulfur-F-ethene (2.553 g, 13.4 mmol) were condensed in at -196°. The vessel was sealed, allowed to warm to room temperature, and stirred for two hours. The resulting yellow solution was filtered under vacuum to remove residual silver fluoride, and the unreacted olefin along with the acetonitrile solvent was removed by pumping the filtrate. The white, solid product, $AgCH(SF_5)CF_3$,was isolated as the solvate. Calcd. mass for $AgCH(SF_5)CF_3 \cdot 0.5CH_3CN$: 1.677 g. Found: 1.677 g.

Treatment of $AgCH(SF_5)CF_3$ with a slight deficiency of anhydrous HCℓ (4.71 mmol) over a 14 hr period gave a volatile mixture that was fractionated at -80, -115, -196°. Upon further separation by GLPC (¼" x 4', 10% DCQF-1, 30/60 Chromosorb P, 30°, 50 ml/min He), the contents of the traps held at -115° and -196° yielded 1,1-dihydro-1-pentafluorosulfur-F-ethane (0.720 g, 69%) which was identified by its characteristic infrared spectrum[12]. Since our infrared spectrum covers a broader range than that reported earlier[12], our data are reported here along with those for the Raman spectrum. $HCH(SF_5)CF_3$. Infrared, vapor phase, cm^{-1}: 3047(vvw), 3005(vvw), 1424(mw), 1353(ms), 1300(ms), 1272(ms), 1150(vs), 915(s), 878(vs), 858(vs), 740(m), 683(w), 654(w), 615(w), 572(w), 529 (sh,w), 513(vw), 402(vvw), 298(vvw). Raman, liquid phase, cm^{-1}: 3030(6), 3003(36), 1423(2), 1355(2), 1298(1), 1265(1), 1135(3), 908(4), 870(2), 848(6), 733(100), 681(88), 650(20), 607(12), 567(2), 530(3), 519(8), 482(3), 452(?), 408(6), 294(43), 268(3), 238(13), 156(1). In addition, a small amount of the starting material ($SF_5CH=CF_2$, 0.1083 g, 9%) was recovered along with a minor unidentified product which infrared and mass spectral data suggested was 1-trifluorosulfur-2-hydro-F-ethane (0.192 g, 20%). Infrared spectrum, vapor phase, cm^{-1}: 1400(m), 1265(m), 1170(s), 1148(s), 1030(w)(SiF_4?), 880(m), 850(s), 795(m), 705(w), 630(w), 590(w). Mass spectrum, 70 eV, m/e (I/Io x 100): 190, p^+?(28), 171(15), 107(8), 91(8), 89(100), 85(5), 83(10), 82(18), 81(5), 71(8), 70(13), 69(13), 64(23), 63(13), 57(15), 55(15), 51(39), 48(13), 45(13), 44(8), 43(18), 41(26).

The white solid residue remaining in the reaction vessel after the previous treatment weighed 0.6955 g (4.85 mmol, 103% of the theoretical amount of AgCℓ).

Preparation of 1-deutero-1-hydro-1-pentafluorosulfur-F-ethane

A quantity of $AgCH(SF_5)CF_3$ (approx. composition $AgCH(SF_5)CF_3 \cdot 2 \cdot 0\ CD_3CN$, 1.59 mmol) was prepared as described previously except that CD_3CN was used as the solvent. Anhydrous DCℓ(0.0424 g, 1.13 mmol) was condensed into the reaction vessel containing the $AgCH(SF_5)CF_3$ solvate, and the mixture was allowed to warm slowly to room temperature with stirring. A reaction took place immediately as evidenced by a lightening of the gray color of the solid (formation of AgCℓ) and after 30 min., the volatile material was removed. Fractional condensation at -80 and -196° resulted in the isolation of CD_3CN (-80° trap, 0.1201 g, 2.73 mmol) and a mixture (-196° trap which was further separated by GLPC (¼" x 8', 20% OV-210 on 80/100 Chromosorb W-HP, 70 ml/min He) and contained $DCH(SF_5)CF_3$, $SF_5CH=CF_2$, and a small amount of CD_3CN. The yield of $DCH(SF_5)CF_3$ was close to 41% (0.0971 g, 0.46 mmol) based on DCℓ, but the best sample was still slightly impure with small amounts of unidentified substances. The gray residue (0.3957 g) remaining in the reaction vessel contained AgCℓ, unreacted $AgCH(SF_5)CF_3$ and probably AgF. $DCH(SF_5)CF_3$: M. Calcd: 211. Found: 215. Mass spectrum: m/e (I/Io x 100) species: 192(20) $SF_5CHDCF_2^+$, 191(9) $SF_5CDCF_2^+$, 172(5) SF_5CDCF^+, 129(4) $^{34}SF_5^+$, 127(91) $^{32}SF_5^+$,

123(8) SF_5CHD^+, 108(1) SF_4^+, 102(2) CF_3CDF^+, 101(1) CF_3CHD^+, 91(6) $^{34}SF_3^+$, 83(100) $^{32}SF_3^+$, 85(2) SiF_3^+, 84(71) CF_3CHD^+, 83(8) CF_3CD^+, 82(2) CF_3CH^+, 70(11) SF_2^+, 69(30) CF_3^+, 66(3) SiF_2^+, 65(16) CF_2CHD^+, 64(10) CF_2CD^+, 63(3) CF_2CH^+, 52(14) CF_2D^+, 51(6) SF^+ and CF_2H^+, 47(1) SiF^+, 46(9) $CFCHD^+$, 45(6) $CFCD^+$, 44(4) $CFCH^+$ and CO_2^+, 43(2) C_2F, 34(53) $CFHD^+$, 33(5) CFD^+, 32(4) CHF^+ and S^+, 31(13) CF^+, 28(9) N_2^+ and CO^+, 18(5) H_2O^+ and OD^+, 15(2) CDH. Infrared, vapor phase, cm^{-1}: 3060(vvw), 2920(vvvw), 2420 (vvvw), 2350(vvvw), 2280(vvw), 1465(vvw), 1406(ms), 1363(ms), 1270(ms), 1212(w), 1170(vs), 1145(vs), 935(ms), 880(ms), 850(vvs), 794(s), 705(m), 630(w), 590(w), 575(sh,vw), 530(vw), 475(vvw). A satisfactory Raman spectrum was not obtained.

Preparation of 1-deutero-1-pentafluorosulfur-F-ethane

A quantity of anhydrous DCℓ (0.0243 g, 0.65 mmol) was condensed into a 30 cm^3 Pyrex reaction vessel which contained $AgCF(SF_5)CF_3 \cdot CD_3CN$ (0.67 mmol) prepared as described previously[5]. The reaction mixture was stirred for 30 min. in subdued light and the volatile material was removed under vacuum. The clear, volatile liquid was separated by fractional condensation at -78, -118, and -196°C. The -78° and -118° fractions were further separated by GLPC (¼" x 4', 15% DC-200 on 80/100 Chromosorb P, 23°, 150 mℓ/min He), and a sample of $DCF(SF_5)CF_3$ was isolated (overall yield 49%). $DCF(SF_5)CF_3$: M. Calcd.: 229. Found: 220. Mass spectrum, m/e (I/Io x 100) species: 129(2) $^{34}SF_5^+$, 127 (42) $^{32}SF_5^+$, 108 (4) SF_4^+, 102 (56) CF_3CDF^+, 101 (7) CF_3CHF^+, 91 (6) $^{34}SF_3^+$, 89 (100) $^{32}SF_3^+$, 83 (5) CF_3CD^+, 82 (≪ 1) CF_3CH^+, 70 (6) SF_2^+, 69 (18) CF_3^+ 64 (2) CF_2CD^+, 63 (1) CF_2CH^+, 52 (1) $^{13}CF_2D^+$, 52 (86) $^{12}CF_2D^+$, 51 (12) SF^+, CF_2H^+, 50 (1) CF_2^+, 46 (2) $CFCHD^+$, 45 (1) $CFCD^+$, 44 (2) $CFCH^+$, CO_2^+, 43 (2) C_2F^+, 33 (8) CFD^+, 32 (3) CFH^+, O_2^+, S^+, 31 (13) CF^+, 28 (5) N_2^+ CO^+. Infrared and Raman data are presented in Table II.

Preparation of 1-chloro-1-pentafluorosulfur-F-ethane

A sample of $AgCF(SF_5)CF_3 \cdot 2\,CH_3CN$ (1.9619 g, 4.70 mmol) was prepared and dry, high purity $C\ell_2$ (6.07 mmol) was added. The reaction was allowed to proceed in the dark at room temperature for 3 hr. with stirring. After this time, the grayish solid had turned white (AgCℓ) indicating that a reaction had taken place. The volatile material was removed and separated by fractional condensation and GLPC (DCQF-1) as described previously. After exhaustive purification a pure sample of $C\ell CF(SF_5)CF_3$ (0.0969 g, 0.39 mmol) was obtained (8% based on $AgCF(SF_5)CF_3 \cdot 2CH_3CN$). $C\ell CF(SF_5)CF_3$. % S,F. Calcd.: 12.2, 65.1. Found: 12.3, 65.3. Mass spectrum, 70 eV, m/e (I/Io x 100) species: 193 (2) $SF_5CFC\ell^+$, 138 (.6) $SF_2CF^{35}C\ell^+$, 137 (30) $CF_3F^{37}C\ell^+$, 136 (2) $SF_2CF^{35}C\ell^+$, 135 (100) $CF_3CF^{35}C\ell^+$, 131 (3)?, 129 (.3) $^{34}SF_5^+$, 127 (9) $^{32}SF_5^+$, 119 (12) $C_2F_5^+$, 118 (2) $CF_2CF^{37}C\ell^+$, 116 (5) $CF_2CF^{35}C\ell^+$, 108 (.2) SF_4^+, 91 (1) $^{34}SF_3^+$, 89 (37) $^{32}SF_3^+$, 87 (17) $CF_2^{37}C\ell^+$, 85 (56) $CF_2^{35}C\ell^+$, 70 (16.4) $^{32}SF_2^+$, 69 (44) CF_3^+, 68 (1) $CF\,^{37}C\ell^+$, 67 (3) $^{35}SC\ell^+$, 66 (8) $CF^{35}C\ell^+$, 55 (2)?, 51 (4) $^{32}SF^+$, 50 (4) CF_2^+, 47 (3) $^{35}C\ell^+$, 44 (2) CO_2^+, 37 (1) $^{37}C\ell^+$, 35(2) $^{35}C\ell^+$, 32 (6) $^{32}S^+$, O_2, 31(14) CF^+, 28 (22) N_2^+, CO^+. The vapor phase infrared spectrum was similar to that obtained earlier for $BrCF(SF_5)CF_3$ [5]. Infrared spectrum, vapor phase, cm^{-1}: 1273(m), 1242(vs), 1220(s), 1135(s), 960(m), 935(m), 898(vvs), 829(vs), 778(m), 686(w), 607(m), 578(vw), 555(vvw).

Spectra

Infrared spectra for the purpose of identification were taken on a Perkin-Elmer Model 457 infrared spectrophotometer. High resolution infrared spectra were recorded on a Perkin-Elmer Model 621 infrared spectrophotometer which was purged with dry air. Gaseous samples were held in 7 or 10 cm Pyrex cells equipped with either potassium bromide or cesium iodide windows.

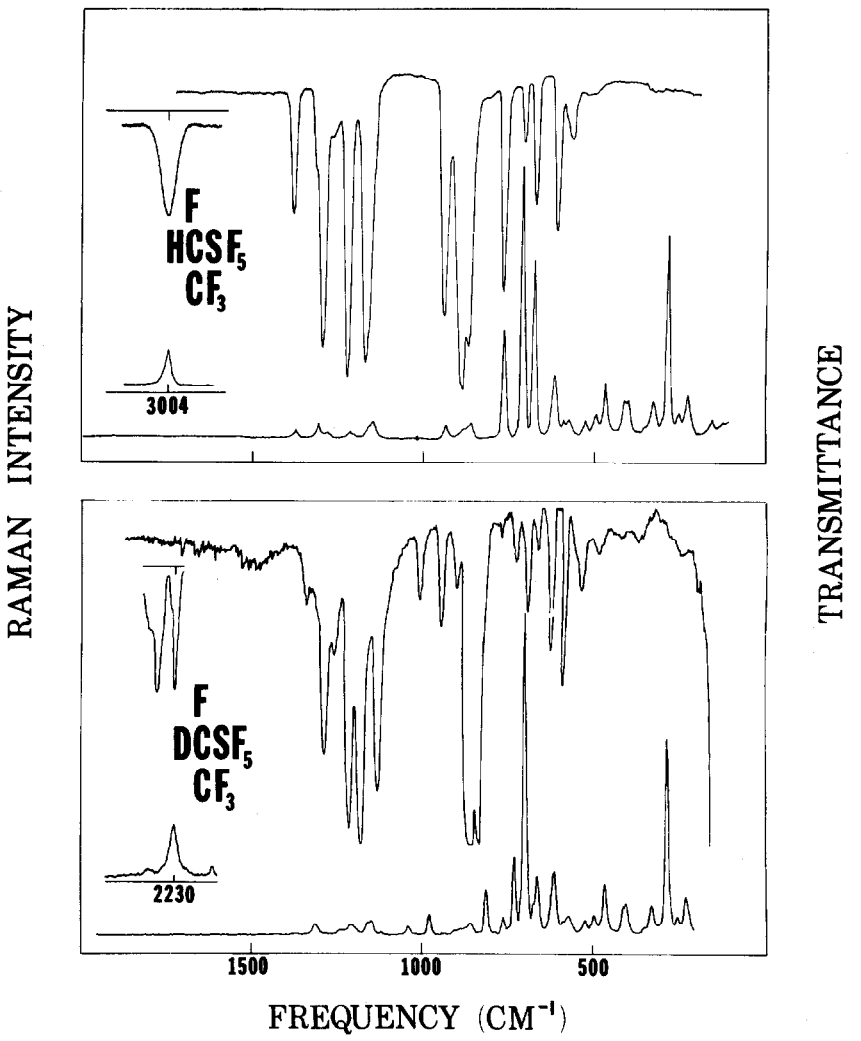

FIG. I. VIBRATIONAL SPECTRA OF $HCF(SF_5)CF_3$ AND $DCF(SF_5)CF_3$

Top: Infrared spectra; gas phase, ca. 5 torr.; gain, 4.5; attenuator speed, 1100; suppression, 4; slit program, auto; scan time, 32 min; source current, 0.8 amp.

Bottom: Raman spectra; liquid (cap.); sensitivity, 55; time constant, auto; slits, 8 -8 -8; height, 12; scan rate, 50 cm^{-1}/min.; laser power, 300 mw (4880 Å).

TABLE I

Vibrational Frequencies and Assignments for $HCF(SF_5)CF_3$

Raman (ℓ)			Infrared (g)	Assignment
$\nu(cm^{-1})$	I	ρ	$\nu(cm^{-1})$	
3004	11	0.23	3007 vw	C-H stretching
2734	0.2			2 x 1376 = 2752
2600	0.2			2 x 1308 = 2616
			2572 vvw	2 x 1294 = 2588
			2529 vvw	1376 + 1161 = 2537
			2457 vvw	1294 + 1161 = 2455
			2425 vvw	2 x 1217 = 2434
			2382 vvw	1217 + 1161 = 2378
2328	0.5		2325 vvw	2 x 1161 = 2322
			2299 vvw	1376 + 935 = 2311
			2235 vvw	1376 + 865 = 2241
			2152 vvw	1217 + 935 = 2152
			2078 vvw	1217 + 865 = 2082
			2027 vvw	1161 + 865 = 2026
			1935 vvw	1332 + 611 = 1943
1901	1			1148 + 761 = 1909
			1704 vvw	1294 + 409 = 1703
			1620 vvw	1294 + 327 = 1621, 1217 + 409 = 1626
			1597 vvw	885 + 710 = 1595, 1376 + 218 = 1594
			1562 vw	1161 + 400 = 1561, 885 + 675 = 1560
			1501 vw	1217 + 283 = 1500, 1376 + 123 = 1499
			1421 vvw	2 x 710 = 1420
1376	0.4	0.44	1376 m	C-C + CF_3 stretching
1308	3	0.32	1332 w	C-H bending
1285	1	0.44	1294 vs	CF_3 stretching
			1242 vvw	675 + 572 = 1247
1212	1	0.37	1217 vs	CF_3 stretching(C-H bending?)
1157	3	0.43	1161 vs	C-F stretching
1148	3	0.38		586 + 568 = 1154
			1113 vvw	710 + 400 = 1110, 710 + 409 = 1119
			1048 vvw	2 x 523 = 1046 766 + 283 = 1049, 935 + 123 = 1058
			991 vvw	2 x 494 = 988 710 + 283 = 993, 865 + 123 = 988
937	3	0.28	935 s	CF_3 + C-C stretching
884	1	0.71	885 vvs	SF_4 stretching
861	2	0.38	865 vs	S-F stretching
801	0.1		814 w	2 x 409 = 818, 523 + 283 = 806, 400 + 409 = 809
761	22	0.10	766 s	CF_3 deformation
706	100	0.05	710 m	SF_4 stretching
672	44	0.05	675 ms	SF_4 deformation
612	9	0.63	611 ms	CF_3 deformation
586	3	0.63		SF_4 stretching
568	2	0.75	572 w	S-F wagging
524	3	0.48	523 w	CF_3 deformation
494	4	0.72		SF_4 deformation
465	12	0.33	464 vw	SF_4 deformation
410	6	0.50	409 vw	CF_3 rocking
399	6	0.50	400 vw	CF_3 rocking
352	1	0.48		1212 - 861 = 351
326	5	0.64	327 vw	SF_5 rocking
281	49	0.20	283 vw	C-S stretching
248	4	0.60		SF_4 deformation
223	6	0.36	218 vvw	CCF bending
155	1	0.24		CSF bending
123	0.2			CCS bending

TABLE II

Vibrational Frequencies and Assignments for $DCF(SF_5)CF_3$

Raman (ℓ)			Infrared(g)		
$\nu(cm^{-1})$	I	ρ	$\nu(cm^{-1})$	I	
			2560	vvw	1318 + 1240 = 2558
			2530	vvw	1318 + 1212 = 2530
			2480	vvw	2 x 1240 = 2480
			2410	vvw	2 x 1212 = 2424
			2320	vvw	2 x 1160 = 2320
2230	12	0.42	2230	vvw	C-D stretching
			2124	vvw	1240 + 897 = 2137
2112	1		2115	vvw	1240 + 877 = 2117
			2080	vvw	1212 + 877 = 2089, 2 x 1040 = 2080
			2058	vvw	1160 + 897 = 2057
			1863	vvw	1240 + 625 = 1865
			1768	vvw	1040 + 730 = 1770, 897 + 877 = 1774
			1739	vvw	981 + 760 = 1741, 1040 + 701 = 1741
			1714	vvw	1318 + 398 = 1716
			1620	vvw	1212 + 409 = 1621, 1160 + 460 = 1620
			1593	vvw	1318 + 276 = 1594
			1555	vvw	1160 + 398 = 1558, 897 + 663 = 1560, 1318 + 245 = 1563, 1240 + 320 = 1560
			1486	vvw	1212 + 276 = 1488, 760 + 730 = 1490
1375	0.6		1375	vvw	981 + 398 = 1379, 1160 + 223 = 1383
1314	7	0.59	1318	ms	C-C + CF_3 stretching
			1288	vvw	663 + 625 = 1288
1236	0.5		1240	s	CF_3 stretching
1208	11	0.63	1212	vs	CF_3 stretching
1153	11	0.74	1160	s,b	C-F stretching
1140	11	0.31			580 + 560 = 1140
1038	6	0.20	1040	w	C-D bending
975	9	0.35	981	m	C-D bending
925	0.1		938	vvw	CF_3 + C-C stretching
906	?				
895	0.6		897	vvs	SF_4 stretching
873	1		877	vs	S-F stretching
855	2				580 + 275 = 855
817	15	0.25	815	vvw	701 + 125 = 826, 2 x 409 = 818
760	6	0.25	760	vw	1160 - 398 = 762*
723	26	0.28	730	w	CF_3 deformation
701	6				455 + 241 = 696*
692	100	0.20	720	w	SF_4 stretching
670	7	0.18	669	ms	398 + 276 = 674*
655	21	0.28	663	ms	SF_4 deformation
610	30	0.81	625	m	CF_3 deformation
580	1				SF_4 stretching
560	8 br	0.61	575	w	S-F wagging
520	5	0.48	532	vw	CF_3 deformation
487	5	0.51			SF_4 deformation
463	0.5				241 + 223 = 464
455	16	0.54	460	vw	SF_4 deformation
402	10	0.49	409	vw	CF_3 rocking
394	11	0.55	398	vvw	CF_3 rocking
338	1				1208 - 873 = 335
320	12	0.66			SF_5 rocking
275	75	0.22	276	vvvw	C-S stretching*
241	3	0.55	245	vvvw	SF_4 deformation
223	4	0.65			CCF bending
158	4	0.62			CSF bending
125	0.5				CCS bending

*may be due in part to trace impurity of $HCF(SF_5)CF_3$

Raman spectra were taken using a Beckman Model 700 laser-Raman spectrophotometer equipped with a Spectra-Physics 2-watt argon-ion laser. In order to ensure the identification of "grating ghosts", spectra were obtained at the 4880 Å and 5145 Å exciting lines from which other discharge lines were removed by means of a narrow band pass filter (10 Å). The spectrometer was calibrated against the emission lines of Ne. Data are presented in Tables I and II and Fig. I.

Mass spectra were recorded on either a CVC MA-2 TOF or a CEC 21-110 mass spectrometer operating at an ionizing potential of 70 eV.

RESULTS AND DISCUSSION

Synthesis

In a previous communication, the facile addition of silver fluoride to 1-pentafluorosulfur-F-ethene (I) was reported[5]. In this work it was found that 1-hydro-1-pentafluorosulfur-F-ethene (II) also reacts readily with silver fluoride to form 1-hydro-1-pentafluorosulfur-F-ethylsilver which was isolated as the acetonitrile solvate.

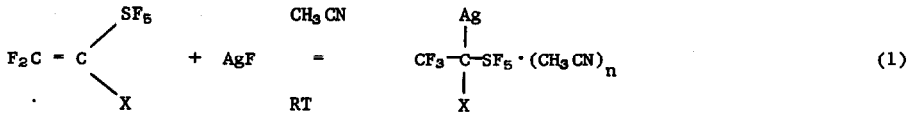

(1)

I X = F

II X = H

The number of solvent molecules associated with the silver complex was found to range from 0.5 to 2 but was variable within these limits. Attempts to completely remove the solvent resulted in varying degrees of decomposition of the silver complex.

Reactive fluoroalkylsilver complexes of the type $AgCX(SF_5)CF_3$ (X = H, F) appear to be generally useful intermediates for the synthesis of halo- hydro- and deutero- substituted pentafluorosulfurethanes by reaction with halogens and substances containing acidic hydrogen (deuterium). Earlier the reaction of $AgCF(SF_5)CF_3$ with Br_2, HCl, and H_2O was reported[5]. In this work, we have extended our study to include the reactions of $AgCH(SF_5)CF_3$ with HCl and DCl and of $AgCF(SF_5)CF_3$ with Cl_2 and DCl.

$$AgCH(SF_5)CF_3 + HCl = HCH(SF_5)CF_3 + AgCl \quad (2)$$

$$AgCH(SF_5)CF_3 + DCl = DCH(SF_5)CF_3 + AgCl \quad (3)$$

$$AgCF(SF_5)CF_3 + Cl_2 = ClCF(SF_5)CF_3 + AgCl \quad (4)$$

$$AgCF(SF_5)CF_3 + DCl = DCF(SF_5)CF_3 + AgCl \quad (5)$$

The reaction of $AgCH(SF_5)CF_3$ with HCl produced the known compound $HCH(SF_5)CH_3$[12] in good yield indicating that the silver complex exists as formulated above. A minor by-product also formed in this reaction, and mass spectral evidence indicated that it contained an SF_3 rather than an SF_5 group. (The most intense peak was at m/e = 89 (SF_3^+); no peak was observed at m/e = 127 (SF_5^+)). If the peak at m/e = 190 is that for the molecule-ion, the mass corresponds to the composition C_2F_7S which may have the structure $SF_3CH(F)CF_3$. Another peak, at m/e = 101, corresponds to a fragment (CF_3CHF^+) consistent with this interpretation as do others in the spectrum. Since definitive data are lacking, this suggestion should be regarded as tentative.

Mass and infrared spectra, and vapor density measurements are consistent with the formulations of the other reaction products. Peaks appearing in all of the mass spectra at m/e corresponding to the fragment CF_2X (where X = H, D, Cl) are probably due to rearrangement or combination of fragments in the mass spectrometer since a strong peak for CF_2Br^+ was observed in the mass spectrum of $BrCF(SF_5)CF_3$ for which ^{19}F nmr spectroscopy had demonstrated the presence of the CF_3CF- group[5]. Infrared spectra of the derivatives

showed intense absorptions in the regions associated with vibrations involving CF_3 and SF_5 groups (see analysis of $HCF(SF_5)CF_3$ below). The analytical data for $C\ell CF(SF_5)CF_3$ are in good agreement with its calculated elemental composition. The vapor density measurements for the other derivatives are all within 4% of the calculated values.

Vibrational Spectra of $HCF(SF_5)CF_3$ and $DCF(SF_5)CF_3$

Reference Raman and infrared spectra of $HCF(SF_5)CF_3$ (designated hereafter as "H") and the isotopically substituted derivative, $DCF(SF_5)CF_3$, (designated hereafter as "D") are shown in Fig. I. Vibrational data and assignments are presented in Tables I and II. Eggers and Wright[13] and later Griffiths[9] concluded from vibrational studies of CF_3SF_5 that the data were in best accord with the assumption of free rotation about the C-S bond. They analyzed the spectrum in terms of local C_{4v} symmetry at the SF_5 group and C_{3v} symmetry at the CF_3 group.

If free rotation about the C-S bond in $HCF(SF_5)CF_3$ is assumed, then, for the SF_5-C moeity, the 3N-6 rule predicts 15 fundamentals and group theory indicates that these will be of symmetry $4a_1$, $2b_1$, b_2 and 4e. The a_1 and e modes are both infrared and Raman active but the b modes are Raman active only. Absence of free rotation about the C-S bond would result in lowering the local symmetry to that of the molecule as a whole, point group C_1. The 15 vibrational modes would then all be singly degenerate of species a, and all modes would be both infrared and Raman active. Even in C_1 symmetry, however, it is possible that the group frequency concept would have some validity for SF_5 in view of the large mass difference between it and the rest of the molecule. Published assignments of the vibrational modes for $SF_5C\ell$[7,9,14], SF_5Br[7,15], and SF_5CF_3[9,13] as well as the diagnostic bands observed by Cross et al.[10] were used as a guide for the assignment of $HCF(SF_5)CF_3$ and $DCF(SF_5)CF_3$. The polyfluorocarbon portion of the molecule (18 normal modes of symmetry a) was assigned by comparison with assignments for somewhat similar species such as CF_3CH_2X (X = F, Cℓ, Br, I)[16,17] $CF_3CHC\ell Br$[18] and CF_3CHFX (X = Cℓ, Br)[19]. Isotopic substitution of hydrogen by deuterium allowed us to assign the C-H bonding modes.

Vibrations of the SF_5 Group -

"a_1" The four totally symmetric vibrations for the SF_5 group are the S-F axial stretch, the symmetrical SF_4 square stretch, the SF_4 out-of-plane deformation, and the C-S stretch.

The S-F axial stretching mode appears as an intense infrared absorption at 865 cm^{-1} in the spectrum of "H" and at 877 cm^{-1} in that of "D". The bands are weak in the Raman spectra of both compounds, but they appear to be more strongly polarized than other bands in the vicinity. This mode has been observed near 855 cm^{-1} for $SF_5C\ell$[5,9], near 849 cm^{-1} for SF_5Br[5,15], and at 883 cm^{-1} for CF_3SF_5[9].

The symmetrical SF_4 square-stretching mode is usually one of the strongest bands in the Raman spectra of SF_5 compounds[5,15]. No exception was found for compounds "H" and "D" for which the SF_4 square-stretching modes were observed at 706 cm^{-1} and 692 cm^{-1} respectively as strongly polarized bands (ρ = 0.05, 0.17). This mode has been assigned to a band at 707 cm^{-1} in $SF_5C\ell$[9], 692 cm^{-1} in SF_5Br[15] and 692 in CF_3SF_5[9].

The SF_4 out-of-plane deformation is a bending motion of four of the S-F bonds out of the plane determined by the SF_4 square; two bands appear which are candidates for this assignment: 672 and 612 cm^{-1} in the spectrum of "H" and 655 and 610 cm^{-1} in that of "D". The SF_4 symmetric deformation is usually observed near 600 cm^{-1} [10] and has been reported to occur at 602 cm^{-1} for $SF_5C\ell$[7,9,14], 591 cm^{-1} for SF_5Br[15], 613 cm^{-1} for SF_5CF_3[9], and 637 cm^{-1} for SF_5OF[25]. Both bands exhibit PQR structure in each case (P-R separation ca.

10 cm^{-1} for "H") although that for "D" is not well resolved; thus, a decision cannot be made on this basis. Since the bands at 672 cm^{-1} for "H" and 655 cm^{-1} for "D" are strongly polarized, while those at 612 cm^{-1} and 610 cm^{-1} are weakly polarized and depolarized respectively, we have assigned the bands of higher frequency to the SF_4 symmetric deformation (a_1).

The bands of lower frequency are assigned to one of the antisymmetric CF_3 deformations (see below).

The C-S stretching mode is similar to the S-Cℓ stretch in $SF_5Cℓ$. It is expected to occur at low frequency due to the large masses involved. A very strongly polarized Raman band at 281 cm^{-1} for "H" and at 275 cm^{-1} for "D" is assigned to this vibration. Griffiths[9] observed this mode at 324 cm^{-1} in the spectrum of CF_3SF_5.

"b_1" The two b_1 vibrational modes involving the SF_4 square are similar to the a_1 modes, the difference being that the b_1 vibrations are antisymmetric with respect to the principal axis of the SF_5 group.

The SF_4 antisymmetric stretching mode is Raman active only and is of relatively low energy. It is assigned to a weak, depolarized Raman band at 586 cm^{-1} for "H" and at 580 cm^{-1} for "D". The SF_4 antisymmetric stretch has been assigned to depolarized Raman bands at 625 cm^{-1} and 627 cm^{-1} for $SF_5Cℓ$ and CF_3SF_5[9] and 620 cm^{-1} for SF_5Br[15].

The other b_1 mode is the antisymmetric out-of-plane deformation. It is observed as a weakly polarized Raman band ($\rho = 0.60$) at 248 cm^{-1} for "H" and at 241 cm^{-1} for "D". The analogous modes for $SF_5Cℓ$ and SF_5CF_3 have been observed at 273 cm^{-1} and 262 cm^{-1} [9].

"b_2" The b_2 mode is antisymmetric with respect to the principal axis (of SF_5) and a reflection plane and, thus, is the SF_4 antisymmetric in-plane deformation. It should be Raman active only. A weak depolarized Raman band at 494 cm^{-1} for "H" and one at 487 cm^{-1} for "D" is assigned to this mode. No absorptions appear at these frequencies in the infrared spectrum. The antisymmetric SF_4 in-plane deformation has been observed at 504 cm^{-1} and 501 cm^{-1} in $SF_5Cℓ$ and SF_5CF_3 [9].

"e" The degenerate stretching and bending modes are both infrared and Raman active.

The degenerate SF_4 square stretching vibration is usually very intense in the infrared spectra of SF_5-containing compounds and weak in the Raman spectra. A very intense infrared band at 885 cm^{-1} for "H" and at 897 cm^{-1} for "D" was assigned to this mode. The Raman band was weak in the first case and was not detected in the second. In $SF_5Cℓ$, SF_5Br, and CF_3SF_5, this mode has been assigned to bands at 909, 894, and 912 cm^{-1} [9,15].

The degenerate SF_4 in-plane deformation usually occurs at lower frequency in the region of 400 to 500 cm^{-1} [10]. For "H" it is found in the Raman spectrum at 465 cm^{-1} and for "D" at 455 cm^{-1}. The infrared counterparts of both vibrations were observed although it was necessary to record the spectrum of "H" at 100 mm pressure in order to observe the very weak absorption at 465 cm^{-1}. For $SF_5Cℓ$, SF_5Br, and CF_3SF_5, this vibration was observed at 440, 419, and 427 cm^{-1} [7,9,15].

The degenerate SF-wag involves motion of the axial S-F fluorine atom off the four-fold axis, and it appears at 569 cm^{-1} for "H" and at 650 cm^{-1} for "D". It has been assigned to bands at 592, and 588 cm^{-1} in $SF_5Cℓ$, SF_5Br, and SF_5CF_3 [7,9,15].

The degenerate SF_5 rocking vibration involves movement of the SF_5 group off the S-C axis. A weakly polarized band at 326 cm^{-1} in the Raman spectrum of "H" and one at 320 cm^{-1} in that of "D" was tentatively assigned to this mode. The infrared counterpart was not observed for "D". Supporting this assignment is the fact that this vibration was observed at 319 cm^{-1} for SF_5CF_3 [9]. On the other hand, the infrared counterpart in SF_5CF_3 was observed to be of medium-strong intensity. The analogous vibrations for $SF_5Cℓ$ and

SF_5Br were found at considerably lower frequencies, 271 and 222 cm^{-1} [9,15].

Vibrations of the CF_3CHF Group -

In C_1 symmetry, all 18 fundamentals associated with the CF_3CHF-moiety are singly degenerate and both infrared and Raman active. Although the normal modes are undoubtedly extensively mixed owing to the similar masses of most of the atoms, an attempt was made to identify each mode in terms of the motion deemed to contribute most heavily to the vibration. Most of these assignments should be regarded as tentative.

The antisymmetric CF_3 stretching vibrations, which are degenerate in an environment of higher symmetry, are well separated; they occur as strong infrared bands at 1294 and 1217 cm^{-1} for "H" and at 1240 and 1212 cm^{-1} for "D". The corresponding Raman emissions are weak as expected for C-F stretching motions. Crowder[16], who studied the series of compounds CF_3CH_2X (where X = F, Cl, Br, I), found that the asymmetric CF_3 stretching modes were well separated in the species of higher molecular weight (for example: 1275 and 1223 cm^{-1} for CF_3CH_2I).

In the case of the symmetric CF_3 stretch, Crowder[16] has concluded from normal coordinate calculations that this mode is coupled with the carbon-carbon stretching mode in the series CF_3CH_2X. Earlier, Tuazon et al.[20] had called attention to the fact that there is extensive interaction between $\nu_s CF_3$ and ν_{C-C} in fluoroalkanes with the result that the higher frequency component usually has a larger contribution from ν_{C-C}. We have, therefore, assigned the infrared band at 1376 cm^{-1} for "H" and at 1318 cm^{-1} for "D" to the carbon-carbon stretching mode and that at 935 cm^{-1} for "H" and at 938 cm^{-1} for "D" to the CF_3 symmetric stretching mode. In the related compounds CF_3CHFBr and CF_3CDFBr, the high frequency modes at 865 and 810 cm^{-1}, respectively[19]. It is not clear why the lower frequency component in "H" and "D" is higher than is usually found (855 - 840 cm^{-1} for CF_3CH_2X)[16] but no other bands in the 900 to 800 cm^{-1} range are more likely candidates.

There are three out-of-plane deformations associated with the CF_3 group; two are antisymmetric and one is symmetric. The antisymmetric deformations (in higher symmetry degenerate) occur at 612 and 524 cm^{-1} for "H" and 610 and 520 cm^{-1} for "D". These vibrations occur at 552 and 520 cm^{-1} for $CF_3CHClBr$ [18] and at 570 and 525 cm^{-1} for CF_3CHFBr [19]. They are not separated as much in the CF_3CH_2X series[16]. The symmetric CF_3 deformation is usually a main feature of the infrared and Raman spectra of trifluoromethyl compounds and has been observed at 755 cm^{-1} for SF_5CF_3[9]. It appears as a strongly polarized band at 761 cm^{-1} for "H" and at 723 cm^{-1} for "D". The infrared counterparts are both present but the band for "D" is weak. This frequency is somewhat higher than those assigned to $\pi_s CF_3$ in the CF_3CH_2X series (666-632 cm^{-1})[16] and $CF_3CHClBr$ (665 cm^{-1})[18] but is not so greatly different from those observed for CF_3CHFCl and CF_3CHFBr (698 and 691 cm^{-1})[19]. Infrared data for the compound CF_3CHFI, which has the same molecular weight as $HCF(SF_5)CF_3$, have been reported[21] but not assigned. It is probable that the very strong band at 694 cm^{-1} is $\pi_s CF_3$, which is in line with these assignments.

The CF_3 rocking vibrations are expected to occur at low frequencies and are assigned to bands at 410 and 399 cm^{-1} for "H" and at 402 and 394 cm^{-1} for "D". Crowder has assigned bands at 409 and 350 cm^{-1} to these modes in CF_3CH_2F and 289 and 355 cm^{-1} in CF_3CH_2I [16].

The CF_3 torsion is expected to occur at very low frequency and has been observed by Lopata and Durig[17] for the series CF_3CH_2X (where X = F, Cl, Br, I) at 107, 93, 89, and 82 cm^{-1} respectively. A strong band centered at 92 cm^{-1} in the Raman spectrum which was determined to be due to our optical system and not the sample probably obscured the torsion.

The vibrations associated with the -C(H,D)F- portion of the molecule are due to C-F and C-H stretching and bending motions. The C-F stretching mode is easily identified as the

very strong infrared band at 1161 cm^{-1} for "H" and at 1160 cm^{-1} for "D" and is close to the region found for other substances containing the -CFH- group[16,19,22].

The C-H stretching vibration for "H" is observed at 3004 cm^{-1} in the Raman spectrum which is within the usual range for a C-H stretch in fluoroalkanes[23], and it is the only band in the region. The C-H stretch is rather weak in the infrared spectrum which again is usual for this mode in a fluoroalkane[23]. The corresponding C-D stretch for "D" occurs at 2230 cm^{-1} yielding an isotopic lowering of 0.742 (harmonic oscillator approximation 0.707). The band was of medium intensity in the Raman spectrum and was very weak in the infrared spectrum. An infrared scan of "D" at 100 mm pressure gave a strong sharp band at 2233 cm^{-1}; an overtone ($2\nu_5$) showed up at 2320 cm^{-1}.

The C-H bending modes occur in the same region as the C-F stretching modes[23] and are often difficult to identify. One of the C-H bends is tentatively assigned to a band at 1308 cm^{-1}, but the other bend is not observed. Since the C-D bending modes for "D" were found at 1040 and 981 cm^{-1}, the position of the second C-H bend for "H" can be calculated if it is assumed that the isotopic shift [0.795] is the same for both modes. This places the second C-H bend at 1233 cm^{-1}, and thus, it probably overlaps the intense infrared band at 1217 (νCF_3). In a study of HCFCℓBr, Diem and Burow found the CH bends at 1305 and 1205 cm^{-1}; upon deuteration, the bends shifted to 974 and 916 cm^{-1} [24].

The in-plane C-C-F deformation is assigned to a band at 223 cm^{-1} in the Raman spectrum of "H" and one also at 223 cm^{-1} in that of "D". This mode appears at 230 cm^{-1} for CF_3CH_2F [16,17].

The S-C-F and C-C-S deformations should appear at the lowest frequencies save for the torsions. A weak Raman emission at 155 cm^{-1} for "H" and one at 158 cm^{-1} for "D" are assigned to the former while a very weak band at 122 cm^{-1} for "H" and one at 125 cm^{-1} for "D" are assigned to the latter. The C-C-I bend for CF_3CH_2I occurs at 134 cm^{-1} [16,17].

Finally, a band which could be ascribed to the SF_5 torsional mode was not observed in the spectrum of either derivative. This mode would be both infrared and Raman inactive if our assumptions are correct.

A Raman band at 817 cm^{-1} in the spectrum of $DCF(SF_5)CF_3$ was of the intensity expected for a fundamental, but no likely candidates emerged. The combination of the weak CCS bending mode (125 cm^{-1}) with the most intense vibration in the spectrum, the SF_4 deformation (a_1, 692 cm^{-1}), could produce a band of the magnitude observed, and we have assigned it on that basis.

In general, all of the bands could be attributed to fundamentals and overtones or reasonable combinations. Therefore, the assignment is internally consistent; however, there is no guarantee that it is unique.

The vibrational spectrum of the SF_5 group attached to the radical CF_3CHF- is consistent with local C_{4v} symmetry. All of the vibrational modes associated with the SF_5 group except the inactive torsion were observed and could be assigned on this basis. If the local symmetry at the SF_5 group were lower than C_{4v}, the e modes would be expected to split; no indications of splitting were observed. Furthermore, the a_1, b_1, b_2, and e modes generally followed the selection rules expected for C_{4v} local symmetry. It appears from these results, that, as a first approximation, the SF_5 group in two-carbon pentafluorosulfurfluoroalkyl derivatives may be treated separately in assigning the spectrum.

The fluorocarbon portion of the molecule presents a more difficult problem, however. The vibrational modes are highly mixed and, in the absence of a complete normal coordinate analysis, are difficult to assign in terms of the vibration which contributes the largest percentage to the mode. Assignments of the stretching vibrations are on firmer ground;

assignments of the deformations are less certain.

Acknowledgements: We are indebted to Dr. R. A. DeMarco for the mass spectra of $HCF(SF_5)CF_3$ and $DCF(SF_5)CF_3$. We wish to thank Dr. W. B. Fox for some technical assistance in the very preliminary stages of this work while REN was a visiting scientist and HFE was an NRC Postdoctoral Fellow at the Naval Research Lab., Wash. D.C. We acknowledge the support of the Wake Forest University Research and Publication Fund for the photographic work. This work taken in part from: M. Uhrig, M.S. Thesis, Wake Forest University, 1979.

REFERENCES

[1]Present Address: Phillips Res. Center, Phillips Petroleum Co., Bartlesville, OK, U.S.A.

[2]W. T. Miller and R. T. Burnard, J. Am. Chem. Soc., 90 (1968) 7367.

[3]W. T. Miller, R. H. Snider, and R. J. Hummel, J.Am. Chem. Soc., 91 (1969) 6532.

[4]K. K. Sun and W. T. Miller, J. Am. Chem. Soc., 92 (1970) 6985.

[5]R. E. Noftle and W. B. Fox, J. Fluorine Chem., 9 (1977) 219.

[6]R. E. Noftle, R. R. Smardzewski, and W. B. Fox, Inorg. Chem., 16 (1977) 3380.

[7]R. R. Smardzewski, R. E. Noftle, and W. B. Fox, J. Molec. Spectrosc., 62 (1976) 449.

[8]R. D. Dresdner and T. R. Hooper in "Fluorine Chem. Rev." P. Tarrant, ed., Vol. 4, Marcel Dekker, New York, 1969.

[9]J. E. Griffiths, Spectrochim. Acta, 23A (1967) 2145.

[10]L. H. Cross, G. Cushing, and H. L. Roberts, Spectrochim. Acta, 17A (1961) 344.

[11]J. Stewart, L. Kegley, H. F. White, and G. L. Gard, J. Org. Chem., 34 (1969) 760.

[12]R. A. DeMarco and W. B. Fox, J. Fluorine Chem., 12 (1978) 137.

[13]D. Eggers and H. Wright, J. Chem. Phys., 35 (1961) 1045.

[14]L. H. Cross, H. L. Roberts, P. Goggin, and L. A. Woodward, Trans. Faraday Soc., 56 (1960) 945.

[15]K. O.Christe, E. C. Curtis, and C. J. Schack, Spectrochim. Acta., 33A (1977) 69.

[16]G. A. Crowder, J. Fluorine Chem., 3 (1973/74) 125.

[17]A. D. Lopata and J. R. Durig, J. Raman Spectrosc., 6 (1977) 61.

[18]R. Theimer and J. R. Nielsen, J. Chem. Phys., 27 (1957) 887.

[19]R. E. Noftle, C. Ellis, G. Johnson, and S. F. Bush, 4th Winter Fluorine Conf., Daytona Beach, Florida, Jan. 28 - Feb. 2, 1979.

[20]E. C. Tuazon, W. G. Fateley, and F. F. Bentley, Appl. Spectrosc., 25 (1971) 374.

[21]M. Hauptschein and M. Braid, J. Amer. Chem. Soc., 83 (1961) 2383.

[22]J. R. Durig, C. J. Wurrey, W. E. Bucy, and A. E. Sloan, Spectrochim. Acta., 32A(1) (1976) 175.

[23]J. K. Brown and K. J. Morgan in "Advances in Fluorine Chemistry", M. Stacey, J. C. Tatlow, and A. G. Sharpe, eds., Vol. 4, Butterworths, London, 1965.

[24]M. Diem and D. F. Burow, J. Chem. Phys., 64 (1976) 5179.

[25]W. H. Hale and S. M. Williamson, Inorg. Chem., 4 (9)(1965) 1342.

Polyhedron Vol. 1, No. 9-10, pp. 735-736, 1982
Printed in Great Britain.

0277-5387/82/090735-02$03.00/0
Pergamon Press Ltd.

REACTION OF SCANDIUM TRIFLUORIDE WITH HYDRAZINE

P. GLAVIČ

"J. Stefan" Institute, YU-61001 Ljubljana, P.O.Box 199

(Received 14 May 1982)

Abstract - ScF_3 reacts with anhydrous hydrazine yielding $ScF_3.N_2H_4$; upon heating the compound in inert atmosphere ScF_3 is regained. With hydrazine hydrate $N_2H_5Sc(OH)F_3$ is obtained with solid ScF_3; it decomposes to ScF_3 in two steps.

Hydrazine complexes of ScF_3 have not been isolated so far. Although ScF_3 does not react directly with NH_3[1], the reaction of $4ScF_3.H_2O$ with gaseous NH_3 under pressure yields $5ScF_3.2NH_3$[2]. Therefore, in the continuation of our work on metal fluoride-hydrazine systems[3], we investigated reactions of ScF_3 with anhydrous hydrazine and hydrazine hydrate in the hope of isolating some ScF_3-hydrazine complexes.

ScF_3 was prepared by dissolving Sc_2O_3 in hot, concentrated HCl; the solvent was evaporated and the remaining solid digested several times with large excess of 40 % HF. The solid ScF_3 was dried and heated in vacuum at 200 °C for 5 hours (Found: Sc, 44.2; F, 55.7; Calc.: Sc, 44.10; F, 55.90 %). Scandium was determined by EDTA titration at pH = 4.5 with Methyl-Thymol Blue as indicator[4].

The preparation of anhydrous hydrazine, the experimental technique and the other methods of analysis were described elsewhere[5].

a) ScF_3-N_2H_4 system

Solid ScF_3 reacted with liquid anhydrous N_2H_4 in a stirred glass reactor under vacuum. The reaction was slow - 96 hours at 50 °C were needed to obtain the product with a constant composition. Excess N_2H_4 had to be removed at -30°C to prevent decomposition of the product, which was $ScF_3.N_2H_4$ (Found: Sc, 33.0; F, 40.0; N_2H_4 23.7; Calc.: Sc, 33.55; F, 42.53; N_2H_4 23.92 %). Although most scandium compounds are six-coordinated, no higher ScF_3-hydrazines could be isolated in contrast with the most of the previously investigated systems[3].

$ScF_3.N_2H_4$ is stable in vacuum and in dry air. In open air it hydrolyses, the product contains $N_2H_5ScF_4$[6] as shown by chemical analysis and IR spectroscopy. In 5 % HF the reaction proceeds to the solvated $2N_2H_5ScF_4.HF.H_2O$[6], which was identified by the same methods.

The thermal decomposition of $ScF_3.N_2H_4$ in argon atmosphere started slowly at 40 °C and hastened at 90 °C. One strong exothermic peak at 140 °C was observed, followed by a weak one at 220 °C. The decomposition was concluded at 430 °C, the residue being pure ScF_3 (Found: Sc, 44.4; F, 55.4 %).

The IR spectrum of $ScF_3.N_2H_4$ exhibits all the bands which are characteristic for the hydrazine adducts. The spectrum has well resolved bands at the following frequencies (in cm^{-1}): 3365 m,sh, 3337 vs, 3293 s, 1625 and 1600 s, 1530 w, 1370 w,1304 m, 1195 w,sh, 1140 vs, 1100 w,sh, 985 w,sh, 955 s, 670 w, 590 w,sh and 490 vs,b†. The shoulder at 985 cm^{-1} is the only indication that bidentate $ScF_3.2N_2H_4$ might exist, but we were not able to isolate it.

b) ScF_3-N_2H_4-H_2O system

Solid ScF_3 was reacted with 80 % solution of hydrazine hydrate in a polyethylene container.No colour or temperature changes were observed. The solid was allowed to react for several days, the product was filtered and washed with methanol to separate water and N_2H_5F. The product was $N_2H_5Sc(OH)F_3$ (Found: Sc, 31.6; F, 37.5; N_2H_4 21.0; Calc.: Sc, 29.75; F, 37.49; N_2H_4 21.08 %). The IR spectrum of $N_2H_5Sc(OH)F_3$ differs from the spectra of $ScF_3.N_2H_4$ or $2N_2H_5ScF_4.HF.H_2O$[6] and in the skeletal wavelength region it is also different from the spectrum of $N_2H_5ScF_4$[6]. The presence of $N_2H_5^+$ ions is demonstrated by the strong (NH_3^+) stretching vibrations. The spectrum has well resolved peaks (in cm^{-1}) at: 3370 w,sh, 3358 vs, 3110 vs,vb, 1612 s,1598 m,sh,1538 m, 1270 w, 1190 w,sh, 1087 s, 949 s, 821 w,b and 480 vs,b. The OH^-modes are superimposed on the (NH_2) ones.

Thermal decomposition of the solid is different from the thermal decomposition of $ScF_3.N_2H_4$ and also from the thermoanalytical course of the hydrazinium fluoroscandates[7]. It decomposes in two steps, starting at 150 °C and ending at 440 °C. Two endothermic peaks were resolved, a strong one at 185°C and a medium one at 340°C. The end product was somewhat unpure ScF_3 with 45.6 % Sc and 53.1 % F.

Acknowledgements - The present work was carried out with the financial supports of the Research Community of Slovenia and the National Bureau of Standards, Washington, which are gratefully acknowledged. The author wishes to thank Mr.A. Bole and Miss B.Sedej for their help.

References

1. I. V. Tananaev and V. P. Orlovskii, Zh. Neorg. Khim. 1962, 7, 2299.
2. V. P. Orlovskii, Zh. Neorg. Khim. 1967, 12, 20.
3. P. Glavič, J. Slivnik and A. Bole, J. Inorg. Nucl, Chem. 1980, 42, 617 and 1782.
4. T.S. West, Complexometry with EDTA and Related Reagents,BDH Chemicals Ltd, Poole,1969,p.202.
5. P. Glavič and J. Slivnik, J. Inorg. Nucl. Chem. 1970, 39. 2939.
6. J. Slivnik, M. Bohinc and A. Ranten, Monatsh. Chem.1974, 105, 951.
7. J. Slivnik, J. Maček, A. Rahten and B. Sedej, Thermochimica Acta 1980, 39, 21.

---

†w-weak, m-medium, s-strong, v-very, sh-shoulder, b-broad.

Polyhedron Vol. 1, No. 9-10, pp. 737-738, 1982
Printed in Great Britain.

0277-5387/82/090737-02$03.00/0
Pergamon Press Ltd.

COMMUNICATION

AN ANIONIC SIX-COORDINATE HIGH-SPIN IRON(III) PORPHYRIN

(*Received* 24 *August* 1982)

Abstract - Isolation and characterisation of the tetrabutylammonium salt of difluoro iron(III) tetraphenylporphyrin are described.

All known iron(III) tetraphenylporphyrin compounds having a high spin (S = 5/2) ground state can be classified in two categories : (1) the well known neutral five-coordinate complexes of the type FeX(tpp), where X is an uninegative anion, and (2) the recently described cationic six-coordinate complexes $[Fe(L)_2(tpp)]^+$, in which L is an oxygen-donor molecule such as water, ethanol or dimethylsulfoxide[1,2]. We now report that axial ligation of iron(III) tetraphenylporphyrin by two fluoride anions gives rise to isolable anionic six-coordinate complexes in which the ferric ion is high-spin.

EXPERIMENTAL

Preparation of fluoro(tetraphenylporphyrinato) iron(III)

Tetraphenylporphyrin (H_2tpp) was prepared by a literature method[3]. Direct insertion of the FeF^{2+} moiety from FeF_3 gave FeF(tpp) in a single step, a significant improvement with respect to previous methods[4]. H_2tpp (3g) and $FeF_3.3H_2O$ (1.5g) were dissolved in 1 l of dimethylformamide which had been dried over 4A molecular sieves for 4 days. The mixture was refluxed for 6 hours, and the solvent was then distilled off until a residual volume of ca. 200 ml was obtained. Overnight crystallisation gave the expected complex. After filtration and washing with ethanol, this crude product was dissolved in dichloromethane (200 ml) and recrystallised by slow addition of cyclohexane (300 ml). Yield : 3.17g (94 %). Found : C, 76.79 ; H, 4.19 ; N, 8.21 ; $C_{44}H_{28}N_4FeF$ requires C, 76.86 ; H, 4.10 ; N, 8.15. IR : 615 cm^{-1} (ν_{Fe-F}[5]).

Preparation of tetrabutylammonium difluoro(tetraphenylporphyrinato)ferrate(III)

Addition of 150 mg of tetrabutylammonium fluoride trihydrate to 200 mg of FeF(tpp) in 15 ml of dichloromethane changed the colour of the solution from brown to green. Acetonitrile (30 ml) was then added, and the volume of the mixture was reduced to 10 ml with a rotating evaporator. The dark violet crystals which were obtained were filtered and dried in air. Yield : 220 mg (79 %). Found : C, 75.15 ; H, 6.80 ; N, 7.33 ; Fe, 5.97 ; F, 4.55. Calculated for $[(C_4H_9)_4N]$ $[FeF_2(C_{44}H_{28}N_4)]$: C, 75.94 ; H, 6.80 ; N, 7.38 ; Fe, 5.88 ; F, 4.00. Electronic spectra were recorded on a Beckman Acta MVI spectrophotometer. Infrared spectra of KBr pellets were obtained on a Beckman 4250 instrument. A Varian E-104 A spectrometer was used for EPR spectra. Magnetic susceptibility measurements were made by the Faraday method.

RESULTS AND DISCUSSION

Analytical data indicate that the anionic difluoro complex of iron(III) tetraphenylporphyrin can be isolated as a crystalline solid with a tetrabutylammonium counter ion. The formation of a similar complex of deuteroporphyrin IX in solution had been inferred by Momenteau, Mispelter, and Lexa on the basis of spectroscopic studies[6].

$[NBu_4]$ $[FeF_2(tpp)]$ shows absorption maxima at 415,588, and 628 nm in dichloromethane solution. The Fe-F stretching frequency observed at 615 cm^{-1} in FeF(tpp) is not found in the infrared spectrum of the difluoro complex. Instead, a broad, strong absorption is observed at 485 cm^{-1}, which we assign to a trans F-Fe-F vibrational mode.

EPR spectra in frozen dichloromethane solution at 80 K show the usual pattern of high-spin iron(III) porphyrins : $g_{\perp} = 5.7$, $g_{//} = 2.0$. In contrast to the report concerning the deuteroporphyrin IX complex[6], we have not been able to detect a hyperfine splitting of the $g = 2$ line by the two fluorine nuclei of $[FeF_2(tpp)]^-$. Magnetic susceptibility measurements on the microcrystalline solid confirmed the $S = 5/2$ state : the value of the effective magnetic moment at room temperature is 5.95 BM.

The varied spin states of ferric porphyrins are known to be controlled by the nature and number of their axial ligands[1]. The present characterisation of $[FeF_2(tpp)]^-$, the first anionic six-coordinate ferric porphyrin with a high spin state, provides a further illustration of this concept. X-ray structure determination of this complex, crystallised as the 2-methyl-imidazolium salt[7], confirms the trans difluoro configuration, and it shows a planar, radially expanded porphyrin core with long iron-nitrogen bond distances (2.064(3)Å), as expected for a high spin iron(III) porphyrin complex[1].

Aknowledgements - Partial support of this research by the Centre National de la Recherche Scientifique (LA 321) is acknowledged.

PIERRE GANS
JEAN-CLAUDE MARCHON*
JEAN-MARC MOULIS

Laboratoires de Chimie
Département de Recherche Fondamentale
Centre d'Etudes Nucléaires de Grenoble
85 X, 38041 Grenoble cedex, France

REFERENCES

1 W.R. Scheidt and C.A. Reed, Chem. Rev., 1981, 81, 543.

2 W.R. Scheidt and M. Gouterman, in "Iron Porphyrins", A.B.P. Lever and H.B. Gray, Eds., Addison-Wesley, Reading, in the press.

3 A.D. Adler, F.R. Longo, J.D. Finarelli, J. Goldmacher, J. Assour and L. Korsakoff, J. Org. Chem., 1967, 32, 476.

4 K. Anzai, K. Hatano, Y.J. Lee, and W.R. Scheidt, Inorg. Chem., 1981, 20, 2337 ; I.A. Cohen, D.A. Summerville, and S.R. Su, J. Am. Chem. Soc., 1976, 98, 5813.

5 H. Ogoshi, E. Watanabe, Z. Yoshida, J. Kincaid, and K. Nakamoto, J. Am. Chem. Soc., 1973, 93, 2845.

6 M. Momenteau, J. Mispelter, and D. Lexa, Bioch. Biophys. Acta, 1973, 320, 652.

7 W.R. Scheidt, Y.J. Lee, S. Tamai, K. Hatano, preprint.

Polyhedron Vol. 1, No. 11–12, pp. 739–777, 1982
Printed in Great Britain.

0277-5387/82/110739-39$19.50/0
Pergamon Press Ltd.

POLYHEDRON REPORT NUMBER 2

THE PREPARATION AND PROPERTIES OF METALLACYCLIC COMPOUNDS OF THE TRANSITION ELEMENTS

S. DAVID CHAPPELL* and DAVID J. COLE-HAMILTON

Department of Inorganic, Physical and Industrial Chemistry, University of Liverpool, P.O. Box 147, Liverpool L69 3BX, England

CONTENTS

This review covers the literature up to the end of 1981. Although it does not claim to be a fully comprehensive treatise, all areas of metallacycle formation are covered and an effort has been made to ensure that all important literature has been included. However, only the chemistry of isolated and characterised metallacyclic complexes is discussed. We concentrate on synthetic procedures for the production of metallacyclic compounds but also, where appropriate, discuss the reaction chemistry of such compounds. The very large number of mechanistic schemes for various catalytic reactions, which invoke metallacyclic compounds as intermediates has been referred to in passing, where appropriate, but further details of these schemes may be found elsewhere and in some cases have been reviewed.[1–17]

During recent years, metallacyclic compounds of the transition elements have been the subject of considerable research as it is now recognised that they play an important role in a number of catalytic reactions, e.g. alkene metathesis,[1–5] isomerisation of strained carbocyclic rings,[6–9] cycloaddition of alkenes,[10–11] and oligomerisation of dienes.[12–15] Recently they have also been suggested as intermediates in polymerisation reactions.[16, 17] However, despite their discovery in the mid-fifties, metallacyclic compounds did not become intensively studied until their role in catalysis was appreciated. Several synthetic routes have been used for their production and these will now be considered in some depth.

1. INSERTION INTO C–C BONDS

The first metallacyclic complex was prepared by Tipper[18] in 1955. He treated chloroplatinic acid with cyclopropane in acetic anhydride to give a compound of formula $[PtCl_2(C_3H_6)]_n$. The complex was later shown[19] to be a chloride bridged tetramer, with a structure analogous to Pt(IV) alkyls, in which platinum has inserted into the cyclopropane ring. Subsequent research has shown this method of synthesis to be useful for a small number of transition metals and many metallacycles have now been made *via* the reaction of platinum compounds with cyclopropanes. A better route to substituted Tipper complexes has since been shown to be the metathetical reaction between Zeise's dimer, $[(C_2H_4)PtCl_2]_2$, and the relevant substituted cyclopropane.[20–22] An electrophilic attack on the organic ring has been proposed[22] and it is found that with aryl cyclopropanes insertions are always into the most substituted C–C bond on the ring. However, the most stable isomer thermodynamically has the platinum bonded to the least substituted carbon atoms.

The general area of platinacyclobutane chemistry has been one of the most intensively studied areas of metallacyclic chemistry and as this field has already been reviewed[23] it will not be covered in depth. A wide variety of both Pt(II) and Pt(IV) metallacycles has now been made[24–29] and many of their reactions

studied, including isomerisation,[30,31] conversion to ylide[32,33] or alkene[34,35] complexes and decomposition studies both thermal[26,36,37] and photochemical[38,39].

A more recent example of the insertion of Zeise's dimer into C–C bonds is its reaction with bicyclo-[1.1.0]-butane[40] to give a polymeric platinacyclobutane which when reacted with pyridine affords **1**.

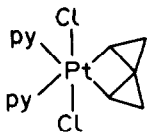

1

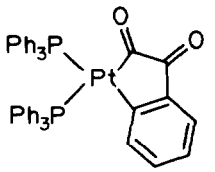

2

A further less related example is the reaction of *tetrakis*(triphenylphosphine)platinum(0) with 1,2-benzocyclobutadienequinone[41] in which a $Pt(PPh_3)_2$ unit inserts into one phenyl-carbon bond of the cyclic dione giving **2**. As may be expected similar reactions are observed for palladium but are much less common than for platinum due to the fact that palladium is less able to accept electron density from the ring. Hence it is found that palladium will only insert into cyclopropanes containing good electron-withdrawing substituents. Lenarda *et al.*[42] have demonstrated the formation of palladacyclobutanes **3** from tetracyanocyclopropane and *tetrakis*(triphenylphosphine)palladium (0).

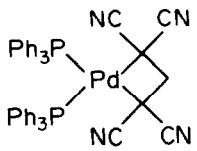

3

Here the Pd(0) species is a nucleophilic centre and so it inserts into the C–C bond containing the CN substituents.

The compound, $[Rh(CO)_2Cl]_2$, has also been shown to insert into a wide range of organic molecules. The first report of this occurring appeared in 1968, although in this case, further insertion of CO into a Rh–C bond gave a rhodacyclopentanone ring when it was reacted with cyclopropane.[43] Spectroscopic data was taken to indicate structure **4** in which both the CO groups and the keto-groups can be *cis* or *trans* to one another. The presence of chlorine

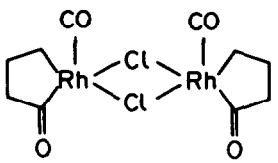

4

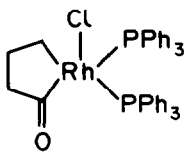

5

bridges was confirmed by the cleavage reactions with donors such as triphenylphosphine which also eliminate CO to give **5**.

Soon after this, the reaction of the same compound with cubane,[44] (eqn 1) giving **1** was reported. A similar reaction has been shown to

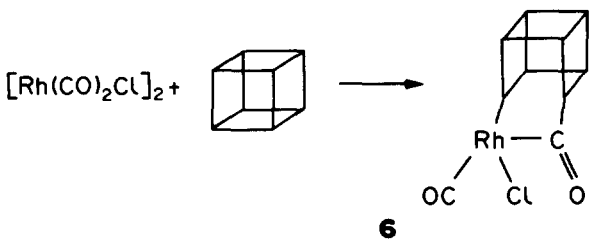

(1)

6

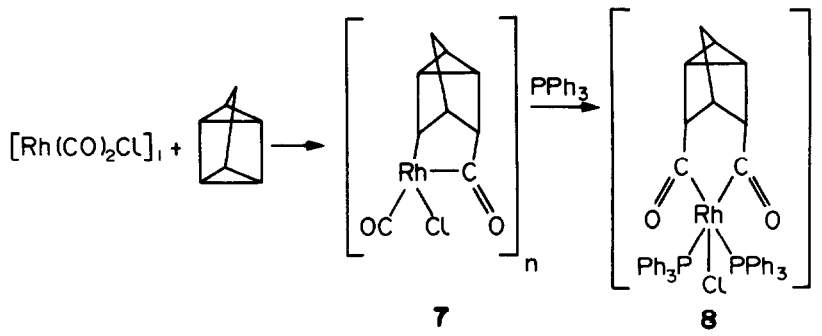

7 8 (2)

occur with quadricyclene,[45,46] (eqn 2). The product 7 presumably arises from oxidative addition of quadricyclene to the rhodium and this product then undergoes a CO insertion reaction to give the acyl complex. A polymeric chlorine-bridged structure has been assigned on the basis that Rh(III) has a preference for coordination numbers greater than four. Under CO, this compound then undergoes a rapid stoichiometric reaction with triphenylphosphine to yield **8**, in which a further CO unit has inserted into the ring. The oxidative addition reaction observed here is seen as evidence that the rhodium-(I) catalysed valence isomerisation of quadricyclene to norbornadiene[47] proceeds via a similar pathway, (eqn 3), with oxidative addition being the rate determining step.

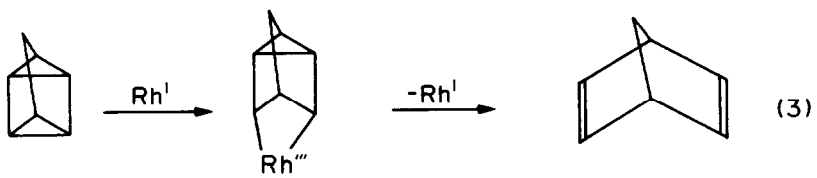

(3)

A similar mechanism has been proposed for the rearrangement of cubane[44] to tricyclooctadiene. A rhodacyclohexane unit **9** can also be produced by the reaction of 1,3-bishomocubane with $[Rh(CO)_2Cl]_2$,[48] (eqn 4).

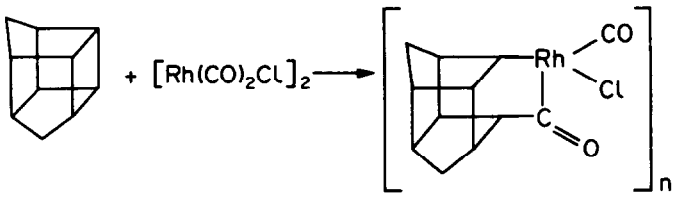

(4)

9

It was shown that the insertion occurs exclusively at the central bond of the bicyclo[2.2.0] hexane system and the final product is again believed to be polymeric. The same research group have reported a similar reaction for the dimer $[Ir(CO)_3Cl]_2$,[49] although in this case the product **10** contains a five membered ring system and CO insertion does not occur (eqn 5).

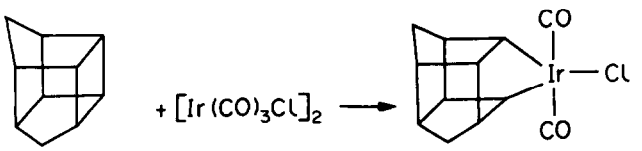

(5)

10

None of the previously reported metallacycles could be truly said to be intermediates in the metal assisted isomerisation as their thermolysis leads to carbonyl compounds rather than rearranged hydro-

carbons. However, **10** can be further converted into tricyclooctadiene lending further evidence to the postulated mechanism shown in eqn (3).

In addition to the reaction with cyclopropane mentioned earlier, $[Rh(CO)_2Cl]_2$ has been shown to react with fused ring cyclopropanes such as dibenzosemibullvalene[50] **11** (eqn 6).

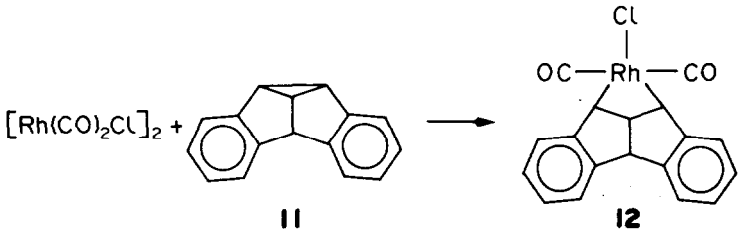

11 **12** (6)

Although there is no direct evidence, the product **12** is thought to be dimeric on the basis of the mass spectrum obtained together with the preference of Rh(III) for 6-coordination. The exact geometry is unsure as the two CO groups may be *cis* or *trans* to one another. By passing CO through a suspension of the compound in dichloromethane it is thought that CO groups insert into both the Rh-C bonds giving a six membered ring structure. An identical reaction to this has been reported for diironnonacarbonyl[51, 52] (eqn 7).

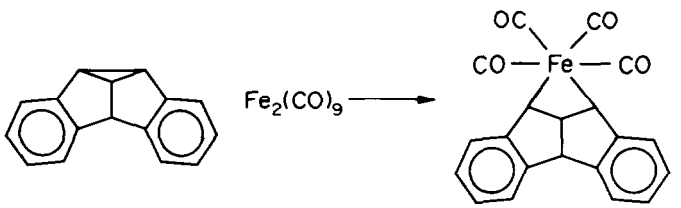

(7)

13

The final product **13**, for which the structure is confirmed by single crystal X-ray diffraction, reacts further with 1,2-*bis*(diphenylphosphino)ethane to yield a similar product in which two CO's have been replaced by the phosphine. The complex **13** is kinetically very stable, no reaction being observed with *conc.* HCl at 80° after three days. This is probably due to the fact that the normal decomposition pathways such as β-elimination are unavailable.

When $Fe_2(CO)_9$ is reacted with semibullvalene **15**, the product is **18** (eqn 9). The difference between this reaction and the reaction with dibenzosemibullvalene is probably due to the fact that **14** can do little else but close to **13** whereas **16** can and does rearrange to **17** which ultimately yields **18**.

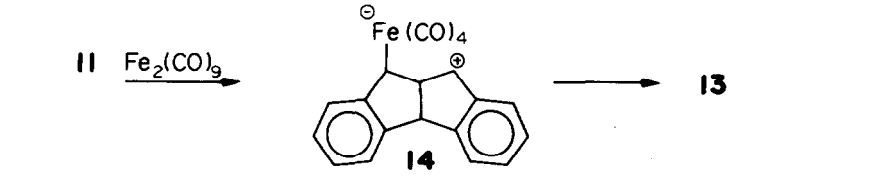

14 (8)

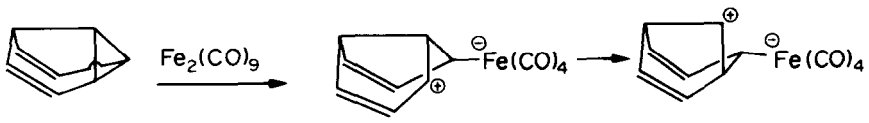

15 **16** **17**

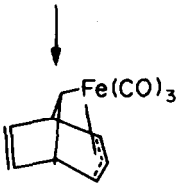

(9)

18

Later, Tam[53] showed that under slightly different conditions a further product in which a CO unit inserts into the metallacyclic ring can be obtained from dibenzosemibullavalene. The product then obtained is similar to the Rh(III) compound 5.

Other insertion reactions have been observed for iron complexes by two different groups. On photolysing $Fe(CO)_5$ with 1-2a(6a)-η-benzocyclobutadiene-tricarbonyliron[54] **19** a mixture of products including metallacycles formed *via* insertion into C–C bonds is obtained (eqn 10).

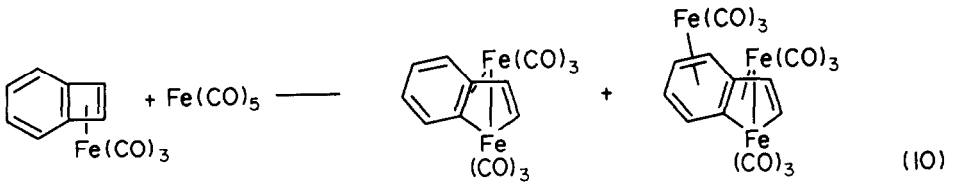

(10)

19 **20** **21**

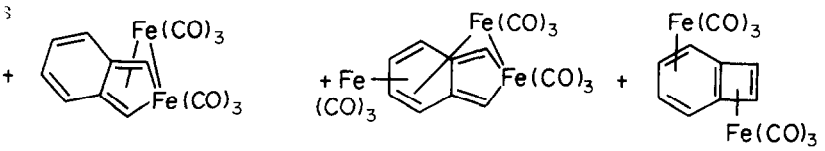

22 **23** **24**

Two of these products, **20** and **21**, had previously been synthesised in a different photolytic reaction of $Fe(CO)_5$ with *o*-bromostyrene.[55] The metallacyclic complexes result *via* an unusual opening of the cyclobutadiene ring in **19**. An analogous ring-opening takes place in the formation of **25** by photochemical reaction of (cyclobutadiene)(cyclopentadienyl)cobalt

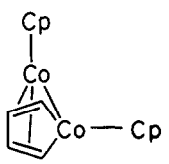

25

with dicarbonylcyclopentadienylcobalt.[56–58] Compounds **20** and **22** in equation (10) have been synthesised independently[59] on reacting $Fe_3(CO)_{12}$ with benzocyclobutadienetricarbonyliron.

Iron has also been shown to insert into a cyclopropene ring. The reaction of $Fe_2(CO)_9$ with naphtho[b]cyclopropene results in the formation of the ferracyclopentenone[60] complex **26** for which the structure is

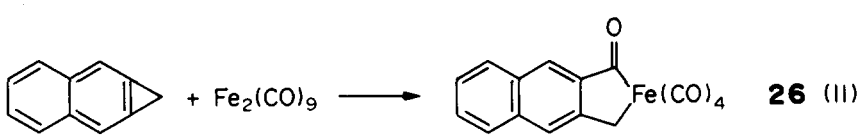

26 (11)

confirmed by single crystal X-ray studies. The complex may be formally regarded as resulting from the addition of an Fe–C bond of $Fe(CO)_5$ across one edge of the three membered ring of the cyclopropene and hence the iron atom is coordinated in a distorted octahedral fashion. A similar reaction, this time for a cyclopropane, is observed in the photochemical reaction of $Fe(CO)_5$ with 1,2-diphenyl-4,4-diacetyltrifulvene to give **27**.[61] It is formed by insertion of a

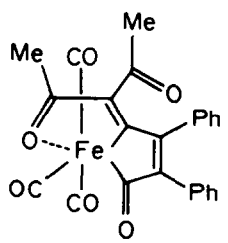

27

photochemically generated $Fe(CO)_4$ group into the three membered ring system. Simultaneously an O–Fe donor bond involving one acetyl group is formed. The same reaction is observed when $Fe_3(CO)_{12}$ reacts photochemically with 1,2-dimethyl-4,4-dicyanotrifulvene.[62]

A further isolated reaction producing a compound analogous to those shown for iron is that of cyclooctatetraene with dimethyltetracarbonylosmium(II).[63] A carbon–carbon bond of the alkene is broken and two hydrogen atoms are lost to give **28**. The corresponding compound for

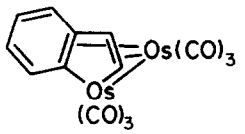

28

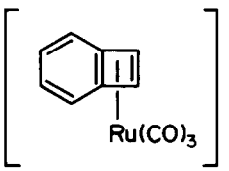

29

ruthenium is formed by the reaction of 1,4-dibromocyclooctatetraene with $Ru_3(CO)_{12}$ which presumably forms from benzocyclobutadiene(tricarbonyl)ruthenium **29** as an intermediate *via* a type of reaction already discussed for iron.[54]

2. DILITHIO AND DI-GRIGNARD REAGENTS

The insertions of metals into C–C bonds, described above, appear to be limited to the class 'B' metals, whereas lithium or magnesium reagents offer a far more generalised route to metallacycles for metals throughout the transition series. One of the earliest examples of such a reaction is that reported by Braye *et al.*[64] for the reaction of *bis*-cyclopentadienylzirconium dichloride with 1,4-dilithio-1,2,3,4-tetraphenylbutadiene (eqn 12).

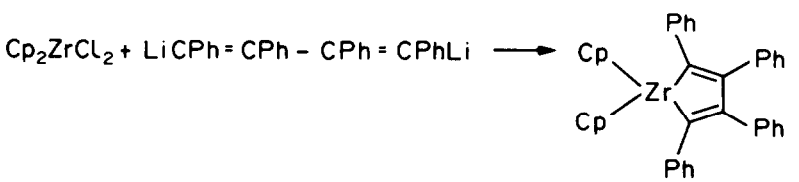

(12)

30

In fact, reactions of a related metal, titanium, are amongst the most common in this category. In 1967 Cohen and Massey[65] reported the reaction of Cp_2TiCl_2 with 2,2-dilithiooctafluorobiphenyl (eqn 13).

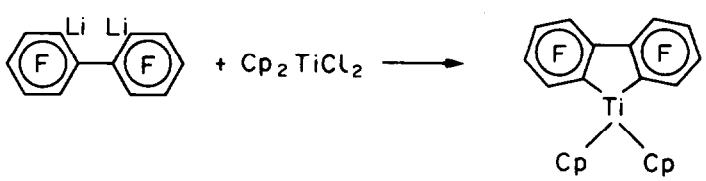

(13)

31

The product, containing a titanacyclopentene unit, shows reasonable thermal stability being decomposed *in vacuo* only after 24 hr at temperatures in excess of 330°C. Reactions using the same lithium reagent have been reported for Pt, Co, Rh, Ir and Zr[66] (eqn 14). For the cobalt triad, the yields observed decrease in

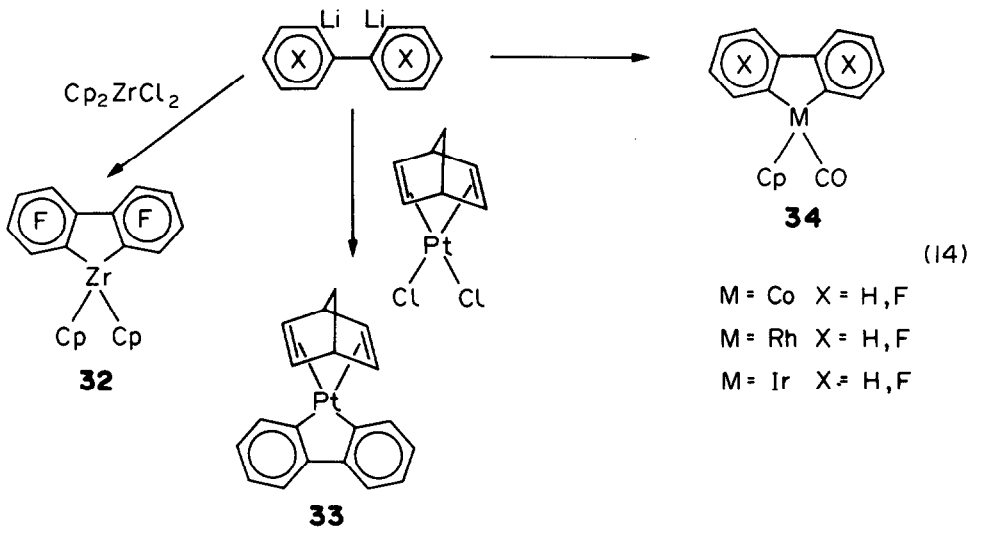

the order Co ≥ Rh > Ir with yields being below 5% for the last two metals, both when X = H and F. Triphenylphosphine is found to replace the CO ligand in experiments on both the cobalt complexes. The hafnium complex reported had been previously synthesised.[67]

Titanocenedichloride, Cp_2TiCl_2, appears to be a general starting material for the formation of titanium metallacycles. Rausch[68] has demonstrated its reaction with two lithium reagents (eqn 15).

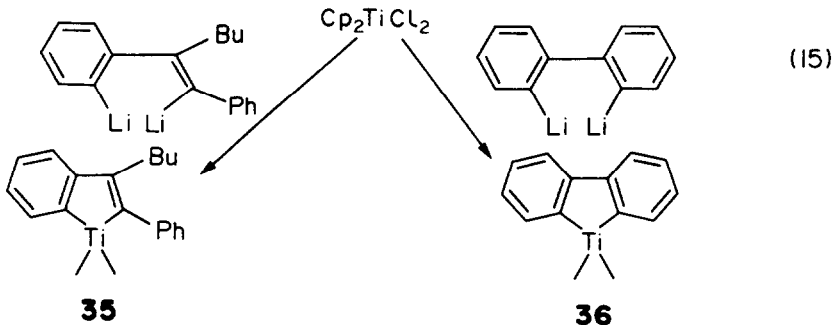

Compound **36** is found to be stable at room temperature in air although *bis*-cyclopentadienyl(*bis o*-phenyl)titanium must be stored at low temperatures, preferably under nitrogen, to prevent decomposition. Such enhanced stability of metallacycles with respect to their non-cyclic counterparts may be due to electronic factors associated with incorporation of the metal into an unsaturated ring system, or possibly, to the relative steric requirements of the metallacycle ligand compared with the two aryl substituents. Unsubstituted titanacyclopentanes have been made[69,70] by reacting Cp_2TiCl_2 with 1,4-dilithiobutane at low temperature (eqn 15).

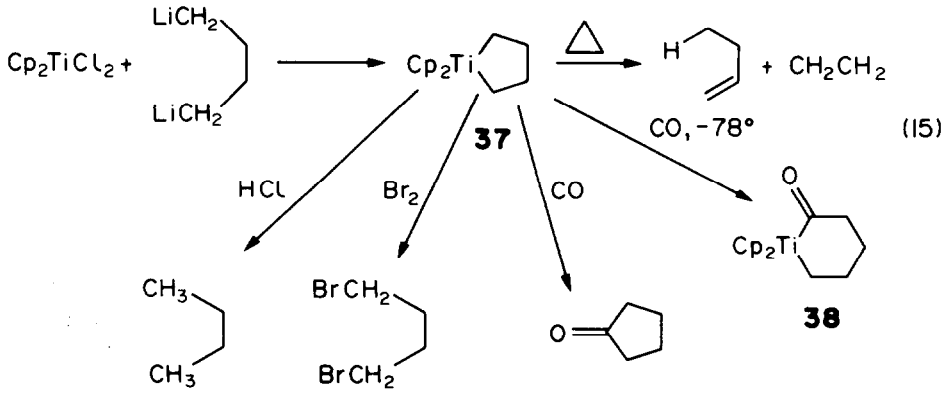

The bright orange solid, **37**, is stable only below −30°C and its structural assignment results on the reactions outlined. Carbonylation of **37** at −40°C at a pressure of 10 atmospheres, followed by warming to room temperature yields cyclopentanone. However under one atmosphere of CO at −78°C **38** is produced. It is assigned the structure of a CO insertion product on the basis of IR(C = O stretch at 1730 cm^{-1}) and NMR studies. Again this product decomposes at room temperature having a half-life in CH_2Cl_2 of ~ 15 min. at 35°C. The chemistry of **37** differs markedly from that of an acyclic analogue Cp_2TiBu_2 in several respects.

Firstly the metallacycle is somewhat more stable and also its decomposition products are somewhat different. Cp_2TiBu_2 yields butane and 1-butene on decomposition whereas the metallacycle yields the analogous 1-butene and ethene. Although the mechanism of formation of the latter has not been established it probably includes a carbon–carbon bond cleavage encouraged by the ~0°C Ti–C–C–C dihedral angle (the crystal structure of $L_2Pt(CH_2)_4$ has been reported[72] but shows slight puckering of the ring). A similar complex for platinum, has been reported, **39** and is found to be far more stable than the titanium complex.[71] This and several other

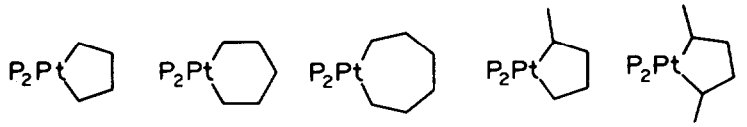

39 **40** **41** **42** **43**

metallacyclic complexes **40–43** are prepared by the reaction of the appropriate di-Grignard reagent with dichloro(1,5-cyclooctadiene)platinum(II) in ether, followed by displacement of 1,5-cyclooctadiene by tertiary phosphines (P). Thermal decompositions were carried out and two features are significant. Firstly, the metallacycles are again found to be markedly more thermally stable than are acyclic platinum(II) alkyls (the larger and more mobile platinacycle (**41**) apart). It is also interesting that the presence of one (**42**), or two (**43**) secondary Pt–C bonds results in little decrease of this thermal stability as organometallic derivatives of secondary alkyl groups are often less stable than those of primary alkyls. Secondly, the decomposition products suggest that the mechanism is one similar to that established for $L_2Pt(n\text{-}Bu)_2$ (eqn 16).

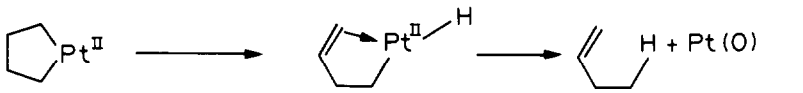

(16)

One of the above complexes $[(PPh_3)_2Pt(CH_2)_4]$ has been structurally characterised[72]. The square planar geometry about the platinum atom is found to be distorted. One possible explanation could be the result of a contribution to the bonding from the canonical form **44** (eqn 17).

To test this hypothesis iodine was reacted with the complex[73] to give the

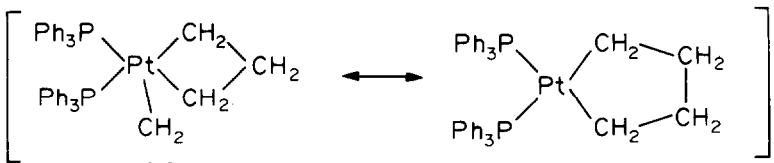

44 **45**

analogous Pt(IV) compound (eqn 18). This has no vacant stereochemical position and is already an 18-electron complex and so a canonical form analogous to **44** can play no part.

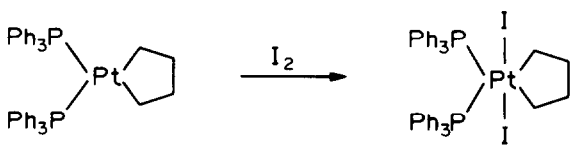

46

It was found that the disorder in the butanediyl ligand of the Pt(IV) complex is a result of the two central carbon atoms alternating between the two forms indicated schematically in **47**. This puckering of the ring relieves the crowding of the

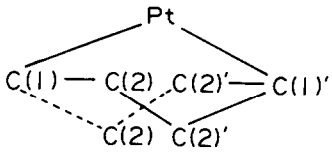

47

hydrogen atoms on adjacent carbon atoms and the two conformations are equivalent as far as the immediate neighbours of platinum are concerned. For the puckering of the ring no lack of symmetry with respect to the platinum atom is observed in contrast to the result reported for the Pt(II) complex **45** and therefore supports the equilibrium suggested in eqn (17).

Palladium may also be used to make metallacyclopentanes by reaction of 1,4-dilithiobutane with $PdCl_2(dppe)$[74,75] at $-70°C$ giving the palladacycle **48**. This compound is thermally very stable considering that it contains β-hydrogen atoms available for hydride elimination and decomposes in about 12 hr in toluene ($Pd(Bu^n)_2(dppe)$ decomposes in about 1 hr). On reaction with CO at room temperature **48** gives only decomposition products (*n*-butenes); no insertion

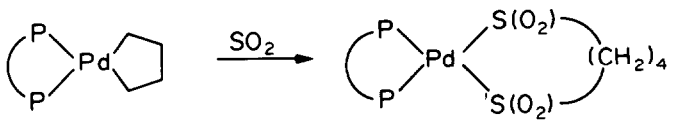

48 **49** (19)

or keto products are observed. However, when reacted with liquid SO_2 at $-40°C$ a stable cyclic compound **49** is observed (eqn 19). The difference in reactivity between CO and SO_2 can be attributed to the greater electrophilicity of the latter. When **48** is treated with Ph_3CBF_4 the η^3-allylic compound **51** is obtained (eqn 20). (Interestingly the reverse reaction, giving metallacyclic

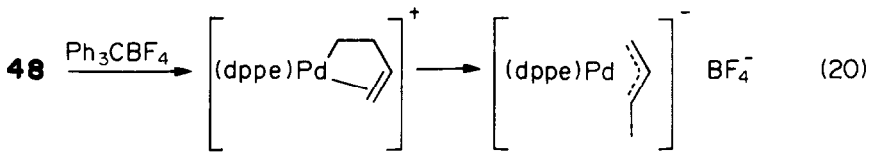

50 **51** (20)

compounds *via* nucleophilic attack by H^- on allylic compounds, has been previously reported.[76] AN initial β-hydrogen abstraction by the trityl cation would give the intermediate **50** which would then rearrange to give the more stable η^3-allylic derivative. Such a β-hydrogen abstraction appears to be closely related to the mechanism of thermal decomposition giving *n*-butenes which is thought to proceed *via* an inter-or intra-molecular abstraction of hydrogen from one of the β-carbons, see eqn (16) above.

Slightly previously to the palladium work Grubbs *et al.*[77] produced analogous complexes using nickel by the same method. Complexes containing different phosphine ligands were made and they appear to be somewhat more air sensitive than the platinum and palladium examples. Furthermore, whilst thermal decomposition of both platina- and pallada-cyclopentanes gives mainly *n*-butenes, it is found that on thermal decomposition of the nickelacyclopentane, cyclobutane elimination occurs.

Reactions of $RhI_2(PPh_3)(\eta^5\text{-}C_5Me_5)$ with di-Grignard reagents $BrMg(CH_2)_nMgBr$ have been shown to produce rhodacycloalkanes[78] (eqn 21).

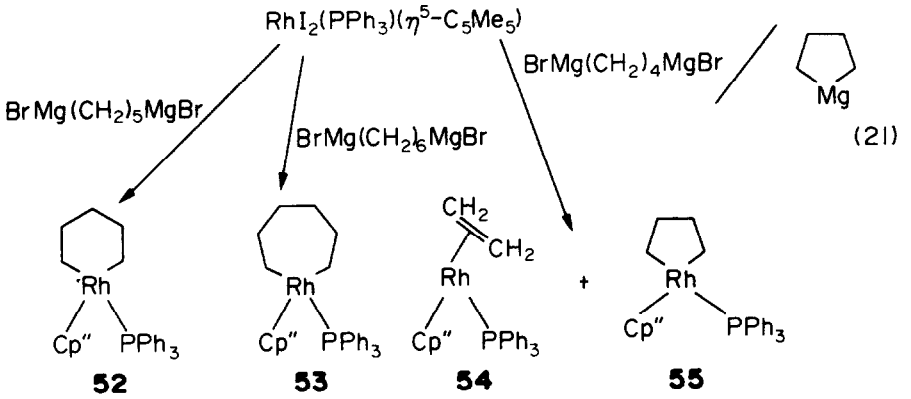

When $n = 5$ and 6 the rhodacycloalkanes **52** and **53** are produced as expected. Both decompose under argon at 160°C; no carbon–carbon bond cleavage is observed, the only volatile products being *n*-pentenes and *n*-hexenes. However, reaction of the starting material with the di-Grignard ($n = 4$) leads to a mixture of **54** (yield 40%) and **55** (*ca.* 10%). Ethene is detected in the reaction mixture by g.l.c. The same results are obtained by using magnesacyclopentane as the alkylating agent. The method of preparation of **54** and the subsequent evolution of ethene suggests that the metallacyclopentane **55** is the precursor of **54** undergoing carbon–carbon σ-bond cleavage. The fact that carbon–carbon σ-bond cleavage is not observed in **52** or **53** demonstrates the importance of ring size in determining the properties of rhodacycloalkanes. Although similar fragmentations have been suggested[70] this is the first example of the resulting alkene complex being isolated. It has subsequently been found[79] that the analogous reactions of the isostructural derivatives of cobalt **56** and iridium **57** with $Mg(CH_2)_4$ or $[BrMgCH_2CH_2]_2$ give the metallacycles, **58** and **59**, in a pure form with no free ethene or ethene-metal complexes being observed (eqn 21)

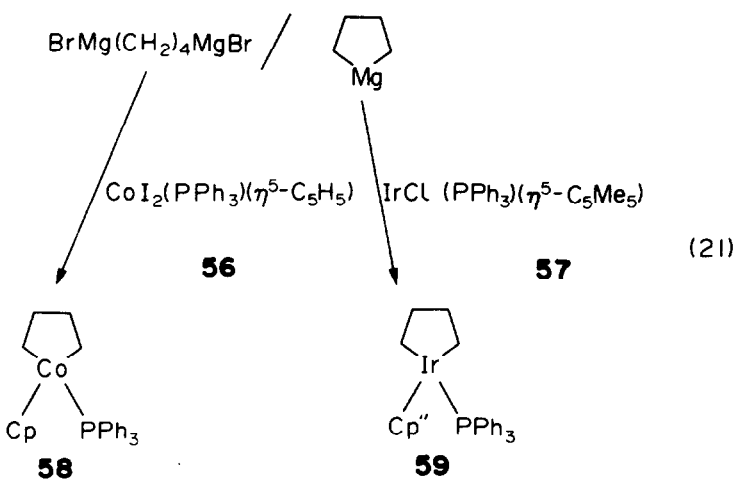

Furthermore, when **58** and **59** are thermally decomposed in mesitylene at 110°C, C_4 hydrocarbons are obtained as the only volatile products. X-ray crystallographic studies of the Rh, Ir and Co complexes have subsequently shown[80] that there is a puckering of the metallacyclic ring for these complexes and the carbon–carbon bond distances are extremely short for the $C(sp^3)$–$C(sp^3)$ bonds of a metallacyclic ring.

More recently a detailed study of the syntheses of metallabenzocyclopentene compounds has been carried out. Lappert *et al.*[81–85] have synthesised such compounds for niobium, titanium, zirconium and hafnium **60** (eqn 23). The niobium complexes so produced appear to be the first examples of d^1 metallacycles.

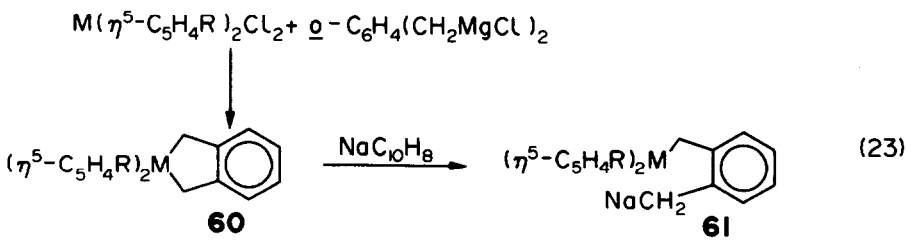

M = Nb	R = Me_3Si, H	M = Ti	R = Me_3Si, H
M = Ti	R = Me_3Si, H	M = Zr	R = Me_3Si, H
M = Zr	R = Me_3Si, H	M = Hf	R = Me_3Si
M = Hf	R = Me_3Si		

Addition of sodium naphthalide at room temperature to the d^0 metallacycles causes reductive cleavage giving a black (Ti) or brown (Zr, Hf) solution of the substituted benzyl carbanion **61**. The d^0 metallacycles are found to be quite thermally stable (e.g. M = Ti, R = H mp 132°C)[82] by comparison with saturated analogues, e.g. $Ti(\eta\text{-}C_5H_5)_2(CH_2)_4$ decomposes by β-elimination above $-20°C$[70]. Under an atmosphere of CO insertion occurs into the hafnium complex to give a metallabenzocyclohepta-2,7-dione, **62** (eqn 24).

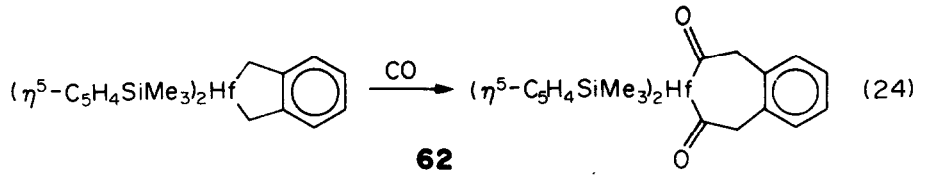

Furthermore it is possible to isolate complexes free from π-acceptor ligands for Ti, Zr and Hf (eqn 25). The insolubility of the compounds suggests

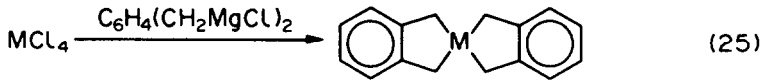

63

that they may be polymers with the *o*-xylylidene ligand bridging successive metal atoms. Platinacyclic compounds have also been prepared from the same Grignard reagent (eqn 26)

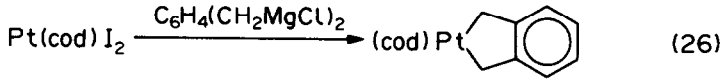

64

Work has been done by the same group on an apparently similar system where the alkylating agent is *o*-$C_6H_4[CH(SiMe_3)Li(tmeda)]_2$[83] (eqn 27). The incorporation of the α,α'-trimethylsilylmethyl substituents into the

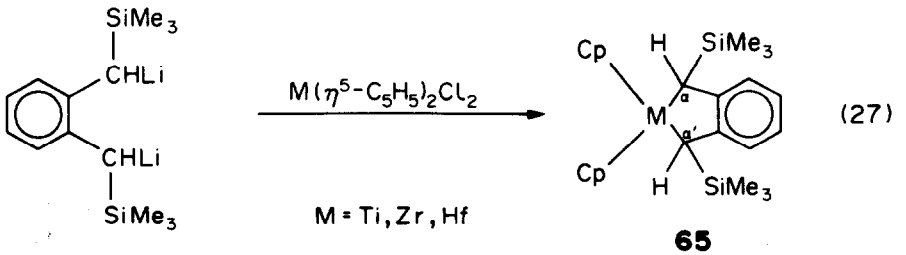

metallacycle introduce some interesting features. Firstly the complexes are thermally and to a certain

extent, aerobically stable, the enhanced stability probably being a result of increased shielding of the metal centre by the large $SiMe_3$ groups. By virtue of the chiral centres at Cα and Cα' metallacycle formation proceeds stereospecifically to give only the meso diastereomers. This assignment is based on the NMR inequivalence of the two $(\eta^5\text{-}C_5H_5)^-$ ligands and the equivalence of the α- and α'-hydrogen atoms and $SiMe_3$ groups. It is also found that reversible one electron reductions to the metallate(III) benzocyclopentenes **66** occur.

$$[\overline{M\{CH(SiMe_3)C_6H_4CH(SiMe_3)\text{-}o\}}(\eta\text{-}(C_5H_5)_2]^-.$$

66

The ease of reduction falls in the order Ti ≥ Zr > Hf. Evidence that the resulting complexes **66** are d^1 complexes derives from ESR studies. 2,3-benzometallacyclopentene complexes of tungsten have also been prepared. Thus reaction of WCl_4O with $C_6H_4(CH_2MgCl)_2$[84] gives the tungsten (V) complex **67**. Again this is a rare example of a d^1 metallacycle and its preparation also

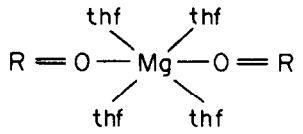

67

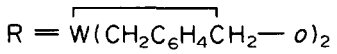

demonstrates that the *o*-xylylidene ligand is capable of stabilising high oxidation states.

Furthermore when WCl_4O is reacted with an excess of the di-Grignard reagent, $W(\overline{CH_2C_6H_4CH_2}\text{-}o)_3$, **68**, results.[85] This establishes a new class of organometallic compound, the metallatricycle. It is a surprisingly thermally robust complex being sublimable at 160°C with minimal decomposition. (C.f. another W(VI) complex, $W(CH_3)_6$, which decomposes slowly at −35°C[86]). The enhanced stability is probably a result of folding of the *o*-xylylidene ligand which allows significant $W(d^0)$-π interaction.

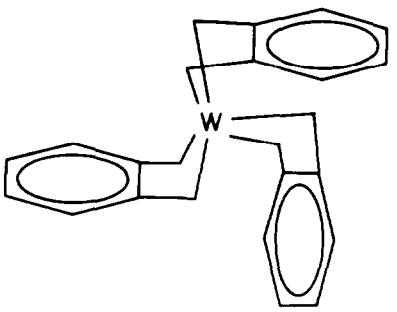

68

3. METALLACYCLES DERIVED FROM COUPLING REACTIONS OF ALKENES OR ALKYNES

Reactions of metal complexes with alkenes giving metallacycloalkanes, or alkynes giving metallacycloalkadienes represent the most common method for synthesis of metallacyclic compounds. A large amount of work has been carried out on alkyne reactions as many transition metals act as catalysts for the cyclotrimerisation of alkynes to benzene derivatives. This method of synthesis yields almost exclusively five membered ring systems.

The earliest examples of such reactions involve iron complexes. The reaction of but-2-yne with the monoanion of iron carbonyl hydride[87] produced a complex whose structure was not fully clear at the time. Soon afterwards however, X-ray crystallographic analysis[88] showed structure **69** to be the true representation, a ferracyclopentene complex. A similar compound **70** was subsequently prepared[89]

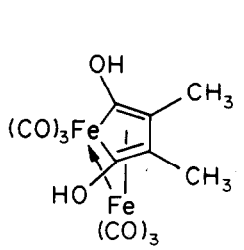

69

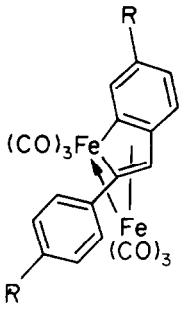

70

from diphenylacetylene and dodecacarbonyltriiron. More recently a monomeric metallacyclopentadiene complex of iron has been synthesised from the reduction of $FeCl_2(PMe_3)_2$ in the presence of 2-butyne.[90] The product is **71** a highly volatile

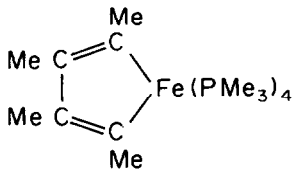

71

solid of high thermal reactivity.

The fluorinated iron metallacycle **72** has been made by two different groups at about the same time from the reaction of tetrafluoroethene with $Fe(CO)_5$[91] or $Fe_3(CO)_{12}$[92]. Confirmation that the complex is a tetracarbonyl comes from its mass spectrum ($M^+ = 368$ a.m.u.) and its reaction with iodine at 150°C releasing four moles of CO.

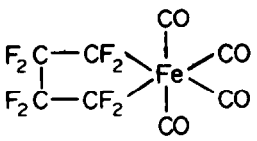

72

Another ferracyclopentane has been synthesised[93] on photolysis of an iron methylacrylate complex with further alkene (eqn 28). Isomers **74a** and **74b** are formed although **74a** predominates. At low reaction temperatures the

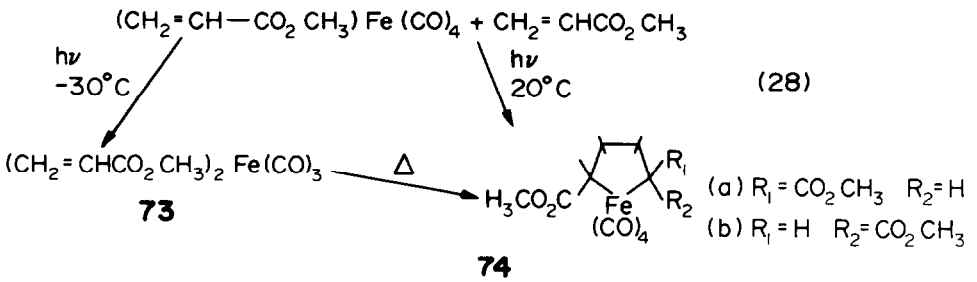

(28)

dialkene complex **73** is obtained which has been shown to convert to **74** at room temperature. Compounds such as **73** and **74** have been proposed as intermediates in the photochemical formation of cyclopentanones from $Fe(CO)_5$[94] and cyclic alkenes and the fact that such products are observed in the reaction of **74** with CO(40 atmospheres, 60°C) lends support to that view. More recently a further photochemical reaction of $Fe(CO)_5$ with an alkene to give a ferracyclopentane complex **75** (eqn 29), has

been reported[95] and the reaction is found to be stereospecific. An isomeric complex is obtained

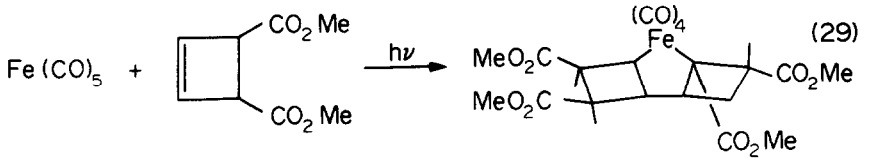

(29)

from the same cyclobutene when $Fe_2(CO)_9$ is used under non-photolytic conditions. A complex of ruthenium **76** somewhat related to the iron complexes **69** and **70** has been made[96] by the reaction of diphenylacetylene with $Ru_3(CO)_{12}$ at 200°C.

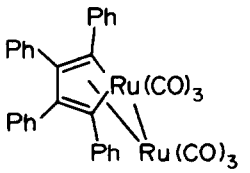

76

Further work on iron, ruthenium and osmium with hexafluorobut-2-yne[97] has been carried out using the complexes *trans*-$M(CO)_3L_2$. Ultraviolet irradiation of *trans*-$Fe(CO)_3L$ with excess hexafluorobut-2-yne gives **77**. Similar treatment of *trans*-$Ru(CO)_3L_2$ with an equimolar amount of hexafluorobut-2-yne gives **78** although when an excess of the alkyne is used complexes **79–81** result. Over longer periods of irradiation **82** is also a product. When an excess of

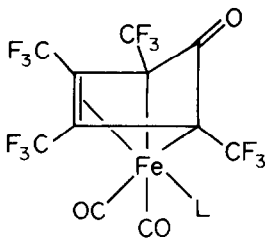

77

L = $PhMe_2P$, $(EtO)_3P$

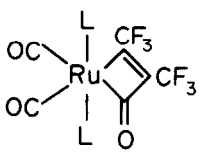

78

L = $(MeO)_3P$

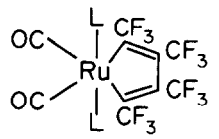

79

L = $(MeO)_3P$, $PhMe_2P$

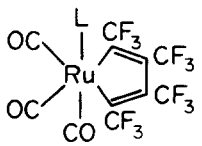

80

L = $PhMe_2P$

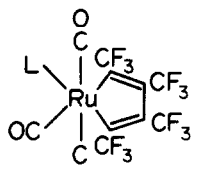

81

L = $PhMe_2P$

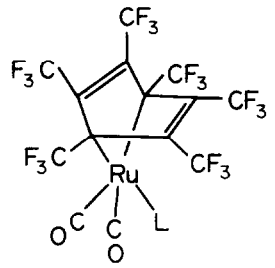

82

L = $(MeO)_3P$

83

hexafluorobut-2-yne is irradiated with *trans*-$Os(CO)_3L_2$ complex **83** is the only isolated product. Thus the nature of the metal has a significant bearing upon how the reaction proceeds. However, it is reasonable to suggest that certain common pathways exist and a plausible reaction scheme which accounts for all of the observed products has been outlined (eqn 30).

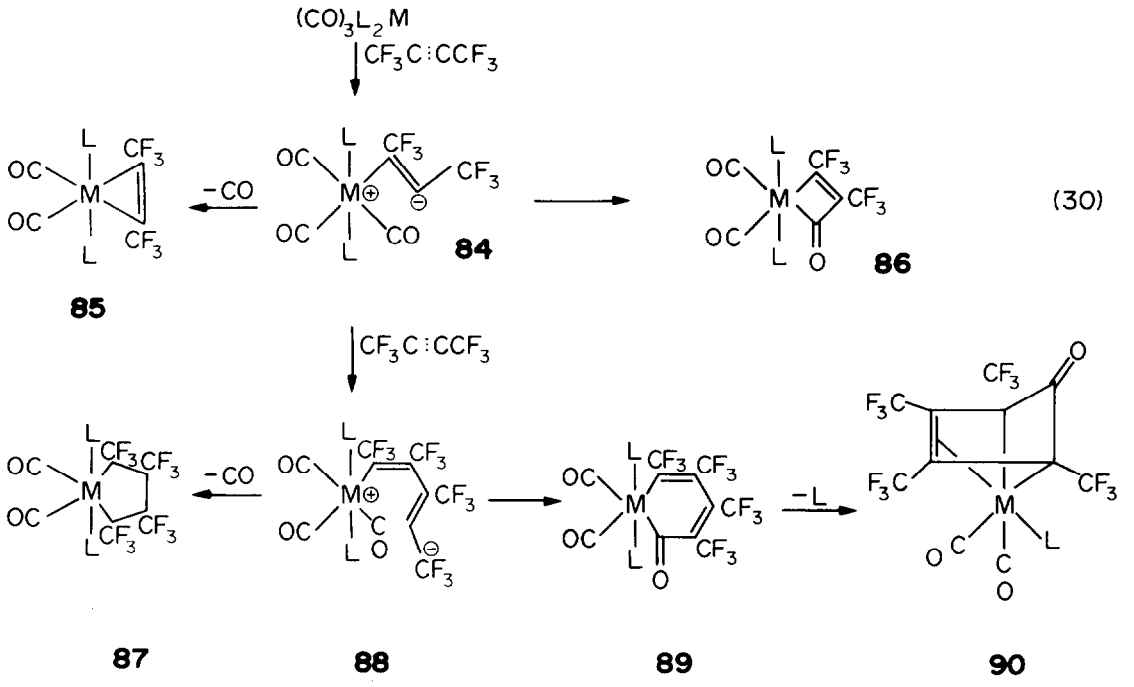

Initially an ionic intermediate **84** is formed. This either ring closes to form a three membered ring compound **85**, or intramolecular nucleophilc attack by the carbanion on coordinated CO may give a metallacyclobutenone **86**. Alternatively at higher alkyne concentrations the intermediate **84** can be intercepted by a further molecule of alkyne to form an ionic intermediate **88** which can ring close to a metallacyclopentadiene **87** or attack coordinated CO and lead to the cyclopentadienone **90**. A scheme parallel to that established in iridium chemistry[98] (*see later*) appears to be invalidated for several reasons. Firstly, it was found that a vacant site is necessary to allow the second molecule of alkyne to enter the coordination sphere, which is clearly unlikely for the Fe, Ru, Os system. Furthermore it has been observed[99, 100] that σ-bonded alkyl groups bearing electronegative substituents do not easily migrate onto coordinated CO again invalidating the iridium mechanism for this system.

An unusual six membered ruthenacycle has been synthesised *via* an alkyne type reaction. When a mixture of $RuH_2(PPh_3)_3(CO)$ and methyl propiolate (1:6 molar ratio) are refluxed in benzene[101], an air stable complex **91** results. The interesting feature of this molecule is the existence of a six membered metallacyclohexadiene

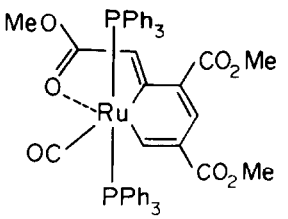

91

ring consisting of three methylpropiolate molecules and a ruthenium, instead of a seven membered metallacycloheptatriene ring. The reaction may proceed *via*

$$Ru(H)_2(CO)(PPh_3)_3 \longrightarrow Ru(CO)(PPh_3)_3 \longrightarrow$$

92 **93**

$$Ru(H)(C{\equiv}CCO_2CH_3)(CO)(PPh_3)_3 \longrightarrow Ru(C{\equiv}CHCO_2CH_3)(CO)(PPh_3)_3 \longrightarrow \mathbf{91} \quad (31)$$

94 **95**

formation of coordinatively unsaturated species such as **93**, oxidative addition of methyl propiolate to give a hydridoethynyl ruthenium complex **94** followed by a 1,3-hydrogen shift to give the vinylidene ruthenium complex **95** and ring expansion by successive addition of two molecules of methyl propiolate to give the observed product **91** (eqn 31).

Another substituted ruthenacyclopentane[102] has been synthesised via the reaction of $Ru_3(CO)_{12}$ with *o*-styryldiphenylphosphine (eqn 32).

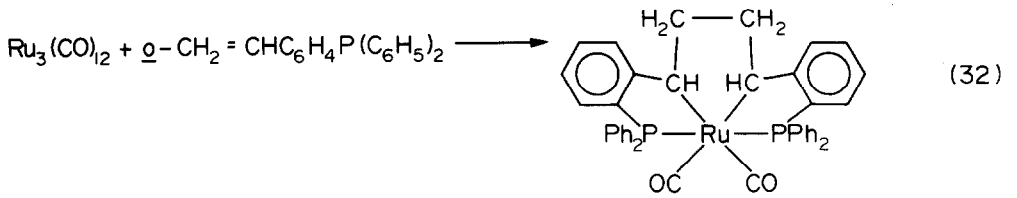

(32)

The complex has been shown by single crystal X-ray diffraction studies to be an octahedral σ-bonded dicarbonyl complex of Ru(II) containing a puckered ruthenacyclopentane ring formed by the coupling of two vinyl residues at the β-carbon atoms. A very similar reaction to this has been observed in a rhodium system. Reaction of $RhCl(PPh_3)_3$ with 2 mols of *o*-phenylethynyldiphenylphosphine[103] **97** leads to the formation of **98**.

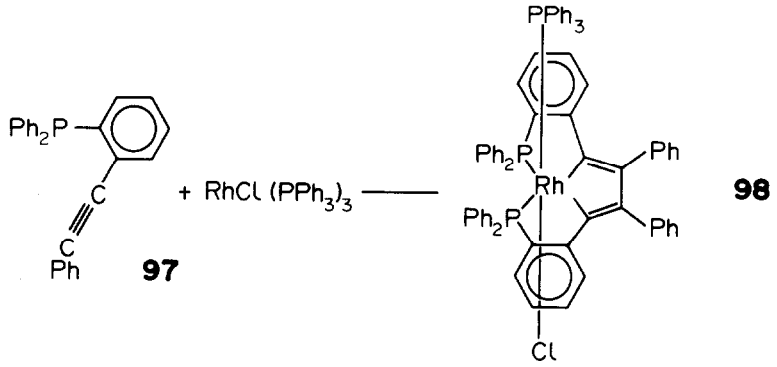

On reaction with diphenylacetylene an ionic η^6-arene chelate Rh(1) complex **99** forms almost instantaneously

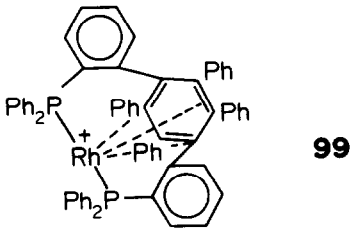

This (**99**) is the first reported isolation of the Rh-arene intermediate[97] long suspected to occur in the Rh-catalysed trimerisation of acetylene.

Hexafluorobut-2-yne readily reacts with cyclopentadienyldicarbonylrhodium giving a mixture of two products[104] (eqn 33). Both complexes are extremely stable being inert in both air and in solution and remain unchanged on dissolving in concentrated acids.

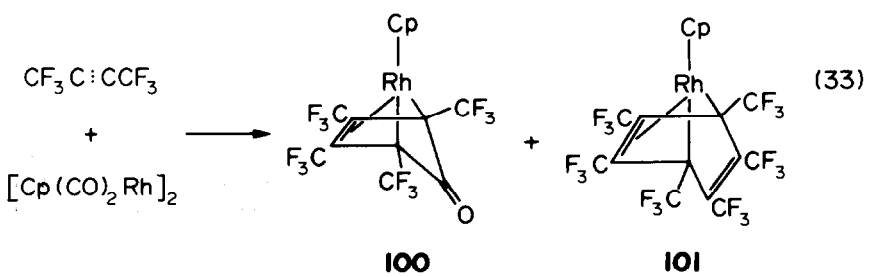

(33)

When a similar rhodium complex is reacted with a different alkyne, hex-3-yne,[105] the reaction proceeds in rather a different manner (eqns 34 and 35).

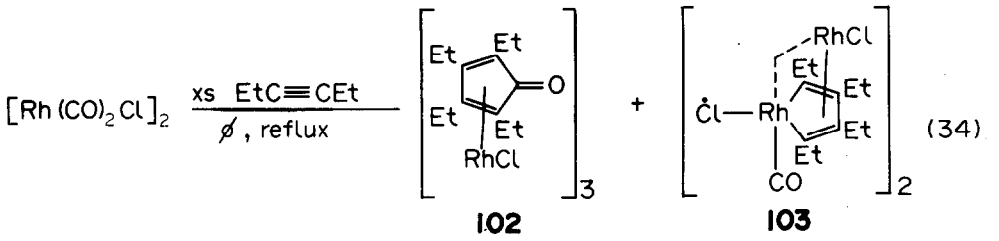

102 103 (34)

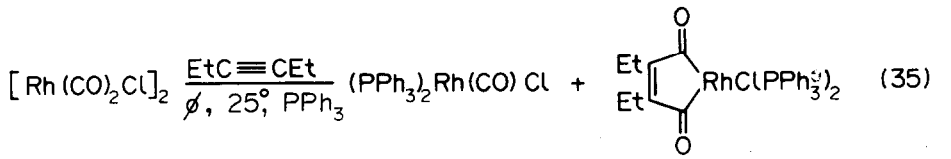

104 (35)

In refluxing benzene the products are **102** and the thermally very stable dimer **103** which reacts with a variety of ligands to give adducts, $[(C_4Et_4)Rh_2(CO)Cl_2L_3]$. The adducts, however, are not very stable and either revert to **103** (L = CO, pyridine) or decompose further ($L = PPh_3$). When the reaction is carried out at 25°C in the presence of PPh_3 the rhodacyclopentene **104** may be isolated. But-2-yne had previously been shown to react with $[Rh(CO)_2Cl]_2$ in the same way to give an analogous complex to **104**.[106]

An unusual reaction of hexafluorobut-2-yne has been reported with the complex $[Rh(cod)Cl]_2$ in the presence of sodium acetylacetonate.[107,108] It is found that the alkyne adds 1,4 to the coordinated cycloocta-1,5-diene giving **105** which contains a rhodacyclopentane ring.

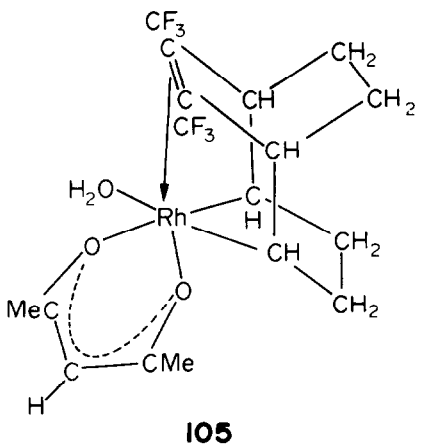

105

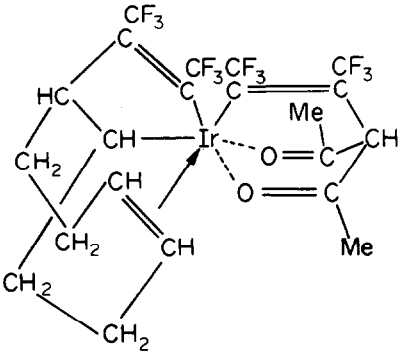

106

An alternative mode of addition is observed in **106** made from the reaction of hexafluorobut-2-yne with [Ir(acac)cod)]. Here one molecule of hexafluorobut-2-yne inserts between the metal and one olefinic carbon atom to form an iridacyclopentene ring. The second olefinic bond of the diene remains π-bonded to the metal. A second molecule of the alkyne adds 1,4 to the iridium acetylacetonato ring. These addition reactions presumably involve an intermediate metal-alkyne complex. In the case of the rhodium example, the close proximity of the coordinated alkyne to cyclooctadiene held in the correct conformation by the metal, would then facilitate 1,4-addition to give the observed product. The iridium reaction does not produce a 1,4-addition product presumably because the initial reaction involves 1,4-addition of C_4F_6 across the metal-acac ring to produce a five-coordinated intermediate in which the

metal formally achieves 18 electrons in its valence shell. Formation of a second acetylene complex is thus unlikely and the reaction follows a different course.

Hexafluorobut-2-yne has also been shown to react with *tris*(triphenylstibine)chlororhodium(I)[109,110] in benzene at 80°C to give **107**.

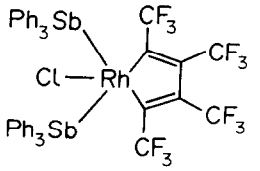

107

The complex adds one mol. of CO at ambient temperatures to give $RhCl(CO)(C_8F_{12})(SbPh_3)_2$. It also reacts with pyridine, trifluorophosphine, and (in the presence of a large cation) cyanide ion to give similar adducts. The analogous triphenylarsine complex to **107** has been prepared but unlike the triphenylstibine complex does not form stable adducts with CO, PF_3, etc.

A little previously to this work, Collman *et al.*[98] had reported the production of irida- and rhodacyclopentadienes from alkynes (eqn 36).

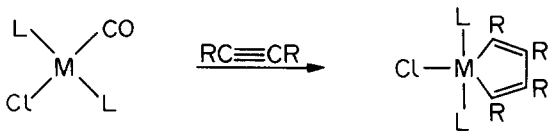

108

(36)

M = Ir L = PPh_3

M = Rh L = $AsPh_3$

(a) M = Ir L = PPh_3 R = CO_2Me, CO_2Et

M = Rh L = $AsPh_3$ R = CO_2Me

The metallacyclopentadiene structures **108** are assigned on the basis of spectral evidence. The iridium complex possesses a latent site of unsaturation and takes up one mol. of CO. to form a coordinatively saturated complex. (Similar experiments were not performed on the rhodium complex.) Furthermore, it is found to catalyse the trimerisation of dimethylacetylene-dicarboxylate at a reasonable rate in boiling toluene. The rhodacycle is found to be effective in boiling benzene. On the evidence of results obtained, a scheme has been postulated (eqn 37). That a latent site of coordination must be present is supported by the observation of almost total inhibition of alkyne trimerisation under 60 psi of CO. Also maleic anhydride does not react with **108** arguing against a Diels–Alder mechanism. Furthermore, the cyclisation mechanism appears to be sensitive to steric hinderance as no catalytic activity is observed when diphenylacetylene is used in place of dimethylacetylenedicarboxylate.

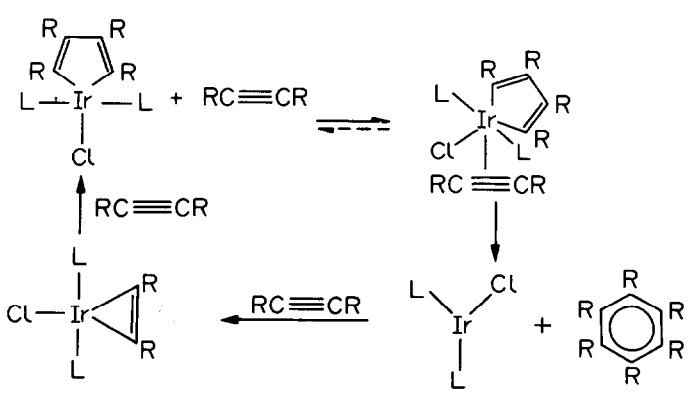

(37)

Other iridium metallacycles containing two different acetylenic units were also subsequently shown to act as alkyne trimerisation catalysts[111] (eqn 38).

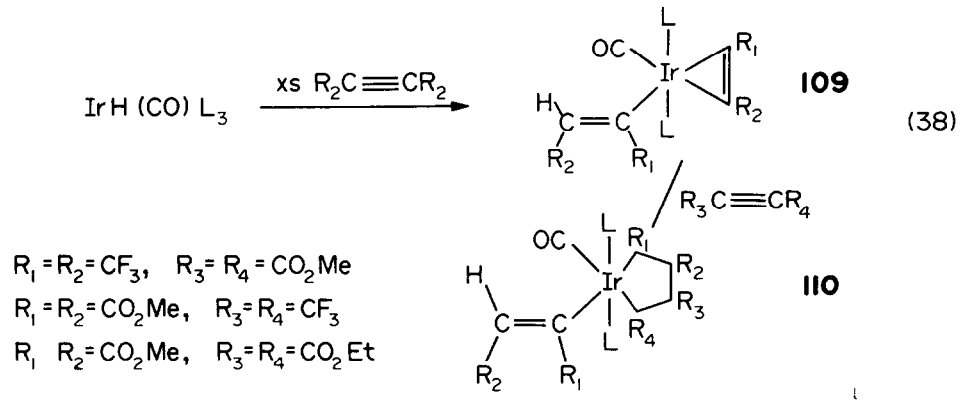

(38)

The reaction of $IrH(CO)(PPh_3)_3$ with an excess of an alkyne at 50–80°C leads to the formation of **109** which can react further with other alkynes giving **110**. **110a** is apparently a far more effective catalyst than those reported by Collman *et al.* Thus in C_6D_6 at 80°C with a 2 mole% concentration of **110a** there is a 70% conversion of dimethylacetylenedicarboxylate into $C_6(COOMe)_6$ after 8 hr, compared with figures of 11 and 5% for Collman's catalysts. The fact that a coordinatively saturated molecule such as **110a** is so effective as a catalyst appears to bring into question the theory that a vacant coordination site is necessary for activity, although it is possible that a coordinatively unsaturated species derives from **110a** and it is this which is the active catalyst. Similar reactions to those reported for other rhodium complexes have been reported using an unusual starting material $Rh(C_6H_4PPh_2)(PPh_3)_2$[112] (eqn 39).

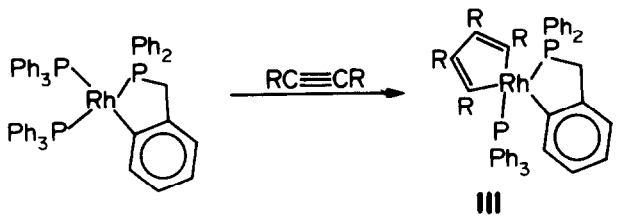

(39)

Again a rhodacyclopentadiene complex is observed, the metallated phosphine remaining unchanged.

Alkyne reactions have also been observed[13] in cobalt systems. Reaction of $C_6F_5C \equiv CC_6F_5$ with $CpCo(PPh_3)_2$ gives a metallacyclopentadiene complex **112** similar to those discussed above for Rh and Ir. Again the reaction can be performed in a two stage process[114] so as to incorporate two different alkyne groups (eqn 40)

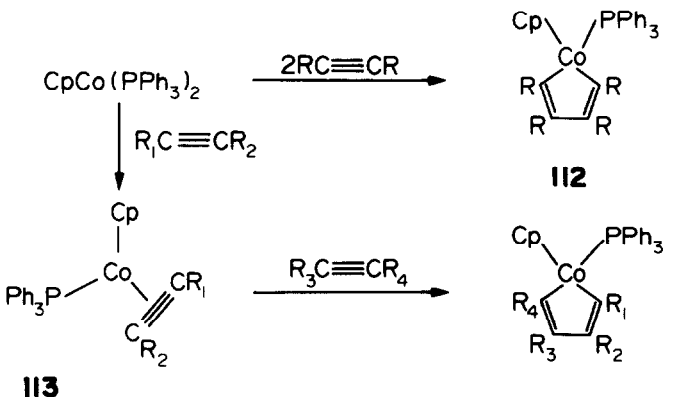

(40)

It is found that in the one step process first reported in 1967[115] only two of the expected three isomers are obtained.[114] Furthermore, when the alkyne complex **113** is reacted with unsymmetrical alkynes, only one isomer is obtained. Obviously the first step of the cobaltacyclopentadiene formation from $CpCo(PPh_3)_2$ is replacement of one of the phosphines by an alkyne molecule giving a π-alkyne complex **115** (eqn 41). For the further

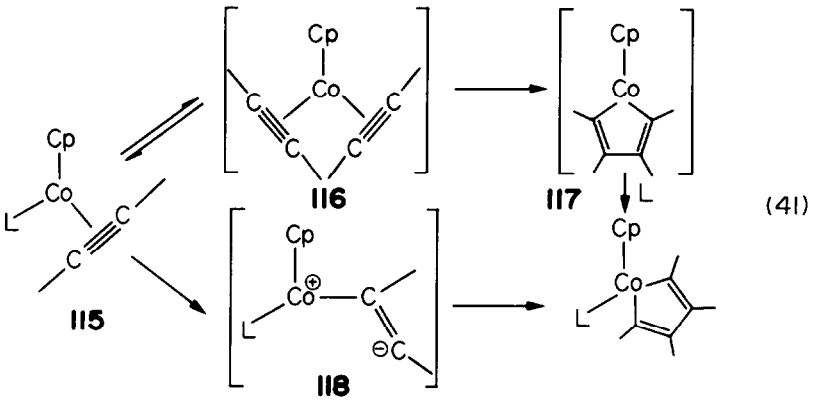

reaction of **115** with an alkyne, two mechanisms may be proposed. In the first an attacking alkyne replaces the phosphine to give a *bis* alkyne complex, **116**, which undergoes oxidative coupling to give a coordinatively unsaturated Co(III) metallacycle **117** which then adds phosphine. Similar intermediates have been proposed[70] in the reaction of titanocene with alkenes. The second pathway involves a thermally excited ionic monohapto-alkyne intermediate **118** to supply a vacant coordination site for an attacking alkyne molecule.

The first pathway appears to be the more likely as polar solvents which should stabilize **118** are shown not to increase the rate of reaction. Furthermore, addition of free triphenylphosphine to **115** with diphenylacetylene markedly decreases the rate and so it seems that **116**→**117** is the rate determining step, and that a preequilibrium is attained between **115** and **116**. When asymmetrically substituted alkynes are used the isomers obtained will be governed by the arrangements of the two alkyne molecules in **116** which might well be affected by dipole–dipole interactions between them.

The acetylene complex **113** has also been shown[116] to react with alkenes (eqn 42). *Trans*-disubstituted alkenes lead to a mixture of two isomeric cobaltacyclopentenes, whereas *cis*-alkenes yield only one isomer.

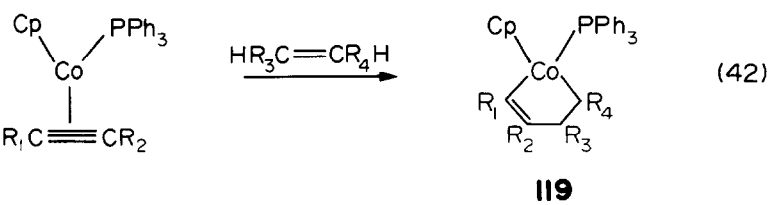

The same group has carried out reactions of **120*** with other Lewis Bases. Reaction of **120** with 2 mols. of phenylisocyanide leads to the formation of **122** (eqn 43), for which the structure is confirmed by X-ray diffraction studies on a single crystal. When the ratio of phenylisocyanide to **120** is low the products are **122** and **121**. Addition of an excess of PPh_3 to the initial reaction mixture increases the observed yield of **121**.

Fewer examples of alkyne reactions leading to metallacyclopentadienes are known for Ni, Pd and Pt as these metals generally prefer to form monoalkyne complexes which tend to be inert to further acetylenic attack. However, a series of palladacyclopentadienes has been made[118] using a zerovalent palladium starting material. Thus, reaction of dibenzylideneacetonepalladium, $[Pd(dba)_2]$, with

*120 is an alternative way of drawing 113.

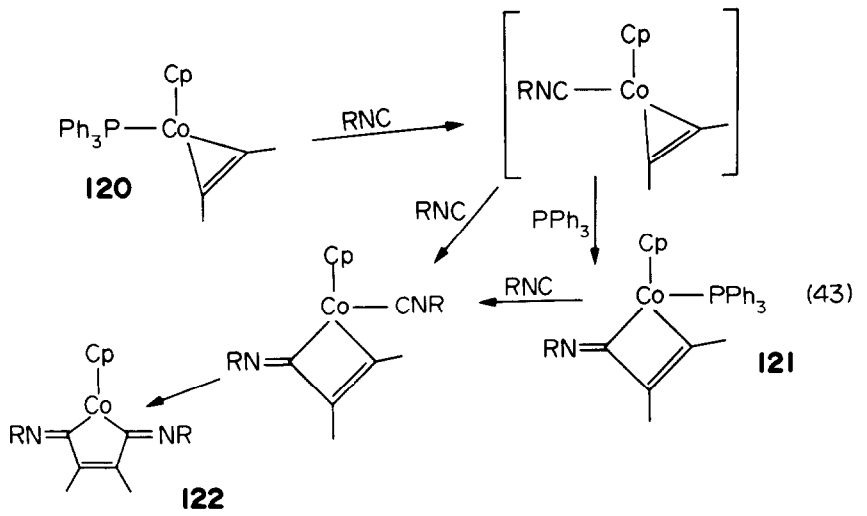

dimethylacetylenedicarboxylate at room temperature leads to the formation of **123** which forms adducts **124** with either monodentate or bidentate donor ligands (eqn 44)

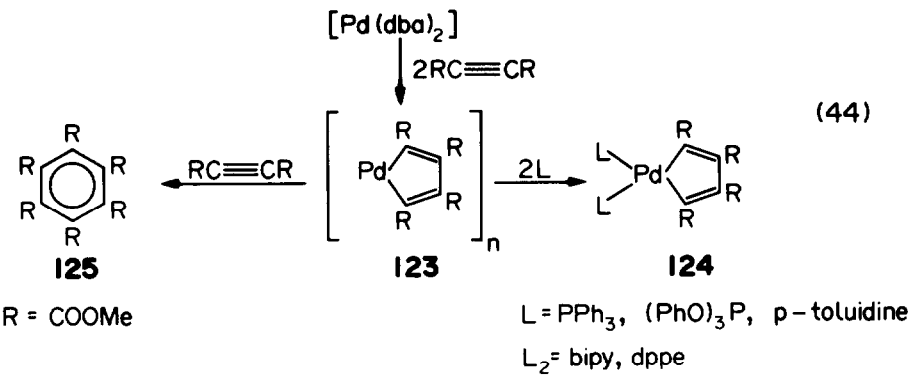

Interestingly, on further reaction with the alkyne, **123** gives the benzene derivative **125**, with 60 equivalents of acetylene being trimerised per equivalent of **123**. This is the first example of the trimerisation reaction being observed for platinum or palladium and the reaction is probably induced by the nucleophilicity of the metal in **123**.

Reaction of the nickel complex $Ni[C_6(CF_3)_6][P(OMe)_3]_2$[119] with three molar equivalents of hexafluorobut-2-yne leads to the formation of the unusual nickelacycloheptatriene[120], **126** (eqn 45), for which the structure is confirmed by an X-ray crystal structure study.

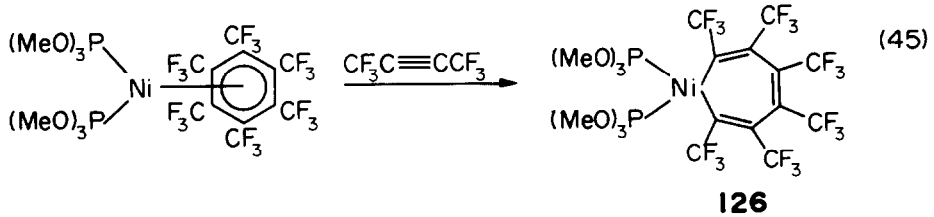

Analogous products have since been reported from the reaction of $NiCl(H)(Cy_3P)_2$ with $CF_3C \equiv CCF_3$,[121]

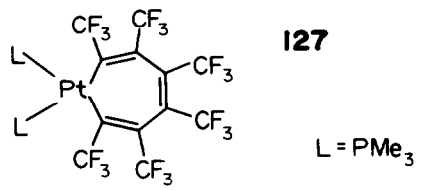

and from the reaction[122] of *trans*-stilbene*bis*(trimethylphosphine)platinum with hexakis(trifluoromethyl)benzene **127**. It is reasonable to suggest that an initially formed 1,2-η-bonded species undergoes a ring opening reaction. An alternative explanation is that this species rearranges with C–C bond cleavage to form a Pt(0) dicarbene complex which transforms electronically to the observed product. That the ring-opening reaction is very dependent on the nature of the ligands coordinated to platinum, is shown by the absence of such a reaction when the same reaction is performed with PEt_3 being the coordinating ligand.

Zerovalent nickel complexes have been shown[123] to react with tetrafluoroethene affording nickelacyclopentanes (eqn 46). In the corresponding reaction $(PPh_3)_4Pt$ affords the simple alkene complex $(PPh_3)_2Pt(C_2F_4)$[124]. It is suggested

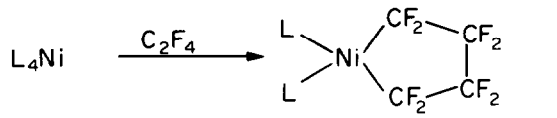

(46)

128

that the nickel system forms an analogous complex initially and this then reacts further to give the nickelacycles. This further reaction is probably only seen for nickel as this metal adds further alkene to form a 5-coordinate intermediate far more readily than platinum(II) for which five coordination is very rare.

Doyle *et al.*[125] have reported the reaction of 2,2'-bipyridyl(cycloocta-1,5-diene)nickel with several alkenes at room temperature to give substituted nickelacyclopentanes (eqn 47). The corresponding unsubstituted

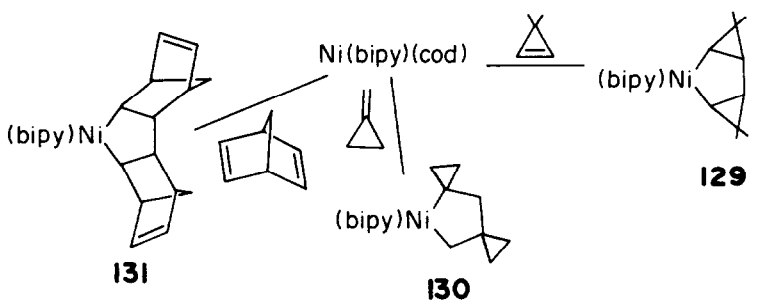

(47)

131 **130** **129**

nickelacyclopentane complex can be isolated from the reaction with 1,4-dibromobutane but not with ethene. Reaction of **129**, **130** or **131** with activated alkenes, such as maleic anhydride, results in reductive elimination of cyclobutanes, behaviour somewhat different from that observed for a palladacyclopentane derivative which decomposes to give *n*-butenes.[75] Furthermore, at temperatures above 90°C, reaction of **129**, **130** or **131** with the appropriate alkene leads to cyclodimer formation and regeneration of the nickel complex. Thus the complexes are acting catalytically, with fifty turnovers per nickel atom having been reported.

The group IVB metals are also reported to yield metallacyclic compounds from alkyne reactions. The first such example was that of titanocene, Cp_2Ti, with diphenylacetylene[126] (eqn 48). This complex has very recently been made by eliminating propene from Cp_2Ti(allyl) on reaction with diphenylacetylene[127].

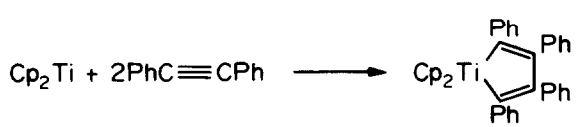

(48)

132

The corresponding zirconacycle, originally made via the reaction of Cp_2ZrCl_2 with a dilithium reagent,[64] has subsequently been made by a similar alkyne route.[128] Both the titanium and zirconium metallacyclo-

pentadiene complexes have been made by a slightly different route[129](eqn 49) which is rather convenient.

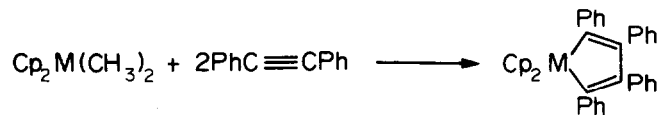

(49)

133

Photochemical reaction of the dimethyl derivatives of titanocene or zirconocene with diphenylacetylene gives **133** in yields of 35–50% *via* homolytic cleavage of a Me–M bond. In the original work, the yellow hafnacycle was apparently prepared by this route, but not fully characterised. Under the photochemical conditions employed, the methyl radicals react not only to produce methane but also undergo reaction with diphenylacetylene to yield a variety of other compounds including *cis*- and *trans*-methylstilbenes. However, it has subsequently been shown[130] that it is possible to produce the hafnacycle in a pure form by this method and an X-ray crystallographic study has confirmed the postulated structure.

More recently, the thermally induced reactions of bis(η^5-cyclopentadienyl)diphenyltitanium with symmetrical and unsymmetrical alkynes have been studied[131, 132] (eqn 50). This reaction with diphenylacetylene has been shown[133] to give

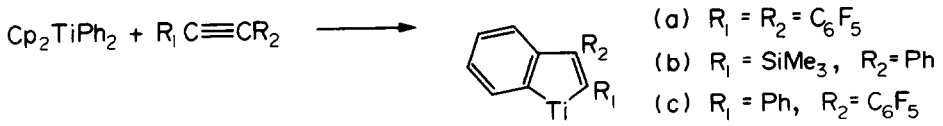

(a) $R_1 = R_2 = C_6F_5$
(b) $R_1 = SiMe_3$, $R_2 = Ph$
(c) $R_1 = Ph$, $R_2 = C_6F_5$
(d) $R_1 = C_6F_5$, $R_2 = Ph$

134

(50)

134 ($R_1 = R_2 = Ph$), *via* insertion of the alkyne into the carbon-titanium σ bond of an intermediate $Ph_2Ti(C_6H_4)$ species.[134] The complexes are formally metallacyclopentadienes containing an unsymmetrically fused benzene ring which has important consequences for the structure of the molecule (see **135**). It is found that the C(1)–C(2) bond lengths are substantially shorter than

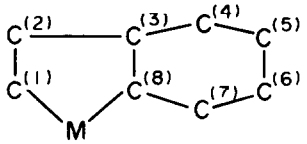

135

those of C(3)–C(8) in accordance with the idea of a full double bond between C(1) and C(2) but only a delocalised double bond of an aromatic nature between C(3) and C(8). There is found to be no localisation of the π-electron density in the six-membered ring and C(2)–C(3) appears to be a normal bond between two sp^2 hybridised carbon atoms. In **134b** the two Ti–C bond lengths are nearly equal but in **134a** they are quite different. This is probably due to the fact that the interactions between cyclopentadienyl groups and the ligand bound to C(1) are important for specification of the Ti–C(1) bond length. With the more bulky C_6F_5 ligand this bond is thus weakened. A similar reaction has been performed using phenyl(pentafluorophenyl)acetylene[135] with products **134(c)** and **134(d)** being formed in 44% and less than 1% yield respectively.

One unusual reaction of a titanium complex with an acetylene to give a titanacyclobutene complex has recently been reported[136] (eqn 51). **136**

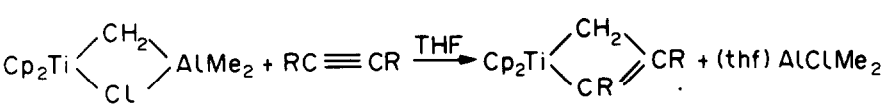

(51)

136 **137** (a) R = Ph (b) R = $SiMe_3$

reacts with diphenylacetylene or *bis*(trimethylsilyl)acetylene in THF to produce **137a** and **137b** respectively. THF is found to assist the synthesis of **137** by complexing with aluminium and freeing the Cp_2TiCH_2 group for addition to alkyne. Diphenylacetylene converts **137** to **137a** at elevated temperatures although the reverse reaction does not seem to occur. Furthermore, 2-methylpropene-1-^{13}C and **137b** react to yield **137b**-^{13}C with enrichment in the methylene position. One possible mechanism is that the alkyne is substituted by alkene to give **138** which then reverts back to **137b** (eqn 52). This exchange reaction shows

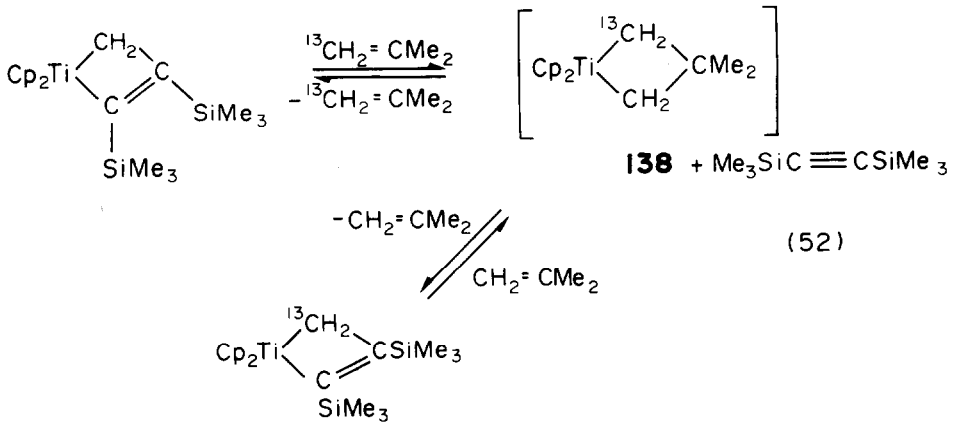

(52)

that the titanacyclobutene **137b** is considerably more stable than the titanacyclobutane **138**. Intermediate **138** is also postulated in a scheme describing CH_2 exchange between $Cp_2TiCH_2AlClMe_2$.[137] A recent X-ray crystallographic study[138] suggests that **137b** is more reactive than **137a** as **137b** shows a partial fragmentation of the metallacyclobutane ring and incipient formation of separate titanium-methylene and titanium-alkyne bonds. This is consistent with the greater chemical lability of the alkyne unit as compared with that of complex **137a**.

Similar reactions have since been performed with a variety of alkenes[139] again giving titanacyclobutanes. Several systems have been studied and one in particular (see eqn 53) suggests a role in metathesis reactions. Pyridine removes Me_2AlCl from $Cp_2TiCH_2AlClMe_2$ and the reactive $[Cp_2TiCH_2]$

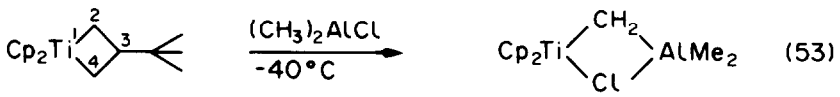

139 **140** (53)

fragment is immediately trapped by alkene to give the titanacyclobutane. This reaction coupled with the one shown above provides the necessary steps for this metathesis system. Complex *trans*-**139**-d_1 (d is on C(4)) on treatment with Me_2AlCl in toluene gave a mixture of **140** and **140**-d_1 thus completing the metathesis cycle. Subsequent X-ray diffraction structural studies suggest the titanacyclobutanes involved in metathesis to be planar and symmetrical.[140] If this is the case then the source of stereoselection in alkene metathesis may result from factors other than those arising from the conformational effects due to puckering of the intermediate, which had previously been suggested.

A metallacyclobutene structure **141** has also been reported[141] for the complex resulting from the reaction of phenylethynylsodium, $Na(C\equiv CC_6H_5)$, with chloro*bis*(methylcyclopentadienyl)titanium(III) (eqn 54), the structure being confirmed by a single crystal X-ray diffraction study.

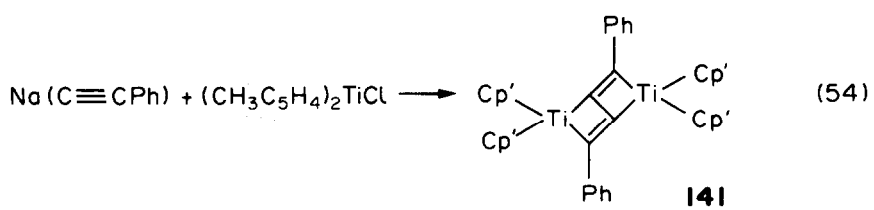

(54)

Thus, the previously reported analogous reaction in which $Cp = C_5H_5$[142] may now be looked upon as giving a metallacyclobutene rather than one of the postulated alkyne complexes.

The zirconocene derivative $[(\eta^5\text{-}C_5Me_5)_2ZrN_2]_2$ has been shown to absorb ethene[143] with evolution of dinitrogen to afford **142** in almost quantitative yield. The complex is also obtained from $(\eta^5\text{-}C_5Me_5)_2ZrH_2$ and ethylene at 25°C according to eqn (55).

142

The complex reacts with both HCl and H_2 to yield predominantly butane. Furthermore, on reaction with CO, complex **144** in which the carbonyl oxygen is bound to the zirconium, is obtained. This is presumably formed *via* intermediate **143** from which migratory insertion of CO into a Zr-alkyl occurs with remarkable facility. Subsequent steps are as shown in eqn (56).

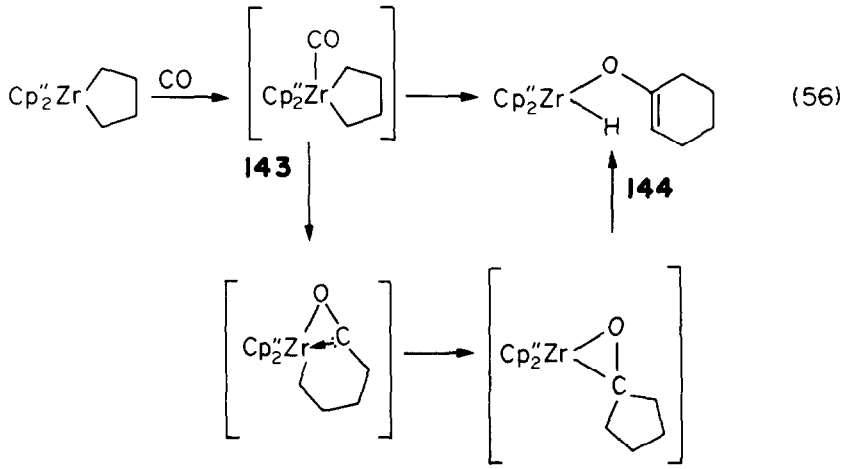

Diphenylzirconocene, Cp_2ZrPh_2, also reacts with ethylene on heating to give a zirconacyclopentene complex[144] *via* a zirconium benzyne intermediate (eqn 57).

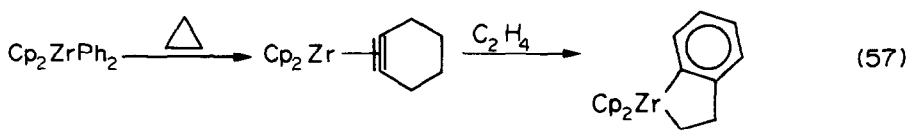

145

It is found that exchange of alkenes occurs enabling synthesis of a range of such zirconium metallacycles. This exchange presumably occurs via benzyne-alkene intermediates (eqn 58). The exact position of the equilibrium depends upon the nature of the alkene; with excess norbornene **146** is almost exclusively obtained whereas conversion is only about 50% with the less reactive alkene, 1-octene. Furthermore, work using substituted products of **145** shows the reaction to be sensitive to steric hinderance.

A series of tantalacyclopentanes has been made[145, 146] by the reaction of the neopentylidene complex $Ta(\eta^5\text{-}C_5H_5)Cl_2(CHCMe_3)$ with alkenes at −30°C (eqn 59). This represents one of the first examples in which metallacyclopentanes are formed from two simple alkenes (see also Ref. 42).

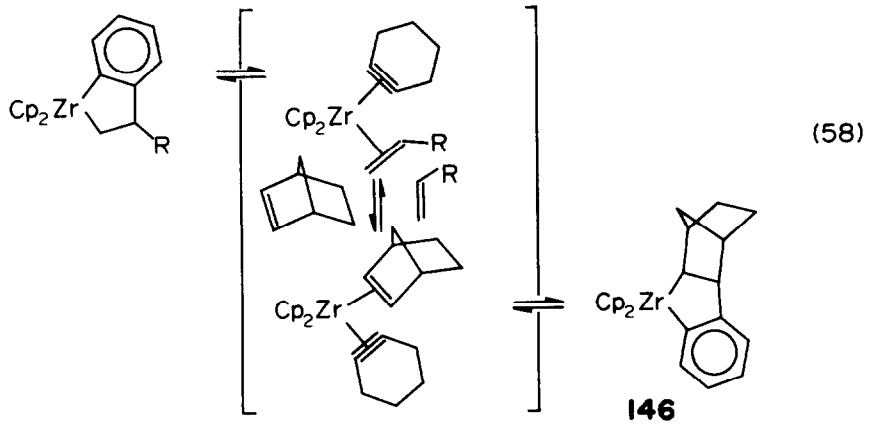

(58)

146

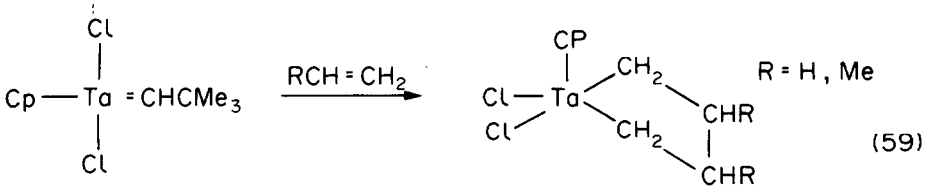

(59)

147

Similar tantalacyclopentanes are also produced from the reaction of alkenes with (η^5-C_5Me_5)Ta(alkene)Cl_2 (eqn 60). It appears that all these metallacycles are in equilibrium with the alkene complex and free alkene, as even **149** easily

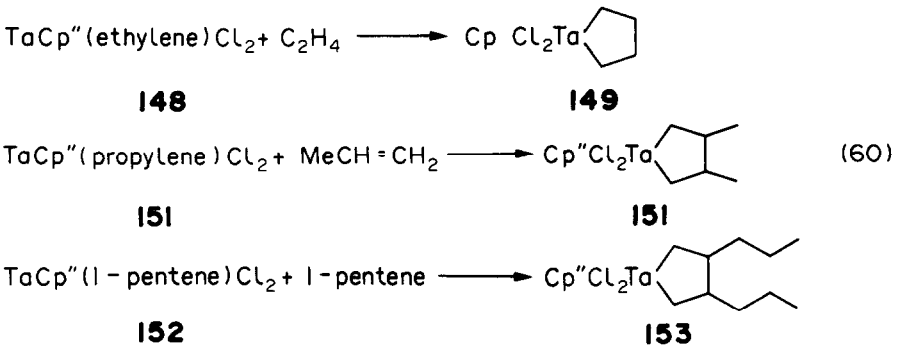

(60)

reverts to **148** and ethylene in toluene at 25°C under partial vacuum. However, the equilibrium lies well towards **149**. A mixed metallacycle, **154**, may be obtained when 1 mol. of propene is added to **148** at −35°C (eqn 61) and the two isomers (**154a** and **b**) may be observed by NMR at low temperature.

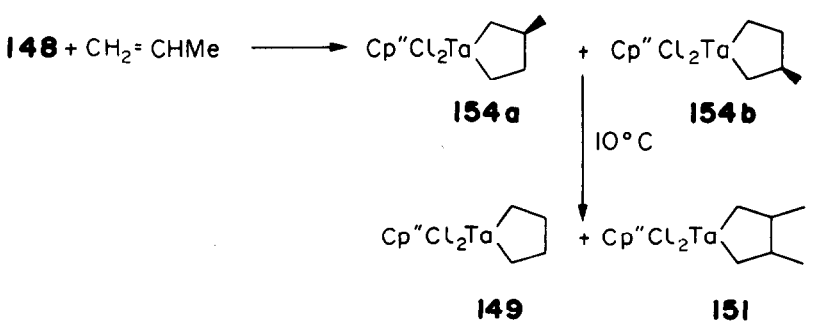

On warming to 10°C for two hours **154** disproportionates to give **149** and **151**. Single crystal X-ray diffraction studies have been performed on **149** and a related complex $Ta(\eta^5\text{-}C_5Me_5)(C_7H_{12})Cl_2$[147, 148] which contains a tantalabicyclo-[3.3.0]-octane framework. These results show the tantalacyclopentane ring to have an unusual "opened-envelope" conformation **155**, which may reduce interactions between the metallacyclopentane ring and the C_5Me_5 ligand.

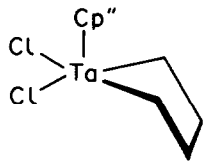

155

Furthermore, the alignment of the tantalacyclopentane ligand may in some way facilitate the observed reversible loss of alkene.

Compounds of the type **151** have been shown to be the active intermediates in the catalytic dimerisation of alkenes.[148b] The same group has carried out related work on benzyne complexes of tantalum.[149] The benzyne complex **156** formed from the reaction of phenyllithium with $Ta(\eta^5\text{-}C_5Me_5)Me_3Cl$ eliminating methane, has been shown to react with ethene at 30°C giving a benzotantalacyclopentene complex **157** in 86% yield (eqn 62).

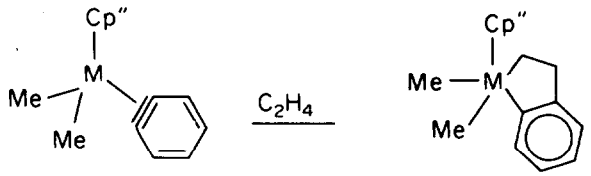

156 **157** (62)

The corresponding niobium complex is similarly prepared in 75% yield. It is surprising that the complexes **156** do not react more readily with ethene in view of the facility of the reaction of $TaCp''(C_2H_4)Cl_2$ with ethene. One possible explanation could be that there is delocalisation of electrons throughout the $Ta\text{–}C_6H_4$ system.

A niobium metallacyclopentadiene had been synthesised as early as 1968[150] by the reaction of **158** with diphenylacetylene giving **159** (eqn 63).

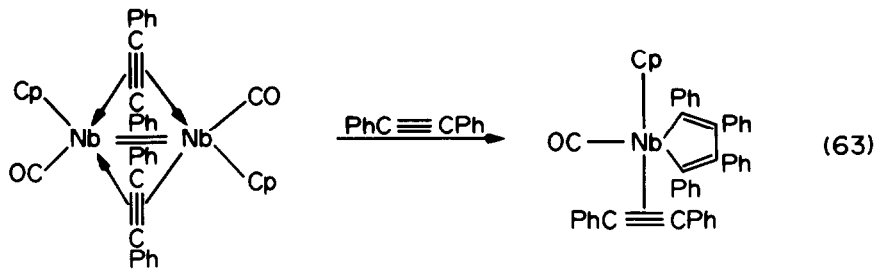

158 **159** (63)

4. POLYALKENE OR POLYALKYNE REACTIONS

Apart from reactions involving coupling of simple alkenes metallacycles can be prepared from polyalkene or polyalkyne reactions. One such early example is the reaction of 1,7-cyclododecadiyne with $Fe(CO)_5$[151] (eqn 64) which gives primarily a complex assigned the structure **160** based on spectroscopic evidence.

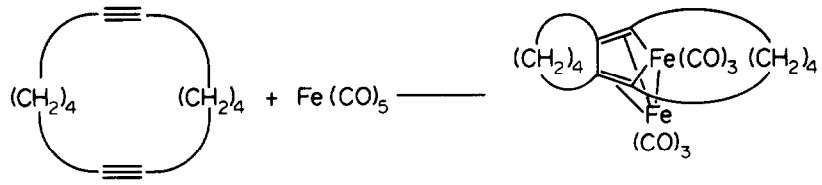

(64)

160

Single crystal X-ray diffraction studies have since shown[152] the structure to be represented by **161**. The most remarkable feature of this structure is that

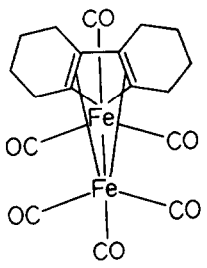

161

gross skeletal rearrangement of the starting diyne has occurred upon complexation. This reaction probably occurs *via* the formation of a metallacycle of type **160** which then rearranges to the observed type **161**. (Evidence for this type of process has been reported previously.[115]) Isolation of trace amounts of a compound of structure **162** from the reaction mixture indicates that cyclobutadiene

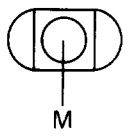

162

formation may also play a part. This appears to be supported by the results of another group[59] (see above).

Two unusual reactions of $Fe(CO)_5$ are those with *o*-di-iodobenzene and *cis*-2,3-dibromobut-2-ene on photolysis[153] (eqn 65). The reactions proceed *via* photochemical loss of halogen from the halo-moieties followed by attack of pentacarbonyliron.

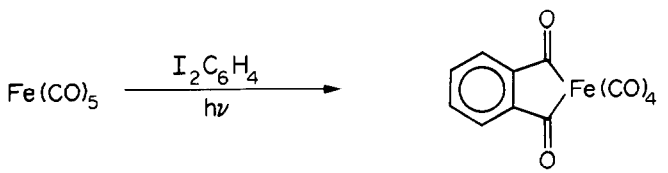

(65)

163

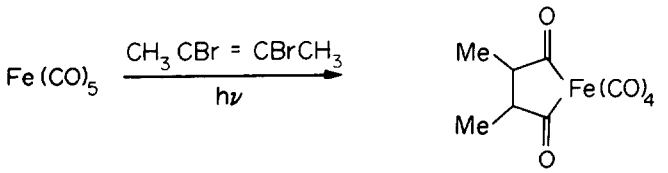

164

It is possible that the product of the related reaction of $Ni(CO)_4$ with *o*-diiodobenzene[154] which was assigned the dimeric benzyne structure **165** may be the polymeric complex **166** which contains an

analogous metallacyclopentene structure to **163**.

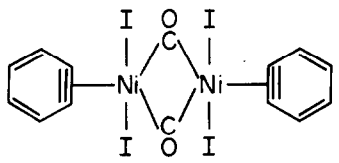

165

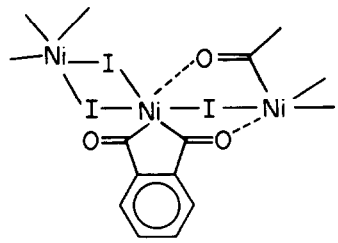

166

The osmium trimer, $Os_3(CO)_{12}$, has been reacted with 2,3-dimethylbuta-1,3-diene[155] giving a complex initially assigned a diolefinic structure. Subsequent single crystal X-ray diffraction studies[156] have shown a metallacyclopentadiene unit to be incorporated into the dimeric structure in a manner similar to that observed with iron (**167**)

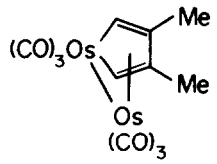

167

$Fe(CO)_5$ had been previously reacted with perfluorobutadiene[157] under UV irradiation to give a ferracyclopentene, **168**, whose structure is confirmed by X-ray crystallographic studies.[158] The same alkene has since been shown to react in a similar way with $[(CO)_2RhCl]_2$[43] to give the chlorine bridged dimeric

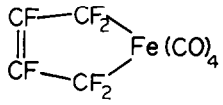

168

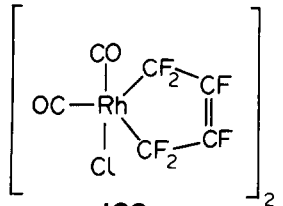

169

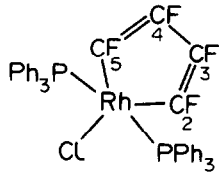

170

species **169**. Furthermore, the monomeric rhodacycle, **170**, may be obtained from hexafluorobuta-1,3-diene and $RhCl(PPh_3)_3$ or $RhCl(C_2H_4)(PPh_3)_2$ with subsequent evolution of fluorine. ^{19}F NMR studies indicate that the molecule is non-fluxional while the fluorines on C(3) and C(4) [and hence those on C(2) and C(5)] are non-equivalent. This is probably because the two metal-carbon σ-bond lengths are unequal as a result of the differing *trans*-effects of different groups *trans* or approximately *trans* to them.

The versatility of the reaction of butadiene to give metallacycles is illustrated by the fact that zerovalent platinum species will also react in a similar manner.[159] Reaction of an excess of 2,3-dimethylbuta-1,3-diene with *bis*(cycloocta-1,5-diene)platinum affords **171a** which reacts with tert-butylisocyanide displacing

171

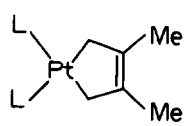

(a) L = 1,5-C_8H_{12}

(b) L = t-BuNC

cycloocta-1,5-diene to give **171b**. Thus the reaction involves an oxidative 1,4-addition of the 1,3-diene to a Pt(0) species and probably involves the intermediacy of (cod)(2,3-dimethylbuta-1,3-diene)platinum(0) which undergoes an electronic rearrangement to form the Pt(II) five membered ring species. However, all conjugated diene complexes can be considered to have a contribution from a resonance form such as **171**. (The same group had previously reported the analogous reaction for nickel using hexafluorobuta-1,3-diene.)[160, 161] In contrast buta-1,3-diene reacts with $Pt(cod)_2$ to give **172a**,

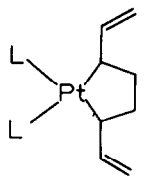

172 (a) L = 1, 5-C_8H_{12}
(b) L = t-BuNC

a 2,5-divinylplatinacyclopentane, which again reacts with *t*-BuNC to give **172b**. The reaction has been shown to proceed *via* an allyl complex **173** which has been isolated for the trimethylphosphine system (eqn 66).

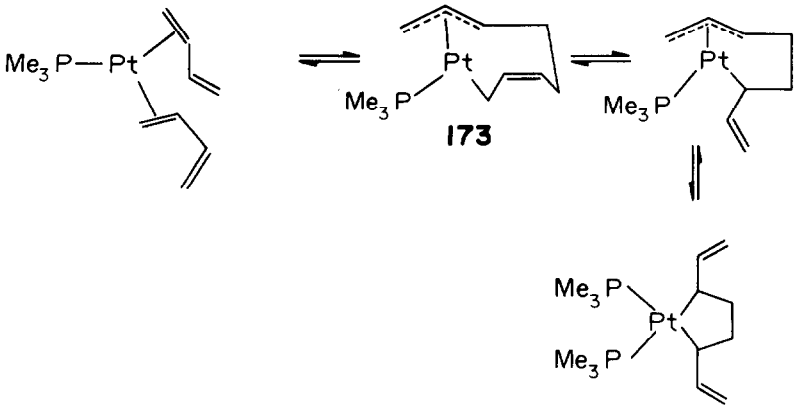

173

(66)

More recently longer chain dienes have been used for metallacyclic synthesis. Reaction of Cp_2ZrL_2 (where L = variety of donor ligands) with octa-1,7-diene[162] gives the bicycloalkane complex **174** in high yield.

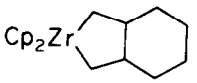

174

From this *cis*-and *trans*-1,2-dimethylcyclohexane are formed on hydrolysis. The analogous titanium complex has been similarly prepared.[163]

A similar series of reactions has subsequently been reported for $Ta(\eta^5\text{-}C_5Me_5)(olefin)Cl_2$ with 1,6-heptadiene, 1,7-octadiene and 1,8-nonadiene[164] (eqn 67). For

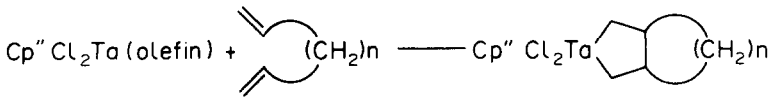

(67)

175 (a) n = 3 (b) n = 4 (c) n = 5

175a only the *cis* isomer is obtained, **175b** occurs as a mixture of *cis* and *trans* isomers and **175c** is found to consist entirely of the *trans* isomer. The stability of the complexes is found to decrease in the order a > b > c. As mentioned previously, a single crystal X-ray diffraction study of **175a**[147] shows an "opened-envelope" conformation of the metallacyclic ligand (see **155**). This had been proposed as being due to steric effects and is now suggested as being due to the fact that the 14 electron metal is attracting

electron density from the CαCβ bonds. It has been proposed that distortions in alkylidene ligands in certain Ta and Nb complexes can be attributed to the same phenomenon.[165]

Metallacyclic derivatives have also been made from allene reactions of transition metal complexes. If the reaction of allene with $Rh(acac)(C_2H_4)_2$ is carried out at −78°C[166] a complex assigned the structure **176**, which contains a 3,4-dimethylenerhodacyclopentane moiety is formed. The complex is thermally very unstable and decomposes violently above 0°C.

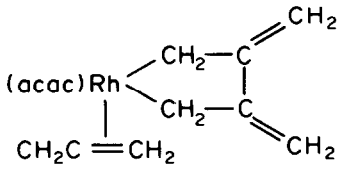

176

Furthermore reaction with more allene at −35°C leads to the formation of a *bis*(π-allylic)complex. However, the instability of **176** is probably due to the reactivity of the lone allene rather than the rhodacyclopentane unit, as reaction of **176** with pyridine or triphenylphosphine leads to the isolation of stable complex **177** and **178**.

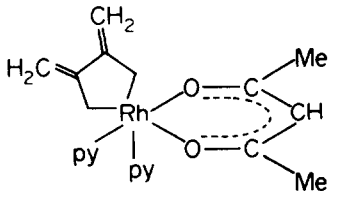

177

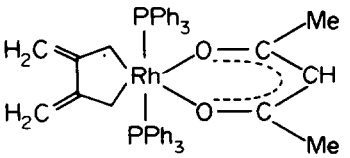

178

The structure of **177** is confirmed by X-ray examination of single crystals.[167] The fact that allene can enter into an "oxidative coupling" reaction accounts for the transformation of Rh(I) to Rh(III) and this reaction is most probably the first step in the formation of *bis*-(π-allylic) complexes of rhodium. Similar reactions to those observed for rhodium have subsequently been reported to occur for iridium.[168, 169] The reaction of $Ir(acac)(\eta\text{-}C_8H_{14})_2$ with allene at −78°C again gives a thermally unstable complex assigned as **179** which on reaction with pyridine affords the more stable complex **180** (eqn 67).

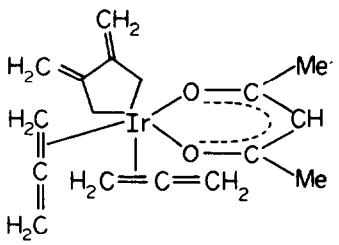

179

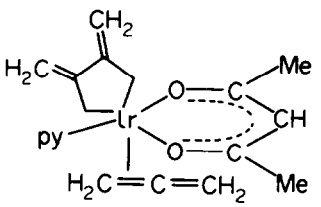

(67)

180

Again **179** is seen as a precursor of a *bis*(π-allylic) complex of iridium. Metallacyclopentanes of the kind isolated here had been previously postulated as intermediates in the cyclooligomerisation and polymerisation of allenes by nickel complexes.[170]

A model intermediate for the dimerisation of allene which contains a nickelacyclopentane structure has been synthesised.[171] Reaction of *bis*(cycloocta-1,5-diene)nickel with *bis*(dicyclohexylphosphino)ethane and allene at −20°C to 0°C leads to the formation of **181**. The complex reacts with hydrogen in the presence of Raney nickel to give 2,3-dimethylbutane and with CO at room

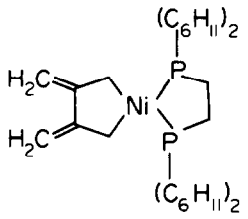

181

temperature to give the cyclic ketone, 3,4-dimethylenecyclopentanone. More recently assymmetric metallacycles have been synthesised from allenes,[172] a class of compound which has been suggested as showing analogies to the organometallic reactions of CO_2,[173] carbodiimides[174] and ketenes.[175] The reaction of $[(C_5Me_5)_2ZrN_2]_2N_2$ with allene results in release of all dinitrogen and isolation of the zirconacyclopentane, **182** (only this isomer is obtained)

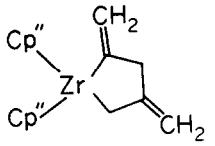

182

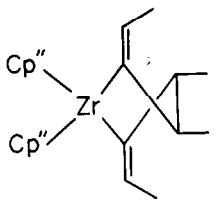

183

for which the structure is confirmed by X-ray diffraction studies on a single crystal. When it is carried out using 1,3-dimethylallene, the reaction proceeds in a slightly different manner to give **183**, in which the ethylidene groups substitute the zirconacyclopentane ring in the 2 an 5 positions. Again only one of the 48 possible isomers is obtained suggesting a high degree of chiral selectivity.

Metallacyclobutane derivatives of molybdenum and tungsten have been synthesised from allylic derivatives.[76,176] Treatment of the *bis*-η^1-allyltungsten compound **184** with dilute acid gives the η^3-allylic compound **185** which reacts with MeLi or $NaBH_4$ to give the metallacylobutanes **186** and **187** (eqn 68).

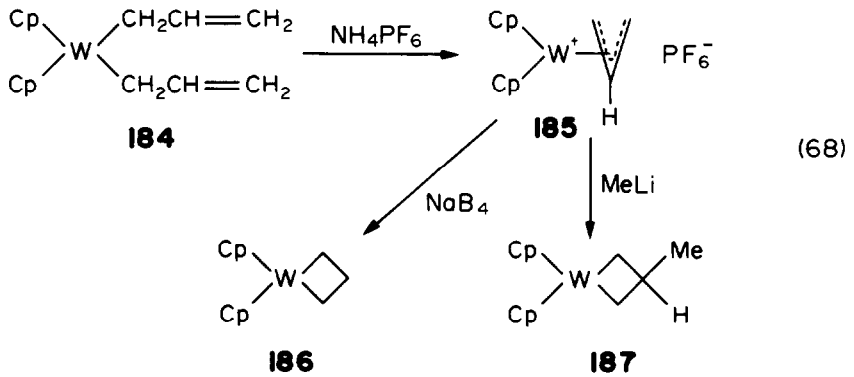

(68)

Similar reactions are observed for the molybdenum analogue of **185**, made from the reaction of $[Cp_2MoH_3]PF_6$ with buta-1,3-diene. It is clear from the above reactions and others using sodium borodeuteride that the formation of the metallacyclobutane complexes from the η^3-allylic precursors proceeds *via* nucleophilic attack exclusively on the central carbon atom of the η^3-allylic group. A possible explanation is that when the metal centre of an organometallic cation is relatively electron rich, then, in the absence of marked steric effects, nucleophilic addition occurs so that the electron density at the metal centre is either reduced or subjected to the minimal increase. For an allyl group, attack will therefore occur at the central carbon atom, as in this case.

The thermolysis of several of these metallacycles has been studied[177] and minor amounts of products containing fewer carbon atoms than were in the metallacycle are found. However, on photolysis substantial amounts of such compounds are observed. This can be accounted for by invoking a ring opening mechanism for the decomposition of the type generally agreed to occur for alkene metathesis.

Thus the role of the photolysis step would be to provide a suitable vacant site on the metal centre, which could be achieved by a photo-induced η^5-η^3 shift of a η-cyclopentadienyl ring (eqn 69). It appears that in these

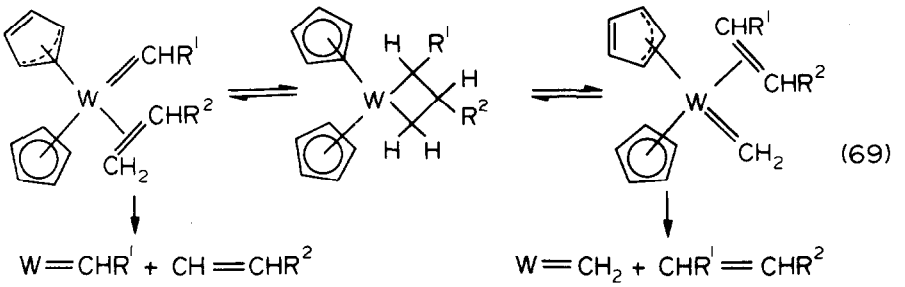

(69)

systems the substituent has a marked effect on the direction of ring opening explaining why certain products predominate. For example with both the 2-phenyl- and 2-methyltungstenacyclobutane complexes the substituted ethene is the dominant carbon deficient product.

A series of reactions of $[Ir(COD)Cl]_2$ with norbornadiene[12,178] have yielded metallacycles giving valuable information on the mechanism of cyclodimerisation of alkenes. Complex **188**, formed on reacting $[Ir(COD)Cl]_2$ with excess norbornadiene at room temperature, gives the acetylacetonate derivative **190** when refluxed with 2,4-pentanedione and Na_2CO_3 (eqn 70).

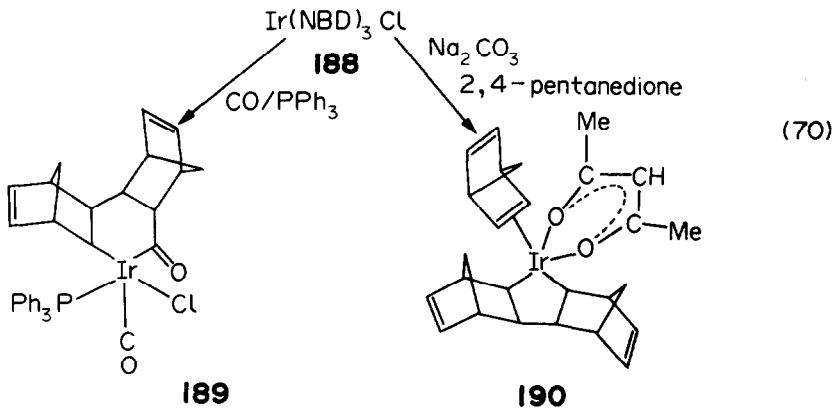

(70)

A single crystal X-ray diffraction study shows that two NBD groups form a saturated metallacycle by insertion of the iridium atom into the four membered ring of an incipient norbornadiene dimer molecule of *exo-trans-exo* stereochemistry. As a result of this crystal structure, complex **188** has been assigned an analogous structure. A further related complex **189** is obtained by bubbling CO through a solution of **188** followed by addition of one mol of triphenylphosphine. This, however, contains an iridacyclohexane ring formed by insertion of CO into one of the Ir–C bonds of the iridacycle. When **189** is refluxed with a five-fold excess of triphenylphosphine ring closure is induced and the norbornadiene dimer is displaced from the iridium atom in about 35% yield. Complexes of this type had previously been suggested as intermediates for various catalytic processes[3,8,9] but no metal-carbon σ-bonded species had been isolated and then proven to be a genuine intermediate.

5. FORMATION OF METALLACYCLES VIA CYCLOMETALLATION REACTIONS

Recently, several metallacycles have been prepared *via* decomposition of alkyl complexes of the transition elements, in which the well known decomposition pathway, β-elimination, is blocked by substitution at the β-carbon atom. Cyclometallation involving coordinated ligands has been known for a long time[179] but only recently has its application to hydrocarbyl systems been recognised. The first such example involved the decomposition of methyl(1-naphthylmethyl)*bis*(triphenylphosphine)platinum(II) **191** in refluxing toluene[180] to give **192** (eqn 71) with evolution of methane.

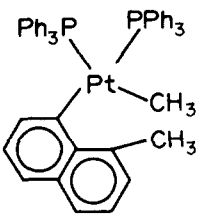

191

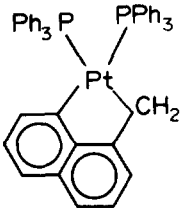

192

(71)

Subsequently $Ru_2(O_2CMe)_4Cl$ has been shown to react with $Mg(CH_2Bu^t)_2$ and PMe_3[181] to produce the metallacyclobutane **193**.

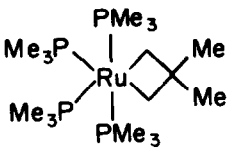

193

The reaction presumably proceeds *via* the *bis*-neopentyl derivative which spontaneously decomposes to give the observed product. An analogous reaction to this is observed in a platinum system[182,183] which is found to require far more forcing conditions (eqn 72). The origin of the hydrogen atom

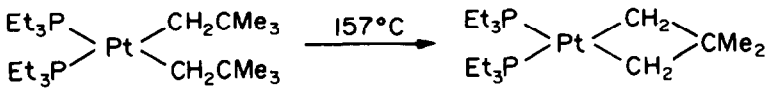

194 195

(72)

consumed in conversion of a neopentyl group of **194** to neopentane is established as a methyl group of a second neopentyl group by deuterium labelling experiments. Furthermore, the reaction is thought to proceed *via* dissociation of one of the phosphine ligands since in the presence of excess phosphine, the rate of reaction is reduced. Hence the mechanism shown in eqn (73) has been suggested.

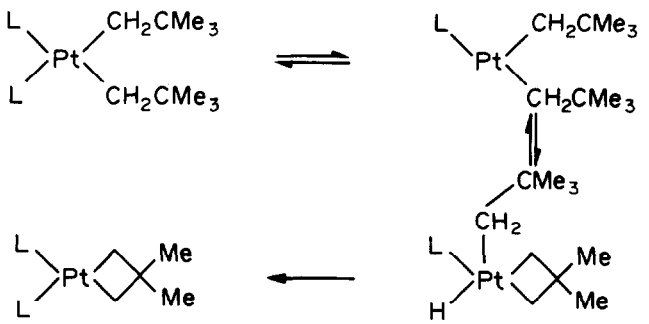

(73)

The same group have recently expanded this study to produce platinacyclopentanes and platinacyclohexanes.[184] The thermal decompositions of **196** and **197** have been studied and found to produce the platinacycles **198–201**. (Eqn 74.)

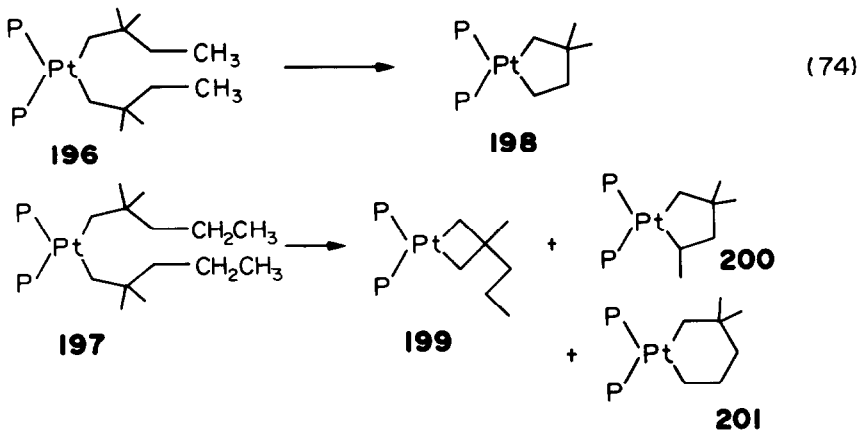

All are *bis*(triethylphosphine) complexes. In the second reaction, **200** is the major product (68%), with **199** and **201** being produced in 23 and 9% yield respectively. These percentage yields are seen as being somewhat related to the amount of ring strain in each of the products. These results also strongly suggest that ring strain in platinacyclobutanes is much smaller than in cyclobutane itself. This may help to explain why isomerisation of five-membered to four-membered metallacycles[185] appears to be more facile than the corresponding reaction in all carbon systems.

Platinacyclopentenes have also been made on thermolysis of *o*-methylbenzyl derivatives[186] (eqn 75). The reaction proceeds *via* a δ-hydrogen abstraction

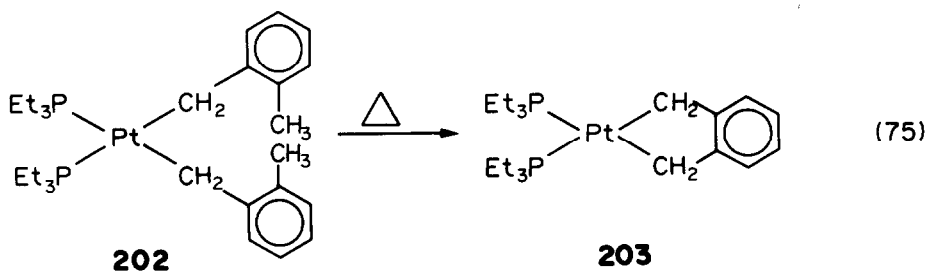

liberating xylene and again forcing conditions are necessary (refluxing xylene for 16 hr). The structure of the complex is confirmed by spectroscopic means and by the reaction with excess iodine liberating 1,2-*bis*(iodomethyl) benzene.

Very recently an iridium alkyl has been shown to decompose on formation at room temperature to give an iridacyclobutane[187]. Reaction of $Ir(PMe_3)_4Cl$ with $LiCH_2CMe_2$ in hexane affords *fac-tris*(trimethylphosphine)hydrido(2,2-dimethyl-1,3-propanediyl)iridium (III), **204**, in high yield. The presumed alkyl precursor is not detected in this system except as a transient orange solution

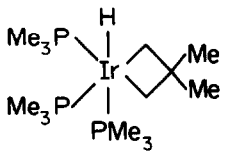

but when the reaction is carried out using $LiCH_2SiMe_3$ the intermediate can be isolated. The difference in reactivity may arise from the decreased steric demand of the (trimethylsilyl)methyl ligand as compared to that of the neopentyl group.

Intramolecular oxidative additions also proceed readily with other alkyl groups. Thus, reaction of $Ir(PMe_3)_4Cl$ with benzylmagnesium chloride gives the benzometallacyclobutene complex **205**. Cyclisation can be seen to result from Ir insertion into a γ C–H bond. Facile insertion at the aryl δ-position of the neophyl (CH_2CMe_2Ph) ligand has also been observed on reaction of $Ir(PMe_3)_4Cl$ with $LiCH_2CMe_2Ph$ in hexane to give the benzoiridacyclopentene complex **206**.

Rapid cyclisation is also observed *via* oxidative addition to a distal C–H bond of functionalised alkyl groups. $Ir(PMe_3)_4Cl$ reacts with the enolate salt of acetone giving the iridacyclobutan-3-one complex **207**.

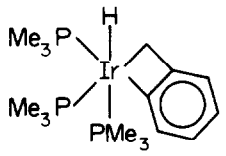

205

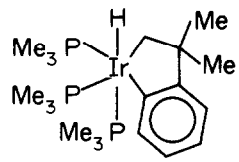

206

A similar reaction has been observed in platinum and palladium complexes[188] whereby dimethyl 3-oxoglutarate reacts with the zerovalent complexes L_4Pt and L_4Pd to give **208**. It may also be noted that the trimethylphosphite analogue of **205** has been reported[189] to form *via* the corresponding Ir(I) *o*-tolyl complex. This complex has now been reformulated, due to single crystal X-ray studies, as an iridaindanone[190] **209** formed *via* ring closure and CO insertion.

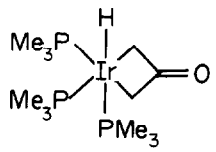

207

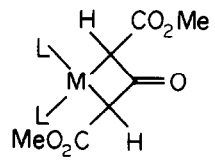

208

The facility for iridium to perform these reaction derives from the ability of Ir(I) centres to undergo facile oxidative addition reactions and the formation of Ir(III)-H bonds acts as an additional driving force.

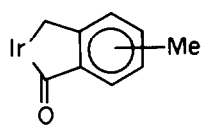

209

REFERENCES

[1]T. J. Katz, *Adv. in Organometal Chem.* 1977, **16**, 283.
[2]C. G. Biefeld, H. A. Eick and R. H. Grubbs, *Inorg. Chem.* 1973, **12**, 2166.
[3]R. H. Grubbs and T. K. Brunck, *J. Am. Chem. Soc.* 1972, **94**, 2538.
[4]R. J. Haines and G. J. Leigh, *Chem. Soc. Rev.* 1974, **4**, 155.
[5]N. Calderon, J. P. Lawrence and E. A. Ofstead, *Adv. Organometal Chem.* 1979, **17**, 449.
[6]L. Cassar, P. E. Eaton and J. Halpern, *J. Am. Chem. Soc.* 1970, **92**, 3515.
[7]T. J. Katz and N. Acton, *Tett Lett.* 1967, 2601.
[8]P. W. Hall, R. J. Puddephatt, K. R. Seddon and C. F. H. Tipper, *J. Organometal Chem.* 1974, **81**, 423.
[9]K. C. Bishop, *Chem. Rev.* 1976, **76**, 461.
[10]A. R. Fraser, P. H. Bird, S. A. Bezman, J. R. Shapley, R. White and J. A. Osborn, *J. Am. Chem. Soc.* 1973, **95**, 597.
[11]M. J. Doyle, J. McMeeking and P. J. Binger, *J. Chem. Soc.* 1976, 376.
[12]M. A. Bennett, R. N. Johnson and I. B. Tomkins, *J. Am. Chem. Soc.* 1974, **96**, 61.
[13]G. K. Barker, M. Green, J. A. K. Howard, J. L. Spencer and F. G. A. Stone, *J. Am. Chem. Soc.* 1976, **98**, 3373.
[14]P. Diversi, G. Ingrosso, A. Immirzi, W. Porzio and M. Zocchi, *J. Organometal Chem.* 1977, **122**, 253.
[15]P. W. Jolly, C. Kruger, R. Saltz and J. K. Sekutowski, *J. Organometal Chem.* 1979, **165**, C39.
[16]K. J. Ivin, J. J. Rooney, C. D. Stewart, M. L. H. Green and R. Mahtab, *J. Chem. Soc. Chem. Comm.* 1978, 604.
[17]R. J. McKinney, *J. Chem. Soc. Chem. Comm.* 1980, 490.
[18]C. F. H. Tipper, *J. Chem. Soc.* 1955. 2045.
[19]S. E. Binns, R. H. Cragg, R. D. Gillard, B. T. Heaton and M. F. Pilbrow, *J. Chem. Soc.* (*A*), 1969, 1227.
[20]W. J. Irwin and F. J. McQuillin, *Tett Lett.* 1968, 1937.
[21]K. G. Powell and F. J. McQuillin, *Tett Lett.* 1971, 3313.
[22]F. J. McQuillin and K. G. Powell, *J. Chem. Soc. Dalton*, 1972, 2123.
[23]R. J. Puddephatt, *Coord. Chem. Rev.* 1980, 149.
[24]D. B. Brown and V. A. Viens, *J. Organometal Chem.* 1977, **142**, 117.
[25]R. J. Al-Essa, R. J. Puddephatt, M. A. Quyser and C. F. H. Tipper, *J. Organometal Chem.* 1978, **150**, 295.
[26]F. Iwanciw, M. A. Quyser, R. J. Puddephatt and C. F. H. Tipper, *J. Organometal Chem.* 1976, **113**, 91.
[27]M. Lenarda, R. Ros, M. Graziani and V. Belluco, *J. Organometal Chem.* 1972, **46**, C29.

[28]J. Rajaram and J. A. Ibers, *J. Am. Chem. Soc.* 1978, **100**, 829.
[29]J. P. Visser and J. E. Ramakers-Blom, *J. Organometal Chem.* 1972, **44**, C63.
[30]R. J. Al-Essa, R. J. Puddephatt, M. A. Quyser and C. F. H. Tipper, *J. Am. Chem. Soc.* 1979, **101**, 364.
[31]R. J. Puddephatt, M. A. Quyser and C. F. H. Tipper, *J. Chem. Soc. Chem. Comm.*, 1976, 626.
[32]M. Keeton, R. Mason and D. R. Russell, *J. Organometal Chem.* 1971, **33**, 259.
[33]R. J. Al-Essa and R. J. Puddephatt, *J. Chem. Soc. Chem. Comm.* 1980, 45.
[34]B. M. Cushman and D. B. Brown, *J. Organometal Chem.* 1978, **152**, C42.
[35]T. H. Johnson and S-S. Cheng, *J. Am. Chem. Soc.* 1979, **101**, 5277.
[36]P. W. Hall, R. J. Puddephatt, K. R. Seddon and C. F. H. Tipper, *J. Organometal Chem.* 1974, **81**, 423.
[37]T. H. Johnson and E. C. Hefty, *J. Org. Chem.* 1979, **44**, 4896.
[38]D. C. L. Perkins, R. J. Puddephatt and C. F. H. Tipper, *J. Organometal Chem.* 1978, **154**, C16.
[39]G. Phillips, R. J. Puddephatt and C. F. H. Tipper, *J. Organometal Chem.* 1977, **131**, 467.
[40]A. Miyashita, M. Takahashi and H. Takaya, *J. Am. Chem. Soc.* 1981, **103**, 6257.
[41]J. A. Evans, G. F. Everitt, R. D. W. Kemmitt and D. R. Russell, *J. Chem. Soc. Chem. Comm.* 1973, 158.
[42]M. Lenarda, R. Ros, M. Graziani and U. Belluco, *J. Organometal Chem.* 1974, **65**, 407.
[43]D. M. Roundhill, D. N. Lawson and G. Wilkinson, *J. Chem. Soc.* (*A*), 1968, 845.
[44]J. Halpern, P. Eaton and L. Cassar, *J. Am. Chem. Soc.* 1965, **91**, 2405.
[45]L. Cassar and J. Halpern, *J. Chem. Soc. Chem. Comm.* 1970, 1082.
[46]P. G. Gassman and J. A. Nikora, *J. Organometal Chem.* 1975, **92**, 81.
[47]H. Hogeveen and H. C. Volger, *J. Am. Chem. Soc.* 1967, **89**, 2486.
[48]J. Blum, C. Zlotogorski and A. Zoran, *Tett Lett*, 1975, 1117.
[49]J. Blum, C. Zlotogorski, H. Schwarz and G. Hohne, *Tett Lett*, 1978, 3501.
[50]B. F. G. Johnson, J. Lewis and S. W. Tam, *J. Organometal Chem.* 1976, **105**, 271.
[51]R. M. Moriarty, K-N. Chen, C. L. Yeh, J. L. Flippen and J. Karle, *J. Am. Chem. Soc.* 1972, **94**, 8944.
[52]J. L. Flippen, *Inorg. Chem.* 1974, **13**, 1054.
[53]S. W. Tam, *Tett Lett.* 1974, 2385.
[54]R. Victor and R. Ben Shoshan, *J. Chem. Soc. Chem. Comm.* 1974, 93.
[55]R. Victor, R. Ben Shoshan and S. Sarel, *J. Chem. Soc. Chem. Comm.* 1971, 1241.
[56]M. Rosenblum and B. North, *J. Am. Chem. Soc.* 1968, **90**, 1060.
[57]M. Rosenblum, W. P. Giering, B. North and D. Wells, *J. Organometal Chem.* 1971, **28**, C17.
[58]M. Rosenblum. B. North, D. Wells and W. P. Giering, *J. Am. Chem. Soc.* 1972, **94**, 1239.
[59]R. E. Davis, B. L. Barnett, R. G. Amiet, W. Merk, J. S. McKennis and R. Pettit, *J. Am. Chem. Soc.* 1974, **96**, 7108.
[60]F. A. Cotton, J. M. Troup, W. E. Billups, L. P. Lin and C. V. Smith, *J. Organometal Chem.* 1975, **102**, 345.
[61]G. Dettlaf, U. Behrens, T. Eicher and E. Weiss, *J. Organometal Chem.* 1978, **152**, 197.
[62]G. Dettlaf, U. Behrens, T. Eicher and E. Weiss, *J. Organometal Chem.* 1978, **152**, 203.
[63]P. J. Harris, J. A. K. Howard, S. A. R. Knox, R. P. Phillips, F. G. A. Stone and P. Woodward, *J. Chem. Soc. Dalton*, 1976, 377.
[64]E. H. Brayne, W. Hubel and I. Calpier, *J. Am. Chem. Soc.* 1961, **83**, 4406.
[65]S. C. Cohen and A. G. Massey, *J. Organometal Chem.* 1967, **10**, 471.
[66]S. A. Gardner, H. B. Gordon and M. D. Rausch, *J. Organometal Chem.* 1973, **60**, 179.
[67]M. D. Rausch, H. B. Gordon and E. Samuel, *J. Coord. Chem.* 1971, **1**, 141.
[68]M. D. Raush and L. P. Klemann, *J. Chem. Soc. Chem. Comm.* 1971, 354.
[69]J. X. McDermott and G. M. Whitesides, *J. Am. Chem. Soc.* 1974, **96**, 947.
[70]J. X. McDermott, M. E. Wilson and G. M. Whitesides, *J. Am. Chem. Soc.* 1976, **98**, 6529.
[71]J. X. McDermott, J. F. White and G. M. Whitesides, *J. Am. Chem. Soc.* 1973, **95**, 4451.
[72]C. G. Biefeld, H. A. Eick and R. H. Grubbs, *Inorg. Chem.* 1973, **12**, 2166.
[73]A. K. Cheetham, R. J. Puddephatt, A. Zalkin, D. H. Templeton and L. K. Templeton, *Inorg. Chem.* 1976, **15**, 2997.
[74]P. Diversi, G. Ingrosso and A. Lucherini. *J. Chem. Soc. Chem. Comm* 1978, 735.
[75]P. Diversi, G. Ingrosso, A. Lucherini and S. Murtas, *J. Chem. Soc. Dalton*, 1980, 1633.
[76]M. Ephritikhine, B. R. Francis, M. L. H. Green, R. E. Mackenzie and M. J. Smith, *J. Chem. Soc. Dalton*, 1977, 1131.
[77]R. H. Grubbs, A. Miyashita, M-I. M. Liu and P. Burk, *J. Am. Chem. Soc.* 1977, **99**, 3863.
[78]P. Diversi, G. Ingrosso and A. Lucherini, *J. Chem. Soc. Chem. Comm.* 1977, **52**.
[79]P. Diversi, G. Ingrosso, A. Lucherini, W. Porzio and M. Zocchi, *J. Chem. Soc. Chem. Comm.* 1977, 811.
[80]P. Diversi, G. Ingrosso. A. Lucherini. W. Porzio and M. Zocchi, *Inorg. Chem.* 1980. **19**. 3590.
[81]M. F. Lappert, T. R. Martin, C. R. C. Milne, J. L. Atwood, W. E. Hunter and R. E. Pentilla, *J. Organometal Chem.* 1980, **192**, C35.
[82]M. F. Lappert, T. R. Martin, J. L. Atwood and W. E. Hunter, *J. Chem. Soc. Chem. Comm.* 1980, 476.
[83]M. F. Lappert and C. L. Raston, *J. Chem. Soc. Chem. Comm.* 1980, 1284.
[84]M. F. Lappert, C. L. Raston, G. L. Rowbottom and A. H. White, *J. Chem. Soc. Chem. Comm.* 1981, 6.
[85]M. F. Lappert, C. L. Raston, B. W. Skelton and A. H. White, *J. Chem. Soc. Chem. Comm.* 1981, 485.
[86]A. J. Shortland and G. Wilkinson, *J. Chem. Soc. Dalton*, 1973, 872.
[87]R. Clarkson, E. R. H. Jones, P. C. Wailes and M. C. Whiting, *J. Am. Chem. Soc.*, 1956, **78**, 6206.
[88]A. A. Hock and O. S. Mills, *Proc. Chem. Soc.* 1958, 223.
[89]W. Hubel and E. H. Braye, *J. Inorg. Nucl. Chem.* 1959, **10**, 250.
[90]J. W. Rathke and E. L. Muetterties, *J. Am. Chem. Soc.* 1975, **97**, 3272.
[91]T. A. Manuel, S. L. Stafford and F. G. A. Stone, *J. Am. Chem. Soc.* 1961, **83**, 249.
[92]H. H. Hoehn, L. Pratt, K. F. Watterson and G. Wilkinson, *J. Chem. Soc* 1961, 2738.
[93]F. W. Grevels, D. Schulz and E. A. Koerner von Gustorf, *Angew. Chem. Int. Edn. Engl.* 1974, **13**, 534.
[94]J. Granjean, P. Laszlo and A. Stockis, *J. Am. Chem. Soc.* 1974, **96**, 1622.
[95]B. E. Foulyer, F. W. Grevels, D. Hess, E. A. Koerner von Gustorf and J. Leitich, *J. Chem. Soc. Dalton* 1979, 1451.
[96]C. T. Sears and F. G. A. Stone, *J. Organometal Chem.* 1968, **11**, 644.
[97]R. Burt, M. Cooke and M. Green, *J. Chem. Soc.* (*A*) 1970, 2981.
[98]J. P. Collman, J. W. Kang, W. F. Little and M. F. Sullivan, *Inorg. Chem.* 1968, **7**, 1298.
[99]P. M. Treichel and F. G. A. Stone, *Adv. Organometal Chem.* 1964, **1**, 143.
[100]R. S. Nyholm, *Quart Rev.* 1970, **24**, 1.
[101]H. Yamazaki and K. Aoki, *J. Organometal Chem.* 1976, **122**, C54.

[102]M. A. Bennett, R. N. Johnson and I. B. Tomkins, *J. Am. Chem. Soc.* 1974, **96**, 61.
[103]W. Winter, *Angew Chem. Int. Edn. (Eng)* 1976, **15**, 241.
[104]R. S. Dickson and G. Wilkinson, *J. Chem. Soc.* 1964, 2699.
[105]S. McVey and P. M. Maitlis, *J. Organometal Chem.* 1969, **19**, 169.
[106]J. W. Kang, S. McVey and P. M. Maitlis, *Can. J. Chem.* 1968, **46**, 3189.
[107]A. C. Jarvis, R. D. Kemmitt, B. Y. Kimura, D. R. Russell and P. A. Tucker, *J. Chem. Soc. Chem. Comm.* 1974, 797.
[108]D. R. Russell and P. A. Tucker, *J. Chem. Soc. Dalton*, 1976, 841.
[109]J. T. Mague and G. Wilkinson, *Inorg. Chem.* 1968, 7, 542.
[110]J. T. Mague, *J. Am. Chem. Soc.* 1969, **91**, 3983.
[111]W. H. Baddley and G. B. Tupper, *J. Organometal Chem.* 1974, **67**, C16.
[112]W. Keirn, *J. Organometal Chem.* 1969, **16**, 191.
[113]R. G. Gastinger, M. D. Rausch, D. A. Sullivan and G. J. Palenik, *J. Am. Chem. Soc.* 1976, **98**, 719.
[114]H. Yamazaki and Y. Wakatsuki, *J. Organometal Chem.* 1977, **139**, 157.
[115]H. Yamazaki and N. Hagihara, *J. Organometal Chem.* 1967, **7**, P22.
[116]Y. Wakatsuki, K. Aoki and H. Yamazaki, *J. Am. Chem. Soc.* 1979, **101**, 1123.
[117]H. Yamazaki, K. Aoki, Y. Yamamoto and Y. Wakatsuki, *J. Am. Chem. Soc.* 1975, **97**, 3546.
[118]K. Moseley and P. M. Maitlis, *J. Chem. Soc. Dalton*, 1974, 169.
[119]J. Browning, C. S. Cundy, M. Green and F. G. A. Stone, *J. Chem. Soc. (A)* 1971, 448.
[120]J. Browning, M. Green, B. R. Penfold, J. L. Spencer and F. G. A. Stone, *J. Chem. Soc. Chem. Comm.* 1973, 31.
[121]H. C. Clark and A. Shaver, *Can J. Chem.* 1975, **53**, 3462.
[122]J. Browning, M. Green, A. Laguna, L. E. Smart, J. L. Spencer and F. G. A. Stone, *J. Chem. Soc. Chem. Comm.* 1975, 723.
[123]C. S. Cundy, M. Green and F. G. A. Stone, *J. Chem. Soc. (A)* 1970, 1647.
[124]M. Green, R. B. L. Osborn, A. J. Rest and F. G. A. Stone, *J. Chem. Soc. (A)*, 1968, 2525.
[125]P. Binger, M. Doyle, J. McMeeking, C. Kruger and Y-H. Tsay, *J. Organometal Chem.* 1977, **135**, 405.
[126]M. E. Vol'pin, V. A. Dubovitsker, O. V. Nigina and D. N. Kurnasov, *Dokl Akad Nauk SSSR* 1963, **151**, 1100.
[127]B. Klei, J. H. Teuben and H. J. de Liefde Meijer, *J. Chem. Soc. Chem. Comm.* 1981, 342.
[128]G. W. Watt and F. O. Drummond Jr. *J. Am. Chem. Soc.* 1970, **92**, 826.
[129]H. Alt and M. D. Rausch, *J. Am. Chem. Soc.* 1974, **96**, 5936.
[130]J. L. Atwood, W. E. Hunter, H. Alt and M. D. Rausch, *J. Am. Chem. Soc.* 1976, **98**, 2454.
[131]J. Mattia, M. B. Humphrey, R. D. Rogers, J. L. Atwood and M. D. Rausch, *Inorg. Chem.* 1978, **17**, 3257.
[132]I. R. Butler, W. E. Lindsell and P. N. Preston, *J. Chem. Res. (synopses)* 1981, 185.
[133]H. Massai, K. Sonogashira and N. Hagihara, *Bull. Chem. Soc. Japan* 1968, **41**, 750.
[134]J. Dvorak, R. J. O'Brien and W. Santo, *J. Chem. Soc. Chem. Comm.* 1970, 411.
[135]J. Mattia, D. J. Sikora, D. W. Mascomber, M. D. Rausch, J. P. Hickey, G. D. Friesen and L. J. Todd, *J. Organometal Chem.* 1981, **213**, 441.
[136]F. N. Tebbe and R. L. Harlow, *J. Am. Chem. Soc.* 1980, **102**, 6149.
[137]F. N. Tebbe, G. W. Parshall and D. W. Ovenall, *J. Am. Chem. Soc.* 1979, **101**, 5074.
[138]R. J. McKinney, T. H. Tulip, D. L. Thorn, T. S. Coolbaugh and F. N. Tebbe, *J. Am. Chem. Soc.* 1981, **103**, 5584.
[139]T. R. Howard, J. B. Lee and R. H. Grubbs, *J. Am. Chem. Soc.* 1980, **102**, 6876.
[140]J. B. Lee, G. J. Gajda, W. P. Schaefer, T. R. Howard, T. Ikariya, D. A. Straus and R. H. Grubbs, *J. Am. Chem. Soc.* 1981, **103**, 7358.
[141]D. G. Sekutowski and G. D. Sticky, *J. Am. Chem. Soc.* 1976, **98**, 1376.
[142]J. H. Teuben and H. J. de Liefde Meijer, *J. Organometal Chem.* 1969, **17**, 87.
[143]J. M. Manriquez, D. R. McAlister, R. D. Sanner and J. E. Bercaw, *J. Am. Chem. Soc.* 1978, **100**, 2716.
[144]G. Erker and K. Kropp, *J. Am. Chem. Soc.* 1979, **101**, 3659.
[145]S. J. McLain, C. D. Wood and R. R. Schrock, *J. Am. Chem. Soc.* 1977, **99**, 3519.
[146]S. J. McLain, C. D. Wood and R. R. Schrock, *J. Am. Chem. Soc.* 1979, **101**, 4558.
[147]M. R. Churchill and W. J. Youngs, *J. Am. Chem. Soc.* 1979, **101**, 6462.
[148]M. R. Churchill and W. J. Youngs, *Inorg. Chem.* 1980, **19**, 3106. [148b]S. J. McLain, J. Sancho and R. R. Schrock, *J. Am. Chem. Soc.* 1980, **102**, 5610.
[149]S. J. McLain, R. R. Schrock, P. R. Sharp, M. R. Churchill and W. J. Youngs, *J. Am. Chem. Soc.* 1979, **101**, 263.
[150]A. N. Nesmeyanov, A. I. Gusev, A. A. Pasynskii, K. N. Anisimov, N. E. Kolobova and Yu T. Struchkov, *J. Chem. Soc. Chem. Comm.* 1968, 1356.
[151]R. B. King and I. Haiduc, *J. Am. Chem. Soc.* 1972, **94**, 4044.
[152]H. B. Chin and R. Bau, *J. Am. Chem. Soc.* 1973, **95**, 5068.
[153]F-W. Grevels, J. Buchkremer and E. A. Koerner von Gustorf, *J. Organometal Chem.* 1976, **111**, 235.
[154]E. W. Gowling, S. F. A. Kettle and G. M. Sharples, *J. Chem. Soc. Chem. Comm.* 1968, 21.
[155]E. O. Fischer, K. Bittler and H. P. Fritz, *Z. Naturforsch*, 1963, **18B**, 83.
[156]R. P. Dodge, O. S. Mills and V. Schomaker, *Proc. Chem. Soc.* 1963, 380.
[157]R. L. Hunt, D. M. Roundhill and G. Wilkinson, *J. Chem. Soc. (A)* 1967, 982.
[158]R. Mason, quoted in Ref. 157.
[159]G. K. Barker, M. Green, J. A. K. Howard, J. L. Spencer and F. G. A. Stone, *J. Am. Chem. Soc.* 1976, **98**, 3373.
[160]J. Browning, M. Green and F. G. A. Stone, *J. Chem. Soc. (A)* 1971, 453.
[161]M. Green, S. K. Shakshooki and F. G. A. Stone, *J. Chem. Soc. (A)* 1971, 2828.
[162]K. I. Gell and J. Schwartz, *J. Chem. Soc. Chem. Comm* 1979, 244.
[163]R. H. Grubbs and A. Miyashita, *J. Chem. Soc. Chem. Comm.* 1977, 864.
[164]G. Smith, S. J. McLain and R. R. Schrock, *J. Organometal Chem.* 1980, **202**, 269.
[165]A. J. Schultz, J. M. Williams, R. R. Schrock, G. A. Rupprecht and J. D. Fellman, *J. Am. Chem. Soc.* 1979, **101**, 1593.
[166]G. Ingrosso, L. Porri, G. Pantini and P. Racanelli, *J. Organometal Chem.* 1975, **84**, 75.
[167]G. Ingrosso, A. Immirzi and L. Porri, *J. Organometal Chem.* 1973, **60**, C35.
[168]P. Diversi, G. Ingrosso, A. Immirzi, W. Porzio and M. Zocchi, *J. Organometal Chem.* 1977, **125**, 253.
[169]P. Diversi, G. Ingrosso, A. Immirzi and M. Zocchi, *J. Organometal Chem.* 1976, **104**, C1.
[170]R. J. Pasquale. *J. Organometal Chem.* 1971, **32**, 381.
[171]P. W. Jolly, C. Kruger, R. Salz and J. C. Sekutowski, *J. Organometal Chem.* 1979, **165**, C39.

[172]R. J. Schmidt and D. M. Duggan, *Inorg. Chem.* 1981, **20**, 318.
[173]T. Herskowitz and L. Guggenberger, *J. Am. Chem. Soc.* 1976, **98**, 1615.
[174]D. M. Duggan, *Inorg. Chem.* 1979, **18**, 903.
[175]G. Fachinetti, C. Biran, C. Floriani, A. Chiesi-Villa and C. J. Guastini, *J. Am. Chem. Soc.* 1978, **100**, 1921.
[176]M. Ephritikhine, M. L. H. Green and R. E. Mackenzie, *J. Chem. Soc. Chem. Comm.* 1976, 619.
[177]G. J. A. Adam, S. G. Davies, K. A. Ford, M. Ephritikhine, P. F. Todd and M. L. H. Green, *J. Mol. Catal.* 1980, **8**, 15.
[178]S. A. Bezman, P. H. Bird, A. R. Fraser and J. A. Osborn, *Inorg. Chem.* 1980, **19**, 3755.
[179]G. W. Parshall, *Acc. Chem. Res.* 1970, **3**, 139.
[180]J. A. Duff, B. L. Shaw and B. L. Turtle, *J. Organometal Chem.* 1974, **66**, C18.
[181]R. A. Andersen, R. A. Jones and G. Wilkinson, *J. Chem. Soc. Dalton* 1978, 446.
[182]P. Foley and G. M. Whitesides, *J. Am. Chem. Soc.* 1979, **101**, 2732.
[183]P. Foley, R. DiCosimo and G. M. Whitesides, *J. Am. Chem. Soc.* 1980, **102**, 6713.
[184]S. S. Moore, R. DiCosimo, A. F. Sowinski and G. M. Whitesides, *J. Am. Chem. Soc.* 1981, **103**, 948.
[185]S. J. McLain, J. Sancho and R. R. Schrock, *J. Am. Chem. Soc.* 1979, **101**, 5451.
[186]S. D. Chappell and D. J. Cole-Hamilton, *J. Chem. Soc. Chem. Comm.* 1980, 238.
[187]T. H. Tulip and D. L. Thorn, *J. Am. Chem. Soc.* 1981, **103**, 2448.
[188]D. A. Clarke, R. D. W. Kemmitt, M. A. Mazid, M. D. Schilling and D. R. Russell, *J. Chem. Soc. Chem. Comm* 1978, 744.
[189]L. Dahlenburg, U. Sinnwell and D. Thoennes, *Chem. Ber* 1978, **111**, 3367.
[190]K. von Deuten and L. Dahlenburg, *Trans. Met. Chem.* 1980, **5**, 222.

Polyhedron Vol. 1, No. 11-12, pp. 779-780, 1982
Printed in Great Britain.

0277-5387/82/110779-02$03.00/0
Pergamon Press Ltd.

NOVEL FEATURES IN THE STEREOCHEMISTRY OF OCTACYANIDES: PHASE TRANSITION IN TETRA-*n*-BUTYLAMMONIUM OCTACYANOTUNGSTATE(V)

A. SAMOTUS*, A. KANAS, S. HODOROWICZ and J. CZERWONKA
Institute of Chemistry, Jagiellonian University, Kraków, Poland

J. ŚCIESIŃSKI
Institute of Nuclear Physics, Kraków, Poland

and

Cz. PALUSZKIEWICZ
Regional Laboratory of Physicochemical Analysis and Structural Research, Kraków, Poland

(*Received* 31 *July* 1981)

Abstract—Tetra-*n*-butylammonium octacyanotungstate(V) has been found to exist in three phases at the temperature range 90–353 K. The IR and ^{1}H-NMR spectra as well as thermogravimetric and powder diffraction studies support these structural changes. The phase transitions were found in the temperature range 273–283 K (T_1) and 333–343 K (T_2).

INTRODUCTION

Octacyanometalates [M = Mo(IV, V); W(IV, V); Nb(III, IV)] are known to have tendency for two stereochemical arrangements, dodecahedral (D_{2d}) and antiprismatic (D_{4d}). Solid $[(n\text{-Bu})_4N]_3[Mo(CN)_8]$ is known to contain a D_2 anion differing little from D_{2d} symmetry[1] and $[(n\text{-Bu})_4N]_3[W(CN)_8]$ is isomorphous to its molybdenum analogue.[2] Infrared and Raman spectra of both tetrabutylammonium salts in solid state are unexpectedly simple and very similar to those of antiprismatic $Na_3[W(CN)_8]\ 4H_2O$.[3,4] Electron spin resonance spectra seem to indicate that the solid and solution geometries of the tetra-*n*-butylammonium salt are not the same and that in the acetonitrile glass, $[(n\text{-Bu})_4N]_3[W(CN)_8]$ is "more square antiprismatic" than in the crystalline state.[5] It was found, however, that the use of ESR parameters to determine the structure of 8-coordinate complexes does not have a general validity.[6]†

In the course of our study on the structure and reactivity of octacyanotungstate(V) we have found for $[(n\text{-Bu})_4N]_3[W(CN)_8]$ two phase transitions at the temperature range 263–353 K identified by thermal measurements, IR and NMR spectra and X-ray powder diffraction studies. The present note is the first report on the phase transition in octacyano-complexes of transition metals.

EXPERIMENTAL

Tetra-*n*-butylammonium octacyanotungstate(V) was made by the literature method.[2] To avoid photochemical reactions the synthesis procedure and all manipulations with the solid sample were carried out in a red light of photographic lamp.

The thermogravimetric (TG) and differential thermal analyses (DTA) were performed under argon with a heating rate of 5 K/min on a Mettler Thermoanalyser. The DTA and TG curves of $[(n\text{-Bu})_4N]_3[W(CN_8]$ in the temperature range 293–373 K exhibit a single endothermic peak at T_{max} 337 K without the weight loss, thus suggesting a phase transition.

Middle range IR spectra (400–3800 cm^{-1}) were carried out in the temperature range 90–353 K (heating rate 1 K/min) with the interferometric spectrometer FTS-14 "Digilab". The samples were prepared as Nujol mull and/or as a thin film (obtained by evaporation of ethanolic solution) on KRS-5.‡

Proton magnetic resonance spectra of $[(n\text{-Bu})_4N]_3[W(CN)_8]$ were obtained for a polycrystalline sample with a broad line spectrometer operating with a Robinson type marginal oscillator at the frequency of 17 MHz.

X-Ray powder diffraction analysis was performed with the DRON-2 diffractometer (CuK_α radiation) equipped with the high-temperature camera and a special low-temperature attachment.[8] Calculations of the unit cell parameters were carried our with the CDC CYBER computer using 20 successive Bragg's maxima.

RESULTS AND CONCLUSIONS

Infrared spectra of $[(n\text{-Bu})_4N]_3[W(CN)_8]$ *at various temperatures*

The most useful region for identification purposes is the region between 2100–2160 and 420–460 cm^{-1} characteristic for C–N stretching and W–C stretching vibrations, respectively.[3,4] Our measurements at various temperatures were started at room temperature, then the sample was gradually heated up to 353 K and then cooled down to 90 K. As can be seen in Fig. 1 $[(n\text{-Bu})_4N]_3[W(CN)_8]$ exhibits two phase transitions in the temperature range 273–283 K(T_1) and 333–343 K(T_2) characterized by a sudden change of the number and peak position of absorption bands. The changes are fully reversible although the temperature ranges of transformation found upon heating are shifted in respect to those upon cooling (expected hysteresis of transition). The changes of middle range IR bands related to $[(N\text{-Bu})_4N]^+$ cation are insignificant.

*Author to whom correspondence should be addressed.

†ESR experiments for polycrystalline sample of $[(n\text{-Bu})_4N]_3[W(CN)_8]$ at various temperatures did not show remarkable changes but only slight differences in broadening of the signal from room temperature to about 373 K.[7]

‡The KBr pellet technique was not convenient because, under pressure, the metathetical reaction occurred.

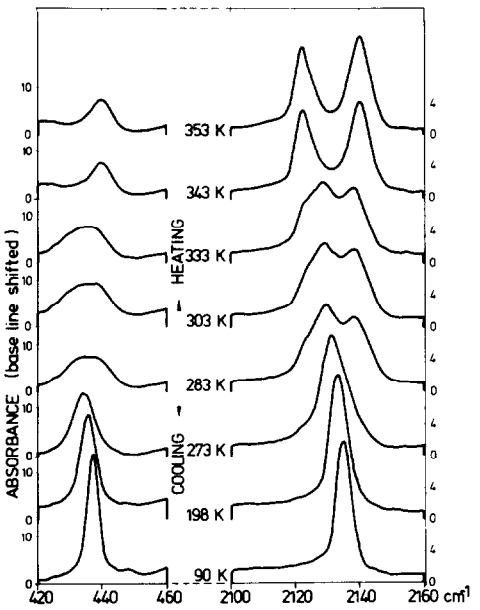

Fig. 1. The IR profile of ν(CN) and ν(WC) bands at various temperature (KRS-5 technique, resolution 2 cm^{-1}).

Proton magnetic resonance spectra

Three selected spectra recorded at temperature below T_1 (phase I), between T_1 and T_2 (phase II) and above T_2 (phase III) are presented in Fig. 2. Basing on these spectra it can be concluded that in the phase I (at temperature not so far below T_1) *n*-butylammonium groups are not fixed in the space but undergo a rotational motion which leads to the narrowing of absorption line. In the intermediate phase II the motion of complex cations is essentially axial rotation and, finally, in the high temperature phase III molecules reorient almost spherically. It seems possible that the change of symmetry of complex anion with temperature results from the different kinds of motions of organic cation.

X-Ray powder diffractograms

The existence of three phases found strong support in X-ray powder diffraction study. On heating and on cooling through the transition region established previously the changes of diffraction pattern were observed. The diffractograms of the different phases I–III are shown in Fig. 3.

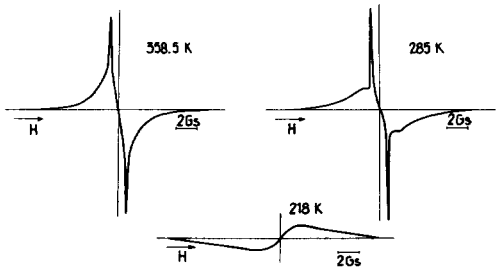

Fig. 2. First derivatives of the ^{1}H NMR spectra of [(*n*-Bu)$_4$N]$_3$[W(CN)$_8$].

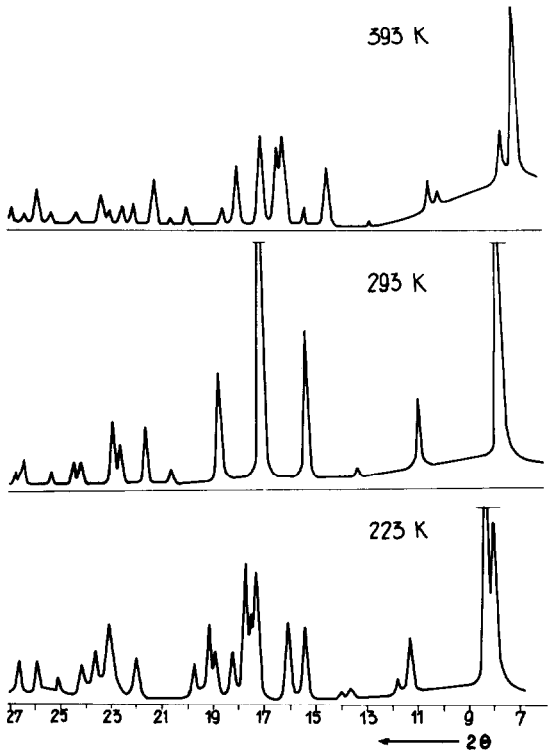

Fig. 3. X-Ray powder diffraction patterns of the phase I–III of [(*n*-Bu)$_4$N]$_3$[W(CN)$_8$].

At room temperature the complex was found to crystallize in a tetragonal system with the lattice constants $a = 16.72(5)$ Å and $c = 23.71(5)$ Å which are in agreement with the previous data for [(*n*-Bu)$_4$N]$_3$[Mo(CN)$_8$].[1] But, the observed reflection indices do not show systematic absences of $l = 2n + 1$ for *hkl* corresponding to the space group P4/ncc determined for molybdenum analogue.[1] It seems possible that the sample of monocrystal investigated by Corden *et al.*[1] is not representative for room-temperature phase of [(*n*-Bu)$_4$N]$_3$[M(CN)$_8$] (M = Mo, W). The detailed investigation on the phase transitions and structural aspect of the separate phases in octacyanides of transition metals are in progress.

Acknowledgement—This work was supported in part by Polish Academy of Sciences.

REFERENCES

[1] B. J. Corden, J. A. Cunningham and R. Eisenberg, *Inorg. Chem.* 1970, **9**, 356.
[2] A. Samotus and A. Kanas, *Proc. 8th Conf. Coord. Chem.*, Smolenice–Bratislava (Czechoslovakia) p. 361 (1980).
[3] P. M. Kiernan and W. P. Griffith, *J. Chem. Soc. Dalton* 1975, **23**, 2489.
[4] A. Kanas and A. Samotus, *Proc. III SOPTROCC*, Mogilany–Kraków, (Poland) p. 37 (1980).
[5] R. A. Pribush and R. D. Archer, *Inorg. Chem.* 1974, **13**, 2556.
[6] C. D. Garner and F. E. Mabbs, *J. Inorg. Nucl. Chem.* 1979, **41**, 1125 and references therein.
[7] R. D. Archer, private communication.
[8] S. Hodorowicz, M. Ciechanowicz-Rutkowska, J. M. Janik and J. A. Janik, *Phys. Status. Solidi* (a) 1977, **43**, 53.

Polyhedron Vol. 1, No. 11-12, pp. 781-783, 1982
Printed in Great Britain.

0277-5387/82/110781-03$03.00/0
Pergamon Press Ltd.

LIGATING PROPERTIES OF TERTIARY PHOSPHINE/ ARSINE SULPHIDES OR SELENIDES—VI. ADDITION COMPOUNDS OF ZINC(II), CADMIUM(II) AND MERCURY(II) WITH SULPHIDES OR SELENIDES OF TRIPHENYL- AND TRI-p-TOLYLPHOSPHINES AND 1,3-TRIMETHYLENEBIS (DIPHENYLPHOSPHINE)

T. S. LOBANA,* T. R. GUPTA and S. S. SANDHU
Department of Chemistry, Guru Nanak Dev University, Amritsar-143005, India

(*Received* 26 *October* 1981)

Abstract—Post-transition elements react with ligands, triphenylphosphine sulphide or selenide (Ph_3PS or Ph_3PSe), tri-*p*-tolylphosphine sulphide or selenide (T_3PS or T_3PSe) and 1,3-trimethylene*bis*-(diphenylphosphine sulphide or selenide) (PDPS or PDPSe) in suitable organic solvents forming complexes of compsoitions: MX_2. L(M = Zn, X = I, L = all except Ph_3PS: M = Cd, X = I, L = T_3PS, T_3PSe, M = Hg, L = T_3PSe, X = Cl, Br, I); $ZnI_2.2Ph_3PS$, $Hg(NO_3)_2.2Ph_3PS$, $CdBr_2.3T_3PSe$ and $3Hg(NO_3)_2.4Ph_3PSe$. All these have been characterized through elemental analyses, ir spectra (4000–200 cm^{-1}) and molar conductance (nitrobenzene). Complexes are essentially nonelectrolytes. Tetrahedral structures have been assigned to all except a 1 : 3 complex which has been assigned a bridged octahedral structure.

INTRODUCTION

Mono- and di-tertiaryphosphines and their oxides are known to form a large number of complexes with different metal ions. However, relatively much less attention has been paid to coordination chemistry of tertiaryphosphine sulphides and selenides which contain sulphur and selenium as the donor atoms.[1-8]

In this paper, we are reporting the coordination compounds of triphenylphosphine sulphide or selenide, (Ph_3PS or Ph_3PSe), tri-*p*-tolylphosphine sulphide or selenide (Ph_3PS or Ph_3PSe), tri-*p*-tolylphosphine sulphide or selenide (T_3PS or T_3PSe) and 1,3-trimethylene*bis*-(diphenylphosphine sulphide or selenide) (PDPS, PDPSe) with zinc(II) iodide, cadmium(II) halides and mercury(II) halides and nitrate.

EXPERIMENTAL

Ligands

The ligands were prepared by a published method.[1] The melting points are: Ph_3PS, 158–59°C, Ph_3PSe, 187–88°C; T_3PS, 181–82°C, T_3PSe, 198°C, PDPS, 110–112°C and PDPSe, 112°C.

Complexes

Zinc(II) iodide complexes were prepared by the addition of a ligand solution in dry benzene to metal iodide solution in a mixture of ether–benzene (2 : 1), followed by refluxing, reducing volume and treatment with petroleum–ether (40–60°C). In some cases complex separated during refluxing. The complexes were recrystallised from benzene-alcohol mixtures.

Cadmium(II) and mercury(II) halide complexes were obtained by adding a ligand solution in benzene or benzene–absolute alcohol mixture (1 : 2) to that of metal salt in absolute alcohol. The complexes were separated either immediately or during refluxing or after reducing the volume. These were recrystalised from benzene-alcohol mixtures. In case of mercury(II) nitrate, the ligand and metal salt solution were taken in acetone. The reaction mixture was allowed to stand for 1–2 hr to obtain the solid.

Techniques

The elemental analyses for carbon and hydrogen were carried out by Australian Microanalytical Service, Melbourne. Zinc(II) and cadmium(II) were estimated using EDTA method.[9] Zinc(II) iodide was prepared by a published method.[10] The molar conductivity was measured on Toshniwal Conductivity Bridge type CIOI/02A. The IR spectra in the range, 4000–200 cm^{-1} was recorded in solid KBr by the Defence Research and Development Established, Gwalior, India. Lack of solubility in the suitable solvent prevents the use of techniques like ^1H NMR etc.

RESULTS AND DISCUSSION

Elemental analyses show that most of the complexes are of 1 : 1 ratio. However, 1 : 2, 1 : 3 and 3 : 4 (metal : ligand) complexes were also formed in some cases (Table 1). The adducts are white crystalline powders, quite stable and decompose above 200°C. However, the adduct $3Hg(NO_3)_2.4Ph_3PSe$ changes its colour slowly after several days. The conductance shows the adducts to be essentially nonelectrolytes. However, the conductance values in some cases are indicative of partial ionization of the adducts in nitrobenzene:

$$[MX_2.nL] \rightleftharpoons [MX.nL]^+ + {}^-X.$$

The 3 : 4 adduct is insoluble in nitrobenzene indicating its probable polymeric nature.

The IR spectra in the range (4000–650 cm^{-1}) indicate that the ν(P–C) aromatic bands in the free ligands remain unchanged on coordination except in one or two cases where a small upward shift has been noticed (Table 2). In the nitrate complexes, this band occurs at about 1110 cm^{-1} which may be attributed to coupling with a vibration due to nitrate group having same region of absorption.

In the far IR region, 650–200 cm^{-1} ν(P=S), ν(P=Se) and ν(M–S) have been assigned. The ν(P=Se) bands record a downward shift of 13–20 cm^{-1} in the complexes. The ν(P=S) bands in the complexes, $ZnI_2.2Ph_3PS$, $ZnI_2.PDPS$ and $Hg(NO_3)_2.2Ph_3PS$ occur at 585, 580 and 530 cm^{-1}

*Author to whom correspondence should be addressed.

Table 1. Analytical data, melting points and molar conductance

S. No.	Complex	Found (Required) C%	H%	M%	M.P °C	Molar conductance ohm^{-1}cm^{2}mole^{-1}
1.	$ZnI_2.2Ph_3PS$	46.77(47.62)	3.40(3.31)	8.35(7.21)	180	16.19
2.	$ZnI_2.T_3PS$	39.30(38.46)	3.52(3.21)	11.74(10.00)	200	18.17
3.	$ZnI_2.PDPS$	38.40(40.75)	3.13(3.27)	-	248-53	16.20
4.	CdI_2T_3PS	36.01(35.88)	3.09(2.99)	14.90(16.00)	265	13.99
5.	$Hg(NO_3)_2.2Ph_3PS$	45.89(47.34)	3.24(3.29)	-	250(d)	14.65
6.	$3Hg(NO_3)_2.4Ph_3PSe$	36.03(36.96)	2.76(2.57)	-	235-45(d)	b
7.	$ZnI_2.Ph_3PSe$	32.88(32.72)	2.15(2.27)	11.46(9.91)	240	17.70
8.	$ZnI_2.T_3PSe$	36.97(35.89)	3.17(2.99)	10.35(9.32)	278(d)	15.88
9.	$ZnI_2.PDPSe$	36.95(36.44)	3.03(2.92)	-	262-63(d)	14.58
10.	$CdBr_2.3T_3PSe$	54.19(53.19)	4.81(4.43)	7.31(7.91)	234	6.20
11.	$CdI_2.T_3PSe$	34.00(33.63)	2.96(2.80)	16.8(15.0)	263	3.85
12.	$HgCl_2.T_3PSe$	38.27(38.50)	3.18(3.21)	-	205-20(d)	3.56
13.	$HgBr_2.T_3PSe$	34.06(33.89)	2.85(2.82)	-	225-38(d)	4.75
14.	HgI_2T_3PSe	30.54(30.09)	2.56(2.51)	-	214(d)	3.78

d-decomposition, b-complex insoluble in nitrobenzene.

respectively. However, in the case of T_3PS, the bands at 675, 572 cm^{-1} in the free ligand occur at 640 and 555 cm^{-1} respectively in its complexes. The shifts in ν(P=S) are higher in case of Ph_3PS adducts as compared to those of T_3PS adducts, probably due to difference in inductive effects of phenyl and tolyl groups.

The decrease in ν(P=S) and ν(P=Se) indicate coordination through sulphur and selenium atoms. The larger ν(P=S) shifts as compared to ν(P=Se) are due to stronger p_π–d_π bond in ligands like Ph_3PS because P and S are small and similar in size whereas there is considerable size difference in P and Se atoms and hence weaker p_π–d_π bond. Also, vibrations of heavy Se atoms would be less sensitive to coordination. Morgan *et al.*[2] have shown with the help of X-ray photolectron spectroscopy that in the adducts of Ph_3PO, Ph_3PS and Ph_3PSe with HgI_2 while going from O to Se, there is essentially no change in the "2*p*"-bonding energy and is attributed to charge localization through π-bond feedback. This may account for low changes in ν(P=S) and ν(P=Se) as the pi-bonding would tend to increase the observed frequencies.

Table 2. The IR spectra of ligands and complexes (4000–200 cm^{-1})

S. No.	Ligand/complex	ν(P–C$_{ar.}$) cm^{-1}	ν(P=S/P=Se) cm^{-1}	ν(M–S) cm^{-1}
	Ph_3PS	1095s	638s	-
	Ph_3PSe	1090s	545s	-
	T_3PS	1095s	675s, 572s	-
	T_3PSe	1095s	535s	-
	PDPS	1080s	626s	-
	PDPSe	1080s	540s	-
1.	$ZnI_2.2Ph_3PS$	1095s	585s	300w
2.	$ZnI_2.T_3PS$	1095s	640, 555s	375w
3.	ZnI_2PDPS	1100s	580s	320w
4.	CdI_2T_3PS	1190	640, 555s	380vw, 350w
5.	$Hg(NO_3)_2.2Ph_3PS$	1110	530s	330w
6.	$3Hg(NO_3)_2.4Ph_3PSe$	1115	530s	-
7.	$ZnI_2.Ph_3PSe$	1090s	532s	-
8.	$ZnI_2.T_3PSe$	1090s	520s	-
9.	$ZnI_2.PDPSe$	1095s	520s	-
10.	$CdBr_2.3T_3PSe$	1095s	525s	-
11.	$CdI_2.T_3PSe$	1090s	520s	-
12.	$HgCl_2.T_3PSe$	1090s	520s	-
13.	$HgBr_2.T_3PSe$	1095s	522s	-
14.	$HgI_2.T_3PSe$	1090s	520s	-

s=strong; w=weak, ms=moderately strong.

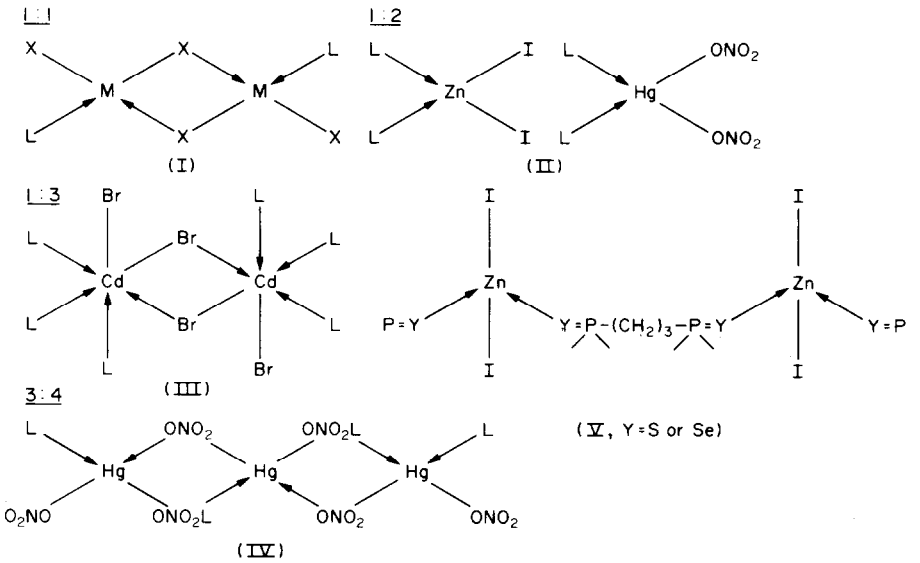

Fig. 1.

Tentative assignments to ν(M–S) bands between 300 and 380 cm^{-1} have been made. A weak band at 345 cm^{-1} in $ZnI_2.T_3PSe$ complex has been assigned to Zn–Se bond. The other M–Se bands could not be detected. A band of medium intensity at 280 cm^{-1} was obtained in case of $HgCl_2.T_3PSe$ which has been assigned to Hg–Cl bond. The ν_1, ν_2, ν_3 and ν_4 bands due to nitrate occur at 945; 810; 1350, 1290, 1230 and 715 cm^{-1} respectively in the complex, $Hg(NO_3)_2.2Ph_3PS$. The ν_3 bands in $3Hg(NO_3)_2.4Ph_3PSe$ occur at 1430, 1378 and 1178 cm^{-1}; while ν_4 band occurs at 712 cm^{-1}. The ν_3 band gives a single peak in ionic nitrate and the splitting of ν_3 band is indicative of coordinated nitrate in the complexes. The ν_1 and ν_2 bands in the latter complex appear to have been obscured by the ligand bands.

On the basis of the above studies, the following structures have been assigned (I–V).

In all the structural assignments except (IV), the metal is tetrahedrally or nearly tetrahedrally surrounded. Structure(I) is corroborated by similar structure of $HgCl_2.Ph_3PSe$ determined by X-ray.[1] In structure V, the ligands PDPS and PDPSe containing three $-CH_2-$ groups connecting the functional groups have been shown as bridging one because chelation would lead to formation of eight membered unstable rings. Moreover, the distant P=Se groups shall have higher probability to join two metal ions from either end. Thus a polymeric structure appears most likely which is supported by insolubility in organic solvents. Moreover, the analogous ligand, EDPO (1,2-dimethylene*bis*-(diphenylphosphine oxide)) containing one $-CH_2-$ group less than in PDPS or PDPSe has been shown by X-ray crystal studies to act as a bridge.[11,12]

Acknowledgement—One of us (TRG) thanks the Guru Nanak Dev University authorities for providing research facilities.

REFERENCES

[1]T. S. Lobana and S. S. Sandhu, *J. Chem. Sci.* 1978, **4**, 37; C.A. 1979, **91**, 67636j (Review).
[2]W. E. Morgan, W. J. Stec, R. G. Albridge and J. R. Van Wazar, *Inorg. Chem.* 1971, **10**, 926.
[3]E. W. Ainscough, H. A. Bergen, A. M. Brodie and K. A. Brown, *J. Chem. Soc. Dalton Trans.* 1976, 1649.
[4]M. G. B. Drew, G. W. A. Fowles, R. J. Hobson and D. A. Rice, *Inorg. Chim. Acta* 1976, **20**, L35.
[5]S. O. Grim and J. D. Mitchell, *Inorg. Chem.* 1977, **16**, 1762.
[6]F. Caballero and P. Royo, *J. Organomet. Chem.* 1977, **137**, 229.
[7]J. Rimbault, J. C. Pierrard and R. P. Hugel, *J. Chem. Res.(S)* 1978, 74.
[8]K. C. Malhotra, Gita Malhotra and S. C. Chaudhary, *Indian J. Chem.* 1978, **16A**, 905.
[9]A. I. Vogel, *Quantitative Inorganic Analysis*, 3rd Edn, pp. 443, 444.
[10]H. Brauer, *Handbook of Preparative Inorganic Chemistry*, Vol. 2, 2nd Edn. Academic Press, New York (1965).
[11]M. Mathew and G. J. Palenik, *Can. J. Chem.* 1969, **47**, 1093.
[12]M. Mathew and G. J. Palenik, *Inorg. Chim. Acta* 1971, **5**, 573.

Polyhedron Vol. 1, No. 11-12, pp. 785-790, 1982
Printed in Great Britain.

0277-5387/82/110785-06$03.00/0
Pergamon Press Ltd.

ADSORPTION HPLC OF TETRADENTATE β-KETOIMINE COPPER, NICKEL AND PALLADIUM CHELATES†

PAUL J. CLARK,‡ IMOGENE E. TREBLE§ and PETER C. UDEN*
Department of Chemistry, GRC Towers, University of Massachusetts, Amherst, MA 01003, U.S.A.

(*Received* 14 *December* 1981)

Abstract—High Pressure Liquid Chromatography (HPLC), utilizing adsorption on microparticulate silica, provides analytical resolution of copper, nickel, and palladium chelates of tetradentate β-ketoimines. The chelates investigated are those of non-fluorinated, semi-fluorinated and fluorinated ligands derived from condensation of acetylacetone and trifluoroacetyl-acetone with ethylenediamine, 1,2-diaminopropane and 2,3-diaminobutane. Novel chelates are described for the latter ligand group with various geometrical isomers being prepared. HPLC separations are described related to the increase in extent of chelate fluorination, the nature of the chelated metal and the geometrical isomer forms of the complexes.

INTRODUCTION

While the separation of metals as coordination complexes has frequently been accomplished by liquid–liquid partition extraction, the development of higher efficiency liquid phase separations has resulted from the establishment of the technique of High Performance Liquid Chromatography (HPLC). A significant advantage of HPLC is its ability to resolve multi-component mixtures at ambient temperatures by modes such as liquid–liquid partition, liquid-solid adsorption, size exclusion and ion exchange. Mobile phase solvent changes provide high column efficiencies comparable with those seen in gas chromatography.

The application of HPLC separations to organometallic and coordination chemistry has been recently reviewed by Veening and Willeford.[1] Various HPLC modes have been utilized for transition metal chelate separations; liquid–liquid partition was employed by Huber *et al.*[2] for β-diketonates, while adsorption was used for resolution of *bis*acetyl*bis*thiobenzoylhydrazones of Hg(II), Cu(II), Pd(II) and Zn(II) with nanogram detection limits.[3] We have reported adsorption HPLC of *bis*diethyldithiocarbamates,[4] and of geometric trifluoracetylacetonate isomers using gradient elution.[5] We have reported preliminary data on chelates of representative Schiff base ligands, N,N ethylene-*bis*acetylacetoneimine ($H_2(enAA_2)$) and N,N′ ethylene *bis*salicylaldimine ($H_2(enSal_2)$).[6] The reverse phase partition mode employing water/methanol/acetonitrile solvents on octadecyl bonded substrates was also employed in the HPLC separation of several compounds of the tetradentate β-ketoimine series.[7,8]

The present study extends these investigations to include fluorinated, semi-fluorinated and non-fluorinated tetradentate β-ketoimine chelates of copper, nickel and palladium, having ethylenediamine (en), propylenediamine (pn) or butylenediamine (bn) bridging groups in the ligand (Fig. 1). For the latter chelates resolution of racemic and meso isomers is accomplished, paralleling that noted in some cases by gas chromatography.[9] A number of these compounds were synthesized for the first time; the gas chromatographic separations of these and related chelates will be reported in later publications.

EXPERIMENTAL

Preparation of ligands

Ligands were synthesized according to the method of Martell,[10] in which an ethanolic solution of the appropriate diamine is added dropwise to a refluxing solution of the β-diketone(s) in ethanol. Purification was generally by recrystallization from 95% ethanol followed by vacuum sublimation at *ca.* 0.1 torr. Specific details of ligands not previously reported are noted.

N,N′-*butylenebis*(*acetylacetoneimine*), $H_2(bnAA_2)$

Racemic and meso isomers of this ligand were recovered as follows. The first crop of crystals recovered from the reaction mother liquor and washed with cold 95% ethanol were found by gas chromatography to be greater than 99% racemic. The filtrate was enriched with the meso isomer which was recovered by *n*-hexane extraction of the brown oil obtained by evaporation of the ethanol. Further enrichment (to *ca.* 50 : 1, meso: racemic) was obtained by dry column silica gel chromatography with chloroform eluent.

N,N′-*butylenebis*(*trifluoroacetylacetoneimine*), $H_2(bnTFA_2)$

The mixed isomer ligand was made as previously reported.[9] A first crop of crystals recovered from the mother liquor and washed with 95% ethanol was found by gas chromatography to be almost completely racemic. After evaporation of the mother liquor a second crop of crystals was found to be greater than 90% meso; a third crop was almost purely meso.

N,N′-*ethylene*(*acetylacetoneimine*)(*trifluoroacetylacetoneimine*), H_2(enAA-TFA)

Equimolar ratios of ethylenediamine, acetylacetone and trifluoroacetylacetone were reacted. The first crop of white crystals contained about 70% H_2(enAA-TFA) and about 30% $H_2(enTFA_2)$. No $H_2(enAA_2)$ was noted. The mixture was used for chelate preparation without further separation.

N,N′-*propylene*(*acetylacetoneimine*)(*trifluoroacetylacetoneimine*), H_2(pnAA-TFA)

A similar procedure to that used for H_2(enAA-TFA) was employed. Gas chromatographic examination of the product indicated the ligand mixture to be *ca.* 70% H_2(pnAA-TFA) with the two symmetrical ligands also being formed. $H_2(pnTFA_2)$ was removed by successive recrystallizations from 95% ethanol. The mixture was used for chelate preparation without further separation.

N,N′-*butylene*(*acetylacetoneimine*)(*trifluoroacetylacetoneimine*), H_2(bnAA-TFA)

A similar procedure to that used for H_2(enAA-TFA) was

†Abstracted in part from the Ph.D. Dissertations of P. J. Clark (1977), Imogene E. Bigley (Treble) (1978). University of Massachusetts, Amherst, Massachusetts.

‡Present address: Loctite Corporation, Newington, CT 06111, U.S.A.

§Present address: Union Carbide Corporation, Bound Brook, NJ 08805, U.S.A.

*Author to whom correspondence should be addressed.

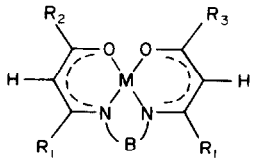

R_1	R_2	R_3	B	Abbreviation
CH_3	CH_3	CH_3	en	M(II)(enAA$_2$)
CH_3	CF_3	CF_3	en	M(II)(enTFA$_2$)
CH_3	CH_3	CF_3	en	M(II)(enAA–TFA)
CH_3	CH_3	CH_3	pn	M(II)(pnAA$_2$)
CH_3	CF_3	CF_3	pn	M(II)(pnTFA$_2$)
CH_3	CH_3	CF_3	pn	M(II)(pnAA–TFA)
CH_3	CH_3	CH_3	bn	M(II)(bnAA$_2$)
CH_3	CF_3	CF_3	bn	M(II)(bnTFA$_2$)
CH_3	CH_3	CF_3	bn	M(II)(bnAA–TFA)

en = $-CH_2CH_2-$ pn = $-CH(CH_3)CH_2-$
bn = $-CH(CH_3)CH(CH_3)-$

Fig. 1. General structure of tetradentate β-ketoimine complexes.

employed. The mother liquor was used for chelate preparation with no further purification. Gas chromatography showed the two isomeric semifluorinated ligand species to be the most abundant (*ca.* 60%).

Preparation of metal chelates

The non-fluorinated metal chelates of copper(II) and nickel(II) was prepared by reaction of a 1.5% aqueous sodium carbonate solution of the ligand with an excess of metal salt. The metal complex formed was extracted into chloroform. The fluorinated and semifluorinated chelates of these metals were formed by reaction of the ligand with the tetramine complex in a ternary phase system of water, chloroform and ethanol (1:1:2.5, v:v:v) as described previously.[11] All palladium(II) complexes were synthesized by refluxing a benzene solution of the ligand with a slightly greater than stoichiometric amount of palladium *bis*(benzonitrile) chloride complex. Chelates were recovered by filtration from hot solution and recrystallization. Specific preparative details of chelates not previously reported are described below and elemental analytical data is shown in Table 1.

N,N'-*butylenebis*(*acetylacetoneiminato*)Cu(II), Cu(bnAA$_2$)

Racemic and meso isomers, prepared as noted above from either purified ligands or the crude unresolved H$_2$(bnAA$_2$) mother liquor, were purified by repeated dry column silica gel chromatography. The racemic chelate eluted first as a purple band followed by the meso form as a blue-green band. Final purification by sublimation (0.1 Torr) was carried out for the racemic isomer at 65°C and for the meso isomer at 110°C.

N,N'-*ethylene*(*acetylacetoneiminato-trifluoroacetylacetoneiminato*)Cu(II), Cu(enAA–TFA)

A 70:30 mixture of Cu(enAA–TFA) and Cu(enTFA$_2$) was prepared from the crude ligand noted above. Cu(enAA–TFA) was isolated in greater than 98% purity by repeated recrystal lizations from 95% ethanol. This selectively removed the less soluble Cu(enTFA$_2$) and concentrated Cu(enAA–TFA) in the filtrate. Enriched crystals were sublimed slowly at 95–100°C at

Table 1. Elemental microanalytical data for tetradentate β-ketoimine chelates

	% Carbon		% Hydrogen		% Nitrogen	
Chelate	Calculated	Found	Calculated	Found	Calculated	Found
Cu(enAA-TFA)	42.4	42.6	4.5	4.7	8.2	8.3
Ni(enAA-TFA)	43.0	42.6	4.5	4.4	8.4	8.4
Pd(enAA-TFA)	37.7	36.7	3.9	3.6	7.3	7.1
Cu(bnAA$_2$) dl	53.6	53.7	7.1	7.3	8.9	8.8
Cu(bnAA$_2$) m	53.6	53.5	7.1	7.0	8.9	8.7
Ni(bnAA$_2$) dl	54.4	55.0	7.2	7.4	9.1	9.2
Ni(bnAA$_2$) m	54.4	- *	7.2	- *	9.1	- *
Pd(bnAA$_2$) dl	47.1	47.7	6.2	6.1	7.9	7.9
Pd(bnAA$_2$) m	47.1	- *	6.2	- *	7.9	- *
Cu(bnTFA$_2$) dl	39.9	40.0	3.8	3.7	6.6	6.7
Cu(bnTFA$_2$) m	39.9	40.5	3.8	3.9	6.6	6.6
Ni(bnTFA$_2$) dl	40.3	40.6	3.9	3.9	6.7	6.7
Ni(bnTFA$_2$) m	40.3	40.5	3.9	3.8	6.7	6.6
Pd(bnTFA$_2$) dl	36.2	36.5	3.5	3.5	6.0	6.0
Pd(bnTFA$_2$) m	36.2	36.4	3.5	3.5	6.0	6.0

* Insufficient sample isolated for analysis but results for purified unresolved mixtures of dl and m chelates chelates substantiate their identities. (Ni(bnAA$_2$) C, 54.8; H, 7.3; N, 9.2; Pd(bnAA$_2$) C, 47.5; H, 6.2; N, 7.9)

Elemental analytical data for the following chelates is given in reference 12; Cu(enAA$_2$), Ni(enAA$_2$), Pd(enAA$_2$), Cu(enTFA$_2$), Ni(enTFA$_2$), Pd(enTFA$_2$), Cu(pnAA$_2$), Ni(pnAA$_2$), Pd(pnAA$_2$), Cu(pnTFA$_2$), Ni(pnTFA$_2$), Pd(pnTFA$_2$).

which temperature the Cu(enAA-TFA) volatilized preferentially (0.1 Torr).

N,N'-*propylene(acetylacetoneiminato-trifluoroacetylacetoneiminato)*Cu(II), Cu(pnAA-TFA)

The chelation reaction from the crude H_2(pnAA-TFA) mother liquor gave products in the ratio Cu(pnAA-TFA) 72%, Cu(pnTFA$_2$) 25%, and Cu(pnAA$_2$) 3%. Sufficient complex was isolated for chromatographic investigation but not for elemental analysis.

N,N'-*butylene(acetylacetoneiminato-trifluoroacetylacetoneiminato)*Cu(II), Cu(bnAA-TFA)

The chelation reaction from the crude H_2(bnAA-TFA) mother liquor gave a mixture of the Cu(bnAA-TFA) isomers as the predominant product (*ca.* 60%). The recemic and meso isomers of Cu(bnAA$_2$) and Cu(bnTFA$_2$) were present at *ca.* 40%. The Cu(bnAA-TFA) isomers were not further preparatively resolved.

N,N'*butylene bis(acetylacetoneiminato)*Ni(II), Ni(bnAA$_2$)

A mixture of racemic and meso isomers was readily prepared from the H_2(bnAA$_2$) mother liquor and an excess of a 1.5% sodium carbonate solution of nicken(II) chloride. Silica gel column chromatography was insufficiently selective for full isomer resolution. Pure samples of racemic isomer were prepared from pure racemic ligand, but enriched meso ligand gave a sample with a 2.5 : meso : racemic composition. The pure meso complex could only be isolated in very small amounts by gas chromatography and its elemental analysis was not determined.

N,N'-*butylenebis(trifluoroacetylacetoneiminato*(Ni(II), Ni(bnTFA$_2$)

Pure meso and racemic samples were prepared from pure isomeric ligands. Sublimation temperatures for racemic (blue-green) and meso (olive green) forms were 155 and 175°C respectively (0.1 Torr).

N,N'-*ethylene(acetylacetoneiminato-trifluoroacetylacetoneiminato)*Ni(II), Ni(enAA-TFA)

A similar procedure to that employed for Cu(enAA-TFA) was employed. Repeated recrystallization from 95% ethanol gave the product which was separated from the less volatile Ni(enTFA$_2$) by slow sublimation at 105°C (0.1 Torr).

N,N'-*propylene(acetylacetoneiminato-trifluoroacetylacetoneiminato)*Ni(II), Ni(pnAA-TFA)

The preparation was similar to that of Cu(pnAA-TFA). Similar product proportions were obtained but insufficient material was isolated for elemental analysis.

N,N'-*butylene(acetylacetoneiminato-trifluoroacetylacetoneiminato)*Ni(II), Ni(bnAA-TFA)

The preparation was similar to that of Cu(bnAA-TFA). The reaction rate with Ni(II) chloride hexahydrate was much slower than for the "en" and "pn" bridged analogs, 7 days being allowed before phase separation. Gas chromatography again showed the two product isomers of the desired complex to be present as approximately 60% of volatile nickel chelates.

N,N'-*butylenebis(acetylacetoneiminato)*Pd(II), Pd(bnAA$_2$)

Pure racemic chelate was prepared from racemic ligand by the Pd(II) benzonitrile chloride method with sublimation of the product at 112°C (0.1 Torr). The meso chelate was prepared from the enriched meso ligand, but in insufficient quantity for elemental analysis.

N,N'-*butylenebis(trifluoroacetylacetoneiminato)*Pd(II), Pd(bnTFA$_2$)

Racemic chelate of greater than 99% purity was prepared from racemic ligand, sublimation being carried out at 165°C (0.1 Torr). Meso chelate was obtained in *ca.* 90% purity by reaction with meso enriched ligand, the remaining product was the racemic chelate.

N,N'-*ethylene(acetylacetoniminato-trifluoroacetylacetoneiminato)*Pd(II), Pd(enAA-TFA)

The product from the reaction with a 70 : 30, H_2(enAA-TFA): H_2(enTFA$_2$) ligand mixture was found to yield a sublimate which was *ca.* 90% in Pd(enAA-TFA) and 10% in Pd(enTFA$_2$) in a fraction obtained at 165–175°C over 72 hr (0.1 Torr).

N,N'-*propylene(acetylacetoneiminato-trifluoroacetylacetoneiminato)*Pd(II), Pd(pnAA-TFA)

The preparation was similar to that of Pd(enAA-TFA), yielding a product with a ratio of Pd(pnAA-TFA) to Pd(pnTFA$_2$) of 7.5 : 1. Insufficient product was isolated for elemental analysis.

N,N'-*butylene(acetylacetoneiminato-trifluoroacetylacetoneinimato)*Pd(II), Pd(bnAA-TFA)

Both isomers of this chelate were prepared from the crude H_2(bnAA-TFA) mother liquor. The product contained mostly the isomers together with some unreacted ligands and racemic and meso Pd(bnAA$_2$) and Pd(bnTFA$_2$). Chromatographic examination was carried out without further separation of the small amount of material obtained.

Characterization of ligands

It has been previously established that in the reaction of 2,3-diaminobutane with trifluoroacetylacetone,[12] the meso and racemic forms of the former persist on condensation to produce the isomeric forms of the tetradentate ligand, H_2(bnTFA$_2$). These forms in turn retain their identity on complexation with divalent transition metal ions. The reactions were followed by NMR spectroscopy of the resolved diamine isomers, and adsorption column and gas chromatographic resolution of ligand and chelates. In every case the species derived from racemic structures were found to be more volatile than those with meso structures and eluted first from the gas chromatographic column.

Further, it has been established that in all cases both ligands and chelates containing non-fluorinated groups show greater gas chromatographic retention than those with fluorinated groups present. In addition, ligands and chelates with ethylene bridges are retained longer than those with propylene bridges. Likewise those with racemic butylene bridges have even less retention. Those with meso butylene bridges always elute gas chromatographically between those with propylene and ethylene bridges.

In the present study, similar gas chromatographic behavior was observed for all ligands, with the noted trends being seen. In each preparation the chelates formed from ligands at different stages of isolation gave confirmatory evidence on their nature or isomeric structure. For none of the isomers was there any evidence of isomerization after the tetradentate ligand was formed in the initial condensation.

Characterization of chelates

All metal chelates were characterized by mass spectrometry of pure samples, using a Hitachi-Perkin-Elmer RMU 6L magnetic sector instrument, and direct probe insertion. Elemental analysis was used to verify composition (Table 1) with the exception of the semifluorinated "pn" and "bn" bridged species which were isolated in insufficient quantities. (Elemental analysis was performed in the University of Massachusetts Microanalytical Laboratory). Gas chromatographic analysis for reaction product composition was performed as previously reported.[11]

High pressure liquid chromatography

A Tractor-Chromatec Model 3100 instrument equipped with a 254 nm UV detector was used for initial studies. Later, results were obtained on an HPLC system consisting of LDC Constametric I and 11G pumps and a Model 1601 Gradient Master (Laboratory Data Control, Inc.). An LDC Spectromonitor II variable wavelength detector with an 8 μL flow cell was employed. Two different microparticulate silica columns were used which gave similar results. Those were a 30 cm × 4 cm I.D. column packed with Spherisorb SGP 8 μm silica (Spherisorb, Hauppauge, New York), by a balanced density slurry technique utilizing 1 : 1 bromoform: tetrachlorethylene; and a 25 cm × 4 mm I.D. column packed with Partisil 10 μm silica (Whatman, Inc.,

Clifton, New Jersey). Columns were of stainless steel with zero dead volume fittings. Solvents used were HPLC grade (Fisher).

RESULTS AND DISCUSSION

Initial investigation of the adsorption HPLC of the tetradentate β-ketoimine chelates of copper, nickel and palladium was carried out on a column packed with Partisil 10 micrometer diameter irregular particle silica. Solvent systems with successively increasing acetonitrile modifier in methylene chloride, 0, 2.5 and 5%, were employed. Table 2 lists retention volumes for fluorinated, semi-fluorinated and non-fluorinated complexes. The resolvable geometric isomers of the butylene bridged complexes are designated as dl (racemic) and *m* (meso) for the symmetrical substituted species, but as [1] and [2] for the semi-fluorinated chelates. This designation is made because, unlike the M(bnAA$_2$) and M(bnTFA$_2$) chelates which possess a plane of symmetry, the M(bnAA-TFA) complexes have no such symmetry. Consequently their meso isomers, although they contain the meso diamine group residue, are in fact non-superimposable mirror images and are therefore racemic pairs of enantiomers (Fig. 2). Nevertheless, it will be noted that the [2] isomers behave chromatographically in a fashion analogous to the meso M(bnAA$_2$) and M(bnTFA$_2$) isomers while the [1] isomers behave similarly to their racemic analogs.

A number of trends in retention are clear from Table 2. For all complexes, the introduction of small percentages of acetonitrile into methylene chloride results in major decreases in retention, allowing elution of non-fluorinated chelates. For all solvent systems a clear trend is seen for the effect of fluorination on retention behavior. The non-fluorinated chelates of the three metals are much more strongly retained than the semi-fluorinated or fluorinated analogs. The former elute close to the column void volume. Fully fluorinated complexes

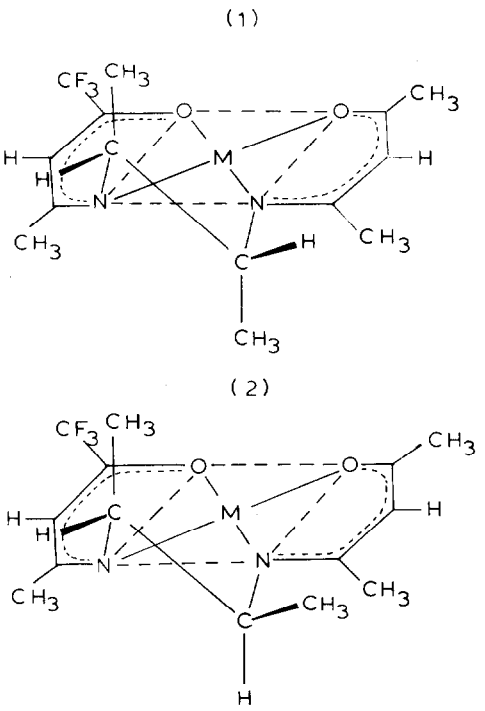

Fig. 2. Structures of butylene bridged semi-fluorinated chelates.

Table 2. Retention volumes (ml) for tetradentate β-ketoimine chelates. Column 30 cm × 0.4 mm I.D. Partisil 10 μm irregular silica

Complex	CH_2Cl_2			2.5% CH_3CN in CH_2Cl_2			5% CH_3CN in CH_2Cl_2		
Metals	Cu	Ni	Pd	Cu	Ni	Pd	Cu	Ni	Pd
H_2enAA$_2$	-	-	-	42.2	24.2	15.7	19.4	12.0	8.4
H_2enAATFA	25.2	16.0	12.0	5.4	4.8	3.9	4.1	3.9	3.3
H_2enTFA$_2$	6.1	4.7	4.6	3.6	3.5	3.6	3.2	3.2	3.2
H_2pnAA$_2$	-	-	-	39.8	24.9	16.0	17.3	11.9	8.0
H_2pnAATFA	22.1	15.1	11.9	5.2	4.8	3.9	3.9	3.3	3.2
H_2pnTFA$_2$	5.0	4.5	4.4	3.5	3.4	3.4	3.1	3.0	3.1
H_2bnAA$_2$ dl	-	-	-	34.3	23.9	16.0	16.5	12.4	7.1
H_2bnAA$_2$ meso	-	-	-	66.8	28.7	18.6	29.6	14.6	9.2
H_2bnAATFA (1)	19.3	15.2	12.1	4.5	4.5	3.7	3.5	3.5	3.3
H_2bnAATFA (2)	32.5	19.1	*	5.2	4.7	#	3.8	#	#
H_2bnTFA$_2$ dl	4.6	4.5	4.4	3.2	3.3	3.3	3.2	3.1	3.1
H_2bnTFA$_2$ meso	5.8	4.7	4.6	#	#	#	#	#	#
	Void volume 3.1 ml			Void volume 3.1 ml			Void volume 3.0 ml		

* broad shoulder, identity doubtful (see Figure 7.)

\# isomers unresolved.

Mobile phase flow rates approximately 1,5 ml / minute.

are always least retained, in contrast to their behavior on ODS columns with a 1 : 1, methanol: water mobile phase where they are retained longest.[7] Separation of the ethylene bridged copper complexes is shown in Fig. 3, using the Spherisorb silica column (see Experimental Section) which is somewhat more efficiencient than the Partisil silica column. Comparative resolution of nickel and palladium species is shown in Fig. 4. The substitution of a single CF_3 group greatly reduces column interaction but a second group substitution only marginally further reduces retention. However, the selectivity differences introduced by fluorination become more pronounced as the mobile phase polarity is reduced to pure methylene chloride. This effect is seen in the retention volumes of the ethylene and propylene bridged complexes in Column A of Table 2, where semi-fluorinated and fluorinated complexes are very well separated.

Another general trend is the significant decrease seen in the retention volumes of the copper chelates as the diamine bridge is changed successively from ethylene to propylene to racemic butylene. This trend is clear for fluorinated, semi-fluorinated and non-fluorinated chelates, but the effect on the nickel and palladium analogs is much less pronounced. In fact the retention times for the non-fluorinated complexes of nickel and palladium are very similar regardless of which bridging group is present. This enhanced selectivity for copper chelates with differing bridging groups is in agreement with some earlier data reported by Walters.[13] By contrast, baseline resolution with reversal of elution order for both copper and nickel chelates differing by the diamine bridge composition was observed on ODS.[7] The latter observation is explicable from the increased hydrocarbon content introduced by increasing the carbon number of the bridge which changes affinity for the hydrocarbon substrate.

The effects of fluorination on retention selectivity depend greatly on solvent polarity, but the effects of change in the diamine bridge are relatively minor, with the exception of the case of the meso isomers of the butylene bridged complexes which is discussed subsequently.

In Table 2 the effect which the chelated metal has on retention behavior is demonstrated. Under the conditions employed here, the palladium chelate is always eluted first among analogous complexes followed by the nickel and copper complexes. It is noteworthy that the nickel–copper elution order is the same for both non-fluorinated and fluorinated compounds; this contrasts with the reversal of nickel–copper elution order for fluorinated compounds on the ODS columns[7] with methanol : water solvent.

Adsorptive HPLC on silica was also effective for the separation of chelate isomers. When the bridging group of the tetradentate β-ketoimines is butylene, the possibility of three isomers exists, two being enantiomers (racemic or *dl*) and one being optically active (meso). Figure 5 shows the resolution of the pairs of racemic and meso isomers of the palladium, nickel and copper N,N'-butyl-ene*bis*(acetylacetoneimine){H_2(bnAA_2)} chelates on silica, with a mobile phase of 5% acetonitrile in methylene chloride. While it must be noted that the meso isomers of the nickel and palladium complexes had not been isolated in a pure form, the preparative procedure employed and the chromatographic separation sequence both gave the strongest indication of identity of the isomers in question. In each case, the racemic isomer elutes before the meso isomer and the elution order is palladium, nickel and copper. Baseline resolutions of Pd(bnAA_2) isomers is obtainable with a less polar mobile phase. Although the resolution of the copper isomers ($R_s = 2.9$) is greater than that of the nickel isomers

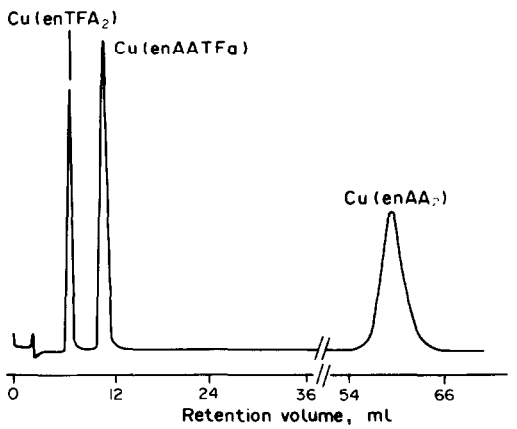

Fig. 3. HPLC separation of Cu(enTFA$_2$), Cu(enAA-TFA) and Cu(enAA$_2$) on Spherisorb 8 μm silica. Column 30 cm × 4 mm I.D. stainless steel. Mobile phase 2.5% acetonitrile in methylene chloride, flow rate 1.5 mL/min.

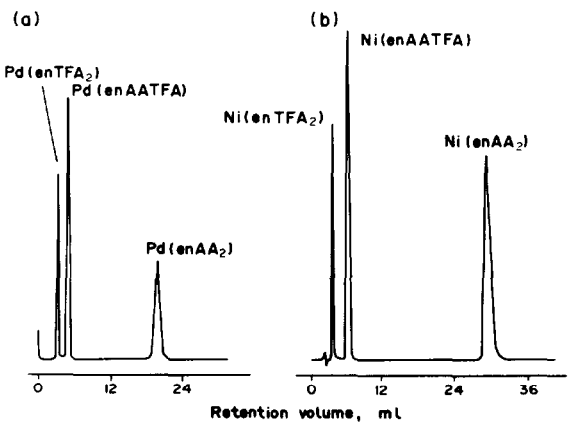

Fig. 4. HPLC separation of nickel and palladium chelates on Spherisorb silica. Conditions as in Fig. 3.

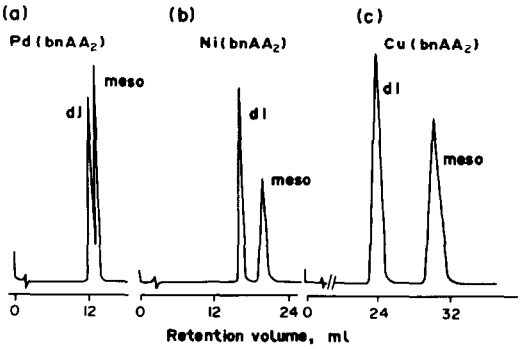

Fig. 5. HPLC resolution of racemic and meso isomer pairs for palladium, nickel and copper chelates of H_2(bnAA_2) on Spherisorb silica. Mobile phase 5% acetonitrile in methylene chloride, flow rate 1.5 mL/min.

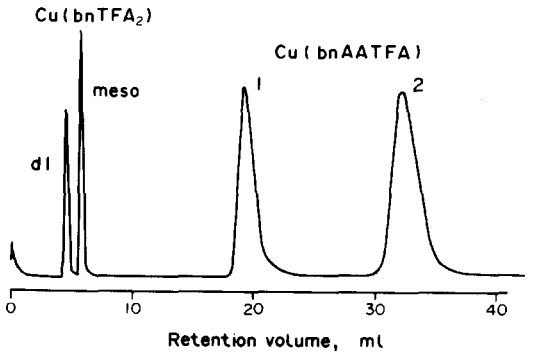

Fig. 6. Resolution of isomer pairs of fluorinated and semifluorinated butylene bridged chelates of copper(II). Mobile phase methylene chloride flow rate 1.45 mL/min.

(R_s = 1.8) the retention of the former is almost double that of the latter. Under similar conditions, no resolution of the isomers of the semi-fluorinated or fluorinated species is obtained except for those of Cu(bnAA–TFA) which show a small retention difference. An unmodified methylene chloride solvent gives resolution of both the racemic and meso pairs of the fluorinated complexes of all three metals and also the [1] and [2] isomer pairs of the semi-fluorinated chelates. The somewhat improved peak shapes obtained with the Spherisorb column compared with the Partisil column is again depicted in Fig. 6 for the copper chelates and in Fig. 7 for nickel and palladium complexes. The resolution of racemic from meso forms decreases from copper to palladium for the fluorinated chelates, this trend being the opposite of that observed in their gas chromatographic resolution on a Dexsil column.[9] It is not certain whether the [2] form of Pd(bnAA–TFA) is observed since only a partially resolved shoulder is noted in the chromatogram (Fig. 7b).

For all three butylene species, non-fluorinated, semi-fluorinated and fluorinated, the resolution between racemic and meso [1] and [2] isomers of copper chelates is much greater than between those of nickel or palladium, the difference being most pronounced for the non-fluorinated species. It is suggested that the color difference between the racemic (purple) and meso (green) isomers of the copper chelates may relate to the

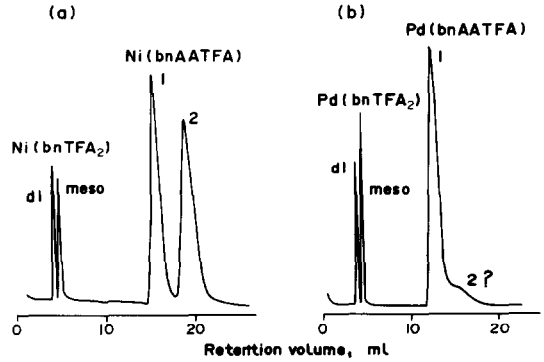

Fig. 7. Resolution of palladium and nickel isomer pairs as in Fig. 6.

difference in retention behavior of the butylene bridged isomers in general, the argument being derived from a series of papers by Waters *et al.*,[14–18] relating color isomerism to structure for some tetradentate β-ketosimine chelates.

On the basis of two and three dimensional X-ray analysis of purple $Cu(enAA_2)$.[14] green $Cu(enAA_2)\cdot H_2O$[15,16], green $Cu(pnSal_2)\cdot H_2O$ (N,N'-propylene *bis*(salicylideneiminato)Cu(II) monohydrate)[17] and green $Cu(enSal_2)$,[18] Waters *et al.* concluded that a purple color generally indicated a species containing four coordinate Cu(II), while green usually indicated a five coordinate species. Of most significance to the study described here is the structure of $Cu(enSal_2)$ which, unlike $Cu(enAA_2)\cdot H_2O$ and $Cu(pnSal_2)H_2O$, has its fifth coordination site between the copper atom of one molecule and the oxygen of another rather than between copper and an oxygen of water, i.e. the compound is dimeric.

It is hoped that the interesting, and in some cases, anomalous HPLC behavior observed together with the gas chromatographic behavior of these chelates to be described in a later publication will prompt structural investigations of this family of chelates similar to those performed by Waters *et al.* and more recently to that by Scaringe and Hodgson of $Ni(enTFA_2)$.[19] In this fashion the relationship between refined structural features of a family of chelates and liquid chromatographic adsorption and partition separations may be more clearly defined.

Acknowledgements—We wish to thank Dr. F. H. Walters for his contribution to initial stages of this study. The work was supported in part by the National Science Foundation (Grant CHE73-05201).

REFERENCES

[1]H. Veening and B. R. Willeford, *Rev. Inorg. Chem.* 1979 **1(3)**, 281.
[2]J. F. K. Huber, J. C. Kraak and H. Veening, *Anal. Chem.* 1972 **44**, 1554.
[3]P. Heinzman and K. Ballschmiter, *J. Chromatog.* 1977 **137**, 153.
[4]P. C. Uden and I. E. Bigley, *Anal. Chim Acta* 1977 **94**, 29.
[5]P. C. Uden, I. E. Bigley and F. H. Walters, *Anal. Chim. Acta* 1978, **100**, 555.
[6]P. C. Uden and F. H. Walters, *Anal. Chim. Acta* 1975 **79**, 175.
[7]P. C. Uden, D. M. Parees and F. H. Walters, *Anal. Lett.* 1975 **8**, 795.
[8]D. M. Parees, Ph. D. Dissertation. University of Massachusetts (1976).
[9]P. C. Uden and K. Blessel, *Inorg. Chem.* 1973 **12**, 352.
[10]A. E. Martell, R. L. Belford and M. Calvin, *J. Inorg. Nucl. Chem.* 1958 **5**, 170.
[11]R. Belcher, R. J. Martin, W. I. Stephen, D. E. Henderson, A. Kamalizad and P. C. Uden, *Anal. Chem.* 1973 **45**, 1197.
[12]R. Belcher, K. Blessel, T. J. Cardwell, M. Pravica, W. I. Stephen and P. C. Uden, *J. Inorg. Nucl. Chem.* 1973 **35**, 1127.
[13]F. H. Walters, Ph. D. Dissertation. University of Massachusetts (1975).
[14]D. Hall, A. D. Rae and T. N. Waters, *J. Chem. Soc.* 1963 5897.
[15]D. Hall, H. J. Morgan and T. N. Waters, *J. Chem. Soc.* (A) 1966 677.
[16]G. R. Clark, D. Hall and T. N. Waters, *J. Chem. Soc.* (A) 1969 823.
[17]F. J. Llewellen and T. N. Waters, *J. Chem. Soc.* (A) 1960 2939.
[18]D. Hall and T. N. Waters, *J. Chem. Soc.* 1960 2644.
[19]R. P. Scaringe and D. J. Hodgson, *Inorg. Chem.* **15**, 1193.

Polyhedron Vol. 1, No. 11-12, pp. 791-798, 1982
Printed in Great Britain.

0277-5387/82/110791-08$03.00/0
Pergamon Press Ltd.

COMPLEXES OF VITAMIN B_6 XII†

MIXED LIGAND COMPLEXES OF SOME DIVALENT METAL IONS WITH PYRIDOXAMINE AND HISTIDINE

MOHAMED S. El-EZABY* and FAWZIA M. Al-SOGAIR
Department of Chemistry, Kuwait University, Kuwait

(*Received* 5 *January* 1982)

Abstract—Potentiometric pH titrations ($I = 0.15$ M $NaNO_3$; 37°C) have been employed to study the various complex equilibria in the systems involving pyridoxamine and histidine with Co(II), Ni(II), Cu(II), and Zn(II). The stoichiometry and formation constants of different species have been determined with the aid of MINIQUAD-75. The complexes obtained were mostly protonated and positively charged. The formation of the ternary species is discussed in terms of the binary species. They were also correlated with the quaternary species involving pyridoxamine, glycine, and imidazole. Spectral analysis of the complex solutions of different compositions are also reported. The relevance of these ternary complex equilibria to some biological functions is discussed.

INTRODUCTION

Histidine, His, is an essential amino acid which constitutes an integral part of many proteins. Many features of histidine coordination chemistry have been revealed in many reports.[1-3] The anionic form is bound as a terdentate ligand and the neutral form predominantly as a substituted glycinate. The importance of histidine interactions with many metal ions in biological systems has been recognized quite recently since its imidazole nitrogen provides a means by which metal ions may be bound to the proteins. In addition, the histidyl residue in many peptides provides an anchor for metal ions, promoting deprotonation of the peptidic proton. Glycylglycine-L-histidine, for instance, was used in a model study for the carrying of plasma exchangeable Cu^{2+} by the amino terminal of aspartyl alanine-L-histidyl residues of human plasma albumin.[4]

Pyridoxamine, Pm, a vitamin B_6 compound, acts as a coenzyme for reactions of carbonyl compounds.[5] It forms quite stable binary complexes in solutions[6] and it has been reported recently that it was involved in many ternary complex formation reactions as one of the ligands.[6-9] The ligands used in these investigations were primarily bidentate. However, ternary complex formation involving Pm and terdentate ligands has not been studied. These complex equilibria may serve as a model for the interaction of vitamin B_6 with proteins in biological systems. They may also provide a model for the bioavailability of these metal complexes.

EXPERIMENTAL

Materials

L-Histidine (Schuchardt, München) and pyridoxamine dihydrochloride (Fluka) were used as provided. Stock solutions of these ligands (0.1M) were standardized potentiometrically against standard carbonate-free NaOH (0.1M). Histidine was made 0.1M in HNO_3. Co(II), Ni(II), Cu(II), and Zn(II) nitrates (BDH) were used. The concentration of the stock solutions of these metals salts were checked complexiметrically by standard solution of EDTA using potentiometric methods utilizing cupric selective electrode.[10]

Equipment

Orion Research Microprocessor Ionalyzer type 901, (provided with Radiometer combined glass electrode type GK2301C) was used in monitoring the pH during the titration. The ionalyzer in the pH mode was calibrated using two Radiometer buffers at pH's 6.98 and 4.03 at 37°C. Radiometer autoburette model ABU12 was used to deliver the titrant (0.1M NaOH carbonate-free). Spectral measurements were taken on Pye Unicam model SP8-100.

The pH-metric titrations were carried out as previously described.[7] The ionic strength of all titration solutions was adjusted to 0.15 M in NO_3^-. The temperature of the titration cell was kept constant at 37°C. The titrant in most cases was a solution of 0.1 M carbonate-free NaOH which was 0.15 M in $NaNO_3$ and in few cases was 0.1 M HNO_3. In all titrations, purified nitrogen was surged in the solution before and during the titration time. The metal ions concentrations were in the range $(1.0-3.0)\ 10^{-3}$ M. The ligand concentrations did not exceed 3 times the concentration of the metal ions in the binary systems. In the ternary systems, the concentration of each ligand was not more than 3 times the concentration of the metal ions.

The direct pH meter readings were used in the calculations. The pK_w of water was taken as equal to 13.38 at $I = 0.15$ and 37°C.[11]

Method of calculation

Titration data were analysed by using MINIQUAD-75 programme.[12] Different equilibrium reaction models have been tested. The results were assessed by observing the values of chi square (Xi^2), crystallographic factor (R) and sum of squared residuals.[5]

A choice of an equilibrium model was based on adopting the lowest values of Xi^2, R and S, taking into consideration the errors in experimental quantities and rules of propagation of errors.

In calculating the stability constants of the binary complexes using MINIQUAD-75, the protonation constants were kept constant while varying the values of the binary species. In case of the ternary systems, the formation constants of the protonated species and those of binary species were kept constant while varying those of the ternary species.

RESULTS AND DISCUSSION

Binary systems

The protonation constants for the free pyridoxamine and the formation constants of its binary complexes with

†Part XI. Ternary complexes of some bivalent metal ions with ethylenediamine and pyridoxamine, submitted for publication, Ref. 9.

*Author to whom correspondence should be addressed.

Table 1. Reported formation constants for the binary complexes of Co(II), Ni(II), Cu(II), and Zn(II) with pyridoxamine at I = 0.15 and T = 37°C (Ref. 12). *l*, *p*. *q* and *s* are the stoichiometric coefficients corresponding to Pm, His, M, and H

M^{2+}	*l p q s*	log β
H^+	1 0 0 1	10.407
	1 0 0 2	18.562
	1 0 0 3	22.063
Co^{2+}	1 0 1 0	5.591
	1 0 1 1	13.330
	2 0 1 0	10.255
	2 0 1 2	27.435
Ni^{2+}	1 0 1 0	6.464
	1 0 1 1	14.203
	2 0 1 0	10.521
	2 0 1 2	28.137
Cu^{2+}	1 0 1 0	10.805
	1 0 1 1	17.225
	1 0 1 2	21.337
	2 0 1 3	38.914
	2 0 1 0	17.471
	2 0 1 1	25.458
	2 0 1 2	32.535
Zn^{2+}	1 0 1 0	6.411
	2 0 1 0	11.874.

the metal ions have been reported earlier, Table 1.[12] The protonation constants for the histidine and the formation constants for its binary complexes have been redetermined under the conditions used in this work, Table 2. Several new binary complexes of histidine have been determined, for all metal ions studied, such as M(His·H) and M(His)(His·H), (M stands for the metal ion). The species M(His·H) implies that histidine may act as a bidentate ligand ligating the metal ions through the imidazole nitrogen and the amino nitrogen or through the carboxyl group and the amino group, or through the imidazole nitrogen and carboxyl group.

On the other hand, the species M(His) implies that His acts as a terdentate ligand. The species M(His)(His·H) indicates a sort of mixed ligand complex showing the bidentate and terdentate characters of His emphasizing the existence of penta-coordinated structural species in solution. Those species were observed for all metal ions studied, in contradiction to what have been previously reported by Perrin and Sharma in case of the Co(II)-histidine complexes.[13] The presence of $M(His)_2$ species may indicate that these metal ions are hexa-coordinated utilizing fully the terdentate character of His ligand.

It is worth mentioning that the mixed ligand complexes involving glycine and imidazole are more stable than the binary complexes of M(His),[12] Tables 2, and 3. This may be rationalized as due to the steric character exhibited by His in the latter complexes.

Table 2. Formation constants for the binary complexes of Co(II), Ni(II), Cu(II), and Zn(II) with histidine (n = no. of titration points, s = standard deviation) at I = 0.15 and T = 37°C

M^{2+}	Stoichiometric Coefficients *l p q s*	log β(s)	*n*	pH range	Reported values	Reference I, T
H^+	0 1 0 1	9.086(0.006)	322	4.6–10.3	8.92	(i), 0.15, 37°C
	0 1 0 2	15.150(0.011)			14.88	(i), 0.15, 37°C
	0 1 0 3	17.120(0.023)	312	1.9–3.3	17.12	(i), 0.15, 37°C
Co^{2+}	0 1 1 0	6.518(0.015)	405	4.2–7.0	6.70	(i), 0.15, 37°C
	0 1 1 1	12.056(0.015)				
	0 2 1 0	12.053(0.016)			12.06	(i), 0.15, 37°C
	0 2 1 1	19.042(0.008)				
Ni^{2+}	0 1 1 0	8.533(0.007)	277	3.9–5.9	8.43	(i), 0.15, 37°C
	0 1 1 1	12.913(0.026)				
	0 2 1 0	15.100(0.025)			15.14	(i), 0.15, 37°C
	0 2 1 1	20.869(0.034)				
Cu^{2+}	0 1 1 0	10.190(0.007)	280	3.1–6.9	9.79, 9.77	(i), (iv), 0.15, 37°C
	0 1 1 1	14.262(0.015)			14.18, 13.94	(ii), 0.15, 25°C
	0 2 1 0	16.234(0.050)			17.41, 17.38	(i), (iv), 0.15, 37°C
	0 2 1 1	22.801(0.054)			24.01, 23.12	(ii), 0.15, 25°C
Zn^{2+}	0 1 1 0	6.051(0.025)	376	5.0–6.9	6.34	(i), 015, 37°C
	0 1 1 1	11.821(0.038)			10.72	(iii), 0.15, 37°C
	0 2 1 0	—			11.69	(i), 0.15, 37°C
	0 2 1 1	17.991(0.035)			16.92	(iii), 0.15, 37°C

(i) Ref. 13.
(ii) T. P. A. Kruck and B. Sarkar, *Can. J. Chem.* 1973, **51**, 3549.
(iii) A. Kayali and G. Berthon, *J. Chem. Soc. Dalton* 1980, 2374.
(iv) G. E. Jackson, P. M. May and D. R. Williams, *J. Inorg. Nucl. Chem.* 1981, **43**, 825.

Table 3. Reported formation constants* of the mixed ligand complexes involving pyridoxamine, glycine, and imidazole at I = 0.15 and T = 37°C. *l*, *p*, *q*, *r* and *s* are the stoichiometric coefficients for Pm, gly, Imd, M, and H.

M^{2+}	*l*	*p*	*q*	*r*	*s*	log β
Co^{2+}	0	1	1	1	0	7.889
	1	1	1	1	1	21.958
	1	1	1	1	2	29.321
Ni^{2+}	0	1	1	1	0	8.849
	1	1	1	1	1	23.080
	1	1	1	1	2	29.543
Cu^{2+}	0	1	1	1	0	11.860
	1	1	1	1	0	20.083
	1	1	1	1	1	29.860
	1	1	1	1	2	37.230
Zn^{2+}	0	1	1	1	0	7.911
	1	1	1	1	1	24.560
	1	1	1	1	2	31.020

*Ref. 12.

Ternary systems

Figure 1 shows typical titration curves for 1:1:1 composition ratios of Pm:His:M of the ternary systems under consideration. Several inflections occur in the pH range 4.7–8.0 depending on the type of the ternary system. Although these inflections may give some information about the stoichiometries of some species in solution, yet they are not useful in such systems where protonation constant of the ligands are of different values. Generally, complex formation starts at pH > 3.0 in Cu(II) ternary system, and at pH > 3.5 in Co(II), Ni(II), and Zn(II) systems. Precipitation occurs only in Zn(II) system at pH's > 8.2. Table 4 depicts the values of the formation constants of the ternary systems using only titration data from 1:1:1 composition ratios. These constants stand for the following equilibrium reaction:

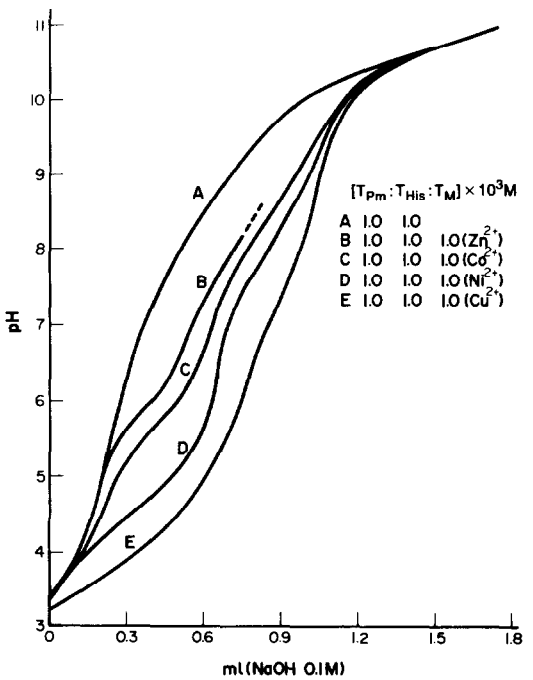

Fig. 1. pH titration curves of the 1:1:1 (Pm:His:M) ternary systems. $T_{Pm} = T_{His} = T_M = 1 \times 10^{-3}$ M.

$$lPm^- + pHis^- + qM^{2+} + rH^+ \leftrightharpoons (M_qPm_lHis_pH_r)^z;$$

$$\beta_{qlpr} = (M_qPm_lHis_pH_r)/(Pm)^l(His)^p(M)^q(H)^r \quad (1)$$

where *l*, *p*, *q* and *r* are the stoichiometric coefficients and $z = (2q + r) - (l + p)$. Protonated complexes are more predominant than nonprotonated complexes. The presence of 1:1:1:1 (Pm:His:M:H) species indicate that penta-coordinated species (His is terdentate and Pm is bidentate) are well exhibited by all metal ions except Zn(II). This is true, of course, if we assume that Pm is singly protonated with the proton located on the pyridinic nitrogen similar to the protonated species of the binary complexes of Pm with the metal ions. Irving–Williams order of stability for these species is obeyed. The existence of the species 1:1:1:4, on the other hand, indicates that both Pm and His may act as monodentate ligands. The site of ligating atoms cannot be easily predicted. However, a good guess may give the notion that the site of the ligating atoms varies with the various affinities of different metal ions especially when the Irving–Williams order of stability is not held, Table 4. Of course, these species are stable in acidic medium where competitions are strong between H^+ and the metal ions towards different ligating sites of the ligands. The other ternary species 1:1:1:2 and 1:1:1:3 show more or less the same order of stability exhibited by the species 1:1:1:4. The formation of the ternary species 1:1:1:*s* may be visualized as if they were formed from binary species as follows:

$$MLH_m + ML'H_n \leftrightharpoons MLL'H_s + M;$$

$$K^I = \beta_{1TH_s}/\beta_{1MLH_m}\beta_{1ML'H_n} \quad (2)$$

where β_{1TH_s}, β_{1MLH_m} and $\beta_{1ML'H_n}$ are the formation constants of the ternary species, mono-binary species of the first ligand, LH_m, and mono-binary species of the second ligand $L'H_n$, respectively, and $s = m + n$. Table 5 listed the calculated values of $\log K^I$ ($= \Delta \log K$ reported by Sigel[14]) whenever the binary constants are available. There are two values for the $\log K^I$ of the 1:1:1:1 depending on whether the proton is located on Pm or His moieties, i.e.

$$M(Pm{\cdot}H) + M(His) \rightleftarrows M(Pm)(His)H + M;$$

$$K_i^I = \beta_{1TH}/\beta_{1MPmH}\beta_{1MHis} \quad (3a)$$

or

$$M(Pm) + M(His{\cdot}H) \rightleftarrows M(Pm)(His)H + M;$$

$$K_{ii}^I = \beta_{1TH}/\beta_{1MPm}\beta_{1MHisH}. \quad (3b)$$

Although, it appears from Table 5 that equilibrium reactions (3b) are more favourable than those of (3a), however, the protonation equilibrium constants of His are less in values than those of Pm in absence of metal ions. A fact which may give one the notion that proton should be located on Pm moiety in the ternary complex species. In both cases, however, the formation of the ternary complex species are favourable over that of the

Table 4. MINIQUAD-75 formation constants of the ternary species of Co(II), Ni(II), Cu(II), and Zn(II) with Pm and His using 1:1:1 ($T_{pm}:T_{His}:T_B$) composition ratio at I = 0.15 and T = 37°C, σ = standard deviation, S = sum of squared residuals, Xi^2 = chi square, R = crystallographic factor; *l*, *p*, *q*, and *s* are the stoichiometric coefficients (Pm, His, M, and H)

M^{2+}	*l p q s*	log $\beta(\pm\sigma)$	S	Xi^2	R	*n*	pH range
Co^{2+}	1 1 1 0	—					
	1 1 1 1	21.155(0.002)					
	1 1 1 2	30.032(0.001)	9.7E-7	183	0.019	197	3.4–9.4
	1 1 1 3	36.938(0.001)					
	1 1 1 4	42.414(0.001)					
Ni^{2+}	1 1 1 0	—					
	1 1 1 1	23.420(0.003)					
	1 1 1 2	31.666(0.002)	9.6E-7	53	0.021	230	3.7–10.3
	1 1 1 3	37.288(0.002)					
	1 1 1 4	42.131(0.001)					
Cu^{2+}	1 1 1 0	16.708(0.012)					
	1 1 1 1	25.698(0.001)					
	1 1 1 2	31.441(0.002)	8.4E-7	413	0.010	276	3.1–8.4
	1 1 1 3	35.630(0.002)					
	1 1 1 4	38.007(0.027)					
Zn^{2+}	1 1 1 0	—					
	1 1 1 1	—					
	1 1 1 2	28.798(0.001)	2.3E-7	274	0.024	266	3.5–8.3
	1 1 1 3	35.656(0.001)					
	1 1 1 4	41.655(0.001)					

Table 5. Log K^I values for the reactions 3(*a* & *b*)

M^{2+}	*l p q s*	log K^I
Co^{2+}	1 1 1 1	+1.31*
		+3.51**
	1 1 1 2	+4.64*
Ni^{2+}	1 1 1 1	+0.69*
		+4.05**
	1 1 1 2	+4.56*
Cu^{2+}	1 1 1 1	−1.71*
		+0.63**
	1 1 1 2	−0.04*

*eq. 3a
**eq. 3b

mono-binary complex species (log K^I values are positive), except in Cu(II) systems. This may indicate that penta-coordinated structure are more allowable in Co(II) and Ni(II) ternary 1:1:1:1 complex species than that in Cu(II) system.

It is quite interesting to notice that 1:1:1:0 complex species are not easily detected in all systems except in the Cu(II) system. Even in the latter, the enhancement of the ternary complex formation of 1:1:1:0 species from the corresponding binary species is not favoured as evidenced by the value of −4.29 for the log K^1.

If histidine is assumed to behave like a combination of two ligands, glycine and imidazole, one may compare the quarternary complex formation involving glycine (Gly), imidazole (Imd) and pyridoxamine, Table 3, with the ternary complex formation involving histidine and pyridoxamine. It is noticed that the formation constants of the 1:1:1:1:1 quaternary species are more or less comparable in magnitude to those of the ternary species 1:1:1:1 except in Cu(II) system where the formation constants of the latter are much smaller than the former. This finding may indicate how far histidine affected the stability of the ternary species of Cu(II) in comparison to the Co(II) and Ni(II) species. It gives much insight about the weight of steric effect exhibited by histidine in presence of pyridoxamine in the Cu(II) system in which the metal ion is unable to overcome the structural allowances permitted for Co(II) and Ni(II) metal ions. Composition ratios in addition to 1:1:1 ratios were utilized in calculating the formation constants of the equilibrium reactions described by eqn (1). The formation constants are listed in Table 6.

Stoichiometric species other than those shown in Table 4 were also obtained. The formation constants of the 1:1:1:s species shown in Table 6 are identical to those obtained only from 1:1:1 composition ratios except in very few cases. These exceptions, however, may indicate that the pH range used for the 1:1:1 composition ratios is not as quite adequate for the calculation of the formation constants as other compositions or may be due to statistical reasons. Increasing the ligand concentration usually prohibit the possibility of undetected slight precipitation. The ternary species obtained are protonated such as 1:2:1:3, 1:2:1:4 and 2:1:1:4, species. The number of protons exceeds the possibility that Pm is the only protonated moiety in these ternary complexes. One may think that His is also protonated in such complexes. The 1:2:1:3 are probably octahedral in structure and 1:2:1:4 are likely trigonal bipyramidal or square pyramidal if water molecule is excluded from these complexes. It is surprising that these species contain two molecules of histidine rather than one. This may be rationalized on the basis that His coordinate the metal ions through the carboxyl and amino groups forming five-membered metal complex which is more stable than the six-membered metal com-

Table 6. MINIQUAD-75 formation constants of the ternary species of Co(II), Ni(II), Cu(II), and Zn(II) with Pm and His using different composition ratios including 1:1:1 ($T_{Pm}:T_{His}:T_M$) at I = 0.15 and T = 37°C. σ = standard deviation, S = sum of the squared residuals, Xi^2 = chi square R = crystallographic factor, *l*, *p*, *q*, *s* are the stoichiometric coefficients (Pm:His:M:H)

M^{2+}	*l* *p* *q* *s*	log $\beta(\pm\sigma)$	S	Xi^2	R	*n*	pH range
Co^{2+}	1 1 1 0	—					
	1 1 1 1	21.089(0.008)					
	1 1 1 2	29.743(0.003)					
	1 1 1 3	37.027(0.002)	2.7E-6	291	0.017	229	3.4–9.3
	1 1 1 4	43.028(0.001)					
	1 2 1 3	43.489(0.002)					
	1 2 1 4	49.963(0.002)					
Ni^{2+}	1 1 1 0	—					
	1 1 1 1	23.044(0.013)					
	1 1 1 2	32.317(0.003)					
	1 1 1 3	37.936(0.001)	2.1E-5	137	0.059	215	3.4–8.5
	1 1 1 4	41.309(0.004)					
	1 2 1 3	—					
	1 2 1 4	50.298(0.010)					
	2 1 1 4	54.027(0.003)					
Cu^{2+}	1 1 1 0	16.387(0.024)					
	1 1 1 1	25.674(0.001)					
	1 1 1 2	31.123(0.006)	3.4E-7	131	0,009	144	3.0–8.6
	1 1 1 3	35.798(0.002)					
	1 1 1 4	38.007(0.041)					
	1 2 1 3	45.129(0.002)					
Zn^{2+}	1 1 1 0	—					
	1 1 1 1	—					
	1 1 1 2	28.494(0.005)					
	1 1 1 3	35.812(0.003)	1.2E-6	82	0.014	228	−5.0–8.5
	1 1 1 4	42.000(0.001)					
	1 2 1 3	41.998(0.002)					
	1 2 1 4	48.404(0.004)					

plex involving Pm. In other words, His does not utilize the pyridinic nitrogen of imidazole on ligation with the metal ions.

In Figs. 2(a–d), the concentration of complex species present in the systems Co(II)–Pm–His, Ni(II)–Pm–His, Cu(II)–Pm–His, and Zn(II)–Pm–His for 1:1:1 composition ratios are shown in their dependence on pH as they are obtained from MINIQUAD-75 program. It is worth mentioning that these distribution diagrams are not independent of the initial concentrations of the ligands and metal ions in solutions, since increasing the concentration of one of the ligands with respect to another may enhance the formation of some species which are not present under different concentration conditions. The enhancement or de-enhancement, of course, depends on the formation constants of different species under identical conditions. Generally, these plots serve two purposes. Firstly, the plots indicate the relevance of minor species which may be obtained as a result of experimental errors. Secondly, these plots provides a model for different equilibria which may be present in biological systems, e.g. intestinal equilibria involving these ligands or their complexes when they are orally administered.

The distribution diagrams shown in Fig. 2, indicate that free cupric ions in Cu(II)–His–Pm exist in higher concentration than Co(II), Ni(II), and Zn(II) metal ions in their corresponding ternary systems. This may be rationalized on the basis that electrostatic repulsions are higher between His and Pm moieties in Cu(II) ternary system (assuming square planar structure) than in the other ternary systems. In addition, some binary complex species of histidine with Cu(II) exist at significant concentration at different pH's specifically at pH's lower than 6 and higher than 7.5. The binary species of Cu(II) with Pm mainly exist at acidic pH's with concentration lower than that of Cu(II) with His. In Co(II), Ni(II), and Zn(II) ternary systems, the concentration of the binary species are less significant than in Cu(II) ternary system. On the other hand, ternary species are predominant in wide pH range in the Co(II), Ni(II), and Zn(II) systems, in particular, where various protonated species coexist. In the Cu(II) ternary system, only the species 1:1:1:1 and 1:1:1:2 exist with the former present at maximum concentration at pH ≃ 7.5. The latter exist at acidic pH's with the maximum concentration at pH ≃ 5.3. These complexes are positively charged which make them less susceptible to intestinal absorption. The ligands themselves will only be absorbed at moderate pH values (~ 6.5) where the dipolar forms are the predominant species. The ternary species which may be readily absorbed is the neutrally-charged species of Cu–Pm–His (1:1:1:0) as well as the binary species $Cu(His)_2$ and $Cu(Pm)_2$. The ternary Cu(II) species is found to be of significant concentration at pH's higher than 8.0. These pH's are likely to be suitable for intestinal absorption where the medium pH is ~8.0.

Spectral analysis of the binary and ternary systems

Figure 3(a–c) show the spectra of the binary and ternary systems at specified conditions in the wavelength range 350–850 nm. There are hypsochromic shifts in the

spectra of the binary complexes (of the Cu(II) systems) when the composition ratios changed from 1:1 to 2:1, Table 7. The shifts amount to 53 and 47 nm in the Cu(II)–Pm and Cu(II)–His systems, respectively, Table 7. Another hypsochromic shift was observed in the ternary Cu(II) system with respect to 2:1 binary spectra which amount to 30 and 18 nm relative to $Cu(Pm)_2$ and $Cu(His)_2$ respectively. This shift confirms the presence of ternary species in solution. Generally, these bands are less broad than that of the aquated Cu(II). The latter has

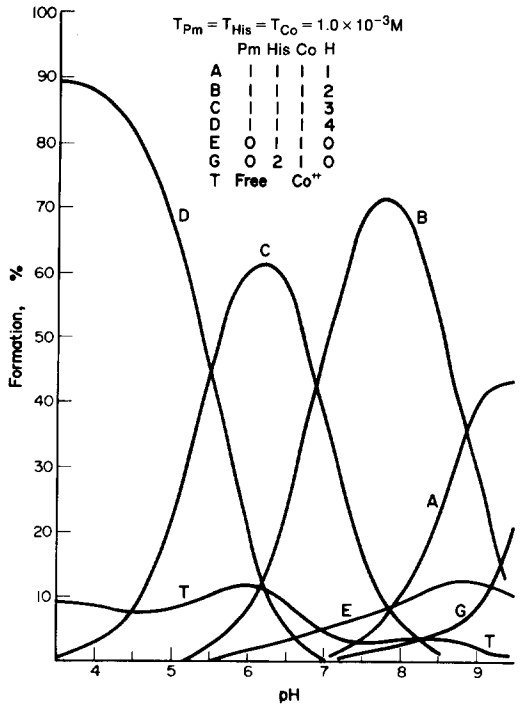

(a)

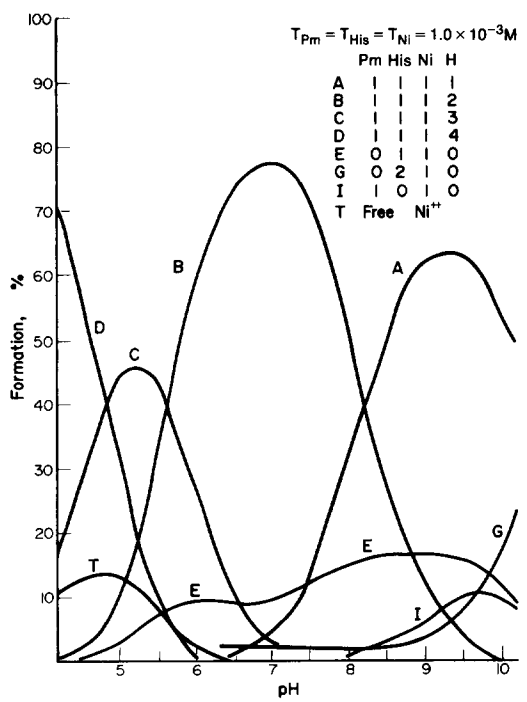

(b)

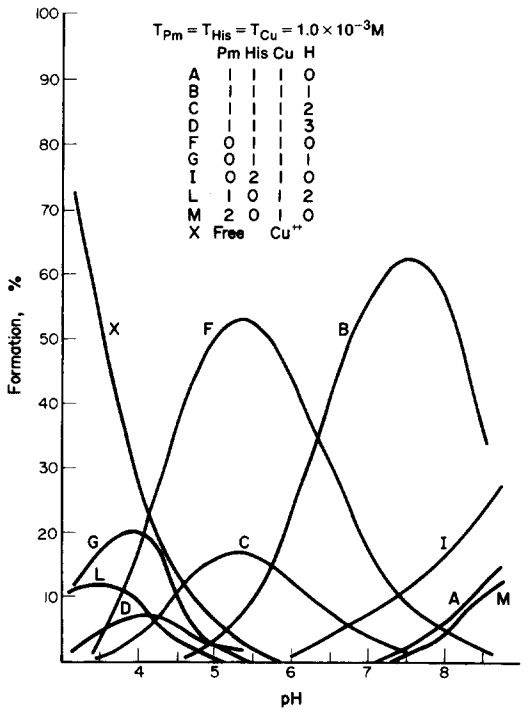

(c)

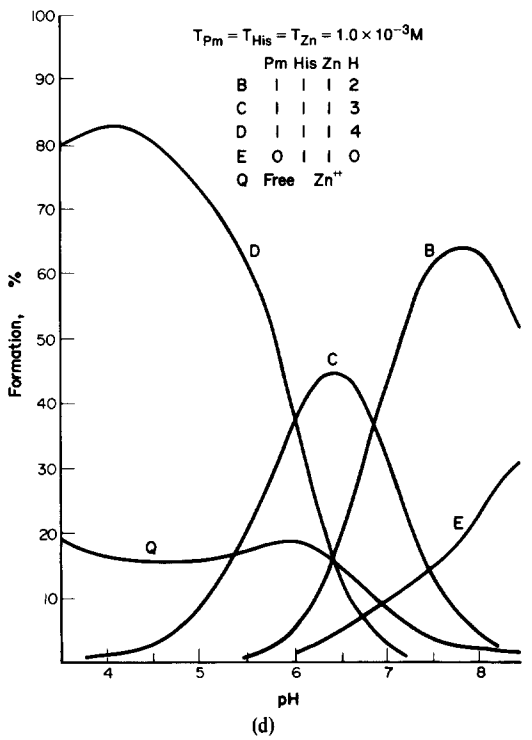

(d)

Fig. 2. Distribution diagrams of the metal complexes as function of pH in the systems; (a) Co(II)–Pm–His. (b) Ni(II)–Pm–His. (c) Cu(II)–Pm–His. (d) Zn(II)–Pm–His.

a weak, broad, asymmetric band with maximum wavelength (λ_{max}) at 833 nm ($\epsilon = 11$). This band was attributed to $^2T_{2g} \leftarrow {}^2E_g$ transition.[15] The spectral bands observed in the binary and ternary systems may be also assigned to the same transition of the aquated Cu(II). In such case, however, the energy is greater due to the increase in electron density in the vicinity of the Cu(II)

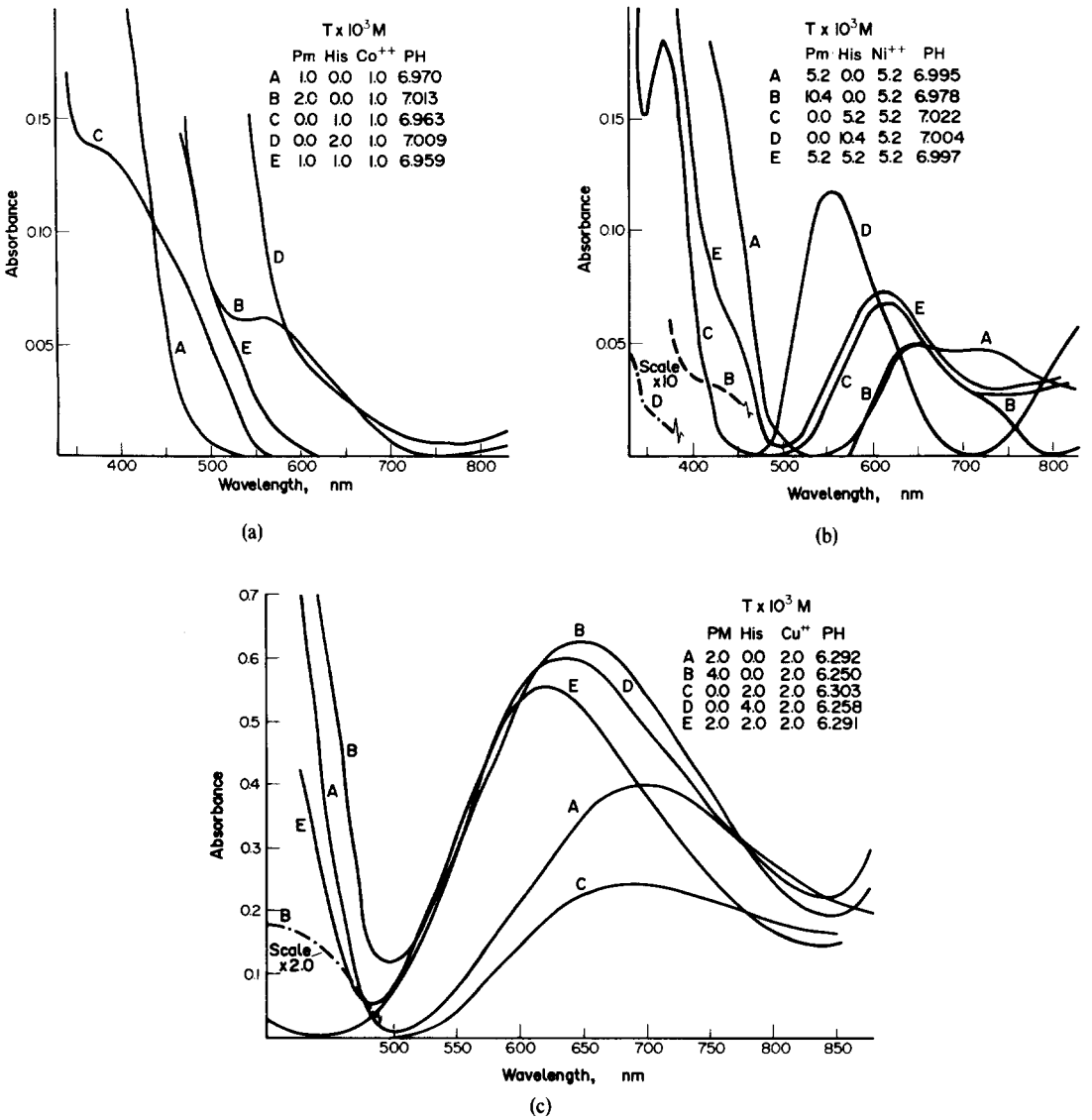

Fig. 3. Spectra of the binary and ternary systems in the wavelength range 350–850 nm for: (a) Co(II)–Pm–His. (b) Ni(II)–Pm–His. (c) Cu(II)–Pm–His.

Table 7. Spectral bands of the binary and ternary complexes involved in the system M-Pm-His. T = concentration, $\bar{\epsilon}$ = average molar absorptivity. T × 10^3 M

M^{2+}	Pm	His	M	pH	λ_{max}(nm)($\bar{\epsilon}$)
Cu^{2+}	2.0	—	2.0	6.3	698(50)
	4.0	—	2.0	6.3	645(78)
	—	2.0	2.0	6.3	680(30)
	—	4.0	2.0	6.3	633(75)
	2.0	2.0	2.0	6.3	615(70)
Ni^{2+}	5.2	—	5.2	7.0	650(2.4), 720(2.2), 454(sh), >900
	10.4	—	5.2	7.0	645(2.4), 725(1.15), 422, >900
	—	5.2	5.2	7.0	610(3.2), 760(1.4), 370(9.0), >900
	—	10.4	5.2	7.0	553(5.7), 785(sh), 354(sh), >900
	5.2	5.2	5.2	7.0	610(3.5), 760(1.7), 458(sh), >900
Co^{2+}	1.0	—	1.0	7.0	430(sh), >900
	—	2.0	1.0	7.0	375(sh), >900
	1.0	1.0	1.0	7.0	430(sh), >900

ions relative to that of water molecules as a result of ligand coordination, Table 7.

The Ni(II) ternary system exhibits a spectrum which is identical to that of the 1:1 Ni(II)–His binary system in the wavelength range above 500 nm but they are quite different at wavelength range less than 500 nm, Table 7. The overlap is considerable between the bands at 610 and 760 nm for the ternary species similar to that of the 1:1 binary species (650 and 720 nm for Ni(II)–Pm and 610 and 760 nm for Ni(II)–His binary species). A hypsochromic shift is observed in the spectra of the binary species when the composition is changed from 1:1 to 2:1 ratios. The shift is slight in the Ni(II)–Pm system and large in the Ni(II)-His system in the wavelength range above 500 nm. These bands are weak as in the aquated Ni(II) ions. The latter has three weak bands at 395, 690 (overlapped band) and 1149 nm which may be attributed to $^3T_{1g}(P) \leftarrow {}^3A_{2g}(F)$, $^3T_{1g}(F) \leftarrow {}^3A_{2g}(F)$ and $^3T_{2g}(F) \leftarrow {}^3A_{2g}(F)$, respectively.[15] One may expect that ternary and binary species will have the same type of transitions except that they have higher energies as a result of substituting water molecules by ligands of higher electron density. The relative shift of the spectral bands of the ternary species with respect to that of the 2:1 binary species confirm the formation of such species in solution. The overlapped band in the wavelength range 610–760 nm may be assigned to the transition $^3T_{2g}(F) \leftarrow {}^3A_{2g}(F)$, while the band at $\lambda_{max} > 900$ nm to the transition $^3T_{2g}(F) \leftarrow {}^3A_{2g}(F)$. The band at 458 nm cannot be assigned simply to the transition $^3T_{1g}(P) \leftarrow {}^3A_{2g}(F)$ since it may be attributed to the charge transfer type between the metal and ligands.

The spectral bands observed in the spectra of Co(II) systems cannot be simply correlated with the spectral bands of the aquated Co(II) ions. The latter exhibit three bands at 1250 nm ($\epsilon = 1.3$), 510 nm ($\epsilon = 4.8$) and 463 nm ($\epsilon = 2.1$).[15] The spectra of Co(II) system only show a shoulder in the wavelength range 555–375 nn and a band at wavelength greater than 900 nm. The shoulders in the wavelength range 555–375 nm may be attributed to the two latter transitions in the spectra of the aquated Co(II) ions and the band at $\lambda > 900$ is attributed to that at 1250 nm. Inclusion of the effect of charge transfer spectra on the shoulder band cannot, however, be ignored. Further analysis of the spectral bands at $\lambda > 900$ nm is required.

Acknowledgement—This investigation was supported by Kuwait University Research Council Grant No. SC010.

REFERENCES

[1]R. J. Sundberg and R. B. Martin, *Chem. Rev.* 1974, **74**, 471.
[2]R. B. Martin, *Metal Ions in Biological Systems* (Edited by H. Sigel), Vol. 9. New York, Marcel Dekker (1979).
[3]S. T. Chow and C. A. McAuliffe, *Progress in Chemistry*, (Edited by Lippard) Vol. 19. Interscience, New York (1975).
[4]N. Camerman, A. Camerman and B. Sarker, *Can. J. Chem.* 1976, **54**, 1309.
[5]D. E. Metzler, *Biochemistry*. Academic Press, New York (1977).
[6]B. A. Abd-El-Nabey and M. S. El-Ezaby, *J. Inorg. Nucl. Chem.* 1978, **40**, 739.
[7]M. S. El-Ezaby, H. M. Marafie and S. Fareed, *J. Inorg. Biochem.* 1979, **11**, 317.
[8]M. S. El-Ezaby and T. E. El-Khalafawy, *J. Inorg. Nucl. Chem.* 1981, **43**, 831.
[9]H. M. Marafie, M. S. El-Ezaby, B. A. Abd-El-Nabey and N. Kittaneh, *Transition Met. Chem.* 1982, **7**, 227.
[10]Instruction Manual for Cupric Electrode Type F1112Cu, Radiometer A/S, Copenhagen, 1972.
[11]G. Berthon, P. M. May and D. R. Williams, *J. Chem. Soc. Dalton*, 1978, 1433.
[12]M. S. El-Ezaby and M. Rashad, 21*st Int. Conf. on Coord. Chem.* Toulouse, France (1980).
[13]D. D. Perrin and V. S. Sharma, *J. Chem. Soc. A* 1967, 724.
[14]H. Sigel, *Chimia* 1967, **21**, 489.
[15]B. N. Figgis, *Introduction to Ligand Fields*. Interscience, New York (1966).

Polyhedron Vol. 1, No. 11-12, pp. 799-801, 1982
Printed in Great Britain.

0277-5387/82/110799-03$03.00/0
Pergamon Press Ltd.

THE NATURE OF THE PRODUCT FROM THE REACTION OF TETRACYANOETHYLENE WITH IRON PENTACARBONYL

JAMES C. FANNING*, PATRICIA A. HUDSON, LAWRENCE A. SANDERS and EDWARD JONES

Department of Chemistry and Geology, Clemson University, Clemson, SC 29631, U.S.A.

(*Received* 18 *March* 1982)

Abstract—The reaction of tetracyanoethylene with iron pentacarbonyl in mesitylene at 90° gave an insoluble product, $Fe_2C_{16}H_{12}N_8O_7$. The Mössbauer and IR spectra, the magnetic susceptibilities over the temperature range 95–298 K, and the thermal decomposition temperatures in a nitrogen atmosphere were measured. The solid is best described as an iron (III) ketoamine polymer with hydroxo bridges between iron atoms.

INTRODUCTION

The reaction of tetracyanoethylene (TCNE) with metal compounds was studied extensively by Berlin *et al.*[1-4] in the 1960's in an attempt to prepare metal polymers with tetraazaporphine-metal monomeric units. The proposed structure of the iron units is shown in I.

The polymers were formed by reacting metal compounds, primarily those of copper, iron, and magnesium, with TCNE, usually in a ratio of 1:2, under a variety of conditions. The polymers had varying percent analyses (C, H, N, and metal), not totaling a hundred, indicating the presence of oxygen or other elements in the polymer. The percent compositions and the C/N ratios were variable. Also, the C/N ratio was not equal to 1.5, the value expected if the tetraazaporphine polymer formed. A recent preparation,[4,5] using $FeCl_3$ and TCNE as starting materials heated together for 10 hr in urea at 250°, resulted in a product which had a low percent iron, and a C/N ratio of approx. 1.5. However, two types of iron were present in the product, as shown by the Mössbauer spectrum.

Since there was some doubt about the exact nature of the products resulting from heating TCNE in the presence of metal compounds, we decided to investigate the preparation of the polymer and its nature. The TCNE–iron compound reactions were selected for study since they enabled the Mössbauer spectrometer to be used to follow the reactions. Iron pentacarbonyl was used as a reactant. The previously reported iron products had been made starting with either iron (III) acetylacetonate or iron (III) chloride. The product from the iron (iii) chloride reaction retained a portion of the chloride (Cl/Fe = 0.87)[4]. It is also possible that some of the acetylacetonate anion was retained by the product of that reaction.

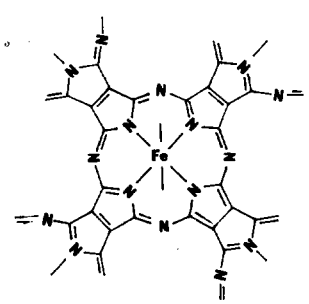

I - tetraazaporphine $[Fe(OH)(C_{12}N_8)]_x$

*Author to whom correspondence should be addressed.

EXPERIMENTAL

Chemicals. Iron pentacarbonyl and mesitylene were distilled prior to use. TCNE was sublimed under reduced pressure at 97°.

The Reaction. 455 mg (2.32 mmoles) of iron pentacarbonyl was dissolved in 30 mL of mesitylene and 388 mg (3.03 mmoles) of TCNE added. The solution was placed in a reaction tube fitted with inlet and outlet ports. The tube was covered with aluminum foil to prevent any light effects. Nitrogen was bubbled through the red solution for a few minutes and the tube sealed, placed into a 90° oven, and allowed to stand for 24 hr. At that time a fine, black powder was present along with a clear, light yellow supernatant solution. The solid was collected and extracted using a Soxhlet extraction apparatus for 24 hr with benzene and 24 hr, with acetone. It was dried under vacuum over P_2O_5 resulting in a product yield of 376 mg.

The product

(a) *Analysis*[6] *Found*: %C, 35.21; %H, 2.47; %N, 20.94; %Fe, 21.05; %O (by difference), 20.33. Calc. for $Fe_2C_{16}H_{12}N_8O_7$: %C, 35.58; %H, 2.24: %N, 20.75; %Fe, 20.68; %O, 20.74.

(b) IR *spectrum.* The spectrum was obtained on a Perkin-Elmer Model 621 IR Spectrophotometer using both a mineral oil mull and KBr disc. The spectra were essentially identical except for the mulling agent bands. Spectral bands: 3300vs, br; 2950sh, s, br; 2200s; 2150sh, m; 2080sh, m; 1760w; 1570vs, br; 1440sh, br, s; 1350sh, br, s; 950w; 680s; 500w, br.

(c) *Magnetic measurements.* The corrected molar magnetic susceptibilities (χ_M) and magnetic moments (μ_B) were determined using equipment previously described.[7] The diamagnetic correction used was -1.09×10^{-4} cgs units. The values of T(K), $\chi_M \times 10^3$(cgs units), and μ_B(B.M.) were: 298, 5.09, 3.48; 274, 5.33, 3.42; 255, 5.57, 3.37; 244, 5.68, 3.33; 224, 5.98, 3.27; 216, 6.02, 3.23; 195, 6.46, 3.18; 181, 6.61, 3.10; 179, 6.72, 3.10; 170, 6.85, 3.05; 155, 7.16, 2.98; 142, 7.46, 2.91; 133, 7.74, 2.87; 118, 8.25, 2.79; 105, 8.95, 2.74; 100, 9.34, 2.74; 97, 9.47, 2.71; 95, 9.65, 2.70.

(d) *Mössbauer spectrum.* The spectrum was obtained at room temperature using equipment and computer analysis programs which have been described.[8] The center shift values are referenced to sodium nitroprusside. The spectral parameters for

the two-line spectrum are: center shift, 0.60 mms^{-1}; quadrupole splitting, 0.88 mms^{-1}; average width at half-height, 0.71; percent effect, 3.4; and ratio of low velocity peak intensity to high velocity peak intensity, 1.35.

(e) *Thermal decomposition.* The product was heated in a nitrogen atmosphere using previously described equipment.[9]

RESULTS

When TCNE and iron pentacarbonyl in a 2.5–3.00 ratio, were allowed to react in mesitylene under a nitrogen atmosphere for 24 hr at 90°, a fine black powder resulted. The powder was extracted with benzene and acetone. Analysis of the powder showed it to have: a high percentage of iron; hydrogen present; a C/N ratio equal to 2.0; and oxygen present since the percentages did not total to a hundred. A formula, $Fe_2C_{16}H_{12}N_8O_7$, was calculated for the product.

The IR spectrum of the product showed a very strong 2200 cm^{-1} band, indicating the presence of CN groups. The very strong, broad 1570 cm^{-1} band was probably due to either C=C or C=N stretch or both. The weak, broad peak at 950 cm^{-1} possibly resulted from $Fe_2(OH)_2^{4+}$ units.[10] Since there was no strong peak around 2000 cm^{-1} it was assumed that all of the CO groups have been displaced from the iron.

A two-line Mössbauer spectrum showed the presence of only one type of iron. The center shift, δ, and the quadrupole splitting, Δ, values at room temperature were 0.60 and 0.88 mms^{-1}, respectively. These values were similar to those for one of the pairs of lines in the product formed between TCNE and iron (III) chloride mentioned above[5] (δ: 0.73 mms^{-1}; and Δ: 0.90 mms^{-1}) and those expected for iron (III).

The black product has an unusual room temperature magnetic moment, 3.48 B.M., that decreased with temperature. If the iron (III) was high spin, a temperature-independent magnetic moment of 5.92 B.M. was expected. A plot of the reciprocal of the molar magnetic susceptibility vs the absolute temperature gave a curve that could be fitted[11] with the Van Vleck equation for high-spin Fe(III) (total spin quatum number, $S = 5/2$) having an exchange coupling constant, J, equal to $-25\ cm^{-1}$. The low, negative J value indicated that the product was weakly antiferromagnetic with no oxo bridges between iron atoms.[12] Antiferromagnetic interaction might occur through dihydroxy bridges.

Heating the polymer in a nitrogen atmosphere resulted in a gradual loss of weight from about 80 to about 290° with a 26% total weight loss. No further weight change occurred until 360°, at which temperature the material underwent significant decomposition. If CN is lost (as HCN or $(CN)_2$) during the initial decomposition step, then the high C/N ratios found in the previously reported preparations may result from using high temperatures for the preparations.

The reaction between TCNE and iron pentacarbonyl was carried out under many different conditions, varying solvent, temperature, and ratio of reactants. The reaction in mesitylene at 90° with a small excess of iron pentacarbonyl gave the most uniform product and the best yield. If excess TCNE or a 1:2 metal to TCNE ratio was used, the iron content was low. At 90°, in a nitrogen atmosphere, and in the absence of light, iron pentacarbonyl was not expected to decompose (b pt 103°). The yellow supernatant solution remaining after the reaction contained excess carbonyl. Both the benzene and acetone extracts of the product contained some iron carbonyl.

Attempts were made to keep moisture and air out of the reaction and product work-up; however, the product always had some oxygen and hydrogen present no matter how carefully it was treated. In order to obtain a satisfactory analysis, extractions were required. This could not be done without some exposure to air. Therefore, once the reaction had been carried out in an inert atmosphere, no special precaution was taken to avoid contact with air.

Two of the reactions were unusual. In dimethylsulfoxide at 90°, a reaction did not take place until a 0.5% of water was added, then Prussian Blue, as shown by the Mössbauer spectrum, was formed. When benzyl alcohol was used as the reaction medium at 90°, a white product resulted which immediately changed to Prussian Blue when exposed to air.

DISCUSSION

Tetracyanoethylene is a very reactive compound[13] and is polymerized by a variety of reagents.[13,14] Since nucleophiles displace CN groups, it is not unexpected that if polymerization occurs in the presence of a nucleophile, CN groups are lost and the nucleophile incorporated into the polymer.[15] Metal compounds react with TCNE especially when the metal is in a low oxidation state.[16–18] A variety of products may result since TCNE may bind to the metal through an ethylenic carbon or through a CN nitrogen. Therefore, it is not surprising to find polymer formation occurring in the reaction described here and to have iron incorporated into the polymer.

Considering the reactivity of TCNE and the possibility of including oxygen, hydrogen, and iron (III) with bridging OH groups into the polymer structure, there are at least three possible types of polymers that might be proposed. These are: (a) the ketoamine (II); (b) the tetraazaporphine (I); and (c) the hydroxamate (III) structures.

The ketoamine structure is made up of two TCNE molecules, each having lost two CN groups. The molecules are joined together and each has formally added a water molecule. The oxygen replaces one CN group and two hydrogens bind to each of the atoms of one CN group. The entire group ($C_8H_4N_4O_2$) bridges two iron

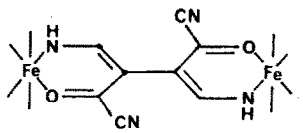

II - ketoamine $[Fe(OH)(C_8H_4N_4O_2)]_x$

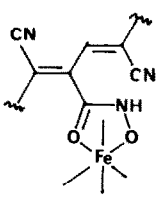

III - hydroxamate
$[Fe(OH)_2(C_8HN_4O_2)]_x$

(III) ions. Each iron is bound to two of these ketoamine groups and two bridging OH groups, giving six ligands about the iron. This structural arrangement is the simplest ketoamine type to fit the empirical formula. The formula for the polymer would be $Fe(C_8H_4N_4O_2)(OH)\cdot 1/2H_2O$. More complex ketoamine structures might possibly be formulated.

Such a structure as II would be expected on the basis of the work of Storbecke and Starke.[15] They heated TCNE in quinoline for 5 hr at 200° with a trace of moisture and obtained a polymer. The polymer was described as TCNE units linked together through the loss of CN groups with some CN groups on the chain replaced by OH groups. Anionic polymerization of TCNE in the gas phase has been shown to occur through the loss of CN groups.[19] Thus, TCNE polymerization through CN loss may possibly be occurring in the TCNE-iron pentacarbonyl reaction. IR[20,21] and Mössbauer spectra and magnetic susceptibility data are not in disagreement with the ketoamine structure.

The "sought-after" tetraazaporphine structure (I) is less likely since the C/N ratio is too high and it is difficult to incorporate hydrogen and oxygen into the structure, except as an OH group bound to each iron and as lattice bound water. The Mössbauer spectral parameters of the polymer are not those expected for iron (III) bound in a tetraazaporphine site. The spectral parameters for iron (III) tetrasulfophthalocyanine have been determined[7] and the δ values are smaller ($\sim$0.4 mms^{-1}) and the Δ values, larger (1.5–3.0 mms^{-1}) than the values obtained for the iron polymer. The CN stretch found in the IR spectrum cannot be accounted for by this structure.

Another type of polymer to be considered is the hydroxamate (III) one. This would involve the loss of CN groups, linkage of TCNE molecules, and oxidation and hydrolysis of CN groups. Hydroxamate bidentate type ligand sites result which complex iron (III). Most hydroxamates have a strong IR band around 1600 cm^{-1}[22] which is not found in the IR spectrum of the product. Also the hydroxamate structure would give a very low hydrogen content. These points, however, are not conclusive enough to rule out the hydroxamate structure.

TCNE reacts with iron carbonyl compounds to produce dicyanovinyl groups, $C{=}C(CN)_2$, bound to iron.[16,23] This does not appear to be occurring in the reaction described here since the iron would be expected to be in a low oxidation state and low spin state. The Mössbauer spectrum and magnetic susceptibility data do not support the formation of a dicyanovinyl polymer.

At this time the ketoamine structure is the favored one for the iron polymer; however other structures, such as the hydroxamate, cannot be ruled out. The results do show that the tetraazaporphine is not a likely one and other structures need to be considered.

REFERENCES

[1] A. A. Berlin and A. I. Sherle, *Inorg. Macromol. Rev.*, 1971, **1**, 235.

[2] A. A. Berlin, N. G. Matveyeva, A. I. Sherle and N. D. Kostrova, *Vysokomol. Soedin.*, 1962, **4**, 860. (Eng. trans. p. 260).

[3] A. A. Berlin, A. I. Sherle, G. V. Belova and O. M. Boreyev, *Vysokomol. Soedin.*, 1965, **7**, 88. (Eng. trans. p. 92).

[4] T. I. Andrianova, A. I. Sherle and A. A. Berlin, *Izv. Akad. Nauk SSSR Ser. Khim.*, 1973, 531 (Eng. trans. p. 509).

[5] N. I. Shapiro, I. P. Suzdalev, V. I. Gol'Danskii, A. I. Sherle and A. A. Berlin, *Teor. Exsp. Khim.*, 1975, **11**, 330. (Eng. trans. p. 272).

[6] Analyses were carried out by Galbraith Laboratories, Inc., Knoxville, TN.

[7] J. C. Fanning, G. B. Park, C. J. James and W. R. Heatley, Jr., *J. Inorg. Nucl. Chem.*, 1980, **42**, 343.

[8] C. P. Monaghan and J. C. Fanning, *J. Phys. Chem.*, 1978, **82**, 1045.

[9] J. C. Fanning, C. D. Elrod, B. S. Franke and J. D. Melnik, *J. Inorg. Nucl. Chem.*, 1972, **34**, 139.

[10] H. J. Schugar, G. R. Rossman and H. B. Gray, *J. Am. Chem. Soc.*, 1969, **91**, 4564.

[11] The computer program for these calculations was kindly supplied by Dr. S. Vitale of the Libra Universita' Degli Studi Di Trento.

[12] R. S. Drago, Physical Methods in Chemistry. Saunders, Philadelphia, p. 429, 1977.

[13] D. N. Dhar, *Chem. Rev.*, 1967 **61**, 611.

[14] A. A. Berlin and N. G. Matveeva, *Dokl. Akad. Nauk SSSR*, 1961, **140**, 368. (Eng. trans. p. 899).

[15] I. Storbeck and M. Starke, *Ber. Bunsenges. Phy. Chem.*, 1965, **69**, 343.

[16] R. B. King and M. S. Saran, *J. Am. Chem. Soc.*, 1973, **95**, 1811.

[17] S. R. Su and A. Wojcicki, *Inorg. Chem.*, 1975, **14**, 89.

[18] P. J. Krusic, H. Stoklosa, L. E. Manzer and P. Meakin, *J. Am. Chem. Soc.*, 1975, **97**, 667.

[19] J. H. Bowie, *Austr. J. Chem.* 1977, **30**, 2161.

[20] H. F. Holtzclaw, Jr., J. P. Collman and R. M. Alire, *J. Am. Chem. Soc.*, 1958, **80**, 1100.

[21] A. K. Srivastava, V. B. Rava and M. Mohan, *J. Inorg. Nucl. Chem.*, 1974, **36**, 3864.

[22] J. Lueng and K. N. Raymond, *J. Am. Chem. Soc.*, 1974, **96**, 1757.

[23] K. Wallenfels, K. Friedrich, J. Rieser, W. Ertel and H. K. Thieme, *Angew. Chem. Int. Ed. Engl.*, 1976, **15**, 261.

Polyhedron Vol. 1, No. 11-12, pp. 803-808. 1982
Printed in Great Britain.

0277-5387/82/110803-06$03.00/0
Pergamon Press Ltd.

t-BUTYL ISOCYANIDE COMPLEXES OF RHENIUM(I), CHROMIUM(O), TUNGSTEN(O,I) AND PLATINUM(II); X-RAY CRYSTAL STRUCTURES OF BIS(*t*-BUTYLISOCYANIDE)-TRIS(TRIMETHYLPHOSPHINE)CHLORORHENIUM(I) AND TRIS(*t*-BUTYLISOCYANIDE)BIS(TRIMETHYL-PHOSPHINE)CHLORORHENIUM(I)

KWOK W. CHIU, CHRISTOPHER G. HOWARD and GEOFFREY WILKINSON*
Chemistry Department, Imperial College, London, SW7 2AY, England

and

ANITA M. R. GALAS and MICHAEL B. HURSTHOUSE*
Chemistry Department, Queen Mary College, London, E1 4NS, England

(*Received* 27 *February* 1982)

Abstract—The reduction of $ReCl_4(THF)_2$ in the presence of excess *t*-butylisocyanide by sodium amalgam produces *pentakis*(*t*-butylisocyanide)chlororhenium(I), which has been converted to the corresponding methyl and ethyl derivatives. The reaction of pentakis(trimethylphosphine)chlororhenium(I) with Bu^{t}NC gives partially substituted complexes, $ReCl(CNBu^t)_2(PMe_3)_3$ and $ReCl(CNBu^t)_3(PMe_3)_2$. The structures of both compounds have been determined by X-ray methods. Octahedral $ReCl(CNBu^t)_2(PMe_3)_3$ has *trans* isocyanide groups with one linear [C–N–C = 175(1)°] and one slightly bent [C–N–C = 159(1)°]. The Re–C bond lengths are equal within experimental error [2.004(7), 2.003(7)Å]. In the octahedral $ReCl(CNBu^t)_3(PMe_3)_2$, for which the structure is not well defined, due to disorder, the unique isocyanide *trans* to chlorine is considerably bent at the nitrogen atom [C–N–C = 141(6)°] and appears to show the shortest Re–C bond length, 1.94(5) *vs* 2.02(5)Å for the other two isocyanides which are mutually *trans*.

Protonation of these two isocyanide complexes with fluoroboric acid gives, respectively, the salts $[ReCl(CNBu^t)CNHBu^t(PMe_3)_3]BF_4$ and $[ReCl(CNBu^t)_2CNHBu^t(PMe_3)_2]BF_4$, whose configurations have been determined by NMR spectroscopy.

The reduction by sodium amalgam of $Cr_2(CO_2Me)_4$ in tetrahydrofuran in presence of Bu^{t}NC gives a high yield of $Cr(CNBu^t)_6$ while similar reduction of the dimeric tungsten(II) complex of the anion (mhp) of 2-methyl-6-hydroxypyridine gives $W(CNBu^t)_6$. Interaction of $W_2(mhp)_4$ in methanol–ether with Bu^{t}NC gives a tungsten(I) complex $W_2(\mu\text{-mhp})_2(Bu^tNC)_4$, which may be an intermediate in the reductive cleavage reaction.

Interaction of *cis*-$PtMe_2(PMe_3)_2$ with Bu^{t}NC leads only to replacement of one PMe_3 group to give the complex *cis*-$PtMe_2(PMe_3)(CNBu^t)$.

We have synthesised the zerovalent molybdenum isocyanide complex, $Mo(CNBu^t)_6$, by reductive cleavage of dimolybdenum(II) tetraacetate, $Mo_2(CO_2Me)_4$, using sodium amalgam in presence of Bu^{t}NC.[1] Additionally, the binuclear carboxylates or chloro carboxylates of Mo, Re, Ru and Rh have been shown to undergo cleavage with Bu^{t}NC to give mono-nuclear species such as $[Re(CNBu^t)_6]Cl$.[2]

We now report related studies on *t*-butylisocyanide complexes of rhenium, chromium, tungsten and platinum. The X-ray diffraction studies on $ReCl(CNBu^t)_2(PMe_3)_3$ and $ReCl(CNBu^t)_3(PMe_3)_2$ are described.

1. RHENIUM COMPLEXES

(a) *Pentakis*(t-*butylisocyanide*) *compounds*

The isocyanide complexes $ReX[CN(p\text{-tolyl})]_5$, X = Cl, Br and I have been obtained from $ReX(CO)_5$;[3] the rhenium(III) complex $ReBr_3(CNp\text{-tolyl})_4$[4] and the $[Re(CNBu^t)_6]^+$ cation[2] are known. Isocyanide cations, $[Re(CNR)_4(PR_3)_2]^+$ have been made recently by interaction of isocyanides in presence of KPF_6 with $ReH_7(PR_3)_2$ (PR_3 = PPh_3, PEt_2Ph).[5]

The compound $ReCl(CNBu^t)_5$ is readily obtained in high yield by sodium amalgam reduction of tetrachlororhenium-*bis*(tetrahydrofuran) in tetrahydrofuran containing excess *t*-butylisocyanide. The compound forms pale yellow diamagnetic crystals and is air-sensitive, particularly in solution in ether and in aromatic hydrocarbons.

Although the interaction of methyllithium with $ReX(CO)_5$ gives $Li[cis\text{-}ReX\{C(O)Me\}(CO)_4]$[6], alkylation of the isocyanide complex gives only the methyl, $ReMe(CNBu^t)_5$, as petroleum-soluble orange crystals. The Re–CH_3 proton resonance occurs at δ 1.09 ppm while the $^{13}C\{^1H\}$ peak is at δ 27.15 ppm.

Relatively few ethyl complexes of transition metal are known except where coordination sites are blocked by firmly held ligands that inhibit β-hydride transfer.[7] The compound $ReEt(CNBu^t)_5$ is, as expected, reasonably thermally stable but is air sensitive. The Re–Et resonance is at δ 3.26 *q*, ^3J(H–H) = 9 Hz (CH_2CH_3) and 2.25 *t*, ^3J(H–H) = 9 Hz (CH_2CH_3). In the $^{13}C\{^1H\}$ spectrum the carbons of C_2H_5 are at δ 23.7 ppm, *s* (CH_3) and 27.1 *s* (CH_2), the assignment being confirmed by the off set proton decoupled spectrum where CH_2 is a triplet and CH_3 a quartet.

(b) t-*Butylisocyanide-trimethylphosphine complexes*

The interaction of pentakis(trimethylphosphine)-

*Authors to whom correspondence may be addressed.

chlororhenium(I)[8] with an excess of Bu^{t}NC gives an air-sensitive, petroleum soluble, orange crystalline complex whose ^{1}H, ^{13}C{^{1}H} and ^{31}P{^{1}H} NMR spectra and analysis indicate that it is the octahedral $ReCl(CNBu^t)_2(PMe_3)_3$ with *trans*-isocyanide and *mer*-PMe_3 groups.

The molecular structure of the *bis*-isocyanide is shown in Fig. 1 and selected geometry parameters are given in Table 1. Although numerous structures of transition metal isocyanides are known, only two rhenium complexes, the rhenium(IV) salt $(Bu_4^nN)[ReCl_5(CNMe)]$[9] and the rhenium(III) complex $ReBr_3(CNp\text{-}tolyl)_4$[4] appear to have been studied. In both of these compounds the isocyanides are essentially linear at nitrogen and the Re–C distances are 2.14(3)Å for the chloride and 1.964(6)–2.014(7)Å for the bromide. In the present complex, the two Bu^{t}NC ligands are mutually *trans* and although the angle at nitrogen differs considerably [175(1)° for N(111) and 159(1)° for N(112)], the corresponding Re–C distances are equal within the limits of experimental error at 2.004(7) and 2.003(7)Å. Accordingly, it seems reasonable to assume that both ligands bond in the "normal", i.e. linear fashion, Re–$\bar{C}\equiv\overset{+}{N}$–R, with bending at N(112) a consequence of steric factors. This model is in agreement with the position of the isocyanide stretch in the infrared spectrum where a band due to linear isocyanide occurs.[10] The Re–P distances show the expected differences, with those mutually *trans* to each other (and hence competing in the π-back bonding process) considerably longer, *ca.* 0.1Å, than that *trans* to the Re–Cl bond.

Table 1. Selected bond lengths and angles for $ReCl(CNBu^t)_2(PMe_3)_3$

(a) Bond lengths (Å)			
Re–P(1)	2.385(2)	Re–Cl	2.570(2)
Re–P(2)	2.371(2)	Re–C(111)	2.004(7)
Re–P(3)	2.289(2)	Re–C(211)	2.003(7)
C(111)–N(111)	1.128(9)	C(211)–N(211)	1.151(9)
C(112)–N(111)	1.438(10)	C(212)–N(211)	1.484(9)
P–C(Me)	1.825(10)–1.890(10)	Avge	1.85
(b) Bond angles (deg)			
Cl–Re–P(1)	84.7(1)	P(1)–Re–P(3)	95.2(1)
Cl–Re–P(2)	85.3(1)	P(2)–Re–P(3)	95.8(1)
Cl–Re–P(3)	171.5(1)	P(1)–Re–P(2)	167.1(1)
C(111)–Re–Cl	94.2(3)	C(211)–Re–Cl	83.8(2)
C(111)–Re–P(3)	94.3(3)	C(211)–Re–P(3)	87.7(2)
C(111)–Re–P(1)	86.1(2)	C(211)–Re–P(1)	93.0(2)
C(111)–Re–P(2)	86.5(2)	C(211)–Re–P(2)	94.1(2)
Re–P–C(Me)	114.1(4)–120.7(4)	Avge	117.9

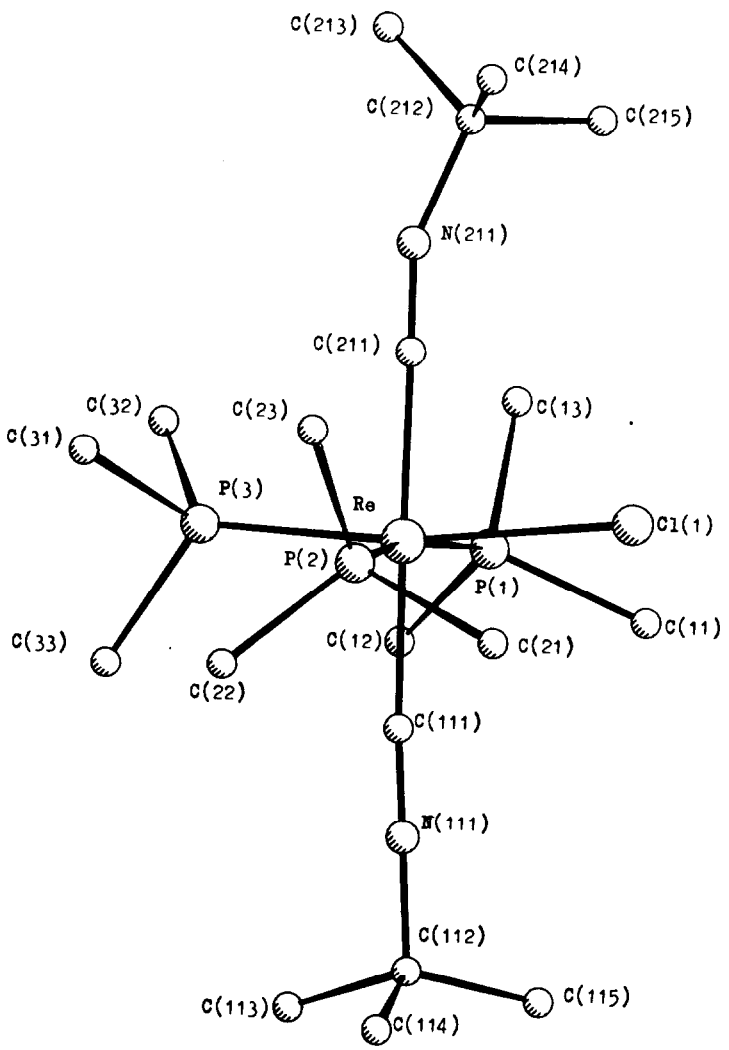

Fig. 1.

Interaction of the above complex with additional Bu^{t}NC under more forcing conditions in toluene at 90°C for 16 hr gives a similar monomeric orange complex, $ReCl(CNBu^t)_3(PMe_3)_2$, for which NMR data indicates *trans*-PMe_3 and *mer*-Bu^{t}NC groups. Unlike the *bis*-isocyanide which has linear M–C–N groups (CN stretches in IR at 2080m, 1900vs, br, and 1780m) the *tris* species has bands at 2080s, 2010vs, br, 1940s, 1830s, and 1791s cm^{-1}. The low C–N stretch can be attributed to a bent isocyanide.[2,10] The ^1H NMR also has two singlets for the Bu^t group in a ratio 2:1 indicating two types of Bu^{t}NC groups, but spectroscopic data does not indicate which of the *mer* Bu^{t}NC groups is bent. The structure of the complex has been investigated by X-ray crystallography but serious disorder has made it impossible to obtain a well defined set of parameters (see Experimental).

At the present stage of refinement the three isocyanide ligands are seen to have a *mer* configuration, and show three different geometries. The ligand *trans* to chlorine is significantly bent at the nitrogen atom, with C–N̂–C = 141(6)° and also at carbon, with Re–Ĉ–N = 155(5)°. Of the other two ligands, which are *trans* to each other, one is quite linear with Re–Ĉ–N = 173(4)° and C–N̂–C = 175(5)° while the other shows a small degree of bending, with Re–Ĉ–N = 167(5) and C–N̂–C = 155(5)°. The Re–C distances to those ligands are essentially equal at 2.00(5) and 2.03(6)Å and are similar to those in previous compounds, but are longer than the distance involving the "bent" ligand where Re–C is 1.94(5)Å. This is presumably a reflection of a greater degree of π-back bonding to the ligand *trans* to chlorine, and the geometry of this ligand corresponds to a significant contribution from the canonical form.

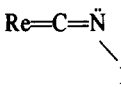

Whether the bending of these ligands is due in the first instance to steric or electronic factors, the greater the bending at nitrogen, the more basic will this atom become. It is therefore logical to propose that it is the ligand *trans* to chlorine which is protonated as discussed below.

(c) *Protonation of trimethylphosphine isocyanide complexes*

(i) $ReCl(CNBu^t)_2(PMe_3)_3$. Interaction of this complex with one equivalent of fluoroboric acid in diethylether at −78°C led to the yellow air stable crystalline salt $[ReCl(CNBu^t)(CNHBu^t)(PMe_3)_3]BF_4$, which is soluble in THF and methanol in which it is a 1:1 electrolyte. The $^{31}P\{^1H\}$ NMR spectrum indicates a *mer* configuration for the PMe_3 groups as in (1). The $^{13}C\{^1H\}$ spectrum shows

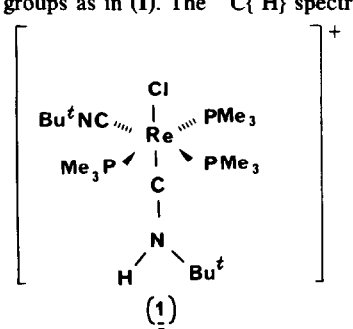

(1)

the Bu^{t}NC group to be *trans* to a phosphine (δ 146.0 ppm) while the carbyne carbon of the CNHBu^t group is *cis* to all phosphines giving a quartet (δ 226.8 ppm). The ^{13}C spectrum also shows "virtual coupling"[11] as the resonances of the carbon atom of the phosphine *trans* to each other are an apparent 1:2:1 triplet. This effect is also seen in the proton resonance spectra for the protons on the *trans* phosphines. The configurational change from that of the starting material accords with the best π-accepting ligand being *trans* to a non-π-bond ligand, i.e., chloride. Other examples of this situation are well known, one case being *trans*-$CrBr(CNEt_2)(CO)_4$.[12]

The IR spectrum of the salt has bands at 3238 cm^{-1} (NH) and 1560 cm^{-1} (C=N). Together with the position of the $^{13}C\{^1H\}$ carbyne resonances it indicates that the bonding lies between the canonical forms

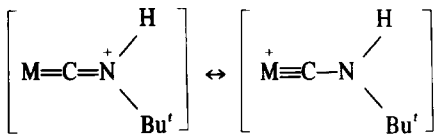

as discussed for Mo and W compounds.[13]

(ii) $ReCl(CNBu^t)_3(PMe_3)_2$. Protonation here gives the pale green air-stable salt $[ReCl(CNBu^t)_2(CNHBu^t)(PMe_3)_2]BF_4$ which is soluble in THF and methanol. The NMR data confirm the structure (2) with *trans*-CNBu^t

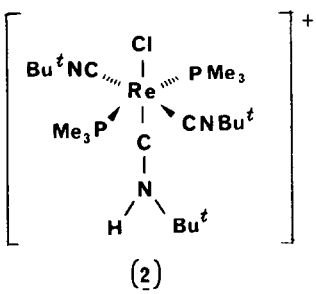

(2)

and *trans* PMe_3 groups. The CNHBu^t group is *trans* to chlorine. Both ^1H and $^{13}C\{^1H\}$ spectra again show virtual coupling due to *trans* phosphines.

The two isocyanides can be protonated only once, presumably due to the lowered basicity of nitrogen in these systems. For *trans*-$M(CNR)_2(dppe)_2$ M=Mo, W, mono or diprotonation can occur,[13] whereas for $Fe(CNBu^t)_5$ protonation occurs at the metal.[14]

2. HEXAKIS(*t*-BUTYLISOCYANIDE)CHROMIUM(0)

Although this compound was first made from $Cr_2(C_8H_8)_3$,[15] which in turn was made by metal atom vapour techniques, it is much more readily obtained by the method used[1] for $Mo(CNBu^t)_6$, namely reduction of the acetate $Cr_2(CO_2Me)_4$ by sodium amalgam in tetrahydrofuran containing excess ligand.

3. TUNGSTEN COMPLEXES

A similar reaction to the above, but using $W_2(mhp)_4$ (mhpH = 2-methyl-6-hydroxypyridine)[16] gave the dark red, very petroleum soluble and air-sensitive *hexakis*(*t*-butylisocyanide)tungsten(0); this completes the isoleptic Group VI compounds. Other zerovalent isocyanides, can probably be made similarly, indeed, after completion of our studies, $W(CNPh)_6$ has been made from $W_2(dmhp)_4$, dmhp being the anion of

2,4-dimethyl-6-hydroxypyrimidine[17] in 30% yield, but in the absence of sodium amalgam.

The reaction of $W_2(mhp)_4$ with excess Bu^{t}NC in ether–methanol (the procedure used for cleavage of the dimeric acetates by isocyanide[2]) gives by contrast a binuclear ditungsten(I) compound of stoichiometry $W_2(mhp)_2(CNBu^t)_4$. This is a diamagnetic air-stable orange crystalline solid, slightly soluble in petroleum, but very soluble in aromatic hydrocarbons. So far attempts to obtain crystals of X-ray quality from these and other solvents have not been successful. The spectroscopic data however, are consistent with a structure having mhp bridges and terminal isocyanide groups as in (3); since

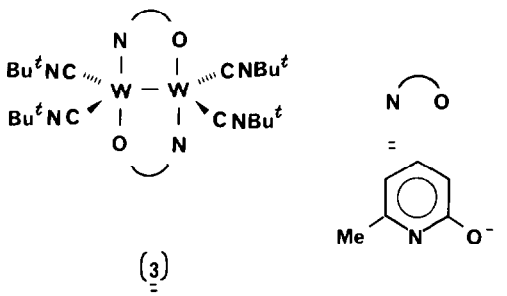

(3)

there are two sets of equivalent Bu^{t}NC groups; the bridge ligands are probably at 90° or thereabouts. Attempts to detect the metal–metal bond absorption by laser Raman spectroscopy failed due to fluorescence and decomposition.

4. *t*-BUTYLISOCYANIDE(TRIMETHYLPHOSPHINE) CIS-DIMETHYLPLATINUM(II)

Although methyl complexes can undergo insertion reactions[1] with Bu^{t}NC and other isocyanides, the interaction of *cis*-$PtMe_2(PMe_3)_2$ with Bu^{t}NC gives the air stable *cis*-$PtMe_2(PMe_3)(CNBu^t)$, where only one PMe_3 group has been substituted. The structure of the compound is fully established by ^1H, $^{13}C\{^1H\}$ and $^{31}P\{^1H\}$ NMR spectra. In these spectra weak bands due to ^{195}Pt couplings are observed except for resonances of the Bu^{t}NC ligand; there is no appreciable coupling or broadening of the $^{13}C\{^1H\}$ spectra due to ^{14}N. No ^{13}C signal was observed for the carbon of the isocyanide, which is consistent with the long relaxation time and low Overhauser effect associated with this carbon atom. The $^{195}Pt\{^1H\}$ spectrum consists of a doublet of 1:1:1 triplets, centred at $\delta + 210.6$ (in ppm to high frequency of Ξ $^{195}Pt = 21.4$ MHz[18]) with $J(^{195}Pt–^{31}P) = 1686$ Hz and $^2J(^{195}Pt–^{14}N) = 62$ Hz; there are relatively few examples of Pt–N splitting through two bonds.

EXPERIMENTAL

Microanalyses by Pascher (Bonn) and Imperial College Laboratories. Molecular weights were determined cryoscopically in benzene. Melting points (uncorrected) were determined in sealed tubes under nitrogen. All operations were carried out under oxygen-free nitrogen or argon or in vacuum. Solvents were dried over sodium or sodium-benzophenone and were distilled under nitrogen before use. The petroleum used had b.p. 40–60°C unless otherwise stated.

Spectrometers

NMR. Perkin-Elmer R32 (^1H, 90 MHz); Bruker WM-250 (^1H,250; $^{13}C\{^1H\}$, 62.9; $^{31}P\{^1H\}$ 101.27; ^{195}Pt, 53.8 MHz): data in δ ppm referenced to $SiMe_4$ and 85% H_3PO_4 (external) at 36°C in deuteriobenzene unless otherwise stated. *IR.* Perkin-Elmer 683; spectra in Nujol mulls unless otherwise stated; data in cm^{-1}, PMe_3 bands omitted.

(1) Pentakis(t-*butylisocyanide*)*chlororhenium*(*I*)

A suspension of $ReCl_4(THF)_2$ (1.8 g, 3.8 mmol) in THF (100 cm^3) was added to excess Bu^{t}NC (3 cm^3, 30 mmol) in THF (50 cm^3) with excess Na/Hg (1 g in 5 cm^3 Hg) and the mixture stirred for 18 hr at room temperature. The orange-yellow solution was filtered, concentrated to *ca.* 2 cm^3 and cooled at −20°C to give yellow crystals. Yield: 2.0 g, 85%; m.p., 184–185°C. [Found: C 46.1 (47.1); H 7.0 (7.1); Cl 5.3 (5.6); N 10.8 (10.0)%. *M* 620 (635.5).]

NMR. ^1H: 1.36 s (9); 1.16 s (36) C*Me*$_3$.

$^{13}C\{^1H\}$: 31.46 s (12), 32.90 s (3), C*Me*$_3$; 55.40 s, 55.49 s, *C*Me$_3$; 156.76, 190.37 *C*NBu^t.

IR. 2100s, 2010br,s, 1830br,s, 1770sh, 1455s, 1365m, 1230m, 1200s, 1115m, 1045w, 1032, 970w, 925w, 892w, 745m, 725s, 632w, 556s, 500w, 430s.

(2) Pentakis(t-*butylisocyanide*)*methylrhenium*(*I*)

To $ReCl(CNBu^t)_5$ (0.42 g, 0.65 mmol) in diethylether (40 cm^3) at −78°C was added MeLi (0.25 cm^3, 2.5 M in Et_2O) and the mixture allowed to warm to room temperature with stirring. After 4 hr the mixture was evaporated, the residue extracted with petroleum (30 cm^3), the solution filtered, concentrated to *ca.* 2 cm^3 and cooled at −20°C to give orange crystals. Yield: 0.33 g, 80%; m.p., 96–97°C. [Found: C 50.1 (50.6); H 7.8 (7.8); N 10.9 (11.3)%. *M* 610 (616).]

NMR. ^1H: 1.45 s (9), 1.29 s (36), C*Me*; 1.09 s (3) Re-*Me*.

$^{13}C\{^1H\}$: 27.15 s Re-*Me*; 32.00 s (12), 32.5 s (3) C*Me*$_3$; 55.01 s 55.10 s, *C*Me$_3$; 165.87 s, 185.30 s, Re-*C*-N.

IR. 2100s, 2010br,s, 1830br,s, 1770sh, 1460s, 1365m, 1230m, 1200s, 1115w, 1035w, 888w, 875w, 742w, 730s, 556s, 432s.

(3) Pentakis(t-*butylisocyanide*)*ethylrhenium*(*I*)

As for the methyl compound but using $ReCl(CNBu^t)_5$ (1.14 g, 1.75 mmol) in petroleum (100 cm^3) and ethyllithium (2.0 cm^3, 0.95 M in toluene) to give orange crystals. Yield: 0.94 g, 83%; m.p., 80–81°C. [Found: C 50.4 (51.4); H 7.9 (7.9); N 11.2 (11.1)%. M, 620 (630).]

NMR. ^1H: 32.6 q (2), $^3J(H–H) = 8$ Hz, C*H*$_2$Me; 2.25 t (3), $^3J(H–H) = 9$ Hz, CH$_2$*Me*, 1.34 s (9), 1.20 s (36), C*Me*$_3$.

$^{13}C\{^1H\}$: 23.70 s, ReCH$_2$*Me*$_3$; 27.11 s, ReCH$_2$Me; 31.89 s (12), 32.67 s (3), C*Me*$_3$; 54.83 s, 54.94 s, *C*Me$_3$; 165.42 s, 186.34 s, Re-*C*-N.

IR. 2100s, 2010s, 2010br,s, 1800br,s, 1755sh,s, 1368m, 1230m, 1200s, 1118w, 1035w, 910w, 882w, 875w, 742m, 730s, 659w, 558s, 435s.

(4) *a,f* - Bis(t - *butylisocyanide*) - c,d,e - tris(*trimethylphosphine*) - *chlororhenium*(*I*)

To $ReCl(PMe_3)_5$ (1.0 g, 1.7 mmol) in Et_2O (50 cm^3) was added Bu^{t}NC (1.0 cm^3, 10 mmol) at room temperature and the mixture stirred for *ca.* 12 hr. After evaporation in vacuum the residue was extracted into petroleum (2 × 30 cm^3), the solution filtered, concentrated to *ca.* 3 cm^3 and cooled to −20°C to give orange crystals. Yield: 0.8 g, 80%; m.p., 164–5°C. [Found: C 37.6 (37.0); H 7.1 (7.3); Cl 6.0 (5.8); N 4.2 (4.5); P 15.6 (15.1)%. *M* 590 (615.5).]

NMR. ^1H: 12.1 s (18) C*Me*$_3$; 1.45 d (9), $^2J(P–H) = 6$Hz, 1.70 "*t*" (18) $^2J(P–H) + {}^4J(P–H) = 6$ Hz, P*Me*$_3$.

$^{13}C\{^1H\}$: 170.8 $t^2J(C–P) = 10$ Hz, *C*NBu^t; 54.9 s, *C*Me$_3$; 31.8 s *C*Me$_3$; 27.5 d $^1J(P–C) = 26.9$ Hz, 30.6 "*t*" $^1J(P–C) + {}^3J(P–C) = 29.4$ Hz, P*Me*$_3$.

$^{31}P\{^1H\}$: −35.7 s (2); −37.9 s(1).

IR. 2080m,sh, 1930vbr,s, 1780m,sh.

(5) c,d,e - Tris(t - *butylisocyanide*) - a,f - bis(*trimethylphosphine*)-*chlororhenium*(*I*)

To $ReCl(CNBu^t)_2(PMe_3)_3$ (0.4 g, 0.6 mmol) in toluene (70 cm^3) was added Bu^{t}NC (0.5 cm^3, 5.0 mmol) and the solution stirred at 90°C for 18 hr. The solution was filtered, evaporated and the residue extracted into petroleum (40 cm^3) which was filtered, concentrated to *ca.* 2 cm^3 and cooled at −20°C to give yellow crystals. Yield: 0.3 g, 80%; m.p., 196–7°C. [Found: C 40.3 (40.5);

H 7.1 (7.2); Cl 5.8 (5.7); N 7.0 (6.7); P 9.7 (10.0)%. *M* 610 (622.5).]

NMR. ^{1}H: 1.35 s (18), 1.57 s(9), C*Me*$_3$; 2.0 "*t*" (18) ^2J(P–H) + ^4J(P–H) = 7.0 Hz, P*Me*$_3$.

^{13}C{^{1}H}: 163.0 s *C*NCMe$_3$; 55.1 s, 53.6 s, *C*Me$_3$; 33.1 s, 32.0 s, C*Me*$_3$; 18.8 "*t*" ^1J(P–C) + ^3J(P–C) = 29.6 Hz, P*Me*$_3$.

^{31}P{^{1}H}: −33.2 s, *P*Me$_3$.

IR. 2080s,sh, 2010vbr,s, 1940s,sh, 1830s,br, 1791s.

(6) a - (t - *butylaminomethylidyne*) - f - (t - *butylisocyanide*)tris(*trimethylphosphine*) - *chlororhenium*(*I*) *tetrafluoroborate*

To a solution of ReCl(CNBu^t)$_2$(PMe$_3$)$_3$ (0.4 g, 0.67 mmol) in diethyl ether (50 cm^3) at −78°C was added fluoroboric acid (0.1 cm^3 of 40% aqueous, 0.67 mmol) to give a yellow precipitate on warming to room temperature. The mixture was evaporated in vacuum, washed with petroleum (50 cm^3), diethylether (30 ml) and dissolved in THF (50 cm^3). On filtering, concentrating to 15 cm^3 and cooling to −20°C yellow crystals were obtained. Yield: 80%; m.p., 207°C. [Found: C 31.2 (31.6); H 6.1 (6.4); N 3.8 (3.8); Cl 4.9 (5.1)%.] Λ_M (MeOH, 25°C), 95 Ω^{-1} cm^2 mol^{-1}.

NMR. ^{1}H (d$_4$-MeOH): 1.76 "*t*" (18) ^2J(P–H) + ^4J(P–H) = 7.36 Hz, 1.67 d (9) ^2J(P–H) = 8.42 Hz, P*Me*$_3$; 1.62 s (9), CNC*Me*$_3$, 1.37 s (9), CNHC*Me*$_3$.

^{13}C{^{1}H}: 226.8 q ^2J(C–P) = 11.8 Hz, *C*NHCMe$_3$; 146.0 d m ^2J(C–P) = 64 Hz, *C*NCMe$_3$; 59.3 s, CN*C*Me$_3$; 53.5 s, CNH*C*Me$_3$; 30.7 CNC*Me*$_3$; 30.6 s, CNHC*Me*$_3$; 20.1 d, ^1J(C–P) = 30.8 Hz; 18.9 "*t*" ^1J(C–P) + ^3J(C–P) = 32.8 Hz, P*Me*$_3$.

^{31}P{^{1}H}: −35.9 *t*, ^2J(P–P) = 21 Hz; −38.9 d.

IR. 3238s, N–H; 2150 s C≡N; 1560 brs, C=N.

(7) a - (t - *butylaminomethylidyne*) - *b,d* - bis(t-*butylisocyanide*) - *c,e*-bis(*trimethylphosphine*)*chlororhenium*(*I*)*tetrafluoroborate*

To a solution of ReCl(CNBu^t)$_3$(PMe$_3$)$_2$ (0.24 g, 0.38 mmol) in THF (50 cm^3) at −78°C was added fluoroboric acid (7×10^{-2} cm^3 of 40% aqueous, 0.38 mmol) to give a green precipiate which dissolved at room temperature. After stirring overnight the solution was evaporated in vacuum and the solid washed with petroleum (50 cm^3) and ether (30 cm^3). The resulting solid was dissolved in THF (40 cm^3), concentrated to 10 cm^3 and cooled to −20°C to give pale green crystals. Yield: 80%; m.p., 207°C dec. [Found: C 34.5 (35.4); H 6.6 (6.6); N 5.3 (5.9)%.] Λ_M (MeOH, 25°C), 88 Ω^{-1} cm^2 mol^{-1}.

NMR. ^{1}H (d$_4$-MeOH): 1.71 "*t*" (9) ^2J(P–H) + ^4J(P–H) = 7.98 Hz, P*Me*$_3$; 1.55 s (18), CNC*Me*$_3$; 1.31 s (9) CNHC*Me*$_3$.

^{13}C{^{1}H}: 228.6 t, ^2J(P–C) = 10.3 Hz, *C*NHCMe$_3$, 149.3 br *C*NCMe$_3$; 59.3 s, CN*C*Me$_3$; 53.7 s, CNH*C*Me$_3$; 30.75 s, CNC*Me*$_3$; 30.68 (CNHC*Me*$_3$; 18.0 "*t*", ^1J(P–C) + ^3J(P–C) = 32.8 Hz, P*Me*$_3$.

^{31}P{^{1}H}: −32.1 s *P*Me$_3$.

IR. 3220s, N–H; 2130s, C≡N; 1570br,s C=N.

(8) Hexakis(t-*butylisocyanide*)*chromium*(*O*)

To a suspension of Cr$_2$(CO$_2$Me)$_4$ (1.0 g, 2.84 mmol) in THF (60 cm^3) with Na/Hg (1.0 g, in 100 g Hg) was added Bu^{t}NC (3.5 cm^3, 35 mmol) and the mixture stirred for 24 hr at room temperature. After filtration and evaporation the solid residue was extracted into petroleum (60 cm^3) which was filtered, reduced to *ca.* 20 cm^3 and cooled to −20°C to give red brown crystals, which were collected and dried in vacuum. Yield: 1.4 g, 90%, decomp. 139–141°C. [Found: C 65.0 (65.6); H 9.8 (9.8); N 14.9 (15.3)%. *M* 540 (550).]

NMR. ^{1}H: 1.40 s C*Me*$_3$.

^{13}C{^{1}H}: 192.2 s *C*NBu^t; 55.22 s, *C*Me$_3$; 32.36 s C*Me*$_3$.

IR. 2100w, 1960vbr,s, 1870v,br,s, 1360s, 1230s, 1200br,s, 1032w, 880m, 736s, 630br,w, 622br,w, 430s.

(9) Hexakis(t-*butylisocyanide*)*tungsten*(*O*)

To a suspension of W$_2$(mhp)$_4$[16] (1.0 g, 1.24 mmol) in THF (70 cm^3) with Na/Hg (1.0 g, in 100 g Hg) was added Bu^{t}NC (2.0 cm^3, 20 mmol) and the mixture stirred (24 hr) at room temperature. After filtration and evaporation the residue was extracted into petroleum (50 cm^3) which was filtered, reduced to *ca.* 15 cm^3 and cooled at −20°C to yield red crystals which were collected and dried in vacuum. A second batch of crystals were obtained on further concentration and cooling of the solution. Yield: 0.76 g, 88%; m.p., 82–84°C. [Found: C 51.2 (51.4); H 7.6 (7.7); N 11.8 (12.0)%. *M* 690 (682).]

NMR. ^{1}H. 1.43 s, C*Me*$_3$.

^{13}C{^{1}H}: 193.15 s *C*NBu^t; 55.40 s, *C*Me$_3$; 32.25 s, C*Me*$_3$.

IR. 2100w, 1955v,br,s, 1865v,br,s, 1360s, 1228s, 1210br,s, 1032w, 875m, 735s, 630br,w, 625br,w, 432s.

(10) Tetrakis (t - *butylisocyanide*)bis(*μ* - 2 - *oxo* - 6 - *methylpyridinato*)*ditungsten*(*I*), (*W–W*)

Excess Bu^{t}NC (1.5 cm^3, 15 mmol) was added to W$_2$(mhp)$_4$ (1.2 g, 1.5 mmol) in Et$_2$O (60 cm^3) and MeOH (10 cm^3), and the mixture refluxed for 48 hr. The volatile materials were removed under vacuum and the residue extracted with petroleum (3 × 40 cm^3). The extract was filtered, concentrated to *ca.* 60 cm^3 and cooled to give an orange crystalline solid. Yield: 0.59 g, 70%; m.p., 204–5°C. [Found: C 41.1 (41.9); H 5.3 (5.2); N 8.7 (9.2); O 4.7 (3.5)%. M 850 (916)].

NMR. ^{1}H: 7.0 m, 6.3 m, 5.7 m, protons on pyridine; 2.9 s, 2.8 s, Me on pyridine; 1.6 s, 1.57 s, 1.0 s, 0.8 s, C*Me*$_3$.

^{13}C{^{1}H}: 219.4, 217.2 m *C*NBu^t; 61.6, 61.2, 56.2, 55.3, *C*Me$_3$; 31.9, 30.7, C*Me*$_3$; 24.6, 23.7, C*H*$_3$ on pyridine; 110.9, 109.0, 108.0, 107.1, aromatic carbons of pyridine.

IR. 3030w, 3010w, 2110w, 2080s, 2050s, 1607m, 1600m, 1554w, 1519w, 1485s, 1470s, 1449s, 1361m, 1352m, 1260w, 1230w, 1200m, 1150w, 1009w, 970m, 875w, 795m, 790, 779m, 742m, 740m, 720m, 574w, 530m, 515m.

(11) t-*Butylisocyanide*(*trimethylphosphine*)cis-*dimethylplatinum*-(*II*)

Excess Bu^{t}NC (2 cm^3, 20 mmol) was added to *cis*-PtMe$_2$(PMe$_3$)$_2$[19] (1.0 g, 2.65 mmol) in petroleum (20 cm^3) and the mixture stirred for 5 hr at room temperature. After evaporation, the residue was washed with petroleum and extracted into toluene (2 × 20 cm^3), the solution filtered, concentrated to *ca.* 5 cm^3 and cooled at −20°C to give colourless crystals. Yield: 0.8 g, 80%; m.p., 106–107°C. [Found: C 30.9 (31.3); H 6.3 (6.3); N 3.6 (3.6); P 7.7 (8.1)%. *M* 370 (384).]

NMR.^{1}H: 0.95 s (9) C*Me*$_3$; 1.17 d (9), ^2J(P–H) = 8.5 Hz, ^3J(P–H) = 20.6 Hz, P*Me*$_3$; 0.87 d (3), ^3J(P–H) = 9.7 Hz, ^2J(Pt–H) = 70 Hz, *Me* (*trans*-P); 1.3 d (3), ^3J(P–H) = 7.7 Hz, ^2J(Pt–H) = 71 Hz, *Me*(*cis*-P).

^{13}C{^{1}H}: 30.2 s C*Me*$_3$; 56.1 s *C*Me$_3$; 15.6 d, ^1J(P–C) = 28 Hz, ^2J(Pt–C) = 56 Hz, P*Me*$_3$; −1.6 d ^2J(P–C) = 106 Hz, ^2J(Pt–C) = 570 Hz, *C*H$_3$ (*trans*-P); −2.7 d, ^2J(P–C) = 7.4 Hz, ^1J(Pt–C) = 606 Hz, *C*H$_3$ (*cis*-P).

^{31}P{^{1}H}: −23.6, ^1J(Pt–P) = 1690 Hz, *P*Me$_3$.

^{195}Pt{^{1}H} see text.

IR. 2175vs, 2062s, 1465s, 1420m, 1410w, 1390m, 1305w, 1285m, 1230m, 1200vs, 1043w, 945vs, 850m, 730s, 678m, 544m, 525m, 508, 460w.

CRYSTALLOGRAPHIC STUDIES

Crystal data

(a) ReCl(CNBu^t)$_2$(PMe$_3$)$_3$, M = 616.16. Monoclinic, space group $P2_1/a$, a = 25.855(3), b = 9.855(4), c = 11.387(2)Å, β = 98.71(1)°, Z = 4, D_c = 1.42 g cm^{-3}, μ(MoK_α) = 42.98 cm^{-1}.

(b) ReCl(CNBu^t)$_3$(PMe$_3$)$_2$, M = 623.2. Orthorhombic, space group $P2_12_12_1$, a = 9.679(4), b = 10.882(1), c = 29.155(4), Z = 4, D_c = 1.35 g cm^{-3}, μ(MoK_α) = 39.68 cm^{-1}.

Data collection

CAD4 diffractometer, graphite monochromated MoK_α radiation, λ = 0.71069Å, $\omega/2\theta$ scan mode. ReCl(CNBu^t)$_2$(PMe$_3$)$_3$, $1.5 \le \theta \le 28.0°$, ω scan width = $0.85 + 0.35 \tan \theta$, ω scan speed 1.27–6.77 deg min^{-1}, T = 298 K, 6886 unique data measured, 4747 observed [$I > 1.5\sigma(I)$]. ReCl(CNBu^t)$_3$(PMe$_3$)$_2$, $1.5 \le \theta \le 25.0°$, ω scan width = $0.65 + 0.35 \tan \theta$, ω scan speed 1.27–6.77 deg min^{-1}, T = 298 K, 3239 unique data measured, 2327 observed [$I > 1.5\sigma(I)$].

Both sets of data were corrected for absorption empirically.[20]

Structure solution and refinement

Both analyses gave problems. For $ReCl(CNBu^t)_2(PMe_3)_3$ the solution was straightforward, but refinement was difficult due to excessive anisotropic thermal motion and/or positional disorder in the Bu^t groups. Eventually, a reasonably stable model was obtained, although some of the carbon atom temperature factors are extremely anisotropic. Unfortunately it did not prove possible to establish a model in which the Bu^t groups could be represented by multiple positioning and fractional occupancy. Nevertheless, the reasonably low R values (see below) suggest that the model presented may be considered an acceptable one, in spite of its deficiencies.

For $ReCl(CNBu^t)_3(PMe_3)_2$ the structure solution and refinement were extremely difficult due to heavy atom pseudo-symmetry. The pseudo special positioning of the rhenium atom very close to 1/4, O, Z produced $2/m$ pseudo symmetry in the electron density maps. Development of the structure was eventually achieved by not refining any atomic parameters until the whole molecule had been identified. Subsequent refinement has still proved difficult even after using the DFIX facility in SHELX[21] to fix the lengths of P–C(Me) and C–C(Me) bonds to standard values, and we have not yet achieved an acceptable model. We believe this to be due to a mixture of excessive disorder and the residual effects of pseudo symmetry. Accordingly, we defer presenting these results until data has been recollected at low temperature.

Final $R(=\Sigma||F|/\Sigma|F_0|)$ and $R\omega$ $(=\Sigma\omega^{1/2}|\Delta F|/\Sigma\omega^{1/2}|F_0|)$ values for $ReCl(CNBu^t)_2(PMe_3)_3$, are 0.043 and 0.044.

Final atomic coordinates, thermal parameters and a list of F_0/F_0 values have been deposited with the Editor as supplementary data.†

Acknowledgement—We thank the S.E.R.C. for support.

†Copies are available on request from the Editor at Queen Mary College. Tables of atomic coordinates have also been deposited with the Cambridge Crystallographic Data Centre, University Chemical Laboratory, Lensfield Road, Cambridge, CB2 1EW.

REFERENCES

[1] K. W. Chiu, R. A. Jones, G. Wilkinson, A. M. R. Galas and M. B. Hursthouse, *J. Chem. Soc., Dalton Trans.* 1981, 2088.

[2] G. S. Girolami and R. A. Andersen, *Inorg. Chem.* 1981, **20**, 2040.

[3a] M. Freni and P. Romiti, *J. Organometal. Chem.* 1975, **87**, 241; [b] P. M. Treichel and J. P. Williams, *J. Organometal. Chem.* 1977, **135**, 39.

[4] P. M. Treichel, J. P. Williams, W. A. Freeman and J. I. Gelder, *J. Organomet. Chem.* 1979, **170**, 247.

[5] J. D. Allison, C. J. Cameron, R. E. Wild and R. A. Walton, *J. Organometal. Chem.* 1981, **218**, C62.

[6] K. P. Darst and C. M. Lukehart, *J. Organometal. Chem.* 1979, **171**, 65.

[7] See $(\eta^5\text{-}C_5H_5)M(CO)_3Et$, M = Cr, Mo, W, T. S. Piper and G. Wilkinson, *J. Inorg. Nucl. Chem.* 1956, **3**, 104.

[8] K. W. Chiu, C. G. Howard, H. S. Rzepa, R. N. Sheppard, G. Wilkinson, A. M. R. Galas and M. B. Hursthouse, *Polyhedron* 1982, **1**, 441.

[9] K. W. Chiu, C. G. Howard, M. S. Rzepa, R. N. Sheppard, G. Wilkinson, A. M. R. Galas and M. B. Hursthouse, *Polyhedron* 1982, 1 in press.

[10] J. M. Bassett, M. Green, J. A. K. Howard and F. G. A. Stone, *J. Chem. Soc., Dalton Trans.* 1979, 1003; J. Chatt, A. J. L. Pombeiro, R. L. Richards, G. H. D. Royston, K. W. Muir and R. Walker, *J. Chem. Soc., Chem. Commun.* 1975, 708.

[11] R. K. Harris, *Can. J. Chem.* 1964, **42**, 2275; D. E. Axelson and C. E. Holloway, *J. Chem. Soc., Chem. Commun.* 1973, 455; D. A. Redfield, J. H. Nelson and L. W. Cary, *Inorg. Nuclear Chem. Letts.* 1974, **10**, 727.

[12] E. O. Fischer and U. Schubert, *J. Organometal. Chem.* 1975, **100**, 49; E. O. Fischer, G. Hutner, W. Kleine and A. Frank, *Angew. Chem. Int. Ed. Eng.* 1975, **14**, 700.

[13] J. Chatt, A. J. L. Pombeiro and R. L. Richards, *J. Chem. Soc., Dalton Trans.* 1980, 492.

[14] J. M. Bassett, L. J. Farrugia and F. G. A. Stone, *J. Chem. Soc. Dalton Trans.* 1980, 1789.

[15] P. L. Timms and T. W. Turney, *J. Chem. Soc., Dalton Trans.* 1976, 2021.

[16] F. A. Cotton, P. E. Fanwide, R. H. Niswander and J. C. Sekutowski, *J. Am. Chem. Soc.* 1978, **100**, 4725.

[17] D. D. Klenworth, W. W. Welters III and R. A. Walton, *J. Organometal. Chem.* 1981, **213**, C13.

[18] R. K. Harris and B. E. Mann, *NMR and the Periodic Table.* Academic Press, New York (1978).

[19] D. M. Adams, J. Chatt and B. L. Shaw, *J. Chem. Soc.* 1960, 2047.

[20] A. C. T. North, D. C. Phillips and F. S. Mathews, *Acta Cryst.* 1968, **A24**, 351.

[21] SHELX structure determinations program package, G. M. Sheldrick, University of Cambridge, 1976.

Polyhedron Vol. 1, No. 11-12, pp. 809-817, 1982
Printed in Great Britain.

0277-5387/82/110809-09$03.00/0
Pergamon Press Ltd.

BIS(DIPHENYLPHOSPHINO)METHANE TRIMETHYLPHOSPHINE ALKYL AND η^5-CYCLOPENTADIENYL COMPOUNDS OF RHODIUM(I); $^{31}P\{^1H\}$ TWO DIMENSIONAL δ/J RESOLVED AND OVERHAUSER EFFECT NUCLEAR MAGNETIC RESONANCE SPECTROSCOPY

KWOK W. CHIU, HENRY S. RZEPA,* RICHARD N. SHEPPARD, GEOFFREY WILKINSON* and WAI-KWOK WONG

Chemistry Department, Imperial College of Science and Technology, London, SW7 2AY, England

(*Received* 28 *April* 1982)

Abstract—Neutral mononuclear tertiary phosphine rhodium(I) complexes of the formula $RhX(PMe_3)(dppm)$, X = Cl, CH_2SiMe_3, CH_2CMe_3, CH_2CMe_2Ph, η^5-C_5H_5, dppm = *bis*(diphenylphosphino)methane, $RhCl(PPh_3)(dppm)$, $RhX(dppm)_2$, X = Cl, Me and $Rh(\eta^5$-$C_5H_5)(dppm)$ have been synthesised. In $Rh(\eta^5$-$C_5H_5)(PMe_3)(dppm)$, the dppm ligand is unidentate according to $^{31}P\{^1H\}$ NMR and X-ray data.

The $^{31}P\{^1H\}$ NMR spectral parameters of $RhX(PR_3)(dppm)$ have been determined by a combination of two dimensional δ/J resolved spectroscopy and heteronuclear nuclear Overhauser effect difference spectroscopy (NOEDS) in conjunction with iterative analysis of the one dimensional spectra.

INTRODUCTION

Although there is a variety[1-4] of mono- and bi-nuclear rhodium *bis*(diphenylphosphino)methane(dppm) complexes, neutral mononuclear species are rare. The neutral η^3-2-methylallyl *bis*(diphenylphosphino)methane rhodium(I)[2] exists as a dimer in solution, but is said to be monomeric, based on mass spectral evidence, in the solid state. Here we describe the synthesis and characterisation of several neutral mononuclear rhodium *bis*(diphenylphosphino)methane complexes.

The interaction of excess dppm with $[Rh(PMe_3)_4]Cl$ gives $RhCl(PMe_3)(dppm)$ and with $RhCl(PPh_3)_3$ gives $RhCl(PPh_3)(dppm)$ or $RhCl(dppm)_2$[3], depending on the conditions. In toluene solution, $RhCl(PMe_3)(dppm)$ reacts with Me_3SiCH_2Li, Me_3CCH_2MgBr, $PhMe_2CCH_2MgCl$ and C_5H_5Na to give, respectively, $Rh(CH_2SiMe_3)(PMe_3)(dppm)$, $Ph(CH_2CMe_3)(PMe_3)$-$(dppm)$, $Rh(CH_2CMe_2Ph)(PMe_3)(dppm)$ and $Rh(\eta^5$-$C_5H_5)(PMe_3)(dppm)$. In toluene solution, $RhCl(dppm)_2$ reacts with MeLi and C_5H_5Na to give $RhMe(dppm)_2$ and $Rh(\eta^5$-$C_5H_5)(dppm)$, respectively; the latter compound is also obtained by refluxing $Rh(\eta^5$-$C_5H_5)(PMe_3)(dppm)$ in toluene.

The ^{31}P proton decoupled spectra of these complexes can be complicated, due to the presence of both J_{PP} and J_{RhP} coupling. Since J_{PP} can be as large as 500 Hz in these systems, assignment with the aid of selective homonuclear double resonance experiments can be difficult or impossible to achieve by ordinary r.f. decoupling, due to the high power levels required. A more general approach is to obtain *J*-resolved 2D spectra, using the pulse sequence $90° - \tau_1 - 180° - \tau_1$-acquire ($\tau_2$) with a suitable set of values for τ_1, followed by successive Fourier transformations with respect to τ_2 (to achieve $\delta \pm J$ dispersion) and to τ_1 (to achieve *J* dispersion only). A rotation of 45° of the resulting data matrix gives a 2D spectrum which (in the weak coupling limit) can be projected onto one axis (the "δ" axis) to give the effect of a broadband homonuclear decoupled spectrum and onto the other axis (the "*J*" axis) to show only the homonuclear couplings.[5] A valuable feature of this approach is its ability to separate the homo- and heteronuclear coupling and to simplify the analysis of the chemical shifts associated with the different phosphorus sites. Although such a separation of variables depends on the spin system being weakly coupled, a substantial degree of strong coupling can in fact be tolerated, and its effects when present can be readily recognised and calculated.[5]

The application of this 2D technique to the complex $RhCl(PMe_3)(dppm)$ enabled the spectrum to be readily analysed for the phosphorus chemical shifts, the ^{31}P-^{31}P and the ^{31}P-^{103}Rh couplings. These could be transferred by analogy to the other complexes in this series, as the starting point in an iterative analysis of the conventional one dimensional spectra.[5]

RESULTS AND DISCUSSION

(1) *Bis* (*diphenylphosphino*)*methane*(*trimethylphosphine*)-*chlororhodium*(*I*)

The complex $[Rh(PMe_3)_4]Cl$[6] reacts with excess dppm in refluxing toluene to give the air-sensitive orange crystalline complex $RhCl(PMe_3)(dppm)$ in high yield (95%); it is monomeric in benzene.

Application of the two-dimensional δ/J resolved NMR method enabled the $^{32}P\{^2H\}$ spectrum of this compound (Fig. 1) to be readily analysed for the approximate values of the coupling constants and phosphorus chemical shifts.[5] These were then used as the starting point for an iterative analysis of the $^{31}P\{^1H\}$ one dimensional spectrum. The values obtained for the homonuclear ^{31}P-^{31}P coupling constants, the heteronuclear ^{31}P-^{103}Rh coupling constants and the ^{31}P chemical shifts are shown in Table 1. Good agreement between the calculated and the observed spectrum (Fig. 2a, b) could be obtained only by setting the relative values of J_{PP}^{trans} and J_{PP}^{cis} to be opposite in sign.

Although the large (J_{PP} = 407.7 Hz) coupling can be assumed to correspond to a *trans* interaction, there,

*Authors to whom correspondence should be addressed.

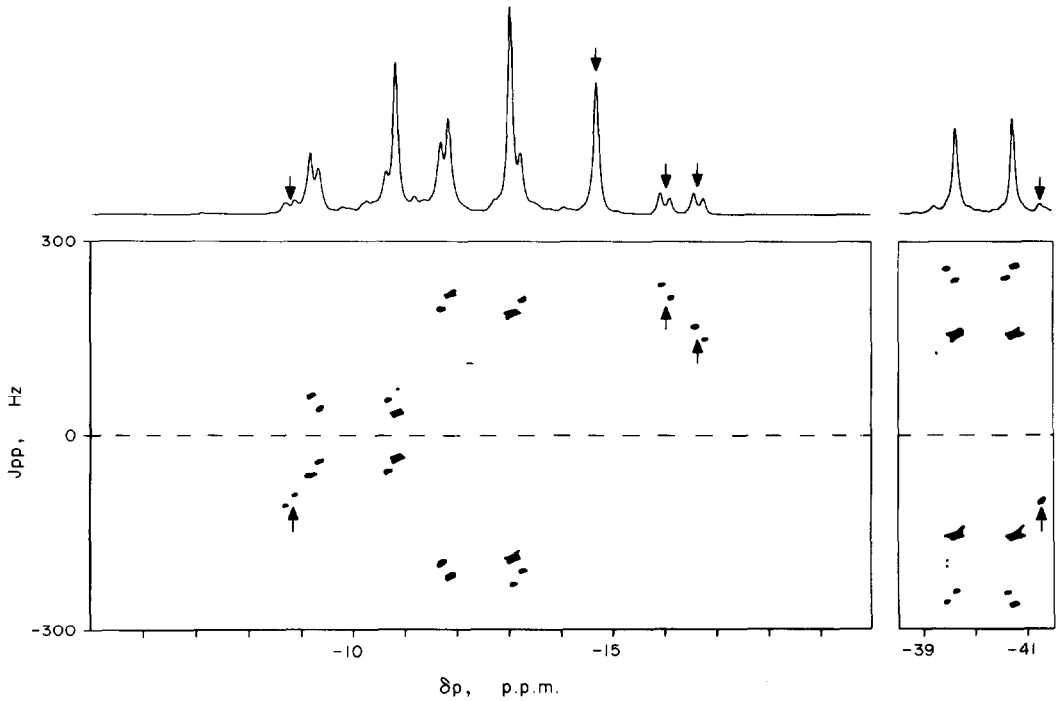

Fig. 1. Two dimensional $^{31}P\{^1H\}$ δ/J resolved spectrum of *ca.* 10 mM solution of $RhCl(PMe_3)dppm$ in benzene. The spectrum was tilted by 45° and is shown as a contour plot with a projection showing the ^{31}P chemical shift positions. Peaks marked with arrows are instrumental artifacts, and can be identified since they do not correctly reflect in the plane of symmetry in the J dimension (shown by a dashed line in the contour plot). Their positions and intensities also change according to the acquisition parameters, unlike the genuine peaks. Several such artifacts shown in the projection (e.g. at δ − 14.6) are off the vertical scale in the contour representation.

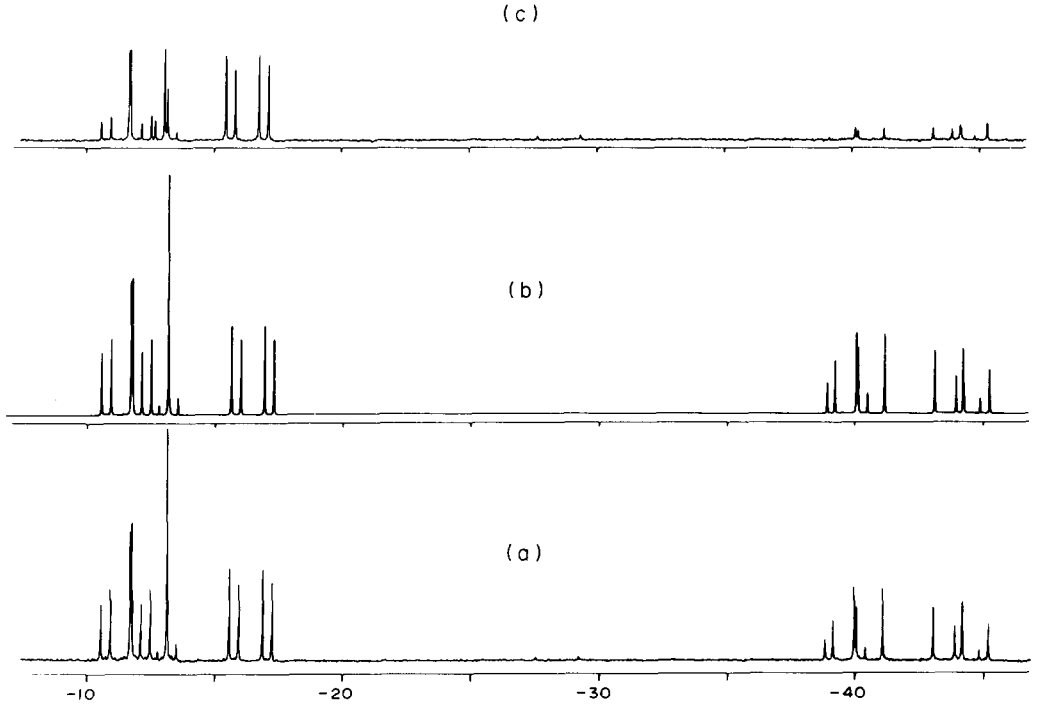

Fig. 2. $^{31}P\{^1H\}$ NMR spectrum of $RhCl(PMe_3)(dppm)$, (a) observed, (b) calculated, (c) n.O.e. difference spectrum obtained by pre-irradiation at the PMe_3 proton resonance, and subtraction of a control spectrum obtained with off-resonance ^1H pre-irradiation.

Table 1. Spectral parameters for $RhX(PR_3)(dppm)$, R = Me, Ph

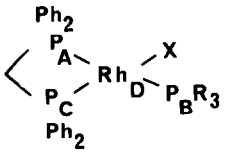

X	Cℓ[a]	CH_2SiMe_3[a]	CH_2CMe_2Ph[a]	CH_2CMe_3[a]	Cℓ[b]
δ_A[c]	-40.2	-24.1	-26.8	-22.9	-38.5[d]
δ_B	-12.7	-13.7	-16.9	-14.3	+32.7
δ_C	-10.2	-19.7	-11.6	-17.4	-13.3
$\pm J_{AB}$[e]	407.7	378.8	343.7	371.1	382.9
$\pm J_{AC}$	-96.4	-63.3	-57.6	-56.7	-99.6
$\pm J_{AD}$	-112.7	-135.2	-148.8	-145.6	-118.8
$\pm J_{BC}$	-37.1	-38.0	-38.5	-38.0	-33.7
$\pm J_{BD}$	-131.1	-156.3	-170.1	-168.1	-134.8
$\pm J_{CD}$	-158.2	-103.9	-96.1	-94.5	-159.5

[a] $RhX(PMe_3)(dppm)$, [b] $RhCℓ(PPh_3)(dppm)$, [c] in benzene, containing 10% benzene, and referenced to external 85% H_3PO_4 (δ 0.0) at 101.25 MHz,

[d] In $CH_2Cℓ_2$ - 10% d_6-acetone and referenced to external 85% H_3PO_4 (δ 0.0) at 101.25 MHz,

[e] Coupling constants are determined by iterative spectral analysis. The standard deviation in the calculated transition frequency was < 0.2 Hz in all cases. Good agreement between the observed and calculated spectra can be obtained only by setting the relative values of $\pm J_{PP}^{(trans)}$ and $\pm J_{PP}^{(cis)}$ to be opposite in sign. The absolute signs could not be determined by this approach and we have assumed $\pm J_{PP}^{(trans)}$ to be positive.

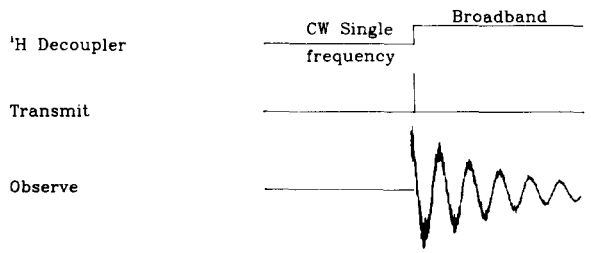

Fig. 3. Pulse sequence for observation of the heteronuclear $^{31}P\{^1H\}$ nuclear Overhauser effect. To obtain the n.O.e., the CW decoupling is tuned to the appropriate proton resonance. To obtain a control spectrum for subtraction, the CW decoupling is moved far off resonance but left operating to minimise sample temperature variation. To minimize the effects of long term instabilities, both sets of data are collected simultaneously by switching the CW frequency from one frequency to the other at regular intervals and storing the two sets of data separately.

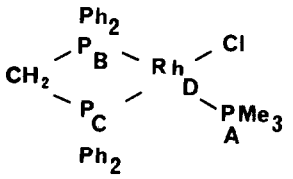

(1a)

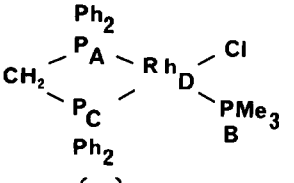

(1b)

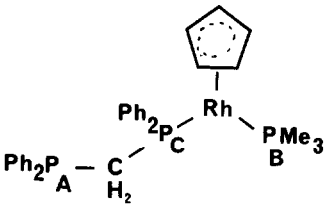

(2)

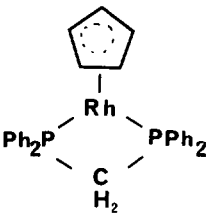

(3)

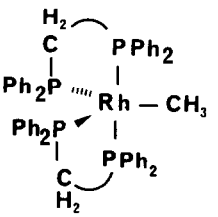

(4)

nevertheless, remains an ambiguity in assigning these spectral constants to specific phosphorus atoms (1a vs 1b).

Although in principle these could be distinguished by selective proton decoupling experiments, the presence of long range ^{1}H–^{31}P coupling to the phenyl groups results in very complex spectra. We instead made use of the significant $^{31}P\{^{1}H\}$ nuclear Overhauser effect,[7] using the experimental sequence shown in Fig. 3. Single frequency ^{1}H pre-irradiation at a specific proton resonance allows a selective $^{31}P\{^{1}H\}$ n.O.e. to build up, and allows the non-selective n.O.e. from the broadband irradiation in the cycle to decay between transients. From a spectrum obtained in this way is subtracted a control in which the single frequency ^{1}H decoupling is off-resonance, giving a difference spectrum which shows only the effects due to the $^{31}P\{^{1}H\}$ n.O.e. Pre-irradiation of the proton resonance corresponding to the PMe_3 gave a difference spectrum (Fig. 2c) which shows only enhancement ($\eta \simeq 1.10$) of the low field signals, indicating that the high field signals ($\eta \simeq 1.017$) are *not* due to the PMe_3 group and therefore, that assignment 1*b* is correct. We note that the actual transitions enhanced are complex due to the significant degree of second order character present in the spectrum, and the probable presence of three spin effects,[8] although this does not affect our qualitative conclusions. This experiment represents, as far as we are aware, the first such application of heteronuclear n.O.e. difference spectroscopy.

$RhCl(PMe_3)$(dppm) does not react with hydrogen (2 atm., 70°C), ethylene (2 atm., 25°C), $NaBH_4$ and Na metal (25°C). It reacts with $LiAlH_4$, MeLi, and EtLi, but complex mixtures were obtained and attempts to isolate pure compounds were unsuccessful.

(2) *Bis(diphenylphosphino)methane(trimethylphosphine)-trimethylsilylmethylrhodium(I)*

In toluene, $RhCl(PMe_3)$(dppm) reacts with one equivalent of Me_3SiCH_2Li to give the air-sensitive complex $RhCH_2SiMe_3(PMe_3)$(dppm) which can be readily crystallised from 40 to 60° petroleum as red crystals in 80% yield; it is monomeric in benzene.

The observed and simulated $^{31}P\{^{1}H\}$ spectra are shown in Fig. 4 and spectral parameters are given in the Table.

Unlike the parent compound, $Rh(CH_2SiMe_3)(PMe_3)$-(dppm) reacts readily with hydrogen at 1 atm. pressure at room temperature to give a mixture from which no crystalline product could be isolated. The ^{1}H NMR spectrum of the mixture shows the absence of the trimethylsilylmethyl group on the rhodium, but no hydride is observed in either IR or ^{1}H NMR spectra.

Since $Rh(CH_2SiMe_3)(PMe_3)$(dppm) slowly (*ca.* 12 hr) catalyses the isomerisation of hex-1-ene to hex-2-ene under 1 atm. of hydrogen (but not N_2 or Ar) at room

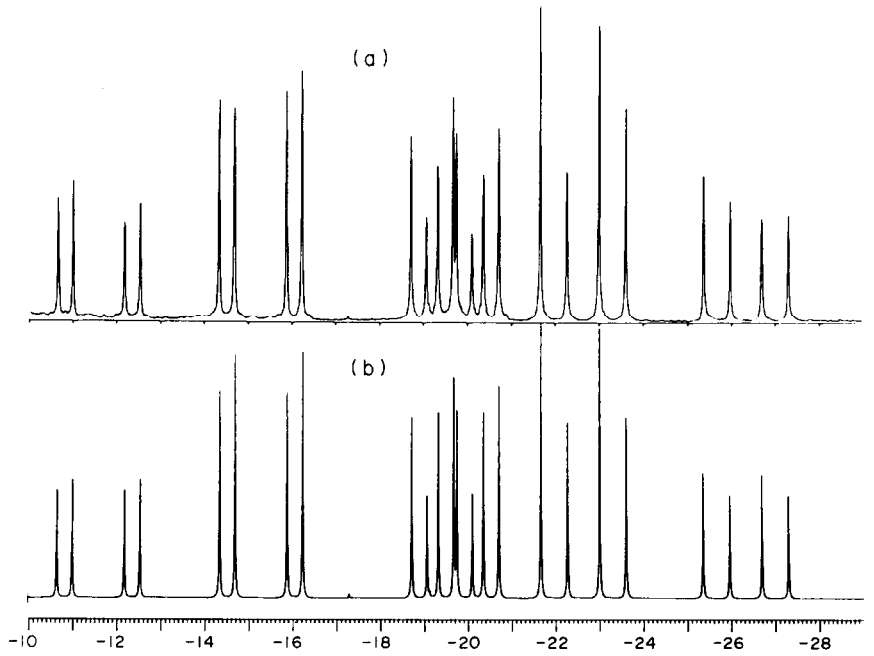

Fig. 4. Observed (a) and calculated (b) $^{31}P\{^1H\}$ spectrum of $Rh(CH_2SiMe_3)(PMe_3)$(dppm).

temperature a transient hydrido species is presumably involved. At 100°C with 20 atm. hydrogen $Rh(CH_2SiMe_3)(PMe_3)$(dppm) slowly (*ca.* 12 hr) hydrogenates hex-1-ene to hexane (100% conversion). Hydroformylation of hex-1-ene to a mixture of 2-methylhexanol and heptaldehyde (straight branched chain isomer, ratio 3:1) under 30 atm. of CO/H_2 (1:1) also occurs slowly. The solution IR spectrum of the residual solution shows a terminal CO stretch at 1960 cm^{-1}; interaction of the complex with CO alone at 1 atm. gives a mixture with CO stretches at 1960 and 1940 cm^{-1}. Attempts to isolate these carbonyl species in a pure state have failed.

(3) *Bis(diphenylphosphino)methane(trimethylphosphine) -neopentyl- and neophylrhodium(I)*

Alkylation with one equivalent of neopentylmagnesium bromide or of neophylmagnesium chloride in THF give high yields of the corresponding alkyls which can be obtained from petroleum as orange air-sensitive crystals. Both compounds are monomeric in benzene.

The $^{31}P\{^1H\}$ observed and simulated spectra for the

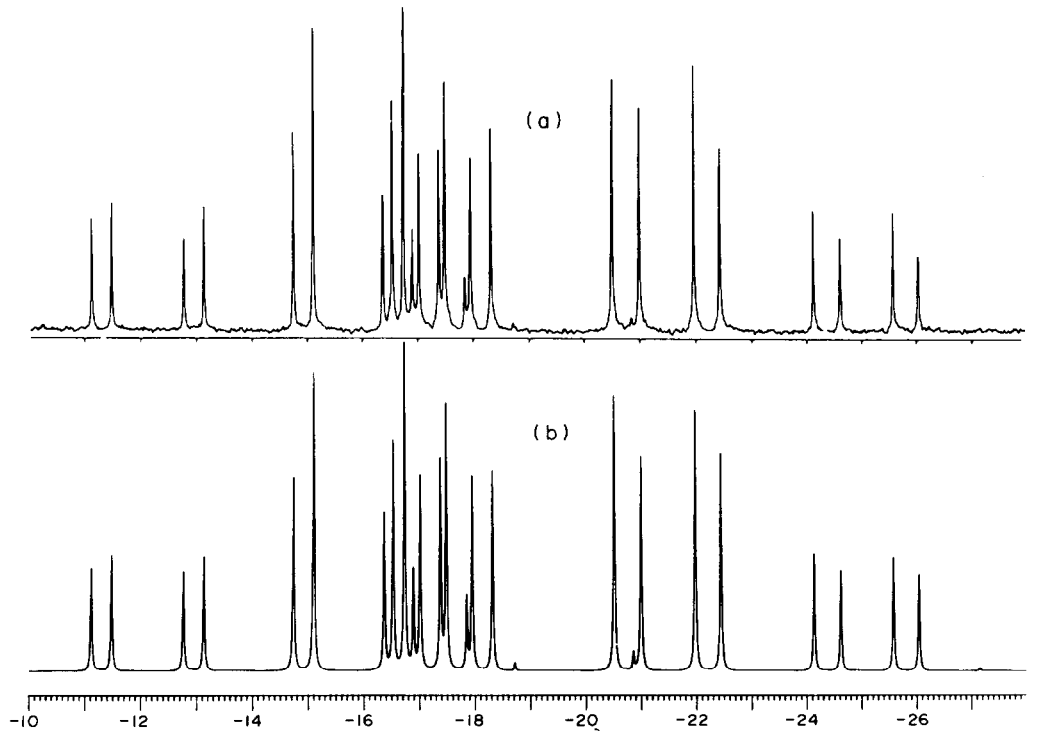

Fig. 5. Observed (a) and calculated (b) $^{31}P\{^1H\}$ spectrum of $Rh(CH_2CMe_3)(PMe_3)$(dppm).

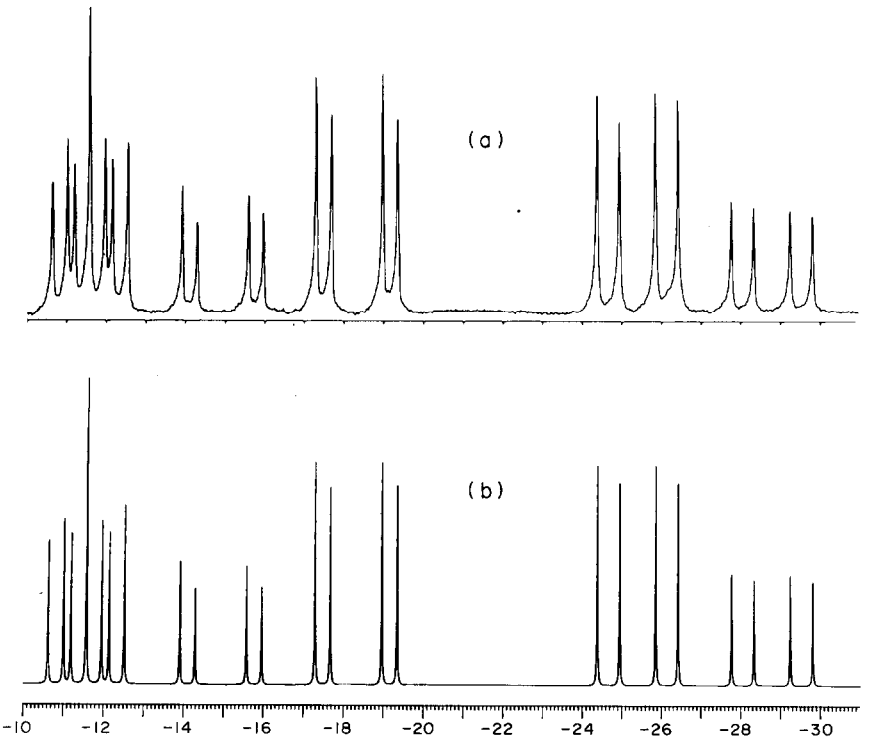

Fig. 6. Observed (a) and calculated (b) $^{31}P\{^1H\}$ spectrum of $Rh(CH_2CMe_2Ph)(PMe_3)(dppm)$.

alkyls are shown in Figs. 5 and 6 respectively. Spectral parameters are in Table 1.

For all the complexes $RhX(PR_3)(dppm)$ we can conclude that the magnitude of the homonuclear ^{31}P–^{31}P coupling constants are in the order $J(P_A–P_B) \gg J(P_A–P_C) > J(P_B–P_C)$ and also that the signs of the coupling constants $J(trans)$ and $J(cis)$ are opposite to each other.

(4) *Bis(diphenylphosphino)methane(trimethylphosphine)-η^5-cyclopentadienylrhodium(I) and Bis(diphenylphosphino)methane η^5-cyclopentadienylrhodium(I)*

The interaction of $RhCl(PMe_3)(dppm)$ in toluene with one equivalent of C_5H_5Na leads to orange–red air-sensitive crystals of $Rh(\eta^5\text{-}C_5H_5)(PMe_3)(dppm)$. The NMR data indicate unidentate dppm as in (2) and the structure has been confirmed by X-ray diffraction[9] (Fig. 7).

The $^{31}P\{^1H\}$ spectrum shows a doublet at δ −23.21 [$J(P_A - P_C) = \pm 97.6$ Hz], a doublet of doublets at δ −2.20 [$J(Rh\text{-}P_B) = \pm 208.6$ Hz; $J(P_B - P_C) = \pm 55.3$ Hz] and a doublet of doublet of doublets at δ 47.94 [$J(Rh\text{-}P_C = \pm 231.9$ Hz; $J(P_A - P_C) = \pm 97.6$ Hz; $J(P_B - P_C) = \pm 55.3$ Hz]. Heteronuclear ^{31}P–^{103}Rh coupling is not observed for the δ −23.21 resonance so that this can be assigned to the non-bonded phosphorus atom. These spectral parameters are consistent with those observed for the other complexes studied (Table 1).

On heating the complex in refluxing toluene, PMe_3 is lost and $Rh(\eta^5\text{-}C_5H_5)(dppm)$ is formed quantitatively. The compound forms orange–red air-sensitive crystals and is monomeric in benzene. The NMR data is consistent with the chelate structure (3). Thus, the $^{31}P\{^1H\}$ NMR spectrum shows a doublet with heteronuclear ^{31}P–^{103}Rh coupling of 190.2 Hz at δ −11.72 ppm. The ^1H NMR spectrum shows a doublet [$J(^{103}Rh\text{-}C_5H_5) = 0.7$ Hz] for the cyclopentadienyl protons.

(5) *Bis(diphenylphosphino)methane(triphenylphosphine chlororhodium(I)*

Interaction of excess dppm with $RhCl(PPh_3)_3$ in toluene at room temperature for 18 hr gives $RhCl(PPh_3)(dppm)$ in 90% yield. The compound is sparingly soluble in toluene but can be crystallised as orange crystals from CH_2Cl_2 in which it is monomeric; it is a non-conductor in $MeNO_2$.

Assignment of the $^{31}P\{^1H\}$ parameters is subject to the same ambiguity as for $RhCl(PMe_3)(dppm)$. Three distinct sets of signals were observed (Figs. 8a, b). The two sets due to the dppm ligand were assigned by carrying out a heteronuclear n.O.e. experiment similar to that described for $RhCl(PMe_3)(dppm)$, but in which the CH_2 protons in the dppm ligand were pre-irradiated. Significant ($\eta \simeq 1.12$) enhancements are seen in the difference spectrum (Fig. 8c) for the two sets of high field signals, suggesting the assignment of these to the dppm ligand and of the low field set ($\eta = 1.01$) to the PPh_3 phosphorus atom. These assignments are completely consistent with those made for $RhCl(PMe_3)(dppm)$ (Table 1).

(6) *Bis[bis(diphenylphosphino)methane] methylrhodium-(I)*

Interaction of excess *bis*(diphenylphosphino)methane with $RhCl(PPh_3)_3$ in toluene at room temperature for four days gives the known[3] $RhCl(dppm)_2$ in 90% yield. It is monomeric in benzene. The compound reacts with one equivalent of methyl lithium in toluene to give orange–red crystals of $RhMe(dppm)_2$ which is monomeric in benzene and is a non-conductor in nitromethane and hence must be 5-coordinate. The room temperature $^{31}P\{^1H\}$ NMR spectrum shows essentially an AB quartet with further heteronuclear ^{31}P–^{103}Rh coupling; at −60°C a complicated AA'BB'X pattern is observed in which the AB' and A'B couplings are approx. 300 Hz.

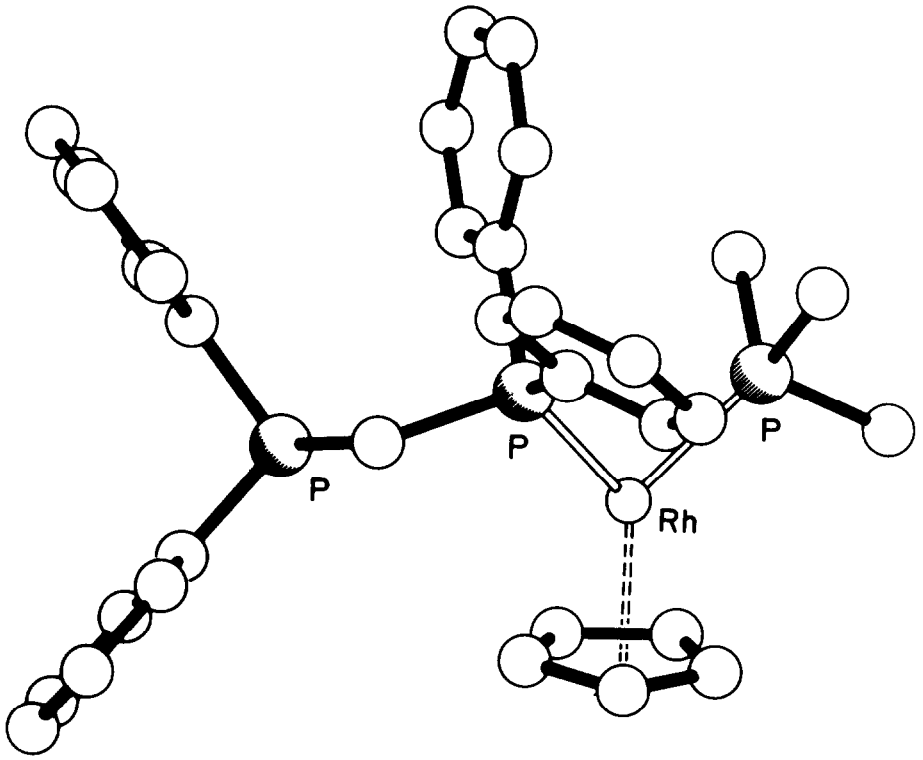

Fig. 7. The structure of Rh(η^5-C_5H_5)(PMe_3)(dppm) as determined by X-ray diffraction. Rh–P(PMe_3) = 2.214(2)Å; Rh–P(dppm) = 2.188(2)Å; Rh–C = 2.251–2.313(8)Å.

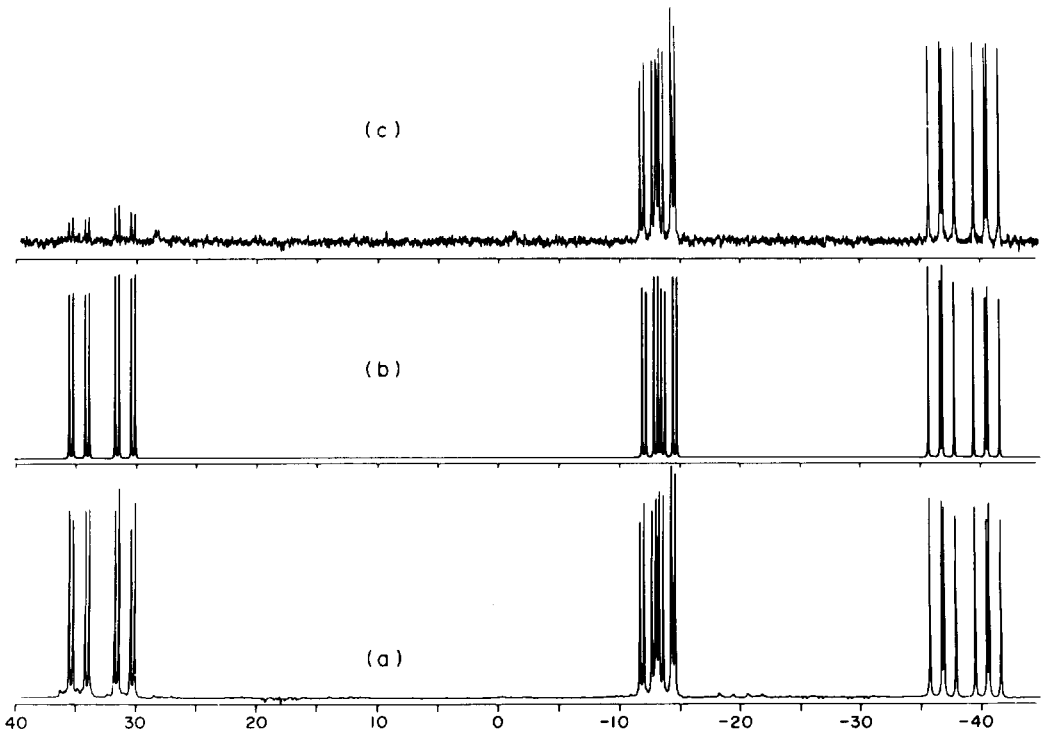

Fig. 8. Observed (a) and calculated (b) $^{31}P\{^1H\}$ spectrum of RhCl(PPh_3)(dppm), (c) n.O.e. difference spectrum obtained by pre-irradiation at the dppm CH_2 proton resonance, and subtraction of a control spectrum obtained with off-resonance ^1H pre-irradiation.

Unfortunately, an accurate analysis of this spectrum could not be obtained, possibly as a result of the effects of fluxionality still present in the spectrum. The ^{31}P data are, however, consistent with a trigonal bipyramidal geometry (**4**) and non-rigidity at room temperature. The tbp geometry should produce an AA'BB'X pattern whereas a square pyramidal geometry should show a doublet (i.e. an A_4X pattern) resulting from heteronuclear ^{31}P–^{103}Rh splitting of the four equivalent phosphorus nuclei. An X-ray diffraction study[4] on a related cationic complex, $[Rh(dppm)_2CO]BF_4$, has confirmed a trigonal bipyramidal structure.

With one equivalent of C_5H_5Na, $RhCl(dppm)_2$ in toluene reacts to give high yields of $Rh(\eta\text{-}C_5H_5)(dppm)$.

EXPERIMENTAL

Microanalyses by Pascher, Bonn, and Imperial College laboratories. Molecular weights: cryoscopically in benzene. Melting points were determined in sealed capillaries under vacuum.

All operations were performed under oxygen-free nitrogen or *in vacuo*. Tetrahydrofuran, toluene, benzene and petroleum (b.p. 40–60°C) were dried over sodium–benzophenone and distilled under nitrogen before using.

Instruments

NMR: Perkin–Elmer R32 (^1H, 90 MHz), Bruker WM250 (^1H, 250; $^{31}P\{^1H\}$, 101.25 MHz); data in δ ppm referenced to $SiMe_4$ and 85% H_3PO_4 (external) at 26°C in C_6D_6 unless otherwise stated. IR: Perkin–Elmer 683; spectra in cm^{-1} and Nujol mulls unless otherwise stated. Conductivity data were obtained on a Mullard conductivity bridge type E7566/3 with a matching conductivity cell.

All iterative NMR spectral analysis were performed using an interactive graphical program written by Burgess and Rzepa.

Detailed NMR procedures

Two dimensional δ/J resolved spectra were recorded using a preliminary version of the Bruker ASPECT 2000 software and the following acquisition parameters: data size 512 (F_1) × 4k (F_2), spectral width 760 Hz (F_1) and 6 kHz (F_2) giving a digital resolution of 1.47 Hz (F_1) and 2.94 Hz (F_2). A delay of 40 s (*ca.* $5T_1$) between $90° - \tau_1 - 180° - \tau_1$-acquire ($\tau_2$) pulse cycles was used and four transients were acquired for each value of τ_1 (quadrature detection) to give a total acquisition time of 17 hr. The data was multiplied by half cosine window functions before Fourier transformation and the resulting two dimensional spectrum tilted by 45°. Peak positions in this spectrum could be obtained to an accuracy of ± 1.5 Hz, although the contour representation (Fig. 1) is shown with an exponential weighting function and a deliberately low contour level to improve clarity of presentation.

Nuclear Overhauser effect difference spectra were obtained at ambient temperatures, with 2800 transients being acquired for both the control and the CW ^1H pre-irradiation experiments. The following micro-program sequence was used on the ASPECT 2000:

1 ZE	14 02	27 LO TO 9 TIMES: 700
2 RE PDEC	15 CW	28 DO
3 ZE	16 D1	29 EXIT
4 S1	17 BB	
5 DO	18 S2	D1 3 sec
6 WR PDEC	19 02	D2 0.05 sec
7 IF PDEC	20 D2	S1 24 H
8 LO TO 1 TIMES: 2	21 GO 13	S2 4 H
9 RF PDEC	22 DO	
10 RF	23 WR PDEC	
11 RE PDEC	24 IF PDEC	
12 RL FREQL	25 IF FREQL	
13 S1	26 LO TO 11 TIMES: 2	

The two frequency list files contain the decoupler frequencies for selective and broad-band irradiation.

(1) *Bis(diphenylphosphino)methane(trimethylphosphine)chlororhodium(I)*

Bis(diphenylphosphino)methane (1.74 g, 4.52 mmol) was added to a toluene solution (100 cm^3) of $[Rh(PMe_3)_4]Cl$ (2.0 g, 4.52 mmol). The mixture was refluxed for 24 hr. Volatile materials were removed under vacuum, and the residue extracted into hot toluene (2 × 30 cm^3), filtered, concentrated to *ca.* 50 cm^3 and cooled at −20°C to give orange crystals, which were collected and washed with petroleum. Yield; > 2.6 g, 95%; m.p., 210–1°C. [Found: C, 55.8 (56.1); H, 5.0 (5.2); P, 15.6 (15.5); Cl, 5.6 (5.9)%; *M* 580 (598.5)]. NMR. ^1H: 1.07 s, (9), PMe_3; 3.74 br, s, (2), PCH_2P; 7.0–7.9 m (20) Ph_2P. $^{31}P\{^1H\}$: see Table 1.

IR. 3035w, 3025w, 1670w, 1585w, 1570w, 1480m, 1436s, 1422m, 1360w, 1340w, 1310m, 1300w, 1283m, 1280m, 1185m, 1160w, 1100s, 1080m, 1070m, 1025w, 1000w, 955vs, 940s, 875w, 850w, 840w, 790w, 756s, 740s, 730s, 700s, 670m, 660w, 545s, 510s, 492w, 470w, 460w, 450w, 445w, 420w.

(2) *Bis(diphenylphosphino)methane(triphenylphosphine)chlororhodium(I)*

Bis(diphenylphosphino)methane (1.9 g, 4.95 mmol) was added to a toluene solution (100 cm^3) of $RhCl(PPh_3)_3$ (2.0 g, 2.16 mmol) at room temperature. The solution was stirred for 18 hr. The yellow precipitate was collected, washed with toluene (2 × 20 cm^3) and dried *in vacuo* to give 1.2 g pure RhCl(dppm)(PPh_3). A further 0.3 g was obtained by concentrating the combined filtrate to *ca.* 50 cm^3 and cooling at −20°C. The compound can be recrystallised from CH_2Cl_2 to give orange crystals. Total yield; 1.5 g, 90%; m.p., 170–2°C. [Found: C, 65.9 (65.8); H, 4.7 (4.7); P, 11.8 (11.9); Cl, 4.4 (4.5)%. *M* 780 (784.5)].

NMR. ^1H: ($CDCl_3$): 4.95 s, (2), PCH_2P; 6.7–7.8 br, m (35); $(Ph_2P)_2CH_2$ and Ph_3P. $^{31}P\{^1H\}$: see Table 1.

IR. 3052w, 1584w, 1568w, 1480m, 1435s, 1310m, 1275m, 1182m, 1178m, 1155w, 1092s, 1070m, 1025m, 998m, 915w, 848w, 752s, 735s, 723s, 695s, 672m, sh, 615w, 550m, 520s, 510s, 495s, 478m, 465m, 436m, 420m.

(3) *Bis[bis(diphenylphosphino)methane]chlororhodium(I)*

Bis(diphenylphosphino)methane (2.0 g, 5 mmol) was added to a solution of $RhCl(PPh_3)_3$ (2.0 g, 2.2 mmol) in 200 cm^3 of toluene at room temperature. The solution was stirred for 4 d. The orange solution was evaporated and the residue extracted into toluene (2 × 30 cm^3). The combined filtrated was concentrated to *ca.* 30 cm^3 and cooled at −20°C to give orange–red crystals. Yield; 1.7 g, 90%; m.p., 88–90°C (lit., 97°C dec.) [Found: C, 66.3 (66.2); H, 4.9 (4.9); P, 13.4 (13.7); Cl, 3.8 (3.8 (3.9)%. *M*, 920 (906.5)].

NMR. ^1H: 3.83 br, s (4), PCH_2P; 6.90 and 7.68 br, s (40), Ph_2P. $^{31}P\{^1H\}$: −16.1 d, *J*(Rh-P) = 105.7 Hz.

IR. 3025w, 1585w, 1570w, 1494w, 1482m, 1436s, 1366w, 1306w, 1184w, 1155w, 1096s, 1090msh, 1028w, 998w, 756m, 734s, 729s, sh, 702s, sh, 696s, 670w, 618w, 553w, 522s, 512s, 501m, sh, 492w, 440w, 421w.

(4) *Bis(diphenylphosphino)methane(trimethylphosphine)trimethylsilylmethylrhodium(I)*

Trimethylsilylmethyllithium (1.6 cm^3, 1.7 M in petroleum; 2.68 mmol) was added to a toluene solution (100 cm^3) of RhCl(dppm)(PMe_3) (1.6 g, 2.68 mmol) at −40°C. The mixture was allowed to warm to room temperature slowly and stirred for an additional 8 hr. Volatile materials were removed under reduced pressure and the residue was extracted with petroleum (3 × 40 cm^3). The combined filtrate was concentrated to *ca.* 60 cm^3 and cooled at −20°C to give red crystals. Yield: 1.4 g, 80%; m.p., 115–6°C. [Found: C, 58.7 (59.1); H, 6.5 (6.5); P, 14.4 (14.3); Si, 3.9 (4.3)%. *M*, 640 (650)].

NMR. ^{1}H: 0.29 s (2), CH_2SiMe_3; 0.31 s (9), CH_2SiMe_3; 1.08 d (9), ^2J(P–H) = 6 Hz, PMe_3; 3.93 *t*, (2) ^2J(P–H) = 8 Hz, $PCH_{22}P$; 7.03–7.73 m, (20), Ph_2P. $^{31}P\{^1H\}$: see Table 1.

IR. 3050w, 3030w, 1950br, w, 1895br, w, 1820br, w, 1610m, 1586m, 1497m, 1478s, 1435vs, 1420m, 1306w, 1280w, 1248w, 1180w, 1155w, 1105m, 1095s, 1065w, 1050w, 1026w, 1000w, 945s, 880m, 850s, 835m, 785w, 740s, 728vs, 692vs, 665m, 615w, 545m, 535s, 520s, 510s, 490w, 482w, 469w.

(5) *Bis(diphenylphosphino)methane(trimethylphosphine)neopentylrhodium(I)*

In a similar way from neopentylmagnesium bromide (2.0 cm^3, 0.42 M in Et_2O; 0.82 mmol) and a THF solution (80 cm^3) of RhCl(dppm)(PMe_3) (0.47 g, 0.79 mmol) at −78°C. The petroleum extract was concentrated to *ca.* 60 cm^3 and cooled to −20°C to give orange crystals. Yield: 0.4 g, 75%; m.p., 154–5°C. [Found: C, 62.2 (62.5); H, 6.6 (6.6); P, 14.2 (14.6)%. *M*, 610 (634)].

NMR. ^{1}H: 1.11 d (9), J(P–H) = 6.5 Hz, PMe_3; 1.37 s (9), CH_2CMe_3; 1.93 br, m (2), CH_2CMe_3 3.95 t (2), J(P–CH_2) = 16.8 Hz, PCH_2P; 7.0–7.8 br, m (20) Ph_2P. $^{31}P\{^1H\}$: see Table 1.

IR. 3035w, 3028w, 1585m, 1570w, 1482m, 1434s, 1420w, 1348m, 1307w, 1300w, 1278m, 1229m, 1175w, 1092s, 1081m, 1069w, 1029m, 1000m, 948s, 930m, 842w, 760w, 755m, 740vs, 725s, 715m, 700vs, 665w, 615w, 540m, 509m, 488m, 440m, 430m, 420m.

(6) *Bis(diphenylphosphino)methane(trimethylphosphine)neophylrhodium(I)*

As in (4), but using neophyl magnesium chloride (1.9 cm^3, 0.6 M in Et_2O; 1.14 mmol) and a THF solution (80 cm^3) of RhCl(dppm)(PMe_3) (0.6 g, 1 mmol) at −78°C. The petroleum extract was concentrated to *ca.* 60 cm^3 and cooled to −20°C to give orange crystals. Yield: 0.56 g, 80%; m.p., 168–9°C. [Found: C, 65.5 (65.5); H, 6.5 (6.3); P, 13.3 (13.4)%. *M* 670 (696)].

NMR. ^{1}H: 0.84 d (9), J(P–H) = 7.1 Hz, PMe_3; 1.73 s (8), CH_2CMe_2Ph; 3.9 br, m (2), PCH_2P; 6.8–8.4 br, m (25), Ph_2P and $PhMe_2C$. $^{31}P\{^1H\}$: see Table 1.

IR. 3030m, 3015m, 1970w, 1955w, 1880w, 1810w, 1486m, 1560m, 1480s, 1431s, 1418s, 1345m, 1297m, 1279s, 1233w, 1190w, 1176w, 1095s, 1082s, 1067m, 1040m, 1027m, 1015m, 1000w, 940vs, 930vs, 842m, 767m, 758m, 749s, 735s, sh, 720vs, 692vs, 670m, sh, 662s, 640w, 618w, 560m, 535m, 510m, 485m, 430m, 415w.

(7) *Bis(diphenylphosphino)methane(trimethylphosphine)-η^5-cyclopentadienylrhodium(I)*

Sodium cyclopentadienide (1 cm^3, 1.12 *M* in THF; 1.12 mmol) was added to a toluene solution (50 cm^3) of RhCl(dppm)(PMe_3) (0.65 g, 1.09 mmol) at −50°C. The mixture was allowed to warm and stirred at room temperature for 12 hr. Volatile materials were removed under reduced pressure. The residue was extracted into petroleum (3 × 40 cm^3) and filtered. The combined filtrate was concentrated to *ca.* 60 cm^3 and cooled to −20°C to give red crystals. Yield: 0.5 g, 75%; m.p., 112–3°C. [Found: C, 63.4 (63.0); H, 5.8 (5.7); P, 14.6 (14.8)%. *M* 600 (628)].

NMR. ^{1}H: 0.85 d (9), J(P–H) = 8.7 Hz, PMe_3; 3.3 d (2), J(P–H) = 7.6 Hz, PCH_2P; 5.4 s (5), η^5-C_5H_5; 7.0–8.0 br, m (20), Ph_2P. $^{31}P\{^1H\}$: −23.21 d, J(P–P) = 97.6 Hz, Ph_2P–CH_2(Ph_2)PRh; −2.2 d of d, J(Rh–P) = 208.6 Hz, J(P–P) = 55.3 Hz, PMe_3; 47.9 d of d, J(Rh–P) = 231.9 Hz; (J(P–P) = 97.6; J(P–P) = 55.3 Hz, $RhPPh_2CH_2PPh_2$.

IR. 3020w, 1610w, 1586w, 1486m, 1480m, 1434s, 1420m, 1330w, 1308m, 1298m, 1279m, 1190w, 1180w, 1160w, 1130w, 1095m, sh, 1090s, 1060w, 1040w, 1024m, 1009m, 1000m, 992m, 948vs, 930s, 875m, 848m, 825w, 770m, 759s, 745s, sh, 730vs, 695vs, 675s, 660m, 620w, 550w, 510s, 500s, 471m, 464m, 450m, 390m.

(8) *Bis(diphenylphosphino)methane-η^5-cyclopentadienylrhodium(I)*

(a) A toluene solution (50 cm^3) of (η^5-C_5H_5)Rh(dppm)(PMe_3) (0.3 g, 0.47 mmol) was refluxed for 18 hr. The solution was evaporated to dryness. The residue was washed with petroleum (2 × 30 cm^3), extracted into toluene (20 cm^3) and filtered. The filtrate was concentrated to *ca.* 2 cm^3 and cooled at −78°C to give orange crystals. Yield: 0.25 g, 95%; m.p., 199–200°C. [Found: C, 65.6 (65.2); H, 5.1 (4.9), P, 10.9 (11.2)%. *M* 530 (552)].

NMR. ^{1}H: 3.90 t of d (2), J(P–H) = 10.6 Hz, J(Rh–H) = 1.5 Hz, PCH_2P; 5.50 d (5), J(Rh–C_5H_5) = 0.6 Hz, η^5-C_5H_5; 7.04–7.75 br, m (20), Ph_2P. $^{31}P\{^1H\}$: −11.59 d, J(Rh–P) = 163.4 Hz.

IR. 3070w, 3050w, 1940br, w, 1960br, w, 1825br, w, 1580m, 1570m, 1480m, 1435s, 1327w, 1305w, 1275w, 1260m, 1180m, 1156w, 1100m, 1090s, 1080s, 1025m, 1000m, 870w, 850w, 810w, 770s, 750s, 730s, 695s, 660w, 618w, 550s, 512s, 490w, 482w, 470m, 423m.

(b) Sodium cyclopentadienide (0.5 cm^3, 1.12 *M* in THF; 0.56 mmol) was added to a THF solution (30 cm^3) of RhCl($dppm)_2$ (0.4 g; 0.44 mmol) at 0°C. The solution was warmed and stirred at room temperature for 18 hr. The deep red solution was evaporated and the residue extracted into 20 cm^3 of toluene and filtered. The filtrate was concentrated to *ca.* 10 cm^3 and then 20 cm^3 of diethyl ether were added to the solution and cooled at −20°C. Dppm first crystallised and was removed, after which the filtrated was concentrated to *ca.* 5 cm^3 and cooled at −20°C to give orange crystals. Yield: 0.22 g, 90%.

(9) *Bis[bis(diphenylphosphino)methane]methylrhodium(I)*

Methyllithium (0.5 cm^3, 1.1 *M*; 0.55 mmol) was added to a toluene solution (40 cm^3) of RhCl($dppm)_2$ at 0°C, and the solution stirred at room temperature for 18 hr. when the solvent was removed. The residue was extracted into toluene (2 × 20 cm^3), the combined filtrate concentrated *ca.* 20 cm^3 and cooled at −20°C, to give orange–red crystals. Yield: 0.37 g, 80%; m.p., 218°C. [Found: C, 69.1 (69.1); H, 5.1 (5.3); P, 14.2 (14.0)%. *M* 860 (886)].

NMR. ^{1}H: 0.29 s (3), Rh–CH_3; 3.83 b, s (2), PCH_2P; 4.08 b, t (2), J(P–CH_2) = 9 Hz, PCH_2P; 6.7–6.9, br, m (40) Ph_2P. $^{31}P\{^1H\}$: AA'BB'M spectrum, −19.04, J(Rh–P) = 122 Hz, J(P–P) = 302 Hz; −26.24, J(Rh–P) = 101 Hz, J(P–P) = 302 Hz.

IR. 3025w, 1582w, 1480m, 1432s, 1428s, sh, 1300w, 1272w, 1170w, 1150w, 1110m, 1095s, 1065w, 1025m, 1000w, 992w, 878m, 852m, 740s, 730m, 722m, 696s, 666w, 540m, 521s, 512m, sh, 508s, 483m, 420m.

Acknowledgements—We thank Johnson Matthey Ltd. for loan of rhodium, the S.E.R.C. for support, Miss Sue Johnson for assistance with NMR spectra and David Neuhaus for helpful discussions.

REFERENCES

[1]M. Cowie and T. G. Southern, *Inorg. Chem.* 1982, **21**, 246; W. A. Fordyce and G. A. Crosby, *J. Am. Chem. Soc.* 1982, **104**, 985; B. R. James and D. Mahajan, *Can. J. Chem.* 1980, **58**, 996; M. Cowie and S. K. Dwight, *Inorg. Chem.* 1979, **18**, 1209; A. R. Sanger, *J. Chem. Soc. Dalton Trans.* 1977, 120.

[2]M. D. Fryzuk, *Inorg. Chim. Acta* 1981, **54**, L265.

[3]B. R. James and D. Mahajan, *Can. J. Chem.* 1979, **57**, 180.

[4]L. H. Pignolet, H. D. Doughty, S. C. Nowicki and A. L. Casalnuovo, *Inorg. Chim.* 1980, **19**, 2172.

[5]*Preliminary Note*: K. W. Chiu, H. S. Rzepa, R. N. Sheppard, G. Wilkinson and W. K. Wong, *J. Chem. Soc. Chem. Commun.* 1982, 482; see also J. J. Colquhoun and W. McFarlane, *J. Chem. Soc. Chem. Commun.* 1982, 484.

[6]R. A. Jones, F. Mayor Real, G. Wilkinson, M. B. Hursthouse, A. M. R. Galas and K. M. A. Malik, *J. Chem. Soc., Dalton Trans.* 1980, 511.

[7]W. McFarlane and D. S. Rycroft, *Nuclear Magnetic Resonance* (Edited by G. A. Webb), Specialist Periodical Report, Vol. 10, p. 180. Royal Society of Chemistry, London (1981).

[8]J. H. Noggle and R. E. Shirmer, The Nuclear Overhauser Effect. Academic Press, New York (1971).

[9]J. I. Davies and A. C. Skapski, Imperial College, private communication.

Polyhedron Vol. 1, No. 11-12, pp. 819-820, 1982
Printed in Great Britain.

0277-5387/82/110819-02$03.00/0
Pergamon Press Ltd.

NOTES

Coordination compounds of $[Hg\{PPh_2[M(CO)_5]\}_2]$, (M = Cr, Mo, W)

(*Received* 25 *February* 1982)

Abstract—Coordination of various neutral N and O ligands causes drastic changes in $^1J(^{31}P-^{199}Hg)$ (increase up to the threefold) and $\delta(^{31}P)$ (shifts up to 30 ppm to low frequencies), which are due to the presence of the $M(CO)_5$ groups. The complexes with DMSO, phen and bipy were isolated in the solid state. No coordination of $[Hg\{PCy_2[Cr(CO)_5]\}_2]$ with the above ligands is observed.

INTRODUCTION

Whilst the coordination behaviour of mercury(II) halides, pseudohalides and organomercury compounds is well investigated,[1] there is only limited information on the coordination of Hg–P bonded species: Cationic $[Hg(PR_3)_2]^{2+}$ is known[2] to coordinate two more PR_3 to form $[Hg(PR_3)_4]^{2+}$, and phosphine coordination compounds of the Hg–P bonded $[Hg\{P(O)(OEt)_2\}_2]$ have recently been reported.[3] On the other hand no coordination compounds between $[Hg\{PPh_2[M(CO)_5]\}_2]$, (M = Cr, Mo, W), (1) and PPh_3 are formed.[4]

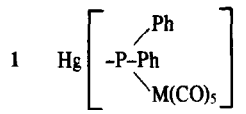

RESULTS AND DISCUSSION

This fact seems to be due to steric reasons rather than to the electronic acceptor qualities of mercury in 1 since we were able to detect, and isolate in part, a number of coordination compounds with N and O donor ligands.

1 forms isolable 1:1 complexes with bidentate phen (1,10-phenanthroline) and bipy (2,2'-bipyridyl) and 1:2 complexes with monodentate DMSO (dimethyl sulphoxide) (Table 1). On the other hand the new compound $[Hg\{PCy_2[Cr(CO)_5]\}_2]$ (Cy = Cyclohexyl) forms no complexes with the above ligands presumably due to steric reasons.

Coordination of 1 results in large effects upon $^1J(^{31}P-^{199}Hg)$ and $\delta(^{31}P)$ (Table 2). For example the coupling constant $^1J(^{31}P-^{199}Hg)$ of $[Hg\{PPh_2[Cr(CO)_5]\}_2]$ increases from 640 Hz for the pure compound to 2046 Hz for its phen complex, i.e. by more than a factor of 3. The ^{31}P chemical shift decreases from 77.2 ppm to 47.7 ppm by the unusually large amount of 30 ppm. No comparable effects were noted for the corresponding reactions of the Hg–P bonded $[Hg\{P(O)(Oet)_2\}_2]$ and $[Hg\{P(O)t\text{-}Bu)_2\}_2]$. The effects seem thus to be associated with the electronic properties of the $M(CO)_5$ group.

Mercury(II) compounds are known to form Lewis acid-base adducts with various basic transition metal (e.g. group VI B) compounds[5] and hence the N and O donors may possibly compete with an interaction between mercury and the metal M = Cr, Mo or W of 1.

Table 1. Analytical data of $[Hg\{PPh_2[M(CO)_5]\}_2L_n]$

M	L	n	C[a]	H[a]	N[a]
Cr	DMSO	2	41..2 (41.1)	3.0 (2.9)	
Cr	bipy	1	47.8 (47.6)	2.5 (2.5)	2.6 (2.5)
Cr	phen	1	48.8 (48.7)	2.6 (2.5)	2.4 (2.5)
Mo	DMSO	2	38.2 (38.1)	2.8 (2.7)	
Mo	bipy	1	44.0 (44.1)	2.5 (2.4)	2.3 (2.3)
Mo	phen	1	45.4 (45.2)	2.2 (2.3)	2.4 (2.3)
W	DMSO	2	33.2 (33.2)	2.5 (2.3)	
W	bipy	1	38.4 (38.4)	2.0 (2.1)	1.9 (2.0)
W	phen	1	39.8 (39.5)	2.3 (2.0)	2.0 (2.0)

[a] Found (calc.).

Table 2. NMR parameters of $[Hg\{PPh_2[M(CO)_5]\}_2L_n]$[a]

M	L	n	solvent	$\delta(^{31}P)$	$^1J(^{31}P-^{199}Hg)$
Cr			CH_2Cl_2	77.2[b]	640[b]
Mo			Ch_2Cl_2	50.5[b]	525[b]
W			CH_2Cl_2	27.4[b]	725[b]
Cr	phen	1	CH_2Cl_2	47.7	2046
Mo	phen	1	CH_2Cl_2	22.8	1958
W	phen	1	CH_2Cl_2	0.9	2231
Cr	bipy	1	CH_2Cl_2	53.9	1742
Mo	bipy	1	CH_2Cl_2	31.6	1488
W	bipy	1	CH_2Cl_2	6.8	1879
Cr		1	pyridine	63.4	1433
Mo			pyridine	37.3	1318
W			pyridine	14.8	1582

[a] 10^{-4} mol/cm^3, 301 K, chemical shifts in ppm to high frequency of 85% H_3PO_4, coupling constants in Hz.
[b] Taken from Ref. 4.

The complexation by N and O donors is associated with a decrease in $\nu(CO)$ absorptions of 1 up to 10 wavenumbers. Shifts to high frequencies were observed for Lewis acid–base interactions between substituted group VI B carbonyl compounds and mercury(II) compounds.[5]

The ^{199}Hg chemical shift of 1 (M = Cr) changes from 1278 ppm in CH_2Cl_2[4] to 1335 ppm in pyridine [reference aqueous $Hg(ClO_4)_2$], this difference being small in comparison with other mercury(II) compounds.

The complexes of 1 with bipy and phen are essentially non-dissociated in solution, whilst the DMSO complexes are considerably dissociated (decrease of $\delta(^{31}P)$ and increase of $^1J(^{31}P-^{199}Hg)$ upon cooling or presence of excess ligand.) The monodentate ligands pyridine-N-oxide and pyridine behave in the same way. No complexation was observed with Ph_2S as indicated by unchanged $\delta(^{31}P)$ and $^1J(^{31}P-^{199}Hg)$ values of 1.

Solutions of one half equivalent phen or bipy and 1 exhibit one broad (W1/2 = 200 Hz) ^{31}P resonance at ambient temperature which resolves to the sharp signals of the uncomplexed 1 and its phen or bipy complex upon cooling below 263 K. This is due to the ligand exchange reaction (1),

$$[Hg\{PPh_2[M(CO)_5]\}_2L] + [Hg\{PPh_2[M(CO)_5]\}_2] \rightleftharpoons [Hg\{PPh_2[M(CO)_5]\}_2] + [Hg\{PPh_2[M(CO)_5]\}_2L] \quad L = \text{phen or bipy} \quad (1)$$

and proves the stoicheiometry of the co-ordination complexes in solution.

EXPERIMENTAL

NMR spectra were recorded on a Bruker WP-80 in the FT mode, chemical analyses were obtained with a Heraeus EA-415.

All operations were carried out under dinitrogen in dried solvents.

The compounds 1 were prepared as described previously,[4] the new $[Hg\{PCy_2[Cr(CO)_5]\}_2]$ was obtained analogously to 1: yellowish-white crystals, dec. above 200°C; found: C 41.7, H 4.6, calc. for $C_{34}H_{44}Cr_2HgO_{10}P_2$: C 41.7, H 4.5; Molecular weight: 978 (MS, based on ^{52}Cr and ^{200}Hg), $\delta(^{31}P)$: 90.6, $^1J(^{31}P-^{199}Hg)$: 603 Hz (5×10^{-5} mol/cm^3 CH_2Cl_2, reference 85% H_3PO_4).

The DMSO complexes crystallize upon addition of excess DMSO to CH_2Cl_2 solutions of 1. They are only sparingly soluble in DMSO and better in CH_2Cl_2. The bipy and phen complexes were obtained by slow evaporation of equimolar solutions of the ligands and 1 in toluene. (The crystallisation tendency of the phen complexes is rather low.)

Acknowledgement—Thanks are due to the Fonds zur Förderung der Wissenschaft, Vienna, for making available the NMR spectrometer.

PAUL PERINGER

Institut für Anorg. und Analyt. Chemie der Universität Innsbruck
Innrain 52a,
A-6020 Innsbruck, Austria

REFERENCES

[1]C. A. McAuliffe, *The Chemistry of Mercury*. McMillan, London, 1977.
[2]H. Schmidbaur and K. H. Raethlein, *Chem. Ber.* 1973, **106**, 2491.
[3]J. Eichbichler and P. Peringer, *Inorg. Nucl. Chem. Lett.* 1981, **17**, 305.
[4]P. Peringer and J. Eichbichler, *J. Chem. Soc. Dalton*, 1982, 667.
[5]K. Edgar, B. F. G. Johnson, J. Lewis and S. B. Wild, *J. Chem. Soc. (A)* **1968**, 2851.

Polyhedron Vol. 1, No. 11-12, pp. 820-822, 1982
Printed in Great Britain.

0277-5387/82/110820-03$03.00/0
Pergamon Press Ltd.

Fragmentation of μ_4-oxohexa-μ-nitratotetraberyllium, $Be_4O(NO)_3)_6$, under electron impact

(*Received* 18 *March* 1982)

Abstract—The behaviour of $Be_4O(NO_3)_6$ under electron impact is similar to that of its carboxylato analogues, $Be_4O(RCO_2)_6$ where R is H, alkyl or halogenated alkyl. In all these systems, the dissociation of the molecular ions is dominated by steric interactions. The major fragmentations involve the elimination of N_2O_5 or $(RCO)_2O$ and $Be(NO_3)_2$ or $Be(RCO_2)_2$ from the ions $[M-NO_3]^+$ or $[M-RCO_2]^+$. The results obtained confirm the structural similarity of the nitrato complex to tetra-nuclear beryllium oxocarboxylates.

μ_4-Oxohexa-μ-nitratotetraberyllium (beryllium oxonitrate) was first synthesized by Addison and Walker.[1] The product composition, its volatility and IR spectrum in the region of NO_3 stretches enabled the authors to suggest a structure similar to the more familiar beryllium oxocarboxylates, with bridge ligands linking pairs of metal ions along 6 OBe_4 tetrahedron edges. This structure was later confirmed by X-ray diffraction.[2]

Earlier, electron impact induced fragmentations of a number of tetranuclear metal oxoacido complexes[3-6] and metal nitrates[7] have been studied. We now report the results of a mass spectrometric study of $Be_4O(NO_3)_6$ undertaken in order to determine the molecular composition of this compound in the gas phase for the purpose of interpreting its electron diffraction pattern. The spectrum was recorded on an AEI MS-30 instrument equipped with a DS-50 data processing system. The conditions were: direct inlet system temperature 30°C, ionizing chamber temperature 250°C, ionizing electron energy 70 eV, emission current 100 mcA. The compound was prepared by nitration of $BeCl_2$ with nitric anhydride followed by sublimation of the product at 130–140°C.[8]

The metal-containing fragment ions observed in the spectrum are shown in Scheme 1. On the whole, the spectrum is analogous to the spectra of beryllium and zinc carboxylato complexes[3-6] on the one hand and to those of Group IV metal tetranitrates[7] on the other. None of these spectra contains the molecular ion; the heaviest ions are formed by the elimination of one acido ligand radical from $[M]^+$. Further fragmentations of transition metal nitrates (Ti, Zr, Hf, Sn, V[7]) involve the loss of N_2O_5, N_2O_6, NO and NO_2. The relative intensities of fragment ions formed from $[Be_4O(NO_3)_6]^+$ (with retention of its tetranuclear core) and from $[Ti(NO_3)_4]^+$ in sequential fragmentation steps are compared in Table 1. The spectra are obviously similar which, probably, reflects similarity in the nature of nitrato group interactions with heavy cations and the tetra-nuclear cluster OBe_4. The presence of ions *d* in the spectrum of $Ti(NO_3)_4$ was explained[7] by the change of Ti valency state to 2+; the absence of the corresponding ions in the spectrum of $Be_4O(NO_3)_6$ confirms this explanation. With titanium, steps *e* and *f* lead to the intense oxo-ions $[TiO_3]^+$ and $[TiO_2]^+$ whose further fragmentations are impeded by the absence of intact ligands. Fragment ions formed from $[Be_4O(NO_3)_6]^+$ at the corresponding steps still contain NO_3 groups and are for that reason less stable. In spite of that, the *e*/*f* intensity ratios (i.e. the relative probabilities of the formation of ions *e* and *f*, see Scheme 1) are approximately the same in the two spectra. Lastly, the fragmentation chain is longer with $Be_4O(NO_3)_6$ because of the presence of a larger number of ligands in the parent ion.

The other fragmentation path of beryllium oxonitrate naturally absent in the spectra of mononuclear complexes involves the loss of the $Be(NO_3)_2$ molecule from $[Be_4O(NO_3)_5]^+$ (the corresponding transition was proved by metastables for beryllium oxocarboxylato complexes) and leads directly to the most intense metal-containing ion, $[Be_3O(NO_3)_3]^+$. The further dissociation of this ion proceeds as with tetra-nuclear fragments. Similar in nature and intensity processes are observed in all the beryllium and zinc μ_4-oxoderivatives studied.[3-6] The summed intensities of tri- and tetra-nuclear fragments in the spectra of beryllium oxonitrate and its structural analogues are compared in Table 2.

The data given in that table are indicative of comparative independence of cluster unit fragmentations on the ligand electronic properties. This substantiates the stereochemical rationalization of the stabilization processes in electron impact induced mass spectra of inorganic coordination compounds suggested in our earlier works.[3-6] This typically inorganic type of behaviour depends probably on predominantly ionic nature of interactions between ligands and the inorganic core.

A detailed comparison of the data on beryllium compounds lends further support to this conclusion. Thus, $[Be_4OX_5]^+$ ions, where X is an acido ligand, all fragment by two mechanisms, by splitting off of the corresponding acid anhydride with the formation of the ions $[Be_4OX_3O]^+$ and by the loss of the BeX_2

All operations were carried out under dinitrogen in dried solvents.

The compounds 1 were prepared as described previously,[4] the new $[Hg\{PCy_2[Cr(CO)_5]\}_2]$ was obtained analogously to 1: yellowish-white crystals, dec. above 200°C; found: C 41.7, H 4.6, calc. for $C_{34}H_{44}Cr_2HgO_{10}P_2$: C 41.7, H 4.5; Molecular weight: 978 (MS, based on ^{52}Cr and ^{200}Hg), $\delta(^{31}P)$: 90.6, $^1J(^{31}P-^{199}Hg)$: 603 Hz (5×10^{-5} mol/cm^3 CH_2Cl_2, reference 85% H_3PO_4).

The DMSO complexes crystallize upon addition of excess DMSO to CH_2Cl_2 solutions of 1. They are only sparingly soluble in DMSO and better in CH_2Cl_2. The bipy and phen complexes were obtained by slow evaporation of equimolar solutions of the ligands and 1 in toluene. (The crystallisation tendency of the phen complexes is rather low.)

Acknowledgement—Thanks are due to the Fonds zur Förderung der Wissenschaft, Vienna, for making available the NMR spectrometer.

PAUL PERINGER

Institut für Anorg. und Analyt. Chemie der Universität Innsbruck
Innrain 52a,
A-6020 Innsbruck, Austria

REFERENCES

[1]C. A. McAuliffe, *The Chemistry of Mercury*. McMillan, London, 1977.
[2]H. Schmidbaur and K. H. Raethlein, *Chem. Ber.* 1973, **106**, 2491.
[3]J. Eichbichler and P. Peringer, *Inorg. Nucl. Chem. Lett.* 1981, **17**, 305.
[4]P. Peringer and J. Eichbichler, *J. Chem. Soc. Dalton*, 1982, 667.
[5]K. Edgar, B. F. G. Johnson, J. Lewis and S. B. Wild, *J. Chem. Soc. (A)* **1968**, 2851.

Polyhedron Vol. 1, No. 11-12, pp. 820-822, 1982
Printed in Great Britain.

0277-5387/82/110820-03$03.00/0
Pergamon Press Ltd.

Fragmentation of μ_4-oxohexa-μ-nitratotetraberyllium, $Be_4O(NO)_3)_6$, under electron impact

(*Received* 18 *March* 1982)

Abstract—The behaviour of $Be_4O(NO_3)_6$ under electron impact is similar to that of its carboxylato analogues, $Be_4O(RCO_2)_6$ where R is H, alkyl or halogenated alkyl. In all these systems, the dissociation of the molecular ions is dominated by steric interactions. The major fragmentations involve the elimination of N_2O_5 or $(RCO)_2O$ and $Be(NO_3)_2$ or $Be(RCO_2)_2$ from the ions $[M-NO_3]^+$ or $[M-RCO_2]^+$. The results obtained confirm the structural similarity of the nitrato complex to tetra-nuclear beryllium oxocarboxylates.

μ_4-Oxohexa-μ-nitratotetraberyllium (beryllium oxonitrate) was first synthesized by Addison and Walker.[1] The product composition, its volatility and IR spectrum in the region of NO_3 stretches enabled the authors to suggest a structure similar to the more familiar beryllium oxocarboxylates, with bridge ligands linking pairs of metal ions along 6 OBe_4 tetrahedron edges. This structure was later confirmed by X-ray diffraction.[2]

Earlier, electron impact induced fragmentations of a number of tetranuclear metal oxoacido complexes[3-6] and metal nitrates[7] have been studied. We now report the results of a mass spectrometric study of $Be_4O(NO_3)_6$ undertaken in order to determine the molecular composition of this compound in the gas phase for the purpose of interpreting its electron diffraction pattern. The spectrum was recorded on an AEI MS-30 instrument equipped with a DS-50 data processing system. The conditions were: direct inlet system temperature 30°C, ionizing chamber temperature 250°C, ionizing electron energy 70 eV, emission current 100 mcA. The compound was prepared by nitration of $BeCl_2$ with nitric anhydride followed by sublimation of the product at 130–140°C.[8]

The metal-containing fragment ions observed in the spectrum are shown in Scheme 1. On the whole, the spectrum is analogous to the spectra of beryllium and zinc carboxylato complexes[3-6] on the one hand and to those of Group IV metal tetranitrates[7] on the other. None of these spectra contains the molecular ion; the heaviest ions are formed by the elimination of one acido ligand radical from $[M]^+$. Further fragmentations of transition metal nitrates (Ti, Zr, Hf, Sn, V[7]) involve the loss of N_2O_5, N_2O_6, NO and NO_2. The relative intensities of fragment ions formed from $[Be_4O(NO_3)_6]^+$ (with retention of its tetranuclear core) and from $[Ti(NO_3)_4]^+$ in sequential fragmentation steps are compared in Table 1. The spectra are obviously similar which, probably, reflects similarity in the nature of nitrato group interactions with heavy cations and the tetra-nuclear cluster OBe_4. The presence of ions *d* in the spectrum of $Ti(NO_3)_4$ was explained[7] by the change of Ti valency state to 2+; the absence of the corresponding ions in the spectrum of $Be_4O(NO_3)_6$ confirms this explanation. With titanium, steps *e* and *f* lead to the intense oxo-ions $[TiO_3]^+$ and $[TiO_2]^+$ whose further fragmentations are impeded by the absence of intact ligands. Fragment ions formed from $[Be_4O(NO_3)_6]^+$ at the corresponding steps still contain NO_3 groups and are for that reason less stable. In spite of that, the *e*/*f* intensity ratios (i.e. the relative probabilities of the formation of ions *e* and *f*, see Scheme 1) are approximately the same in the two spectra. Lastly, the fragmentation chain is longer with $Be_4O(NO_3)_6$ because of the presence of a larger number of ligands in the parent ion.

The other fragmentation path of beryllium oxonitrate naturally absent in the spectra of mononuclear complexes involves the loss of the $Be(NO_3)_2$ molecule from $[Be_4O(NO_3)_5]^+$ (the corresponding transition was proved by metastables for beryllium oxocarboxylato complexes) and leads directly to the most intense metal-containing ion, $[Be_3O(NO_3)_3]^+$. The further dissociation of this ion proceeds as with tetra-nuclear fragments. Similar in nature and intensity processes are observed in all the beryllium and zinc μ_4-oxoderivatives studied.[3-6] The summed intensities of tri- and tetra-nuclear fragments in the spectra of beryllium oxonitrate and its structural analogues are compared in Table 2.

The data given in that table are indicative of comparative independence of cluster unit fragmentations on the ligand electronic properties. This substantiates the stereochemical rationalization of the stabilization processes in electron impact induced mass spectra of inorganic coordination compounds suggested in our earlier works.[3-6] This typically inorganic type of behaviour depends probably on predominantly ionic nature of interactions between ligands and the inorganic core.

A detailed comparison of the data on beryllium compounds lends further support to this conclusion. Thus, $[Be_4OX_5]^+$ ions, where X is an acido ligand, all fragment by two mechanisms, by splitting off of the corresponding acid anhydride with the formation of the ions $[Be_4OX_3O]^+$ and by the loss of the BeX_2

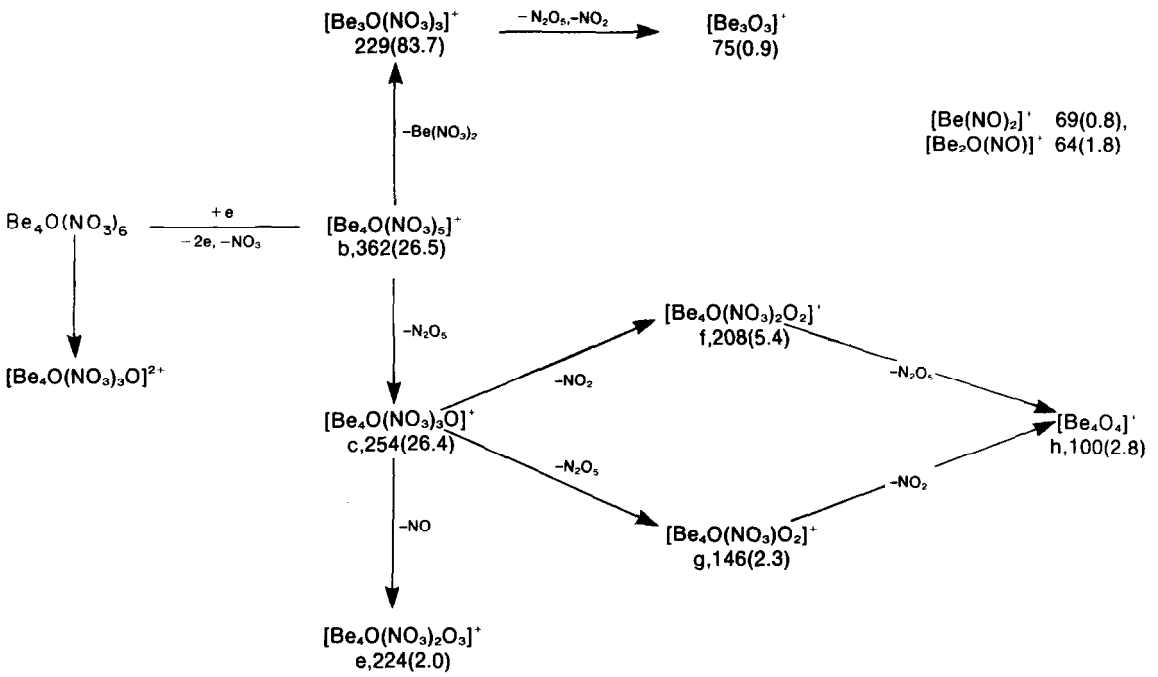

Scheme 1. Fragmentation of $Be_4O(NO_3)_6$ under electron impact. The *m/e* values and relative intensities (in parentheses) are given. The ions included in Table 1 are labelled by letters. The intensities are related to $[NO_2]^+$ as base ion.

Table 1. Relative intensities of metal-containing ions in the spectra of $Ti(NO_3)_4$[7] and $Be_4O(NO_3)_6$* (in per cent of the summed intensities)

	Ion	$Ti(NO_3)_4$	$Be_4O(NO_3)_6$
a	$[M]^+$	-	-
b	$[M-NO_3]^+$	35.7	40.5
c	$[b-N_2O_5]^+$	15.5	40.4
d	$[b-N_2O_6]^+$	3.0	-
e	$[c-NO]^+$	13.7	3.1
f	$[c-NO_2]^+$	32.1	8.3
g	$[c-N_2O_5]^+$	-	3.5
h	$[f-N_2O_5]^+$ $[g-NO_2]^+$	-	4.3
	Total	100	100

*Tetranuclear ions only are included.

molecule and formation of the planar $[Be_3OX_3]^+$ ion,[6] the most stable particle in all the spectra studied. In the further fragmentations, the major process is the elimination of NO_2 ($CHal_2CO_2$ from halogenated beryllium oxoacetates) with oxygen (halogen) transfer to the free coordination site on the inorganic core (with hydrogen-containing ligands such as carboxylato and alkoxo groups, the corresponding process involves proton shift to oxygen and splitting off of ketene or olefinic fragments). The specific feature of the spectrum of beryllium oxonitrate, the elimination of NO and like fragments, may reasonably well be explained by the presence of a variable valence element in the ligand (for details see Ref. [7]). The appearance of double charged ions in the spectra of zinc and halogenated beryllium oxocarboxylates (see the ion $[Be_4O(NO_3)_3O]^{2+}$, Scheme 1) is discussed in the work.[5]

The absence of the ions whose origin from $[M]^+$ is doubtful or merely does not fit the schemes usual for beryllium complexes and metal nitrates has two important implications. First, it points to the uniformity of the molecular composition of $Be_4O(NO_3)_6$ in the gas phase which is important for the interpretation of its gas phase electron diffraction pattern we are now completing. Second, the striking similarity of the mass spectra of all beryl-

Table 2. Intensities of tetra- and trinuclear ions in the mass spectra of Be_4OX_6 (X is an acido ligand)

X	Be_4	Be_3	Refs.
NO_3	39.7	60.3	This work
HCO_2	54.2	41.2	[3]
CH_3CO_2	63.1	33.1	[3]
CF_3CO_2	76.2	23.8	[5]
CCl_3CO_2	54.9	35.9	[5]

lium μ_4-oxoacido complexes presupposes a similarity in the structures of these compounds.

To conclude, we wish to emphasize once more that the mass spectrometric evidence collected in this work and in those cited above shows that with inorganic coordination compounds, ligand electronic effects are of only minor importance in determining the direction of ion stabilization processes. In return and in part as a consequence, mass spectra of inorganic complexes are an especially useful source of structural information.

Department of Chemistry
Moscow State University
Moscow 117234
U.S.S.R.

VIKTOR A. SIPACHEV*
NIKOLAI I. TUSEEV

A. N. Nesmeyanov Institute of Organo-Element Compounds of the U.S.S.R. Academy of Sciences
Moscow 117813
U.S.S.R.

YURII S. NEKRASOV

*Author to whom correspondence should be addressed.

R. F. GALIMZYANOV
V. I. Vernadskii Institute of Geochemistry and Analytical Chemistry of the U.S.S.R. Academy of Sciences
Moscow 117334
U.S.S.R.

REFERENCES

[1]C. C. Addison and A. Walker, *Proc. Chem. Soc.*, 1961, 242.
[2]B. Duffin, M. J. Haley and S. C. Wallwork, private communication.
[3]Yu. S. Nekrasov, S. Yu. Sil'vestrova, A. I. Grigor'ev, L. N. Reshetova and V. A. Sipachev, *Org. Mass Spectrom.*, 1978, **13**, 491.
[4]V. A. Sipachev, L. N. Reshetova, Yu. S. Nekrasov and S. Yu. Sil'vestrova, *Org. Mass Spectrom.*, 1980, **15**, 192.
[5]V. A. Sipachev, Yu. S. Nekrasov and S. Yu. Sil'vestrova, *Org. Mass Spectrom.*, in press.
[6]V. A. Sipachev and I. P. Gloriozov, *Org. Mass Spectrom.*, 1979, **14**, 29.
[7]Yu. S. Nekrasov, V. A. Sipachev and N. I. Tuseev, *J. Inorg. Nucl. Chem.*, 1980, **42**, 1677.
[8]N. I. Tuseev, A. S. Izmailovich and L. N. Komissarova, *Vestnik Moskov. Univ., Ser. Khim.*, 1979, 284.

Polyhedron Vol. 1, No. 11-12, pp. 822-824, 1982
Printed in Great Britain.

0277-5387/82/110822-03$03.00/0
Pergamon Press Ltd.

A ^{11}B NMR study of 5,6-Dicarba-nido-decaborane (12)

(*Received* 19 *April* 1982)

Abstract—Final assignment of all eight signals in the ^{11}B NMR spectrum (64.2 MHz) of 5,6-dicarba-nido-decaborane (12) is reported on the basis of its substituted derivatives.

5,6-Dicarba-nido-decaborane (12), 5,6-$C_2B_8H_{12}$ (I), was prepared independently by two different methods by Rietz *et al.*[1] and in our laboratory.[2,3] On the basis of ^{1}H and ^{11}B NMR results, both groups suggested for (I) the same asymmetrical structure isoelectronic with the $[B_{10}H_{12}]^{2-}$ anion. The molecular structure of (I), shown in Scheme 1, has recently been unambiguously confirmed by an X-ray diffraction study[4] on *iso*-$B_{18}H_{22}$, which is the 8-substituted derivative of (I).[5,6] First attempts to assign the ^{11}B NMR spectrum of (I), based on its certain analogy with that of $B_{10}H_{14}$, were made by Rietz[7] and in our laboratory,[8,9] but a more rigorous assignment should be done only on the basis of specifically substituted derivatives of (I). Their syntheses are based on an oxidative degradation[2,3,10] of the B(9 or 11) atom in the framework of [7,8-$C_2B_9H_{12}]^-$ (see Scheme 1) or on a direct substitution of (I).

We report herein a final assignment of the ^{11}B NMR spectrum of (I) (see Fig. 1a) consisting of eight doublets of equal intensity. The *C*, *E* and *F* signals exhibit coupling to hydrogen bridges and should therefore be associated with the B(8, 9, 10) atoms. In accord with this finding is an evident sharpening and narrowing of these signals in the spectrum of μ-D_2-5,6-$C_2B_8H_{10}$(II) prepared by the exchange reaction of (I) with D_2O in ether. Line narrowing in the ^{11}B NMR spectrum of (I) (see Fig. 1b) revealed a distinct splitting[7] of the doublet *F*, which is typical of a C–B–μH arrangement[8] and the resonance *F* should therefore be due to the B(10) atom. The doublet *E* is distinctly split by an apparent ^{11}B–^{11}B coupling and can be attributed to the B(9) atom.

Ferric chloride oxidation of the [5-Cl-7,8-$C_2B_9H_{11}]^-$ anion[10] produced the mixture of 4-Cl-5,6-$C_2B_8H_{11}$ (III) and 8-Cl-$C_2B_8H_{11}$ (IV) from which pure compounds were isolated using

Table 2. Intensities of tetra- and trinuclear ions in the mass spectra of Be_4OX_6 (X is an acido ligand)

X	Be_4	Be_3	Refs.
NO_3	39.7	60.3	This work
HCO_2	54.2	41.2	[3]
CH_3CO_2	63.1	33.1	[3]
CF_3CO_2	76.2	23.8	[5]
CCl_3CO_2	54.9	35.9	[5]

lium μ_4-oxoacido complexes presupposes a similarity in the structures of these compounds.

To conclude, we wish to emphasize once more that the mass spectrometric evidence collected in this work and in those cited above shows that with inorganic coordination compounds, ligand electronic effects are of only minor importance in determining the direction of ion stabilization processes. In return and in part as a consequence, mass spectra of inorganic complexes are an especially useful source of structural information.

Department of Chemistry
Moscow State University
Moscow 117234
U.S.S.R.

VIKTOR A. SIPACHEV*
NIKOLAI I. TUSEEV

A. N. Nesmeyanov Institute of Organo-Element Compounds of the U.S.S.R. Academy of Sciences
Moscow 117813
U.S.S.R.

YURII S. NEKRASOV

*Author to whom correspondence should be addressed.

R. F. GALIMZYANOV
V. I. Vernadskii Institute of Geochemistry and Analytical Chemistry of the U.S.S.R. Academy of Sciences
Moscow 117334
U.S.S.R.

REFERENCES

[1]C. C. Addison and A. Walker, *Proc. Chem. Soc.*, 1961, 242.
[2]B. Duffin, M. J. Haley and S. C. Wallwork, private communication.
[3]Yu. S. Nekrasov, S. Yu. Sil'vestrova, A. I. Grigor'ev, L. N. Reshetova and V. A. Sipachev, *Org. Mass Spectrom.*, 1978, **13**, 491.
[4]V. A. Sipachev, L. N. Reshetova, Yu. S. Nekrasov and S. Yu. Sil'vestrova, *Org. Mass Spectrom.*, 1980, **15**, 192.
[5]V. A. Sipachev, Yu. S. Nekrasov and S. Yu. Sil'vestrova, *Org. Mass Spectrom.*, in press.
[6]V. A. Sipachev and I. P. Gloriozov, *Org. Mass Spectrom.*, 1979, **14**, 29.
[7]Yu. S. Nekrasov, V. A. Sipachev and N. I. Tuseev, *J. Inorg. Nucl. Chem.*, 1980, **42**, 1677.
[8]N. I. Tuseev, A. S. Izmailovich and L. N. Komissarova, *Vestnik Moskov. Univ., Ser. Khim.*, 1979, 284.

Polyhedron Vol. 1, No. 11-12, pp. 822-824, 1982
Printed in Great Britain.

0277-5387/82/110822-03$03.00/0
Pergamon Press Ltd.

A ^{11}B NMR study of 5,6-Dicarba-nido-decaborane (12)

(*Received* 19 *April* 1982)

Abstract—Final assignment of all eight signals in the ^{11}B NMR spectrum (64.2 MHz) of 5,6-dicarba-nido-decaborane (12) is reported on the basis of its substituted derivatives.

5,6-Dicarba-nido-decaborane (12), 5,6-$C_2B_8H_{12}$ (I), was prepared independently by two different methods by Rietz *et al.*[1] and in our laboratory.[2,3] On the basis of ^{1}H and ^{11}B NMR results, both groups suggested for (I) the same asymmetrical structure isoelectronic with the $[B_{10}H_{12}]^{2-}$ anion. The molecular structure of (I), shown in Scheme 1, has recently been unambiguously confirmed by an X-ray diffraction study[4] on *iso*-$B_{18}H_{22}$, which is the 8-substituted derivative of (I).[5,6] First attempts to assign the ^{11}B NMR spectrum of (I), based on its certain analogy with that of $B_{10}H_{14}$, were made by Rietz[7] and in our laboratory,[8,9] but a more rigorous assignment should be done only on the basis of specifically substituted derivatives of (I). Their syntheses are based on an oxidative degradation[2,3,10] of the B(9 or 11) atom in the framework of [7,8-$C_2B_9H_{12}]^-$ (see Scheme 1) or on a direct substitution of (I).

We report herein a final assignment of the ^{11}B NMR spectrum of (I) (see Fig. 1a) consisting of eight doublets of equal intensity. The *C*, *E* and *F* signals exhibit coupling to hydrogen bridges and should therefore be associated with the B(8, 9, 10) atoms. In accord with this finding is an evident sharpening and narrowing of these signals in the spectrum of μ-D_2-5,6-$C_2B_8H_{10}$(II) prepared by the exchange reaction of (I) with D_2O in ether. Line narrowing in the ^{11}B NMR spectrum of (I) (see Fig. 1b) revealed a distinct splitting[7] of the doublet *F*, which is typical of a C–B–μH arrangement[8] and the resonance *F* should therefore be due to the B(10) atom. The doublet *E* is distinctly split by an apparent ^{11}B–^{11}B coupling and can be attributed to the B(9) atom.

Ferric chloride oxidation of the [5-Cl-7,8-$C_2B_9H_{11}]^-$ anion[10] produced the mixture of 4-Cl-5,6-$C_2B_8H_{11}$ (III) and 8-Cl-$C_2B_8H_{11}$ (IV) from which pure compounds were isolated using

preparative HPLC technique. Analogous oxidation of [9-Cl-7,8-$C_2B_9H_{11}$]$^-$ and [3-Ph-7,8-$C_2B_9H_{11}$]$^-$ afforded respectively 10-Cl-5,6-$C_2B_8H_{11}$ (V) and a mixture in which 2-Ph-5,6-$C_2B_8H_{11}$ (VI) predominated. ^{11}B NMR spectra of compounds (III)–(VI) (see Table 1), in which the resonances of substituted atoms collapsed to downfield shifted singlets, allowed us to identify the signals due to the B(4,8,10,2) atoms. Ferric chloride oxidation of the [1,5,6,10-10-D_4-7,8-$C_2B_9H^8$]$^-$ anion, obtained by base degradation of the 8,9,10,12-D_4-1,2-$C_2B_{10}H_8$ dicarbaborane, resulted in the isolation of 3,4,8,9-D_4-5,6-$C_2B_8H_9$ (VII). Replacement of four hydrogens for deuterium caused the resonances *C*, *D*, *E* and *H* to collapse to sharp singlets, which enabled us to assign the signal *D* to the B(3) atom. Only resonances due to B(1) and B(7) atoms remain to be assigned.

The following order of reactivity toward electrophilic substitution can be expected from the CNDO/2 atomic charges (in *e*): B(7) (−0.05) > B(4) (−0.03) > B(3), B(9) (+0.02) > B(8), B(10) (+0.04) > B(2) (+0.05) > B(1) (+0.06). Strong preference for electrophilic substitution at the B(7) site is also indicated by the character of the highest occupied molecular orbital. Direct

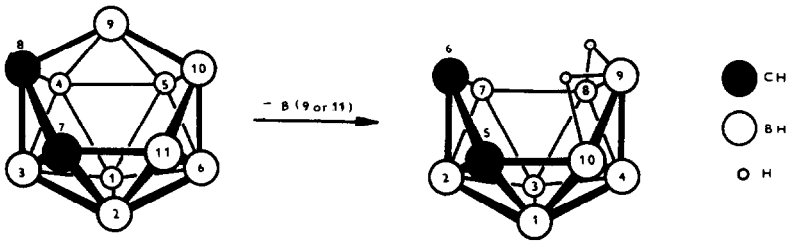

Scheme 1

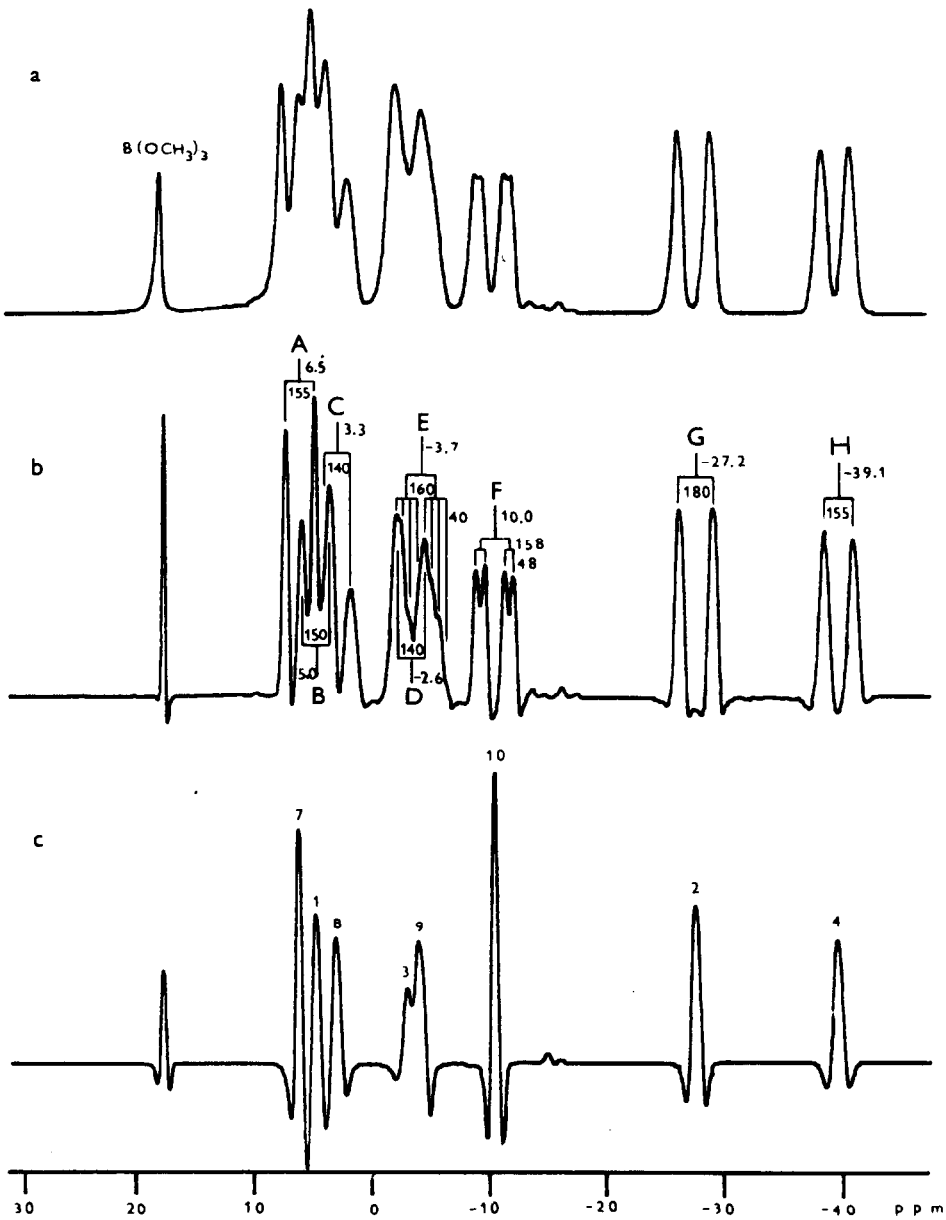

Fig. 1. ^{11}B NMR (64.2 MHz, $CDCl_3$) spectrum of 5,6-$C_2B_8H_{12}$ (a) normal (b) line narrowed (c) line narrowed, ^{1}H decoupled.

Table 1. Assignment of signals in the ^{11}B NMR spectra of substituted derivatives of 5,6-$C_2B_8H_{12}$

Compound	δ^{11}_B*							
	B(7)	B(1)	B(8)	B(3)	B(9)	B(10)	B(2)	B(4)
(II)	6.8	5.2	3.6	−2.1	−4.2	−9.1	−27.0	−38.8
(III)	7.2	6.4	4.0	−0.8	−3.2	−10.0	−26.9	−21.8[s]
(IV)	9.3	5.3	11.7[s]	−2.4	−6.2	−15.5	−27.2	−37.5
(V)	7.6	6.7	−0.2	−0.2	−6.7	−0.2[s]	−27.1	−38.0
(VII)	6.5	5.0	3.3[s]	−2.6[s]	−3.7[s]	−10.0	−27.2	−39.1[s]
(VIII)	9.6[s]	7.4	5.7	−1.0	−2.5	−8.8	−26.3	−39.2
(IX)	−4.5[s]	6.8	6.7	0.0	−2.8	−9.5	−26.0	−38.3
(X)	6.5[s]	5.0	3.3	−2.6[s]	−3.7	−10.0	−27.2	−39.1[s]

*In ppm relative to $BF_3.OEt_2$ at 64.2 MHz in $CDCl_3$
[s]singlet.

bromination and iodination of (I) in the $AlCl_3/CS_2$ system produced[10] monohalogenated species the structure of which was, accepting the above quantum chemical arguments, assigned to 7-Br (VIII) and 7-I-5,6-$C_2B_8H_{11}$ (IX). The 7-substitution caused the low field signal A to collapse to downfield and upfield shifted singlets in the spectra of (VIII) and (IX), respectively. Consistent with the CNDO/2 atomic charges is also the result of a prolonged deuteration of (I) with DCl/$AlCl_3$ to obtain a trideuterated species (X) the ^{11}B NMR spectrum of which confirmed a quantitative deuteration of the B(3,4,7) atoms. Consequently, the remaining doublet B is associated with the B(1) atom.

BOHUMIL ŠTÍBR*
STANISLAV HEŘMÁNEK
ZBYNĚK JANOUŠEK
ZBYNĚK PLZÁK
JIŘÍ DOLANSKÝ
JAROMÍR PLEŠEK

Institute of Inorganic Chemistry Prague, Czechoslovak Academy of Sciences, 250 68 Řež near Prague, Czechoslovakia

REFERENCES

[1]R. R. Rietz and R. Schaeffer, *J. Am. Chem. Soc.* 1971, **93**, 1263.
[2]J. Plešek and S. Heřmánek, *Chem. and Ind.* 1971, 1267.
[3]J. Plešek and S. Heřmánek, *Collect. Czech. Chem. Commun.* 1974, **39**, 821.
[4]V. Šurbrtová, A. Línek and J. Hašek, *Acta Cryst. Sect. (B)*, in press.
[5]Z. Janoušek, Thesis, *Institute of Inorganic Chemistry*, Prague, 1971.
[6]Z. Janoušek, J. Plešek, B. Štíbr and S. Heřmánek, *Collect. Czech. Chem. Commun.* in press.
[7]R. R. Rietz, Thesis, Indiana University, Bloomington, Indiana, 1971.
[8]J. Plešek and S. Heřmánek, *Pure Appl. Chem.* 1974, **39**, 431.
[9]H. M. Colquhoun, T. J. Greenhough, M. G. H. Wallbridge S. Heřmánek and J. Plešek, *J. Chem. Soc. (Dalton)* 1978, 944.
[10]B. Štíbr, S. Heřmánek and Z. Janoušek, *Collect. Czech. Chem. Commun.*, in press.

Polyhedron Vol. 1, No. 11-12, pp. 824-826, 1982
Printed in Great Britain.

0277-5387/82/110824-03$03.00/0
Pergamon Press Ltd.

Optically active (−)-5,6-dicarba-nido-decaborane (12)

(*Received* 19 *April* 1982)

Abstract—One-way conversion of the racemic (±)-5,6-dicarba-nido-decaborane (12) to its laevorotatory enantiomer by (+)-N-methylcamphidine is reported.

In 1969 we reported the resolution of 5-Br-6,9-$(Me_2S)_2B_{10}H_{11}$ (I) into enantiomers.[1] Its laevorotatory isomer was later converted to the dextrorotatory enantiomer[2] of 4-Br-1,2-$C_2B_{10}H_{11}$ (II). Later we published[3] the resolution of iso-$B_{18}H_{22}$ (III) into its antipodes, which were remarkable by having extreme values of specific rotation, especially that of its mono and dianion. Until recently, no absolute configuration of any optically active compound with a borane skeleton was known. However, the absolute configuration of the (+)-(I) enantiomer was established not long ago by an X-ray diffraction study,[4] which should reflect even on current nomenclature of borane compounds. Thus, the correlation of (I) and (II) families is now established, while the absolute configuration of (III) is hitherto unknown.

We report herein a high yield and one-way conversion of the racemic[5] (±)-5,6-$C_2B_8H_{12}$ (IV) to its laevorotatory enantiomer (−)-(IV). The conversion is based on the reaction of (+)-N-methylcamphidine, (+)-NMC, (+)-(V), with racemate (IV) to form a diastereomeric $[(+)\text{-NMCH}]^+$ $[(-)\text{-}5,6\text{-}C_2B_8H_{11}]^-$ salt (VI) from which the (−)-(IV) enantiomer is released by hydrochloric acid. The (+)-NMC, $[\alpha]_D^{20} + 34.0°$, was prepared by the reduction of (+)-N-methylcamphorimide with $NaAlH_2(OCH_2CH_2OCH_3)_2$ in benzene in 93% yield. According to our observations, the reaction of racemate (IV) and base (+)-(V) can be rationalized in terms of an equilibrium precipitation of the salt (VI) (see Scheme). The equilibrium is then regulated by the solubility product of (VI) (1.6×10^{-2} in *n*-hexane, estimated) and can be shifted in favour of (VI) by slow evaporation of solvents. In many experiments aimed at isolating the dextrorotatory form of (IV) from the solution remaining on the l.h.s. of the equilibrium after removing diastereomer (VI), only racemate (IV) was obtained which can be reused for further (IV)→(−)-(IV) conversion. Maximum yields of the total conversion ranged 85% in *n*-hexane using 1 : 2 molar ratio of (IV) and (+)-(V).

The results so far presented are in agreement with an evident fluxionality of the [5,6-$C_2B_8H_{11}$] anion in the solution. Indeed, a complete racemization of pure (−)-(IV) was achieved by the action of triethylamine in dichloromethane-*n*-hexane solution.

As seen in Tables 1 and 2, both ^1H and ^{11}B n.m.r. spectra of the diastereomer (VI) in $DCDl_3$ show only minor changes in comparison with those of compounds (IV) and (+)-(V), which strongly supports the idea that the diastereomer (VI), as the salt of a weak base (+)-(V) and a weak acid[6] (−)-(IV) (pK_a 6.18), is extensively dissociated in the solution.

The observed maximum $[\alpha]_D^{20}$ value for the isolated (−)-(IV) enantiomer is very high and we feel that this is not only a consequence of a formal replacement of two BH^- groups for two isoelectronic CH vertices in $[B_{10}H_{12}]^{2-}$, but also the consequence of a gross distortion[7] of the 5,6-$C_2B_8H_{12}$ framework caused by such a skeletal substitution.

Due to its equilibrium character, the discussed (IV)→(−)-(IV)

Table 1. Assignment of signals in the ^{11}B NMR spectra of substituted derivatives of 5,6-$C_2B_8H_{12}$

Compound	δ^{11}_B*							
	B(7)	B(1)	B(8)	B(3)	B(9)	B(10)	B(2)	B(4)
(II)	6.8	5.2	3.6	−2.1	−4.2	−9.1	−27.0	−38.8
(III)	7.2	6.4	4.0	−0.8	−3.2	−10.0	−26.9	−21.8[s]
(IV)	9.3	5.3	11.7[s]	−2.4	−6.2	−15.5	−27.2	−37.5
(V)	7.6	6.7	−0.2	−0.2	−6.7	−0.2[s]	−27.1	−38.0
(VII)	6.5	5.0	3.3[s]	−2.6[s]	−3.7[s]	−10.0	−27.2	−39.1[s]
(VIII)	9.6[s]	7.4	5.7	−1.0	−2.5	−8.8	−26.3	−39.2
(IX)	−4.5[s]	6.8	6.7	0.0	−2.8	−9.5	−26.0	−38.3
(X)	6.5[s]	5.0	3.3	−2.6[s]	−3.7	−10.0	−27.2	−39.1[s]

*In ppm relative to $BF_3.OEt_2$ at 64.2 MHz in $CDCl_3$
[s]singlet.

bromination and iodination of (I) in the $AlCl_3/CS_2$ system produced[10] monohalogenated species the structure of which was, accepting the above quantum chemical arguments, assigned to 7-Br (VIII) and 7-I-5,6-$C_2B_8H_{11}$ (IX). The 7-substitution caused the low field signal A to collapse to downfield and upfield shifted singlets in the spectra of (VIII) and (IX), respectively. Consistent with the CNDO/2 atomic charges is also the result of a prolonged deuteration of (I) with DCl/$AlCl_3$ to obtain a trideuterated species (X) the ^{11}B NMR spectrum of which confirmed a quantitative deuteration of the B(3,4,7) atoms. Consequently, the remaining doublet B is associated with the B(1) atom.

BOHUMIL ŠTÍBR*
STANISLAV HEŘMÁNEK
ZBYNĚK JANOUŠEK
ZBYNĚK PLZÁK
JIŘÍ DOLANSKÝ
JAROMÍR PLEŠEK

Institute of Inorganic Chemistry Prague, Czechoslovak Academy of Sciences, 250 68 Řež near Prague, Czechoslovakia

REFERENCES

[1]R. R. Rietz and R. Schaeffer, *J. Am. Chem. Soc.* 1971, **93**, 1263.
[2]J. Plešek and S. Heřmánek, *Chem. and Ind.* 1971, 1267.
[3]J. Plešek and S. Heřmánek, *Collect. Czech. Chem. Commun.* 1974, **39**, 821.
[4]V. Šurbrtová, A. Línek and J. Hašek, *Acta Cryst. Sect. (B)*, in press.
[5]Z. Janoušek, Thesis, *Institute of Inorganic Chemistry*, Prague, 1971.
[6]Z. Janoušek, J. Plešek, B. Štíbr and S. Heřmánek, *Collect. Czech. Chem. Commun.* in press.
[7]R. R. Rietz, Thesis, Indiana University, Bloomington, Indiana, 1971.
[8]J. Plešek and S. Heřmánek, *Pure Appl. Chem.* 1974, **39**, 431.
[9]H. M. Colquhoun, T. J. Greenhough, M. G. H. Wallbridge S. Heřmánek and J. Plešek, *J. Chem. Soc. (Dalton)* 1978, 944.
[10]B. Štíbr, S. Heřmánek and Z. Janoušek, *Collect. Czech. Chem. Commun.*, in press.

Polyhedron Vol. 1, No. 11-12, pp. 824-826, 1982
Printed in Great Britain.

0277-5387/82/110824-03$03.00/0
Pergamon Press Ltd.

Optically active (−)-5,6-dicarba-nido-decaborane (12)

(*Received* 19 *April* 1982)

Abstract—One-way conversion of the racemic (±)-5,6-dicarba-nido-decaborane (12) to its laevorotatory enantiomer by (+)-N-methylcamphidine is reported.

In 1969 we reported the resolution of 5-Br-6,9-$(Me_2S)_2B_{10}H_{11}$ (I) into enantiomers.[1] Its laevorotatory isomer was later converted to the dextrorotatory enantiomer[2] of 4-Br-1,2-$C_2B_{10}H_{11}$ (II). Later we published[3] the resolution of iso-$B_{18}H_{22}$ (III) into its antipodes, which were remarkable by having extreme values of specific rotation, especially that of its mono and dianion. Until recently, no absolute configuration of any optically active compound with a borane skeleton was known. However, the absolute configuration of the (+)-(I) enantiomer was established not long ago by an X-ray diffraction study,[4] which should reflect even on current nomenclature of borane compounds. Thus, the correlation of (I) and (II) families is now established, while the absolute configuration of (III) is hitherto unknown.

We report herein a high yield and one-way conversion of the racemic[5] (±)-5,6-$C_2B_8H_{12}$ (IV) to its laevorotatory enantiomer (−)-(IV). The conversion is based on the reaction of (+)-N-methylcamphidine, (+)-NMC, (+)-(V), with racemate (IV) to form a diastereomeric $[(+)\text{-NMCH}]^+$ $[(-)\text{-}5,6\text{-}C_2B_8H_{11}]^-$ salt (VI) from which the (−)-(IV) enantiomer is released by hydrochloric acid. The (+)-NMC, $[\alpha]_D^{20} + 34.0°$, was prepared by the reduction of (+)-N-methylcamphorimide with $NaAlH_2(OCH_2CH_2OCH_3)_2$ in benzene in 93% yield. According to our observations, the reaction of racemate (IV) and base (+)-(V) can be rationalized in terms of an equilibrium precipitation of the salt (VI) (see Scheme). The equilibrium is then regulated by the solubility product of (VI) (1.6×10^{-2} in *n*-hexane, estimated) and can be shifted in favour of (VI) by slow evaporation of solvents. In many experiments aimed at isolating the dextrorotatory form of (IV) from the solution remaining on the l.h.s. of the equilibrium after removing diastereomer (VI), only racemate (IV) was obtained which can be reused for further (IV)→(−)-(IV) conversion. Maximum yields of the total conversion ranged 85% in *n*-hexane using 1 : 2 molar ratio of (IV) and (+)-(V).

The results so far presented are in agreement with an evident fluxionality of the [5,6-$C_2B_8H_{11}$] anion in the solution. Indeed, a complete racemization of pure (−)-(IV) was achieved by the action of triethylamine in dichloromethane-*n*-hexane solution.

As seen in Tables 1 and 2, both ^1H and ^{11}B n.m.r. spectra of the diastereomer (VI) in $DCDl_3$ show only minor changes in comparison with those of compounds (IV) and (+)-(V), which strongly supports the idea that the diastereomer (VI), as the salt of a weak base (+)-(V) and a weak acid[6] (−)-(IV) (pK_a 6.18), is extensively dissociated in the solution.

The observed maximum $[\alpha]_D^{20}$ value for the isolated (−)-(IV) enantiomer is very high and we feel that this is not only a consequence of a formal replacement of two BH^- groups for two isoelectronic CH vertices in $[B_{10}H_{12}]^{2-}$, but also the consequence of a gross distortion[7] of the 5,6-$C_2B_8H_{12}$ framework caused by such a skeletal substitution.

Due to its equilibrium character, the discussed (IV)→(−)-(IV)

solution precipitate

$$(\pm)\text{-}5,6\text{-}C_2B_8H_{12} + (+)\text{-NMC} \rightleftarrows (+)\text{-NMCH}^{+}[(-)\text{-}5,6\text{-}C_2B_8H_{11}^{-}]$$
(IV) (+)-(V) (VI)

↓ dil. HCl

$[\alpha]_D^{20}$ for (−)-(IV) −841.23° (−)-5,6-$C_2B_8H_{12}$

(petrolether c 1.4) (−)-(IV)

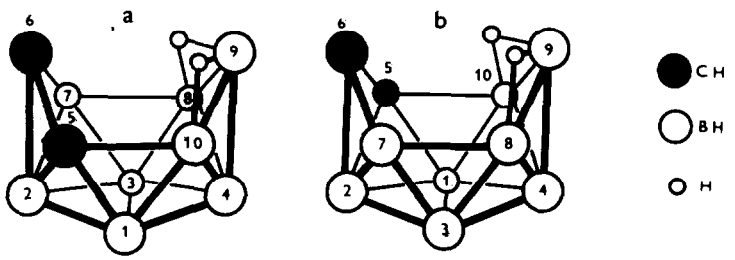

Fig. 1. Numbering system[1] for two 5,6-$C_2B_8H_{12}$ enantiomers (a) *p*-(IV) (counterclockwise numbering). (b) *σ*-(IV) (clockwise numbering).

Table 1.

^{11}B n.m.r. spectra (64.2 MHz)

Compound	Solvent	δ_B^*
(IV)	$CDCl_3$	6.5(1), 5.0(1), 3.3(1), -2.6(1), -10.0(1), -27.2(1), -39.1(1)
(VI)	$CDCl_3$	6.6(1), 5.1(1), 3.4(1), -2.9(1) -10.0(1), -27.1(1), -39.0(1)
$Na^+[5,6\text{-}C_2B_8H_{11}]^-$	CD_3CN	17.5(1), 8.2(1), -1.9(1), -11.5(1), -14.1(1), -15.0(1), -28.7(1), -31.0(1)

*In ppm relative to $BF_3.OEt_2$; relative intensity in parentheses.

Table 2.

^{1}H n.m.r. spectra (60 MHz)

Compound	Solvent	δ^*
(IV)	$CDCl_3$	6.51(1)(CH skel.), 4.99(1)(CH skel.), -2.4(2)(B-μH)
(VI)	$CDCl_3$	6.47(1)(CH skel.), 4.97(CH skel.), 2.71(2)(CH_2N), 2.68(2)(CH_2N), 2.35 (3)(CH_3N), 1.72(5)(CH_2,CH), 0.96 (3)(CH_3), 0.90(3)(CH_3), 0.84(3)(CH_3), -2.4(2)(B-μH)
(+)-(V)	$CDCl_3$	2.52(2)(CH_2N), 2.48(2)(CH_2N), 2.25 (3)(CH_3N), 1.64(5)(CH_2,CH), 0.91 (3)(CH_3), 0.87(3)(CH_3), 0.79(3)(CH_3)
$Na^+[5,6\text{-}C_2B_8H_{11}]^-$	CD_3CN	4.56(CH skel.)

*In ppm relative to TMS; relative intensity and assignment in parentheses.

conversion represents a rare reaction in which a racemate can be converted to only one optically active form. From the above results it follows that the missing (+)-(IV) antipode can be isolated by the use of (−)-NMC or a different optically active base as the precipitating agent. The relevant experiments along with those aimed at determining the absolute configuration in the 5,6-$C_2B_8H_{12}$ series are now in progress.

REFERENCES

1. J. Plešek, S. Heřmánek and B. Štíbr, *Collect. Czech. Chem. Commun.* 1969, **34**, 3233.
2. J. Plešek, V. Gregor and S. Heřmánek, *Collect. Czech. Chem. Commun.* 1970, **35**, 346.
3. S. Heřmánek and J. Plešek, *Collect. Czech. Chem. Commun.* 1970, **35**, 2488.
4. E. Císařová and A. Línek, *Acta Cryst. Sect.* (*B*), in press.
5. J. Plešek and S. Heřmánek, *Collect. Czech. Chem. Commun.* 1974, **39**, 821.
6. S. Heřmánek, H. Plotová and J. Plešek, *Collect. Czech. Chem. Commun.* 1975, **40**, 3593.
7. V. Šubrtová, A. Línek and J. Hašek, *Acta Cryst. Sect.* (*B*), in press.

*Author to whom correspondence should be addressed.

Institute of Inorganic Chemistry Prague, Czechoslovak Academy of Sciences, BOHUMIL ŠTÍBR*
250 68 *Řež near Prague,* JAROMÍR PLEŠEK
Czechoslovakia
Laboratory of Monosacharides, ALENA ZOBÁČOVÁ
Prague Institute of Chemical Technology, Suchbátarova 5,
166 28 *Prague* 6,
Czechoslovakia

Polyhedron Vol. 1, No. 11-12, pp. 826-827, 1982
Printed in Great Britain.

0277-5387/82/110826-02$03.00/0
Pergamon Press Ltd.

Evidence for trifluoromethyltin(II) compounds

(*Received* 17 *May* 1982)

Abstract—The products of several reactions between $(CF_3)_2Cd \cdot$ glyme and SnI_2 in tetrahydrofuran have been examined by ^{19}F NMR. Resonances representing the new compounds CF_3CdI, CF_3SnI and $(CF_3)_2Sn$ were assigned based on NMR parameters and ^{119}Sn Mössbauer spectra.

Although trifluoromethyl-tin (IV) compounds have been prepared by a variety of routes including reaction of $(CH_3)_6Sn_2$ with CF_3I[1,2], of CF_3 radicals with SnI_4,[3] of $(CH_3)_2Hg$ with $SnBr_4$[4,5] and of $(CF_3)_2Cd$ with SnX_4(X = Br, I)[6,7], corresponding tin(II) compounds have not been reported. One attempt to prepare them from CF_3I and SnI_2 at elevated temperature was unsuccessful yielding only fluorocarbons suggestive of CF_2 extrusion from a transient Sn–CF_3 species[8].

We wish to report spectroscopic evidence for $(CF_3)_2Sn$ and CF_3SnI prepared by reactions between $(CF_3)_2Cd \cdot$ glyme and SnI_2. When freshly prepared THF solutions of $(CF_3)_2Cd \cdot$ glyme and SnI_2 were combined in a 1:1 molar ratio, the SnI_2 was rapidly decolourized at −14°C and a small amount of an off-white precipitate appeared. After 2 hr, the solution was filtered and a sample diverted into an NMR tube and sealed. The ^{19}F FT-NMR spectrum of that solution 2 hr. later contained resonances at $\delta - 33.9$, -34.5, -41.3 and -46.3 (relative to $CFCl_3$). Satellites corresponding to $^{19}F-^{113}Cd$ and $^{19}F-^{111}Cd$ of 473/453 and 507/483 Hz helped identify the downfield resonances as $(CF_3)_2Cd$ (I) ($\delta - 34.5$) (Lit. For $(CF_3)_2Cd \cdot$ glyme: $\delta - 35.4$, $j = 466/445$ Hz) and CF_3CdI (II), a new compound. The $\delta - 41.3$ resonance exhibits satellites ($j = 233/225$ Hz) attributable to $^{19}F-^{119}Sn$(8.68%, I = 1/2) and $^{19}F-^{117}Sn$ (7.67%, I = 1/2) and we tentatively assign the signal to CF_3SnI (III).

The resonance at $\delta - 46.3$ lacks satellites and is a tansient species, diminishing with time as new resonances form (*vide infra*).

Several additional reactions were carried out to help identify the new species formed. $(CF_3)_2Cd \cdot$ glyme and SnI_2 were combined in a 1.5:1 molar ratio with THF as solvent, stirred at −78°C for 2 hr. at −14°C for 1 hr. and at 25° for 72 hr. after which a small amount of white precipitate was filtered off and the solvent removed *in vacuo*. The solid residue was extracted with CH_2Cl_2 to remove any unreacted $(CF_3)_2Cd \cdot$ glyme[7] and a portion of the residue redissolved in THF giving ^{19}F resonances at $\delta - 33.9$ ($j = 498/476$ Hz) (II), -41.3 ($j = 234/225$ Hz) (III), -43.9 ($j = 368/357$ Hz), -46.5 and -51.2. The absence of the $\delta - 34.5$ resonance confirms its identity as I.

The new resonance at $\delta - 43.9$ is tentatively assigned as $(CF_3)_2Sn$ (IV) owing to its later appearance in the spectrum of the products and its larger coupling constants. A reaction with a 2:1 ratio of $(CF_3)_2Cd \cdot$ glyme and SnI_2 in THF_{d8} was prepared directly in an NMR tube. The spectrum obtained immediately upon warming to room temperature contained signals of I and II, a small signal at $\delta - 41.3$(III) along with the major peak at $\delta - 46.8$ and it had not noticeably changed after 40 min. However, after two weeks the $\delta - 46.8$ resonance had been replaced by resonances at $\delta - 43.2$(IV) -45.1, -49.1 and -51.1($j = = 553$, 528) (Fig. 1). Evidently the $\delta - 46.8$ resonance which appears immediately in the reaction represents an intermediate, probably bimetallic, through which the CF_3 exchange occurs. In the normal course of such exchange reactions, a nomosubstituted product is expected to be formed first (eqn 1)

$$(CF_3)_2Cd + SnI_2 \leftrightarrows CF_3CdI + CF_3SnI \quad (1)$$

and subsequently the disubstituted product should appear (eqns 2 and 3):

$$(CF_3)_2Cd + CF_3SnI \rightleftharpoons CF_3CdI + (CF_3)_2Sn \quad (2)$$

$$CF_3CdI + CF_3SnI \rightleftharpoons CdI_2 + (CF_3)_2Sn. \quad (3)$$

This sequence supports the assignments of the $\delta - 41.3$ and $\delta - 43.2$ resonances as III and IV respectively. Some confirmation of this assignment comes from $^{19}F-^{31}P$ coupling constants of $P(CF_3)_3$ (85.5 ± 0.10 Hz) and $P(CF_3)_2I$(73.2 ± 0.4 Hz)[9]. Substituting iodine for CF_3 lowers the coupling constant which is the same relationship seen in IV (368/357 Hz) and (III) (234/235 Hz) according to our assignment[10].

conversion represents a rare reaction in which a racemate can be converted to only one optically active form. From the above results it follows that the missing (+)-(IV) antipode can be isolated by the use of (−)-NMC or a different optically active base as the precipitating agent. The relevant experiments along with those aimed at determining the absolute configuration in the 5,6-$C_2B_8H_{12}$ series are now in progress.

REFERENCES

1. J. Plešek, S. Heřmánek and B. Štíbr, *Collect. Czech. Chem. Commun.* 1969, **34**, 3233.
2. J. Plešek, V. Gregor and S. Heřmánek, *Collect. Czech. Chem. Commun.* 1970, **35**, 346.
3. S. Heřmánek and J. Plešek, *Collect. Czech. Chem. Commun.* 1970, **35**, 2488.
4. E. Císařová and A. Línek, *Acta Cryst. Sect.* (*B*), in press.
5. J. Plešek and S. Heřmánek, *Collect. Czech. Chem. Commun.* 1974, **39**, 821.
6. S. Heřmánek, H. Plotová and J. Plešek, *Collect. Czech. Chem. Commun.* 1975, **40**, 3593.
7. V. Šubrtová, A. Línek and J. Hašek, *Acta Cryst. Sect.* (*B*), in press.

*Author to whom correspondence should be addressed.

Institute of Inorganic Chemistry Prague, Czechoslovak Academy of Sciences, BOHUMIL ŠTÍBR*
250 68 *Řež near Prague,* JAROMÍR PLEŠEK
Czechoslovakia
Laboratory of Monosacharides, ALENA ZOBÁČOVÁ
Prague Institute of Chemical Technology, Suchbátarova 5,
166 28 *Prague* 6,
Czechoslovakia

Polyhedron Vol. 1, No. 11-12, pp. 826-827, 1982
Printed in Great Britain.

0277-5387/82/110826-02$03.00/0
Pergamon Press Ltd.

Evidence for trifluoromethyltin(II) compounds

(*Received* 17 *May* 1982)

Abstract—The products of several reactions between $(CF_3)_2Cd \cdot$ glyme and SnI_2 in tetrahydrofuran have been examined by ^{19}F NMR. Resonances representing the new compounds CF_3CdI, CF_3SnI and $(CF_3)_2Sn$ were assigned based on NMR parameters and ^{119}Sn Mössbauer spectra.

Although trifluoromethyl-tin (IV) compounds have been prepared by a variety of routes including reaction of $(CH_3)_6Sn_2$ with CF_3I[1,2], of CF_3 radicals with SnI_4,[3] of $(CH_3)_2Hg$ with $SnBr_4$[4,5] and of $(CF_3)_2Cd$ with SnX_4(X = Br, I)[6,7], corresponding tin(II) compounds have not been reported. One attempt to prepare them from CF_3I and SnI_2 at elevated temperature was unsuccessful yielding only fluorocarbons suggestive of CF_2 extrusion from a transient Sn–CF_3 species[8].

We wish to report spectroscopic evidence for $(CF_3)_2Sn$ and CF_3SnI prepared by reactions between $(CF_3)_2Cd \cdot$ glyme and SnI_2. When freshly prepared THF solutions of $(CF_3)_2Cd \cdot$ glyme and SnI_2 were combined in a 1:1 molar ratio, the SnI_2 was rapidly decolourized at −14°C and a small amount of an off-white precipitate appeared. After 2 hr, the solution was filtered and a sample diverted into an NMR tube and sealed. The ^{19}F FT-NMR spectrum of that solution 2 hr. later contained resonances at $\delta - 33.9$, -34.5, -41.3 and -46.3 (relative to $CFCl_3$). Satellites corresponding to $^{19}F-^{113}Cd$ and $^{19}F-^{111}Cd$ of 473/453 and 507/483 Hz helped identify the downfield resonances as $(CF_3)_2Cd$ (I) ($\delta - 34.5$) (Lit. For $(CF_3)_2Cd \cdot$ glyme: $\delta - 35.4$, $j = 466/445$ Hz) and CF_3CdI (II), a new compound. The $\delta - 41.3$ resonance exhibits satellites ($j = 233/225$ Hz) attributable to $^{19}F-^{119}Sn$(8.68%, I = 1/2) and $^{19}F-^{117}Sn$ (7.67%, I = 1/2) and we tentatively assign the signal to CF_3SnI (III).

The resonance at $\delta - 46.3$ lacks satellites and is a tansient species, diminishing with time as new resonances form (*vide infra*).

Several additional reactions were carried out to help identify the new species formed. $(CF_3)_2Cd \cdot$ glyme and SnI_2 were combined in a 1.5:1 molar ratio with THF as solvent, stirred at −78°C for 2 hr. at −14°C for 1 hr. and at 25° for 72 hr. after which a small amount of white precipitate was filtered off and the solvent removed *in vacuo*. The solid residue was extracted with CH_2Cl_2 to remove any unreacted $(CF_3)_2Cd \cdot$ glyme[7] and a portion of the residue redissolved in THF giving ^{19}F resonances at $\delta - 33.9$ ($j = 498/476$ Hz) (II), -41.3 ($j = 234/225$ Hz) (III), -43.9 ($j = 368/357$ Hz), -46.5 and -51.2. The absence of the $\delta - 34.5$ resonance confirms its identity as I.

The new resonance at $\delta - 43.9$ is tentatively assigned as $(CF_3)_2Sn$ (IV) owing to its later appearance in the spectrum of the products and its larger coupling constants. A reaction with a 2:1 ratio of $(CF_3)_2Cd \cdot$ glyme and SnI_2 in THF_{d8} was prepared directly in an NMR tube. The spectrum obtained immediately upon warming to room temperature contained signals of I and II, a small signal at $\delta - 41.3$(III) along with the major peak at $\delta - 46.8$ and it had not noticeably changed after 40 min. However, after two weeks the $\delta - 46.8$ resonance had been replaced by resonances at $\delta - 43.2$(IV) -45.1, -49.1 and -51.1($j = = 553$, 528) (Fig. 1). Evidently the $\delta - 46.8$ resonance which appears immediately in the reaction represents an intermediate, probably bimetallic, through which the CF_3 exchange occurs. In the normal course of such exchange reactions, a nomosubstituted product is expected to be formed first (eqn 1)

$$(CF_3)_2Cd + SnI_2 \leftrightarrows CF_3CdI + CF_3SnI \quad (1)$$

and subsequently the disubstituted product should appear (eqns 2 and 3):

$$(CF_3)_2Cd + CF_3SnI \rightleftharpoons CF_3CdI + (CF_3)_2Sn \quad (2)$$

$$CF_3CdI + CF_3SnI \rightleftharpoons CdI_2 + (CF_3)_2Sn. \quad (3)$$

This sequence supports the assignments of the $\delta - 41.3$ and $\delta - 43.2$ resonances as III and IV respectively. Some confirmation of this assignment comes from $^{19}F-^{31}P$ coupling constants of $P(CF_3)_3$ (85.5 ± 0.10 Hz) and $P(CF_3)_2I$(73.2 ± 0.4 Hz)[9]. Substituting iodine for CF_3 lowers the coupling constant which is the same relationship seen in IV (368/357 Hz) and (III) (234/235 Hz) according to our assignment[10].

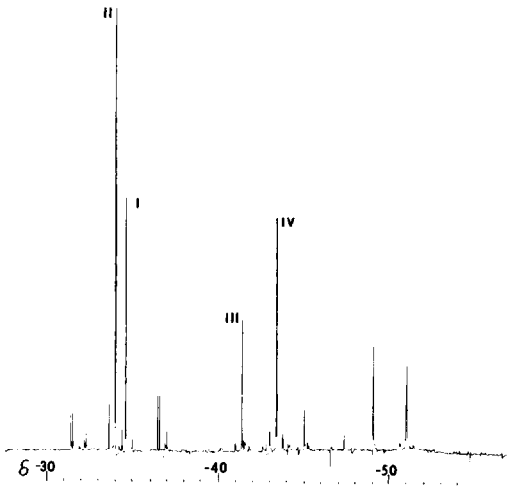

Fig. 1. ^{19}F NMR spectrum of $2(CF_3)_2Cd \cdot glyme + SnI_2$ reaction in THF_{d8} after two weeks at room temperature. Chemical shifts are relative to $CFCl_3$, upfield being negative δ.

The $\delta - 51.1$ resonance appears in spectra of exchange reactions maintained in the THF solution only after extended periods but it is always present when the solvent is removed and the solid redissolved to obtain a spectrum. (Even when the solvent is not removed, some solid eventually forms in the reaction.) The magnitude of the coupling constants falls in the range of those reported for CF_3–Sn(IV) compounds[3,7] suggesting the resonance might represent $[(CF_3)_2Sn]_x$ species resulting from association as seen in organotin(II) compounds[11].

The solid product mixture obtained by removing solvent from a 1:1 $(CF_3)_2Cd:SnI_2$ reaction was found to contain CdI_2 by comparison of its X-ray powder diffraction pattern with that of an authentic sample but no other crystalline species were present[12]. Mössbauer spectra (78K) of solids from several 1:1 reactions after vacuum transfer of solvent all consisted of asymmetric doublets (I.S. = 3.49 ± 0.02 relative to $BaSnO_3$, Q.S. = 1.40 ± 0.2 mmsec^{-1}). It appears that the spectra of III and IV are not resolved under these conditions since both are believed to be present. The Mössbauer parameters closely resemble those of monoclinic SnF_2 (I.S. = 3.51, Q.S. = 1.60 mmsec^{-1}, our system) which could be expected from CF_2 extrusion by the CF_3–Sn(II) species, however no lines corresponding to SnF_2 appear in the powder pattern of the solid product mixture. Evidently there is a coincidental similarity of Mössbauer parameters.

*Author to whom correspondence should be addressed.

Diorganostannylenes usually form insoluble oligomers, $(R_2Sn)_x$, which exhibit isomer shift values characteristic of Sn(IV)[11]. In particular, $[(C_6F_5)_2Sn]_x$, perhaps the closest analog of III, has a reported isomer shift of 1.69 mmsec^{-1}, clearly in the Sn(IV) region[13]. CF_3-stannylenes apparently behave somewhat differently inasmuch as no Sn(IV) species appeared in our Mössbauer spectra. It is tempting to attribute the difference to the high group electronegativity of CF_3 but further comparison must await isolation and a more thorough characterization of the products.

Acknowledgement—The support of this investigation by the Robert A. Welch Foundation under grant E-439 is gratefully acknowledged. Helpful information concerning the chemical characteristics of $(CF_3)_2Cd \cdot glyme$ provided prior to publication by Professor J. A. Morrison is appreciated.

R. HANI
R. A. GEANANGEL*

Department of Chemistry
University of Houston Central Campus
Houston, TX 77004
U.S.A.

REFERENCES

[1]H. C. Clark, C. J. Willis, *J. Am. Chem. Soc.* 1960 **82** 1888.
[2]H. D. Kaesz, J. R. Phillips, F. G. A. Stone, *J. Am. Chem. Soc.* 1960 **82**, 6228.
[3]R. J. Lagow, L. L. Gerchman, R. A. Jacob, J. A. Morrison, *J. Am. Chem. Soc.* 1975 **97**, 518.
[4]J. A. Morrison, L. L. Gerchman, R. Eujen, R. J. Lagow, *J. Fluorine Chem.* 1977 **10**, 333.
[5]R. J. Lagow, R. Eujen, L. L. Gerchman, J. A. Morrison, *J. Am. Chem. Soc.* 1978 **100**, 1722.
[6]L. J. Krause, J. A. Morrison, *J. C. S. Chem. Comm.* 1980, 671.
[7]L. J. Krause, J. A. Morrison, *J. Am. Chem. Soc.* 1981, **103**, 2995.
[8]H. C. Clark, C. J. Willis, *J. Am. Chem. Soc.* 1962, **84**, 898.
[9]V. Mark, C. H. Dungan, M. M. Crutchfield, J. R. VanWazer, ^{31}P *Nucl. Mag. Res.* 1967, **5**, 227.
[10]Although the phosphines are the closest analogues we could find to the proposed tin compounds, it should be recognized that there may be unexpected factors affecting comparison of coupling constants in the two systems.
[11]J. W. Connolly, C. Hoff, *Adv. Organomet. Chem.* 1981, **19**, 123.
[12]Dark bands characteristic of polymetric substances lacking long range order were present in the X-ray powder pattern along with CdI_2 lines.
[13]M. P. Bigwood, P. J. Corvan, J. J. Zuckerman, *J. Am. Chem. Soc.* 1981, **103**, 7643.

Polyhedron Vol. 1, No. 11-12, pp. 827-830, 1982
Printed in Great Britain.

0277-5387/82/110827-04$03.00/0
Pergamon Press Ltd.

The determination of the stability constants of uranyl and thorium with aminopolycarboxylic acids

(*Received* 19 *May* 1982)

Abstract—The stability of uranyl and thorium ions with ligands N-(2'-carboxy phenyl) iminodiacetic acid (ADA), iminodiacetic acid (IDA) and [(ethylenedioxy)diethylenedinitrilo]tetraacetic acid (EGRA) have been studied using the potentiometric technique in 0.1M, KNO_3 solution at 25°C. The complexes of thorium (IV) ions with IDA and ADA are shown to be more stable than those for uranyl ions, while EGTA forms more stable complexes with uranyl ion.

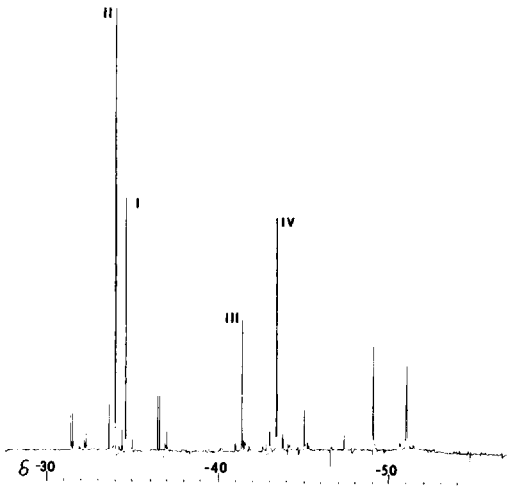

Fig. 1. ^{19}F NMR spectrum of $2(CF_3)_2Cd \cdot glyme + SnI_2$ reaction in THF_{d8} after two weeks at room temperature. Chemical shifts are relative to $CFCl_3$, upfield being negative δ.

The $\delta - 51.1$ resonance appears in spectra of exchange reactions maintained in the THF solution only after extended periods but it is always present when the solvent is removed and the solid redissolved to obtain a spectrum. (Even when the solvent is not removed, some solid eventually forms in the reaction.) The magnitude of the coupling constants falls in the range of those reported for CF_3–Sn(IV) compounds[3,7] suggesting the resonance might represent $[(CF_3)_2Sn]_x$ species resulting from association as seen in organotin(II) compounds[11].

The solid product mixture obtained by removing solvent from a 1:1 $(CF_3)_2Cd:SnI_2$ reaction was found to contain CdI_2 by comparison of its X-ray powder diffraction pattern with that of an authentic sample but no other crystalline species were present[12]. Mössbauer spectra (78K) of solids from several 1:1 reactions after vacuum transfer of solvent all consisted of asymmetric doublets (I.S. = 3.49 ± 0.02 relative to $BaSnO_3$, Q.S. = 1.40 ± 0.2 mmsec^{-1}). It appears that the spectra of III and IV are not resolved under these conditions since both are believed to be present. The Mössbauer parameters closely resemble those of monoclinic SnF_2 (I.S. = 3.51, Q.S. = 1.60 mmsec^{-1}, our system) which could be expected from CF_2 extrusion by the CF_3–Sn(II) species, however no lines corresponding to SnF_2 appear in the powder pattern of the solid product mixture. Evidently there is a coincidental similarity of Mössbauer parameters.

*Author to whom correspondence should be addressed.

Diorganostannylenes usually form insoluble oligomers, $(R_2Sn)_x$, which exhibit isomer shift values characteristic of Sn(IV)[11]. In particular, $[(C_6F_5)_2Sn]_x$, perhaps the closest analog of III, has a reported isomer shift of 1.69 mmsec^{-1}, clearly in the Sn(IV) region[13]. CF_3-stannylenes apparently behave somewhat differently inasmuch as no Sn(IV) species appeared in our Mössbauer spectra. It is tempting to attribute the difference to the high group electronegativity of CF_3 but further comparison must await isolation and a more thorough characterization of the products.

Acknowledgement—The support of this investigation by the Robert A. Welch Foundation under grant E-439 is gratefully acknowledged. Helpful information concerning the chemical characteristics of $(CF_3)_2Cd \cdot glyme$ provided prior to publication by Professor J. A. Morrison is appreciated.

R. HANI
R. A. GEANANGEL*

Department of Chemistry
University of Houston Central Campus
Houston, TX 77004
U.S.A.

REFERENCES

[1]H. C. Clark, C. J. Willis, *J. Am. Chem. Soc.* 1960 **82** 1888.
[2]H. D. Kaesz, J. R. Phillips, F. G. A. Stone, *J. Am. Chem. Soc.* 1960 **82**, 6228.
[3]R. J. Lagow, L. L. Gerchman, R. A. Jacob, J. A. Morrison, *J. Am. Chem. Soc.* 1975 **97**, 518.
[4]J. A. Morrison, L. L. Gerchman, R. Eujen, R. J. Lagow, *J. Fluorine Chem.* 1977 **10**, 333.
[5]R. J. Lagow, R. Eujen, L. L. Gerchman, J. A. Morrison, *J. Am. Chem. Soc.* 1978 **100**, 1722.
[6]L. J. Krause, J. A. Morrison, *J. C. S. Chem. Comm.* 1980, 671.
[7]L. J. Krause, J. A. Morrison, *J. Am. Chem. Soc.* 1981, **103**, 2995.
[8]H. C. Clark, C. J. Willis, *J. Am. Chem. Soc.* 1962, **84**, 898.
[9]V. Mark, C. H. Dungan, M. M. Crutchfield, J. R. VanWazer, ^{31}P *Nucl. Mag. Res.* 1967, **5**, 227.
[10]Although the phosphines are the closest analogues we could find to the proposed tin compounds, it should be recognized that there may be unexpected factors affecting comparison of coupling constants in the two systems.
[11]J. W. Connolly, C. Hoff, *Adv. Organomet. Chem.* 1981, **19**, 123.
[12]Dark bands characteristic of polymetric substances lacking long range order were present in the X-ray powder pattern along with CdI_2 lines.
[13]M. P. Bigwood, P. J. Corvan, J. J. Zuckerman, *J. Am. Chem. Soc.* 1981, **103**, 7643.

Polyhedron Vol. 1, No. 11-12, pp. 827-830, 1982
Printed in Great Britain.

0277-5387/82/110827-04$03.00/0
Pergamon Press Ltd.

The determination of the stability constants of uranyl and thorium with aminopolycarboxylic acids

(*Received* 19 *May* 1982)

Abstract—The stability of uranyl and thorium ions with ligands N-(2'-carboxy phenyl) iminodiacetic acid (ADA), iminodiacetic acid (IDA) and [(ethylenedioxy)diethylenedinitrilo]tetraacetic acid (EGRA) have been studied using the potentiometric technique in 0.1M, KNO_3 solution at 25°C. The complexes of thorium (IV) ions with IDA and ADA are shown to be more stable than those for uranyl ions, while EGTA forms more stable complexes with uranyl ion.

INTRODUCTION

There have been reports on diaminocarboxylic acid complexes with uranyl and thorium ions using ionic exchange or redox electrode technique,[1,2] but little work has been published using the potentiometric titration method. Only recent studies of mixed ligand complexes of uranyl with amino-acids and some monocarboxylic acids were reported (using potentiometric titration method) each suggesting a relatively strong bond formation between uranyl ion and oxygen or nitrogen in the ligand molecule.

We wish to report the results for UO_2^{2+} and Th^{4+} complexes of iminodiacetic acid (H_2IDA), N-(2'-carboxphenyl) iminodiacetic acid (H_3ADA) and [(ethylenedioxy) diethylenedinitrilo] tetra acetic acid (H_4EGTA) each having one or more oxygen and nitrogen as the donor atoms in their molecules able to form strong bonds with uranyl and thorium ions. The effects of various oxygen and nitrogen donor atoms on the stabilities of metal chelates are compared with the chelating behaviour of compounds containing additional coordinating group other than carboxylate group (i.e. IDA vs EGTA).

Typical of the formation constants found are those for uranyl complexes of nitrilotriacetic acid and thorium complexes of EDTA reported as $\log KMl = 9.56 \pm 0.03$ and $\log KMHL = 25.3$ respectively,[5,2] using different methods than potentiometric titration.

Equilibrium studies on uranyl (VI) ion with IDA have been already reported at 20°C and at ionic strength I = 0.1 M;[10] since it is desirable to compare all the systems under the same experimental conditions, we have calculated the stability constants for IDA at I = 0.1M (KNO_3) and at 25°C. However, Dasilva and Simones[6] have studied a series of amino polycarboxylic acids (including EGTA and ADA) complexes of UO_2^{2+} and gave KMHL values only.

EXPERIMENTAL

Standard solutions of uranium and thorium were prepared from $UO_2(NO_3)_2 \cdot 6H_2O$ (Analar grade, BDH). The ligands EGTA and ADA were of Hopkin and Williams and IDA of Fluka; all were used as such. The ligands were standardized with carbonated free sodium hydroxide solution (0.1M). All pH measurements were made with an automatic Mettler pH meter with a combined glass and calomel electrode assembly at 25 ± 0.1°C and ionic strength of 0.1M(KNO_3). The pH meter was standardized before each titration by potassium hydrogen phthalate buffer (5×10^{-2} M with a pH value of 4.00 at 25°C). A value of 0.80 for the activity coefficient of 0.1M[H^+] was used[7] in the conversion of pH values to hydrogen ion concentrations. A steady stream of nitrogen gas freed from carbon dioxide was passed over the solution during the titrations.

Methods

Stability constants of the complexes, $\log KML_1$, and $\log KML_2$ evaluated from the formation curves of the systems were only approximate when they did not differ greatly in magnitude (2.5 log units)[8,9]; exact values were determined by eqn (1) according to Irving and Rossotti[8,9] where KML_1, KML_2... are successive stability constants, L = free ligand anion concentration, $\bar{n}$ = formation function of the system.

$$\frac{\bar{n}}{(\bar{n}-1)[L]} = KML_1 + KML_1 \cdot KML_2 \frac{(2-n)[L]}{(1-n)}$$

$$+ \sum_{n=3}^{N} KML_1, KML_2 \ldots KML_n \cdot \frac{(n-\bar{n})[L]^{n-1}}{(1-n)}. \qquad (1)$$

From the plot of $\bar{n}/(1-\bar{n})[L]$ vs $(2-\bar{n})[L]/(1-\bar{n})$ the intercept ($\log KML_1$) and gradient ($\log \beta 2$) were obtained.

The titration curves for free ligands and in the presence of metal ions are given in Figs. 1–3.

RESULTS AND DISCUSSION

Calculated values for proton and metal complex formation constants are given in Table 1 with those reported for iminodiacetic acid.[10,11] As expected, the benzyl group in H_3ADA reduces the donor power of the nitrogen atom in the ligand resulting in a lower $\log K_1$ value for ADA, in contrast to its analogue ligands (IDA) and (EGTA). The values of $\log K_2$ correspond to the protonation of the carboxy group; these are lower for aliphatic ligands than for those with aromatic groups in consequence of the inductive effect of the substituents in the latter. This general trend has resulted and is shown in Table 1.

Again, a comparison of results for ADA and IDA complexes with metals show that complexes of the latter are stronger in spite of ADA being more acidic than IDA. This could be attributed to the extra bonding group in ADA molecule.

Structure of EGTA resembles that of EDTA, having four carboxylic groups and two nitrogens to form strong complexes through its oxygen and nitrogen atoms with uranyl and thorium ions. As it appears, the complexes of this ligand with uranyl ion are more stable while thorium complexes are somehow less stable with respect to other ligands studied in this work. This could be explained in terms of UO_2^{2+} ion being much larger than Th^{4+} favored by a larger ligand like EGTA. Miyake and Nurnberg[12] have also concluded that the maximum number of ligands coordinated to the UO_2^{2+} ion in aqueous solution to increase with the length of carbon-chain of the ligand, and that complexes with a different coordination number can be formed. However, a maximum coordination of 8 has been suggested for uranyl ion,[13]

Table 1. Proton and metal complex formation constants at 25°C and I = 0.1M (KNO_3). Standard deviation (σ values) in parentheses

Ligand	H^+		UO_2^{2+}		Th^{4+}	
	Log K_1	*Log* K_2	*Log* K_1	*Log* K_2	*Log* K_1	*Log* K_2
H_2IDA	9.299(4)	2.812 (4)	8.73 (2)	8.55 (6)	10.66 (6)	9.07 (7)
	9.33*	2.58*	8.93 †			
H_3ADA	8.473(7)	3.768 (5)	9.71 (3)	8.28 (8)	12.93 (6)	8.40 (4)
H_4EGTA	9.126(1)	2.959 (5)	11.23(7)	7.80 (2)	9.89 (3)	—

* *Ref. 9*

† *Ref. 10*

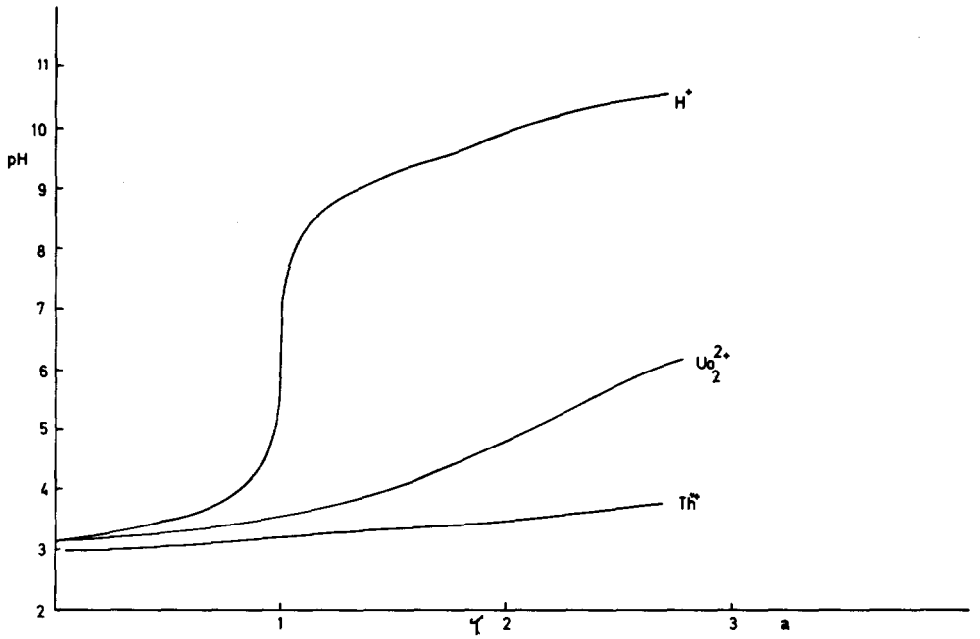

Fig. 1. Titration curves for iminodiacetic acid (H_2IDA) and its metal complexes at 25°C I = 0.1 (KNO_3).

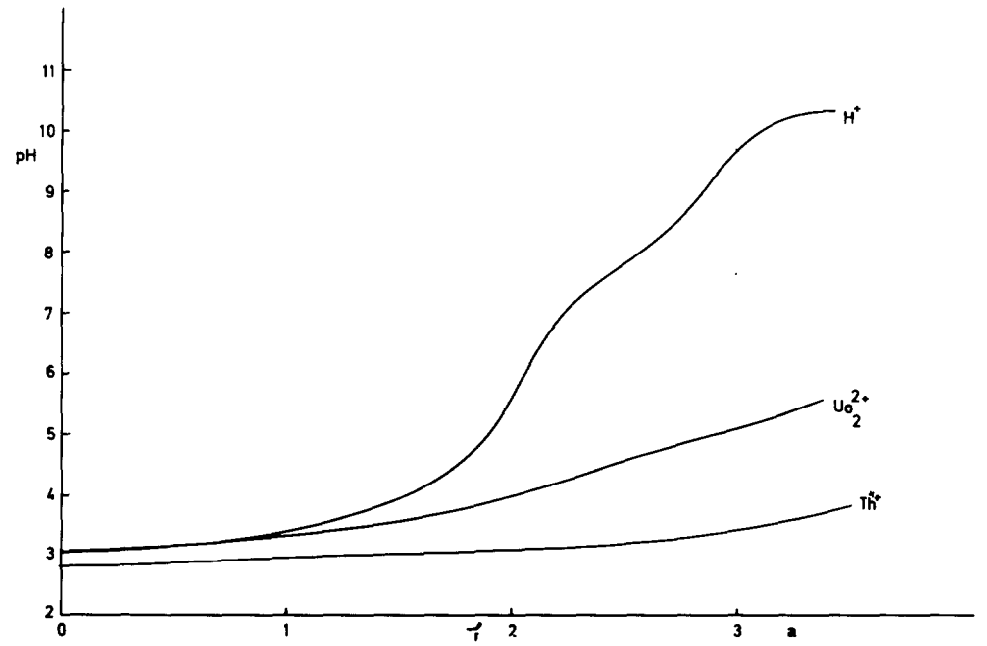

Fig. 2. Titration curves for N-(2-carboxy phenyl)iminodiacetic (H_3ADA) and its metal complexes at 25°C and I = 0.1M (KNO_3).

that is a maximum of six donor atoms (one EGTA or two tridentate ligand molecules) are sufficient to coordinate with UO_2^{2+} to reach the specified coordination number. This idea would result in an hexagonal bipyramidal structure for UO_2^{2+} complexes as has been pointed out by this author. In this case, only five donor atoms would take place in coordination with the central ion (UO_2^{2+}). Since the maximum metal:ligand ratio used was 1:2, therefore according to Ebele's[13] statement, all complexes investigated in this work may exhibit an hexagonal bipyramidal structure.

A possible structure of iminodiacetic acid chelate compatible with experimental evidence is indicated by I.

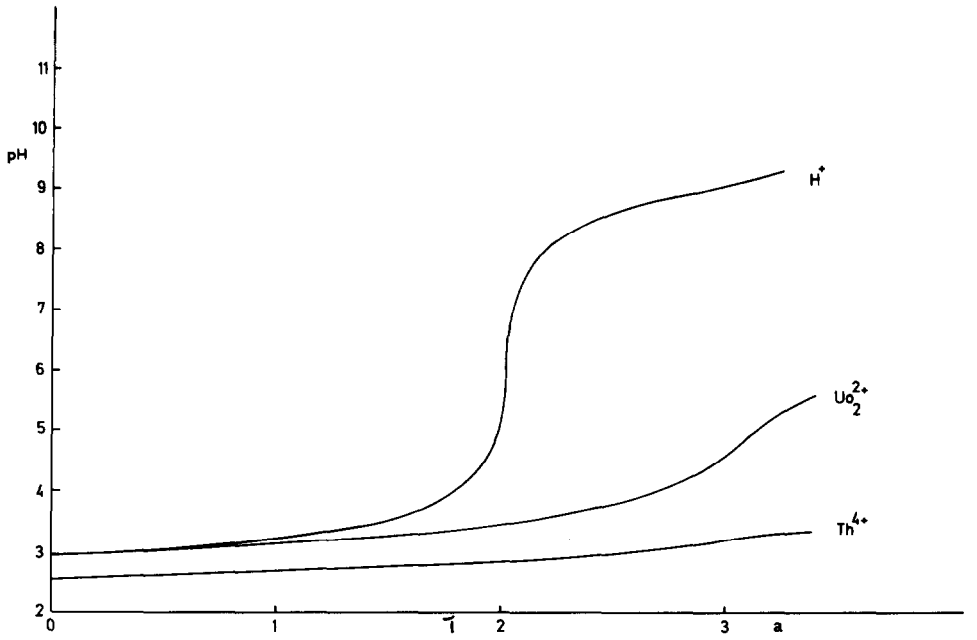

Fig. 3. Titration curves for [(ethylene dioxy)diethylenedinitrilo]tetraacetic acid (H_4EGTA) and its metal complexes at 25°C and I = 0.1 (KNO_3).

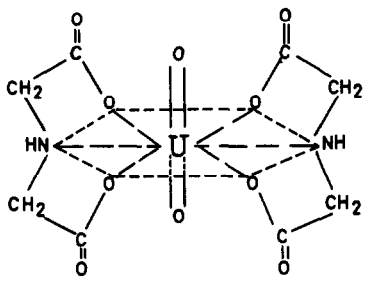

I

Since ADA is the less basis ligand, this correlation has been taken to indicate involvement of the phenolic carboxy group in the coordination with Th^{4+} giving a possible structure like II.

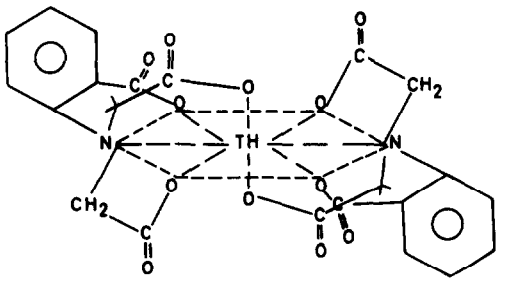

II

However, on the basis of potentiometric data alone, it is not possible to conclude a real structure for these complexes therefore, an X-ray diffraction study is required.

Acknowledgement—The authors are grateful to Mr. N. Meissami for his valuable suggestions on several aspects of this paper.

Nuclear Research Centre
P.P. Box 3327
Tehran
Iran

M. NOURMAND*
I. BAYAT
S. YOUSEFI†

REFERENCES

[1]G. H. Garey and A. E. Martell, *J. Am. Chem. Soc.* 1968, **90**, 32.
[2]E. Bottari and G. Anderegg, *Helv. Chem. Acta.* 1967, **50**, 234.
[3]P. V. Selvaraj and Santapa, *J. Inorg. Nucl. Chem.* 1977, **39**, 119.
[4]D. N. Shelke and D. V. Jahagirdar, *J. Inorg. Nucl. Chem.* 1981, **43**, 757.
[5]M. Cefola, R. C. Taylor, P. S. Gentile and A. V. Celiano, *J. Phys. Chem.* 1962, **66**, 790.
[6]J. Da Silva and M. Simoes, *Rev. Port. Qium.* 1969, **11**, 54.
[7]H. M. Irving, M. G. Miles and L. D. Pettit, *Anal. Chim. Acta.* 1967, **38**, 475.
[8]H. M. Irving and H. S. Rossotti, *J. Chem. Soc.* 1953, 3397.
[9]H. M. Irving and H. S. Rossotti, *J. Chem. Soc.* 1954, 2904.
[10]N. A. Skorik and V. N. Komok, *J. Gen. Chem.* 1967, **37**, 1461.
[11]K. S. Rajan and A. E. Martell, *J. Inorg. Nucl. Chem.* 1964, **26**, 789.
[12]C. Miyake and H. W. Nurneberg, *J. Inorg. Nucl. Chem.* 1967, **29**, 2411.
[13]S. H. Eberle, *Komplexverbindungen der Actiniden mit Organishen Liganden*, K.F.K. 1136 (Oct. 1970).

*Author to whom correspondence should be addressed.
†Abstracted in part from the M.Sc. thesis of S. Yousefi, Tehran University.

Polyhedron Vol. 1, No. 11-12, pp. 831-833, 1982
Printed in Great Britain.

0277-5387/82/110831-03$03.00/0
Pergamon Press Ltd.

Complexes of Zn(II) and Mn(II) with biacetyldihydrazone

(*Received* 22 *June* 1982)

Abstract—The complexes $[Zn(BdH)_2Cl_2]$ and $[Mn(BdH)_2Cl_2]$ have been prepared and studied by IR, electronic and ESR spectroscopies and by magnetic measurements. All results agree with a molecular formula for both complexes and a distorted octahedral environment for the metal atoms.

INTRODUCTION

The biacetyldihydrazone (BdH) is a bidentate ligand with two imine N-atoms as donors. Among the first transition series elements only the complexes of Fe(II), Co(II) and Ni(II) have been reported[1-4]. They are similar to the pyridine, *o*-phenanthroline and α-diimine complexes, except those of Fe(II).

In the present paper the preparation and studies by spectroscopic and magnetic techniques of $[Zn(BdH)_2Cl_2]$ and $[Mn(BdH)_2Cl_2]$ are reported.

EXPERIMENTAL

Sample preparations and analytical data. The ligand was prepared according to the method of Busch and Bailar[5]. Found: C, 42.39; H, 9.04; N, 49.39; Calc. for $C_4H_{10}N_4$: C, 42.09; H, 8.83; N, 49.08%.

The synthesis of complexes followed the method described by Stoufer and Busch[1] for other BdH complexes, by reaction of the metal chloride with BdH in methanol. $[Zn(BdH)_2Cl_2]$. White solid, m.p., 220°. Found: C, 26.50; H, 5.42; N, 30.99; Zn, 17.82. Calc. C, 26.33; H, 5.48; N, 30.72; Zn, 17.93% $[Mn(BdH)_2Cl_2]$. Pink brown solid, d. 215°. Found: C, 27.32; H, 5.66; N, 15.38; Mn, 31.84. Calc. C, 27.11; H, 5.65; N, 15.51; Mn, 31.63.

Both are air stable, insoluble in methanol and ethanol, soluble in water and dimethylformamide. The complex of Zn(II) is soluble in acetone while Mn(II) complex is slightly soluble.

Conductivity measurements. The electrical conductivities were determined using a Philips GM 4144/01 conductivimeter with a PR 9512/00 cell.

IR spectra. The spectra were obtained with a Perkin-Elmer 325 spectrophotometer using potassium bromide pellets and nujol mulls.

Magnetic susceptibility. The Gouy method was used to determine the magnetic susceptibility. The instrumental system was formed by a Bruker B-M4 electromagnet, a Sartorius electronic microbalance and a Leybold VNK 3-300 cryostat.

ESR spectra. The spectra were recorded on a Varian model E-12, in the X-band and a resonant cavity E-231. The field modulation frequency was 10^5 Hz. For the accurate determination of magnetic field value, standard PITCH ($g = 2.0028$) was employed.

Table 1. IR absorption bands (cm^{-1}) for BdH and its complexes

Assignment	BdH	$[Zn(BdH)_2Cl_2]$	$[Mn(BdH)_2Cl_2]$
		3380 (s)	3390 (s)
$\nu_a(NH_2)$	3325 (s)	3350 (s)	3355 (s)
		3295 (m)	3295 (m)
		3260 (s)	3270 (s)
$\nu_s(NH_2)$	3182 (s)	3207 (s)	3210 (s)
ν(CH)	3000 (w)	2910 (w)	2920 (w)
	2920 (m)	2900 (w)	2890 (w)
$\delta_s(NH_2)$	1630 (s)	1650 (w)	1645 (w)
		1627 (s)	1615 (s)
ν(C=N)	1570 (ms)	1560 (w)	1550 (w)
$\delta_a(C-CH_3)$	1450 (s)	1435 (m)	1435 (m)
		1373 (s)	1380 (m)
$\delta_s(C-CH_3)$	1358 (s)	1355 (m)	1367 (m)
			1350 (w)
	1302 (w)		
	1273 (m)		
	1120 (s)	1147 (ms)	1140 (ms)
	1073 (s)	1095 (ms)	1090 (ms)
	1010 (w)		
	936 (s)	957 (w)	951 (w)
		787	783 (w)
$\rho_r(NH_2)$	720-730	760 (m)	757 (s)
		591 (mw)	586 (mw)
		552 (w)	542 (w)
	450 (m)	461 (m)	461 (m)
		345 (w)	338 (w)
		283 (s)	270 (m)
	230 (s)	230 (s)	242 (w)
			226 (mw)
			208 (w)

s: strong; m: medium; w: weak.

Electronic spectra. The spectra were obtained in dimethylformamide solutions, with a Kontron Uvikon 820 Spectrophotometer with Uvikon Recorder 21 register.

RESULTS AND DISCUSSION

Conductivity measurements. The molar conductivity values of 4.3 and 0.76 $\Omega^{-1}\,cm^2\,mol^{-1}$, obtained for the Zn(II) and Mn(II) complexes, respectively, indicate that are not electrolytes[6]. In both cases, the chloride ions must be directly bonded to the metal atom, according to the formula $[M(BdH)_2Cl_2]$ (M = Zn, Mn).

IR spectra. In Table 1 are given the IR absorption bands for biacetyldihydrazone and its complexes. The absorptions of the free ligand are in agreement with those reported by Stoufer and Busch[3].

The most significant variation between free ligand and complexes refers to the C=N stretching frequency. Whereas this band is at 1570 cm^{-1} in the spectrum of ligand, it occurs at 1627 cm^{-1} for $[Zn(BdH)_2Cl_2]$ and at 1615 cm^{-1} for $[Mn(BdH)_2Cl_2]$. A similar shift for the C=N stretching frequency has been observed for other complexes with BdH[3].

There are two features that may cause opposite shifts in this frequency. The *cis* conformation of BdH as a bidentate ligand in complexes has higher $\nu_{C=N}$ frequency than the *trans* form of the free ligand, because of its lower degree of conjugation. In the opposite trend, the back donation from metal d orbitals to the π^* (antibonding) orbitals of C=N group of ligand, shifts the $\nu_{C=N}$ frequency to lower values.

Our results agree with the behavior of BdH as bidentate, since the increasing of $\nu_{C=N}$ frequency confirms the transition from *trans* to *cis* form. As a consequence of this consideration and the values of molar conductivity, it can be supposed, for both complexes, distorted octahedral coordination, involving two bidentate BdH molecules and two chloride ions.

In $[Mn(BdH)_2Cl_2]$ there is a certain π-interaction, since the $\nu_{C=N}$ increases by 45 cm^{-1} compared with 57 cm^{-1} for $[Zn(BdH)_2Cl_2]$.

Magnetic susceptibility. The Mn(II) complex is paramagnetic, with $\mu_{eff} = 5.98$BM, and presents a lineal variation of $1/\chi$ with temperature. This is the normal case of a high spin d^5 configuration, with ground state $^6A_1$, without orbital contribution because there is no excited state with the same spin multiplicity.

ESR spectra. In the spectrum of solid $[Mn(BdH)_2Cl_2]$ (Fig. 1a) there is only a very broad signal ($\Delta H = 450$ G) with $g = 2.07$. In dimethylformamide (Fig. 1b) the signal splits into six equivalent components, with $g = 2.01$. The hyperfine structure due to ^{55}Mn (I = 5/2, abundance 100%) corresponds to an isotropic hyperfine coupling constant $A_{iso} = 87.10^{-4}\,cm^{-1}$. The g-value is close to the free spin value of 2.0023, as corresponds to the absence of spin-orbit coupling in the ground state $^6A_1$ without another sextet term of higher energy. The A_{iso} value is consistent with the octahedral coordination since the A_{iso} (^{55}Mn) in tetrahedral sites is 20–25% lower than in octahedral sites[7].

Electronic spectra. In high spin complexes of Mn(II) all d–d transitions are spin forbidden as deduced from the Tanabe-Sugano diagram for a d^5 configuration and, accordingly, they are very weak in intensity. The transitions to spin doublets are highly forbidden. In Table 2 are given the absorption maxima and molar extinction coefficients for BdH and its Mn(II) complex. The band at 274 nm corresponds to a $\pi \rightarrow \pi^*$ transition in the ligand. The band at 490 nm is assigned to a $^4T_1(G) \leftarrow {}^6A_1$ transition.

For octahedral complexes of Mn(II), the d–d transitions have ϵ values of some $10^{-2} - 10^3$ 1 $cm^{-1}\,mol^{-1}$. However, in non-centrosymmetric molecules the Laporte rule is relaxed and with organic ligands intensity may increase[8]. The relatively high value of ϵ for the Mn(II) complex agrees with the metal-ligand π interaction deduced from the IR spectra.

Table 2. Absorption band maxima and molar extinction coefficients

	λ_{max} (nm)	ϵ (1 $cm^{-1}\,mol^{-1}$)
BdH	270	$1{,}84 \cdot 10^4$
$[Mn(BdH)_2Cl_2]$	274	$3{,}96 \cdot 10^4$
	490	6,72

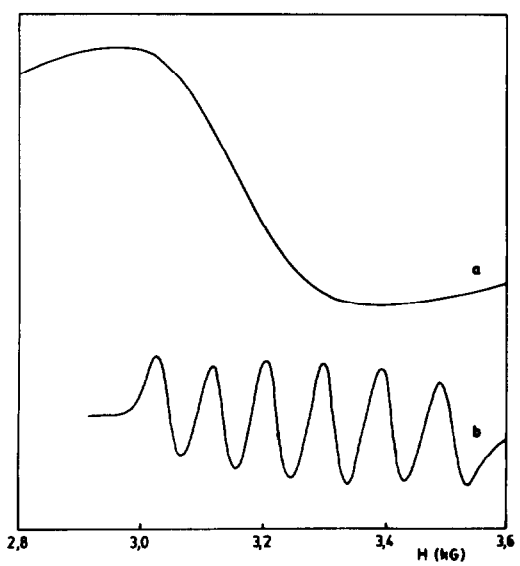

Fig. 1. ESR spectra of $[Mn(BdH)_2Cl_2]$: (a) solid; (b) in dimethylformamide solution.

Acknowledgements—The authors wish to thank the Facultad de Ciencias of the Universidad Autonoma of Madrid for the access to the ESR equipment.

A. E. SANCHEZ PELAEZ
Departamento de Química Inorgánica,
Facultad de Ciencias Químicas,
Universidad Complutense,
Madrid,
Spain

M. J. GONZALEZ GARMENDIA*
Departamento de Química Inorgánica,
Facultad de Ciencias Químicas,
Universidad del País Vasco,
San Sebastián,
Spain

*Author to whom correspondence should be addressed.

REFERENCES

[1]R. C. Stoufer and D. H. Busch, *J. Am. Chem. Soc.* 1956, **78**, 6016.
[2]R. C. Stoufer, D. W. Smith, E. A. Clevenger and T. E. Norris, *Inorg. Chem.* 1967, **5**, 1167.
[3]R. C. Stoufer and D. H. Busch, *J. Am. Chem. Soc.* 1960, **82**, 3491.
[4]L. F. Lindoy and S. E. Livingstone, *Coord. Chem. Rev.* 1967, **2**, 173.
[5]D. H. Busch and J. C. Bailar Jr., *J. Am. Chem. Soc.* 1956, **78**, 1137.
[6]W. J. Geary, *Coord. Chem. Rev.* 1971, **7**, 81.
[7]B. A. Goodman and J. B. Raynor, *Adv. Inorg. Chem. Radiochem.* 1970, **13**, 135.
[8]A. B. P. Lever, *Inorganic Electronic Spectroscopy*. American Elsevier, New York (1968).

Polyhedron Vol. 1, No. 11–12, pp. 833–834, 1982
Printed in Great Britain

0277–5387/82/110833–02$03.00/0
Pergamon Press Ltd.

Preparation of closo-10-vertex transition metal carbaboranes

(*Received* 24 *June* 1982)

Abstract—The synthesis of the ten-vertex closo-metallacarbaboranes 10-η^5-C_5H_5Ni-η^4-1-CB_8H_9, 6-η^5-C_5H_5Ni-η^5-1-CB_8H_9, (η^5-C_5H_5Ni)$_2$-1-CB_7H_8, and [2-η^5-C_5H_5Co-η^5-1-CB_8H_9]$^-$ from 4-CB_8H_{14} is reported.

The first representative of the ten-vertex metallacarbaborane family, 10-η^5-C_5H_5Ni-η^4-1-CB_8H_9, was isolated by Hawthorne *et al.*[1] as a minor by-product in the reaction of the [7-$CB_{10}H_{13}$]$^-$ anion with nickelocene. Based on polyhedral expansion of the [6-η^5-C_5H_5Co-η^5-1-CB_7H_8]$^-$ anion,[2] the same group also elaborated the route for preparing mixed neutral bimetallacarbaboranes.[3] Our recent high yield preparation of the 4-CB_8H_{14} carbaborane[4,5] enabled us to use it for a convenient synthesis of metallacarbaboranes isoelectronic with the $B_{10}H_{10}^{2-}$ anion.

Treatment of 4-$CB_8H_{13}Na$ with nickelocene in diglyme at 130–140°C for 8 hr resulted in the formation of an orange–yellow complex (I), R_F 0.34 (TLC, Sulifol silica-gel plates, benzene-*n*-hexane 1:2), M^+ 236, which slowly rearranged to another isomeric orange–yellow compound (II), R_F 0.58, M^+ 236 (corresponding to $^{62}Ni^{12}C_6{}^{11}B_8{}^1H_{14}{}^+$), under the conditions of dry column chromatography on silica-gel in benzene–*n*-hexane (1:2) during the work up of the reaction mixture. Column chromatography allowed us to isolate pure complex (II) [15% yield; ^{1}H n.m.r. (200 MHz, $CDCl_3$, ppm relative to tetramethylsilane) δ 5.96 (5 H, s, C_5H_5), 8.07 (1 H, s, CH skel.); ^{11}B NMR (64.2 MHz, $CDCl_3$, ppm relative to BF_3 etherate) δ_B 2.35 (4 B, d, $^1J_{B-H}$ 160 Hz), 26.87 (4 B, d, 145)]. The data are consistent with those found for 10-η^5-C_5H_5Ni-η^4-1-CB_8H_9 by Hawthorne *et al.*[1] We were, however unable to obtain pure complex (I) due to its progressive rearrangement to compound (II) under relatively mild conditions. The NMR data of (I) [^{1}H NMR (200 MHz, $CDCl_3$) δ 5.01 (5 H, s, C_5H_5), 5.48 (1 H, s, CH skel.); ^{11}B NMR (64.2 MHz, $CDCl_3$) δ_B 76.5 (1 B, d), 2.0 (2 B, d), −1.4 (1 B, d), −17.0 (2 B, d), −19.1 (2 B, d)], obtained by subtracting the signals of (II) from the spectrum of the isolated ca. 1:10 mixture of (I) and (II), were in agreement with the 6-η^5-C_5H_5Ni-η^5-1-CB_8H_9 gross symmetry. For the complex (I) can be smoothly rearranged to the compound (II) without any detectable intermediate, the 6,1-arrangement for (I) should be preferred to the 2,1-structural alternative.

In contrast to the preceding reaction, treatment of 4-$CB_8H_{13}NMe_4$ (preheated to 160°C) with nickelocene in acetonitrile produced, besides complexes (I) and (II), a dark green paramagnetic species the mass spectrum of which (M^+ 347) is consistent with a bimetallic (C_5H_5Ni)$_2$$CB_7H_8$ complex (III). Considering the electron count arguments,[6] a neutral compound of such a formula should contain two nickel atoms in different oxidation states, Ni^{4+} and Ni^{3+}, the latter being responsible for paramagnetism. The green colour of (III), which is usually indicative of metal–metal bonding,[7] should signify the preference for the 6,10-(η^5-C_5H_5Ni)$_2$-1-CB_7H_8 structure; an X-ray diffraction study on (III) is in progress.

Reaction of 4-CB_8H_{14} with $CoCl_2 \cdot 6H_2O$ and cyclopentadiene in concentrated ethanolic KOH afforded a red–orange complex (IV) in 20% yield. Elemental analysis of its tetramethylammonium salt and the NMR data [^{1}H NMR (200 MHz, $(CD_3)_2CO$) δ 6.56 (1 H, s, CH skel.), 4.75 (5 H, s, C_5H_5), 3.46 (12 H, s, NMe_4^+); ^{11}B NMR (64.2 MHz, $(CD_3)_2CO$) δ_B 34.20 (1 B, d, 148), 2.31 (1 B, d, 142), 0.39 (2 B, d, 136), −21.33 (2 B, d, 140), −25.52 (2 B, d, 136)] correspond well to the [2-η^5-C_5H_5Co-η^5-1-CB_8H_9]$^-$ NMe_4^+ structure for (IV), which has recently been determined by

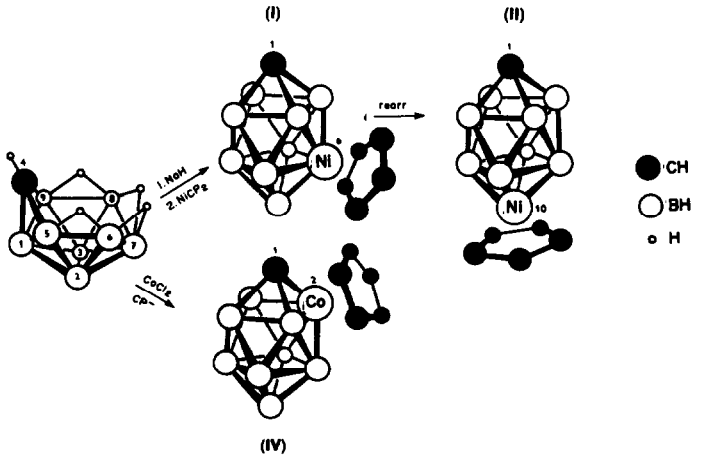

REFERENCES

[1]R. C. Stoufer and D. H. Busch, *J. Am. Chem. Soc.* 1956, **78**, 6016.
[2]R. C. Stoufer, D. W. Smith, E. A. Clevenger and T. E. Norris, *Inorg. Chem.* 1967, **5**, 1167.
[3]R. C. Stoufer and D. H. Busch, *J. Am. Chem. Soc.* 1960, **82**, 3491.
[4]L. F. Lindoy and S. E. Livingstone, *Coord. Chem. Rev.* 1967, **2**, 173.
[5]D. H. Busch and J. C. Bailar Jr., *J. Am. Chem. Soc.* 1956, **78**, 1137.
[6]W. J. Geary, *Coord. Chem. Rev.* 1971, **7**, 81.
[7]B. A. Goodman and J. B. Raynor, *Adv. Inorg. Chem. Radiochem.* 1970, **13**, 135.
[8]A. B. P. Lever, *Inorganic Electronic Spectroscopy*. American Elsevier, New York (1968).

Polyhedron Vol. 1, No. 11–12, pp. 833–834, 1982
Printed in Great Britain

0277–5387/82/110833–02$03.00/0
Pergamon Press Ltd.

Preparation of closo-10-vertex transition metal carbaboranes

(*Received* 24 *June* 1982)

Abstract—The synthesis of the ten-vertex closo-metallacarbaboranes 10-η^5-C_5H_5Ni-η^4-1-CB_8H_9, 6-η^5-C_5H_5Ni-η^5-1-CB_8H_9, (η^5-C_5H_5Ni)$_2$-1-CB_7H_8, and [2-η^5-C_5H_5Co-η^5-1-CB_8H_9]$^-$ from 4-CB_8H_{14} is reported.

The first representative of the ten-vertex metallacarbaborane family, 10-η^5-C_5H_5Ni-η^4-1-CB_8H_9, was isolated by Hawthorne *et al.*[1] as a minor by-product in the reaction of the [7-$CB_{10}H_{13}$]$^-$ anion with nickelocene. Based on polyhedral expansion of the [6-η^5-C_5H_5Co-η^5-1-CB_7H_8]$^-$ anion,[2] the same group also elaborated the route for preparing mixed neutral bimetallacarbaboranes.[3] Our recent high yield preparation of the 4-CB_8H_{14} carbaborane[4,5] enabled us to use it for a convenient synthesis of metallacarbaboranes isoelectronic with the $B_{10}H_{10}^{2-}$ anion.

Treatment of 4-$CB_8H_{13}Na$ with nickelocene in diglyme at 130–140°C for 8 hr resulted in the formation of an orange–yellow complex (I), R_F 0.34 (TLC, Sulifol silica-gel plates, benzene-*n*-hexane 1:2), M^+ 236, which slowly rearranged to another isomeric orange–yellow compound (II), R_F 0.58, M^+ 236 (corresponding to $^{62}Ni^{12}C_6{}^{11}B_8{}^1H_{14}{}^+$), under the conditions of dry column chromatography on silica-gel in benzene–*n*-hexane (1:2) during the work up of the reaction mixture. Column chromatography allowed us to isolate pure complex (II) [15% yield; ^{1}H n.m.r. (200 MHz, $CDCl_3$, ppm relative to tetramethylsilane) δ 5.96 (5 H, s, C_5H_5), 8.07 (1 H, s, CH skel.); ^{11}B NMR (64.2 MHz, $CDCl_3$, ppm relative to BF_3 etherate) δ_B 2.35 (4 B, d, $^1J_{B-H}$ 160 Hz), 26.87 (4 B, d, 145)]. The data are consistent with those found for 10-η^5-C_5H_5Ni-η^4-1-CB_8H_9 by Hawthorne *et al.*[1] We were, however unable to obtain pure complex (I) due to its progressive rearrangement to compound (II) under relatively mild conditions. The NMR data of (I) [^{1}H NMR (200 MHz, $CDCl_3$) δ 5.01 (5 H, s, C_5H_5), 5.48 (1 H, s, CH skel.); ^{11}B NMR (64.2 MHz, $CDCl_3$) δ_B 76.5 (1 B, d), 2.0 (2 B, d), −1.4 (1 B, d), −17.0 (2 B, d), −19.1 (2 B, d)], obtained by subtracting the signals of (II) from the spectrum of the isolated ca. 1:10 mixture of (I) and (II), were in agreement with the 6-η^5-C_5H_5Ni-η^5-1-CB_8H_9 gross symmetry. For the complex (I) can be smoothly rearranged to the compound (II) without any detectable intermediate, the 6,1-arrangement for (I) should be preferred to the 2,1-structural alternative.

In contrast to the preceding reaction, treatment of 4-$CB_8H_{13}NMe_4$ (preheated to 160°C) with nickelocene in acetonitrile produced, besides complexes (I) and (II), a dark green paramagnetic species the mass spectrum of which (M^+ 347) is consistent with a bimetallic (C_5H_5Ni)$_2$$CB_7H_8$ complex (III). Considering the electron count arguments,[6] a neutral compound of such a formula should contain two nickel atoms in different oxidation states, Ni^{4+} and Ni^{3+}, the latter being responsible for paramagnetism. The green colour of (III), which is usually indicative of metal–metal bonding,[7] should signify the preference for the 6,10-(η^5-C_5H_5Ni)$_2$-1-CB_7H_8 structure; an X-ray diffraction study on (III) is in progress.

Reaction of 4-CB_8H_{14} with $CoCl_2 \cdot 6H_2O$ and cyclopentadiene in concentrated ethanolic KOH afforded a red–orange complex (IV) in 20% yield. Elemental analysis of its tetramethylammonium salt and the NMR data [^{1}H NMR (200 MHz, $(CD_3)_2CO$) δ 6.56 (1 H, s, CH skel.), 4.75 (5 H, s, C_5H_5), 3.46 (12 H, s, NMe_4^+); ^{11}B NMR (64.2 MHz, $(CD_3)_2CO$) δ_B 34.20 (1 B, d, 148), 2.31 (1 B, d, 142), 0.39 (2 B, d, 136), −21.33 (2 B, d, 140), −25.52 (2 B, d, 136)] correspond well to the [2-η^5-C_5H_5Co-η^5-1-CB_8H_9]$^-$ NMe_4^+ structure for (IV), which has recently been determined by

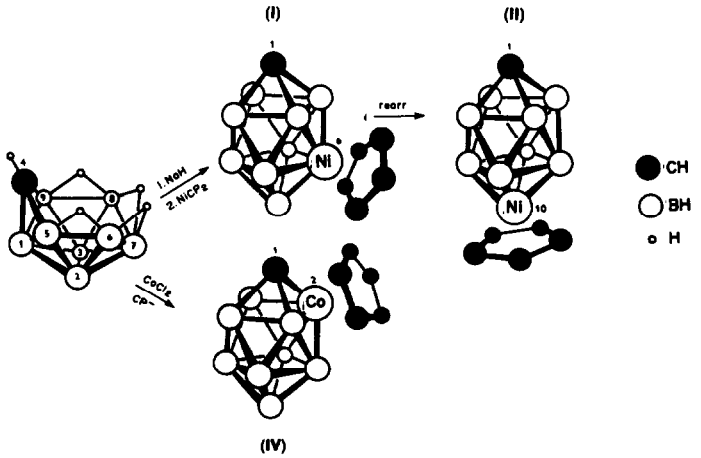

an X-ray diffraction study.[8] The same complex can also be obtained in the reaction of $CoCl_2$ with 4-$CB_8H_{13}Na$ in ether.

The formation of the discussed monometallic complexes can be envisaged as an insertion of the metal atom above the B(6, 7, 8) triangular face of the $[4\text{-}CB_8H_{13}]^-$ anion to form the (I) and (IV) complexes upon dehydrogenation and reorganization of the skeleton. In contrast to the cobalt complex (IV), the nickel species (I) is unstable due to unfavourable location of the Ni^{4+} central ion in the equatorial belt,[9] which accounts for the observed (I)→(II) rearrangement. Similar facile equatorial-apex rearrangement of the skeletal nickel atom was observed with the isoelectronic $[2\text{-}\eta^5\text{-}C_5H_5Ni\text{-}\eta^5\text{-}B_9H_9]^-$ anion.[9]

BOHUMIL ŠTIBR*
ZBYNĚK JANOUŠEK
Institute of Inorganic Chemistry Prague, KAREL BAŠE
Czechoslovak Academy of Sciences, JIŘÍ DOLANSKÝ
250 68 *Řež near Prague,* STANISLAV HEŘMÁNEK
Czechoslovakia

KONSTANTIN A. SOLNTSEV
LEV A. BUTMAN
N. S. Kurnakov Institute of General IGOR I. KUZNETSOV
and Inorganic Chemistry, NICOLAI T. KUZNETSOV
Academy of Sciences of the USSR,
117 071 *Moscow,*
Leninski Prospect 31,
U.S.S.R.

*Author to whom correspondence should be addressed.

REFERENCES

[1]C. G. Salentine, R. R. Rietz and M. F. Hawthorne, *Inorg. Chem.* 1974, **13**, 3025.
[2]D. F. Dustin and M. F. Hawthorne, *Inorg. Chem.* 1973, **12**, 1380.
[3]C. G. Salentine and M. F. Hawthorne, *J. Am. Chem. Soc.* 1975, **97**, 6382.
[4]B. Štíbr, K. Baše, S. Heřmánek and J. Plešek, *J. Chem. Soc. Chem. Commun.* 1976, 150.
[5]K. Baše, B. Štíbr, J. Dolanský and J. Duben, *Collect. Czech. Chem. Commun.* 1981, **46**, 2385.
[6]K. Wade, *Adv. Inorg. Chem. Radiochem.* 1976, **18**, 1 and refs. therein; C. J. Jones, W. J. Evans and M. F. Hawthorne, *J. Chem. Soc. Chem. Commun.* 1973, 543.
[7]W. J. Evans, C. J. Jones, B. Štíbr and M. F. Hawthorne, *J. Organomet. Chem.* 1973, **60**, C 27; W. J. Evans, C. J. Jones, B. Štíbr, R. A. Grey and M. F. Hawthorne, *J. Am. Chem. Soc.* 1974, **96**, 7405.
[8]K. A. Solntsev, L. A. Butman, I. I. Kuznetsov, N. T. Kuznetsov, B. Štíbr, Z. Janoušek and K. Baše, *Izv. Akad. Nauk USSR, Ser. Khim.*, in press.
[9]R. N. Leyden and M. F. Hawthorne, *J. Chem. Soc. Chem. Commun.* 1975, 311.

Polyhedron Vol. 1, No. 11-12, pp. 834–835, 1982
Printed in Great Britain.

0277-5387/82/110834-02$03.00/0
Pergamon Press Ltd.

Photosynthesis of a cyanocomplex containing molybdenum(IV) and molybdenum(VI): Photosynthesis of $K_6[Mo_2^{IV}Mo^{VI}(CN)_8O_6]2H_2O$

(*Received* 24 *June* 1982)

Abstract—A photochemical method for the preparation of $K_6[Mo_2^{IV}Mo^{VI}(CN)_8O_6]2H_2O$ is discussed. The synthesis of this complex was achieved by photolysing aqueous solutions of $K_4Mo(CN)_8$ in contact with atmospheric oxygen.

INTRODUCTION

Cyano complexes of molybdenum have been reported with the molybdenum in the valency states of II–V.[1] Preparation of a new compound $K_6[Mo_2^{IV}Mo^{VI}(CN)_8O_6]2H_2O$ was reported by Poel and Neumann.[2] We report the photolytic synthesis of this compound.

EXPERIMENTAL

The potassium octacyanomolybdate(IV) was obtained by the method of Furman and Miller.[3] The molybdenum (IV) content was determined by titration with standard permaganate solution potentiometrically. Found: K, 31.4; C, 19.2; N, 22.4; H_2O, 7.3. Calc. for $K_4Mo(CN)_8 2H_2O$; K, 31.49; Mo 19.34; C, 19.35; N, 22.57; H_2O 7.26%.

Photolysis was carried out using a Phillips medium pressure mercury arc lamp with a filter which transmitted radiations of wavelength in the range 340–430 nm. Solutions were contained in Pyrex reaction vessels.

Infrared spectra were recorded on a Perkin–Elmer Model 137 spectrophotometer as nujol mulls and were checked using KBr disc technique also. The visible spectra were recorded using Kϕ-10 spectrophotometer.

K_3 type Leeds and Northrup potentiometer with lamp and scale arrangement was used for potentiometric redox titrations. Bright platinum electrodes in conjunction with saturated calomel electrode were used.

RESULTS AND DISCUSSIONS

When a light yellow coloured aqueous solution of $K_4Mo(CN)_8$ was photolysed in contact with atmospheric oxygen at 10°C, it became red and the characteristic absorption peak of the red species $[Mo(CN)_7H_2O]^{3-}$ appeared at 512 nm;[4–6] on further irradiation, the 512 nm peak decreased and a new absorption peak at 618 nm appeared which grew to a maximum. At this stage, titration of an aliquot with $KMnO_4$ showed that 1.5 equivalents of the latter was used up per molybdenum atom when photolysis was done in an inert atmosphere, 2.0 equivalent per Mo atom were required at this stage. Apparently some of the molybdenum had been oxidised in contact with atmospheric oxygen. When the peak at 618 nm in the absorption spectrum of the solution photolysed in contact with atmospheric oxygen reached its maximum, alcohol was added to the blue solution and a blue precipitate separated out. After recrystallization, a blue solid was obtained which, on analysis gave: K, 27.2: Mo(total), 33.5; Mo(IV), 22.2; C, 11.1; N, 12.7; H_2O, 4.2.

an X-ray diffraction study.[8] The same complex can also be obtained in the reaction of $CoCl_2$ with 4-$CB_8H_{13}Na$ in ether.

The formation of the discussed monometallic complexes can be envisaged as an insertion of the metal atom above the B(6, 7, 8) triangular face of the $[4\text{-}CB_8H_{13}]^-$ anion to form the (I) and (IV) complexes upon dehydrogenation and reorganization of the skeleton. In contrast to the cobalt complex (IV), the nickel species (I) is unstable due to unfavourable location of the Ni^{4+} central ion in the equatorial belt,[9] which accounts for the observed (I)→(II) rearrangement. Similar facile equatorial-apex rearrangement of the skeletal nickel atom was observed with the isoelectronic $[2\text{-}\eta^5\text{-}C_5H_5Ni\text{-}\eta^5\text{-}B_9H_9]^-$ anion.[9]

BOHUMIL ŠTIBR*
ZBYNĚK JANOUŠEK
Institute of Inorganic Chemistry Prague, KAREL BAŠE
Czechoslovak Academy of Sciences, JIŘÍ DOLANSKÝ
250 68 *Řež near Prague,* STANISLAV HEŘMÁNEK
Czechoslovakia

KONSTANTIN A. SOLNTSEV
LEV A. BUTMAN
N. S. Kurnakov Institute of General IGOR I. KUZNETSOV
and Inorganic Chemistry, NICOLAI T. KUZNETSOV
Academy of Sciences of the USSR,
117 071 *Moscow,*
Leninski Prospect 31,
U.S.S.R.

*Author to whom correspondence should be addressed.

REFERENCES

[1]C. G. Salentine, R. R. Rietz and M. F. Hawthorne, *Inorg. Chem.* 1974, **13**, 3025.
[2]D. F. Dustin and M. F. Hawthorne, *Inorg. Chem.* 1973, **12**, 1380.
[3]C. G. Salentine and M. F. Hawthorne, *J. Am. Chem. Soc.* 1975, **97**, 6382.
[4]B. Štíbr, K. Baše, S. Heřmánek and J. Plešek, *J. Chem. Soc. Chem. Commun.* 1976, 150.
[5]K. Baše, B. Štíbr, J. Dolanský and J. Duben, *Collect. Czech. Chem. Commun.* 1981, **46**, 2385.
[6]K. Wade, *Adv. Inorg. Chem. Radiochem.* 1976, **18**, 1 and refs. therein; C. J. Jones, W. J. Evans and M. F. Hawthorne, *J. Chem. Soc. Chem. Commun.* 1973, 543.
[7]W. J. Evans, C. J. Jones, B. Štíbr and M. F. Hawthorne, *J. Organomet. Chem.* 1973, **60**, C 27; W. J. Evans, C. J. Jones, B. Štíbr, R. A. Grey and M. F. Hawthorne, *J. Am. Chem. Soc.* 1974, **96**, 7405.
[8]K. A. Solntsev, L. A. Butman, I. I. Kuznetsov, N. T. Kuznetsov, B. Štíbr, Z. Janoušek and K. Baše, *Izv. Akad. Nauk USSR, Ser. Khim.*, in press.
[9]R. N. Leyden and M. F. Hawthorne, *J. Chem. Soc. Chem. Commun.* 1975, 311.

Polyhedron Vol. 1, No. 11-12, pp. 834–835, 1982
Printed in Great Britain.

0277-5387/82/110834-02$03.00/0
Pergamon Press Ltd.

Photosynthesis of a cyanocomplex containing molybdenum(IV) and molybdenum(VI): Photosynthesis of $K_6[Mo_2^{IV}Mo^{VI}(CN)_8O_6]2H_2O$

(*Received* 24 *June* 1982)

Abstract—A photochemical method for the preparation of $K_6[Mo_2^{IV}Mo^{VI}(CN)_8O_6]2H_2O$ is discussed. The synthesis of this complex was achieved by photolysing aqueous solutions of $K_4Mo(CN)_8$ in contact with atmospheric oxygen.

INTRODUCTION

Cyano complexes of molybdenum have been reported with the molybdenum in the valency states of II–V.[1] Preparation of a new compound $K_6[Mo_2^{IV}Mo^{VI}(CN)_8O_6]2H_2O$ was reported by Poel and Neumann.[2] We report the photolytic synthesis of this compound.

EXPERIMENTAL

The potassium octacyanomolybdate(IV) was obtained by the method of Furman and Miller.[3] The molybdenum (IV) content was determined by titration with standard permaganate solution potentiometrically. Found: K, 31.4; C, 19.2; N, 22.4; H_2O, 7.3. Calc. for $K_4Mo(CN)_8 2H_2O$; K, 31.49; Mo 19.34; C, 19.35; N, 22.57; H_2O 7.26%.

Photolysis was carried out using a Phillips medium pressure mercury arc lamp with a filter which transmitted radiations of wavelength in the range 340–430 nm. Solutions were contained in Pyrex reaction vessels.

Infrared spectra were recorded on a Perkin–Elmer Model 137 spectrophotometer as nujol mulls and were checked using KBr disc technique also. The visible spectra were recorded using Kϕ-10 spectrophotometer.

K_3 type Leeds and Northrup potentiometer with lamp and scale arrangement was used for potentiometric redox titrations. Bright platinum electrodes in conjunction with saturated calomel electrode were used.

RESULTS AND DISCUSSIONS

When a light yellow coloured aqueous solution of $K_4Mo(CN)_8$ was photolysed in contact with atmospheric oxygen at 10°C, it became red and the characteristic absorption peak of the red species $[Mo(CN)_7H_2O]^{3-}$ appeared at 512 nm;[4–6] on further irradiation, the 512 nm peak decreased and a new absorption peak at 618 nm appeared which grew to a maximum. At this stage, titration of an aliquot with $KMnO_4$ showed that 1.5 equivalents of the latter was used up per molybdenum atom when photolysis was done in an inert atmosphere, 2.0 equivalent per Mo atom were required at this stage. Apparently some of the molybdenum had been oxidised in contact with atmospheric oxygen. When the peak at 618 nm in the absorption spectrum of the solution photolysed in contact with atmospheric oxygen reached its maximum, alcohol was added to the blue solution and a blue precipitate separated out. After recrystallization, a blue solid was obtained which, on analysis gave: K, 27.2: Mo(total), 33.5; Mo(IV), 22.2; C, 11.1; N, 12.7; H_2O, 4.2.

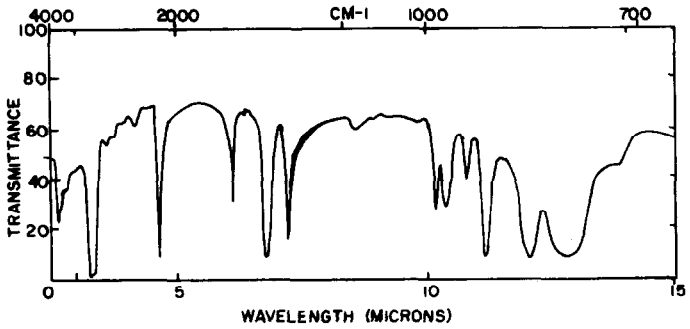

Fig. 1. IR spectra of $K_6[Mo_2(IV)Mo(VI)(CN)_8O_6]2H_2O$(Nujol Mull).

$K_6(Mo^{IV}Mo^{VI}(CN)_8O_6]2H_2O$ requires: K, 27.18; Mo(total). 33.36; Mo (IV), 22.24; C, 11.14; N, 12.99; H_2O, 4.16%.

The molybdenum in the solid was present in two oxidation states. Redox titration with $KMnO_4$ was done to determine the content of Mo(IV). It was assumed that in these titrations two equivalents of the reagent would be used up per Mo(IV). This assumption was made in the light of our experience with blue hydroxo compounds of Mo(IV) obtained in an inert atmosphere.[7] Total molybdenum in the above blue compound was obtained by analysis. There was no molybdenum in the 5-oxidation state, as was seen from the fact that the substance was not paramagnetic. The molybdenum was, therefore, in either four or six oxidation states. Mo(total): Mo(IV) remained unchanged upon repeated precipitation from aqueous solution with methanol or ethanol, indicating that the solid was a compound and not a mixture.

The IR spectrum of the compound is shown in Fig. 1. Poel and Neumann[2] published a similar IR spectrum of a molybdenum compound which they had prepared by a synthetic method and not by the photodecomposition of $K_4Mo(CN)_8$, as has been done by us. Similarity between their spectrum and the part of our spectrum on the extreme right of Fig. 1 is obvious. They formulated their compounds as $K_6[Mo_2^{IV}Mo^{VI}(CN)_8O_6]2H_2O$ and analysis of our blue solid agrees with this formula.

Using this method the deep blue solid can be prepared on a large scale. This complex compound is an example of mixed oxidation state. Deep intense colour is often observed for substances containing an element in two different oxidation states such as Prussian blue.

Department of Chemistry A. E. NYA
University of Calabar HARI MOHAN*
Calabar
Nigeria

*Author to whom correspondence should be addressed.

REFERENCES

[1]M. H. Ford-Smith, *The Chemistry of Complex Cyanides*, p. 38. Her Majesty's Stationary Office, London, 1964.
[2]J. V. Poel, and H. M. Neumann, *Inorg. Chem.* 1968, 3, 2086.
[3]N. H. Furman, and C. O. Miller, *Inorg. Syn.* 1950, 3, 160.
[4]R. P. Mitra, B. K. Sharma, and Hari Mohan, *Can. J. Chem.* 1969, 47, 2317.
[5]R. P. Mitra, B. K. Sharma, and Hari Mohan, *Ind. J. Chem.* 1969, 7, 1162.
[6]R. P. Mitra, B. K. Sharma, and Hari Mohan, *Aust. J. Chem.* 1972, 25, 449.
[7]Hari Mohan, Ph.D. Thesis, University of Delhi, 1969.

Polyhedron Vol. 1, No. 11-12, pp. 835-836, 1982
Printed in Great Britain.

0277-5387/82/110835-02$03.00/0
Pergamon Press Ltd.

$UO_2F_4^{2-}$: A new uranyl complex ion

Abstract—The synthesis, vibrational and electronic spectra of $[(CH_3)_4N]_2\ UO_2F_4$ are described. The data indicate that this compound contains the previously unknown $UO_2F_4^{2-}$ ion which has D_{4h} symmetry.

(*Received* 2 *August* 1982)

INTRODUCTION

We have recently reported and analysed the IR, Raman, luminescence and electronic absorption spectra of numerous compounds containing the monomeric $UO_2F_5^{3-}$ ion[1] and various dimeric[2] and polymeric fluoro and aquofluoro complex anions.[3,4] In every case the uranyl ion is surrounded by five fluoride ions or water molecules in a plane giving a pentagonal bipyramidal coordination about the uranium atom. We have now prepared the compound $[(CH_3)_4N]_2UO_2F_4$ for which spectroscopic measurements indicate that the uranyl ion is coordinated by four fluoride ions in a plane giving an approx. D_{4h} $UO_2F_4^{2-}$ structure. Whilst the analogous $UO_2Cl_4^{2-}$ and $UO_2Br_4^{2-}$ ions are well known[5-10] this anion has not been previously described.

EXPERIMENTAL

Slow evaporation of a highly concentrated aqueous solution of uranyl nitrate containing a nine-fold molar excess of $(CH_3)_4NF{\cdot}5H_2O$ at room temperature gave deliquescent green

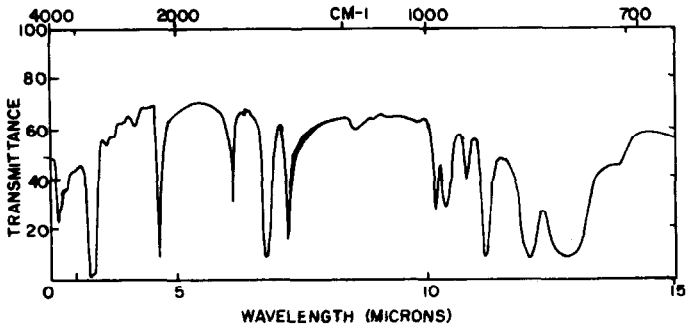

Fig. 1. IR spectra of $K_6[Mo_2(IV)Mo(VI)(CN)_8O_6]2H_2O$(Nujol Mull).

$K_6(Mo^{IV}Mo^{VI}(CN)_8O_6]2H_2O$ requires: K, 27.18; Mo(total). 33.36; Mo (IV), 22.24; C, 11.14; N, 12.99; H_2O, 4.16%.

The molybdenum in the solid was present in two oxidation states. Redox titration with $KMnO_4$ was done to determine the content of Mo(IV). It was assumed that in these titrations two equivalents of the reagent would be used up per Mo(IV). This assumption was made in the light of our experience with blue hydroxo compounds of Mo(IV) obtained in an inert atmosphere.[7] Total molybdenum in the above blue compound was obtained by analysis. There was no molybdenum in the 5-oxidation state, as was seen from the fact that the substance was not paramagnetic. The molybdenum was, therefore, in either four or six oxidation states. Mo(total): Mo(IV) remained unchanged upon repeated precipitation from aqueous solution with methanol or ethanol, indicating that the solid was a compound and not a mixture.

The IR spectrum of the compound is shown in Fig. 1. Poel and Neumann[2] published a similar IR spectrum of a molybdenum compound which they had prepared by a synthetic method and not by the photodecomposition of $K_4Mo(CN)_8$, as has been done by us. Similarity between their spectrum and the part of our spectrum on the extreme right of Fig. 1 is obvious. They formulated their compounds as $K_6[Mo_2^{IV}Mo^{VI}(CN)_8O_6]2H_2O$ and analysis of our blue solid agrees with this formula.

Using this method the deep blue solid can be prepared on a large scale. This complex compound is an example of mixed oxidation state. Deep intense colour is often observed for substances containing an element in two different oxidation states such as Prussian blue.

Department of Chemistry A. E. NYA
University of Calabar HARI MOHAN*
Calabar
Nigeria

*Author to whom correspondence should be addressed.

REFERENCES

[1]M. H. Ford-Smith, *The Chemistry of Complex Cyanides*, p. 38. Her Majesty's Stationary Office, London, 1964.
[2]J. V. Poel, and H. M. Neumann, *Inorg. Chem.* 1968, 3, 2086.
[3]N. H. Furman, and C. O. Miller, *Inorg. Syn.* 1950, 3, 160.
[4]R. P. Mitra, B. K. Sharma, and Hari Mohan, *Can. J. Chem.* 1969, 47, 2317.
[5]R. P. Mitra, B. K. Sharma, and Hari Mohan, *Ind. J. Chem.* 1969, 7, 1162.
[6]R. P. Mitra, B. K. Sharma, and Hari Mohan, *Aust. J. Chem.* 1972, 25, 449.
[7]Hari Mohan, Ph.D. Thesis, University of Delhi, 1969.

Polyhedron Vol. 1, No. 11-12, pp. 835-836, 1982
Printed in Great Britain.

0277-5387/82/110835-02$03.00/0
Pergamon Press Ltd.

$UO_2F_4^{2-}$: A new uranyl complex ion

Abstract—The synthesis, vibrational and electronic spectra of $[(CH_3)_4N]_2\ UO_2F_4$ are described. The data indicate that this compound contains the previously unknown $UO_2F_4^{2-}$ ion which has D_{4h} symmetry.

(*Received* 2 *August* 1982)

INTRODUCTION

We have recently reported and analysed the IR, Raman, luminescence and electronic absorption spectra of numerous compounds containing the monomeric $UO_2F_5^{3-}$ ion[1] and various dimeric[2] and polymeric fluoro and aquofluoro complex anions.[3,4] In every case the uranyl ion is surrounded by five fluoride ions or water molecules in a plane giving a pentagonal bipyramidal coordination about the uranium atom. We have now prepared the compound $[(CH_3)_4N]_2UO_2F_4$ for which spectroscopic measurements indicate that the uranyl ion is coordinated by four fluoride ions in a plane giving an approx. D_{4h} $UO_2F_4^{2-}$ structure. Whilst the analogous $UO_2Cl_4^{2-}$ and $UO_2Br_4^{2-}$ ions are well known[5-10] this anion has not been previously described.

EXPERIMENTAL

Slow evaporation of a highly concentrated aqueous solution of uranyl nitrate containing a nine-fold molar excess of $(CH_3)_4NF{\cdot}5H_2O$ at room temperature gave deliquescent green

crystals. These crystals have not yet been obtained in a pure form or studied in detail but their spectroscopic properties suggest that they should be formulated as $[(CH_3)_4N]_2[UO_2F_4(OH_2)]$ containing a monomeric anion with an in-plane coordination number of five. Calc. for $[(CH_3)_4N]_2[UO_2F_4(OH_2)]$: C, 18.8; H, 5.1; N, 5.5. Found: C, 17.7; H, 4.7; N, 5.4%. Heating these crystals at 100°C *in vacuo* yielded a deliquescent yellow powder $[(CH_3)_4N]_2\ UO_2F_4$. Calc. for $[(CH_3)_4N]_2UO_2F_4$: C, 19.4; H, 4.9; N, 5.7; U, 48.1; F, 15.4. Found: C, 19.1; H, 4.8; N, 5.5; U, 47.4; F, 14.8%. Exposure of this powder to moist air produced a green powder which analytical and spectroscopic measurements suggest is identical to the original green crystals.

Luminescence and vibrational spectra[10] were recorded as previously described.

RESULTS AND DISCUSSION

The vibrational spectra of $[(CH_3)_4N]_2UO_2F_4$ showed three single sharp bands at 848, 412 and 266 cm^{-1} in the IR spectrum and four sharp single bands at 798, 445, 253 and 178 cm^{-1} in the Raman spectrum due to the anion. The simplicity of the spectrum and the mutal exclusion immediately eliminate the possibility that the anion is dimeric [as in $M_4(UO_2)_2F_8{\cdot}2H_2O$[2]] or polymeric.[3,4] It is more difficult to eliminate the possibility of the presence of $UO_2F_5^{3-}$ because the exclusion rule also applies to D_{5h} symmetry. It is difficult however to devise a reasonable formulation based on this anion which accounts for the observed stoichiometry and spectra. The vibrational spectra give no evidence for the presence of water. The vibrational spectra are however readily interpreted in terms of a D_{4h} $UO_2F_4^{2-}$ structure, the three IR active bands being assigned as ν_2 a_{2u}(U–O), ν_6 e_u(U–F) and ν_3 $e_u\delta$(O–U–O) and the four Raman active bands as ν_1 a_{1g}(U–O), ν_4 a_{1g}(U–F) ν_{11} $e_g\delta$(O–U–F) and ν_7 $b_{1g}\delta$(F–U–F) respectively. It is noteworthy that both the IR and Raman active U–F stretching modes are at significantly higher wavenumber than the corresponding modes of the $UO_2F_5^{3-}$ anion.[1]

The luminescence spectrum of $[(CH_3)_4N]_2UO_2F_4$ is well resolved and significantly different from that of all other uranyl fluoride complex ions we have studied. The electronic origin appears with moderate intensity at 19,240 cm^{-1}. This is, we believe, the lowest energy luminescence origin reported for any uranyl complex. Sixteen other compounds,[4] containing monomeric, dimeric or polymeric anions based on the $UO_2F_5^{3-}$ or $UO_2F_4(OH_2)^{2-}$ chromophores and K, Rb, Cs, NH_4^+ and $(C_2H_5)_4N^+$ cations have this origin between 19,790 and 20,070 cm^{-1}. Whilst several factors contribute to the energy of this origin, it is interesting to note that six coordinate uranyl complex ions such as $[UO_2(O_2NO)_3]^-$ have electronic origins in the region of 21,000 cm^{-1}. The observation of a single origin in the low temperature and 80 K luminescence spectra (and in the 20 K mull absorption spectrum) shows the presence of a single type of uranyl ion of high symmetry. The absorption spectrum is distinctly different from that of the $UO_2F_5^{3-}$ ion, but the sensitivity and resolution in the mull spectra are not sufficient for detailed analysis.

In the luminescence spectrum the intensity of the vibronic origins is higher (relative to the origin and $n\nu_1$ progression thereupon) for $[(CH_3)N]_2\ UO_2F_4$ than for $M_3UO_2F_5$ compounds. This also indicates a highly symmetrical anion, but in addition it is noteworthy that the out-of-plane bending mode (ν_{11} in D_{5h}, ν_{10} in D_{4h}) is prominent in the luminescence spectrum of $[(CH_3)_4N]_2UO_2F_4$ but not readily observed in the spectra of other fluoro-anions. We have argued previously[1] that this mode should occur strongly in the spectra of D_{4h} uranyl anions but only weakly in the spectra of D_{5h} anions and this is supported by the luminescence of the $UO_2Cl_4^{2-}$ and $UO_2Br_4^{2-}$ anions.

Progressions in the symmetric U–F stretching mode ν_4 based on the origin and vibronic origins are much more intense in $[(CH_3)_4N]_2UO_2F_4$ than in $M_3UO_2F_5$ compounds showing that a large change (ca. 3.5 pm) occurs in the U–F bond distance in the excited Π_u state compared with the ground state. This together with the relatively high wavenumber of the ν_4 and ν_6 modes shows the presence of a stronger U–F bond in $[(CH_3)_4N]_2UO_2F_4$ than in the $UO_2F_5^{3-}$ anion.

The spectroscopic evidence then strongly suggests that $[(CH_3)_4N]_2UO_2F_4$ contains a monomeric anion of near D_{4h} symmetry. Unfortunately our preparative procedure yields a fine powder quite unsuitable for detailed X-ray structural analysis. If a method of preparaing large single crystals could be devised the polarized electronic absorption spectrum would be of considerable interest.

Acknowledgement—We thank the SERC for financial support. We thank Dr. T. J. Dines (University College, London) and Mr. N. Campbell (Imperial College, London) for recording Raman spectra under the ULIRS scheme.

Department of Chemistry
Birkbeck College
Malet Street
London WC1E 7HX
England

COLIN D. FLINT*
PETER A. TANNER

REFERENCES

[1]C. D. Flint and P. A. Tanner, *Mol. Phys.* 1981, **43**, 933.
[2]C. D. Flint and P. A. Tanner, *J. Chem. Soc., Faraday* 2 1981, **77**, 2339.
[3]C. D. Flint and P. A. Tanner, *J. Chem. Soc., Faraday* 2 1982, **78**, 832.
[4]P. A. Tanner, Thesis, University of London, 1980.
[5]C. D. Flint and P. A. Tanner, *J. Chem. Soc., Faraday* 2 1978, **74**, 2210.
[6]R. Denning, T. Snellgrove and D. Woodward, *Molec. Phys.* 1976, **32**, 419.
[7]C. D. Flint and P. A. Tanner, *J. Chem. Soc., Faraday* 2 1981, **77**, 1865.
[8]C. D. Flint and P. A. Tanner, *Inorg. Chem.* 1981, **20**, 4405.
[9]C. D. Flint and P. A. Tanner, *J. Chem. Soc., Faraday* 2 1982, **78**, 103.
[10]C. D. Flint and P. A. Tanner, *J. Chem. Soc., Faraday* 2 1982, **78**, 953.

*Author to whom correspondence should be addressed.

Polyhedron Vol. 1, No. 11–12, pp. 836–838, 1982
Printed in Great Britain.

0277-5387/82/110836-03$03.00/0
Pergamon Press Ltd.

The polynuclear complex formation between lead(II) and 2-mercaptoethanol reinvestigated

(*Received* 21 *September* 1982)

Abstract—The thermodynamics of complex formation between lead(II) and 2-mercaptoethanol has been reinvestigated at I = 150 mmol dm^{-3} $NaNO_3$ and at lower metal:ligand ratios in order to determine the mononuclear formation constants.

crystals. These crystals have not yet been obtained in a pure form or studied in detail but their spectroscopic properties suggest that they should be formulated as $[(CH_3)_4N]_2[UO_2F_4(OH_2)]$ containing a monomeric anion with an in-plane coordination number of five. Calc. for $[(CH_3)_4N]_2[UO_2F_4(OH_2)]$: C, 18.8; H, 5.1; N, 5.5. Found: C, 17.7; H, 4.7; N, 5.4%. Heating these crystals at 100°C *in vacuo* yielded a deliquescent yellow powder $[(CH_3)_4N]_2\ UO_2F_4$. Calc. for $[(CH_3)_4N]_2UO_2F_4$: C, 19.4; H, 4.9; N, 5.7; U, 48.1; F, 15.4. Found: C, 19.1; H, 4.8; N, 5.5; U, 47.4; F, 14.8%. Exposure of this powder to moist air produced a green powder which analytical and spectroscopic measurements suggest is identical to the original green crystals.

Luminescence and vibrational spectra[10] were recorded as previously described.

RESULTS AND DISCUSSION

The vibrational spectra of $[(CH_3)_4N]_2UO_2F_4$ showed three single sharp bands at 848, 412 and 266 cm^{-1} in the IR spectrum and four sharp single bands at 798, 445, 253 and 178 cm^{-1} in the Raman spectrum due to the anion. The simplicity of the spectrum and the mutal exclusion immediately eliminate the possibility that the anion is dimeric [as in $M_4(UO_2)_2F_8{\cdot}2H_2O$[2]] or polymeric.[3,4] It is more difficult to eliminate the possibility of the presence of $UO_2F_5^{3-}$ because the exclusion rule also applies to D_{5h} symmetry. It is difficult however to devise a reasonable formulation based on this anion which accounts for the observed stoichiometry and spectra. The vibrational spectra give no evidence for the presence of water. The vibrational spectra are however readily interpreted in terms of a D_{4h} $UO_2F_4^{2-}$ structure, the three IR active bands being assigned as ν_2 a_{2u}(U–O), ν_6 e_u(U–F) and ν_3 $e_u\delta$(O–U–O) and the four Raman active bands as ν_1 a_{1g}(U–O), ν_4 a_{1g}(U–F) ν_{11} $e_g\delta$(O–U–F) and ν_7 $b_{1g}\delta$(F–U–F) respectively. It is noteworthy that both the IR and Raman active U–F stretching modes are at significantly higher wavenumber than the corresponding modes of the $UO_2F_5^{3-}$ anion.[1]

The luminescence spectrum of $[(CH_3)_4N]_2UO_2F_4$ is well resolved and significantly different from that of all other uranyl fluoride complex ions we have studied. The electronic origin appears with moderate intensity at 19,240 cm^{-1}. This is, we believe, the lowest energy luminescence origin reported for any uranyl complex. Sixteen other compounds,[4] containing monomeric, dimeric or polymeric anions based on the $UO_2F_5^{3-}$ or $UO_2F_4(OH_2)^{2-}$ chromophores and K, Rb, Cs, NH_4^+ and $(C_2H_5)_4N^+$ cations have this origin between 19,790 and 20,070 cm^{-1}. Whilst several factors contribute to the energy of this origin, it is interesting to note that six coordinate uranyl complex ions such as $[UO_2(O_2NO)_3]^-$ have electronic origins in the region of 21,000 cm^{-1}. The observation of a single origin in the low temperature and 80 K luminescence spectra (and in the 20 K mull absorption spectrum) shows the presence of a single type of uranyl ion of high symmetry. The absorption spectrum is distinctly different from that of the $UO_2F_5^{3-}$ ion, but the sensitivity and resolution in the mull spectra are not sufficient for detailed analysis.

In the luminescence spectrum the intensity of the vibronic origins is higher (relative to the origin and $n\nu_1$ progression thereupon) for $[(CH_3)N]_2\ UO_2F_4$ than for $M_3UO_2F_5$ compounds. This also indicates a highly symmetrical anion, but in addition it is noteworthy that the out-of-plane bending mode (ν_{11} in D_{5h}, ν_{10} in D_{4h}) is prominent in the luminescence spectrum of $[(CH_3)_4N]_2UO_2F_4$ but not readily observed in the spectra of other fluoro-anions. We have argued previously[1] that this mode should occur strongly in the spectra of D_{4h} uranyl anions but only weakly in the spectra of D_{5h} anions and this is supported by the luminescence of the $UO_2Cl_4^{2-}$ and $UO_2Br_4^{2-}$ anions.

Progressions in the symmetric U–F stretching mode ν_4 based on the origin and vibronic origins are much more intense in $[(CH_3)_4N]_2UO_2F_4$ than in $M_3UO_2F_5$ compounds showing that a large change (ca. 3.5 pm) occurs in the U–F bond distance in the excited Π_u state compared with the ground state. This together with the relatively high wavenumber of the ν_4 and ν_6 modes shows the presence of a stronger U–F bond in $[(CH_3)_4N]_2UO_2F_4$ than in the $UO_2F_5^{3-}$ anion.

The spectroscopic evidence then strongly suggests that $[(CH_3)_4N]_2UO_2F_4$ contains a monomeric anion of near D_{4h} symmetry. Unfortunately our preparative procedure yields a fine powder quite unsuitable for detailed X-ray structural analysis. If a method of preparaing large single crystals could be devised the polarized electronic absorption spectrum would be of considerable interest.

Acknowledgement—We thank the SERC for financial support. We thank Dr. T. J. Dines (University College, London) and Mr. N. Campbell (Imperial College, London) for recording Raman spectra under the ULIRS scheme.

Department of Chemistry
Birkbeck College
Malet Street
London WC1E 7HX
England

COLIN D. FLINT*
PETER A. TANNER

REFERENCES

[1]C. D. Flint and P. A. Tanner, *Mol. Phys.* 1981, **43**, 933.
[2]C. D. Flint and P. A. Tanner, *J. Chem. Soc., Faraday* 2 1981, **77**, 2339.
[3]C. D. Flint and P. A. Tanner, *J. Chem. Soc., Faraday* 2 1982, **78**, 832.
[4]P. A. Tanner, Thesis, University of London, 1980.
[5]C. D. Flint and P. A. Tanner, *J. Chem. Soc., Faraday* 2 1978, **74**, 2210.
[6]R. Denning, T. Snellgrove and D. Woodward, *Molec. Phys.* 1976, **32**, 419.
[7]C. D. Flint and P. A. Tanner, *J. Chem. Soc., Faraday* 2 1981, **77**, 1865.
[8]C. D. Flint and P. A. Tanner, *Inorg. Chem.* 1981, **20**, 4405.
[9]C. D. Flint and P. A. Tanner, *J. Chem. Soc., Faraday* 2 1982, **78**, 103.
[10]C. D. Flint and P. A. Tanner, *J. Chem. Soc., Faraday* 2 1982, **78**, 953.

*Author to whom correspondence should be addressed.

Polyhedron Vol. 1, No. 11–12, pp. 836–838, 1982
Printed in Great Britain.

0277-5387/82/110836-03$03.00/0
Pergamon Press Ltd.

The polynuclear complex formation between lead(II) and 2-mercaptoethanol reinvestigated

(*Received* 21 *September* 1982)

Abstract—The thermodynamics of complex formation between lead(II) and 2-mercaptoethanol has been reinvestigated at I = 150 mmol dm^{-3} $NaNO_3$ and at lower metal:ligand ratios in order to determine the mononuclear formation constants.

INTRODUCTION

Recently the chelate effect model[1] has been extended from nitrogen and oxygen coordination to include the sulphur donor ligands. Several metal systems with 2-mercaptoethanol (LH) have already been studied[2-5] but for the lead(II) system only polynuclear complexes were detected.[6] Since the chelate effect model can only predict mononuclear formation constants, this system was reinvestigated at a lower ionic strength (0.15 mol dm^{-3} $NaNO_3$) and at lower metal:ligand ratios with the view to isolating these constants.

EXPERIMENTAL

A stock solution of redistilled 2-mercaptoethanol (Merck) was prepared and standardised by potentiometric titration using a Gran plot.[7] All other reagents were of analytical grade and were used without further purification. The lead(II) nitrate stock solution (0.05 mol dm^{-3}) was standardised volumetrically by complexometric (EDTA) titration. All solutions were prepared using degassed, glass-distilled water.

Potentiometric titrations were carried out using a glass electrode and the procedure described before,[8] all studies being performed at 25.00 ± 0.05°C and I = 150 mmol dm^{-3} in $NaNO_3$. Protonation constants were obtained for the ligand at different total ligand concentrations and the absence of metal ions. Similarly the metal complex formation curves were obtained at different metal ligand ratios and at different total ligand and total metal concentrations. The data were treated by MINIQUAD[9] and SCOGS[10] least squares analysis and the resulting "best" set of constants checked using the PSEUDOPLOT[11] approach. Infrared spectra were recorded as a nujol mull between polyethylene plates (500–80 cm^{-1}) on a Digilab FTS 16 B/D inteferometer.

RESULTS AND DISCUSSION

The formation curves for the lead(II)-2-mercaptoethanol system (Fig. 1) are similar to those obtained by de Brabander *et al.*,[6] except that precipitation was detected at a much earlier stage. This was particularly so at low metal:ligand ratios. The complex formation curves were not superimposable indicating the presence of polynuclear complex species.

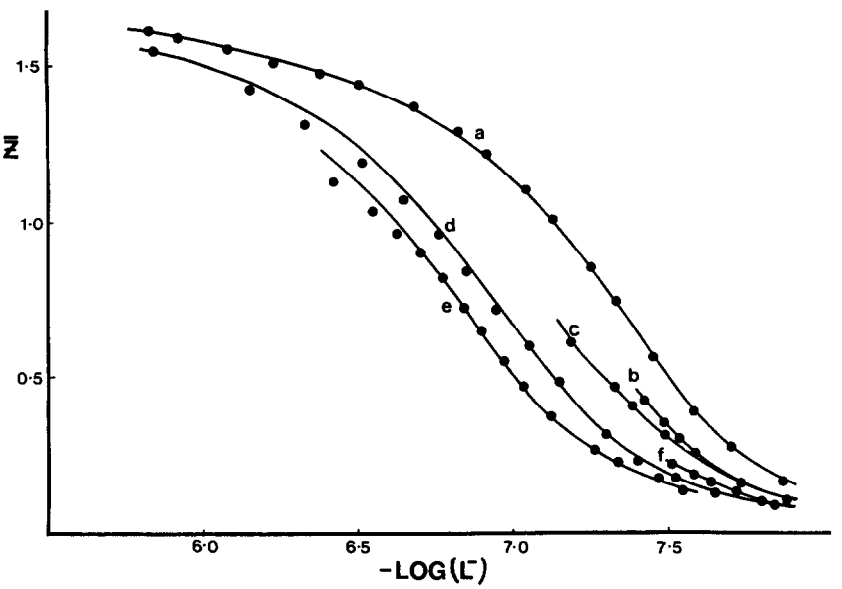

Fig. 1. Formation curves for the Pb(II)-2-mercaptoethanol system. Solid lines are theoretical curves calculated using the constants given in Table 1. Total metal and total ligand concentrations are (mmole dm^{-3}); (a) 16; 89 (b) 8; 4 (c) 8; 9 (d) 2; 10 (e) 1; 5 and (f) 4; 2 respectively.

Table 1. Formation constants determined for the lead(II)-2-mercaptoethanol system at 25°C and I = 0.15 mol dm^3 $NaNO_3$, together with literature data for this system. βpqr is the formation constant for the species $Pb_pL_qH_r$ defined by $\beta pqr = [Pb_pL_qH_r]/[Pb]^p[L]^q[H]^r$. n is the number of experimental points, R the crystallographic R factor and χ^2 the statistical χ^2 of MINIQUAD

p	q	r	log βpqr	n	R	χ^2	Reference
0	1	1	9.412 ± 0.001[a]	33	0.0037	15.6	present study
0	1	1	9.49				(6) 0.5M KNO_3, 25°C
3	5	0	39.88 ± 0.03	147	0.0029	38.6	present study
3	5	0	38.500				(6) 0.5M KNO_3, 25°C
3	4	0	33.31 ± 0.05	147	0.0029	38.6	present study
3	4	0	32.654				(6) 0.5M KNO_3^-, 25°C
1	1	0	6.74 ± 0.11	147	0.0029	38.6	present study
1	1[b]	0	6.634				(6) 0.5M KNO_3, 25°C
2	1	0	8.73 ± 0.13	147	0.0029	38.6	present study
2	1	0	8.937				(6) 0.5M KNO_3, 25°C

[a] standard deviation in log β

[b] LH = 3-mercapto-1,2-propanediol

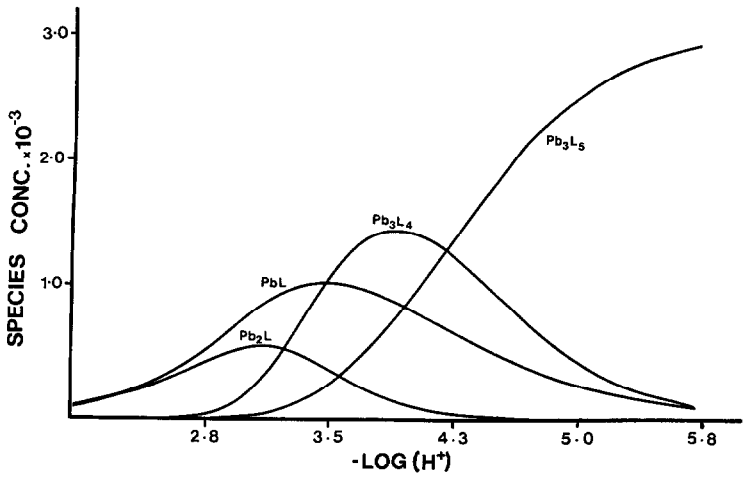

Fig. 2. Species distribution graph of the Pb(II)-2-mercaptoethanol system. Total metal = 0.01 mole dm^{-3} and total ligand = 0.05 mole dm^{-3}.

As a first attempt at refinement of the data, de Brabander's model[6] of Pb_3L_5, Pb_3L_4, Pb_2L, Pb_2L_2 and Pb_2L_3 was used. From this model the minor species Pb_2L_2 and Pb_2L_3 were eliminated. The introduction of an PbL species to the model led to a significant[12] improvement, particularly at low metal concentrations. As a check on this model the literature model for 3-mercapto-1,2-propanediol[6] was used. From this model the PbL_2 and PbL_3 species were understandably (maximum $\bar{Z} \simeq 1$) eliminated, leaving the same model as before. The resulting formation constants, given in Table 1, are in good agreement with the literature, considering differences in ionic strength and calibration procedures. As a final check the experimentally obtained formation curves were compared (Fig. 1) with theoretical curves, calculated using the above constants and the computer program PSEUDOPLOT. The literature model[6] was also "pseudo-plotted" but when compared to both our data and those in the literature, gave marked deviations at low metal concentrations.

Using the constants given in Table 1, a species distribution diagram was constructed (Fig. 2). This shows that, under the experimental conditions used, the ML species is appreciably formed ($\sim 10\%$) and cannot be ignored.

One difficulty encountered in the determination of mononuclear stability constants in this system is the early advent of precipitation, particularly at low metal:ligand concentration ratios. Elemental analysis of the precipitate is consistent with the empirical formulae $Pb(SCH_2CH_2OH)_2$ (obs. C 13.3%; H 2.8%; Calc. C 13.3%; H 2.3%). The far-infrared spectrum of the complex (νPb–O 311, νPb–S 246 cm^{-1}) is not consistent with a polymeric structure with bridging S atoms that has been proposed for the Ni(II) complex.[5] We suggest instead that Pb(II) sits in a tetrahedral environment and the ligand is bidentate. This structure is similar to that found for the Bi(III) complex.[13] The previous suggestion of metal–metal bonding is discounted.[6]

*Author to whom correspondence should be addressed.

Department of Inorganic Chemistry GRAHAM E. JACKSON*
University of Cape Town
South Africa

Department of Chemistry ROBERT D. HANCOCK
University of the Witwatersrand
South Africa

REFERENCES

[1]R. D. Hancock and F. Marzicano, *J.C.S. Dalton*, 1976, 1096.
[2]R. Tunaboylu and G. Schwarzenbach, *Helv. Chim. Acta* 1972, **55**, 2065.
[3]R. Tunaboylu and G. Schwarzenbach, *Helv. Chim. Acta* 1971, **54**, 2166.
[4]G. Schwarzenbach and M. Schellenberg, *Helv. Chim. Acta* 1965, **8**, 83.
[5]H. F. de Brabander, L. C. Van Poucke and Z. Eeckhaut, *Inorg. Chim. Acta* 1972, **6**, 459.
[6]H. F. de Brabander, J. J. Tombeux and L. C. Van Poucke, *J. Coord. Chem.* 1974, **4**, 87.
[7]G. Gran, *International Congress on Analytical Chemistry* 1952, **77**, 661.
[8]G. V. Fazakerley, G. E. Jackson and P. W. Linder, *J. Inorg. Nucl. Chem.* 1976, **38**, 1397.
[9]A. Sabatini, A. Vacca and P. Gans, *Talanta* 1974, **21**, 53.
[10]I. G. Sayce, *Talanta*, 1968, **15**, 1397.
[11]A. M. Corrie, G. K. R. Makar, M. L. D. Touche and D. R. Williams, *J. Chem. Soc. Dalton* 1975, 105.
[12]A. Vacca, A. Sabatini and M. A. Gristina, *Coord. Chem. Rev.* 1972, **8**, 45.
[13]G. E. Jackson, L. R. Nassimbeni and M. L. Niven, *Acta Cryst.* submitted.

Polyhedron Vol. 1, No. 11-12, pp. 839-840, 1982
Printed in Great Britain

0277-5387/82/110839-02$03.00/0
Pergamon Press Ltd.

COMMUNICATIONS

The photochemical decomposition of alcohols catalysed by tri(isopropyl) phosphine complexes of rhodium(I)

(*Received* 19 *April* 1982)

Abstract—Photolysis of $RhH(P^iPr_3)_3$ or $RhH(CO)(P^iPr_3)_2$ in solution in primary alcohols (RCH_2OH) produces H_2, CO and RH, whereas hydrogen and acetone are produced from propan-2-ol; in the presence of hex-1-ene, this last reaction gives acetone and hexane in the absence of illumination.

Although the photochemical production of hydrogen from water has received considerable study in recent years,[1,2] the related energy storing photochemical production of hydrogen from alcohols has been little studied.

Heterogeneous reactions have been reported in which platinized TiO_2 catalyses[3] the production of hydrogen and aldehydes or ketones from primary or secondary alcohols and in which TiO_2 catalyses[4] the formation of hydrogen and CO_2 from aqueous methanol. Both of these reactions occur under UV illumination and the latter is a mildly exoergonic process.

The thermal decomposition of alcohols to give carbonyls, hydrogen and/or metal hydrides has been well documented.[5,6]

We now report that certain rhodium complexes give hydrogen on photolysis in alcohols. Thus, photolysis of $RhH(P^iPr_3)_3$[7] or of $RhH(CO)(P^iPr_3)_2$[8] in methanol with light from a 500 w tungsten halogen lamp passing through pyrex and water filters catalytically produces hydrogen and carbon monoxide in 2:1 molar ratios. In the absence of either illumination or catalyst, neither hydrogen nor carbon monoxide is produced.

Although we have not yet completed a full kinetic study of this system, it is clear that the reaction has a moderately high activation energy (~30 kJ $mole^{-1}$) and hence that there must be a slow thermal step or a pre-equilibrium whose position is temperature dependent.

With ethanol, H_2, CO and CH_4 are the major products, whereas propan-2-ol gives hydrogen and acetone. For both of these systems, illumination is essential and the reactions proceed faster at higher temperatures.

Since $RhH(P^iPr_3)_3$ is known[8] to react thermally with methanol to give $RhH(CO)(P^iPr_3)_2$, it seems reasonable to suppose that the mechanism of decomposition of primary alcohols is the same for both catalysts.

We propose then, that the key photochemical step is the loss of CO from $RhH(CO)(P^iPr_3)_2$ ($\lambda_{max} = 360$ nm), a reaction which has many precedents in organometallic chemistry[9], and that $RhH(P^iPr_3)_2$ reacts by a series of thermal steps with the alcohol to regenerate $RhH(CO)(P^iPr_3)_2$ giving two moles of hydrogen or one of hydrogen and one of methane (see Scheme 1).

For the dehydrogenation of propan-2-ol, a similar mechanism (Scheme 2) accounts for the formation of acetone and a trihydridorhodium species but in this case, hydrogen loss occurs photochemically rather than thermally.† At present, it is not clear why the loss of hydrogen in this case should be photochemical, whereas for primary alcohols, it is thermal‡, although production of hydrogen from species of this kind is known[8,10] to depend markedly on the nature of the other ligands in the coordination sphere. Thus, hydrogen does not evolve thermally from $[RhH_2(py)_2P^iPr_3)_2)_2]^+$ but, when one pyridine (py) molecule is replaced by CO, smooth hydrogen evolution is observed in the dark at room temperature.

Further support for the idea that hydrogen loss is the photochemical step in the dehydrogenation of propan-2-ol comes from the observation that when the reaction is carried out in the presence of a hydrogen acceptor such as hex-1-ene, $RhH(P^iPr_3)_3$ catalyses transfer hydrogenation from propan-2-ol to give acetone and hexane, the reaction occuring thermally and not being enhanced by illumination. Intermediate (A) in Scheme 2 presumably coordinates hexene after loss of acetone and transfers two hydrogen atoms to the alkene to give hexane and $RhH(P^iPr_3)_2$, a series of reactions which are exoergonic and unlikely to be light assisted.

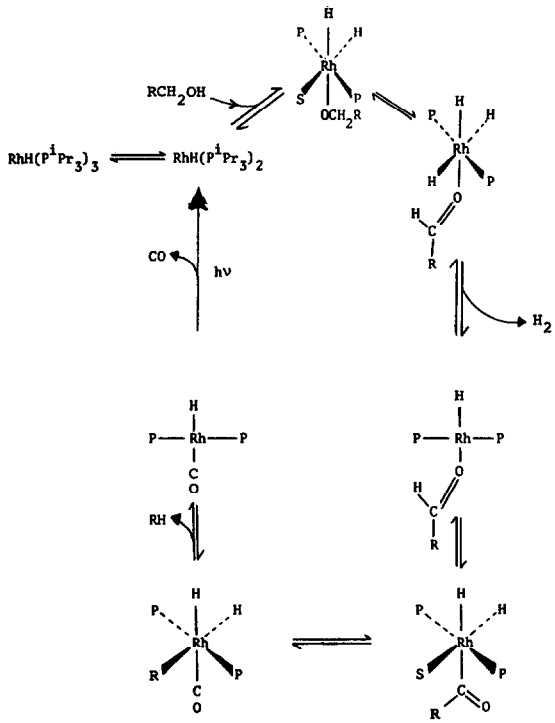

Scheme 1. Proposed mechanism for the photochemical dehydrocarbonylation of primary alcohols catalysed by $RhH(P^iPr_3)_3$ or $RhH(CO)(P^iPr_3)_2$. (R = H or Me, P = P^iPr_3, S = solvent.)

†We are currently investigating whether light also speeds up the loss of hydrogen from $RhH_3(P^iPr_3)_2(OCHMe)$, although we know that this can occur thermally.

‡We note, however, that since dehydrogenation of isopropanol is endoergonic, light absorption must occur to drive the reaction. (For primary alcohols the formation of the metal carbonyl is exoergonic so light is not a necessary requirement for the hydrogen loss in these cases.)

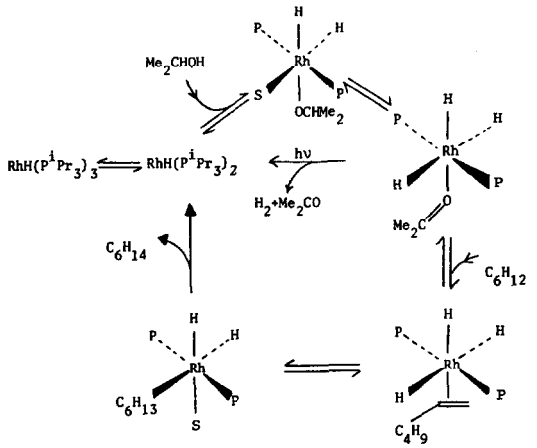

Scheme 2. Proposed mechanisms for the photochemical dehydrogenation of propan-2-ol and for the thermal transfer of hydrogen between propan-2-ol and hex-1-ene catalysed by $RhH(P^iPr_3)_3$. ($P = P^iPr_3$, S = solvent).

Although these reactions may find some use in increasing the fuel content of waste alcohols, they are perhaps likely to be of greater significance in organic synthesis for the formation of specialist alkanes by the dehydrocarbonylation of alcohols.

*Author to whom correspondence should be addressed.

ESTHER DELGADO-LIETA
MICHAEL A. LUKE
RODNEY F. JONES
DAVID J. COLE-HAMILTON*

Donnan Laboratories,
University of Liverpool,
PO Box 147, Liverpool,
L69 3BX,
England

Acknowledgements—We thank the University of Madrid (E.S.D.) and the S.R.C.(R.F.J.) for support and Johnson Matthey Ltd. for loans of rhodium salts.

REFERENCES

[1]M. Gratzel, *Acc. Chem. Res.* 1981, 376 and references therein.
[2]R. F. Jones and D. J. Cole-Hamilton, *J. Chem. Soc. Chem. Commun.* 1981, 58.
[3]P. Pichat, J-M. Herrmann, J. Disdier, H. Courbon and M-N. Mozzanega, *Nouv. J. Chim.* 1981, **5**, 627.
[4]T. Kawai and T. Sakata, *J. Chem. Soc. Chem. Commun.* 1980, 694.
[5]J. Chatt, B. L. Shaw and A. E. Field, *J. Chem. Soc.* 1964, 3466.
[6]E. Benedetti, G. Bracci, G. Sbrana, F. Salvetti and G. Grassi, *J. Organomet. Chem.* 1972, **37**, 361.
[7]T. Yoshida, T. Okano, D. L. Thorn, T. H. Tulip, S. Otsuka and J. A. Ibers, *J. Organomet. Chem.* 1979, **181**, 183.
[8]T. Yoshida, T. Okano and S. Otsuka, *J. Am. Chem. Soc.* 1980, **102**, 5966.
[9]See F. A. Cotton and G. Wilkinson, *Advanced Inorganic Chemistry*, 4th Edn, p. 1070. Wiley, New York 1980.
[10]T. Yoshida, T. Okano, Y. Ueda and S. Otsuka, *J. Am. Chem. Soc.* 1981, **103**, 3411.

Polyhedron Vol. 1, No. 11-12, pp. 840-841, 1982
Printed in Great Britain.

0277-5387/82/110840-02$03.00/0
Pergamon Press Ltd.

X-Ray crystal structure of the tris(acetato)dioxoosmate(VI) anion

(*Received* 13 *July* 1982)

Abstract—X-ray crystallographic study of $K[OsO_2(O_2CMe)_3].\ 2MeCO_2H$ shows that the anion has *cis* dioxo, one chelate and two *trans* monodentate acetato groups.

Although only recently there has been interest in non-carbon monoxide containing carboxylato complexes of osmium, with the synthesis of osmium(III) species, $[OsCl(\mu\text{-}O_2CR)_2]_2$ for which the X-ray structure of the butyrate has been confirmed,[1,2] of osmium(IV) oxo species, $Os_2(\mu\text{-}O)\ (\mu\text{-}O_2CR)_2X_4(PR_3)_2$ for which X-ray confirmation has been obtained[3] and osmium(III) species, $OsX_2(O_2CR)(PR_3)_2$,[4] the first osmium carboxylate complex of osmium(VI), $K[OsO_2(O_2CMe)_3]$, was made many years ago by Criegee.[5] During synthetic studies using this salt as starting material, we have obtained deep blue air-sensitive crystals of the solvate $K[OsO_2(O_2CMe)_3]\cdot 2MeCO_2H$ from acetic acid.

Measurements on a crystal, of approximate size 0.13 × 0.40 × 0.45 mm, sealed in a Lindemann tube showed the compound to be triclinic, with unit-cell dimensions $a = 7.669(1)$, $b = 11.638(2)$, $c = 11.709(1)$Å, $\alpha = 111.51(1)$, $\beta = 98.49(1)$, $\gamma = 106.61(1)°$, $U = 893.5(2)$Å^3 (at 19° C), space group $P\bar{1}$ and $Z = 2$. X-Ray diffraction data were collected on a Nicolet R3m/Eclipse S140 diffractometer system using an ω-scan technique with graphite-monochromated Cu-$K\alpha$ radiation. A total of 1839 independent reflections were measured (to $\theta = 50°$), of which 14 were judged to be "unobserved", and the data were corrected for absorption [μ(Cu-$K\alpha$) = 161.2 cm^{-1}]. The structure was solved by Patterson and Fourier methods, and least-squares refinement has now reached $R = 0.052$. The program system SHELXTL[6] was used throughout the calculations.

There are three species in the structure: potassium cations, the $[OsO_2(O_2CMe)_3]^-$ anions, and acetic acid molecules of solvation. In the complex anion, shown in Fig. 1, the osmium atom is coordinated to two terminal oxygen atoms, to two *trans* monodentate acetate groups, and to a bidentate acetate. The geometry is very markedly distorted away from octahedral, with the angle between *cis* terminal oxygen atoms of 125.2(3)° and the angle subtended by the bidentate acetate of 59.2(3)°. The anion has almost perfect $mm2(C_{2v})$ point symmetry.

There are three types of Os–O bonds in the coordination sphere. The Os–O(terminal) distances are 1.700(7) and 1.722(8)Å

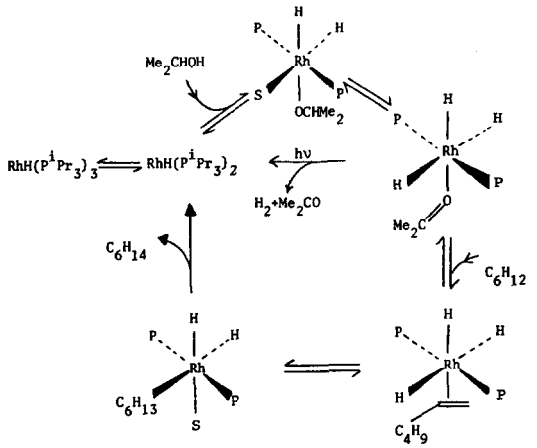

Scheme 2. Proposed mechanisms for the photochemical dehydrogenation of propan-2-ol and for the thermal transfer of hydrogen between propan-2-ol and hex-1-ene catalysed by $RhH(P^iPr_3)_3$. ($P = P^iPr_3$, S = solvent).

Although these reactions may find some use in increasing the fuel content of waste alcohols, they are perhaps likely to be of greater significance in organic synthesis for the formation of specialist alkanes by the dehydrocarbonylation of alcohols.

*Author to whom correspondence should be addressed.

ESTHER DELGADO-LIETA
MICHAEL A. LUKE
RODNEY F. JONES
DAVID J. COLE-HAMILTON*

Donnan Laboratories,
University of Liverpool,
PO Box 147, Liverpool,
L69 3BX,
England

Acknowledgements—We thank the University of Madrid (E.S.D.) and the S.R.C.(R.F.J.) for support and Johnson Matthey Ltd. for loans of rhodium salts.

REFERENCES

[1]M. Gratzel, *Acc. Chem. Res.* 1981, 376 and references therein.
[2]R. F. Jones and D. J. Cole-Hamilton, *J. Chem. Soc. Chem. Commun.* 1981, 58.
[3]P. Pichat, J-M. Herrmann, J. Disdier, H. Courbon and M-N. Mozzanega, *Nouv. J. Chim.* 1981, **5**, 627.
[4]T. Kawai and T. Sakata, *J. Chem. Soc. Chem. Commun.* 1980, 694.
[5]J. Chatt, B. L. Shaw and A. E. Field, *J. Chem. Soc.* 1964, 3466.
[6]E. Benedetti, G. Bracci, G. Sbrana, F. Salvetti and G. Grassi, *J. Organomet. Chem.* 1972, **37**, 361.
[7]T. Yoshida, T. Okano, D. L. Thorn, T. H. Tulip, S. Otsuka and J. A. Ibers, *J. Organomet. Chem.* 1979, **181**, 183.
[8]T. Yoshida, T. Okano and S. Otsuka, *J. Am. Chem. Soc.* 1980, **102**, 5966.
[9]See F. A. Cotton and G. Wilkinson, *Advanced Inorganic Chemistry*, 4th Edn, p. 1070. Wiley, New York 1980.
[10]T. Yoshida, T. Okano, Y. Ueda and S. Otsuka, *J. Am. Chem. Soc.* 1981, **103**, 3411.

Polyhedron Vol. 1, No. 11-12, pp. 840-841, 1982
Printed in Great Britain.

0277-5387/82/110840-02$03.00/0
Pergamon Press Ltd.

X-Ray crystal structure of the tris(acetato)dioxoosmate(VI) anion

(*Received* 13 *July* 1982)

Abstract—X-ray crystallographic study of $K[OsO_2(O_2CMe)_3].\ 2MeCO_2H$ shows that the anion has *cis* dioxo, one chelate and two *trans* monodentate acetato groups.

Although only recently there has been interest in non-carbon monoxide containing carboxylato complexes of osmium, with the synthesis of osmium(III) species, $[OsCl(\mu\text{-}O_2CR)_2]_2$ for which the X-ray structure of the butyrate has been confirmed,[1,2] of osmium(IV) oxo species, $Os_2(\mu\text{-}O)\ (\mu\text{-}O_2CR)_2X_4(PR_3)_2$ for which X-ray confirmation has been obtained[3] and osmium(III) species, $OsX_2(O_2CR)(PR_3)_2$,[4] the first osmium carboxylate complex of osmium(VI), $K[OsO_2(O_2CMe)_3]$, was made many years ago by Criegee.[5] During synthetic studies using this salt as starting material, we have obtained deep blue air-sensitive crystals of the solvate $K[OsO_2(O_2CMe)_3]\cdot 2MeCO_2H$ from acetic acid.

Measurements on a crystal, of approximate size 0.13 × 0.40 × 0.45 mm, sealed in a Lindemann tube showed the compound to be triclinic, with unit-cell dimensions $a = 7.669(1)$, $b = 11.638(2)$, $c = 11.709(1)$Å, $\alpha = 111.51(1)$, $\beta = 98.49(1)$, $\gamma = 106.61(1)°$, $U = 893.5(2)$Å^3 (at 19° C), space group $P\bar{1}$ and $Z = 2$. X-Ray diffraction data were collected on a Nicolet R3m/Eclipse S140 diffractometer system using an ω-scan technique with graphite-monochromated Cu-$K\alpha$ radiation. A total of 1839 independent reflections were measured (to $\theta = 50°$), of which 14 were judged to be "unobserved", and the data were corrected for absorption [μ(Cu-$K\alpha$) = 161.2 cm^{-1}]. The structure was solved by Patterson and Fourier methods, and least-squares refinement has now reached $R = 0.052$. The program system SHELXTL[6] was used throughout the calculations.

There are three species in the structure: potassium cations, the $[OsO_2(O_2CMe)_3]^-$ anions, and acetic acid molecules of solvation. In the complex anion, shown in Fig. 1, the osmium atom is coordinated to two terminal oxygen atoms, to two *trans* monodentate acetate groups, and to a bidentate acetate. The geometry is very markedly distorted away from octahedral, with the angle between *cis* terminal oxygen atoms of 125.2(3)° and the angle subtended by the bidentate acetate of 59.2(3)°. The anion has almost perfect $mm2(C_{2v})$ point symmetry.

There are three types of Os–O bonds in the coordination sphere. The Os–O(terminal) distances are 1.700(7) and 1.722(8)Å

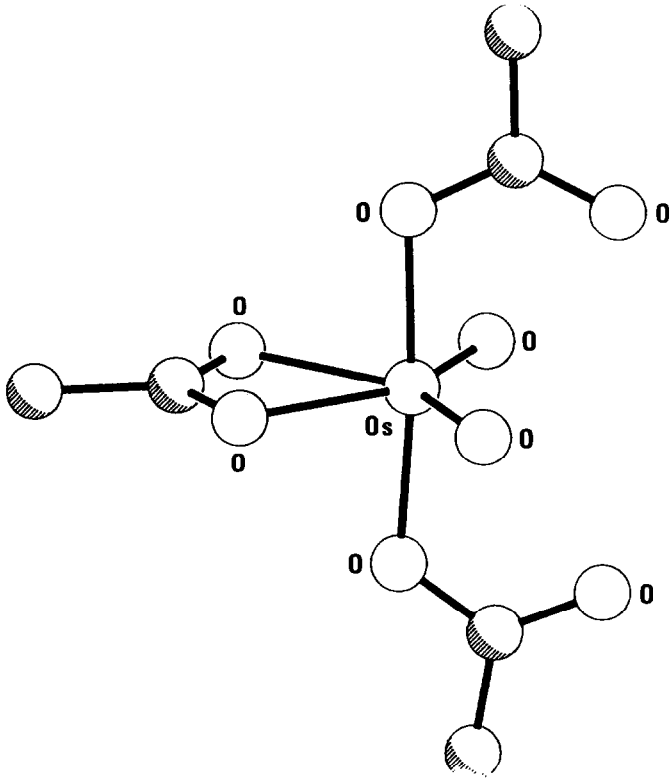

Fig. 1. Structure of the tris(acetato)dioxoosmate(VI) anion.

(mean 1.711Å) comparable to those found in other oxo-osmium complexes.[7] Bond lengths Os–O to the monodentate acetates are normal, 2.019(7) and 2.032(8)Å (mean 2.026Å), while those to the bidentate acetate are, as expected, longer at 2.127(6) and 2.169(6)Å (mean 2.148Å).

A *cis* arrangement of terminal oxo groups is very unusual for a d^2 dioxo system, and can be better rationalised by thinking of the anion as a pseudo trigonal bipyramidal species, with the bidentate acetate occupying one coordination site.[8] Indeed, a trigonal-bipyramidal complex was postulated to exist in solution on the basis of the weakly and asymmetrically bridged dimeric structure of $[OsO_2$(cyclohexane-1,2-diolato) (quinuclidine)$]_2$.[9] In that complex the distorted coordination observed for the osmium atom in the solid state was thought to arise from the approach of two trigonal bipyramidal molecules opening out the equatorial O=Os=O angle to 154°. In the title anion the O=Os=O angle is close to that expected for equatorial *tbp* positions.

The acetic acid molecules of solvation take part in hydrogen bonding of the type O–H . . . O but do not otherwise impinge on the complex anion.

The IR spectrum of the non-solvated salt[10] is consistent with the structure now determined.

TORSTEN BEHLING
MARIO V. CAPPARELLI
ANDRZEJ C. SKAPSKI*
GEOFFREY WILKINSON*

Chemistry Department,
Imperial College of Science and Technology,
London, SW7 2AY,
England

*Authors to whom correspondence should be addressed.

Acknowledgements—We thank the SERC for the diffractometer system and the Central University of Venezuela (M.V.C.) for study leave.

REFERENCES

[1]D. S. Moore, A. S. Alves and G. Wilkinson, *J. Chem. Soc., Chem. Commun.* 1981, 1164.
[2]T. A. Stephenson, P. A. Rocher and M. D. Walkinshaws, *J. Organomet. Chem.* 1982, **232**, C51.
[3]J. E. Armstrong, W. R. Robinson and R. A. Walton, *J. Chem. Soc., Chem. Commun.* 1981, 1120.
[4]D. S. Moore and S. D. Robinson, *Inorg. Chem.* 1979, **18**, 2307.
[5]R. Criegee, *Liebigs Ann. Chem.* 1936, **522**, 75; R. Criegee, B. Marchand and H. Wannovius, *Liebigs Ann. Chem.* 1942, **550**, 99.
[6]G. M. Sheldrick, SHELXTL—an integrated system for solving, refining, and displaying crystal structures from diffraction data. Revision 3, July 1981, Nicolet Instruments Ltd., Warwick, England.
[7]B. A. Cartwright, W. P. Griffith, M. Schröder and A. C. Skapski, *Inorg. Chim. Acta* 1981, **53**, L129; T. Prangé and C. Pascard, *Acta Cryst.* 1977, **B33**, 621; T. J. Kistenmacher, L. G. Marzilli and M. Rossi, *Bioinorg. Chem.* 1976, **6**, 347; J. F. Conn, J. J. Kim, F. L. Suddath, P. Blattman and A. Rich, *J. Am. Chem. Soc.* 1976, **96**, 7152.
[8]F. A. Cotton, D. M. L. Goodgame and R. H. Soderberg, *Inorg. Chem.* 1963, **2**, 1162; J. C. Taylor, M. H. Mueller and R. L. Hitterman, *Acta Cryst.* 1966, **20**, 842.
[9]B. A. Cartwright, W. P. Griffith, M. Schröder and A. C. Skapski, *J. Chem. Soc., Chem. Commun.* 1978, 853.
[10]W. P. Griffith and R. Rossetti, *J. Chem. Soc., Dalton Trans.* 1972, 1449.

Polyhedron Vol. 1, No. 11-12, pp. 842-843, 1982
Printed in Great Britain.

0277-5387/82/110842-02$03.00/0
Pergamon Press Ltd.

Electrophilic attacks on μ_3-bridging acetyl in a triiron carbonyl cluster; C–O bond cleavage to give μ_3-ethylidyne and μ-methoxo groups

(*Received* 6 *August* 1982)

Abstract—The triiron carbonyl cluster anion, $[Fe_3(CO)_9(\mu_3\text{-}CH_3CO)]^-$ reacts with fluoroboric acid to give the neutral cluster $Fe_3(CO)_9(\mu\text{-}H)(\mu_3\text{-}CH_3CO)$. Methylfluorosulphate reacts to give the compound $Fe_3(CO)_9(\mu_3\text{-}CCH_3)(\mu_3\text{-}OCH_3)$ in which the μ_3-acetyl group has undergone stoichiometric C–O bond cleavage.

The reaction of the iron carbonylate anion, $[Fe_2(CO)_8]^{2-}$, with methyl iodide produces the cluster $[Fe_3(CO)_9\mu_3\text{-}MeCO]^-$ which has a unique bridging acetyl group.[1] The tetraalkylammonium salt of this ion reacts with fluoroboric or trifluoroacetic acid in tetrahydrofuran and with methyl fluorosulphate in dichloromethane to give neutral triiron clusters that have been characterised spectroscopically and by X-ray crystallography.[2] As in the reaction of $[Fe_2(CO)_8]^{2-}$ with electrophiles the nature of the product here also depends on the electrophile.

The product from proton attack, $Fe_3(CO)_9(\mu\text{-}H)\mu_3\text{-}MeCO$ (1) retains the unique bridge acyl group in which the C–O bond has considerable double bond character (Fig. 1). However, the $MeSO_3F$ reaction product (2) (Fig. 2) has a triply bridged ethylidyne, $\mu\text{-}CMe_3$, group and a triply bridged methoxo, μ-OMe, group. By contrast with the hydrido species (1) which has a closo structure, (2) has an open structure. If we consider the μ_3-OMe group as a five-electron ligand then the cluster is a 50-electron one and an open structure is expected.[3]

The formation of (2) probably occurs via initial attack on the lone pair of acyl oxygen (eqn 1) to give the species (3) in which the C–O bond would be much weakened and lengthened and thus susceptible to ready cleavage.

Although C–O bond scission has long been considered a potential step in Fischer–Tropsch type reactions and many examples of C–O bond lengthening are known, the mechanism of C–O bond cleavages in acyl and related compounds such as (4)[5] is obscure.

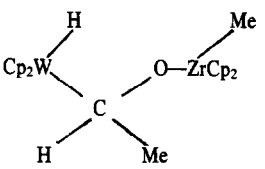

(4)

The present work provides direct evidence for such a C–O scission in an electrophilic attack to give alkylidyne and alcoxo

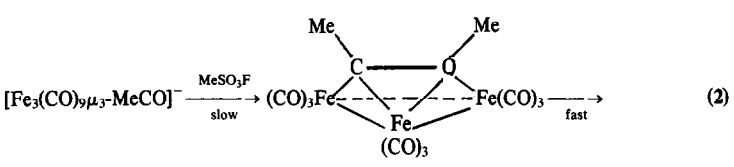

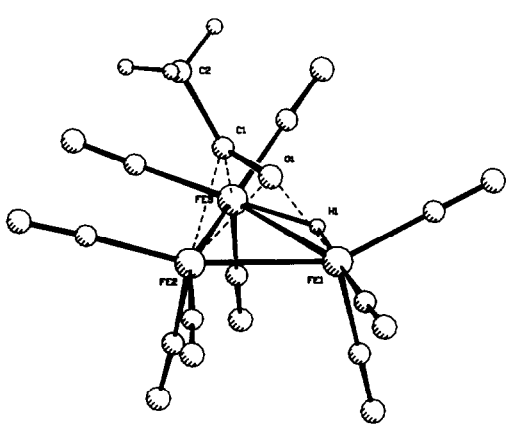

Fig. 1. The structure of the bridged hydrido acyl compound. Important bond lengths (Å) are: Fe(1)–Fe(2)

Fe(1)–Fe(2)	2.485(1),	Fe(1)–Fe(3)	2.737(1),
Fe(2)–Fe(3)	2.578(1),	Fe(1)–H(1)	1.68(5),
Fe(3)–H(1)	1.51(5),	Fe(1)–O(1),	1.958(4),
Fe(2) O(1)	2.003(4),	Fe(2)–C(1)	2.073(5),
Fe(3)–C(1)	1.910(4),	C(1)–O(1)	1.33(1),

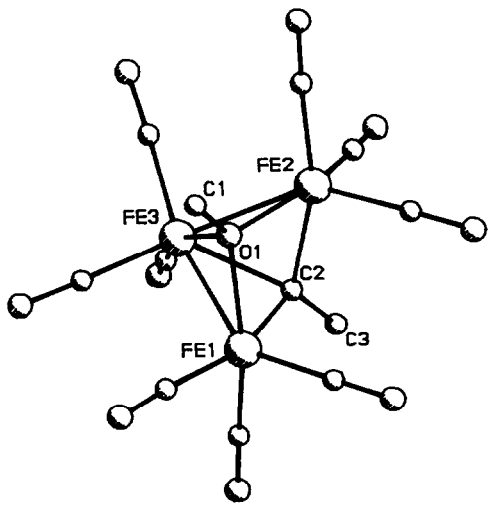

Fig. 2. The structure of the alcoxo alkylidyne compound. Important lengths (Å) are:

Fe(1)–Fe(2)	3.059(1),	Fe(1)–Fe(3)	2.472(1),
Fe(2)–Fe(3)	2.459(1),	C(2)–Fe(1)	1.937(3),
C(2)–Fe(2)	1.942(3),	C(2)–Fe(3)	2.063(3),
C(2)–C(3)	1.509(4),	O(1)–Fe(1)	1.984(2),
O(1)–Fe(2)	1.989(4),	O(1)–Fe(3)	1.941(2),
O(1)–C(1)	1.435(4),		

groups; it also provides support for the proposal of the intermediacy of surface bound alkylidynes.[6]

Electrophilic attacks on other acyl compounds are under study.

Acknowledgement—We thank the S.E.R.C. for support.

Chemistry Department
Imperial College
London, SW7 2AY
England
WAI-KWOK WONG
GEOFFREY WILKINSON*

Chemistry Department
Queen Mary College
Mile End Road
London, E1 4NS
England
ANITA M. R. GALAS
MARK A. THORNTON-PETT
MICHAEL B. HURSTHOUSE*

REFERENCES

[1]W. K. Wong, G. Wilkinson, A. M. R. Galas, M. B. Hursthouse and M. A. Thornton-Pett, *J. Chem. Soc., Dalton Trans.* 1981, 2496.

[2]*Crystal Data.* Compound **1**, $C_{11}H_4O_{10}Fe_3$, M = 463.69, triclinic, $a = 7.884(1)$, $b = 8.257(1)$, $c = 12.941(2)$Å, $\alpha = 96.03(2)$, $\beta = 99.46(2)$, $\gamma = 106.85(2)°$, space group $P\bar{1}$, $Z = 2$, $D_c = 1.96\ g\ cm^{-3}$, $\mu(Mo\text{-}K\alpha) = 27.84\ cm^{-1}$, F(000) = 456.

Compound **2**. $C_{12}H_6O_{10}Fe_3$, M = 477.72, triclinic, $a = 7.659(4)$ $b = 9.051(1)$, $c = 13.142(1)$Å, $\alpha = 98.77(2)$, $\beta = 100.03(2)$, $\gamma = 108.86(2)°$, space group $P\bar{1}$, $Z = 2$, $D_c = 1.87\ g\ cm^{-3}$, $\mu(Mo\text{-}K\alpha) = 27.10\ cm^{-1}$, $F(000) = 464$.

Intensity data for both compounds were recorded on an automatic diffractometer using Mo-$K\alpha$ radiation, the structures solved by direct methods and refined by least squares. For compound **1**, R is 0.029 for 2250 observed [$I > 1.5\sigma(I)$] data out of 3065 recorded, and for compound **2**, R is 0.038 for 2582/2973 data.

Full lists of atomic parameters and bond lengths and angles have been deposited as supplementary data with the Editor, from whom copies are available. Atomic coordinates have also been deposited with the Cambridge Crystallographic Data Base.

[3]K. Wade in *Transition Metal Clusters*, (Edited by B. F. G. Johnson) Chap. 3. Wiley, New York (1980).

[4]C. Masters, *Adv. Organomet. Chem.* 1979, **17**, 80; Ch. K. Rofer-Depoorter, *Chem. Rev.* 1981, **81**, 447; K. G. Caulton, *J. Mol. Catal.* 1981, **13**, 71; W. A. Herrmann, *Angew. Chem. Int. Ed., Engl.* 1982, **21**, 117.

[5]J. A. Marsella, K. Folting, J. C. Huffman and K. G. Caulton, *J. Am. Chem. Soc.* 1981, **103**, 5596.

[6]M. A. Beno, J. M. Williams, M. Tachikawa and E. L. Muetterties, *J. Am. Chem. Soc.* 1981, **103**, 1485; J. E. Demuth and H. Ibach, *Surf. Sci.* 1978, **78**, *L*238.

*Authors to whom correspondence should be addressed.

Polyhedron Vol. 1, No. 11-12, p. 845, 1982. Pergamon Press Ltd. Printed in Great Britain.

BOOK REVIEW

Gmelin Handbook of Inorganic Chemistry. 8th Edn. *Sn–Organotin Compounds. Part 9. Triorganotin–sulphur Compounds.* Published by the Gmelin Institute for Inorganic Chemistry of the Max Planck Society for the Advancement of Science. Springer-Verlag. Berlin-Heidelberg-New York. 1982. xii + 276 pp. DM 727. US approx. $323.

Inorganic and organometallic chemists will be familiar with the general format of the Gmelin volumes, but the text is now wholly in English, and the type-face is larger.

Until 1960, only about 1000 papers had been published on organotin chemistry, but about 1500 are now published annually, and the compounds are finding increasing application in technology and agriculture. The problem of keeping abreast of this rapidly expanding field is mitigated by Herbert and Ingeborg Schumann's steady output of the Gmelin volumes on tin. Beginning in 1975, the tetraalkyltin compounds were covered in Parts 1–3, the alkyltin hydrides in Part 4, and the alkyltin halides and pseudohalides in Parts 5–8.

The present volume (Part 9) deals with mononuclear triorganotin sulphur compounds, that is particularly the derivatives of thiols and thiocarboxylic acids; compounds containing more than one tin atom, such as the bistrialkyltin sulphides and the oligomeric dialkyltin sulphides are not included. The literature is covered up to the end of 1980.

The book begins with 4 pages of references to the general literature on organometallic chemistry, particularly organotin chemistry, published in 1979 and 1980, bringing up to date the list in Part 8. This is followed by 19 pages of general references to reviews, research papers, and patents, in chronological order from the middle 1960's on organotin–sulphur compounds.

Data on the individual trialkyltin–sulphur compounds then constitute the bulk of the value. The information listed for each compound covers, in order, the synthetic methods, the structure, spectroscopic data, physical properties, chemical reactions, biological activity, applications, and, finally, references. Related information (e.g. the reactions of Me_3SnSMe, or the compounds Ph_3SnSR, where R is heterocyclic), are often collected into tables.

The style is less telegraphic than that in Beilstein. If an X-ray diffraction study has been carried out, the structure of the molecule is illustrated, and the bond lengths and angles are all listed. Similarly, NMR, IR, Raman, m.s. and Mössbauer data are given in detail. The final 44 pages carry a formula index of the compounds in the book.

I could not find any significant error or omission in the references, or indeed in the English. Anyone working in the organotin field who can obtain access to this series will be grateful to the service which the Schumanns are doing for the subject.

A. G. DAVIES